TAYLOR ENGINEERING, INC.

Flood Protection Level of Service Provided by Existing Infrastructure for Current and Future Sea Level Conditions in the C8 and C9 Watersheds Draft Final Comprehensive Report

Deliverable 5.2

CONTRACT 4600004085

Work Order 03

South Florida Water Management District
3301 Gun Club Road
West Palm Beach, Florida 33406

Submitted 1/19/2021

14499 N. Dale Mabry Hwy, Suite 290,
Tampa, Florida 33618
813-963-6469 | www.taylorengineering.com

Flood Protection Level of Service Provided by
Existing Infrastructure for Current and Future Sea Level Conditions in the C8 and C9 Watersheds

Final Comprehensive Report
Deliverables 5.2
CONTRACT 4600004085
Work Order 03

Prepared for the

South Florida Water Management District

by

Taylor Engineering, Inc.
14499 N. Dale Mabry Hwy, Suite 290
Tampa, FL 33618
(904) 731-7040

January 2021

C2020-025

Michael DelCharco, P.E. FL 57423

Table of Contents

List of Figures

List of Tables

List of Appendix Figures

List of Appendix Tables

EXECUTIVE SUMMARY

Introduction

The South Florida Water Management District (SFWMD) is conducting a system-wide review of its regional water management infrastructure to determine the flood protection level of service (FPLOS) currently provided by existing infrastructure. The FPLOS describes the level of protection provided by the water management facilities within a watershed under both current and future conditions, where future conditions FPLOS considers sea level rise (SLR) and future development. This information can be used by local governments, SFWMD, and other state and federal agencies to identify areas where improvements or upgrades of water management facilities are required, the appropriate entity or entities responsible for making improvements, and funding and technical resources available to support these efforts.

Taylor Engineering developed an integrated groundwater and surface water model of the C-8 and C-9 watersheds, using MIKE SHE and MIKE HYDRO, to determine the flood protection level of service provided by existing infrastructure under current and future sea level conditions for the 72-hour design storm events of 5, 10, 25, and 100-year recurrence frequency. The flood protection level of service was determined through six performance metrics that are derived from the outputs of the watershed-scale flood event modeling. These performance metrics include analysis of canal bank exceedance, maximum discharge capacity through the canals, the effects of sea level rise on the effective capacity of tidal structures, the effects of sea level rise on the maximum conveyance capacity of a watershed at the tidal structures, depth of flooding, and duration of flooding. Together, these performance metrics highlight deficiencies of the system and assign a flood protection level of service rating.

This final comprehensive report describes the development and application of the 2019 SFWMD C8 C9 FPLOS Model, which is a physically-based integrated hydrologic / hydraulic model that includes a thorough representation of the hydrologic system and drainage network within the C8 and C9 Basins in northern Miami-Dade County and southern Broward County. This report combines relevant information from previous deliverables, including data collection and assimilation, model calibration and validation, and design storm model set-up and parameterization, with the results of the FPLOS study by existing infrastructure under current and future sea level conditions. This report summarizes each deliverable to provide background information without obscuring the report with excessive information. These interim documents are provided separately, as appendices.

Model Setup and Calibration

Taylor Engineering developed the 2019 SFWMD C8 C9 FPLOS Model using the latest available data, such as the 2019 Broward County Model, professional surveys (2019), Miami-Dade County GIS databases, and SFWMD XP SWMM models. Applying MIKE HYDRO, Taylor Engineering developed a thorough and accurate representation of the canal conveyance network in a 1D model of the primary canal system with many secondary/tertiary systems included. The MIKE HYDRO model includes approximately 100 canals, 300 culverts, 50 bridges, 10 pumps, and 10 gated structures. Applying MIKE SHE, Taylor Engineering developed a detailed 2D overland flow model and 3D groundwater model. Significant areas of development in the 2D overland flow model include incorporating the latest available topographic, land use, and rainfall data, applying a fine computational grid (250 ft) in conjunction with the multi-cell overland feature (125 ft), and applying a simplified representation of stormwater management practices required by permit. The 3D groundwater model applies the top 3 layers of the 5-layer groundwater model from the 2019 Broward County Model.

This study calibrated the 2019 SFWMD C8 C9 FPLOS Model to Subtropical Depression Leslie (October 2-4, 2000). Ultimately, rainfall data from 5 local gauges were used in model calibration with total rainfall depths from 7.5 inches on the west side to 16.01 inches on the east side of the model domain. Based on NOAA Atlas 14 rainfall depths, this event could be described as less than a 5-year 3-day storm on the west side or as high as a 100-year 3-day storm on the east side. Model simulated peak surface water stages and groundwater elevations generally agreed to within 0.5 ft of the observed values, with an absolute average difference of 0.3 ft for both surface water and groundwater. Model simulated peak discharge and total discharge volume agreed to within 10% and 17% of observed values, respectively, with an absolute average difference of 6% of peak discharge and 14% of total volume.

After calibration, the study validated the 2019 SFWMD C8 C9 FPLOS Model to Hurricane Irma (September 9-11, 2017). The model validation applied NEXRAD 2km gridded rainfall data across 247 pixels with total rainfall depths varying between approximately 6 inches and 10 inches. Based on NOAA Atlas 14 rainfall depths, this event was less than a 5-year 3-day storm in some areas and about a 10-year 3-day storm in other areas. Model simulated peak surface water stages generally agreed to within 0.4 ft of the observed values, with an absolute average difference of 0.2 ft. Model simulated peak discharge and total discharge volume agreed to within 17% and 14% of observed values, respectively, with an absolute average difference of 13% peak discharge and 10% total volume. The model simulated groundwater elevations generally agreed to within 1 ft of observed values, with an absolute average difference of 0.8 ft. The calibration and validation results provide confidence in the model setup and parameterization and suggest that the model is a reliable predictor of current condition water levels and flows.

Current Conditions Design Storm Simulations

The study simulated current conditions with the 5, 10, 25, and 100-year 3-day design storms, with rainfall derived from NOAA Atlas 14 rainfall depths distributed temporally based on the normalized SFWMD 3-day distribution. Boundary conditions at the tidal structures applied storm-surge tidal stages with the peak surge coinciding with peak rainfall intensity. The study examined the six FPLOS performance metrics for the current conditions simulation results. These metrics provided a model-based assessment of the current level of flood protection provided by the C-8 and C-9 watershed's primary canal network and associated control structures. These performance metrics indicate potential level of service deficiencies by highlighting areas that failed multiple performance metrics, with emphasis placed on performance metrics #1 (bank exceedance) and #5 (overland inundation). In some cases, PM #1 bank exceedances did not manifest as significant overland inundation and therefore were considered insignificant localized FPLOS deficiencies. In other cases, flooding shown by PM #5 did not correspond to bank exceedances in PM #1, suggesting that flooding could be due to problems with secondary and tertiary drainage systems.

Under current conditions, the C-8 Canal generally provides a 10-year level of service, with some areas providing 25-year level of service or better. The C-9 Canal generally provides a 25-year level of service under current conditions, with some areas providing 100-year level of service or better. The current condition design storm results serve as a baseline for comparison with future conditions under three sea level rise scenarios.

Future Conditions Design Storm Simulations

The model simulations represented future conditions through land use changes and the addition of the C-9 Impoundment. The land use, updated to reflect projected areas of future development identified by Broward and Miami-Dade counties, included about 4,000 acres of undeveloped, agricultural, recreational, forests, disturbed, and open lands. The model projected future land use changes by changing the land use classification and the associated model parameters such as overland Manning's roughness coefficient. The MIKE HYDRO model was updated to represent the two largest areas of land use change through the addition of canals and pump stations, which represent the required on-site storage and control off-site discharge to existing permitted allowances. Additionally, Taylor Engineering explicitly modeled the C-9 Impoundment based on the latest available information and conceptually represented its interactions with the C-11 impoundment outside of the model domain. This FPLOS study assumed the C-9 Impoundment has 50% of its designed capacity available for storage, which provided approximately 3,500 ac-ft of capacity during the future condition design storm simulations.

The study simulated future conditions with the 5, 10, 25, and 100-year 3-day design storms for 1, 2, and 3 ft sea level rise (SLR), driven by the same NOAA Atlas 14 rainfall depths as current conditions, distributed temporally based on the normalized SFWMD 3-day distribution. Storm-surge tidal stages with SLR, applied at the tailwater boundary of the tidal structures, assume the peak surge coincide with peak rainfall intensity. The future conditions simulation results were evaluated using the same six performance metrics and followed the same procedure that was used to evaluate the current conditions results. Under future conditions with sea level rise, the C-8 Canal would generally provide a 5-year level of service, especially for the 2 and 3 ft sea level rise scenarios. Although the model predicts that some localized areas will provide a 25-year level of service or better, the system as a whole would likely be overwhelmed by lower intensity storms. The model predicts that many segments of the C-8 Canal will be overwhelmed for each sea level rise scenario, largely due to its low bank elevations and the reduced discharge capacity of the S-28 tidal structure. The model predicts that structure S-28 on the C-8 Canal will be overtopped during the each of the SLR scenarios, with nearly 2,300 cfs of reverse flow during the 100-year SLR3 scenario.

Under future conditions with sea level rise, the C-9 Canal would generally provide a 10-year level of service for the 1 and 2 ft SLR scenarios, and a 5-year level of service or less for the 3 ft SLR scenario. Although the model predicts that some localized areas will provide a 25-year level of service or better, the system as a whole would likely be overwhelmed by lower intensity storms. The model predicts that many segments of the C-9 Canal will be overwhelmed for each sea level rise scenario, largely due to its low bank elevations and the reduced discharge capacity of the S-29 tidal structure. The model predicts that structure S-29 on the C-9 Canal will be overtopped during the each of the SLR scenarios, with nearly 3,750 cfs of reverse flow during the 100-year SLR3 scenario. Both the S-28 and S-29 structures would experience overtopping from the high tide portion of the normal tide cycle for SLR2 and SLR3 scenarios.

1 INTRODUCTION

The South Florida Water Management District, herein referred to as SFWMD or District, is conducting a system-wide review of its regional water management infrastructure to determine the flood protection level of service (FPLOS) currently provided by existing infrastructure. The FPLOS describes the level of protection provided by the water management facilities within a watershed under both current and future conditions, where future conditions FPLOS considers sea level rise (SLR) and future development. This information can be used by local governments, SFWMD, and other state and federal agencies to identify areas where improvements or upgrades of water management facilities are required, the appropriate entity or entities responsible for making improvements, and funding and technical resources available to support these efforts.

This final comprehensive report combines the relevant information from the previous deliverables, including data collection and availability, model calibration and validation, and design storm model set-up and parameterization, with the results of the FPLOS study by existing infrastructure for the C-8 and C-9 Basins under current and future sea level conditions. The two watersheds, along with the canal network and tidal outfall structures, are depicted in **Figure 1-1.** Interim documents describing prior tasks completed as part of this study effort are available in their entirety as appendices. Each deliverable was summarized in this report to provide background information without obscuring the report with excessive information. These interim documents are provided separately as listed in the appendices.

Taylor Engineering has developed an integrated groundwater and surface water model of the C-8 and C-9 watersheds, using MIKE SHE and MIKE HYDRO, to determine the flood protection level of service provided by existing infrastructure under current and future sea level conditions for the 72-hour design storm events of 1 in 5, 10, 25, and 100-year recurrence frequency. The flood protection level of service was determined through several metrics, the majority of which are derived from the outputs of the watershed-scale flood event modeling. The flood protection metrics are defined in **Section 7**.

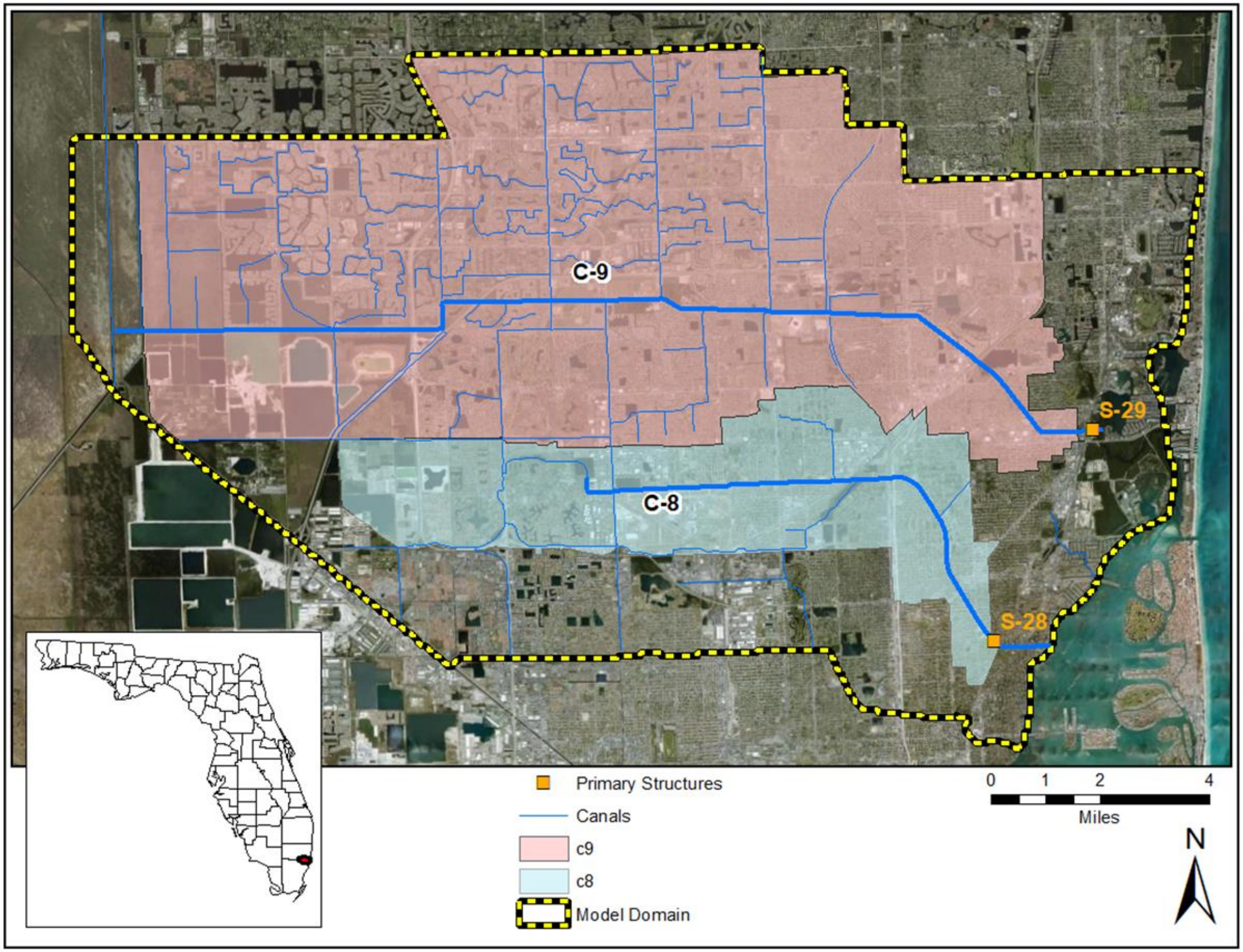

Figure 1-1: C-8 and C-9 Watersheds, Canal Network, and Primary Structures

2 DATA COLLECTION AND ASSIMILATION

This chapter details the data used to develop the SFWMD C-8 & C-9 MIKE SHE and MIKE HYDRO models for use in the C8-C9 FPLOS Study. Specifically, this section details the availability of topography, land use, culvert, gate, bridge, pump, and cross section data, survey requirements, calibration and validation simulation periods, the availability of groundwater data, the availability of district stage, flow, and gate operations, design storm rainfall, and initial groundwater levels for design storms.

2.1 Topography

Taylor Engineering made the topography for this project by merging the Miami-Dade County 5ft DEM (2015 Miami-Dade County DEM 5ft, 2017) with the 5-ft composite DEM of Broward County created by Geosyntec Consultants (2018). The portion of the composite DEM used was developed using the following sources:

- Broward County DEM – 2007 – 5' cell size source – base source
- SFWMD 50' cell size source – west area extension

To minimize/eliminate seams in the overland flow module, the DEMs were merged along the C-9 canal and through the levees in the water conservation area to the west, as shown in **Figure 2.1-1.** In **Figure 2.1-1**, the DEM was filtered between 0-25 ft NAVD88 for visual clarity (200+ ft elevation landfill causes color palette distortion).

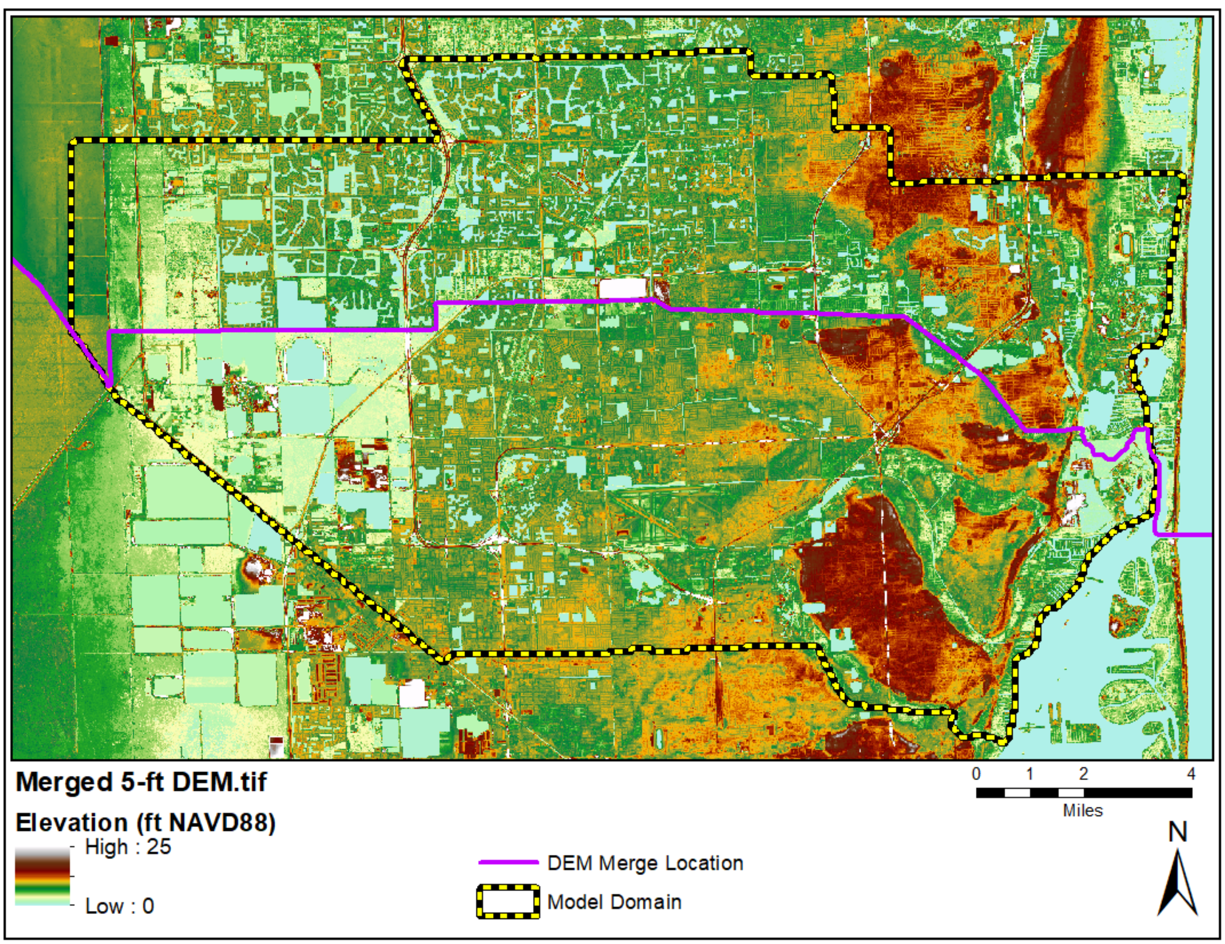

Figure 2.1-1: Merged 5-ft DEM

2.2 Land Use

The land use data for this project is based on the SFWMD 2014-2016 Land Use dataset (SFWMD LCLU, 2017). Preliminary comparisons with aerial imagery from 1999 to 2019 showed little to no significant changes in land use, such as segments of open land being developed into high density residential areas. Land use change resulting in areas such as commercial and services to high density residential were not considered a significant change in terms of the runoff potential. To confirm this observation, a spatial comparison was made in GIS using the SFWMD 1999 and the 2014-2016 land use shapefiles. Less than 2% of the total model area was identified as having a significant land use change during this period of time. Because these land use changes have occurred after the Broward County stormwater ordinance of the 1980s, there should be no impact to the flood protection level of service. The relatively unchanged land use over the past 20 years or so was an important consideration in evaluating potential historical storm events for calibration and validation, as discussed in **Section 2.4**.

2.3 MIKE HYDRO River 1D Model

The MIKE HYDRO 1D model was developed from several sources with emphasis placed on gates, pumps, culverts, bridges, and cross sections. The available data came from the following sources:

- Broward County: Updated 2019 MIKE SHE & MIKE HYDRO models, Ref: Current Conditions Model Update and Validation Draft Report (Taylor Engineering, 2019), & 5-ft DEM
- Stoner & Associates Inc: 2019 Survey (completed for Broward County Future Floodplain Modeling and Mapping project)
- South Broward Drainage District: GIS database & 2013 Facilities Report and Water Control Plan
- SFWMD: Structure Books (OCC, 2018) (S28, 2019) (S29, 2019) (MD North Central Basin Atlas v3, 2016) for operable structure dimensions, elevations, and operating criteria. DBHYDRO for water levels, discharges, and structure operations.
- Miami-Dade County: C-8 and C-9 XP SWMM Models, 5-ft DEM, & GIS Database:
  - Pipes: https://gis-mdc.opendata.arcgis.com/datasets/stormwater-line
  - Points (canal cross sections, structures, etc.): https://gis-mdc.opendata.arcgis.com/datasets/stormwater-point
  - Water bodies: https://gis-mdc.opendata.arcgis.com/datasets/water-p

Upon initial investigation, Taylor Engineering noticed that there were some 1D model components such as culverts and cross sections that had available data from multiple sources. In instances where this occurred and the details differed (such as different culvert diameters), the data was used in the following order of priority: (1) survey, (2) Broward County 2019 MIKE HYDRO model, (3) reports & documentation, (4) GIS databases, and (5) Miami-Dade C8 and C-9 XP SWMM models. The order of priority was determined based on the freshness of the data and Taylor Engineering's confidence/exposure with the data/sources. Survey had the highest level of confidence as it was recently completed or was to be completed in the near future and should capture any changes to infrastructure that may not have yet been included other data sets. The 2019 Broward County MIKE HYDRO model had the second highest level of confidence as the data that went into it was analyzed and refined over the last several months leading up to this project, and Taylor Engineering is very familiar with the areas that have up-to-date data and the areas that are questionable. Reports and documentation had the third highest level of confidence as they were used to build parts of the 2019 Broward County MIKE HYDRO model. The Miami-Dade GIS databases was assigned the fourth highest level of confidence as Taylor Engineering hadn't yet had the opportunity to see how well the data lines up with other confirmed sources. The Miami-Dade XP SWMM models that Taylor Engineering had access to had the lowest level of confidence as they were older versions and there were several areas that did not match what is in the Miami-Dade GIS databases. Taylor Engineering assumes that the discrepancies between the Miami-Dade GIS databases and the C-8 and C-9 XP SWMM models that we had access to were due to changes in infrastructure that had not been updated in the XP SWMM models; therefore, the GIS database had higher priority than the XP SWMM models for instances of data differences.

Figure 2.3-1 shows the location of the available 1-D model data. It should be noted that some of the data items shown are not complete; for example, culverts included in the Miami-Dade GIS databases that are missing inverts, dimensions, or both; bridges missing low chord elevations, etc. These and other data gaps were assessed and included in the survey scope of work described in **Section 2.5**.

For model calibration and validation, structure operations were based on recorded operations from DBHYDRO where available (primary structures), and operational criteria were used where recorded observations were unavailable (secondary structures). For design storms, the operational criteria for District structures come from the District's structure books. The operational criteria for Broward County and South Broward Drainage District structures come from the 2019 Broward County Current Conditions model, which has operating criteria that is both inherited from the 2014 FEMA model and verified/updated based on stakeholder data and documents (such as the SBDD Facilities Report, 2013). There were no known Miami-Dade County operated structures in the model. Structure flow rating parameters were used where applicable, which come from the various flow rating analysis reports (2011-2019) and Atlas of Flow Computation (2015) that were provided by the SFWMD.

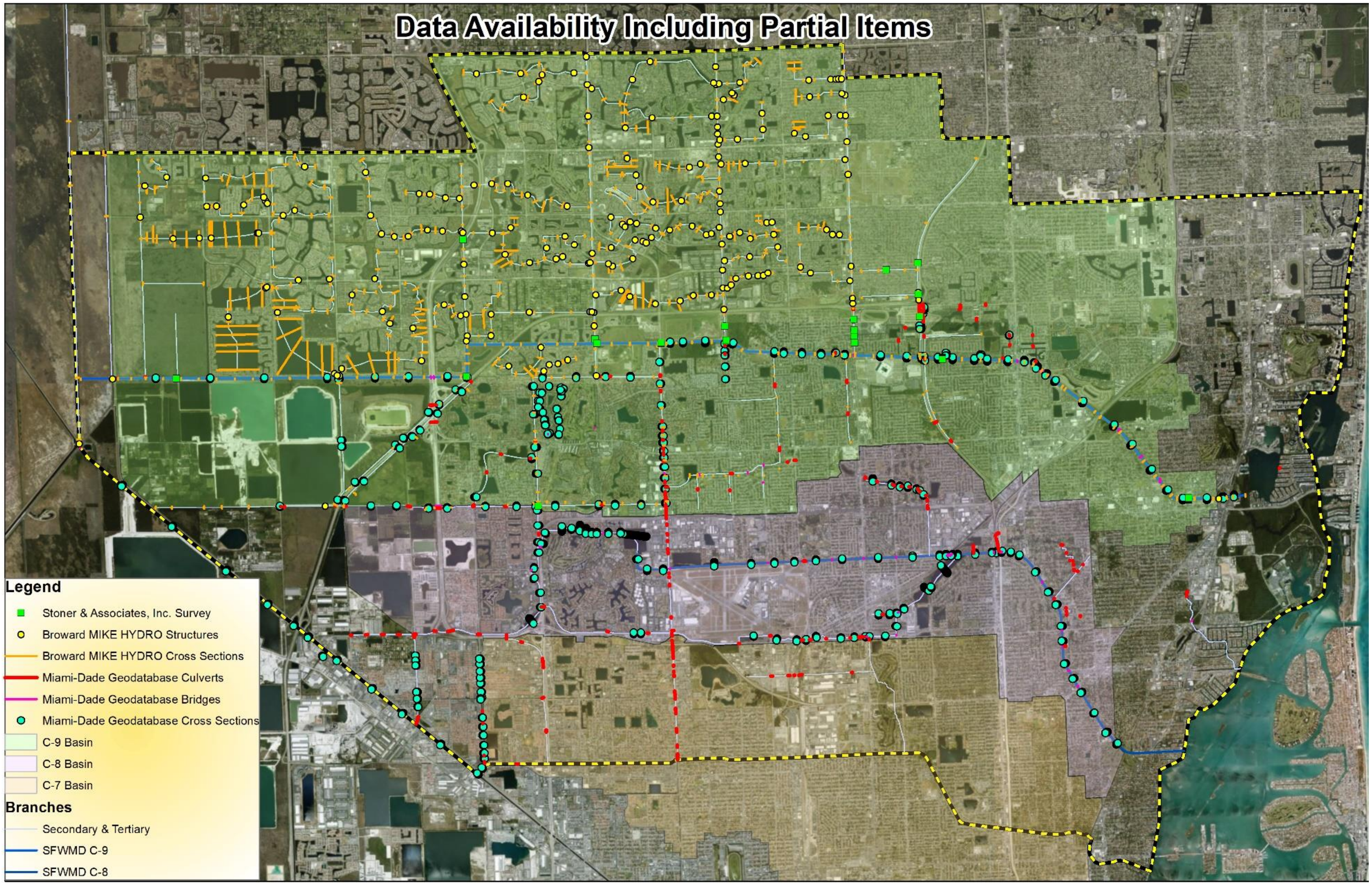

Figure 2.3-1: Map of the Available Data at the Beginning of C-8 and C-9 FPLOS Study (Originally Proposed Domain)

2.4 Field Survey

The available data was quite extensive, however, there were several areas lacking detail. **Figure 2.4-1** shows the location of the initial items identified for field survey. These items included 30 culverts, 23 cross sections, and 21 bridges. Taylor Engineering and the District tried to anticipate all the surveying needs of the project, but inevitable field variations caused changes and one culvert was omitted. Some items in the survey request had partial data available, such as culvert diameter or elevation of channel bottom under bridge but were missing information such as culvert inverts or low chord elevation of bridge.

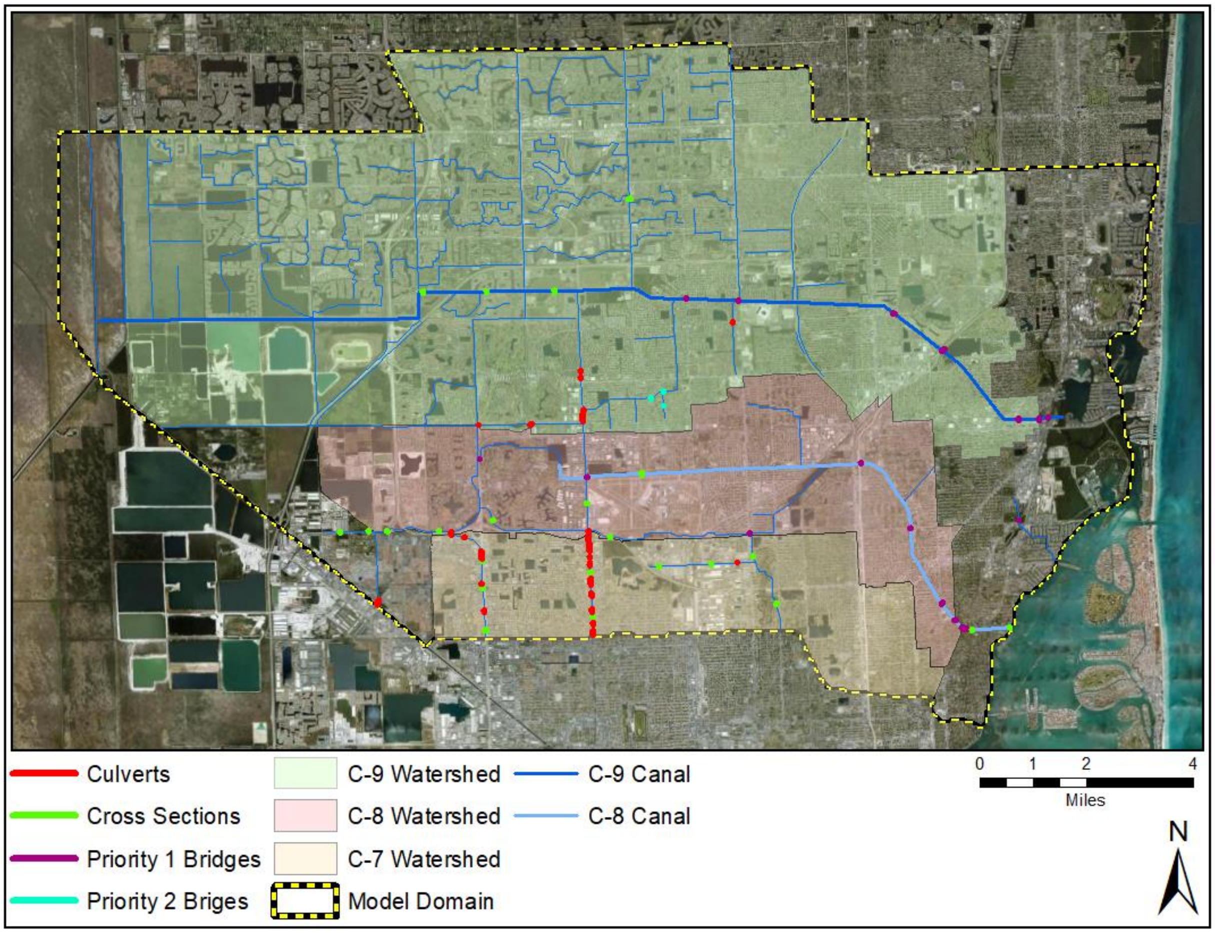

Figure 2.4-1: Inventory of Field Surveyed Items

2.5 Storm Event Selection

Average daily discharge data for the S-28 and S-29 outfall structures (C-8 and C-9 basins, respectively) were analyzed to identify the largest storm events since 1999. Then, instantaneous stage and discharge data were analyzed to identify the events that produced the largest headwater and tailwater elevation and discharge rate. Preference was given to storm events producing strong responses in both watersheds. The selection was narrowed to the storms during the following dates:

- Hurricane Irene (October 14-16, 1999)
- Subtropical Depression Leslie (October 2-4, 2000)
- Hurricane Gabrielle (September 13-15, 2001)
- Unnamed Storm (June 6-7, 2017)
- Hurricane Irma (September 9-10, 2017)

Subtropical Depression Leslie, which later became Tropical Storm Leslie, was chosen as the calibration event and Hurricane Irma as the validation event. Subtropical Depression Leslie resulted in the largest discharge response at both the C-8 and C-9 outfall structures in the past 20 years, as well as some of the highest canal water elevations. Hurricane Irma produced large discharge responses at both outfall structures and had a storm surge which resulted in the highest water elevations. **Figure 2.5-1** through **Figure 2.5-4** compare the discharge, headwater elevation, and tailwater elevation at the C-8 and C-9 outfall structures.

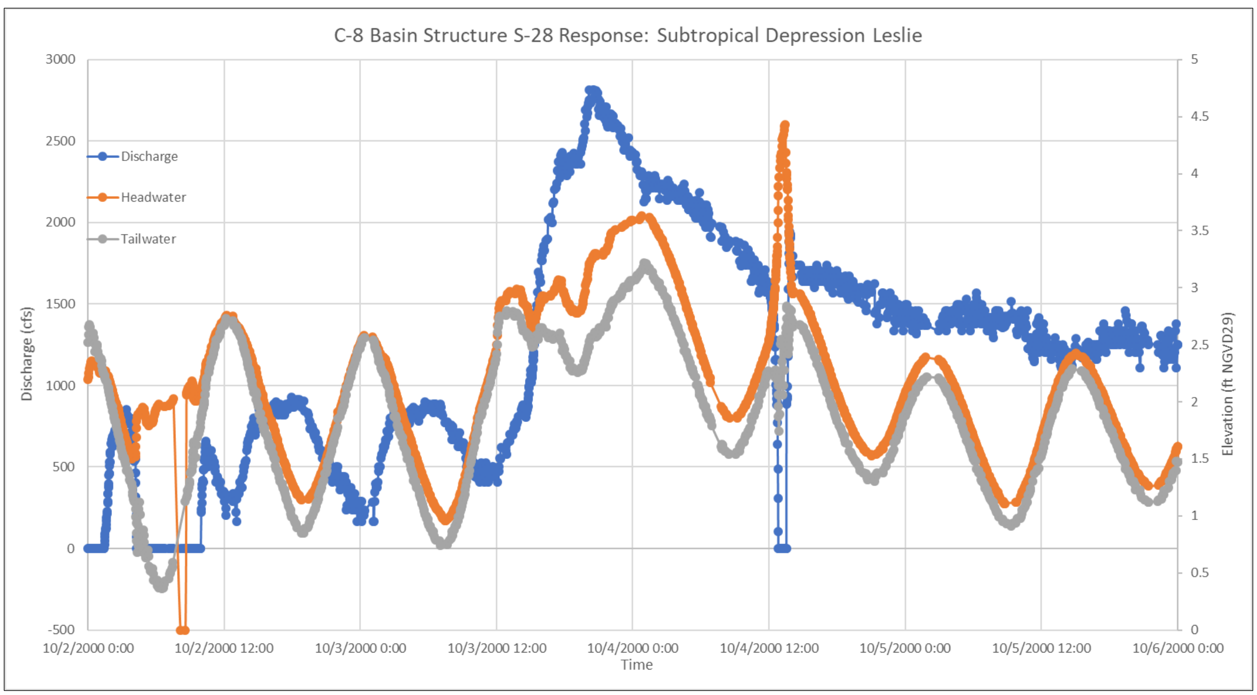

Figure 2.5-1: C-8 Basin Structure S-28 Response to Subtropical Depression Leslie

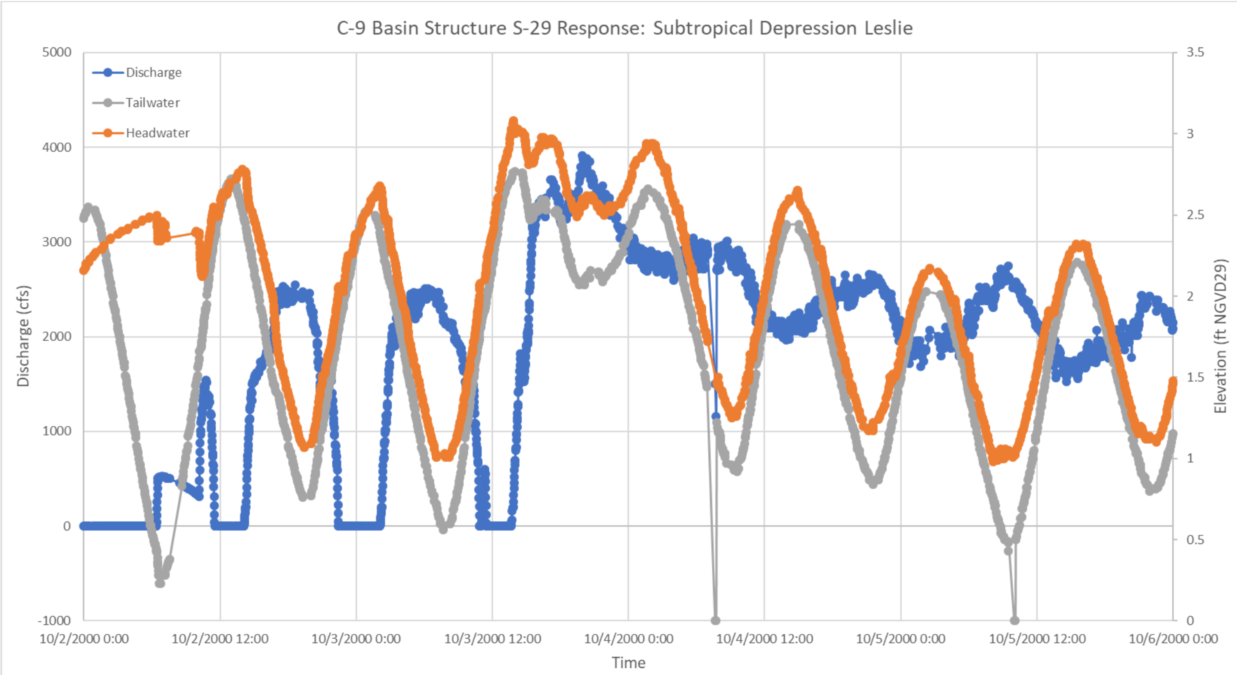

Figure 2.5-2: C-9 Basin Structure S-29 Response to Subtropical Depression Leslie

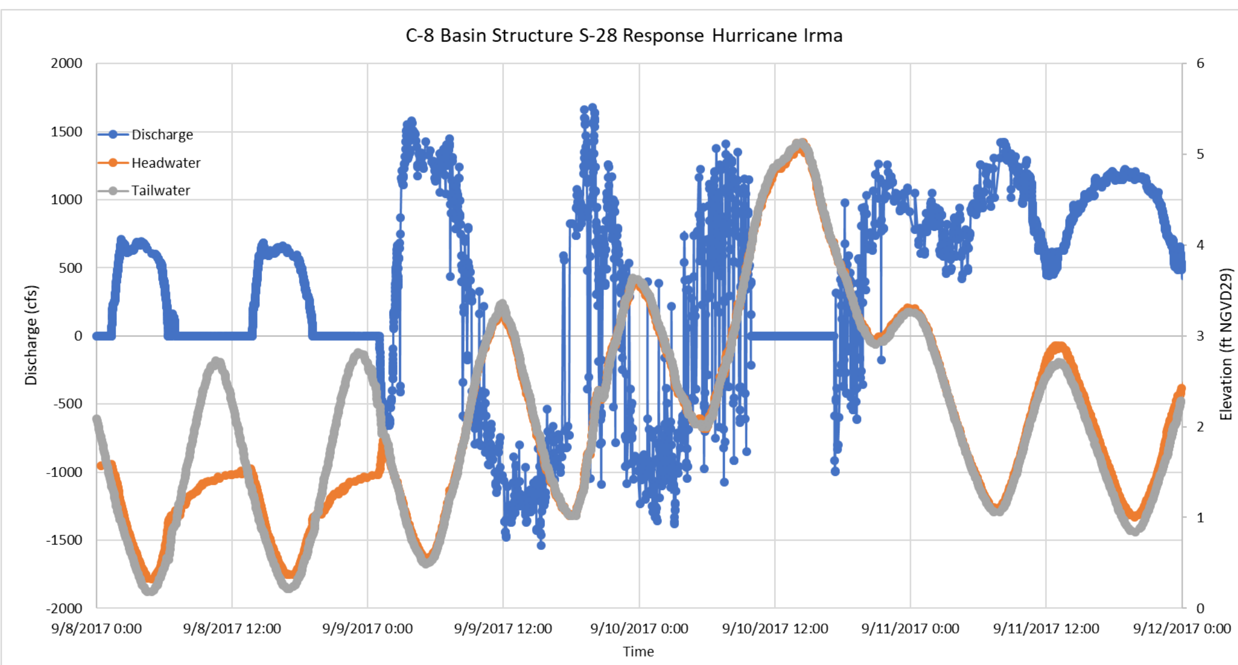

Figure 2.5-3: C-8 Basin Structure S-28 Response to Hurricane Irma

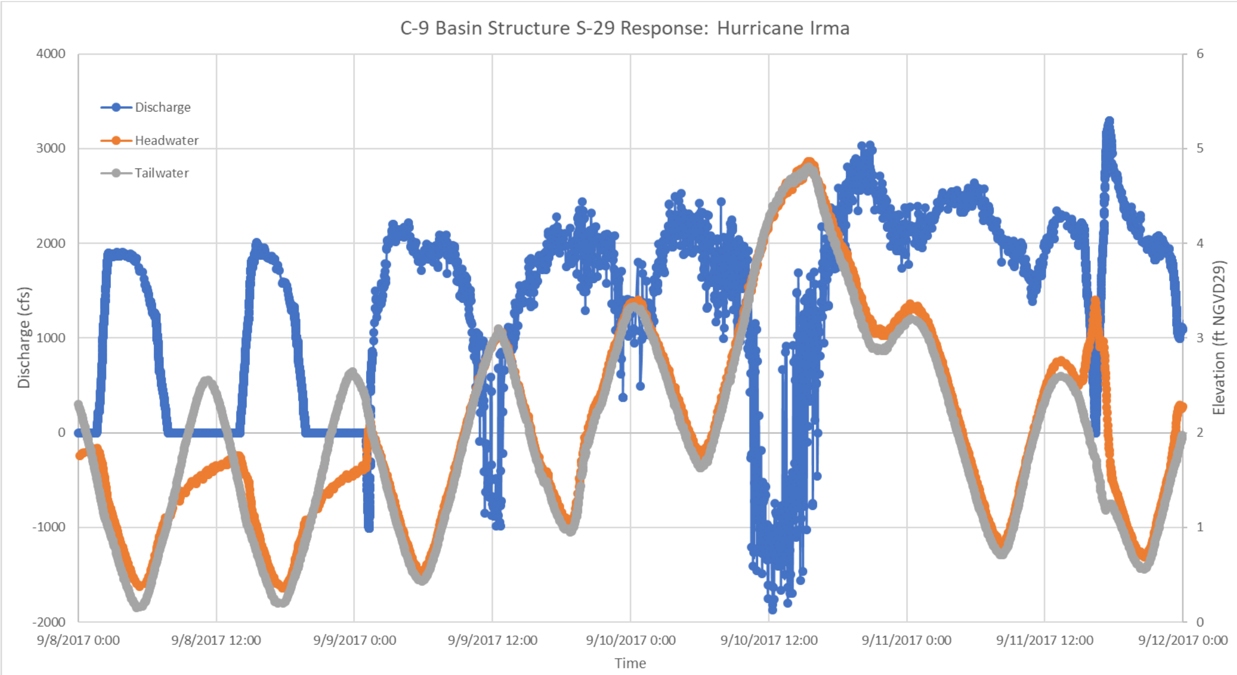

Figure 2.5-4: C-9 Basin Structure S-29 Response to Hurricane Irma

Available rainfall data for Subtropical Storm Leslie was called into question as NEXRAD data in the early 2000s was less accurate than it is today. Therefore, rain gauge data (DBHYDRO) was compared to the NEXRAD data for the pixel(s) that they were in or bordered against. This exercise suggested that the NEXRAD data and gauge data were similar in terms of total rainfall, however, there were some differences as far as the timing of the rainfall. **Figure 2.5-5** and **Figure 2.5-6** show different comparisons relating to NEXRAD rainfall, gauge rainfall, and structure discharge.

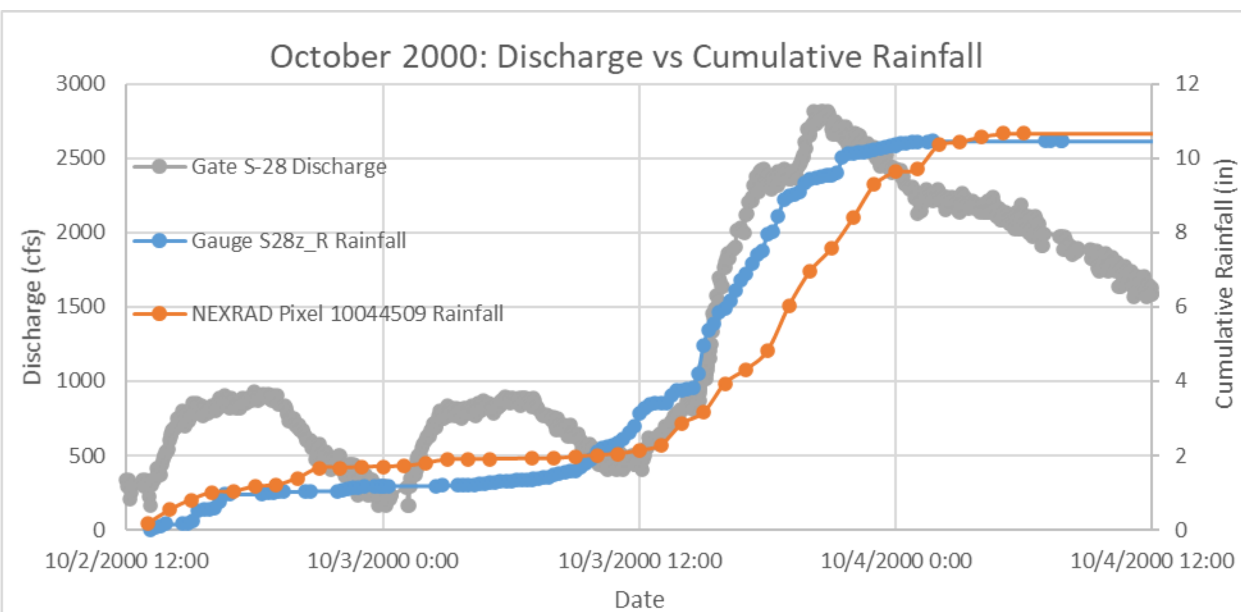

Figure 2.5-5: Discharge vs Cumulative Rainfall for Gate S-28 (NEXRAD Pixel and Rain Gauge Located Centrally in C-8 Basin)

The cumulative rainfall totals for the rain gauge and the associated NEXRAD pixel are only off by about 0.2 inches, which is about 2%. This was a negligible amount and well within the accuracy of either measurement method. More concerning was the temporal shift in the rainfall, which was about 3-hours. Based on the timing of rainfall relative to the discharge, it is believed that the rainfall gauges are more accurate. Simply put, the NEXRAD data shows a rainfall response after the runoff response, which goes against rainfall-runoff principles. **Figure 2.5-6** compares the same rainfall as **Figure 2.5-5**, but plotted as rainfall intensity.

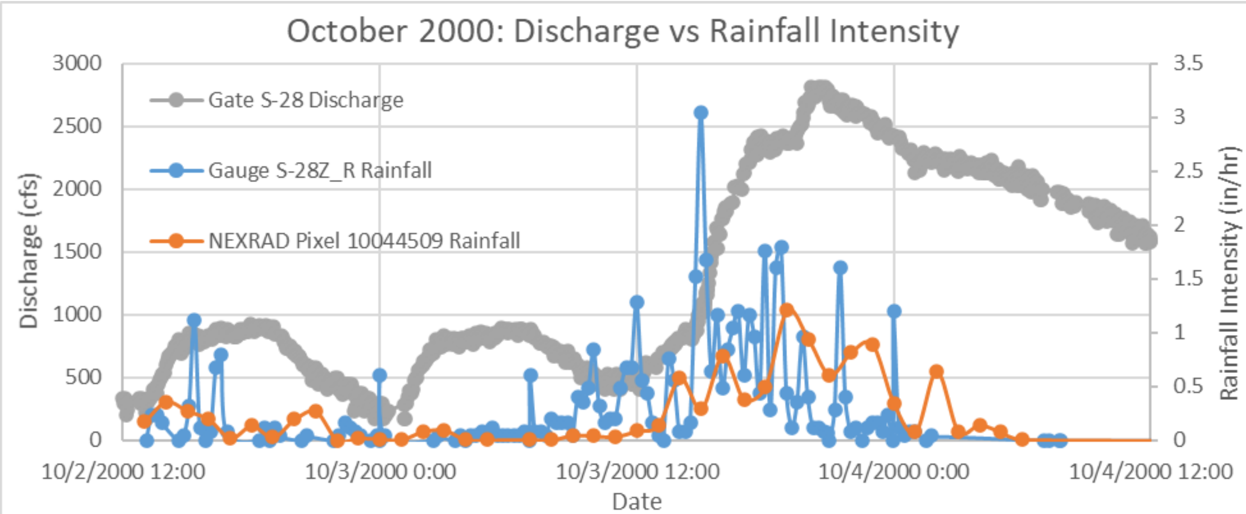

Figure 2.5-6: Discharge vs Rainfall Intensity for Gate S-28 (NEXRAD Pixel and Rain Gauge Located Centrally in C-8 Basin)

Figure 2.5-6 shows there is a large difference in rainfall intensity when comparing the rain gauge to the NEXRAD data. The rain gauge data was recorded in 15-minute intervals whereas the NEXRAD data was recorded in hourly intervals, as 15-minute NEXRAD data was not available until 2002. Therefore, the NEXRAD data was unable to capture the high intensity short duration part of the storm. It was noted that this limitation could have some effect on calibration efforts. **Figure 2.5-7** compares the rain gauge located centrally in the C-9 basin with NEXRAD data for the two pixels it borders.

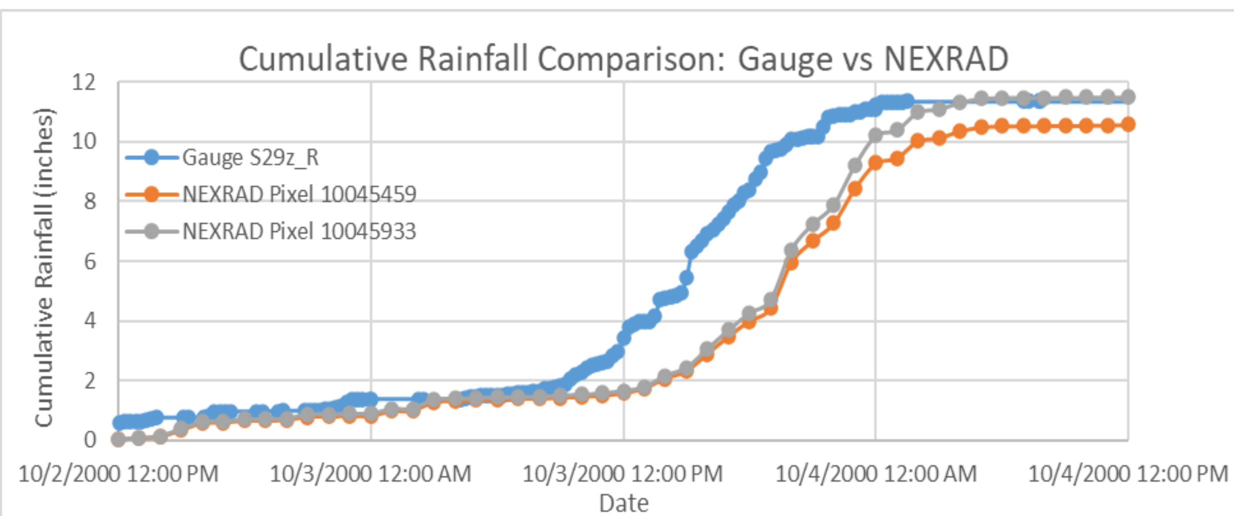

Figure 2.5-7: Cumulative Gauge Rainfall vs Cumulative NEXRAD Rainfall (NEXRAD Pixel and Rain Gauge Located Centrally in C-9 Basin)

The cumulative rainfall totals were fairly close, with NEXRAD data being between 0.2 and 0.7 inches different, or about 2-6%. Again, there was a temporal lag of about 4 hours. **Figure 2.5-8** compares the rain gauge located in the western part of the C-9 Basin with NEXRAD data.

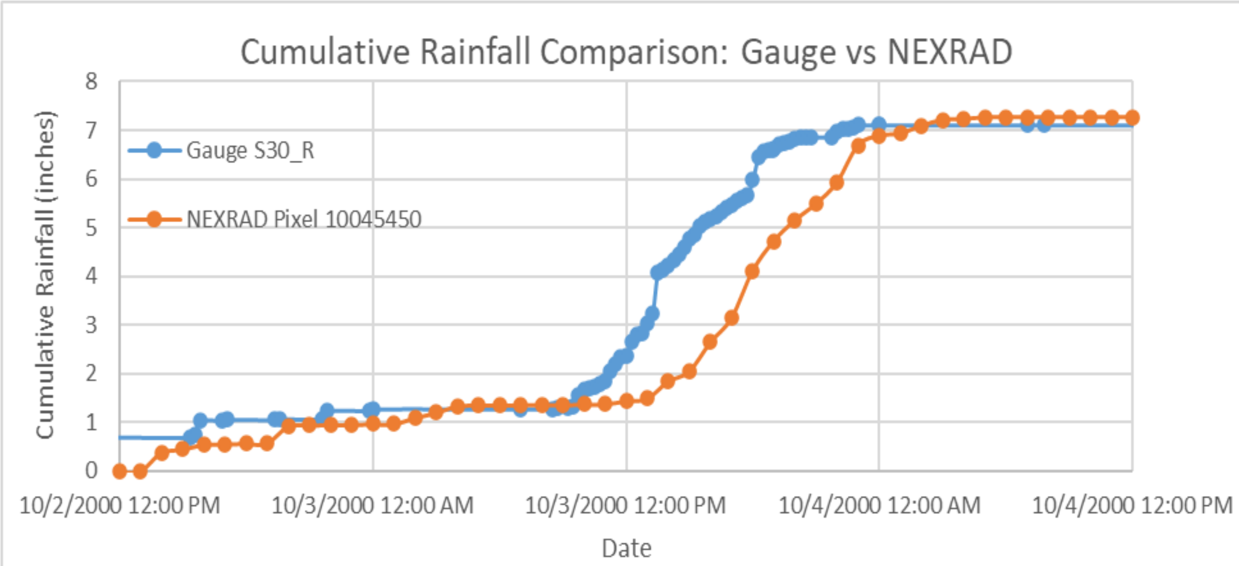

Figure 2.5-8: Cumulative Gauge Rainfall vs Cumulative NEXRAD Rainfall (NEXRAD Pixel and Rain Gauge Located in Western C-9 Basin)

The cumulative rainfall totals are within 0.2 inches apart which is about 2%. Again, there is a temporal lag of about 4 hours. **Figure 2.5-9** compares the rain gauge located at the tidal outfall of the C-7 Basin with NEXRAD data.

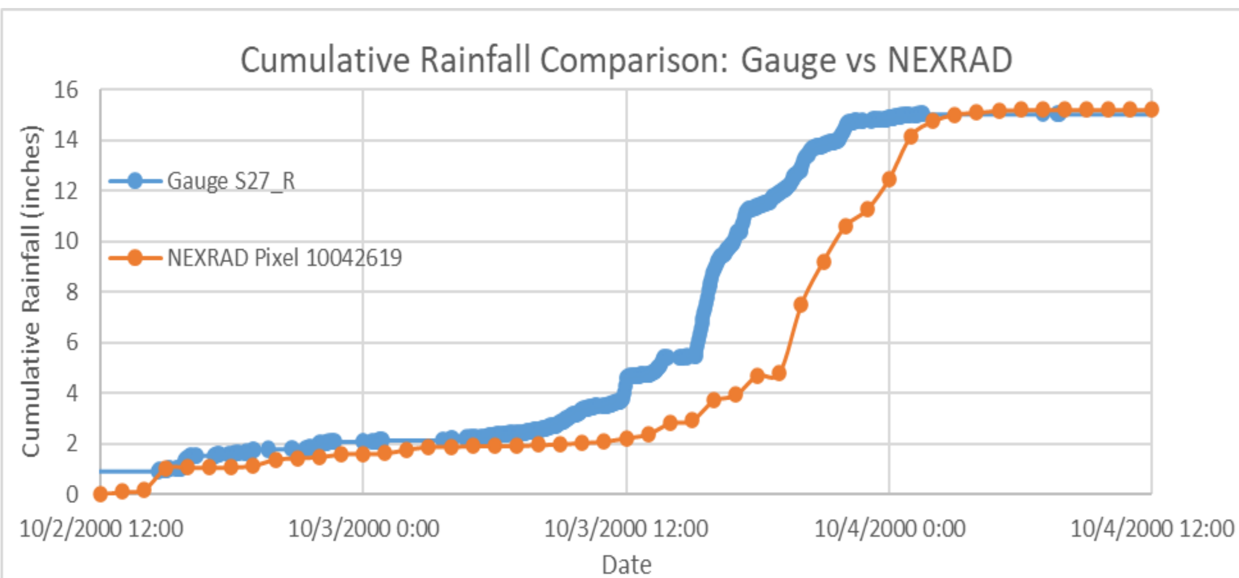

Figure 2.5-9: Cumulative Gauge Rainfall vs Cumulative NEXRAD Rainfall (NEXRAD Pixel and Rain Gauge Located at C-7 Basin Tidal Outfall)

The cumulative rainfall totals are within 0.2 inches apart which is only about 1%. Again, there is a temporal lag of about 4-5 hours.

The NEXRAD data appeared to capture the total rainfall well compared to the gauge data, however, there were some concerns with using it. As mentioned, the 1-hour interval of the NEXRAD data averages-out the highest-intensity parts of the storm. Additionally, there are some temporal differences. These two issues were further discussed before any decisions were made on whether or not to use it for the calibration event. It was originally noted that it was not advisable to use the existing rain gauges to make Thiessen polygons for calibration use as: (1) the rain gauges do not capture the significant spatial differences that were noticed in the NEXRAD data and (2) it is likely that one rain gauge was not functioning properly during the storm. **Figure 2.5-10** shows the variation of total rainfall depth in randomly selected NEXRAD pixels and the rain gauges.

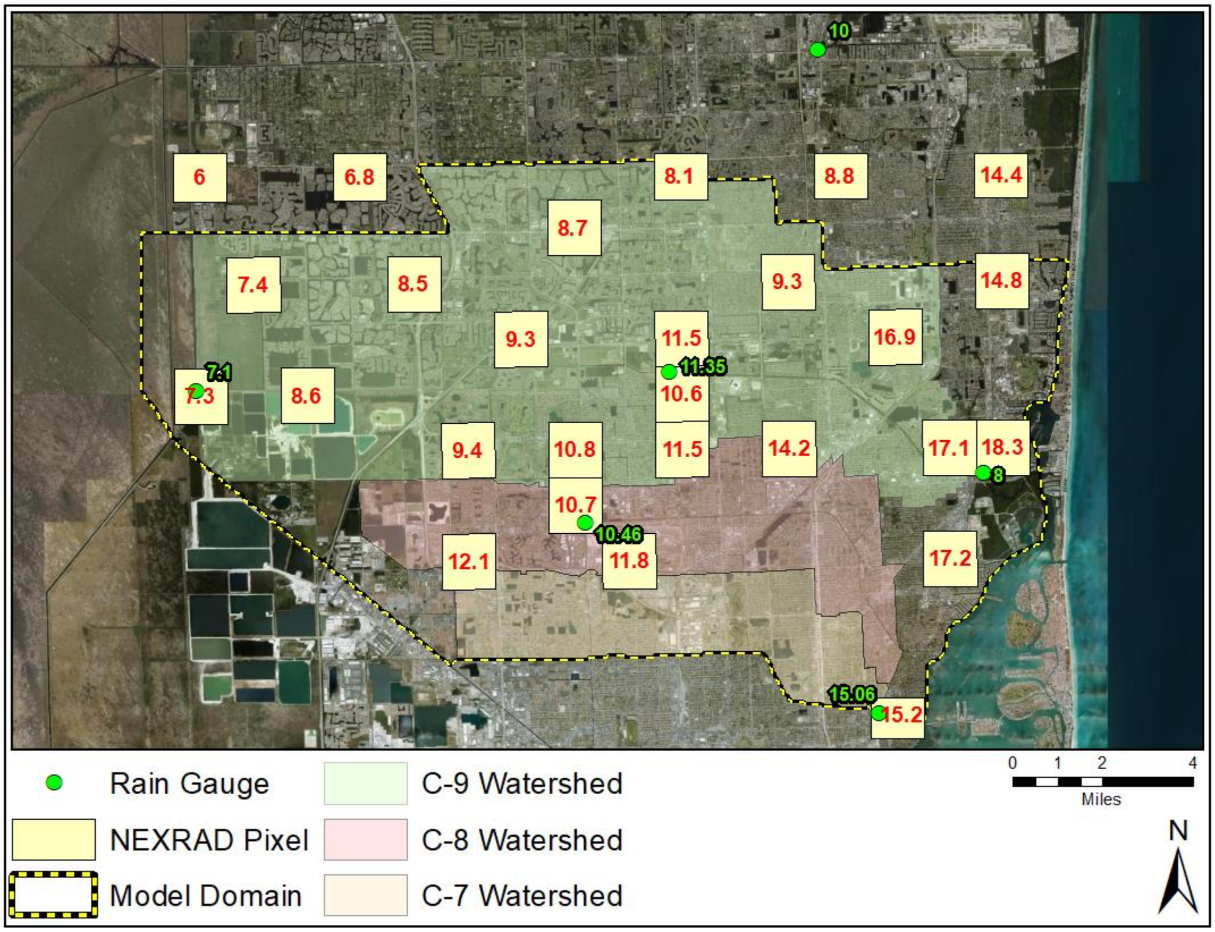

Figure 2.5-10: Randomly Selected NEXRAD Pixel and Rain Gauge Rainfall Summary

The NEXRAD rainfall data for October 2000 showed a spatial difference ranging from about 7 inches in the northwestern part of the C-9 basin to upwards of 18 inches in the southeastern part of the C-8 basin. There was some concern initially that the rain gauges alone may not adequately define the spatial distribution. It appeared that the rain gauges captured the timing of the rainfall better than NEXRAD, while NEXRAD appeared to capture the spatial variation in rainfall depths better than the rain gauges. Therefore, Taylor Engineering initially recommended using the total rainfall depths from each NEXRAD pixel and distributing it temporally based on a rain gauge that is assigned by Thiessen polygons, which would result in shifting the NEXRAD timing of the rainfall to match the rain gauges while maintaining spatial variation in rainfall totals of the NEXRAD pixels. This approach was originally attempted for model calibration but ultimately was discarded and replaced with unmodified rain gauge data. For more information regarding the NEXRAD temporal manipulation, refer to Deliverable 1.1, *Data Availability Memorandum* (Taylor Engineering, 2019). Aside from Gauge S-29_R, all rain gauges were within 0.2 inches of the NEXRAD pixel bordering it. Gauge S-29_R only recorded about 8 inches during the storm while surrounding NEXRAD pixels show between 17 and 18 inches. This indicated the gauge was malfunctioning during the storm; therefore, this gauge was not considered. **Figure 2.5-11** shows the Thiessen Polygons of the rain gauges used to distribute rainfall.

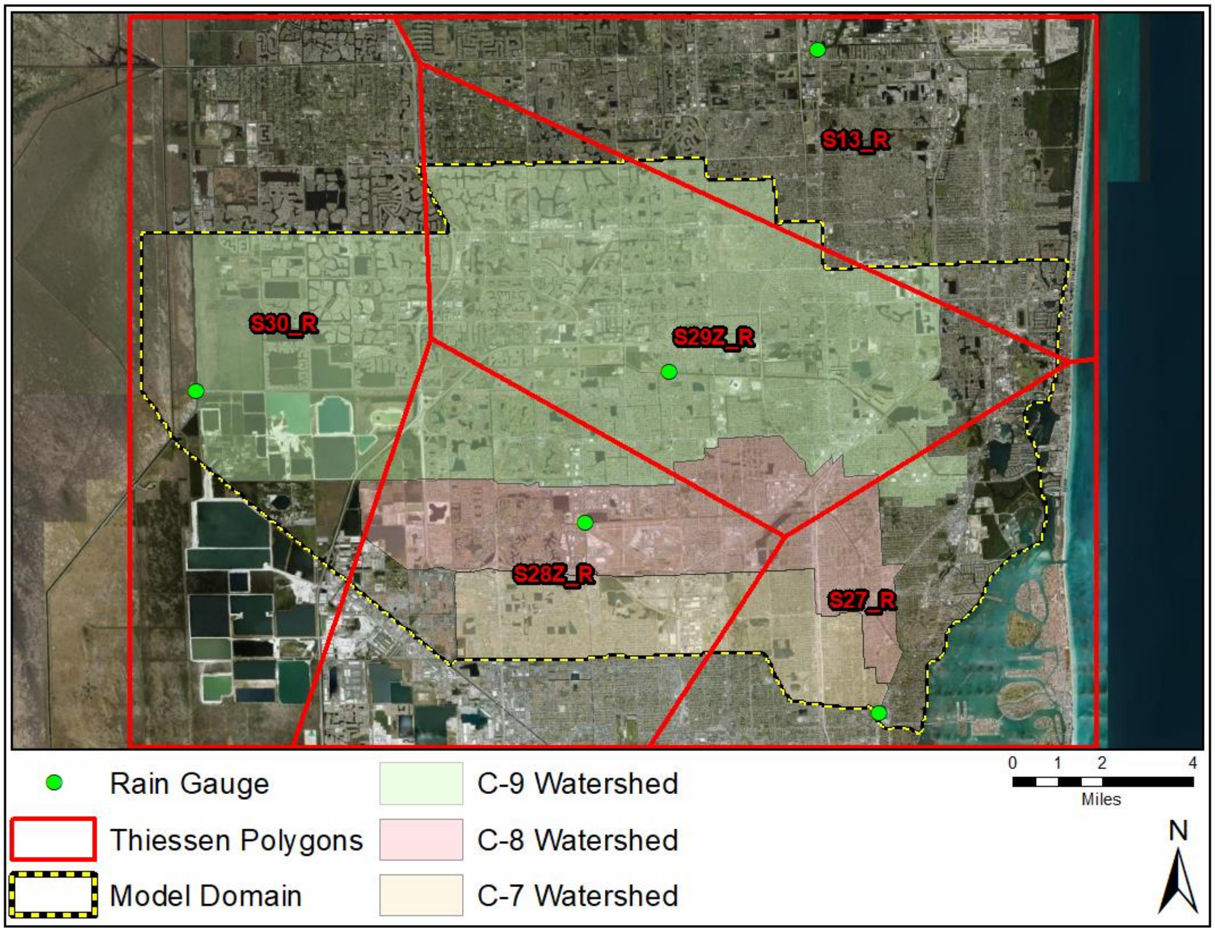

Figure 2.5-11: Thiessen Polygons of the Rainfall Gauges with Available Data during the Calibration Period

2.6 Calibration/Validation Data Availability and Collection

In addition to accurate rainfall, data needed for model calibration and validation included gate openings, breakpoint stage, and breakpoint discharge for all primary operational structures, and groundwater levels for the wells within the surficial aquifer and the model domain. When breakpoint data was unavailable, the best available data (hourly, daily max, etc.) was used. **Figure 2.6-1** shows the location of the primary structures and wells analyzed for data availability and gaps.

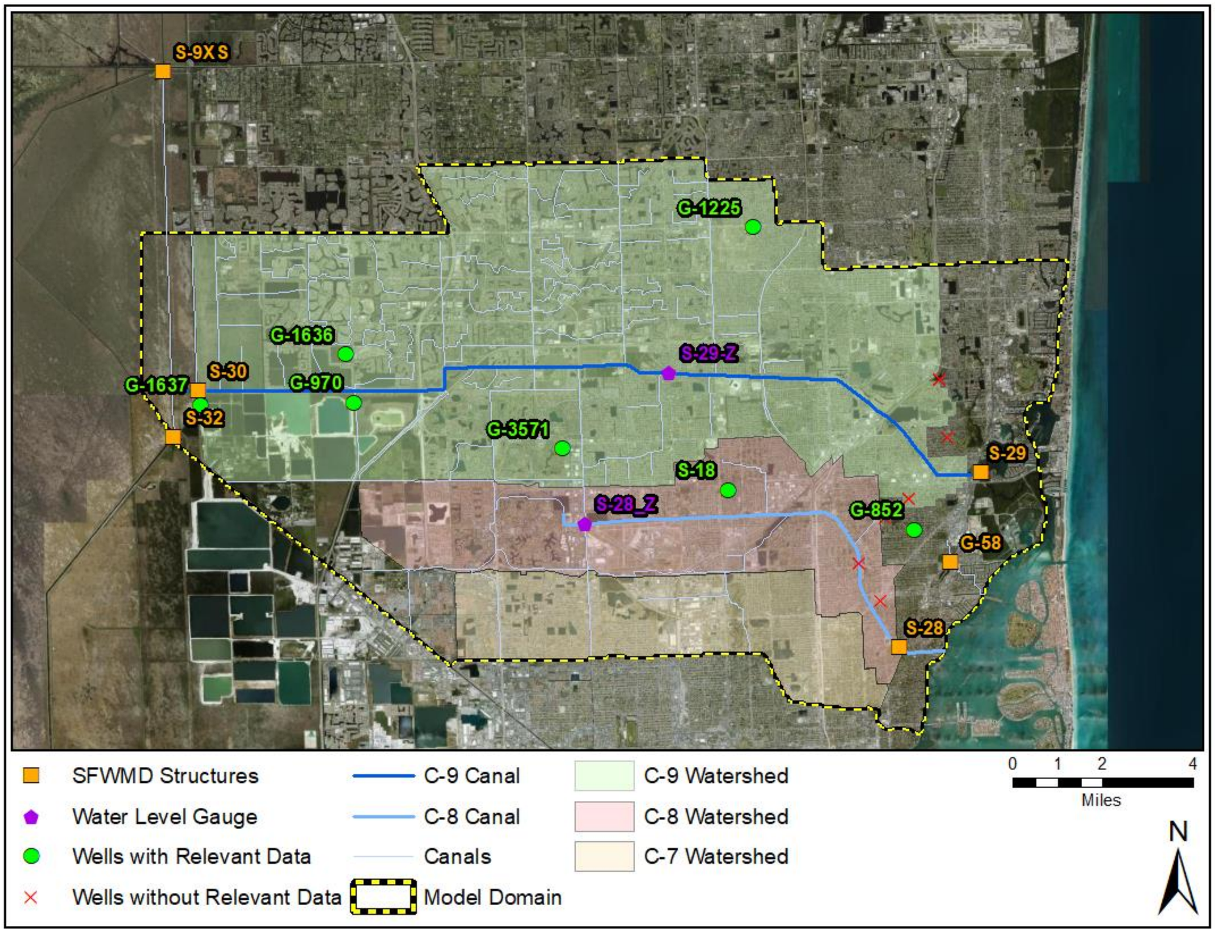

Figure 2.6-1: Calibration/Validation Locations Analyzed for Data Availability and Gaps

Stage, flow, and groundwater level data were graphed to visually analyze data for gaps and outliers. **Table 2-1** shows the completeness of data for the storm events in October 2000, June 2017, and September 2017.

Table 2-1: Structure Data Availability Summary

NAME	BASIN	CONTROL	DBKEY	DATA TYPE	STATUS
S-28	C-8	Gated	65070	Breakpoint Discharge	Complete
			6627	Breakpoint HW Stage	
			6628	Breakpoint TW Stage	
			LT203 & LS856	Breakpoint Gate Opening	
S-29	C-9	Gated	65071	Breakpoint Discharge	Complete
			6631	Breakpoint HW Stage	
			6632	Breakpoint TW Stage	
			LS491, LS857, LS858, & LS859	Breakpoint Gate Opening	
S-30	C-9	Gated	65074	Breakpoint Discharge	Complete
			6686	Breakpoint HW Stage	
			6639	Breakpoint TW Stage	
			LS493, LS862, & LS863	Breakpoint Gate Opening	
S-32	L-33 CC	Gated	65077	Breakpoint Discharge	Complete
			SP543	Breakpoint HW Stage	
			6643 & AI581	Breakpoint TW Stage	
			LS495, LS867, SP544 & SP545	Breakpoint Gate Opening	
G-58	North Biscayne Bay	Gated	64715	Breakpoint Discharge	No September 2017
			IX539	Breakpoint HW Stage	No September 2017
			N/A	Breakpoint TW Stage	Not in DBHYDRO
			LS376, LS693, LS694, & LS695	Breakpoint Gate Opening	No September 2017
S-9XS	L-33 CC	Boarded	90829	15-Minute Discharge	Complete
			SO013	15-Minute to Hourly HW Stage	Complete
			OH925 & OH924	15-minute and Breakpoint TW Stage	Complete
			LD575 & LS966	Other Board Elevation	Other

Although there were several wells within the model domain, many of them contained no useful data as it pertains to the purpose of this project because of infrequent or random interval sampling. **Table 2-2** and **Table 2-3** shows the wells that were within the model domain and the surficial aquifer system (SAS) that have concurrent data available to three of the aforementioned storm events.

Table 2-2: Wells within SAS with Complete Groundwater Level Data for October 2000

WELL NAME	BASIN	DBKEY	DATA TYPE
G-1225	C-9	1758	Daily Max
G-1636	C-9	1716	Daily Max
G-1637	C-9	1698	Daily Max
G-3571	C-9	LP668	Daily Max
G-852	North Biscayne Bay	1662	Daily Max
G-970	C-9	1703	Daily Max
S-18	C-8	1673	Daily Max

Table 2-3: Wells within SAS with Complete Groundwater Level Data for June-September 2017

WELL NAME	BASIN	DBKEY	DATA TYPE
G-1225	C-9	1758	Hourly GW Level (missing data during Irma)
G-1636	C-9	1716	Hourly GW Level
G-1637	C-9	1698	Hourly GW Level (missing data during Irma)
G-3571	C-9	LP668	Hourly GW Level
G-852	North Biscayne Bay	1662	Hourly GW Level
G-970	C-9	1703	Hourly GW Level
S-18	C-8	1673	Hourly GW Level
G-1166R	C-7	88676	Hourly GW Level

2.7 Groundwater Data Availability

There were two sources of groundwater data that were available. The first source was the 2019 Broward County Current Conditions Model, and the second source was a groundwater study authored by J. D Hughes and J. T White, which was documented in a United States Geological Survey (USGS) report titled *Hydrologic Conditions in Urban Miami-Dade County, Florida, and the Effect of Groundwater Pumpage and Increased Sea Level on Canal Leakage and Regional Groundwater Flow* (2016). The majority of the 2019 Broward County model's groundwater data was inherited from previous versions of the model, which has been around since the early 2000s. The earlier versions of this model were intended for long-term water supply simulations, so the 5-layer groundwater model has been parameterized and calibrated over the years and is assumed to be a good representation of the aquifer system. The groundwater model by Hughes and White is several years newer and used a different modeling approach, in which they discretized the groundwater model into 3 layers: an upper and lower permeable layer separated by a layer about 100 times less permeable. A significant amount of data from this study was available, including but not limited to year 2000 wet season heads, horizontal hydraulic conductivity, transmissivity, specific storage, specific yield, aquifer thickness, and bottom of aquifer layer elevations. Some of this data was available as figures with contours while others were raster data. Taylor Engineering reached out to Hughes and received the data needed to create shapefiles of the data in the USGS report.

As the groundwater study by Hughes and White (2016) is several years newer, is an approved dataset, and is well documented, Taylor Engineering originally proposed to use a 3-layer groundwater model based on this study. The groundwater model was intended to include the following data from the USGS: (1) layer bottom elevations, (2) horizontal hydraulic conductivity, (3) vertical hydraulic conductivity, (4) specific yield, (5) specific storage, and (6) initial groundwater elevations based on 2000 wet season head (calibration model only). However, after initial calibration attempts, the groundwater model was reparametrized based on the 2019 Broward County Current Conditions model. This is discussed more in **Section 4.2**, and for additional detail refer to **Appendix J**.

2.8 Boundary Conditions

2.8.1 Calibration

For the October 2000 calibration event, the eastern surface and groundwater boundary conditions come from the Virginia Key tidal station. The southern boundary conditions are time-stage relationship along the C6 and C7 canal for surface water and a general head for groundwater (based on observed canal stages from DBHYDRO). Observed stage in Water Conservation Area 3B serves as the western boundary conditions with a time-stage relationship for surface water, and a general head boundary for groundwater (based on observed water level recorder data from DBHYDRO). The northern groundwater boundary was developed based on observed heads from the USGS study (Hughes and White, 2016). Tidal boundaries at the S-28 and S-29 structures are forced using observed tailwater data from DBHYDRO.

2.8.2 Validation

For the September 2017 validation event, the eastern surface and groundwater boundary conditions come from the Virginia Key tidal station. The southern boundary conditions are time-stage relationships along the C6 and C7 canal for surface water and a general head for groundwater (based on observed canal stages from DBHYDRO). Observed stage in Water Conservation Area 3B serves as the western boundary conditions with a time-stage relationship for surface water, and a general head boundary for groundwater (based on observed water level recorder data from DBHYDRO). The northern boundary was developed using simulated groundwater elevations from of the 2019 Broward County Current Conditions Validation Model, which was originally developed for the June 2017 event but was extended to run through September 2017. Tidal boundaries at the S-28 and S-29 structures are forced using observed tailwater data from DBHYDRO.

2.8.3 Design Storms

For all design storm events, the eastern surface and groundwater boundary conditions come from the District-provided tidal data with storm surge and/or sea level rise, depending on the specific scenario. The southern boundary conditions are time-stage relationships along the C6 and C7 canal for surface water and a general head for groundwater (District-provided design storm model results from XP SWMM and HEC RAS models). Observed stage in Water Conservation Area 3B serves as the western boundary conditions with a time-stage relationship for surface water, and a general head boundary for groundwater (based on observed water level recorder data from DBHYDRO). The northern boundary was developed using simulated groundwater elevations from of the 2019 Broward County Current Conditions Design Storm Models. Tidal boundaries at the S-28, S-29, and G-58 structures are forced using District-provided tidal data with storm surge and/or sea level rise, depending on the specific scenario.

2.9 Initial Conditions

2.9.1 Overland Depths

For all simulations, any grid cell within a drainage basin that are lower than the basin's water control elevation were set to an initial depth equal to the difference of the water control elevation and the elevation of the cell. Essentially, this will bring the water elevation in any "sinks" to the water control elevation. This eliminates excess "dead storage" and ensures that water is not being routed via ponded drainage or flood codes at the start of the simulation. This is a fair assumption as both the calibration and validation events occurred late in the wet season so it is expected that low areas would be wet, and design storms are intended to be conservative

2.9.2 Groundwater and Canal Stages- Calibration

The initial groundwater elevations for calibration were developed by making localized adjustments to the 2000 wet season heads from the MODFLOW model developed as part of the USGS study (Hughes and White, 2016). The initial surface water levels in the main canals were based on observed data. Initial stages in the secondary/tertiary canal systems that are controlled by structures were set based on water control elevations.

2.9.3 Groundwater and Canal Stages- Validation

The initial groundwater elevation for the validation event was created by extending the 2019 Broward County Current Conditions Model groundwater elevation map (which includes part of Miami-Dade County) south to cover the remaining area of the model extent. The 2019 Broward County model's initial groundwater map was developed from Broward County's average 1990-1999 wet season map (Broward County, 2000). Average September groundwater elevation contours from the USGS (Fish and Stewart, 1991) were used to extend the initial groundwater elevation map south to cover the remaining model domain. The groundwater elevations were compared with available well data. Early wet-season (June 2017) groundwater elevations were a close match with the average wet-season elevations from the 1990s, therefore, no adjustments to the contours were applied. The initial stages in the main canals were based on observed data. Initial stages in the secondary/tertiary canal systems that are controlled by structures were set based on water control elevations.

2.9.4 Groundwater and Canal Stages- Design Storms

2.9.4.1 <u>Groundwater Stages</u>

There were two options available for developing the initial groundwater elevations for the design storms. The first option was to simply use the same initial groundwater elevations from the validation model, which was the approach used for the 2019 Broward County Current Condition Design Storm models. This is the preferred methodology as the storm event is from recent history and there is observed data available that could be used for boundary conditions if needed. Additionally, there was generally a good match between the initial groundwater elevations map (based on typical late wet season conditions) and the observed data at well locations at the beginning of the event. This provides realistic initial groundwater elevations.

The second option, although not recommended, would be to use simulated groundwater elevations from the validation simulation. Essentially, the groundwater elevations at some point in time during the validation simulation, such as 12 hours after the peak rainfall, could be extracted and used as a new starting point for the design storms. This approach would provide higher initial groundwater elevations, which would provide a more conservative starting point for the design storm simulation. However, this approach should only be considered IF the simulated groundwater elevations during the validation simulation are a close match with observed well data, model wide.

2.9.4.2 Canal Stages

The initial surface water levels were based on water control elevations when known, or operational rules. For example, if a particular area was controlled at elevation 4.0 feet, then every branch within that drainage area was given an initial condition of 4.0 feet. If there was no established control elevation, then the initial water level was set equal to the level in which the controlling structure (could be several miles away) begins to operate.

3 MODEL DEVELOPMENT

This section details the development and initial parameterization of the SFWMD C-8 & C-9 MIKE SHE and MIKE HYDRO River models for use in the C8-C9 FPLOS Study. Please note that several of the data inputs were modified during model calibration and only the final values are shown. Refer to Deliverable 2.1, *C8-C9 Calibration and Validation Memorandum Final Draft* (Taylor Engineering, 1/21/2020) for the original values used in developing the model, before any adjustments were made during calibration.

3.1 Model Domain and Grid

The model domain extends from the C-9 and C-11 basin boundary in the north to the C-6 and C-7 canals in the south, and from just west of the L-33 canal in the west to the intercoastal in the east, as shown in **Figure 3.1-1**. A computational grid size of 250-ft was chosen and coupled with the multi-cell overland feature using a 125-ft grid. This further refines the storage and conveyance characteristics of each computational grid cell. Although the model computations are based on a 250-ft grid cell, the conveyance and storage characteristics of each cell are calculated based on the finer 125-ft grid. This provides a high level of topographic detail and overland storage definition, which is sufficient for this sub-regional scale model. The computational grid size and multi-cell overland definition are consistent with the 2019 Broward County Current Conditions model (Taylor Engineering, 2019). Additionally, the C8-C9 model grid origin is aligned so that it is an exact integer of grid cells away from the 2019 Broward County model origin, meaning that the data input and outputs are compatible between both models.

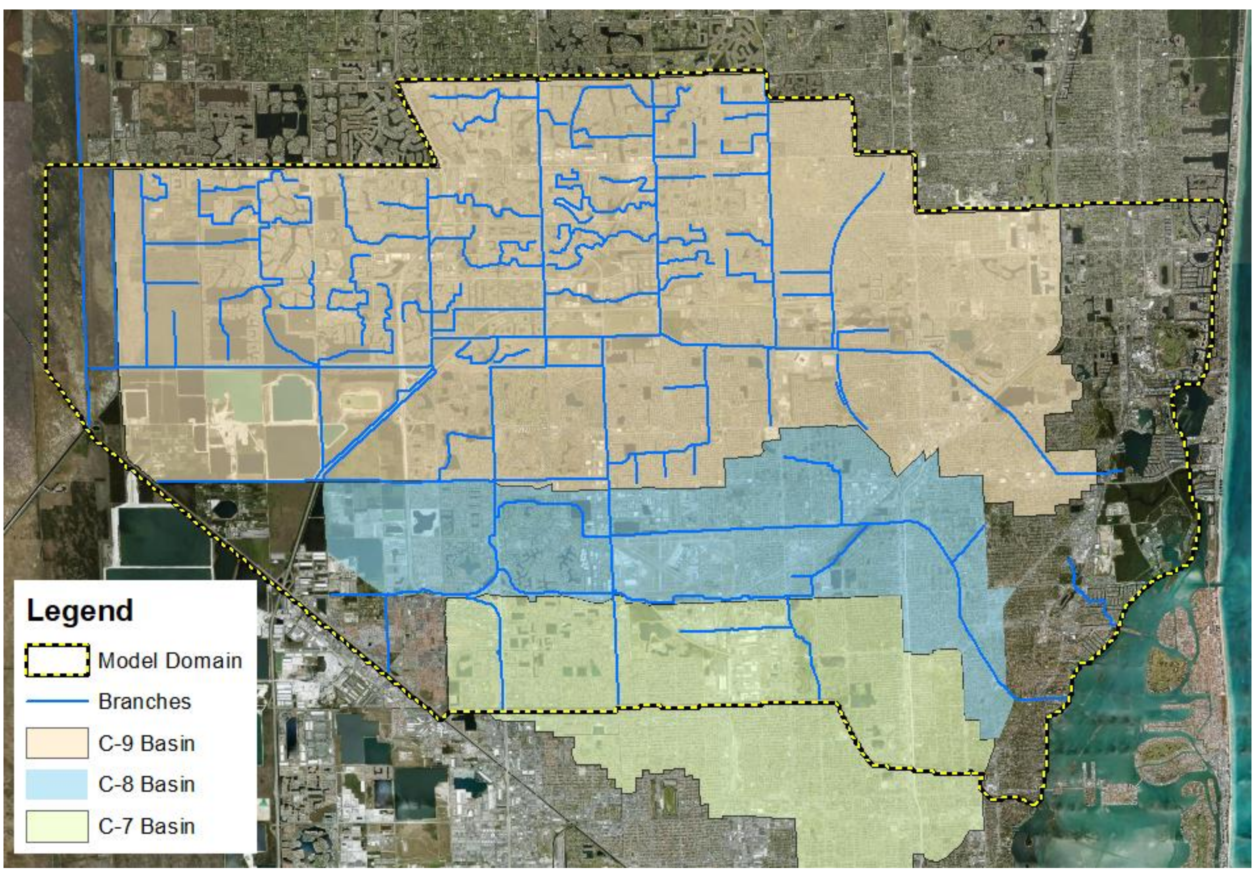

Figure 3.1-1: Model Domain and SFWMD Basin Map

3.2 Topography

The topography input file was made from the merged DEM presented in **Figure 2.1-1**. The 125-ft DEM was made by taking the median values from the 5-ft DEM within each 125-ft grid cell. Areas with elevations greater than 25 ft NAVD88 (typically landfills or high bridges) were reduced to 25 ft to eliminate the possibility of having numerical stability issues in the 2D model (such as flow from 200-ft elevation cell to 10-ft elevation cell). Areas with elevations less than -2 ft NAVD88 were increased to -2 ft (typically intercoastal areas- bathymetry likely built into DEM). The topography was converted from NAVD88 to NGVD29 by adding 1.57 ft, the conversion from CorpsCon6 tool. Several areas were tested, and the differences were minimal. A uniform conversion of 1.57 ft was deemed appropriate and efficient.

3.3 Simulation Specification

The simulation period for the calibration event was a three-week period from October 1st, 2000 12am to October 21st, 2000 12am. The verification event was a nearly four-month period from June 2nd, 2017 12am to September 27th 12am. The design storm events were given a start date of June 4th, 2017 12am, as it provides a realistic starting point for initial conditions and boundary conditions based on recent observed data. The initial groundwater elevations at this point in time were a good match with observed groundwater well elevations, with most locations agreeing to within +/- 0.25 ft. In addition, this start date aligns with the validation model and the 2019 Broward County Design Storm models, which provides observed (western boundary) and simulated boundary condition data (northern boundary). June 4th at 12am was chosen specifically as this aligns the peak of the design storm with the peak of the storm in the boundary conditions. This approach is consistent with the 2019 Broward County Model. Although the design storm rainfall has a duration of only 3 days, the design storm simulation period was set to 16 days. A 2-day spin-up period was chosen to allow any discontinuities within the boundary conditions or initial conditions to come to equilibrium before the start of the design storm rainfall. The design storm period was given a duration of 14 days, 11 of which occur after the rainfall ends. The purpose for running the simulation an additional 11 days was so that results existed that could be used to generate a model-simulated water table map that could be useful as an alternative input for initial groundwater level conditions and to determine duration of flooding in areas of the model where potential flooding damages may need to be evaluated as part of mitigation alternatives.

3.4 Climate

3.4.1 Rainfall

The storm event from October 2nd-4th, 2000, was used to calibrate the model. Originally, temporally modified NEXRAD rainfall was attempted, but ultimately was replaced with rain gauge data (as shown in **Figure 2.5-11**). This is discussed in greater detail in **Section 4.4**. **Table 3-1** shows the rain gauge recorded rainfall totals for October 1st-21st, 2000, with most of it occurring during between October 2-4.

Table 3-1: Rain Gauge based Total Rainfall Depths

Rain Gauge	Total Rainfall (in)
S-13_R	10.46
S-27_R	16.01
S-28Z_R	12.57
S-29Z_R	13.65
S-30_R	7.5

The verification event rainfall comes from unmodified NEXRAD data, which had been QA/QC by Geosyntec Consultants (2018) as part of the 2019 Broward County modeling project. The design storm simulation uses NOAA Atlas 14 rainfall depths (**Table 3-2**) that are temporally distributed based on the normalized cumulative SFWMD 3-day distribution and spatially distributed based on Thiessen Polygons of the NOAA stations (**Figure 3.4-1**), which is consistent with the 2019 Broward County model approach.

Table 3-2: Design Storm Rainfall Depths per NOAA Atlas 14 Station

NOAA Station	3-Day Storm Rainfall Depth (inches)			
	5-Year	*10-Year*	*25-Year*	*100-Year*
PENNSUCO 5 WNW	8.12	9.66	12.1	16.3
MRF114	8.9	10.7	13.5	18.4
MRF117	8.85	10.5	13.1	17.7
MIAMI BEACH	8.48	10.1	12.6	16.9
HIALEAH	8.91	10.6	13.2	17.8
FT LAUDERDALE INTL AP	8.95	10.8	13.5	18.3

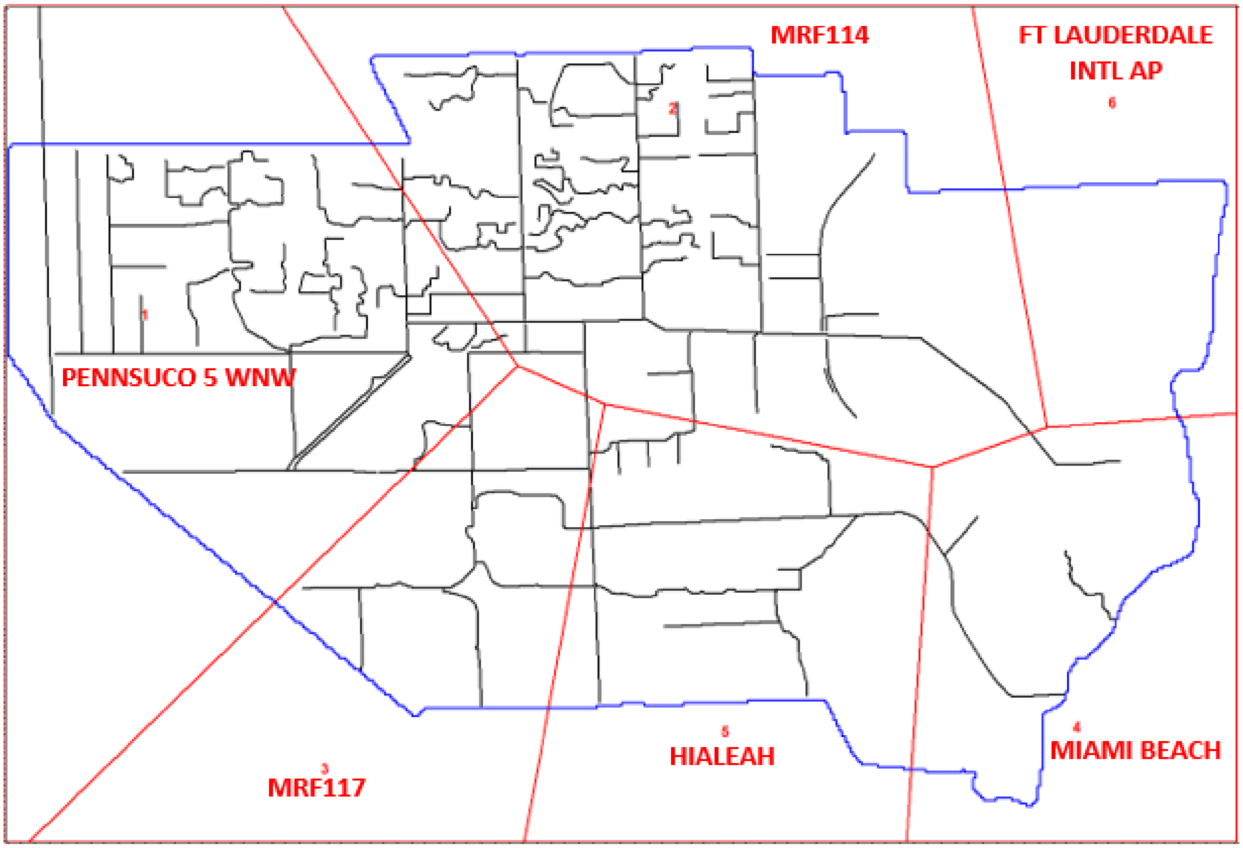

Figure 3.4-1 Design Storm Thiessen Polygons based on NOAA Atlas 14 Rainfall Stations

3.4.2 Reference Evapotranspiration

Short term simulations are typically not very sensitive to this parameter and reference ET does not vary significantly across relatively small areas, such as this model domain. Therefore, a uniform spatial distribution was chosen for the calibration and validation simulations. Time varying SFWMD Reference ET (NEXRAD Viewer, 2020) for pixel #10045457 (centrally located) was applied model-wide. **Figure 3.4-2** & **Figure 3.4-3** show the reference ET used for the calibration and validation simulations, respectively. For the design storms, the reference ET was set to a constant 2 mm/d, which is the minimum daily wet season value rounded to the nearest mm, in year 2017, including during Hurricane Irma (USGS Reference and Potential Evapotranspiration, 2018). Minimum wet season reference ET values were deemed sufficient as ET will be rather insignificant compared to design storm rainfall depths. This is a conservative approach. Evapotranspiration is a relatively small fraction of a design storm water budget, with an even smaller fraction of that fraction occurring during the time to peak (time to peak is a few days; most design storm ET occurs during hydrograph recession).

Reference ET is based on a reference "crop", typically well-watered grass. Reference ET is adjusted by crop coefficients, which vary by land use. **Table 3-3** shows the final crop coefficients used in the model, based on the 2019 Broward County Current Conditions model. Adjusted reference ET is further reduced based on water availability, root depth and leaf area index, although these parameters are not important for event-based simulations.

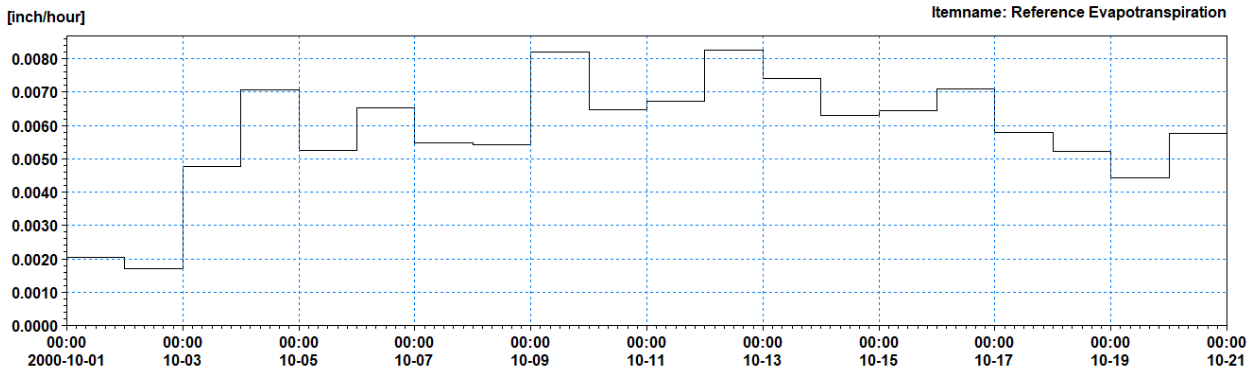

Figure 3.4-2: Reference ET for Pixel 10045457 for Calibration Simulation

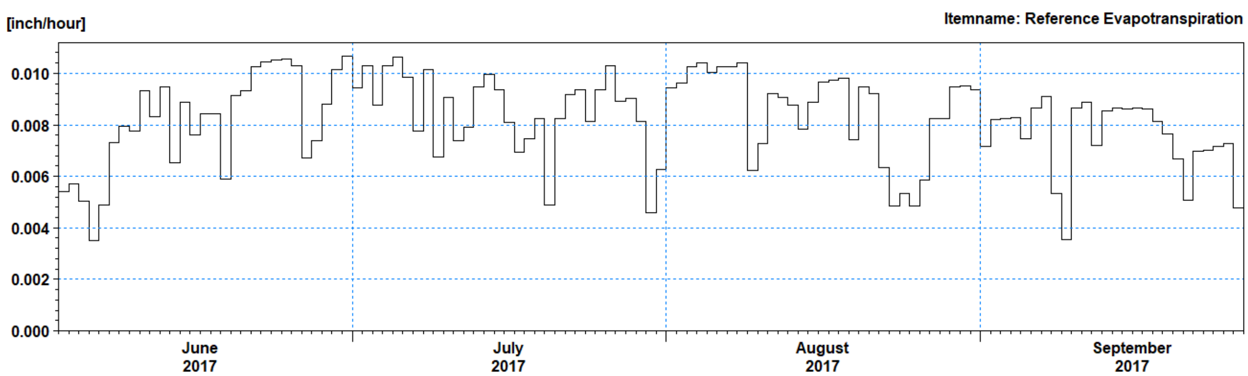

Figure 3.4-3: Reference ET for Pixel 10045457 for Validation Simulation

Table 3-3: Crop Coefficients by FLUCCS Code

FLUCCS Code	Land Use	Crop Coefficient (Kc)	FLUCCS Code	Land Use	Crop Coefficient (Kc)
1100	Residential, Low Density	0.67	**3200**	Upland Shrub and Brushland	0.8
1200	Residential, Medium Density	0.58	**3300**	Mixed Rangeland	0.8
1300	Residential, High Density	0.48	**4200**	Upland Hardwood Forests	0.8
1400	Commercial and Services	0.48	**4300**	Upland Mixed Forests	0.8
1500	Industrial	0.4	**5100**	Streams and Waterways	0.8
1700	Institutional	0.48	**5200**	Lakes	0.8
1800	Recreational	0.72	**5300**	Reservoirs	0.8
1900	Open Land	0.8	**5400**	Bays and Estuaries	0.8
2100	Cropland and Pastureland	0.8	**5700**	Ocean and Gulf	0.8
2200	Tree Crops	0.8	**6100**	Wetland Hardwood Forests	0.8
2300	Feeding Operations	0.8	**6400**	Vegetated Non-Forested Wetlands	0.8
2400	Nurseries and Vineyards	0.8	**7400**	Disturbed Land	0.8
2500	Specialty Farms	0.8	**8100**	Transportation	0.4
2600	Other Open Lands - Rural	0.8	**8200**	Communications	0.4
3100	Herbaceous (Dry Prairie)	0.8	**8300**	Utilities	0.4

3.5 Land Use

To be consistent with the 2019 Broward County Current Conditions model, the land use/vegetation map was created by merging the 2019 Broward County model's land use map with the SFWMD Land Use Land Cover data (SFWMD LCLU, 2017). The 2019 Broward County Current Conditions model's land use map was created using the same data from SFWMD, but some additional changes were made throughout the county after comparing satellite imagery from 2015 with 2018. Therefore, by merging the Broward County land use map with the SFWMD land use data, it ensured that any changes in the C-9 basin from the 2019 Broward County Model were incorporated.

As suggested by SFWMD, this study changed extractive land use areas to reservoirs as they are filled with water. This change is consistent across all of the land use-based parameters. Land use values are assigned based on the 250-ft computation grid. The land use grid was made from a polygon shapefile of land use areas based on the maximum area of land use(s) in the 250-ft grid cell. As discussed in **Section 2.2**, there were less than 2% change in land use classification since 2000, so this dataset was used for the calibration, validation, and design storm events. Refer to **Table 3-4** for land use description by Florida Land Use Cover Classification System (FLUCCS) codes (Florida Natural Areas Inventory, 2012) and **Figure 3.5-1** for the spatial distribution.

Table 3-4: Land Use by FLUCCS Code

FLUCCS Code	Land Use	Area-Weighted %
1100	Residential, Low Density	1.7
1200	Residential, Medium Density	32.9
1300	Residential, High Density	12.1
1400	Commercial and Services	9
1500	Industrial	2.9
1700	Institutional	4
1800	Recreational	4
1900	Open Land	1.3
2100	Cropland and Pastureland	0.7
2200	Tree Crops	0
2300	Feeding Operations	0
2400	Nurseries and Vineyards	0.8
2500	Specialty Farms	0
2600	Other Open Lands - Rural	0
3100	Herbaceous (Dry Prairie)	0.1

FLUCCS Code	Land Use	Area-Weighted %
3200	Upland Shrub and Brushland	0.3
3300	Mixed Rangeland	0
4200	Upland Hardwood Forests	0.8
4300	Upland Mixed Forests	0.3
5100	Streams and Waterways	1.7
5200	Lakes	0.3
5300	Reservoirs	10.2
5400	Bays and Estuaries	0.3
5700	Ocean and Gulf	0
6100	Wetland Hardwood Forests	4.1
6400	Vegetated Non-Forested Wetlands	4.7
7400	Disturbed Land	0.7
8100	Transportation	6.2
8200	Communications	0.1
8300	Utilities	0.9

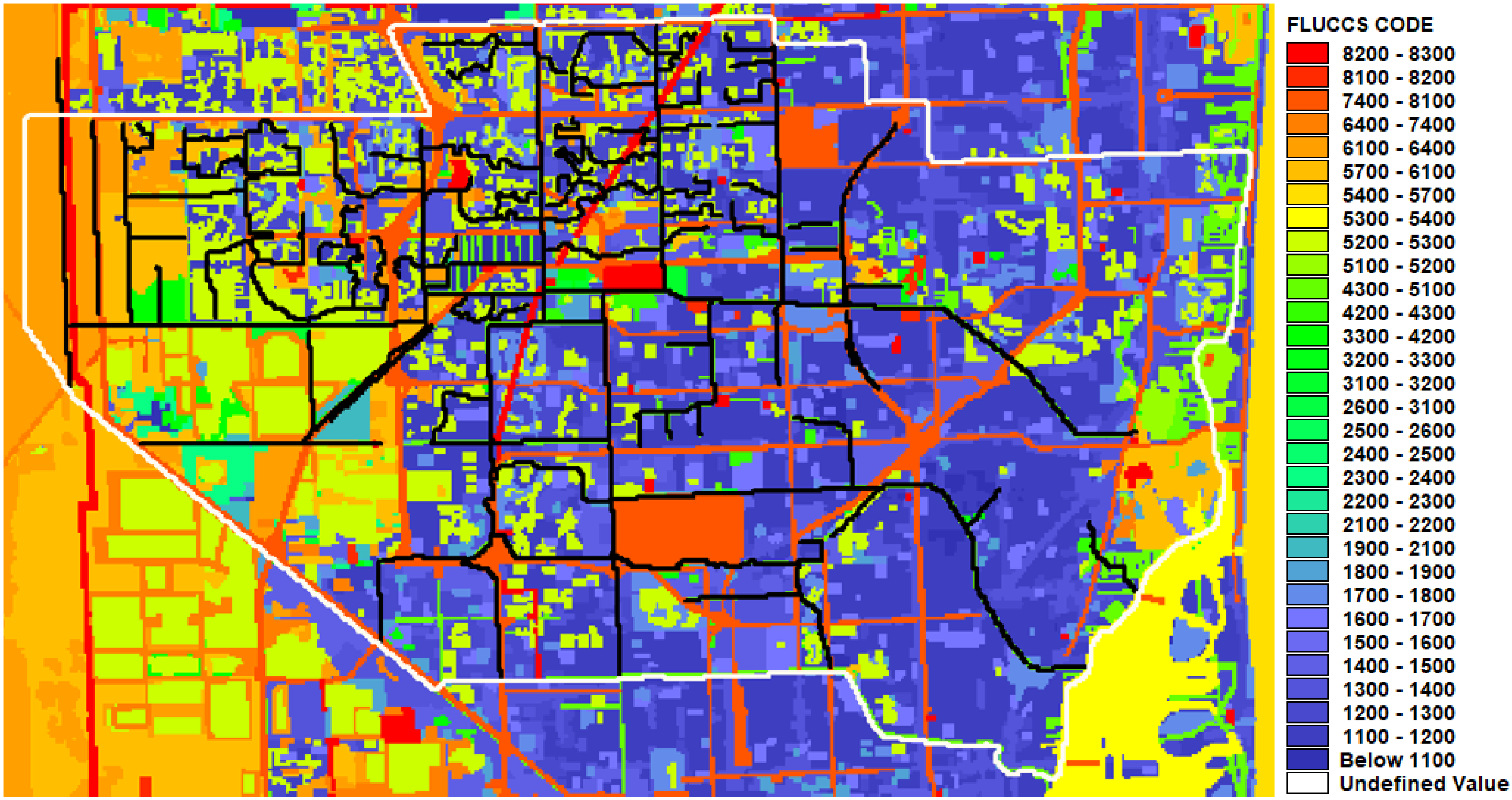

Figure 3.5-1: Land Use/Vegetation by FLUCCS Code

3.6 Rivers and Lakes (1D Model)

The 1D model was developed using MIKE HYDRO. The 1D network in the C-9 basin was mainly based on the 2019 Broward County Current Conditions model. The 1D network in the C-8 and C-7 basins were developed for this project. District, County, survey (Stoner and Associates, 2019), and South Broward Drainage District (SBDD) data were used when and where applicable and available. Additional survey (BDH Consulting Group, 2019) was completed for this project. The data used and parameterization of the river network are discussed in **Section 3.6.1** through **Section 3.6.1.3**.

3.6.1 1D River Network

The 1D river network is composed of 95 branches, 93 of which could be considered secondary or tertiary systems. The purpose of this study is to determine the flood protection level of service for the C-8 and C-9 Canals. Although the focus of this study is on the two primary canals, C-8 and C-9, a high level of detail was placed on the secondary/tertiary canal systems, as they are both a major source of discharge into the primary system and storage prior to discharging into the primary system. Many of the secondary/tertiary canal systems were setup to simulate the connectivity between lakes and other discontinuous (from DEM) water bodies, which are connected through a series of hydraulic structures. Water bodies that are not explicitly represented via a branch may still be connected to the 1D river network through the use of flood codes, which is discussed in section **3.6.3.1.**

3.6.1.1 Hydraulic Control Structures

The 1D network is controlled through a series of culverts, weirs, gates, and pumps. Specifically, there are 309 culverts, 8 weirs, 8 gated structures, and 8 pump stations. There are also 46 bridges explicitly modeled, which may control flow if they become submerged. The data for these structures came from a variety of sources, including South Broward Drainage District's Facilities Report, Miami-Dade Stormwater Geodatabase, SFWMD Operations Control Center Structure Books, SFWMD Flow Rating Analysis reports, SFWMD XP SWMM models, and professional survey. In areas where specific data was unavailable, an approximation was made. Specifically, South Broward Drainage District's (SBDD) Facilities Report lacked invert elevations for approximately 200 of the culverts included in the model, therefore, an approximation was made by matching the top of the culvert with the water control elevation, with respect to the specific drainage basin, as suggested by SBDD (Email provided in **Appendix A**).

There are four SFWMD control structures within the C-8 and C-9 basins (S-28, S-29, S-30, and S-32), and two outside the basins (S-9XS and G-58). S-9XS was used for boundary conditions on the L-33 Canal and G-58 controls Arch Creek. The four SFWMD control structures within the basins were represented as sluice gates. This was done so that the District's flow rating parameters could be incorporated, which provide the closest model calculation representation of the actual stage-discharge relationship of the structures as it uses the same set of equations.

3.6.1.2 Cross Sections

The availability of cross section data was limited to mainly the Miami-Dade portion of the model domain. Both the Miami-Dade County GIS Geodatabase as well as the SFWMD XP SWMM C-7, C-8, and C-9 models had cross section data for branches within Miami-Dade County. Cross sections for the C-9 Canal were available from both survey data and the C-9 XP SWMM model. For many secondary/tertiary canals in

Broward County, cross section data was essentially nonexistent. Therefore, the secondary/tertiary system cross sections within the Broward County portion of the model was carried over from the 2019 Broward County Current Conditions Model, which are mainly estimates based on the DEM. Most of the secondary/tertiary canal cross sections in the Broward County portion of the model were cut using the latest available 5-ft DEM (a composite DEM made by Geosyntec consultants, as discussed in **Section 2.1**). This means that the DEM was used for cross section elevation and geometry, from the bank to the water surface. An assumed geometry was used below the water surface (**Figure 3.6-1**), typically, from the last bank point down to an elevation of -2/-3 ft was assumed to have a side slope of 4(h):1(v), and then a side slope of 2:1 from -2/-3 ft to -8 ft. The water surface elevation varied across the model domain due to water control elevation differences, so the channel geometry may appear different for the "cut" cross sections. It is important to note that "cut" cross sections from the DEM were not used to "cut" cross sections for C-8 and C-9 Canal. The DEM was only used for C-8 and C-9 Canals to extend the channel banks as needed. Additional cross section data for this project was collected via professional survey.

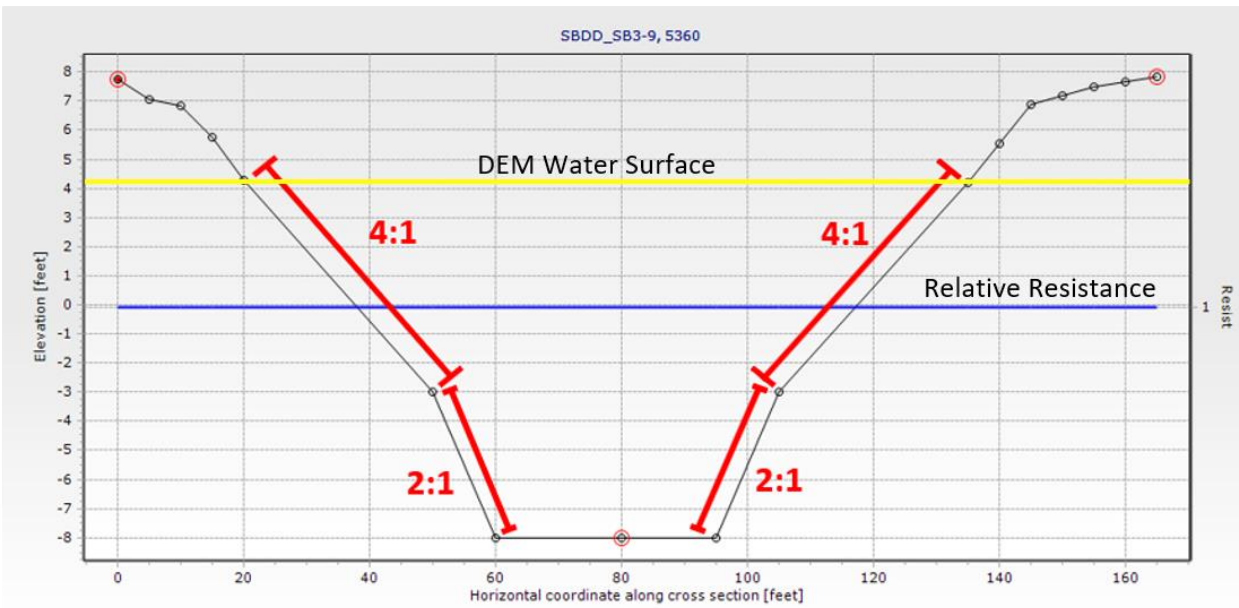

Figure 3.6-1: Example of a "Cut" Cross Section from DEM

3.6.1.3 <u>Survey Data</u>

Survey for this project focused on areas with little or no available data. Refer to **Figure 2.4-1** for a map of the surveyed items collected as a part of this project. These items were incorporated into the 1D model.

3.6.2 Canal-Aquifer Interactions

The 1D river network is coupled with the 2D groundwater model by MIKE SHE couplings. Essentially, at each grid cell along either side of a river branch, the exchange is calculated by multiplying the head difference between the grid cell (groundwater level in the cell(s) adjacent to the river link) and the river with the conductance. The model calculates the conductance based on the options assigned. For each branch or branch segment in the model, 1 of 3 conductance options were chosen, either (1) aquifer + riverbed, (2) aquifer only, or (3) riverbed only. These options change the way the model calculates the exchange between the groundwater and the river, where the aquifer conductance depends on the horizontal hydraulic conductivity and the riverbed conductance depends on an assigned leakage coefficient. Only aquifer + riverbed and riverbed only were used. A leakage coefficient of 1E-5/s was assigned (the model default value) for all branches, with a few localized adjustments made during model calibration.

3.6.3 Canal-Overland Flow Interactions

The 1D river network is coupled with the 2D overland flow model by MIKE SHE couplings. In this model, both coupling options were used, which are (1) flood codes and (2) overbank spilling. These options are discussed in **Section 3.6.3.1** and **Section 3.6.3.2**

3.6.3.1 Flood Codes

On secondary and tertiary canals, flood codes are used to allow communication between MIKE HYDRO and MIKE SHE when water levels in MIKE HYDRO exceed the adjacent floodplain elevations. Flood codes also allow MIKE SHE to communicate directly with MIKE HYDRO whenever the water elevation of flood code cells exceed the water elevation in the river branch, as long as the water elevation in the branch is higher than the grid cell's topographic elevation. Flood codes were also used in areas where direct connections were not explicitly represented, such as ponds or lakes within proximity of a river branch, or water bodies that become disconnected in the DEM. An example of flood code placement is shown in **Figure 3.6-2**. It is important to note that the specific value of the flood code is not important, it is just a unique identifier.

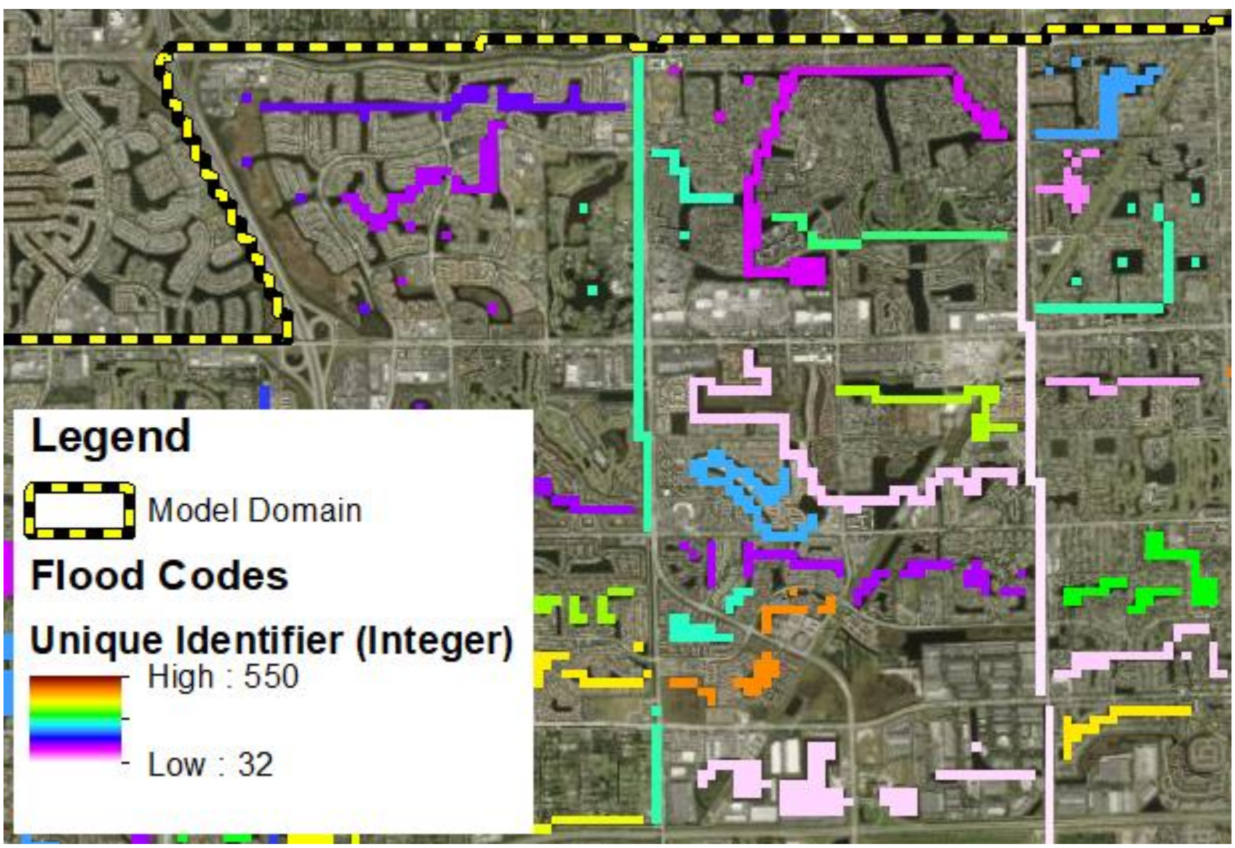

Figure 3.6-2: Example of Flood Code Placement

Flood code cells are excluded from 2D overland flow computations, so it is important to place them wisely, such as the lowest cell in an area. Covering an entire lake with flood code cells would turn off the overland computations for the entire lake. Therefore, the only time entire water features were covered with flood codes was when the storage was accounted for in the 1D model, such as a branch going through a lake (the lake water levels are computed in the 1-D model and the cross sections extend to the edges of the lake). Flood codes along secondary and tertiary canals are generally limited to one cell along each bank.

The detailed surface topography provided an opportunity to take advantage of the flood code feature and account for storage that would otherwise be lost in a larger resolution topographic map. The flood code setup is shown in **Figure 3.6-3**. Although the specific value of the flood code does not matter, as they are just an identifier that relate a cell to a specific branch, the flood code values in the C-9 basin were kept the same as the 2019 Broward County Model for consistency. New flood code areas were assigned identifiers not used in the 2019 Broward County model, which should eliminate any issues in the future if the models are merged.

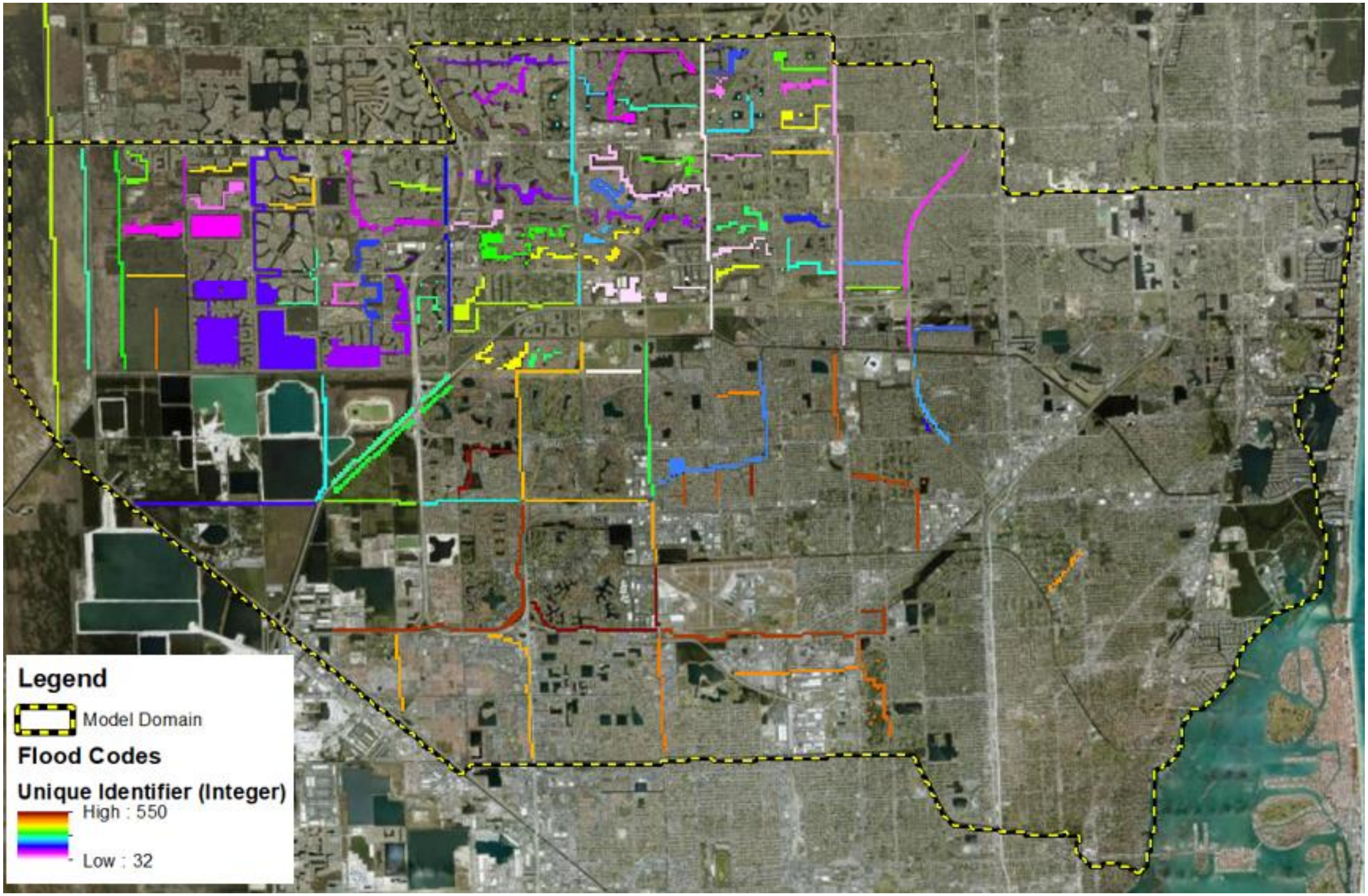

Figure 3.6-3: Map of Flood Codes (Specific Values do not Matter- Unique Identifiers)

3.6.3.2 Overbank Spilling

The C-8 and C-9 primary canals rely on overbank spilling instead of flood codes, which allows communication between MIKE SHE and MIKE HYDRO via the weir equation, whenever the water level in the canals becomes greater than the cross-section bank elevations. Overbank spilling is based on the cross section and the 2D grid, whichever is higher. In most instances, the berms are not represented well in the 125-ft or 250-ft topography grid, as median values are used. Therefore, the berm elevations should be and were included in the cross sections. In instances where the 2D grid is higher than the cross section, the water will “glass wall” in the cross section until it reaches the 2D grid elevation. Overbank spilling provides a more physically based representation of the exchange between canal and 2D grid, which is more important on the C-8 and C-9 canal than the secondary and tertiary canal system as they are the focus of this FPLOS project. Therefore C-8 and C-9 will only spill out to the 2D model when water levels exceed bank elevations, whereas branches with flood codes may exchange whenever the water level in the canal is greater than the water level on the 2D grid (ignores bank elevations- assumes it has connectivity such as culverts). For numerical stability purposes, some secondary canal segments within close proximity of the primary canals were switched to overbank spilling.

3.6.4 Hydrodynamic Initial Conditions

The 1D model’s initial water levels were set based on two different categories, which are (1) based on observed data and (2) based on control elevations. In areas where there is observed data, such as water elevation upstream of the C-8 and C-9 tidal structures for calibration and validation simulations, the initial conditions were set to match the observed data. In areas that are controlled via operable control structures such as SBDD, the initial conditions were set to match the control elevation, which differ from the gate open or pump on elevations. This is consistent with the approach used in the 2019 Broward County Model. For the design storms, the 1D model’s initial water levels were set based on control elevations.

3.6.5 Boundary Conditions (1D Model)

3.6.5.1 Calibration / Validation Model

On the west side of the model, the boundary structures (S-9XS and S-32) were assigned a time varying water level boundary based on observed stage data obtained from the District. On the east side of the model, the tailwater stage at the primary canal outfall structures were forced as a user-specified boundary condition based on observed data obtained from the District. At the intercoastal waterway, water levels were forced based on the Virginia Key tide station. On the south side of the model, water levels were forced at the downstream boundary of the 1-D branches connecting to the C-6 and C-7 Canals based on observed data obtained from the District.

3.6.5.2 Design Storm Model

On the west side of the model, the boundary structures (S-9XS and S-32) have a time varying water level boundary based on simulated design storms from other models (2019 Broward County MIKE SHE / MIKE HYDRO model for S-9XS and C-6 XP SWMM for S-32). On the east side of the model, the tailwater stage at the primary canal outfall structures were forced as a user-specified boundary condition based on District provided year 2015 tidal boundary data at the S-28 and S-29 structures, which include storm surge effects for the design storms of interest. The dates of the District provided time series data were relative for the purposes of design storms. Therefore, for each boundary condition using SFWMD provided data, the dates were adjusted so that the peak stages occur at the same time as the peak rainfall, as agreed upon with the District. The 1D tidal boundaries, which force the tailwater at structures S-28, S-29, and G-58, were set up to use the SFWMD provided design storm stages. G-58 was assigned the same tidal data as structure S-28. The design storm tidal boundaries for current sea level (CSL) are shown in **Figure 3.6-4** (S-28) **and Figure 3.6-5** (S-29).

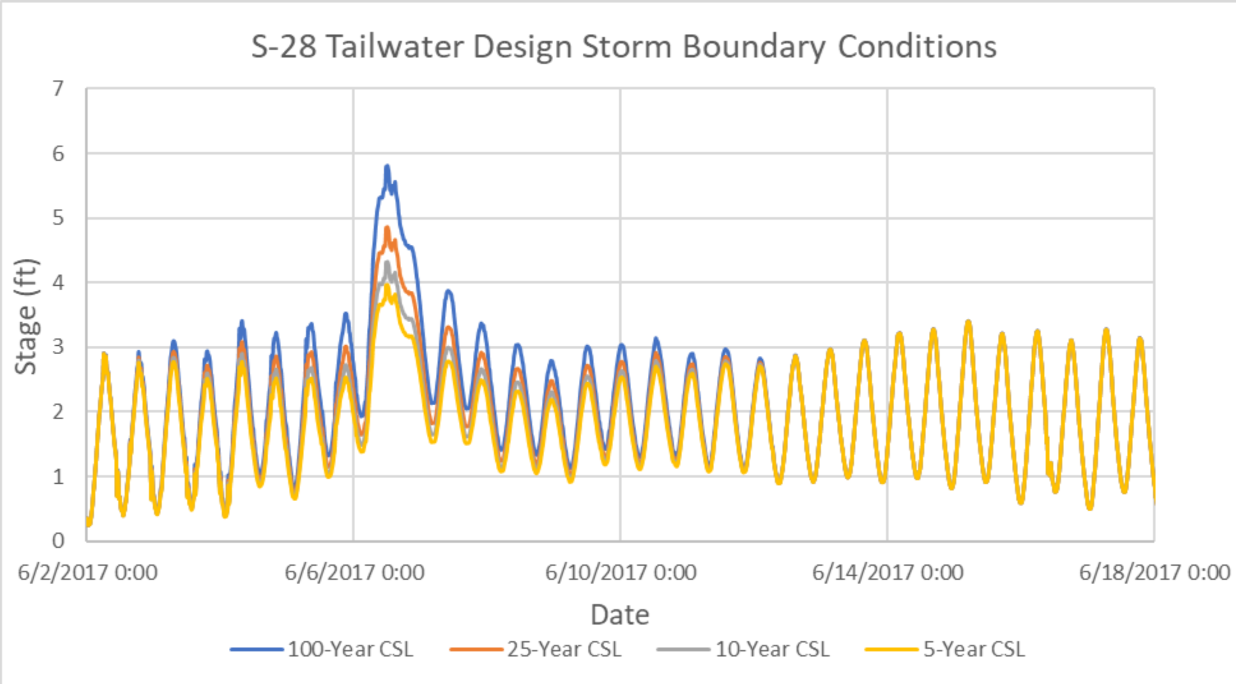

Figure 3.6-4: Design Storm Current Sea Level Tidal Boundary Stages for S-28

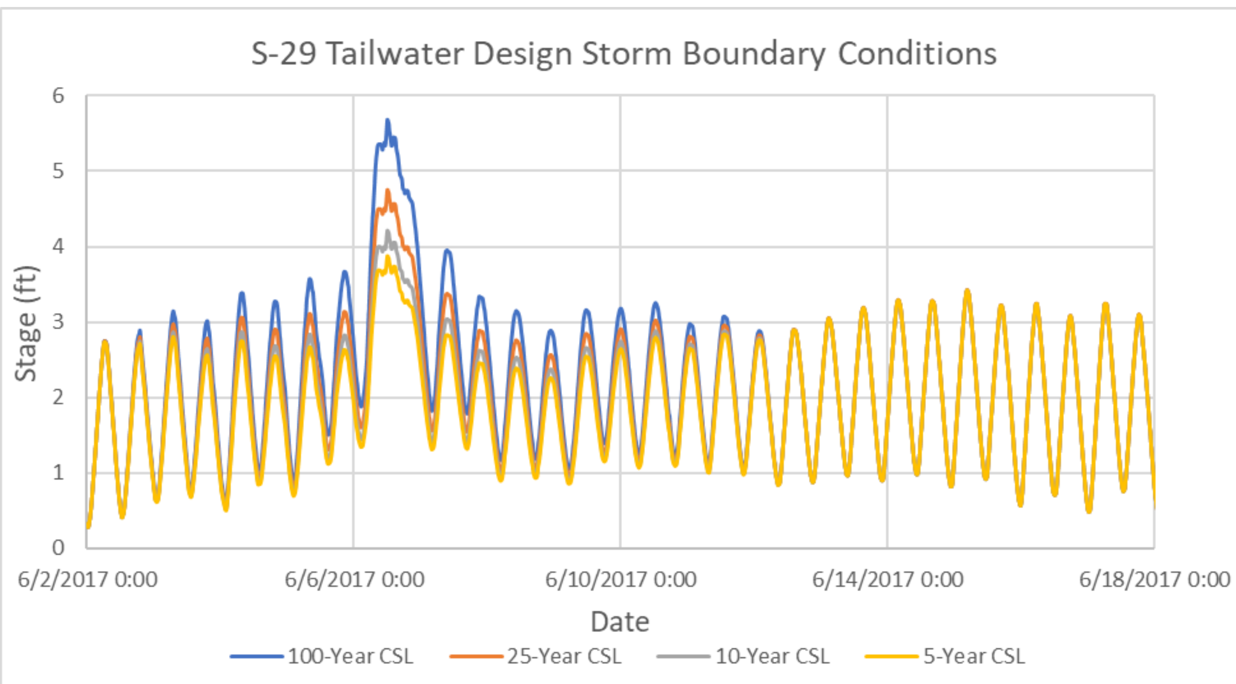

Figure 3.6-5: Design Storm Current Sea Level Tidal Boundary Stages for S-29

At the intercoastal waterway, water levels were forced based on the District-provided storm stage time series data. On the south side of the model, water levels were forced at the downstream boundary of the 1-D branches connecting to the C-6 and C-7 Canals based on simulated design storm data obtained from the District (XP SWMM and HEC-RAS models).

3.7 Overland Flow

The overland flow module, or 2D model, is essentially parameterized by district drainage basins. The C-9 basin, which mainly lies within Broward County, was parameterized to be consistent with the 2019 Broward County model, which was based on two major categories: (1) land use and (2) ERP permitted areas. The C-8 Basin, which is in Miami-Dade County, was parameterized in a similar way but based on different data. This parameterization is explained in **Section 3.7.1** through **Section 3.7.7**.

3.7.1 Overland Flow in Broward County

Most of the parameters in the overland flow model are spatially varied by land use, while other parameters are spatially varied by land use within ERP permitted areas. A large portion of Broward County is made up of permitted areas that are required to retain some volume of rainfall, whether it be the first 1-inch of rainfall or 2.5-inches over the impervious area, or a more stringent requirement to retain the runoff resulting from the 25-year 3-day storm, with no discharge. For the 2019 Broward County model, Taylor Engineering proposed to separate the permitted areas into the following categories: (1) areas controlled by operable structures such as pumps or gates, (2) areas that had at least 10% waterbody land coverage such as lakes or ponds, (3a) areas with less than 10% waterbody land coverage and have at least 2.5-feet depth to water table, and (3b) areas with less than 10% waterbody land coverage and have less than 2.5-feet depth to water table. Depth to groundwater was estimated by subtracting the initial groundwater elevation from the topography elevation. The assumption behind this is that areas with an initial depth to groundwater greater than 2.5-feet would have the ability to infiltrate more rainfall than areas with less than 2.5-feet. This was the assumed threshold for where exfiltration areas would likely be located. It is important to note that this assumption does not in any way affect the actual infiltration ability of the model, it was just a way to select which areas to parameterize to account for what cannot be explicitly modeled.

Permit areas classified as category 1, those behind operable structures, were parameterized just based on land use, as if they were unpermitted. Flow to the canal network from these areas is controlled by operable structures (gates and pumps), which are designed to limit discharge to permitted values and at permitted threshold water levels. Therefore, runoff rates within the respective drainage areas are ultimately limited by the operable structure. Although there may in fact be permitted areas within an overall drainage area that are held to a higher level of stormwater retention, for the purposes of this sub-regional scale model, if the operable structure is within its permitted allowance than it can be assumed that so are the areas draining to it. These areas classified as category 1 are controlled by permitted pumps and gates, that retain water on-site until the water levels reach the permitted discharge elevation, which means they often have a large amount of “dead storage” or on-site retention. Permit areas classified as category 2, those with at least 10% waterbody land coverage, were parameterized to account for the required detention storage, potential surface water storage, and sub-grid scale drainage features. Permit areas classified as category 3a, those with less than 10% waterbody land coverage and on average more than 2.5-feet depth to water table, were parameterized to account for the required detention storage and the likelihood of exfiltration trenches and other stormwater management features. Permit areas classified as category 3b, those with less than 10% waterbody land coverage and on average less than 2.5-feet depth to water table, would have been parameterized to only account for the required on-site retention. There are currently no category 3b areas within the C-9 basin. **Table 3-5** shows the criteria used to develop these stormwater management categories and the parameterization changes applied to these areas. It is important to note that these categories are unofficial and were developed to simplify the ERPs. A map of these stormwater management categories (SMC) developed by Taylor Engineering is shown in **Figure 3.7-1**.

Table 3-5: SMC Criteria and Parametrization within Broward County

Stormwater Management Category	Criteria	Parametrization
1	-Located in Broward County -Controlled by pump/gate	No change- only parameterized based on land use
2	-Located in Broward County -Greater than 10% water cover	- Increased detention storage based on 1” of the entire area or 2.5”x impervious area (whichever is greater) -Maximum storage change rate based on SFWMD CSM rating
3a	-Located in Broward County -Less than 10% water cover and greater than 2.5 feet depth to water table	-Increased detention storage based on 1” of the entire area or 2.5”x impervious area (whichever is greater) -paved runoff coefficient decreased by 50%

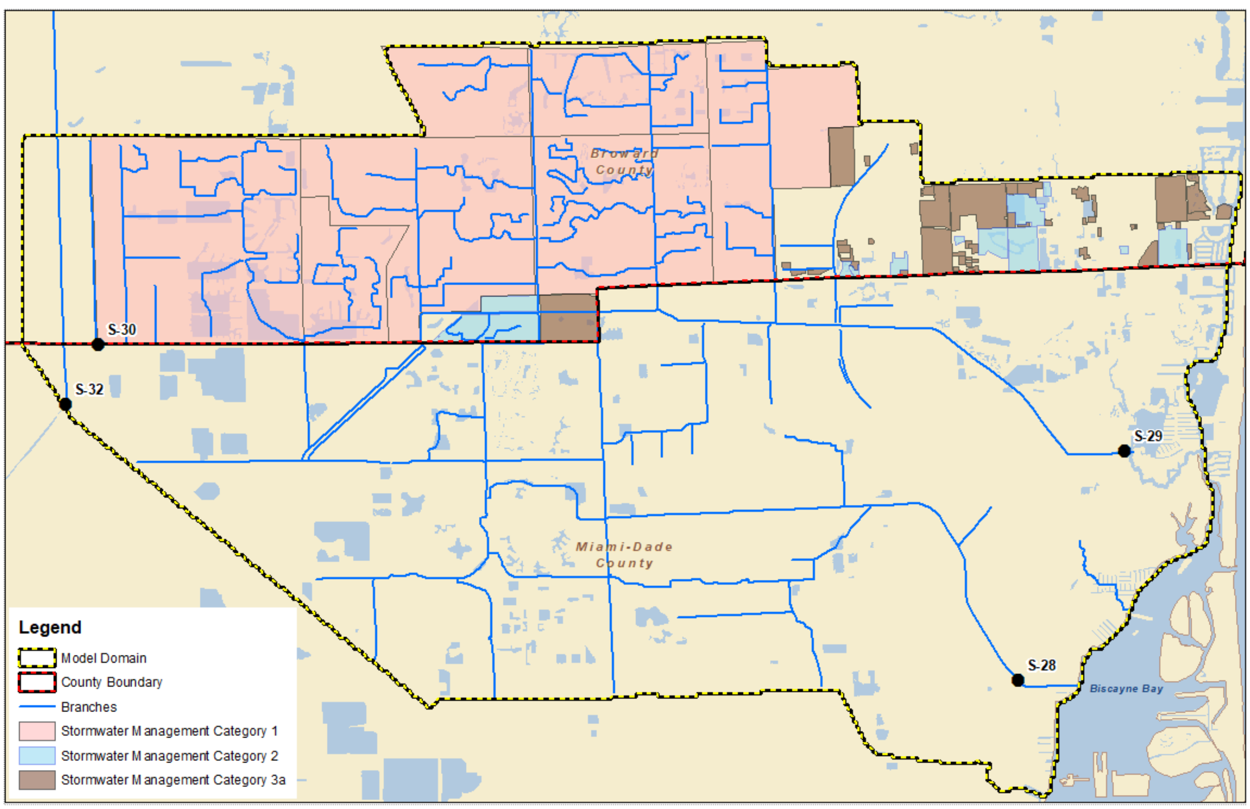

Figure 3.7-1: SMCs Used to Parameterize Overland Flow in Broward County

3.7.2 Overland Flow in Miami-Dade County

Within the Miami-Dade portion of the model, most of the parameters in the overland flow model are spatially varied by land use, while other parameters are spatially varied by land use within areas that are internally drained. Several areas within the C-8 drainage basin are either internally drained or have a large network of French drains, both of which reduce the amount of runoff making its way to the C-8 and C-9 Canals. Although the capacity of the French drain systems in Miami-Dade County was unknown, they were designed to retain/infiltrate some volume of rainfall before discharging into the canal system. Taylor Engineering proposed to the District to separate drainage areas into the following categories: (5) areas draining directly to MIKE Hydro branches, (6) areas internally drained or that have a large number of French drains relative to area served, and (7) areas both draining to branches and having French drains.

Areas classified as category 5, those draining to a branch, were parameterized just based on land use. Areas classified as category 6, those internally drained or have a large number of French drains, were parameterized by land use and adjusted to account for features that route and store water within the drainage basin. Areas classified as category 7, were parameterized by land use and adjusted to account for potential water storage and sub-grid scale drainage features like exfiltration trenches and other stormwater management features. Although based on different criteria, these categories are similar to the stormwater management categories developed for the 2019 Broward County model. **Table 3-6** shows the criteria used to develop these stormwater management categories and the parameterization changes applied to these areas. It is important to note that these categories are unofficial and were developed to simplify French drains and areas internally drained. A map of these stormwater management categories (SMC) developed by Taylor Engineering is shown in **Figure 3.7-2**.

Table 3-6: SMC Criteria and Parametrization within Miami-Dade County

Stormwater Management Category	Criteria	Parametrization
5	-Located in Miami-Dade County -Drains directly to canal	No change- only parameterized based on land use
6	- Located in Miami-Dade County -Internally drained or has a large number of French drains	-Increased detention storage based on 1" over entire area or 2.5"x impervious area (whichever is greater) -Paved runoff coefficient decreased by 50% -not allowed to drain directly to canal
7	-Located in Miami-Dade County -Drains directly to canal AND has a large number of French Drains	-Increased detention storage based on 1" over entire area or 2.5"x impervious area (whichever is greater) -Paved runoff coefficient decreased by 50% -allowed to drain directly to canal

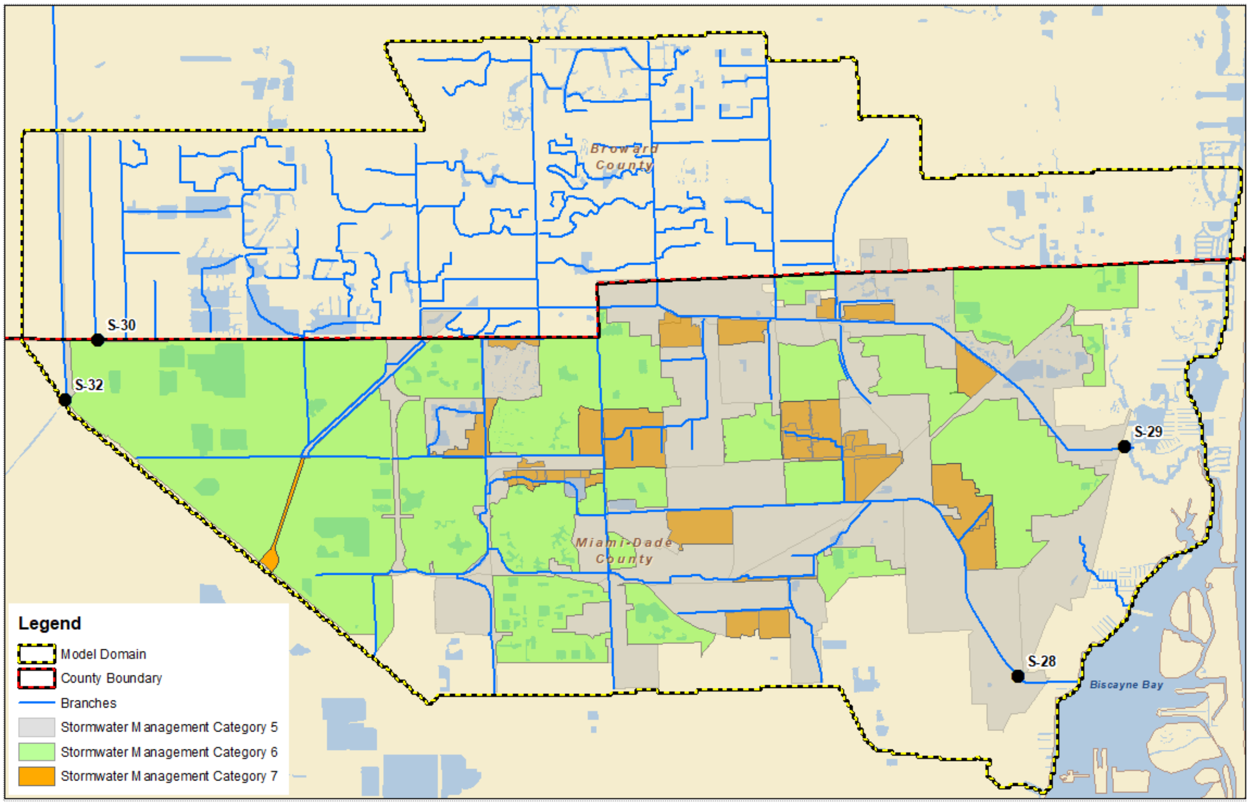

Figure 3.7-2: SMCs Used to Parameterize Overland Flow in Miami-Dade County

As shown in **Figure 3.7-3**, the areas in green are assumed to be internally drained for the purpose of parameterizing the ponded and saturated zone drainage routines. These areas either drain to local water bodies or have a large number of French drains. However, it is important to note that runoff from these areas can still reach the MIKE Hydro branches via the 2-D overland flow module. The areas in yellow are areas that drain to branches, however, several areas in yellow also have a large number of French drains, as shown by the red lines. The areas in yellow that have little to no French drains are considered category 5, areas that are green are considered category 6, and areas in yellow that have a large number of French drains are considered category 7. The area in purple drains to the boundary, so the specific overland flow parameterization is less likely to affect the model results and were only parameterized based on land use.

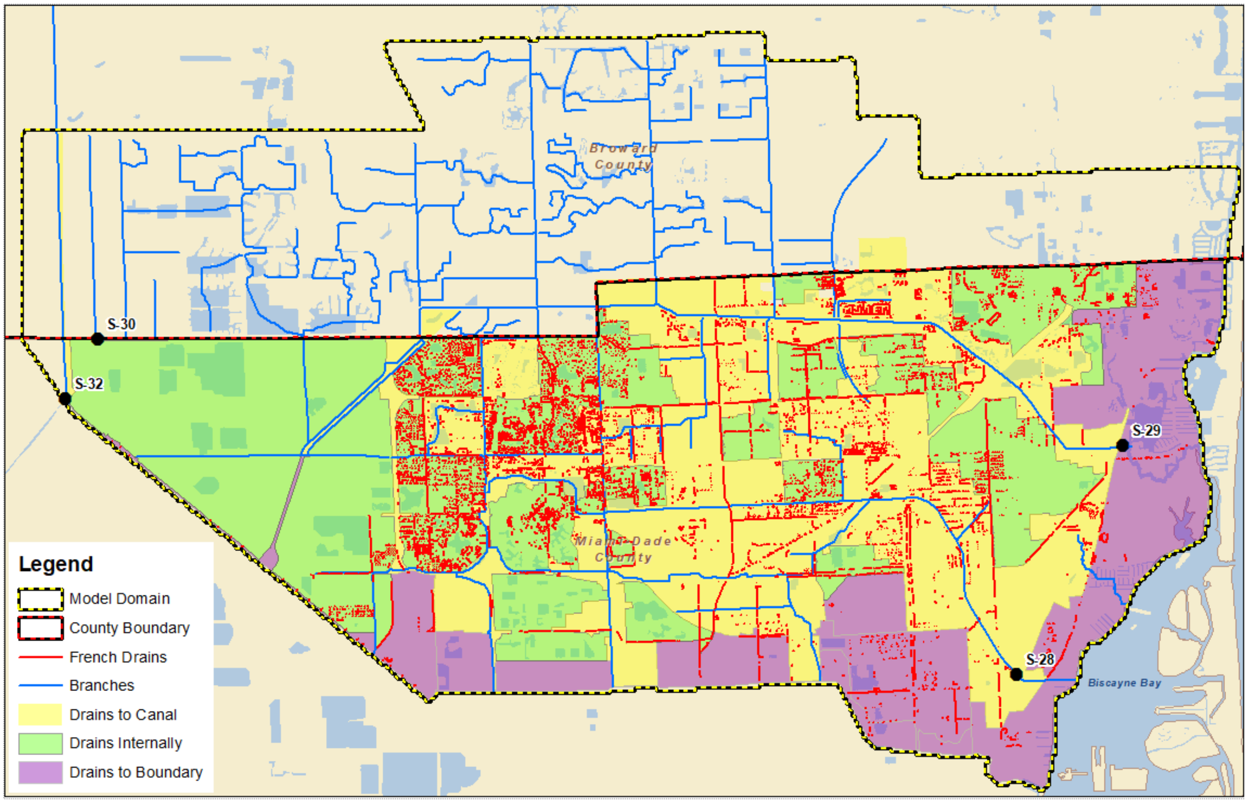

Figure 3.7-3: Drainage Categories in the Miami-Dade Portion of the Model Domain

3.7.3 Overland Manning's Roughness Coefficient

This parameter, used in the MIKE SHE 2-D overland flow component, is spatially distributed based on land use, with values ranging from 0.06 to 0.45, based previous models, literature (Environmental Protection Agency, 2015), and professional experience. **Table 3-7** provides FLUCCS Code based Manning's roughness coefficients. Please note that Manning's "M" is equal to 1/n.

Table 3-7: Land Use Based Manning's Roughness Coefficients

FLUCCS Code	Land Use	Manning's Roughness (n)	Manning's Roughness (M)
1100	Residential, Low Density	0.14	7.14
1200	Residential, Medium Density	0.12	8.33
1300	Residential, High Density	0.11	9.09
1400	Commercial and Services	0.07	14.29
1500	Industrial	0.07	14.29
1700	Institutional	0.13	7.69
1800	Recreational	0.13	7.69
1900	Open Land	0.14	7.14
2100	Cropland and Pastureland	0.17	5.88
2200	Tree Crops	0.17	5.88
2300	Feeding Operations	0.17	5.88
2400	Nurseries and Vineyards	0.17	5.88
2500	Specialty Farms	0.17	5.88
2600	Other Open Lands - Rural	0.14	7.14
3100	Herbaceous (Dry Prairie)	0.13	7.69
3200	Upland Shrub and Brushland	0.3	3.33
3300	Mixed Rangeland	0.3	3.33
4200	Upland Hardwood Forests	0.45	2.22
4300	Upland Mixed Forests	0.45	2.22
5100	Streams and Waterways	0.06	16.67
5200	Lakes	0.06	16.67
5300	Reservoirs	0.06	16.67
5400	Bays and Estuaries	0.06	16.67
5700	Ocean and Gulf	0.06	16.67
6100	Wetland Hardwood Forests	0.45	2.22
6400	Vegetated Non-Forested Wetlands	0.3	3.33
7400	Disturbed Land	0.14	7.14
8100	Transportation	0.11	9.09
8200	Communications	0.14	7.14
8300	Utilities	0.14	7.14

3.7.4 Detention Storage

This parameter is spatially distributed, based on both land use and the categories defined for Broward County and Miami-Dade County. Within Broward County, the non-permitted area's detention storage was spatially distributed based on land use with values ranging from 0 to 0.4 inches, as shown in **Table 3-8.**

Table 3-8: Land Use Based Detention Storage

FLUCCS Code	Land Use	Detention Storage (in)	Runoff Coefficient	"Permit Based" Detention Storage (in)
1100	Residential, Low Density	0.1	0.075	1
1200	Residential, Medium Density	0.1	0.22	1
1300	Residential, High Density	0.1	0.45	1.125
1400	Commercial and Services	0.1	0.72	1.8
1500	Industrial	0.1	0.4	1
1700	Institutional	0.1	0.3	1
1800	Recreational	0.3	0	No Change
1900	Open Land	0.15	0	No Change
2100	Cropland and Pastureland	0.15	0	No Change
2200	Tree Crops	0.25	0	No Change
2300	Feeding Operations	0.25	0	No Change
2400	Nurseries and Vineyards	0.25	0	No Change
2500	Specialty Farms	0.25	0	No Change
2600	Other Open Lands - Rural	0.15	0	No Change
3100	Herbaceous (Dry Prairie)	0.15	0	No Change
3200	Upland Shrub and Brushland	0.15	0	No Change
3300	Mixed Rangeland	0.15	0	No Change
4200	Upland Hardwood Forests	0.4	0	No Change
4300	Upland Mixed Forests	0.4	0	No Change
5100	Streams and Waterways	0	0	No Change
5200	Lakes	0	0	No Change
5300	Reservoirs	0	0	No Change
5400	Bays and Estuaries	0	0	No Change
5700	Ocean and Gulf	0	0	No Change
6100	Wetland Hardwood Forests	0.4	0	No Change
6400	Vegetated Non-Forested Wetlands	0.4	0	No Change
7400	Disturbed Land	0.1	0	No Change
8100	Transportation	0.1	0.56	1.4
8200	Communications	0.1	0	No Change
8300	Utilities	0.1	0	No Change

No change implies that the detention storage is based on land use

Even at a fine grid size of 125-ft, not all storage can be accounted for. This detention storage represents microtopography not represented in the DEM, such as potholes, bird baths, pools, street-side swales, etc. First, detention storage values of 0.1-0.4 inches (based on previous models, professional experience, and literature) were applied model-wide to account for sub-grid scale storage features. In areas controlled by operable control structures (SMC 1), such as SBDD, no additional changes to detention storage were made. In the remaining permitted areas or French drain areas, detention storage was increased to represent the small-scale on-site stormwater treatment or storage areas that are not explicitly modeled. This is expanded upon in the next few paragraphs.

In permitted areas within Broward County, the detention storage was spatially distributed by land use, but adjusted to account for the required retention. The permitted areas fall under an ordinance requiring retention of the 1st 1-inch of rainfall over the entire area or 2.5-inches of rainfall over the impervious area, whichever is greater. Within the permitted areas, the detention storage for impervious areas were increased by multiplying the directly connected impervious area (DCIA, defined by the paved area runoff coefficients discussed in **Section 3.7.7**) by 2.5 inches, and any of the resulting values less than 1-inch were increased to 1-inch. Therefore, within category 2, and 3a permitted areas, the detention storage increased from 0.1-0.4 inches to 1-1.8 inches, dependent on the land use (**Table 3-8**). This helps represent the on-site retention that permitted areas are required to have.

Within the Miami-Dade County portion of the model domain, the drainage categories were treated in a similar way to the permitted areas within Broward County. In stormwater management category 5 areas, those that drain to a canal and have little to no French drains, the detention storage was treated the same as non-permitted areas in Broward County and only parameterized based on land use, with values ranging from 0-0.4 inches (**Table 3-8**). In stormwater management category 6 areas, those that are internally drained to water bodies or low areas or have a large number of French drains, the detention storage was treated the same as permitted areas in Broward County and parameterized basin on land use and adjusted to account for retention. Although these areas are forced to drain to local depressions within the ponded drainage routine, the detention storage was increased to hold that drained water on site, representing the internal storage of local depressions and exfiltration areas. Otherwise, ponded water above the detention storage can still flow via the 2D overland flow routine into other drainage areas and then be routed to a branch. These category 6 areas were adjusted from 0.1-0.4 inches to 1-1.8 inches, based on land use. In drainage category 7 areas, those that drain to a canal and have a relatively large number of French drains, the detention storage was treated the same as permitted areas in Broward County and parameterized basin on land use and adjusted to account for retention provided by exfiltration areas, with values being increased from 0.1-0.4 inches to 1-1.8 inches. Category 7 areas differ from category 6 areas as they can drain to a branch within the ponded drainage routine, after the detention storage has been met. These values for stormwater management categories 6 and 7 areas were an initial model parameterization subject to change during model calibration but was not required.

3.7.5 Initial Water Depth (2D Overland Model)

The initial water depth defines the initial water depth on the ground surface in the 2-D overland module, also known as ponded water. This parameter was developed using an approach based on topography and basin control elevation, which is consistent with the 2019 Broward County model. Any cells within a drainage basin that are lower than the basin's water control elevation have an initial depth equal to the difference of the water control elevation and the elevation of the cell. This eliminates "dead storage" and ensures that water is not being routed via ponded drainage or flood codes at the start of the simulation. Specifying an initial depth will result in ponded water, which will eliminate the "dead storage" associated with a local sink. This also provides consistency between 1D and 2D model initial water elevations. The initial water depths for the 2D model are shown in **Figure 3.7-4.**

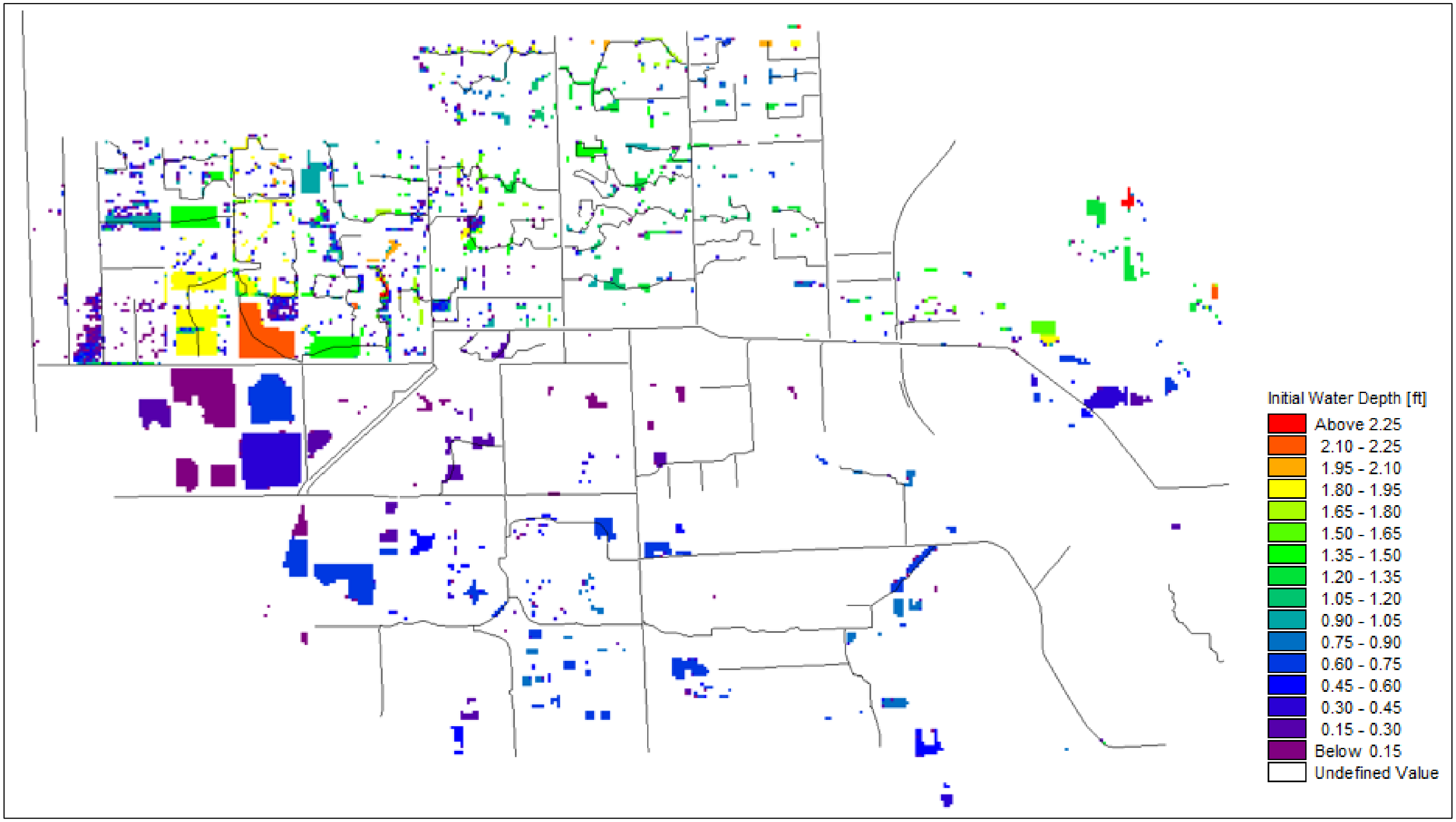

Figure 3.7-4: Initial Water Depths in the 2D Overland Flow Model

3.7.6 Surface-Subsurface Leakage Coefficient

This parameter reduces the exchange between land surface and the unsaturated or saturated zone, which can help account for near-surface soil compaction or fine sediment deposits. The model can be very sensitive to this parameter; too small of a value can essentially act as if there is an impermeable layer and allow for little to no infiltration. The leakage coefficient was set to a uniform spatial distribution using the model default value of 1E-4. No permanent changes to spatial distribution or magnitude were made during model calibration.

3.7.7 Ponded Drainage

This is a relatively new feature introduced in the 2017 release of MIKE SHE that simulates routing of ponded water from impervious surfaces via features that are not explicitly modeled, such as curb inlets and local-scale storm drains. The ponded drainage routine routes runoff from directly connected impervious areas to canals based on user-specified drainage basins (subbasins). The volume that is allowed to be routed is determined by a paved area runoff coefficient, which was assigned based on land use, and a maximum storage change rate. The rate at which the volume is routed is controlled by time constants. These ponded drainage parameters are discussed in **Section 3.7.7.1** through **Section 3.7.7.4**.

3.7.7.1 Maximum Storage Change Rate

For this study, the maximum storage change rate was set to a uniform spatial distribution with a value of 0.095 ft3/s (each grid cell limited to 40 mm/day), and then adjusted in specific areas where there was evidence suggesting a different value. Choosing realistic values ensures proper drainage representation and prevents drainage rates from exceeding sub-grid scale drainage capacities. For example, if sub-grid scale drainage features such as roadside swales and culverts are designed to handle 5-inches of rainfall over the course of a day, then the maximum storage rate should correspond. Within the Broward County portion of the model, the stormwater management category 2 area's maximum storage change rate was spatially distributed based on the permitted cubic feet per second per square mile (CSM) allowance per SFWMD drainage basin (**Appendix B**). In the western portion of the C-9 drainage basin, the allowable discharge is 20 CSM pumped, which is equivalent to 0.045 ft3/s based on the model grid size (each grid cell limited to 18.9 mm/day). This parameterization ensures that the permitted areas do not discharge more than their permitted allowance. Only category 2 permitted areas were based on the district's CSM allowance as these were the area's most likely holding water back in their surface waterbodies and discharging through structures at a permitted rate. Based on location, this 20 CSM pumped criteria only applies to one permit area in the western C-9 basin based on the way the stormwater management categories were developed. However, this one permit area happens to be explicitly simulated and is known to drain via gravity connection only, therefore, there were no areas where this 20 CSM pumped criteria applies. However, this categorization and criteria should be applied when considering future development and land use changes. It is important to note that this parameter is used to represent features not explicitly modeled. Therefore, areas such as the SBDD drainage basins were not included as they are physically represented by pump stations which follow permitted discharge rates.

The C-8 canal has "essentially unlimited inflow by gravity connection" **(Appendix B**), so no restrictions were necessarily required. This parameter could have been restricted in category 7 areas during model calibration, to help reduce the volume of runoff making it to the branch (capacity of exfiltration areas unknown), but changes were deemed unnecessary. Similarly, the initial value of 0.095 ft3/s, which is equivalent to about 43 CSM, could have been increased for the C-8 basin during model calibration, but again was deemed unnecessary.

This parameter will only limit discharge in the ponded drainage routine, which is meant to represent sub-grid scale drainage features (e.g., local-scale storm drains). Therefore, this will limit the ponded drainage discharge during bigger storm events, but this is appropriate. If the local small-scale drainage features were only designed to handle a 25-year storm, then the discharge will be limited during a 100-year storm. This does not limit discharge by 2-D overland flow. This parameter only limits the ponded drainage discharge, which is only responsible for routing a portion of the runoff occurring over the paved area fraction (i.e., directly connected impervious).

3.7.7.2 Paved Runoff Coefficient

This parameter, similar to DCIA, is spatially distributed based on land use and stormwater management categories (SMC). Essentially, the paved runoff coefficient is the fraction of *ponded* water (not precipitation) that drains to storm sewers and other surface drainage features in paved areas (DHI, 2017). Within Broward County, the paved runoff coefficients were parameterized based on land use. In SMC 3a areas, the coefficients were distributed based on land use like everywhere else, but then decreased by half. Since these permitted areas are assumed to use management features such as exfiltration trenches, the paved runoff coefficients were adjusted to reduce the amount of runoff and increase the infiltration, as one would expect in areas served by exfiltration features. Within Miami-Dade County, the paved runoff coefficients were parameterized based on land use. In areas served by a relatively large number of French drains, the coefficients were distributed based on land use, but then decreased by half, just like SMC 3a areas within Broward County. Decreasing the paved runoff coefficient reduces runoff which provides the opportunity for increased infiltration. This parameterization was done as an attempt to simulate what cannot be explicitly represented in this scale of a model. The land use areas that were included in the ponded drainage routine can be seen in **Table 3-9** . All other land use categories, such as forests, were set to 0, which “turns off” the ponded drainage routine for those areas. These paved runoff coefficients were derived from previous models and professional experience.

Table 3-9: Land Use Based Paved Runoff Coefficients

FLUCCS Code	Land Use	Paved Runoff Coefficient	Paved Runoff Coefficient for SMC 3a, 6, & 7 Areas
1100	Residential, Low Density	0.075	0.0375
1200	Residential, Medium Density	0.22	0.11
1300	Residential, High Density	0.45	0.225
1400	Commercial and Services	0.72	0.36
1500	Industrial	0.4	0.2
1700	Institutional	0.3	0.15
8100	Transportation	0.56	0.28

3.7.7.3 Inflow and Outflow Constant

These parameters can be adjusted to speed up or slow down the rate at which ponded drainage is routed to the river branches. Making the inflow constant larger than the outflow constant will create artificial storage, so this was avoided. An initial value of 0.001 (model default) was used as a starting point for both inflow and outflow constants. No permanent changes were made during model calibration.

3.7.7.4 Drain Codes

Each drain code represents an individual subbasin, for the purpose of draining water internally or to a branch via the ponded and saturated zone drain routines. It should be noted that these “subbasins” do not prevent overland exchange between areas. In areas of uncertainty, drainage basins were left as larger areas so that the 2-D overland flow model could determine drainage divides. Basins were only further refined if there was clear evidence in the DEM, such as visible berms or water bodies with differing elevations. In the Broward County portion of the model, the majority of the area was defined based on data provided by South Broward Drainage District and their permitted drainage basins. In the Miami-Dade portion of the model, subbasins were developed from data provided digitally by Miami-Dade County. Miami-Dade County provided very detailed subbasin data, much too refined for this scale model. Therefore, new subbasins were developed by defining and aggregating basins based on drainage categories (as discussed in **Section 3.7.2**) and drainage destination (such as a specific canal). Essentially, areas with the same classification that shared a common boundary and destination, were merged into one basin. This process resulted in the number of basins in the Miami-Dade portion of the model to be decreased from about 830 basins down to about 40, while maintaining drainage characteristics.

Cells assigned an initial depth or a flood code, were assigned a drain code of 0 (dark blue cells in **Figure 3.7-5**), which turns off drainage from that cell. Not doing so would create feedback loops, as the drained water would return back to the cell via flood code, only to be drained back to the branch again and so on. **Figure 3.7-5** shows a map of the drain codes, where each unique color represents a drainage basin (areas in yellow drain to boundary). Although the specific value of the positive drain codes do not matter (negative drains internally or to boundary) as they are just an identifier that define a drainage area, the drain code values in the C-9 basin were kept the same as the 2019 Broward County Model for consistency. New drain codes were assigned identifiers not used in the 2019 Broward County model, which should eliminate any issues in the future if the models are merged together.

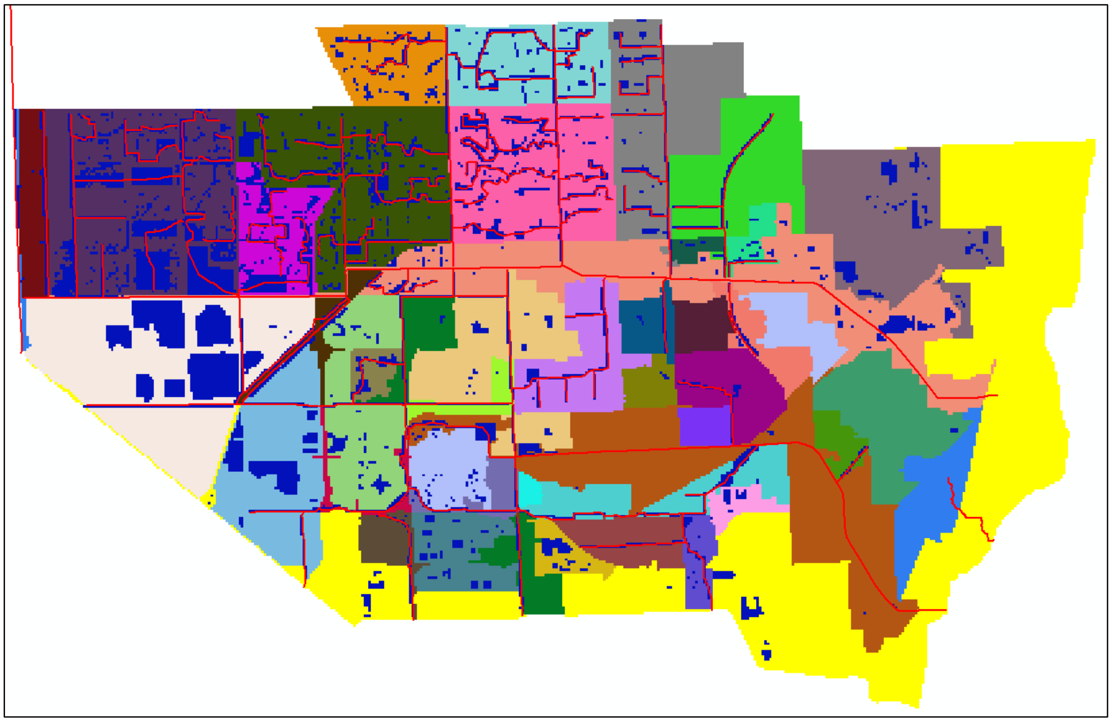

Figure 3.7-5: Drain Codes used to Delineate Common Drainage Areas

3.7.8 Boundary Conditions (2D Model)

For the calibration and validation model, no 2-D overland boundary conditions were applied. However, a 2-D overland tidal boundary was included in the design storm simulations using the spatial distribution shown in **Figure 3.7-6** based on the District-provided time series for S-28 and S-29 (**Figure 3.6-4** and **Figure 3.6-5**).

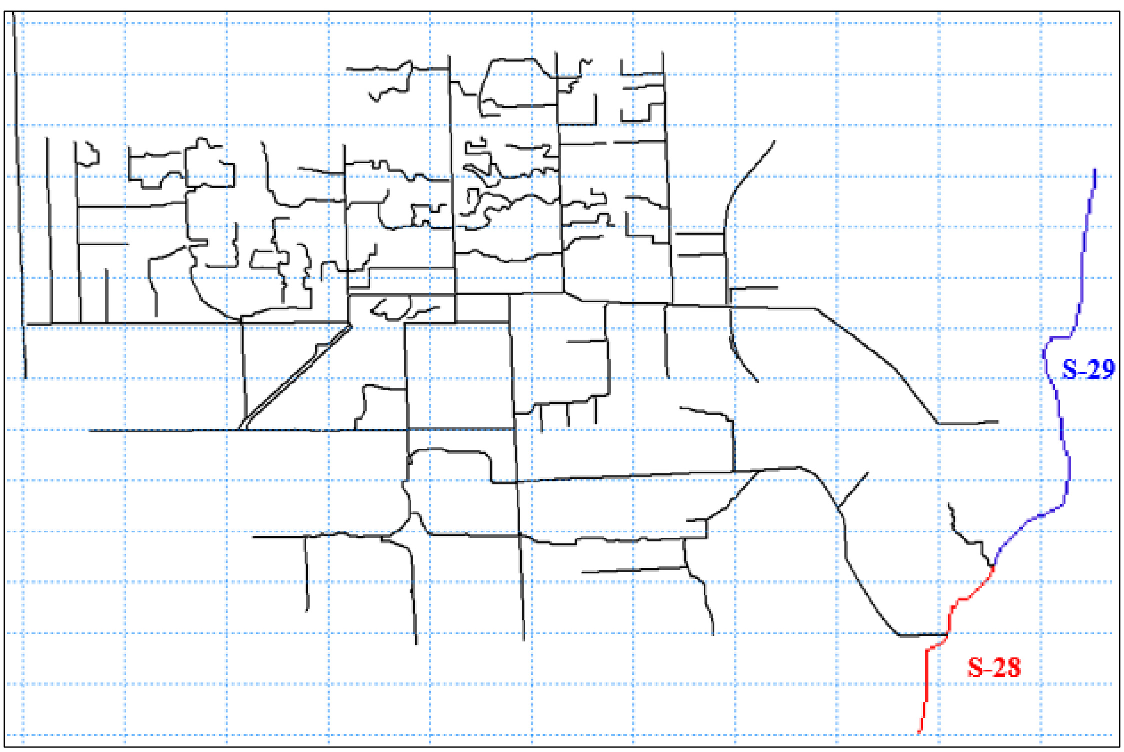

Figure 3.7-6: Spatial Distribution of 2-D Overland Flow Tidal Boundary

3.8 Unsaturated Zone

The soil distributions and unsaturated zone parameters were carried over from the 2019 Broward County Current Conditions model (which were mainly inherited from the Broward County 2014 FEMA model) (**Figure 3.8-1**). The 2019 Broward County model's soil parameters that were changed were the saturated water content and field capacity for Margate Fine Sand and the field capacity for urban land, which were adjusted during model validation in an effort to improve the groundwater response to rainfall. These are incorporated in this model from the start. This model uses the simple 2-layer water balance method for unsaturated zone calculations, which is consistent with the 2019 Broward County model. **Table 3-10** shows the final soil parameters.

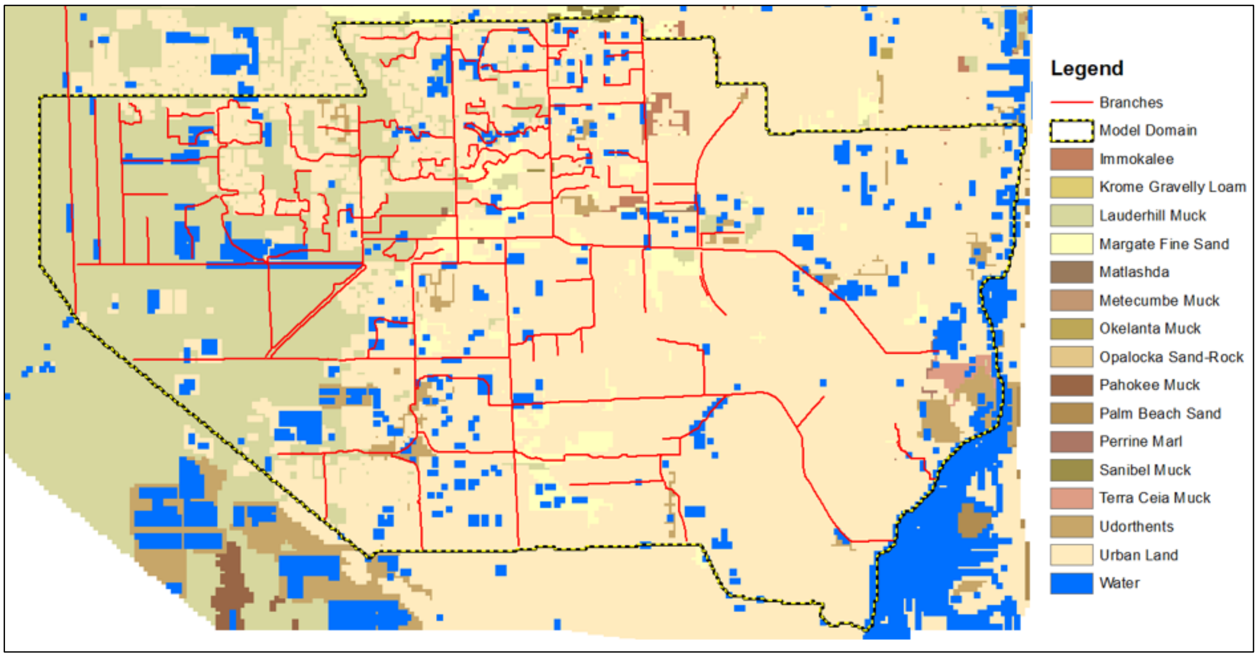

Figure 3.8-1: Map of Soils

Table 3-10: Unsaturated Zone Soil Parameters

2-Layer Unsaturated Zone Soil Profiles	Water content at saturation	Water content at field capacity	Water content at wilting point	Saturated hydraulic conductivity (ft/day)
Immokalee	0.44	0.14	0.06	85.0
Krome Gravelly Loam	0.45	0.17	0.08	28.3
Margate Fine Sand	0.35	0.18	0.06	28.3
Matlashda	0.42	0.09	0.04	198.4
Opalocka Sand-Rock	0.42	0.09	0.06	198.4
Palm Beach Sand	0.42	0.09	0.06	198.4
Perrine Marl	0.47	0.25	0.13	28.3
Muck	0.7	0.59	0.18	141.7
Udorthents	0.3	0.13	0.08	28.3
Urban Land	0.3	0.2	0.08	28.3

3.9 Saturated Zone

As previously mentioned, this model was initially parameterized based on the 3-layer MODFLOW model developed by the USGS (Hughes and White, 2016). The final saturated zone configuration was based on the 5-layer 2019 Broward County Current Conditions model. Although the C-8 and C-9 model is based on the 2019 Broward County Current Conditions model, there are still setup differences between the two. In the C-8 and C-9 model, only the first 3 of the 5 layers of the 2019 Broward County groundwater model were used. The top 3-layers are adequate for short-term flood event modeling, whereas the 5-layer model was designed for long-term water supply modeling. This would prevent the C-8 and C-9 model from being merged directly, but a simple solution would be to just add the last 2 groundwater layers into the C-8 and C-9 model if merging them is desired in the future.

3.9.1 Lower Levels of Computation Layers

This parameter was originally spatially distributed based on data from Hughes and White (2016) (refer to Deliverable 1.2, *C8-C9 Model Development Memorandum* (Taylor Engineering, 11/4/2019)). The final configuration is based on the 2019 Broward County Current Conditions model. **Figure 3.9-1** through **Figure 3.9-3** show the lower levels of the three saturated zone layers.

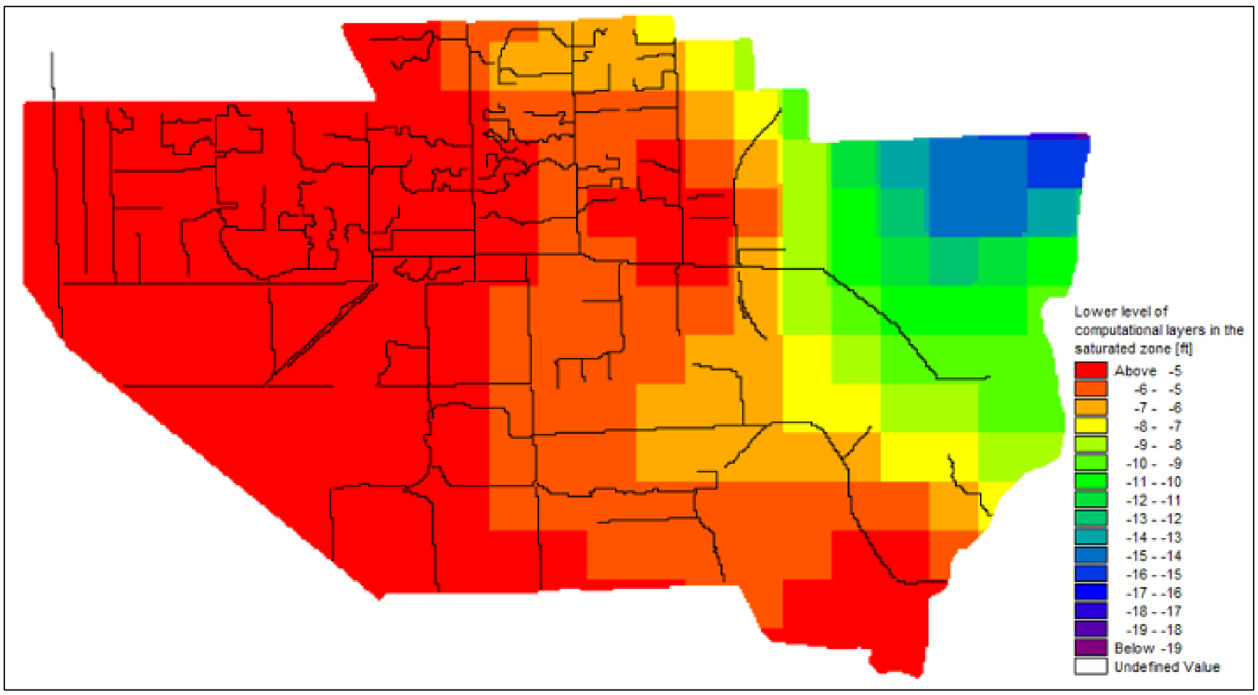

Figure 3.9-1: Lower Level of Computational Layer 1

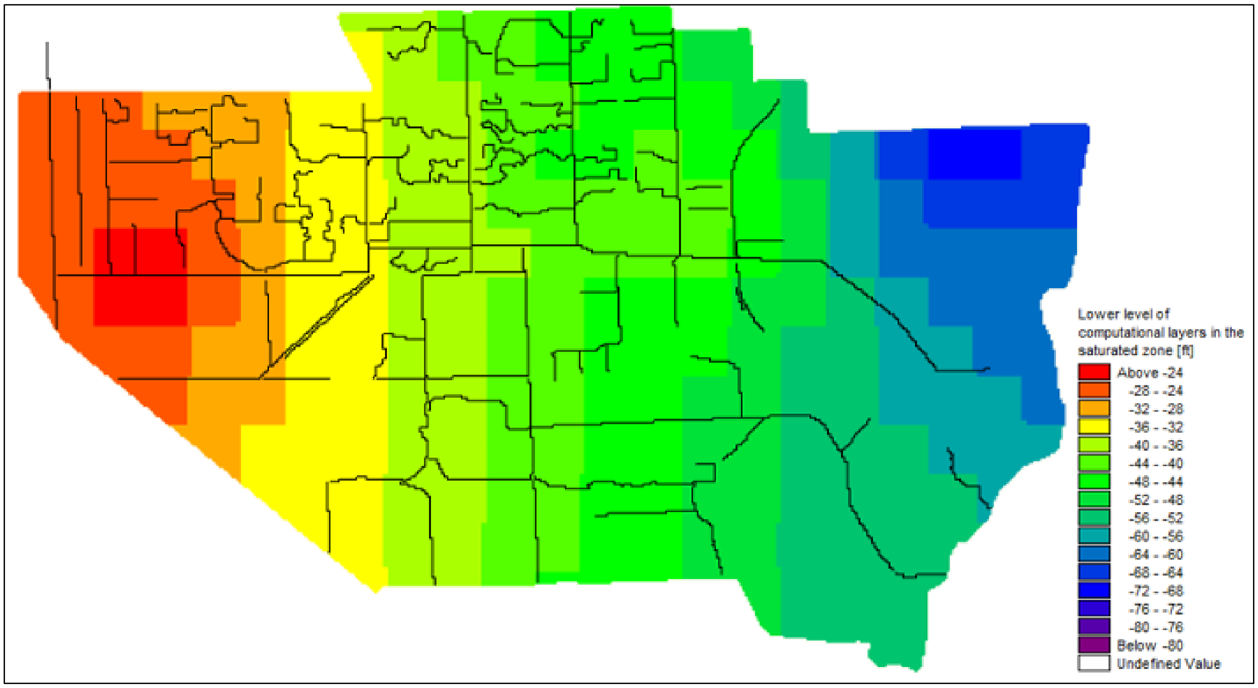

Figure 3.9-2: Lower Level of Computational Layer 2

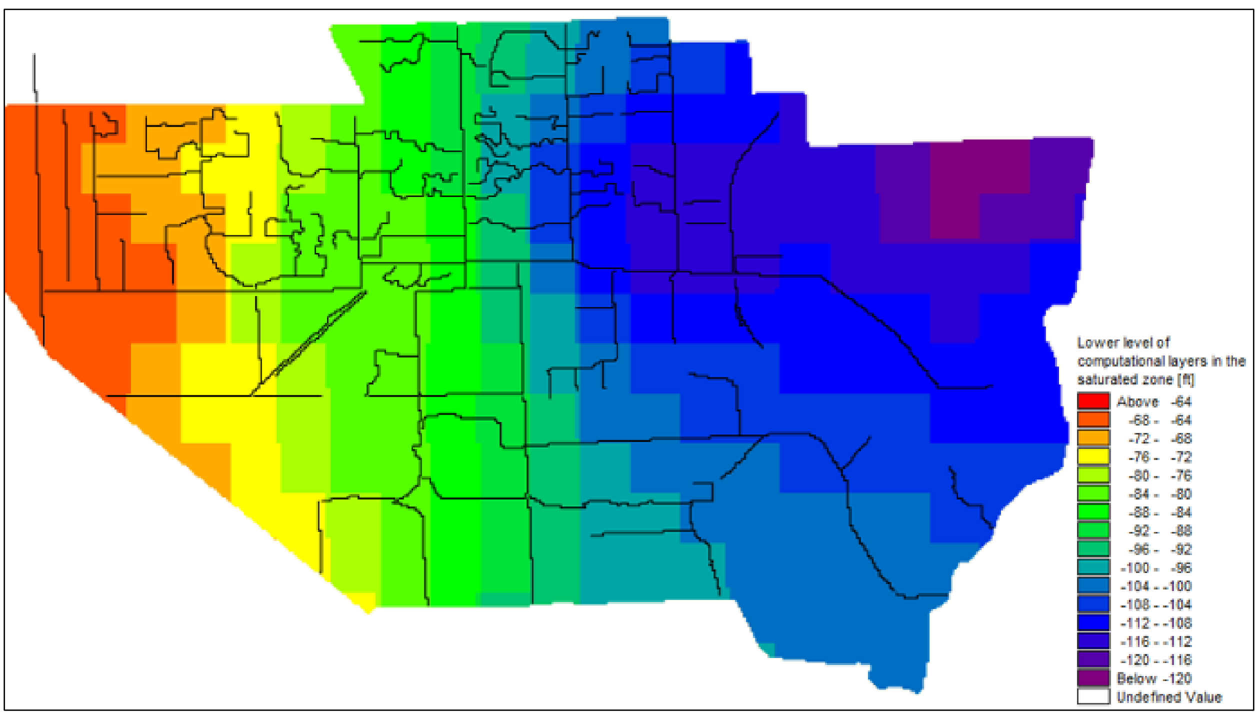

Figure 3.9-3: Lower Level of Computational Layer 3

3.9.2 Horizontal Hydraulic Conductivity

This parameter was originally spatially distributed based on data from Hughes and White (2016) (refer to Deliverable 1.2, *C8-C9 Model Development Memorandum* (Taylor Engineering, 11/4/2019), **Appendix I**). The final configuration is based on the 2019 Broward County Current Conditions model. **Figure 3.9-4** through **Figure 3.9-6** show the horizontal hydraulic conductivity of the three saturated zone layers.

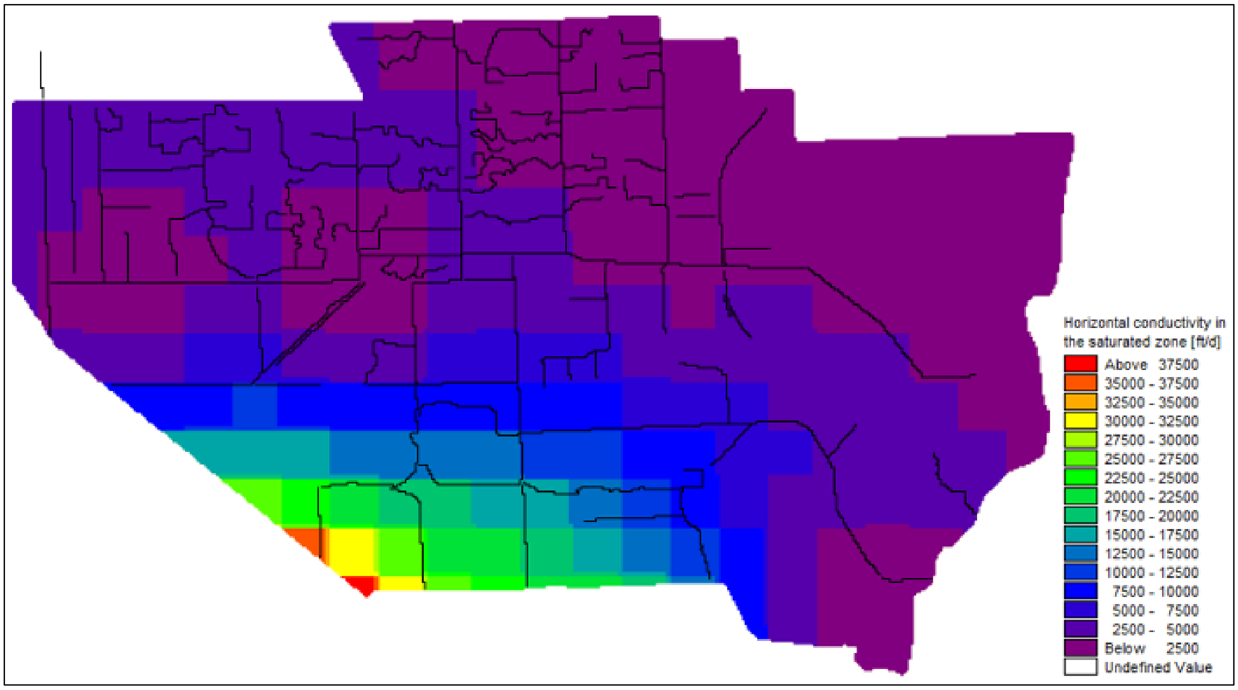

Figure 3.9-4: Horizontal Hydraulic Conductivity in Layer 1

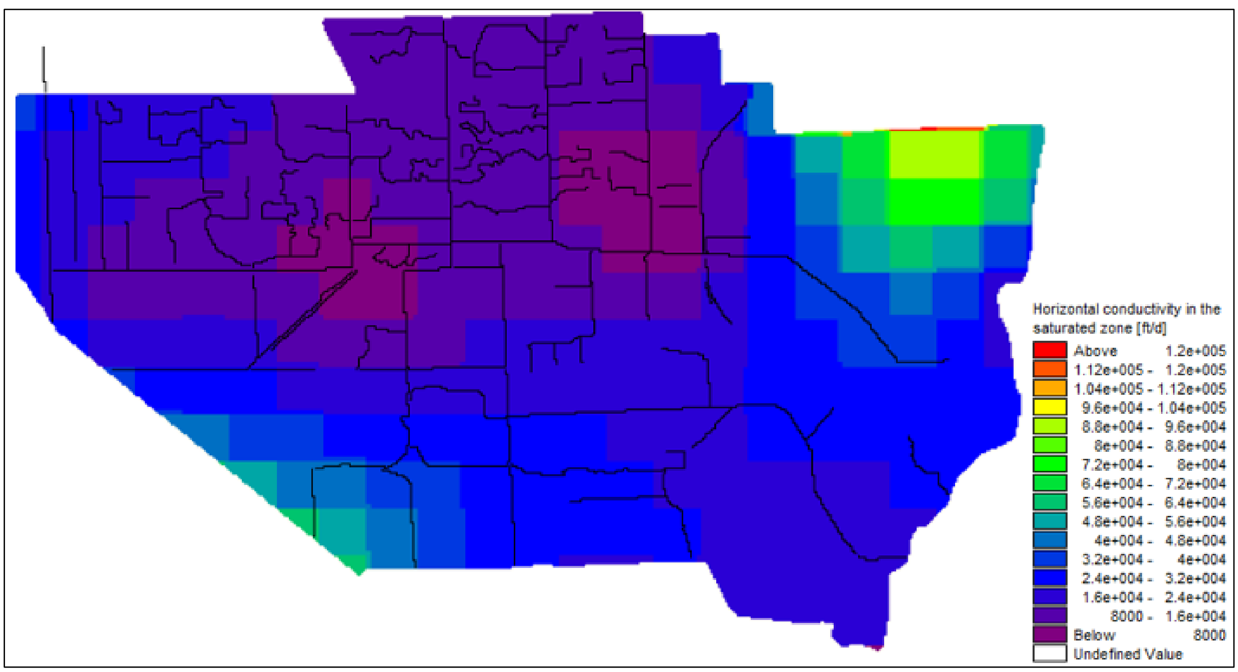

Figure 3.9-5: Horizontal Hydraulic Conductivity in Layer 2

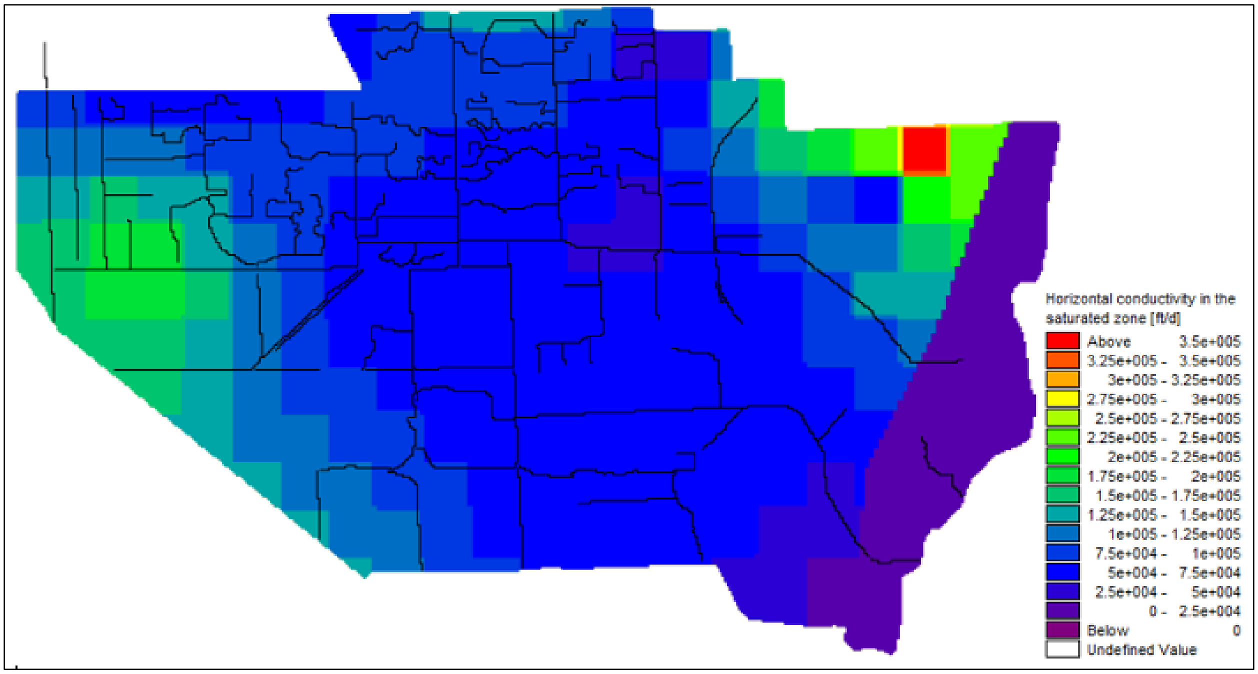

Figure 3.9-6: Horizontal Hydraulic Conductivity in Layer 3

3.9.3 Vertical Hydraulic Conductivity

This parameter was originally spatially distributed based on data from Hughes and White (2016) (refer to Deliverable 1.2, *C8-C9 Model Development Memorandum* (Taylor Engineering, 11/4/2019)). The final configuration is based on the 2019 Broward County Current Conditions model. **Figure 3.9-7** through **Figure 3.9-9** show the vertical hydraulic conductivity of the three saturated zone layers.

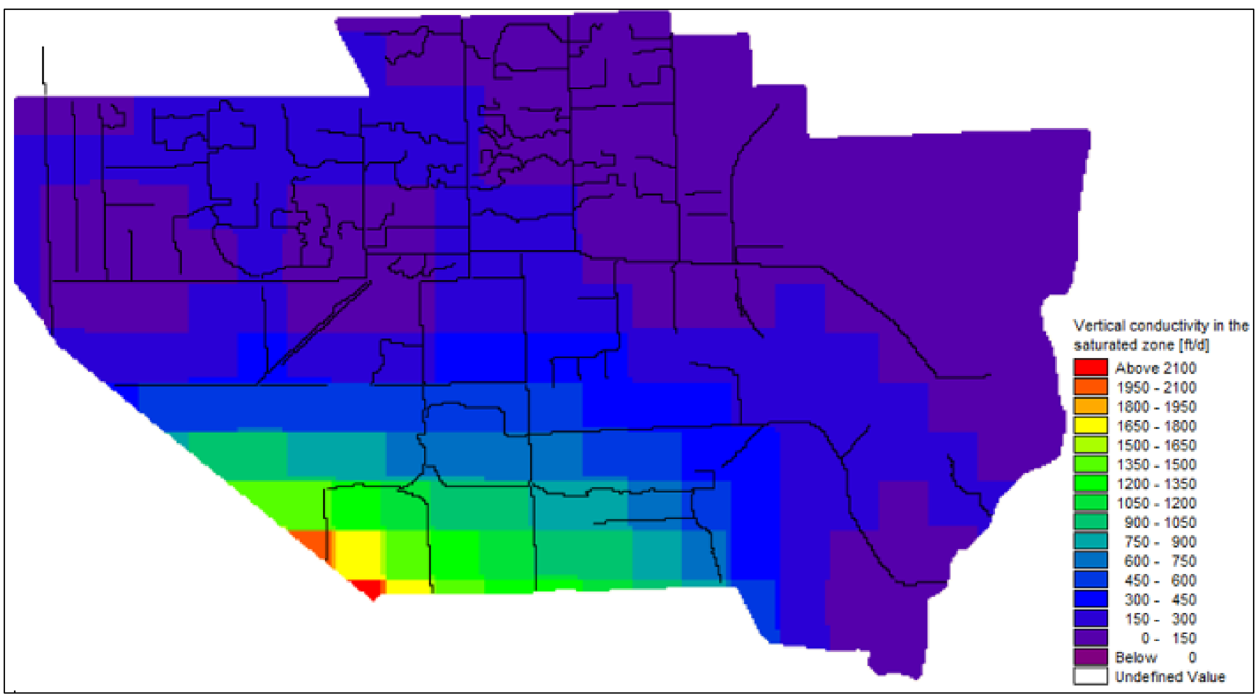

Figure 3.9-7: Vertical Hydraulic Conductivity in Layer 1

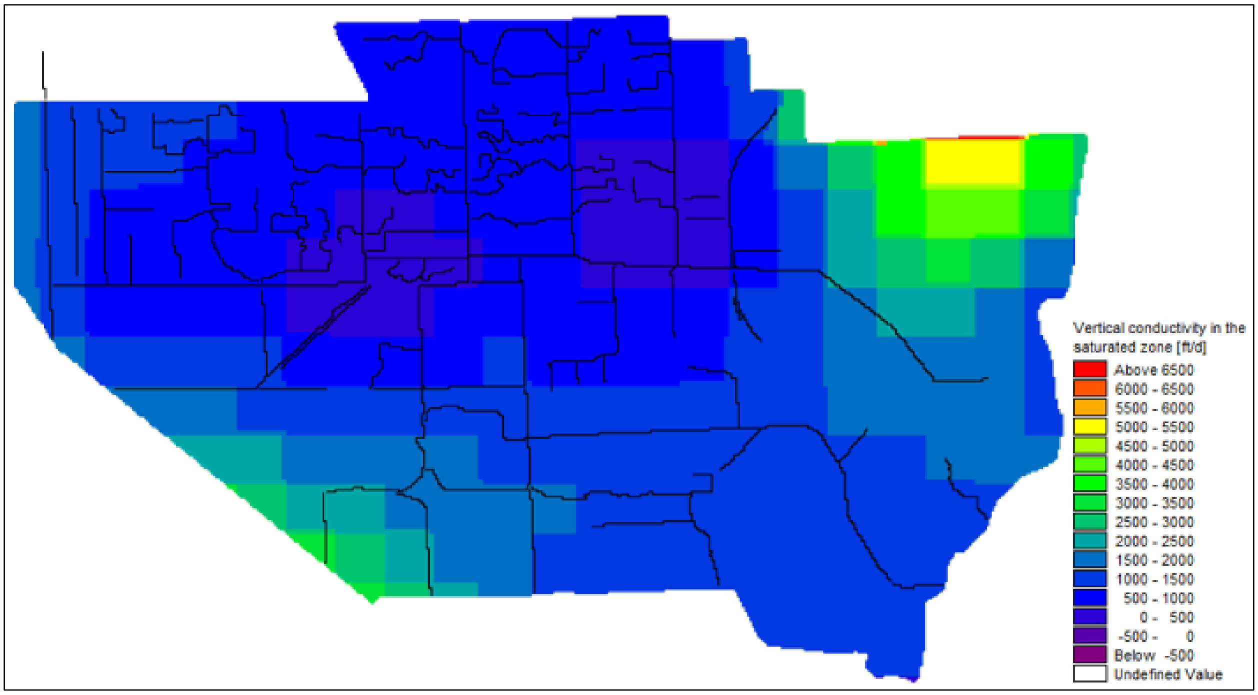

Figure 3.9-8: Vertical Hydraulic Conductivity in Layer 2

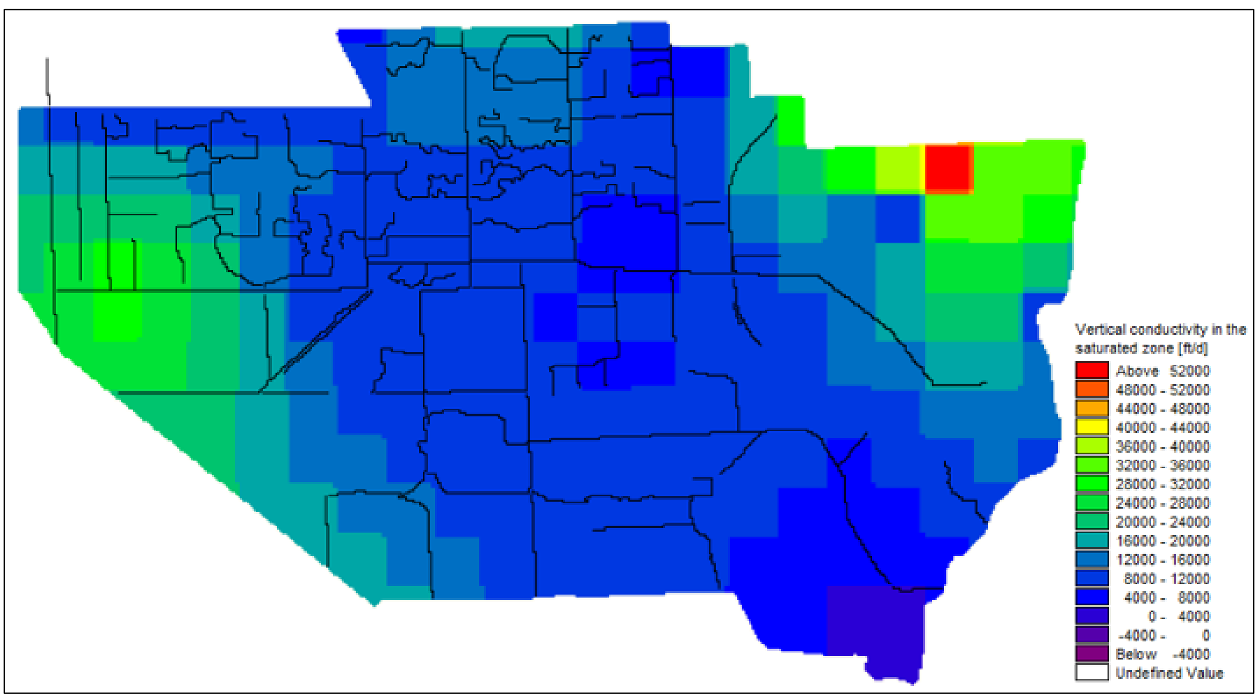

Figure 3.9-9: Vertical Hydraulic Conductivity in Layer 3

3.9.4 Specific Yield

This parameter was originally spatially distributed based on data from Hughes and White (2016) (refer to Deliverable 1.2, *C8-C9 Model Development Memorandum* (Taylor Engineering, 11/4/2019)). The final configuration is based on the 2019 Broward County Current Conditions model. **Figure 3.9-10** shows the user-specified specific yield of the three saturated zone layers. During model preprocessing, MIKE SHE adjusts the specific yield layer one of the saturated zone based on the difference between the water content at saturation and field capacity, based on the two-layer UZ soil type (**Figure 3.9-11**).

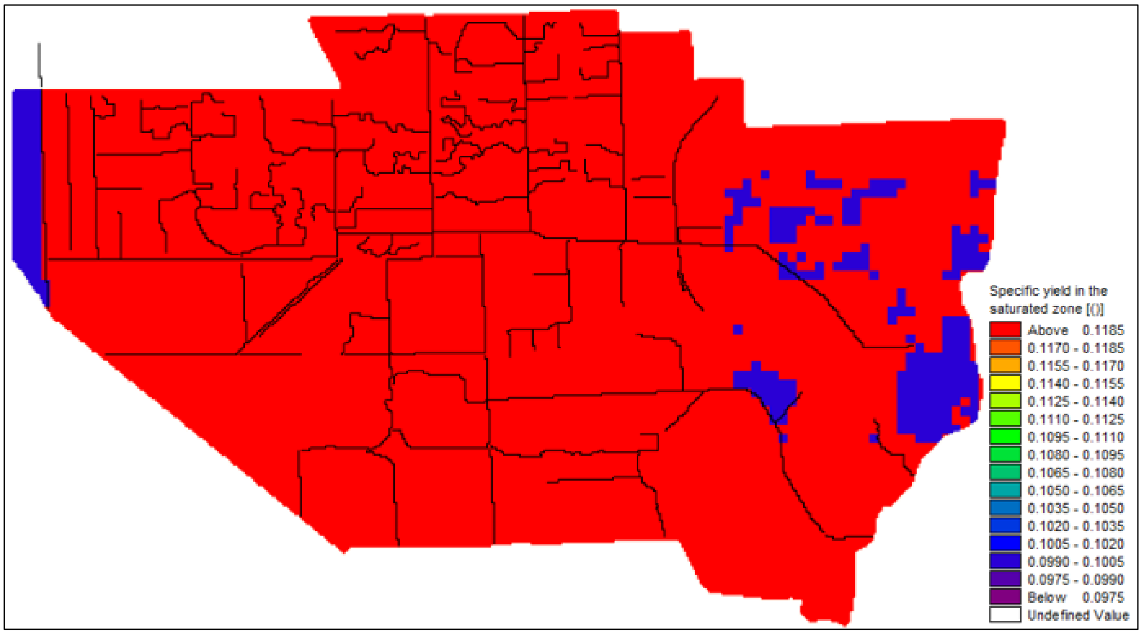

Figure 3.9-10: User Specified Specific Yield in Layers 1, 2, and 3

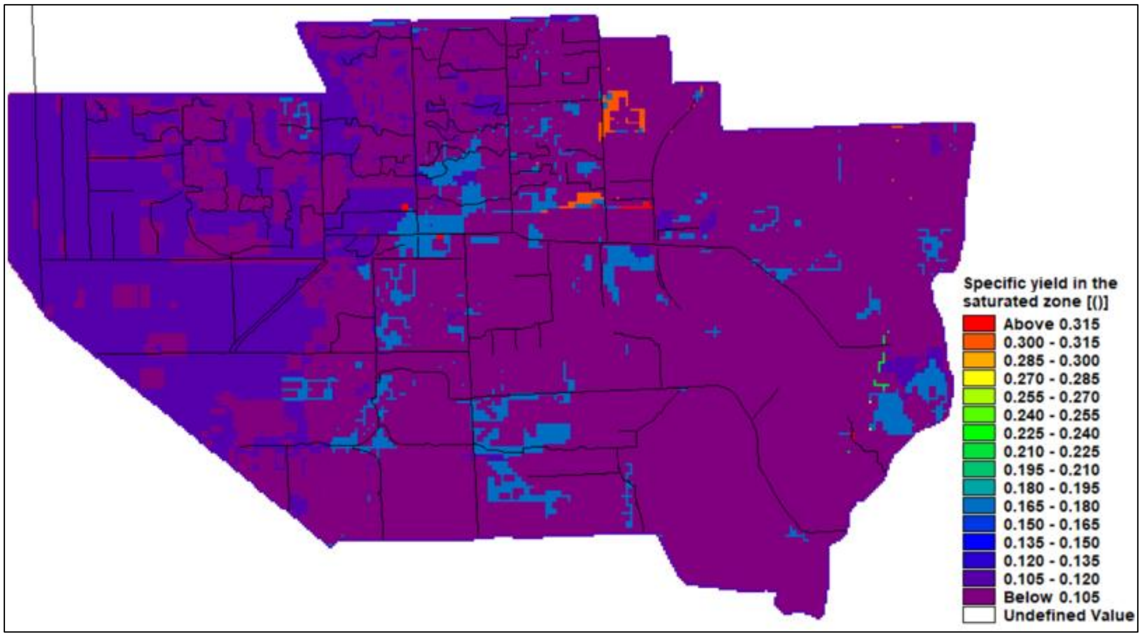

Figure 3.9-11: Model-Adjusted Specific Yield in Layer 1

3.9.5 Specific Storage

This parameter was originally spatially distributed based on data from Hughes and White (2016) (refer to Deliverable 1.2, C8-C9 Model Development Memorandum (Taylor Engineering, 11/4/2019)). The final configuration is based on the 2019 Broward County Current Conditions model. Layer 1 was given a uniform specific storage of 0.06096/ft, based on the 2019 Broward County Current Conditions model. **Figure 3.9-12** and **Figure 3.9-13** show the specific storage of the bottom two saturated zone layers.

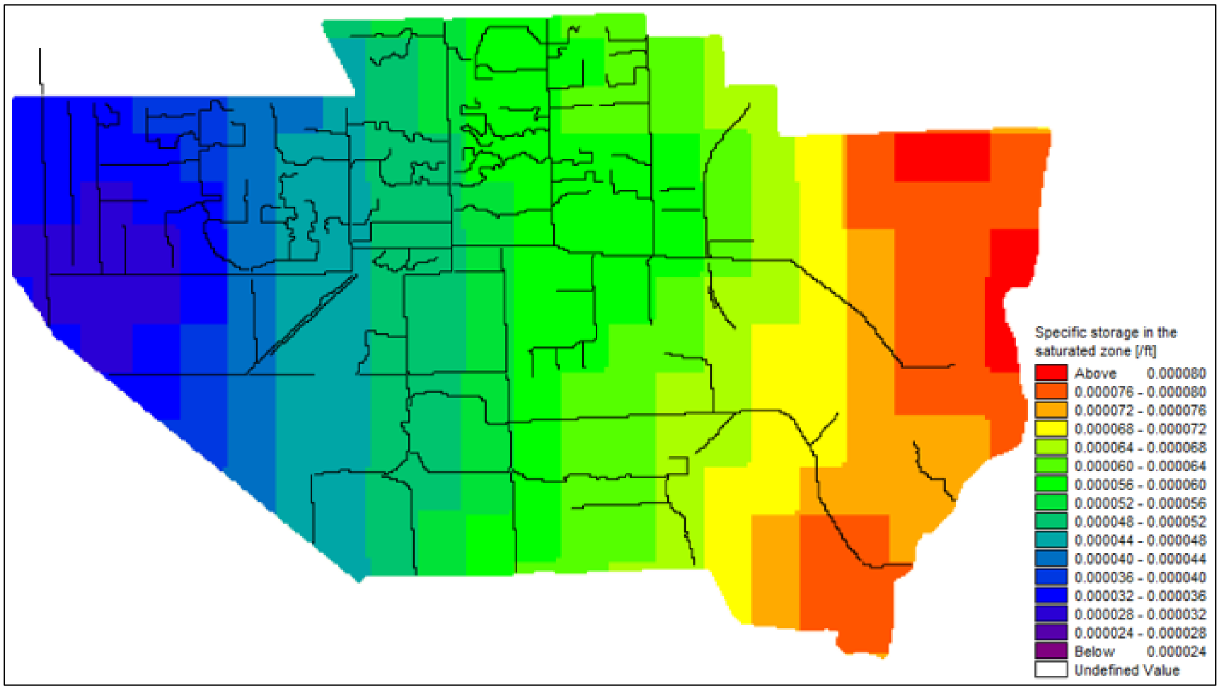

Figure 3.9-12: Specific Storage in Layer 2

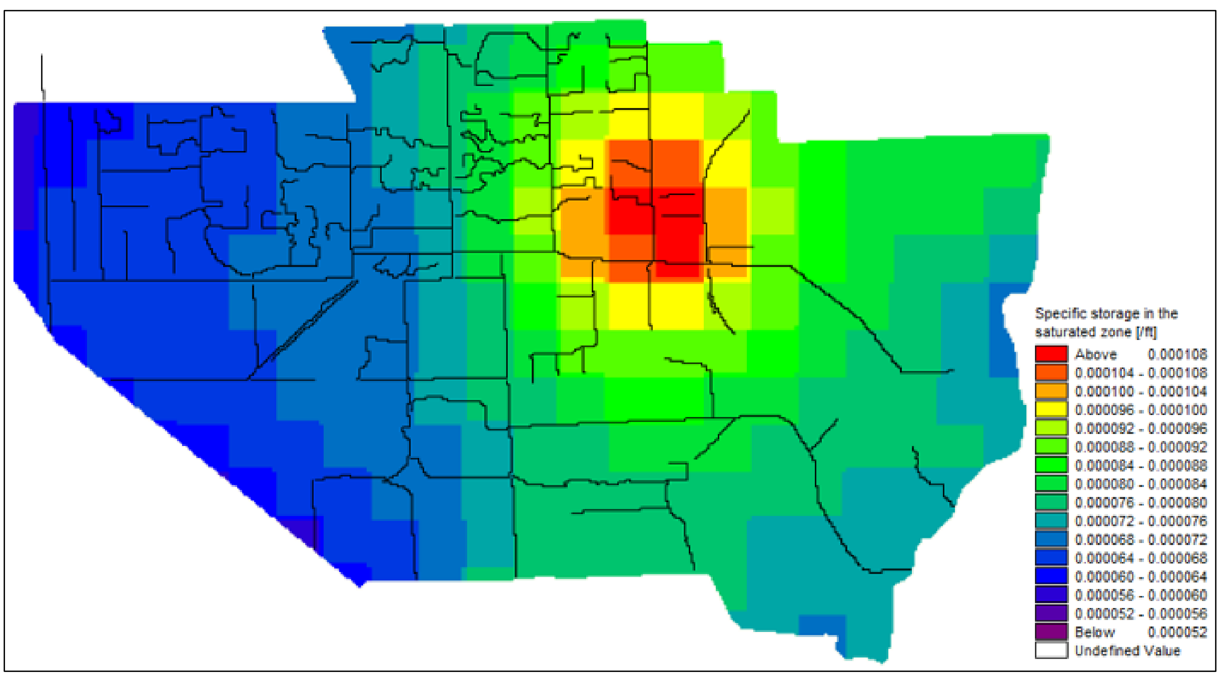

Figure 3.9-13: Specific Storage in Layer 3

3.9.6 Initial Potential Head

3.9.6.1 Calibration Model

Although there were groundwater wells within the model domain that had data available, there were not enough locations to generate a high confidence surface. Therefore, this parameter is spatially distributed based on results from Hughes and White (2016), with slight modification. The initial potential head from the USGS model was a close match at many of the observed points and had what appeared to be realistic "drawdown" near major branches. Therefore, the USGS data was used as a starting point and some localized adjustments were so that made it was a closer match to the observed data. The initial potential head map (**Figure 3.9-14**) is within about +0.25 ft of the observed well elevations at the start of the simulation period.

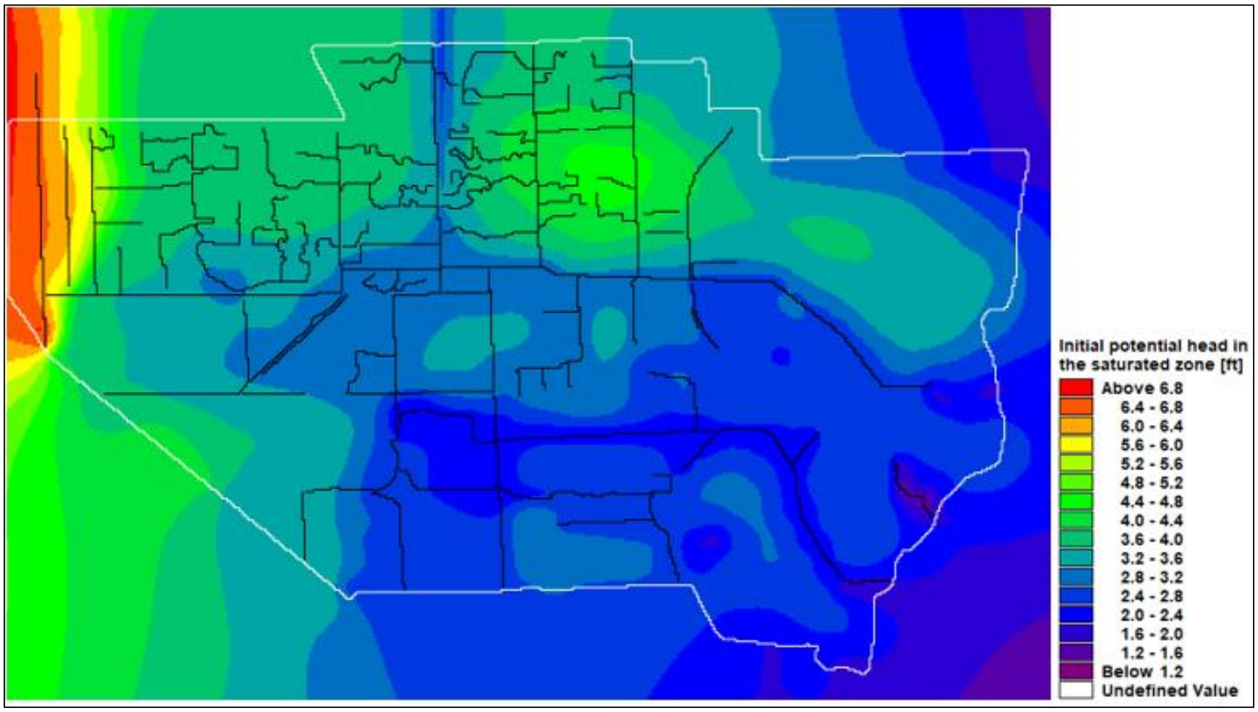

Figure 3.9-14: Initial Potential Head in Saturated Zone for October 2nd, 2000

3.9.6.2 Validation Model

The initial potential head for the validation simulation is spatially distributed based on data from Broward County's average wet season head map (Broward County, 2000) (used to generate the initial potential head for the 2019 Broward County Current Conditions Model) and USGS wet season groundwater contours (Fish and Stewart, 1991). **Figure 3.9-15** shows how the initial potential head for the validation simulation was generated and **Figure 3.9-16** shows the final initial potential head. The initial potential head is within about +/- 0.5 ft of observed well elevations near the start of the validation simulation, which is part of the 3+ month spin-up period.

Figure 3.9-15: Development of Initial Potential Head for Validation Simulation

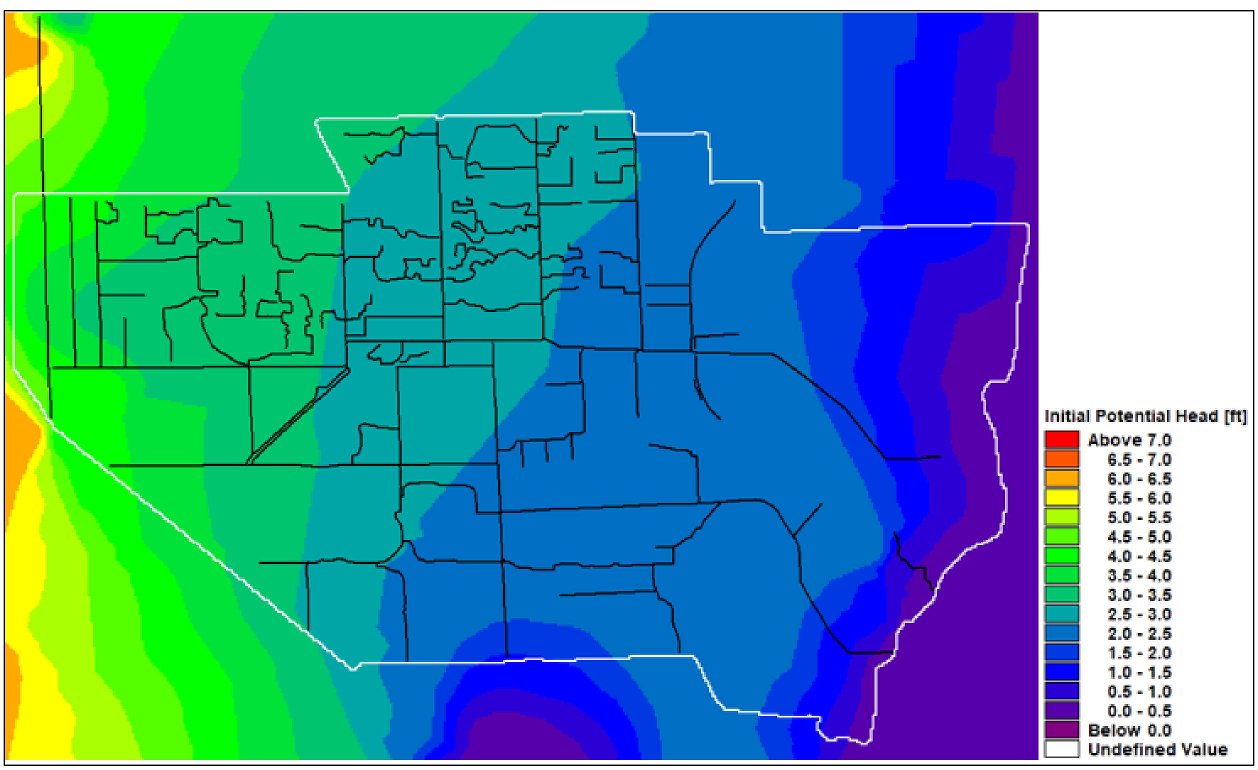

Figure 3.9-16: Initial Potential Head in Saturated Zone for Validation Simulation

3.9.6.3 Design Storm Model

The design storm initial groundwater elevations were developed by making localized adjustments to the initial potential head from the validation simulation. Although the initial potential head matched the observed groundwater elevations within +/- 0.5 ft, there were some areas where the groundwater levels were upwards of 1 ft lower than the water bodies within an area of established control elevations. This difference was not significant for the validation model as this was at the start of the 3-month spin-up period. However, for the design storm scenarios, which were only given a 2-day spin-up period, it is significant. Therefore, for the design storms, the initial groundwater levels were adjusted so that they closely matched basin control elevations, where they existed. This was done by changing initial water levels in areas that have established basin control elevations, and then running the model without any rainfall for a brief period of time so that any discontinuities resulting from differences in basin water control elevations smooth out. After 6 hours of simulation with no rainfall, this approach resulted in an initial potential head that matched basin control elevations closely in areas where they existed, eliminated elevation discontinuities, and created smooth gradients. This was done to prevent the water levels in the lakes to drop (or rise) due to lower (or higher) initial groundwater elevations. **Figure 3.9-17** shows the final initial potential head developed for the current condition design storm simulations.

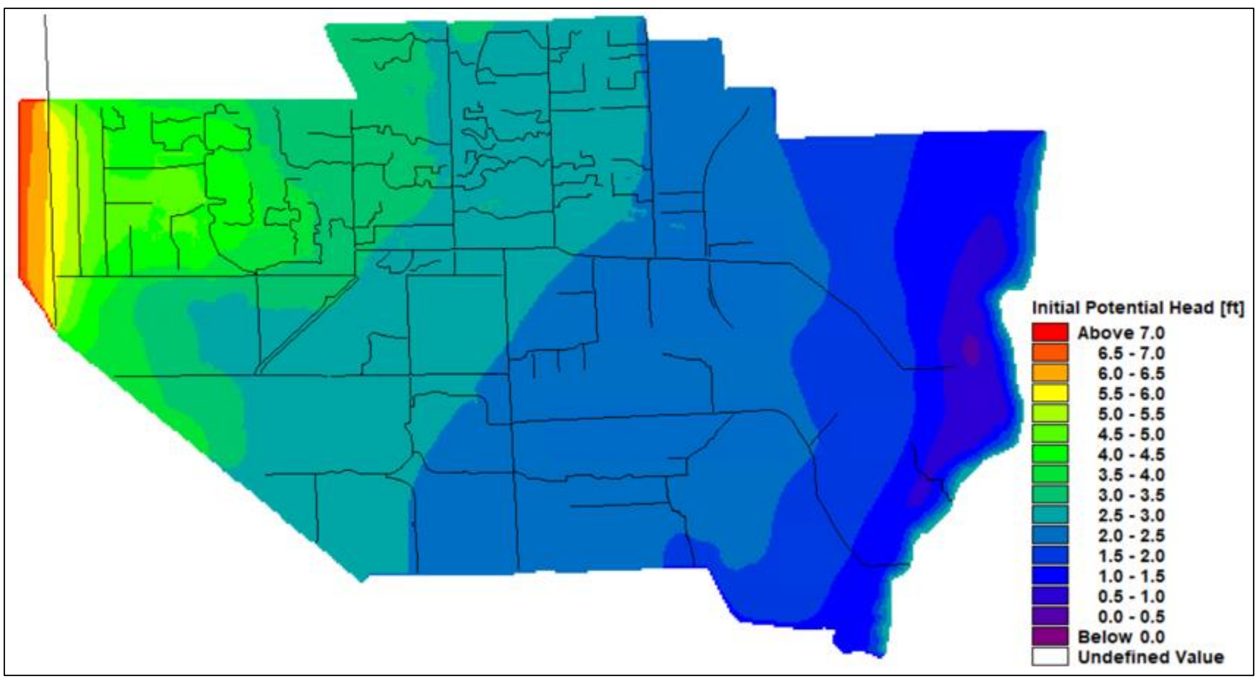

Figure 3.9-17: Initial Potential Head in Saturated Zone for Design Storm Simulations

3.9.7 Boundary Conditions

Refer to **Section 2.8.1** & **2.8.2** for boundary condition set up for the calibration and validation simulations. For the design storm simulations, SFWMD provided year 2015 tidal boundary data at the S-28 and S-29 structures, which include storm surge effects for the design storms of interest. The saturated zone tidal boundaries were assigned the same spatial distribution as the 2-D overland flow boundary shown in **Figure 3.7-6** using the District-provided time series for S-28 and S-29 (**Figure 3.6-4** and **Figure 3.6-5**).

The western boundary (**Figure 3.9-18**) and western internal boundary (**Figure 3.9-19**) were set to observed data from the June 2017 storm event. As June 2017 was wetter than normal in the weeks leading up to it, Water Conservation Area 3B stage was already elevated. Taylor Engineering proposed to use the observed data (**Figure 3.9-20**) as an assumed design storm boundary as the elevated levels may be equivalent to what could be expected during a design storm, and the District agreed this is a reasonable approach.

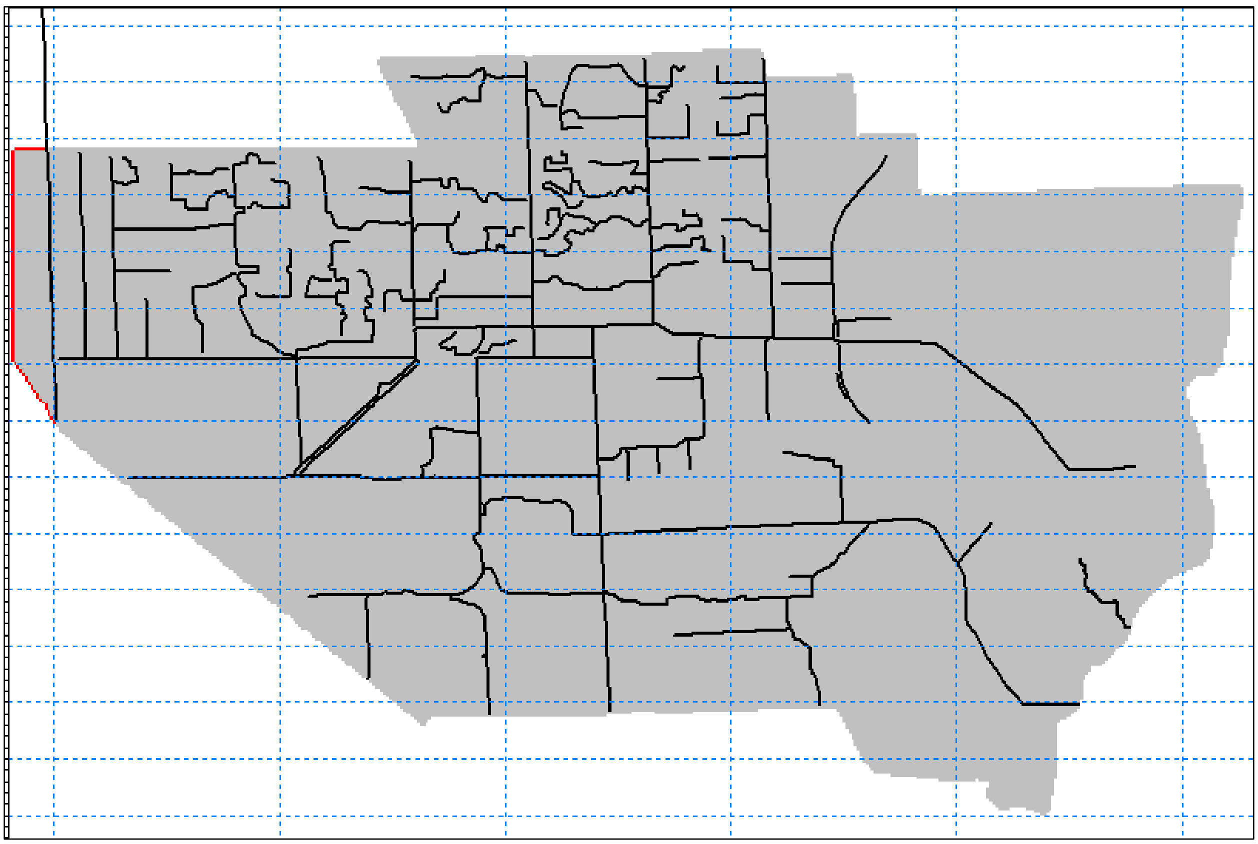

Figure 3.9-18: Western General Head Groundwater Boundary Location

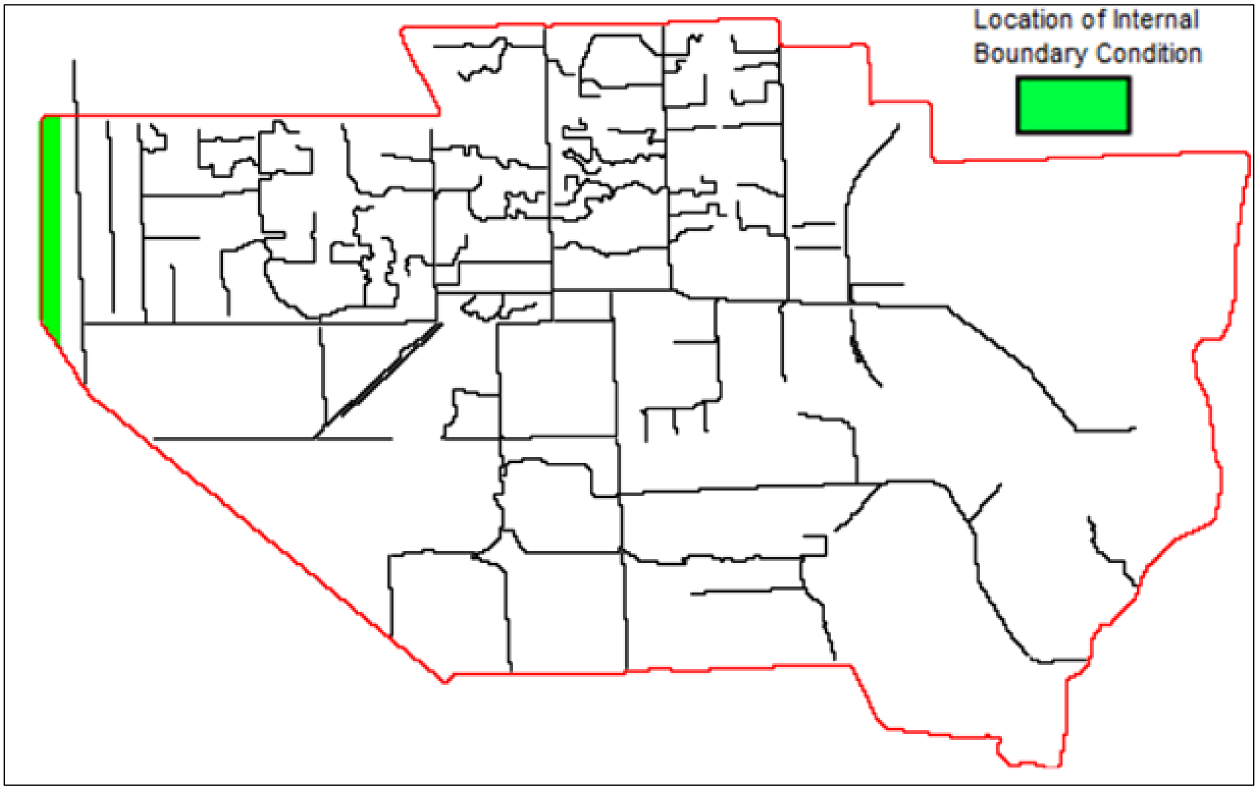

Figure 3.9-19: Western Internal Head-Controlled Flux Boundary Location

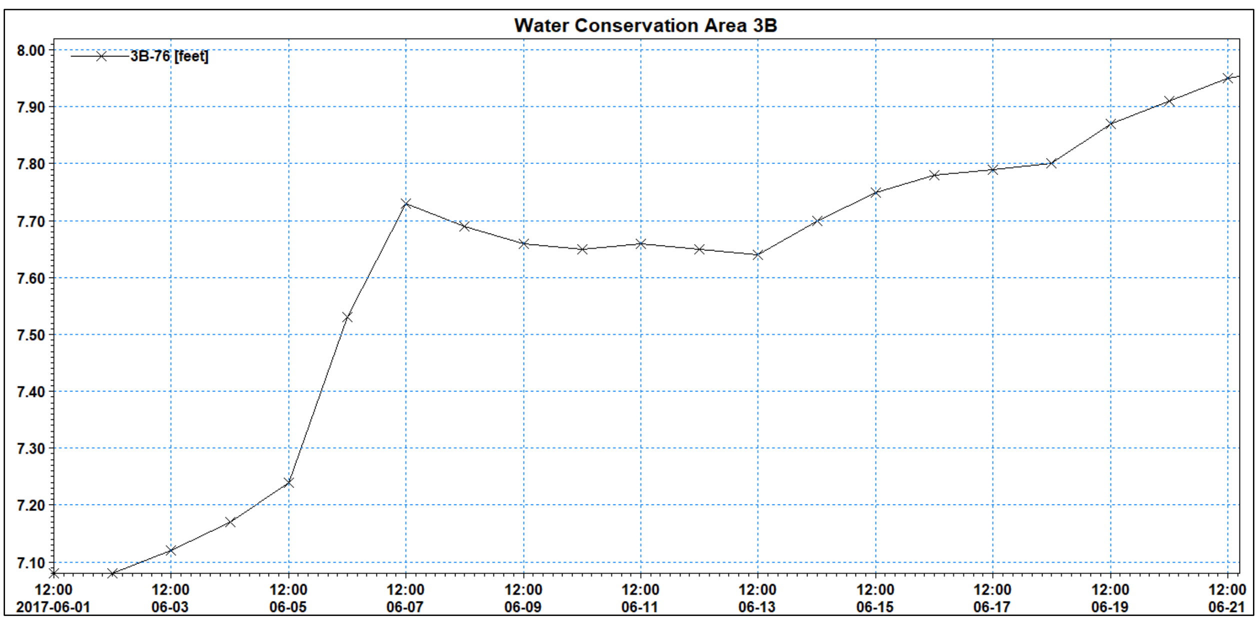

Figure 3.9-20: Western General Head Groundwater Boundary Stage Time-Series

The northern general head groundwater boundary used simulated groundwater elevations from the 2019 Broward County design storm models, which is based on the same storm event. The southern general head groundwater boundary was split into 4 sections and was assigned District-provided simulated canal stage data from XP SWMM and HEC RAS models for the C-6 and C-7 canals. The four sections are S-27 headwater and G-72 tailwater on the C-7 Canal and G-72 headwater and S-31 tailwater on the C-6 canal. The time series for the groundwater general head boundaries for the four segments also served as the downstream boundary conditions for the 1-D branches connecting to the C7 and C6 Canals. The spatial distribution and time-series data for S-27 headwater are shown in **Figure 3.9-21** and **Figure 3.9-22**, respectively.

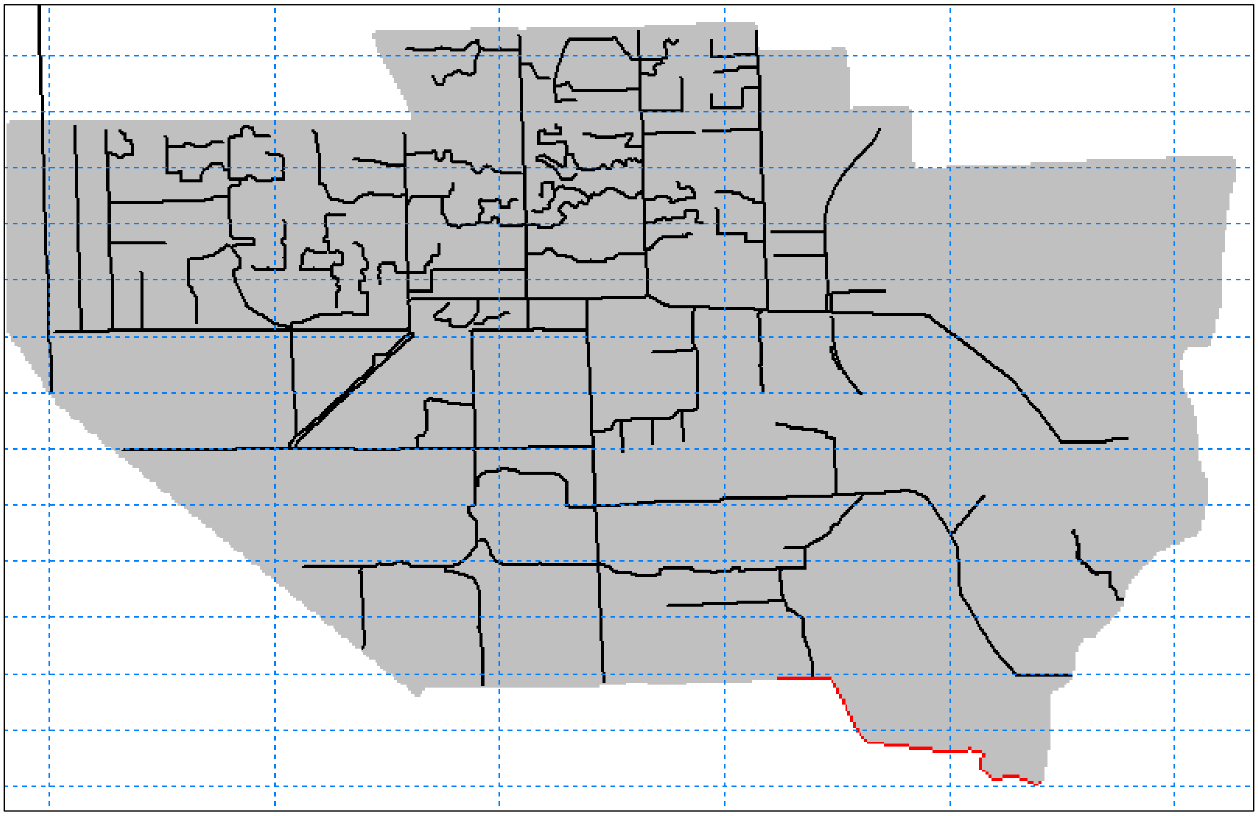

Figure 3.9-21: General Head Groundwater Boundary Using S-27 HW Simulated Design Storm Stages

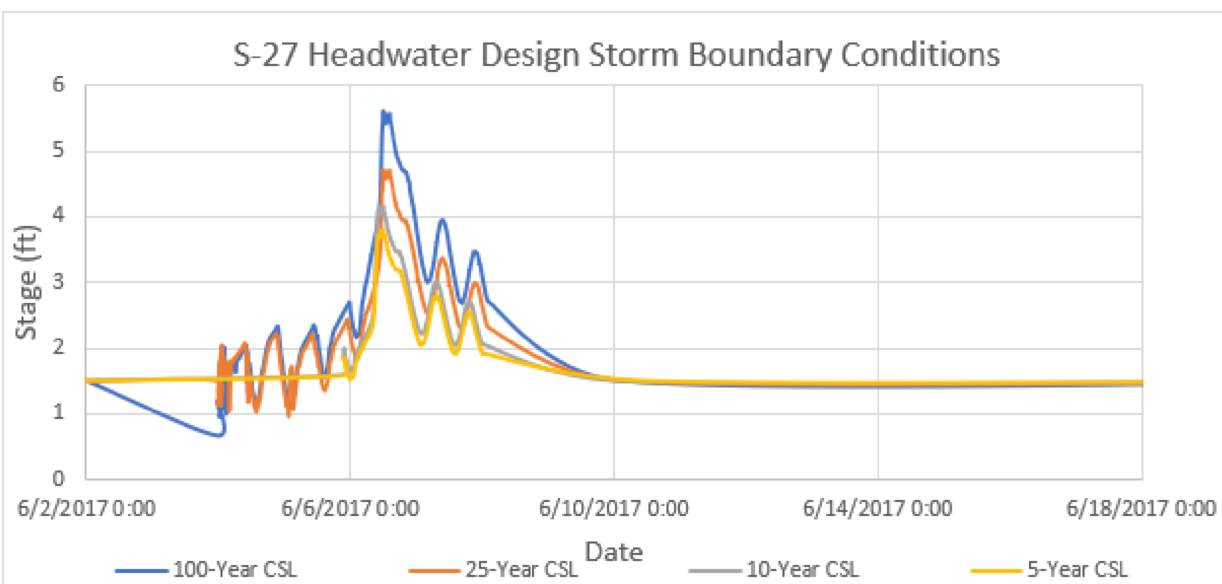

Figure 3.9-22: District Provided Simulated Design Storm Stages for S-27 HW

The spatial distribution and time-series data for G-72 tailwater are shown in **Figure 3.9-23** and **Figure 3.9-24**, respectively.

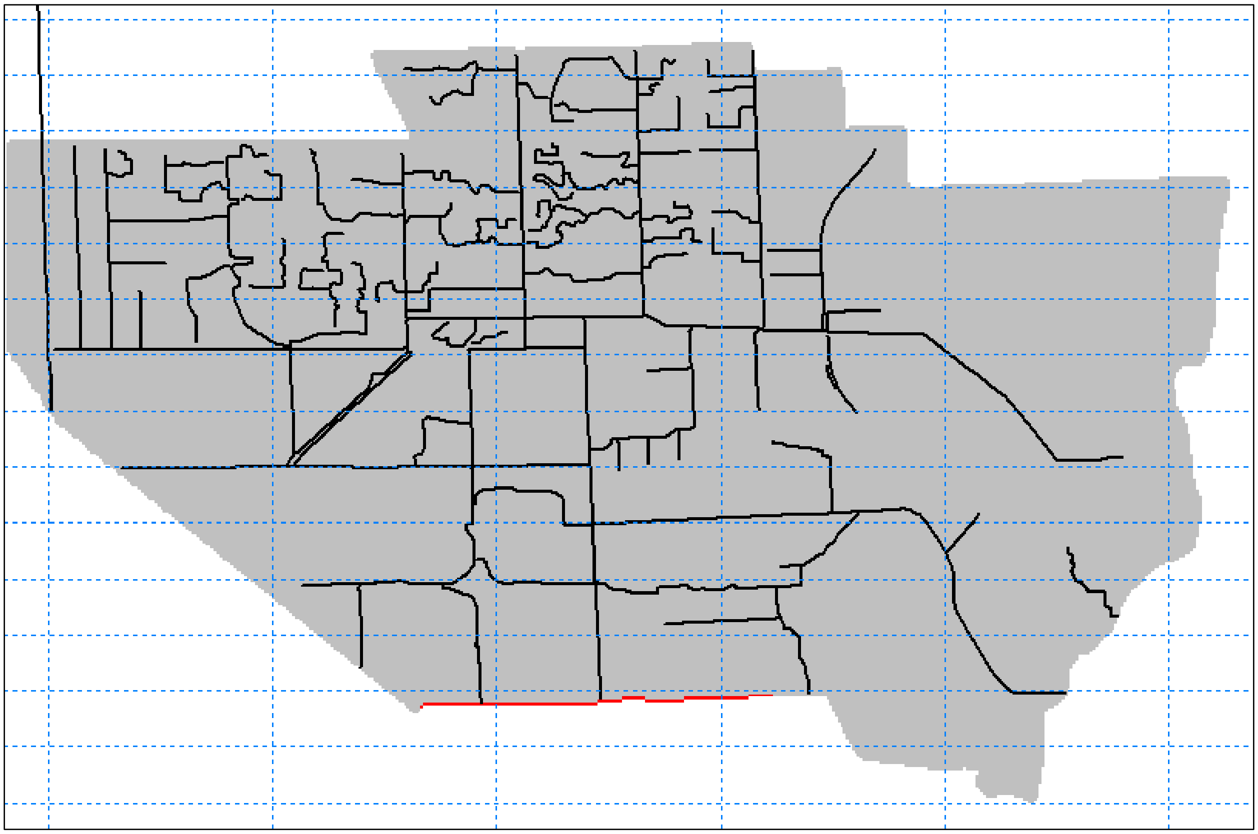

Figure 3.9-23: General Head Groundwater Boundary Using G-72 TW Simulated Design Storm Stages

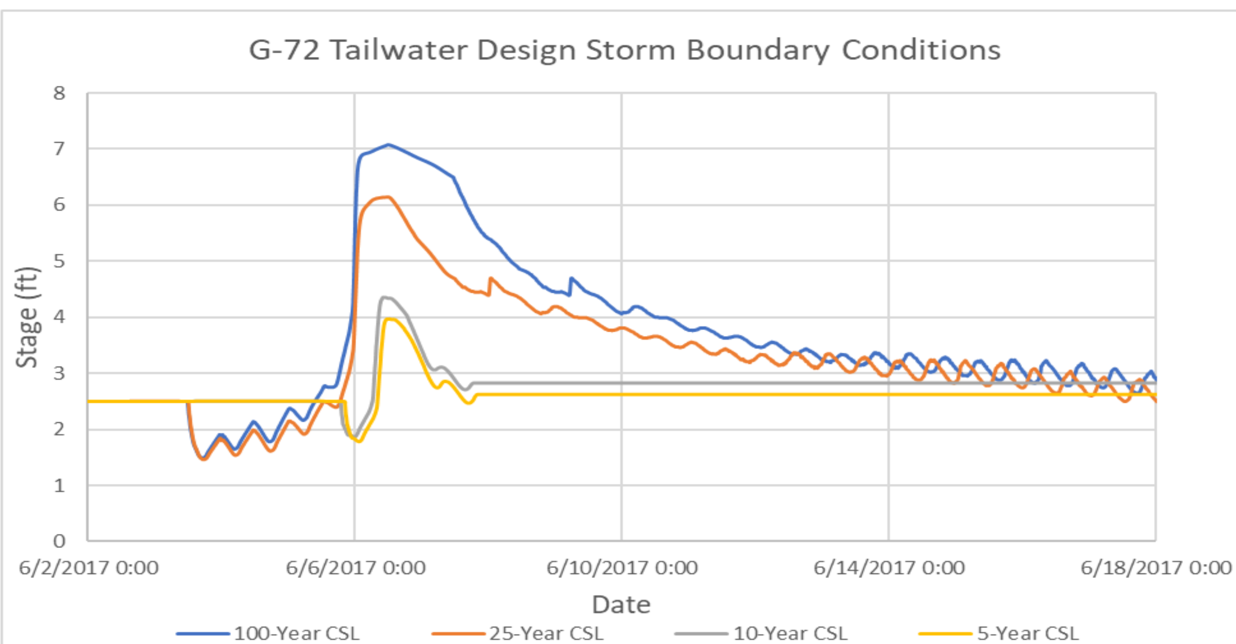

Figure 3.9-24: District Provided Simulated Design Storm Stages for G-72 TW

The spatial distribution for G-72 headwater is shown in **Figure 3.9-25**.

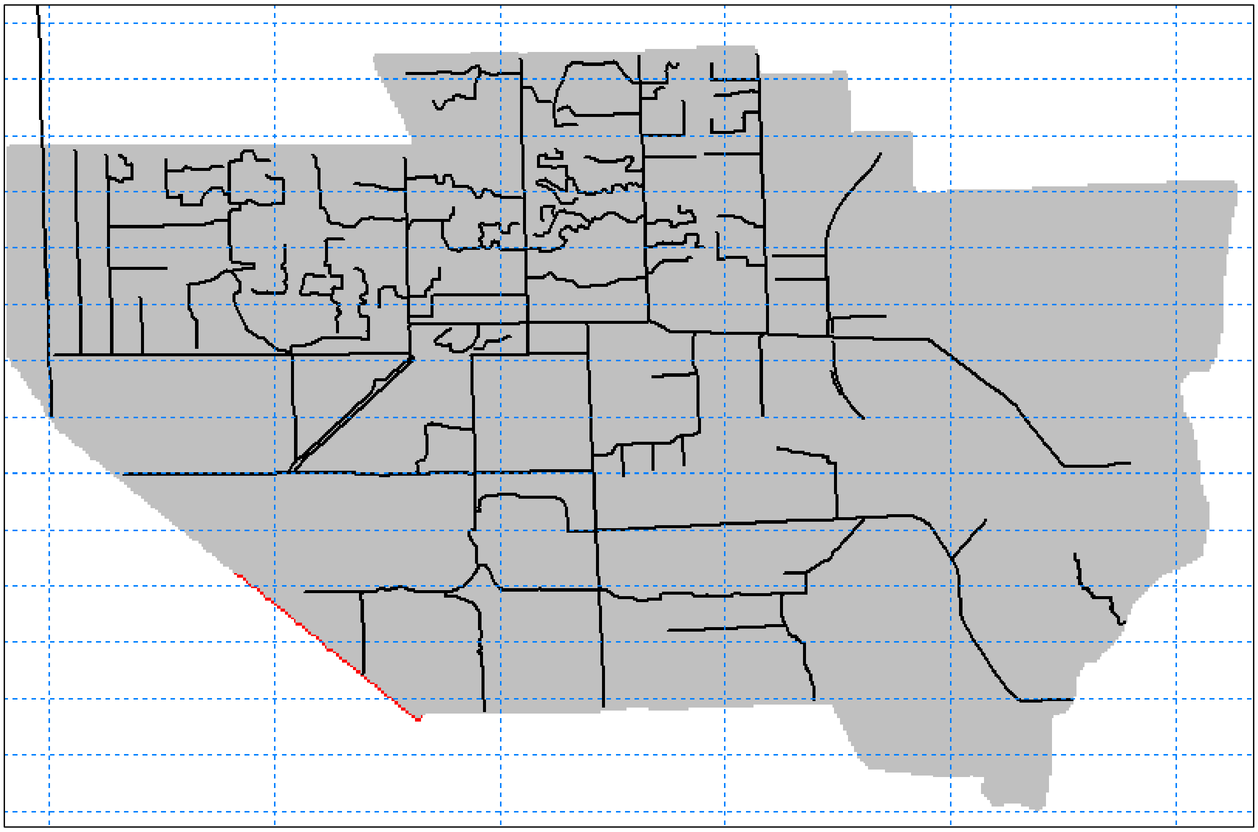

Figure 3.9-25: General Head Groundwater Boundary Using G-72 HW Simulated Design Storm Stages

For the G-72 HW boundary condition, there was only simulated data for the 10, 25, and 100-year design storms. As there was no data for the 5-year design storm, SFWMD suggested a scale-down approach. Therefore, the G-72 HW peak stage (NGVD29) was plotted against the 3-day rainfall depth for the nearest NOAA Atlas 14 station and fitted with a trendline. The best-fitting trendline (highest R^2 coefficient) was determined to be logarithmic. **Table 3-11** and **Figure 3.9-26** show the data used and the corresponding graph, respectively.

Table 3-11: Data Used to Scale-Down G-72 HW Peak Stage

Return period (Yr)	Rainfall depth (in)	Peak Stage (ft NGVD29)
5-yr	8.85	5.25 (calculated)
10-yr	10.5	5.59
25-yr	13.1	6.47
100-yr	17.7	7

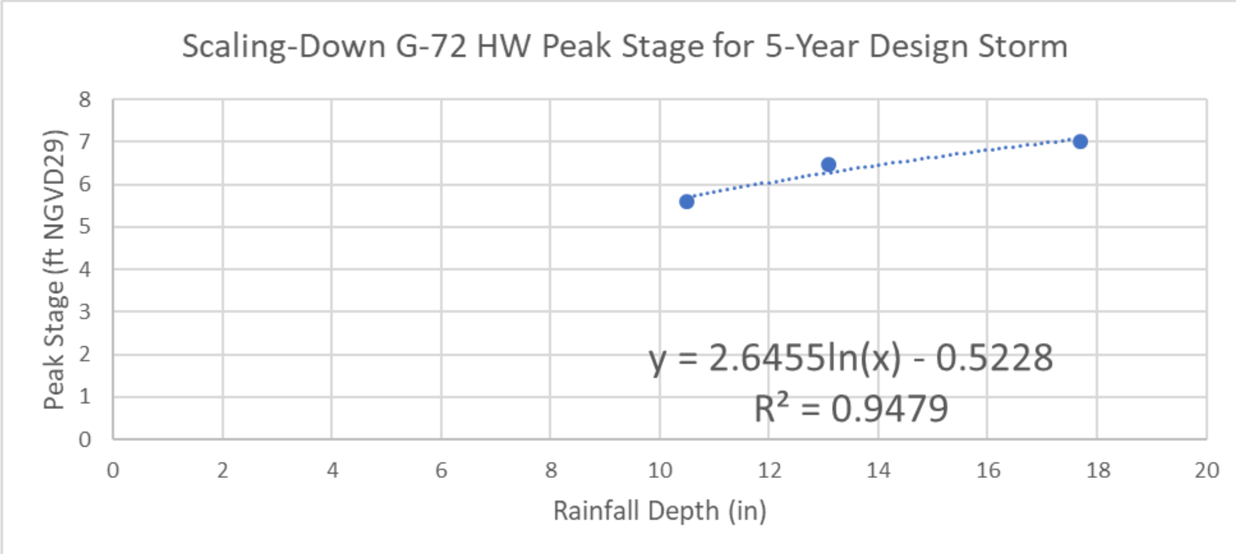

Figure 3.9-26: Scale-Down Approach for G-72 Headwater

With this approach, the peak stage for the 5-year design storm at G-72 HW was determined to be 5.25 feet. Therefore, a correction factor of 0.939 (5 year stage divided by 10 year stage) was applied to the 10-year time series data for all values greater than 2.52 feet (this is the lowest value possible before the correction factor would reduce stage to below the control elevation of 2.5 feet).

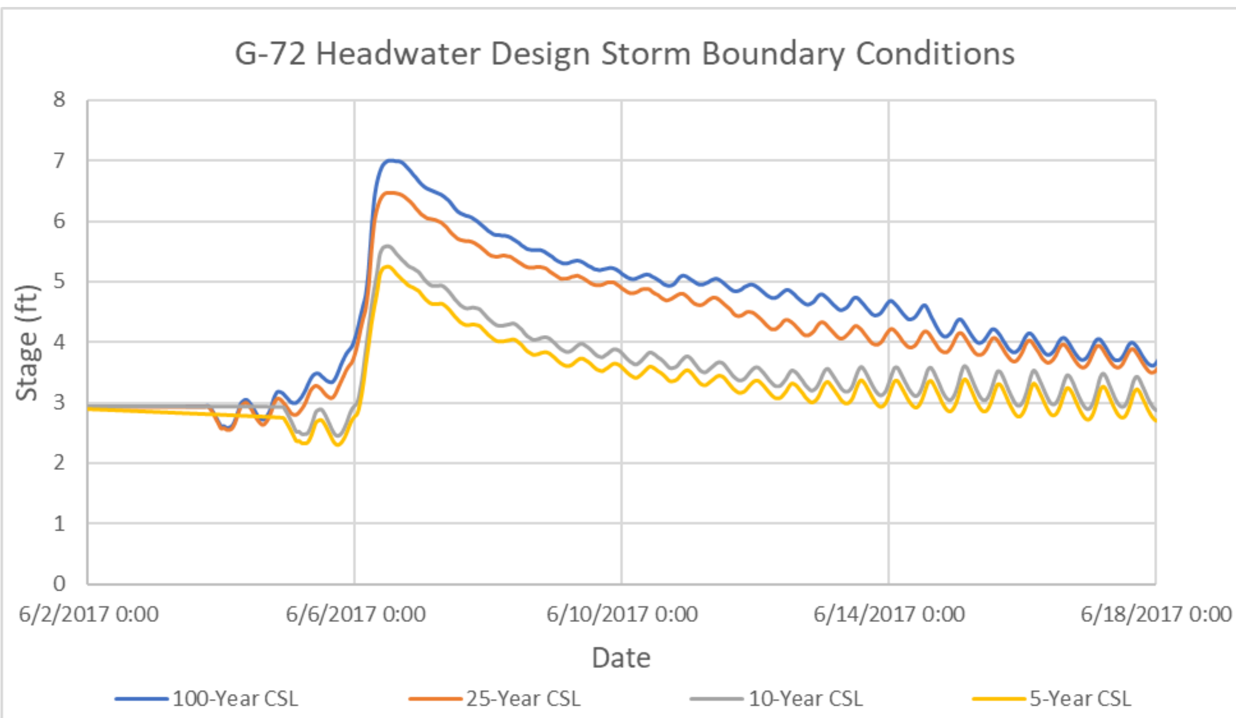

Figure 3.9-27: District Provided and Scaled-Down Simulated Design Storm Stages for G-72 HW

The spatial distribution for S-31 tailwater is shown in **Figure 3.9-28**.

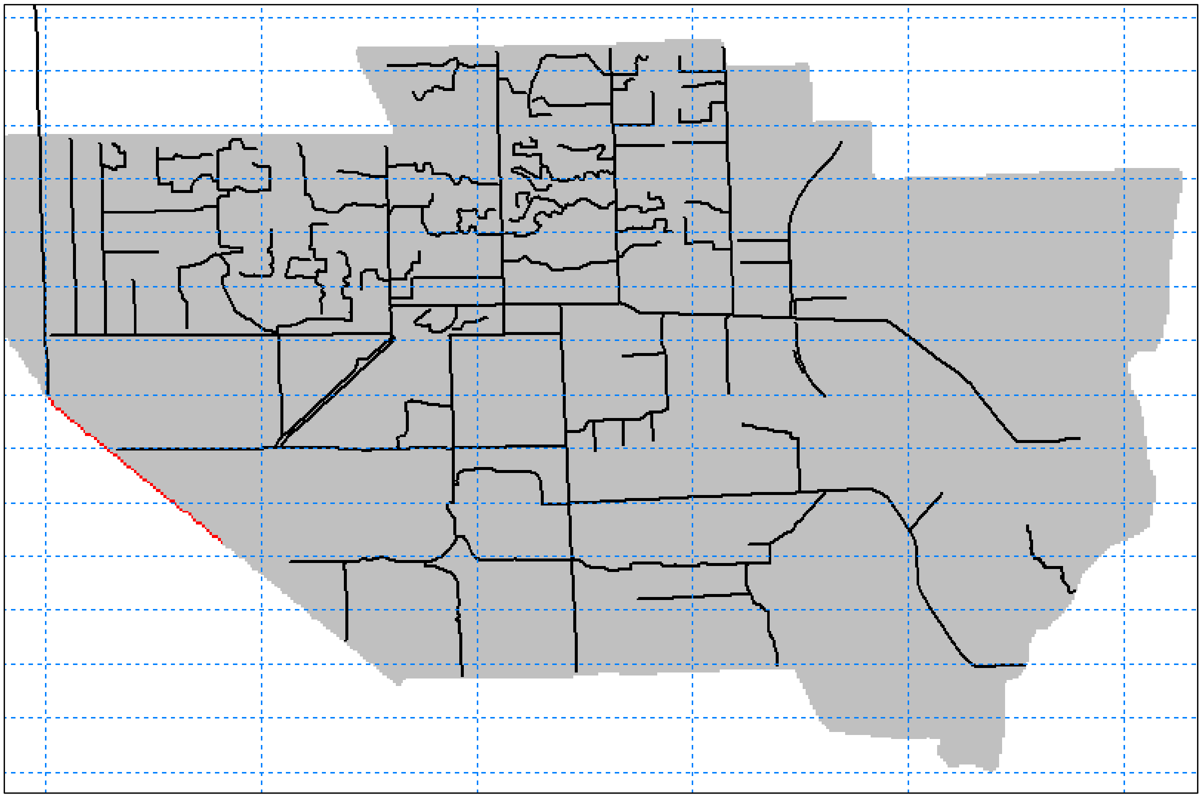

Figure 3.9-28: General Head Groundwater Boundary Using S-31/32 TW Simulated Design Storm Stages

For the S-31 TW boundary condition, there was only simulated data for the 10, 25, and 100-year design storms. As there was no data for the 5-year design storm, SFWMD suggested a scale-down approach. Therefore, the S-31 TW peak stage (NGVD29) was plotted against the 3-day rainfall depth for the nearest NOAA Atlas 14 station and fitted with a trendline. The best-fitting trendline (highest R^2 coefficient) was determined to be logarithmic. **Table 3-12** and **Figure 3.9-29** show the data used and the corresponding graph, respectively.

Table 3-12: Data Used to Scale-Down S-31 TW Peak Stage

Return period (Yr)	Rainfall depth (in)	Peak Stage (ft NGVD29)
5	8.12	5.43 (calculated)
10	9.66	5.84
25	12.1	6.97
100	16.3	7.56

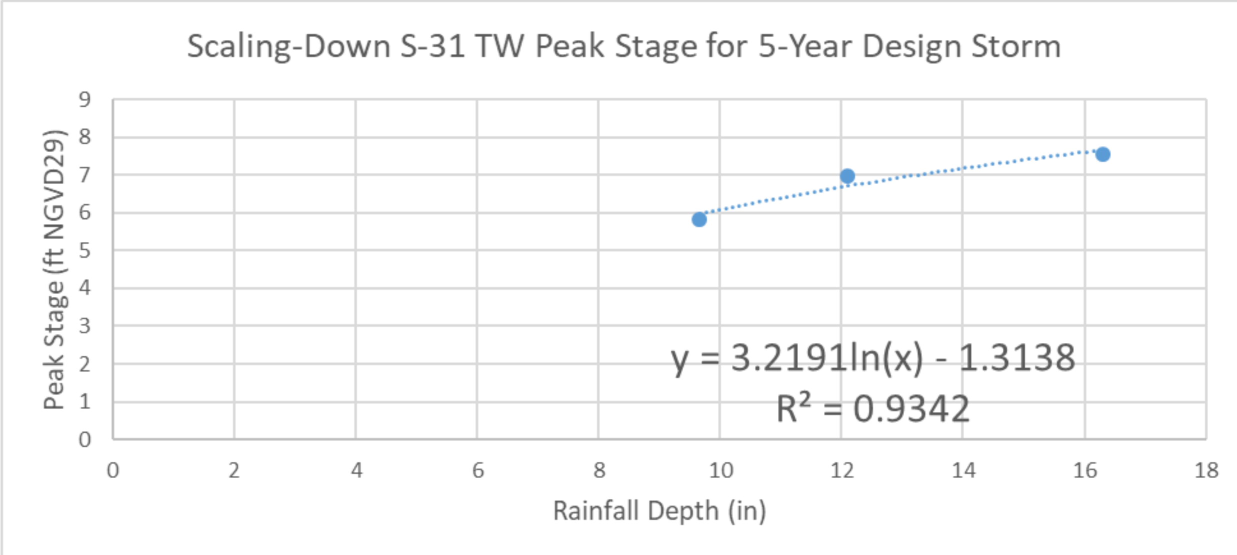

Figure 3.9-29: Scale-Down Approach for S-31 Tailwater

With this approach, the peak stage for the 5-year design storm at S-31 TW was determined to be 5.43 ft NGVD29. Therefore, a correction factor of 0.929 (5 year stage divided by 10 year stage) was applied to the 10-year time series data for all values greater than 4.18 ft (this is the lowest value possible before the correction factor would reduce stage to below the initial elevation of 3.88 feet) and values greater than 3.88 but less than 4.18 were set to 3.88 feet.

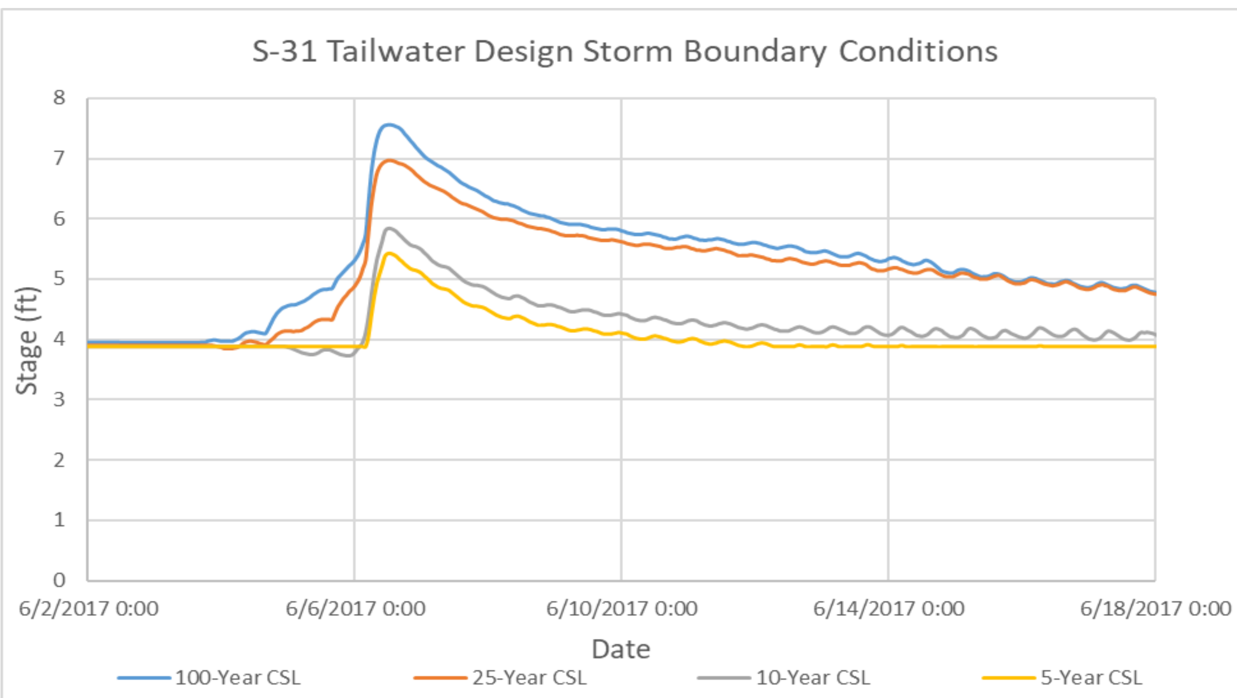

Figure 3.9-30: District Provided and Scaled-Down Simulated Design Storm Stages for S-31/32 TW

3.9.8 Drainage Level

The saturated zone drainage routine conceptually represents local-scale drainage features such as roadside underdrains, shallow swales, and field-scale agricultural ditches not explicitly represented elsewhere in the model setup. The saturated zone drainage level was developed based on land use, with urban areas set to 1.5 ft below ground, rural/agricultural areas set to 2.5 ft below ground, and 0 ft (turn saturated zone drainage off) for water and undeveloped areas. The spatial distribution of the saturated zone drainage levels are shown in **Figure 3.9-31**.

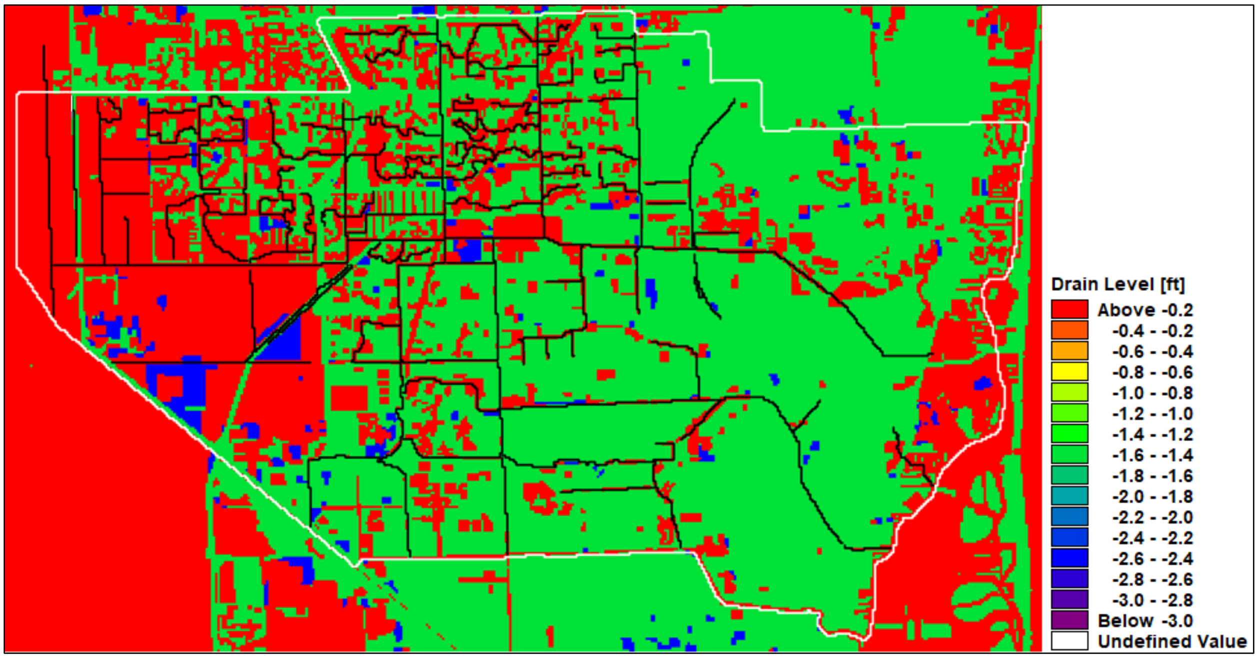

Figure 3.9-31: Drain Levels in the Saturated Zone

3.9.9 Drainage Time Constants

This parameter was set to the final calibrated value from the 2019 Broward County model (within the C-9 basin), with a value of 5E-07/s for developed land use areas. The saturated zone drainage is calculated as a linear reservoir based on the head difference between the water table and the drain level and a time constant. The time constant characterizes the "density" of the drainage network. In areas with several drainage features, such as a basin with a lot of underdrains, the time constant could be increased as part of the calibration process. A larger time constant would allow the saturated zone to drain faster to the specified sink (local depression, boundary, or nearest branch within same drain code). In undeveloped land areas and water bodies, the time constant was set to 0, to shut off the saturated zone drainage routine. No permanent changes to spatial distribution or magnitude were made during model calibration.

3.9.10 Drain Codes

The saturated zone drainage routine used the same drain codes as the ponded drainage layer (**Figure 3.7-5**), without the initial depth or flood code cells set to drain code 0.

4 MODEL CALIBRATION

The model calibration process focused on attaining the best-fit for the peak water levels, total discharge volume, and peak discharge. This study set a calibration target of +/- 10-20% peak discharge and total discharge volume and +/- 0.5 ft headwater/tailwater and groundwater elevation. This approach allows a more comprehensive assessment of the model's simulated hydrologic and hydraulic response to rainfall, as compared to only matching peak stages or peak discharges. Refer to **Figure 2.6-1** for the locations of the SFWMD structures and groundwater wells used to calibrate the model. The operable structures (gates) used recorded gate openings and the tidal tailwater elevations were forced with the recorded water levels obtained from DBHYDRO. The model's simulated peak headwater/tailwater, peak discharge, total discharge volume, and groundwater levels were compared with observed data from SFWMD's DBHYDRO database.

4.1 Calibration Summary

Model calibration started with reparameterizing the groundwater model based on the 2019 Broward County Current Conditions model and expanding the model domain so that an internal boundary condition could be included. This inclusion was done for consistency with the 2019 Broward County Model, and to attempt to improve the hydrologic response in the western part of the model domain. These adjustments could be viewed as a model setup correction more so than a calibration alteration. These modifications resulted in improved model simulated surface water and groundwater responses throughout the model domain. However, the model was significantly overpredicting the peak discharge rates and the total volume discharged through the tidal structures and subsequent calibration efforts were primarily focused on improving these simulated values. Several adjustments were made to the following parameters in an effort to reduce the runoff volume and shift the timing of the runoff to better simulate the "peaks":

- Surface-subsurface leakage coefficient
- Paved area runoff coefficient
- Manning's roughness coefficient (overland flow)
- Manning's roughness coefficient (channel flow)
- Ponded drainage time constants
  - Maximum storage change rate
  - Inflow / Outflow time constant
- Saturated zone drainage time constants
  - Maximum storage change rate
  - Inflow / Outflow time constant

However, these parametric changes resulted in little to no improvement in model performance and often led to a worse agreement between simulated and observed surface water stages and groundwater levels.

This suggested that inaccurate rainfall inputs may be a factor. As noted previously in **Section 2.5,** the year 2000 NEXRAD rainfall data was highly uncertain, due to both the questionability of NEXRAD DATA between 2000-2005 and the temporal adjustments made to the rainfall time series. Therefore, the adjusted NEXRAD data was replaced with the rain gauge data. Subsequent model simulations showed significant improvements in simulated peak discharge rates and total discharge volumes. This, in combination with the validation results described in **Section 5**, suggests the initial rainfall setup was responsible for the aforementioned overpredictions in the calibration model.

After the change in rainfall data, model calibration goals were met at most calibration points. In the areas not meeting calibration goals, localized adjustments were made but resulted in no significant improvement in model performance. The only adjustments that resulted in improvements were changes to Manning's roughness coefficient in three canals. At this point in the calibration process, three things were evident:

- for the calibration period, gauge-based rainfall data was more reliable than NEXRAD data, but still does not fully capture spatial-temporal patterns in rainfall
- overall, there was a very good match between simulated and observed data
- additional reasonable parametric changes are not resulting in further improvement in model performance.

Therefore, Taylor Engineering felt confident that the model setup and parameterization was a reasonable representation of the conditions that existed within the area if interest in October of 2000.

At this point, it was determined to use the calibrated model to simulate the chosen independent validation storm event, which was Hurricane Irma. Good model performance during an independent storm event further validates the adequacy of the model setup and parameterization approach. The validation storm event was relatively recent, compared to 20 years ago for the calibration event. As such, the NEXRAD rain data associated with the validation event was expected to have a lower level of uncertainty. As discussed in **Section 5**, during the validation event, model-simulated hydrologic and hydraulic conditions were in close agreement with the observed data. Excellent model performance during the validation simulation further confirms the adequacy of the model setup and parameterization approach. **Section 4.2** through **Section 4.5** provide details on the model setup and parameterization changes made during calibration.

4.2 Saturated Zone

During the initial calibration runs, it was noticed that groundwater wells G-1636, G-1637, and G-970 had a very subdued response to rainfall, whereas the recorded data showed a quite pronounced response. Adjustments were made to try to increase the groundwater response, including increased surface-subsurface leakage coefficient and decreased saturated zone drainage time constant. These changes resulted in almost no change, which is quite unusual as models are typically quite sensitive to these parameters. Therefore, this study reexamined the saturated zone inputs derived from the USGS. The USGS groundwater model was configured differently than the 2019 Broward County Current Conditions model. The USGS groundwater model (Hughes & White, 2016) used a second layer with low conductivity, whereas the 2019 Broward County model had a highly conductive second layer representing the Biscayne aquifer. Taylor Engineering decided to reparametrize the entire groundwater model based on the 2019 Broward County Current Conditions MIKE SHE model, which happened to extend far enough south to cover the entire C-8 C-9 model domain. Therefore, the first major change during model calibration was reparameterizing the saturated zone based on the 2019 Broward County MIKE SHE model, with the exception of the initial potential head. These changes to the groundwater model resulted in better simulated groundwater levels throughout the model when compared to the observed data. Refer to **Figure 3.9-1** through **Figure 3.9-13** for the final aquifer parameters.

4.3 Boundary Conditions

After changing the groundwater model configuration, the simulated data was a closer match to the observed data in most parts of the study area. However, the western groundwater wells were still a little less responsive than observed data. The 2019 Broward County Current Conditions model had an internal boundary condition, just west of the SFWMD L-33 canal, which is where the original C-8 C-9 model domain ended. Therefore, the model domain was extended about 1 mile west so that the internal boundary condition could be included, as shown in **Figure 3.9-19**. This internal boundary condition is based on the stage in Water Conservation Area 3B and is a head-controlled flux boundary with a leakage coefficient of 3E-6, as characterized in the 2019 Broward County Current Conditions model. This change helped the groundwater respond more closely to the observed data.

4.4 Rainfall

The storm event from October 2nd-4th, 2000 was used to calibrate the model, with a simulation period of October 1st-21st. Both point rain measurements and spatially distributed NEXRAD data were available for the October 2000 storm event. Initially, hourly NEXRAD rainfall data with a spatial resolution of 2 km x 2 km was used for total rainfall depth and spatial distribution. The temporal distribution of each NEXRAD pixel was adjusted based on recorded rain gauge data. A rain gauge was assigned to each NEXRAD pixel based on Thiessen polygons that were delineated using the rain gauge locations present in the area. The calibration scenario using NEXRAD rainfall resulted in a reasonable match between simulated and observed groundwater levels and surface water stages throughout the model. However, the simulated peak discharge rates and the total discharge volume differed by upwards of +30%. Calibration efforts included varying parameters such as surface-subsurface leakage coefficient, paved area runoff coefficient, Manning's roughness for both overland and channel flow, ponded drainage time constants, and saturated zone drainage time constants, which resulted in no significant improvement in model performance. Considering there was a reasonable match between simulated and observed data for groundwater levels and surface water stages, it was suspected there was simply too much rainfall being simulated. It is well known by the District that the quality of the NEXRAD data is questionable for the 2000 -2005 period, given that the collection and application of NEXRAD data in Florida during that time was an emerging technology. It was entirely possible that NEXRAD data was simply not an accurate representation of actual rainfall. Therefore, the NEXRAD data replaced with raw rain gauge data. Although there are still rainfall data limitations by using only 5 reference points, the rain gauge data led to significantly improved peak discharge rates and total discharge volumes.

4.5 Manning's Roughness Coefficient

After switching the rainfall data and vastly reducing the overprediction of peak discharge rates and total discharge volume, some localized adjustments to the 1D model's Manning's roughness coefficients were made in an attempt to improve the peak surface water stage, as well as the overall shape of the hydrographs. Throughout the model, only a few canals were adjusted, as shown in the table below.

Table 4-1: Manning's Roughness Calibration Adjustments

Branch	Original Manning's n	Adjusted Manning's n
SFWMD C-8 Ext	0.033	0.04
Peter S Pike Canal	0.033	0.04
Grahams Dairy Canal	0.033	0.04

4.6 Calibration Results

Overall, the calibrated model sufficiently simulated surface water and groundwater responses to rainfall and were a good match to recorded observations at multiple locations throughout the model domain. Model simulated peak surface water stages generally agreed to within 0.5 ft of the observed stages, with an absolute average difference of 0.3 ft. Model simulated peak discharge rates agreed to within 10% of the observed peak discharge, with an absolute average difference of 6%. Model simulated total discharge volume agreed to within 17% of observed discharge volume, with an absolute average difference of 14%. Model simulated groundwater elevations generally agreed to within 0.5 ft of the observed elevations, with an absolute average difference of 0.3 ft. **Table 4-2** provides a detailed summary of the simulated vs. observed differences, **Table 4-3** provides a comparison between simulated and observed peak stages, **Table 4-4** provides a comparison between simulated and observed peak discharges and time of peak discharge, **Table 4-5** and **Table 4-6** provide water budgets for the C-8 and C-9 basins, respectively for the calibration period of October 1st-21st, 2000. **Table 4-7** provides simulation statistics for both the entire simulation period and the first 7 days of simulation.

Table 4-2: Calibration Results Comparison

Calibration Point	Total Volume Difference	Peak Discharge Difference (cfs)	Peak Headwater Difference (ft)	Peak Tailwater Difference (ft)	Groundwater Elevation Difference (ft)
S-28	-10.6%	3%	0.45	Forced	
S-29	16.8%	9%	0.56	Forced	
S-30			0.15	0.38	
S-32			0.05	Forced	
S-9XS			0.35	Forced	
S-28Z			0.67		
S-29Z			0.01		
G-1225					0.57
G-1636					-0.12
G-1637					-0.10
G-3571					-0.81
G-852					-0.18
G-970					-0.21
S-18					0.05

Table 4-3: Calibration Peak Stage Comparison

Calibration Point	Peak Stage (ft NGVD29)		
	Simulated	Observed	Difference
S-28	4.87	4.42	0.45
S-29	3.75	3.19	0.56
S-30 HW	6.74	6.59	0.15
S-30 TW	5.2	4.82	0.38
S-32	6.73	6.68	0.05
S-9XS	6.83	6.48	0.35
S-28Z	5.53	6.2	-0.67
S-29Z	4.95	4.94	0.01
G-1225	7.36	6.79	0.57
G-1636	4.8	4.93	-0.13
G-1637	5.34	5.44	-0.1
G-3571	6.62	7.43	-0.81
G-852	7.1	7.28	-0.18
G-970	4.57	4.78	-0.21
S-18	7.19	7.14	0.05

Table 4-4: Calibration Peak Discharge Comparison

Calibration Point	Peak Discharge (cfs)			Time of Peak Discharge	
	Simulated	Observed	Difference	Simulated	Observed
S-28	2835	2743	92	10/4/2000 5:50	10/3/2000 20:30
S-29	4151	3792	359	10/4/2000 7:50	10/3/2000 20:00

Table 4-5: Calibration Water Budget for C-8 Basin

Water Budget Term	Inches (Average Over C-8 Basin)	
	Inflows	Outflows and Storage
Rainfall	13.4	
Evapotranspiration		1.4
Surface runoff		8.2
Groundwater flow to canals		4.4
Groundwater boundary inflow	0.3	
Change in surface storage		0.2
Change in groundwater storage	0.4	

Table 4-6: Calibration Water Budget for C-9 Basin

Water Budget Term	Inches (Average Over C-9 Basin)	
	Inflows	Outflows and Storage
Rainfall	11.8	
Evapotranspiration		1.6
Surface runoff		10.9
Groundwater flow to canals		4.0
Groundwater boundary inflow	6.1	
Change in surface storage		1.2
Change in groundwater storage		0.2

After **Table 4-7**, **Figure 4.6-1** through **Figure 4.6-17** present a visual comparison between model simulated and observed conditions throughout the model domain. Structure headwater/tailwater that were used as boundary conditions are not included as they are identical (i.e., S-28 tailwater was a forced boundary).

Table 4-7: Calibration Model Statistics for Simulated vs Observed Data

Calibration Point	7-day Simulation (Oct 1st -7th, 2000)						21-day Simulation (Oct 1st -21st, 2000)					
	ME	MAE	RMSE	STDres	R (Correlation)	Nash Sutcliffe	ME	MAE	RMSE	STDres	R (Correlation)	Nash Sutcliffe
S-29 Q (cfs)	-272	499	613	549	0.92	0.64	-217	317	440	383	0.94	0.75
S-29 HW (ft)	-0.037	0.19	0.21	0.21	0.92	0.83	-0.08	0.13	0.18	0.16	0.97	0.88
S-28 Q (cfs)	-102	223	310	293	0.96	0.8	86	239	329	318	0.89	0.65
S-28 HW (ft)	-0.047	0.09	0.13	0.13	0.98	0.95	-0.0009	0.05	0.08	0.08	0.99	0.98
S-30 HW (ft)	-0.17	0.17	0.2	0.11	0.96	0.44	-0.086	0.109	0.15	0.13	0.88	0.65
S-30 TW (ft)	-0.21	0.34	0.41	0.35	0.99	0.78	0.45	0.49	0.52	0.26	0.96	0.4
S-32 HW (ft)	-0.086	0.12	0.15	0.12	0.96	0.7	-0.001	0.1	0.11	0.11	0.88	0.71
S-9XS HW (ft)	-0.19	0.23	0.26	0.18	0.96	0.33	-0.3	0.31	0.33	0.13	0.91	-4.95
S-29Z Stage (ft)	0.05	0.28	0.39	0.38	0.94	0.81	-0.02	0.32	0.38	0.38	0.87	0.71
S-28Z Stage (ft)	0.34	0.35	0.39	0.18	0.99	0.9	0.35	0.36	0.39	0.16	0.99	0.89
G-1225 (ft)	-0.035	0.37	0.43	0.43	0.98	0.93	-0.19	0.32	0.36	0.31	0.98	0.9
G-1636 (ft)	-0.03	0.26	0.35	0.35	0.88	0.76	-0.01	0.19	0.25	0.25	0.9	0.77
G-1637 (ft)	0.19	0.2	0.3	0.24	0.92	0.75	0.13	0.13	0.19	0.15	0.93	0.77
G-970 (ft)	0.14	0.33	0.4	0.38	0.91	0.76	-0.1	0.33	0.42	0.41	0.82	0.6
G-3571 (ft)	0.93	1	1.4	1	0.83	0.43	0.59	0.62	0.91	0.69	0.9	0.56
S-18 (ft)	0.56	0.66	1.23	1.1	0.84	0.63	0.14	0.33	0.73	0.72	0.89	0.76
G-852 (ft)	0.55	0.81	1.26	1.13	0.88	0.71	0.6	0.68	0.94	0.73	0.91	0.68

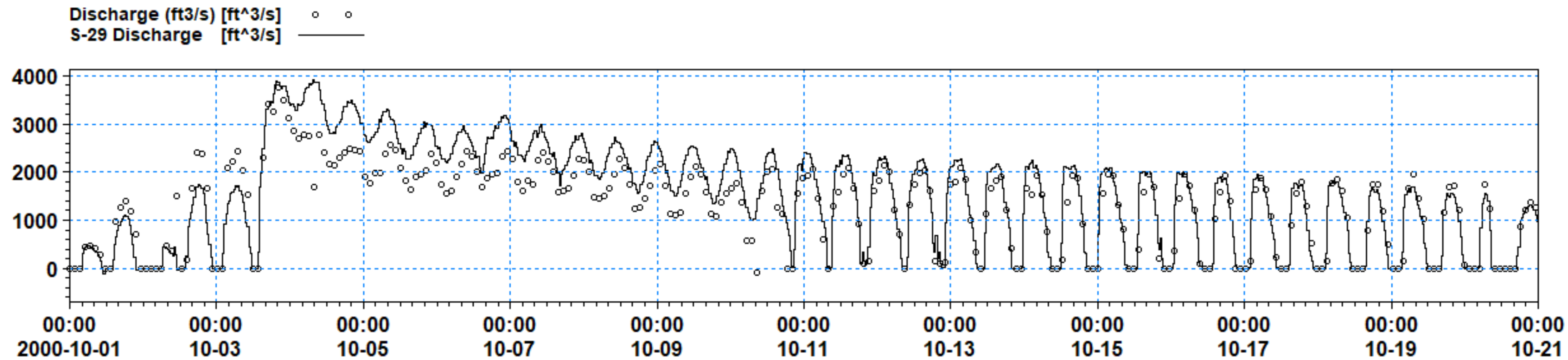

Figure 4.6-1: Simulated (line) vs Observed (dots) Discharge Comparison for SFWMD C-9 Structure S-29, October 1st-21st, 2000

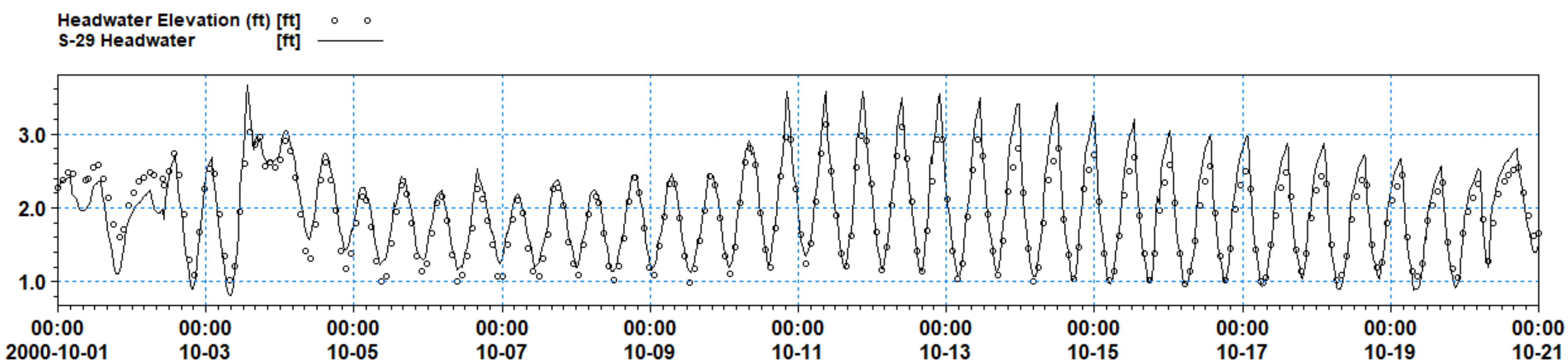

Figure 4.6-2: Simulated (line) vs Observed (dots) Headwater Comparison for SFWMD C-9 Structure S-29, October 1st-21st, 2000

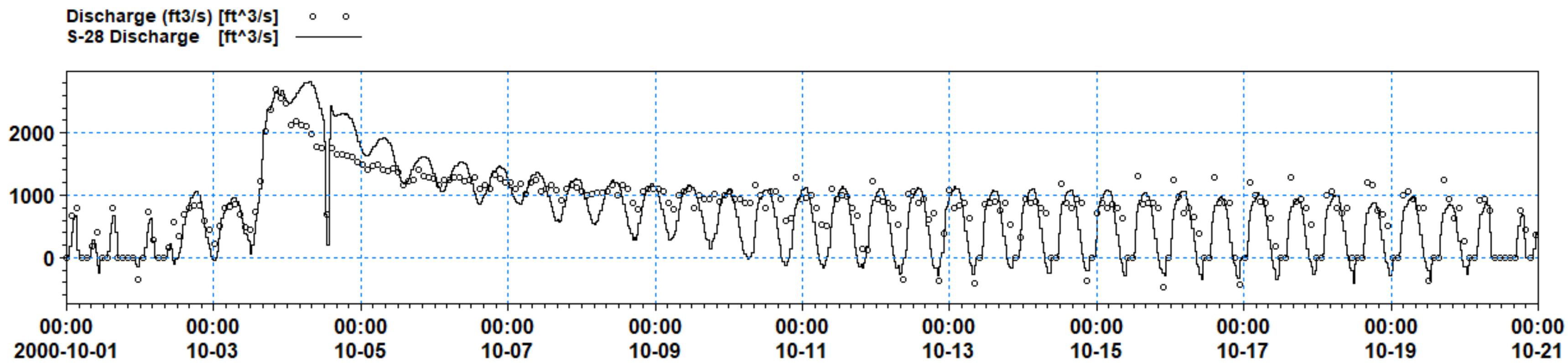

Figure 4.6-3: Simulated (line) vs Observed (dots) Discharge Comparison for SFWMD C-8 Structure S-28, October 1st-21st, 2000

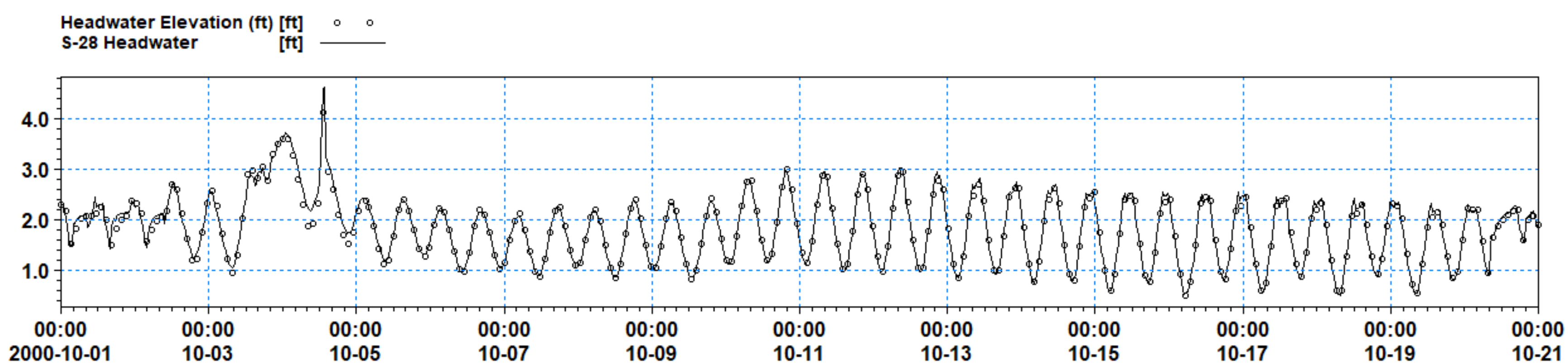

Figure 4.6-4: Simulated (line) vs Observed (dots) Headwater Comparison for SFWMD C-8 Structure S-28, October 1st-21st, 2000

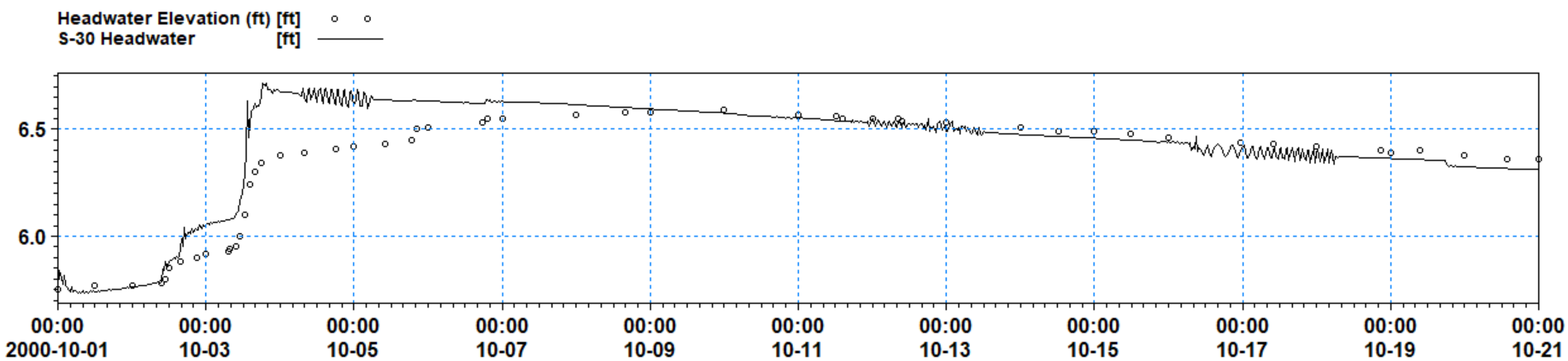

Figure 4.6-5: Simulated (line) vs Observed (dots) Headwater Comparison for SFWMD C-9 Structure S-30, October 1st-21st, 2000

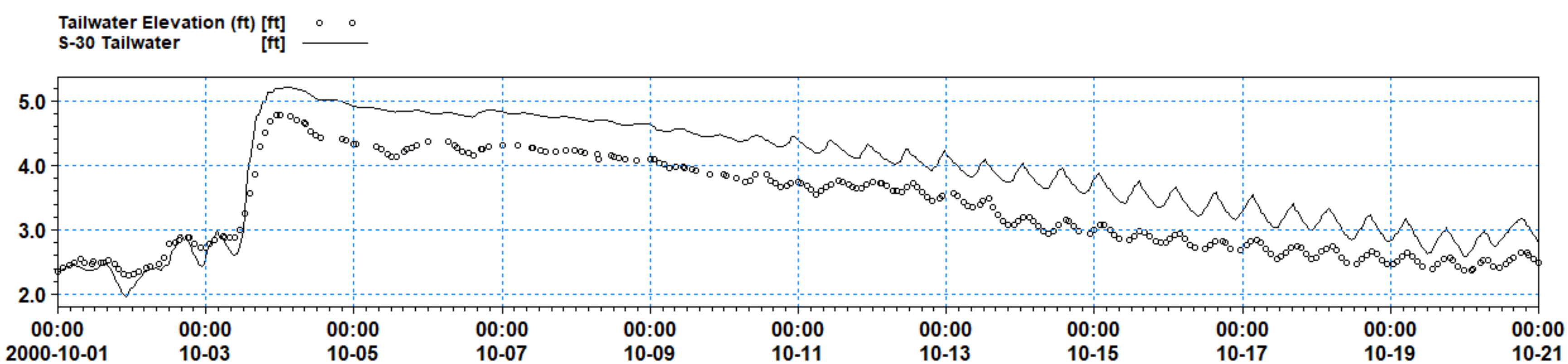

Figure 4.6-6: Simulated (line) vs Observed (dots) Tailwater Comparison for SFWMD C-9 Structure S-30, October 1st-21st, 2000

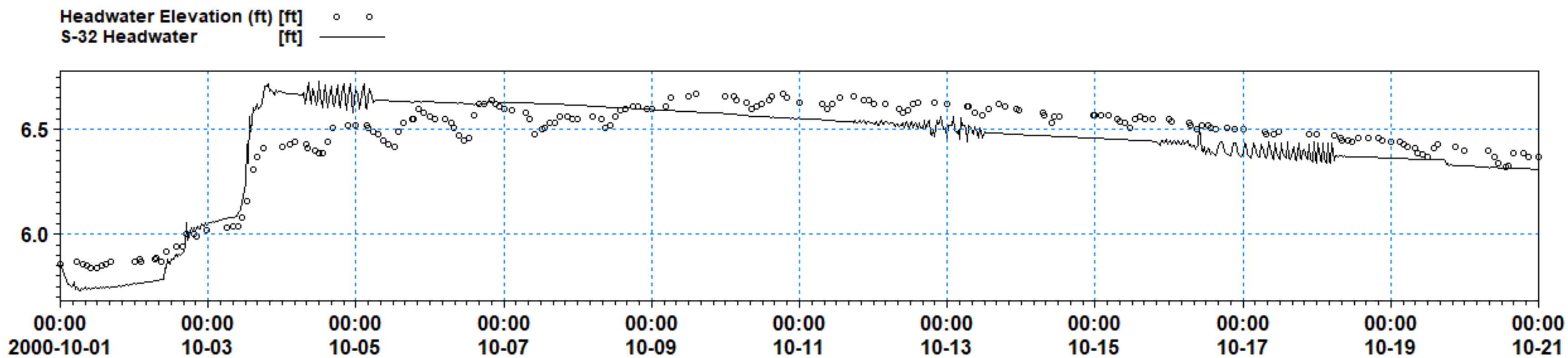

Figure 4.6-7: Simulated (line) vs Observed (dots) Headwater Comparison for SFWMD L-33 Structure S-32, October 1st-21st, 2000

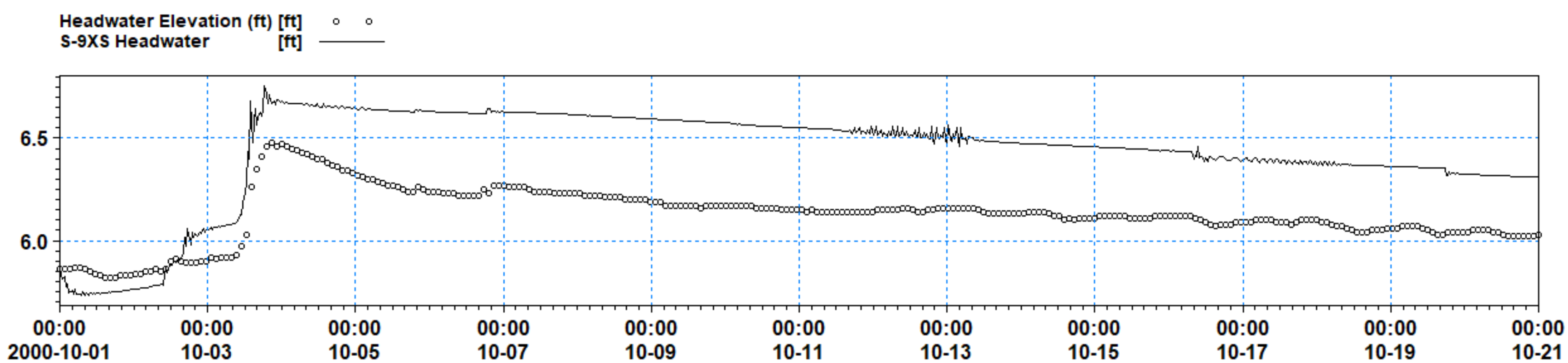

Figure 4.6-8: Simulated (line) vs Observed (dots) Headwater Comparison for SFWMD L-33 Structure S-9XS, October 1st-21st, 2000

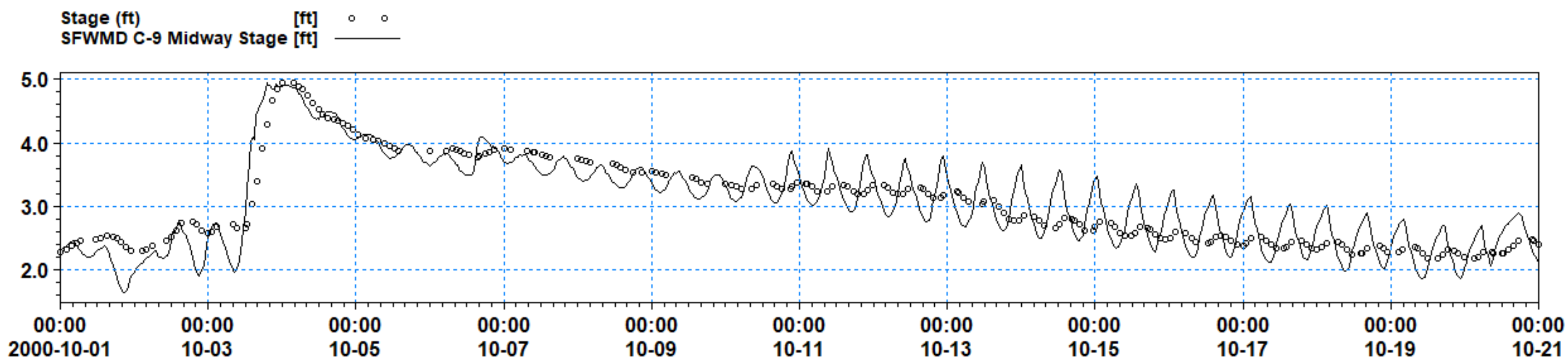

Figure 4.6-9: Simulated (line) vs Observed (dots) Stage Comparison for SFWMD C-9 Water Level Recorder S-29Z, October 1st-21st, 2000

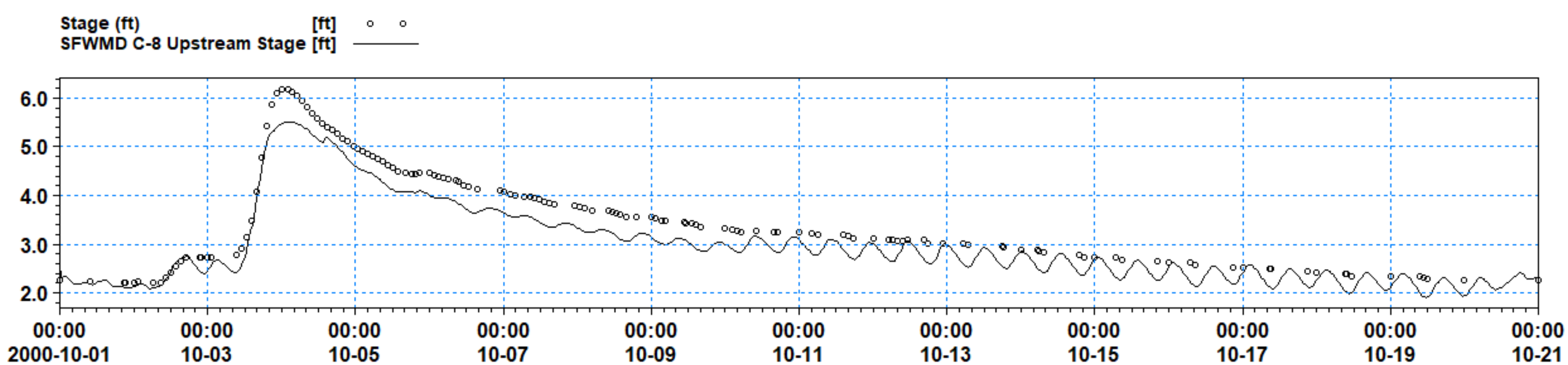

Figure 4.6-10: Simulated (line) vs Observed (dots) Stage Comparison for SFWMD C-8 Water Level Recorder S-28Z, October 1st-21st, 2000

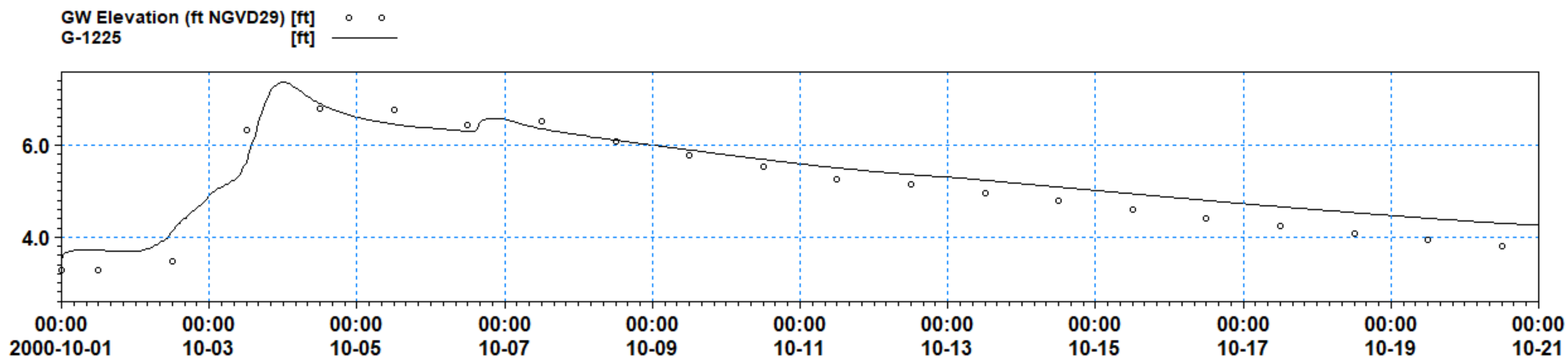

Figure 4.6-11: Simulated (line) vs Observed (dots) Groundwater Elevation Comparison for Well G-1225, October 1st-21st, 2000

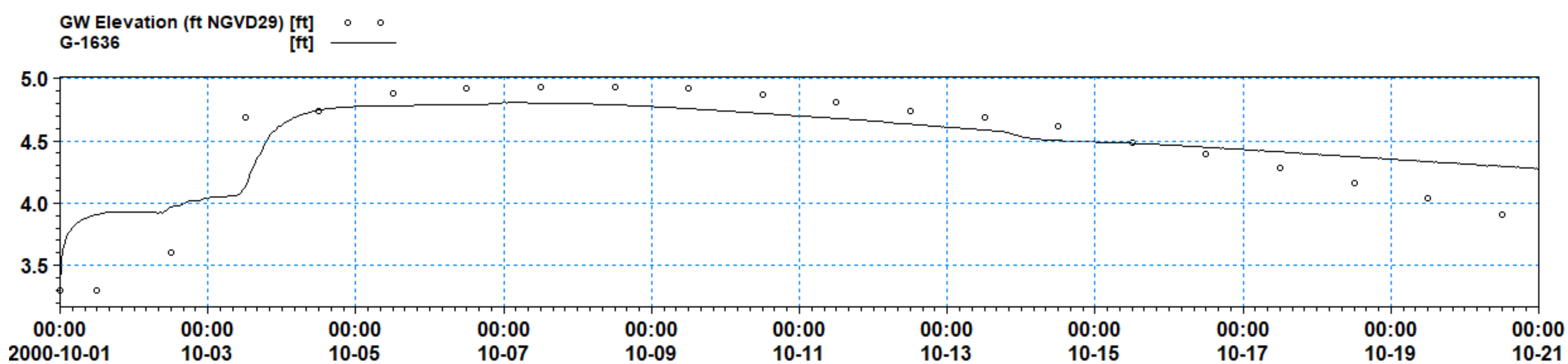

Figure 4.6-12: Simulated (line) vs Observed (dots) Groundwater Elevation Comparison for Well G-1636, October 1st-21st, 2000

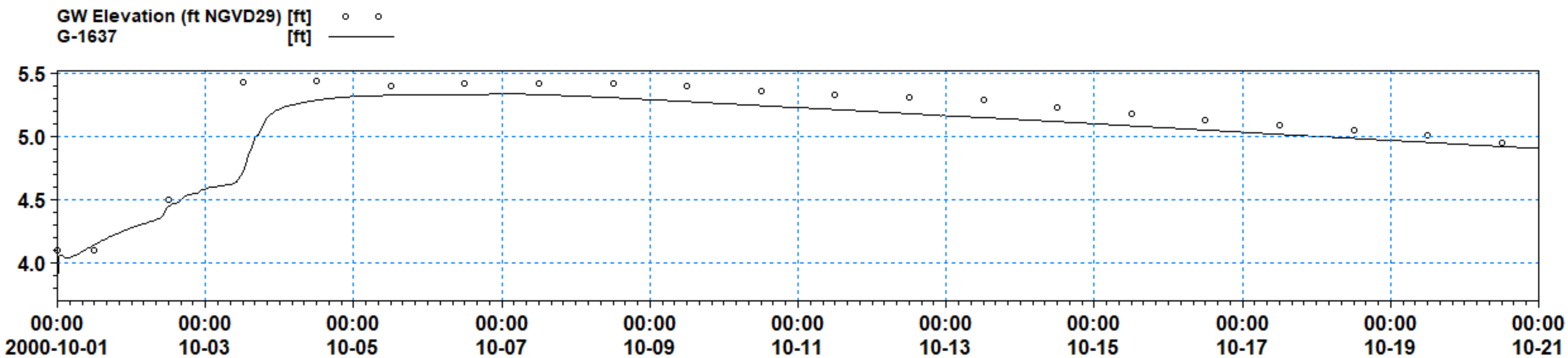

Figure 4.6-13: Simulated (line) vs Observed (dots) Groundwater Elevation Comparison for Well G-1637, October 1st-21st, 2000

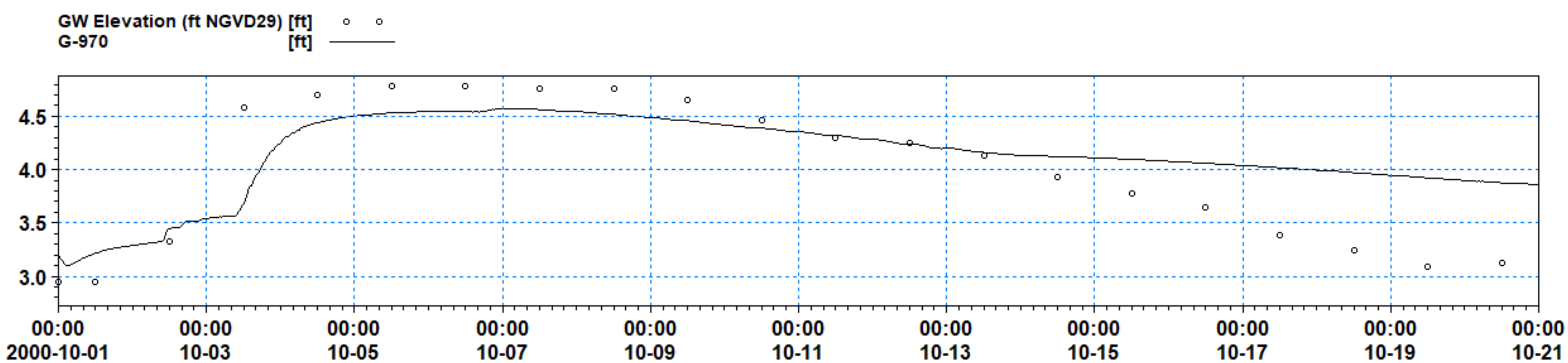

Figure 4.6-14: Simulated (line) vs Observed (dots) Groundwater Elevation Comparison for Well G-970, October 1st-21st, 2000

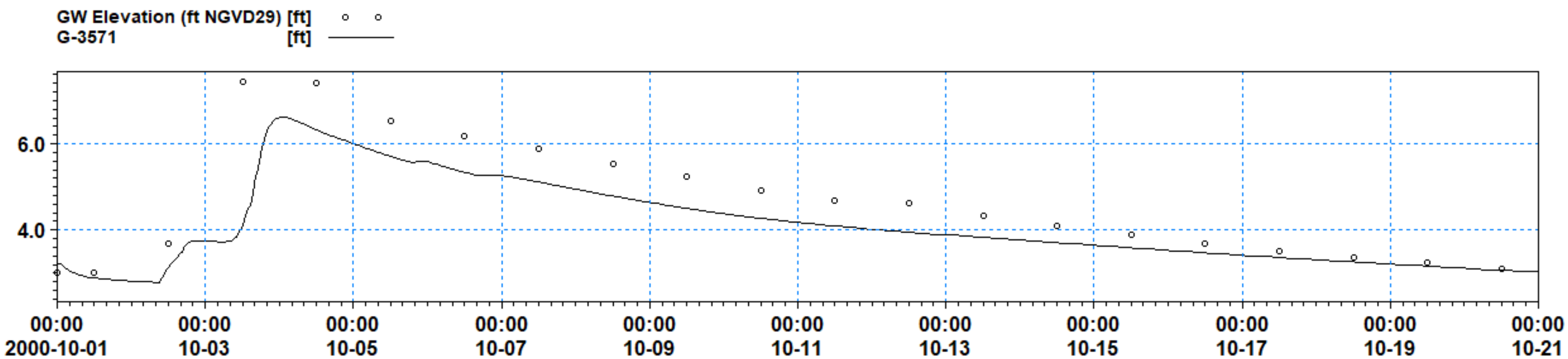

Figure 4.6-15: Simulated (line) vs Observed (dots) Groundwater Elevation Comparison for Well G-3571, October 1st-21st, 2000

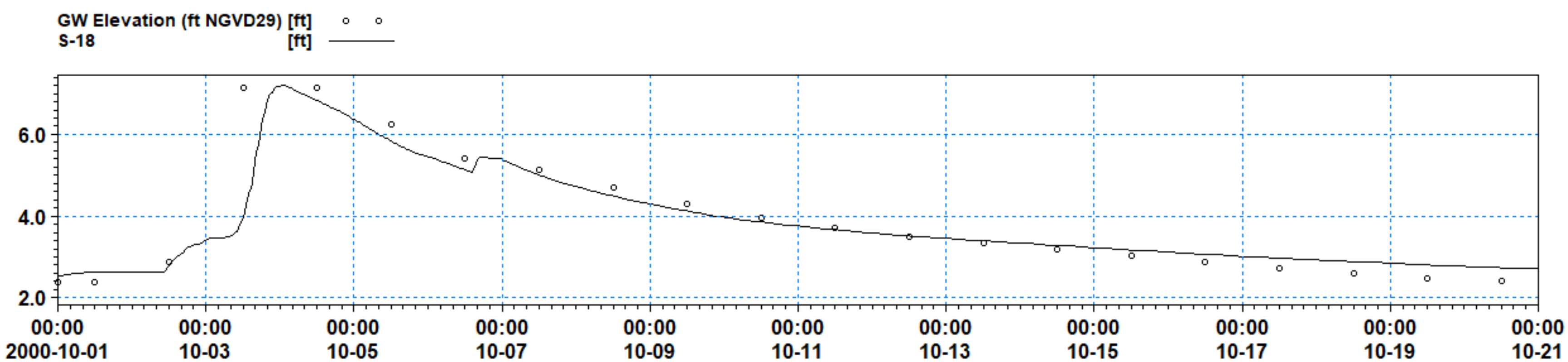

Figure 4.6-16: Simulated (line) vs Observed (dots) Groundwater Elevation Comparison for Well S-18, October 1st-21st, 2000

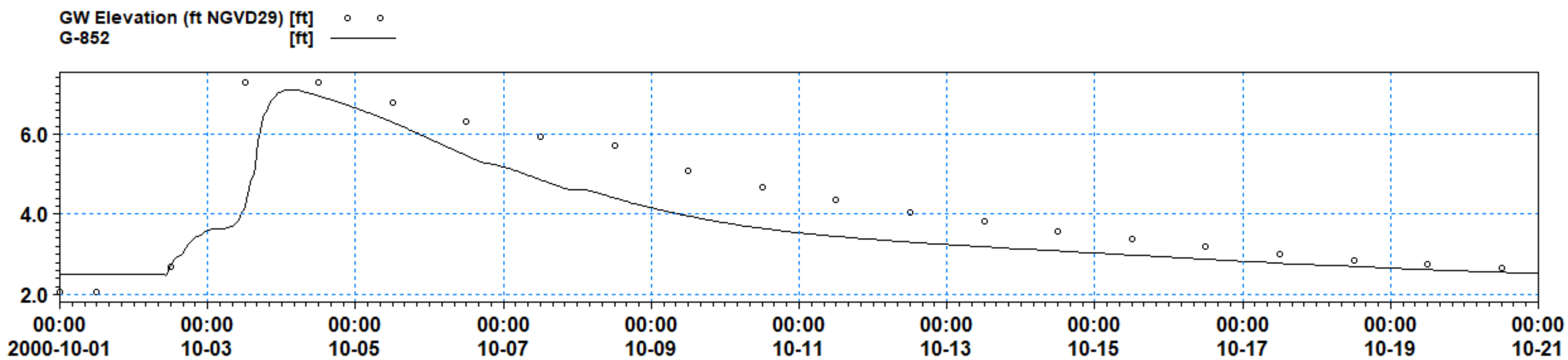

Figure 4.6-17: Simulated (line) vs Observed (dots) Groundwater Elevation Comparison for Well G-852, October 1st-21st, 2000

5 MODEL VALIDATION

Refer to **Figure 2.6-1** for the locations of the SFWMD structures and groundwater wells used to validate the model. The operable structures (gates) used recorded gate openings and the tidal tailwater elevations were forced with the recorded water levels obtained from DBHYDRO. The model's simulated peak headwater/tailwater, peak discharge, total discharge volume, and groundwater levels were compared with observed data which was obtained from SFWMD's DBHYDRO database. Overall, the model adequately simulated surface water and groundwater responses to rainfall and were a good match to recorded observations at multiple locations throughout the model domain. Model simulated surface water stages generally agreed to within 0.4 ft of observed stages, with an absolute average difference of 0.2 ft. Model simulated peak discharge rates agreed to within about 17% of observed peak discharges, with an absolute average difference of 13%. Model simulated discharge volumes agreed to within 14% of observed discharge volumes, with an absolute average difference of 10%. Model simulated groundwater elevations generally agreed to within 1 ft of observed elevations, with an absolute average difference of 0.8 ft. **Table 5-1** provides a detailed summary of the simulated vs. observed differences, **Table 5-2** provides a comparison between simulated and observed peak stages, **Table 5-3** provides a comparison between simulated and observed peak discharges and time of peak discharge, **Table 5-4** and **Table 5-5** provide water budgets for the C-8 and C-9 basins, respectively, for the validation period of September 9th-16th, 2017. **Table 5-6** provides simulation statistics for both the entire simulation period of June-September 2017 and the 7-day period around the time of Hurricane Irma (9th-16th).

Table 5-1: Validation Results Comparison

Calibration Point	Total Volume Difference	Peak Discharge Difference (cfs)	Peak Headwater Difference (ft)	Peak Tailwater Difference (ft)	Groundwater Elevation Difference (ft)
S-28	14.4%	-17.4%	-0.01	Forced	
S-29	-5.5%	8.8%	-0.05	Forced	
S-30			0.32	0.43	
S-32			0.23	Forced	
S-9XS			0.44	Forced	
S-28Z			-0.10		
S-29Z			0.15		
G-1225					-1.26
G-1636					0.24
G-1637					0.77
G-3571					-1.59
G-852					-0.28
G-970					-0.64
S-18					0.7

Table 5-2: Validation Peak Stage Comparison

Calibration Point	Peak Stage (ft NGVD29)		
	Simulated	Observed	Difference
S-28	5.12	5.13	-0.01
S-29	4.82	4.87	-0.05
S-30 HW	6.91	6.59	0.32
S-30 TW	5.25	4.82	0.43
S-32	6.91	6.68	0.23
S-9XS	6.92	6.48	0.44
S-28Z	5.08	5.18	-0.1
S-29Z	5.09	4.94	0.15
G-1225	5.23		
G-1636	4.93	4.73	0.2
G-1637	5.52		
G-3571	5.71	7.27	-1.56
G-852	5.53	5.81	-0.28
G-970	4.56	5.14	-0.58
S-18	5.79	5.08	0.71

Table 5-3: Validation Peak Discharge Comparison

Calibration Point	Peak Discharge (cfs)			Time of Peak Discharge	
	Simulated	Observed	Difference	Simulated	Observed
S-28	1591	2010	-419	9/11/2017 6:20	9/9/2017 5:10
S-29	3393	3119	274	9/11/2017 17:35	9/11/2017 17:35

Table 5-4: Validation Water Budget for C-8 Basin

Water Budget Term	Inches (Average Over C-8 Basin)	
	Inflows	Outflows and Storage
Rainfall	7.7	
Evapotranspiration		0.7
Surface runoff		2.4
Groundwater flow to canals		1.6
Groundwater boundary inflow		0.3
Change in surface storage		0.6
Change in groundwater storage		2.0

Table 5-5: Validation Water Budget for C-9 Basin.

Water Budget Term	Inches (Average Over C-9 Basin)	
	Inflows	Outflows and Storage
Rainfall	8.1	
Evapotranspiration		0.8
Surface runoff		4.8
Groundwater flow to canals		1.1
Groundwater boundary inflow	1.4	
Change in surface storage		0.9
Change in groundwater storage		1.8

After **Table 5-6**, **Figure 4.6-1** through **Figure 4.6-16** presents a visual comparison between model simulated and observed conditions throughout the model domain during a 1-week portion of the validation period coinciding with Hurricane Irma and the following few days. Again, structure headwater/tailwater that were used as boundary conditions are not included as they are identical (i.e., S-28 tailwater was a forced boundary). Note that a few of the groundwater wells had no observed data during the period of September 9th-16th, 2017. Comparison plots for the full 4-month simulation period are provided in **Appendix C**.

Table 5-6: Validation Model Statistics for Simulated vs Observed Data

Calibration Point	7-day Simulation (September 9th -16th, 2017)						4-month Simulation (June 2nd -September 27th, 2017)					
	ME	MAE	RMSE	STDres	R (Correlation)	Nash Sutcliffe	ME	MAE	RMSE	STDres	R (Correlation)	Nash Sutcliffe
S-29 Q (cfs)	87	304	499	491	0.83	0.61	67	119	210	199	0.96	0.92
S-29 HW (ft)	-0.002	0.04	0.06	0.06	0.998	0.996	0.013	0.13	0.19	0.19	0.96	0.89
S-28 Q (cfs)	-75	364	608	604	0.59	0.30	-9	49	159	159	0.91	0.82
S-28 HW (ft)	0.01	0.05	0.05	0.05	0.998	0.997	-0.06	0.1	0.13	0.12	0.98	0.95
S-30 HW (ft)	-0.47	0.47	0.49	0.15	0.87	-2.78	-0.23	0.43	0.47	0.41	0.90	0.26
S-30 TW (ft)	-0.44	0.45	0.54	0.31	0.93	0.60	-0.64	0.65	0.73	0.34	0.85	0.38
S-32 HW (ft)	-0.55	0.55	0.58	0.17	0.89	-3.1	-0.32	0.48	0.53	0.42	0.89	-0.018
S-9XS HW (ft)	-0.87	0.87	0.89	0.19	0.91	-7.5	-0.53	0.80	0.85	0.66	0.57	-7.37
S-29Z Stage (ft)	-0.07	0.15	0.21	0.20	0.97	0.93	-0.13	0.22	0.28	0.25	0.87	0.64
S-28Z Stage (ft)	0.02	0.10	0.13	0.13	0.99	0.98	-0.12	0.16	0.19	0.14	0.95	0084
G-1225 (ft)	-	-	-	-	-	-	0.55	0.6	0.73	0.48	0.78	0.096
G-1636 (ft)	-0.38	0.38	0.52	0.36	0.96	0.09	-0.75	0.75	0.83	0.35	0.74	-2.06
G-1637 (ft)	-	-	-	-	-	-	-0.88	0.88	0.97	0.42	0.47	-3.87
G-970 (ft)	-0.32	0.42	0.54	0.43	0.90	0.26	-0.83	0.84	0.89	0.32	0.78	-2.82
G-3571 (ft)	0.49	0.60	0.75	0.57	0.96	0.67	-0.057	0.26	0.33	0.32	0.94	0.83
S-18 (ft)	-0.35	0.35	0.42	0.24	0.97	0.78	-0.36	0.36	0.43	0.23	0.93	0.34
G-852 (ft)	0.56	0.56	0.61	0.23	0.98	0.61	0.47	0.48	0.55	0.29	0.92	0.42

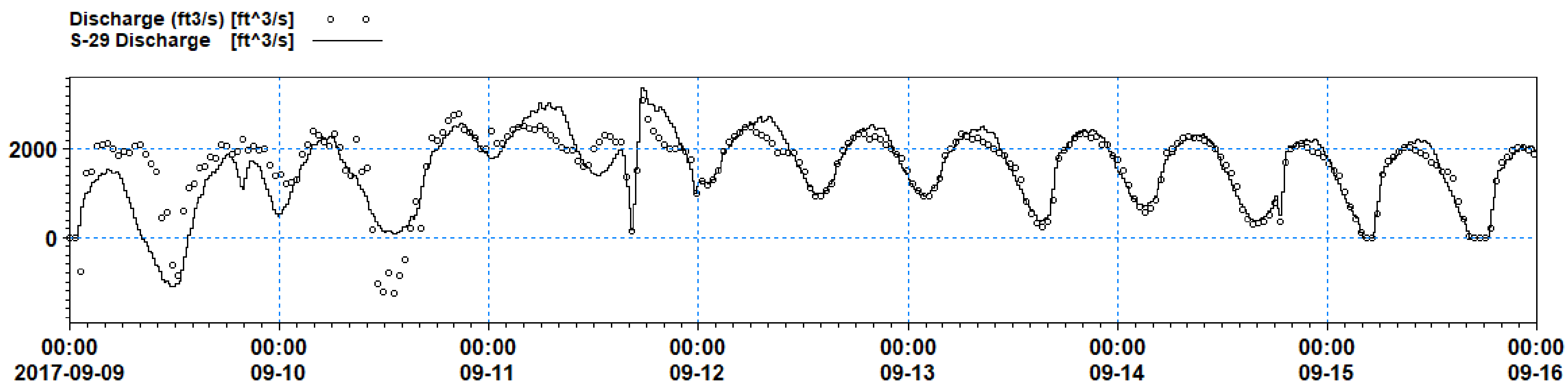

Figure 4.6-1: Simulated (line) vs Observed (dots) Discharge Comparison for SFWMD C-9 Structure S-29, September 9th-16th, 2017

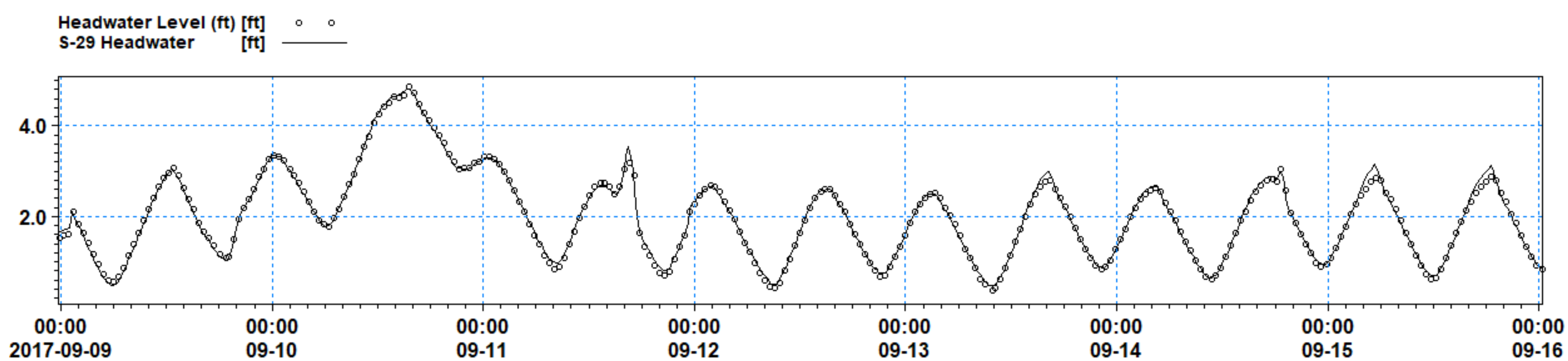

Figure 4.6-2: Simulated (line) vs Observed (dots) Headwater Comparison for SFWMD C-9 Structure S-29, September 9th-16th, 2017

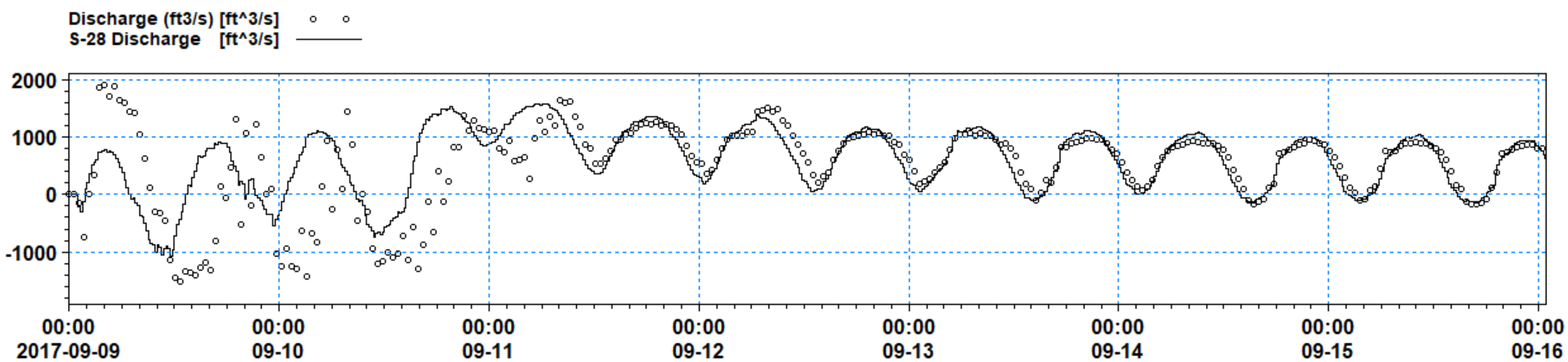

Figure 4.6-3: Simulated (line) vs Observed (dots) Discharge Comparison for SFWMD C-8 Structure S-28, September 9th-16th, 2017

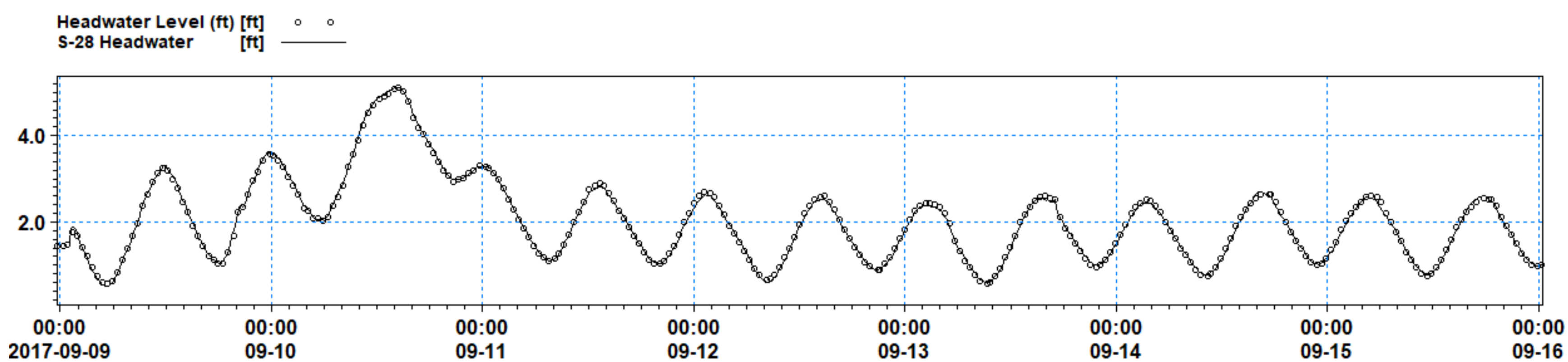

Figure 4.6-4: Simulated (line) vs Observed (dots) Headwater Comparison for SFWMD C-8 Structure S-28, September 9th-16th, 2017

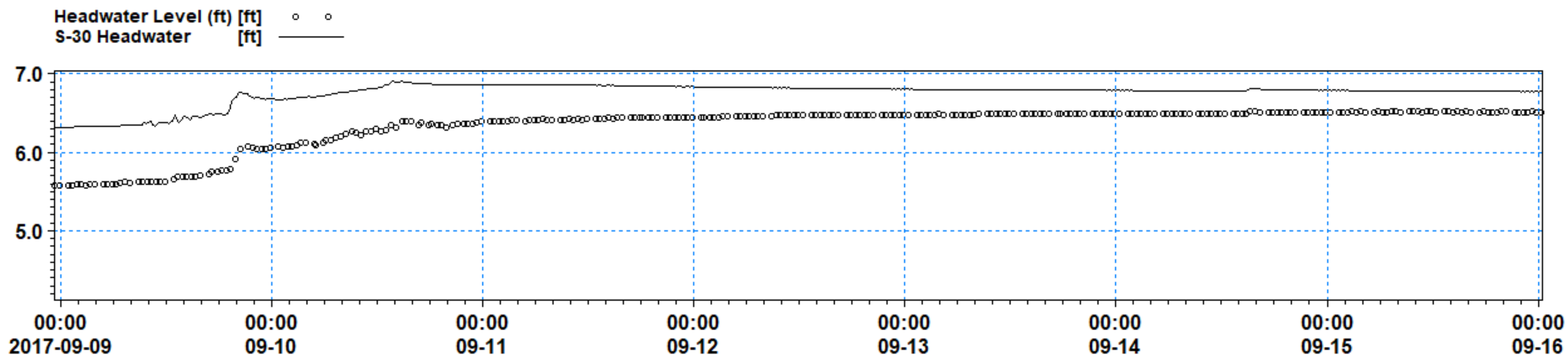

Figure 4.6-5: Simulated (line) vs Observed (dots) Headwater Comparison for SFWMD C-9 Structure S-30, September 9th-16th, 2017

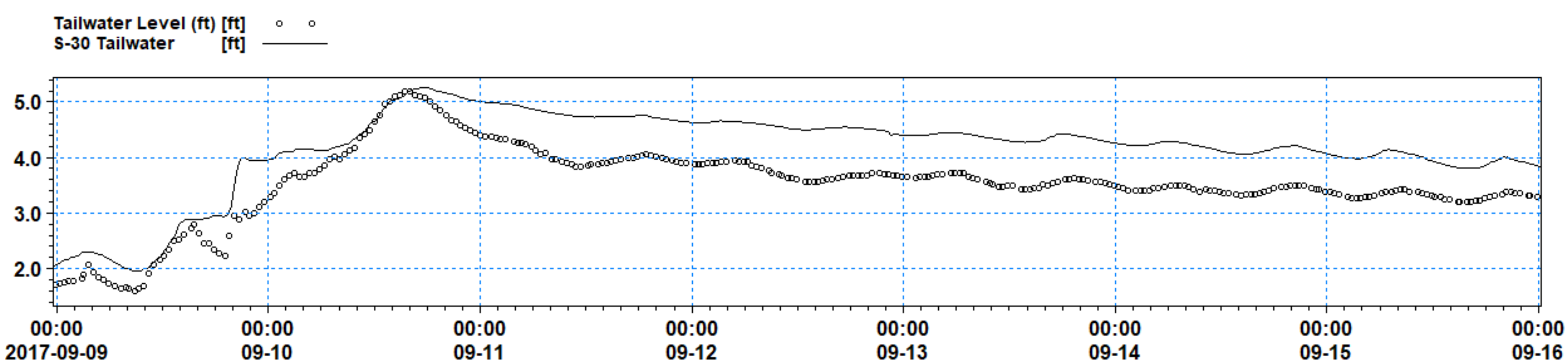

Figure 4.6-6: Simulated (line) vs Observed (dots) Tailwater Comparison for SFWMD C-9 Structure S-30, September 9th-16th, 2017

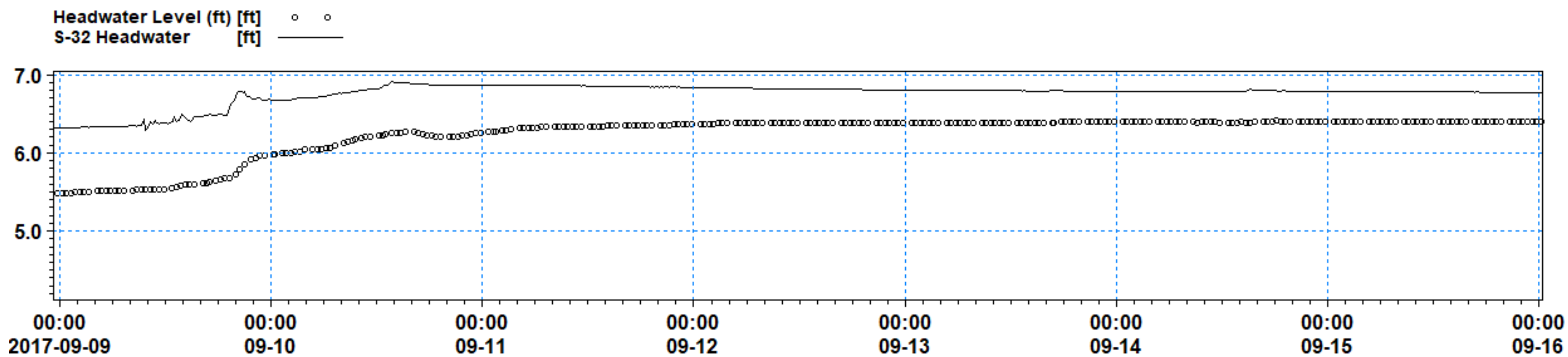

Figure 4.6-7: Simulated (line) vs Observed (dots) Headwater Comparison for SFWMD L-33 Structure S-32, September 9th-16th, 2017

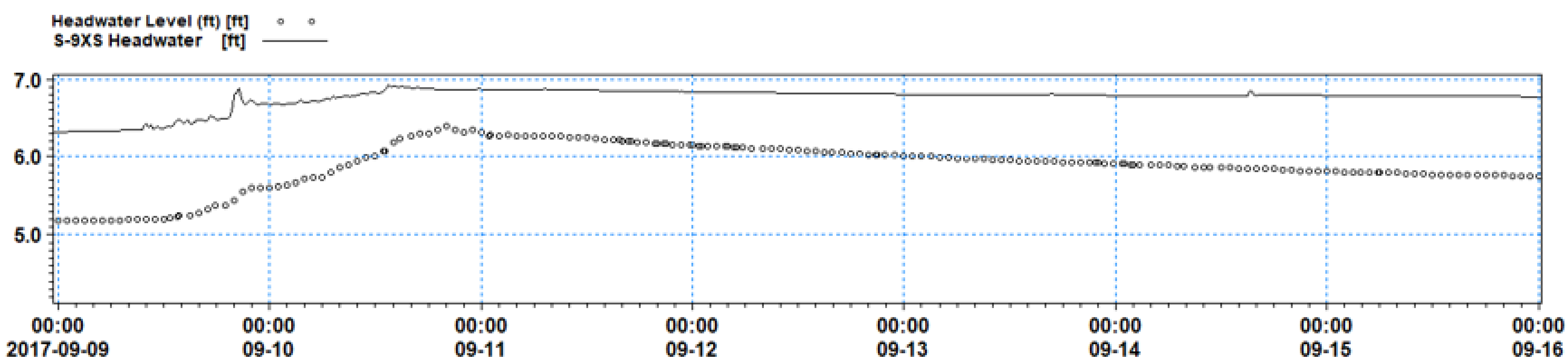

Figure 4.6-8: Simulated (line) vs Observed (dots) Headwater Comparison for SFWMD L-33 Structure S-9XS, September 9th-16th, 2017

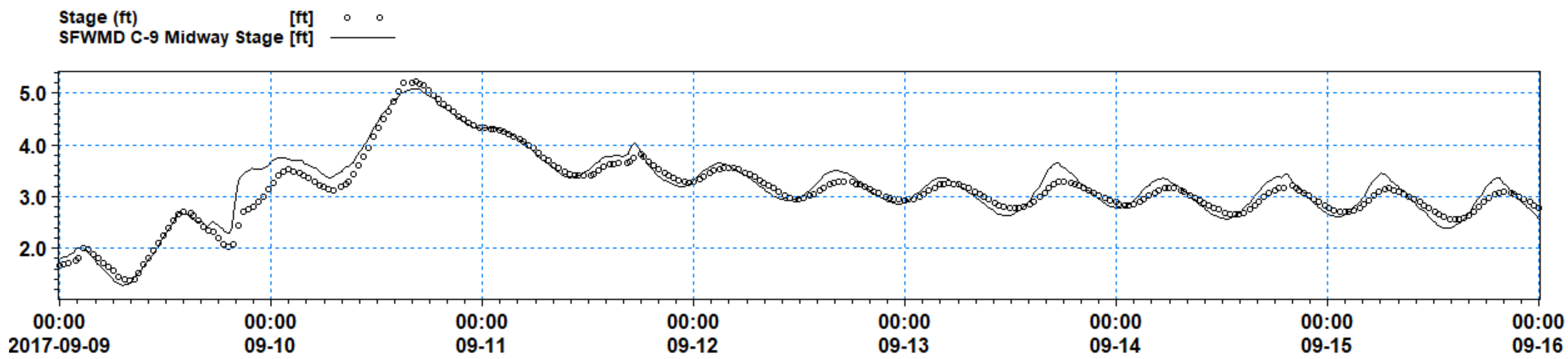

Figure 4.6-9: Simulated (line) vs Observed (dots) Stage Comparison for SFWMD C-9 Water Level Recorder S-29Z, September 9th-16th, 2017

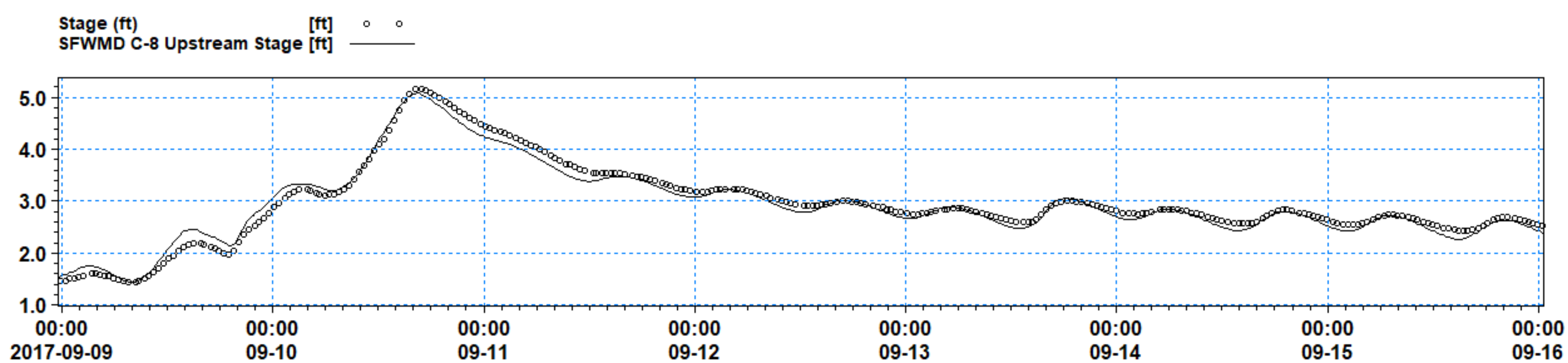

Figure 4.6-10: Simulated (line) vs Observed (dots) Stage Comparison for SFWMD C-8 Water Level Recorder S-28Z, September 9th-16th, 2017

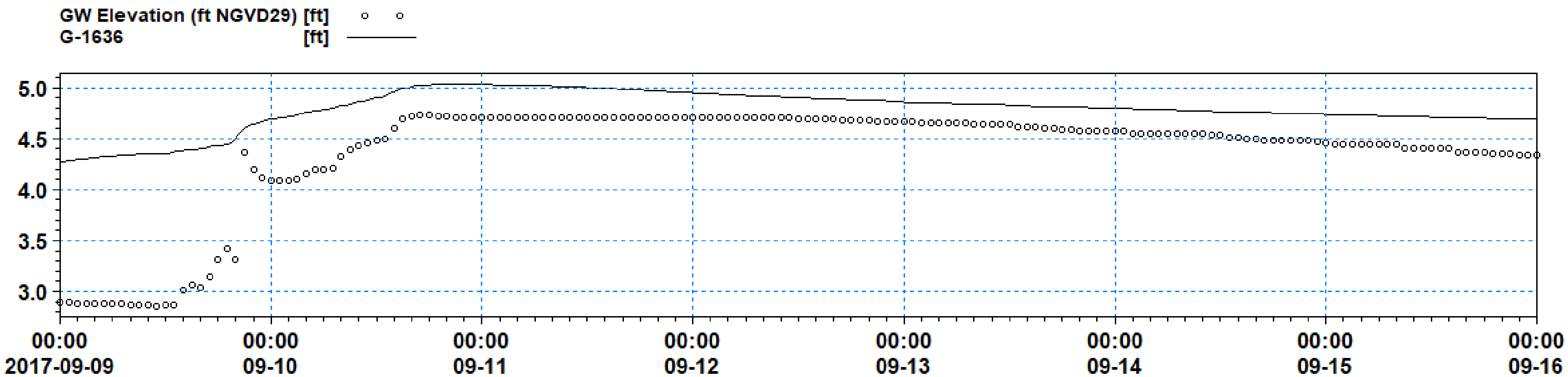

Figure 4.6-11: Simulated (line) vs Observed (dots) Groundwater Elevation Comparison for Well G-1636, September 9th-16th, 2017

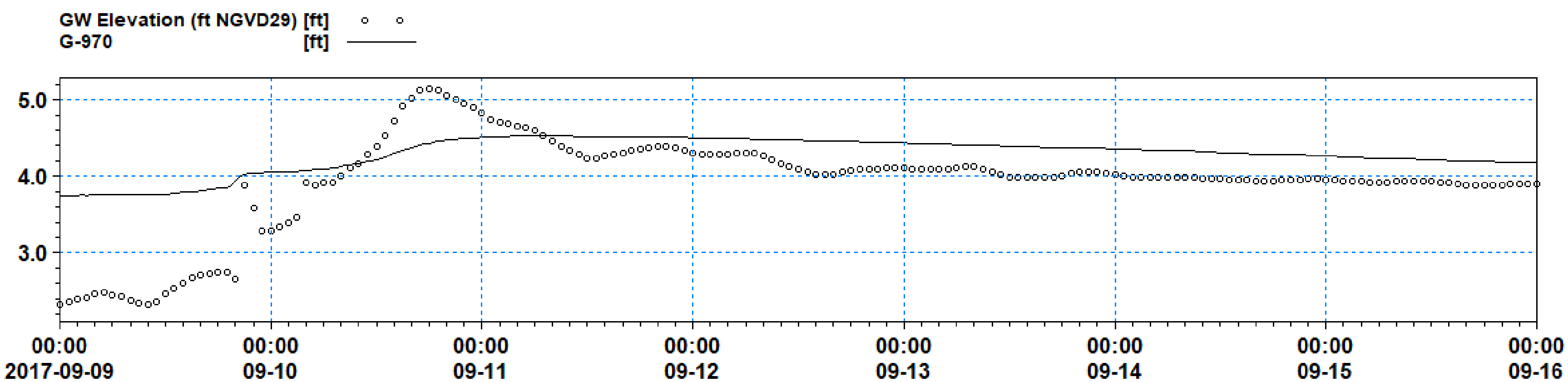

Figure 4.6-12: Simulated (line) vs Observed (dots) Groundwater Elevation Comparison for Well G-970, September 9th-16th, 2017

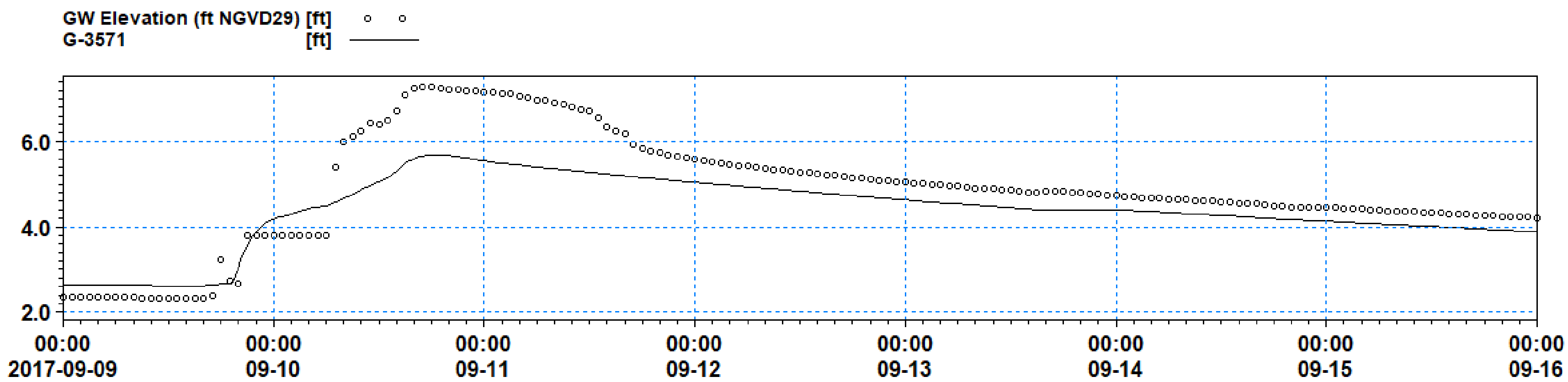

Figure 4.6-13: Simulated (line) vs Observed (dots) Groundwater Elevation Comparison for Well G-3571, September 9th-16th, 2017

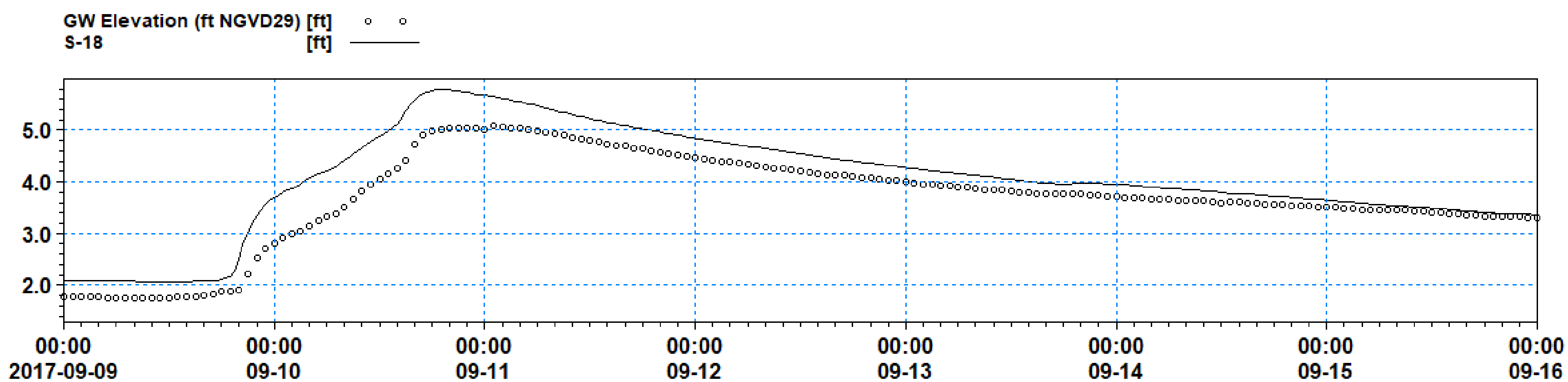

Figure 4.6-14: Simulated (line) vs Observed (dots) Groundwater Elevation Comparison for Well S-18, September 9th-16th, 2017

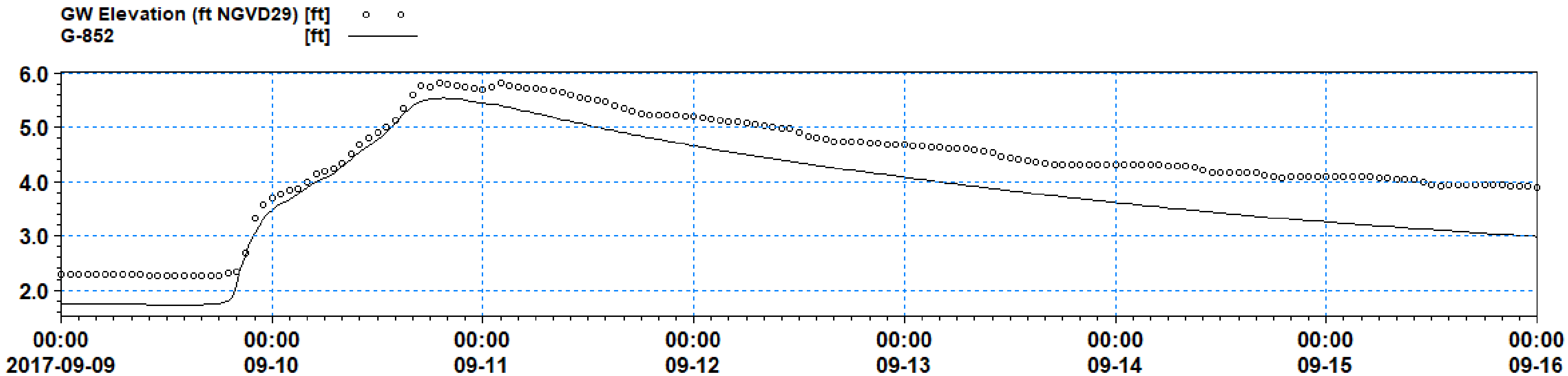

Figure 4.6-15: Simulated (line) vs Observed (dots) Groundwater Elevation Comparison for Well G-852, September 9th-16th, 2017

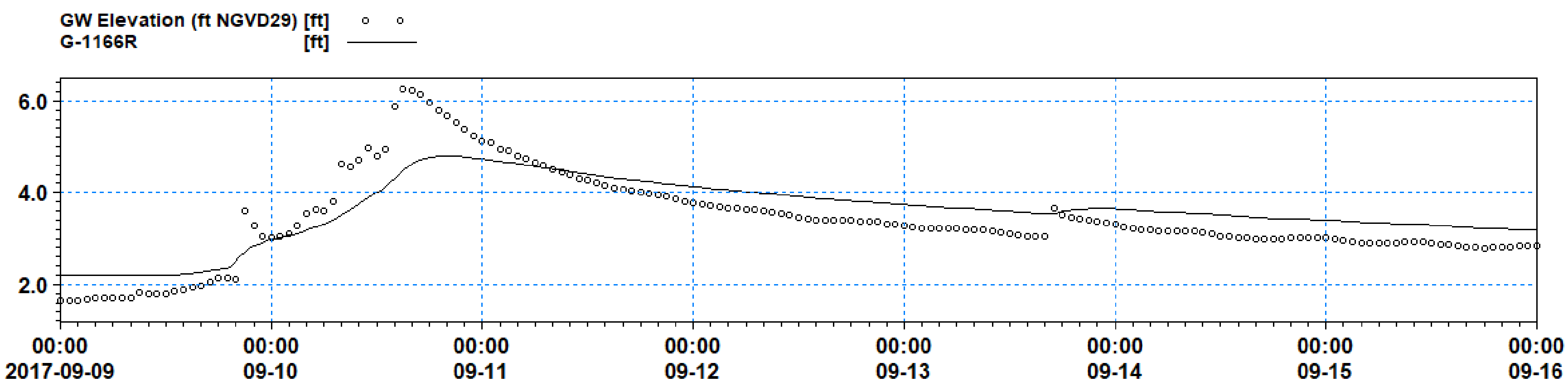

Figure 4.6-16: Simulated (line) vs Observed (dots) Groundwater Elevation Comparison for Well G-1166R, September 9th-16th, 2017

5.1 Conclusions

The C-8 C-9 calibration/validation model is a physically based integrated hydrologic and hydraulic model that includes a thorough representation of the hydrologic system and drainage network within the C-8 and C-9 basins, in Broward County and Miami-Dade County. Although a large portion of this model was inherited from the 2019 Broward County Current Conditions model, a lot of additional detail provided by Miami-Dade County and SFWMD, along with the survey collected specifically for this project by BDH Consulting Group, was incorporated into this model. Considering the scale of this model, the amount of detail is quite high, and most secondary and tertiary canal systems are modeled, including hundreds of culverts. The C-8 C-9 model was calibrated using the October 2nd-4th, 2000 storm event, which for the most part produced simulated canal stage results as well as groundwater elevations within 0.5 ft of observed. Likewise, the calibrated model produced simulated peak discharges and volumes within 10% and 17% of observed values, respectively. The C-8 C-9 model was validated using the September 9th-11th, 2017 storm event, which for the most part produced simulated canal stage results to within 0.4 ft. Additionally, the validation model produced simulated peak discharges and volumes to within about 15% of observed values. The validation model simulated groundwater elevations that were generally within 1 ft of observed values, which is a little higher than what was desired. It is worth mentioning that the areas with the largest differences were typically closer to the model boundary and might be adversely affected by uncertainty in the boundary conditions. The groundwater wells more centrally located in the model domain typically had simulated elevations closer to observed.

Overall, these results provide confidence in the model setup and parameterization, and further confidence that the model is a reliable predictor of water levels and flows based on current conditions. In the calibration model, the largest source of uncertainty comes from the rainfall data. Originally, temporally modified NEXRAD rainfall was used, which caused calibration challenges as it was likely providing significantly too much rainfall, as well as timing issues. With the rainfall input switched to rain gauges, significantly better results were achieved. However, there is still some uncertainty with the rainfall as there was data for only 5 rain gauges in the area, which could introduce some error in the spatial distribution. It is possible, and perhaps even likely, that the largest difference in simulated vs. observed stage is due to not simulating enough rainfall in the immediate upstream drainage area. In the validation model, the largest source of uncertainty comes from rating parameter issues, including how sensitive the rating equations are to negligible differences in head. Looking at structure S-28 during validation, there is a discrepancy between simulated and observed discharge, however, the headwater is a near perfect match, tailwater is forced, and the rating parameters are matched. The observed discharge is calculated based on a set of equations using rating parameters and the head difference between upstream and downstream of the structure. It has been determined that the rating equation used to characterize flow through these gates are particularly sensitive to the head difference between headwater and tailwater, especially during uncontrolled submerged conditions. So, although the model is simulating a near-perfect headwater, it is often slightly underpredicting, even as little as 0.001-0.05ft, which significantly reduced the head gradient through the structure. This is the cause for the model simulating discharges that are significantly smaller than the observed data. One example of this is on September 9th, 2017 at 6:55am. The observed discharge is 1420 cfs calculated based on a 0.037 ft gradient (keep in mind that is less than 0.5 inches), whereas the calculated discharge is around 75 cfs because the head gradient drops to less than 0.001 ft. The headwater is well within the target of +/- 0.5ft, as it is only about -0.5 inches, however, this causes the discharge to become extremely underpredicted, both in the model and verified by hand calculations using the same uncontrolled submerged equations with SFWMD rating parameters. This issue appears to be limited to uncontrolled submerged conditions, which is a rare occurrence. From 1985 to 2016, this structure operated in controlled submerged conditions 96% of the time (SFWMD, 2016). Likewise, the other major tidal outfall structure in this model (S-29), has been reported to have operated in controlled submerged conditions 99.14% of the time during 2011-2016 (SFWMD, 2016). So, although there is a sensitivity issue with uncontrolled submerged discharge, it historically has been a rare occurrence and it must be kept in mind that simulated vs observed discharge discrepancies during uncontrolled submerged operation are due to extremely small head differences that would otherwise be considered negligible.

In summary, Taylor Engineering believes that the C-8 C-9 model is setup and parameterized in a way that accurately represents the current drainage characteristics and will be a reliable predictor of water levels and flows in the design storm scenarios. However, it is important to keep in mind that any predictions by this computer model (or any other computer models) show only what could happen, not necessarily what will happen. Model outputs can only be as good as the data input, and this model is no exception. The limitations of this model and its ability to predict what could happen should be known and considered when interpreting the results.

6 MODEL DEVELOPMENT FOR CURRENT CONDITIONS

6.1 Overview

For this study's current conditions design storm model, Taylor Engineering modified the calibrated/validated model (2017 conditions) and updated it with all applicable changes to the model setup including structure operations, rainfall, evapotranspiration, tidal boundaries, and initial conditions. The recorded structure operations were replaced with rule-based operations. The observed NEXRAD rainfall was replaced with Thiessen polygon-based 3-day design storm rainfall depths from NOAA Atlas 14 using the SFWMD 3-day temporal distribution. The reference evapotranspiration was updated to a constant 2 mm/d, which is the minimum daily wet season value in year 2017 (USGS Reference and Potential Evapotranspiration, 2018). The 1-D tidal boundaries (forced tailwater at tidal structures) were updated to the SFWMD-provided design storm stage hydrographs. The SFWMD design storm stage hydrographs were also applied to the eastern general-head groundwater boundary. A time varying 2-D overland flow boundary was included along the coastal portion of the eastern boundary using the SFWMD design storm stage hydrographs. Localized adjustments to the initial groundwater levels were performed to ensure a close match between the groundwater levels and water control elevations.

6.2 Rules-Based Operations

The operable structure rules were based on standard operating procedure as detailed in the District's Operations Control Center Structure Books. The control rules for S-28 and S-29 are shown in **Figure 6.2-1** and **Figure 6.2-2**, respectively.

	Description	Condition	Control type	Value type
1		[s:hUS:S-28] - [s:hDS:S-28] <=0.09144	Direct setting	Close
2		[s:hUS:S-28] >0.64008	Direct setting	Fully open
3		[s:hUS:S-28] > 0.4572 && [s:hUS:S-28] <0.54864	Unchanged	Absolute value
4		[s:hUS:S-28] <0.4572	Direct setting	Close

Figure 6.2-1: Control Rules for S-28 (SI Units)

	Description	Condition	Control type	Value type
1		[s:hUS:S-29] - [s:hDS:S-29] <=0.09144	Direct setting	Close
2		[s:hUS:S-29] >0.762	Direct setting	Fully open
3		[s:hUS:S-29] > 0.4572 && [s:hUS:S-29] <0.6096	Unchanged	Absolute value
4		[s:hUS:S-29] <0.4572	Direct setting	Close

Figure 6.2-2: Control Rules for S-29 (SI Units)

6.3 Rainfall

The rainfall method for the design storm simulations was a Thiessen Polygon approach, which is the same approach used for design storms in the 2019 Broward County model and the 2016 BCB FPLOS (Taylor Engineering, 2016). The centroid of each polygon corresponds to a NOAA Atlas 14 station (**Figure 3.4-1**). Rainfall 3-day totals for each return period were based on NOAA Atlas 14 depths. The NOAA rainfall depths were distributed temporally based on the normalized cumulative SFWMD 3-day distribution. Total rainfall values per NOAA station are reported in **Table 3-2**.

6.4 Boundary Conditions

The 1-D tidal boundaries were updated using the District-provided time series for S-28 and S-29 (**Figure 3.6-4** and **Figure 3.6-5**). The SFWMD design storm stage hydrographs were also applied to the 2-D overland tidal boundary and the eastern general-head groundwater boundary (**Figure 3.7-6**). **Section 3.9.7** details the spatial distribution of the saturated zone boundary conditions and the various time series data applied.

6.5 Initial Groundwater Elevation

As described in **Section 3.9.6**, the design storm initial groundwater elevations were developed by making localized adjustments to the initial potential head from the validation simulation so that they closely matched basin control elevations. **Figure 3.9-17** shows the final initial potential head developed for the current condition design storm simulations.

7 FLOOD PROTECTION LEVEL OF SERVICE PERFORMANCE METRICS

The District relies on six (6) formal performance metrics (PMs) to evaluate the flood protection level of service provided by the primary water management infrastructure. These metrics, defined briefly in this section, were derived from the District publication *Flood Protection LOS Analysis for the C-4 Watershed, Appendix A: LOS Basic Concepts* (SFWMD H&H Bureau, December 29, 2015). **Section 8** provides the results of the FPLOS evaluation for existing conditions and **Section 10** provides the results of the FPLOS evaluation for future conditions with sea level rise.

PM #1 Maximum Stage in Primary Canals – This is the peak stage profile in the primary canal system. The profile is developed for the 72-hour duration, 5-year, 10-year, 25-year, and 100-year recurrence frequency design storms. The largest design storm that stays within the canal banks establishes the FPLOS of the primary canal system.

PM #2 Maximum Daily Discharge Capacity through the Primary Canals – This is the maximum discharge capacity throughout the primary canal network. Discharge is calculated as area weighted flow, in units of cubic feet per second per square mile of contributing area for the 25-year design event. Tidal effects are filtered by using a 12-hour moving average of discharge. Although the peak of the 25-year net discharge hydrographs are referred to in this report as the calculated discharge capacity, the true capacity of the canal segment is the net discharge corresponding to the largest design flood event that remains within the banks of the canal using the results of the 5-year, 10-year, 25-year, and 100-year events.

PM #3 – Structure Performance – Effects of Sea Level Rise – This metric shows the effective capacity of a tidal structure. It is comparable to the static design condition assumed in the original design but compares structure flow over a range of storm surge events and a range of sea level rise scenarios. Structure performance during current conditions with no effects of sea level rise is discussed in **Section 8.3**. Structure performance during future conditions with 1, 2, and 3 ft sea level rise is discussed in **Section 10.3**, and is compared with the current condition results.

PM #4 Peak Storm Runoff – Effects of Sea Level Rise – This is the maximum conveyance capacity of a watershed at the tidal structure for a range of design storms. It shows the maximum conveyance (moving 12-hour average) for a specific design storm and a specific tidal boundary condition. This metric examines the behavior of the system under severe stress and can be used to check if conditions exceed design limits. With respect to evaluating this PM, it is assumed that design rainfall and design storm surge occur simultaneously, or with a temporal offset that maximizes stress on the structure. Structure performance during current conditions with no effects of sea level rise is discussed in **Section 8.4**. Structure performance during future conditions with 1, 2, and 3 ft sea level rise is discussed in **Section 10.4**, and is compared with the current condition results.

PM #5 Frequency of Flooding – Stage-based FPLOS for Subwatersheds – In this metric, the flood elevations or depths of overland flooding are evaluated for the 72-hour duration, 5-year, 10-year, 25-year, and 100-year recurrence frequency design storms. These flood depths/elevations can then be compared with elevations of build features such as buildings and roadways, where such information exists. For the purposes of this C-8 and C-9 FPLOS evaluation, flood inundation maps were developed from the model output for each storm event.

PM #6 Duration of Flooding – This metric quantifies the duration of flooding across the entire watershed. The length of time the flood elevation is projected to be above a threshold depth of 0.25 ft was mapped over the study area using the multi-cell gridded model output files for the 2-D overland flow component.

8 CURRENT CONDITION FLOOD PROTECTION LEVEL OF SERVICE ASSESSMENT

After model calibration and validation, the model was setup to represent design storm conditions using District-provided time series data as described in **Section 3**, and executed for the 72-hour 5-year, 10-year, 25-year, and 100-year storm events. Model results were evaluated for stability and reasonableness prior to proceeding with the FPLOS evaluation. **Appendix D** provides a summary of the model results at primary control structures. The remainder of this section describes the results of the FPLOS evaluations for all relevant performance metrics, which for current conditions include PM #1, PM #2, PM #5, and PM #6. PM #3 and #4 results presented in this section are partial, as the complete results were dependent on future condition simulations from Phase 1B of this project and were not available for comparison with current conditions at the time of evaluating current conditions. Complete results with future conditions for PM #3 and #4 are presented in **Section 10.3** and **10.4**.

8.1 PM #1 – Maximum Stage in Primary Canals

This is the peak stage profile in the primary canal system. The profile is developed for the 72-hour 5-year, 10-year, 25-year, and 100-year design storms. The largest design storm that stays within the canal banks establishes the FPLOS of the primary canal system.

To evaluate this PM under current conditions within the C-8 and C-9 watersheds, instantaneous peak stage profiles were prepared for the primary canals within the watersheds, which are the C-8 and C-9 Canals, respectively. Bank elevations on the profile figures are based on the MIKE HYDRO cross-section data. For the purposes of this metric, several cross-section banks were modified/extended (based on the current LiDAR data) before model simulation to better capture levees or the areas at which the canals would be considered out-of-bank. Also shown in the figures are major roadway landmarks, control structures, and primary canal junctions.

Table 8-1 summarizes the PM #1 results shown graphically in **Figure 8.1-1** and **Figure 8.1-2**, listing the maximum return period profile that is contained within the canal banks. Although the C-8 Canal contained the 5-year and 10-year profiles along the majority of the canal length, the bank elevation was exceeded for the 5-year event over short segments at multiple locations. Similarly, although the C-9 Canal contained the 10-year and 25-year profiles along the majority of the canal length, the bank elevation was exceeded for the 10-year event over short segments at a few locations. Therefore, if a strict interpretation of this criteria is used, then both the C8 and C9 Canal have a 5-year FPLOS. However, as discussed in the Conclusions, the determination of FPLOS should consider the results of all applicable performance metrics. With careful consideration of PM #1 and PM #5, both the C8 and C9 Canals provide a 10-year and 25-year FPLOS, respectively.

Table 8-1: PM #1 Summary Results

Canal Segment	Figure Number	FPLOS Localized	FPLOS Overall	Comment
C-8	**Figure 8.1-1**	5-year	10-year	Overall FPLOS from **Section 8.7.1**
C-9	**Figure 8.1-2**	5-year	25-year	Overall FPLOS from **Section 8.7.2**

The PM #1 performance of the C-8 Canal is generally worse east of its confluence with the Opa Locka Canal compared to the western segment. Notable areas of bank exceedances include the following:

- Just west of NE 6th Avenue (CR915), south bank exceeded for 5-year event, north bank exceeded for 10-year event.
- Downstream of NE 135th St. (CR 916), north bank exceeded for 5-year event, south bank for 25-year event.
- From North Miami Avenue to NE 135th St., south bank exceeded for 10-year event.
- Downstream of Opa Locka Canal, south bank exceeded for 10-year event.

Notable areas of bank exceedances in the C-9 Canal include:

- Halfway between I-95 and S-29 to S-29, south bank exceeded for 25-year event, north bank for the 100-year event.
- Downstream of US Hwy 441, north bank exceeded for 25-year event.
- From SBDD pumps S-4 and S-5 to the Ronald Reagan Turnpike, south bank exceeded for the 25-year event.

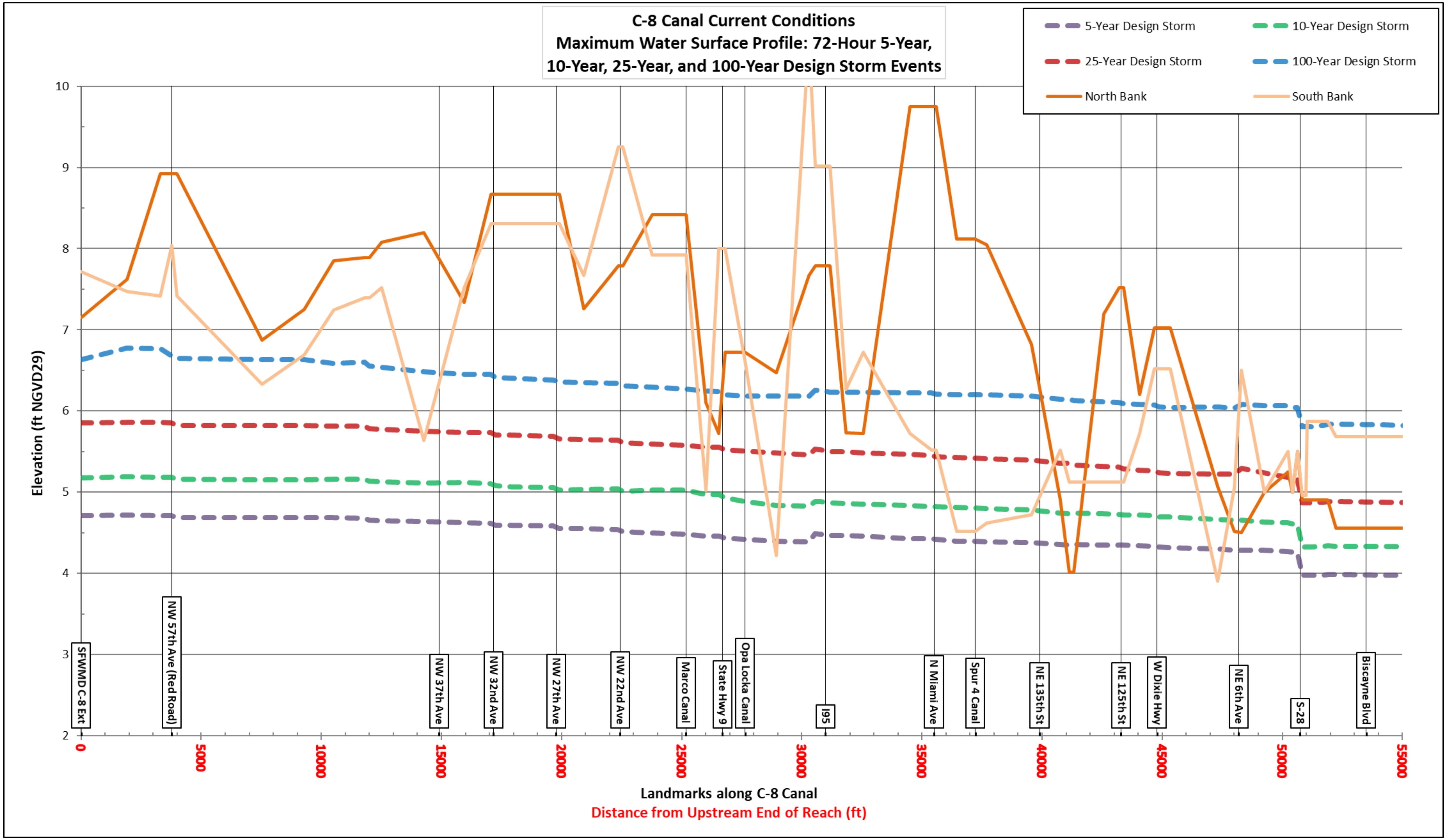

Figure 8.1-1: C-8 Canal Peak Stage Profiles

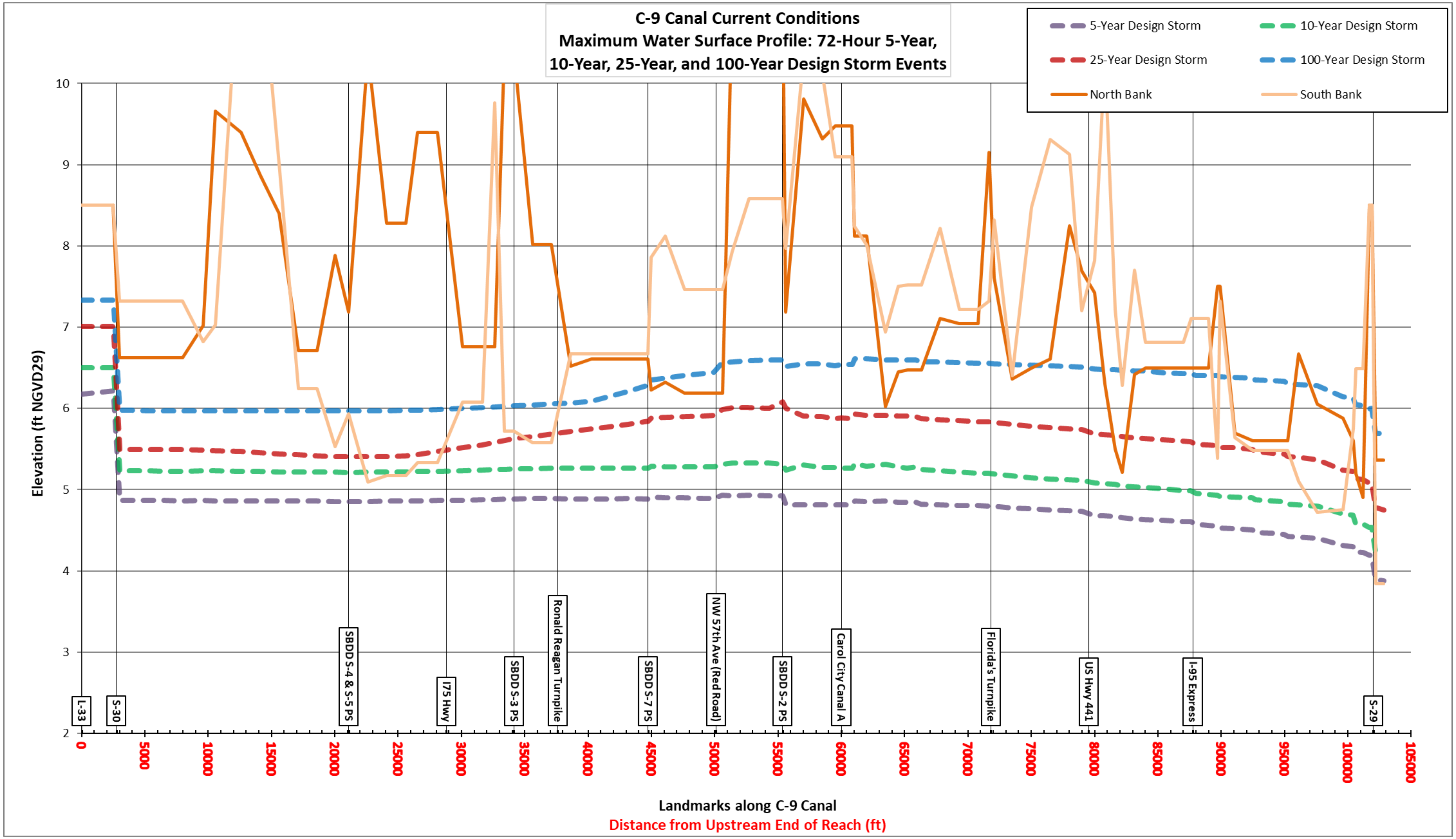

Figure 8.1-2: C-9 Canal Peak Stage Profiles

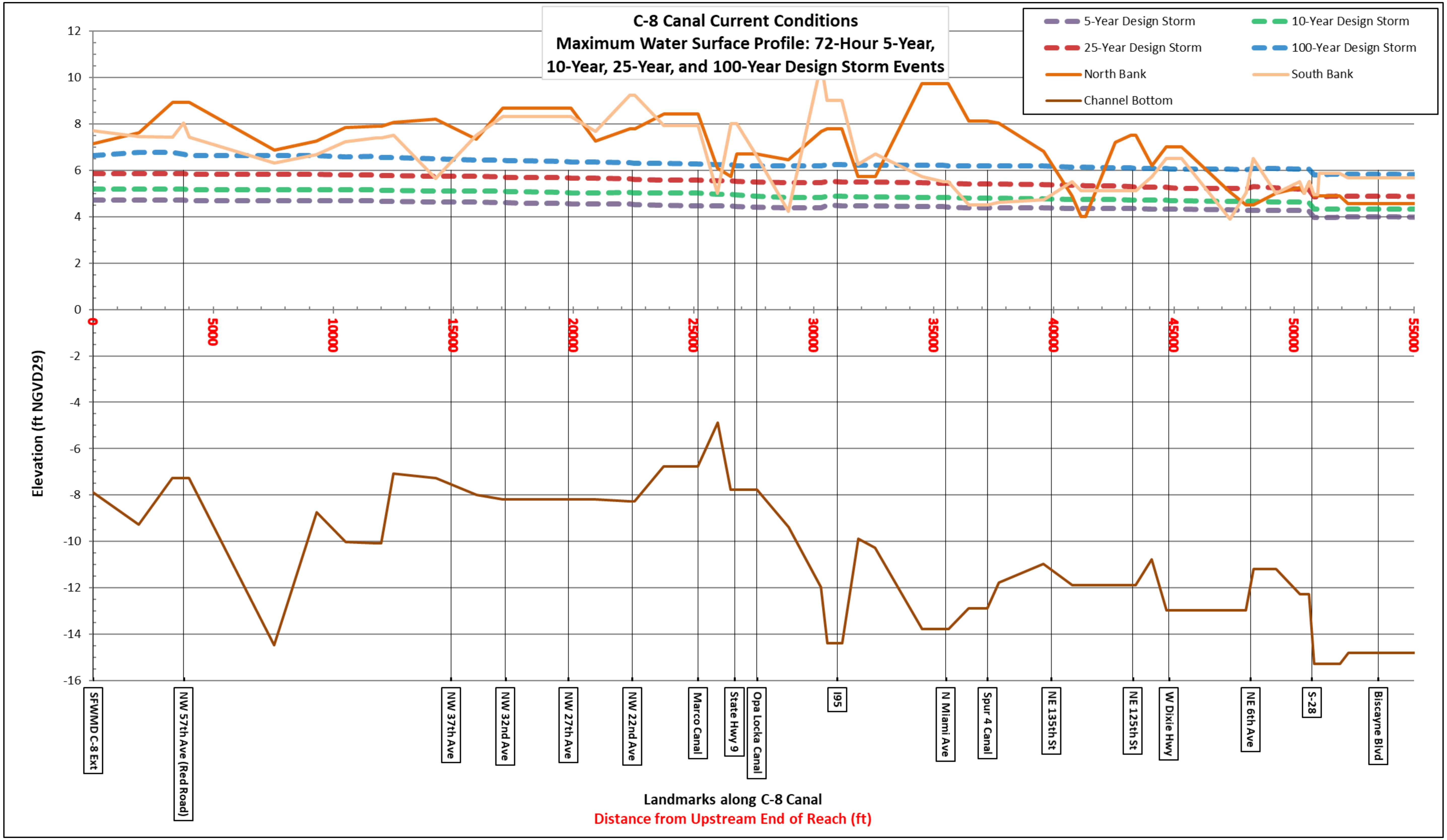

Figure 8.1-3: C-8 Canal Peak Stage Profiles with Canal Bottom

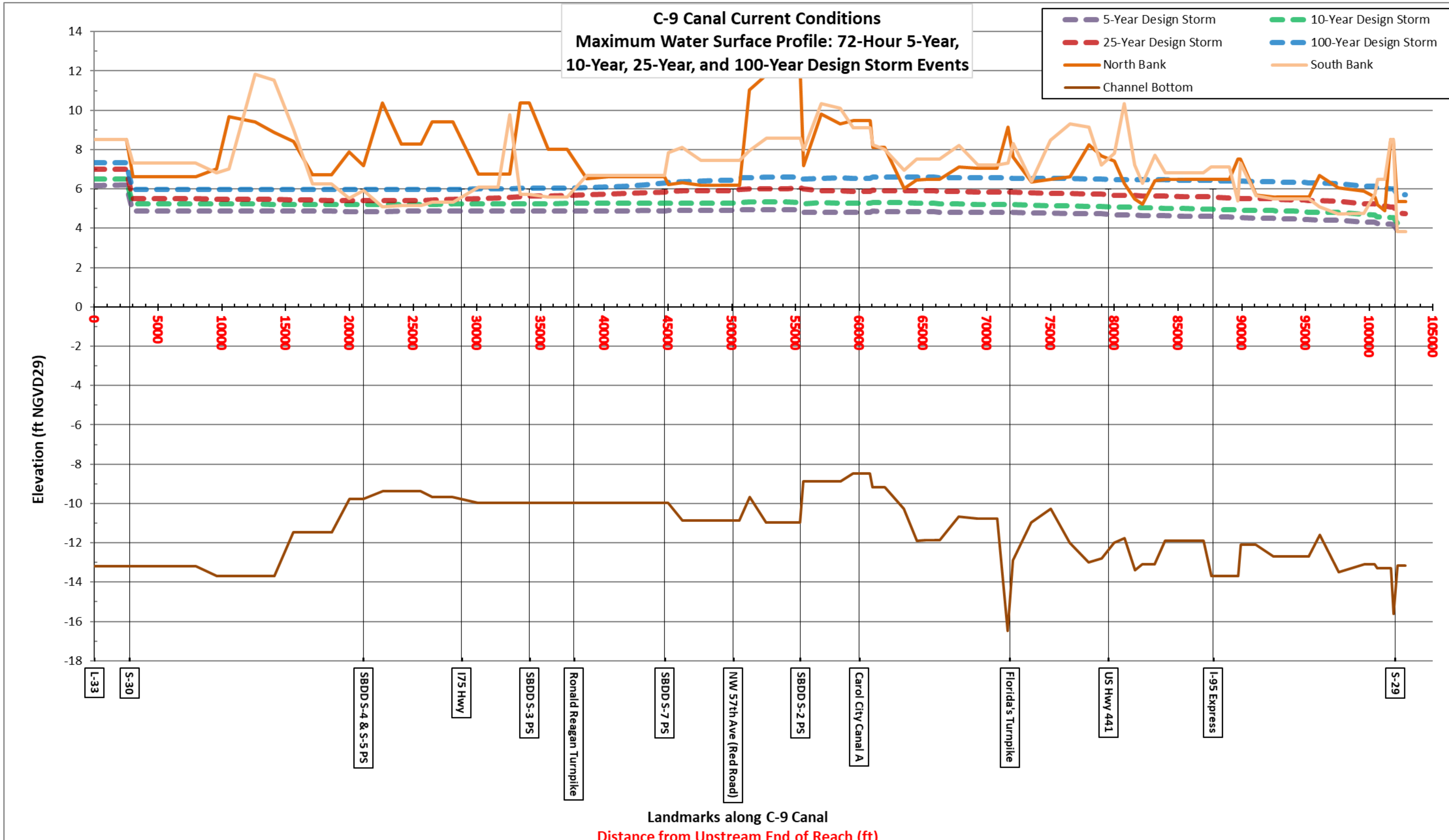

Figure 8.1-4: C-9 Canal Peak Stage Profiles with Canal Bottom

Table 8-2 shows the peak stages at the major landmarks along the C-8 Canal for each of the design storms. Bridge low cord elevations were specified were applicable. Although the water level in the C-8 Canal exceeded bank elevations in several locations for the various design storms (**Figure 8.1-1**), the water level did not get high enough to become restricted by the low cord elevation of any bridge.

Table 8-2: C-8 Canal Peak Stage at Landmarks

Landmark	Peak Stage (ft NGVD29)				Bridge Low Cord Elevation (ft NGVD29)
	5-Yr	10-Yr	25-Yr	100-Yr	
SFWMD C-8 Ext	4.71	5.18	5.86	6.63	
NW 57th Ave (Red Road)	4.71	5.18	5.85	6.68	9.2
NW 37th Ave	4.64	5.12	5.75	6.49	
NW 32nd Ave	4.62	5.11	5.73	6.45	9.18
NW 27th Ave	4.58	5.06	5.69	6.38	7.02
NW 22nd Ave	4.54	5.04	5.64	6.34	8
Macro Canal	4.48	5.02	5.57	6.27	
Rail Road / State Hwy 9	4.46	4.97	5.55	6.24	7.44
NW 7th Ave Bridge	4.39	4.83	5.46	6.18	8.53
I-95	4.48	4.89	5.52	6.25	8.05
North Miami Ave	4.42	4.83	5.45	6.22	9.62
Spur 4 Canal	4.39	4.81	5.42	6.20	
NE 135th St	4.37	4.78	5.40	6.19	7.38
NE 125th St	4.34	4.73	5.31	6.11	11.47
W Dixie Hwy	4.33	4.71	5.26	6.07	10.57
NE 6th Ave	4.28	4.65	5.22	6.03	9.02
S-28	4.26	4.61	5.16	6.04	
Biscayne Blvd	3.98	4.33	4.88	5.83	

Table 8-2 shows the peak stages at the major landmarks along the C-9 Canal for each of the design storms. Bridge low cord elevations were specified were applicable. For the 5-yr and 10-yr design storm events, the water level in the C-9 Canal exceeded bank elevations in a couple locations (**Figure 8.1-2**), however, the water level did not get high enough to become restricted by the low cord elevation of any bridge. For the 25-yr and 100-yr design storms, the water level in the C-9 Canal exceeded bank elevations in a couple additional areas and became elevated enough to become restricted by the low cord elevation of bridges, as shown in red in **Table 8-3**. None of the bridges were overtopped.

Table 8-3: C-9 Canal Peak Stage at Landmarks

Landmark	Peak Stage (ft NGVD29)				Bridge Low Cord Elevation (ft NGVD29)
	5-Yr	10-Yr	25-Yr	100-Yr	
L-33	6.17	6.50	7.0	7.34	
S-30	4.87	5.23	5.50	5.97	
SBDD S-4 & S-5 PS	4.86	5.21	5.41	5.97	
I75 Hwy	4.87	5.23	5.47	5.96	
SBDD S-3 PS	4.88	5.25	5.63	6.03	
Ronald Reagan Turnpike	4.9	5.26	5.68	6.05	
SBDD S-7 PS /Flaming Rd	4.88	5.27	5.84	6.29	9.76
NW 57th Ave (Red Road)	4.89	5.28	5.92	6.43	9.54
SBDD S-2 PS / NW 47th Ave	4.93	5.31	6.08	6.60	8.9
Carol City Canal A	4.81	5.27	5.88	6.54	
NW 37th Ave	4.81	5.26	5.87	6.54	8.6
NW 27th Ave	4.84	5.28	5.90	6.60	7.93
Florida's Turnpike	4.8	5.20	5.83	6.56	
US Hwy 441	4.73	5.11	5.74	6.51	7.53
NW 199th St	4.67	5.06	5.67	6.48	8.6
I-95 Express	4.60	4.98	5.59	6.43	8.43
Miami Gardens Dr	4.55	4.93	5.54	6.40	8.96
NE 15th Ave	4.45	4.85	5.44	6.33	8.87
NW 19th Ave	4.40	4.80	5.37	6.28	5.6
NE 22nd Ave	4.3	4.69	5.23	6.13	4.9
Rail Road at Biscayne Blvd	4.23	4.57	5.12	6.03	5.77
S-29	4.19	4.54	5.08	6.0	

8.2 PM #2 – Maximum Daily Discharge Capacity through the Primary Canals

PM #2 is the maximum discharge capacity throughout the primary canals. Discharge is calculated for canals as area weighted flow, in units of cubic feet per second per square mile of contributing area. Canal segments are generally defined as areas between water control structures, however, there are no intermittent control structures along the C-8 and C-9 Canals. Therefore, the segment associated with structures S-28 and S-29, is the entire C-8 and C-9 Canals, respectively. This means that the contributing area for S-28 and S-29 is the entire C-8 basin and C-9 basin, respectively. Structure S-30, which is on the C-9 Basin boundary, was closed during the design storms (based on control rules), so there was no additional inflow into the C-9 basin. Within the C-9 Basin, there are two areas with different allowable runoff rates based on the District's ERP Handbook; (1) "essentially unlimited inflow by gravity connections east of Red Road", and (2) "20 CSM pumped and essentially unlimited inflow by gravity connections west of Red Road or Flamingo BLVD". Therefore, the C-9 Basin discharge capacity was estimated for the entire C-9 Basin, as well as for the respective areas east and west of Red Road. **Table 8-4** lists the canal segments identified for this analysis. The table also identifies the contributing area for each canal segment, and the discharge capacity calculated for each segment associated with each design storm event.

Discharge capacity was calculated by dividing the peak of the discharge hydrograph by the canal segments contributing area. For structures S-28 and S-29, discharge capacity was calculated by dividing the peak discharge by the entire basin area. For the C-9 Basin, two additional estimates were made for the respective areas east and west of Red Road. These two additional estimates were necessitated by the presence of two different allowable runoff rates within the C-9 Basin. For the drainage area west of Red Road, the peak discharge at the Q-point located at Red Road (shown as a green dot in **Figure 8.2-1**) was divided by the contributing drainage area (highlighted in green in **Figure 8.2-1**). For the drainage area east of Red Road, the peak discharge at the Q-point located at Red Road was subtracted from the peak discharge at structure S-29, and then divided by the contributing drainage area east of Red Road. Tidal effects were filtered by using a 12-hour moving average of discharge.

Table 8-4: Water Control Catchment Inflow and Outflow Points and Discharge Capacity

Discharge west and east of Red Road is an estimate due to interconnected outfalls on both sides of Red Road

Structure / Segment	Inflow	Outflow	Water Control Catchment Area (sq.mi)	Peak Discharge Capacity (cfs/sq.mi)			
				5-Yr	10-Yr	25-Yr	100-Yr
S-28	Beginning of C-8	S-28	28.22	51	61.9	82.8	115.3
S-29	Beginning of C-9/ Structure S-30	S-29	99.37	21.5	24.5	29.3	37.5
C-9 west of Red Road	Beginning of C-9/ Structure S-30	Q-point at Red Road	61.24	13.5	15.2	17.9	20.9
C-9 east of Red Road	Q-point at Red Road	S-29	38.13	46.7	51.6	65.8	89.1

Figure 8.2-1 shows the contributing areas draining to each canal segment. The C-8 catchment polygon was based on the District's Arc Hydro Enhanced Database (AHED). The C-9 catchment polygons were based on both the District's AHED as well as SBDD and Miami-Dade County subbasins. It is important to note that the C-9 Basin is technically one drainage area and does not have a real drainage divide. The two drainage areas shown within the C-9 Basin represent the spatial variability in the District's allowable discharge rates within the C-9 Basin. The area-weighted discharge presented for the areas east and west of Red Road are an approximation due to the uncertainty in the exact location of this allowable runoff-based basin divide. Additionally, the drainage areas east and west of Red Road are interconnected. Although the drainage divide is specified as Red Road, the contributing drainage area on the north side of the C-9 Canal extends east of Red Road and has two outfalls that are interconnected, one east of Red Road and one west of Red Road. For this analysis, the discharge at Red Road was used, so some discharge from the contributing drainage area is not included as it discharges further downstream. It should be noted that comparing the discharge in the western half of the C-9 Canal to the permitted rates does not have significant meaning as there are several gravity connections to the C-9 Canal west of Red Road and two pumped connections east of Red Road.

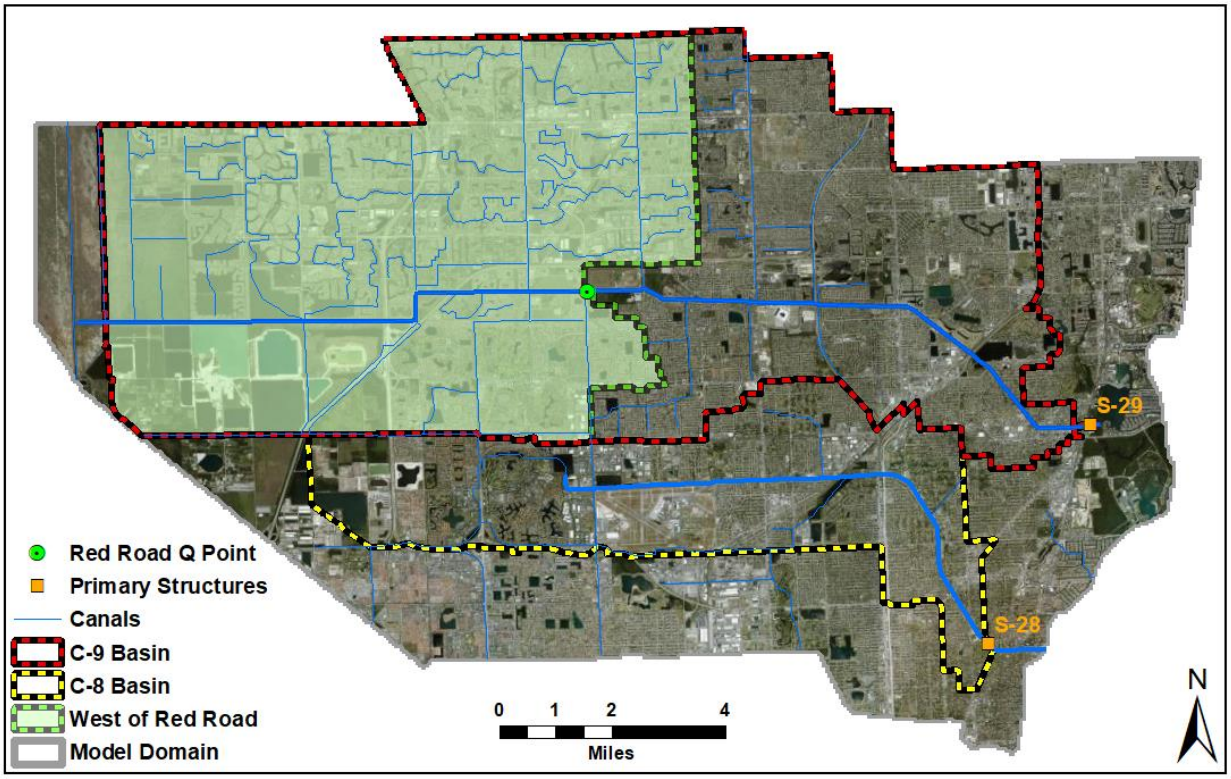

Figure 8.2-1: Catchment Areas for Calculating PM #2

Figure 8.2-2 through **Figure 8.2-5** present a visual comparison of the area-weighted discharge hydrographs for each canal segment with respect to the 72-hour 5-year, 10-year, 25-year, and 100-year design storms. Although the peak discharge during each design storm event are referred to in this section as the calculated discharge capacity, the true capacity of the canal segment is the net discharge corresponding to the largest design flood event that remains within the banks of the canal. Therefore, the results of PM #2 must be evaluated in conjunction with the results of PM #1 (Maximum Stage in Primary Canals) and PM #5 (Frequency of Flooding). As discussed in **Section 8.1**, peak stages in all canals exceeded the canal banks for the 100-year event. In several canal locations, a 10-year event was sufficient to cause water levels to exceed the canal bank elevations (see **Figure 8.1-1** and **Figure 8.1-2**) but these generally appear to be localized flooding instances that do not extend far from the canal banks. This is based on an examination of the PM #5 results (**Section 8.3**).

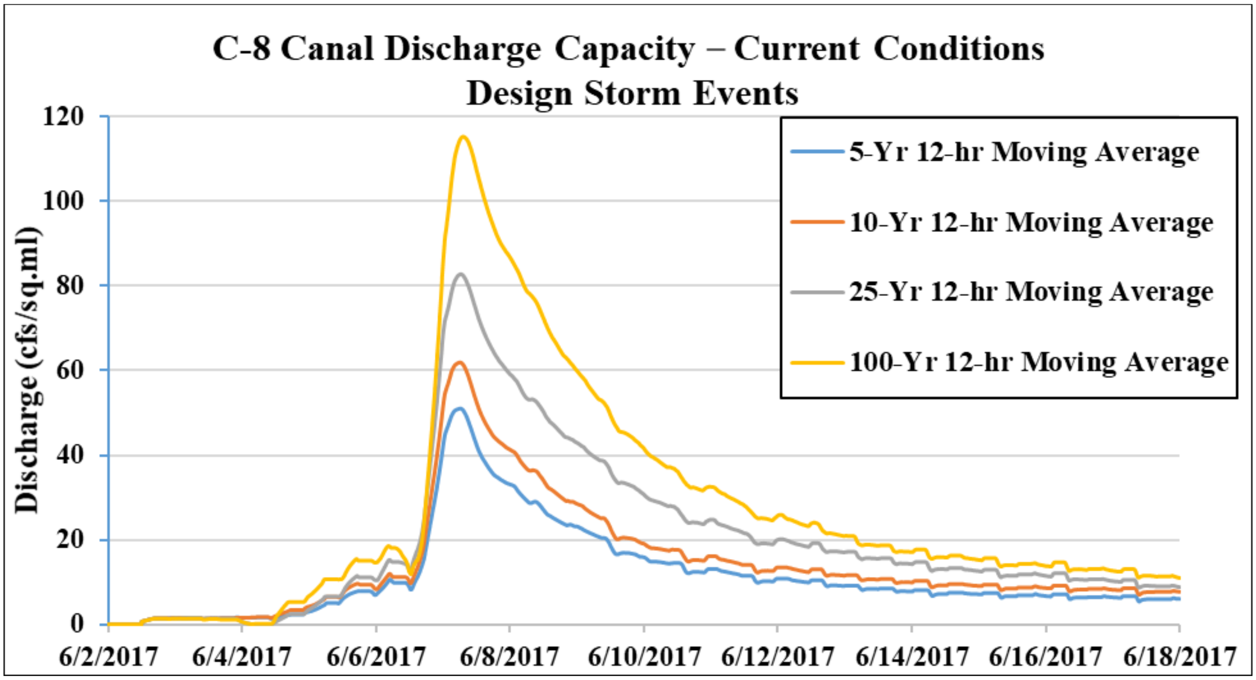

Figure 8.2-2: Area-Weighted Discharge Hydrograph for C-8 Canal Structure S-28

The C-8 canal is allowed "essentially unlimited inflow by gravity connections", as is the area draining to the C-9 Canal east of Red Road. Therefore, the only canal segment in the model that is subject to District discharge limitations is the area draining to the C-9 Canal west of Red Road, which has a limit of 20 CSM pumped.

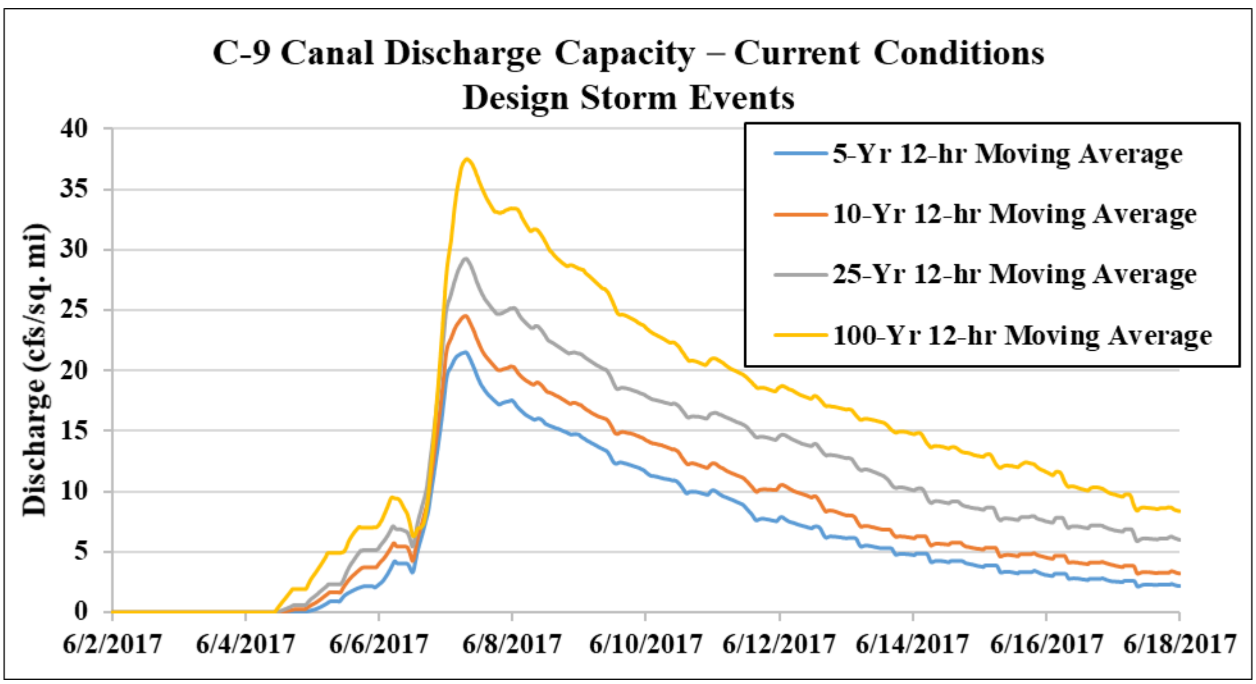

Figure 8.2-3: Area-Weighted Discharge Hydrograph for C-9 Canal Structure S-29

The peak discharge capacity of the C-9 Canal west of Red Road was 20.9 CSM for the 100-year design storm. However, it cannot be said that the area west of Red Road is exceeding the permitted allowance as there are several gravity connections contributing to that discharge capacity. Additionally, there are pumped connections east of Red Road that share a common drainage area with west of Red Road due to the interconnectivity of the drainage system. Therefore, the discharge capacity of the C-9 Canal, with respect to east or west of Red Road, is strictly an estimate and should not be used for regulatory purposes. With that said, the SBDD pump discharge and operation rules are based on their permitted allowance from the District. Considering there are gravity connections west of Red Road, the 100-year peak discharge capacity of 20.9 CSM compared to the permitted allowance of 20 CSM pumped sounds reasonable.

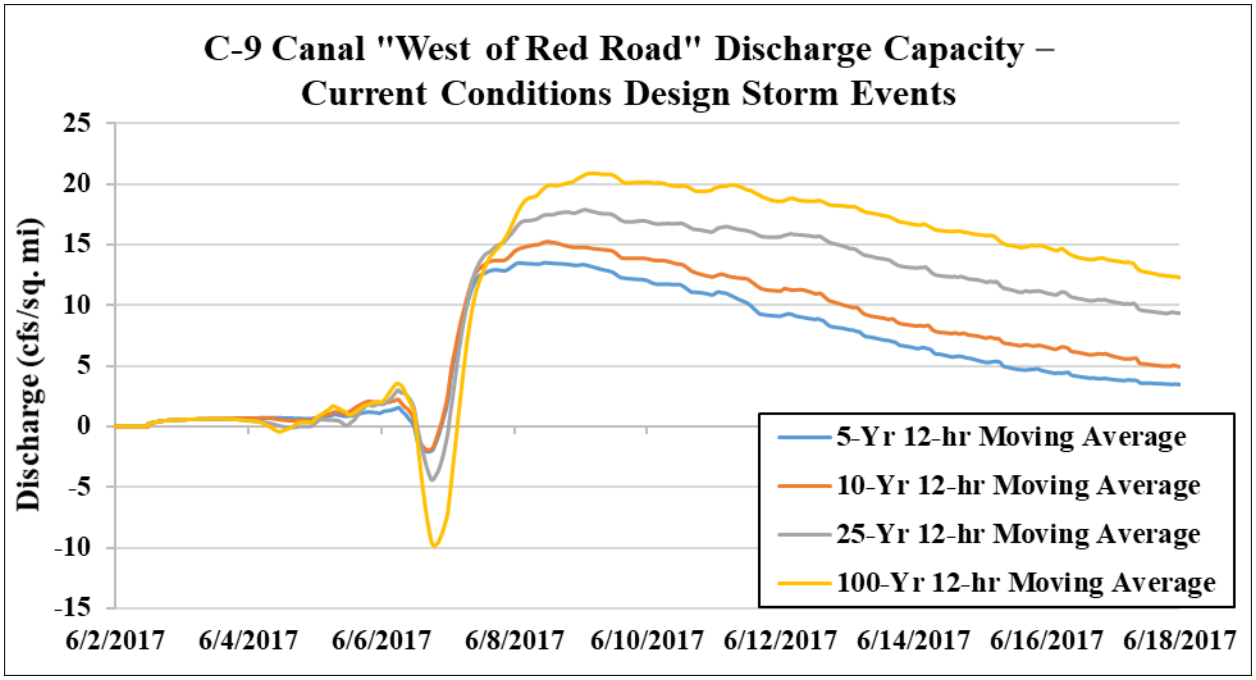

Figure 8.2-4: Area Weighted Discharge Hydrograph for C-9 Canal West of Red Road

Discharge west of Red Road is an estimate due to interconnected outfalls on both sides of Red Road

Figure 8.2-4 has negative discharge during peak rainfall. This occurs because there is a delayed response in the west side as there is a significant amount of dead storage (large lakes in SBDD). The storage in the west side is controlled by pumps that turn on at an elevation higher than control elevation. As the pumps turn on, the discharge becomes positive.

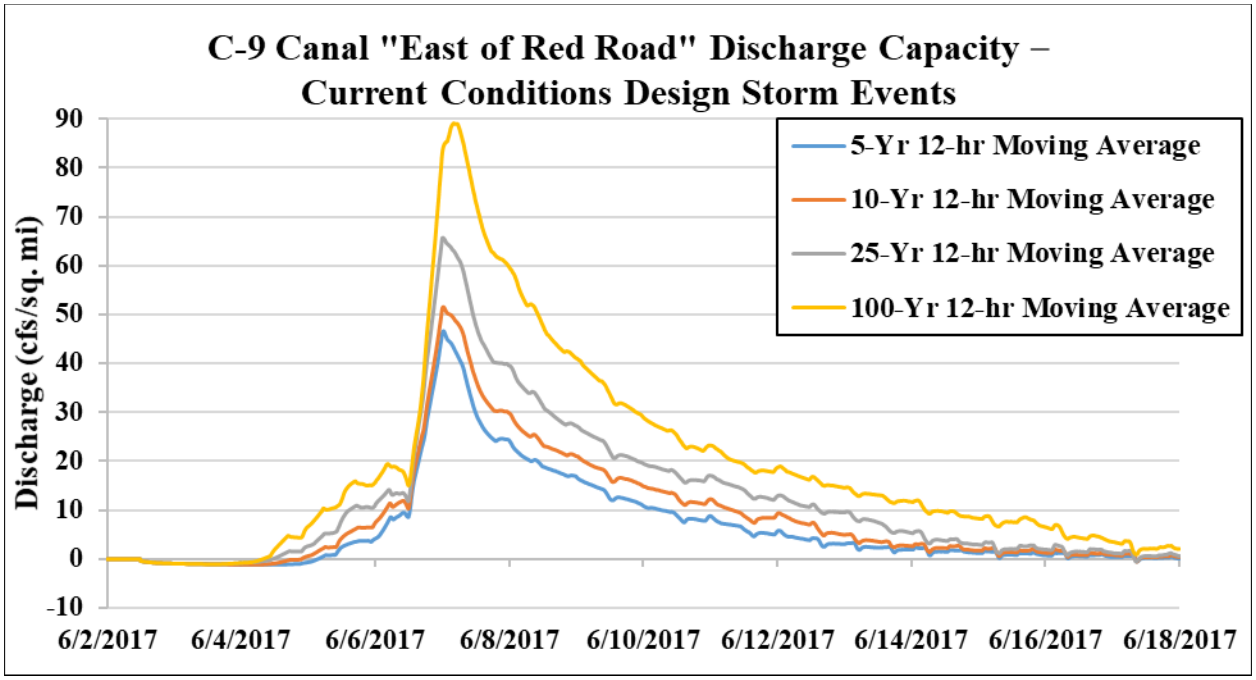

Figure 8.2-5: Area-Weighted Discharge Hydrograph for C-9 Canal East of Red Road

Discharge east of Red Road is an estimate due to interconnected outfalls on both sides of Red Road

Figure 8.2-6 shows the location of inter-basin connections, where discharge between the C-8 and C-9 watersheds occur, as well as between the C-8 and C-7 watersheds.

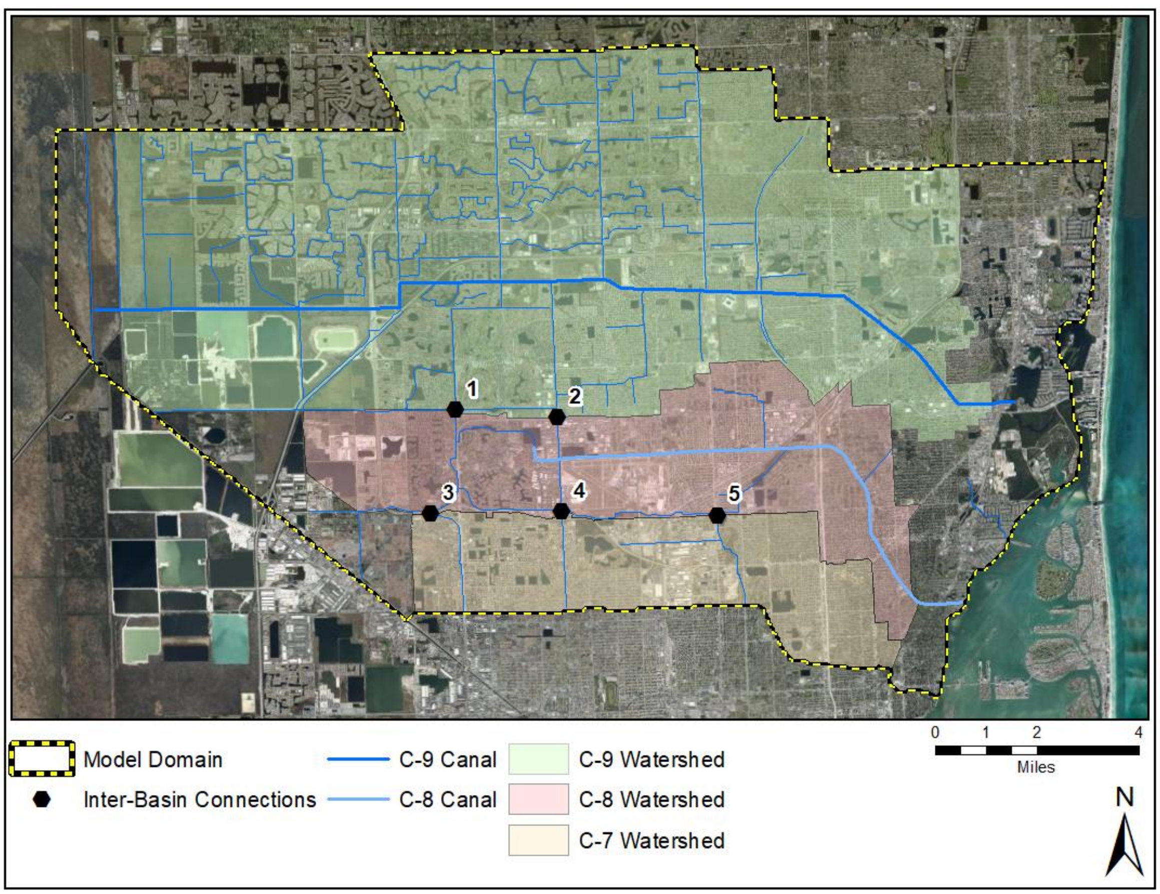

Figure 8.2-6: Location of Inter-Basin Connections

Connection 1 is a culvert under NW 78th Ave. **Figure 8.2-7** shows the inter-basin discharge, with positive values representing flow from the C-8 to the C-9 watershed and negative values indicating flow from the C-9 to the C-8 watershed. For the 100-year design storm, the peak discharge from C-8 to C-9 watershed at this inter-basin connection is about 60 cfs, whereas the peak discharge at Red Road on the C-9 Canal is around 1300 cfs. Relative to the flow in the C-9 Canal, this inter-basin exchange is small, contributing less than 5% of the peak discharge.

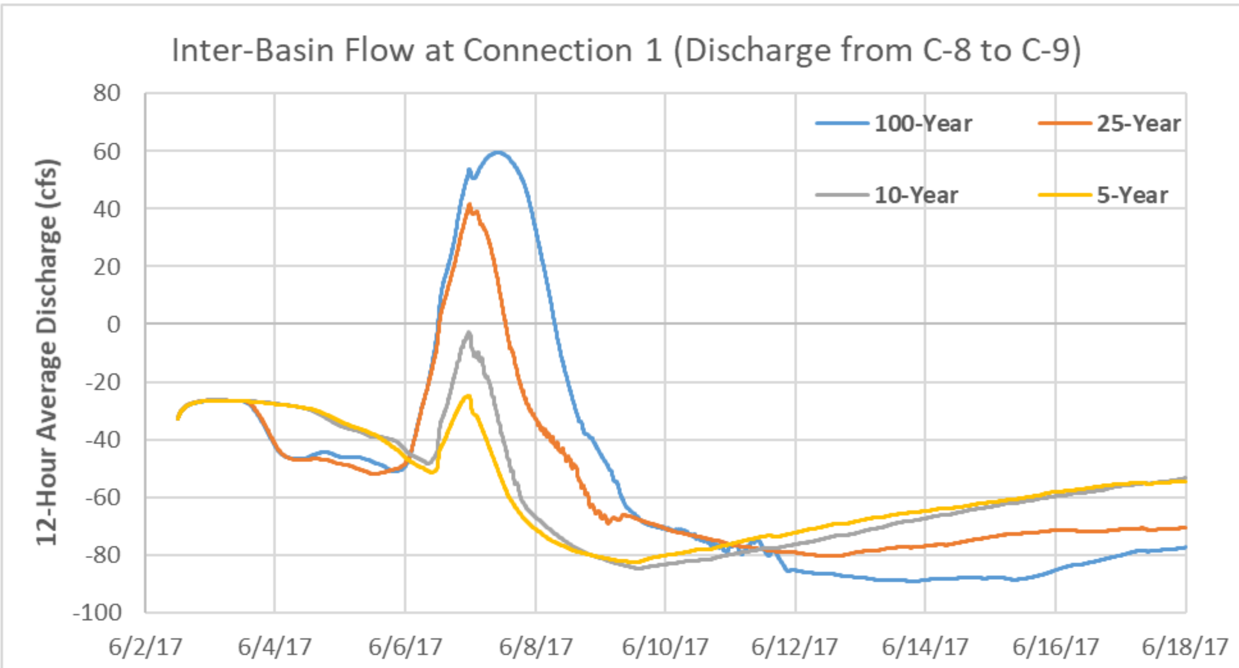

Figure 8.2-7: Inter-Basin Discharge Between C-8 and C-9 Watersheds at Connection 1

For the 100-year design storm, the peak discharge from C-9 to C-8 watershed at this inter-basin connection is about 90 cfs. However, this occurs several days after the peak discharge and does not contribute to peak discharge rates in the C-8 Canal.

Connection 2 is a culvert under Palmetto Expressway, just west of Red Road. **Figure 8.2-8** shows the inter-basin discharge, with positive values representing flow from the C-9 to the C-8 watershed and negative values indicating flow from the C-8 to the C-9 watershed. For the 100-year design storm, the peak discharge from C-9 to C-8 watershed at this inter-basin connection is about 125 cfs, however, it occurs several days after the peak discharge in the C-8 Canal. During the peak discharge at S-28, this basin interconnect is contributing a relatively small amount during the 25 and 100-year events. During the 5 and 10-year storms, the inter-basin flow during peak discharge at S-28 is more significant than during the 25 and 100-year storms, with approximately 10% and 8%, respectively.

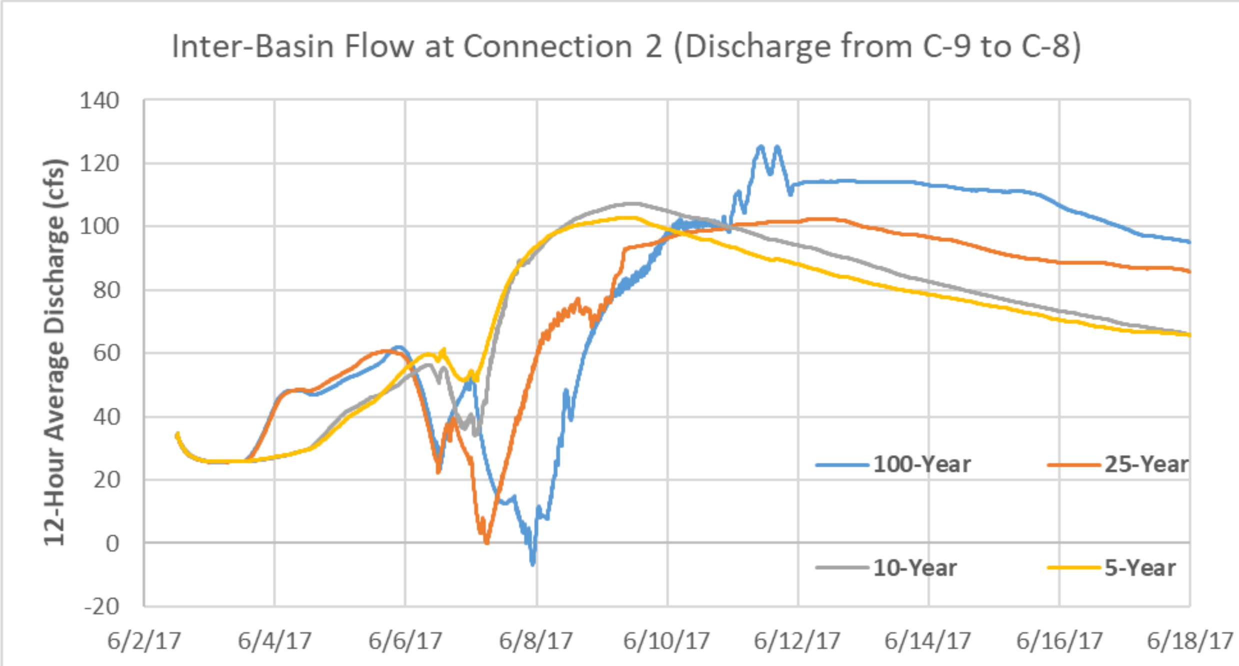

Figure 8.2-8: Inter-Basin Discharge Between C-8 and C-9 Watersheds at Connection 2

Connection 3 is a culvert under I75. **Figure 8.2-9** shows the inter-basin discharge, with positive values representing flow from the C-8 to the C-7 watershed and negative values indicating flow from the C-7 to the C-8 watershed. Flows from C-8 to C-7 watershed reduces the burden on the C-8 canal, peaking at about 100 cfs during the 25 and 100-year storms. During the 5 and 10-year storms, the discharge leaving the C-8 watershed is higher, at about 170 cfs. This relieves the C-8 canal system of some stress.

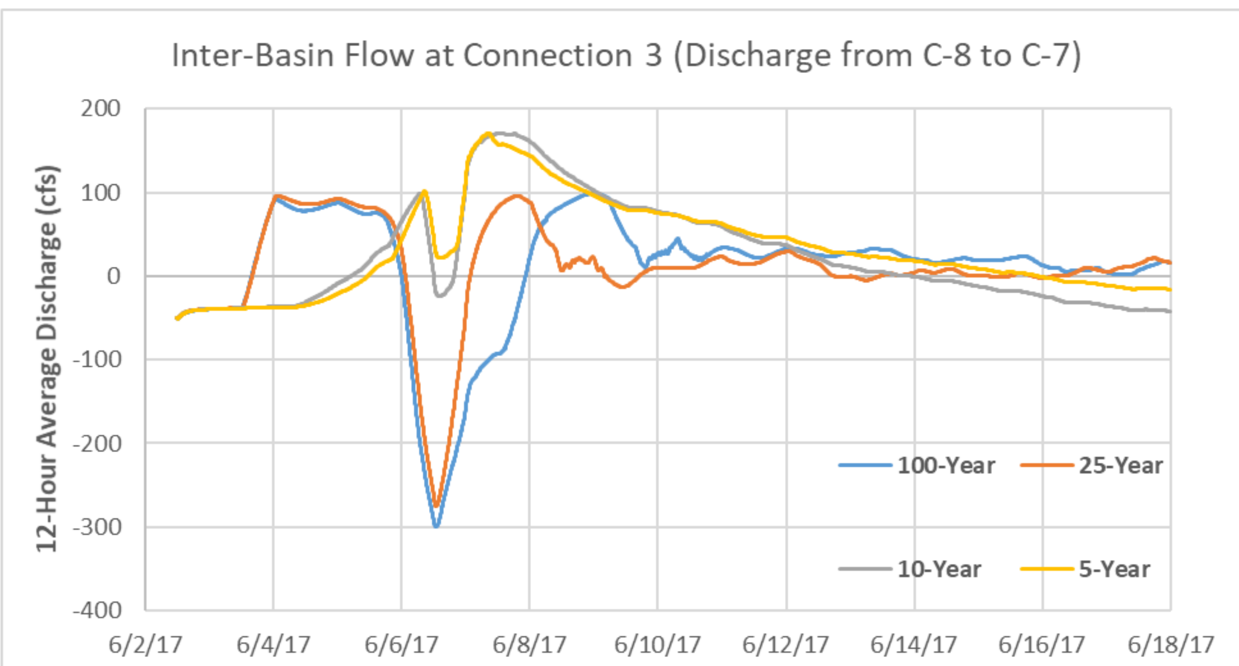

Figure 8.2-9: Inter-Basin Discharge Between C-8 and C-7 Watersheds at Connection 3

For the 25 and 100-year design storm, the peak discharge from C-7 to C-8 watershed at this inter-basin connection is about 300 cfs and occurs about 18 hours prior to peak discharge at S-28. Relative to the peak discharge at S-28, this inter-basin flow is about 9% for the 100-year event and 13% for the 25-year event. This adds stress to the C-8 Canal system.

Connection 4 is a culvert under NE 135th St at Red Road. **Figure 8.2-10** shows the inter-basin discharge, with positive values representing flow from the C-8 to the C-7 watershed and negative values indicating flow from the C-7 to the C-8 watershed. Flows from C-8 to C-7 watershed reduces the burden on the C-8 canal, peaking at about 50 cfs during the 100-year storm. This relieves the C-8 canal system of some stress.

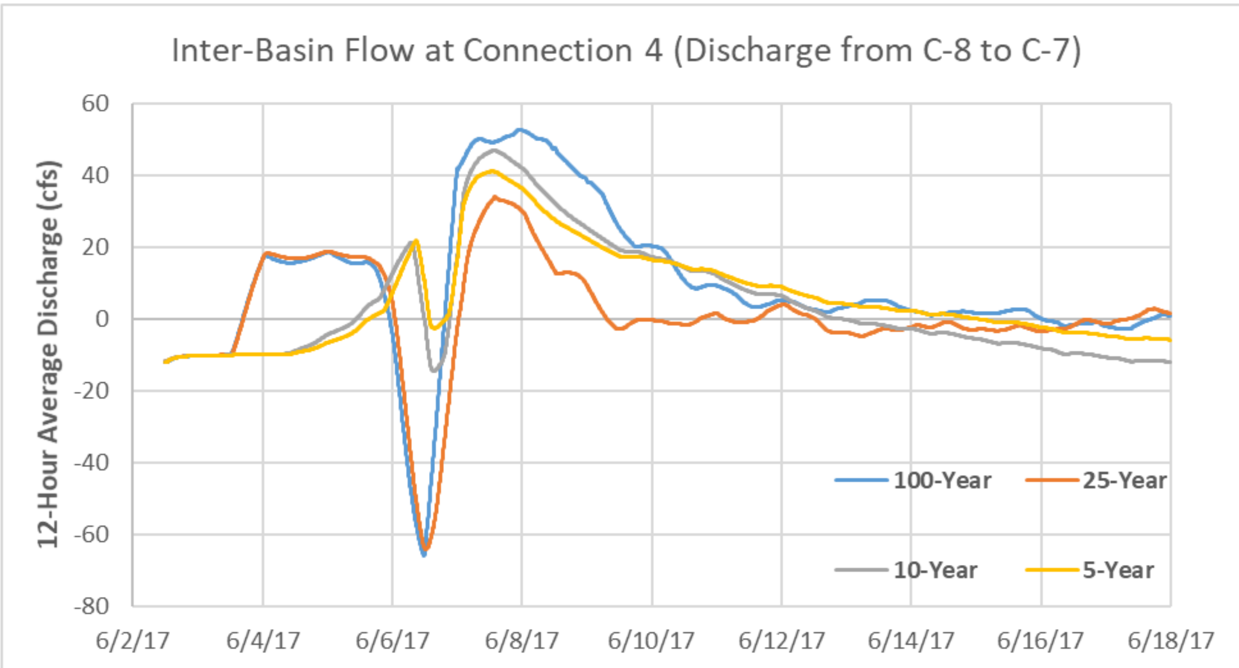

Figure 8.2-10: Inter-Basin Discharge Between C-8 and C-7 Watersheds at Connection 4

For the 25 and 100-year design storm, the peak discharge from C-7 to C-8 watershed at this inter-basin connection is about 65 cfs and occurs about 18 hours prior to peak discharge at S-28. Relative to the peak discharge at S-28, this inter-basin flow is rather insignificant, with about 2% for the 100-year event and 3% for the 25-year event.

Connection 5 is a culvert under NE 135th St just east of NW 27th Ave. **Figure 8.2-11** shows the inter-basin discharge, with negative values indicating flow from the C-8 to the C-7 watershed. Flows from C-8 to C-7 watershed reduces the burden on the C-8 canal, peaking at about 120 cfs during the 100-year storm. This relieves the C-8 canal system of some stress.

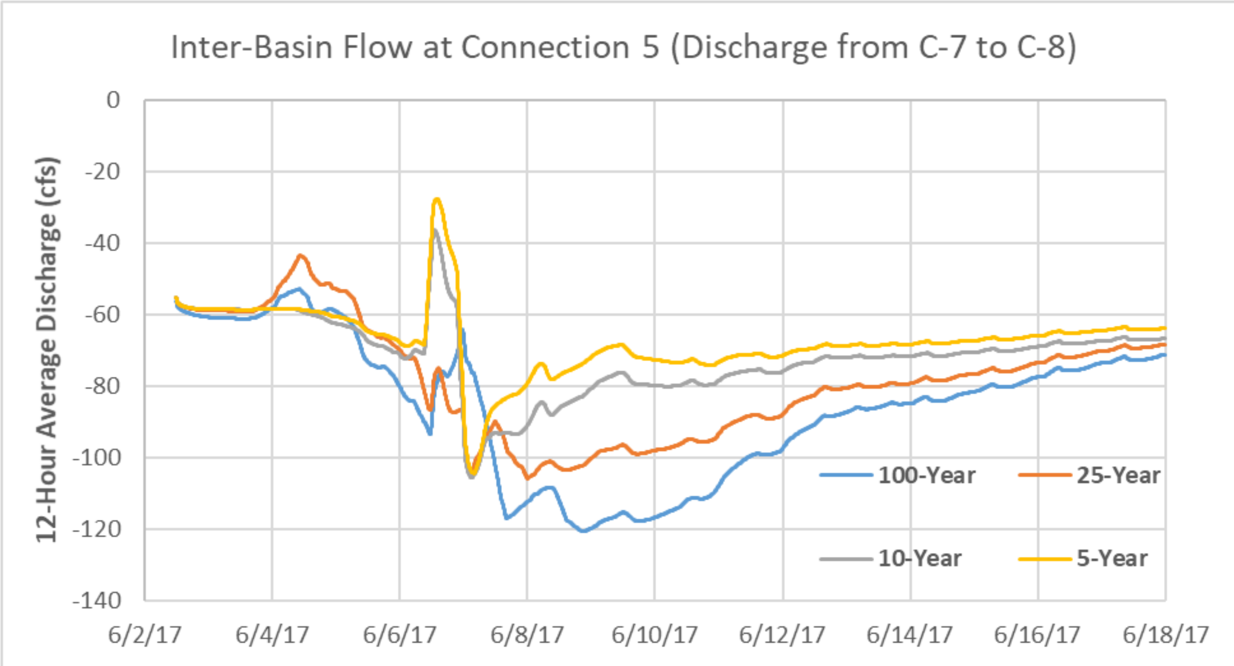

Figure 8.2-11: Inter-Basin Discharge Between C-8 and C-7 Watersheds at Connection 5

8.3 PM #3 – Structure Performance

PM #3 shows the effective capacity of a tidal structure. For this metric, structure discharge over a range of storm events and sea level rise scenarios is compared with the original static design condition. In this section, PM #3 only evaluates current condition design storms with no sea level rise; this section provides insight on the current structure performance. **Section 10.3** compares the results from this section with the structure performance under three sea level rise conditions to determine what degradation in performance occurs, if any, under sea level rise scenarios.

SFWMD has completed a similar evaluation for the S-28 and S-29 structures in reports titled, *The Effects of Sea Level Rise on S28 Performance* (Zhang, 2017) and *The Effects of Sea Level Rise on S29 Performance* (Zhang, 2017). In these evaluations, a simple hydraulic model was used with fixed headwater stage based on design headwater and a tailwater that oscillates tidally. To add to the work that has already been done, this PM is evaluated using the full MIKE SHE / MIKE HYDRO model results. Essentially, the main difference is that headwater is not forced, rather it is simulated using the fully dynamic model. Please note that this analysis is for informational purposes and is not intended to replace the previous work done by the District, but rather supplement it and analyze it using a different method.

Structure S-28 has a static design headwater and tailwater of 2.2 ft and 1.7 ft, respectively. The static design discharge is 3220 cfs based on 0.5 ft head gradient (Zhang, 2017). **Figure 8.3-1** and **Figure 8.3-2** show instantaneous values and 12-hour moving average values, respectively, for S-28 based on a 25-year design storm.

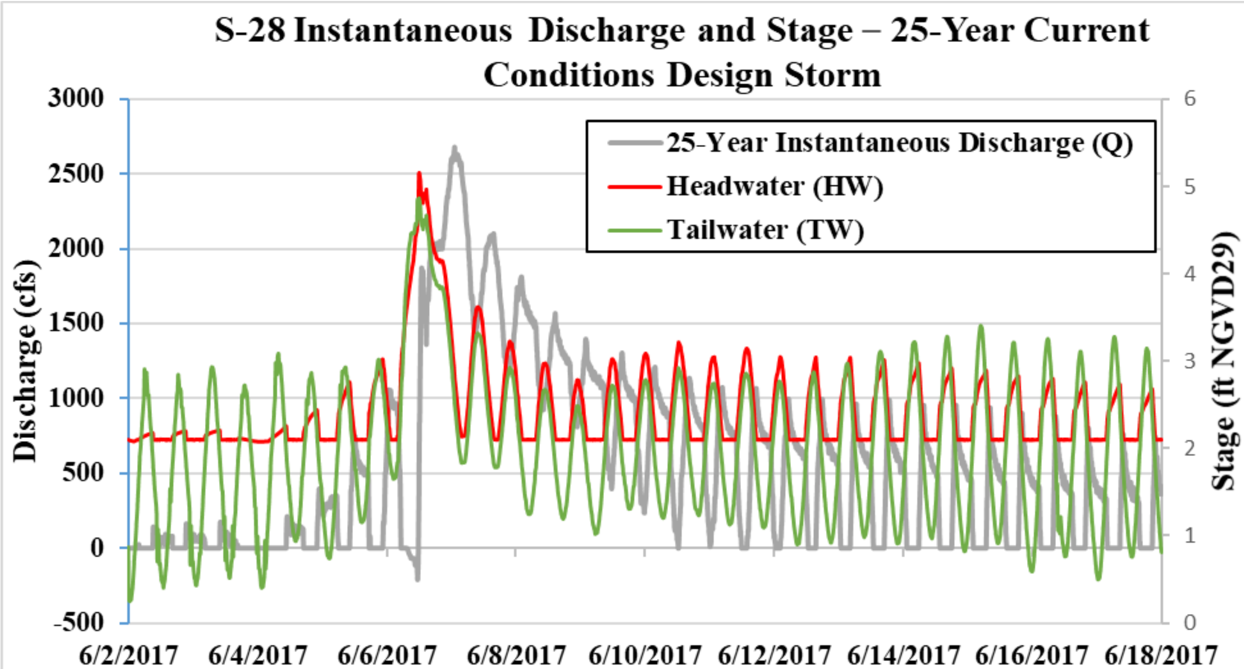

Figure 8.3-1: Instantaneous Discharge and Stage at S-28 Structure for 25-Year Current Conditions Design Storm

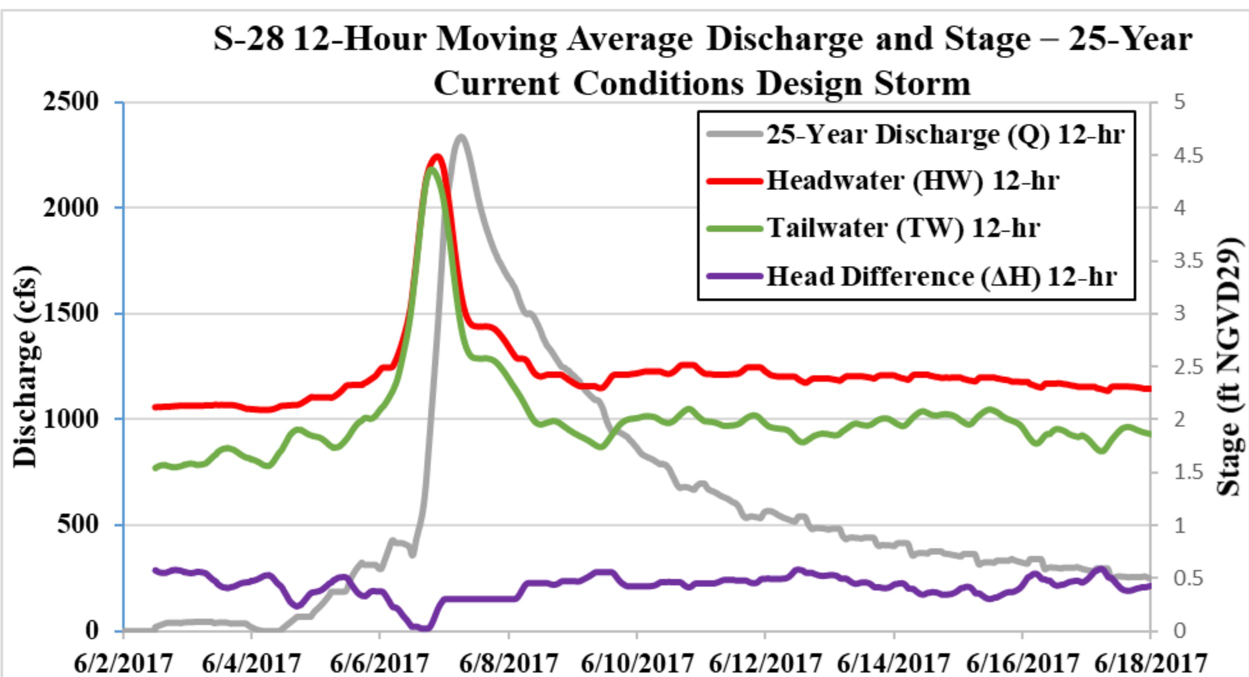

Figure 8.3-2: Tidally Averaged (12-hour) 25-Year Design Storm Discharge, Stage, and Head Gradient for Structure S-28

Figure 8.3-3 and **Figure 8.3-4** show instantaneous values and 12-hour moving average values, respectively, for S-28 based on a 100-year design storm.

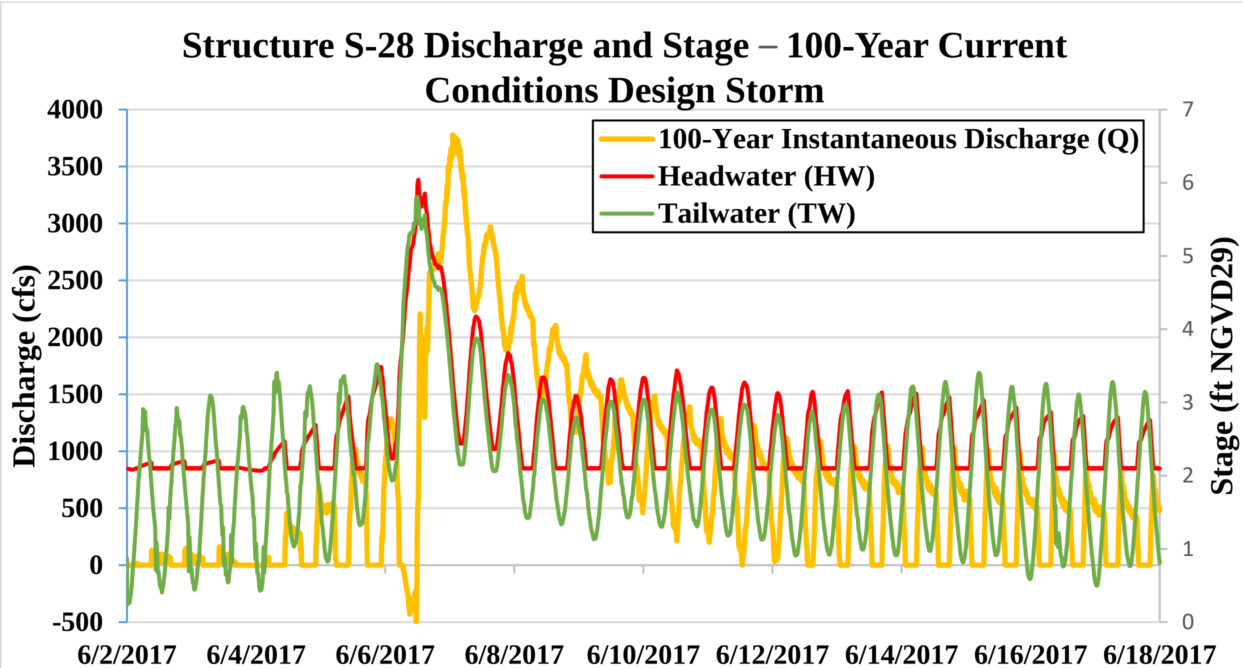

Figure 8.3-3: Instantaneous Discharge and Stage at S-28 Structure for 100-Year Current Conditions Design Storm

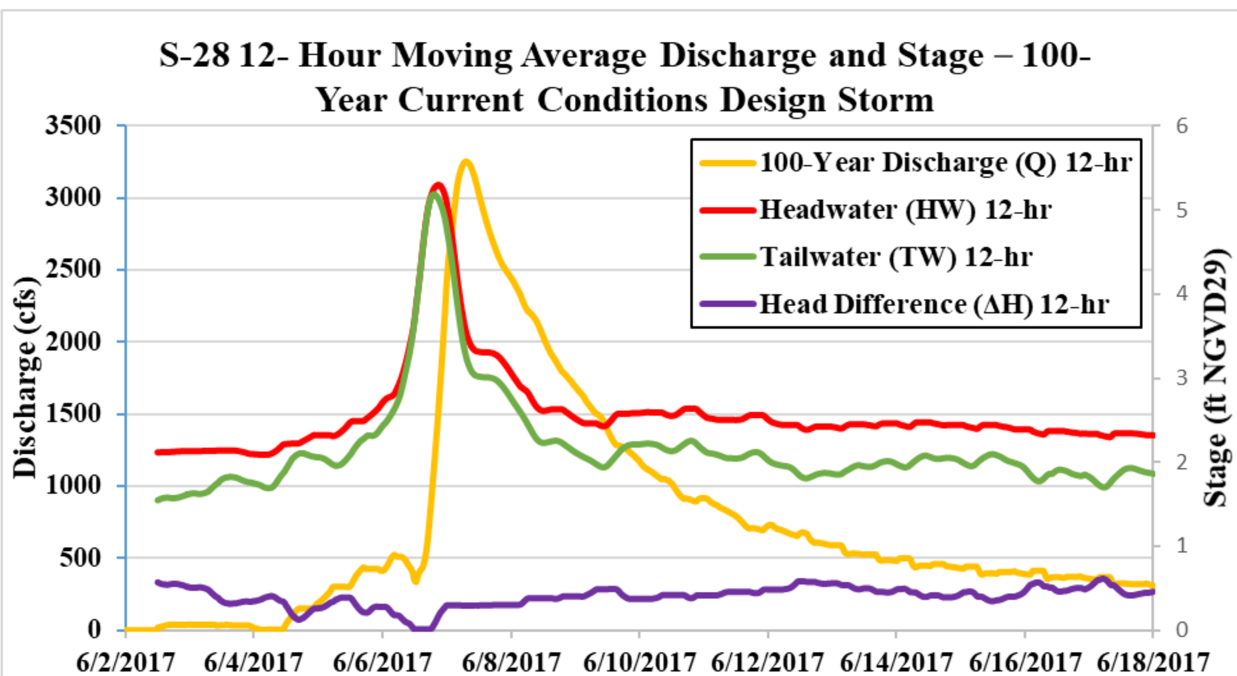

Figure 8.3-4: Tidally Averaged (12-hour) 100-Year Design Storm Discharge, Stage, and Head Gradient for Structure S-28

As shown in **Figure 8.3-4,** the S-28 structure slightly exceeds the design discharge of 3220 cfs, with a 12-hour moving average peak of 3250 cfs. While this discharge occurs with a 12-hour average head difference of only 0.3 feet, the design headwater assumption is violated. The assumed design headwater stage is 2.2 feet, while the predicted headwater is 3.5 feet. **Table 8-5** summarizes the simulated 12-hour moving average peak discharge, headwater, tailwater, and head differential for S-28, for each of the design storms.

Table 8-5: Summary of the 12-Hour Moving Average Discharge and Stage at S-28

S-28	12-Hour Moving Average			
	Peak Discharge (cfs)	Peak Headwater (ft NGVD29)	Peak Tailwater (ft NGVD29)	Head Differential (ft)
5-Year	1441	2.75	2.39	0.36
10-Year	1748	2.93	2.61	0.32
25-Year	2337	3.17	2.87	0.3
100-Year	3254	3.55	3.25	0.3

Structure S-29 has a static design headwater and tailwater of 2.4 ft and 1.9 ft, respectively. The static design discharge is 4780 cfs based on 0.5 ft head difference (Zhang, 2017). **Figure 8.3-5** and **Figure 8.3-6 s**how instantaneous values and 12-hour moving average values, respectively, for S-29 based on a 25-year design storm.

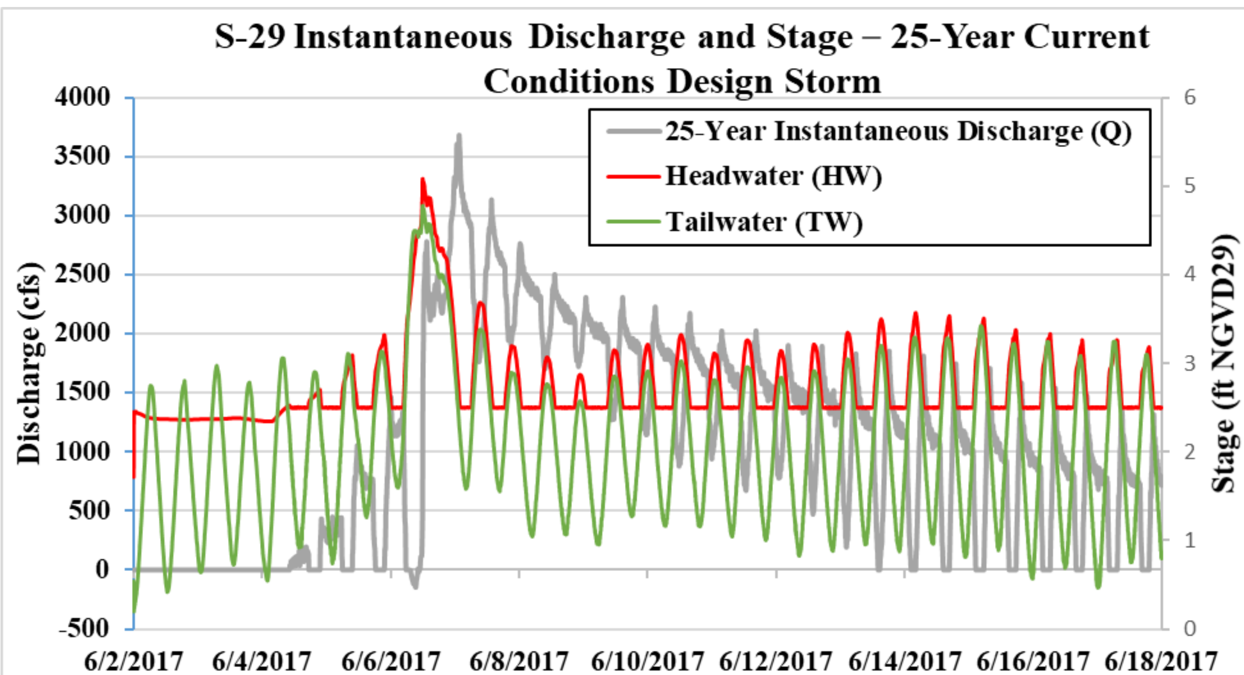

Figure 8.3-5: Instantaneous Discharge and Stage at S-29 Structure for 25-Year Current Conditions Design Storm

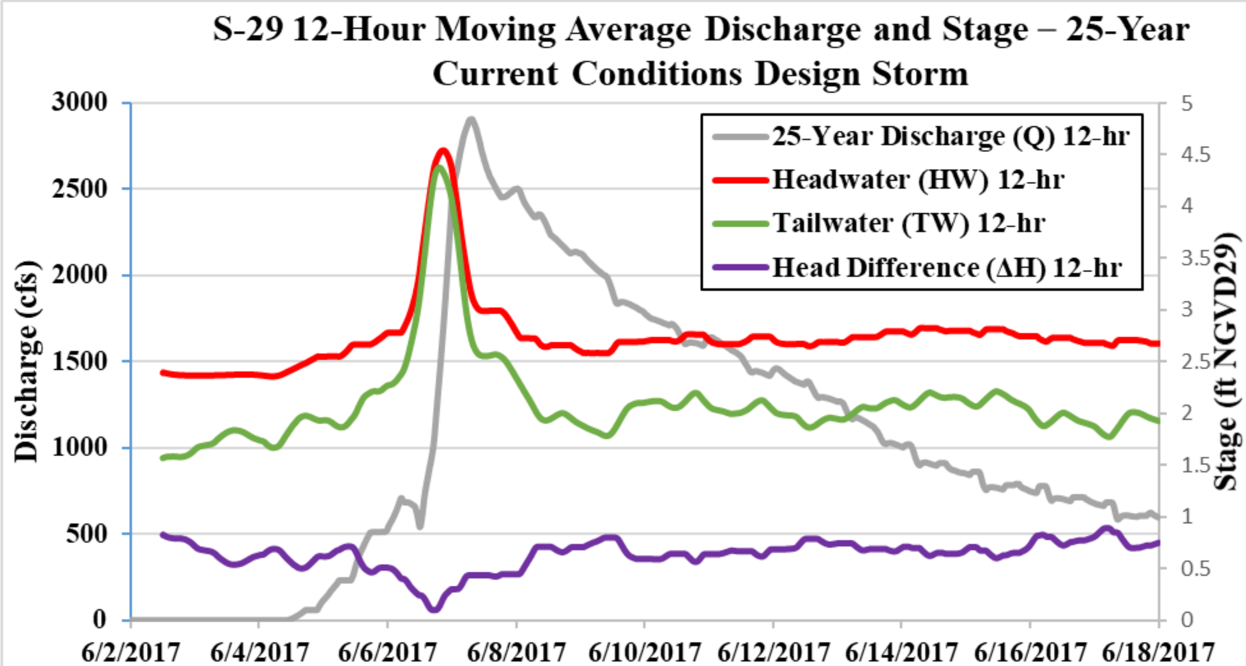

Figure 8.3-6: Tidally Averaged (12-hour) 25-Year Design Storm Discharge, Stage, and Head Gradient for Structure S-29

Figure 8.3-7 and **Figure 8.3-8** show instantaneous values and 12-hour moving average values, respectively, for S-29 based on a 100-year design storm.

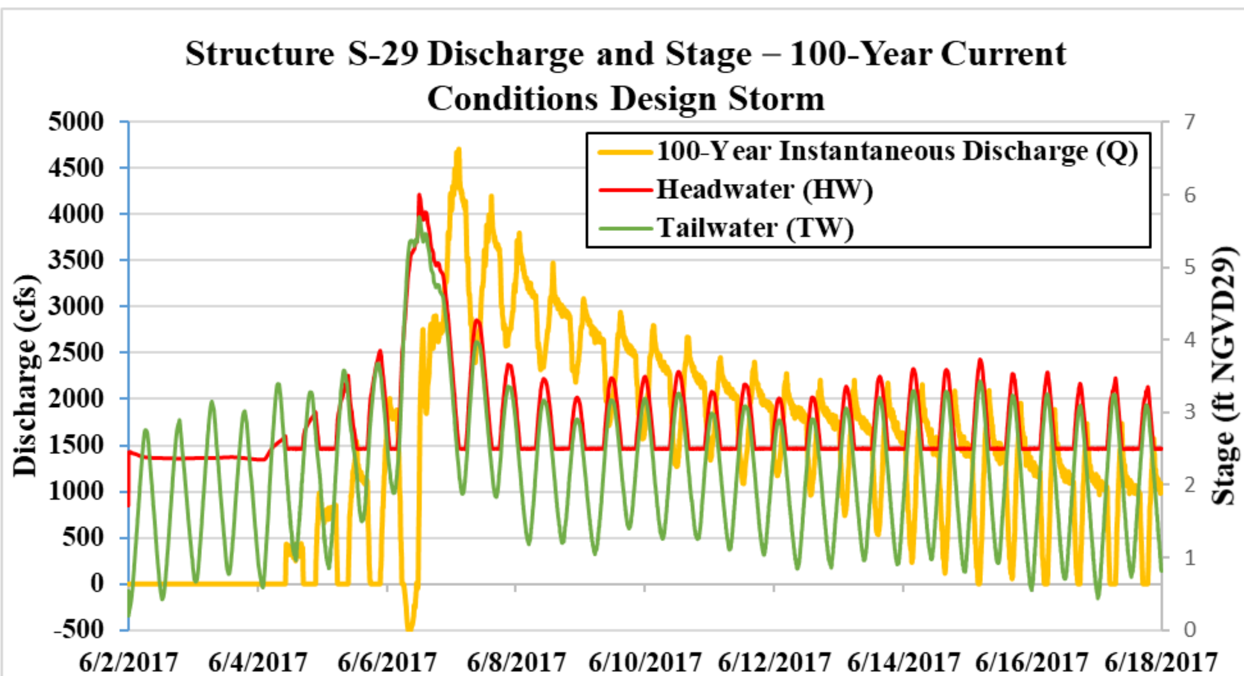

Figure 8.3-7: Instantaneous Discharge and Stage at S-29 Structure for 100-Year Current Conditions Design Storm

During the 100-year design storm, structure S-29 has an instantaneous peak discharge of 4710 cfs, which is just shy of the static design discharge of 4780. While this discharge occurs with an instantaneous head difference of 0.31 feet, the design headwater assumption is slightly violated. The assumed design headwater stage is 2.4 feet, while the predicted headwater is 2.5 feet.

As shown in **Figure 8.3-8**, the S-29 structure falls significantly short of the design discharge of 4780 cfs, with a 12-hour moving peak of just 3728 cfs. The 12-hour moving average head difference was only 0.35 ft, compared to 0.5 ft in the static design condition. This indicated that the current conditions storm surge was preventing S-29 from reaching its design condition. Additionally, the design headwater assumption is violated with a 12-hour average headwater elevation of 3.5 feet, compared to 2.4 feet for the static design condition assumption. **Section 10.3** evaluates this structure under three sea level rise scenarios and discusses if sea level rise causes any further degradation in performance.

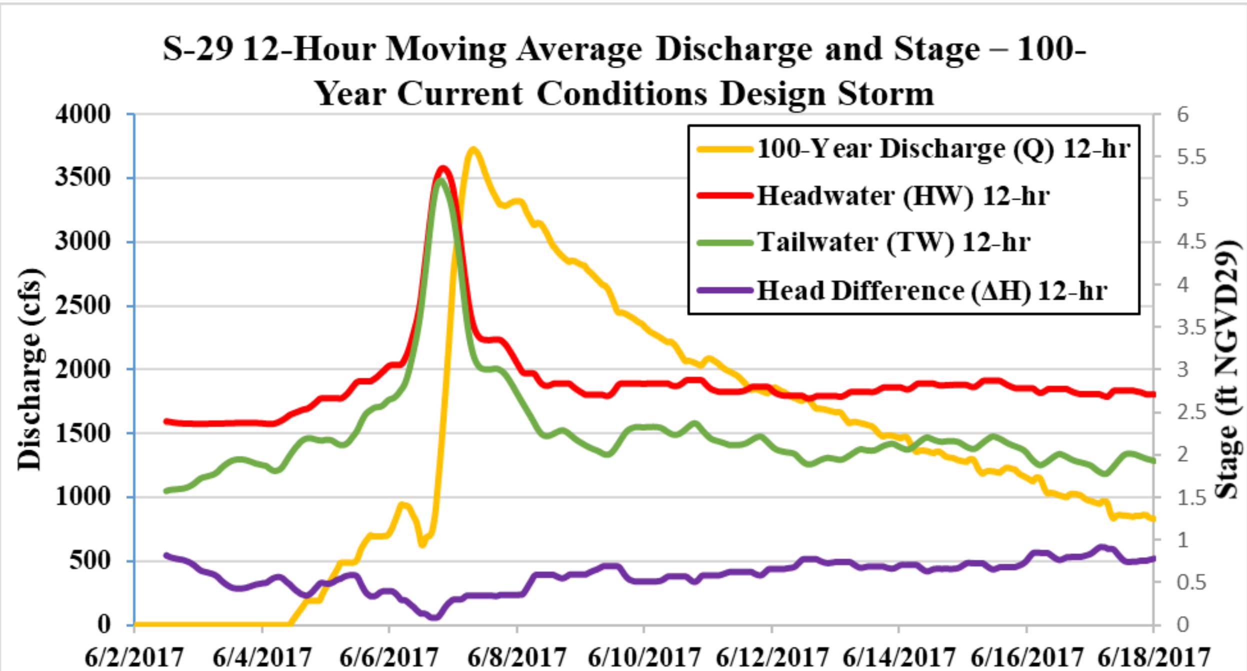

Figure 8.3-8: Tidally Averaged (12-hour) 100-Year Design Storm Discharge, Stage, and Head Gradient for Structure S-29

Table 8-6 summarizes the simulated 12-hour moving average peak discharge, headwater, tailwater, and head differential for S-28, for each of the design storms.

Table 8-6: Summary of the 12-Hour Moving Average Discharge and Stage at S-29

S-29	12-Hour Moving Average			
	Peak Discharge (cfs)	Peak Headwater (ft NGVD29)	Peak Tailwater (ft NGVD29)	Head Differential (ft)
5-Year	2140	2.84	2.27	0.57
10-Year	2437	2.95	2.44	0.51
25-Year	2908	3.14	2.71	0.43
100-Year	3728	3.52	3.17	0.35

8.4 PM #4 – Peak Storm Runoff

PM #4 is the maximum conveyance capacity of a watershed at the tidal structure for a range of design storms. It shows the maximum conveyance (moving 12-hr average) for a specific design storm and a specific tidal boundary condition. The results presented in this section are limited to current condition design storms. This metric was further evaluated during Phase 1B of this project and is presented in **Section 10.3**, in which structure performance during current conditions was compared with performance during three sea level rise scenarios. **Figure 8.4-1** and **Figure 8.4-2** represent the design storm discharge at tidal structures S-28 and S-29, respectively, for current conditions. These discharge hydrographs, specifically the peak discharge, are compared with the peak discharge under future sea level rise scenarios in **Section 10.3**.

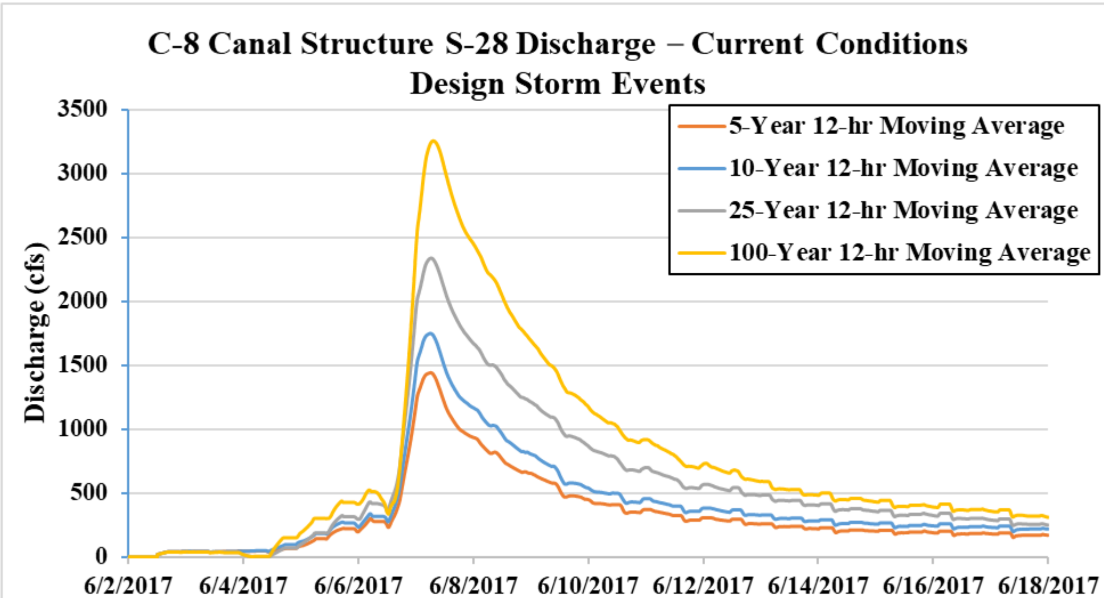

Figure 8.4-1: C-8 Canal Structure S-28 Discharge Hydrographs

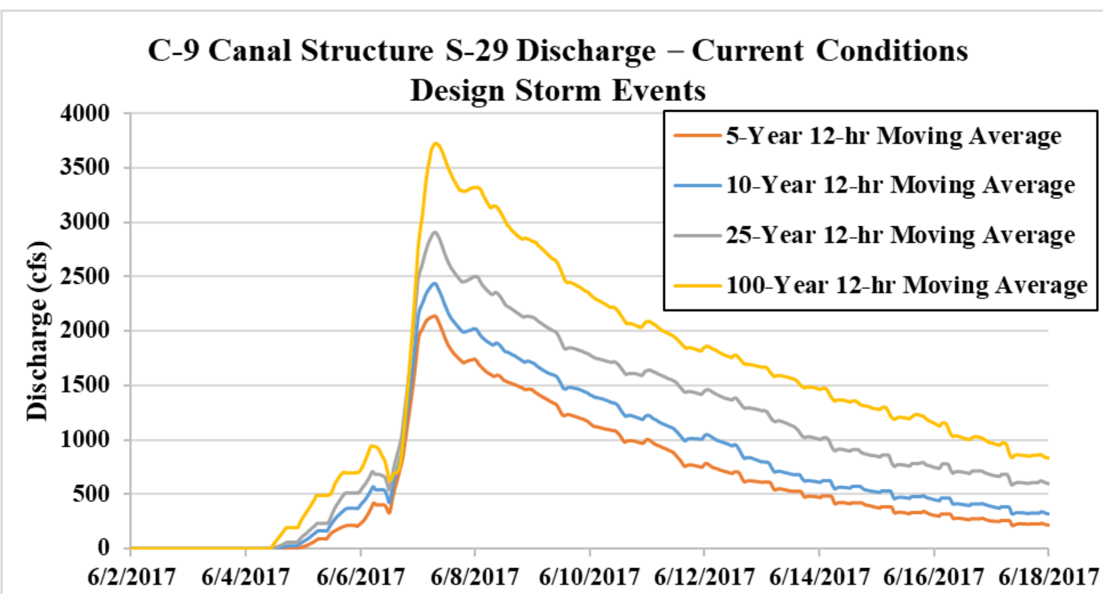

Figure 8.4-2: C-9 Canal Structure S-29 Discharge Hydrographs

Figure 8.4-3 shows the 12-hour average peak discharge versus the design storm return period for S-28 and **Table 8-7** shows the instantaneous and 12-hour average peak discharge. **Figure 8.4-3** was further developed in **Section 10.4** to compare changes in peak discharge for each design storm under future conditions with three sea level rise scenarios.

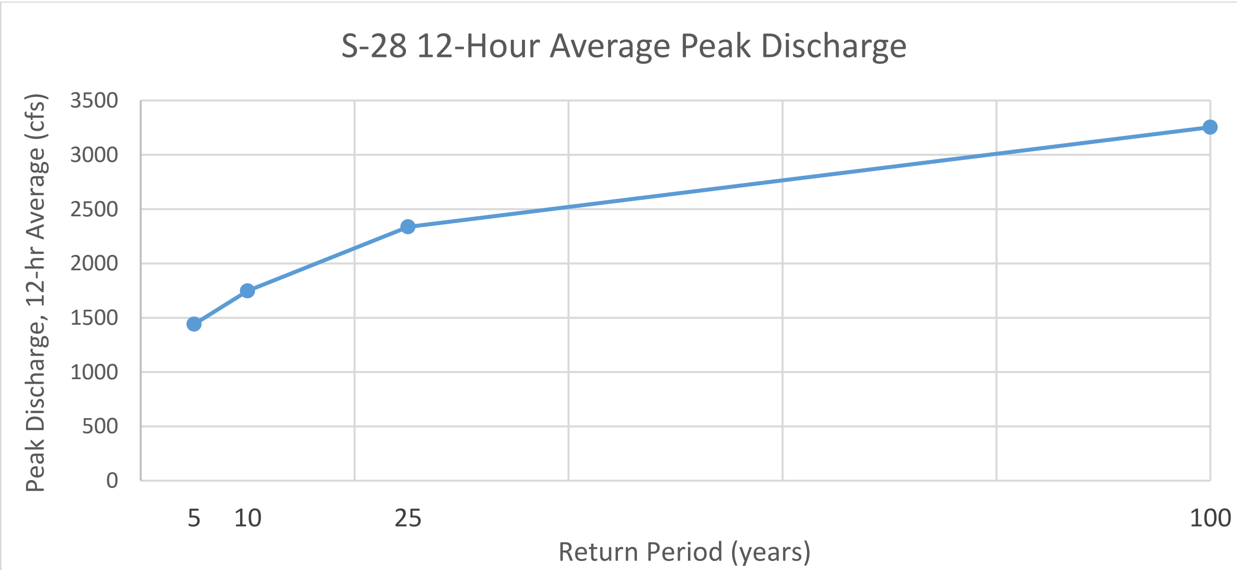

Figure 8.4-3: Structure S-28 12-Hour Average Peak Discharge

Table 8-7: S-28 Peak Discharge Summary

S-28	Peak Discharge (cfs)	
	Instantaneous	Moving Average (12-hr)
5-Year	1720	1441
10-Year	2059	1748
25-Year	2679	2337
100-Year	3777	3254

Figure 8.4-4 shows the 12-hour average peak discharge versus the design storm return period for S-29 and **Table 8-8** shows the instantaneous and 12-hour average peak discharge. **Figure 8.4-4** was further developed in **Section 10.4** to compare changes in peak discharge for each design storm under future conditions with three sea level rise scenarios.

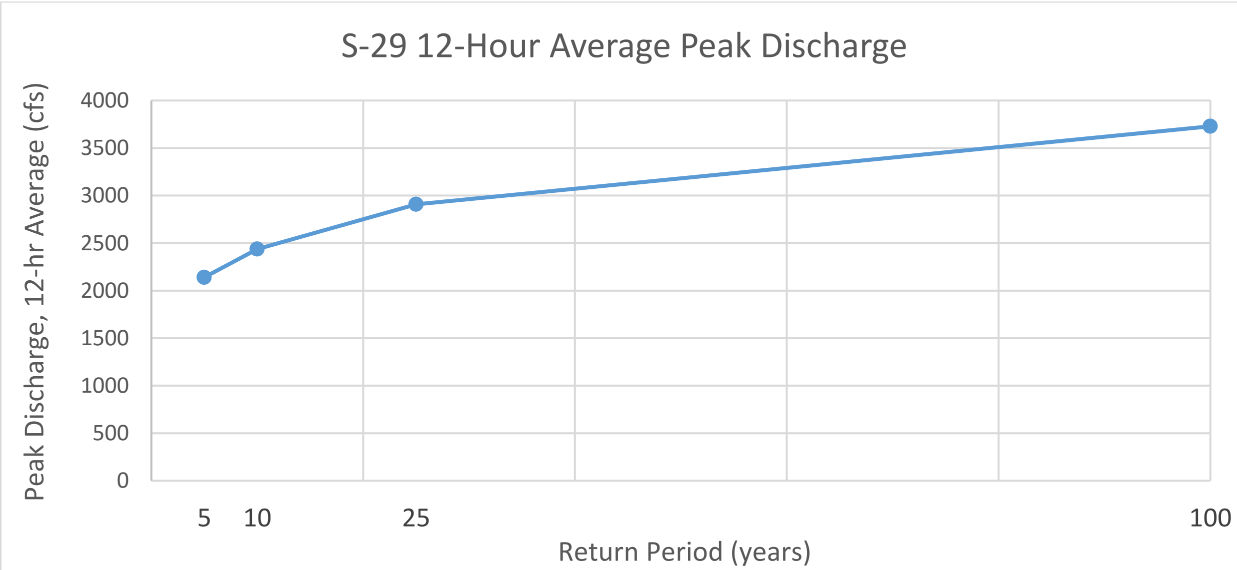

Figure 8.4-4: Structure S-29 12-Hour Average Peak Discharge

Table 8-8: S-29 Peak Discharge Summary

S-29	Peak Discharge (cfs)	
	Instantaneous	Moving Average (12-hr)
5-Year	2647	2140
10-Year	3052	2437
25-Year	3681	2908
100-Year	4710	3728

8.5 PM #5 – Frequency of Flooding

For this PM, the depths of overland flooding were evaluated for the 72-hour design storms with the return period of 5-year, 10-year, 25-year, and 100-year. These flood depths, or elevations, can be compared with elevations of features such as buildings and roadways, where such information exists. For the purposes of this C8/C9 FPLOS evaluation, flood inundation maps were prepared using MIKE SHE gridded model output for each storm event, in the form of depth of overland water. Flooding depths were representative of the overland water depths on the 125-ft grid. The resulting flood inundation maps over the entire model domain are shown in **Figure 8.5-1** through **Figure 8.5-4** for each of the four design storm events. **Figure 8.5-5** through **Figure 8.5-8** show the flood duration maps for each of the design storm events for urban areas only. **Figure 8.5-9** through **Figure 8.5-11** show up close examples of flood duration along the C-8 Canal and **Figure 8.5-12** through **Figure 8.5-15** show up close examples of flood duration along the C-9 Canal.

The southwest portion of the C-9 Basin is undeveloped (as of the date of current condition model development, or year 2020), and thus were not served by stormwater collection and conveyance facilities. These undeveloped areas show the greatest extents and depths of flooding for the design storm events.

Notable developed areas also show flooding under PM #5. For example, residential areas along the C-8 Canal upstream and downstream of NE 135th St (CR 916), show extensive spatial extents of flooding in PM #5, which is most evident for the 25-year and 100-year events. This flooding is corroborated by PM #1 results, which show the south canal bank is exceeded for the 10-year event over a long segment upstream of CR916, while the north bank is exceeded for the 5-year event downstream of CR916.

In the C-9 Watershed, extensive flooding is shown along a 1-mile segment of the canal, on the south side of the canal west of Red Road (a.k.a. CR823 or 57th Ave.) for the 25-and 100-year events. However, PM #1 does not show a canal bank exceedance in this location. The flooding in this area could be due to the topography being lower than the canal bank and/or inadequate secondary drainage infrastructure. Other areas of flooding include residential areas further upstream, on the north side of the C-9 Canal upstream of the Ronald Reagan Turnpike. Again, the PM #1 results do not show a bank exceedance in this area. The flooding shown in this area could be from under-performing secondary/tertiary drainage systems.

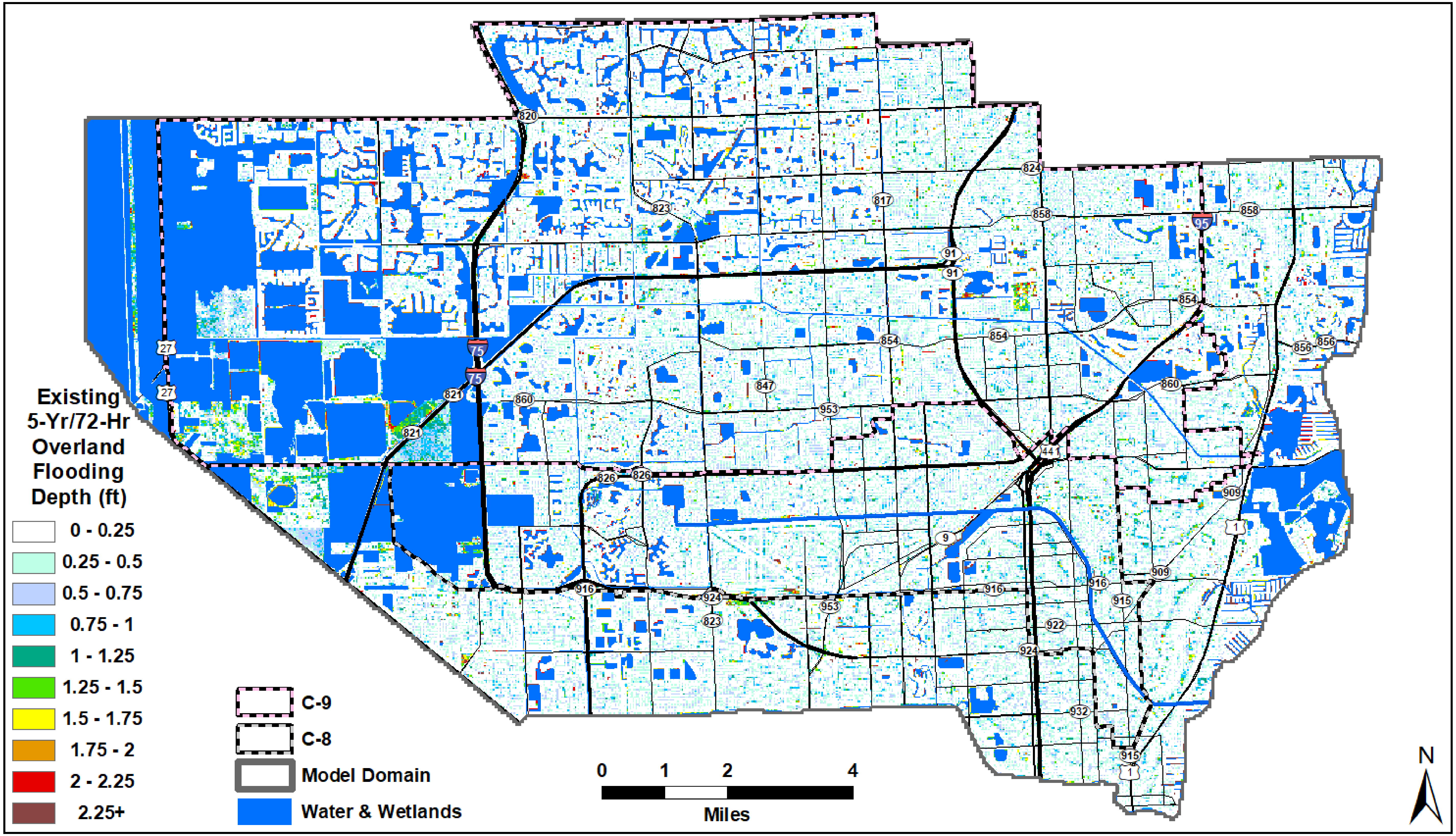

Figure 8.5-1: Flood Inundation Map for 5-Year Design Storm Event

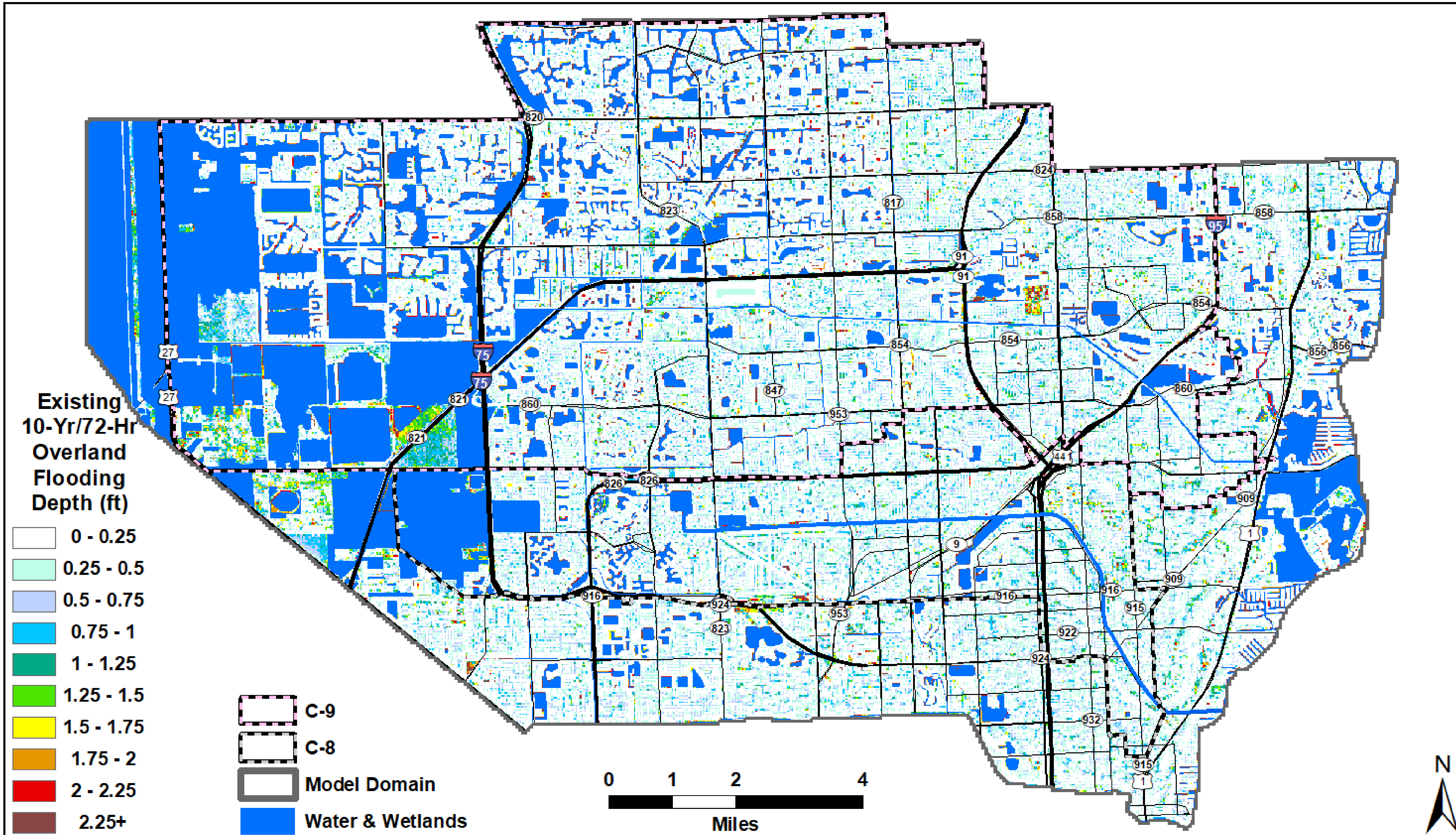

Figure 8.5-2: Flood Inundation Map for 10-Year Design Storm Event

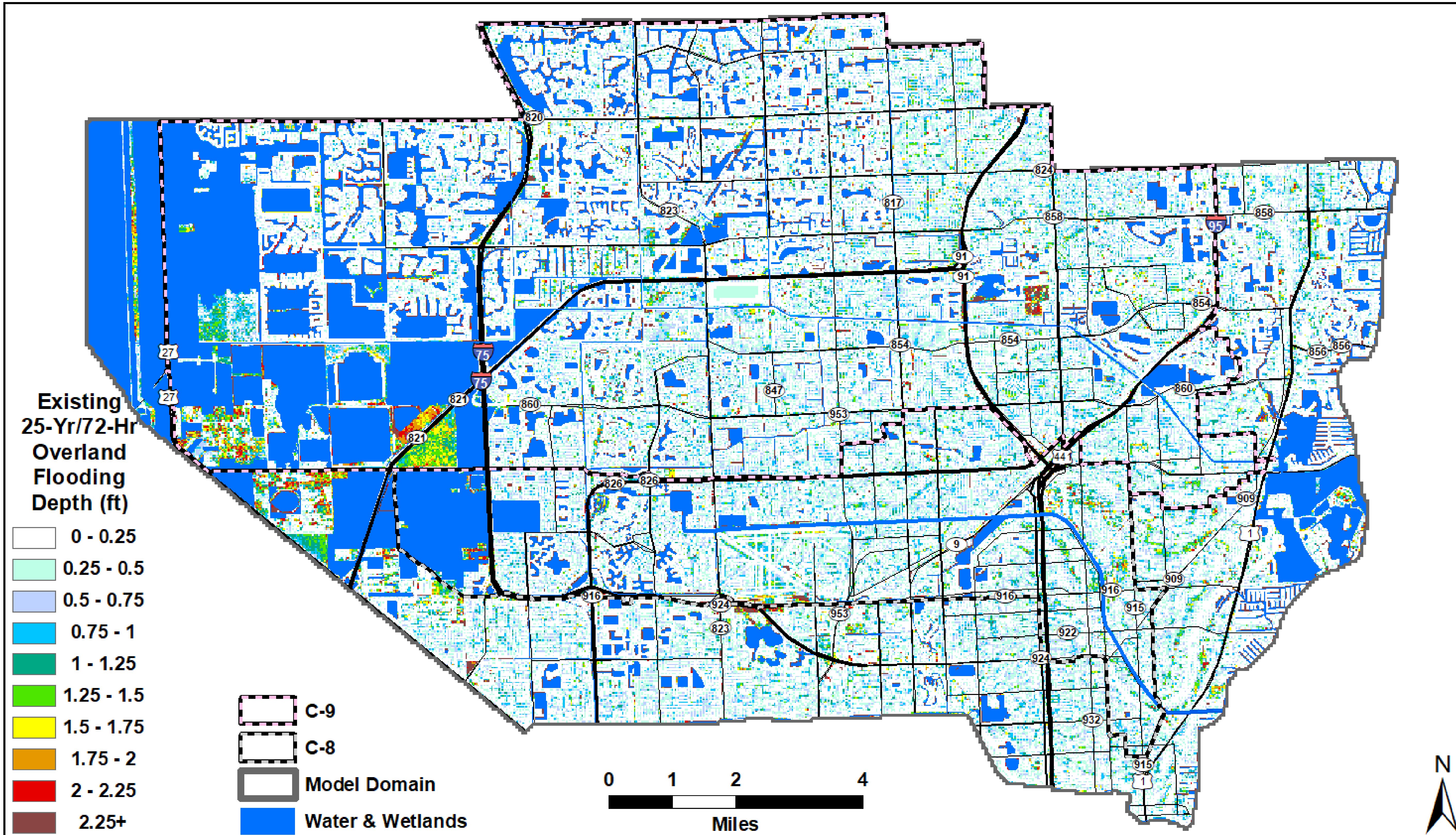

Figure 8.5-3: Flood Inundation Map for 25-Year Design Storm Event

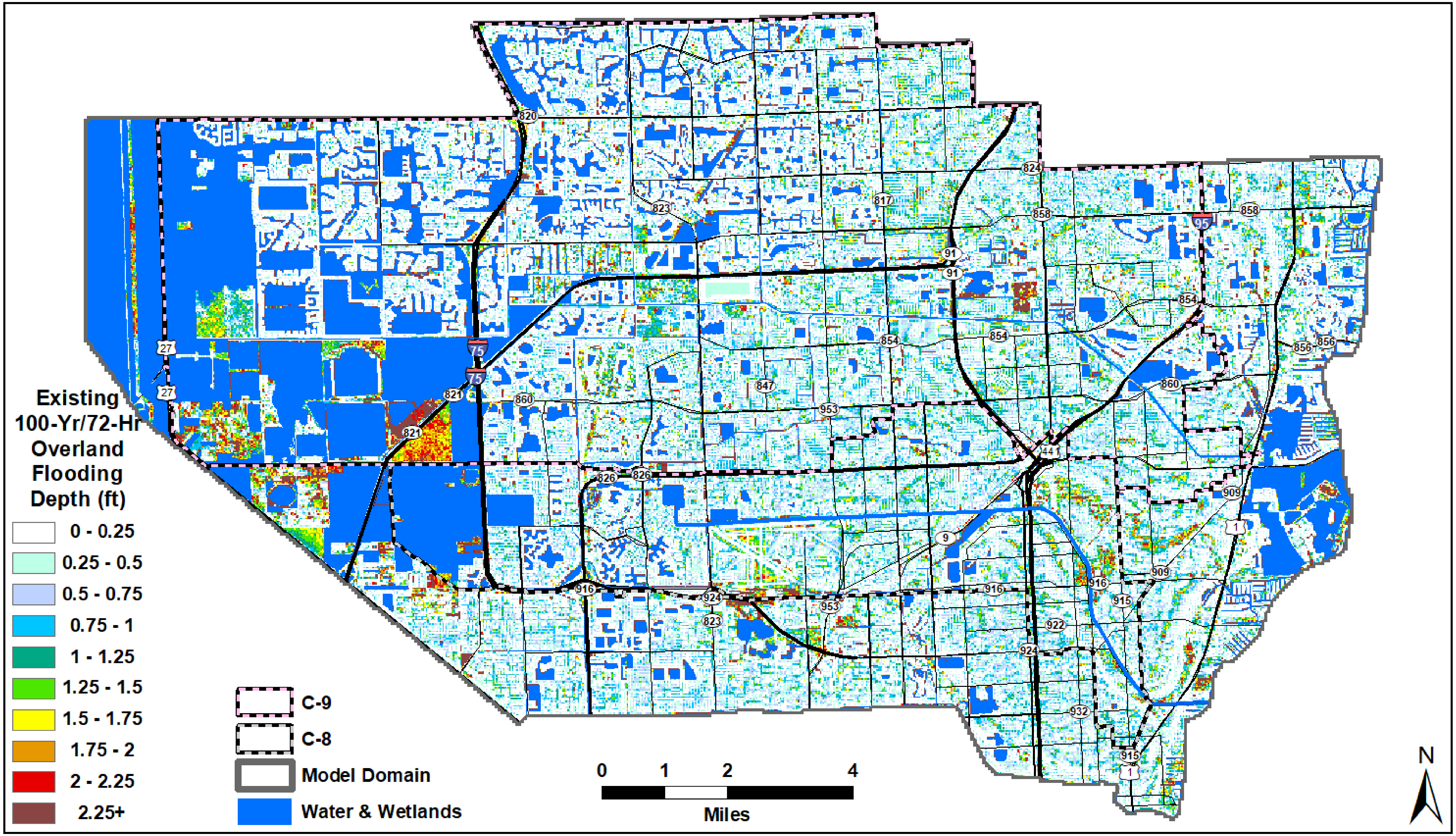

Figure 8.5-4: Flood Inundation Map for 100-Year Design Storm Event

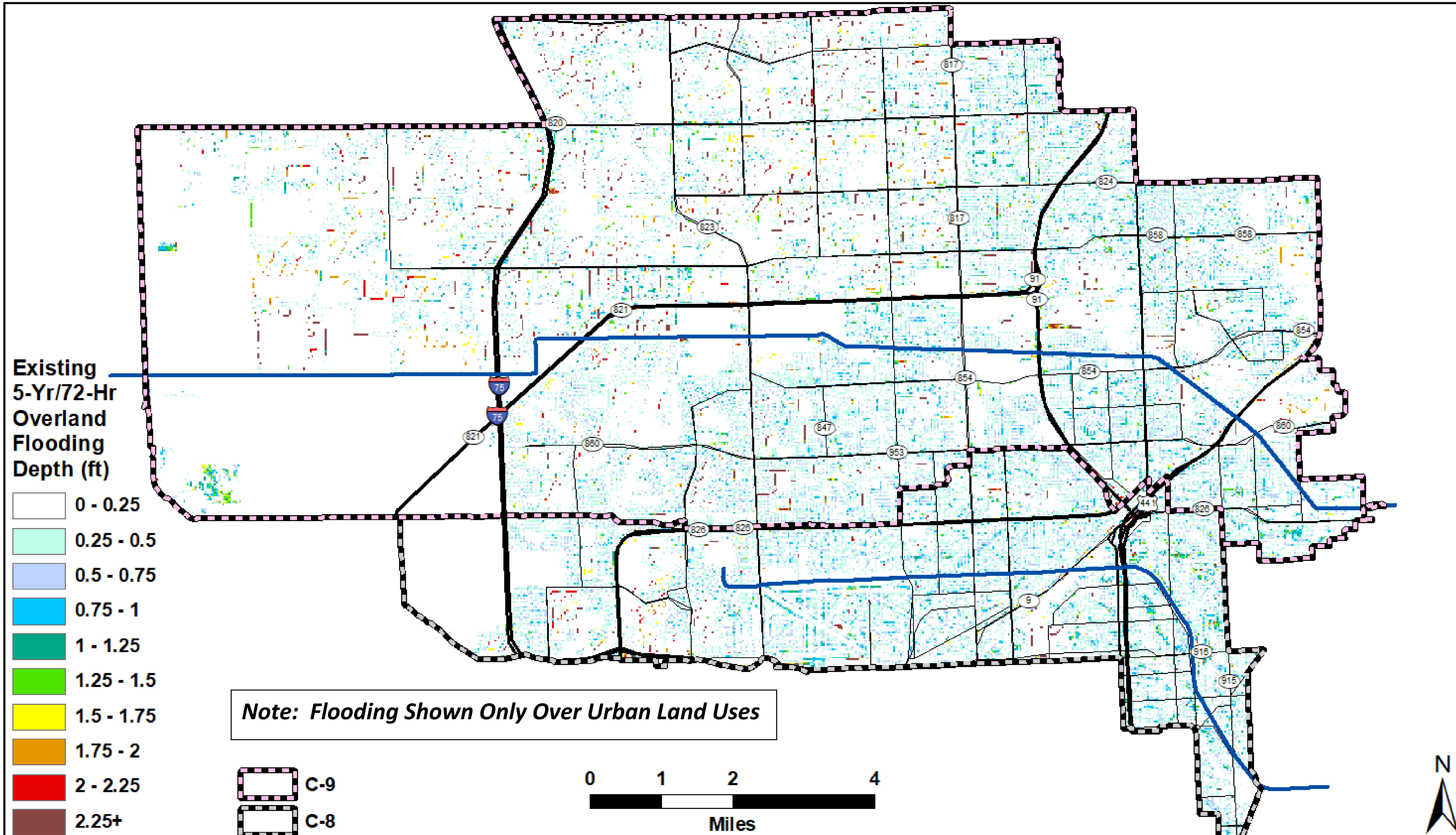

Figure 8.5-5: Flood Inundation Map for 5-Year Design Storm Event in Urban Land Use Areas

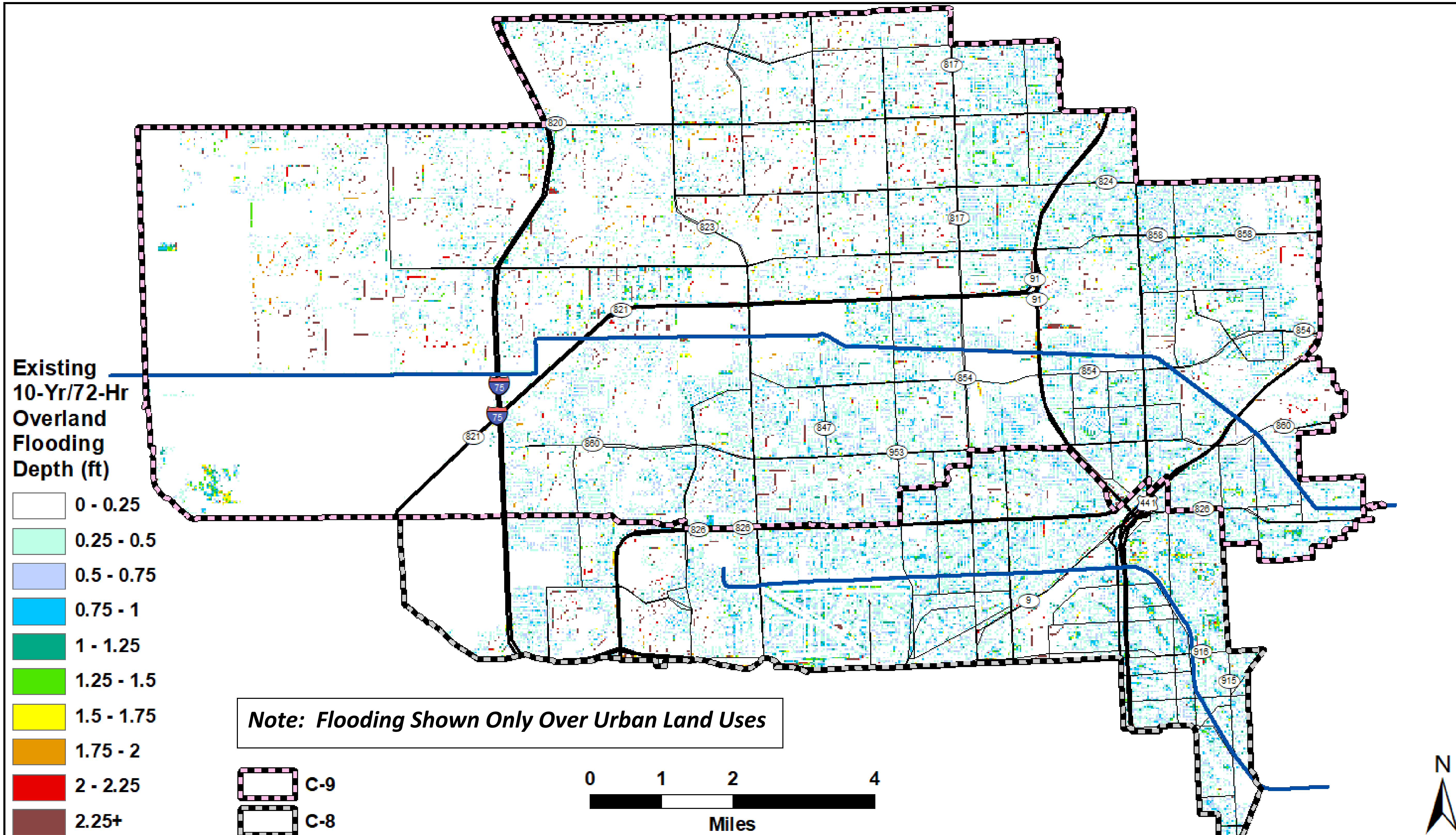

Figure 8.5-6 Flood Inundation Map for 10-Year Design Storm Event in Urban Land Use Areas

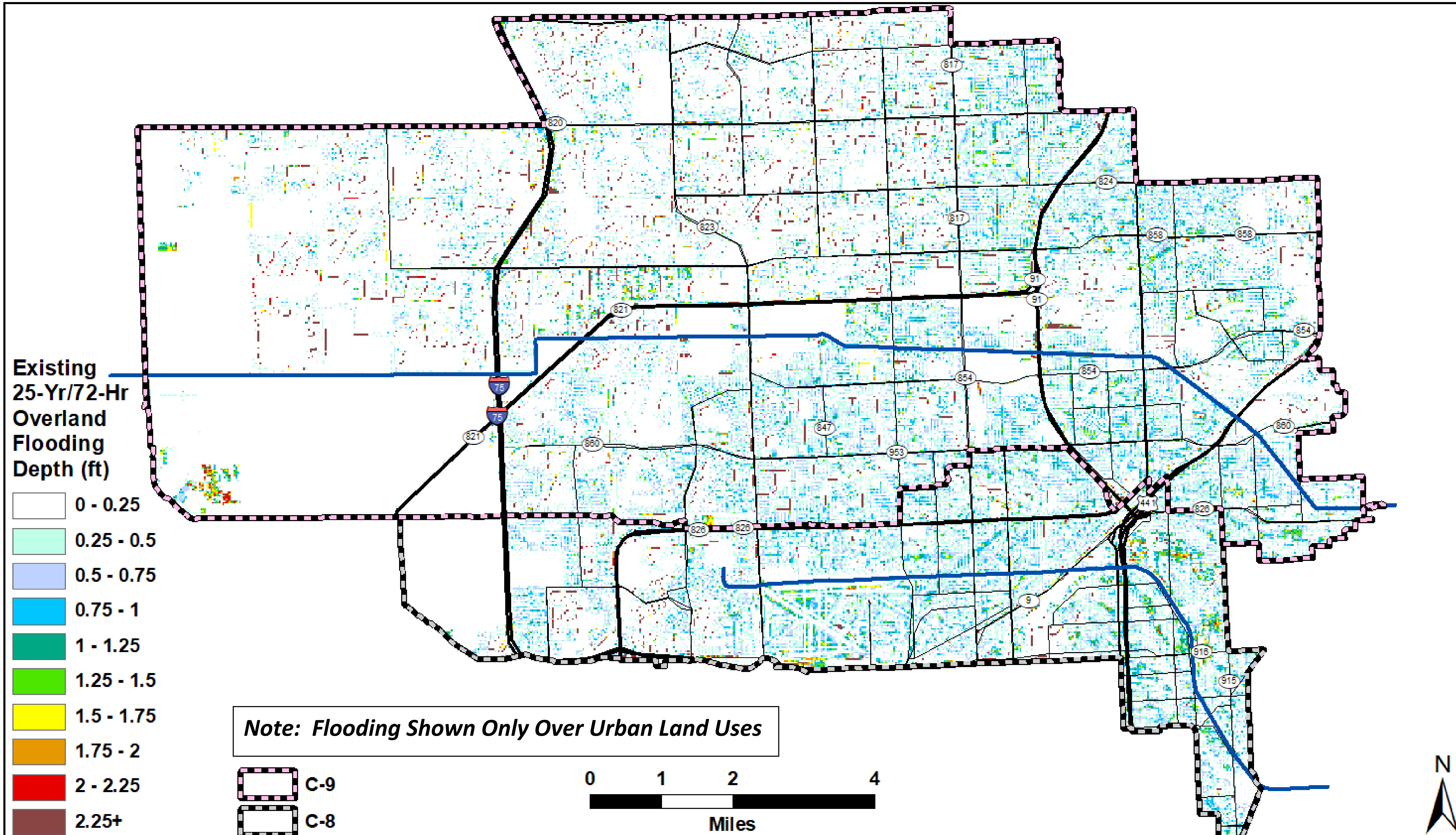

Figure 8.5-7: Flood Inundation Map for 25-Year Design Storm Event in Urban Land Use Areas

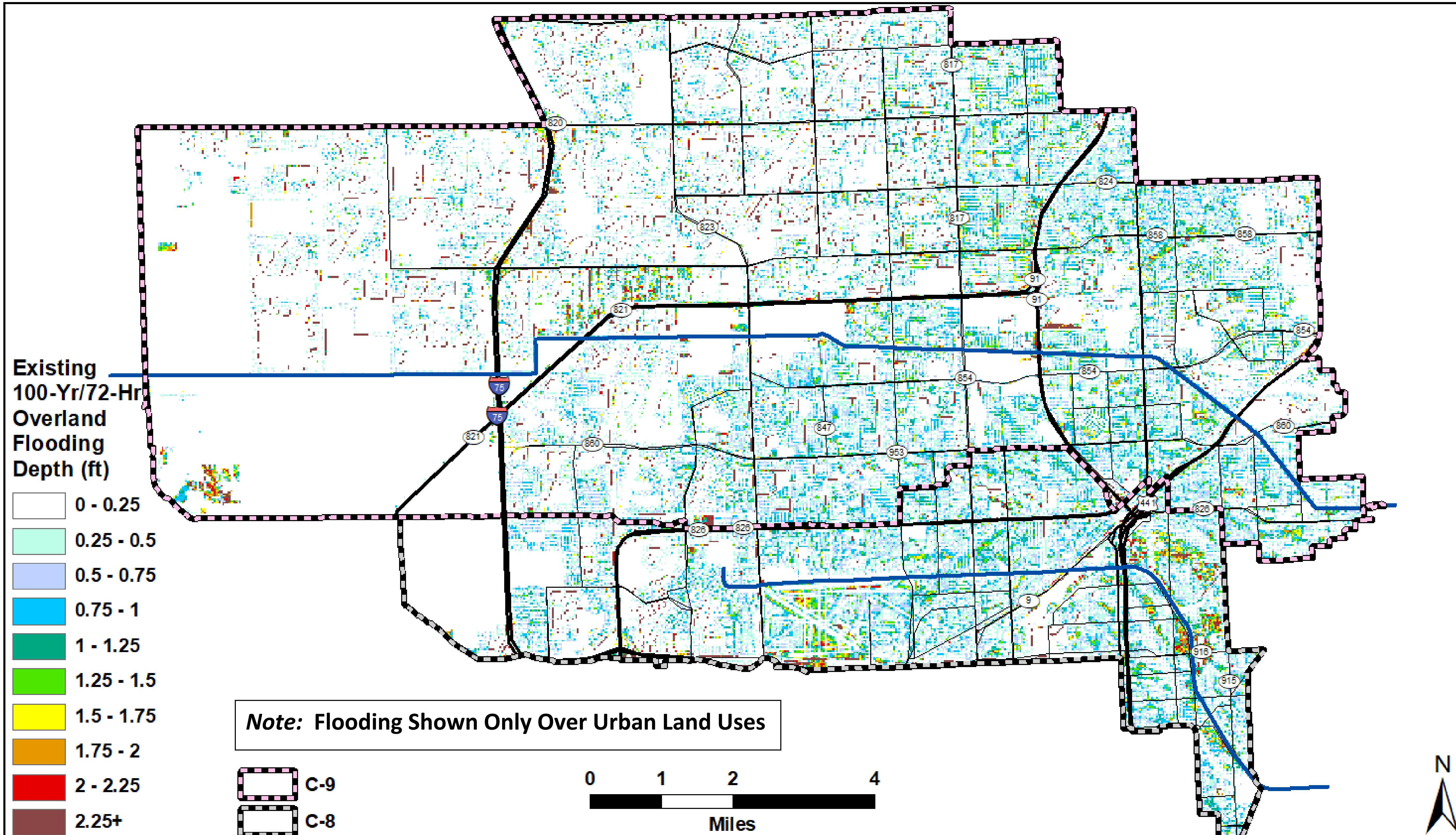

Figure 8.5-8: Flood Inundation Map for 100-Year Design Storm Event in Urban Land Use Areas

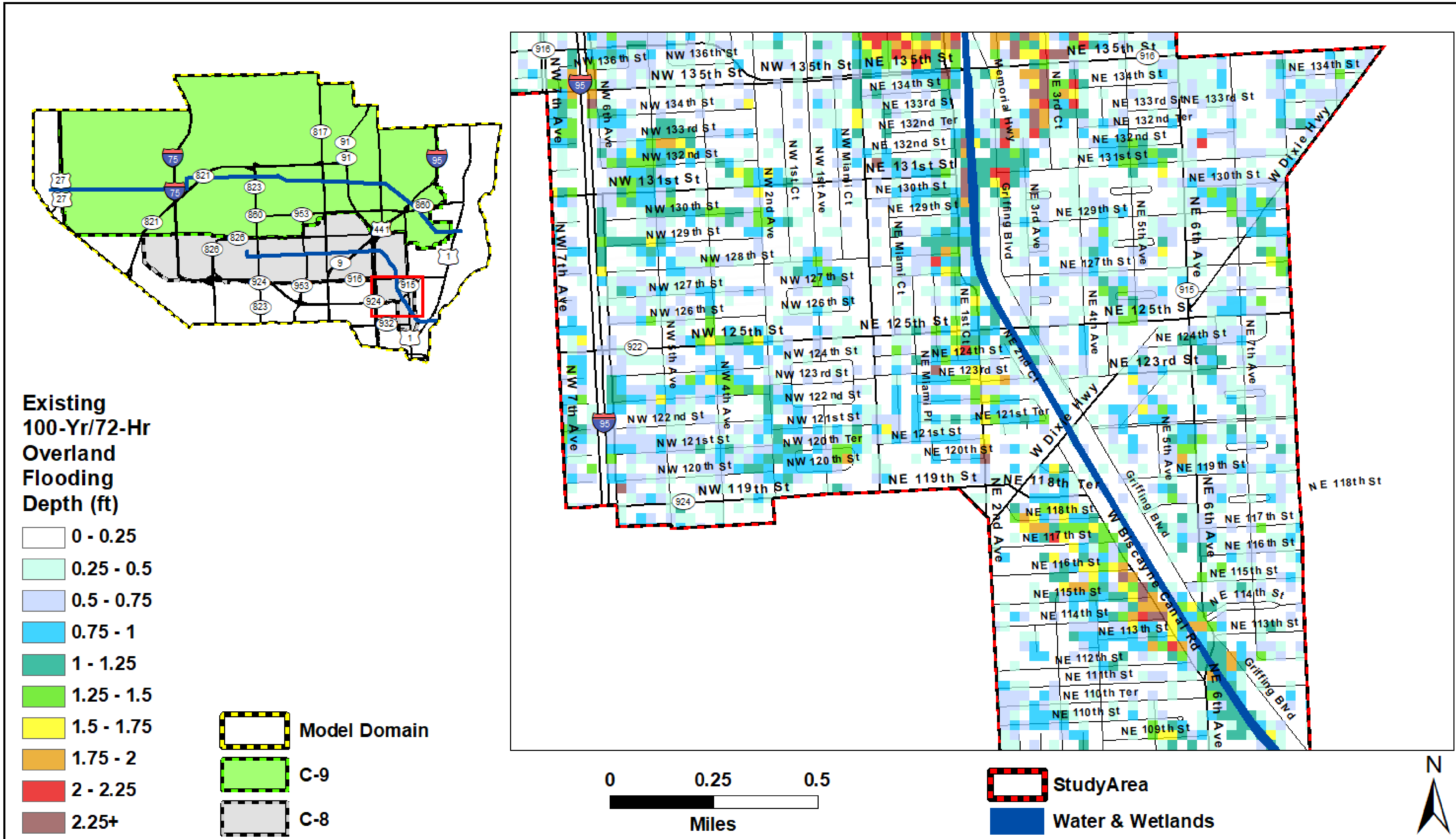

Figure 8.5-9: Up Close Flood Inundation Map for 100-Year Design Storm Event C-8 Canal Between and NE 135th St (CR916) and NE 6th Ave (CR915)

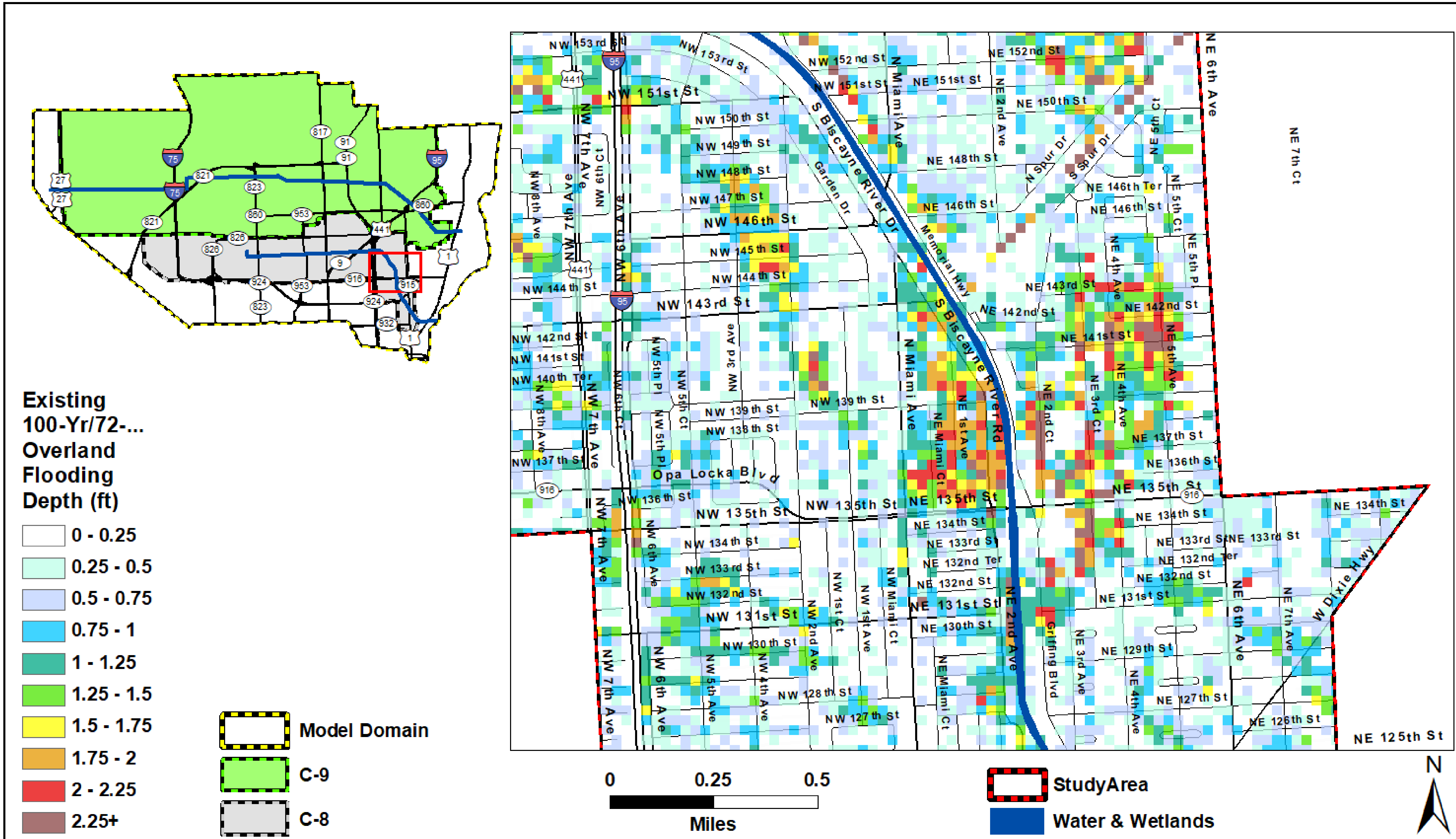

Figure 8.5-10: Up Close Flood Inundation Map for 100-Year Design Storm Event C-8 Canal Between North Miami Ave and NE 135th St (CR916)

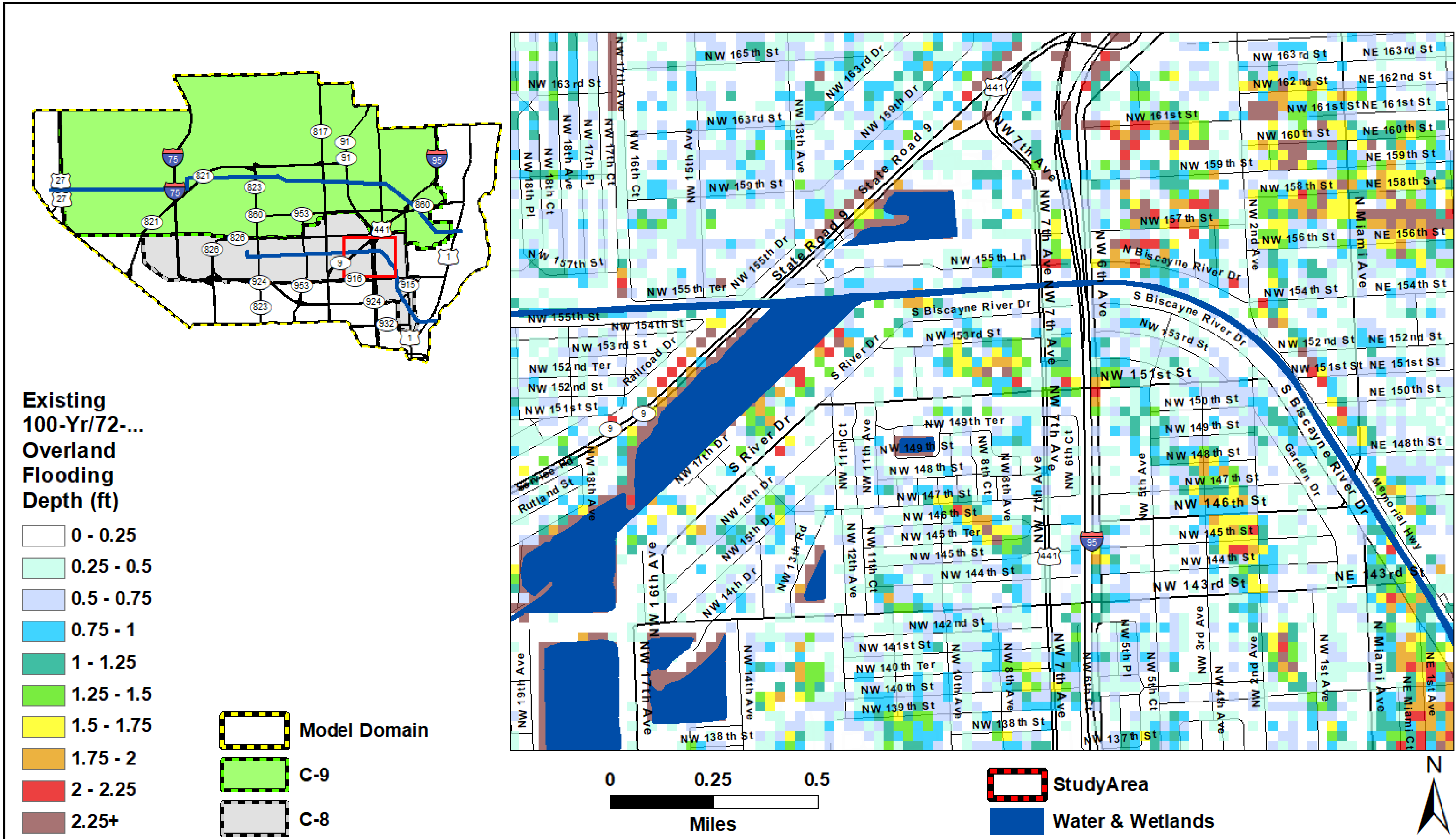

Figure 8.5-11: Up Close Flood Inundation Map for 100-Year Design Storm Event C-8 Canal Near Opa Locka Canal

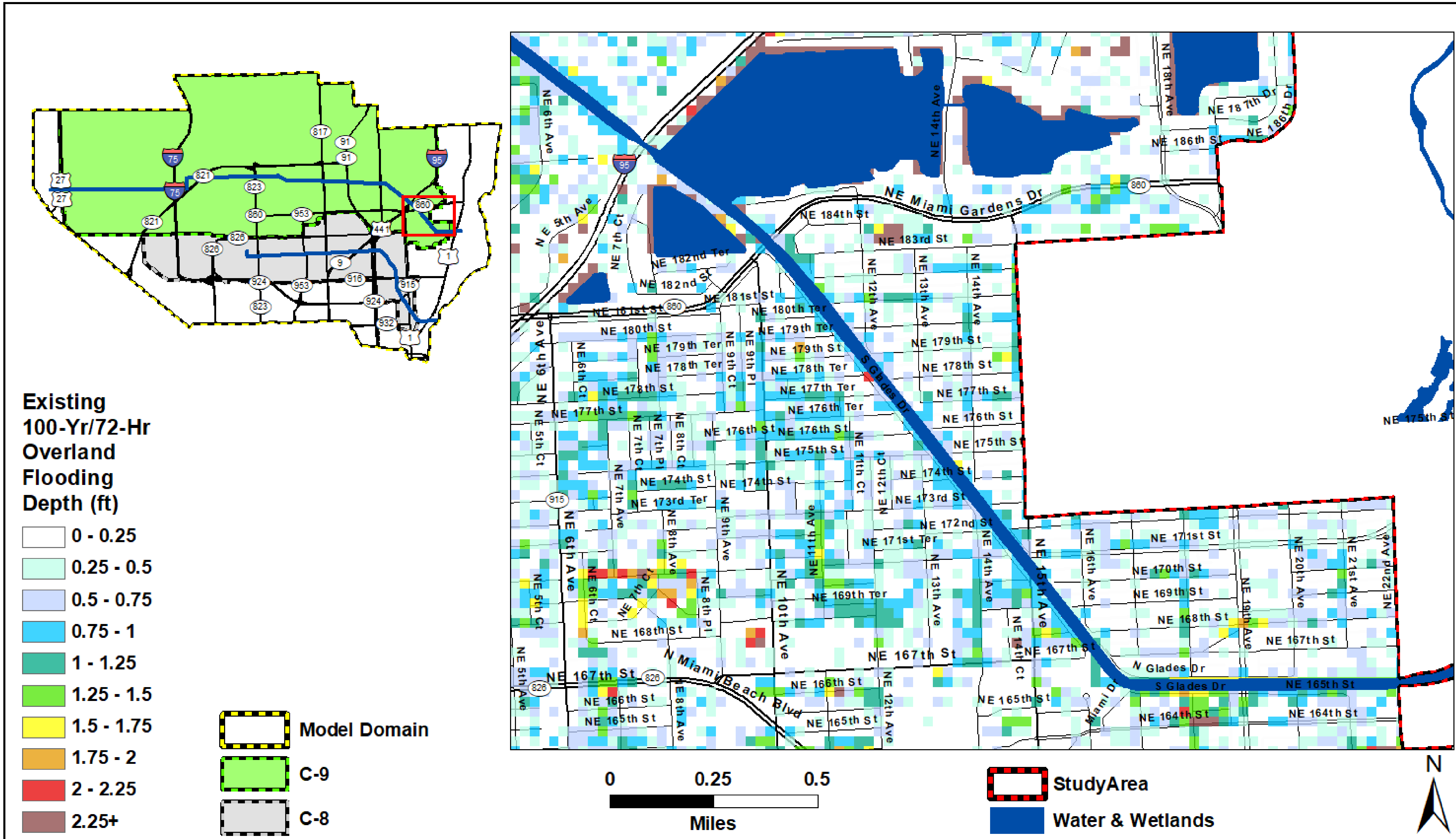

Figure 8.5-12: Up Close Flood Inundation Map for 100-Year Design Storm Event C-9 Canal Between I-95 and S-29

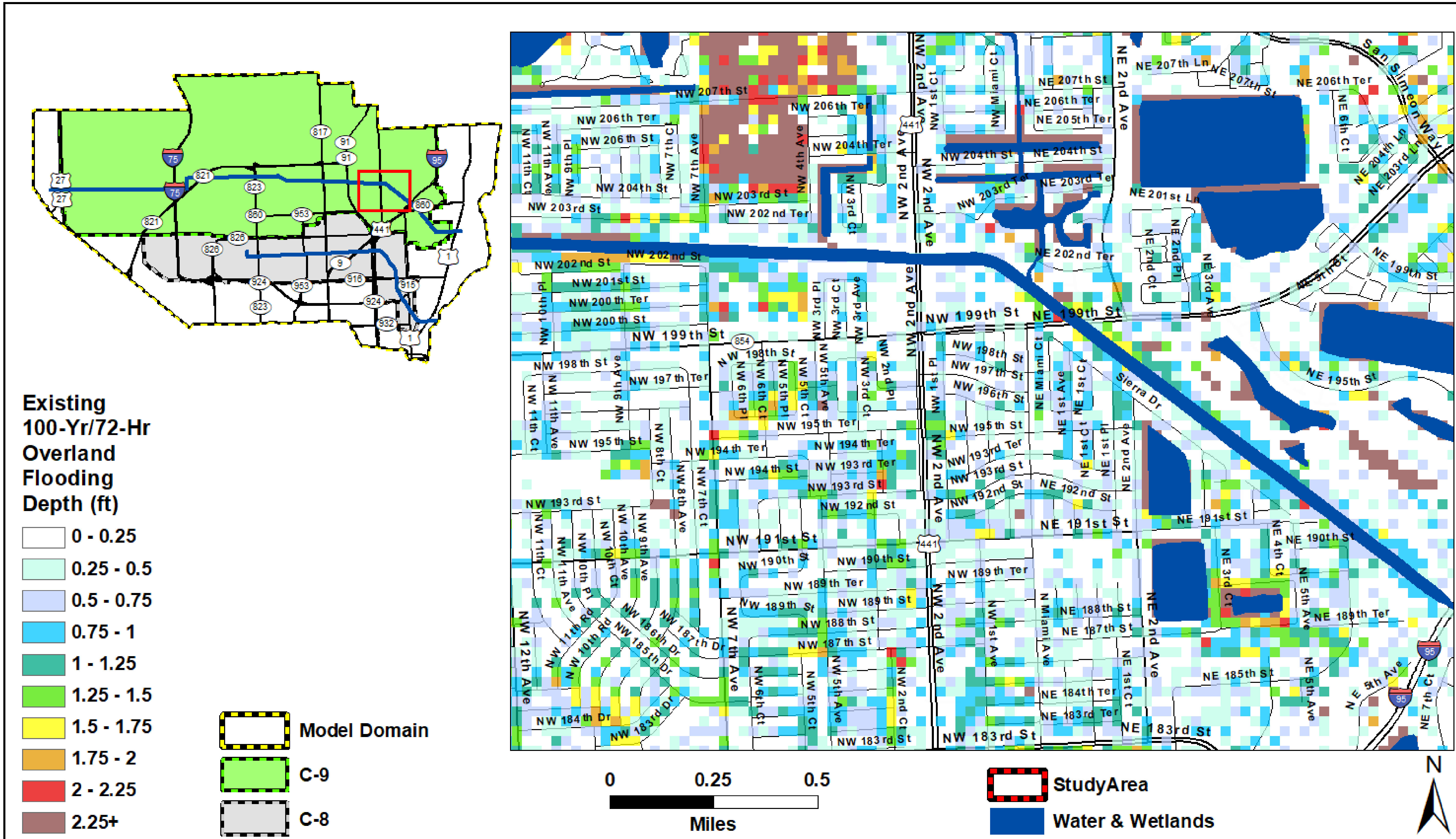

Figure 8.5-13: Up Close Flood Inundation Map for 100-Year Design Storm Event C-9 Canal Near US Hwy 441

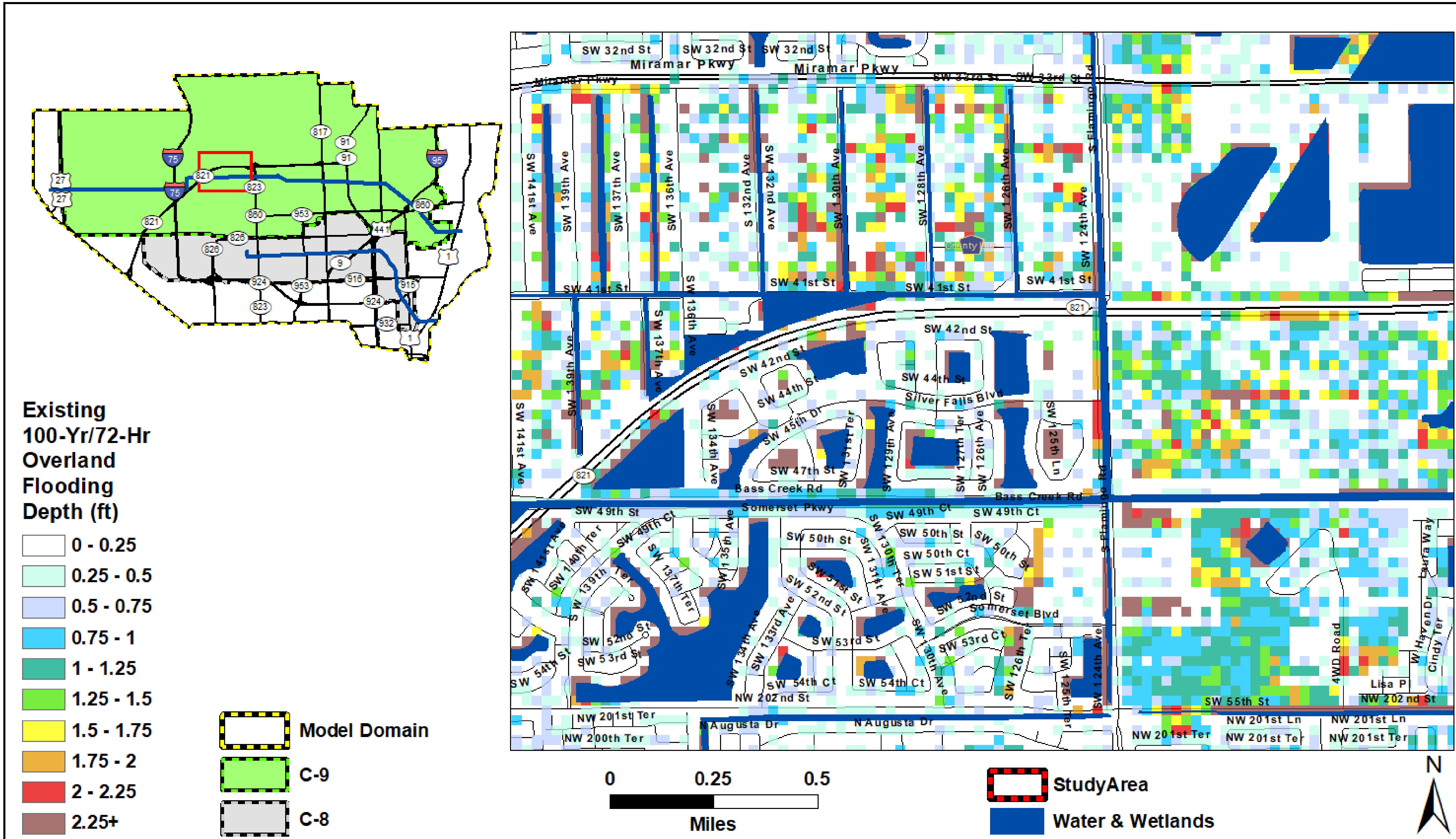

Figure 8.5-14: Up Close Flood Inundation Map for 100-Year Design Storm Event C-9 Canal Near Ronald Reagan Turnpike

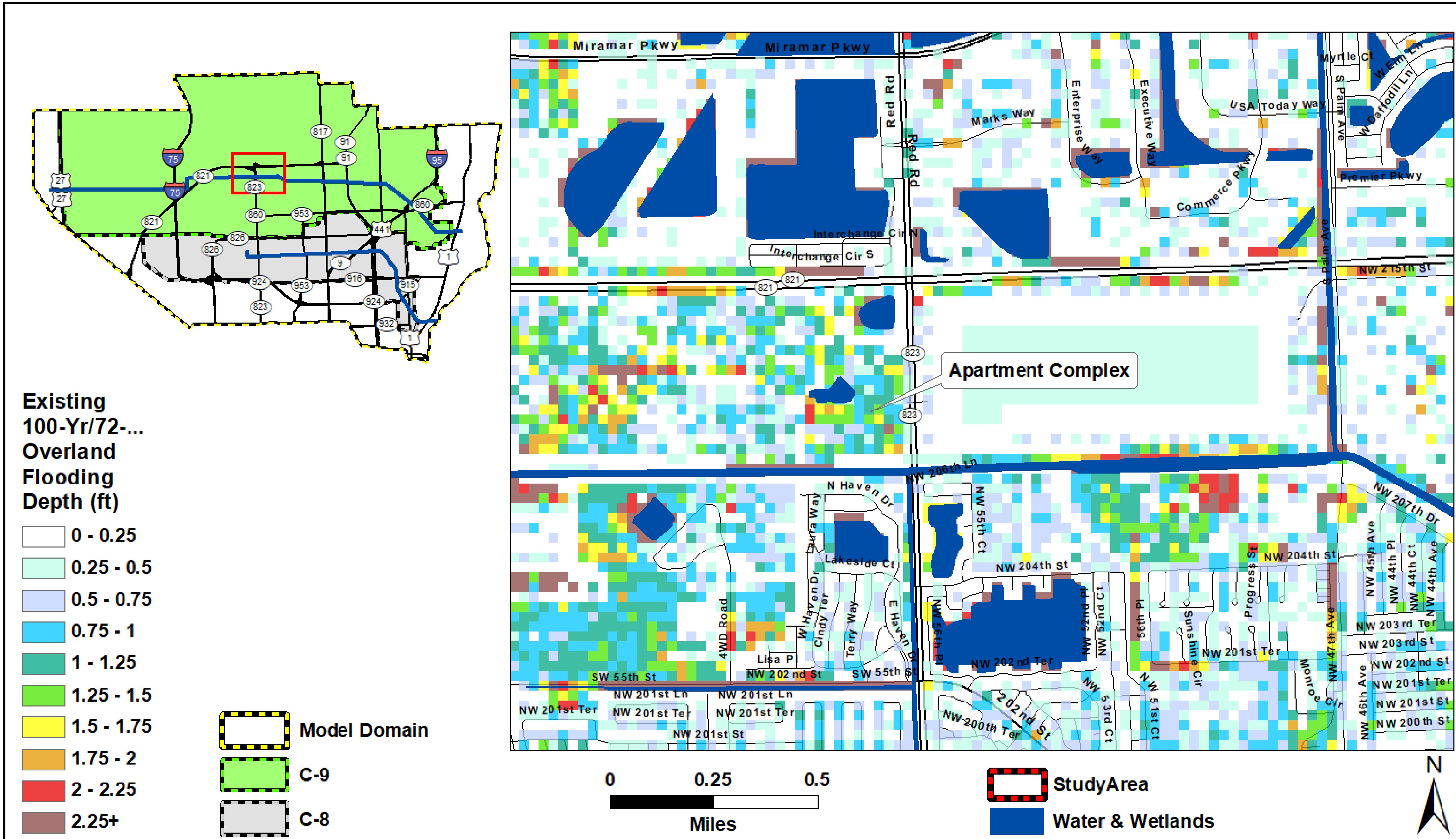

Figure 8.5-15: Up Close Flood Inundation Map for 100-Year Design Storm Event C-9 Canal Near Red Road

8.6 PM #6 – Duration of Flooding

For PM #6, the duration of flooding maps were developed by estimating the duration over which water depth exceeds a given threshold value. In this study, the duration of overland flooding was estimated using model simulated water depths and a threshold flooding depth of 0.25 ft. Additionally, the duration of flooding in the District Canals were estimated as the amount of time it takes for the water levels to return to target stage. The target stages of 3.6 ft for S-28Z and 3.5 ft for S-29Z were provided by the District (Email from Hongying Zhao, 5/12/2020). **Table 8-9** shows the duration of time taken for the headwater at S-28 and S-29 to return to target stage.

Table 8-9: Duration for Water Levels to Return to Target Stage

Design Storm	Duration to Return to Target Stage (hr)	
	S-28Z	S-29Z
5-Year	27	55
10-Year	40	92
25-Year	95	158
100-Year	140	242

The duration of overland flooding was estimated for all four design storm events based on the length of time the flood depth was predicted to exceed the threshold value (0.25 ft) within each MIKE SHE 125-ft grid cell using the statistics tool in MIKE ZERO. The flood duration maps for each of the design storm events are shown in **Figure 8.6-1** through **Figure 8.6-4** for the 5-year, 10-year, 25-year, and 100-year design storm events, respectively.

Based on model simulations, large areas were inundated for over 72 hours, even for the 5-year design storm (**Figure 8.6-1)**. These areas are comprised primarily of lakes and wetlands and other low-lying undeveloped areas. An increase in flooding extent and duration was observed as the magnitude of the design storms increased (**Figure 8.6-2** through **Figure 8.6-4**). A vast majority of the watershed was inundated for at least a small duration during the 100-year design storm. Developed areas with the largest flood duration generally tend to coincide with the highest depths of flooding determined from PM#5. **Figure 8.6-5** through **Figure 8.6-8** show the flood duration maps for each of the design storm events for urban areas only. **Figure 8.6-9** through **Figure 8.6-11** show up close examples of flood duration along the C-8 Canal and **Figure 8.6-12** through **Figure 8.6-15** show up close examples of flood duration along the C-9 Canal.

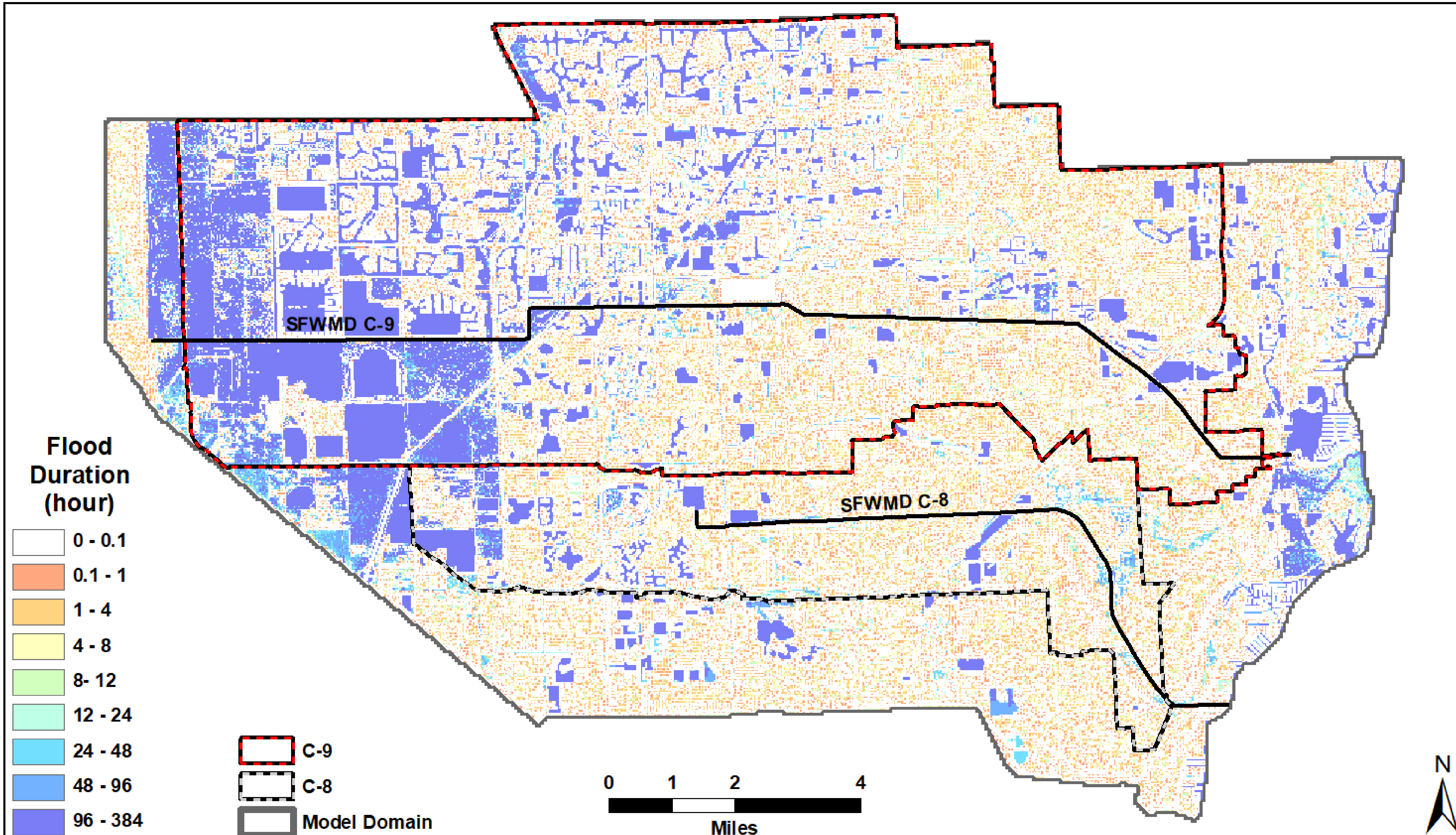

Figure 8.6-1: Flood Duration Map for 5-Year Current Conditions Design Storm Event

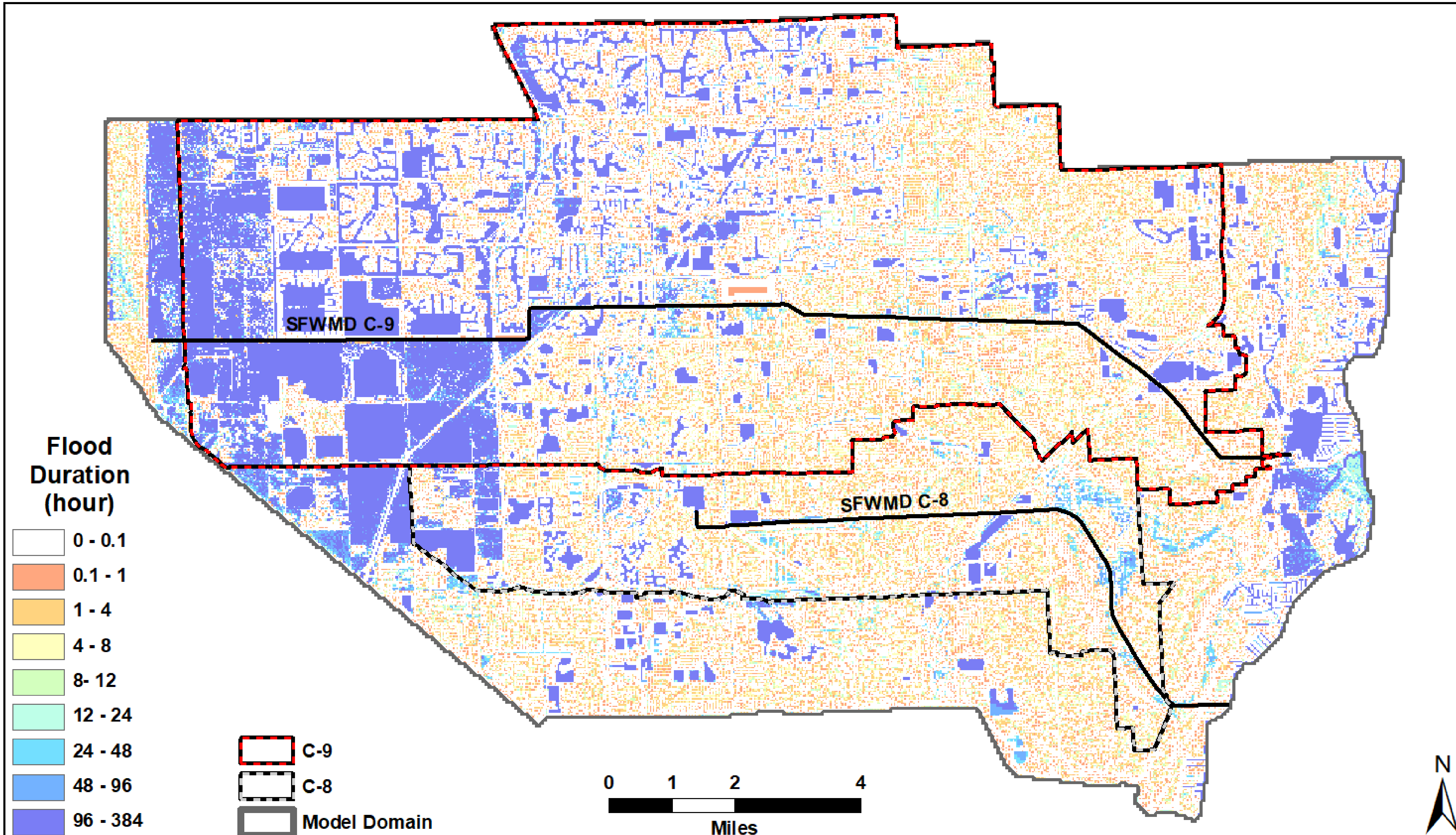

Figure 8.6-2: Flood Duration Map for 10-Year Current Conditions Design Storm Event

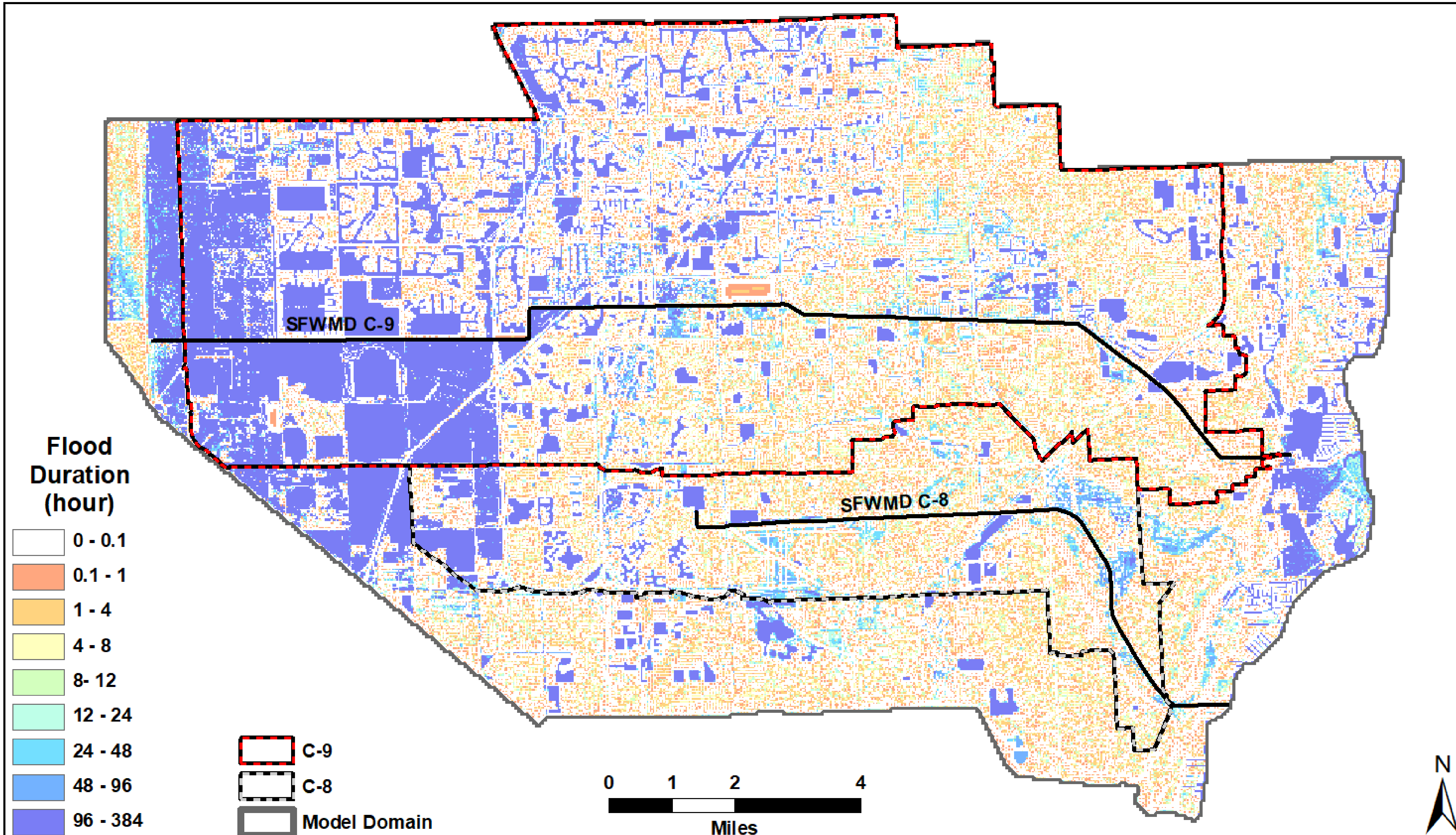

Figure 8.6-3: Flood Duration Map for 25-Year Current Conditions Design Storm Event

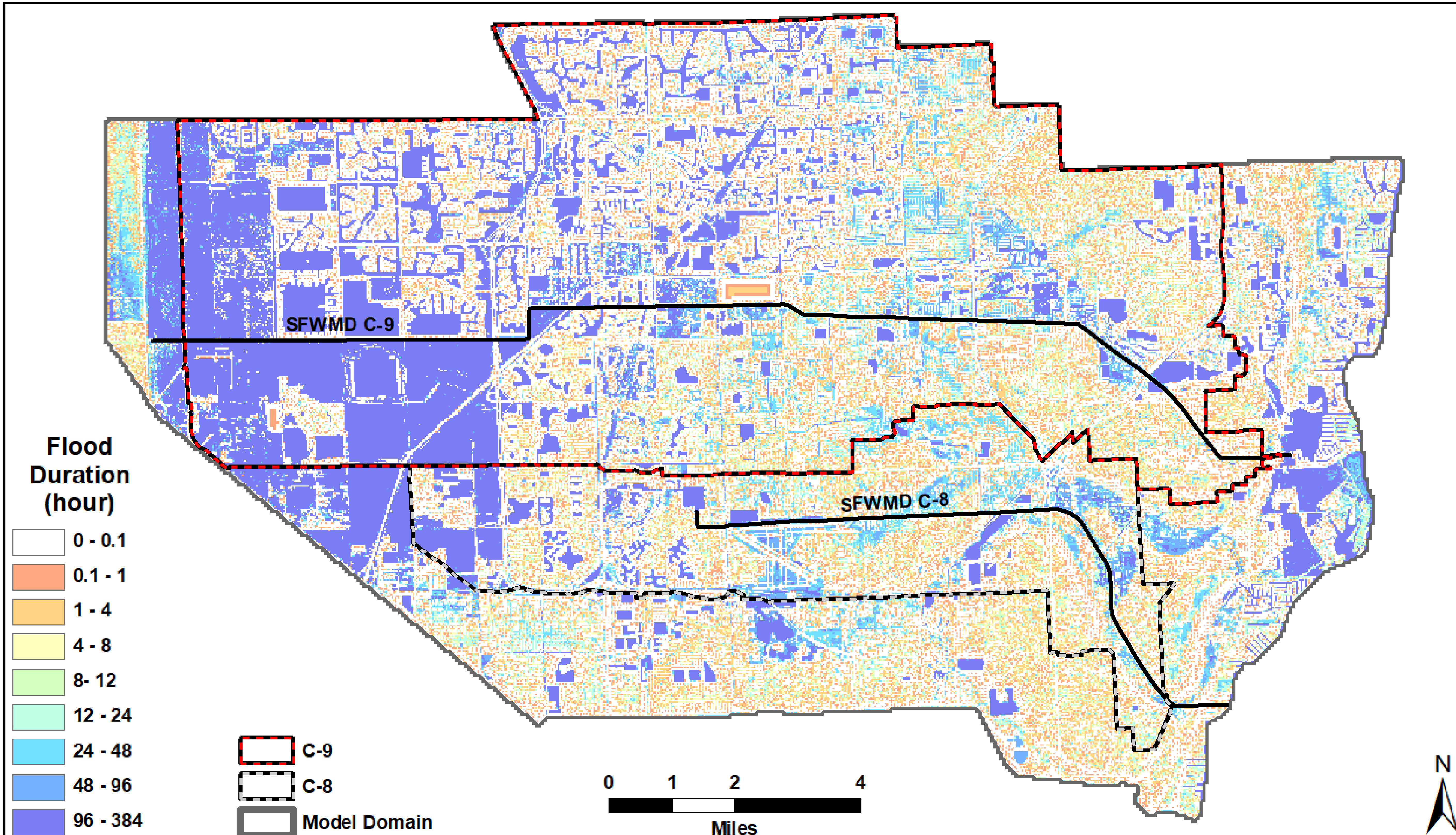

Figure 8.6-4: Flood Duration Map for 100-Year Current Conditions Design Storm Event

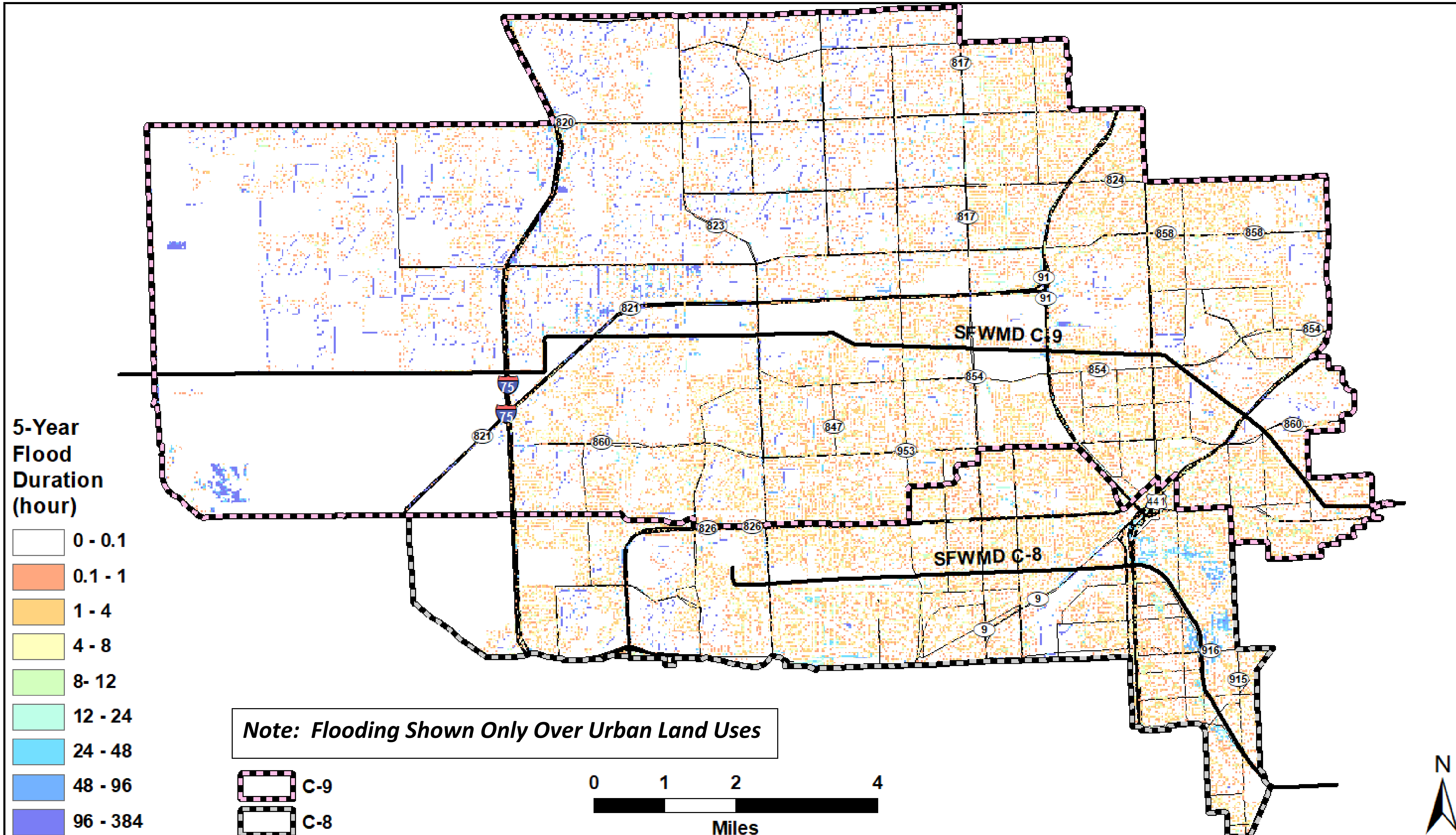

Figure 8.6-5: Flood Duration Map for 5-Year Design Storm Event in Urban Land Use Areas

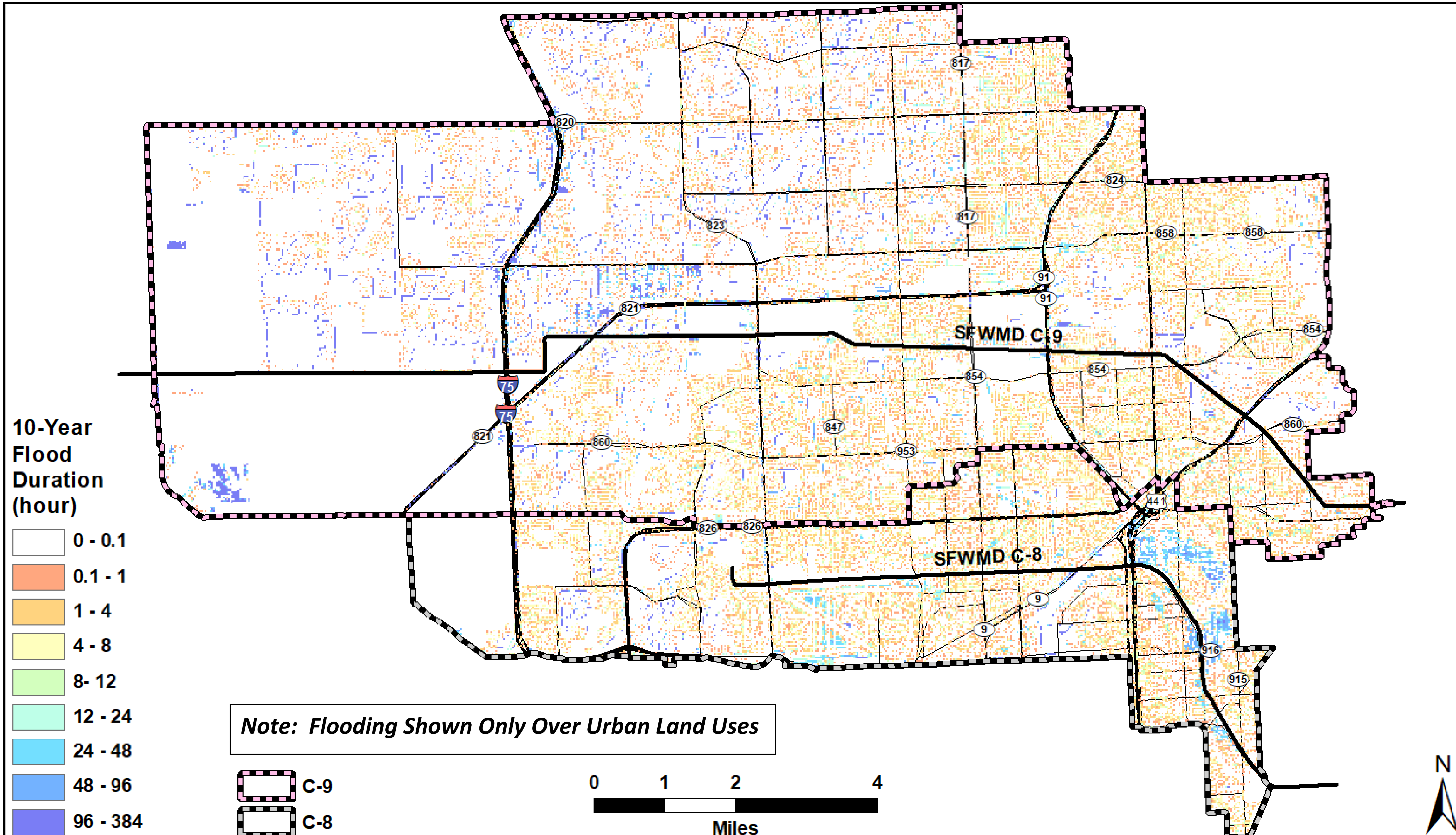

Figure 8.6-6 Flood Duration Map for 10-Year Design Storm Event in Urban Land Use Areas

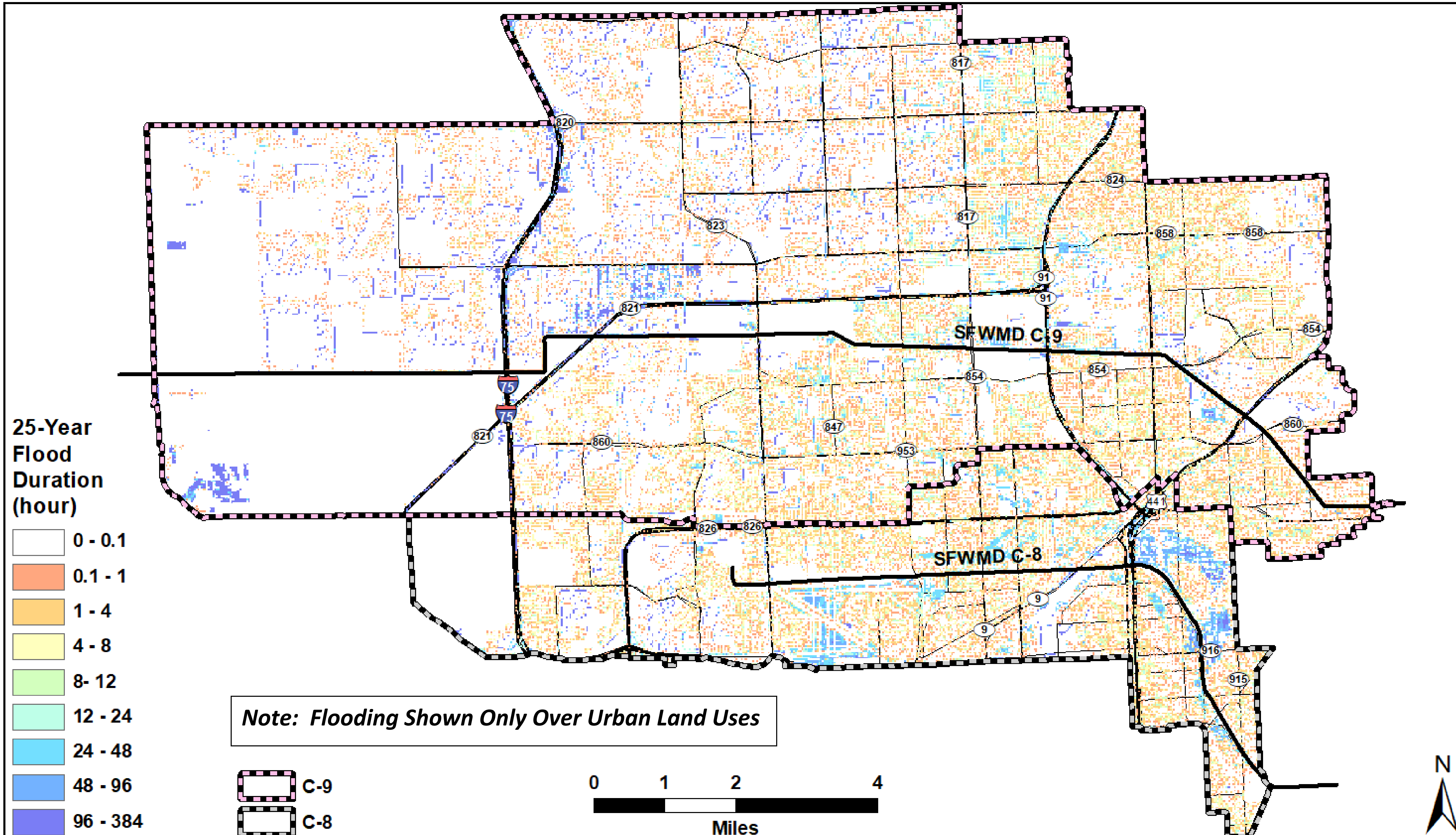

Figure 8.6-7: Flood Duration Map for 25-Year Design Storm Event in Urban Land Use Areas

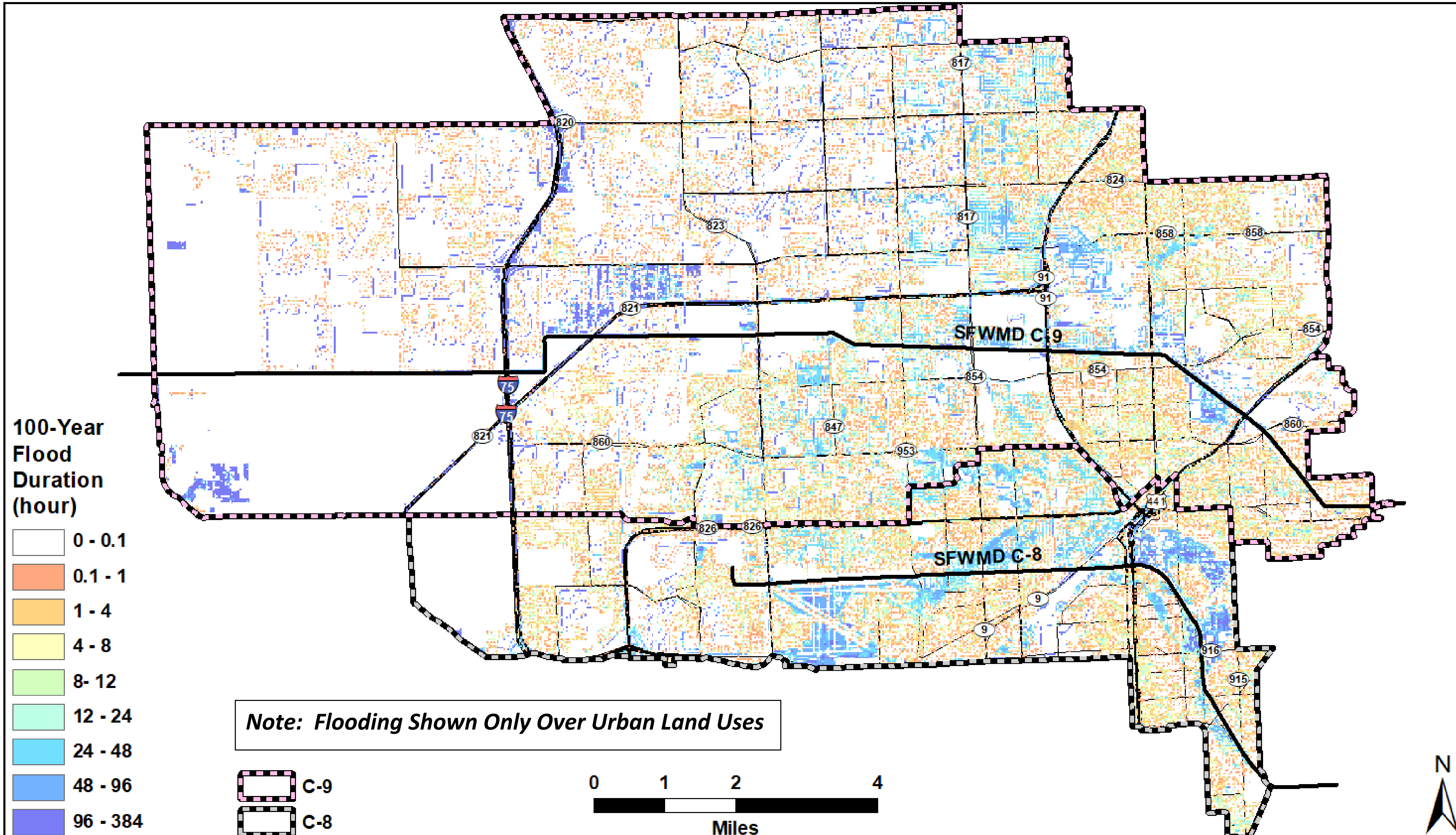

Figure 8.6-8: Flood Duration Map for 100-Year Design Storm Event in Urban Land Use Areas

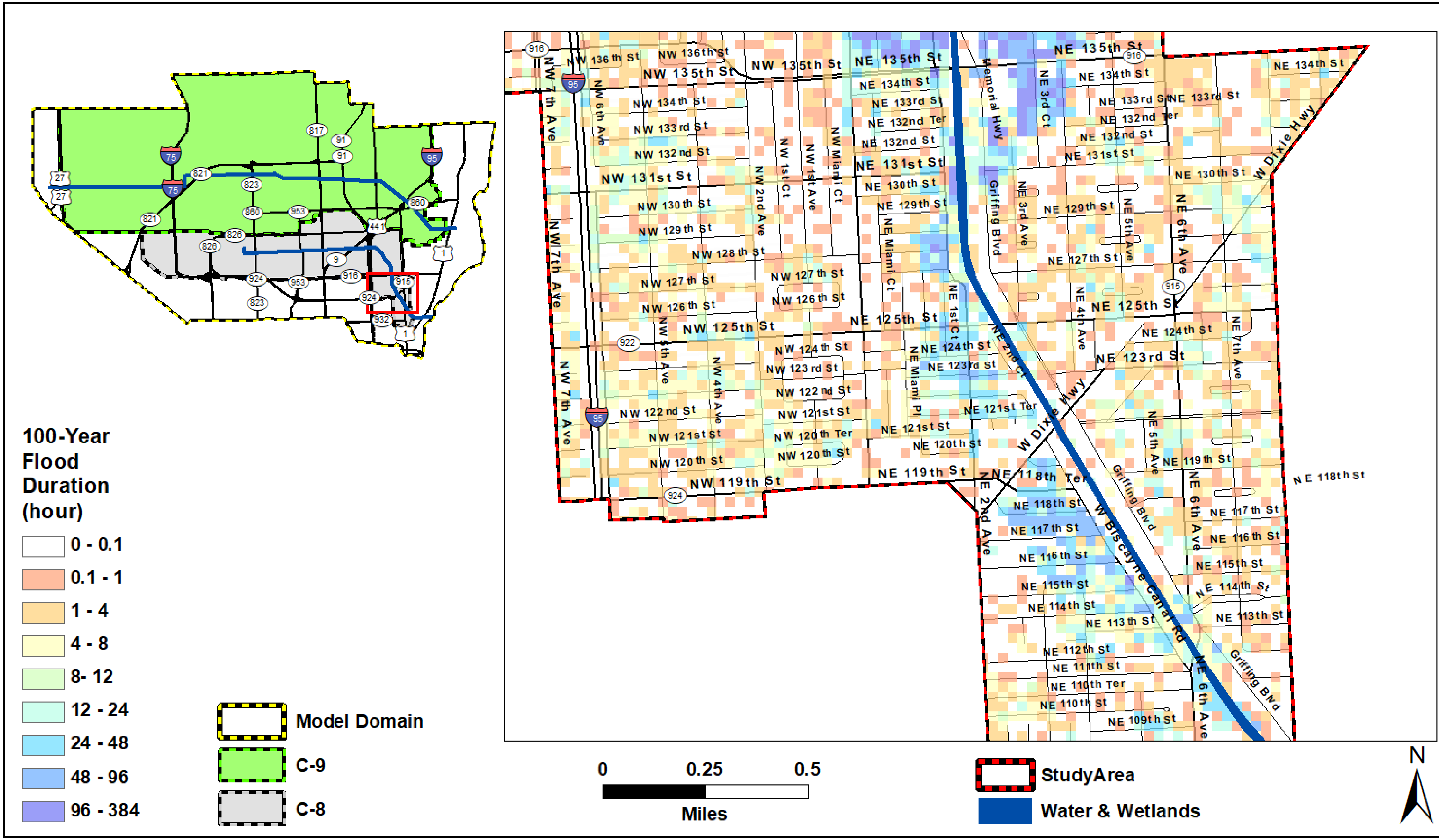

Figure 8.6-9: Up Close Flood Duration Map for 100-Year Design Storm Event C-8 Canal Between and NE 135th St (CR916) and NE 6th Ave (CR915)

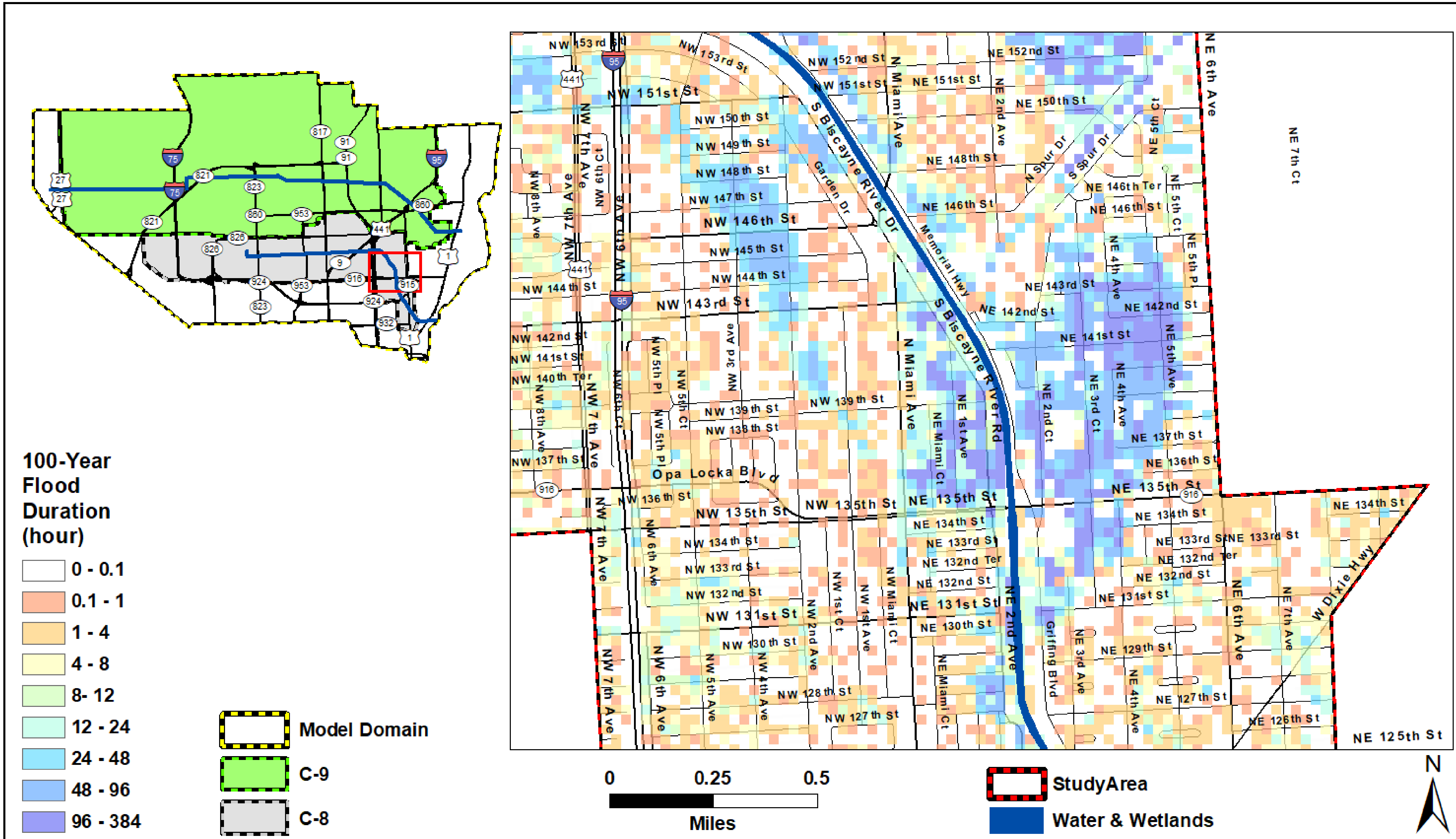

Figure 8.6-10: Up Close Flood Duration Map for 100-Year Design Storm Event C-8 Canal Between North Miami Ave and NE 135th St (CR916)

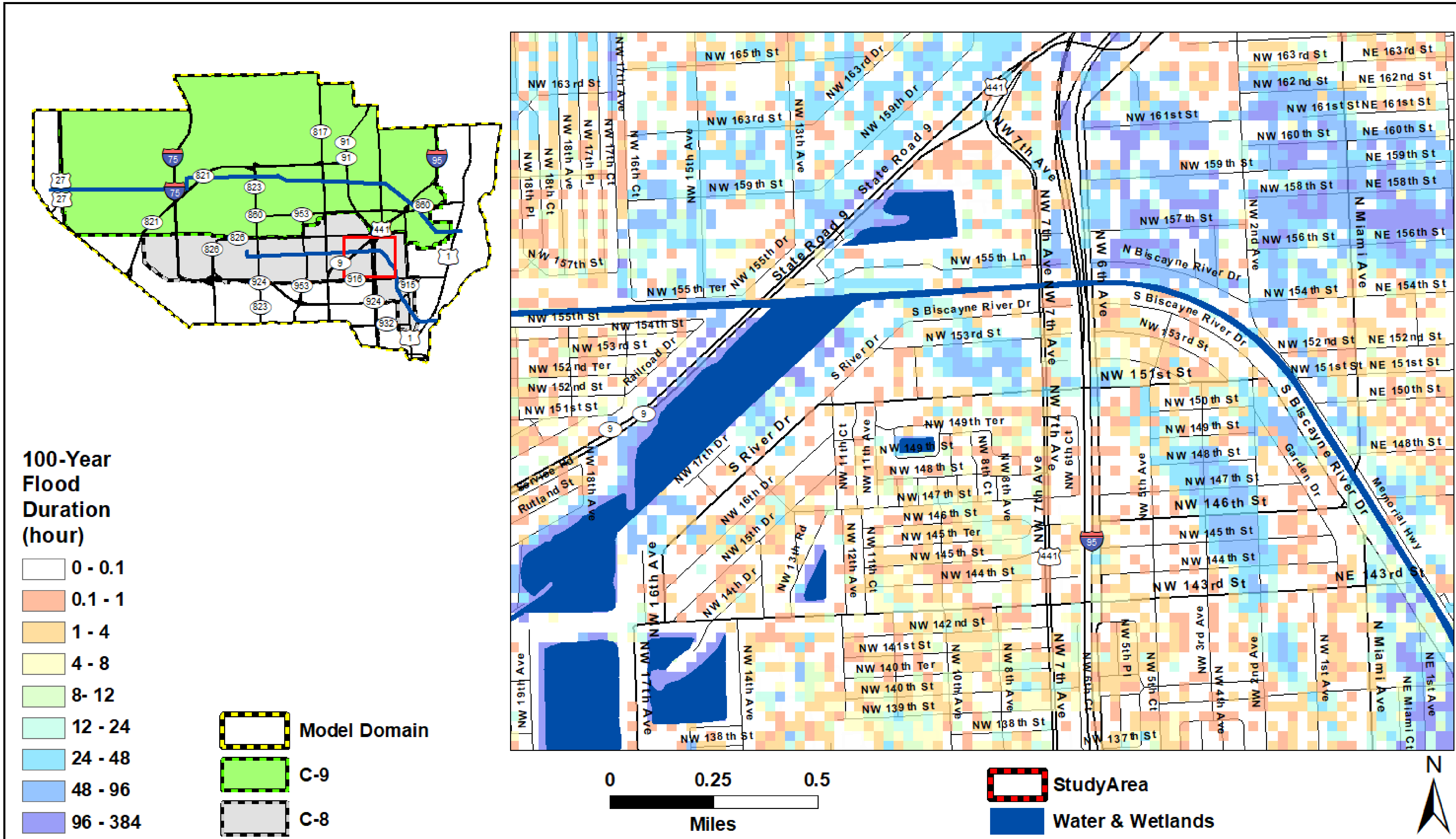

Figure 8.6-11: Up Close Flood Duration Map for 100-Year Design Storm Event C-8 Canal Near Opa Locka Canal

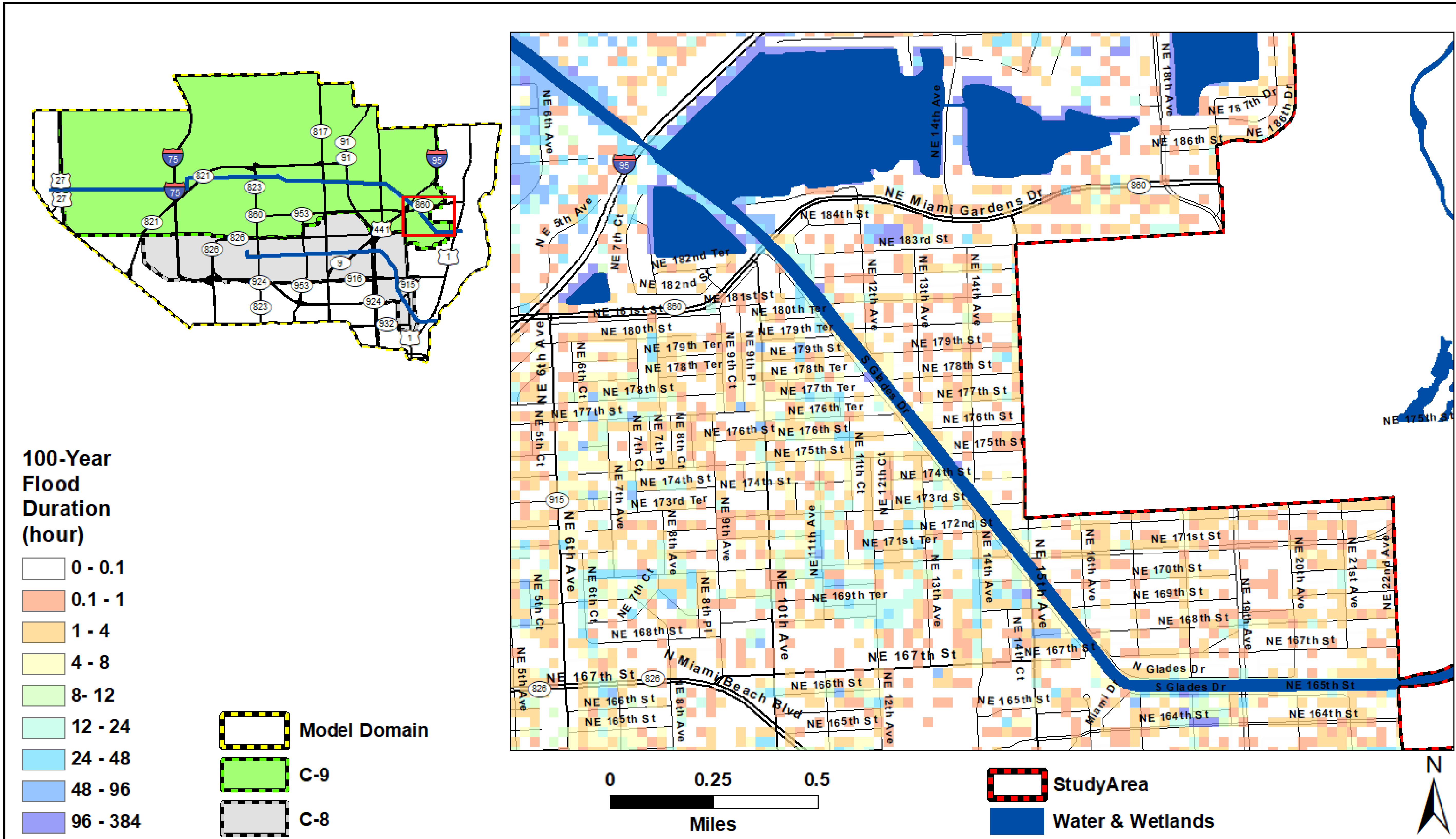

Figure 8.6-12: Up Close Flood Duration Map for 100-Year Design Storm Event C-9 Canal Between I-95 and S-29

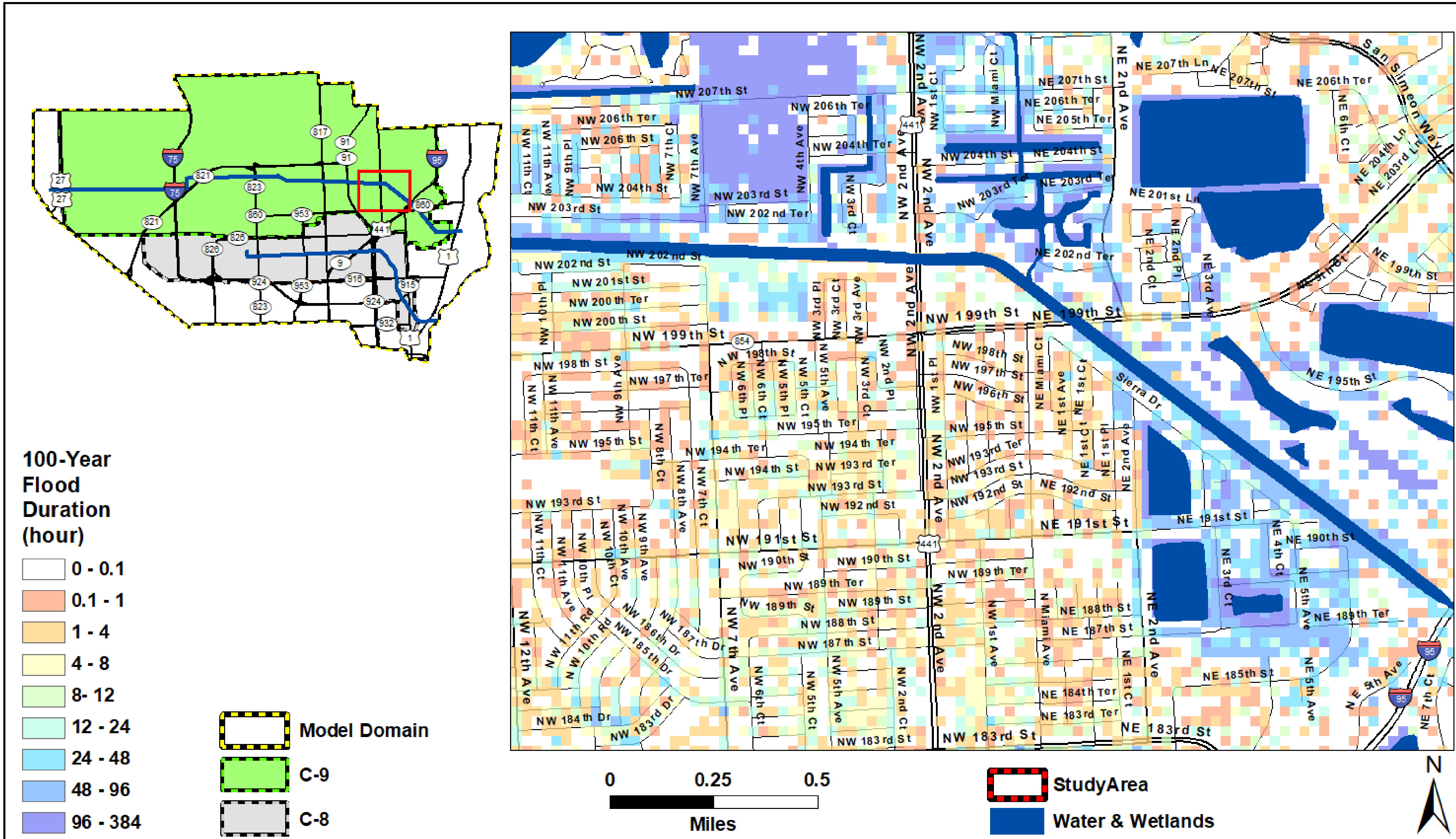

Figure 8.6-13: Up Close Flood Duration Map for 100-Year Design Storm Event C-9 Canal Near US Hwy 441

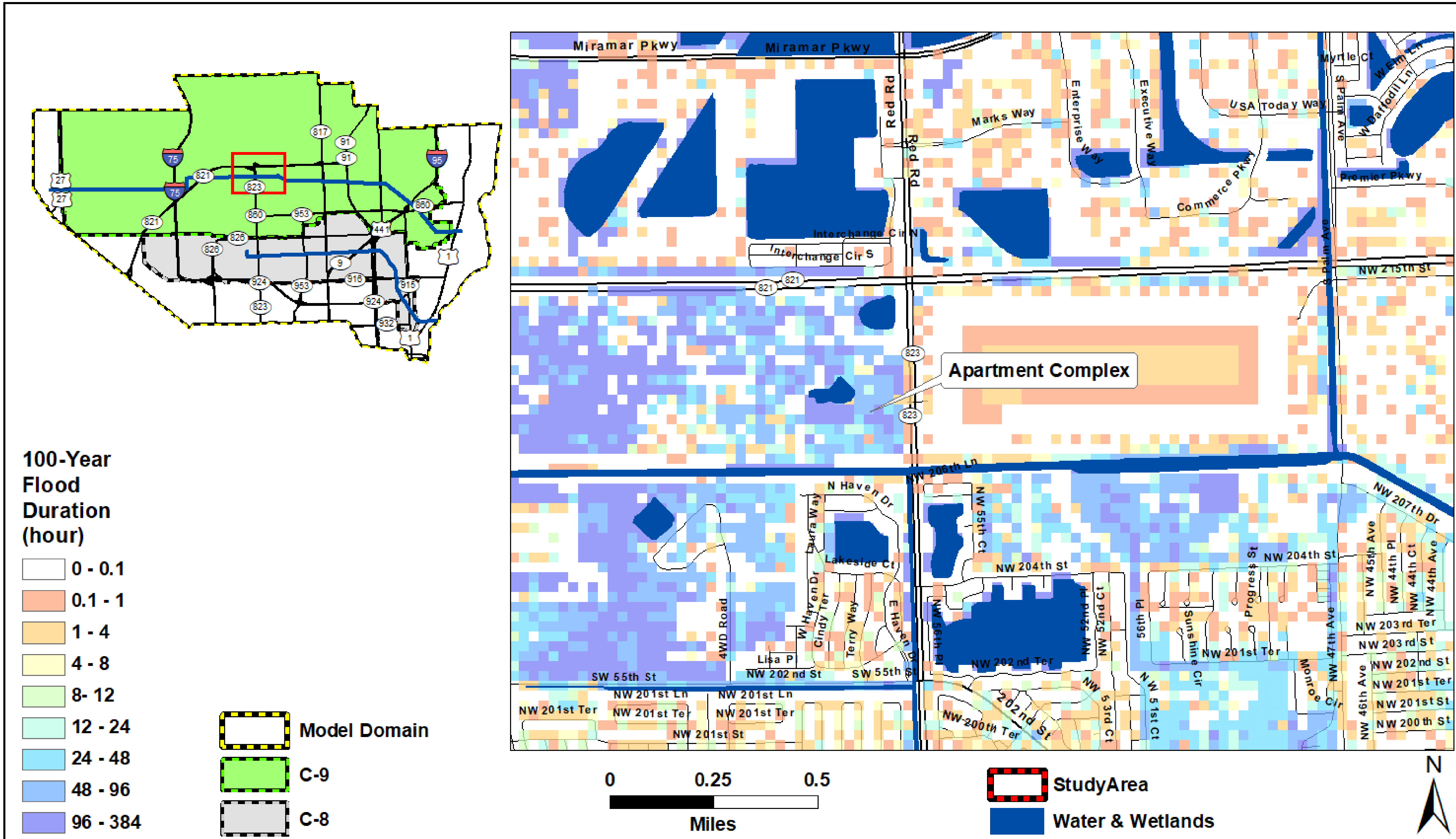

Figure 8.6-14: Up Close Flood Duration Map for 100-Year Design Storm Event C-9 Canal Near Red Road

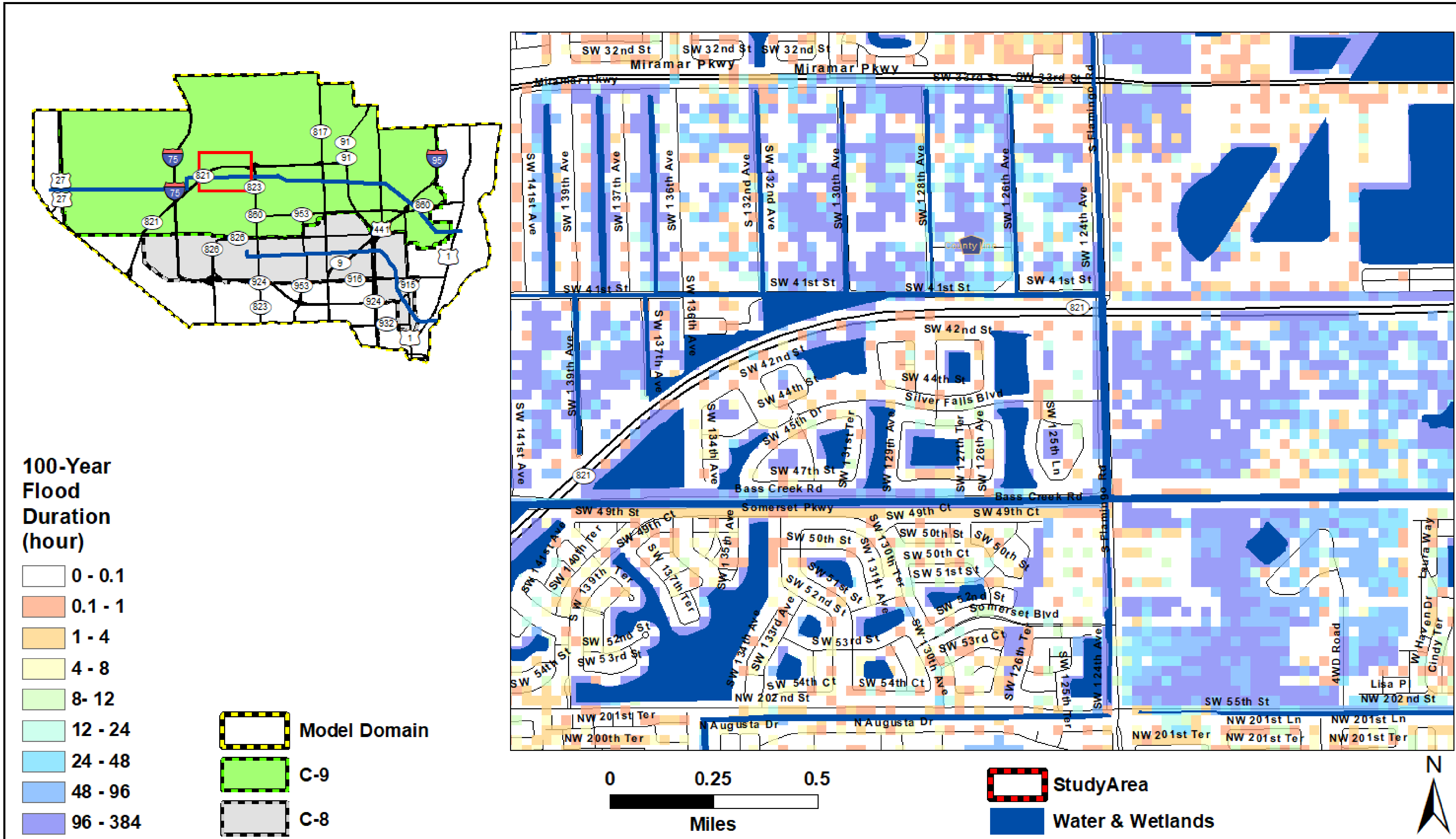

Figure 8.6-15: Up Close Flood Duration Map for 100-Year Design Storm Event C-9 Canal Near Ronald Reagan Turnpike

8.7 Current Condition FPLOS Assessment Conclusions

The current conditions design storm simulation results were evaluated using six performance measures. The analysis presented in this report provides a model-based assessment of the current level of flood protection provided by the C-8 and C-9 watershed's primary canal network and associated control structures. These results were used to determine potential FPLOS deficiencies by highlighting areas that failed multiple performance measures such as bank exceedances that corresponded to overland inundation (PM #5 and/or PM #6). In some cases, PM #1 bank exceedances did not manifest as significant overland inundation and thus were considered insignificant localized FPLOS deficiencies. In other cases, flooding was shown by PM #5 and PM #6 that did not correspond to bank exceedances in PM #1, suggesting that flooding could be due to problems with secondary and tertiary drainage systems.

It should also be noted that the model results are subjected to certain limitations associated with the scale of the 2-dimensional model grid. Although the model uses a 125-ft grid that is suitable for the sub-regional scale flood protection level of service evaluation, the results should not be extended to local-scale evaluations or regulatory determinations of flooding extents, where considerable variations in topography can occur within the area of each grid cell.

8.7.1 Current Condition FPLOS Assessment Conclusion for C-8 Watershed

Based on the results of this study, it appears that the C-8 canal generally provides a 10-year level of service, with some areas receiving a 25-year level of service or better. There were a few localized areas where the water levels exceeded the canal banks for the 5-year event as shown in PM #1 (**Figure 8.1-1**), however, it does not correspond to a significant area of flood inundation as shown in PM #5 (**Figure 8.5-1**)**.** For the 25-year design storm, the model results suggest that several segments of the C-8 Canal would be overwhelmed during peak flood conditions, with the western segment (west of Opa Locka Canal) generally performing better than the eastern segment. For the 100-year design storm, the model results suggest that most of the C-8 Canal would be overwhelmed during peak flood conditions, while most of the watershed would be inundated to some degree.

8.7.2 Current Condition FPLOS Assessment Conclusion for C-9 Watershed

Based on the results of this study, it appears that the C-9 canal generally provides a 25-year level of service, with some areas receiving a 100-year level of service or better. There were a few localized areas where the water levels exceeded the canal banks for the 10-year event as shown in PM #1 (**Figure 8.1-2**), however, it typically does not correspond to a significant area of flood inundation east of Interstate I-75 as shown in PM #5 (**Figure 8.5-2**). West of Interstate I-75, the water level exceedance corresponds to a significant amount of area of flood inundation, although it is in undeveloped areas. For the 100-year design storm, the model results suggest that several segments of the C-9 Canal would be overwhelmed during peak flood conditions, while most of the watershed would be inundated to some degree. Some areas of this watershed appear to have deficiencies in secondary and/or tertiary drainage systems that result in flooding of developed areas, as these flooded areas generally do not correspond to canal bank exceedances.

9 MODEL DEVELOPMENT FOR FUTURE CONDITIONS

This section documents the development and initial parameterization of the South Florida Water Management District (SFWMD) C-8 C-9 Future Conditions MIKE SHE and MIKE HYDRO models. The developed models were used in the C-8 C-9 future conditions flood protection level-of-service (FPLOS) study. Several model inputs and parameters used in the future condition model were obtained from the final version of the current conditions model. This section focuses on the development and parameterization changes that were made to the model for the future conditions' simulations. For details on model development and setup of the existing conditions model, please refer to the report *Flood Protection Level of Service Provided by Existing Infrastructure for Current Sea Level Conditions in the C8 and C9 Watersheds* (Taylor Engineering, 6/17/2020).

9.1 Rainfall

The design storms used in the future conditions model used the same NOAA Atlas 14 rainfall depths as used in the current conditions model. The design storms were temporally distributed based on the SFWMD 3-day distribution and spatially distributed based on Thiessen Polygons of the NOAA stations. The sensitivity run, to be completed only for the 10-year design storm, will have a 9% increase in rainfall. This increase comes from the Broward County DDF Change Factor Ensemble Analysis (Yin, Li, & Urich, 2019).

9.2 Land Use

The future conditions land use map was developed by modifying the current conditions land use map to reflect projected future changes. Areas of future change were identified by comparing undeveloped, agricultural, and lower density development areas (such as low density residential) to future conditions land use maps from the Broward County Planning Council (2020) and Miami-Dade County (n.d.). The future conditions land use maps from these sources were generalized, whereas the current conditions land use map was very detailed. Therefore, by starting with the current conditions land use map and applying changes identified from the future land use map, there was no significant loss in spatial detail. The future land use changes were most often applied to areas classified as open land, recreational, cropland and pastureland, forests, and disturbed land. Areas classified as wetlands in current conditions were not changed due to their protected status.

Within the Broward County portion of the model, about 805 acres were changed to represent future land use conditions. Within the Miami-Dade County portion of the model, about 3180 acres were changed to represent future land use conditions. The areas with future land use changes are shown in **Figure 9.2-1**. The C-9 Impoundment area is represented as reservoir land use for future conditions.

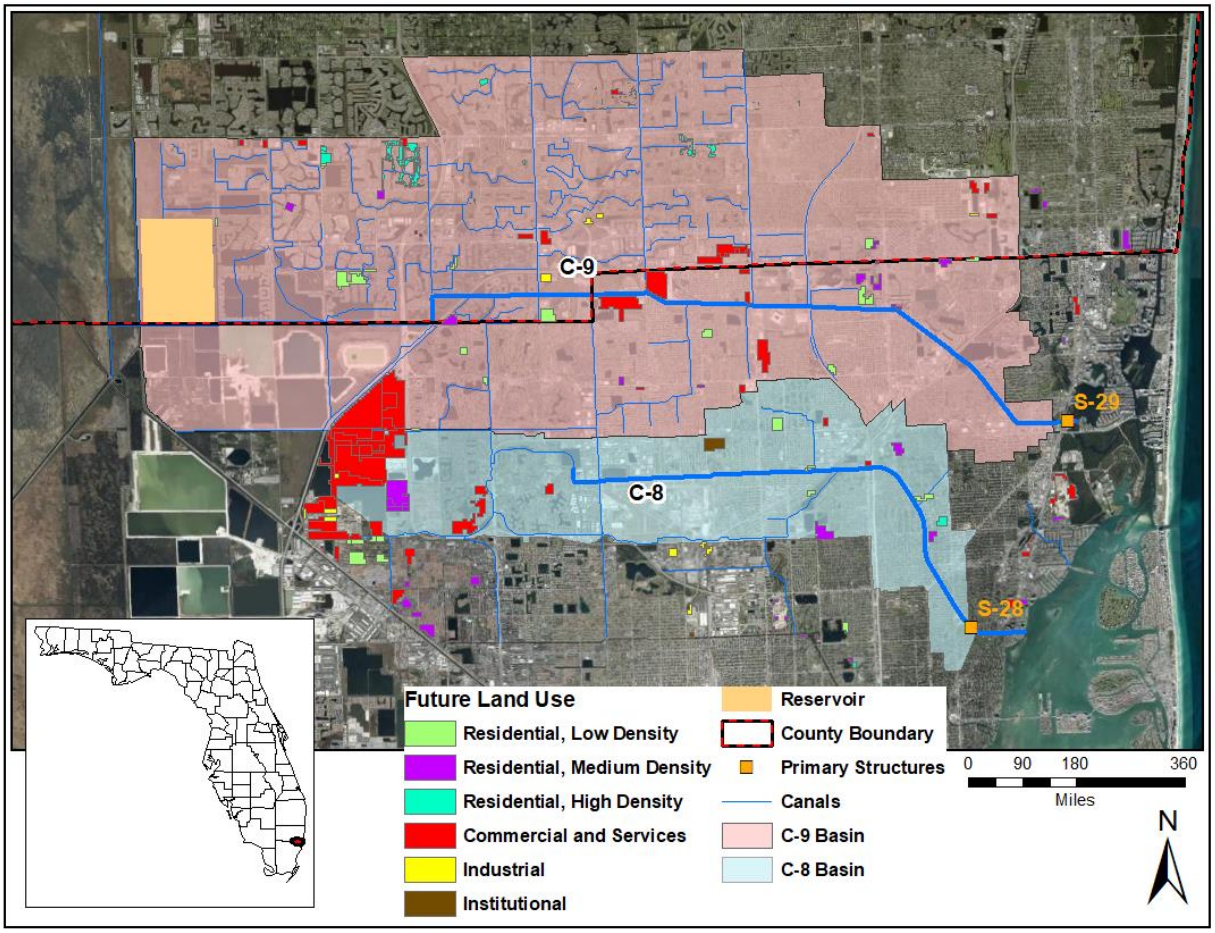

Figure 9.2-1: Areas of Future Land Use Changes

9.3 Topography

The land surface elevation of the areas with future land use change were compared with the FEMA Base Flood Elevation (BFE) and increased where the current elevation is less than the BFE. For the larger areas with land use change that do not have storage explicitly modeled in the MIKE HYDRO model, a portion of the area was lowered to account for floodplain compensation. Many of the areas with land use change were only a small cluster of grid cells, in which case it was not feasible or necessary to lower any of the grid cells once raised to BFE. These areas were relatively small and widely spread throughout the model domain, so they should have negligible hydrologic impact. Also, detention storage in these areas was accounted for in the overland flow module as discussed in **Section 9.4.2**. For the area of the C-9 impoundment (discussed in **Section 9.5.1.2**), the topography was adjusted so that the levees were accounted for (19.5 ft NGVD29) and the elevation inside the impoundment was set to the average impoundment ground elevation (4.5 ft NGVD29), per the Army Corps Project Implementation Report (USACE, 2012).

9.4 Overland Flow

In the current conditions model, most of the parameters in the overland flow module within Broward County were spatially varied by land use, while other parameters were spatially varied by land use within ERP permitted areas. Within Miami-Dade County, most of the parameters were spatially varied by land use, while other parameters were spatially varied by land use within areas that are internally drained (e.g., via exfiltration trenches, French drains, etc.). For the areas of land use that were changed to represent future conditions, the associated parameterization changes to the overland flow layers were applied the same way as in the current conditions. Refer to Section 3.7 in the C8 C9 FPLOS by Existing Infrastructure for CSL Conditions Draft Report (Taylor Engineering, 6/17/2020) for the specific details regarding parameterization of the overland flow module. For the purposes of this study, the following assumptions are applied:

- Each of the areas identified as having land use change is an “ERP permitted area” and must comply with the stormwater quality ordinance of retaining the greater of the first 1 inch of rainfall or 2.5 inches over the impervious area.
- Within Broward County, the areas of land use change that are not considered Stormwater management category (SMC) 1 are considered SMC 3b (most conservative approach)
- Within Miami-Dade County, the areas of land use change have the same SMC classification as current conditions, such as internally drained or drains to branch
    - Undeveloped internally drained areas that are were developed still drain internally unless the drainage network was explicitly modeled in MIKE Hydro (such as the new Mega Mall)

A brief summary of the parameterization changes applied to the overland flow layers is provided in **Section 9.4.1** through **Section 9.4.3**.

9.4.1 Manning’s Number

The Manning’s roughness coefficient for the overland module was developed for the areas of land use change the same way as the current conditions model and was based on land use. Refer to Table 3-7 in the C8 C9 FPLOS by Existing Infrastructure for CSL Conditions Draft Report (Taylor Engineering, 6/17/2020) for the Manning’s roughness coefficients based on land use by FLUCCS codes.

9.4.2 Detention Storage

The areas identified for land use change were assigned detention storage based on the new land use type. For the areas of land use change that were in areas directly controlled by operable structures represented in the model, no additional change to detention storage was made. For the areas of land use change that were not in areas directly controlled by operable structures, the detention storage was increased based on the assumption that all areas of future development will require an ERP. Therefore, detention storage in these areas of land use was increased the same way as in ERP areas (and internally drained areas within Miami-Dade County) in the current conditions model. This involved multiplying the paved area runoff coefficient (represents DCIA) by 2.5 inches and any of the resulting values which were less than 1” were increased to 1”.

9.4.3 Paved Area Runoff Coefficient

The areas identified for land use change were assigned a paved area runoff coefficient based on the new land use type. For the areas of land use change that were in areas directly controlled by operable structures, no additional change to the paved area runoff coefficient was made. For the areas of land use change that were not in areas directly controlled by operable structures, the paved area runoff coefficient was decreased based on the assumption that all areas of future development will require an ERP. Therefore, paved area runoff coefficients in these areas of land use were decreased the same way as in ERP areas (and internally drained areas within Miami-Dade County) in the current conditions study, which was to reduce the values by half. Refer to Table 3-7 in the C8 C9 FPLOS by Existing Infrastructure for CSL Conditions Draft Report (Taylor Engineering, 6/17/2020) for the runoff coefficients based on land use by FLUCCS codes.

9.5 Rivers and Lakes (1D Model)

9.5.1 1D Model Configuration Updates

In the future conditions model, two major changes to the 1D network were made, which are (1) explicitly representing the discharge from the two largest areas of land use change and (2) including the C-9 Impoundment. Although these two major changes are explicitly represented in the model, the specific details regarding the implementation are conceptual. These updates are discussed in **Section 9.5.1.1** and **Section 9.5.1.2**.

9.5.1.1 Areas of Land Use Change

Based on the identified areas of land use change, it was decided that only the two largest areas would be explicitly modeled in the 1D network. **Figure 9.5-1** shows the location of the two largest land use change areas.

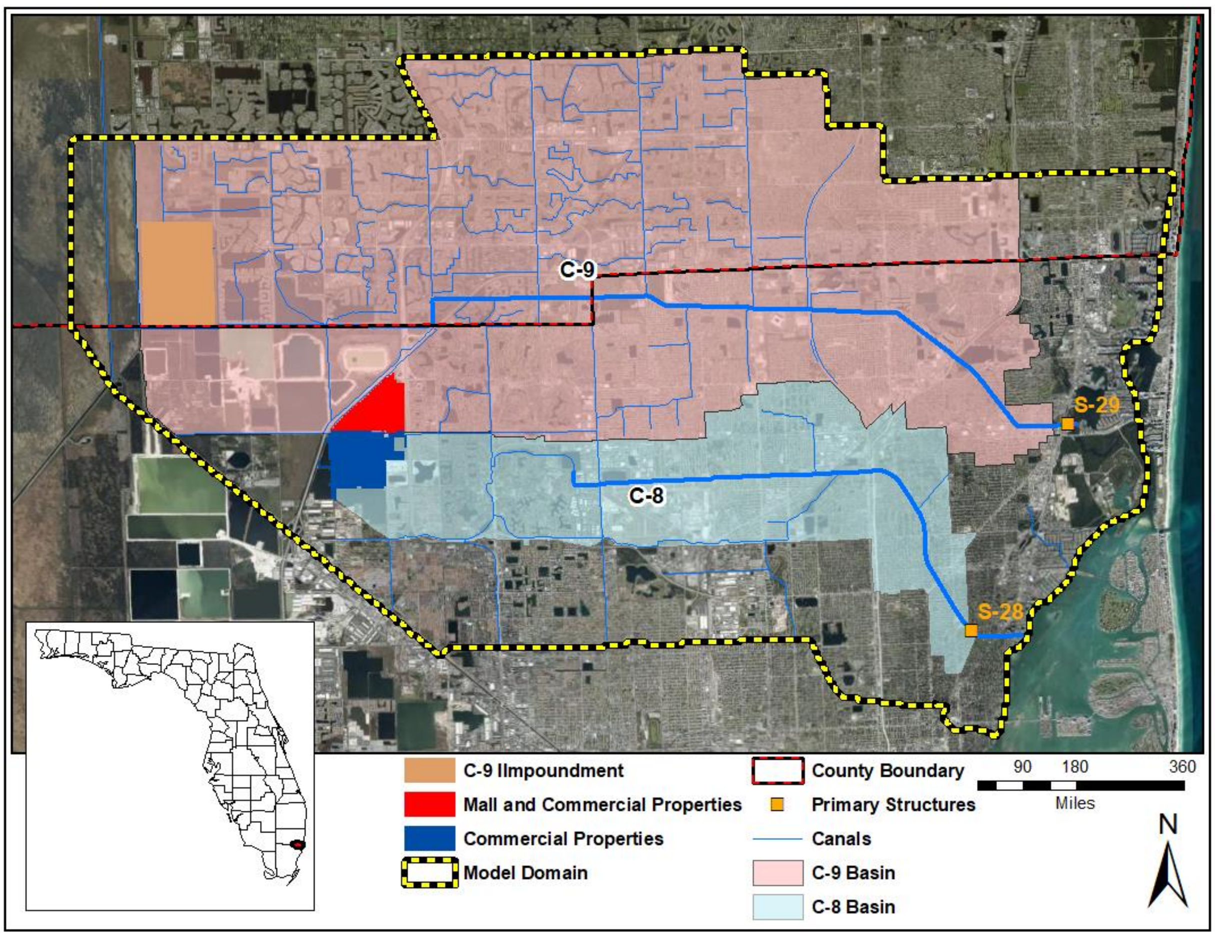

Figure 9.5-1: Areas of Land Use Change with Explicit MIKE HYDRO Changes

The first location (shown in red) is where the American Dream Miami Mall ("Mega Mall") and other commercial properties will be located. The second location (shown in blue) will be developed into other commercial properties. For these two locations, a conceptual MIKE HYDRO branch has been added to represent storage and to control discharge. To control the discharge, a pump that is limited to the District's CSM allowance is proposed. Although peak discharge from a developed property should not be greater than predeveloped conditions, these two areas are internally drained under current conditions. To be conservative, Taylor Engineering represented these two areas as being controlled by a pump that limits the total discharge to the District's allowance, with the assumption that in future conditions these properties will have a positive outfall and ultimately drain to the C-9 Canal (area in red) and C-8 Canal (area in blue). Areas draining to the C-9 Canal have an allowance of 20 CSM pumped. There is currently no set allowance for areas draining to the C-8 Canal. For the purposes of this study, Taylor used the same discharge allowance for the area draining to the C-8 Canal as the area draining to the C-9 Canal. The pumps have an "on" elevation equal to 1 ft above the control elevation, which was set at 0.5 feet below the existing property grade (Ref: 40E-41.063 F.A.C., Conditions for Issuance of Permits in the Western Canal 9 Basin). For the mall and commercial properties segment, the control elevation was 3.2 ft NGVD29 and the pump "on" elevation was set to 4.2 ft NGVD29. For the commercial properties segment, the control elevation was 3.4 ft NGVD29 and the pump "on" elevation was set to 4.4 ft NGVD29. The mall and commercial properties pump follows the same operating criteria as the pump stations in western South Broward Drainage District, which requires the pump to turn off when water levels in the C-9 Canal reach an elevation of 6.8 ft NGVD29. Based on the 20 CSM allowance, the mall and commercial properties segment draining to the C-9 Canal has a discharge limit of 17.9 cfs and the commercial properties segment draining to the C-8 Canal has a discharge limit of 11.25 cfs.

The conceptual branches/lakes have an area equal to 20% of the property segment. The two large property segments were conceptually broken down into five categories for the purposes of determining the available storage. Each property was considered to have 20% lake, 20% parking, 10% road, 5% open space (10% by net area; total area minus lake, parking, and road) and 45% area available for development. Conceptually, the parking areas were assumed to be built on top of stormwater detention vaults at average topography elevation and are responsible for capturing the required runoff from the parking areas. The open space topography elevation was lowered to the average groundwater elevation.

For the mall and commercial properties segment, the average topography elevation was 3.7 ft NGVD29 and the average current condition groundwater elevation was 2.9 ft NGVD29. This provided 0.8 ac-ft of storage per acre of land that was converted to lake, parking area, and open space. For the commercial properties segment, the average topography elevation was 3.9 ft NGVD29 and the average current conditions groundwater elevation was 2.9 ft NGVD29. This provided 1 ac-ft of storage per acre of land that was converted to lake, parking area, and open space.

The amount of additional storage provided by the lake, under the parking areas, and in the open space was calculated by multiplying the area by the difference between the average topography elevation and average groundwater elevation. This storage volume (ac-ft) was divided by the difference between the FEMA BFE elevation and the average topography elevation, which resulted in the amount of land area (ac) that could be increased to the FEMA BFE. For the mall and commercial properties area draining to the C-9 Canal, only about 60 acres of the developed land could be raised to the FEMA BFE. For the commercial properties area draining to the C-8 Canal, about 120 acres of the developed land could be raised to the FEMA BFE. As this land segment was originally internally drained and draining to one of the nearby major lakes, it was assumed that part of the property would still drain internally in the future. With a large part of this property now being drained to the C-8 Canal, there is a reduced load on the lakes that were originally being drained to. Therefore, it was assumed that the remainder of the property segment lower than the FEMA BFE (about 50 acres) could be raised to the FEMA BFE without the need for additional compensation.

9.5.1.2 C-9 Impoundment

The C-9 Impoundment is a project being designed with the intentions of capturing excess storm water. This will reduce the amount of water pumped to the water conservation areas and lost to tide and sometimes reduce water levels in the C-9 Canal. This project has the ability to reduce peak flood stages during major storms by pumping water from the C-9 Canal into an above-ground storage reservoir. The C-11 Impoundment is intended to operate the same way in the C-11 basin. These two projects are being designed to operate together in the future. The C-11 Impoundment project will have the ability to transfer water into the C-9 Impoundment, both for water management and for storm water control. However, the C-9 Impoundment project will only be able to "capture available storm runoff in the C-9 West Basin ***or*** to lift discharges from the C-11 West Basin (released from the C-11 Impoundment) to the C-9 Impoundment" (Burns & McDonnell, 2006). Therefore, it seems that during a major storm event, the two impoundments would operate independently, as the C-9 Impoundment will be pumping stormwater runoff from the C-9 basin. However, it is possible that the C-11 Impoundment could need to divert water to the C-9 Impoundment during a major storm. Instead of speculating on how to explicitly represent the interaction between the two projects, Taylor Engineering did not explicitly represent inter-impoundment transfer in the future conditions model and instead represented it by limiting how long the C-9 Impoundment accepts water from the C-9 Basin.

The C-11 Impoundment project is planned to have a storage capacity of 4,592 ac-ft and a pumping rate of 1,050 cfs and the C-9 impoundment project is planned to have a storage capacity of 7,056 ac-ft and a pumping rate of 1,000 cfs (USACE, 2012). Therefore, if starting empty, the C-11 Impoundment could receive water at the maximum allowed rate for 53 hours and the C-9 Impoundment could receive water at the maximum allowed rate for about 85 hours. To simulate a reasonable worst case scenario, Taylor Engineering assumed that both impoundments start at 50% capacity and that once full, the C-11 Impoundment diverts water to the C-9 Impoundment, at which point the C-9 Impoundment could no longer pump water from the C-9 basin. To eliminate the need to explicitly model the transfer of water from the C-11 Impoundment, Taylor Engineering implemented the following approach:

- Start the C-9 Impoundment at 50% capacity and assume the C-11 Impoundment is at 50% capacity (this means the C-11 could receive water for 26.5 hours before it is full)
- Allow the C-9 Impoundment to start receiving water from C-9 Canal when the water level in the western portion of the C-9 Canal reaches 3.5 ft NGVD29 (Burns & McDonnell, 2006)
- Stop the C-9 Impoundment from receiving water from C-9 Canal after 26.5 hours of pumping at 1000 cfs (or equivalent volume) (assumes the C-9 and C-11 Impoundments would be pumping at the same time) (C-11 Impoundment full after 26.5 hours when starting at 50% capacity)
    - The remaining volume is conceptual storage available for the water transfer from the C-11 Impoundment

This is a very simple and efficient way to represent the C-9 Impoundment in a worst case scenario, where it exists in future conditions but cannot be fully utilized. The explicit representation of water seepage from the C-9 Impoundment is not required as it can be assumed that any seepage that results from higher stages in the impoundment is captured and returned. Within MIKE HYDRO and MIKE SHE, the C-9

Impoundment components will be represented with low leakage coefficients. By setting the canal and overland leakage coefficients to low values, the seepage collection and return system can be left out as it is being conceptually represented by reducing or eliminating any seepage from occurring within the C-9 Impoundment area. As "The Savings Clause requires assurance that no negative impact will occur to existing levels of flood protection and is demonstrated in project design" (USACE, 2012), it can be assumed that the design of the Impoundment will have little to no negative impact, and reducing or eliminating the leakage is the simplest way to represent this complex system.

Sensitivity tests were conducted for the 10-year 1 ft sea level rise and 100-year 2 ft sea level rise scenarios, in which the C-9 Impoundment was represented as only having 50% storage capacity, as well as 100% full. These four simulations showed that the C-9 Impoundment having 50% storage capacity has negligible effects on the overall FPLOS in the C-9 Basin. Although the model results were more sensitive to the C-9 Impoundment for the 10-year 1 ft sea level rise scenario that it was for the 100-year 2 ft sea level rise scenario, the sensitivity was not large enough to warrant not simulating potential storage in the C-9 Impoundment. For the 10-year 1 ft sea level rise C-9 Impoundment sensitivity test, there was a 0.15 ft stage reduction at the western side of the C-9 Canal (where the impoundment is) (**Figure 9.5-2**), 0.0 ft stage reduction at S-29 (**Figure 9.5-3**), and a total discharge difference of 8% at S-29 (**Figure 9.5-4**).

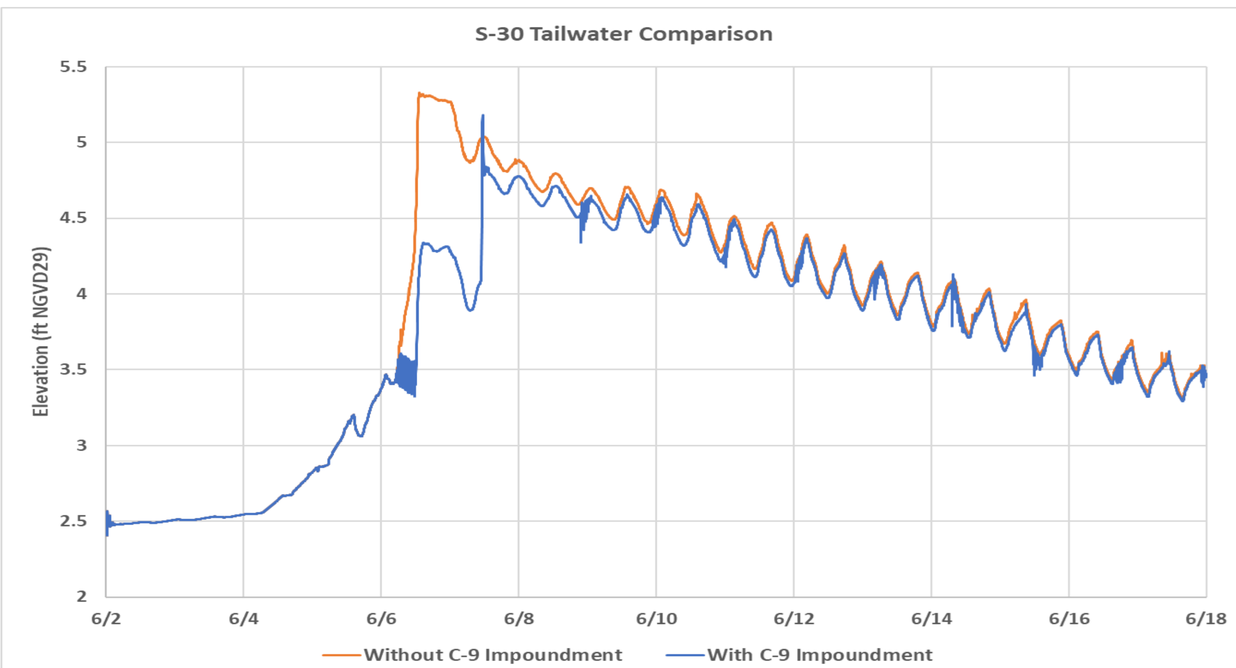

Figure 9.5-2: C-9 Impoundment Sensitivity Test for S-30 Tailwater During 10-Year Design Storm with 1 ft Sea Level Rise (with Impoundment= 50% Capacity)

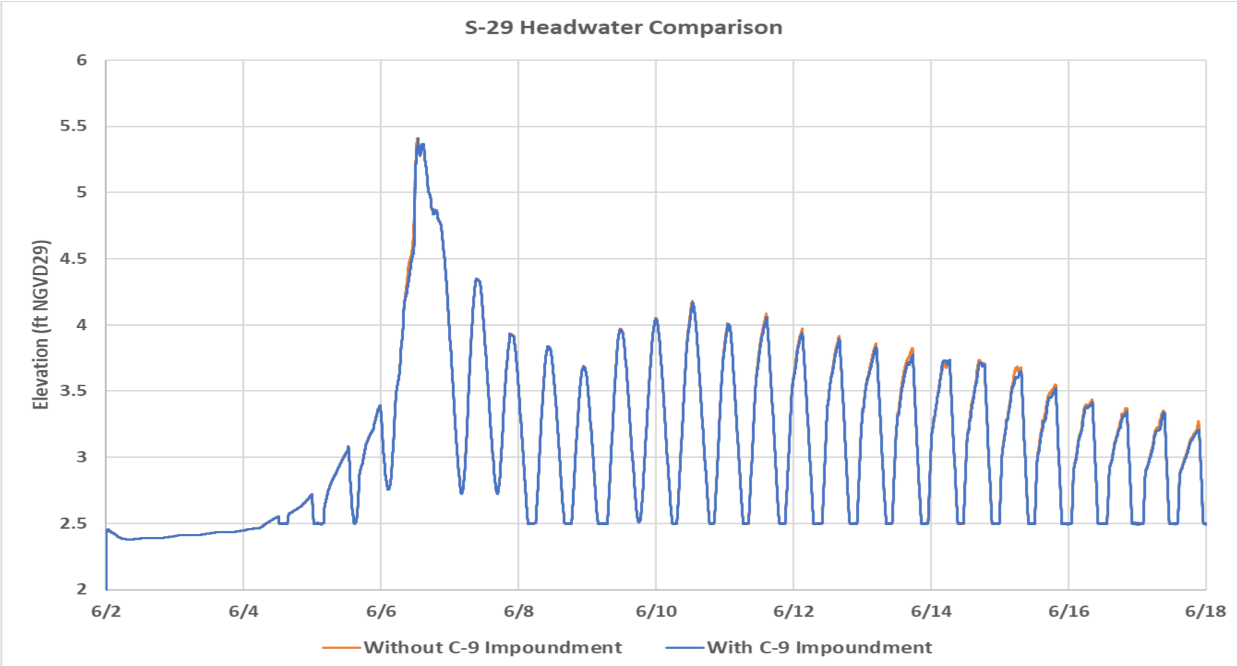

Figure 9.5-3: C-9 Impoundment Sensitivity Test for S-29 Headwater During 10-Year Design Storm with 1 ft Sea Level Rise (with Impoundment= 50% Capacity)

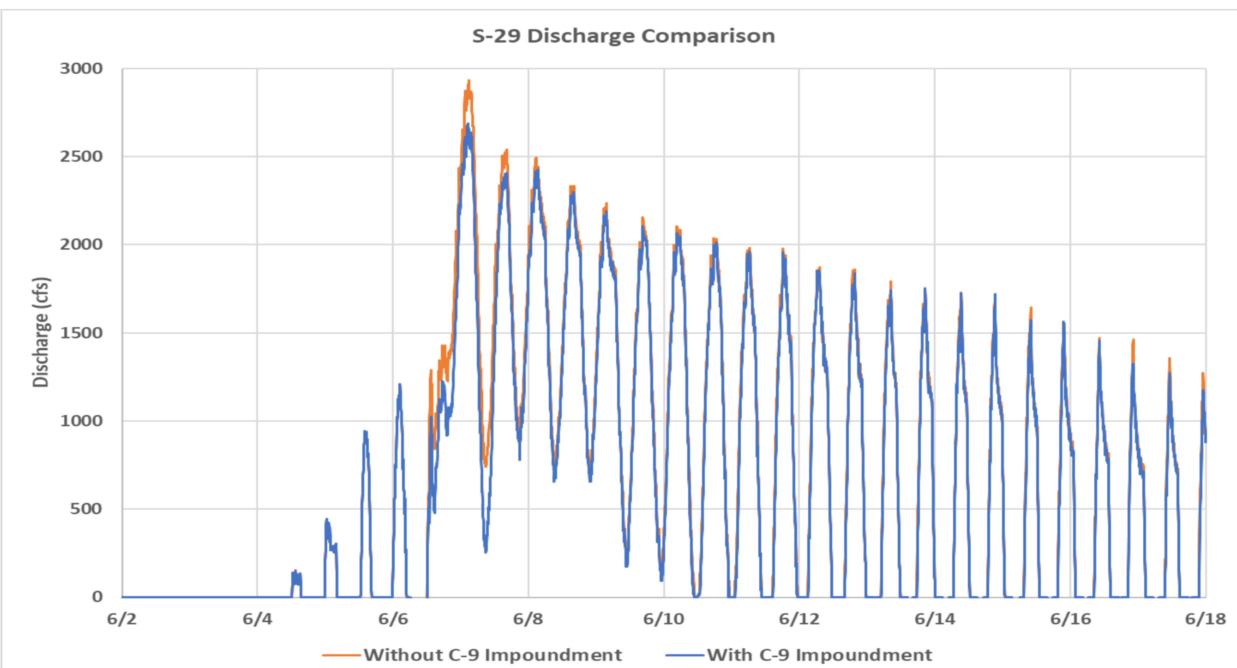

Figure 9.5-4: C-9 Impoundment Sensitivity Test for S-29 Discharge During 10-Year Design Storm with 1 ft Sea Level Rise (with Impoundment= 50% Capacity)

Comparatively, the 100-year 2 ft sea level rise scenario only had a 0.06 ft stage reduction at the western side of the C-9 Canal (**Figure 9.5-5**), 0.03 ft stage reduction at S-29 (**Figure 9.5-6**), and 1% total discharge difference at S-29 (**Figure 9.5-7**).

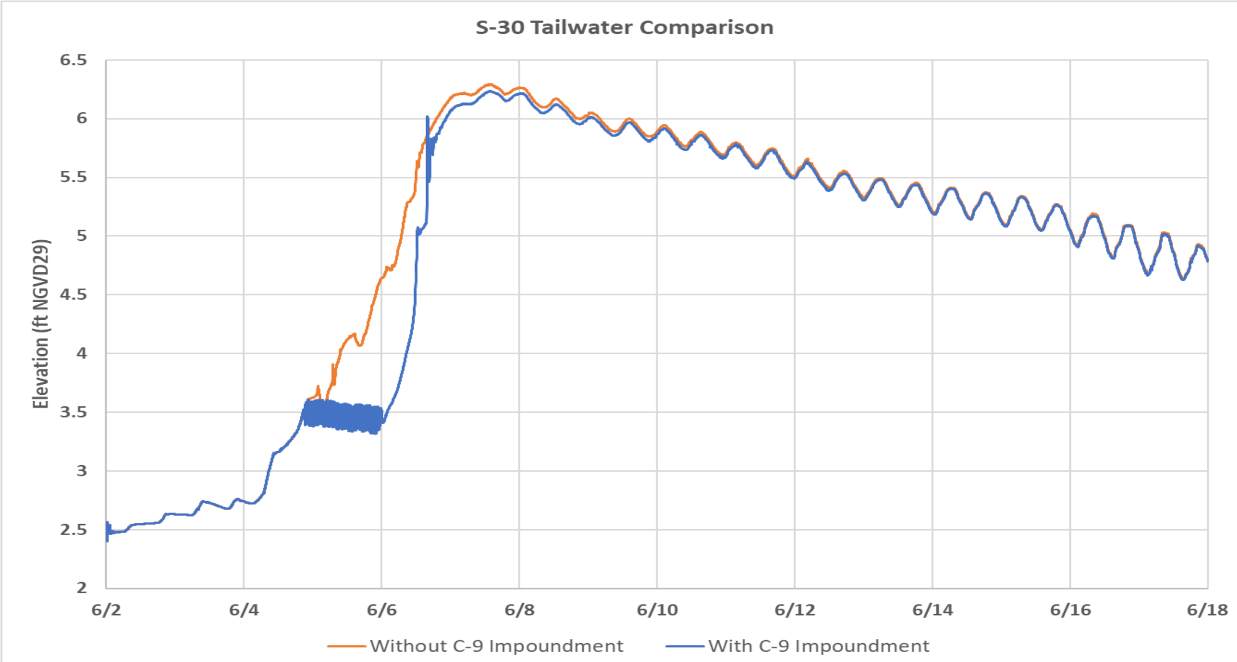

Figure 9.5-5: C-9 Impoundment Sensitivity Test for S-30 Tailwater During 100-Year Design Storm with 2 ft Sea Level Rise (with Impoundment= 50% Capacity)

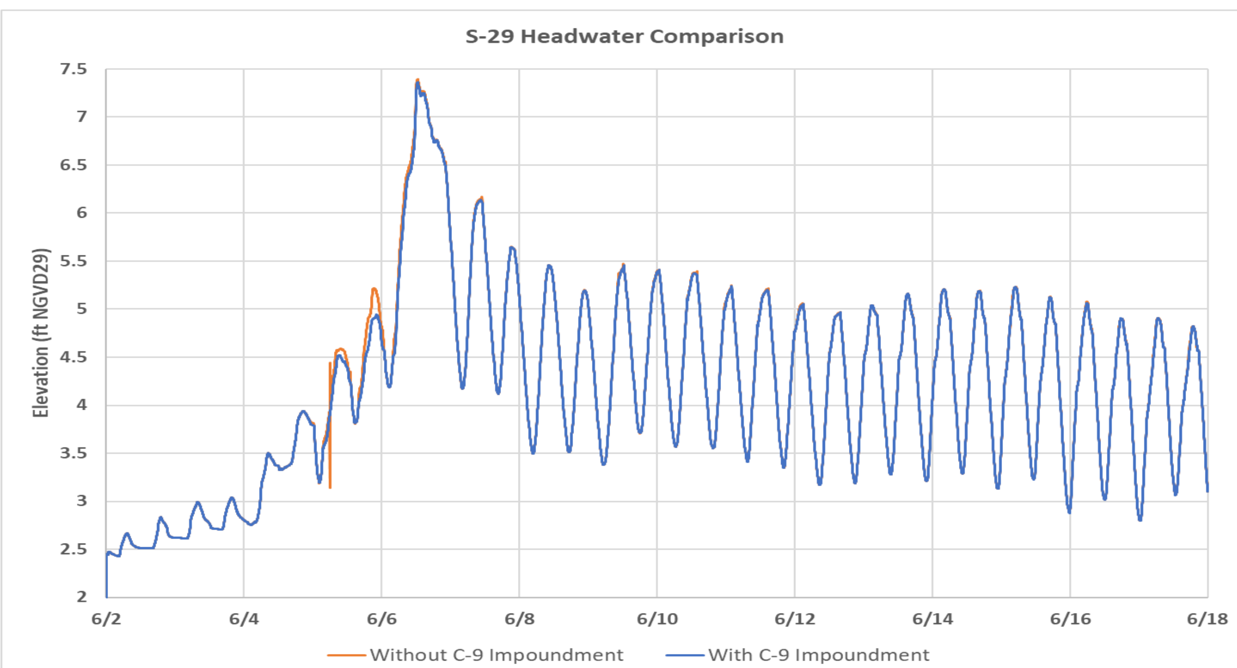

Figure 9.5-6: C-9 Impoundment Sensitivity Test for S-29 Headwater During 100-Year Design Storm with 2 ft Sea Level Rise (with Impoundment= 50% Capacity)

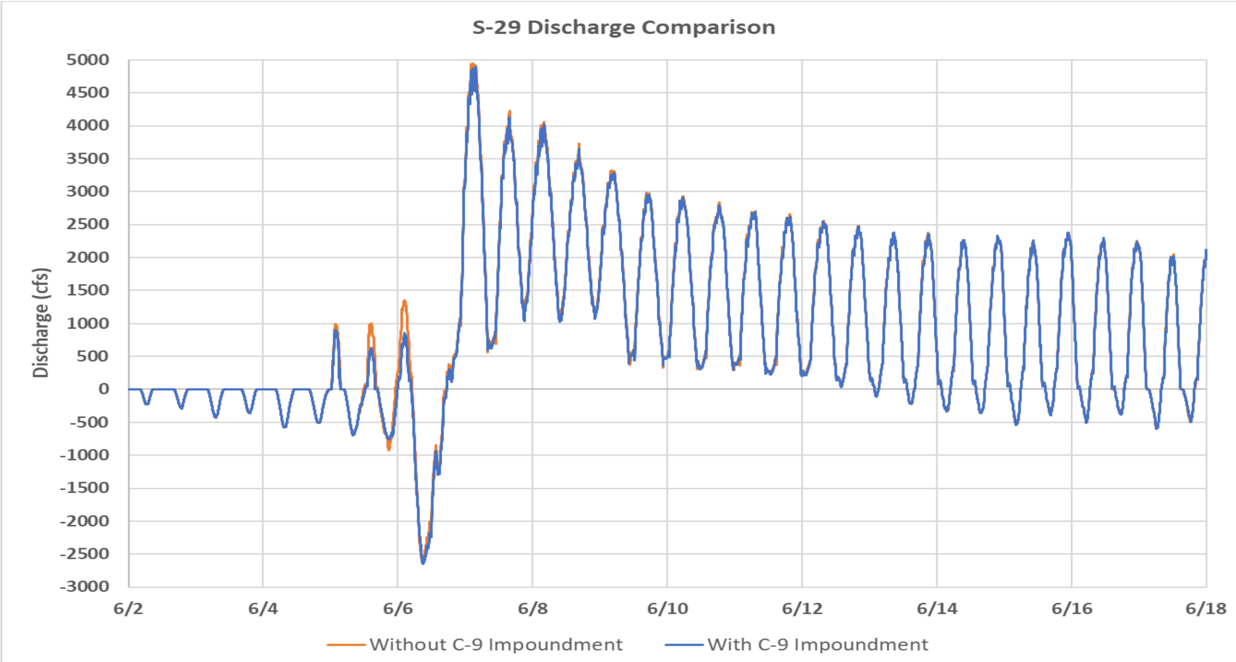

Figure 9.5-7: C-9 Impoundment Sensitivity Test for S-29 Discharge During 100-Year Design Storm with 2 ft Sea Level Rise (with Impoundment= 50% Capacity)

After analyzing the results of these sensitivity tests, Taylor Engineering suggested to keep the original recommendation of starting the C-9 Impoundment with 50% capacity, and the District agreed.

Comparatively, the 100-year 2 ft sea level rise scenario only had a 0.06 ft stage reduction at the western side of the C-9 Canal, 0.03 ft stage reduction at S-29, and 1% total discharge difference at S-29. After analyzing the results of these sensitivity tests, Taylor Engineering suggested to keep the original recommendation of starting the C-9 Impoundment with 50% capacity, and the District agreed.

9.5.2 Boundary Conditions (1D Model)

The 1-D tidal boundaries (forced tailwater at tidal structures) used the SFWMD-provided design storm surge stage hydrographs. These are the same hydrographs from the current condition design storms, but increased by 1, 2, and 3 ft to represent various sea level rise scenarios. The design storm tidal boundaries for the future seal level rise scenarios are shown in **Figure 9.5-8** through **Figure 9.5-15**.

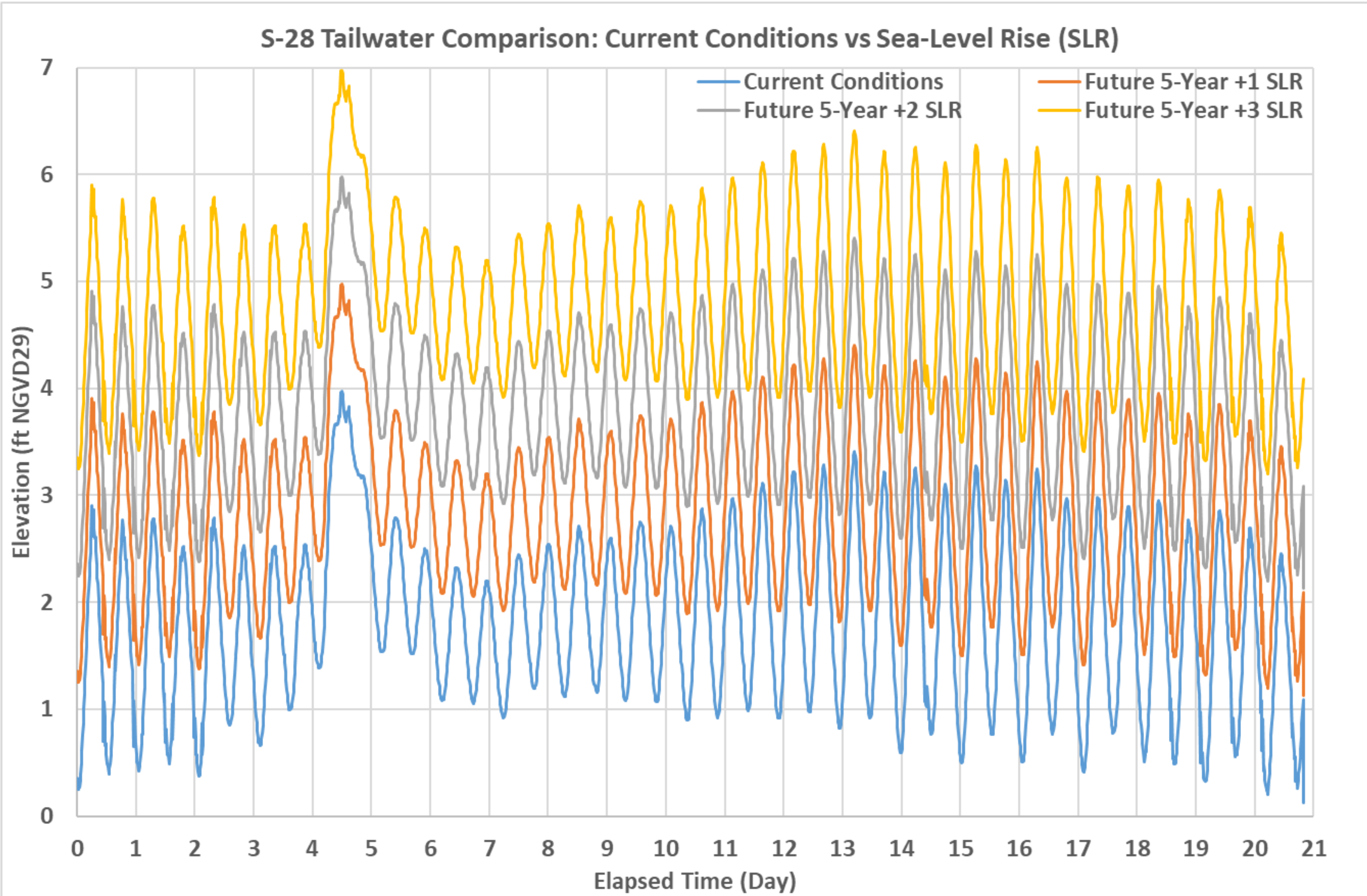

Figure 9.5-8: Future Conditions Sea Level Rise 5-Year Design Storm Tidal Boundary Stages for S-28

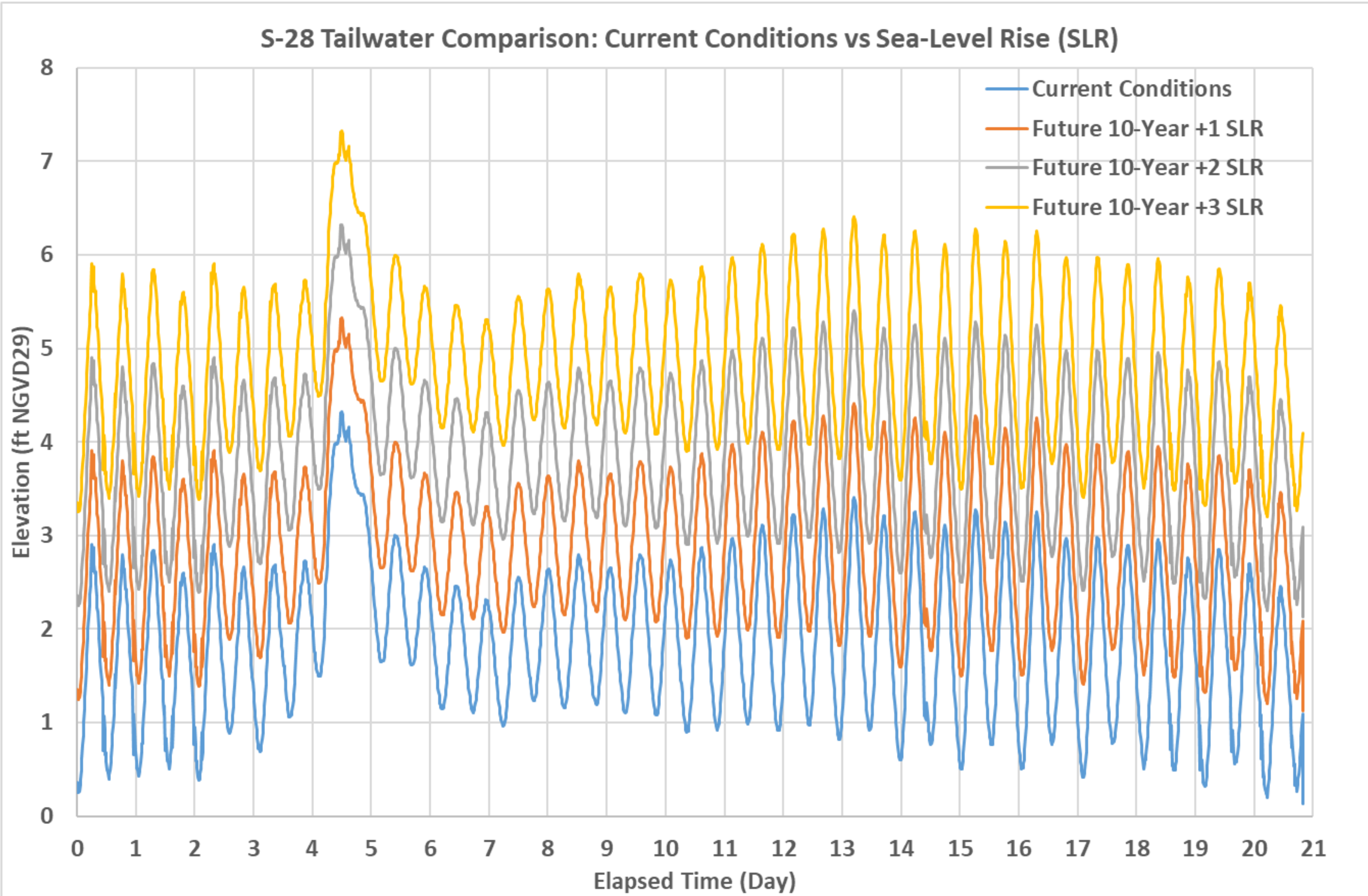

Figure 9.5-9: Future Conditions Sea Level Rise 10-Year Design Storm Tidal Boundary Stages for S-28

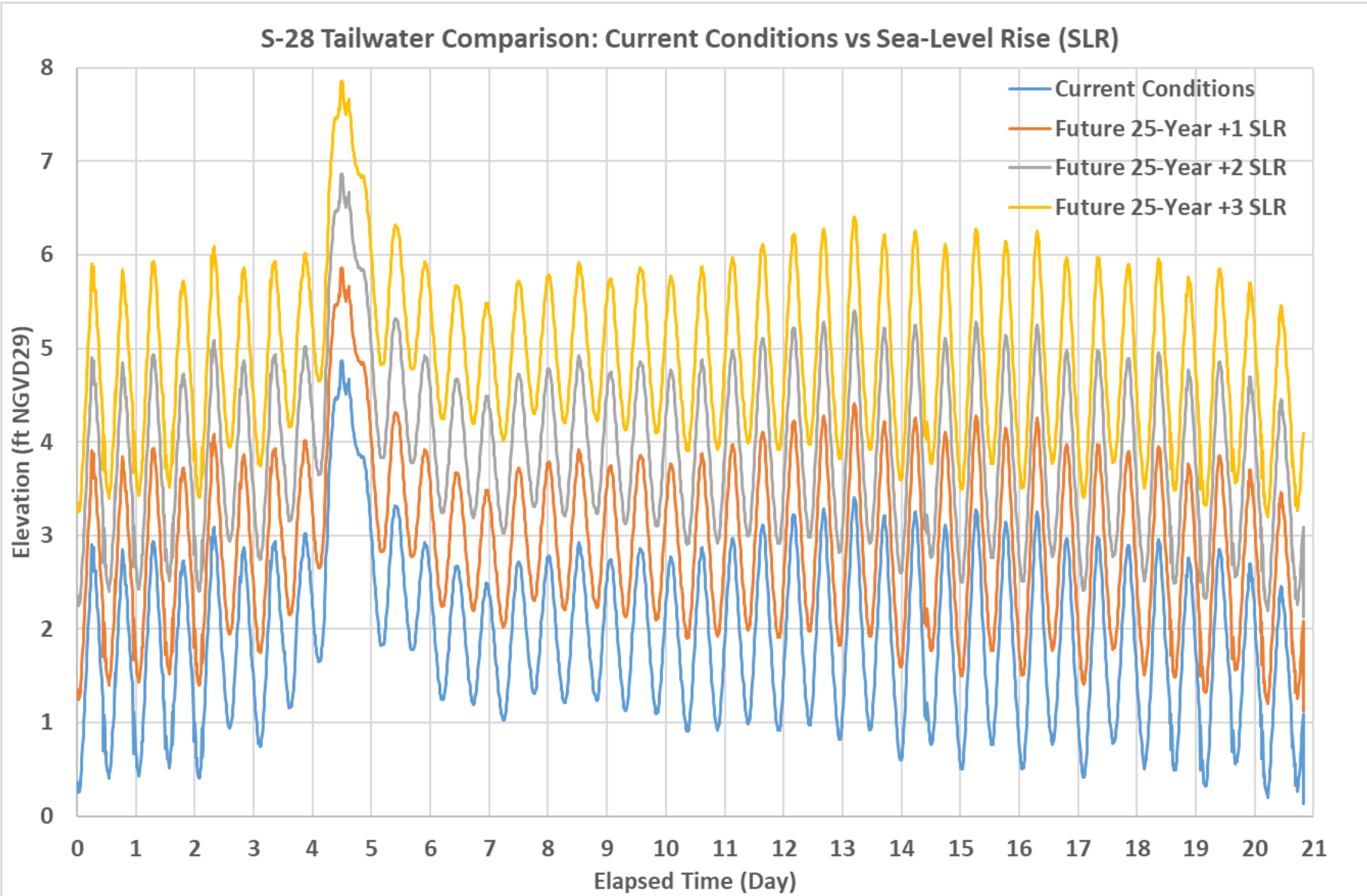

Figure 9.5-10: Future Conditions Sea Level Rise 25-Year Design Storm Tidal Boundary Stages for S-28

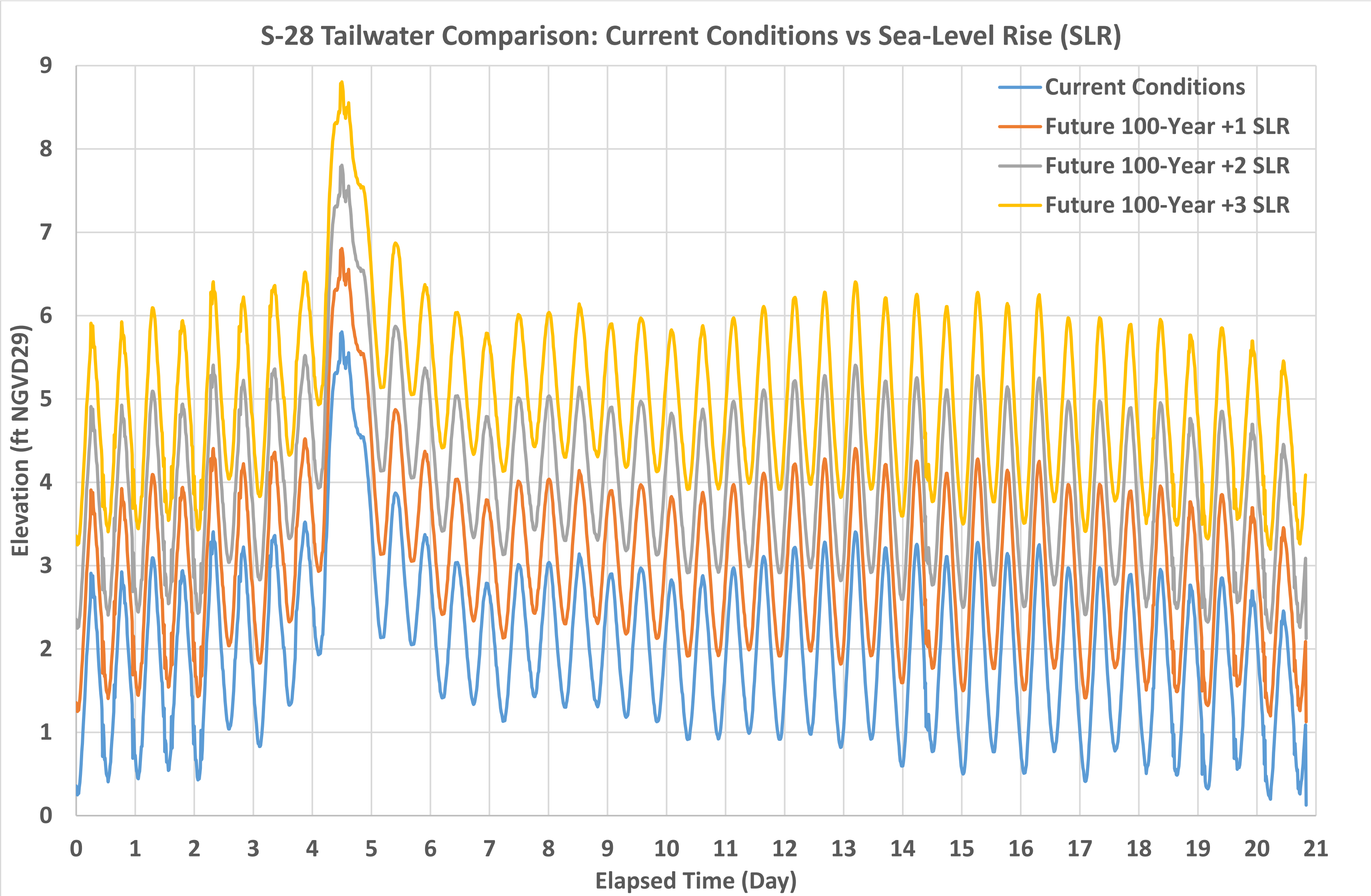

Figure 9.5-11: Future Conditions Sea Level Rise 100-Year Design Storm Tidal Boundary Stages for S-28

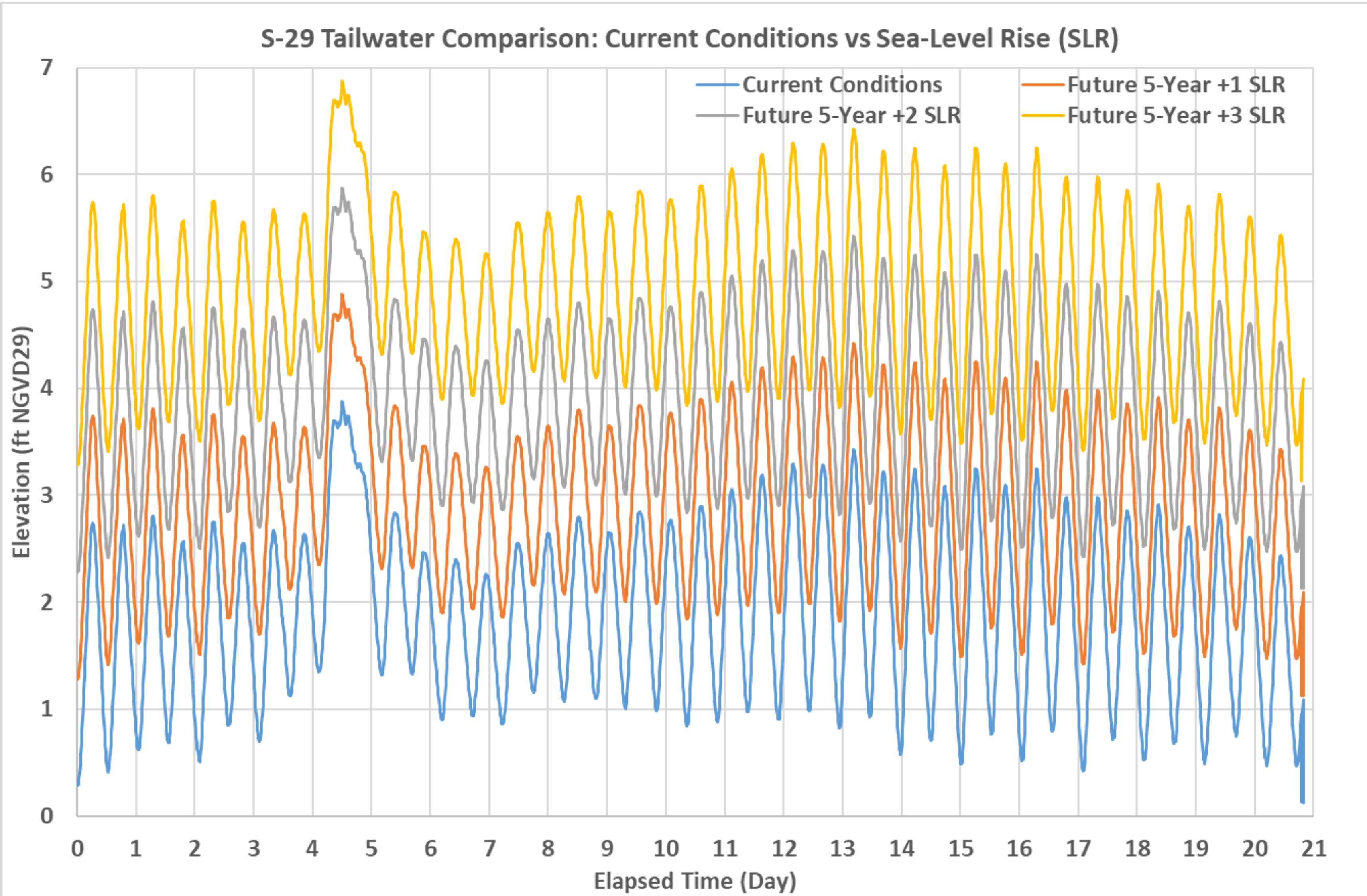

Figure 9.5-12: Future Conditions Sea Level Rise 5-Year Design Storm Tidal Boundary Stages for S-29

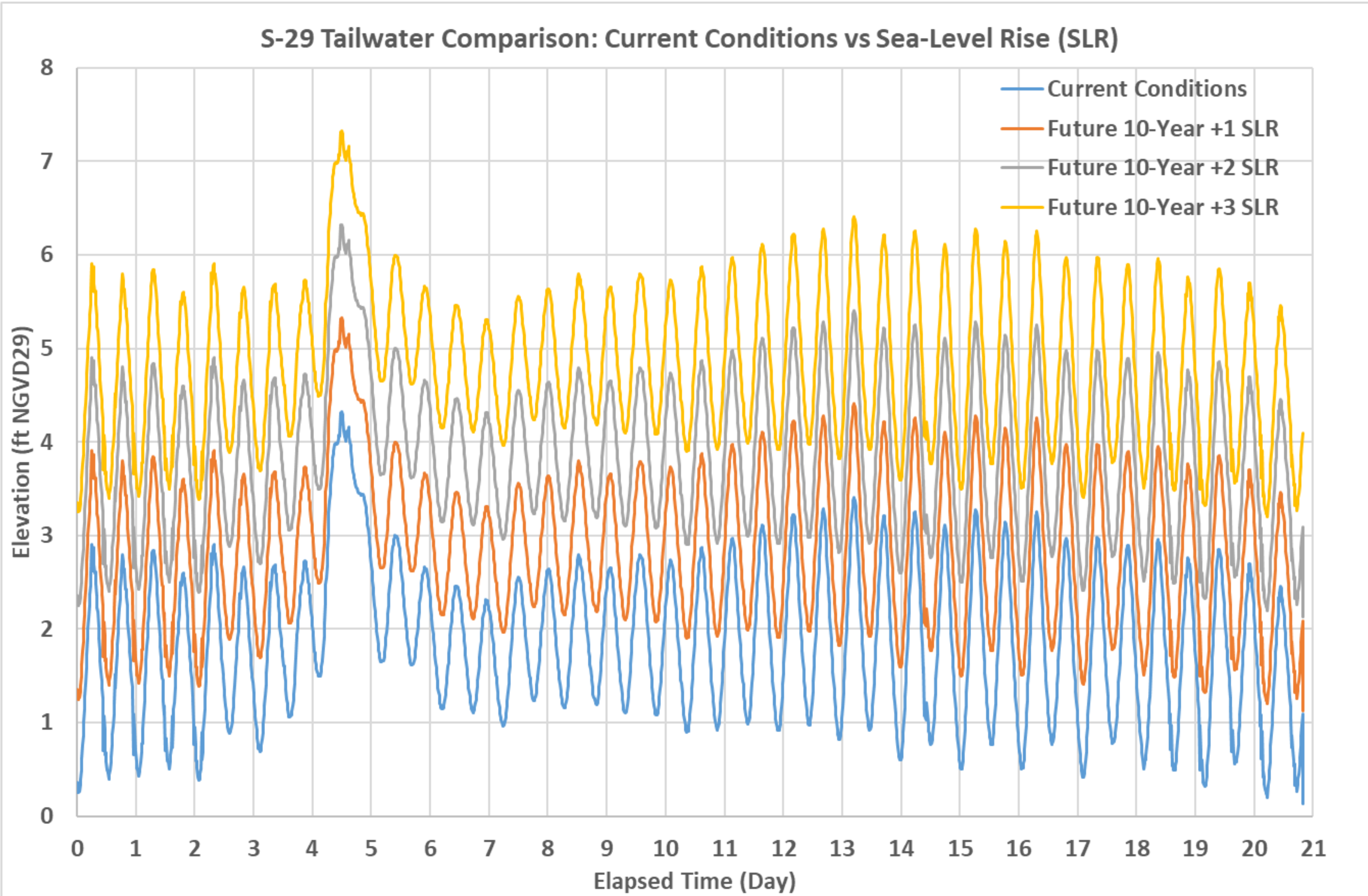

Figure 9.5-13: Future Conditions Sea Level Rise 10-Year Design Storm Tidal Boundary Stages for S-29

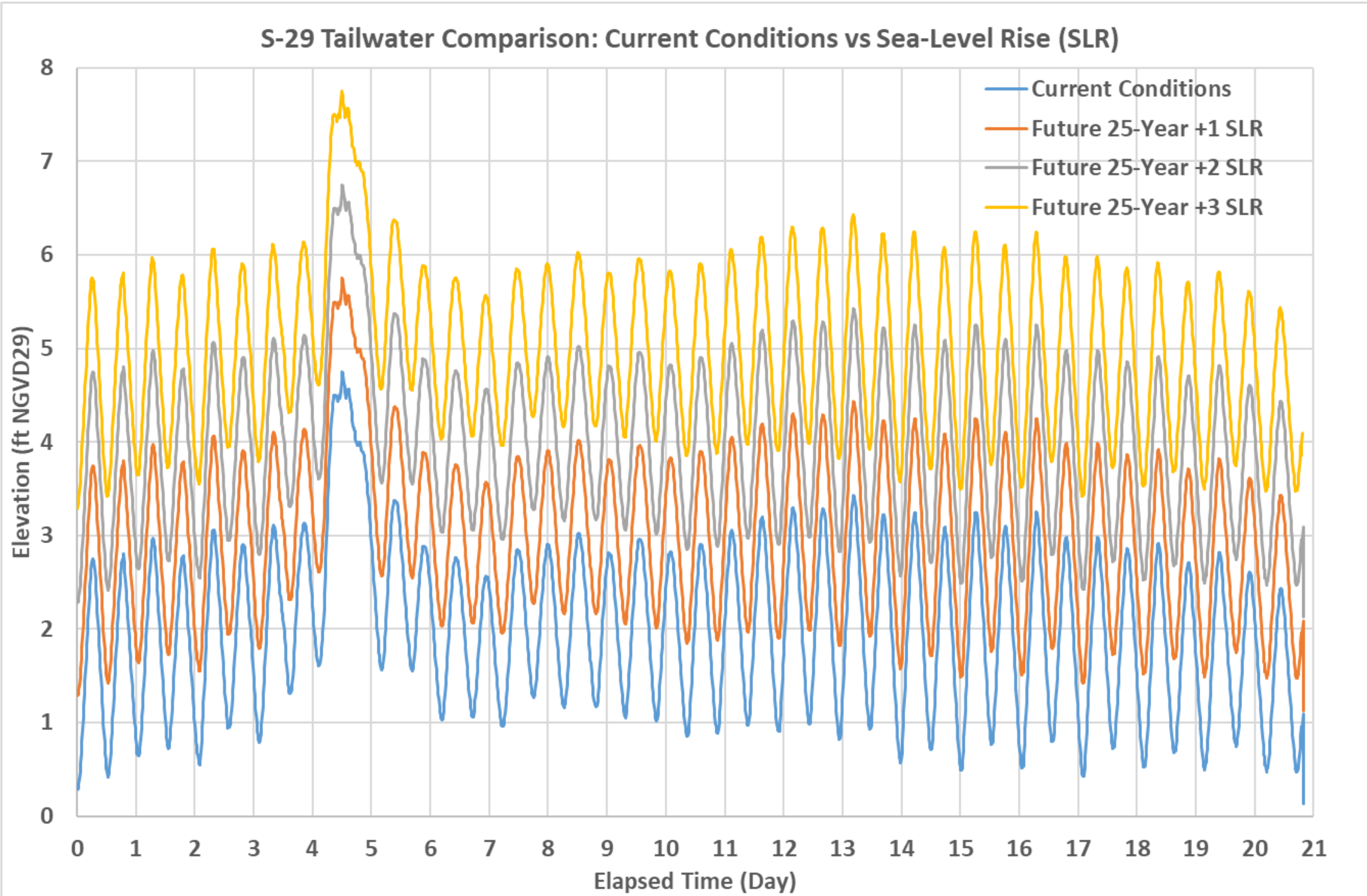

Figure 9.5-14: Future Conditions Sea Level Rise 25-Year Design Storm Tidal Boundary Stages for S-29

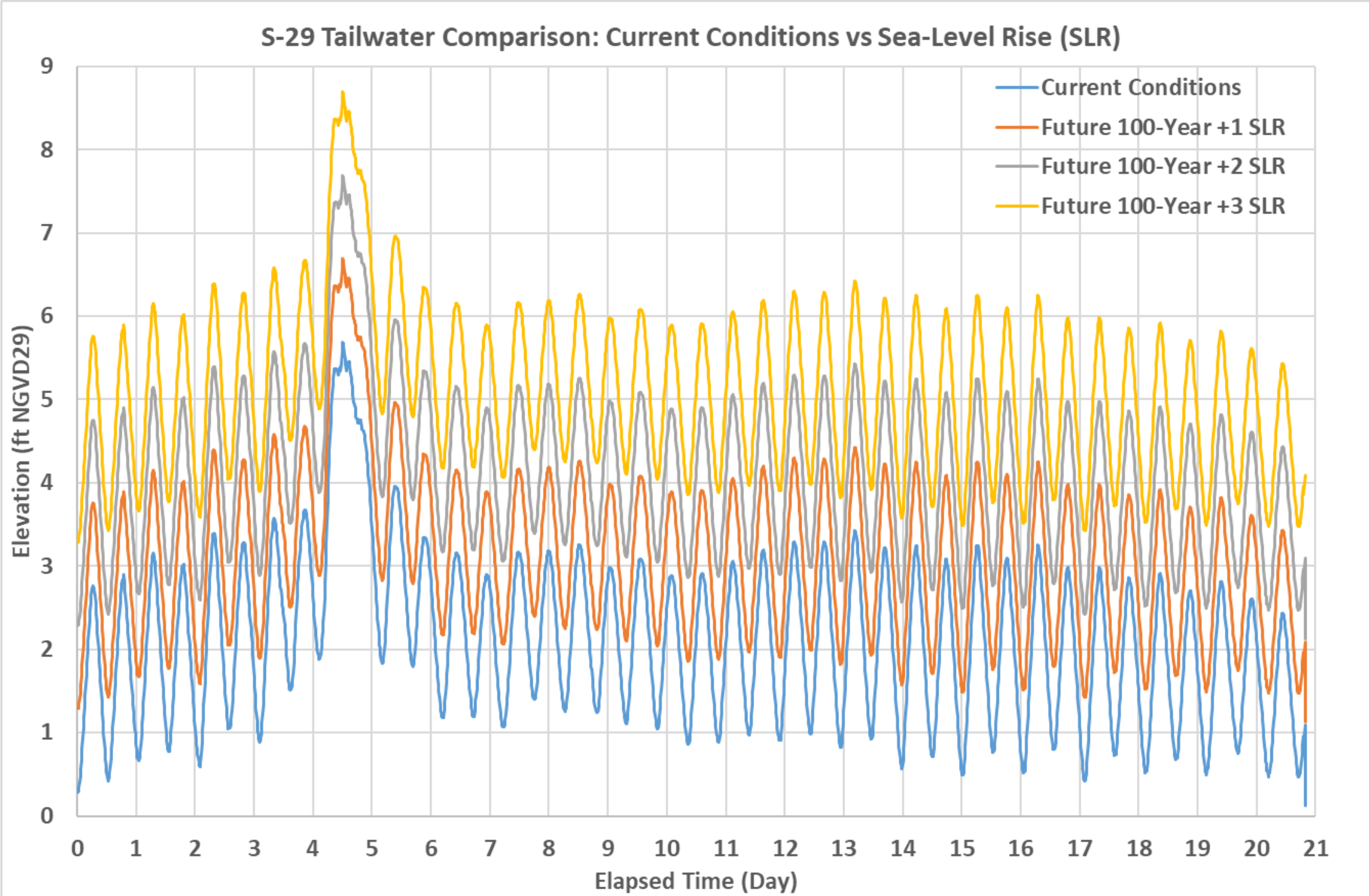

Figure 9.5-15: Future Conditions Sea Level Rise 100-Year Design Storm Tidal Boundary Stages for S-29

At the intercoastal waterway, water levels were forced based on the District-provided design storm surge stage time series data (**Figure 9.5-8** through **Figure 9.5-15**). On the southeast side of the model, the forced water levels (based on S-27 headwater) at the downstream boundary of the 1-D branches connecting to the C-7 Canals were updated to represent future conditions. Taylor Engineering proposed two methods for updating S-27 headwater to reflect the future conditions; (1) adding 1, 2, and 3 feet to the current conditions headwater (District's XPSWMM model simulated data) level to reflect the three sea level rise conditions while ensuring pre/post storm headwater is never lower than the low tide tailwater, and (2) increasing the headwater level by a factor determined through regression analysis of simulated future condition headwater levels based on the District's XPSMM model.

9.5.2.1 S-27 Headwater- Method 1

This method of developing future conditions headwater levels for the S-27 structure simply adds 1, 2, and 3 feet to the current condition's hydrograph, which was provided by the District (assumptions had to be made about pre/post storm water levels). As previously stated, this approach assumes that the S-27 structure maintains the same headwater/tailwater relationship that was observed in the District's XPSWMM current condition models. Adding 1, 2, and 3 feet to the current condition's headwater is the same as applying the current conditions headwater/tailwater ratio to the future conditions storm surge tailwater that includes 1, 2, and 3 feet of sea level rise. Slight adjustment to the pre/post storm water levels were made so that they do not drop below the minimum low tide tailwater elevation. This was done as it is unrealistic for a tidal spillway structure's headwater elevation to drop below the low tide tailwater elevation unless mitigation measures (i.e., a pump station) were to be implemented. An example of the proposed boundary condition hydrographs resulting from this method are shown in **Figure 9.5-16**.

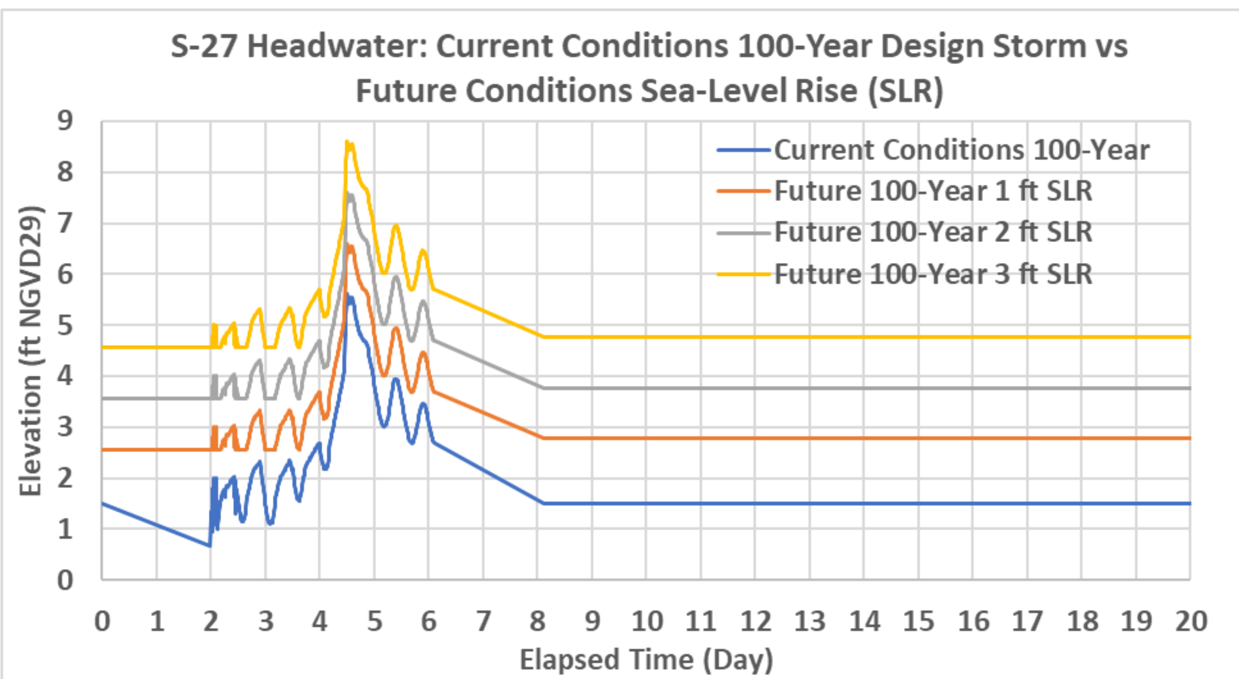

Figure 9.5-16: Example of S-27 Future Condition Headwater Stage Developed by Adding 1, 2, and 3 Feet to Current Conditions Stages

9.5.2.2 S-27 Headwater- Method 2

This method of developing future conditions headwater levels for the S-27 structure is based on a regression analysis of future conditions simulated data from the District's XPSWMM model. The District provided simulated future condition headwater levels for S-27 that for sea level rise scenarios of 0, 0.76, 1.09, and 2.21 feet, as shown in **Table 9-1**.

Table 9-1: SFWMD Future Conditions S-27 Peak Stage Under Various Sea Level Rise Conditions

Sea Level Rise in District's Future Conditions XPSWMM Model (ft)	Simulated Future Conditions Peak Water Level (ft NGVD29)
0 (base value)	5.941 (base value)
0.76	6.43
1.09	6.68
2.21	7.36

For this study, the sea level rise conditions are 1, 2, and 3 feet. Therefore, a regression analysis was conducted. The District's simulated future peak water levels were plotted against the amount of sea level rise and assigned the best-fitting trendline based on R^2 value, as shown in **Figure 9.5-17**.

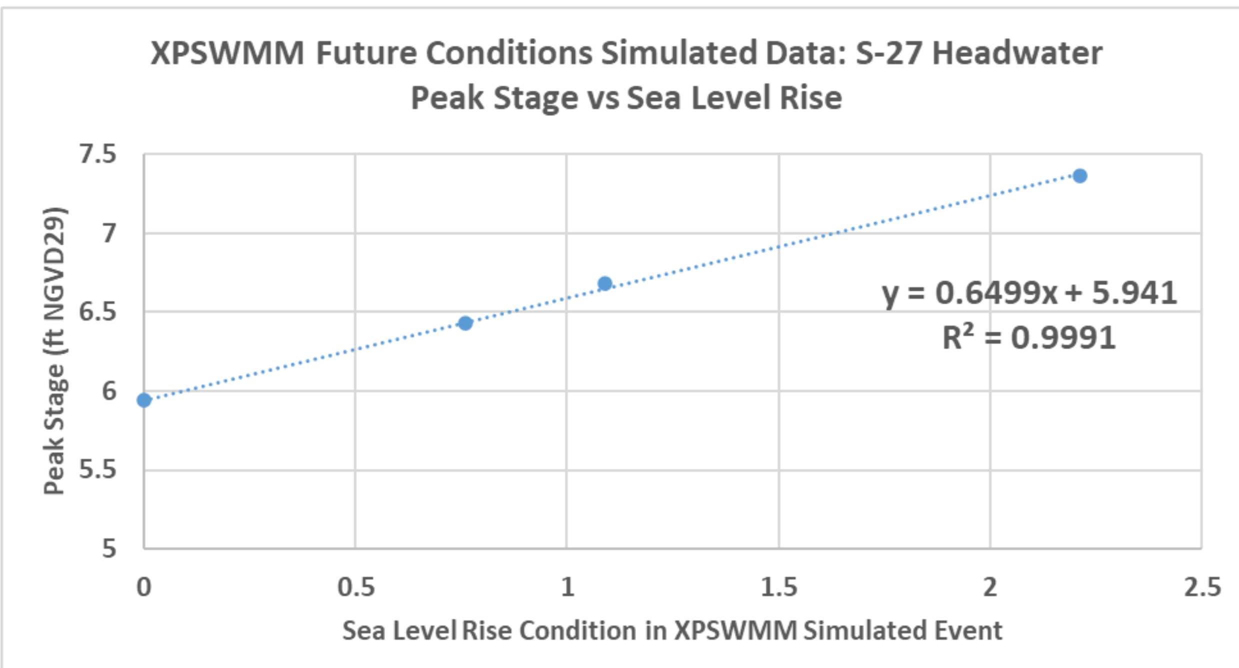

Figure 9.5-17: Regression Analysis of S-27 Future Conditions Headwater Stage vs Sea Level Rise

From the equation of the trendline, interpolated and extrapolated peak water levels for 1, 2, and 3 feet sea level rise were calculated. Then, a multiplication factor was calculated for each of the sea level rise conditions based on the simulated peak water level (peak water level with SLR divided by base peak water level), as shown in **Table 9-2**.

Table 9-2: Interpolated/Extrapolated Peak Water Levels from XPSWMM Future Conditions 100-Year Design Storm

Sea Level Rise Conditions (ft)	Interpolated/Extrapolated Peak Water Level based on XPSWMM Simulated Data (ft NGVD29)	Multiplication Factor
0 (base value)	5.94 (base value)	1.000
1	6.59	1.109
2	7.24	1.219
3	7.89	1.328

The multiplication factors shown in **Table 9-2** were multiplied with the current conditions' headwater hydrograph for S-27. The peak water levels for S-27 headwater for future conditions sea level rise scenarios of 1, 2, and 3 feet are shown in **Table 9-3**. The S-27 headwater hydrographs for future condition sea level rise scenarios are shown in **Figure 9.5-18**.

Table 9-3: Peak Water Levels for S-27 Headwater for Future Conditions 100-Year Design Storms

Sea Level Rise Conditions (ft)	Current Conditions Peak Water Level	Multiplication Factor	Future Conditions Peak Water Level (ft NGVD29)
1	5.61	1.109	6.22
2		1.219	6.84
3		1.328	7.45

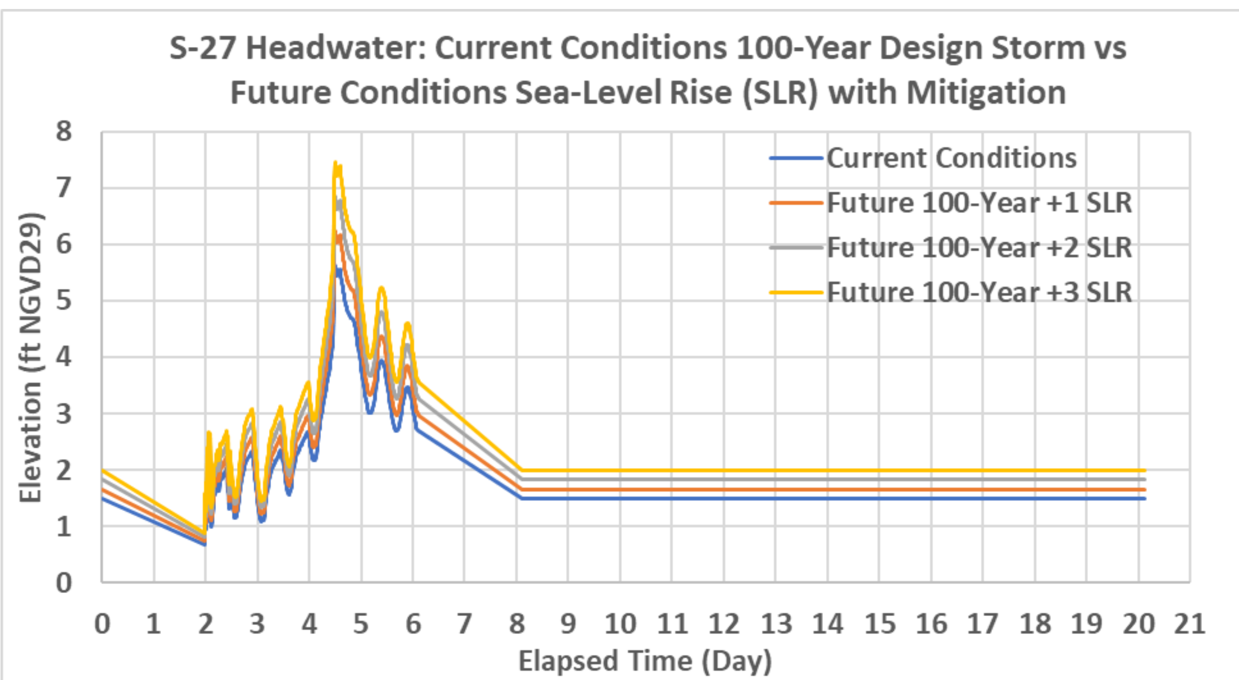

Figure 9.5-18: S-27 Future Conditions Headwater for 100-Year Design Storm Based on Regression Analysis of Future Conditions Simulated Data with Mitigation Measures

9.5.2.3 S-27 Headwater- Method Comparison and Sensitivity

The two methods of developing the S-27 headwater boundary represent different levels of conservativeness, with the higher boundary representing the most conservative scenario in terms of worst case flooding in the model. When this model was developed, the C-7 Canal was chosen as a boundary condition for two reasons: (1) There was observed data that was useful for calibrating/validating the model, and perhaps more importantly, (2) It was believed to be at a distance from the area of interest (C-8 basin/canal) such that any uncertainty in the boundary condition should have minimal effect on the outcome of the simulations. As there are two different levels of conservativeness that could be made for the future conditions water levels in the C-7 Canal, a sensitivity test was performed for the S-27 headwater boundary.

The sensitivity test was conducted using the current conditions model, with modified tailwater levels at S-28 and S-29 (to represent sea level rise) and the new headwater levels at S-27 headwater. The current conditions model was used so that the effects of the boundary condition could be determined without the effects of any other changes to the model such as land use and increased groundwater levels. Therefore, two model simulations were completed using the 100-year design storm with 3 ft of sea level rise. **Figure 9.5-19** shows the two S-27 headwater hydrographs and the respective tailwater hydrograph. The peak water level under the second method is about 1.2 ft lower than the more conservative approach of applying the current conditions headwater/tailwater ratio to the 3 ft storm surge tailwater hydrograph.

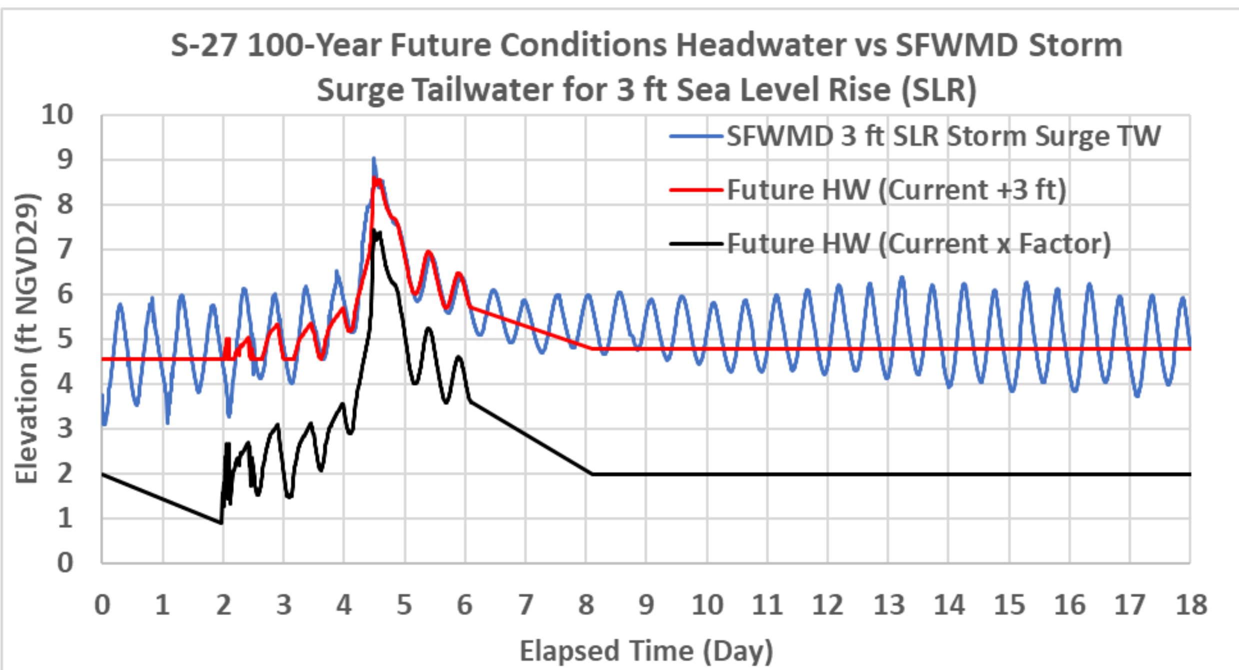

Figure 9.5-19: Comparison of the Developed 100-Year Design Storm S-27 Headwater Hydrographs and the SFWMD Storm Surge Design Storm Tailwater for 3 ft Sea Level Rise

Although the two approaches were significantly different, there was no significant difference indicated by the sensitivity test. The method of applying 3 ft to the current conditions hydrograph resulted in only 0.1 ft higher peak stages at S-28Z (upstream) and S-28 (downstream) of the C-8 Canal (**Figure 9.5-20** and

Figure 9.5-21, respectively), when compared to the method of applying a multiplication factor. This small increase did not propagate into the C-9 Canal, which maintained the same levels. Additionally, there were no notable differences in duration of high-water levels in the C-8 Canal. The method of applying 3 ft to the current conditions hydrograph resulted in reduced inter-basin discharge from the C-8 to the C-7, when compared to the multiplication factor approach, although it was larger than under current conditions.

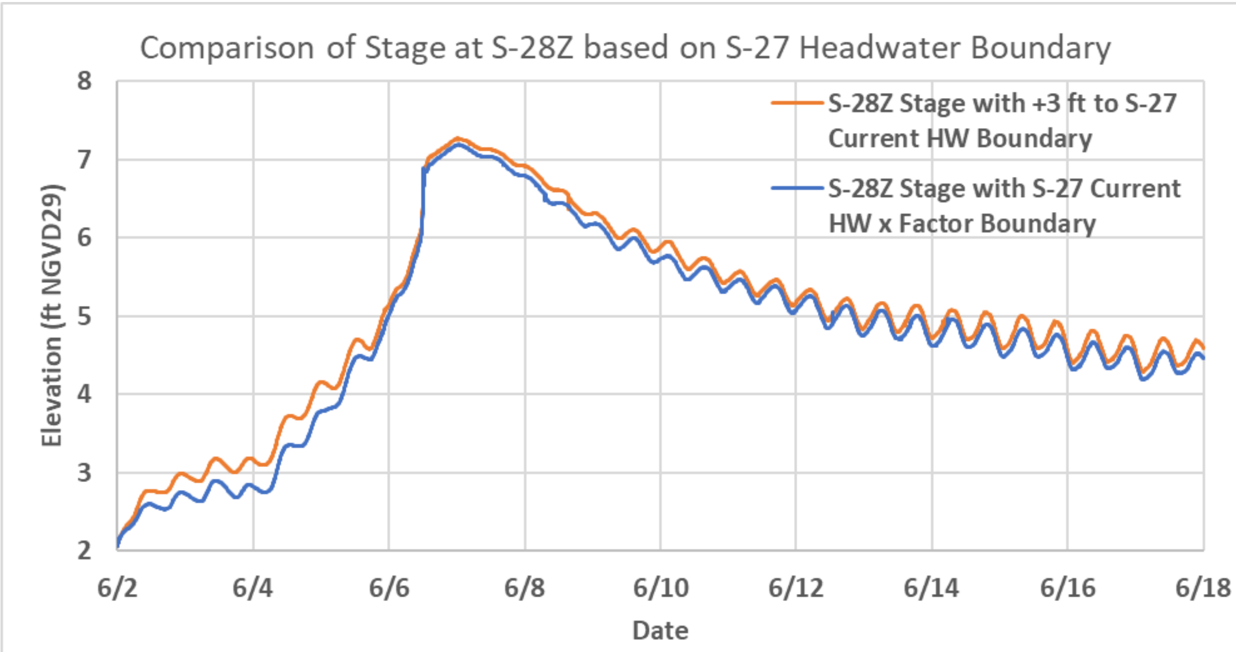

Figure 9.5-20: Headwater Stage Comparison at S-28 for Sensitivity Test

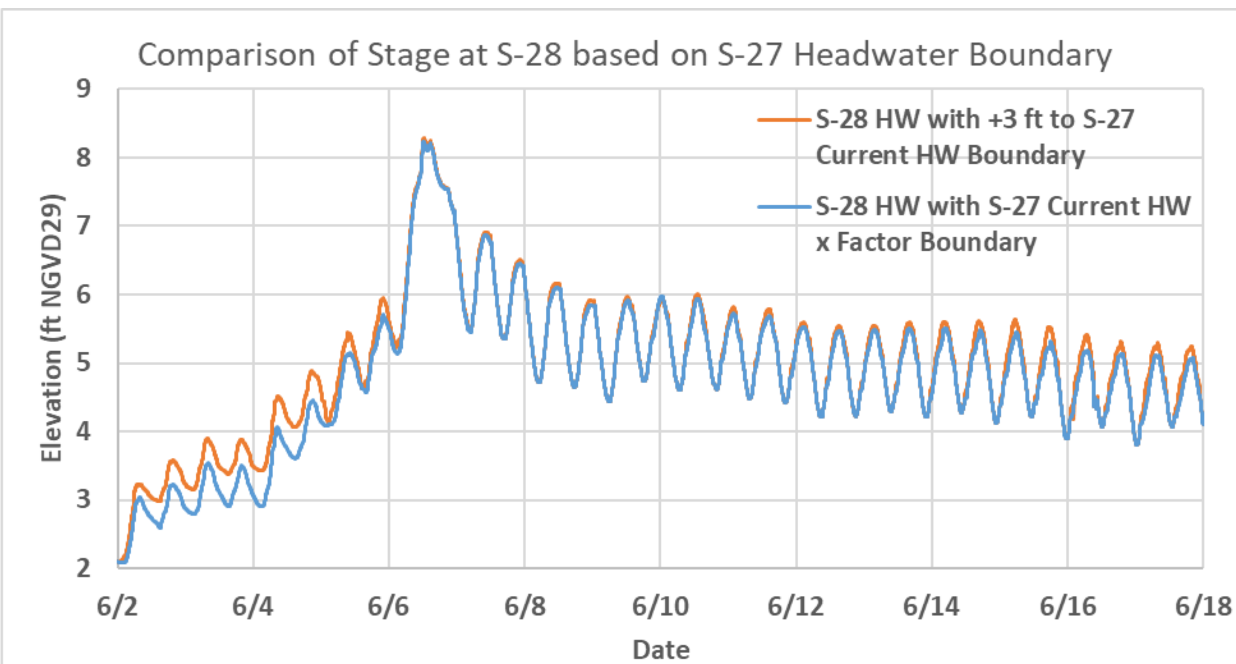

Figure 9.5-21: Stage Comparison at S-28Z for Sensitivity Test

The sensitivity test accomplished two things: (1) It demonstrated that either boundary could be used, as there was no significant difference in the C-8 model results and (2) It validated the assumption that the boundary was far enough from the area of interest that uncertainty in the boundary conditions had minimal effect on the outcome.

Both methods of developing future conditions headwater levels for S-27 were reasonable. Taylor Engineering, supported by the District, decided to use the first method, which increased the current conditions headwater by 1, 2, and 3 feet. This aligned with the District's direction of using the conservative approach. This approach was reasonable as it was believed that the S-27 structure would likely be overtopped/bypassed for each sea level rise condition unless mitigative measures are implemented in the future.

The recommended S-27 headwater boundary hydrographs for each of the design storms are shown in **Figure 9.5-22** through **Figure 9.5-25**.

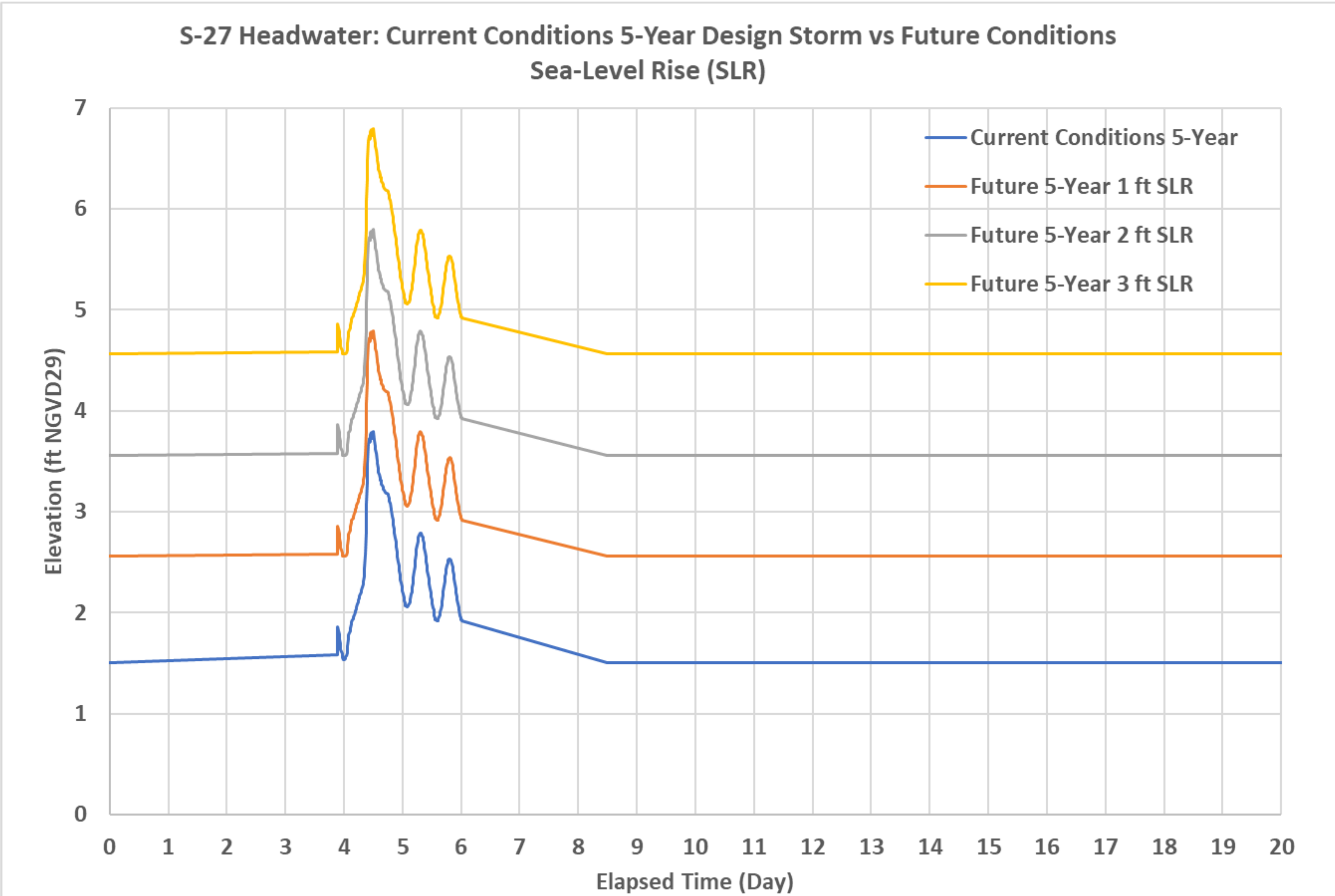

Figure 9.5-22: S-27 Future Condition Headwater Stages for 5-Year Design Storm under 3 Sea Level Rise Scenarios

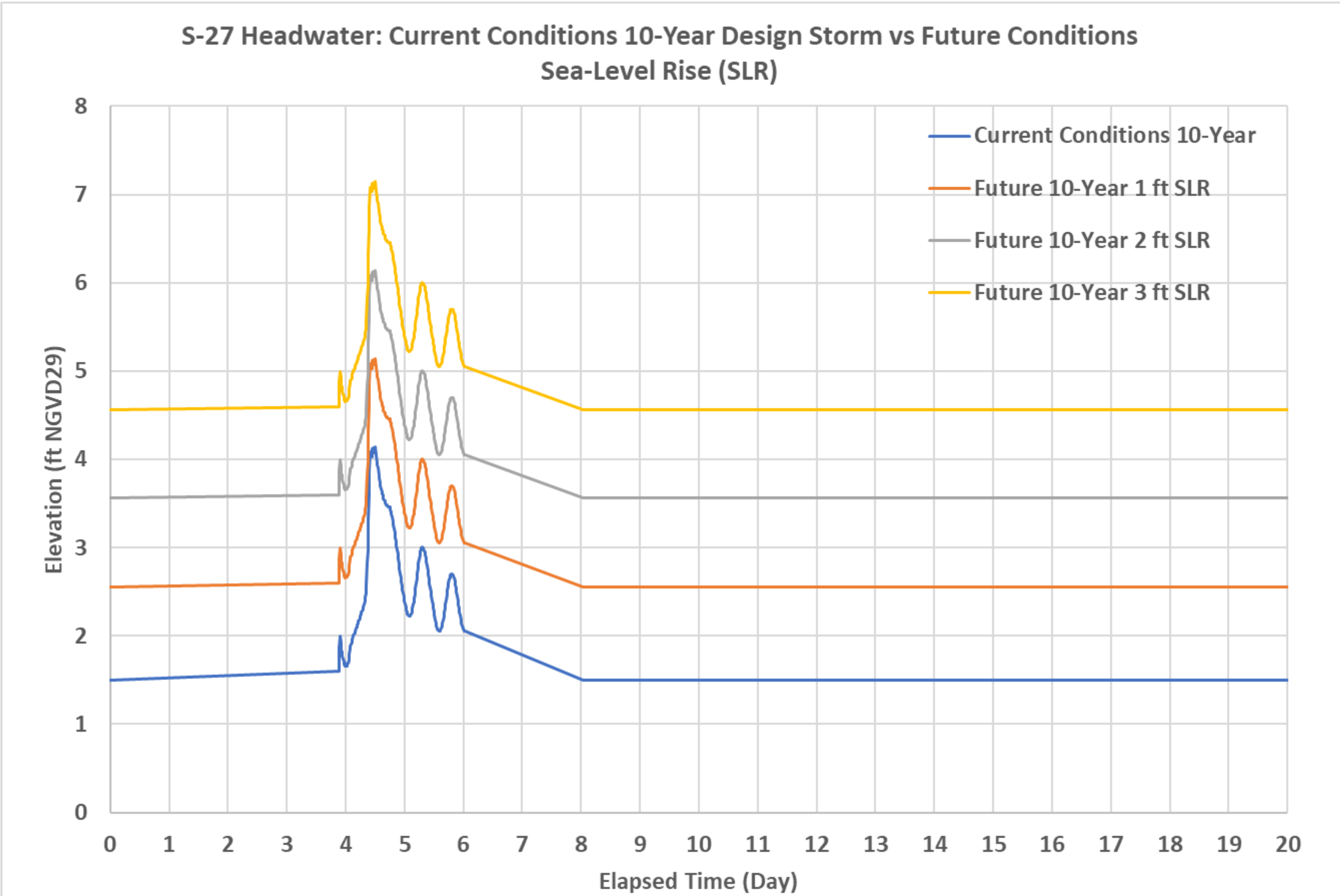

Figure 9.5-23: S-27 Future Condition Headwater Stages for 10-Year Design Storm under 3 Sea Level Rise Scenarios

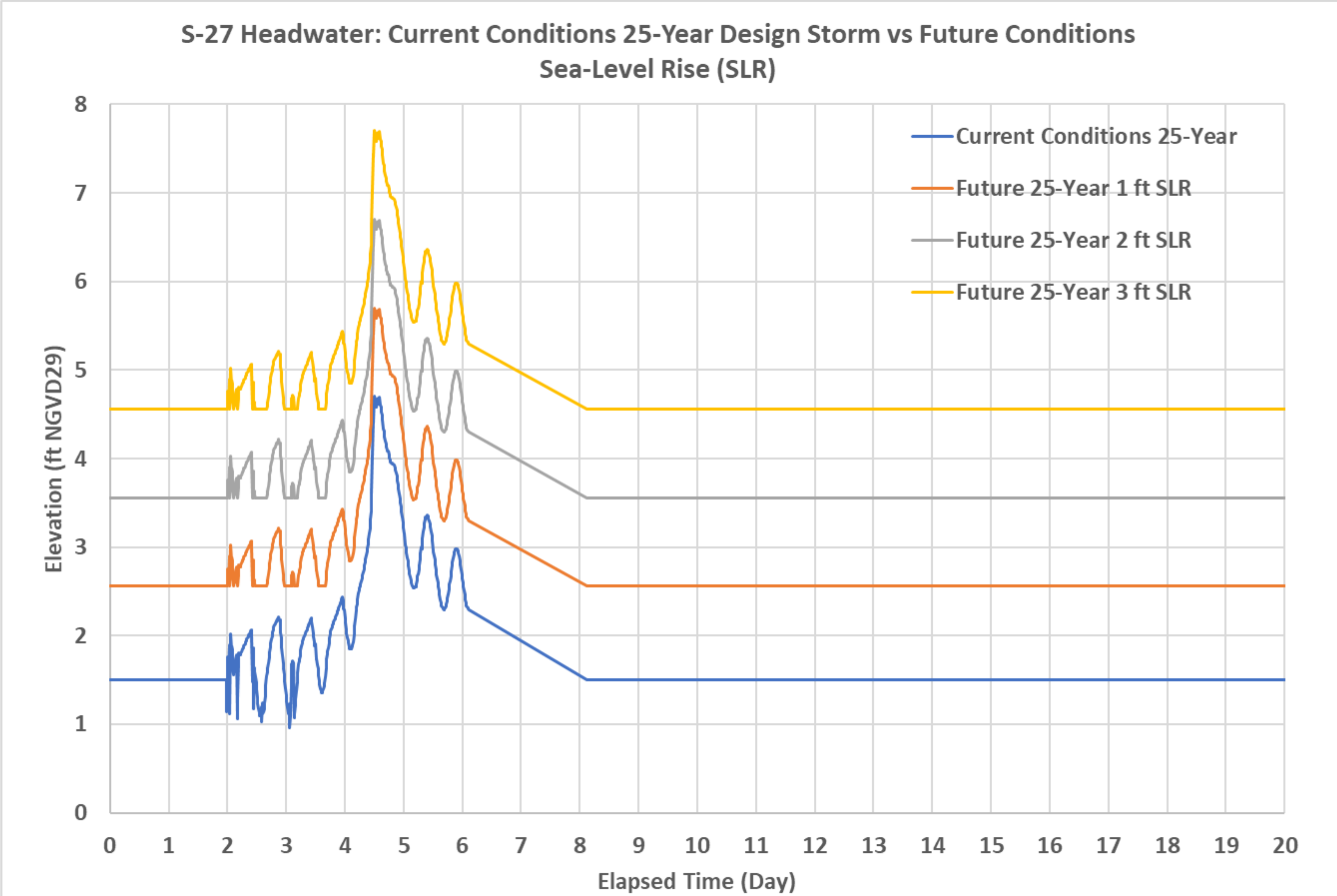

Figure 9.5-24: S-27 Future Condition Headwater Stages for 25-Year Design Storm under 3 Sea Level Rise Scenarios

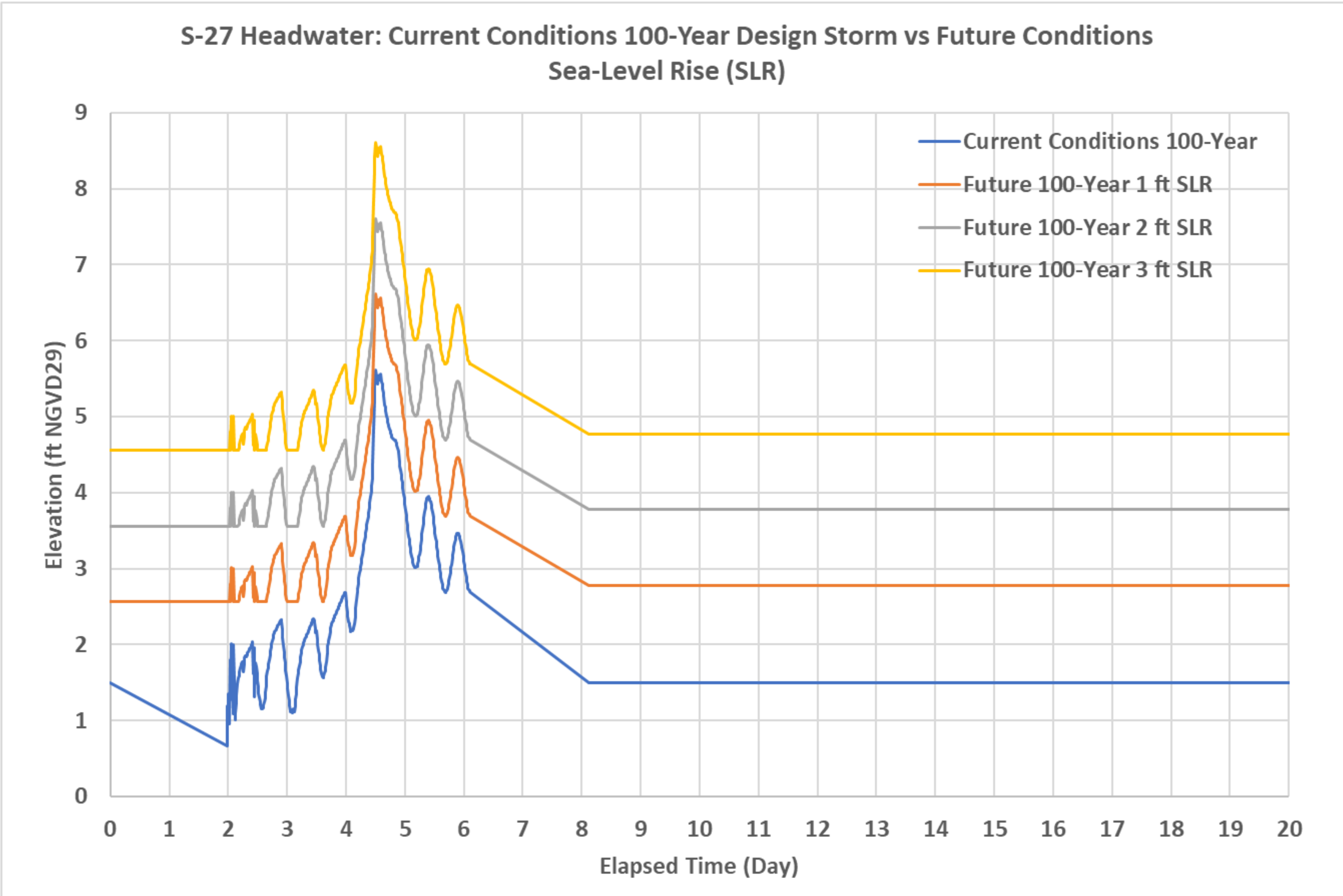

Figure 9.5-25: S-27 Future Condition Headwater Stages for 100-Year Design Storm under 3 Sea Level Rise Scenarios

9.6 Initial Groundwater

For this study, the initial groundwater levels for future conditions were developed using the Broward County Future Groundwater Map (from the 2019 Broward County MIKE SHE Future Conditions 2060 model) and merging it with adjusted Miami-Dade potentiometric surface contours for the current conditions. Then, any area in the future conditions map that was lower than current conditions was replaced with the current condition groundwater level. The Broward County Future Initial Potential Head Map was based on a 26" of sea level rise. The Miami-Dade County potentiometric surface contours were adjusted by shifting the current condition contours to align with the contours created from the Broward County future conditions data. The Broward County Future Conditions Initial Potential Head Map covered the majority of the model domain.

As the Broward County data was based on 26" of sea level rise, the map described in the preceding paragraph was deemed appropriate to be used as the future conditions potentiometric surface map for the 2 ft sea level rise scenario. To develop the future potentiometric surface map for the 1 and 3 ft sea level rise scenarios, the current conditions groundwater surface elevation was subtracted from the future groundwater surface elevation for the 2 ft SLR scenario. The result of this was a difference map that showed how much the groundwater levels would increase from current conditions. This difference map was multiplied by 50% to represent the increase in groundwater due to 1 ft of sea level rise. To develop the future conditions potentiometric surface map for the 1 and 3 ft SLR scenario, the 50% difference map was subtracted and added to the 2 ft SLR future groundwater map, respectively. **Figure 9.6-1** through **Figure 9.6-3** show the future conditions initial potentiometric surface maps for each of the three sea level rise scenarios. Please note that the discontinuous groundwater elevations and checkered pattern are artifacts of the source data and the process of merging different datasets. These artifacts disappeared within the first few minutes of the simulation and there is a 2-day spin-up period prior to the design storms, which allows the groundwater to come to a dynamic equilibrium before the start of the design storm rainfall.

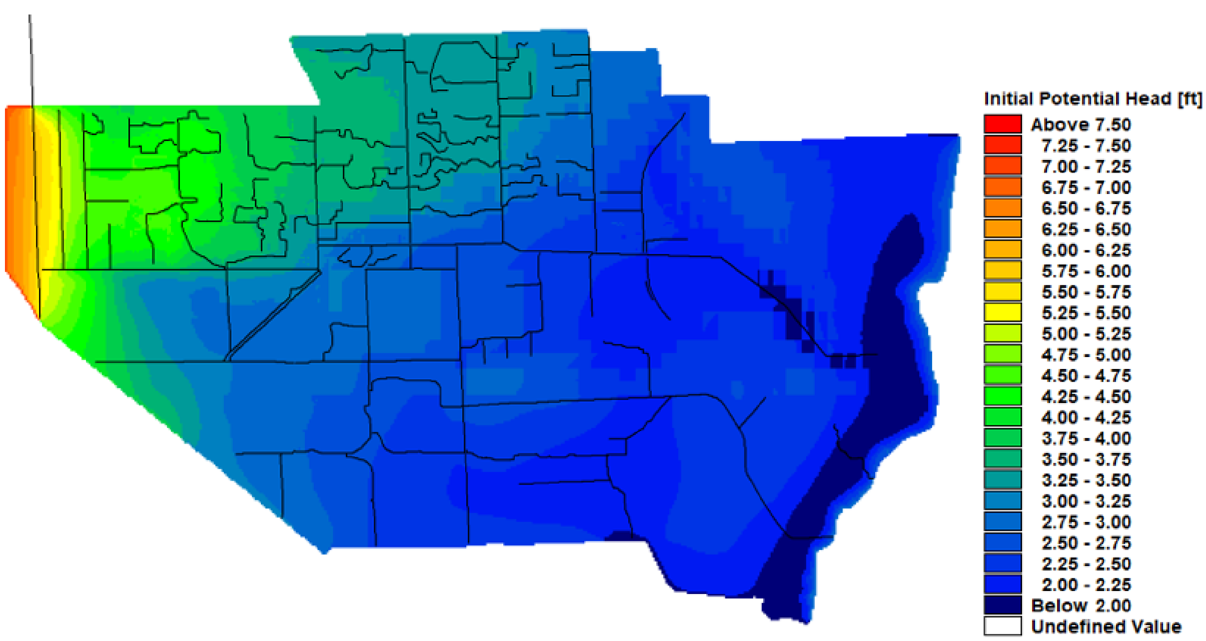

Figure 9.6-1: Future Conditions Initial Groundwater Levels for 1 ft Sea Level Rise

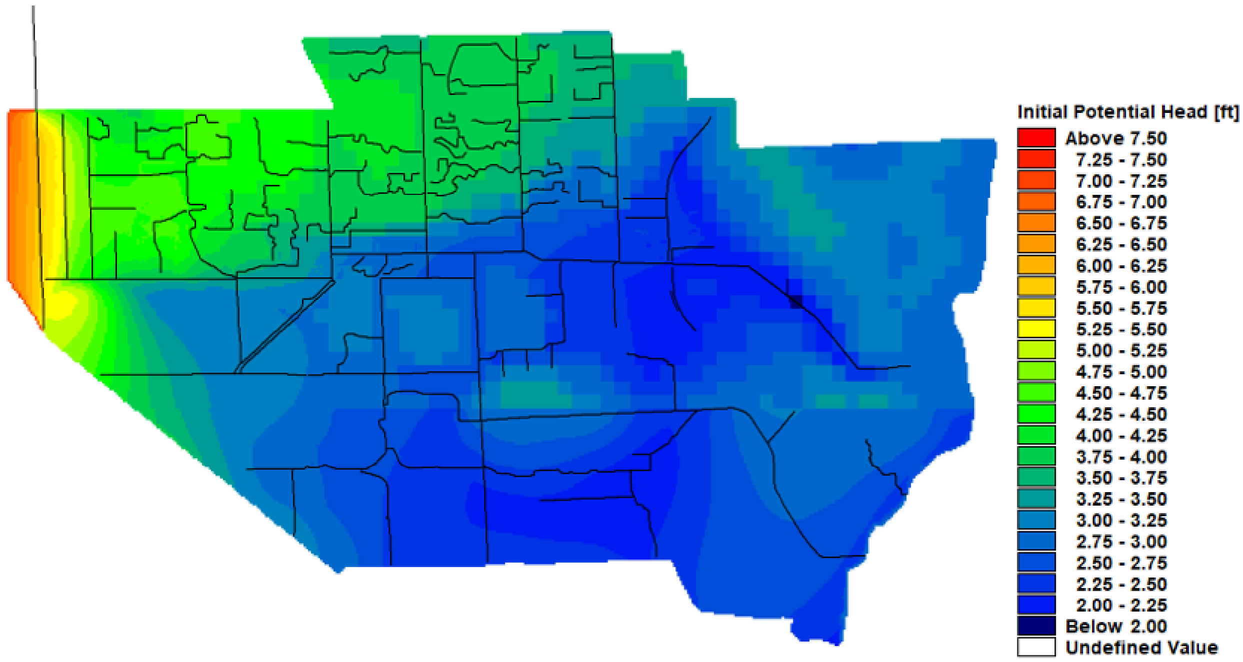

Figure 9.6-2: Future Conditions Initial Groundwater Levels for 2 ft Sea Level Rise

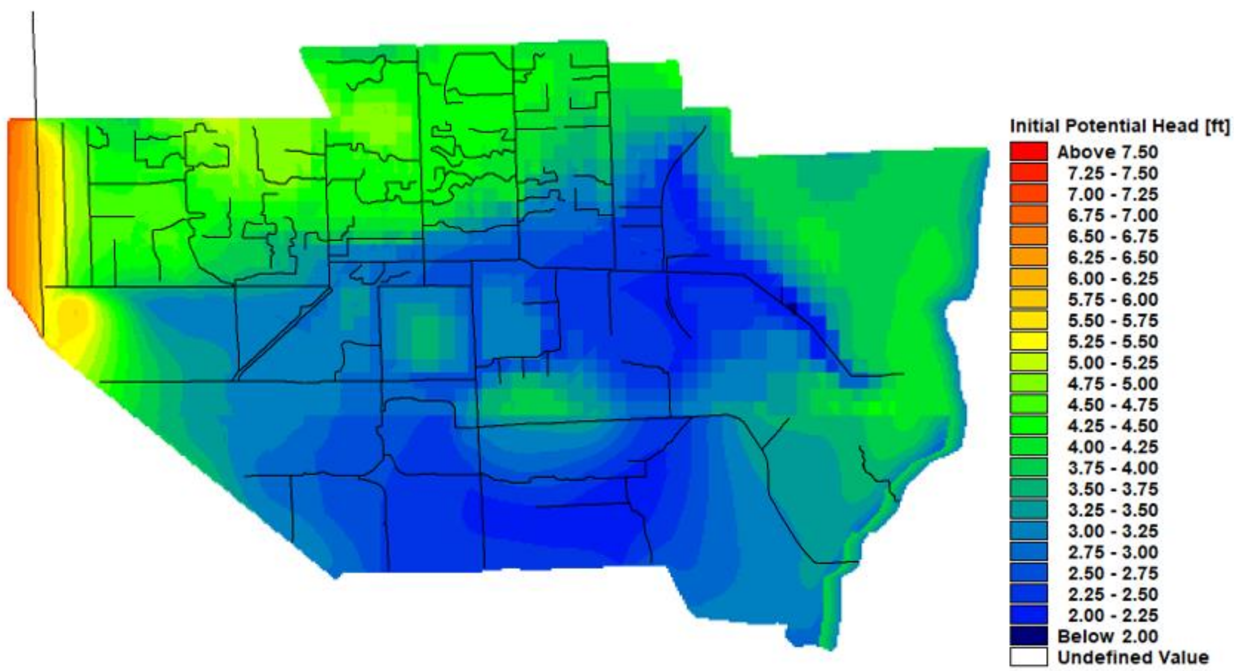

Figure 9.6-3: Future Conditions Initial Groundwater Levels for 3 ft Sea Level Rise

10 FUTURE CONDITION FLOOD PROTECTION LEVEL OF SERVICE ASSESSMENT

Future conditions with sea level rise was simulated for the 72-hour 5-year, 10-year, 25-year, and 100-year 3-day design storm events. For each design storm, three future sea level rise scenarios, 1, 2, and 3 ft, were simulated (SLR1, SLR2, and SLR3). The model setup for these scenarios was previously described in **Section 9**. **Appendix E** provides a summary of the model results at primary control structures. The remainder of this section describes the results of the FPLOS evaluations. For comparison purposes, figures in PM #1, #2, and #4 present future conditions results with the current conditions results.

10.1 PM #1 – Maximum Stage in Primary Canals

This is the peak stage profile in the primary canal system. The profile is developed for the 72-hour 5-year, 10-year, 25-year, and 100-year design storms. The largest design storm that stays within the canal banks establishes the FPLOS of the primary canal system.

To evaluate this PM under future conditions within the C-8 and C-9 watersheds, instantaneous peak stage profiles were prepared for the primary canals within the watersheds, which are the C-8 and C-9 Canals, respectively. Bank elevations on the profile figures are based on the MIKE HYDRO cross-section data. Also shown in the figures are major roadway landmarks, control structures, and primary canal junctions.

Table 10-1 through **Table 10-3** summarize the PM #1 results for SLR 1, SLR2, and SLR3, respectively, which are shown graphically in **Figure 10.1-2** through **Figure 10.1-9**. These tables list the maximum return period profile that is contained within the canal banks.

Although the C-8 Canal contained the 5-year and 10-year profiles along the majority of the canal length under current conditions, the banks were exceeded in several locations for the 5-year SLR1 event. Similarly, although the C-9 Canal contained the 10-year and 25-year profiles along the majority of the canal length under current conditions, the bank elevation was exceeded for the 5-year SLR1 event at a few locations. Therefore, if a strict interpretation of this criteria is used, then both the C8 and C9 Canal have less than a 5-year FPLOS. However, as summarized in the Conclusions, the determination of FPLOS should consider the results of all applicable performance metrics. With careful consideration of PM #1 and PM #5, the C8 and C9 Canals provide a 5-year and 10-year FPLOS for SLR1 and SLR2, respectively. For SLR3, both the C8 and C9 Canals provide less than a 5-year FPLOS. With respect to **Table 10-1** through **Table 10-3**, "FPLOS Localized" is the return period that any bank exceedances are noticed, even if it doesn't correspond to a significant area of flood inundation as shown in PM #5. FPLOS overall is the return period in which there are several bank exceedances and/or the bank exceedances correspond to a significant area of flood inundation as shown in PM #5.

Table 10-1: PM #1 Summary Results for Sea Level Rise 1

Canal Segment	Figure Number	FPLOS Localized	FPLOS Overall	Comment
C-8	**Figure 10.1-2**	5-year	5-Year	Overall FPLOS from **Section 10.7.1**
C-9	**Figure 10.1-3**	5-year	10-year	Overall FPLOS from **Section 10.7.2**

Table 10-2: PM #1 Summary Results for Sea Level Rise 2

Canal Segment	Figure Number	FPLOS Localized	FPLOS Overall	Comment
C-8	**Figure 10.1-2**	5-year	5-year	Overall FPLOS from **Section 10.7.1**
C-9	**Figure 10.1-3**	5-year	10-year	Overall FPLOS from **Section 10.7.2**

Table 10-3: PM #1 Summary Results for Sea Level Rise 3

Canal Segment	Figure Number	FPLOS Localized	FPLOS Overall	Comment
C-8	**Figure 10.1-2**	5-year	5-year	Overall FPLOS from **Section 10.7.1**
C-9	**Figure 10.1-3**	5-year	5-year	Overall FPLOS from **Section 10.7.2**

The PM #1 performance of the C-8 Canal under future conditions is generally worse east of its confluence with the Opa Locka Canal compared to the western segment. Notable areas of bank exceedances as shown in **Figure 10.1-2** include:

- Downstream of NE 6th Avenue (CR915) south bank exceeded for 5-year SLR1 event.
- Just west of NE 6th Avenue (CR915), north and south bank exceeded for 5-year SLR1 event.
- Downstream of NE 135th St. (CR 916), north and south bank exceeded for 5-year SLR1 event.
- From North Miami Avenue to NE 135th St., south bank exceeded for 5-year SLR1-year event.
- Downstream of Opa Locka Canal, south bank exceeded for 5-year SLR1 event.
- Halfway between Marco Canal and State Highway 9, south bank exceeded for 5-year SLR1.

Under current conditions, the hydraulic grade line of the C-8 Canal typically had a positive gradient downstream towards the tidal structure. However, under future sea level rise conditions, this gradient becomes zero and often negative. The inflection point is the point at which the slope of the hydraulic grade line changes from positive to negative. For the 5-year SLR1 and SLR2 events, the hydraulic grade line becomes flat, or zero, in a few locations. This suggests that the effects of sea level rise are in equilibrium with the effects of increased initial groundwater elevations and higher runoff potential. However, for the 5-year SLR3 event, there is no inflection point as everything upstream of S-28 has a negative gradient. This suggests that the effects of 3 feet of sea level rise are more influential than the increase in initial groundwater and runoff potential, which is what causes the flow direction to shift from west to east (inland to tide) to east to west (tide to inland). A similar trend is shown for each design storm under the 3 ft sea level rise condition. For the 25-year 2 ft sea level rise event, the inflection point was shifted about 8000 ft upstream from NE 6th Ave for SLR1 to NE 135th St, compared to the 25-year SLR1 event.

The PM #1 performance of the C-9 Canal under future conditions is generally worse east of its confluence with Carol City Canal A compared to the western segment. Notable areas of bank exceedances in the C-9 Canal as shown in **Figure 10.1-3** include:

- Upstream of S-29, south bank exceeded for 5-year SLR1 event.
- Halfway between I-95 and S-29 to S-29, south bank exceeded for 5-year SLR1 event, north bank for the 5-year SLR2 event.
- Downstream of US Hwy 441, north bank exceeded for 10-year SLR1 event and 5-year SLR2 event, south bank exceeded for 10-year SLR3 event and 25-year SLR2 event
- From SBDD pumps S-4 and S-5 to Highway I75, south bank exceeded for the 5-year SLR3 event and 10-year SLR2 event.
- From SBDD pumps S-3 to the Ronald Reagan Turnpike, south bank exceeded for the 5-year SLR3 event and the 25-year SLR1 event

Under current conditions, the C-9 Canal typically had a positive gradient downstream towards the tidal structure for the 5-year and 10-year design storms. For both the 25-year and 100-year current condition design storms, inflection points could be seen in multiple locations, including near the SBDD S-4/S-5 pump stations and near the SBDD S-2 pump station. Under current conditions, these inflection points appear to be mostly caused by the discharge from the pump stations, causing localized high water levels that cause flow both west (towards inland) and east (towards tide). Under future conditions, although the pump discharge still contributes, the inflection points become influenced by the increase in sea level rise as well. Please note that the reason that SLR1 peak stage in the western C-9 Canal is lower than current conditions is because of the C-9 Impoundment pulling water from the western end of the C-9 Canal.

It is important to note that the maximum water levels presented in the maximum surface water profiles do not occur at the same time; they are the maximum stage at each location regardless of timing. For the 5-year and 10-year future conditions SLR1 design storms, an inflection point or dip in the profile between the SBDD S-4/S-5 pump stations and Highway I75 can be seen. **Figure 10.1-1** shows two instantaneous moments of the water surface profile for the C-9 Canal. The right side of the dip, between Highway I75 and SBDD S-7 pump station, occurs at the peak of the design storm, which has the highest rainfall and the highest storm surge levels (pink portion of the graph). At the peak of the design storm, the C-9 Impoundment is pumping which caused lower water levels in the western C-9 Canal. This results in a steep hydraulic grade line from east to west. About 24 hours later, the rainfall has finished, the maximum storm surge has passed, the C-9 Impoundment has stopped pumping, the S-29 structure is near peak discharge, and there is still discharge into the C-9 Canal. This causes the water levels in the western C-9 Canal to rebound and results in a steep hydraulic grade line from west to east (blue portion of the graph). At some point during the simulation, the water level where the two grade lines overlap were higher than it was during the two instantaneous moments captured in the figure, however, it was lower than current conditions. The dip in the profile, which is lower than current conditions, is in part a result of the two "extremes" causing lower levels in the canal.

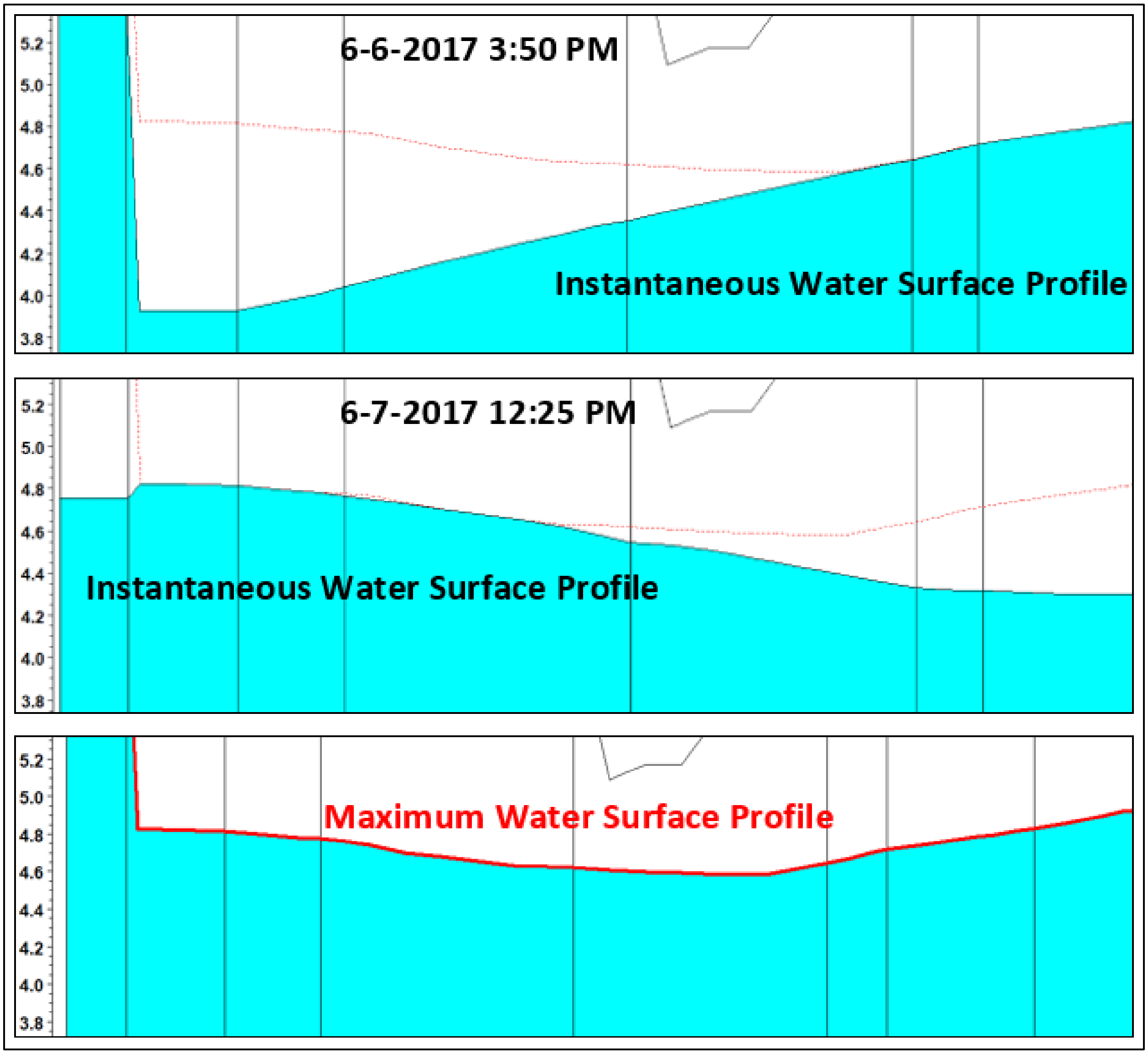

Figure 10.1-1: Visual representation of C-9 Canal Stage at Two Moments During the 5-Year SLR1 Event

For the 5, 10, and 25-year 1 ft sea level rise scenarios, the effects of the C-9 Impoundment appear to have more influence on the western C-9 Canal stages than sea level rise. This is not the case for the 100-year SLR1 scenario or any of the SLR2 or SLR3 scenarios. Like the C-8 Canal, the C-9 Canal mostly has a negative grade line for each design storm under the 3 ft sea level rise scenario. This shows that 3 ft of sea level rise is more influential than the increased initial groundwater levels and increased runoff potential for both canals.

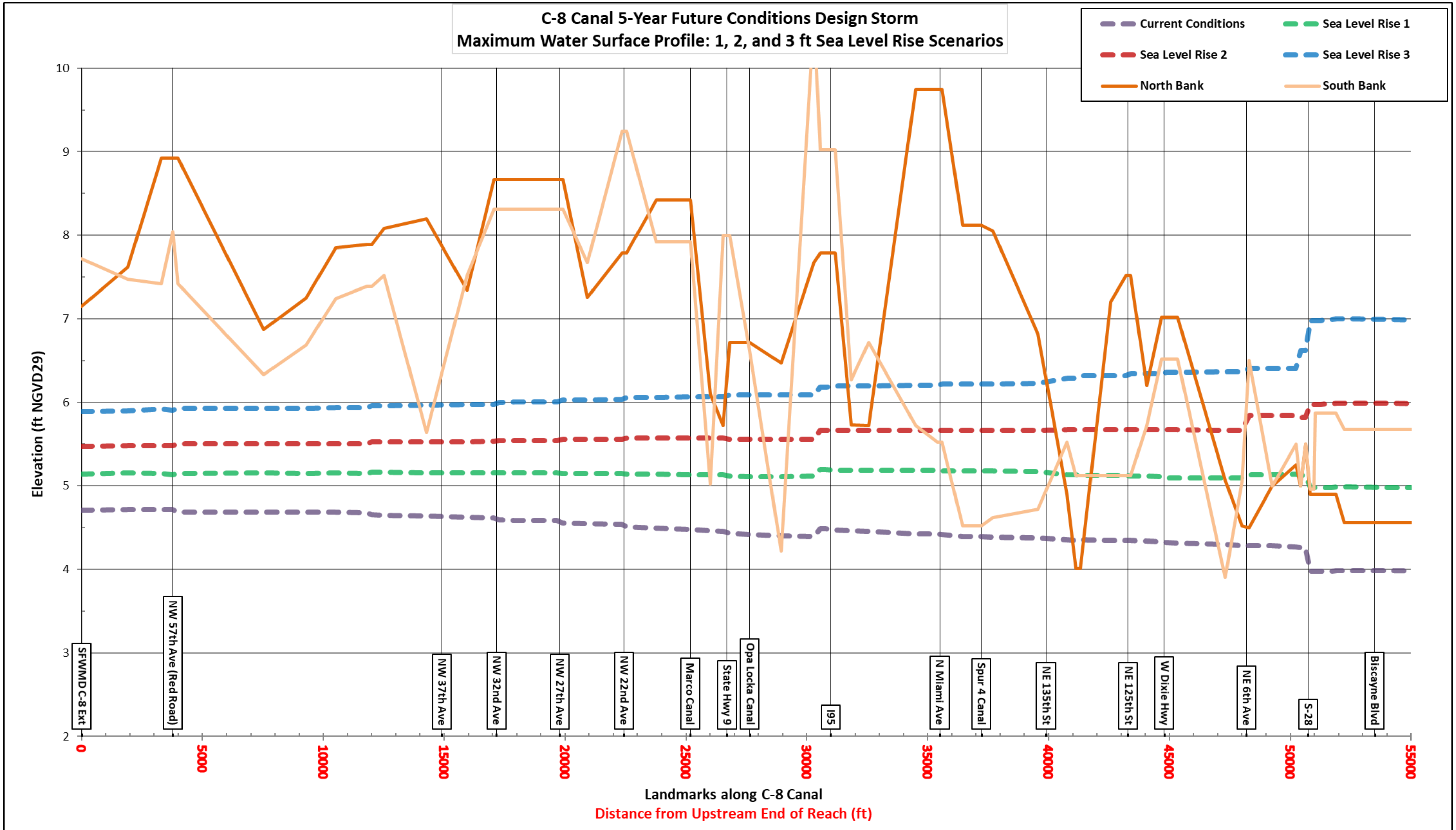

Figure 10.1-2: C-8 Canal Peak Stage Profiles for 5-Year Design Storm – Current vs Future Sea Level Rise Scenarios

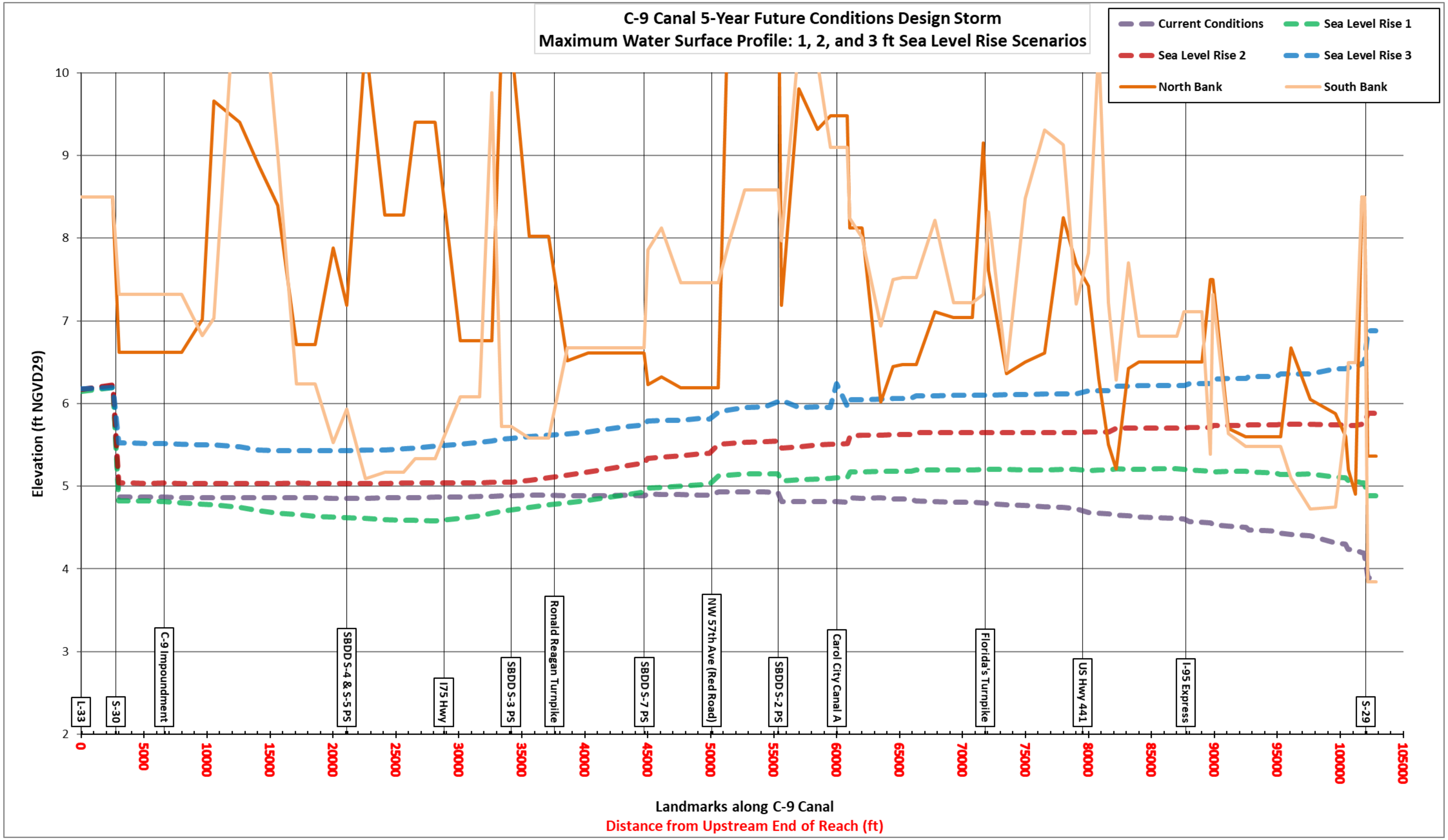

Figure 10.1-3: C-9 Canal Peak Stage Profiles for 5-Year Design Storm – Current vs Future Sea Level Rise Scenarios

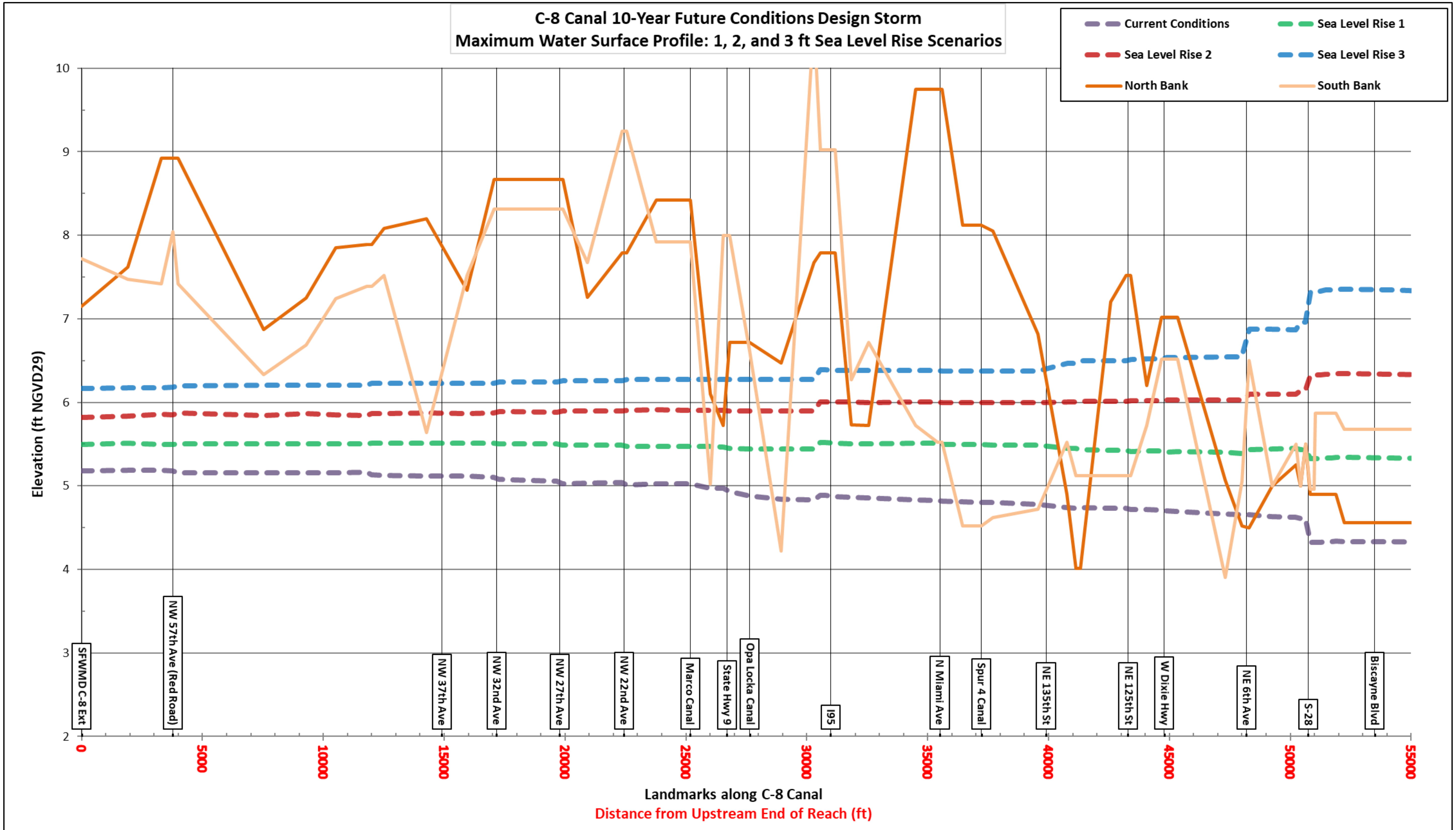

Figure 10.1-4: C-8 Canal Peak Stage Profiles for 10-Year Design Storm – Current vs Future Sea Level Rise Scenarios

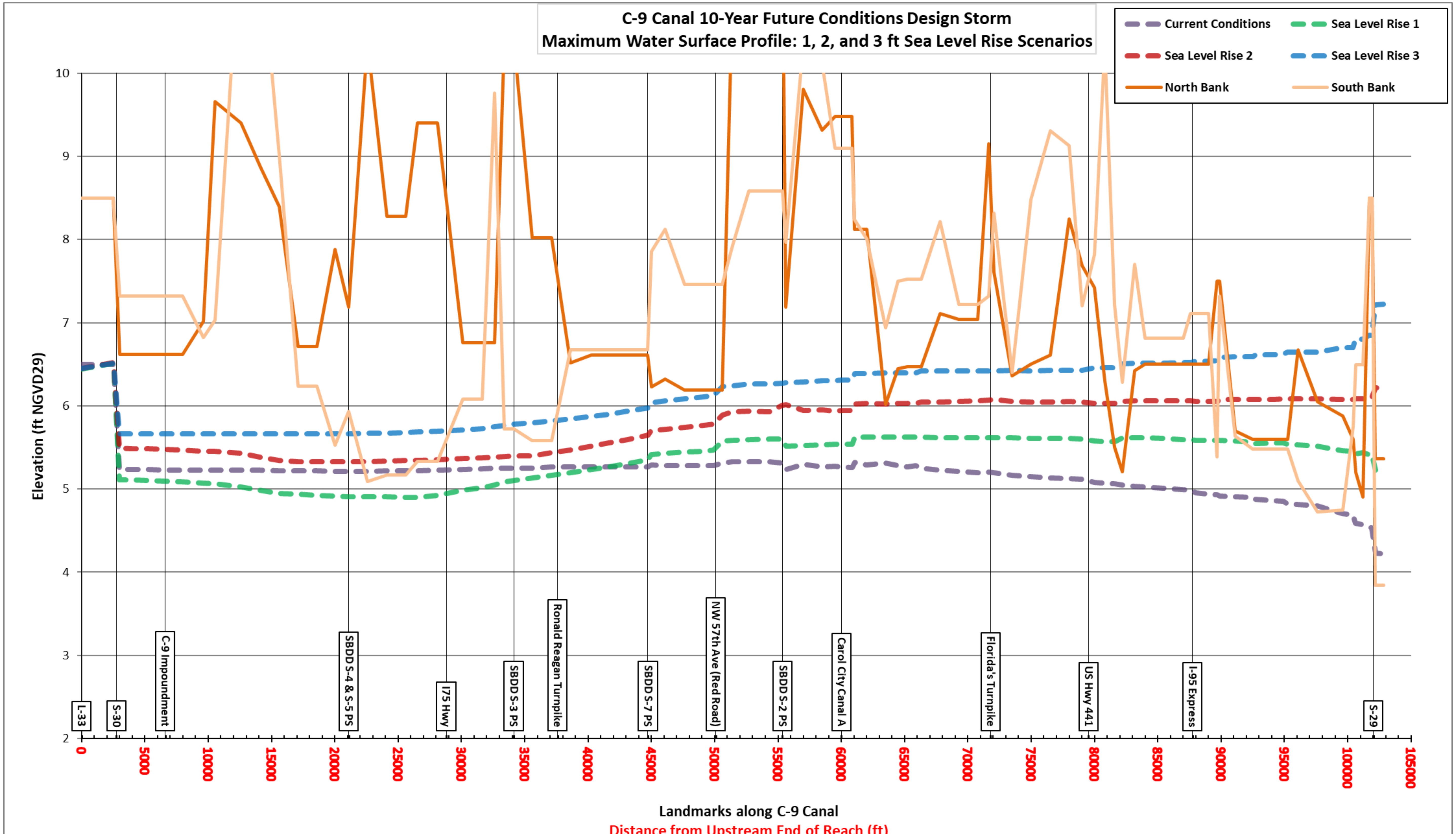

Figure 10.1-5: C-9 Canal Peak Stage Profiles for 10-Year Design Storm – Current vs Future Sea Level Rise Scenarios

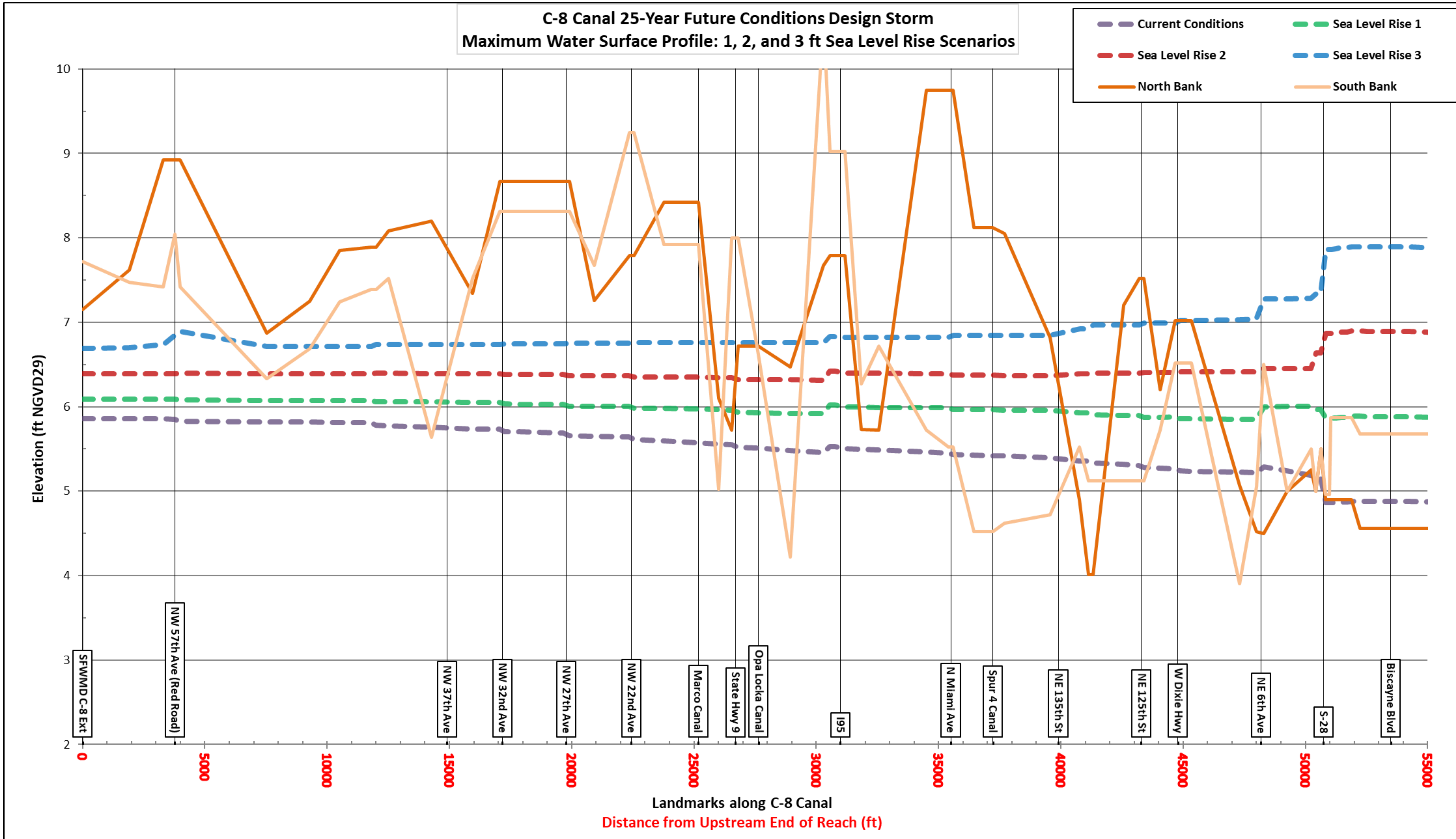

Figure 10.1-6: C-8 Canal Peak Stage Profiles for 25-Year Design Storm – Current vs Future Sea Level Rise Scenarios

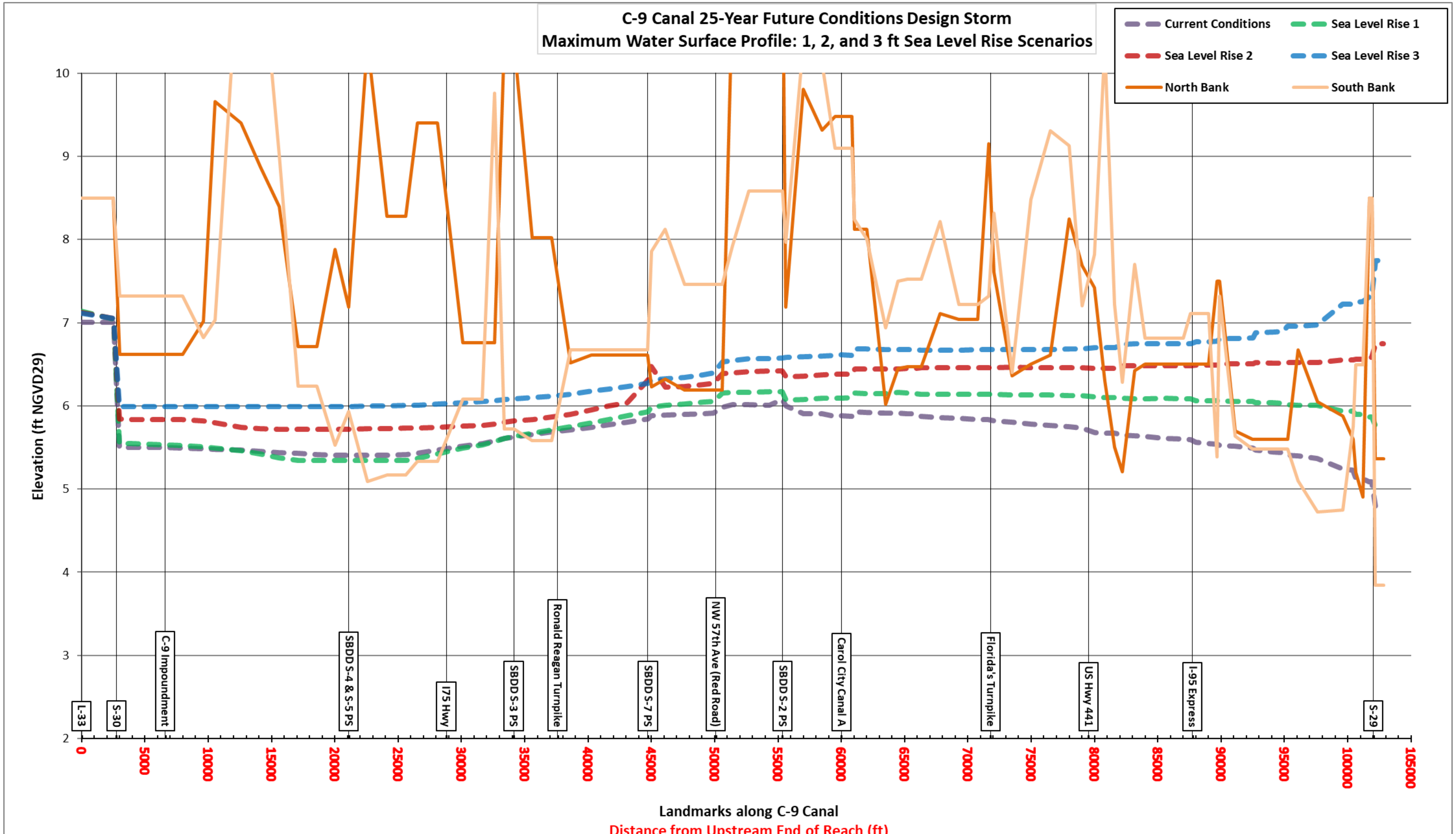

Figure 10.1-7: C-9 Canal Peak Stage Profiles for 25-Year Design Storm – Current vs Future Sea Level Rise Scenarios

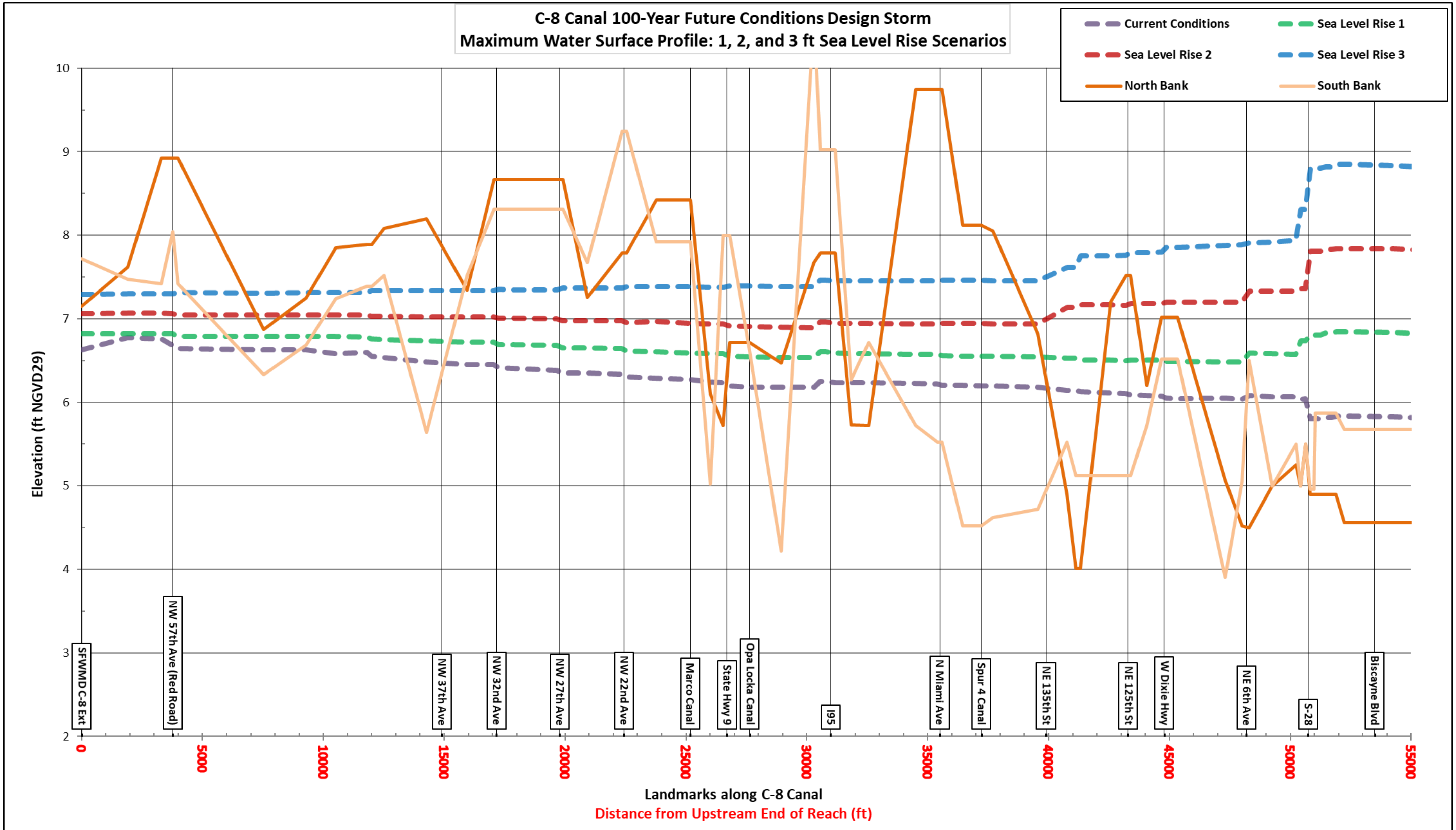

Figure 10.1-8: C-8 Canal Peak Stage Profiles for 100-Year Design Storm – Current vs Future Sea Level Rise Scenarios

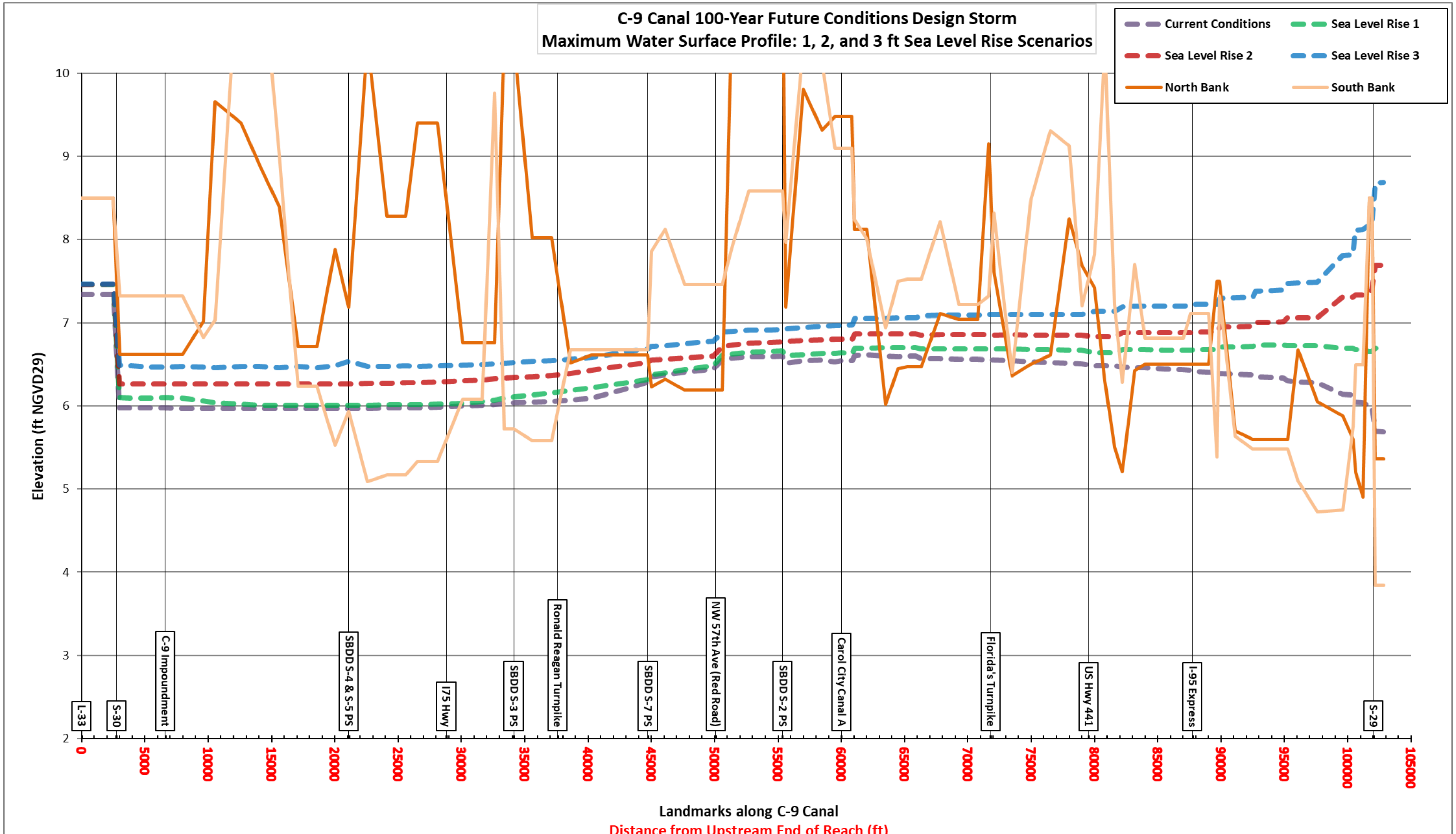

Figure 10.1-9: C-9 Canal Peak Stage Profiles for 100-Year Design Storm – Current vs Future Sea Level Rise Scenarios

Table 10-4 through **Table 10-6** show the peak stages at the major landmarks along the C-8 Canal for each of the future condition sea level rise scenario design storms. Bridge low cord elevations were specified where applicable. Although the water level in the C-8 Canal exceeded bank elevations in several locations for the various design storms, the water level did not get high enough to become restricted by the low cord elevation of any bridge for SLR1 and SLR2 scenarios. For the 100-year 2 ft sea level rise scenario, the water level in the C-8 canal was elevated enough to be within 0.02 ft of becoming restricted by the low cord of a bridge, as shown in orange in **Table 10-5**. Although not restricted in the model simulation, it is close enough and well within the error of margin that it should be considered at risk. For the 100-year 3 ft sea level rise scenario, the water level in the C-8 Canal exceeded bank elevations in several areas and became elevated enough to become restricted by the low cord elevation of two bridges, as shown in red in **Table 10-6**. None of the bridges were overtopped.

Table 10-4: C-8 Canal Peak Stage at Landmarks for SLR1

Landmark	Peak Stage (ft NGVD29)				Bridge Low Cord Elevation (ft NGVD29)
	5-Yr	10-Yr	25-Yr	100-Yr	
SFWMD C-8 Ext	5.14	5.49	6.09	6.82	
NW 57th Ave (Red Road)	5.14	5.5	6.09	6.82	9.2
NW 37th Ave	5.16	5.51	6.06	6.74	
NW 32nd Ave	5.16	5.5	6.03	6.69	9.18
NW 27th Ave	5.16	5.5	6.03	6.68	7.02
NW 22nd Ave	5.15	5.49	6	6.64	8
Macro Canal	5.14	5.47	5.97	6.59	
Rail Road / State Hwy 9	5.13	5.47	5.96	6.58	7.44
NW 7th Ave Bridge	5.11	5.45	5.93	6.54	8.53
I-95	5.2	5.52	6.02	6.61	8.05
North Miami Ave	5.19	5.51	5.99	6.58	9.62
Spur 4 Canal	5.18	5.49	5.96	6.55	
NE 135th St	5.17	5.49	5.96	6.55	7.38
NE 125th St	5.13	5.43	5.9	6.5	11.47
W Dixie Hwy	5.11	5.42	5.88	6.5	10.57
NE 6th Ave	5.13	5.43	6	6.59	9.02
S-28 (HW)	5.13	5.43	5.97	6.74	
Biscayne Blvd	4.98	5.34	5.88	6.84	

Table 10-5: C-8 Canal Peak Stage at Landmarks for SLR2

Landmark	Peak Stage (ft NGVD29)				Bridge Low Cord Elevation (ft NGVD29)
	5-Yr	10-Yr	25-Yr	100-Yr	
SFWMD C-8 Ext	5.48	5.82	6.39	7.06	
NW 57th Ave (Red Road)	5.48	5.85	6.39	7.06	9.2
NW 37th Ave	5.53	5.87	6.39	7.03	
NW 32nd Ave	5.55	5.89	6.38	7.0	9.18
NW 27th Ave	5.55	5.88	6.38	7.0	7.02
NW 22nd Ave	5.56	5.9	6.37	6.97	8
Macro Canal	5.57	5.91	6.35	6.95	
Rail Road / State Hwy 9	5.57	5.91	6.35	6.94	7.44
NW 7th Ave Bridge	5.56	5.89	6.32	6.9	8.53
I-95	5.66	6.01	6.42	6.96	8.05
North Miami Ave	5.67	6	6.39	6.94	9.62
Spur 4 Canal	5.67	6	6.37	6.94	
NE 135th St	5.67	6	6.37	6.94	7.38
NE 125th St	5.67	6.01	6.4	7.16	11.47
W Dixie Hwy	5.67	6.02	6.41	7.18	10.57
NE 6th Ave	5.84	6.1	6.45	7.33	9.02
S-28 (HW)	5.82	6.14	6.64	7.36	
Biscayne Blvd	5.99	6.34	6.89	7.84	

Table 10-6: C-8 Canal Peak Stage at Landmarks for SLR3

Landmark	Peak Stage (ft NGVD29)				Bridge Low Cord Elevation (ft NGVD29)
	5-Yr	10-Yr	25-Yr	100-Yr	
SFWMD C-8 Ext	5.89	6.17	6.69	7.29	
NW 57th Ave (Red Road)	5.9	6.18	6.84	7.3	9.2
NW 37th Ave	5.97	6.23	6.74	7.34	
NW 32nd Ave	6	6.25	6.75	7.35	9.18
NW 27th Ave	6	6.25	6.75	7.35	7.02
NW 22nd Ave	6.03	6.26	6.75	7.37	8
Macro Canal	6.06	6.28	6.76	7.38	
Rail Road / State Hwy 9	6.07	6.28	6.76	7.38	7.44
NW 7th Ave Bridge	6.09	6.27	6.76	7.39	8.53
I-95	6.18	6.39	6.83	7.46	8.05
North Miami Ave	6.2	6.38	6.82	7.45	9.62
Spur 4 Canal	6.22	6.37	6.84	7.46	
NE 135th St	6.23	6.37	6.84	7.46	7.38
NE 125th St	6.32	6.5	6.97	7.76	11.47
W Dixie Hwy	6.34	6.52	6.99	7.8	10.57
NE 6th Ave	6.41	6.87	7.28	7.91	9.02
S-28 (HW)	6.62	6.96	7.34	8.31	
Biscayne Blvd	7	7.35	7.89	8.85	

Table 10-7 through **Table 10-9** shows the peak stages at the major landmarks along the C-9 Canal for each of the design storms. Bridge low cord elevations were specified where applicable. For the 5-year and 10-year SLR1 design storm events, the water level in the C-9 Canal exceeded bank elevations in a couple locations (**Figure 10.1-3**) and the water level became high enough to become restricted by the low cord of one bridge, as shown in red in **Table 10-7.** For the 25-year and 100-year SLR1 design storms, the water level in the C-9 Canal exceeded bank elevations in several areas and became elevated enough to become restricted by the low cord elevation of three bridges, as shown in red in **Table 10-7**. Canal bank exceedances increased with both design storm frequency and sea level rise. For the sea level rise 3 scenario, the three bridges that became submerged under the 25 and 100-year SLR1 scenarios became submerged for each design storm, as shown in red in **Table 10-9**. It is unknown if any of the submerged bridges would become overtopped as the overflow elevations are unknown (these were not surveyed, and bridge decks were scrubbed from the DEM).

Table 10-7: C-9 Canal Peak Stage at Landmarks for SLR1

Landmark	Peak Stage (ft NGVD29)				Bridge Low Cord Elevation (ft NGVD29)
	5-Yr	10-Yr	25-Yr	100-Yr	
L-33	6.15	6.44	7.14	7.46	
S-30 (TW)	4.82	5.11	5.55	6.1	
SBDD S-4 & S-5 PS	4.62	4.91	5.34	6.01	
I75 Hwy	4.58	4.92	5.42	6.02	
SBDD S-3 PS	4.72	5.11	5.63	6.11	
Ronald Reagan Turnpike	4.77	5.17	5.71	6.16	
SBDD S-7 PS /Flaming Rd	4.93	5.35	5.93	6.32	9.76
NW 57th Ave (Red Road)	5.03	5.47	6.05	6.48	9.54
SBDD S-2 PS / NW 47th Ave	5.15	5.6	6.17	6.66	8.9
Carol City Canal A	5.1	5.54	6.1	6.64	
NW 37th Ave	5.11	5.54	6.1	6.63	8.6
NW 27th Ave	5.18	5.63	6.15	6.7	7.93
Florida's Turnpike	5.2	5.62	6.14	6.68	
US Hwy 441	5.19	5.58	6.11	6.64	7.53
NW 199th St	5.21	5.62	6.09	6.68	8.6
I-95 Express	5.2	5.58	6.06	6.68	8.43
Miami Gardens Dr	5.18	5.59	6.06	6.71	8.96
NE 15th Ave	5.14	5.54	6.01	6.72	8.87
NW 19th Ave	5.11	5.46	5.94	6.7	5.6
NE 22nd Ave	5.07	5.42	5.89	6.68	4.9
Rail Road at Biscayne Blvd	5.04	5.42	5.87	6.66	5.77
S-29 (HW)	5.04	5.42	5.87	6.65	

Table 10-8: C-9 Canal Peak Stage at Landmarks for SLR2

Landmark	Peak Stage (ft NGVD29)				Bridge Low Cord Elevation (ft NGVD29)
	5-Yr	10-Yr	25-Yr	100-Yr	
L-33	6.17	6.45	7.12	7.46	
S-30 (TW)	5.04	5.49	5.84	6.26	
SBDD S-4 & S-5 PS	5.03	5.33	5.72	6.26	
I75 Hwy	5.04	5.36	5.74	6.29	
SBDD S-3 PS	5.05	5.4	5.82	6.34	
Ronald Reagan Turnpike	5.1	5.44	5.86	6.37	
SBDD S-7 PS /Flaming Rd	5.28	5.64	6.31	6.52	9.76
NW 57th Ave (Red Road)	5.4	5.78	6.27	6.6	9.54
SBDD S-2 PS / NW 47th Ave	5.54	6	6.42	6.77	8.9
Carol City Canal A	5.51	5.95	6.38	6.8	
NW 37th Ave	5.51	5.94	6.38	6.8	8.6
NW 27th Ave	5.62	6.03	6.45	6.87	7.93
Florida's Turnpike	5.65	6.07	6.46	6.85	
US Hwy 441	5.66	6.03	6.45	6.84	7.53
NW 199th St	5.7	6.06	6.48	6.88	8.6
I-95 Express	5.71	6.05	6.49	6.89	8.43
Miami Gardens Dr	5.74	6.07	8.52	6.95	8.96
NE 15th Ave	5.75	6.08	6.52	7.06	8.87
NW 19th Ave	5.74	6.08	6.55	7.31	5.6
NE 22nd Ave	5.74	6.09	6.56	7.33	4.9
Rail Road at Biscayne Blvd	5.75	6.1	6.58	7.38	5.77
S-29 (HW)	5.75	6.1	6.58	7.38	

Table 10-9: C-9 Canal Peak Stage at Landmarks for SLR3

Landmark	Peak Stage (ft NGVD29)				Bridge Low Cord Elevation (ft NGVD29)
	5-Yr	10-Yr	25-Yr	100-Yr	
L-33	6.18	6.45	7.11	7.46	
S-30 (TW)	5.52	5.67	5.99	6.49	
SBDD S-4 & S-5 PS	5.43	5.67	5.99	6.54	
I75 Hwy	5.48	5.69	6.02	6.48	
SBDD S-3 PS	5.58	5.78	6.09	6.52	
Ronald Reagan Turnpike	5.62	5.82	6.11	6.55	
SBDD S-7 PS /Flaming Rd	5.75	5.97	6.27	6.69	9.76
NW 57th Ave (Red Road)	5.82	6.12	6.39	6.78	9.54
SBDD S-2 PS / NW 47th Ave	6.03	6.27	6.57	6.92	8.9
Carol City Canal A	6.24	6.31	6.61	6.97	
NW 37th Ave	5.96	6.31	6.61	6.97	8.6
NW 27th Ave	6.06	6.4	6.68	7.06	7.93
Florida's Turnpike	6.1	6.42	6.68	7.1	
US Hwy 441	6.15	6.46	6.7	7.14	7.53
NW 199th St	6.21	6.51	6.74	7.19	8.6
I-95 Express	6.24	6.54	6.77	7.22	8.43
Miami Gardens Dr	6.3	6.59	6.81	7.29	8.96
NE 15th Ave	6.36	6.65	6.96	7.47	8.87
NW 19th Ave	6.42	6.7	7.22	7.81	5.6
NE 22nd Ave	6.44	6.8	7.25	8.11	4.9
Rail Road at Biscayne Blvd	6.48	6.85	7.31	8.17	5.77
S-29 (HW)	6.48	6.85	7.31	8.17	

10.2 PM #2 – Maximum Daily Discharge Capacity through the Primary Canals

PM #2 is the maximum discharge capacity throughout the primary canals. Discharge is calculated for canals as area weighted flow, in units of cubic feet per second per square mile of contributing area. Canal segments are generally defined as areas between water control structures, however, there are no intermittent control structures along the C-8 and C-9 Canals. Therefore, the segment associated with structures S-28 and S-29, is the entire C-8 and C-9 Canals, respectively. This means that the contributing area for S-28 and S-29 is the entire C-8 basin and C-9 basin, respectively. Structure S-30, which is on the C-9 Basin boundary, was closed for the majority or entirety of the design storms (based on control rules), so there was negligible/no additional inflow into the C-9 basin. Within the C-9 Basin, there are two areas with different allowable runoff rates based on the District's ERP Handbook; (1) "essentially unlimited inflow by gravity connections east of Red Road", and (2) "20 CSM pumped and essentially unlimited inflow by gravity connections west of Red Road or Flamingo BLVD". Therefore, the C-9 Basin discharge capacity was estimated for the entire C-9 Basin, as well as for the respective areas east and west of Red Road. **Table 10-10** through **Table 10-13** lists the canal segments identified for this analysis, the contributing area for each canal segment, and the discharge capacity calculated for each segment associated with each design and sea level rise scenario.

Discharge capacity was calculated by dividing the 12-hour moving average peak of the discharge hydrograph by the canal segments contributing area. For structures S-28 and S-29, discharge capacity was calculated by dividing the peak 12-hour discharge by the entire basin area. For the C-9 Basin, two additional estimates were made for the respective areas east and west of Red Road. These two additional estimates were necessitated by the presence of two different allowable runoff rates within the C-9 Basin. For the drainage area west of Red Road, the peak discharge at the Q-point (model discharge calculation point) located at Red Road (shown as a green dot in **Figure 10.2-1**) was divided by the contributing drainage area (highlighted in green in **Figure 10.2-1**). For the drainage area east of Red Road, the peak discharge at the Q-point located at Red Road was subtracted from the peak discharge at structure S-29, and then divided by the contributing drainage area east of Red Road. Tidal effects were filtered by using a 12-hour moving average of discharge.

Table 10-10: Water Control Catchment Discharge Capacity for 5-Year Future Conditions Design Storms

Structure / Segment	Inflow	Outflow	Water Control Catchment Area (sq.mi)	5-Year Design Storm Peak Discharge Capacity (cfs/sq.mi)			
				Current	SLR1	SLR2	SLR3
S-28	Beginning of C-8	S-28	28.22	51	48.2	44.2	39
S-29	Beginning of C-9/ Structure S-30	S-29	99.37	21.5	16.7	11.7	9.1
C-9 west of Red Road	Beginning of C-9/ Structure S-30	Q-point at Red Road	61.24	13.5	10.6	7.3	3.9
C-9 east of Red Road	Q-point at Red Road	S-29	38.13	46.7	45.7	39.6	32.7

Discharge west and east of Red Road is an estimate due to interconnected outfalls on both sides of Red Road

Table 10-11: Water Control Catchment Discharge Capacity for 10-Year Future Conditions Design Storms

Structure / Segment	Inflow	Outflow	Water Control Catchment Area (sq.mi)	10-Year Design Storm Peak Discharge Capacity (cfs/sq.mi)			
				Current	SLR1	SLR2	SLR3
S-28	Beginning of C-8	S-28	28.22	61.9	60.3	57.4	50.5
S-29	Beginning of C-9/ Structure S-30	S-29	99.37	24.6	19.2	15.9	12.5
C-9 west of Red Road	Beginning of C-9/ Structure S-30	Q-point at Red Road	61.24	15.2	12.1	8.5	4.5
C-9 east of Red Road	Q-point at Red Road	S-29	38.13	51.3	51.5	47.9	45.5

Discharge west and east of Red Road is an estimate due to interconnected outfalls on both sides of Red Road

Table 10-12: Water Control Catchment Discharge Capacity for 25-Year Future Conditions Design Storms

Structure / Segment	Inflow	Outflow	Water Control Catchment Area (sq.mi)	25-Year Design Storm Peak Discharge Capacity (cfs/sq.mi)			
				Current	SLR1	SLR2	SLR3
S-28	Beginning of C-8	S-28	28.22	82.8	82	82	66.1
S-29	Beginning of C-9/ Structure S-30	S-29	99.37	29.3	25.2	21.7	16.6
C-9 west of Red Road	Beginning of C-9/ Structure S-30	Q-point at Red Road	61.24	17.9	15.3	11.9	7.6
C-9 east of Red Road	Q-point at Red Road	S-29	38.13	65.8	68	65.5	58

Discharge west and east of Red Road is an estimate due to interconnected outfalls on both sides of Red Road

Table 10-13: Water Control Catchment Discharge Capacity for 100-Year Future Conditions Design Storms

Structure / Segment	Inflow	Outflow	Water Control Catchment Area (sq.mi)	100-Year Design Storm Peak Discharge Capacity (cfs/sq.mi)			
				Current	SLR1	SLR2	SLR3
S-28	Beginning of C-8	S-28	28.22	115.3	115.5	103.4	82.6
S-29	Beginning of C-9/ Structure S-30	S-29	99.37	37.5	34	29.7	23.1
C-9 west of Red Road	Beginning of C-9/ Structure S-30	Q-point at Red Road	61.24	20.9	18.1	14.1	8.7
C-9 east of Red Road	Q-point at Red Road	S-29	38.13	89.1	90.9	88.7	80.9

Discharge west and east of Red Road is an estimate due to interconnected outfalls on both sides of Red Road

Figure 10.2-1 shows the contributing areas draining to each canal segment. The C-8 catchment polygon was based on the District's Arc Hydro Enhanced Database (AHED). The C-9 catchment polygons were based on both the District's AHED as well as SBDD and Miami-Dade County subbasins. It is important to note that the C-9 Basin is technically one drainage area and does not have a real drainage divide. The two drainage areas shown within the C-9 Basin represent the spatial variability in the District's allowable discharge rates within the C-9 Basin. The area-weighted discharge presented for the areas east and west of Red Road are an approximation due to the uncertainty in the exact location of this allowable runoff-based basin divide. Additionally, the drainage areas east and west of Red Road are interconnected. Although the drainage divide is specified as Red Road, the contributing drainage area on the north side of the C-9 Canal extends east of Red Road and has two outfalls that are interconnected, one east of Red Road and one west of Red Road. For this analysis, the discharge at Red Road was used, so some discharge from the contributing drainage area is not included as it discharges further downstream. It should be noted that comparing the discharge in the western half of the C-9 Canal to the permitted rates does not have significant meaning as there are several gravity connections to the C-9 Canal west of Red Road and two pumped connections east of Red Road.

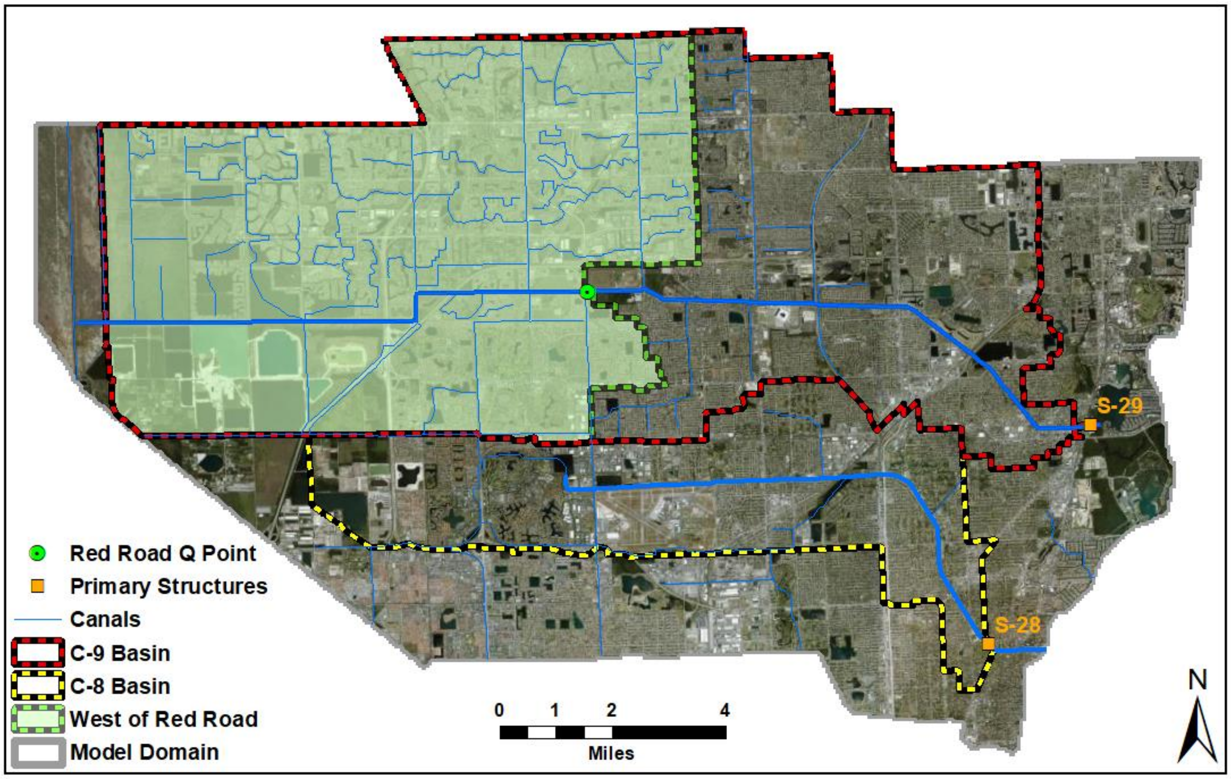

Figure 10.2-1: Catchment Areas for Calculating PM #2

The figures in **Section 10.2.1** through **Section 10.2.4** present visual comparisons of the area-weighted discharge hydrographs for the C-8 and C-9 Canal for each design storm under three sea level rise conditions vs current conditions. An additional two hydrographs are presented for areas east and west of Red Road. Areas east of Red Road are allowed unlimited discharge by gravity and areas west of Red Road have a pumped discharge limitation equal to 20 CSM. It is important to note that the discharge capacity east and west of Red Road is approximate as there are several gravity connections west of Red Road and pumped connections east of Red Road. Additionally, there are pumped connections east of Red Road that share a common drainage area with west of Red Road due to the interconnectivity of the drainage system. Therefore, the discharge capacity of the C-9 Canal, with respect to east or west of Red Road, is strictly an estimate and should not be used for regulatory purposes.

Although the peak discharge during each design storm event are referred to in this section as the calculated discharge capacity, the true capacity of the canal segment is the net discharge corresponding to the largest design flood event that remains within the banks of the canal. Therefore, the results of PM #2 must be evaluated in conjunction with the results of PM #1 (Maximum Stage in Primary Canals) and PM #5 (Frequency of Flooding).

10.2.1 5-Year Design Storms

Figure 10.2-2 through **Figure 10.2-5** present a visual comparison of the area-weighted discharge hydrographs for each canal segment with respect to the 5-year 72-hour design storm for each sea level rise scenario.

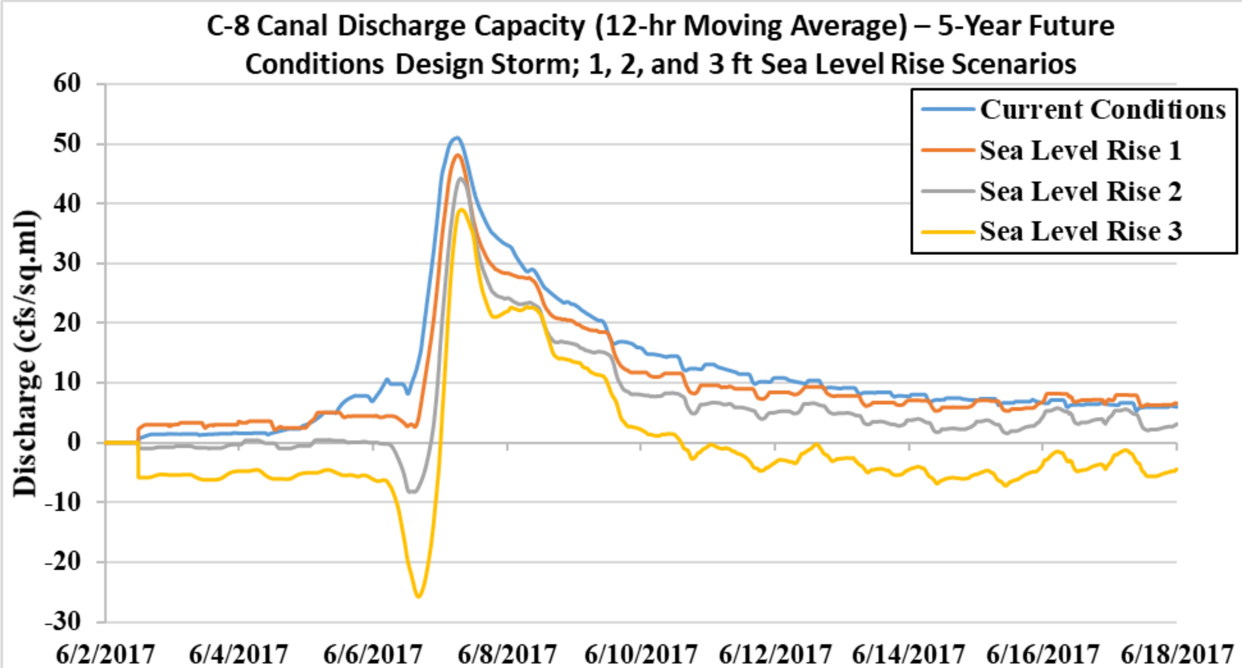

Figure 10.2-2: Area-Weighted Discharge Hydrograph for C-8 Canal (S-28) for 5-Year Design Storms

For both the C-8 and C-9 Canals, the discharge capacity for the 5-year design storm is reduced with the increase in sea level rise. This was expected as it was believed that the increased tidal water levels would reduce the structures ability to discharge and at some point, cause a flow reversal. Although the tidal structures are designed to prevent backwater through gate operation (gates are closed when tailwater stage is higher than headwater stage), the increase tailwater stages due to sea level rise allow the tidal water to overtop and/or bypass the structure. In the C-8 Canal, a flow reversal can be seen during the 5-year SLR2 scenario and is significantly larger during the SLR3 scenario.

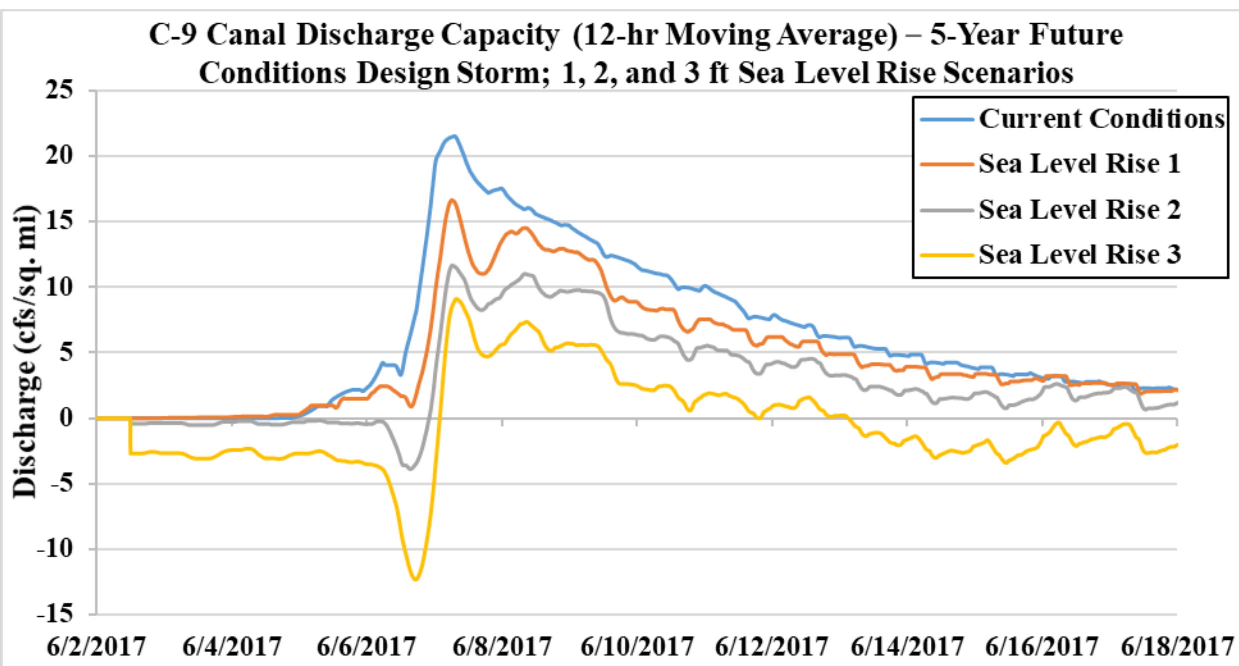

Figure 10.2-3: Area-Weighted Discharge Hydrograph for C-9 Canal (S-29) for 5-Year Design Storms

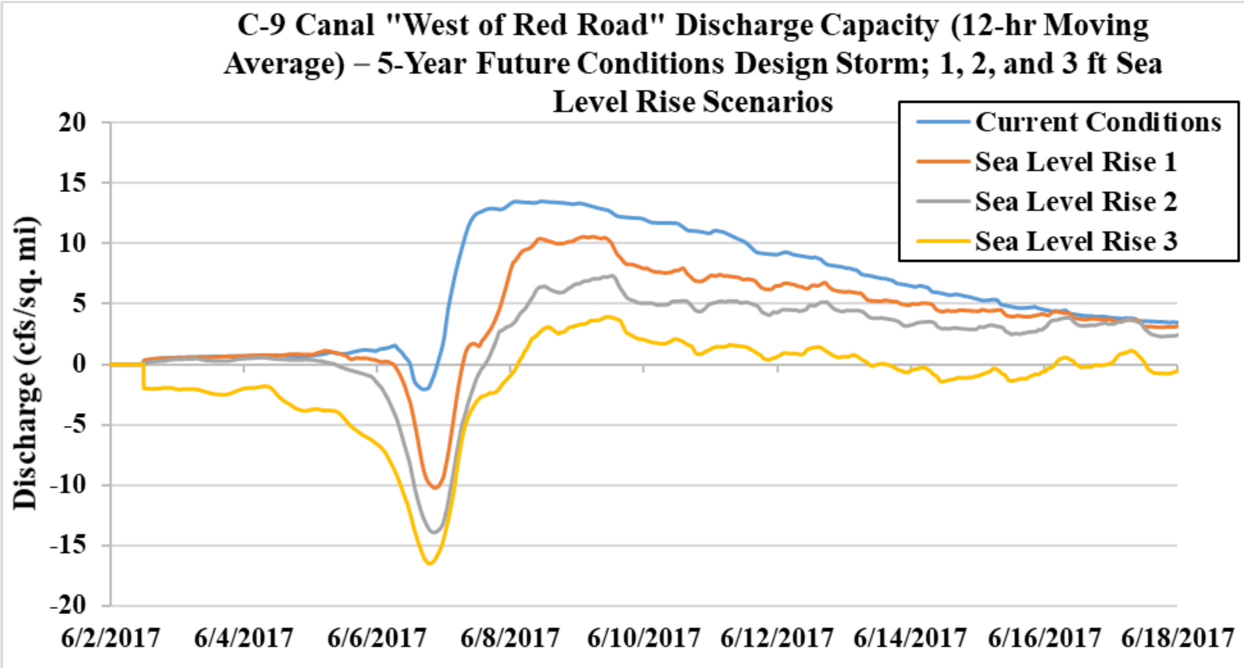

Figure 10.2-4: Area Weighted Discharge Hydrograph for C-9 Canal West of Red Road for 5-Year Design Storms

Discharge west of Red Road is an estimate due to interconnected outfalls on both sides of Red Road

The peak discharge capacity of the C-9 Canal west of Red Road was 13.5 CSM for the 5-year current conditions scenario and is further reduced for each sea level rise scenario, resulting in less than 5 CSM for SLR3. This reduction is caused by higher water levels east of Red Road, which is a result of sea level rise. The western C-9 basin is drained by pumps on the secondary canals. Based on simulated stages in the C-9 canal, the future conditions pumping duration was not limited by current permit conditions requiring pumps to shut off when stages in C-9 reach a certain level (between 6.5 - 7.0 ft NGVD29, depending on location). Therefore the total discharge to the C-9 canal under future sea level rise scenarios would likely be greater than current conditions due to increased groundwater levels, which tends to increase runoff. This shows that the simulated reduction in discharge capacity of the C-9 Canal was not caused by a reduction in discharge to the canal but is caused by higher tailwater conditions in the eastern segment of C-9. The future discharge capacity is inversely related to sea level.

Figure 10.2-4 shows negative discharge during peak rainfall. This occurs because there is a delayed response in the west side of C-9 as there is a significant amount of dead storage (large lakes in SBDD) and because of the C-9 Impoundment, which is pulling water from the western C-9 Canal. The storage in the west side is controlled by pumps that turn on at an elevation higher than control elevation (See **Appendix E**) . As the pumps turn on and the C-9 Impoundment pumps turn off, the discharge becomes positive. For the area east of Red Road, as shown in **Figure 10.2-5**, a negative discharge during peak rainfall is seen during the SLR3 scenario. This indicates that under the 3 ft sea level rise scenario, the inflection point is shifted west, past Red Road, which can be seen in **Figure 10.1-3**. The inflection point is the point in which the slope of the hydraulic grade line changes from positive to negative.

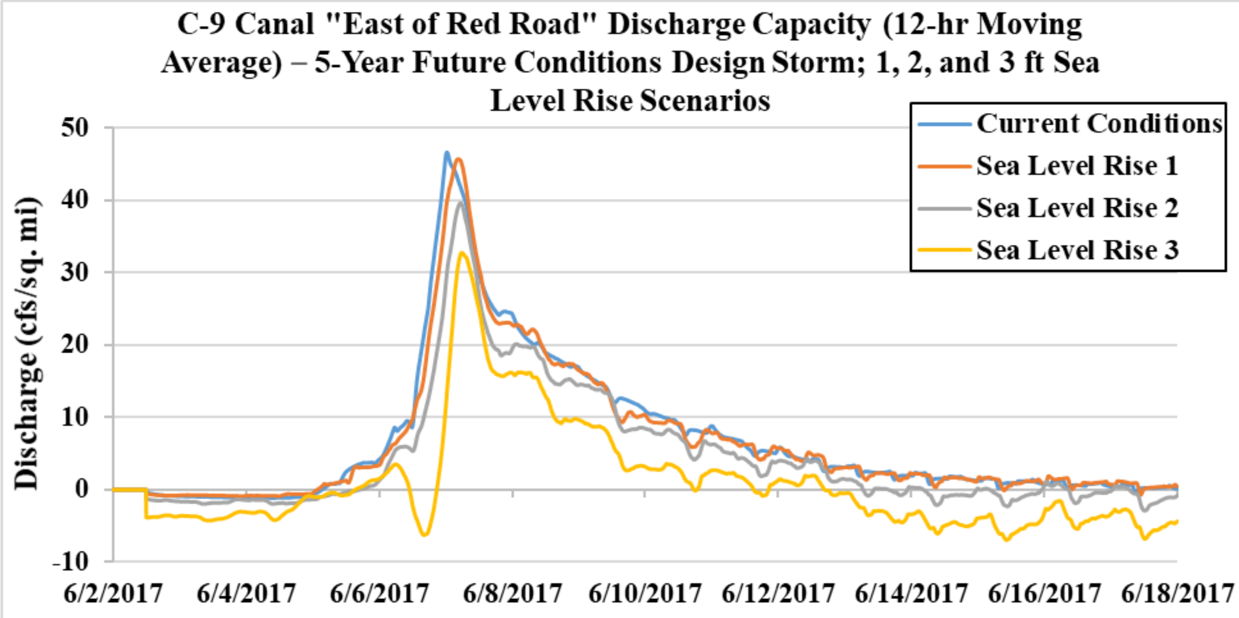

Figure 10.2-5: Area-Weighted Discharge Hydrograph for C-9 Canal East of Red Road for 5-Year Design Storms

Discharge east of Red Road is an estimate due to interconnected outfalls on both sides of Red Road

10.2.2 10-Year Design Storms

Figure 10.2-6 through **Figure 10.2-9** present a visual comparison of the area-weighted discharge hydrographs for each canal segment with respect to the 10-year 72-hour design storm for each sea level rise scenario.

For both the C-8 and C-9 Canals, the discharge capacity for the 10-year design storm is reduced with the increase in sea level rise. For both the C-8 and C-9 Canals, a flow reversal can be seen during the SLR2 scenario and is significantly larger during the SLR3 scenario.

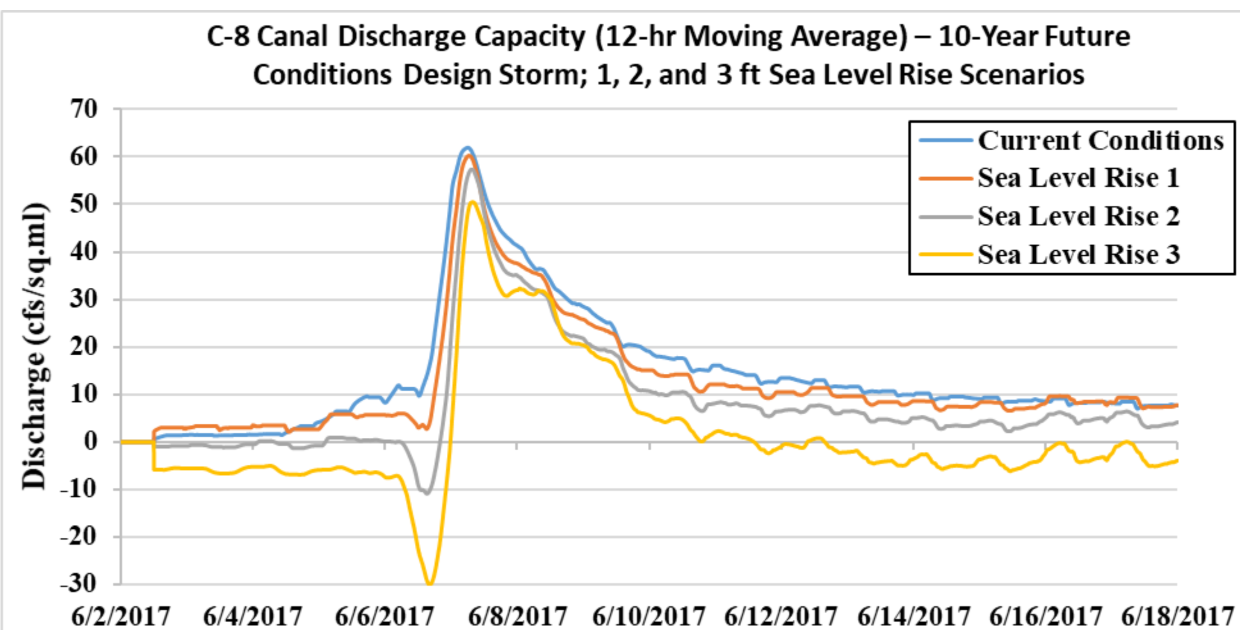

Figure 10.2-6: Area-Weighted Discharge Hydrograph for C-8 Canal (S-28) 10-Year Design Storms

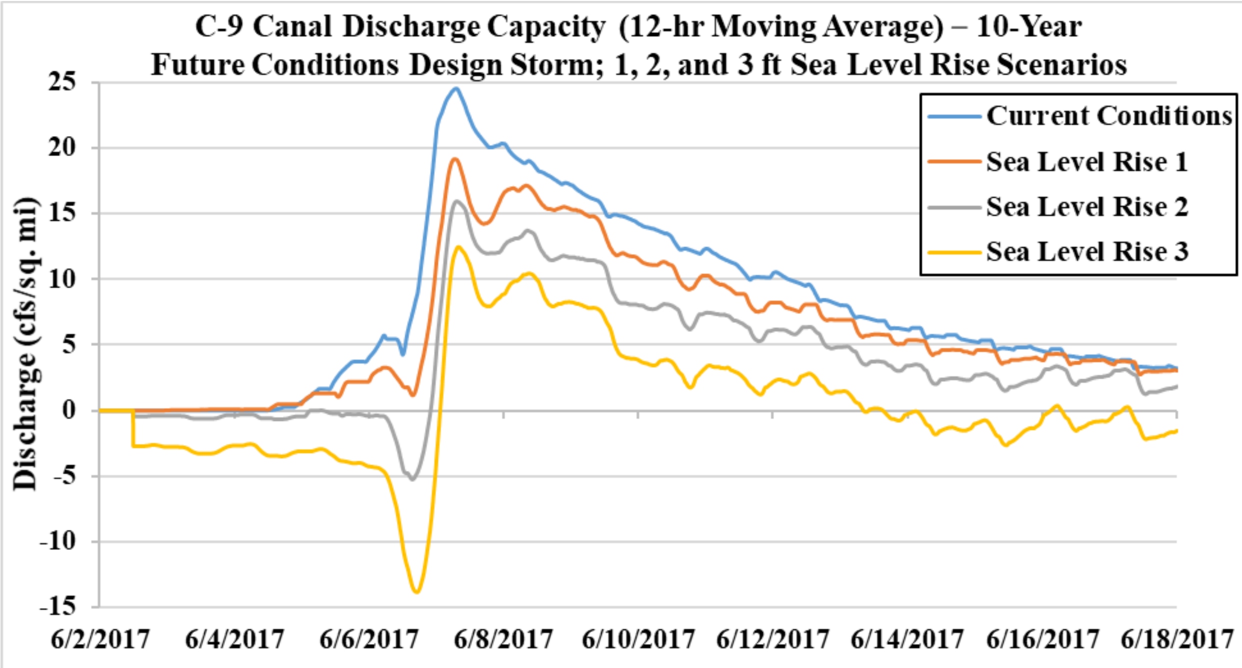

Figure 10.2-7: Area-Weighted Discharge Hydrograph for C-9 Canal (S-29) 10-Year Design Storms

The peak discharge capacity of the C-9 Canal west of Red Road was 15.2 CSM for the 10-year current conditions scenario and is further reduced for each sea level rise scenario, resulting in less than 5 CSM for SLR3. This reduction is caused by higher water levels east of Red Road, which is a result of sea level rise. The western C-9 basin is drained by pumps and based on simulated stages in the C-9 canal, the pumping duration was not limited, so total discharge to the C-9 canal under sea level rise scenarios were equivalent or greater than current conditions due to increased groundwater levels. This shows that the reduction in discharge capacity of the C-9 Canal was not caused by a reduction in discharge to the canal.

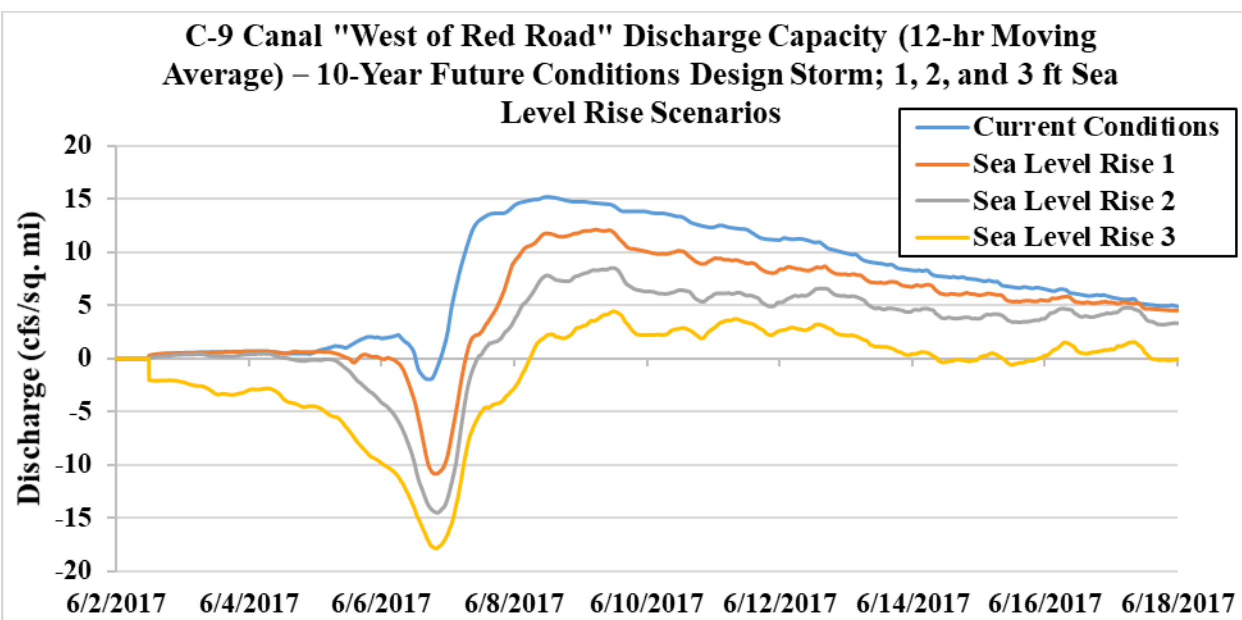

Figure 10.2-8: Area Weighted Discharge Hydrograph for C-9 Canal West of Red Road for 10-Year Design Storms

Figure 10.2-8 shows negative discharge during peak rainfall, similar to the 5-year storm results. Again, this occurs because there is a delayed response in the west side as there is a significant amount of dead storage (large lakes in SBDD) and because of the C-9 Impoundment, which is pulling water from the western C-9 Canal. The storage in the west side is controlled by pumps that turn on at an elevation higher than control elevation. As the pumps turn on and the C-9 Impoundment pumps turn off, the discharge becomes positive. For the area east of Red Road, as shown in **Figure 10.2-9**, a negative discharge during peak rainfall is seen during the SLR3 scenario. This indicates that under the 3 ft sea level rise scenario, the inflection point is shifted west, past Red Road, which can be seen in **Figure 10.1-5**.

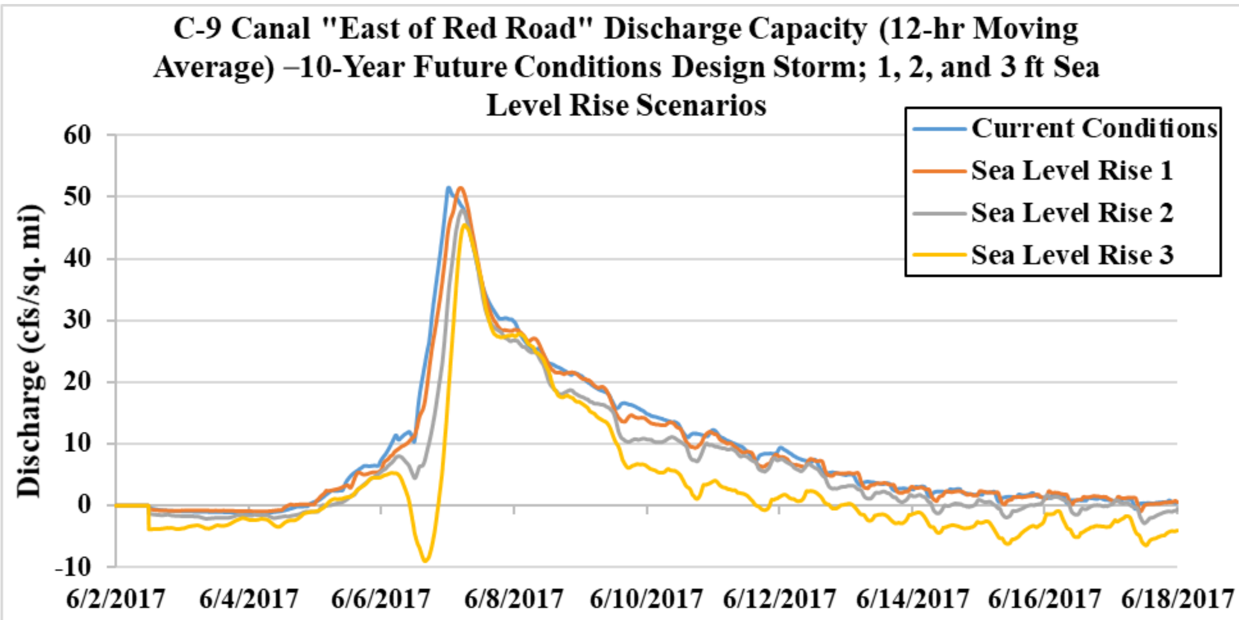

Figure 10.2-9: Area-Weighted Discharge Hydrograph for C-9 Canal East of Red Road for 10-Year Design Storms

10.2.3 25-Year Design Storms

Figure 10.2-13, and **Figure 10.2-14** present a visual comparison of the area-weighted discharge hydrographs for each canal segment with respect to the 25-year 72-hour design storm for each sea level rise scenario.

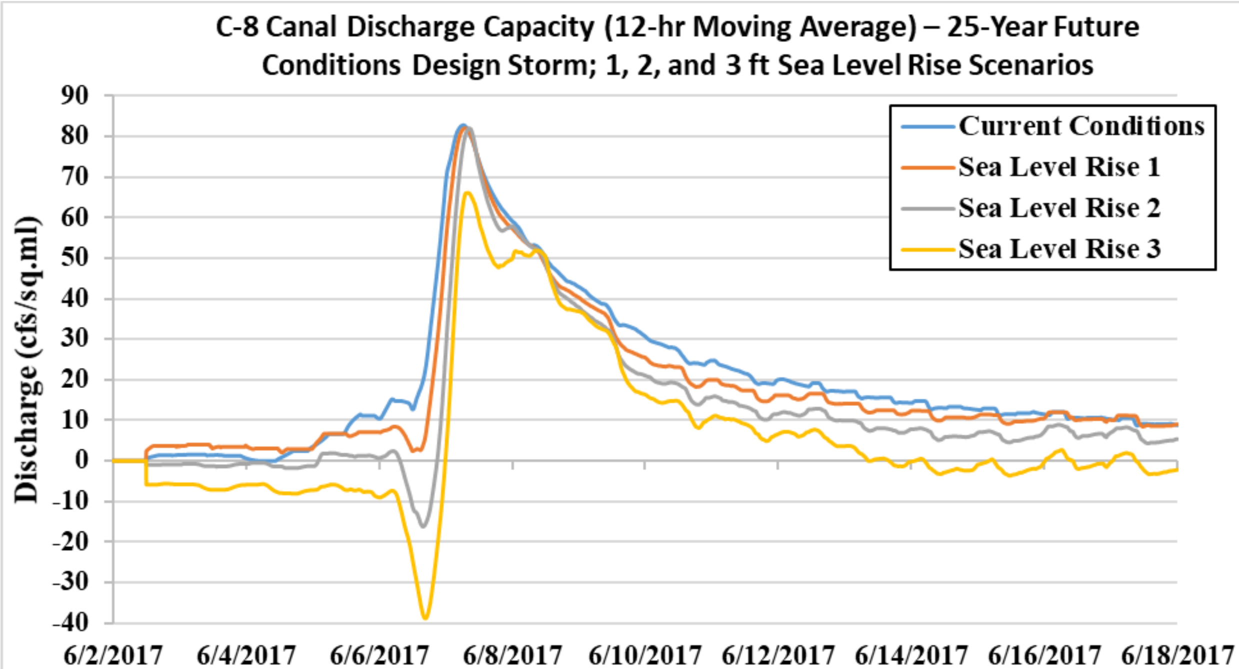

Figure 10.2-10: Area-Weighted Discharge Hydrograph for C-8 Canal (S-28) 25-Year Design Storms

For both the C-8 and C-9 Canals, the discharge capacity for the 25-year design storm is reduced with the increase in sea level rise. For both the C-8 and C-9 Canals, a flow reversal can be seen during the SLR2 scenario and is significantly larger during the SLR3 scenario.

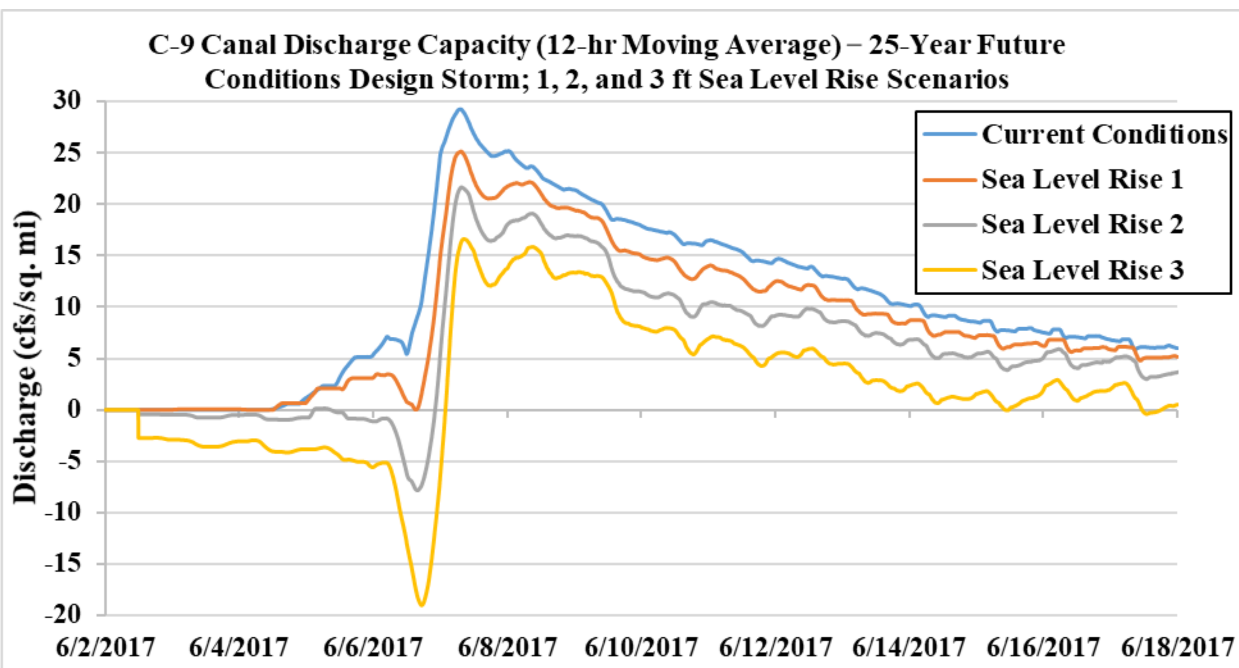

Figure 10.2-11: Area-Weighted Discharge Hydrograph for C-9 Canal (S-29) 25-Year Design Storms

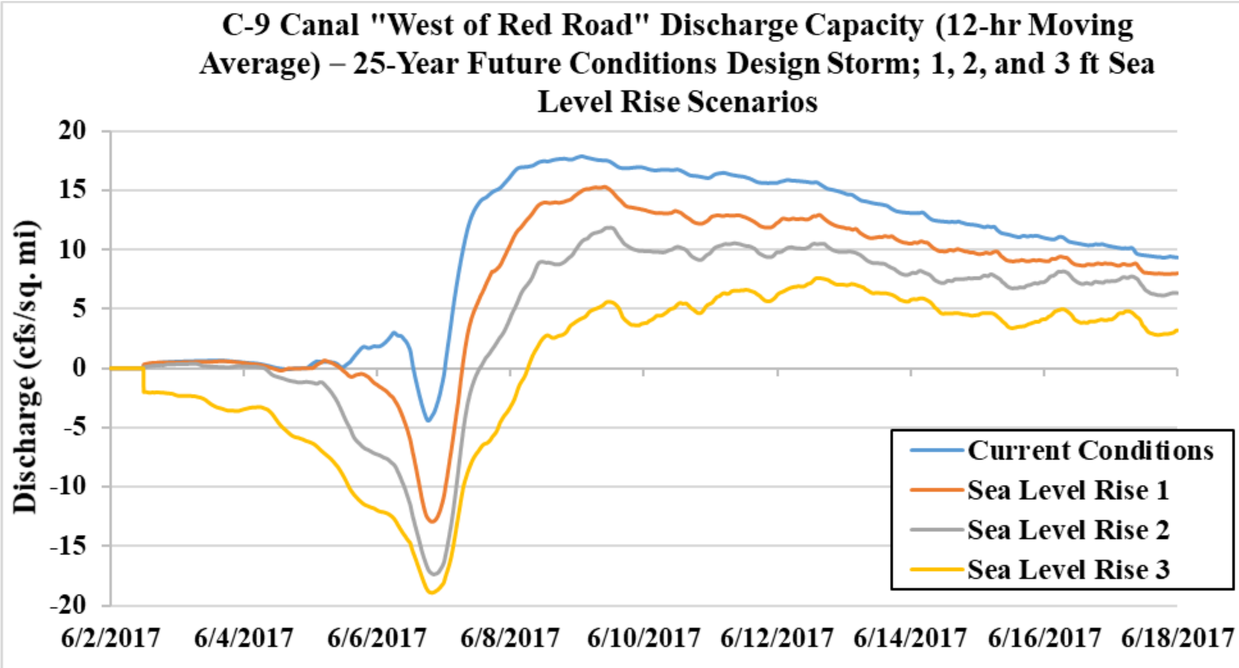

Figure 10.2-12: Area Weighted Discharge Hydrograph for C-9 Canal West of Red Road for 25-Year Design Storms

The peak discharge capacity of the C-9 Canal west of Red Road was 17.9 CSM for the 25-year current conditions scenario and is further reduced for each sea level rise scenario, resulting in less than 8 CSM for SLR3. This reduction is caused by higher water levels east of Red Road, which is a result of sea level rise. Like the 5-year and 10-year design storms, the drainage by pumps to the western C-9 canal was not limited by simulated stage, therefore, the reduction in discharge capacity was not caused by a reduction in discharge to the C-9 Canal.

Figure 10.2-12 shows negative discharge during peak rainfall. This occurs for the same reasons previously described in the discussion of the 5-year and 10-year storm events. For the area east of Red Road, as shown in **Figure 10.2-13**, a negative discharge during peak rainfall is seen during the SLR3 scenario. This indicates that under the 3 ft sea level rise scenario, the inflection point is shifted west, past Red Road, which can be seen in **Figure 10.1-7**. Interestingly, the peak discharge capacity for SLR1 is greater than current conditions, which could indicate that the changes in future conditions runoff potential and initial groundwater elevation is more influential than the increase in sea level for the 25-year design storm. For the 3 ft sea level rise scenario, there was 1 pump station east of Red Road that had limited pumping duration due to simulated stages in the C-9 Canal.

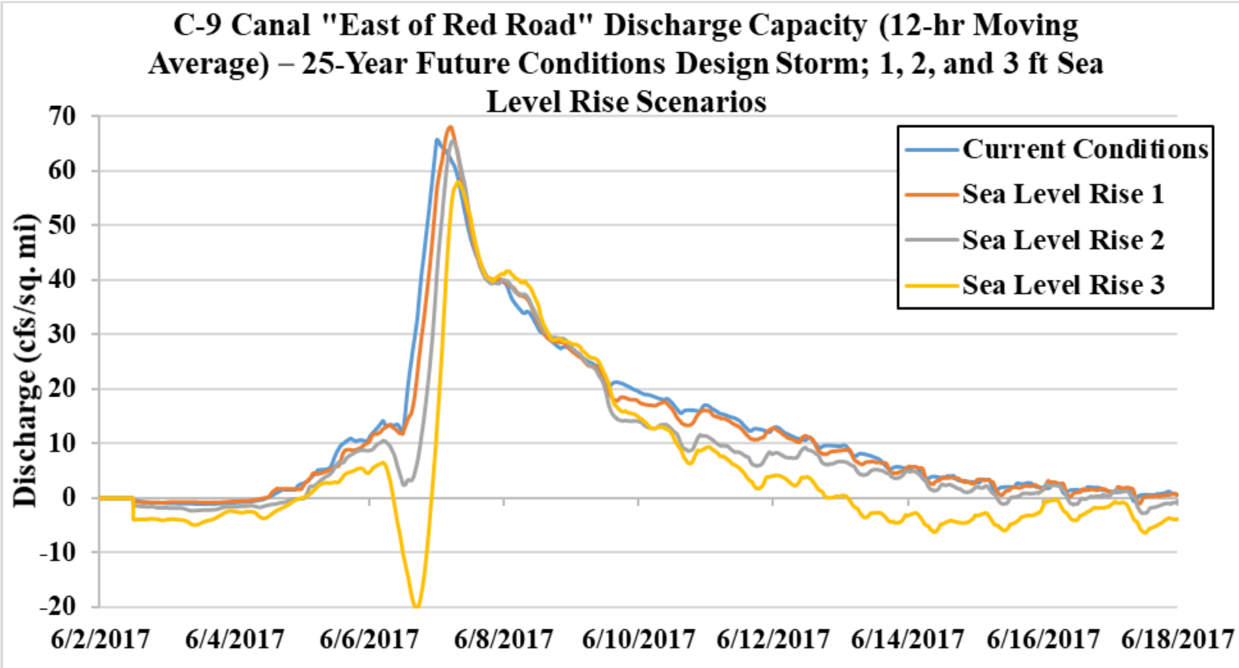

Figure 10.2-13: Area-Weighted Discharge Hydrograph for C-9 Canal East of Red Road for 25-Year Design Storms

10.2.4 100-Year Design Storms

Figure 10.2-14 through **Figure 10.2-17** presents a visual comparison of the area-weighted discharge hydrographs for each canal segment with respect to the 100-year 72-hour design storm for each sea level rise scenario.

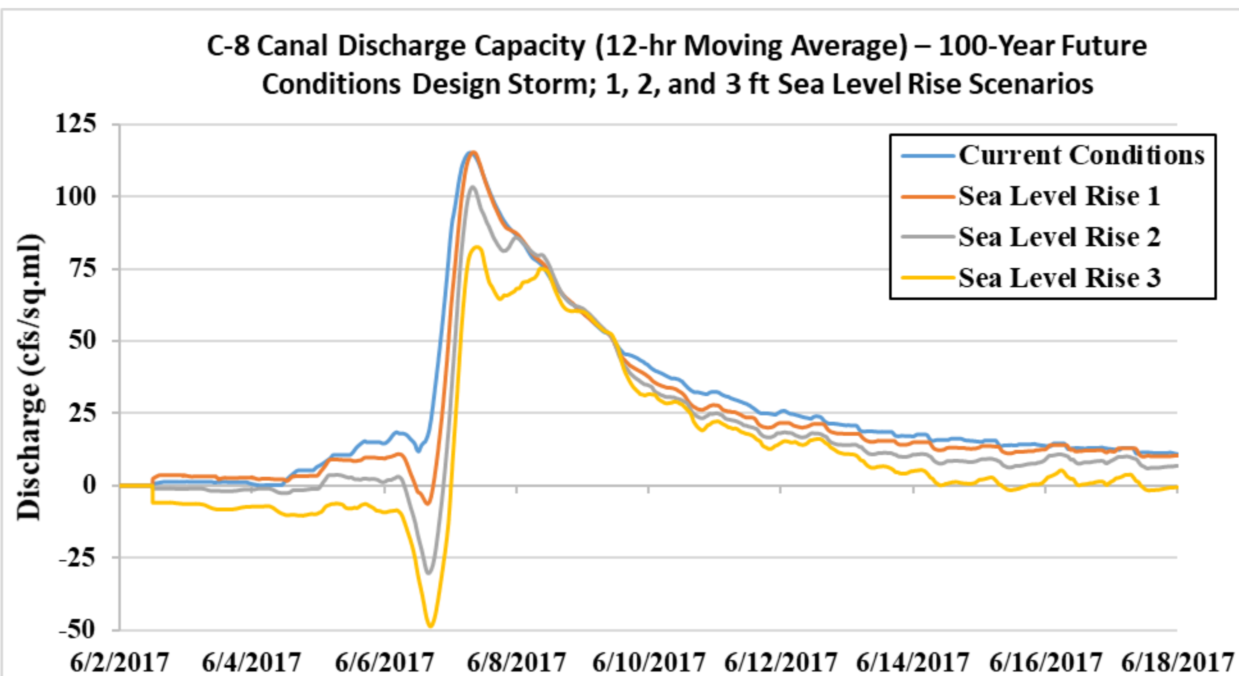

Figure 10.2-14: Area-Weighted Discharge Hydrograph for C-8 Canal (S-28) 100-Year Design Storms

For the C-8 Canal, the discharge capacity for the 100-year design storm is slightly higher (0.17 CSM) for the SLR1 scenario than current conditions but is reduced with further increase in sea level rise. For the C-

9 Canal, the discharge capacity for the 100-year design storm is reduced with the increase in sea level rise. For both the C-8 and C-9 Canals, a flow reversal can be seen during the SLR1 scenario and is significantly larger during the SLR3 scenario.

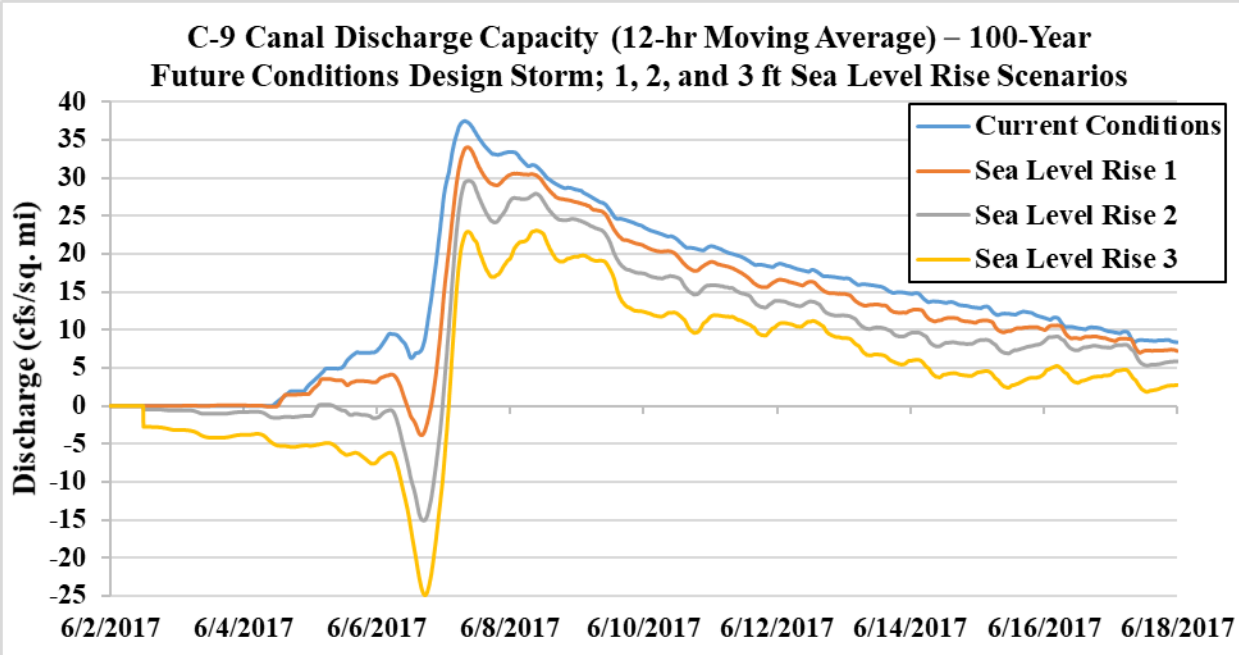

Figure 10.2-15: Area-Weighted Discharge Hydrograph for C-9 Canal (S-29) 100-Year Design Storms

The peak discharge capacity of the C-9 Canal west of Red Road was 20.9 CSM for the 25-year current conditions scenario and is further reduced for each sea level rise scenario, resulting in less than 9 CSM for SLR3.

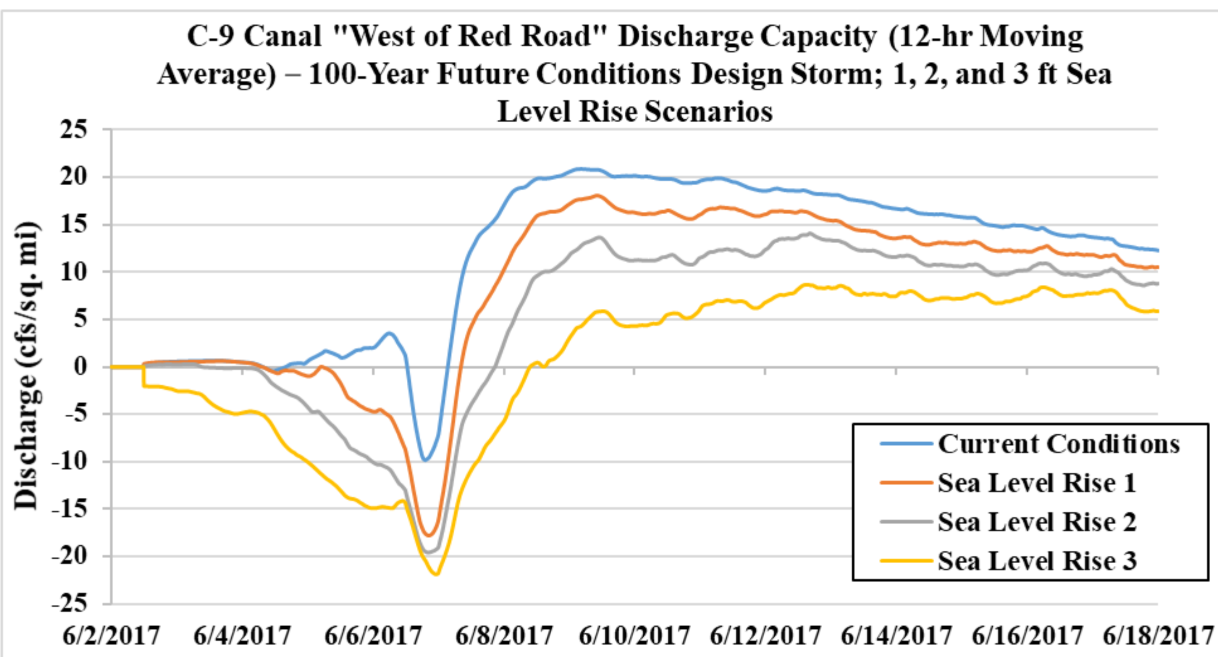

Figure 10.2-16: Area Weighted Discharge Hydrograph for C-9 Canal West of Red Road for 100-Year Design Storms

Figure 10.2-16 shows negative discharge during peak rainfall. This occurs for the same reasons previously described in the discussion of the 5, 10, and 25-year storm events.

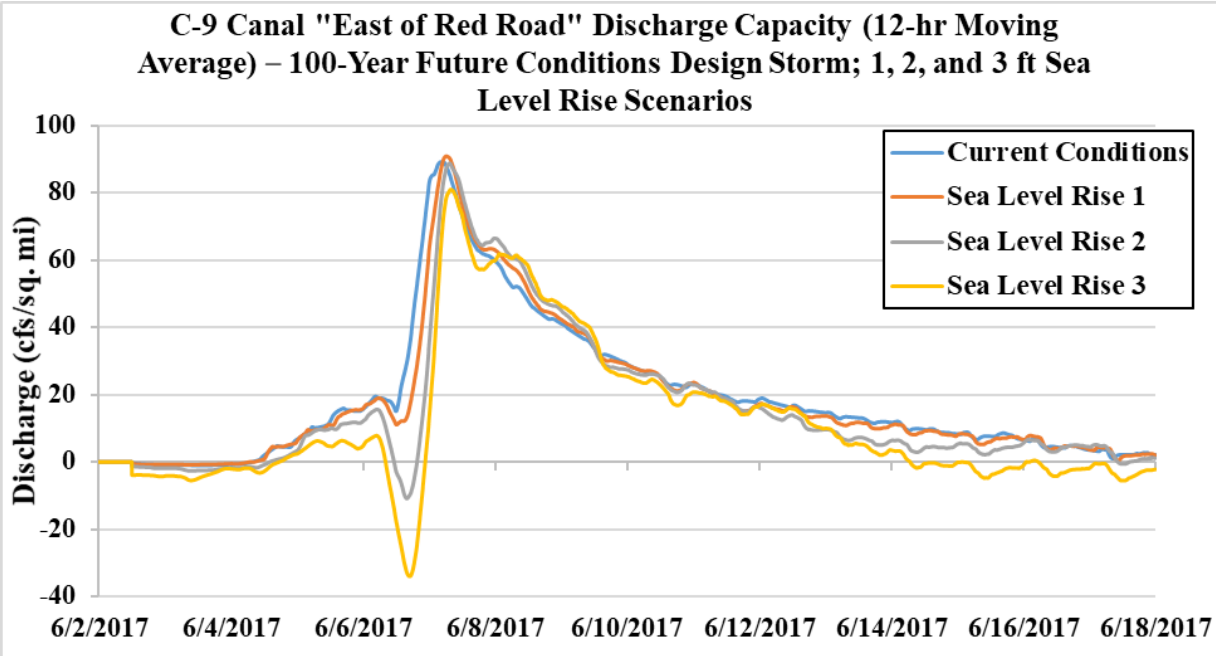

Figure 10.2-17: Area-Weighted Discharge Hydrograph for C-9 Canal East of Red Road for 100-Year Design Storms

For the area east of Red Road, as shown in **Figure 10.2-17**, a negative discharge during peak rainfall is seen during the SLR2 and SLR3 scenarios. This indicates that under the 2 ft and 3 ft sea level rise scenarios, the inflection point is shifted west, past Red Road, which can be seen in **Figure 10.1-9**. Interestingly, the peak discharge capacity for SLR1 is greater than current conditions, which could indicate that the changes in future conditions runoff potential (as a result of higher initial groundwater elevation) is more influential than the 1 ft increase in sea level for the 100-year design storm. For the 1 ft and 2 ft sea level rise scenarios, there was 1 pump station east of Red Road that had limited pumping duration due to simulated stages in the C-9 Canal. For the 3 ft sea level rise scenario, there were 2 pump stations east of Red Road that had limited pumping duration.

10.2.5 Inter-basin Discharge

Figure 10.2-18 shows the location of inter-basin connections, where discharge between the C-8 and C-9 watersheds occur, as well as between the C-8 and C-7 watersheds.

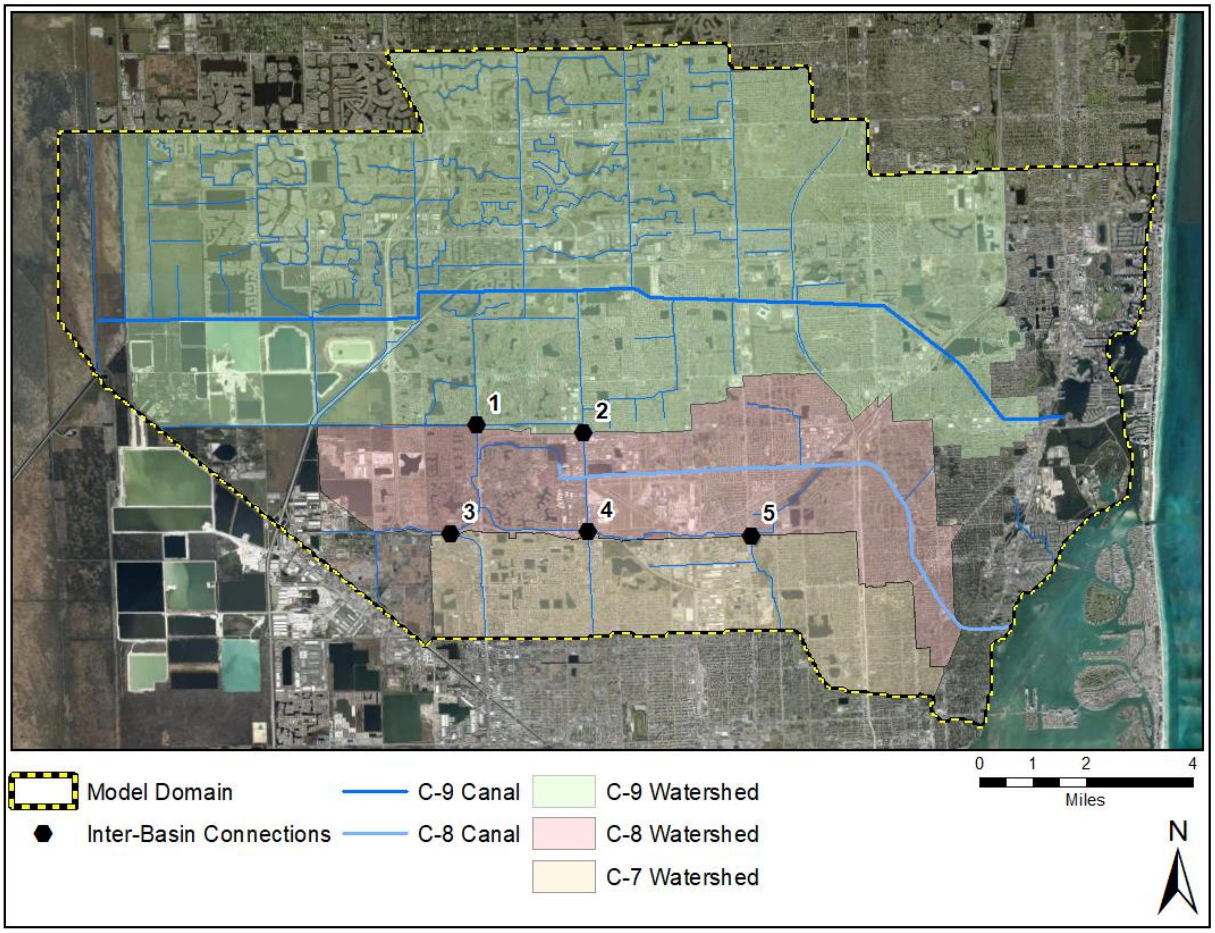

Figure 10.2-18: Location of Inter-Basin Connections

Connection 1 is a culvert under NW 78th Ave. **Figure 10.2-19** and **Figure 10.2-20** show the inter-basin discharge for the 5-year and 100-year design storms, with positive values representing flow from the C-8 to the C-9 watershed and negative values indicating flow from the C-9 to the C-8 watershed. For the 5-year current conditions design storm, there was no discharge from the C-8 to the C-9 Canal, as the flow direction was from the C-9 Canal to the C-8 Canal. Under all three future conditions sea level rise scenarios, there is inter-basin discharge in the direction from the C-8 to C-9 Canal. This is likely due to the C-9 Impoundment, which reduces stage in the C-9 Canal, creating a head gradient from C-8 to C-9.

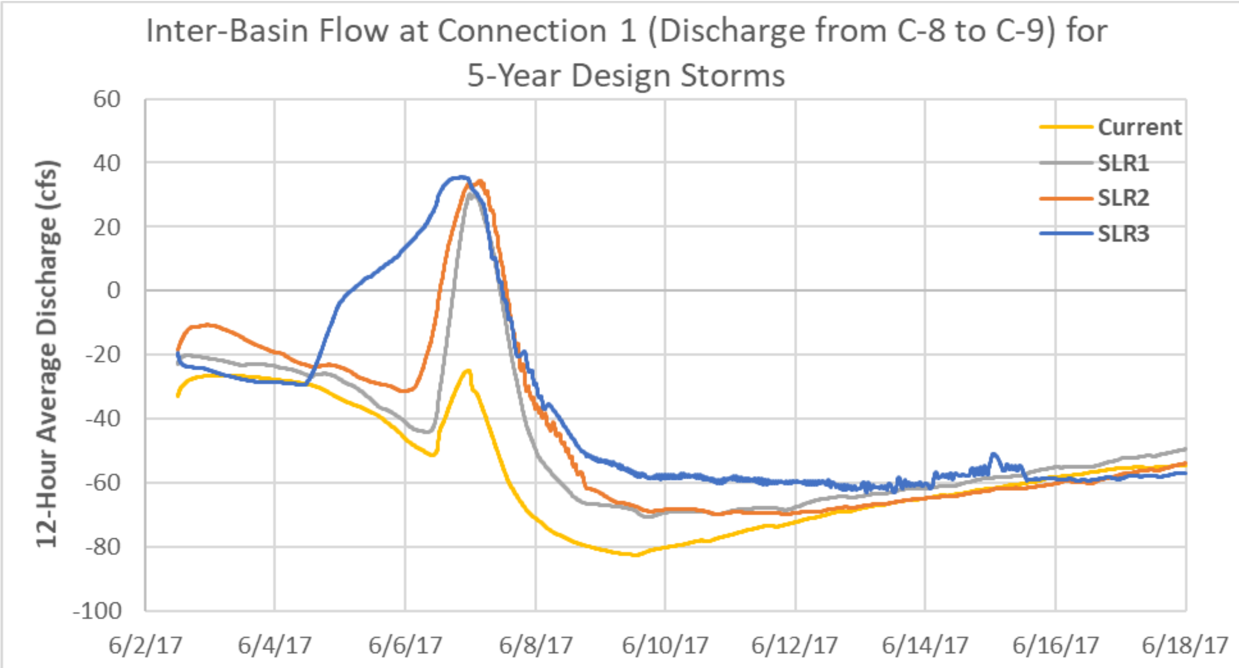

Figure 10.2-19: 5-Year Inter-Basin Discharge Between C-8 and C-9 Watersheds at Connection 1

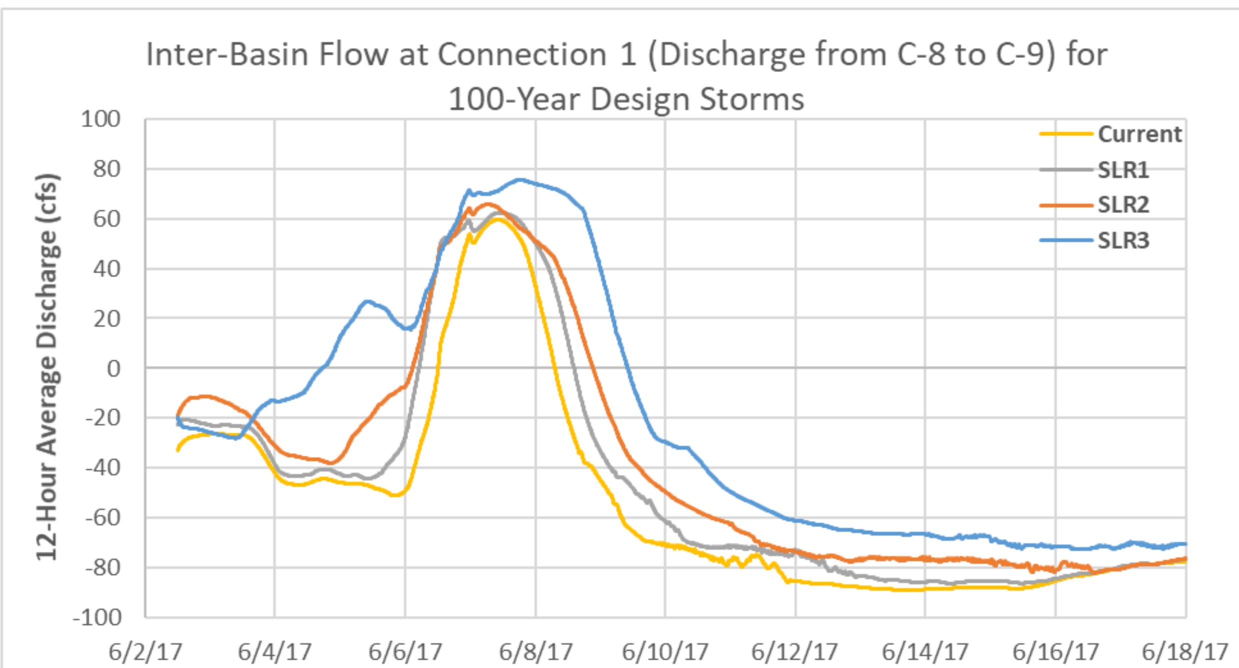

Figure 10.2-20: 100-Year Inter-Basin Discharge Between C-8 and C-9 Watersheds at Connection 1

For the 100-year future conditions design storms, the peak discharge from C-8 to C-9 watershed at this inter-basin connection doesn't change much compared to current conditions. Current conditions peak discharge was about 60 cfs, whereas the future conditions peak discharge for SLR1, SLR2, and SLR3 is 62, 66, and 76 cfs, respectively. Relative to the flow in the C-9 Canal at Red Road (1300 cfs for SLR1, 1200 cfs for SLR2, and 1100 cfs SLR3), this inter-basin exchange is small, contributing around 5-7%, respectively.

The peak discharge from C-9 to C-8 watershed at this inter-basin connection is reduced from about 90 cfs under current conditions to 70-86 cfs depending on SLR. However, this occurs several days after the peak discharge and does not contribute to peak discharge rates in the C-8 Canal.

Connection 2 is a culvert under Palmetto Expressway, just west of Red Road. **Figure 10.2-21** and **Figure 10.2-22** show the inter-basin discharge for the 5-year and 100-year design storms, with positive values representing flow from the C-9 to the C-8 watershed and negative values indicating flow from the C-8 to the C-9 watershed. For the 5-year design storm, the peak discharge from C-9 to C-8 watershed at this inter-basin connection was reduced from about 100 cfs under current conditions to about 70-90 cfs under future conditions sea level rise scenarios. The peak inter-basin discharge occurs several days after the peak discharge in the C-8 Canal. For the 5-year design storm, there was no discharge from C-8 to C-9 watershed at this inter-basin connection under current conditions, however, under SLR2 and SLR3, the peak inter-basin discharge is 30 cfs and 50 cfs, respectively. Relative to the peak flow in the C-9 Canal at Red Road (850 cfs for SLR2 and 620 cfs SLR3), this inter-basin exchange is small, contributing no more than 8%.

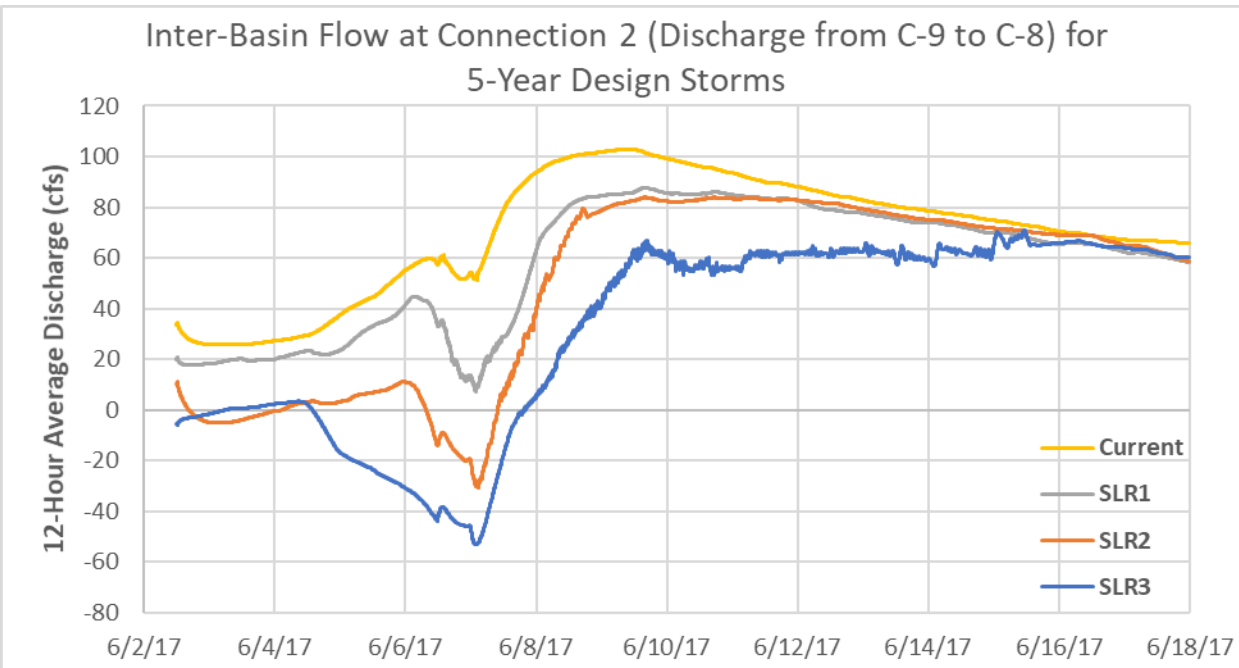

Figure 10.2-21: 5-Year Inter-Basin Discharge Between C-8 and C-9 Watersheds at Connection 2

For the 100-year design storm, the peak discharge from C-9 to C-8 watershed at this inter-basin connection was reduced from about 125 cfs under current conditions to about 80-110 cfs under future conditions sea level rise scenarios. The peak inter-basin discharge occurs several days after the peak discharge in the C-8 Canal. For the 100-year design storm, there was almost no discharge from C-8 to C-9 watershed at this inter-basin connection under current conditions, however, under all sea level rise scenarios, the peak inter-basin discharge is larger, between 30-50 cfs. Relative to the peak flow in the C-9 Canal at Red Road (1340 cfs for SLR1, 850 cfs for SLR2, and 620 cfs SLR3), this inter-basin exchange is small, contributing between 2% and 8%.

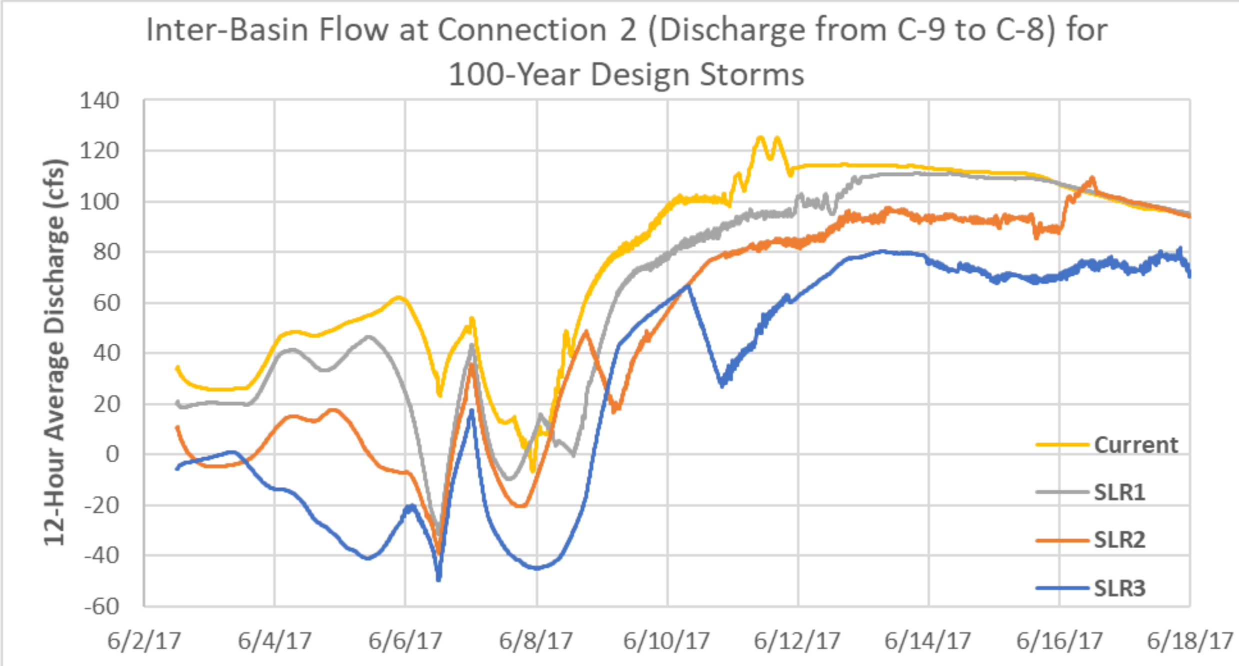

Figure 10.2-22: 100-Year Inter-Basin Discharge Between C-8 and C-9 Watersheds at Connection 2

Connection 3 is a culvert under I75. **Figure 10.2-23** and **Figure 10.2-24** show the inter-basin discharge for the 5-year and 100-year design storms, with positive values representing flow from the C-8 to the C-7 watershed and negative values indicating flow from the C-7 to the C-8 watershed. Flows from C-8 to C-7 watershed reduces the burden on the C-8 canal, peaking at 189 cfs, 237 cfs, and 266 cfs for SLR1, SLR2, and SLR3, respectively, compared to 171 cfs under current conditions.

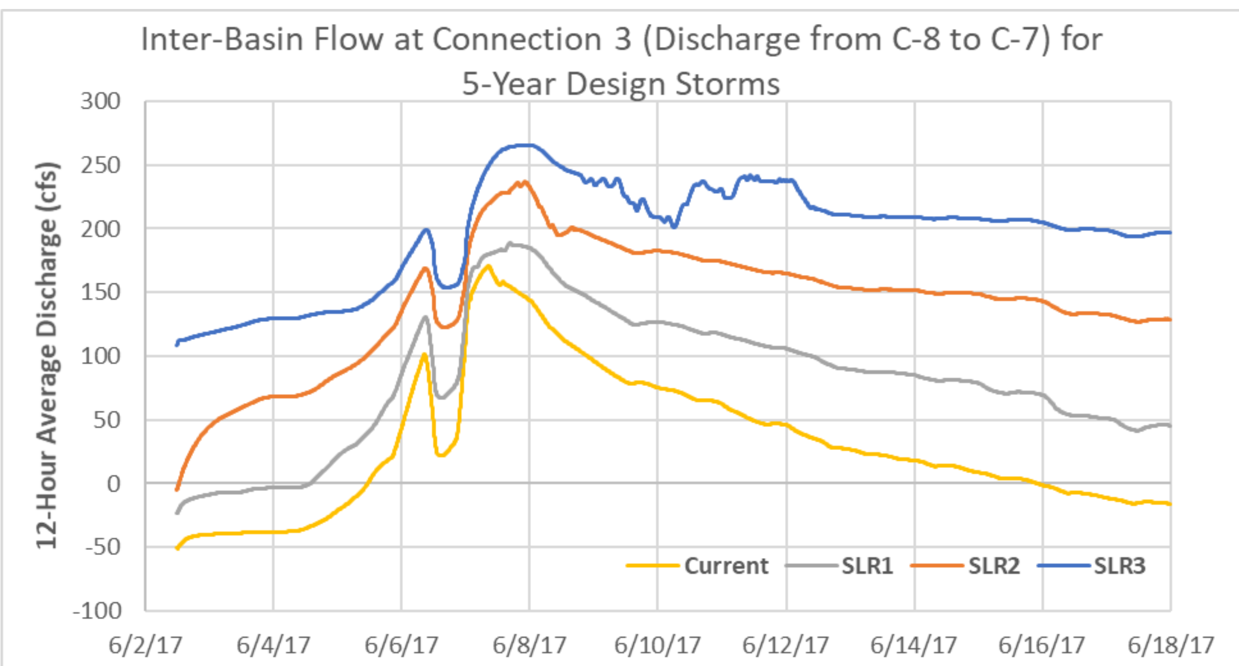

Figure 10.2-23: 5-Year Inter-Basin Discharge Between C-8 and C-7 Watersheds at Connection 3

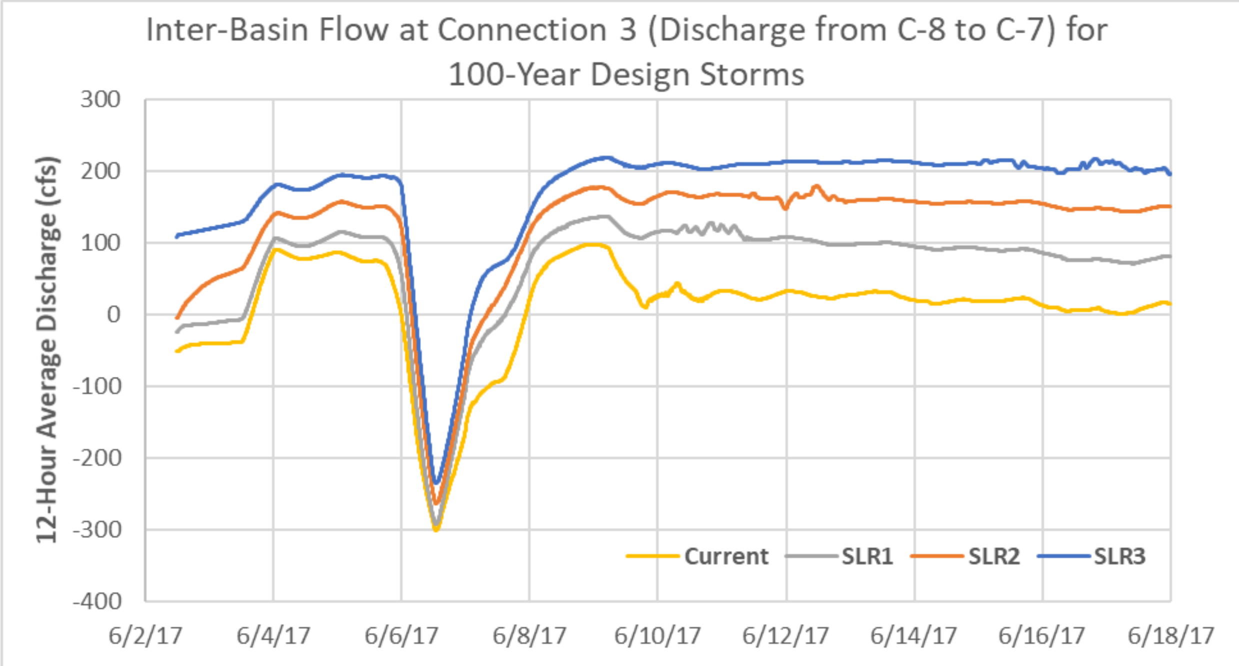

Figure 10.2-24: 100-Year Inter-Basin Discharge Between C-8 and C-7 Watersheds at Connection 3

For the 100-year design storm, the peak discharge from C-7 to C-8 watershed at this inter-basin connection was about 300 cfs for current conditions and occurs about 18 hours prior to peak discharge at S-28. For future conditions, the inter-basin discharge from C-7 to C-8 was reduced to 235 cfs for SLR1, 264 cfs for SLR2, and 291 cfs for SLR3. The reduced peak inter-basin discharge from C-7 to C-8 reduces the stress on the C-8 Canal system, as does the increased post-storm inter-basin discharge.

Connection 4 is a culvert under NE 135th St at Red Road. **Figure 10.2-25** and **Figure 10.2-26** show the inter-basin discharge for the 5-year and 100-year design storms, with positive values representing flow from the C-8 to the C-7 watershed and negative values indicating flow from the C-7 to the C-8 watershed. Flows from C-8 to C-7 watershed reduces the burden on the C-8 canal, peaking at about 50 cfs for SLR1, 60 cfs for SLR2, and 70 cfs for SLR3, compared to 40 cfs current conditions. This relieves the C-8 canal system of some stress.

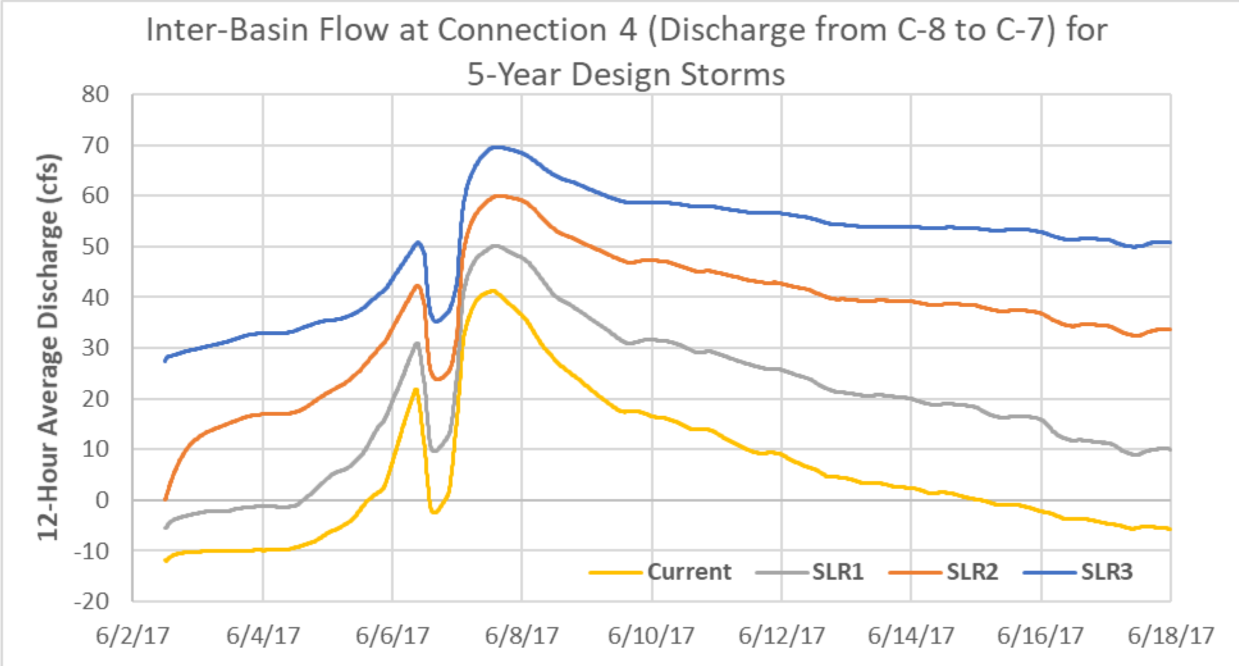

Figure 10.2-25: 5-Year Inter-Basin Discharge Between C-8 and C-7 Watersheds at Connection 4

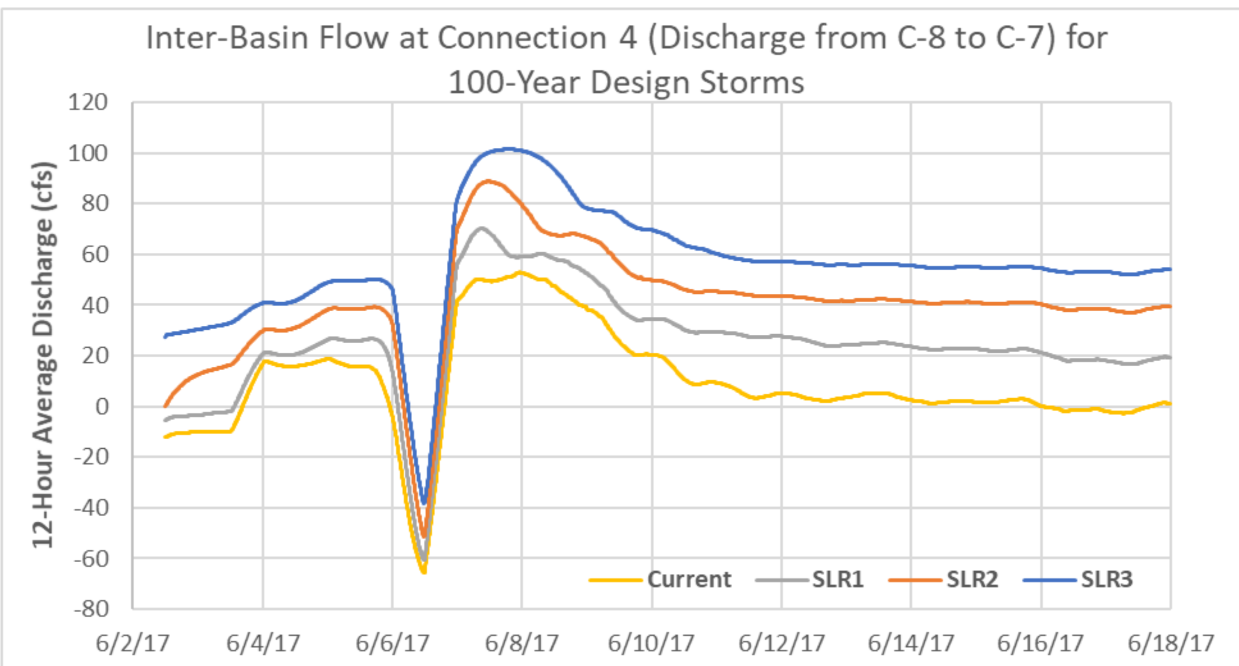

Figure 10.2-26: 100-Year Inter-Basin Discharge Between C-8 and C-7 Watersheds at Connection 4

For the 100-year design storm, the peak discharge from C-7 to C-8 watershed at this inter-basin connection was about 65 cfs for current conditions and occurs about 18 hours prior to peak discharge at S-28. For future conditions, the inter-basin discharge from C-7 to C-8 was reduced to 61 cfs for SLR1, 52 cfs for SLR2, and 39 cfs for SLR3. The reduced peak inter-basin discharge from C-7 to C-8 reduces the stress on the C-8 Canal system, as does the increased post-storm inter-basin discharge.

Connection 5 is a culvert under NE 135th St just east of NW 27th Ave. **Figure 10.2-27** and **Figure 10.2-28** show the inter-basin discharge for the 5-year and 100-year design storms, with negative values indicating flow from the C-8 to the C-7 watershed. Flow from C-8 to C-7 watershed reduces the burden on the C-8 Canal. For the 5-year design storms, there was not much change in inter-basin flow from the C-7 to C-8 Canal, staying around 100 cfs. For the 100-year SLR2 and SLR3 design storms, there was increased inter-basin flow from C-7 to C-8 during peak rainfall, which adds stress to the C-8 Canal system.

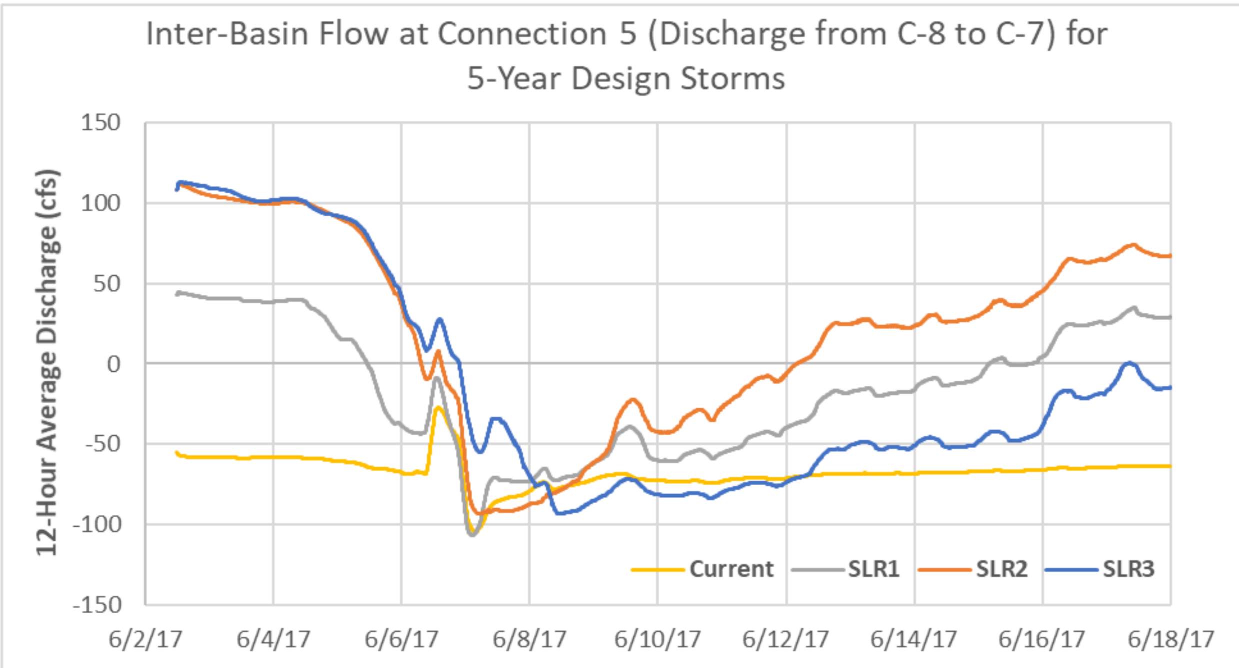

Figure 10.2-27: 5-Year Inter-Basin Discharge Between C-8 and C-7 Watersheds at Connection 5

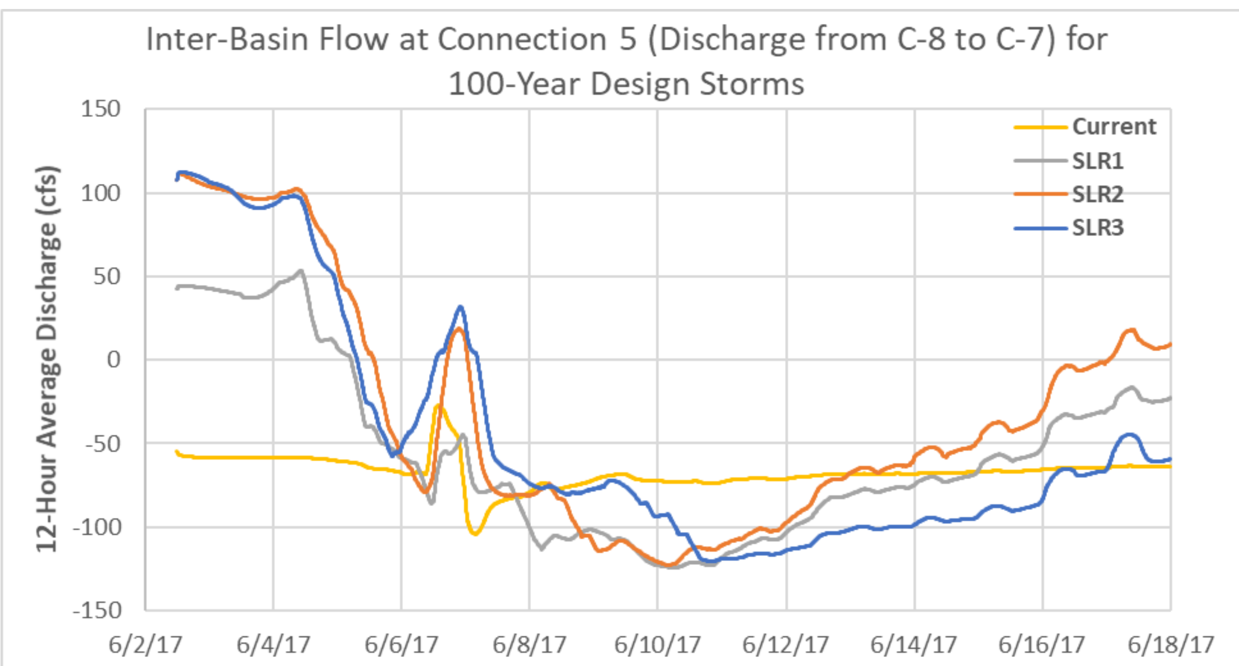

Figure 10.2-28: 100-Year Inter-Basin Discharge Between C-8 and C-7 Watersheds at Connection 5

10.3 PM #3 – Structure Performance

PM #3 shows the effective capacity of a tidal structure. For this metric, structure discharge over a range of storm events and sea level rise scenarios is compared with the original static design condition. Future condition design storms simulated three sea level rise scenarios. This PM provides insight on the structure performance under future sea level rise conditions and compares it with current conditions to determine what degradation in performance occurs, if any.

SFWMD has completed a similar evaluation for the S-28 and S-29 structures in reports titled, *The Effects of Sea Level Rise on S28 Performance* (Zhang, 2017) and *The Effects of Sea Level Rise on S29 Performance* (Zhang, 2017). In these evaluations, a simple hydraulic model was used with fixed headwater stage based on design headwater and a tailwater that oscillates tidally. To add to the work that has already been done, this PM is evaluated using the full MIKE SHE / MIKE HYDRO model results. Essentially, the main difference is that headwater is not forced, rather it is simulated using the fully dynamic model. Please note that this analysis is for informational purposes and is not intended to replace the previous work done by the District, but rather supplement it and analyze it using a different method.

10.3.1 S-28

Structure S-28 has a static design headwater and tailwater of 2.2 ft and 1.7 ft, respectively. The static design discharge is 3220 cfs based on 0.5 ft head gradient (Zhang, 2017). **Figure 10.3-1** and **Figure 10.3-2** show instantaneous values and 12-hour moving average values, respectively, for S-28 based on a 25-year design storm with 1 ft of sea level rise. Although the instantaneous peak discharge for the 25-year SLR1 is greater than current conditions, it is short lived.

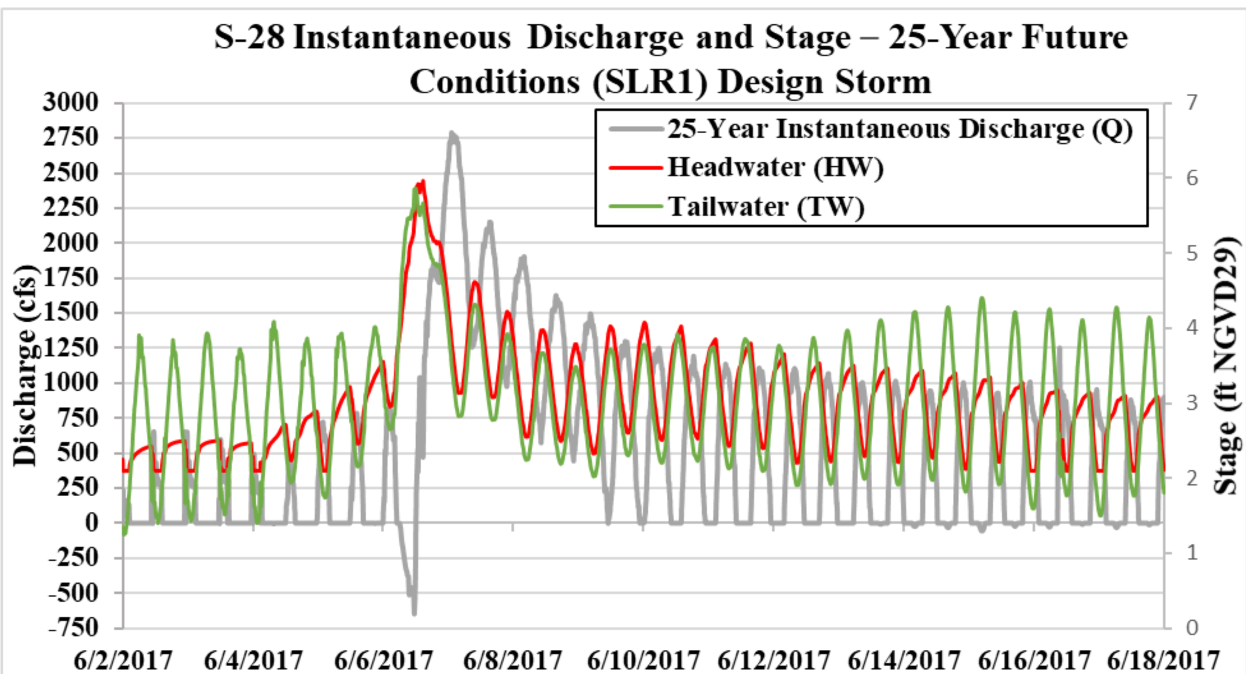

Figure 10.3-1: Instantaneous Discharge and Stage at S-28 Structure for 25-Year Future Conditions Sea Level Rise 1 Design Storm

At the peak of the storm, there is about 650 cfs of reversed flow, which is likely what caused the increased peak discharge, as there was more water “stacked” on the upstream side of the structure. Filtering out the effects of the tide reveals that the peak discharge decreased compared to current conditions.

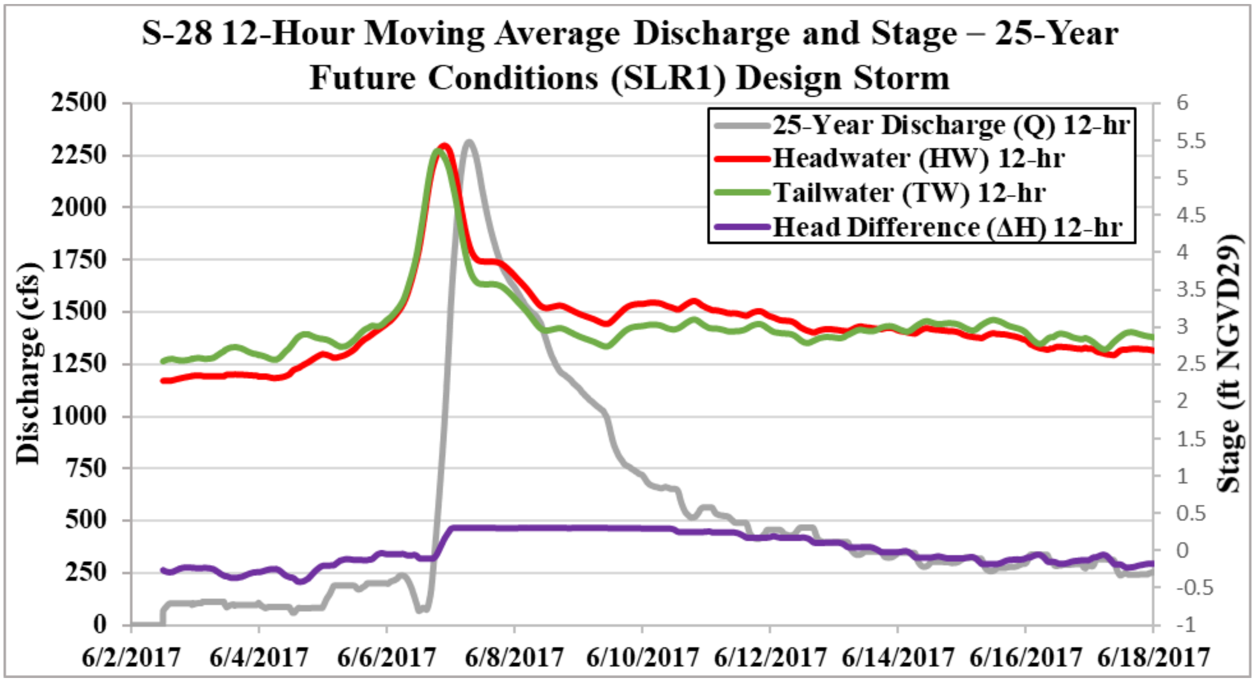

Figure 10.3-2: Tidally Averaged (12-hour) 25-Year Future Conditions Sea Level Rise 1 Design Storm Discharge, Stage, and Head Difference for Structure S-28

Figure 10.3-3 and **Figure 10.3-4** show instantaneous values and 12-hour moving average values, respectively, for S-28 based on a 100-year design storm with 1 ft of sea level rise. Although the instantaneous peak discharge for the 100-year SLR1 is greater than current conditions, it is short lived. At the peak of the storm, there is over 1,000 cfs of reversed flow, which is likely what caused the increased peak discharge, as there was more water “stacked” on the upstream side of the structure. Filtering out the effects of the tide reveals that the peak discharge slightly increased (5 cfs) compared to current conditions.

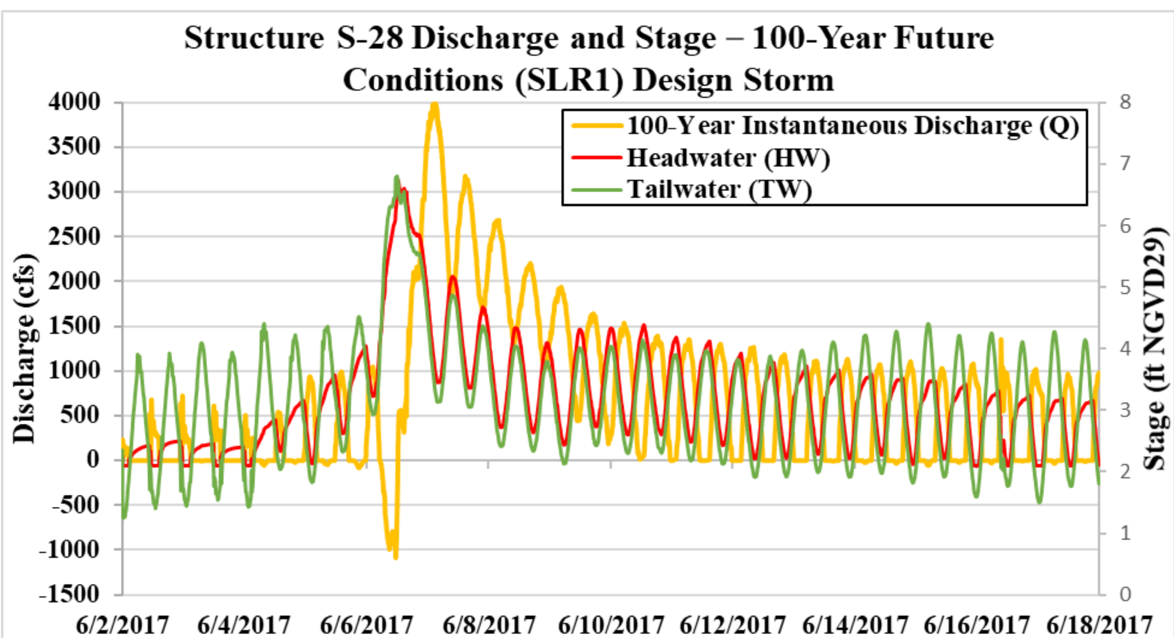

Figure 10.3-3: Instantaneous Discharge and Stage at S-28 Structure for 100-Year Future Conditions Sea Level Rise 1 Design Storm

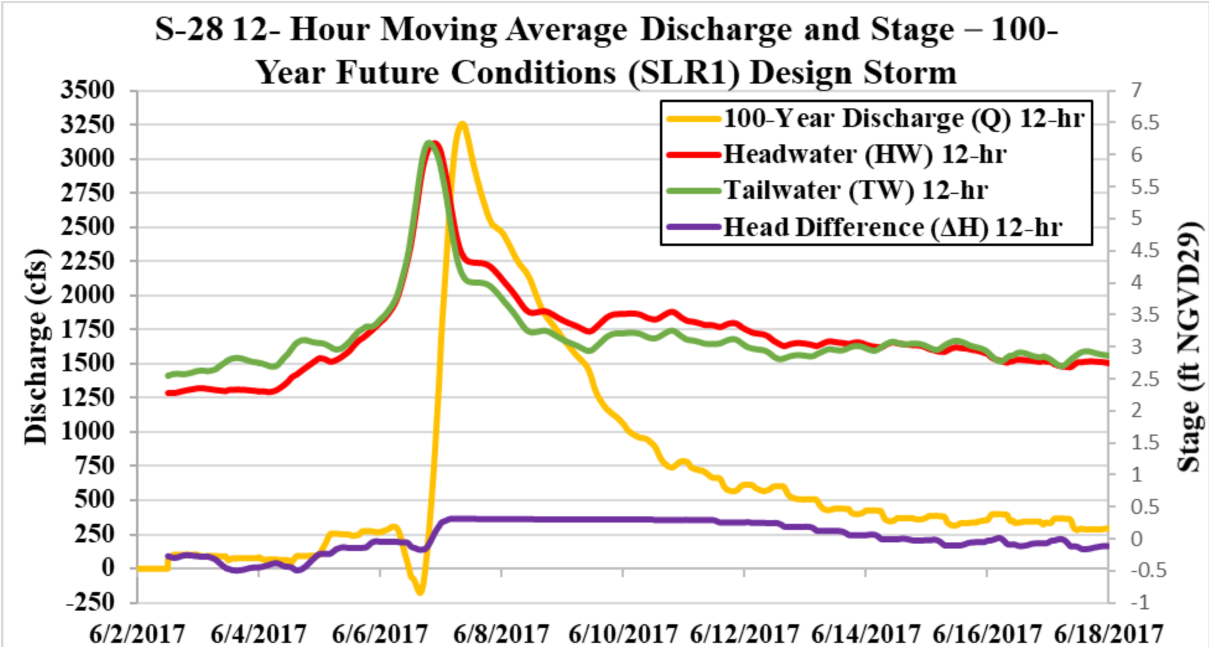

Figure 10.3-4: Tidally Averaged (12-hour) 100-Year Future Conditions Sea Level Rise 1 Design Storm Discharge, Stage, and Head Difference for Structure S-28

As shown in **Figure 10.3-4,** the S-28 structure slightly exceeds the design discharge of 3220 cfs, with a 12-hour moving average peak of 3260 cfs. While this discharge occurs with a 12-hour average head difference of only 0.31 feet, the design headwater assumption is violated. The assumed design headwater stage is 2.2 feet, while the predicted headwater is 4.4 feet at the time of peak discharge. Additionally, there is a flow reversal, peaking at 178 cfs due to a -0.17 ft headwater/tailwater gradient.

Figure 10.3-5 and **Figure 10.3-6** show instantaneous values and 12-hour moving average values, respectively, for S-28 based on a 25-year design storm with 2 ft of sea level rise. Although the instantaneous peak discharge for the 25-year SLR2 is about 500 cfs greater than current conditions, it is short lived. At the peak of the storm, there is nearly 1200 cfs of reversed flow, which is likely what caused the increased peak discharge, as there was more water “stacked” on the upstream side of the structure.

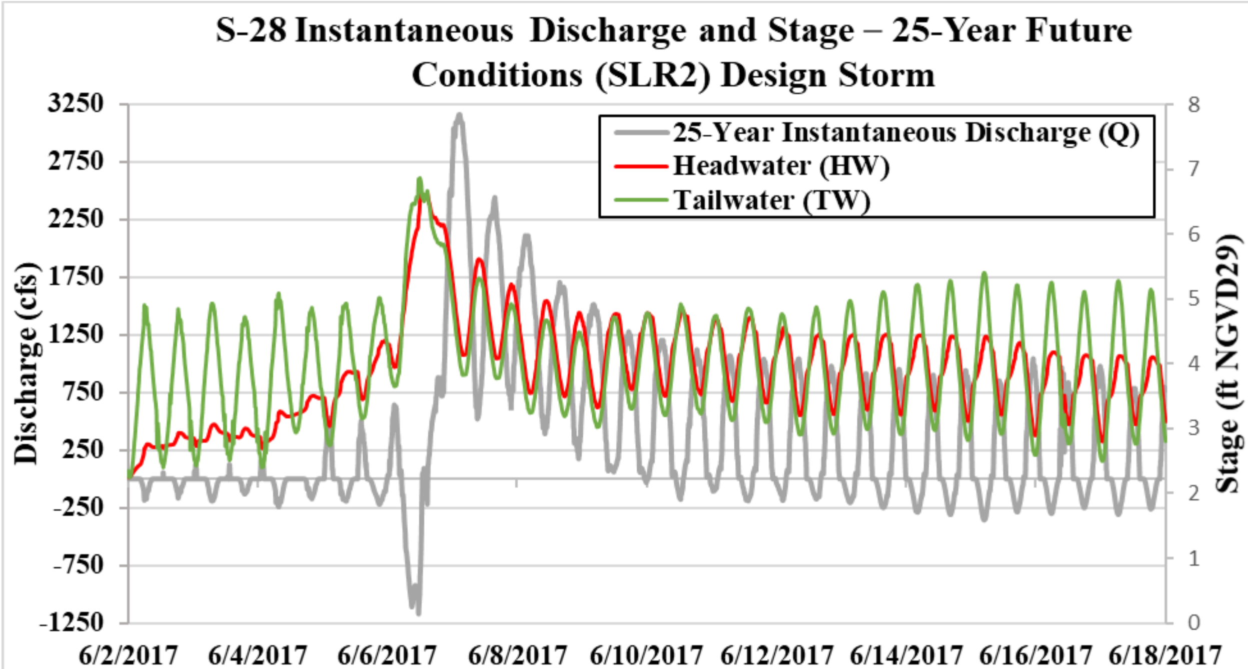

Figure 10.3-5: Instantaneous Discharge and Stage at S-28 Structure for 25-Year Future Conditions Sea Level Rise 2 Design Storm

Filtering out the effects of the tide reveals that the peak discharge decreased compared to current conditions.

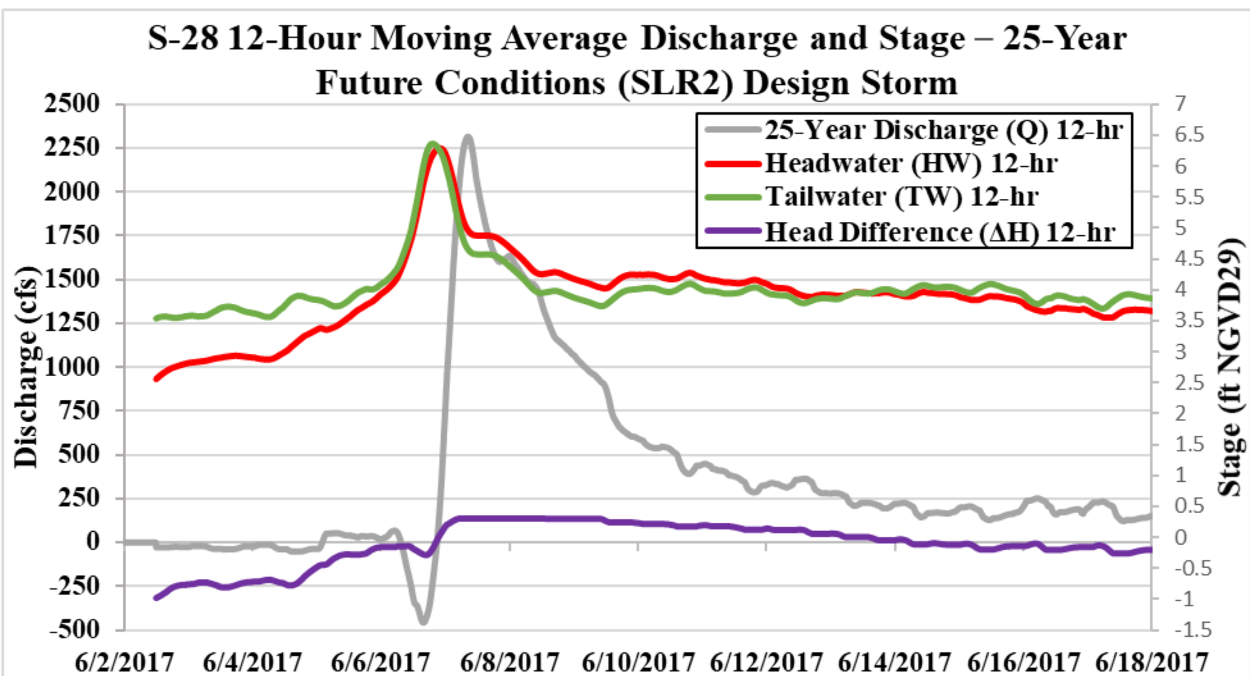

Figure 10.3-6: Tidally Averaged (12-hour) 25-Year Future Conditions Sea Level Rise 2 Design Storm Discharge, Stage, and Head Difference for Structure S-28

Figure 10.3-7 and **Figure 10.3-8** show instantaneous values and 12-hour moving average values, respectively, for S-28 based on a 100-year design storm with 2 ft of sea level rise.

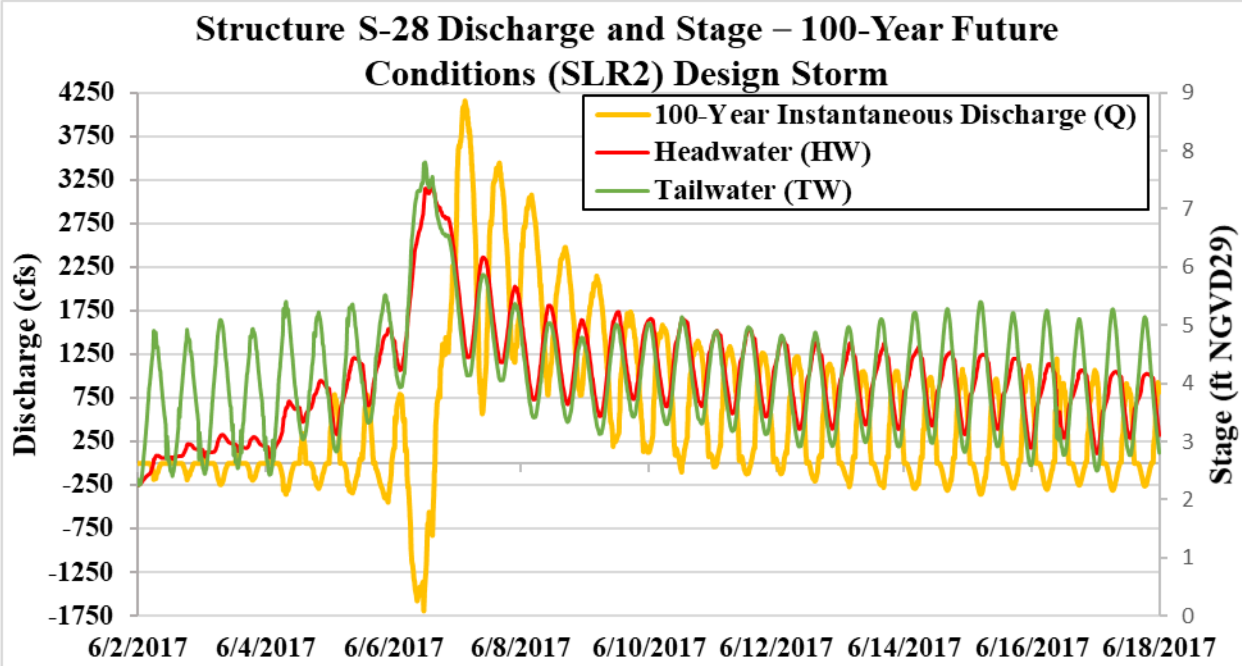

Figure 10.3-7: Instantaneous Discharge and Stage at S-28 Structure for 100-Year Future Conditions Sea Level Rise 2 Design Storm

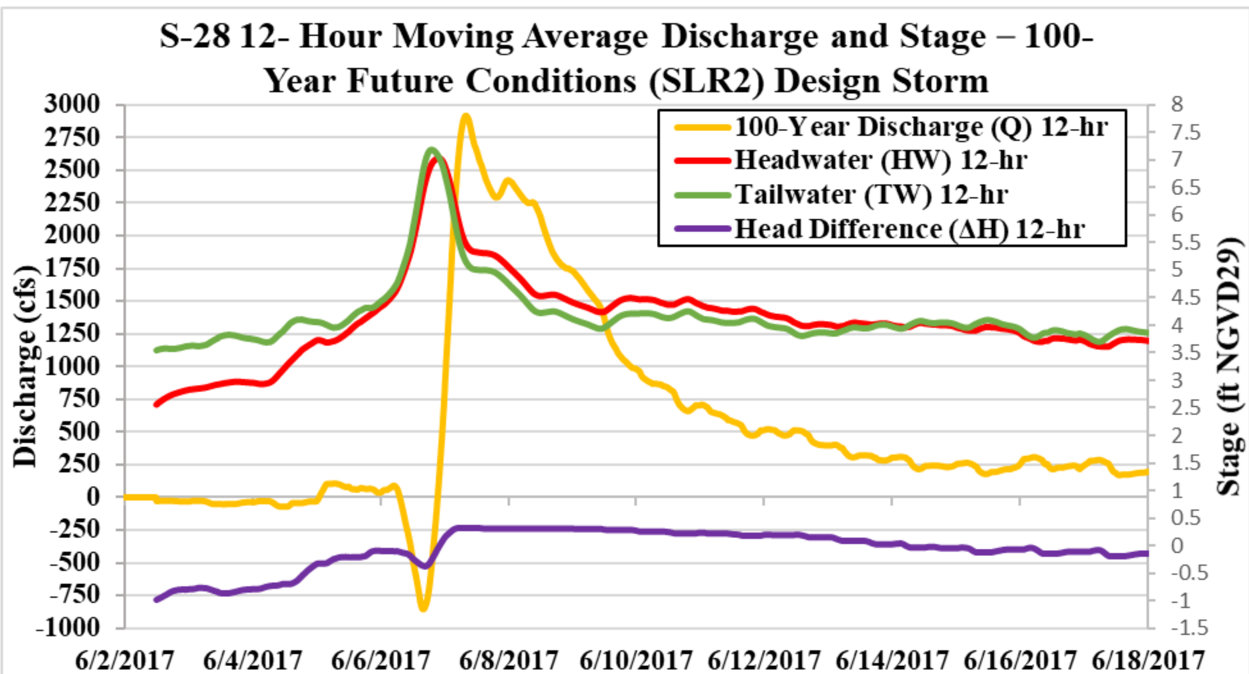

Figure 10.3-8: Tidally Averaged (12-hour) 100-Year Future Conditions Sea Level Rise 2 Design Storm Discharge, Stage, and Head Difference for Structure S-28

As shown in **Figure 10.3-8,** the S-28 structure is unable to reach the design discharge of 3220 cfs, with a 12-hour moving average peak of 2919 cfs. While this discharge occurs with a 12-hour average head difference of only 0.32 feet, the design headwater assumption is violated. The assumed design headwater stage is 2.2 feet, while the predicted headwater is 5.5 feet at the time of peak discharge. Additionally, there is a flow reversal, peaking at 855 cfs due to a -0.37 ft headwater/tailwater gradient.

Figure 10.3-9 and **Figure 10.3-10** show instantaneous values and 12-hour moving average values, respectively, for S-28 based on a 25-year design storm with 3 ft of sea level rise. Although the instantaneous peak discharge for the 25-year SLR3 is about 600 cfs greater than current conditions, it is short lived. At the peak of the storm, there is 1722 cfs of reversed flow. Filtering out the effects of the tide reveals that the peak discharge decreased.

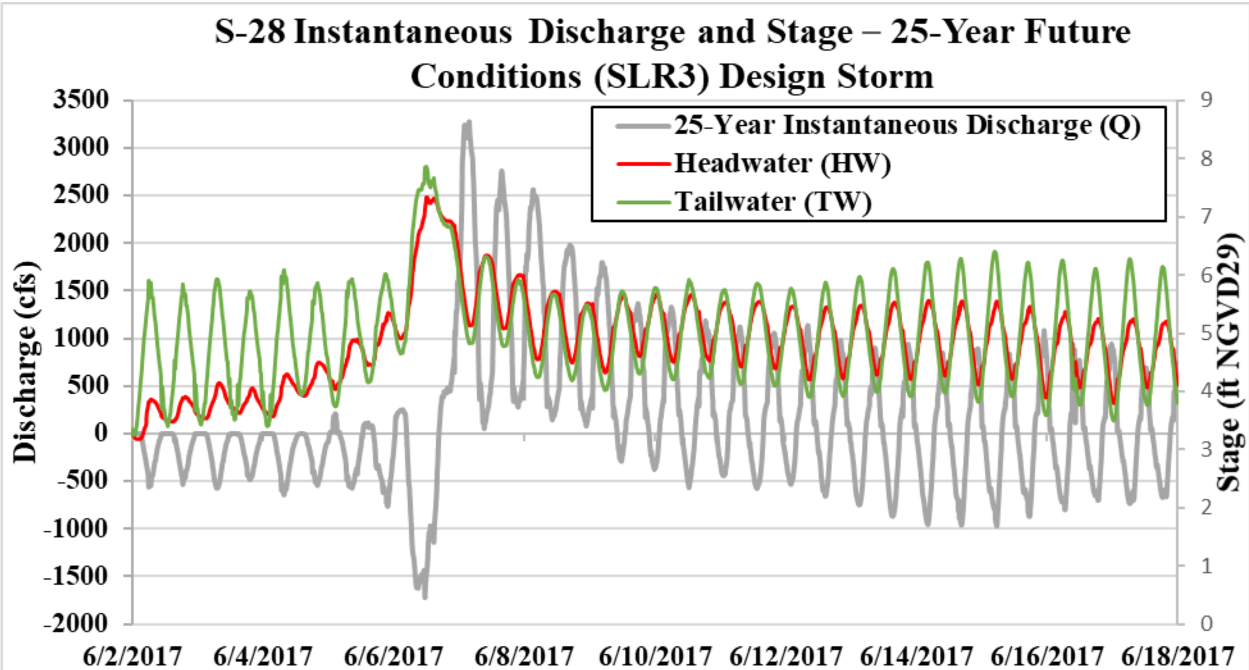

Figure 10.3-9: Instantaneous Discharge and Stage at S-28 Structure for 25-Year Future Conditions Sea Level Rise 3 Design Storm

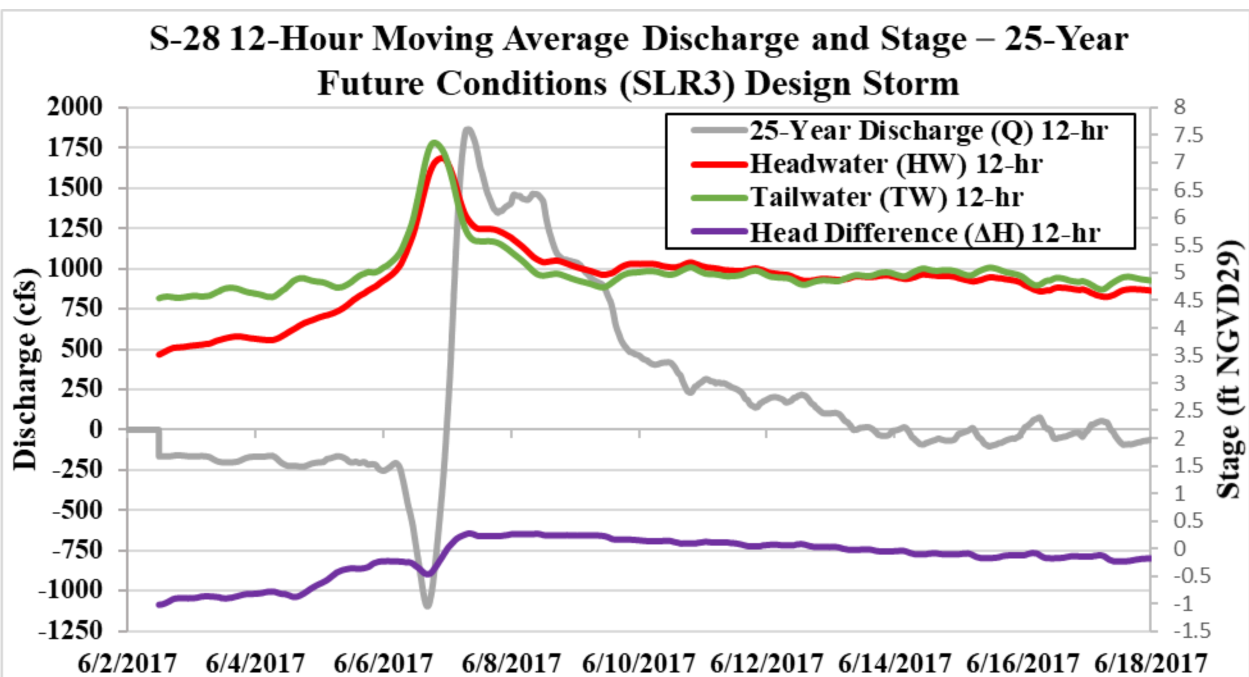

Figure 10.3-10: Tidally Averaged (12-hour) 25-Year Future Conditions Sea Level Rise 2 Design Storm Discharge, Stage, and Head Gradient for Structure S-28

Figure 10.3-11 and **Figure 10.3-12** show instantaneous values and 12-hour moving average values, respectively, for S-28 based on a 100-year design storm with 3 ft of sea level rise.

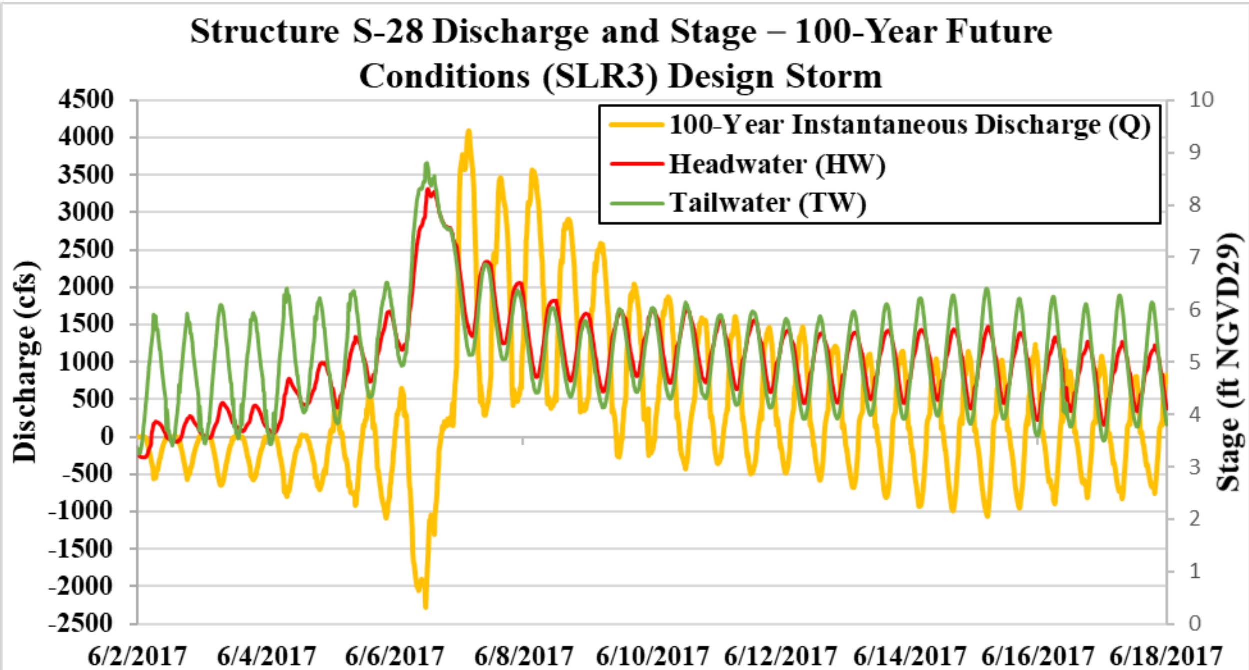

Figure 10.3-11: Instantaneous Discharge and Stage at S-28 Structure for 100-Year Future Conditions Sea Level Rise 3 Design Storm

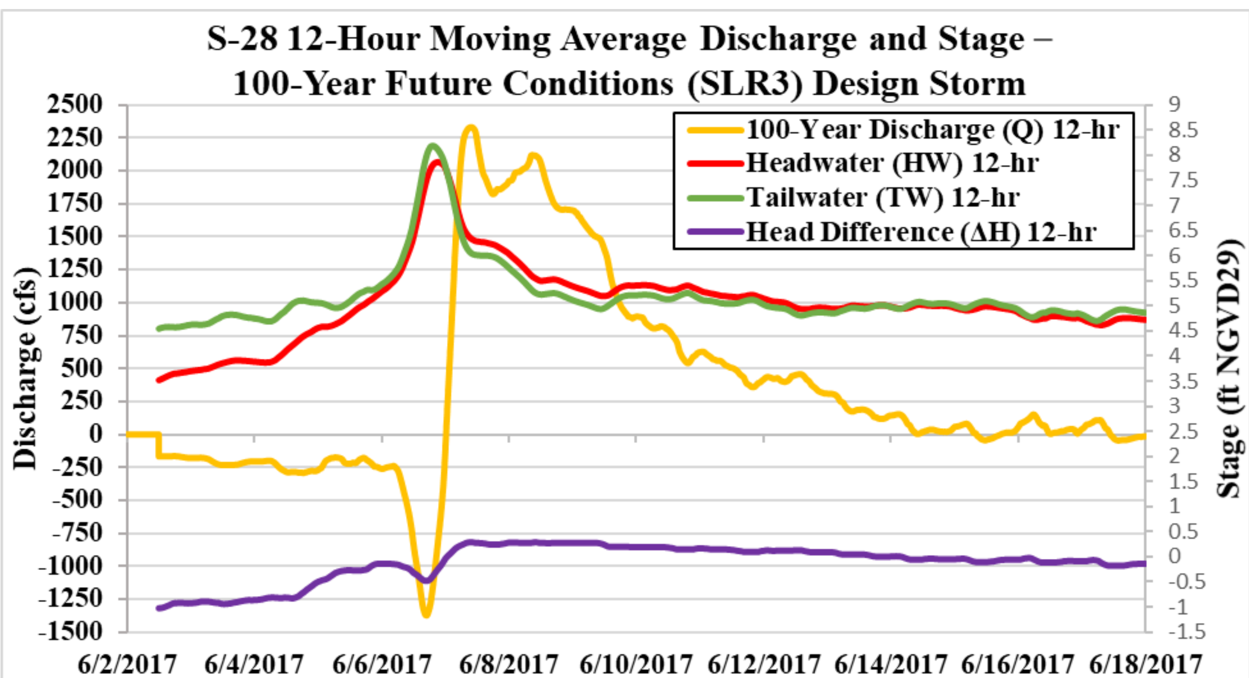

Figure 10.3-12: Tidally Averaged (12-hour) 100-Year Future Conditions Sea Level Rise 3 Design Storm Discharge, Stage, and Head Gradient for Structure S-28

As shown in **Figure 10.3-12,** the S-28 structure is unable to reach the design discharge of 3220 cfs, with a 12-hour moving average peak of 2331 cfs. While this discharge occurs with a 12-hour average head difference of only 0.29 feet, the design headwater assumption is violated. The assumed design headwater stage is 2.2 feet, while the predicted headwater is 6.4 feet at the time of peak discharge. Additionally, there is a flow reversal, peaking at -1374 cfs due to a -0.48 ft headwater/tailwater gradient. Looking at instantaneous discharge (**Appendix F**), the S-28 structure reaches the design discharge for all 100-year design storm scenarios; however, the increased headwater stage causes flooding in the watershed.

Table 10-14 through **Table 10-17** summarize the simulated 12-hour moving average peak discharge, headwater, tailwater, and head differential for S-28, for each of the design storms. From the tables, an inverse relationship is evident between the peak discharge and rising sea level, which is to be expected.

Table 10-14: Summary of the 12-Hour Moving Average Discharge and Stage at S-28 for 5-Year Future Conditions Design Storms

Design Storm Scenario	5- Year Design Storm 12-Hour Moving Average at S-28			
	Peak Discharge (cfs) [Q	Headwater (ft NGVD29) at Peak Q	Tailwater (ft NGVD29) at Peak Q	Head Differential (ft) at Peak Q
Current	1441	2.75	2.39	0.36
SLR1	1359	3.68	3.38	0.30
SLR2	1248	4.58	4.28	0.30
SLR3	1101	5.5	5.26	0.24

Table 10-15: Summary of the 12-Hour Moving Average Discharge and Stage at S-28 for 10-Year Future Conditions Design Storms

Design Storm Scenario	10- Year Design Storm 12-Hour Moving Average at S-28			
	Peak Discharge (cfs) [Q]	Headwater (ft NGVD29)	Tailwater (ft NGVD29) at Peak Q	Head Differential (ft) at Peak Q
Current	1748	2.93	2.61	0.32
SLR1	1700	3.87	3.56	0.31
SLR2	1619	4.76	4.46	0.30
SLR3	1424	5.69	5.44	0.25

Table 10-16: Summary of the 12-Hour Moving Average Discharge and Stage at S-28 for 25-Year Future Conditions Design Storms

Design Storm Scenario	25- Year Design Storm 12-Hour Moving Average at S-28			
	Peak Discharge (cfs) [Q]	Headwater (ft NGVD29) at Peak Q	Tailwater (ft NGVD29) at Peak Q	Head Differential (ft) at Peak Q
Current	2337	3.17	2.87	0.30
SLR1	2315	4.09	3.78	0.31
SLR2	2315	4.96	4.66	0.30
SLR3	1865	5.96	5.69	0.27

Table 10-17: Summary of the 12-Hour Moving Average Discharge and Stage at S-28 for 100-Year Future Conditions Design Storms

Design Storm Scenario	100- Year Design Storm 12-Hour Moving Average at S-28			
	Peak Discharge (cfs) [Q]	Headwater (ft NGVD29) at Peak Q	Tailwater (ft NGVD29) at Peak Q	Head Differential (ft) at Peak Q
Current	3254	3.55	3.25	0.30
SLR1	3259	4.44	4.13	0.31
SLR2	2919	5.48	5.16	0.32
SLR3	2331	6.36	6.07	0.29

10.3.2 S-29

Structure S-29 has a static design headwater and tailwater of 2.4 ft and 1.9 ft, respectively. The static design discharge is 4780 cfs based on 0.5 ft head difference (Zhang, 2017). **Figure 10.3-13** and **Figure 10.3-14 s**how instantaneous values and 12-hour moving average values, respectively, for S-29 based on a 25-year design storm with 1 ft sea level rise.

The instantaneous peak discharge for the 25-year SLR1 scenario is smaller than current conditions and is short lived. At the peak of the storm, there is nearly 750 cfs of reversed flow. Filtering out the effects of the tide reveals a more significant decrease in the peak discharge compared to current conditions.

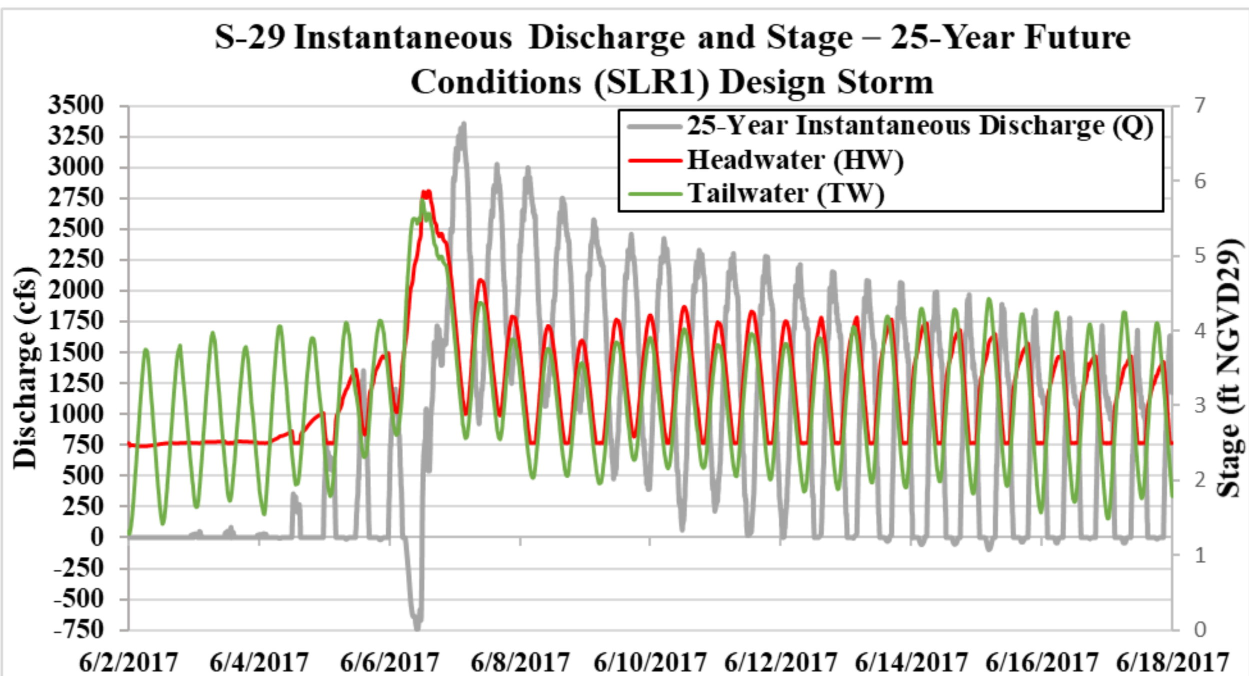

Figure 10.3-13: Instantaneous Discharge and Stage at S-29 Structure for 25-Year Future Conditions Sea Level Rise 1 Design Storm

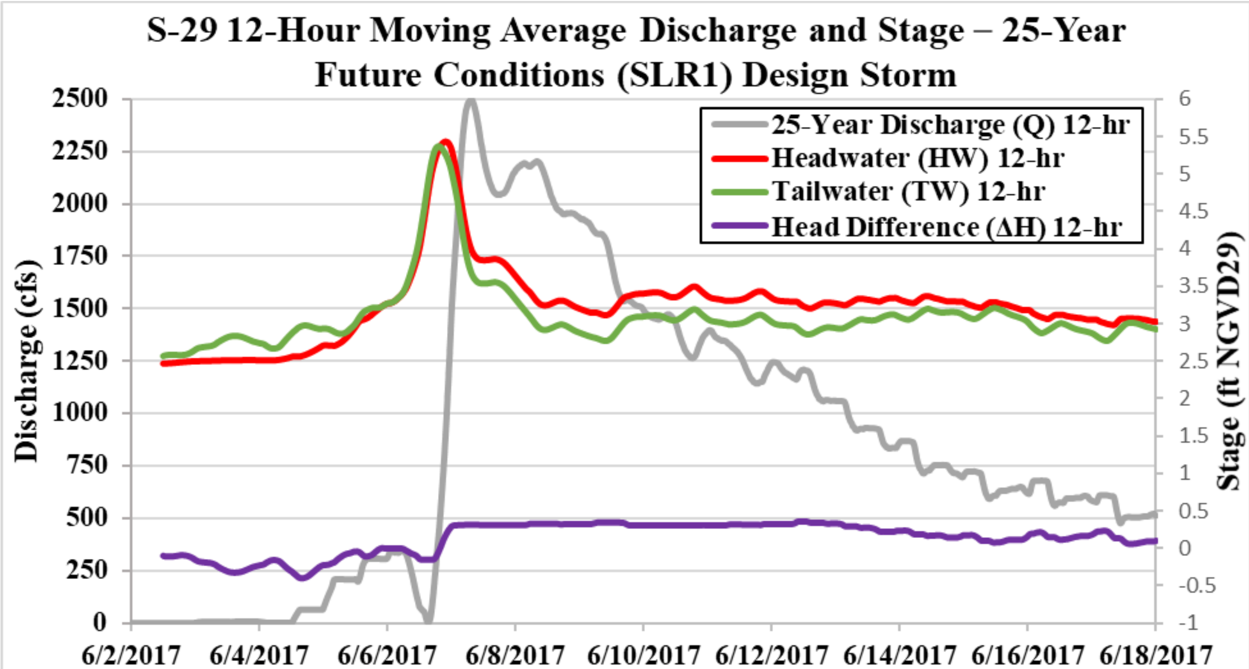

Figure 10.3-14: Tidally Averaged (12-hour) 25-Year Future Conditions Sea Level Rise 1 Design Storm Discharge, Stage, and Head Gradient for Structure S-29

Figure 10.3-15 and **Figure 10.3-16** show instantaneous values and 12-hour moving average values, respectively, for S-29 based on a 100-year design storm with 1 ft of sea level rise.

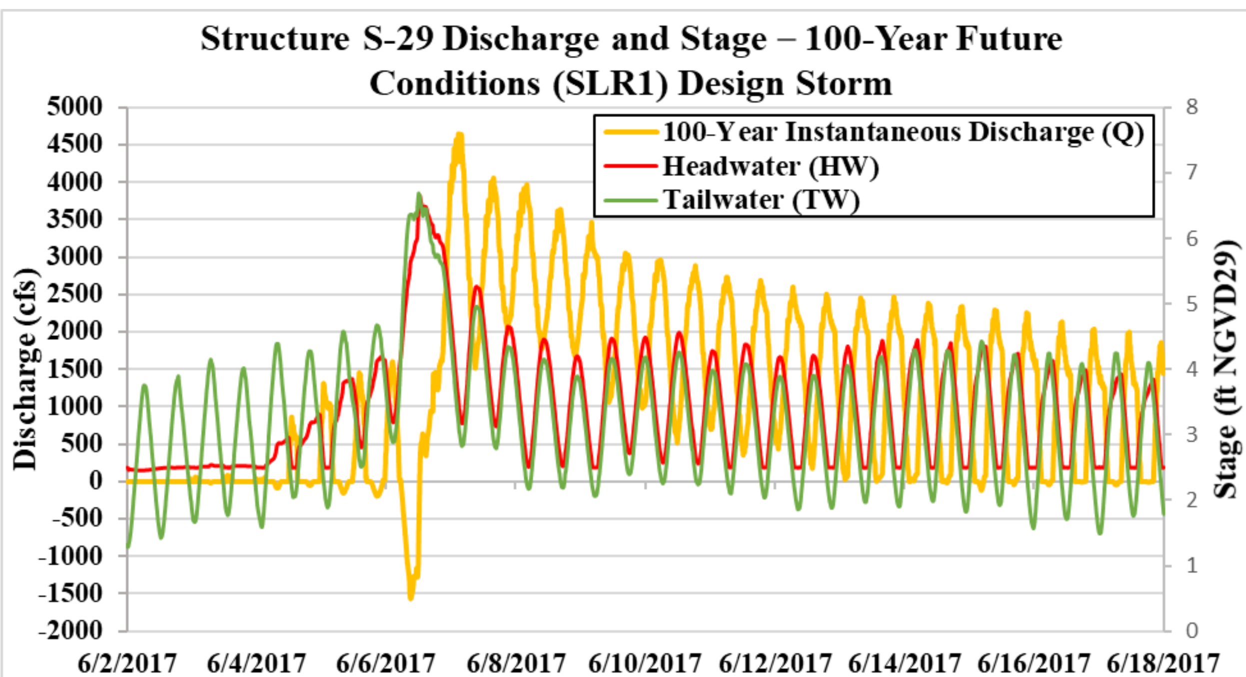

Figure 10.3-15: Instantaneous Discharge and Stage at S-29 Structure for 100-Year Future Conditions Sea Level Rise 1 Design Storm

The instantaneous peak discharge for the 100-year SLR1 scenario is smaller than current conditions and is short lived. At the peak of the storm, there is over 1500 cfs of reversed flow. Filtering out the effects of the tide reveals a more significant decrease in the peak discharge compared to current conditions.

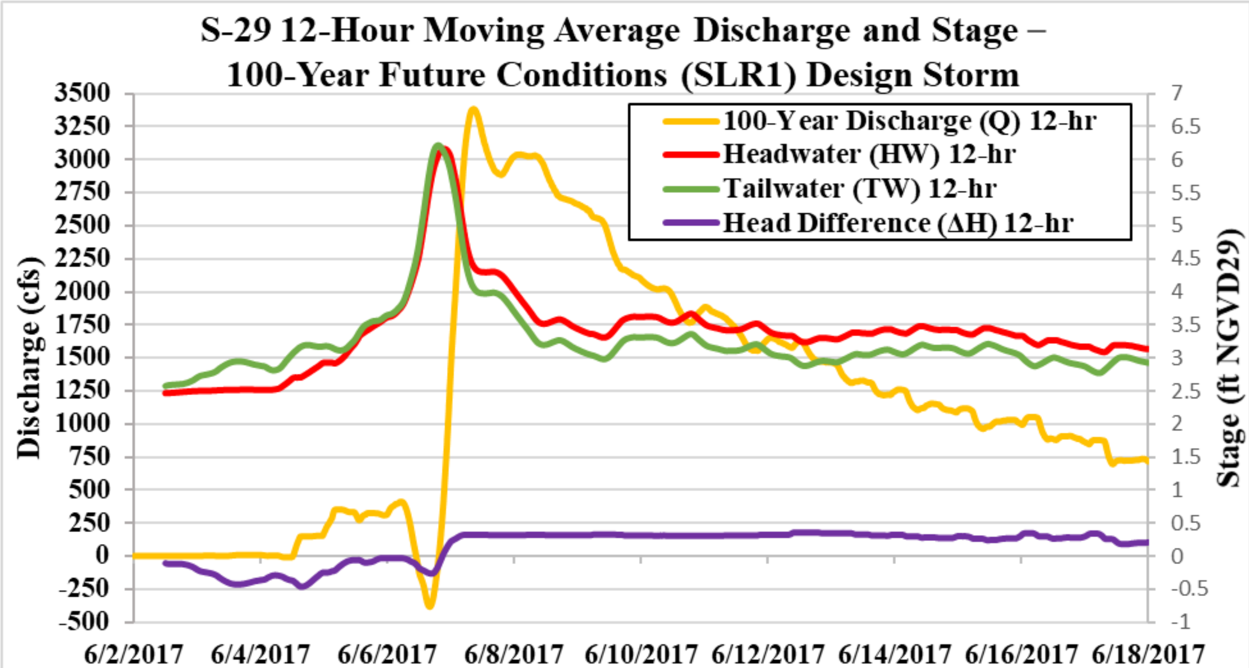

Figure 10.3-16: Tidally Averaged (12-hour) 100-Year Future Conditions Sea Level Rise 1 Design Storm Discharge, Stage, and Head Gradient for Structure S-29

As shown in **Figure 10.3-16,** the S-29 structure falls significantly short of the design discharge of 4780 cfs, with a 12-hour moving peak of just 3384 cfs. While this discharge occurs with a 12-hour average head difference of only 0.32 feet, the design headwater assumption is violated. The assumed design headwater stage is 2.2 feet, while the predicted headwater is 4.4 feet at the time of peak discharge. Additionally, there is a flow reversal, peaking at 384 cfs due to a -0.26 ft headwater/tailwater gradient.

Figure 10.3-17 and **Figure 10.3-18** show instantaneous values and 12-hour moving average values, respectively, for S-29 based on a 25-year design storm with 2 ft of sea level rise. The instantaneous peak discharge for the 25-year SLR2 is about 220 cfs smaller than current conditions. At the peak of the storm, there is nearly 1750 cfs of reversed flow. Filtering out the effects of the tide reveals a more significant decrease in the peak discharge.

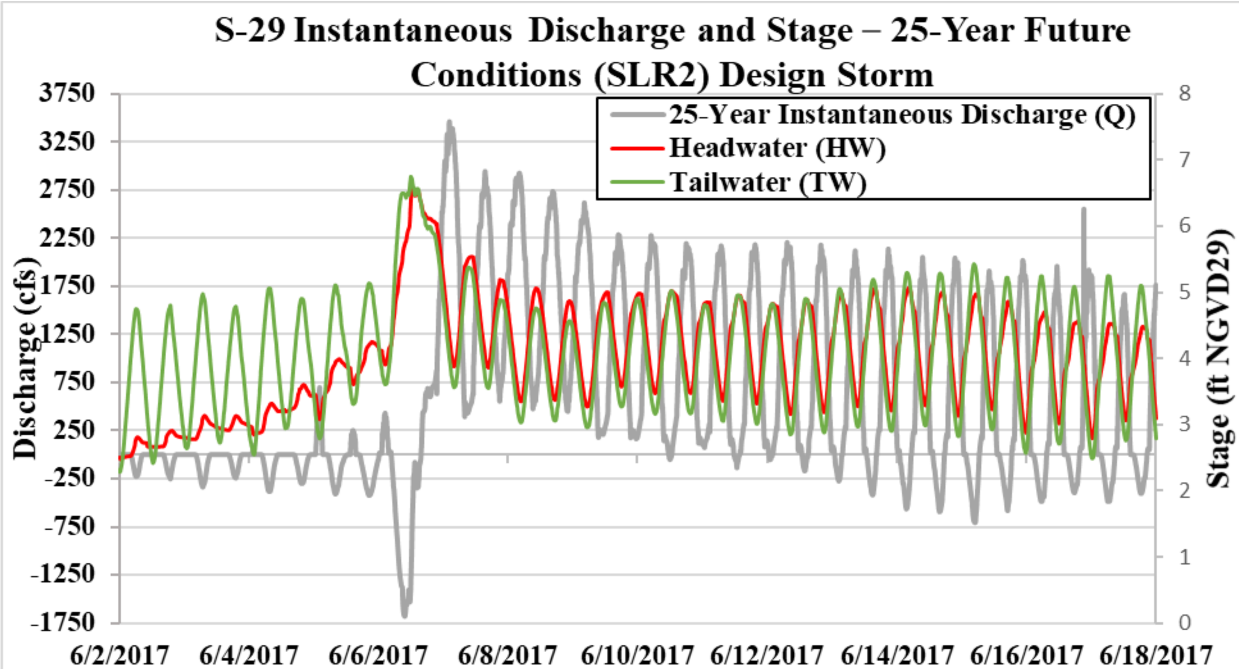

Figure 10.3-17: Instantaneous Discharge and Stage at S-29 Structure for 25-Year Future Conditions Sea Level Rise 2 Design Storm

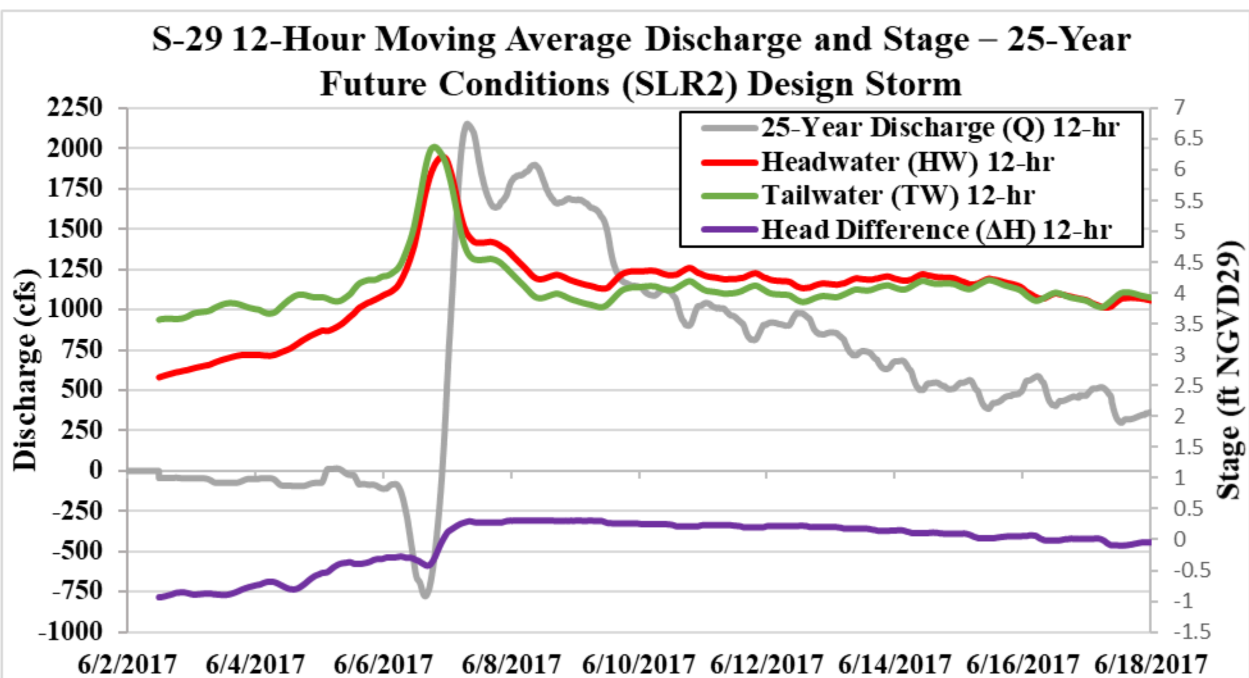

Figure 10.3-18: Tidally Averaged (12-hour) 25-Year Future Conditions Sea Level Rise 2 Design Storm Discharge, Stage, and Head Gradient for Structure S-29

Figure 10.3-19 and **Figure 10.3-20** show instantaneous values and 12-hour moving average values, respectively, for S-29 based on a 100-year design storm with 2 ft of sea level rise.

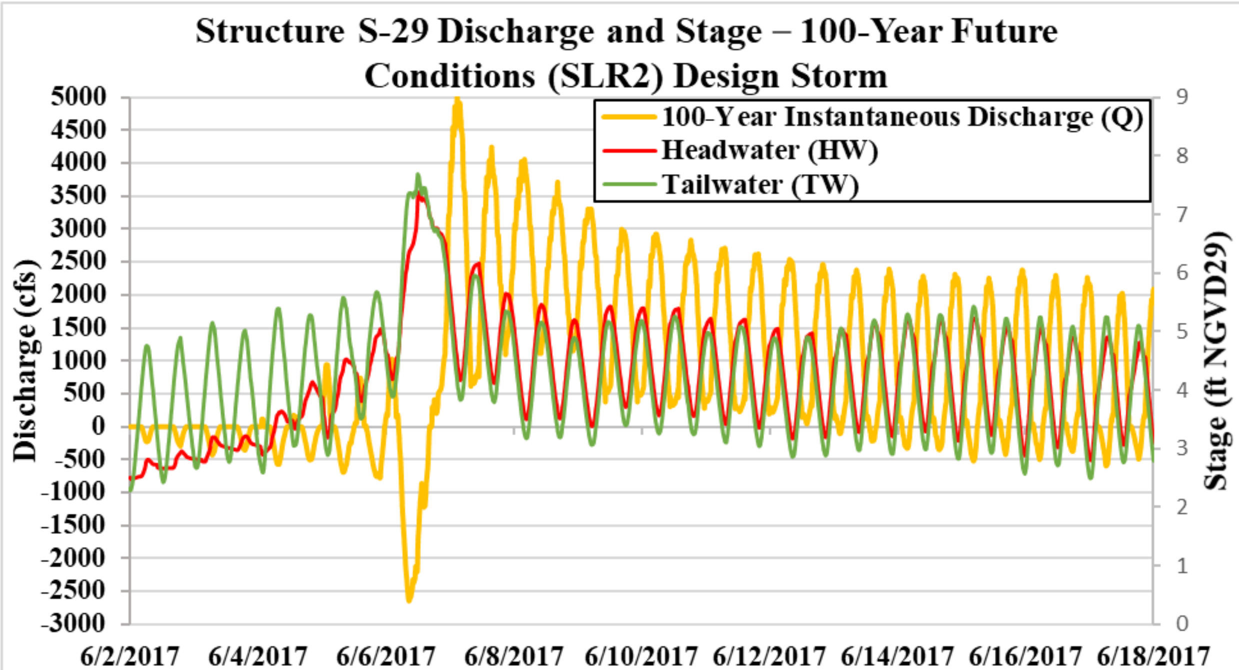

Figure 10.3-19: Instantaneous Discharge and Stage at S-29 Structure for 100-Year Future Conditions Sea Level Rise 2 Design Storm

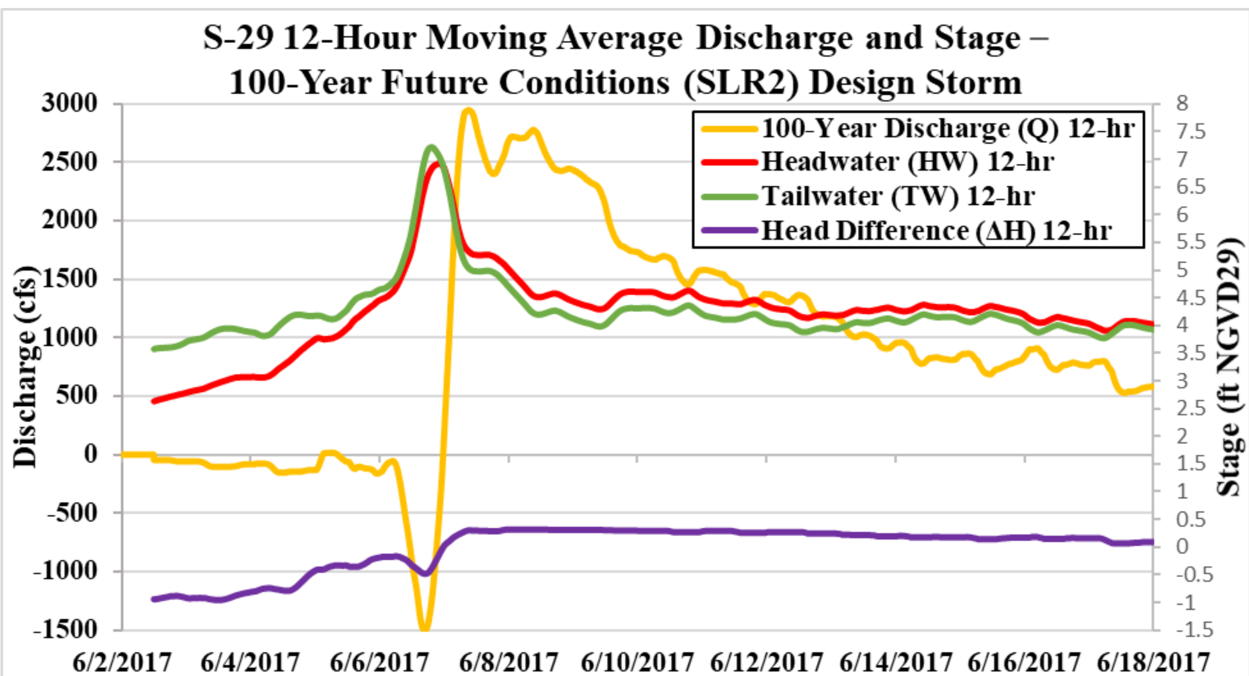

Figure 10.3-20: Tidally Averaged (12-hour) 100-Year Future Conditions Sea Level Rise 2 Design Storm Discharge, Stage, and Head Gradient for Structure S-29

As shown in **Figure 10.3-20,** the S-29 structure falls significantly short of the design discharge of 4780 cfs, with a 12-hour moving peak of just 2947 cfs. While this discharge occurs with a 12-hour average head difference of only 0.3 feet, the design headwater assumption is violated. The assumed design headwater stage is 2.2 feet, while the predicted headwater is 5.3 feet at the time of peak discharge. Additionally, there is a flow reversal, peaking at -1500 cfs due to a -0.48 ft headwater/tailwater gradient.

Figure 10.3-21 and **Figure 10.3-22** show instantaneous values and 12-hour moving average values, respectively, for S-29 based on a 25-year design storm with 3 ft of sea level rise. The instantaneous peak discharge for the 25-year SLR3 is only about 50 cfs smaller than current conditions, however, filtering out the effects of the tide reveals a more significant decrease in the peak discharge. At the peak of the storm, there is nearly 1900 cfs of reversed flow.

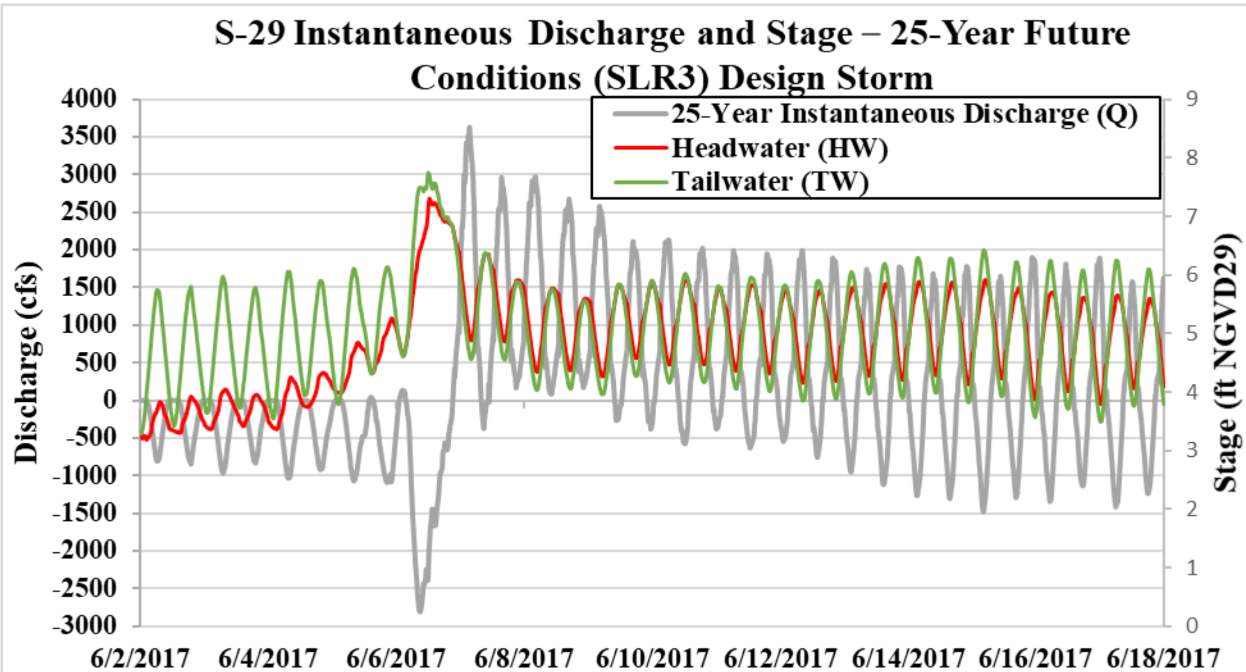

Figure 10.3-21: Instantaneous Discharge and Stage at S-29 Structure for 25-Year Future Conditions Sea Level Rise 3 Design Storm

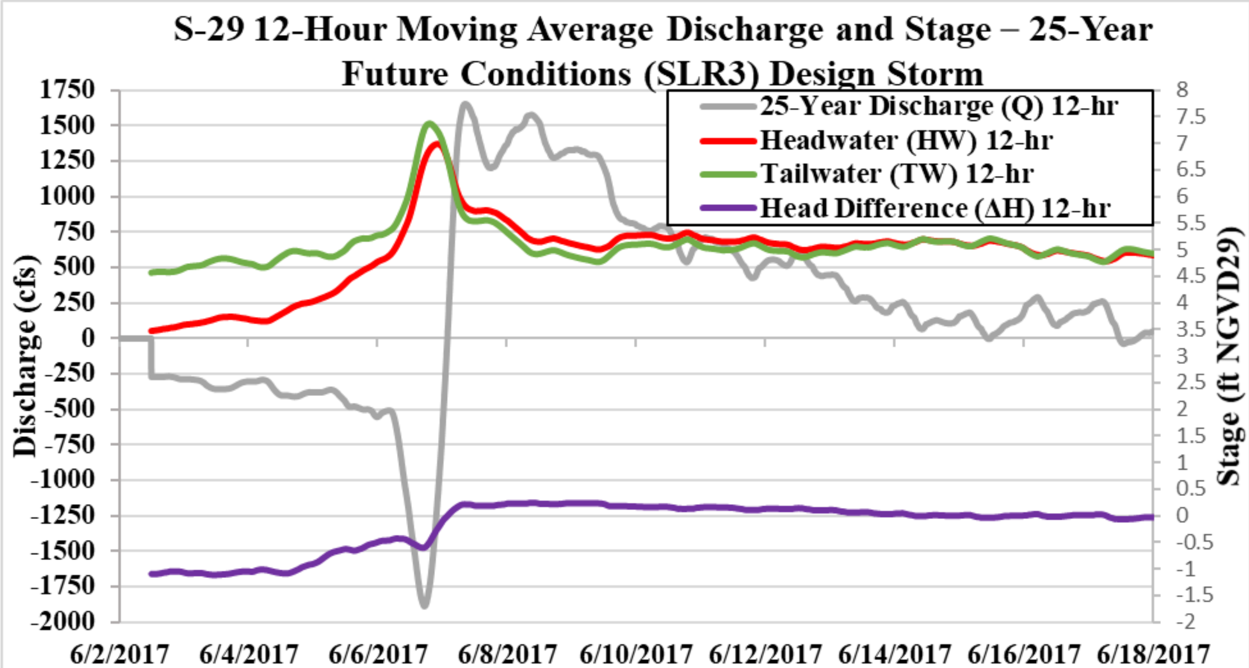

Figure 10.3-22: Tidally Averaged (12-hour) 25-Year Future Conditions Sea Level Rise 3 Design Storm Discharge, Stage, and Head Gradient for Structure S-29

Figure 10.3-23 and **Figure 10.3-24** show instantaneous values and 12-hour moving average values, respectively, for S-29 based on a 100-year design storm with 3 ft of sea level rise.

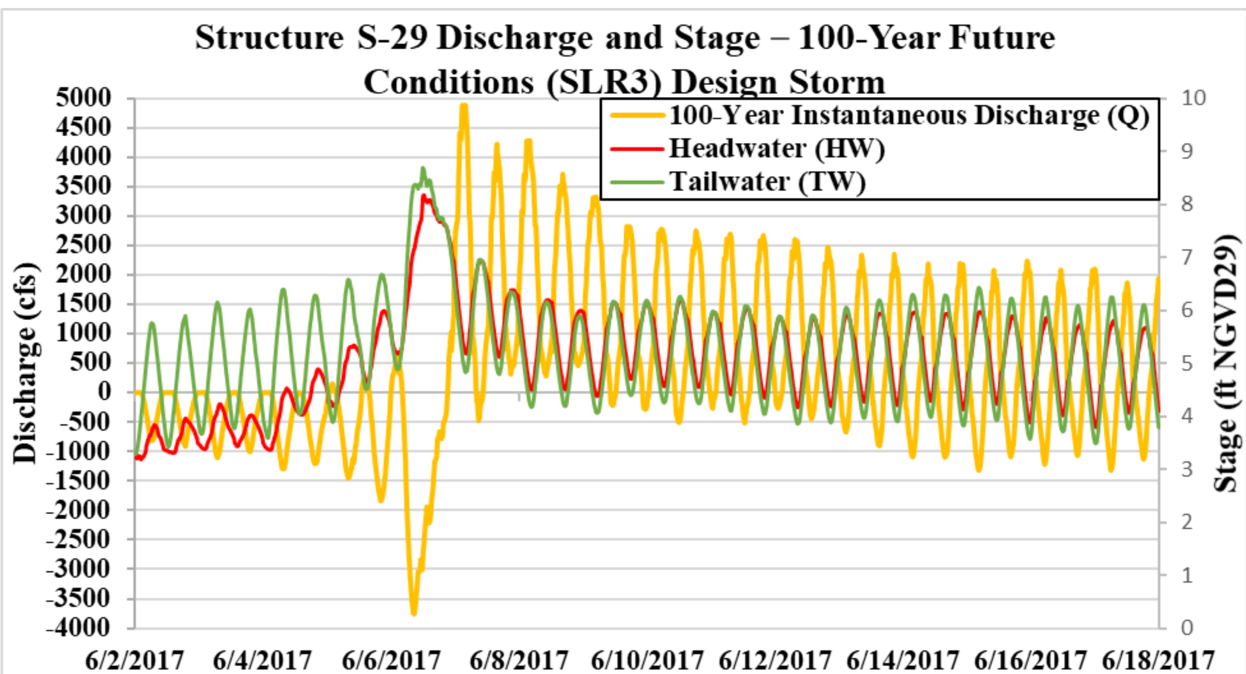

Figure 10.3-23: Instantaneous Discharge and Stage at S-29 Structure for 100-Year Future Conditions Sea Level Rise 3 Design Storm

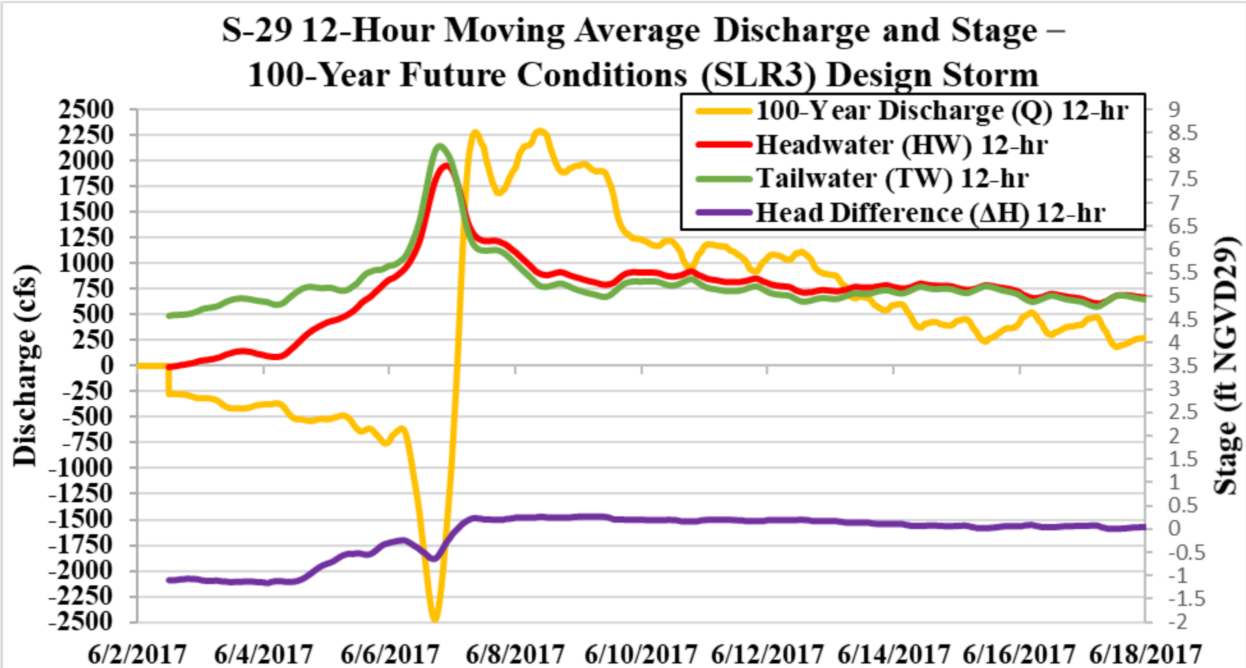

Figure 10.3-24: Tidally Averaged (12-hour) 100-Year Future Conditions Sea Level Rise 3 Design Storm Discharge, Stage, and Head Gradient for Structure S-29

As shown in **Figure 10.3-24,** the S-29 structure falls significantly short of the design discharge of 4780 cfs, with a 12-hour moving peak of just 2294 cfs. This discharge occurs with a 12-hour average head difference of only 0.26 feet and the design headwater assumption is violated. The assumed design headwater stage is 2.2 feet, while the predicted headwater is 5.5 feet at the time of peak discharge. Before the peak positive flow, there is a flow reversal, peaking at -2477 cfs (larger than the peak outflow) due to a -0.64 ft headwater/tailwater difference. Looking at instantaneous discharge (**Appendix F**), the S-29 structure reaches the design discharge for all 100-year design storm scenarios; however, the increased headwater stage causes flooding in the watershed.

Table 10-18 through **Table 10-21** summarizes the simulated 12-hour moving average peak discharge, headwater, tailwater, and head differential for S-29, for each of the design storms. Similar to the trend at S-28, the numbers show an inverse relationship between sea level and peak discharge. However, this trend is even more pronounced at S-29 compared to S-28. This is partially due to the C-9 Impoundment providing some relief by pumping up to 1000 cfs out of the canal for a total of volume of about 713.6 million gallons.

Table 10-18: Summary of the 12-Hour Moving Average Discharge and Stage at S-29 for 5-Year Future Conditions Design Storms

Design Storm Scenario	5- Year Design Storm 12-Hour Moving Average at S-29			
	Peak Discharge (cfs) [Q]	Headwater (ft NGVD29) at Peak Q	Tailwater (ft NGVD29) at Peak Q	Head Differential (ft) at Peak Q
Current	2140	2.84	2.27	0.57
SLR1	1655	3.65	3.34	0.31
SLR2	1159	4.58	4.33	0.25
SLR3	905	5.39	5.21	0.18

Table 10-19: Summary of the 12-Hour Moving Average Discharge and Stage at S-29 for 10-Year Future Conditions Design Storms

Design Storm Scenario	10- Year Design Storm 12-Hour Moving Average at S-29			
	Peak Discharge (cfs) [Q]	Headwater (ft NGVD29) at Peak Q	Tailwater (ft NGVD29) at Peak Q	Head Differential (ft) at Peak Q
Current	2437	2.95	2.44	0.51
SLR1	1904	3.80	3.49	0.31
SLR2	1584	4.70	4.42	0.28
SLR3	1238	5.58	5.38	0.20

Table 10-20: Summary of the 12-Hour Moving Average Discharge and Stage at S-29 for 25-Year Future Conditions Design Storms

Design Storm Scenario	25- Year Design Storm 12-Hour Moving Average at S-29			
	Peak Discharge (cfs) [Q]	Headwater (ft NGVD29) at Peak Q	Tailwater (ft NGVD29) at Peak Q	Head Differential (ft) at Peak Q
Current	2908	3.14	2.71	0.43
SLR1	2500	3.99	3.68	0.31
SLR2	2153	4.96	4.67	0.29
SLR3	1653	5.82	5.61	0.21

Table 10-21: Summary of the 12-Hour Moving Average Discharge and Stage at S-29 for 100-Year Future Conditions Design Storms

Design Storm Scenario	100- Year Design Storm 12-Hour Moving Average at S-29			
	Peak Discharge (cfs) [Q]	Headwater (ft NGVD29) at Peak Q	Tailwater (ft NGVD29) at Peak Q	Head Differential (ft) at Peak Q
Current	3728	3.52	3.17	0.35
SLR1	3384	4.38	4.06	0.32
SLR2	2947	5.34	5.04	0.30
SLR3	2294	5.48	5.22	0.26

10.4 PM #4 – Peak Storm Runoff

PM #4 is the maximum conveyance capacity of a watershed at the tidal structure for a range of design storms. It shows the maximum conveyance (moving 12-hr average) for a specific design storm and a specific tidal boundary condition. **Figure 10.4-1** and **Figure 10.4-2** represent the 5-year design storm discharge at tidal structures S-28 and S-29, respectively. These discharge hydrographs, specifically the peak discharge, are evaluated under three future sea level rise scenarios and compared with current conditions. **Figure 10.3-3** through **Figure 10.3-8** present the discharge at tidal structures S-28 and S-29 for the 10, 25, and 100-year design storms.

10.4.1 5-Year Design Storm

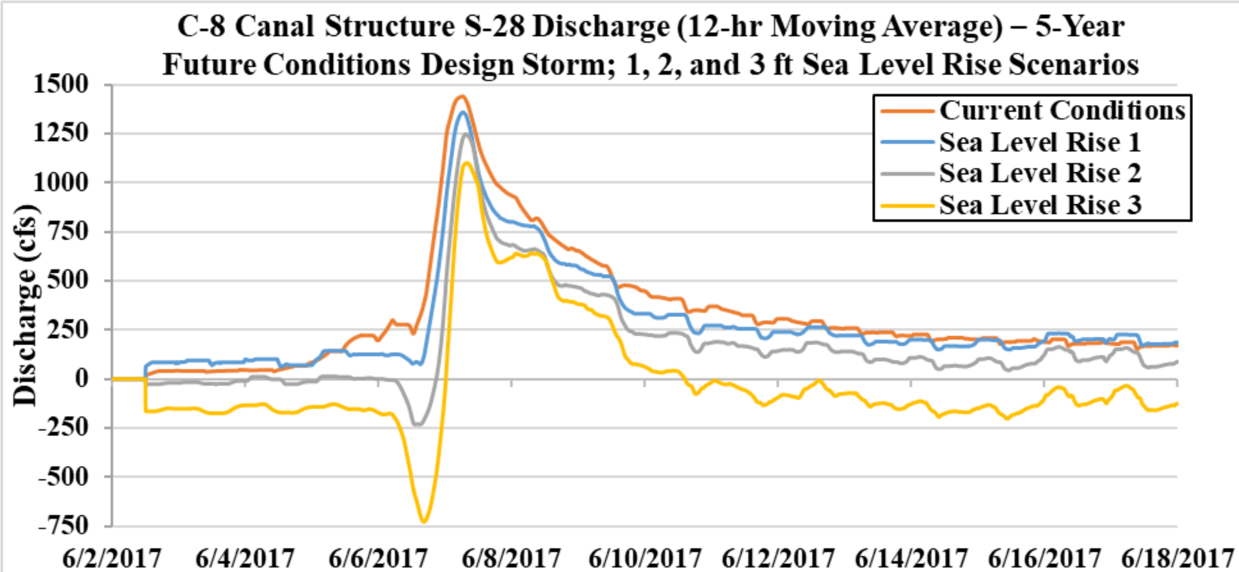

Figure 10.4-1: C-8 Canal Structure S-28 Discharge Hydrographs for 5-Year Design Storms

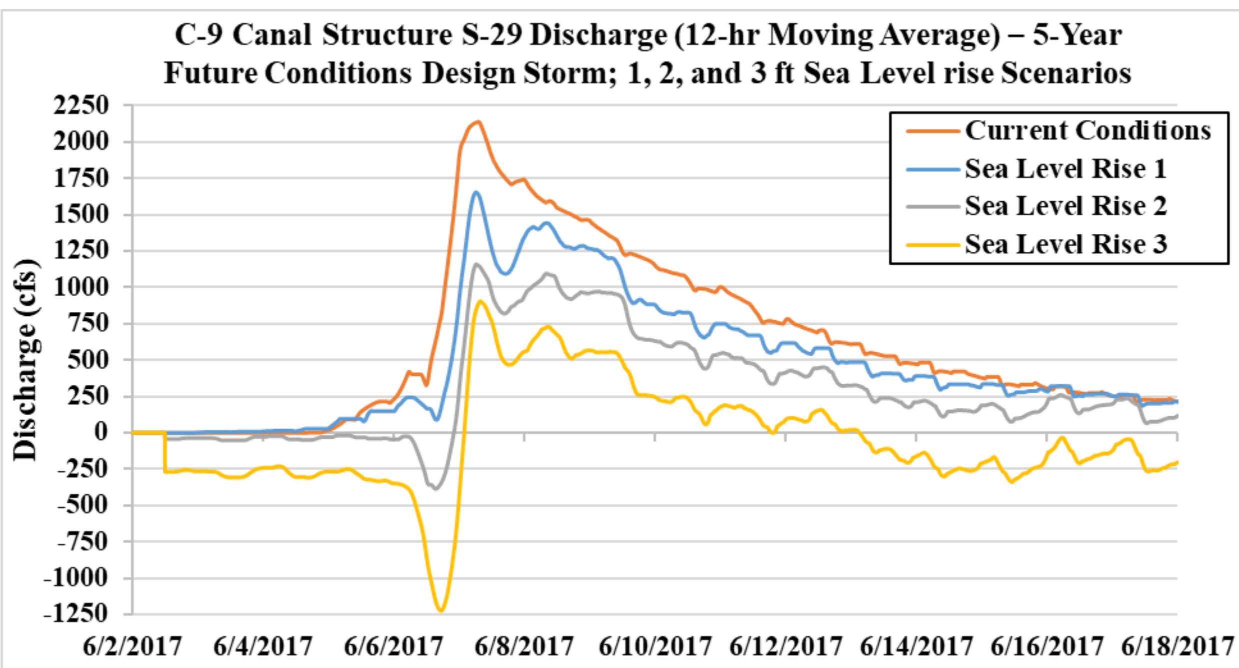

Figure 10.4-2: C-9 Canal Structure S-29 Discharge Hydrographs for 5-Year Design Storms

10.4.2 10-Year Design Storm

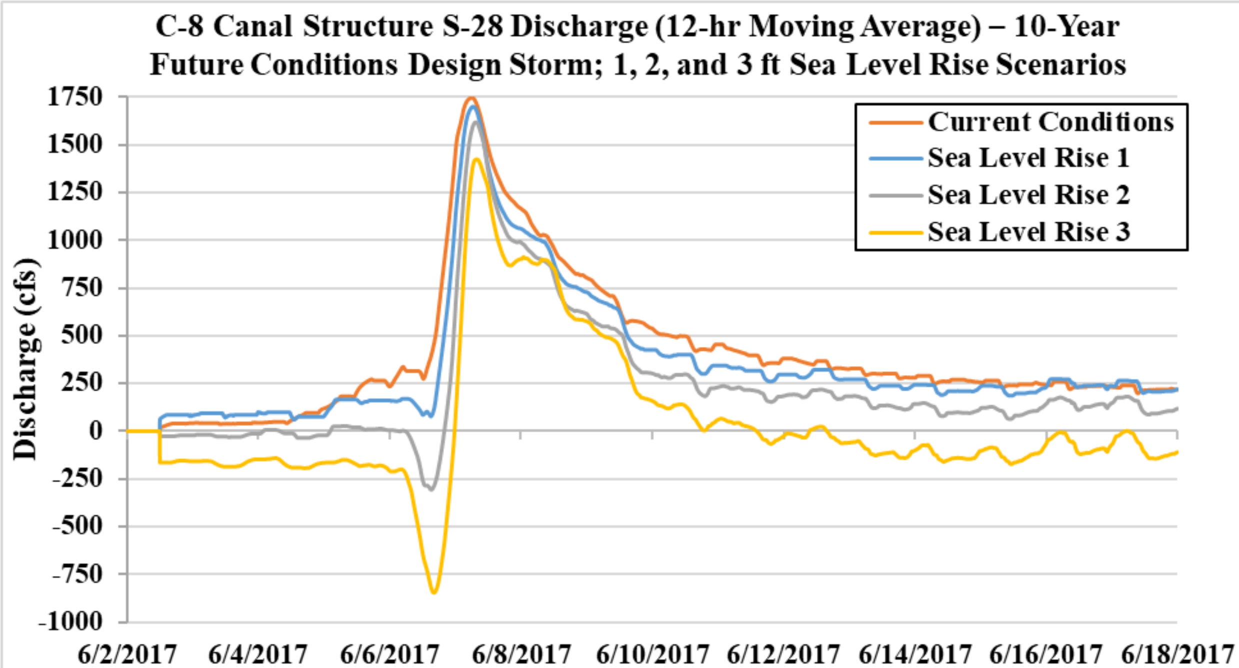

Figure 10.4-3: C-8 Canal Structure S-28 Discharge Hydrographs for 10-Year Design Storms

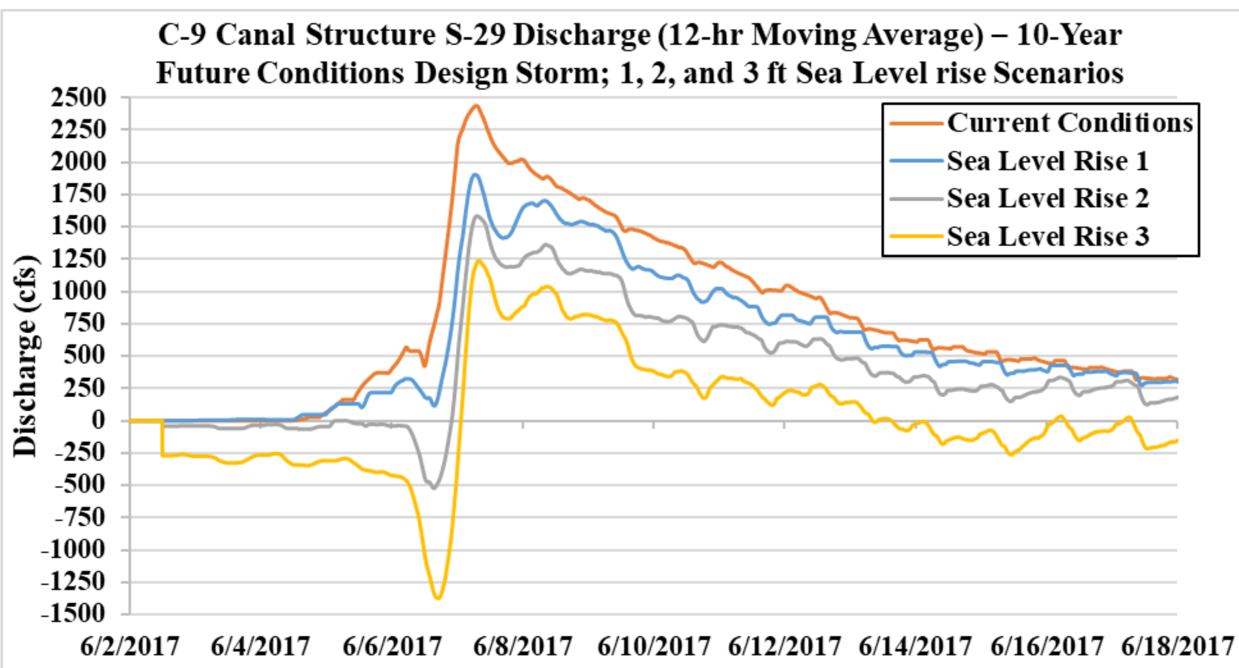

Figure 10.4-4: C-9 Canal Structure S-29 Discharge Hydrographs for 10-Year Design Storms

10.4.3 25-Year Design Storm

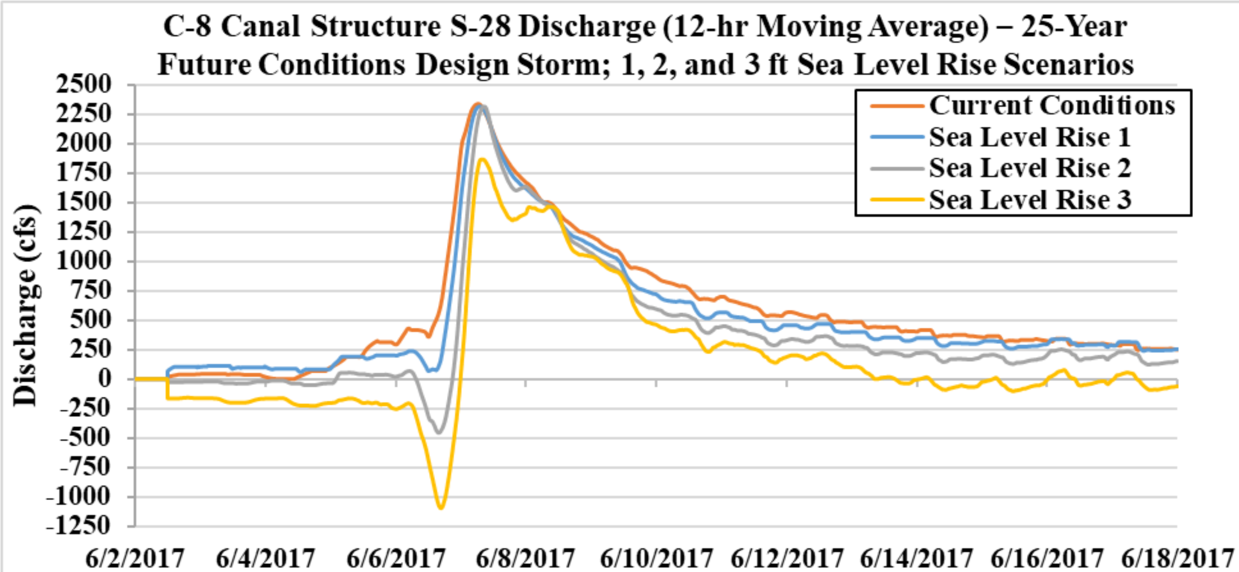

Figure 10.4-5: C-8 Canal Structure S-28 Discharge Hydrographs for 25-Year Design Storms

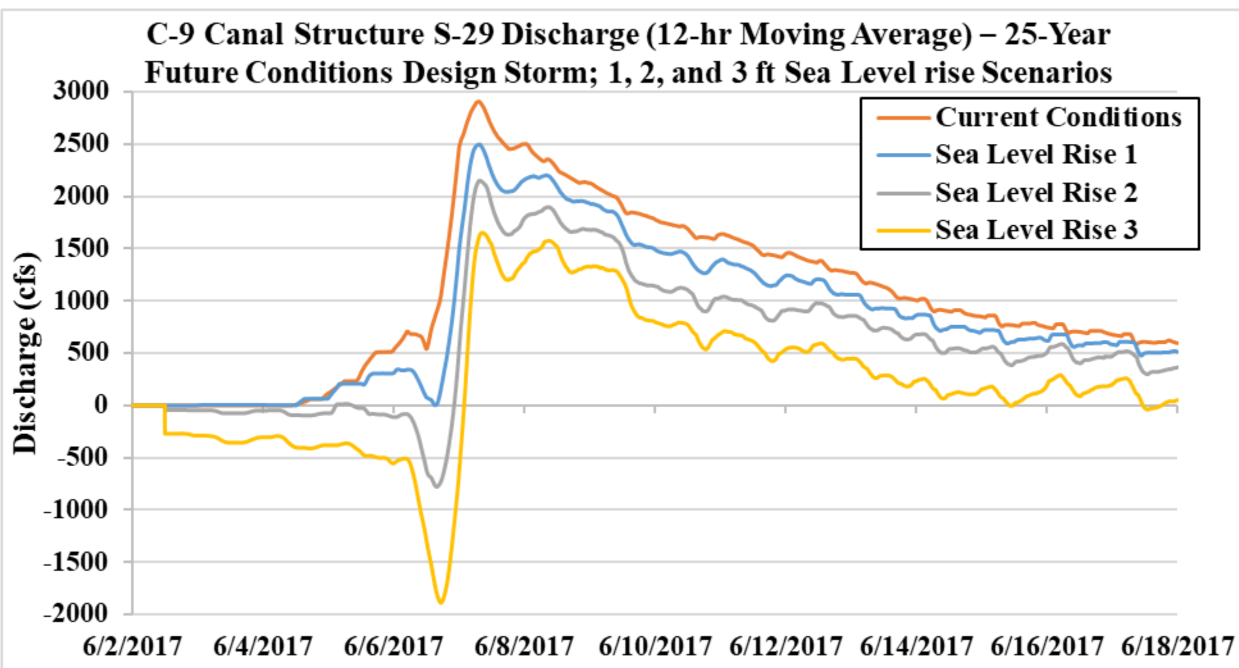

Figure 10.4-6: C-9 Canal Structure S-29 Discharge Hydrographs for 25-Year Design Storms

10.4.4 100-Year Design Storm

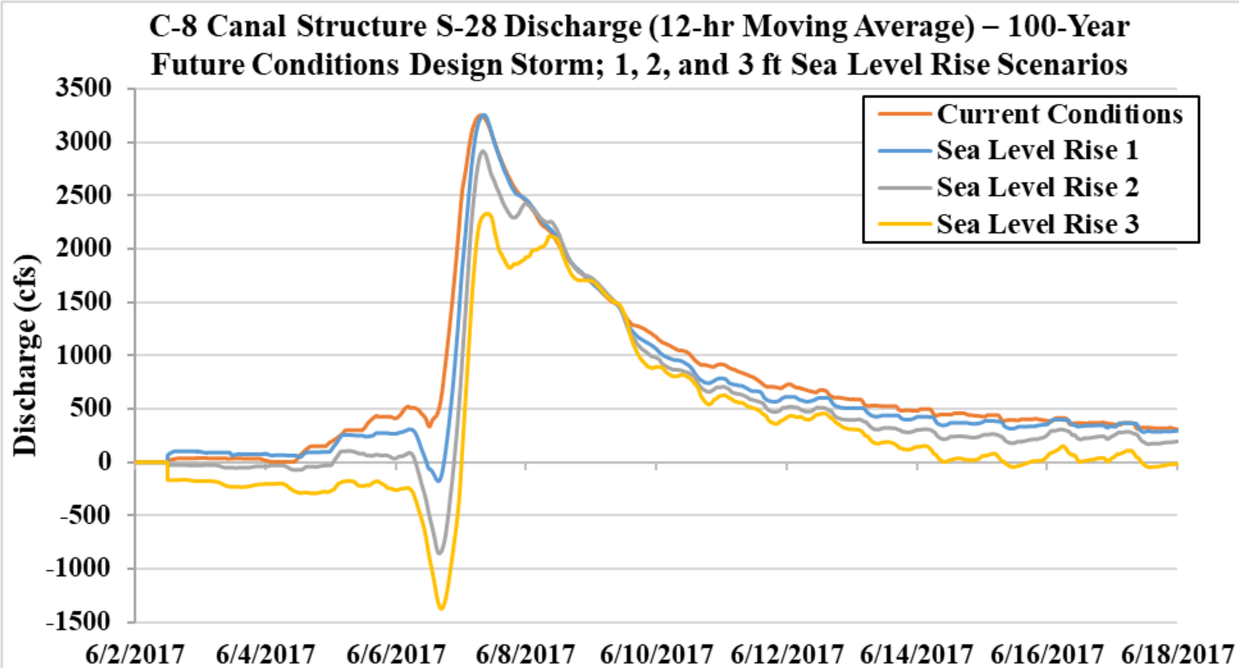

Figure 10.4-7: C-8 Canal Structure S-28 Discharge Hydrographs for 100-Year Design Storms

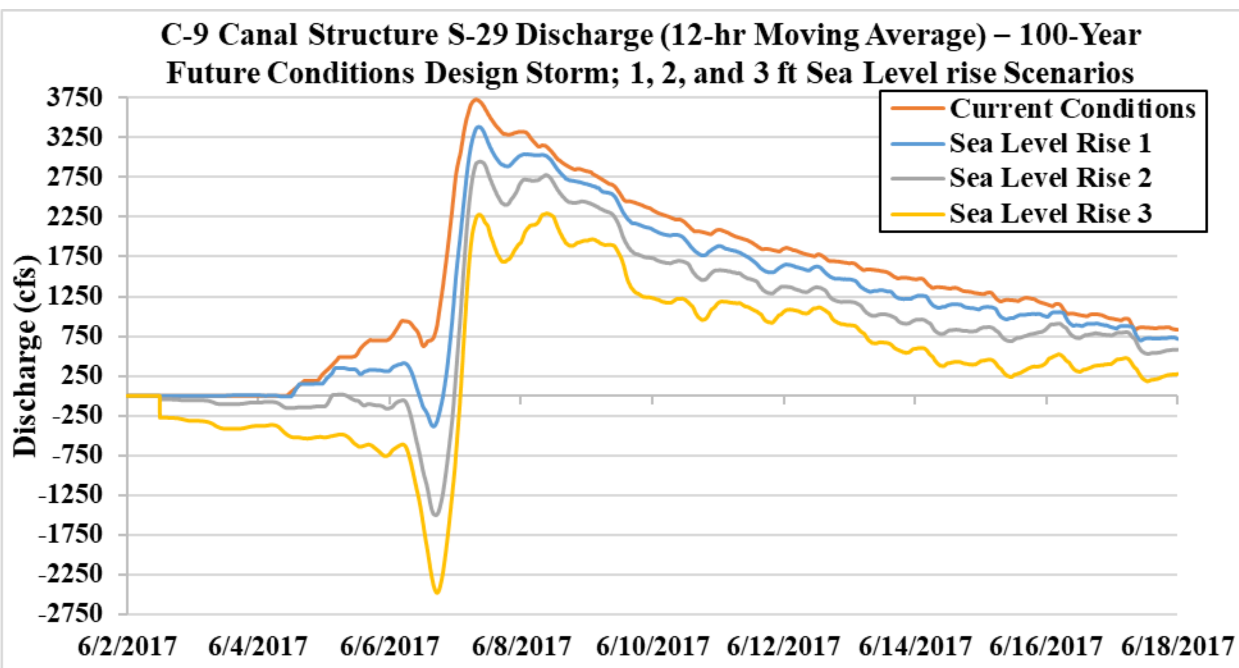

Figure 10.4-8: C-9 Canal Structure S-29 Discharge Hydrographs for 100-Year Design Storms

10.4.5 Peak Discharge Summary

Figure 10.4-9 shows the S-28 12-hour average peak discharge versus the design storm return period for three sea level rise scenarios. From the figure, it can be seen that the 5, 10, and 25-year 12-hour average peak discharges are relatively insensitive to sea level rise up to and including the 2 feet SLR scenarios. However, the discharges are all reduced significantly in the 3-foot SLR Scenario. **Table 10-22** through **Table 10-25** show the instantaneous and 12-hour average peak discharge for each design storm and sea level rise scenario.

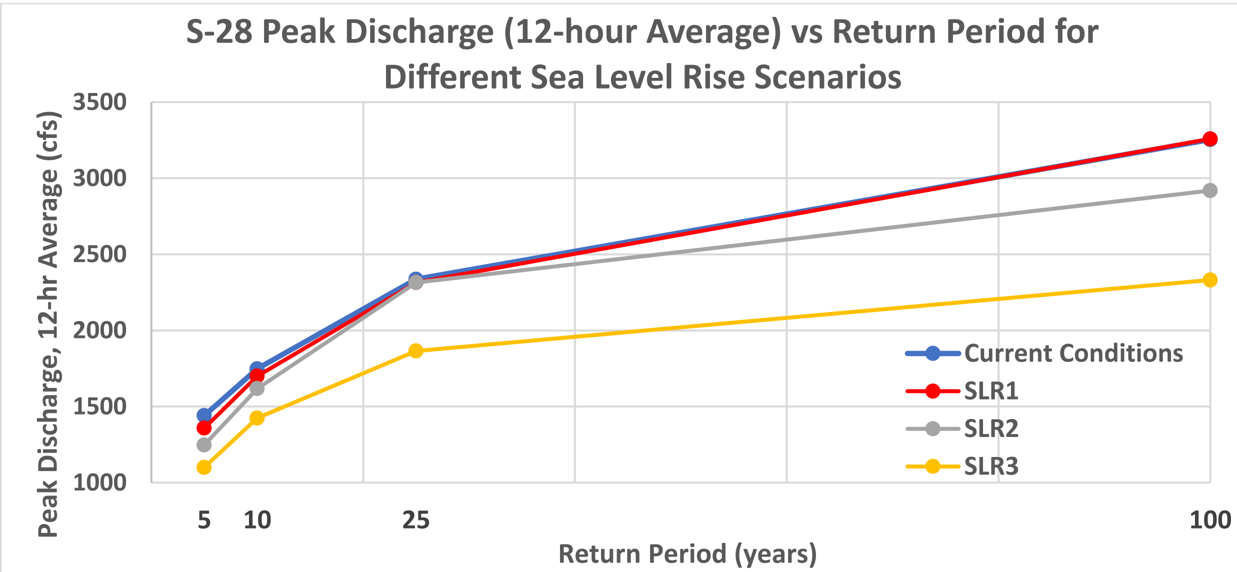

Figure 10.4-9: Structure S-28 12-Hour Average Peak Discharge for Different Sea Level Rise Scenarios

Table 10-22: S-28 Peak Discharge Summary for 5-Year Design Storms

Sea Level Rise Scenario	S-28 5-Year Design Storm Peak Discharge (cfs)		12-hr Moving Average Discharge Reduction Percentage
	Instantaneous	Moving Average (12-hr)	
Current	1720	1441	N/A
SLR1	1695	1359	5.7%
SLR2	1839	1248	13.4%
SLR3	2087	1101	23.6%

Table 10-23: S-28 Peak Discharge Summary for 10-Year Design Storms

Sea Level Rise Scenario	S-28 10-Year Design Storm Peak Discharge (cfs)		12-hr Moving Average Discharge Reduction Percentage
	Instantaneous	Moving Average (12-hr)	
Current	2059	1748	N/A
SLR1	2103	1700	2.7%
SLR2	2268	1619	7.4%
SLR3	2615	1424	18.5%

Table 10-24: S-28 Peak Discharge Summary for 25-Year Design Storms

Sea Level Rise Scenario	S-28 25-Year Design Storm Peak Discharge (cfs)		12-hr Moving Average Discharge Reduction Percentage
	Instantaneous	Moving Average (12-hr)	
Current	2679	2337	N/A
SLR1	2789	2315	0.9%
SLR2	3163	2315	0.9%
SLR3	3278	1865	20.2%

Table 10-25: S-28 Peak Discharge Summary for 100-Year Design Storms

Sea Level Rise Scenario	S-28 100-Year Design Storm Peak Discharge (cfs)		12-hr Moving Average Discharge Reduction Percentage
	Instantaneous	Moving Average (12-hr)	
Current	3777	3254	N/A
SLR1	3999	3259	-0.2%
SLR2	4157	2919	10.3%
SLR3	4094	2331	28.4%

Figure 10.4-10 shows the S-29 12-hour average peak discharge versus the design storm return period for three sea level rise scenarios. Unlike at S-28, the 12-hour peak discharges at S-29 for all storms are sensitive to all SLR scenarios, including the 1-foot SLR. This is partially due to the C-9 Impoundment and western lakes/prior mine pits attenuating the discharge.

Table 10-26 and **Table 10-29** shows the instantaneous and 12-hour average peak discharge for each design storm and sea level rise scenario.

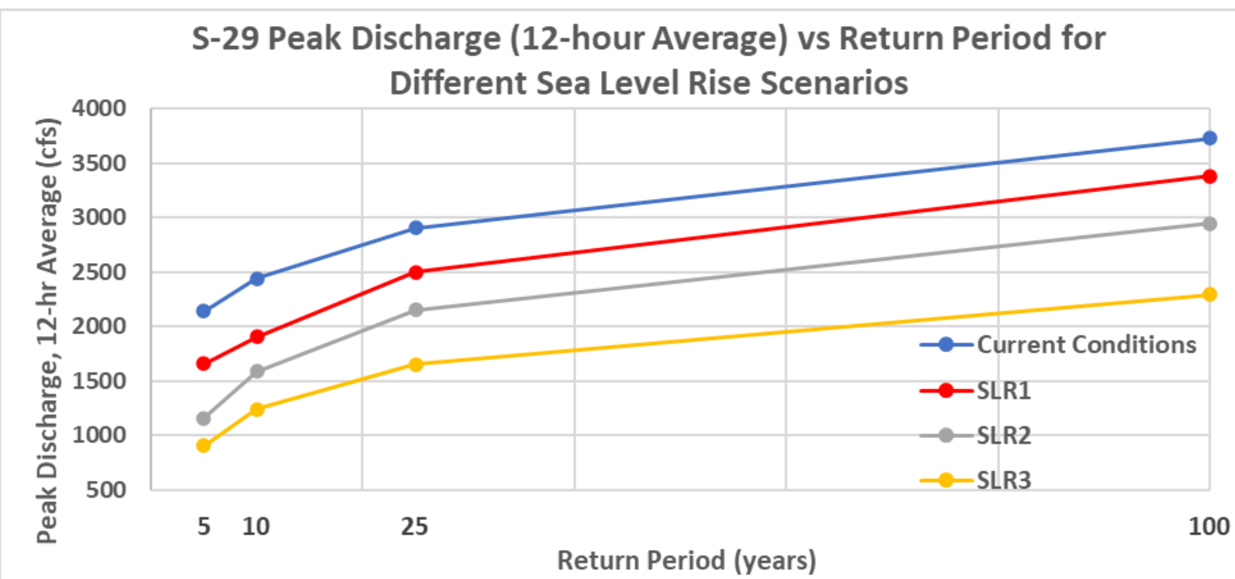

Figure 10.4-10: Structure S-29 12-Hour Average Peak Discharge for Different Sea Level Rise Scenarios

Table 10-26: S-29 Peak Discharge Summary for 5-Year Design Storms

Sea Level Rise Scenario	S-29 5-Year Design Storm Peak Discharge (cfs)		12-hr Moving Average Discharge Reduction Percentage
	Instantaneous	Moving Average (12-hr)	
Current	2647	2140	N/A
SLR1	2417	1656	22.6%
SLR2	2190	1159	45.8%
SLR3	2186	905	57.7%

Table 10-27: S-29 Peak Discharge Summary for 10-Year Design Storms

Sea Level Rise Scenario	S-29 10-Year Design Storm Peak Discharge (cfs)		12-hr Moving Average Discharge Reduction Percentage
	Instantaneous	Moving Average (12-hr)	
Current	3052	2437	N/A
SLR1	2698	1904	21.9%
SLR2	2526	1584	35.0%
SLR3	2631	1238	49.2%

Table 10-28: S-29 Peak Discharge Summary for 25-Year Design Storms

Sea Level Rise Scenario	S-29 25-Year Design Storm Peak Discharge (cfs)		12-hr Moving Average Discharge Reduction Percentage
	Instantaneous	Moving Average (12-hr)	
Current	3681	2908	N/A
SLR1	3360	2500	14.0%
SLR2	3460	2153	26.0%
SLR3	3632	1653	43.2%

Table 10-29: S-29 Peak Discharge Summary for 100-Year Design Storms

Sea Level Rise Scenario	S-29 100-Year Design Storm Peak Discharge (cfs)		12-hr Moving Average Discharge Reduction Percentage
	Instantaneous	Moving Average (12-hr)	
Current	4710	3728	N/A
SLR1	4645	3384	9.2%
SLR2	5074	2947	20.9%
SLR3	4883	2294	38.5%

10.5 PM #5 – Frequency of Flooding

For this PM, the depths of overland flooding were evaluated for the 72-hour design storms with the return period of 5-year, 10-year, 25-year, and 100-year with sea level rise conditions of 1, 2, and 3 ft. These flood depths, or elevations, can be compared with elevations of features such as buildings and roadways, where such information exists. For the purposes of this C-8/C-9 FPLOS evaluation, flood inundation maps were prepared using MIKE SHE gridded model output for each storm event, in the form of depth of overland water. Flooding depths were representative of the overland water depths on the 125-ft grid. **Table 10-30** through **Table 10-33** summarize the area of flooding shown in the flood inundation maps for each of the design storms, as presented in **Figure 10.5-1** through **Figure 10.5-24**.

Table 10-30: Summary of the PM #5 Flood Inundation Area for the 5-Year Design Storm

Water depth (ft)	CSL	SLR1	SLR2	SLR3	CSL	SLR1	SLR2	SLR3
	C-8 Watershed Area of Flooding (acres)				C-9 Watershed Area of Flooding (acres)			
< 0.25	3665	3824	3781	3752	14514	14231	13975	13862
>= 0.25	6574	6526	6661	6844	33647	31567	32182	32578
>= 0.50	3593	3600	3753	4005	20011	18417	19220	19863
>= 0.75	2221	2279	2409	2705	11927	10852	11638	12513
>= 1.00	1661	1760	1888	2143	7633	7002	7740	8648
>= 1.25	1391	1516	1642	1830	5064	4746	5376	6201
>= 1.50	1270	1288	1472	1665	3517	3389	3777	4495
>= 1.75	1187	1172	1222	1523	2484	2418	2670	3161
>= 2.00	1053	1093	1155	1258	1606	1589	1758	2070
>= 2.25	840	878	1066	1150	987	1017	1134	1317
>= 2.50	394	419	603	850	557	592	661	787
	Flooding in Urban Areas Within C-8 Watershed (acres)				**Flooding in Urban Areas Within C-9 Watershed (acres)**			
>= 0.25	3055	3570	3535	3515	11346	12251	12185	12153
>= 0.25	5302	5003	5109	5267	23882	22306	22494	22735
>= 0.50	2620	2234	2358	2571	13073	11471	11706	12019
>= 0.75	1198	1001	1100	1354	6903	5766	5996	6329
>= 1.00	596	528	629	834	3973	3321	3524	3815
>= 1.25	343	326	421	569	2626	2250	2415	2662
>= 1.50	235	227	295	443	1928	1673	1792	1996
>= 1.75	182	185	216	343	1545	1339	1416	1550
>= 2.00	150	148	177	243	1247	1010	1082	1189
>= 2.25	115	94	148	182	988	753	835	913
>= 2.50	91	54	83	114	756	504	569	664

Table 10-31: Summary of the PM #5 Flood Inundation Area for the 10-Year Design Storm

Water depth (ft)	CSL	SLR1	SLR2	SLR3	CSL	SLR1	SLR2	SLR3
	C-8 Watershed Area of Flooding (acres)				C-9 Watershed Area of Flooding (acres)			
< 0.25	3406	3546	3517	3451	13612	13357	13275	13183
>= 0.25	7359	7324	7457	7697	37550	35310	35716	36164
>= 0.50	4353	4299	4506	4754	23829	22036	22652	23193
>= 0.75	2709	2736	2946	3212	14936	13670	14400	15137
>= 1.00	1958	2042	2205	2492	9788	9023	9717	10621
>= 1.25	1601	1718	1865	2105	6586	6175	6842	7784
>= 1.50	1410	1545	1682	1854	4521	4318	4911	5733
>= 1.75	1285	1355	1524	1705	3236	3106	3457	4184
>= 2.00	1222	1204	1251	1553	2269	2226	2450	2889
>= 2.25	1076	1149	1202	1292	1476	1502	1630	1869
>= 2.50	906	1021	1145	1217	915	937	1004	1129
	Flooding in Urban Areas Within C-8 Watershed (acres)				**Flooding in Urban Areas Within C-9 Watershed (acres)**			
>= 0.25	3262	3316	3291	3238	11868	11674	11657	11612
>= 0.25	4647	5734	5847	6059	21129	25266	25464	25766
>= 0.50	2015	2877	3048	3267	10699	14089	14323	14678
>= 0.75	840	1398	1578	1810	5308	7577	7822	8201
>= 1.00	406	758	889	1142	3074	4413	4631	4983
>= 1.25	233	474	595	792	2093	2903	3070	3379
>= 1.50	172	338	441	581	1559	2124	2254	2502
>= 1.75	131	242	325	464	1252	1681	1769	1955
>= 2.00	103	200	231	361	935	1350	1412	1535
>= 2.25	73	170	198	260	692	1082	1136	1233
>= 2.50	50	135	171	206	451	814	882	958

Table 10-32: Summary of the PM #5 Flood Inundation Area for the 25-Year Design Storm

Water depth (ft)	CSL	SLR1	SLR2	SLR3	CSL	SLR1	SLR2	SLR3
	C-8 Watershed Area of Flooding (acres)				C-9 Watershed Area of Flooding (acres)			
< 0.25	3048	3122	3060	2960	12708	12527	12429	12330
>= 0.25	8449	8466	8690	8985	42357	39960	40343	40893
>= 0.50	5457	5391	5627	6027	29068	26991	27499	28194
>= 0.75	3575	3545	3787	4166	19713	18038	18607	19286
>= 1.00	2564	2555	2872	3159	13632	12414	13095	13678
>= 1.25	2010	2060	2309	2625	9588	8819	9595	10150
>= 1.50	1720	1821	1976	2307	6797	6337	7082	7691
>= 1.75	1542	1664	1816	2042	4712	4484	5158	5745
>= 2.00	1412	1536	1689	1849	3213	3114	3661	4149
>= 2.25	1314	1291	1537	1721	2162	2073	2367	2771
>= 2.50	1263	1239	1291	1447	1362	1339	1433	1604
	Flooding in Urban Areas Within C-8 Watershed (acres)				Flooding in Urban Areas Within C-9 Watershed (acres)			
>= 0.25	2747	2923	2870	2769	10896	11169	11134	11067
>= 0.25	6236	6784	6987	7259	27560	29144	29432	30016
>= 0.50	3524	3882	4093	4453	16672	17943	18299	18921
>= 0.75	1824	2117	2333	2681	9581	10565	10903	11479
>= 1.00	974	1201	1481	1738	5602	6378	6674	7137
>= 1.25	558	748	963	1244	3578	4136	4390	4758
>= 1.50	374	543	674	963	2544	2925	3130	3416
>= 1.75	278	411	540	727	1977	2220	2381	2609
>= 2.00	217	314	439	563	1614	1771	1889	2051
>= 2.25	185	244	327	463	1317	1418	1495	1612
>= 2.50	162	212	245	356	1099	1156	1207	1272

Table 10-33: Summary of the PM #5 Flood Inundation Area for the 100-Year Design Storm

Water depth (ft)	CSL	SLR1	SLR2	SLR3	CSL	SLR1	SLR2	SLR3
	C-8 Watershed Area of Flooding (acres)				C-9 Watershed Area of Flooding (acres)			
< 0.25	2531	2539	2473	2377	11567	11383	11295	11166
>= 0.25	10053	10167	10415	10773	49123	46711	46893	46979
>= 0.50	7183	7211	7553	7993	36421	34263	34548	34752
>= 0.75	5025	5013	5418	5867	26351	24460	24778	25060
>= 1.00	3674	3676	4032	4538	18964	17424	17737	17984
>= 1.25	2834	2921	3159	3665	13764	12613	12859	13037
>= 1.50	2351	2414	2705	3067	10037	9341	9513	9597
>= 1.75	2012	2089	2391	2699	7297	6931	7078	7081
>= 2.00	1763	1895	2107	2448	5041	4860	5049	5057
>= 2.25	1604	1759	1905	2204	3307	3290	3379	3416
>= 2.50	1480	1632	1766	1983	1860	1883	1949	1923
	Flooding in Urban Areas Within C-8 Watershed (acres)				Flooding in Urban Areas Within C-9 Watershed (acres)			
>= 0.25	2294	2382	2325	2236	10063	10278	10203	10138
>= 0.25	7657	8363	8588	8921	33701	35655	36153	36697
>= 0.50	5029	5569	5886	6284	22895	24591	25137	25765
>= 0.75	3054	3461	3830	4244	14698	16122	16651	17323
>= 1.00	1846	2198	2513	2974	9211	10382	10862	11440
>= 1.25	1125	1501	1714	2162	5866	6811	7189	7644
>= 1.50	753	1040	1297	1619	3947	4651	4938	5303
>= 1.75	525	750	1018	1287	2897	3397	3572	3876
>= 2.00	392	588	763	1069	2213	2530	2671	2889
>= 2.25	302	478	599	853	1807	1997	2096	2225
>= 2.50	240	374	491	666	1473	1565	1624	1713

The flood inundation maps over the entire model domain are shown in **Figure 10.5-1** through **Figure 10.5-12** for each of the four design storm events and sea level rise scenarios. **Figure 10.5-13** through **Figure 10.5-24** show the flood inundation maps for each of the design storm and sea level rise scenarios for urban areas only within the C8 and C9 basins. **Figure 10.5-25** through **Figure 10.5-42** show up close examples of flood depth along the C-8 Canal and **Figure 10.5-43** through **Figure 10.5-66** show up close examples of flood depth along the C-9 Canal. **Figure 10.5-67** through **Figure 10.5-69** show the maximum overland water depth difference between future and current conditions for the 25-Year SLR1, SLR2 and SLR3 design storm events.

The southwest portion of the C-9 Basin is mostly undeveloped (even with future land use changes considered), and thus were not served by stormwater collection and conveyance facilities. These undeveloped areas show the greatest extents and depths of flooding for the design storm events.

Notable developed areas also show flooding under PM #5. For example, residential areas along the C-8 Canal upstream and downstream of NE 135th St (CR 916), show extensive spatial extents of flooding in PM #5, which is most evident for the 25-year and 100-year SLR3 events, but is also evident in 5-year and

10-year SLR2 events. This flooding is corroborated by PM #1 results, which show that both the north and south bank is exceeded for the 5-year SLR1 event over a long segment upstream and downstream of CR916. For the 100-year SLR 3 event, flood stage in this area is upwards of 3 ft higher than the bank elevations.

In the C-9 Watershed, extensive flooding is shown upstream of S-29 for the 10-year SLR3 event, as well as downstream of US Highway 441. This flooding is corroborated by PM #1 results, which show that both the north and south bank exceedances for 10-year SLR3 event over long segments. Under current conditions, there were localized areas such as west of Red Road and upstream of the Ronald Reagan Turnpike that showed flooding in PM #5 but did not show canal bank exceedances in PM #1. Flooding in these areas could be due to the topography being lower than the canal bank and/or inadequate secondary drainage infrastructure. However, under future conditions, particularly with 2 ft and 3 ft sea level rise, the canal stage does exceed the bank elevations in these locations. The canal banks exceedances exacerbate the localized flooding that was shown when canal stages were still in-bank.

Both the C-8 and C-9 Canal experience extensive flooding, upwards of 2 to 3 ft in depth, for several miles during the 25-year and 100-year 3 ft sea level rise scenarios. This was an expected result due to the low bypass elevation of the tidal outfall structures, as well as the relatively low canal bank elevations for many parts of the C-8 and C-9 Canals.

10.5.1 5-Year Design Storm Model-Wide Flood Depth Map

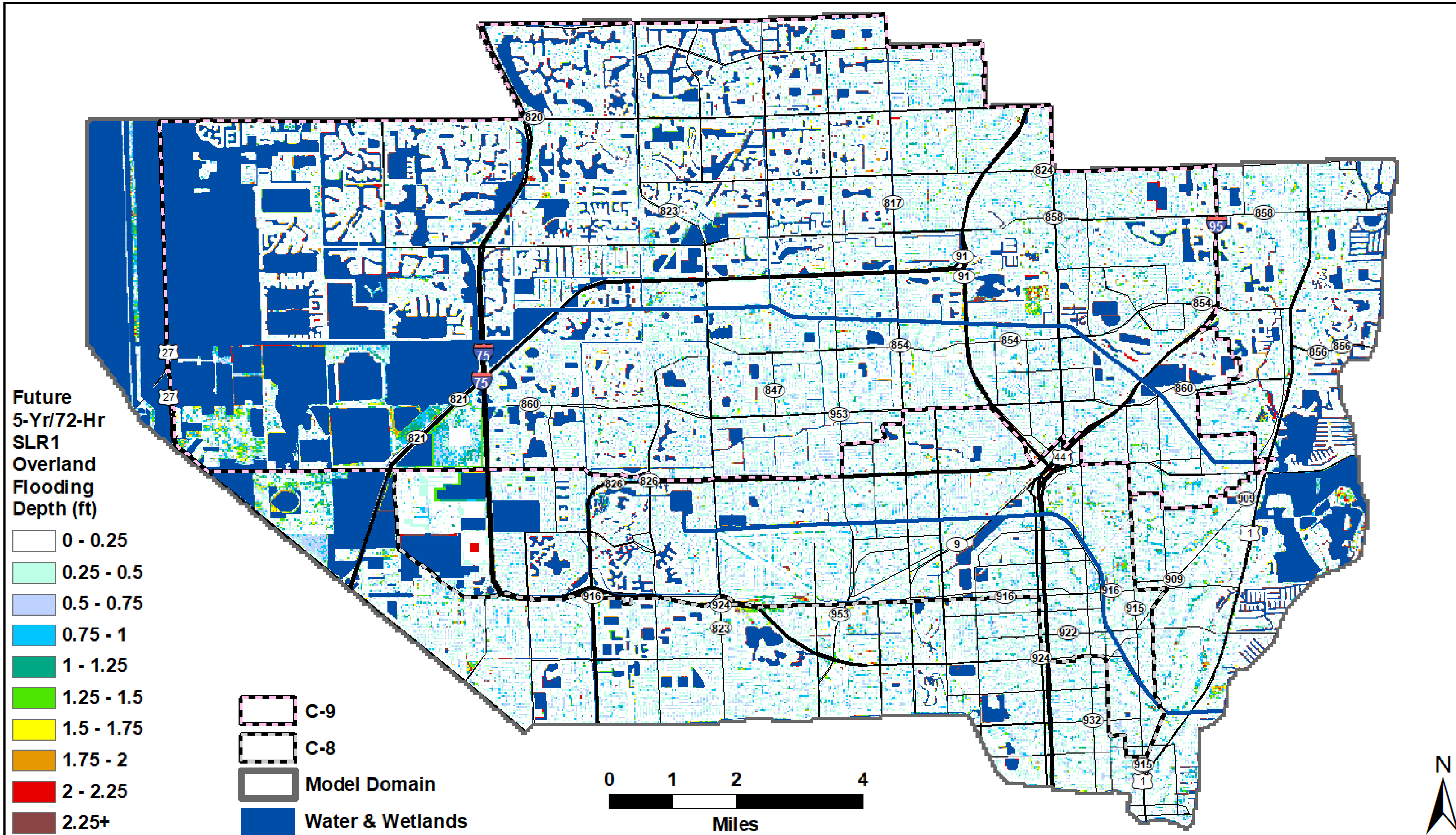

Figure 10.5-1: Flood Inundation Map for 5-Year Sea Level Rise 1 Design Storm Event

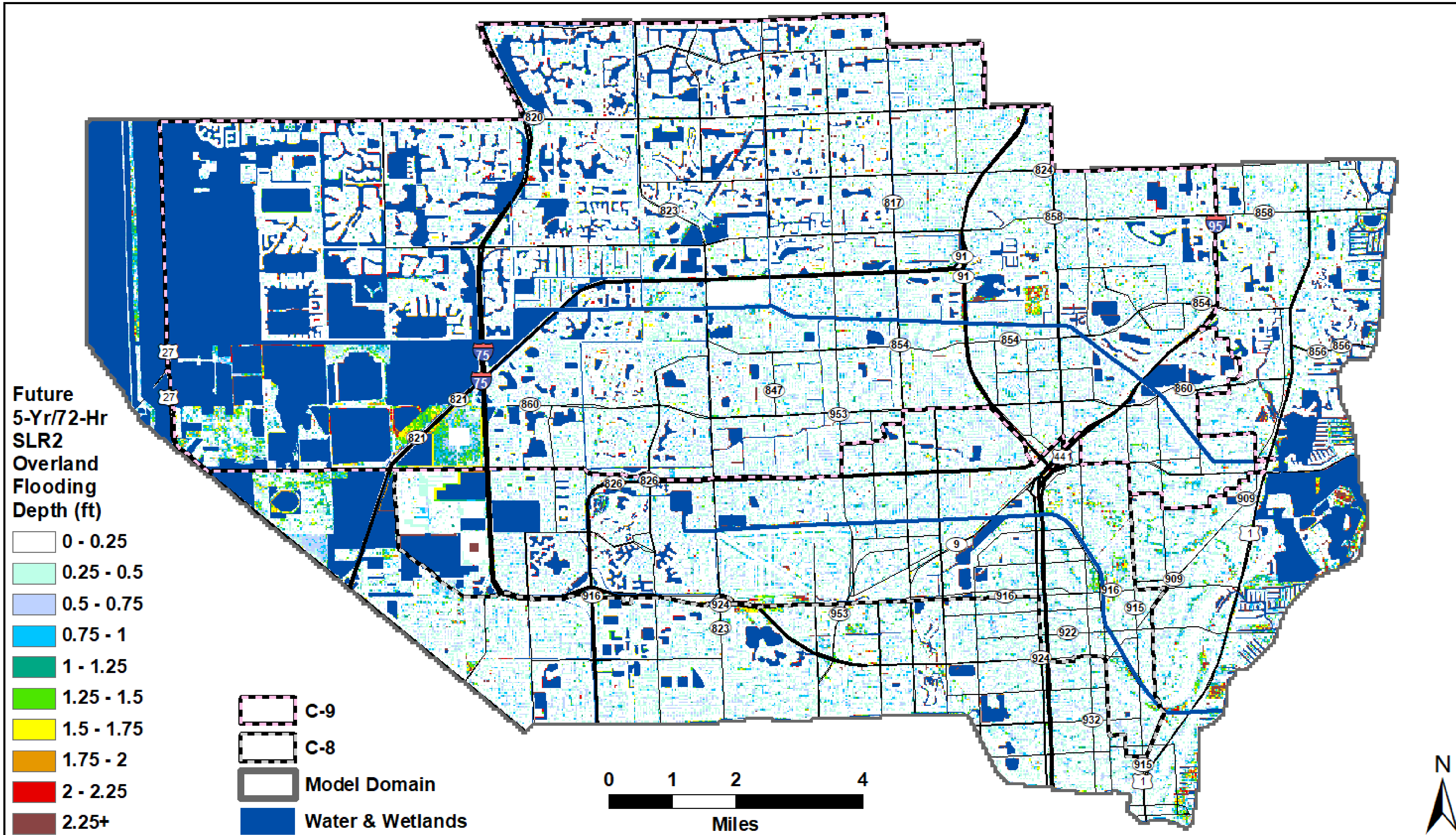

Figure 10.5-2: Flood Inundation Map for 5-Year Sea Level Rise 2 Design Storm Event

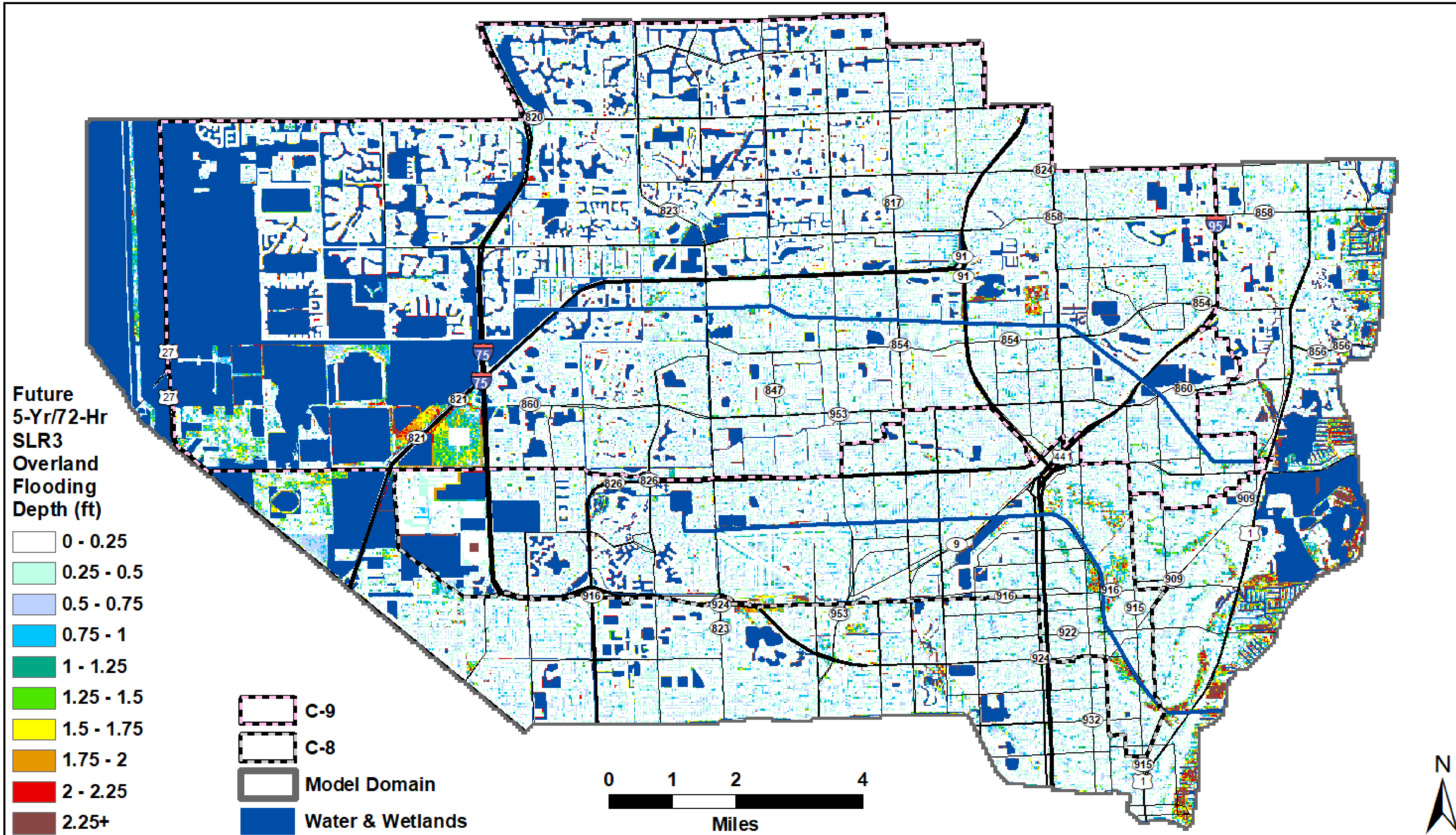

Figure 10.5-3: Flood Inundation Map for 5-Year Sea Level Rise 3 Design Storm Event

10.5.2 10-Year Design Storm Model-Wide Flood Depth Map

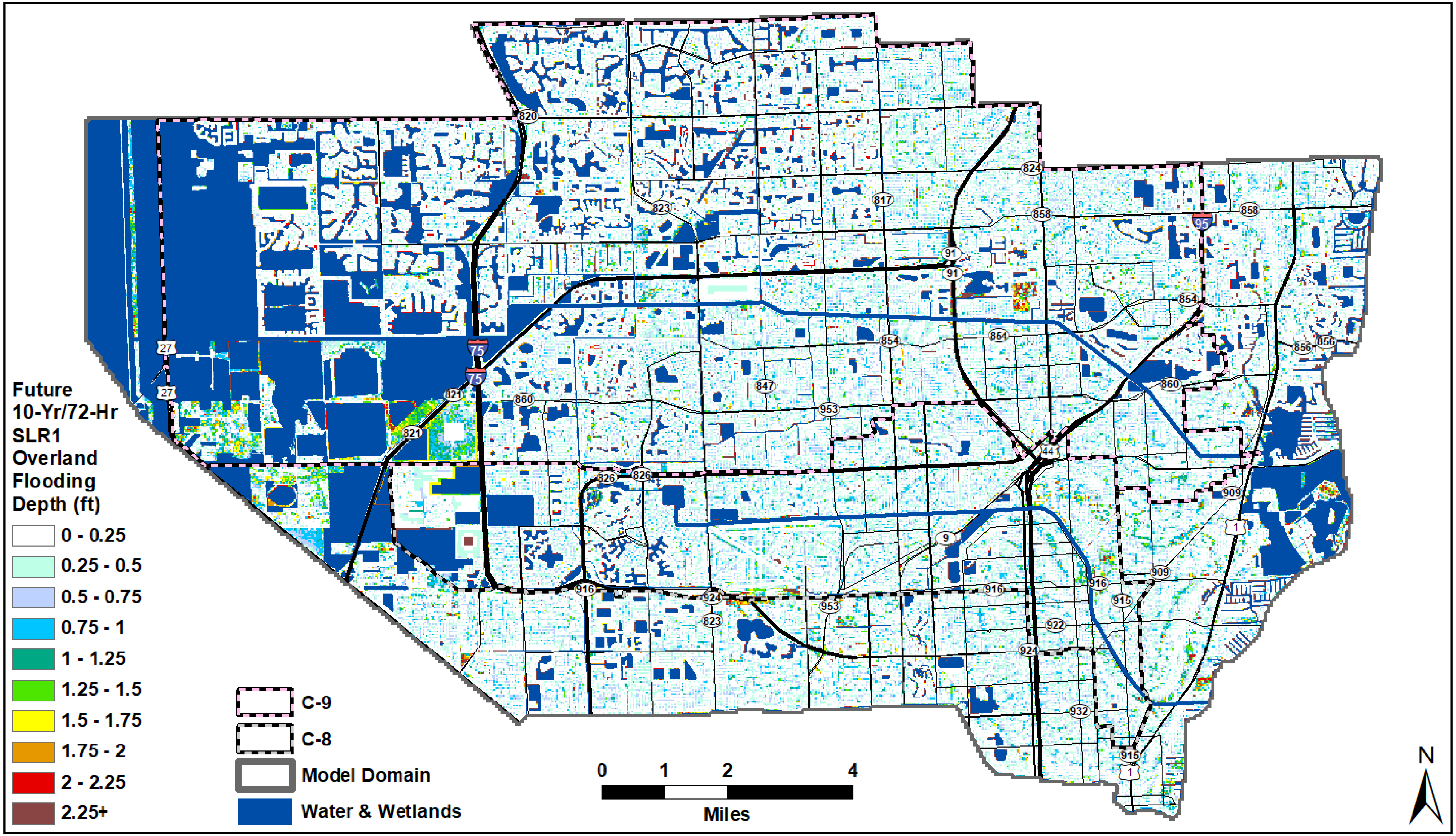

Figure 10.5-4: Flood Inundation Map for 10-Year Sea Level Rise 1 Design Storm Event

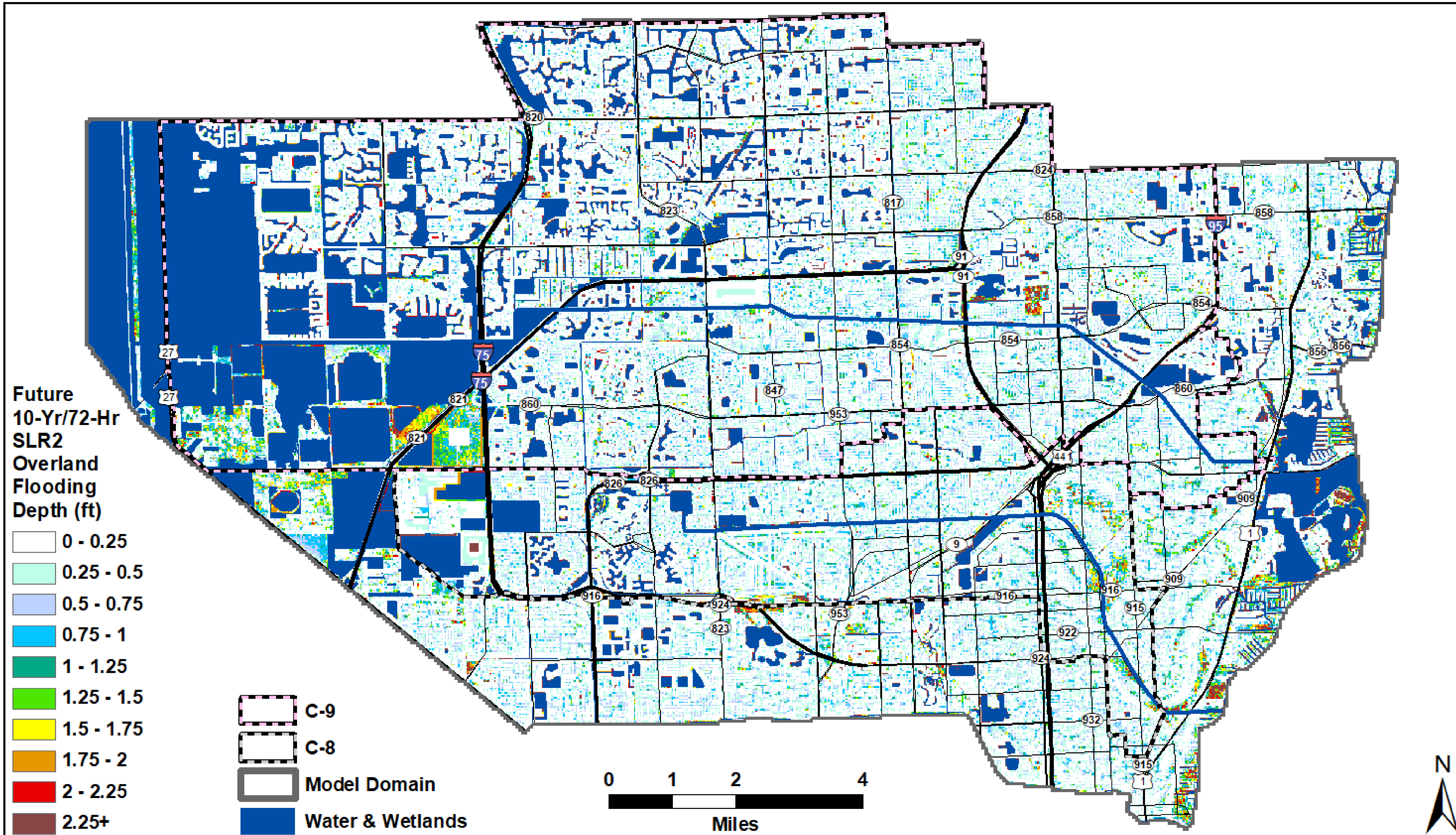

Figure 10.5-5: Flood Inundation Map for 10-Year Sea Level Rise 2 Design Storm Event

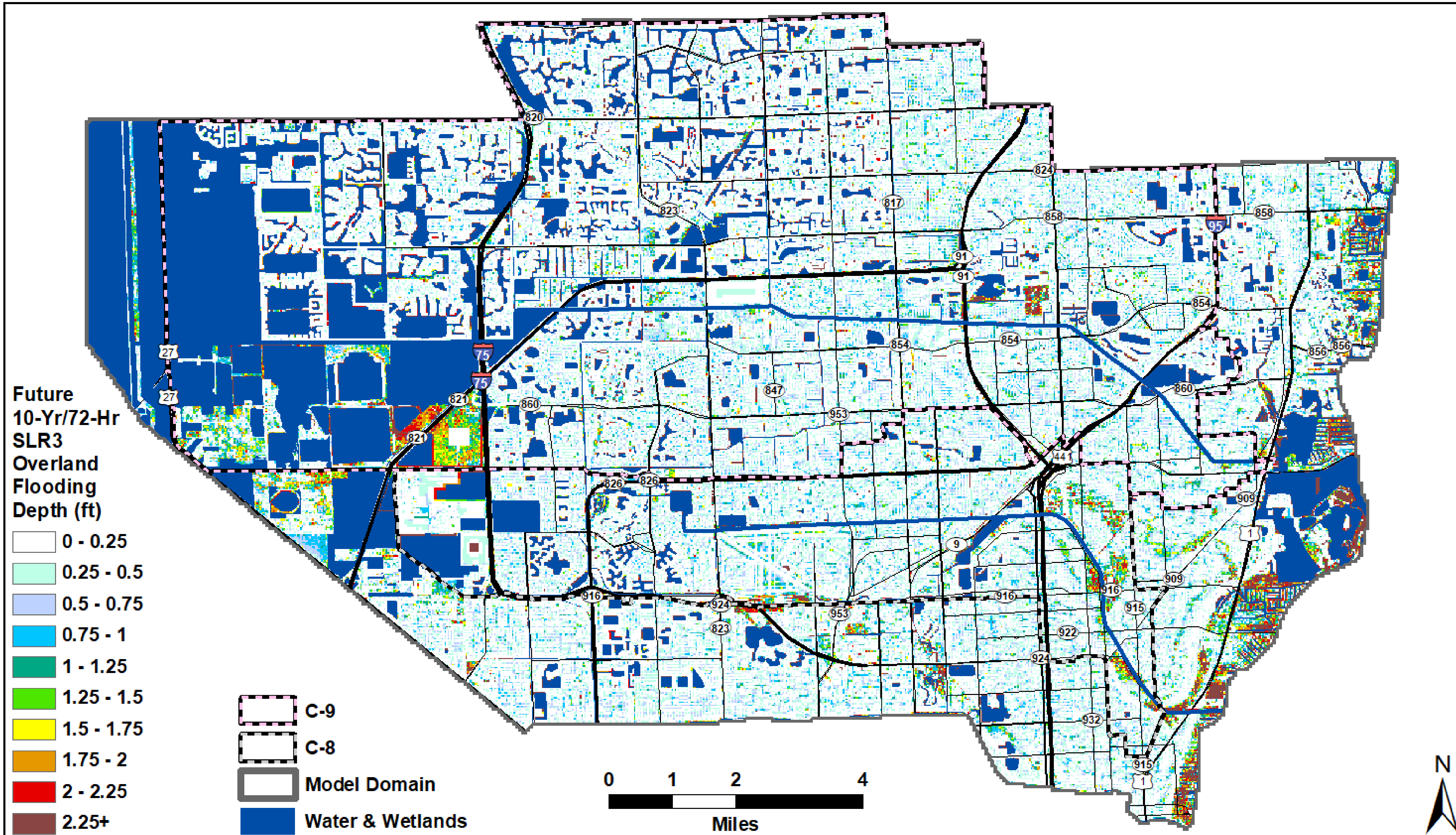

Figure 10.5-6: Flood Inundation Map for 10-Year Sea Level Rise 3 Design Storm Event

10.5.3 25-Year Design Storm Model-Wide Flood Depth Map

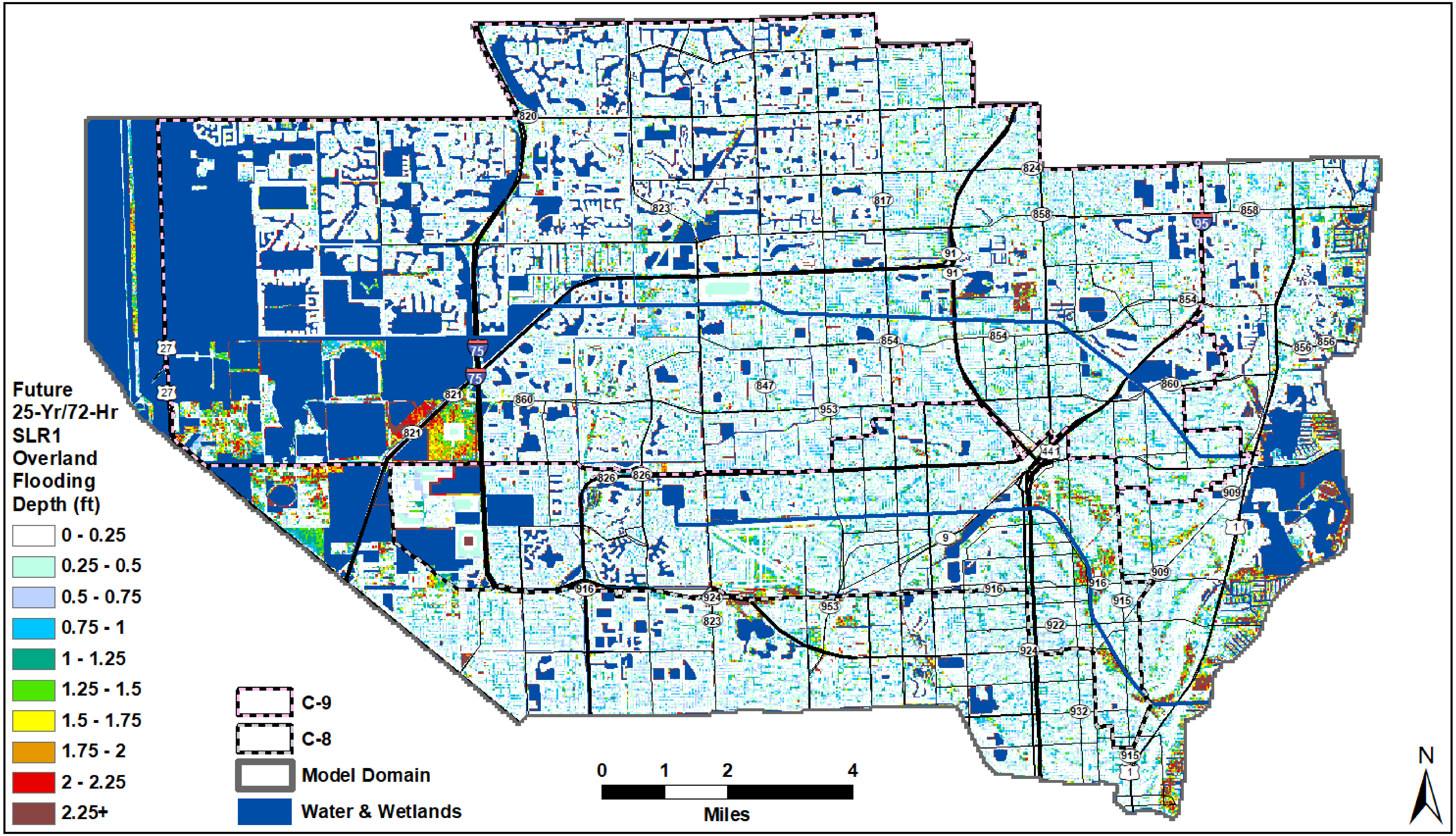

Figure 10.5-7: Flood Inundation Map for 25-Year Sea Level Rise 1 Design Storm Event

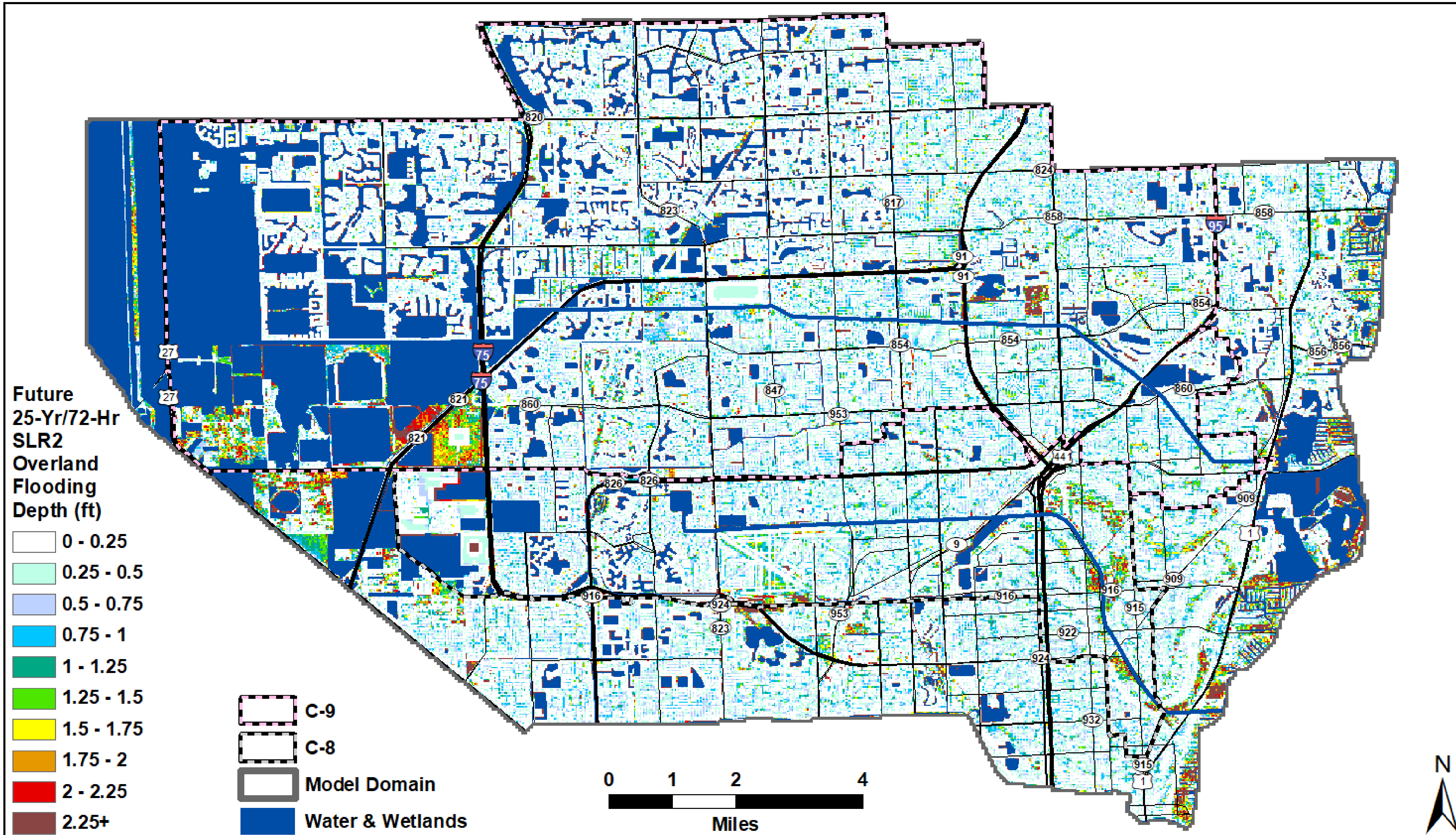

Figure 10.5-8: Flood Inundation Map for 25-Year Sea Level Rise 2 Design Storm Event

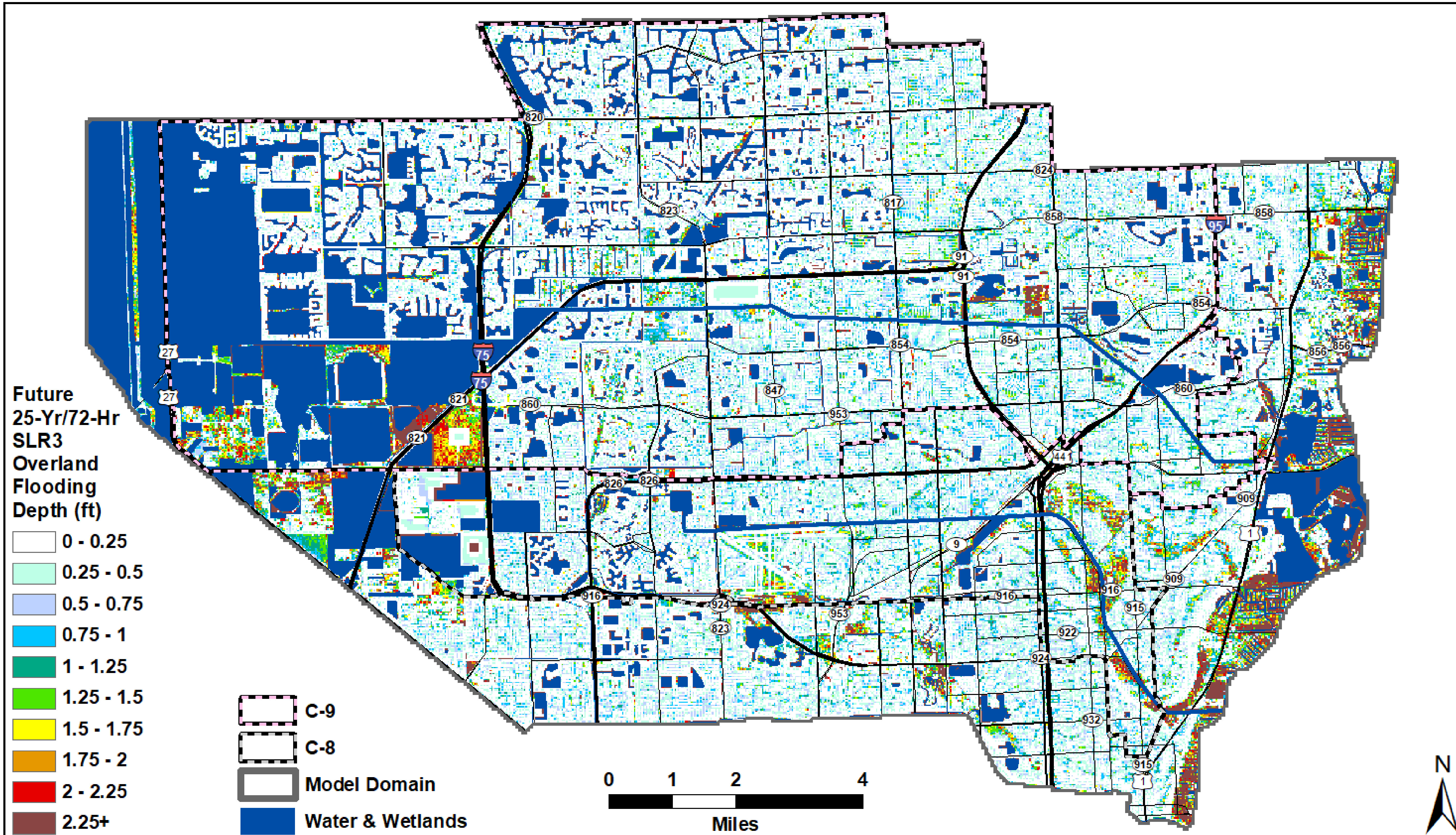

Figure 10.5-9: Flood Inundation Map for 25-Year Sea Level Rise 3 Design Storm Event

10.5.4 100-Year Design Storm Model-Wide Flood Depth Map

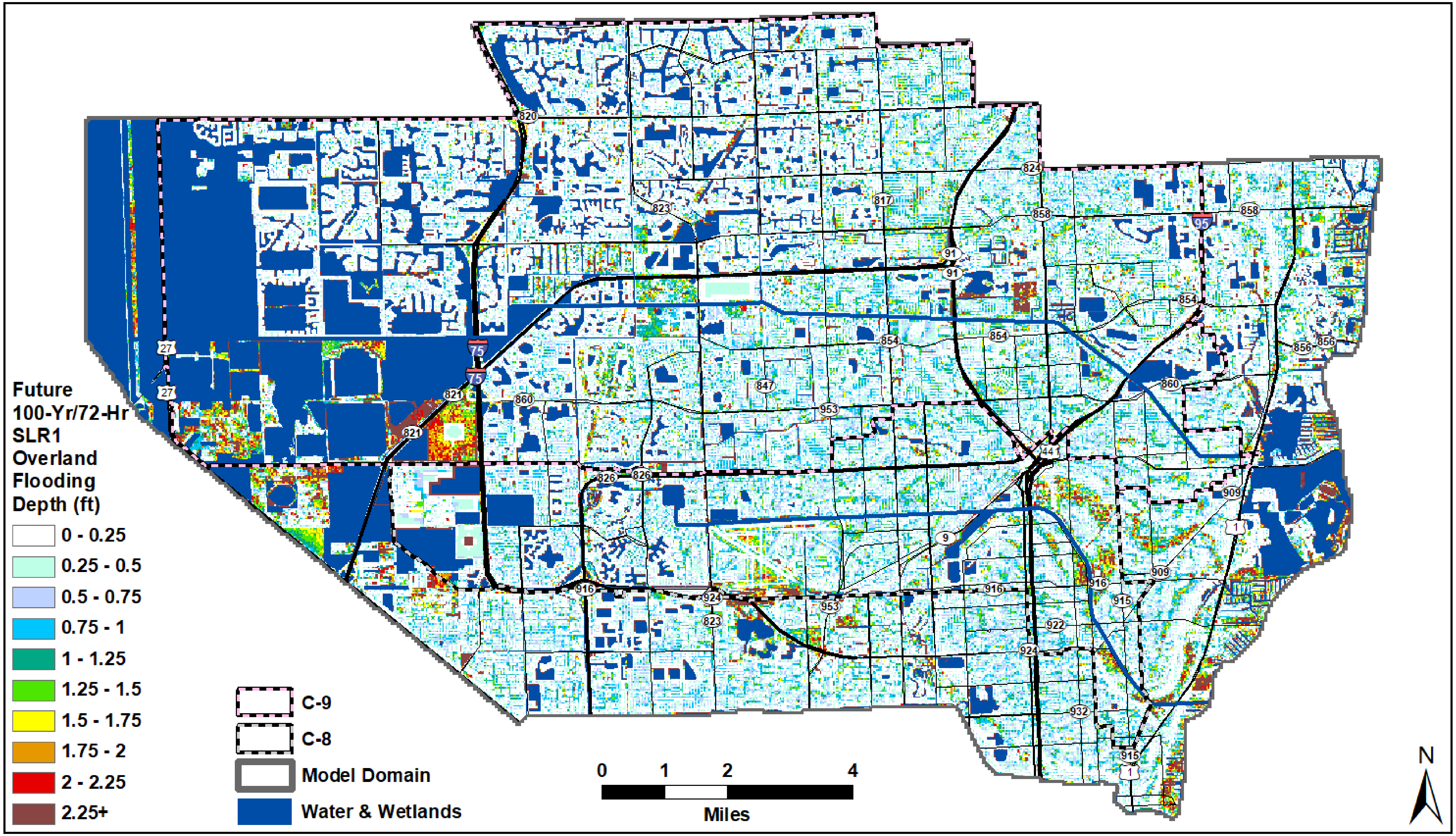

Figure 10.5-10: Flood Inundation Map for 100-Year Sea Level Rise 1 Design Storm Event

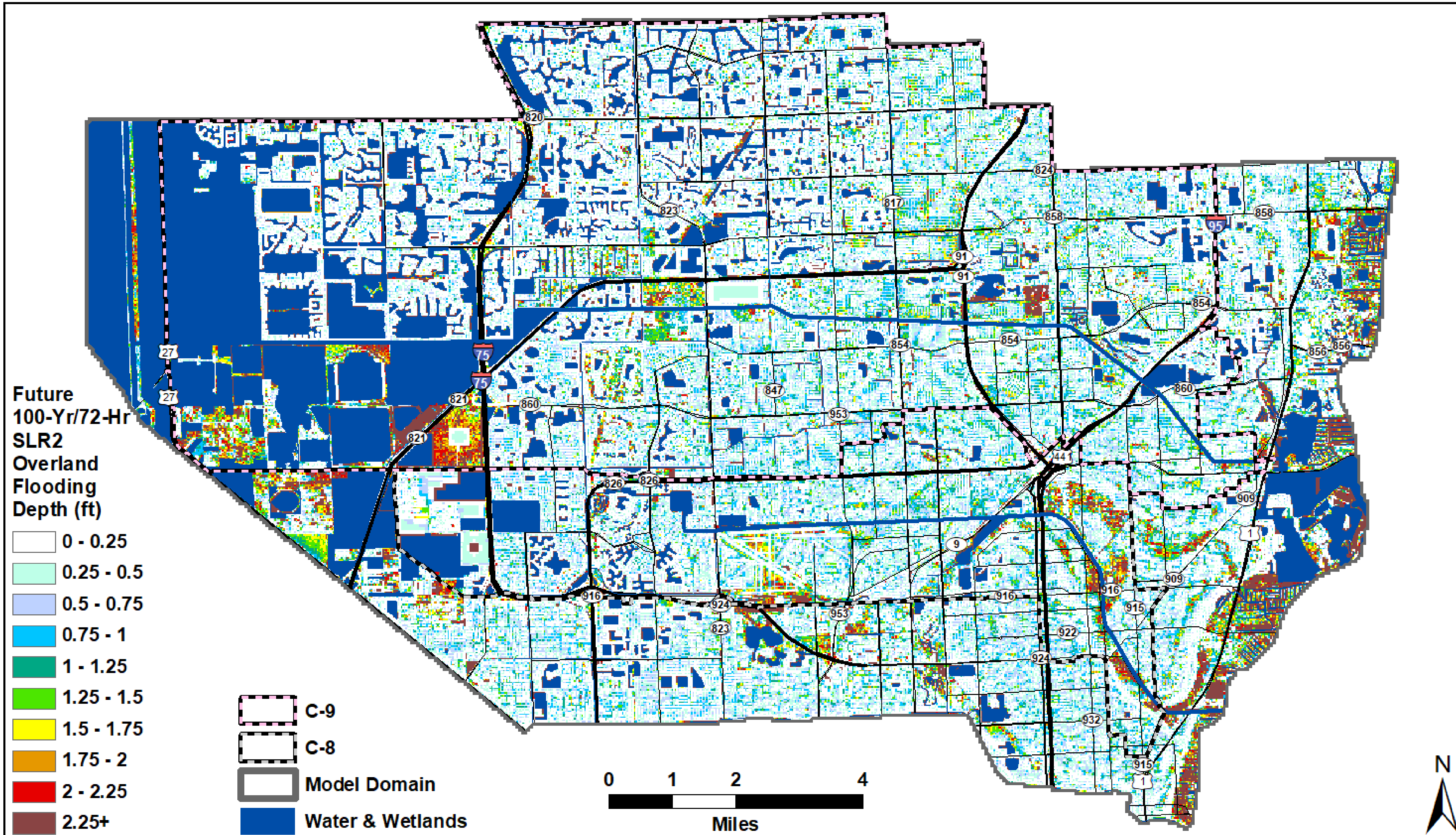

Figure 10.5-11: Flood Inundation Map for 100-Year Sea Level Rise 2 Design Storm Event

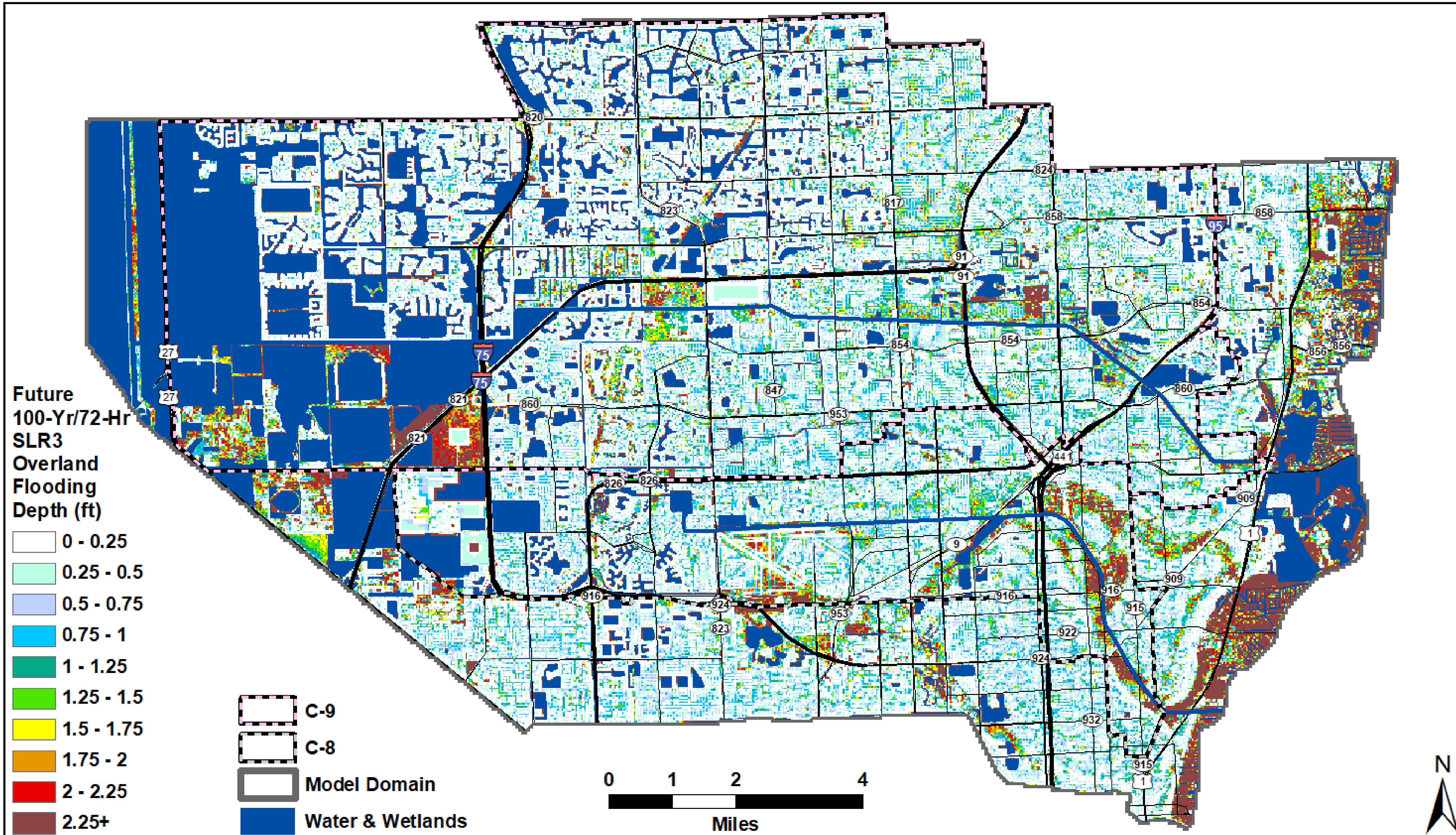

Figure 10.5-12: Flood Inundation Map for 100-Year Sea Level Rise 3 Design Storm Event

10.5.5 5-Year Design Storm Flood Depth Map for Urban Land Use Areas

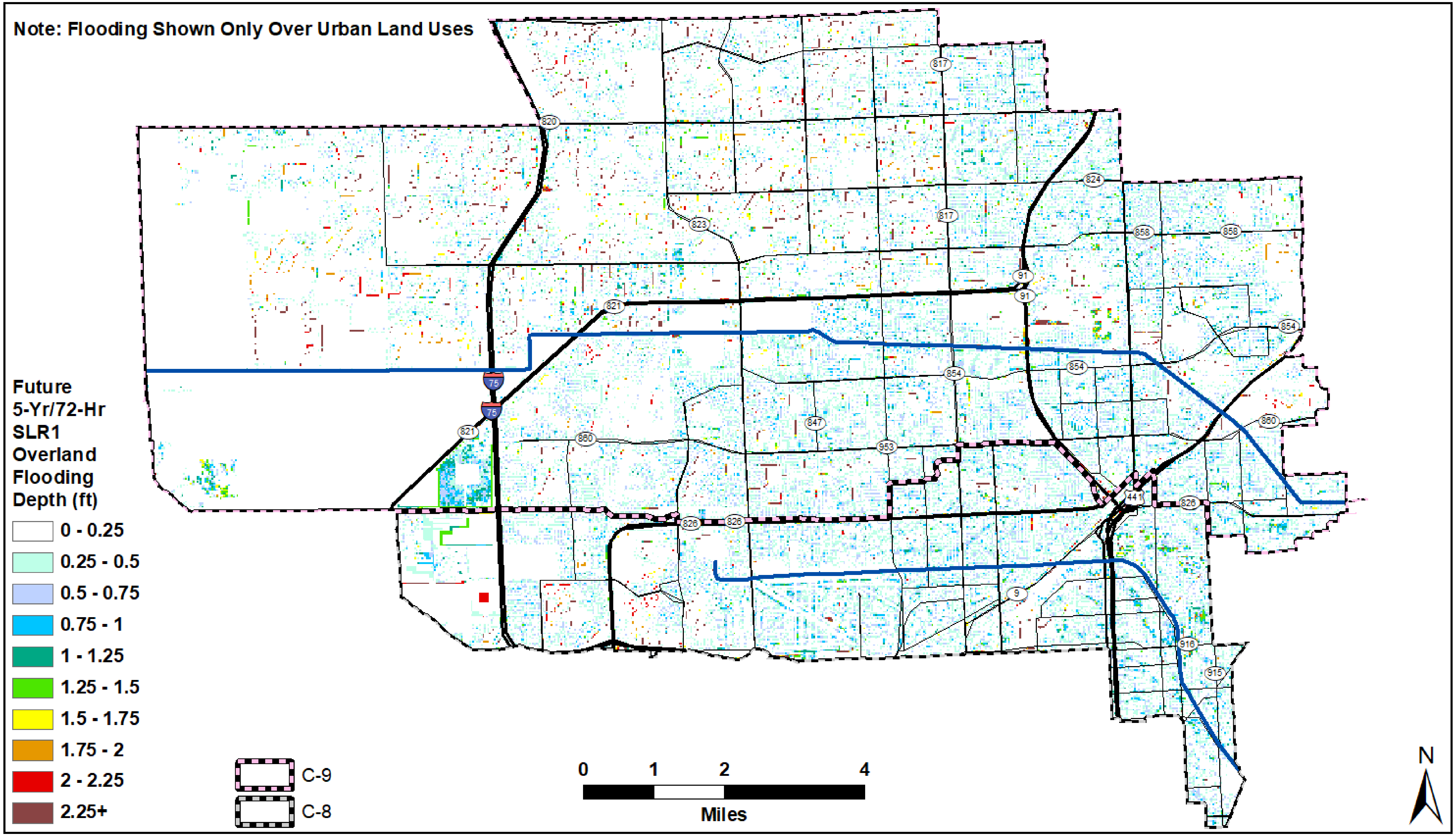

Figure 10.5-13: Flood Inundation Map for 5-Year Sea Level Rise 1 Design Storm Event in Urban Land Use Areas

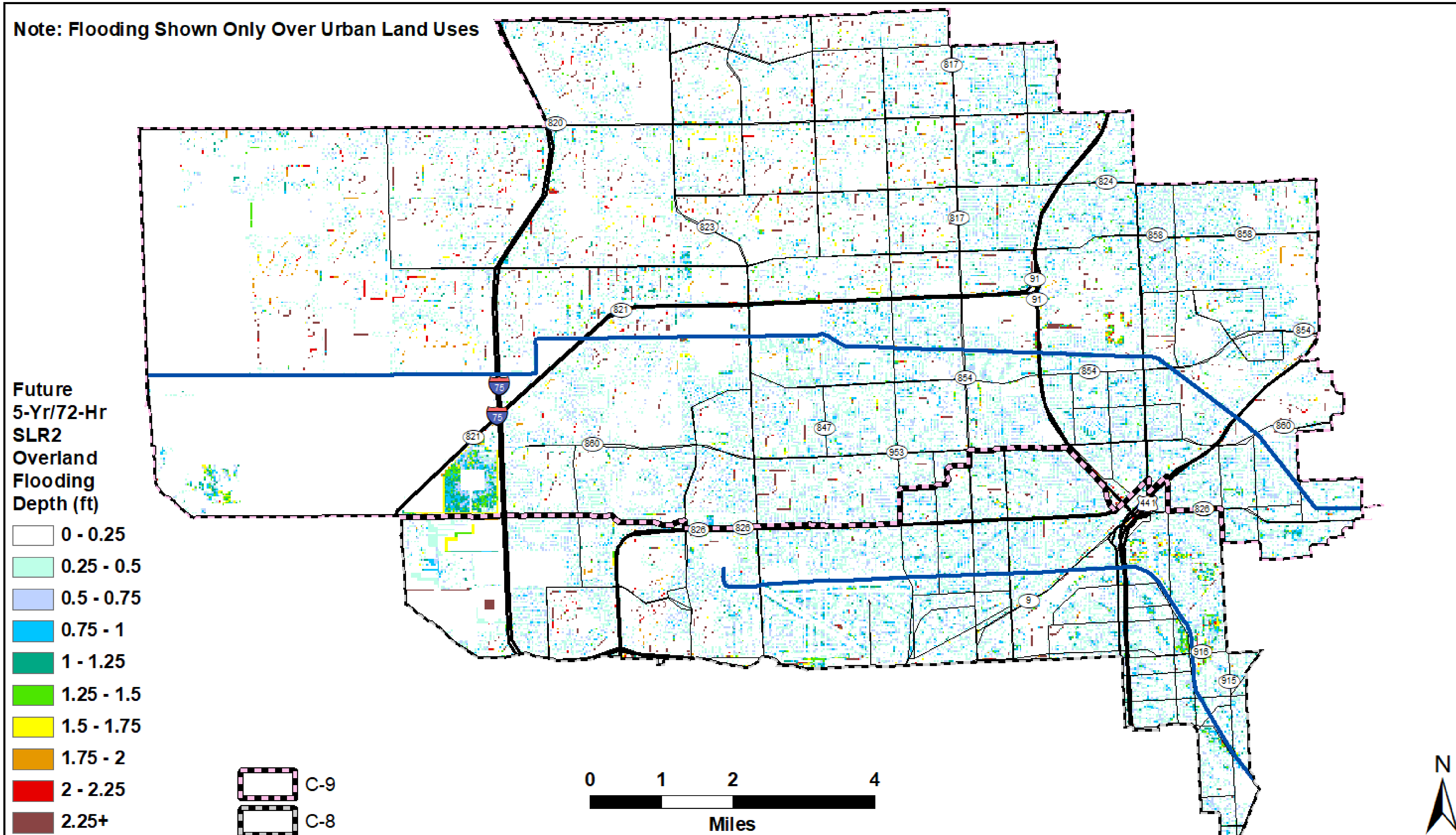

Figure 10.5-14: Flood Inundation Map for 5-Year Sea Level Rise 2 Design Storm Event in Urban Land Use Areas

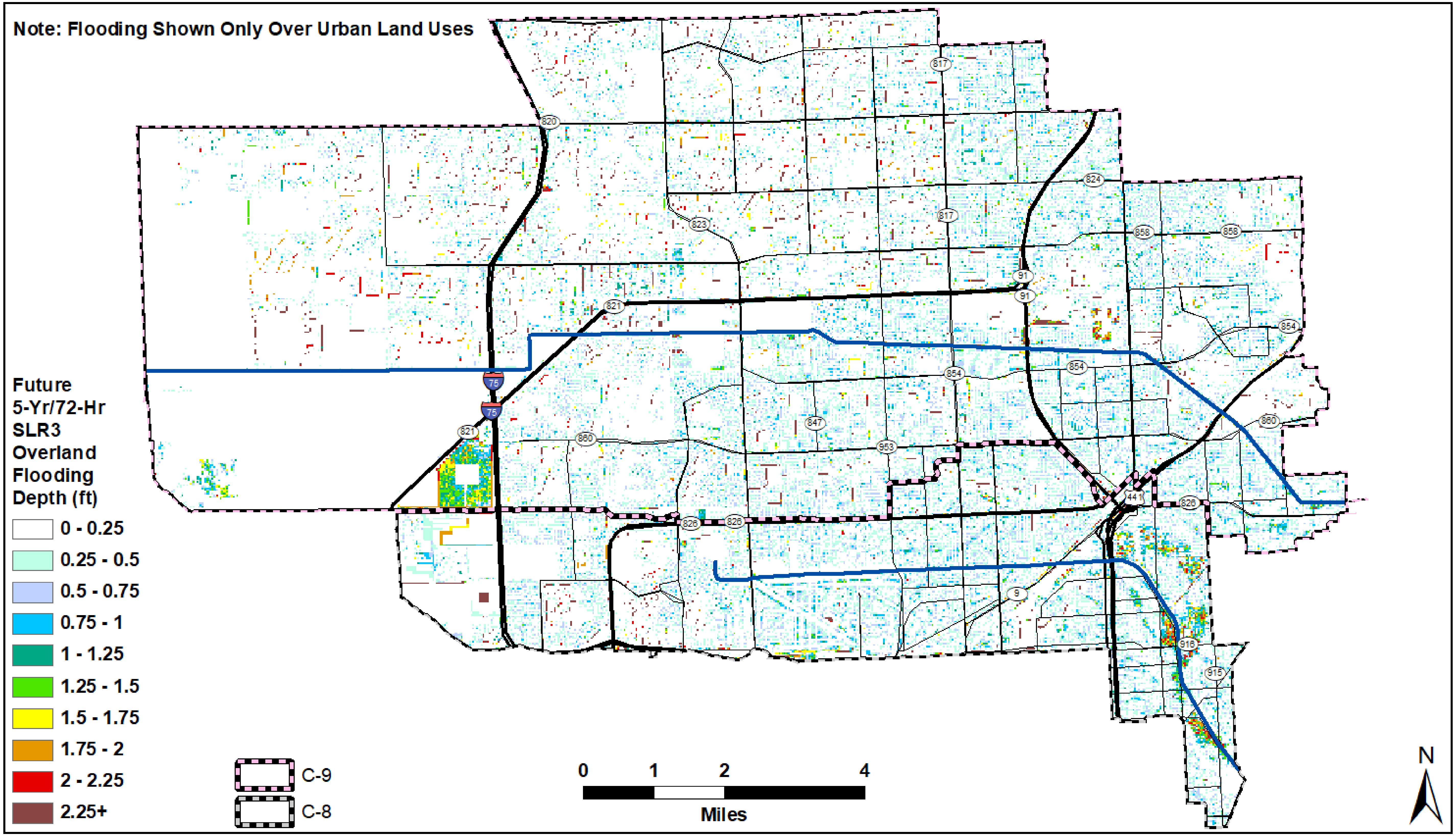

Figure 10.5-15: Flood Inundation Map for 5-Year Sea Level Rise 3 Design Storm Event in Urban Land Use Areas

10.5.6 10-Year Design Storm Flood Depth Map for Urban Land Use Areas

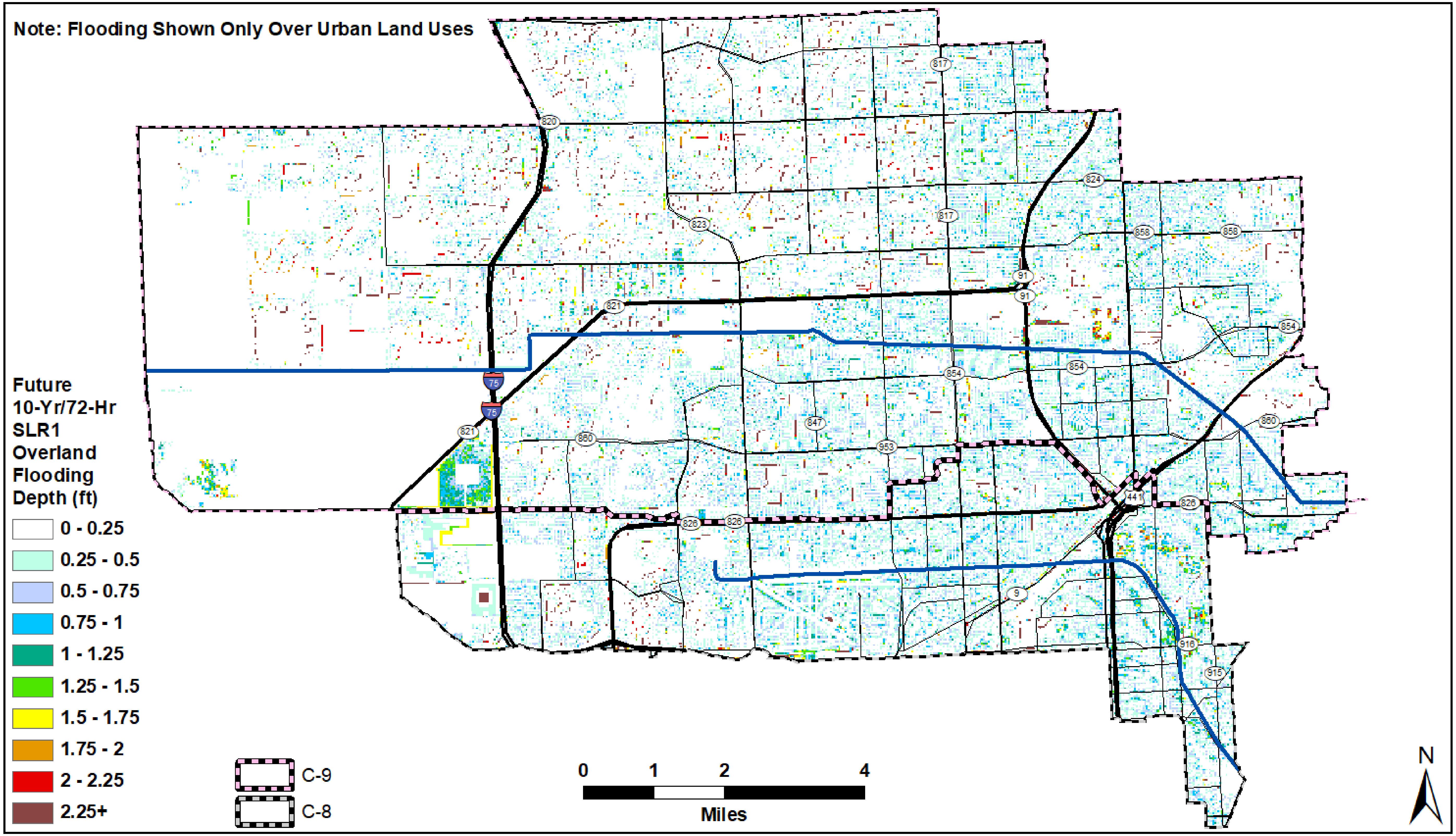

Figure 10.5-16 Flood Inundation Map for 10-Year Sea Level Rise 1 Design Storm Event in Urban Land Use Areas

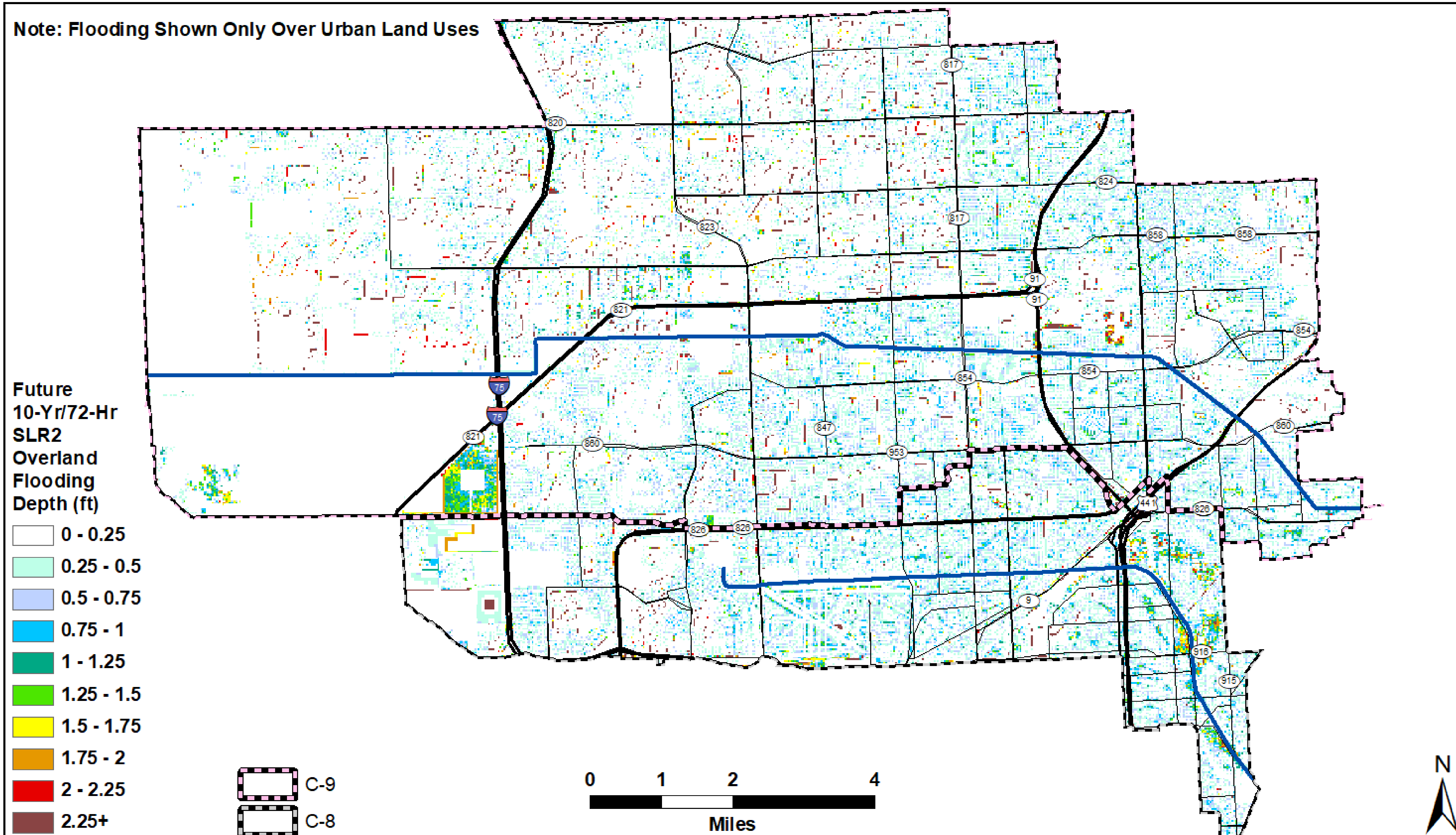

Figure 10.5-17 Flood Inundation Map for 10-Year Sea Level Rise 2 Design Storm Event in Urban Land Use Areas

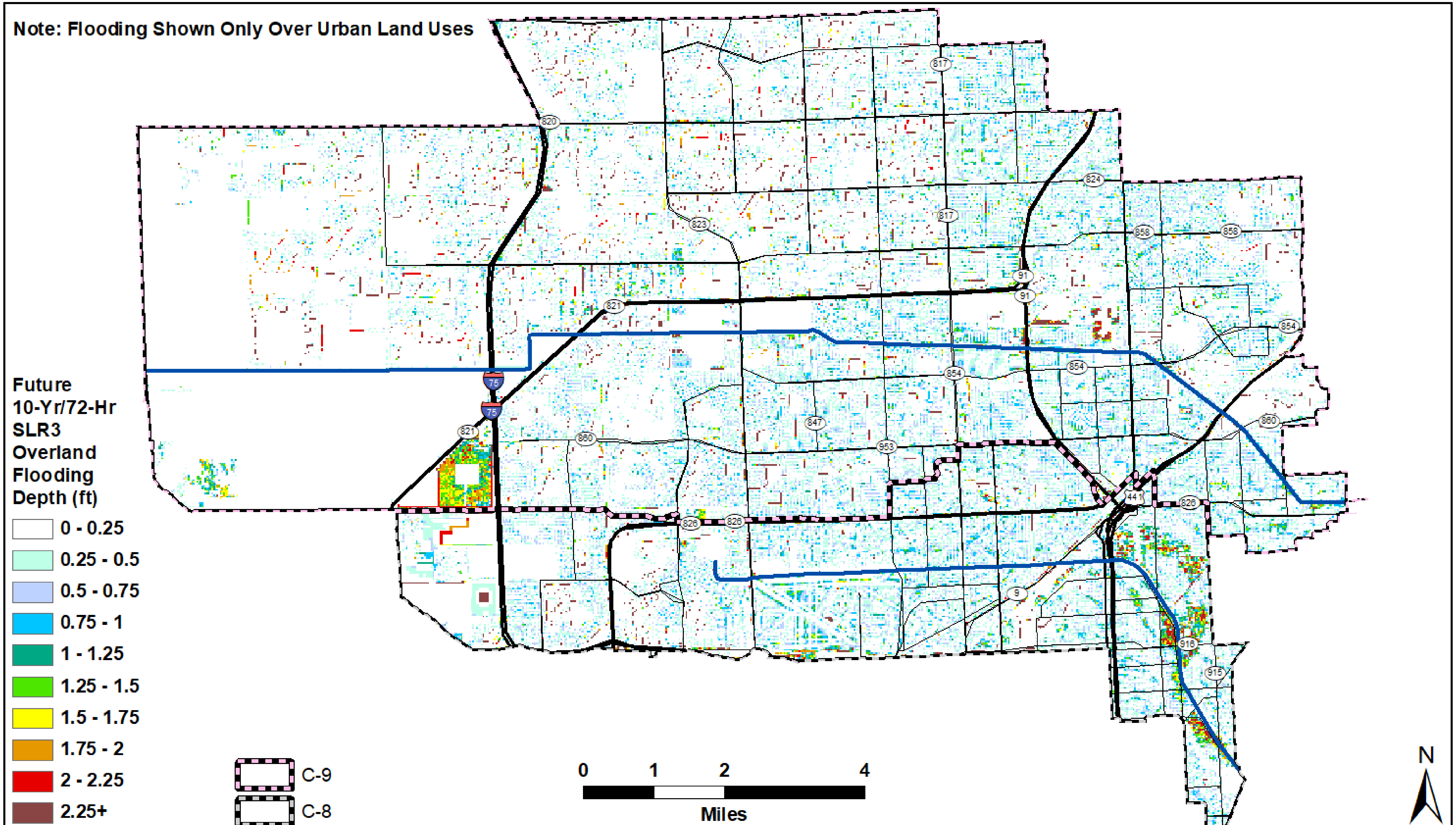

Figure 10.5-18 Flood Inundation Map for 10-Year Sea Level Rise 3 Design Storm Event in Urban Land Use Areas

10.5.7 25-Year Design Storm Flood Depth Map for Urban Land Use Areas

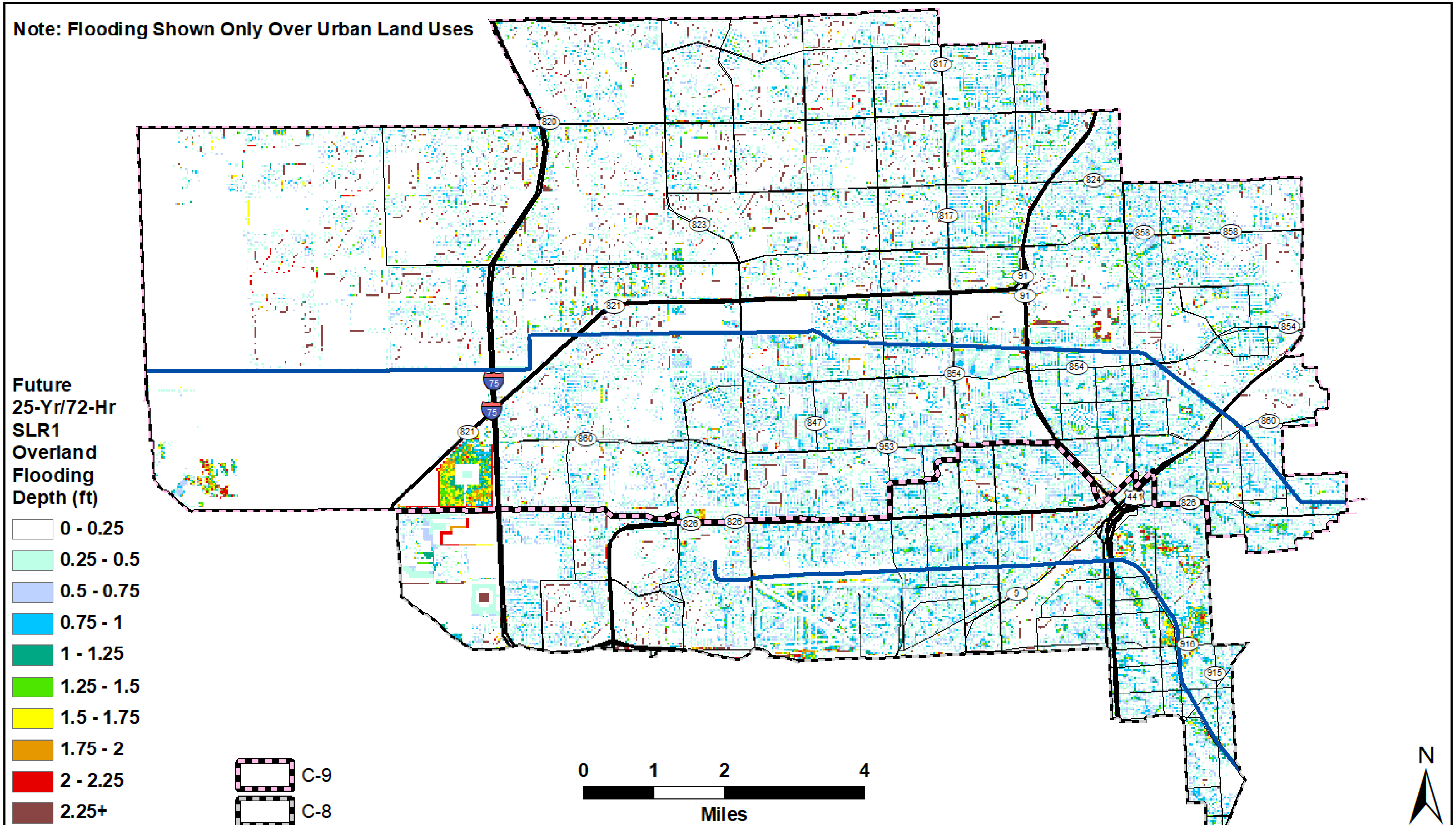

Figure 10.5-19 Flood Inundation Map for 25-Year Sea Level Rise 1 Design Storm Event in Urban Land Use Areas

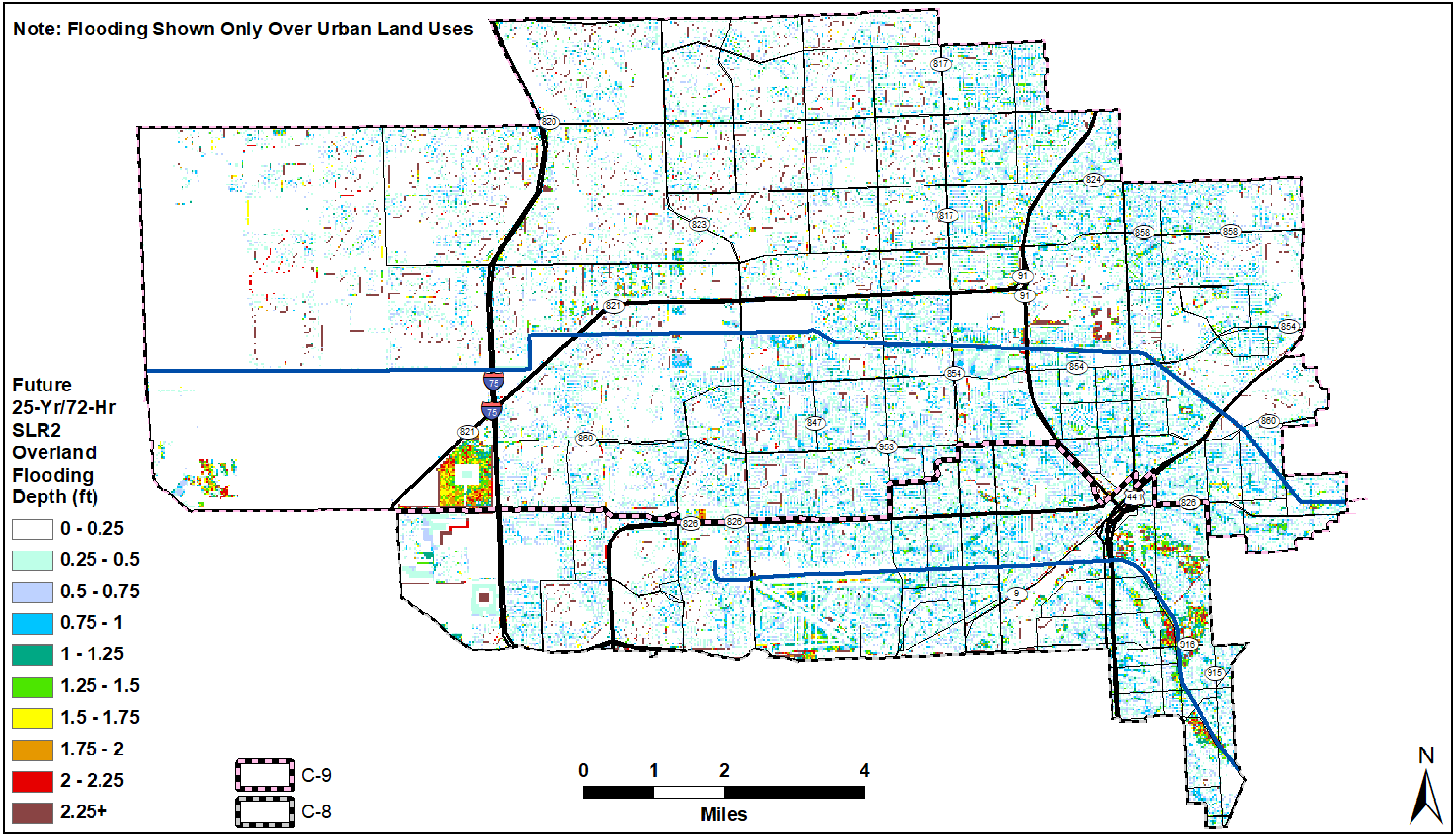

Figure 10.5-20 Flood Inundation Map for 25-Year Sea Level Rise 2 Design Storm Event in Urban Land Use Areas

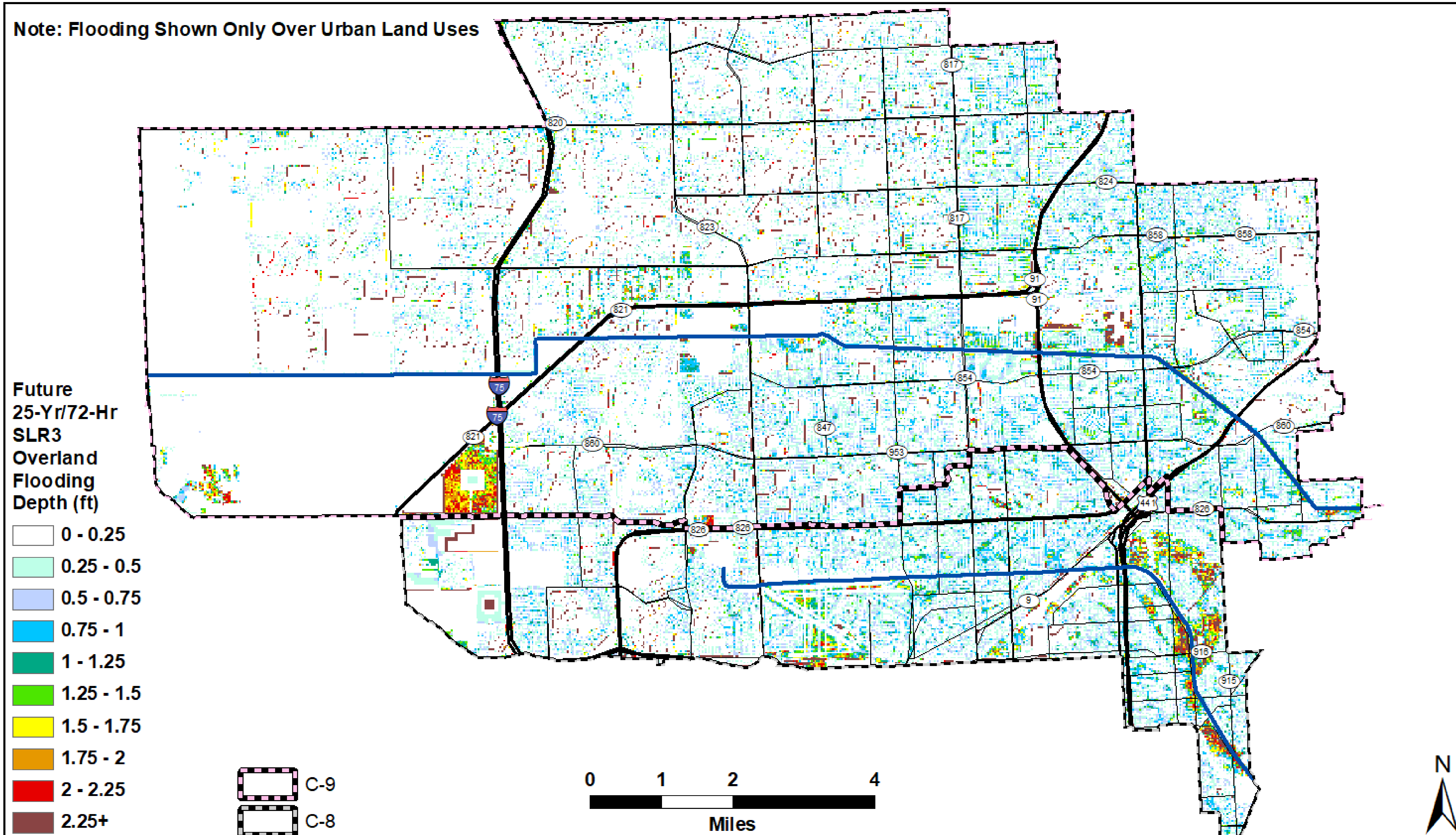

Figure 10.5-21 Flood Inundation Map for 25-Year Sea Level Rise 3 Design Storm Event in Urban Land Use Areas

10.5.8 100-Year Design Storm Flood Depth Map for Urban Land Use Areas

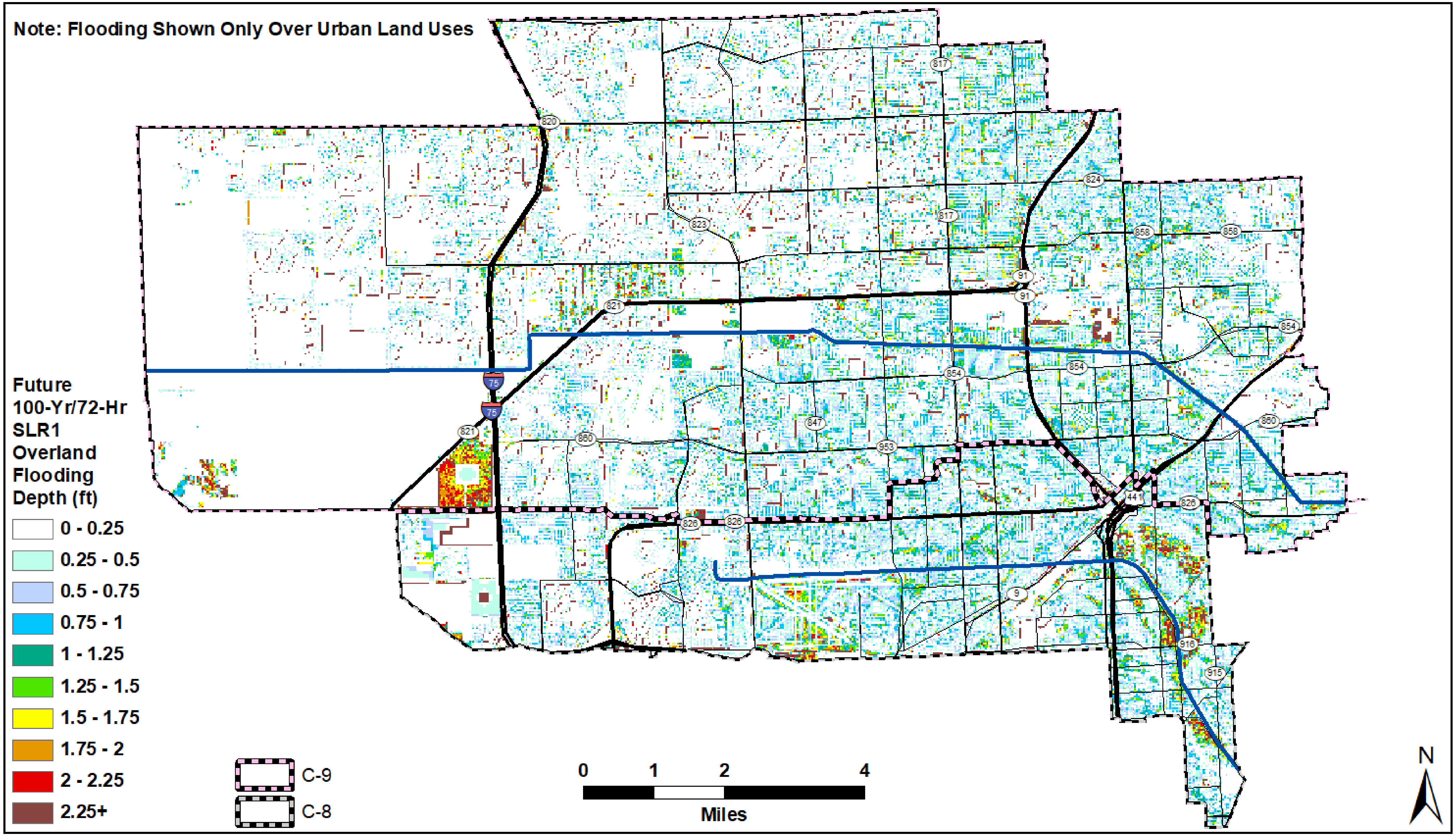

Figure 10.5-22 Flood Inundation Map for 100-Year Sea Level Rise 1 Design Storm Event in Urban Land Use Areas

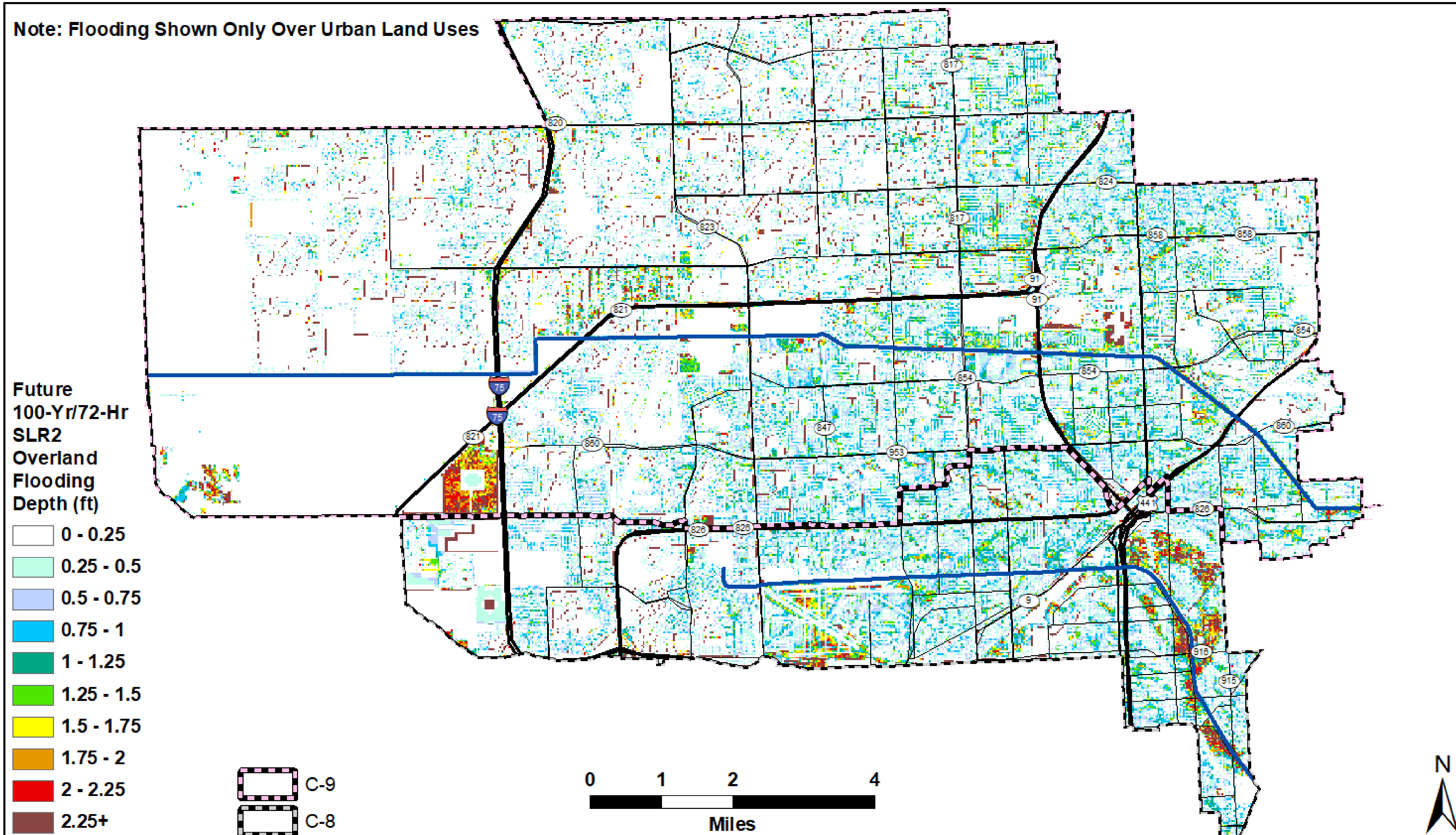

Figure 10.5-23 Flood Inundation Map for 100-Year Sea Level Rise 2 Design Storm Event in Urban Land Use Areas

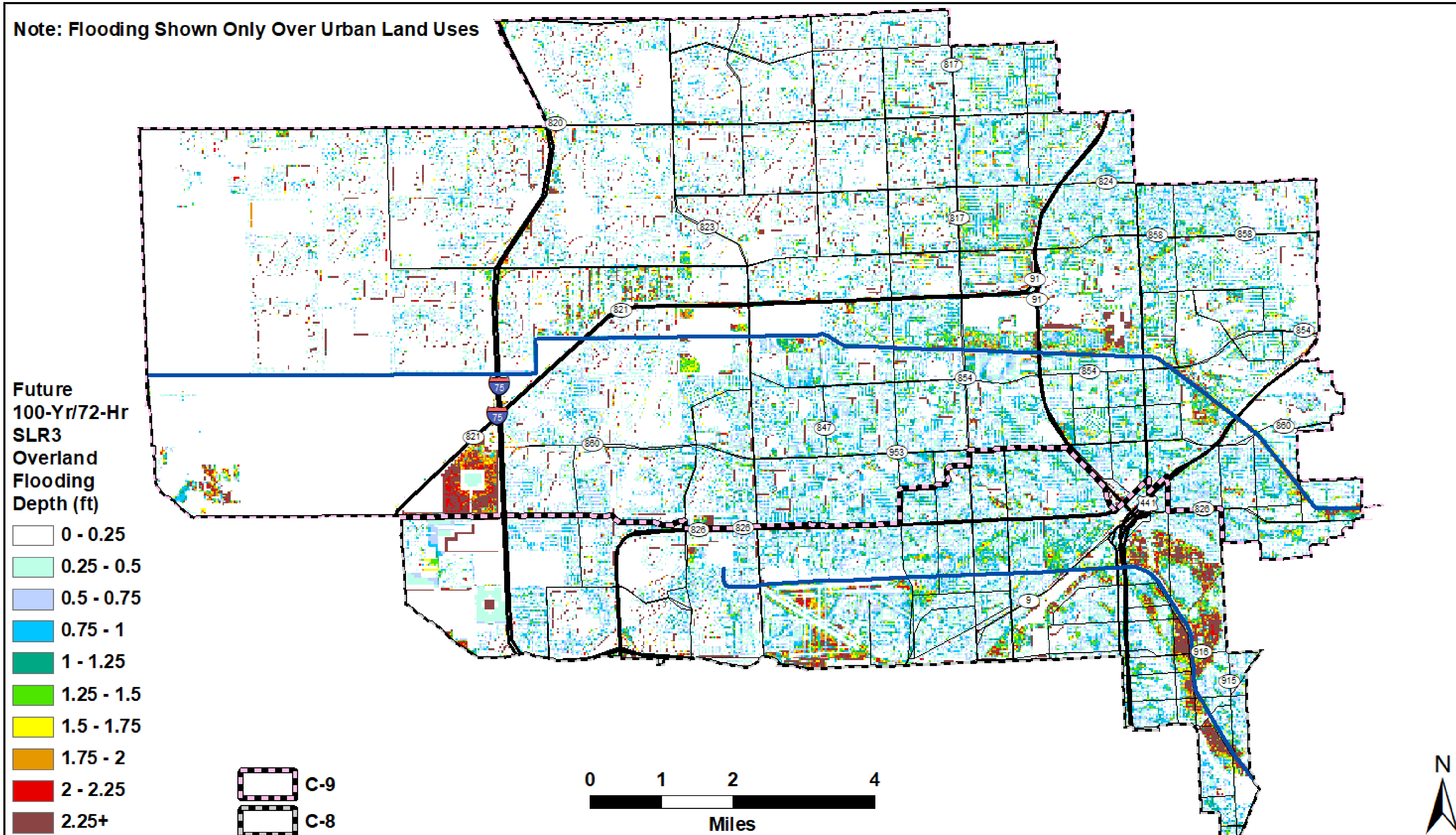

Figure 10.5-24 Flood Inundation Map for 100-Year Sea Level Rise 3 Design Storm Event in Urban Land Use Areas

10.5.9 Up-Close Flood Inundation Maps

For the C-8 Canal, bank exceedances seen in PM #1 caused by the future conditions 5-year design storm with various sea level rise correspond to a significant area of flood inundation as shown in PM #5. For the C-9 Canal, there are only a few areas of bank exceedance for the 5-year design storms, which do not correspond to significant areas of flood inundation, as shown in PM #5. However, the 10-year design storm with various amounts of sea level rise causes additional bank exceedances, some of which do correspond to a significant area of flood inundation. Therefore, for the "up-close" flood inundation maps shown in this section, the 5-year design storms will be shown for the C-8 Canal and the 10-year design storms will be shown for the C-9 Canal. Additionally, the 100-year design storms will be shown for both canals.

Under current conditions, increase in flooding was presented with respect to an increase in design storm rainfall volume and intensity. Intuitively, more rainfall increases the flooding potential under the same conditions. This is a well-established principle; therefore, future conditions results are presented with respect to an increase in sea level rise for a given design storm.

For the C-8 Canal, each design storm intensity and sea level rise combination larger than the 5-year SLR1 event show an increase in flood inundation with respect to the increase in sea level. For example, in the lower reaches of C-8, the floodwaters start to come out of bank and flood the neighboring residential areas for the 5-year SLR2 event and become worse as design storm intensity and sea level rise increase.

Figure 10.5-25 through **Figure 10.5-27** show up-close flood inundation maps for the area between NE 135th St (CR916) and NE 6th Ave (CR915). For the 5-year SLR1 event, little to no flood inundation with respect to an overbank exceedance is shown, however, areas of flood inundation become more pronounced for the SLR2 event. Similarly, the area and depth of the SLR3 flood inundation significantly increases. For these three maps, the same rainfall is used, and the other difference is the amount of sea level rise and the initial groundwater levels that changed to represent the effects of higher tidal levels. **Figure 10.5-28** through **Figure 10.5-30** show the same location but for the 100-year design storm. Although significant flooding is shown for the SLR1 event, distinct increases in the area and depth of flood inundation is seen for the SLR2 and SLR3 events.

Figure 10.5-31 through **Figure 10.5-33** show up-close flood inundation maps for the area between North Miami Ave and NE 135th St (CR916). Localized flood inundation along the west bank is seen in a couple of locations for the 5-year SLR1 event, with significant increases in spatial extent and depth noted for the SLR2 and SLR3 events. Interestingly, there are areas of flood inundation in the SLR1 event that appear to be caused more by localized flooding than by bank exceedances that become worsened by bank exceedances under 2 ft and 3 ft of sea level rise. **Figure 10.5-34** through **Figure 10.5-36** show the same location but for the 100-year design storm. Again, although significant flooding is shown for the SLR1 event, distinct increases in the area and depth of flood inundation is seen for the SLR2 and SLR3 events.

Figure 10.5-37 through **Figure 10.5-39** show up-close flood inundation maps for the area near the Opa Locka Canal. Like the previous two areas, little to no flooding from bank exceedances are seen under SLR1 but become visible and increase in extent and magnitude as sea level rise increases. **Figure 10.5-40** through **Figure 10.5-42** show the same location but for the 100-yar design storm, which also experiences an increase in flood area and depth as sea level rise increases.

Typically, the C-9 Canal has higher bank elevations than the C-8 Canal, which meant less bank exceedances and less area and magnitude of flood inundation under current conditions. Although higher, they are not high enough to prevent flooding under sea level rise conditions. Notable bank exceedances were seen for the 10-year design storm, even with just 1 ft of sea level rise. Like the trend for the C-8 Canal, the extent and magnitude of the flood inundation increases with sea level rise. **Figure 10.5-43** through **Figure 10.5-45** show up-close flood inundation maps for the area between I-95 and S-29. For the 10-year SLR1 event, only a small area of flooding is seen upstream of S-29. For the SLR2 event, this area becomes further inundated and for the SLR3 event, the flooding extends nearly 2 miles upstream. **Figure 10.5-46** through **Figure 10.5-48** show the same location but for the 100-yar design storm.

Figure 10.5-49 through **Figure 10.5-51** show up-close flood inundation maps for the area near US Highway 441. For the 10-year SLR1 event, a notable area of flooding is seen both upstream and downstream of US Highway 441, however, only the segment downstream is caused by bank exceedance. For the SLR2 and SLR3 scenarios, the flooding downstream of US Highway 441 has significant increase in flooding extent and depth, while the area upstream has very little change. The upstream area not changing much with response to sea level rise makes sense as there is not a bank exceedance. **Figure 10.5-52** through **Figure 10.5-54** show the same location but for the 100-yr design storm, however, these figures do show an increase in flooding with response to sea level rise for the area upstream of US Highway 441 as the water level in the canal exceeds the bank elevations.

Figure 10.5-55 through **Figure 10.5-57** show up-close flood inundation maps for the area just west of the Ronald Reagan Turnpike. Like current conditions, this area shows some flooding in PM #5 while showing no bank exceedances in PM #1. The flooding in this area could be due to the topography being lower than the canal bank and/or inadequate secondary drainage infrastructure. For the 10-year design storms, regardless of 1, 2, or 3 ft sea level rise, the flooding in this location does not change much (small changes likely due to initial groundwater elevation differences). On the west side of this up-close example (Near Bass Creek Road), even the 100-year design storm 3-ft scenario does not cause bank exceedance, however, an increase in flood inundation is seen, shown in **Figure 10.5-58** through **Figure 10.5-60**. This is partially due to the increased canal stage limiting the gravity-based discharge from the surrounding area. On the east side of this up-close example, a significant increase in flooding is shown for the 100-year design storm as sea level rise increases, and the bank elevations become further exceeded.

Figure 10.5-61 through **Figure 10.5-63** show up-close flood inundation maps for the area near Red Road. Like the previous up-close example, this area shows flooding in PM #5 without bank exceedances in PM #1, both in current conditions as well as for the 10-year future condition design storms. However, for the 100-year design storm, the banks are exceeded, which leads to an increase in flood inundation as sea level rise increases as shown in **Figure 10.5-64** through **Figure 10.5-66**.

Sea level rise increases the stress on the drainage systems by reducing the discharge capacity of the tidal structures which leads to increased stages in the canals. Aside from making existing areas that exceed canal banks worse, sea level rise can cause new canal segments to exceed bank elevations, which will worsen any flooding that already exists. This section presents up-close examples of flood inundation as sea level rise increases.

10.5.9.1 Up-Close Flood Inundation Maps for the C-8 Canal Between NE 135th St (CR916) and NE 6th Ave (CR915)

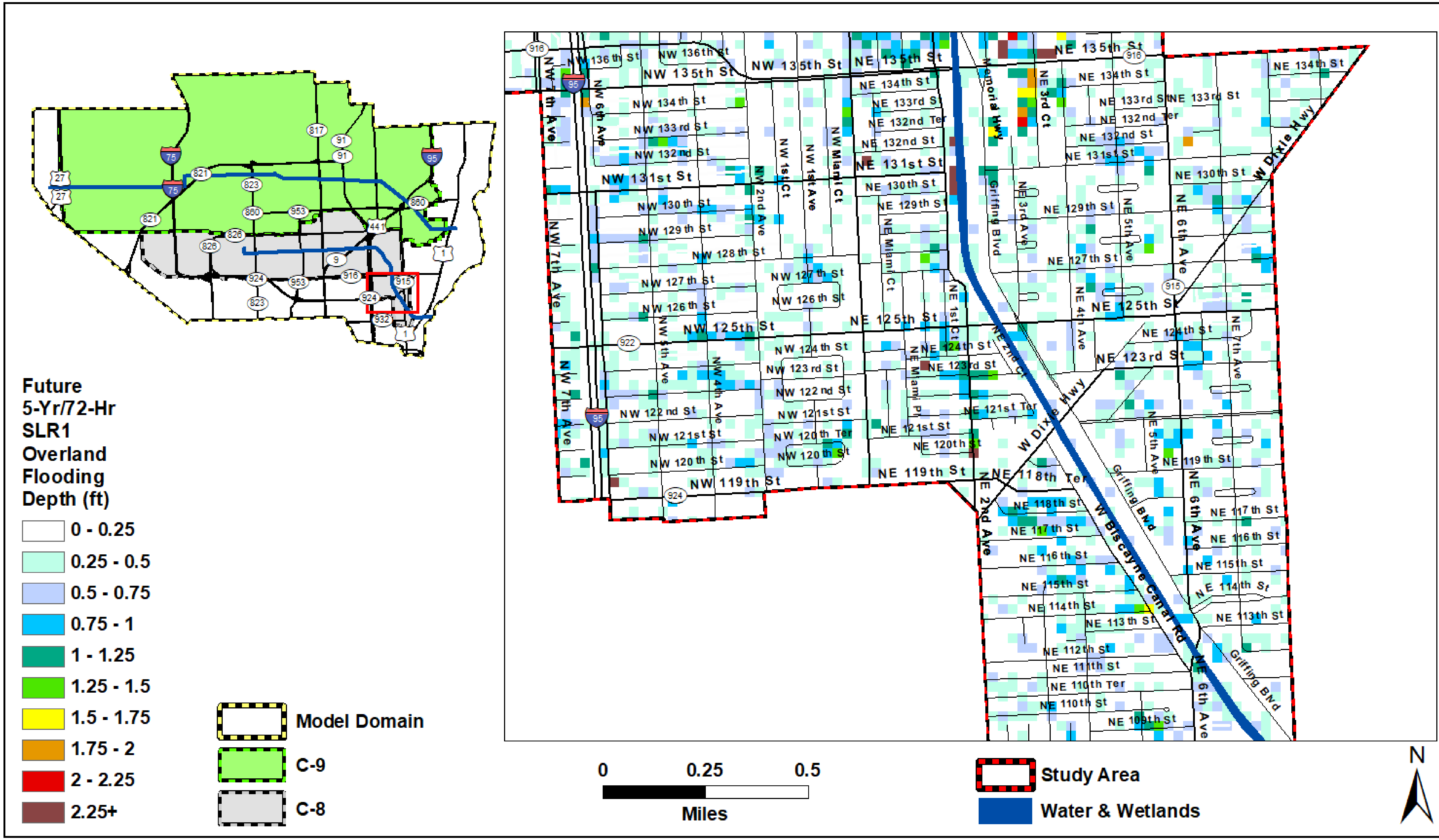

Figure 10.5-25: Up Close 5-Year Sea Level Rise 1 Flood Inundation Map for the C-8 Canal Between and NE 135th St (CR916) and NE 6th Ave (CR915)

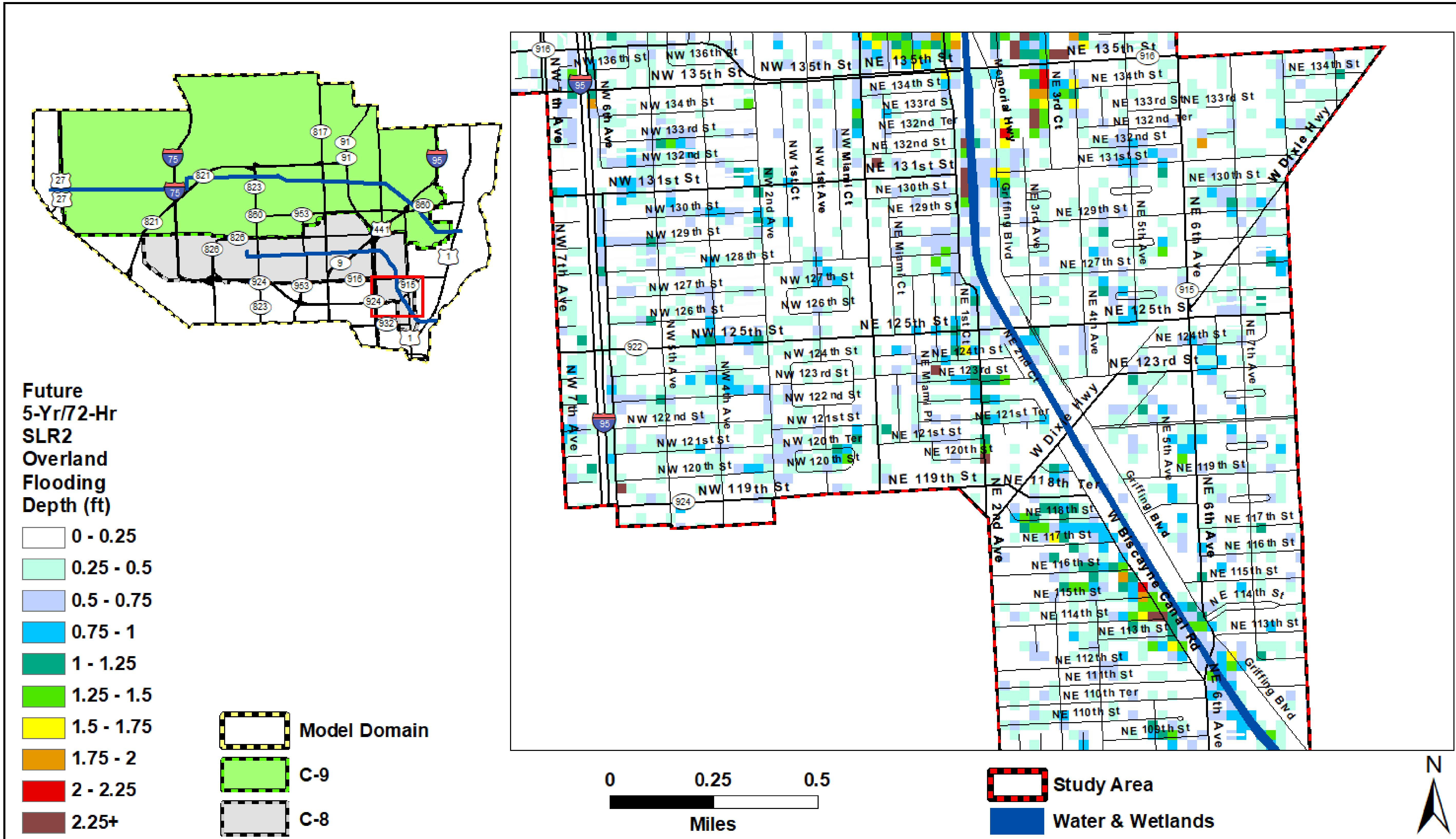

Figure 10.5-26: Up Close 5-Year Sea Level Rise 2 Flood Inundation Map for the C-8 Canal Between and NE 135th St (CR916) and NE 6th Ave (CR915)

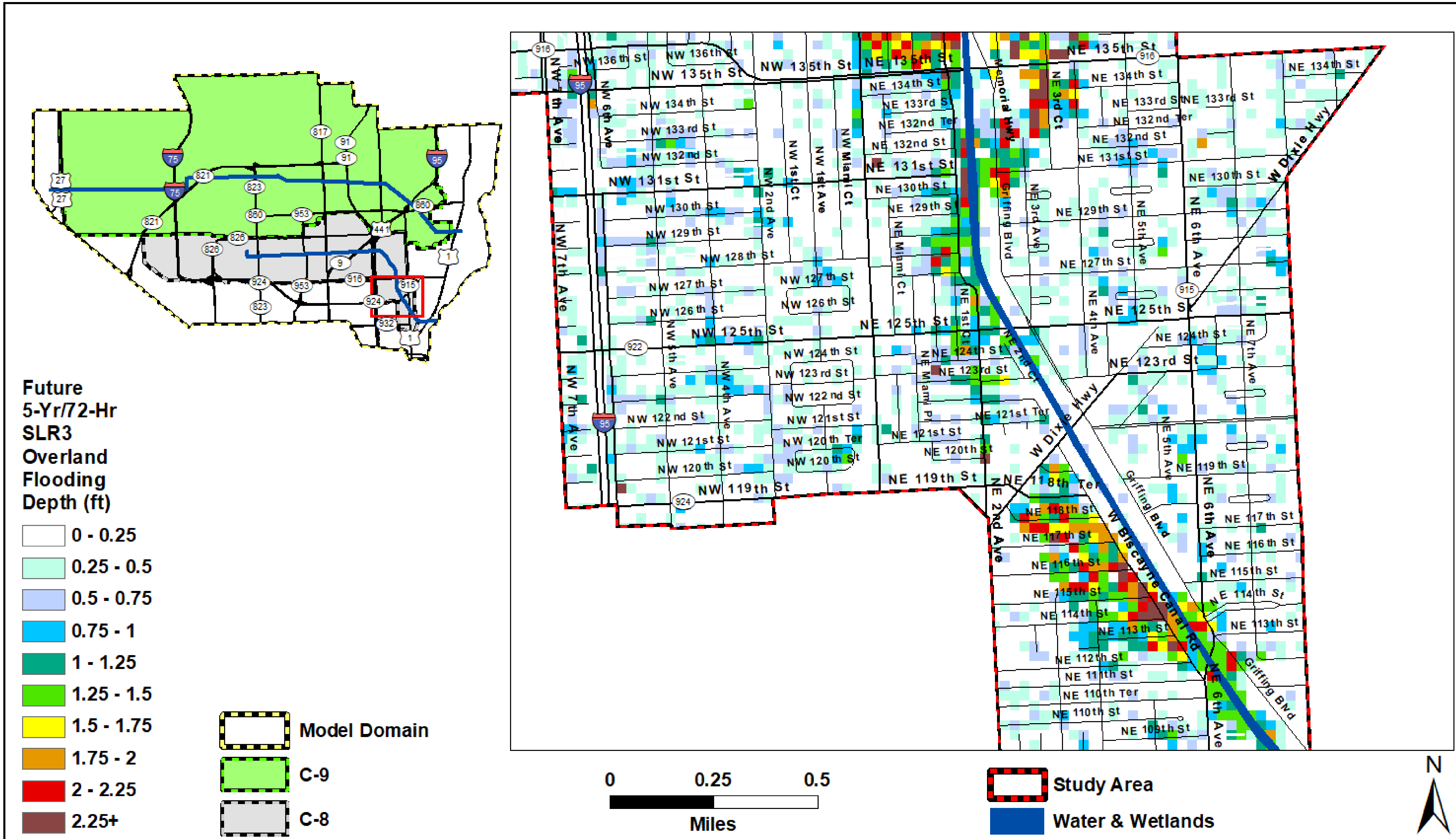

Figure 10.5-27: Up Close 5-Year Sea Level Rise 3 Flood Inundation Map for the C-8 Canal Between and NE 135th St (CR916) and NE 6th Ave (CR915)

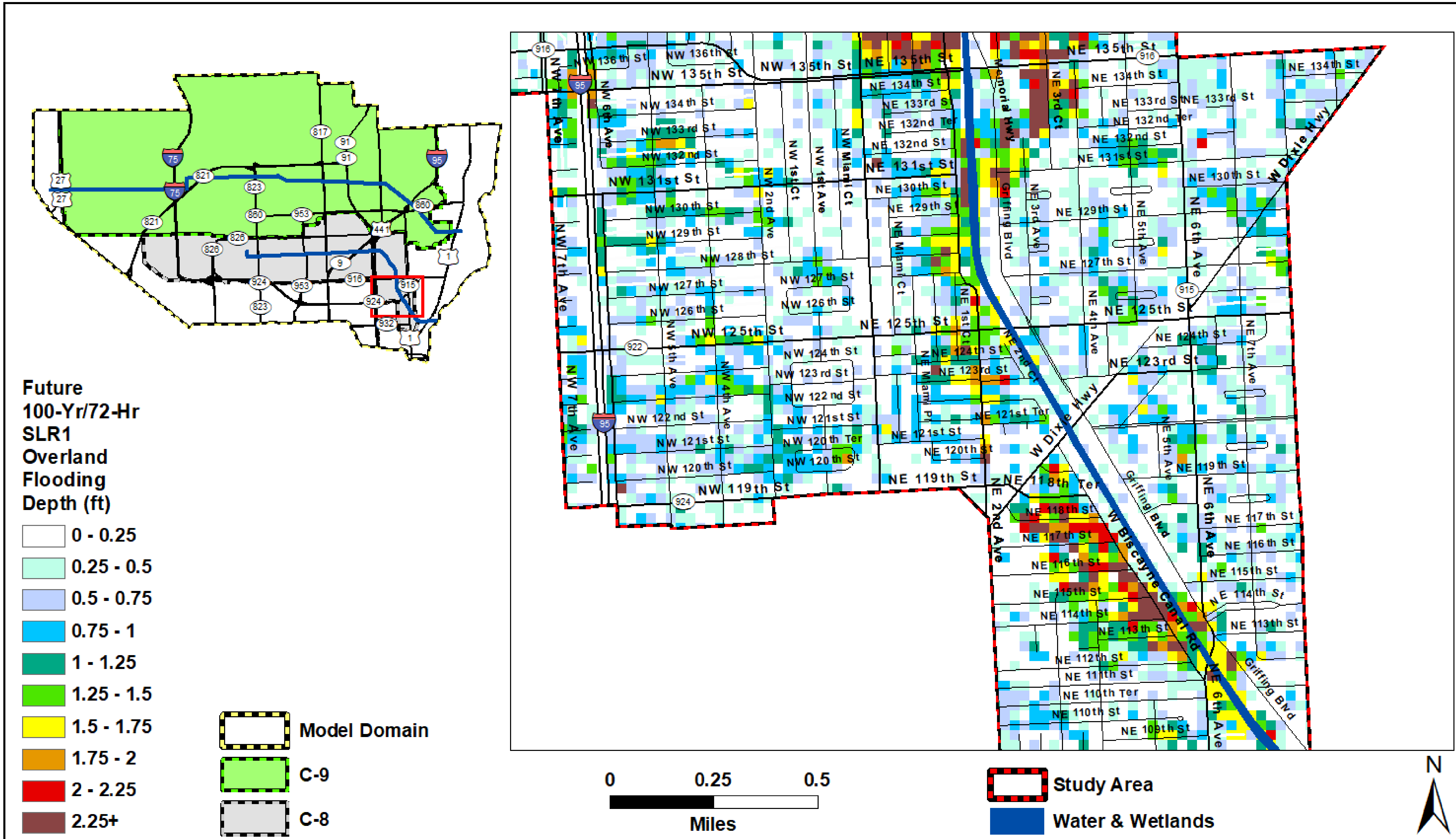

Figure 10.5-28: Up Close 100-Year Sea Level Rise 1 Flood Inundation Map for the C-8 Canal Between and NE 135th St (CR916) and NE 6th Ave (CR915)

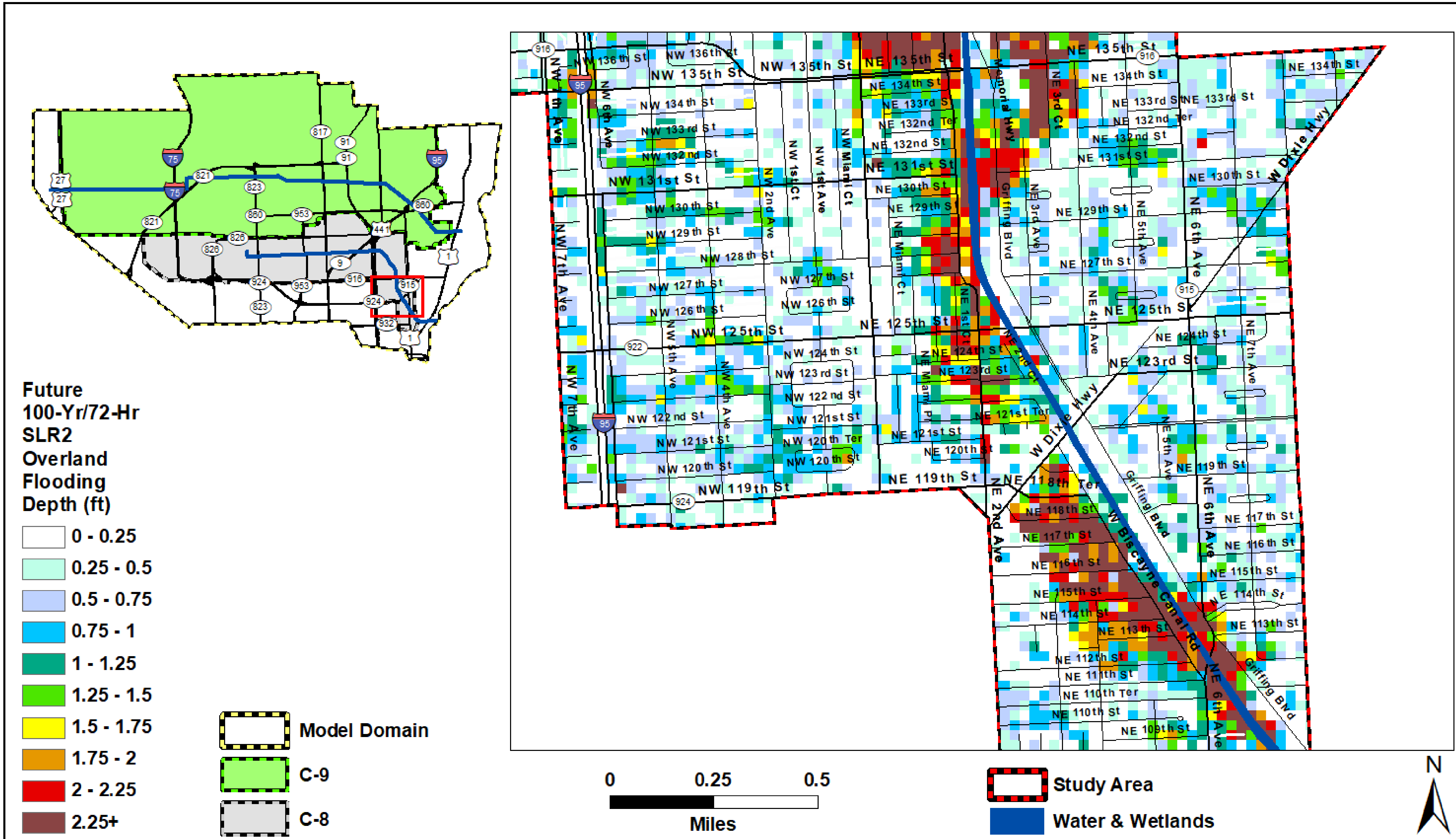

Figure 10.5-29: Up Close 100-Year Sea Level Rise 2 Flood Inundation Map for the C-8 Canal Between and NE 135th St (CR916) and NE 6th Ave (CR915)

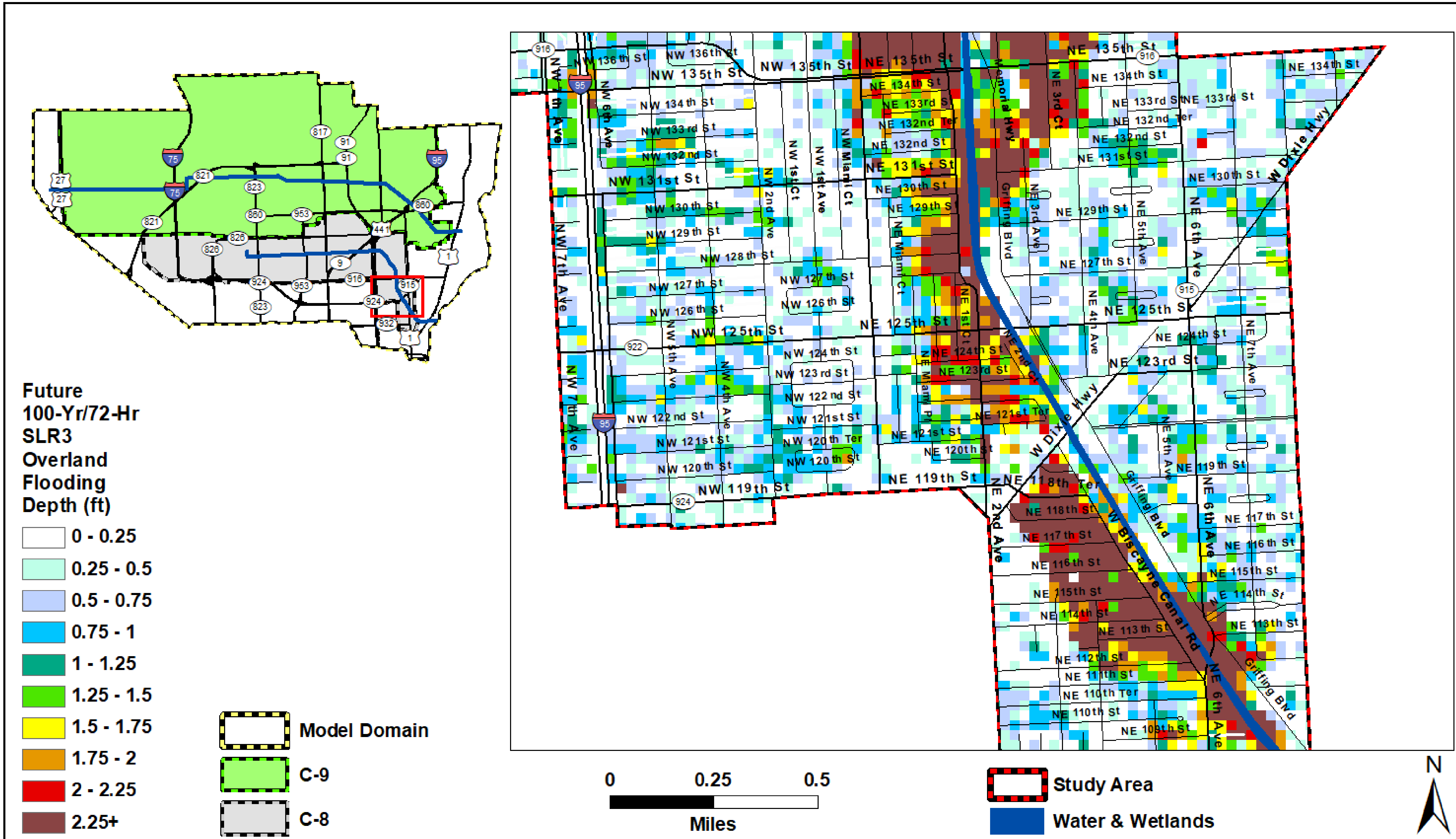

Figure 10.5-30: Up Close 100-Year Sea Level Rise 3 Flood Inundation Map for the C-8 Canal Between and NE 135th St (CR916) and NE 6th Ave (CR915)

10.5.9.2 Up-Close Flood Inundation Maps for the C-8 Canal Between North Miami Ave and NE 135th St (CR916)

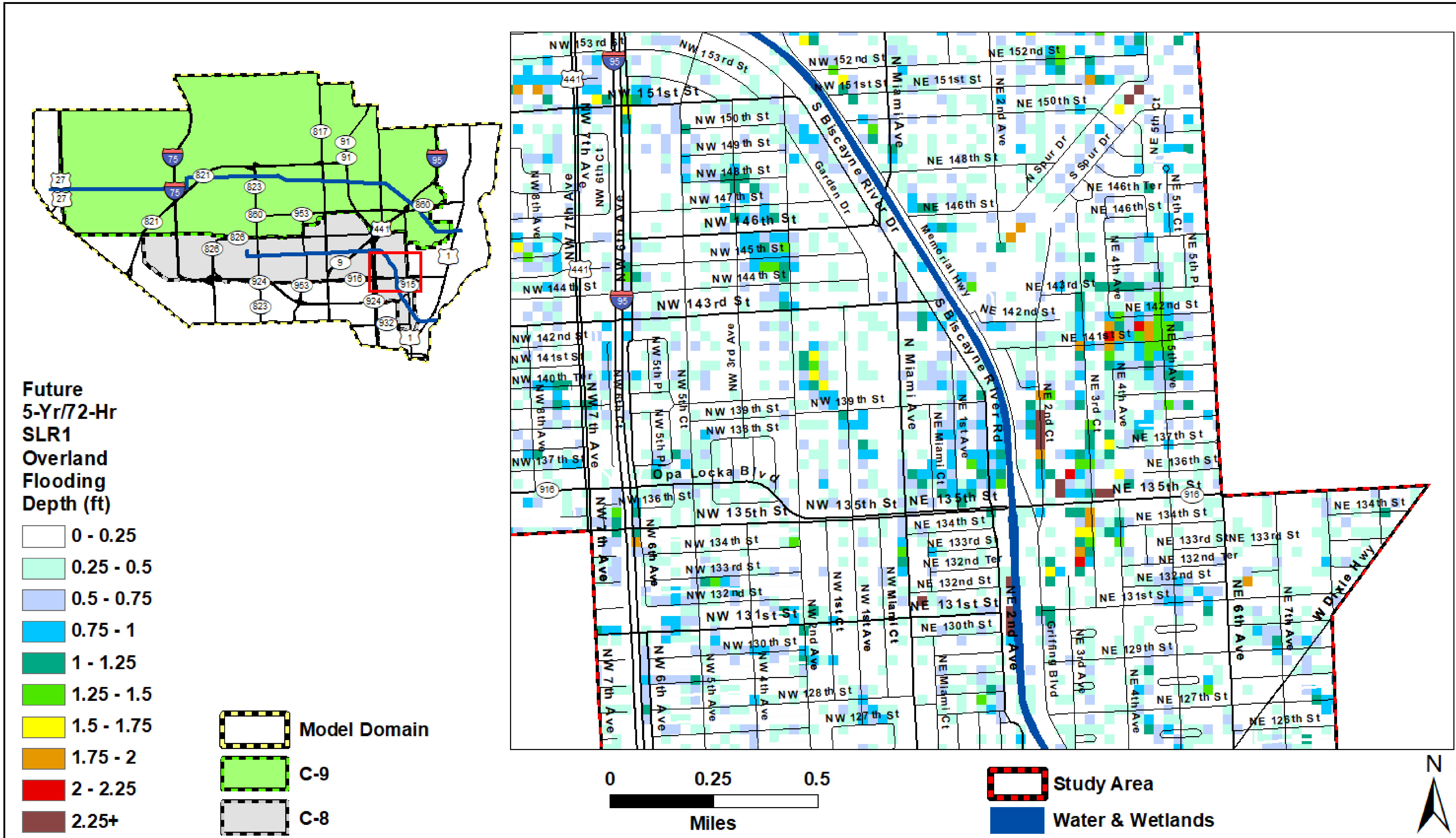

Figure 10.5-31: Up Close 5-Year Sea Level Rise 1 Flood Inundation Map for the C-8 Canal Between North Miami Ave and NE 135th St (CR916)

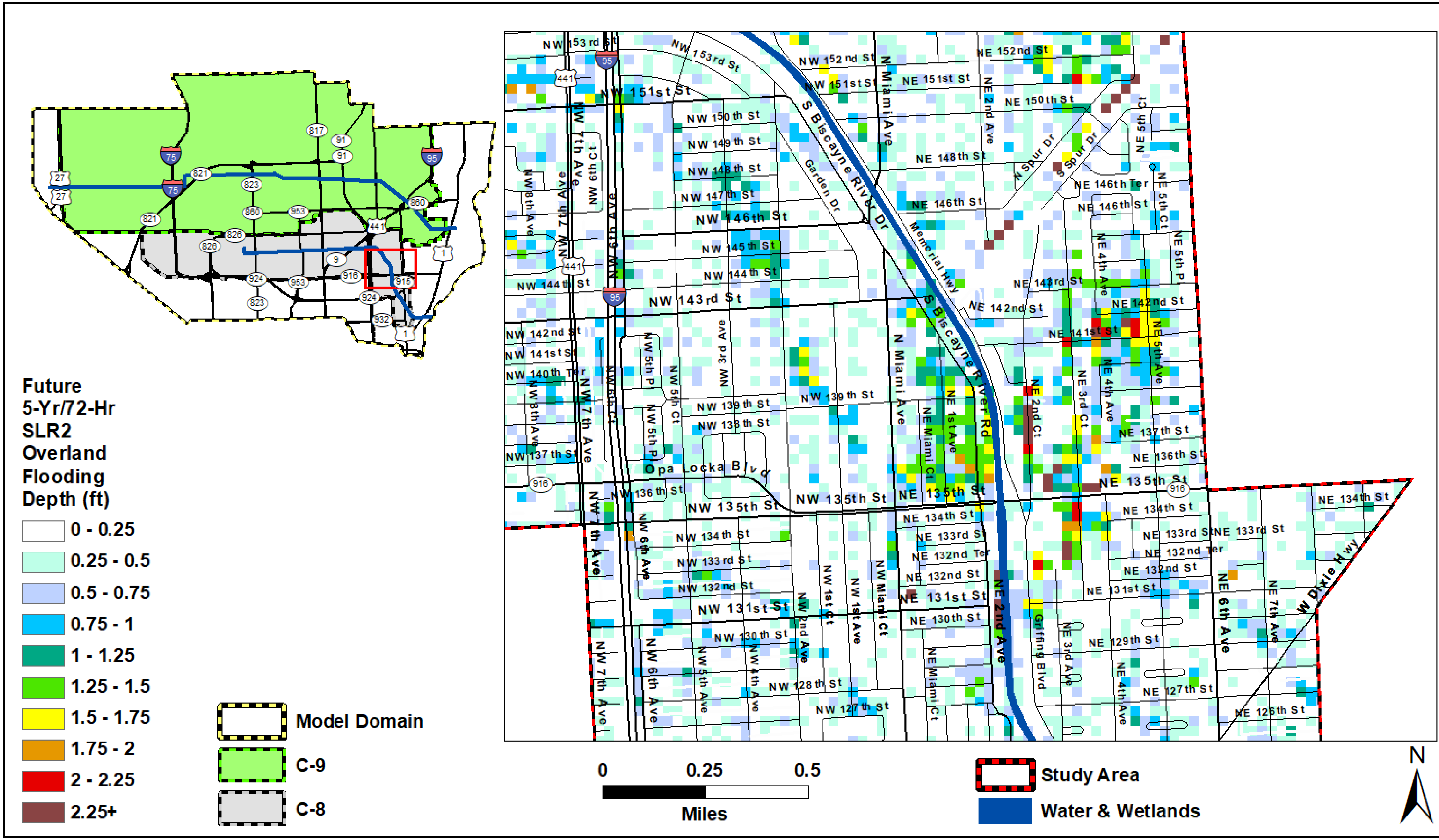

Figure 10.5-32: Up Close 5-Year Sea Level Rise 2 Flood Inundation Map for the C-8 Canal Between North Miami Ave and NE 135th St (CR916)

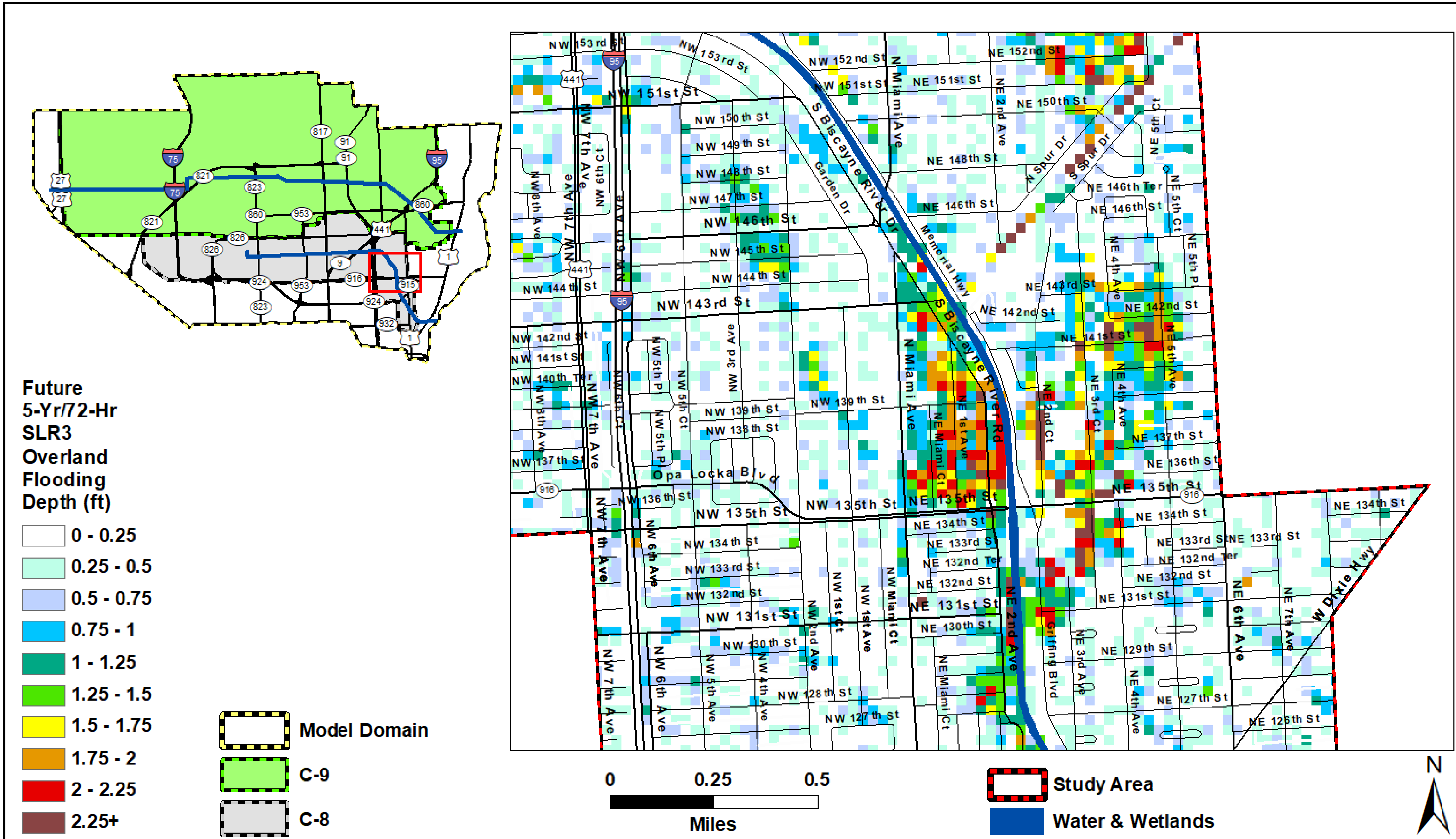

Figure 10.5-33: Up Close 5-Year Sea Level Rise 3 Flood Inundation Map for the C-8 Canal Between North Miami Ave and NE 135th St (CR916)

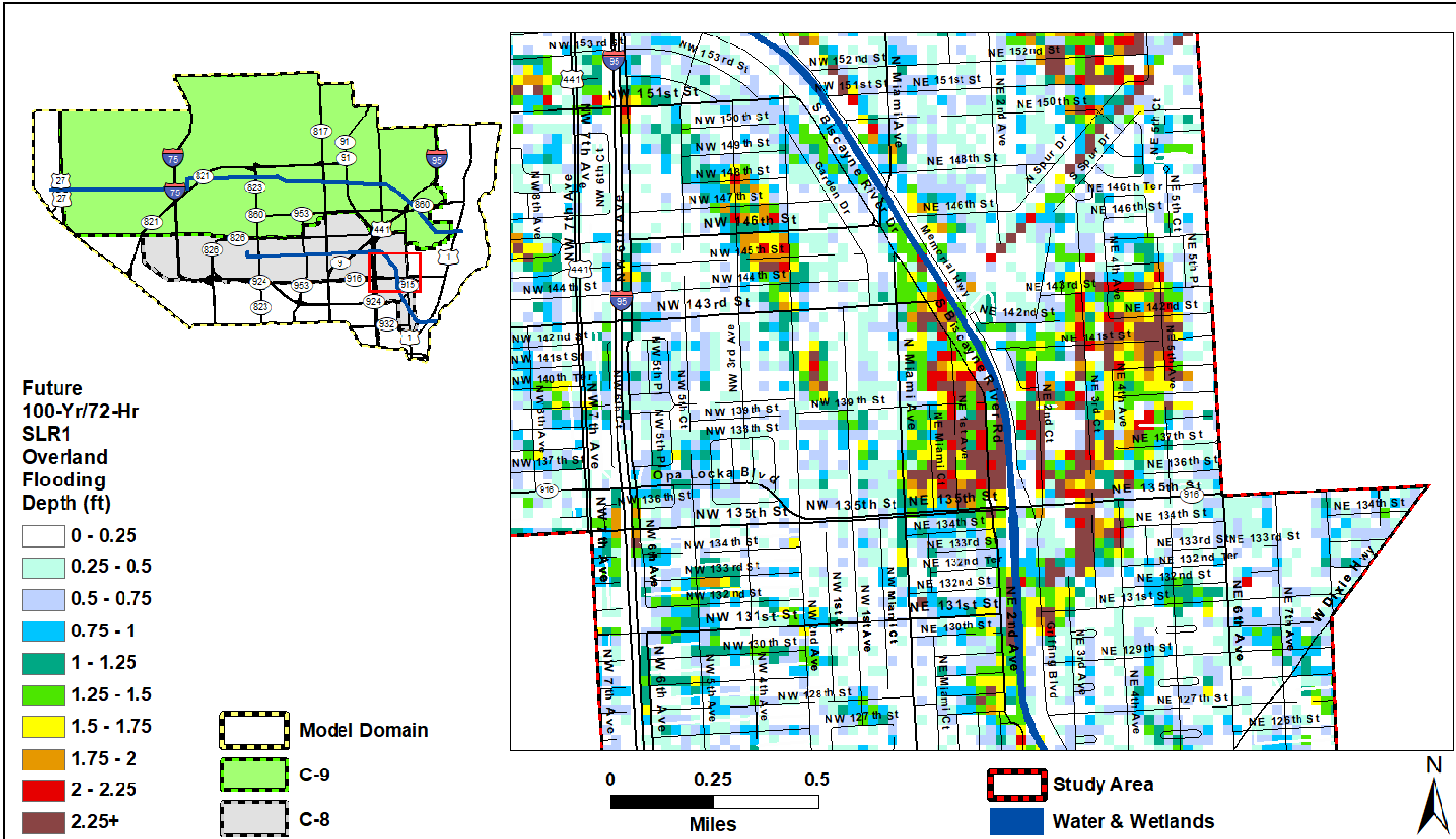

Figure 10.5-34: Up Close 100-Year Sea Level Rise 1 Flood Inundation Map for the C-8 Canal Between North Miami Ave and NE 135th St (CR916)

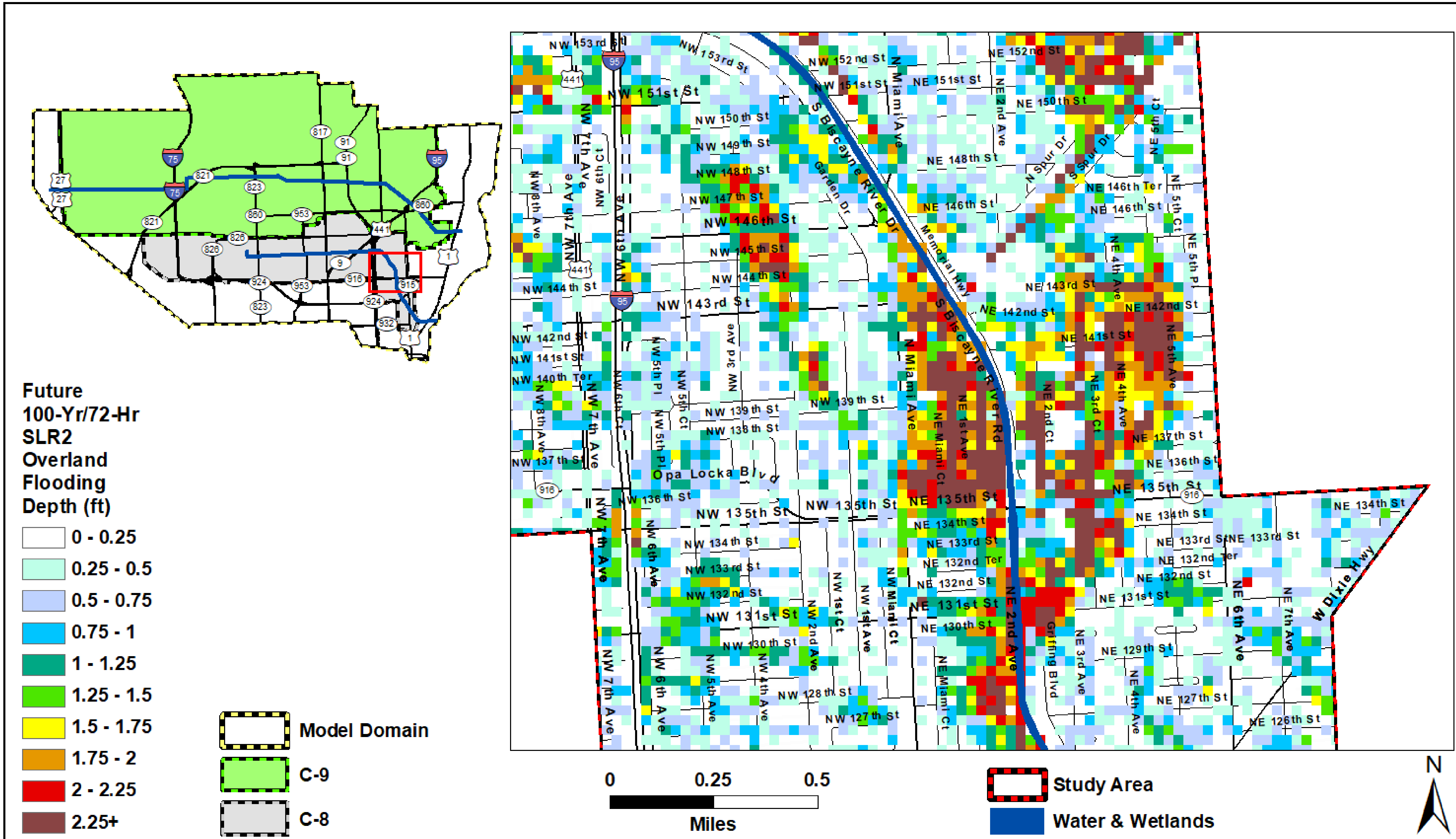

Figure 10.5-35: Up Close 100-Year Sea Level Rise 2 Flood Inundation Map for the C-8 Canal Between North Miami Ave and NE 135th St (CR916)

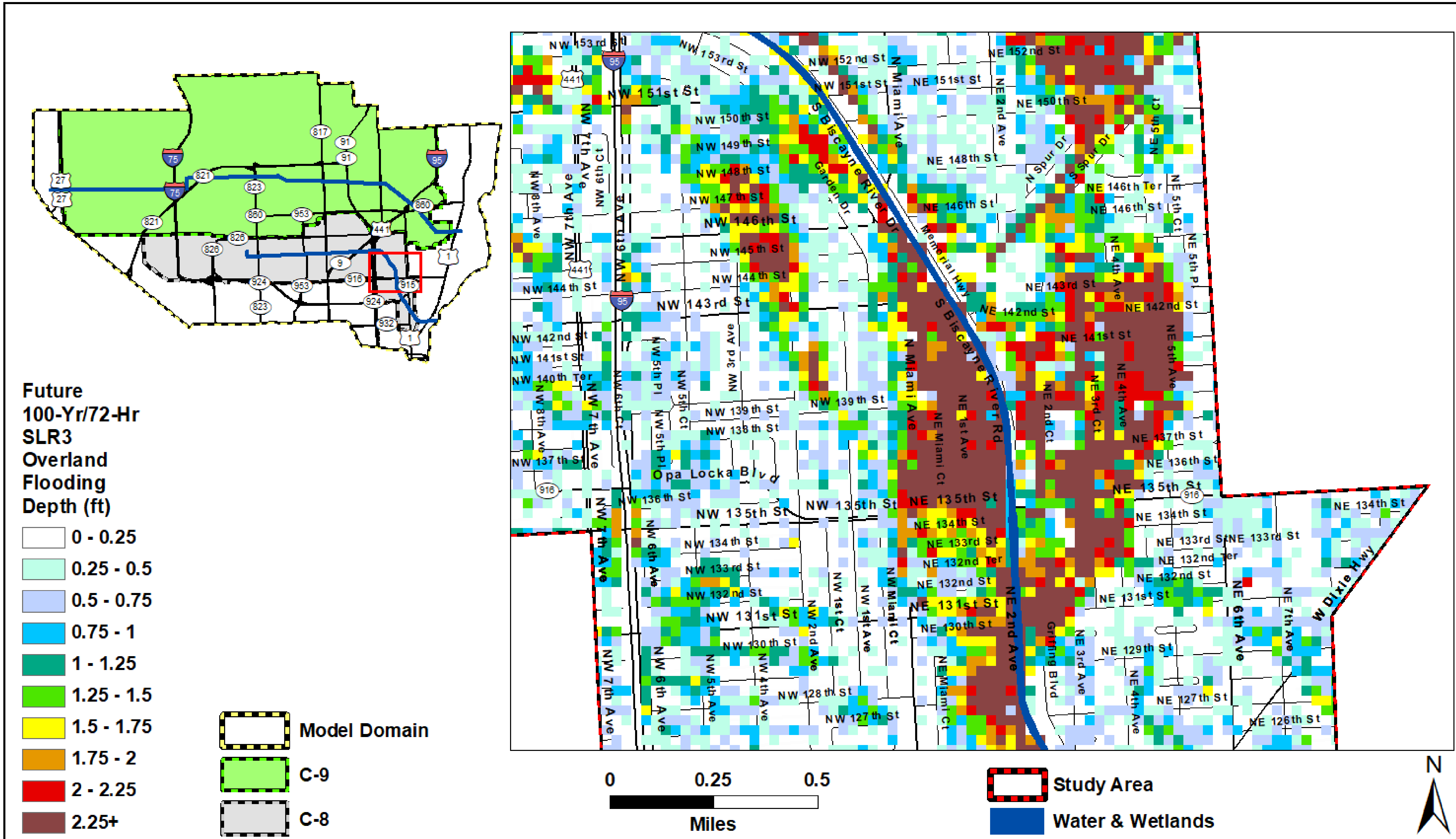

Figure 10.5-36: Up Close 100-Year Sea Level Rise 3 Flood Inundation Map for the C-8 Canal Between North Miami Ave and NE 135th St (CR916)

10.5.9.3 Up-Close Flood Inundation Maps for the C-8 Canal Near Opa Locka Canal

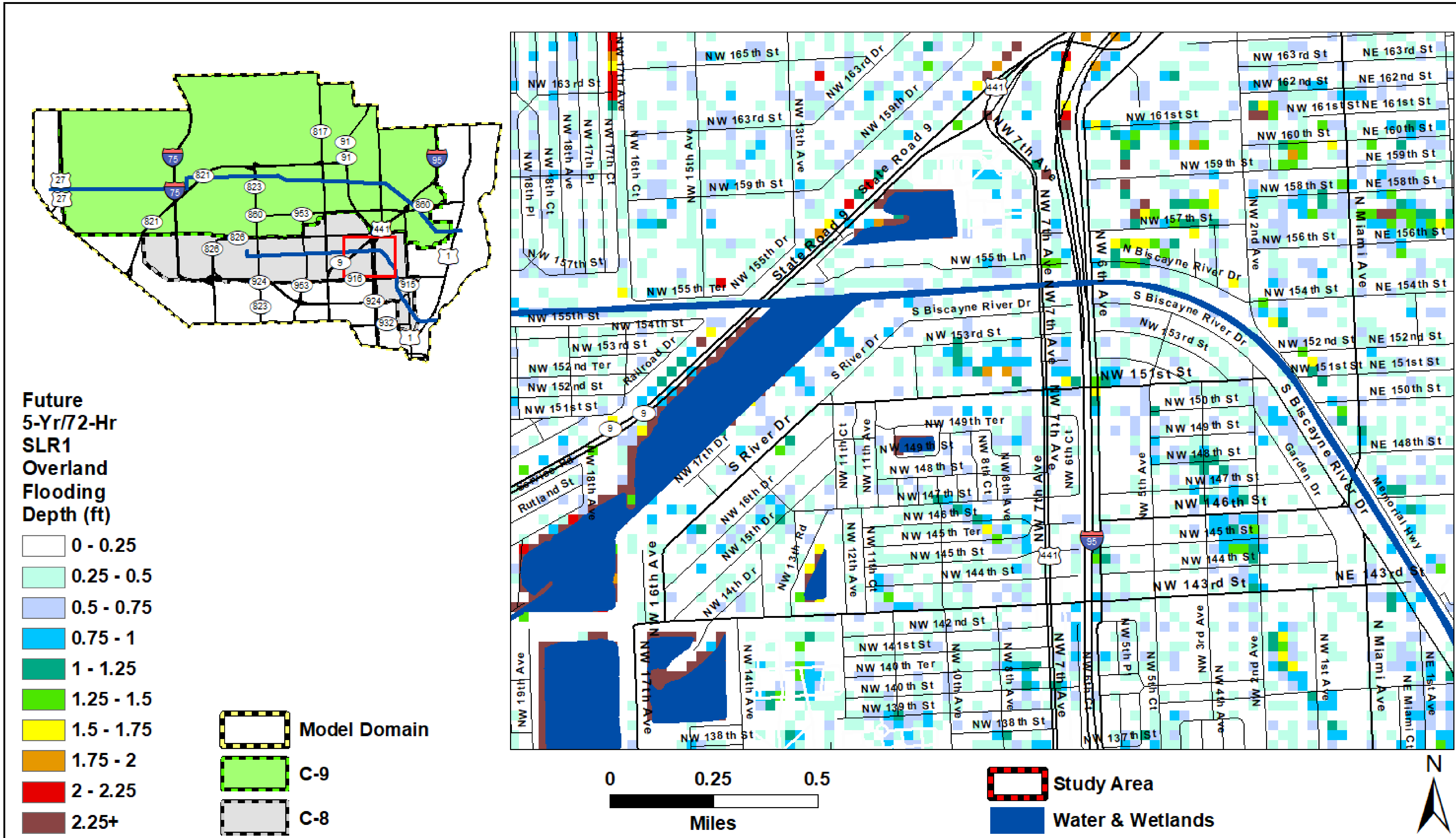

Figure 10.5-37: Up Close 5-Year Sea Level Rise 1 Flood Inundation Map for the C-8 Canal Near Opa Locka Canal

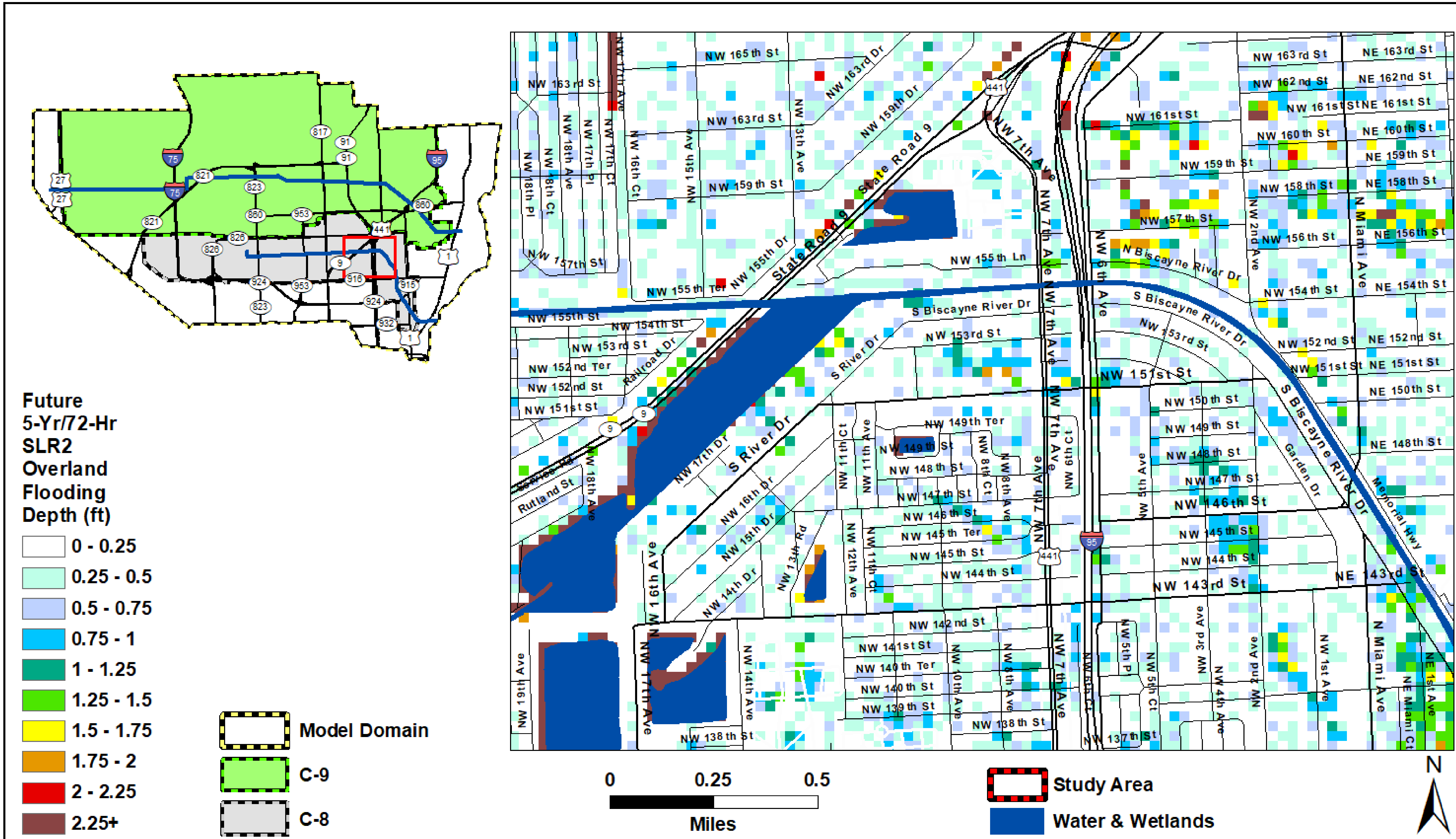

Figure 10.5-38: Up Close 5-Year Sea Level Rise 2 Flood Inundation Map for the C-8 Canal Near Opa Locka Canal

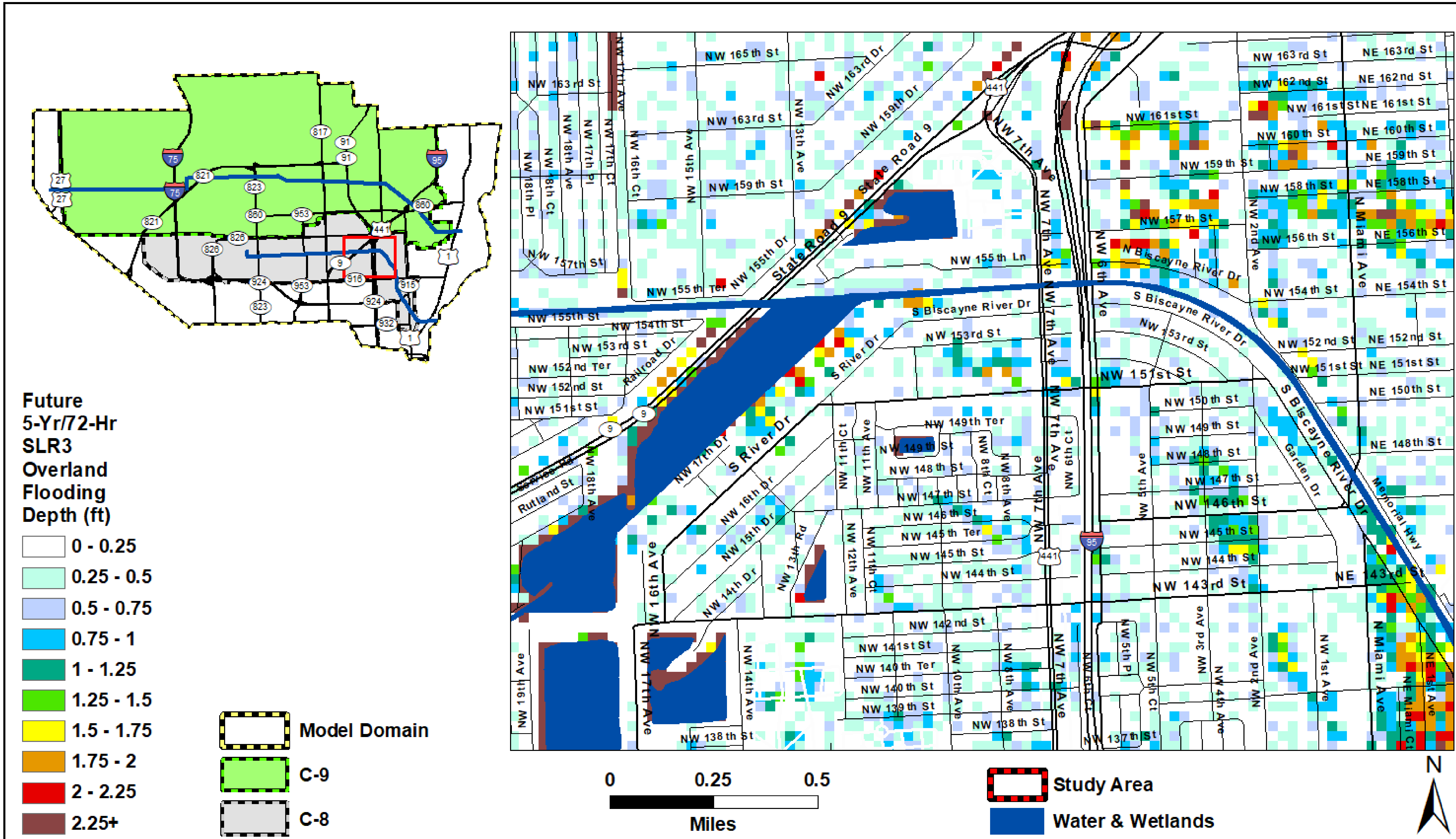

Figure 10.5-39: Up Close 5-Year Sea Level Rise 3 Flood Inundation Map for the C-8 Canal Near Opa Locka Canal

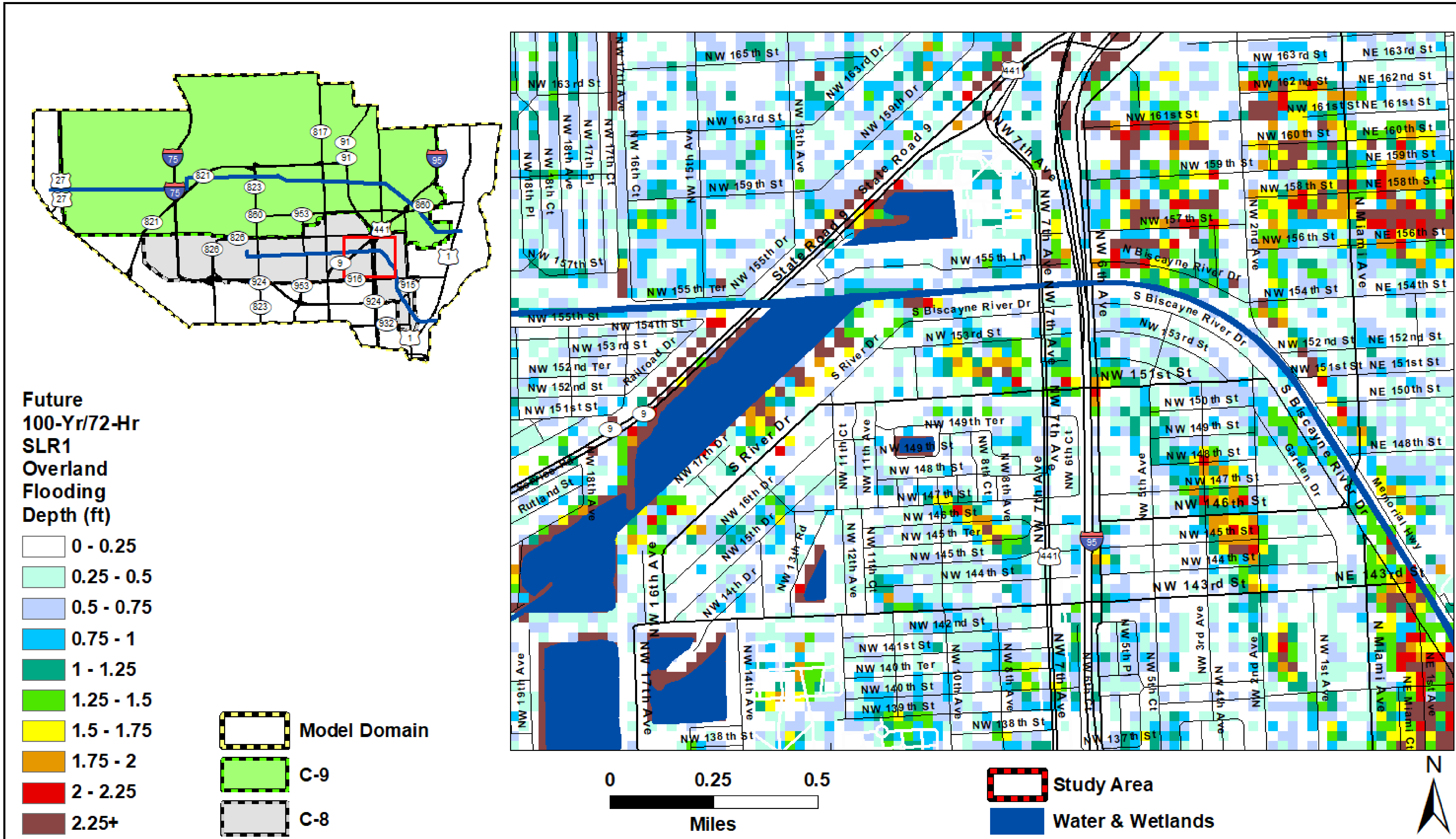

Figure 10.5-40: Up Close 100-Year Sea Level Rise 1 Flood Inundation Map for the C-8 Canal Near Opa Locka Canal

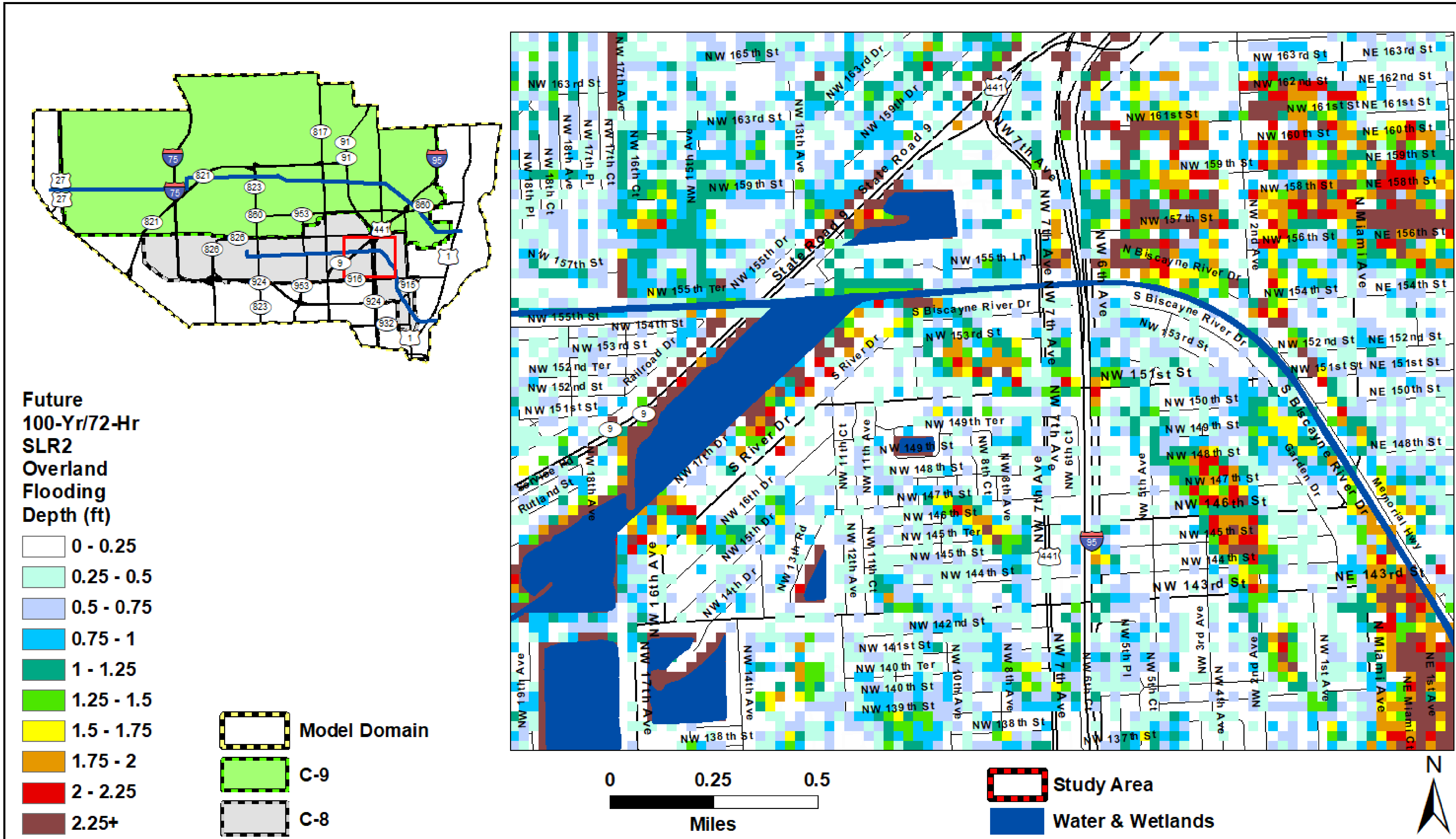

Figure 10.5-41: Up Close 100-Year Sea Level Rise 2 Flood Inundation Map for the C-8 Canal Near Opa Locka Canal

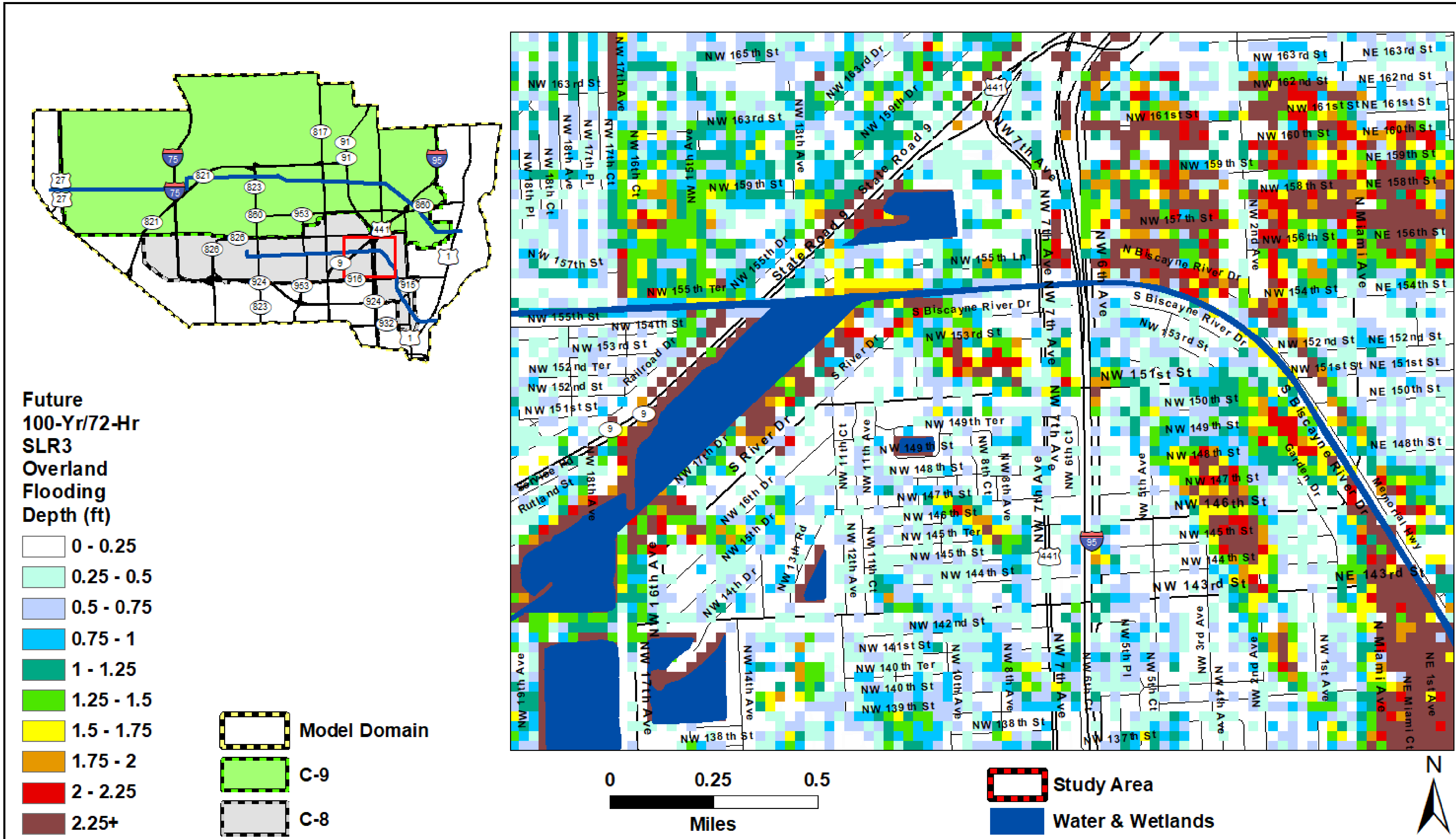

Figure 10.5-42: Up Close 100-Year Sea Level Rise 3 Flood Inundation Map for the C-8 Canal Near Opa Locka Canal

10.5.9.4 Up-Close Flood Inundation Maps for the C-9 Canal Between I-95 and S-29

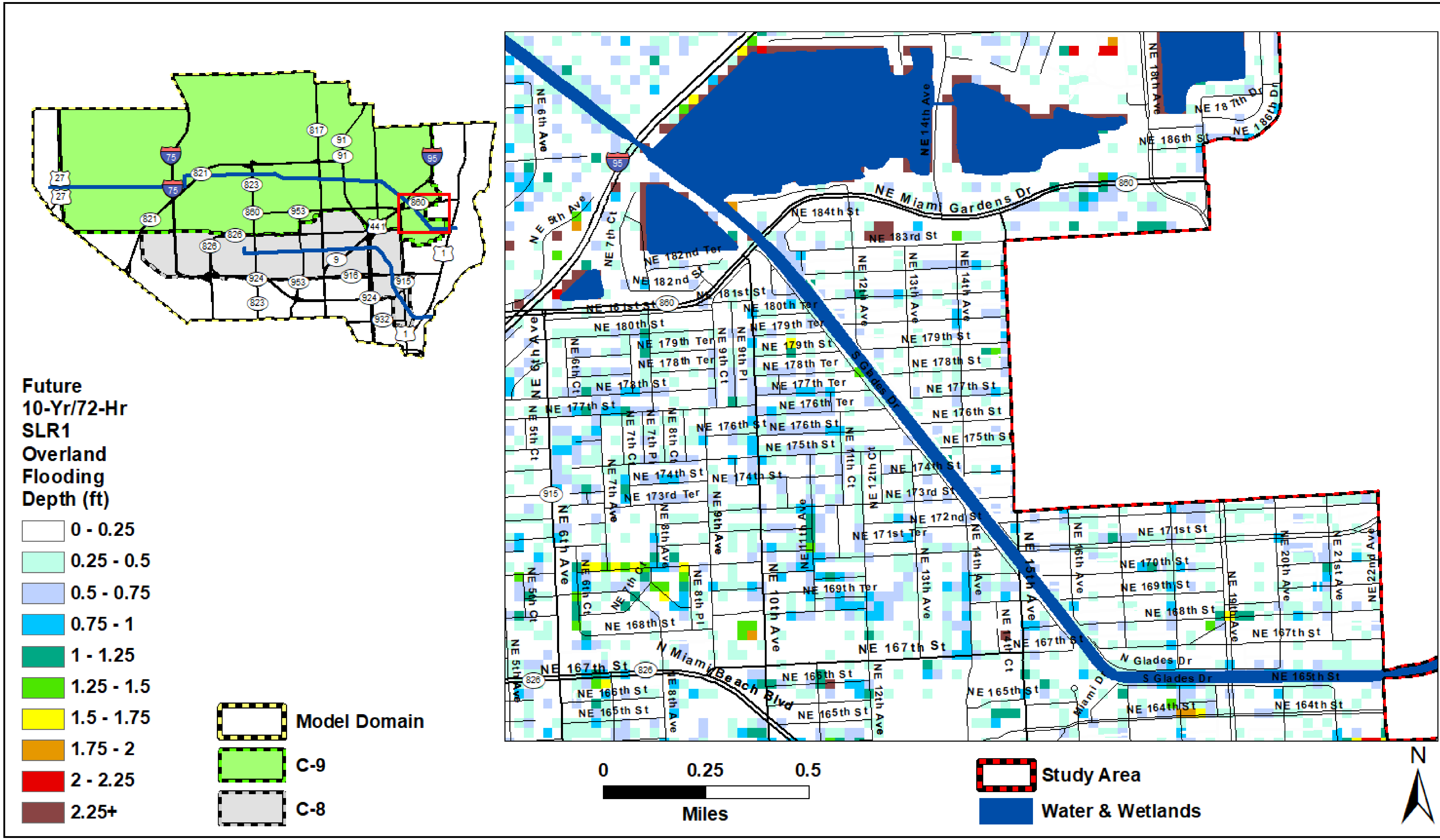

Figure 10.5-43: Up Close 10-Year Design Storm Sea Level Rise 1 Flood Inundation Map for the C-9 Canal Between I-95 and S-29

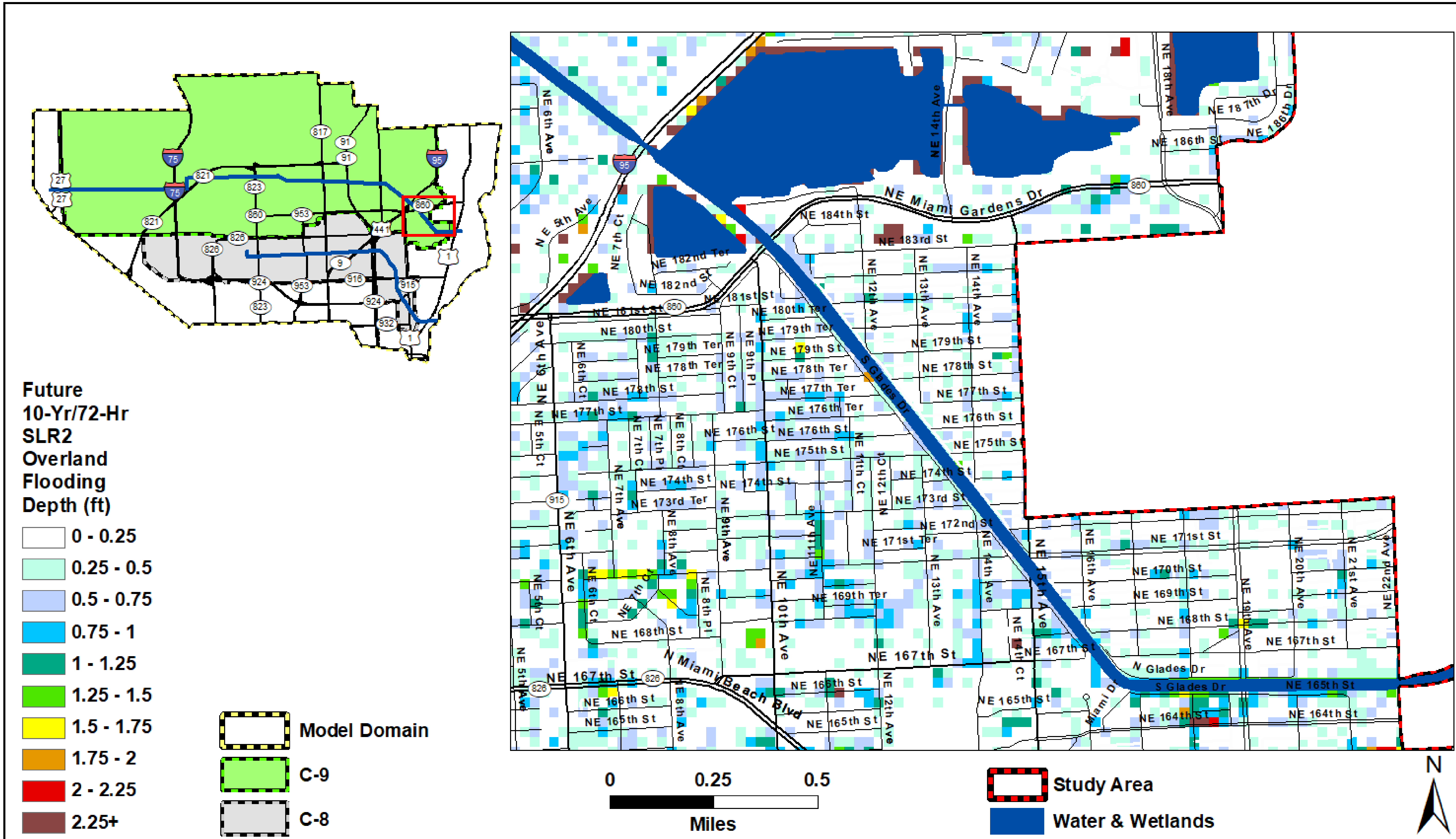

Figure 10.5-44: Up Close 10-Year Design Storm Sea Level Rise 2 Flood Inundation Map for the C-9 Canal Between I-95 and S-29

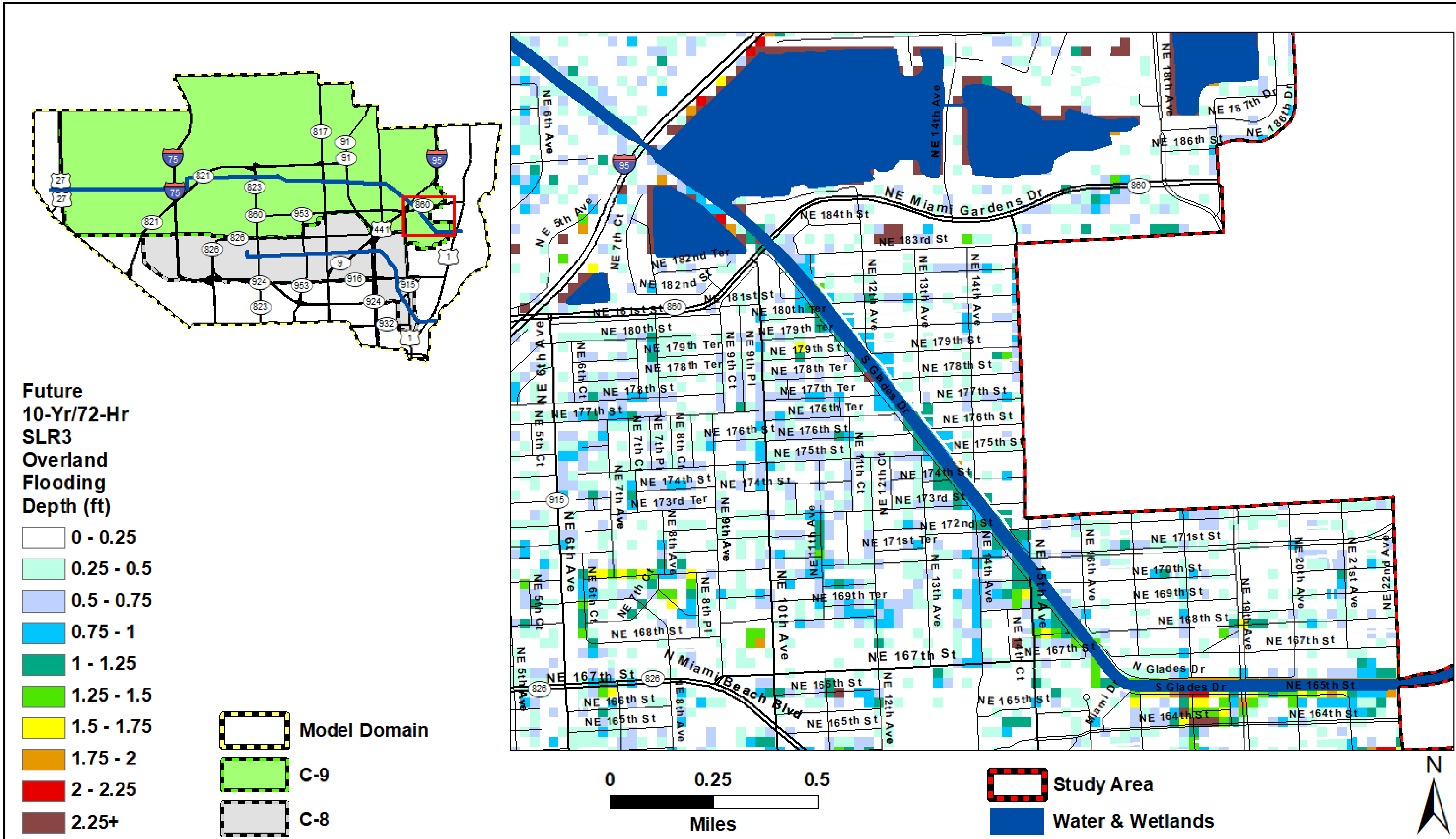

Figure 10.5-45: Up Close 10-Year Design Storm Sea Level Rise 3 Flood Inundation Map for the C-9 Canal Between I-95 and S-29

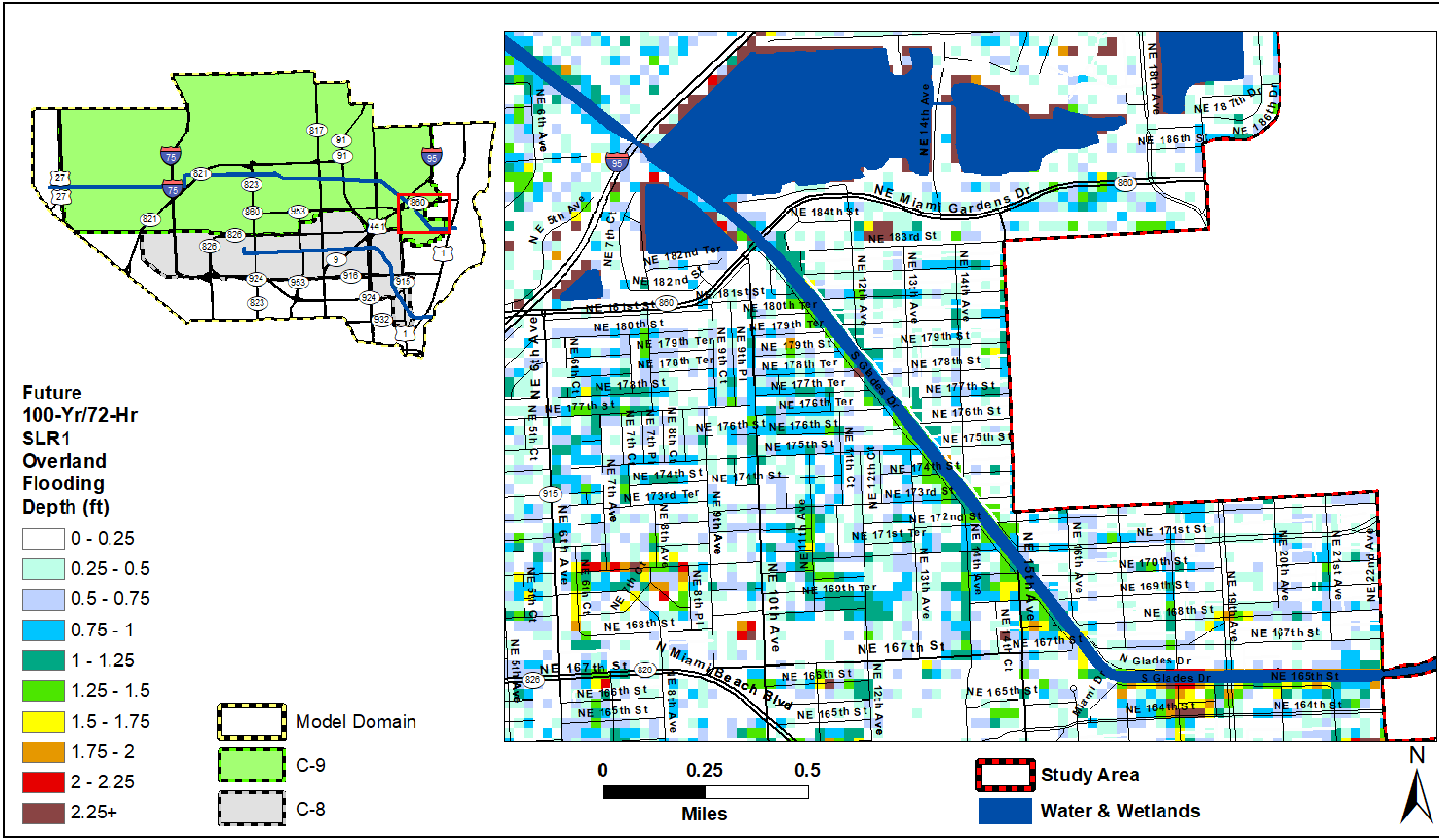

Figure 10.5-46: Up Close 100-Year Design Storm Sea Level Rise 1 Flood Inundation Map for the C-9 Canal Between I-95 and S-29

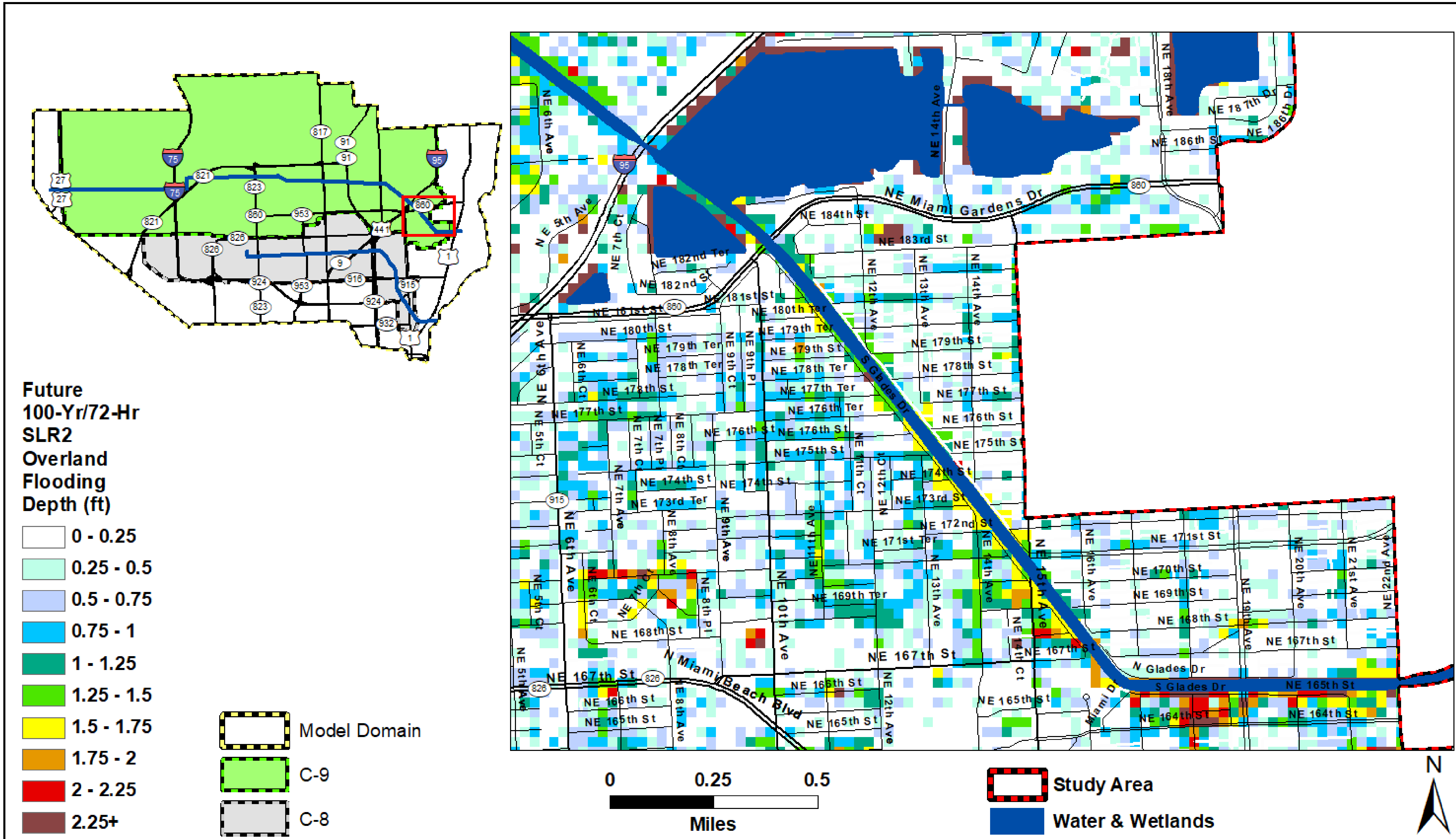

Figure 10.5-47: Up Close 100-Year Design Storm Sea Level Rise 2 Flood Inundation Map for the C-9 Canal Between I-95 and S-29

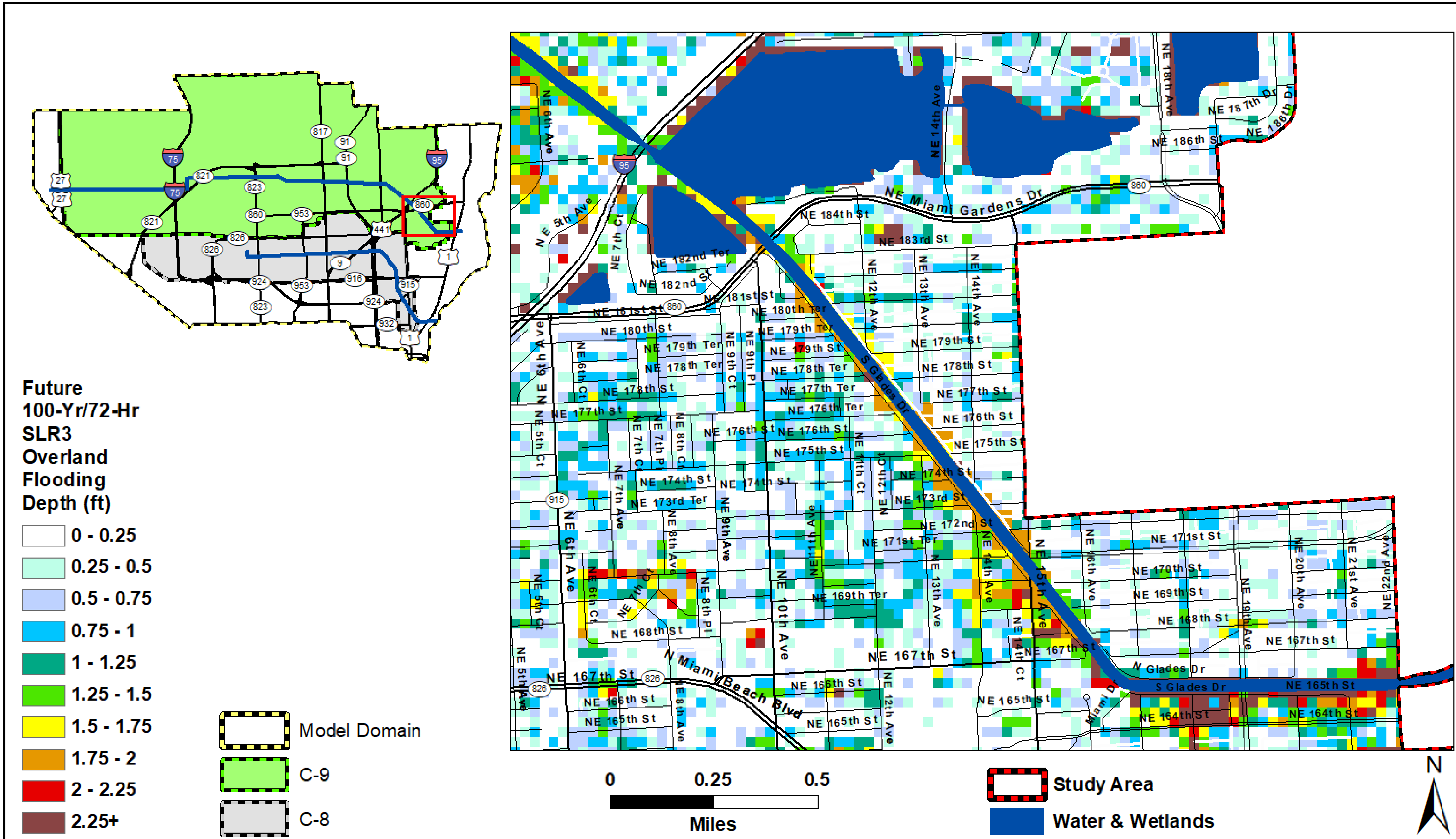

Figure 10.5-48: Up Close 100-Year Design Storm Sea Level Rise 3 Flood Inundation Map for the C-9 Canal Between I-95 and S-29

10.5.9.5 Up-Close Flood Inundation Maps for the C-9 Canal Near US Hwy 441

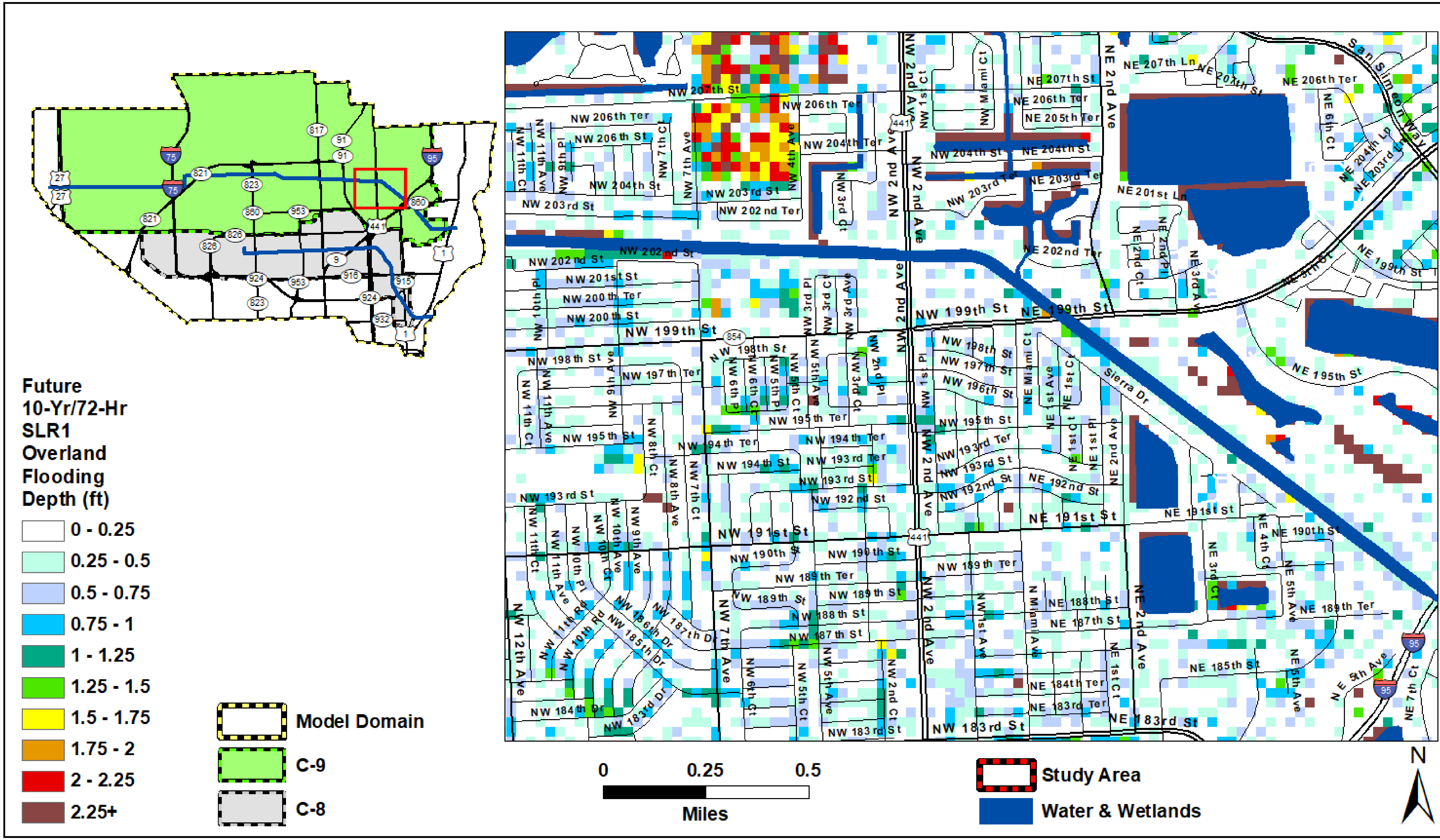

Figure 10.5-49: Up Close 10-Year Sea Level Rise 1 Flood Inundation Map for the C-9 Canal Near US Hwy 441

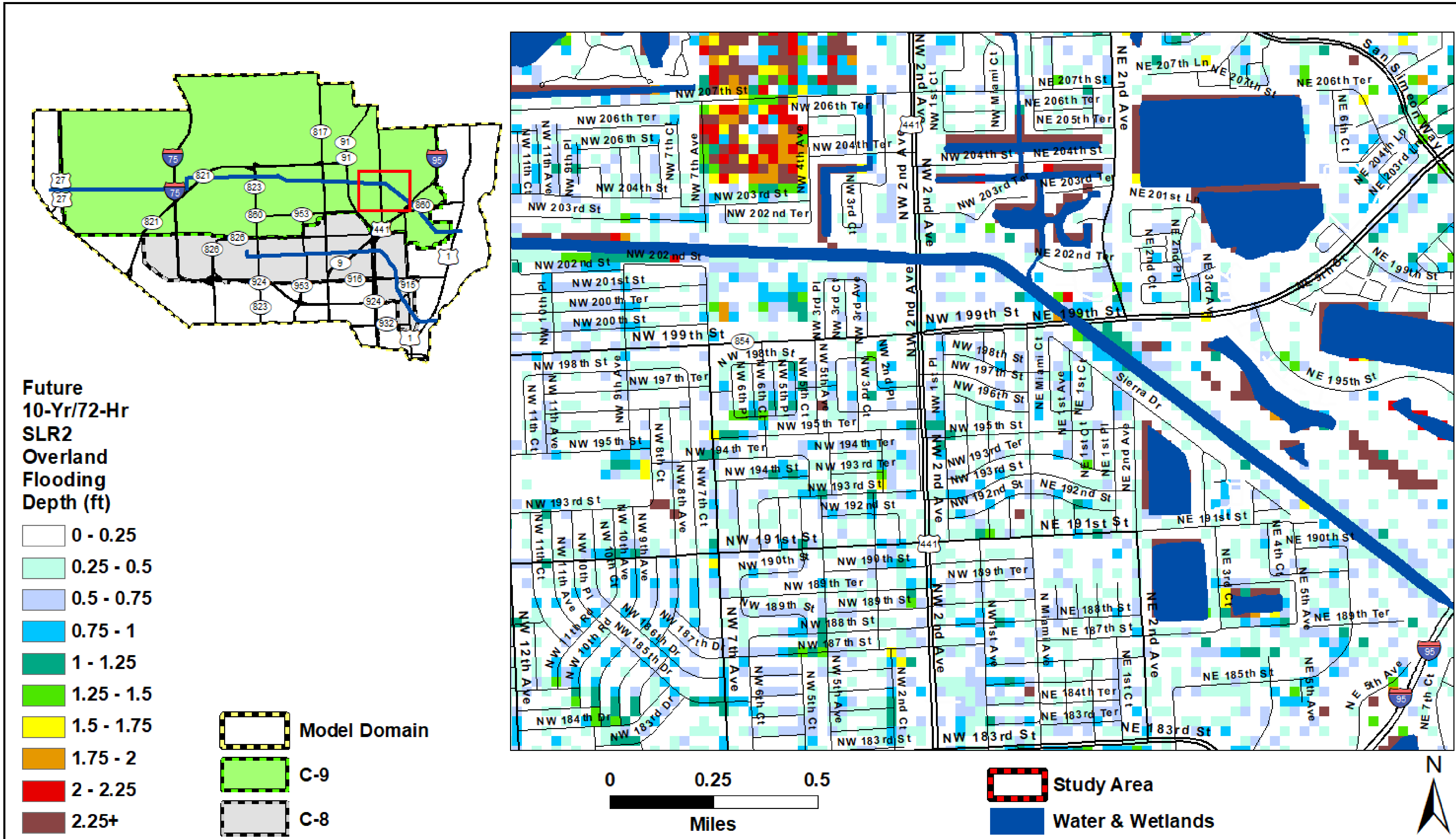

Figure 10.5-50: Up Close 10-Year Sea Level Rise 2 Flood Inundation Map for the C-9 Canal Near US Hwy 441

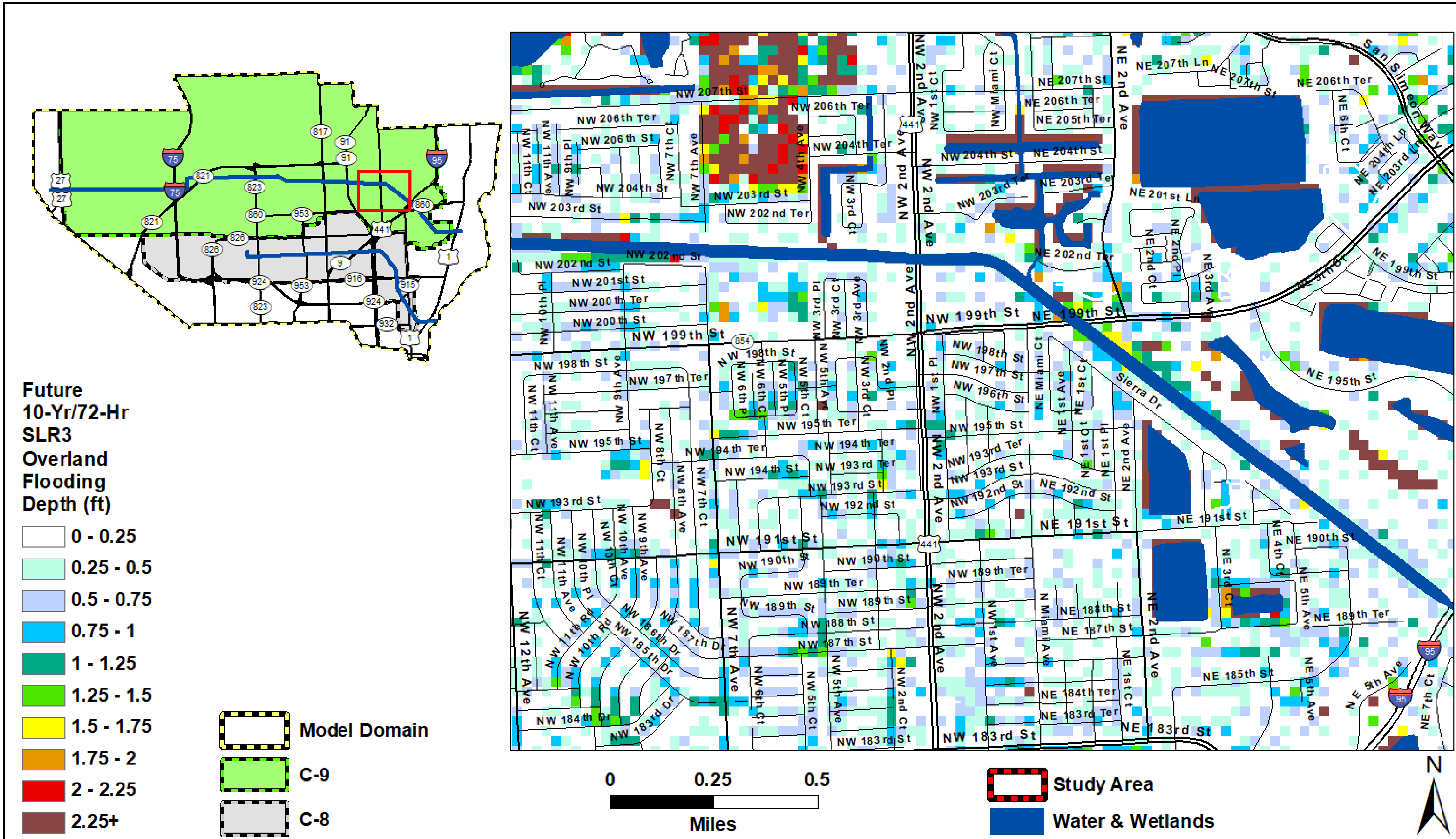

Figure 10.5-51: Up Close 10-Year Sea Level Rise 3 Flood Inundation Map for the C-9 Canal Near US Hwy 441

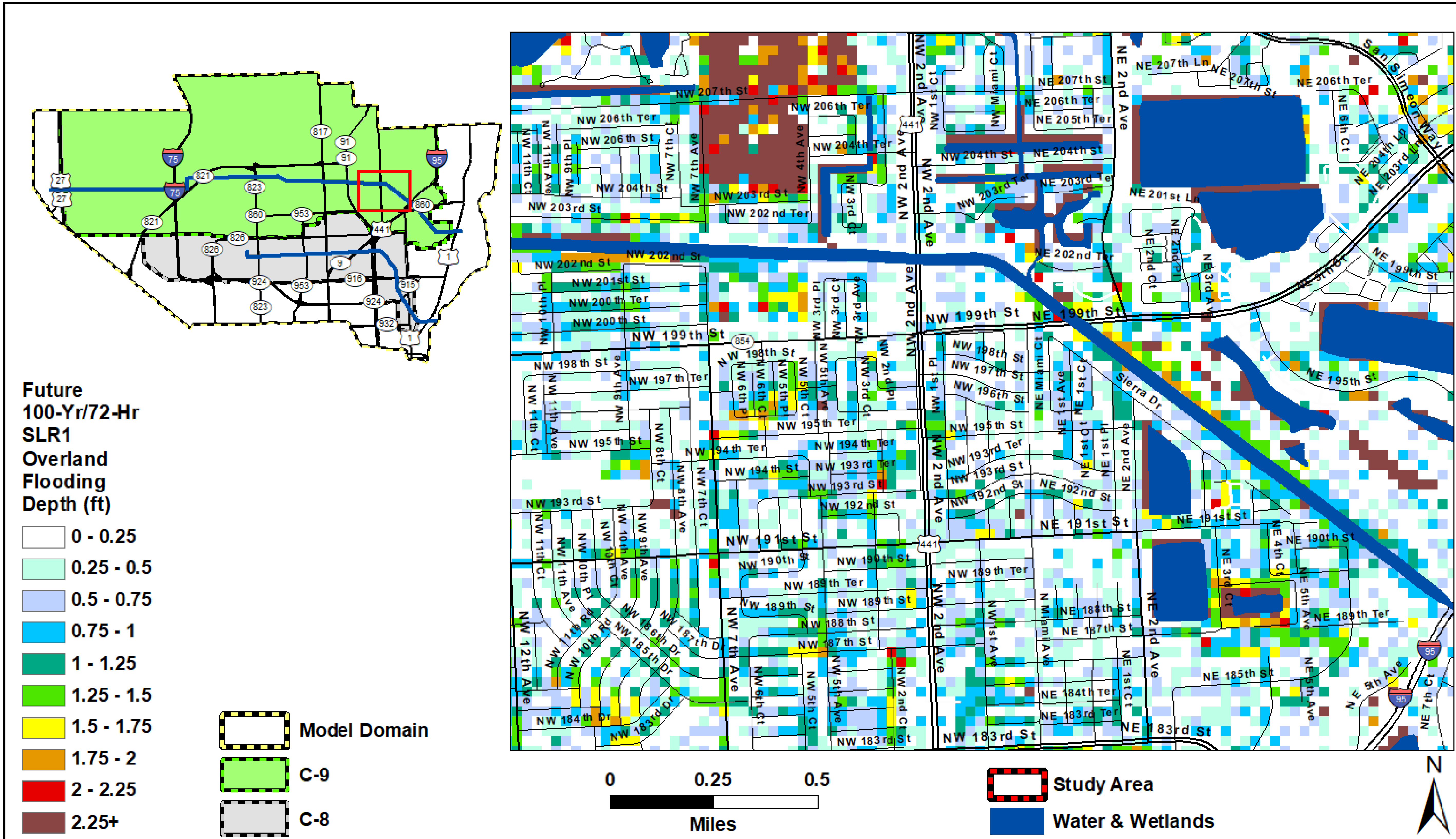

Figure 10.5-52: Up Close 100-Year Sea Level Rise 1 Flood Inundation Map for the C-9 Canal Near US Hwy 441

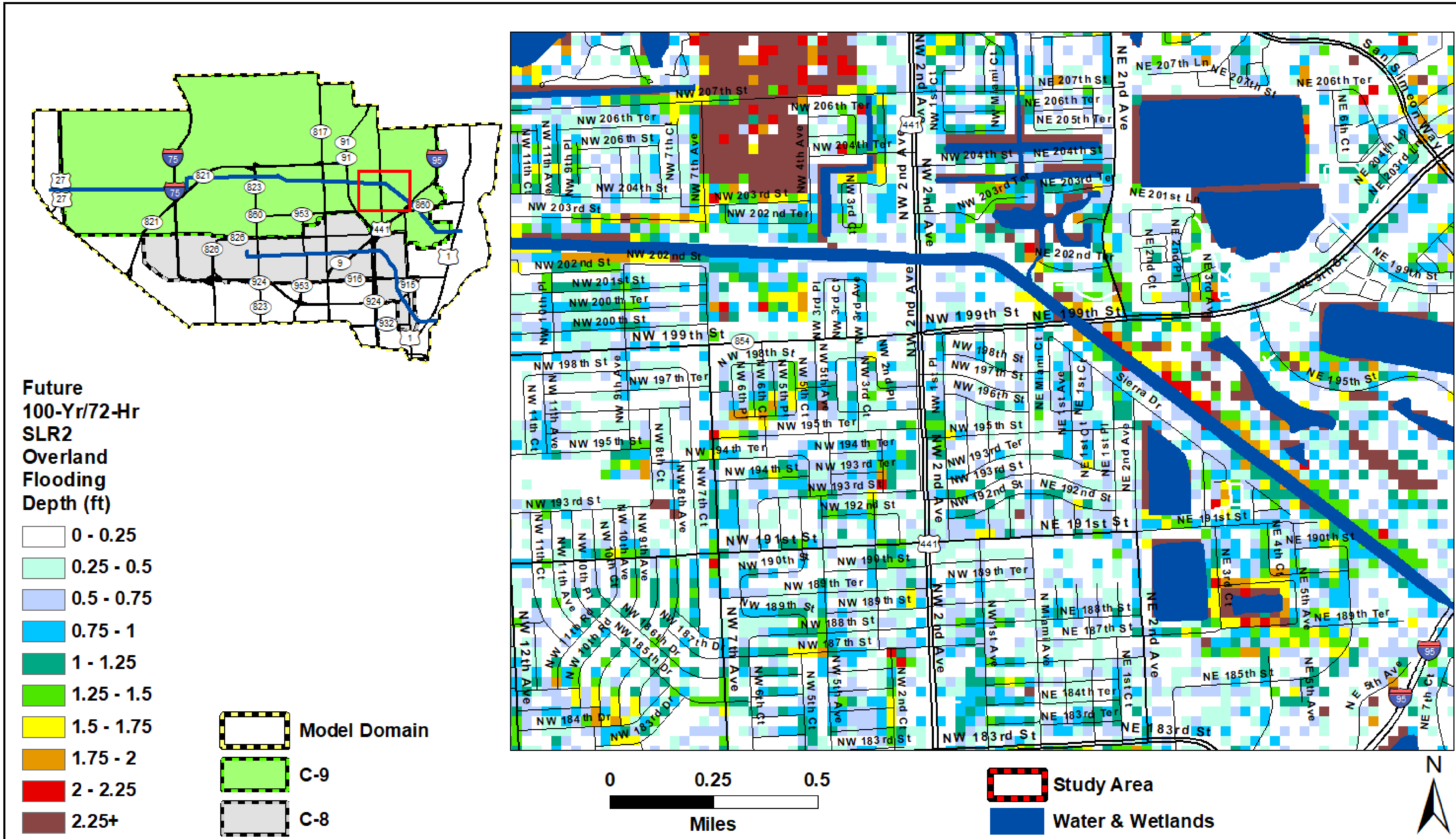

Figure 10.5-53: Up Close 100-Year Sea Level Rise 2 Flood Inundation Map for the C-9 Canal Near US Hwy 441

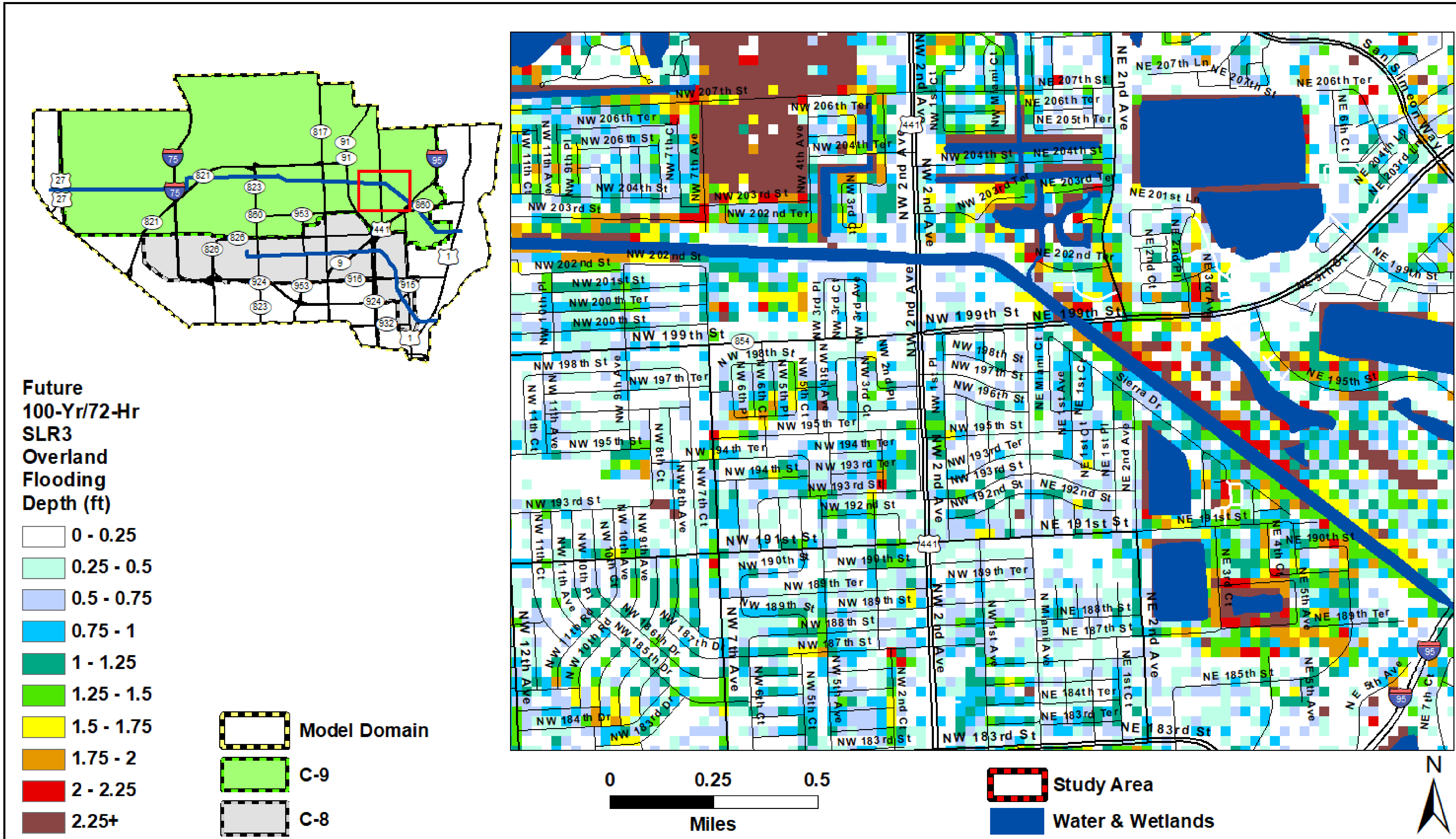

Figure 10.5-54: Up Close 100-Year Sea Level Rise 3 Flood Inundation Map for the C-9 Canal Near US Hwy 441

10.5.9.6 Up-Close Flood Inundation Maps for the C-9 Canal Near Ronald Reagan Turnpike

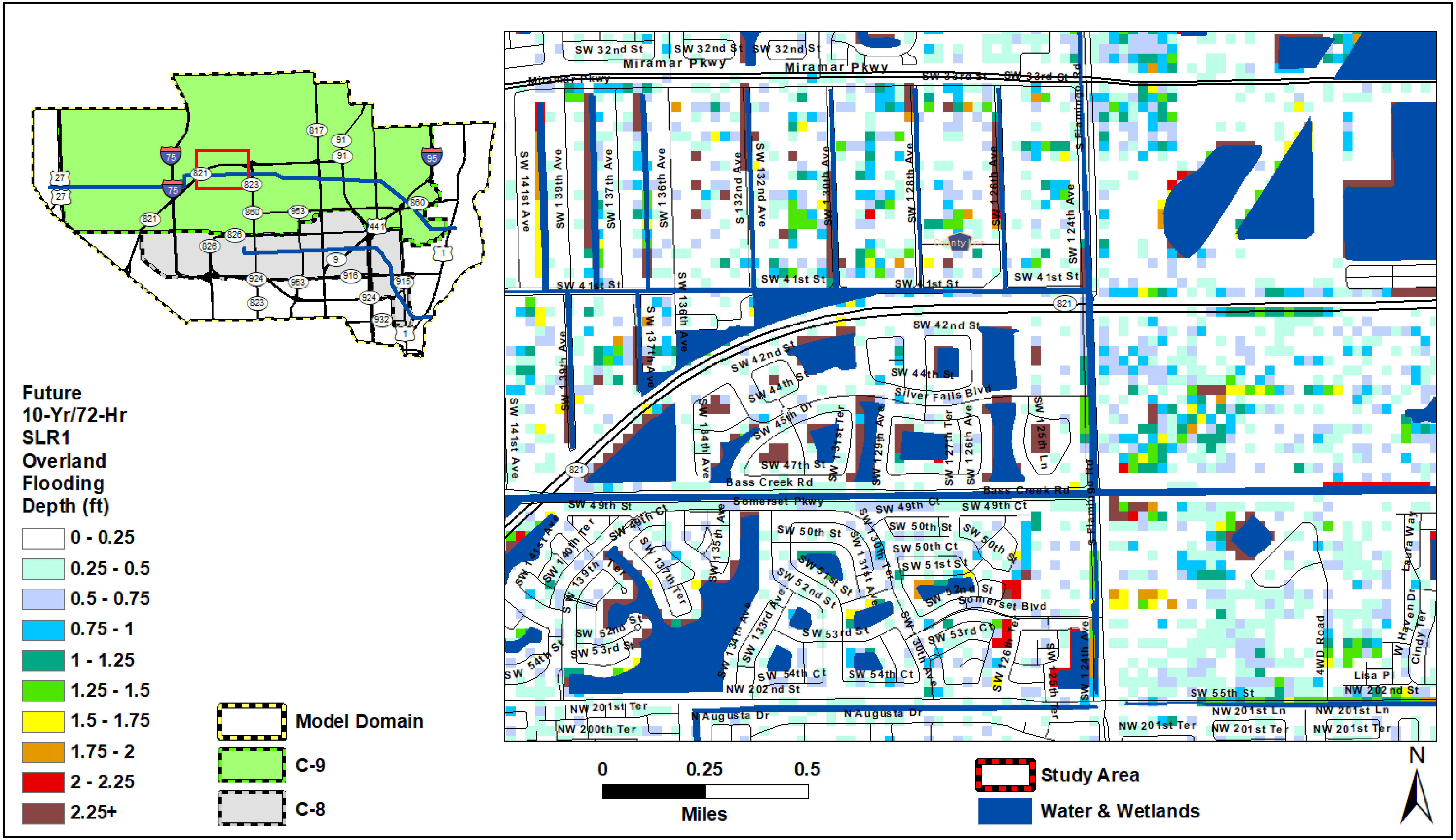

Figure 10.5-55: Up Close 10-Year Sea Level Rise 1 Flood Inundation Map for the C-9 Canal Near Ronald Reagan Turnpike

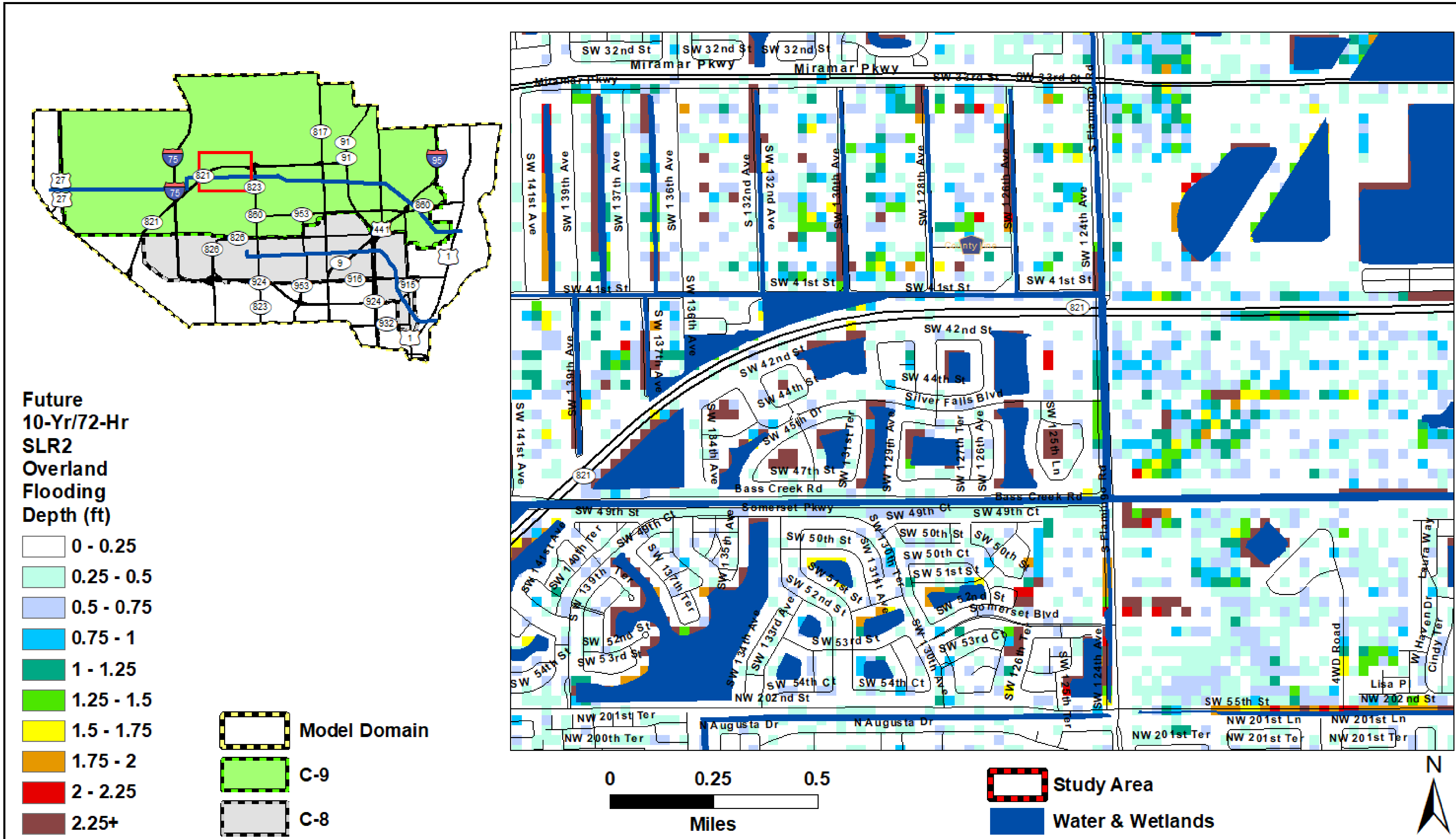

Figure 10.5-56: Up Close 10-Year Sea Level Rise 2 Flood Inundation Map for the C-9 Canal Near Ronald Reagan Turnpike

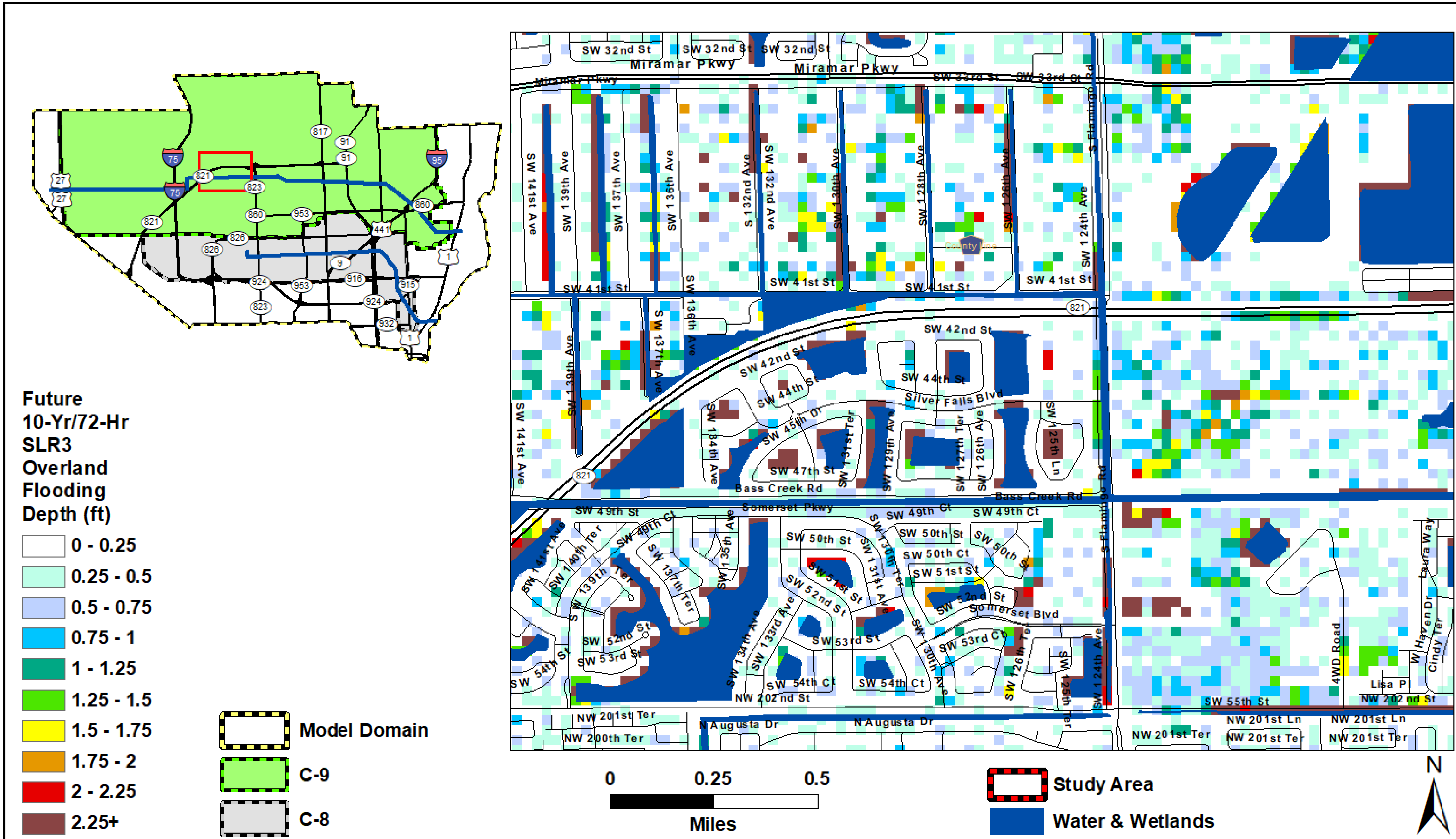

Figure 10.5-57: Up Close 10-Year Sea Level Rise 3 Flood Inundation Map for the C-9 Canal Near Ronald Reagan Turnpike

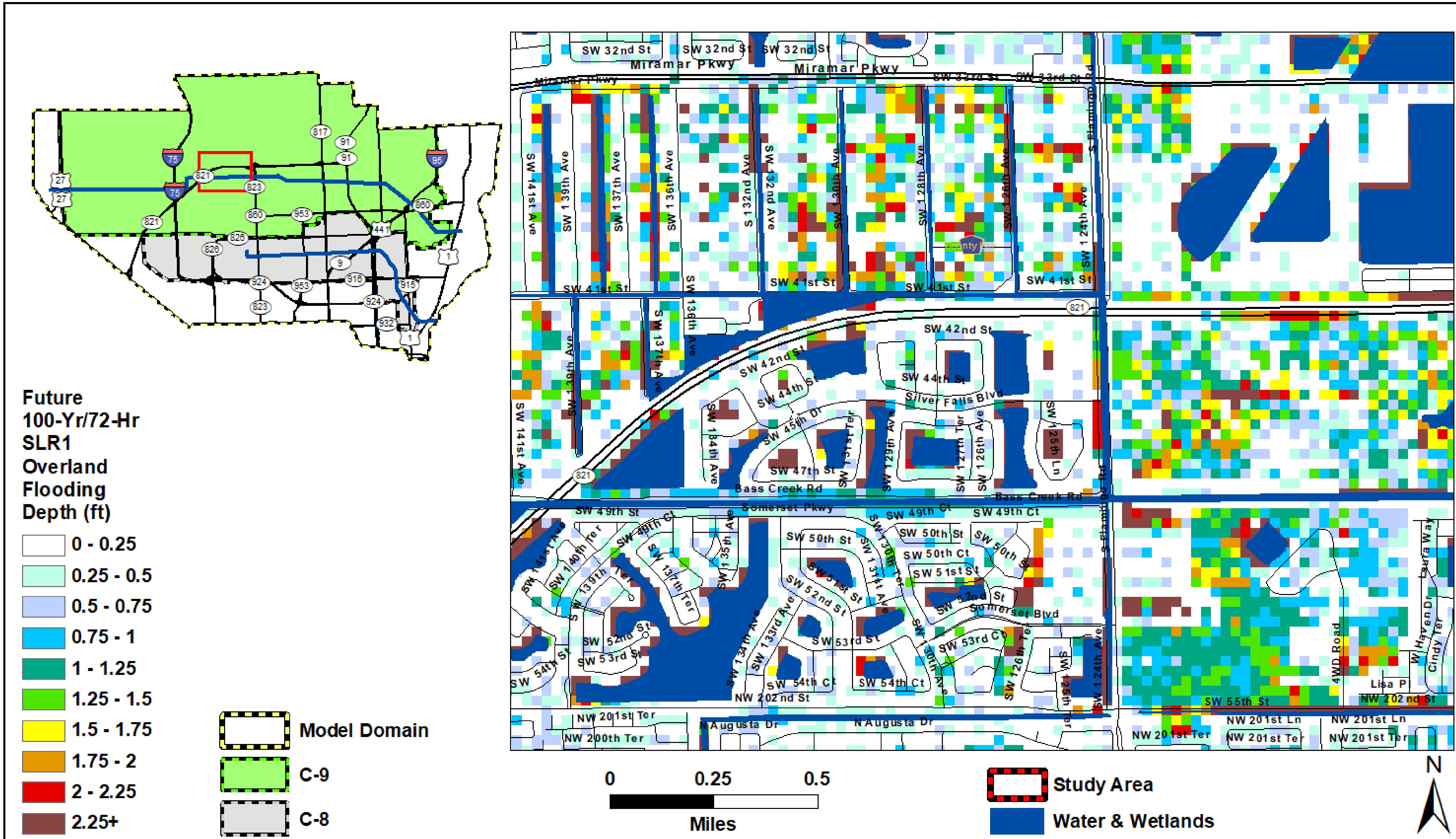

Figure 10.5-58: Up Close 100-Year Sea Level Rise 1 Flood Inundation Map for the C-9 Canal Near Ronald Reagan Turnpike

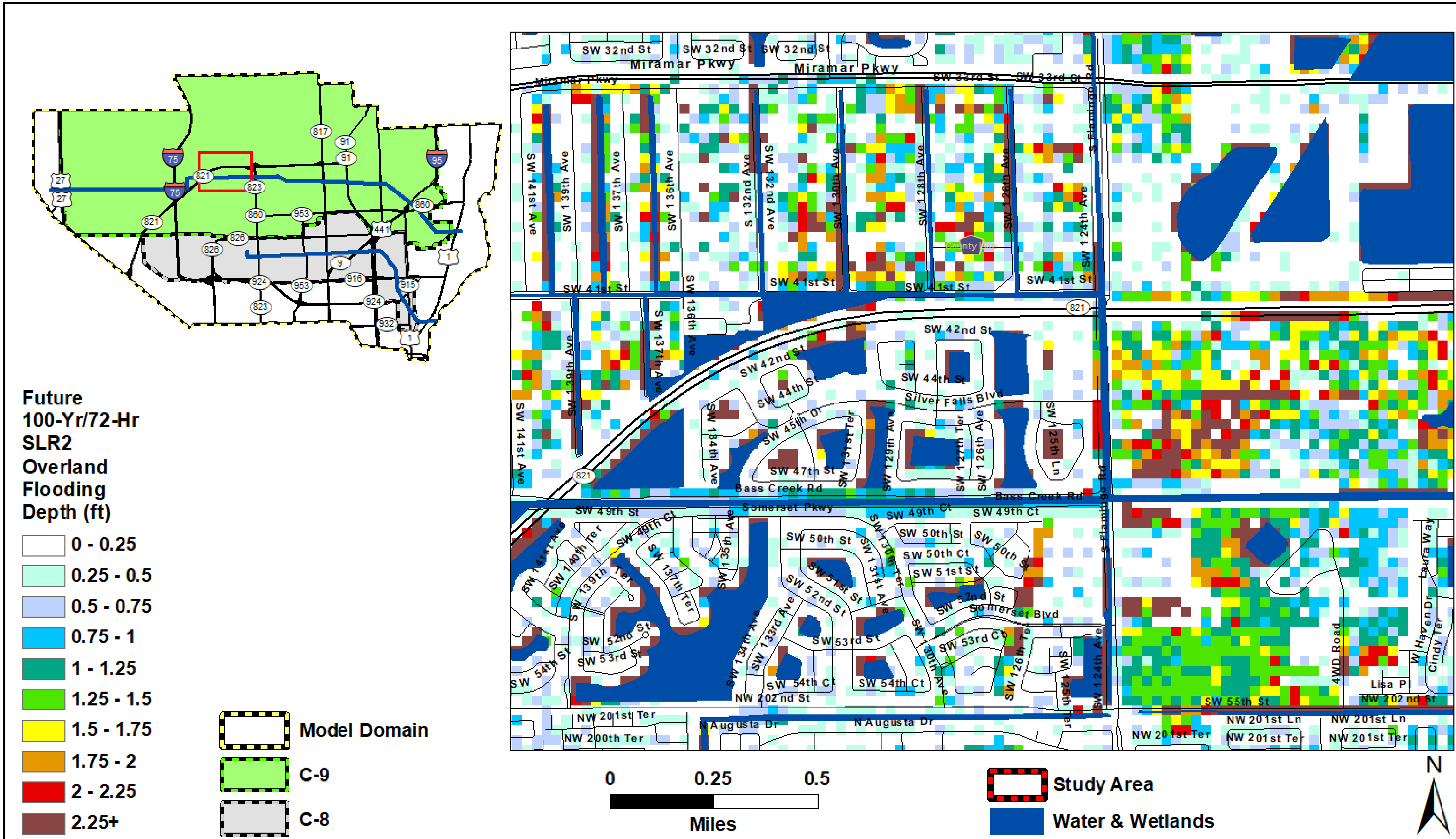

Figure 10.5-59: Up Close 100-Year Sea Level Rise 2 Flood Inundation Map for the C-9 Canal Near Ronald Reagan Turnpike

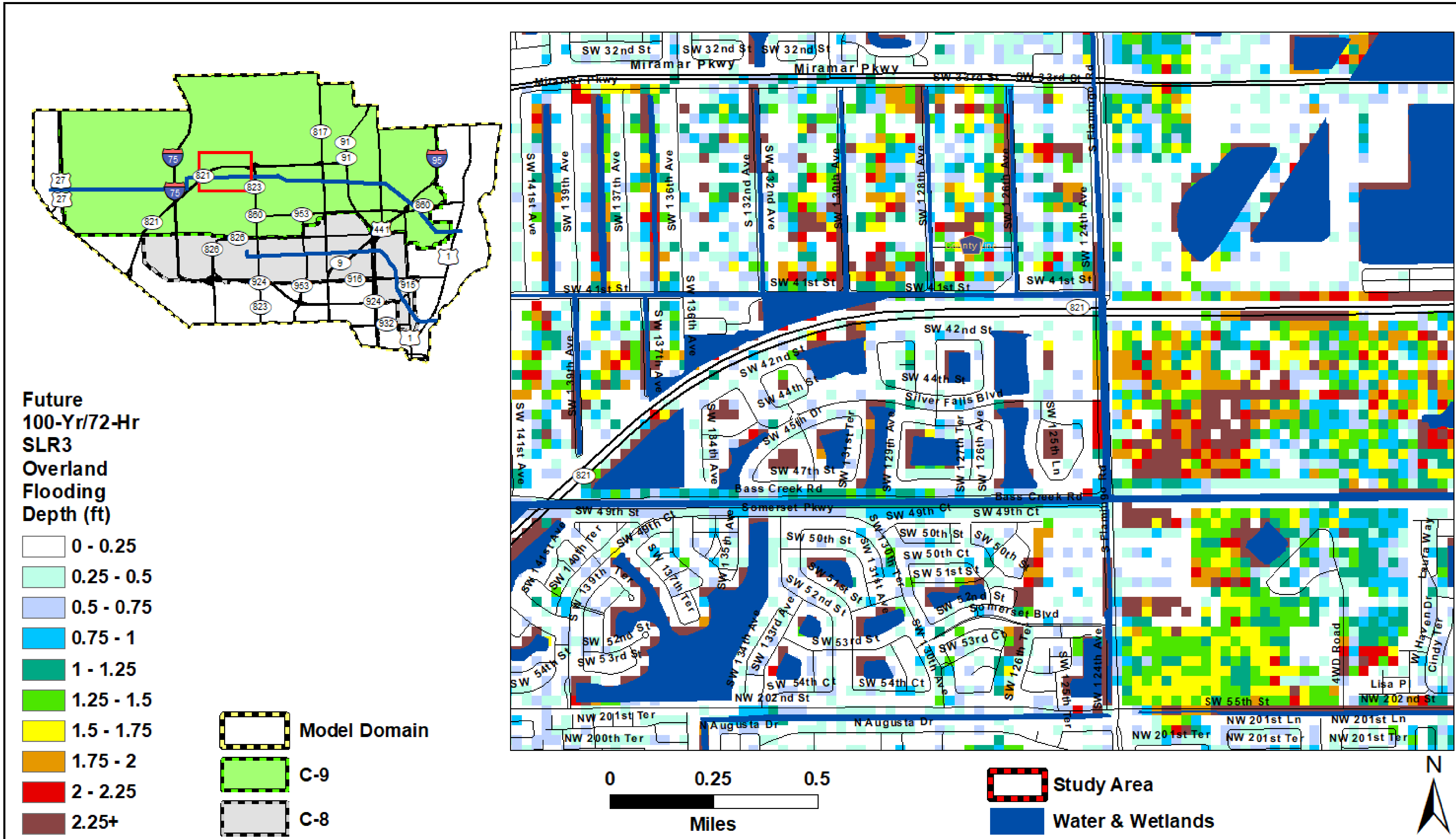

Figure 10.5-60: Up Close 100-Year Sea Level Rise 3 Flood Inundation Map for the C-9 Canal Near Ronald Reagan Turnpike

10.5.9.7 Up-Close Flood Inundation Maps for the C-9 Canal Near Red Road

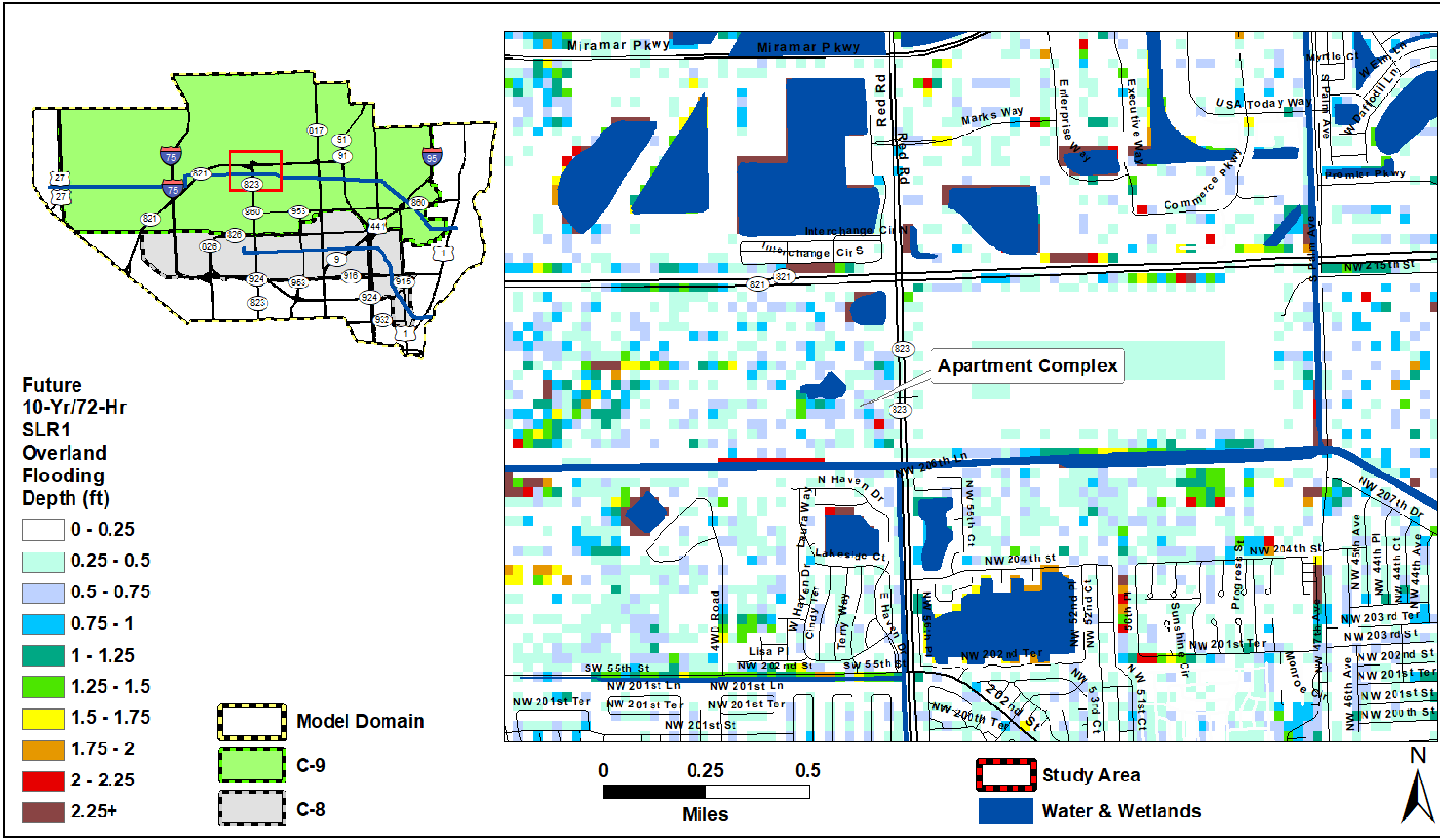

Figure 10.5-61: Up Close 10-Year Sea Level Rise 1 Flood Inundation Map for the C-9 Canal Near Red Road

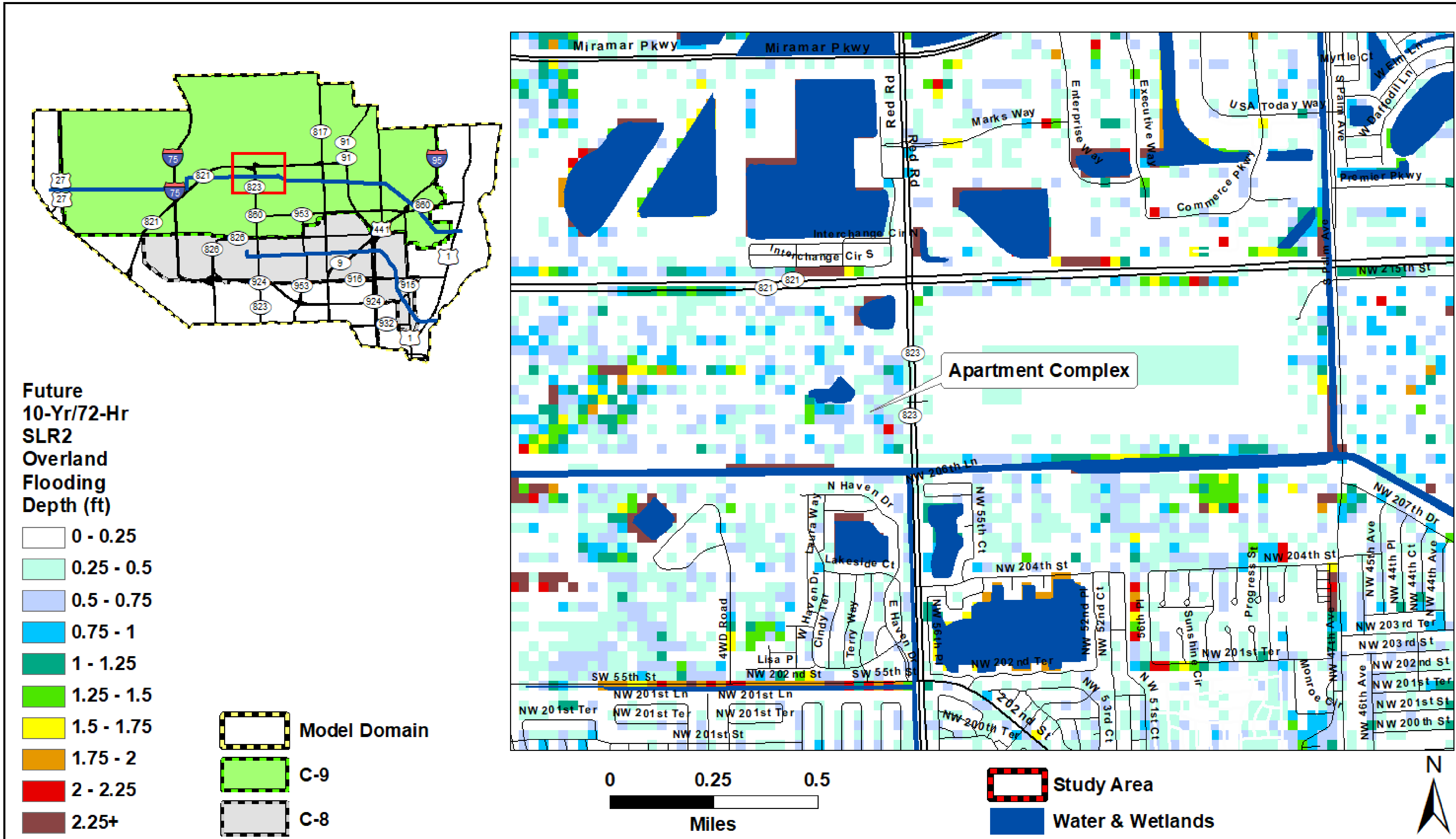

Figure 10.5-62: Up Close 10-Year Sea Level Rise 2 Flood Inundation Map for the C-9 Canal Near Red Road

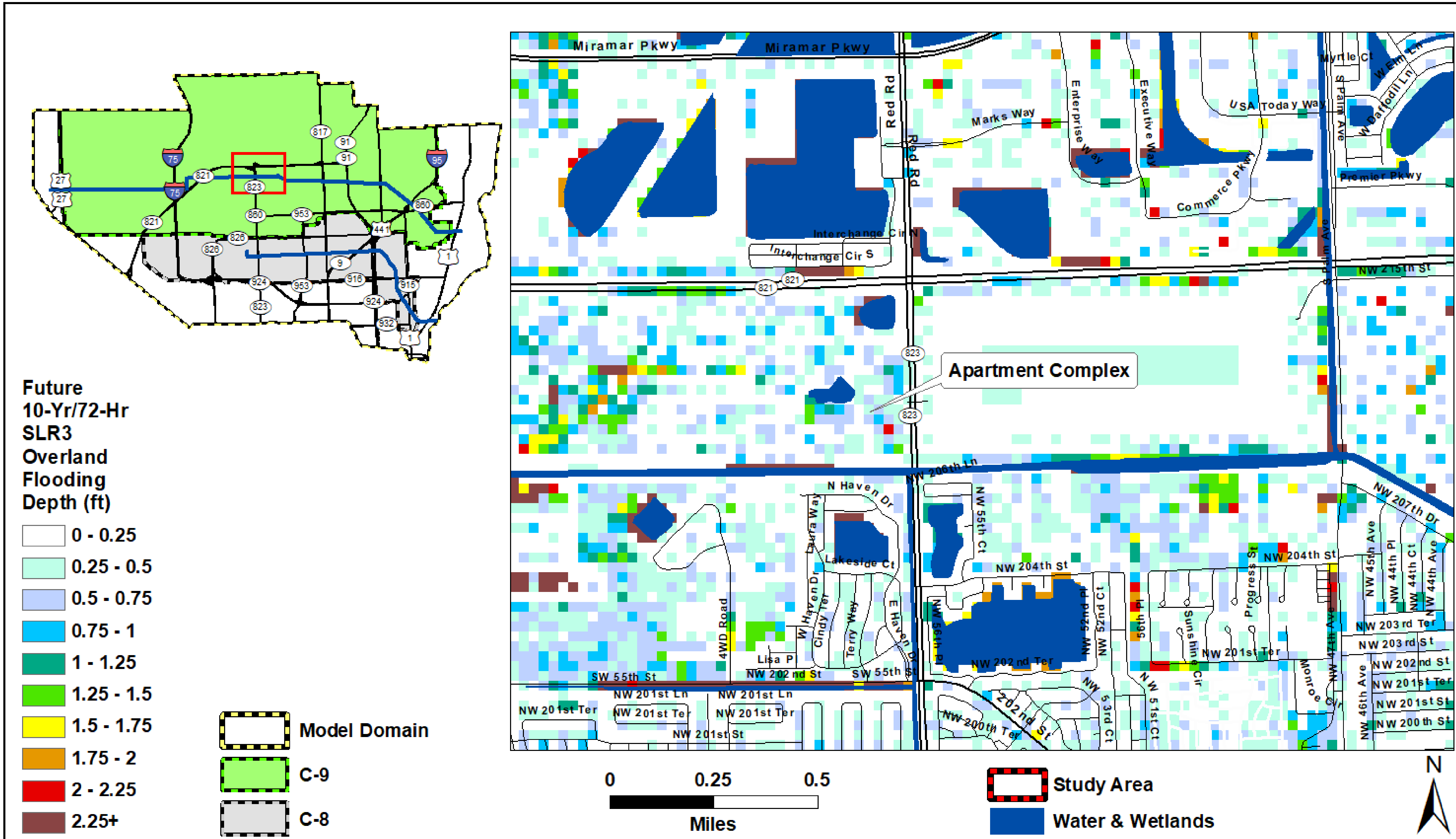

Figure 10.5-63: Up Close 10-Year Sea Level Rise 3 Flood Inundation Map for the C-9 Canal Near Red Road

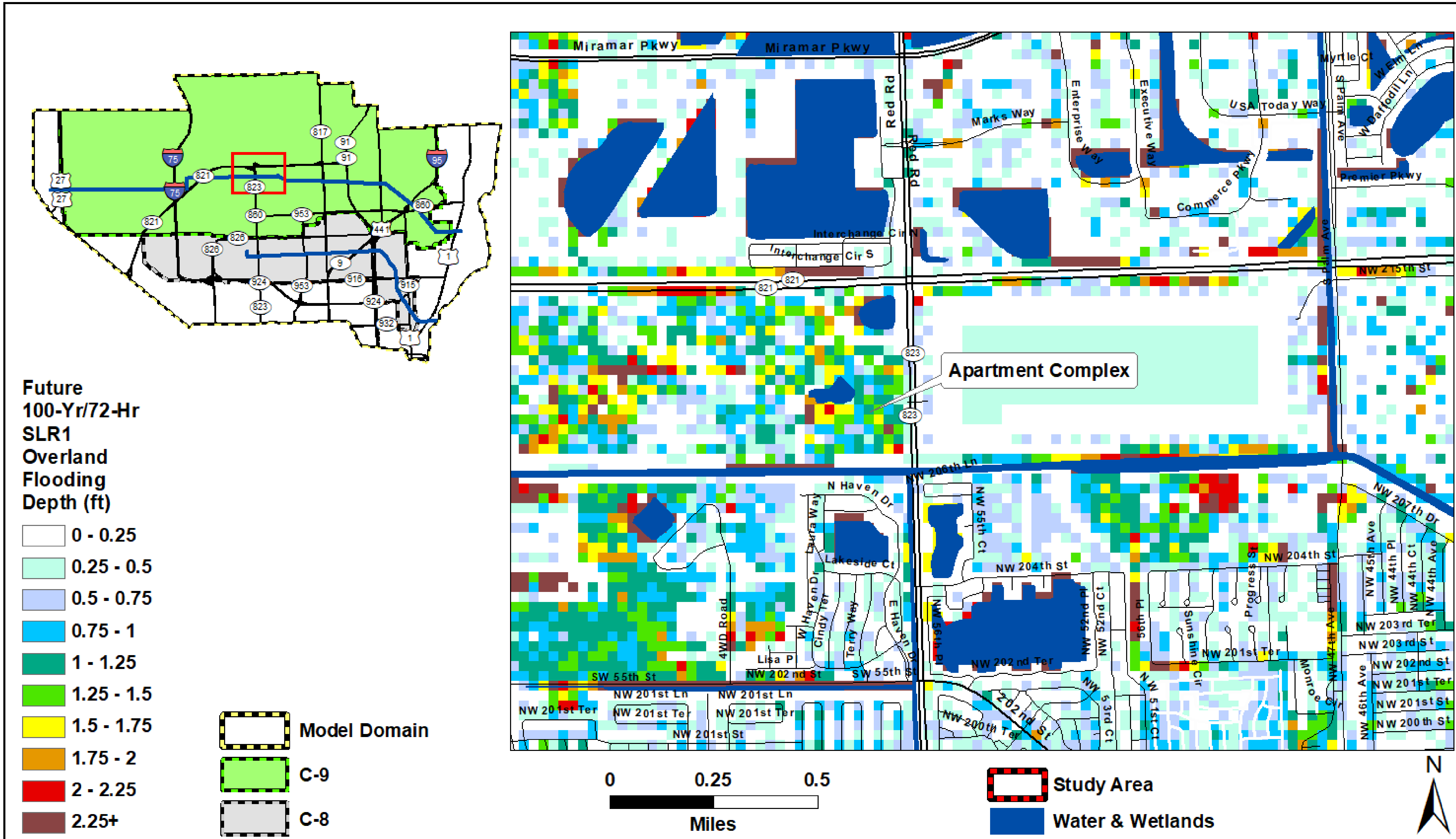

Figure 10.5-64: Up Close 100-Year Sea Level Rise 1 Flood Inundation Map for the C-9 Canal Near Red Road

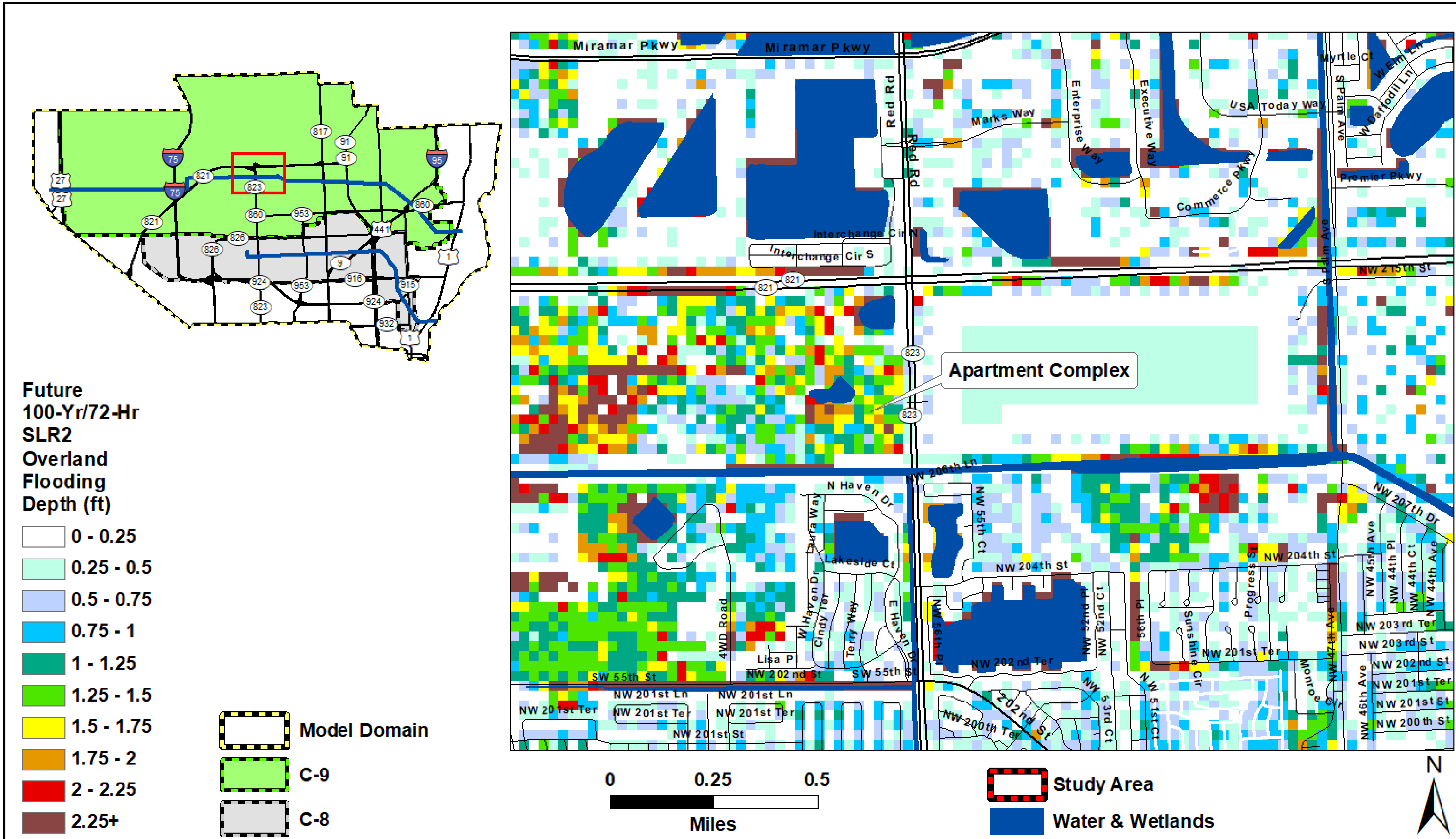

Figure 10.5-65: Up Close 100-Year Sea Level Rise 2 Flood Inundation Map for the C-9 Canal Near Red Road

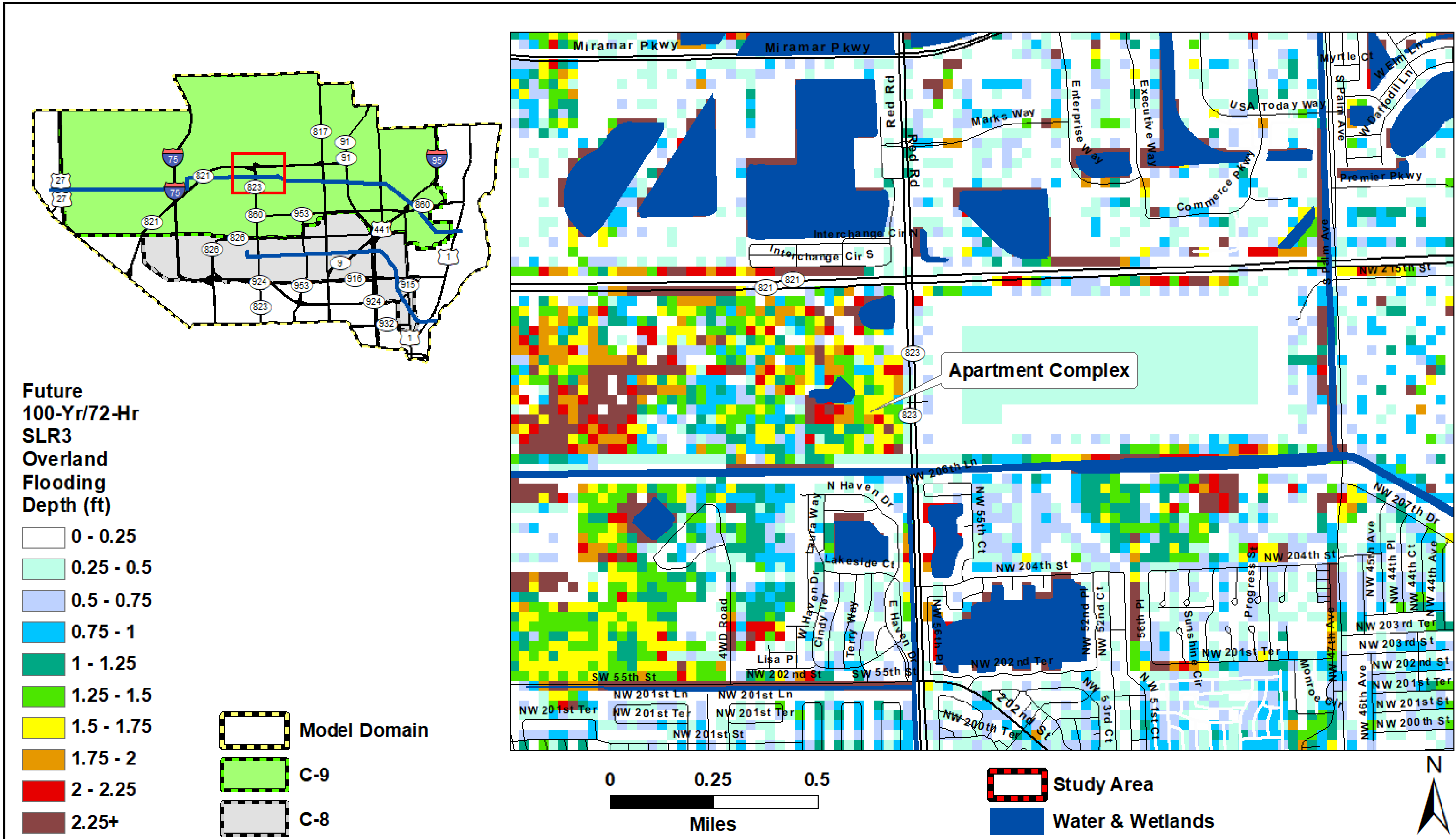

Figure 10.5-66: Up Close 100-Year Sea Level Rise 3 Flood Inundation Map for the C-9 Canal Near Red Road

10.5.10 Flood Inundation Difference Maps for Urban Land Use Areas

This section presents depth difference maps between the future conditions 25-year design storm with 1, 2, and 3 ft sea level rise and current conditions. These maps provide another way to interpret the PM #5 results by depicting the increases in flood elevations and extents that can be expected with increasing sea level. Under current conditions, increase in flooding was presented with respect to an increase in design storm intensity. Intuitively, more rainfall increases the flooding potential under the same conditions. This is a well-established principle; therefore, instead of presenting difference maps between two design storms of different intensities, future conditions results are presented with respect to an increase in sea level rise for a given design storm. For any given design storm (same rainfall), the effect of the increase in sea level rise does not necessarily act the same way as the increase in rainfall does. For instance, an increase in rainfall mostly leads to a model-wide increase in flood depth. However, an increase in sea level rise has varying effects on the area and depth of flood inundation. **Figure 10.5-67** through **Figure 10.5-69** show the maximum overland water depth difference between future conditions and current conditions for the 25-year design storm for all three sea level rise scenarios, for urban land use only. It is important to note that there is no difference in rainfall. It is also important to note that areas of future land use change that have increased topography elevation will mostly show up as negative values as they are no longer low points that accumulate water.

Figure 10.5-67 presents the difference in maximum water depth between the 25-year SLR1 and the current conditions 25-year design storm. Although there are changes in the maximum flood depth, the differences are typically in close proximity of the C-8 and C-9 Canal, or areas of topography elevation change. There is noticeably less flood depth difference in the C-9 basin than there is in the C-8 basin, which makes sense as the C-9 basin in drained by pumps and the C-8 basin is gravity-driven. This suggests that the C-8 basin *should* be more sensitive to sea level rise as any changes in the C-8 Canal stage directly correspond to a change in the ability for the C-8 basin to drain.

Figure 10.5-68 presents the difference in maximum water depth between the 25-year SLR2 and the current conditions 25-year design storm. Compared to the SLR1 difference, there are more changes in the maximum flood depth, with the largest differences still being in close proximity of the C-8 and C-9 Canal. Aside from the larger spatial extent of increased flood depths, the flood depths are also significantly higher, especially along the C-8 Canal. This was also observed in the maximum stage profiles in PM #1 and the up-close flooding in PM #5. Under SLR2, parts of the C-9 Basin, away from the C-9 Canal, are starting to show increases in flood depth.

Figure 10.5-69 presents the difference in maximum water depth between the 25-year SLR3 and the current conditions 25-year design storm. The changes in the maximum flood stage are significant, both in terms of extent and depth. Under SLR3, significant lengths of the C-8 and C-9 Canals, as well as inland areas, “feel the effects” of 3 ft of sea level rise. Increased flooding is seen in parts of Broward County that are normally drained by pumps. In the 3 ft sea level rise scenario, parts of the secondary system in eastern SBDD experience increased flooding as the SBDD pumps are forced to stop pumping due to the high water level in the C-9 Canal. Flooding in the C-8 Basin increases as stage in the C-8 Canal increase, as it is drained by gravity. Therefore, increases in stage in the C-8 Canal from increases in sea level rise will have a direct effect on flood levels in the C-8 Basin.

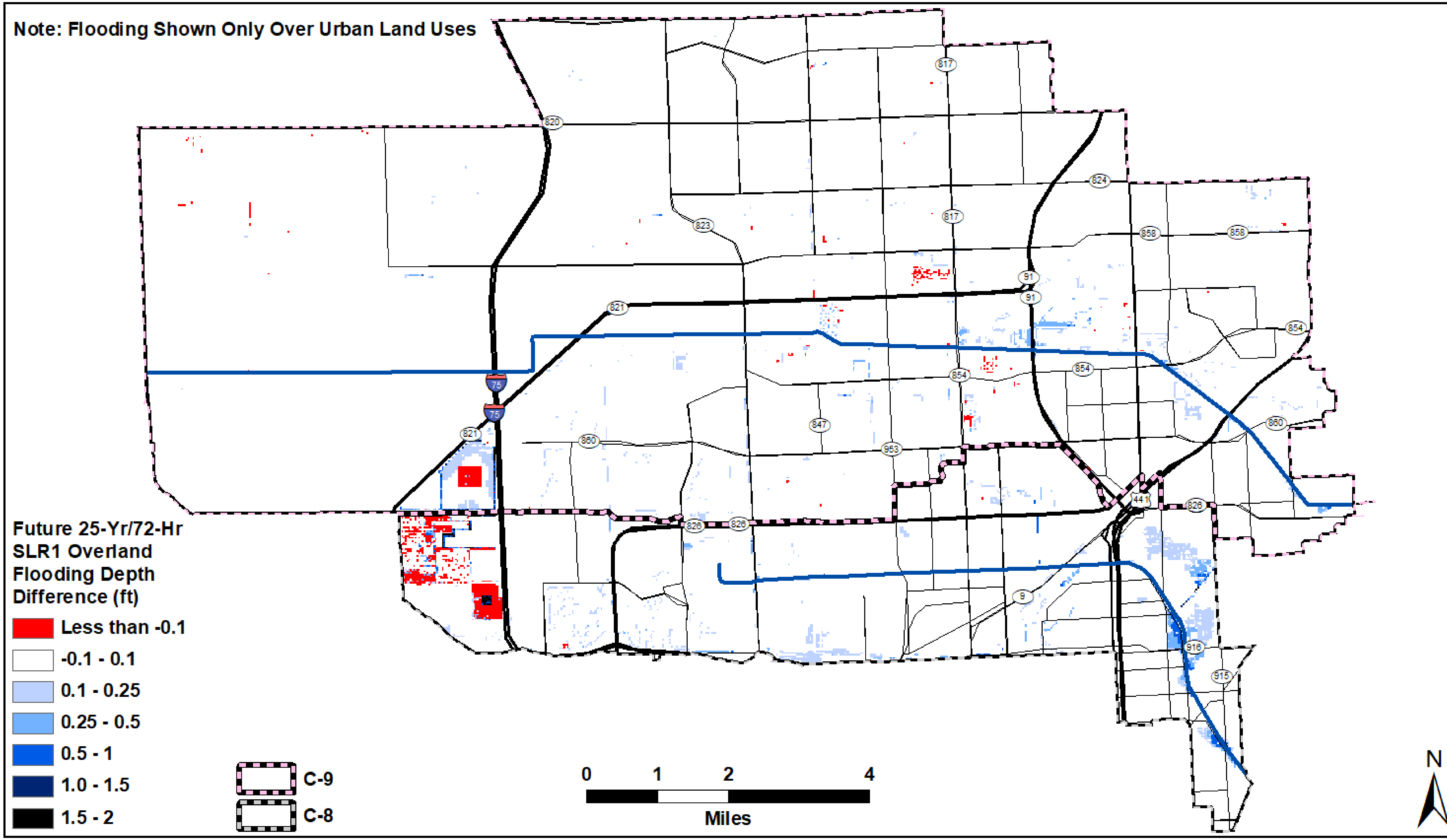

Figure 10.5-67: Flood Inundation Difference Map for 25-Year Sea Level Rise 1 Design Storm Event in Urban Land Use Areas (Future minus Current Conditions)

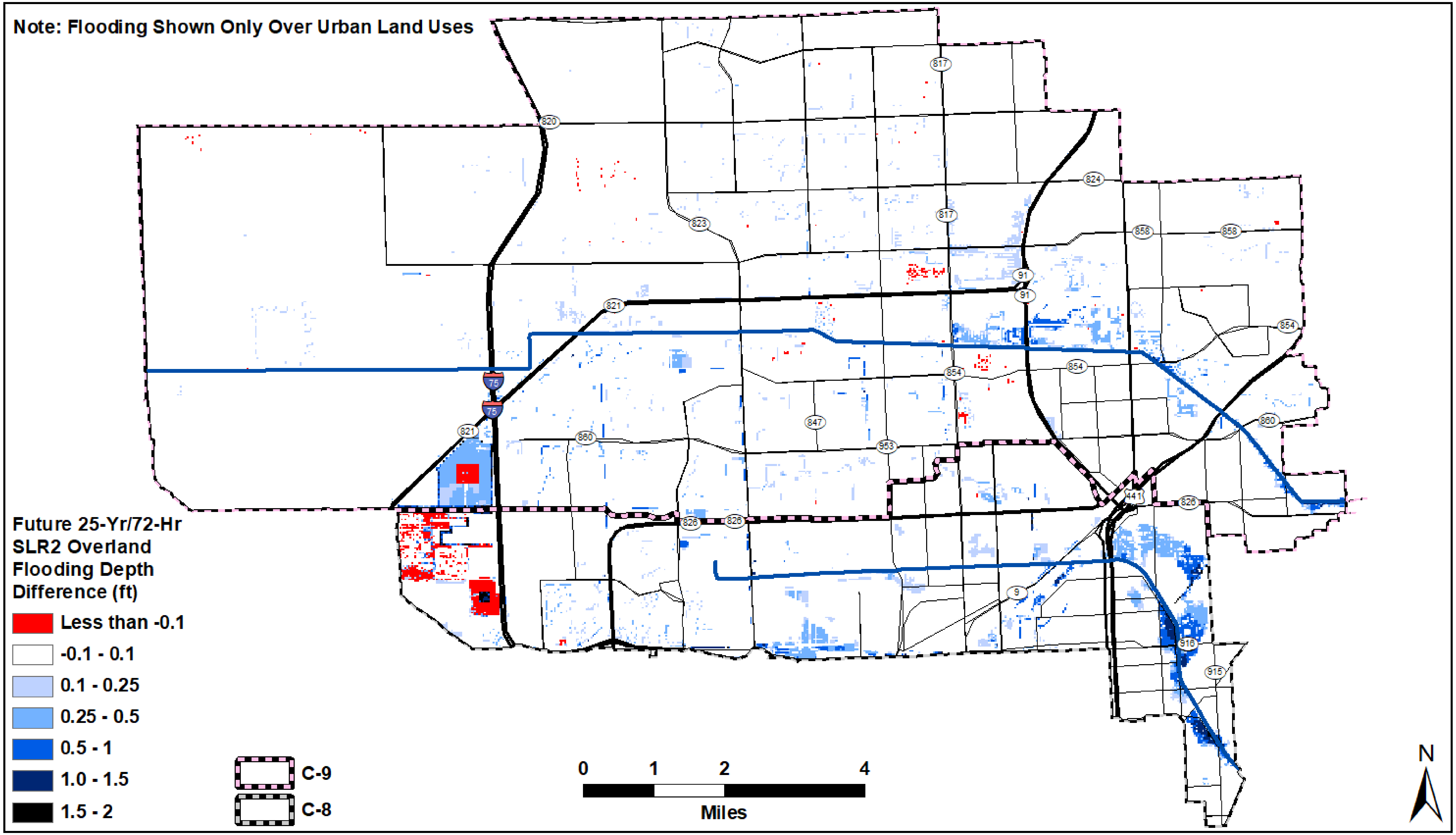

Figure 10.5-68: Flood Inundation Difference Map for 25-Year Sea Level Rise 2 Design Storm Event in Urban Land Use Areas (Future minus Current Conditions)

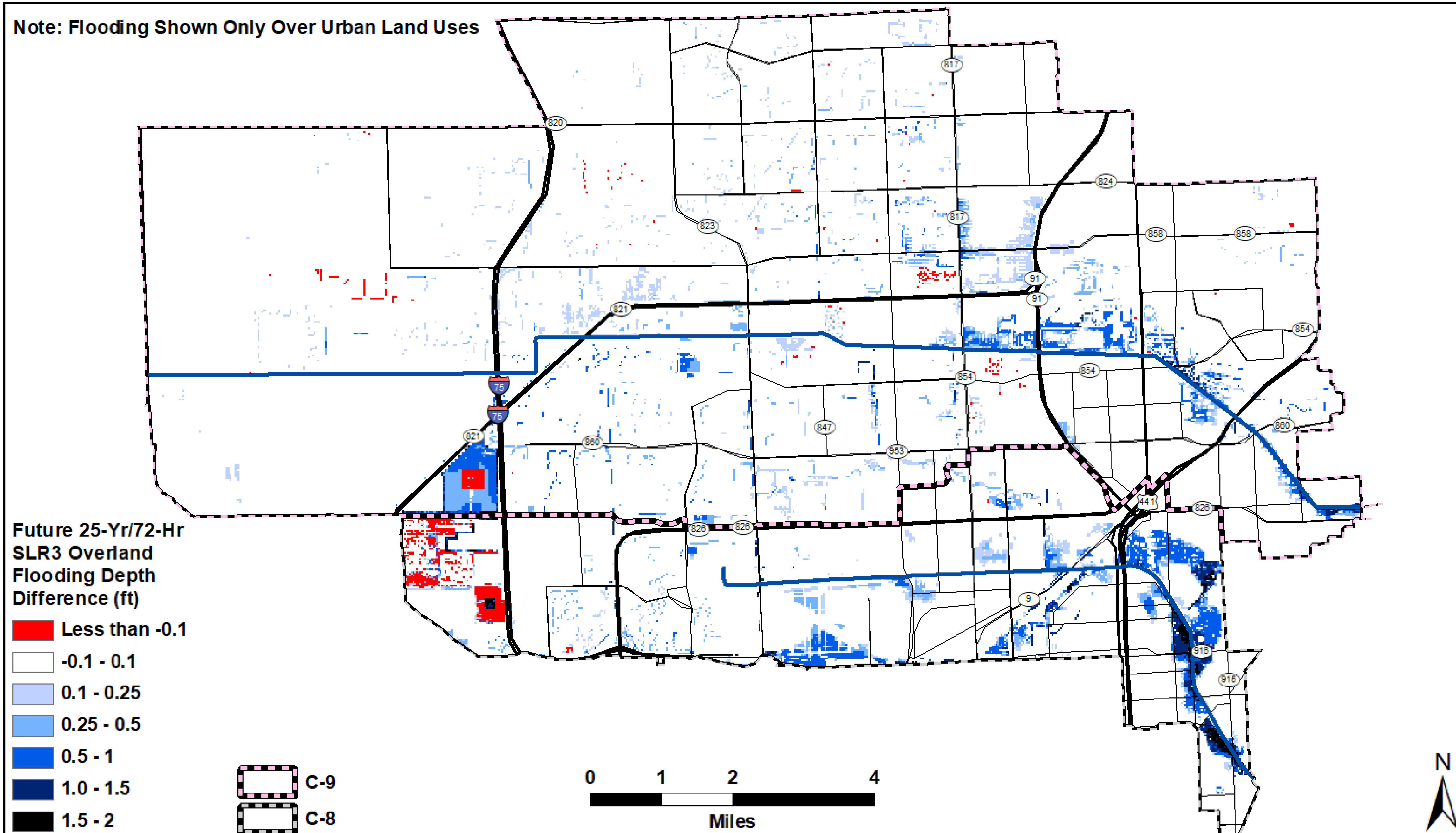

Figure 10.5-69: Flood Inundation Difference Map for 25-Year Sea Level Rise 3 Design Storm Event in Urban Land Use Areas (Future minus Current Conditions)

10.6 PM #6 – Duration of Flooding

For PM #6, the duration of flooding maps were developed by estimating the duration over which water depth exceeds a given threshold value. In this study, the duration of overland flooding was estimated using model simulated water depths and a threshold flooding depth of 0.25 ft. Additionally, the duration of flooding in the District Canals were estimated as the amount of time it takes for the water levels to return to target stage. The target stages of 3.6 ft for S-28Z and 3.5 ft for S-29Z were provided by the District (Email from Hongying Zhao, 5/12/2020). **Table 10-34** shows the duration of time taken for the water level in the C-8 and C-9 Canal to return to target stage, based on the first instance. For the 2 ft and 3 ft sea level rise scenarios, the C-8 and C-9 Canals do not return to target stage during the model simulation period if based upon the crest of the tidal signal. As shown in Table 10-34, even the lowest portion the tidal cycle is higher than target stage for the 3 ft sea level rise scenario.

Table 10-34: Duration for Water Levels to Return to Target Stage

Design Storm	Duration for S-28Z Return to Target Stage (hr)				Duration for S-29Z Return to Target Stage (hr)			
	5-Year	10-Year	25-Year	100-Year	5-Year	10-Year	25-Year	100-Year
Current	27	40	95	140	55	92	158	242
SLR1	44	60	128	181	60	98	182	247
SLR2	163	217	255	N/A	245	279	N/A	N/A
SLR3	N/A	N/A	N/A	N/A	N/A	N/A	N/A	N/A

N/A means that the stage did not return to target stage within the model simulation period

The duration of overland flooding was estimated for all four design storm events based on the length of time the flood depth was predicted to exceed the threshold value (0.25 ft) within each MIKE SHE 125-ft grid cell using the statistics tool in MIKE ZERO. The flood duration maps for each of the design storm events are shown in **Figure 10.6-1** through **Figure 10.6-12**.

Based on model simulations, large areas were inundated for over 72 hours, even for the 5-year sea level rise 1 design storm (**Figure 10.6-1**). These areas are comprised primarily of lakes and wetlands and other low-lying undeveloped areas. An increase in flooding extent and duration was observed as the magnitude of the design storms increased. Additionally, an increase in flooding extent and duration was observed as the magnitude of sea level rise increased, even across the same return period design storm. A vast majority of the watershed was inundated for at least a small duration during the 100-year SLR1 design storm, with notable increases for the 100-year SLR3 storm. Developed areas with the largest flood duration generally tend to coincide with the highest depths of flooding determined from PM#5. **Figure 10.6-13** through **Figure 10.6-24** show the flood duration maps for each of the design storm and sea level rise scenario for urban areas only. **Figure 10.6-25** through **Figure 10.6-42** show up-close examples of flood duration along the C-8 Canal and **Figure 10.6-43** through **Figure 10.6-66** show up-close examples of flood duration along the C-9 Canal. **Figure 10.6-67** through **Figure 10.6-69** show the maximum flood duration difference between future and current conditions for the 25-Year SLR1, SLR2 and SLR3 design storm events.

10.6.1 5-Year Design Storm Model-Wide Flood Duration Map

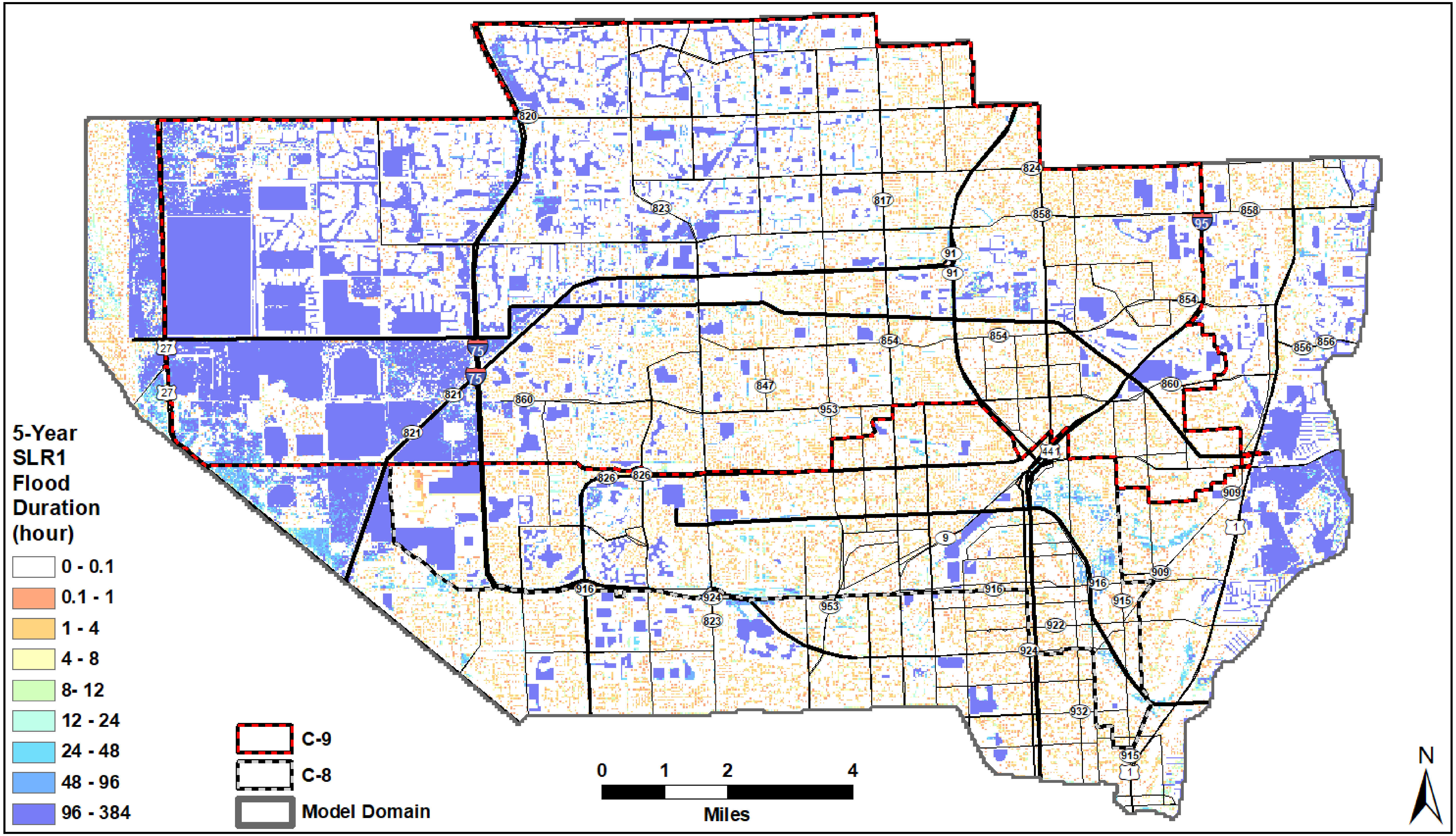

Figure 10.6-1: Flood Duration Map for 5-Year Sea Level Rise 1 Design Storm Event

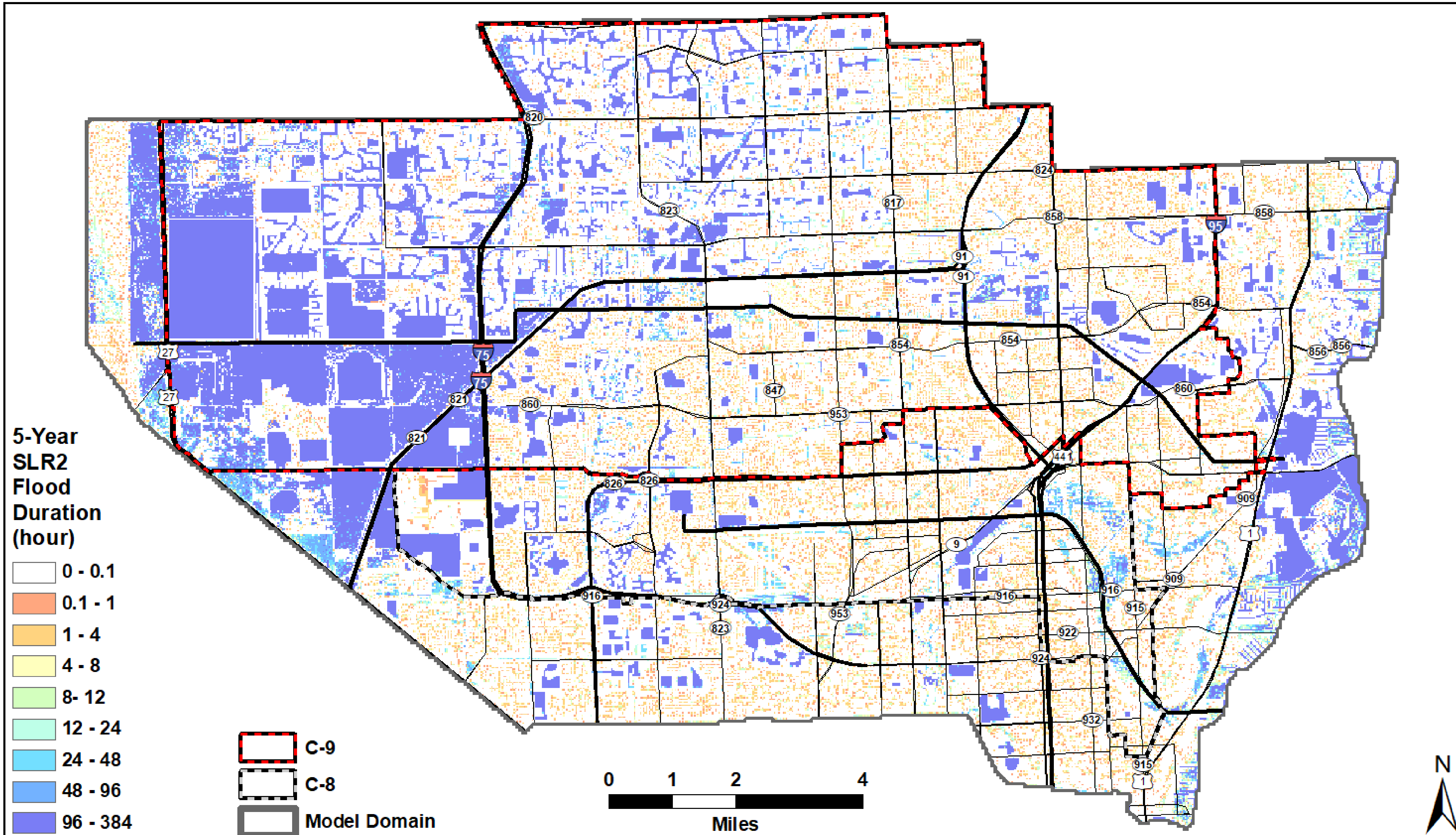

Figure 10.6-2: Flood Duration Map for 5-Year Sea Level Rise 2 Design Storm Event

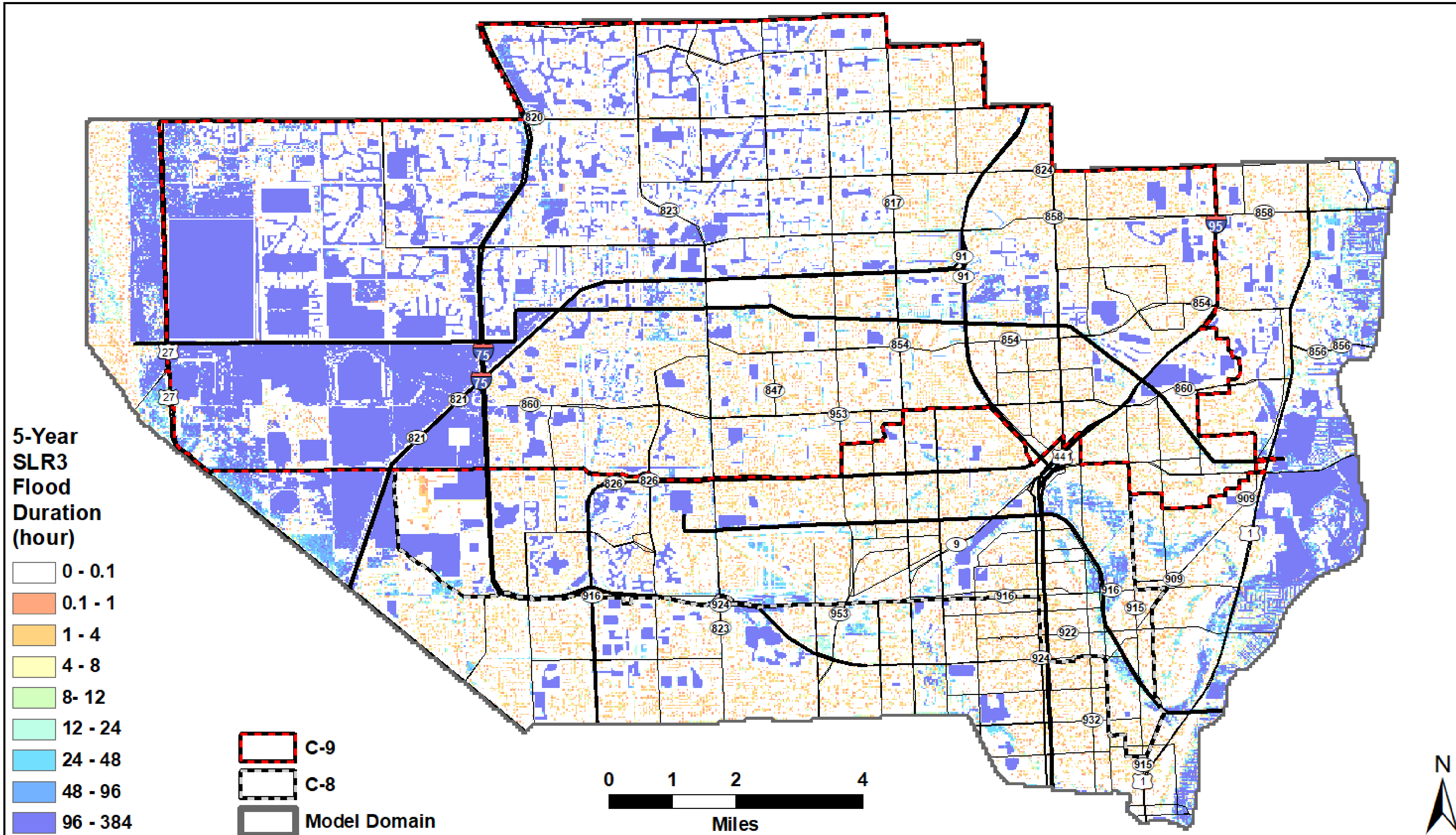

Figure 10.6-3: Flood Duration Map for 5-Year Sea Level Rise 3 Design Storm Event

10.6.2 10-Year Design Storm Model-Wide Flood Duration Map

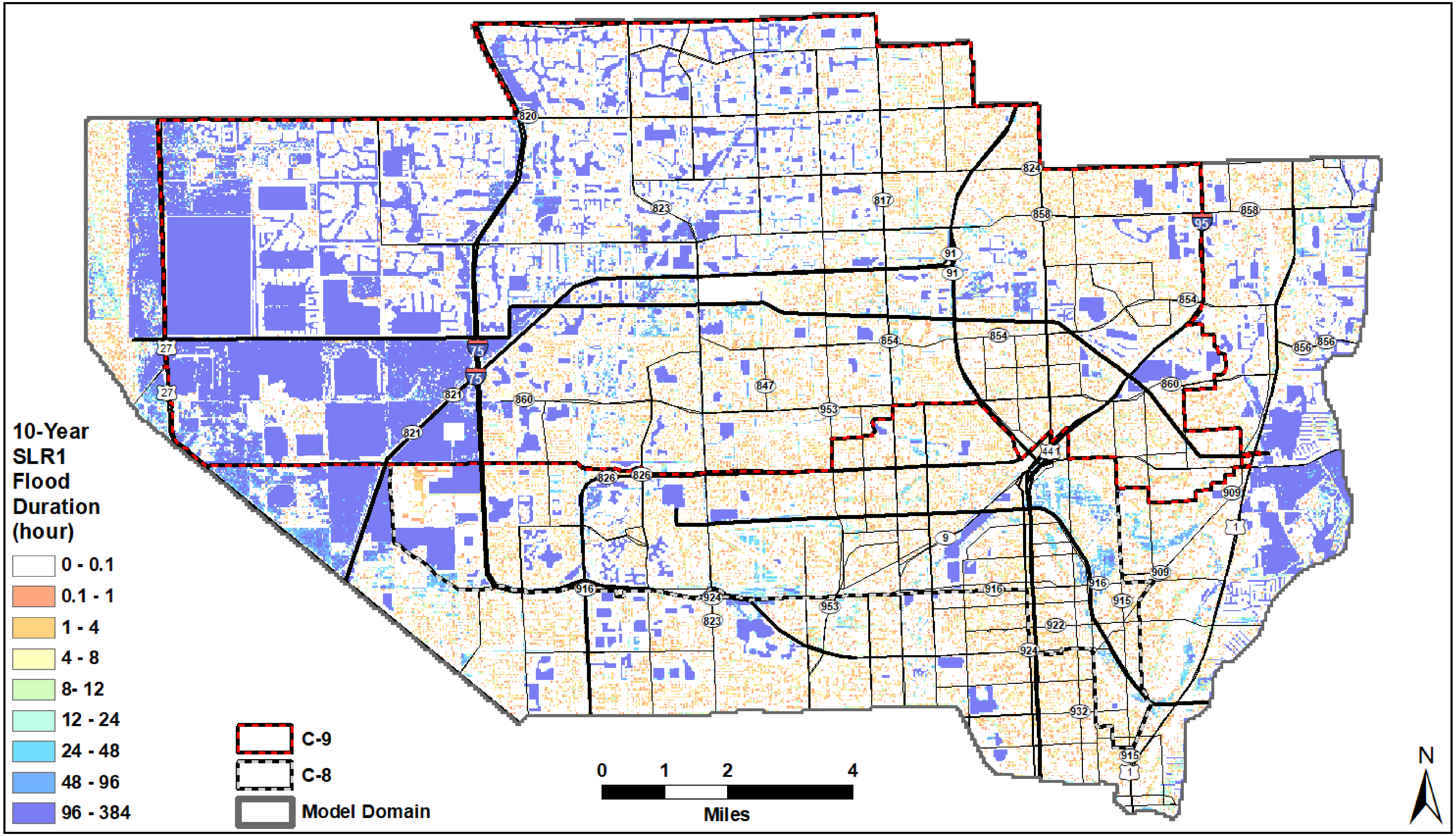

Figure 10.6-4: Flood Duration Map for 10-Year Sea Level Rise 1 Design Storm Event

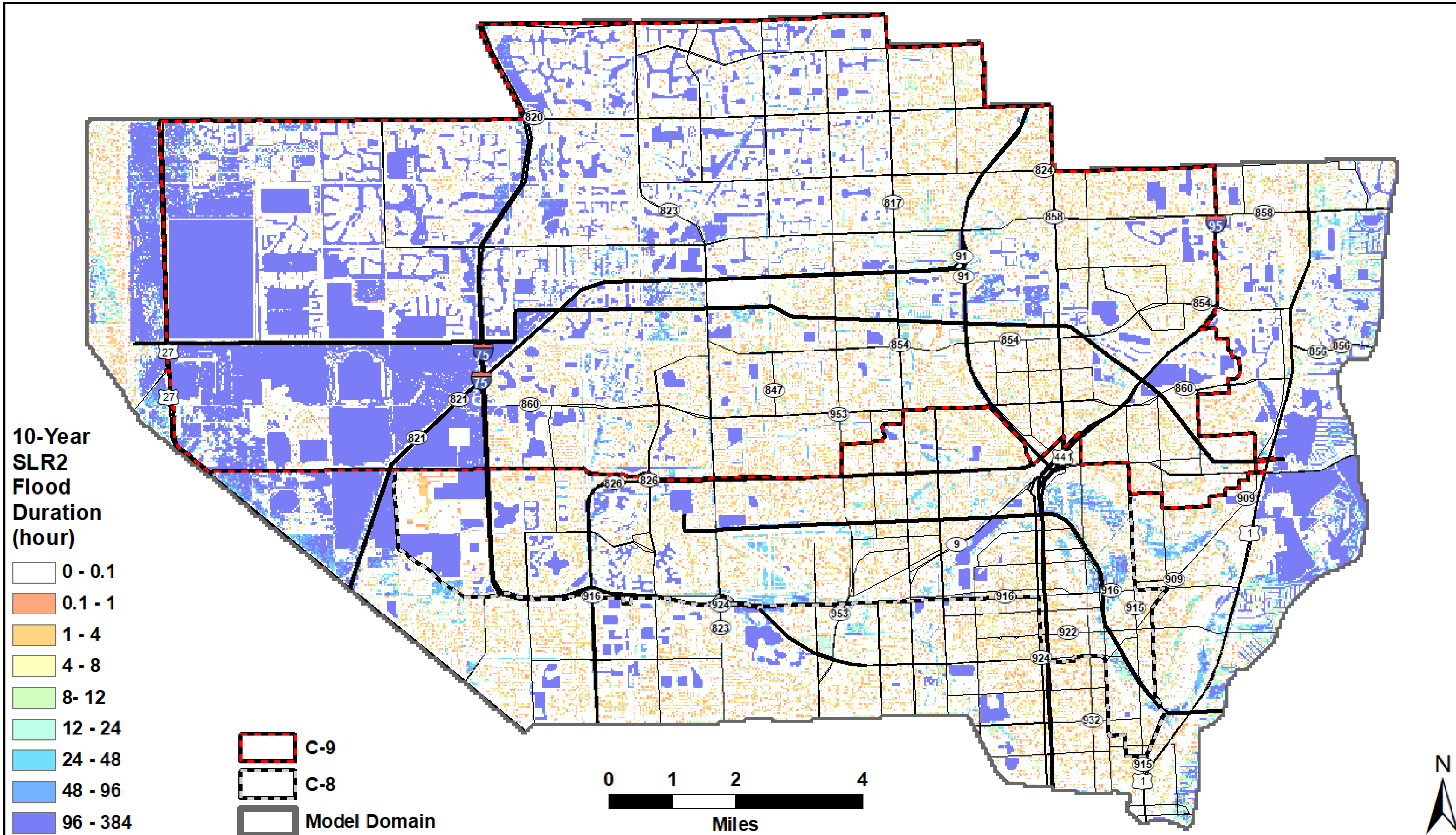

Figure 10.6-5: Flood Duration Map for 10-Year Sea Level Rise 2 Design Storm Event

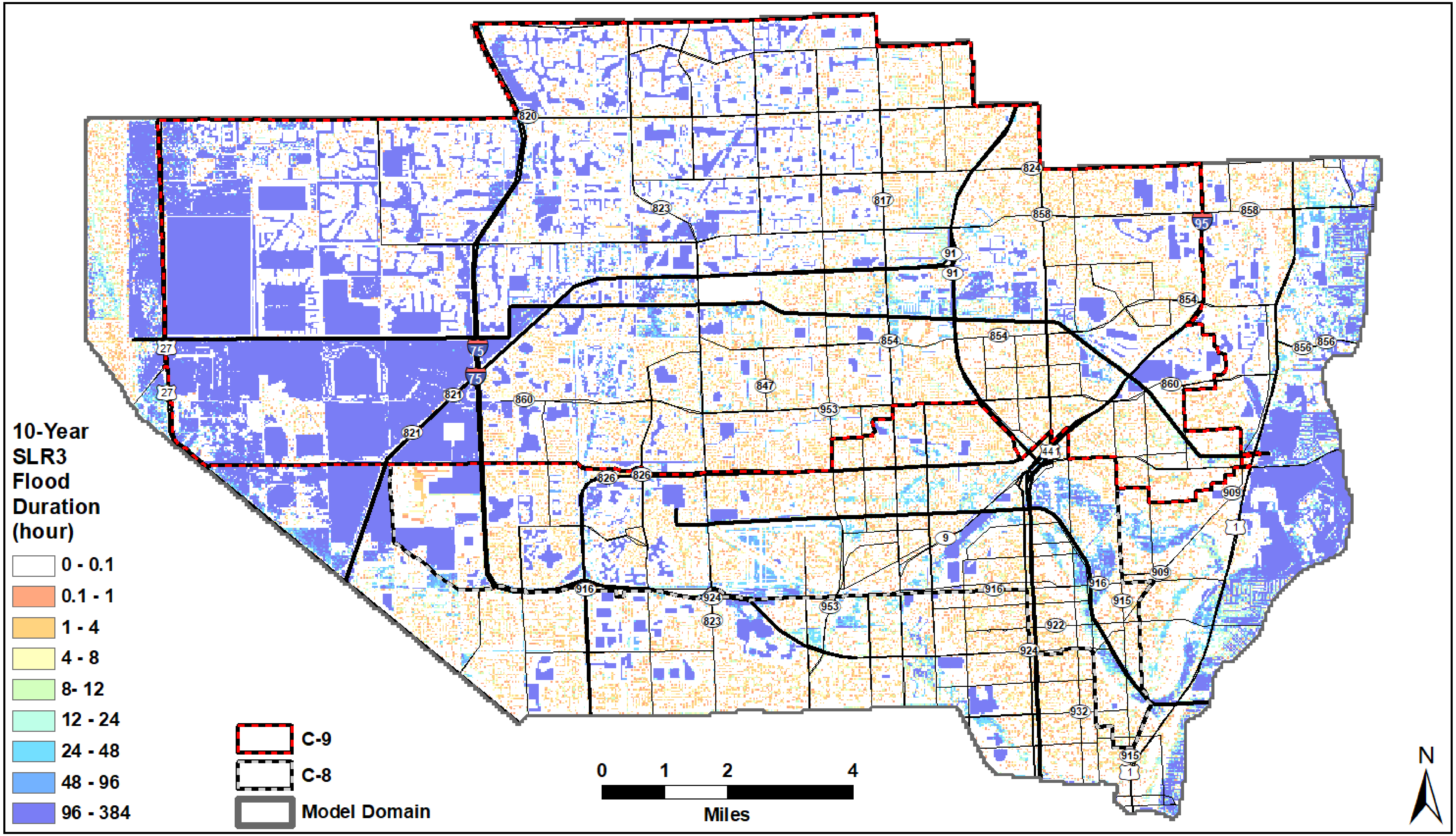

Figure 10.6-6: Flood Duration Map for 10-Year Sea Level Rise 3 Design Storm Event

10.6.3 25-Year Design Storm Model-Wide Flood Duration Map

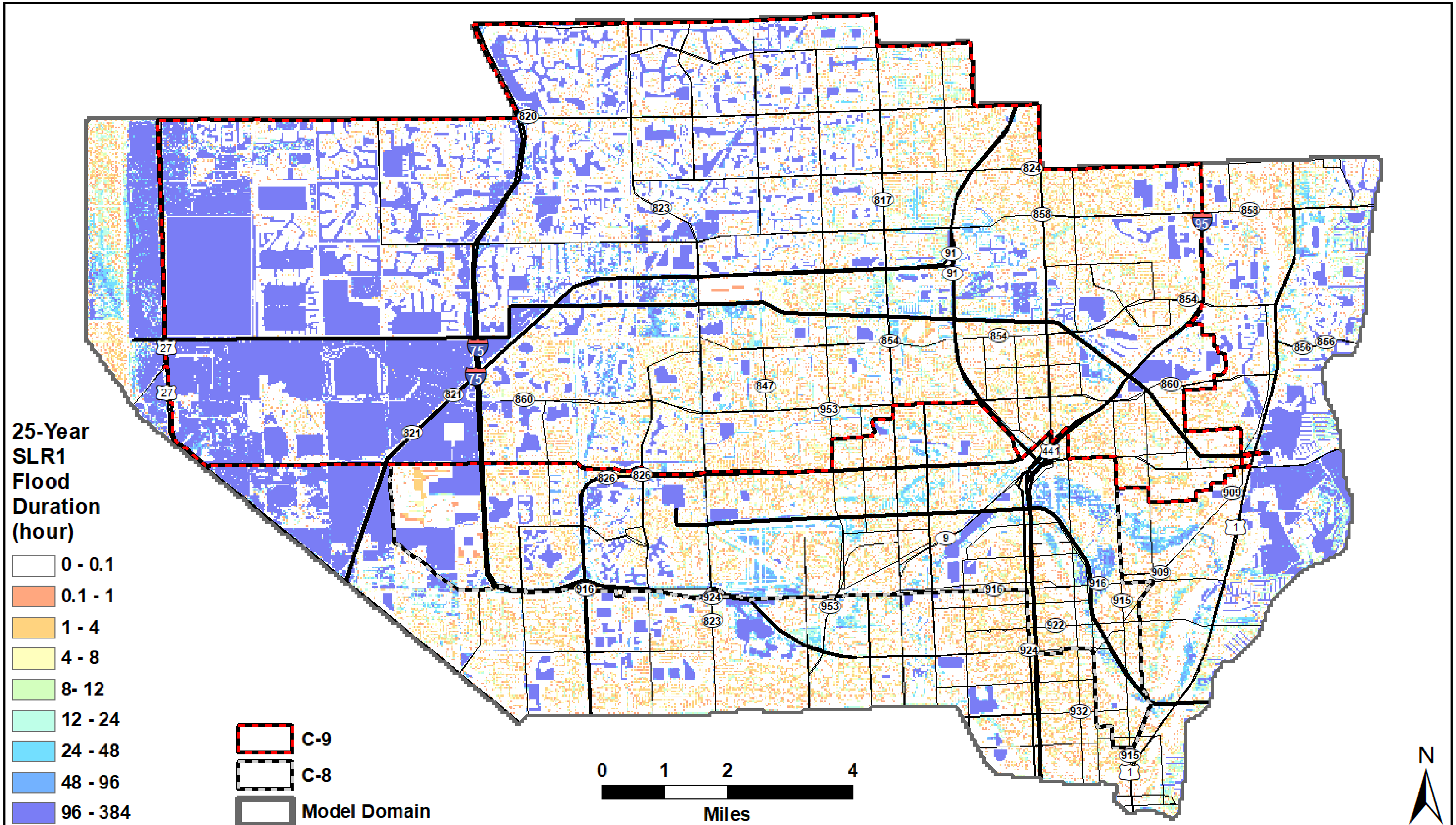

Figure 10.6-7: Flood Duration Map for 25-Year Sea Level Rise 1 Design Storm Event

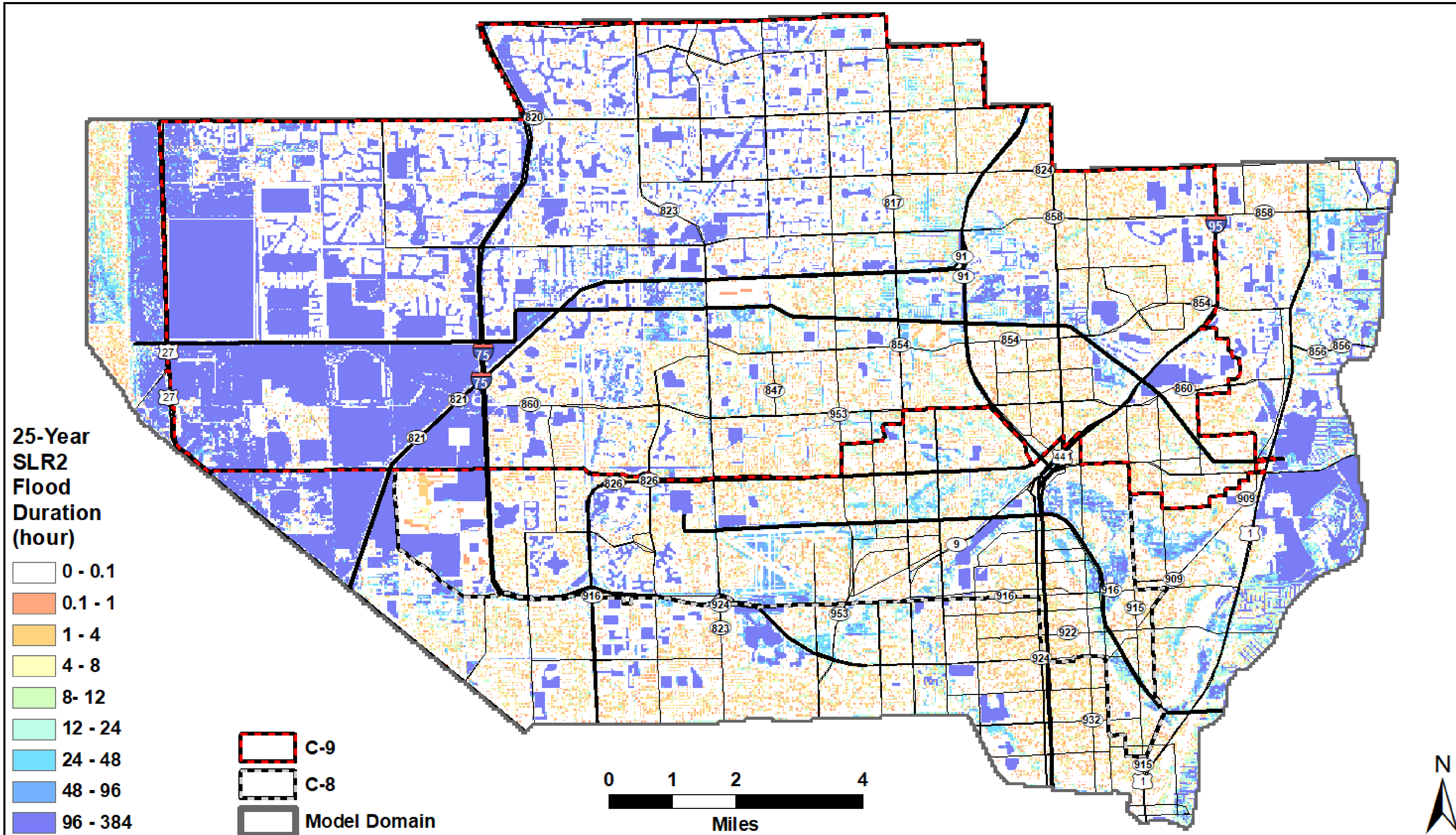

Figure 10.6-8: Flood Duration Map for 25-Year Sea Level Rise 2 Design Storm Event

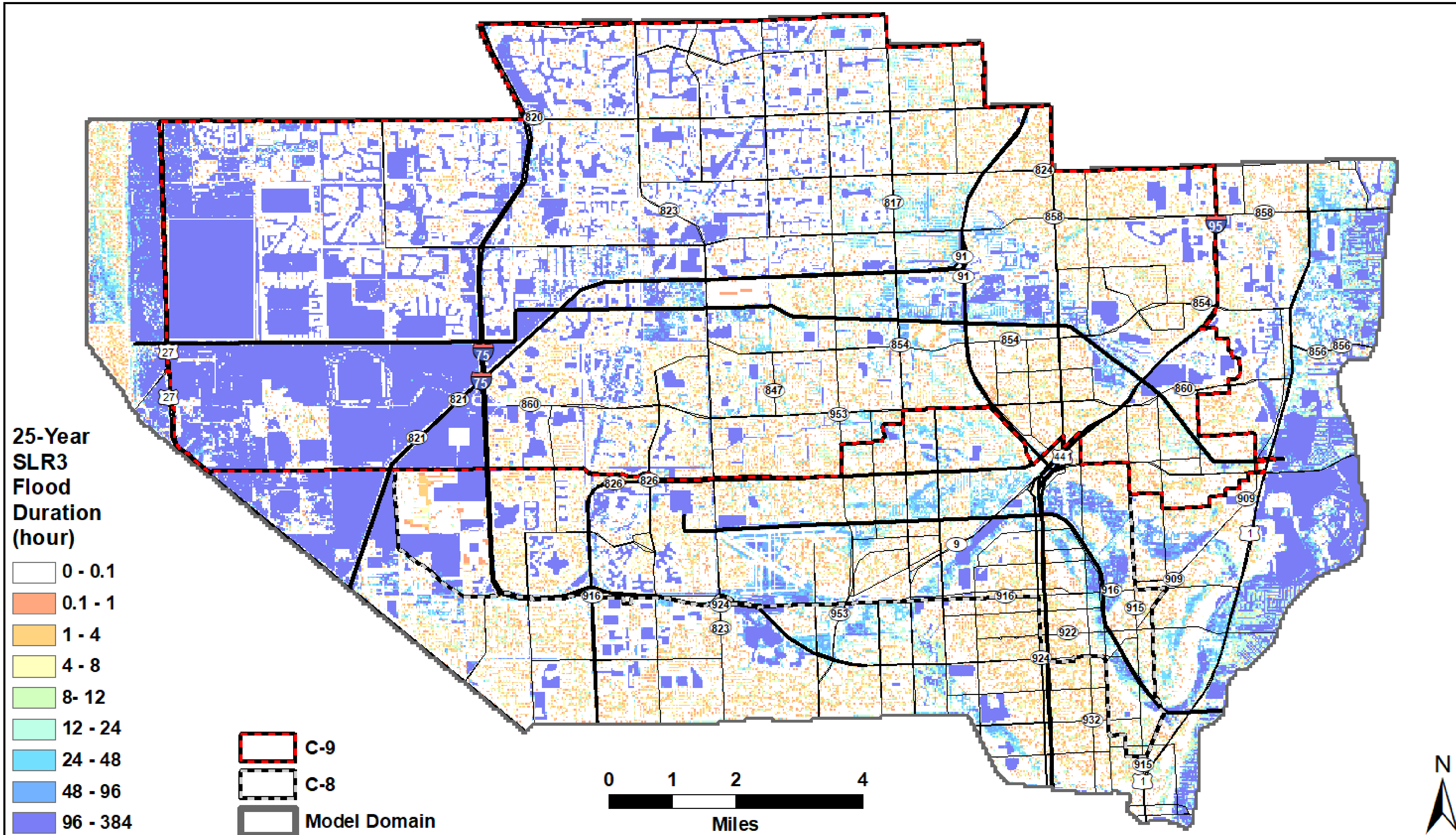

Figure 10.6-9: Flood Duration Map for 25-Year Sea Level Rise 3 Design Storm Event

10.6.4 100-Year Design Storm Model-Wide Flood Duration Map

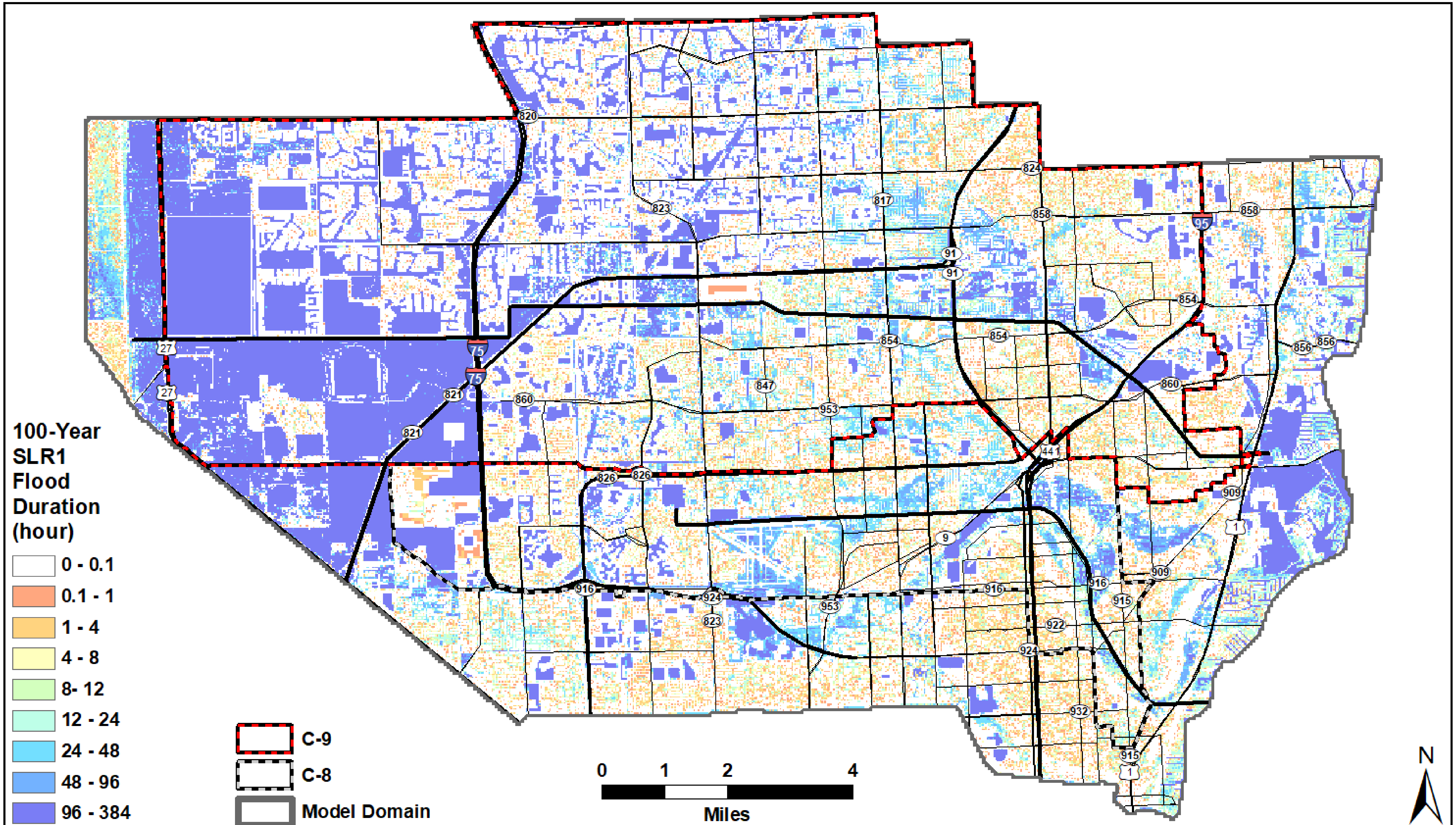

Figure 10.6-10: Flood Duration Map for 100-Year Sea Level Rise 1 Design Storm Event

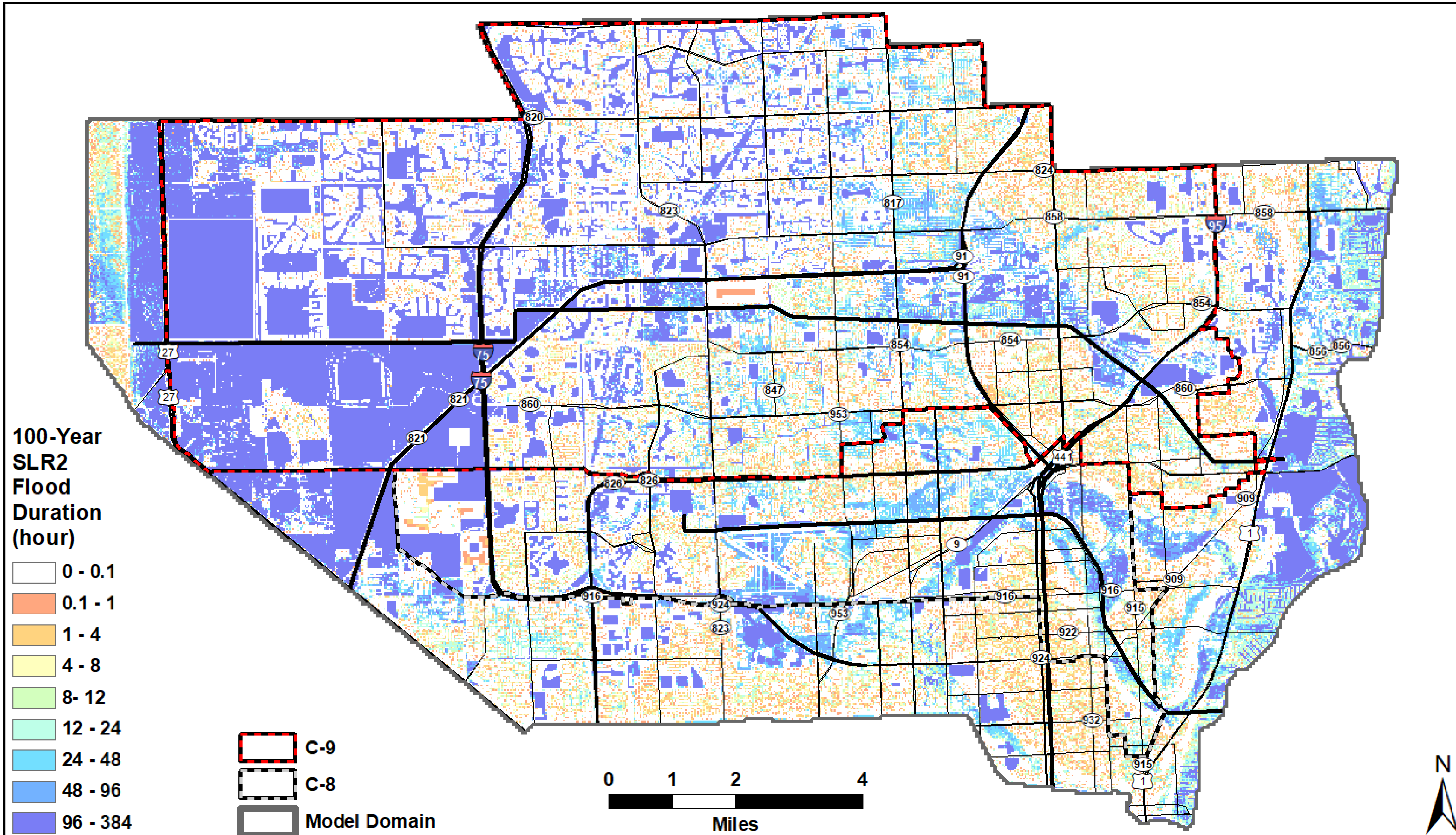

Figure 10.6-11: Flood Duration Map for 100-Year Sea Level Rise 2 Design Storm Event

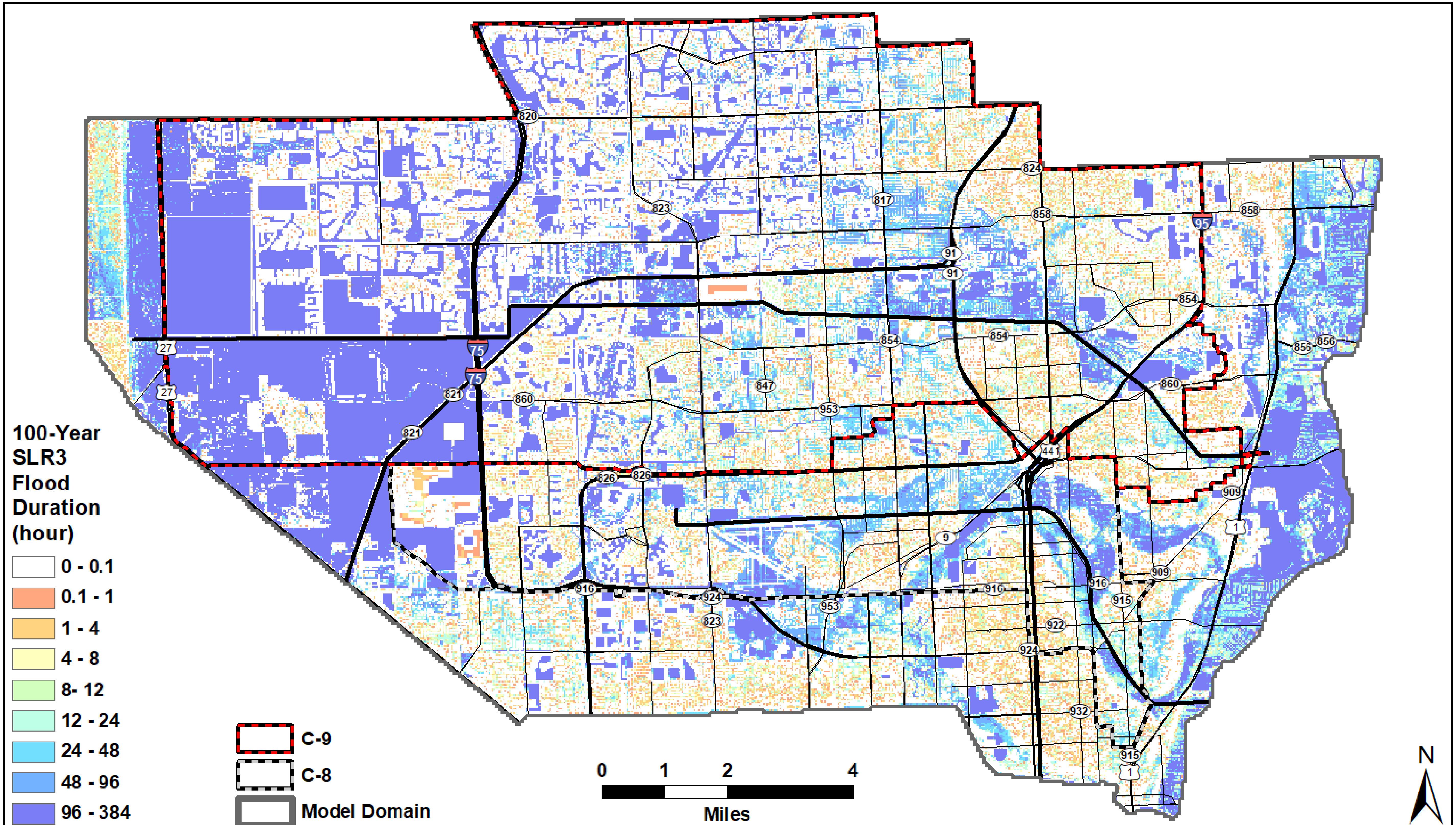

Figure 10.6-12: Flood Duration Map for 100-Year Sea Level Rise 3 Design Storm Event

10.6.5 5-Year Design Storm Flood Duration Map for Urban Land Use Areas

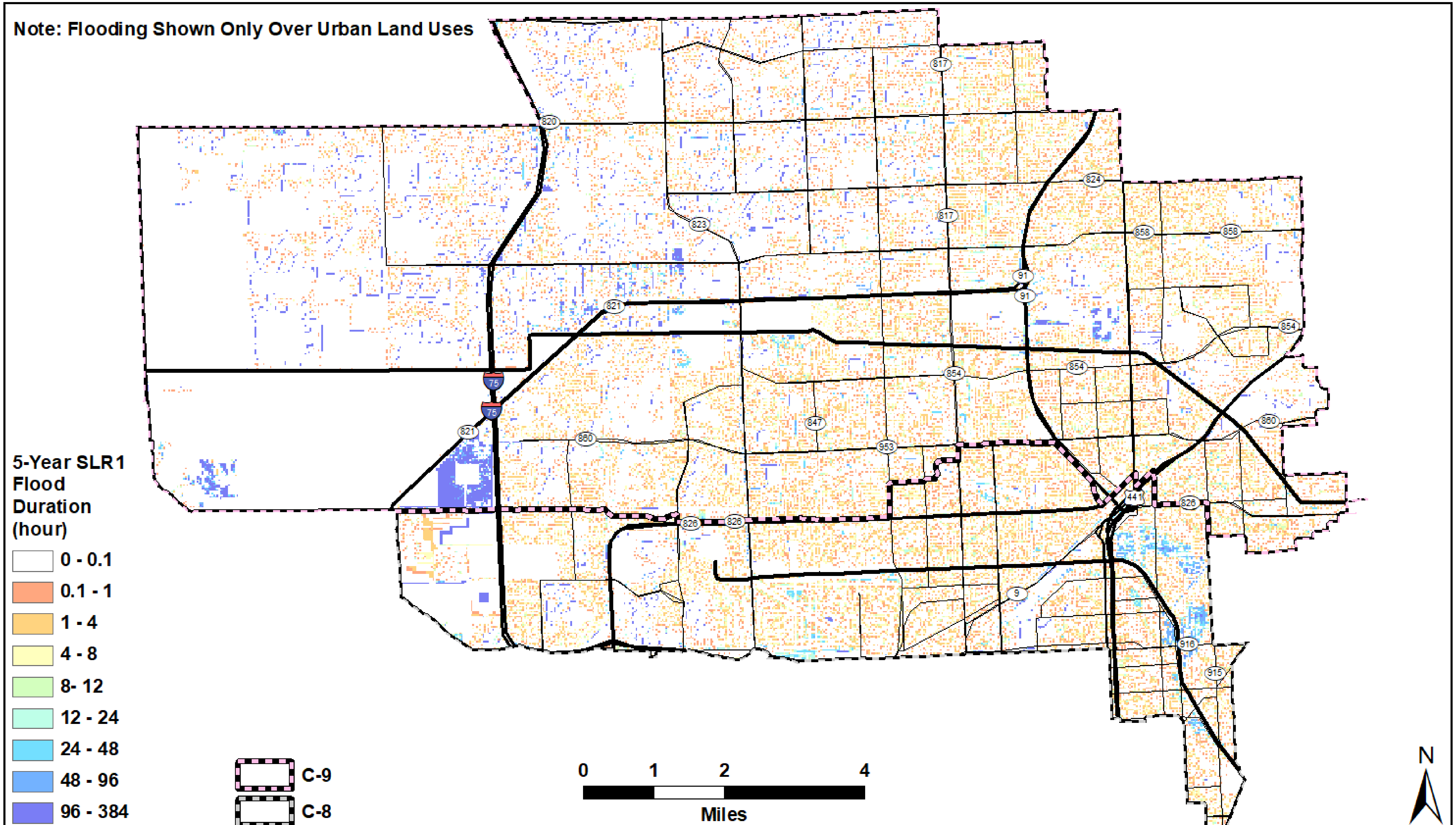

Figure 10.6-13: Flood Duration Map for 5-Year Sea Level Rise 1 Design Storm Event in Urban Land Use Areas

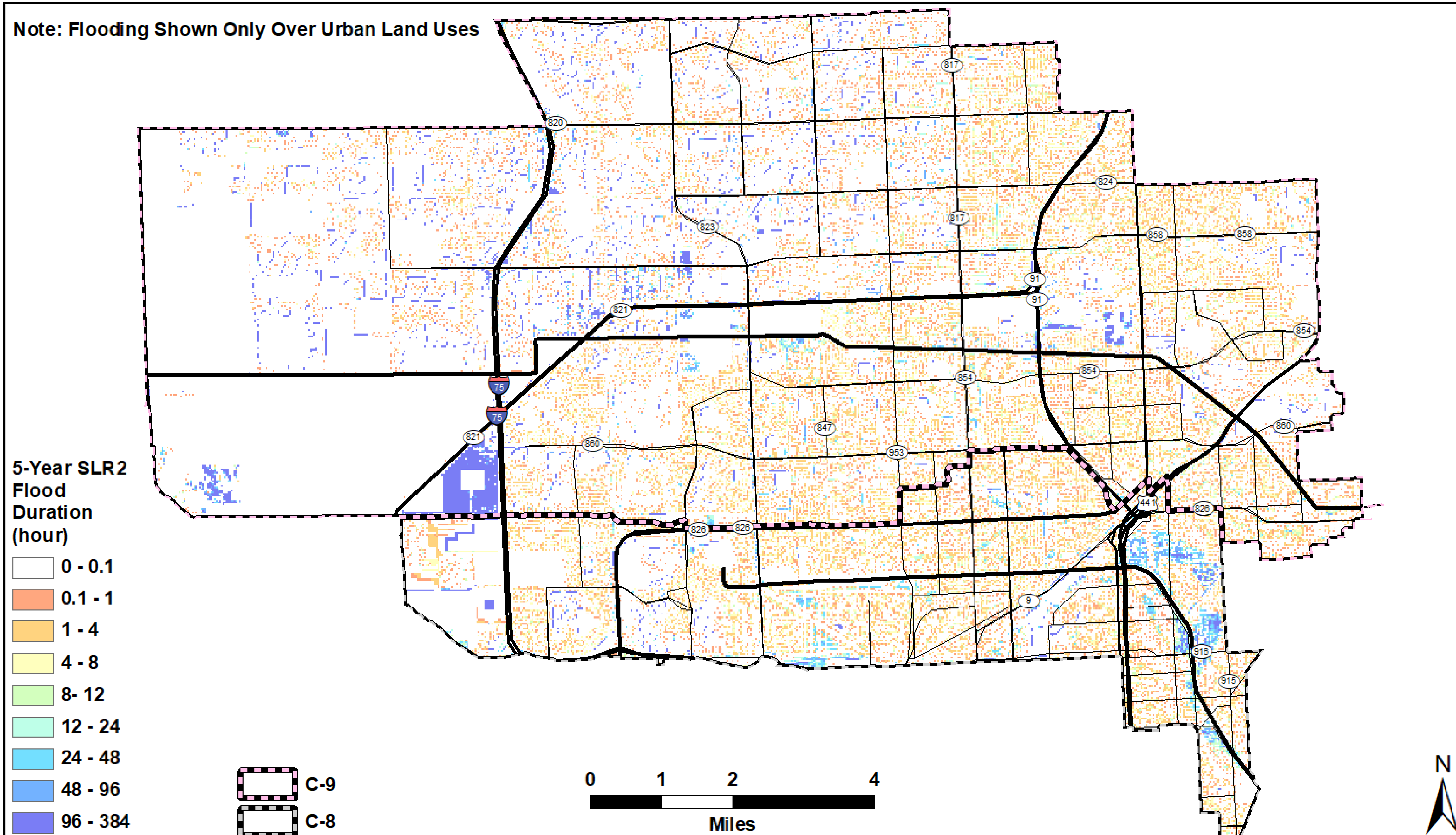

Figure 10.6-14: Flood Duration Map for 5-Year Sea Level Rise 2 Design Storm Event in Urban Land Use Areas

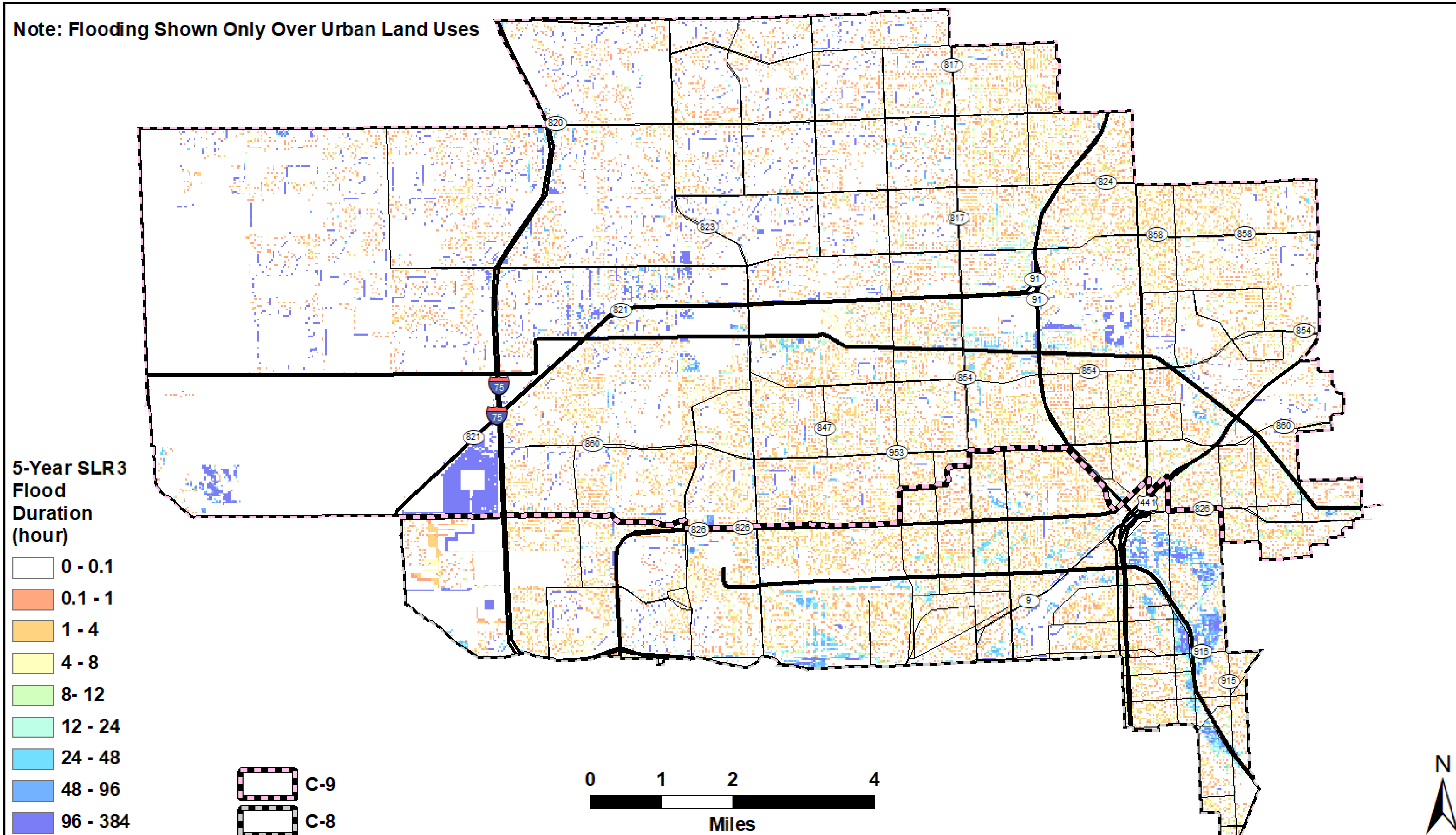

Figure 10.6-15: Flood Duration Map for 5-Year Sea Level Rise 3 Design Storm Event in Urban Land Use Areas

10.6.6 10-Year Design Storm Flood Duration Map for Urban Land Use Areas

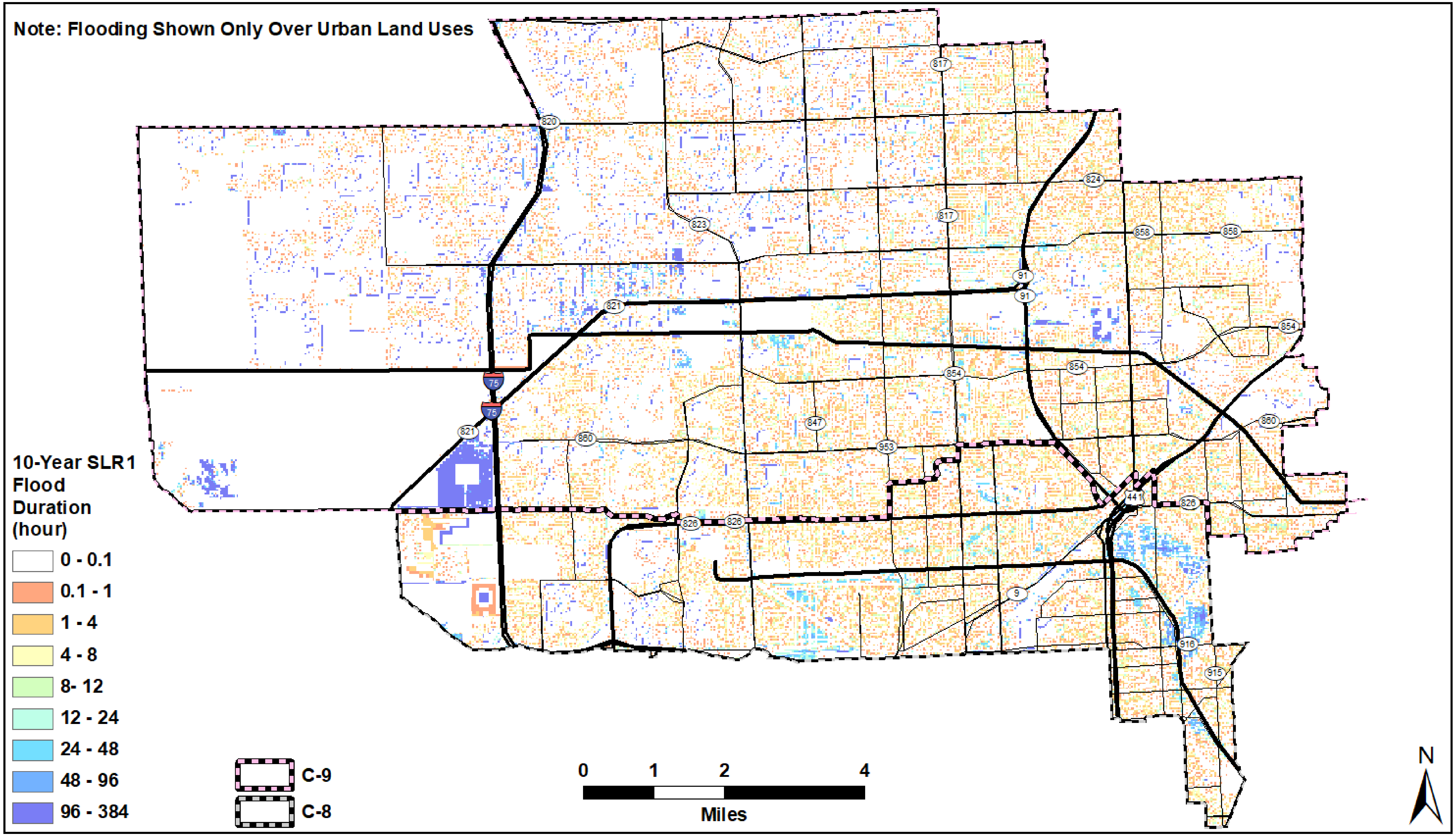

Figure 10.6-16: Flood Duration Map for 10-Year Sea Level Rise 1 Design Storm Event in Urban Land Use Areas

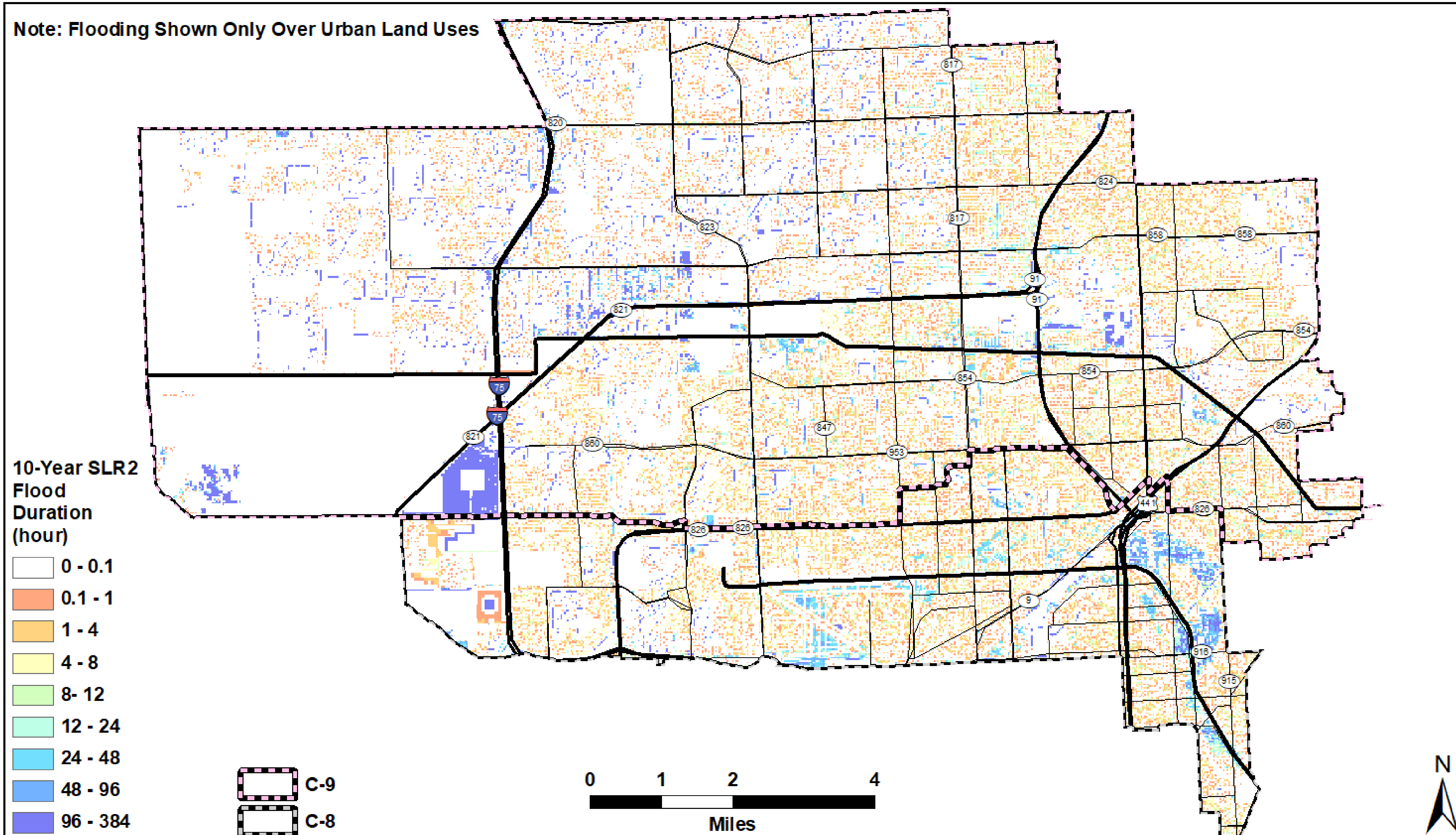

Figure 10.6-17: Flood Duration Map for 10-Year Sea Level Rise 2 Design Storm Event in Urban Land Use Areas

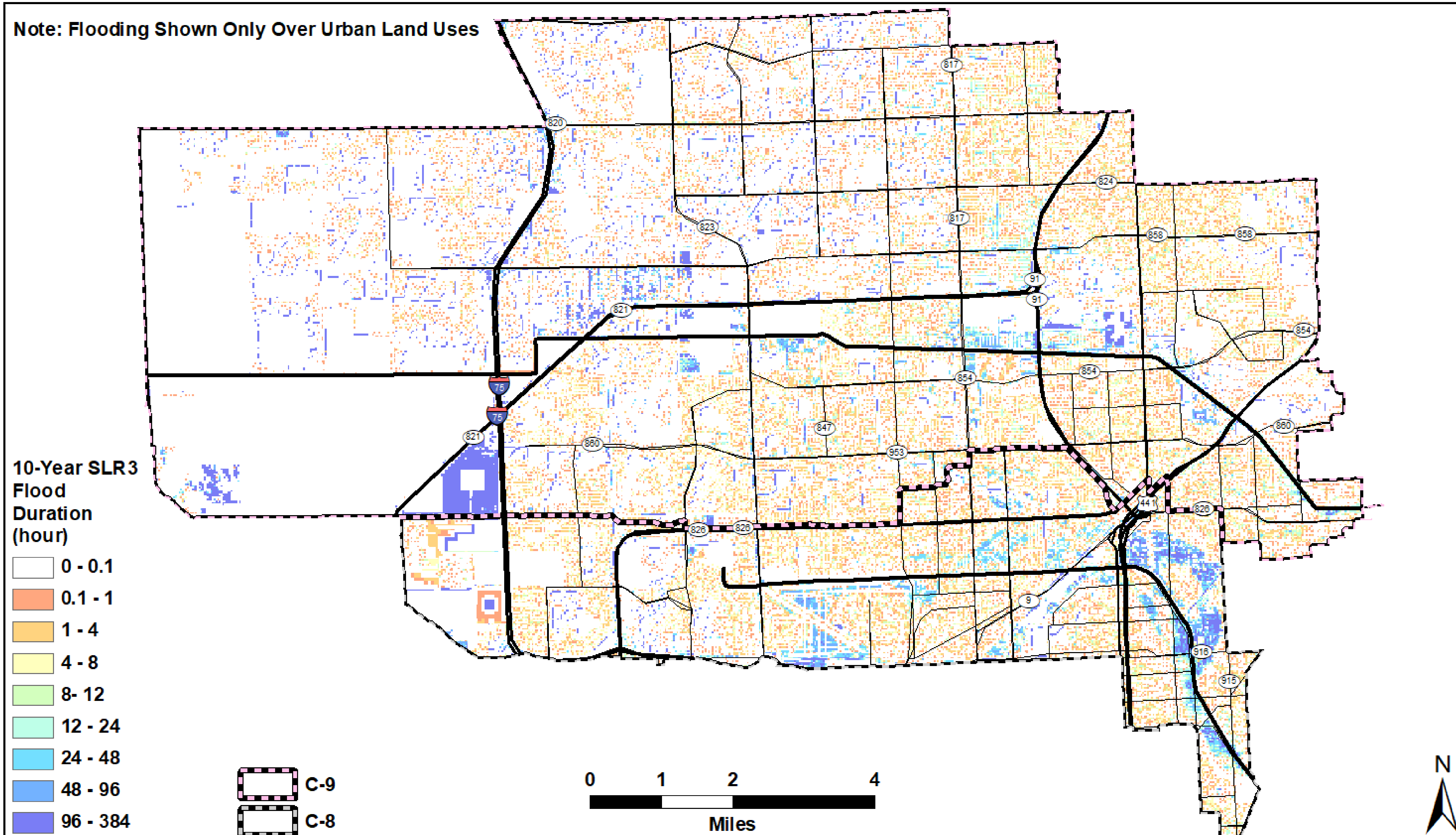

Figure 10.6-18: Flood Duration Map for 10-Year Sea Level Rise 3 Design Storm Event in Urban Land Use Areas

10.6.7 25-Year Design Storm Flood Duration Map for Urban Land Use Areas

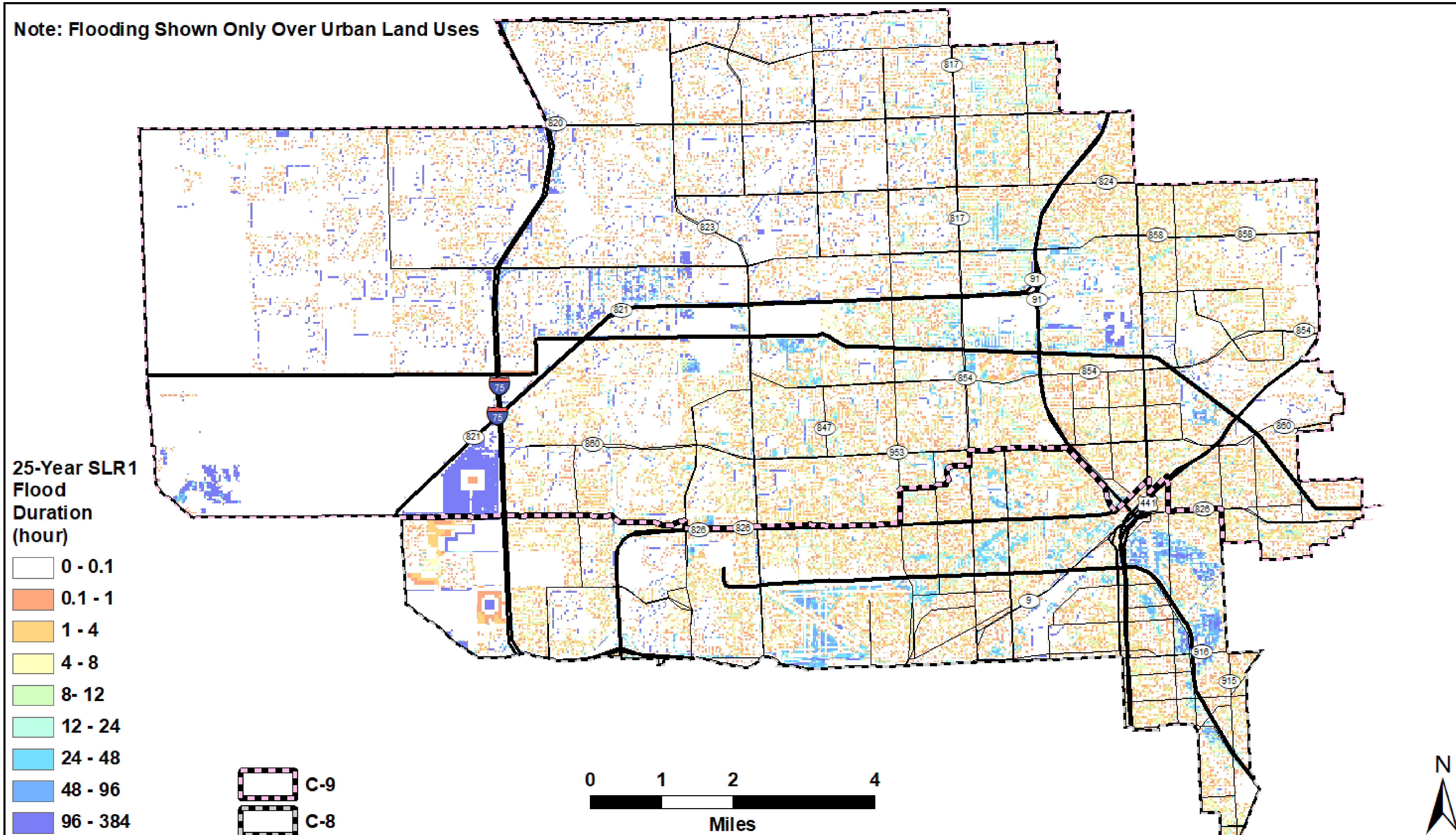

Figure 10.6-19: Flood Duration Map for 25-Year Sea Level Rise 1 Design Storm Event in Urban Land Use Areas

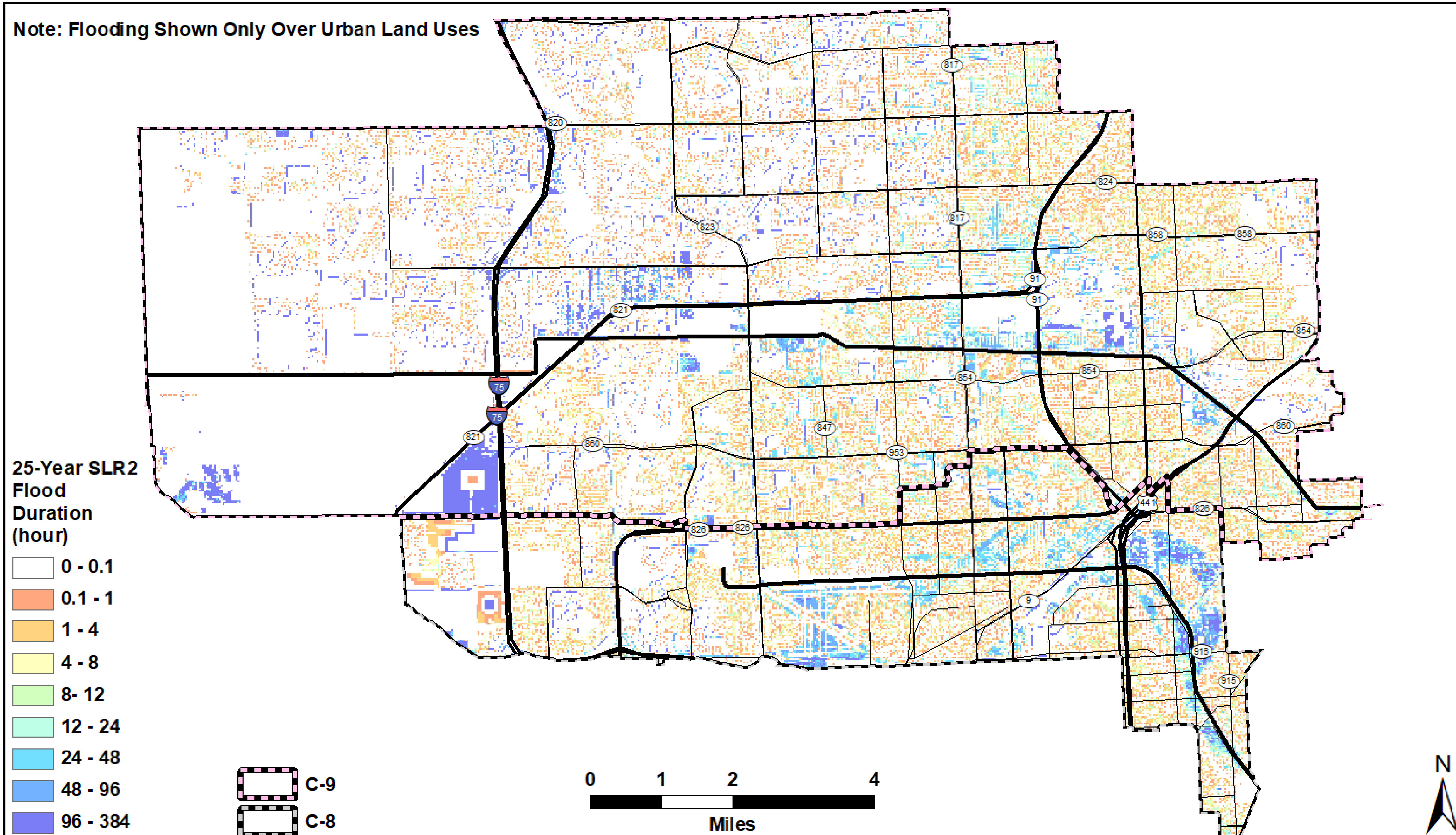

Figure 10.6-20: Flood Duration Map for 25-Year Sea Level Rise 2 Design Storm Event in Urban Land Use Areas

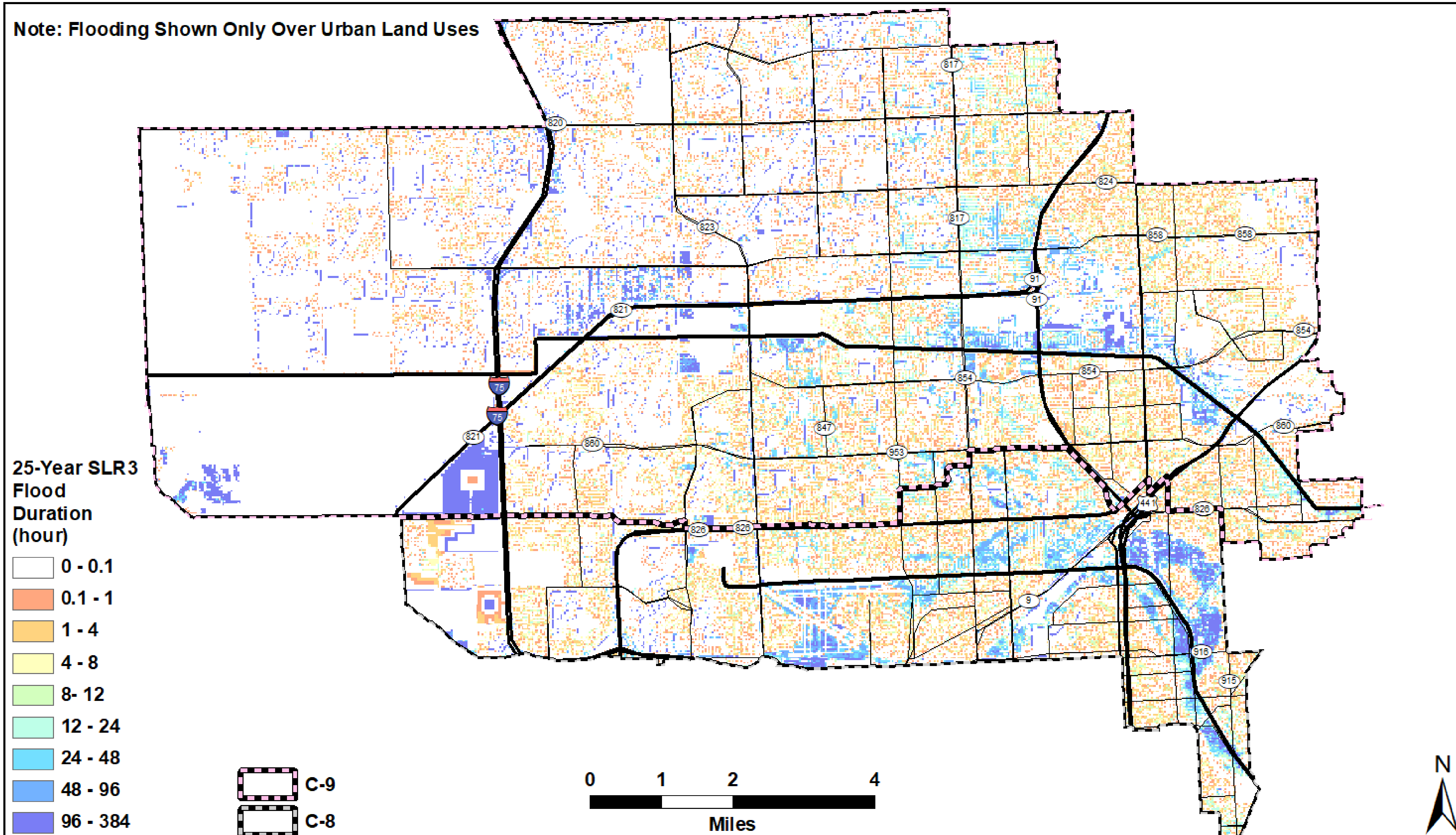

Figure 10.6-21: Flood Duration Map for 25-Year Sea Level Rise 3 Design Storm Event in Urban Land Use Areas

10.6.8 100-Year Design Storm Flood Duration Map for Urban Land Use Areas

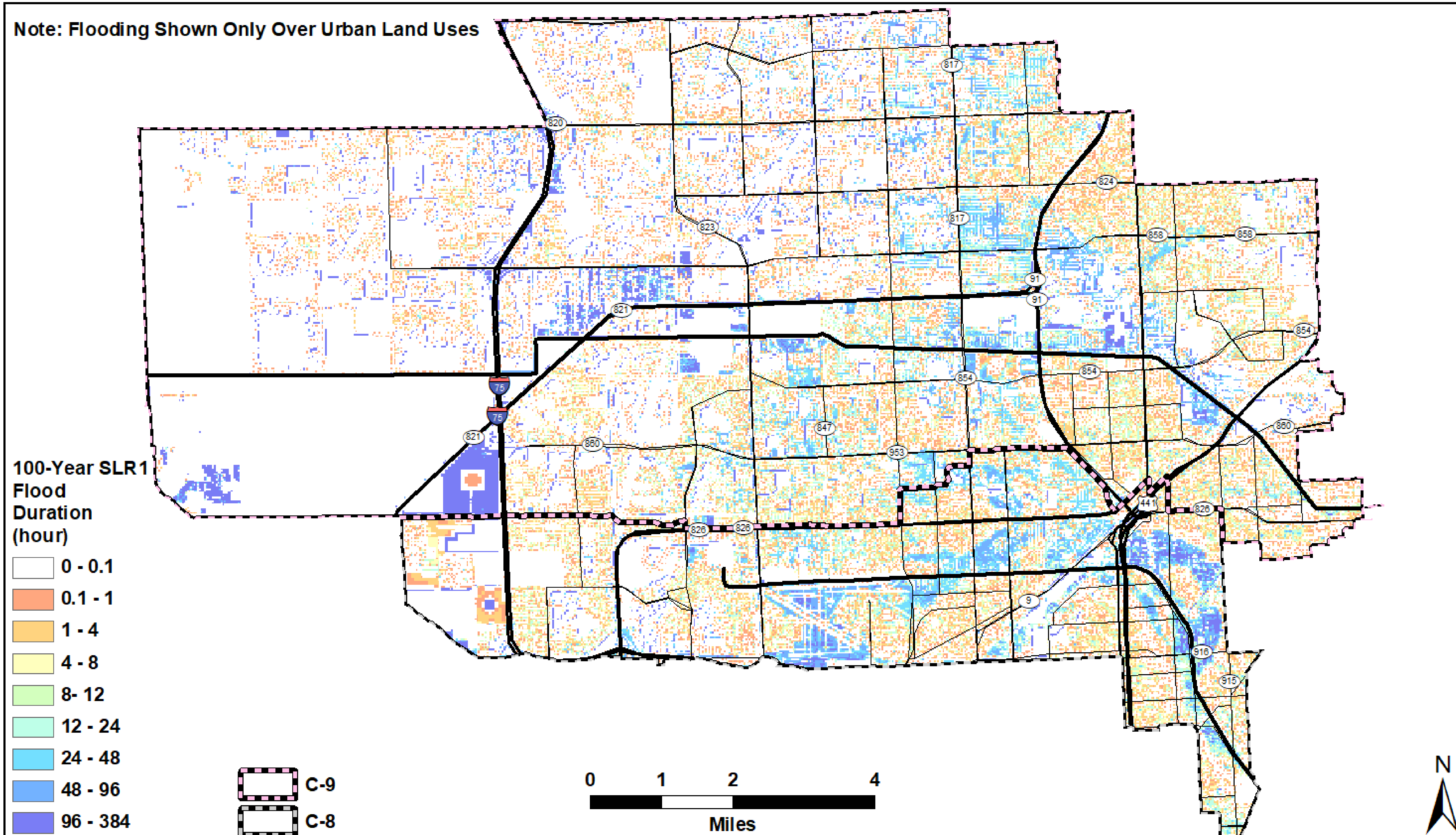

Figure 10.6-22: Flood Duration Map for 100-Year Sea Level Rise 1 Design Storm Event in Urban Land Use Areas

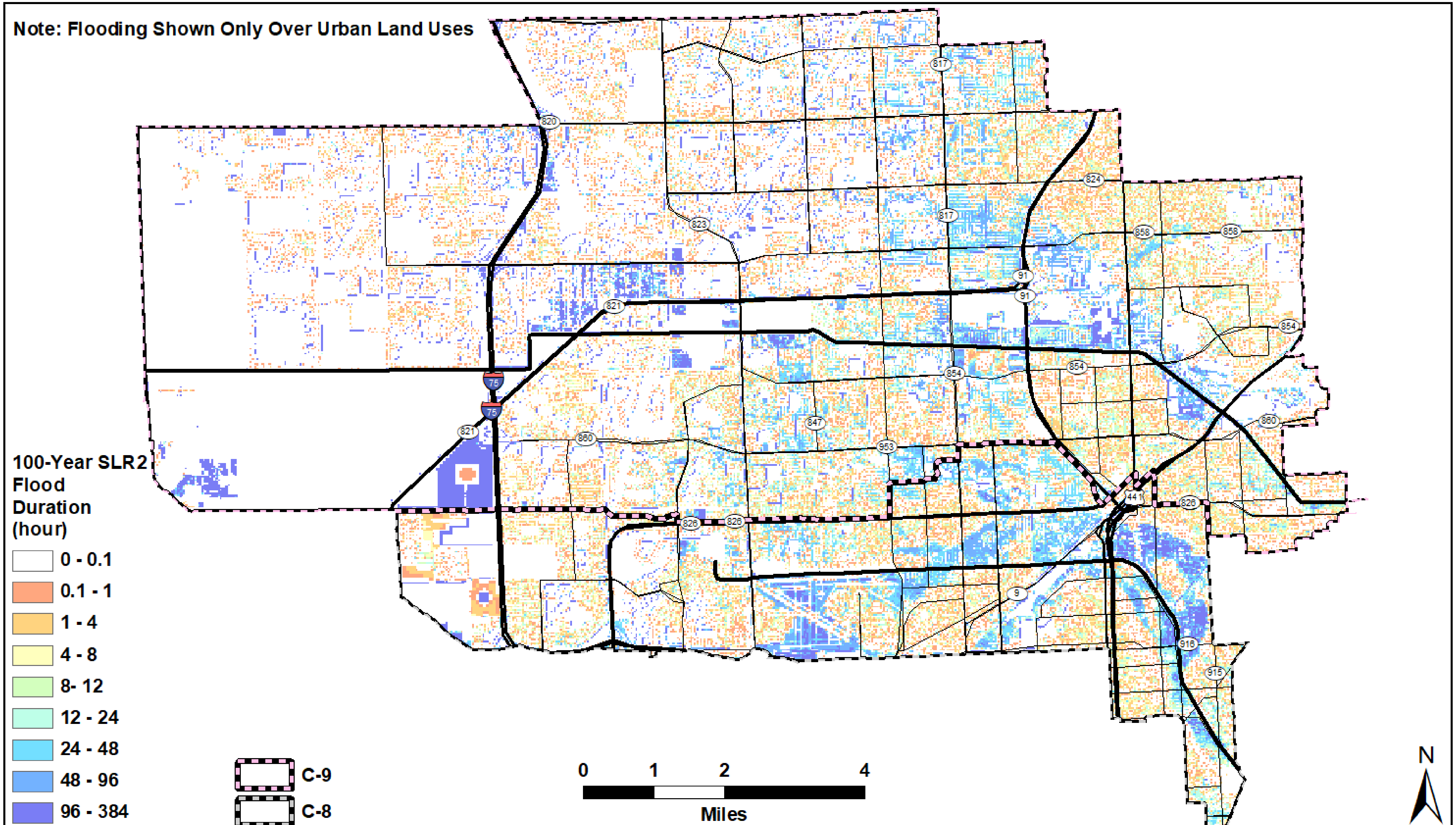

Figure 10.6-23: Flood Duration Map for 100-Year Sea Level Rise 2 Design Storm Event in Urban Land Use Areas

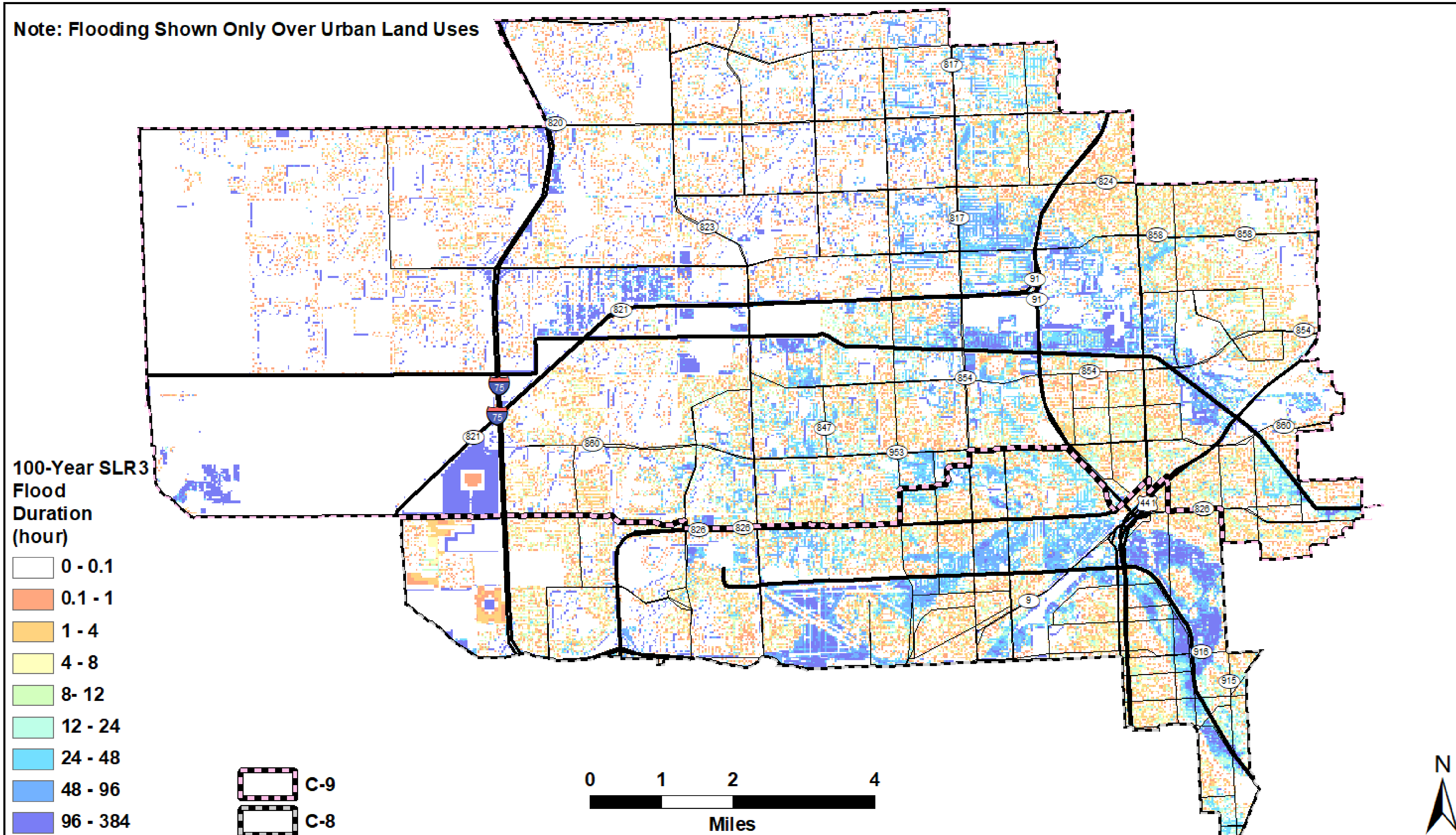

Figure 10.6-24: Flood Duration Map for 100-Year Sea Level Rise 3 Design Storm Event in Urban Land Use Areas

10.6.9 Up-Close Flood Duration Maps

10.6.9.1 Up-Close Flood Duration Maps for the C-8 Canal Between NE 135th St (CR916) and NE 6th Ave (CR915)

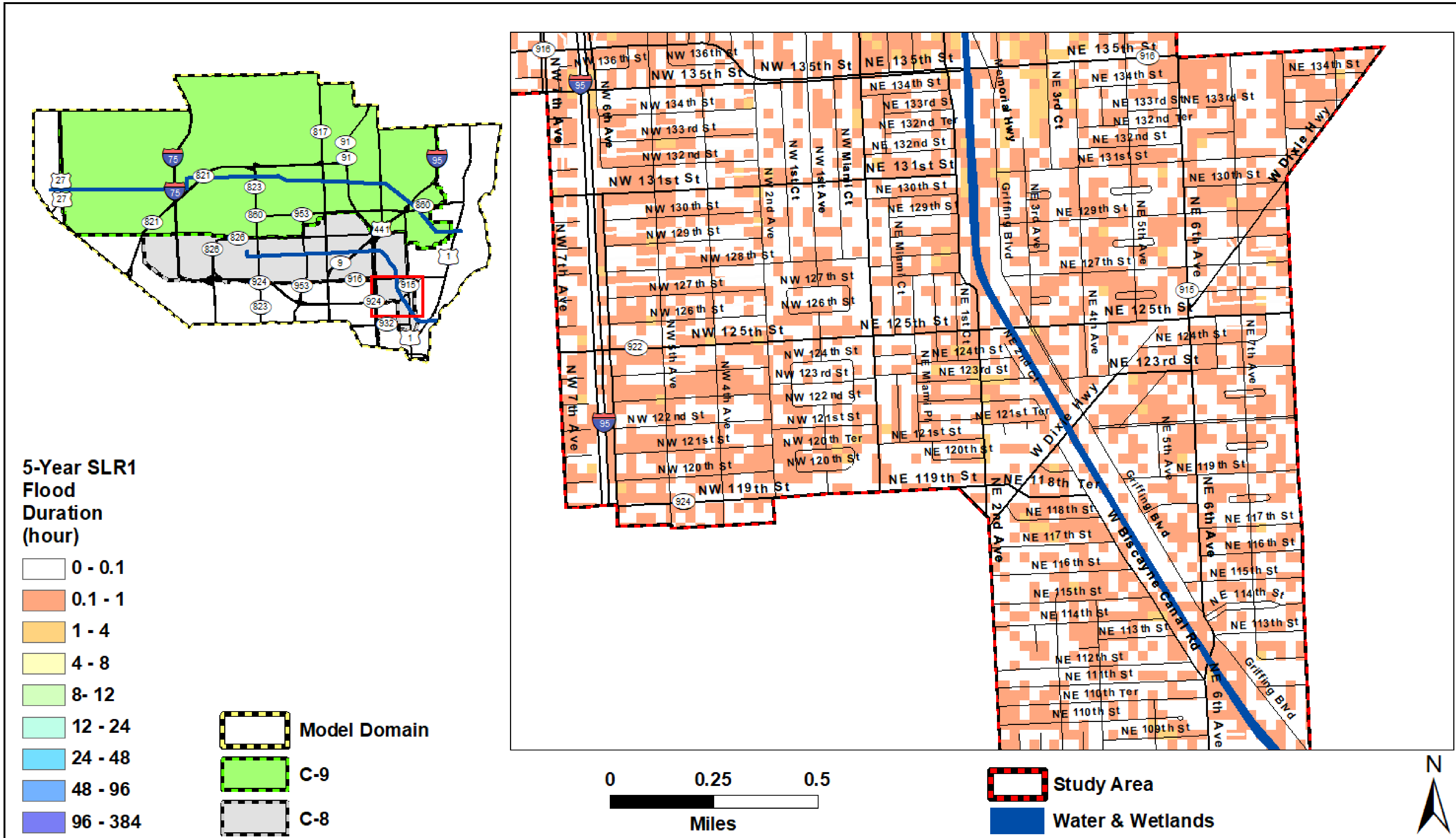

Figure 10.6-25: Up Close 5-Year Sea Level Rise 1 Flood Duration Map for the C-8 Canal Between and NE 135th St (CR916) and NE 6th Ave (CR915)

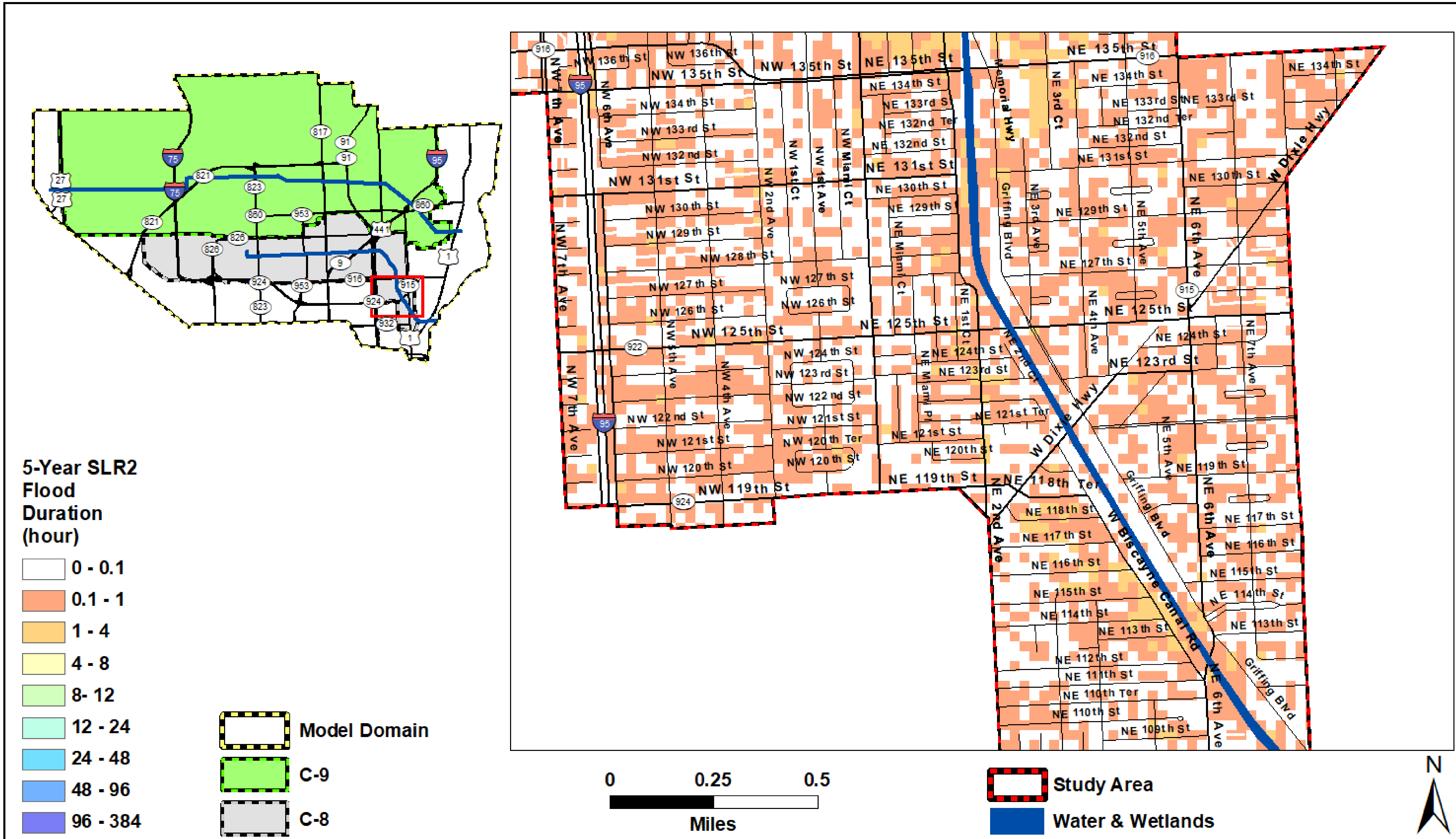

Figure 10.6-26: Up Close 5-Year Sea Level Rise 2 Flood Duration Map for the C-8 Canal Between and NE 135th St (CR916) and NE 6th Ave (CR915)

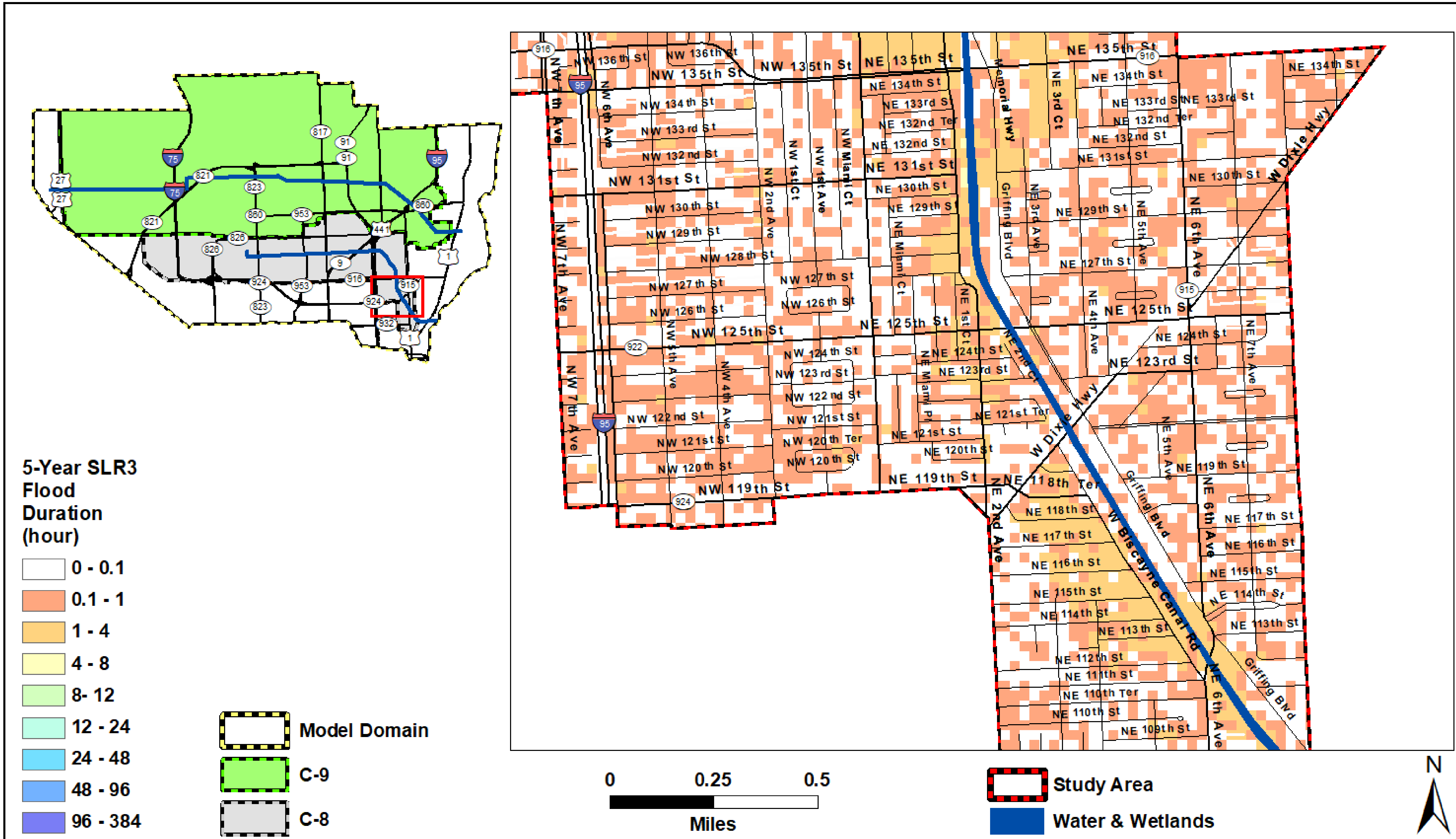

Figure 10.6-27: Up Close 5-Year Sea Level Rise 3 Flood Duration Map for the C-8 Canal Between and NE 135th St (CR916) and NE 6th Ave (CR915)

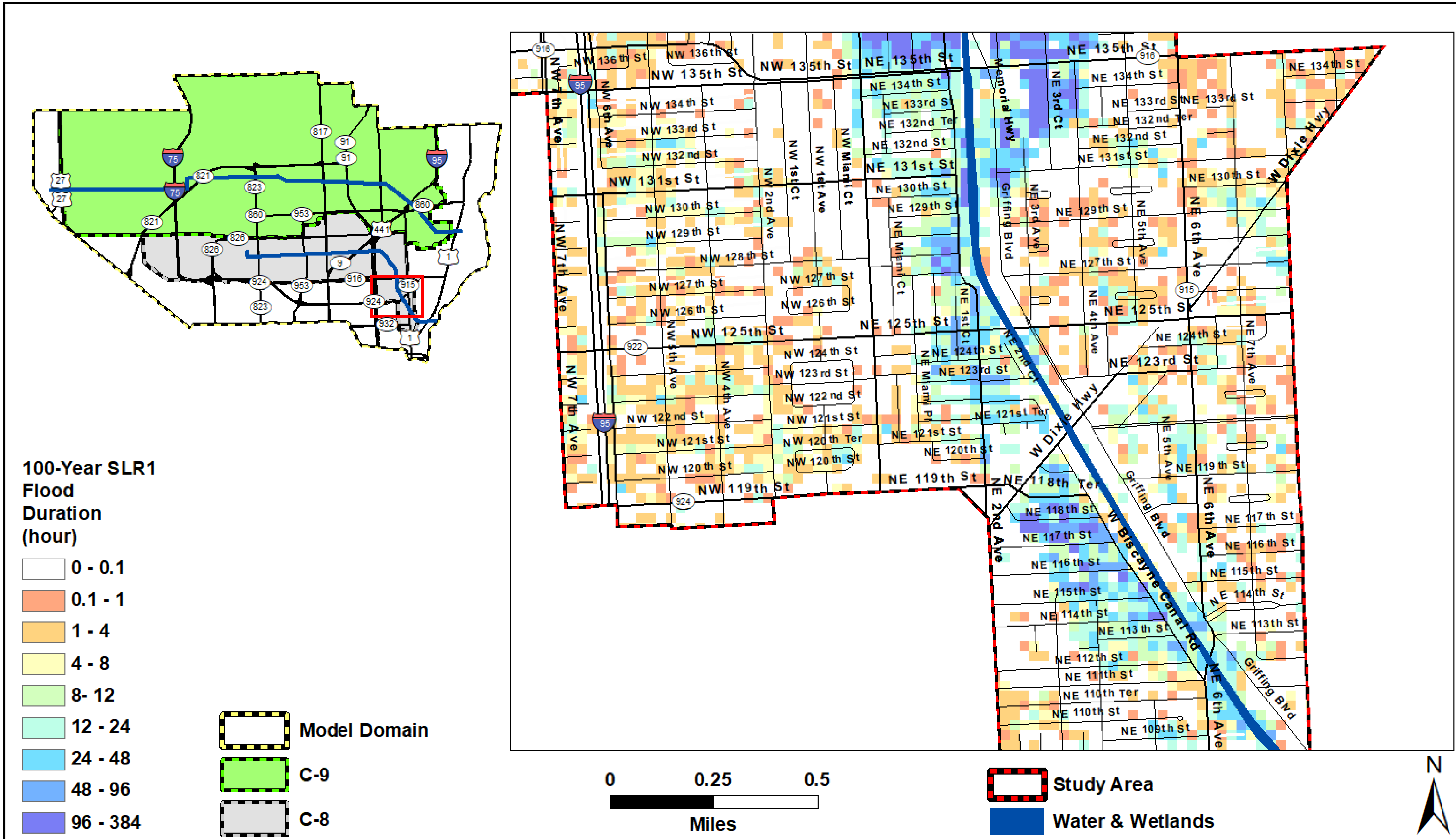

Figure 10.6-28: Up Close 100-Year Sea Level Rise 1 Flood Duration Map for the C-8 Canal Between and NE 135th St (CR916) and NE 6th Ave (CR915)

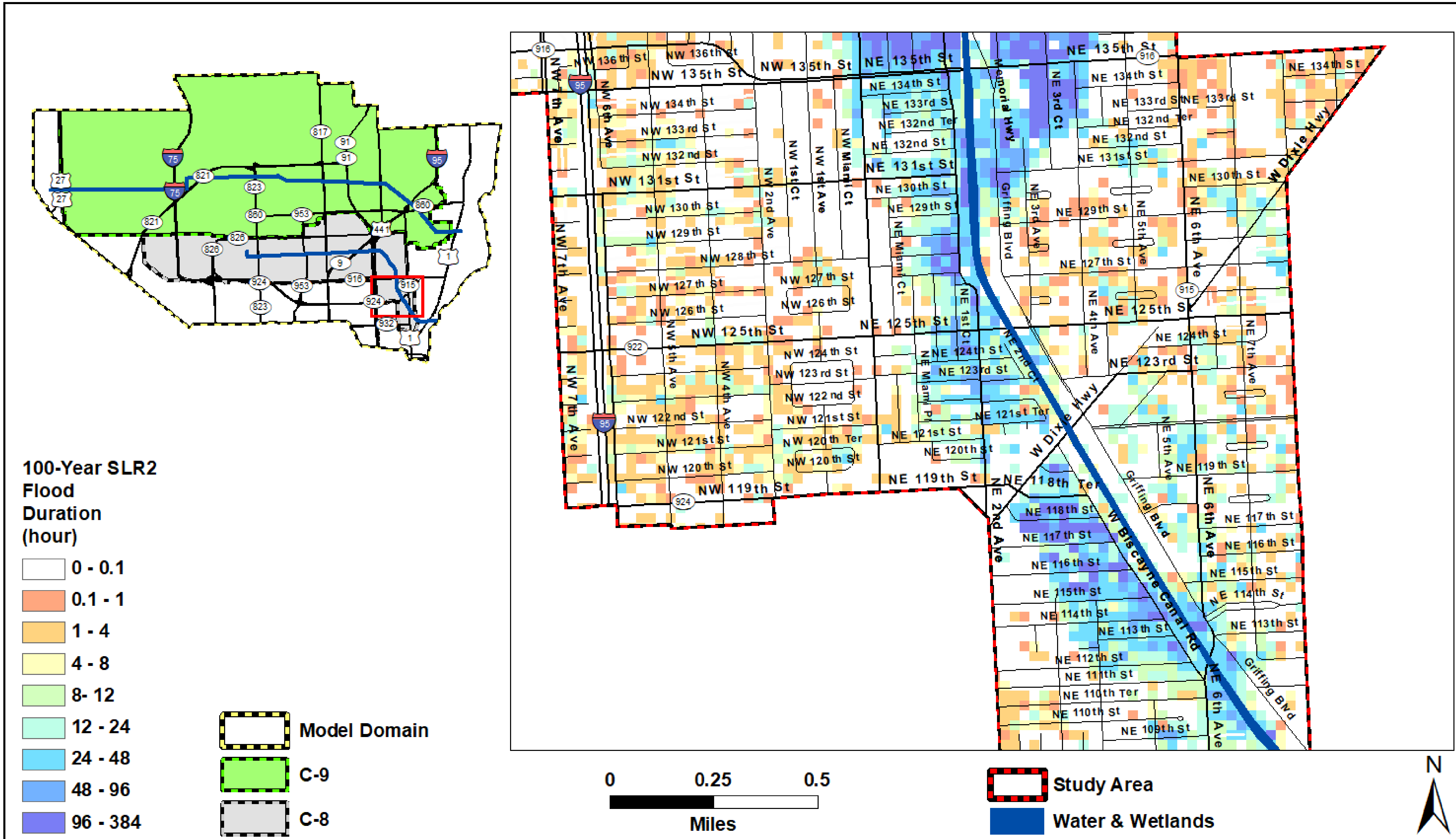

Figure 10.6-29: Up Close 100-Year Sea Level Rise 2 Flood Duration Map for the C-8 Canal Between and NE 135th St (CR916) and NE 6th Ave (CR915)

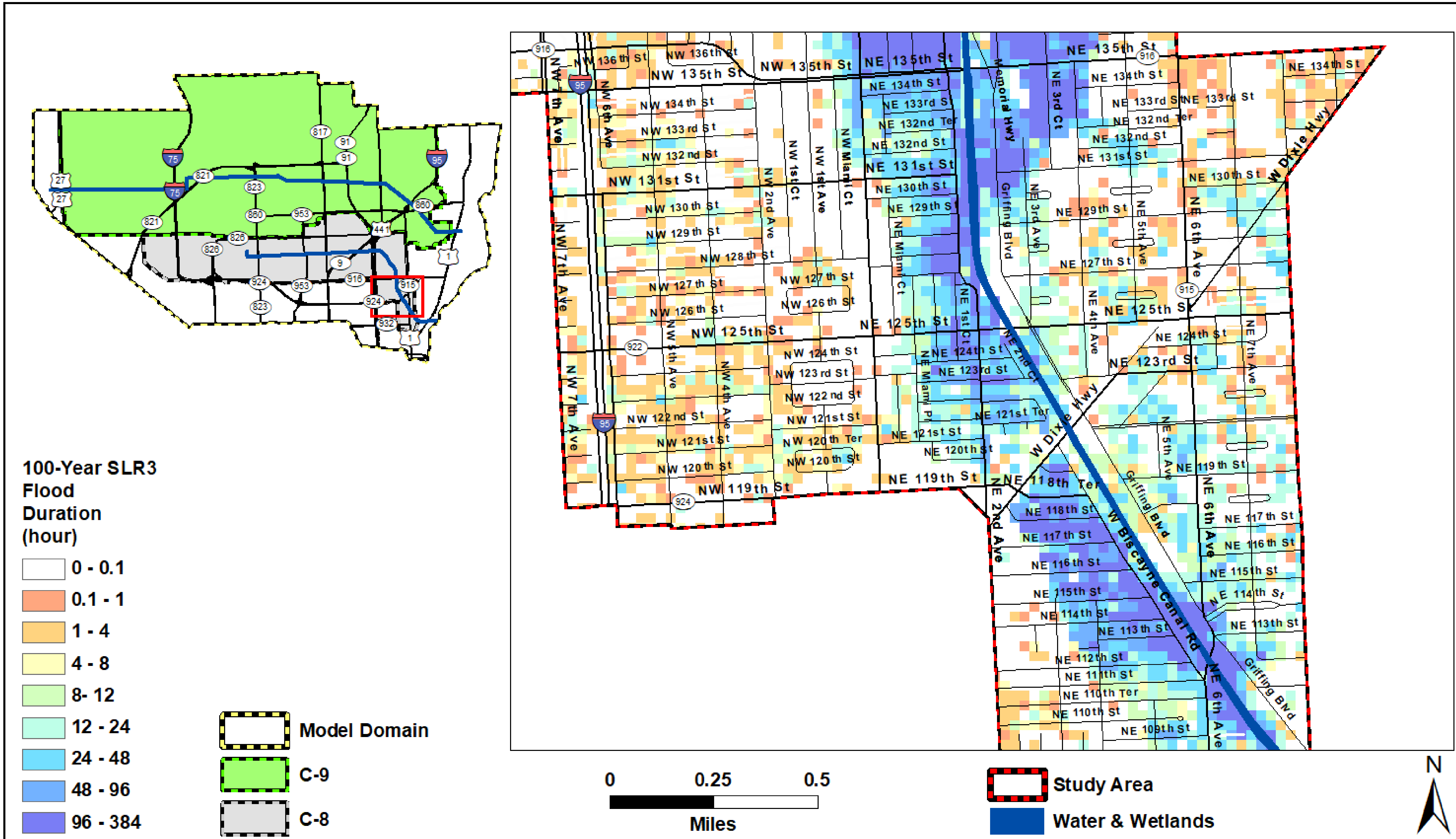

Figure 10.6-30: Up Close 100-Year Sea Level Rise 3 Flood Duration Map for the C-8 Canal Between and NE 135th St (CR916) and NE 6th Ave (CR915)

10.6.9.2 Up-Close Flood Duration Maps for the C-8 Canal Between North Miami Ave and NE 135th St (CR916)

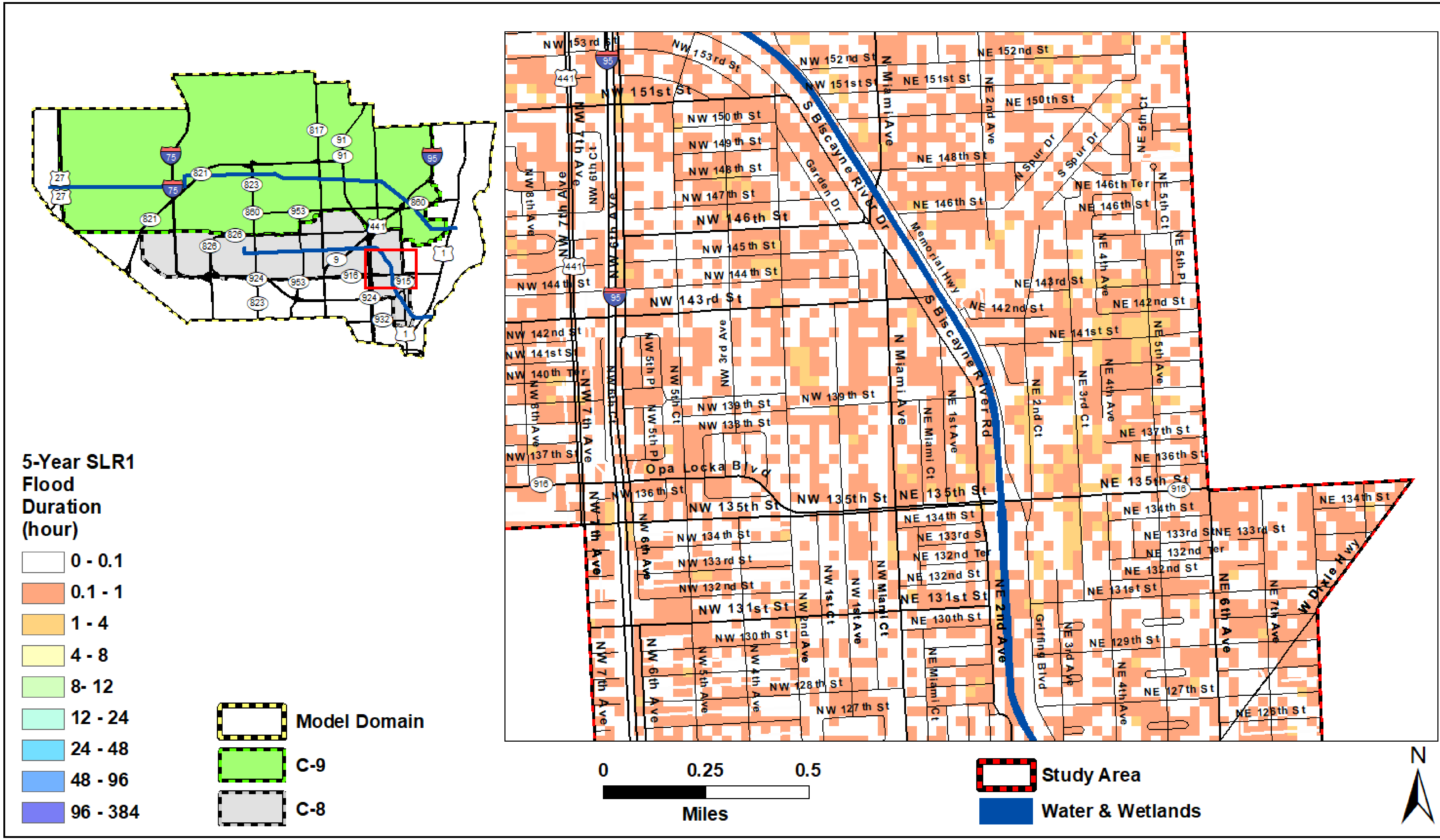

Figure 10.6-31: Up Close 5-Year Sea Level Rise 1 Flood Duration Map for the C-8 Canal Between North Miami Ave and NE 135th St (CR916)

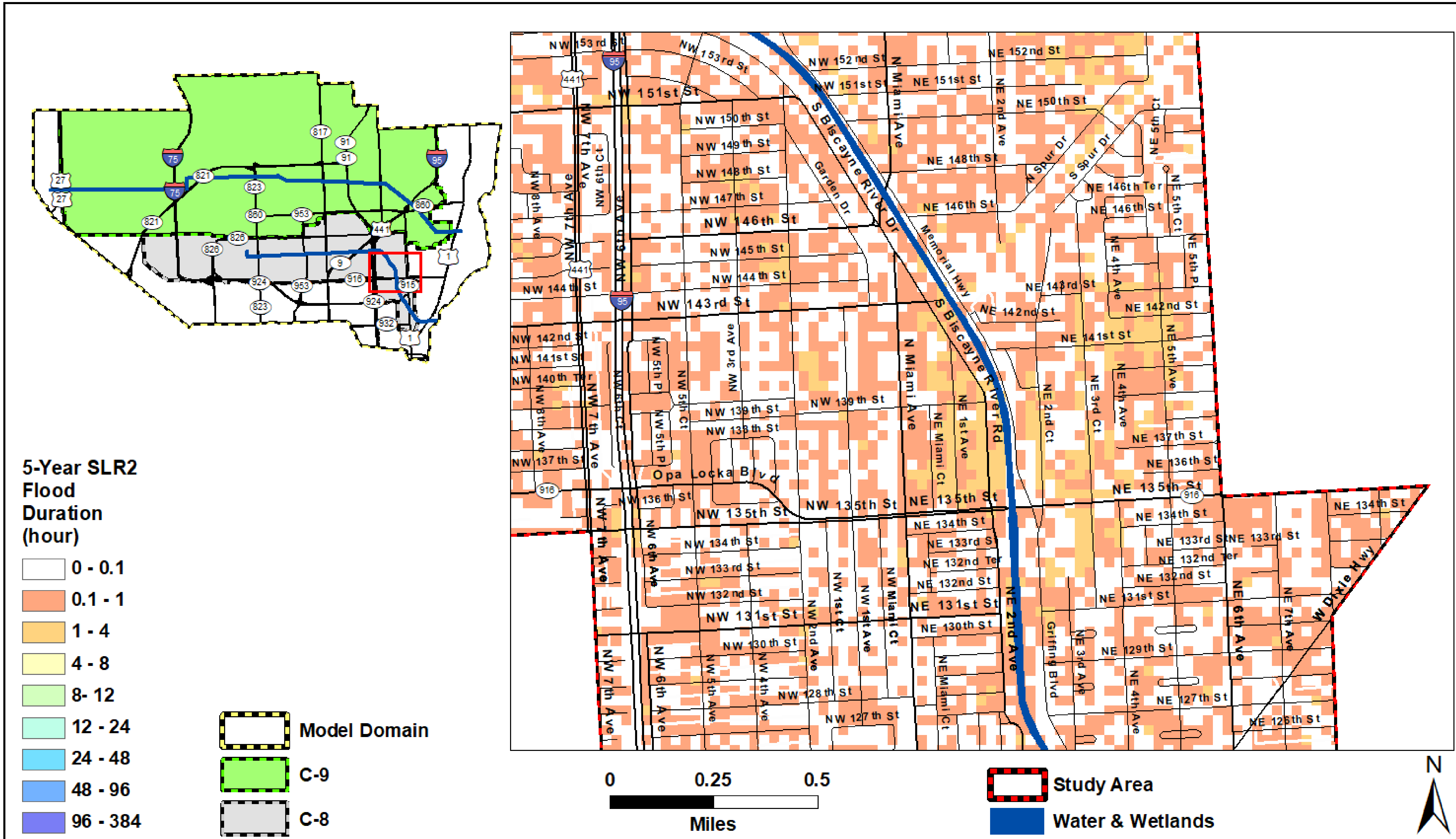

Figure 10.6-32: Up Close 5-Year Sea Level Rise 2 Flood Duration Map for the C-8 Canal Between North Miami Ave and NE 135th St (CR916)

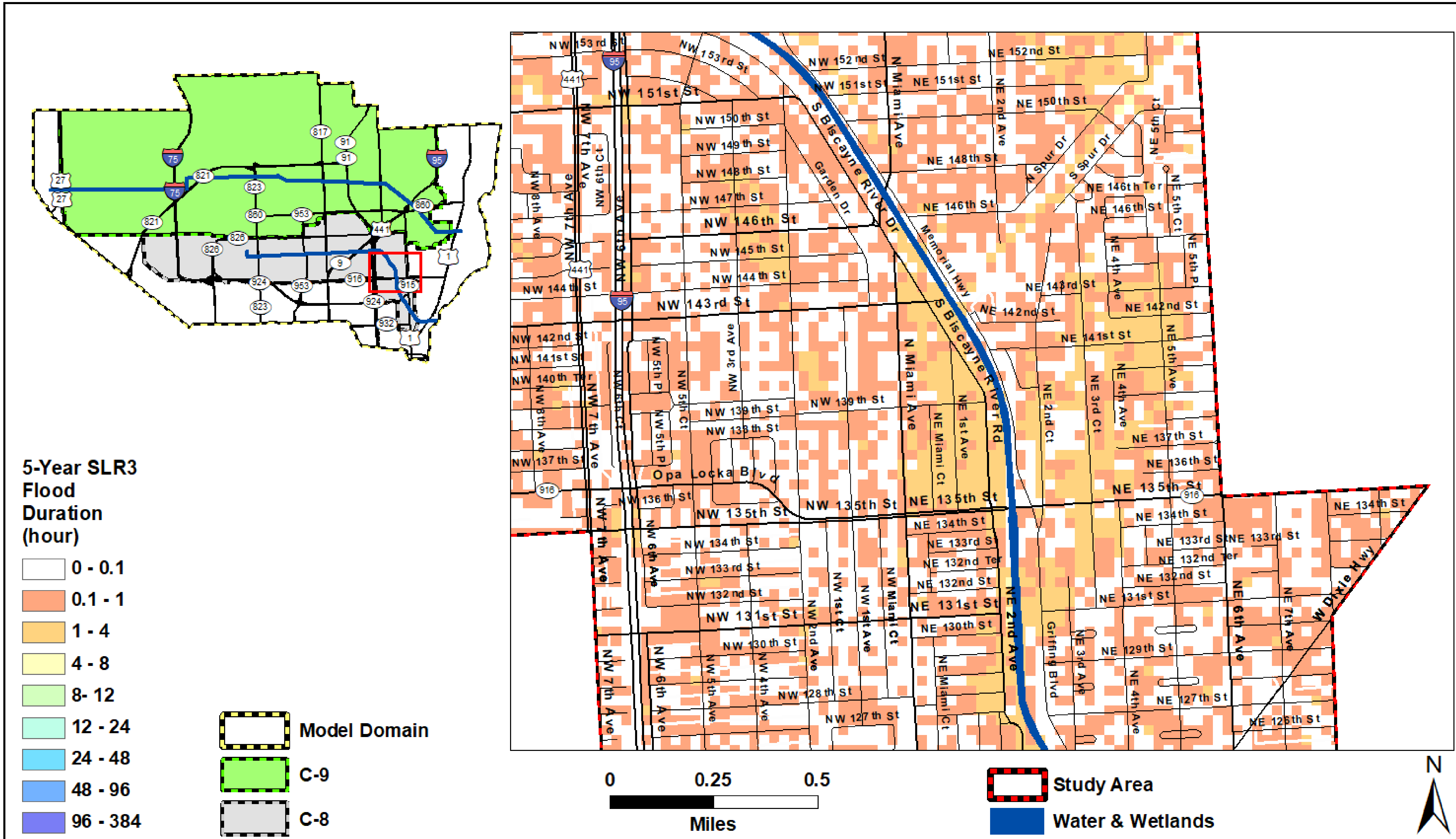

Figure 10.6-33: Up Close 5-Year Sea Level Rise 3 Flood Duration Map for the C-8 Canal Between North Miami Ave and NE 135th St (CR916)

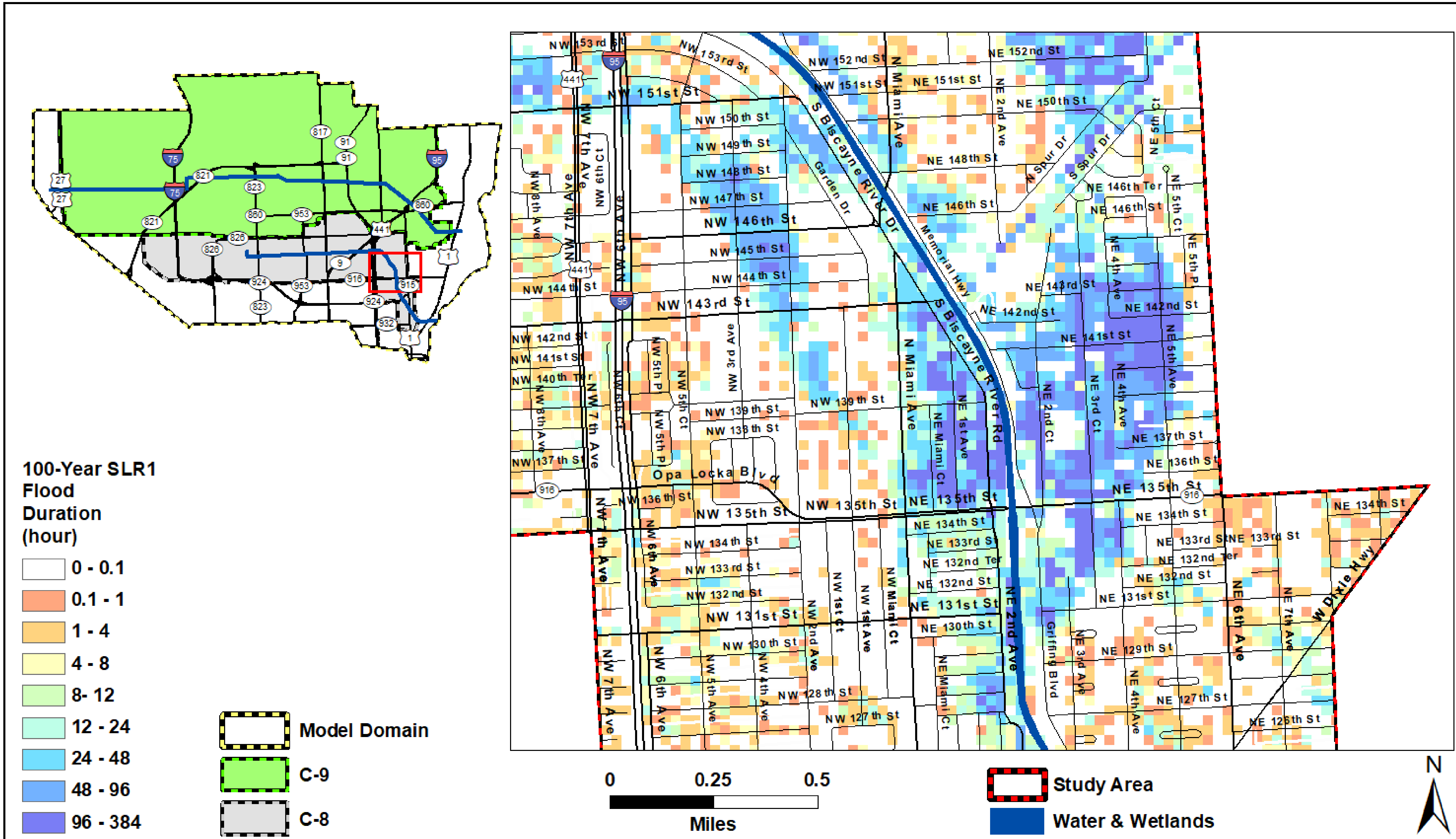

Figure 10.6-34: Up Close 100-Year Sea Level Rise 1 Flood Duration Map for the C-8 Canal Between North Miami Ave and NE 135th St (CR916)

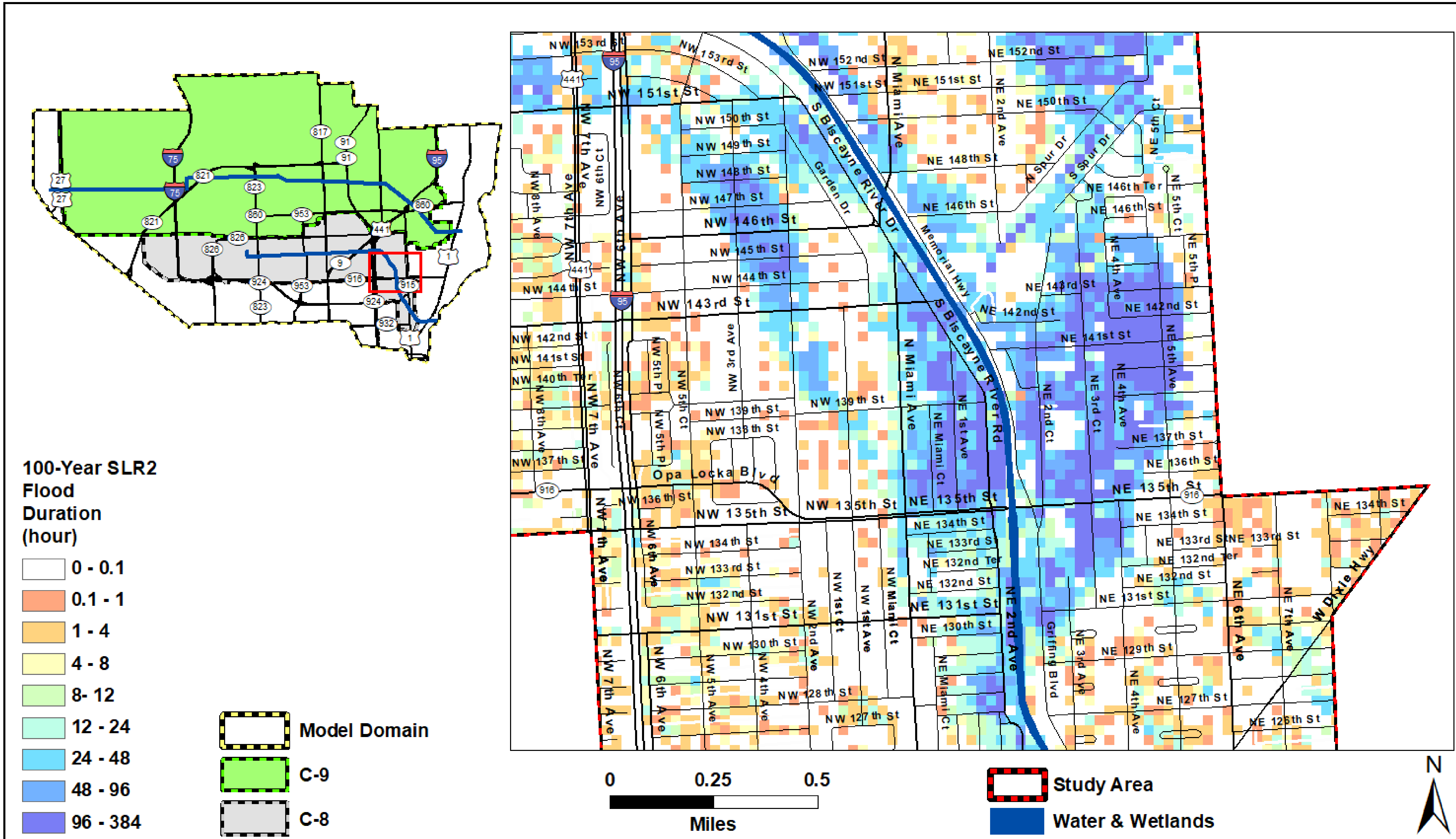

Figure 10.6-35: Up Close 100-Year Sea Level Rise 2 Flood Duration Map for the C-8 Canal Between North Miami Ave and NE 135th St (CR916)

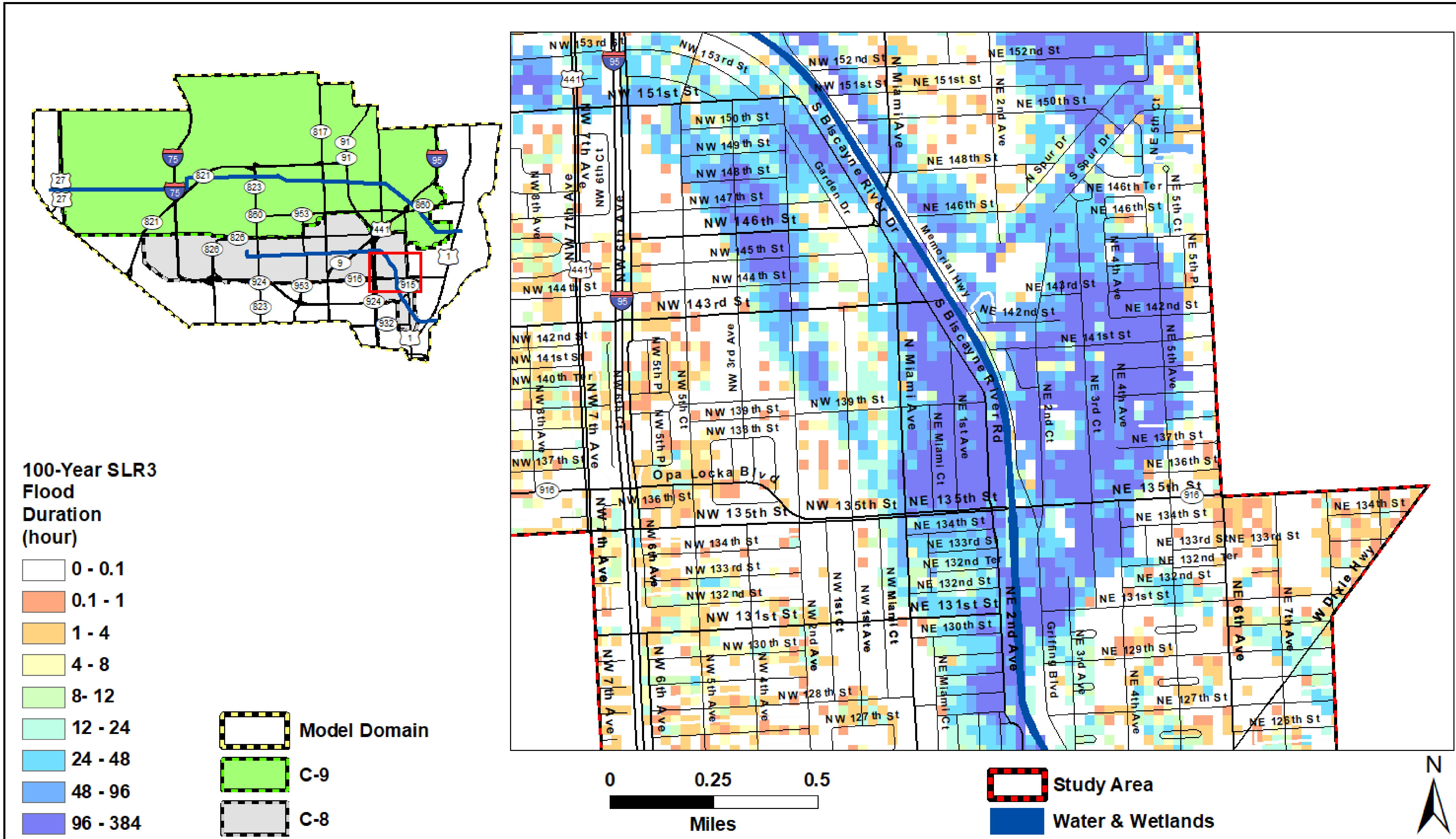

Figure 10.6-36: Up Close 100-Year Sea Level Rise 3 Flood Duration Map for the C-8 Canal Between North Miami Ave and NE 135th St (CR916)

10.6.9.3 Up-Close Flood Duration Maps for the C-8 Canal Near Opa Locka Canal

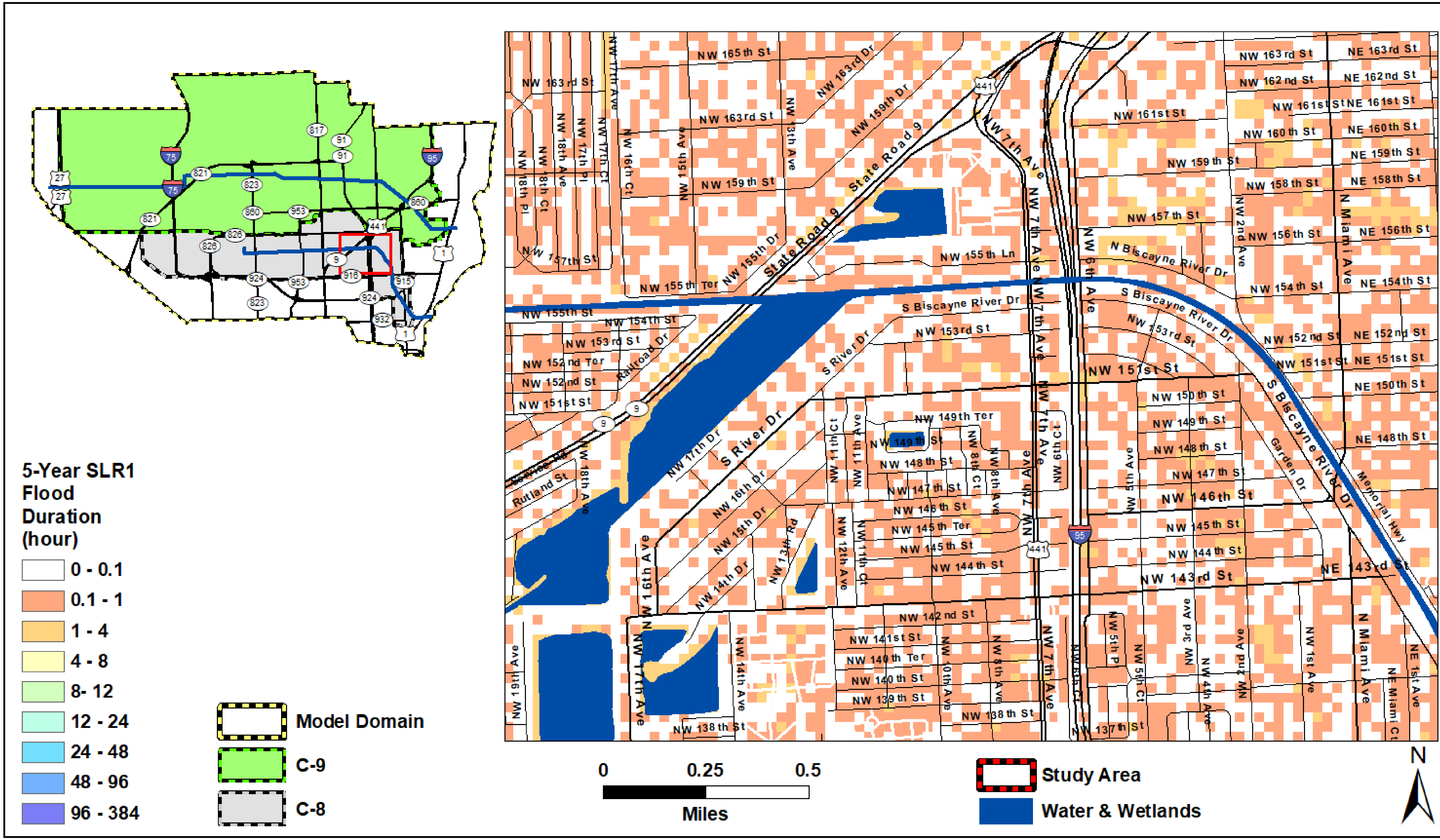

Figure 10.6-37: Up Close 5-Year Sea Level Rise 1 Flood Duration Map for the C-8 Canal Near Opa Locka Canal

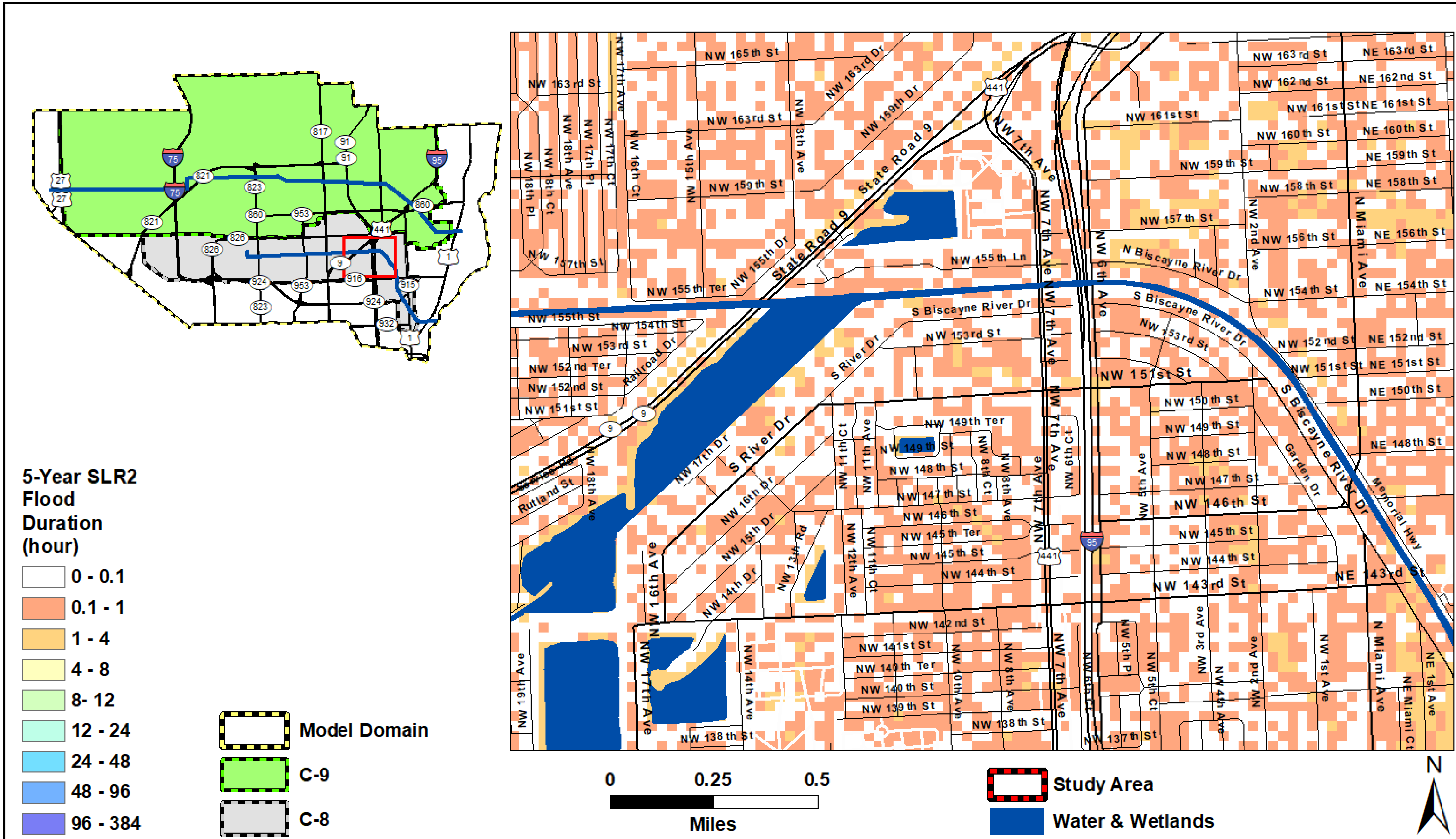

Figure 10.6-38: Up Close 5-Year Sea Level Rise 2 Flood Duration Map for the C-8 Canal Near Opa Locka Canal

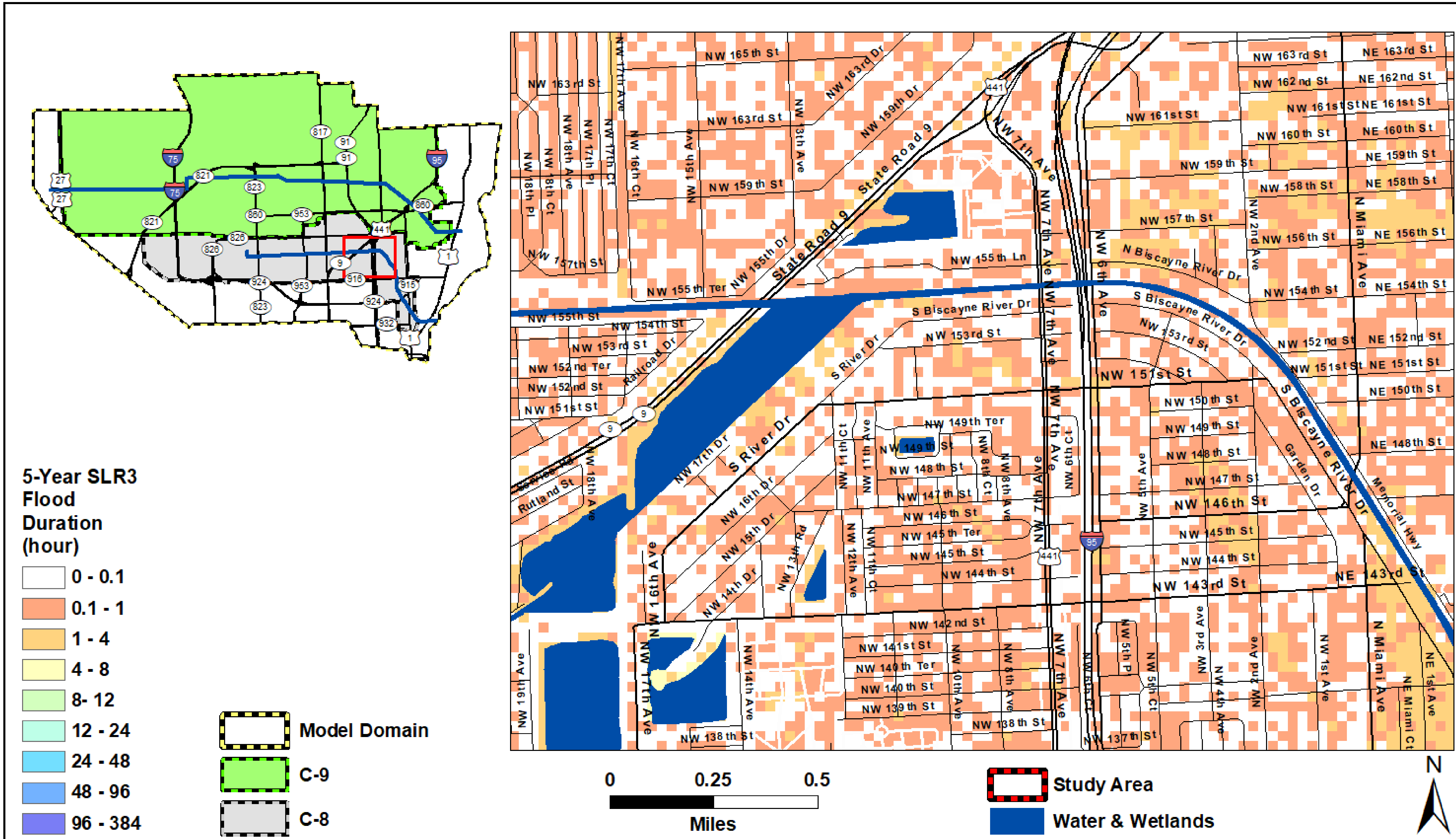

Figure 10.6-39: Up Close 5-Year Sea Level Rise 3 Flood Duration Map for the C-8 Canal Near Opa Locka Canal

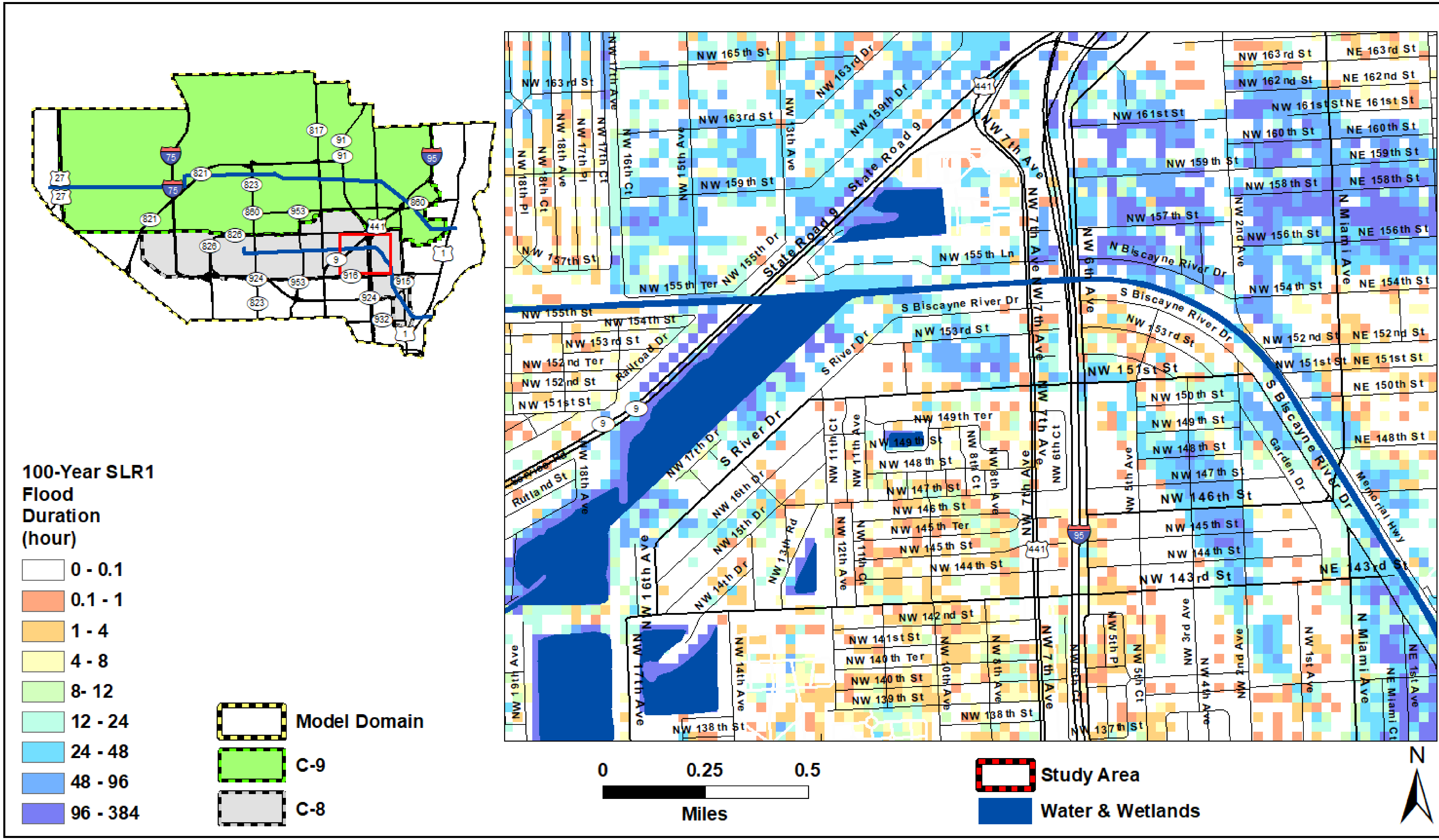

Figure 10.6-40: Up Close 100-Year Sea Level Rise 1 Flood Duration Map for the C-8 Canal Near Opa Locka Canal

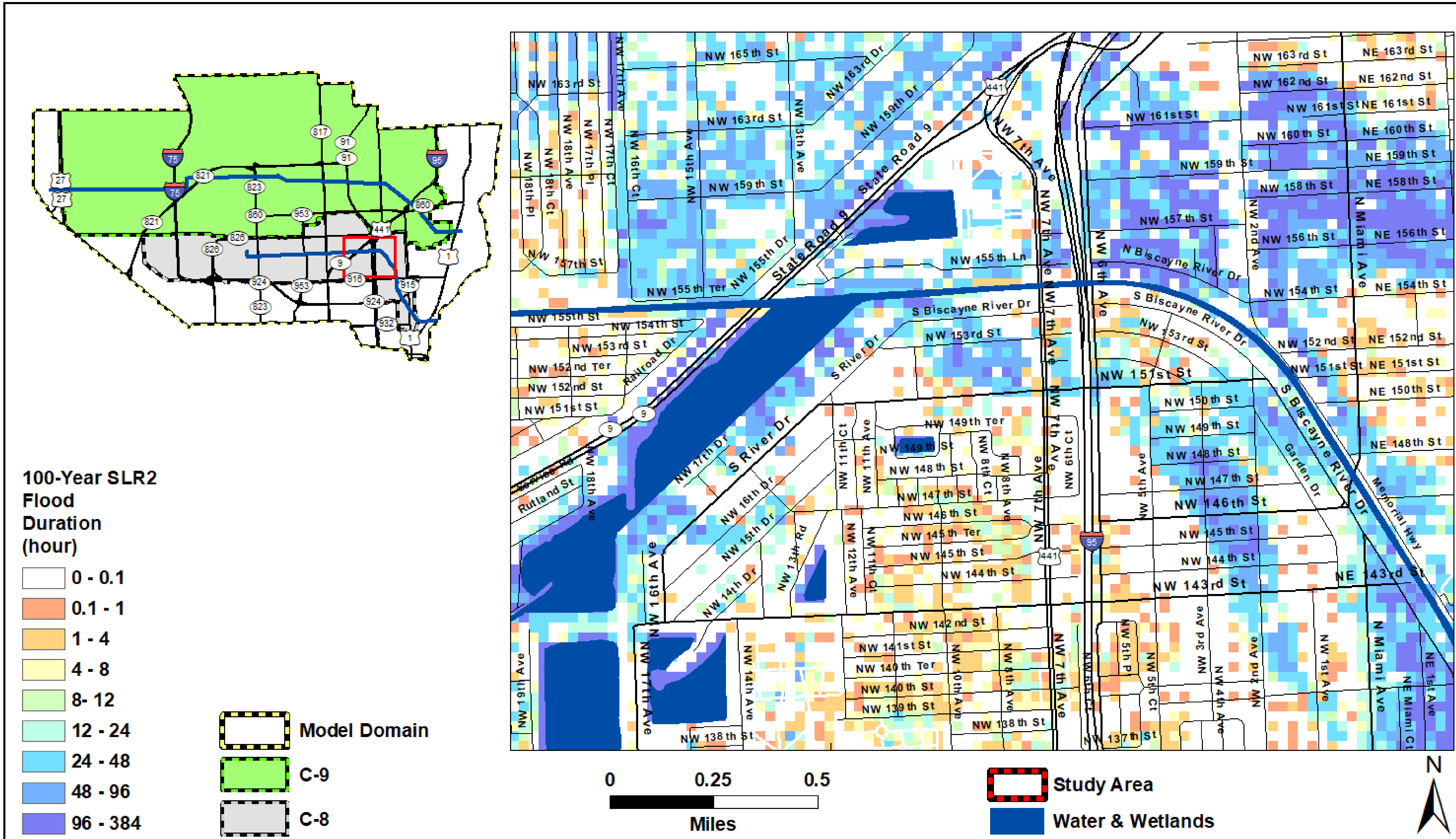

Figure 10.6-41: Up Close 100-Year Sea Level Rise 2 Flood Duration Map for the C-8 Canal Near Opa Locka Canal

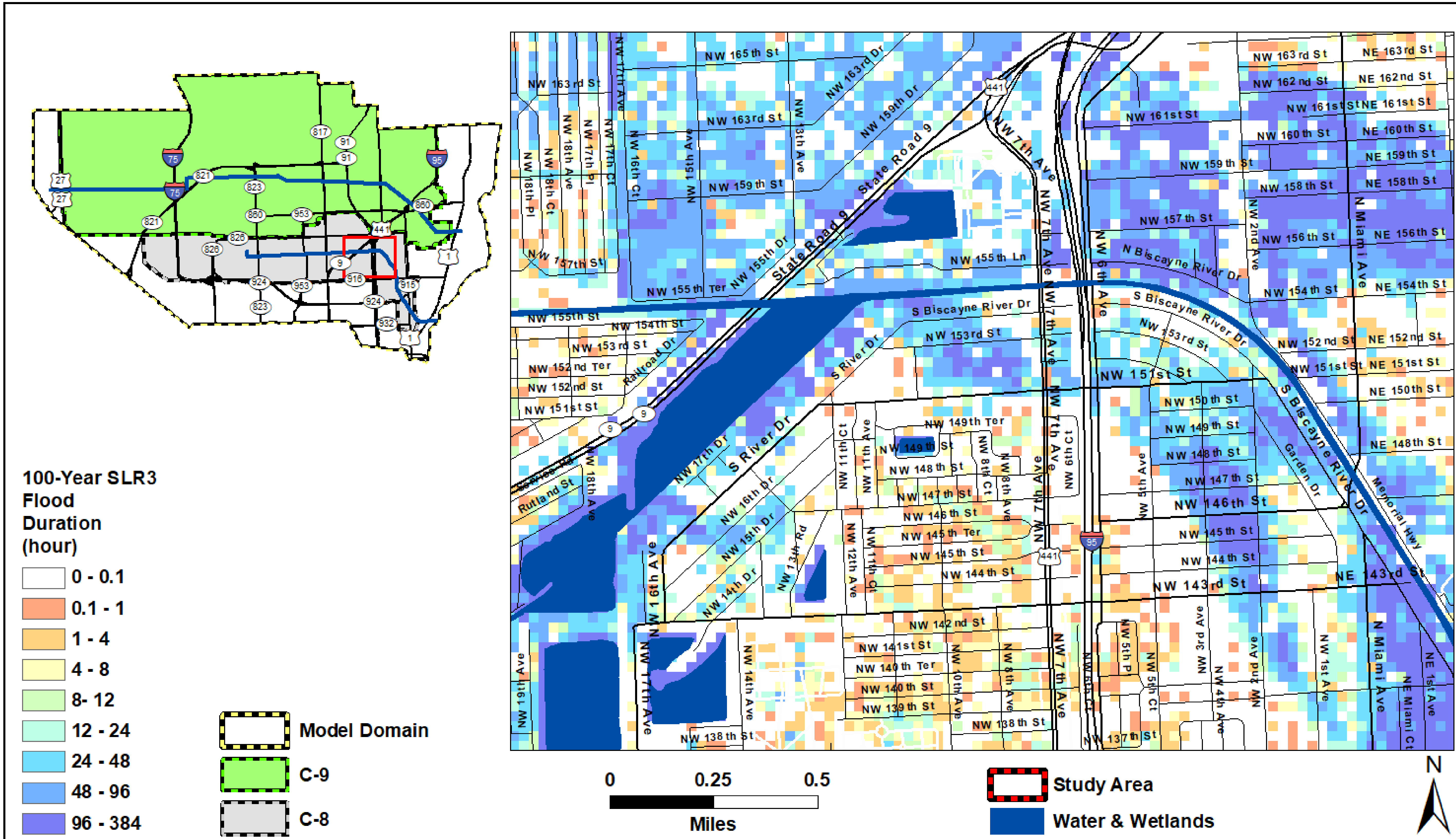

Figure 10.6-42: Up Close 100-Year Sea Level Rise 3 Flood Duration Map for the C-8 Canal Near Opa Locka Canal

10.6.9.4 Up-Close Flood Duration Maps for the C-9 Canal Between I-95 and S-29

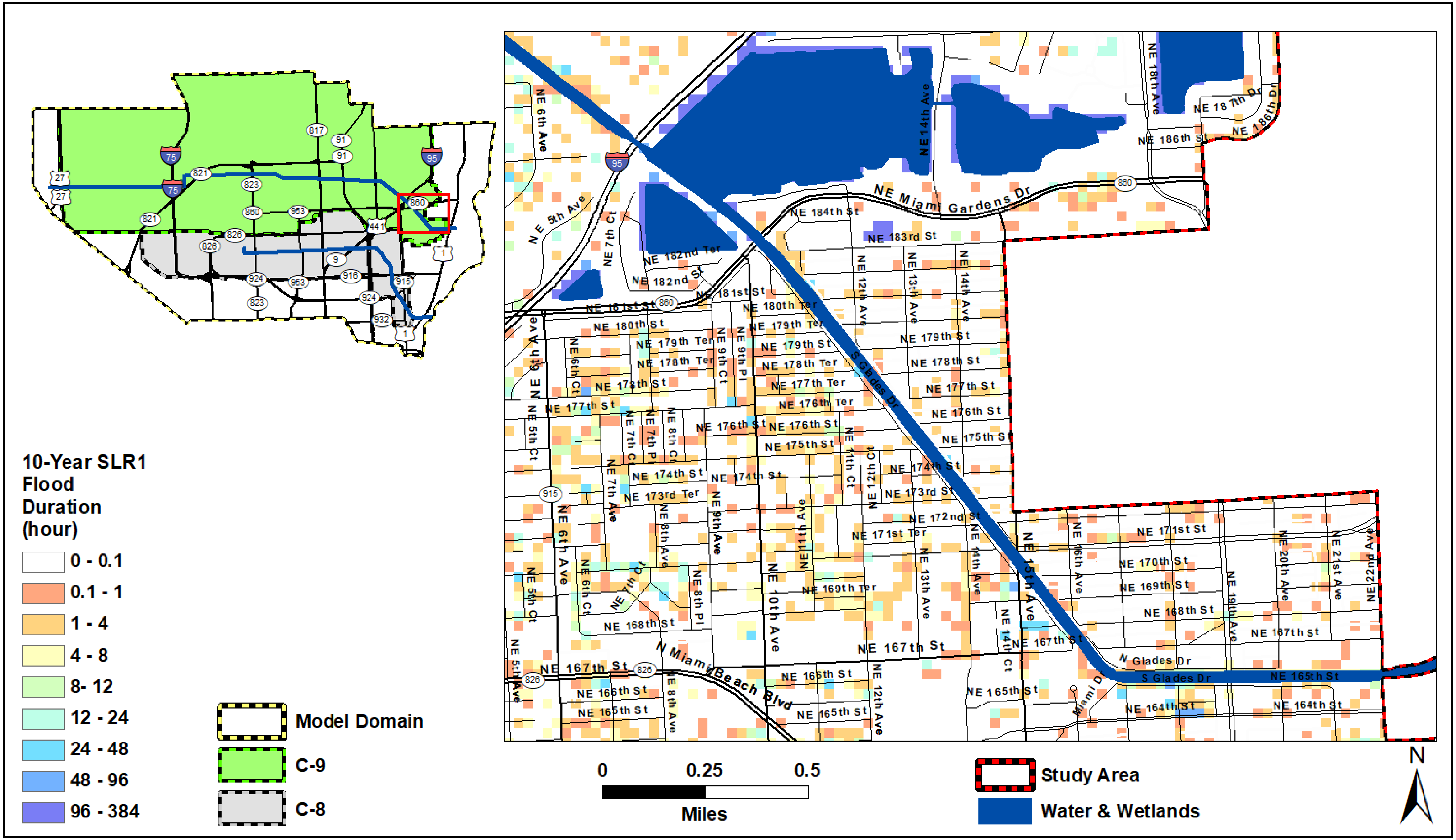

Figure 10.6-43: Up Close 10-Year Design Storm Sea Level Rise 1 Flood Duration Map for the C-9 Canal Between I-95 and S-29

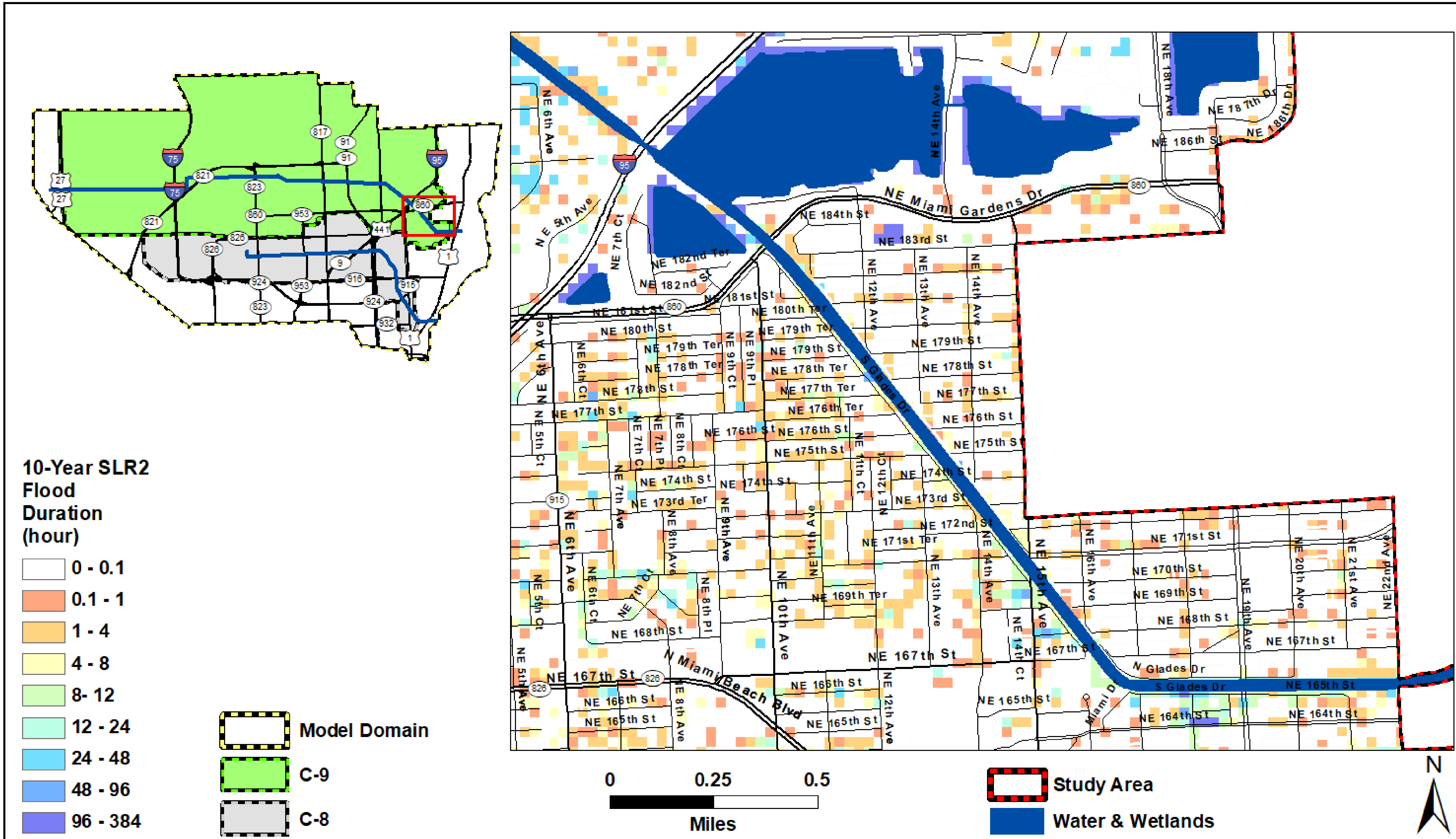

Figure 10.6-44: Up Close 10-Year Design Storm Sea Level Rise 2 Flood Duration Map for the C-9 Canal Between I-95 and S-29

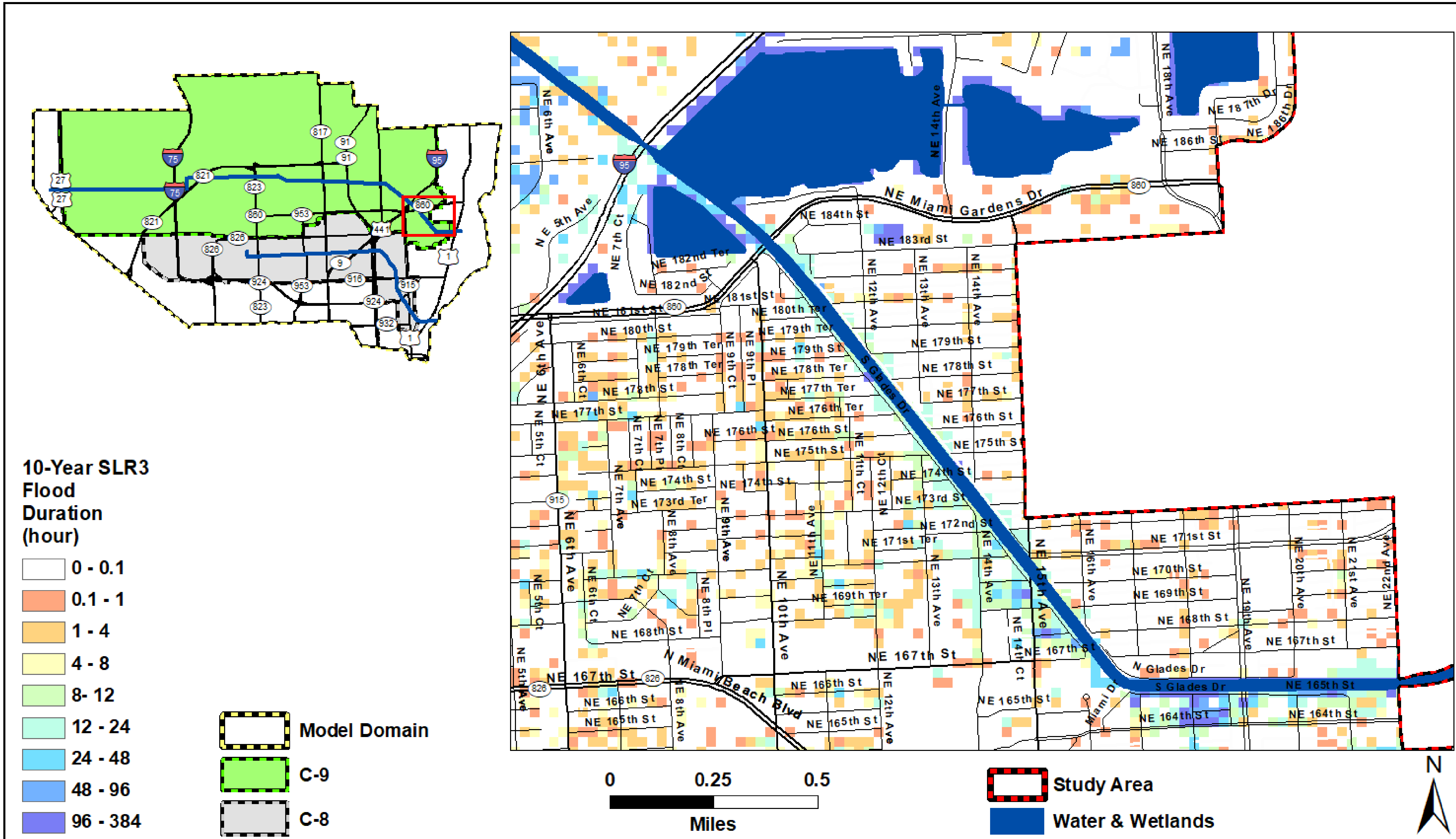

Figure 10.6-45: Up Close 10-Year Design Storm Sea Level Rise 3 Flood Duration Map for the C-9 Canal Between I-95 and S-29

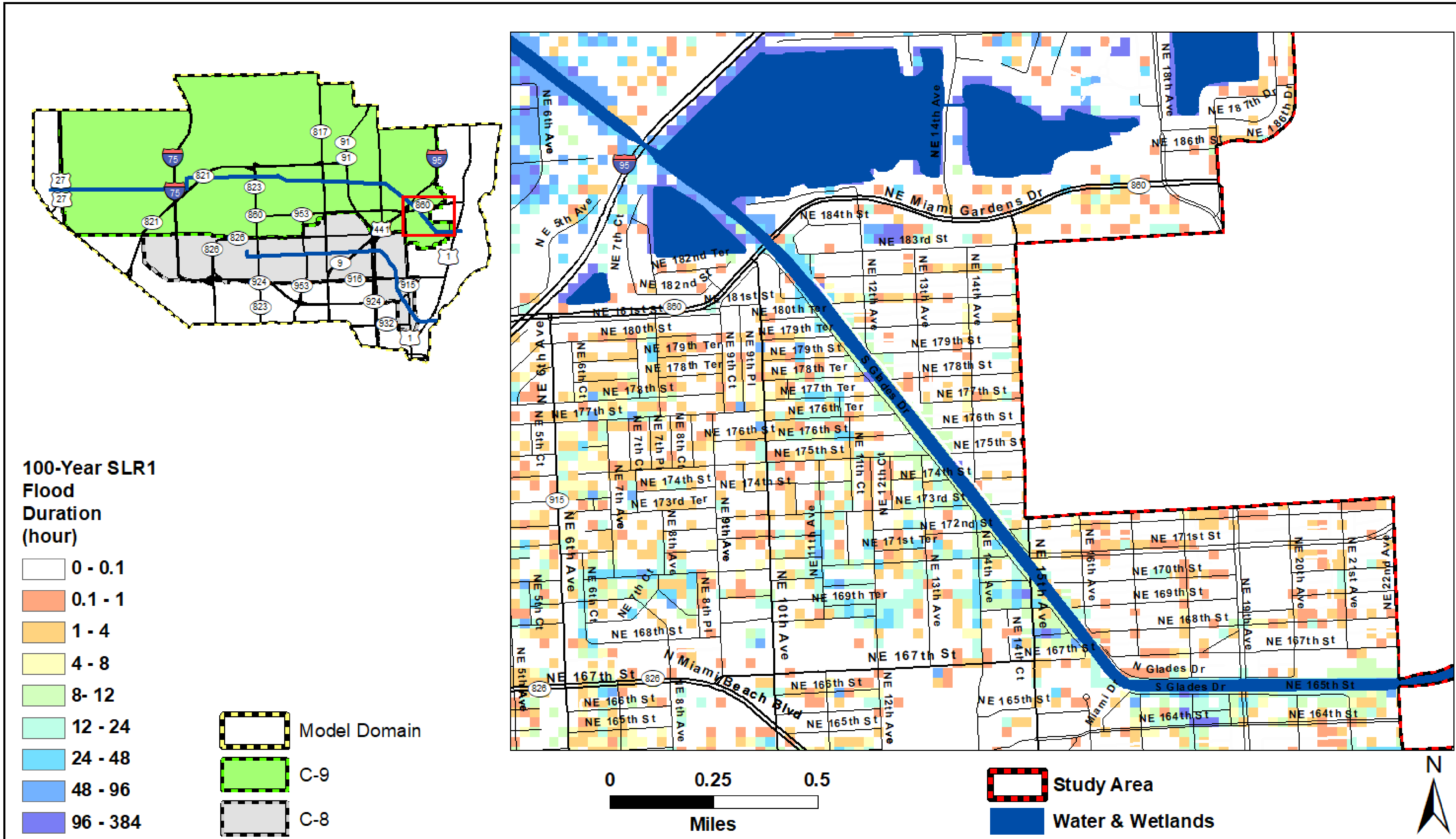

Figure 10.6-46: Up Close 100-Year Design Storm Sea Level Rise 1 Flood Duration Map for the C-9 Canal Between I-95 and S-29

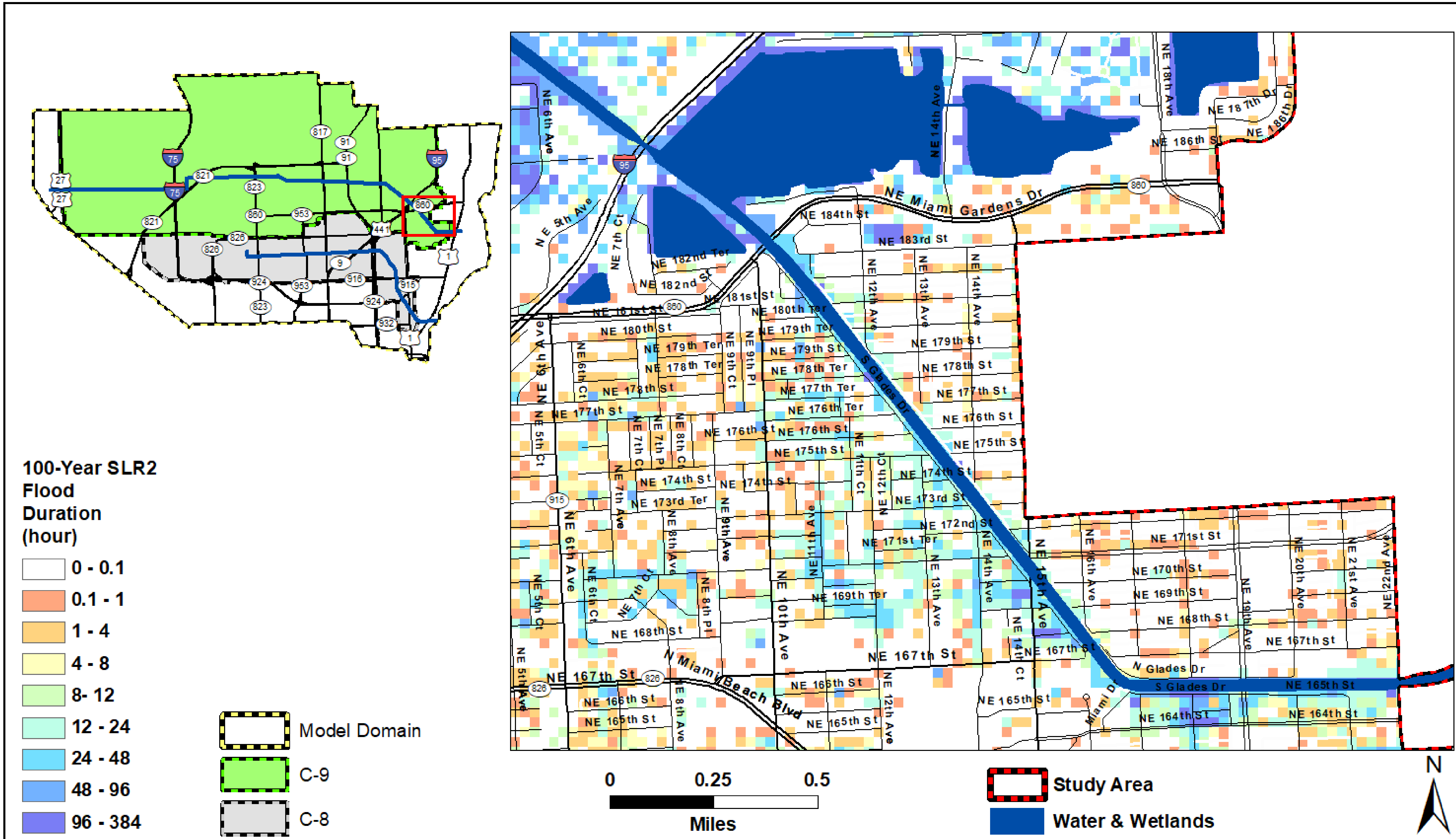

Figure 10.6-47: Up Close 100-Year Design Storm Sea Level Rise 2 Flood Duration Map for the C-9 Canal Between I-95 and S-29

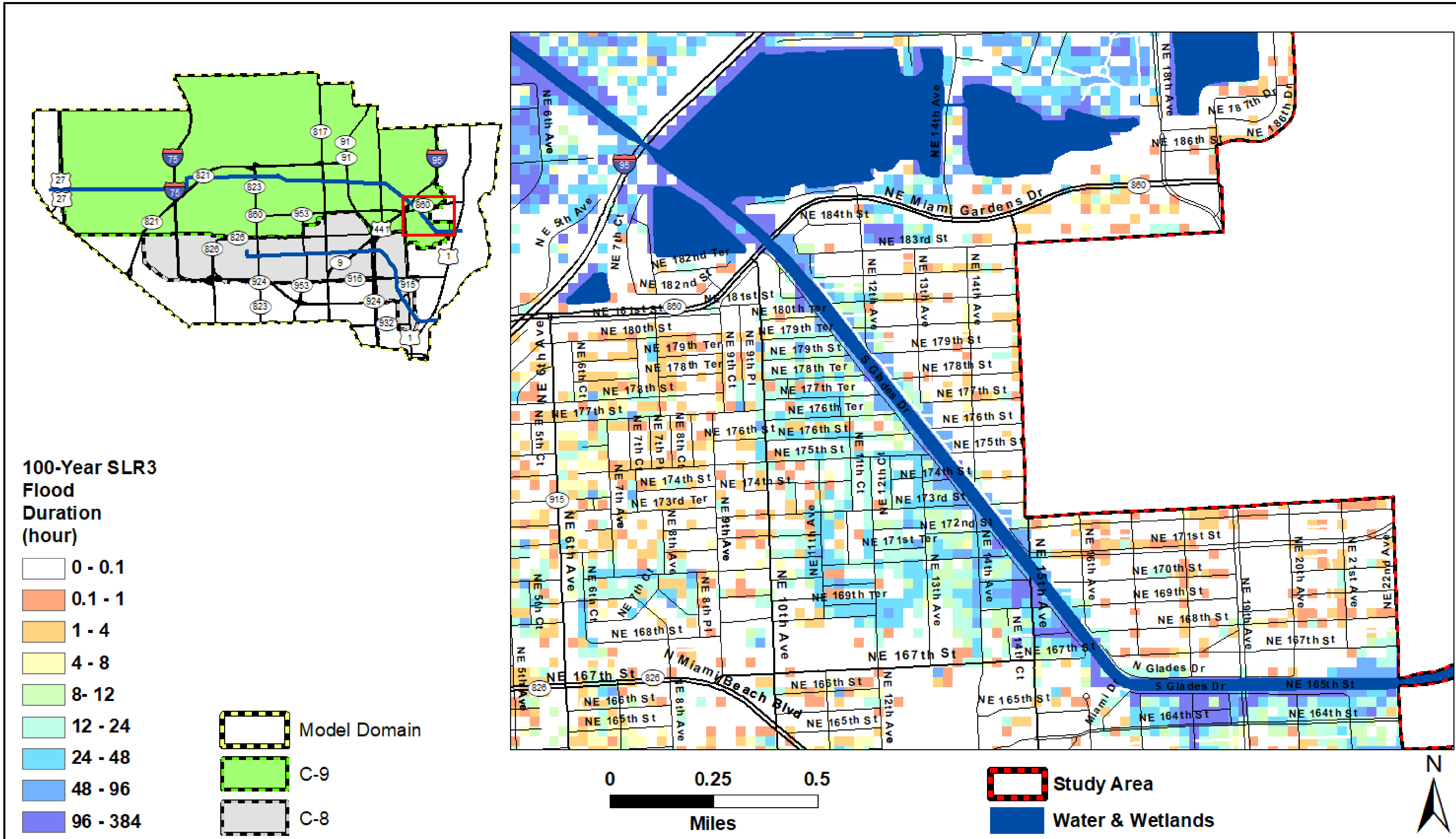

Figure 10.6-48: Up Close 100-Year Design Storm Sea Level Rise 3 Flood Duration Map for the C-9 Canal Between I-95 and S-29

10.6.9.5 Up-Close Flood Duration Maps for the C-9 Canal Near US Hwy 441

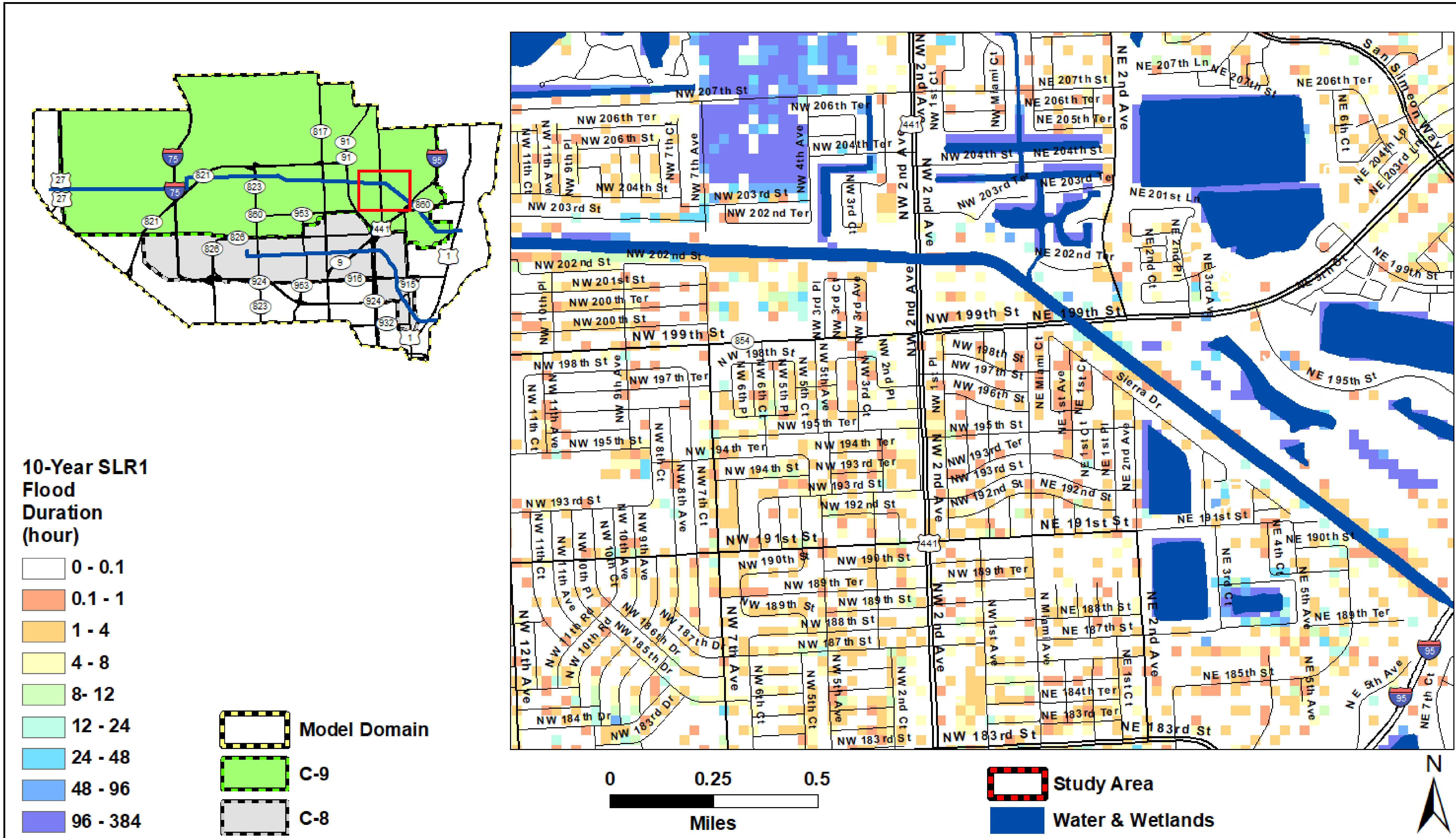

Figure 10.6-49: Up Close 10-Year Sea Level Rise 1 Flood Duration Map for the C-9 Canal Near US Hwy 441

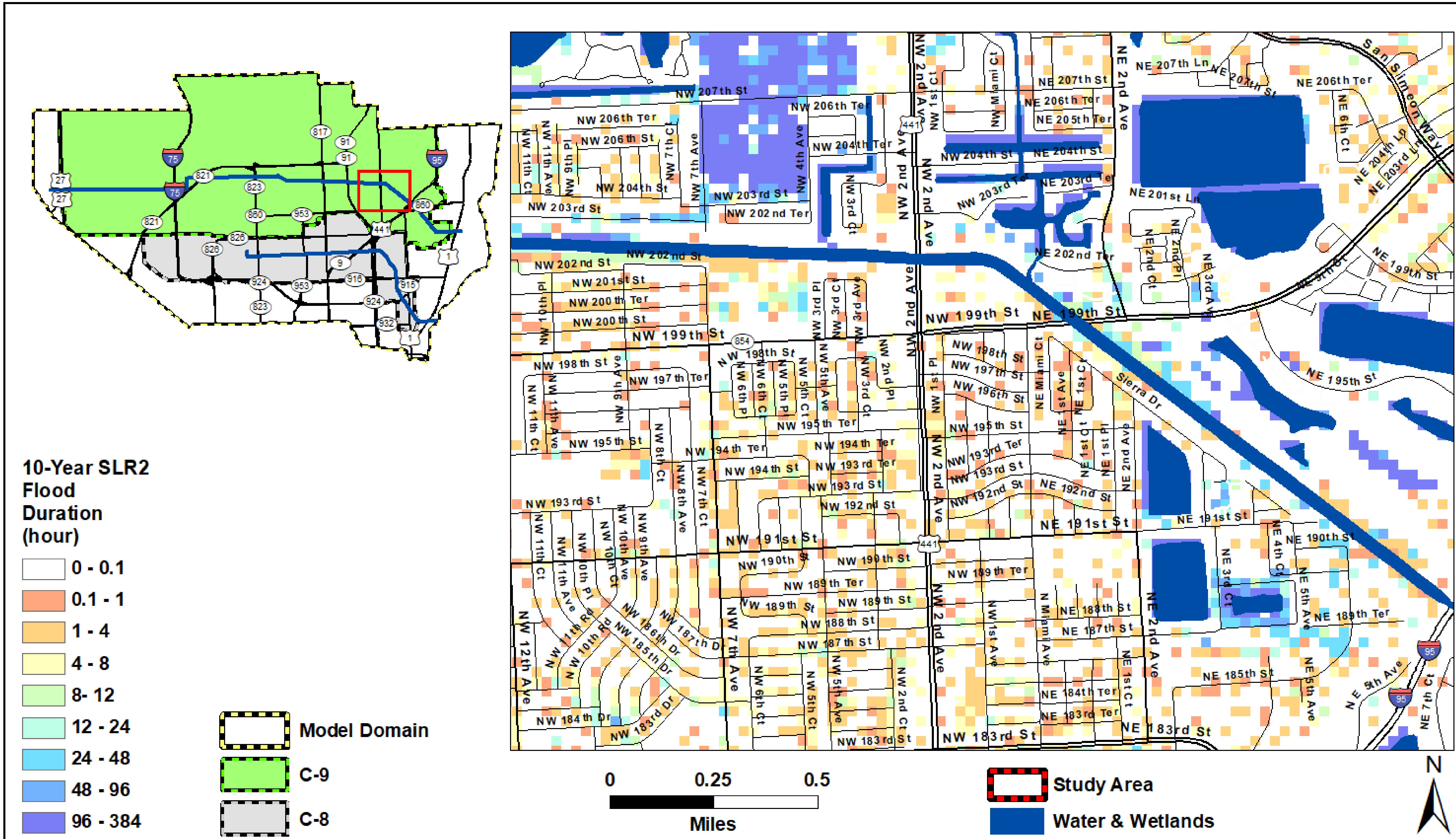

Figure 10.6-50: Up Close 10-Year Sea Level Rise 2 Flood Duration Map for the C-9 Canal Near US Hwy 441

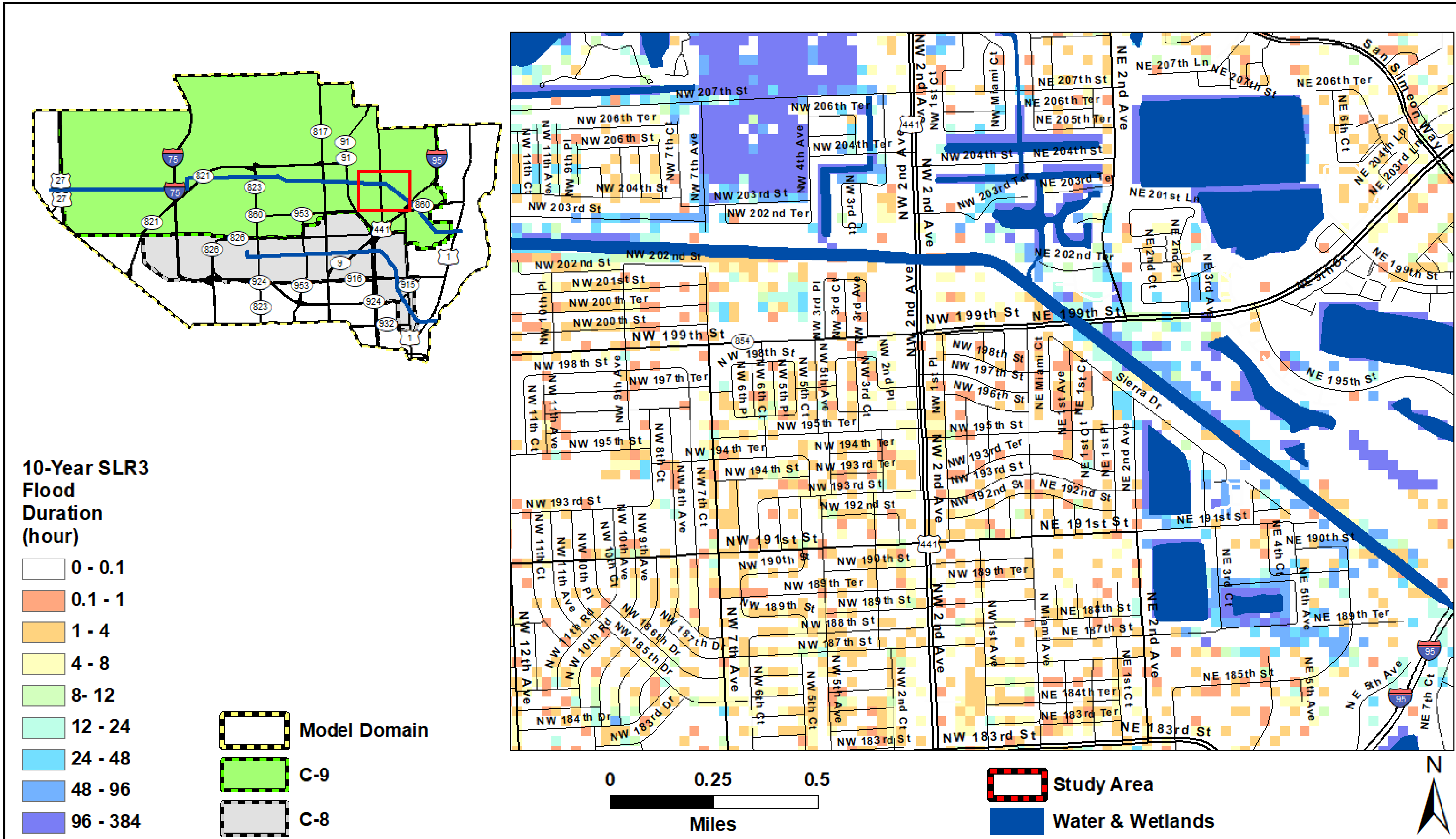

Figure 10.6-51: Up Close 10-Year Sea Level Rise 3 Flood Duration Map for the C-9 Canal Near US Hwy 441

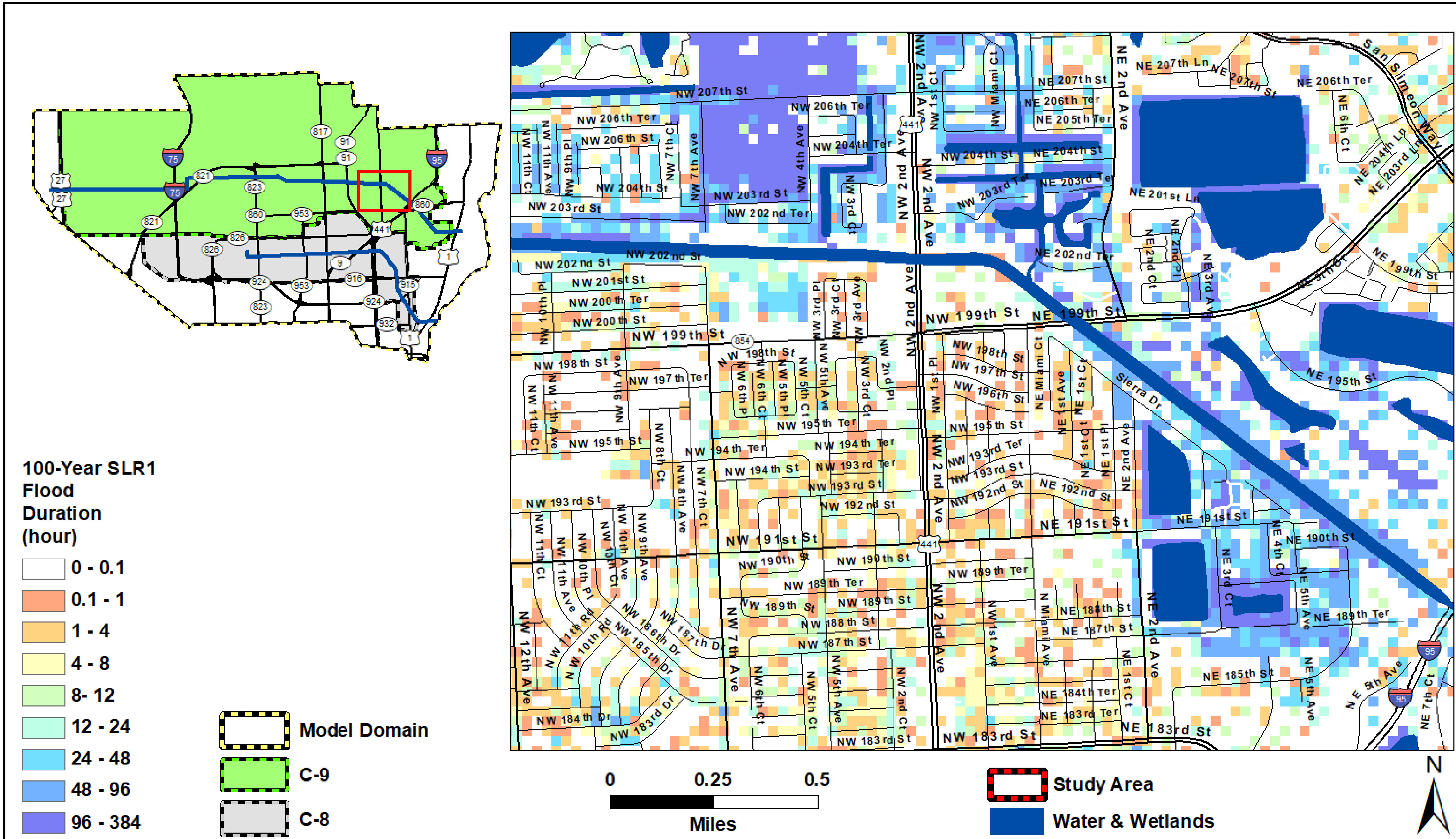

Figure 10.6-52: Up Close 100-Year Sea Level Rise 1 Flood Duration Map for the C-9 Canal Near US Hwy 441

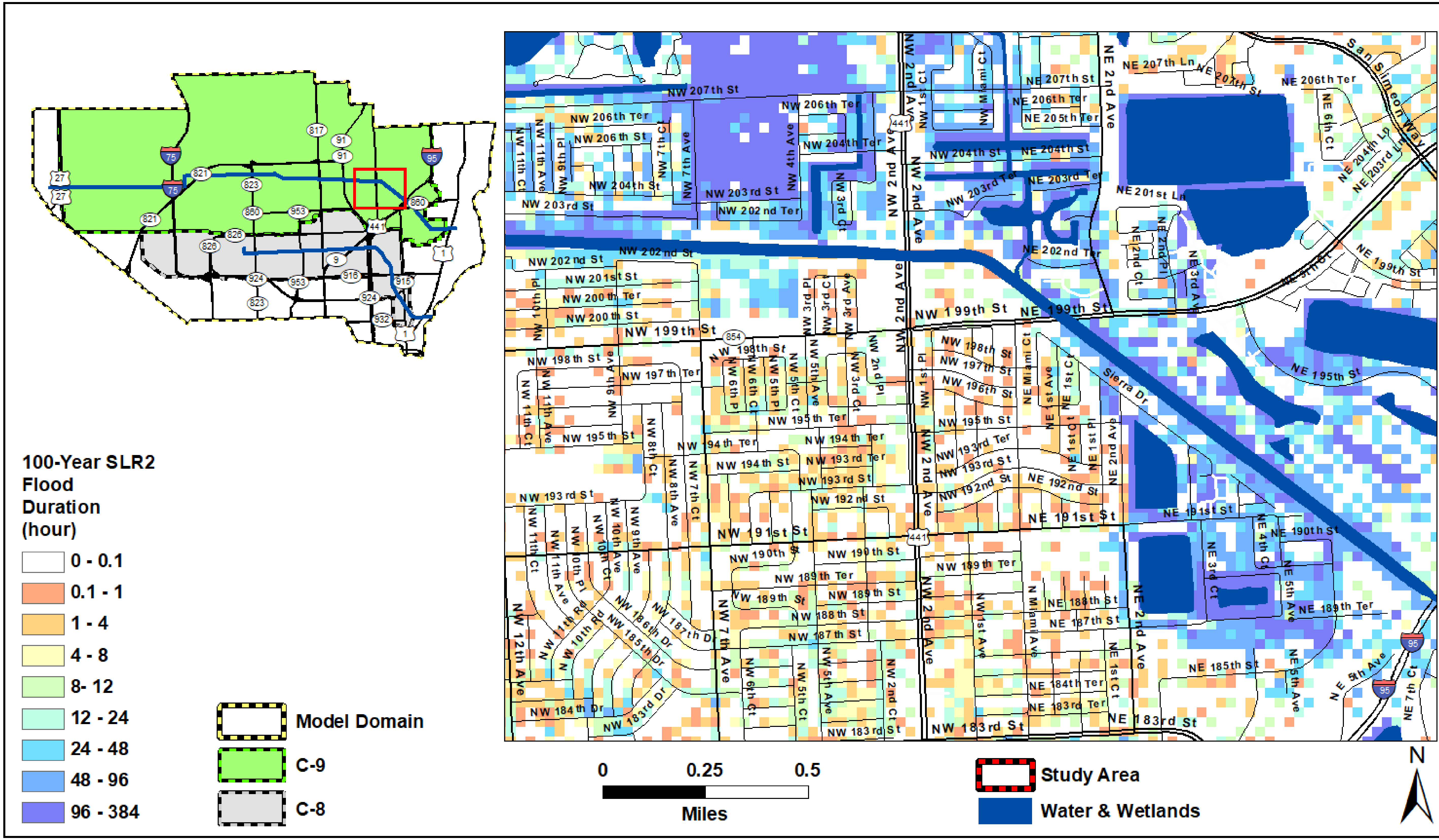

Figure 10.6-53: Up Close 100-Year Sea Level Rise 2 Flood Duration Map for the C-9 Canal Near US Hwy 441

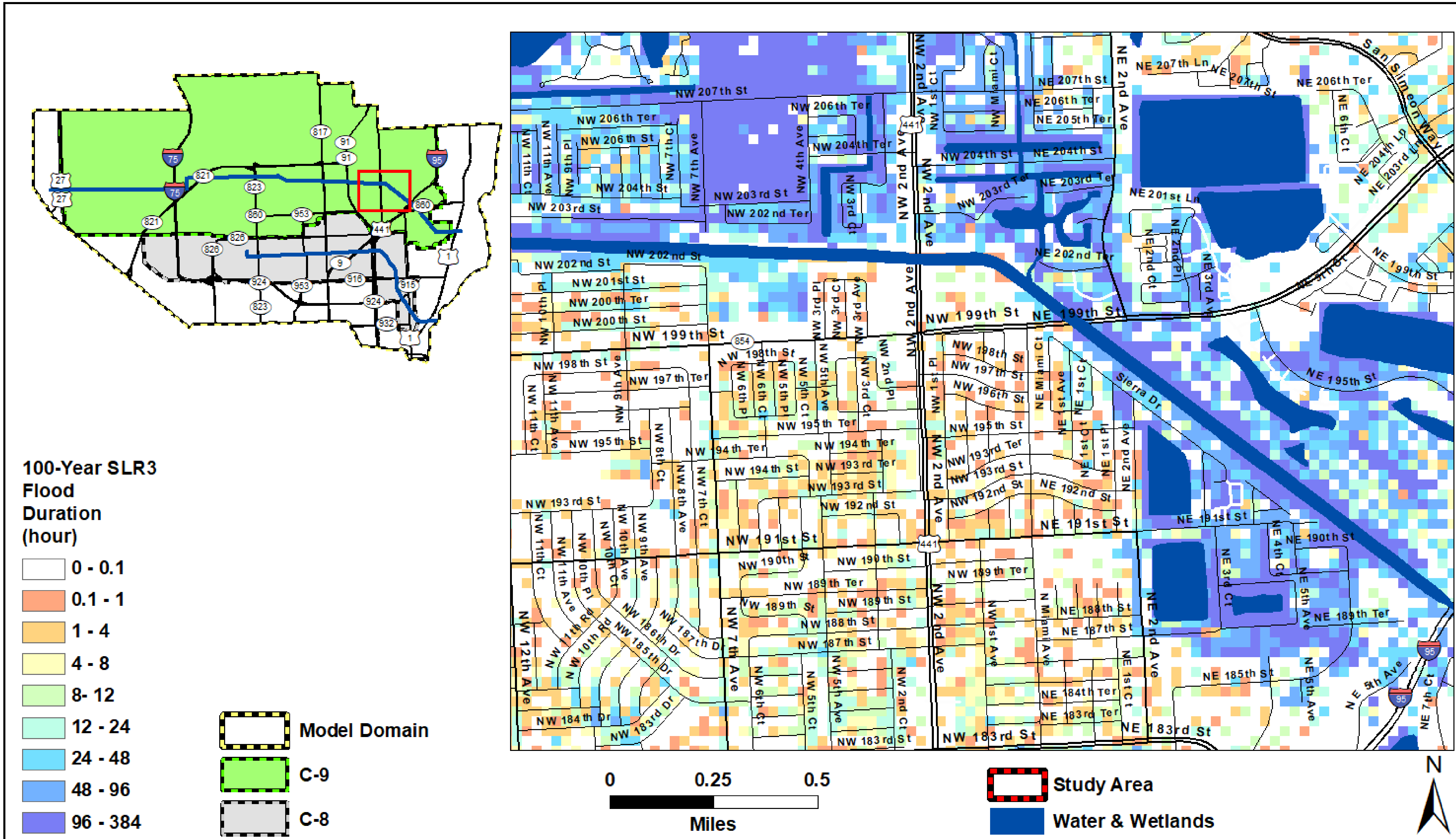

Figure 10.6-54: Up Close 100-Year Sea Level Rise 3 Flood Duration Map for the C-9 Canal Near US Hwy 441

10.6.9.6 Up-Close Flood Duration Maps for the C-9 Canal Near Ronald Reagan Turnpike

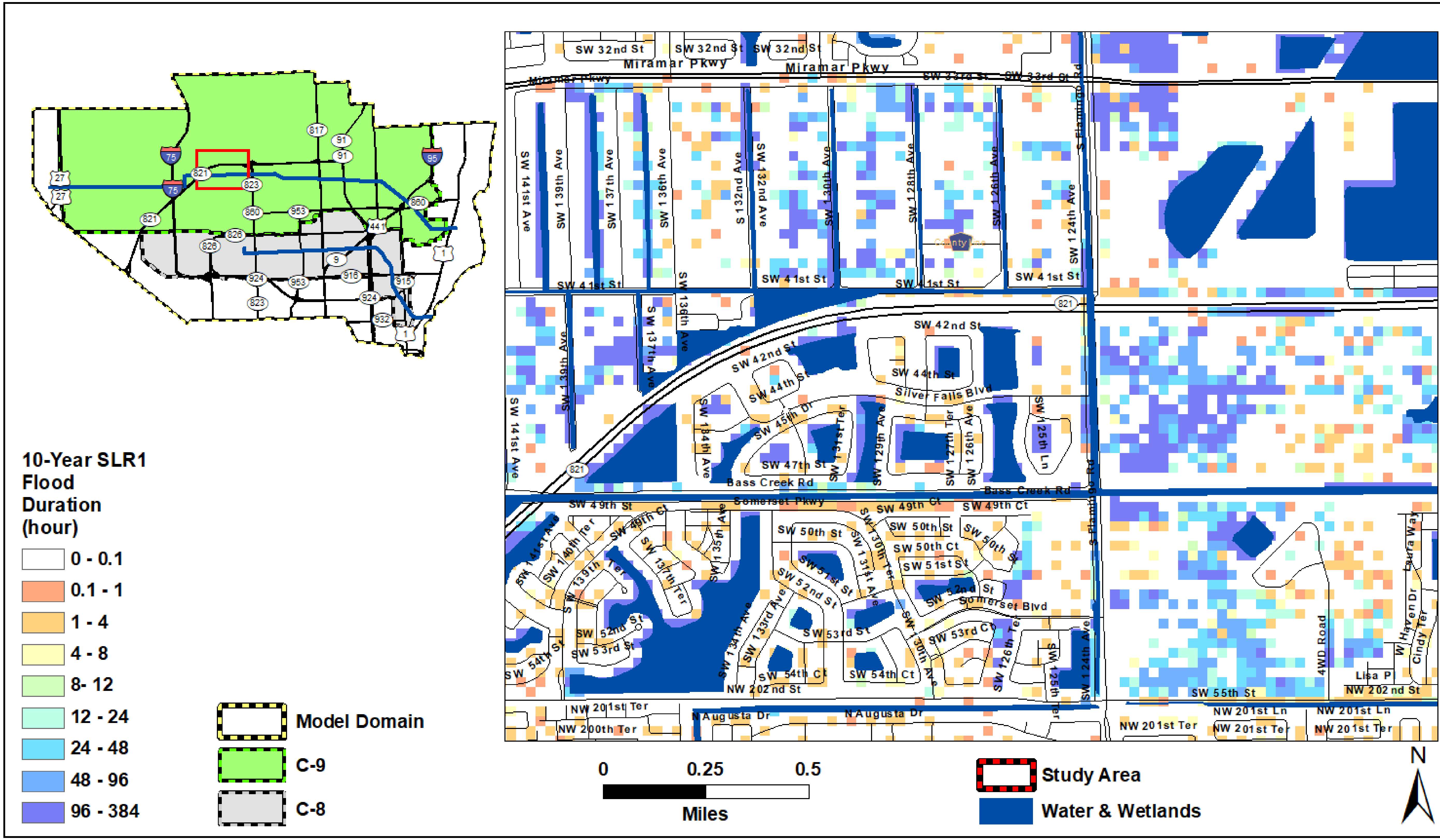

Figure 10.6-55: Up Close 10-Year Sea Level Rise 1 Flood Duration Map for the C-9 Canal Near Ronald Reagan Turnpike

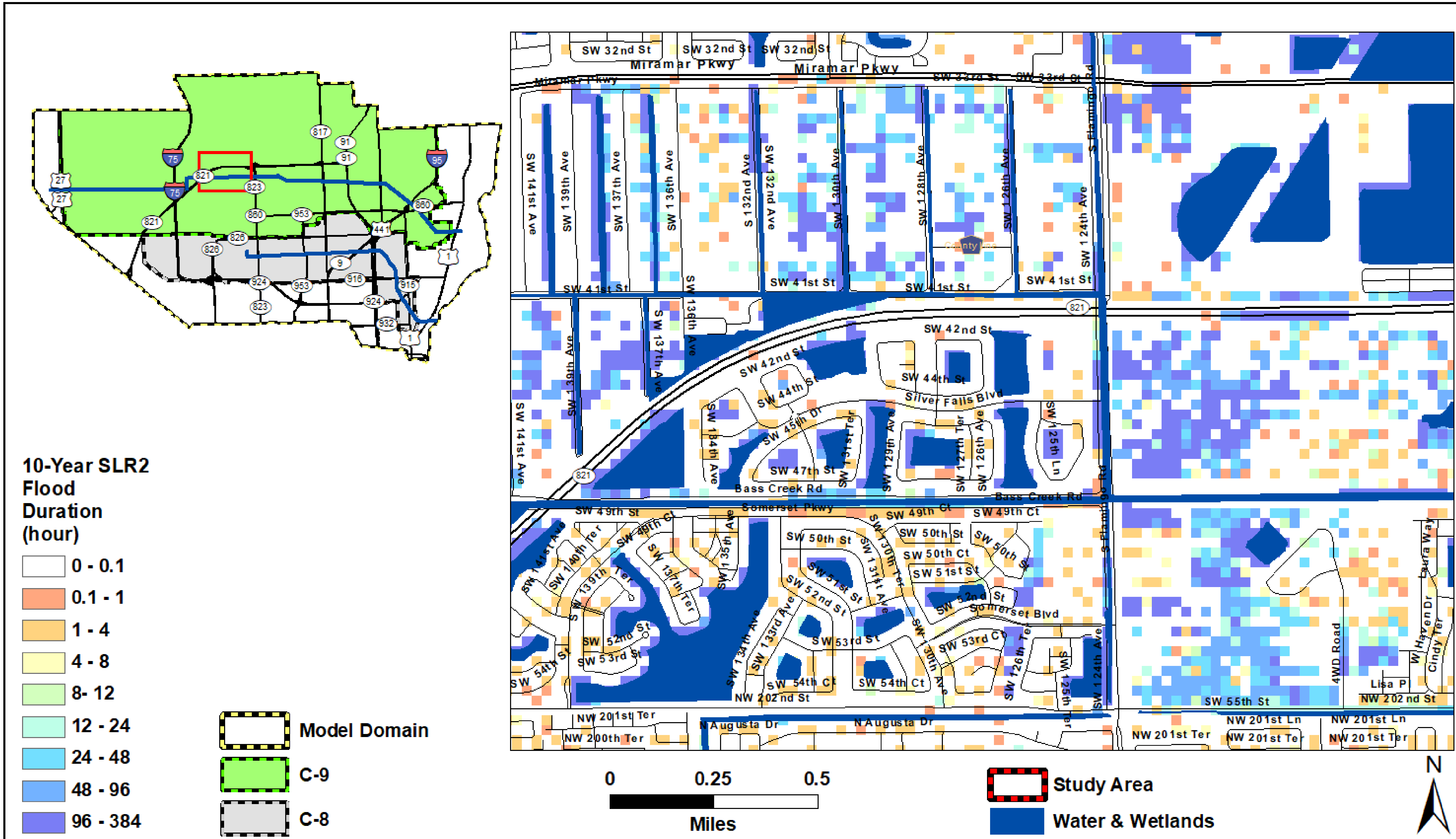

Figure 10.6-56: Up Close 10-Year Sea Level Rise 2 Flood Duration Map for the C-9 Canal Near Ronald Reagan Turnpike

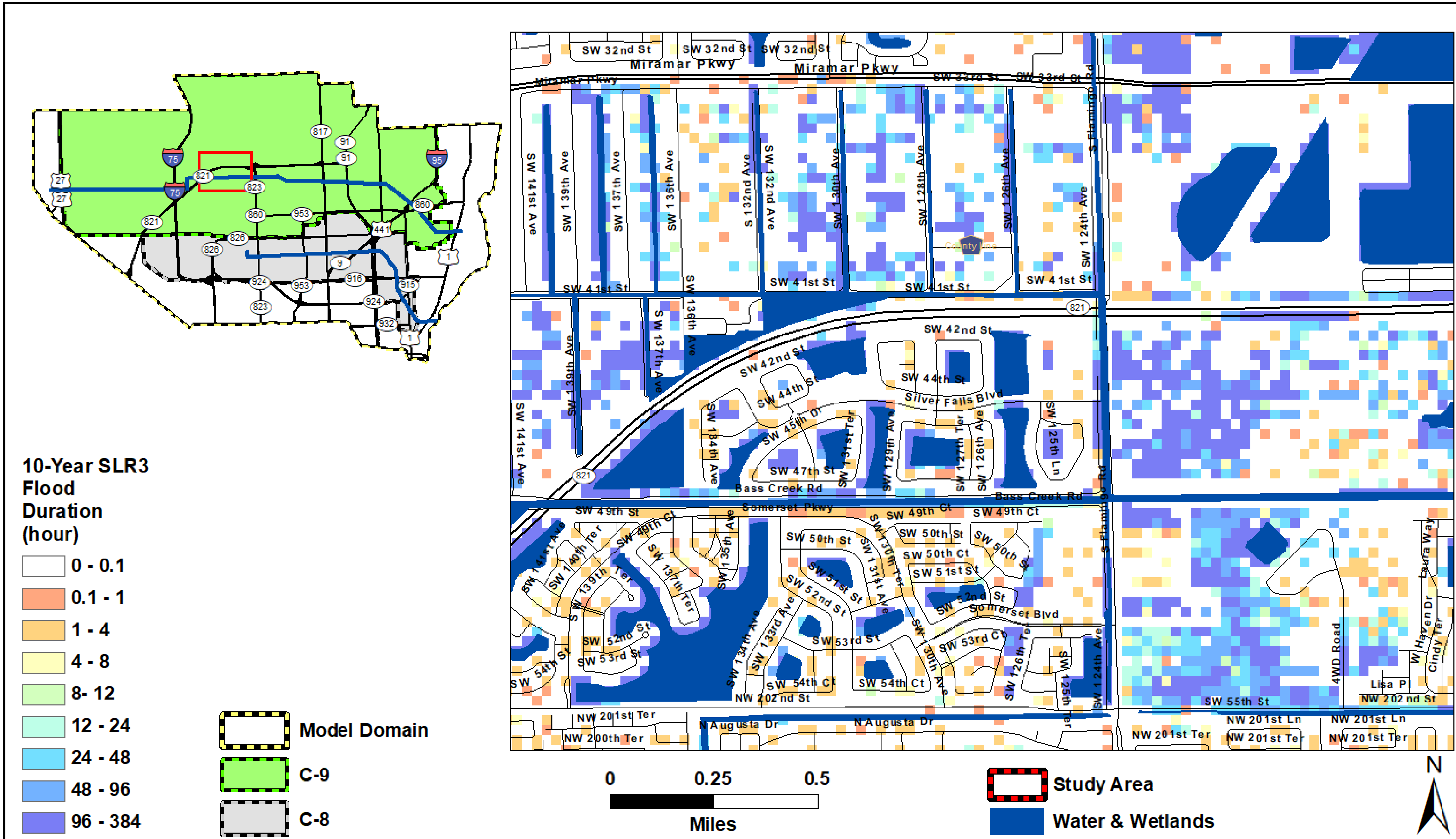

Figure 10.6-57: Up Close 10-Year Sea Level Rise 3 Flood Duration Map for the C-9 Canal Near Ronald Reagan Turnpike

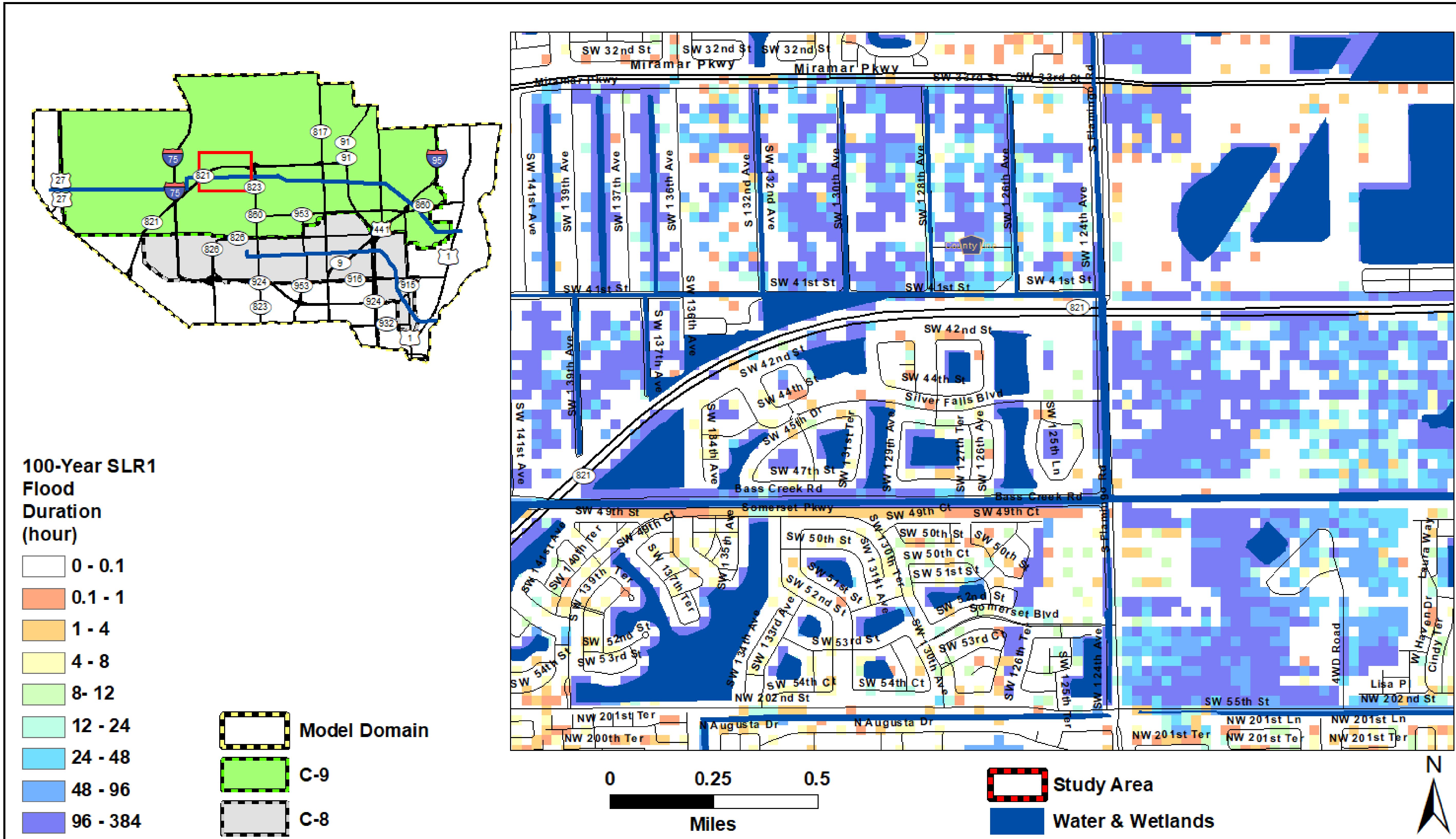

Figure 10.6-58: Up Close 100-Year Sea Level Rise 1 Flood Duration Map for the C-9 Canal Near Ronald Reagan Turnpike

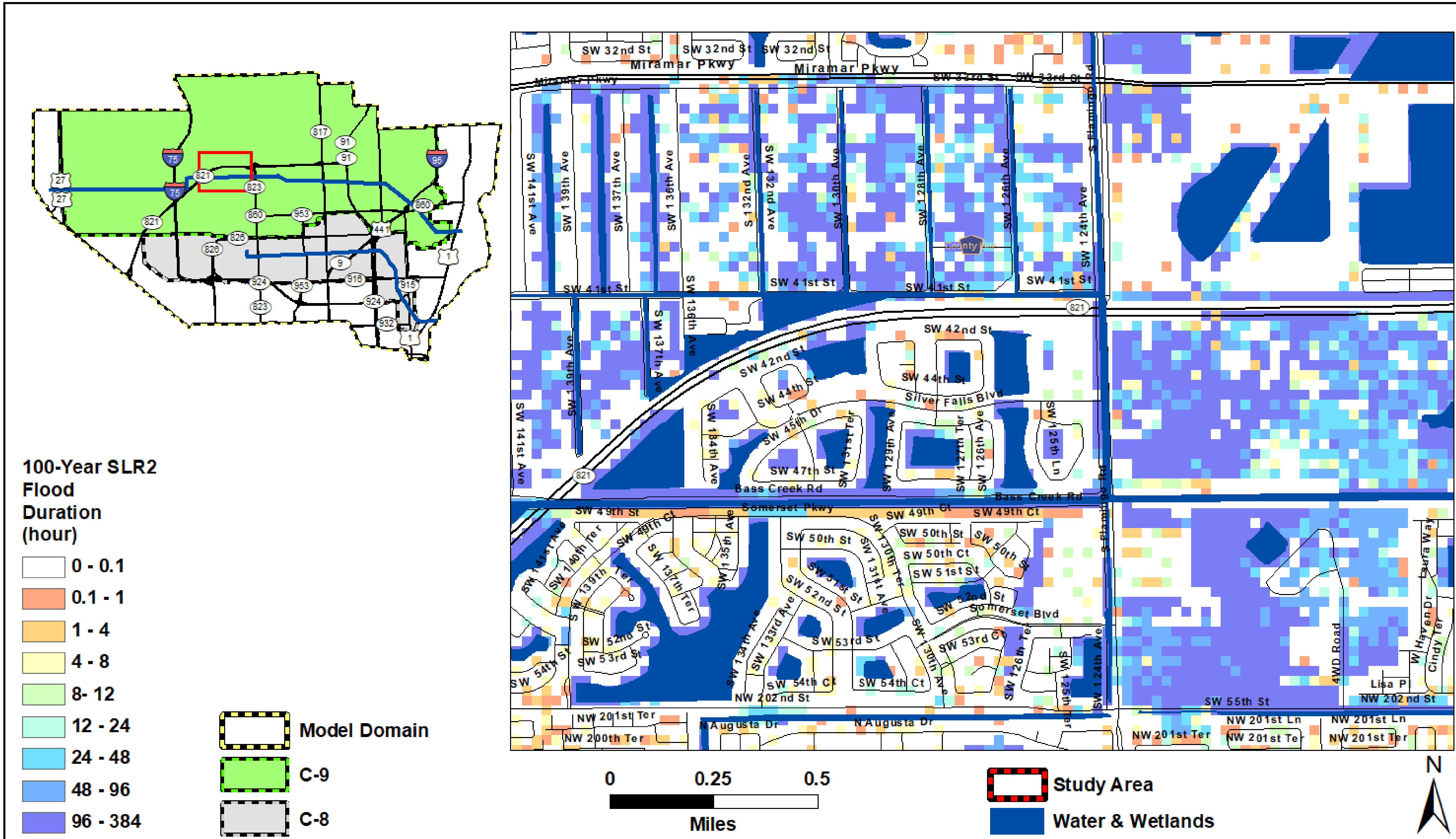

Figure 10.6-59: Up Close 100-Year Sea Level Rise 2 Flood Duration Map for the C-9 Canal Near Ronald Reagan Turnpike

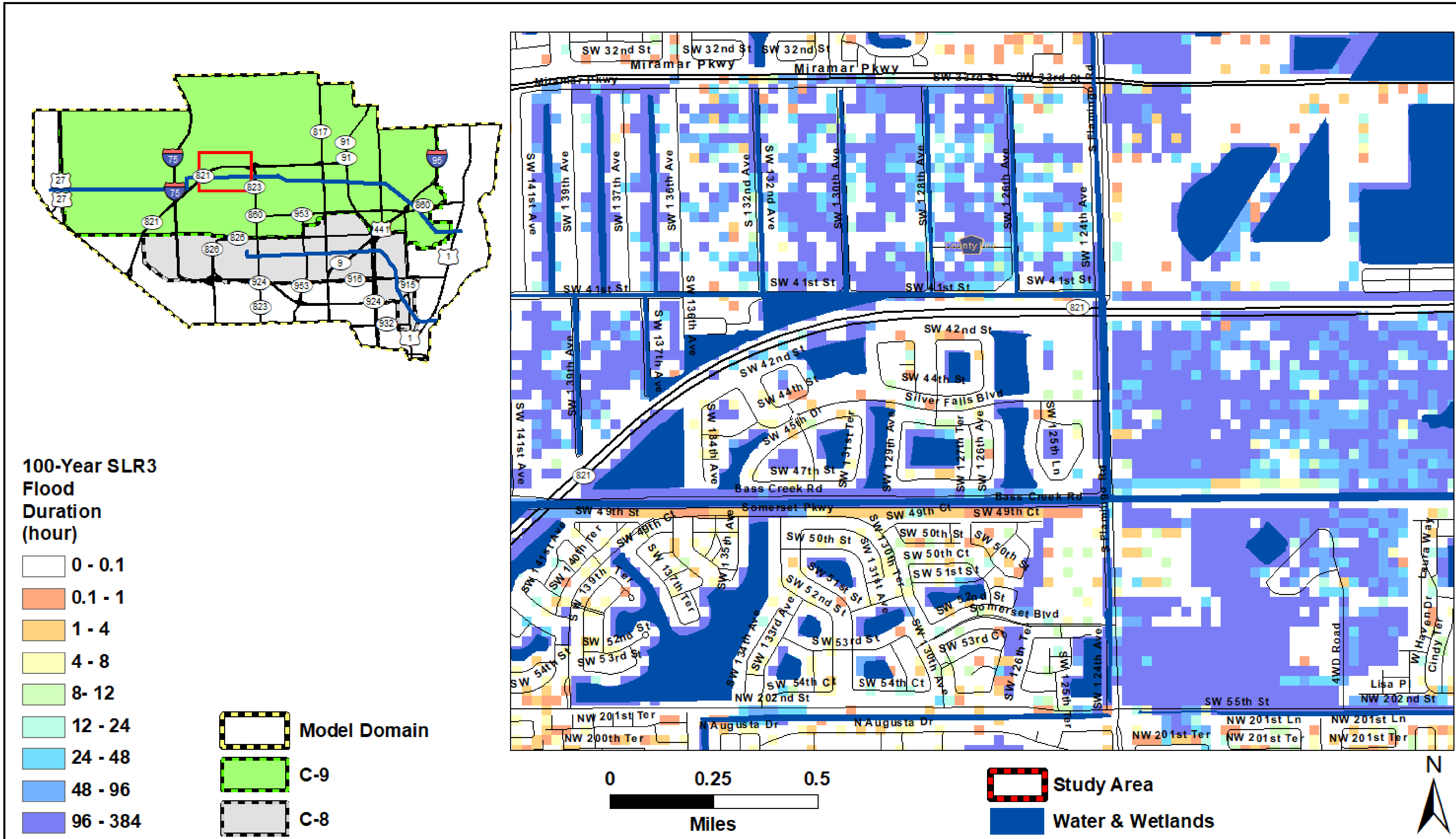

Figure 10.6-60: Up Close 100-Year Sea Level Rise 3 Flood Duration Map for the C-9 Canal Near Ronald Reagan Turnpike

10.6.9.7 Up-Close Flood Duration Maps for the C-9 Canal Near Red Road

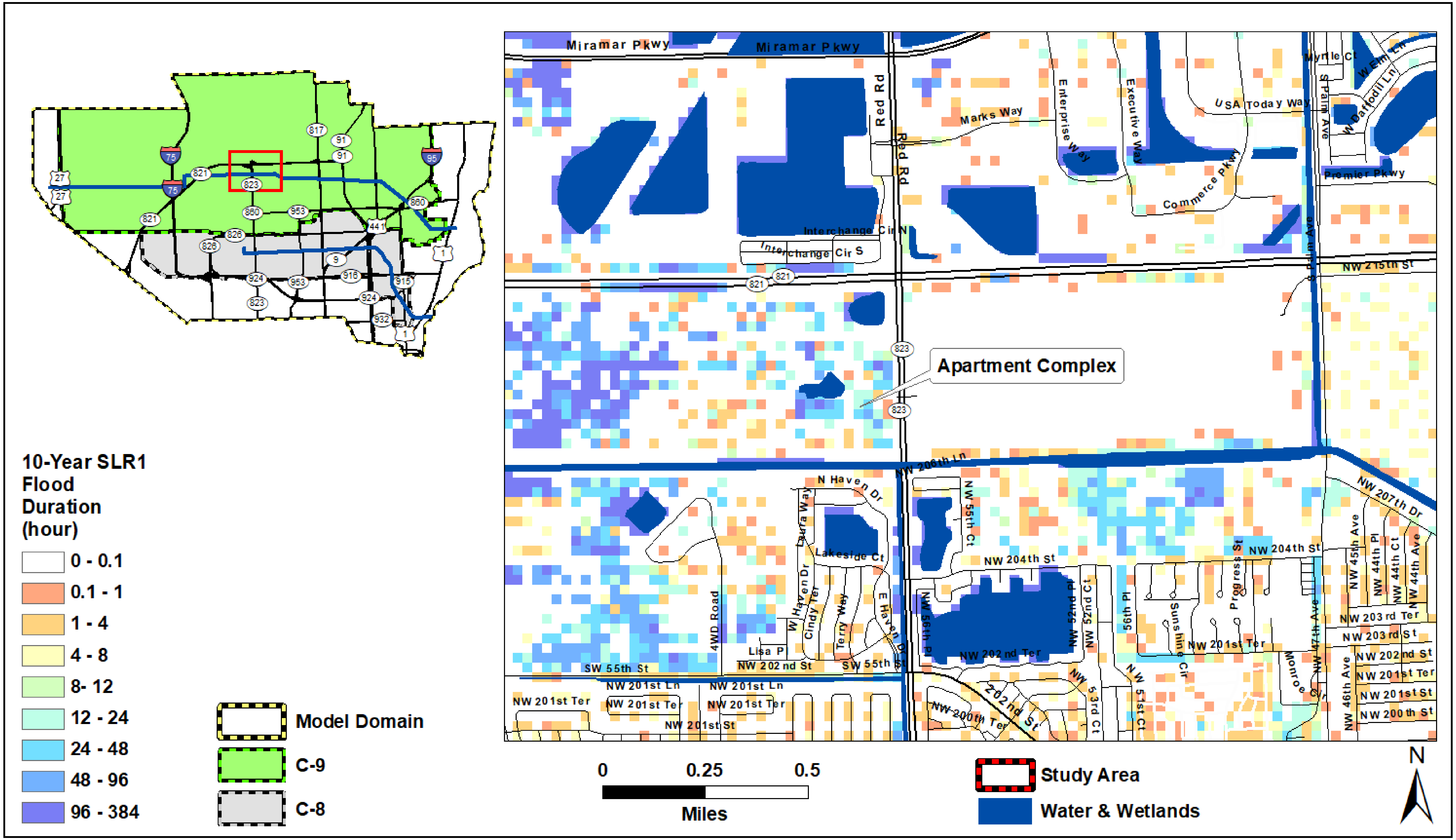

Figure 10.6-61: Up Close 10-Year Sea Level Rise 1 Flood Duration Map for the C-9 Canal Near Red Road

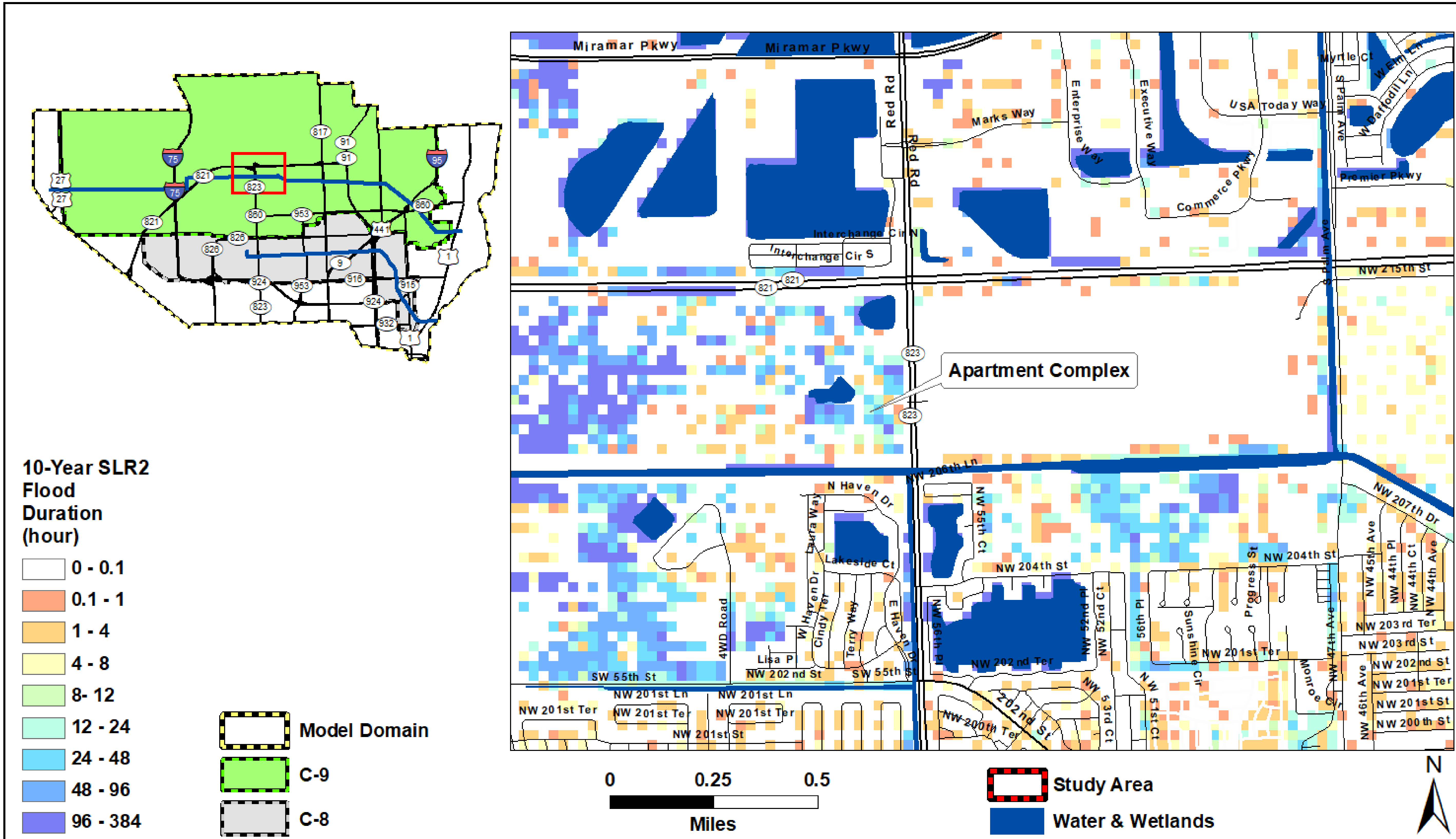

Figure 10.6-62: Up Close 10-Year Sea Level Rise 1 Flood Duration Map for the C-9 Canal Near Red Road

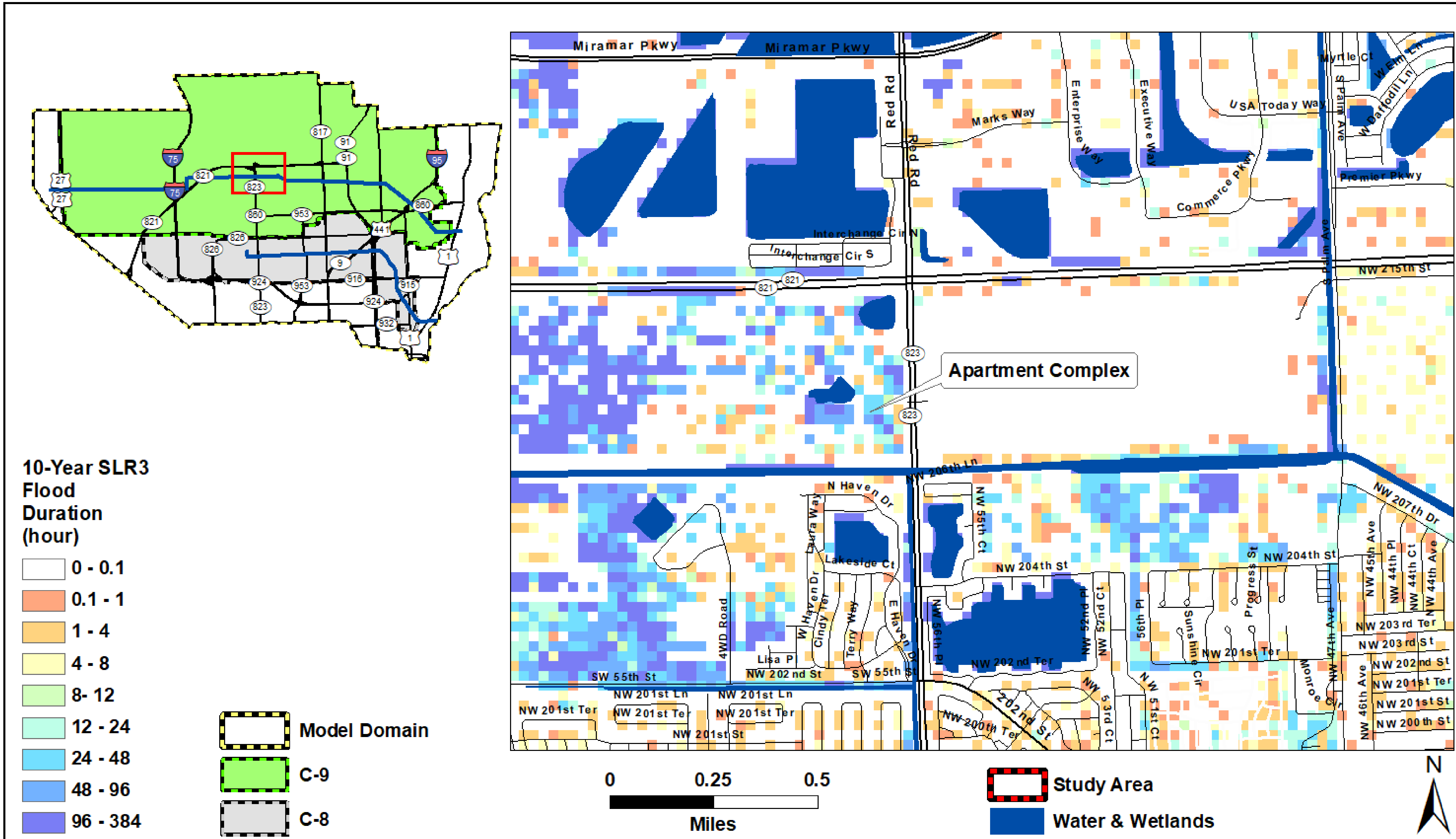

Figure 10.6-63: Up Close 10-Year Sea Level Rise 1 Flood Duration Map for the C-9 Canal Near Red Road

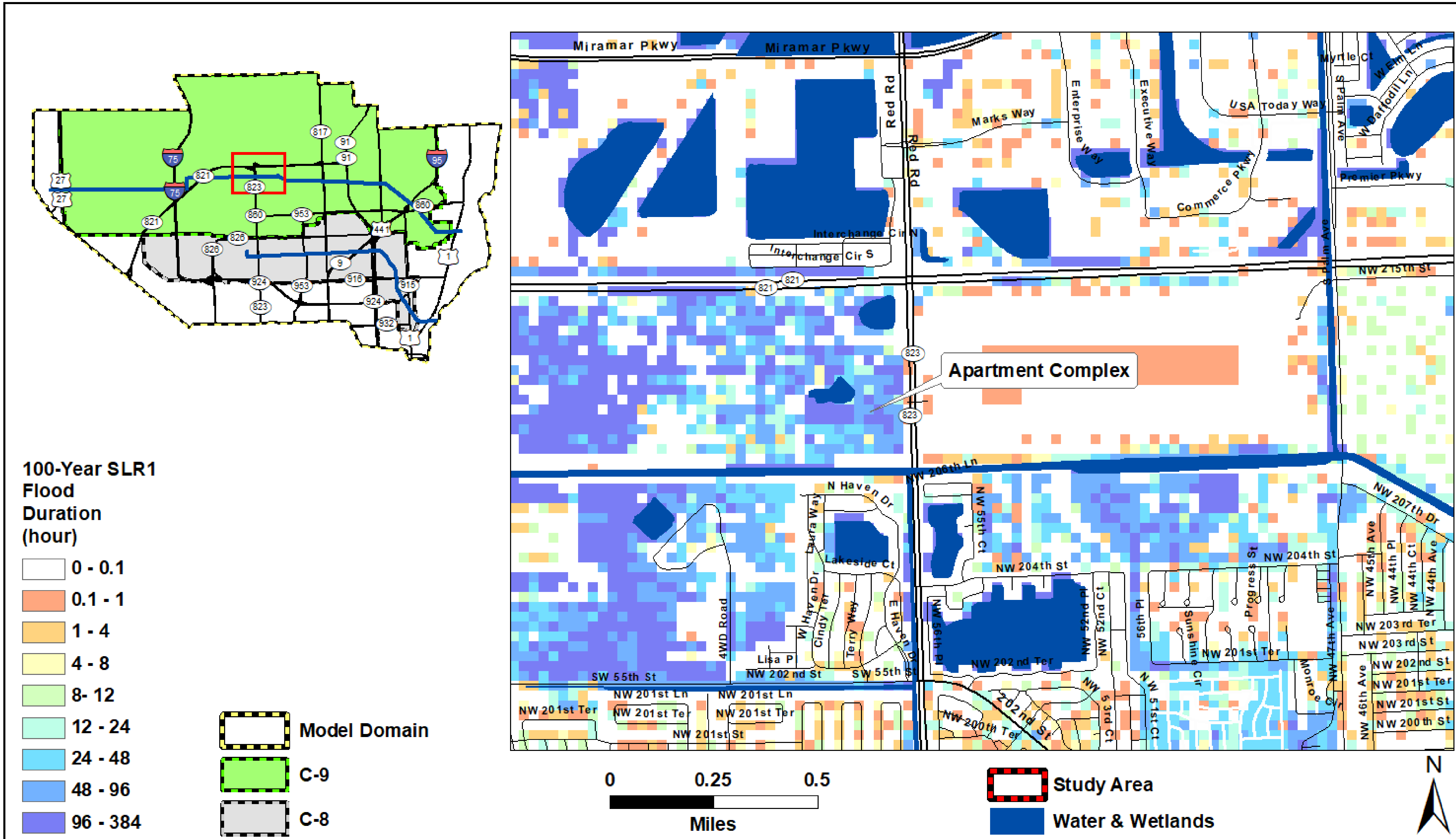

Figure 10.6-64: Up Close 100-Year Sea Level Rise 1 Flood Duration Map for the C-9 Canal Near Red Road

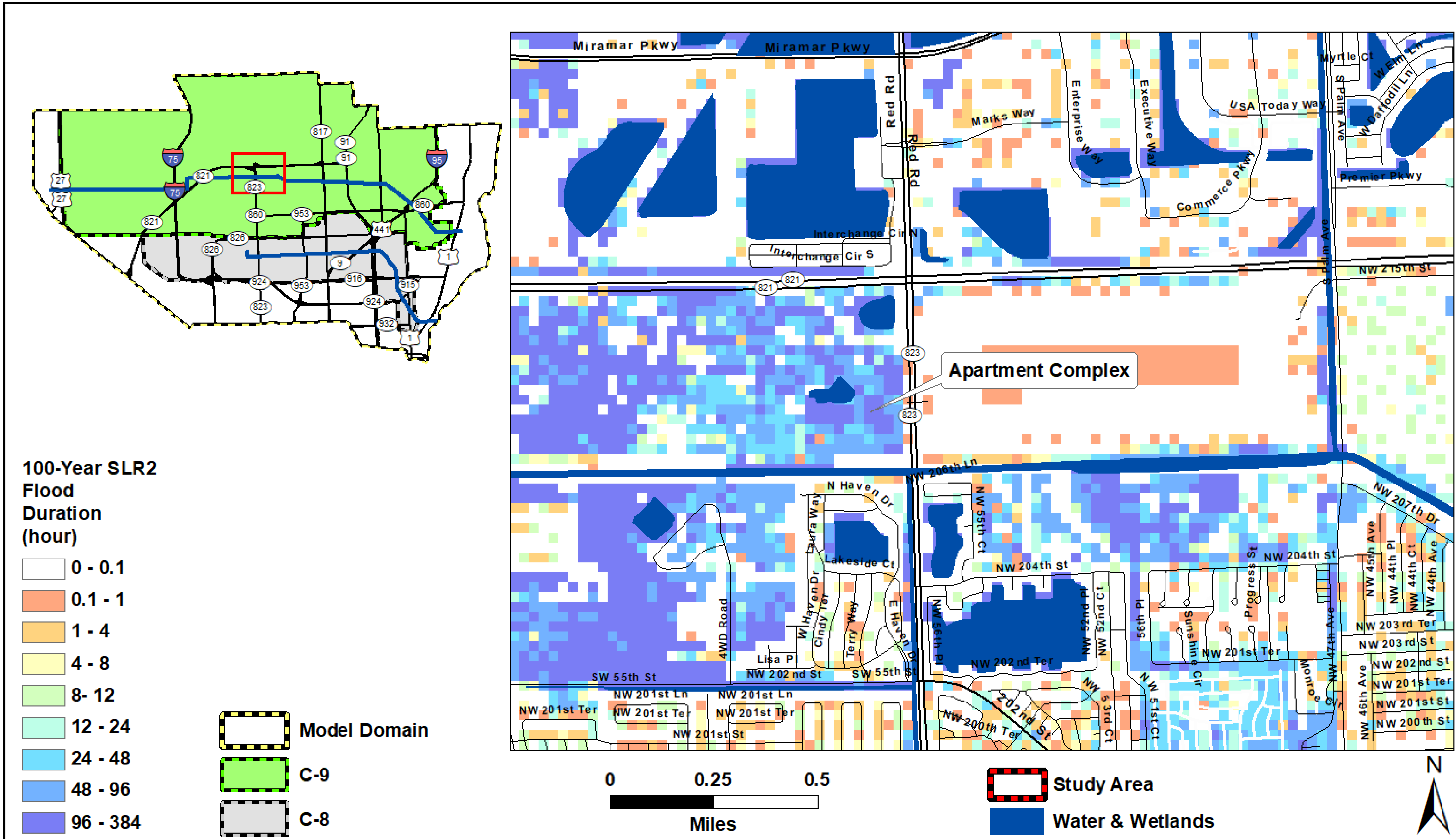

Figure 10.6-65: Up Close 100-Year Sea Level Rise 1 Flood Duration Map for the C-9 Canal Near Red Road

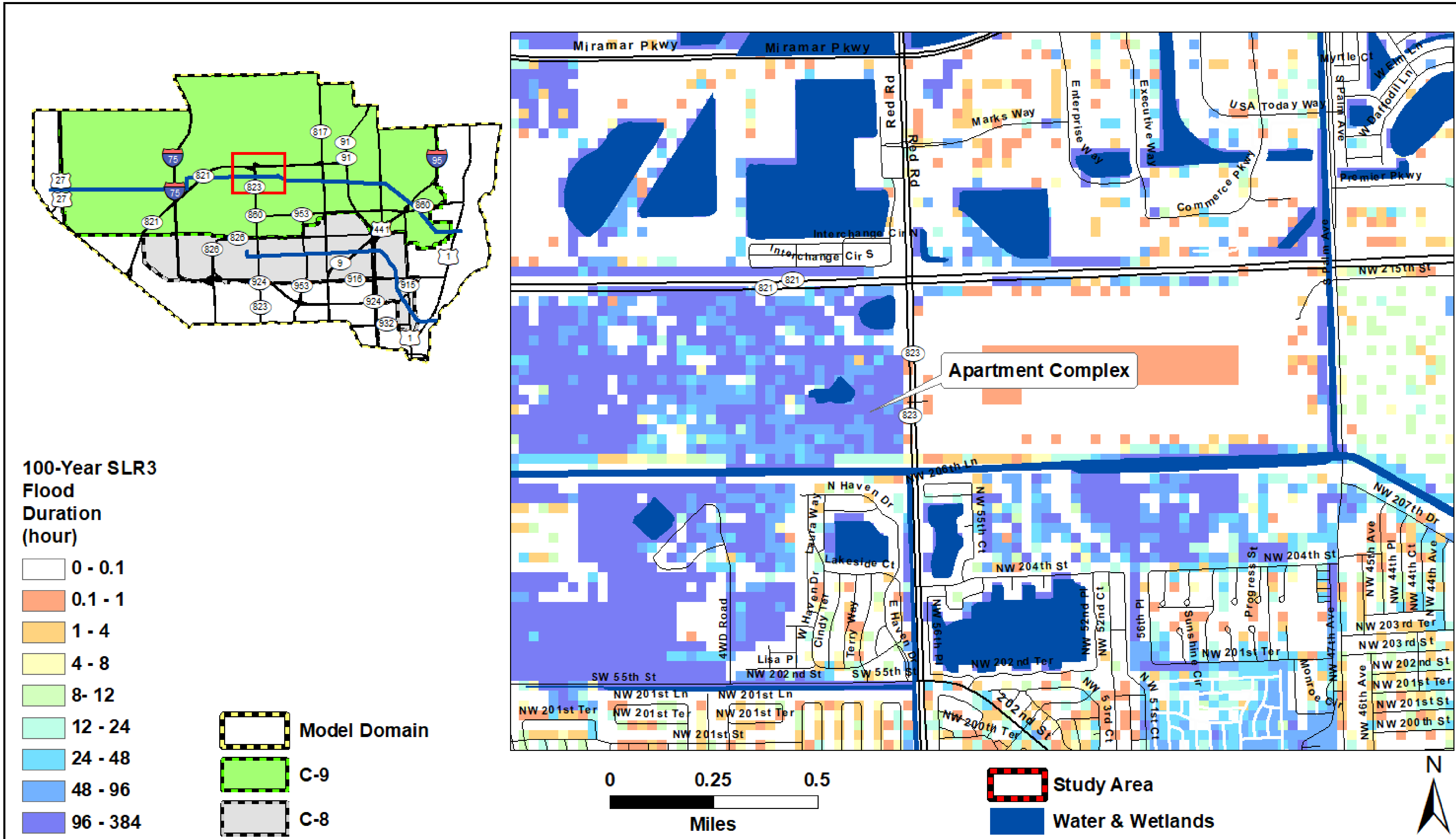

Figure 10.6-66: Up Close 100-Year Sea Level Rise 1 Flood Duration Map for the C-9 Canal Near Red Road

10.6.10 Flood Duration Difference Maps for Urban Land Use Areas

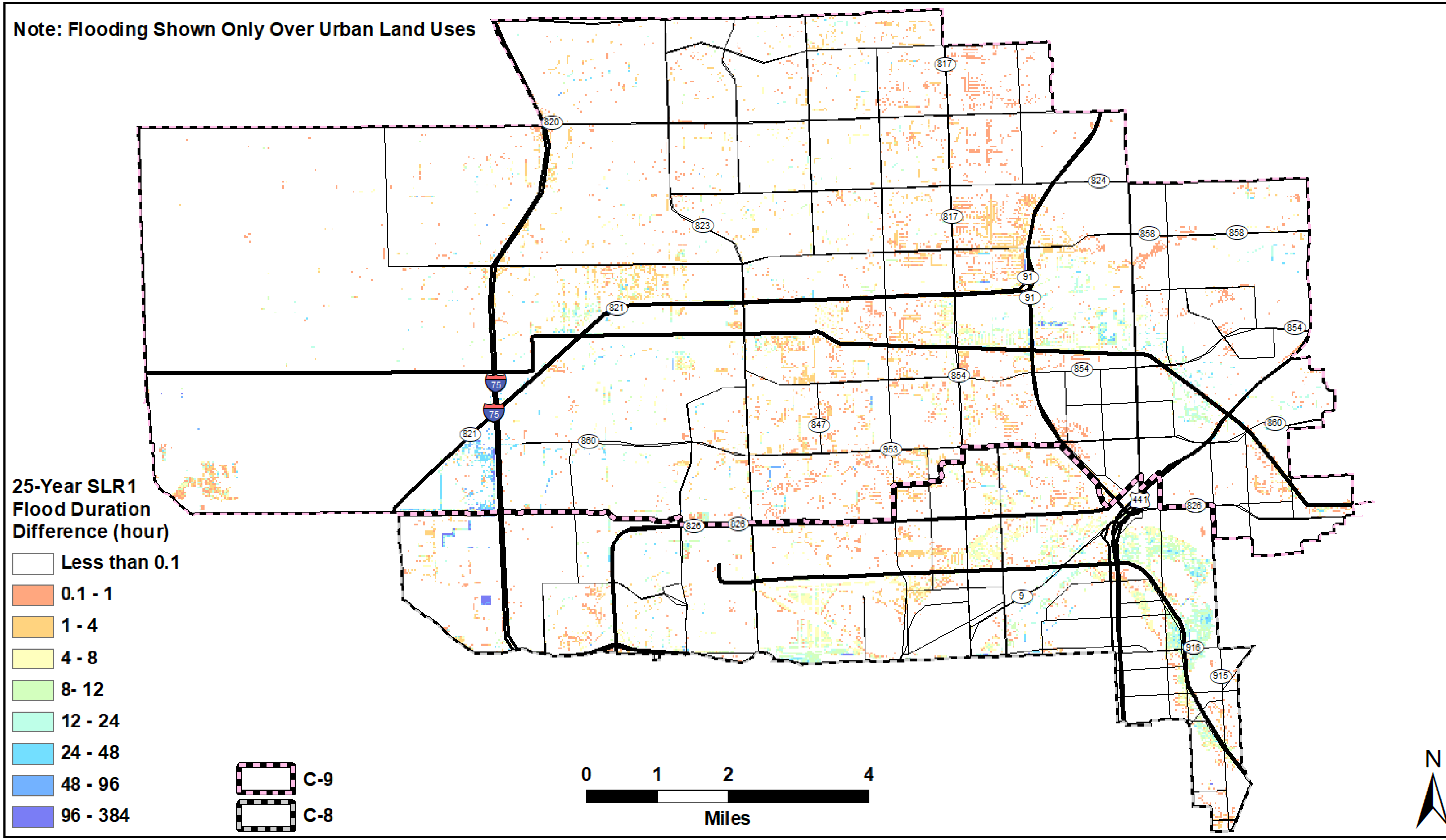

Figure 10.6-67: Flood Duration Difference Map for 25-Year Sea Level Rise 1 Design Storm Event in Urban Land Use Areas (Future minus Current Conditions)

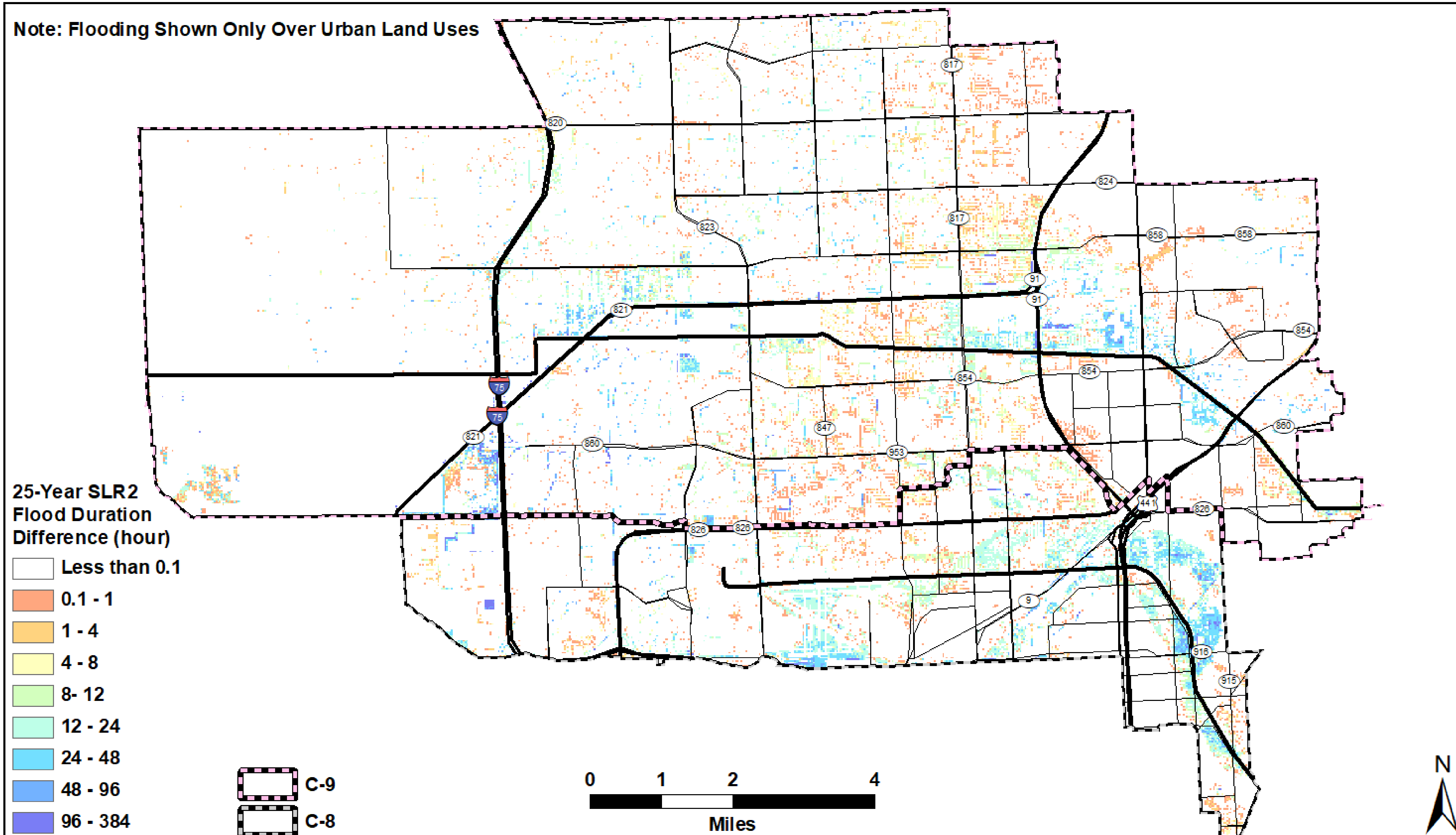

Figure 10.6-68: Flood Duration Difference Map for 25-Year Sea Level Rise 2 Design Storm Event in Urban Land Use Areas (Future minus Current Conditions)

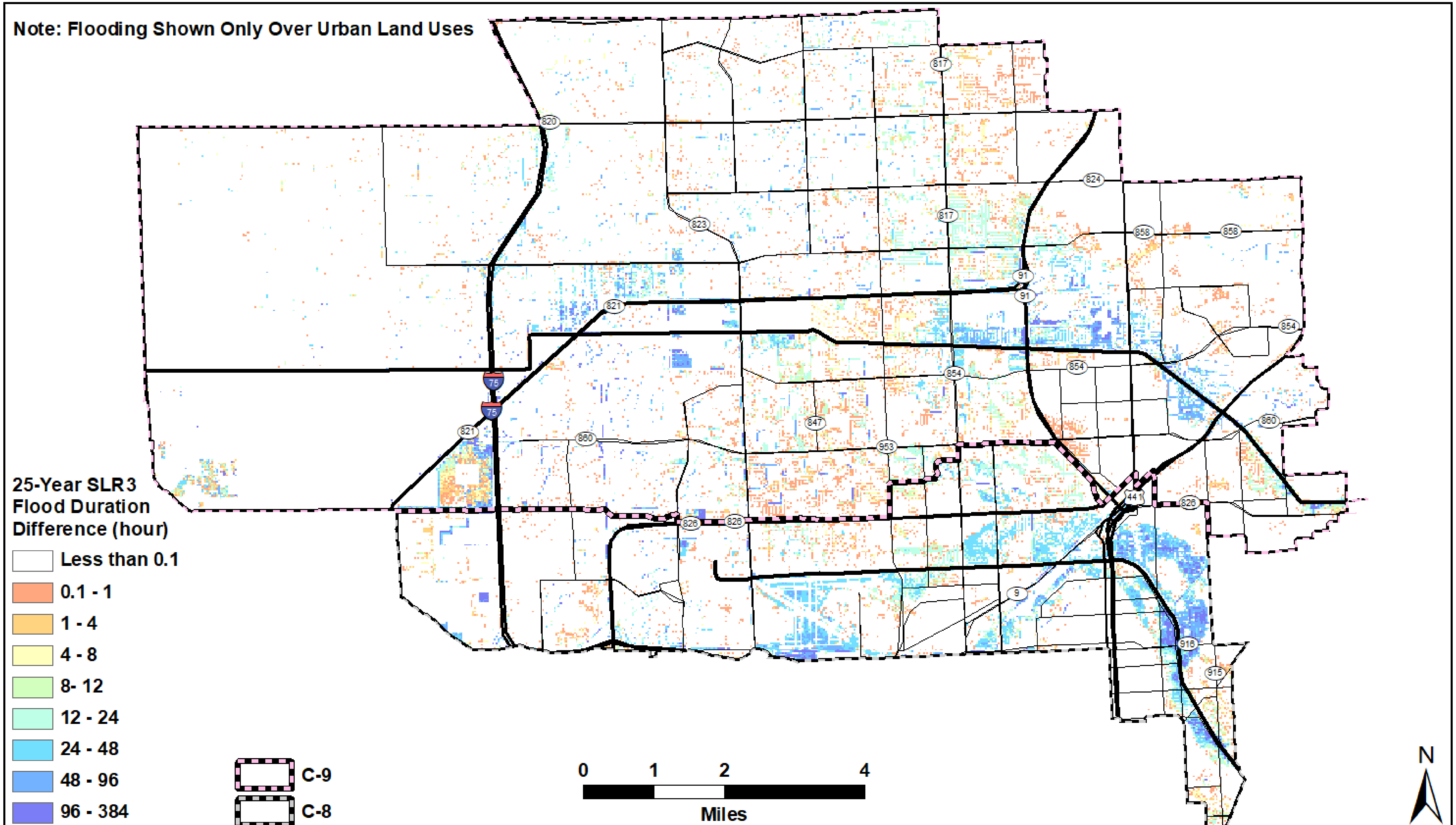

Figure 10.6-69: Flood Duration Difference Map for 25-Year Sea Level Rise 3 Design Storm Event in Urban Land Use Areas (Future minus Current Conditions)

10.7 Future Sea Level Conditions FPLOS Assessment Conclusions

The future conditions design storm simulation results were evaluated using six performance measures. The analysis presented in this report provides a model-based assessment of the future level of flood protection provided by the existing C-8 and C-9 watershed's primary canal network and associated control structures. These results were used to determine potential FPLOS deficiencies by highlighting areas that failed multiple performance measures, such as bank exceedances that result in overland inundation (PM #5 and/or PM #6). In many cases, PM #1 bank exceedances did manifest as significant overland inundation, shown in PM #5, and thus were considered significant localized FPLOS deficiencies.

It should also be noted that the model results are subjected to certain limitations associated with the scale of the 2-dimensional model grid. Although the model uses a 125-ft grid that is suitable for the sub-regional scale flood protection level of service evaluation, the results should not be extended to local-scale evaluations or regulatory determinations of flooding extents since considerable variations in topography can occur within the area of each grid cell.

10.7.1 Future Sea Level Conditions FPLOS Assessment Conclusions for C-8 Watershed

Based on the results of the future condition simulations, the C-8 Canal generally provides a 5-year or less level of service, especially for the 2 ft and 3 ft sea level rise conditions. Although some localized areas have a 25-year level of service or better with respect to bank exceedances, the system as a whole is overwhelmed for the design storms of lower intensity. Under the 3 ft sea level rise scenario, even a 5-year design storm was enough to flood a significant portion of the system. There were a few localized areas where the water levels exceeded the canal banks for the 5-year 1 ft sea level rise event as shown in PM #1 (**Figure 10.1-2)**, however, it does not correspond to a significant area of flood inundation as shown in PM #5 (**Figure 10.5-1).** For the 25-year design storm, regardless of the amount of sea level rise, the model results suggest that a significant portion of the eastern half of the C-8 Canal would be overwhelmed during peak flood conditions, with the western segment (west of Marco Canal) generally performing better. For the 100-year design storm, regardless of the amount of sea level rise, the model results suggest that most of the C-8 Canal would be overwhelmed during peak flood conditions, while most of the watershed would be inundated to some degree. As expected, the 100-year 3 ft sea level rise event was the worst-case scenario simulated and it shows that nearly half of the C-8 Canal would be out-of-bank (**Figure 10.1-8)** and a significant portion of the watershed would inundated, with large areas experiencing over 2 feet of flood depth (**Figure 10.5-12**).

The C-8 Canal is overwhelmed in large segments for the majority of the design storm and sea level rise combinations, which can be in-part attributed to its low bank elevations. However, the S-28 tidal outfall structure also has a significant role in the performance of the C-8 Canal. Under future conditions sea level rise scenarios, the discharge capacity of the S-28 structure is reduced. Looking at the 12-hour moving average peak discharge, it becomes apparent that S-28 is unable to maintain design capacity under certain sea level rise conditions. Although peak discharge is not reduced drastically for the SLR 1 and 2 foot scenarios for design storms up to and including the 25-year event, the peak discharge is reduced by 24%, 19%, 20%, and 28%, from current conditions to the 3 ft sea level rise scenario for the 5, 10, 25, and 100-year design storms, respectively. The peak discharge response is different at S-29, which starts to "feel the effects" of sea level rise for even the 1 ft SLR scenario and for the smaller storm events (discussed in the next subsection). Interestingly, the instantaneous peak discharge is larger under future conditions, however, this is a result of the increased surge-induced reverse flow which is bypassing the structure and causing the water to "stack", which provides the opportunity for increased instantaneous discharge once the tide level falls. The design discharge of 3220 cfs was only reached during the 100-year design storm events, however, the design headwater assumption is violated by 2.2 ft. The assumed design headwater stage is 2.2 feet, while the predicted headwater is 4.4 feet at the time of peak discharge. Although the design discharge can be passed, the resulting increased headwater elevation causes flooding within the C-8 watershed.

10.7.2 Future Sea Level Conditions FPLOS Assessment Conclusions for C-9 Watershed

Based on the results of this study, it appears that the C-9 Canal generally provides a 10-year or less level of service for the 1 ft and 2 ft sea level rise conditions and a 5-year level of service for the 3 ft sea level rise scenario. Although some localized areas have a 25-year or 100-year level of service with respect to bank exceedances, the system as a whole is overwhelmed for the design storms of lower intensity. Under the 3 ft sea level rise scenario, a 10-year design storm was enough to overwhelm a significant portion of the system. There were a few localized areas where the water levels exceeded the canal banks for the 10-year 1 ft sea level rise event as shown in PM #1 (**Figure 10.1-5**), however, it does not correspond to a significant area of flood inundation as shown in PM #5 (**Figure 10.5-4**). For the 25-year design storm, regardless of the amount of sea level rise, the model results suggest that a large portion of the C-9 Canal would be overwhelmed during peak flood conditions, with the western segment (west of Carol City Canal A) generally performing better. For the 100-year design storm, regardless of the amount of sea level rise, the model results suggest that most of the C-9 Canal would be overwhelmed during peak flood conditions, while most of the watershed would be inundated to some degree. The 100-year 3 ft sea level rise event was the worst-case scenario simulated, and it shows that nearly half of the C-9 Canal would be out-of-bank (**Figure 10.1-9**) and a significant portion of the watershed would inundated, with large areas experiencing over 2 feet of flood depth (**Figure 10.5-12**).

The C-9 Canal is overwhelmed in localized segments for the majority of the design storm and sea level rise combinations, which can be attributed to its low bank elevations and higher tailwater conditions under sea level rise scenarios. The discharge capacity of the S-29 structure is reduced under all of the future sea level rise scenarios. Looking at the 12-hour moving average peak discharge, it becomes apparent that S-29 is unable to maintain design capacity under all sea level rise conditions. For the 5, 10, 25, and 100-year design storms, the peak discharge is reduced by 23%, 22%, 14%, and 9%, respectively, from current conditions to the 1 ft sea level rise scenario. Similarly, a reduction of 46%, 35%, 26%, and 21%, respectively, is seen for the 2 ft sea level rise scenario and 58%, 49%, 43%, and 38%, respectively, is seen for the 3 ft sea level rise scenario. These reductions are due to a combination of factors: (1) the C-9 Impoundment removing water from the western C-9 Canal will ultimately reduce the total volume discharged to tide, (2) discharge from some of the eastern SBDD pump stations will be limited due to stages in the C-9 Canal triggering "pump off" conditions required by permit, and (3) the storage characteristics of the western C-9 basin, namely the prevalence of large lakes (former mine pits) ,which have the ability to attenuate peak discharge rates and accommodate storm surge-induced flow reversals.

11 RAINFALL SENSITIVITY TEST – 10-YEAR SLR1 DESIGN STORM

A rainfall sensitivity test was conducted for the future conditions design storms using the 10-year 1 ft sea level rise scenario. A 9% increase was applied to the NOAA Atlas 14 10-year rainfall depths based on the Broward County DDF Change Factor Ensemble Analysis (Yin, Li, & Urich, 2019). The sensitivity test used the same SFWMD 3-day temporal distribution and Thiessen Polygon spatial distribution used in the previous design storm simulations. The total rainfall depth was the only parameter change for the sensitivity test. **Section 11.1** through **Section 11.5** describe the applicable results of the FPLOS evaluation on the 10-year SLR1 rainfall sensitivity simulation.

11.1 PM #1 – Maximum Stage in Primary Canals

This is the peak stage profile in the primary canal system. The profile was developed for the 10-year 72-hour design storm with 1 ft sea level rise and a 9% increase in rainfall. To evaluate this PM under future conditions within the C-8 and C-9 watersheds, instantaneous peak stage profiles were prepared for the primary canals within the watersheds, which are the C-8 and C-9 Canals, respectively. Bank elevations on the profile figures are based on the MIKE HYDRO cross-section data. Also shown in the figures are major roadway landmarks, control structures, and primary canal junctions. **Figure 11.1-1** and **Figure 11.1-2** show the maximum stage in the C-8 and C-9 Canals, respectively.

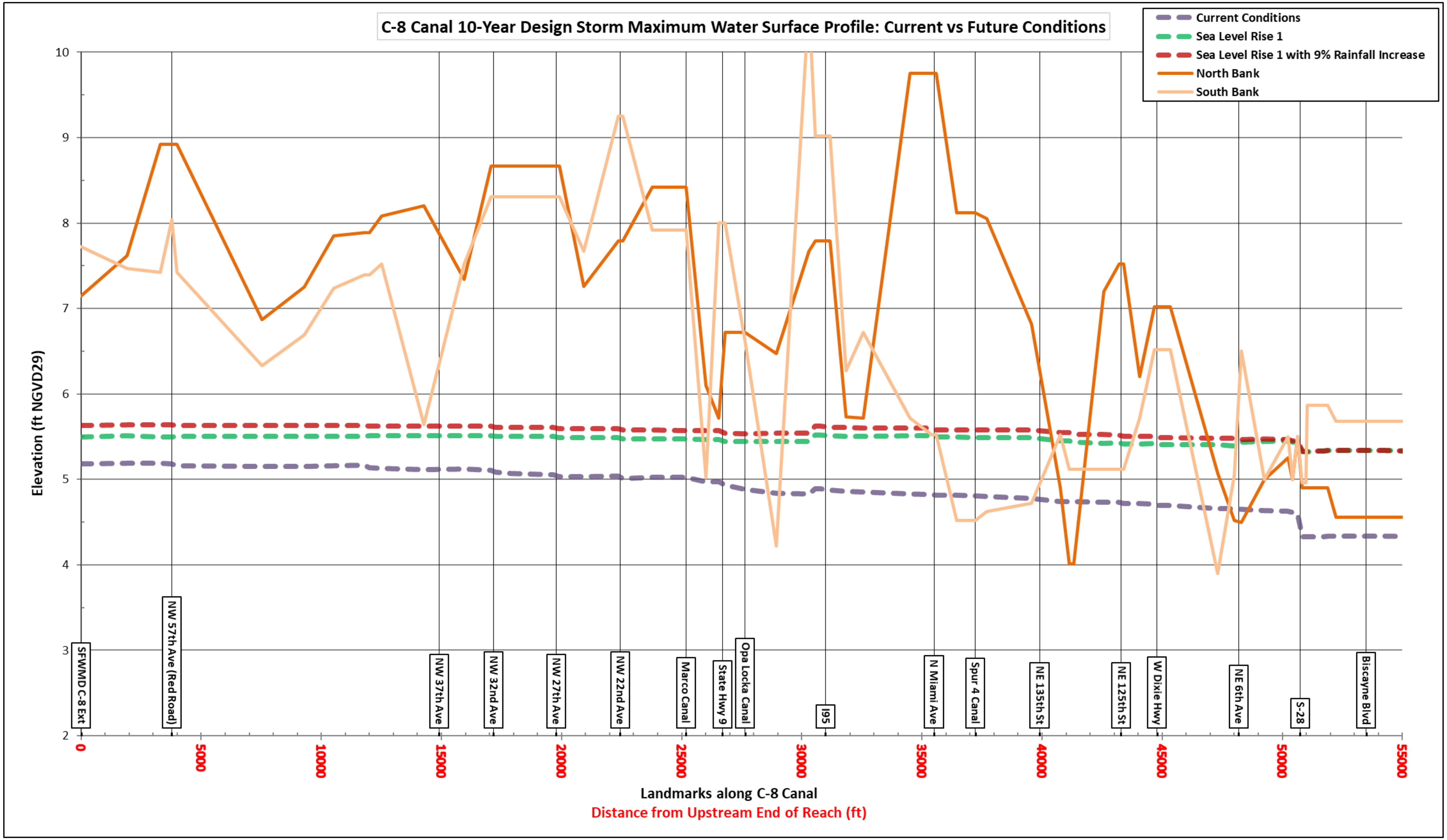

Figure 11.1-1: C-8 Canal Peak Stage Profiles for 10-Year Design Storm – Current vs Future Sea Level Rise and Rainfall Scenarios

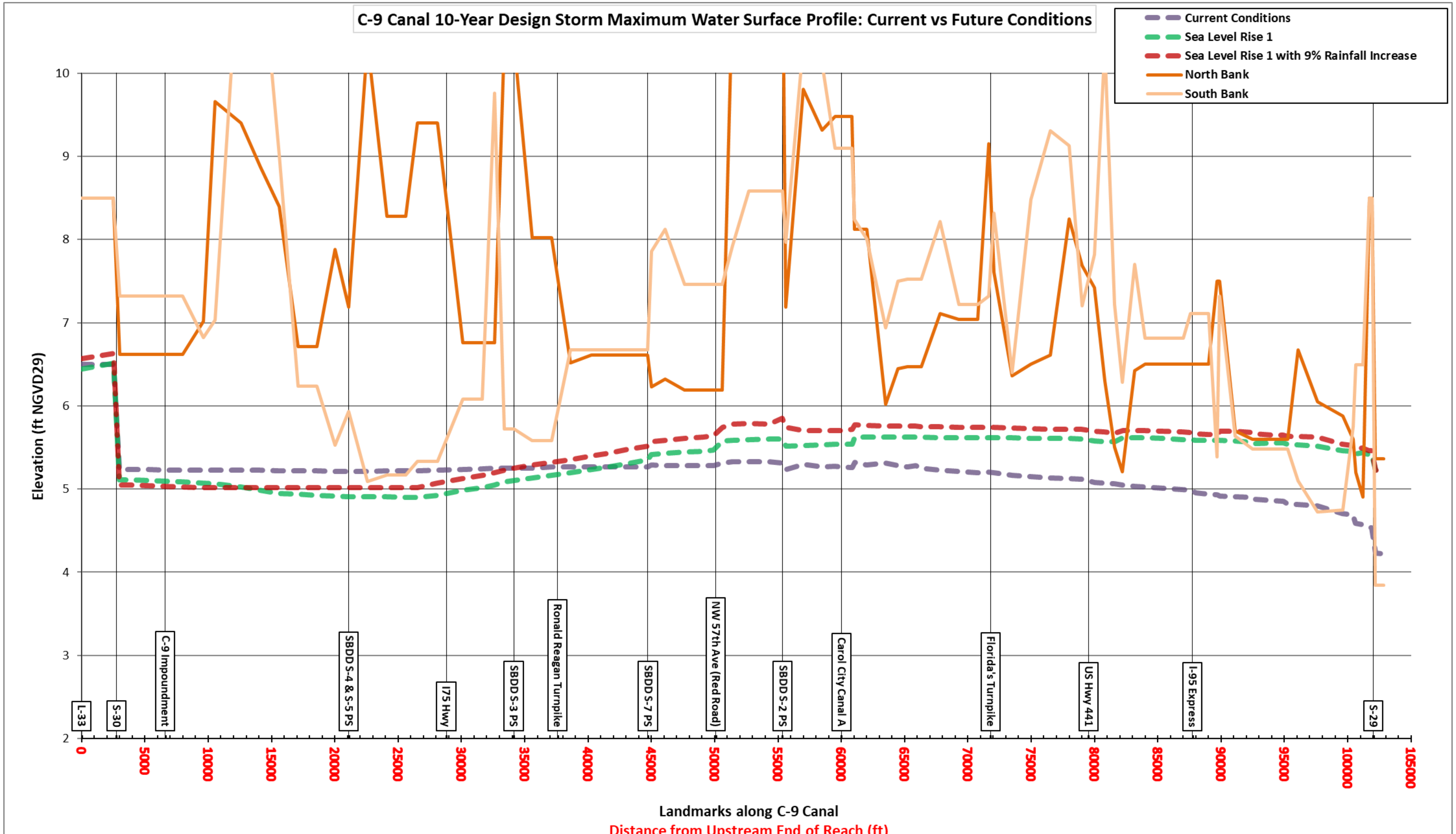

Figure 11.1-2: C-9 Canal Peak Stage Profiles for 10-Year Design Storm – Current vs Future Sea Level Rise and Rainfall Scenarios

11.2 PM #2 – Maximum Daily Discharge Capacity through the Primary Canals

Discharge capacity was calculated by dividing the peak of the discharge hydrograph by the canal segments contributing area. For structures S-28 and S-29, discharge capacity was calculated by dividing the peak discharge by the entire basin area. For the C-9 Basin, two additional estimates were made for the respective areas east and west of Red Road. These two additional estimates were necessitated by the presence of two different allowable runoff rates within the C-9 Basin. For the drainage area west of Red Road, the peak discharge at the Q-point located at Red Road (shown as a green dot in **Figure 10.2-1**) was divided by the contributing drainage area (highlighted in green in **Figure 10.2-1**). For the drainage area east of Red Road, the peak discharge at the Q-point located at Red Road was subtracted from the peak discharge at structure S-29, and then divided by the contributing drainage area east of Red Road. Tidal effects were filtered by using a 12-hour moving average of discharge.

Table 11-1 lists the canal segments identified for this analysis, the contributing area for each canal segment, and the discharge capacity calculated for each segment associated with each of the 10-year design scenarios analyzed.

Table 11-1: Water Control Catchment Discharge Capacity for 10-Year Future Conditions Design Storms

Structure / Segment	Inflow	Outflow	Water Control Catchment Area (sq.mi)	10-Year Design Storm Peak Discharge Capacity (cfs/sq.mi)		
				Current	SLR1	SLR1 w/ Rainfall Increase
S-28	Beginning of C-8	S-28	28.22	61.9	60.3	66.7
S-29	Beginning of C-9/ Structure S-30	S-29	99.37	24.6	19.2	21.2
C-9 west of Red Road	Beginning of C-9/ Structure S-30	Q-point at Red Road	61.24	15.2	12.1	13.0
C-9 east of Red Road	Q-point at Red Road	S-29	38.13	51.3	51.5	56.6

Discharge west and east of Red Road is an estimate due to interconnected outfalls on both sides of Red Road

Figure 11.2-1 through **Figure 11.2-4** present visual comparisons of the area-weighted discharge hydrographs for the C-8 and C-9 Canal for the future conditions 10-year design storm with 1 ft sea level rise and 9% increase in rainfall. An additional two hydrographs are presented for areas east and west of Red Road. With the higher rainfall, the structure discharge capacities increased by 6.4 cfs/sq.mi and 2.0 cfs/sq.mi for S-28 and S-29, respectively compared to SLR1 with current rainfall.

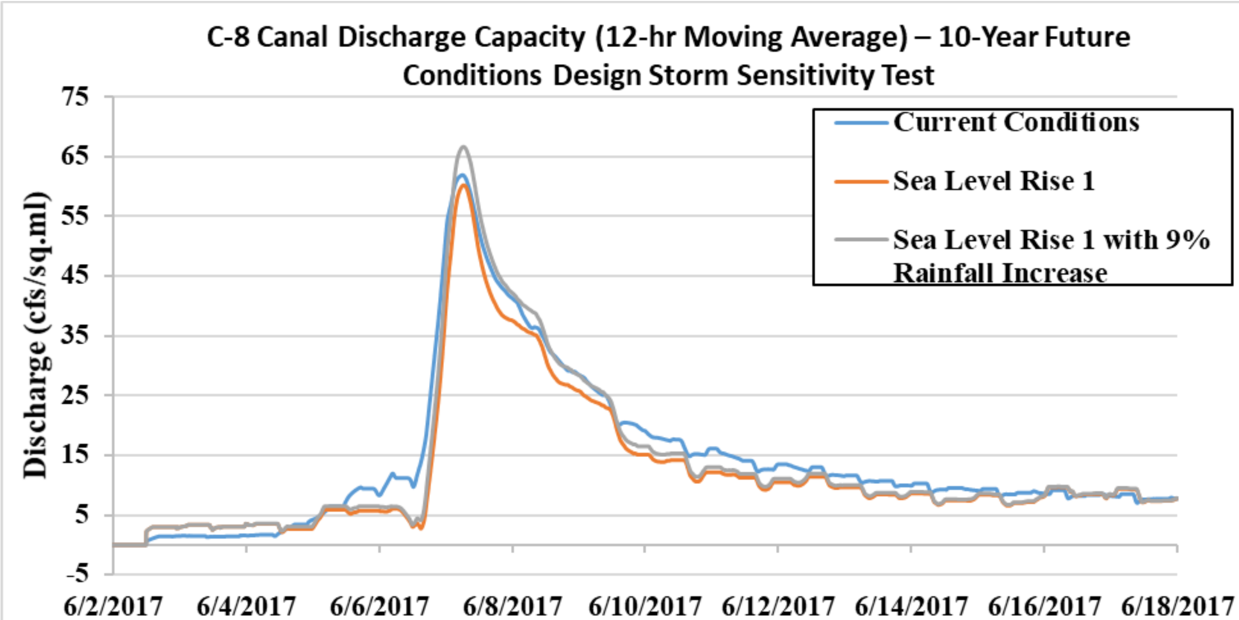

Figure 11.2-1: Area-Weighted Discharge Hydrograph for C-8 Canal (S-28) 10-Year Design Storm Sensitivity Test

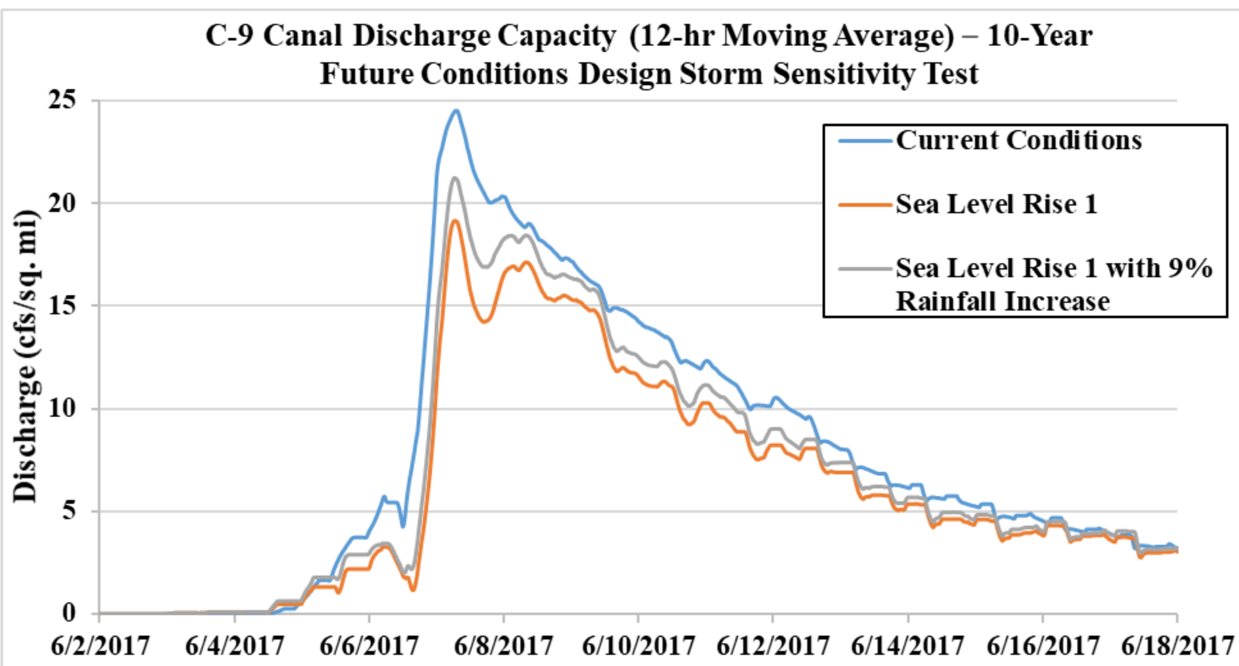

Figure 11.2-2: Area-Weighted Discharge Hydrograph for C-9 Canal (S-29) 10-Year Design Storm Sensitivity Test

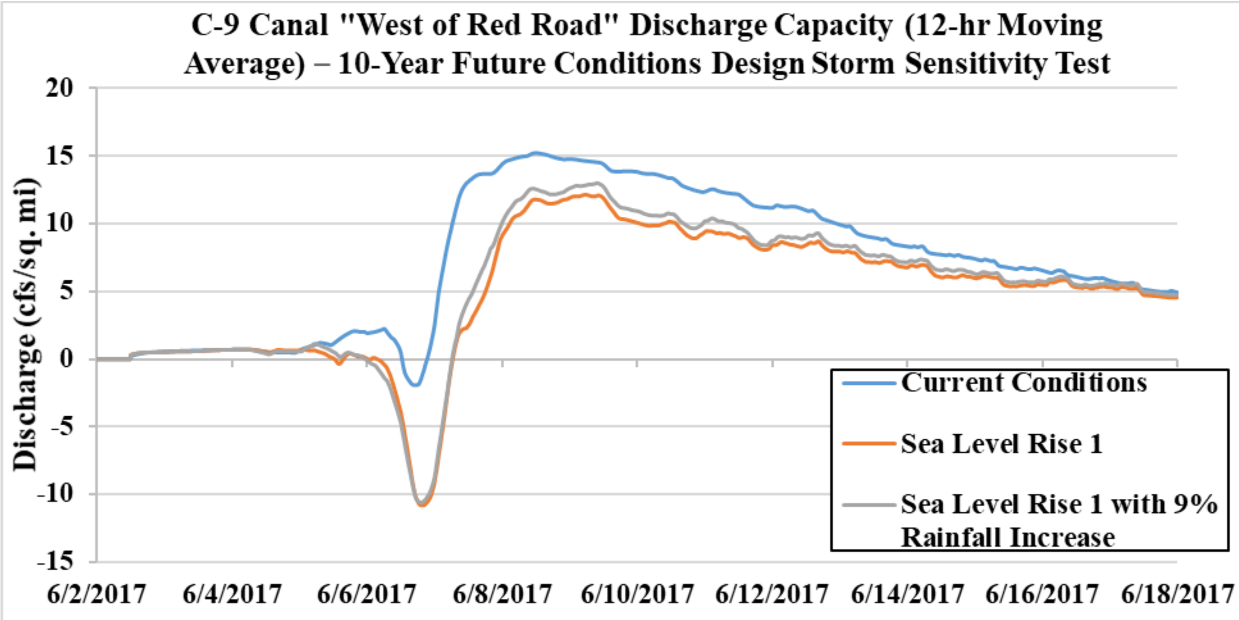

Figure 11.2-3: Area Weighted Discharge Hydrograph for C-9 Canal West of Red Road for 10-Year Design Storms

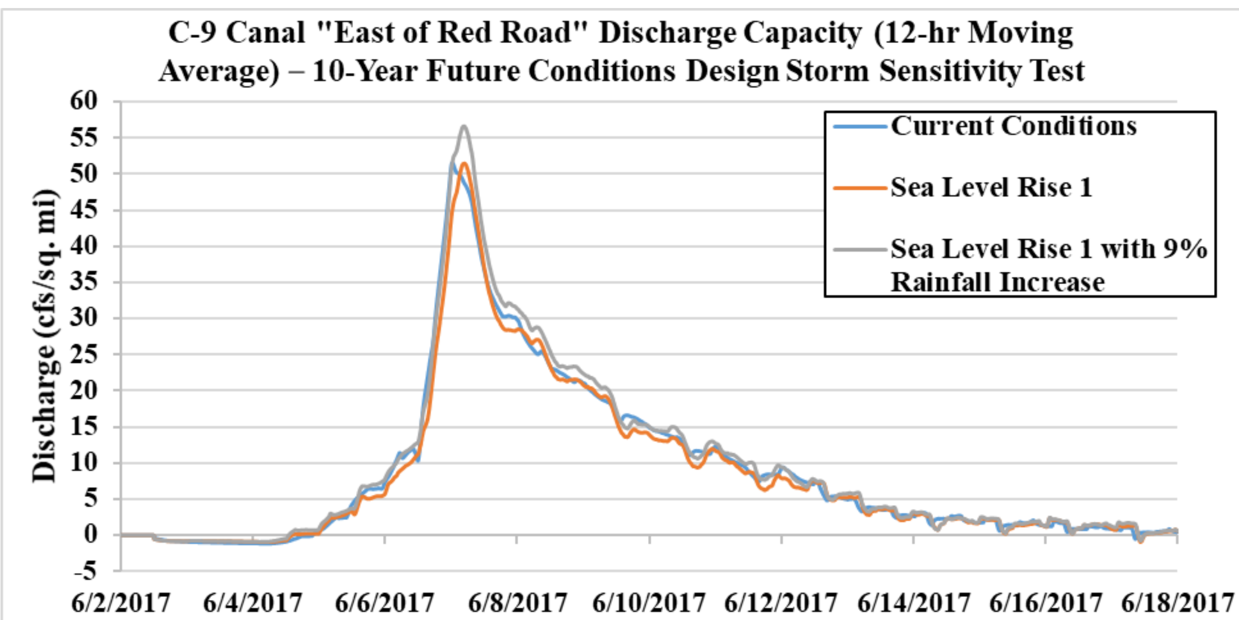

Figure 11.2-4: Area-Weighted Discharge Hydrograph for C-9 Canal East of Red Road for 10-Year Design Storms

11.3 PM #4 – Peak Storm Runoff

PM #4 is the maximum conveyance capacity of a watershed at the tidal structure. It shows the maximum conveyance (moving 12-hr average) for a specific design storm and a specific tidal boundary condition. **Figure 10.4-1** and **Figure 10.4-2** represent the design storm discharge at tidal structures S-28 and S-29, respectively. These discharge hydrographs, specifically the peak discharge, were evaluated for the 10-year future conditions SLR1 scenario with 9% increase in rainfall and compared with the current conditions and future conditions SLR1 design storm. With the higher rainfall, the peak structure discharge increased by 181 cfs and 207 cfs for S-28 and S-29, respectively, compared to SLR1 with current rainfall.

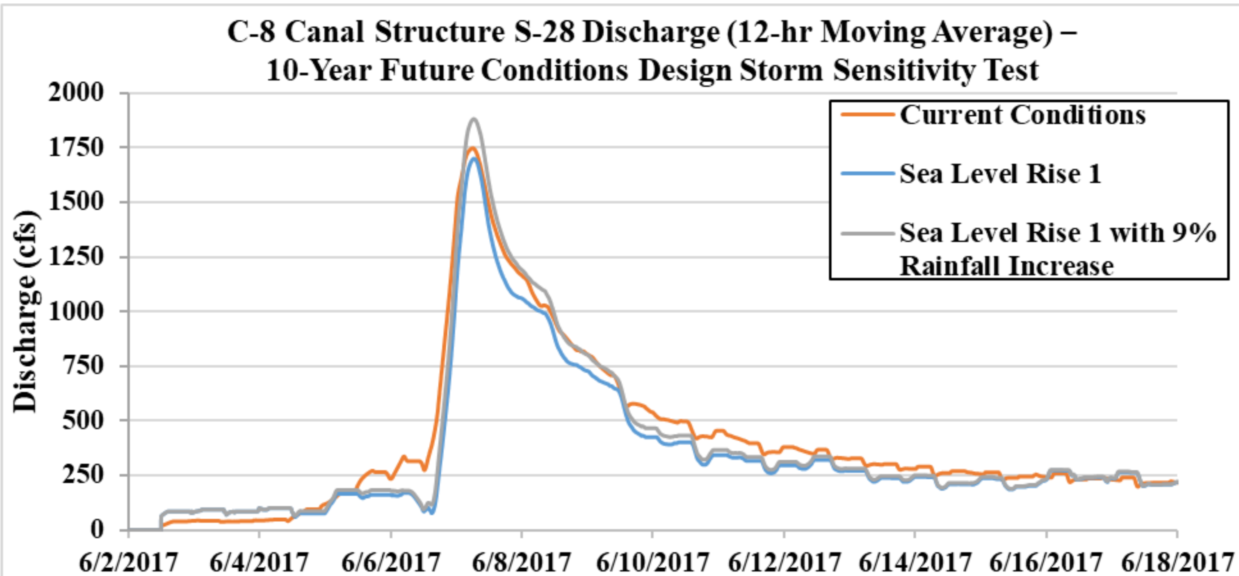

Figure 11.3-1: C-8 Canal Structure S-28 Discharge Hydrographs for 10-Year Design Storm Sensitivity Test

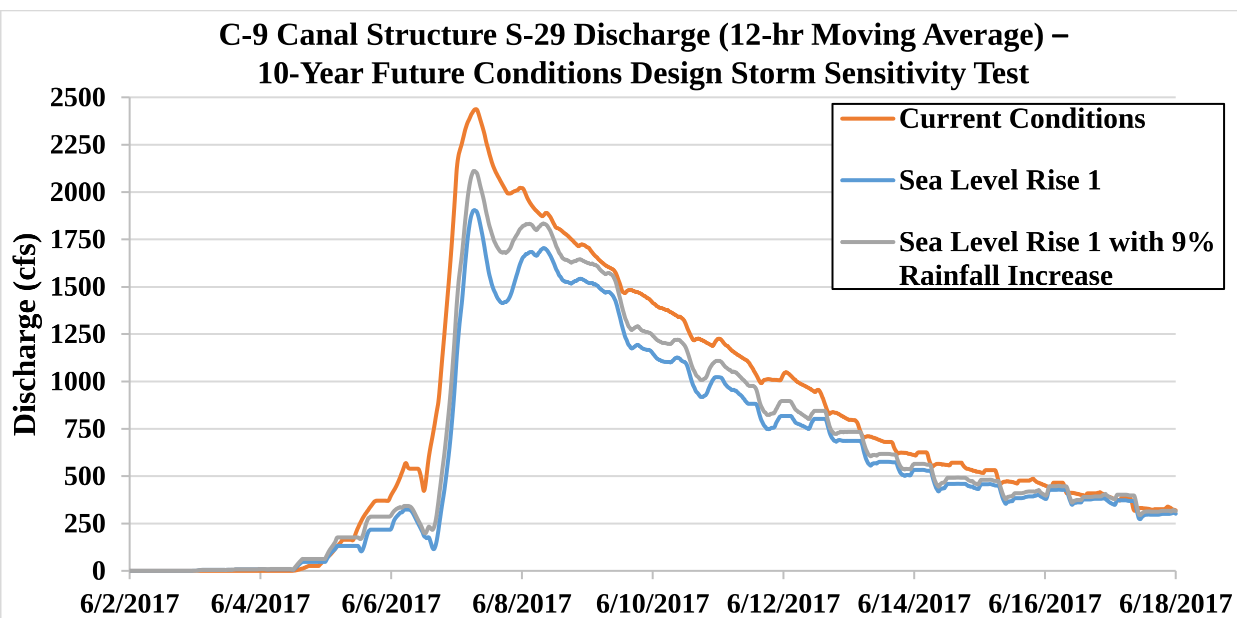

Figure 11.3-2: C-9 Canal Structure S-29 Discharge Hydrographs for 10-Year Design Storm Sensitivity Test

11.4 PM #5 – Frequency of Flooding

For this PM, the depths of overland flooding were evaluated for the 10-year design storm with 1 ft sea level rise and 9% increase in rainfall. These flood depths, or elevations, can be compared with elevations from the 10-year SLR1 design storm to see how sensitive the model is to changes in rainfall under future conditions. For the purposes of this C-8/C-9 FPLOS evaluation, flood inundation maps were prepared using MIKE SHE gridded model output for each storm event, in the form of depth of overland water. Flooding depths were representative of the overland water depths on the 125-ft grid. The resulting flood inundation map over the entire model domain is shown in **Figure 11.4-1** and the flood inundation map over urban areas only is shown in **Figure 11.4-2. Figure 11.4-3** shows the maximum overland water depth difference between future conditions with rainfall increase and future conditions without rainfall increase for the 10-Year SLR1, design storm events.

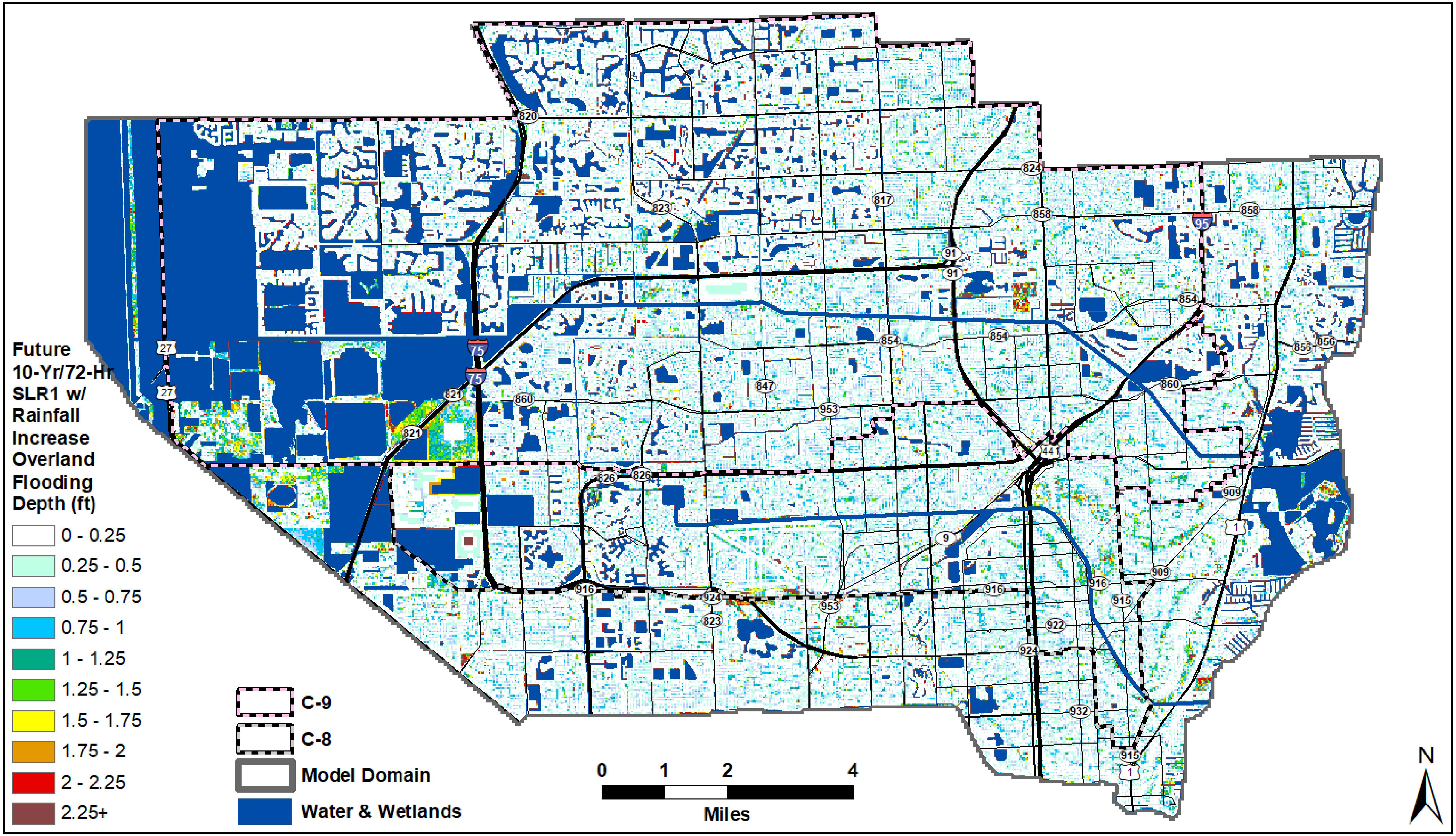

Figure 11.4-1: Flood Inundation Map for 10-Year Sea Level Rise 1 Design Storm Event with 9% Increase in Rainfall

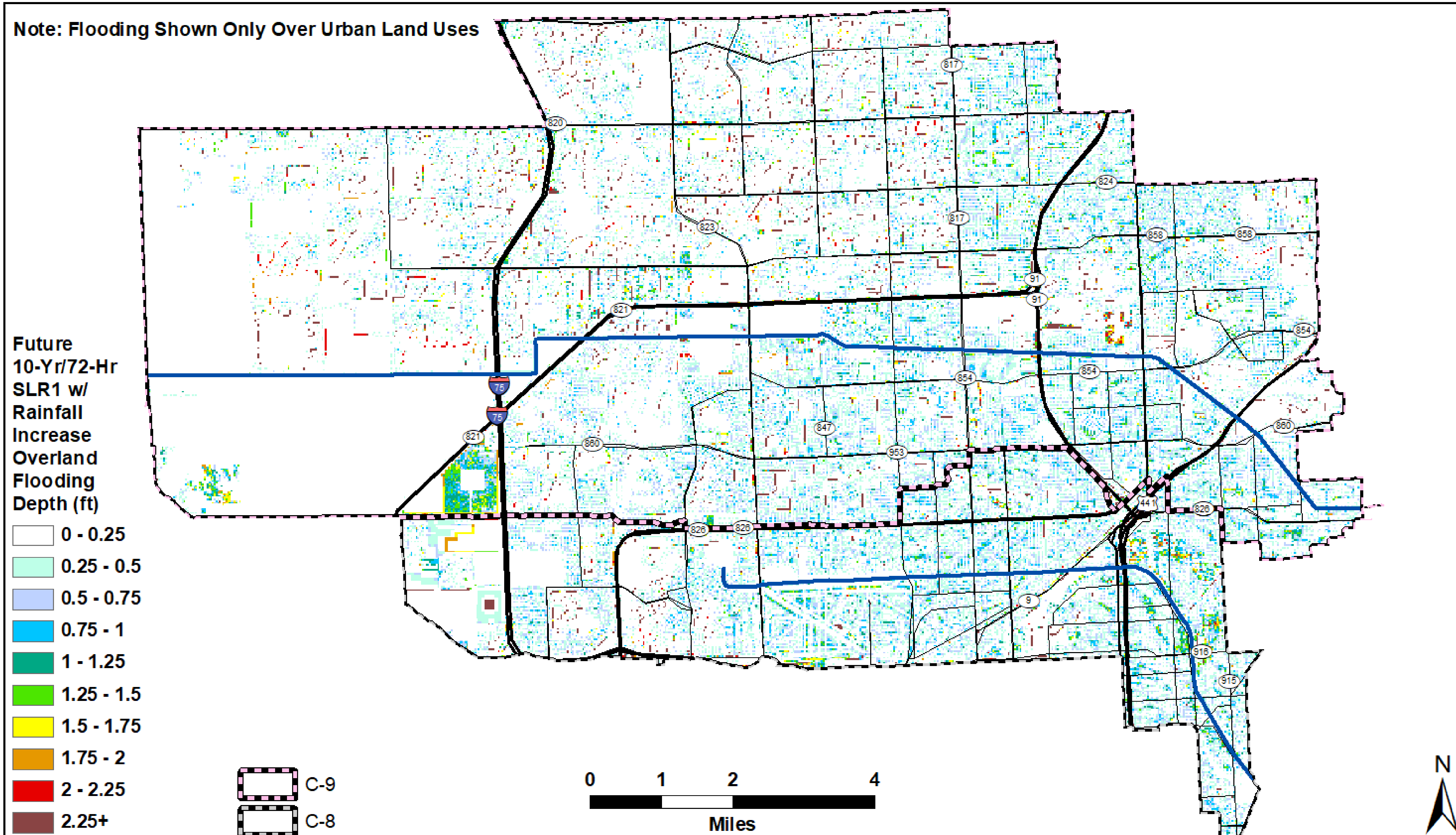

Figure 11.4-2: Flood Inundation Map for 10-Year Sea Level Rise 1 Design Storm Event with 9% Increase In Rainfall in Urban Land Use Areas

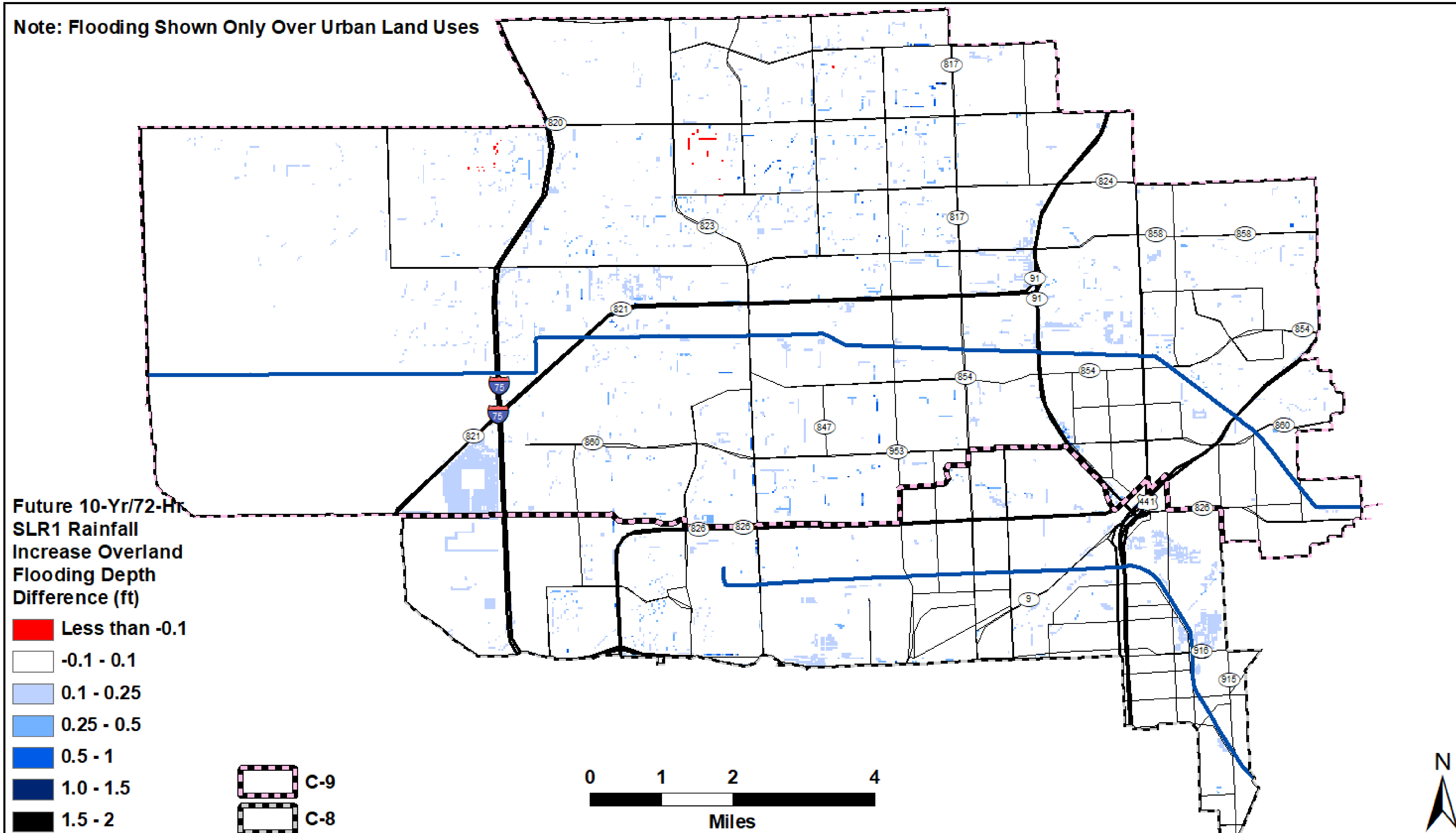

Figure 11.4-3: Flood Inundation Difference Map for 10-Year Sea Level Rise 1 Design Storm Event with Increased Rainfall, in Urban Land Use Areas (Future Conditions with Rainfall Increase minus Future Conditions without)

11.5 PM #6 – Duration of Flooding

For PM #6, the duration of flooding maps were developed by estimating the duration over which water depth exceeds a given threshold value. In this study, the duration of overland flooding was estimated using model simulated water depths and a threshold flooding depth of 0.25 ft. Additionally, the duration of flooding in the District Canals was estimated as the amount of time it takes for the water levels to return to target stage. The target stages of 3.6 ft for S-28Z and 3.5 ft for S-29Z were provided by the District (Email from Hongying Zhao, 5/12/2020). **Table 11-2** shows the duration of time taken for the water level in the C-8 and C-9 Canal to return to target stage, based on the first instance.

Table 11-2: Duration for Water Levels to Return to Target Stage for 10-Year Design Storms

Design Storm	Duration for S-28Z Return to Target Stage (hr) 10-Year	Duration for S-29Z Return to Target Stage (hr) 10-Year
Current	40	92
SLR1	60	98
SLR1 with 9% Rainfall Increase	70	123

The duration of overland flooding was estimated for all four design storm events based on the length of time the flood depth was predicted to exceed the threshold value (0.25 ft) within each MIKE SHE 125-ft grid cell using the statistics tool in MIKE ZERO. The flood duration map over the entire model domain for the 10-year SLR1 design storm with 9% increase in rainfall is shown in **Figure 11.5-1** and the flood duration map over urban area only is shown in **Figure 11.5-2. Figure 11.5-3** shows the flood duration difference between future conditions with rainfall increase and future conditions without rainfall increase for the 10-Year SLR1, design storm events.

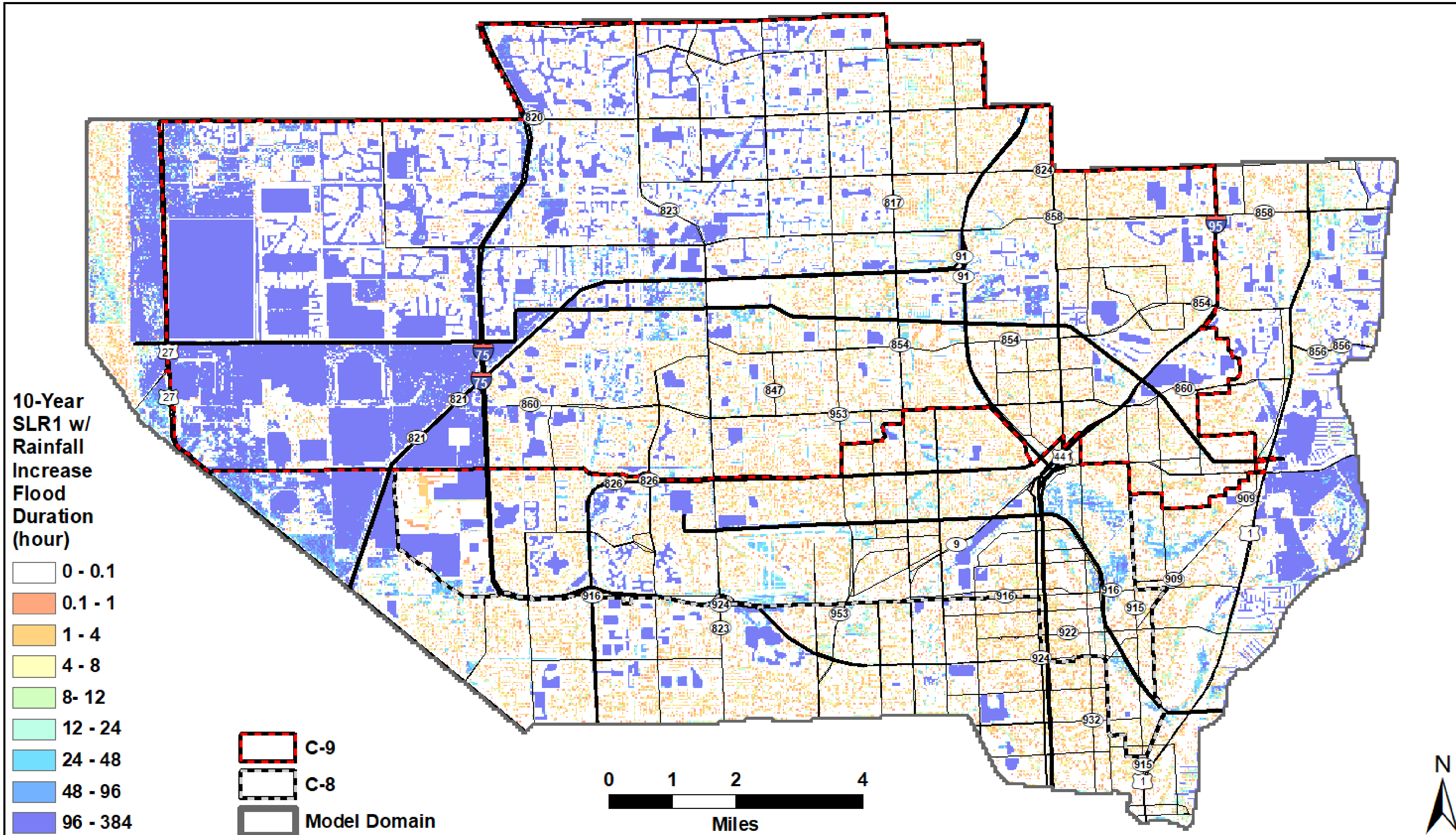

Figure 11.5-1: Flood Duration Map for 10-Year Sea Level Rise 1 Design Storm Event with 9% Increase in Rainfall

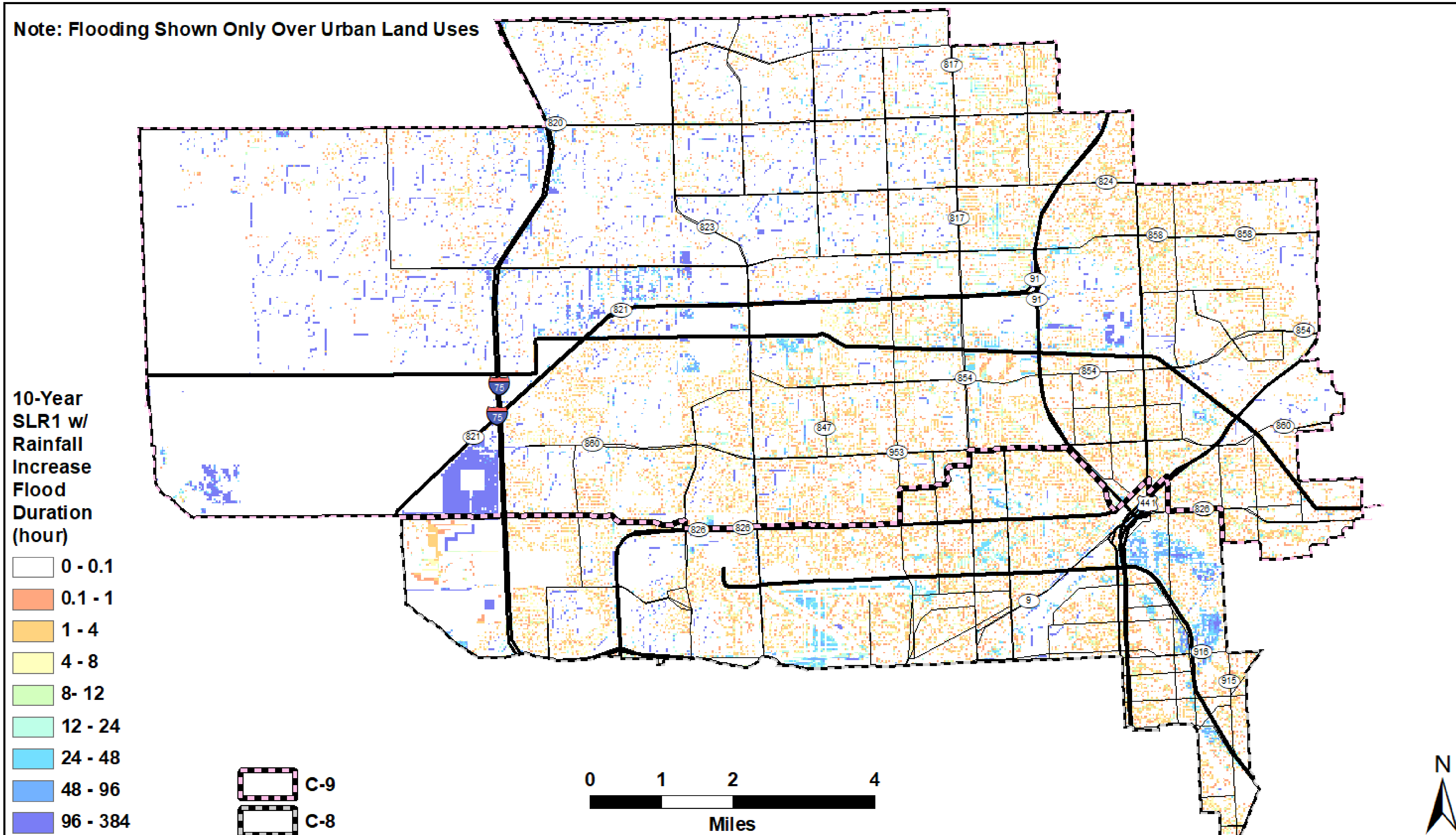

Figure 11.5-2: Flood Duration Map for 10-Year Sea Level Rise 1 Design Storm Event with 9% Increase in Rainfall in Urban Land Use Areas

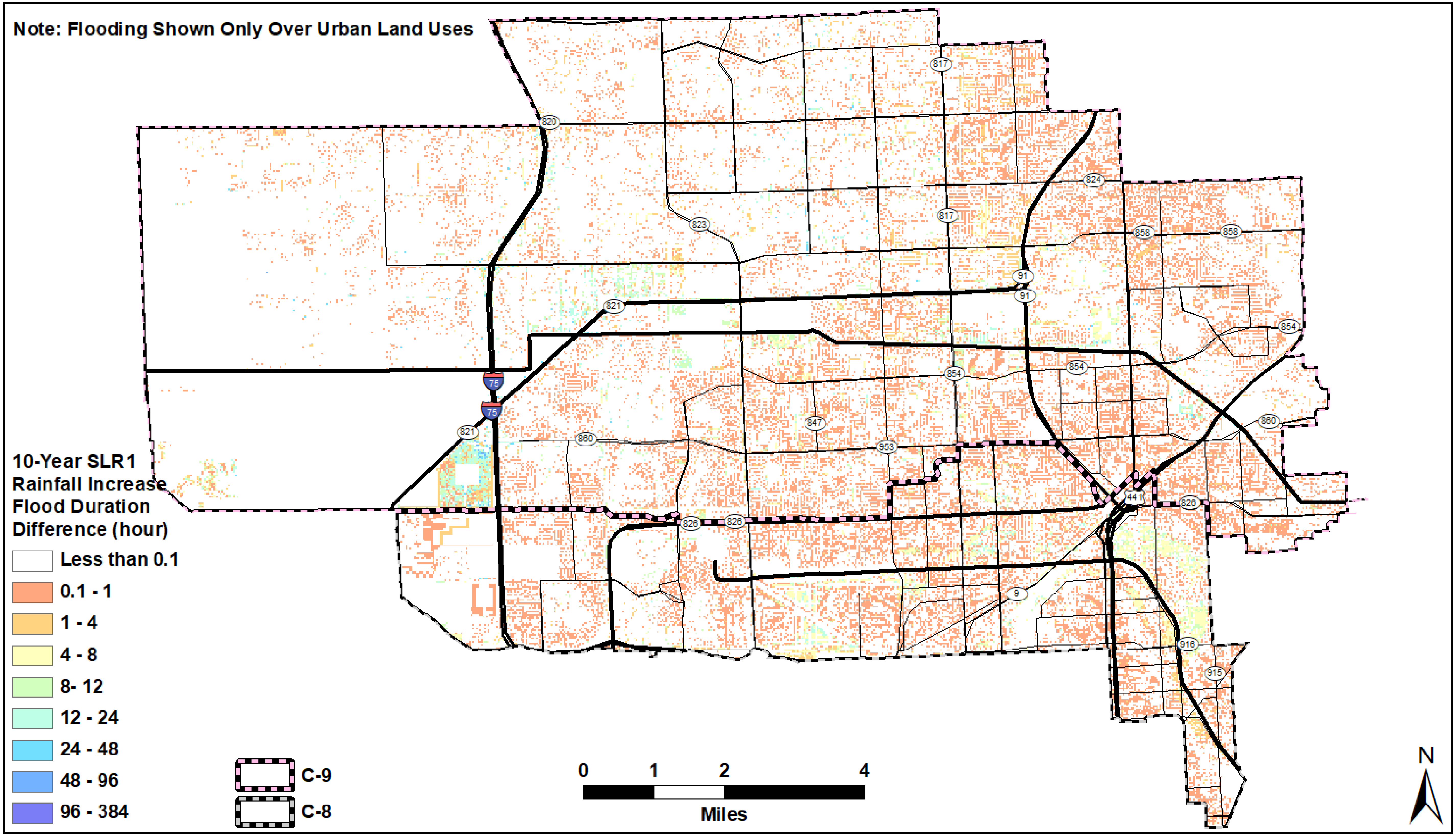

Figure 11.5-3: Flood Duration Difference Map for 10-Year Sea Level Rise 1 Design Storm Event with Increased Rainfall, in Urban Land Use Areas (Future Conditions with Rainfall Increase minus Future Conditions without)

12 SUMMARY AND CONCLUSIONS

Flood protection level of service provided by existing infrastructure was evaluated for current conditions and future conditions with three sea level rise scenarios, using six performance measures. The effects of both rainfall-induced flooding and storm surge flooding were assumed to occur simultaneously. The detailed results of the current and future conditions FPLOS are presented in **Section 8** and **10**, respectively, with current condition conclusions presented in **Section 8.7** and future condition conclusions presented in **Section 10.7**. This section summarizes the overall conclusions from the current and future conditions FPLOS and presents them as key-takeaway points.

12.1 C-8 Watershed

12.1.1 Basin Level of Service

- The C-8 Basin generally provides a 10-year level of service under current conditions.
  - Some localized canal banks are exceeded for 5-year storm (does not correspond to significant flood inundation).
  - Some areas provide a 25-year level of service or better, but several segments are exceeded (resulting in significant flood inundation).
- The C-8 Basin is generally predicted to provide a 5-year (SLR1) or less (SLR2 & SLR3) level of service under future conditions sea level rise.
  - Localized bank exceedances will likely occur for 5-year SLR1 event (not likely to result in significant flood inundation).
  - Bank exceedances for 5-year SLR2 and SLR3 events are predicted to result in significant flood inundation.
  - Some localized areas will likely provide a 25-year level or service or better.
  - The 25-year event will likely overwhelm much of the eastern C-8 basin for all three SLR scenarios.

12.1.2 Effects of Sea Level Rise

- Sea level rise is predicted to result in increased flooding depth and duration in the C-8 Basin.
  - SLR will likely increase the groundwater elevations which reduces available soil storage.
  - SLR will increase the canal elevation downstream of the S-28 structure, which will result in a higher upstream canal stage required to discharge to tide.
    - Increased canal stage will result in increased bank exceedances.
    - Increased canal stage will result in increased duration of flood waters.
- Sea level rise is predicted to decrease the discharge ability of the S-28 tidal outfall structure.
  - SLR will likely always result in a decrease in the 12-hour average peak discharge, with the most dramatic decreases predicted to occur under the SLR3 scenarios.
    - For the 5-year event, SLR1, SLR2, and SLR3 are predicted to result in a 5.7%, 13.4%, and 23.6% decrease in peak discharge, respectively.

        - For the 10-year event, SLR1, SLR2, and SLR3 are predicted to result in a 2.7%, 7.4%, and 18.5% decrease in peak discharge, respectively.
        - For the 25-year event, SLR1, SLR2, and SLR3 are predicted to result in a 0.9%, 0.9%, and 20.2% decrease in peak discharge, respectively.
        - For the 100-year event, SLR1, SLR2, and SLR3 are predicted to result in a -0.2%, 10.3%, and 28.4% decrease in peak discharge, respectively.

- Sea level rise is predicted to result in a violation of the 2.2 ft NGVD29 design headwater assumption for S-28, with peak discharges likely to occur with headwaters as high as 6.4 ft NGVD29.
- Sea level rise will result in increased structure bypass and/or overtopping of the S-28 tidal outfall structure.
    - For the 25-year event, SLR1, SLR2, and SLR3 are predicted to result in about 650 cfs, 1170 cfs, and 1720 cfs peak negative discharge, respectively.
    - For the 100-year event, SLR1, SLR2, and SLR3 are predicted to result in about 1100 cfs, 1700 cfs, and 2300 cfs peak negative discharge, respectively.

12.1.3 Coastal Structure

- The S-28 tidal outfall structure's 12-hour average discharge and stage is unable to meet design criteria under current conditions and is predicted to significantly deviate from design criteria under future condition sea level rise scenarios.
    - S-28 has a static design discharge of 3220 cfs with a 2.2 ft NGVD29 headwater (0.5 ft headwater/tailwater differential).
        - The design headwater assumption is violated for all current condition simulations, with a 12-hr average headwater at time of peak discharge 0.55 ft, 0.71 ft, 0.97 ft, and 1.35 ft higher than design conditions, respectively, for the 5, 10, 25, and 100-year events.
        - The 100-year current conditions design storm was able to achieve the design discharge (simulated headwater 1.3 ft higher than design).
        - The headwater assumption is predicted to be violated for all future condition simulations, with a headwater at time of peak discharge up to 4.16 ft higher than design.
        - The 100-year SLR1 design storm is predicted to be able to achieve the design discharge (simulated headwater 2.2 ft higher than design).
- The S-28 tidal outfall structure's instantaneous peak discharge is predicted to be larger under future conditions and will likely be able to achieve design discharge for the 25-year SLR3 event and all 100-year SLR scenarios.
    - This will be a result of increased surge-induced reverse flow, which will bypass and/or overtop the structure and cause water to "stack" on the upstream side. This provides the opportunity for increased instantaneous discharge once tide levels fall.

- Increased runoff to the canal, due to higher water table conditions and the associated loss of soil storage, may also contribute to the higher discharge rates through S-28.

12.1.4 Canal Capacity

- The C-8 Canal's peak discharge capacity is predicted to almost always decreased as sea level rise increases (exceptions are likely so small they can be considered negligible).
- SLR will cause increased tailwater levels and flow reversals, which will both reduce the S-28 structure's ability to discharge to tide and reduce the discharge capacity of the canal.
- For both current and future conditions, the western segment (west of Marco Canal) is generally predicted to perform better, as the eastern half of the canal will likely be overwhelmed during peak flood conditions.
- The capacity of the C-8 Canal will be limited by its low bank elevations and increased tailwater conditions under sea level rise scenarios. S-28 will experience overtopping during the high tide portion of the normal tide cycle for SLR2 and SLR3.

12.2 C-9 Watershed

12.2.1 Basin Level of Service

- The C-9 Basin generally provides a 25-year level of service under current conditions.
    - Canal banks are exceeded for 10-year storm in a few localized areas (does not correspond to significant flood inundation).
    - Some areas provide a 100-year level of service or better.
- The C-9 Basin is generally predicted to provide a 10-year level of service under future conditions SLR1 and SLR2, and a 5-year level of service under SLR3.
    - Localized bank exceedances will likely occur for 5-year SLR1 and SLR2 (not likely to result in significant flood inundation).
    - Bank exceedances for 10-year SLR3 event is predicted to result in significant flood inundation.
    - Some localized areas will likely provide a 25-year level or service or better under all SLR scenarios.
    - The 25-year SLR3 event will likely overwhelm much of the eastern C-9 basin.

12.2.2 Effects of Sea Level Rise

- Sea level rise is predicted to result in increased flooding depth and duration in the C-9 Basin.
    - SLR will likely increase the groundwater elevations which reduces available soil storage.
    - SLR will increase the canal elevation downstream of the S-29 structure, which will result in a higher upstream stage required to discharge to tide.
        - Increased canal stage will result in increased bank exceedances.

        - Increased canal stage results in increased duration of flood waters.

- Sea level rise is predicted to decrease the discharge ability of the S-29 tidal outfall structure.
    - SLR will likely always result in a decrease in the 12-hour average peak discharge, with the most dramatic decreases predicted to occur under the SLR3 scenarios.
        - For the 5-year event, SLR1, SLR2, and SLR3 are predicted to result in a 22.6%, 45.8%, and 57.7% decrease in peak discharge, respectively.
        - For the 10-year event, SLR1, SLR2, and SLR3 are predicted to result in a 21.9%, 35.0%, and 49.2% decrease in peak discharge, respectively.
        - For the 25-year event, SLR1, SLR2, and SLR3 are predicted to result in a 14.0%, 26.0%, and 43.2% decrease in peak discharge, respectively.
        - For the 100-year event, SLR1, SLR2, and SLR3 are predicted to result in a 9.2%, 20.9%, and 38.5% decrease in peak discharge, respectively.
- Sea level rise is predicted to result in a violation of the 2.4 ft NGVD29 design headwater assumption for S-29, with peak discharges likely to occur with headwaters as high as 5.8 ft NGVD29.
- Sea level rise will result in increased structure bypass and/or overtopping of the S-29 tidal outfall structure.
    - For the 25-year event, SLR1, SLR2, and SLR3 are predicted to result in about 750 cfs, 1750 cfs, and 2800 cfs peak negative discharge, respectively.
    - For the 100-year event, SLR1, SLR2, and SLR3 are predicted to result in about 1550 cfs, 2650 cfs, and 3750 cfs peak negative discharge, respectively.

12.2.3 Coastal Structure

- The S-29 tidal outfall structure's 12-hour average discharge and stage is unable to meet design criteria under current conditions and is predicted to significantly deviate from design criteria under future condition sea level rise scenarios.
    - S-29 has a static design discharge of 4780 cfs with a 2.4 ft NGVD29 headwater (0.5 ft headwater/tailwater differential).
        - The design headwater assumption is violated for all current condition simulations, with a 12-hr average headwater at time of peak discharge 0.44 ft, 0.55 ft, 0.74 ft, and 1.12 ft higher than design conditions, respectively, for the 5, 10, 25, and 100-year events.
        - The design discharge was not achieved for any current condition simulations, with the 100-year design storm discharge peaking at more than 1050 cfs less than design (based on 12-hour moving average).
        - The headwater assumption is predicted to be violated for all future condition scenarios, with a headwater at time of peak discharge up to 3.42 ft higher than design.

        - The 100-year future condition design storms are predicted to peak at about 1400 cfs, 1800 cfs, and 2500 cfs less than design discharge, respectively, for SLR1, SLR2, and SLR3 (based on 12-hour moving average).
    - The S-29 tidal outfall structure is predicted to be unable to achieve design discharge, even on an instantaneous basis. The largest instantaneous peak discharge is predicted to occur for the 100-year SLR2 event, with a peak discharge about 600 cfs less than design.
- The discharge capacity of the S-29 structure is predicted to be smaller under all future sea level rise scenarios.
    - The C-9 Impoundment will remove water from the western C-9 Canal (about 3500 ac-ft), which will result in a reduced the total volume discharged to tide.
    - Discharge from some of the eastern SBDD pump stations are predicted to be limited due to elevated stage in the C-9 Canal triggering “pump off” conditions that are required by permit.
    - The storage characteristics of the western C-9 basin, namely the prevalence of large lakes (former mine pits), will likely help attenuate peak discharge rates and accommodate storm surge-induced flow reversals.

12.2.4 Canal Capacity

- The C-9 Canal’s peak discharge capacity is predicted to decrease as sea level rise increases.
- SLR will cause increased tailwater levels and flow reversals, which will both reduce the S-29 structure’s ability to discharge to tide and reduce the discharge capacity of the canal.
- For both current and future conditions, the western segment (west of Carol City Canal) is generally predicted to perform better, as the eastern half of the canal will likely be overwhelmed during peak flood conditions.
- The capacity of the C-9 Canal will be limited by its low bank elevations and increased tailwater conditions under sea level rise scenarios. S-29 will experience overtopping during the high tide portion of the normal tide cycle for SLR2 and SLR3.

REFERENCES

BDH Consulting Group. (2019). *Survey Work for C8 and C9 FPLOS Models*

Broward County. (2000). *Broward County Average Wet Season Water Table Map*. Broward County office of Environmental Services Water Management Division.

Broward County Planning Council. (2020). *Broward County Future Land Use Plan (2040)* https://www.broward.org/PlanningCouncil/Pages/Maps.aspx

Burns & McDonnell. (2006). *Flood Protection Analysis for Broward County Water Preserve Areas C-11 and C-9 Impoundments (Final Report)*

Environmental Protection Agency. (2015). *Storm Water Management Model User's Manual Version 5.1*.

DHI. (2017). *MIKE SHE User Guide v1*.

Fish, J.E., & Stewart, M.T. (1991). *Hydrogeology of the surficial aquifer system, Dade County, Florida*.

Florida Natural Areas Inventory. (2012). *Florida Land Cover Classification System Definitions for the Cooperative Land Cover Map v2.3*.

Hughes, J. D., & White, J. T. (2016). *Hydrologic conditions in urban Miami-Dade County, Florida, and the effect of groundwater pumpage and increased sea level on canal leakage and regional groundwater flow* (No. 2014-5162 Version 1.2 July 2016). US Geological Survey.

Miami-Dade County. (2017). *2015_ITD_LiDAR Project*; 5-ft Digital Elevation Model (DEM)

Miami-Dade County. (n.d). *Miami Dade County Future Land Use (2030)*

NEXRAD Viewer. (2020). South Florida Water Management District NEXRAD Viewer App https://apps.sfwmd.gov/nexrad2

SBDD. (2013). *South Broward Drainage District Facilities Report and Water Control Plan*.

SFWMD LCLU. (2017). *South Florida Water Management District Land Cover Land Use 2014-2016 dataset*.

SFWMD H&H Bureau. (2015). *Flood Protection LOS Analysis for the C-4 Watershed, Appendix A: LOS Basic Concepts*.

Stoner and Associates. (2019). *Surveyors Report As-Built Survey*. For Project: Broward County 100 Year Flood Elevation Map & Associated Modeling

Taylor Engineering. (2019) *Broward County 100-Yr Flood Elevation Map & Associated Modeling Project*.

Taylor Engineering. (2019). *Broward County Current Conditions MIKE SHE and MIKE HYDRO Models*. Developed for Broward County 100-Year Flood Elevation Map & Associated Modeling Project.

Taylor Engineering. (2019) *Broward County Draft Model Update and Validation Report* (For Broward County 7/26/2019)

Taylor Engineering. (2019). *Deliverable 1.1, Data Availability Memorandum* (For SFWMD 8/26/2019)

Taylor Engineering. (2019). *Deliverable 1.2, C8-C9 Model Development Memorandum* (For SFWMD 11/4/2019)

Taylor Engineering. (2020). *Deliverable 2.1, C8-C9 Calibration and Validation Memorandum Final Draft* (For SFWMD 1/21/2020)

USACE. (2012). *Central and Southern Florida Project Broward County Water Preserve Areas Revised Final Integrated Project Implementation Report and Environmental Impact Statement*

USGS. (2018) *Reference and Potential Evapotranspiration Reference and Potential Evapotranspiration*. https://www.usgs.gov/centers/car-fl-water/science/reference-and-potential-evapotranspiration?qt-science_center_objects=0#qt-science_center_objects.

Yin, C., Li, Y., & Urich, P. (2019). *Broward County DDF Change Factor Ensemble Analysis*.

Zhang. (2017). *The Effects of Sea Level Rise on S28 Performance*

Zhang. (2017). *The Effects of Sea Level Rise on S29 Performance*

Appendix A Email from SBDD

From: Kevin Hart <kevin@sbdd.org>
Sent: Wednesday, January 2, 2019 2:32 PM
To: Mark Ellard <MEllard@Geosyntec.com>
Cc: John Loper <jloper@taylorengineering.com>; Zygnerski, Michael <MZYGNERSKI@broward.org>; Maran, Carolina <CMARAN@broward.org>; Luis Ochoa <luis@sbdd.org>
Subject: RE: Broward Future 100-Year Model Follow Up - SBDD

Mark,

Attached is the latest SFWMD permit for CS12, CS13, CS13-A, ICS12, ISC13 and ISC13-A.

Basically, the permit states the following:

- CS12, CS13, CS13-A are operated to allow the canal stages downstream of the intermediate gates to fluctuate with the C-11 Canal, but no lower that Elev. 3.00' NGVD (except with prior authorization from SFWMD).
- The maximum, combined discharge rate for CS12, CS13, CS13-A is 363 cfs.
- The intermediate gates (internal gate structures) are operated to maintain the permitted control elevation of 4.0' NGVD, within the upstream areas of the S-9/S-10 Basin (upstream of the gates). These gates are only opened when the tail water exceeds Elevation 4.0' NGVD.

The B-1 and B-2 pump stations are operated on a manual basis only. These two pump stations are operated by SBDD on an as-needed basis, and as determined by staff, during extreme rainfall events. Just as an FYI, neither station has operated during the past 7 years (except for maintenance purposes). Both stations have a gravity culvert connection to SBDD's C-1 Canal. For modeling purposes, the two pumps can be activated at Elevation 4.0' NGVD with a pumping capacity of 15,000 GPM. The pumps are used to reduce peak stages and durations within the sub-basins they serve.

The Silver Lakes Flood Gate is an emergency, basin inter-connect between Basins S-9/S-10 and S-5. This gate is operated to allow SBDD to move water from the C-11 Basin to C-9 Basin on an as-needed (emergency) basis. The operation of this gate is performed in conjunction with approval and authority from SFWMD. For modeling purposes, this gate should be closed. However, under adaptation strategies/scenarios, you are welcome to incorporate the use of this gate to manage stages between the C-11 and C-9 basin as applicable. As an FYI, there have been a handful of occasions where SFWMD has asked SBDD to discharge south through the S-5 Basin in order to limit discharges to the C-11 Canal.

The Nautica/Silver Lakes culvert (ID 408) is a basin inter-connect that is operated on an as-needed, emergency basis only. For modeling purposes, this gate should be closed. However, under adaptation strategies/scenarios, you are welcome to incorporate the use of this gate to manage stages between the S-4 and S-5 basins as applicable.

You're probably aware that SBDD has 2 other basin inter-connects that are operated on an as-needed, emergency basis only as well.......... between Basins S-3 and S-2.

On the pipe inverts, we do not have any additional information at this time. For modeling purposes, we suggest that you set the pipe inverts such that the top of pipe matches the Control Water Elevation (CWE), as that is SBDD's standard practice.

Let me know if you need any additional information.

Thanks.

Kevin Hart, P.E., CFM
District Director
South Broward Drainage District
6591 Southwest 160th Avenue
Southwest Ranches, FL 33331
954-680-3337 (office)
e-mail: kevin@sbdd.org

Figure A- 1: Email from SBDD

Appendix B SFWMD ERP Allowable Runoff

ENVIRONMENTAL RESOURCE PERMIT APPLICANT'S HANDBOOK VOLUME II
Effective: MAY 22, 2016

Appendix A: SFWMD - ALLOWABLE DISCHARGE FORMULAS

Canal	Allowable Runoff	Design Frequency
C-1	$Q = \left(\frac{112}{\sqrt{A}} + 31\right) A$	10 year
C-2	Essentially unlimited inflow by gravity connections southeast of Sunset Drive: 54 CSM northwest of Sunset Drive	200 year +
C-4	Essentially unlimited inflow by gravity connections east of S.W. 87th Avenue	200 year +
C-6	Essentially unlimited inflow by gravity connections east of FEC Railroad	200 year +
C-7	Essentially unlimited inflow by gravity connection	100 year +
C-8	Essentially unlimited inflow by gravity connection	200 year +
C-9	Essentially unlimited inflow by gravity connection east of Red Road; 20 CSM pumped, unlimited gravity with development limitations west of Red Road or Flamingo Blvd.	100 year +
C-10	--	200 year +
C-11	20 CSM west of 13A;40 CSM east of 13A	------------
C-12	90.6 CSM	25 year
C-13	75.9 CSM	25 year
C-14	69.2 CSM	25 year
C-15	70.0 CSM	25 year
C-16	62.6 CSM	25 year
C-17	62.7 CSM	25 year
C-18	41.6 CSM	25 year
C-19	57.8 CSM	------------
C-23	31.5 CSM	10 year

Figure B- 1: SFWMD ERP Allowable Runoff by Canal

Appendix C Simulated vs Observed Discharge Comparison for Four Month Calibration/Validation Simulation

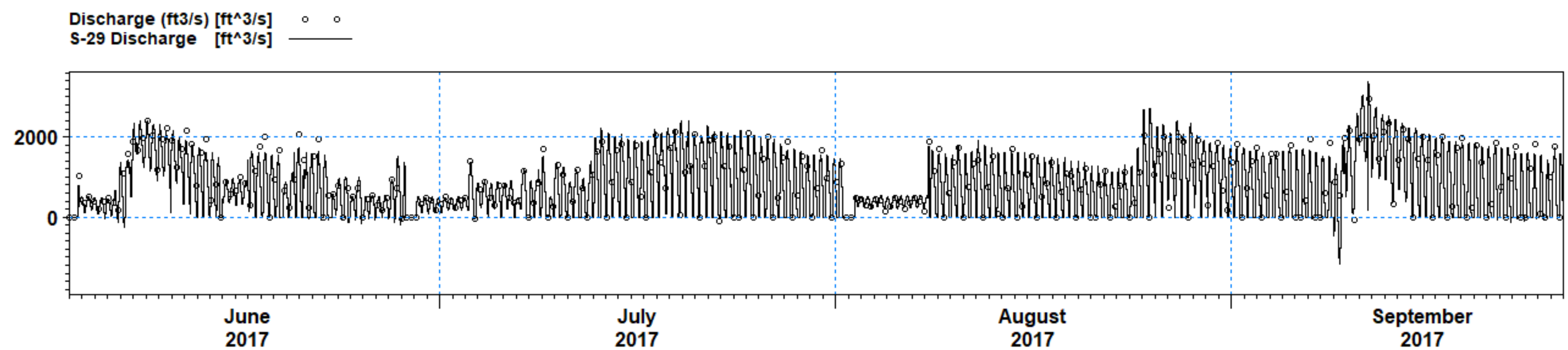

Figure C- 1: Simulated (line) vs Observed (dots) Discharge Comparison for SFWMD C-9 Structure S-29, June 2nd-September 27th, 2017

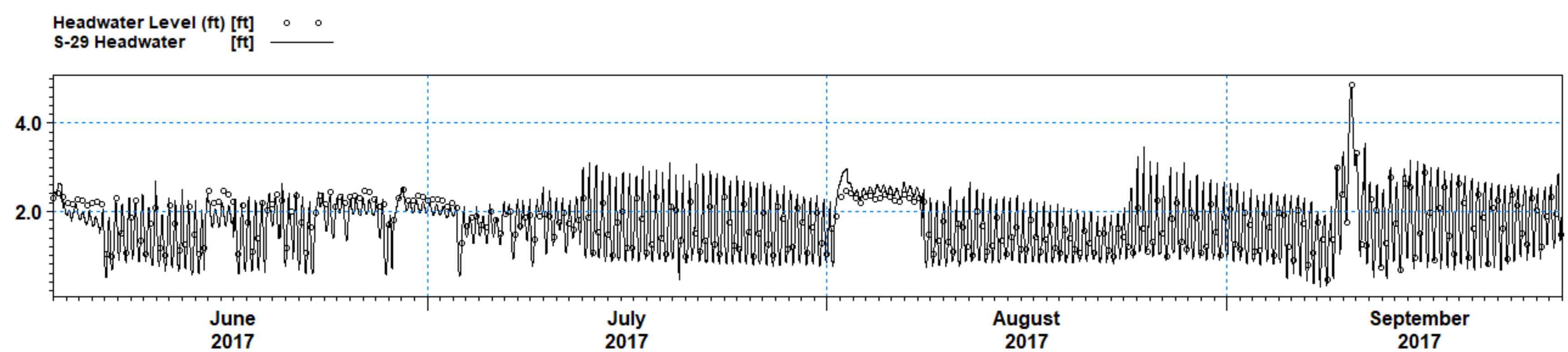

Figure C- 2: Simulated (line) vs Observed (dots) Headwater Comparison for SFWMD C-9 Structure S-29, June 2nd-September 27th, 2017

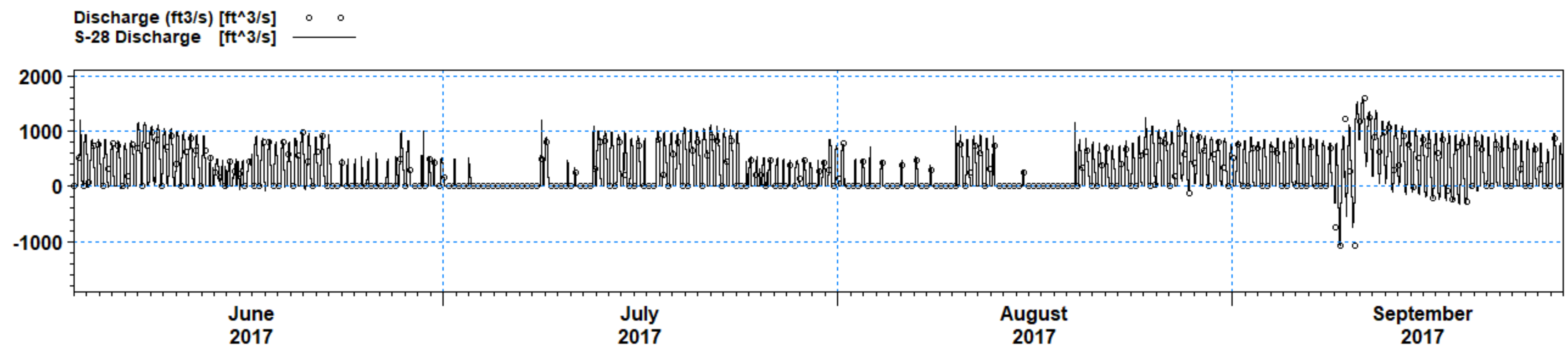

Figure C- 3: Simulated (line) vs Observed (dots) Discharge Comparison for SFWMD C-8 Structure S-28, June 2nd-September 27th, 2017

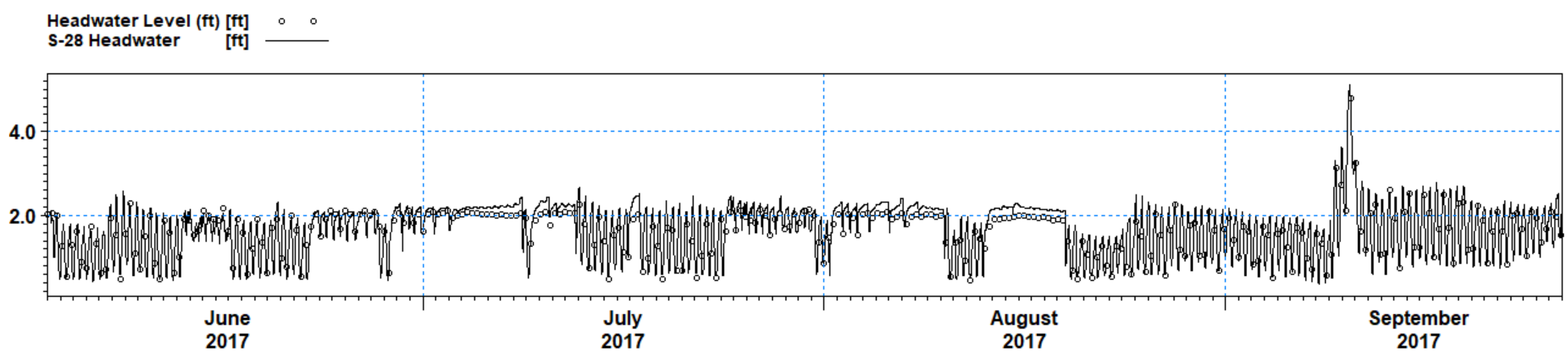

Figure C- 4: Simulated (line) vs Observed (dots) Headwater Comparison for SFWMD C-8 Structure S-28, June 2nd-September 27th, 2017

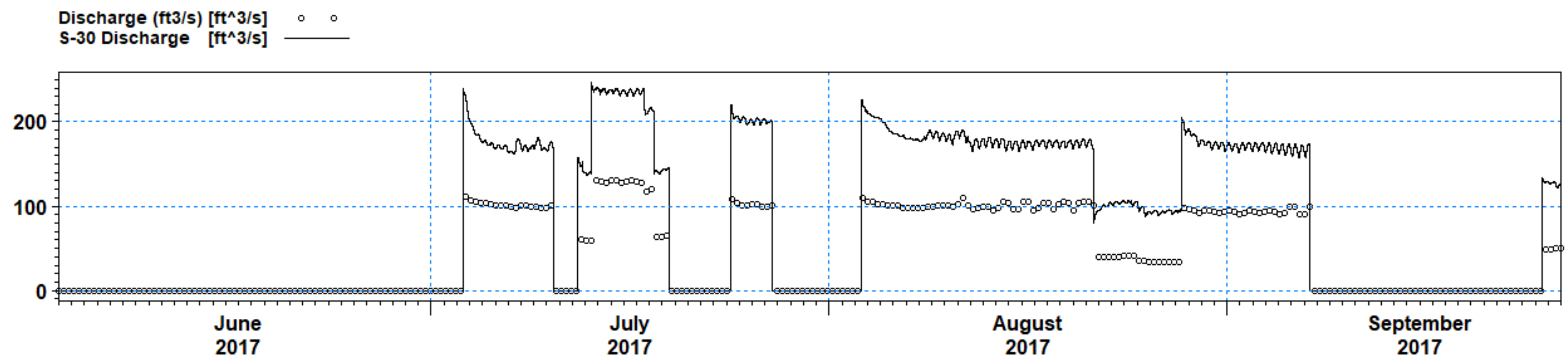

Figure C- 5: Simulated (line) vs Observed (dots) Discharge Comparison for SFWMD C-9 Structure S-30, June 2nd-September 27th, 2017

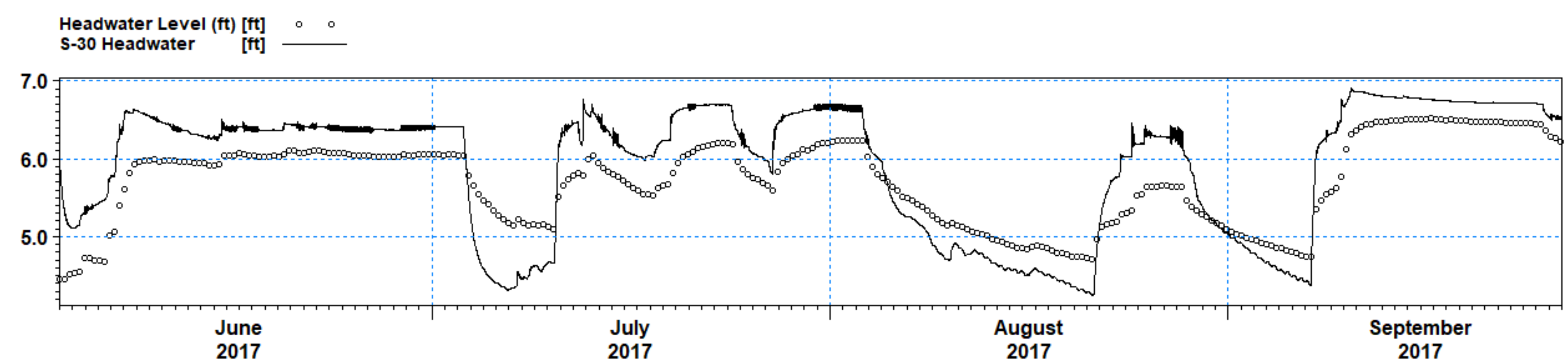

Figure C- 6: Simulated (line) vs Observed (dots) Headwater Comparison for SFWMD C-9 Structure S-30, June 2nd-September 27th, 2017

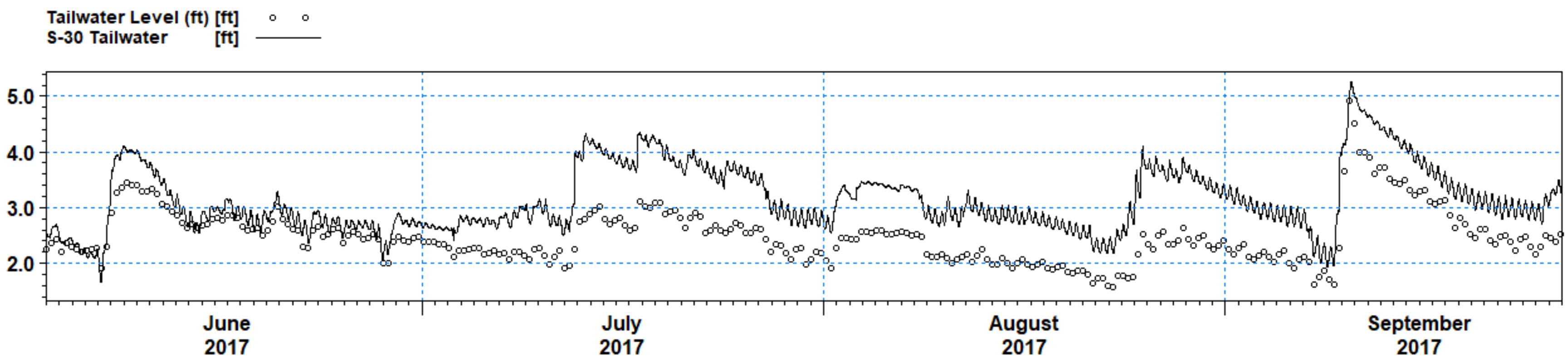

Figure C- 7: Simulated (line) vs Observed (dots) Tailwater Comparison for SFWMD C-9 Structure S-30, June 2nd-September 27th, 2017

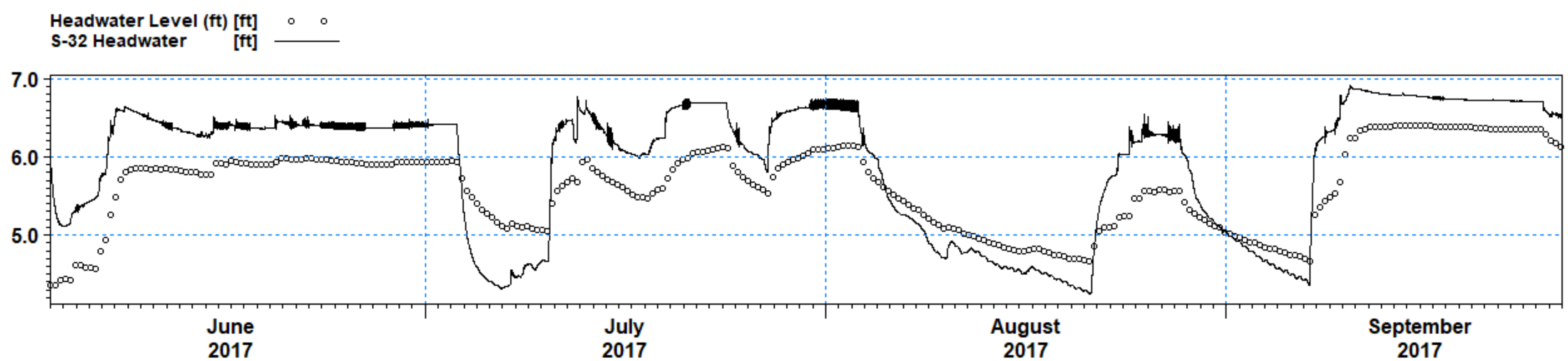

Figure C- 8: Simulated (line) vs Observed (dots) Headwater Comparison for SFWMD L-33 Structure S-32, June 2nd-September 27th, 2017

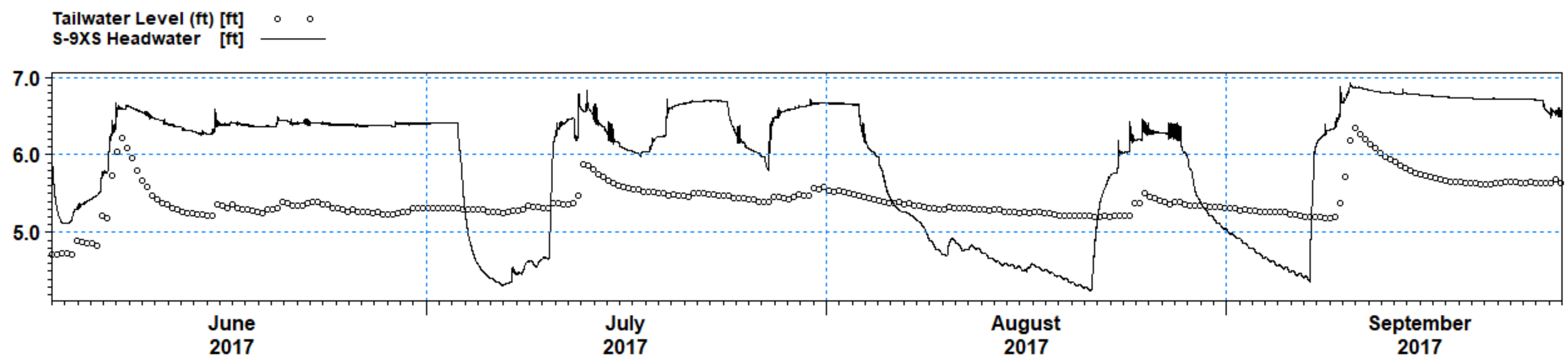

Figure C- 9: Simulated (line) vs Observed (dots) Headwater Comparison for SFWMD L-33 Structure S-9XS, June 2nd-September 27th, 2017

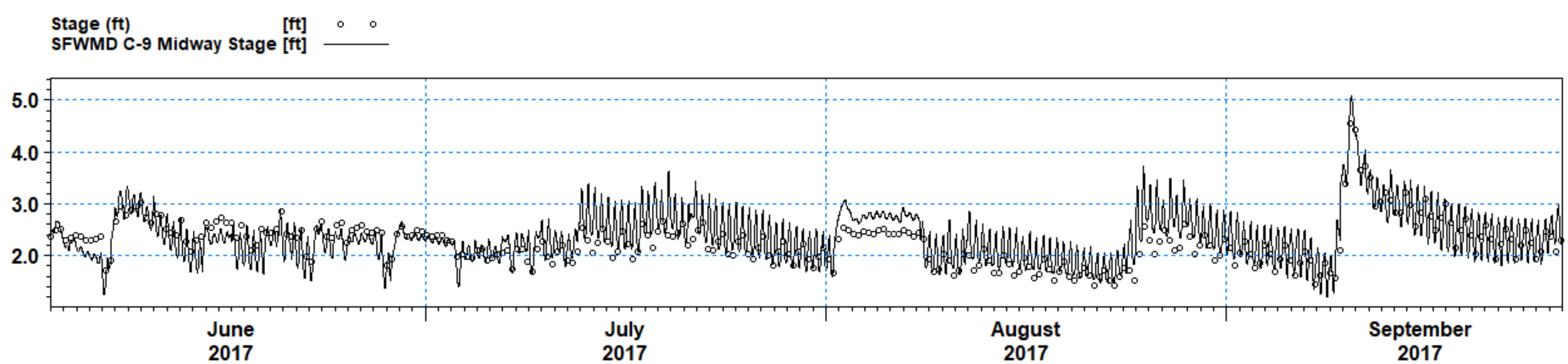

Figure C- 10: Simulated (line) vs Observed (dots) Stage Comparison for SFWMD C-9 Water Level Recorder S-29Z, June 2nd-September 27th, 2017

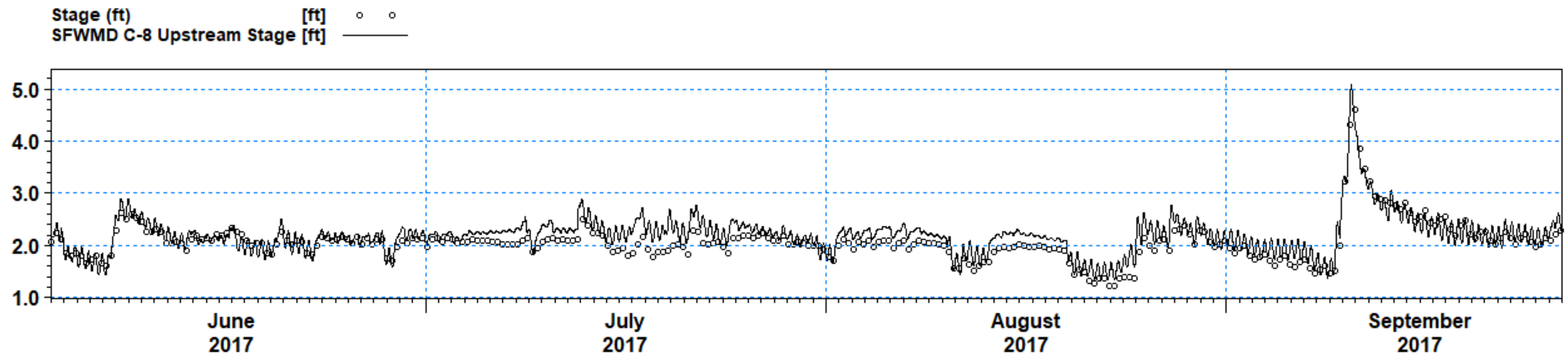

Figure C- 11: Simulated (line) vs Observed (dots) Stage Comparison for SFWMD C-8 Water Level Recorder S-28Z, June 2nd-September 27th, 2017

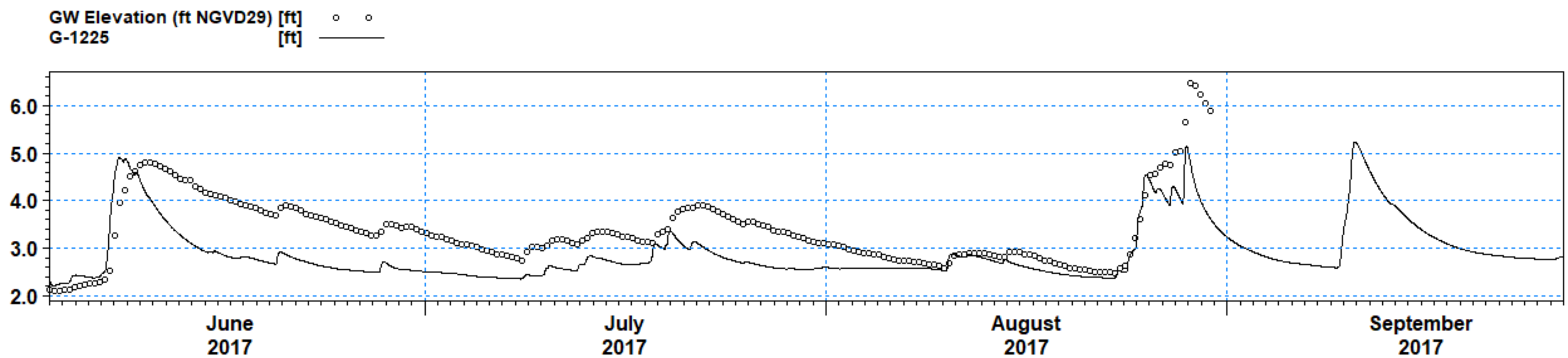

Figure C- 12: Simulated (line) vs Observed (dots) Groundwater Elevation Comparison for Well G-1225, June 2nd-September 27th, 2017

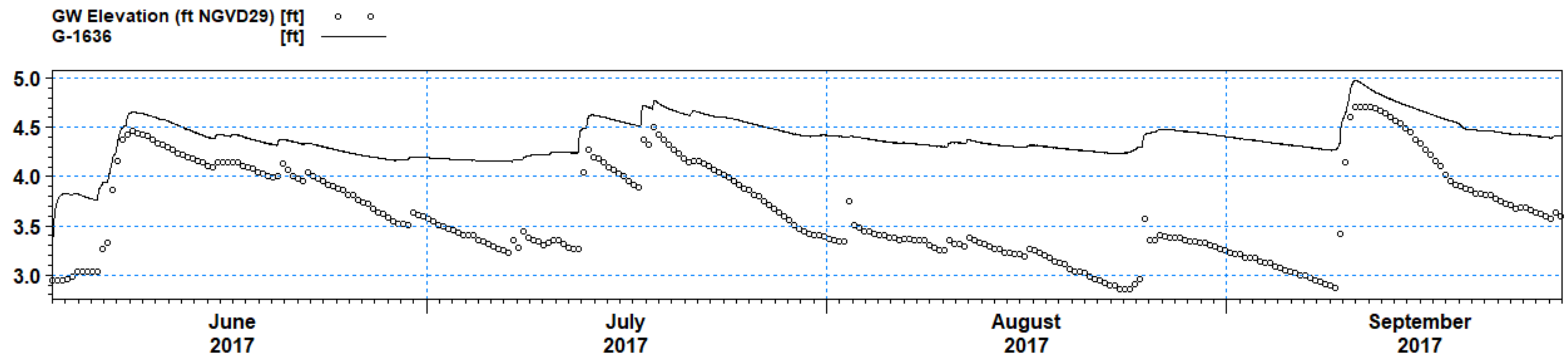

Figure C- 13: Simulated (line) vs Observed (dots) Groundwater Elevation Comparison for Well G-1636, June 2nd-September 27th, 2017

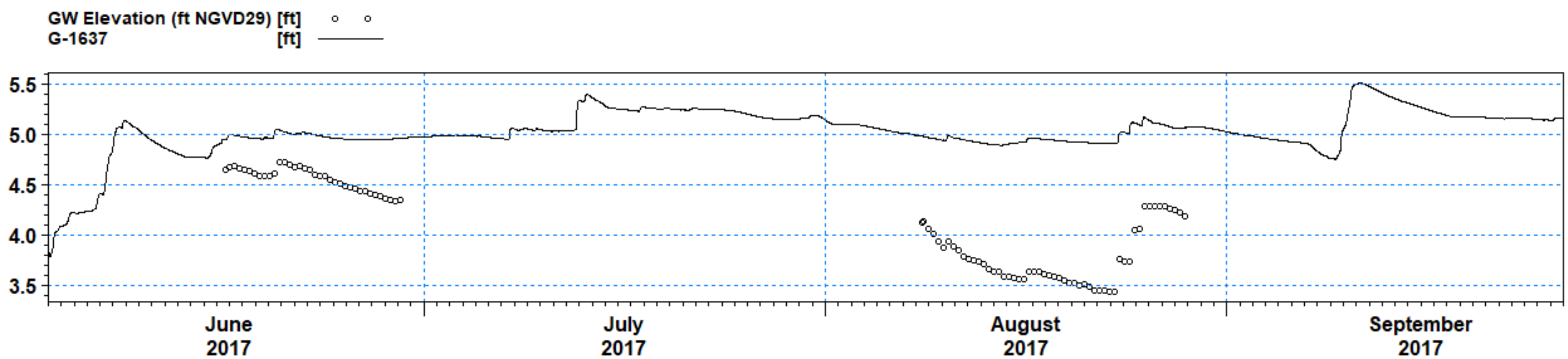

Figure C- 14: Simulated (line) vs Observed (dots) Groundwater Elevation Comparison for Well G-1637, June 2nd-September 27th, 2017

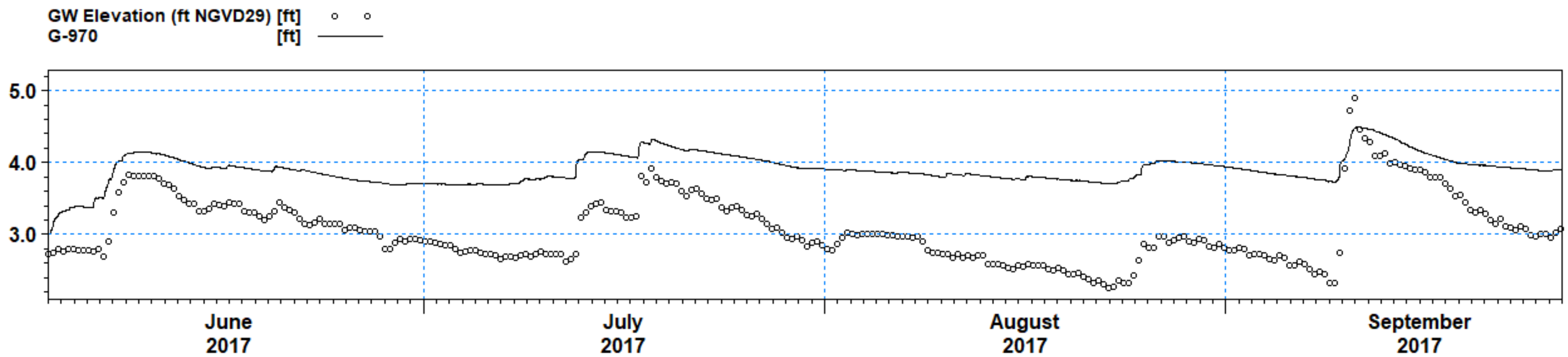

Figure C- 15: Simulated (line) vs Observed (dots) Groundwater Elevation Comparison for Well G-970, June 2nd-September 27th, 2017

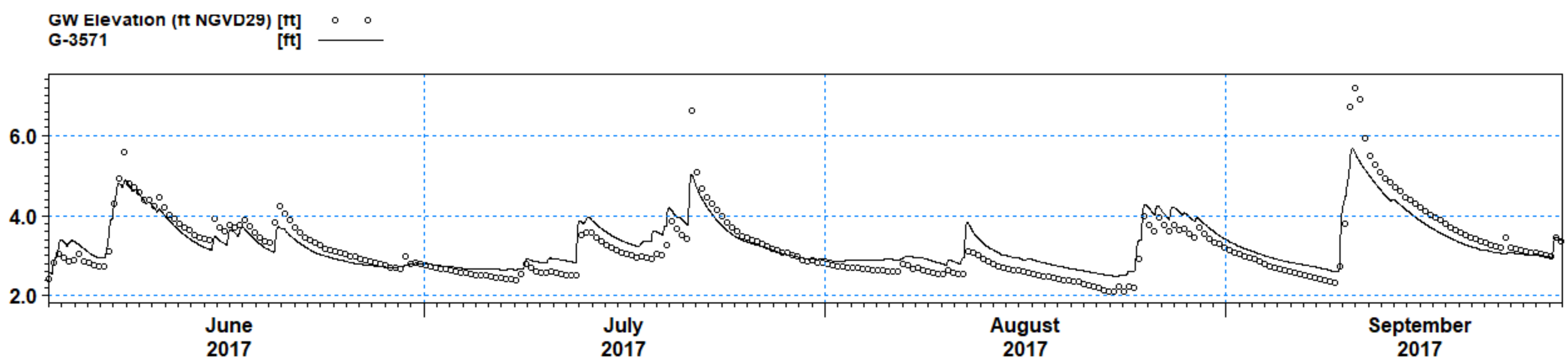

Figure C- 16: Simulated (line) vs Observed (dots) Groundwater Elevation Comparison for Well G-3571, June 2nd-September 27th, 2017

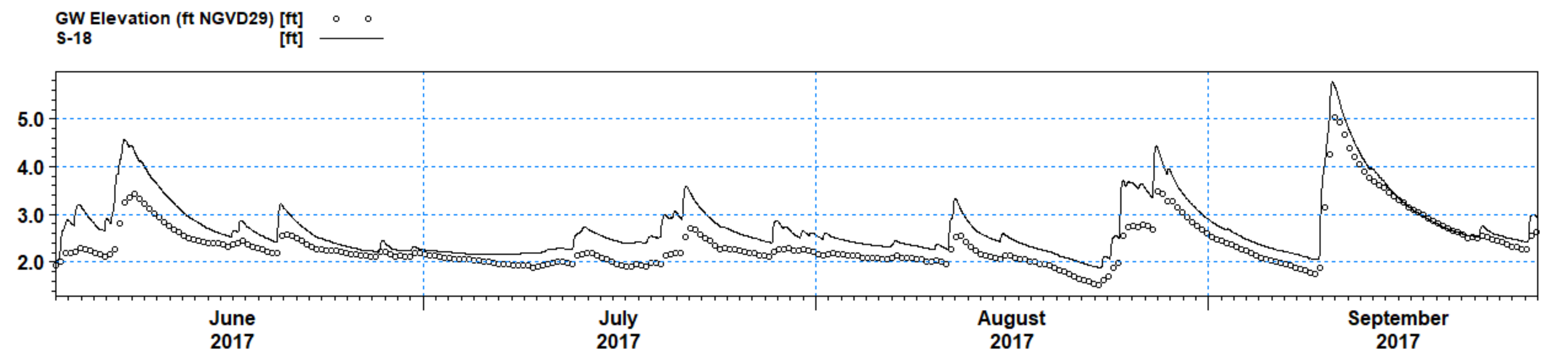

Figure C- 17: Simulated (line) vs Observed (dots) Groundwater Elevation Comparison for Well S-18, June 2nd-September 27th, 2017

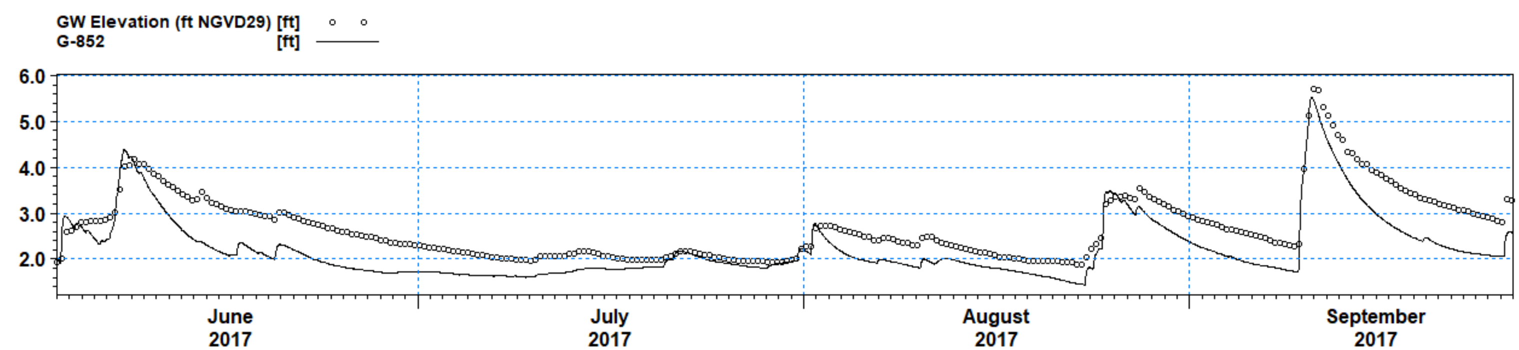

Figure C- 18: Simulated (line) vs Observed (dots) Groundwater Elevation Comparison for Well G-852, June 2nd-September 27th, 2017

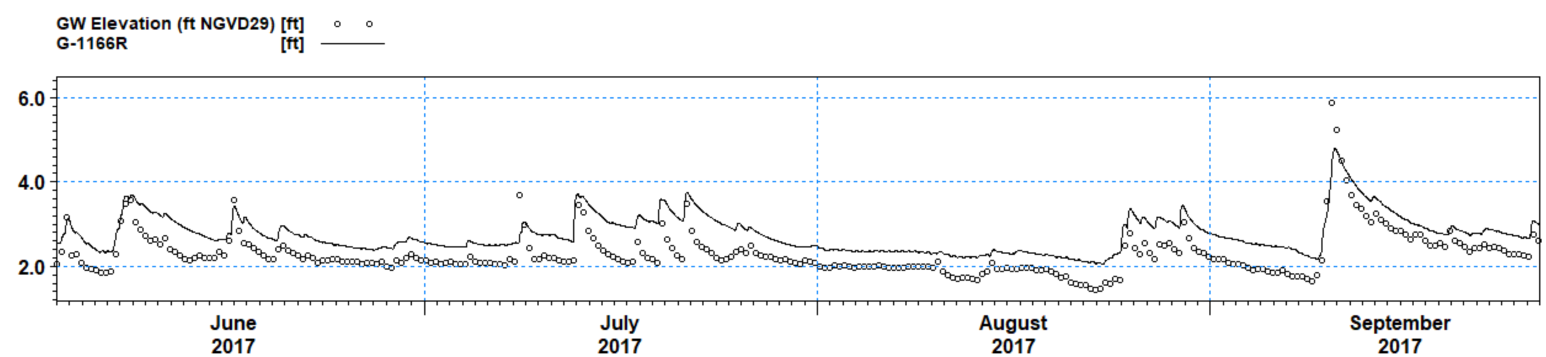

Figure C- 19: Simulated (line) vs Observed (dots) Groundwater Elevation Comparison for Well G-1166R, June 2nd-September 27th, 2017

Appendix D Current Conditions Design Storm Stage and Discharge Summary

Table D- 1: Peak Stage and Discharge Summary

Structure	Peak Stage (ft NGVD29)				Peak Discharge (cfs)			
	5-Year	10-Year	25-Year	100-Year	5-Year	10-Year	25-Year	100-Year
S-28	4.26	4.61	5.16	6.04	1721	2059	2679	3777
S-29	4.19	4.54	5.08	6.0	2647	3052	3681	4710
S-30 TW	4.87	5.23	5.49	5.97				

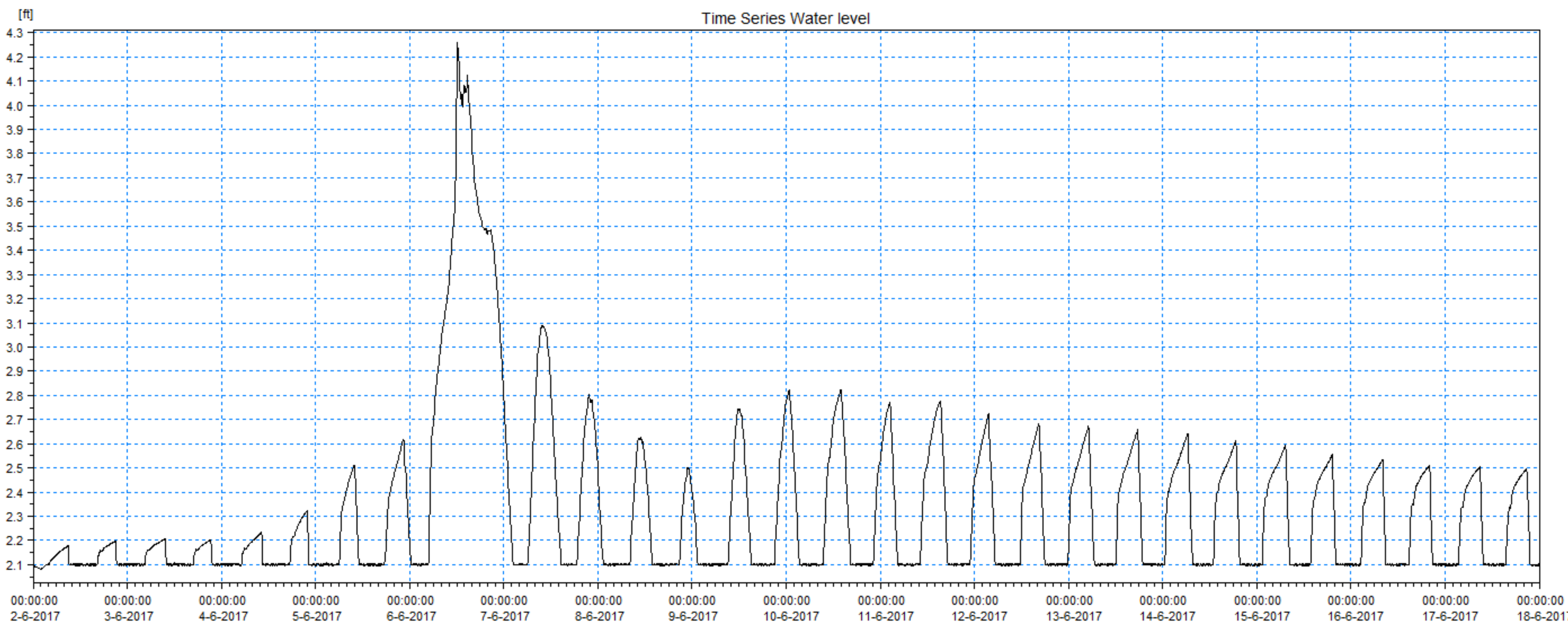

Figure D- 1: S-28 5-Year Design Storm Headwater Stage

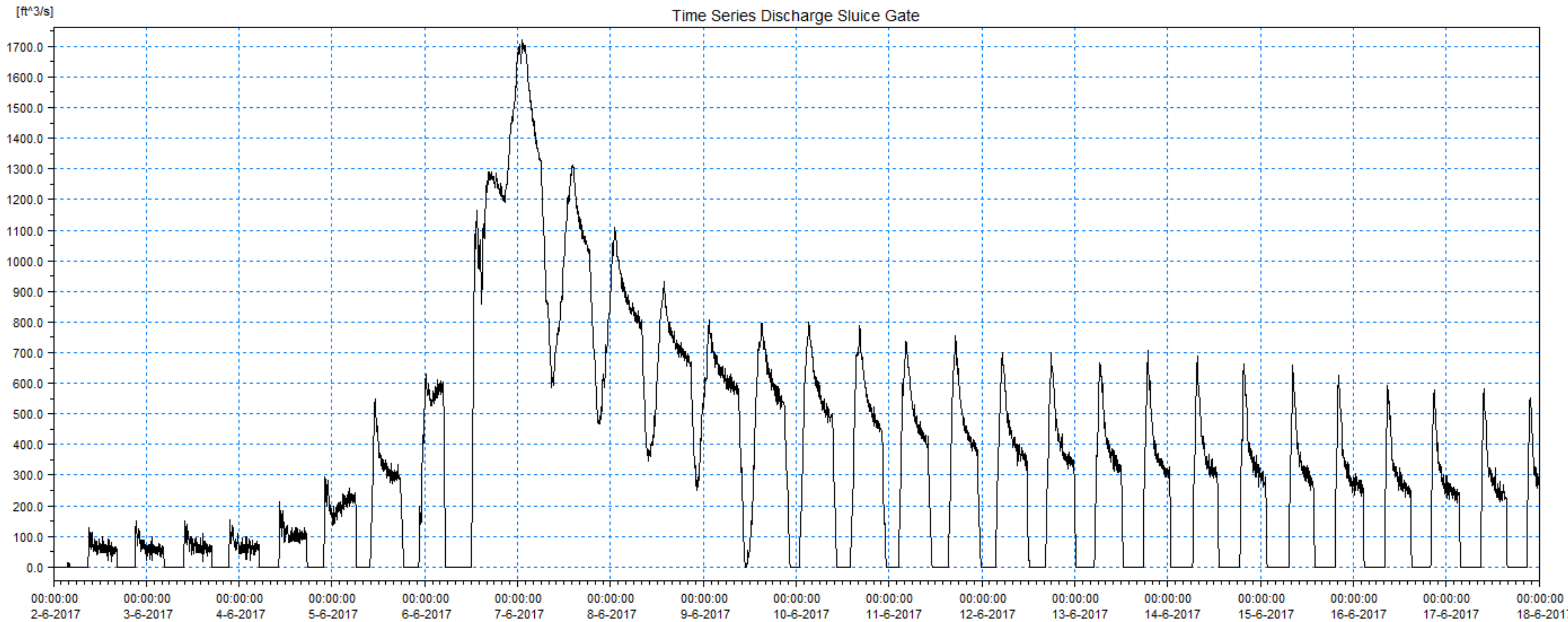

Figure D- 2: S-28 5-Year Design Storm Discharge (cfs)

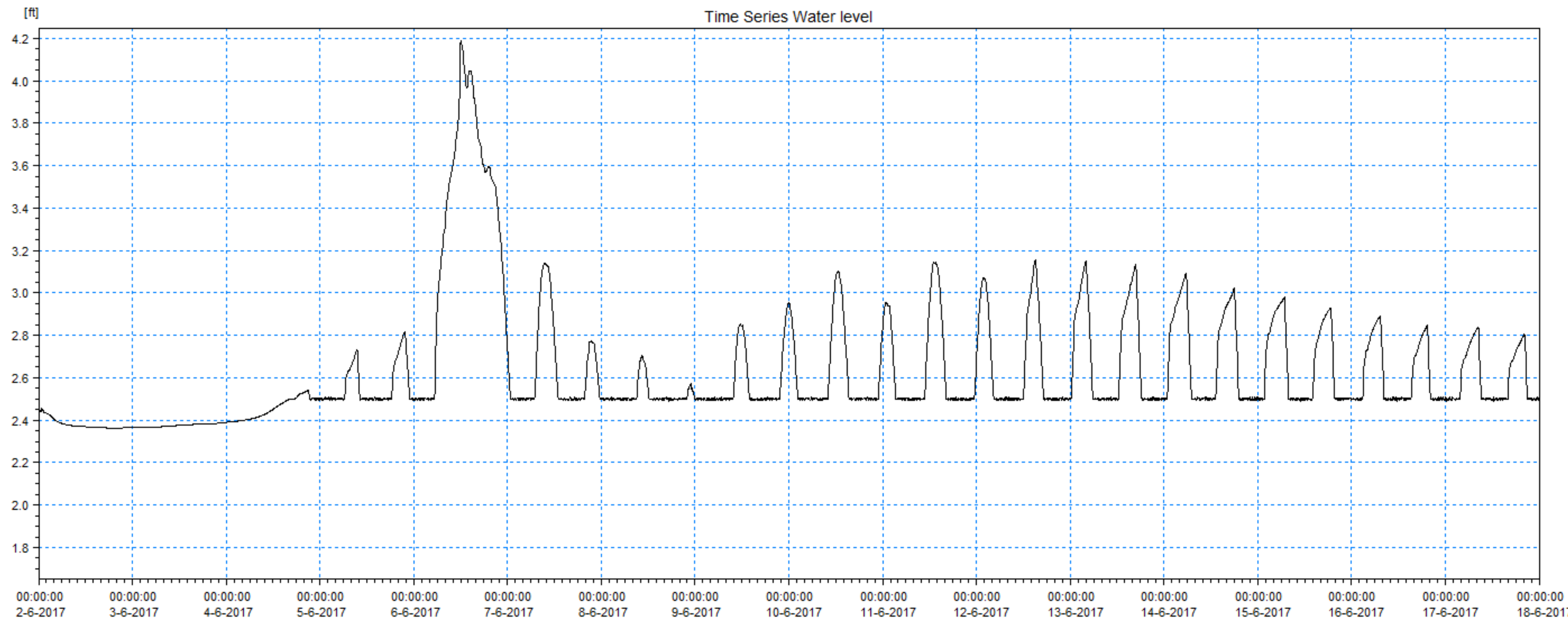

Figure D- 3: S-29 5-Year Design Storm Headwater Stage

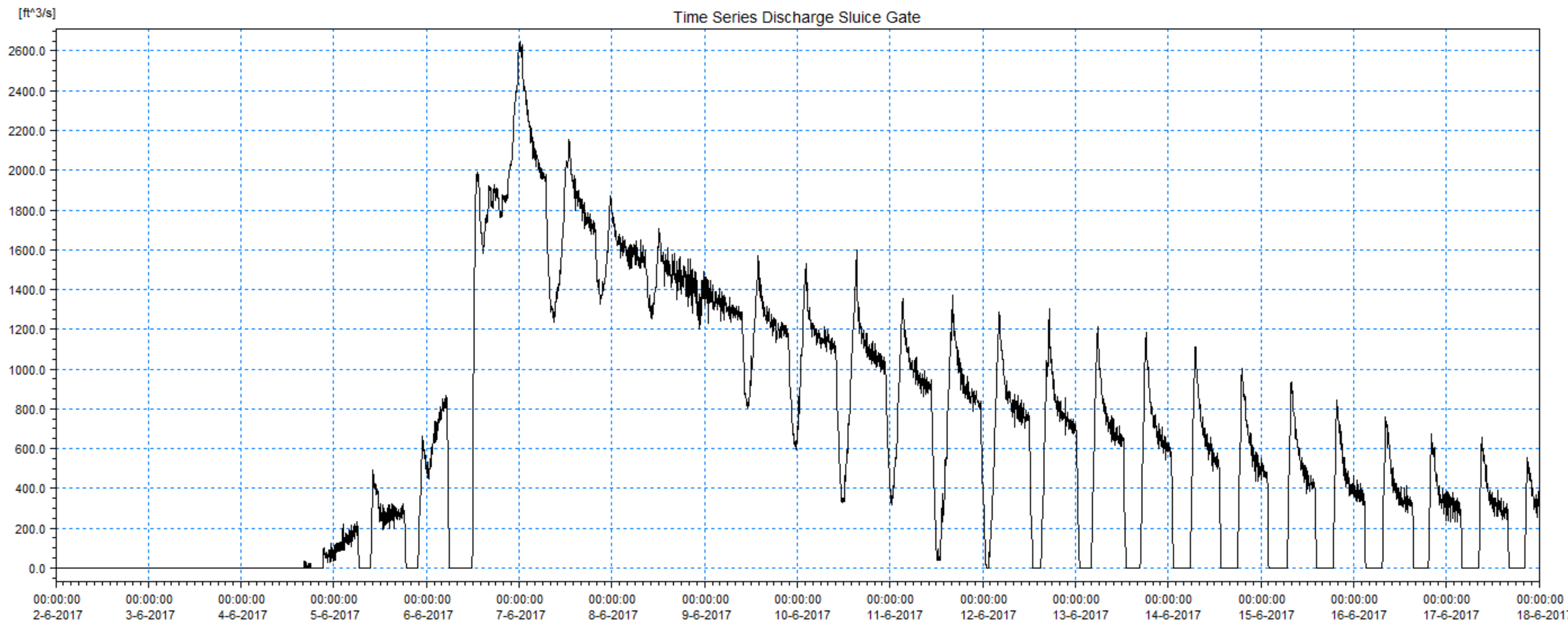

Figure D- 4: S-29 5-Year Design Storm Discharge (cfs)

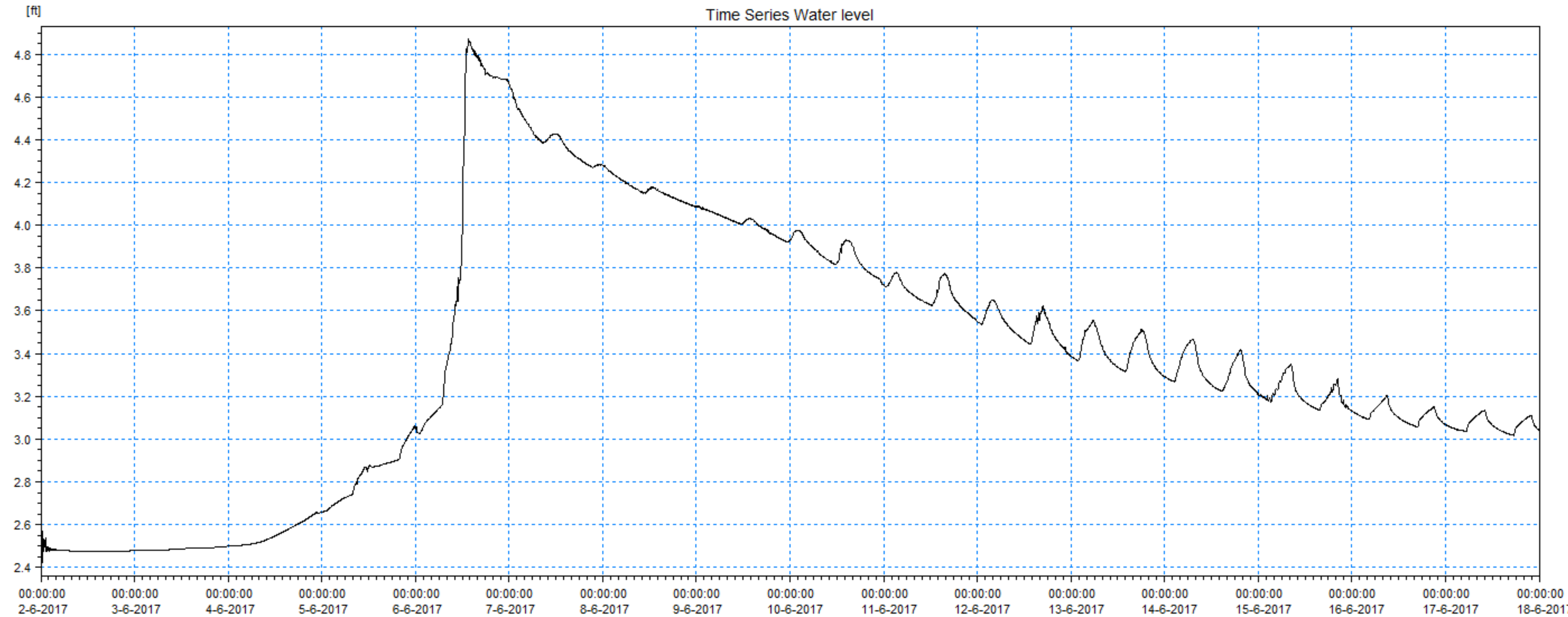

Figure D- 5: S-30 5-Year Design Storm Tailwater Stage

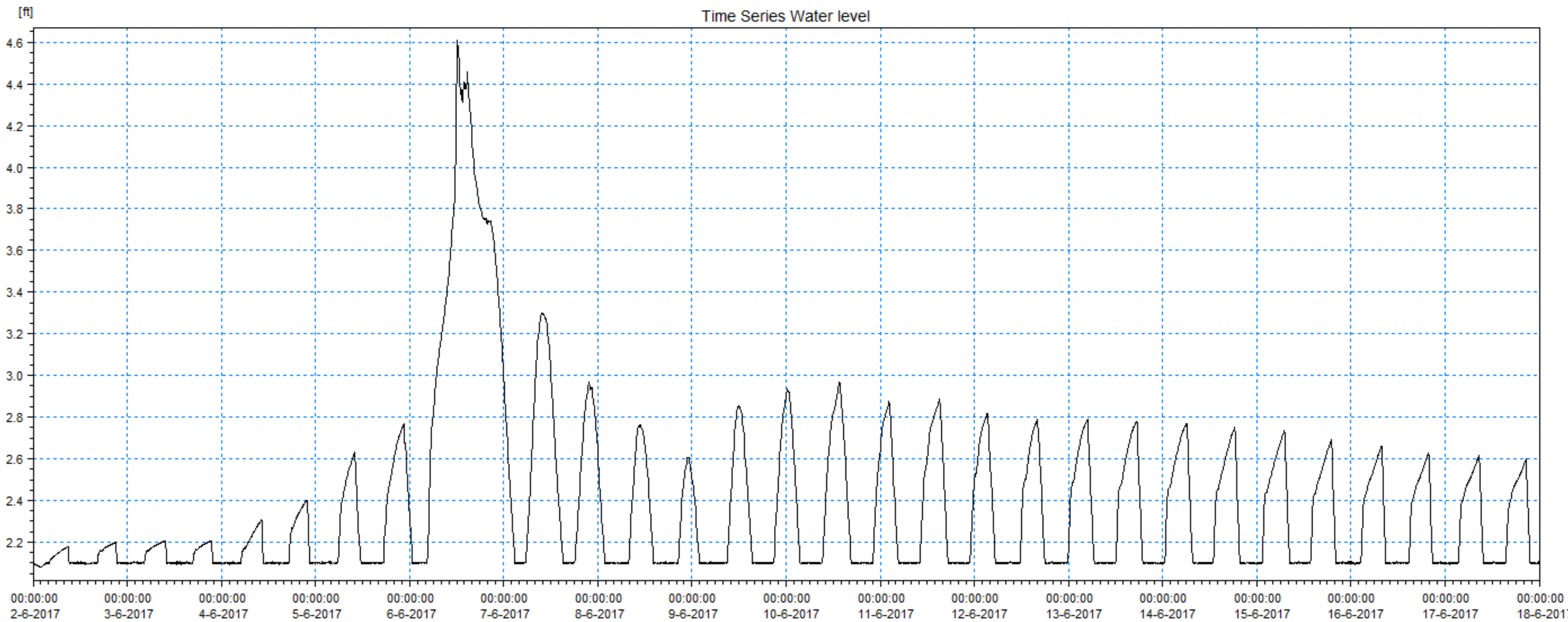

Figure D- 6: S-28 10-Year Design Storm Headwater Stage

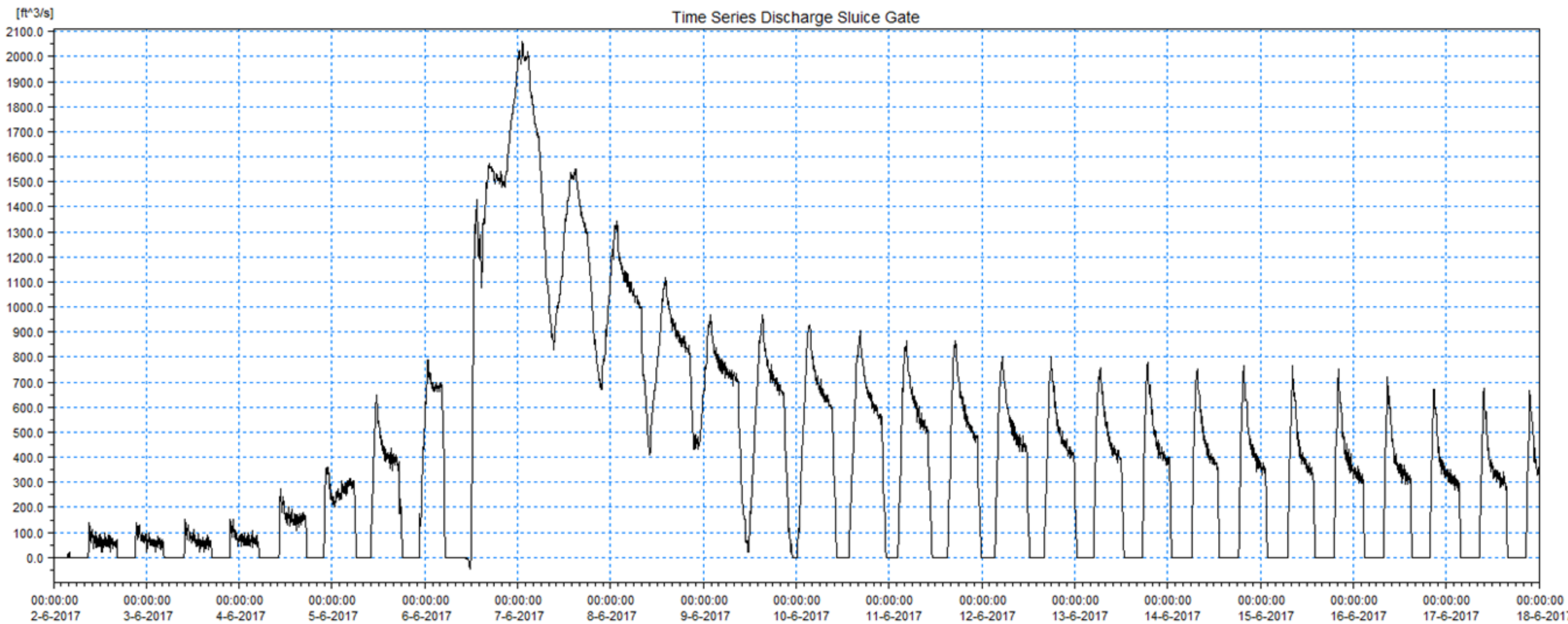

Figure D- 7: S-28 10-Year Design Storm Discharge (cfs)

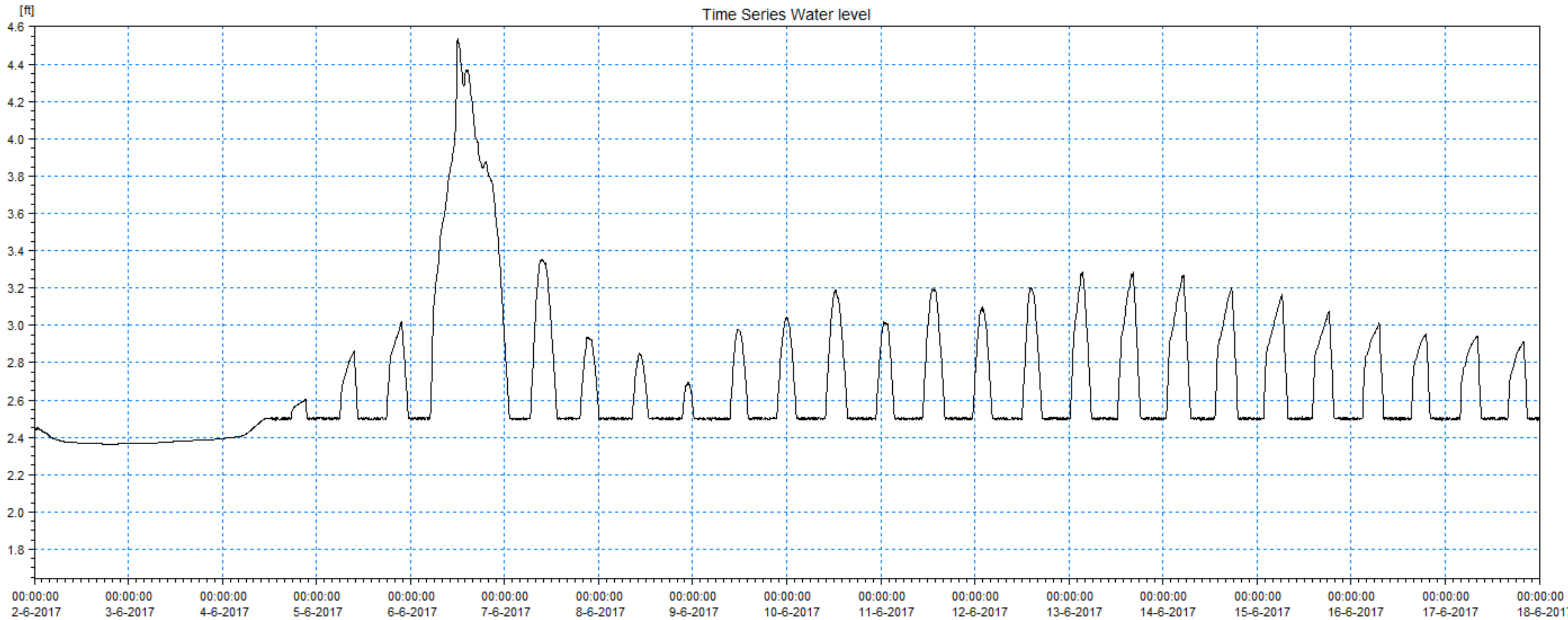

Figure D- 8: S-29 10-Year Design Storm Headwater Stage

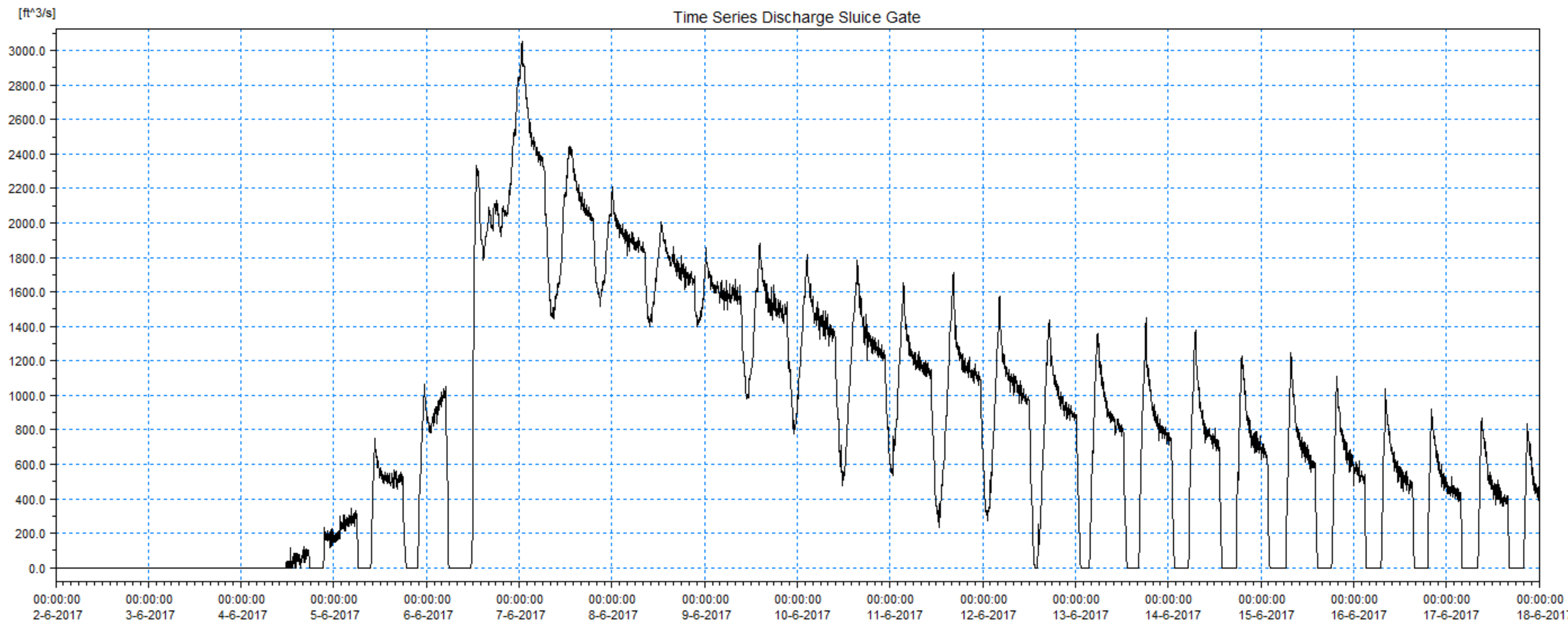

Figure D- 9: S-29 10-Year Design Storm Discharge (cfs)

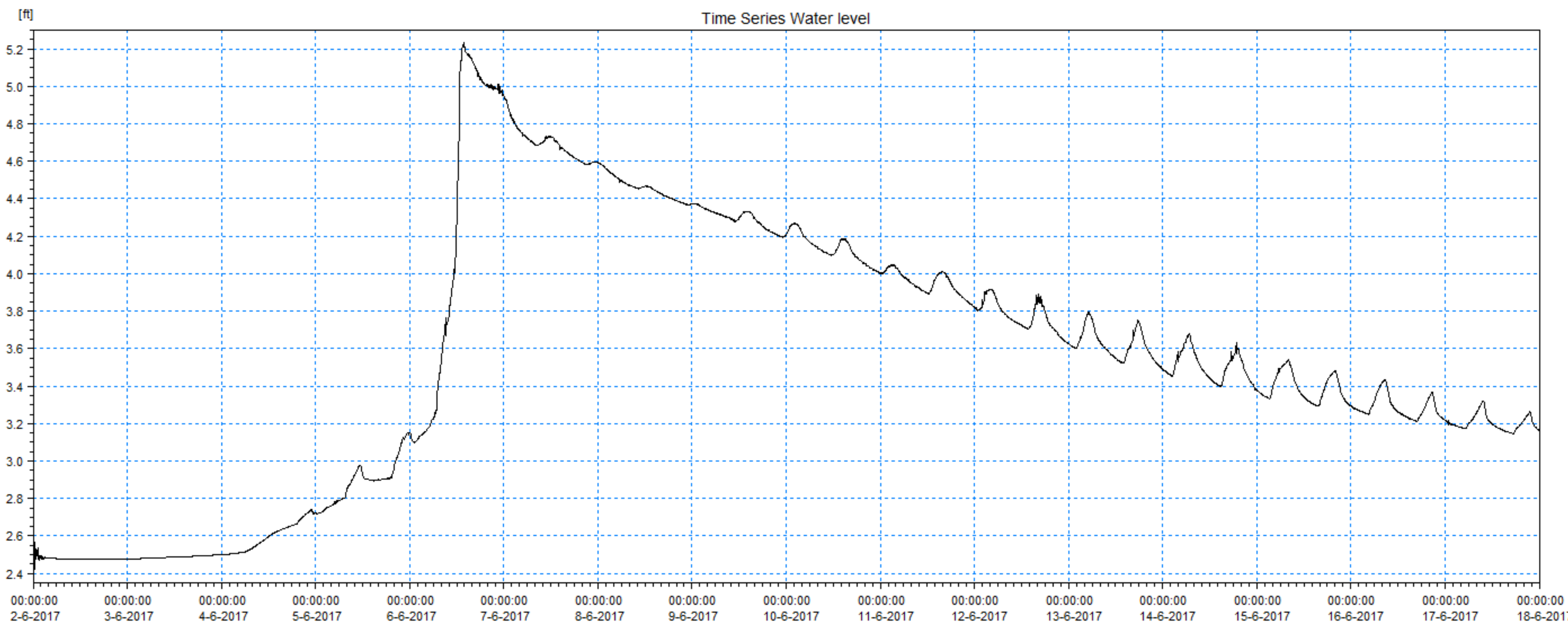

Figure D- 10: S-30 10-Year Design Storm Tailwater Stage

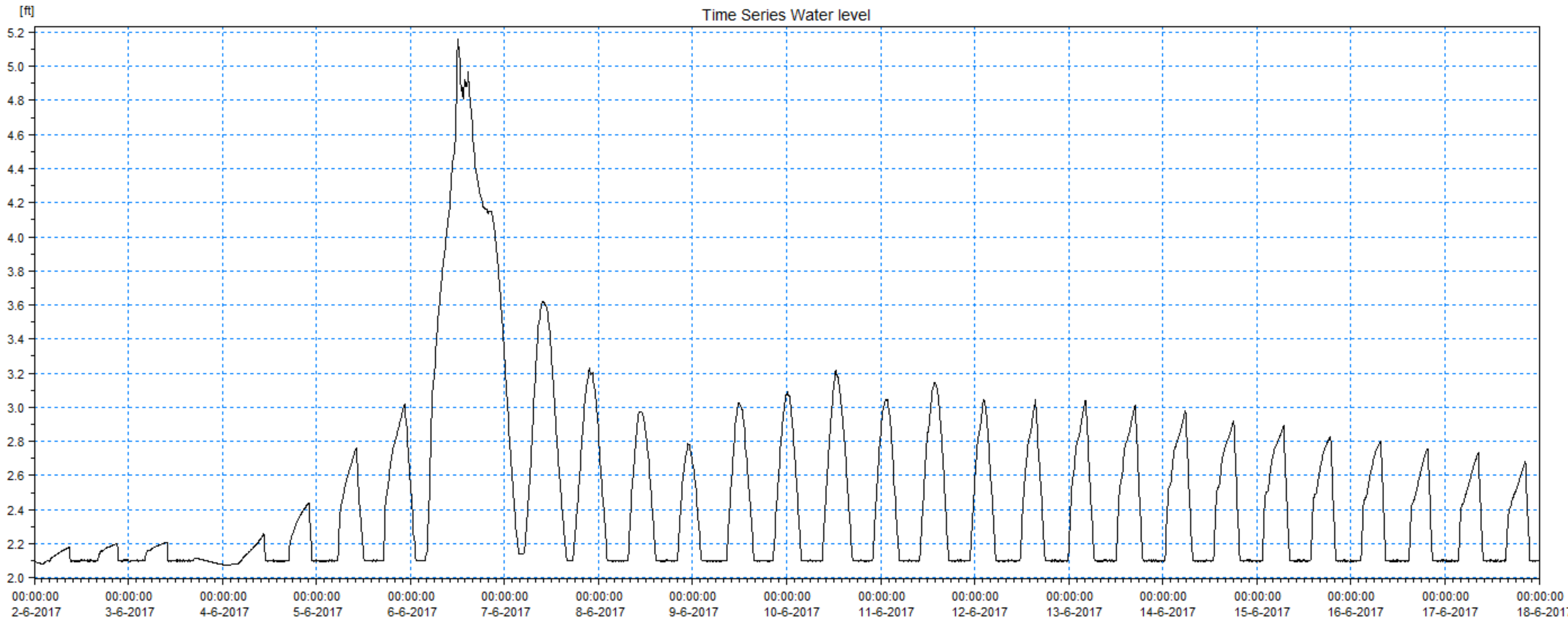

Figure D- 11: S-28 25-Year Design Storm Headwater Stage

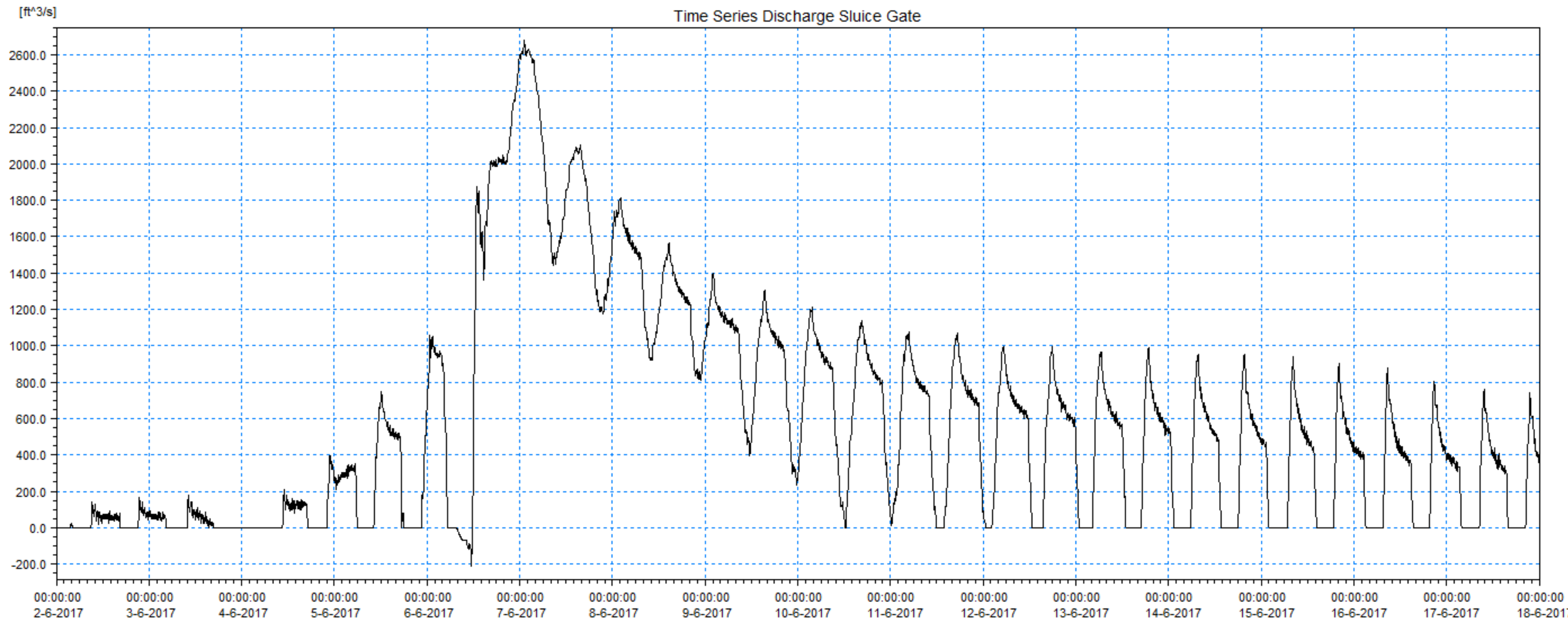

Figure D- 12: S-28 25-Year Design Storm Discharge (cfs)

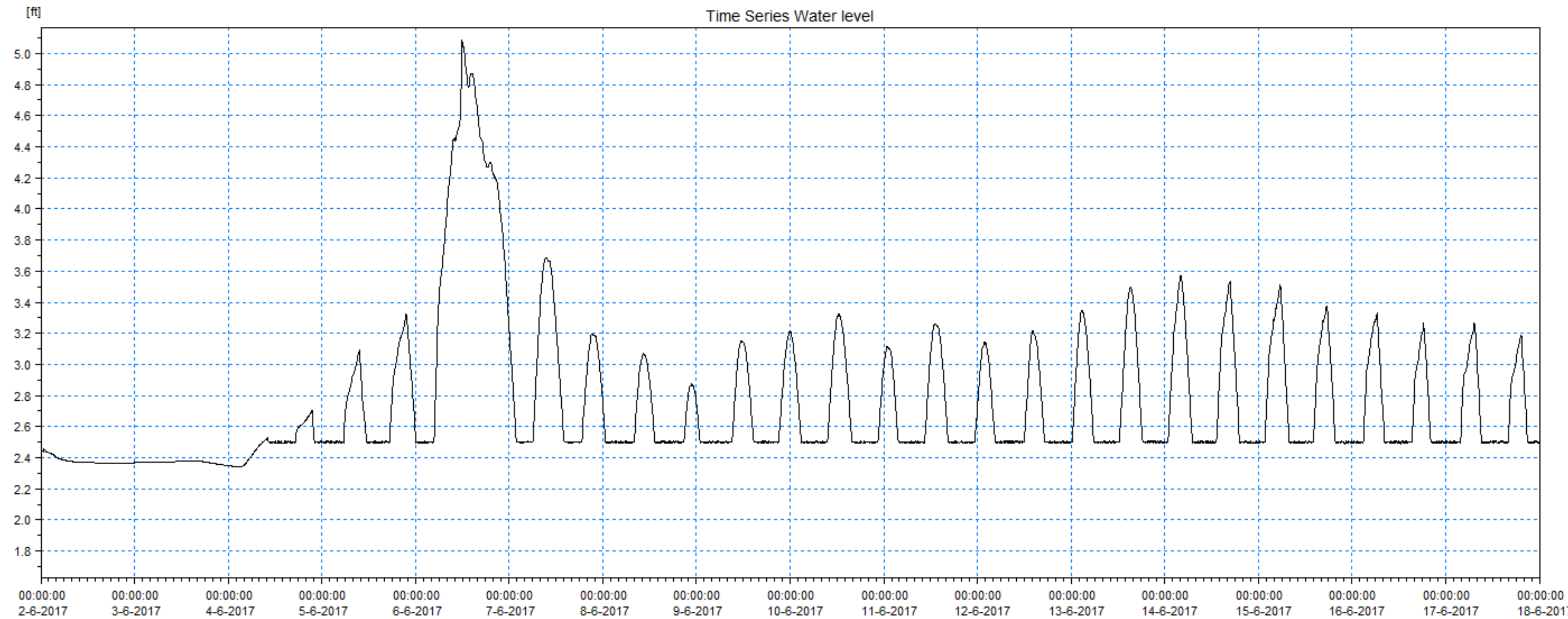

Figure D- 13: S-29 25-Year Design Storm Headwater Stage

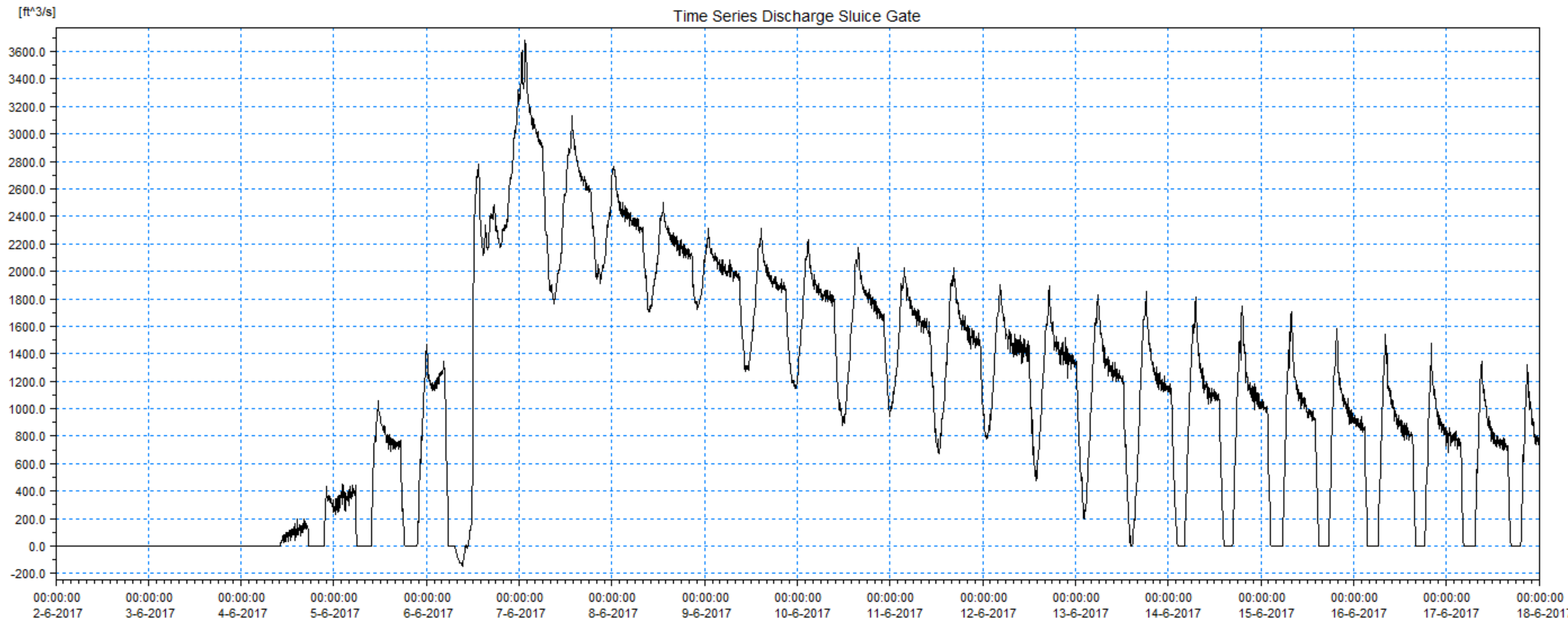

Figure D- 14: S-29 25-Year Design Storm Discharge (cfs)

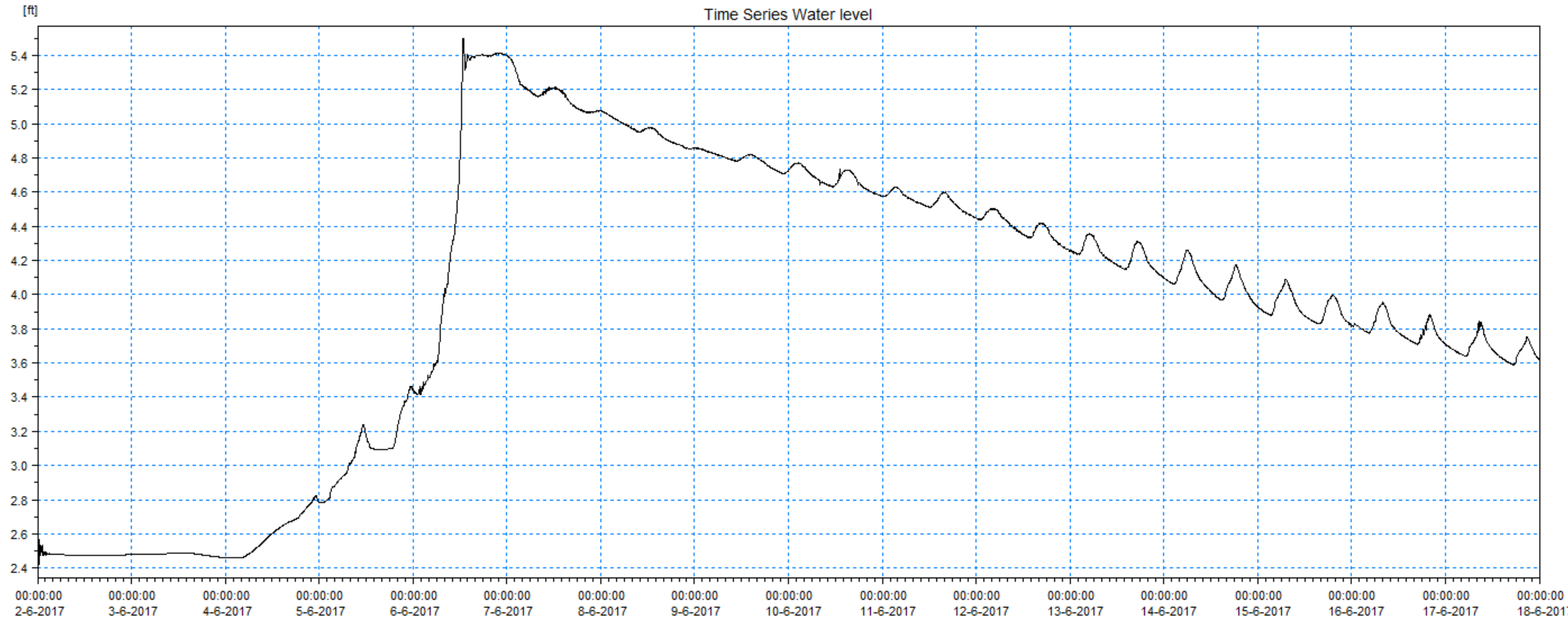

Figure D- 15: S-30 25-Year Design Storm Tailwater Stage

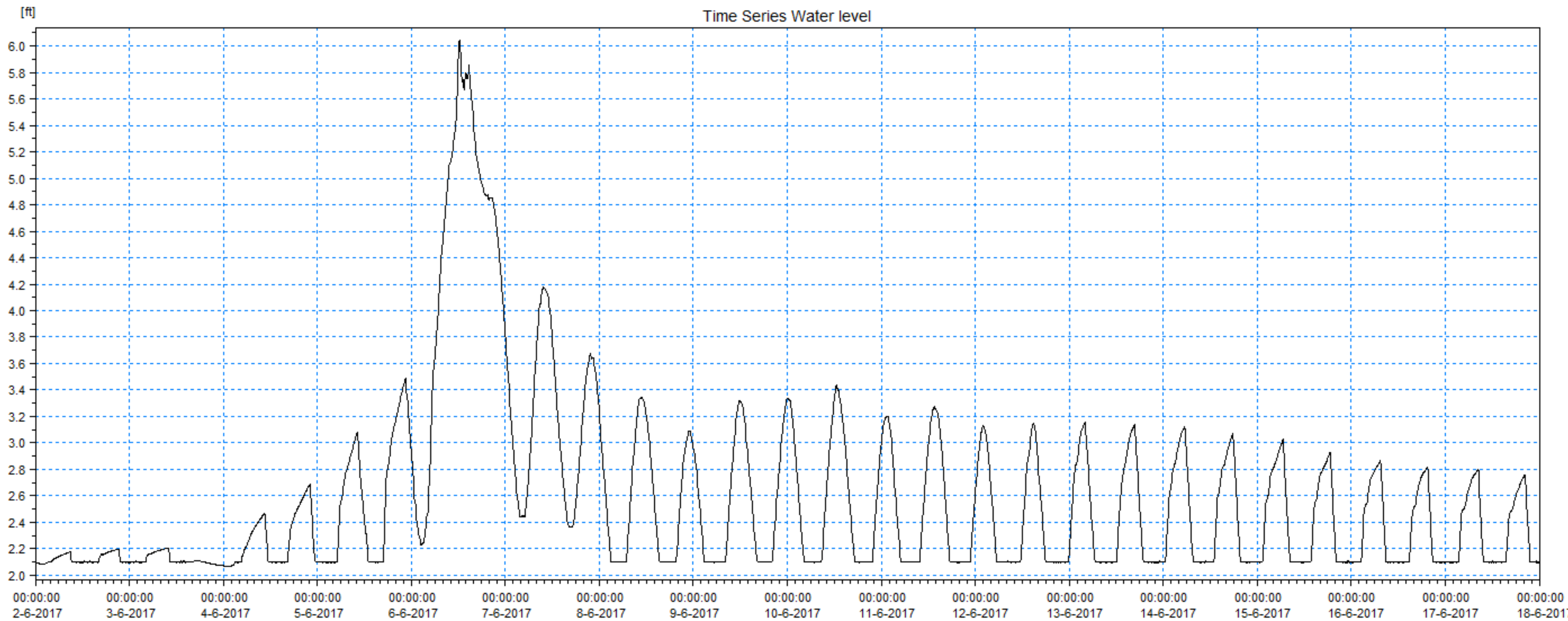

Figure D- 16: S-28 100-Year Design Storm Headwater Stage

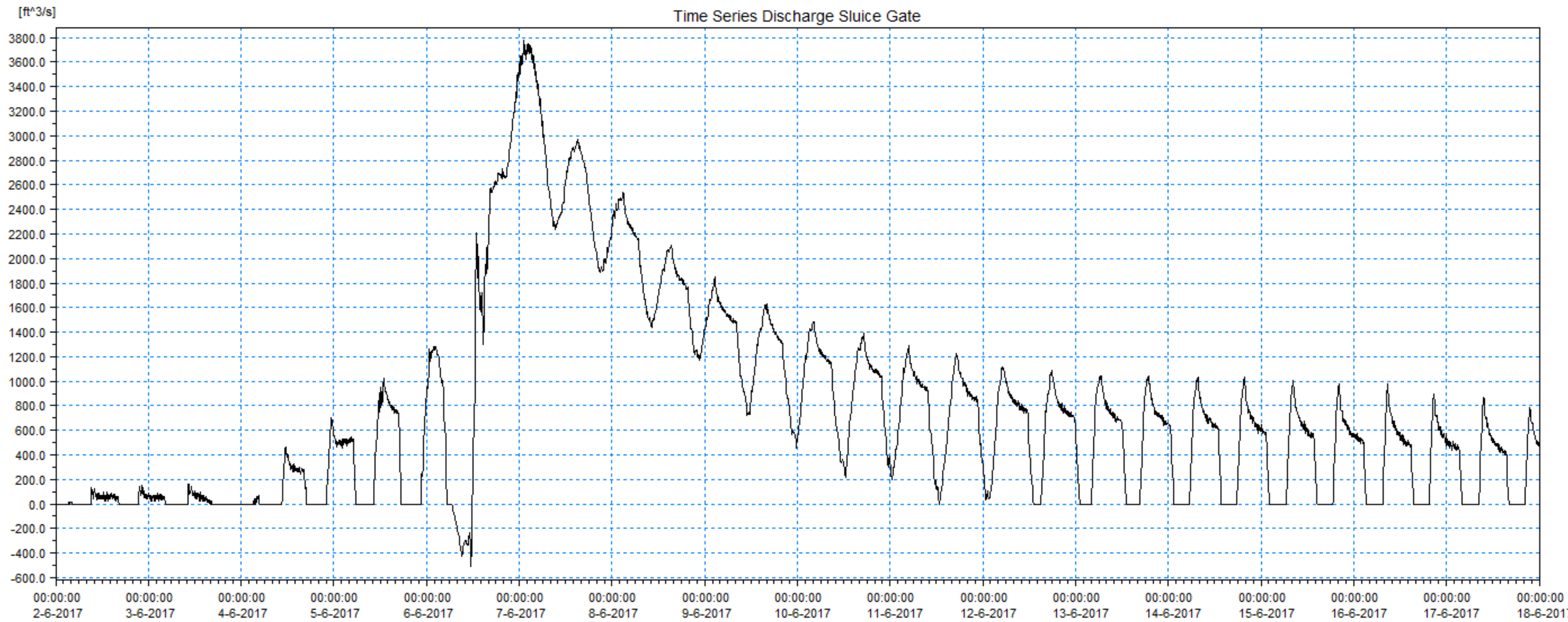

Figure D- 17: S-28 100-Year Design Storm Discharge (cfs)

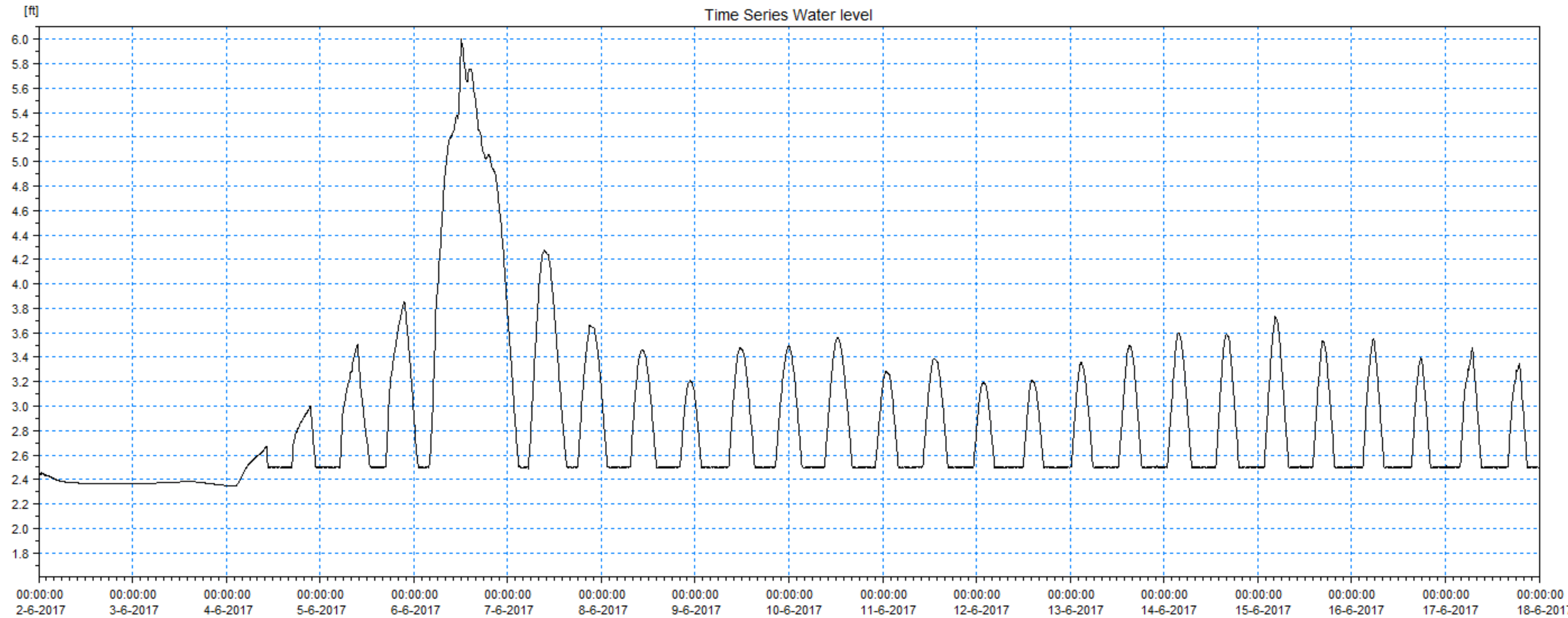

Figure D- 18: S-29 100-Year Design Storm Headwater Stage

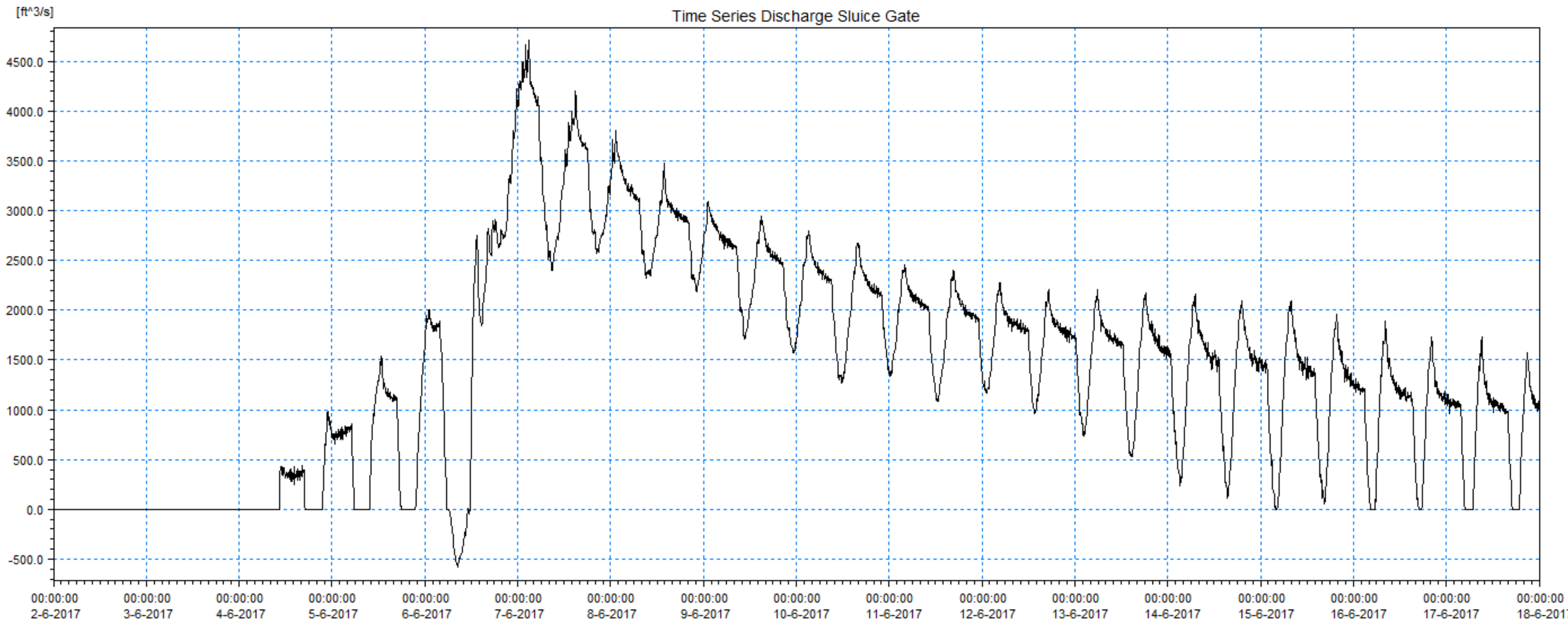

Figure D- 19: S-29 100-Year Design Storm Discharge (cfs)

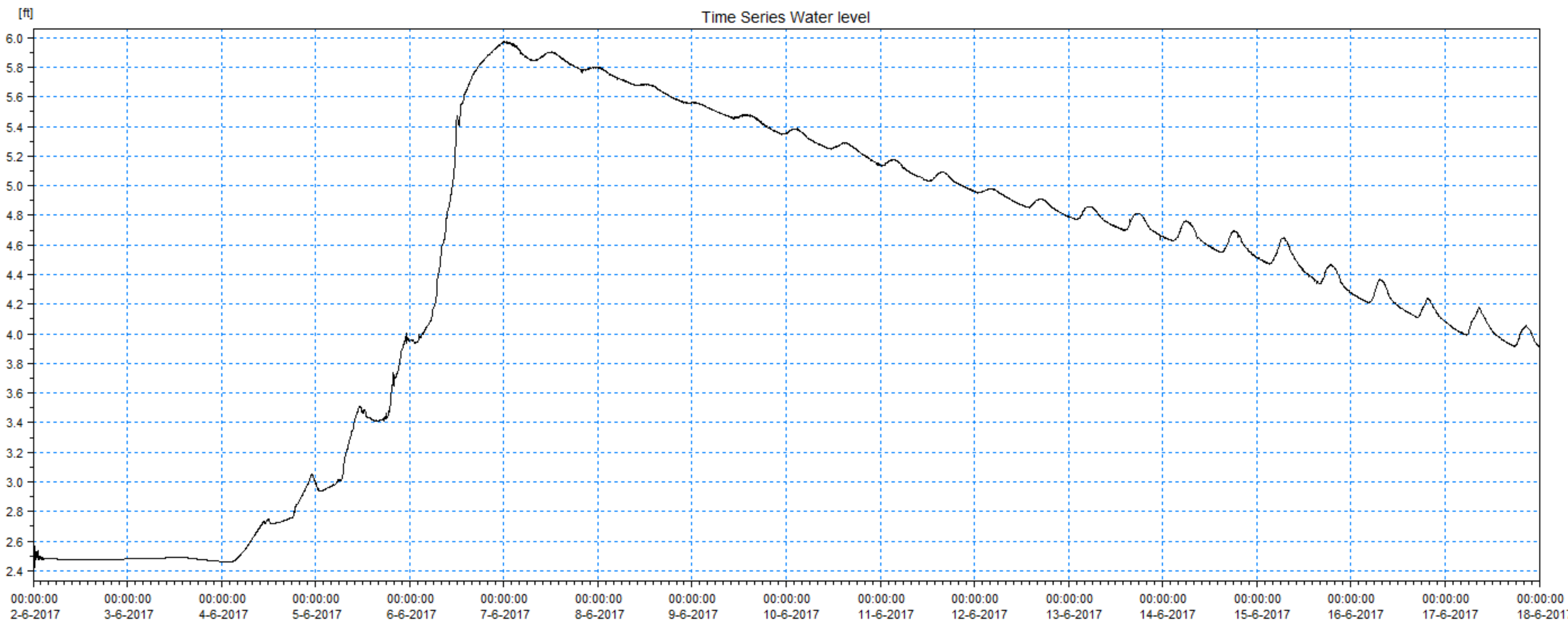

Figure D- 20: S-30 100-Year Design Storm Tailwater Stage

Appendix E South Broward Drainage District Control Elevations and Pump-On Elevations

Per permit, here are SBDD's pump on elevations at all its stormwater pump stations:

Pump Station	CWE	Pump On Elevation	Pump Capacity	Total Allowable Q
S-1 - First Pump	2.50' NGVD	2.75' NGVD	47, 500 GPM	425 cfs (all pumps off at tailwater Elev. of 6.5' NGVD)
S-1 – Second Pump		3.00' NGVD	47, 500 GPM	
S-1 – Third Pump		3.00' NGVD	47, 500 GPM	
S-1 – Fourth Pump (spare)				
S-2 (3 pumps)	2.70' NGVD	3.30' NGVD	45,000 GPM EA.	524 cfs (S-2 & S-7 combined; pumping ceases when the C-9 Canal = Elev. 6.8' NGVD)
S-7 (3 pumps)	2.70' NGVD	3.30' NGVD	50,000 GPM EA.	524 cfs (S-2 & S-7 combined; pumping ceases when the C-9 Canal = Elev. 6.8' NGVD)
S-3 (3 pumps)	3.00' NGVD	3.60' NGVD	45,000 GPM EA.	200 cfs (pumping ceases when the C-9 Canal = Elev. 6.8' NGVD)
S-4 (2 pumps)	3.50' NGVD	4.00' NGVD	31,000 GPM	70 cfs (pumping ceases when the C-9 Canal = Elev. 6.8' NGVD)
S-5 (3 pumps)	4.00' NGVD (Sub-Basin 1) 4.25' NGVD (Sub-Basin 2) 4.50' NGVD (Sub-Basin 3)	4.50' NGVD	40,000 GPM EA.	180 cfs (pumping ceases when the C-9 Canal = Elev. 6.8' NGVD) Pumps Off at Elev 4.00' NGVD
S-8 – First Pump	3.50' NGVD	4.30' NGVD	75,000 GPM	167 cfs (from Elev. 4.3' – 4.55')
S-8 – Second Pump	3.50' NGVD	4.55' NGVD	75,000 GPM	334 cfs (from Elev. 4.55 to 5.70'; discontinue pumping when C-11 Canal = Elev. 5.7' NGVD)
S-8 – Third pump (spare)				

The pump off elevation at all pump stations is equal to the CWE unless otherwise noted. SBDD operates its pump stations such that the pumps/engines rotate and there is always one pump/engine that serves as a spare pump/engine.

Feel free to contact me with any questions.

Thanks.

Kevin Hart, P.E., CFM
District Director
South Broward Drainage District
6591 Southwest 160th Avenue
Southwest Ranches, FL 33331
954-680-3337 (office)
e-mail: kevin@sbdd.org

Figure E- 1: South Broward Drainage Control Elevations and Pump Station Information

Appendix F Instantaneous Stage and Discharge Summary

Table F- 1: Peak Stage and Discharge Summary for 5-Year Design Storms

Structure	Peak Stage (ft NGVD29)			Peak Discharge (cfs)		Minimum Discharge (cfs)	
	S-28	S-29	S-30 TW	S-28	S-29	S-28	S-29
Current	4.26	4.19	4.87	1721	2647	0	0
SLR1	5.12	5.04	4.82	1696	2417	-238	-323
SLR2	5.82	5.75	5.04	1839	2190	-773	-1057
SLR3	6.62	6.48	5.52	2087	2186	-1301	-1962

Table F- 2: Peak Stage and Discharge Summary for 10-Year Design Storms

Structure	Peak Stage (ft NGVD29)			Peak Discharge (cfs)		Minimum Discharge (cfs)	
	S-28	S-29	S-30 TW	S-28	S-29	S-28	S-29
Current	4.61	4.54	5.23	2059	3052	-45	-1
SLR1	5.43	5.42	5.11	2103	2698	-407	-489
SLR1 + 9% Rainfall	5.45	5.46	5.05	2268	2884	-430	-429
SLR2	6.14	6.10	5.49	2268	2526	-1016	-1215
SLR3	6.96	6.85	5.67	2615	2631	-1534	-2225

Table F- 3: Peak Stage and Discharge Summary for 25-Year Design Storms

Structure	Peak Stage (ft NGVD29)			Peak Discharge (cfs)		Peak Reverse Discharge (cfs)	
	S-28	S-29	S-30 TW	S-28	S-29	S-28	S-29
Current	5.16	5.08	5.49	2679	3681	-210	-146
SLR1	5.97	5.86	5.55	2789	3360	-647	-744
SLR2	6.64	6.58	5.84	3163	3460	-1171	-1680
SLR3	7.34	7.31	5.99	3278	3632	-1722	-2812

Table F- 4: Peak Stage and Discharge Summary for 100-Year Design Storms

Structure	Peak Stage (ft NGVD29)			Peak Discharge (cfs)		Peak Reverse Discharge (cfs)	
	S-28	S-29	S-30 TW	S-28	S-29	S-28	S-29
Current	6.04	6.00	5.97	3777	4710	-507	-578
SLR1	6.74	6.65	6.10	3999	4645	-1087	-1566
SLR2	7.36	7.38	6.26	4157	5073	-1692	-2649
SLR3	8.31	8.17	6.49	4094	4883	-2281	-3756

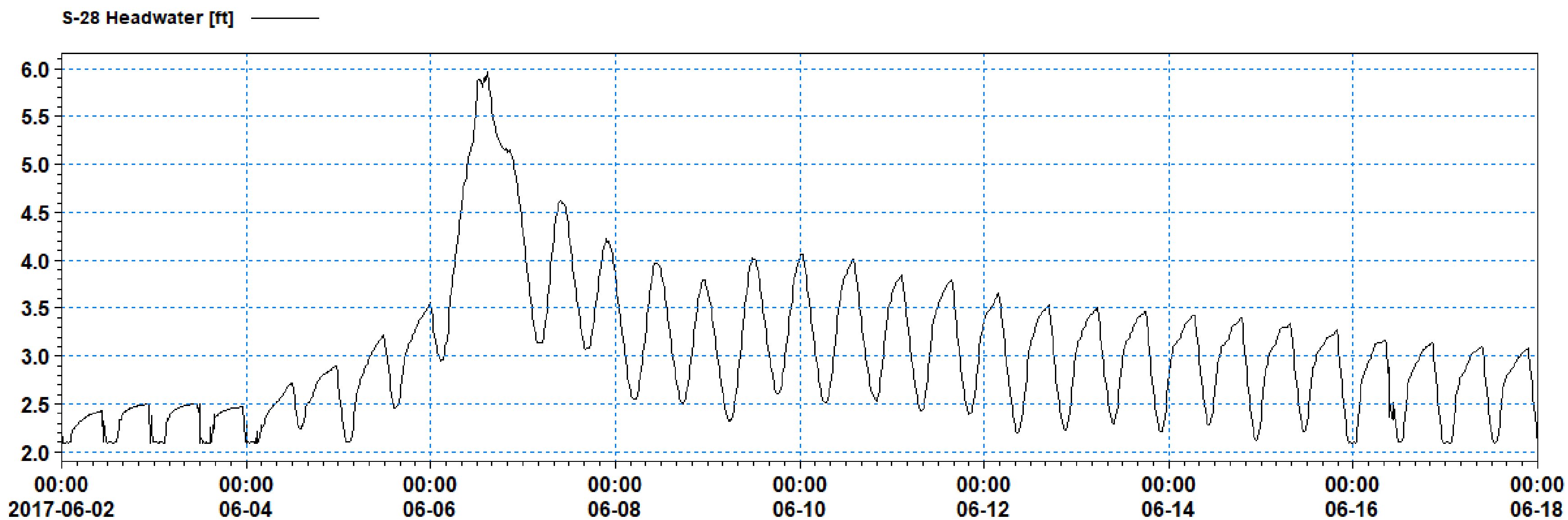

Figure F- 1: S-28 25-Year SLR1 Design Storm Headwater Stage

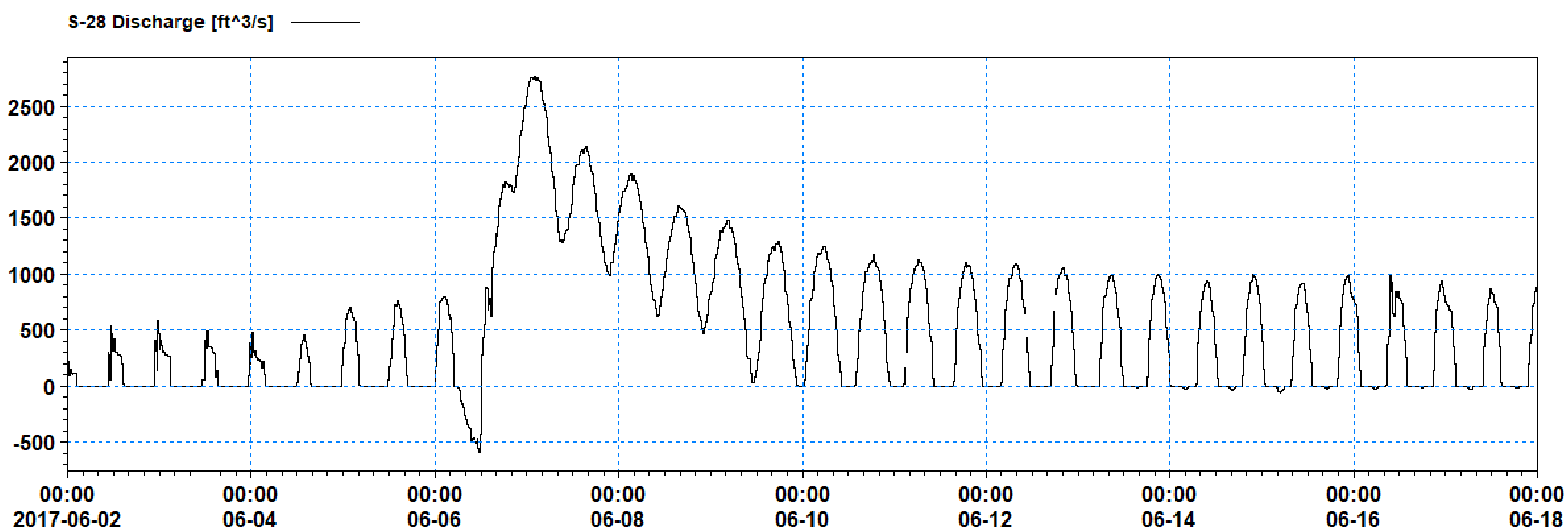

Figure F- 2: S-28 25-Year SLR1 Design Storm Discharge

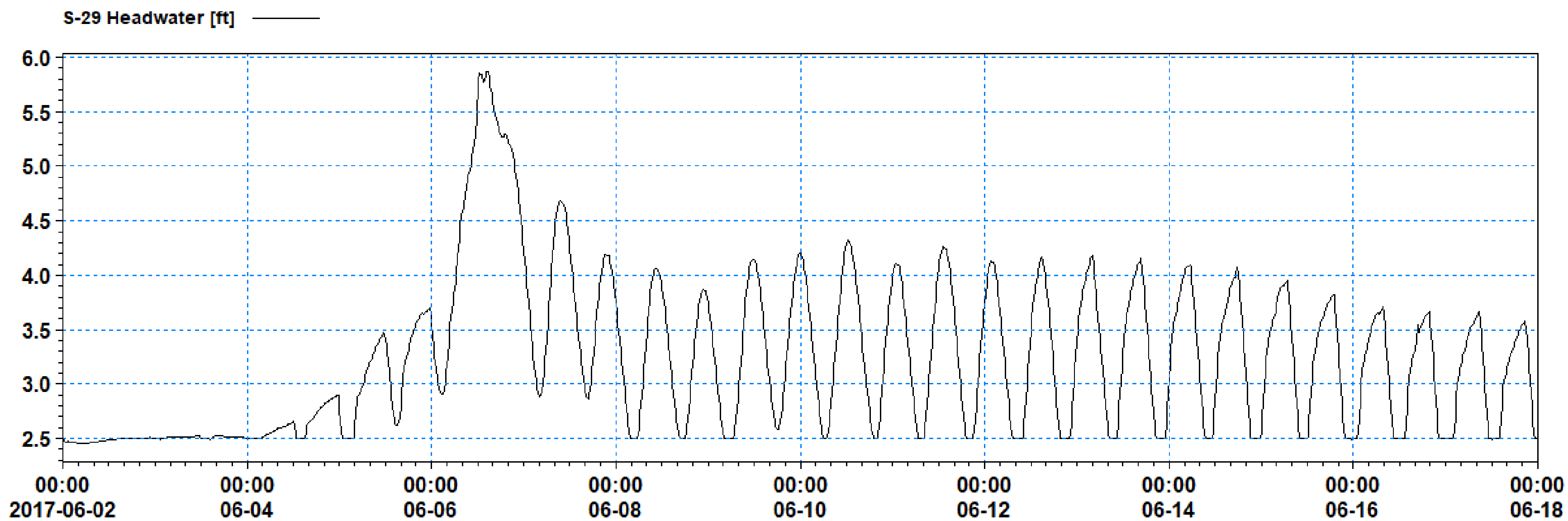

Figure F- 3: S-29 25-Year SLR1 Design Storm Headwater Stage

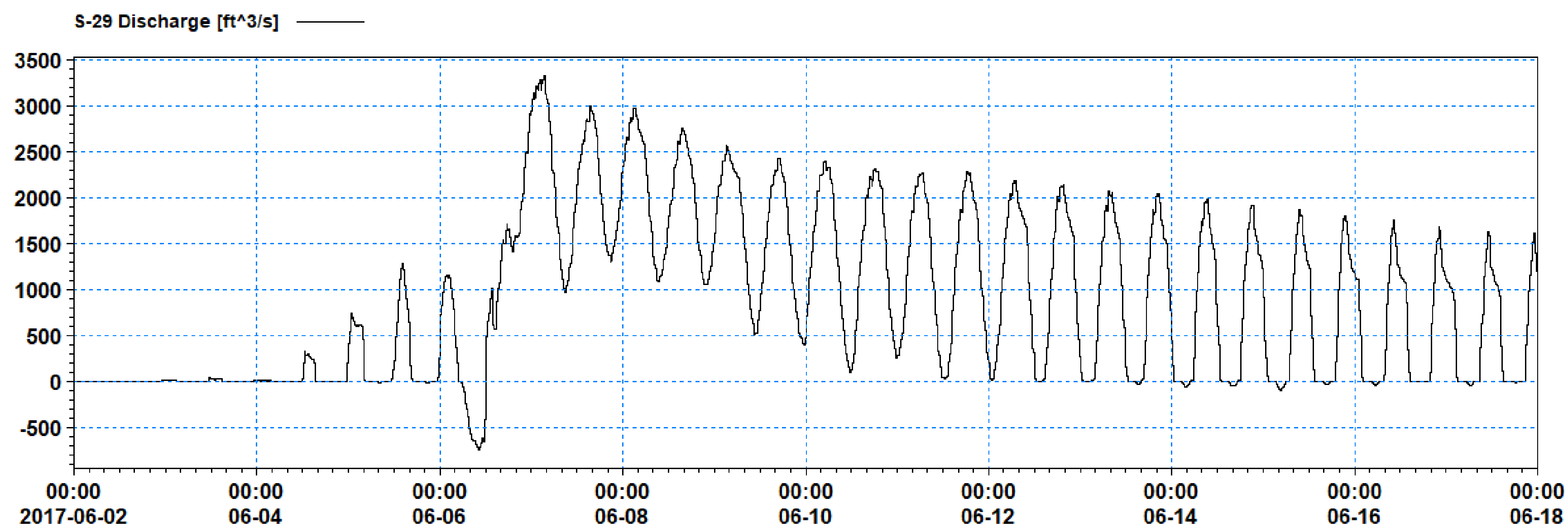

Figure F- 4: S-29 25-Year SLR1 Design Storm Discharge

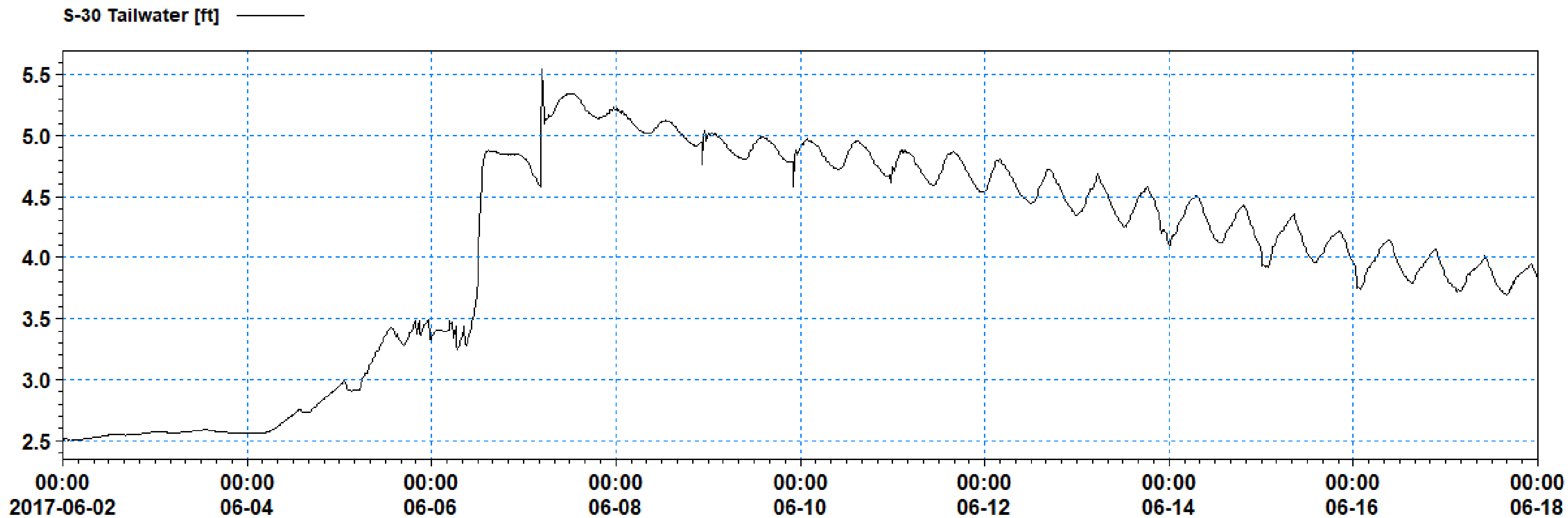

Figure F- 5: S-30 25-Year SLR1 Design Storm Tailwater Stage

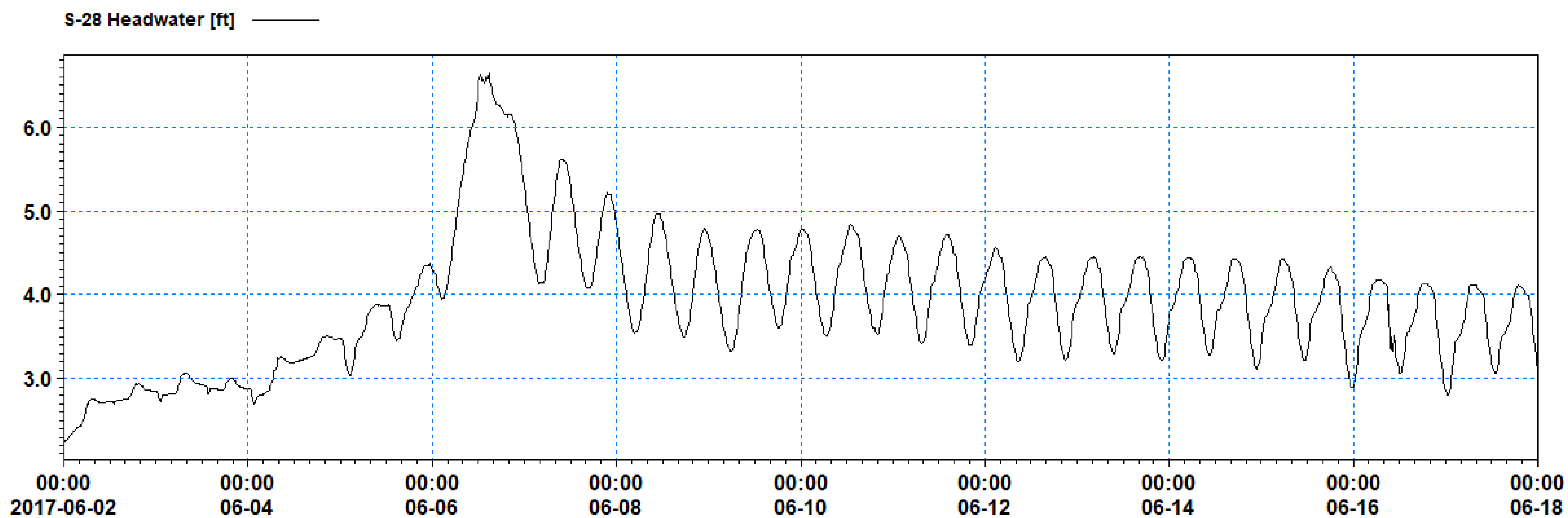

Figure F- 6: S-28 25-Year SLR2 Design Storm Headwater Stage

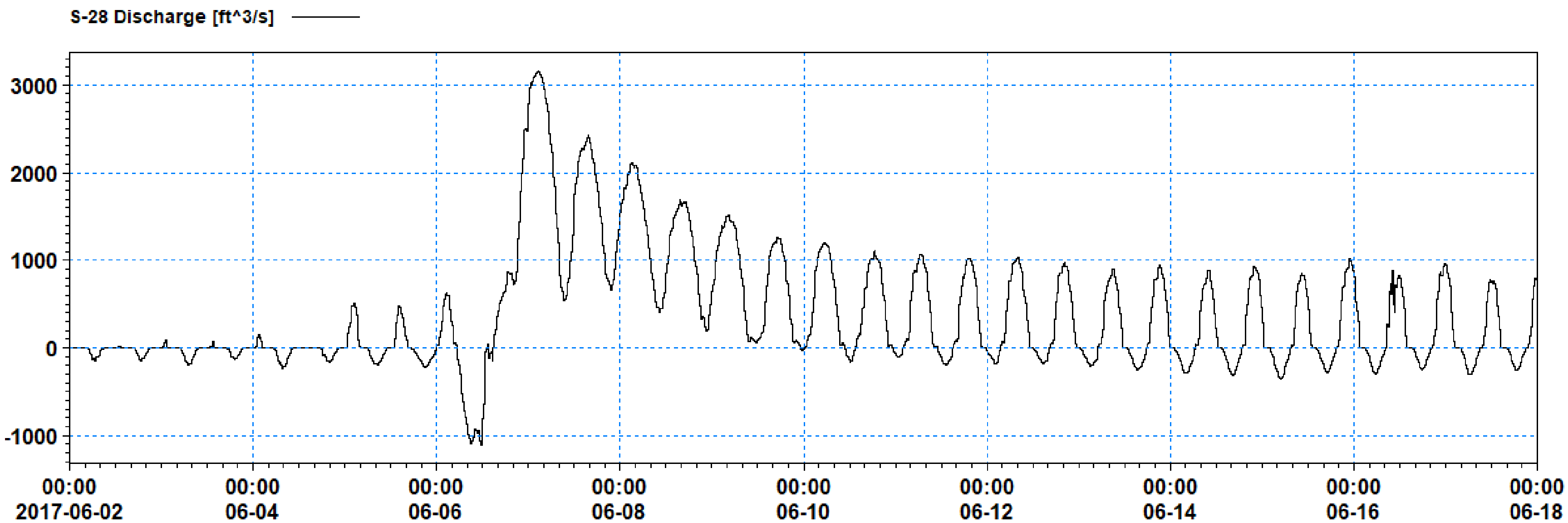

Figure F- 7: S-28 25-Year SLR2 Design Storm Discharge

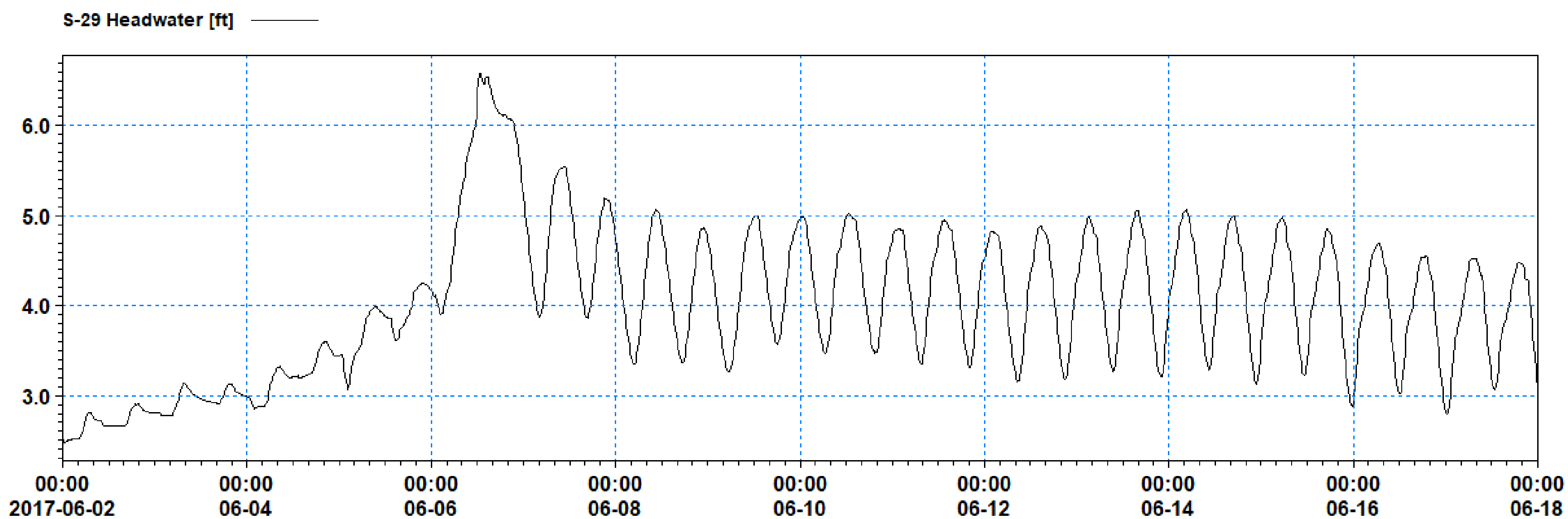

Figure F- 8: S-29 25-Year SLR2 Design Storm Headwater Stage

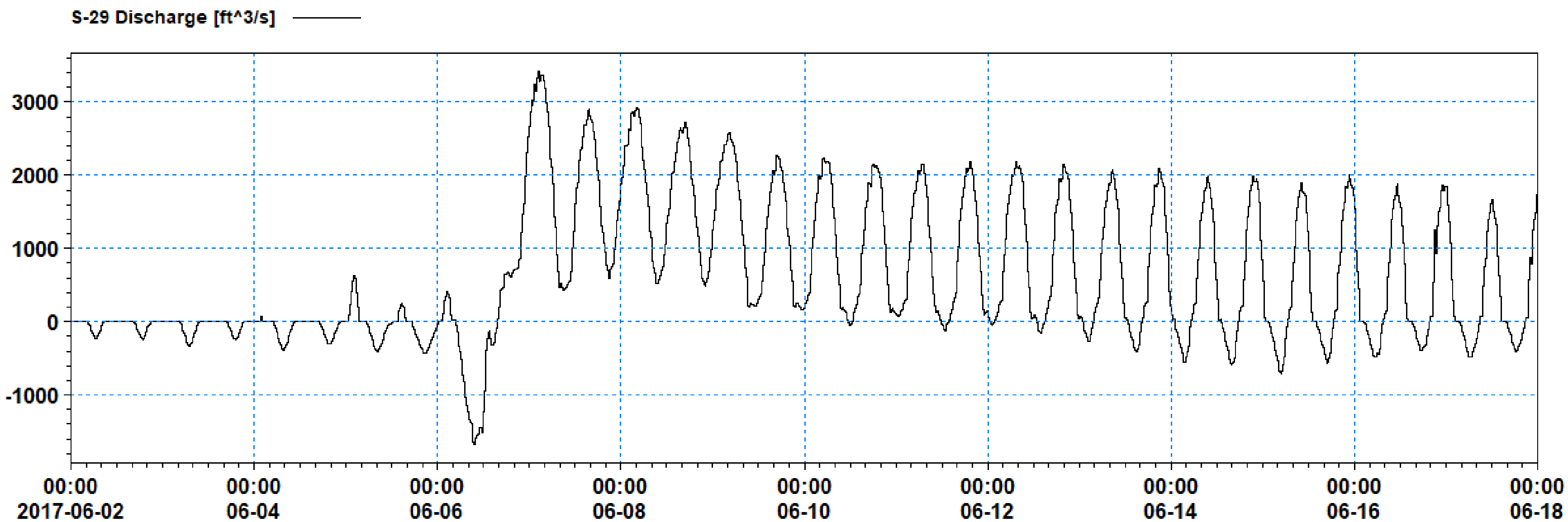

Figure F- 9: S-29 25-Year SLR2 Design Storm Discharge

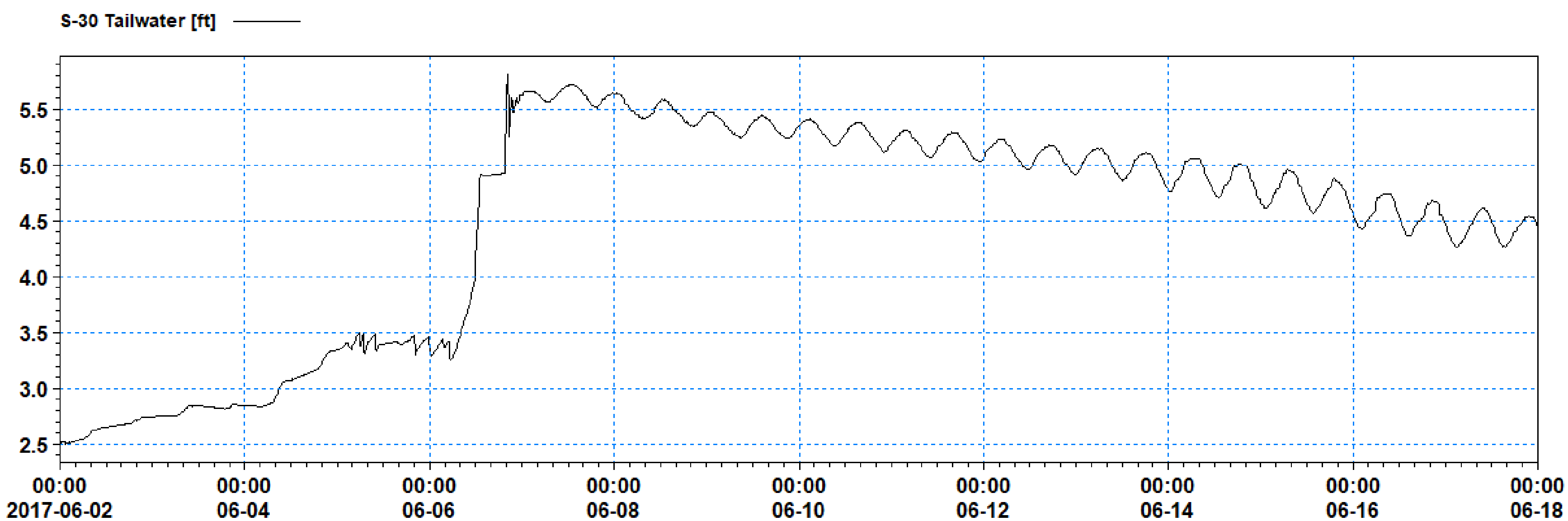

Figure F- 10: S-30 25-Year SLR2 Design Storm Tailwater Stage

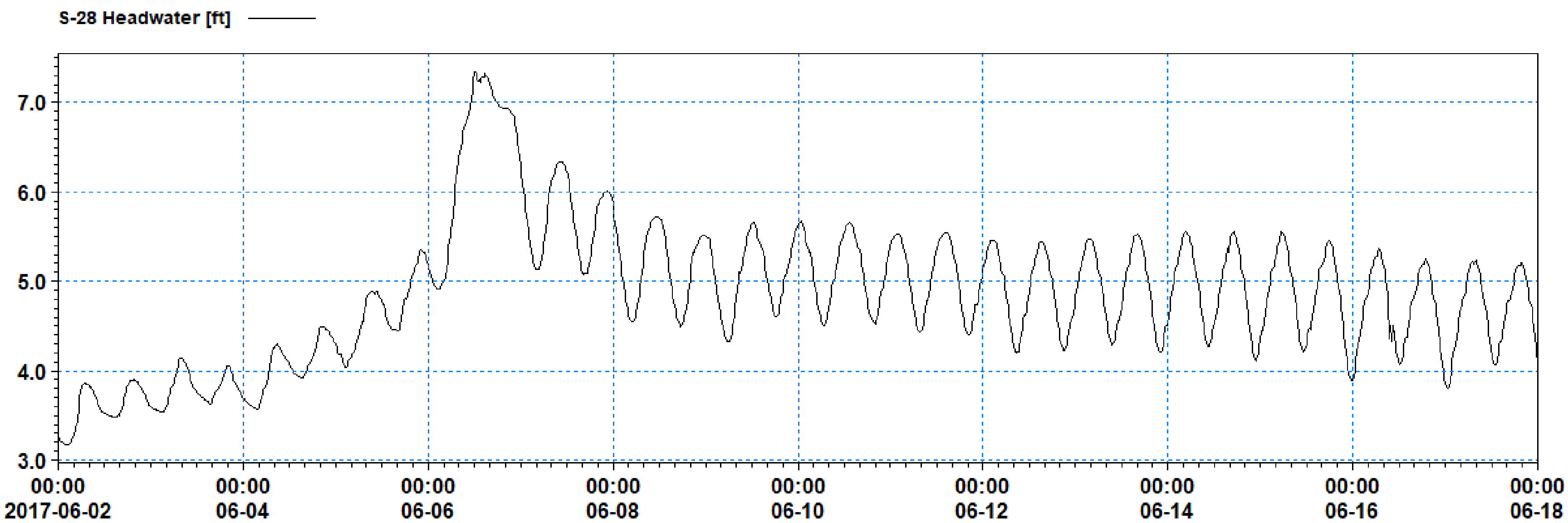

Figure F- 11: S-28 25-Year SLR3 Design Storm Headwater Stage

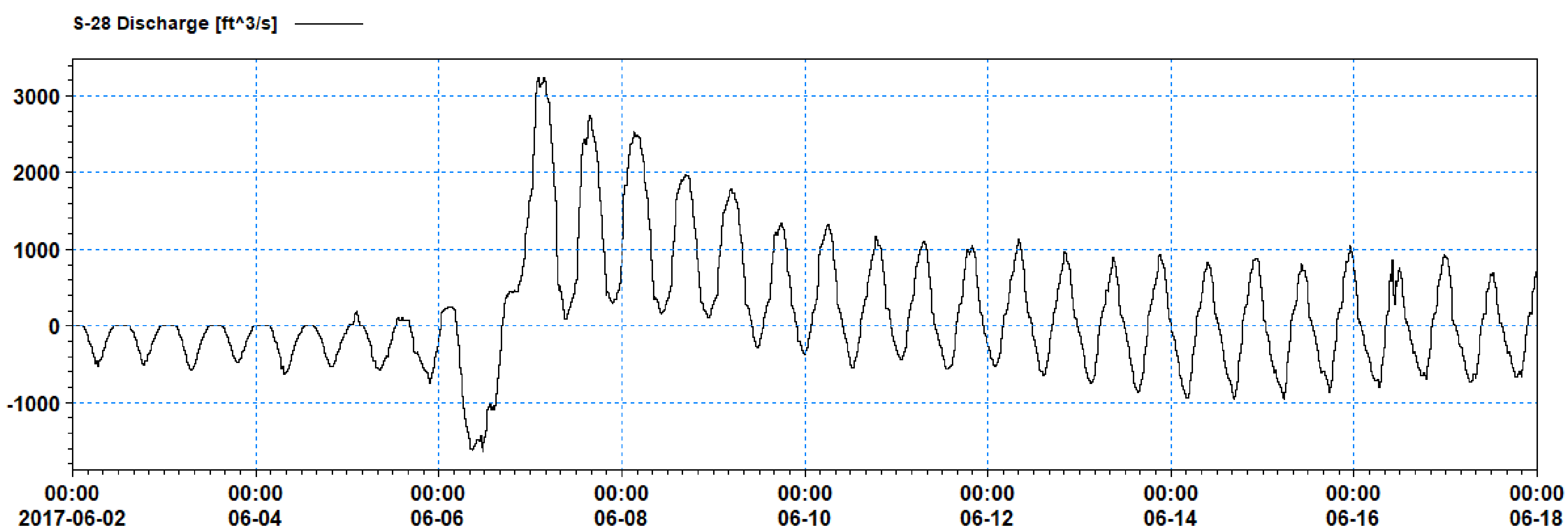

Figure F- 12: S-28 25-Year SLR3 Design Storm Discharge

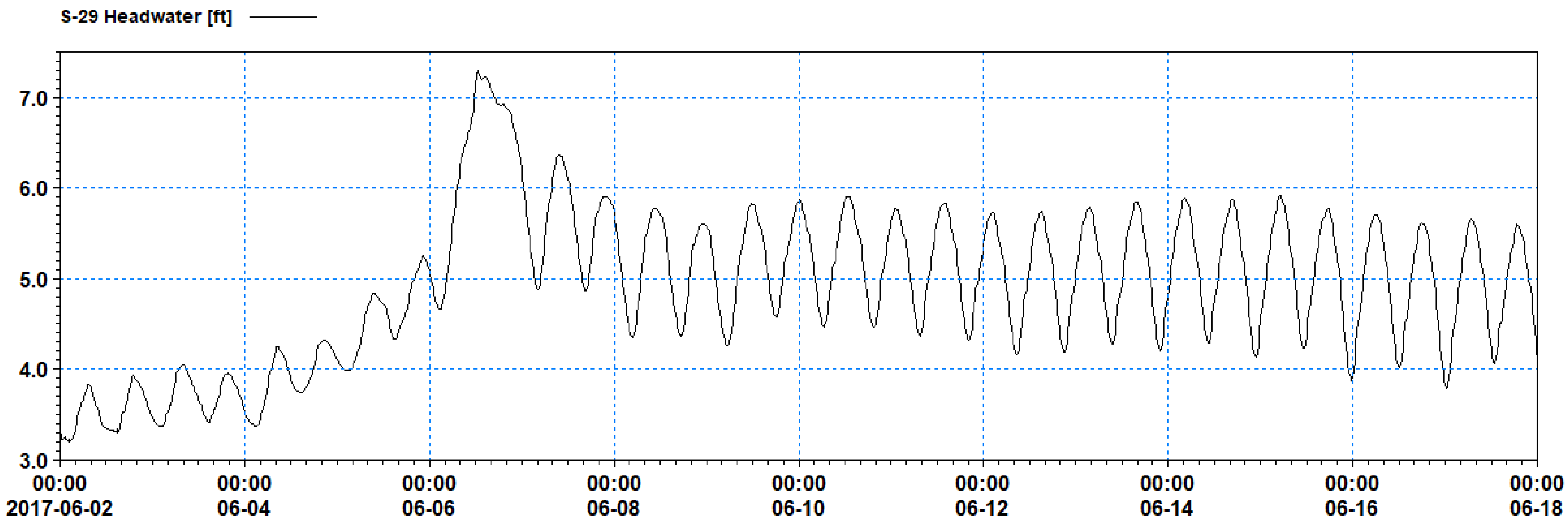

Figure F- 13: S-29 25-Year SLR3 Design Storm Headwater Stage

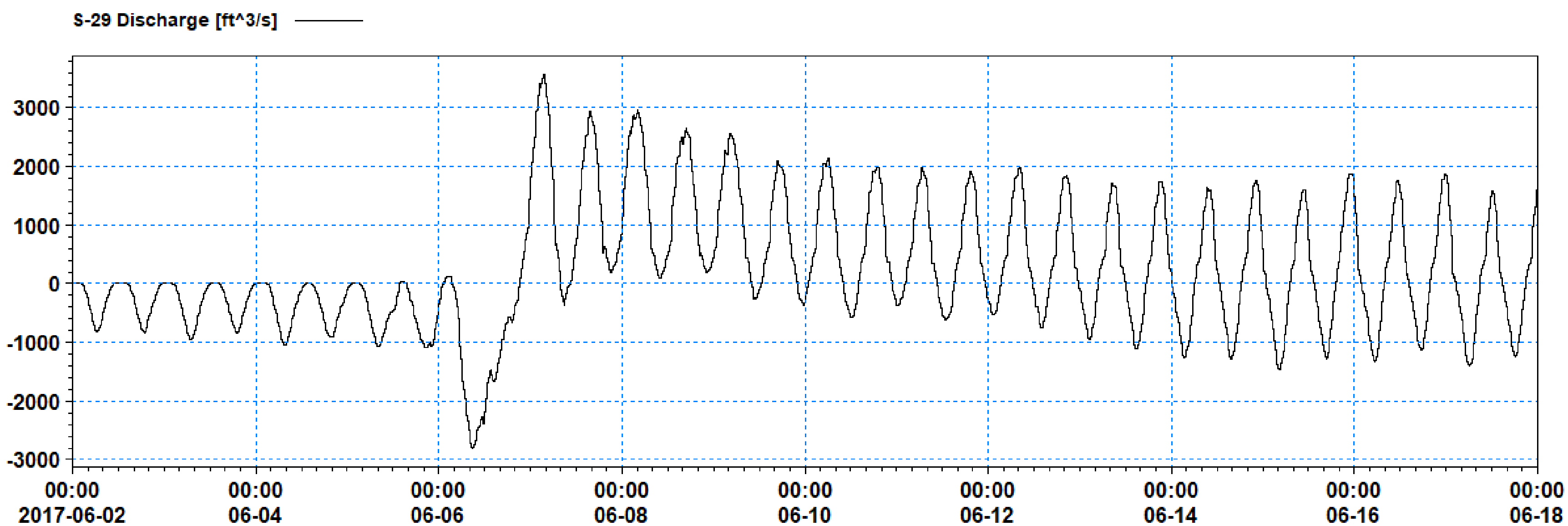

Figure F- 14: S-29 25-Year SLR3 Design Storm Discharge

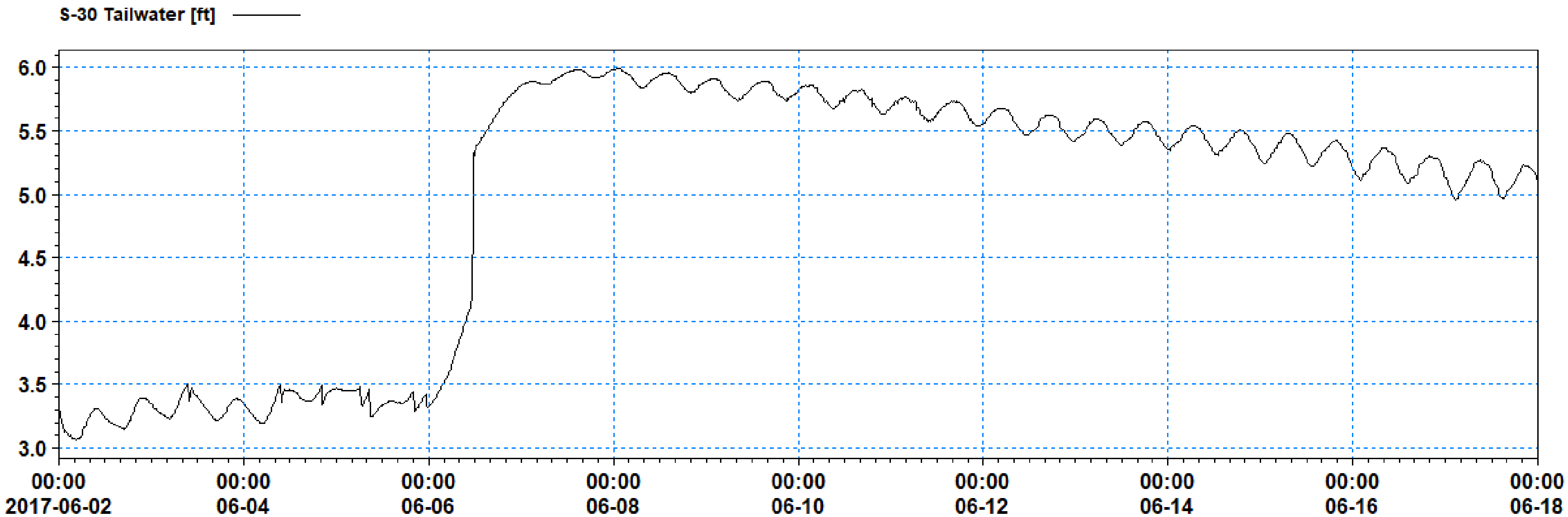

Figure F- 15: S-30 25-Year SLR3 Design Storm Tailwater Stage

Appendix G Water Budget for C-8 and C-9 Basins

Table G- 1: 10-Year Design Storm Water Budget for the C-8 Basin

Water Budget Term	C-8 Basin Average (inches)									
	Inflows					Outflows and Storage				
	Current	SLR1	SLR1 + 9% Rainfall	SLR2	SLR3	Current	SLR1	SLR1 + 9% Rainfall	SLR2	SLR3
Rainfall	10.4	10.4	11.4	10.4	10.4					
Evapotranspiration						0.7	0.6	0.6	0.6	0.7
Surface Runoff						3.7	3.8	4.4	3.9	3.6
Groundwater flow to canals						2.8	2.5	2.6	1.4	0.2
Groundwater boundary flow						2.2	2.1	2.2	2.3	3
Change in surface storage						0.4	0.5	0.5	0.7	1.1
Change in groundwater storage						1	1.2	1.2	1.6	2.2

Table G- 2: 10-Year Design Storm Water Budget for the C-9 Basin

Water Budget Term	C-9 Basin Average (inches)									
	Inflows					Outflows and Storage				
	Current	SLR1	SLR1 + 9% Rainfall	SLR2	SLR3	Current	SLR1	SLR1 + 9% Rainfall	SLR2	SLR3
Rainfall	10.3	10.3	11.3	10.3	10.3					
Evapotranspiration						0.8	0.7	0.7	0.7	0.7
Surface Runoff						4.3	3.9	4.4	3.4	2.3
Groundwater flow to canals						2.4	2.3	2.3	1.9	1.4
Groundwater boundary flow						0.1	0.9	1.2	1.5	2.4
Change in surface storage						1.3	1.4	1.4	1.7	2.2
Change in groundwater storage						1.6	1.4	1.4	1.3	1.5

Appendix H Deliverable 1.1- Data Availability Memorandum

Please note that **Appendix H** is an independent document.

Appendix I Deliverable 1.2- Model Development Memorandum

Please note that **Appendix I** is an independent document.

Appendix J Deliverable 2.1- C8-C9 Calibration and Validation Memorandum

Please note that **Appendix J** is an independent document.

Appendix K Deliverable 3.1.1 & 3.1.2- Current Conditions Model Setup Meeting Notes

Please note that **Appendix K** is an independent document.

Appendix L Deliverable 3.2.1 & 3.2.2- C8 C9 FPLOS by Existing Infrastructure for CSL Conditions Draft Report

Please note that **Appendix L** is an independent document.

Appendix M Deliverable 4.1- Technical Memorandum for Future Conditions Model Setup

Please note that **Appendix M** is an independent document.

Appendix N Deliverable 4.2.2- C8 C9 FPLOS by Existing Infrastructure for Future SLR Conditions Final Report

Please note that **Appendix N** is an independent document.

Appendix O Deliverable 5.1- Technical Memorandum for Preliminary Mitigation Projects for Each Watershed that Doesn’t meet FPLOS

Please note that **Appendix O** is an independent document.

DRAFT Technical Memorandum

To: CSA Central, Inc. and SFWMD

From: Taylor Engineering

Date: 8/26/2019

Re: Available Data for SFWMD C8-C9 FPLOS Study

1.0 INTRODUCTION

This memorandum details the data that Taylor Engineering plans to use to develop the SFWMD C-8 & C-9 MIKE SHE and MIKE HYDRO models for use in the C8-C9 FPLOS Study. Specifically, this memorandum will detail the availability of topography, land use, culvert, gate, bridge, pump, and cross section data, survey requirements, calibration and validation simulation periods, the availability of groundwater data, the availability of district stage, flow, and gate operations, design storm rainfall, and initial groundwater levels for design storms. Please note that the model domain and hydraulic network shown in the figures in this memorandum are initial renderings that subject to change.

2.0 TOPOGRAPHY

The topography for this project will be made by merging the Miami-Dade County 5ft DEM (Miami-Dade County, 2015) with the 5-ft composite DEM of Broward County that was created by Geosyntec Consultants (2018). Geosyntec Consultants developed the 5-ft composite DEM using the following sources and collection (flight) dates:

- Broward County DEM – 2007 – 5' cell size source – base source
- Palm Beach County DEM – 2006 – 10' cell size source – north area extension
- Miami Dade County DEM – 2015 – 5' cell size source – south area extension
- Ft. Lauderdale City Limits DEM – 2016 – 5' cell size source – new areas in east
- Ft. Lauderdale FDOT – 2017 – 0.5' cell size source – new areas in southeast
- SFWMD 50' cell size source – west area extension

To minimize/eliminate seams in the overland flow module, the DEMs will be merged along the C-9 canal and through the levees in the water conservation area to the west, as shown in **Figure 1.** The DEM was filtered between 0-25 ft NAVD88 for visual clarity (200+ ft elevation landfill causes color palette distortion).

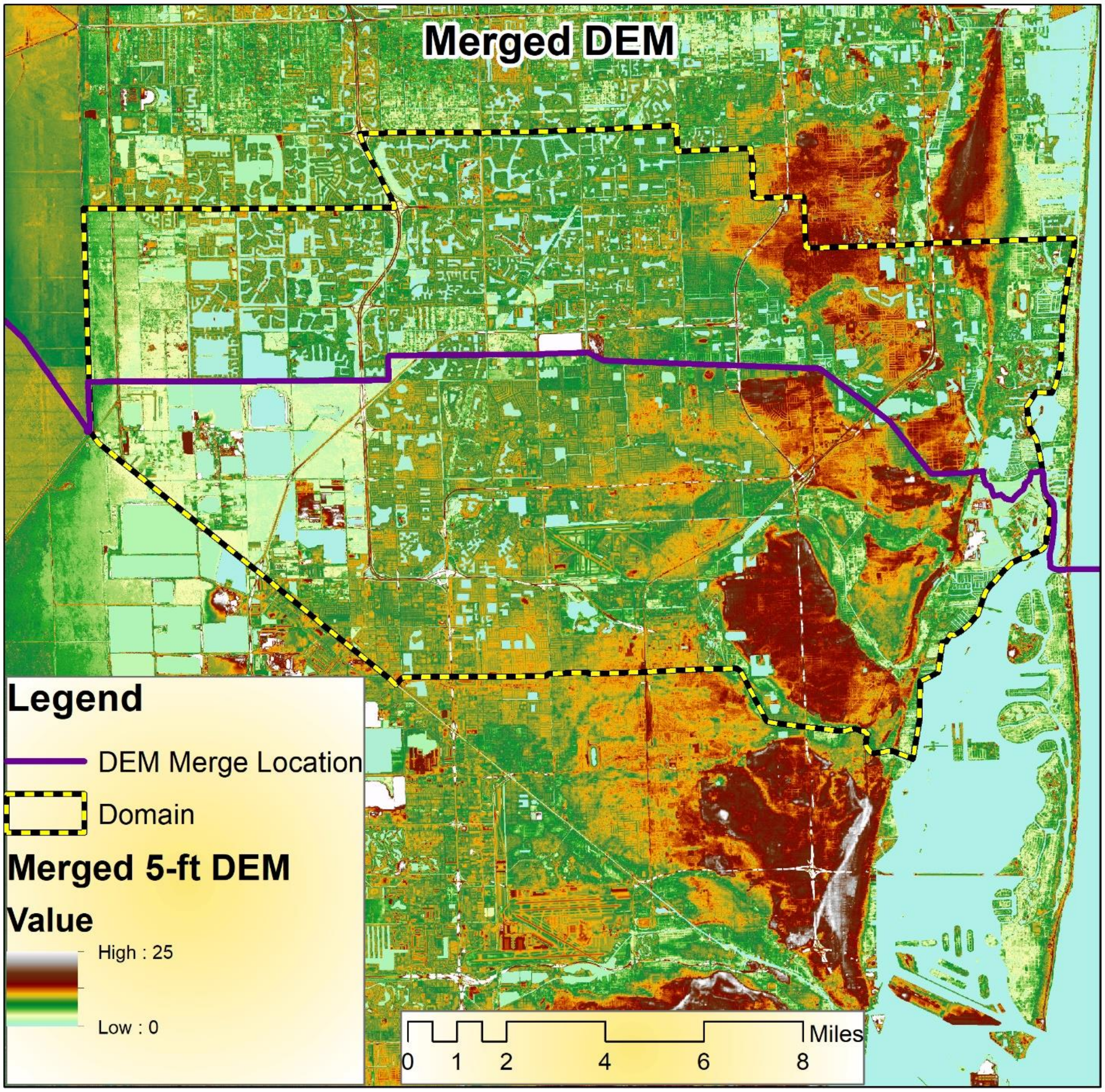

Figure 1: Merged 5-ft DEM

3.0 LAND USE

The land use data for this project will be based on the SFWMD 2014-2016 Land Use dataset. Preliminary comparisons with aerial imagery show little to no significant changes in land use, such as change from open land to high density residential. Updates to the land use may occur if individual areas in excess of 50 acres are identified.

4.0 MIKE HYDRO 1D MODEL

The MIKE HYDRO 1D model will be developed from several sources with emphasis placed on gates, pumps, culverts, bridges, and cross sections. The available data comes from the following sources:

- Broward County: Updated MIKE SHE & MIKE HYDRO models, Ref: Current Conditions Model Update and Validation Draft Report (Taylor Engineering, 2019), & 5-ft DEM

- Stoner & Associates Inc: Survey (completed for Broward County Future Floodplain Modeling and Mapping project)
- South Broward Drainage District: GIS database & 2013 Facilities Report and Water Control Plan
- SFWMD: Structure Book-2018 (for operable structure dimensions, elevations, and operating criteria), DBHYDRO (for water levels, discharges, and structure operations)
- Miami-Dade County: C-8 and C-9 XP SWMM Models, 5-ft DEM, & GIS Database:
    - Pipes: https://gis-mdc.opendata.arcgis.com/datasets/stormwater-line
    - Points (canal cross sections, structures, etc.): https://gis-mdc.opendata.arcgis.com/datasets/stormwater-point
    - Water bodies: https://gis-mdc.opendata.arcgis.com/datasets/water-p

Upon initial investigation, it was noticed that there are some 1D model components such as culverts and cross sections that have available data from multiple sources. In instances where this occurs and the details differ (such as different culvert diameters), the data will be used in the following order of priority: (1) survey, (2) Broward County MIKE HYDRO model, (3) reports & documentation, (4) GIS databases, and (5) Miami-Dade C8 and C-9 XP SWMM models. The order of priority was determined based on the freshness of the data and our confidence/exposure with the data/sources. Survey has the highest level of confidence as it has recently been completed or will be completed in the near future and should capture any changes to infrastructure that may not have yet been included other data sets. The Broward County MIKE HYDRO model has the second highest level of confidence as the data that went into it was analyzed and refined over the last several months, and Taylor Engineering is very familiar with the areas that have up-to-date data and the areas that are questionable. Reports and documentation have the third highest level of confidence as they were used to build parts of the Broward County MIKE HYDRO model. The Miami-Dade GIS databases are assigned the fourth highest level of confidence as Taylor Engineering hasn't yet had the opportunity to see how well the data lines up with other confirmed sources. The Miami-Dade XP SWMM models that Taylor Engineering currently has access to have the lowest level of confidence as they are older versions and there are several areas that do not match what is in the Miami-Dade GIS databases. Taylor Engineering assumes that the discrepancies between the Miami-Dade GIS databases and the C-8 and C-9 XP SWMM models that we have access to are due to changes in infrastructure that have been updated in the GIS databases; therefore, the GIS database has higher priority than the XP SWMM models for instances of data differences.

Figure 2 shows the location of the available 1-D model data. It is noted that some of the data items shown are not complete; for example, culverts included in the Miami-Dade GIS databases that are missing inverts, dimensions, or both; bridges missing low chord elevations, etc. These and other data gaps were assessed and included in the survey scope of work described in the next Section.

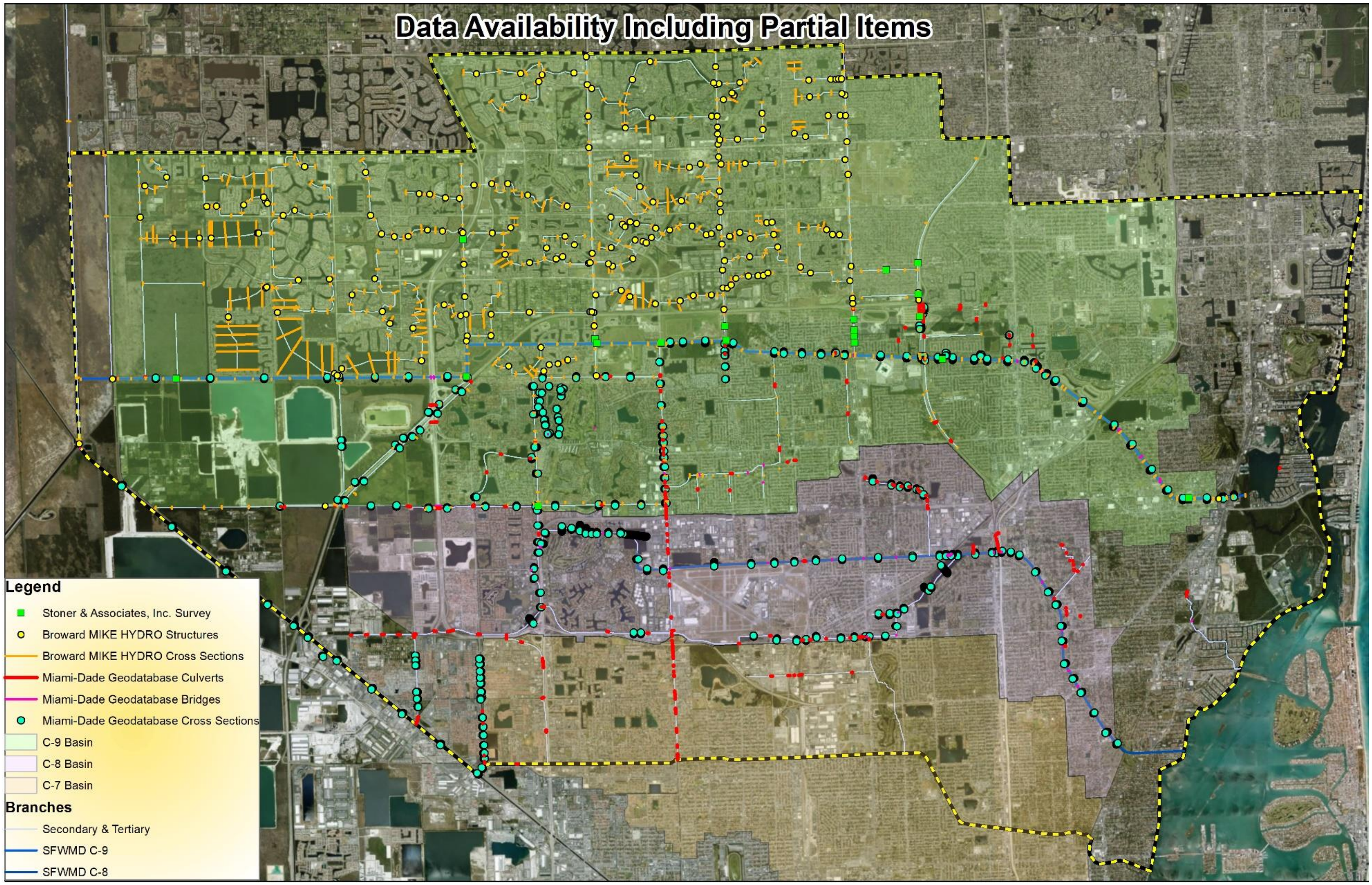

Figure 2: Map of the Available Data

5.0 SURVEY REQUEST

The available data is quite extensive, however, there are several areas lacking detail. The following figure shows the location of the initial items identified for survey. These items are subject to change, but as of now include 30 culverts, 23 cross sections, and 21 bridges (3 of which are lower priority). Some items in the survey request had partial data available, such as culvert diameter or elevation of channel bottom under bridge but were missing information such as culvert inverts or low cord elevation of bridge.

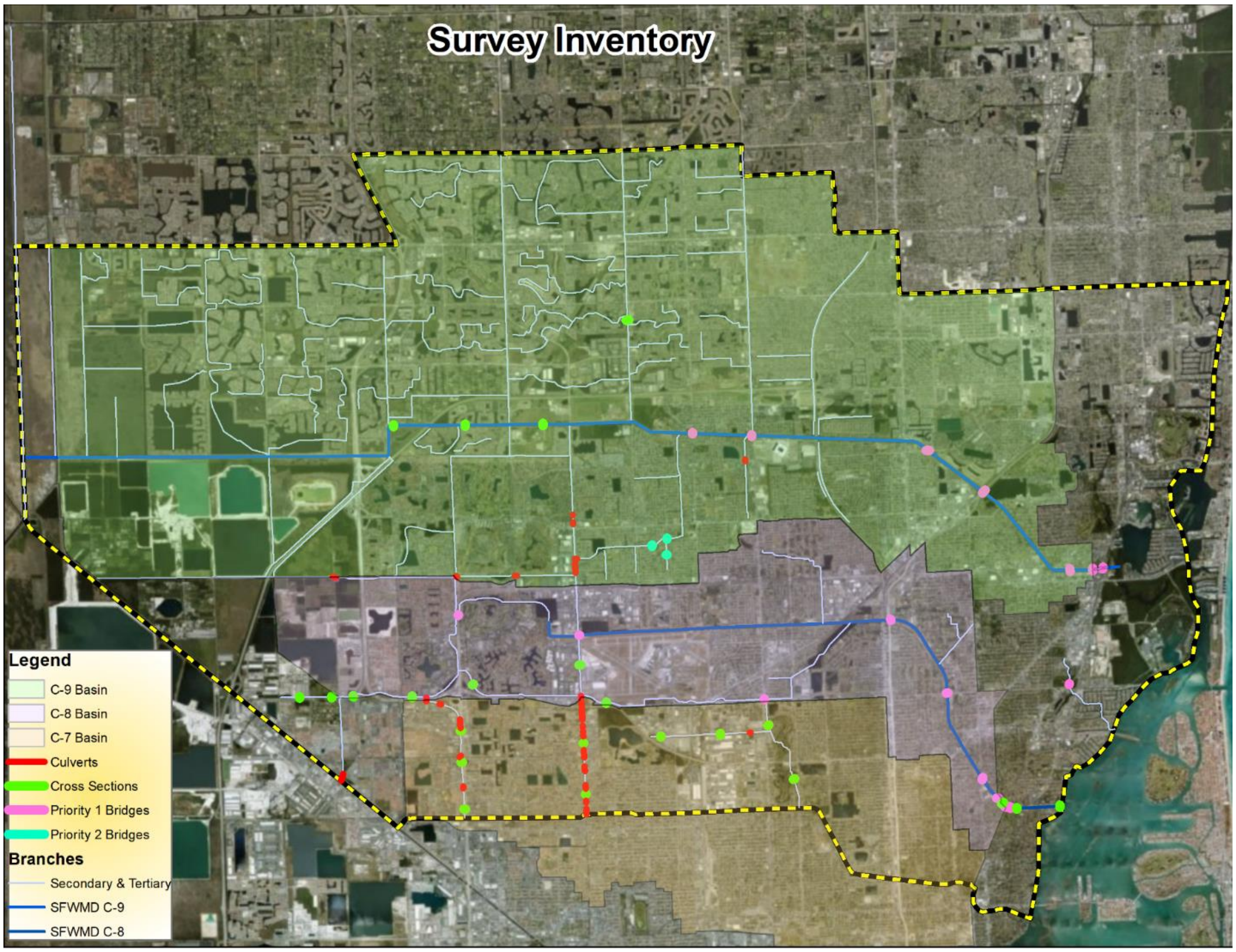

Figure 3: Inventory of Items Proposed for Survey

6.0 STORM EVENTS SELECTION

Average daily discharge data for the S-28 and S-29 outfall structures (C-8 and C-9 basins, respectively) were analyzed to identify the largest storm events since 1999. Then, instantaneous stage and discharge data were analyzed to identify the events that produced the largest headwater and tailwater elevation and discharge rate. Preference was given to storm events producing strong responses in both watersheds. The selection was narrowed to the storms during the following dates:

- Hurricane Irene (October 14-16, 1999)

- Subtropical Depression Leslie (October 2-4, 2000)
- Hurricane Gabrielle (September 13-15, 2001)
- Unnamed Storm June 6-7, 2017
- Hurricane Irma (September 9-10, 2017)

Taylor Engineering recommends the use of Subtropical Depression Leslie, which later became Tropical Storm Leslie, as the calibration event and Hurricane Irma as the validation event. Subtropical Depression Leslie resulted in the largest discharge response at both the C-8 and C-9 outfall structures in the past 20 years, as well as some of the highest canal water elevations. Hurricane Irma produced large discharge responses at both outfall structures and had a storm surge which resulted in the highest water elevations. The following figures compare the discharge, headwater elevation, and tailwater elevation at the C-8 and C-9 outfall structures.

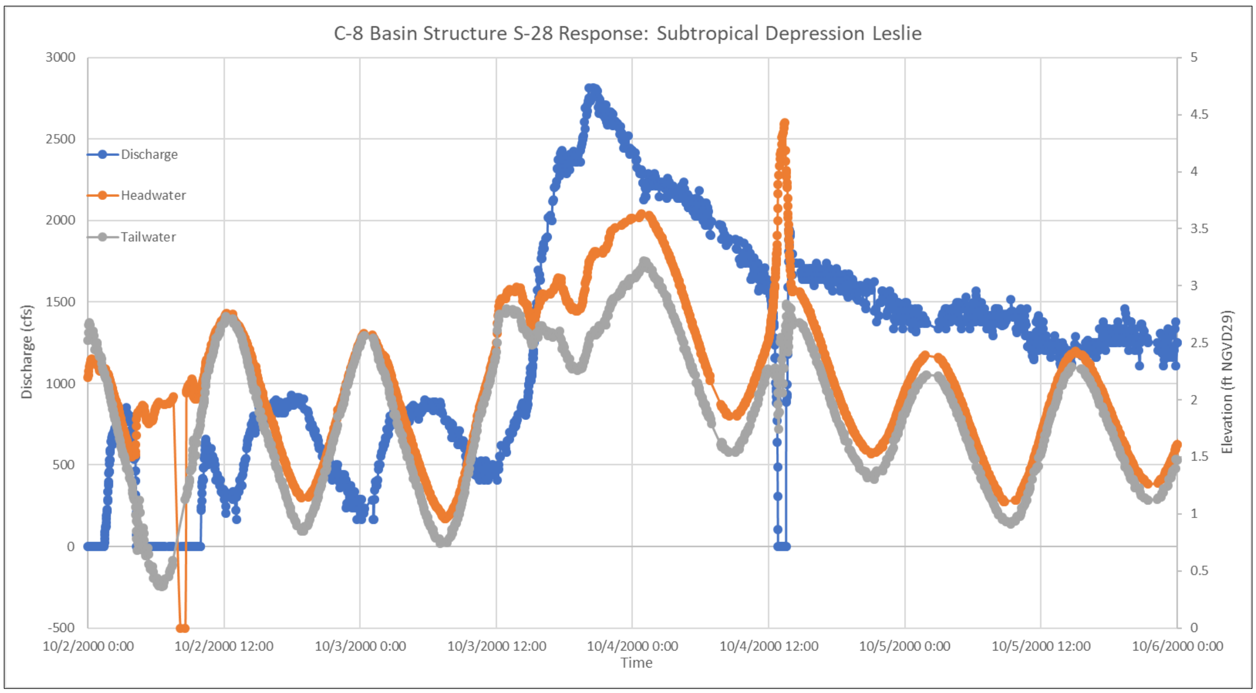

Figure 4: C-8 Basin Structure S-28 Response to Subtropical Depression Leslie

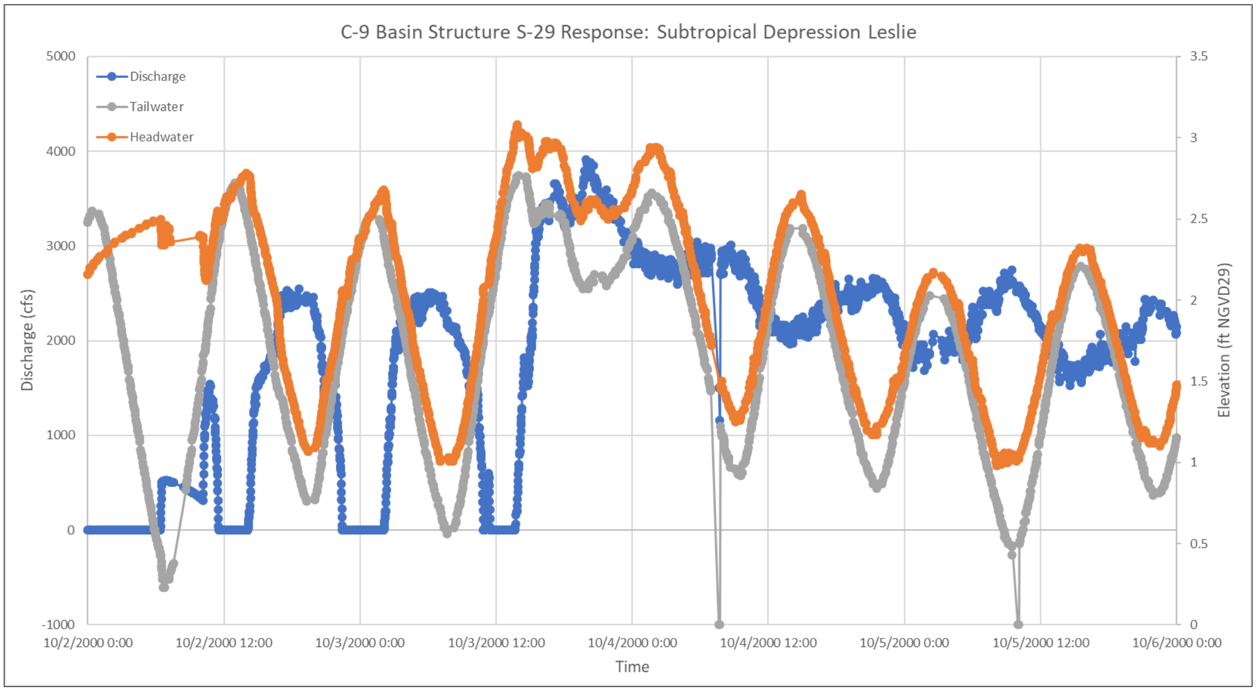

Figure 5: C-9 Basin Structure S-29 Response to Subtropical Depression Leslie

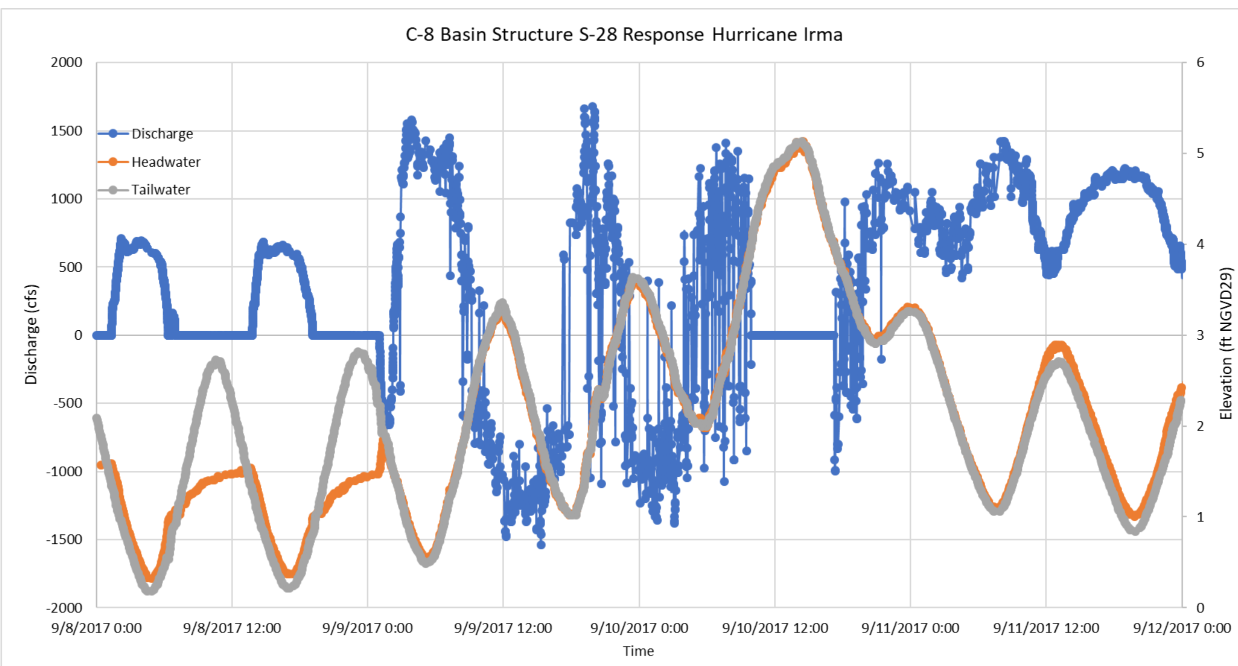

Figure 6: C-8 Basin Structure S-28 Response to Hurricane Irma

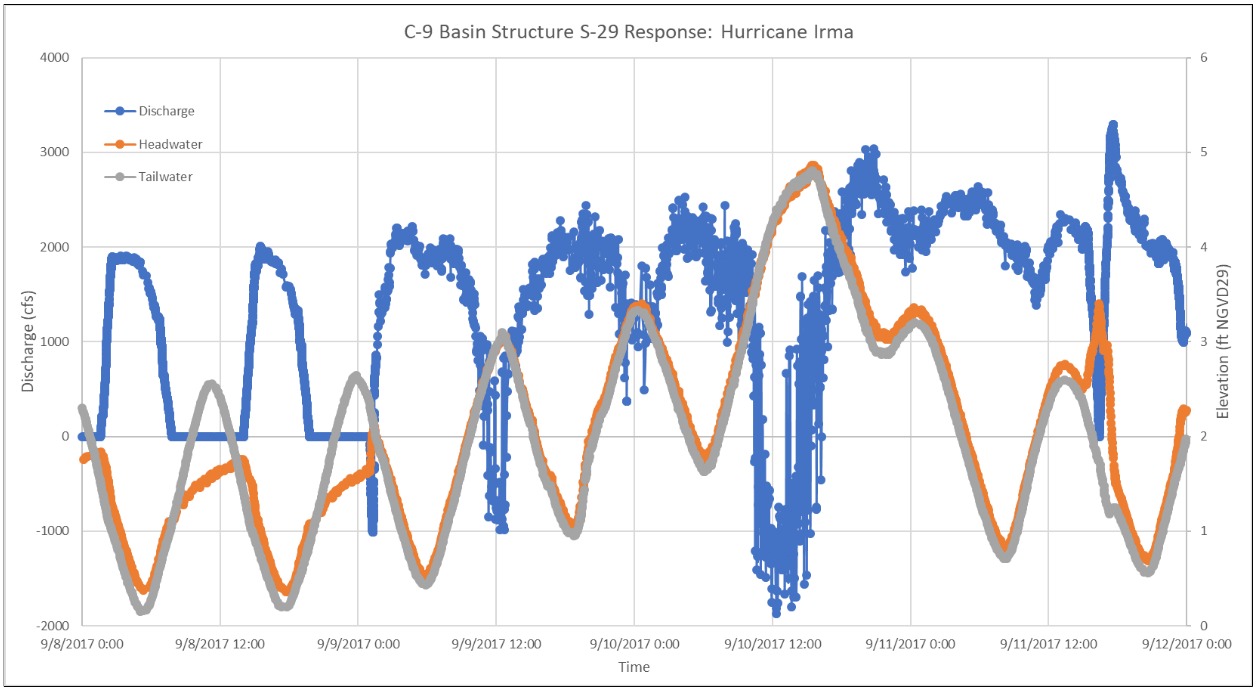

Figure 7: C-9 Basin Structure S-29 Response to Hurricane Irma

Available rainfall data for Subtropical Storm Leslie was called into question as NEXRAD data in the early 2000s was less accurate than it is today. Therefore, rain gauge data (DBHYDRO) was compared to the NEXRAD data for the pixel(s) that they were in or bordered against. This exercise proved that the NEXRAD data and gauge data are very similar in terms of total rainfall, however, there are some differences as far as the timing of the rainfall. The following figures show different comparisons relating to NEXRAD rainfall, gauge rainfall, and structure discharge.

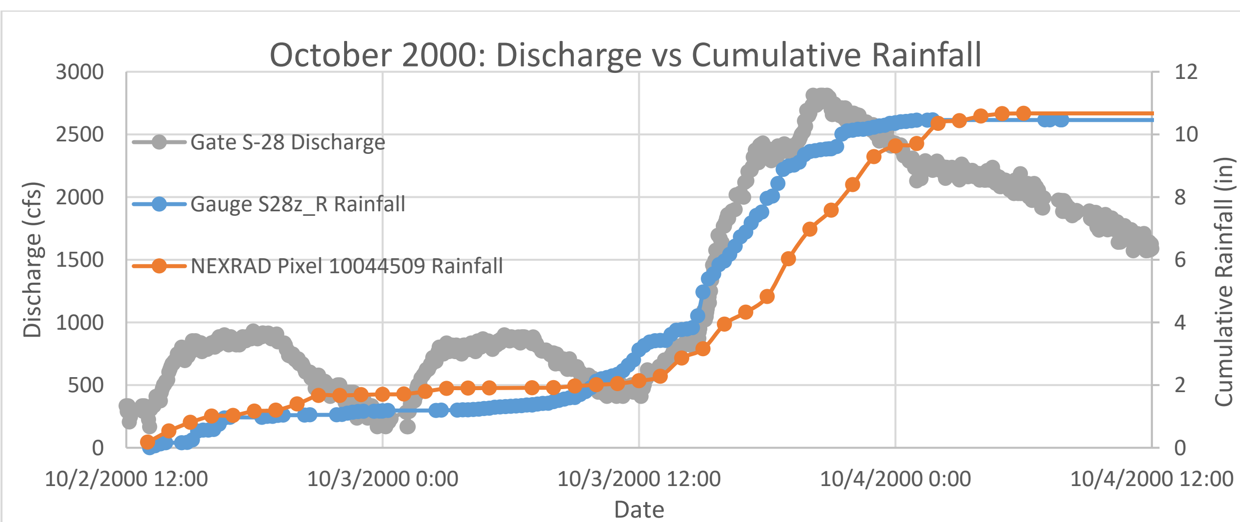

Figure 8: Discharge vs Cumulative Rainfall for Gate S-28 (NEXRAD Pixel and Rain Gauge Located Centrally in C-8 Basin)

The cumulative rainfall totals for the rain gauge and the associated NEXRAD pixel are only off by about 0.2 inches, which is about 2%. This is a negligible amount and well within the accuracy of either measurement method. More concerning is the temporal shift in the rainfall, which is about 3-hours. Comparing the timing of rainfall to the discharge, it is believed that the rainfall gauges are more accurate. Simply put, the NEXRAD data shows a rainfall response after the runoff response, which goes against rainfall-runoff principles. The following figure compares the same rainfall but plotted as rainfall intensity.

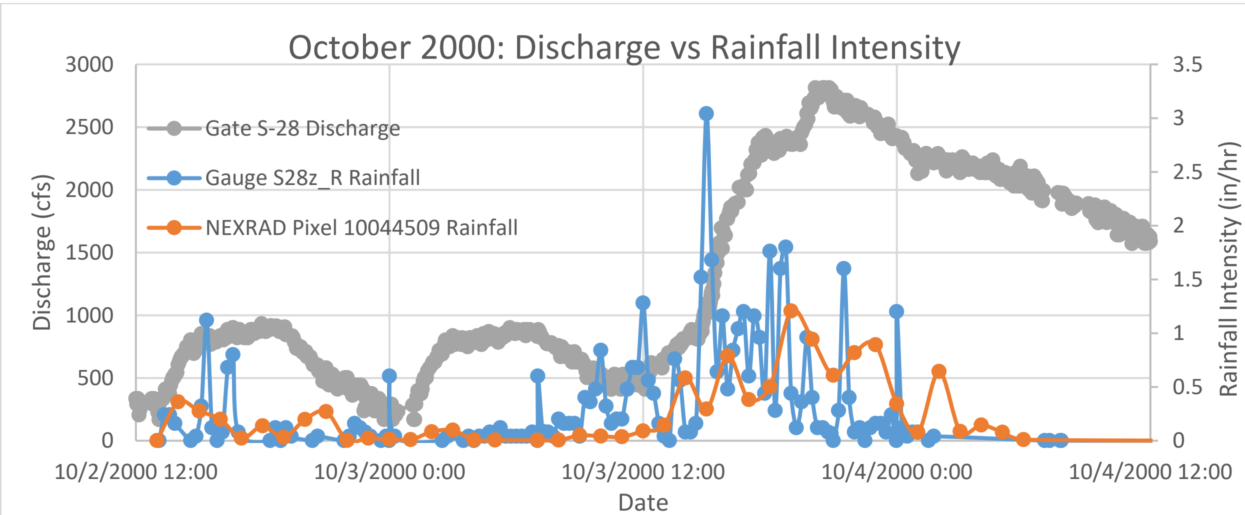

Figure 9: Discharge vs Rainfall Intensity for Gate S-28 (NEXRAD Pixel and Rain Gauge Located Centrally in C-8 Basin)

This figure shows there is a large difference in rainfall intensity when comparing the rain gauge to the NEXRAD data. The rain gauge data was recorded in 15-minute intervals whereas the NEXRAD data was recorded in hourly intervals. Therefore, the NEXRAD data was unable to capture the high intensity short duration part of the storm. It is possible that this could have some effect on calibration efforts. The following figure compares the rain gauge located centrally in the C-9 basin with NEXRAD data for the two pixels it borders.

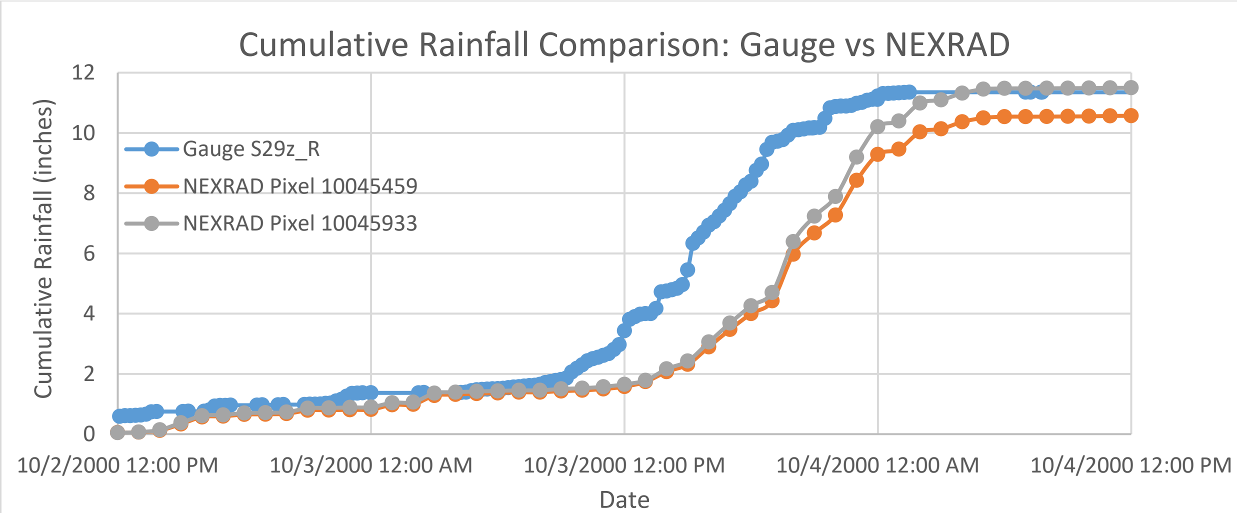

Figure 10:Cumulative Gauge Rainfall vs Cumulative NEXRAD Rainfall (NEXRAD Pixel and Rain Gauge Located Centrally in C-9 Basin)

The cumulative rainfall totals are pretty close, with NEXRAD data being between 0.2 and 0.7 inches different, or about 2-6%. Again, there is a temporal lag of about 4 hours. The following figure compares the rain gauge located in the western part of the C-9 Basin with NEXRAD data.

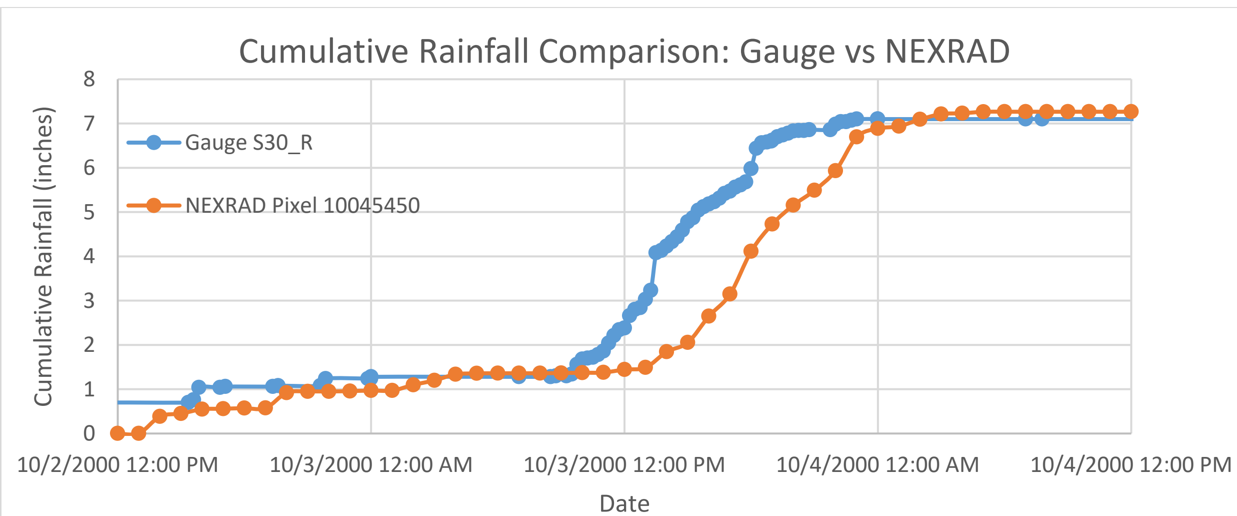

Figure 11:Cumulative Gauge Rainfall vs Cumulative NEXRAD Rainfall (NEXRAD Pixel and Rain Gauge Located in Western C-9 Basin)

The cumulative rainfall totals are within 0.2 inches apart which is about 2%. Again, there is a temporal lag of about 4 hours. The following figure compares the rain gauge located at the tidal outfall of the C-7 Basin with NEXRAD data.

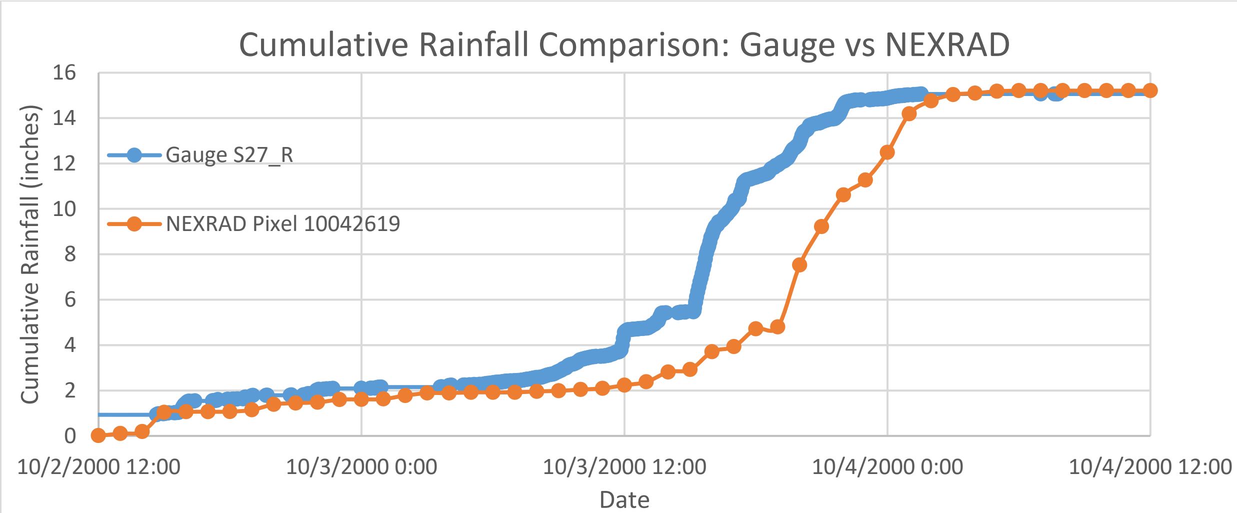

Figure 12: Cumulative Gauge Rainfall vs Cumulative NEXRAD Rainfall (NEXRAD Pixel and Rain Gauge Located at C-7 Basin Tidal Outfall)

The cumulative rainfall totals are within 0.2 inches apart which is only about 1%. Again, there is a temporal lag of about 4-5 hours.

The NEXRAD data captures the total rainfall very well and closely matches gauge data, however, there are some potential concerns with using it. As mentioned, the 1-hour interval of the NEXRAD data averages-out the highest-intensity parts of the storm. Additionally, there are some temporal differences. These two issues should be further discussed before any decisions are made on using it for the calibration event. It should be noted that it is not advisable to use the existing rain gauges to make Thiessen polygons for calibration use as: (1) the rain gauges do not capture the significant spatial differences that were noticed in the NEXRAD data and (2) it is likely that one rain gauge was not been functioning properly during the storm. **Figure 13** shows the variation of total rainfall depth in randomly selected NEXRAD pixels and the rain gauges.

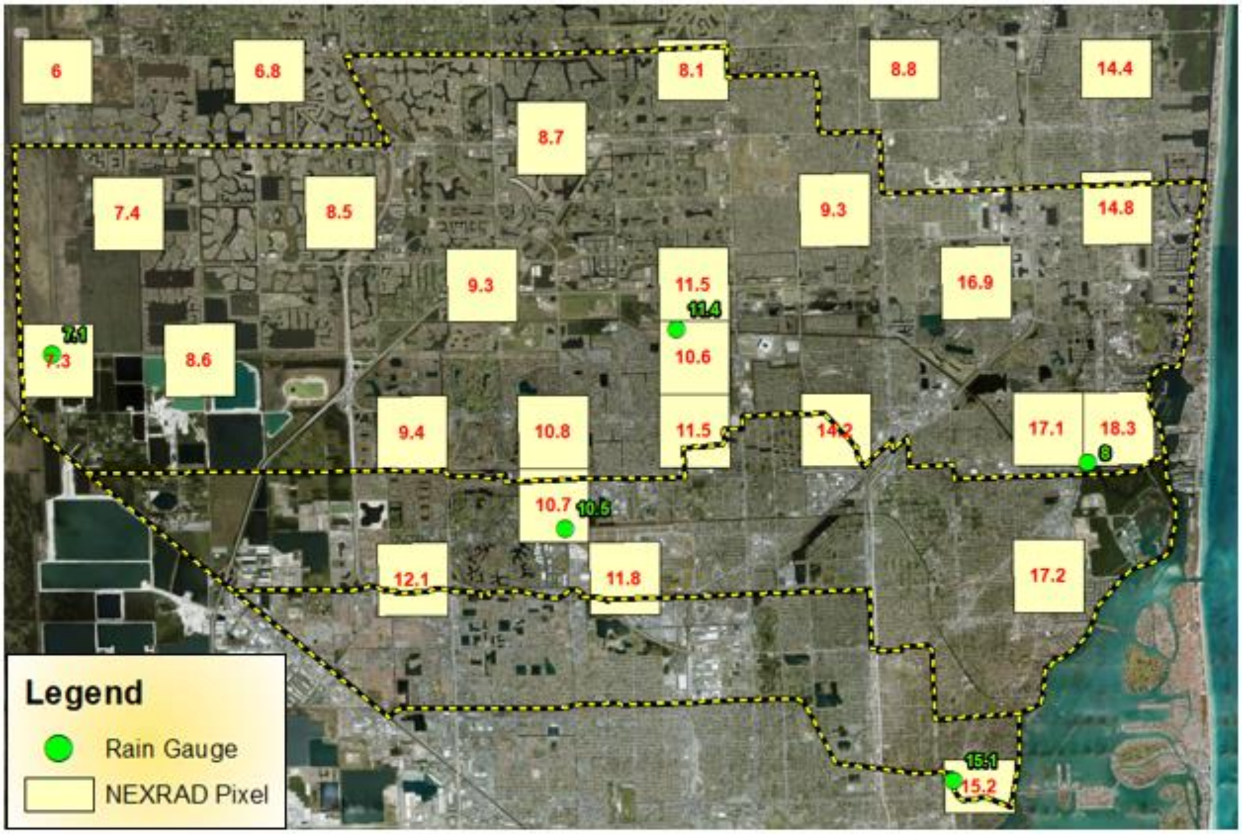

Figure 13: Randomly Selected NEXRAD Pixel and Rain Gauge Rainfall Summary

The NEXRAD rainfall data shows a spatial difference ranging from about 7 inches in the northwestern part of the C-9 basin to upwards of 18 inches in the southeastern part of the C-8 basin. Using the rain gauges alone would significantly alter the spatial distribution and rainfall totals, making an accurate calibration difficult if not impossible. The rain gauges captured the timing of the rainfall better than NEXRAD, while NEXRAD captured the spatial variation in rainfall depths better than the rain gauges. Therefore, Taylor Engineering recommends using the total rainfall depths from each NEXRAD pixel and distribute it temporally based on a rain gauge that is assigned by Thiessen polygons. This will shift the timing of the rainfall to match the rain gauges while maintaining spatial variation in rainfall totals of the NEXRAD pixels. Gauge S-29_R only recorded about 8 inches during the storm while surrounding NEXRAD pixels show between 17 and 18 inches; this gauge will not be considered. The following figure shows the Thiessen Polygons that would be used to assign a rain gauge to the NEXRAD pixels.

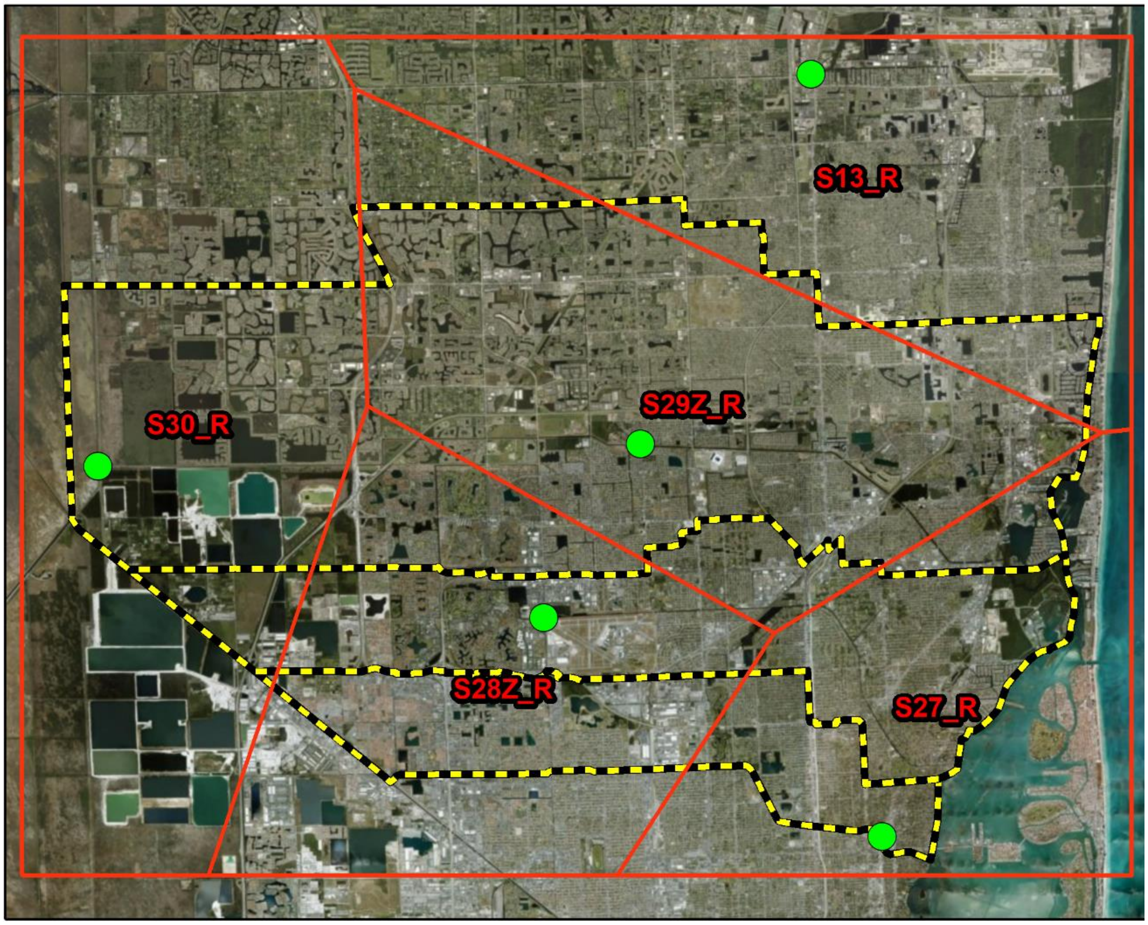

Figure 14: Thiessen Polygons of the Rainfall Gauges

Each NEXRAD pixel within one of the five Thiessen Polygons would use the temporal distribution of the respective rain gauge. This redistribution results in NEXRAD rainfall that aligns well temporally with the discharge response.

7.0 CALIBRATION DATA AVAILABILITY AND COLLECTION

In addition to accurate rainfall, data needed for model calibration includes gate openings, breakpoint stage, and breakpoint discharge for all primary operational structures, and groundwater levels for the wells within the surficial aquifer and the model domain. If breakpoint data is unavailable, the best available data (hourly, etc.) will be used. **Figure 15** shows the location of the primary structures and wells analyzed for data availability and gaps, relative to the initial model domain and 1D hydraulic network.

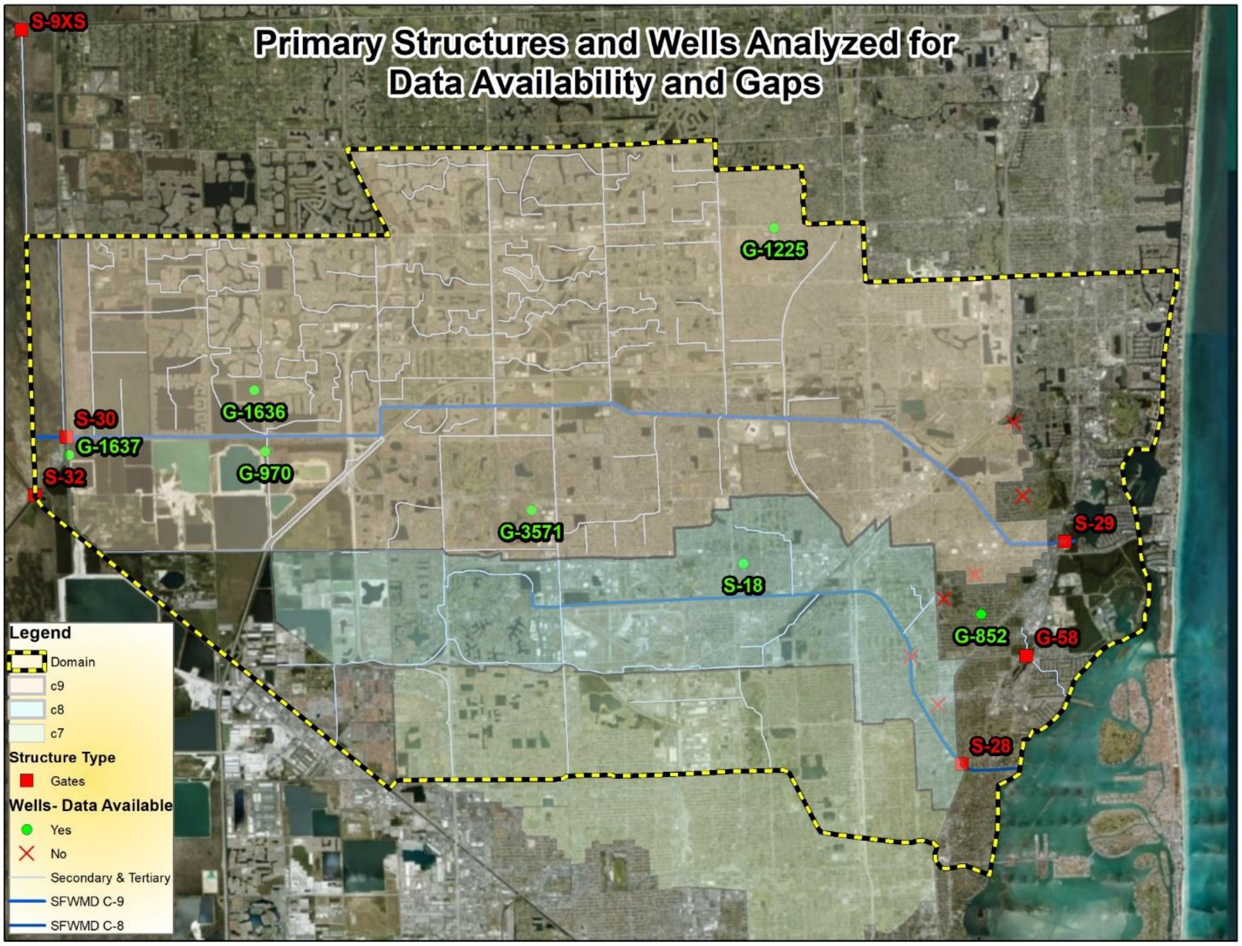

Figure 15: Primary Structures and Wells Analyzed for Data Availability and Gaps

Stage, flow, and groundwater level data were graphed to visually analyze data for gaps and outliers. The following table shows the completeness of data for the storm events in October 2000, June 2017, and September 2017.

Table 1: Structure Data Availability Summary

NAME	BASIN	CONTROL	DBKEY	DATA TYPE	STATUS
S-28	C-8	Gated	65070	Breakpoint Discharge	Complete
			6627	Breakpoint HW Stage	
			6628	Breakpoint TW Stage	
			LT203 & LS856	Breakpoint Gate Opening	
S-29	C-9	Gated	65071	Breakpoint Discharge	Complete
			6631	Breakpoint HW Stage	
			6632	Breakpoint TW Stage	
			LS491, LS857, LS858, & LS859	Breakpoint Gate Opening	
S-30	C-9	Gated	65074	Breakpoint Discharge	Complete
			6686	Breakpoint HW Stage	
			6639	Breakpoint TW Stage	
			LS493, LS862, & LS863	Breakpoint Gate Opening	
S-32	L-33 CC	Gated	65077	Breakpoint Discharge	Complete
			SP543	Breakpoint HW Stage	
			6643 & AI581	Breakpoint TW Stage	
			LS495, LS867, SP544 & SP545	Breakpoint Gate Opening	
G-58	North Biscayne Bay	Gated	64715	Breakpoint Discharge	No September 2017
			IX539	Breakpoint HW Stage	No September 2017
			N/A	Breakpoint TW Stage	Not in DBHYDRO
			LS376, LS693, LS694, & LS695	Breakpoint Gate Opening	No September 2017
S-9XS	L-33 CC	Boarded	90829	15-Minute Discharge	Complete
			SO013	15-Minute to Hourly HW Stage	Complete
			OH925 & OH924	15-minute and Breakpoint TW Stage	Complete
			LD575 & LS966	Other Board Elevation	Other

Although there are several wells within the model domain, many of them contain no useful data as it pertains to the purpose of this project because of infrequent or random interval sampling. The following table shows the wells that are within the model domain and the surficial aquifer system (SAS) that have concurrent data available to three of the aforementioned storm events.

Table 2: Wells with Complete Groundwater Level Data within SAS During October 2000

WELL NAME	BASIN	DBKEY	DATA TYPE
G-1225	C-9	1758	Daily Max
G-1636	C-9	1716	Daily Max
G-1637	C-9	1698	Daily Max
G-3571	C-9	LP668	Daily Max
G-852	North Biscayne Bay	1662	Daily Max
G-970	C-9	1703	Daily Max
S-18	C-8	1673	Daily Max

Table 3: Wells with Complete Groundwater Level Data within SAS During June-September 2017

WELL NAME	BASIN	DBKEY	DATA TYPE
G-1225	C-9	1758	Hourly GW Level
G-1636	C-9	1716	Hourly GW Level
G-1637	C-9	1698	Hourly GW Level
G-3571	C-9	LP668	Hourly GW Level
G-852	North Biscayne Bay	1662	Hourly GW Level
G-970	C-9	1703	Hourly GW Level
S-18	C-8	1673	Hourly GW Level
G-1166R	C-7	88676	Hourly GW Level

8.0 GROUNDWATER DATA AVAILABILITY

A groundwater study authored by J. D Hughes and J. T White was documented in a USGS report titled *Hydrologic Conditions in Urban Miami-Dade County, Florida, and the Effect of Groundwater Pumpage and Increased Sea Level on Canal Leakage and Regional Groundwater Flow* (2016). For modeling purposes, they discretized the Biscayne Aquifer into 3 layers: an upper and lower permeable layer separated by a layer about 100 times less permeable. A significant amount of data from this study is available, including but not limited to year 2000 wet season heads, horizontal hydraulic conductivity, transmissivity, specific storage, specific yield, aquifer thickness, and bottom of aquifer layer elevations. Some of this data is available as figures with contours while others appear to be raster data. Figures with contour data can be georeferenced and recreated in GIS, however, raster data will not be able to be recreated. Taylor Engineering will reach out to the USGS to see if they can provide digital copies of the data used in the modeling and reporting efforts. The following figures are examples of the type of data available from that study.

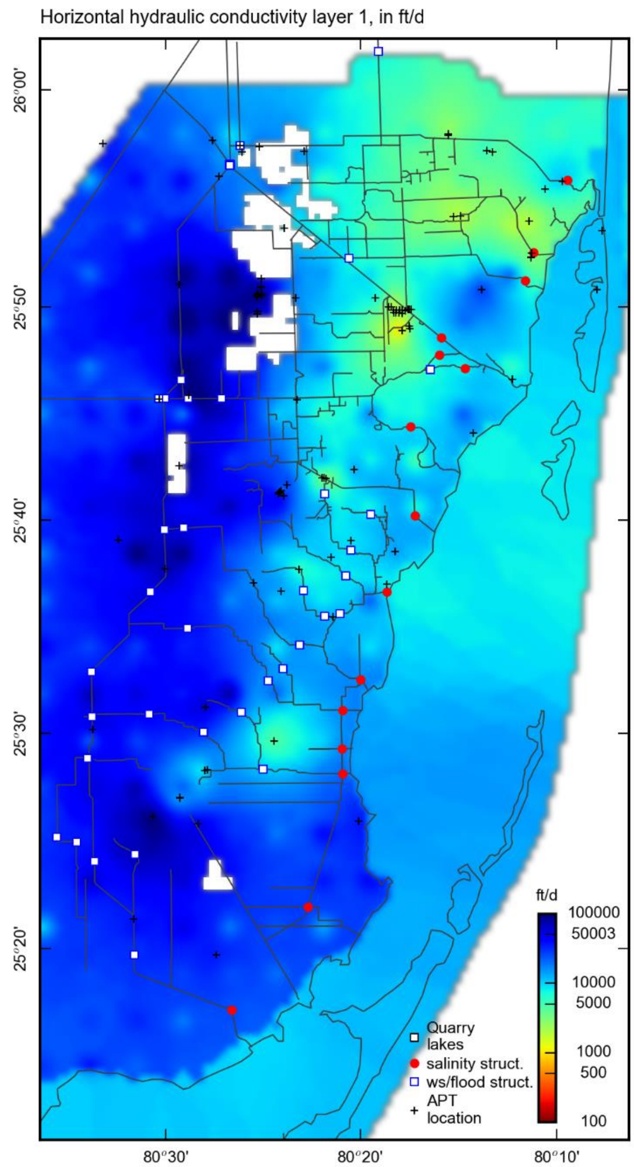

Figure 16: Hydraulic Conductivity of Biscayne Aquifer Layer 1 (Hughes & White, 2016)

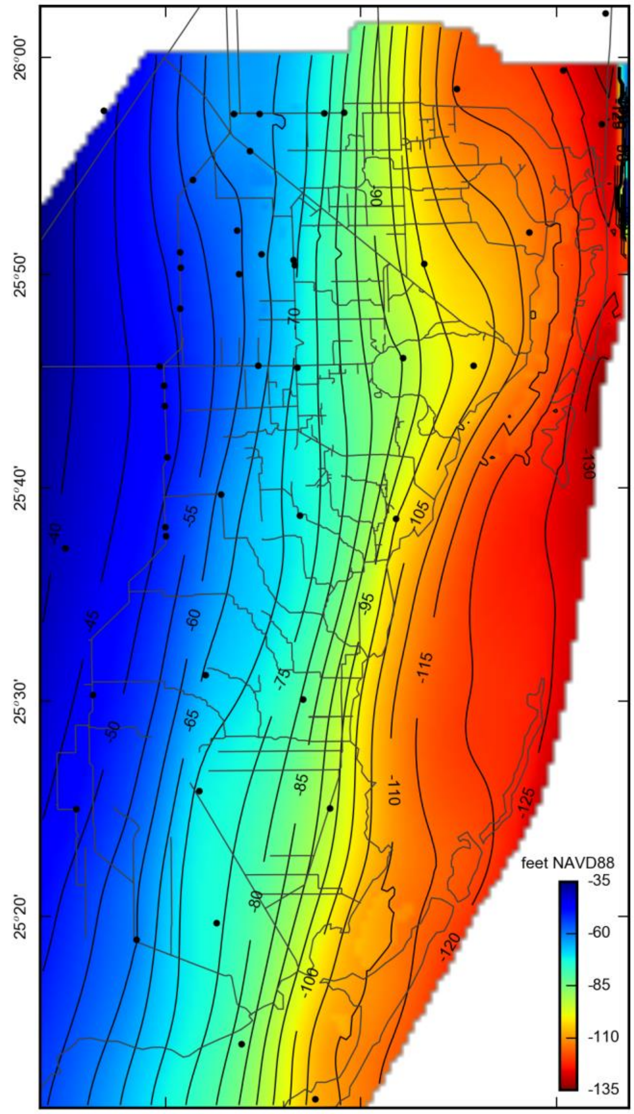

Figure 17:Bottom Elevation of Biscayne Aquifer Layer 3 (Hughes & White, 2016)

DRAFT Technical Memorandum

To: **CSA Central, Inc. and SFWMD**

From: **Taylor Engineering**

Date: **11/4/2019**

Re: **Model Development for SFWMD C8-C9 FPLOS Study**

1.0 INTRODUCTION

This memorandum details the development and initial parameterization of the SFWMD C-8 & C-9 MIKE SHE and MIKE HYDRO models for use in the C8-C9 FPLOS Study. Please note that many of the data inputs are initial values and are subject to change during model calibration.

2.0 MODEL DEVELOPMENT AND PARAMETERIZATION

2.1 Model Domain and Grid

The model domain extends from the C-9 and C-11 basin boundary in the north to the C-6 and C-7 canals in the south, and from the L-33 canal in the west to the intercoastal in the east, as shown in **Figure 1**. A computational grid size of 250-ft was chosen and coupled with the multi-cell overland feature using a 125-ft grid. This further refines the storage and conveyance characteristics of each computational grid cell. Although the model computations are based on a 250-ft grid cell, the conveyance and storage characteristics of each cell are calculated based on the finer 125-foot grid. This provides a high level of topographic detail and overland storage definition, which is sufficient for this sub-regional scale model. The computational grid size and multi-cell overland definition are consistent with the Broward County model (Taylor Engineering, 2019). Additionally, the C-8 C-9 model grid origin is aligned so that it is an exact integer of grid cells away from the Broward County Model origin, meaning that the data input and outputs are compatible between both models.

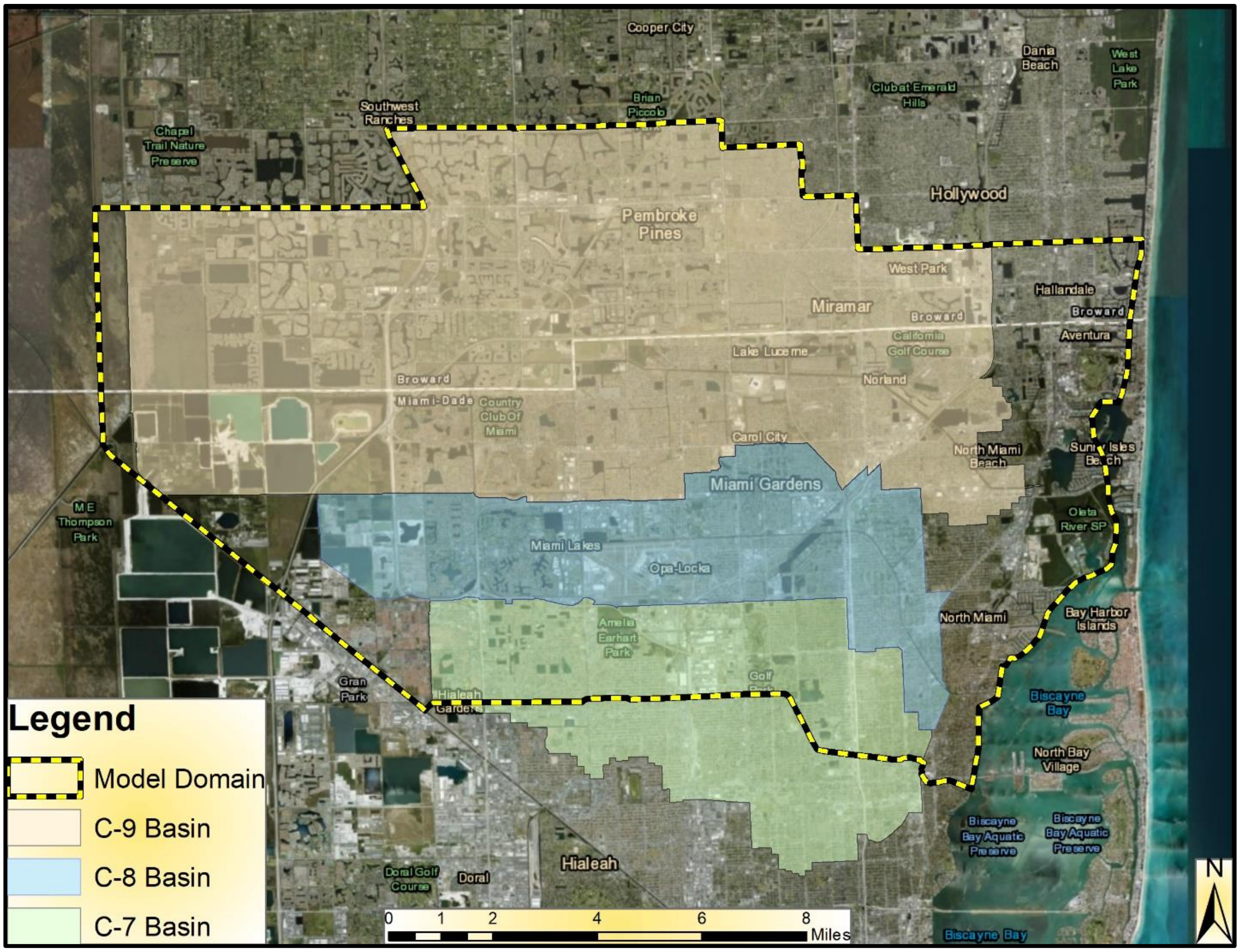

Figure 1: Merged 5-ft DEM

2.2 Topography

The topography input file was made from the merged DEM presented in Figure 1 from the Data Availability Memorandum. Areas with elevations greater than 25 ft NAVD88 (typically landfills or high bridges) were reduced to 25 ft to eliminate the possibility of having numerical stability issues in the 2D model (such as flow from 200-ft elevation cell to 10-ft elevation cell). Areas with elevations less than -2 ft NAVD88 were increased to -2 ft (typically intercoastal areas- bathymetry likely built into DEM). Then the topography was converted from NAVD88 to NGVD29 by adding 1.57 ft, the conversion from CorpsCon6 tool.

2.3 Simulation Specification

The simulation periods differ from one simulation to the next. The simulation period for the calibration model is a three week period from October 1st, 2000 1am to October 22, 2000 12am. The verification event is a three month period from June 2nd, 2017 6am to September 29th 12pm. The design storm will have a starting date that matches the verification event as it provides a realistic starting point for initial conditions and boundary conditions based on recent observed data. The design storm has a rainfall duration of three days; however, the simulation will likely be extended an additional 2-3 weeks. The purpose for running the simulation an additional 2-3 weeks would be to generate a model-simulated water table map that could be useful as an alternative input for initial groundwater level conditions.

2.4 Climate

2.4.1 Rainfall

The calibration event uses NEXRAD rainfall depths that are temporally distributed based on a rain gauge that was spatially assigned via Thiessen Polygons, as discussed in the Data Availability Memorandum. The verification event uses NEXRAD data that is unmodified. The design storm will use NOAA Atlas 14 rainfall depths that are temporally distributed based on the SFWMD 3-day distribution and spatially distributed based on Thiessen Polygons of the NOAA stations (**Figure 2**), which is consistent with the Broward County model.

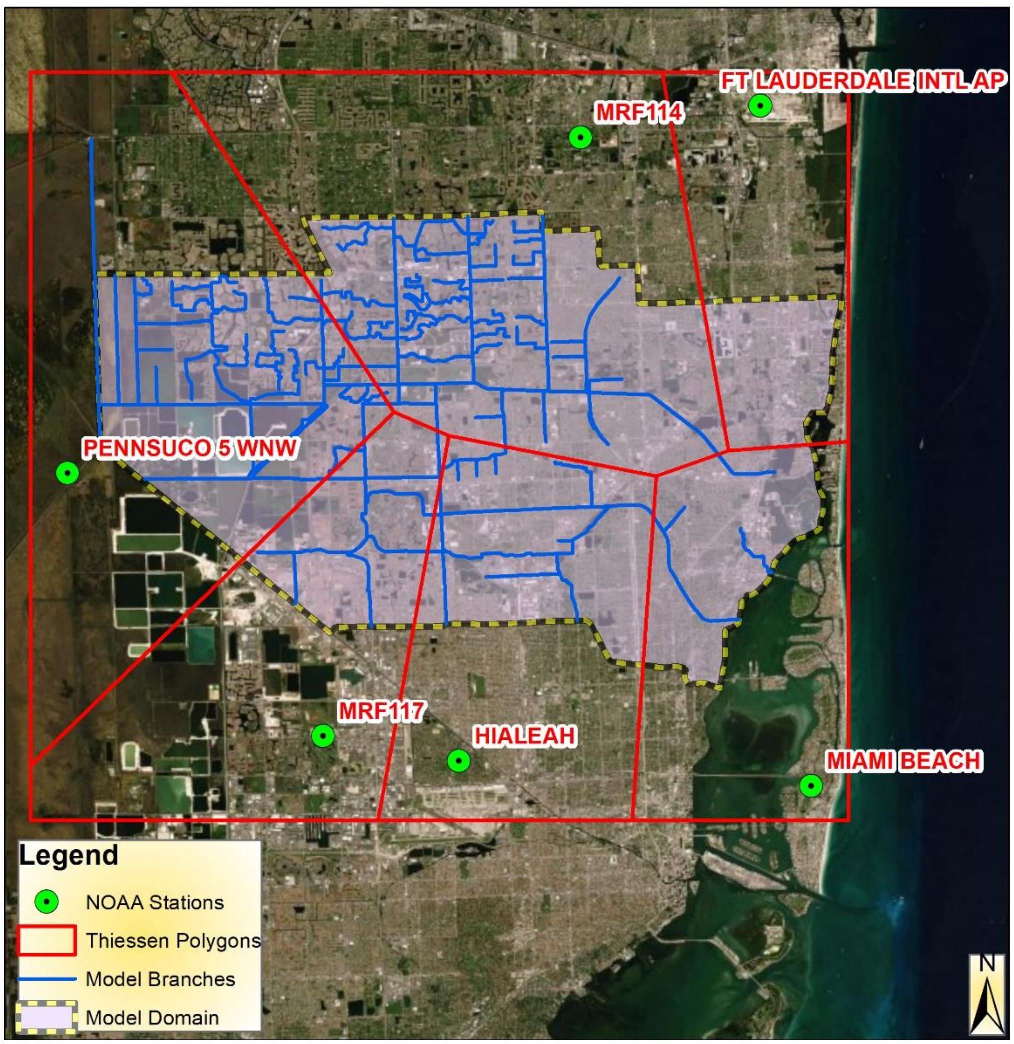

Figure 2: Thiessen Polygons based on NOAA Stations

2.4.2 Reference Evapotranspiration

Short model simulations are typically not very sensitive to this parameter and reference ET does not vary significantly across relatively small areas, such as this model domain. Therefore, a uniform spatial distribution was chosen for the calibration and validation simulations. A time varying temporal distribution will be used based on the SFWMD Reference ET for the specific time period (https://apps.sfwmd.gov/nexrad2), based on a centrally located pixel within the model domain (**Figure 3** & **Figure 4**). For the design storms, the Reference ET will have a uniform spatial distribution and be based on average wet season ET values, developed from the USGS reference ET data.

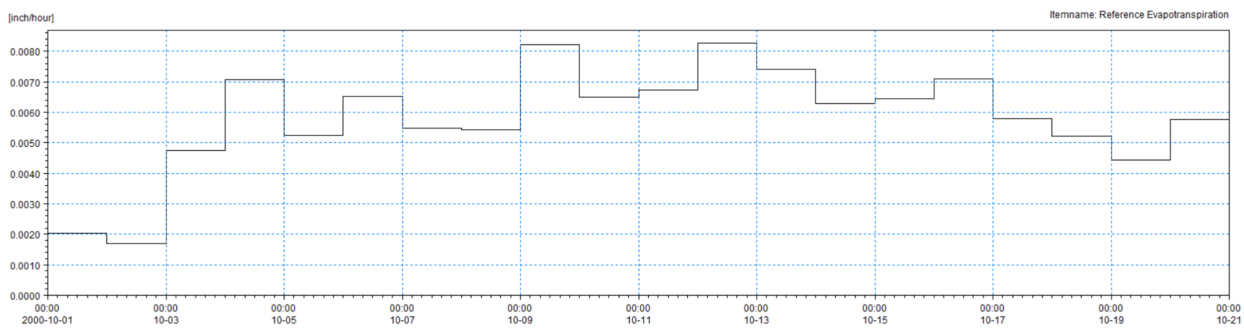

Figure 3: Reference ET for Pixel 10045457 for Calibration Simulation

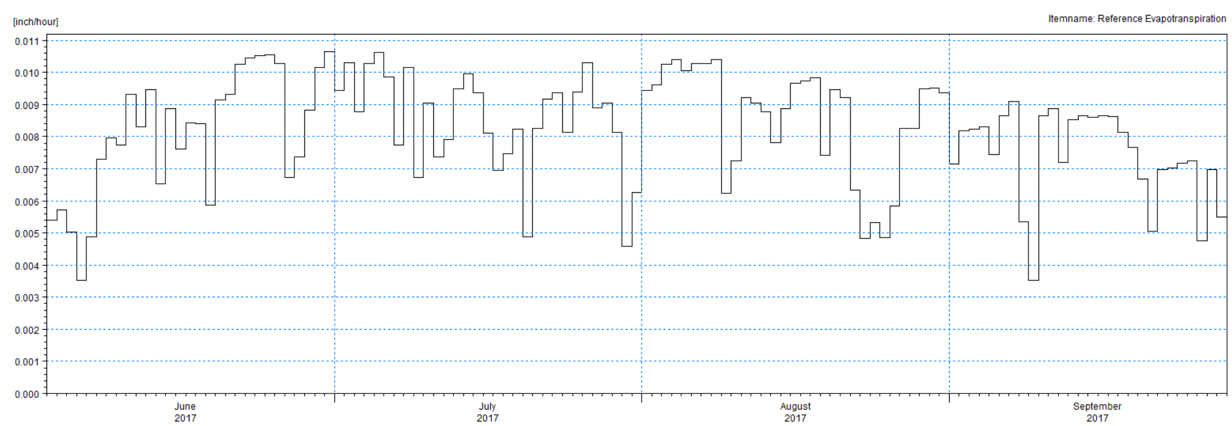

Figure 4: Reference ET for Pixel 10045457 for Validation Simulation

2.5 Land Use

To be consistent with the Broward County Current Conditions model, the land use/vegetation map was created by merging the Broward County model's land use map with the latest available data from SFWMD (2014-2016). The Broward County Current Conditions model's land use map was also created using the latest data from SFWMD, but additional changes to land use were made throughout the county by comparing satellite imagery from 2015 with 2018. Therefore, by merging the Broward County land use map that was updated with the SFWMD land use, it ensured that any changes in the C-9 basin from the Broward County Model were incorporated. As discussed in the data availability memorandum, there were less than 2% change in land use classification since 2000, so this dataset will be used for the calibration event as well as the verification and design storm events. Refer to **Table 1** for land use description by FLUCCS code.

Land Use / Vegetation

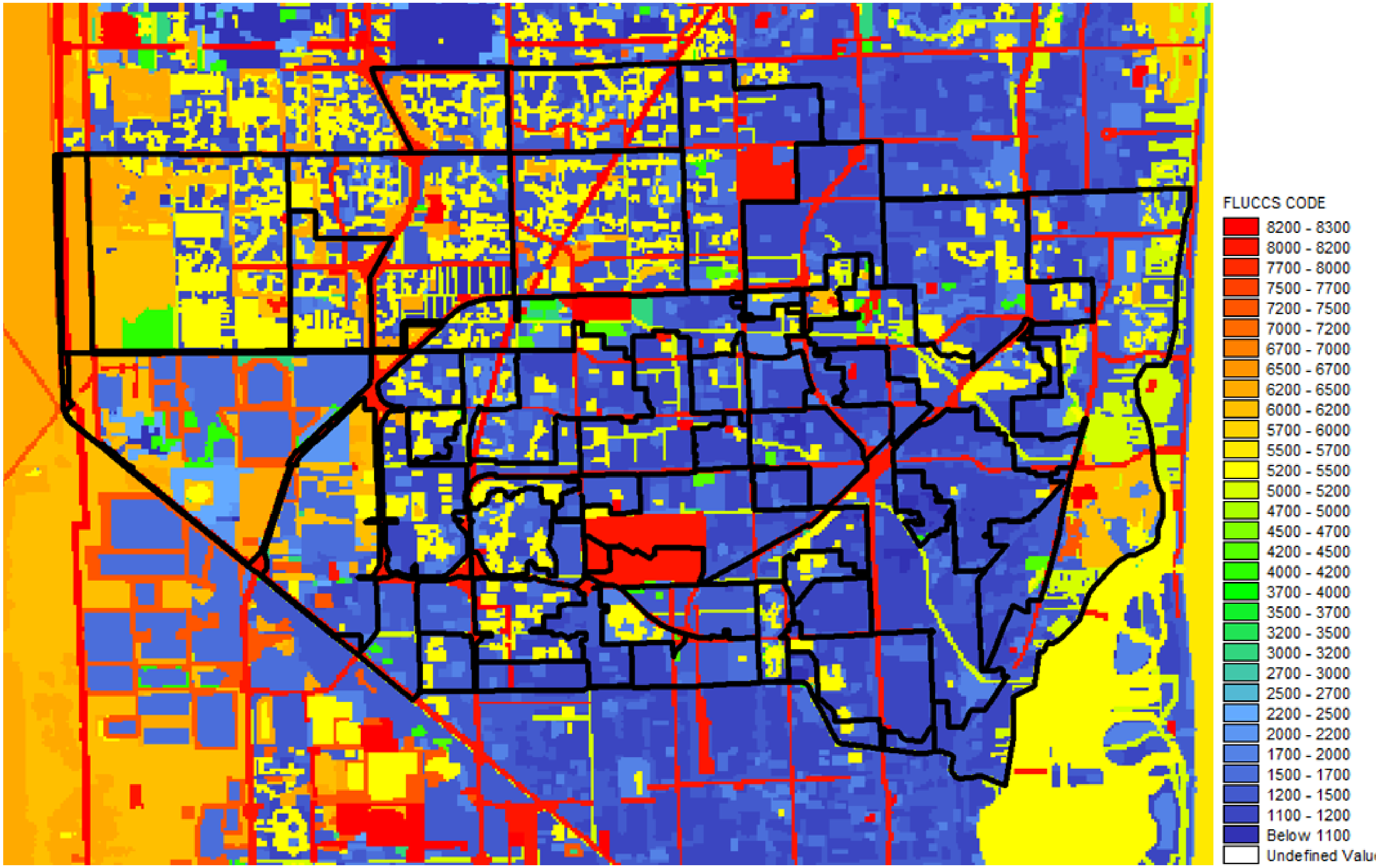

Figure 5: Land Use/Vegetation by FLUCCS Code

Table 1: Land Use by FLUCCS Code

FLUCCS Code	Land Use
1100	Residential, Low Density
1200	Residential, Medium Density
1300	Residential, High Density
1400	Commercial and Services
1500	Industrial
1600	Extractive
1700	Institutional
1800	Recreational
1900	Open Land
2100	Cropland and Pastureland
2200	Tree Crops
2300	Feeding Operations
2400	Nurseries and Vineyards
2500	Specialty Farms
2600	Other Open Lands - Rural
3100	Herbaceous (Dry Prairie)
3200	Upland Shrub and Brushland
3300	Mixed Rangeland
4200	Upland Hardwood Forests
4300	Upland Mixed Forests
5100	Streams and Waterways
5200	Lakes
5300	Reservoirs
5400	Bays and Estuaries
5700	Ocean and Gulf
6100	Wetland Hardwood Forests
6400	Vegetated Non-Forested Wetlands
7400	Disturbed Land
8100	Transportation
8200	Communications
8300	Utilities

2.6 Rivers and Lakes (1D model)

The 1D model was developed using MIKE HYDRO. The 1D network in the C-9 basin was mainly based on the Broward County Current Conditions model. The 1D network in the C-8 and C-7 basins were developed for this project. District, County, survey, and other stakeholder data were used when and where applicable and available. Additional survey was completed for this project. The data used and parameterization of the river network are discussed in the following subsections.

2.6.1 1D River Network

The 1D river network is composed of 95 branches, 93 of which could be considered secondary or tertiary systems. The purpose of this study is to determine the flood protection level of service for the C-8 and C-9 canals. Although the focus of this study is on the two primary canals, C-8 and C-9, a high level of detail was placed on the secondary/tertiary canal systems, as they are both a major source of discharge into the primary system and storage prior to discharging into the primary system. Many of the secondary/tertiary canal systems were setup to simulate the connectivity between lakes and other discontinuous (from DEM) water bodies, which are actually connected through a series of hydraulic structures. Water bodies that are not explicitly represented via a branch may still be connected to the 1D river network, which is discussed in section **2.6.3.1**.

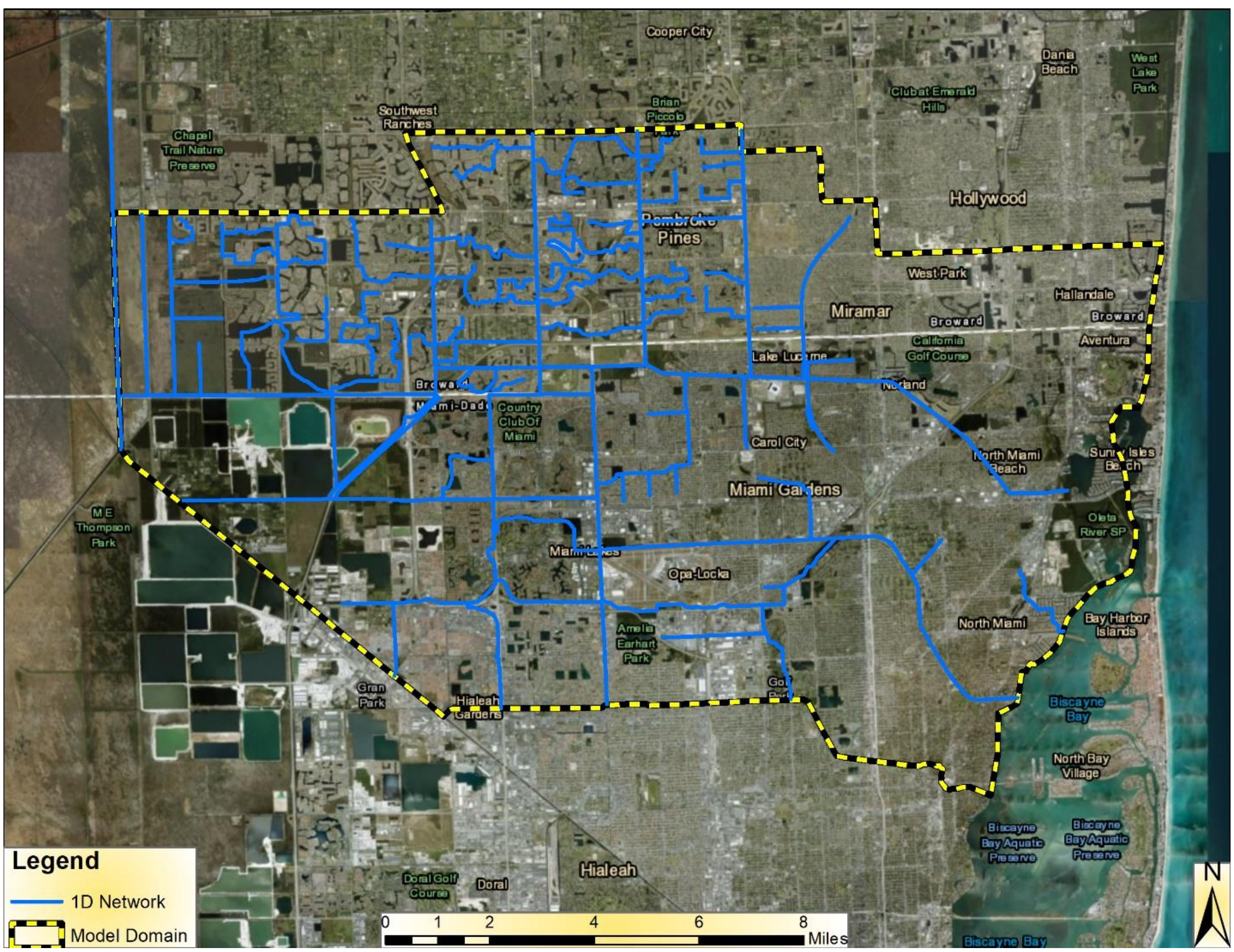

Figure 6: 1D Model Branches

2.6.1.1 Hydraulic Control Structures

The 1D network is controlled through a series of culverts, weirs, gates, and pumps. Specifically, there are 309 culverts, 6 weirs, 8 gated structures, and 8 pump stations. There are also 46 bridges explicitly modeled, which may control flow if they become submerged. The data for these structures came from a variety of sources, including South Broward Drainage District's (SBDD) Facilities Report, Miami-Dade Stormwater Geodatabase, SFWMD Operations Control Center Structure Books, SFWMD Flow Rating Analysis reports, SFWMD XP SWMM models, and professional survey. In areas where specific data was unavailable, an approximation was made. Specifically, South Broward Drainage District's Facilities Report lacked invert elevations for approximately 200 of the culverts included in the model, therefore, an approximation was made by matching the top of the culvert with the water control elevation, with respect to the specific drainage basin, as suggested by SBDD (See **Appendix B**).

There are four SFWMD control structures within the C-8 and C-9 basins, and two outside the basins (one for boundary conditions on the L-33 Canal and one for Arch Creek). The four SFWMD control structures within the basins are represented as sluice gates, so that the District's flow rating parameters could be incorporated, which provide the closest model calculation representation of the actual stage-discharge relationship of the structures.

2.6.1.2 Cross Sections

The availability of cross section data was limited to mainly the Miami-Dade portion of the model domain. Both the Miami-Dade County GIS Geodatabase as well as the SFWMD XP SWMM C-7, C-8, and C-9 models had cross section data for branches within Miami-Dade County. Cross sections for the C-9 canal were available from both survey data and the C-9 XP SWMM model. For secondary/tertiary canals in Broward County, cross section data was essentially nonexistent. Therefore, the cross sections for the branches within the Broward County portion of the model were carried over from the Broward County Current Conditions Model, which are mainly estimates based on the DEM. The majority of the cross sections in the Broward County portion of the model were cut using the latest available 5-ft DEM (a composite DEM made by Geosyntec consultants, as discussed in the data availability memorandum). This means the DEM was used for cross section elevation and geometry, from bank to the water surface. An assumed geometry was used below the water surface. The water surface elevation varied countywide. Additional cross section data for this project was collected via professional survey.

2.6.1.3 Survey Data

Requested survey items focused on areas with little or no available data. A map of the surveyed items and locations can be seen in **Figure 7.** These items were incorporated into the 1D model.

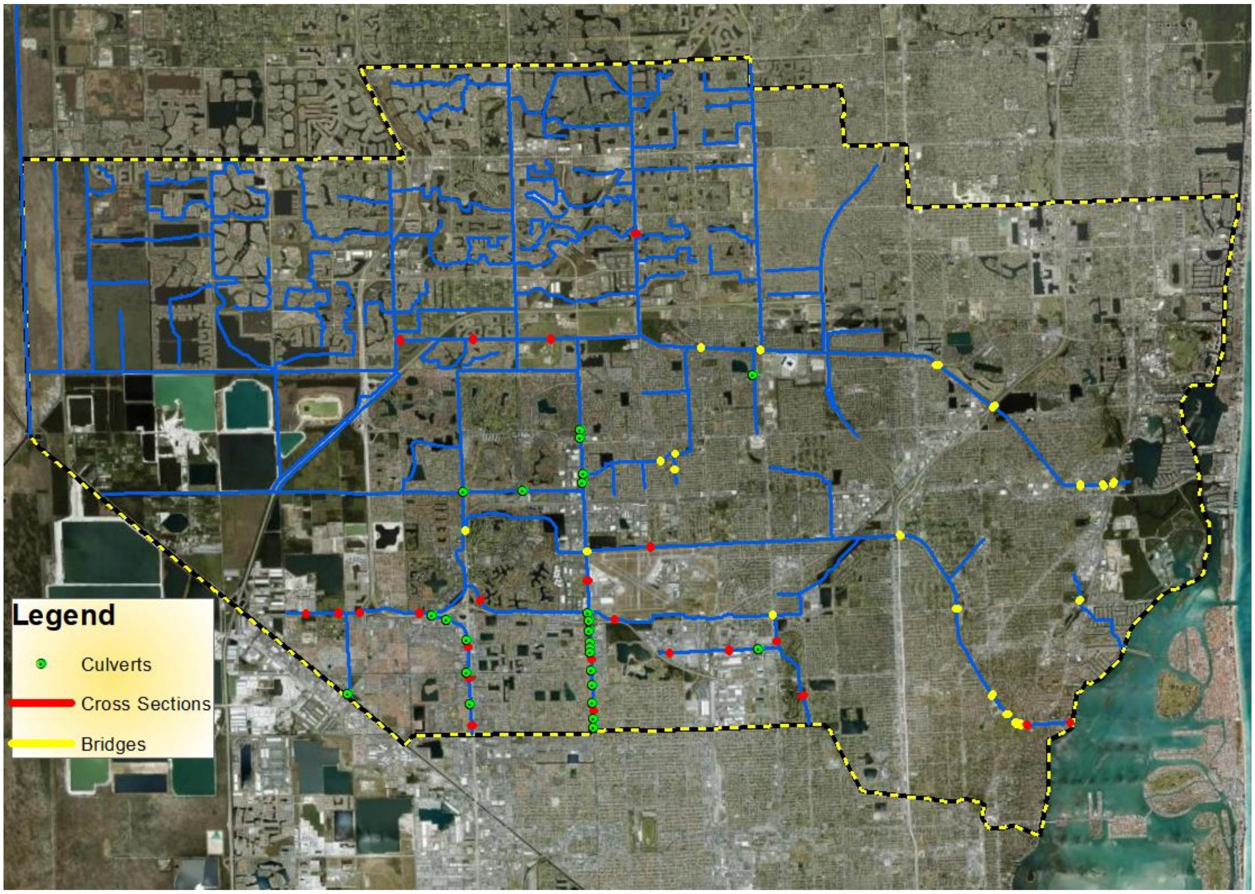

Figure 7: Survey Inventory

2.6.2 Canal-Aquifer Interactions

The 1D river network is coupled with the 2D groundwater model through the use of MIKE SHE couplings. Essentially, at each grid cell along either side of a river branch, the exchange is calculated by multiplying the head difference between the grid cell and the river with the conductance. The model calculates the conductance based on the options assigned. For each branch or branch segment in the model, 1 of 3 conductance options will be chosen, either (1) aquifer + riverbed, (2) aquifer only, or (3) riverbed only. These options change the way the model calculates the exchange between the groundwater and the river, where the aquifer conductance depends on the horizontal hydraulic conductivity and the riverbed conductance depends on an assigned leakage coefficient. Typically, only aquifer + riverbed or riverbed only will be used. In either of these cases, a leakage coefficient is assigned, with 1E-4/s being the model default value. The conductance option and leakage coefficient will likely be adjusted on a case-by-case basis during model calibration.

2.6.3 Canal-Overland Flow Interactions

The 1D river network is coupled with the 2D overland flow model through the use of MIKE SHE couplings. In this model, both coupling options are used, which are (1) flood codes and (2) overbank spilling. These options are discussed in the following two subsections.

2.6.3.1 Flood Codes

On secondary and tertiary canals, flood codes are used to allow communication between MIKE HYDRO and MIKE SHE when water levels in MIKE Hydro exceed the adjacent floodplain elevations. Flood codes also allow MIKE SHE to communicate directly with MIKE HYDRO whenever the water elevation of flood code cells exceed the water elevation in the river branch, as long as the water elevation in the branch is higher than the grid cell's topographic elevation. Flood codes were also used in areas where direct connections were not explicitly represented, such as ponds or lakes within close proximity of a river branch, or water bodies that become disconnected in the DEM. An example of this is shown in **Figure 8**.

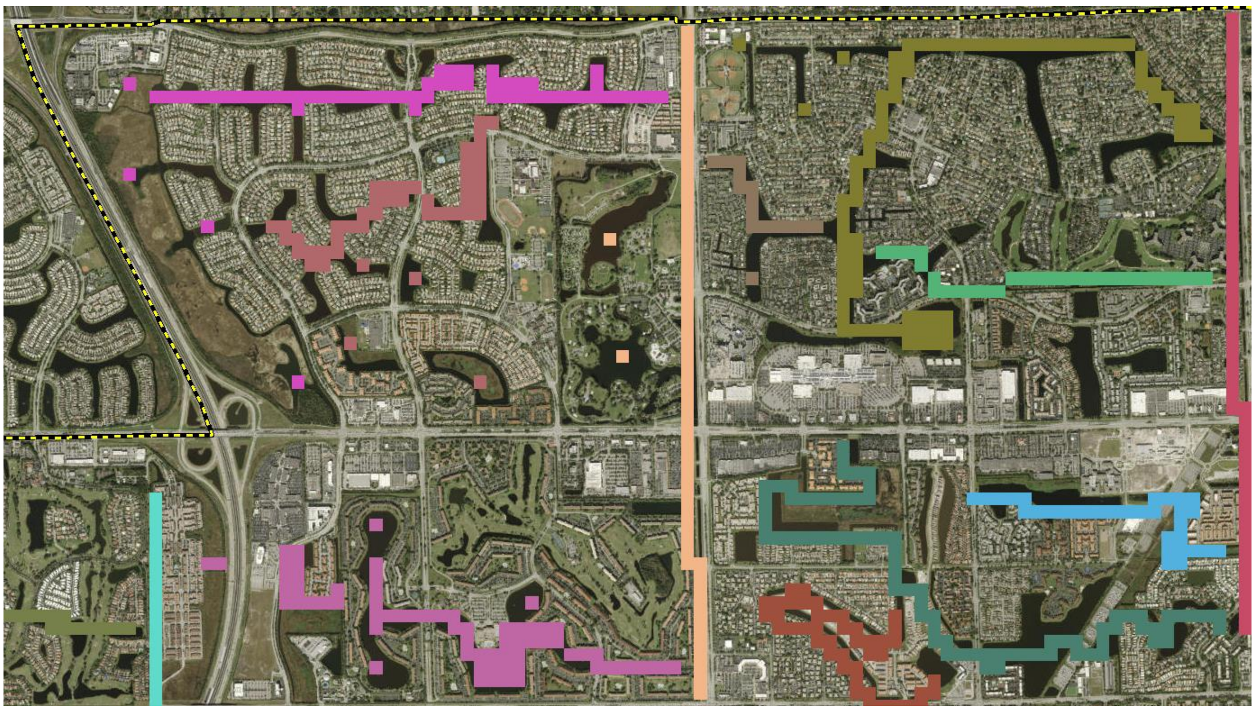

Figure 8: Example of Flood Code Placement

Flood code cells are excluded from 2D overland flow computations, so it is important to place them wisely, such as the lowest cell in a particular area. Covering an entire lake with flood code cells would turn off the overland computations for the entire lake. Therefore, the only time entire water features were covered with flood codes was when the storage was accounted for in the 1D model, such as a branch going through a lake (the lake water levels are computed in the 1-D model). The detailed surface topography provided an opportunity to take advantage of the flood code feature and account for storage that would otherwise be lost in a larger resolution topographic map. The flood code setup is shown in **Figure 9**. Although the specific value of the flood codes do not matter, as they are just an identifier that relate a cell to a specific branch, the flood code values in the C-9 basin were kept the same as the Broward County Model for consistency. New flood code areas were assigned identifiers not used in the Broward County model, which should eliminate any issues in the future if the models are merged together.

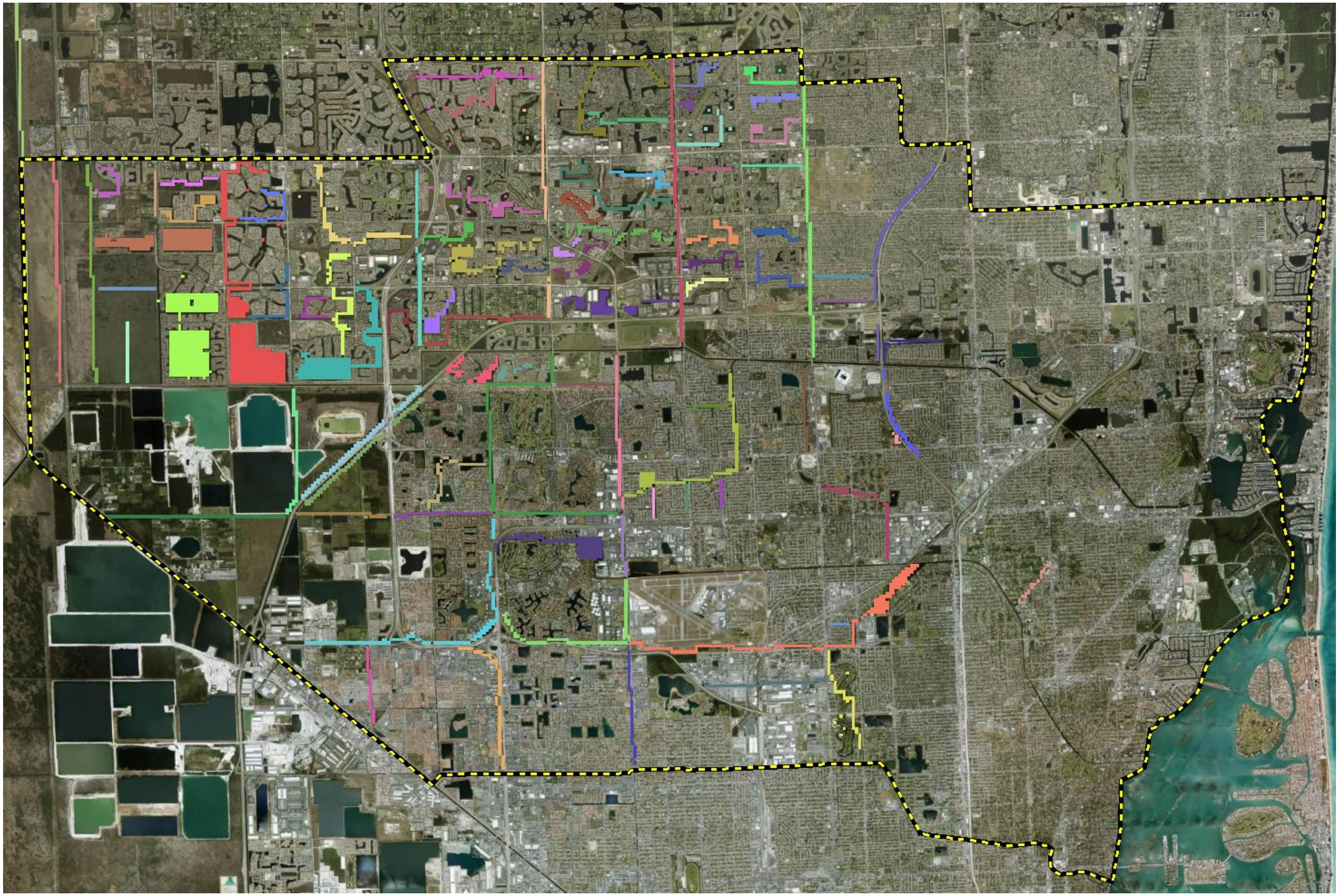

Figure 9: Flood Codes

2.6.3.2 Overbank Spilling

The C-8 and C-9 primary canals rely on overbank spilling instead of flood codes, which allows communication between MIKE SHE and MIKE HYDRO via the weir equation, whenever the water level in the canals become greater than the cross section bank elevations. Overbank spilling provides a more physically based representation of the exchange between canal and 2D grid, which is more important on the C-8 and C-9 canal than the secondary and tertiary canal system.

2.6.4 Hydrodynamic Initial Conditions

The 1D model's initial water levels are set based on two different categories, which are (1) based on observed data and (2) based on control elevations. In areas where there is observed data, such as water elevation upstream of the C-8 and C-9 tidal structures for calibration and validation simulations, the initial conditions are set to match the observed data. In areas that are controlled via operable control structures such as SBDD, the initial conditions are set to match the control elevation, which differ from the gate open or pump on elevations. This is consistent with the approach used in the Broward County Model. The Broward County model also uses a "full bowl" approach in areas where there was no observed data and control elevation was unknown, but the structure operations were known. This meant that if a structure opens when the water level is 4.0 feet, then every branch within that drainage area has an initial water level of 4.0 feet. This approach was not used in this model as there are no areas which fall into that category. For the design storm, the 1D model's initial water levels will be set based on control elevations.

2.7 Overland Flow

The overland flow module, or 2D model, is essentially parameterized by district drainage basin. The C-9 basin, which mainly lies within Broward County, was parameterized to be consistent with the Broward County model, which was based on two major categories: (1) land use and (2) ERP permitted areas. The C-8 Basin, which is in Miami-Dade County, was parameterized in a similar way but based on different data. This is explained in the following subsections.

2.7.1 Overland Flow in Broward County

Most of the parameters in the overland flow model are spatially varied by land use, while other parameters are spatially varied by land use within ERP permitted areas. A large portion of Broward County is made up of permitted areas that are required to retain some volume of rainfall, whether it be the first 1-inch of rainfall or 2.5-inches over the impervious area, or a more stringent requirement to retain the runoff resulting from the 25-year 3-day storm, with no discharge. For the Broward County model, Taylor Engineering proposed to separate the permitted areas into the following categories: (1) areas controlled by operable structures such as pumps or gates, (2) areas that had at least 10% waterbody land coverage such as lakes or ponds, (3a) areas with less than 10% waterbody land coverage and have at least 6 inches of groundwater storage, and (3b) areas with less than 10% waterbody land coverage and have less than 6 inches of groundwater storage. Groundwater storage availability was estimated by subtracting the initial groundwater elevation from the topography elevation, and then multiplying by an assumed specific storage of 0.2. This means that areas with an initial depth to groundwater greater than 2.5-feet had the ability to infiltrate 6+ inches of rainfall, and areas with less than 2.5-feet do not. This was the assumed threshold for where exfiltration areas would likely be located.

Permit areas classified as category 1, those behind operable structures, were parameterized just based on land use, as if they were unpermitted. Flow to the canal network from these areas is controlled by operable structures (gates and pumps), which are designed to limit discharge to permitted values and at permitted threshold water levels. Therefore, runoff rates within the respective drainage areas are ultimately limited by the operable structure. Although there may in fact be permitted areas within an overall drainage area that are held to a higher level of stormwater retention, for the purposes of this sub-regional scale model, if the operable structure is within its permitted allowance than it can be assumed that so are the areas draining to it. These areas classified as category 1 are controlled by permitted pumps and gates, that retain water on-site until the water levels reach the permitted discharge elevation, which means they often have a large amount of "dead storage" or on-site retention. Permit areas classified as category 2, those with at least 10% waterbody land coverage, were parameterized to account for the required detention storage, potential surface water storage, and sub-grid scale drainage features. Permit areas classified as category 3a, those with less than 10% waterbody land coverage and on average more than 6 inches of available groundwater storage, were parameterized to account for the required detention storage and the likelihood of exfiltration trenches and other stormwater management features. Permit areas classified as category 3b, those with less than 10% waterbody land coverage and on average less than 6 inches of available groundwater storage, were parameterized to only account for the required on-site retention. A map of Broward County's permitted areas within the model domain can be seen in **Figure 10**.

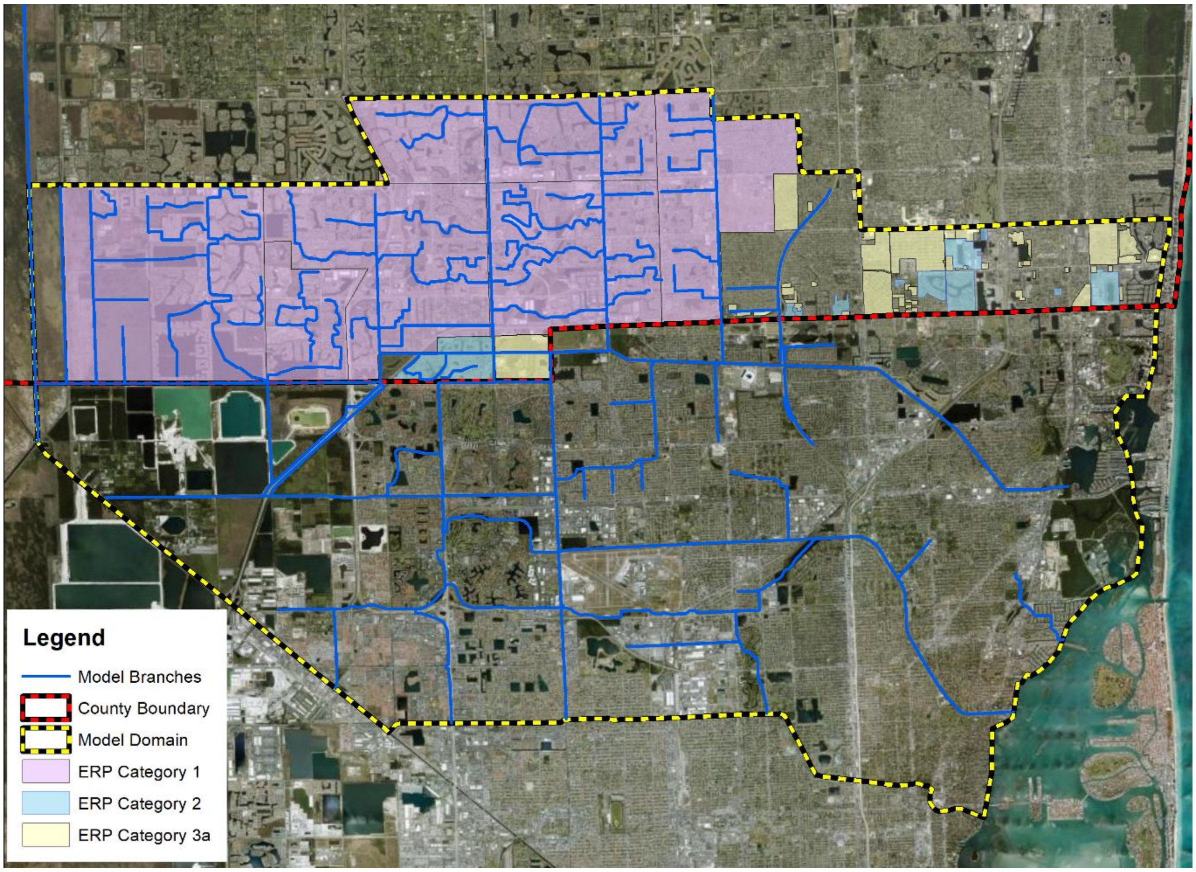

Figure 10: ERP Categories Used to Parameterize Overland Flow in Broward County

2.7.2 Overland Flow in Miami-Dade County

Within the Miami-Dade portion of the model, most of the parameters in the overland flow model are spatially varied by land use, while other parameters are spatially varied by land use within areas that are internally drained. Several areas within the C-8 drainage basin are either internally drained or have a large network of French drains, both of which reduce the amount of runoff making its way to the C-8 and C-9 Canals. Although the capacity of the French drain systems in Miami-Dade County are unknown, they are designed to retain/infiltrate some volume of rainfall before discharging into the canal system. Taylor Engineering proposed to the District to separate drainage areas into the following categories: (5) areas draining directly to MIKE Hydro branches, (6) areas internally drained or that have a large amount of French drains relative to area served, and (7) areas both draining to branches and having French drains.

Areas classified as category 5, those draining to a branch, were parameterized just based on land use. Areas classified as category 6, those internally drained or have a large amount of French drains, were parameterized by land use and adjusted to account for features that route and store water within the drainage basin. Areas classified as category 7, were parameterized by land use and adjusted to account for potential water storage and sub-grid scale drainage features like exfiltration trenches and other stormwater management features. Although based on different criteria, these categories are similar to the ERP areas classified for the Broward County model. A map of the drainage categories developed for the Miami-Dade County portion of the model domain can be seen in **Figure 11**.

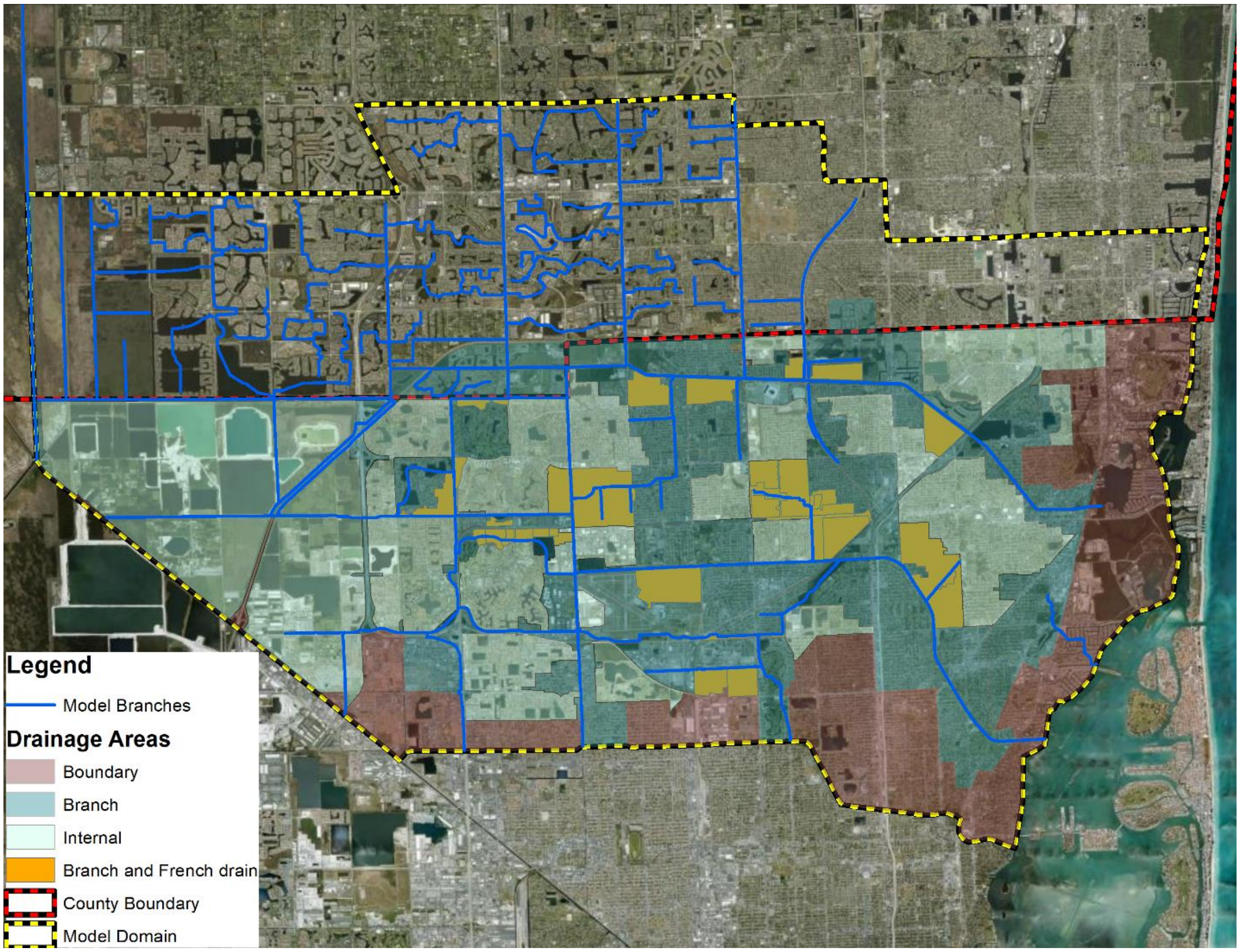

Figure 11: Drainage Categories Used to Parameterized Overland Flow

As shown in **Figure 12,** the areas in green are assumed to be internally drained for the purpose of parameterizing the ponded and saturated zone drain routines as discussed in the following subsections. These areas either drain to local water bodies or have a large amount of French drains. However, it is important to note that runoff from these areas can still be routed to the MIKE Hydro branches via the 2-D overland module.

The areas in yellow are areas that drain to branches, however, several areas in yellow also have a large amount of French drains, as shown by the red lines. In this figure, areas that are green are considered category 6. The areas in yellow that have little to no French drains are considered category 5. The areas in yellow that have a large amount of French drains are considered category 7. The area in purple drains to the boundary, so the specific overland flow parameterization is less likely to affect the model results and were only parameterized based on land use.

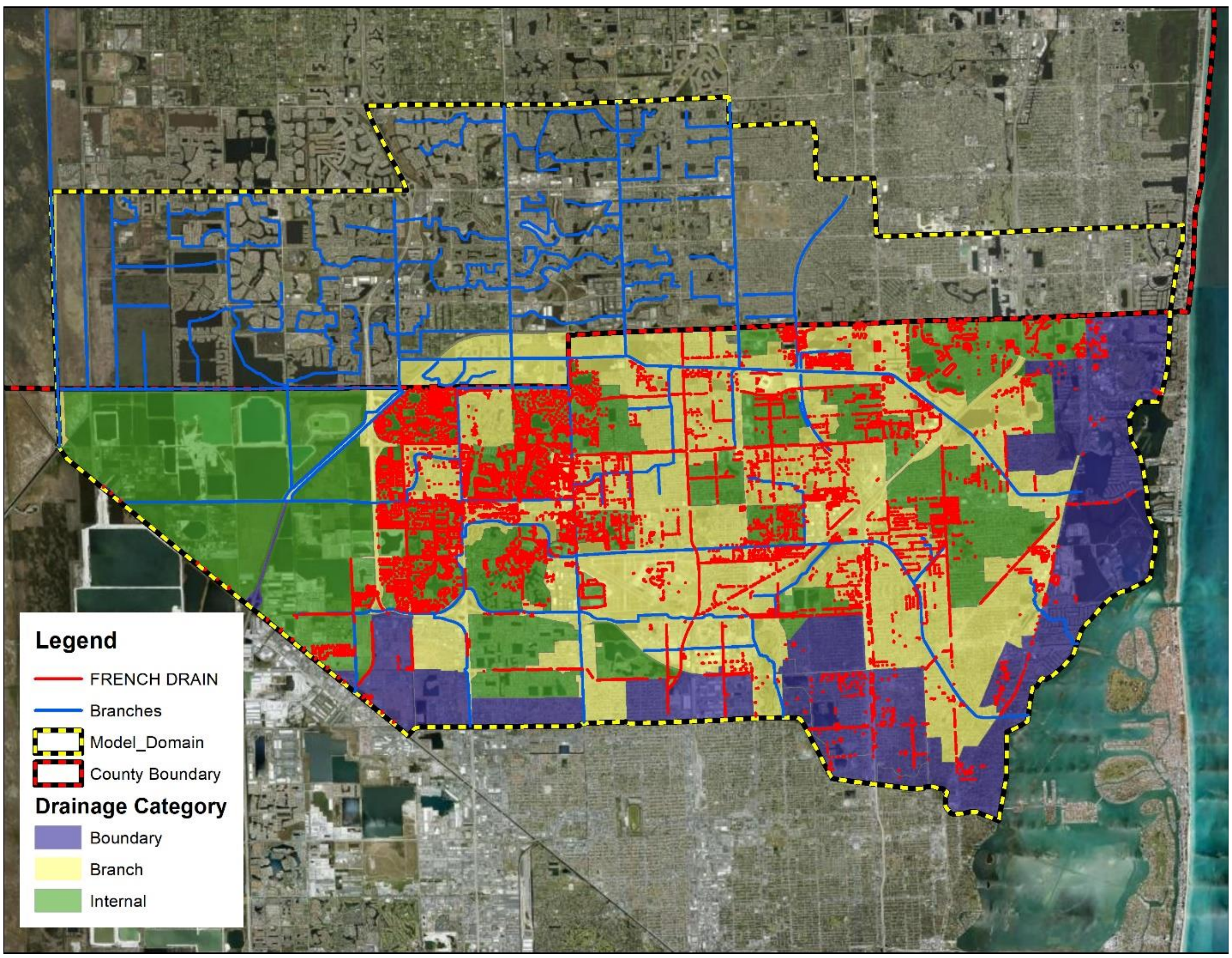

Figure 12: Drainage Categories in the Miami-Dare County Portion of the Model Domain

2.7.3 Overland Manning's Roughness Coefficient (n-value)

This parameter, used in the MIKE SHE 2-D overland flow component, is spatially distributed based on land use, with values ranging from 0.06 to 0.45 (**Table 2**).

Table 2: Land Use Based Manning's Roughness (n) Coefficients

FLUCCS Code	Land Use	Manning's Roughness (n)
1100	Residential, Low Density	0.14
1200	Residential, Medium Density	0.12
1300	Residential, High Density	0.11
1400	Commercial and Services	0.07
1500	Industrial	0.07
1600	Extractive	0.14
1700	Institutional	0.13
1800	Recreational	0.13
1900	Open Land	0.14
2100	Cropland and Pastureland	0.17
2200	Tree Crops	0.17
2300	Feeding Operations	0.17
2400	Nurseries and Vineyards	0.17
2500	Specialty Farms	0.17
2600	Other Open Lands - Rural	0.14
3100	Herbaceous (Dry Prairie)	0.13
3200	Upland Shrub and Brushland	0.3
3300	Mixed Rangeland	0.3
4200	Upland Hardwood Forests	0.45
4300	Upland Mixed Forests	0.45
5100	Streams and Waterways	0.06
5200	Lakes	0.06
5300	Reservoirs	0.06
5400	Bays and Estuaries	0.06
5700	Ocean and Gulf	0.06
6100	Wetland Hardwood Forests	0.45
6400	Vegetated Non-Forested Wetlands	0.3
7400	Disturbed Land	0.14
8100	Transportation	0.11
8200	Communications	0.14
8300	Utilities	0.14

2.7.4 Detention Storage

This parameter is spatially distributed, based on both land use and the categories defined for Broward County and Miami-Dade County. Within Broward County, the non-permitted area's detention storage was spatially distributed based on land use with values ranging from 0 to 0.4 inches, as shown in **Table 3**.

Table 3: Land Use Based Detention Storage

FLUCCS Code	Land Use	Detention Storage (in)
1100	Residential, Low Density	0.1
1200	Residential, Medium Density	0.1
1300	Residential, High Density	0.1
1400	Commercial and Services	0.1
1500	Industrial	0.1
1600	Extractive	0.1
1700	Institutional	0.1
1800	Recreational	0.3
1900	Open Land	0.15
2100	Cropland and Pastureland	0.15
2200	Tree Crops	0.25
2300	Feeding Operations	0.25
2400	Nurseries and Vineyards	0.25
2500	Specialty Farms	0.25
2600	Other Open Lands - Rural	0.15
3100	Herbaceous (Dry Prairie)	0.15
3200	Upland Shrub and Brushland	0.15
3300	Mixed Rangeland	0.15
4200	Upland Hardwood Forests	0.4
4300	Upland Mixed Forests	0.4
5100	Streams and Waterways	0
5200	Lakes	0
5300	Reservoirs	0
5400	Bays and Estuaries	0
5700	Ocean and Gulf	0
6100	Wetland Hardwood Forests	0.4
6400	Vegetated Non-Forested Wetlands	0.4
7400	Disturbed Land	0.1
8100	Transportation	0.1
8200	Communications	0.1
8300	Utilities	0.1

In permitted areas within Broward County, the detention storage was spatially distributed by land use, but adjusted to account for the required retention. The permitted areas have ordinance requiring retention of the 1st 1-inch of rainfall or 2.5-inches of rainfall over the impervious area, whichever is greater. Within the permitted areas, the detention storage for impervious areas were increased by multiplying the paved area runoff coefficients (percentage of DCIA) by 2.5 inches, and any of the resulting values less than 1” was increased to 1”. Therefore, within category 2, 3a, and 3b permitted areas, the detention storage increased from 0.1-0.4 inches to 1-1.8 inches, dependent on the land use. This helps represent the on-site retention that permitted areas are required to have.

Within the Miami-Dade County portion of the model domain, the drainage categories were treated in a similar way to the permitted areas within Broward County. In drainage category 5 areas, those that drain to a canal and have little to no French drains, the detention storage was treated the same as non-permitted areas in Broward County and only parameterized based on land use, with values ranging from 0-0.4 inches (**Table 3**). In drainage category 6 areas, those that are internally drained to water bodies or low areas or have a large amount of French drains, the detention storage was treated the same as permitted areas in Broward County and parameterized basin on land use and adjusted to account for retention. Although these areas are forced to drain to local depressions within the ponded drainage routine, the detention storage was increased to hold that drained water on-site, representing the internal storage of local depressions and exfiltration areas. Otherwise, ponded water above the detention storage can still flow via the 2D overland flow routine into other drainage areas and then be routed to a branch. These category 6 areas were adjusted from 0.1-0.4 inches to 1-1.8 inches, based on land use. These values for category 6 areas were just an initial model parameterization and will likely be further adjusted during model calibration. In drainage category 7 areas, those that drain to a canal and have a relatively large amount of French drains, the detention storage was treated the same as permitted areas in Broward County and parameterized basin on land use and adjusted to account for retention provided by exfiltration areas, with values being increased from 0.1-0.4 inches to 1-1.8 inches. Category 7 areas differ from category 6 areas as they are allowed to drain to a branch within the ponded drainage routine, after the detention storage has been met. These values for category 7 areas were just an initial model parameterization and may be further adjusted during model calibration.

2.7.5 Initial Water Depth

This parameter was developed using an approach based on topography and basin control elevation, which is consistent with the Broward County model. Any cells within a drainage basin that are lower than the basin’s water control elevation have an initial depth equal to the difference of the water control elevation and the elevation of the cell (**Figure 13**). This eliminates excess “dead storage” and ensures that water is not being routed via ponded drainage or flood codes at the start of the simulation.

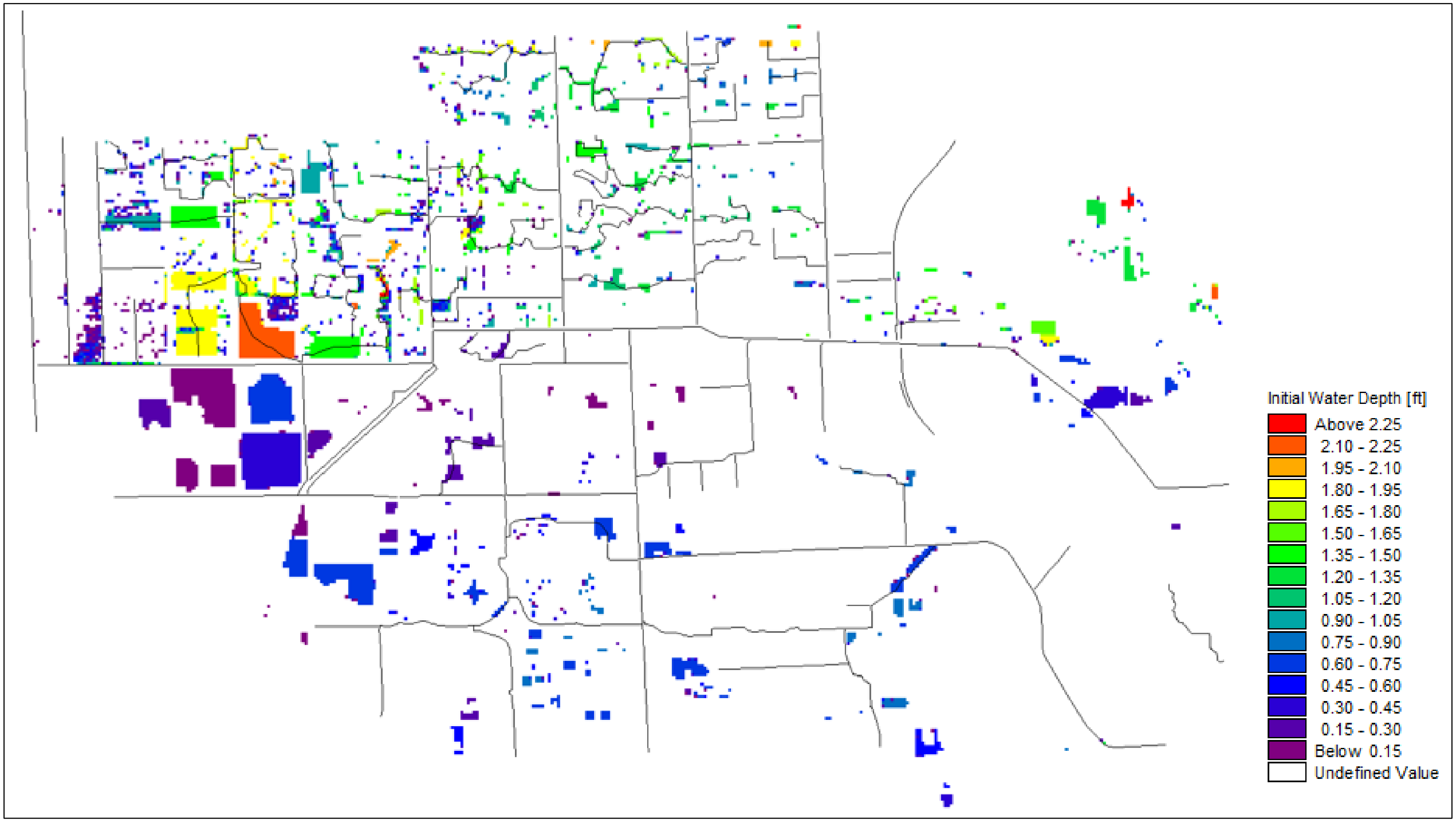

Figure 13: Initial Water Depths in the 2D Model

2.7.6 Surface-Subsurface Leakage Coefficient

This parameter reduces the exchange between land surface and the unsaturated or saturated zone, which can help account for near-surface soil compaction or fine sediment deposits. The model can be very sensitive to this parameter; too small of a value can essentially act as if there is an impermeable layer and allow for little to no infiltration. The leakage coefficient was set to a uniform spatial distribution using the model default value of 1E-4, although it will likely change in both spatial distribution and magnitude during model calibration.

2.7.7 Ponded Drainage

This is a relatively new feature introduced in the 2017 release of MIKE SHE that simulates routing of ponded water from impervious surfaces via features that are not explicitly modeled, such as curb inlets and local-scale storm drains. The ponded drainage routine routes runoff from directly connected impervious areas (DCIA) to canals based on user-specified drainage basins. The volume that is allowed to be routed is determined by a paved area runoff coefficient, which was assigned based on land use, and a maximum storage change rate. The rate at which the volume is routed is controlled by time constants. These parameters are discussed in the following subsections.

2.7.7.1 Maximum Storage Change Rate

This parameter was set to a uniform spatial distribution with a value of 0.095 ft3/s (each grid cell limited to 40mm/day), and then adjusted in specific areas where there was evidence suggesting a different value. Choosing realistic values ensures proper drainage representation and prevents drainage rates from exceeding sub-grid scale drainage capacities. For example, if sub-grid scale drainage features such as roadside swales and culverts are designed to handle 5-inches of rainfall over the course of a day, then the maximum storage rate should correspond. Within the Broward County portion of the model, the category 2 permitted area's maximum storage change rate was spatially distributed based on the permitted cubic feet per second per square mile (CSM) allowance per SFWMD drainage basin (See **Appendix A**). In the western portion of the C-9 drainage basin, the allowable discharge is 20 CSM pumped, which is equivalent to 0.045 ft3/s based on the model grid size (each grid cell limited to 18.9mm/day). This parameterization ensures that the permitted areas do not discharge more than their permitted allowance. Only category 2 permitted areas were based on the district's CSM allowance as these were the areas most likely holding water back in their surface waterbodies and discharging through structures at a permitted rate. The c-8 canal has "essentially unlimited inflow by gravity connection", so no restrictions are necessarily required. However, this parameter may be restricted in category 7 areas during model calibration, to help reduce the volume of runoff making it to the branch (capacity of exfiltration areas unknown). Similarly, the initial value of 0.095 ft3/s, which is equivalent to about 43 CSM, may need to be increased for the C-8 basin during model calibration.

2.7.7.2 Paved Runoff Coefficient

This parameter represents DCIA and is spatially distributed based on land use, permitted areas, and drainage categories. Within Broward County, the paved runoff coefficients were parameterized based on land use. In category 3a permitted areas, the paved area runoff coefficients were distributed based on land use like everywhere else, but then decreased by half. Since these permitted areas are assumed to use management features such as exfiltration trenches, the paved area runoff coefficients were adjusted to reduce the amount of runoff and increase the infiltration, as one would expect in areas served by exfiltration features. Within Miami-Dade County, the paved runoff coefficients were parameterized based on land use. In areas served by a relatively large amount of French drains, the paved area runoff coefficients were distributed based on land use, but then decreased by half, just like category 3a permitted areas within Broward County. Decreasing the runoff coefficient reduced runoff which provides the opportunity for increased infiltration. This parameterization is an attempt to simulate what cannot be explicitly represented in this scale of a model. The land use areas that were included in the ponded drainage routine can be seen in **Table 4**. All other land use categories, such as forests, were set to 0, which "turns off" the ponded drainage routine for those areas.

Table 4: Land Use Based Paved Runoff Coefficients

FLUCCS Code	Land Use	Paved Runoff Coefficient	Paved Runoff Coefficient in Category 3a Permitted Areas and Drainage Category 5 and 7 Areas
1100	Residential, Low Density	0.075	0.0375
1200	Residential, Medium Density	0.22	0.11
1300	Residential, High Density	0.45	0.225
1400	Commercial and Services	0.72	0.36
1500	Industrial	0.4	0.2
1700	Institutional	0.3	0.15
8100	Transportation	0.56	0.28

2.7.7.3 Inflow and Outflow Constant

These parameters can be adjusted to speed up or slow down the rate at which ponded drainage is routed to the river branches. Making the inflow constant larger than the outflow constant will create artificial storage, so this should be avoided. An initial value of 1E-4, the model default, was used as a starting point and may change during model calibration.

2.7.7.4 Drain Codes

Each drain code represents an individual subbasin, for the purpose of draining water internally or to a branch via the ponded and saturated zone drain routines. It should be noted that these "subbasins" do not prevent overland exchange between areas. In areas of uncertainty, drainage basins were left as larger areas so that the 2-D overland flow model could determine drainage divides. Basins were only further refined if there was clear evidence in the DEM, such as visible berms or water bodies with differing elevations. In the Broward County portion of the model, the majority of the area was defined based on data provided by South Broward Drainage District, on their permitted drainage basins. In the Miami-Dade portion of the model, subbasins were developed from data provided by Miami-Dade County. Miami-Dade County provided very detailed subbasin data, much too refined for this scale model. Therefore, new subbasins were developed by defining and aggregating basins based on drainage categories (as discussed in section **2.7.2**) and drainage destination (such as a specific canal). Essentially, areas with the same classification that shared a common boundary and destination, were merged into 1 basin. This process resulted in the number of basins in the Miami-Dade portion of the model to be decreased from about 830 basins down to about 40, while maintaining drainage characteristics.

Cells assigned an initial depth or a flood code, have a drain code of 0 assigned (dark blue cells in **Figure 14**), which turns off drainage from that cell. Not doing so would create feedback loops, as the drained water would return back to the cell via flood code, only to be drained back to the branch again and so on. **Figure 14** shows a map of the drain codes, where each unique color represents a drainage basin (areas in yellow drain to boundary). Although the specific value of the positive drain codes do not matter (negative drains to boundary) as they are just an identifier that define a drainage area, the drain code values in the C-9 basin were kept the same as the Broward County Model for consistency. New drain codes were assigned identifiers not used in the Broward County model, which should eliminate any issues in the future if the models are merged together.

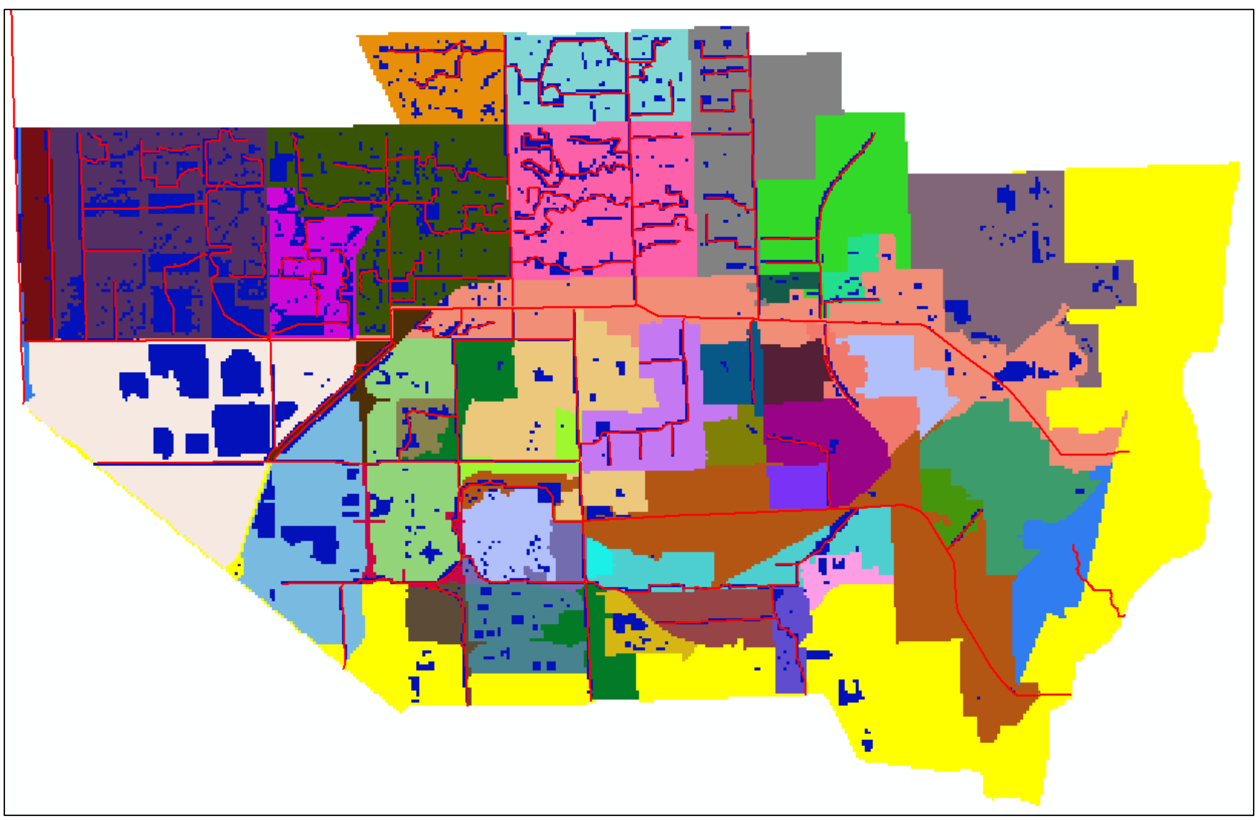

Figure 14: Drain Codes

2.8 Unsaturated Zone

The soil distributions and unsaturated zone parameters were carried over from the Broward County Current Conditions model (which were mainly inherited from the Broward County 2014 FEMA model) (**Figure 15**). The Broward County model's soil parameters that were changed were the saturated water content and field capacity for Margate Fine Sand and the field capacity for urban land, which were adjusted during model validation in an effort to improve the groundwater response to rainfall. These are incorporated in this model from the start. This model uses the simple 2-layer water balance method for unsaturated zone calculations, which is consistent with the Broward County model.

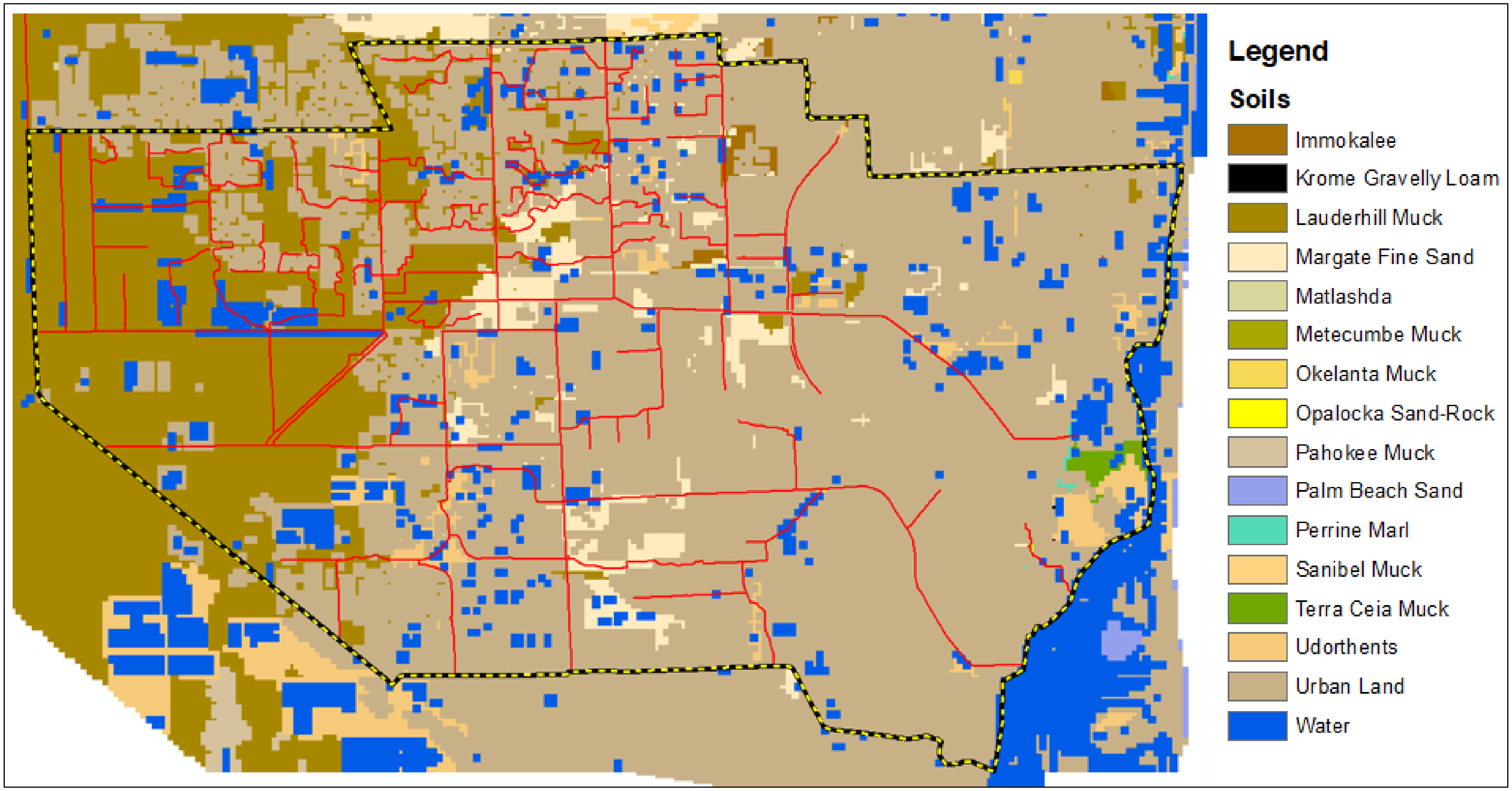

Figure 15: Map of Soils

2.9 Saturated Zone

This model uses a 3-layer groundwater model based on the MODFLOW model developed by the USGS (Hughes and White, 2016). This model represents the Biscayne aquifer with three hydrogeologic layers--two highly permeable layers separated by a less permeable layer. The Broward County model, which originally was developed for long- term water supply simulations, uses a more detailed 5-layer groundwater model. These conceptualization/application differences between the two models may prevent them from being merged into one model at a later time. Although it would be quite an effort, it is believed that the groundwater layers from each model could be massaged into one continuous file.

2.9.1 Lower Levels of Computation Layers in Saturated Zone

This parameter is spatially distributed based on data from Hughes and White (2016). Refer to **Figures 16** through **18** for the lower levels of the three layers representing the Biscayne aquifer.

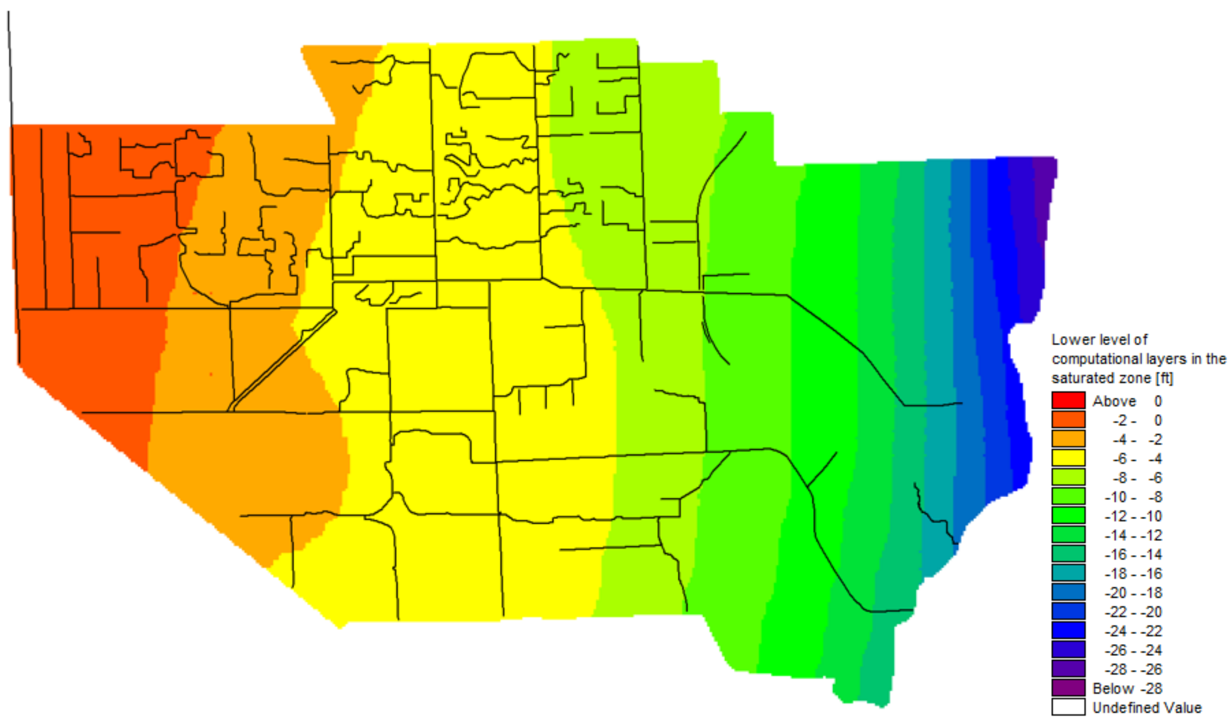

Figure 16: Lower Level of Computational Layer 1

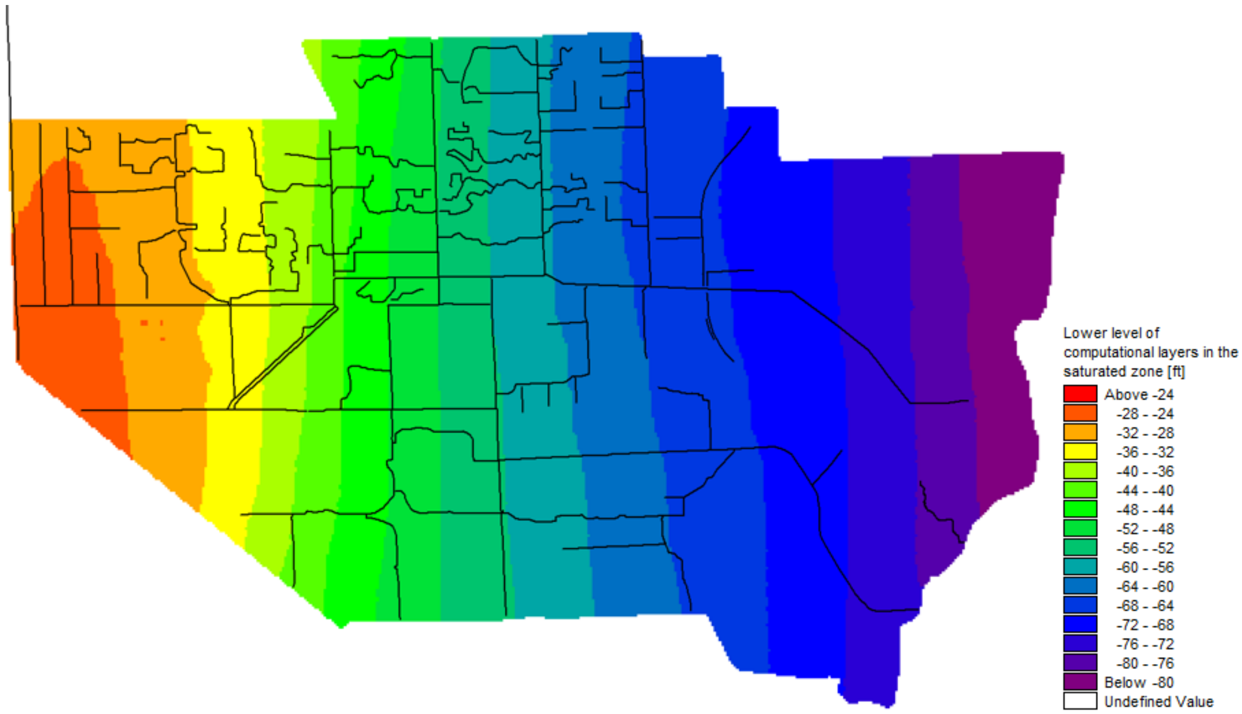

Figure 17: Lower Level of Computational Layer 2

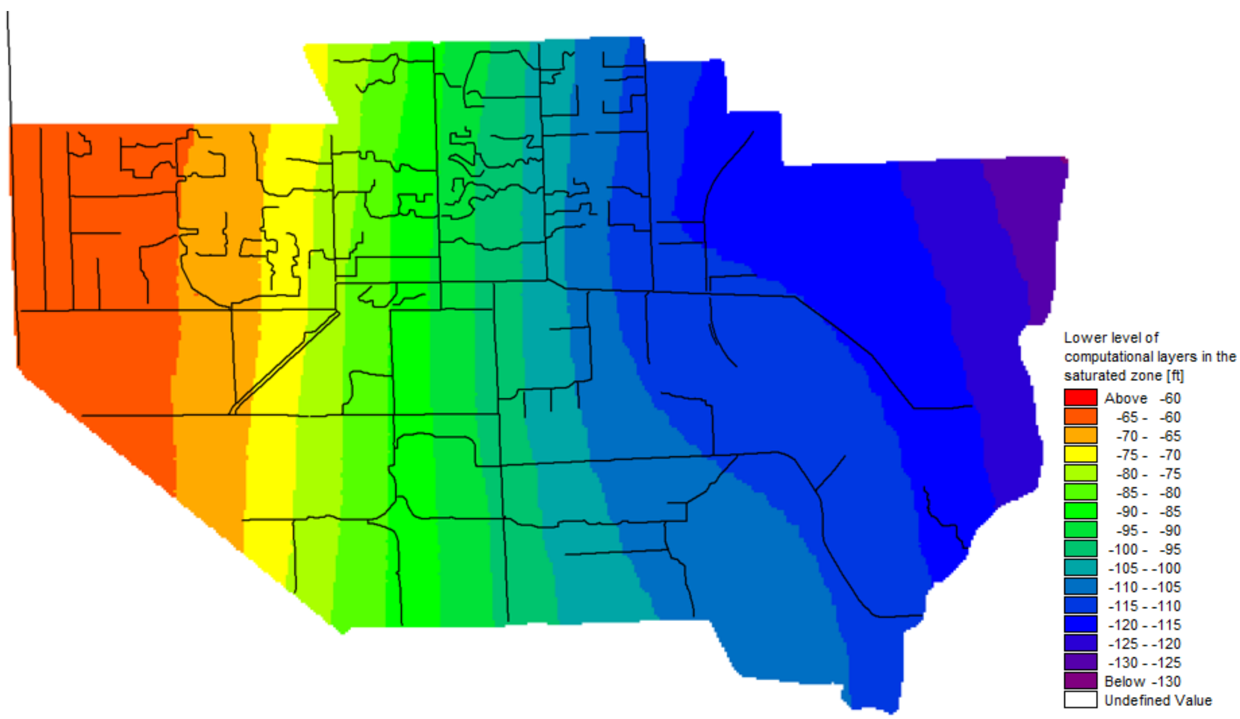

Figure 18: Lower Level of Computational Layer 3

2.9.2 Horizontal Hydraulic Conductivity

Figures 19 through **21** show the distribution of this parameter, adapted from Hughes and White (2016).

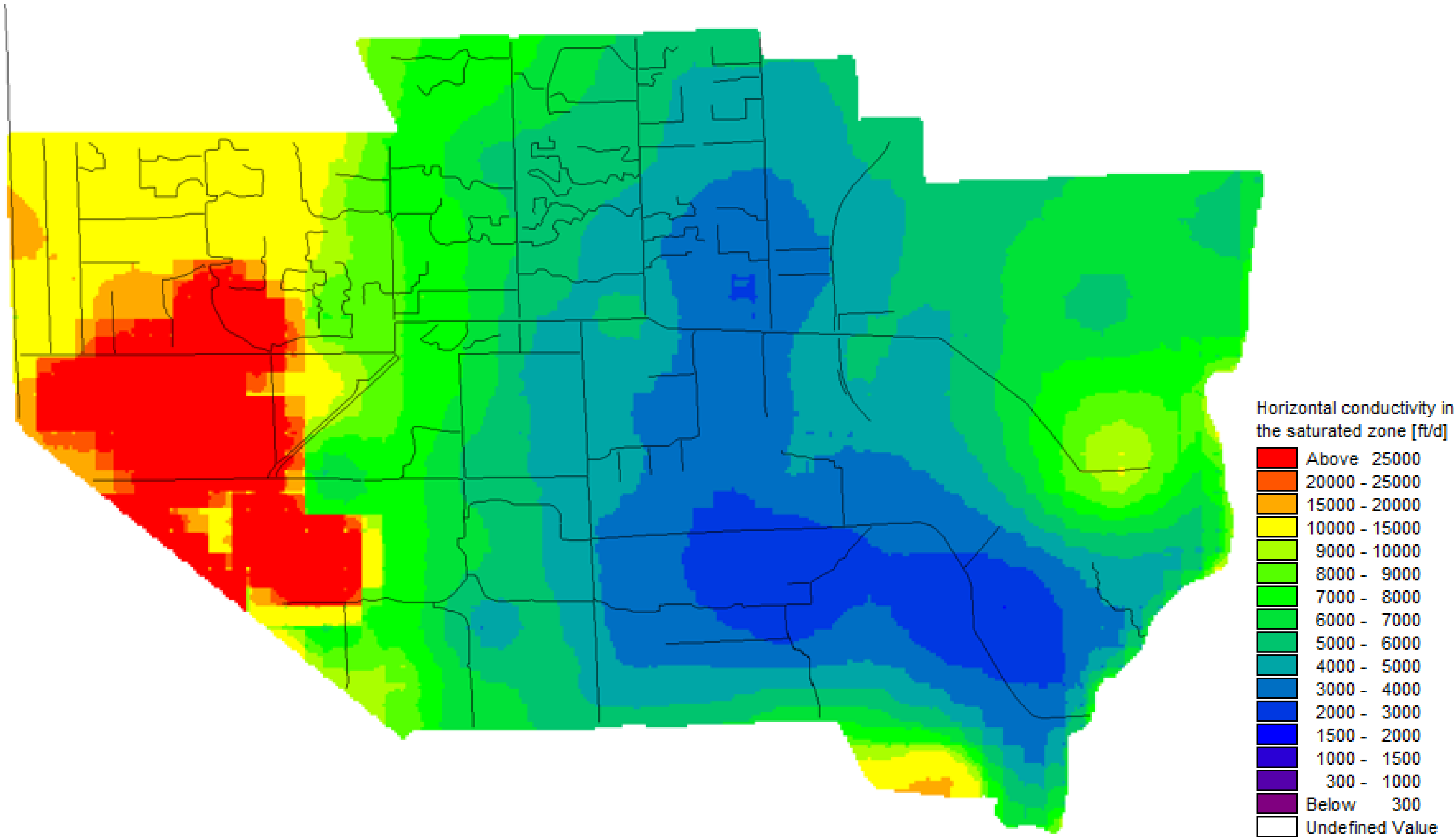

Figure 19: Horizontal Hydraulic Conductivity Layer 1

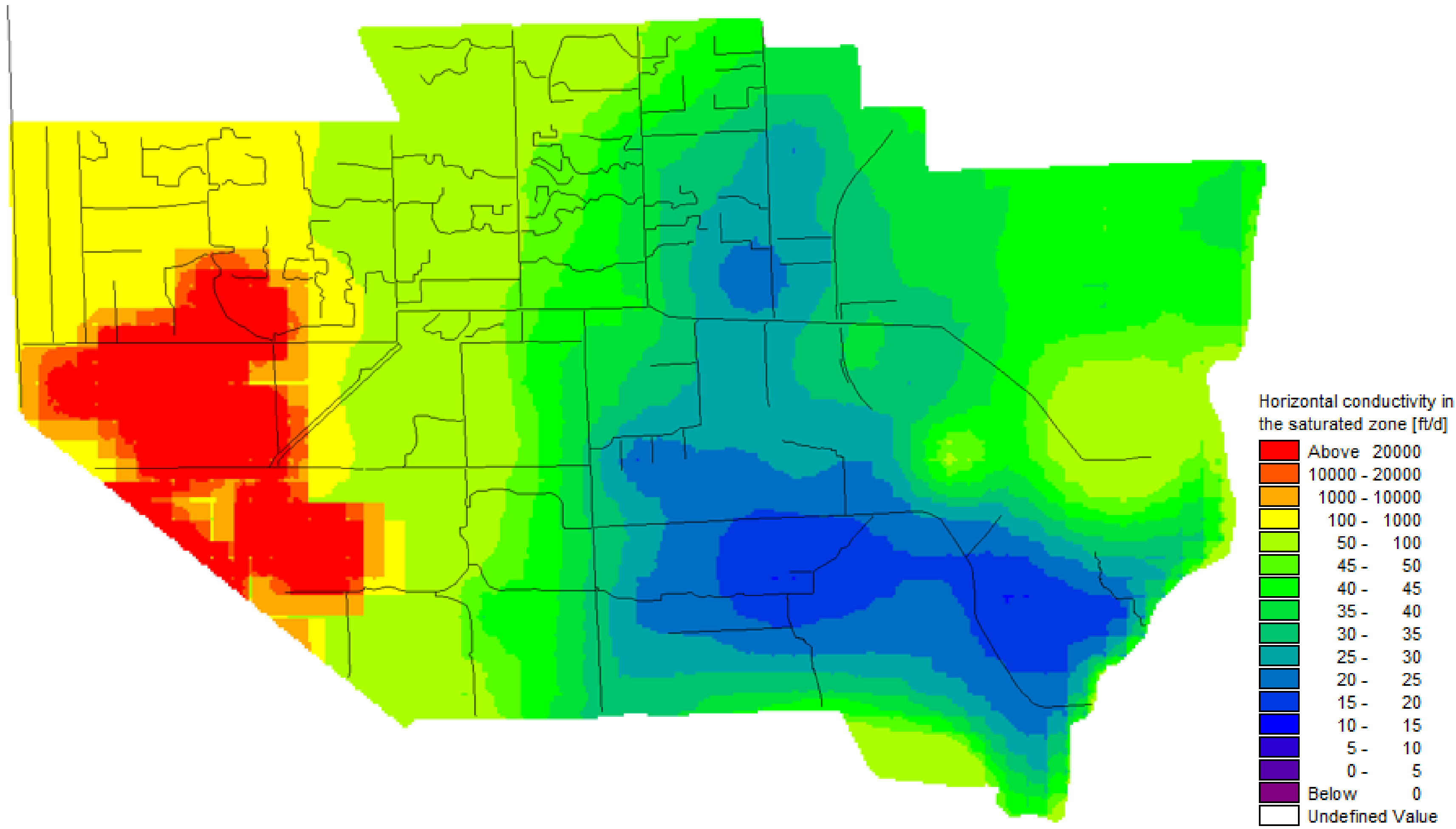

Figure 20: Horizontal Hydraulic Conductivity Layer 2

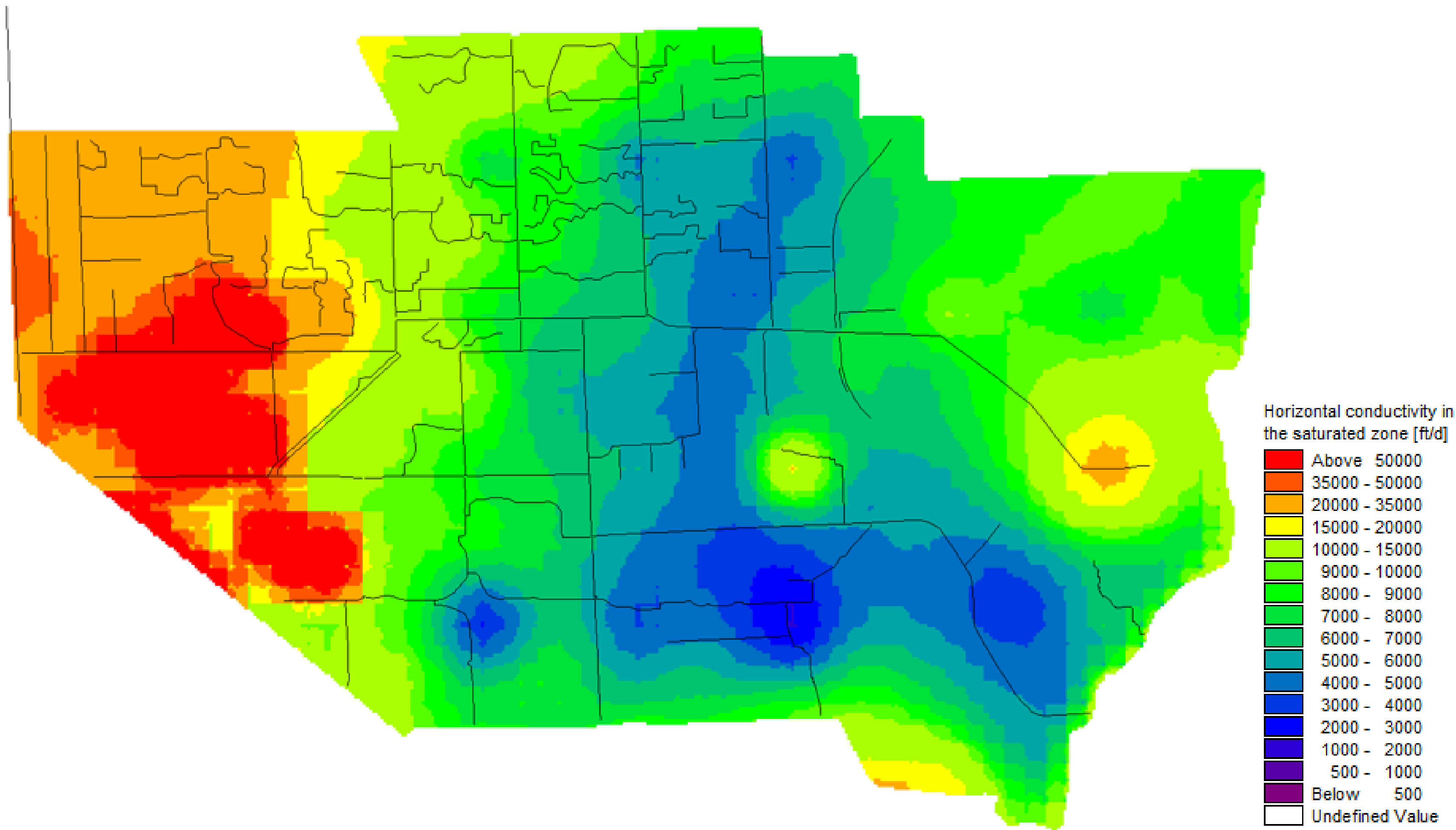

Figure 21: Horizontal Hydraulic Conductivity Layer 3

2.9.3 Vertical Hydraulic Conductivity

This parameter is also spatially distributed based on data from Hughes and White (2016). The spatial distribution and magnitude of the vertical hydraulic conductivity is identical to the horizontal hydraulic conductivity, which are shown in **Figure 19**-**Figure 21.**

2.9.4 Specific Yield

This parameter is spatially distributed based on data from Hughes and White (2016).

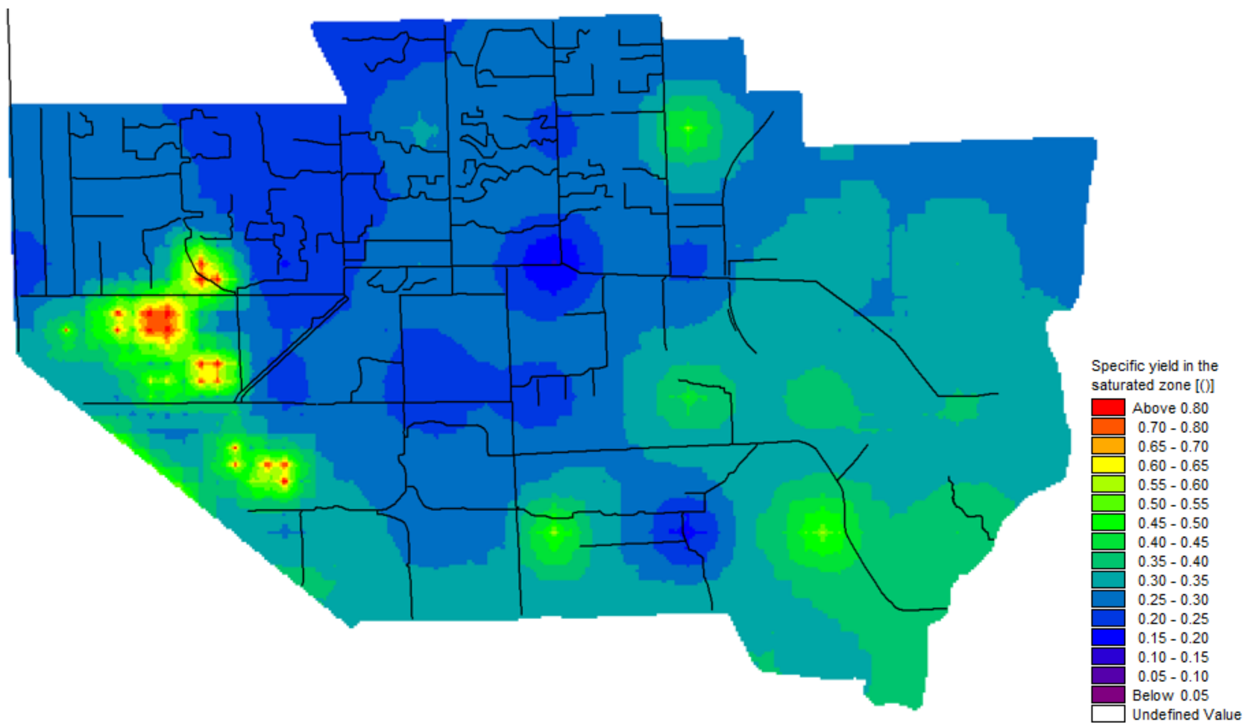

Figure 22: Specific Yield in the Saturated Zone

2.9.5 Specific Storage

This parameter is spatially distributed based on data from Hughes and White (2016).

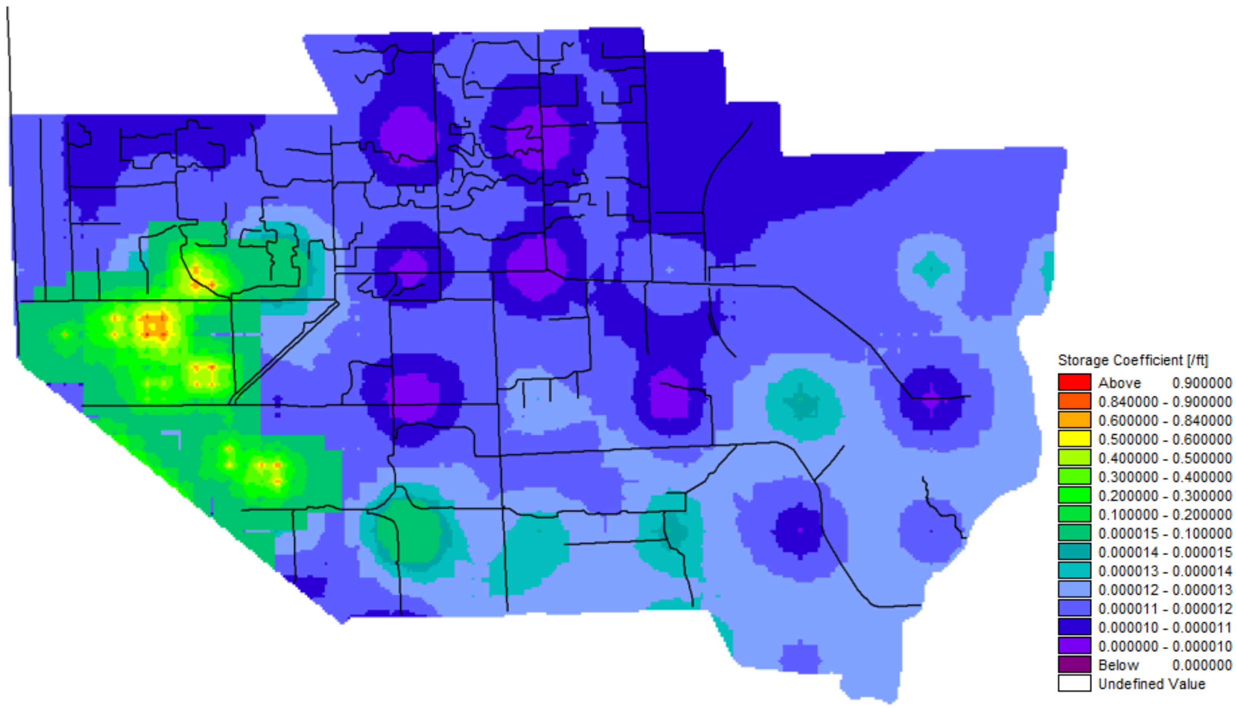

Figure 23: Specific Storage in the Saturated Zone Layer 1

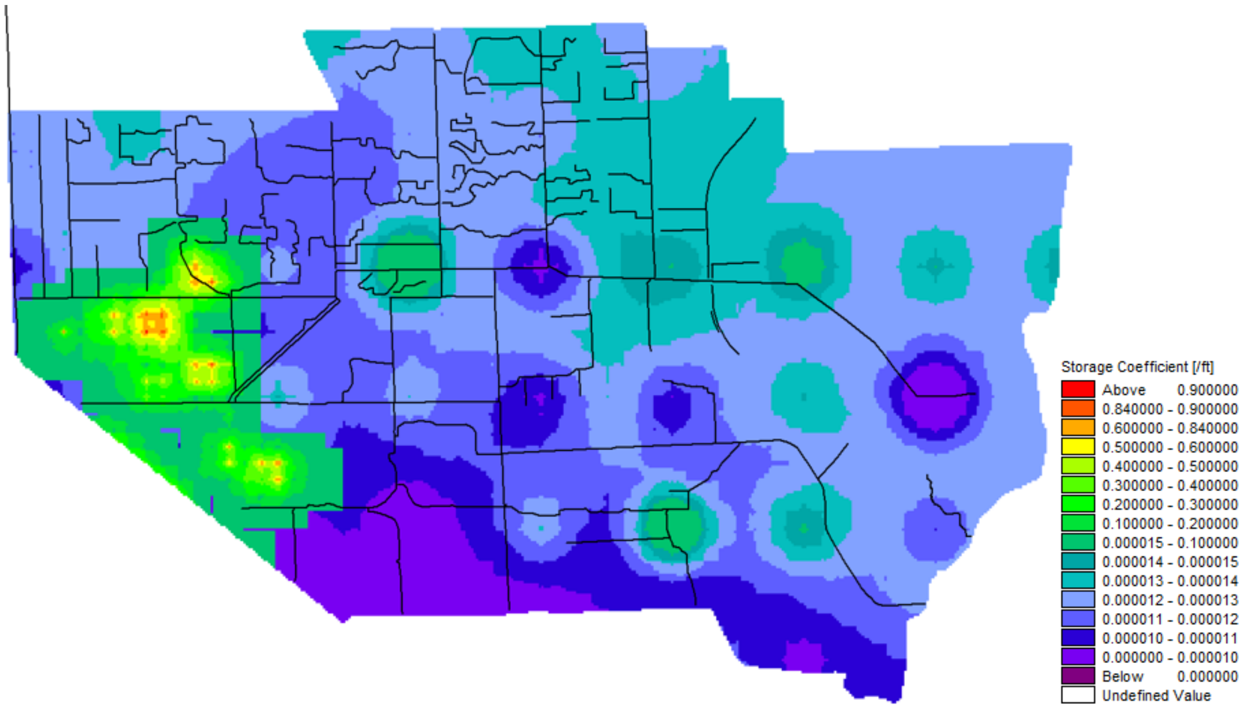

Figure 24: Specific Storage in the Saturated Zone Layer 2

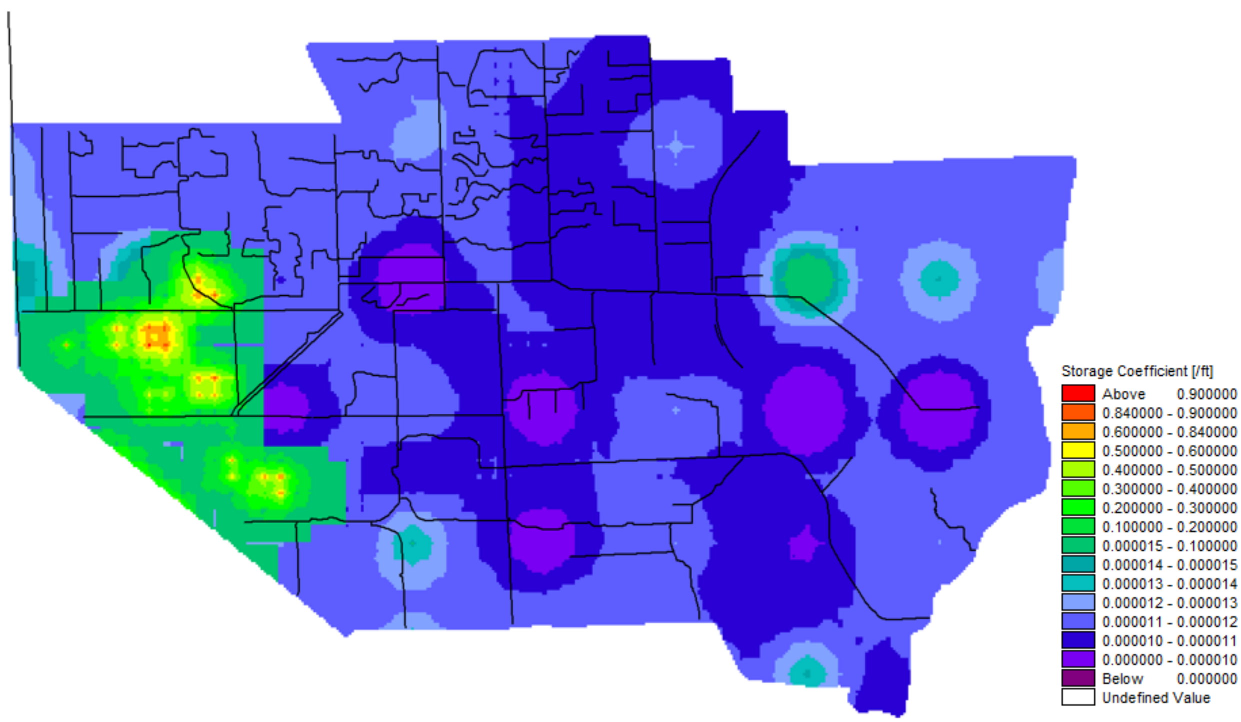

Figure 25: Specific Storage in the Saturated Zone Layer 3

2.9.6 Initial Potential Head

For the calibration model, this parameter is spatially distributed based on results from Hughes and White (2016). This is the initial configuration and is subject to change during model calibration, as groundwater elevations will be compared with observed well data (**Figure 26**).

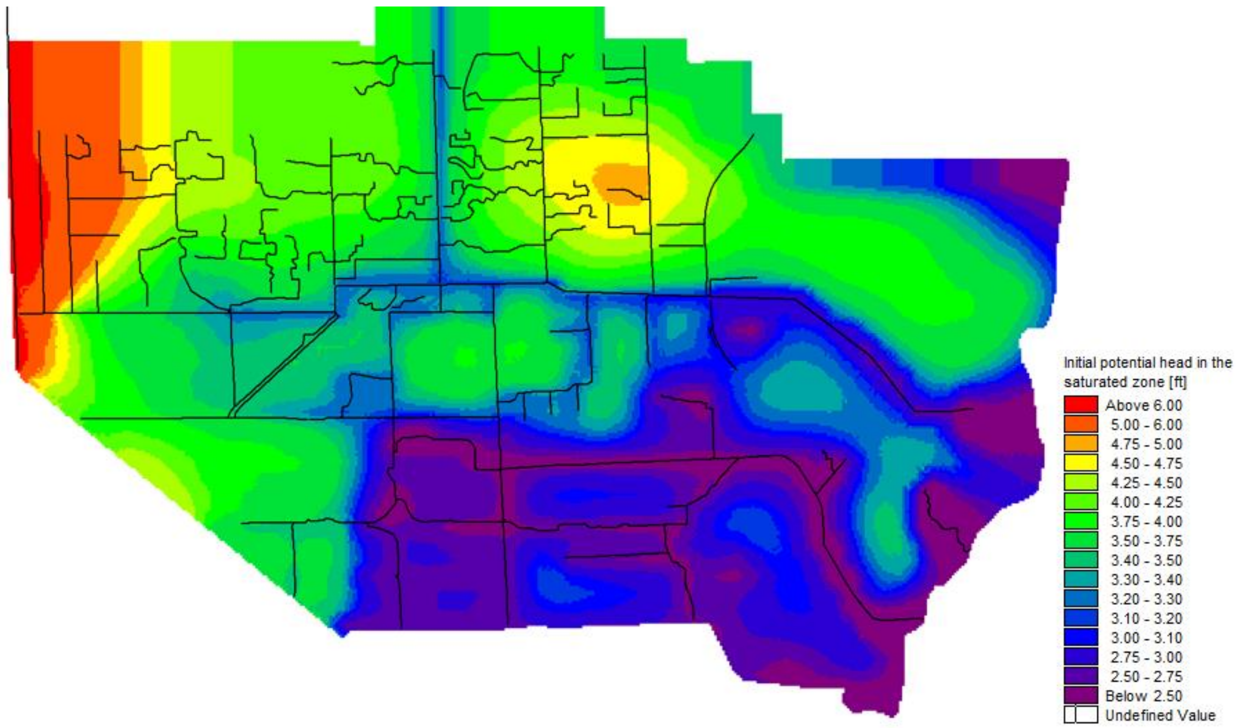

Figure 26: Initial Potential Head in Saturated Zone for October 2000

For the validation and design storm models, the initial potential head is spatially distributed based on data from Broward County's average wet season head map (used for the Broward County model), and then extended south into Miami-Dade County, based on groundwater contours from the USGS (See **Appendix C**), as demonstrated in **Figure 27**. The initial potential head map for these events can be seen in **Figure 28**.

Figure 27: Development of Initial Potential Head for Validation and Design Storm Models

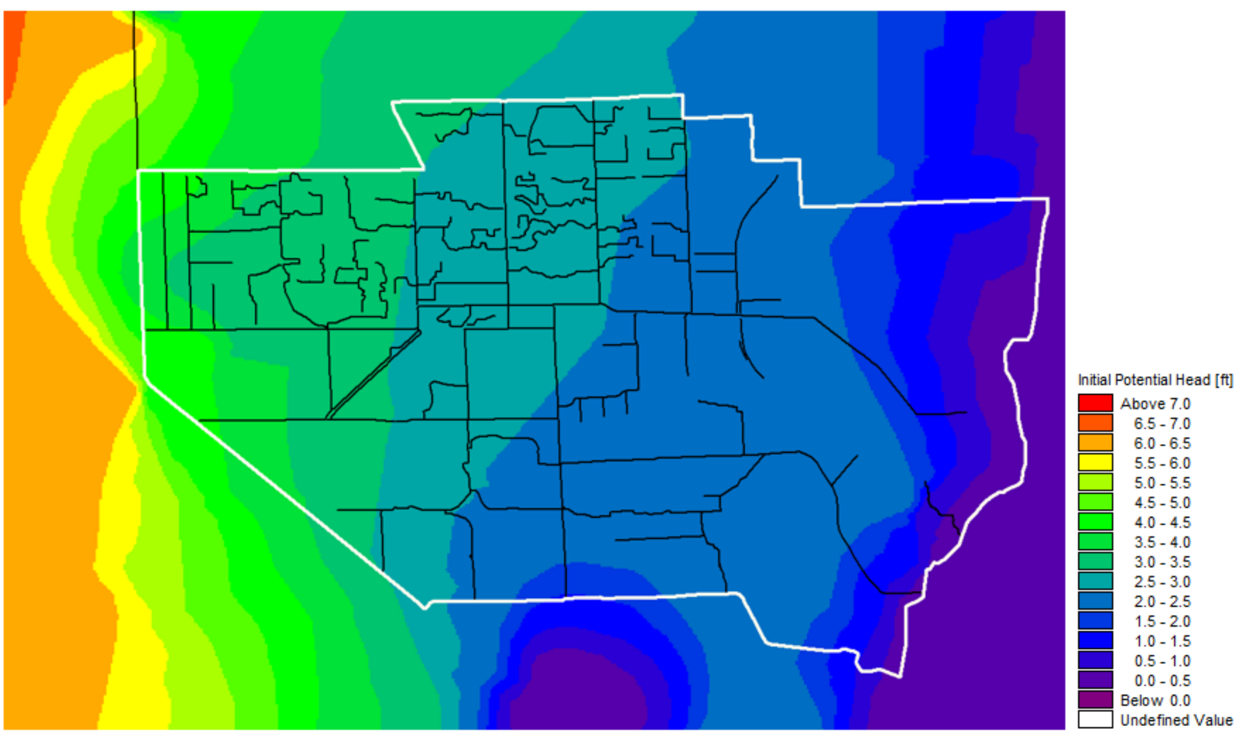

Figure 28: Initial Potential Head in Saturated Zone for June 2017

2.9.7 Boundary Conditions

Refer to the Data Availability Memorandum for boundary conditions.

2.9.8 Drainage Level

The saturated zone drainage level was developed based on land use, with urban areas set to 1.5 ft below ground, rural areas set to 2.5 ft below ground, and 0 feet (turn saturated zone drainage off) for water and undeveloped areas (**Figure 29**).

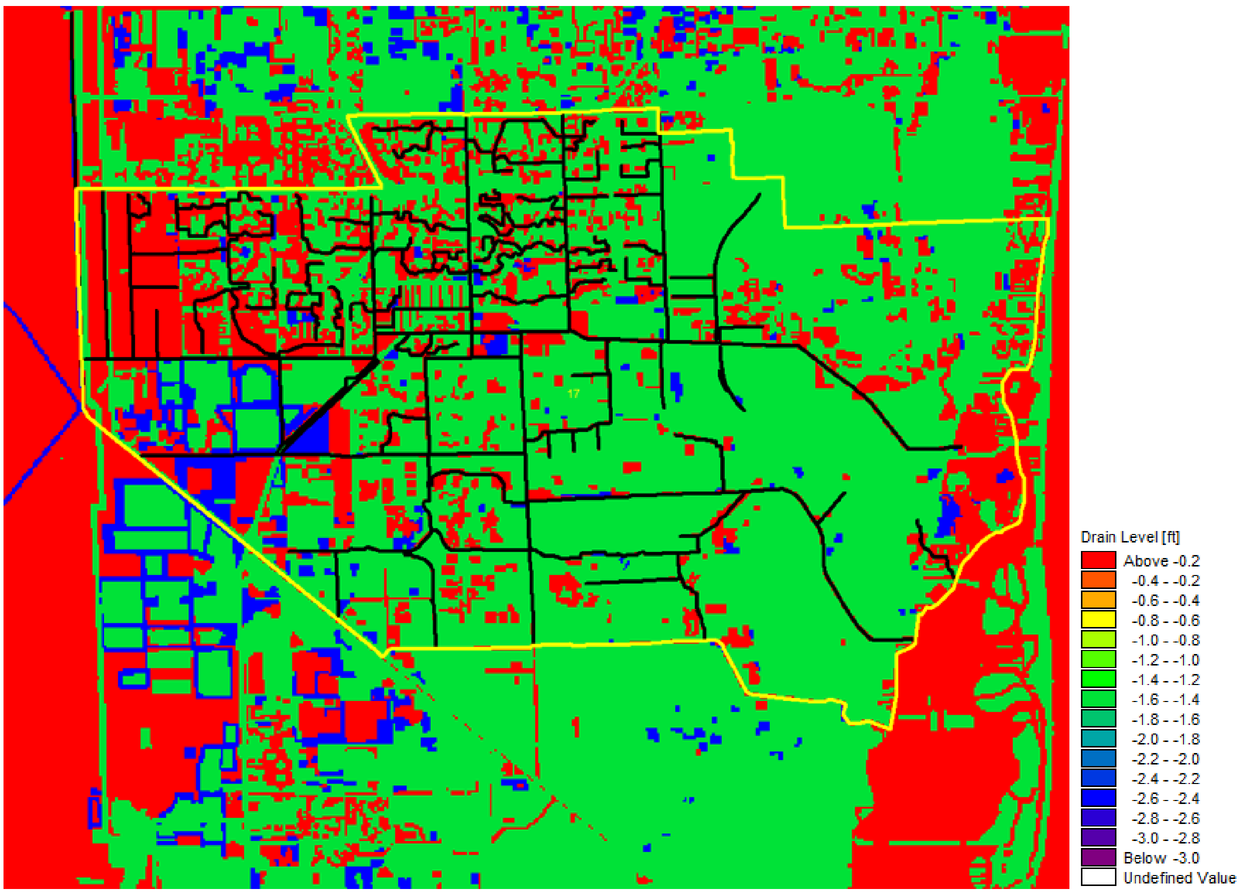

Figure 29: Drain Level in Saturated Zone

2.9.9 Drainage Time Constant

This parameter was set to the model default value of 1E-06/s and will likely be adjusted during model calibration.

2.9.10 Drainage Codes

The saturated zone drainage routine uses the same drain codes as the ponded drainage layer, without the initial depth or flood code cells set to drain code 0.

3.0 APPENDIX A

Appendix A: SFWMD - ALLOWABLE DISCHARGE FORMULAS

Canal	Allowable Runoff	Design Frequency
C-1	$Q = \left(\frac{112}{\sqrt{A}} + 31\right) A$	10 year
C-2	Essentially unlimited inflow by gravity connections southeast of Sunset Drive: 54 CSM northwest of Sunset Drive	200 year +
C-4	Essentially unlimited inflow by gravity connections east of S.W. 87th Avenue	200 year +
C-6	Essentially unlimited inflow by gravity connections east of FEC Railroad	200 year +
C-7	Essentially unlimited inflow by gravity connection	100 year +
C-8	Essentially unlimited inflow by gravity connection	200 year +
C-9	Essentially unlimited inflow by gravity connection east of Red Road; 20 CSM pumped, unlimited gravity with development limitations west of Red Road or Flamingo Blvd.	100 year +
C-10	--	200 year +
C-11	20 CSM west of 13A;40 CSM east of 13A	------------
C-12	90.6 CSM	25 year
C-13	75.9 CSM	25 year
C-14	69.2 CSM	25 year
C-15	70.0 CSM	25 year
C-16	62.6 CSM	25 year
C-17	62.7 CSM	25 year
C-18	41.6 CSM	25 year
C-19	57.8 CSM	------------
C-23	31.5 CSM	10 year

4.0 APPENDIX B

From: Kevin Hart <kevin@sbdd.org>
Sent: Wednesday, January 2, 2019 2:32 PM
To: Mark Ellard <MEllard@Geosyntec.com>
Cc: John Loper <jloper@taylorengineering.com>; Zygnerski, Michael <MZYGNERSKI@broward.org>; Maran, Carolina <CMARAN@broward.org>; Luis Ochoa <luis@sbdd.org>
Subject: RE: Broward Future 100-Year Model Follow Up - SBDD

Mark,

Attached is the latest SFWMD permit for CS12, CS13, CS13-A, ICS12, ISC13 and ISC13-A.

Basically, the permit states the following:

- CS12, CS13, CS13-A are operated to allow the canal stages downstream of the intermediate gates to fluctuate with the C-11 Canal, but no lower that Elev. 3.00' NGVD (except with prior authorization from SFWMD).
- The maximum, combined discharge rate for CS12, CS13, CS13-A is 363 cfs.
- The intermediate gates (internal gate structures) are operated to maintain the permitted control elevation of 4.0' NGVD, within the upstream areas of the S-9/S-10 Basin (upstream of the gates). These gates are only opened when the tail water exceeds Elevation 4.0' NGVD.

The B-1 and B-2 pump stations are operated on a manual basis only. These two pump stations are operated by SBDD on an as-needed basis, and as determined by staff, during extreme rainfall events. Just as an FYI, neither station has operated during the past 7 years (except for maintenance purposes). Both stations have a gravity culvert connection to SBDD's C-1 Canal. For modeling purposes, the two pumps can be activated at Elevation 4.0' NGVD with a pumping capacity of 15,000 GPM. The pumps are used to reduce peak stages and durations within the sub-basins they serve.

The Silver Lakes Flood Gate is an emergency, basin inter-connect between Basins S-9/S-10 and S-5. This gate is operated to allow SBDD to move water from the C-11 Basin to C-9 Basin on an as-needed (emergency) basis. The operation of this gate is performed in conjunction with approval and authority from SFWMD. For modeling purposes, this gate should be closed. However, under adaptation strategies/scenarios, you are welcome to incorporate the use of this gate to manage stages between the C-11 and C-9 basin as applicable. As an FYI, there have been a handful of occasions where SFWMD has asked SBDD to discharge south through the S-5 Basin in order to limit discharges to the C-11 Canal.

The Nautica/Silver Lakes culvert (ID 408) is a basin inter-connect that is operated on an as-needed, emergency basis only. For modeling purposes, this gate should be closed. However, under adaptation strategies/scenarios, you are welcome to incorporate the use of this gate to manage stages between the S-4 and S-5 basins as applicable.

You're probably aware that SBDD has 2 other basin inter-connects that are operated on an as-needed, emergency basis only as well.......... between Basins S-3 and S-2.

On the pipe inverts, we do not have any additional information at this time. For modeling purposes, we suggest that you set the pipe inverts such that the top of pipe matches the Control Water Elevation (CWE), as that is SBDD's standard practice.

Let me know if you need any additional information.

Thanks.

Kevin Hart, P.E., CFM
District Director
South Broward Drainage District
6591 Southwest 160th Avenue
Southwest Ranches, FL 33331
954-680-3337 (office)
e-mail: kevin@sbdd.org

5.0 APPENDIX C

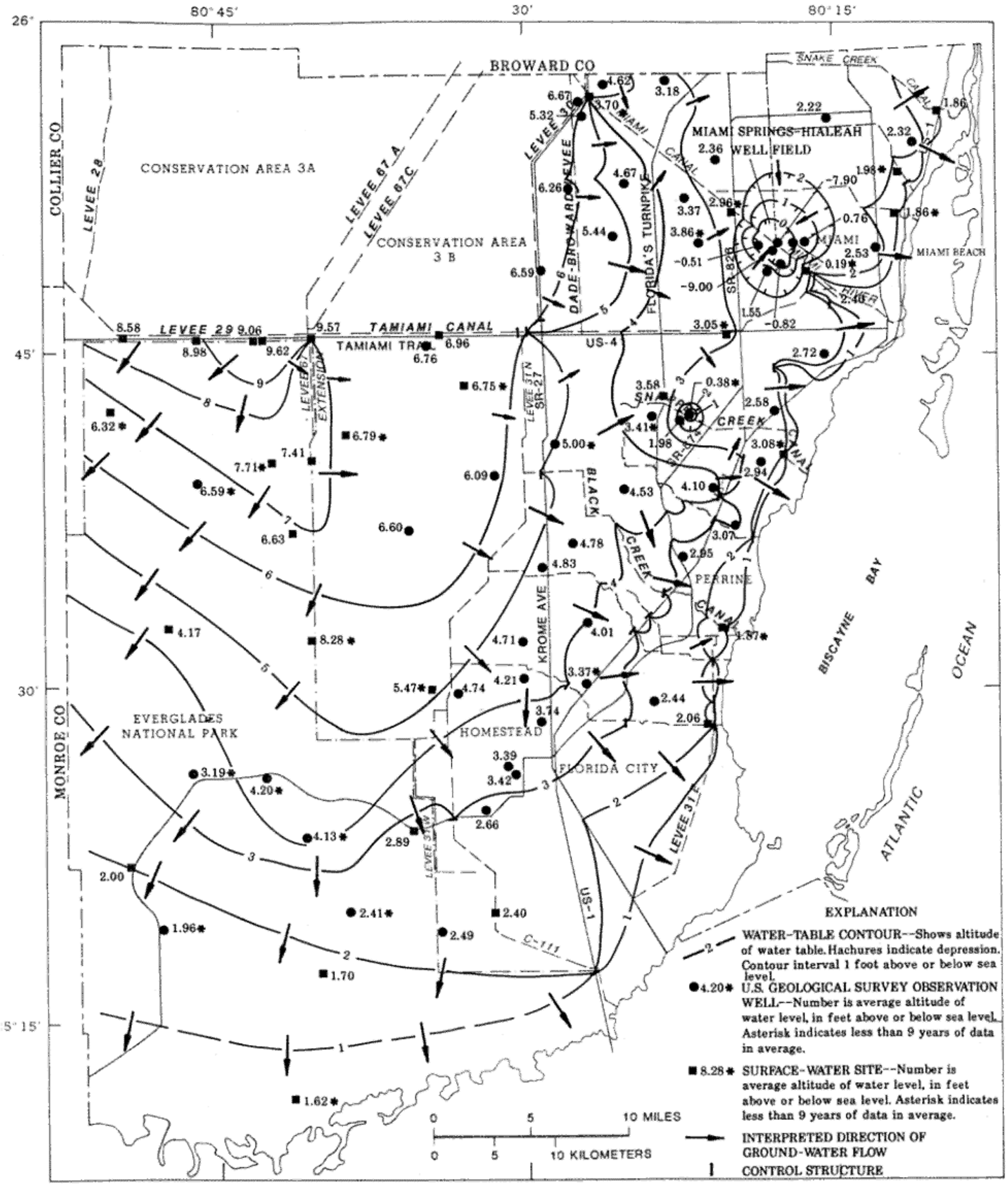

DRAFT Technical Memorandum

To: **CSA Central, Inc. and SFWMD**

From: **Taylor Engineering**

Date: **1/21/2020 REVISED 3/26/2020**

Re: **Model Calibration and Validation for SFWMD C8-C9 FPLOS Study**

1.0 DATA AVAILABILITY AND REVIEW

1.1 Introduction

This section details the data that was used to develop the SFWMD C-8 & C-9 MIKE SHE and MIKE HYDRO models for use in the C8-C9 FPLOS Study. Specifically, this section details the availability of topography, land use, culvert, gate, bridge, pump, and cross section data, survey requirements, calibration and validation simulation periods, the availability of groundwater data, the availability of district stage, flow, and gate operations, design storm rainfall, and initial groundwater levels for design storms. Please note that the model domain and hydraulic network shown in the figures in **Section 1.0** were initial renderings and have been updated, as shown in later sections.

1.2 Topography

The topography for this project was made by merging the Miami-Dade County 5ft DEM (2015 Miami-Dade County DEM 5ft, 2017) with the 5-ft composite DEM of Broward County that was created by Geosyntec Consultants (2018). Geosyntec Consultants developed the 5-ft composite DEM using the following sources and collection (flight) dates:

- Broward County DEM – 2007 – 5’ cell size source – base source
- Palm Beach County DEM – 2006 – 10’ cell size source – north area extension
- Miami Dade County DEM – 2015 – 5’ cell size source – south area extension
- Ft. Lauderdale City Limits DEM – 2016 – 5’ cell size source – new areas in east
- Ft. Lauderdale FDOT – 2017 – 0.5’ cell size source – new areas in southeast
- SFWMD 50’ cell size source – west area extension

To minimize/eliminate seams in the overland flow module, the DEMs were merged along the C-9 canal and through the levees in the water conservation area to the west, as shown in **Figure 1.** The DEM was filtered between 0-25 ft NAVD88 for visual clarity (200+ ft elevation landfill causes color palette distortion).

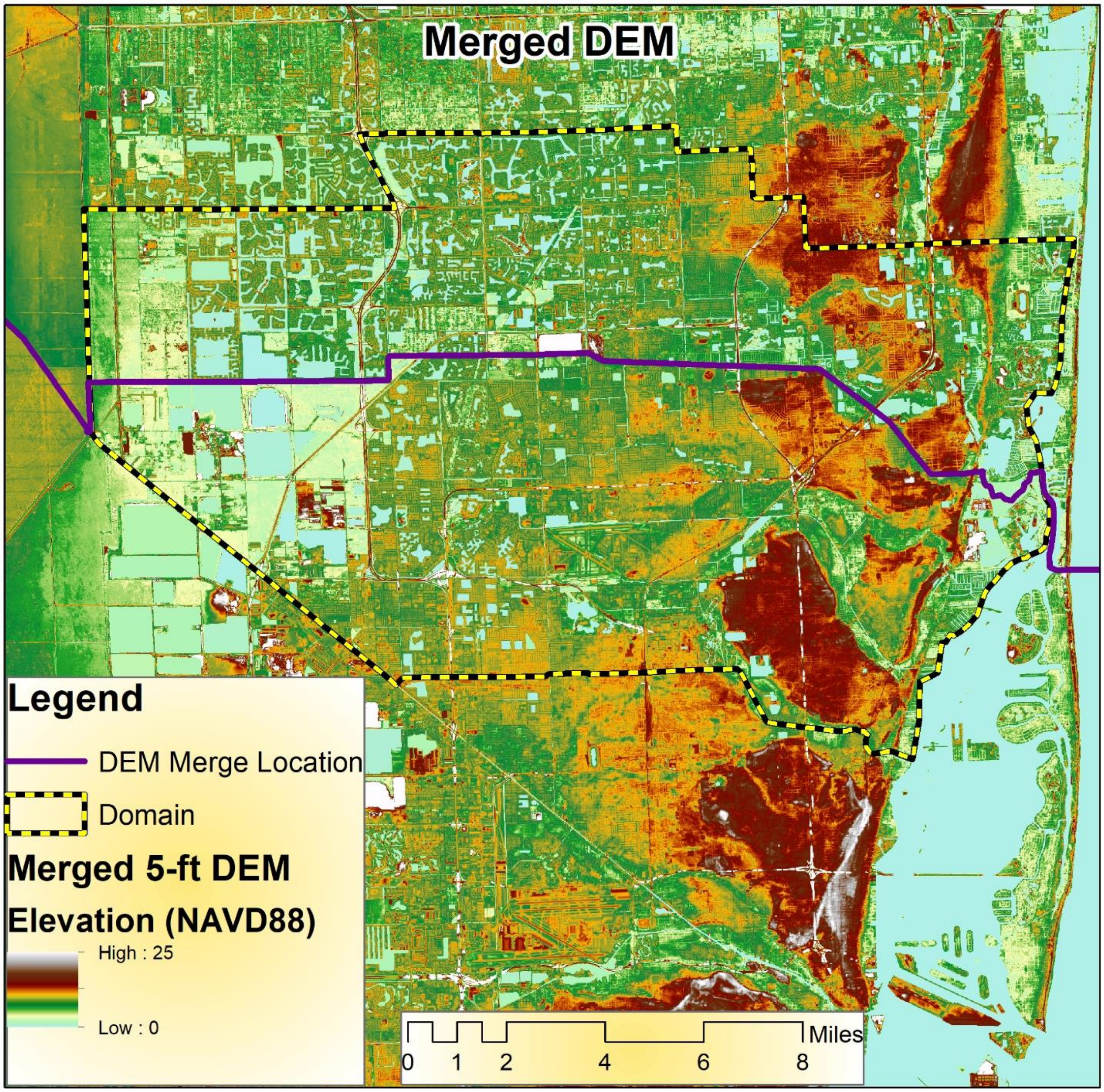

Figure 1: Merged 5-ft DEM

1.3 Land Use

The land use data for this project is based on the SFWMD 2014-2016 Land Use dataset. Preliminary comparisons with aerial imagery from 1999 to 2019 show little to no significant changes in land use, such as segments of open land being developed into high density residential areas. Land use change resulting in areas such as commercial and services to high density residential is not considered a significant change in terms of the runoff potential. To confirm this observation, a spatial comparison was made in GIS using the SFWMD 1999 and the 2014-2016 land use shapefiles. Less than 2% of the total model area was identified as having a significant land use change during this period of time. Because these land use changes have occurred after the Broward County stormwater ordinance of the 1980s, there should be no impact to the flood protection level of service. The relatively unchanged land use over the past 20 years or so is an important consideration in evaluating potential historical storm events for calibration and validation, as discussed in **Section 1.6**.

1.4 MIKE HYDRO River 1D Model

The MIKE HYDRO 1D model was developed from several sources with emphasis placed on gates, pumps, culverts, bridges, and cross sections. The available data comes from the following sources:

- Broward County: Updated 2019 MIKE SHE & MIKE HYDRO models, Ref: Current Conditions Model Update and Validation Draft Report (Taylor Engineering, 2019), & 5-ft DEM
- Stoner & Associates Inc: Survey (completed for Broward County Future Floodplain Modeling and Mapping project)
- South Broward Drainage District: GIS database & 2013 Facilities Report and Water Control Plan
- SFWMD: Structure Books (OCC, 2018) (S28, 2019) (S29, 2019) (MD North Central Basin Atlas v3, 2016) for operable structure dimensions, elevations, and operating criteria. DBHYDRO for water levels, discharges, and structure operations.
- Miami-Dade County: C-8 and C-9 XP SWMM Models, 5-ft DEM, & GIS Database:
    - Pipes: https://gis-mdc.opendata.arcgis.com/datasets/stormwater-line
    - Points (canal cross sections, structures, etc.): https://gis-mdc.opendata.arcgis.com/datasets/stormwater-point
    - Water bodies: https://gis-mdc.opendata.arcgis.com/datasets/water-p

Upon initial investigation, it was noticed that there were some 1D model components such as culverts and cross sections that had available data from multiple sources. In instances where this occurs and the details differ (such as different culvert diameters), the data will be used in the following order of priority: (1) survey, (2) Broward County 2019 MIKE HYDRO model, (3) reports & documentation, (4) GIS databases, and (5) Miami-Dade C8 and C-9 XP SWMM models. The order of priority was determined based on the freshness of the data and our confidence/exposure with the data/sources. Survey has the highest level of confidence as it has recently been completed or will be completed in the near future and should capture any changes to infrastructure that may not have yet been included other data sets. The 2019 Broward County MIKE HYDRO model has the second highest level of confidence as the data that went into it was analyzed and refined over the last several months, and Taylor Engineering is very familiar with the areas that have up-to-date data and the areas that are questionable. Reports and documentation have the third highest level of confidence as they were used to build parts of the 2019 Broward County MIKE HYDRO model. The Miami-Dade GIS databases are assigned the fourth highest level of confidence as Taylor Engineering hasn't yet had the opportunity to see how well the data lines up with other confirmed sources. The Miami-Dade XP SWMM models that Taylor Engineering currently has access to have the lowest level of confidence as they are older versions and there are several areas that do not match what is in the Miami-Dade GIS databases. Taylor Engineering assumes that the discrepancies between the Miami-Dade GIS databases and the C-8 and C-9 XP SWMM models that we have access to are due to changes in infrastructure that have been updated in the GIS databases; therefore, the GIS database has higher priority than the XP SWMM models for instances of data differences.

Figure 2 shows the location of the available 1-D model data. It should be noted that some of the data items shown are not complete; for example, culverts included in the Miami-Dade GIS databases that are missing inverts, dimensions, or both; bridges missing low chord elevations, etc. These and other data gaps were assessed and included in the survey scope of work described in **Section 1.5**.

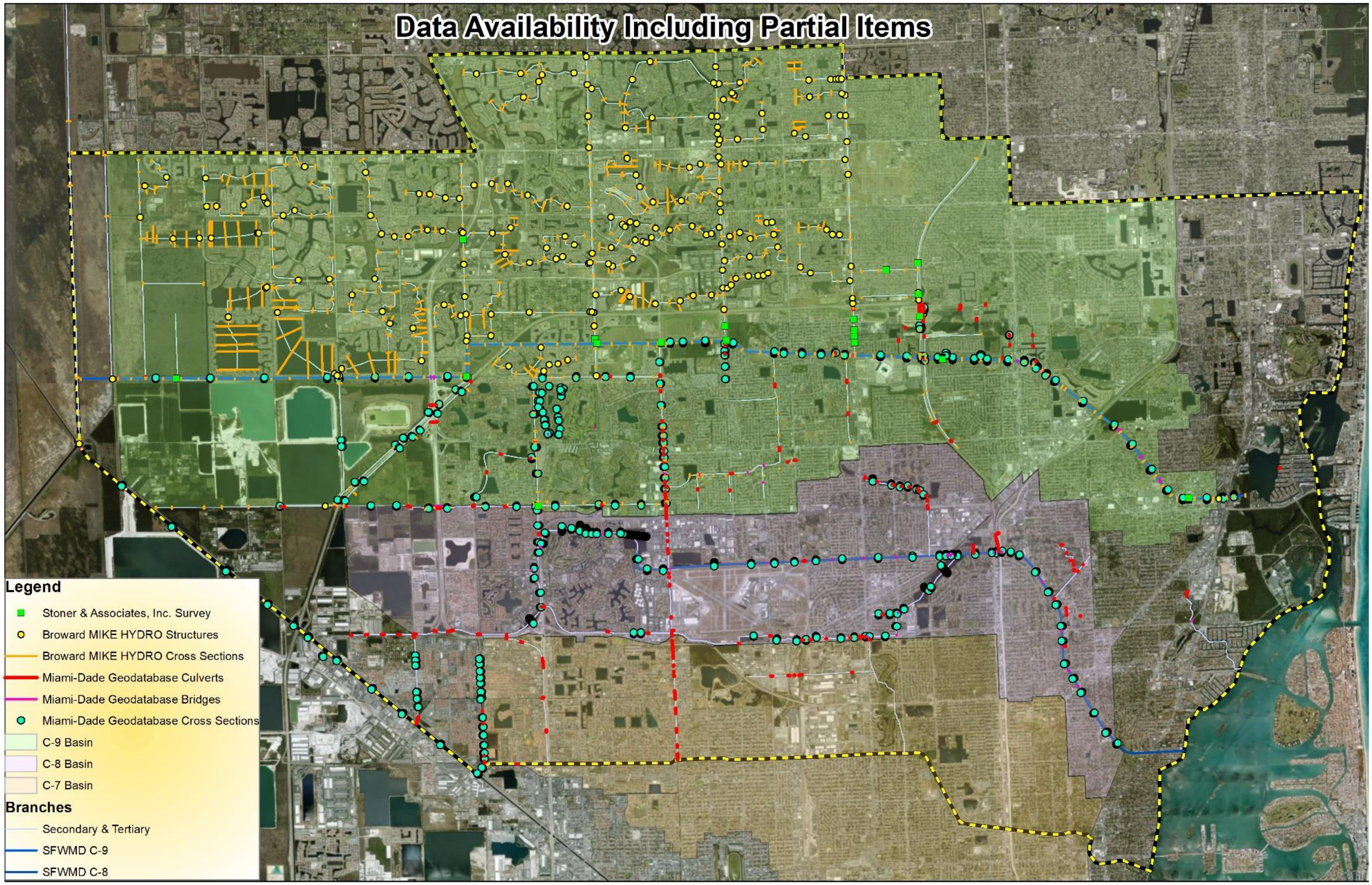

Figure 2: Map of the Available Data

For calibration and validation, structure operations were recorded operations from DBHYDRO where available, and operational criteria were used where recorded observations were unavailable. For design storms, the operational criteria for District structures come from the District's structure books. The operational criteria for Broward County and South Broward Drainage District structures come from the 2019 Broward County Current Conditions model, which has operating criteria that is both inherited from the 2014 FEMA model and verified/updated based on stakeholder data and documents (such as the SBDD Facilities Report, 2013). Any major Miami-Dade structures operating criteria would need to be provided by Miami-Dade; however there are currently no known Miami-Dade operated structures in the model. Structure flow rating parameters are used where applicable, which come from the various flow rating analysis reports (2011-2019) and Atlas of Flow Computation (2015) that were provided by the SFWMD.

1.5 Field Survey

The available data is quite extensive, however, there are several areas lacking detail. The following figure shows the location of the initial items identified for new field survey (with updated model domain). These items included 30 culverts, 23 cross sections, and 21 bridges (3 of which are lower priority). The survey scope was subject to change, and one culvert was omitted as it could not be found; it likely did not exist. Some items in the survey request had partial data available, such as culvert diameter or elevation of channel bottom under bridge but were missing information such as culvert inverts or low chord elevation of bridge.

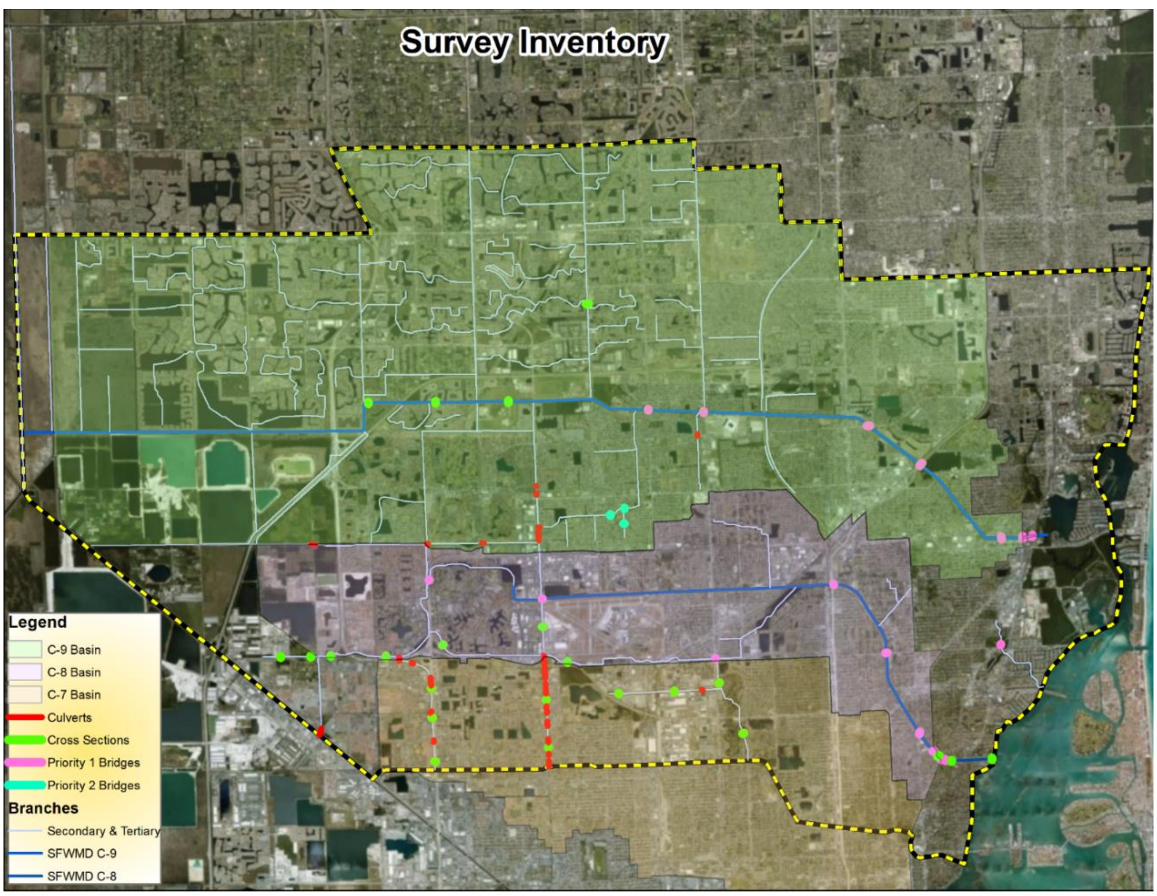

Figure 3: Inventory of Field Surveyed Items

1.6 Storm Events Selection

Average daily discharge data for the S-28 and S-29 outfall structures (C-8 and C-9 basins, respectively) were analyzed to identify the largest storm events since 1999. Then, instantaneous stage and discharge data were analyzed to identify the events that produced the largest headwater and tailwater elevation and discharge rate. Preference was given to storm events producing strong responses in both watersheds. The selection was narrowed to the storms during the following dates:

- Hurricane Irene (October 14-16, 1999)
- Subtropical Depression Leslie (October 2-4, 2000)
- Hurricane Gabrielle (September 13-15, 2001)
- Unnamed Storm June 6-7, 2017
- Hurricane Irma (September 9-10, 2017)

Subtropical Depression Leslie, which later became Tropical Storm Leslie, was chosen as the calibration event and Hurricane Irma as the validation event. Subtropical Depression Leslie resulted in the largest discharge response at both the C-8 and C-9 outfall structures in the past 20 years, as well as some of the highest canal water elevations. Hurricane Irma produced large discharge responses at both outfall structures and had a storm surge which resulted in the highest water elevations. The following figures compare the discharge, headwater elevation, and tailwater elevation at the C-8 and C-9 outfall structures.

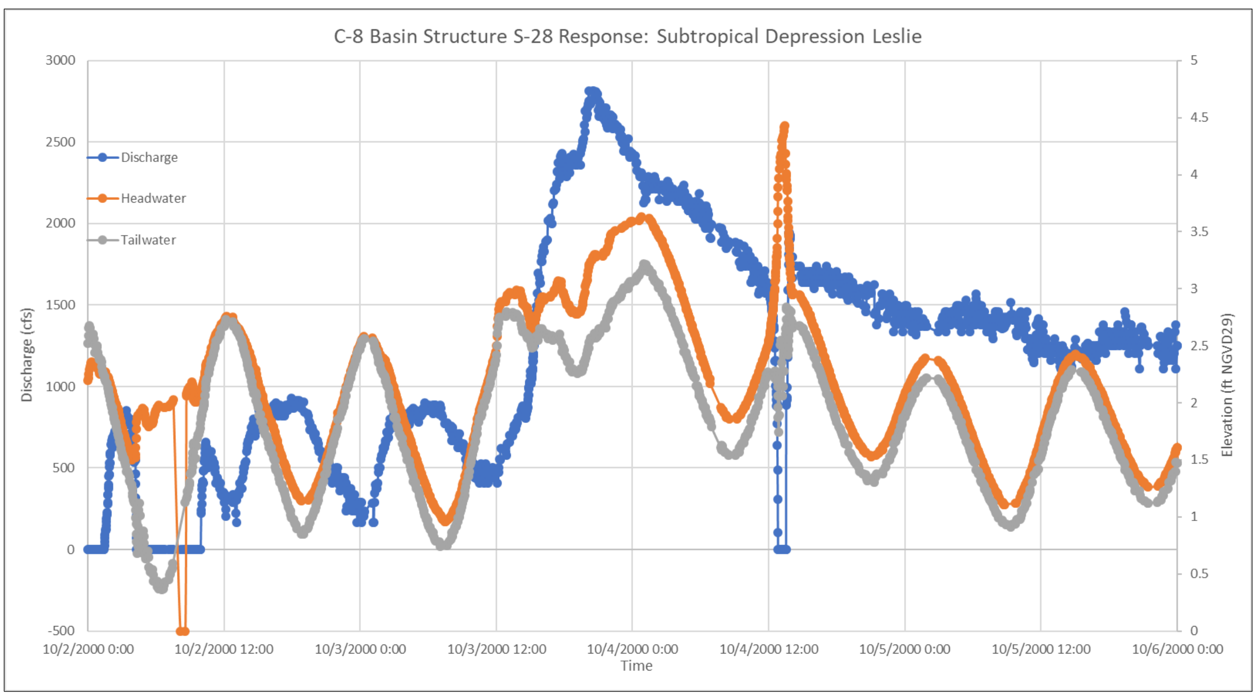

Figure 4: C-8 Basin Structure S-28 Response to Subtropical Depression Leslie

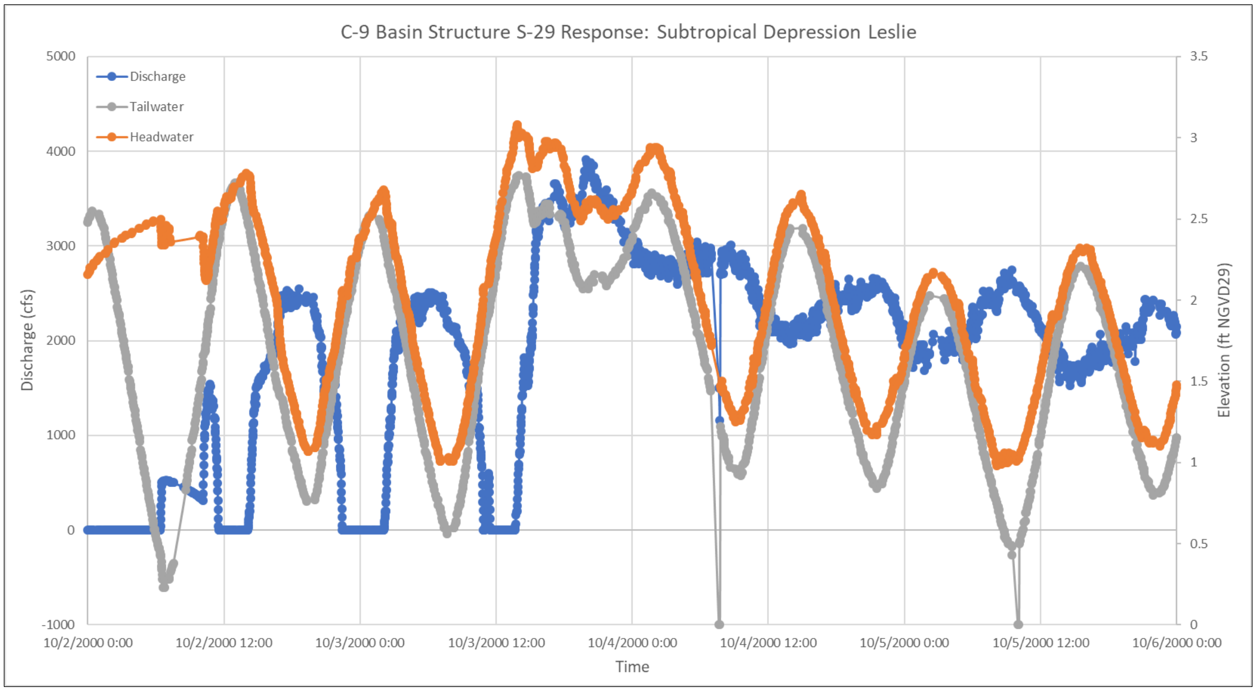

Figure 5: C-9 Basin Structure S-29 Response to Subtropical Depression Leslie

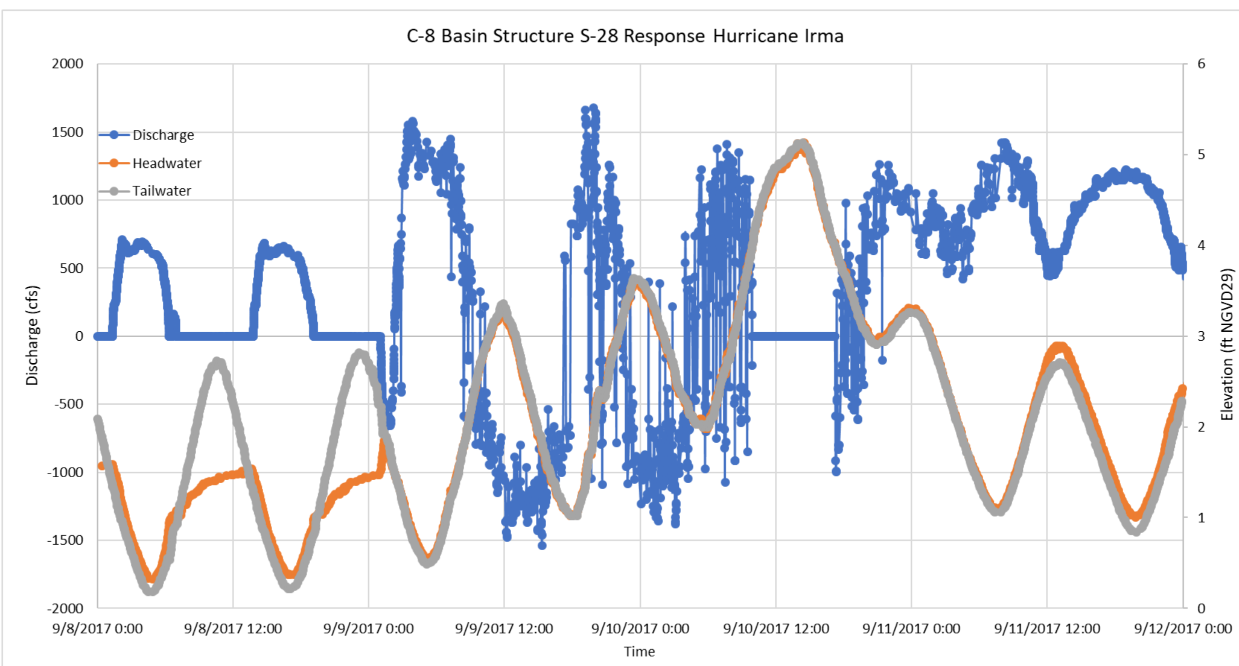

Figure 6: C-8 Basin Structure S-28 Response to Hurricane Irma

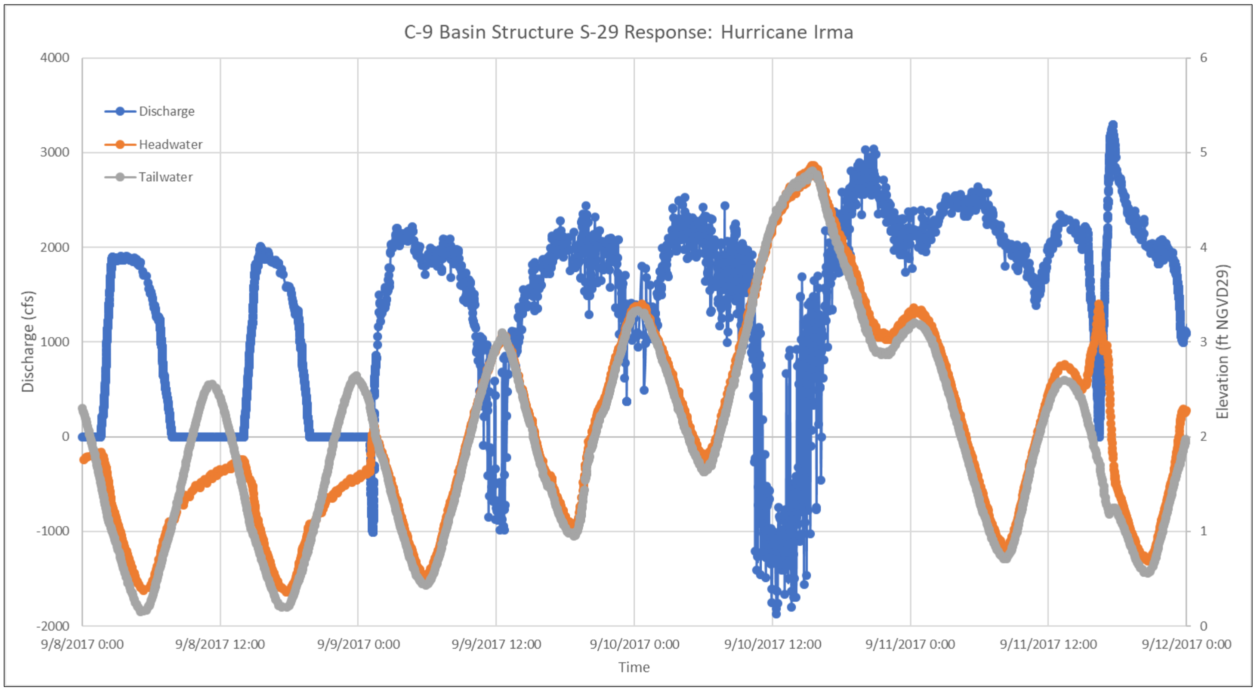

Figure 7: C-9 Basin Structure S-29 Response to Hurricane Irma

Available rainfall data for Subtropical Storm Leslie was called into question as NEXRAD data in the early 2000s was less accurate than it is today. Therefore, rain gauge data (DBHYDRO) was compared to the NEXRAD data for the pixel(s) that they were in or bordered against. This exercise suggested that the NEXRAD data and gauge data are similar in terms of total rainfall, however, there are some differences as far as the timing of the rainfall. The following figures show different comparisons relating to NEXRAD rainfall, gauge rainfall, and structure discharge.

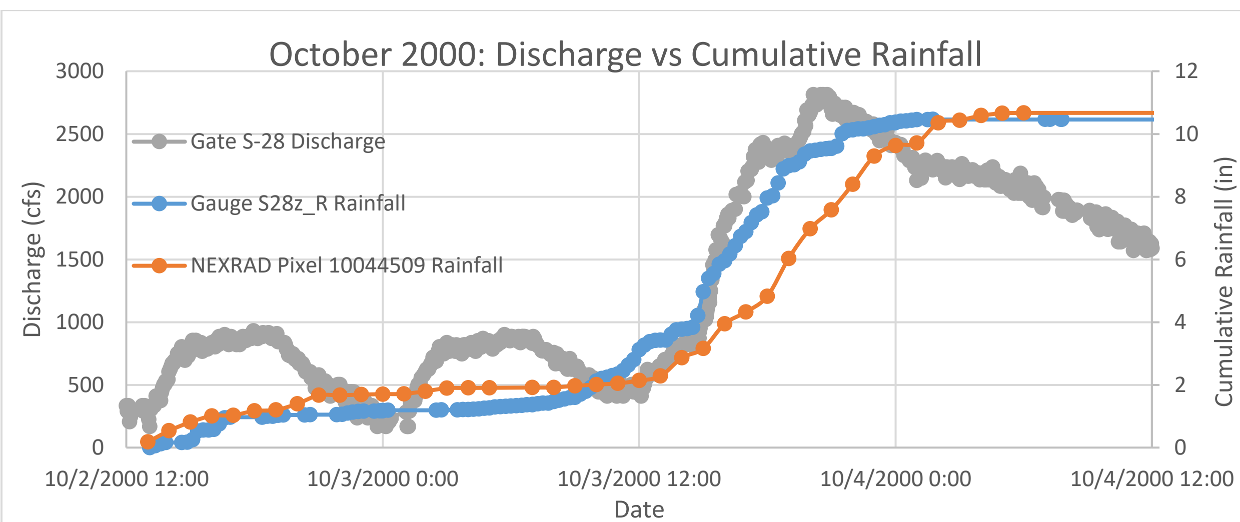

Figure 8: Discharge vs Cumulative Rainfall for Gate S-28 (NEXRAD Pixel and Rain Gauge Located Centrally in C-8 Basin)

The cumulative rainfall totals for the rain gauge and the associated NEXRAD pixel are only off by about 0.2 inches, which is about 2%. This is a negligible amount and well within the accuracy of either measurement method. More concerning is the temporal shift in the rainfall, which is about 3-hours. Comparing the timing of rainfall to the discharge, it is believed that the rainfall gauges are more accurate. Simply put, the NEXRAD data shows a rainfall response after the runoff response, which goes against rainfall-runoff principles. The following figure compares the same rainfall but plotted as rainfall intensity.

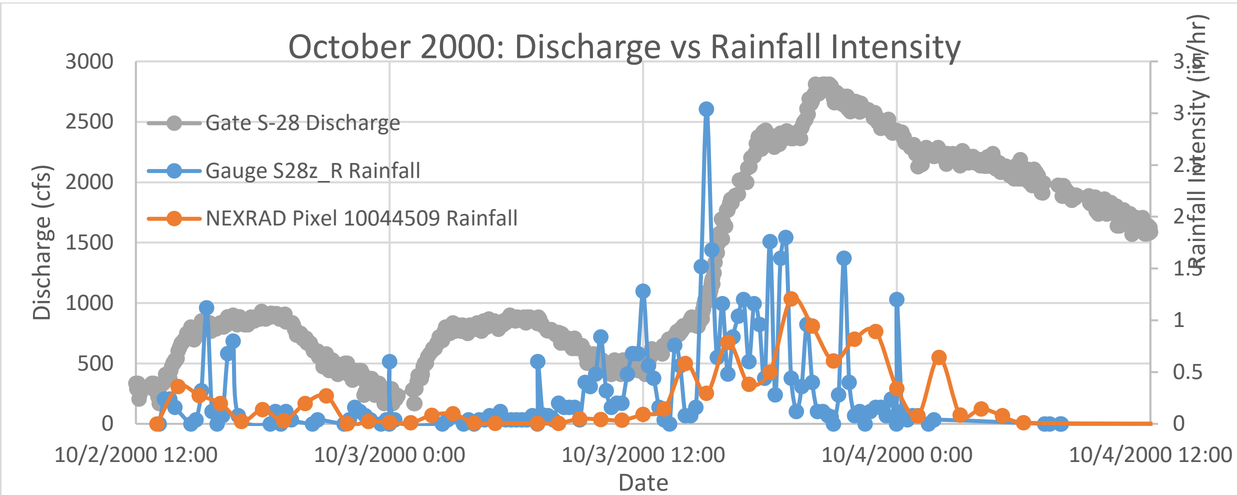

Figure 9: Discharge vs Rainfall Intensity for Gate S-28 (NEXRAD Pixel and Rain Gauge Located Centrally in C-8 Basin)

This figure shows there is a large difference in rainfall intensity when comparing the rain gauge to the NEXRAD data. The rain gauge data was recorded in 15-minute intervals whereas the NEXRAD data was recorded in hourly intervals. Therefore, the NEXRAD data was unable to capture the high intensity short duration part of the storm. It is possible that this could have some effect on calibration efforts. The following figure compares the rain gauge located centrally in the C-9 basin with NEXRAD data for the two pixels it borders.

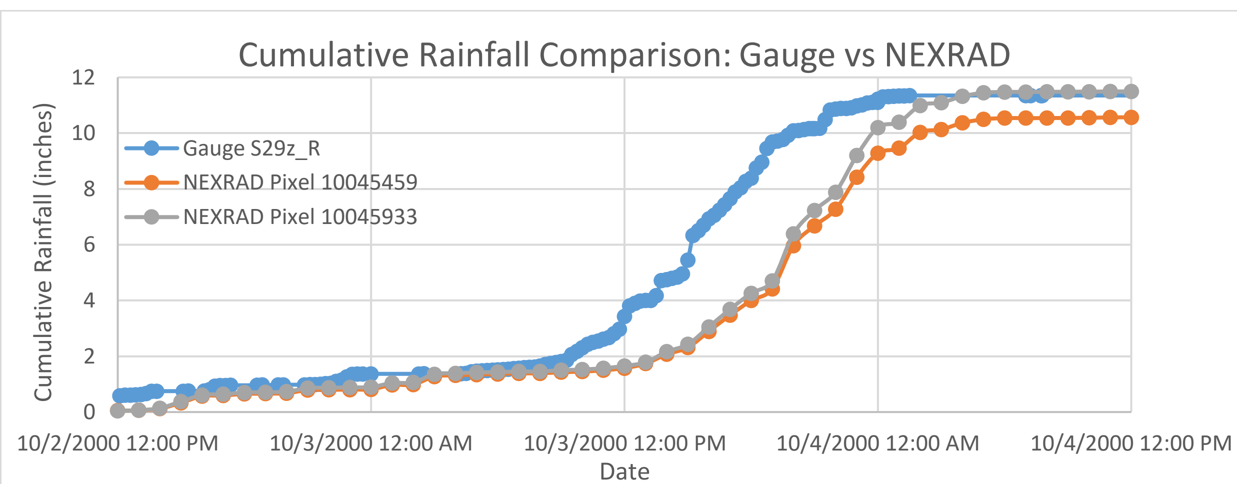

Figure 10:Cumulative Gauge Rainfall vs Cumulative NEXRAD Rainfall (NEXRAD Pixel and Rain Gauge Located Centrally in C-9 Basin)

The cumulative rainfall totals are fairly close, with NEXRAD data being between 0.2 and 0.7 inches different, or about 2-6%. Again, there is a temporal lag of about 4 hours. The following figure compares the rain gauge located in the western part of the C-9 Basin with NEXRAD data.

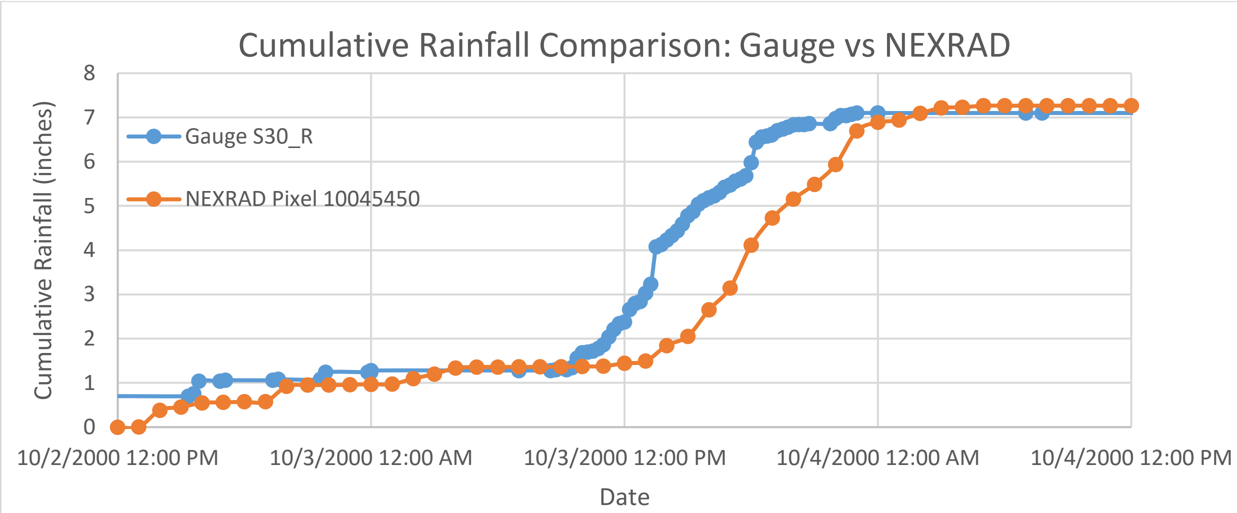

Figure 11:Cumulative Gauge Rainfall vs Cumulative NEXRAD Rainfall (NEXRAD Pixel and Rain Gauge Located in Western C-9 Basin)

The cumulative rainfall totals are within 0.2 inches apart which is about 2%. Again, there is a temporal lag of about 4 hours. The following figure compares the rain gauge located at the tidal outfall of the C-7 Basin with NEXRAD data.

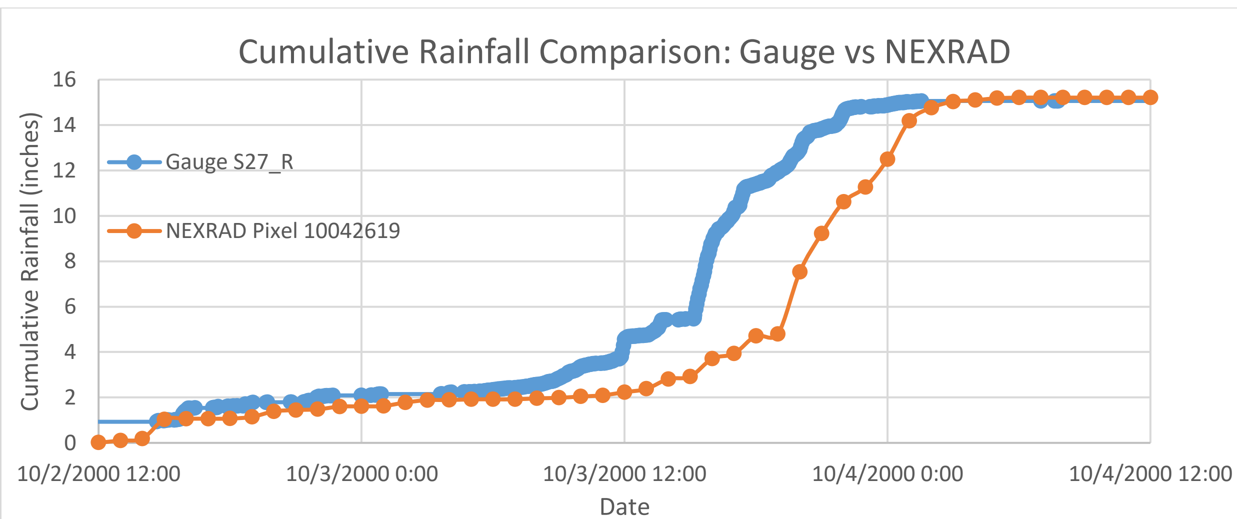

Figure 12: Cumulative Gauge Rainfall vs Cumulative NEXRAD Rainfall (NEXRAD Pixel and Rain Gauge Located at C-7 Basin Tidal Outfall)

The cumulative rainfall totals are within 0.2 inches apart which is only about 1%. Again, there is a temporal lag of about 4-5 hours.

The NEXRAD data captures the total rainfall well compared to the gauge data, however, there were some concerns with using it. As mentioned, the 1-hour interval of the NEXRAD data averages-out the highest-intensity parts of the storm. Additionally, there are some temporal differences. These two issues were further discussed before any decisions were made on using it for the calibration event. It was originally noted that it was not advisable to use the existing rain gauges to make Thiessen polygons for calibration use as: (1) the rain gauges do not capture the significant spatial differences that were noticed in the NEXRAD data and (2) it is likely that one rain gauge was not been functioning properly during the storm. **Figure 13** shows the variation of total rainfall depth in randomly selected NEXRAD pixels and the rain gauges.

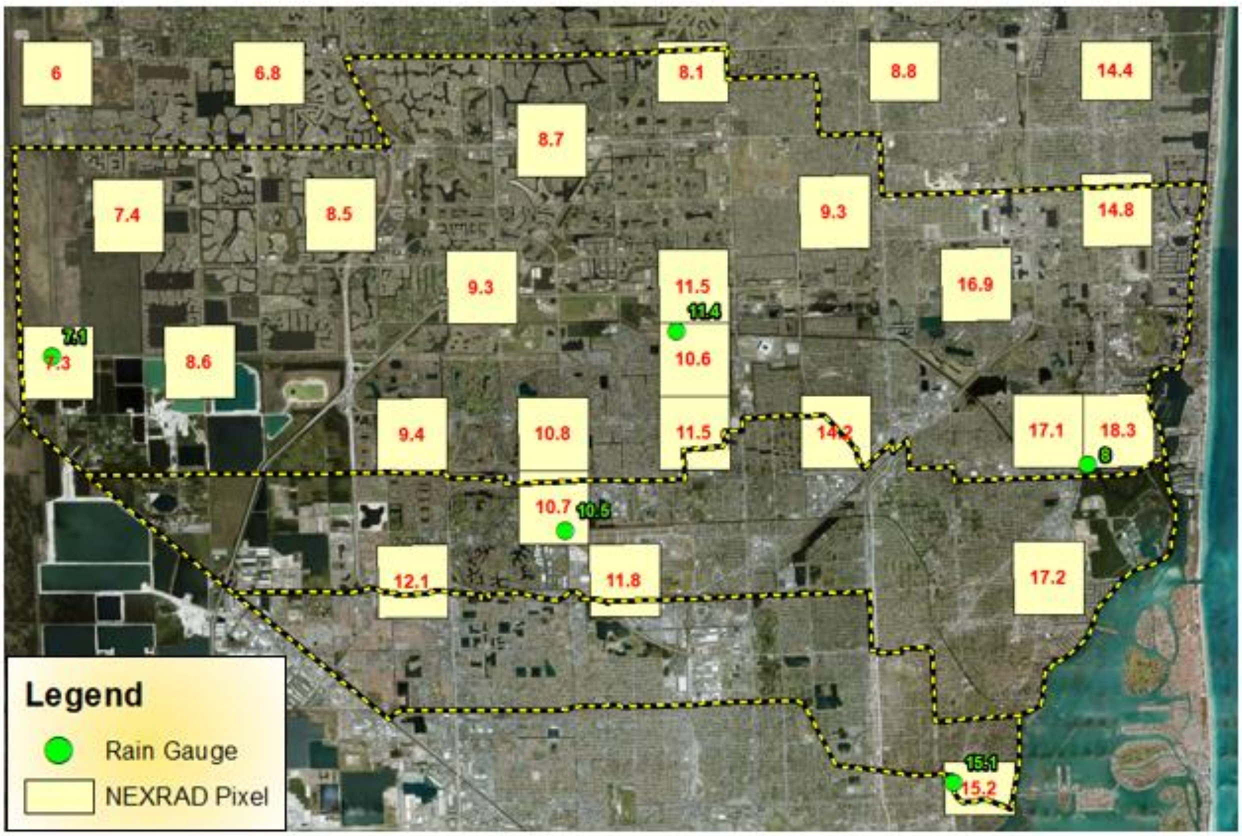

Figure 13: Randomly Selected NEXRAD Pixel and Rain Gauge Rainfall Summary

The NEXRAD rainfall data for October 2000 shows a spatial difference ranging from about 7 inches in the northwestern part of the C-9 basin to upwards of 18 inches in the southeastern part of the C-8 basin. There was some concern initially that the rain gauges alone may not adequately define the spatial distribution. The rain gauges captured the timing of the rainfall better than NEXRAD, while NEXRAD appeared to capture the spatial variation in rainfall depths better than the rain gauges. Therefore, Taylor Engineering initially recommended using the total rainfall depths from each NEXRAD pixel and distributing it temporally based on a rain gauge that is assigned by Thiessen polygons. This results in shifting the timing of the rainfall to match the rain gauges while maintaining spatial variation in rainfall totals of the NEXRAD pixels.

Aside from Gauge S-29_R, all rain gauges were within 0.2 inches of the NEXRAD pixel bordering it. Gauge s-29_R only recorded about 8 inches during the storm while surrounding NEXRAD pixels show between 17 and 18 inches. This indicated the gauge was malfunctioning during the storm; therefore, this gauge was not considered. The following figure shows the Thiessen Polygons created to assign a rain gauge to the NEXRAD pixels.

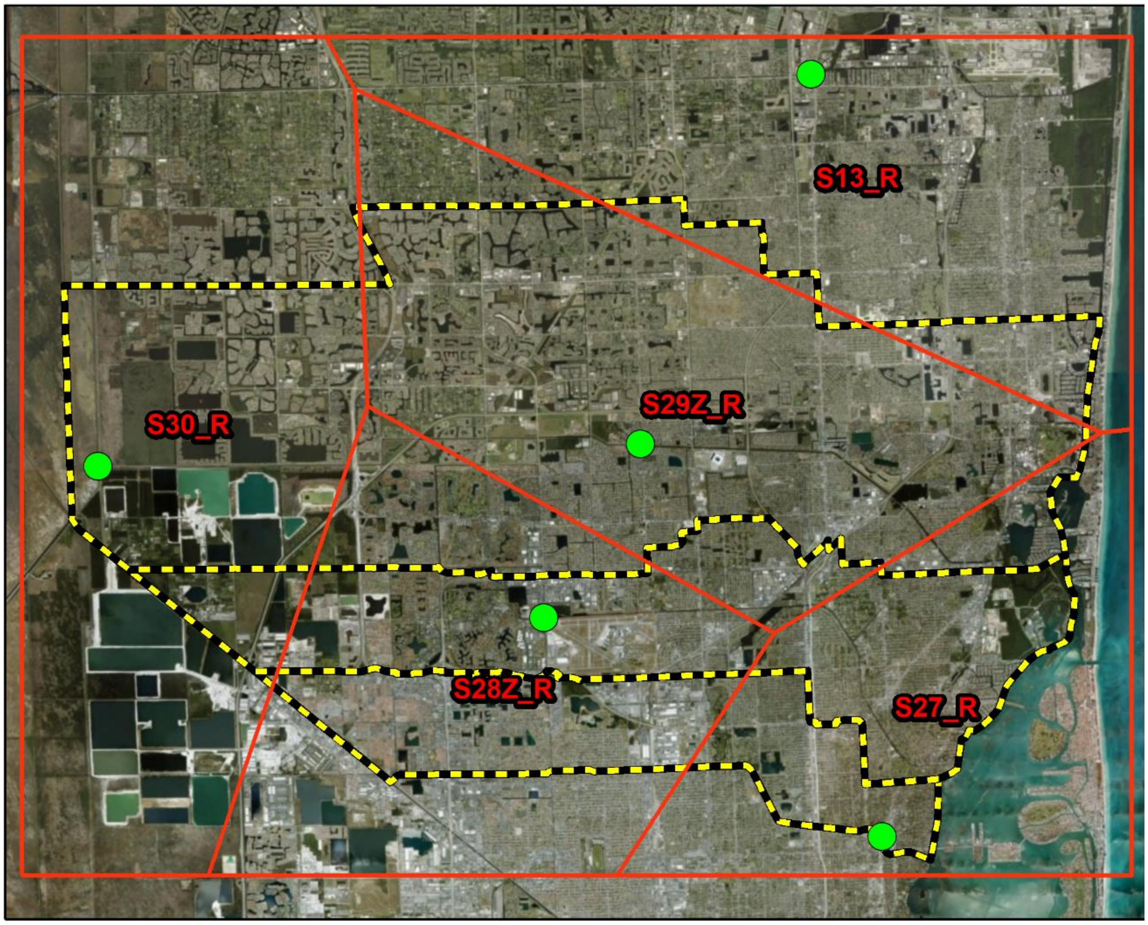

Figure 14: Thiessen Polygons of the Rainfall Gauges

Originally, each NEXRAD pixel within one of the five Thiessen Polygons were assigned the temporal distribution of the respective rain gauge. This redistribution resulted in NEXRAD rainfall that aligns well temporally with the discharge response. However, during initial calibration efforts it became apparent that this methodology was not an accurate representation of rainfall, therefore, Thiessen polygons were used with both the depth and distribution of just the rain gauges. This led to a significantly better calibration. This is further elaborated upon in **Section 3.1.4**.

1.7 Calibration Data Availability and Collection

In addition to accurate rainfall, data needed for model calibration included gate openings, breakpoint stage, and breakpoint discharge for all primary operational structures, and groundwater levels for the wells within the surficial aquifer and the model domain. When breakpoint data was unavailable, the best available data (hourly, etc.) was used. **Figure 15** shows the location of the primary structures and wells analyzed for data availability and gaps, relative to the initial rendering of the model domain and 1D hydraulic network.

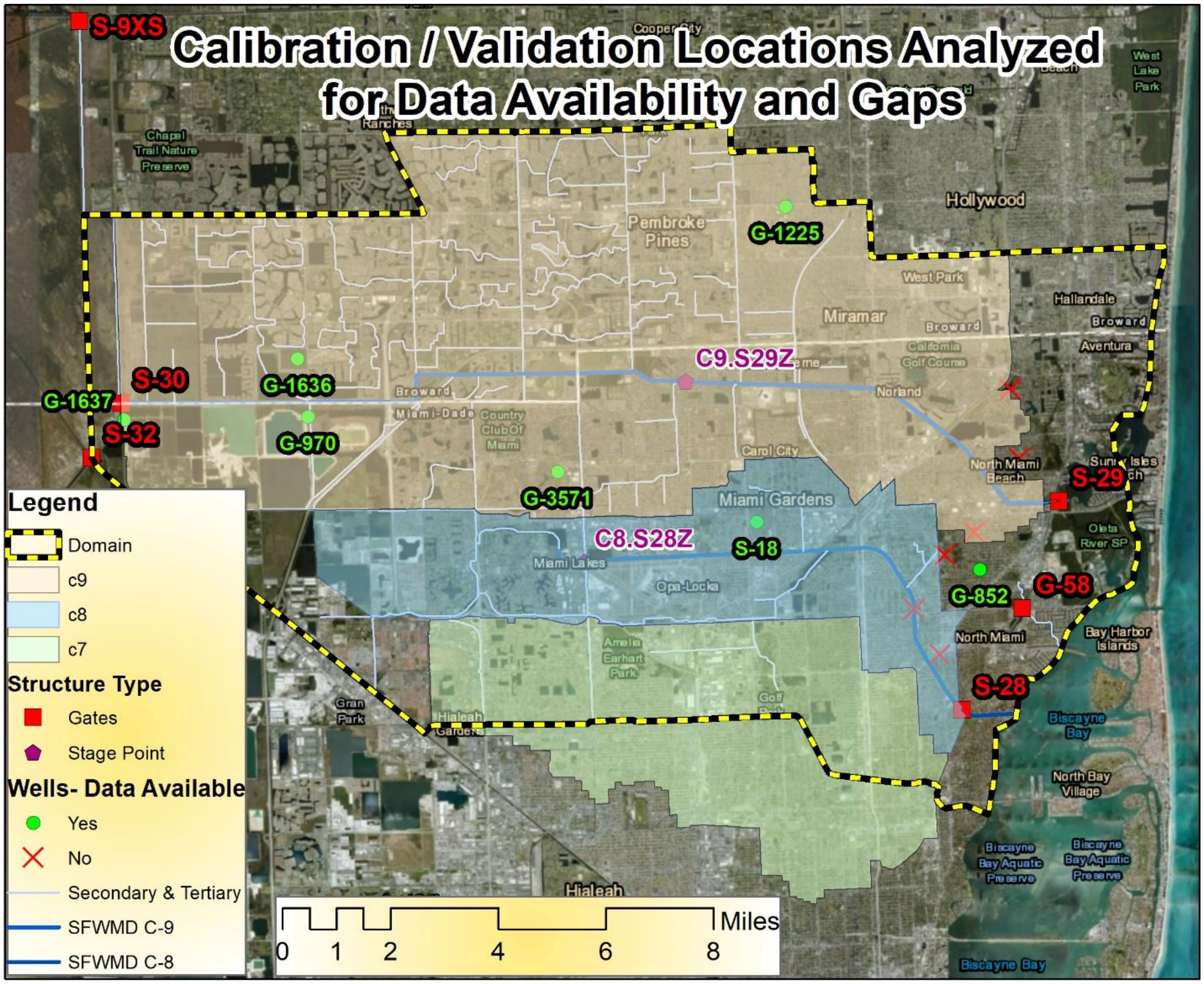

Figure 15: Calibration/Validation Locations Analyzed for Data Availability and Gaps

Stage, flow, and groundwater level data were graphed to visually analyze data for gaps and outliers. The following table shows the completeness of data for the storm events in October 2000, June 2017, and September 2017.

Table 1: Structure Data Availability Summary

NAME	BASIN	CONTROL	DBKEY	DATA TYPE	STATUS
S-28	C-8	Gated	65070	Breakpoint Discharge	Complete
			6627	Breakpoint HW Stage	
			6628	Breakpoint TW Stage	
			LT203 & LS856	Breakpoint Gate Opening	
S-29	C-9	Gated	65071	Breakpoint Discharge	Complete
			6631	Breakpoint HW Stage	
			6632	Breakpoint TW Stage	
			LS491, LS857, LS858, & LS859	Breakpoint Gate Opening	
S-30	C-9	Gated	65074	Breakpoint Discharge	Complete
			6686	Breakpoint HW Stage	
			6639	Breakpoint TW Stage	
			LS493, LS862, & LS863	Breakpoint Gate Opening	
S-32	L-33 CC	Gated	65077	Breakpoint Discharge	Complete
			SP543	Breakpoint HW Stage	
			6643 & AI581	Breakpoint TW Stage	
			LS495, LS867, SP544 & SP545	Breakpoint Gate Opening	
G-58	North Biscayne Bay	Gated	64715	Breakpoint Discharge	No September 2017
			IX539	Breakpoint HW Stage	No September 2017
			N/A	Breakpoint TW Stage	Not in DBHYDRO
			LS376, LS693, LS694, & LS695	Breakpoint Gate Opening	No September 2017
S-9XS	L-33 CC	Boarded	90829	15-Minute Discharge	Complete
			SO013	15-Minute to Hourly HW Stage	Complete
			OH925 & OH924	15-minute and Breakpoint TW Stage	Complete
			LD575 & LS966	Other Board Elevation	Other

Although there are several wells within the model domain, many of them contain no useful data as it pertains to the purpose of this project because of infrequent or random interval sampling. The following table shows the wells that are within the model domain and the surficial aquifer system (SAS) that have concurrent data available to three of the aforementioned storm events.

Table 2: Wells with Complete Groundwater Level Data within SAS During October 2000

WELL NAME	BASIN	DBKEY	DATA TYPE
G-1225	C-9	1758	Daily Max
G-1636	C-9	1716	Daily Max
G-1637	C-9	1698	Daily Max
G-3571	C-9	LP668	Daily Max
G-852	North Biscayne Bay	1662	Daily Max
G-970	C-9	1703	Daily Max
S-18	C-8	1673	Daily Max

Table 3: Wells with Complete Groundwater Level Data within SAS During June-September 2017

WELL NAME	BASIN	DBKEY	DATA TYPE
G-1225	C-9	1758	Hourly GW Level (missing data during Irma)
G-1636	C-9	1716	Hourly GW Level
G-1637	C-9	1698	Hourly GW Level (missing data during Irma)
G-3571	C-9	LP668	Hourly GW Level
G-852	North Biscayne Bay	1662	Hourly GW Level
G-970	C-9	1703	Hourly GW Level
S-18	C-8	1673	Hourly GW Level
G-1166R	C-7	88676	Hourly GW Level

These wells originally appeared to have complete groundwater data, it was realized during model validation that G-1225 and G-1637 were missing data during Hurricane Irma in September 2017.

1.8 Groundwater Data Availability

A groundwater study authored by J. D Hughes and J. T White was documented in a USGS report titled Hydrologic Conditions in Urban Miami-Dade County, Florida, and the Effect of Groundwater Pumpage and Increased Sea Level on Canal Leakage and Regional Groundwater Flow (2016). For modeling purposes, they discretized the Biscayne Aquifer into 3 layers: an upper and lower permeable layer separated by a layer about 100 times less permeable. A significant amount of data from this study is available, including but not limited to year 2000 wet season heads, horizontal hydraulic conductivity, transmissivity, specific storage, specific yield, aquifer thickness, and bottom of aquifer layer elevations. Some of this data is available as figures with contours while others appear to be raster data. Taylor Engineering reached out to Hughes and received the data needed to create shapefiles of the data in the USGS report. Figures with contour data can be georeferenced and recreated in GIS, however, Taylor Engineering was able to produce shapefiles from the USGS data. Taylor Engineering proposed to use a 3-layer groundwater model based on the Hughes and White study. All 3 layers were intended to include the following data from the USGS: (1) layer bottom elevations, (2) horizontal hydraulic conductivity, (3) vertical hydraulic conductivity, (4) specific yield, and (5) specific storage. For the calibration model, the initial groundwater elevations were based on the 2000 wet season head. The following figures from the USGS report are examples of the data available.

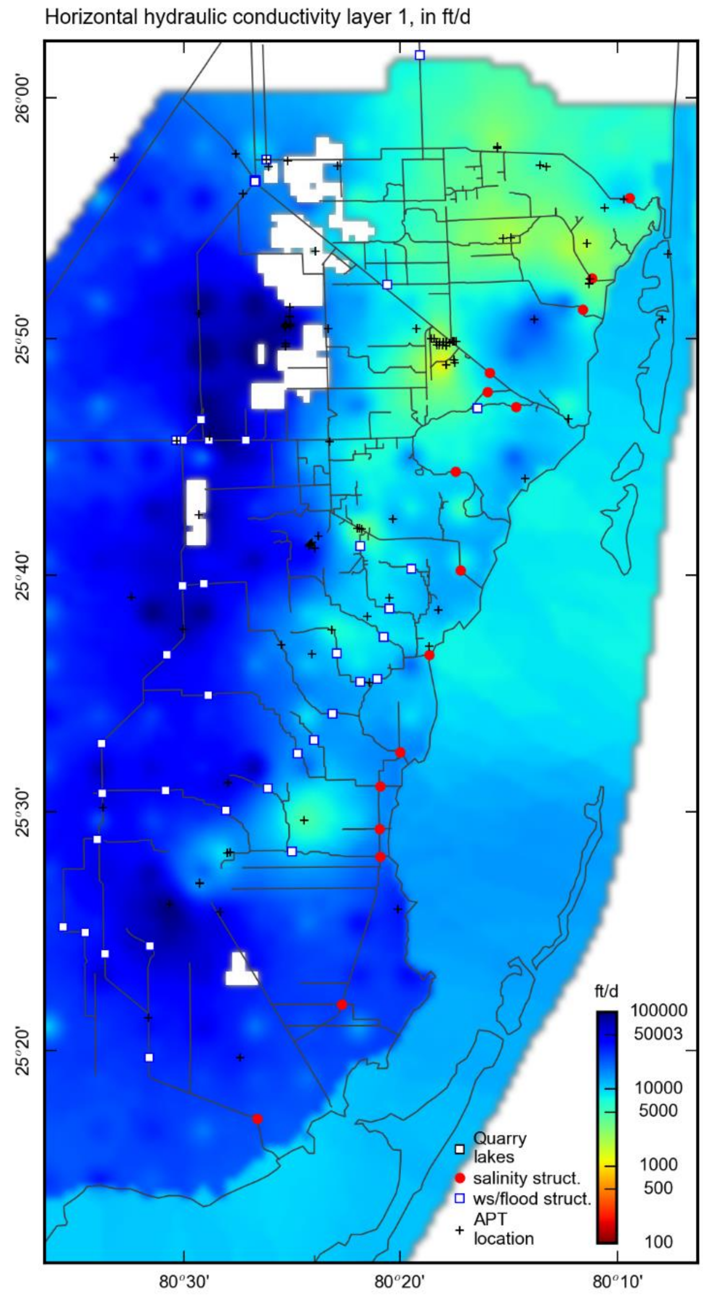

Figure 16: Hydraulic Conductivity of Biscayne Aquifer Layer 1 (Hughes & White, 2016) (not used)

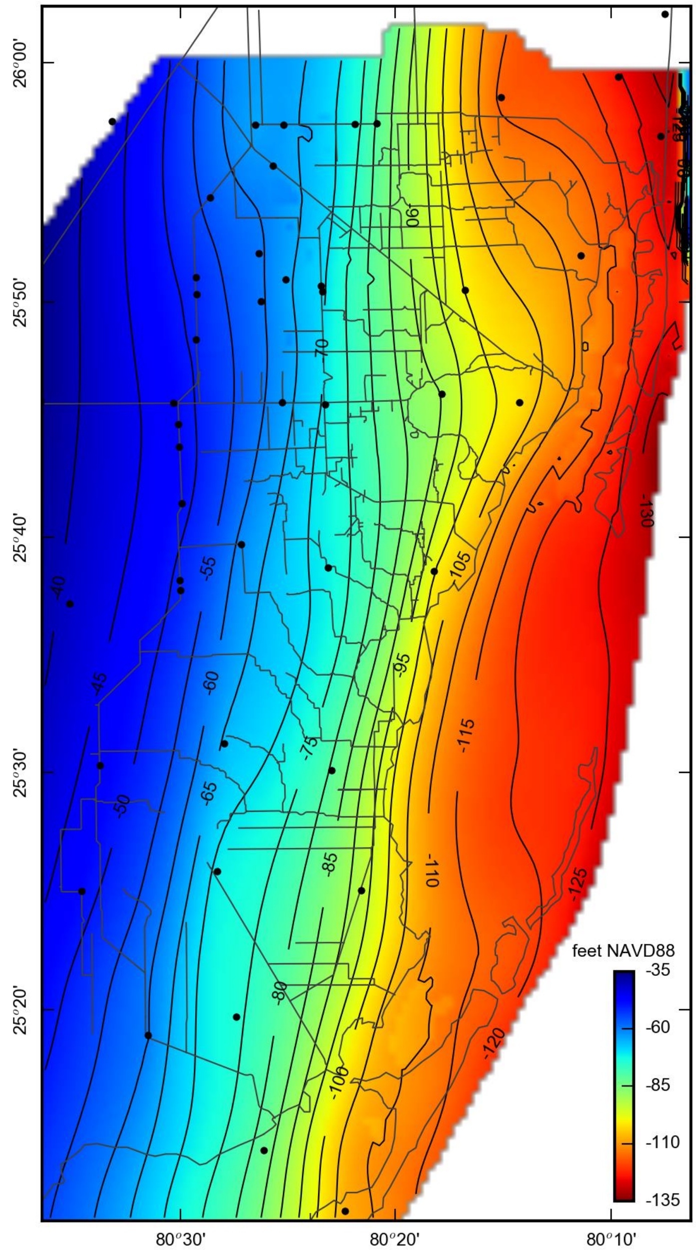

Figure 17: Bottom Elevation of Biscayne Aquifer Layer 3 (Hughes & White, 2016) (not used)

1.9 <u>Boundary Conditions</u>

1.9.1 Calibration

For the October 2000 calibration event, the eastern surface and groundwater boundary conditions come from the Virginia Key tidal station. The southern boundary conditions are time-stage relationship along the C6 and C7 canal for surface water and a general head for groundwater (based on observed canal stages on DBHYDRO). Originally, the L33 canal served as the western boundary condition with time-stage relationship for canal stages at the S9XS and S32 structures. Observed stage in Water Conservation Area

3B now serves as the western boundary conditions with a time-stage relationship for surface water, and a general head boundary for groundwater. The northern groundwater boundary was developed from the USGS study (Hughes and White, 2016). Tidal boundaries at the S-28 and S-29 structures are forced using observed tailwater data.

1.9.2 Validation

For the September 2017 validation event, the northern boundary data comes from the 2019 Broward County Current Conditions Validation Model, which was originally developed for the June 2017 event but was extended to run through September 2017. The eastern surface and groundwater boundary conditions come from the Virginia Key tidal station. The southern boundary conditions are time-stage relationships along the C6 and C7 canal for surface water and a general head for groundwater (based on observed canal stages). Originally, it was planned for the L33 canal to serve as the western boundary with a time-stage relationship for canal stages at the S9XS and S32 structures. This was revised after changes were made to the western calibration boundary conditions during calibration. Observed stage in Water Conservation Area 3B now serves as the western boundary conditions with a time-stage relationship for surface water, and a general head boundary for groundwater. Tidal boundaries at the S-28 and S-29 structures are forced using observed tailwater data.

1.9.3 Design Storm

For all design storm events, the northern groundwater and surface water boundary conditions will come from the results of the 2019 Broward County Current Conditions Design Storm Models. The eastern surface and groundwater boundary conditions will come from the District-provided time series representing the corresponding storm surge heights. The southern boundary conditions will be time-stage relationships along the C6 and C7 canal for surface water and a general head for groundwater (from Miami-Dade County's XP SWMM design storm model results). Water conservation area 3B will serve as western boundary conditions with a time-stage relationship for surface water and a general head boundary for groundwater. Tidal boundaries at the S-28, S-29, and G-58 structures are forced using SFWMD provided tidal data with storm surge and/or sea level rise, depending on the specific scenario.

1.10 Initial Conditions

1.10.1 Overland Depths

For design storm simulations, any cells within a drainage basin that are lower than the basin's water control elevation will be set to an initial depth equal to the difference of the water control elevation and the elevation of the cell. Essentially, this will bring the water elevation in any sinks to the water control elevation. This eliminates excess "dead storage" and ensures that water is not being routed via ponded drainage or flood codes at the start of the simulation. For calibration and validation, the initial overland depths use the same assumption as both events occurred at or near the end of the rainy season.

1.10.2 Groundwater and Canal Stages- Calibration

The initial groundwater elevations for calibration were developed by making localized adjustments to the 2000 wet season heads from the MODFLOW model developed as part of the recent USGS study (Hughes and White, 2016). The initial surface water levels in the main canals are based on observed data. Initial stages in the secondary/tertiary canal systems that are controlled by structures are set based on water control elevations.

1.10.3 Groundwater and Canal Stages- Validation

The initial groundwater elevation for the validation event was created by extending the 2019 Broward County Current Conditions Model groundwater elevation map (which includes part of Miami-Dade County) south to cover the remaining area of the model extent. The 2019 Broward County model's initial groundwater map was developed from Broward County's average wet season map (Broward County, 1990-1999). Average September groundwater elevation contours from the USGS (Fish and Stewart, 1990) (**Appendix A**) were used to extend the initial groundwater elevation map south to cover the remaining model domain. The groundwater elevations were compared with available well data. Early wet-season (June 2017) groundwater elevations were a close match with the average wet-season elevations from the 1990s, therefore, no adjustments to the contours were applied. The initial surface water levels in the main canals were based on observed data. Secondary/tertiary canal system that are controlled by structures were set based on water control elevations.

1.10.4 Groundwater and Canal Stages- Design Storm

There are two options for the initial groundwater elevations for the design storms. The first option would be to use the same initial groundwater elevations from the validation event. An example of this approach would be the 2019 Broward County Current Conditions model. There was generally a good match between the initial groundwater elevations map (based on typical late wet season conditions) and the observed data at well locations at the beginning of the event.. This approach works well since the validation event is from recent history and there are observed data that can be used for some of the boundary conditions. The second option would be to use simulated groundwater elevations from the validation simulation. Depending on the goodness-of-fit on the recession limb of the groundwater hydrographs, this approach could provide higher initial groundwater elevations, which may better represent actual conditions during the latter part of the wet season and have a more conservative starting point for the design storm simulation. This approach would require an overall goodness-of-fit that is fairly uniform throughout the model extent.

The initial surface water levels will be based on water control elevations if known, or operational rules. For example, if a particular area is controlled at elevation 4.0 feet, then every branch within that drainage area will have an initial condition of 4.0 feet. If there is no established control elevation, then the initial level will be set equal to the level in which the controlling structure (could be several miles away) begins to operate.

2.0 MODEL DEVELOPMENT

2.1 <u>Introduction</u>

This section details the development and initial parameterization of the SFWMD C-8 & C-9 MIKE SHE and MIKE HYDRO models for use in the C8-C9 FPLOS Study. Please note that many of the data inputs are initial values and were changed during model calibration.

2.2 Model Development and Parameterization

2.2.1 Model Domain and Grid

The model domain extends from the C-9 and C-11 basin boundary in the north to the C-6 and C-7 canals in the south, and from just west of the L-33 canal in the west to the intercoastal in the east, as shown in **Figure 18**. A computational grid size of 250-ft was chosen and coupled with the multi-cell overland feature using a 125-ft grid. This further refines the storage and conveyance characteristics of each computational grid cell. Although the model computations are based on a 250-ft grid cell, the conveyance and storage characteristics of each cell are calculated based on the finer 125-foot grid. This provides a high level of topographic detail and overland storage definition, which is sufficient for this sub-regional scale model. The computational grid size and multi-cell overland definition are consistent with the Broward County model (Taylor Engineering, 2019). Additionally, the C-8 C-9 model grid origin is aligned so that it is an exact integer of grid cells away from the 2019 Broward County Model origin, meaning that the data input and outputs are compatible between both models.

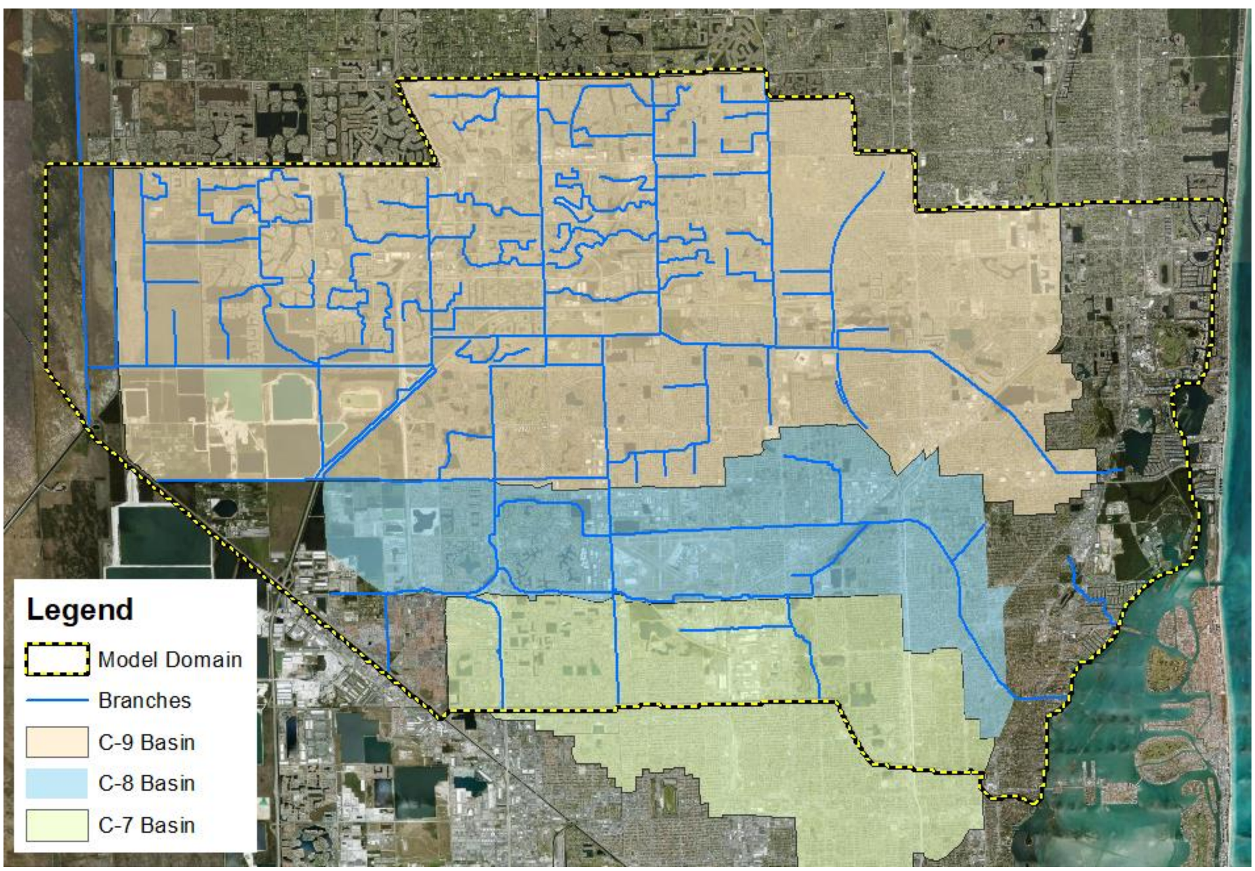

Figure 18: Model Domain and Basin Map

2.2.2 Topography

The topography input file was made from the merged DEM presented in **Figure 1**. The 125-ft DEM was made by taking the median values from the 5-ft DEM within each 125-ft grid cell. Areas with elevations greater than 25 ft NAVD88 (typically landfills or high bridges) were reduced to 25 ft to eliminate the possibility of having numerical stability issues in the 2D model (such as flow from 200-ft elevation cell to 10-ft elevation cell). Areas with elevations less than -2 ft NAVD88 were increased to -2 ft (typically intercoastal areas- bathymetry likely built into DEM). Then the topography was converted from NAVD88 to NGVD29 by adding 1.57 ft, the conversion from CorpsCon6 tool. Several areas were tested, and the differences were minimal. A uniform conversion of 1.57ft was deemed appropriate and efficient.

2.2.3 Simulation Specification

The simulation periods differ from one simulation to the next. The simulation period for the calibration model is a three-week period from October 1st, 2000 12am to October 21st, 2000 12am. The verification event is a nearly four-month period from June 2nd, 2017 12am to September 27th 12am. The design storm will have a similar starting date to the verification event as it provides a realistic starting point for initial conditions and boundary conditions based on recent observed data. The wet season water table map referred to in **Section 1.10.3** was compared to the observed initial groundwater levels on June 2nd, 2017 and was found to be a good match in general, with most locations agreeing to within +/- 0.5'. In addition, this provides observed data from a storm event that are used as boundary conditions. For the design storm, June 4th at 12am was chosen specifically as this aligns the peak of the design storm with the peak of the storm in the boundary conditions. This approach is consistent with the 2019 Broward County Model. Any date during the validation simulation can be used as the starting date for the design storms if the simulated groundwater is a good match to the observed groundwater, in which case the simulated head from the validation event could be used as new initial potential head for the design storm. The design storm has a rainfall duration of three days; however, the simulation will likely be extended an additional 2-3 weeks. The purpose for running the simulation an additional 2-3 weeks would be to generate a model-simulated water table map that could be useful as an alternative input for initial groundwater level conditions and to determine duration of flooding in areas of the model where potential flooding damages may need to be evaluated as part of mitigation alternatives.

2.2.4 Climate

2.2.4.1 Rainfall

The storm event from October 2nd-4th, 2000 was used to calibrate the model, with a simulation period of October 1st-21st. Originally, temporally modified NEXRAD rainfall data (as described in **Section 1.6**) was used. It is well known by the District that the quality of the NEXRAD data is questionable for the 2000 - 2005 period. This limitation was thought to have been overcome by applying the temporal distribution from rain gauges, however, there were rainfall issues during model calibration, so the rainfall methodology was switched to just using rain gauge data. This is described in more detail in **Section 3.1.4**. The verification event uses NEXRAD data that is unmodified. The design storm will use NOAA Atlas 14 rainfall depths that are temporally distributed based on the SFWMD 3-day distribution and spatially distributed based on Thiessen Polygons of the NOAA stations (**Figure 19**), which is consistent with the 2019 Broward County model approach.

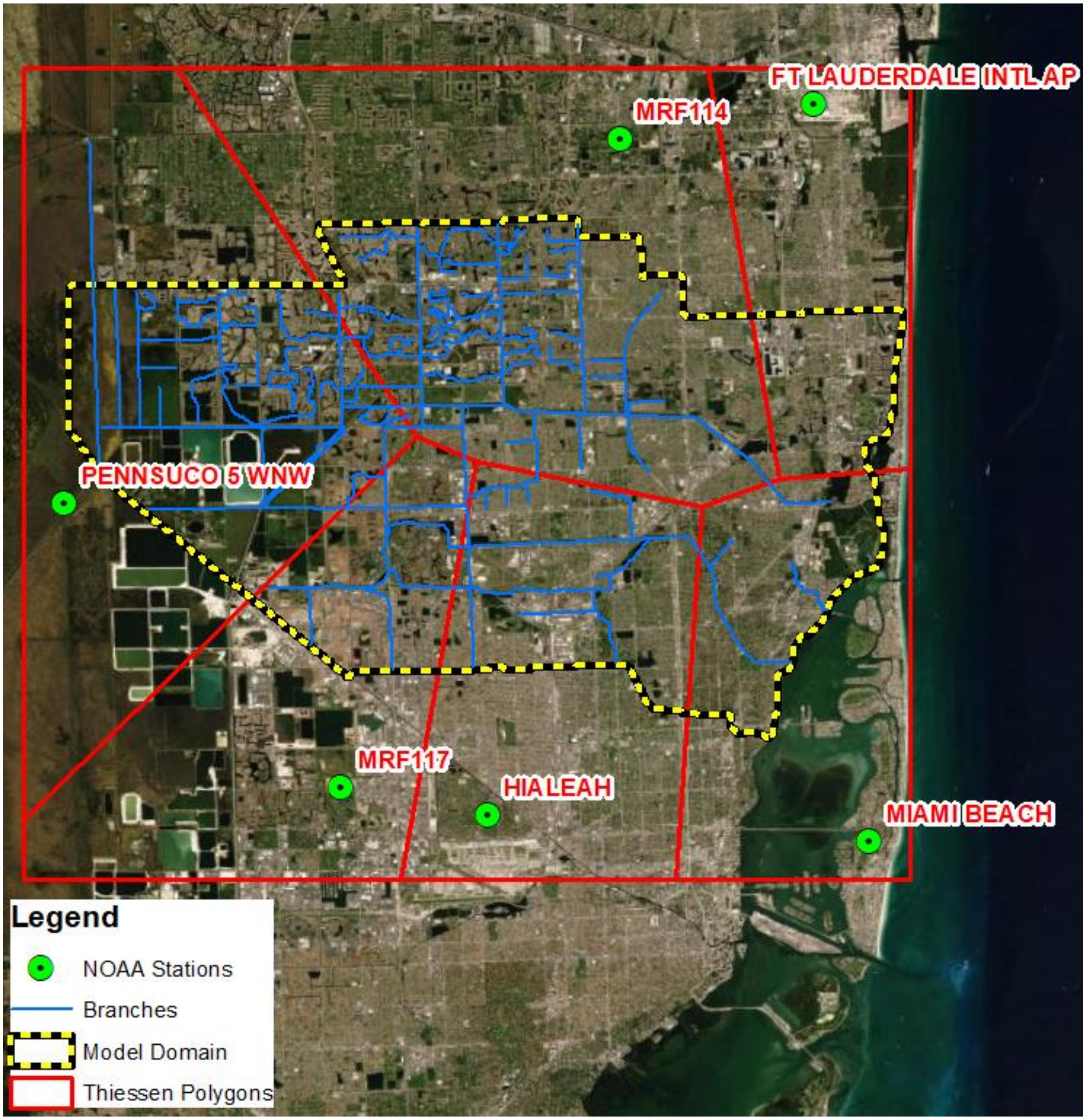

Figure 19: Thiessen Polygons based on NOAA Stations

2.2.4.2 Reference Evapotranspiration

Short term simulations are typically not very sensitive to this parameter and reference ET does not vary significantly across relatively small areas, such as this model domain. Therefore, a uniform spatial distribution was chosen for the calibration and validation simulations. A time varying temporal distribution will be used based on the SFWMD Reference ET for the specific time period (https://apps.sfwmd.gov/nexrad2), based on a centrally located pixel within the model domain (**Figure 20** & **Figure 21**). For the design storms, the Reference ET will have a uniform spatial distribution and be based on average wet season ET values, developed from the USGS reference ET data. Average wet season ET values are sufficient as ET will be rather insignificant compared to design storm rainfall depths.

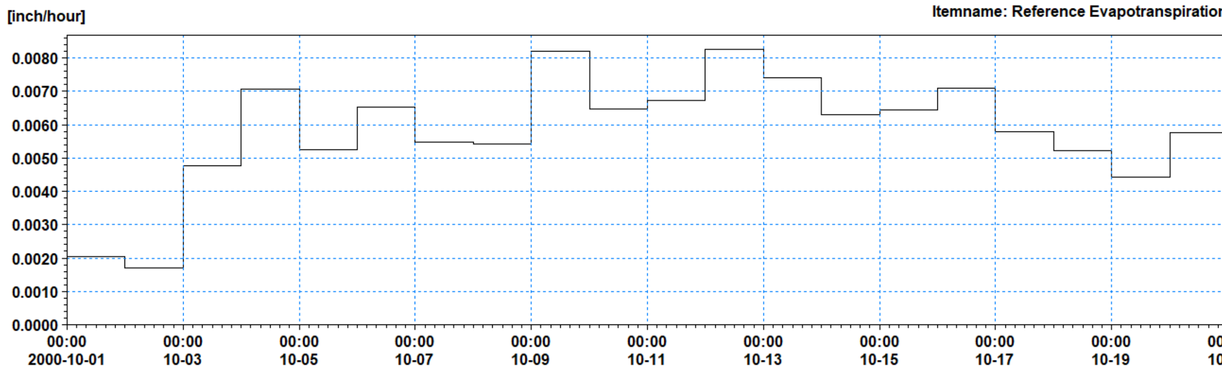

Figure 20: Reference ET for Pixel 10045457 for Calibration Simulation

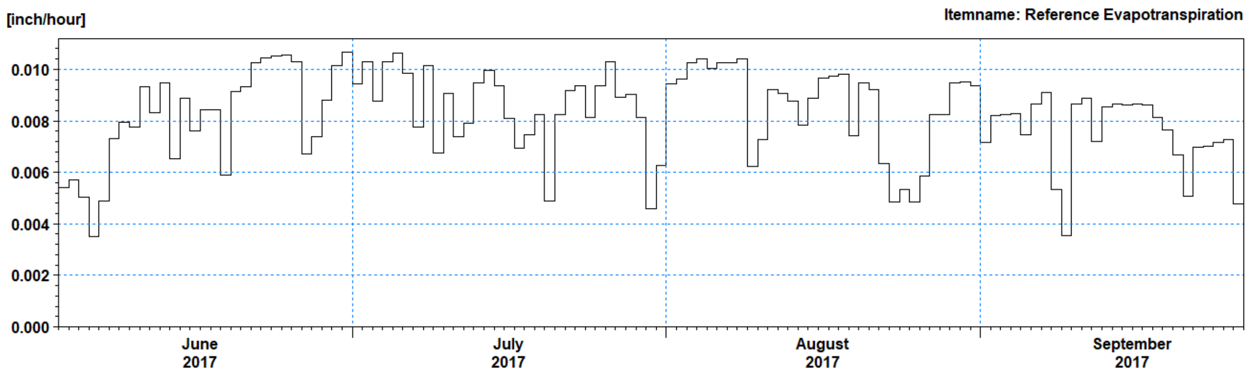

Figure 21: Reference ET for Pixel 10045457 for Validation Simulation

2.2.5 Land Use

To be consistent with the 2019 Broward County Current Conditions model, the land use/vegetation map was created by merging the 2019 Broward County model's land use map with the latest available data from SFWMD (SFWMD, 2018). The 2019 Broward County Current Conditions model's land use map was also created using the latest data from SFWMD, but additional changes to land use were made throughout the county by comparing satellite imagery from 2015 with 2018. Therefore, by merging the Broward County land use map that was updated with the SFWMD land use, it ensured that any changes in the C-9 basin from the 2019 Broward County Model were incorporated. As suggested by SFWMD, the "extractive" land use areas were changed to reservoirs as they are filled with water. All the land use-based parameters have this change accounted for. Land use is assigned based on the 250ft computation grid. The land use grid was made from a polygon shapefile of land use areas based on the maximum area of land use(s) in the 250ft grid cell. As discussed in **Section 1.3**, there were less than 2% change in land use classification since 2000, so this dataset was used for the calibration event as well as the validation and design storm events. Refer to **Table 4** for land use description by Florida Land Use Cover Classification System (FLUCCS) codes (FNAI, 2012).

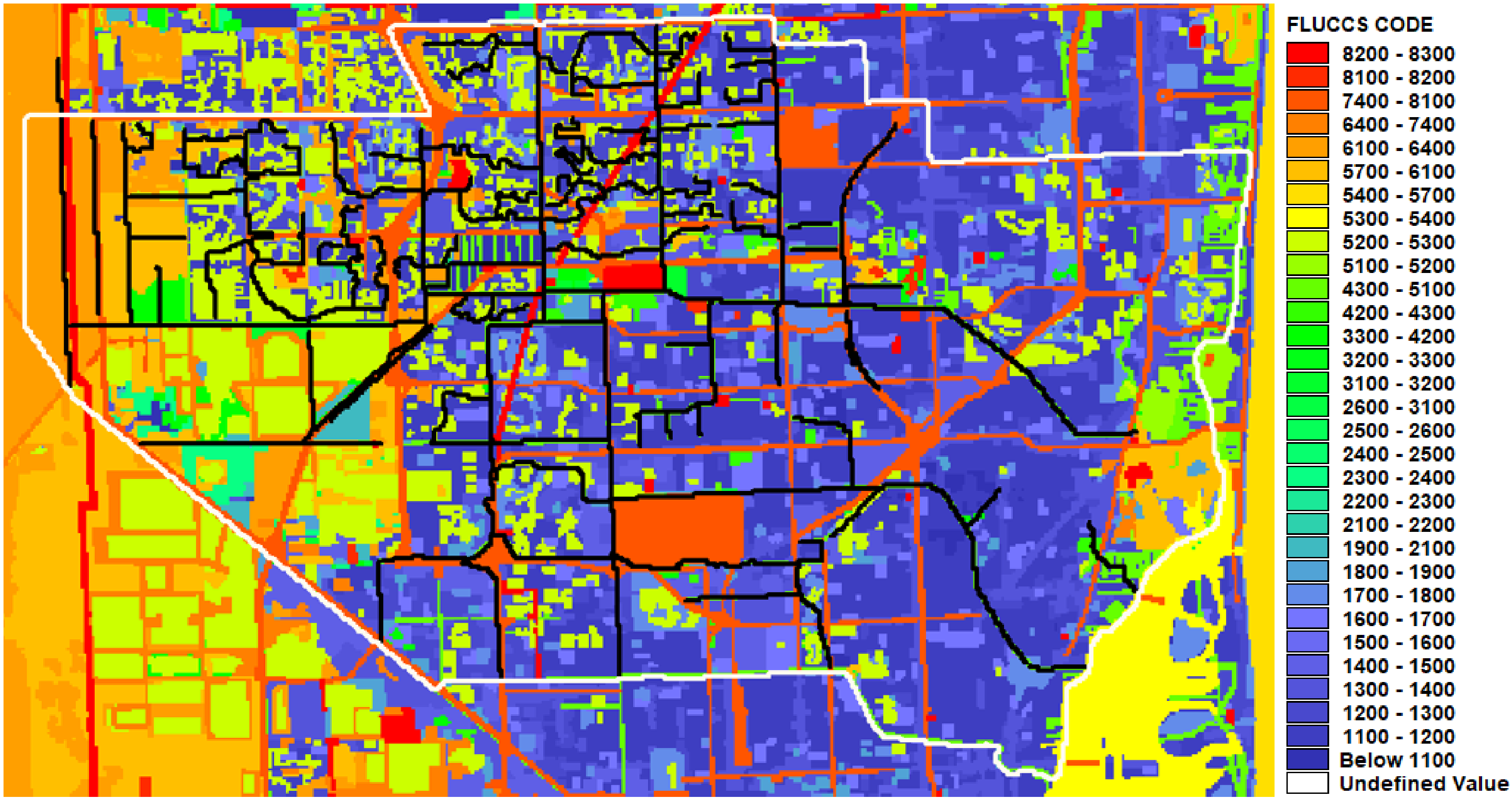

Figure 22: Land Use/Vegetation by FLUCCS Code

Table 4: Land Use by FLUCCS Code

FLUCCS Code	Land Use	Percentage within Model Domain
1100	Residential, Low Density	1.7
1200	Residential, Medium Density	32.9
1300	Residential, High Density	12.1
1400	Commercial and Services	9
1500	Industrial	2.9
1700	Institutional	4
1800	Recreational	4
1900	Open Land	1.3
2100	Cropland and Pastureland	0.7
2200	Tree Crops	0
2300	Feeding Operations	0
2400	Nurseries and Vineyards	0.8
2500	Specialty Farms	0
2600	Other Open Lands - Rural	0
3100	Herbaceous (Dry Prairie)	0.1
3200	Upland Shrub and Brushland	0.3
3300	Mixed Rangeland	0
4200	Upland Hardwood Forests	0.8
4300	Upland Mixed Forests	0.3
5100	Streams and Waterways	1.7
5200	Lakes	0.3
5300	Reservoirs	10.2
5400	Bays and Estuaries	0.3
5700	Ocean and Gulf	0
6100	Wetland Hardwood Forests	4.1
6400	Vegetated Non-Forested Wetlands	4.7
7400	Disturbed Land	0.7
8100	Transportation	6.2
8200	Communications	0.1
8300	Utilities	0.9

2.2.6 *Rivers and Lakes (1D model)*

The 1D model was developed using MIKE HYDRO. The 1D network in the C-9 basin was mainly based on the 2019 Broward County Current Conditions model. The 1D network in the C-8 and C-7 basins were developed for this project. District, County, survey (Stoner and Associates, 2019), and South Broward Drainage District (SBDD) data were used when and where applicable and available. Additional survey (BDH Consulting Group, 2019) was completed for this project. The data used and parameterization of the river network are discussed in the following subsections.

2.2.6.1 1D River Network

The 1D river network is composed of 95 branches, 93 of which could be considered secondary or tertiary systems. The purpose of this study is to determine the flood protection level of service for the C-8 and C-9 canals. Although the focus of this study is on the two primary canals, C-8 and C-9, a high level of detail was placed on the secondary/tertiary canal systems, as they are both a major source of discharge into the primary system and storage prior to discharging into the primary system. Many of the secondary/tertiary canal systems were setup to simulate the connectivity between lakes and other discontinuous (from DEM) water bodies, which are connected through a series of hydraulic structures. Water bodies that are not explicitly represented via a branch may still be connected to the 1D river network through the use of flood codes, which is discussed in section **2.2.6.3.1**.

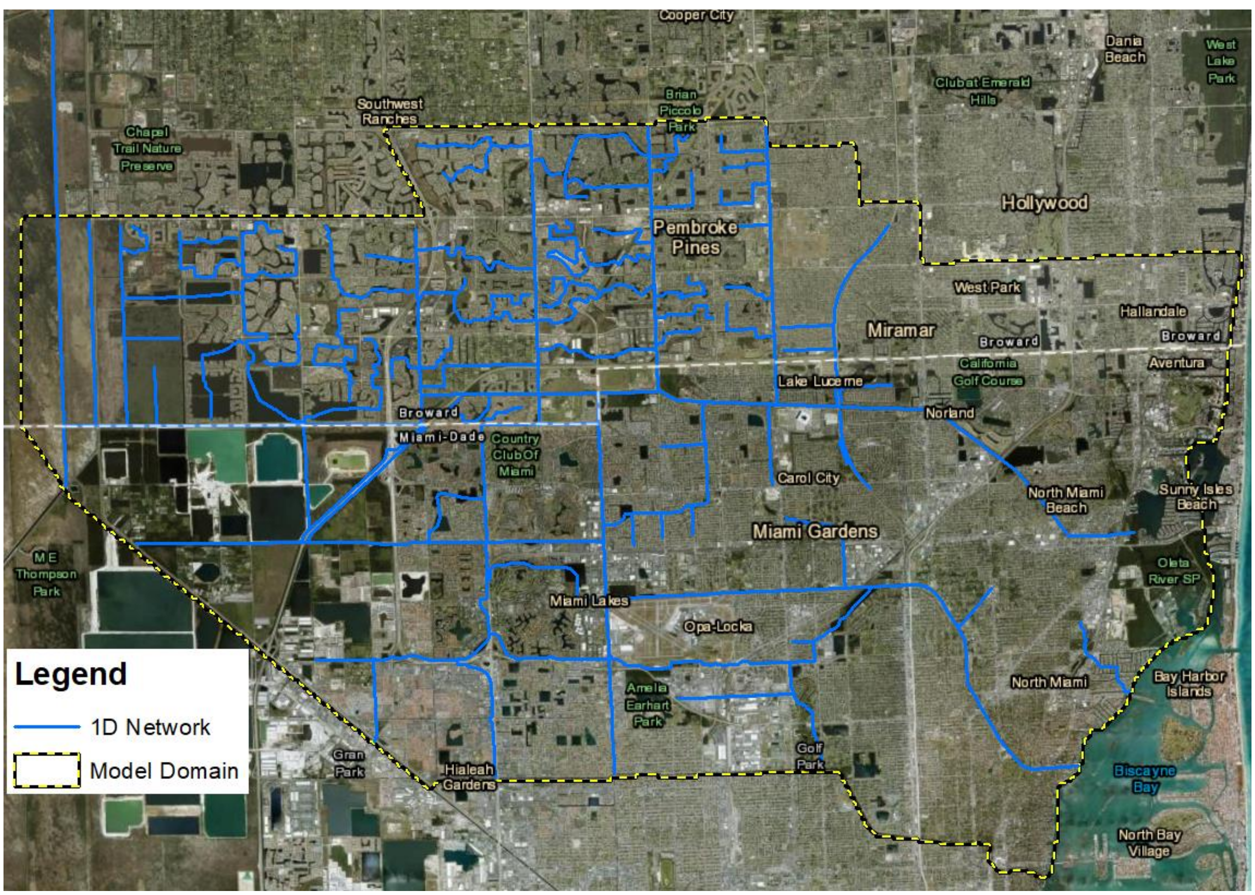

Figure 23: 1D Model Branches

2.2.6.1.1 Hydraulic Control Structures

The 1D network is controlled through a series of culverts, weirs, gates, and pumps. Specifically, there are 309 culverts, 8 weirs, 8 gated structures, and 8 pump stations. There are also 46 bridges explicitly modeled, which may control flow if they become submerged. The data for these structures came from a variety of sources, including South Broward Drainage District's Facilities Report, Miami-Dade Stormwater Geodatabase, SFWMD Operations Control Center Structure Books, SFWMD Flow Rating Analysis reports, SFWMD XP SWMM models, and professional survey. In areas where specific data was unavailable, an approximation was made. Specifically, South Broward Drainage District's Facilities Report lacked invert elevations for approximately 200 of the culverts included in the model, therefore, an approximation was made by matching the top of the culvert with the water control elevation, with respect to the specific drainage basin, as suggested by SBDD (See **Appendix B**).

There are four SFWMD control structures within the C-8 and C-9 basins (S-28, S-29, S-30, and S-32), and two outside the basins (S-9XS and G-58). S-9XS is used for boundary conditions on the L-33 Canal and G-58 controls Arch Creek. The four SFWMD control structures within the basins are represented as sluice gates. This was done so that the District's flow rating parameters could be incorporated, which provide the closest model calculation representation of the actual stage-discharge relationship of the structures as it uses the same set of equations.

2.2.6.1.2 Cross Sections

The availability of cross section data was limited to mainly the Miami-Dade portion of the model domain. Both the Miami-Dade County GIS Geodatabase as well as the SFWMD XP SWMM C-7, C-8, and C-9 models had cross section data for branches within Miami-Dade County. Cross sections for the C-9 canal were available from both survey data and the C-9 XP SWMM model. For many secondary/tertiary canals in Broward County, cross section data was essentially nonexistent. Therefore, the cross sections for the branches within the Broward County portion of the model were carried over from the 2019 Broward County Current Conditions Model, which are mainly estimates based on the DEM. Most of the secondary/tertiary canal cross sections in the Broward County portion of the model were cut using the latest available 5-ft DEM (a composite DEM made by Geosyntec consultants, as discussed in **Section 1.2**). This means the DEM was used for cross section elevation and geometry, from bank to the water surface. An assumed geometry was used below the water surface (**Figure 24**), typically, from the last bank point down to an elevation of -2/-3 was assumed to have a side slope of 4(h):1(v), and then a side slope of 2:1 from -2/-3 ft to -8 ft. The water surface elevation varied across the model domain due to water control elevation differences, so the channel geometry may appear different for the "cut" cross sections. It is important to note that "cut" cross sections from the DEM were not used for the C-8 and C-9 canal. Additional cross section data for this project was collected via professional survey.

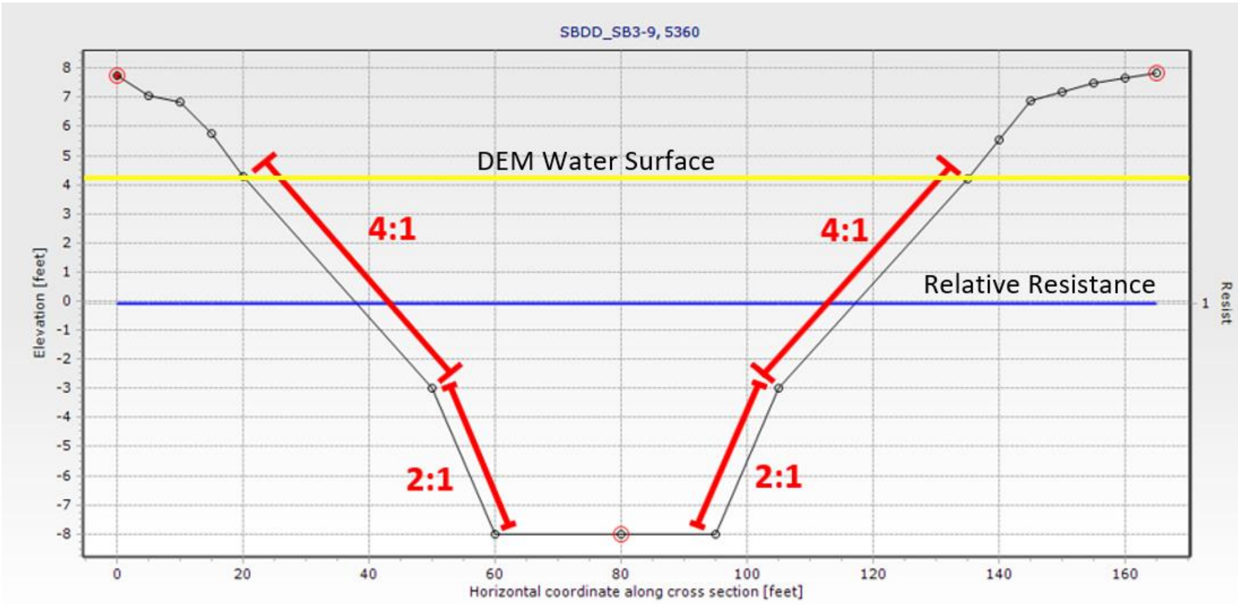

Figure 24: Example of "Cut" Cross Section from DEM

2.2.6.1.3 Survey Data

Requested survey items focused on areas with little or no available data. A map of the surveyed items and locations can be seen in **Figure 25.** These items were incorporated into the 1D model.

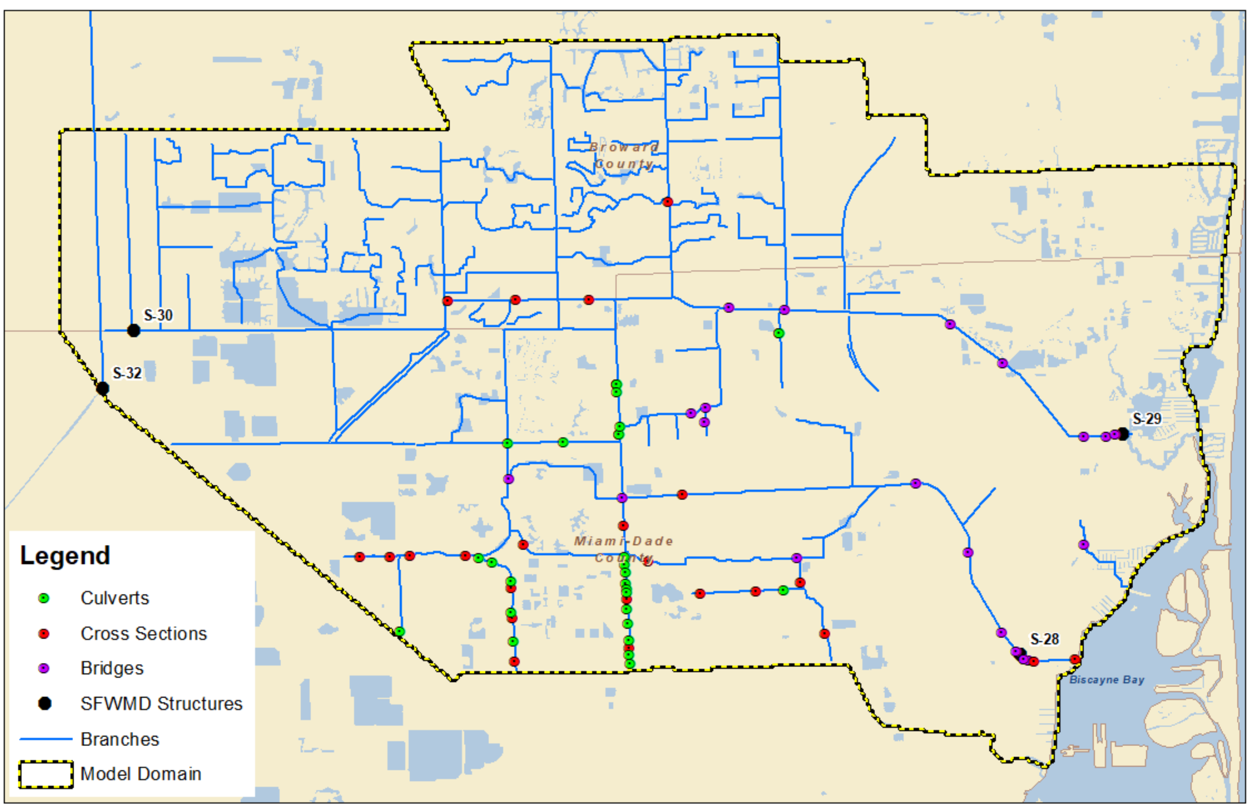

Figure 25: Survey Inventory

2.2.6.2 Canal-Aquifer Interactions

The 1D river network is coupled with the 2D groundwater model by MIKE SHE couplings. Essentially, at each grid cell along either side of a river branch, the exchange is calculated by multiplying the head difference between the grid cell (groundwater level in the cell(s) adjacent to the river link) and the river with the conductance. The model calculates the conductance based on the options assigned. For each branch or branch segment in the model, 1 of 3 conductance options were chosen, either (1) aquifer + riverbed, (2) aquifer only, or (3) riverbed only. These options change the way the model calculates the exchange between the groundwater and the river, where the aquifer conductance depends on the horizontal hydraulic conductivity and the riverbed conductance depends on an assigned leakage coefficient. Typically, only aquifer + riverbed or riverbed only were used. In either of these cases, a leakage coefficient is assigned, with 1E-5/s (time constant) being the model default value. The conductance option and leakage coefficient were adjusted on an as-needed case-by-case basis during model calibration.

2.2.6.3 Canal-Overland Flow Interactions

The 1D river network is coupled with the 2D overland flow model by MIKE SHE couplings. In this model, both coupling options are used, which are (1) flood codes and (2) overbank spilling. These options are discussed in the following two subsections.

2.2.6.3.1 Flood Codes

On secondary and tertiary canals, flood codes are used to allow communication between MIKE HYDRO and MIKE SHE when water levels in MIKE Hydro exceed the adjacent floodplain elevations. Flood codes also allow MIKE SHE to communicate directly with MIKE HYDRO whenever the water elevation of flood code cells exceed the water elevation in the river branch, as long as the water elevation in the branch is higher than the grid cell's topographic elevation. Flood codes were also used in areas where direct connections were not explicitly represented, such as ponds or lakes within proximity of a river branch, or water bodies that become disconnected in the DEM. An example of this is shown in **Figure 26**.

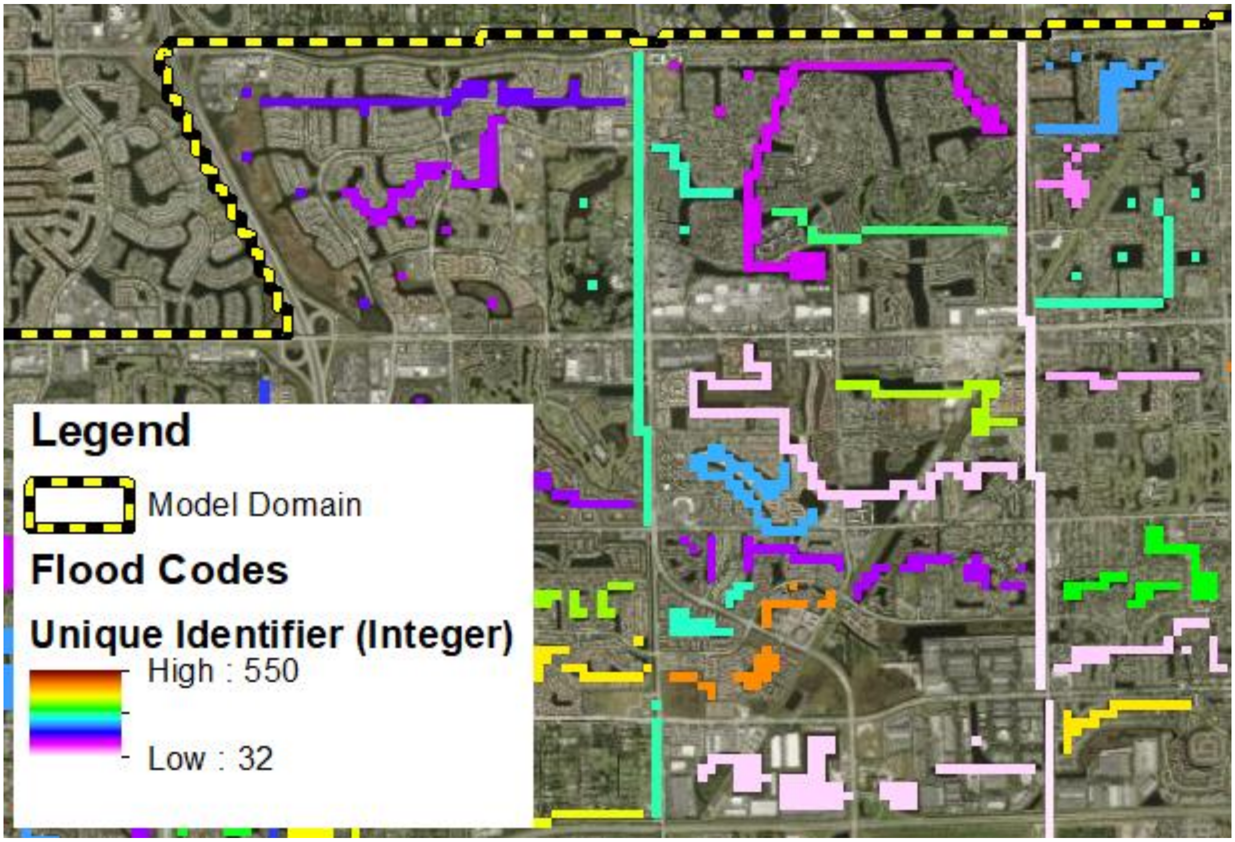

Figure 26: Example of Flood Code Placement

Flood code cells are excluded from 2D overland flow computations, so it is important to place them wisely, such as the lowest cell in an area. Covering an entire lake with flood code cells would turn off the overland computations for the entire lake. Therefore, the only time entire water features were covered with flood codes was when the storage was accounted for in the 1D model, such as a branch going through a lake (the lake water levels are computed in the 1-D model and the cross sections extend to the edges of the lake). Flood codes along secondary and tertiary canals are generally limited to one cell along each bank.

The detailed surface topography provided an opportunity to take advantage of the flood code feature and account for storage that would otherwise be lost in a larger resolution topographic map. The flood code setup is shown in **Figure 27**. Although the specific value of the flood code does not matter, as they are just an identifier that relate a cell to a specific branch, the flood code values in the C-9 basin were kept the same as the 2019 Broward County Model for consistency. New flood code areas were assigned identifiers not used in the 2019 Broward County model, which should eliminate any issues in the future if the models are merged.

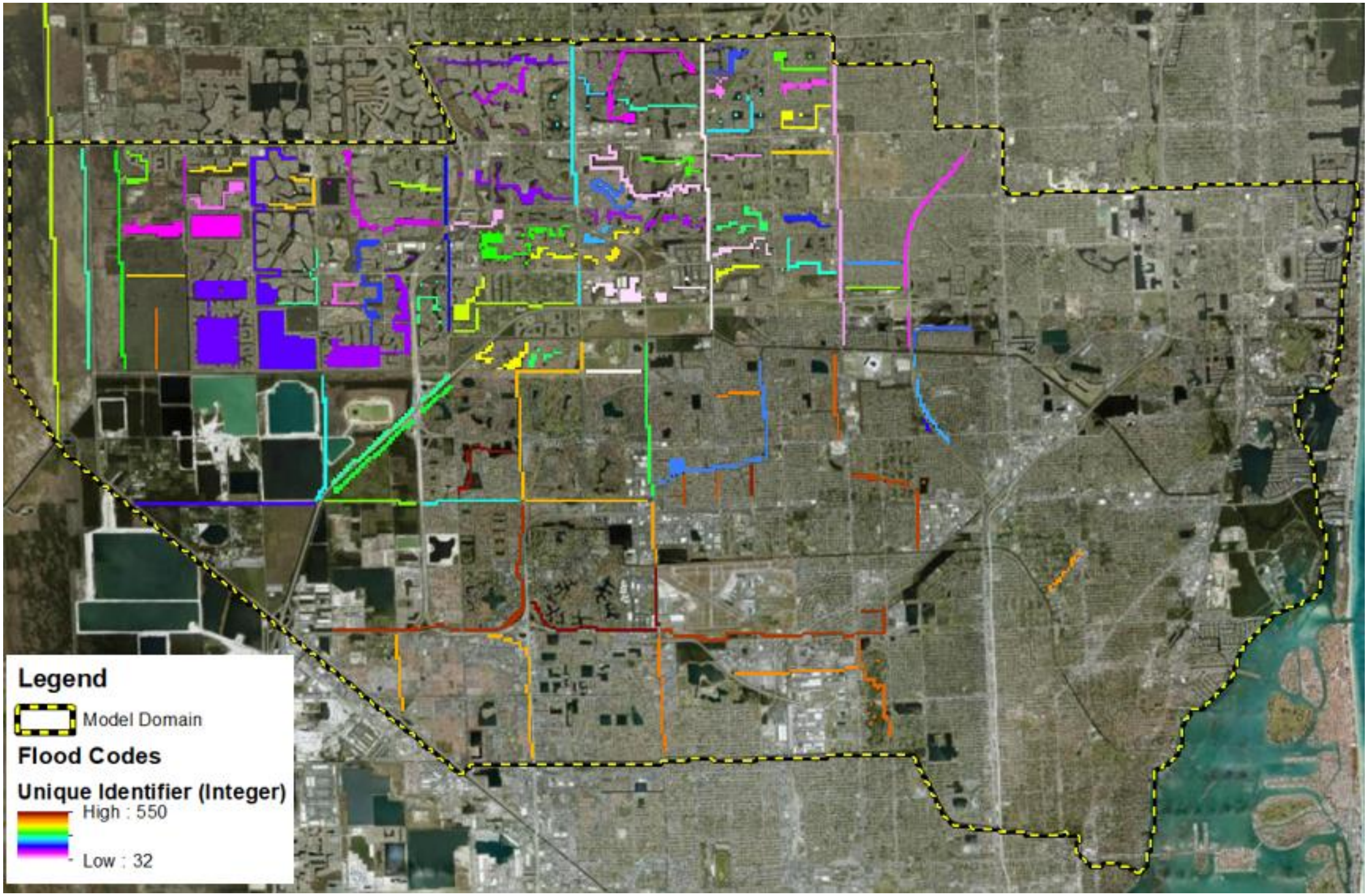

Figure 27: Flood Codes

2.2.6.3.2 Overbank Spilling

The C-8 and C-9 primary canals rely on overbank spilling instead of flood codes, which allows communication between MIKE SHE and MIKE HYDRO via the weir equation, whenever the water level in the canals become greater than the cross section bank elevations. Overbank spilling is based on the cross section and the 2D grid, whichever is higher. In most instances, the berms are not represented well in the 125-ft or 250-ft topo grid, as median values are used, so the berm elevations should be included in the cross sections. In instances where the 2D grid is higher than the cross section, the water will "glass wall" in the cross section until it reaches the 2D grid elevation. Overbank spilling provides a more physically based representation of the exchange between canal and 2D grid, which is more important on the C-8 and C-9 canal than the secondary and tertiary canal system as they are the focus of this FPLOS project. Therefore C-8 and C-9 will only spill out to the 2d model when water levels get above bank elevations, whereas branches with flood codes may exchange whenever the water level in the canal is greater than the water level on the 2D grid (ignores bank elevations- assumes it has connectivity such as culverts).

2.2.6.4 Hydrodynamic Initial Conditions

The 1D model's initial water levels are set based on two different categories, which are (1) based on observed data and (2) based on control elevations. In areas where there is observed data, such as water elevation upstream of the C-8 and C-9 tidal structures for calibration and validation simulations, the initial conditions are set to match the observed data. In areas that are controlled via operable control structures such as SBDD, the initial conditions are set to match the control elevation, which differ from the gate open or pump on elevations. This is consistent with the approach used in the 2019 Broward County Model. For the design storm, the 1D model's initial water levels will be set based on control elevations.

2.2.7 Overland Flow

The overland flow module, or 2D model, is essentially parameterized by district drainage basin. The C-9 basin, which mainly lies within Broward County, was parameterized to be consistent with the 2019 Broward County model, which was based on two major categories: (1) land use and (2) ERP permitted areas. The C-8 Basin, which is in Miami-Dade County, was parameterized in a similar way but based on different data. This is explained in the following subsections.

2.2.7.1 Overland Flow in Broward County

Most of the parameters in the overland flow model are spatially varied by land use, while other parameters are spatially varied by land use within ERP permitted areas. A large portion of Broward County is made up of permitted areas that are required to retain some volume of rainfall, whether it be the first 1-inch of rainfall or 2.5-inches over the impervious area, or a more stringent requirement to retain the runoff resulting from the 25-year 3-day storm, with no discharge. For the 2019 Broward County model, Taylor Engineering proposed to separate the permitted areas into the following categories: (1) areas controlled by operable structures such as pumps or gates, (2) areas that had at least 10% waterbody land coverage such as lakes or ponds, (3a) areas with less than 10% waterbody land coverage and have at least 2.5 feet depth to water table, and (3b) areas with less than 10% waterbody land coverage and have less than 2.5 feet depth to water table. Depth to groundwater was estimated by subtracting the initial groundwater elevation from the topography elevation. The assumption behind this is that areas with an initial depth to groundwater greater than 2.5-feet would have the ability to infiltrate more rainfall than areas with less than 2.5-feet. This was the assumed threshold for where exfiltration areas would likely be located. It is important to note that this assumption does not in any way affect the actual infiltration ability of the model, it was just a way to select which areas to parameterize to account for what cannot be explicitly modeled.

Permit areas classified as category 1, those behind operable structures, were parameterized just based on land use, as if they were unpermitted. Flow to the canal network from these areas is controlled by operable structures (gates and pumps), which are designed to limit discharge to permitted values and at permitted threshold water levels. Therefore, runoff rates within the respective drainage areas are ultimately limited by the operable structure. Although there may in fact be permitted areas within an overall drainage area that are held to a higher level of stormwater retention, for the purposes of this sub-regional scale model, if the operable structure is within its permitted allowance than it can be assumed that so are the areas draining to it. These areas classified as category 1 are controlled by permitted pumps and gates, that retain water on-site until the water levels reach the permitted discharge elevation, which means they often have a large amount of "dead storage" or on-site retention. Permit areas classified as category 2, those with at least 10% waterbody land coverage, were parameterized to account for the required detention storage, potential surface water storage, and sub-grid scale drainage features. Permit areas classified as category 3a, those with less than 10% waterbody land coverage and on average more than 2.5 feet depth to water table, were parameterized to account for the required detention storage and the likelihood of exfiltration trenches and other stormwater management features. Permit areas classified as category 3b, those with less than 10% waterbody land coverage and on average less than 2.5 feet depth to water table, were parameterized to only account for the required on-site retention. There are no 3b areas within the C-9 basin, however, this was the classification used for the 2019 Broward County model, so category 3b was kept to be consistent. A map of Broward County's permitted areas within the model domain can be seen in **Figure 28**.

Stormwater Management Category	Criteria	Parametrization
1	-Located in Broward County -Controlled by pump/gate	No change
2	-Located in Broward County -Greater than 10% water cover	Maximum storage change rate based on SFWMD CSM rating
3a	-Located in Broward County -Less than 10% water cover and greater than 2.5 feet depth to water table	-Increased detention storage based on 1" or 2.5x impervious (whichever is greater) -runoff coefficient decreased by 50%

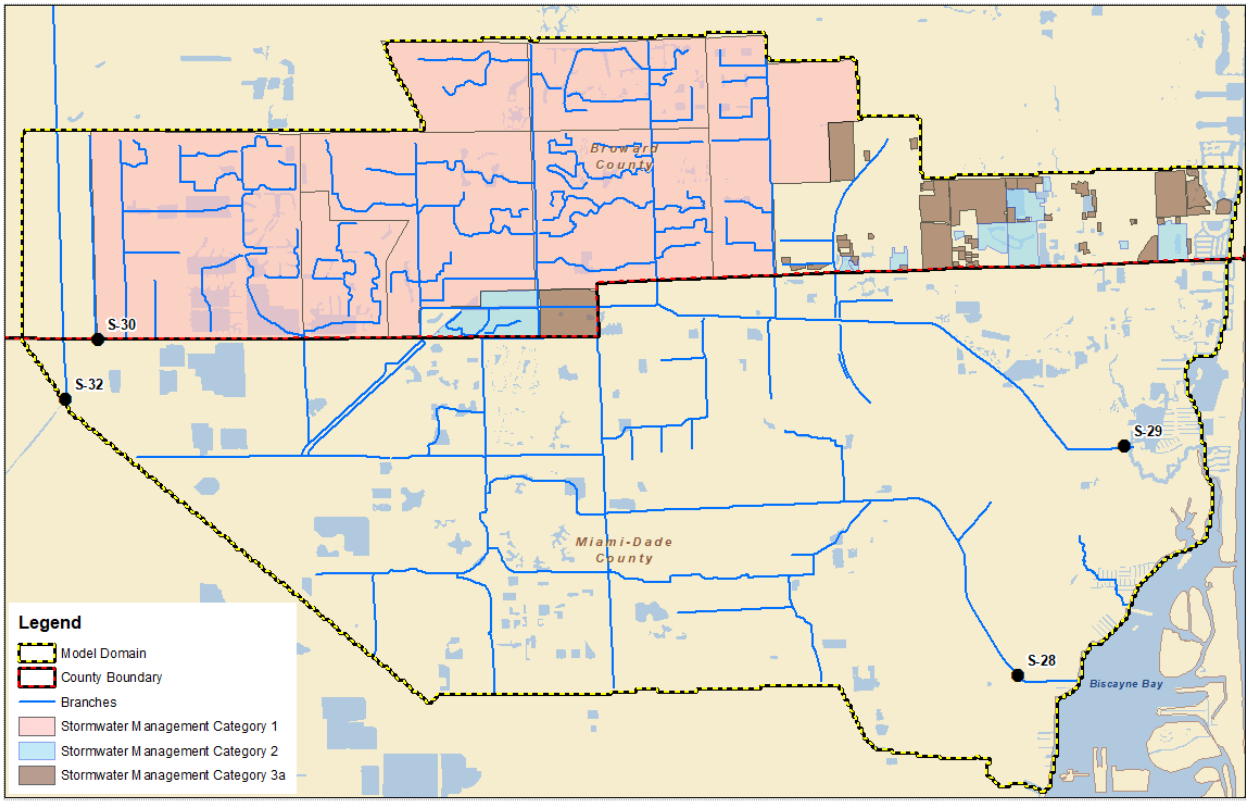

Figure 28: Stormwater Management Categories Used to Parameterize Overland Flow in Broward County

2.2.7.2 Overland Flow in Miami-Dade County

Within the Miami-Dade portion of the model, most of the parameters in the overland flow model are spatially varied by land use, while other parameters are spatially varied by land use within areas that are internally drained. Several areas within the C-8 drainage basin are either internally drained or have a large network of French drains, both of which reduce the amount of runoff making its way to the C-8 and C-9 Canals. Although the capacity of the French drain systems in Miami-Dade County are unknown, they are designed to retain/infiltrate some volume of rainfall before discharging into the canal system. Taylor Engineering proposed to the District to separate drainage areas into the following categories: (5) areas draining directly to MIKE Hydro branches, (6) areas internally drained or that have a large amount of French drains relative to area served, and (7) areas both draining to branches and having French drains.

Areas classified as category 5, those draining to a branch, were parameterized just based on land use. Areas classified as category 6, those internally drained or have a large amount of French drains, were parameterized by land use and adjusted to account for features that route and store water within the drainage basin. Areas classified as category 7, were parameterized by land use and adjusted to account for potential water storage and sub-grid scale drainage features like exfiltration trenches and other stormwater management features. Although based on different criteria, these categories are similar to the stormwater management category areas classified for the 2019 Broward County model. A map of the drainage categories developed for the Miami-Dade County portion of the model domain can be seen in **Figure 29**.

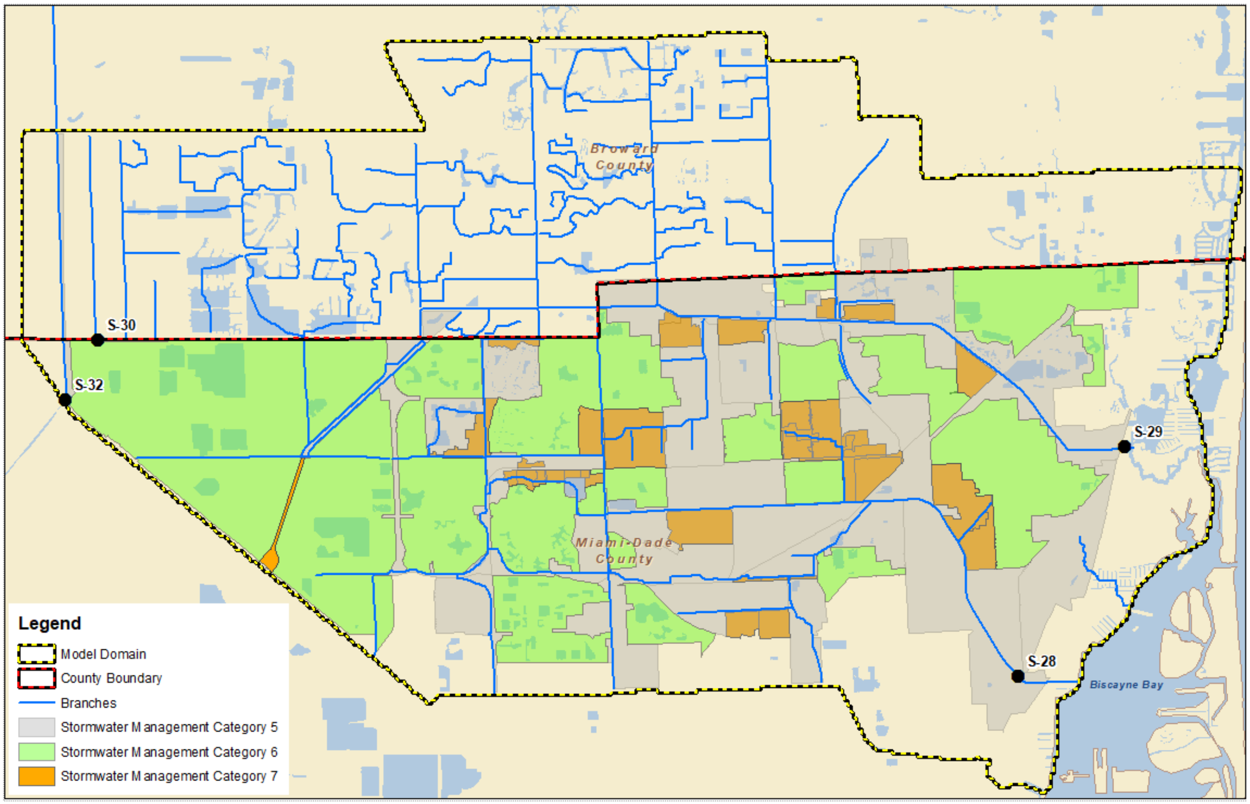

Figure 29: Drainage Categories Used to Parameterized Overland Flow in Miami-Dade County

Stormwater Management Category	Criteria	Parametrization
5	-Located in Miami-Dade County -Drains directly to canal	No change
6	- Located in Miami-Dade County - internally drained or has a large amount of French drains	-Increased detention storage based on 1" or 2.5x impervious (whichever is greater) -Runoff coefficient decreased by 50%
7	-Located in Miami-Dade County -Drains directly to canal AND has a large amount of French Drains	-Increased detention storage based on 1" or 2.5x impervious (whichever is greater) -Runoff coefficient decreased by 50% (differs from category 6 in that ponded drainage routine is allowed to route water directly to canal)

As shown in the next figure (**Figure 30**)**,** the areas in green are assumed to be internally drained for the purpose of parameterizing the ponded and saturated zone drain routines as discussed in the following subsections. These areas either drain to local water bodies or have a large amount of French drains. However, it is important to note that runoff from these areas can still be routed to the MIKE Hydro branches via the 2-D overland module. The areas in yellow are areas that drain to branches, however, several areas in yellow also have a large amount of French drains, as shown by the red lines. In this figure, areas that are green are considered category 6. The areas in yellow that have little to no French drains are considered category 5. The areas in yellow that have a large amount of French drains are considered category 7. The area in purple drains to the boundary, so the specific overland flow parameterization is less likely to affect the model results and were only parameterized based on land use.

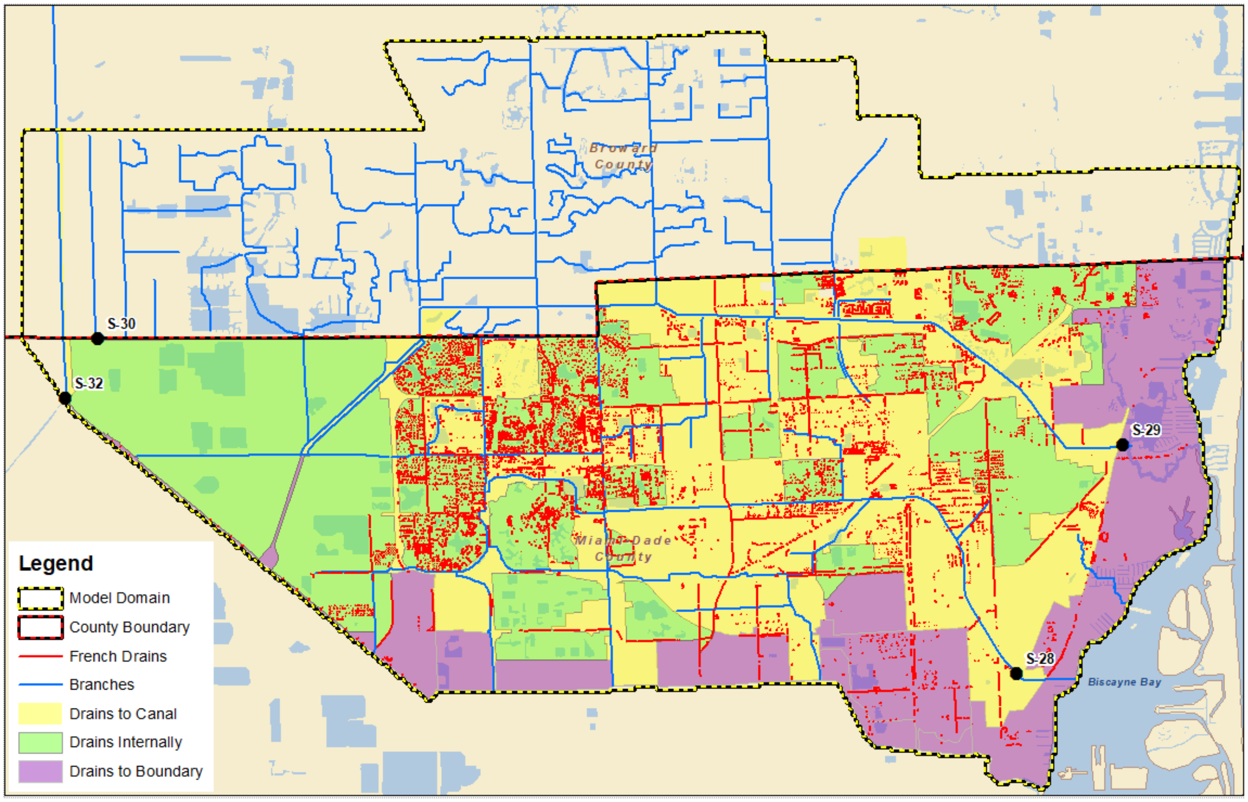

Figure 30: Drainage Categories in the Miami-Dare County Portion of the Model Domain

2.2.7.3 Overland Manning's Roughness Coefficient (n-value)

This parameter, used in the MIKE SHE 2-D overland flow component, is spatially distributed based on land use, with values ranging from 0.06 to 0.45 based both literature (Environmental Protection Agency, 2015) and professional experience (**Table 5**).

Table 5: Land Use Based Manning's Roughness (n) Coefficients

FLUCCS Code	Land Use	Manning's Roughness (n)	Manning's Roughness (M)
1100	Residential, Low Density	0.14	7.14
1200	Residential, Medium Density	0.12	8.33
1300	Residential, High Density	0.11	9.09
1400	Commercial and Services	0.07	14.29
1500	Industrial	0.07	14.29
1700	Institutional	0.13	7.69
1800	Recreational	0.13	7.69
1900	Open Land	0.14	7.14
2100	Cropland and Pastureland	0.17	5.88
2200	Tree Crops	0.17	5.88
2300	Feeding Operations	0.17	5.88
2400	Nurseries and Vineyards	0.17	5.88
2500	Specialty Farms	0.17	5.88
2600	Other Open Lands - Rural	0.14	7.14
3100	Herbaceous (Dry Prairie)	0.13	7.69
3200	Upland Shrub and Brushland	0.3	3.33
3300	Mixed Rangeland	0.3	3.33
4200	Upland Hardwood Forests	0.45	2.22
4300	Upland Mixed Forests	0.45	2.22
5100	Streams and Waterways	0.06	16.67
5200	Lakes	0.06	16.67
5300	Reservoirs	0.06	16.67
5400	Bays and Estuaries	0.06	16.67
5700	Ocean and Gulf	0.06	16.67
6100	Wetland Hardwood Forests	0.45	2.22
6400	Vegetated Non-Forested Wetlands	0.3	3.33
7400	Disturbed Land	0.14	7.14
8100	Transportation	0.11	9.09
8200	Communications	0.14	7.14
8300	Utilities	0.14	7.14

2.2.7.4 *Detention Storage*

This parameter is spatially distributed, based on both land use and the categories defined for Broward County and Miami-Dade County. Within Broward County, the non-permitted area's detention storage was spatially distributed based on land use with values ranging from 0 to 0.4 inches, as shown in **Table 6**.

Table 6: Land Use Based Detention Storage

FLUCCS Code	Land Use	Detention Storage (in)
1100	Residential, Low Density	0.1
1200	Residential, Medium Density	0.1
1300	Residential, High Density	0.1
1400	Commercial and Services	0.1
1500	Industrial	0.1
1700	Institutional	0.1
1800	Recreational	0.3
1900	Open Land	0.15
2100	Cropland and Pastureland	0.15
2200	Tree Crops	0.25
2300	Feeding Operations	0.25
2400	Nurseries and Vineyards	0.25
2500	Specialty Farms	0.25
2600	Other Open Lands - Rural	0.15
3100	Herbaceous (Dry Prairie)	0.15
3200	Upland Shrub and Brushland	0.15
3300	Mixed Rangeland	0.15
4200	Upland Hardwood Forests	0.4
4300	Upland Mixed Forests	0.4
5100	Streams and Waterways	0
5200	Lakes	0
5300	Reservoirs	0
5400	Bays and Estuaries	0
5700	Ocean and Gulf	0
6100	Wetland Hardwood Forests	0.4
6400	Vegetated Non-Forested Wetlands	0.4
7400	Disturbed Land	0.1
8100	Transportation	0.1
8200	Communications	0.1
8300	Utilities	0.1

Even at a fine grid size of 125-ft, not all storage can be accounted for. This detention storage represents microtopography not represented in the DEM, such as potholes, bird baths, pools, street-side swales, etc. First, detention storage values of 0.1”-0.4” (based on professional experience and literature) were applied model-wide to account for sub-grid scale storage features. In areas controlled by operable control structures, such as SBDD, no additional changes to detention storage were made. In the remaining permitted areas or French drain areas, detention storage was increased to represent the small-scale on-site stormwater treatment or storage areas that are not explicitly modeled. This is expanded upon in the next few paragraphs,

In permitted areas within Broward County, the detention storage was spatially distributed by land use, but adjusted to account for the required retention. The permitted areas have ordinance requiring retention of the 1st 1-inch of rainfall or 2.5-inches of rainfall over the impervious area, whichever is greater. Within the permitted areas, the detention storage for impervious areas were increased by multiplying the paved area runoff coefficients (percentage of DCIA) by 2.5 inches, and any of the resulting values less than 1” was increased to 1”. Therefore, within category 2, and 3a permitted areas, the detention storage increased from 0.1-0.4 inches to 1-1.8 inches, dependent on the land use. This helps represent the on-site retention that permitted areas are required to have.

Within the Miami-Dade County portion of the model domain, the drainage categories were treated in a similar way to the permitted areas within Broward County. In drainage category 5 areas, those that drain to a canal and have little to no French drains, the detention storage was treated the same as non-permitted areas in Broward County and only parameterized based on land use, with values ranging from 0-0.4 inches (**Table 6**). In drainage category 6 areas, those that are internally drained to water bodies or low areas or have a large amount of French drains, the detention storage was treated the same as permitted areas in Broward County and parameterized basin on land use and adjusted to account for retention. Although these areas are forced to drain to local depressions within the ponded drainage routine, the detention storage was increased to hold that drained water on-site, representing the internal storage of local depressions and exfiltration areas. Otherwise, ponded water above the detention storage can still flow via the 2D overland flow routine into other drainage areas and then be routed to a branch. These category 6 areas were adjusted from 0.1-0.4 inches to 1-1.8 inches, based on land use. These values for category 6 areas were an initial model parameterization. In drainage category 7 areas, those that drain to a canal and have a relatively large amount of French drains, the detention storage was treated the same as permitted areas in Broward County and parameterized basin on land use and adjusted to account for retention provided by exfiltration areas, with values being increased from 0.1-0.4 inches to 1-1.8 inches. Category 7 areas differ from category 6 areas as they can drain to a branch within the ponded drainage routine, after the detention storage has been met. These values for category 7 areas were also an initial model parameterization, which could have been adjusted during calibration, but were not.

2.2.7.5 Initial Water Depth

The initial water depth defines the initial water depth on the ground surface in the 2-D overland module, also known as ponded water. This parameter was developed using an approach based on topography and basin control elevation, which is consistent with the 2019 Broward County model. Any cells within a drainage basin that are lower than the basin’s water control elevation have an initial depth equal to the difference of the water control elevation and the elevation of the cell (**Figure 31**). This eliminates excess "dead storage" and ensures that water is not being routed via ponded drainage or flood codes at the start of the simulation. Specifying an initial depth will result in ponded water, which will eliminate the "dead storage" associated with a local sink. This also provides consistency between 1D and 2D model initial water elevations.

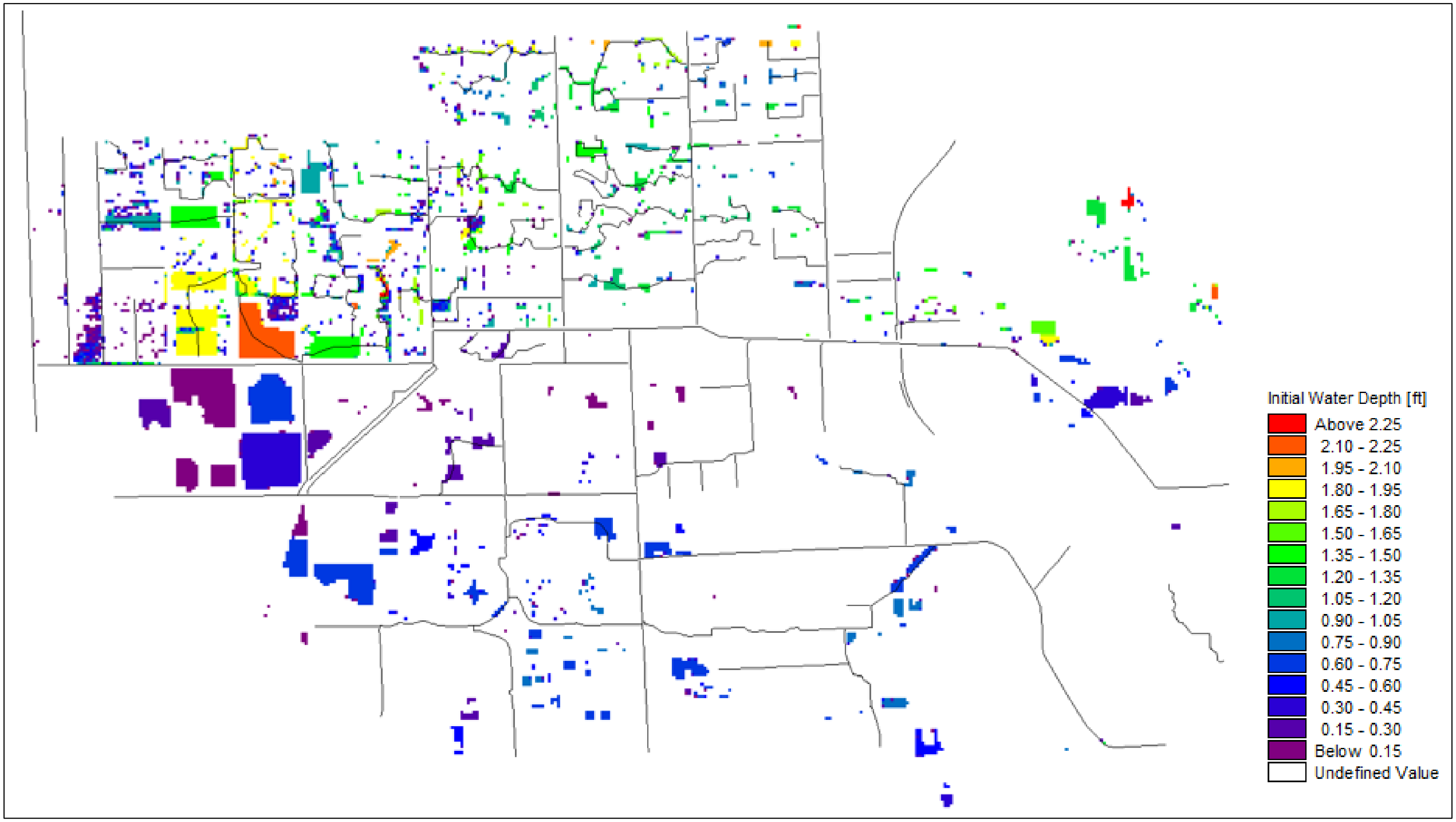

Figure 31: Initial Water Depths in the 2D Model

2.2.7.6 Surface-Subsurface Leakage Coefficient

This parameter reduces the exchange between land surface and the unsaturated or saturated zone, which can help account for near-surface soil compaction or fine sediment deposits. The model can be very sensitive to this parameter; too small of a value can essentially act as if there is an impermeable layer and allow for little to no infiltration. The leakage coefficient was set to a uniform spatial distribution using the model default value of 1E-4. No permanent changes to spatial distribution or magnitude were made during model calibration.

2.2.7.7 Ponded Drainage

This is a relatively new feature introduced in the 2017 release of MIKE SHE that simulates routing of ponded water from impervious surfaces via features that are not explicitly modeled, such as curb inlets and local-scale storm drains. The ponded drainage routine routes runoff from directly connected impervious areas (DCIA) to canals based on user-specified drainage basins. The volume that is allowed to be routed is determined by a paved area runoff coefficient, which was assigned based on land use, and a maximum storage change rate. The rate at which the volume is routed is controlled by time constants. These parameters are discussed in the following subsections.

2.2.7.7.1 Maximum Storage Change Rate

This parameter was set to a uniform spatial distribution with a value of 0.095 ft3/s (each grid cell limited to 40mm/day), and then adjusted in specific areas where there was evidence suggesting a different value. Choosing realistic values ensures proper drainage representation and prevents drainage rates from exceeding sub-grid scale drainage capacities. For example, if sub-grid scale drainage features such as roadside swales and culverts are designed to handle 5-inches of rainfall over the course of a day, then the maximum storage rate should correspond. Within the Broward County portion of the model, the category 2 permitted area's maximum storage change rate was spatially distributed based on the permitted cubic feet per second per square mile (CSM) allowance per SFWMD drainage basin (See **Appendix C**). In the western portion of the C-9 drainage basin, the allowable discharge is 20 CSM pumped, which is equivalent to 0.045 ft3/s based on the model grid size (each grid cell limited to 18.9mm/day). This parameterization ensures that the permitted areas do not discharge more than their permitted allowance. Only category 2 permitted areas were based on the district's CSM allowance as these were the area's most likely holding water back in their surface waterbodies and discharging through structures at a permitted rate. Based on location, this 20 CSM pumped criteria only applies to 1 permit area in the western C-9 basin based on the way we developed the categories. However, this 1 permit area happens to be explicitly simulated and is known to drain via gravity connection only, therefore, there are currently no areas where this 20 CSM pumped criteria applies. However, this categorization and criteria should be applied when considering future development and land use changes.

The C-8 canal has "essentially unlimited inflow by gravity connection", so no restrictions are necessarily required. This parameter could have been restricted in category 7 areas during model calibration, to help reduce the volume of runoff making it to the branch (capacity of exfiltration areas unknown), but changes were deemed unnecessary. Similarly, the initial value of 0.095 ft3/s, which is equivalent to about 43 CSM, could have been increased for the C-8 basin during model calibration.

This parameter will only limit discharge in the ponded drainage routine, which is meant to represent sub-grid scale drainage features (e.g., local-scale storm drains). Therefore, this will limit the ponded drainage discharge during bigger storm events, but this is appropriate. If the local small-scale drainage features were only designed to handle a 25-year storm, then the discharge will be limited during a 100-year storm. This does not limit discharge by 2-D overland flow. This parameter only limits the ponded drainage discharge, which is only responsible for routing a portion of the runoff occurring over the paved area fraction (i.e., directly connected impervious).

2.2.7.7.2 Paved Runoff Coefficient

This parameter represents DCIA and is spatially distributed based on land use and stormwater management categories (SMC). Essentially, the paved area runoff coefficient (ponded drainage runoff coefficient in MIKE SHE) is the fraction of ponded water that drains to storm sewers and other surface drainage features in paved areas (MIKE SHE User Guide V1, 2017, p265). Within Broward County, the paved runoff coefficients were parameterized based on land use. In category 3a permitted areas, the paved area runoff coefficients were distributed based on land use like everywhere else, but then decreased by half. Since these permitted areas are assumed to use management features such as exfiltration trenches, the paved area runoff coefficients were adjusted to reduce the amount of runoff and increase the infiltration, as one would expect in areas served by exfiltration features. Within Miami-Dade County, the paved runoff coefficients were parameterized based on land use. In areas served by a relatively large amount of French drains, the paved area runoff coefficients were distributed based on land use, but then decreased by half, just like category 3a permitted areas within Broward County. Decreasing the runoff coefficient reduced runoff which provides the opportunity for increased infiltration. This parameterization is an attempt to simulate what cannot be explicitly represented in this scale of a model. The land use areas that were included in the ponded drainage routine can be seen in **Table 7**. All other land use categories, such as forests, were set to 0, which "turns off" the ponded drainage routine for those areas. These paved runoff coefficients were derived from the 2019 Broward County Current Conditions model and professional experience.

Table 7: Land Use Based Paved Runoff Coefficients

FLUCCS Code	Land Use	Paved Runoff Coefficient	Paved Runoff Coefficient in Category 3a Permitted Areas and Drainage Category 6 and 7 Areas
1100	Residential, Low Density	0.075	0.0375
1200	Residential, Medium Density	0.22	0.11
1300	Residential, High Density	0.45	0.225
1400	Commercial and Services	0.72	0.36
1500	Industrial	0.4	0.2
1700	Institutional	0.3	0.15
8100	Transportation	0.56	0.28

2.2.7.7.3 Inflow and Outflow Constant

These parameters can be adjusted to speed up or slow down the rate at which ponded drainage is routed to the river branches. Making the inflow constant larger than the outflow constant will create artificial storage, so this was avoided. An initial value of 0.001, the model default, was used as a starting point for both inflow and outflow constants. No permanent changes were made during model calibration.

2.2.7.7.4 Drain Codes

Each drain code represents an individual subbasin, for the purpose of draining water internally or to a branch via the ponded and saturated zone drain routines. It should be noted that these "subbasins" do not prevent overland exchange between areas. In areas of uncertainty, drainage basins were left as larger areas so that the 2-D overland flow model could determine drainage divides. Basins were only further refined if there was clear evidence in the DEM, such as visible berms or water bodies with differing elevations. In the Broward County portion of the model, the majority of the area was defined based on data provided by South Broward Drainage District, and their permitted drainage basins. In the Miami-Dade portion of the model, subbasins were developed from data provided digitally by Miami-Dade County. Miami-Dade County provided very detailed subbasin data, much too refined for this scale model. Therefore, new subbasins were developed by defining and aggregating basins based on drainage categories (as discussed in section **2.2.7.2**) and drainage destination (such as a specific canal). Essentially, areas with the same classification that shared a common boundary and destination, were merged into 1 basin. This process resulted in the number of basins in the Miami-Dade portion of the model to be decreased from about 830 basins down to about 40, while maintaining drainage characteristics.

Cells assigned an initial depth or a flood code, have a drain code of 0 assigned (dark blue cells in **Figure 32**), which turns off drainage from that cell. Not doing so would create feedback loops, as the drained water would return back to the cell via flood code, only to be drained back to the branch again and so on. **Figure 32** shows a map of the drain codes, where each unique color represents a drainage basin (areas in yellow drain to boundary). Although the specific value of the positive drain codes do not matter (negative drains to boundary) as they are just an identifier that define a drainage area, the drain code values in the C-9 basin were kept the same as the 2019 Broward County Model for consistency. New drain codes were assigned identifiers not used in the 2019 Broward County model, which should eliminate any issues in the future if the models are merged together.

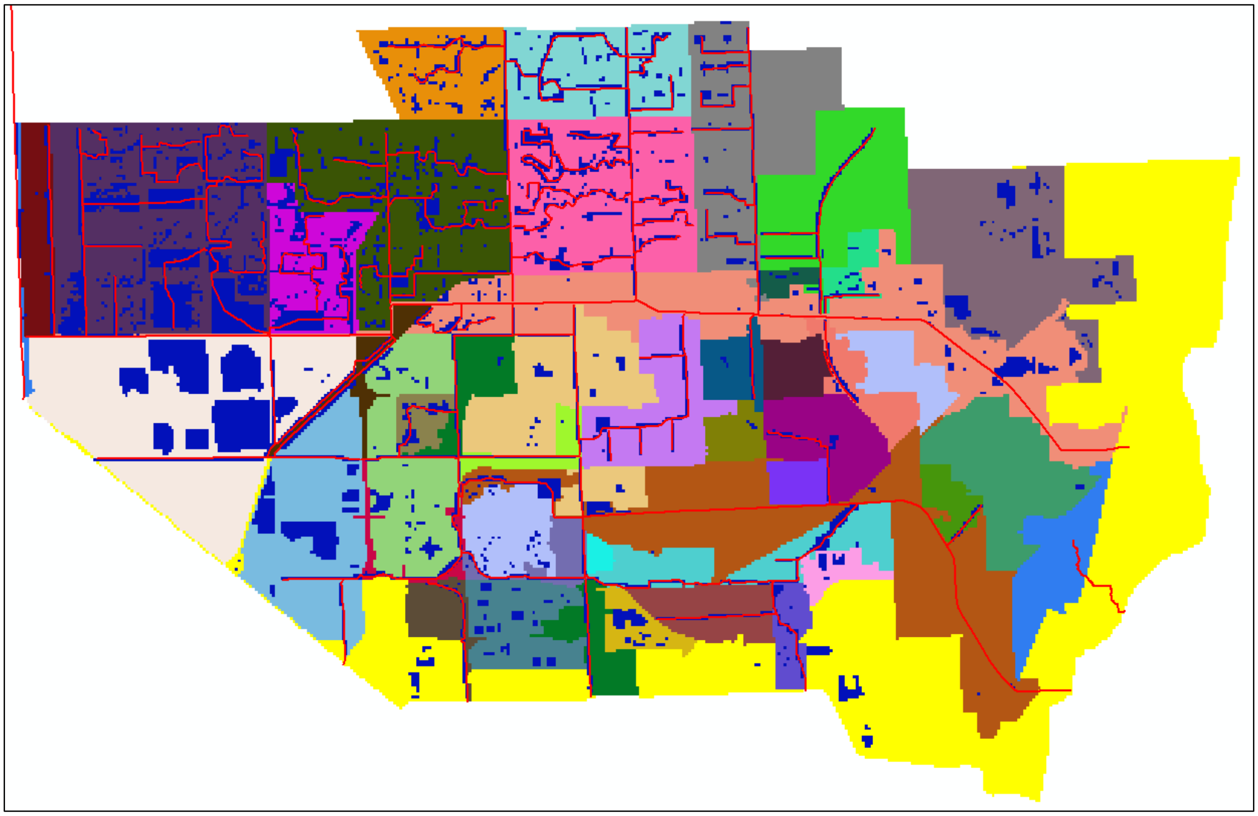

Figure 32: Drain Codes

2.2.8 Unsaturated Zone

The soil distributions and unsaturated zone parameters were carried over from the 2019 Broward County Current Conditions model (which were mainly inherited from the Broward County 2014 FEMA model) (**Figure 33**). The 2019 Broward County model's soil parameters that were changed were the saturated water content and field capacity for Margate Fine Sand and the field capacity for urban land, which were adjusted during model validation in an effort to improve the groundwater response to rainfall. These are incorporated in this model from the start. This model uses the simple 2-layer water balance method for unsaturated zone calculations, which is consistent with the 2019 Broward County model.

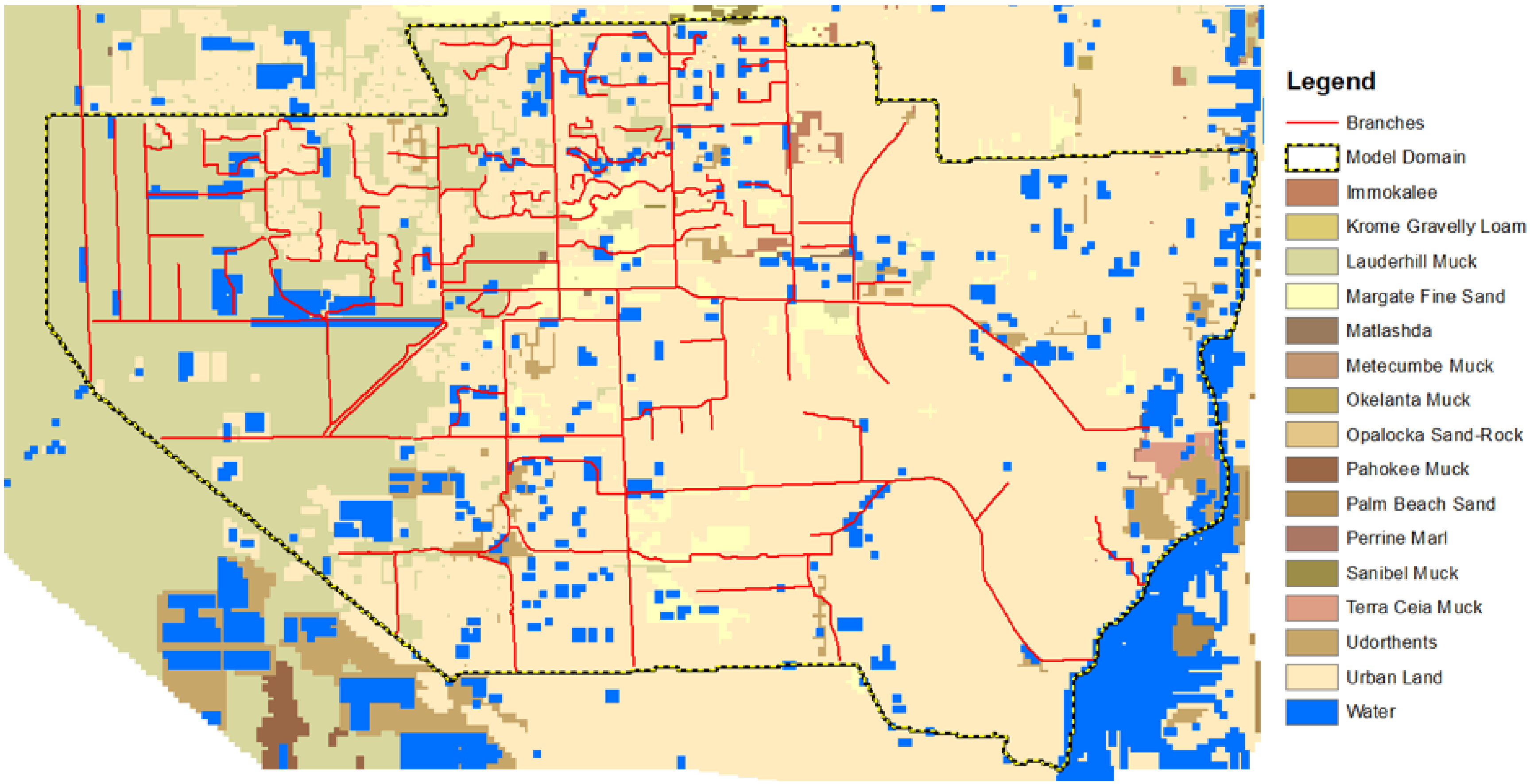

Figure 33: Map of Soils

2.2.9 Saturated Zone

This model initially used a 3-layer groundwater model based on the MODFLOW model developed by the USGS (Hughes and White, 2016). The USGS model represents the Biscayne aquifer with three hydrogeologic layers; two highly permeable layers separated by a less permeable layer. The 2019 Broward County Current Conditions model, which originally was developed for long- term water supply simulations, uses a more detailed 5-layer groundwater model. Although the saturated zone was reparametrized during model calibration using the lower levels, horizontal and vertical hydraulic conductivity, specific yield, and specific storage from the 2019 Broward County Model's input files (refer to **Section 3.1.2**), there are still setup differences between the two. In the C-8 C-9 model, only the first 3 of the 5 layers of the Broward County groundwater model was used. This would prevent the C-8 and C-9 models from being merged directly, but a simple solution would be to just add the last 2 groundwater layers into the C-8 and C-9 model if merging them is desired in the future.

2.2.9.1 Lower Levels of Computation Layers in Saturated Zone

This parameter was originally spatially distributed based on data from Hughes and White (2016) (refer to Deliverable 1.2). These values were modified during model calibration as described in **Section 3.1.2**.

2.2.9.2 Horizontal Hydraulic Conductivity

This parameter was originally spatially distributed based on data from Hughes and White (2016) (refer to Deliverable 1.2). These values were modified during model calibration as described in **Section 3.1.2**.

2.2.9.3 Vertical Hydraulic Conductivity

Initially, this parameter was spatially distributed based on data from Hughes and White (2016) (refer to Deliverable 1.2). However, these layers were modified to use the 2019 Broward County model inputs during model calibration as described in **Section 3.1.2**.

2.2.9.4 Specific Yield

Initially, this parameter was spatially distributed based on data from Hughes and White (2016) (refer to Deliverable 1.2). However, the model input was modified to use the 2019 Broward County specific yield during model calibration as described in **Section 3.1.2**.

2.2.9.5 Specific Storage

Initially, this parameter was spatially distributed based on data from Hughes and White (2016) (refer to Deliverable 1.2). However, these layers were modified to use the 2019 Broward County model inputs during model calibration as described in **Section 3.1.2**.

2.2.9.6 Initial Potential Head

There were not enough observed data points to generate a high confidence surface, so this parameter is spatially distributed based on results from Hughes and White (2016), with slight modification. The initial potential head from the USGS model was a close match at many of the observed points and had what appeared to be realistic “drawdown” near major branches. Therefore, the USGS data was used as a starting point and some localized adjustments were made to closer match the observed data. The initial potential head map is now within about +0.25 ft of the observation points.

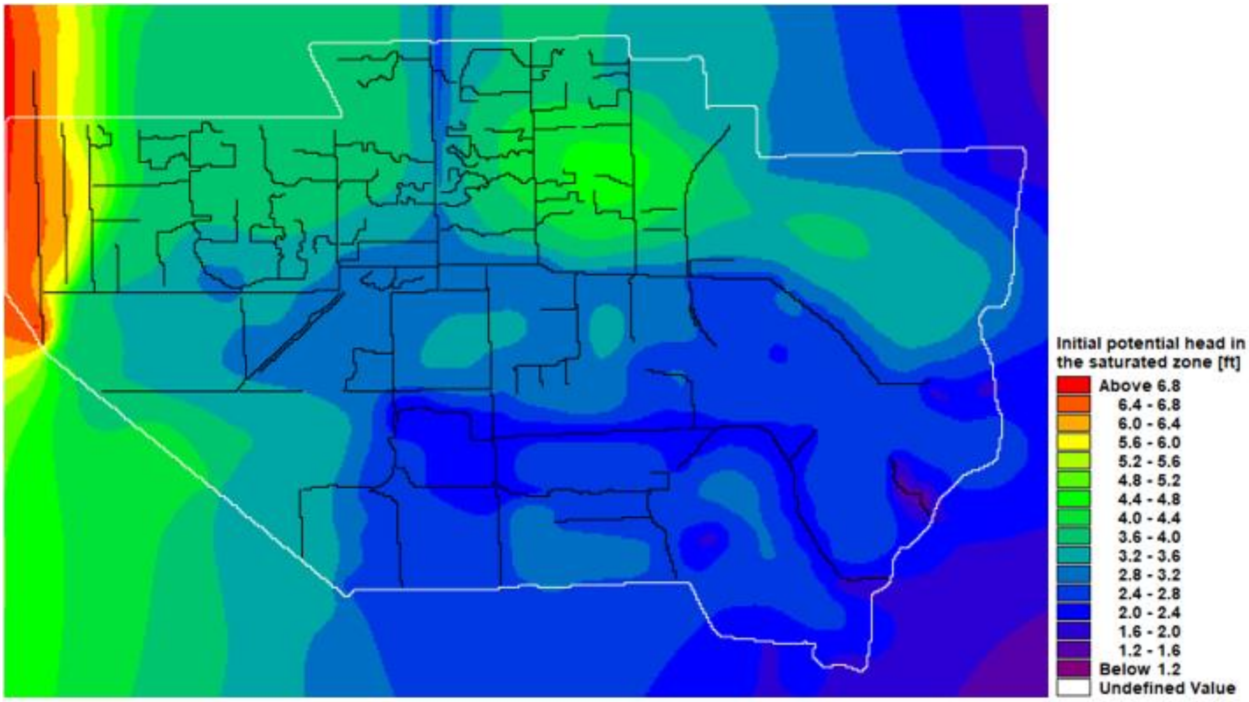

Figure 34: Initial Potential Head in Saturated Zone for October 2000

For the validation and design storm models, the initial potential head is spatially distributed based on data from Broward County’s average wet season head map (used for the 2019 Broward County model), and then extended south into Miami-Dade County, based on groundwater contours from the USGS (See **Appendix A**), as demonstrated in **Figure 35**. The initial potential head map for these events can be seen in **Figure 36**.

Figure 35: Development of Initial Potential Head for Validation and Design Storm Models

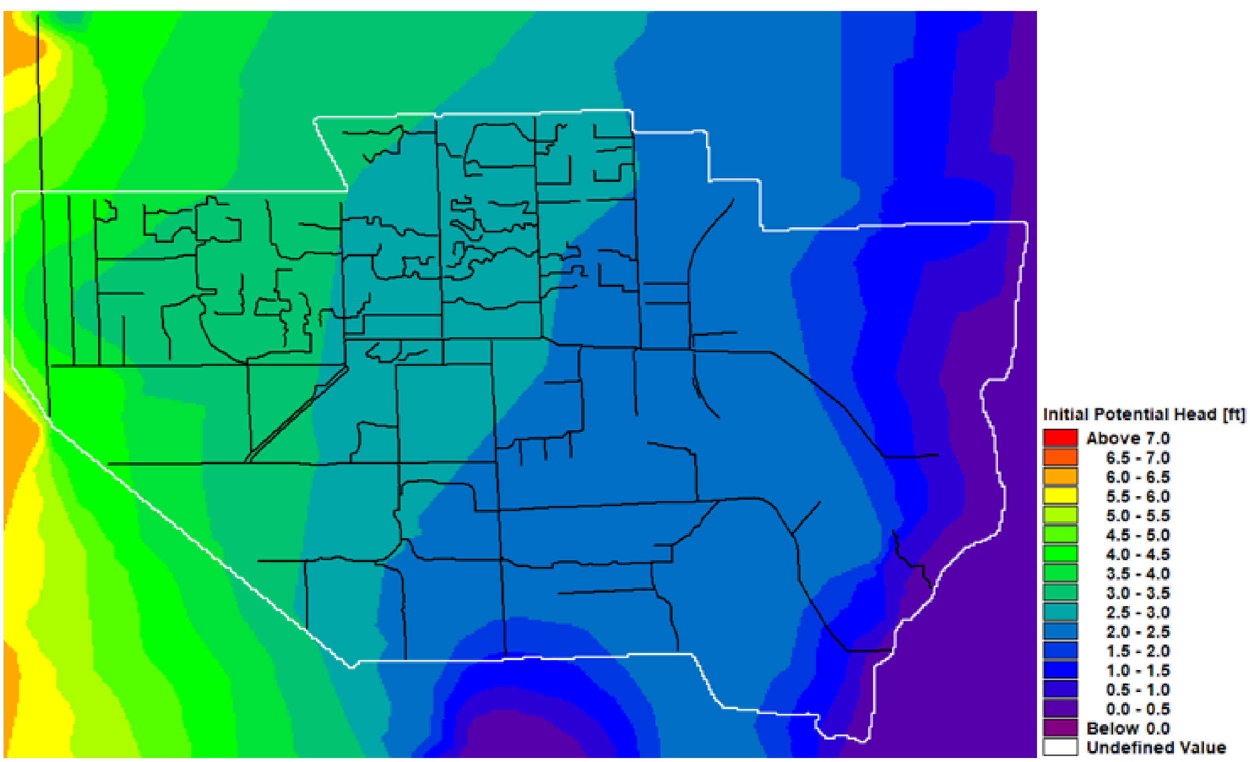

Figure 36: Initial Potential Head in Saturated Zone for June 2017

2.2.9.7 Boundary Conditions

Refer to the Section 1.9 for boundary conditions setup. Additional boundary conditions were added during model calibration (refer to **Section 3.1.3**).

2.2.9.8 Saturated Zone Drainage Level

The saturated zone drainage routine conceptually represents local-scale drainage features such as roadside underdrains, shallow swales, and field-scale agricultural ditches not explicitly represented elsewhere in the model setup. The saturated zone drainage level was developed based on land use, with urban areas set to 1.5 ft below ground, rural/agricultural areas set to 2.5 ft below ground, and 0 feet (turn saturated zone drainage off) for water and undeveloped areas (**Figure 37**).

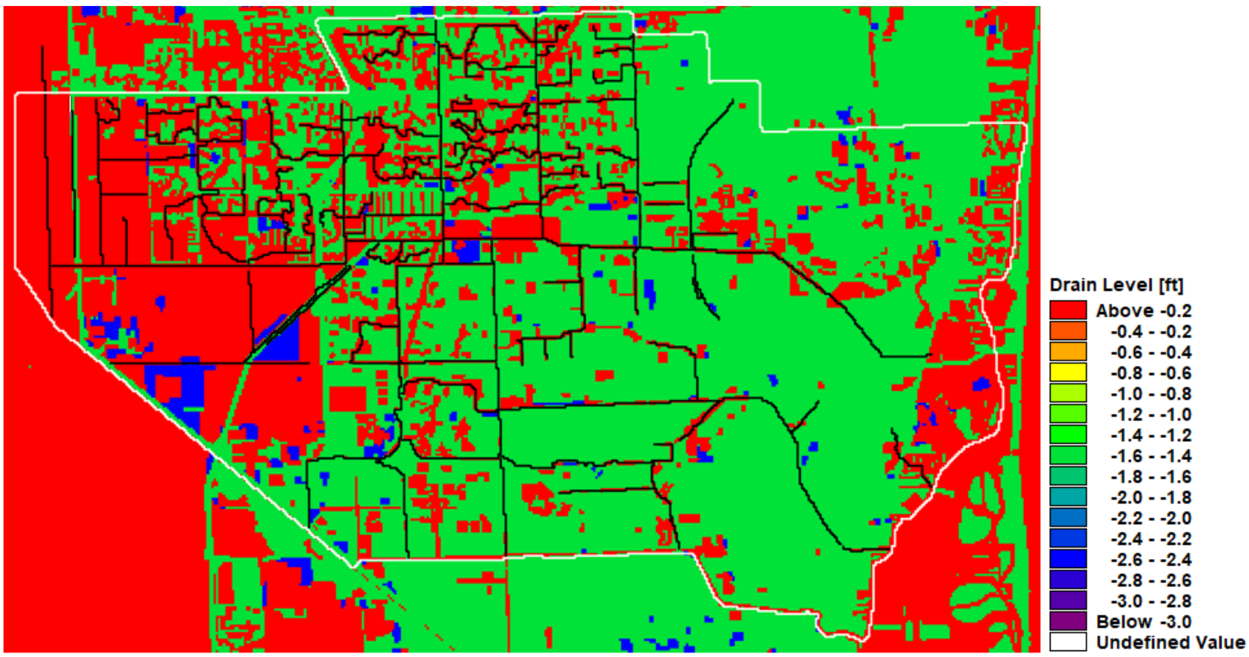

Figure 37: Drain Level in Saturated Zone

2.2.9.9 Saturated Zone Drainage Time Constant

This parameter was set to the final calibrated value from the 2019 Broward County model (within the C-9 basin), with a value of 5E-07/s. The saturated zone drainage is calculated as a linear reservoir based on the head difference between the water table and the drain level and a time constant. The time constant characterizes the "density" of the drainage network. In areas with a lot of drainage features, such as a basin with a lot of underdrains, then the time constant should be higher. The larger time constant allows the saturated zone to drain faster to the specified sink (local depression, boundary, or nearest branch within same drain code). In undeveloped land areas and water bodies, the time constant is set to an extremely small number, or 0, to shut off the saturated zone drainage routine.

2.2.9.10 Drainage Codes

The saturated zone drainage routine uses the same drain codes as the ponded drainage layer, without the initial depth or flood code cells set to drain code 0.

3.0 MODEL CALIBRATION AND VALIDATION

3.1 Model Calibration

The model calibration process focused on attaining the best-fit for the peak water levels, total discharge volume, and peak discharge. A calibration target of +/- 10-20% peak discharge and total discharge volume and +/- 0.5 ft headwater/tailwater and groundwater elevation were set. This approach allows a more comprehensive assessment of the model's simulated hydrologic and hydraulic response to rainfall, as compared to only matching peak stages or peak discharges. The SFWMD structures and groundwater wells used to calibrate the model can be seen in **Figure 38**. The operable structures (gates) used recorded gate openings and the tidal tailwater elevations were forced with the recorded water levels. The model's simulated peak headwater/tailwater, peak discharge, total discharge volume, and groundwater levels were compared with observed data which was obtained from SFWMD's DBHYDRO database.

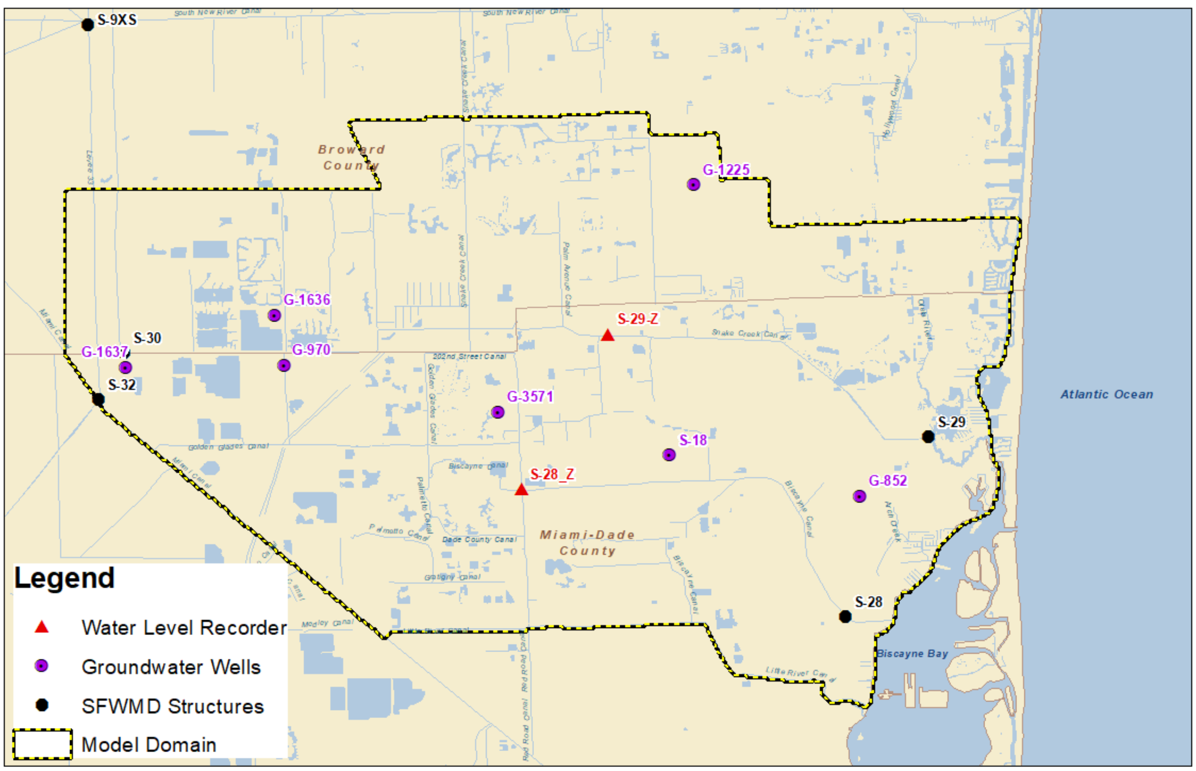

Figure 38: Location Map of Calibration Points

3.1.1 Calibration Summary

Model calibration started with reparameterizing the groundwater model and expanding the model domain so that an internal boundary condition could be included. This inclusion was done for consistency with the 2019 Broward County Model, and to attempt to improve the hydrologic response in the western part of the model domain. These adjustments could be viewed as a model setup correction more so than a calibration alteration. These modifications resulted in improved model simulated surface water and groundwater responses throughout the model domain. However, the model was significantly overpredicting the peak discharge rates and the total volume discharged through the tidal structures and subsequent calibration efforts were primarily focused on improving these simulated values. Several adjustments were made to parameters such as surface-subsurface leakage coefficient, paved area runoff coefficient, Manning's n for both overland and channel flow, ponded drainage time constants, and saturated zone drainage time constants, in an effort to reduce the runoff volume and shift the timing of the runoff to better simulate the "peaks". However, these parametric changes resulted in little to no improvement in model performance and often led to a worse agreement between simulated and observed surface water stages and groundwater levels. This suggested that inaccurate rainfall inputs may be a factor. It was known since the beginning of the project that the NEXRAD rainfall data was highly uncertain, due to both the lack of confidence in 20 year-old NEXRAD data and the temporal adjustments made to the rainfall time series, as discussed in **Section 1.6**. Therefore, the adjusted NEXRAD data was replaced with the rain gauge data. Subsequent model simulations showed significant improvements in simulated peak discharge rates and total discharge volumes. This, in combination with the validation results described in **Section 3.2,** suggests the initial rainfall setup was responsible for the aforementioned overpredictions in the calibration model. After the change in rainfall data, model calibration goals were met at most calibration points. In the areas not meeting calibration goals, localized adjustments were made but resulted in no significant improvement in model performance. The only adjustments that had value were changes to Manning's roughness in three canals. At this point in the calibration process, three things were evident: for the calibration period, gauge-based rainfall data was more reliable than NEXRAD data, but still does not fully capture spatial-temporal patterns in rainfall, (2) overall, there was a very good match between simulated and observed data, and (3) additional reasonable parametric changes are not resulting in further improvement in model performance. Therefore, Taylor Engineering felt confident that the model setup and parameterization was a reasonable representation of the conditions that existed within the model domain in October of 2000. At this point, it was determined to use the calibrated model to simulate the chosen independent validation storm event, which was Hurricane Irma. Good model performance during an independent storm event will further validate the adequacy of the model setup and parameterization approach. The validation storm event is relatively recent, compared to 20 years ago for the calibration event. As such, the NEXRAD rain data associated with the validation event was expected to have a lower level of uncertainty. As discussed in **Section 3.2**, during the validation event, model simulated hydrologic and hydraulic conditions were in close agreement with the observed data. Excellent model performance during the validation simulation further confirms the adequacy of the model setup and parameterization approach. The following sections provide details on the model setup and parameterization changes made during calibration.

3.1.2 Saturated Zone

During the initial calibration runs, it was noticed that groundwater wells G-1636, G-1637, and G-970 had a very subdued response to rainfall, whereas the recorded data showed a quite pronounced response. Adjustments were made to try to increase the groundwater response, including increased surface-subsurface leakage coefficient and decreased saturated zone drainage time constant. These changes resulted in almost no change, which is quite unusual as models are typically quite sensitive to these parameters. Therefore, a closer look was taken at the saturated zone inputs, derived from the USGS. It was noticed that the USGS groundwater model was configured much differently than the way the Broward

County model was set up. The USGS groundwater model (Hughes & White, 2016) used a second layer with low conductivity, whereas the 2019 Broward County model had a highly conductive second layer representing the Biscayne aquifer. It was decided to reparametrize the entire groundwater model based on the data from the 2019 Broward County Current Conditions MIKE SHE model, which happened to extend far enough south. Therefore, the first major change during model calibration was reparameterizing based on the 2019 Broward County MIKE SHE model, with the exception of the initial potential head. With these changes to the groundwater model, the simulated groundwater levels throughout the model were a much better match to the observed data. **Figure 39-Figure 50** show the revised groundwater layer bottoms and aquifer parameters.

3.1.2.1 Lower Level

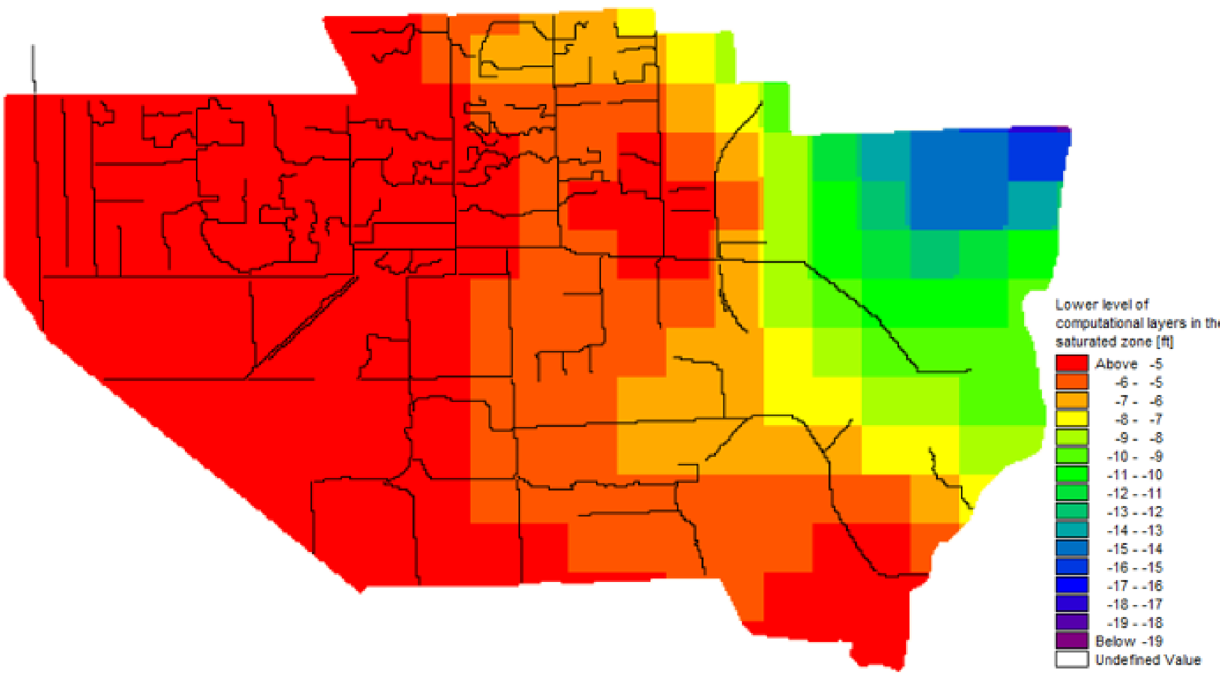

Figure 39: Lower Level of Computational Layer 1- From Broward County Model

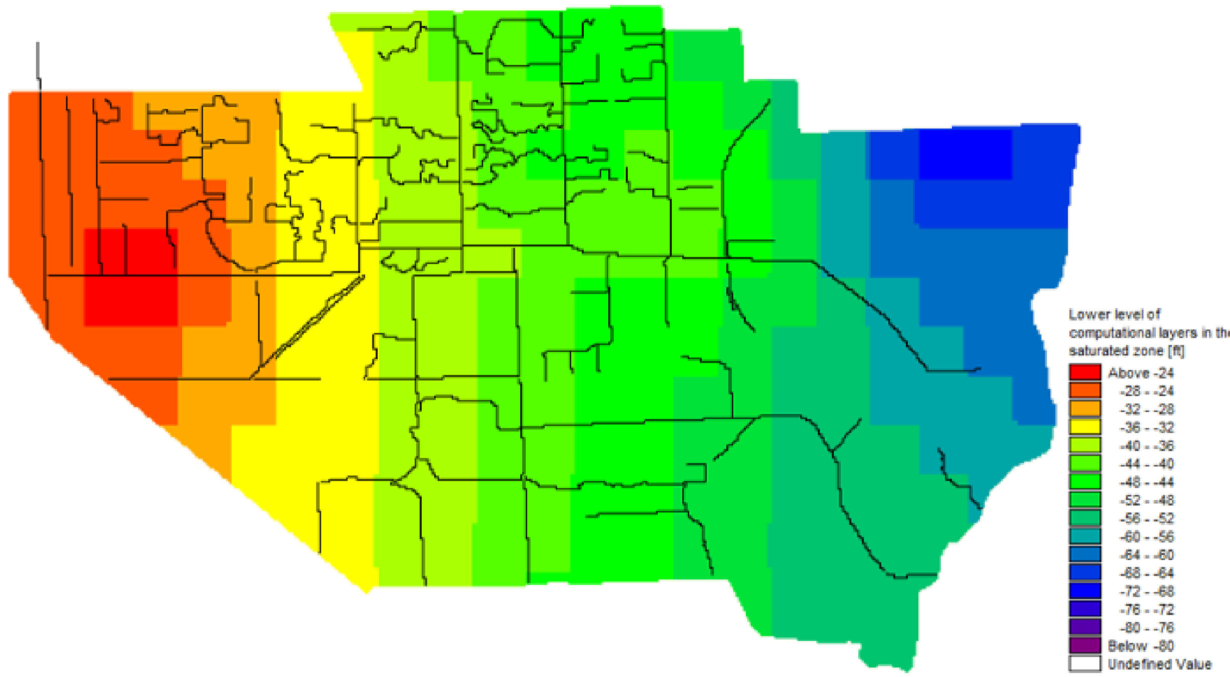

Figure 40: Lower Level of Computational Layer 2- From 2019 Broward County Model

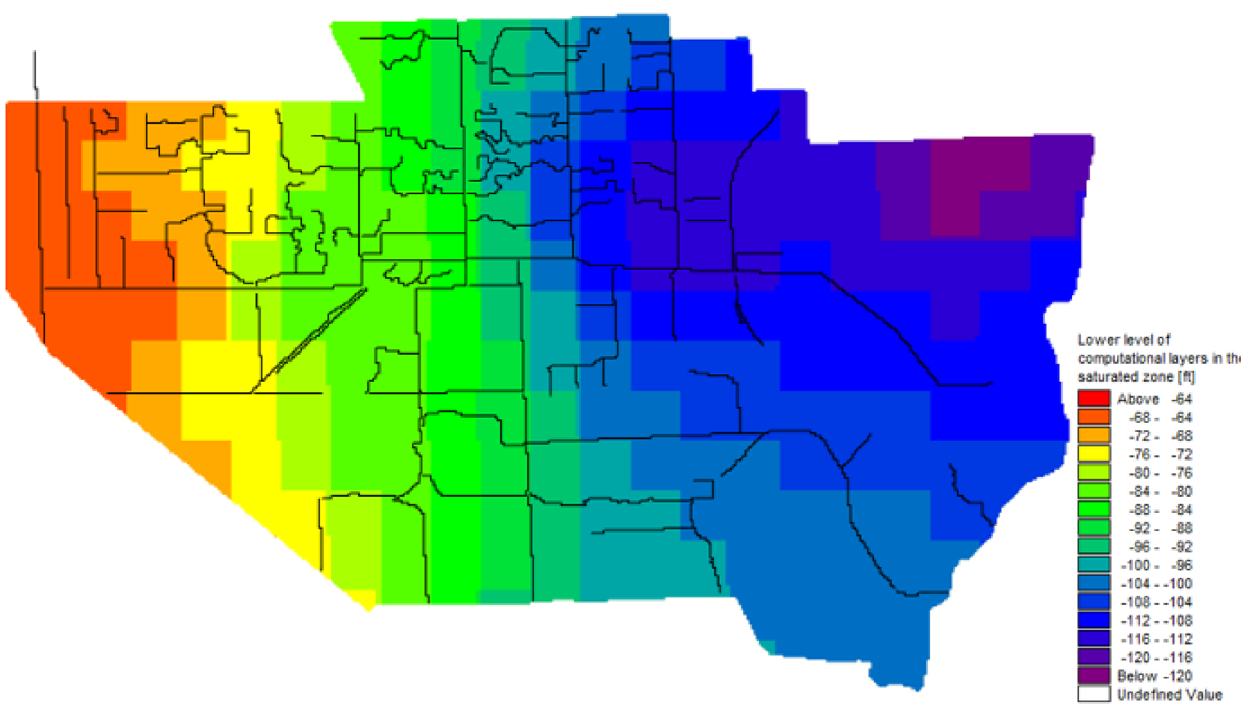

Figure 41: Lower Level of Computational Layer 3- From 2019 Broward County Model

3.1.2.2 Horizontal Hydraulic Conductivity

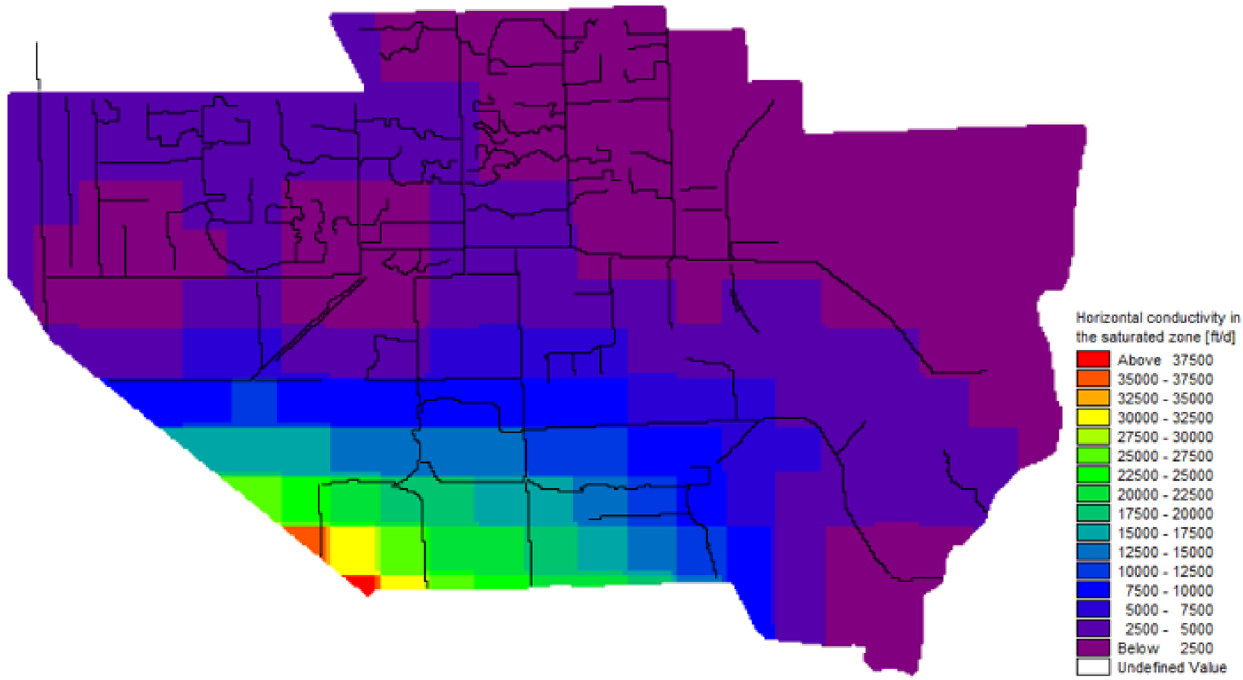

Figure 42: Horizontal Hydraulic Conductivity Layer 1- From 2019 Broward County Model

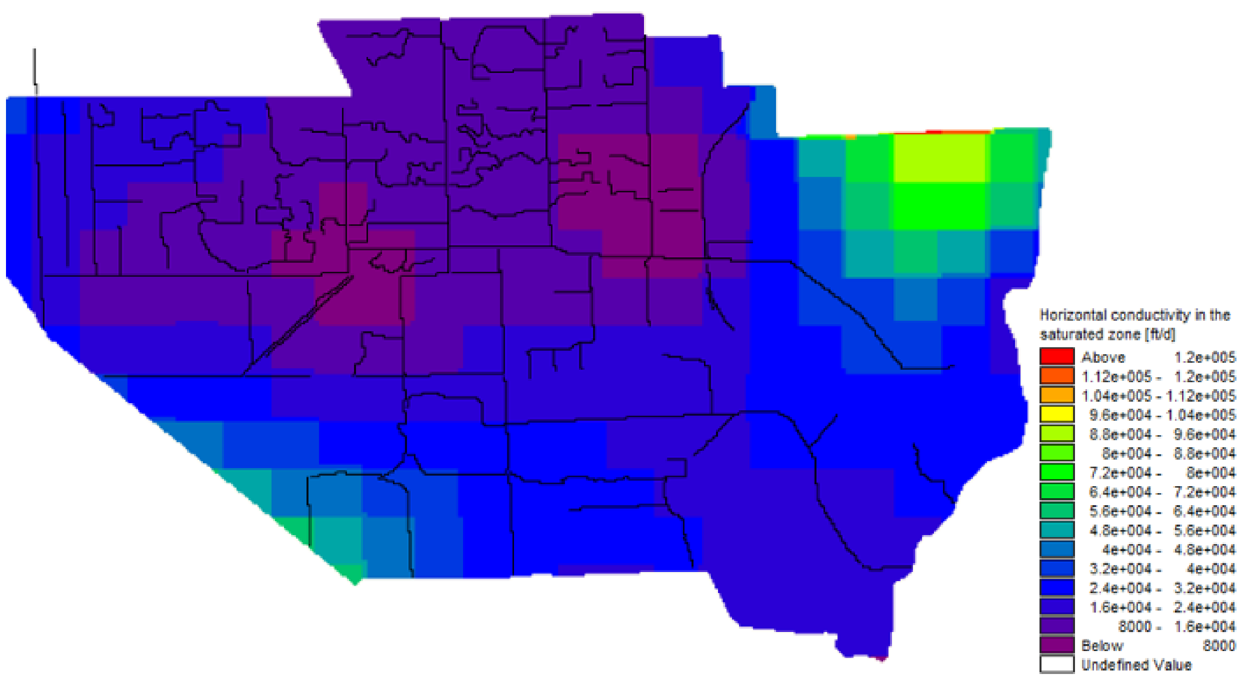

Figure 43: Horizontal Hydraulic Conductivity Layer 2- From 2019 Broward County Model

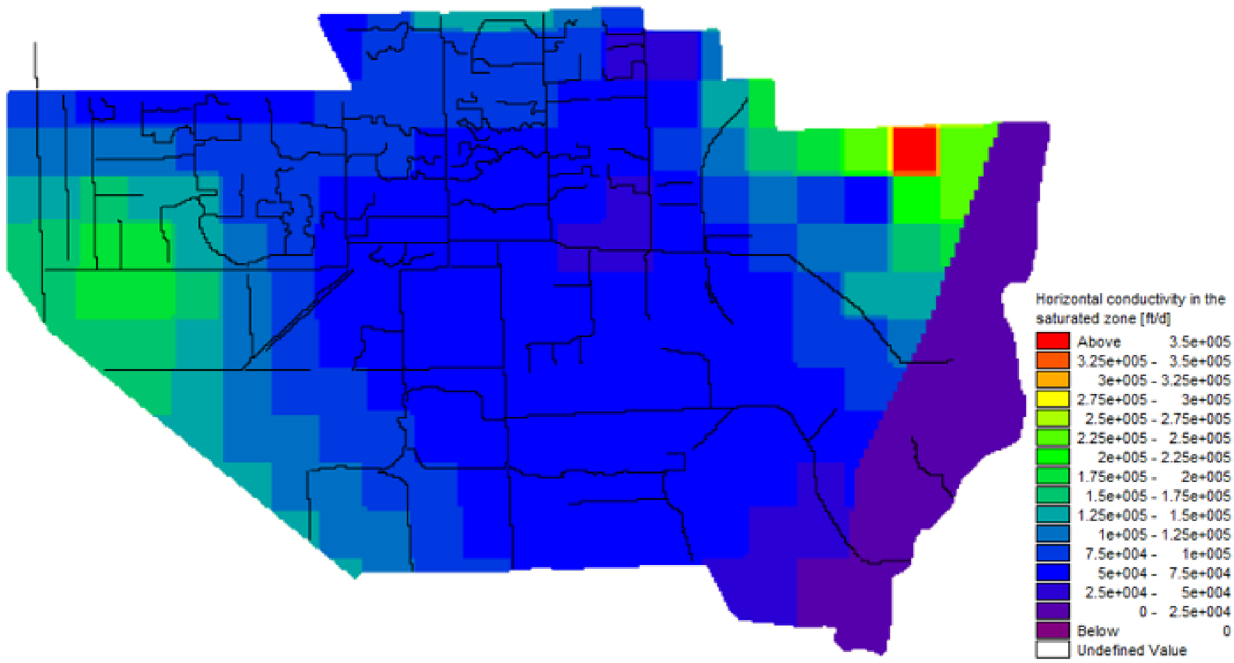

Figure 44: Horizontal Hydraulic Conductivity Layer 3- From 2019 Broward County Model

3.1.2.3 Vertical Hydraulic Conductivity

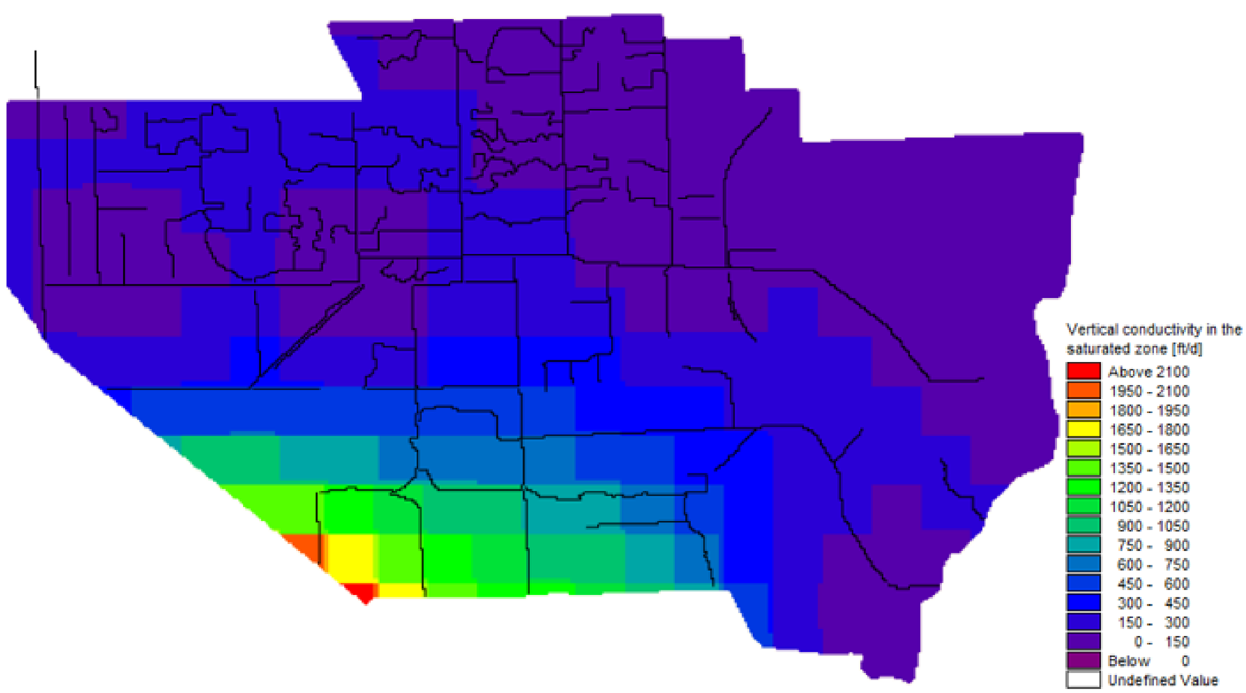

Figure 45: Vertical Hydraulic Conductivity Layer 1- From 2019 Broward County Model

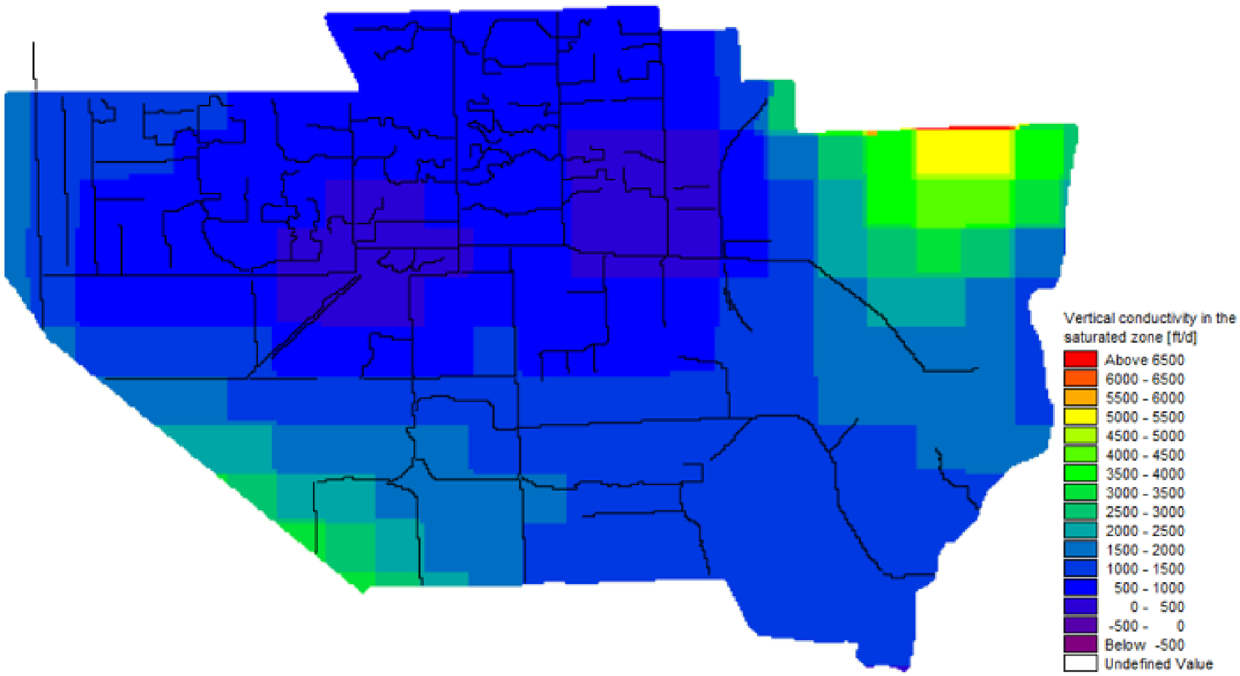

Figure 46: Vertical Hydraulic Conductivity Layer 2- From 2019 Broward County Model

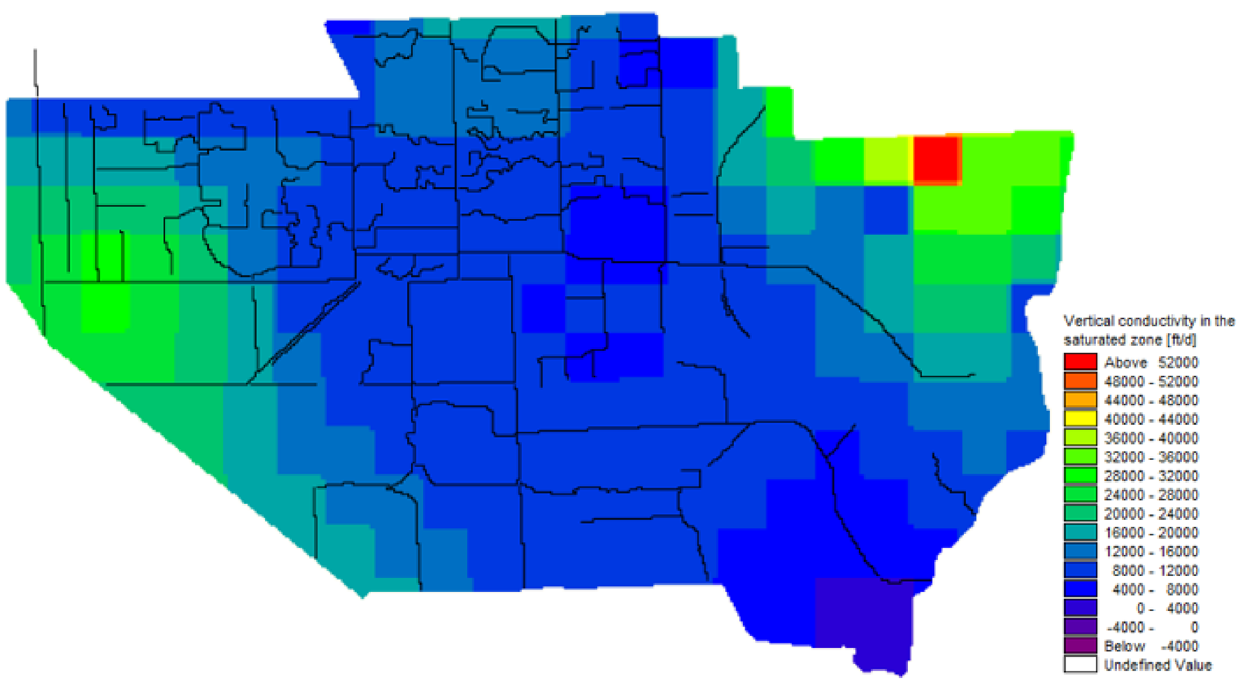

Figure 47: Vertical Hydraulic Conductivity Layer 3- From 2019 Broward County Model

3.1.2.4 Specific Yield

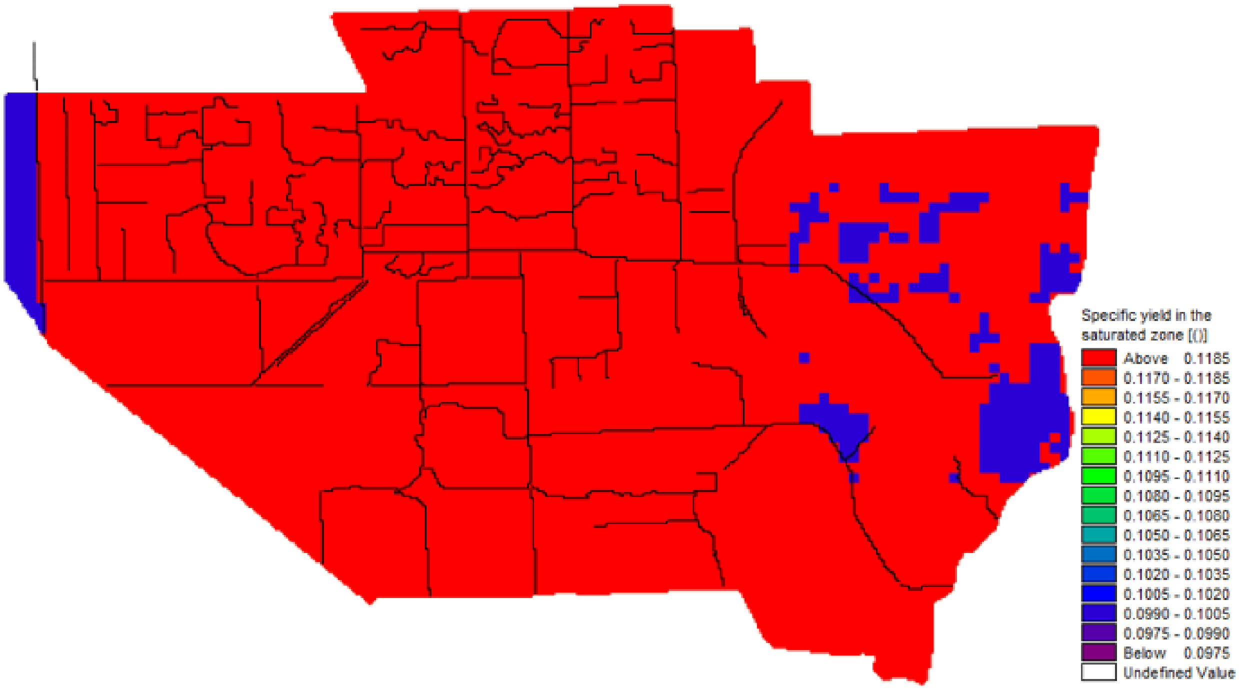

Figure 48: Specific Yield Layers 1, 2, & 3- From 2019 Broward County Model

3.1.2.5 Specific Storage

Layer 1 specific storage had a uniform value of 0.06096/ft, from the 2019 Broward County Model.

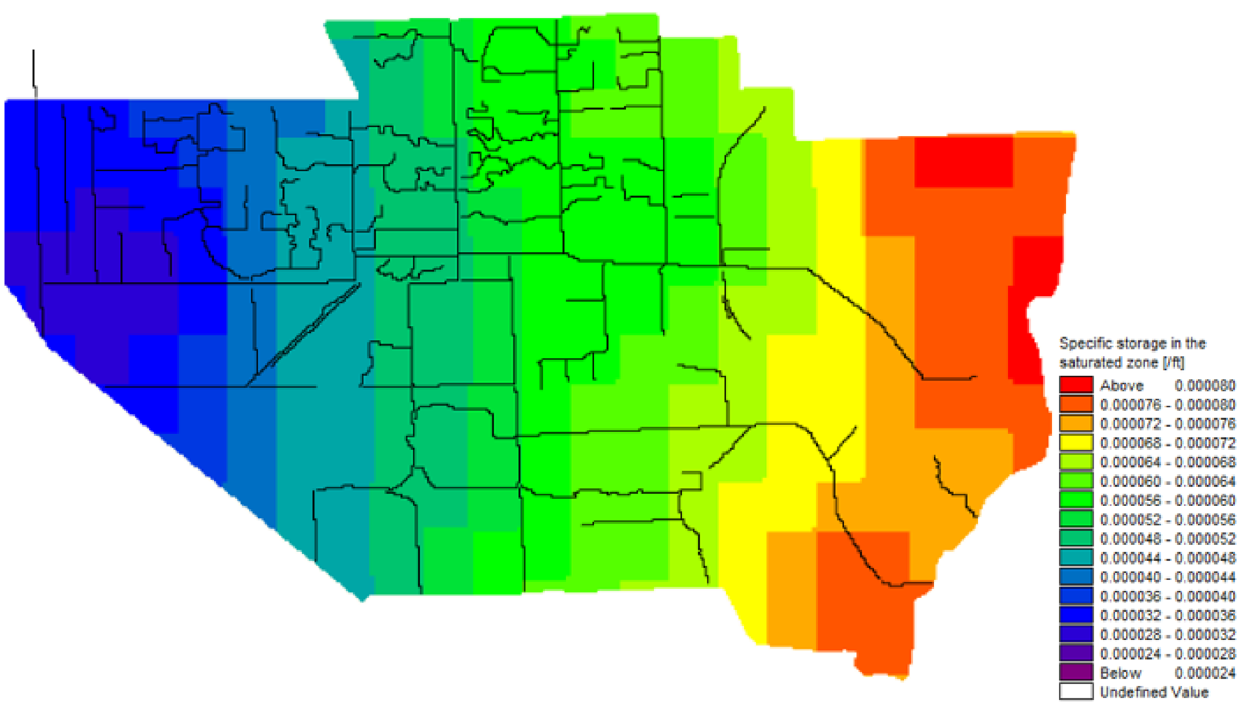

Figure 49: Specific Storage Layer 2- From 2019 Broward County Model

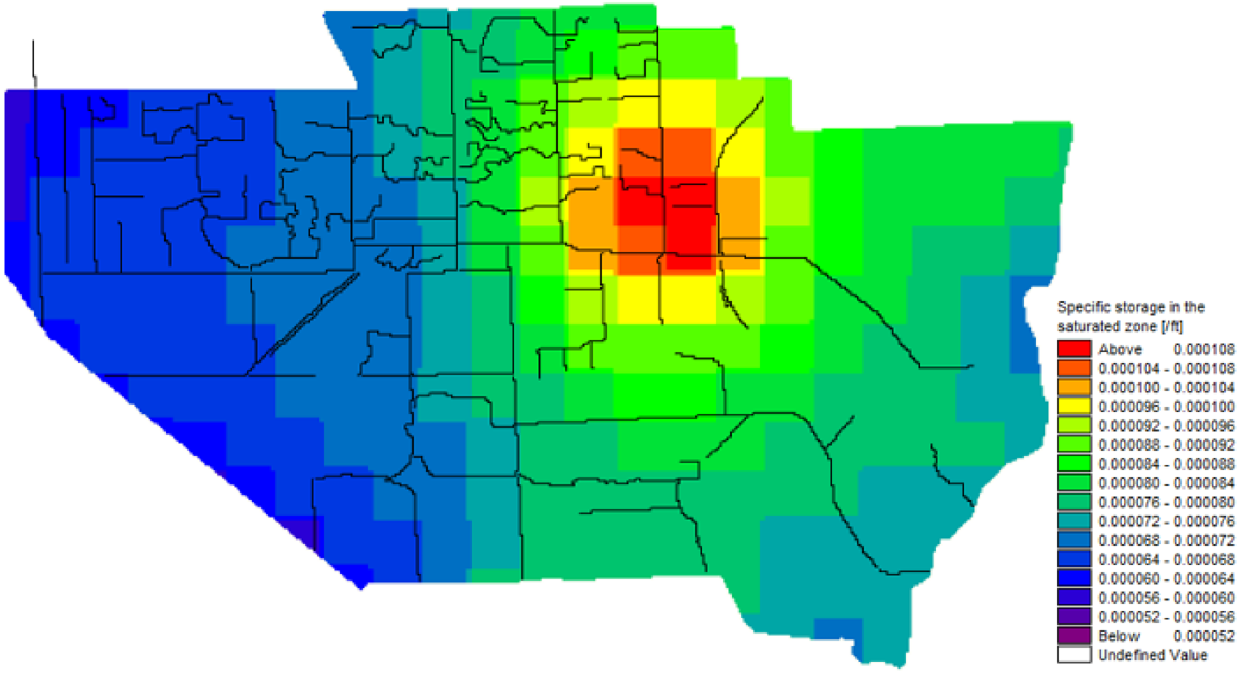

Figure 50: Specific Storage Layer 3- From 2019 Broward County Model

3.1.3 Boundary Conditions

After changing the groundwater model configuration, the simulated data was a closer match to the observed data in most parts of the study area. However, the western groundwater wells were still a little less responsive than observed. The 2019 Broward County model had an internal boundary condition, just west of the SFWMD L-33 canal, which is where the original C8 C9 model domain ended. Therefore, the model domain was extended about 1 mile west so that the internal boundary condition could be included, located as shown in green in the following figure.

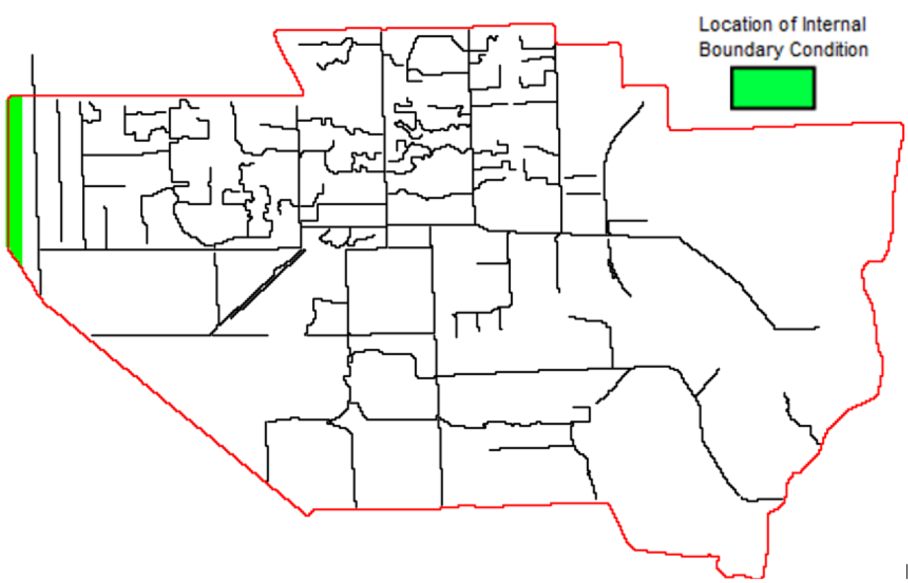

Figure 51: Location of Internal Boundary Condition

This internal boundary condition is based on the stage in Water Conservation Area 3B and is a head-controlled flux boundary with a leakage coefficient of 3E-6, as characterized in the 2019 Broward County Model. This change helped the groundwater respond more closely to the observed data.

3.1.4 Rainfall

The storm event from October 2nd-4th, 2000 was used to calibrate the model, with a simulation period of October 1st-21st. Both point rain measurements and spatially distributed NEXRAD data were available for the October 2000 storm event. Initially, hourly NEXRAD rainfall data with a spatial resolution of 2 km x 2 km was used for total rainfall depth and spatial distribution. The temporal distribution of each NEXRAD pixel was adjusted based on recorded rain gauge data. A rain gauge was assigned to each NEXRAD pixel based on Thiessen polygons that were delineated using the rain gauge locations present in the area (**Figure 14**). The calibration scenario using NEXRAD rainfall resulted in a reasonable match between simulated and observed groundwater levels and surface water stages throughout the model. However, the simulated peak discharge rates and the total discharge volume differed by upwards of +30%. Calibration efforts included varying parameters such as surface-subsurface leakage coefficient, paved area runoff coefficient, Manning's roughness for both overland and channel flow, ponded drainage time constants, and saturated zone drainage time constants, which resulted in no significant improvement in model performance. Considering there was a reasonable match between simulated and observed data for groundwater levels and surface water stages, it was suspected there was simply too much rainfall being simulated. Given that the collection and application of NEXRAD data in Florida during the early 2000s was an emerging technology, it was suspected to have a high level of uncertainty. It was entirely possible that NEXRAD data was simply not an accurate representation of actual rainfall. Therefore, the NEXRAD data was set aside and the raw rain gauge data was used, based on the same Thiessen polygons. Rain gauge S-29_R, although in the model domain, was excluded due to the likeliness that it malfunctioned as described in **Section 1.6.** Although there are still rainfall data limitations by using only 5 reference points, the rain gauge data led to significantly improved peak discharge rates and total discharge volumes. The following table shows the rain gauge recorded rainfall totals for October 1st-21st, 2000.

Table 8: Rain Gauge based Total Rainfall Depth (in) (NOTE: Gauge locations shown on Figure 14)

Rain Gauge	Total Rainfall (in)
S-13_R	10.46
S-27_R	16.01
S-28Z_R	12.57
S-29Z_R	13.65
S-30_R	7.5

3.1.5 Manning's Roughness Coefficient

After switching the rainfall data and vastly reducing the overprediction of peak discharge rates and total discharge volume, some localized adjustments to the Manning's roughness coefficient were made in an attempt to try and improve the peak surface water stage, as well as the overall shape of the hydrographs. Throughout the model, only a few canals were adjusted, as shown in the table below.

Table 9: Manning's Roughness Calibration Adjustments

Branch	Original Manning's n	Adjusted Manning's n
SFWMD C-8 Ext	0.033	0.04
Peter S Pike Canal	0.033	0.04
Grahams Dairy Canal	0.033	0.04

3.1.6 Calibration Results

Overall, the calibrated model sufficiently simulated surface water and groundwater responses to rainfall and were a good match to recorded observations at multiple locations throughout the model domain. Model simulated peak surface water stages generally agreed to within 0.5 ft of the observed stages, with an absolute average difference of 0.3 ft. Model simulated peak discharge rates agreed to within 10% of the observed peak discharge, with an absolute average difference of 6%. Model simulated total discharge volume agreed to within 17% of observed discharge volume, with an absolute average difference of 14%. Model simulated groundwater elevations generally agreed to within 0.5 ft of the observed elevations, with an absolute average difference of 0.3 ft. **Table 10** provides a detailed summary of the simulated vs. observed differences, **Table 11** provides a comparison between simulated and observed peak stages, **Table 12** provides a comparison between simulated and observed peak discharges and time of peak discharge, **Table 13** and **Table 14** provide water budgets for the C-8 and C-9 basins, and **Table 15** provides simulation statistics.

Table 10: Calibration Results Comparison (Simulated minus Observed for October 1st-21st)

Calibration Point	Total Volume Difference Percentage	Peak Discharge Difference Percentage	Peak Headwater Difference (ft)	Peak Tailwater Difference (ft)	Groundwater Elevation Difference (ft)
S-28	-10.6%	3%	0.45	Forced	
S-29	16.8%	9%	0.56	Forced	
S-30			0.15	0.38	
S-32			0.05	Forced	
S-9XS			0.35	Forced	
S-28Z			0.67		
S-29Z			0.01		
G-1225					0.57
G-1636					-0.12
G-1637					-0.10
G-3571					-0.81
G-852					-0.18
G-970					-0.21
S-18					0.05

Table 11: Calibration Peak Stage Comparison (October 1st-21st)

Calibration Point	Peak Stage	
	Simulated	Observed
S-28	4.87	4.42
S-29	3.75	3.19
S-30 HW	6.74	6.59
S-30 TW	5.2	4.82
S-32	6.73	6.68
S-9XS	6.83	6.48
S-28Z	5.53	6.2
S-29Z	4.95	4.94
G-1225	7.36	6.79
G-1636	4.8	4.93
G-1637	5.34	5.44
G-3571	6.62	7.43
G-852	7.1	7.28
G-970	4.57	4.78
S-18	7.19	7.14

Table 12: Calibration Peak Discharge Comparison (October 1st-21st)

Calibration Point	Peak Discharge		Time of Peak Discharge	
	Simulated	Observed	Simulated	Observed
S-28	2835	2743	10/4/2000 5:50 AM	10/3/2000 8:30 PM
S-29	4151	3792	10/4/2000 7:50 AM	10/3/2000 8:00 PM

Table 13: Calibration Water Budget for C-8 Basin (October 1^{st}-21^{st})

Water Budget Term	Inches (Average Over C-8 Basin)	
	Inflows	Outflows and Storage
Rainfall	13.4	
Evapotranspiration		1.4
Surface runoff		8.2
Groundwater flow to canals		4.4
Groundwater boundary inflow	0.3	
Change in surface storage		0.2
Change in groundwater storage	0.4	

Table 14: Calibration Water Budget for C-9 Basin (October 1^{st}-21^{st})

Water Budget Term	Inches (Average Over C-9 Basin)	
	Inflows	Outflows and Storage
Rainfall	11.8	
Evapotranspiration		1.6
Surface runoff		10.9
Groundwater flow to canals		4.0
Groundwater boundary inflow	6.1	
Change in surface storage		1.2
Change in groundwater storage		0.2

Figure 52-Figure 68 present a visual comparison between model simulated and observed conditions throughout the model domain. Structure headwater/tailwater that were used as boundary conditions are not included as they are identical (i.e., S-28 tailwater was a forced boundary).

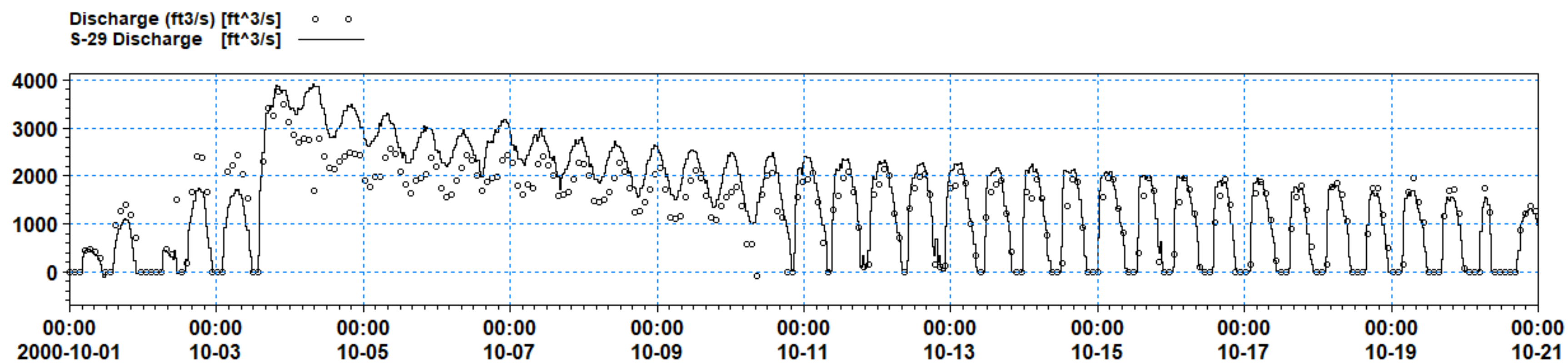

Figure 52: Simulated (line) vs Observed (dots) Discharge Comparison for SFWMD C-9 Structure S-29, October 1st-21st, 2000

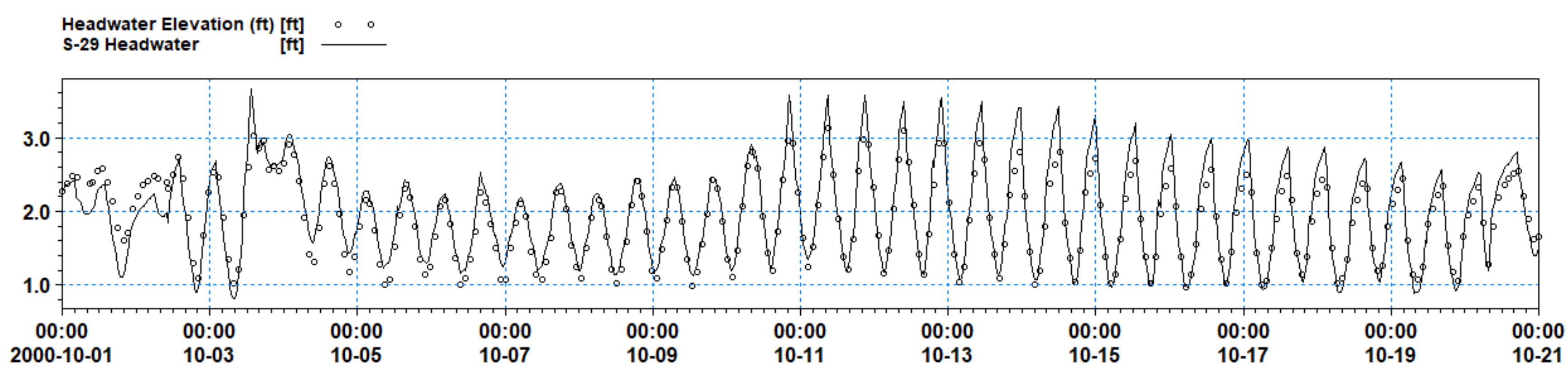

Figure 53: Simulated (line) vs Observed (dots) Headwater Comparison for SFWMD C-9 Structure S-29, October 1st-21st, 2000

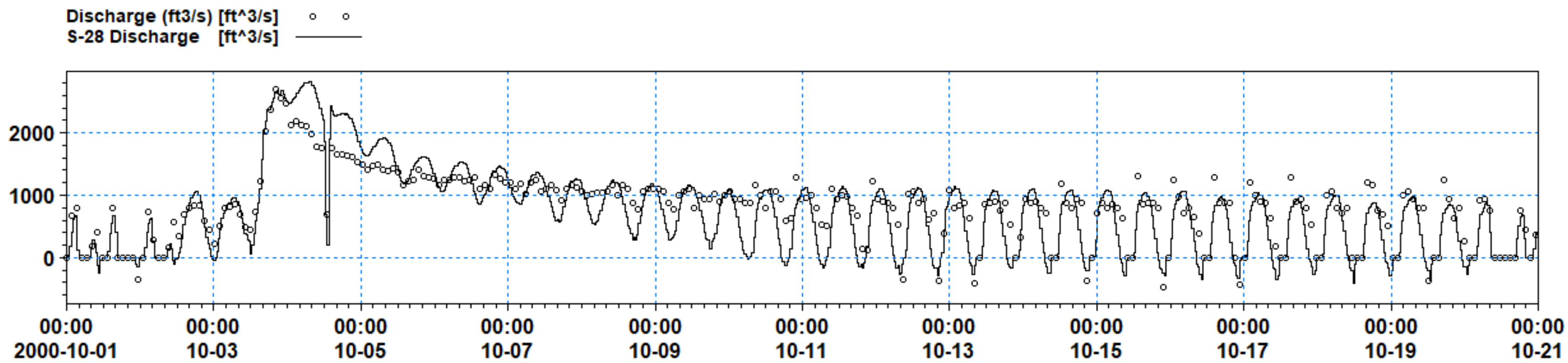

Figure 54: Simulated (line) vs Observed (dots) Discharge Comparison for SFWMD C-8 Structure S-28, October 1st-21st, 2000

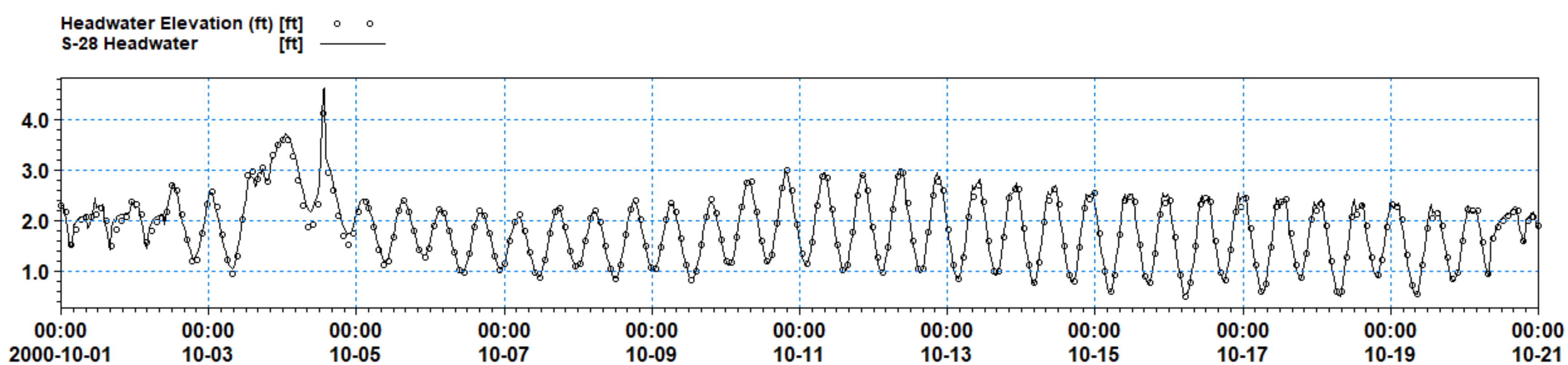

Figure 55: Simulated (line) vs Observed (dots) Headwater Comparison for SFWMD C-8 Structure S-28, October 1st-21st, 2000

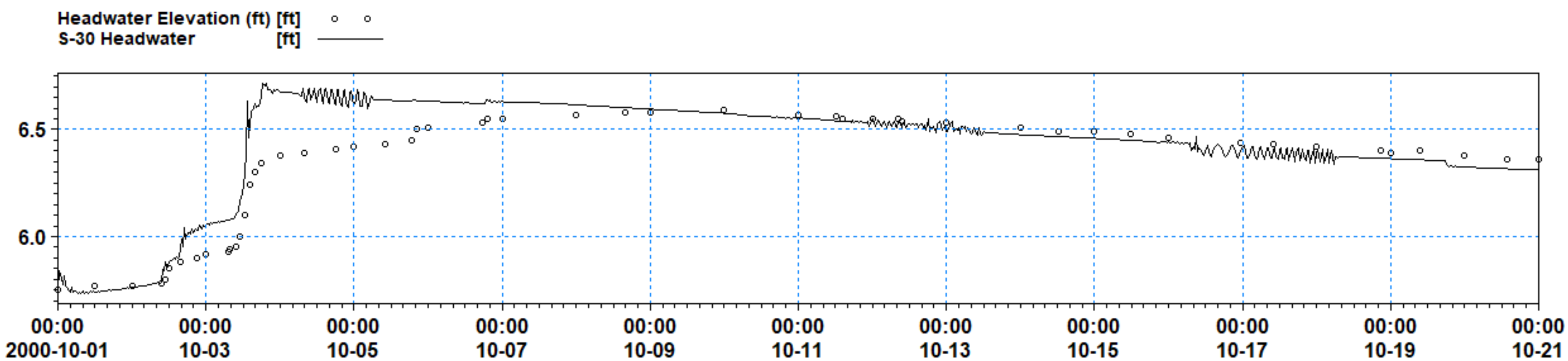

Figure 56: Simulated (line) vs Observed (dots) Headwater Comparison for SFWMD C-9 Structure S-30, October 1st-21st, 2000

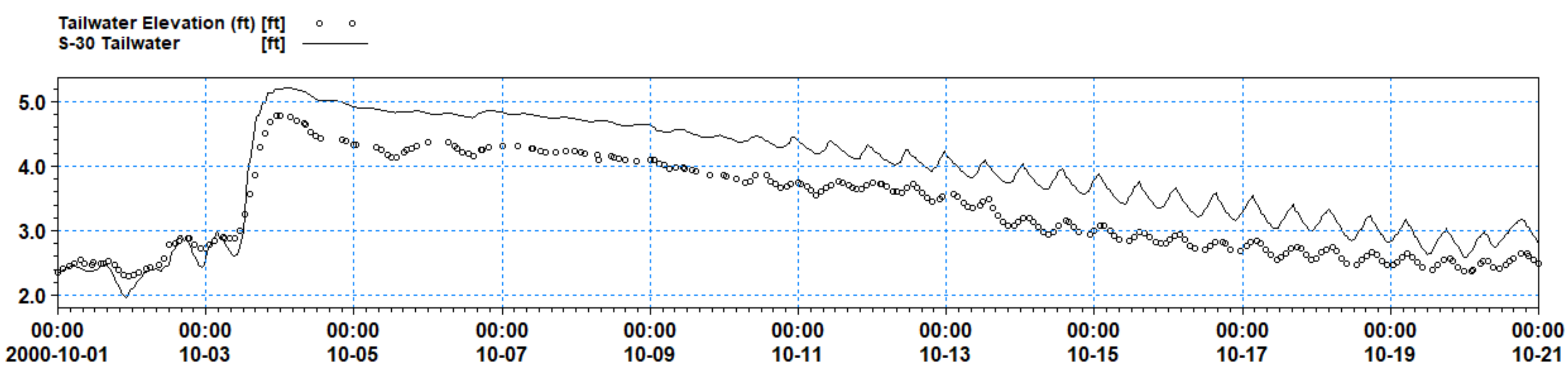

Figure 57: Simulated (line) vs Observed (dots) Tailwater Comparison for SFWMD C-9 Structure S-30, October 1st-21st, 2000

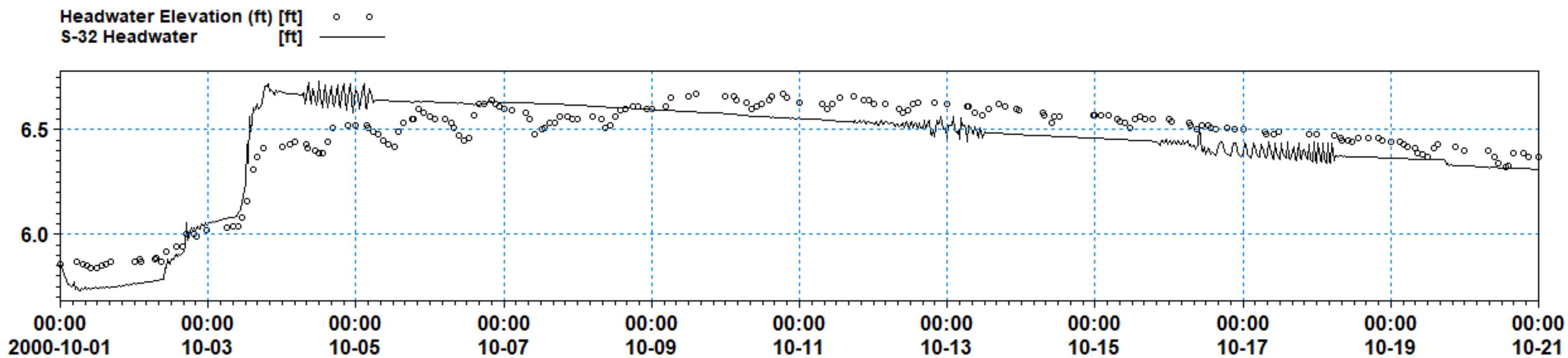

Figure 58: Simulated (line) vs Observed (dots) Headwater Comparison for SFWMD L-33 Structure S-32, October 1st-21st, 2000

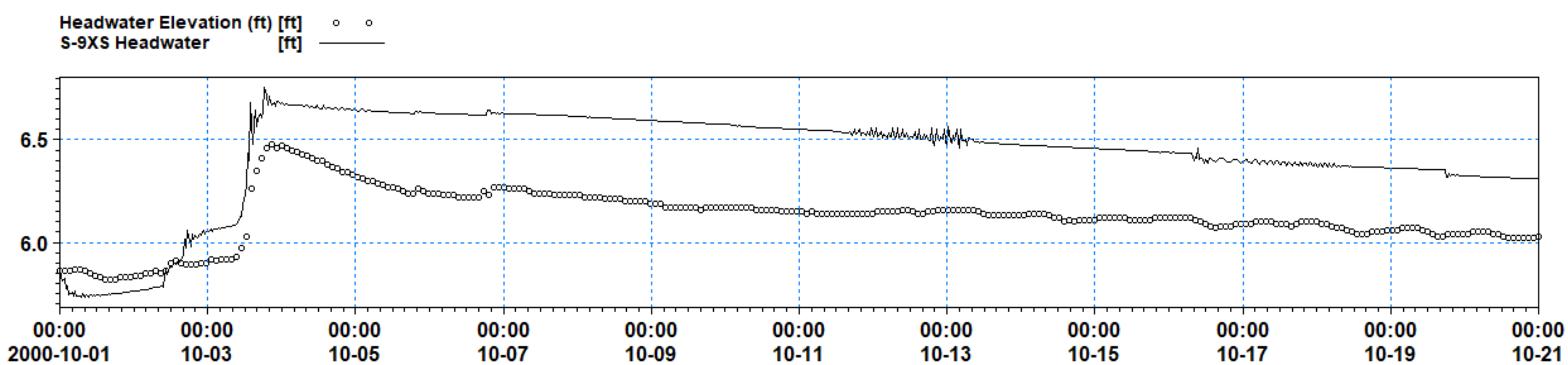

Figure 59: Simulated (line) vs Observed (dots) Headwater Comparison for SFWMD L-33 Structure S-9XS, October 1st-21st, 2000

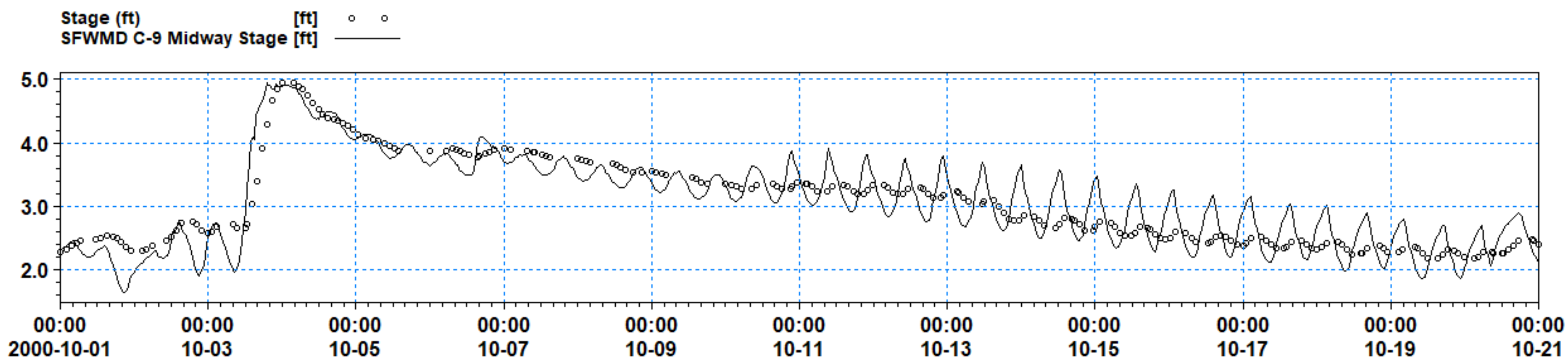

Figure 60: Simulated (line) vs Observed (dots) Stage Comparison for SFWMD C-9 Water Level Recorder S-29Z, October 1st-21st, 2000

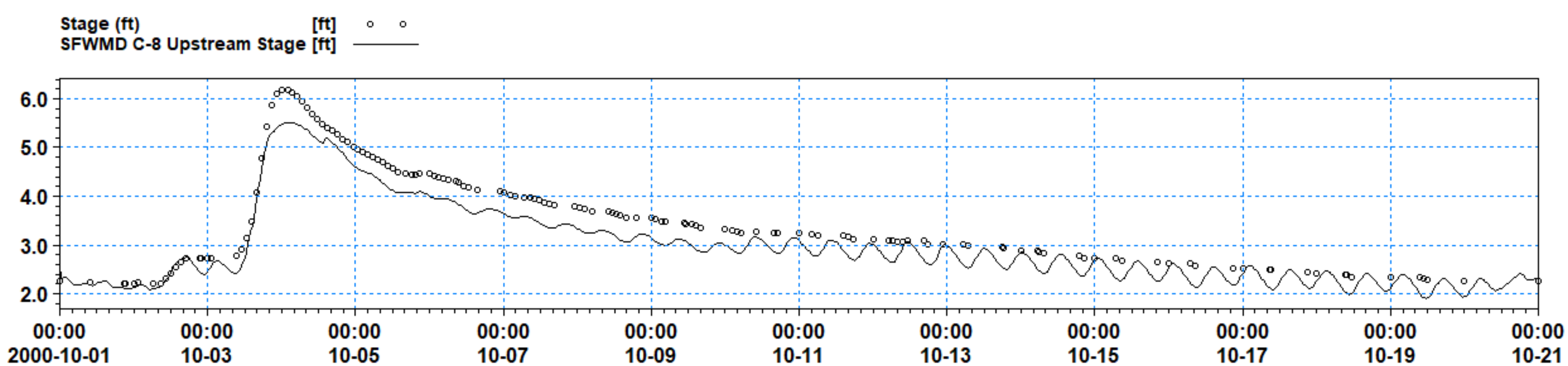

Figure 61: Simulated (line) vs Observed (dots) Stage Comparison for SFWMD C-8 Water Level Recorder S-28Z, October 1st-21st, 2000

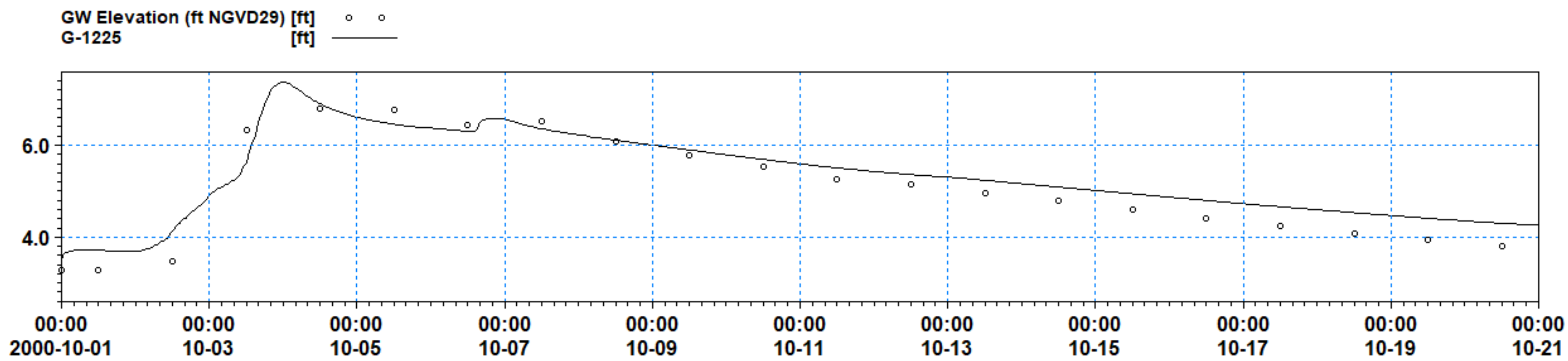

Figure 62: Simulated (line) vs Observed (dots) Groundwater Elevation Comparison for Well G-1225, October 1st-21st, 2000

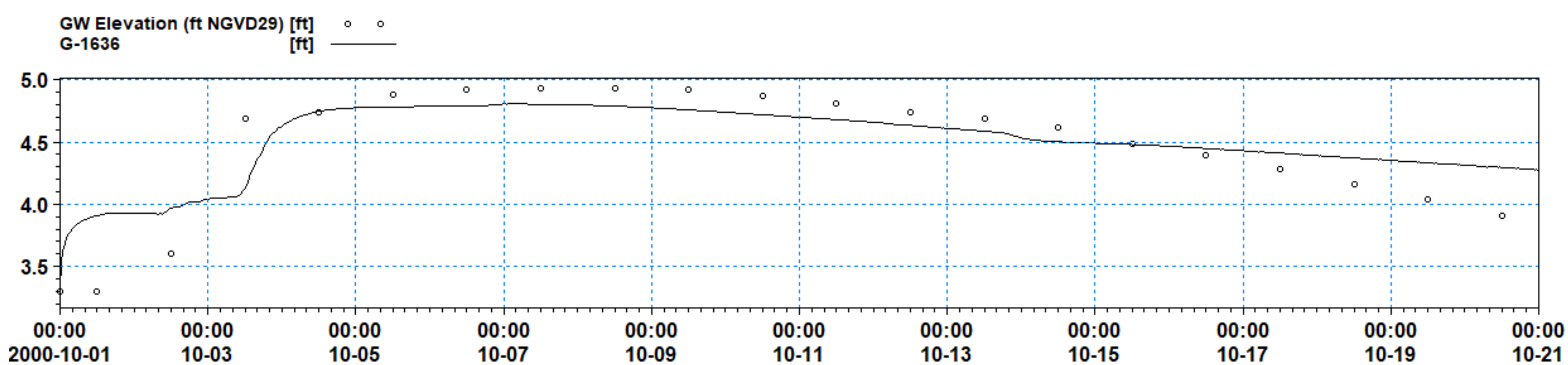

Figure 63: Simulated (line) vs Observed (dots) Groundwater Elevation Comparison for Well G-1636, October 1st-21st, 2000

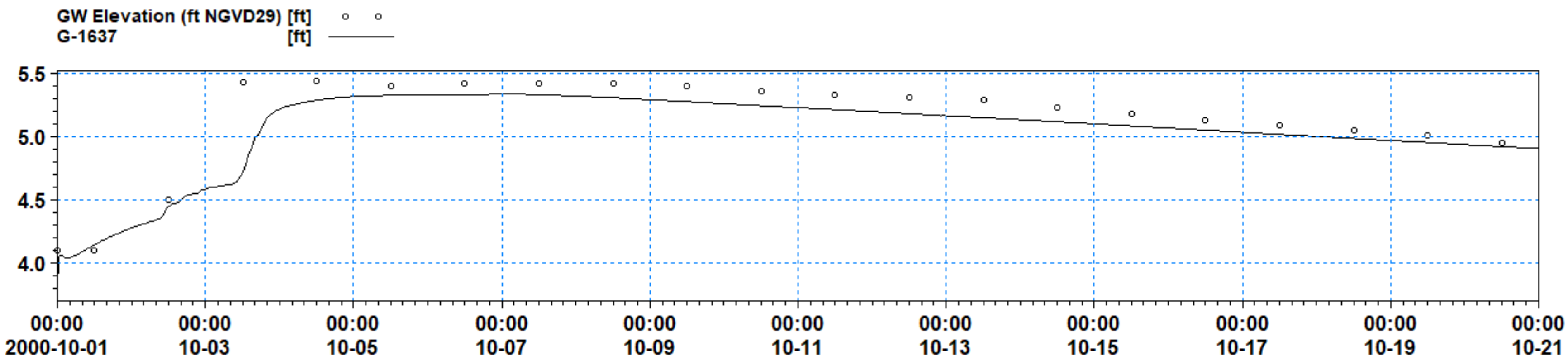

Figure 64: Simulated (line) vs Observed (dots) Groundwater Elevation Comparison for Well G-1637, October 1st-21st, 2000

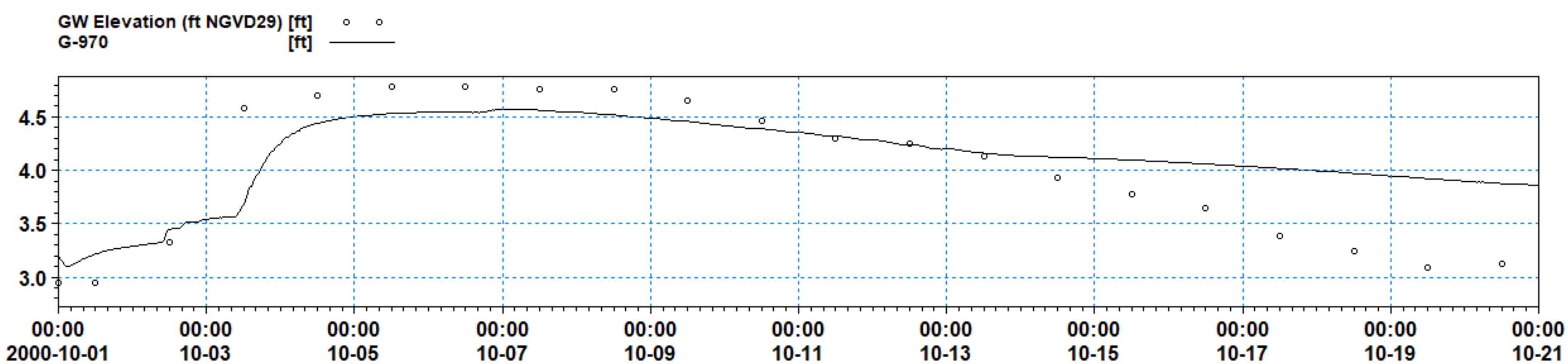

Figure 65: Simulated (line) vs Observed (dots) Groundwater Elevation Comparison for Well G-970, October 1st-21st, 2000

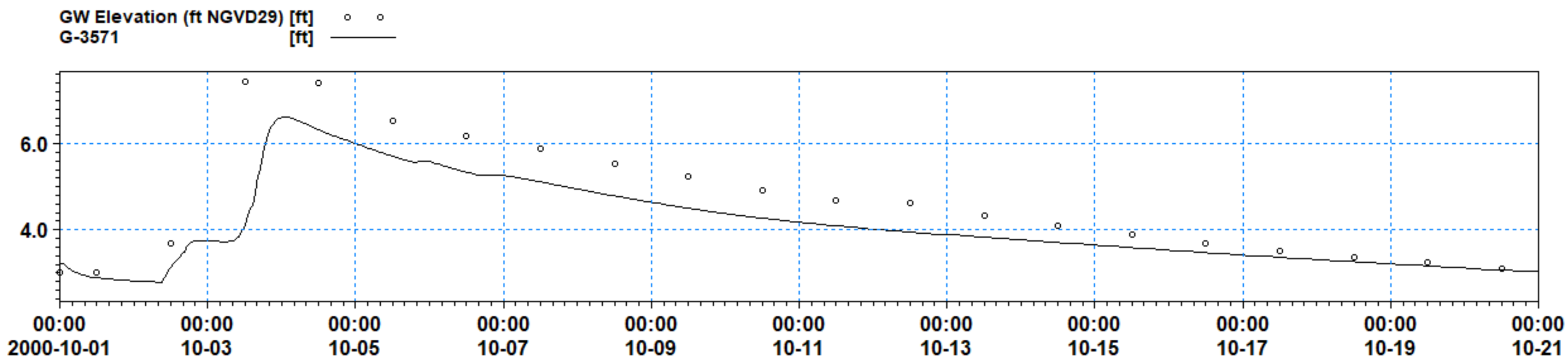

Figure 66: Simulated (line) vs Observed (dots) Groundwater Elevation Comparison for Well G-3571, October 1st-21st, 2000

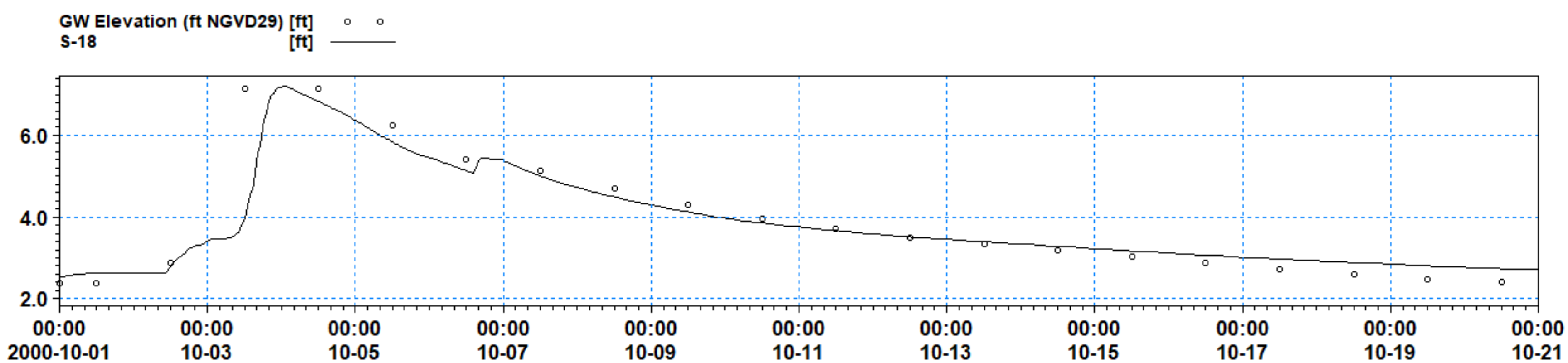

Figure 67: Simulated (line) vs Observed (dots) Groundwater Elevation Comparison for Well S-18, October 1st-21st, 2000

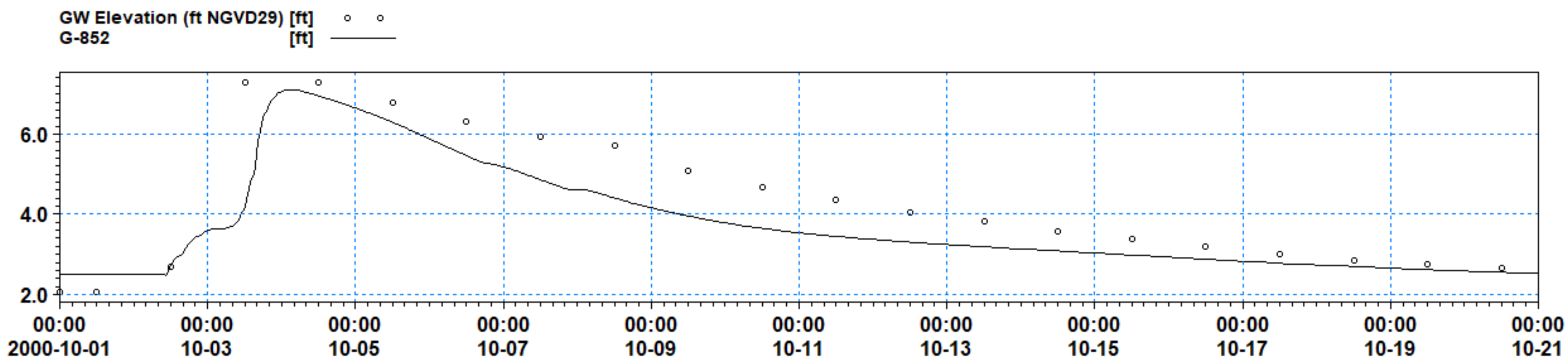

Figure 68: Simulated (line) vs Observed (dots) Groundwater Elevation Comparison for Well G-852, October 1st-21st, 2000

Table 15: Calibration Model Statistics for Simulated vs Observed Data

Calibration Point	7-day Simulation (Oct 1st -7th, 2000)						21-day Simulation (Oct 1st -21st, 2000)					
	ME	MAE	RMSE	STDres	R (Correlation)	Nash_Sutcliffe	ME	MAE	RMSE	STDres	R (Correlation)	Nash_Sutcliffe
S-29 Q (cfs)	-272	499	613	549	0.92	0.64	-217	317	440	383	0.94	0.75
S-29 HW (ft)	-0.037	0.19	0.21	0.21	0.92	0.83	-0.08	0.13	0.18	0.16	0.97	0.88
S-28 Q (cfs)	-102	223	310	293	0.96	0.8	86	239	329	318	0.89	0.65
S-28 HW (ft)	-0.047	0.09	0.13	0.13	0.98	0.95	-0.0009	0.05	0.08	0.08	0.99	0.98
S-30 HW (ft)	-0.17	0.17	0.2	0.11	0.96	0.44	-0.086	0.109	0.15	0.13	0.88	0.65
S-30 TW (ft)	-0.21	0.34	0.41	0.35	0.99	0.78	0.45	0.49	0.52	0.26	0.96	0.4
S-32 HW (ft)	-0.086	0.12	0.15	0.12	0.96	0.7	-0.001	0.1	0.11	0.11	0.88	0.71
S-9XS HW (ft)	-0.19	0.23	0.26	0.18	0.96	0.33	-0.3	0.31	0.33	0.13	0.91	-4.95
S-29Z Stage (ft)	0.05	0.28	0.39	0.38	0.94	0.81	-0.02	0.32	0.38	0.38	0.87	0.71
S-28Z Stage (ft)	0.34	0.35	0.39	0.18	0.99	0.9	0.35	0.36	0.39	0.16	0.99	0.89
G-1225 (ft)	-0.035	0.37	0.43	0.43	0.98	0.93	-0.19	0.32	0.36	0.31	0.98	0.9
G-1636 (ft)	-0.03	0.26	0.35	0.35	0.88	0.76	-0.01	0.19	0.25	0.25	0.9	0.77
G-1637 (ft)	0.19	0.2	0.3	0.24	0.92	0.75	0.13	0.13	0.19	0.15	0.93	0.77
G-970 (ft)	0.14	0.33	0.4	0.38	0.91	0.76	-0.1	0.33	0.42	0.41	0.82	0.6
G-3571 (ft)	0.93	1	1.4	1	0.83	0.43	0.59	0.62	0.91	0.69	0.9	0.56
S-18 (ft)	0.56	0.66	1.23	1.1	0.84	0.63	0.14	0.33	0.73	0.72	0.89	0.76
G-852 (ft)	0.55	0.81	1.26	1.13	0.88	0.71	0.6	0.68	0.94	0.73	0.91	0.68

3.2 Model Validation

The SFWMD structures and groundwater wells used to validate the model are shown in **Figure 38**. The operable structures (gates) used recorded gate openings and the tidal tailwater were forced with the recorded water levels. The model's simulated peak headwater/tailwater, peak discharge, total discharge volume, and groundwater levels were compared with observed data obtained from SFWMD's DBHYDRO database.

Overall, the model adequately simulated surface water and groundwater responses to rainfall and were a good match to recorded observations at multiple locations throughout the model domain. Model simulated surface water stages generally agreed to within 0.4 ft of observed stages, with an absolute average difference of 0.2 ft. Model simulated peak discharge rates agreed to within about 17% of observed peak discharges, with an absolute average difference of 13%. Model simulated discharge volumes agreed to within 14% of observed discharge volumes, with an absolute average difference of 10%. Model simulated groundwater elevations generally agreed to within 1 ft of observed elevations, with an absolute average difference of 0.8 ft. **Table 16** provides a detailed summary of the simulated vs. observed differences, **Table 17** provides a comparison between simulated and observed peak stages, **Table 18** provides a comparison between simulated and observed peak discharges and time of peak discharge, **Table 19 and Table 20** provide water budgets for the C-8 and C-9 basins, and **Table 21** provides simulation statistics.

Table 16: Validation Results Comparison (Simulated minus Observed for September 9th-16th)

Calibration Point	Total Volume Difference Percentage	Peak Discharge Difference Percentage	Peak Headwater Difference (ft)	Peak Tailwater Difference (ft)	Groundwater Elevation Difference (ft)
S-28	14.4%	-17.4%	-0.01	Forced	
S-29	-5.5%	8.8%	-0.05	Forced	
S-30			0.32	0.43	
S-32			0.23	Forced	
S-9XS			0.44	Forced	
S-28Z			-0.10		
S-29Z			0.15		
G-1225					-1.26
G-1636					0.24
G-1637					0.77
G-3571					-1.59
G-852					-0.28
G-970					-0.64
S-18					0.7

Table 17: Validation Peak Stage Comparison (September 9th–16th)

Calibration Point	Peak Stage	
	Simulated	Observed
S-28	5.12	5.13
S-29	4.82	4.87
S-30 HW	6.91	6.59
S-30 TW	5.25	4.82
S-32	6.91	6.68
S-9XS	6.92	6.48
S-28Z	5.08	5.18
S-29Z	5.09	4.94
G-1225	5.23	
G-1636	4.93	4.73
G-1637	5.52	
G-3571	5.71	7.27
G-852	5.53	5.81
G-970	4.56	5.14
S-18	5.79	5.08

Table 18: Validation Peak Discharge Comparison (September 9th–16th)

Calibration Point	Peak Discharge		Time of Peak Discharge	
	Simulated	Observed	Simulated	Observed
S-28	1591	2010	9/11/2017 6:20 AM	9/9/2017 05:10 AM
S-29	3393	3119	9/11/2017 5:35 PM	9/11/2017 5:35 PM

Table 19: Validation Water Budget for C-8 Basin (September 9th–16th)

Water Budget Term	Inches (Average Over C-8 Basin)	
	Inflows	Outflows and Storage
Rainfall	7.7	
Evapotranspiration		0.7
Surface runoff		2.4
Groundwater flow to canals		1.6
Groundwater boundary inflow		0.3
Change in surface storage		0.6
Change in groundwater storage		2.0

Table 20: Validation Water Budget for C-9 Basin (September 9th–16th)

Water Budget Term	Inches (Average Over C-9 Basin)	
	Inflows	Outflows and Storage
Rainfall	8.1	
Evapotranspiration		0.8
Surface runoff		4.8
Groundwater flow to canals		1.1
Groundwater boundary inflow	1.4	
Change in surface storage		0.9
Change in groundwater storage		1.8

Figure 69-Figure 84 present a visual comparison between model simulated and observed conditions throughout the model domain during a 1-week portion of the validation period coinciding with Hurricane Irma and the following few days. Again, structure headwater/tailwater that were used as boundary conditions are not included as they are identical (i.e., S-28 tailwater was a forced boundary). Note that a few of the groundwater wells had no observed data during the period of September 9th-16th, 2017. Comparison plots for the full 4-month simulation period are provided in **Appendix D** .

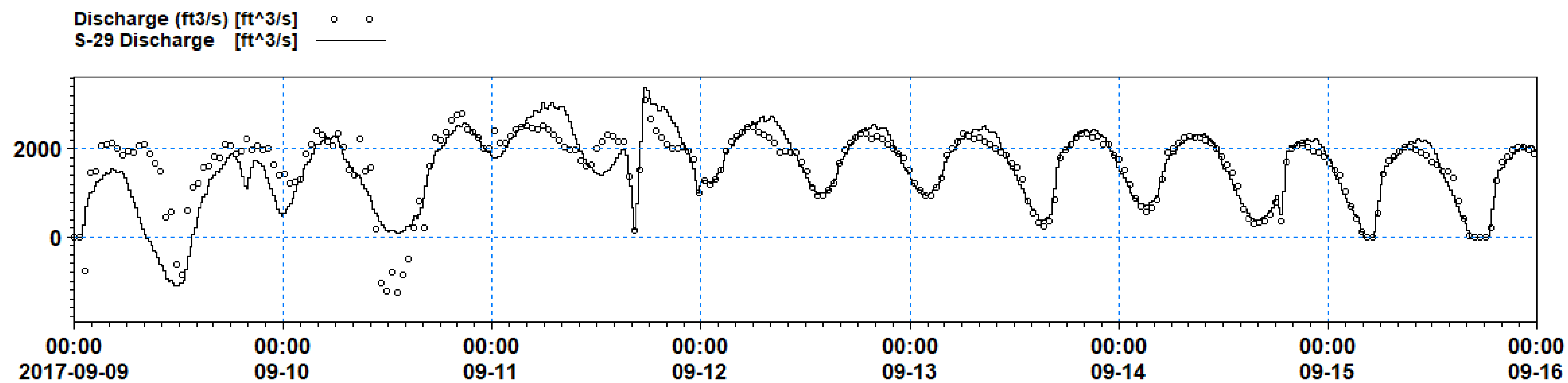

Figure 69: Simulated (line) vs Observed (dots) Discharge Comparison for SFWMD C-9 Structure S-29, September 9th-16th, 2017

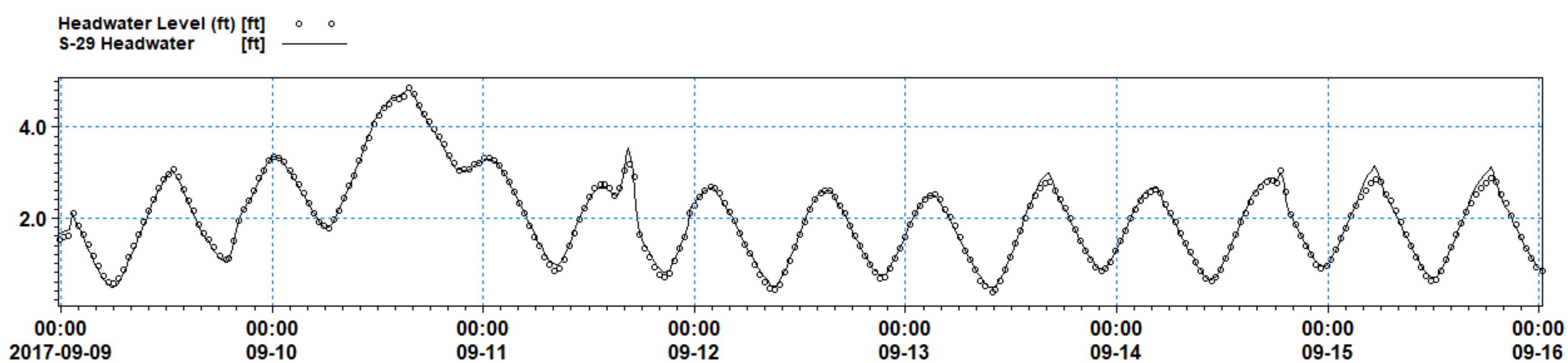

Figure 70: Simulated (line) vs Observed (dots) Headwater Comparison for SFWMD C-9 Structure S-29, September 9th-16th, 2017

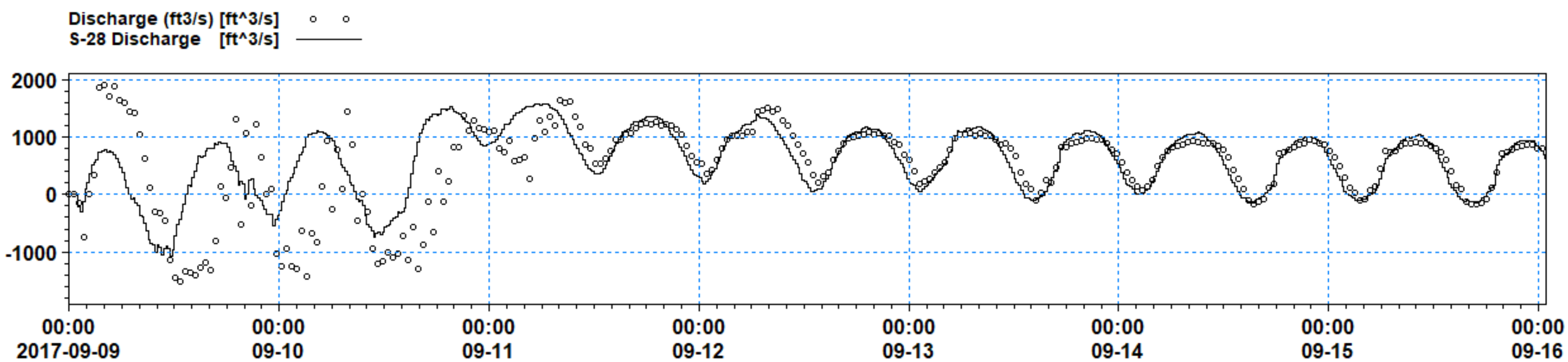

Figure 71: Simulated (line) vs Observed (dots) Discharge Comparison for SFWMD C-8 Structure S-28, September 9th-16th, 2017

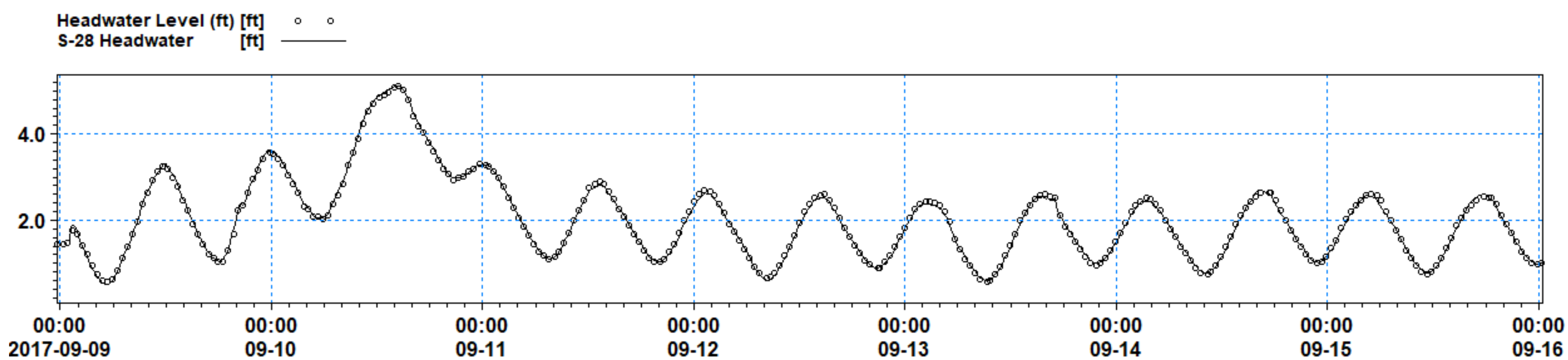

Figure 72: Simulated (line) vs Observed (dots) Headwater Comparison for SFWMD C-8 Structure S-28, September 9th-16th, 2017

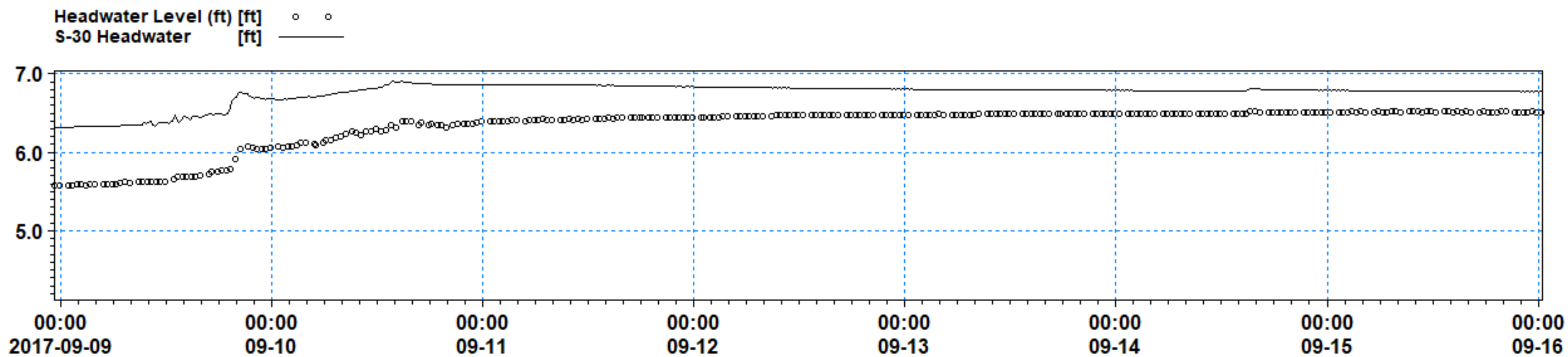

Figure 73: Simulated (line) vs Observed (dots) Headwater Comparison for SFWMD C-9 Structure S-30, September 9th-16th, 2017

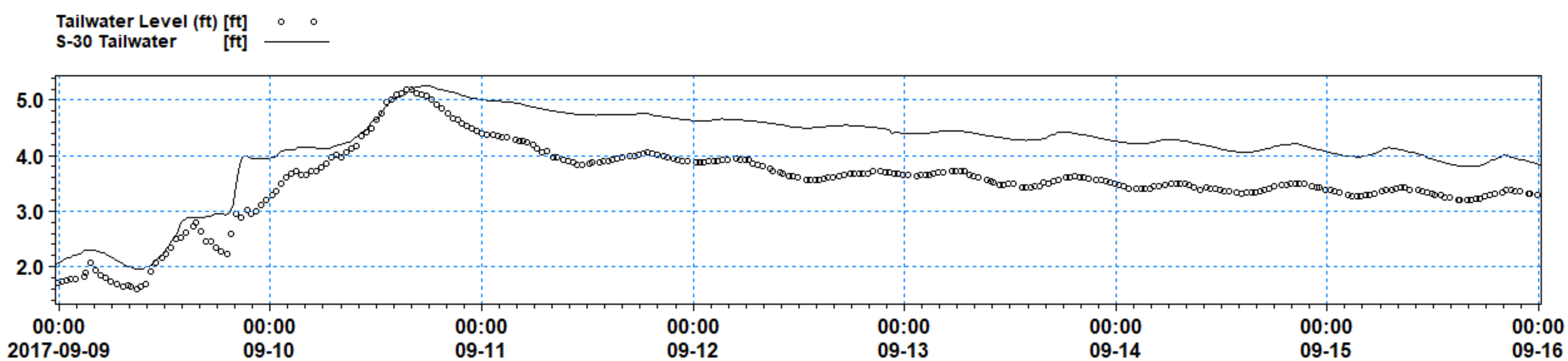

Figure 74: Simulated (line) vs Observed (dots) Tailwater Comparison for SFWMD C-9 Structure S-30, September 9th-16th, 2017

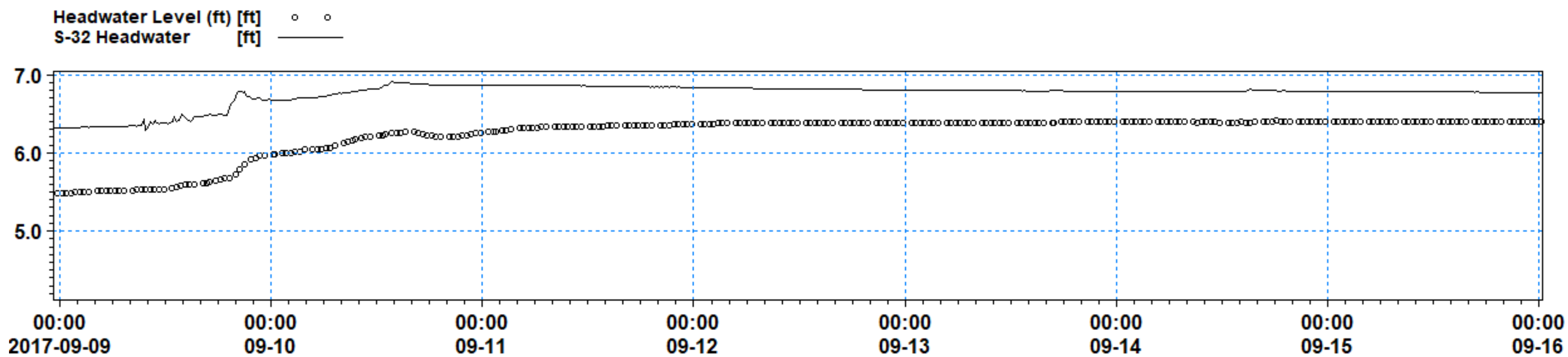

Figure 75: Simulated (line) vs Observed (dots) Headwater Comparison for SFWMD L-33 Structure S-32, September 9th-16th, 2017

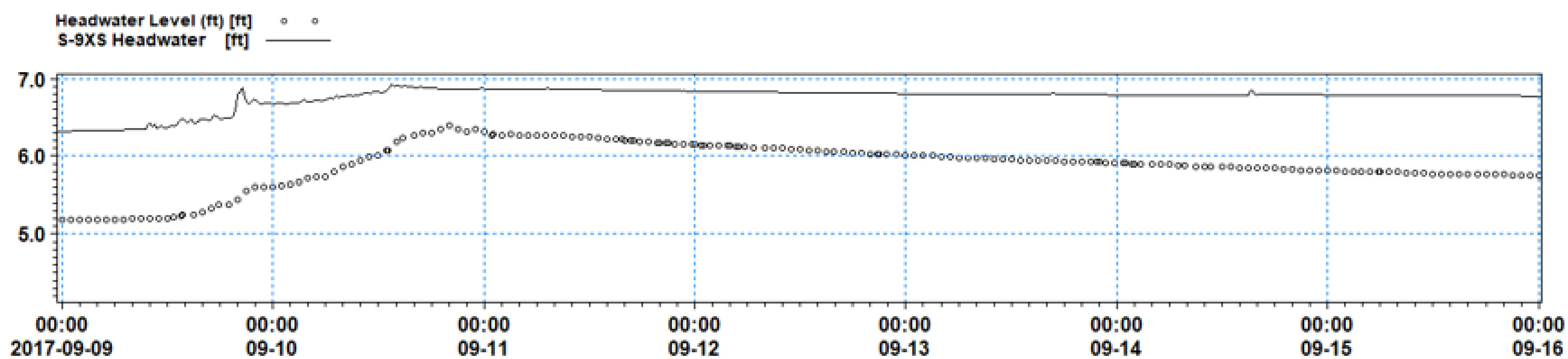

Figure 76: Simulated (line) vs Observed (dots) Headwater Comparison for SFWMD L-33 Structure S-9XS, September 9th-16th, 2017

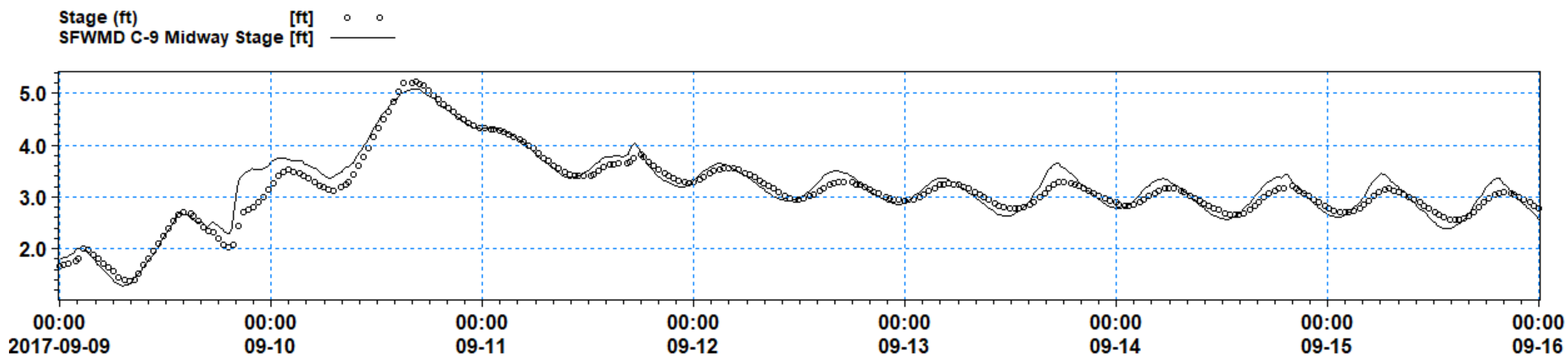

Figure 77: Simulated (line) vs Observed (dots) Stage Comparison for SFWMD C-9 Water Level Recorder S-29Z, September 9th-16th, 2017

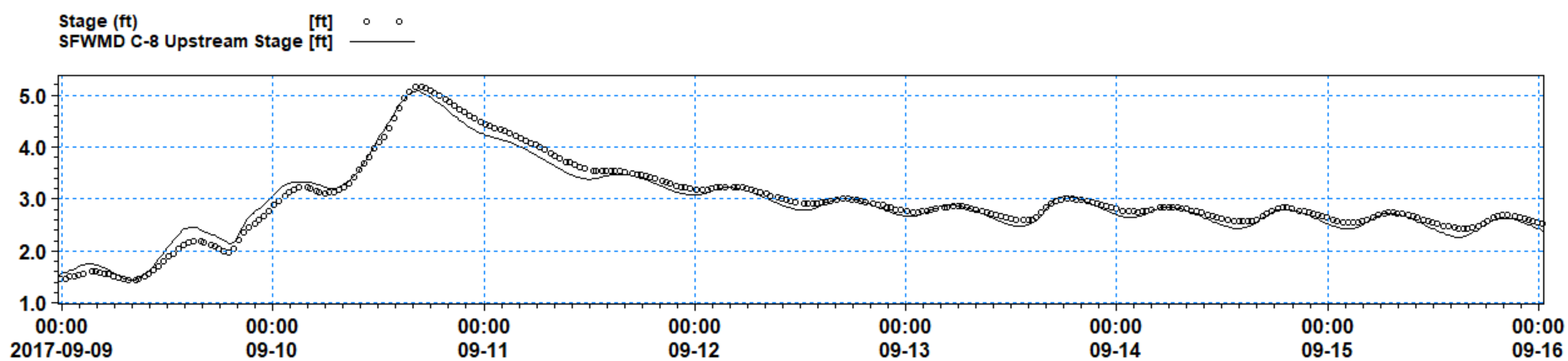

Figure 78: Simulated (line) vs Observed (dots) Stage Comparison for SFWMD C-8 Water Level Recorder S-28Z, September 9th-16th, 2017

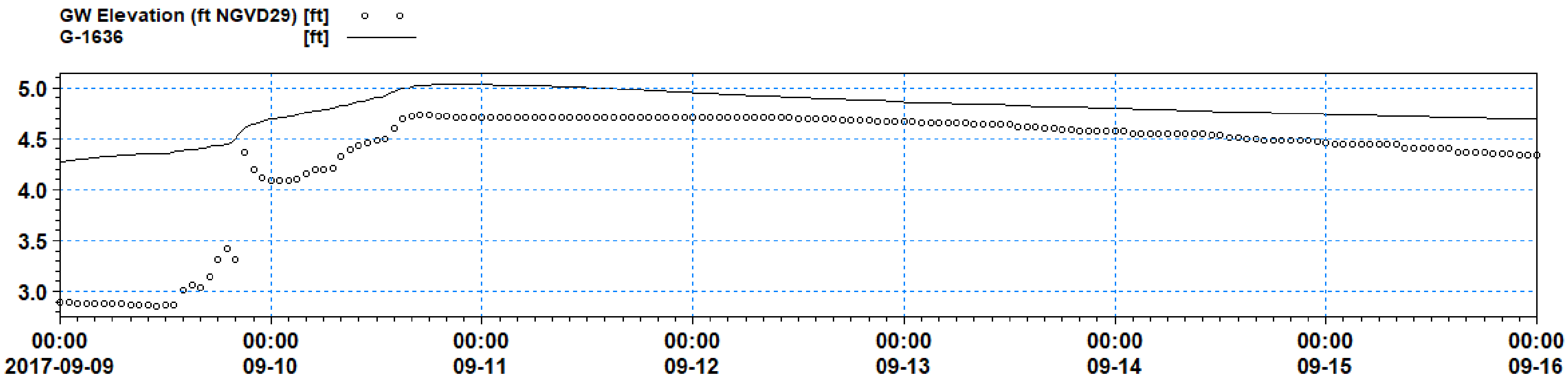

Figure 79: Simulated (line) vs Observed (dots) Groundwater Elevation Comparison for Well G-1636, September 9th-16th, 2017

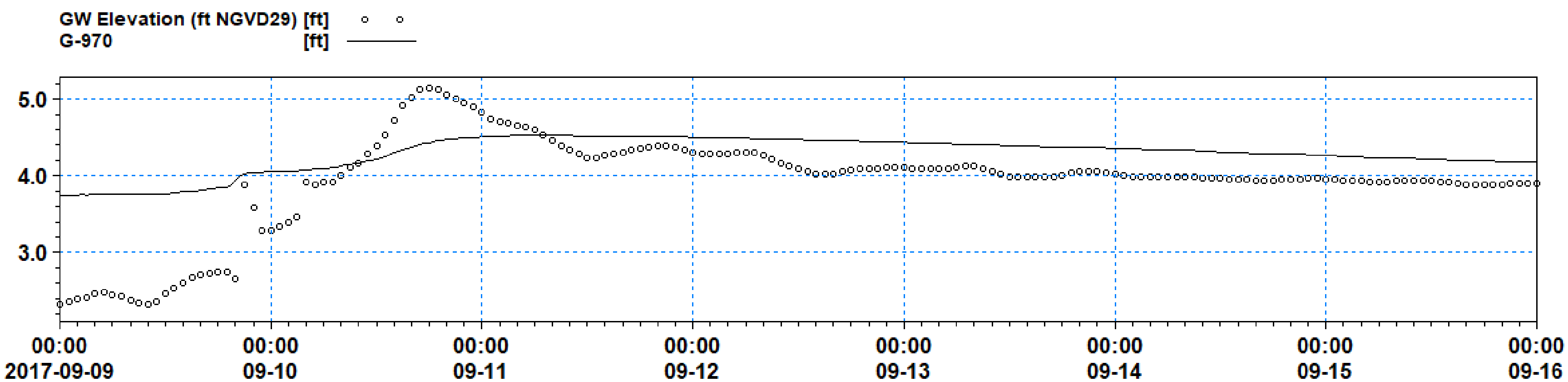

Figure 80: Simulated (line) vs Observed (dots) Groundwater Elevation Comparison for Well G-970, September 9th-16th, 2017

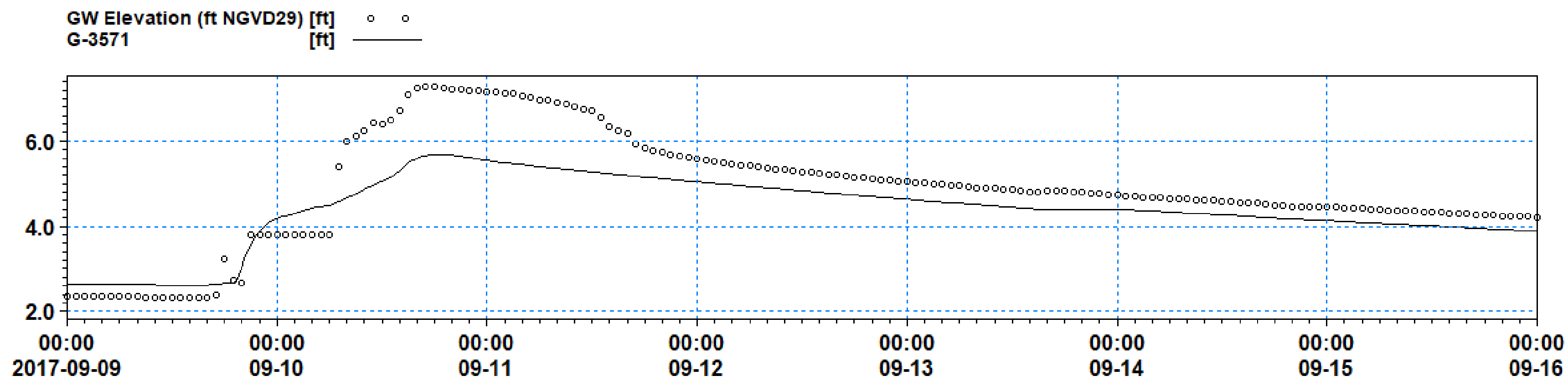

Figure 81: Simulated (line) vs Observed (dots) Groundwater Elevation Comparison for Well G-3571, September 9th-16th, 2017

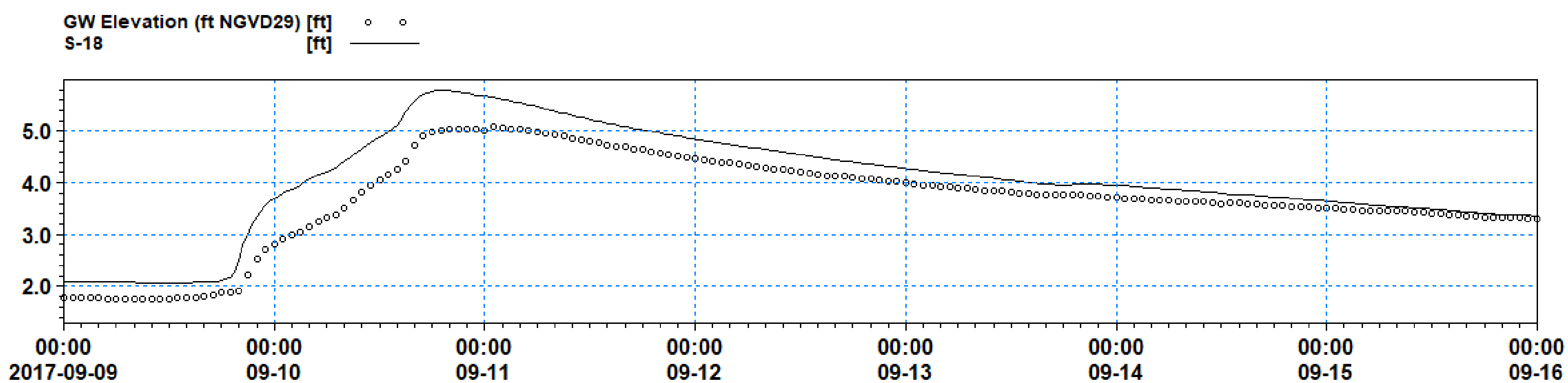

Figure 82: Simulated (line) vs Observed (dots) Groundwater Elevation Comparison for Well S-18, September 9th-16th, 2017

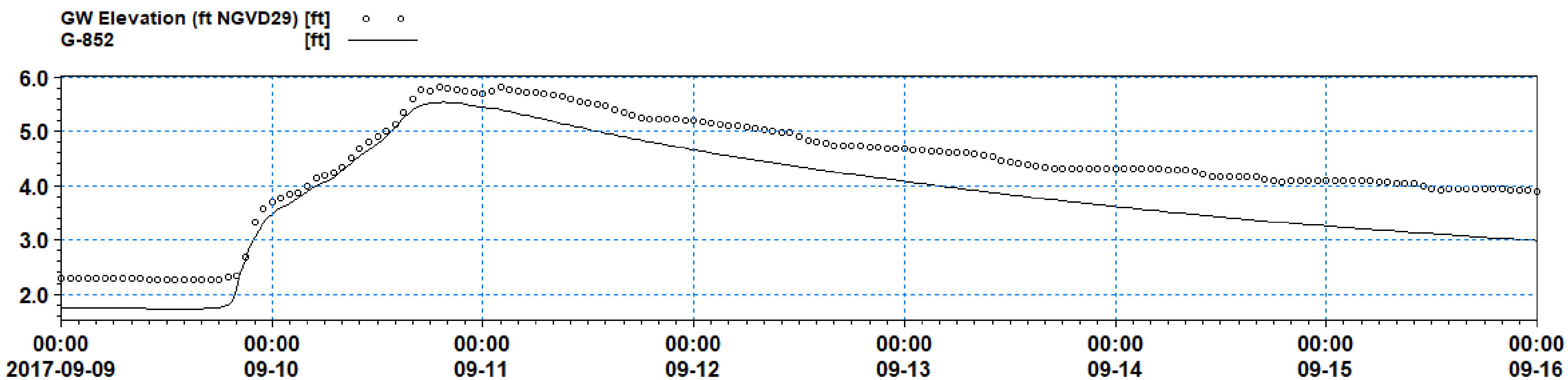

Figure 83: Simulated (line) vs Observed (dots) Groundwater Elevation Comparison for Well G-852, September 9th-16th, 2017

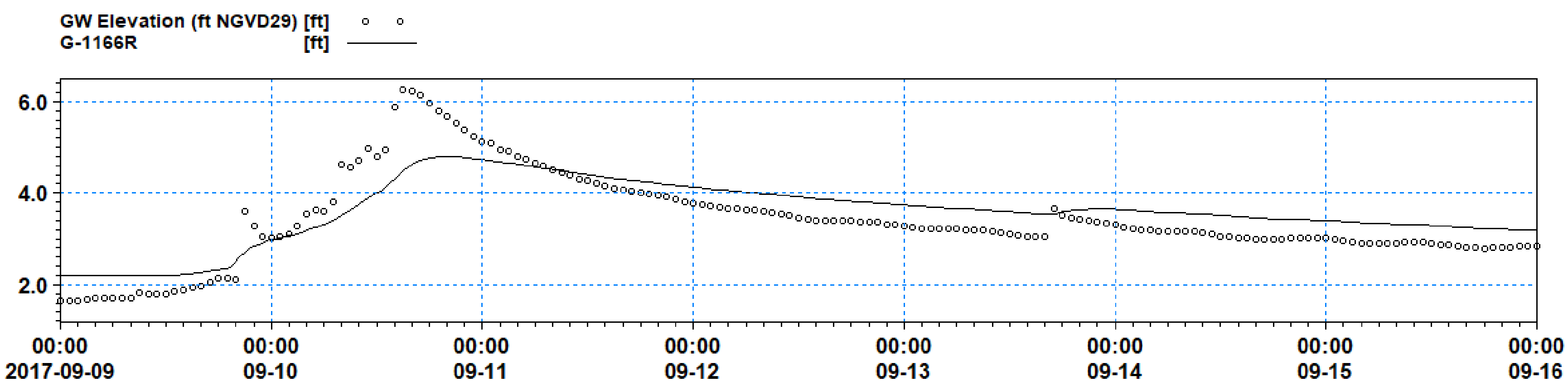

Figure 84: Simulated (line) vs Observed (dots) Groundwater Elevation Comparison for Well G-1166R, September 9th-16th, 2017

Table 21: Validation Model Statistics for Simulated vs Observed Data

Calibration Point	7-day Simulation (September 9th -16th, 2017)						4-month Simulation (June 2nd -September 27th, 2017)					
	ME	MAE	RMSE	STDres	R (Correlation)	Nash_Sutcliffe	ME	MAE	RMSE	STDres	R (Correlation)	Nash_Sutcliffe
S-29 Q (cfs)	87	304	499	491	0.83	0.61	67	119	210	199	0.96	0.92
S-29 HW (ft)	-0.002	0.04	0.06	0.06	0.998	0.996	0.013	0.13	0.19	0.19	0.96	0.89
S-28 Q (cfs)	-75	364	608	604	0.59	0.30	-9	49	159	159	0.91	0.82
S-28 HW (ft)	0.01	0.05	0.05	0.05	0.998	0.997	-0.06	0.1	0.13	0.12	0.98	0.95
S-30 HW (ft)	-0.47	0.47	0.49	0.15	0.87	-2.78	-0.23	0.43	0.47	0.41	0.90	0.26
S-30 TW (ft)	-0.44	0.45	0.54	0.31	0.93	0.60	-0.64	0.65	0.73	0.34	0.85	0.38
S-32 HW (ft)	-0.55	0.55	0.58	0.17	0.89	-3.1	-0.32	0.48	0.53	0.42	0.89	-0.018
S-9XS HW (ft)	-0.87	0.87	0.89	0.19	0.91	-7.5	-0.53	0.80	0.85	0.66	0.57	-7.37
S-29Z Stage (ft)	-0.07	0.15	0.21	0.20	0.97	0.93	-0.13	0.22	0.28	0.25	0.87	0.64
S-28Z Stage (ft)	0.02	0.10	0.13	0.13	0.99	0.98	-0.12	0.16	0.19	0.14	0.95	0084
G-1225 (ft)	-	-	-	-	-	-	0.55	0.6	0.73	0.48	0.78	0.096
G-1636 (ft)	-0.38	0.38	0.52	0.36	0.96	0.09	-0.75	0.75	0.83	0.35	0.74	-2.06
G-1637 (ft)	-	-	-	-	-	-	-0.88	0.88	0.97	0.42	0.47	-3.87
G-970 (ft)	-0.32	0.42	0.54	0.43	0.90	0.26	-0.83	0.84	0.89	0.32	0.78	-2.82
G-3571 (ft)	0.49	0.60	0.75	0.57	0.96	0.67	-0.057	0.26	0.33	0.32	0.94	0.83
S-18 (ft)	-0.35	0.35	0.42	0.24	0.97	0.78	-0.36	0.36	0.43	0.23	0.93	0.34
G-852 (ft)	0.56	0.56	0.61	0.23	0.98	0.61	0.47	0.48	0.55	0.29	0.92	0.42

3.3 Conclusions

The C-8 C-9 calibration/validation model is a physically-based integrated hydrologic / hydraulic model that includes a thorough representation of the hydrologic system and drainage network within the C-8 and C-9 basins, in Broward County and Miami-Dade County. Although a large portion of this model was inherited from the 2019 Broward County model, a lot of additional detail provided by Miami-Dade County and SFWMD, along with the survey collected specifically for this project by BDH Consulting Group, was incorporated into this model. Considering the scale of this model, the amount of detail is quite high, and most secondary and tertiary canal systems are modeled, including hundreds of culverts. The C-8 C-9 model was calibrated using the October 2nd-4th, 2000 storm event, which for the most part produced simulated canal stage results as well as groundwater elevations within 0.5 ft of observed. Likewise, the calibrated model produced simulated peak discharges and volumes within 10% and 17% of observed values, respectively. The C-8 C-9 model was validated using the September 9th-11th, 2017 storm event, which for the most part produced simulated canal stage results to within 0.4 ft. Additionally, the validation model produced simulated peak discharges and volumes to within about 15% of observed values. The validation model simulated groundwater elevations that were generally within 1 ft of observed values, which is a little higher than what was desired. It is worth mentioning that the areas with the largest differences were typically close to the model boundary and might be adversely affected by uncertainty in the boundary conditions. The groundwater wells more centrally located in the model domain typically had simulated elevations closer to observed.

Overall, these results provide confidence in the model setup and parameterization, and further confidence that the model is a reliable predictor of water levels and flows based on current conditions. In the calibration model, the largest source of uncertainty comes from the rainfall data. Originally, temporally modified NEXRAD rainfall was used, which caused calibration challenges as it was likely providing significantly too much rainfall, as well as timing issues. With the rainfall input switched to rain gauges, significantly better results were achieved, even with no other input changes. However, there is still some uncertainty with the rainfall as there was data for only 5 rain gauges in the area, which could introduce some error in the spatial distribution. It is possible, and perhaps even likely, that the largest difference in simulated vs. observed stage is due to not simulating enough rainfall in the immediate upstream drainage area. In the validation model, the largest source of uncertainty comes from what is likely some combination of either rating parameter issues, observed data issues, or issues with how the model calculates flow with nearly zero head difference. Looking at structure S-28 during validation, there is a discrepancy between simulated and observed discharge, however, the headwater is a near perfect match, tailwater is forced, and the rating parameters are matched. The observed discharge is calculated based on a set of equations using rating parameters and the head difference between upstream and downstream of the structure. It has been determined that the rating equation used to characterize flow through these gates are particularly sensitive to the head difference between headwater and tailwater, especially during uncontrolled submerged conditions. So, although the model is simulating a near-perfect headwater, it is often slightly underpredicting, even as little as 0.001-0.05ft, which significantly reduced the head gradient through the structure. This is the cause for the model simulating discharges that are significantly smaller than the observed data. One example of this is on September 9th, 2017 at 6:55am.

The observed discharge is 1420 cfs calculated based on a 0.037 ft gradient (keep in mind that is less than 0.5 inches), whereas the calculated discharge is around 75 cfs because the head gradient drops to 0.001 ft. The headwater is well within the target of +/- 0.5ft, as it is only about -0.5 inches, however, this causes the discharge to become extremely underpredicted, both in the model and verified by hand calculations using the same uncontrolled submerged equations with SFWMD rating parameters. This issue appears to be limited to uncontrolled submerged conditions, which is a rare occurrence. From 1985 to 2016, this structure operated in controlled submerged conditions 96% of the time (SFWMD, 2016). Likewise, the other major tidal outfall structure in this model (S-29), has been reported to have operated in controlled submerged conditions 99.14% of the time during 2011-2016 (SFWMD, 2016). So, although there is a sensitivity issue with uncontrolled submerged discharge, it historically has been a rare occurrence and it must be kept in mind that simulated vs observed discharge discrepancies during uncontrolled submerged operation are due to extremely small head differences that would otherwise be considered negligible.

In summary, Taylor Engineering believes that the C-8 C-9 model is setup and parameterized in a way that accurately represents the current drainage characteristics and will be a reliable predictor of water levels and flows in the design storm scenarios. However, it is important to keep in mind that any predictions by this computer model (or any other) show only what could happen, not necessarily what will happen. Model outputs can only be as good as the data input, and this model is no exception. The limitations of this model and its ability to predict what could happen should be known and considered when interpreting the results.

References

BDH Consulting Group, LLC. (2019). *Survey Work for C8 and C9 FPLOS Models*.

Environmental Protection Agency. (2015). *Storm Water Management Model User's Manual Version 5.1*. Cincinnati: National Risk Management Research Laboratory Office of Research and Development.

Fish, J. E. and M. Stewart, 1990, *Hydrogeology of the Surficial Aquifer System, Dade County, Florida.* U.S. Geological Survey Water Resources Investigations Report 90-4108.

Hughes, J.D., and White, J.T., 2016, *Hydrologic Conditions in Urban Miami-Dade County, Florida, and the Effect of Groundwater Pumpage and Increased Sea Level on Canal Leakage and Regional Groundwater Flow (ver. 1.2, July 2016):* U.S. Geological Survey Scientific Investigations Report 2014–5162, 175 p., http://dx.doi.org/10.3133/sir20145162.

2015 Miami-Dade County DEM 5ft. (2017). Retrieved from https://gis-mdc.opendata.arcgis.com/datasets/32f1de78447c4c958782b1b2b5d47369

South Broward Drainage District. (2013). *South Broward Drainage District Facilities Report and Water Control Plan*.

Stoner & Associates, Inc. (2019). *Surveyors Report As-Built Survey (Bridges, Culverts, & Canal Sections)*. Davie, Florida.

SFWMD. (2016). FLOW RATING ANALYSIS FOR SPILLWAY S28.

SFWMD. (2016). FLOW RATING ANALYSIS FOR SPILLWAY S29.

SFWMD (2018). *Sfwmd.Maps.Arcgis.Com* https://sfwmd.maps.arcgis.com/home/item.html?id=266a64a897514090842e283311c12d30.

Taylor Engineering, Inc., July 2019. *Broward County 100-Year Flood Elevation Map & Associated Modeling: Current Conditions Model Update and Validation Draft Report.* Prepared for Geosyntec, Inc., and Broward County, FL.

FNAI, 2012. https://www.fnai.org/PDF/Cooperative%20Land%20Cover%20v2.3%20Definitions.pdf

Appendix A

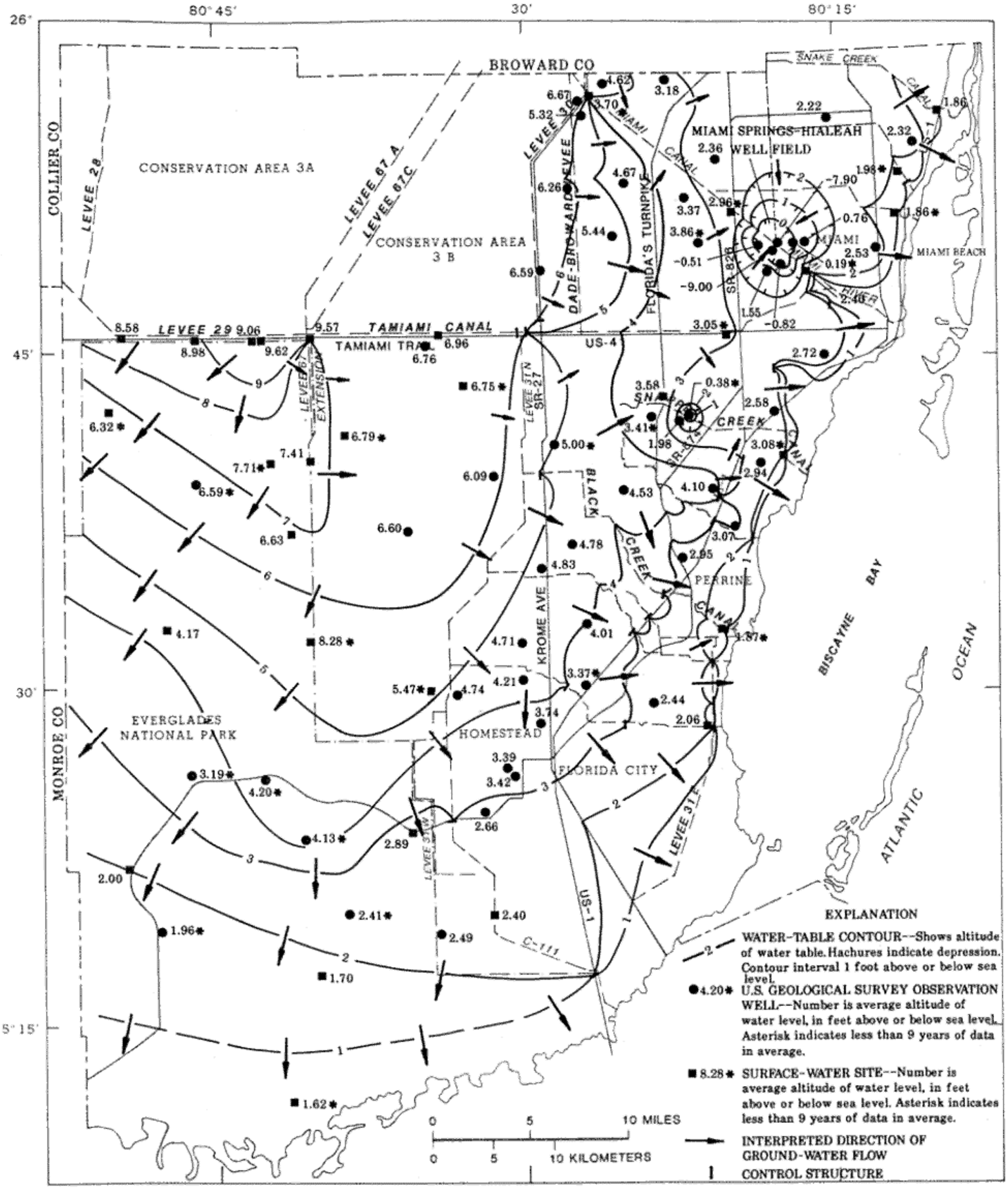
80° 45'
30'
80° 15'
26°
45'
30'
5° 15'
BROWARD CO
COLLIER CO
MONROE CO
LEVEE 28
CONSERVATION AREA 3A
LEVEE 67 A
LEVEE 67C
CONSERVATION AREA 3 B
LEVEE 30
DADE-BROWARD LEVEE
FLORIDA'S TURNPIKE
MIAMI CANAL
SNAKE CREEK
CANAL
MIAMI SPRINGS-HIALEAH WELL FIELD
MIAMI
MIAMI BEACH
SR-826
MIAMI RIVER
LEVEE 29
TAMIAMI CANAL
TAMIAMI TRAIL
US-4
LEVEE 67 EXTENSION
LEVEE 31N
SR-27
SNAPPER CREEK
SR-874
BLACK CREEK
CANAL
KROME AVE
PERRINE
BISCAYNE BAY
OCEAN
ATLANTIC
EVERGLADES NATIONAL PARK
HOMESTEAD
FLORIDA CITY
LEVEE 31W
LEVEE 31E
US-1
C-111
0 5 10 MILES
0 5 10 KILOMETERS
EXPLANATION
WATER-TABLE CONTOUR--Shows altitude of water table. Hachures indicate depression. Contour interval 1 foot above or below sea level.
4.20* U.S. GEOLOGICAL SURVEY OBSERVATION WELL--Number is average altitude of water level, in feet above or below sea level. Asterisk indicates less than 9 years of data in average.
8.28* SURFACE-WATER SITE--Number is average altitude of water level, in feet above or below sea level. Asterisk indicates less than 9 years of data in average.
INTERPRETED DIRECTION OF GROUND-WATER FLOW
CONTROL STRUCTURE

Appendix B

From: Kevin Hart <kevin@sbdd.org>
Sent: Wednesday, January 2, 2019 2:32 PM
To: Mark Ellard <MEllard@Geosyntec.com>
Cc: John Loper <jloper@taylorengineering.com>; Zygnerski, Michael <MZYGNERSKI@broward.org>; Maran, Carolina <CMARAN@broward.org>; Luis Ochoa <luis@sbdd.org>
Subject: RE: Broward Future 100-Year Model Follow Up - SBDD

Mark,

Attached is the latest SFWMD permit for CS12, CS13, CS13-A, ICS12, ISC13 and ISC13-A.

Basically, the permit states the following:

- CS12, CS13, CS13-A are operated to allow the canal stages downstream of the intermediate gates to fluctuate with the C-11 Canal, but no lower that Elev. 3.00' NGVD (except with prior authorization from SFWMD).
- The maximum, combined discharge rate for CS12, CS13, CS13-A is 363 cfs.
- The intermediate gates (internal gate structures) are operated to maintain the permitted control elevation of 4.0' NGVD, within the upstream areas of the S-9/S-10 Basin (upstream of the gates). These gates are only opened when the tail water exceeds Elevation 4.0' NGVD.

The B-1 and B-2 pump stations are operated on a manual basis only. These two pump stations are operated by SBDD on an as-needed basis, and as determined by staff, during extreme rainfall events. Just as an FYI, neither station has operated during the past 7 years (except for maintenance purposes). Both stations have a gravity culvert connection to SBDD's C-1 Canal. For modeling purposes, the two pumps can be activated at Elevation 4.0' NGVD with a pumping capacity of 15,000 GPM. The pumps are used to reduce peak stages and durations within the sub-basins they serve.

The Silver Lakes Flood Gate is an emergency, basin inter-connect between Basins S-9/S-10 and S-5. This gate is operated to allow SBDD to move water from the C-11 Basin to C-9 Basin on an as-needed (emergency) basis. The operation of this gate is performed in conjunction with approval and authority from SFWMD. For modeling purposes, this gate should be closed. However, under adaptation strategies/scenarios, you are welcome to incorporate the use of this gate to manage stages between the C-11 and C-9 basin as applicable. As an FYI, there have been a handful of occasions where SFWMD has asked SBDD to discharge south through the S-5 Basin in order to limit discharges to the C-11 Canal.

The Nautica/Silver Lakes culvert (ID 408) is a basin inter-connect that is operated on an as-needed, emergency basis only. For modeling purposes, this gate should be closed. However, under adaptation strategies/scenarios, you are welcome to incorporate the use of this gate to manage stages between the S-4 and S-5 basins as applicable.

You're probably aware that SBDD has 2 other basin inter-connects that are operated on an as-needed, emergency basis only as well………. between Basins S-3 and S-2.

On the pipe inverts, we do not have any additional information at this time. For modeling purposes, we suggest that you set the pipe inverts such that the top of pipe matches the Control Water Elevation (CWE), as that is SBDD's standard practice.

Let me know if you need any additional information.

Thanks.

Kevin Hart, P.E., CFM
District Director
South Broward Drainage District
6591 Southwest 160th Avenue
Southwest Ranches, FL 33331
954-680-3337 (office)
e-mail: kevin@sbdd.org

Appendix C

ENVIRONMENTAL RESOURCE PERMIT APPLICANT'S HANDBOOK VOLUME II
Effective: MAY 22, 2016

Appendix A: SFWMD - ALLOWABLE DISCHARGE FORMULAS

Canal	Allowable Runoff	Design Frequency
C-1	$Q = \left(\frac{112}{\sqrt{A}} + 31\right) A$	10 year
C-2	Essentially unlimited inflow by gravity connections southeast of Sunset Drive: 54 CSM northwest of Sunset Drive	200 year +
C-4	Essentially unlimited inflow by gravity connections east of S.W. 87th Avenue	200 year +
C-6	Essentially unlimited inflow by gravity connections east of FEC Railroad	200 year +
C-7	Essentially unlimited inflow by gravity connection	100 year +
C-8	Essentially unlimited inflow by gravity connection	200 year +
C-9	Essentially unlimited inflow by gravity connection east of Red Road; 20 CSM pumped, unlimited gravity with development limitations west of Red Road or Flamingo Blvd.	100 year +
C-10	--	200 year +
C-11	20 CSM west of 13A;40 CSM east of 13A	------------
C-12	90.6 CSM	25 year
C-13	75.9 CSM	25 year
C-14	69.2 CSM	25 year
C-15	70.0 CSM	25 year
C-16	62.6 CSM	25 year
C-17	62.7 CSM	25 year
C-18	41.6 CSM	25 year
C-19	57.8 CSM	------------
C-23	31.5 CSM	10 year

Appendix D

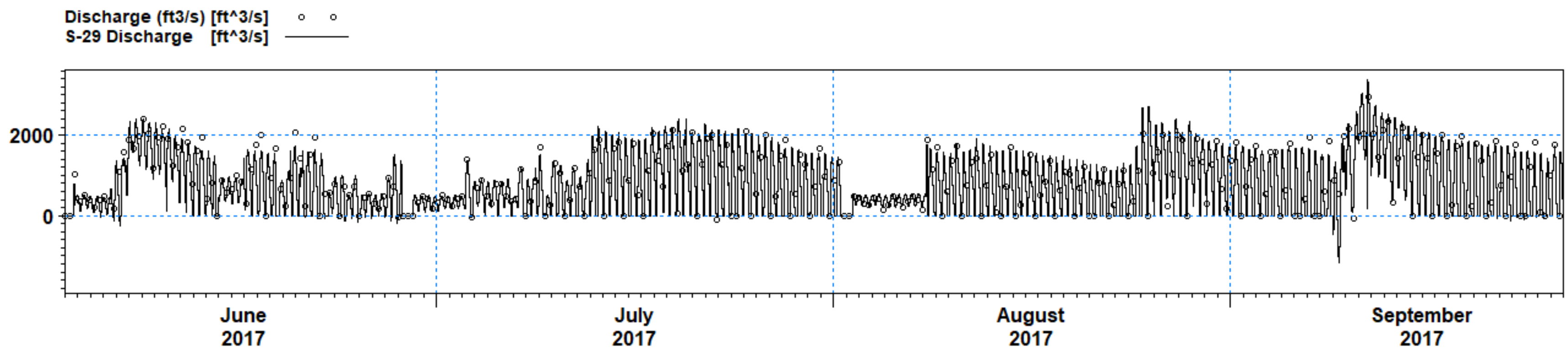

Figure 85: Simulated (line) vs Observed (dots) Discharge Comparison for SFWMD C-9 Structure S-29, June 2nd-September 27th, 2017

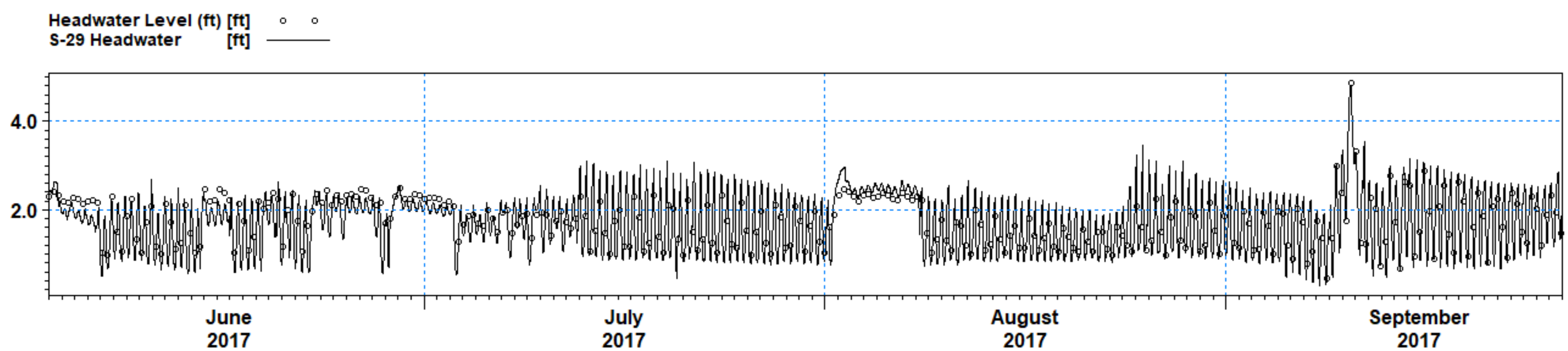

Figure 86: Simulated (line) vs Observed (dots) Headwater Comparison for SFWMD C-9 Structure S-29, June 2nd-September 27th, 2017

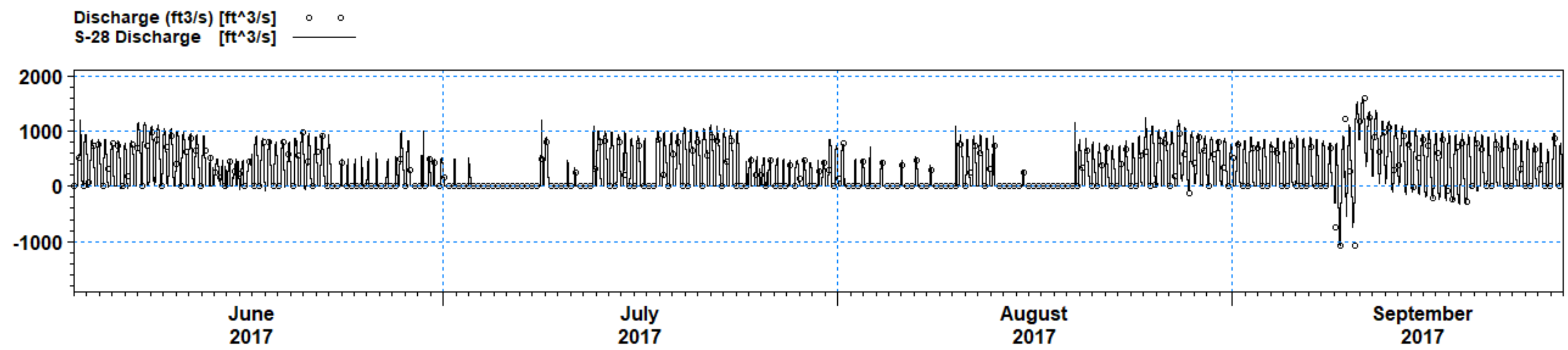

Figure 87: Simulated (line) vs Observed (dots) Discharge Comparison for SFWMD C-8 Structure S-28, June 2nd-September 27th, 2017

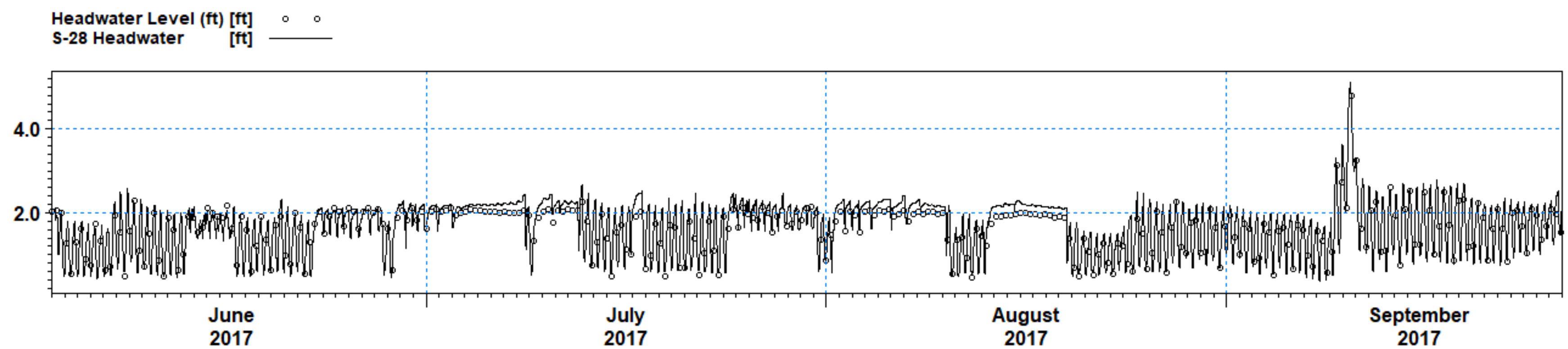

Figure 88: Simulated (line) vs Observed (dots) Headwater Comparison for SFWMD C-8 Structure S-28, June 2nd-September 27th, 2017

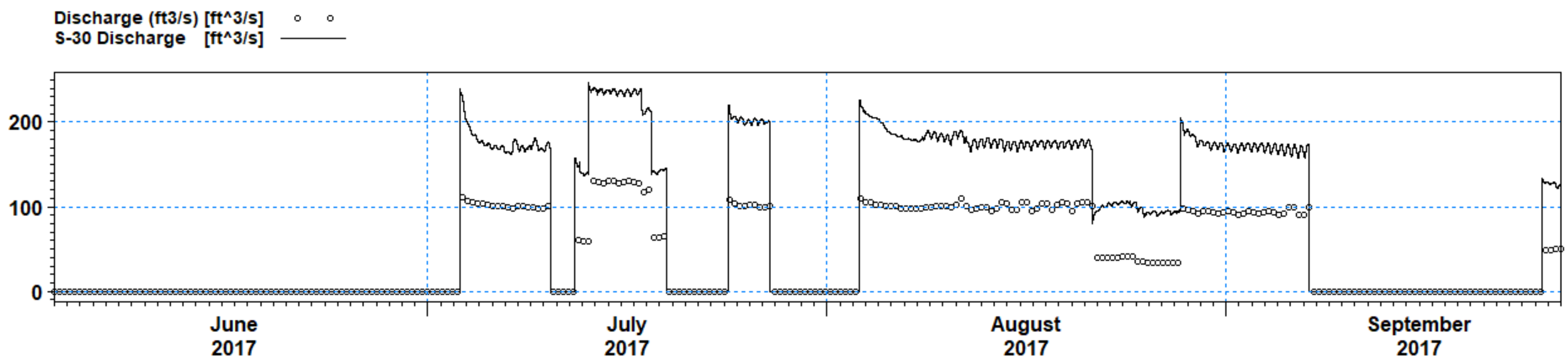

Figure 89: Simulated (line) vs Observed (dots) Discharge Comparison for SFWMD C-9 Structure S-30, June 2nd-September 27th, 2017

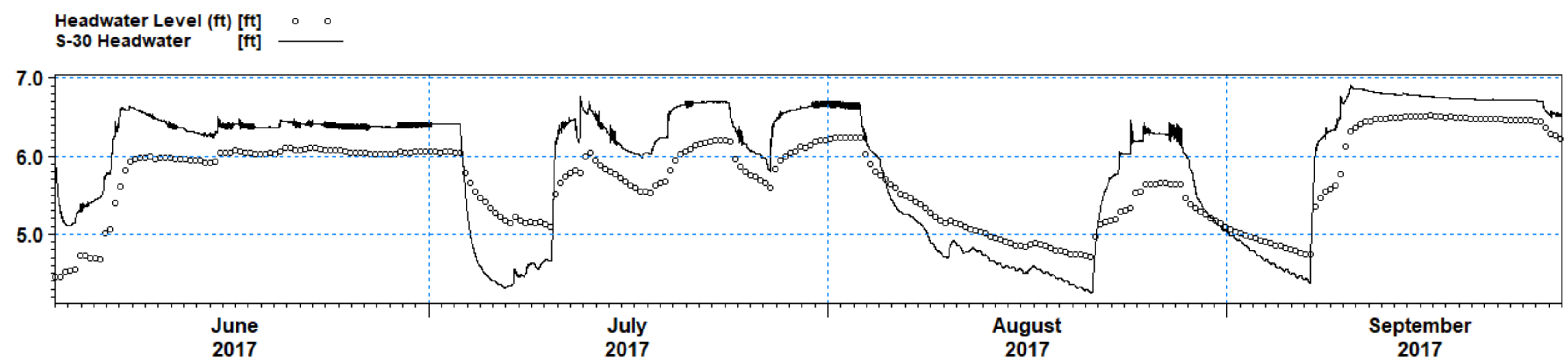

Figure 90: Simulated (line) vs Observed (dots) Headwater Comparison for SFWMD C-9 Structure S-30, June 2nd-September 27th, 2017

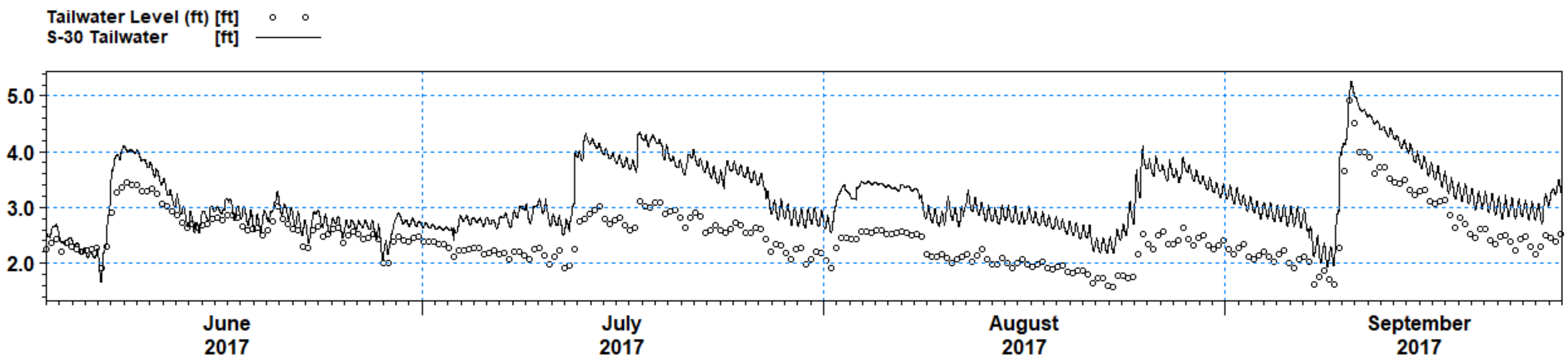

Figure 91: Simulated (line) vs Observed (dots) Tailwater Comparison for SFWMD C-9 Structure S-30, June 2nd-September 27th, 2017

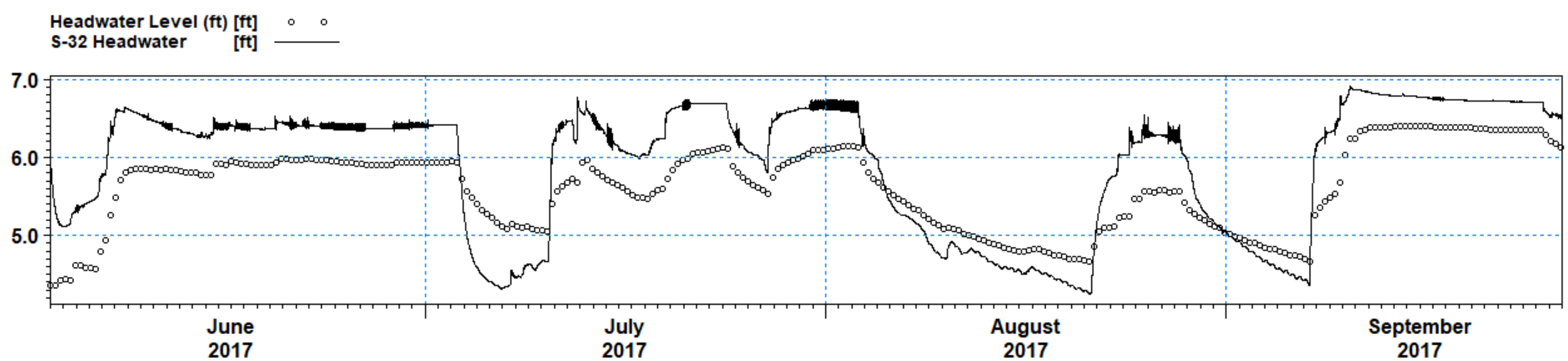

Figure 92: Simulated (line) vs Observed (dots) Headwater Comparison for SFWMD L-33 Structure S-32, June 2nd-September 27th, 2017

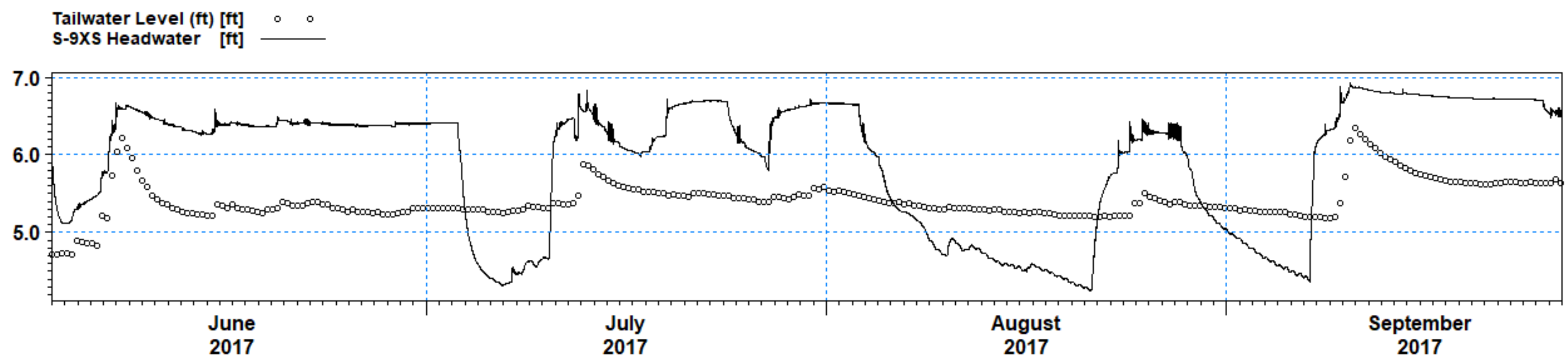

Figure 93: Simulated (line) vs Observed (dots) Headwater Comparison for SFWMD L-33 Structure S-9XS, June 2nd-September 27th, 2017

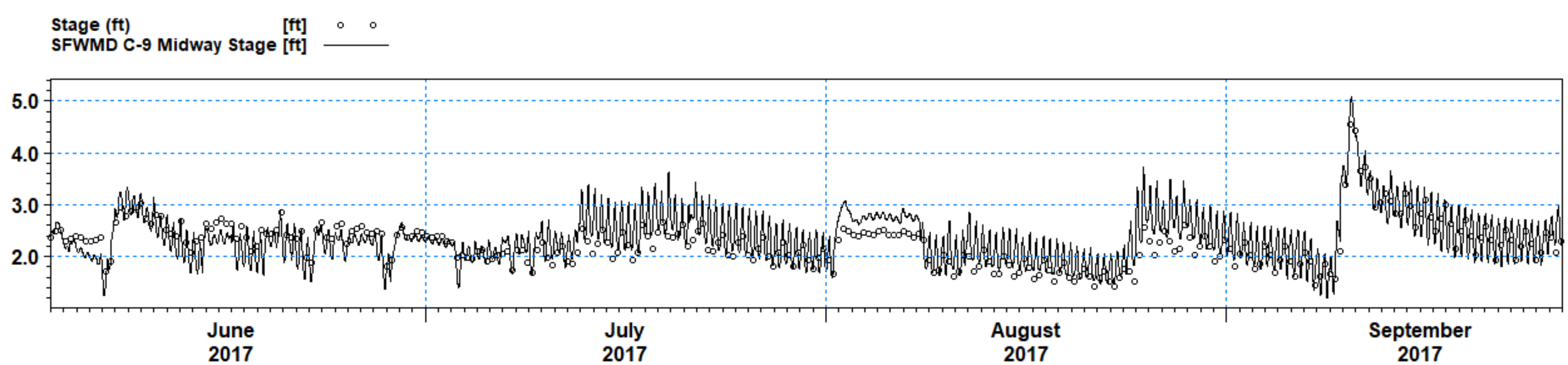

Figure 94: Simulated (line) vs Observed (dots) Stage Comparison for SFWMD C-9 Water Level Recorder S-29Z, June 2nd-September 27th, 2017

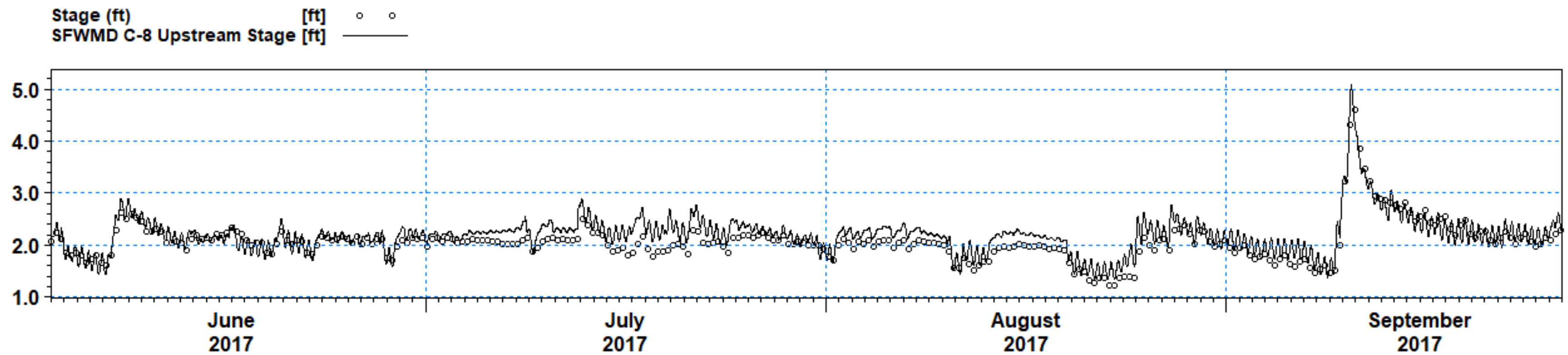

Figure 95: Simulated (line) vs Observed (dots) Stage Comparison for SFWMD C-8 Water Level Recorder S-28Z, June 2nd-September 27th, 2017

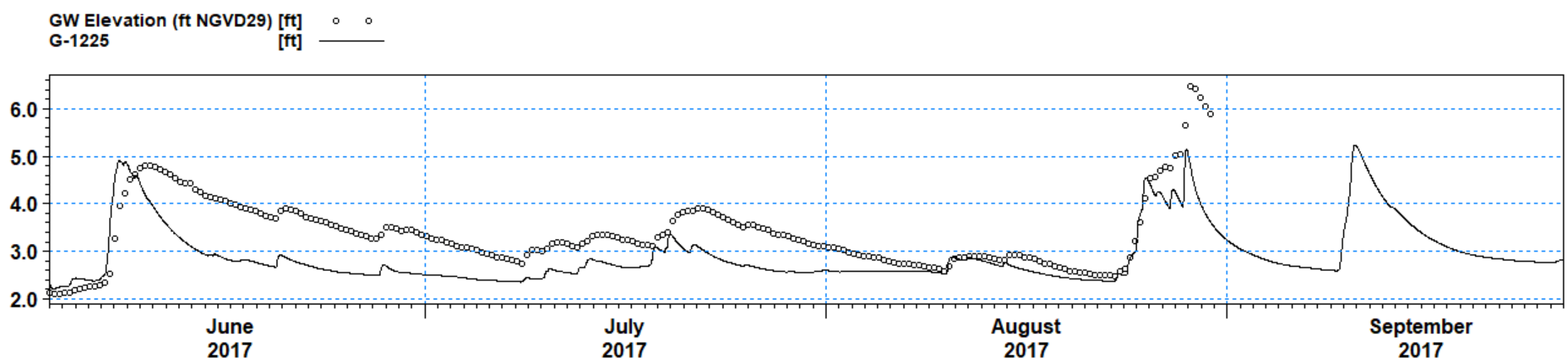

Figure 96: Simulated (line) vs Observed (dots) Groundwater Elevation Comparison for Well G-1225, June 2nd-September 27th, 2017

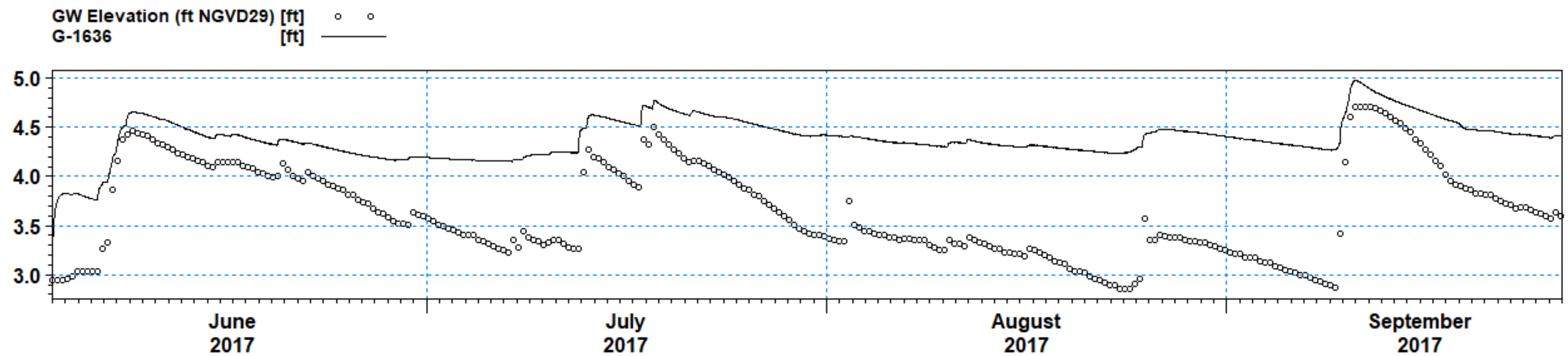

Figure 97: Simulated (line) vs Observed (dots) Groundwater Elevation Comparison for Well G-1636, June 2nd-September 27th, 2017

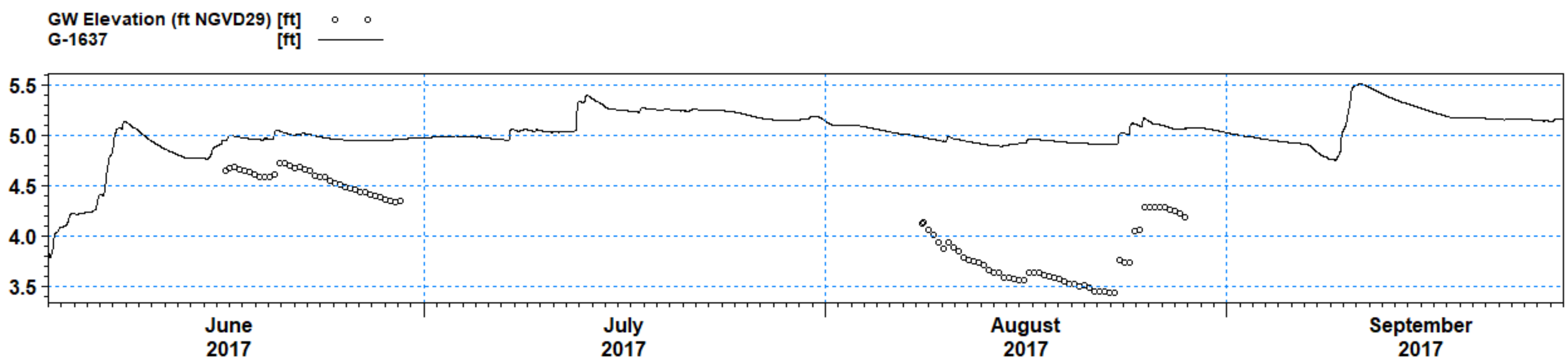

Figure 98: Simulated (line) vs Observed (dots) Groundwater Elevation Comparison for Well G-1637, June 2nd-September 27th, 2017

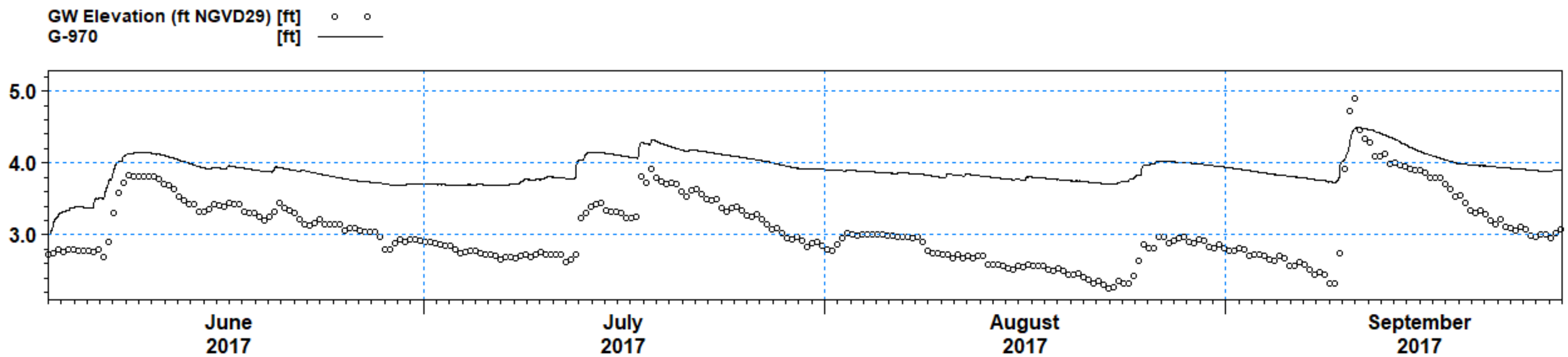

Figure 99: Simulated (line) vs Observed (dots) Groundwater Elevation Comparison for Well G-970, June 2nd-September 27th, 2017

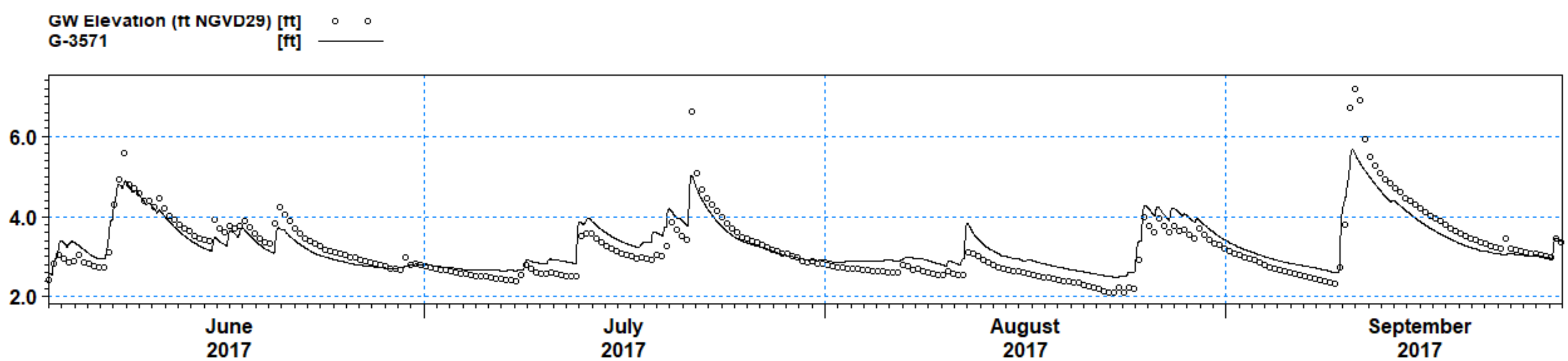

Figure 100: Simulated (line) vs Observed (dots) Groundwater Elevation Comparison for Well G-3571, June 2nd-September 27th, 2017

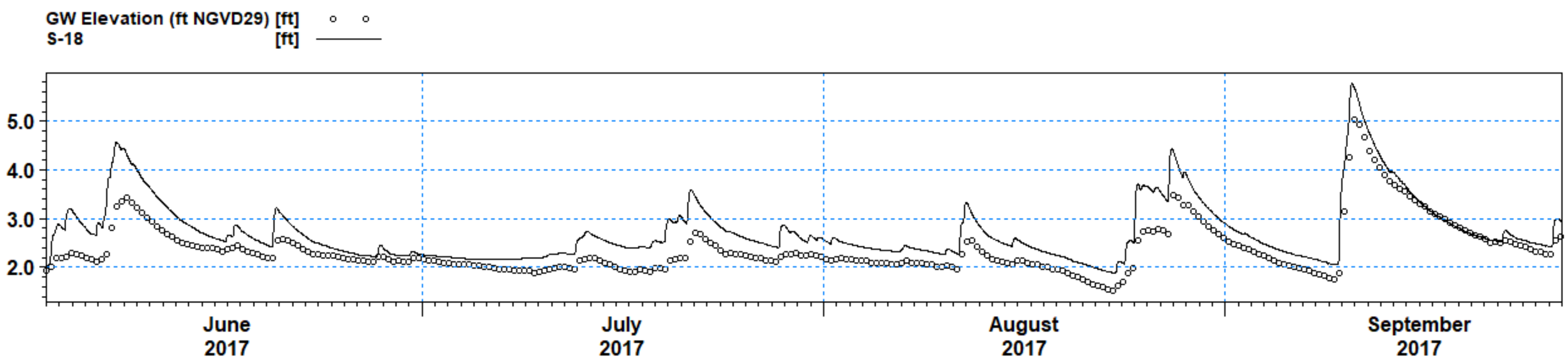

Figure 101: Simulated (line) vs Observed (dots) Groundwater Elevation Comparison for Well S-18, June 2nd-September 27th, 2017

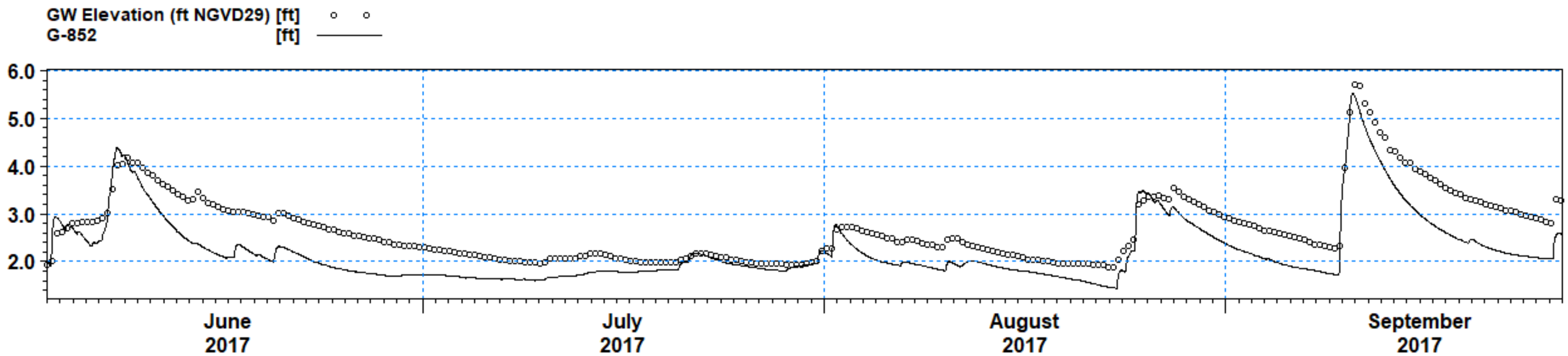

Figure 102: Simulated (line) vs Observed (dots) Groundwater Elevation Comparison for Well G-852, June 2nd-September 27th, 2017

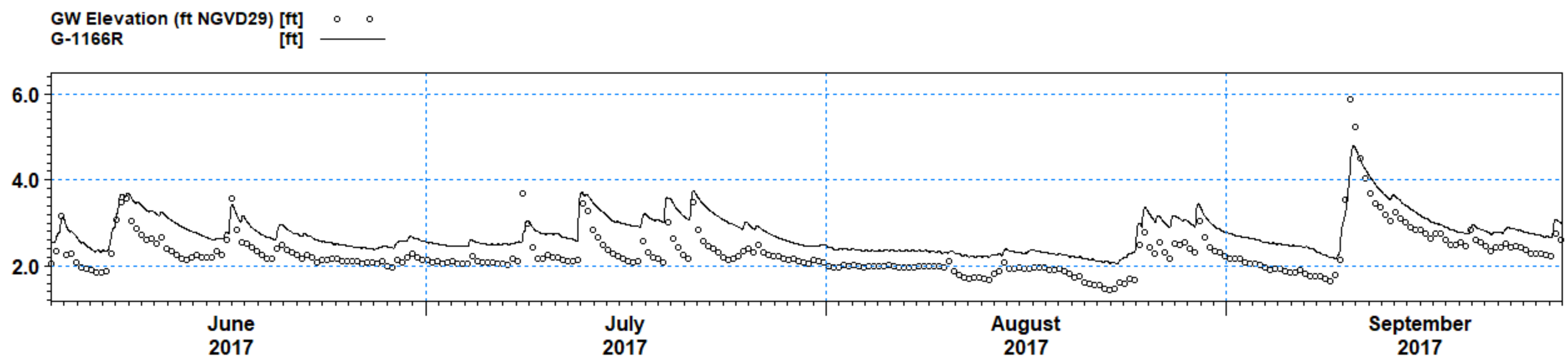

Figure 103: Simulated (line) vs Observed (dots) Groundwater Elevation Comparison for Well G-1166R, June 2nd-September 27th, 2017

Appendix D

Table 22: Unsaturated Zone Soil Parameters

2-Layer Unsaturated Zone Soil Profiles	Water content at saturation	Water content at field capacity	Water content at wilting point	Saturated hydraulic conductivity (ft/day)
Immokalee	0.44	0.14	0.06	85.0
Krome Gravelly Loam	0.45	0.17	0.08	28.3
Margate Fine Sand	0.35	0.18	0.06	28.3
Matlashda	0.42	0.09	0.04	198.4
Opalocka Sand-Rock	0.42	0.09	0.06	198.4
Palm Beach Sand	0.42	0.09	0.06	198.4
Perrine Marl	0.47	0.25	0.13	28.3
Muck	0.7	0.59	0.18	141.7
Udorthents	0.3	0.13	0.08	28.3
Urban Land	0.3	0.2	0.08	28.3

Table 23: Crop Coefficients by FLUCCS Code

FLUCCS Code	Crop Coefficient (Kc)
1100	0.67
1200	0.58
1300	0.48
1400	0.48
1500	0.4
1700	0.48
1800	0.72
1900	0.8
2100	0.8
2200	0.8
2300	0.8
2400	0.8
2500	0.8
2600	0.8
3100	0.8
3200	0.8
3300	0.8
4200	0.8
4300	0.8
5100	0.8
5200	0.8
5300	0.8
5400	0.8
5700	0.8
6100	0.8
6400	0.8
7400	0.8
8100	0.4
8200	0.4
8300	0.4

Meeting Notes: SFWMD C8 C9 FPLOS

Meeting Date: 02/27/2020
Subject: Meeting to discuss current conditions model set-up for design storm simulations
Location: Webex

Attendees:
SFWMD: Ann Springston, Hongying Zhao, Carol Ballard, Ruben Arteaga
CSA Group: Ernesto Marin
Taylor Engineering: John Loper, Joseph Wilder

Current Conditions Model Set-Up

<u>Overview:</u>

The current conditions model started as the calibrated/validated model (2017 conditions) and has been updated with all applicable changes to the model setup including structure operations, rainfall, evapotranspiration, tidal boundaries, and initial conditions. The recorded structure operations have been replaced with rule-based operations. The observed NEXRAD rainfall has been replaced with Thiessen polygon-based 3-day design storm rainfall depths from NOAA Atlas 14 using the SFWMD 3-day temporal distribution. The reference evapotranspiration has been updated to a constant 2 mm/d, which is about the minimum daily wet season value in year 2017, which included Hurricane Irma (USGS Reference and Potential Evapotranspiration, 2018). The 1-D tidal boundaries (forced tailwater at tidal structures) were updated to the SFWMD provided design storm stage hydrographs. The SFWMD design storm stage hydrographs were also applied to the eastern general-head groundwater boundary. A time-varying 2-d overland flow boundary was included along the coastal portion of the eastern boundary using the SFWMD design storm stage hydrographs. Localized adjustments to the initial groundwater levels are being performed to ensure a close match between the groundwater levels and water control elevations, particularly in areas with large lakes such as South Broward Drainage District.

<u>Rule-based Operations:</u>

As agreed, the operable structure rules will be based on standard operating procedure as detailed in the Districts Operations Control Center (OCC) Structure Books (2017). The control rules for S-28 and S-29 are presented in the following two figures.

	Description	Condition	Control type	Value type
1		[s:hUS:S-28] - [s:hDS:S-28] <=0.09144	Direct setting	Close
2		[s:hUS:S-28] >0.64008	Direct setting	Fully open
3		[s:hUS:S-28] > 0.4572 && [s:hUS:S-28] <0.54864	Unchanged	Absolute value
4		[s:hUS:S-28] <0.4572	Direct setting	Close

Figure 1:Control Rules for S-28 (SI Units)

	Description	Condition	Control type	Value type
1		[s:hUS:S-29] - [s:hDS:S-29] <=0.09144	Direct setting	Close
2		[s:hUS:S-29] >0.762	Direct setting	Fully open
3		[s:hUS:S-29] > 0.4572 && [s:hUS:S-29] <0.6096	Unchanged	Absolute value
4		[s:hUS:S-29] <0.4572	Direct setting	Close

Figure 2:Control Rules for S-29 (SI Units)

<u>Rainfall:</u>

The calibration and validation model used rain gauge and NEXRAD radar rainfall, respectively. For the design storm simulations, this has been replaced with a Thiessen polygon approach, identical to the approach used for the design storm runs in the 2019 Broward County model, as well as the 2016 BCB FPLOS (Taylor Engineering, 2016). The centroid of each polygon corresponds to a NOAA Atlas 14 station (Figure 3).

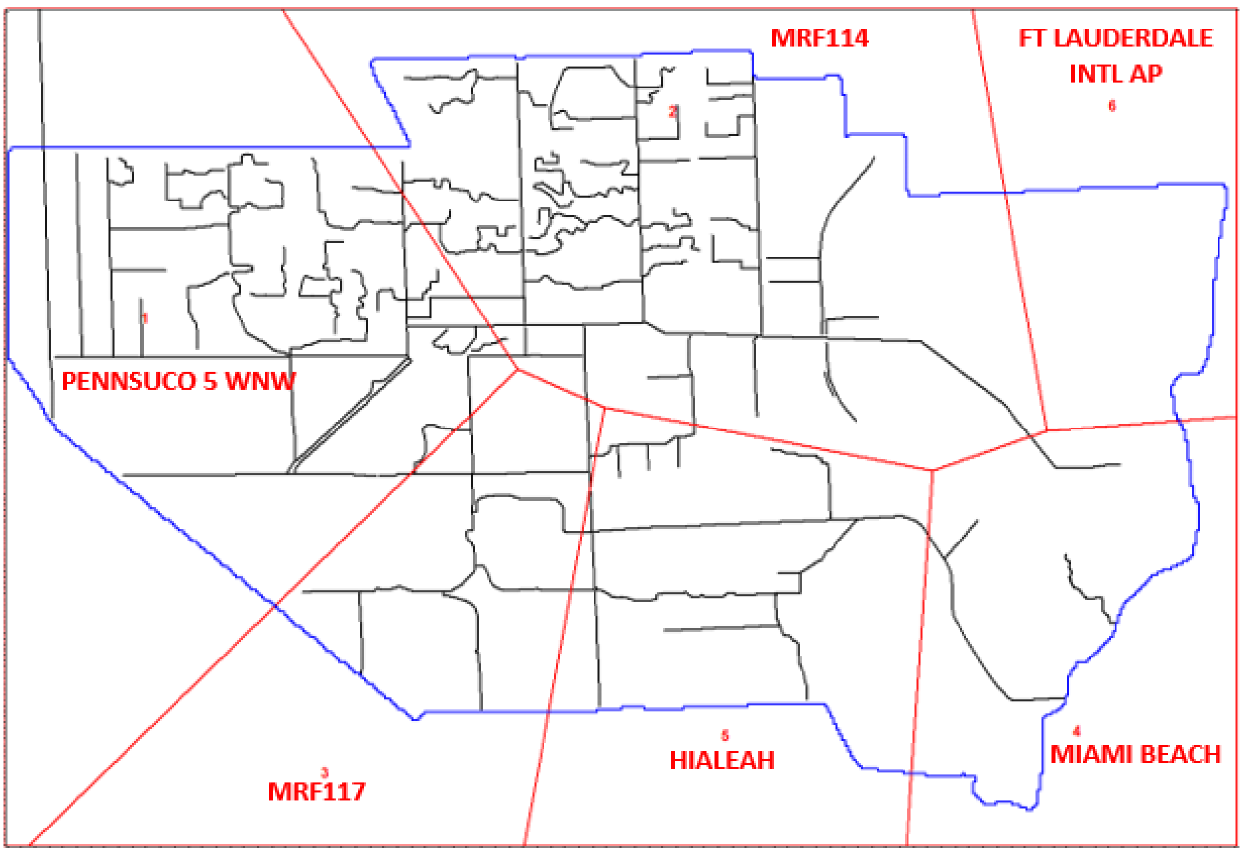

Figure 3: Design Storm Thiessen Polygons based on NOAA Stations

Rainfall 3-day totals for each return period were based on NOAA Atlas 14 depths. The NOAA rainfall depths were distributed temporally based on the SFWMD Environmental Resource Permit Information Manual (2014). Total rainfall are listed in the table below.

Table 1: Design Storm Rainfall Depths per NOAA Atlas 14 Station

NOAA Station	3-Day Storm Rainfall Depth (inches)			
	5-Year	*10-Year*	*25-Year*	*100-Year*
PENNSUCO 5 WNW	8.12	9.66	12.1	16.3
MRF114	8.9	10.7	13.5	18.4
MRF117	8.85	10.5	13.1	17.7
MIAMI BEACH	8.48	10.1	12.6	16.9
HIALEAH	8.91	10.6	13.2	17.8
FT LAUDERDALE INTL AP	8.95	10.8	13.5	18.3

The rainfall is a 72-hour event and specific dates are relative. Therefore, the rainfall was assigned a start date of 6/4/2017, 12am. This aligns the peak rainfall with the overall wettest time during the storm event that was used to develop the northern boundary condition (2019 Broward County Model- the model wide most intense rainfall occurred at 6/6/2017 12pm). The model simulation will start on 6/2/2017 12am, which will result in a 2-day spin-up period with no rainfall.

Boundary Conditions:

SFWMD provided year 2015 tidal boundary data at the S-28 and S-29 structures, which include storm surge effects for the design storms of interest. The dates of the District provided time series data are relative for the purposes of design storms. Therefore, for each boundary condition using SFWMD provided data, the dates were adjusted so that the peak stages occur at the same time as the peak rainfall, as per the Scope of Work. The 1-D tidal boundaries, which force the tailwater at structures S-28, S-29, and G-58, have been updated to use the SFWMD provided design storm stages. The design storm tidal boundaries are shown in the following two figures.

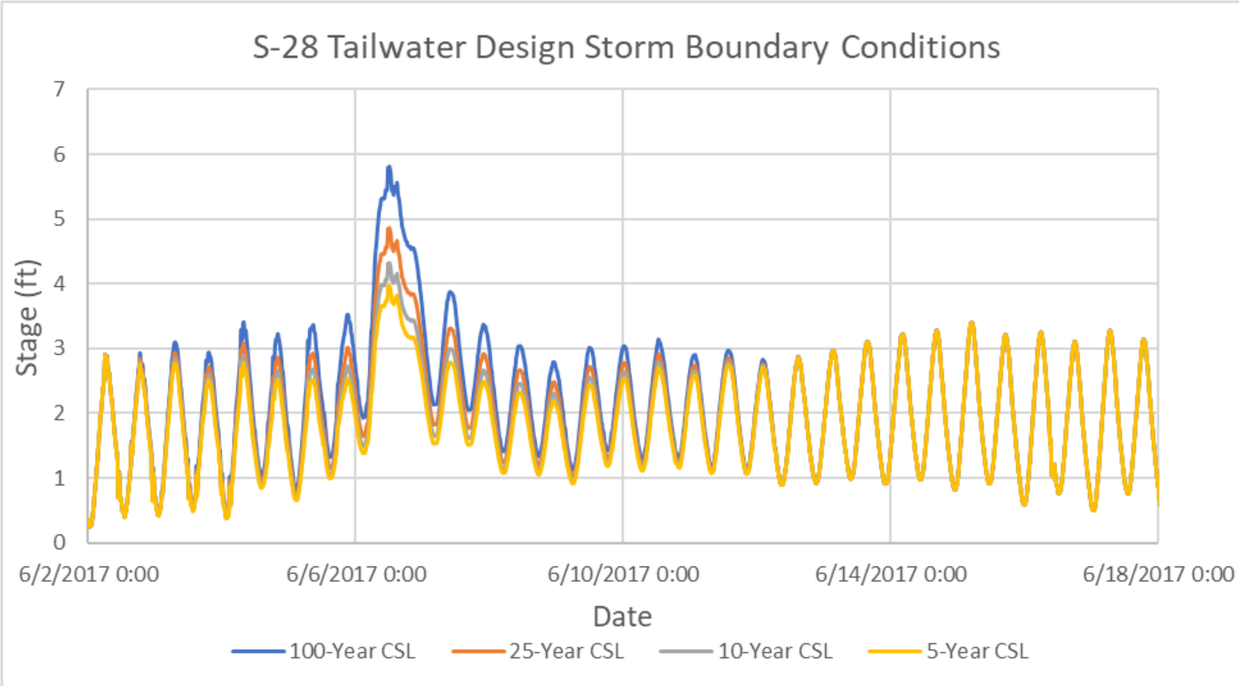

Figure 4: Design Storm Current Sea Level (CSL) Tidal Boundary Stages for S-28

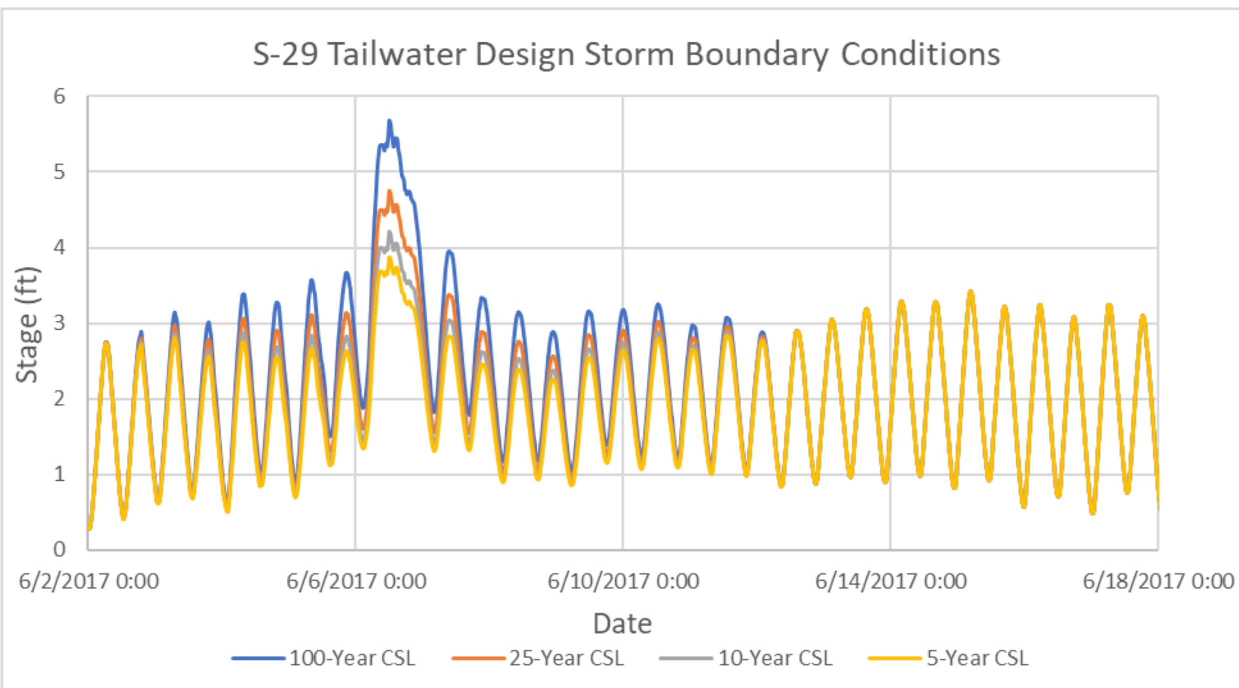

Figure 5: Design Storm Current Sea Level (CSL) Tidal Boundary Stages for S-29

Similarly, the saturated zone tidal boundaries have been updated using the same time-series data, based on the spatial distribution shown in the following figure. Additionally, a 2-D overland tidal boundary has been added using the same time-series data and spatial distribution.

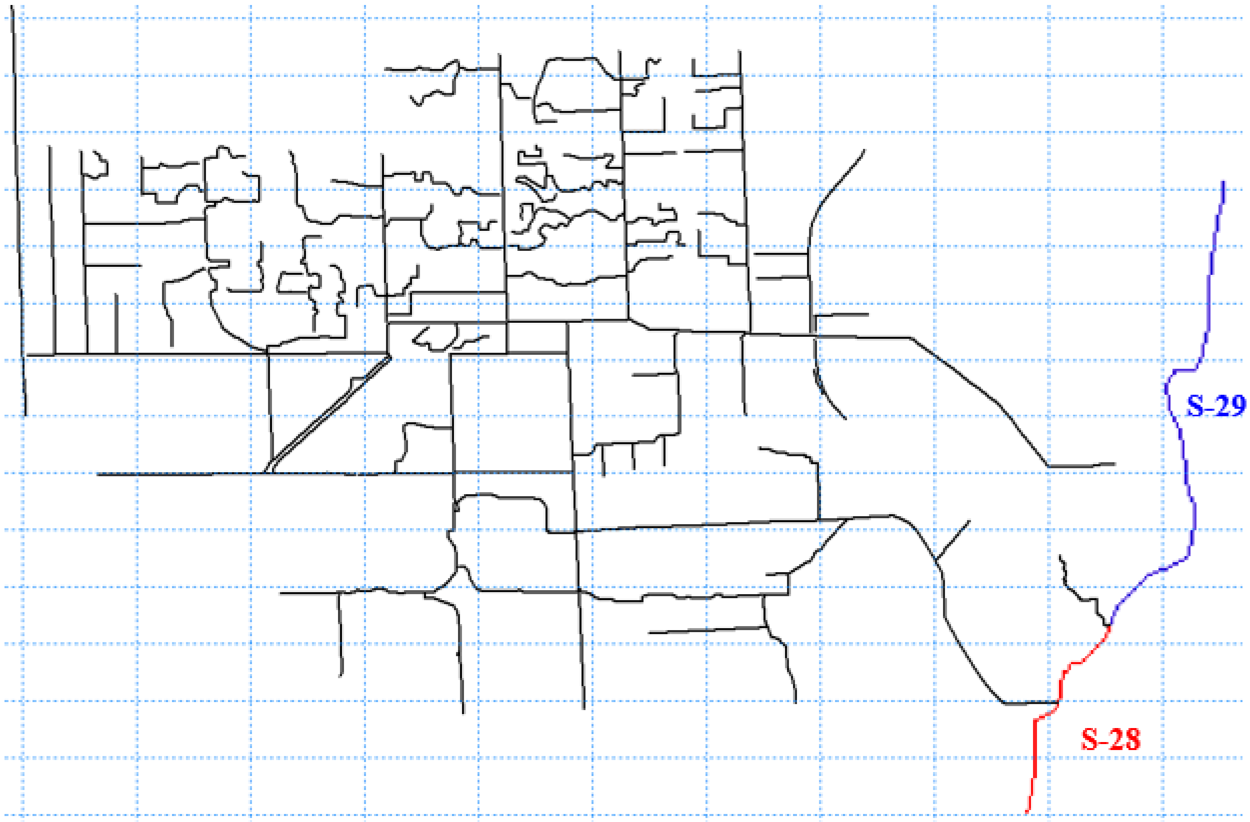

Figure 6: Spatial Distribution of Saturated Zone and 2-D Overland Flow Tidal Boundary

As agreed, the western boundary (**Figure 7**) will continue to use observed data from the June 2017 storm event. As June 2017 was wetter than normal in the weeks leading up to it, Water Conservation Area 3B stage was already elevated. Therefore, the District agreed that it is fair to assume that may be equivalent to an elevated stage that can be used for design storm purposes.

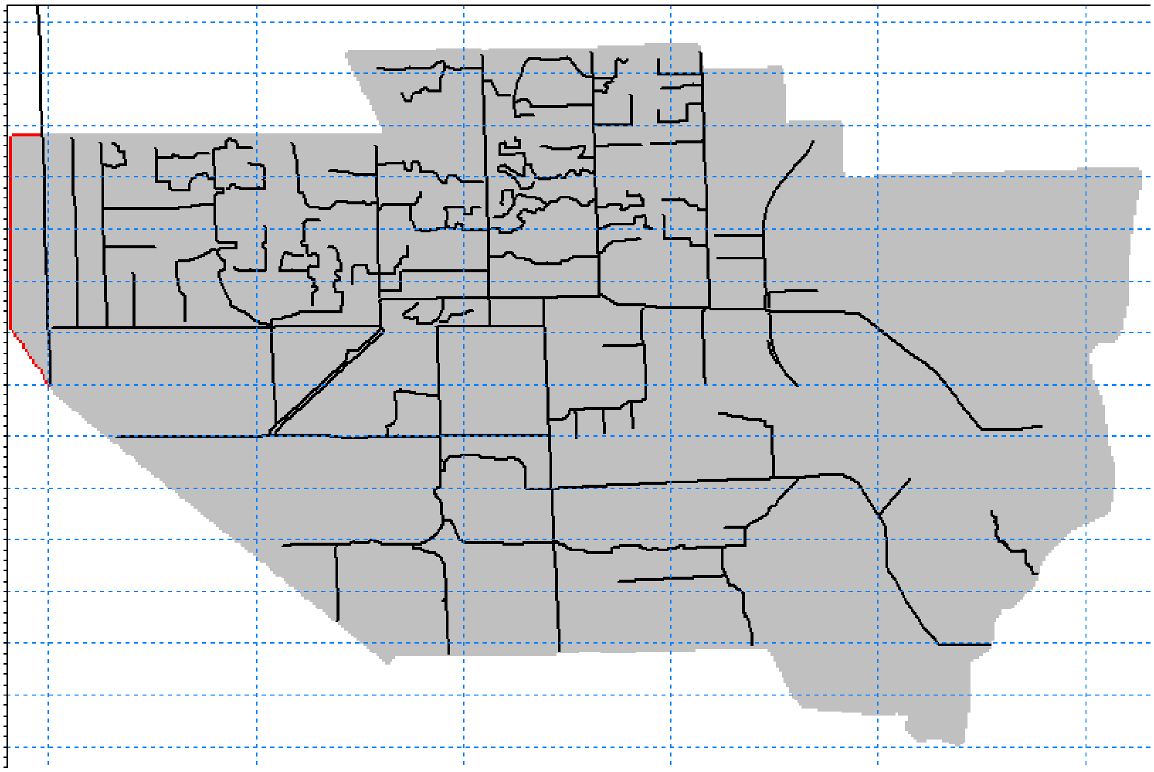

Figure 7: Western General Head Groundwater Boundary Location

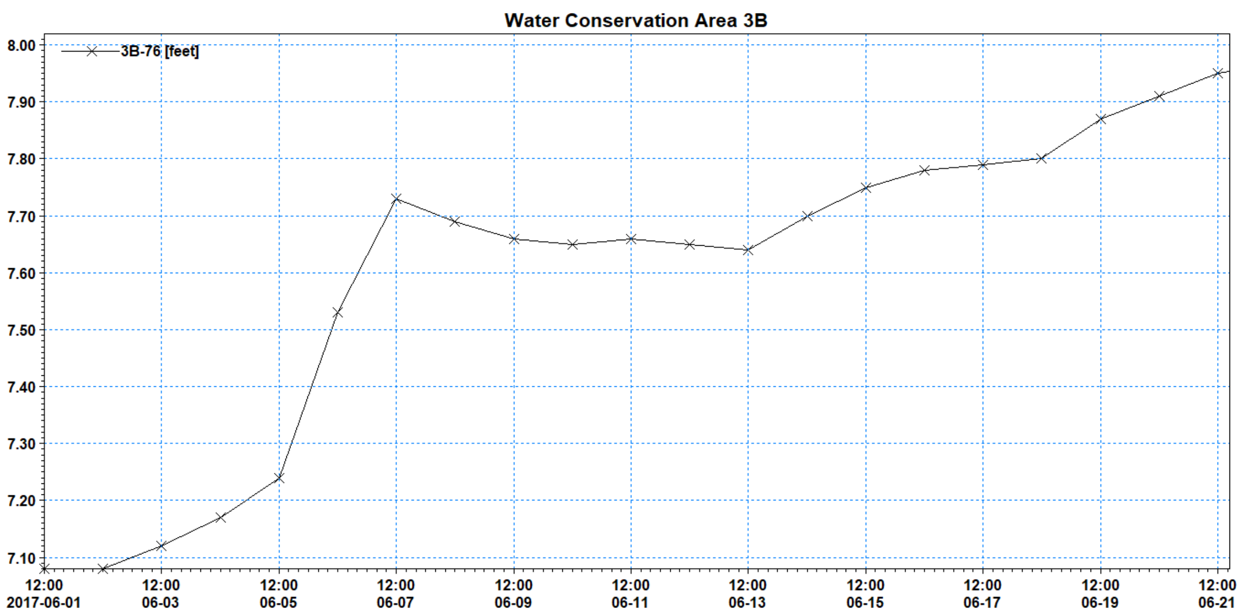

Figure 8: Western General Head Groundwater Boundary Stage Time-Series

The northern general head groundwater boundary uses simulated groundwater elevations from the 2019 Broward County design storm model, which is based on the same storm event. The southern general head groundwater boundary was split into 4 sections and uses District provided simulated canal stage data from XP SWMM and HEC RAS models for the C-6 and C-7 canals. The four sections are S-27 headwater and G-72 tailwater on the C-7 Canal and G-72 headwater and S-31 tailwater on the C-6 canal. The time series for the groundwater general head boundaries for the four segments will also serve as the downstream boundary conditions for the 1-D branches connecting to the C7 and C6 Canals. The spatial distribution and time-series data for S-27 headwater are shown in the following two figures.

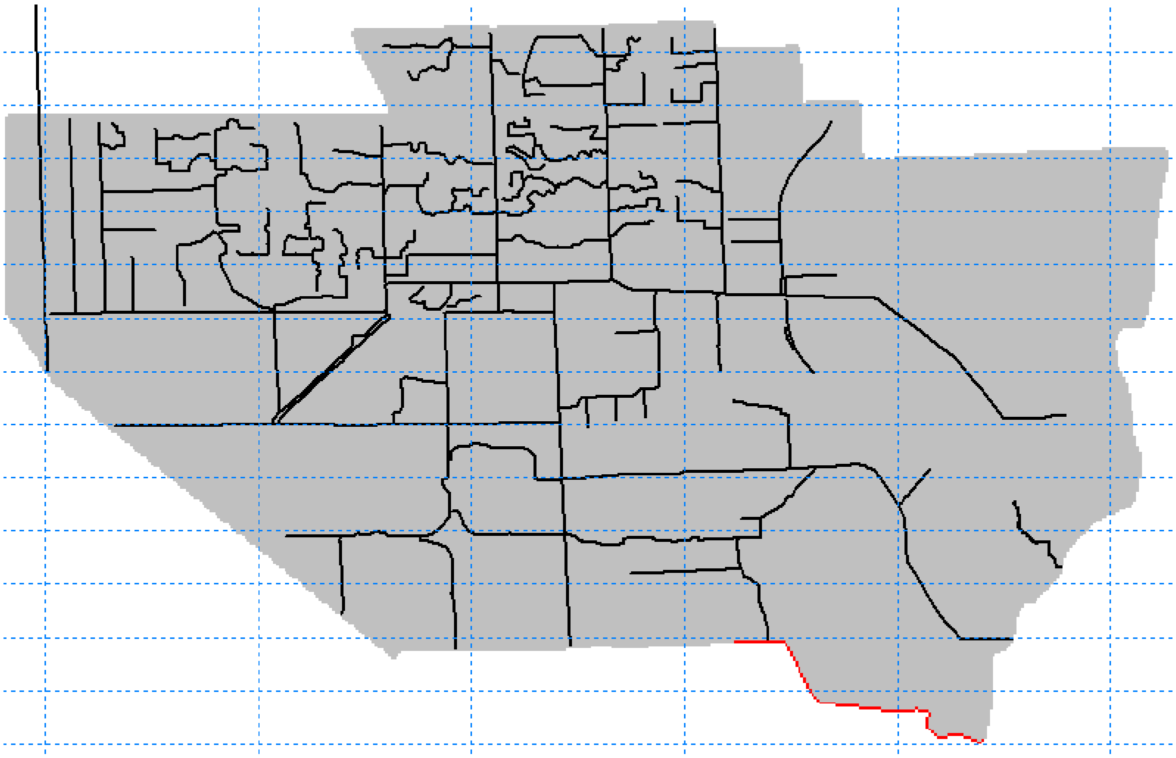

Figure 9: General Head Groundwater Boundary Using S-27 HW Simulated Design Storm Stages

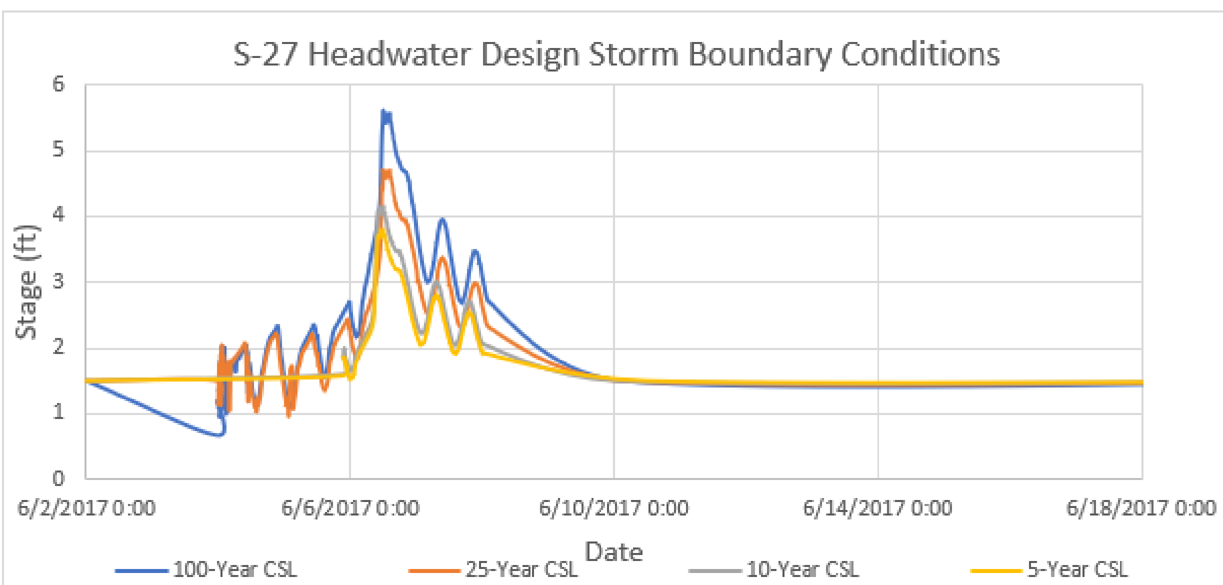

Figure 10: District Provided Simulated Design Storm Stages for S-27 HW

The spatial distribution and time-series data for G-72 tailwater are shown in the following two figures.

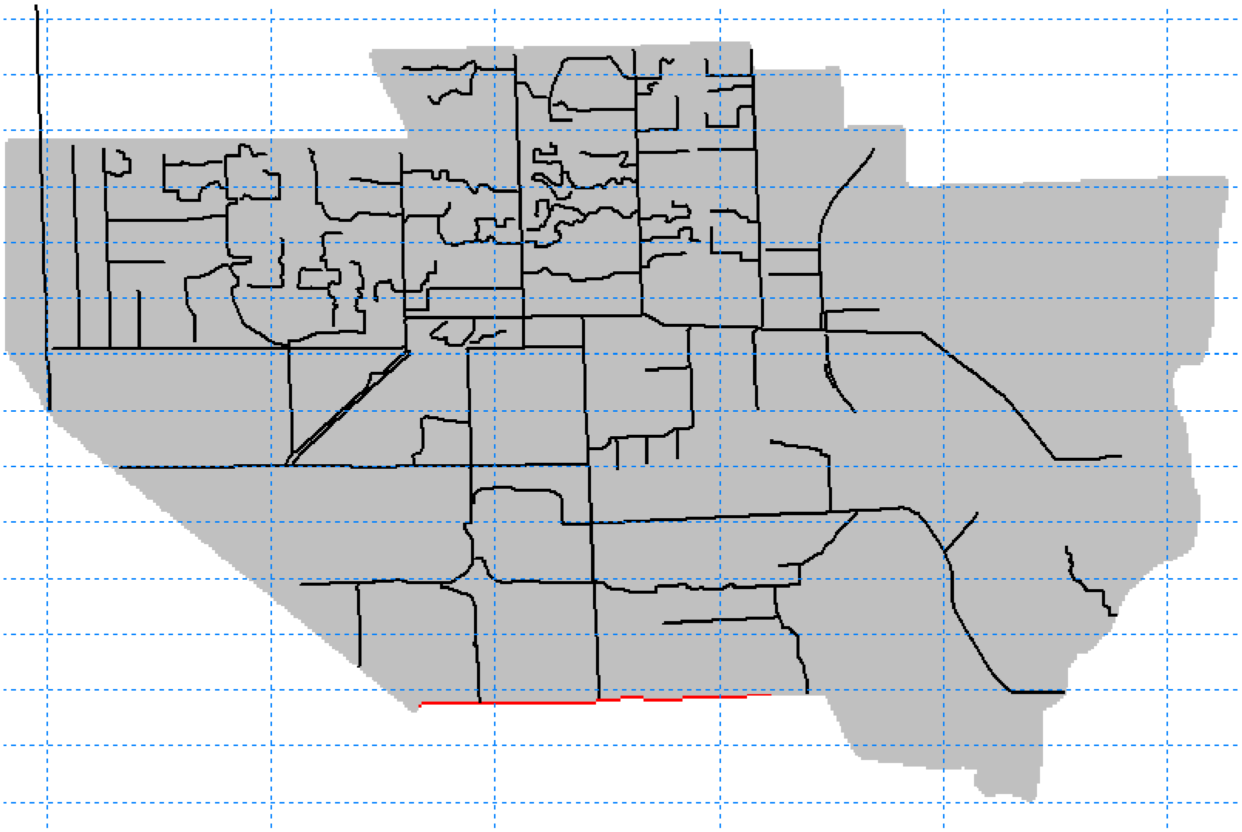

Figure 11: General Head Groundwater Boundary Using G-72 TW Simulated Design Storm Stages

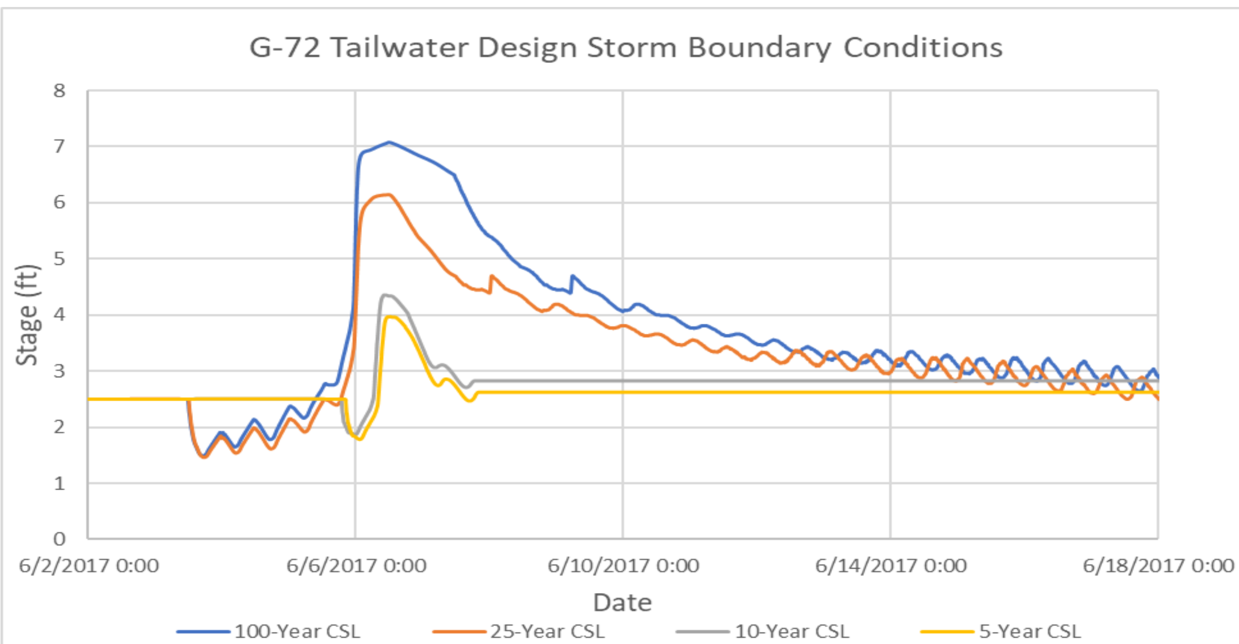

Figure 12: District Provided Simulated Design Storm Stages for G-72 TW

The spatial distribution for G-72 headwater is shown in the following figure.

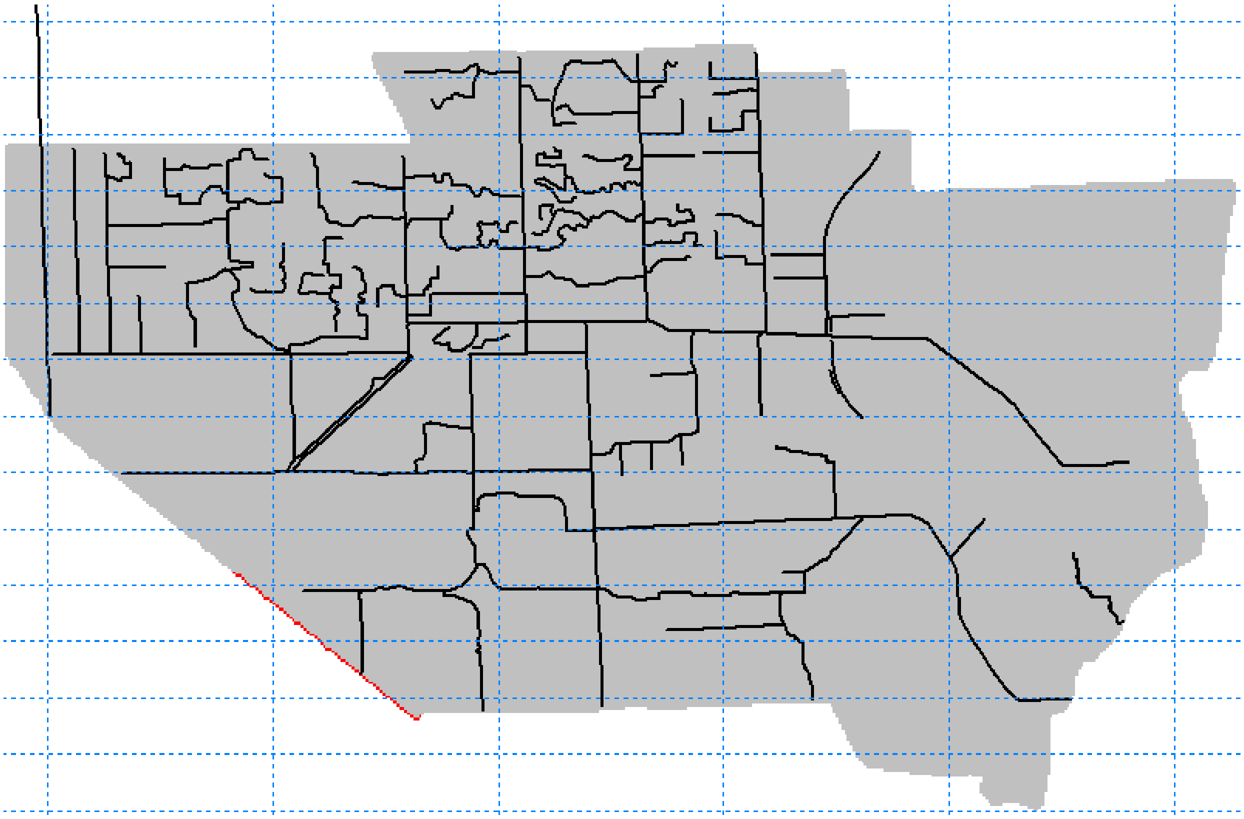

Figure 13: General Head Groundwater Boundary Using G-72 HW Simulated Design Storm Stages

For the G-72 HW boundary condition, there was only simulated data for the 10, 25, and 100-year design storms. As there was no data for the 5-year design storm, SFWMD suggested a scale-down approach. Therefore, the G-72 HW peak stage (NGVD29) was plotted against the 3-day rainfall depth for the nearest NOAA Atlas 14 station and fitted with a trendline. The best-fitting trendline (highest R^2 coefficient) was determined to be logarithmic. The following table and figure show the data used and the corresponding graph.

Table 2:Data Used to Scale-Down G-72 HW Peak Stage

Return period	Rainfall depth (inch)	Peak Stage (ft)
5-yr	8.85	5.25 (calculated)
10-yr	10.5	5.59
25-yr	13.1	6.47
100-yr	17.7	7

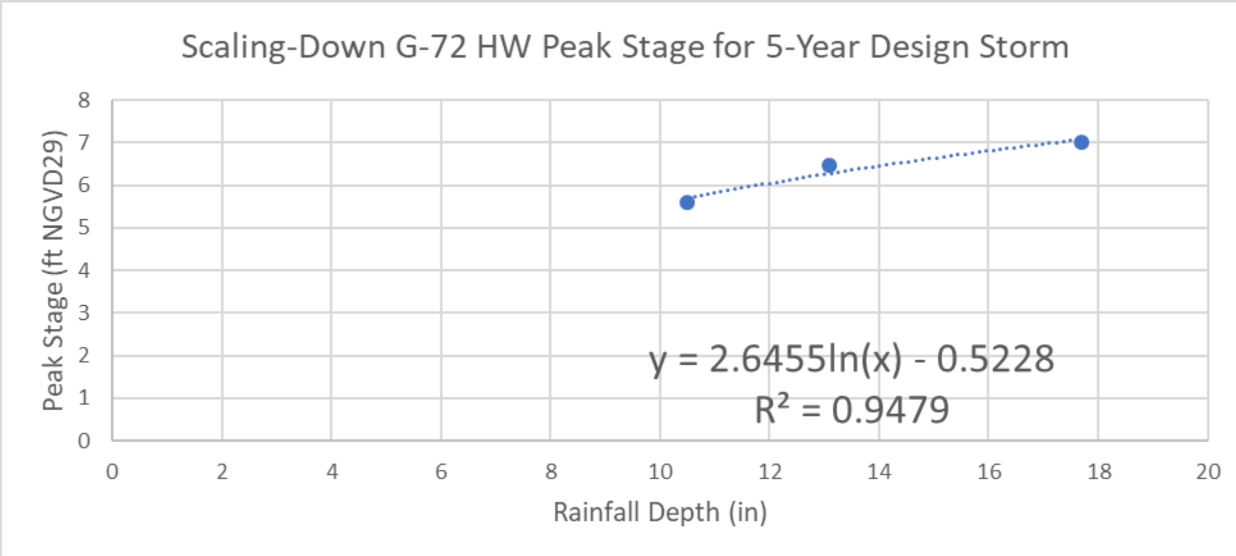

Figure 14: Scale-Down Approach for G-72 Headwater

With this approach, the peak stage for the 5-year design storm at G-72 HW was determined to be 5.25 feet. Therefore, a correction factor of 0.939 (5 year stage divided by 10 year stage) was applied to the 10-year time series data for all values greater than 2.52 feet (this is the lowest value possible before the correction factor would reduce stage to below the control elevation of 2.5 feet).

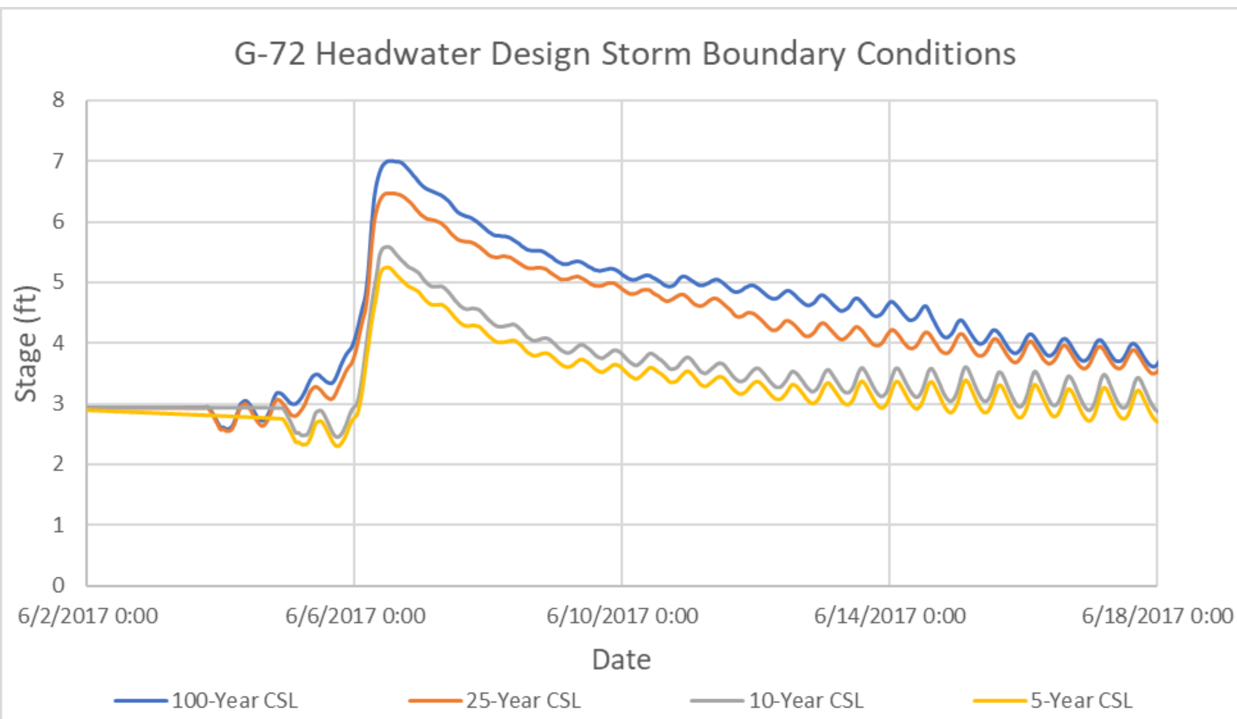

Figure 15: District Provided Simulated Design Storm Stages for G-72 HW

The spatial distribution for S-31 tailwater is shown in the following figure.

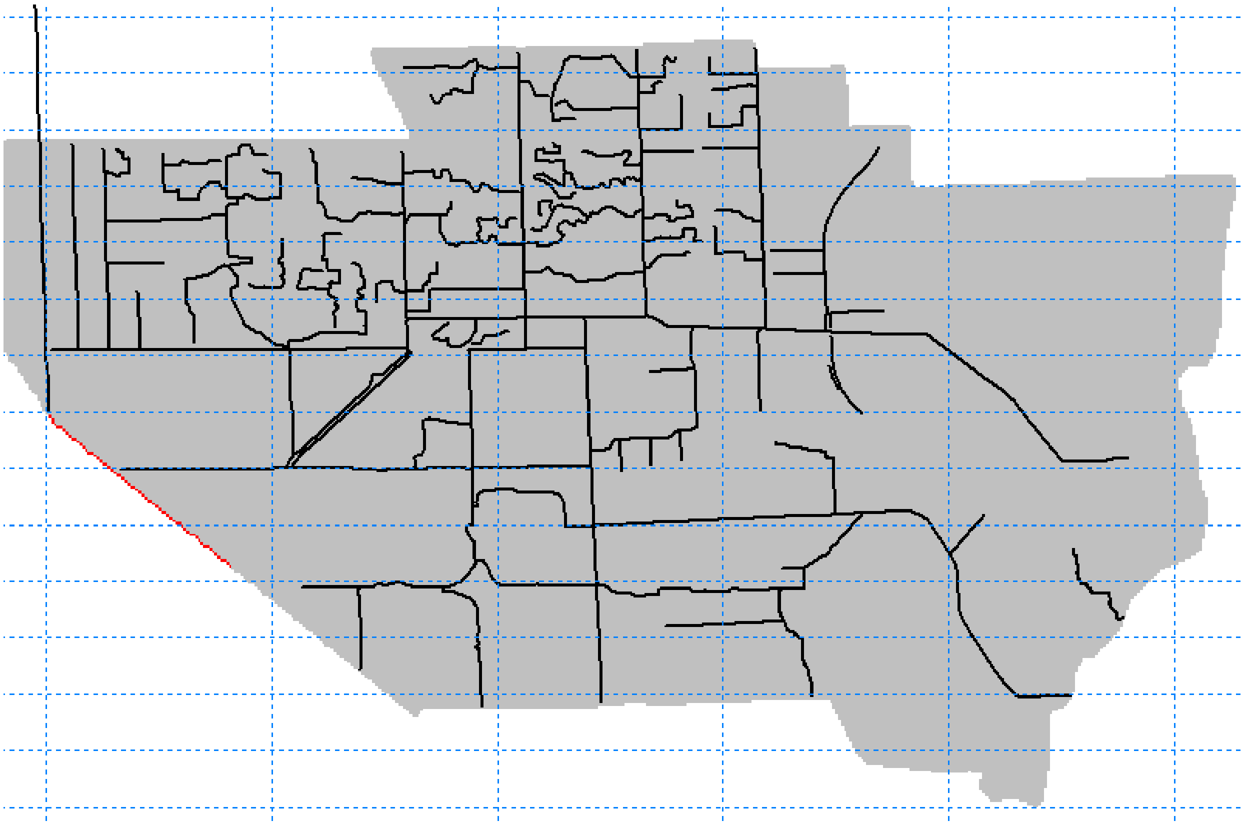

Figure 16: General Head Groundwater Boundary Using S-31/32 TW Simulated Design Storm Stages

For the S-31 TW boundary condition, there was only simulated data for the 10, 25, and 100-year design storms. As there was no data for the 5-year design storm, SFWMD suggested a scale-down approach. Therefore, the S-31 TW peak stage (NGVD29) was plotted against the 3-day rainfall depth for the nearest NOAA Atlas 14 station and fitted with a trendline. The best-fitting trendline (highest R^2 coefficient) was determined to be logarithmic. The following table and figure show the data used and the corresponding graph.

Table 3:Data Used to Scale-Down S-31 TW Peak Stage

Return period	Rainfall depth	Peak Stage
5	8.12	5.43 (calculated)
10	9.66	5.84
25	12.1	6.97
100	16.3	7.56

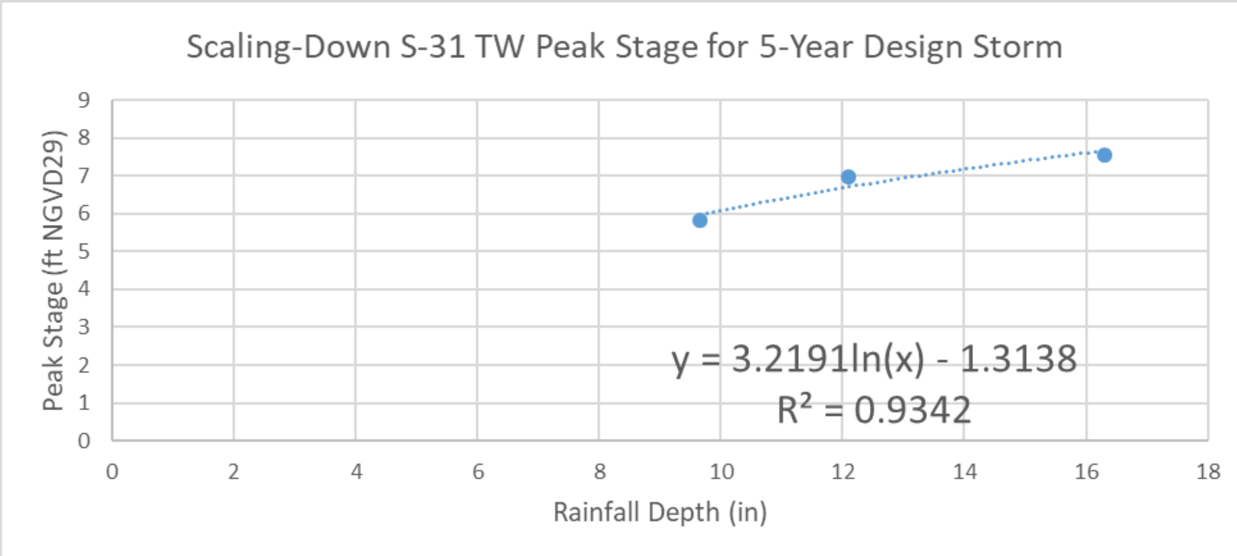

Figure 17: Scale-Down Approach for S-31 Tailwater

With this approach, the peak stage for the 5-year design storm at S-31 TW was determined to be 5.43 ft NGVD29. Therefore, a correction factor of 0.929 (5 year stage divided by 10 year stage) was applied to the 10-year time series data for all values greater than 4.18 ft (this is the lowest value possible before the correction factor would reduce stage to below the initial elevation of 3.88 feet) and values greater than 3.88 but less than 4.18 were set to 3.88 feet.

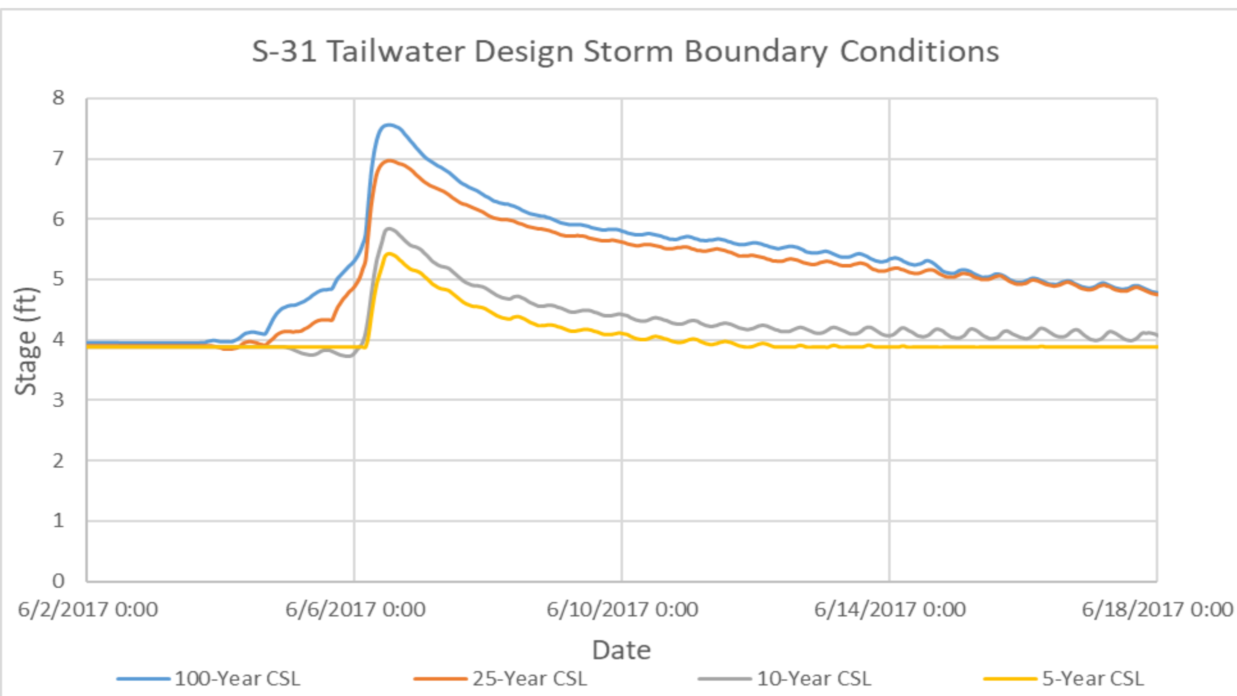

Figure 18: District Provided Simulated Design Storm Stages for S-31/32 TW

Initial Groundwater Levels and Surface Water Depths:

In the calibration model, initial groundwater levels were developed by making localized adjustments to the 2000 wet season heads from the MODFLOW model developed as part of the recent USGS study (Hughes and White, 2016). For the validation model, initial groundwater levels were developed by combining the Broward County Average Wet Season Water Table map with the Miami-Dade County Wet Season Water Table map, which resulted in water levels typically within 0.25 ft of the observation wells. This is identical to the approach used in the Broward County Model, as documented in the Draft Final Modeling Report (Taylor Engineering, 2020). However, there were some areas where the groundwater levels were upwards of 1 ft higher or lower than water bodies with established control elevations near the wells. This difference was not significant for the validation model as this was at the start of the 3-month spin-up period. However, for the design storm which only has a 2-day spin-up period, it is significant. Therefore, for the design storms, the initial groundwater levels will be adjusted so that they closely match basin control elevations, if they exist. For example, if a lake is controlled at 4.0 feet, then the surrounding groundwater should also be at 4.0 feet. This is to prevent the water levels in the lakes to drop (or rise) due to lower (or higher) initial groundwater elevations.

References:

Hughes, J.D., and White, J.T., 2016, *Hydrologic Conditions in Urban Miami-Dade County, Florida, and the Effect of Groundwater Pumpage and Increased Sea Level on Canal Leakage and Regional Groundwater Flow (ver. 1.2, July 2016):* U.S. Geological Survey Scientific Investigations Report 2014–5162, 175 p., http://dx.doi.org/10.3133/sir20145162.

Reference and Potential Evapotranspiration. Usgs.gov. (2018). Retrieved from https://www.usgs.gov/centers/car-fl-water/science/reference-and-potential-evapotranspiration?qt-science_center_objects=0#qt-science_center_objects.

Taylor Engineering. (2016). *BCB FPLOS Final Report*.

Taylor Engineering. (2020). *Broward County Draft Final Modeling Report*.

T A Y L O R   E N G I N E E R I N G ,   I N C .

Flood Protection Level of Service Provided by Existing Infrastructure for Current Sea Level Conditions in the C8 and C9 Watersheds Draft Report (Revised)

Deliverables 3.2.1 and 3.2.2

CONTRACT 4600003098

Work Order 08

Prepared for:

CSA Central, Inc
8200 NW 41st St, Suite 305
Doral, FL 33166

Submitted to:

South Florida Water Management District
3301 Gun Club Road
West Palm Beach, Florida 33406

Submitted 6/17/2020

14499 N. Dale Mabry Hwy, Suite 290,
Tampa, Florida 33618
813-963-6469 | www.taylorengineering.com

Table of Contents

List of Figures

List of Tables

1 INTRODUCTION

The South Florida Water Management District, herein referred to as SFWMD or District, is conducting a system-wide review of its regional water management infrastructure to determine the flood protection level of service (FPLOS) currently provided. The FPLOS describes the level of protection provided by the water management facilities within a watershed under both current and future conditions, where future conditions FPLOS considers sea level rise and future development (part of the next phase of this project). This information can be used by local governments, SFWMD, and other state and federal agencies to identify areas where improvements or upgrades of water management facilities are required, the appropriate entity or entities responsible for making improvements, and funding and technical resources available to support these efforts.

This report combines the relevant information from the previous deliverables including data collection and availability, model calibration and validation, and design storm model set-up and parameterization with the FPLOS by existing infrastructure for the C-8 and C-9 Basins under current sea level conditions. The two watersheds, along with the canal network and tidal outfall structures, are depicted in **Figure 2.1-1.** Interim documents describing prior tasks completed as part of this study effort are available in their entirety but were summarized in this report to provide background information without obscuring the report with irrelevant information, or information that was not used.

Taylor Engineering has developed an integrated groundwater and surface water model of the C-8 and C-9 watersheds, using MIKE SHE and MIKE HYDRO, that was used to determine the flood protection level of service provided by existing infrastructure under current sea level conditions for the 72-hour design storm events of 1 in 5, 10, 25, and 100-year recurrence frequency. The flood protection level of service was determined through several metrics, the majority of which are derived from the outputs of the watershed-scale flood event modeling. The flood protection metrics are defined in **Section 7**.

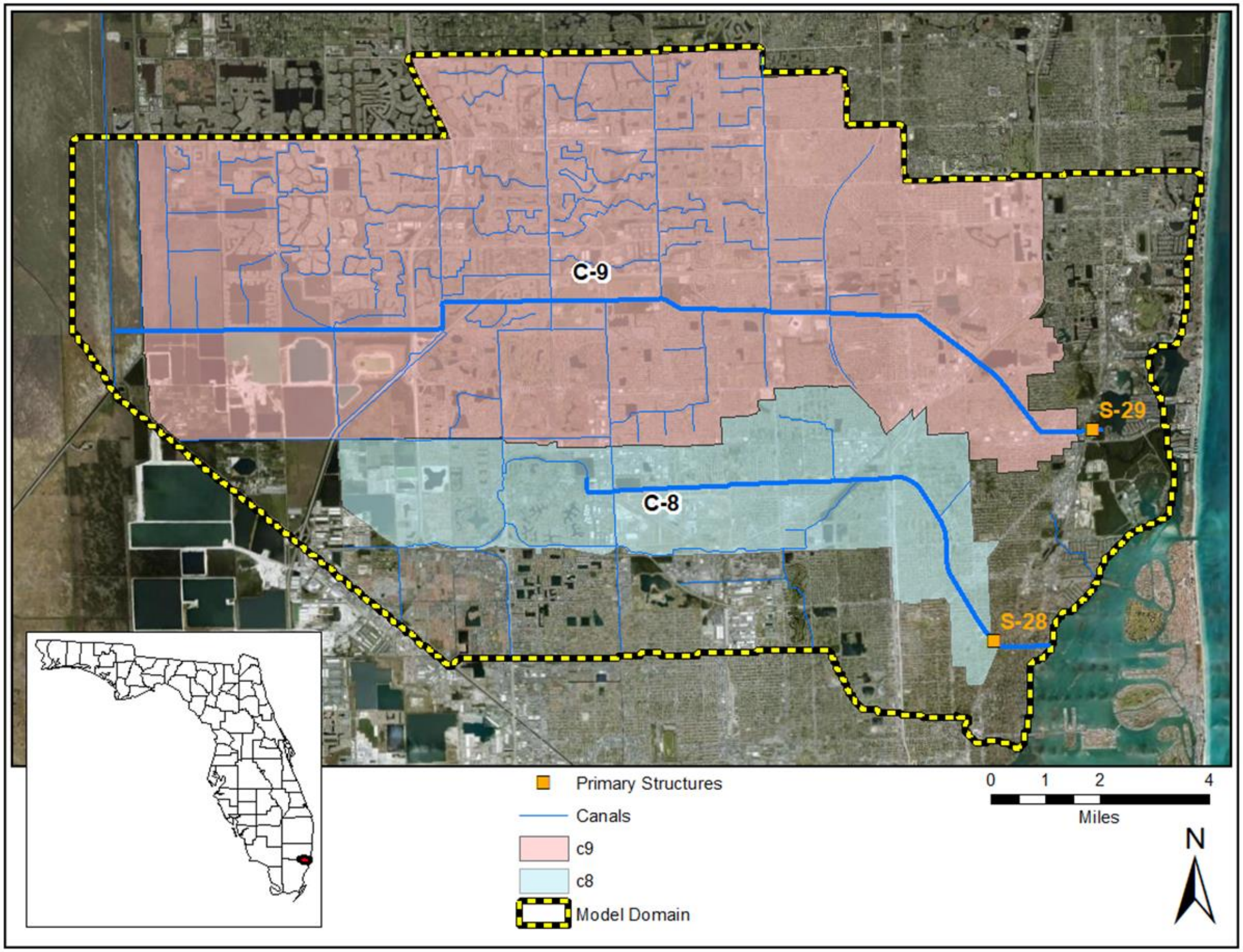

Figure 2.1-1: C-8 and C-9 Watersheds, Canal Network, and Primary Structures

2 DATA COLLECTION AND ASSIMILATION

This chapter details the data that was used to develop the SFWMD C-8 & C-9 MIKE SHE and MIKE HYDRO models for use in the C8-C9 FPLOS Study. Specifically, this section details the availability of topography, land use, culvert, gate, bridge, pump, and cross section data, survey requirements, calibration and validation simulation periods, the availability of groundwater data, the availability of district stage, flow, and gate operations, design storm rainfall, and initial groundwater levels for design storms.

2.1 Topography

The topography for this project was made by merging the Miami-Dade County 5ft DEM (2015 Miami-Dade County DEM 5ft, 2017) with the 5-ft composite DEM of Broward County that was created by Geosyntec Consultants (2018). The portion of the composite DEM used was developed using the following sources:

- Broward County DEM – 2007 – 5' cell size source – base source
- SFWMD 50' cell size source – west area extension

To minimize/eliminate seams in the overland flow module, the DEMs were merged along the C-9 canal and through the levees in the water conservation area to the west, as shown in **Figure 2.1-1.** In this figure, the DEM was filtered between 0-25 ft NAVD88 for visual clarity (200+ ft elevation landfill causes color palette distortion).

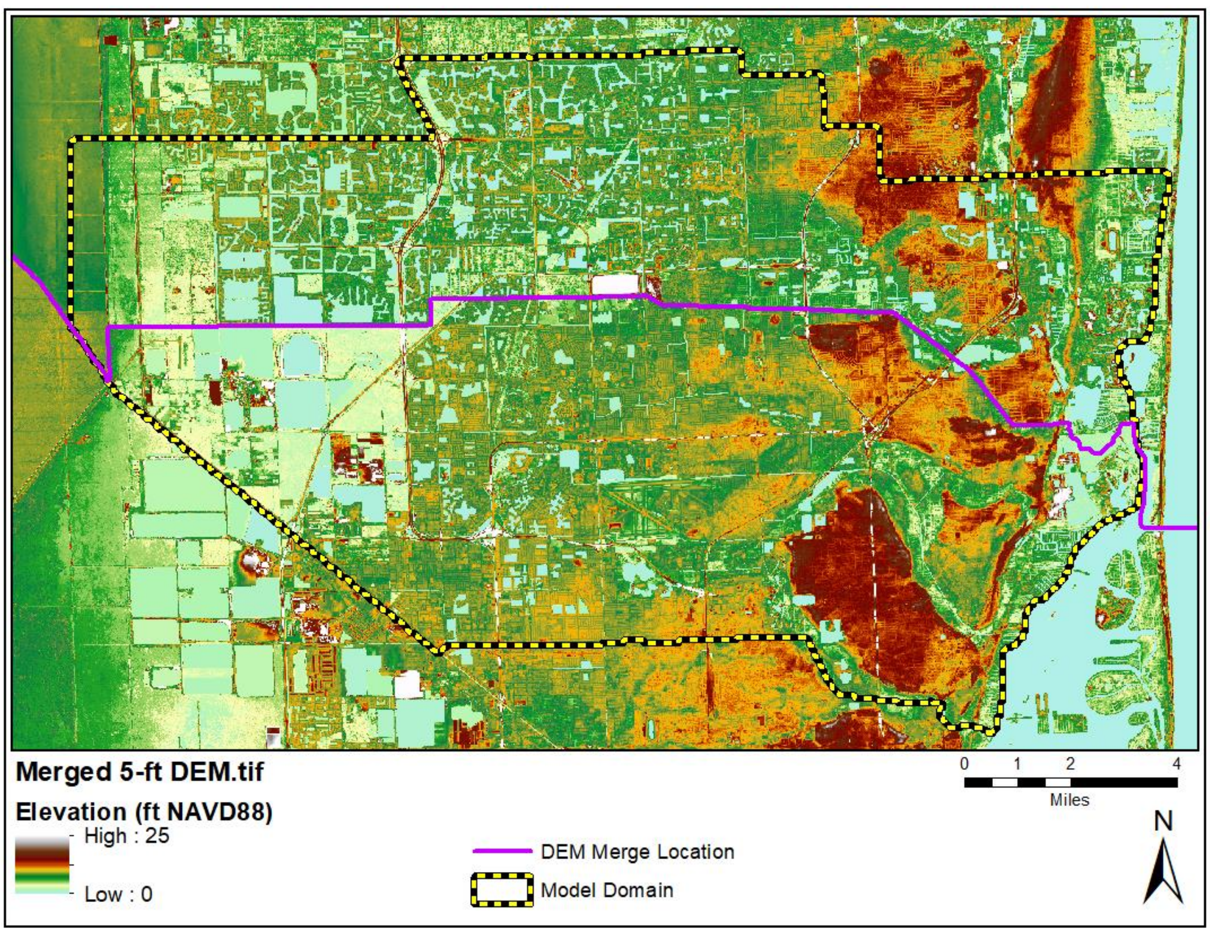

Figure 2.1-1: Merged 5-ft DEM

2.2 Land Use

The land use data for this project is based on the SFWMD 2014-2016 Land Use dataset (SFWMD LCLU, 2017). Preliminary comparisons with aerial imagery from 1999 to 2019 showed little to no significant changes in land use, such as segments of open land being developed into high density residential areas. Land use change resulting in areas such as commercial and services to high density residential were not considered a significant change in terms of the runoff potential. To confirm this observation, a spatial comparison was made in GIS using the SFWMD 1999 and the 2014-2016 land use shapefiles. Less than 2% of the total model area was identified as having a significant land use change during this period of time. Because these land use changes have occurred after the Broward County stormwater ordinance of the 1980s, there should be no impact to the flood protection level of service. The relatively unchanged land use over the past 20 years or so was an important consideration in evaluating potential historical storm events for calibration and validation, as discussed in **Section 2.4**.

2.3 MIKE HYDRO River 1D Model

The MIKE HYDRO 1D model was developed from several sources with emphasis placed on gates, pumps, culverts, bridges, and cross sections. The available data came from the following sources:

- Broward County: Updated 2019 MIKE SHE & MIKE HYDRO models, Ref: Current Conditions Model Update and Validation Draft Report (Taylor Engineering, 2019), & 5-ft DEM
- Stoner & Associates Inc: 2019 Survey (completed for Broward County Future Floodplain Modeling and Mapping project)
- South Broward Drainage District: GIS database & 2013 Facilities Report and Water Control Plan
- SFWMD: Structure Books (OCC, 2018) (S28, 2019) (S29, 2019) (MD North Central Basin Atlas v3, 2016) for operable structure dimensions, elevations, and operating criteria. DBHYDRO for water levels, discharges, and structure operations.
- Miami-Dade County: C-8 and C-9 XP SWMM Models, 5-ft DEM, & GIS Database:
    - Pipes: https://gis-mdc.opendata.arcgis.com/datasets/stormwater-line
    - Points (canal cross sections, structures, etc.): https://gis-mdc.opendata.arcgis.com/datasets/stormwater-point
    - Water bodies: https://gis-mdc.opendata.arcgis.com/datasets/water-p

Upon initial investigation, it was noticed that there were some 1D model components such as culverts and cross sections that had available data from multiple sources. In instances where this occurred and the details differed (such as different culvert diameters), the data was used in the following order of priority: (1) survey, (2) Broward County 2019 MIKE HYDRO model, (3) reports & documentation, (4) GIS databases, and (5) Miami-Dade C8 and C-9 XP SWMM models. The order of priority was determined based on the freshness of the data and Taylor Engineering's confidence/exposure with the data/sources. Survey had the highest level of confidence as it was recently been completed or was to be completed in the near future and should capture any changes to infrastructure that may not have yet been included other data sets. The 2019 Broward County MIKE HYDRO model had the second highest level of confidence as the data that went into it was analyzed and refined over the last several months leading up to this project, and Taylor Engineering is very familiar with the areas that have up-to-date data and the areas that are questionable. Reports and documentation had the third highest level of confidence as they were used to build parts of the 2019 Broward County MIKE HYDRO model. The Miami-Dade GIS databases was assigned the fourth highest level of confidence as Taylor Engineering hadn't yet had the opportunity to see how well the data lines up with other confirmed sources. The Miami-Dade XP SWMM models that Taylor Engineering had access to had the lowest level of confidence as they were older versions and there were several areas that did not match what is in the Miami-Dade GIS databases. Taylor Engineering assumes that the discrepancies between the Miami-Dade GIS databases and the C-8 and C-9 XP SWMM models that we had access to were due to changes in infrastructure that had not been updated in the GIS databases; therefore, the GIS database had higher priority than the XP SWMM models for instances of data differences.

Figure 2.3-1 shows the location of the available 1-D model data. It should be noted that some of the data items shown are not complete; for example, culverts included in the Miami-Dade GIS databases that are missing inverts, dimensions, or both; bridges missing low chord elevations, etc. These and other data gaps were assessed and included in the survey scope of work described in **Section 2.4**.

For model calibration and validation, structure operations were based on recorded operations from DBHYDRO where available (primary structures), and operational criteria were used where recorded observations were unavailable (secondary structures). For design storms, the operational criteria for District structures come from the District's structure books. The operational criteria for Broward County and South Broward Drainage District structures come from the 2019 Broward County Current Conditions model, which has operating criteria that is both inherited from the 2014 FEMA model and verified/updated based on stakeholder data and documents (such as the SBDD Facilities Report, 2013). There were no known Miami-Dade County operated structures in the model. Structure flow rating parameters were used where applicable, which come from the various flow rating analysis reports (2011-2019) and Atlas of Flow Computation (2015) that were provided by the SFWMD.

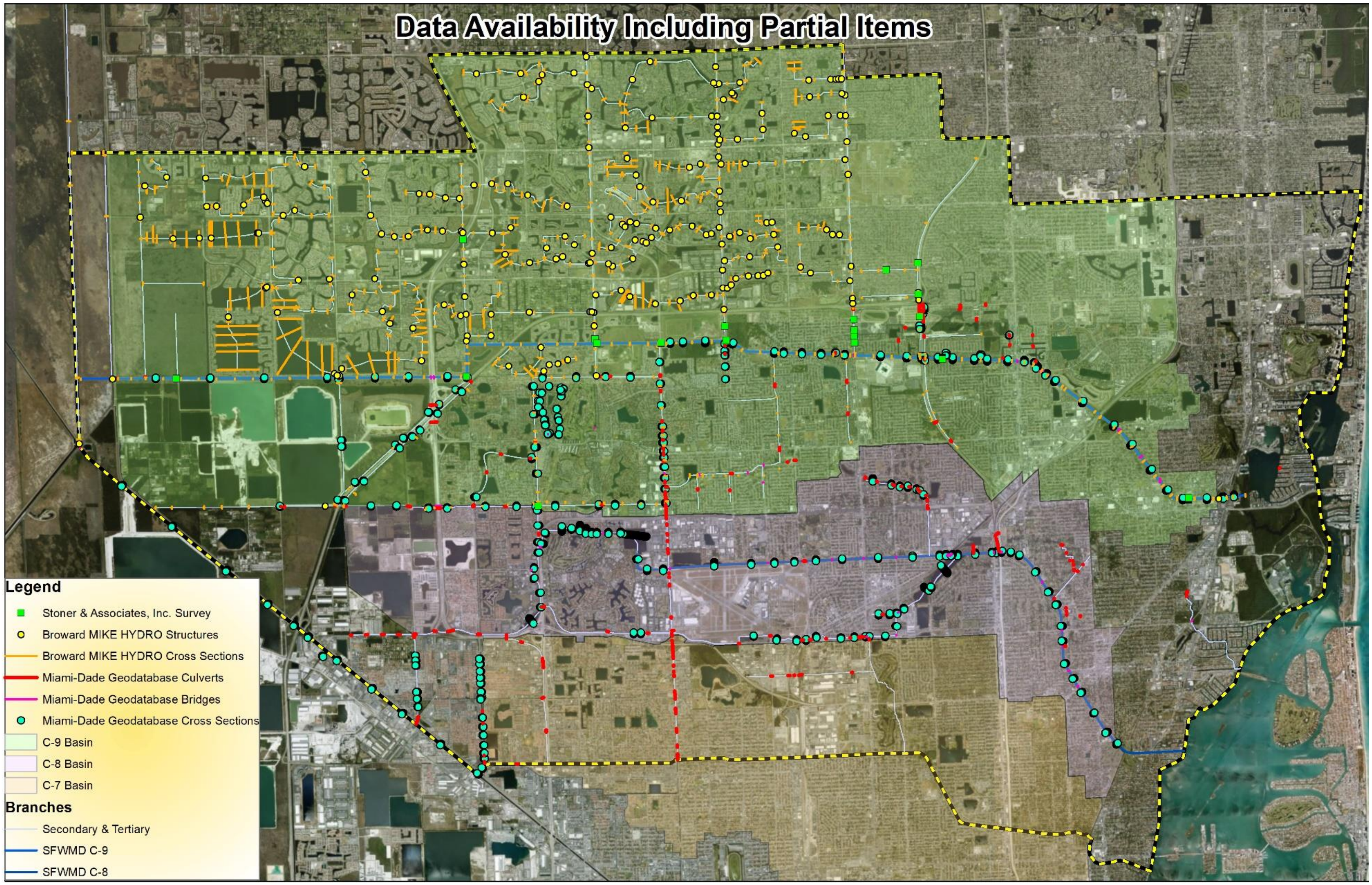

Figure 2.3-1: Map of the Available Data at the Beginning of C-8 and C-9 FPLOS Study (Originally Proposed Domain)

2.4 Field Survey

The available data was quite extensive, however, there were several areas lacking detail. The following figure shows the location of the initial items identified for field survey. These items included 30 culverts, 23 cross sections, and 21 bridges. Taylor Engineering and the District tried to anticipate all the surveying needs of the project, but inevitable field variations caused changes and one culvert was omitted. Some items in the survey request had partial data available, such as culvert diameter or elevation of channel bottom under bridge but were missing information such as culvert inverts or low chord elevation of bridge.

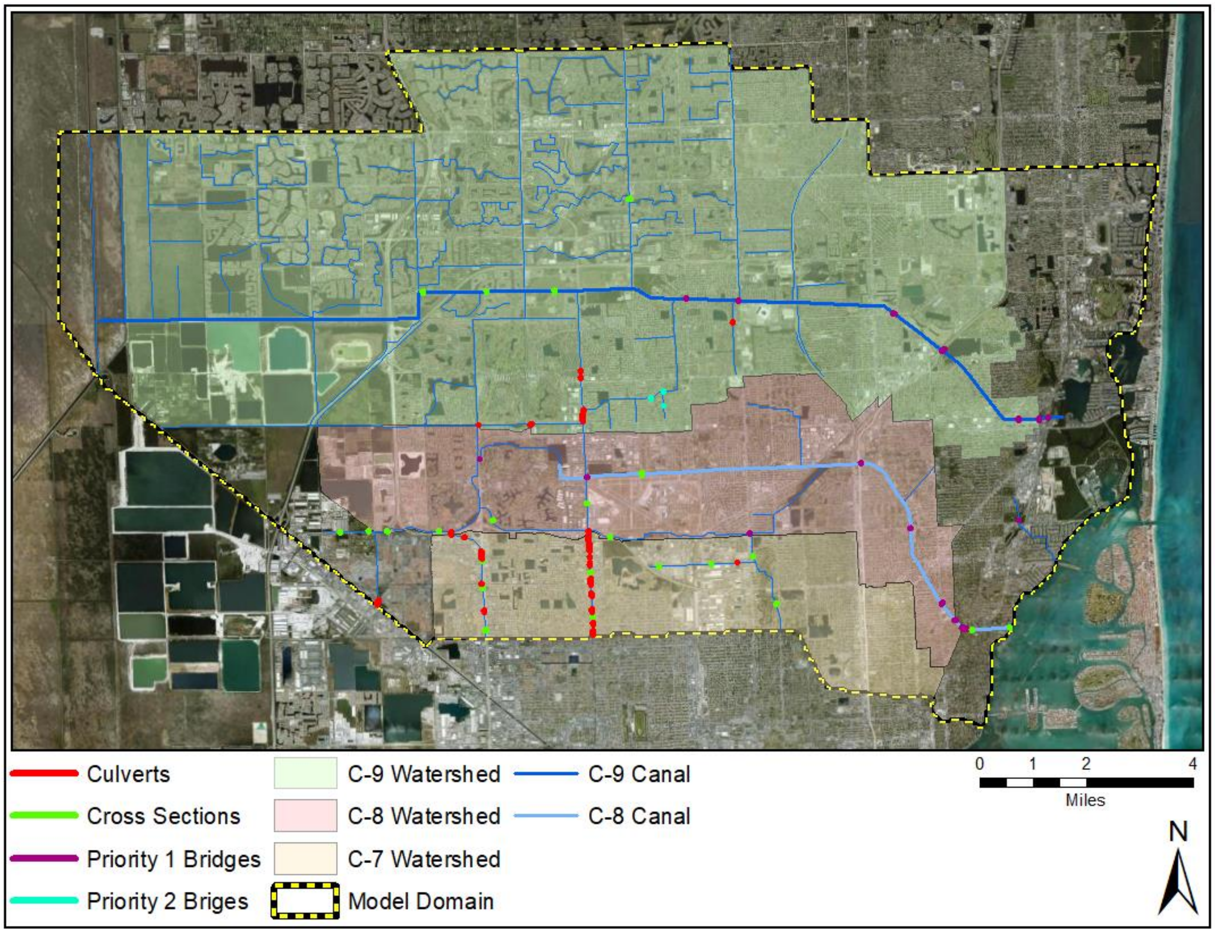

Figure 2.4-1: Inventory of Field Surveyed Items

2.5 Storm Event Selection

Average daily discharge data for the S-28 and S-29 outfall structures (C-8 and C-9 basins, respectively) were analyzed to identify the largest storm events since 1999. Then, instantaneous stage and discharge data were analyzed to identify the events that produced the largest headwater and tailwater elevation and discharge rate. Preference was given to storm events producing strong responses in both watersheds. The selection was narrowed to the storms during the following dates:

- Hurricane Irene (October 14-16, 1999)
- Subtropical Depression Leslie (October 2-4, 2000)
- Hurricane Gabrielle (September 13-15, 2001)
- Unnamed Storm June 6-7, 2017
- Hurricane Irma (September 9-10, 2017)

Subtropical Depression Leslie, which later became Tropical Storm Leslie, was chosen as the calibration event and Hurricane Irma as the validation event. Subtropical Depression Leslie resulted in the largest discharge response at both the C-8 and C-9 outfall structures in the past 20 years, as well as some of the highest canal water elevations. Hurricane Irma produced large discharge responses at both outfall structures and had a storm surge which resulted in the highest water elevations. The following figures compare the discharge, headwater elevation, and tailwater elevation at the C-8 and C-9 outfall structures.

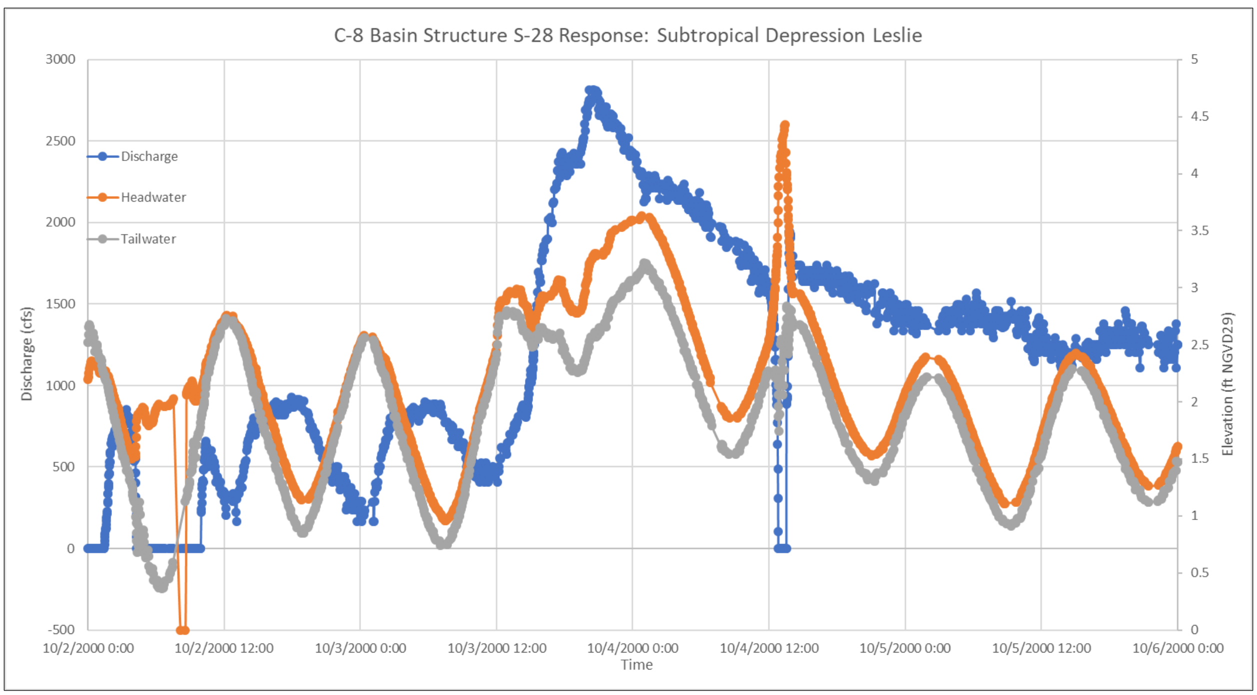

Figure 2.5-1: C-8 Basin Structure S-28 Response to Subtropical Depression Leslie

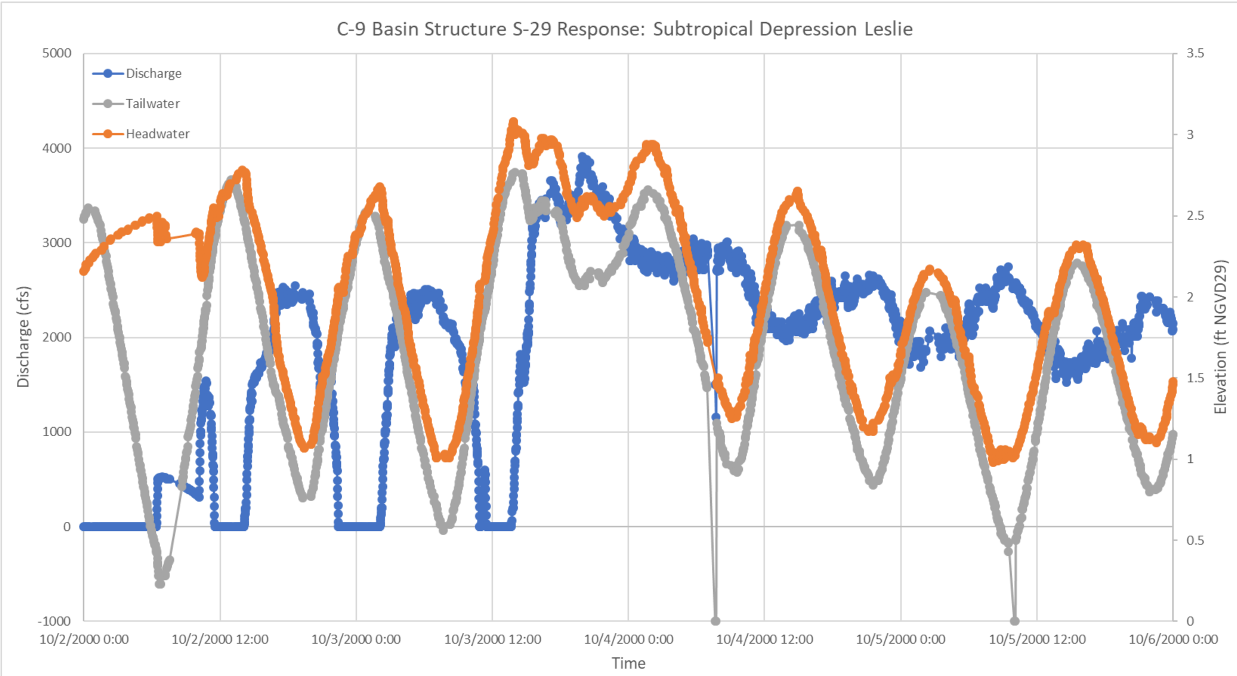

Figure 2.5-2: C-9 Basin Structure S-29 Response to Subtropical Depression Leslie

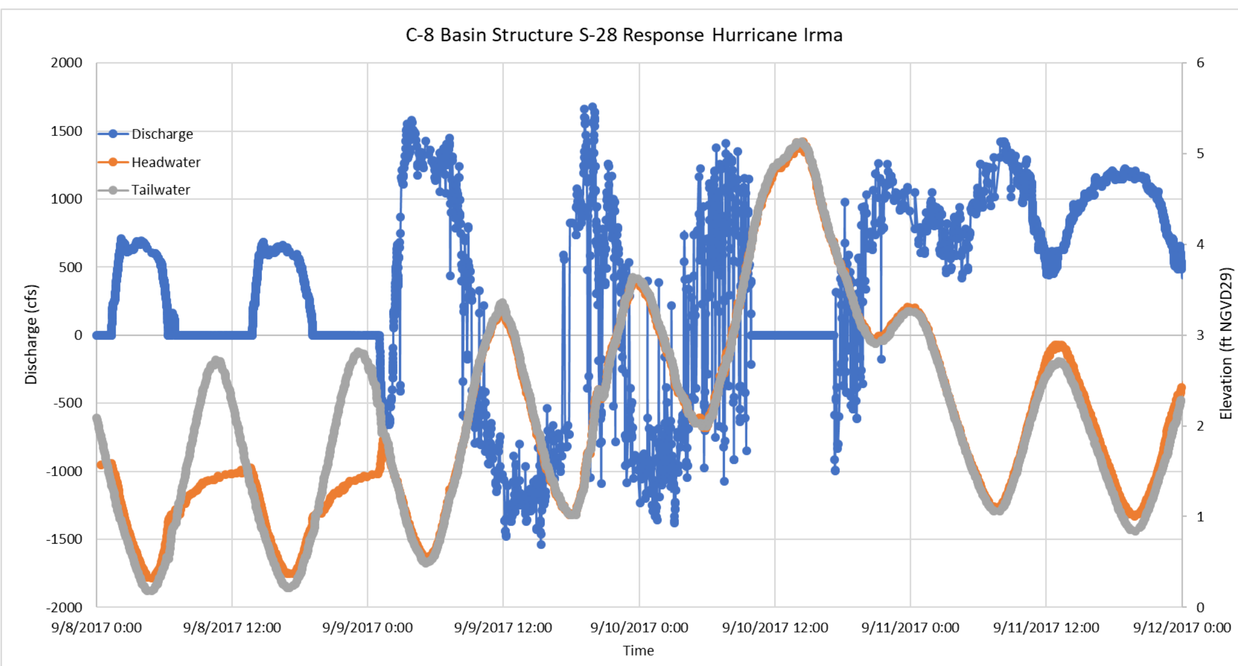

Figure 2.5-3: C-8 Basin Structure S-28 Response to Hurricane Irma

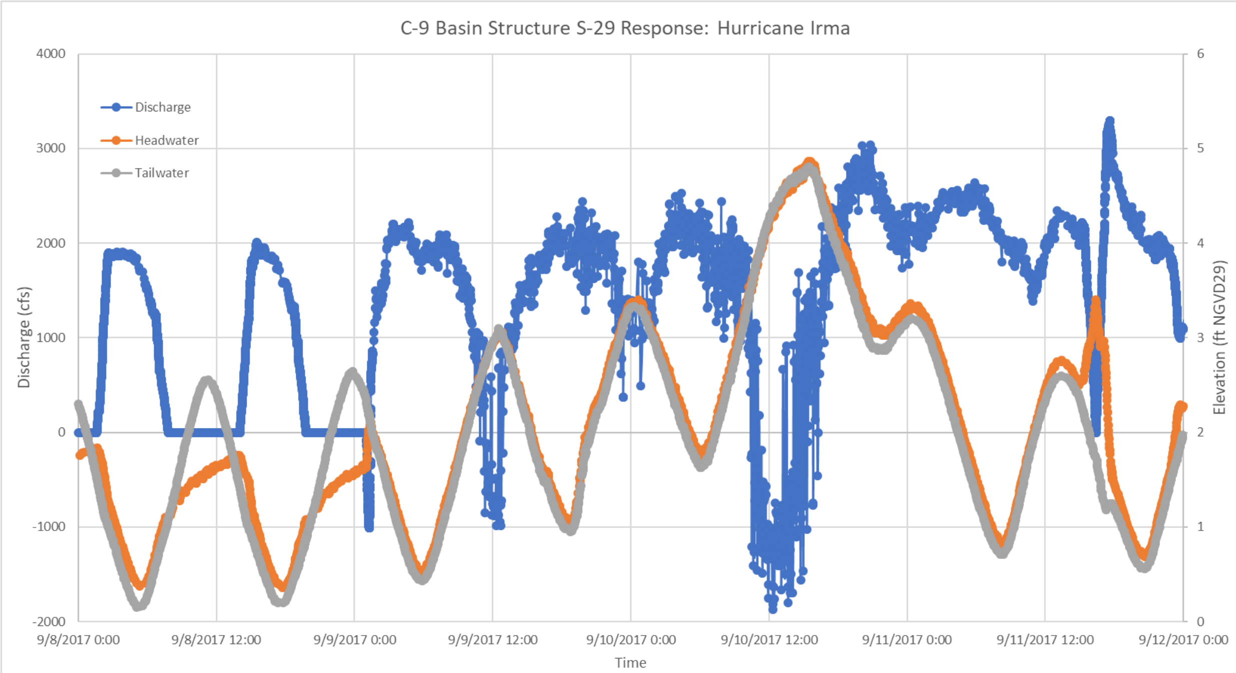

Figure 2.5-4: C-9 Basin Structure S-29 Response to Hurricane Irma

Available rainfall data for Subtropical Storm Leslie was called into question as NEXRAD data in the early 2000s was less accurate than it is today. Therefore, rain gauge data (DBHYDRO) was compared to the NEXRAD data for the pixel(s) that they were in or bordered against. This exercise suggested that the NEXRAD data and gauge data were similar in terms of total rainfall, however, there were some differences as far as the timing of the rainfall. The following figures show different comparisons relating to NEXRAD rainfall, gauge rainfall, and structure discharge.

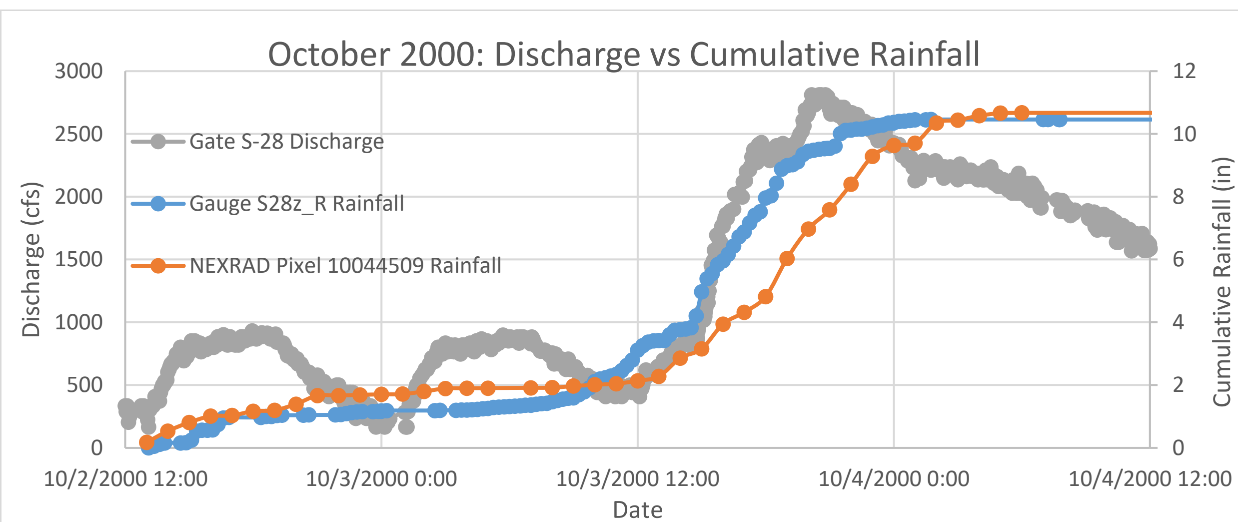

Figure 2.5-5: Discharge vs Cumulative Rainfall for Gate S-28 (NEXRAD Pixel and Rain Gauge Located Centrally in C-8 Basin)

The cumulative rainfall totals for the rain gauge and the associated NEXRAD pixel are only off by about 0.2 inches, which is about 2%. This was a negligible amount and well within the accuracy of either measurement method. More concerning was the temporal shift in the rainfall, which was about 3-hours. Comparing the timing of rainfall to the discharge, it is believed that the rainfall gauges are more accurate. Simply put, the NEXRAD data shows a rainfall response after the runoff response, which goes against rainfall-runoff principles. The following figure compares the same rainfall but plotted as rainfall intensity.

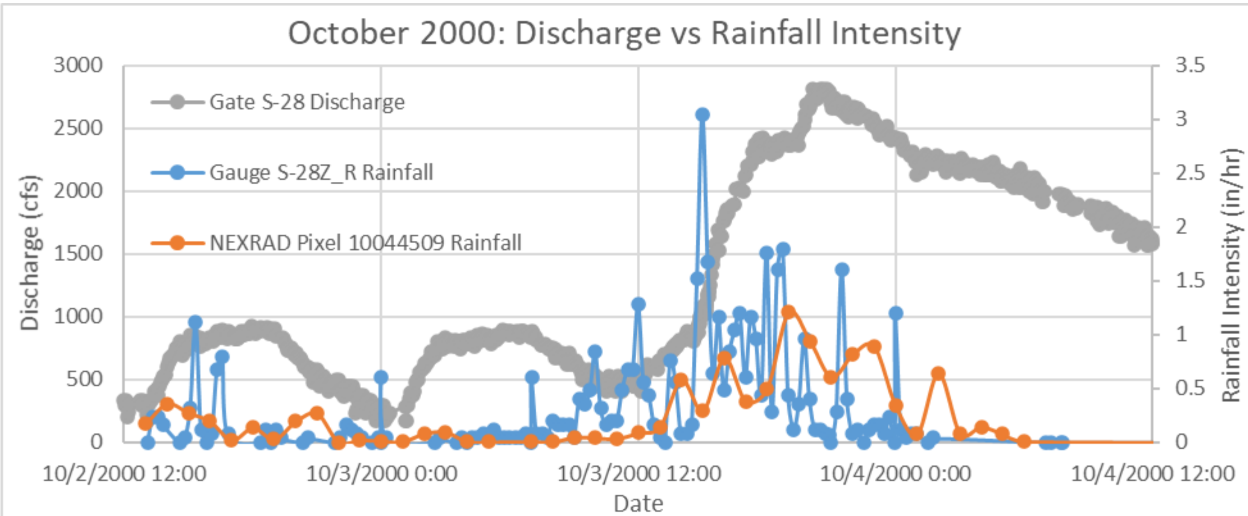

Figure 2.5-6: Discharge vs Rainfall Intensity for Gate S-28 (NEXRAD Pixel and Rain Gauge Located Centrally in C-8 Basin)

This figure shows there is a large difference in rainfall intensity when comparing the rain gauge to the NEXRAD data. The rain gauge data was recorded in 15-minute intervals whereas the NEXRAD data was recorded in hourly intervals, as 15-minute NEXRAD data was not available until 2002. Therefore, the NEXRAD data was unable to capture the high intensity short duration part of the storm. It was noted that this limitation could have some effect on calibration efforts. The following figure compares the rain gauge located centrally in the C-9 basin with NEXRAD data for the two pixels it borders.

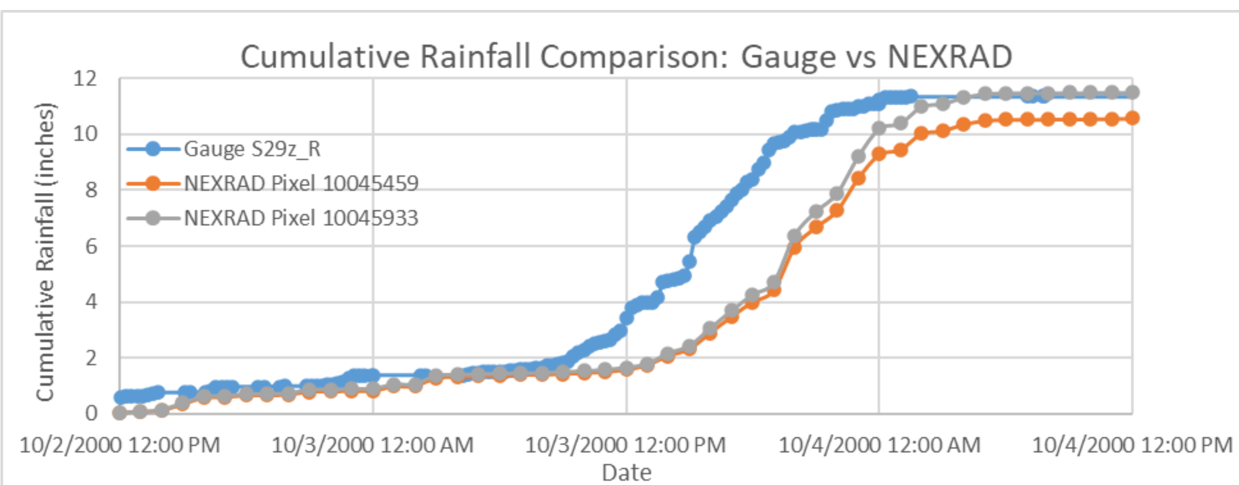

Figure 2.5-7: Cumulative Gauge Rainfall vs Cumulative NEXRAD Rainfall (NEXRAD Pixel and Rain Gauge Located Centrally in C-9 Basin)

The cumulative rainfall totals were fairly close, with NEXRAD data being between 0.2 and 0.7 inches different, or about 2-6%. Again, there was a temporal lag of about 4 hours. The following figure compares the rain gauge located in the western part of the C-9 Basin with NEXRAD data.

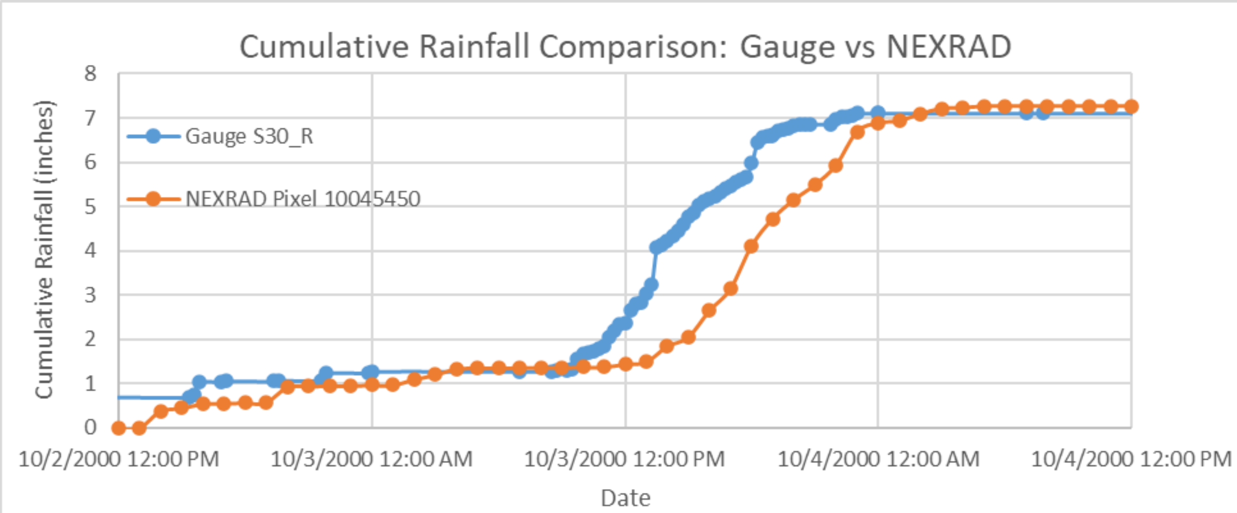

Figure 2.5-8: Cumulative Gauge Rainfall vs Cumulative NEXRAD Rainfall (NEXRAD Pixel and Rain Gauge Located in Western C-9 Basin)

The cumulative rainfall totals are within 0.2 inches apart which is about 2%. Again, there is a temporal lag of about 4 hours. The following figure compares the rain gauge located at the tidal outfall of the C-7 Basin with NEXRAD data.

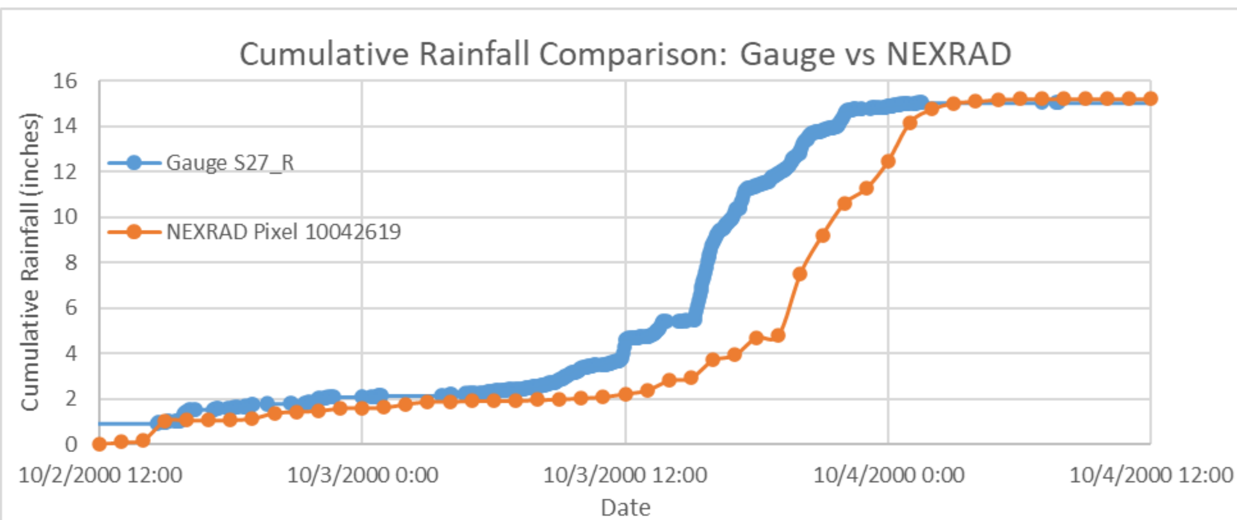

Figure 2.5-9: Cumulative Gauge Rainfall vs Cumulative NEXRAD Rainfall (NEXRAD Pixel and Rain Gauge Located at C-7 Basin Tidal Outfall)

The cumulative rainfall totals are within 0.2 inches apart which is only about 1%. Again, there is a temporal lag of about 4-5 hours.

The NEXRAD data appeared to capture the total rainfall well compared to the gauge data, however, there were some concerns with using it. As mentioned, the 1-hour interval of the NEXRAD data averages-out the highest-intensity parts of the storm. Additionally, there are some temporal differences. These two issues were further discussed before any decisions were made on whether or not to use it for the calibration event. It was originally noted that it was not advisable to use the existing rain gauges to make Thiessen polygons for calibration use as: (1) the rain gauges do not capture the significant spatial differences that were noticed in the NEXRAD data and (2) it is likely that one rain gauge was not been functioning properly during the storm. **Figure 2.5-10** shows the variation of total rainfall depth in randomly selected NEXRAD pixels and the rain gauges.

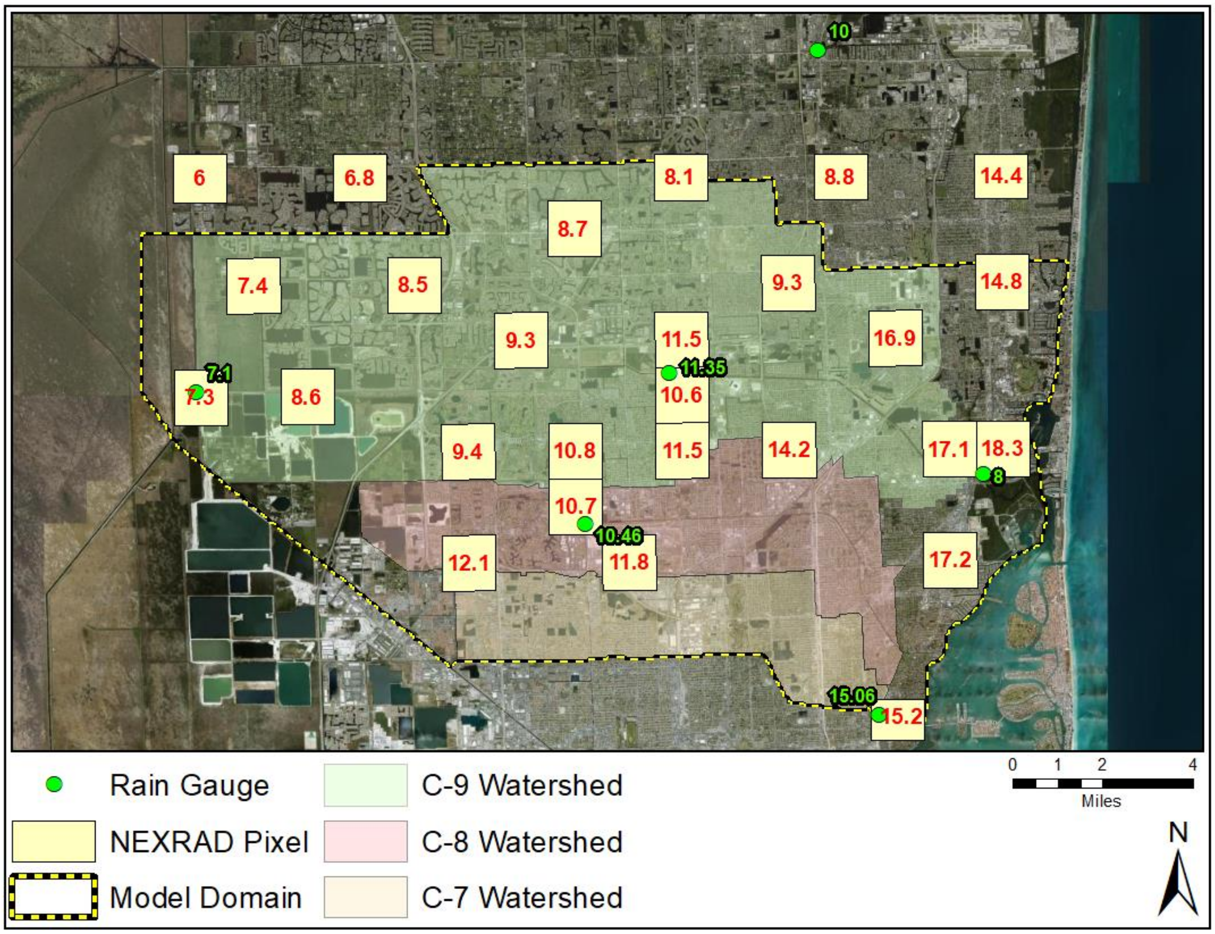

Figure 2.5-10: Randomly Selected NEXRAD Pixel and Rain Gauge Rainfall Summary

The NEXRAD rainfall data for October 2000 showed a spatial difference ranging from about 7 inches in the northwestern part of the C-9 basin to upwards of 18 inches in the southeastern part of the C-8 basin. There was some concern initially that the rain gauges alone may not adequately define the spatial distribution. It appeared that the rain gauges captured the timing of the rainfall better than NEXRAD, while NEXRAD appeared to capture the spatial variation in rainfall depths better than the rain gauges. Therefore, Taylor Engineering initially recommended using the total rainfall depths from each NEXRAD pixel and distributing it temporally based on a rain gauge that is assigned by Thiessen polygons, which would result in shifting the NEXRAD timing of the rainfall to match the rain gauges while maintaining spatial variation in rainfall totals of the NEXRAD pixels. This approach was originally attempted for model calibration but ultimately was discarded and replaced with unmodified rain gauge data. For more information regarding the NEXRAD temporal manipulation, refer to Deliverable 1.1, *Data Availability Memorandum* (Taylor Engineering, 2019). Aside from Gauge S-29_R, all rain gauges were within 0.2 inches of the NEXRAD pixel bordering it. Gauge S-29_R only recorded about 8 inches during the storm while surrounding NEXRAD pixels show between 17 and 18 inches. This indicated the gauge was malfunctioning during the storm; therefore, this gauge was not considered. The following figure shows the Thiessen Polygons of the rain gauges used to distribute rainfall.

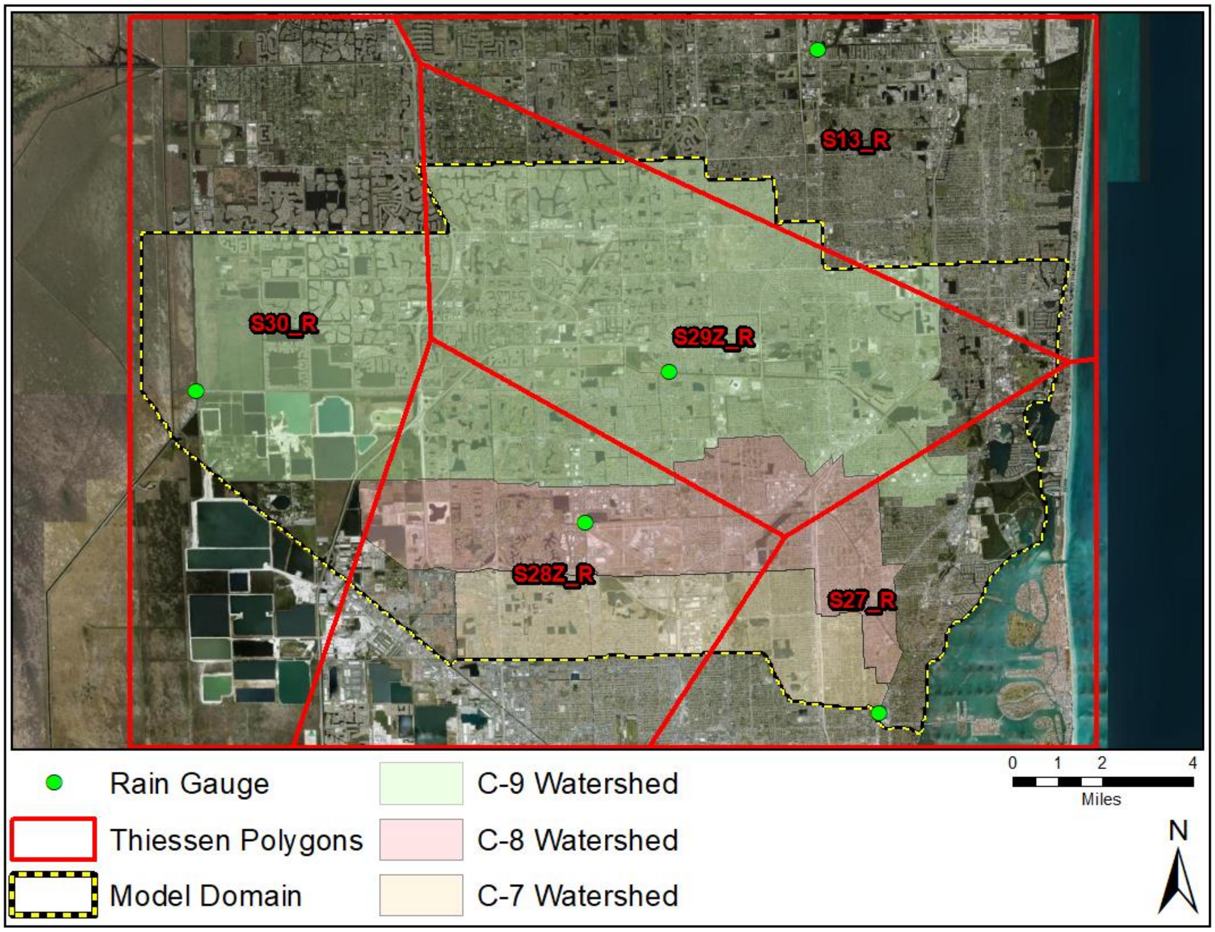

Figure 2.5-11: Thiessen Polygons of the Rainfall Gauges with Available Data during the Calibration Period

2.6 Calibration/Validation Data Availability and Collection

In addition to accurate rainfall, data needed for model calibration and validation included gate openings, breakpoint stage, and breakpoint discharge for all primary operational structures, and groundwater levels for the wells within the surficial aquifer and the model domain. When breakpoint data was unavailable, the best available data (hourly, daily max, etc.) was used. **Figure 2.6-1** shows the location of the primary structures and wells analyzed for data availability and gaps.

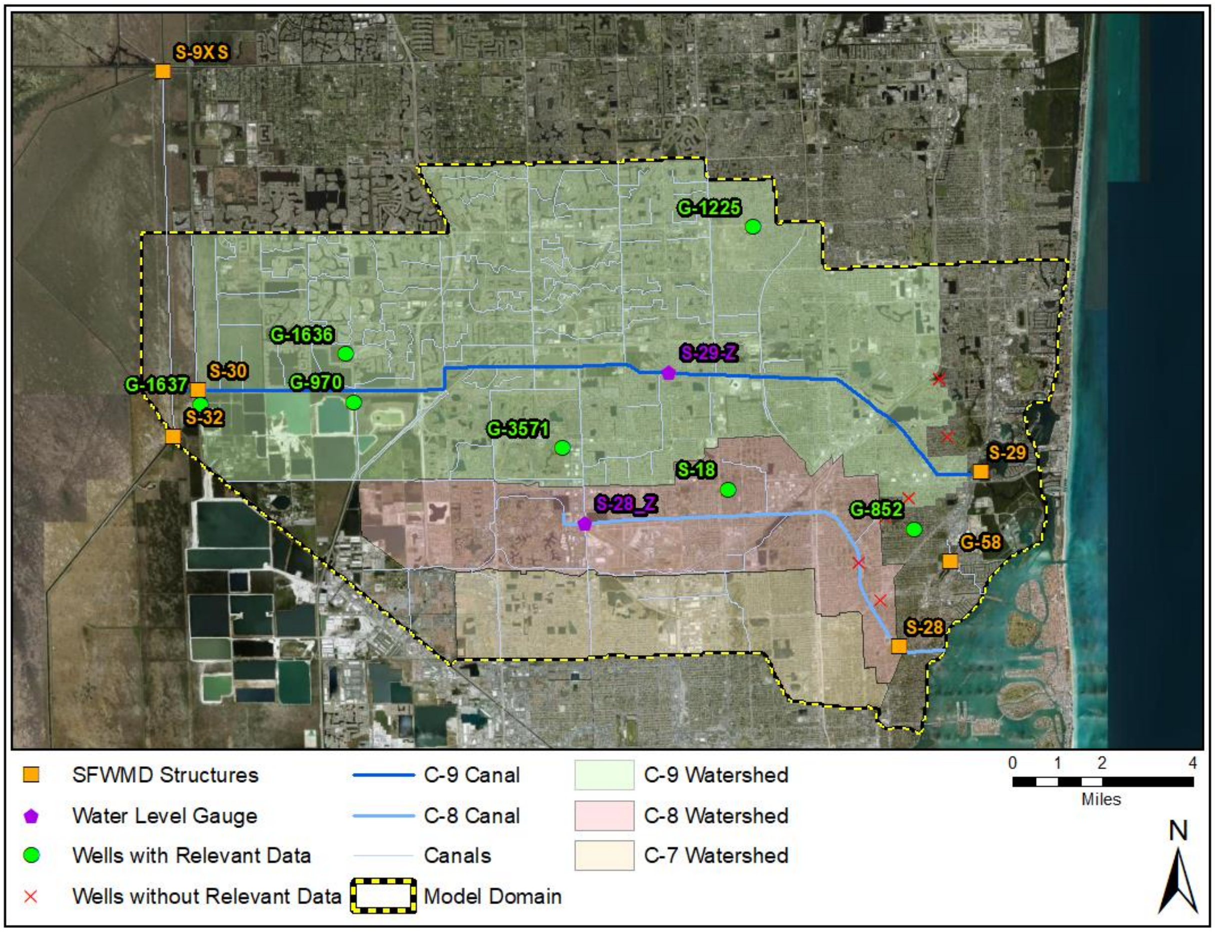

Figure 2.6-1: Calibration/Validation Locations Analyzed for Data Availability and Gaps

Stage, flow, and groundwater level data were graphed to visually analyze data for gaps and outliers. The following table shows the completeness of data for the storm events in October 2000, June 2017, and September 2017.

Table 2-1: Structure Data Availability Summary

NAME	BASIN	CONTROL	DBKEY	DATA TYPE	STATUS
S-28	C-8	Gated	65070	Breakpoint Discharge	Complete
			6627	Breakpoint HW Stage	
			6628	Breakpoint TW Stage	
			LT203 & LS856	Breakpoint Gate Opening	
S-29	C-9	Gated	65071	Breakpoint Discharge	Complete
			6631	Breakpoint HW Stage	
			6632	Breakpoint TW Stage	
			LS491, LS857, LS858, & LS859	Breakpoint Gate Opening	
S-30	C-9	Gated	65074	Breakpoint Discharge	Complete
			6686	Breakpoint HW Stage	
			6639	Breakpoint TW Stage	
			LS493, LS862, & LS863	Breakpoint Gate Opening	
S-32	L-33 CC	Gated	65077	Breakpoint Discharge	Complete
			SP543	Breakpoint HW Stage	
			6643 & AI581	Breakpoint TW Stage	
			LS495, LS867, SP544 & SP545	Breakpoint Gate Opening	
G-58	North Biscayne Bay	Gated	64715	Breakpoint Discharge	No September 2017
			IX539	Breakpoint HW Stage	No September 2017
			N/A	Breakpoint TW Stage	Not in DBHYDRO
			LS376, LS693, LS694, & LS695	Breakpoint Gate Opening	No September 2017
S-9XS	L-33 CC	Boarded	90829	15-Minute Discharge	Complete
			SO013	15-Minute to Hourly HW Stage	Complete
			OH925 & OH924	15-minute and Breakpoint TW Stage	Complete
			LD575 & LS966	Other Board Elevation	Other

Although there were several wells within the model domain, many of them contained no useful data as it pertains to the purpose of this project because of infrequent or random interval sampling. The following table shows the wells that were within the model domain and the surficial aquifer system (SAS) that have concurrent data available to three of the aforementioned storm events.

Table 2-2: Wells within SAS with Complete Groundwater Level Data for October 2000

WELL NAME	BASIN	DBKEY	DATA TYPE
G-1225	C-9	1758	Daily Max
G-1636	C-9	1716	Daily Max
G-1637	C-9	1698	Daily Max
G-3571	C-9	LP668	Daily Max
G-852	North Biscayne Bay	1662	Daily Max
G-970	C-9	1703	Daily Max
S-18	C-8	1673	Daily Max

Table 2-3: Wells within SAS with Complete Groundwater Level Data for June-September 2017

WELL NAME	BASIN	DBKEY	DATA TYPE
G-1225	C-9	1758	Hourly GW Level (missing data during Irma)
G-1636	C-9	1716	Hourly GW Level
G-1637	C-9	1698	Hourly GW Level (missing data during Irma)
G-3571	C-9	LP668	Hourly GW Level
G-852	North Biscayne Bay	1662	Hourly GW Level
G-970	C-9	1703	Hourly GW Level
S-18	C-8	1673	Hourly GW Level
G-1166R	C-7	88676	Hourly GW Level

2.7 Groundwater Data Availability

There were two sources of groundwater data that were available. The first source was the 2019 Broward County Current Conditions model and the second source was a groundwater study authored by J. D Hughes and J. T White, which was documented in a USGS report titled *Hydrologic Conditions in Urban Miami-Dade County, Florida, and the Effect of Groundwater Pumpage and Increased Sea Level on Canal Leakage and Regional Groundwater Flow* (2016). The majority of the 2019 Broward County model's groundwater data was inherited from previous versions of the model, which has been around since the early 2000s. The earlier versions of this model was intended for long-term water supply simulations, so the 5-layer groundwater model has been parameterized and calibrated over the years and is assumed to be a good representation of the aquifer system. The groundwater model by Hughes and White was several years newer and used a different modeling approach, in which they discretized the groundwater model into 3 layers: an upper and lower permeable layer separated by a layer about 100 times less permeable. A significant amount of data from this study was available, including but not limited to year 2000 wet season heads, horizontal hydraulic conductivity, transmissivity, specific storage, specific yield, aquifer thickness, and bottom of aquifer layer elevations. Some of this data was available as figures with contours while others were raster data. Taylor Engineering reached out to Hughes and received the data needed to create shapefiles of the data in the USGS report.

As the groundwater study by Hughes and White (2016) was several years newer, approved dataset, and well documented, Taylor Engineering originally proposed to use a 3-layer groundwater model based on this study. The groundwater model was intended to include the following data from the USGS: (1) layer bottom elevations, (2) horizontal hydraulic conductivity, (3) vertical hydraulic conductivity, (4) specific yield, (5) specific storage, and (6) initial groundwater elevations based on 2000 wet season head (calibration model only). However, after initial calibration attempts, the groundwater model was reparametrized based on the 2019 Broward County Current Conditions model. This is discussed more in **Section 4.2**.

2.8 Boundary Conditions

2.8.1 Calibration

For the October 2000 calibration event, the eastern surface and groundwater boundary conditions come from the Virginia Key tidal station. The southern boundary conditions are time-stage relationship along the C6 and C7 canal for surface water and a general head for groundwater (based on observed canal stages from DBHYDRO). Observed stage in Water Conservation Area 3B serves as the western boundary conditions with a time-stage relationship for surface water, and a general head boundary for groundwater (based on observed water level recorder data from DBHYDRO). The northern groundwater boundary was developed based on observed heads from the USGS study (Hughes and White, 2016). Tidal boundaries at the S-28 and S-29 structures are forced using observed tailwater data from DBHYDRO.

2.8.2 Validation

For the September 2017 validation event, the eastern surface and groundwater boundary conditions come from the Virginia Key tidal station. The southern boundary conditions are time-stage relationships along the C6 and C7 canal for surface water and a general head for groundwater (based on observed canal stages from DBHYDRO). Observed stage in Water Conservation Area 3B serves as the western boundary conditions with a time-stage relationship for surface water, and a general head boundary for groundwater (based on observed water level recorder data from DBHYDRO). The northern boundary was developed using simulated groundwater elevations from of the 2019 Broward County Current Conditions Validation Model, which was originally developed for the June 2017 event but was extended to run through September 2017. Tidal boundaries at the S-28 and S-29 structures are forced using observed tailwater data from DBHYDRO.

2.8.3 Design Storms

For all design storm events, the eastern surface and groundwater boundary conditions will come from the District-provided tidal data with storm surge and/or sea level rise, depending on the specific scenario. The southern boundary conditions will be time-stage relationships along the C6 and C7 canal for surface water and a general head for groundwater (District-provided design storm model results from XP SWMM and HEC RAS models). Observed stage in Water Conservation Area 3B serves as the western boundary conditions with a time-stage relationship for surface water, and a general head boundary for groundwater (based on observed water level recorder data from DBHYDRO). The northern boundary was developed using simulated groundwater elevations from of the 2019 Broward County Current Conditions Design Storm Models. Tidal boundaries at the S-28, S-29, and G-58 structures are forced using District-provided tidal data with storm surge and/or sea level rise, depending on the specific scenario.

2.9 Initial Conditions

2.9.1 Overland Depths

For all simulations, any grid cell within a drainage basin that are lower than the basin's water control elevation will be set to an initial depth equal to the difference of the water control elevation and the elevation of the cell. Essentially, this will bring the water elevation in any "sinks" to the water control elevation. This eliminates excess "dead storage" and ensures that water is not being routed via ponded drainage or flood codes at the start of the simulation. This is a fair assumption as both the calibration and validation events occurred late in the wet season so it is expected that low areas would be wet, and design storms are intended to be conservative

2.9.2 Groundwater and Canal Stages- Calibration

The initial groundwater elevations for calibration were developed by making localized adjustments to the 2000 wet season heads from the MODFLOW model developed as part of the USGS study (Hughes and White, 2016). The initial surface water levels in the main canals were based on observed data. Initial stages in the secondary/tertiary canal systems that are controlled by structures were set based on water control elevations.

2.9.3 Groundwater and Canal Stages- Validation

The initial groundwater elevation for the validation event was created by extending the 2019 Broward County Current Conditions Model groundwater elevation map (which includes part of Miami-Dade County) south to cover the remaining area of the model extent. The 2019 Broward County model's initial groundwater map was developed from Broward County's average 1990-1999 wet season map (Broward County, 2000). Average September groundwater elevation contours from the USGS (Fish and Stewart, 1991) were used to extend the initial groundwater elevation map south to cover the remaining model domain. The groundwater elevations were compared with available well data. Early wet-season (June 2017) groundwater elevations were a close match with the average wet-season elevations from the 1990s, therefore, no adjustments to the contours were applied. The initial stages in the main canals were based on observed data. Initial stages in the secondary/tertiary canal systems that are controlled by structures were set based on water control elevations.

2.9.4 Groundwater and Canal Stages- Design Storms

There were two options available for developing the initial groundwater elevations for the design storms. The first option was to simply use the same initial groundwater elevations from the validation model, which was the approach used for the 2019 Broward County Current Condition Design Storm models. This is the preferred methodology as the storm event is from recent history and there is observed data available that could be used for boundary conditions if needed. Additionally, there was generally a good match between the initial groundwater elevations map (based on typical late wet season conditions) and the observed data at well locations at the beginning of the event. This provides realistic initial groundwater elevations.

The second option, although not recommended, would be to use simulated groundwater elevations from the validation simulation. Essentially, the groundwater elevations at some point in time during the validation simulation, such as 12 hours after the peak rainfall, could be extracted and used as a new starting point for the design storms. This approach would provide higher initial groundwater elevations, which would provide a more conservative starting point for the design storm simulation. However, this approach should only be considered IF the simulated groundwater elevations during the validation simulation are a close match with observed well data, model wide.

For this study, the initial surface water levels were based on water control elevations if known, or operational rules. For example, if a particular area was controlled at elevation 4.0 feet, then every branch within that drainage area was given an initial condition of 4.0 feet. If there was no established control elevation, then the initial water level was set equal to the level in which the controlling structure (could be several miles away) begins to operate

3 MODEL DEVELOPMENT

This section details the development and initial parameterization of the SFWMD C-8 & C-9 MIKE SHE and MIKE HYDRO River models for use in the C8-C9 FPLOS Study. Please note that several of the data inputs were modified during model calibration and only the final values are shown. Refer to Deliverable 2.1, *C8-C9 Calibration and Validation Memorandum Final Draft* (Taylor Engineering, 1/21/2020) for the original values used in developing the model, before any adjustments were made during calibration.

3.1 Model Domain and Grid

The model domain extends from the C-9 and C-11 basin boundary in the north to the C-6 and C-7 canals in the south, and from just west of the L-33 canal in the west to the intercoastal in the east, as shown in **Figure 3.1-1**. A computational grid size of 250-ft was chosen and coupled with the multi-cell overland feature using a 125-ft grid. This further refines the storage and conveyance characteristics of each computational grid cell. Although the model computations are based on a 250-ft grid cell, the conveyance and storage characteristics of each cell are calculated based on the finer 125-foot grid. This provides a high level of topographic detail and overland storage definition, which is sufficient for this sub-regional scale model. The computational grid size and multi-cell overland definition are consistent with the 2019 Broward County Current Conditions model (Taylor Engineering, 2019). Additionally, the C8-C9 model grid origin is aligned so that it is an exact integer of grid cells away from the 2019 Broward County model origin, meaning that the data input and outputs are compatible between both models.

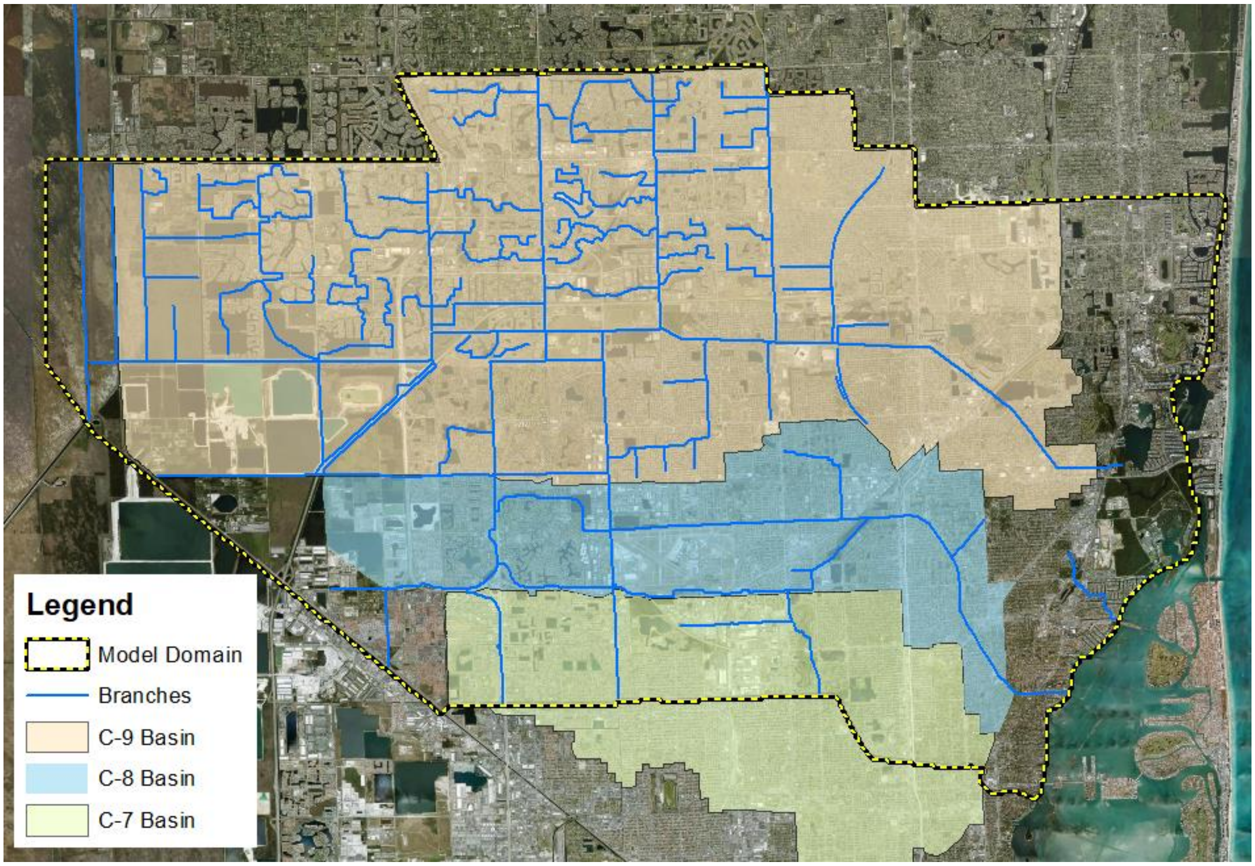

Figure 3.1-1: Model Domain and SFWMD Basin Map

3.2 Topography

The topography input file was made from the merged DEM presented in **Figure 2.1-1**. The 125-ft DEM was made by taking the median values from the 5-ft DEM within each 125-ft grid cell. Areas with elevations greater than 25 ft NAVD88 (typically landfills or high bridges) were reduced to 25 ft to eliminate the possibility of having numerical stability issues in the 2D model (such as flow from 200-ft elevation cell to 10-ft elevation cell). Areas with elevations less than -2 ft NAVD88 were increased to -2 ft (typically intercoastal areas- bathymetry likely built into DEM). The topography was converted from NAVD88 to NGVD29 by adding 1.57 ft, the conversion from CorpsCon6 tool. Several areas were tested, and the differences were minimal. A uniform conversion of 1.57 ft was deemed appropriate and efficient.

3.3 Simulation Specification

The simulation period for the calibration event was a three-week period from October 1st, 2000 12am to October 21st, 2000 12am. The verification event was a nearly four-month period from June 2nd, 2017 12am to September 27th 12am. The design storm events were given a start date of June 4th, 2017 12am, as it provides a realistic starting point for initial conditions and boundary conditions based on recent observed data. The initial groundwater elevations at this point in time were a good match with observed groundwater well elevations, with most locations agreeing to within +/- 0.25 ft. In addition, this start date aligns with the validation model and the 2019 Broward County Design Storm models, which provides observed (western boundary) and simulated boundary condition data (northern boundary). June 4th at

12am was chosen specifically as this aligns the peak of the design storm with the peak of the storm in the boundary conditions. This approach is consistent with the 2019 Broward County Model. Although the design storm rainfall has a duration of only 3 days, the design storm simulation period was set to 16 days. A 2-day spin-up period was chosen to allow any discontinuities within the boundary conditions or initial conditions to come to equilibrium before the start of the design storm rainfall. The design storm period was given a duration of 14 days, 11 of which occur after the rainfall ends. The purpose for running the simulation an additional 11 days was so that results existed that could be used to generate a model-simulated water table map that could be useful as an alternative input for initial groundwater level conditions and to determine duration of flooding in areas of the model where potential flooding damages may need to be evaluated as part of mitigation alternatives.

3.4 Climate

3.4.1 Rainfall

The storm event from October 2nd-4th, 2000, was used to calibrate the model. Originally, temporally modified NEXRAD rainfall was attempted, but ultimately was replaced with rain gauge data (as shown in **Figure 2.5-11**). This is discussed in greater detail in **Section 4.4**. The following table shows the rain gauge recorded rainfall totals for October 1st-21st, 2000, with most of it occurring during between the 2nd-4th.

Table 3-1: Rain Gauge based Total Rainfall Depths

Rain Gauge	Total Rainfall (in)
S-13_R	10.46
S-27_R	16.01
S-28Z_R	12.57
S-29Z_R	13.65
S-30_R	7.5

The verification event rainfall comes from unmodified NEXRAD data, which had been QA/QC by Geosyntec Consultants (2018) as part of the 2019 Broward County modeling project. The design storm simulation uses NOAA Atlas 14 rainfall depths (**Table 3-2**) that are temporally distributed based on the normalized cumulative SFWMD 3-day distribution and spatially distributed based on Thiessen Polygons of the NOAA stations (**Figure 3.4-1**), which is consistent with the 2019 Broward County model approach.

Table 3-2: Design Storm Rainfall Depths per NOAA Atlas 14 Station

NOAA Station	3-Day Storm Rainfall Depth (inches)			
	5-Year	*10-Year*	*25-Year*	*100-Year*
PENNSUCO 5 WNW	8.12	9.66	12.1	16.3
MRF114	8.9	10.7	13.5	18.4
MRF117	8.85	10.5	13.1	17.7
MIAMI BEACH	8.48	10.1	12.6	16.9
HIALEAH	8.91	10.6	13.2	17.8
FT LAUDERDALE INTL AP	8.95	10.8	13.5	18.3

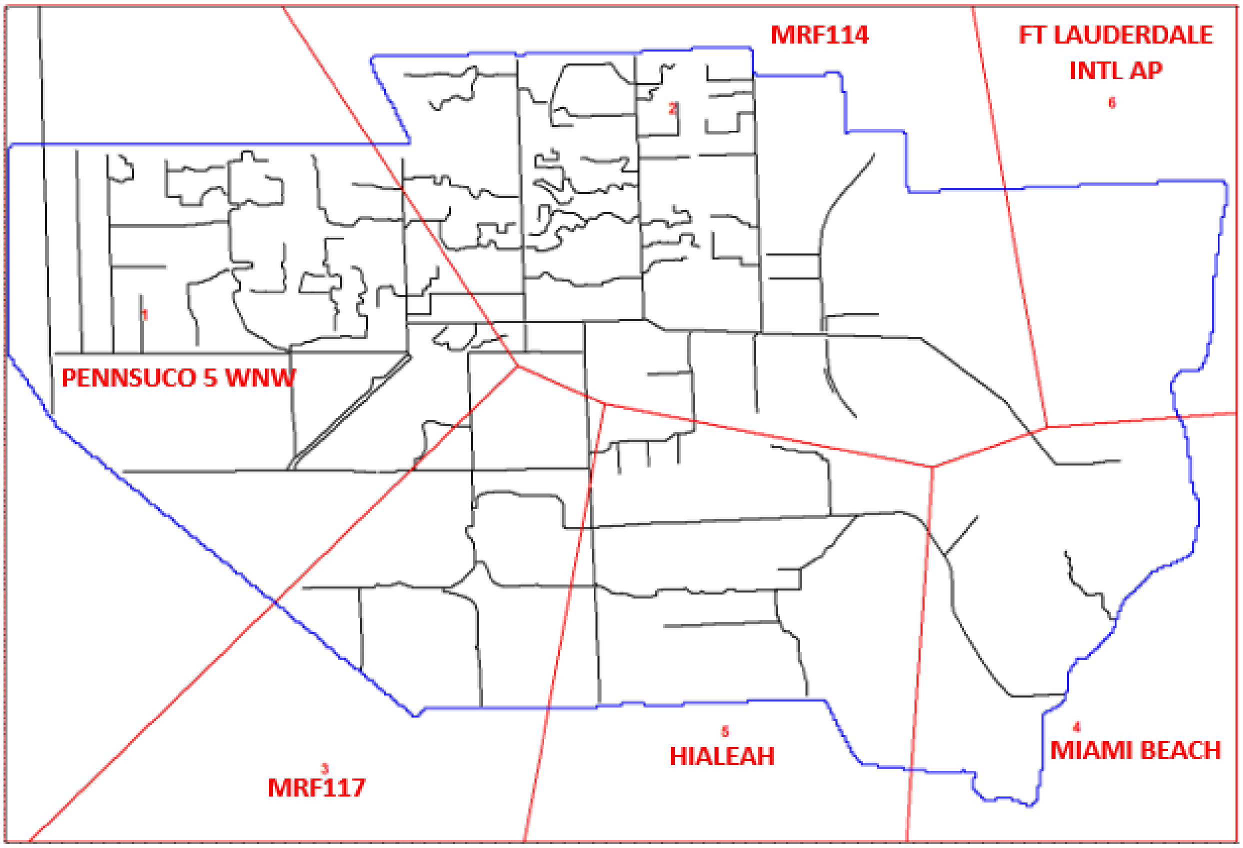

Figure 3.4-1 Design Storm Thiessen Polygons based on NOAA Atlas 14 Rainfall Stations

3.4.2 Reference Evapotranspiration

Short term simulations are typically not very sensitive to this parameter and reference ET does not vary significantly across relatively small areas, such as this model domain. Therefore, a uniform spatial distribution was chosen for the calibration and validation simulations. Time varying SFWMD Reference ET (https://apps.sfwmd.gov/nexrad2) for pixel #10045457 (centrally located) was applied model-wide. **Figure 3.4-2** & **Figure 3.4-3** show the reference ET used for the calibration and validation simulations, respectively. For the design storms, the reference ET was set to a constant 2 mm/d, which is the minimum daily wet season value rounded to the nearest mm, in year 2017, including during Hurricane Irma (USGS Reference and Potential Evapotranspiration, 2018). Minimum wet season reference ET values were deemed sufficient as ET will be rather insignificant compared to design storm rainfall depths. This is a conservative approach. Evapotranspiration is a relatively small fraction of a design storm water budget, with an even smaller fraction of that fraction occurring during the time to peak (time to peak is a few days; most design storm ET occurs during hydrograph recession).

Reference ET is based on a reference "crop", typically well-watered grass. Reference ET is adjusted by crop coefficients, which vary by land use. **Table 3-3** shows the final crop coefficients used in the model, based on the 2019 Broward County Current Conditions model. Adjusted reference ET is further reduced based on water availability, root depth and leaf area index, although these parameters are not important for event-based simulations.

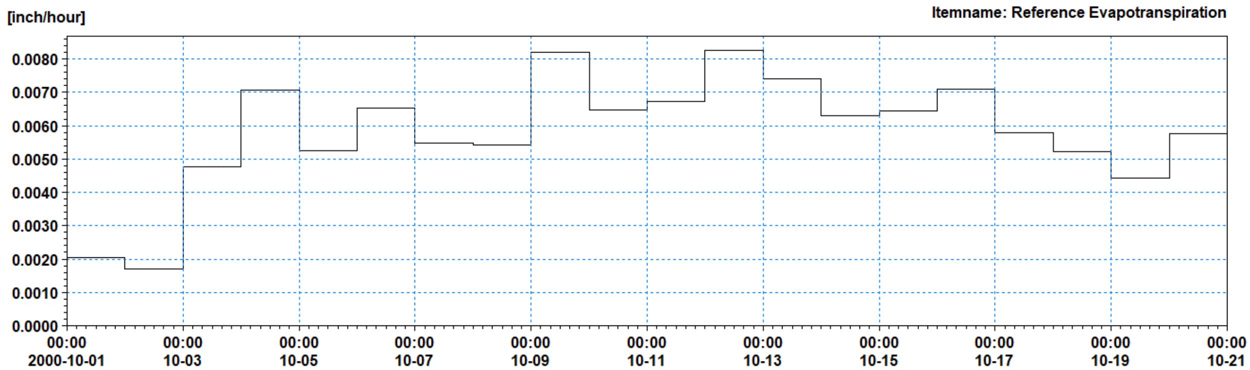

Figure 3.4-2: Reference ET for Pixel 10045457 for Calibration Simulation

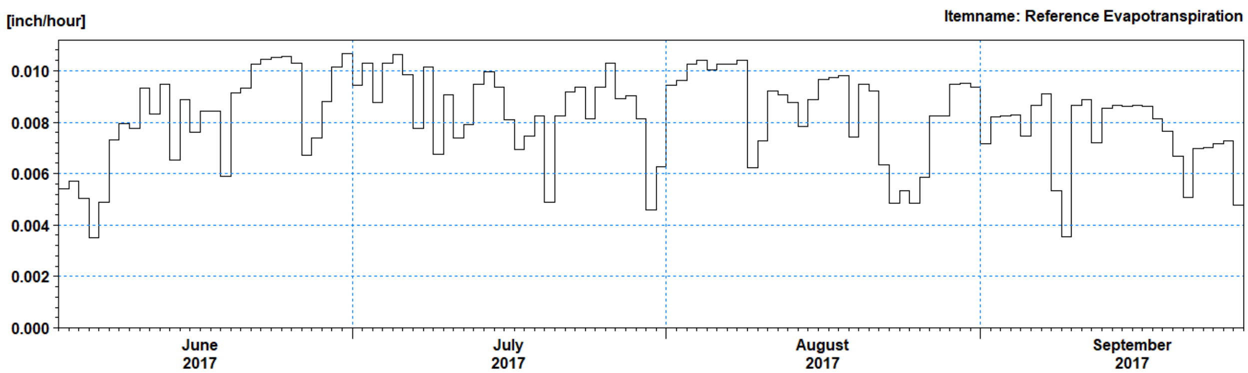

Figure 3.4-3: Reference ET for Pixel 10045457 for Validation Simulation

Table 3-3: Crop Coefficients by FLUCCS Code

FLUCCS Code	Crop Coefficient (Kc)	FLUCCS Code	Crop Coefficient (Kc)	FLUCCS Code	Crop Coefficient (Kc)
1100	0.67	**2300**	0.8	**5200**	0.8
1200	0.58	**2400**	0.8	**5300**	0.8
1300	0.48	**2500**	0.8	**5400**	0.8
1400	0.48	**2600**	0.8	**5700**	0.8
1500	0.4	**3100**	0.8	**6100**	0.8
1700	0.48	**3200**	0.8	**6400**	0.8
1800	0.72	**3300**	0.8	**7400**	0.8
1900	0.8	**4200**	0.8	**8100**	0.4
2100	0.8	**4300**	0.8	**8200**	0.4
2200	0.8	**5100**	0.8	**8300**	0.4

3.5 Land Use

To be consistent with the 2019 Broward County Current Conditions model, the land use/vegetation map was created by merging the 2019 Broward County model's land use map with the SFWMD Land Use Land

Cover data (SFWMD LCLU, 2017). The 2019 Broward County Current Conditions model's land use map was created using the same data from SFWMD, but some additional changes were made throughout the county after comparing satellite imagery from 2015 with 2018. Therefore, by merging the Broward County land use map with the SFWMD land use data, it ensured that any changes in the C-9 basin from the 2019 Broward County Model were incorporated.

As suggested by SFWMD, this study changed "extractive" land use areas to reservoirs as they are filled. This change is consistent across all of the land use-based parameters. Land use values are assigned based on the 250-ft computation grid. The land use grid was made from a polygon shapefile of land use areas based on the maximum area of land use(s) in the 250-ft grid cell. As discussed in **Section 2.2**, there were less than 2% change in land use classification since 2000, so this dataset was used for the calibration, validation, and design storm events. Refer to **Table 3-4** for land use description by Florida Land Use Cover Classification System (FLUCCS) codes (Florida Natural Areas Inventory, 2012) and **Figure 3.5-1** for the spatial distribution.

Table 3-4: Land Use by FLUCCS Code

FLUCCS Code	Land Use	Area-Weighted %
1100	Residential, Low Density	1.7
1200	Residential, Medium Density	32.9
1300	Residential, High Density	12.1
1400	Commercial and Services	9
1500	Industrial	2.9
1700	Institutional	4
1800	Recreational	4
1900	Open Land	1.3
2100	Cropland and Pastureland	0.7
2200	Tree Crops	0
2300	Feeding Operations	0
2400	Nurseries and Vineyards	0.8
2500	Specialty Farms	0
2600	Other Open Lands - Rural	0
3100	Herbaceous (Dry Prairie)	0.1

FLUCCS Code	Land Use	Area-Weighted %
3200	Upland Shrub and Brushland	0.3
3300	Mixed Rangeland	0
4200	Upland Hardwood Forests	0.8
4300	Upland Mixed Forests	0.3
5100	Streams and Waterways	1.7
5200	Lakes	0.3
5300	Reservoirs	10.2
5400	Bays and Estuaries	0.3
5700	Ocean and Gulf	0
6100	Wetland Hardwood Forests	4.1
6400	Vegetated Non-Forested Wetlands	4.7
7400	Disturbed Land	0.7
8100	Transportation	6.2
8200	Communications	0.1
8300	Utilities	0.9

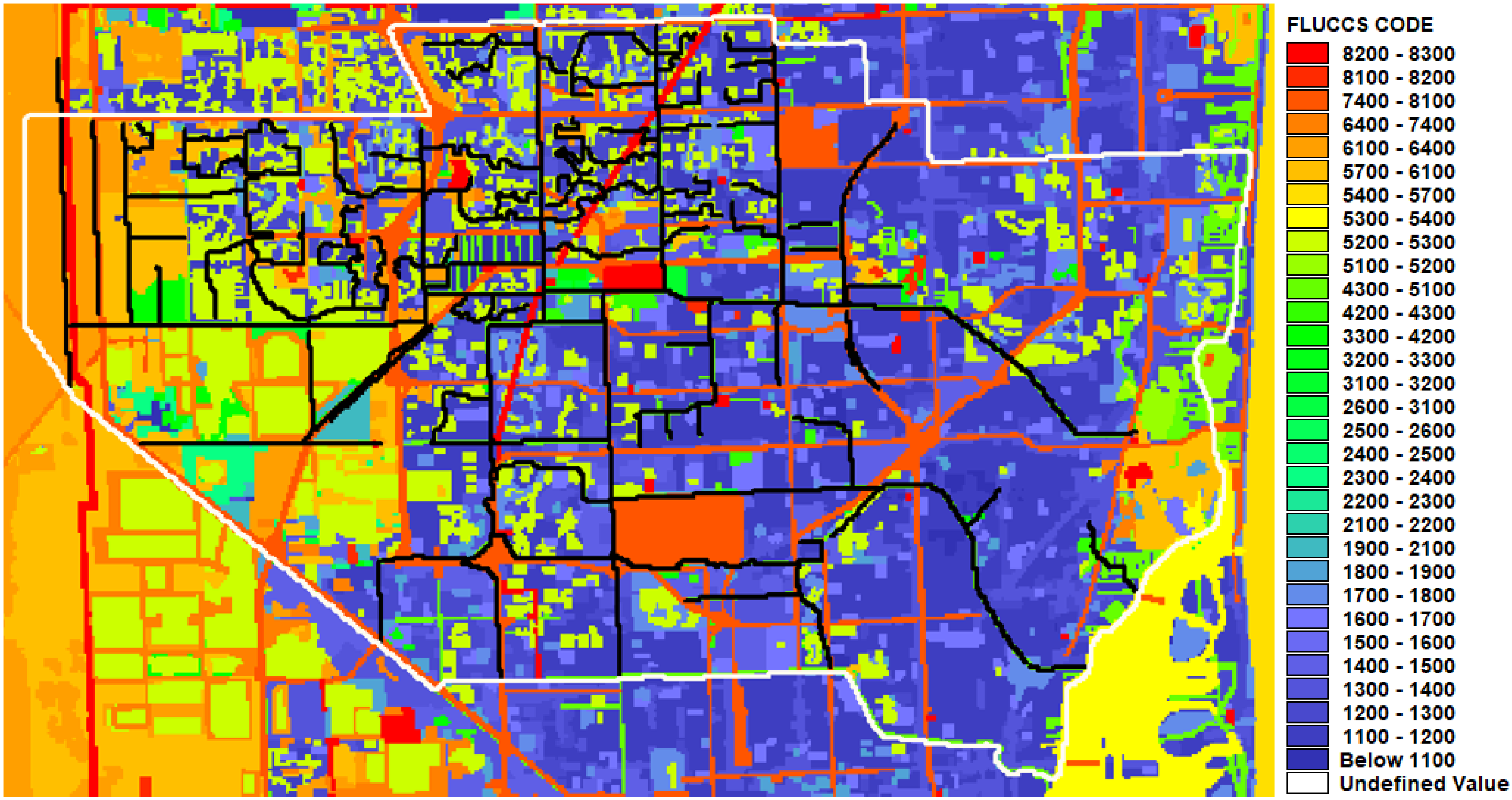

Figure 3.5-1: Land Use/Vegetation by FLUCCS Code

3.6 Rivers and Lakes (1D Model)

The 1D model was developed using MIKE HYDRO. The 1D network in the C-9 basin was mainly based on the 2019 Broward County Current Conditions model. The 1D network in the C-8 and C-7 basins were developed for this project. District, County, survey (Stoner and Associates, 2019), and South Broward Drainage District (SBDD) data were used when and where applicable and available. Additional survey (BDH Consulting Group, 2019) was completed for this project. The data used and parameterization of the river network are discussed in the following subsections.

3.6.1 1D River Network

The 1D river network is composed of 95 branches, 93 of which could be considered secondary or tertiary systems. The purpose of this study is to determine the flood protection level of service for the C-8 and C-9 Canals. Although the focus of this study is on the two primary canals, C-8 and C-9, a high level of detail was placed on the secondary/tertiary canal systems, as they are both a major source of discharge into the primary system and storage prior to discharging into the primary system. Many of the secondary/tertiary canal systems were setup to simulate the connectivity between lakes and other discontinuous (from DEM) water bodies, which are connected through a series of hydraulic structures. Water bodies that are not explicitly represented via a branch may still be connected to the 1D river network through the use of flood codes, which is discussed in section **3.6.3.1.**

3.6.1.1 <u>Hydraulic Control Structures</u>

The 1D network is controlled through a series of culverts, weirs, gates, and pumps. Specifically, there are 309 culverts, 8 weirs, 8 gated structures, and 8 pump stations. There are also 46 bridges explicitly modeled, which may control flow if they become submerged. The data for these structures came from a variety of sources, including South Broward Drainage District's Facilities Report, Miami-Dade Stormwater Geodatabase, SFWMD Operations Control Center Structure Books, SFWMD Flow Rating Analysis reports, SFWMD XP SWMM models, and professional survey. In areas where specific data was unavailable, an approximation was made. Specifically, South Broward Drainage District's (SBDD) Facilities Report lacked invert elevations for approximately 200 of the culverts included in the model, therefore, an approximation was made by matching the top of the culvert with the water control elevation, with respect to the specific drainage basin, as suggested by SBDD (Email provided in **Appendix A**)

There are four SFWMD control structures within the C-8 and C-9 basins (S-28, S-29, S-30, and S-32), and two outside the basins (S-9XS and G-58). S-9XS was used for boundary conditions on the L-33 Canal and G-58 controls Arch Creek. The four SFWMD control structures within the basins were represented as sluice gates. This was done so that the District's flow rating parameters could be incorporated, which provide the closest model calculation representation of the actual stage-discharge relationship of the structures as it uses the same set of equations.

3.6.1.2 <u>Cross Sections</u>

The availability of cross section data was limited to mainly the Miami-Dade portion of the model domain. Both the Miami-Dade County GIS Geodatabase as well as the SFWMD XP SWMM C-7, C-8, and C-9 models had cross section data for branches within Miami-Dade County. Cross sections for the C-9 Canal were available from both survey data and the C-9 XP SWMM model. For many secondary/tertiary canals in

Broward County, cross section data was essentially nonexistent. Therefore, the secondary/tertiary system cross sections within the Broward County portion of the model was carried over from the 2019 Broward County Current Conditions Model, which are mainly estimates based on the DEM. Most of the secondary/tertiary canal cross sections in the Broward County portion of the model were cut using the latest available 5-ft DEM (a composite DEM made by Geosyntec consultants, as discussed in **Section 2.1**). This means that the DEM was used for cross section elevation and geometry, from bank to the water surface. An assumed geometry was used below the water surface (**Figure 3.6-1**), typically, from the last bank point down to an elevation of -2/-3 was assumed to have a side slope of 4(h):1(v), and then a side slope of 2:1 from -2/-3 ft to -8 ft. The water surface elevation varied across the model domain due to water control elevation differences, so the channel geometry may appear different for the "cut" cross sections. It is important to note that "cut" cross sections from the DEM were not used to "cut" cross sections for C-8 and C-9 Canal. The DEM was only used for C-8 and C-9 Canals to extend the channel banks as needed. Additional cross section data for this project was collected via professional survey.

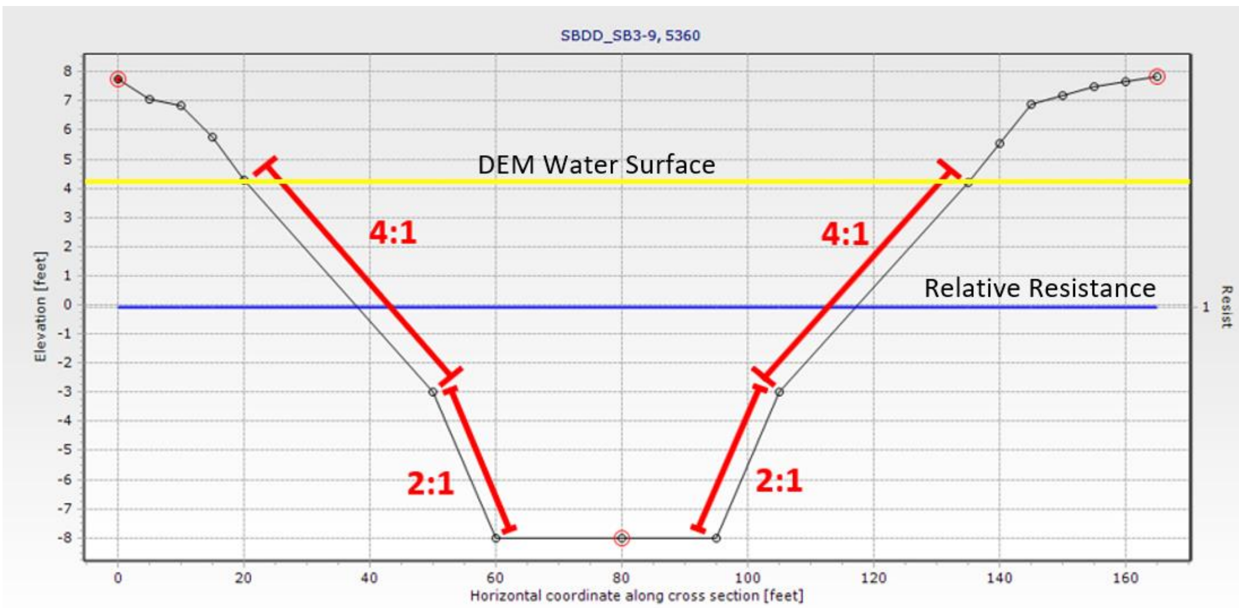

Figure 3.6-1: Example of a "Cut" Cross Section from DEM

3.6.1.3 Survey Data

Survey for this project focused on areas with little or no available data. Refer to **Figure 2.4-1** for a map of the surveyed items collected as a part of this project. These items were incorporated into the 1D model.

3.6.2 Canal-Aquifer Interactions

The 1D river network is coupled with the 2D groundwater model by MIKE SHE couplings. Essentially, at each grid cell along either side of a river branch, the exchange is calculated by multiplying the head difference between the grid cell (groundwater level in the cell(s) adjacent to the river link) and the river with the conductance. The model calculates the conductance based on the options assigned. For each branch or branch segment in the model, 1 of 3 conductance options were chosen, either (1) aquifer + riverbed, (2) aquifer only, or (3) riverbed only. These options change the way the model calculates the exchange between the groundwater and the river, where the aquifer conductance depends on the horizontal hydraulic conductivity and the riverbed conductance depends on an assigned leakage coefficient. Only aquifer + riverbed and riverbed only were used. A leakage coefficient of 1E-5/s was assigned (the model default value) for all branches, with a few localized adjustments made during model calibration.

3.6.3 Canal-Overland Flow Interactions

The 1D river network is coupled with the 2D overland flow model by MIKE SHE couplings. In this model, both coupling options were used, which are (1) flood codes and (2) overbank spilling. These options are discussed in the following two subsections.

3.6.3.1 Flood Codes

On secondary and tertiary canals, flood codes are used to allow communication between MIKE HYDRO and MIKE SHE when water levels in MIKE HYDRO exceed the adjacent floodplain elevations. Flood codes also allow MIKE SHE to communicate directly with MIKE HYDRO whenever the water elevation of flood code cells exceed the water elevation in the river branch, as long as the water elevation in the branch is higher than the grid cell's topographic elevation. Flood codes were also used in areas where direct connections were not explicitly represented, such as ponds or lakes within proximity of a river branch, or water bodies that become disconnected in the DEM. An example of flood code placement is shown in the following figure. It is important to note that the specific value of the flood code is not important, it is just a unique identifier.

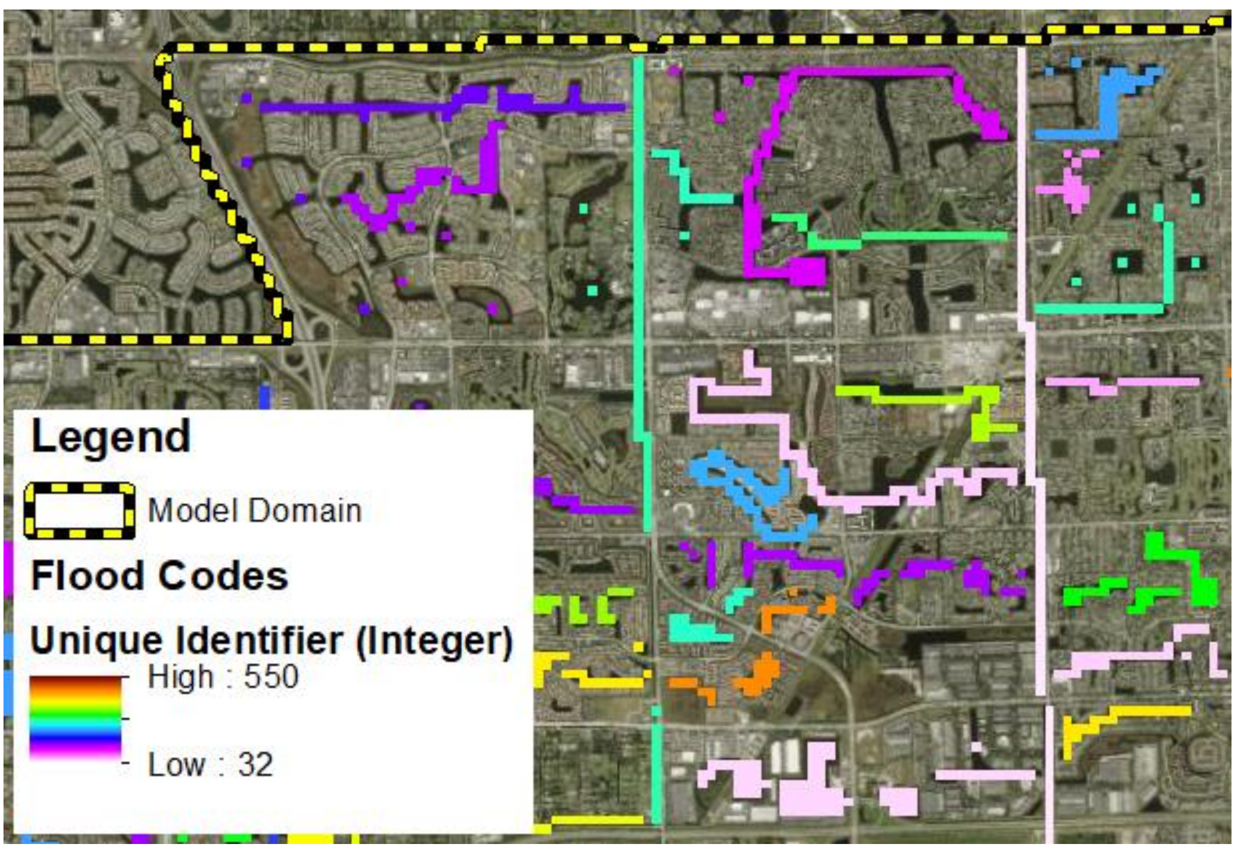

Figure 3.6-2: Example of Flood Code Placement

Flood code cells are excluded from 2D overland flow computations, so it is important to place them wisely, such as the lowest cell in an area. Covering an entire lake with flood code cells would turn off the overland computations for the entire lake. Therefore, the only time entire water features were covered with flood codes was when the storage was accounted for in the 1D model, such as a branch going through a lake (the lake water levels are computed in the 1-D model and the cross sections extend to the edges of the lake). Flood codes along secondary and tertiary canals are generally limited to one cell along each bank.

The detailed surface topography provided an opportunity to take advantage of the flood code feature and account for storage that would otherwise be lost in a larger resolution topographic map. The flood code setup is shown in **Figure 3.6-3**. Although the specific value of the flood code does not matter, as they are just an identifier that relate a cell to a specific branch, the flood code values in the C-9 basin were kept the same as the 2019 Broward County Model for consistency. New flood code areas were assigned identifiers not used in the 2019 Broward County model, which should eliminate any issues in the future if the models are merged.

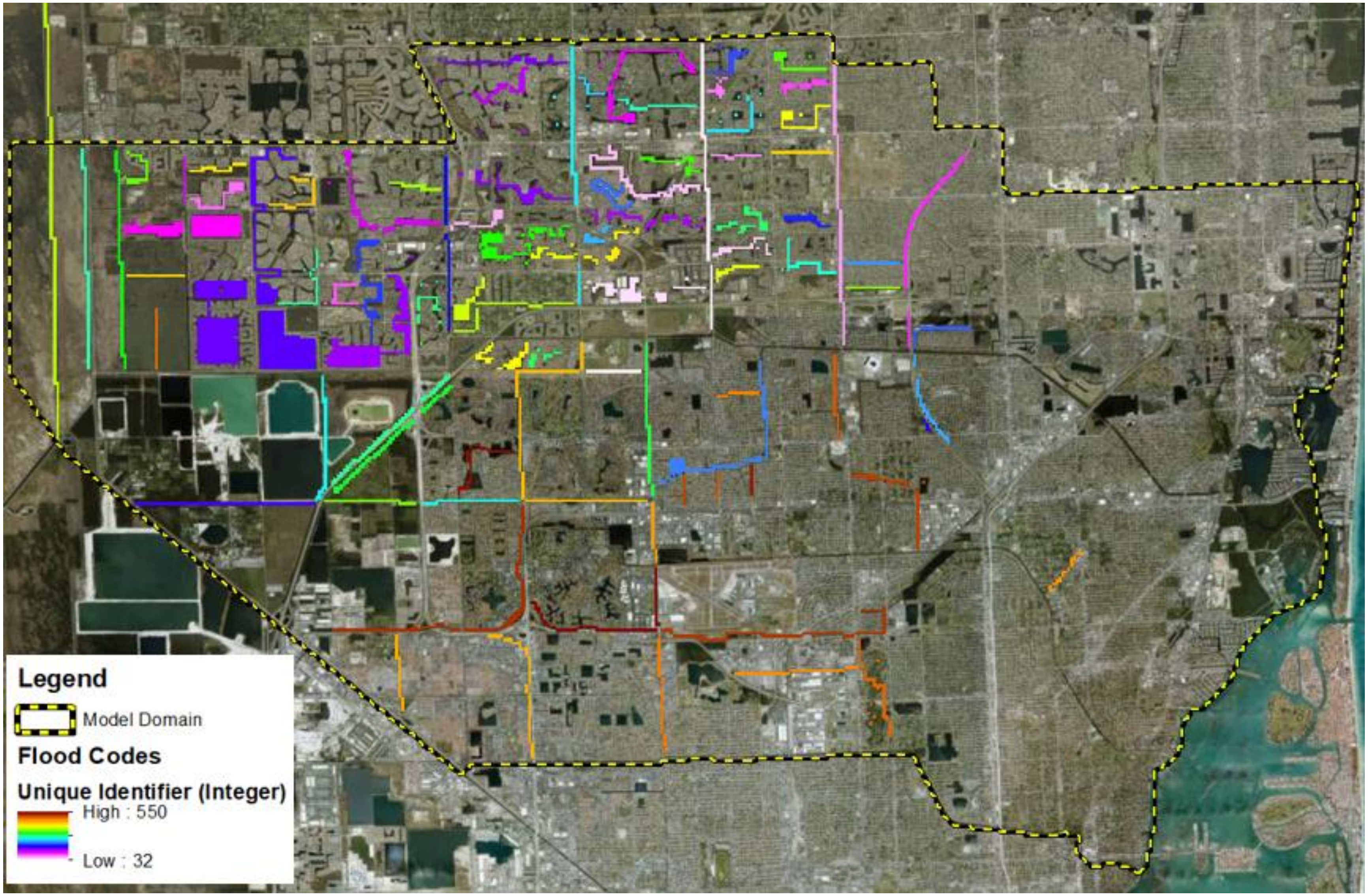

Figure 3.6-3: Map of Flood Codes (Specific Values do not Matter- Unique Identifiers)

3.6.3.2 Overbank Spilling

The C-8 and C-9 primary canals rely on overbank spilling instead of flood codes, which allows communication between MIKE SHE and MIKE HYDRO via the weir equation, whenever the water level in the canals become greater than the cross-section bank elevations. Overbank spilling is based on the cross section and the 2D grid, whichever is higher. In most instances, the berms are not represented well in the 125 ft or 250 ft topography grid, as median values are used. Therefore, the berm elevations should be and were included in the cross sections. In instances where the 2D grid is higher than the cross section, the water will “glass wall” in the cross section until it reaches the 2D grid elevation. Overbank spilling provides a more physically based representation of the exchange between canal and 2D grid, which is more important on the C-8 and C-9 canal than the secondary and tertiary canal system as they are the focus of this FPLOS project. Therefore C-8 and C-9 will only spill out to the 2D model when water levels get above bank elevations, whereas branches with flood codes may exchange whenever the water level in the canal is greater than the water level on the 2D grid (ignores bank elevations- assumes it has connectivity such as culverts). For numerical stability purposes, some secondary canal segments within close proximity of the primary canals were switched to overbank spilling.

3.6.4 Hydrodynamic Initial Conditions

The 1D model’s initial water levels were set based on two different categories, which are (1) based on observed data and (2) based on control elevations. In areas where there is observed data, such as water elevation upstream of the C-8 and C-9 tidal structures for calibration and validation simulations, the initial conditions are set to match the observed data. In areas that are controlled via operable control structures such as SBDD, the initial conditions were set to match the control elevation, which differ from the gate open or pump on elevations. This is consistent with the approach used in the 2019 Broward County Model. For the design storms, the 1D model’s initial water levels were set based on control elevations.

3.6.5 Boundary Conditions (1D Model)

3.6.5.1 Calibration / Validation Model

On the west side of the model, the boundary structures (S-9XS and S-32) were assigned a time varying water level boundary based on observed stage data obtained from the District. On the east side of the model, the tailwater stage at the primary canal outfall structures were forced as a user-specified boundary condition based on observed data obtained from the District. At the intercoastal waterway, water levels were forced based on the Virginia Key tide station. On the south side of the model, water levels were forced at the downstream boundary of the 1-D branches connecting to the C-6 and C-7 Canals based on observed data obtained from the District.

3.6.5.2 Design Storm Model

On the west side of the model, the boundary structures (S-9XS and S-32) have a time varying water level boundary based on simulated design storms from other models (2019 Broward County MIKE SHE / MIKE HYDRO model for S-9XS and C-6 XP SWMM for S-32). On the east side of the model, the tailwater stage at the primary canal outfall structures were forced as a user-specified boundary condition based on District provided year 2015 tidal boundary data at the S-28 and S-29 structures, which include storm surge effects for the design storms of interest. The dates of the District provided time series data were relative for the purposes of design storms. Therefore, for each boundary condition using SFWMD provided data, the dates were adjusted so that the peak stages occur at the same time as the peak rainfall, as agreed upon with the District. The 1D tidal boundaries, which force the tailwater at structures S-28, S-29, and G-58, were set up to use the SFWMD provided design storm stages. G-58 was assigned the same tidal data as structure S-28. The design storm tidal boundaries for current sea level (CSL) are shown in the following two figures.

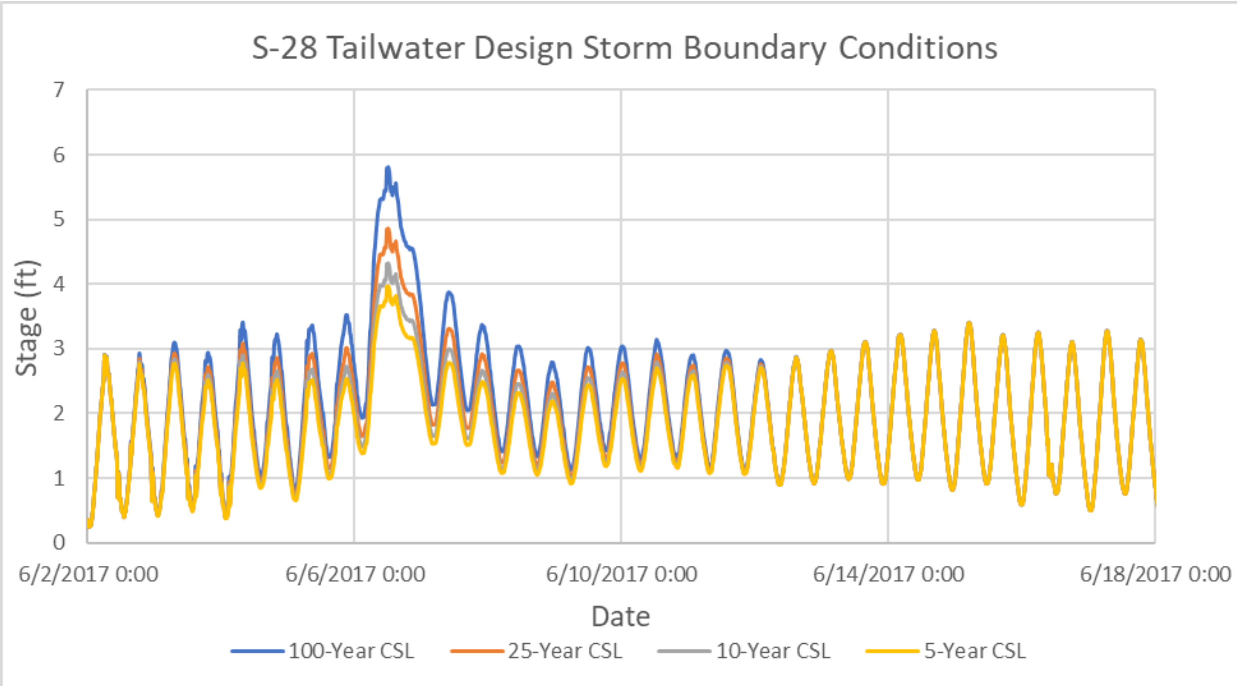

Figure 3.6-4: Design Storm Current Sea Level Tidal Boundary Stages for S-28

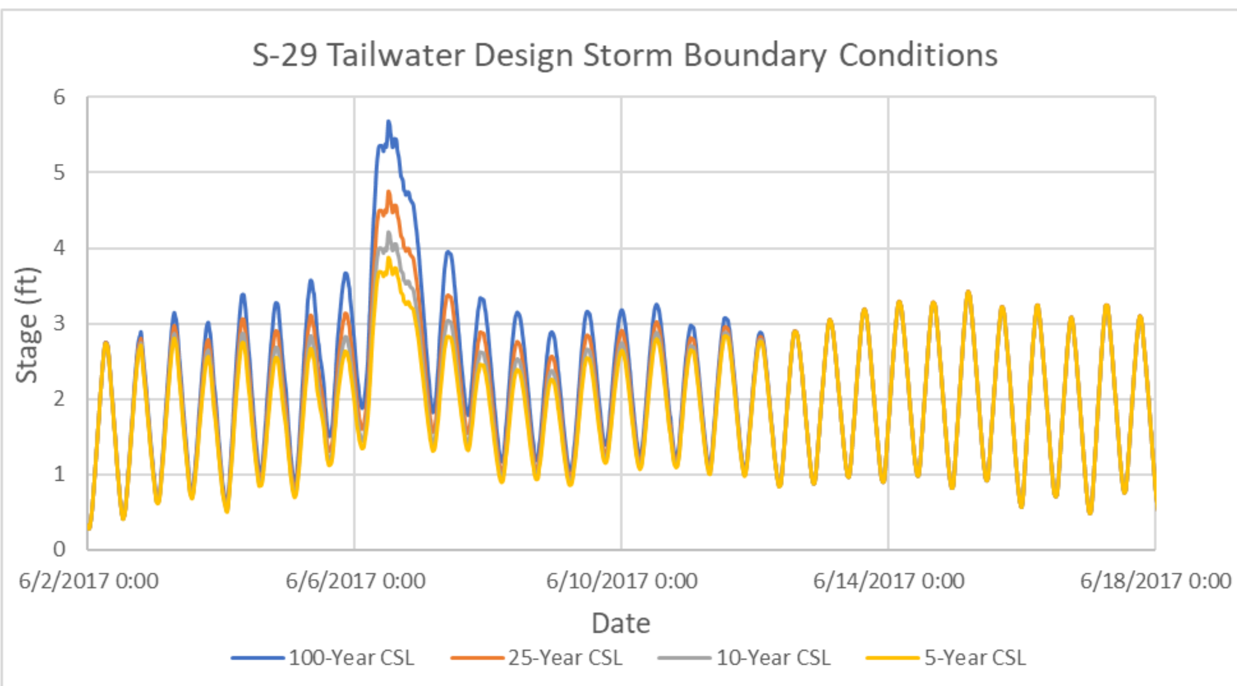

Figure 3.6-5: Design Storm Current Sea Level Tidal Boundary Stages for S-29

At the intercoastal waterway, water levels were forced based on the District-provided storm stage time series data. On the south side of the model, water levels were forced at the downstream boundary of the 1-D branches connecting to the C-6 and C-7 Canals based on simulated design storm data obtained from the District (XP SWMM and HEC-RAS models).

3.7 Overland Flow

The overland flow module, or 2D model, is essentially parameterized by district drainage basins. The C-9 basin, which mainly lies within Broward County, was parameterized to be consistent with the 2019 Broward County model, which was based on two major categories: (1) land use and (2) ERP permitted areas. The C-8 Basin, which is in Miami-Dade County, was parameterized in a similar way but based on different data. This is explained in the following subsections.

3.7.1 Overland Flow in Broward County

Most of the parameters in the overland flow model are spatially varied by land use, while other parameters are spatially varied by land use within ERP permitted areas. A large portion of Broward County is made up of permitted areas that are required to retain some volume of rainfall, whether it be the first 1-inch of rainfall or 2.5-inches over the impervious area, or a more stringent requirement to retain the runoff resulting from the 25-year 3-day storm, with no discharge. For the 2019 Broward County model, Taylor Engineering proposed to separate the permitted areas into the following categories: (1) areas controlled by operable structures such as pumps or gates, (2) areas that had at least 10% waterbody land coverage such as lakes or ponds, (3a) areas with less than 10% waterbody land coverage and have at least 2.5 feet depth to water table, and (3b) areas with less than 10% waterbody land coverage and have less than 2.5 feet depth to water table. Depth to groundwater was estimated by subtracting the initial groundwater elevation from the topography elevation. The assumption behind this is that areas with an initial depth to groundwater greater than 2.5-feet would have the ability to infiltrate more rainfall than areas with less than 2.5-feet. This was the assumed threshold for where exfiltration areas would likely be located. It is important to note that this assumption does not in any way affect the actual infiltration ability of the model, it was just a way to select which areas to parameterize to account for what cannot be explicitly modeled.

Permit areas classified as category 1, those behind operable structures, were parameterized just based on land use, as if they were unpermitted. Flow to the canal network from these areas is controlled by operable structures (gates and pumps), which are designed to limit discharge to permitted values and at permitted threshold water levels. Therefore, runoff rates within the respective drainage areas are ultimately limited by the operable structure. Although there may in fact be permitted areas within an overall drainage area that are held to a higher level of stormwater retention, for the purposes of this sub-regional scale model, if the operable structure is within its permitted allowance than it can be assumed that so are the areas draining to it. These areas classified as category 1 are controlled by permitted pumps and gates, that retain water on-site until the water levels reach the permitted discharge elevation, which means they often have a large amount of “dead storage” or on-site retention. Permit areas classified as category 2, those with at least 10% waterbody land coverage, were parameterized to account for the required detention storage, potential surface water storage, and sub-grid scale drainage features. Permit areas classified as category 3a, those with less than 10% waterbody land coverage and on average more than 2.5 feet depth to water table, were parameterized to account for the required detention storage and the likelihood of exfiltration trenches and other stormwater management features. Permit areas classified as category 3b, those with less than 10% waterbody land coverage and on average less than 2.5 feet depth to water table, would have been parameterized to only account for the required on-site retention. There are currently no category 3b areas within the C-9 basin. **Table 3-5** shows the criteria used to develop these stormwater management categories and the parameterization changes applied to these areas. It is important to note that these categories are unofficial and were developed to simplify the ERPs. A map of these stormwater management categories (SMC) developed by Taylor Engineering is shown in **Figure 3.7-1**.

Table 3-5: SMC Criteria and Parametrization within Broward County

Stormwater Management Category	Criteria	Parametrization
1	-Located in Broward County -Controlled by pump/gate	No change- only parameterized based on land use
2	-Located in Broward County -Greater than 10% water cover	- Increased detention storage based on 1" of the entire area or 2.5"x impervious area (whichever is greater) -Maximum storage change rate based on SFWMD CSM rating
3a	-Located in Broward County -Less than 10% water cover and greater than 2.5 feet depth to water table	-Increased detention storage based on 1" of the entire area or 2.5"x impervious area (whichever is greater) -paved runoff coefficient decreased by 50%

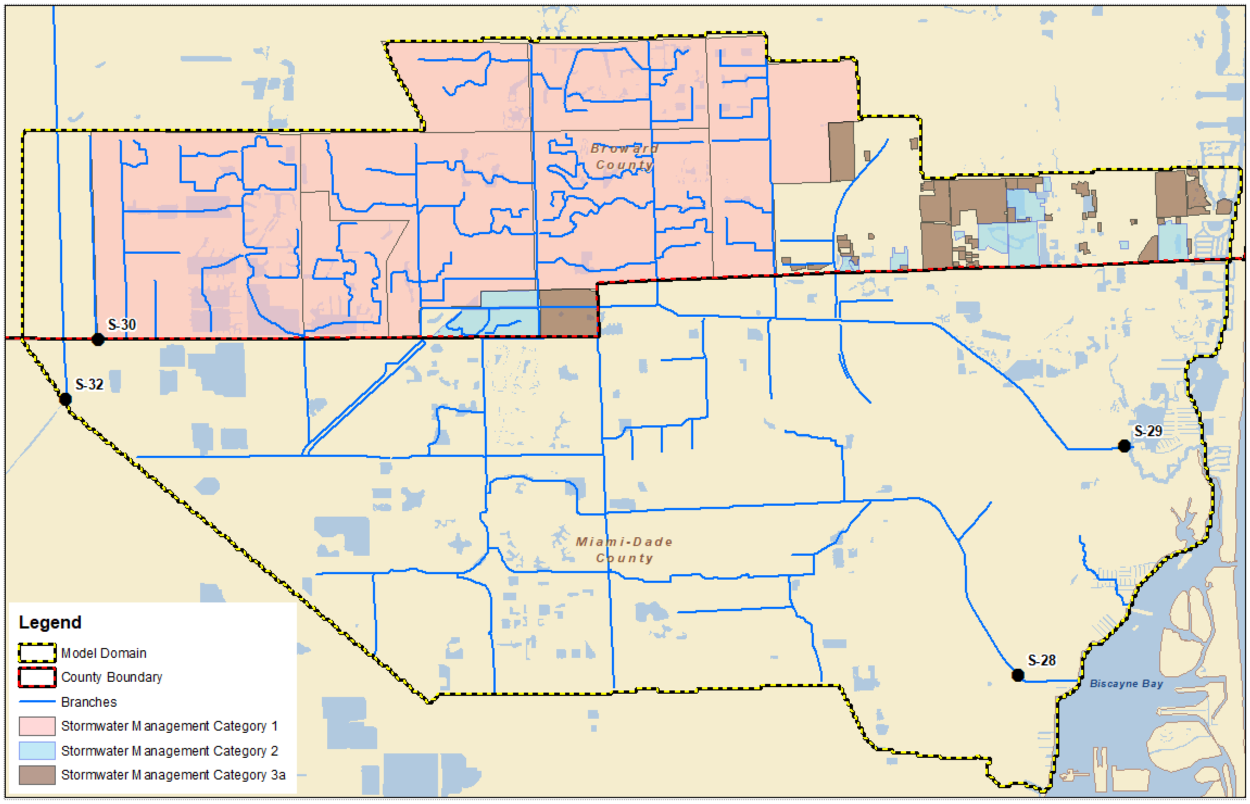

Figure 3.7-1: SMCs Used to Parameterize Overland Flow in Broward County

3.7.2 Overland Flow in Miami-Dade County

Within the Miami-Dade portion of the model, most of the parameters in the overland flow model are spatially varied by land use, while other parameters are spatially varied by land use within areas that are internally drained. Several areas within the C-8 drainage basin are either internally drained or have a large network of French drains, both of which reduce the amount of runoff making its way to the C-8 and C-9 Canals. Although the capacity of the French drain systems in Miami-Dade County was unknown, they were designed to retain/infiltrate some volume of rainfall before discharging into the canal system. Taylor Engineering proposed to the District to separate drainage areas into the following categories: (5) areas draining directly to MIKE Hydro branches, (6) areas internally drained or that have a large amount of French drains relative to area served, and (7) areas both draining to branches and having French drains.

Areas classified as category 5, those draining to a branch, were parameterized just based on land use. Areas classified as category 6, those internally drained or have a large amount of French drains, were parameterized by land use and adjusted to account for features that route and store water within the drainage basin. Areas classified as category 7, were parameterized by land use and adjusted to account for potential water storage and sub-grid scale drainage features like exfiltration trenches and other stormwater management features. Although based on different criteria, these categories are similar to the stormwater management categories developed for the 2019 Broward County model. **Table 3-6** shows the criteria used to develop these stormwater management categories and the parameterization changes applied to these areas. It is important to note that these categories are unofficial and were developed to simplify French drains and areas internally drained. A map of these stormwater management categories (SMC) developed by Taylor Engineering is shown in **Figure 3.7-2**.

Table 3-6: SMC Criteria and Parametrization within Miami-Dade County

Stormwater Management Category	Criteria	Parametrization
5	-Located in Miami-Dade County -Drains directly to canal	No change- only parameterized based on land use
6	- Located in Miami-Dade County -Internally drained or has a large amount of French drains	-Increased detention storage based on 1" over entire area or 2.5"x impervious area (whichever is greater) -Paved runoff coefficient decreased by 50% -not allowed to drain directly to canal
7	-Located in Miami-Dade County -Drains directly to canal AND has a large amount of French Drains	-Increased detention storage based on 1" over entire area or 2.5"x impervious area (whichever is greater) -Paved runoff coefficient decreased by 50% -allowed to drain directly to canal

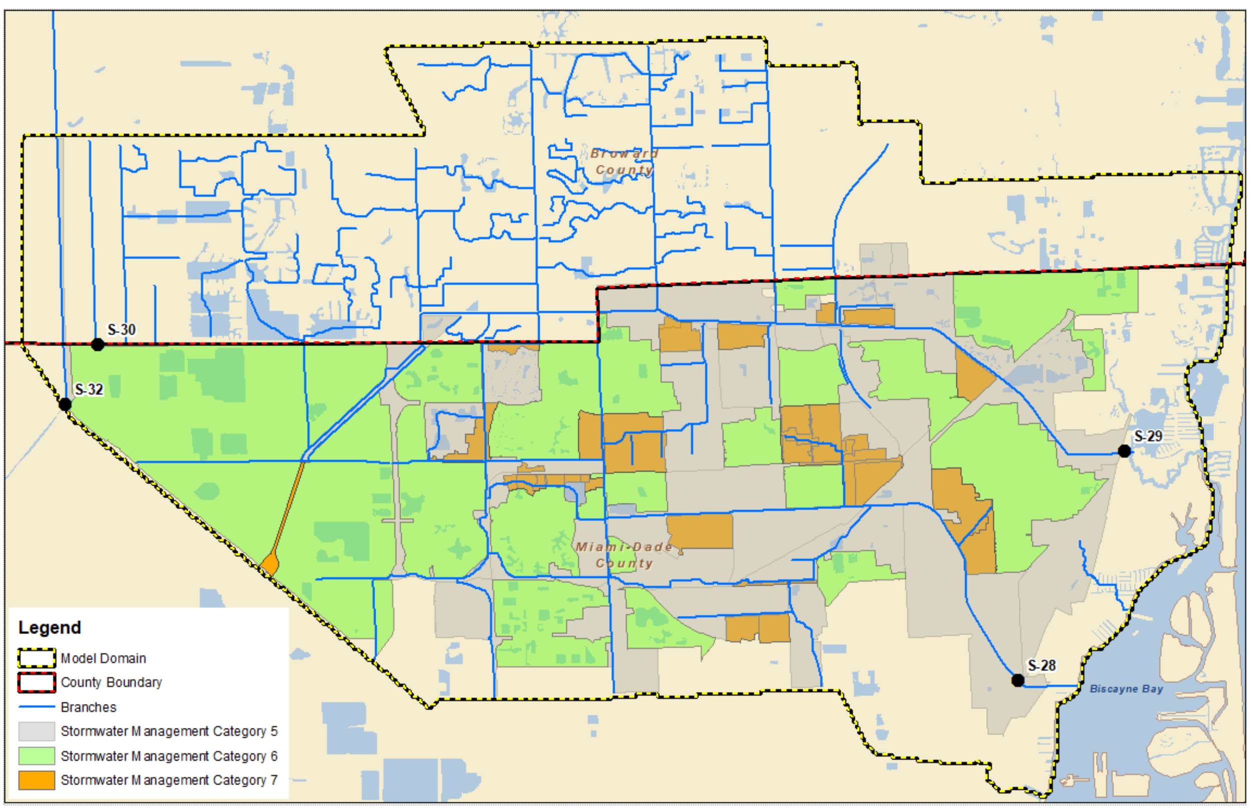

Figure 3.7-2: SMCs Used to Parameterize Overland Flow in Miami-Dade County

As shown in **Figure 3.7-3**, the areas in green are assumed to be internally drained for the purpose of parameterizing the ponded and saturated zone drainage routines. These areas either drain to local water bodies or have a large amount of French drains. However, it is important to note that runoff from these areas can still reach the MIKE Hydro branches via the 2-D overland flow module. The areas in yellow are areas that drain to branches, however, several areas in yellow also have a large amount of French drains, as shown by the red lines. The areas in yellow that have little to no French drains are considered category 5, areas that are green are considered category 6, and areas in yellow that have a large amount of French drains are considered category 7. The area in purple drains to the boundary, so the specific overland flow parameterization is less likely to affect the model results and were only parameterized based on land use.

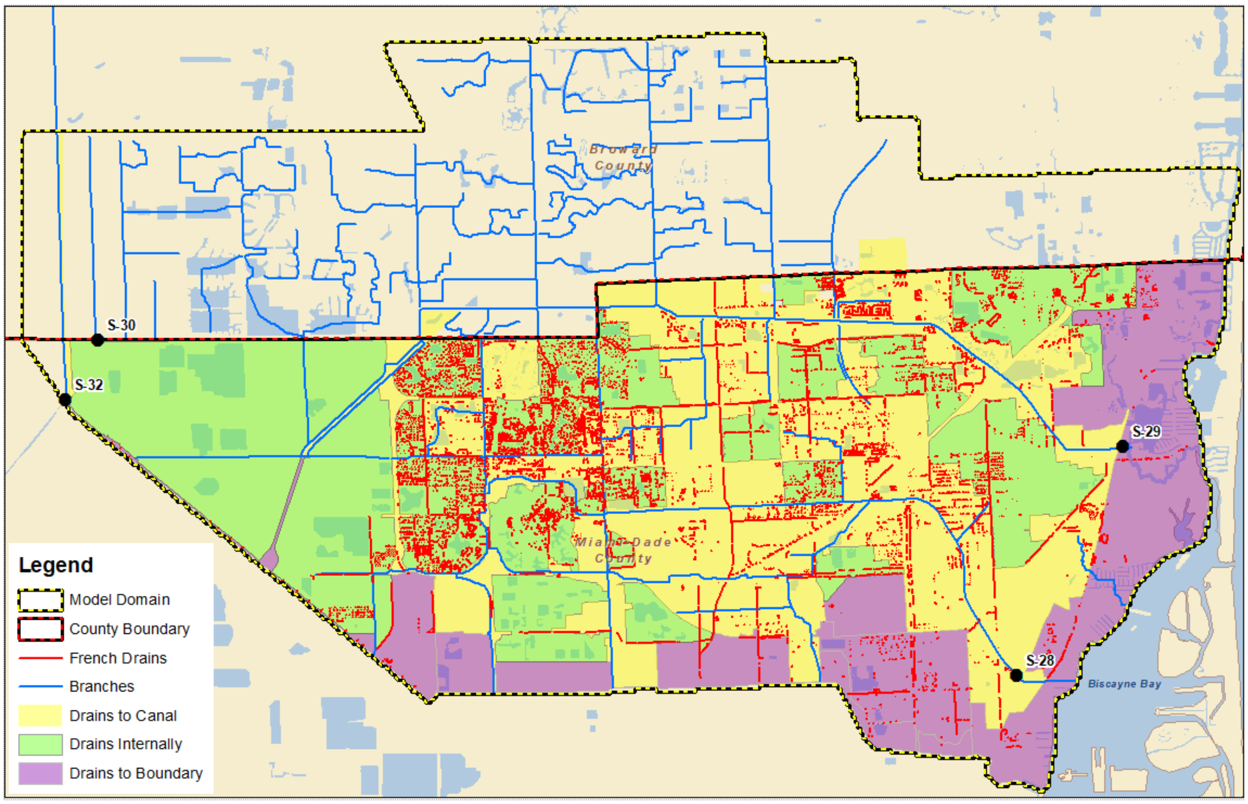

Figure 3.7-3: Drainage Categories in the Miami-Dade Portion of the Model Domain

3.7.3 Overland Manning's Roughness Coefficient

This parameter, used in the MIKE SHE 2-D overland flow component, is spatially distributed based on land use, with values ranging from 0.06 to 0.45, based previous models, literature (Environmental Protection Agency, 2015), and professional experience. Table 3-7 provides FLUCCS Code based Manning's roughness coefficients. Please note that Manning's "M" is equal to 1/n.

Table 3-7: Land Use Based Manning's Roughness Coefficients

FLUCCS Code	Land Use	Manning's Roughness (n)	Manning's Roughness (M)
1100	Residential, Low Density	0.14	7.14
1200	Residential, Medium Density	0.12	8.33
1300	Residential, High Density	0.11	9.09
1400	Commercial and Services	0.07	14.29
1500	Industrial	0.07	14.29
1700	Institutional	0.13	7.69
1800	Recreational	0.13	7.69
1900	Open Land	0.14	7.14
2100	Cropland and Pastureland	0.17	5.88
2200	Tree Crops	0.17	5.88
2300	Feeding Operations	0.17	5.88
2400	Nurseries and Vineyards	0.17	5.88
2500	Specialty Farms	0.17	5.88
2600	Other Open Lands - Rural	0.14	7.14
3100	Herbaceous (Dry Prairie)	0.13	7.69
3200	Upland Shrub and Brushland	0.3	3.33
3300	Mixed Rangeland	0.3	3.33
4200	Upland Hardwood Forests	0.45	2.22
4300	Upland Mixed Forests	0.45	2.22
5100	Streams and Waterways	0.06	16.67
5200	Lakes	0.06	16.67
5300	Reservoirs	0.06	16.67
5400	Bays and Estuaries	0.06	16.67
5700	Ocean and Gulf	0.06	16.67
6100	Wetland Hardwood Forests	0.45	2.22
6400	Vegetated Non-Forested Wetlands	0.3	3.33
7400	Disturbed Land	0.14	7.14
8100	Transportation	0.11	9.09
8200	Communications	0.14	7.14
8300	Utilities	0.14	7.14

3.7.4 Detention Storage

This parameter is spatially distributed, based on both land use and the categories defined for Broward County and Miami-Dade County. Within Broward County, the non-permitted area's detention storage was spatially distributed based on land use with values ranging from 0 to 0.4 inches, as shown in **Table 3-8.**

Table 3-8: Land Use Based Detention Storage

FLUCCS Code	Land Use	Detention Storage (in)	Runoff Coefficient	"Permit Based" Detention Storage (in)
1100	Residential, Low Density	0.1	0.075	1
1200	Residential, Medium Density	0.1	0.22	1
1300	Residential, High Density	0.1	0.45	1.125
1400	Commercial and Services	0.1	0.72	1.8
1500	Industrial	0.1	0.4	1
1700	Institutional	0.1	0.3	1
1800	Recreational	0.3	0	No Change
1900	Open Land	0.15	0	No Change
2100	Cropland and Pastureland	0.15	0	No Change
2200	Tree Crops	0.25	0	No Change
2300	Feeding Operations	0.25	0	No Change
2400	Nurseries and Vineyards	0.25	0	No Change
2500	Specialty Farms	0.25	0	No Change
2600	Other Open Lands - Rural	0.15	0	No Change
3100	Herbaceous (Dry Prairie)	0.15	0	No Change
3200	Upland Shrub and Brushland	0.15	0	No Change
3300	Mixed Rangeland	0.15	0	No Change
4200	Upland Hardwood Forests	0.4	0	No Change
4300	Upland Mixed Forests	0.4	0	No Change
5100	Streams and Waterways	0	0	No Change
5200	Lakes	0	0	No Change
5300	Reservoirs	0	0	No Change
5400	Bays and Estuaries	0	0	No Change
5700	Ocean and Gulf	0	0	No Change
6100	Wetland Hardwood Forests	0.4	0	No Change
6400	Vegetated Non-Forested Wetlands	0.4	0	No Change
7400	Disturbed Land	0.1	0	No Change
8100	Transportation	0.1	0.56	1.4
8200	Communications	0.1	0	No Change
8300	Utilities	0.1	0	No Change

No change implies that the detention storage is based on land use

Even at a fine grid size of 125-ft, not all storage can be accounted for. This detention storage represents microtopography not represented in the DEM, such as potholes, bird baths, pools, street-side swales, etc. First, detention storage values of 0.1"-0.4" (based on previous models, professional experience, and literature) were applied model-wide to account for sub-grid scale storage features. In areas controlled by operable control structures (SMC 1), such as SBDD, no additional changes to detention storage were made. In the remaining permitted areas or French drain areas, detention storage was increased to represent the small-scale on-site stormwater treatment or storage areas that are not explicitly modeled. This is expanded upon in the next few paragraphs.

In permitted areas within Broward County, the detention storage was spatially distributed by land use, but adjusted to account for the required retention. The permitted areas fall under an ordinance requiring retention of the 1st 1-inch of rainfall over the entire area or 2.5-inches of rainfall over the impervious area, whichever is greater. Within the permitted areas, the detention storage for impervious areas were increased by multiplying the directly connected impervious area (DCIA, defined by the paved area runoff coefficients discussed in **Section 3.7.7**) by 2.5 inches, and any of the resulting values less than 1” was increased to 1”. Therefore, within category 2, and 3a permitted areas, the detention storage increased from 0.1-0.4 inches to 1-1.8 inches, dependent on the land use (**Table 3-8**). This helps represent the on-site retention that permitted areas are required to have.

Within the Miami-Dade County portion of the model domain, the drainage categories were treated in a similar way to the permitted areas within Broward County. In stormwater management category 5 areas, those that drain to a canal and have little to no French drains, the detention storage was treated the same as non-permitted areas in Broward County and only parameterized based on land use, with values ranging from 0-0.4 inches (**Table 3-8**). In stormwater management category 6 areas, those that are internally drained to water bodies or low areas or have a large amount of French drains, the detention storage was treated the same as permitted areas in Broward County and parameterized basin on land use and adjusted to account for retention. Although these areas are forced to drain to local depressions within the ponded drainage routine, the detention storage was increased to hold that drained water on site, representing the internal storage of local depressions and exfiltration areas. Otherwise, ponded water above the detention storage can still flow via the 2D overland flow routine into other drainage areas and then be routed to a branch. These category 6 areas were adjusted from 0.1-0.4 inches to 1-1.8 inches, based on land use. In drainage category 7 areas, those that drain to a canal and have a relatively large amount of French drains, the detention storage was treated the same as permitted areas in Broward County and parameterized basin on land use and adjusted to account for retention provided by exfiltration areas, with values being increased from 0.1-0.4 inches to 1-1.8 inches. Category 7 areas differ from category 6 areas as they can drain to a branch within the ponded drainage routine, after the detention storage has been met. These values for stormwater management categories 6 and 7 areas were an initial model parameterization subject to change during model calibration but was not required.

3.7.5 Initial Water Depth (2D Overland Model)

The initial water depth defines the initial water depth on the ground surface in the 2-D overland module, also known as ponded water. This parameter was developed using an approach based on topography and basin control elevation, which is consistent with the 2019 Broward County model. Any cells within a drainage basin that are lower than the basin’s water control elevation have an initial depth equal to the difference of the water control elevation and the elevation of the cell. This eliminates excess “dead storage” and ensures that water is not being routed via ponded drainage or flood codes at the start of the simulation. Specifying an initial depth will result in ponded water, which will eliminate the “dead storage” associated with a local sink. This also provides consistency between 1D and 2D model initial water elevations. The initial water depths for the 2D model are shown in **Figure 3.7-4.**

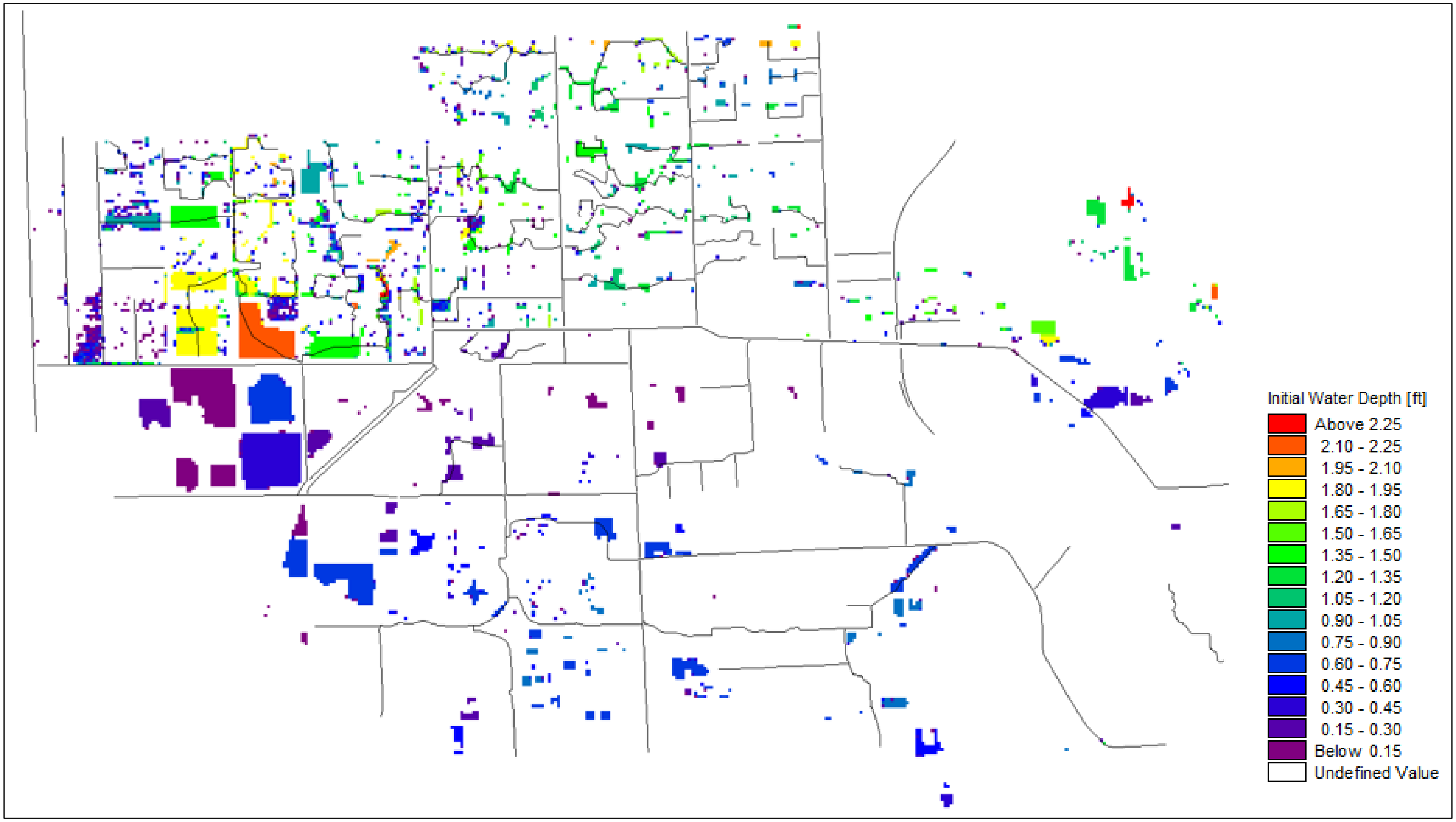

Figure 3.7-4: Initial Water Depths in the 2D Overland Flow Model

3.7.6 Surface-Subsurface Leakage Coefficient

This parameter reduces the exchange between land surface and the unsaturated or saturated zone, which can help account for near-surface soil compaction or fine sediment deposits. The model can be very sensitive to this parameter; too small of a value can essentially act as if there is an impermeable layer and allow for little to no infiltration. The leakage coefficient was set to a uniform spatial distribution using the model default value of 1E-4. No permanent changes to spatial distribution or magnitude were made during model calibration.

3.7.7 Ponded Drainage

This is a relatively new feature introduced in the 2017 release of MIKE SHE that simulates routing of ponded water from impervious surfaces via features that are not explicitly modeled, such as curb inlets and local-scale storm drains. The ponded drainage routine routes runoff from directly connected impervious areas (DCIA) to canals based on user-specified drainage basins (subbasins). The volume that is allowed to be routed is determined by a paved area runoff coefficient, which was assigned based on land use, and a maximum storage change rate. The rate at which the volume is routed is controlled by time constants. These parameters are discussed in the following subsections.

3.7.7.1 <u>Maximum Storage Change Rate</u>

For this study, the maximum storage change rate was set to a uniform spatial distribution with a value of 0.095 ft3/s (each grid cell limited to 40 mm/day), and then adjusted in specific areas where there was evidence suggesting a different value. Choosing realistic values ensures proper drainage representation and prevents drainage rates from exceeding sub-grid scale drainage capacities. For example, if sub-grid scale drainage features such as roadside swales and culverts are designed to handle 5-inches of rainfall over the course of a day, then the maximum storage rate should correspond. Within the Broward County portion of the model, the stormwater management category 2 area's maximum storage change rate was spatially distributed based on the permitted cubic feet per second per square mile (CSM) allowance per SFWMD drainage basin (**Appendix B**). In the western portion of the C-9 drainage basin, the allowable discharge is 20 CSM pumped, which is equivalent to 0.045 ft3/s based on the model grid size (each grid cell limited to 18.9 mm/day). This parameterization ensures that the permitted areas do not discharge more than their permitted allowance. Only category 2 permitted areas were based on the district's CSM allowance as these were the area's most likely holding water back in their surface waterbodies and discharging through structures at a permitted rate. Based on location, this 20 CSM pumped criteria only applies to 1 permit area in the western C-9 basin based on the way the stormwater management categories were developed. However, this 1 permit area happens to be explicitly simulated and is known to drain via gravity connection only, therefore, there were no areas where this 20 CSM pumped criteria applies. However, this categorization and criteria should be applied when considering future development and land use changes. It is important to note that this parameter is used to represent things not explicitly modeled. Therefore, areas such as the SBDD drainage basins were not included as they are physically represented by pump stations which follow permitted discharge rates.

The C-8 canal has "essentially unlimited inflow by gravity connection", so no restrictions were necessarily required. This parameter could have been restricted in category 7 areas during model calibration, to help reduce the volume of runoff making it to the branch (capacity of exfiltration areas unknown), but changes were deemed unnecessary. Similarly, the initial value of 0.095 ft3/s, which is equivalent to about 43 CSM, could have been increased for the C-8 basin during model calibration, but again was deemed unnecessary.

This parameter will only limit discharge in the ponded drainage routine, which is meant to represent sub-grid scale drainage features (e.g., local-scale storm drains). Therefore, this will limit the ponded drainage discharge during bigger storm events, but this is appropriate. If the local small-scale drainage features were only designed to handle a 25-year storm, then the discharge will be limited during a 100-year storm. This does not limit discharge by 2-D overland flow. This parameter only limits the ponded drainage discharge, which is only responsible for routing a portion of the runoff occurring over the paved area fraction (i.e., directly connected impervious).

3.7.7.2 Paved Runoff Coefficient

This parameter, similar to DCIA, is spatially distributed based on land use and stormwater management categories (SMC). Essentially, the paved runoff coefficient is the fraction of *ponded* water (not precipitation) that drains to storm sewers and other surface drainage features in paved areas (DHI, 2017). Within Broward County, the paved runoff coefficients were parameterized based on land use. In SMC 3a areas, the coefficients were distributed based on land use like everywhere else, but then decreased by half. Since these permitted areas are assumed to use management features such as exfiltration trenches, the paved runoff coefficients were adjusted to reduce the amount of runoff and increase the infiltration, as one would expect in areas served by exfiltration features. Within Miami-Dade County, the paved runoff coefficients were parameterized based on land use. In areas served by a relatively large amount of French drains, the coefficients were distributed based on land use, but then decreased by half, just like SMC 3a areas within Broward County. Decreasing the paved runoff coefficient reduces runoff which provides the opportunity for increased infiltration. This parameterization was done as an attempt to simulate what cannot be explicitly represented in this scale of a model. The land use areas that were included in the ponded drainage routine can be seen in **Table 3-9** . All other land use categories, such as forests, were set to 0, which “turns off” the ponded drainage routine for those areas. These paved runoff coefficients were derived from previous models and professional experience.

Table 3-9: Land Use Based Paved Runoff Coefficients

FLUCCS Code	Land Use	Paved Runoff Coefficient	Paved Runoff Coefficient for SMC 3a, 6, & 7 Areas
1100	Residential, Low Density	0.075	0.0375
1200	Residential, Medium Density	0.22	0.11
1300	Residential, High Density	0.45	0.225
1400	Commercial and Services	0.72	0.36
1500	Industrial	0.4	0.2
1700	Institutional	0.3	0.15
8100	Transportation	0.56	0.28

3.7.7.3 Inflow and Outflow Constant

These parameters can be adjusted to speed up or slow down the rate at which ponded drainage is routed to the river branches. Making the inflow constant larger than the outflow constant will create artificial storage, so this was avoided. An initial value of 0.001 (model default) was used as a starting point for both inflow and outflow constants. No permanent changes were made during model calibration.

3.7.7.4 Drain Codes

Each drain code represents an individual subbasin, for the purpose of draining water internally or to a branch via the ponded and saturated zone drain routines. It should be noted that these “subbasins” do not prevent overland exchange between areas. In areas of uncertainty, drainage basins were left as larger areas so that the 2-D overland flow model could determine drainage divides. Basins were only further refined if there was clear evidence in the DEM, such as visible berms or water bodies with differing elevations. In the Broward County portion of the model, the majority of the area was defined based on data provided by South Broward Drainage District and their permitted drainage basins. In the Miami-Dade portion of the model, subbasins were developed from data provided digitally by Miami-Dade County. Miami-Dade County provided very detailed subbasin data, much too refined for this scale model. Therefore, new subbasins were developed by defining and aggregating basins based on drainage categories (as discussed in **Section 3.7.2**) and drainage destination (such as a specific canal). Essentially, areas with the same classification that shared a common boundary and destination, were merged into one basin. This process resulted in the number of basins in the Miami-Dade portion of the model to be decreased from about 830 basins down to about 40, while maintaining drainage characteristics.

Cells assigned an initial depth or a flood code, were assigned a drain code of 0 (dark blue cells in **Figure 3.7-5**), which turns off drainage from that cell. Not doing so would create feedback loops, as the drained water would return back to the cell via flood code, only to be drained back to the branch again and so on. **Figure 3.7-5** shows a map of the drain codes, where each unique color represents a drainage basin (areas in yellow drain to boundary). Although the specific value of the positive drain codes do not matter (negative drains internally or to boundary) as they are just an identifier that define a drainage area, the drain code values in the C-9 basin were kept the same as the 2019 Broward County Model for consistency. New drain codes were assigned identifiers not used in the 2019 Broward County model, which should eliminate any issues in the future if the models are merged together.

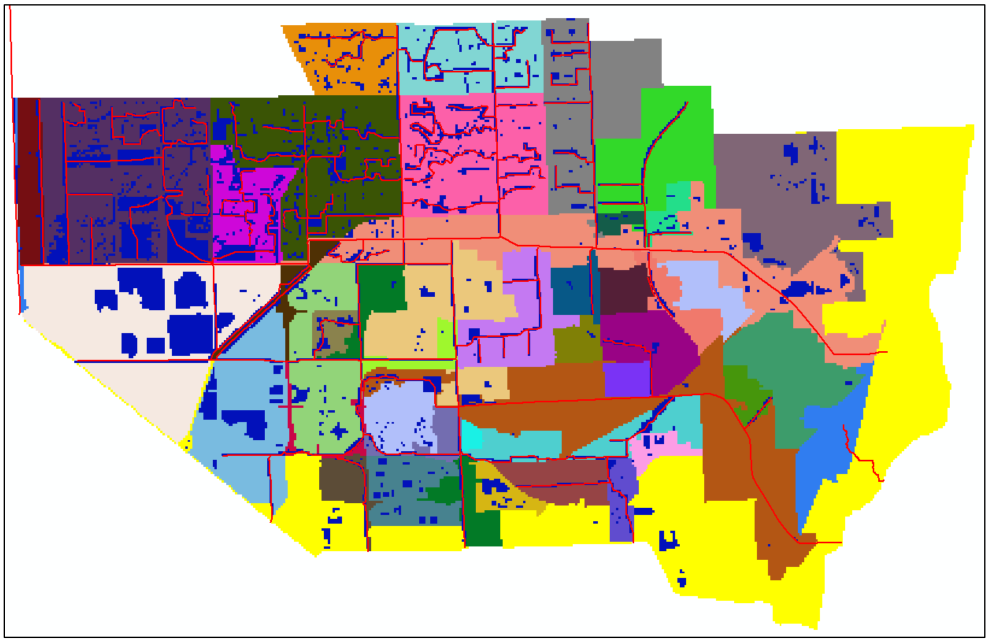

Figure 3.7-5: Drain Codes used to Delineate Common Drainage Areas

3.7.8 Boundary Conditions (2D Model)

For the calibration and validation model, no 2-D overland boundary conditions were applied. However, a 2-D overland tidal boundary was included in the design storm simulations using the spatial distribution shown in **Figure 3.7-6** based on the District-provided time series for S-28 and S-29 (**Figure 3.6-4** and **Figure 3.6-5**).

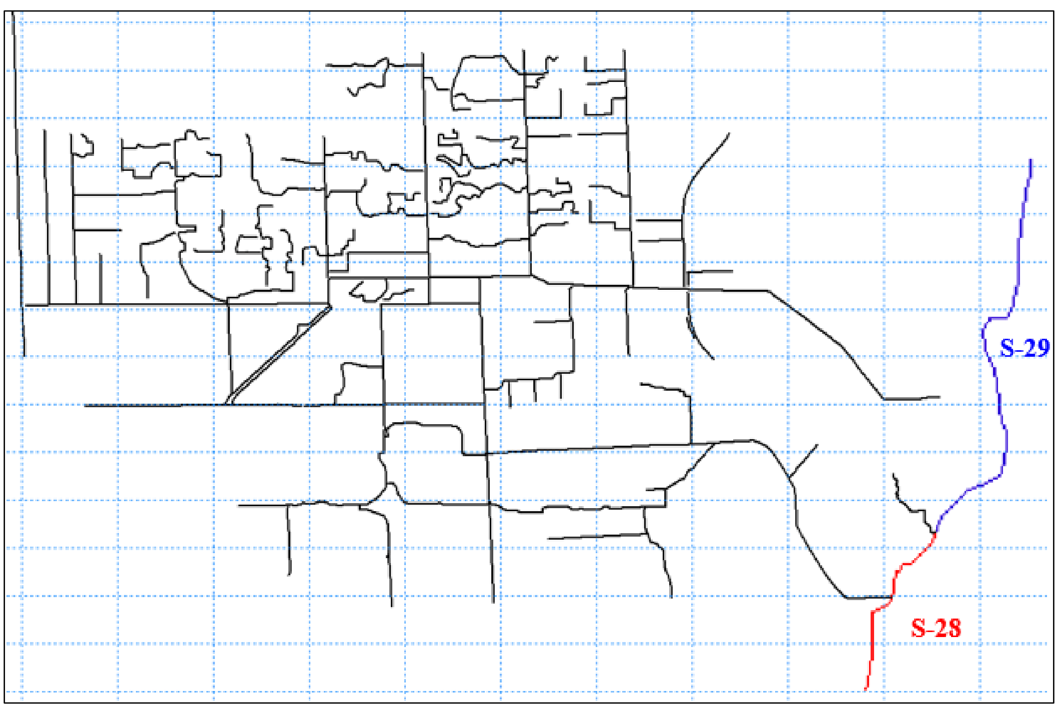

Figure 3.7-6: Spatial Distribution of 2-D Overland Flow Tidal Boundary

3.8 Unsaturated Zone

The soil distributions and unsaturated zone parameters were carried over from the 2019 Broward County Current Conditions model (which were mainly inherited from the Broward County 2014 FEMA model) (**Figure 3.8-1**). The 2019 Broward County model's soil parameters that were changed were the saturated water content and field capacity for Margate Fine Sand and the field capacity for urban land, which were adjusted during model validation in an effort to improve the groundwater response to rainfall. These are incorporated in this model from the start. This model uses the simple 2-layer water balance method for unsaturated zone calculations, which is consistent with the 2019 Broward County model. **Table 3-10** shows the final soil parameters.

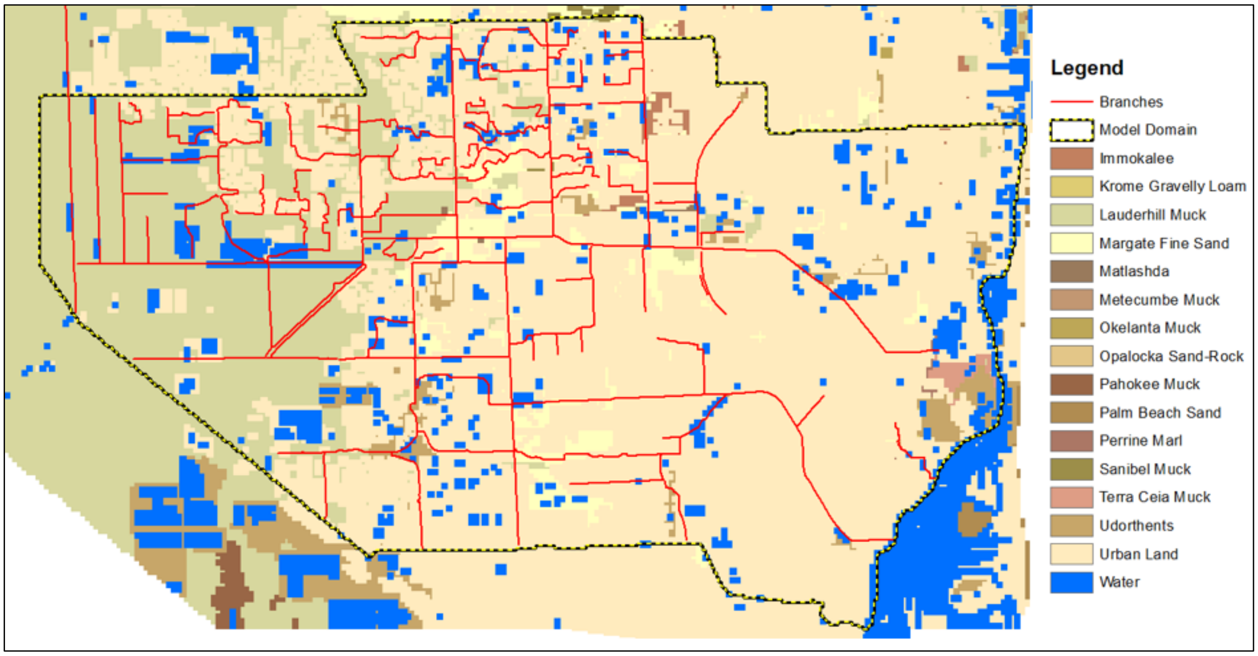

Figure 3.8-1: Map of Soils

Table 3-10: Unsaturated Zone Soil Parameters

2-Layer Unsaturated Zone Soil Profiles	Water content at saturation	Water content at field capacity	Water content at wilting point	Saturated hydraulic conductivity (ft/day)
Immokalee	0.44	0.14	0.06	85.0
Krome Gravelly Loam	0.45	0.17	0.08	28.3
Margate Fine Sand	0.35	0.18	0.06	28.3
Matlashda	0.42	0.09	0.04	198.4
Opalocka Sand-Rock	0.42	0.09	0.06	198.4
Palm Beach Sand	0.42	0.09	0.06	198.4
Perrine Marl	0.47	0.25	0.13	28.3
Muck	0.7	0.59	0.18	141.7
Udorthents	0.3	0.13	0.08	28.3
Urban Land	0.3	0.2	0.08	28.3

3.9 Saturated Zone

As previously mentioned, this model was initially parameterized based on the 3-layer MODFLOW model developed by the USGS (Hughes and White, 2016). The final saturated zone configuration was based on the 5-layer 2019 Broward County Current Conditions model. Although the C-8 C-9 model is based on the 2019 Broward County Current Conditions model, there are still setup differences between the two. In the C-8 C-9 model, only the first 3 of the 5 layers of the 2019 Broward County groundwater model was used. The top 3-layers is adequate for short-term flood event modeling, whereas the 5-layer model was designed for long-term water supply modeling. This would prevent the C-8 and C-9 models from being merged directly, but a simple solution would be to just add the last 2 groundwater layers into the C-8 and C-9 model if merging them is desired in the future.

3.9.1 Lower Levels of Computation Layers

This parameter was originally spatially distributed based on data from Hughes and White (2016) (refer to Deliverable 1.2, *C8-C9 Model Development Memorandum* (Taylor Engineering, 11/4/2019)). The final configuration is based on the 2019 Broward County Current Conditions model. The following three figures show the lower levels of the three saturated zone layers.

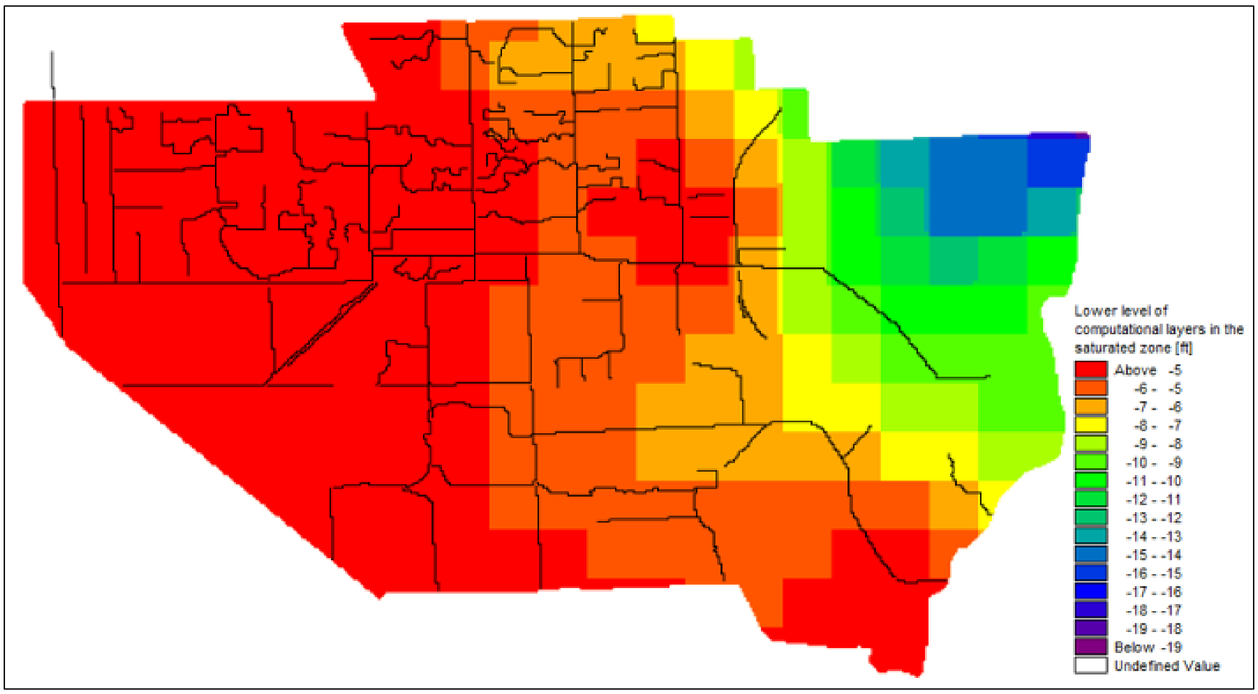

Figure 3.9-1: Lower Level of Computational Layer 1

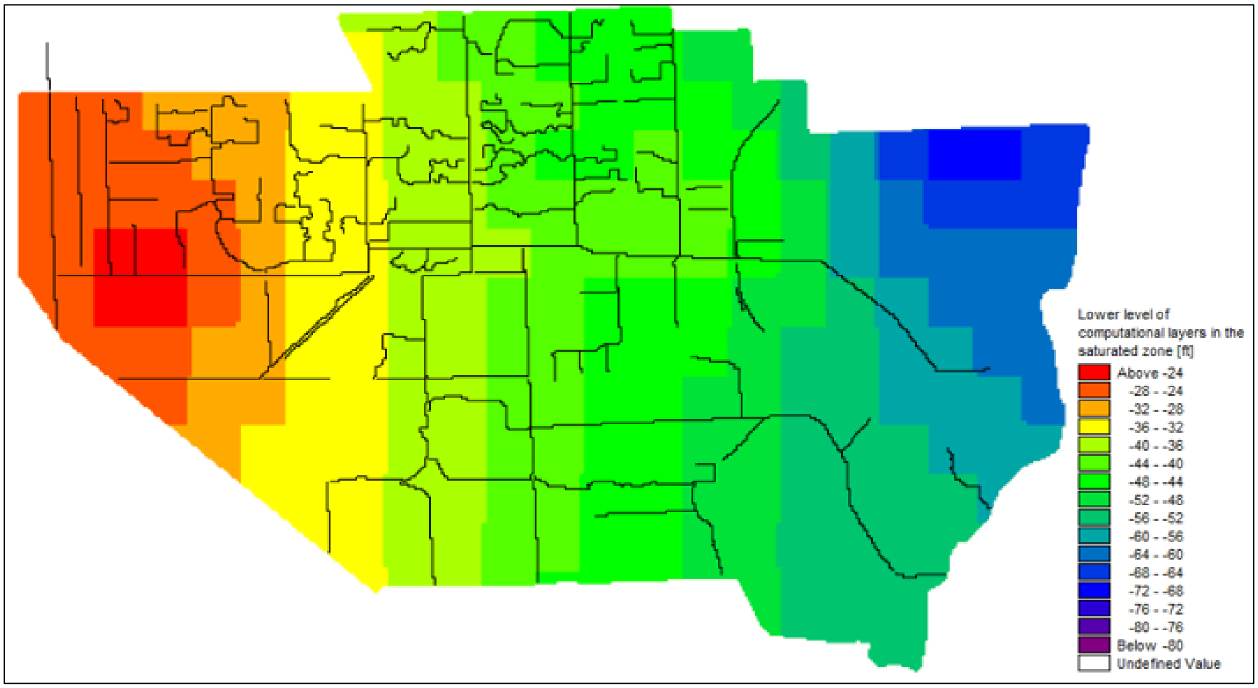

Figure 3.9-2: Lower Level of Computational Layer 2

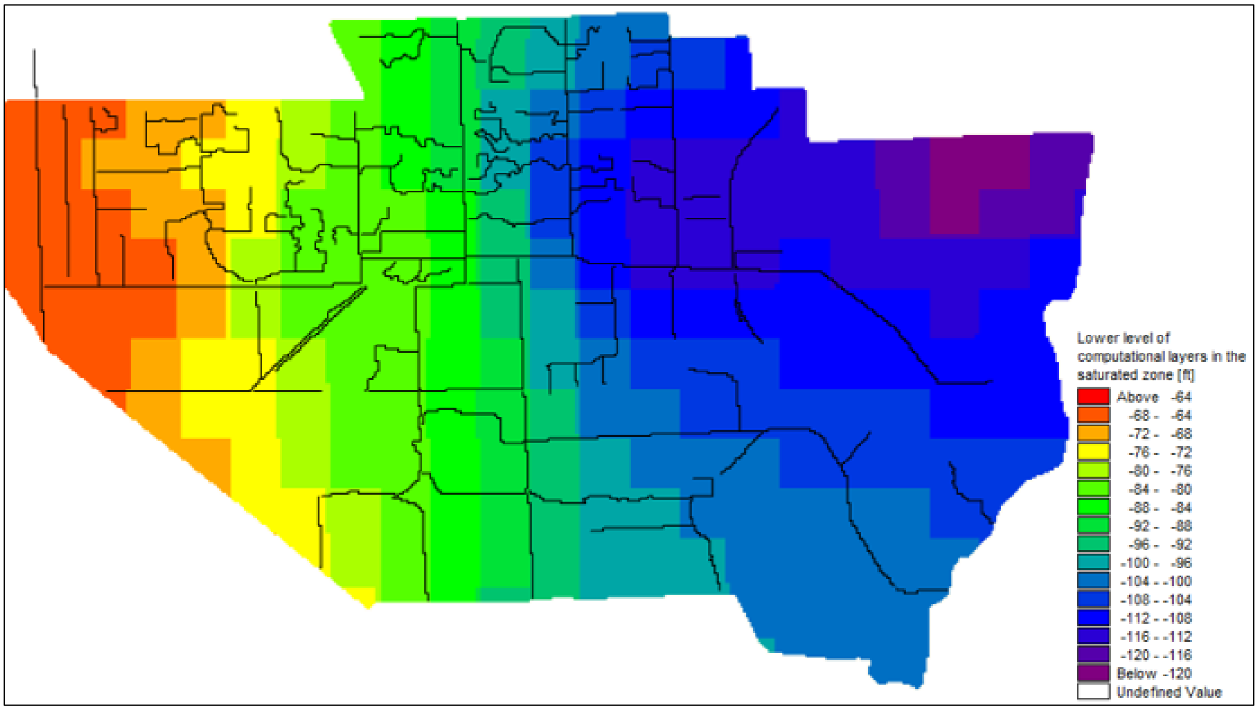

Figure 3.9-3: Lower Level of Computational Layer 3

3.9.2 Horizontal Hydraulic Conductivity

This parameter was originally spatially distributed based on data from Hughes and White (2016) (refer to Deliverable 1.2, *C8-C9 Model Development Memorandum* (Taylor Engineering, 11/4/2019)). The final configuration is based on the 2019 Broward County Current Conditions model. The following three figures show the horizontal hydraulic conductivity of the three saturated zone layers.

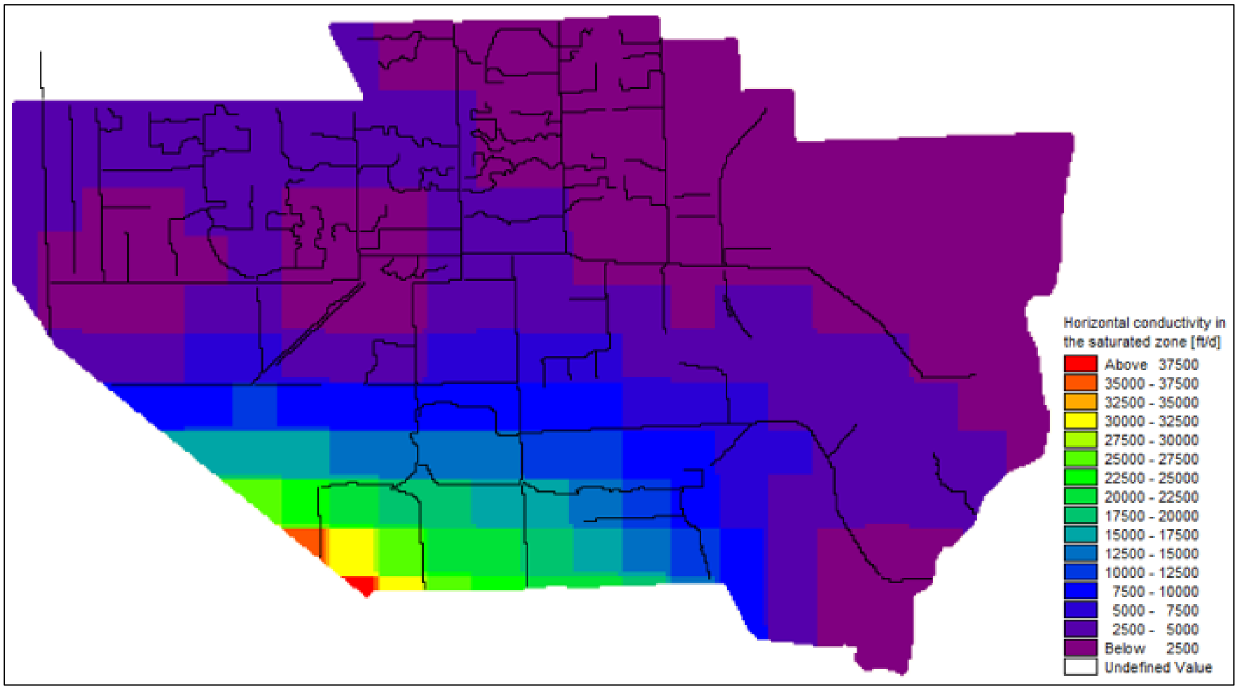

Figure 3.9-4: Horizontal Hydraulic Conductivity in Layer 1

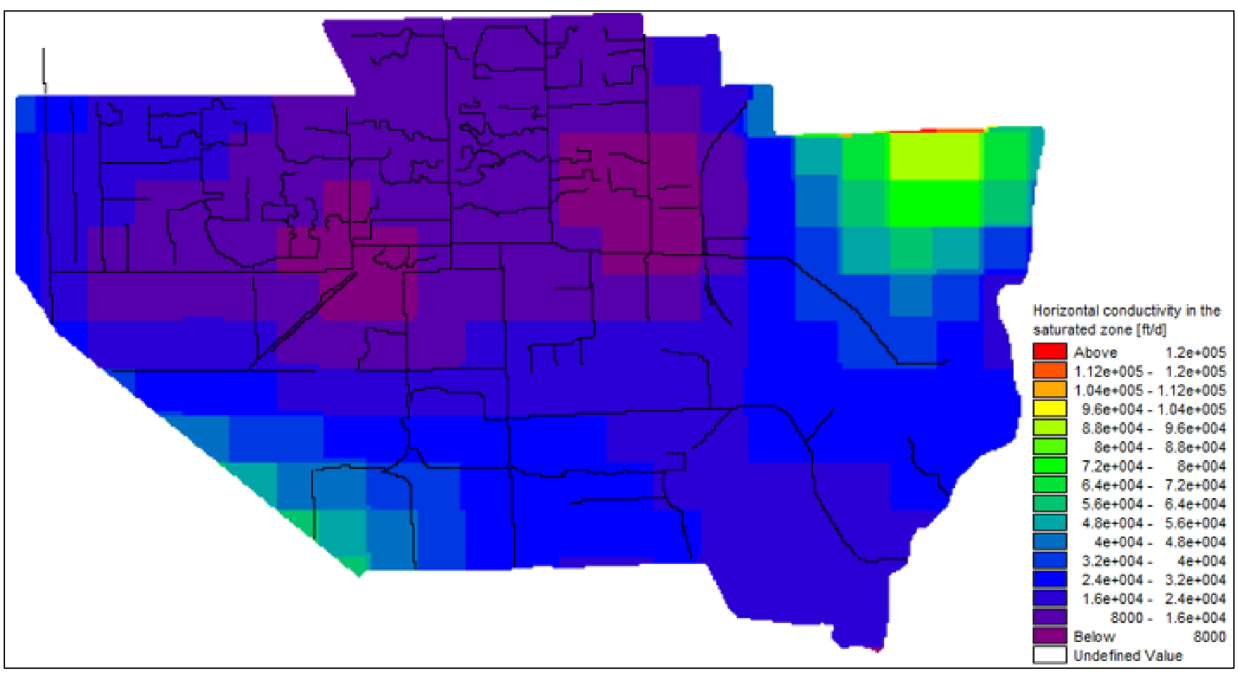

Figure 3.9-5: Horizontal Hydraulic Conductivity in Layer 2

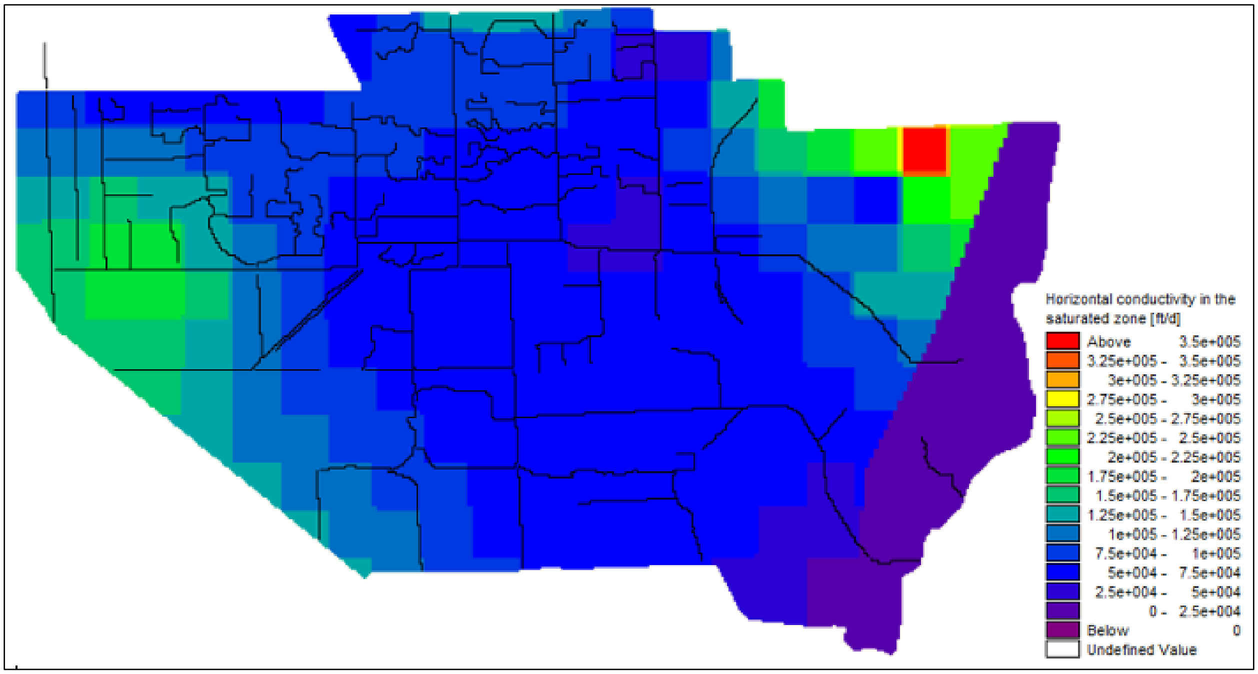

Figure 3.9-6: Horizontal Hydraulic Conductivity in Layer 3

3.9.3 Vertical Hydraulic Conductivity

This parameter was originally spatially distributed based on data from Hughes and White (2016) (refer to Deliverable 1.2, *C8-C9 Model Development Memorandum* (Taylor Engineering, 11/4/2019)). The final configuration is based on the 2019 Broward County Current Conditions model. The following three figures show the vertical hydraulic conductivity of the three saturated zone layers.

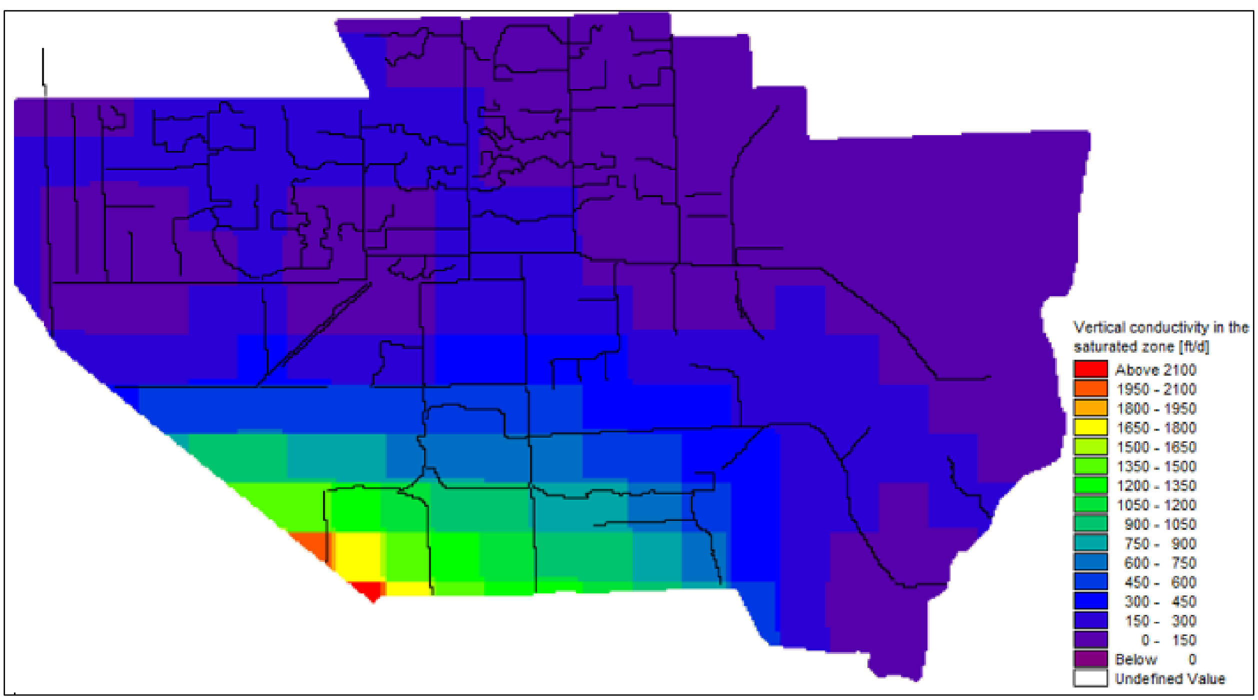

Figure 3.9-7: Vertical Hydraulic Conductivity in Layer 1

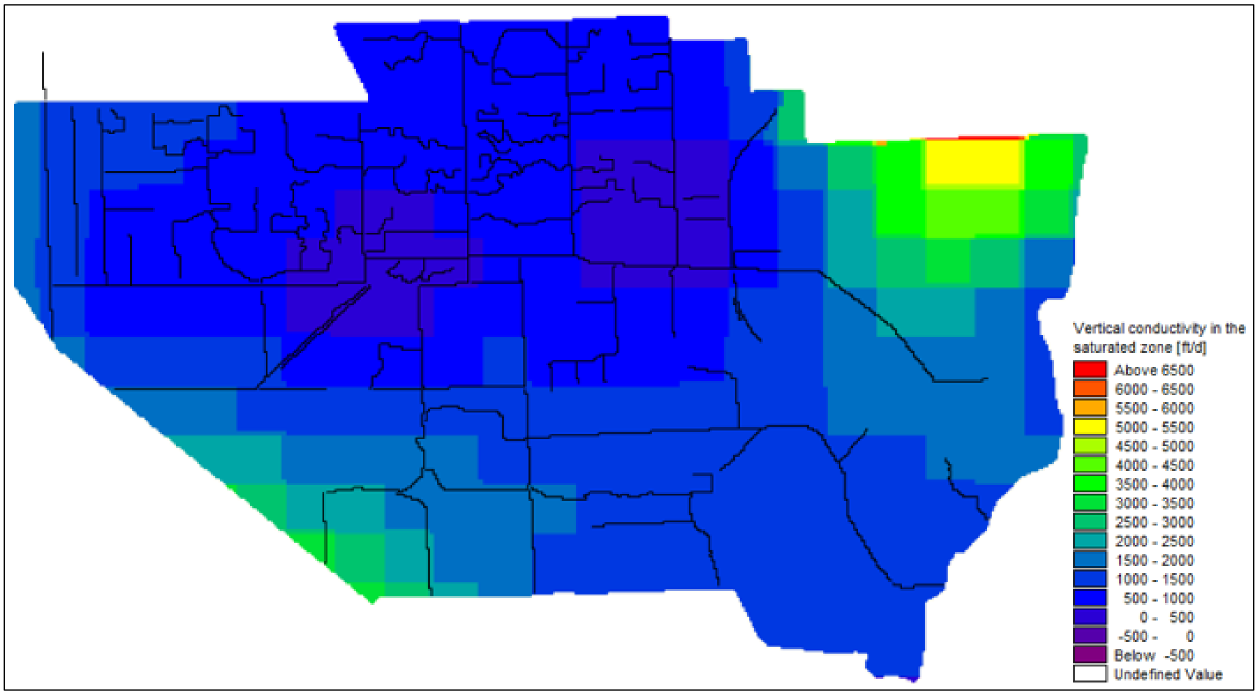

Figure 3.9-8: Vertical Hydraulic Conductivity in Layer 2

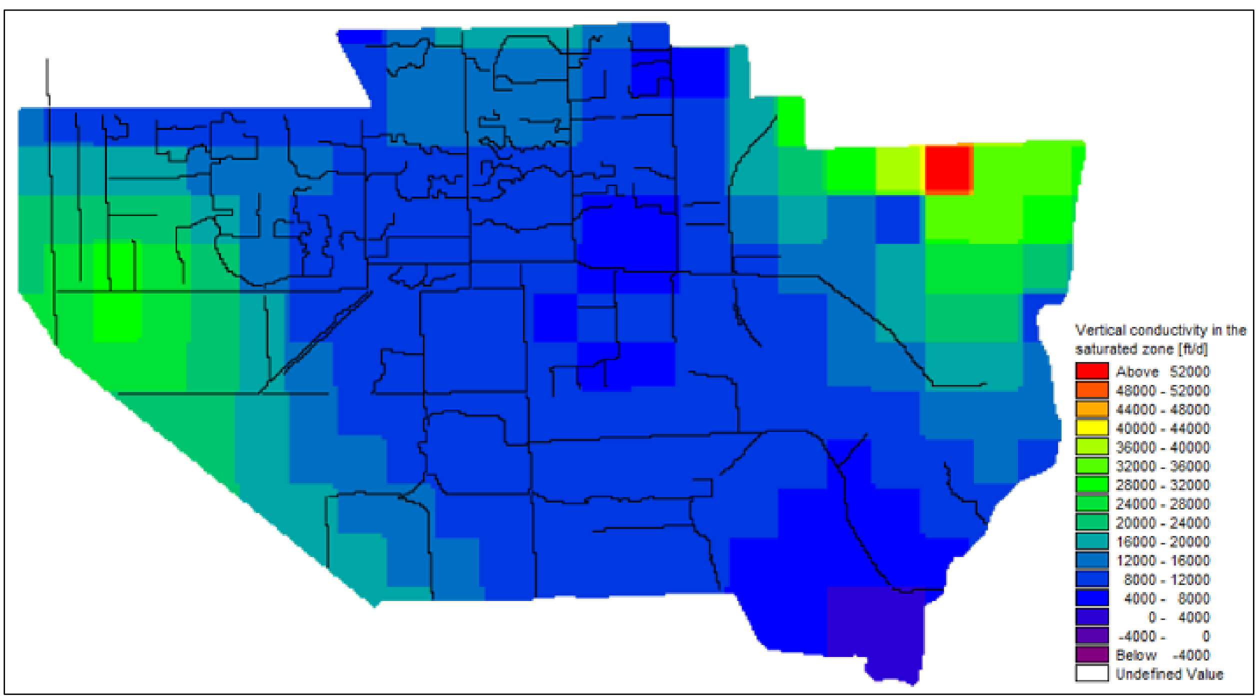

Figure 3.9-9: Vertical Hydraulic Conductivity in Layer 3

3.9.4 Specific Yield

This parameter was originally spatially distributed based on data from Hughes and White (2016) (refer to Deliverable 1.2, *C8-C9 Model Development Memorandum* (Taylor Engineering, 11/4/2019)). The final configuration is based on the 2019 Broward County Current Conditions model. **Figure 3.9-10** shows the user-specified specific yield of the three saturated zone layers. During model preprocessing, MIKE SHE adjusts the specific yield layer one of the saturated zone based on the difference between the water content at saturation and field capacity, based on the two-layer UZ soil type (**Figure 3.9-11**).

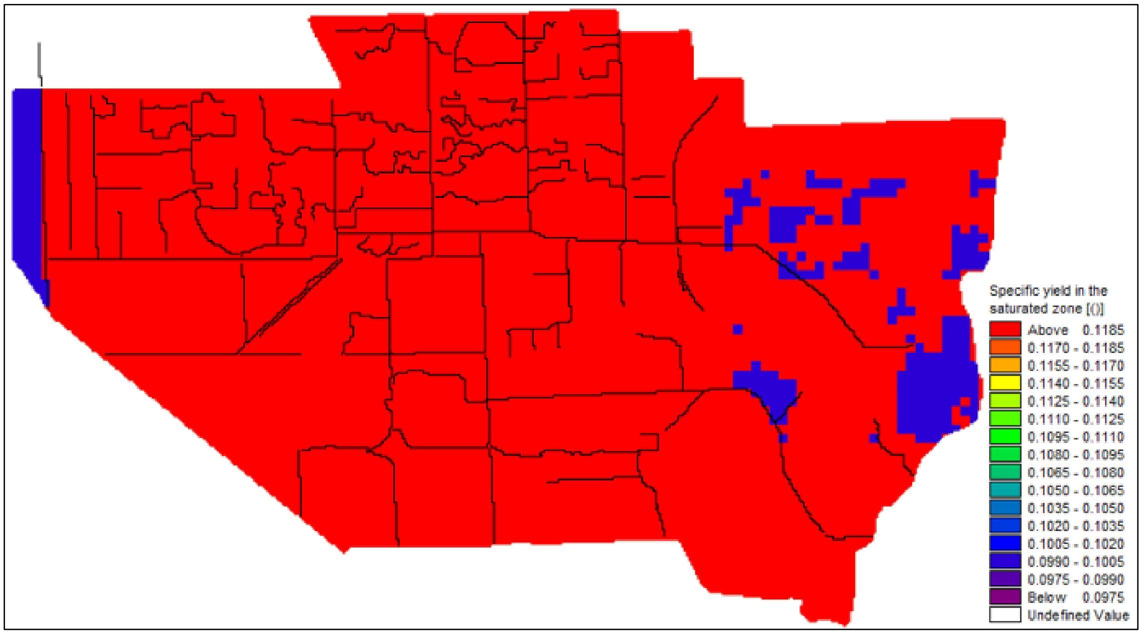

Figure 3.9-10: User Specified Specific Yield in Layers 1, 2, and 3

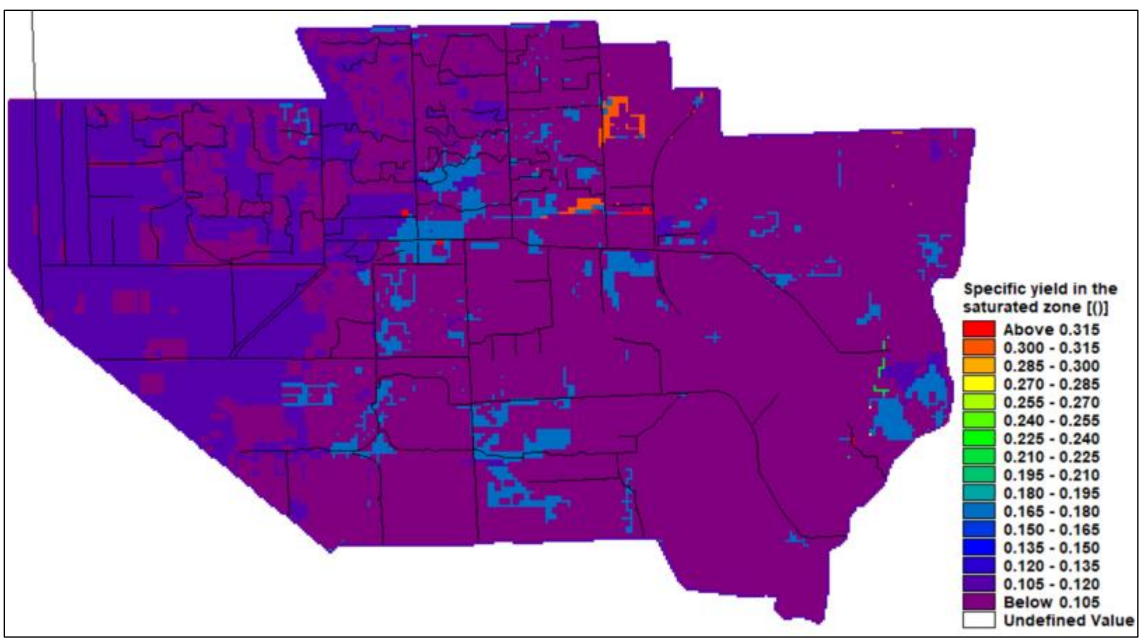

Figure 3.9-11: Model-Adjusted Specific Yield in Layer 1

3.9.5 Specific Storage

This parameter was originally spatially distributed based on data from Hughes and White (2016) (refer to Deliverable 1.2, C8-C9 Model Development Memorandum (Taylor Engineering, 11/4/2019)). The final configuration is based on the 2019 Broward County Current Conditions model. Layer 1 was given a uniform specific storage of 0.06096/ft, based on the 2019 Broward County Current Conditions model. The following figures show the specific storage of the bottom 2 saturated zone layers.

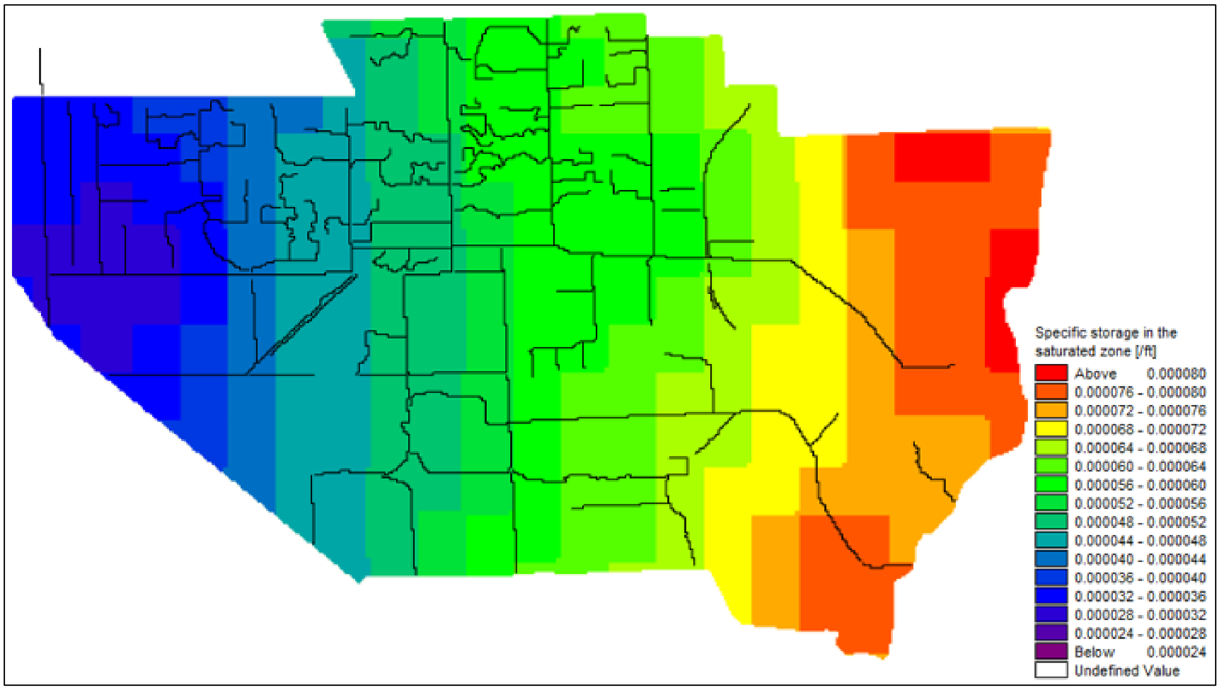

Figure 3.9-12: Specific Storage in Layer 2

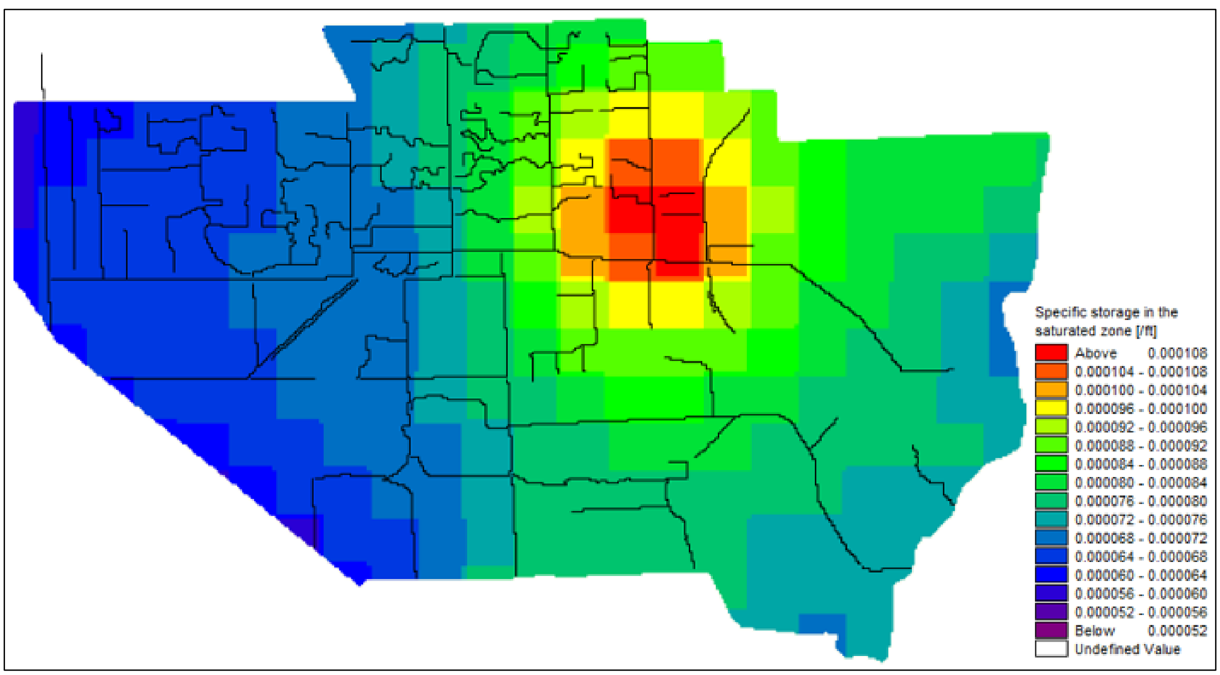

Figure 3.9-13: Specific Storage in Layer 3

3.9.6 Initial Potential Head

3.9.6.1 Calibration Model

Although there were groundwater wells within the model domain that had data available, there were not enough locations to generate a high confidence surface. Therefore, this parameter is spatially distributed based on results from Hughes and White (2016), with slight modification. The initial potential head from the USGS model was a close match at many of the observed points and had what appeared to be realistic "drawdown" near major branches. Therefore, the USGS data was used as a starting point and some localized adjustments were so that made it was a closer match to the observed data. The initial potential head map (**Figure 3.9-14**) is within about +0.25 ft of the observed well elevations at the start of the simulation period.

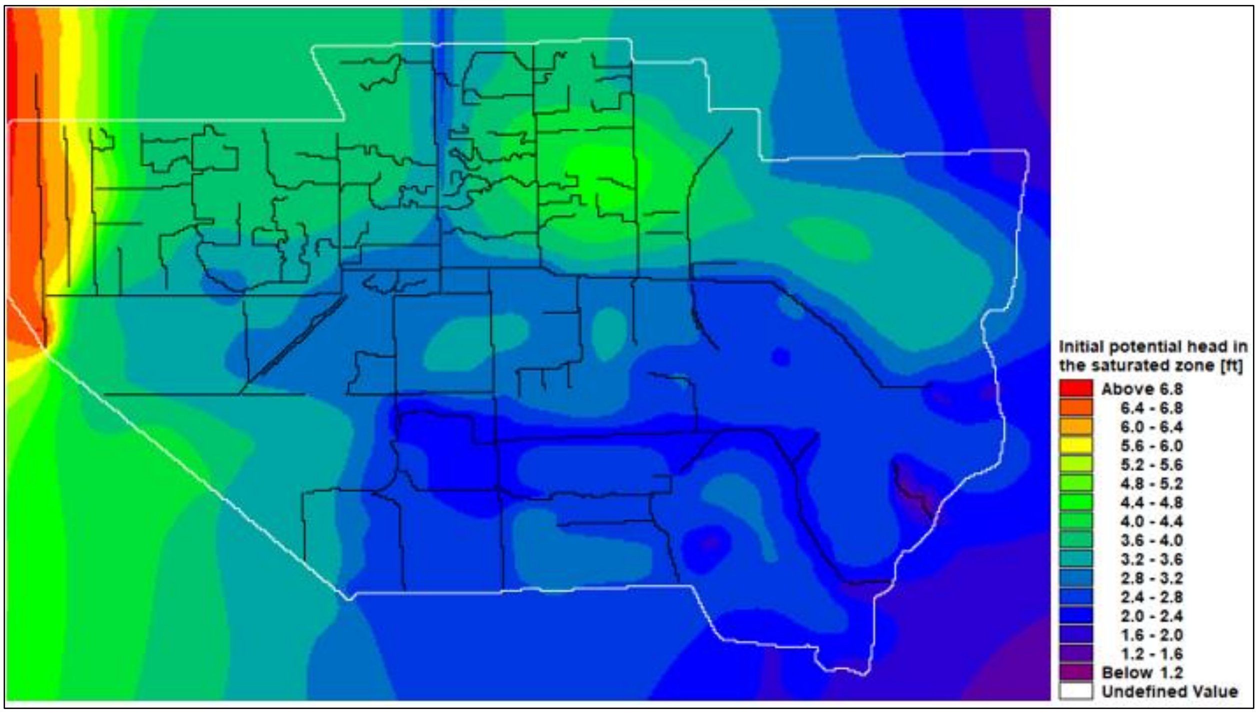

Figure 3.9-14: Initial Potential Head in Saturated Zone for October 2nd, 2000

3.9.6.2 Validation Model

The initial potential head for the validation simulation is spatially distributed based on data from Broward County's average wet season head map (Broward County, 2000) (used to generate the initial potential head for the 2019 Broward County Current Conditions Model) and USGS wet season groundwater contours (Fish and Stewart, 1991). **Figure 3.9-15** shows how the initial potential head for the validation simulation was generated and **Figure 3.9-16** shows the final initial potential head. The initial potential head is within about +/- 0.5 ft of observed well elevations near the start of the validation simulation, which is part of the 3+ month spin-up period.

Figure 3.9-15: Development of Initial Potential Head for Validation Simulation

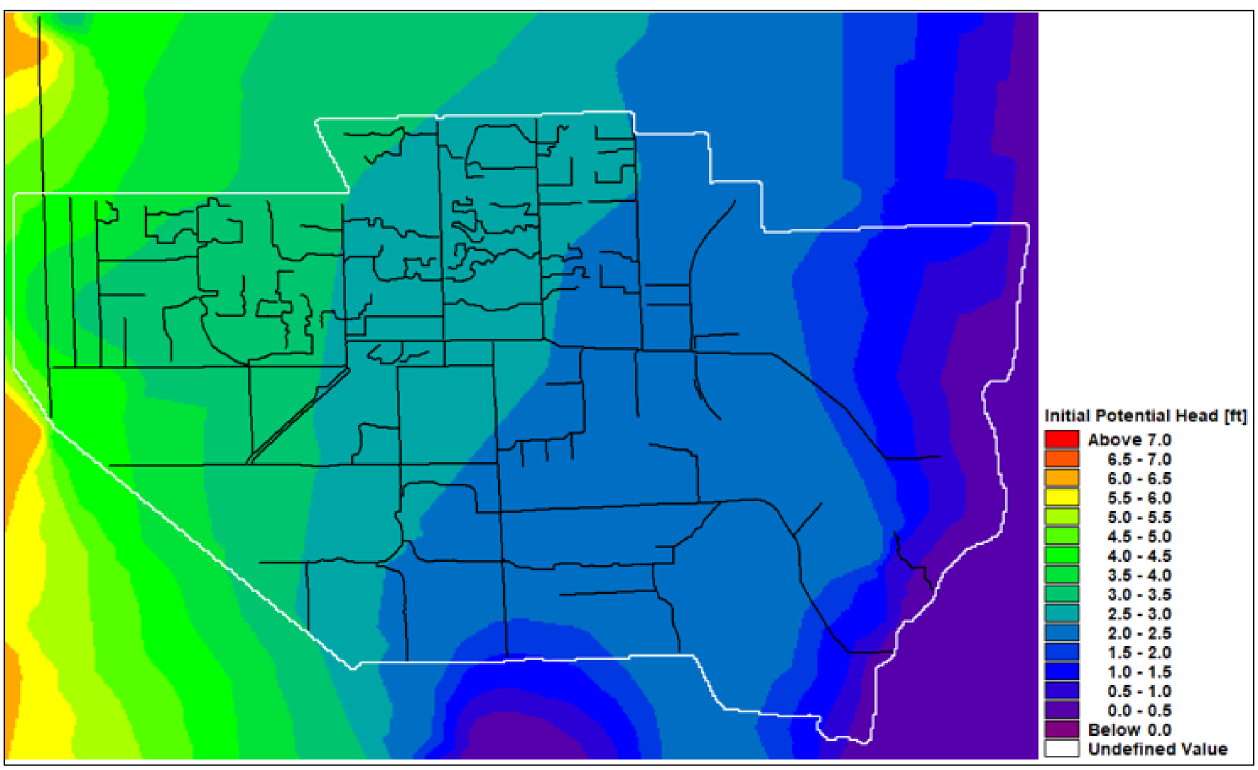

Figure 3.9-16: Initial Potential Head in Saturated Zone for Validation Simulation

3.9.6.3 Design Storm Model

The design storm initial groundwater elevations were developed by making localized adjustments to the initial potential head from the validation simulation. Although the initial potential head matched the observed groundwater elevations within +/- 0.5 ft, there were some areas where the groundwater levels were upwards of 1 ft lower than the water bodies within an area of established control elevations. This difference was not significant for the validation model as this was at the start of the 3-month spin-up period. However, for the design storm scenarios, which were only given a 2-day spin-up period, it is significant. Therefore, for the design storms, the initial groundwater levels were adjusted so that they closely matched basin control elevations, where they existed. This was done by changing initial water levels in areas that have established basin control elevations, and then running the model without any rainfall for a brief period of time so that any discontinuities resulting from differences in basin water control elevations smooth out. After 6 hours of simulation with no rainfall, this approach resulted in an initial potential head that matched basin control elevations closely in areas where they existed, eliminated elevation discontinuities, and created smooth gradients. This was done to prevent the water levels in the lakes to drop (or rise) due to lower (or higher) initial groundwater elevations. **Figure 3.9-17** shows the final initial potential head developed for the current condition design storm simulations.

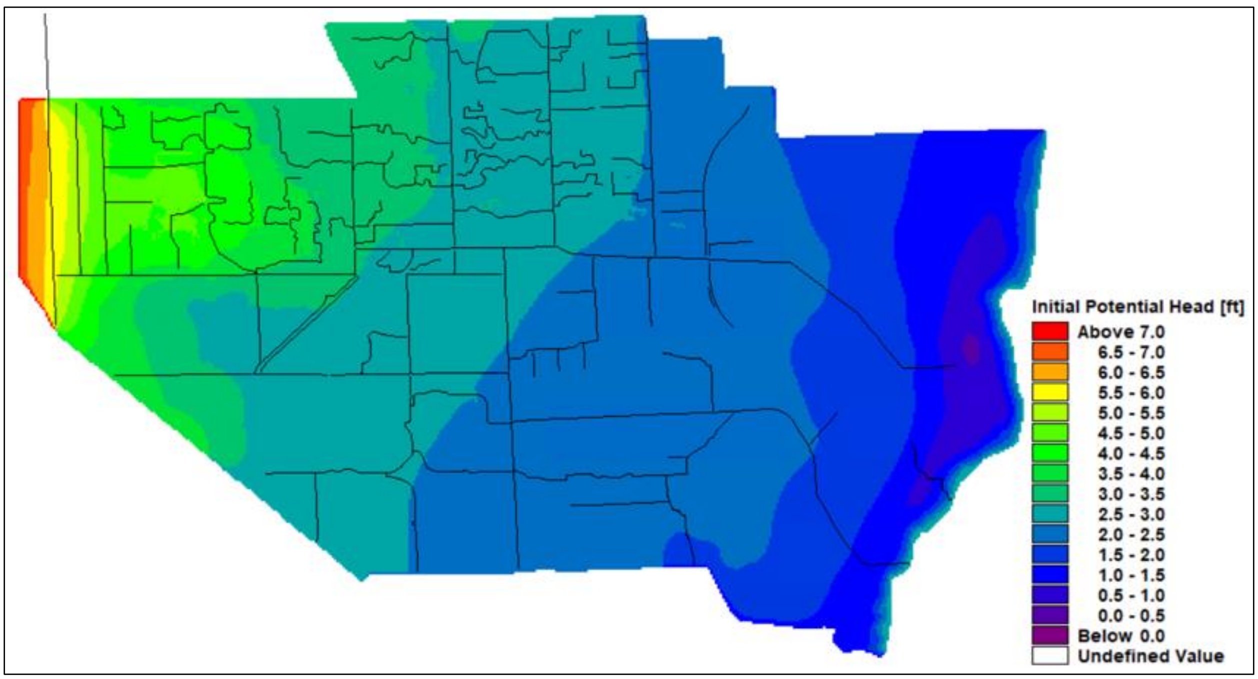

Figure 3.9-17: Initial Potential Head in Saturated Zone for Design Storm Simulations

3.9.7 Boundary Conditions

Refer to **Section 2.8.1** & **2.8.2** for boundary condition set up for the calibration and validation simulations. For the design storm simulations, SFWMD provided year 2015 tidal boundary data at the S-28 and S-29 structures, which include storm surge effects for the design storms of interest. The saturated zone tidal boundaries were assigned the same spatial distribution as the 2-D overland flow boundary shown in **Figure 3.7-6** using the District-provided time series for S-28 and S-29 (**Figure 3.6-4** and **Figure 3.6-5**).

The western boundary (**Figure 3.9-18**) and western internal boundary (**Figure 3.9-19**) was set to observed data from the June 2017 storm event. As June 2017 was wetter than normal in the weeks leading up to it, Water Conservation Area 3B stage was already elevated. Taylor Engineering proposed to use the observed data (**Figure 3.9-20**) as an assumed design storm boundary as the elevated levels may be equivalent to what could be expected during a design storm, and the District agreed this is a reasonable approach.

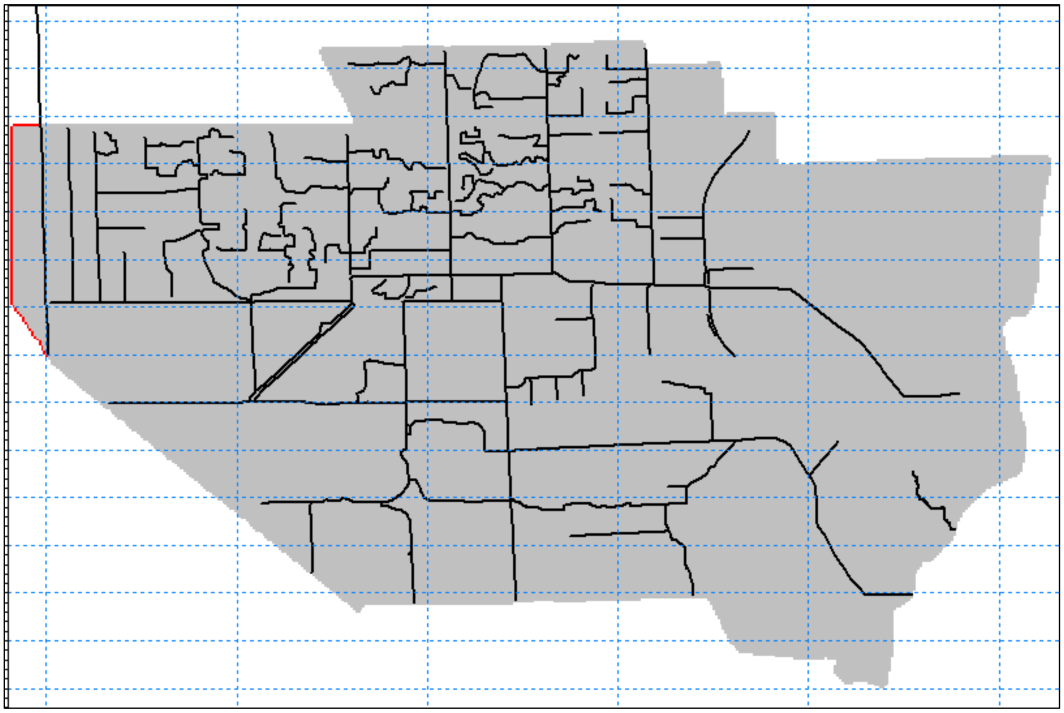

Figure 3.9-18: Western General Head Groundwater Boundary Location

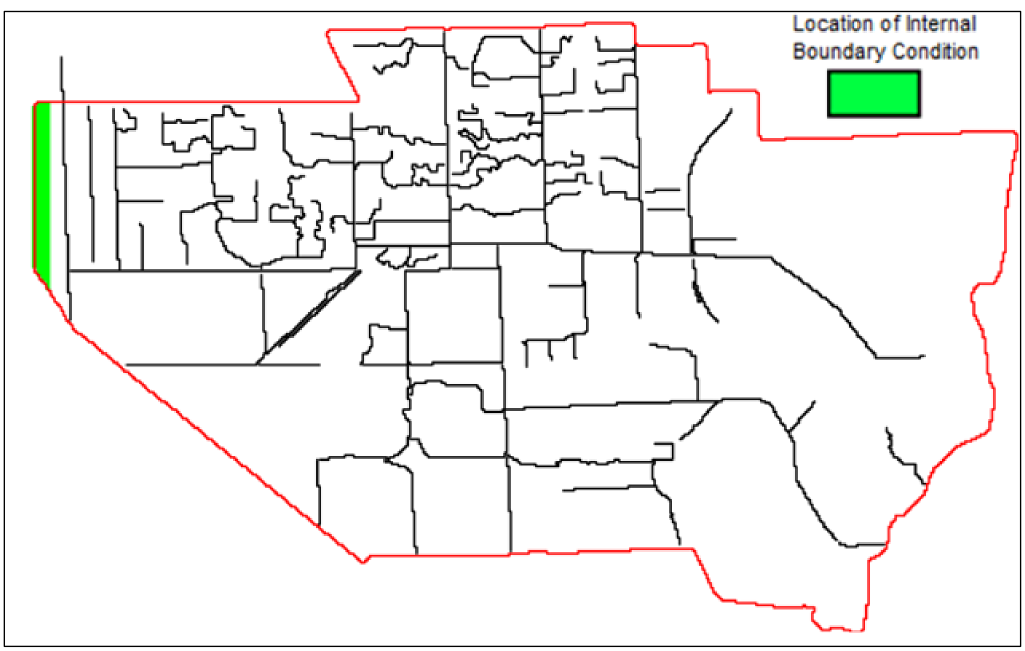

Figure 3.9-19: Western Internal Head-Controlled Flux Boundary Location

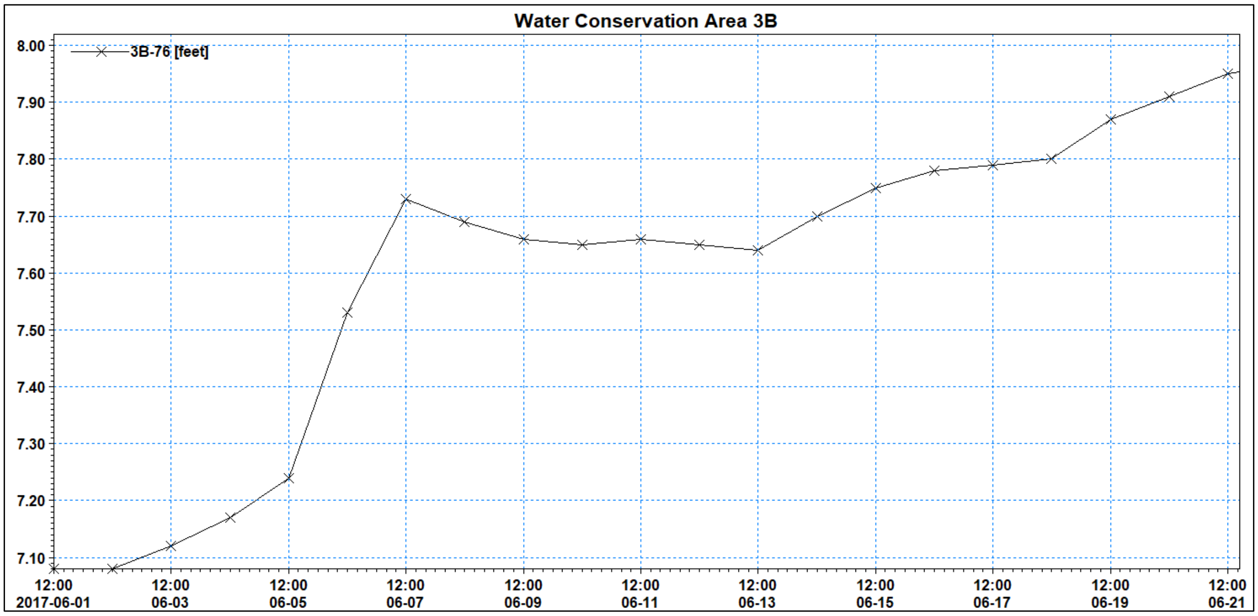

Figure 3.9-20: Western General Head Groundwater Boundary Stage Time-Series

The northern general head groundwater boundary used simulated groundwater elevations from the 2019 Broward County design storm models, which is based on the same storm event. The southern general head groundwater boundary was split into 4 sections and was assigned District provided simulated canal stage data from XP SWMM and HEC RAS models for the C-6 and C-7 canals. The four sections are S-27 headwater and G-72 tailwater on the C-7 Canal and G-72 headwater and S-31 tailwater on the C-6 canal. The time series for the groundwater general head boundaries for the four segments also served as the downstream boundary conditions for the 1-D branches connecting to the C7 and C6 Canals. The spatial distribution and time-series data for S-27 headwater are shown in the following two figures.

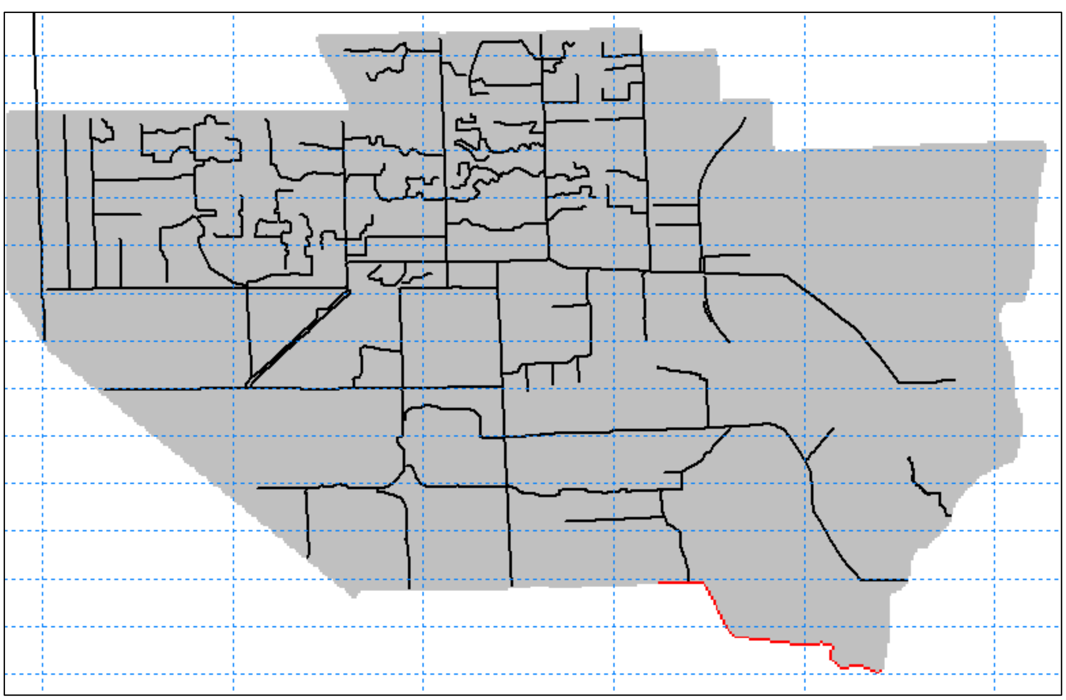

Figure 3.9-21: General Head Groundwater Boundary Using S-27 HW Simulated Design Storm Stages

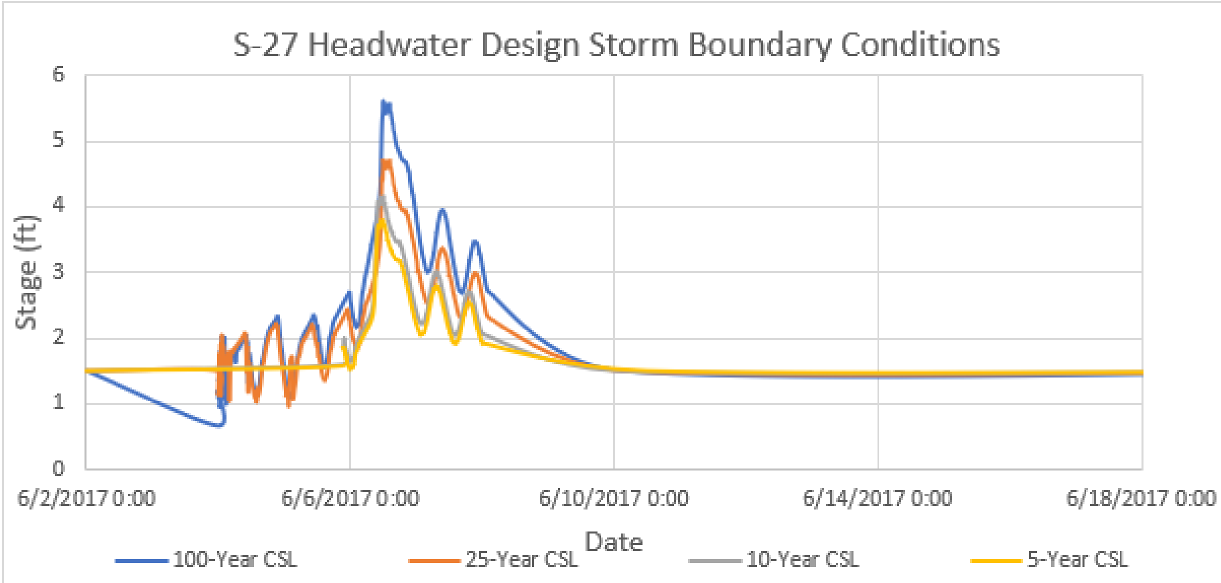

Figure 3.9-22: District Provided Simulated Design Storm Stages for S-27 HW

The spatial distribution and time-series data for G-72 tailwater are shown in the following two figures.

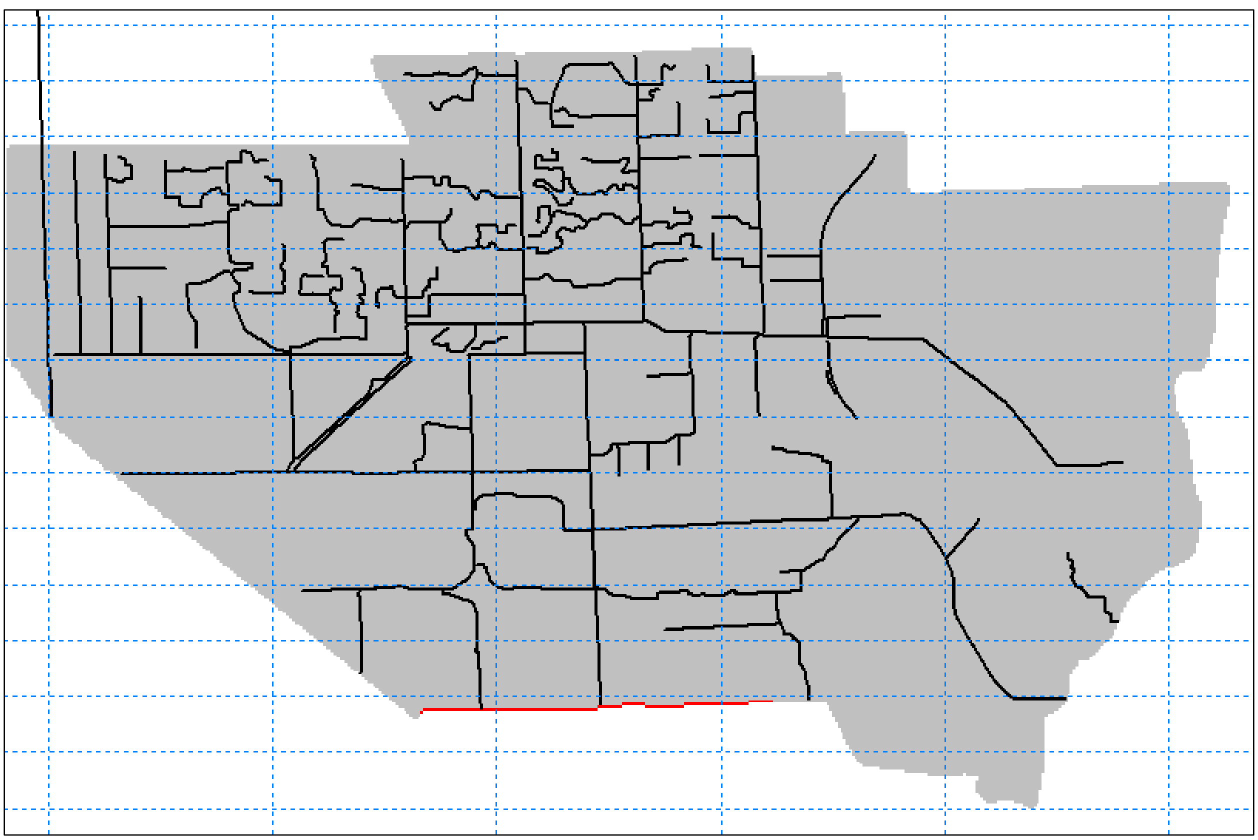

Figure 3.9-23: General Head Groundwater Boundary Using G-72 TW Simulated Design Storm Stages

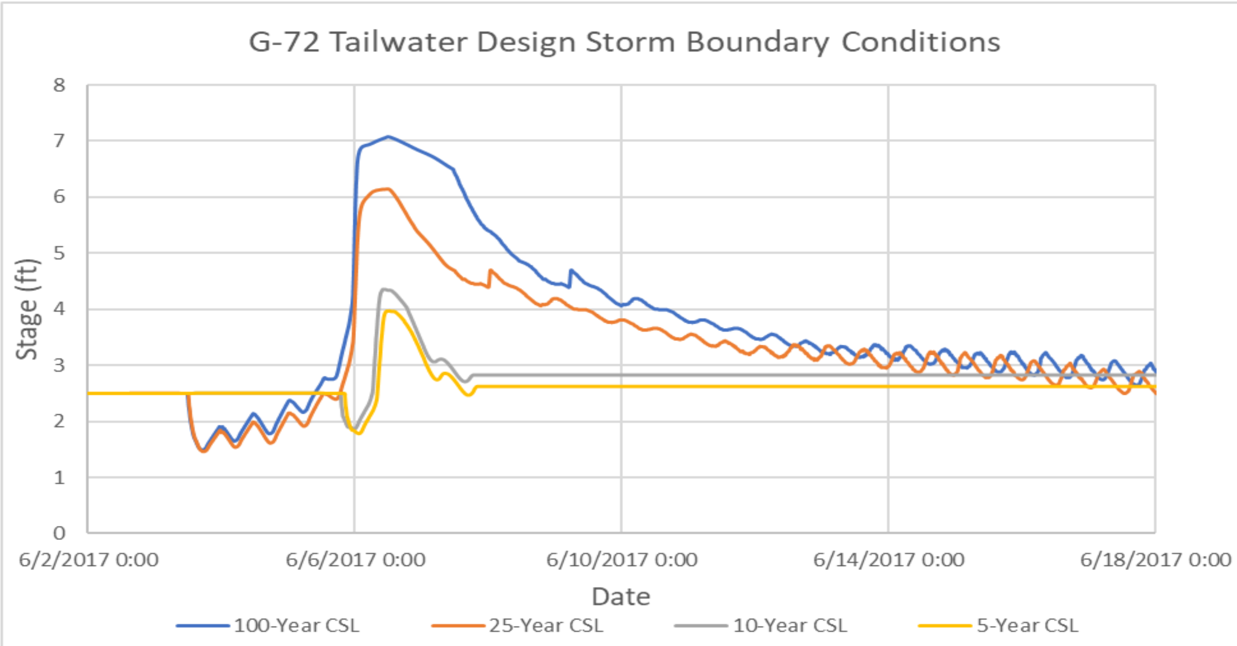

Figure 3.9-24: District Provided Simulated Design Storm Stages for G-72 TW

The spatial distribution for G-72 headwater is shown in the following figure.

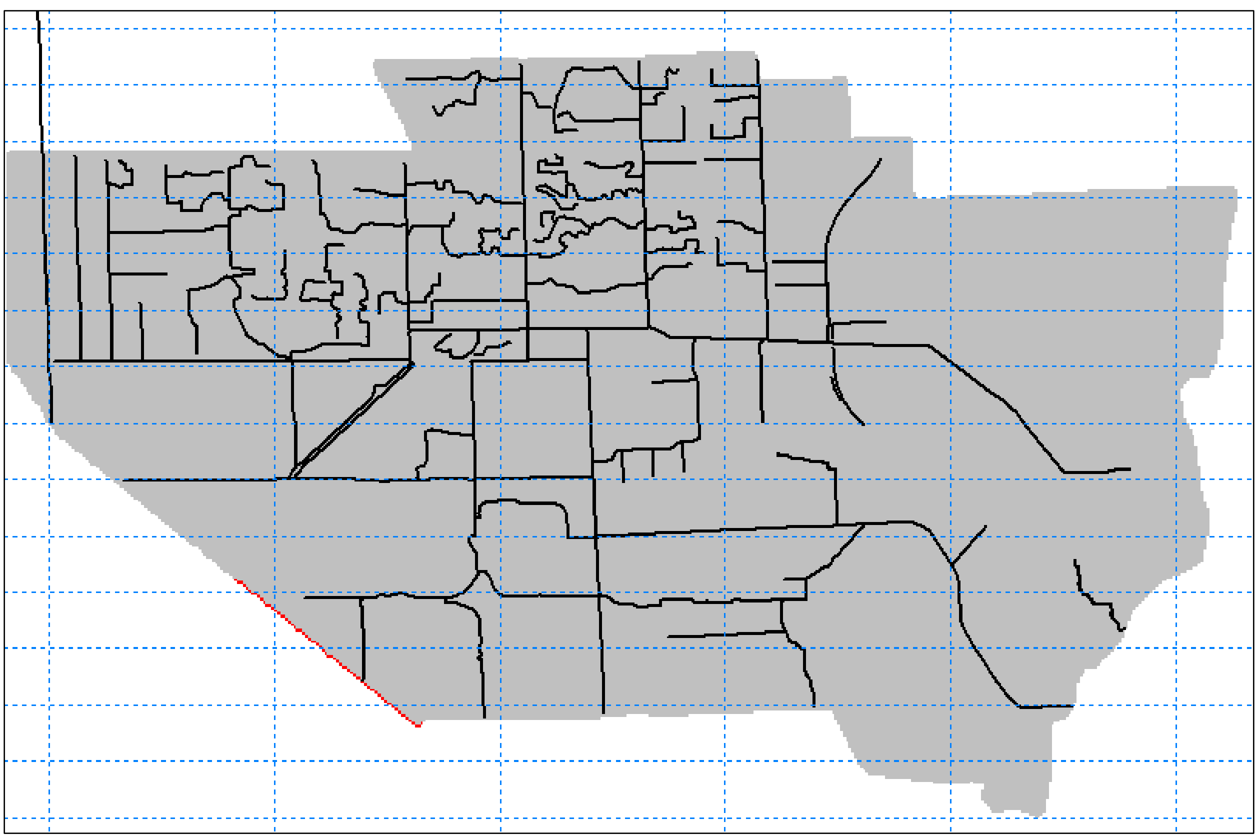

Figure 3.9-25: General Head Groundwater Boundary Using G-72 HW Simulated Design Storm Stages

For the G-72 HW boundary condition, there was only simulated data for the 10, 25, and 100-year design storms. As there was no data for the 5-year design storm, SFWMD suggested a scale-down approach. Therefore, the G-72 HW peak stage (NGVD29) was plotted against the 3-day rainfall depth for the nearest NOAA Atlas 14 station and fitted with a trendline. The best-fitting trendline (highest R^2 coefficient) was determined to be logarithmic. The following table and figure show the data used and the corresponding graph.

Table 3-11: Data Used to Scale-Down G-72 HW Peak Stage

Return period (yr)	Rainfall depth (in)	Peak Stage (ft NGVD29)
5-yr	8.85	5.25 (calculated)
10-yr	10.5	5.59
25-yr	13.1	6.47
100-yr	17.7	7

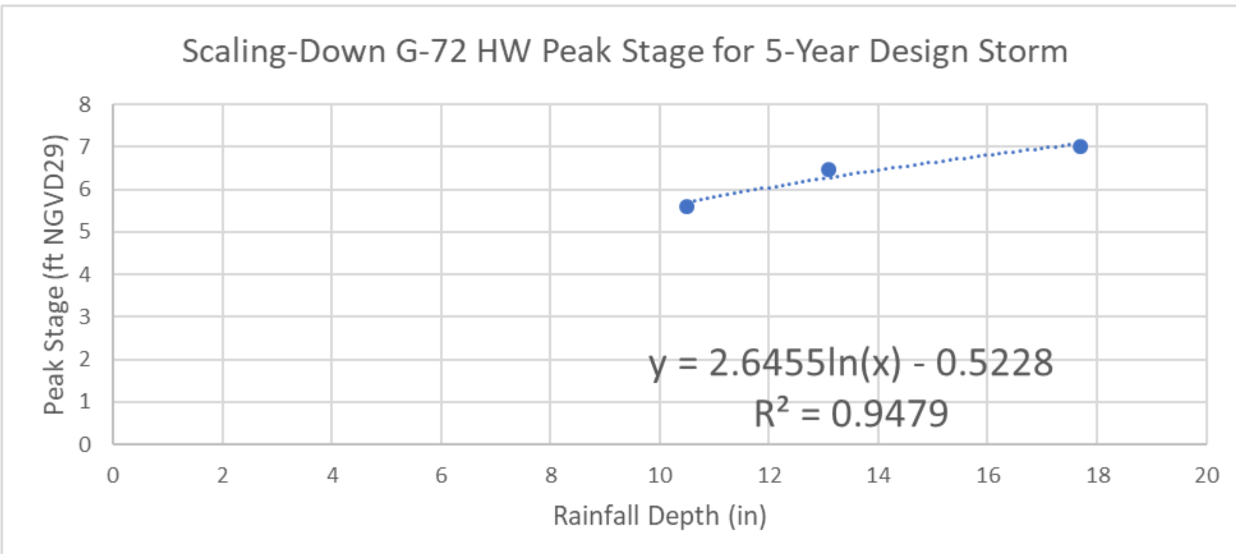

Figure 3.9-26: Scale-Down Approach for G-72 Headwater

With this approach, the peak stage for the 5-year design storm at G-72 HW was determined to be 5.25 feet. Therefore, a correction factor of 0.939 (5 year stage divided by 10 year stage) was applied to the 10-year time series data for all values greater than 2.52 feet (this is the lowest value possible before the correction factor would reduce stage to below the control elevation of 2.5 feet).

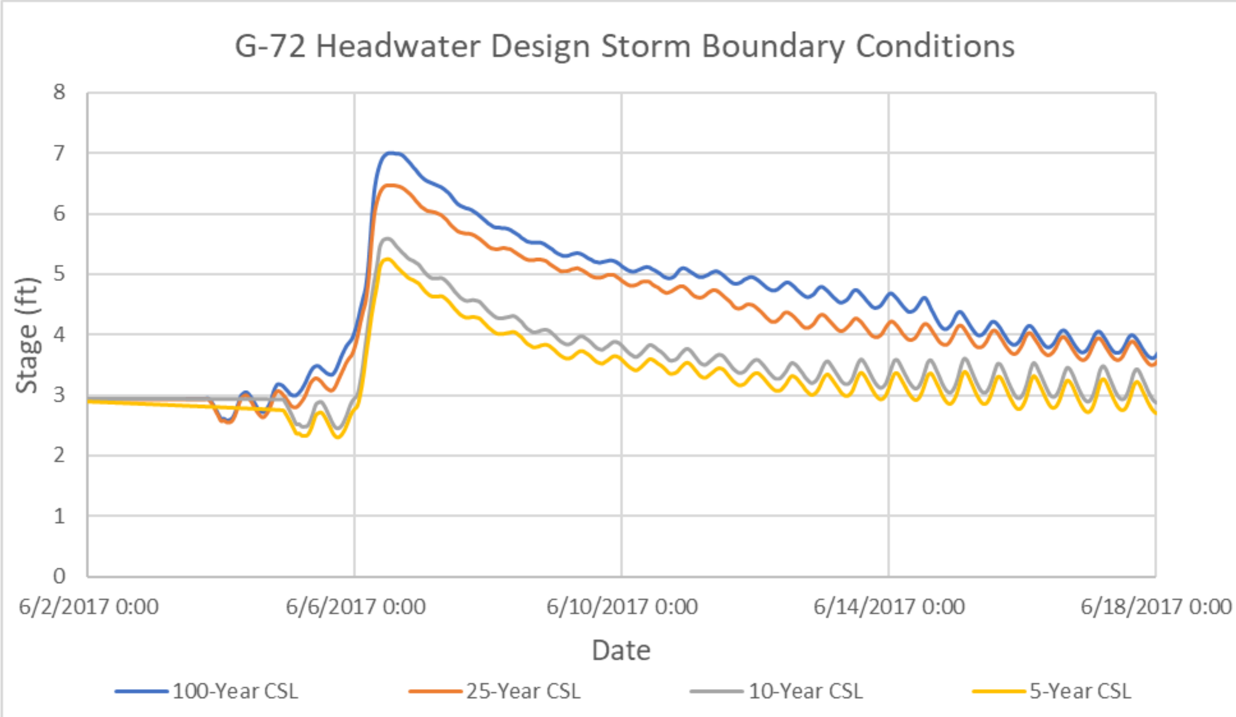

Figure 3.9-27: District Provided and Scaled-Down Simulated Design Storm Stages for G-72 HW

The spatial distribution for S-31 tailwater is shown in the following figure.

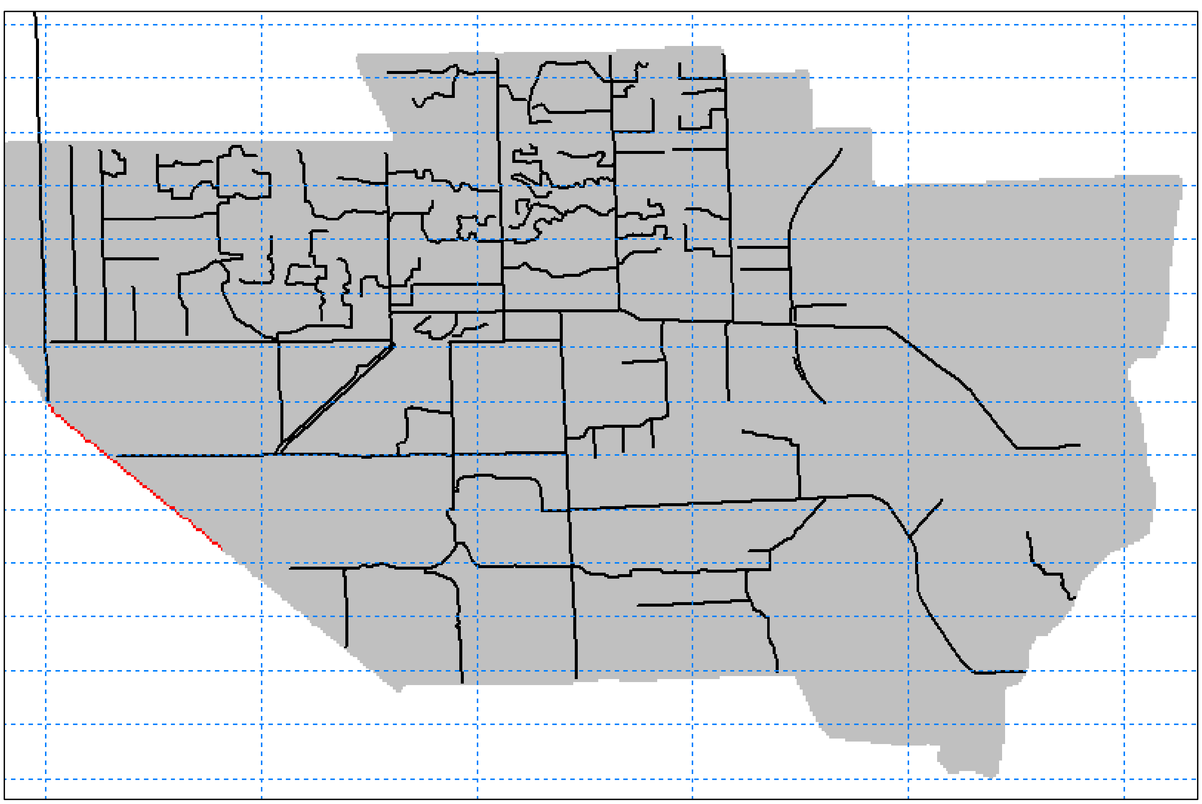

Figure 3.9-28: General Head Groundwater Boundary Using S-31/32 TW Simulated Design Storm Stages

For the S-31 TW boundary condition, there was only simulated data for the 10, 25, and 100-year design storms. As there was no data for the 5-year design storm, SFWMD suggested a scale-down approach. Therefore, the S-31 TW peak stage (NGVD29) was plotted against the 3-day rainfall depth for the nearest NOAA Atlas 14 station and fitted with a trendline. The best-fitting trendline (highest R^2 coefficient) was determined to be logarithmic. The following table and figure show the data used and the corresponding graph.

Table 3-12: Data Used to Scale-Down S-31 TW Peak Stage

Return period (yr)	Rainfall depth (in)	Peak Stage (ft NGVD29)
5	8.12	5.43 (calculated)
10	9.66	5.84
25	12.1	6.97
100	16.3	7.56

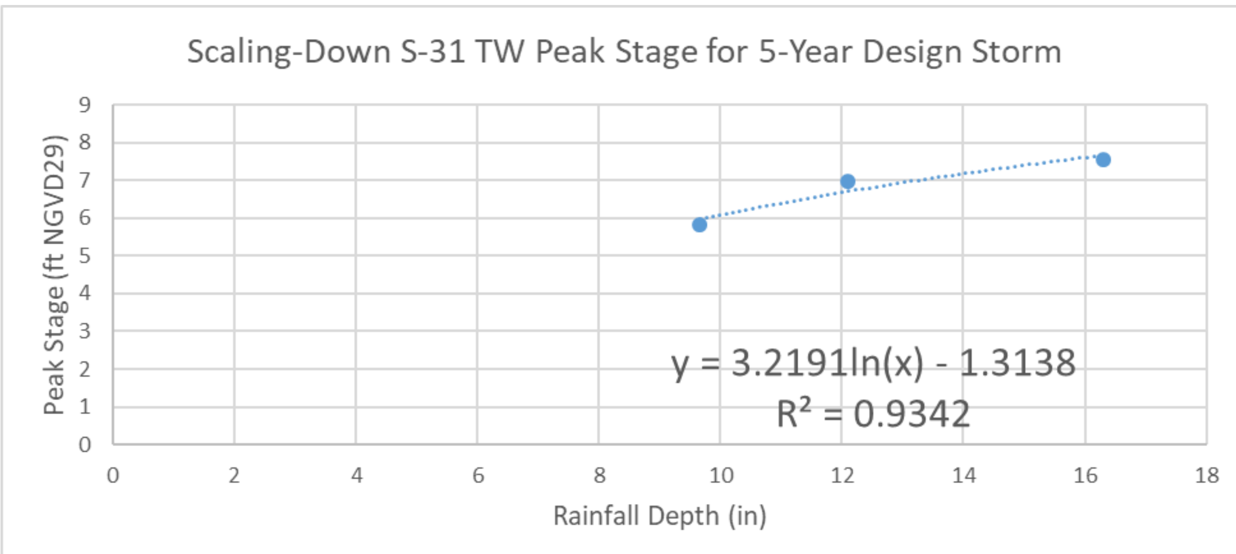

Figure 3.9-29: Scale-Down Approach for S-31 Tailwater

With this approach, the peak stage for the 5-year design storm at S-31 TW was determined to be 5.43 ft NGVD29. Therefore, a correction factor of 0.929 (5 year stage divided by 10 year stage) was applied to the 10-year time series data for all values greater than 4.18 ft (this is the lowest value possible before the correction factor would reduce stage to below the initial elevation of 3.88 feet) and values greater than 3.88 but less than 4.18 were set to 3.88 feet.

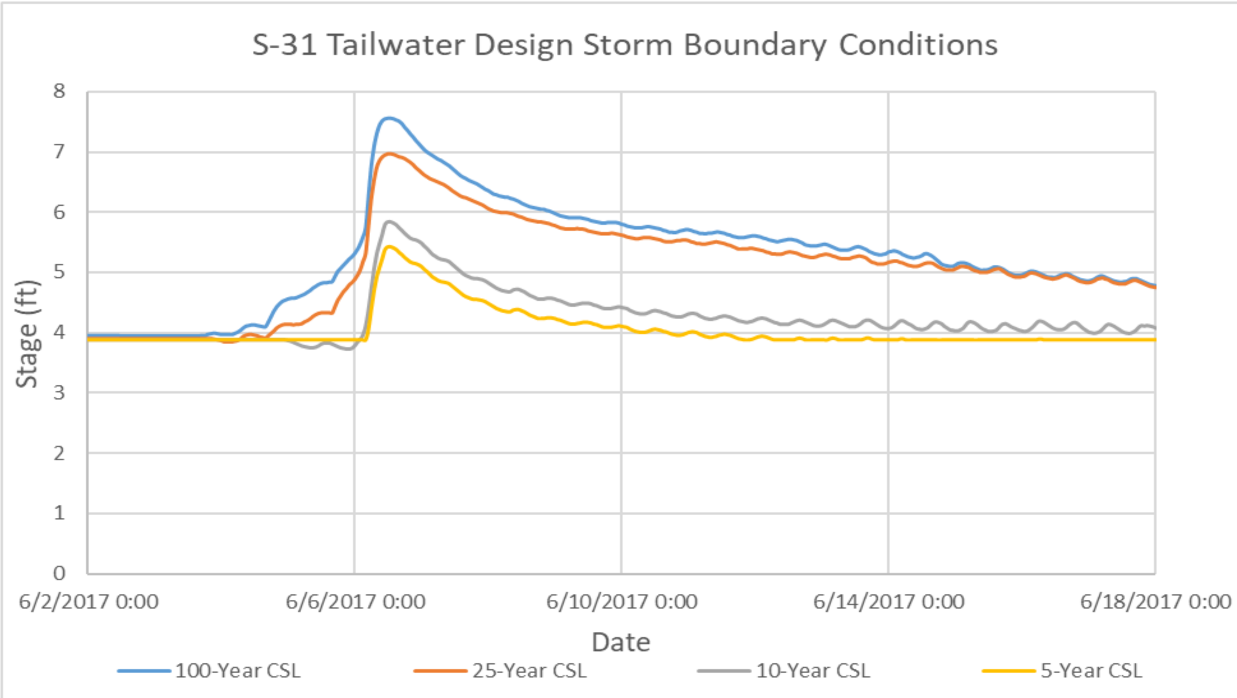

Figure 3.9-30: District Provided and Scaled-Down Simulated Design Storm Stages for S-31/32 TW

3.9.8 Drainage Level

The saturated zone drainage routine conceptually represents local-scale drainage features such as roadside underdrains, shallow swales, and field-scale agricultural ditches not explicitly represented elsewhere in the model setup. The saturated zone drainage level was developed based on land use, with urban areas set to 1.5 ft below ground, rural/agricultural areas set to 2.5 ft below ground, and 0 ft (turn saturated zone drainage off) for water and undeveloped areas. The spatial distribution of the saturated zone drainage levels are shown in **Figure 3.9-31**.

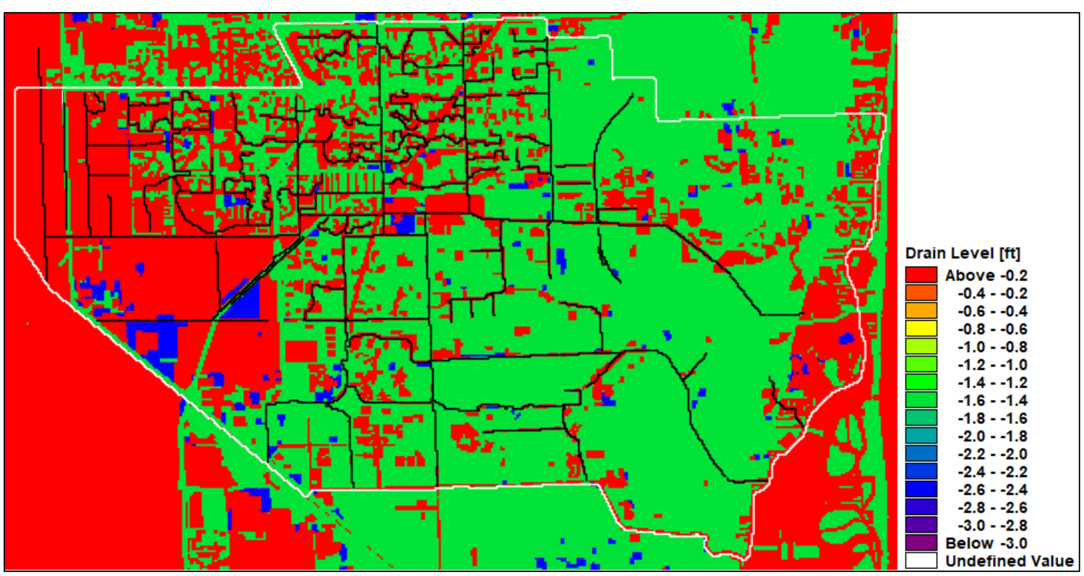

Figure 3.9-31: Drain Levels in the Saturated Zone

3.9.9 Drainage Time Constants

This parameter was set to the final calibrated value from the 2019 Broward County model (within the C-9 basin), with a value of 5E-07/s for developed land use areas. The saturated zone drainage is calculated as a linear reservoir based on the head difference between the water table and the drain level and a time constant. The time constant characterizes the "density" of the drainage network. In areas with a lot of drainage features, such as a basin with a lot of underdrains, the time constant could be increased as part of the calibration process. A larger time constant would allow the saturated zone to drain faster to the specified sink (local depression, boundary, or nearest branch within same drain code). In undeveloped land areas and water bodies, the time constant was set to 0, to shut off the saturated zone drainage routine. No permanent changes to spatial distribution or magnitude were made during model calibration.

3.9.10 Drain Codes

The saturated zone drainage routine used the same drain codes as the ponded drainage layer (**Figure 3.7-5**), without the initial depth or flood code cells set to drain code 0.

4 MODEL CALIBRATION

The model calibration process focused on attaining the best-fit for the peak water levels, total discharge volume, and peak discharge. This study set a calibration target of +/- 10-20% peak discharge and total discharge volume and +/- 0.5 ft headwater/tailwater and groundwater elevation. This approach allows a more comprehensive assessment of the model's simulated hydrologic and hydraulic response to rainfall, as compared to only matching peak stages or peak discharges. Refer to **Figure 2.6-1** for the locations of the SFWMD structures and groundwater wells used to calibrate the model. The operable structures (gates) used recorded gate openings and the tidal tailwater elevations were forced with the recorded water levels obtained from DBHYDRO. The model's simulated peak headwater/tailwater, peak discharge, total discharge volume, and groundwater levels were compared with observed data from SFWMD's DBHYDRO database.

4.1 Calibration Summary

Model calibration started with reparameterizing the groundwater model based on the 2019 Broward County Current Conditions model and expanding the model domain so that an internal boundary condition could be included. This inclusion was done for consistency with the 2019 Broward County Model, and to attempt to improve the hydrologic response in the western part of the model domain. These adjustments could be viewed as a model setup correction more so than a calibration alteration. These modifications resulted in improved model simulated surface water and groundwater responses throughout the model domain. However, the model was significantly overpredicting the peak discharge rates and the total volume discharged through the tidal structures and subsequent calibration efforts were primarily focused on improving these simulated values. Several adjustments were made to the following parameters in an effort to reduce the runoff volume and shift the timing of the runoff to better simulate the "peaks":

- Surface-subsurface leakage coefficient
- Paved area runoff coefficient

- Manning's roughness coefficient (overland flow)
- Manning's roughness coefficient (channel flow)
- ponded drainage time constants
  - Maximum storage change rate
  - Inflow / Outflow time constant
- Saturated zone drainage time constants
  - Maximum storage change rate
  - Inflow / Outflow time constant

However, these parametric changes resulted in little to no improvement in model performance and often led to a worse agreement between simulated and observed surface water stages and groundwater levels.

This suggested that inaccurate rainfall inputs may be a factor. As noted previously in **Section 2.4,** the year 2000 NEXRAD rainfall data was highly uncertain, due to both the questionability of NEXRAD DATA between 2000-2005, and the temporal adjustments made to the rainfall time series. Therefore, the adjusted NEXRAD data was replaced with the rain gauge data. Subsequent model simulations showed significant improvements in simulated peak discharge rates and total discharge volumes. This, in combination with the validation results described in **Section 5**, suggests the initial rainfall setup was responsible for the aforementioned overpredictions in the calibration model.

After the change in rainfall data, model calibration goals were met at most calibration points. In the areas not meeting calibration goals, localized adjustments were made but resulted in no significant improvement in model performance. The only adjustments that resulted in improvements were changes to Manning's roughness coefficient in three canals. At this point in the calibration process, three things were evident:

- for the calibration period, gauge-based rainfall data was more reliable than NEXRAD data, but still does not fully capture spatial-temporal patterns in rainfall
- overall, there was a very good match between simulated and observed data
- additional reasonable parametric changes are not resulting in further improvement in model performance.

Therefore, Taylor Engineering felt confident that the model setup and parameterization was a reasonable representation of the conditions that existed within the area if interest in October of 2000.

At this point, it was determined to use the calibrated model to simulate the chosen independent validation storm event, which was Hurricane Irma. Good model performance during an independent storm event further validates the adequacy of the model setup and parameterization approach. The validation storm event was relatively recent, compared to 20 years ago for the calibration event. As such, the NEXRAD rain data associated with the validation event was expected to have a lower level of uncertainty. As discussed in **Section 5**, during the validation event, model simulated hydrologic and hydraulic conditions were in close agreement with the observed data. Excellent model performance during the validation simulation further confirms the adequacy of the model setup and parameterization approach. The following sections provide details on the model setup and parameterization changes made during calibration.

4.2 Saturated Zone

During the initial calibration runs, it was noticed that groundwater wells G-1636, G-1637, and G-970 had a very subdued response to rainfall, whereas the recorded data showed a quite pronounced response. Adjustments were made to try to increase the groundwater response, including increased surface-subsurface leakage coefficient and decreased saturated zone drainage time constant. These changes resulted in almost no change, which is quite unusual as models are typically quite sensitive to these parameters. Therefore, this study reexamined the saturated zone inputs derived from the USGS. The USGS groundwater model was configured differently than the 2019 Broward County Current Conditions model. The USGS groundwater model (Hughes & White, 2016) used a second layer with low conductivity, whereas the 2019 Broward County model had a highly conductive second layer representing the Biscayne aquifer. Taylor Engineering decided to reparametrize the entire groundwater model based on the 2019 Broward County Current Conditions MIKE SHE model, which happened to extend far enough south to cover the entire C-8 C-9 model domain. Therefore, the first major change during model calibration was reparameterizing the saturated zone based on the 2019 Broward County MIKE SHE model, with the exception of the initial potential head. These changes to the groundwater model resulted in better simulated groundwater levels throughout the model when compared to the observed data. Refer to **Figure 3.9-1** through **Figure 3.9-13** for the final aquifer parameters.

4.3 Boundary Conditions

After changing the groundwater model configuration, the simulated data was a closer match to the observed data in most parts of the study area. However, the western groundwater wells were still a little less responsive than observed data. The 2019 Broward County Current Conditions model had an internal boundary condition, just west of the SFWMD L-33 canal, which is where the original C-8 C-9 model domain ended. Therefore, the model domain was extended about 1 mile west so that the internal boundary condition could be included, as shown in **Figure 3.9-19**. This internal boundary condition is based on the stage in Water Conservation Area 3B and is a head-controlled flux boundary with a leakage coefficient of 3E-6, as characterized in the 2019 Broward County Current Conditions model. This change helped the groundwater respond more closely to the observed data.

4.4 Rainfall

The storm event from October 2^{nd}-4^{th}, 2000 was used to calibrate the model, with a simulation period of October 1st-21st. Both point rain measurements and spatially distributed NEXRAD data were available for the October 2000 storm event. Initially, hourly NEXRAD rainfall data with a spatial resolution of 2 km x 2 km was used for total rainfall depth and spatial distribution. The temporal distribution of each NEXRAD pixel was adjusted based on recorded rain gauge data. A rain gauge was assigned to each NEXRAD pixel based on Thiessen polygons that were delineated using the rain gauge locations present in the area. The calibration scenario using NEXRAD rainfall resulted in a reasonable match between simulated and observed groundwater levels and surface water stages throughout the model. However, the simulated peak discharge rates and the total discharge volume differed by upwards of +30%. Calibration efforts included varying parameters such as surface-subsurface leakage coefficient, paved area runoff coefficient, Manning's roughness for both overland and channel flow, ponded drainage time constants, and saturated zone drainage time constants, which resulted in no significant improvement in model performance. Considering there was a reasonable match between simulated and observed data for groundwater levels and surface water stages, it was suspected there was simply too much rainfall being simulated. It is well known by the District that the quality of the NEXRAD data is questionable for the 2000 -2005 period, given that the collection and application of NEXRAD data in Florida during that time was an emerging technology. It was entirely possible that NEXRAD data was simply not an accurate representation of actual rainfall. Therefore, the NEXRAD data replaced with raw rain gauge data. Although there are still rainfall data limitations by using only 5 reference points, the rain gauge data led to significantly improved peak discharge rates and total discharge volumes.

4.5 Manning's Roughness Coefficient

After switching the rainfall data and vastly reducing the overprediction of peak discharge rates and total discharge volume, some localized adjustments to the 1D model's Manning's roughness coefficients were made in an attempt to improve the peak surface water stage, as well as the overall shape of the hydrographs. Throughout the model, only a few canals were adjusted, as shown in the table below.

Table 4-1: Manning's Roughness Calibration Adjustments

Branch	Original Manning's n	Adjusted Manning's n
SFWMD C-8 Ext	0.033	0.04
Peter S Pike Canal	0.033	0.04
Grahams Dairy Canal	0.033	0.04

4.6 Calibration Results

Overall, the calibrated model sufficiently simulated surface water and groundwater responses to rainfall and were a good match to recorded observations at multiple locations throughout the model domain. Model simulated peak surface water stages generally agreed to within 0.5 ft of the observed stages, with an absolute average difference of 0.3 ft. Model simulated peak discharge rates agreed to within 10% of the observed peak discharge, with an absolute average difference of 6%. Model simulated total discharge volume agreed to within 17% of observed discharge volume, with an absolute average difference of 14%. Model simulated groundwater elevations generally agreed to within 0.5 ft of the observed elevations, with an absolute average difference of 0.3 ft. **Table 4-2** provides a detailed summary of the simulated vs. observed differences, **Table 4-3** provides a comparison between simulated and observed peak stages, **Table 4-4** provides a comparison between simulated and observed peak discharges and time of peak discharge, **Table 4-5** and **Table 4-6** provide water budgets for the C-8 and C-9 basins, respectively for the calibration period of October 1st-21st, 2000. **Table 4-7** provides simulation statistics for both the entire simulation period and the first 7 days of simulation.

Table 4-2: Calibration Results Comparison

Calibration Point	Total Volume Difference	Peak Discharge Difference (cfs)	Peak Headwater Difference (ft)	Peak Tailwater Difference (ft)	Groundwater Elevation Difference (ft)
S-28	-10.6%	3%	0.45	Forced	
S-29	16.8%	9%	0.56	Forced	
S-30			0.15	0.38	
S-32			0.05	Forced	
S-9XS			0.35	Forced	
S-28Z			0.67		
S-29Z			0.01		
G-1225					0.57
G-1636					-0.12
G-1637					-0.10
G-3571					-0.81
G-852					-0.18
G-970					-0.21
S-18					0.05

Table 4-3: Calibration Peak Stage Comparison

Calibration Point	Peak Stage (ft NGVD29)		
	Simulated	Observed	Difference
S-28	4.87	4.42	0.45
S-29	3.75	3.19	0.56
S-30 HW	6.74	6.59	0.15
S-30 TW	5.2	4.82	0.38
S-32	6.73	6.68	0.05
S-9XS	6.83	6.48	0.35
S-28Z	5.53	6.2	-0.67
S-29Z	4.95	4.94	0.01
G-1225	7.36	6.79	0.57
G-1636	4.8	4.93	-0.13
G-1637	5.34	5.44	-0.1
G-3571	6.62	7.43	-0.81
G-852	7.1	7.28	-0.18
G-970	4.57	4.78	-0.21
S-18	7.19	7.14	0.05

Table 4-4: Calibration Peak Discharge Comparison

Calibration Point	Peak Discharge (cfs)			Time of Peak Discharge	
	Simulated	Observed	Difference	Simulated	Observed
S-28	2835	2743	92	10/4/2000 5:50	10/3/2000 20:30
S-29	4151	3792	359	10/4/2000 7:50	10/3/2000 20:00

Table 4-5: Calibration Water Budget for C-8 Basin

Water Budget Term	Inches (Average Over C-8 Basin)	
	Inflows	Outflows and Storage
Rainfall	13.4	
Evapotranspiration		1.4
Surface runoff		8.2
Groundwater flow to canals		4.4
Groundwater boundary inflow	0.3	
Change in surface storage		0.2
Change in groundwater storage	0.4	

Table 4-6: Calibration Water Budget for C-9 Basin

Water Budget Term	Inches (Average Over C-9 Basin)	
	Inflows	Outflows and Storage
Rainfall	11.8	
Evapotranspiration		1.6
Surface runoff		10.9
Groundwater flow to canals		4.0
Groundwater boundary inflow	6.1	
Change in surface storage		1.2
Change in groundwater storage		0.2

After **Table 4-7**, **Figure 4.6-1** through **Figure 4.6-17** present a visual comparison between model simulated and observed conditions throughout the model domain. Structure headwater/tailwater that were used as boundary conditions are not included as they are identical (i.e., S-28 tailwater was a forced boundary).

Table 4-7: Calibration Model Statistics for Simulated vs Observed Data

Calibration Point	7-day Simulation (Oct 1st -7th, 2000)						21-day Simulation (Oct 1st -21st, 2000)					
	ME	MAE	RMSE	STDres	R (Correlation)	Nash Sutcliffe	ME	MAE	RMSE	STDres	R (Correlation)	Nash Sutcliffe
S-29 Q (cfs)	-272	499	613	549	0.92	0.64	-217	317	440	383	0.94	0.75
S-29 HW (ft)	-0.037	0.19	0.21	0.21	0.92	0.83	-0.08	0.13	0.18	0.16	0.97	0.88
S-28 Q (cfs)	-102	223	310	293	0.96	0.8	86	239	329	318	0.89	0.65
S-28 HW (ft)	-0.047	0.09	0.13	0.13	0.98	0.95	-0.0009	0.05	0.08	0.08	0.99	0.98
S-30 HW (ft)	-0.17	0.17	0.2	0.11	0.96	0.44	-0.086	0.109	0.15	0.13	0.88	0.65
S-30 TW (ft)	-0.21	0.34	0.41	0.35	0.99	0.78	0.45	0.49	0.52	0.26	0.96	0.4
S-32 HW (ft)	-0.086	0.12	0.15	0.12	0.96	0.7	-0.001	0.1	0.11	0.11	0.88	0.71
S-9XS HW (ft)	-0.19	0.23	0.26	0.18	0.96	0.33	-0.3	0.31	0.33	0.13	0.91	-4.95
S-29Z Stage (ft)	0.05	0.28	0.39	0.38	0.94	0.81	-0.02	0.32	0.38	0.38	0.87	0.71
S-28Z Stage (ft)	0.34	0.35	0.39	0.18	0.99	0.9	0.35	0.36	0.39	0.16	0.99	0.89
G-1225 (ft)	-0.035	0.37	0.43	0.43	0.98	0.93	-0.19	0.32	0.36	0.31	0.98	0.9
G-1636 (ft)	-0.03	0.26	0.35	0.35	0.88	0.76	-0.01	0.19	0.25	0.25	0.9	0.77
G-1637 (ft)	0.19	0.2	0.3	0.24	0.92	0.75	0.13	0.13	0.19	0.15	0.93	0.77
G-970 (ft)	0.14	0.33	0.4	0.38	0.91	0.76	-0.1	0.33	0.42	0.41	0.82	0.6
G-3571 (ft)	0.93	1	1.4	1	0.83	0.43	0.59	0.62	0.91	0.69	0.9	0.56
S-18 (ft)	0.56	0.66	1.23	1.1	0.84	0.63	0.14	0.33	0.73	0.72	0.89	0.76
G-852 (ft)	0.55	0.81	1.26	1.13	0.88	0.71	0.6	0.68	0.94	0.73	0.91	0.68

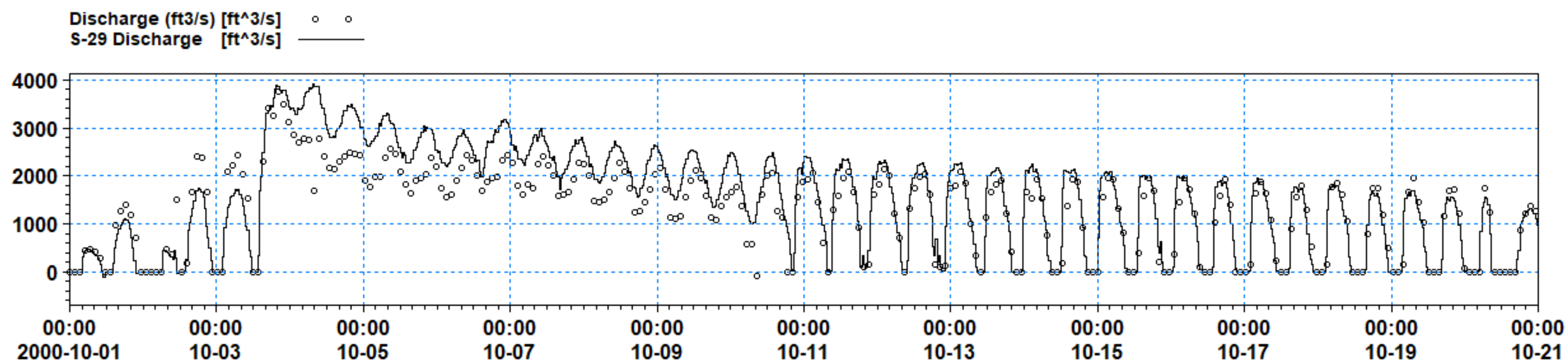

Figure 4.6-1: Simulated (line) vs Observed (dots) Discharge Comparison for SFWMD C-9 Structure S-29, October 1st-21st, 2000

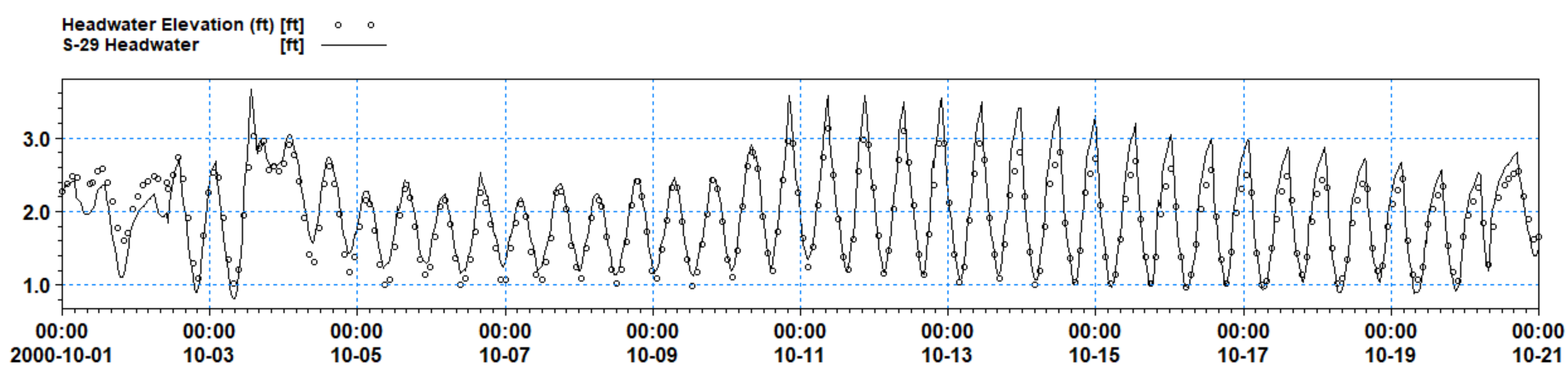

Figure 4.6-2: Simulated (line) vs Observed (dots) Headwater Comparison for SFWMD C-9 Structure S-29, October 1st-21st, 2000

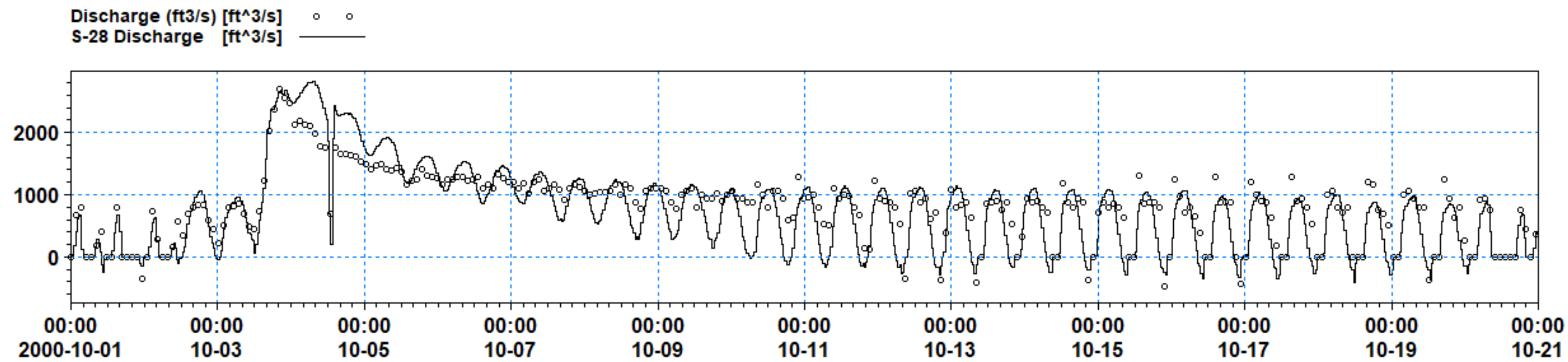

Figure 4.6-3: Simulated (line) vs Observed (dots) Discharge Comparison for SFWMD C-8 Structure S-28, October 1st-21st, 2000

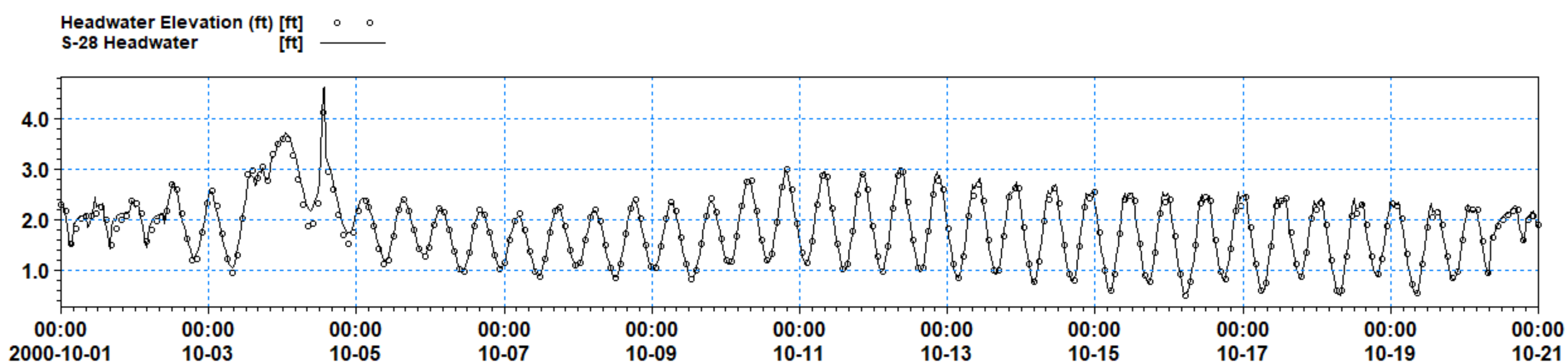

Figure 4.6-4: Simulated (line) vs Observed (dots) Headwater Comparison for SFWMD C-8 Structure S-28, October 1st-21st, 2000

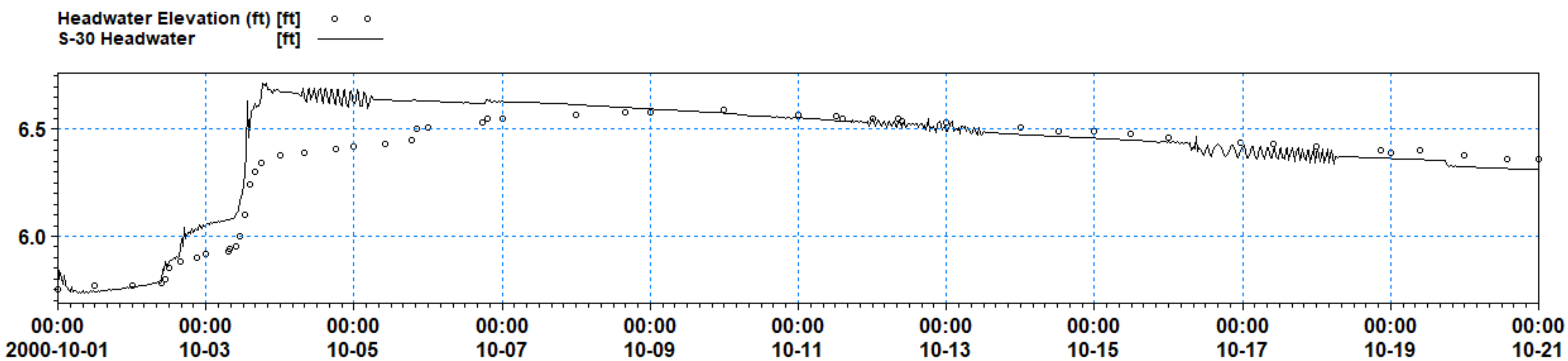

Figure 4.6-5: Simulated (line) vs Observed (dots) Headwater Comparison for SFWMD C-9 Structure S-30, October 1st-21st, 2000

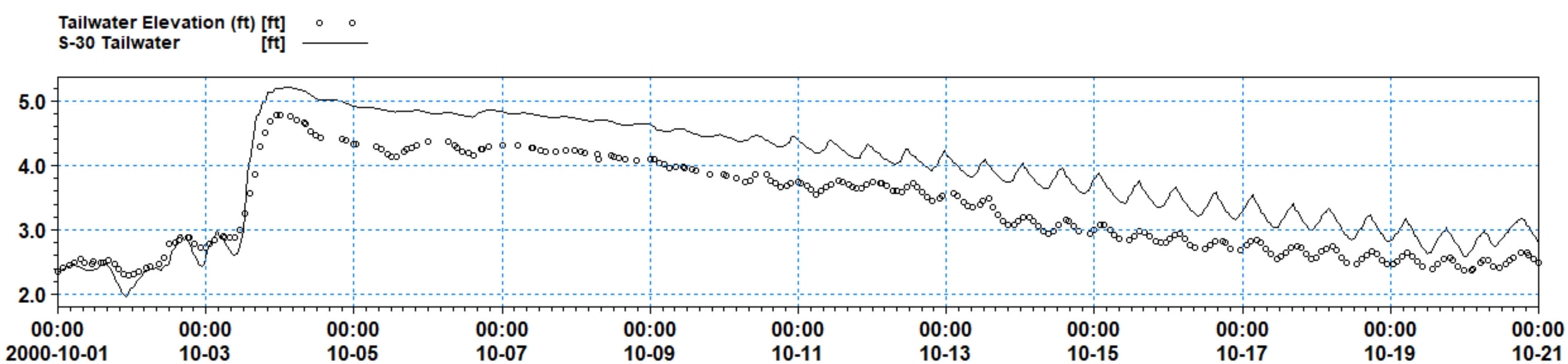

Figure 4.6-6: Simulated (line) vs Observed (dots) Tailwater Comparison for SFWMD C-9 Structure S-30, October 1st-21st, 2000

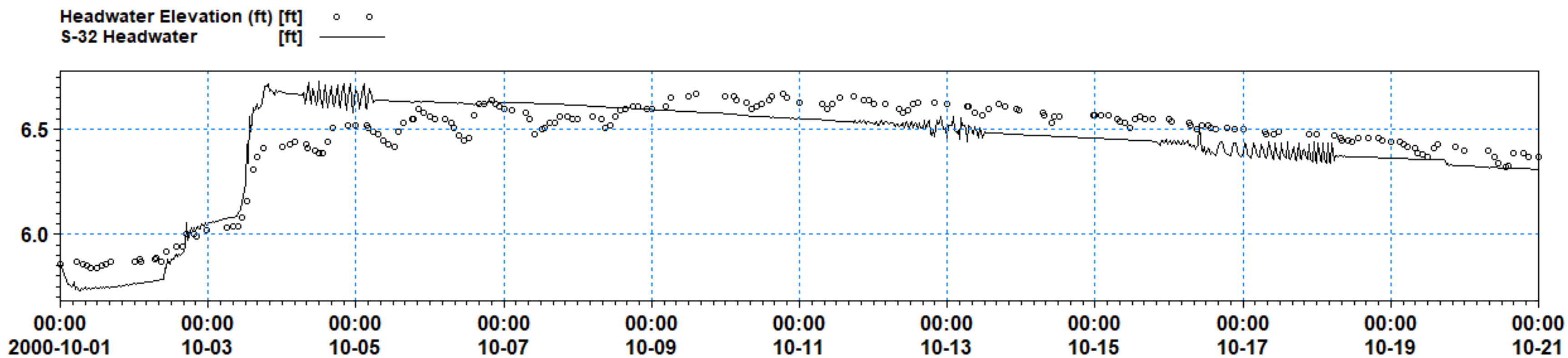

Figure 4.6-7: Simulated (line) vs Observed (dots) Headwater Comparison for SFWMD L-33 Structure S-32, October 1st-21st, 2000

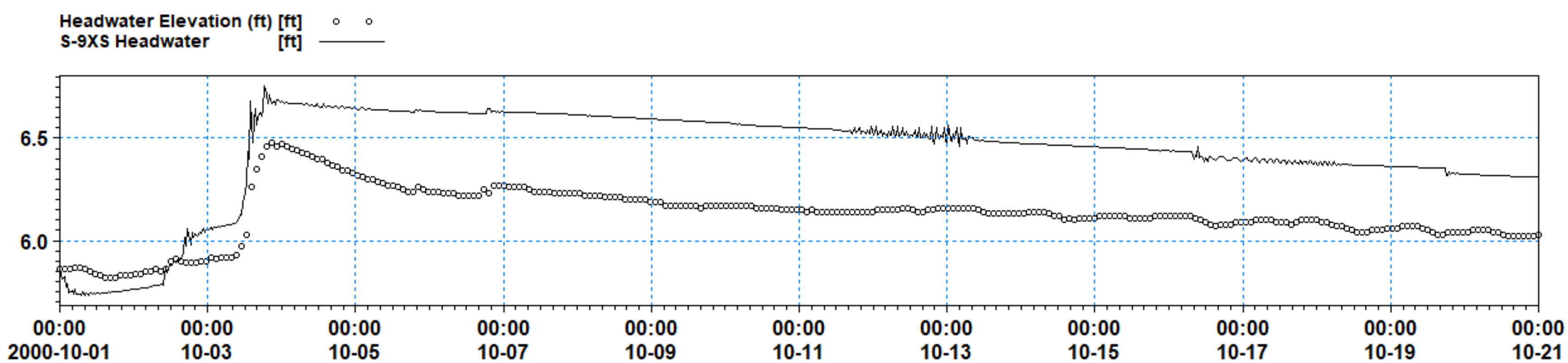

Figure 4.6-8: Simulated (line) vs Observed (dots) Headwater Comparison for SFWMD L-33 Structure S-9XS, October 1st-21st, 2000

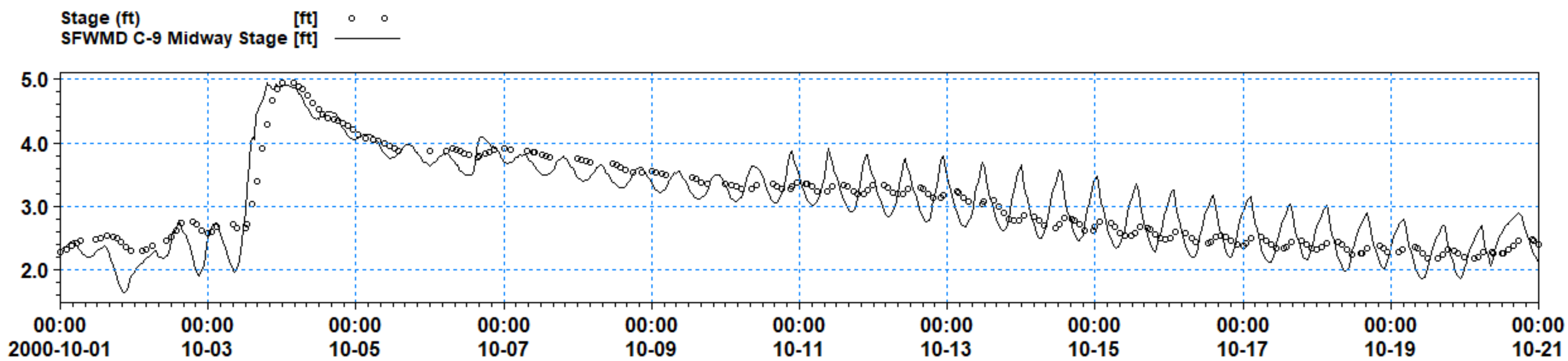

Figure 4.6-9: Simulated (line) vs Observed (dots) Stage Comparison for SFWMD C-9 Water Level Recorder S-29Z, October 1st-21st, 2000

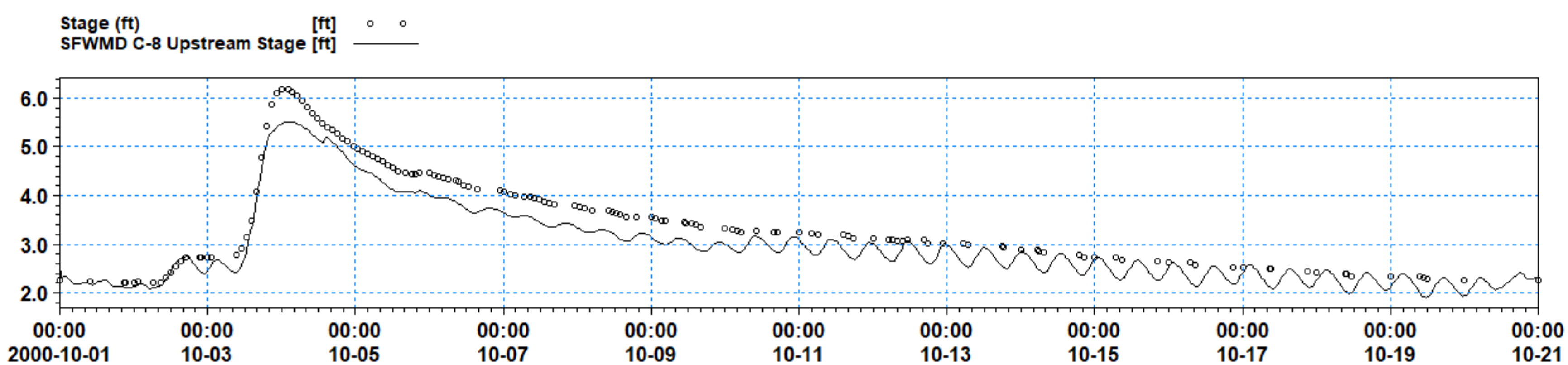

Figure 4.6-10: Simulated (line) vs Observed (dots) Stage Comparison for SFWMD C-8 Water Level Recorder S-28Z, October 1st-21st, 2000

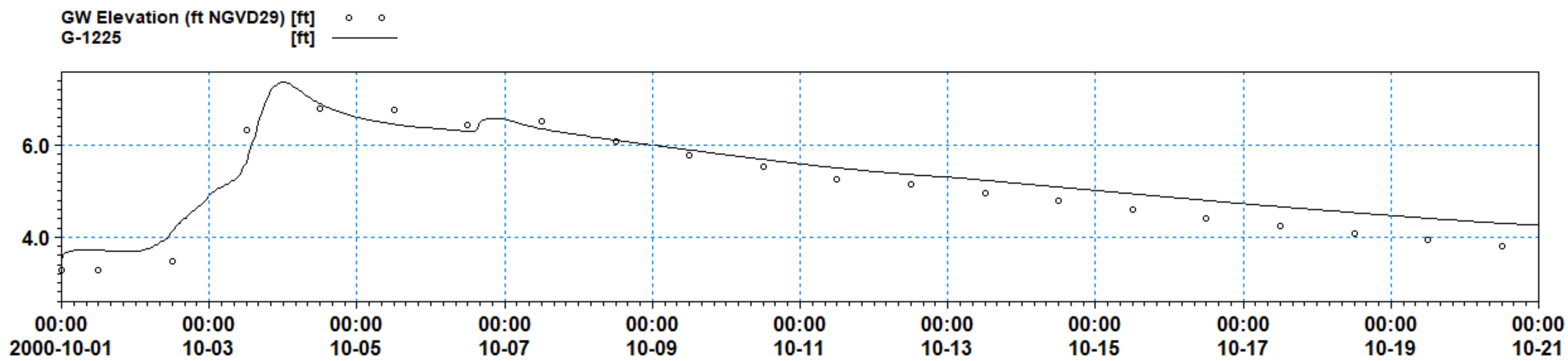

Figure 4.6-11: Simulated (line) vs Observed (dots) Groundwater Elevation Comparison for Well G-1225, October 1st-21st, 2000

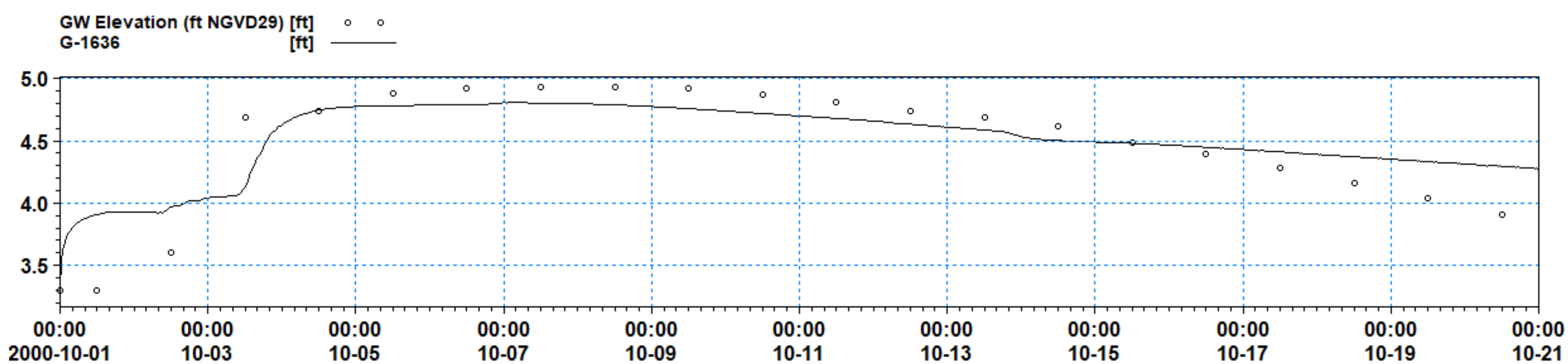

Figure 4.6-12: Simulated (line) vs Observed (dots) Groundwater Elevation Comparison for Well G-1636, October 1st-21st, 2000

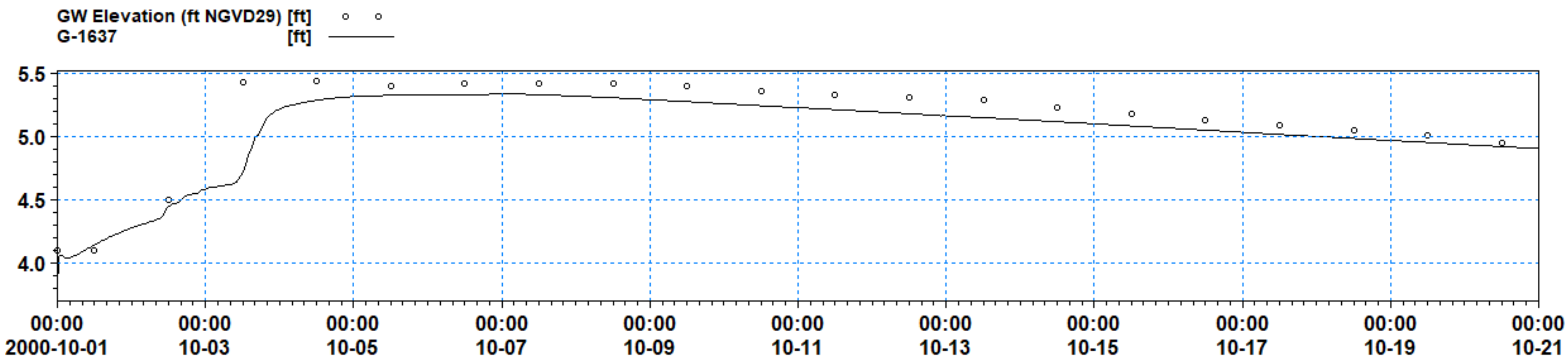

Figure 4.6-13: Simulated (line) vs Observed (dots) Groundwater Elevation Comparison for Well G-1637, October 1st-21st, 2000

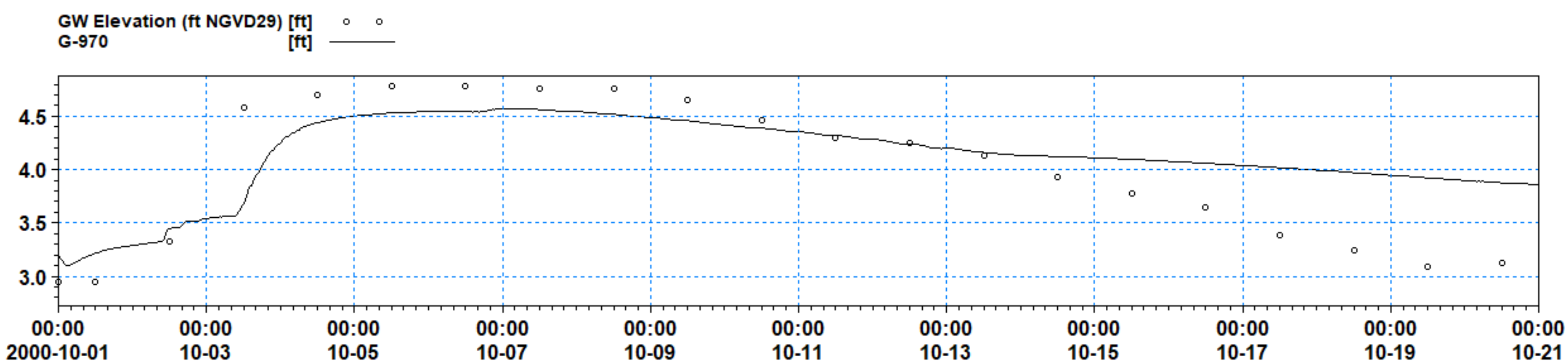

Figure 4.6-14: Simulated (line) vs Observed (dots) Groundwater Elevation Comparison for Well G-970, October 1st-21st, 2000

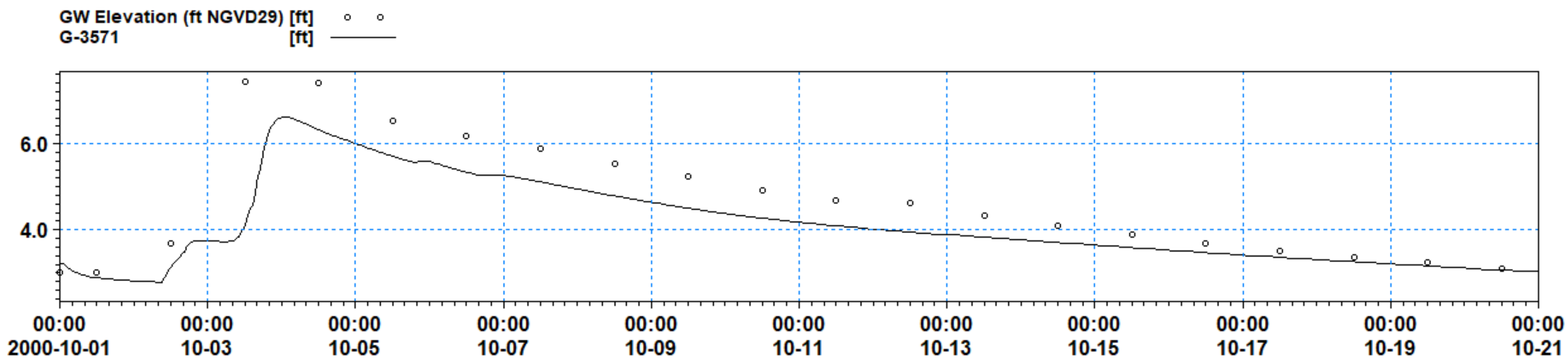

Figure 4.6-15: Simulated (line) vs Observed (dots) Groundwater Elevation Comparison for Well G-3571, October 1st-21st, 2000

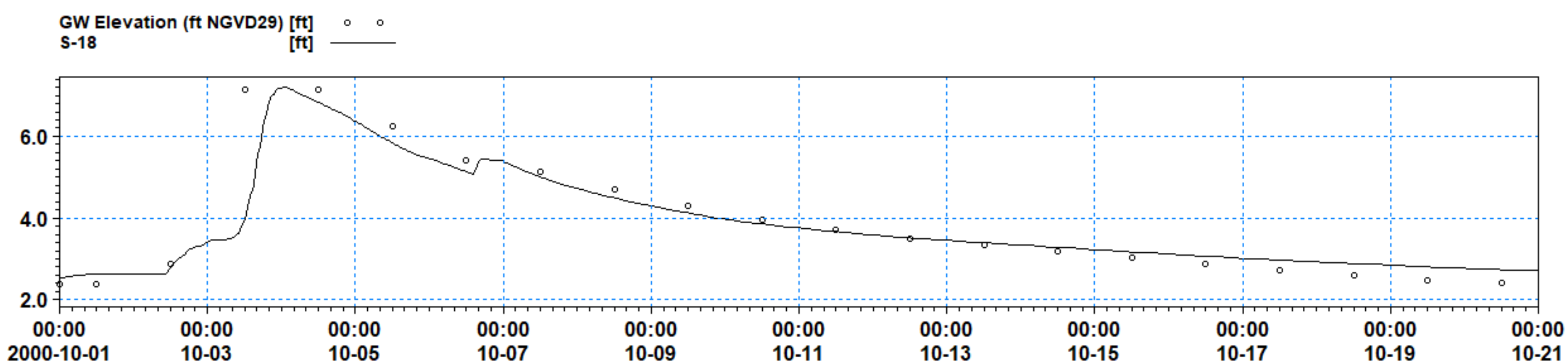

Figure 4.6-16: Simulated (line) vs Observed (dots) Groundwater Elevation Comparison for Well S-18, October 1st-21st, 2000

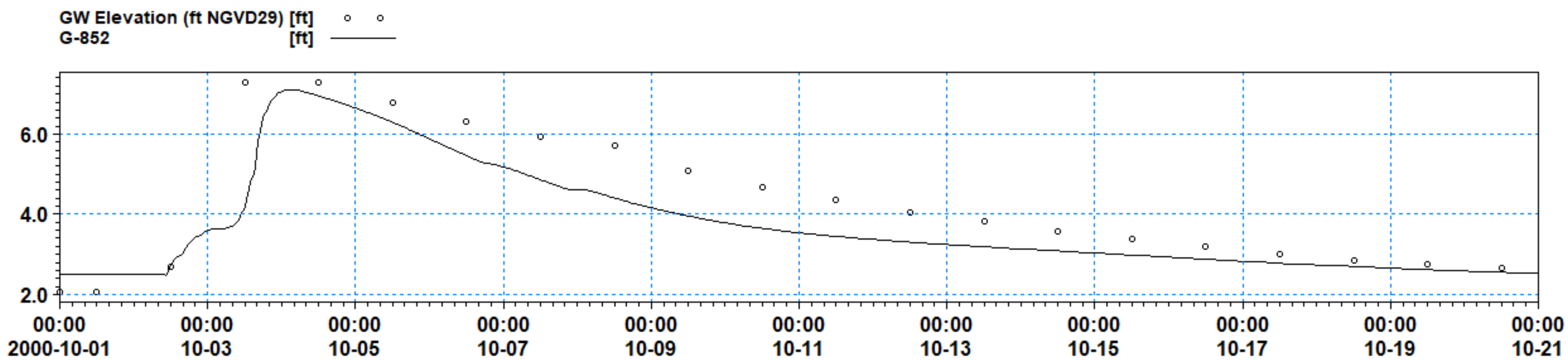

Figure 4.6-17: Simulated (line) vs Observed (dots) Groundwater Elevation Comparison for Well G-852, October 1st-21st, 2000

5 MODEL VALIDATION

Refer to **Figure 2.6-1** for the locations of the SFWMD structures and groundwater wells used to validate the model. The operable structures (gates) used recorded gate openings and the tidal tailwater elevations were forced with the recorded water levels obtained from DBHYDRO. The model's simulated peak headwater/tailwater, peak discharge, total discharge volume, and groundwater levels were compared with observed data which was obtained from SFWMD's DBHYDRO database. Overall, the model adequately simulated surface water and groundwater responses to rainfall and were a good match to recorded observations at multiple locations throughout the model domain. Model simulated surface water stages generally agreed to within 0.4 ft of observed stages, with an absolute average difference of 0.2 ft. Model simulated peak discharge rates agreed to within about 17% of observed peak discharges, with an absolute average difference of 13%. Model simulated discharge volumes agreed to within 14% of observed discharge volumes, with an absolute average difference of 10%. Model simulated groundwater elevations generally agreed to within 1 ft of observed elevations, with an absolute average difference of 0.8 ft. **Table 5-1** provides a detailed summary of the simulated vs. observed differences, **Table 5-2** provides a comparison between simulated and observed peak stages, **Table 5-3** provides a comparison between simulated and observed peak discharges and time of peak discharge, **Table 5-4** and **Table 5-5** provide water budgets for the C-8 and C-9 basins, respectively, for the validation period of September 9th-16th, 2017. **Table 5-6** provides simulation statistics for both the entire simulation period of June-September 2017 and the 7-day period around the time of Hurricane Irma (9th-16th).

Table 5-1: Validation Results Comparison

Calibration Point	Total Volume Difference	Peak Discharge Difference (cfs)	Peak Headwater Difference (ft)	Peak Tailwater Difference (ft)	Groundwater Elevation Difference (ft)
S-28	14.4%	-17.4%	-0.01	Forced	
S-29	-5.5%	8.8%	-0.05	Forced	
S-30			0.32	0.43	
S-32			0.23	Forced	
S-9XS			0.44	Forced	
S-28Z			-0.10		
S-29Z			0.15		
G-1225					-1.26
G-1636					0.24
G-1637					0.77
G-3571					-1.59
G-852					-0.28
G-970					-0.64
S-18					0.7

Table 5-2: Validation Peak Stage Comparison

Calibration Point	Peak Stage (ft NGVD29)		
	Simulated	Observed	Difference
S-28	5.12	5.13	-0.01
S-29	4.82	4.87	-0.05
S-30 HW	6.91	6.59	0.32
S-30 TW	5.25	4.82	0.43
S-32	6.91	6.68	0.23
S-9XS	6.92	6.48	0.44
S-28Z	5.08	5.18	-0.1
S-29Z	5.09	4.94	0.15
G-1225	5.23		
G-1636	4.93	4.73	0.2
G-1637	5.52		
G-3571	5.71	7.27	-1.56
G-852	5.53	5.81	-0.28
G-970	4.56	5.14	-0.58
S-18	5.79	5.08	0.71

Table 5-3: Validation Peak Discharge Comparison

Calibration Point	Peak Discharge (cfs)			Time of Peak Discharge	
	Simulated	Observed	Difference	Simulated	Observed
S-28	1591	2010	-419	9/11/2017 6:20	9/9/2017 5:10
S-29	3393	3119	274	9/11/2017 17:35	9/11/2017 17:35

Table 5-4: Validation Water Budget for C-8 Basin

Water Budget Term	Inches (Average Over C-8 Basin)	
	Inflows	Outflows and Storage
Rainfall	7.7	
Evapotranspiration		0.7
Surface runoff		2.4
Groundwater flow to canals		1.6
Groundwater boundary inflow		0.3
Change in surface storage		0.6
Change in groundwater storage		2.0

Table 5-5: Validation Water Budget for C-9 Basin.

Water Budget Term	Inches (Average Over C-9 Basin)	
	Inflows	Outflows and Storage
Rainfall	8.1	
Evapotranspiration		0.8
Surface runoff		4.8
Groundwater flow to canals		1.1
Groundwater boundary inflow	1.4	
Change in surface storage		0.9
Change in groundwater storage		1.8

After **Table 5-6**, **Figure 4.6-1** through **Figure 4.6-16** presents a visual comparison between model simulated and observed conditions throughout the model domain during a 1-week portion of the validation period coinciding with Hurricane Irma and the following few days. Again, structure headwater/tailwater that were used as boundary conditions are not included as they are identical (i.e., S-28 tailwater was a forced boundary). Note that a few of the groundwater wells had no observed data during the period of September 9th-16th, 2017. Comparison plots for the full 4-month simulation period are provided in **Appendix C**.

Table 5-6: Validation Model Statistics for Simulated vs Observed Data

Calibration Point	7-day Simulation (September 9th -16th, 2017)						4-month Simulation (June 2nd -September 27th, 2017)					
	ME	MAE	RMSE	STDres	R (Correlation)	Nash Sutcliffe	ME	MAE	RMSE	STDres	R (Correlation)	Nash Sutcliffe
S-29 Q (cfs)	87	304	499	491	0.83	0.61	67	119	210	199	0.96	0.92
S-29 HW (ft)	-0.002	0.04	0.06	0.06	0.998	0.996	0.013	0.13	0.19	0.19	0.96	0.89
S-28 Q (cfs)	-75	364	608	604	0.59	0.30	-9	49	159	159	0.91	0.82
S-28 HW (ft)	0.01	0.05	0.05	0.05	0.998	0.997	-0.06	0.1	0.13	0.12	0.98	0.95
S-30 HW (ft)	-0.47	0.47	0.49	0.15	0.87	-2.78	-0.23	0.43	0.47	0.41	0.90	0.26
S-30 TW (ft)	-0.44	0.45	0.54	0.31	0.93	0.60	-0.64	0.65	0.73	0.34	0.85	0.38
S-32 HW (ft)	-0.55	0.55	0.58	0.17	0.89	-3.1	-0.32	0.48	0.53	0.42	0.89	-0.018
S-9XS HW (ft)	-0.87	0.87	0.89	0.19	0.91	-7.5	-0.53	0.80	0.85	0.66	0.57	-7.37
S-29Z Stage (ft)	-0.07	0.15	0.21	0.20	0.97	0.93	-0.13	0.22	0.28	0.25	0.87	0.64
S-28Z Stage (ft)	0.02	0.10	0.13	0.13	0.99	0.98	-0.12	0.16	0.19	0.14	0.95	0084
G-1225 (ft)	-	-	-	-	-	-	0.55	0.6	0.73	0.48	0.78	0.096
G-1636 (ft)	-0.38	0.38	0.52	0.36	0.96	0.09	-0.75	0.75	0.83	0.35	0.74	-2.06
G-1637 (ft)	-	-	-	-	-	-	-0.88	0.88	0.97	0.42	0.47	-3.87
G-970 (ft)	-0.32	0.42	0.54	0.43	0.90	0.26	-0.83	0.84	0.89	0.32	0.78	-2.82
G-3571 (ft)	0.49	0.60	0.75	0.57	0.96	0.67	-0.057	0.26	0.33	0.32	0.94	0.83
S-18 (ft)	-0.35	0.35	0.42	0.24	0.97	0.78	-0.36	0.36	0.43	0.23	0.93	0.34
G-852 (ft)	0.56	0.56	0.61	0.23	0.98	0.61	0.47	0.48	0.55	0.29	0.92	0.42

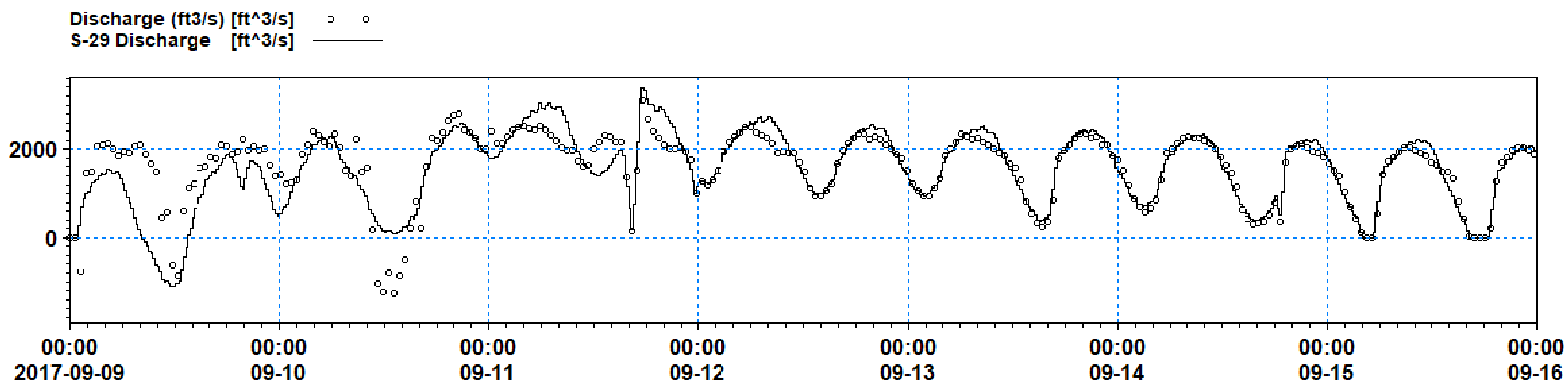

Figure 4.6-1: Simulated (line) vs Observed (dots) Discharge Comparison for SFWMD C-9 Structure S-29, September 9th-16th, 2017

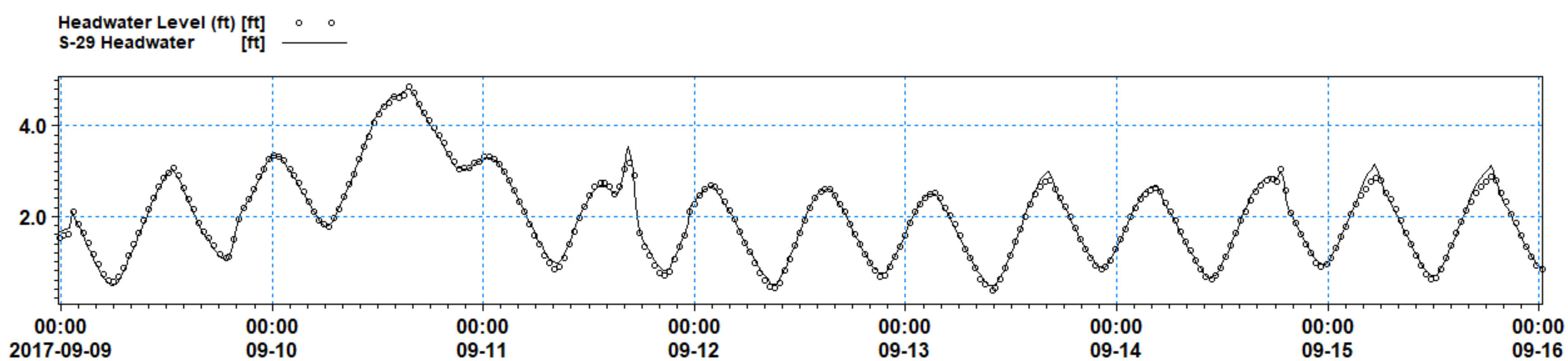

Figure 4.6-2: Simulated (line) vs Observed (dots) Headwater Comparison for SFWMD C-9 Structure S-29, September 9th-16th, 2017

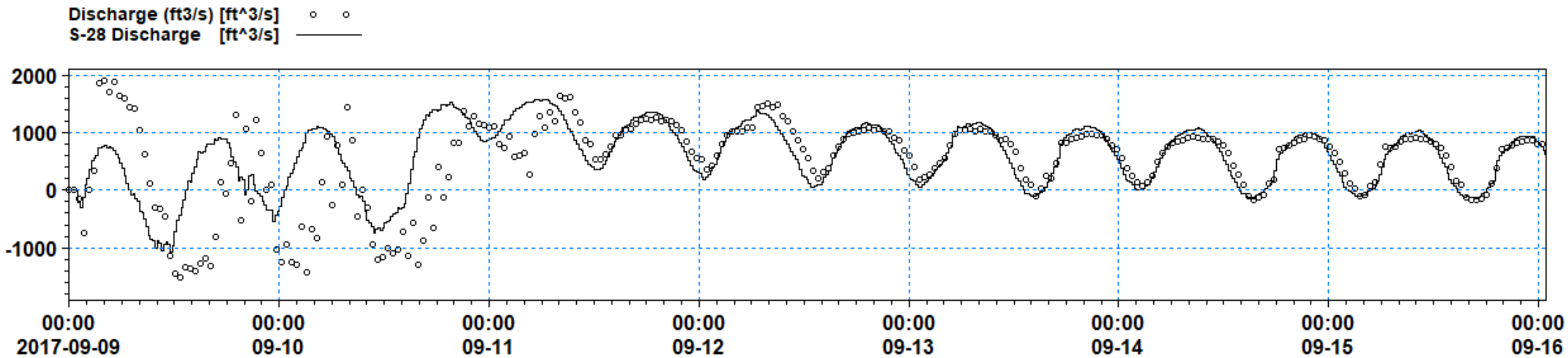

Figure 4.6-3: Simulated (line) vs Observed (dots) Discharge Comparison for SFWMD C-8 Structure S-28, September 9th-16th, 2017

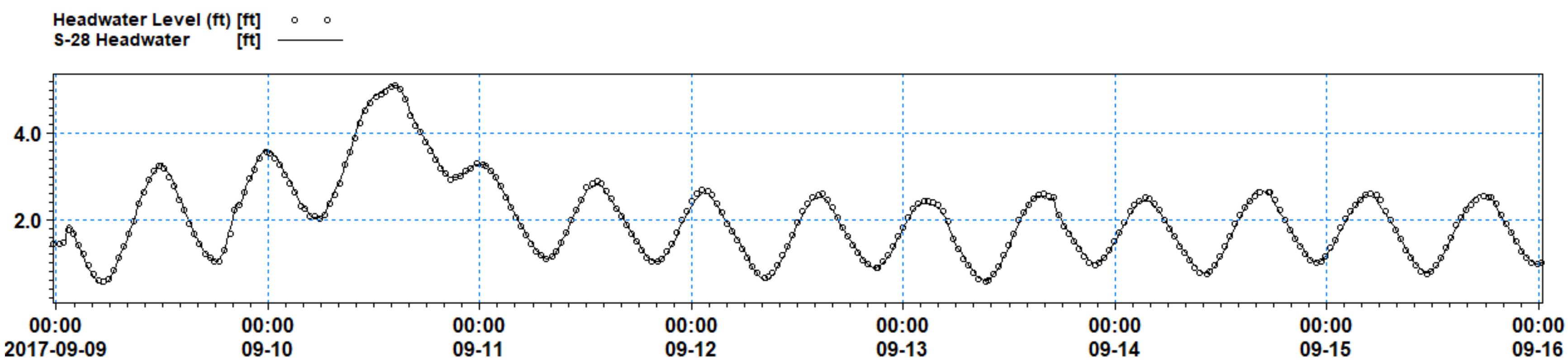

Figure 4.6-4: Simulated (line) vs Observed (dots) Headwater Comparison for SFWMD C-8 Structure S-28, September 9th-16th, 2017

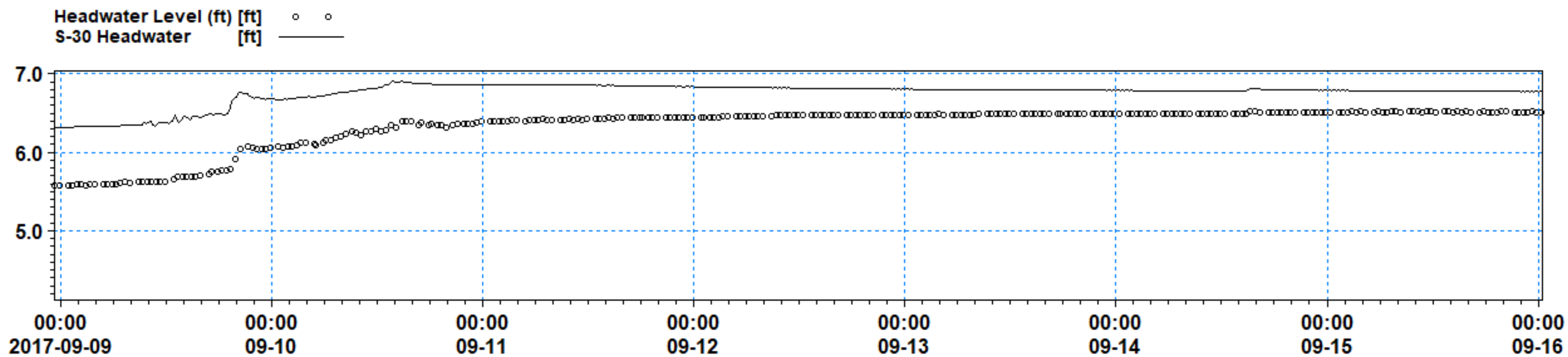

Figure 4.6-5: Simulated (line) vs Observed (dots) Headwater Comparison for SFWMD C-9 Structure S-30, September 9th-16th, 2017

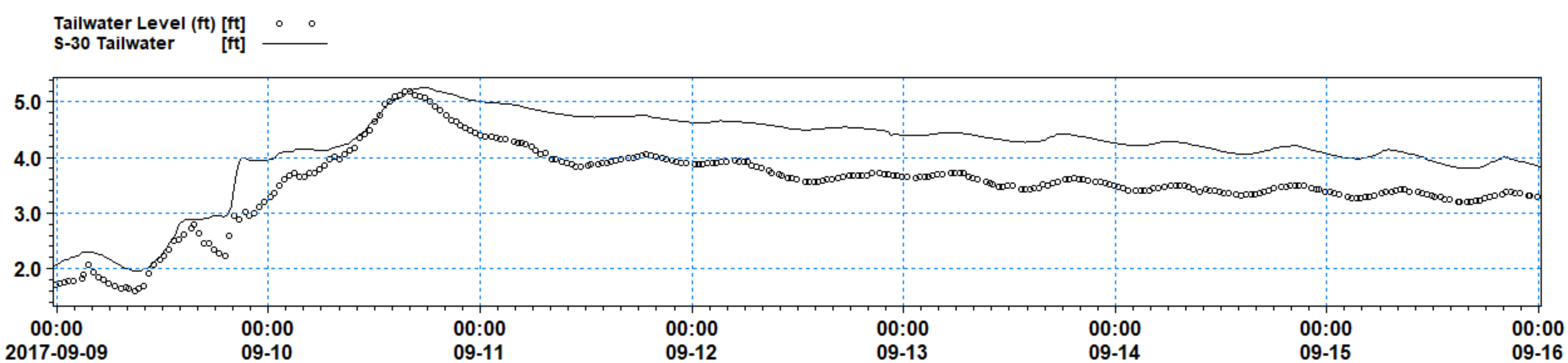

Figure 4.6-6: Simulated (line) vs Observed (dots) Tailwater Comparison for SFWMD C-9 Structure S-30, September 9th-16th, 2017

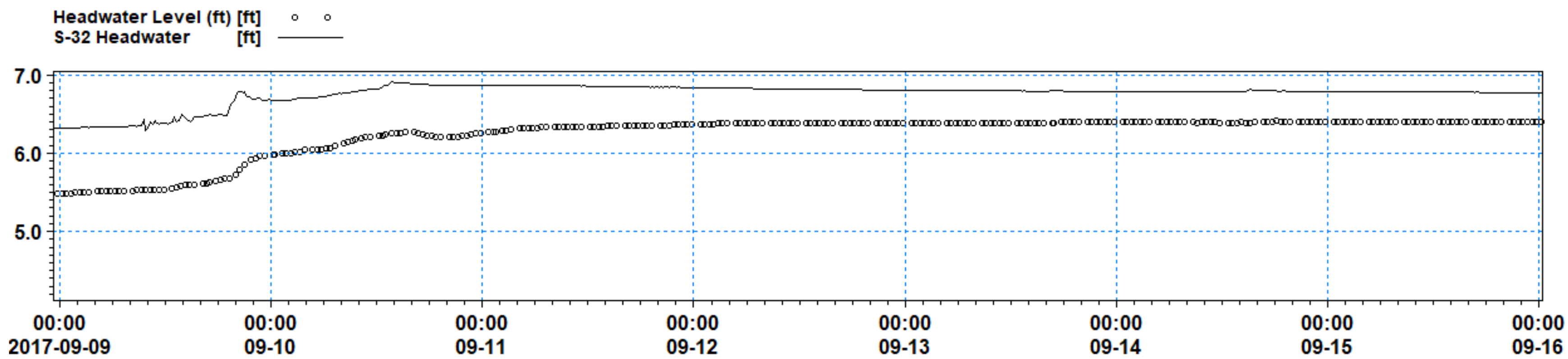

Figure 4.6-7: Simulated (line) vs Observed (dots) Headwater Comparison for SFWMD L-33 Structure S-32, September 9th-16th, 2017

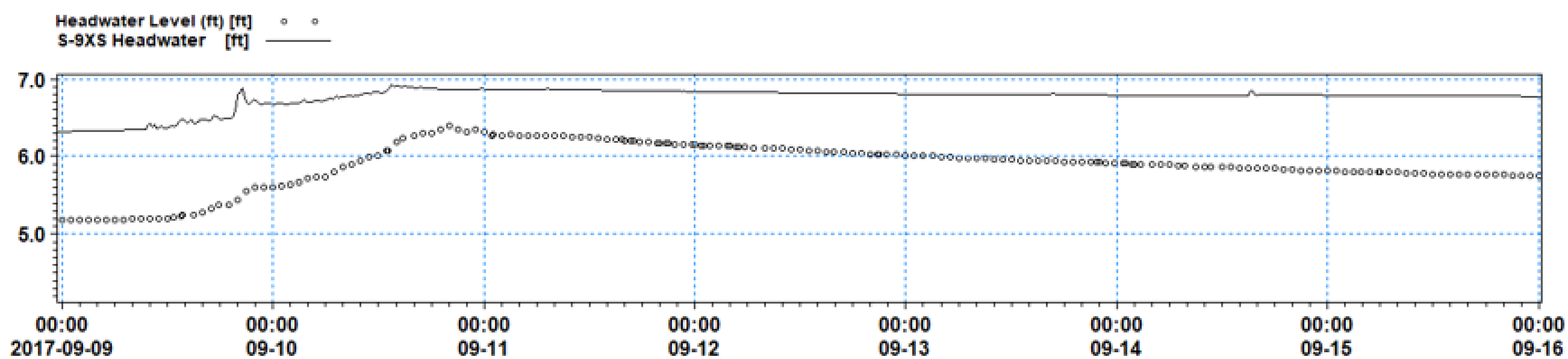

Figure 4.6-8: Simulated (line) vs Observed (dots) Headwater Comparison for SFWMD L-33 Structure S-9XS, September 9th-16th, 2017

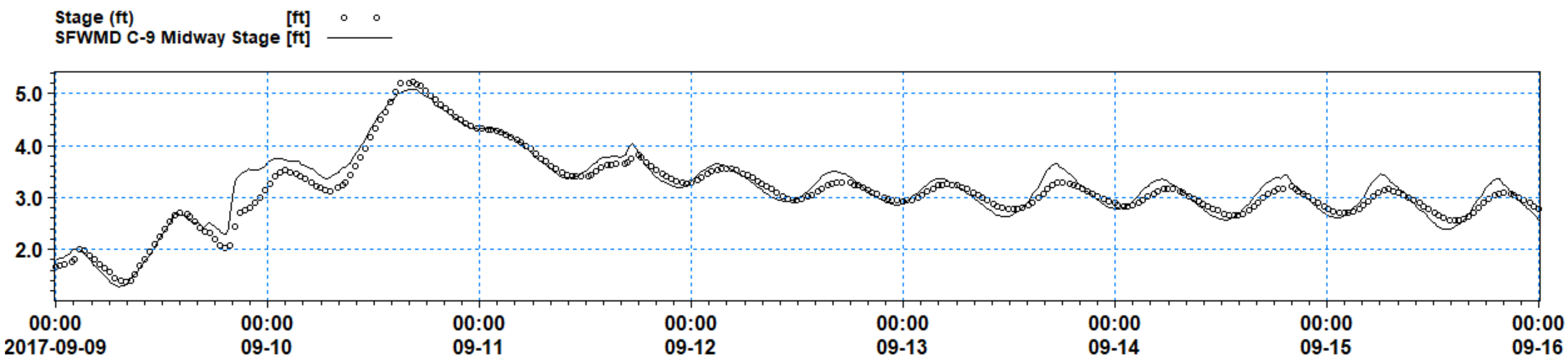

Figure 4.6-9: Simulated (line) vs Observed (dots) Stage Comparison for SFWMD C-9 Water Level Recorder S-29Z, September 9th-16th, 2017

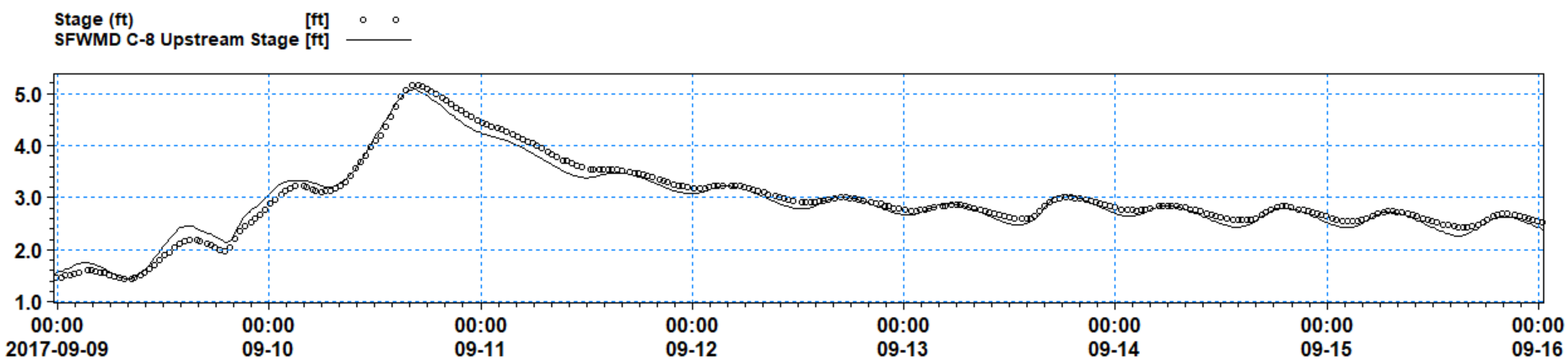

Figure 4.6-10: Simulated (line) vs Observed (dots) Stage Comparison for SFWMD C-8 Water Level Recorder S-28Z, September 9th-16th, 2017

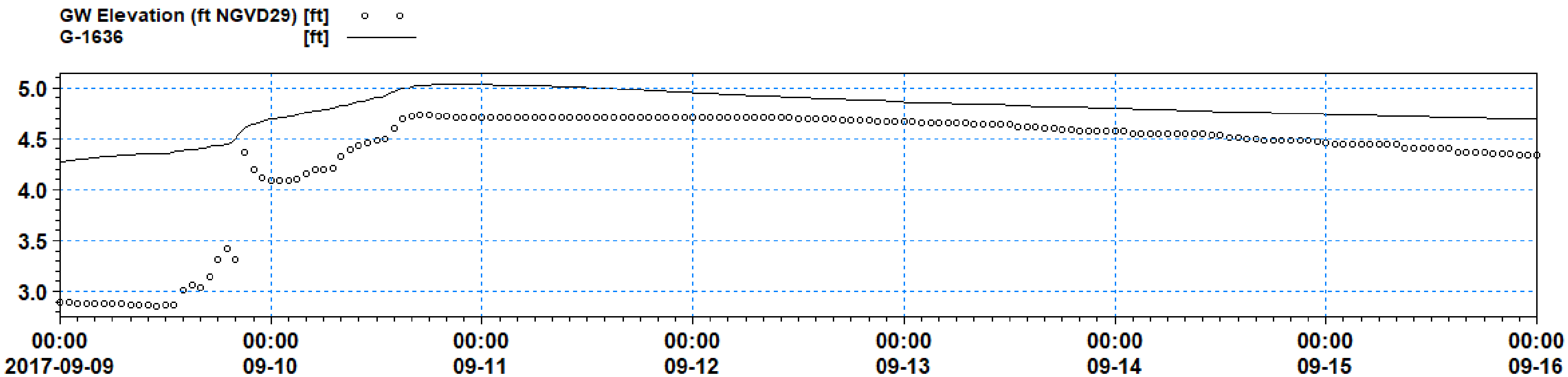

Figure 4.6-11: Simulated (line) vs Observed (dots) Groundwater Elevation Comparison for Well G-1636, September 9th-16th, 2017

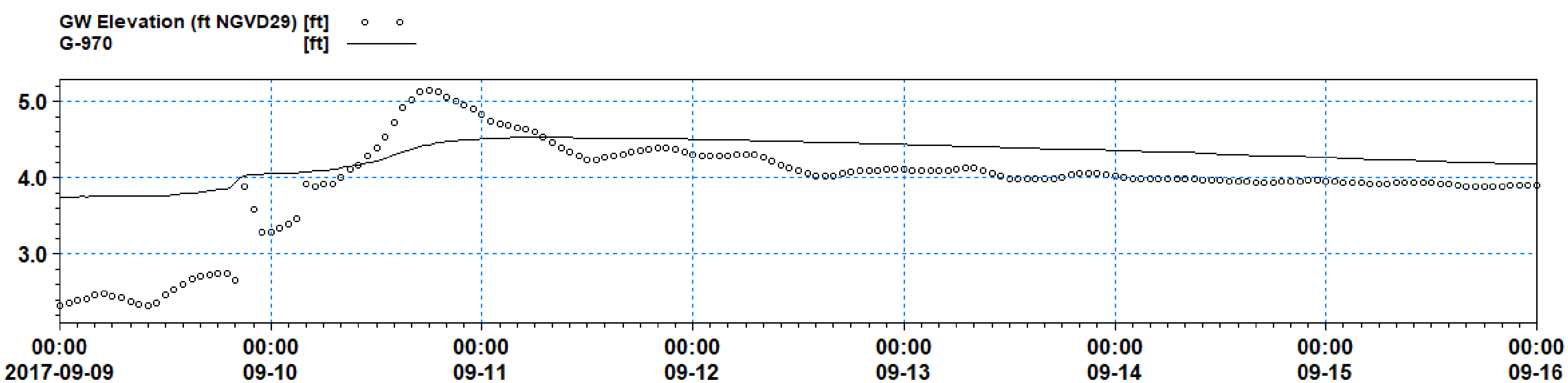

Figure 4.6-12: Simulated (line) vs Observed (dots) Groundwater Elevation Comparison for Well G-970, September 9th-16th, 2017

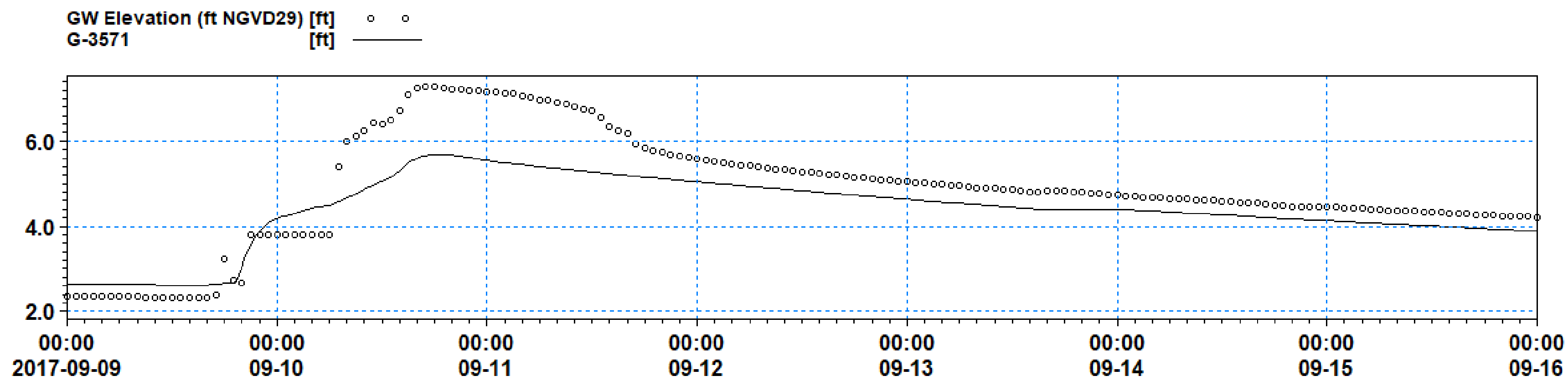

Figure 4.6-13: Simulated (line) vs Observed (dots) Groundwater Elevation Comparison for Well G-3571, September 9th-16th, 2017

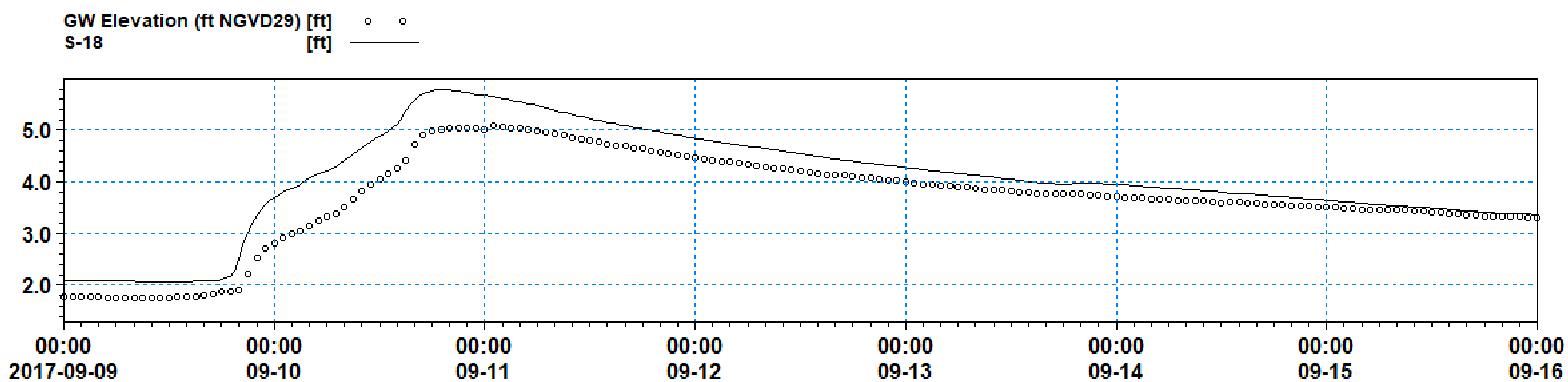

Figure 4.6-14: Simulated (line) vs Observed (dots) Groundwater Elevation Comparison for Well S-18, September 9th-16th, 2017

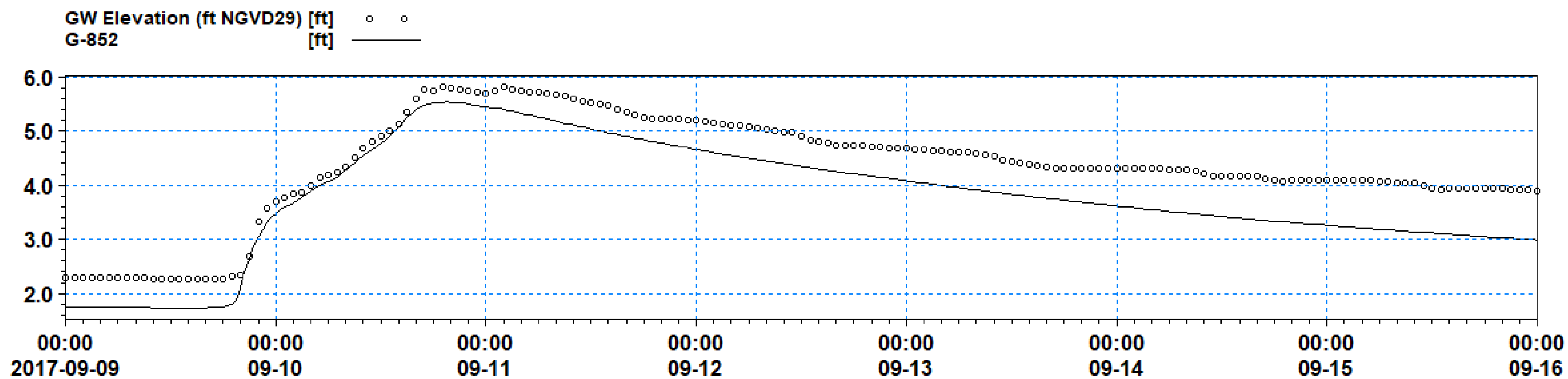

Figure 4.6-15: Simulated (line) vs Observed (dots) Groundwater Elevation Comparison for Well G-852, September 9th-16th, 2017

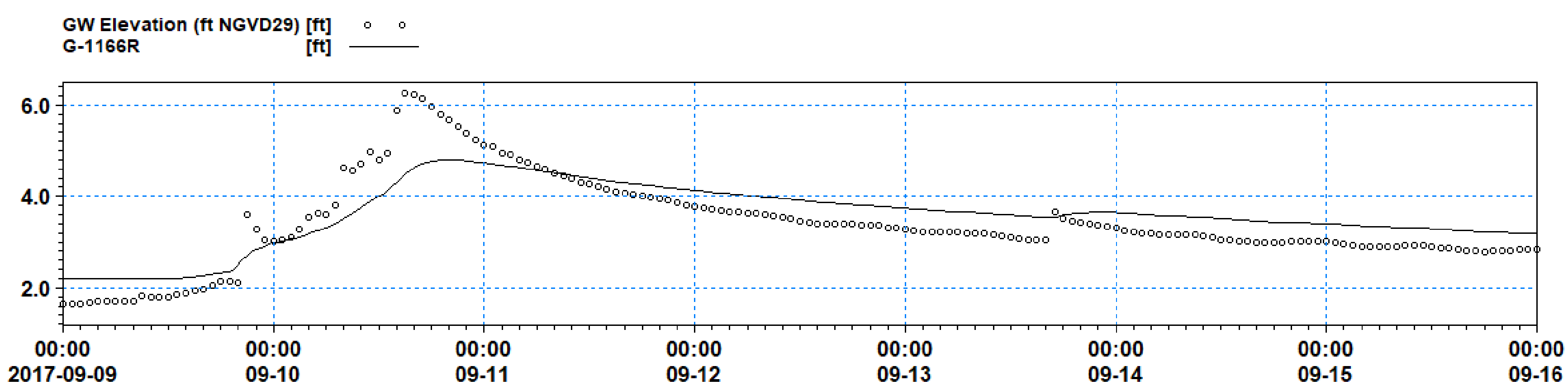

Figure 4.6-16: Simulated (line) vs Observed (dots) Groundwater Elevation Comparison for Well G-1166R, September 9th-16th, 2017

5.1 Conclusions

The C-8 C-9 calibration/validation model is a physically based integrated hydrologic and hydraulic model that includes a thorough representation of the hydrologic system and drainage network within the C-8 and C-9 basins, in Broward County and Miami-Dade County. Although a large portion of this model was inherited from the 2019 Broward County Current Conditions model, a lot of additional detail provided by Miami-Dade County and SFWMD, along with the survey collected specifically for this project by BDH Consulting Group, was incorporated into this model. Considering the scale of this model, the amount of detail is quite high, and most secondary and tertiary canal systems are modeled, including hundreds of culverts. The C-8 C-9 model was calibrated using the October 2nd-4th, 2000 storm event, which for the most part produced simulated canal stage results as well as groundwater elevations within 0.5 ft of observed. Likewise, the calibrated model produced simulated peak discharges and volumes within 10% and 17% of observed values, respectively. The C-8 C-9 model was validated using the September 9th-11th, 2017 storm event, which for the most part produced simulated canal stage results to within 0.4 ft. Additionally, the validation model produced simulated peak discharges and volumes to within about 15% of observed values. The validation model simulated groundwater elevations that were generally within 1 ft of observed values, which is a little higher than what was desired. It is worth mentioning that the areas with the largest differences were typically closer to the model boundary and might be adversely affected by uncertainty in the boundary conditions. The groundwater wells more centrally located in the model domain typically had simulated elevations closer to observed.

Overall, these results provide confidence in the model setup and parameterization, and further confidence that the model is a reliable predictor of water levels and flows based on current conditions. In the calibration model, the largest source of uncertainty comes from the rainfall data. Originally, temporally modified NEXRAD rainfall was used, which caused calibration challenges as it was likely providing significantly too much rainfall, as well as timing issues. With the rainfall input switched to rain gauges, significantly better results were achieved. However, there is still some uncertainty with the rainfall as there was data for only 5 rain gauges in the area, which could introduce some error in the spatial distribution. It is possible, and perhaps even likely, that the largest difference in simulated vs. observed stage is due to not simulating enough rainfall in the immediate upstream drainage area. In the validation model, the largest source of uncertainty comes from rating parameter issues, including how sensitive the rating equations are to negligible differences in head. Looking at structure S-28 during validation, there is a discrepancy between simulated and observed discharge, however, the headwater is a near perfect match, tailwater is forced, and the rating parameters are matched. The observed discharge is calculated based on a set of equations using rating parameters and the head difference between upstream and downstream of the structure. It has been determined that the rating equation used to characterize flow through these gates are particularly sensitive to the head difference between headwater and tailwater, especially during uncontrolled submerged conditions. So, although the model is simulating a near-perfect headwater, it is often slightly underpredicting, even as little as 0.001-0.05ft, which significantly reduced the head gradient through the structure. This is the cause for the model simulating discharges that are significantly smaller than the observed data. One example of this is on September 9th, 2017 at 6:55am. The observed discharge is 1420 cfs calculated based on a 0.037 ft gradient (keep in mind that is less than 0.5 inches), whereas the calculated discharge is around 75 cfs because the head gradient drops to less than 0.001 ft. The headwater is well within the target of +/- 0.5ft, as it is only about -0.5 inches, however, this causes the discharge to become extremely underpredicted, both in the model and verified by hand calculations using the same uncontrolled submerged equations with SFWMD rating parameters. This issue appears to be limited to uncontrolled submerged conditions, which is a rare occurrence. From 1985 to 2016, this structure operated in controlled submerged conditions 96% of the time (SFWMD, 2016). Likewise, the other major tidal outfall structure in this model (S-29), has been reported to have operated in controlled submerged conditions 99.14% of the time during 2011-2016 (SFWMD, 2016). So, although there is a sensitivity issue with uncontrolled submerged discharge, it historically has been a rare occurrence and it must be kept in mind that simulated vs observed discharge discrepancies during uncontrolled submerged operation are due to extremely small head differences that would otherwise be considered negligible.

In summary, Taylor Engineering believes that the C-8 C-9 model is setup and parameterized in a way that accurately represents the current drainage characteristics and will be a reliable predictor of water levels and flows in the design storm scenarios. However, it is important to keep in mind that any predictions by this computer model (or any other) show only what could happen, not necessarily what will happen. Model outputs can only be as good as the data input, and this model is no exception. The limitations of this model and its ability to predict what could happen should be known and considered when interpreting the results.

6 DESIGN STORM SETUP

6.1 Overview

For this study's current conditions design storm model, Taylor Engineering modified the calibrated/validated model (2017 conditions) and updated it with all applicable changes to the model setup including structure operations, rainfall, evapotranspiration, tidal boundaries, and initial conditions. The recorded structure operations were replaced with rule-based operations. The observed NEXRAD rainfall was replaced with Thiessen polygon-based 3-day design storm rainfall depths from NOAA Atlas 14 using the SFWMD 3-day temporal distribution. The reference evapotranspiration was updated to a constant 2 mm/d, which is the minimum daily wet season value in year 2017 (USGS Reference and Potential Evapotranspiration, 2018). The 1-D tidal boundaries (forced tailwater at tidal structures) were updated to the SFWMD-provided design storm stage hydrographs. The SFWMD design storm stage hydrographs were also applied to the eastern general-head groundwater boundary. A time varying 2-D overland flow boundary was included along the coastal portion of the eastern boundary using the SFWMD design storm stage hydrographs. Localized adjustments to the initial groundwater levels were performed to ensure a close match between the groundwater levels and water control elevations.

6.2 Rules-Based Operations

The operable structure rules were based on standard operating procedure as detailed in the District's Operations Control Center Structure Books. The control rules for S-28 and S-29 are shown in **Figure 6.2-1** and **Figure 6.2-2**, respectively.

	Description	Condition	Control type	Value type
1		[s:hUS:S-28] - [s:hDS:S-28] <=0.09144	Direct setting	Close
2		[s:hUS:S-28] >0.64008	Direct setting	Fully open
3		[s:hUS:S-28] > 0.4572 && [s:hUS:S-28] <0.54864	Unchanged	Absolute value
4		[s:hUS:S-28] <0.4572	Direct setting	Close

Figure 6.2-1: Control Rules for S-28 (SI Units)

	Description	Condition	Control type	Value type
1		[s:hUS:S-29] - [s:hDS:S-29] <=0.09144	Direct setting	Close
2		[s:hUS:S-29] >0.762	Direct setting	Fully open
3		[s:hUS:S-29] > 0.4572 && [s:hUS:S-29] <0.6096	Unchanged	Absolute value
4		[s:hUS:S-29] <0.4572	Direct setting	Close

Figure 6.2-2: Control Rules for S-29 (SI Units)

6.3 Rainfall

The rainfall method for the design storm simulations was a Thiessen Polygon approach, which is the same approach used for design storms in the 2019 Broward County model and the 2016 BCB FPLOS (Taylor Engineering, 2016). The centroid of each polygon corresponds to a NOAA Atlas 14 station (**Figure 3.4-1**). Rainfall 3-day totals for each return period were based on NOAA Atlas 14 depths. The NOAA rainfall depths were distributed temporally based on the normalized cumulative SFWMD 3-day distribution. Total rainfall values per NOAA station are reported in **Table 3-2**.

6.4 Boundary Conditions

The 1-D tidal boundaries were updated using the District-provided time series for S-28 and S-29 (**Figure 3.6-4** and **Figure 3.6-5**). The SFWMD design storm stage hydrographs were also applied to the 2-D overland tidal boundary and the eastern general-head groundwater boundary (**Figure 3.7-6**). **Section 3.9.7** details the spatial distribution of the saturated zone boundary conditions and the various time series data applied.

6.5 Initial Groundwater Elevation

As described in **Section 3.9.6**, the design storm initial groundwater elevations were developed by making localized adjustments to the initial potential head from the validation simulation so that they closely matched basin control elevations. **Figure 3.9-17** shows the final initial potential head developed for the current condition design storm simulations.

7 FLOOD PROTECTION LEVEL OF SERVICE METRICS

The District relies on six (6) formal performance metrics (PMs) to evaluate the flood protection level of service provided by the primary water management infrastructure. These metrics, defined briefly in this section, were derived from the District publication *Flood Protection LOS Analysis for the C-4 Watershed,*

Appendix A: LOS Basic Concepts (SFWMD H&H Bureau, December 29, 2015). **Section 8** provides the results of the FPLOS evaluation for existing conditions.

PM #1 Maximum Stage in Primary Canals – This is the peak stage profile in the primary canal system. The profile is developed for the 72-hour duration, 5-year, 10-year, 25-year, and 100-year recurrence frequency design storms. The largest design storm that stays within the canal banks establishes the FPLOS of the primary canal system.

PM #2 Maximum Daily Discharge Capacity through the Primary Canals – This is the maximum discharge capacity throughout the primary canal network. Discharge is calculated as area weighted flow, in units of cubic feet per second per square mile of contributing area for the 25-year design event. Tidal effects are filtered by using a 12-hour moving average of discharge. Although the peak of the 25-year net discharge hydrographs are referred to in this report as the calculated discharge capacity, the true capacity of the canal segment is the net discharge corresponding to the largest design flood event that remains within the banks of the canal using the results of the 5-year, 10-year, 25-year, and 100-year events.

PM #3 – Structure Performance – Effects of Sea Level Rise – This metric shows the effective capacity of a tidal structure. It is comparable to the static design condition assumed in the original design but compares structure flow over a range of storm surge events and a range of sea level rise scenarios. For the C-8 and C-9 FPLOS evaluation, this metric will be evaluated in Task 4.0 of the next Task Order (Phase 1B), where future conditions and sea level rise will be included in the design storms. This metric will then be compared to the reports completed internally by District staff.

PM #4 Peak Storm Runoff – Effects of Sea Level Rise – This is the maximum conveyance capacity of a watershed at the tidal structure for a range of design storms. It shows the maximum conveyance (moving 12-hour average) for a specific design storm and a specific tidal boundary condition. This metric examines the behavior of the system under severe stress and can be used to check if conditions exceed design limits. In evaluating this PM, it is assumed that design rainfall and design storm surge occur simultaneously, or with a temporal offset that maximizes stress on the structure. This metric will be evaluated in Task 4.0 of the next Task Order, where future conditions and sea level rise will be included in the design storms.

PM #5 Frequency of Flooding – Stage-based FPLOS for Subwatersheds – In this metric, the flood elevations or depths of overland flooding are evaluated for the 72-hour duration, 5-year, 10-year, 25-year, and 100-year recurrence frequency design storms. These flood depths/elevations can then be compared with elevations of build features such as buildings and roadways, where such information exists. For the purposes of this C-8 and C-9 FPLOS evaluation, flood inundation maps were developed from the model output for each storm event.

PM #6 Duration of Flooding – This metric quantifies the duration of flooding across the entire watershed. For this Study, the length of time the flood elevation is projected to be above a threshold depth of 0.25 ft was mapped over the entire study area using the multi-cell gridded model output files for the 2-D overland flow component.

8 FLOOD PROTECTION LEVEL OF SERVICE – CURRENT CONDITIONS

After model calibration and validation, the model was setup to represent design storm conditions using District-provided time series data as described in **Section 3**, and executed for the 72-hour 5-year, 10-year, 25-year, and 100-year storm events. Model results were evaluated for stability and reasonableness prior to proceeding with the FPLOS evaluation. **Appendix D** provides a summary of the model results at primary control structures. The remainder of this section describes the results of the FPLOS evaluations for all relevant performance metrics, which for current conditions include PM #1, PM #2, PM #5, and PM #6. PM #3 and #4 cannot be fully evaluated until Phase 1B of this project is completed, which will simulate three future condition sea level rise scenarios; however, the current condition part of the metrics were included.

8.1 PM #1 – Maximum Stage in Primary Canals

This is the peak stage profile in the primary canal system. The profile is developed for the 72-hour 5-year, 10-year, 25-year, and 100-year design storms. The largest design storm that stays within the canal banks establishes the FPLOS of the primary canal system.

To evaluate this PM under current conditions within the C-8 and C-9 watersheds, instantaneous peak stage profiles were prepared for the primary canals within the watersheds, which are the C-8 and C-9 Canals, respectively. Bank elevations on the profile figures are based on the MIKE HYDRO cross-section data. For the purposes of this metric, several cross-section banks were modified/extended (based on the current LiDAR data) before model simulation to better capture levees or the areas at which the canals would be considered out-of-bank. Also shown in the figures are major roadway landmarks, control structures, and primary canal junctions.

Table 8-1 summarizes the PM #1 results shown graphically in **Figure 8.1-3** and **Figure 8.1-4**, listing the maximum return period profile that is contained within the canal banks. Although the C-8 Canal contained the 5-year and 10-year profiles along the majority of the canal length, the bank elevation was exceeded for the 5-year event over short segments at multiple locations. Similarly, although the C-9 Canal contained the 10-year and 25-year profiles along the majority of the canal length, the bank elevation was exceeded for the 10-year event over short segments at a few locations. Therefore, if a strict interpretation of this criteria is used, then both the C8 and C9 Canal have a 5-year FPLOS. However, as discussed in the Conclusions, the determination of FPLOS should consider the results of all applicable performance metrics. With careful consideration of PM #1 and PM #5, both the C8 and C9 Canals provide a 10-year and 25-year FPLOS, respectively.

Table 8-1: PM #1 Summary Results

Canal Segment	Figure Number	FPLOS Localized	FPLOS Overall	Comment
C-8	**Figure 8.1-3**	5-year	10	Overall FPLOS from **Section 9.1.1**
C-9	**Figure 8.1-4**	5-year	25	Overall FPLOS from **Section 9.1.2**

The PM #1 performance of the C-8 Canal is generally worse east of its confluence with the Opa Locka Canal compared to the western segment. Notable areas of bank exceedances include the following:

- Just west of NE 6th Avenue (CR915), south bank exceeded for 5-year event, north bank exceeded for 10-year event.
- Downstream of NE 135th St. (CR 916), north bank exceeded for 5-year event, south bank for 25-year event.
- From North Miami Avenue to NE 135th St., south bank exceeded for 10-year event.
- Downstream of Opa Locka Canal, south bank exceeded for 10-year event.

Notable areas of bank exceedances in the C-9 Canal include:

- Halfway between I-95 and S-29 to S-29, south bank exceeded for 25-year event, north bank for the 100-year event.
- Downstream of US Hwy 441, north bank exceeded for 25-year event.
- From SBDD pumps S-4 and S-5 to the Ronald Reagan Turnpike, south bank exceeded for the 25-year event.

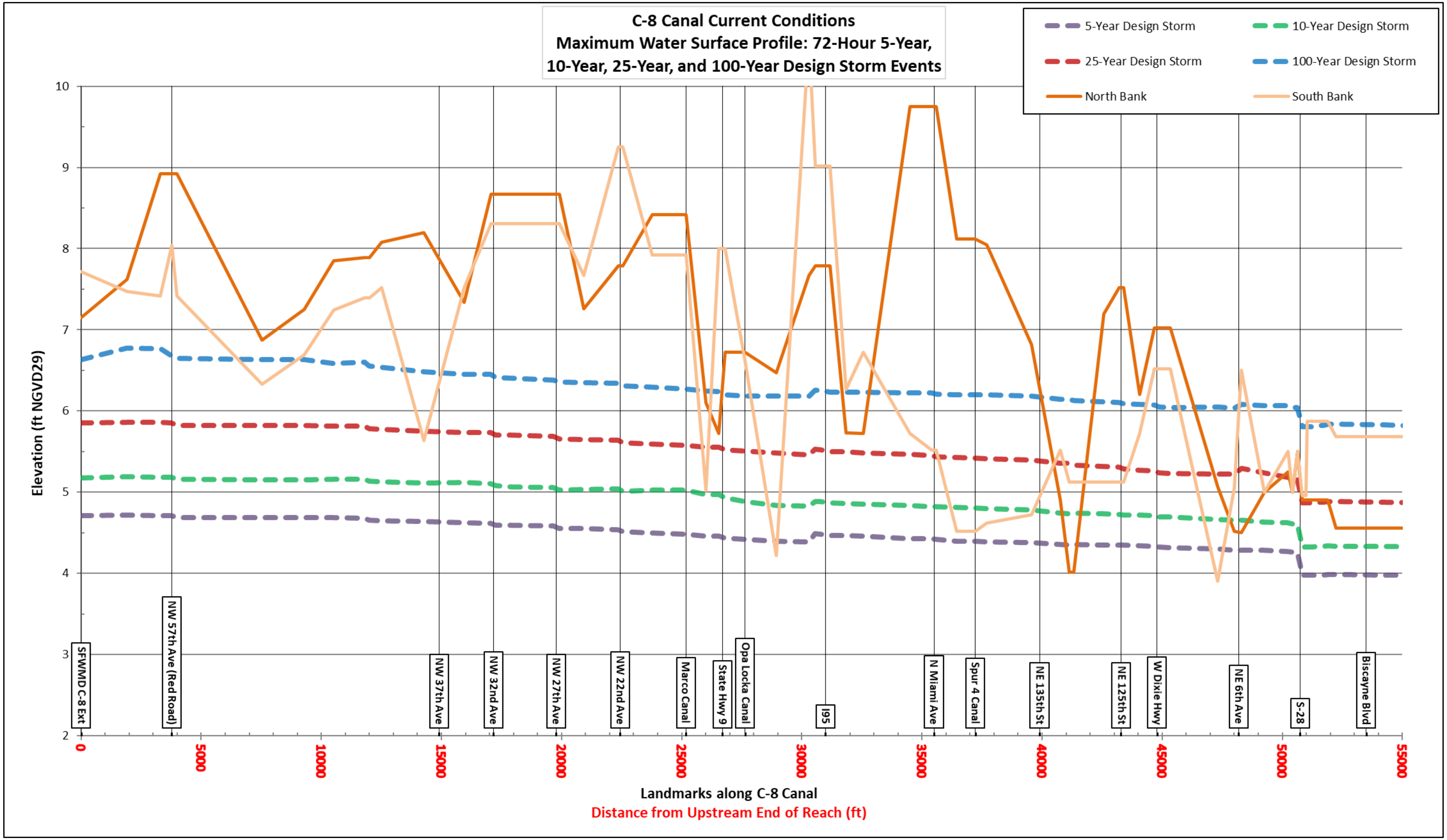

Figure 8.1-1: C-8 Canal Peak Stage Profiles

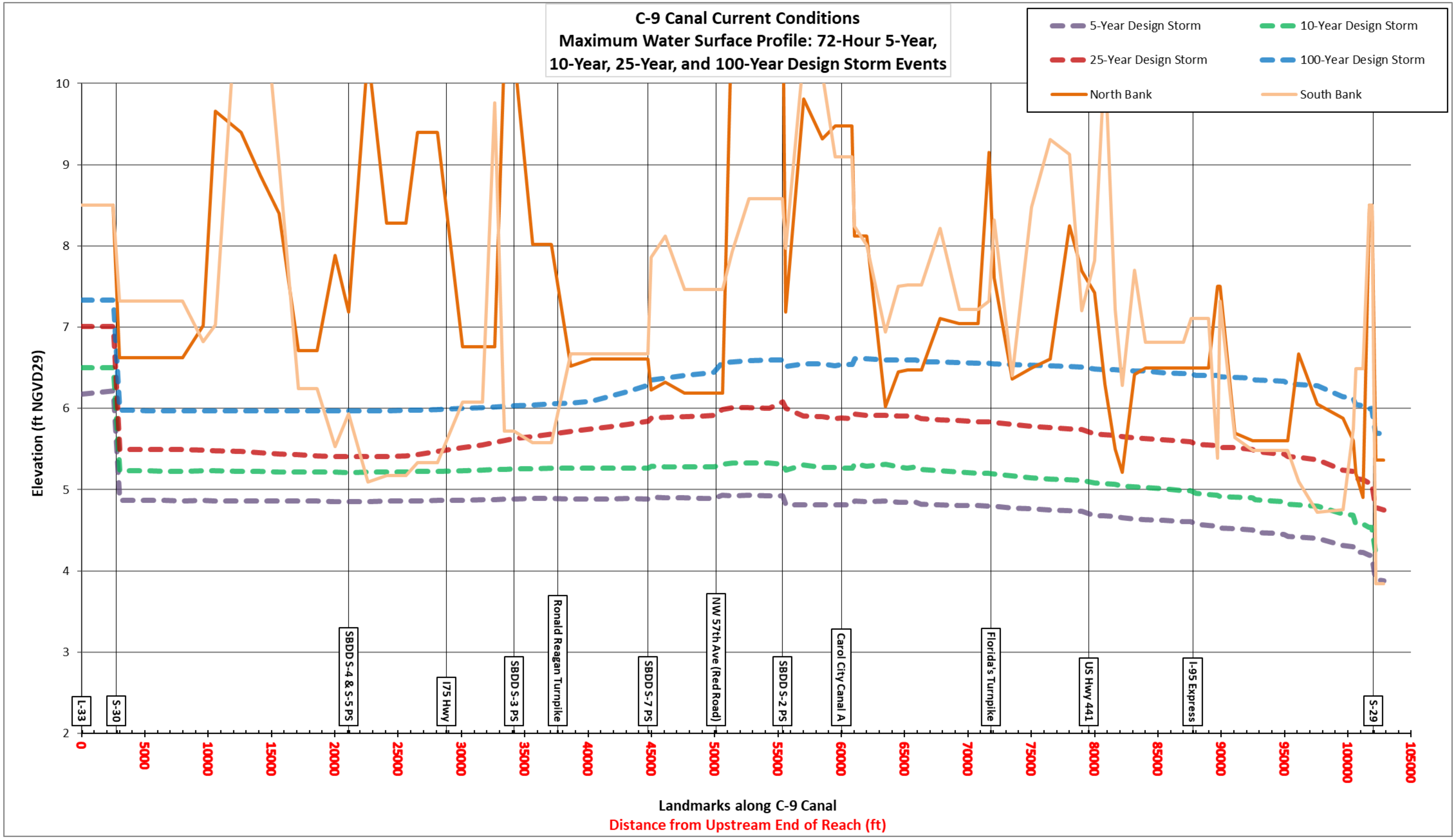

Figure 8.1-2: C-9 Canal Peak Stage Profiles

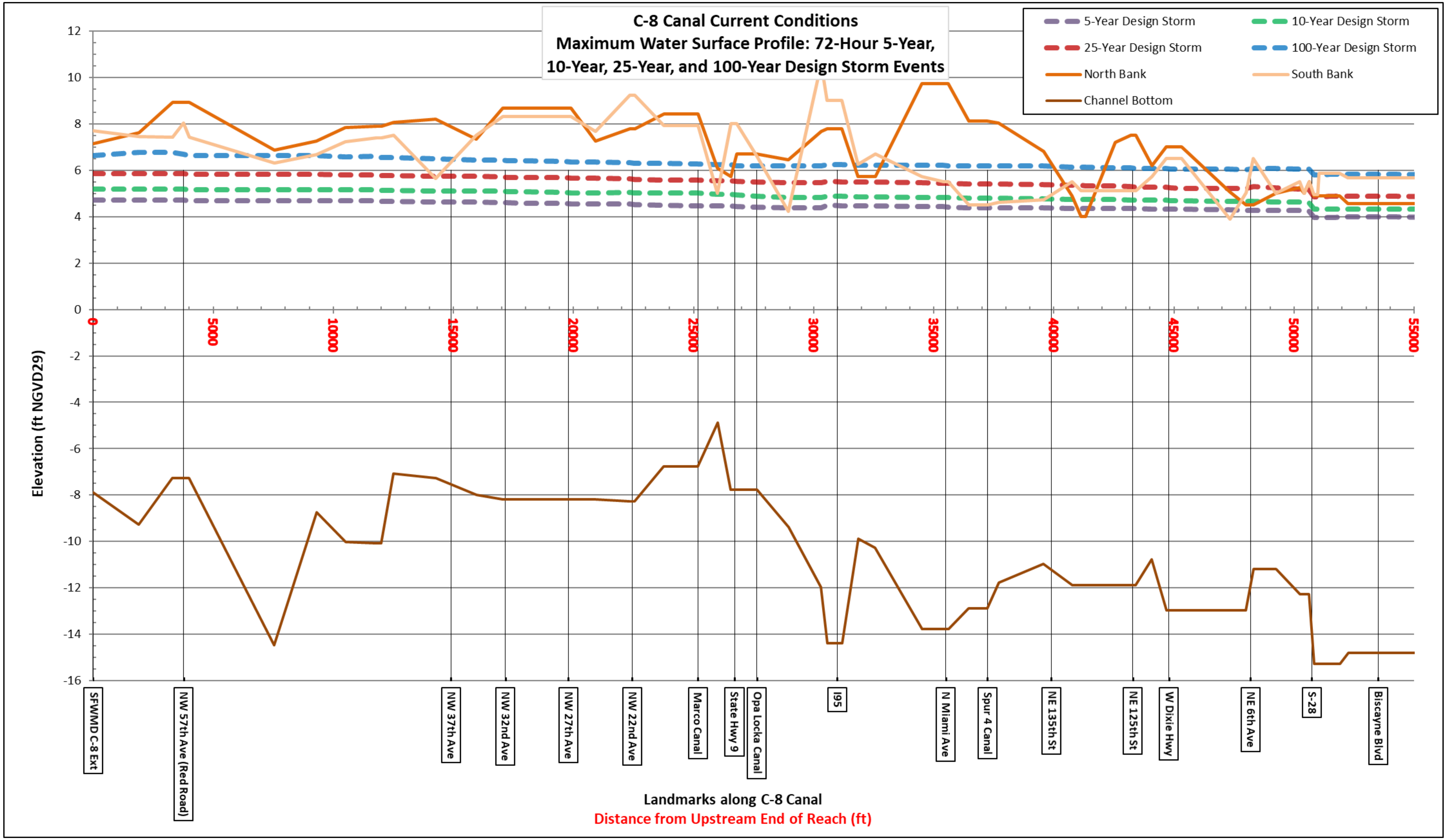

Figure 8.1-3: C-8 Canal Peak Stage Profiles with Canal Bottom

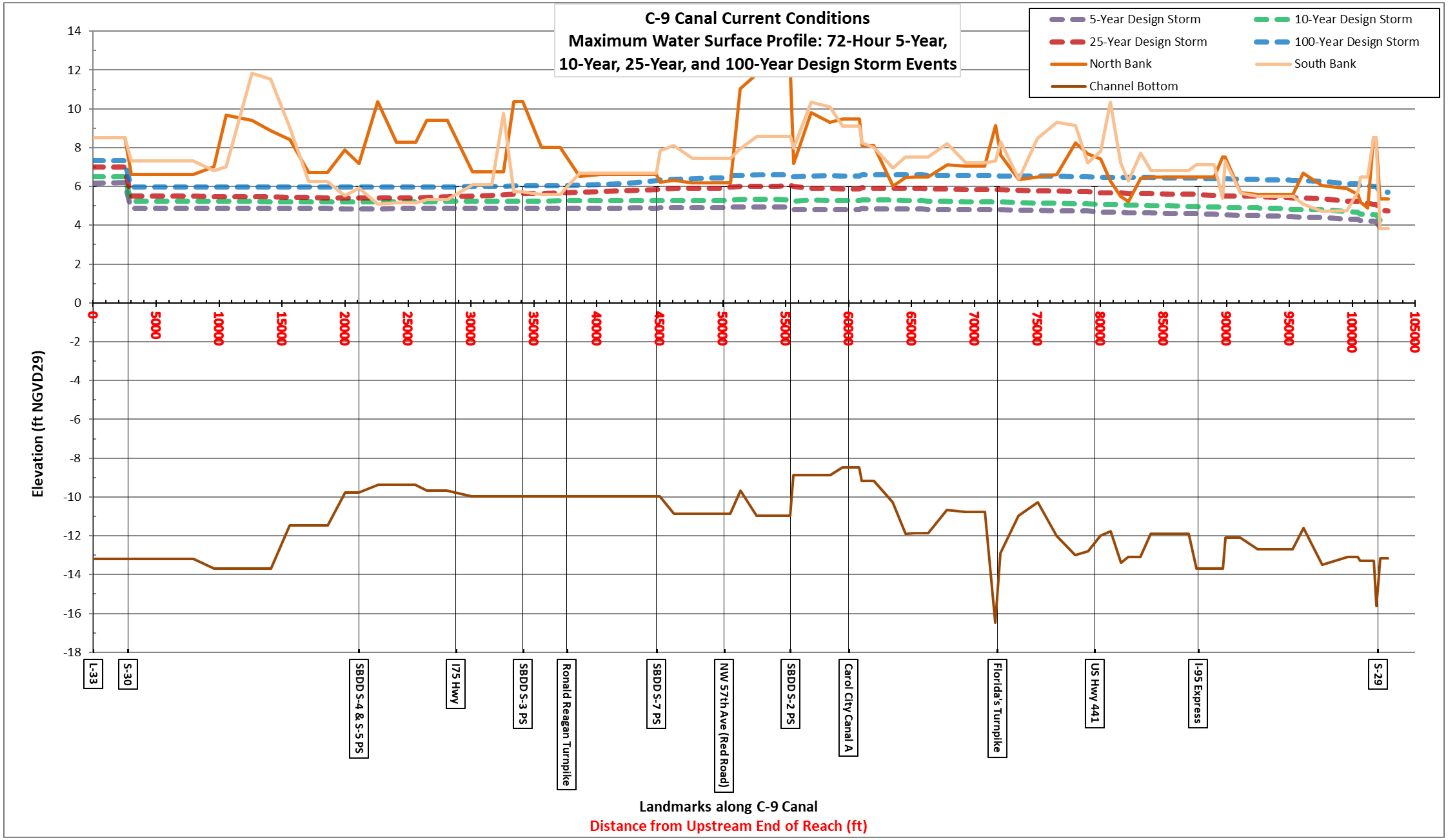

Figure 8.1-4: C-9 Canal Peak Stage Profiles with Canal Bottom

Table 8-2 shows the peak stages at the major landmarks along the C-8 Canal for each of the design storms. Bridge low cord elevations were specified were applicable. Although the water level in the C-8 Canal exceeded bank elevations in several locations for the various design storms (**Figure 8.1-1**), the water level did not get high enough to become restricted by the low cord elevation of any bridge.

Table 8-2: C-8 Canal Peak Stage at Landmarks

Landmark	Peak Stage (ft NGVD29)				Bridge Low Cord Elevation (ft NGVD29)
	5-Yr	10-Yr	25-Yr	100-Yr	
SFWMD C-8 Ext	4.71	5.18	5.86	6.63	
NW 57th Ave (Red Road)	4.71	5.18	5.85	6.68	9.2
NW 37th Ave	4.64	5.12	5.75	6.49	
NW 32nd Ave	4.62	5.11	5.73	6.45	9.18
NW 27th Ave	4.58	5.06	5.69	6.38	7.02
NW 22nd Ave	4.54	5.04	5.64	6.34	8
Macro Canal	4.48	5.02	5.57	6.27	
Rail Road / State Hwy 9	4.46	4.97	5.55	6.24	7.44
NW 7th Ave Bridge	4.39	4.83	5.46	6.18	8.53
I-95	4.48	4.89	5.52	6.25	8.05
North Miami Ave	4.42	4.83	5.45	6.22	9.62
Spur 4 Canal	4.39	4.81	5.42	6.20	
NE 135th St	4.37	4.78	5.40	6.19	7.38
NE 125th St	4.34	4.73	5.31	6.11	11.47
W Dixie Hwy	4.33	4.71	5.26	6.07	10.57
NE 6th Ave	4.28	4.65	5.22	6.03	9.02
S-28	4.26	4.61	5.16	6.04	
Biscayne Blvd	3.98	4.33	4.88	5.83	

Table 8-3 shows the peak stages at the major landmarks along the C-9 Canal for each of the design storms. Bridge low cord elevations were specified were applicable. For the 5-yr and 10-yr design storm events, the water level in the C-9 Canal exceeded bank elevations in a couple locations (**Figure 8.1-2**), however, the water level did not get high enough to become restricted by the low cord elevation of any bridge. For the 25-yr and 100-yr design storms, the water level in the C-9 Canal exceeded bank elevations in a couple additional areas and became elevated enough to become restricted by the low cord elevation of bridges, as shown in red in **Table 8-3**. None of the bridges were overtopped.

Table 8-3: C-9 Canal Peak Stage at Landmarks

Landmark	Peak Stage (ft NGVD29)				Bridge Low Cord Elevation (ft NGVD29)
	5-Yr	10-Yr	25-Yr	100-Yr	
L-33	6.17	6.50	7.0	7.34	
S-30	4.87	5.23	5.50	5.97	
SBDD S-4 & S-5 PS	4.86	5.21	5.41	5.97	
I75 Hwy	4.87	5.23	5.47	5.96	
SBDD S-3 PS	4.88	5.25	5.63	6.03	
Ronald Reagan Turnpike	4.9	5.26	5.68	6.05	
SBDD S-7 PS /Flaming Rd	4.88	5.27	5.84	6.29	9.76
NW 57th Ave (Red Road)	4.89	5.28	5.92	6.43	9.54
SBDD S-2 PS / NW 47th Ave	4.93	5.31	6.08	6.60	8.9
Carol City Canal A	4.81	5.27	5.88	6.54	
NW 37th Ave	4.81	5.26	5.87	6.54	8.6
NW 27th Ave	4.84	5.28	5.90	6.60	7.93
Florida's Turnpike	4.8	5.20	5.83	6.56	
US Hwy 441	4.73	5.11	5.74	6.51	7.53
NW 199th St	4.67	5.06	5.67	6.48	8.6
I-95 Express	4.60	4.98	5.59	6.43	8.43
Miami Gardens Dr	4.55	4.93	5.54	6.40	8.96
NE 15th Ave	4.45	4.85	5.44	6.33	8.87
NW 19th Ave	4.40	4.80	5.37	6.28	5.6
NE 22nd Ave	4.3	4.69	5.23	6.13	4.9
Rail Road at Biscayne Blvd	4.23	4.57	5.12	6.03	5.77
S-29	4.19	4.54	5.08	6.0	

8.2 PM #2 – Maximum Daily Discharge Capacity through the Primary Canals

PM #2 is the maximum discharge capacity throughout the primary canals. Discharge is calculated for canals as area weighted flow, in units of cubic feet per second per square mile of contributing area. Canal segments are generally defined as areas between water control structures, however, there are no intermittent control structures along the C-8 and C-9 Canals. Therefore, the segment associated with structures S-28 and S-29, is the entire C-8 and C-9 Canals, respectively. This means that the contributing area for S-28 and S-29 is the entire C-8 basin and C-9 basin, respectively. Structure S-30, which is on the C-9 Basin boundary, was closed during the design storms (based on control rules), so there was no additional inflow into the C-9 basin. Within the C-9 Basin, there are two areas with different allowable runoff rates based on the District's ERP Handbook; (1) "essentially unlimited inflow by gravity connections east of Red Road", and (2) "20 CSM pumped and essentially unlimited inflow by gravity connections west of Red Road or Flamingo BLVD". Therefore, the C-9 Basin discharge capacity was estimated for the entire C-9 Basin, as well as for the respective areas east and west of Red Road. **Table 8-4** lists the canal segments identified for this analysis. The table also identifies the contributing area for each canal segment, and the discharge capacity calculated for each segment associated with each design storm event.

Discharge capacity was calculated by dividing the peak of the discharge hydrograph by the canal segments contributing area. For structures S-28 and S-29, discharge capacity was calculated by dividing the peak discharge by the entire basin area. For the C-9 Basin, two additional estimates were made for the respective areas east and west of Red Road. These two additional estimates were necessitated by the presence of two different allowable runoff rates within the C-9 Basin. For the drainage area west of Red Road, the peak discharge at the Q-point located at Red Road (shown as a green dot in **Figure 8.2-1**) was divided by the contributing drainage area (highlighted in green in **Figure 8.2-1**). For the drainage area east of Red Road, the peak discharge at the Q-point located at Red Road was subtracted from the peak discharge at structure S-29, and then divided by the contributing drainage area east of Red Road. Tidal effects were filtered by using a 12-hour moving average of discharge.

Table 8-4: Water Control Catchment Inflow and Outflow Points and Discharge Capacity

Discharge west and east of Red Road is an estimate due to interconnected outfalls on both sides of Red Road

Structure / Segment	Inflow	Outflow	Water Control Catchment Area (sq.mi)	Peak Discharge Capacity (cfs/sq.mi)			
				5-Yr	10-Yr	25-Yr	100-Yr
S-28	Beginning of C-8	S-28	28.22	51	61.9	82.8	115.3
S-29	Beginning of C-9/ Structure S-30	S-29	99.37	21.5	24.5	29.3	37.5
C-9 west of Red Road	Beginning of C-9/ Structure S-30	Q-point at Red Road	61.24	13.5	15.2	17.9	20.9
C-9 east of Red Road	Q-point at Red Road	S-29	38.13	46.7	51.6	65.8	89.1

Figure 8.2-1 shows the contributing areas draining to each canal segment. The C-8 catchment polygon was based on the District's Arc Hydro Enhanced Database (AHED). The C-9 catchment polygons were based on both the District's AHED as well as SBDD and Miami-Dade County subbasins. It is important to

note that the C-9 Basin is technically one drainage area and does not have a real drainage divide. The two drainage areas shown within the C-9 Basin represent the spatial variability in the District's allowable discharge rates within the C-9 Basin. The area-weighted discharge presented for the areas east and west of Red Road are an approximation due to the uncertainty in the exact location of this allowable runoff-based basin divide. Additionally, the drainage areas east and west of Red Road are interconnected. Although the drainage divide is specified as Red Road, the contributing drainage area on the north side of the C-9 Canal extends east of Red Road and has two outfalls that are interconnected, one east of Red Road and one west of Red Road. For this analysis, the discharge at Red Road was used, so some discharge from the contributing drainage area is not included as it discharges further downstream. It should be noted that comparing the discharge in the western half of the C-9 Canal to the permitted rates does not have significant meaning as there are several gravity connections to the C-9 Canal west of Red Road and two pumped connections east of Red Road.

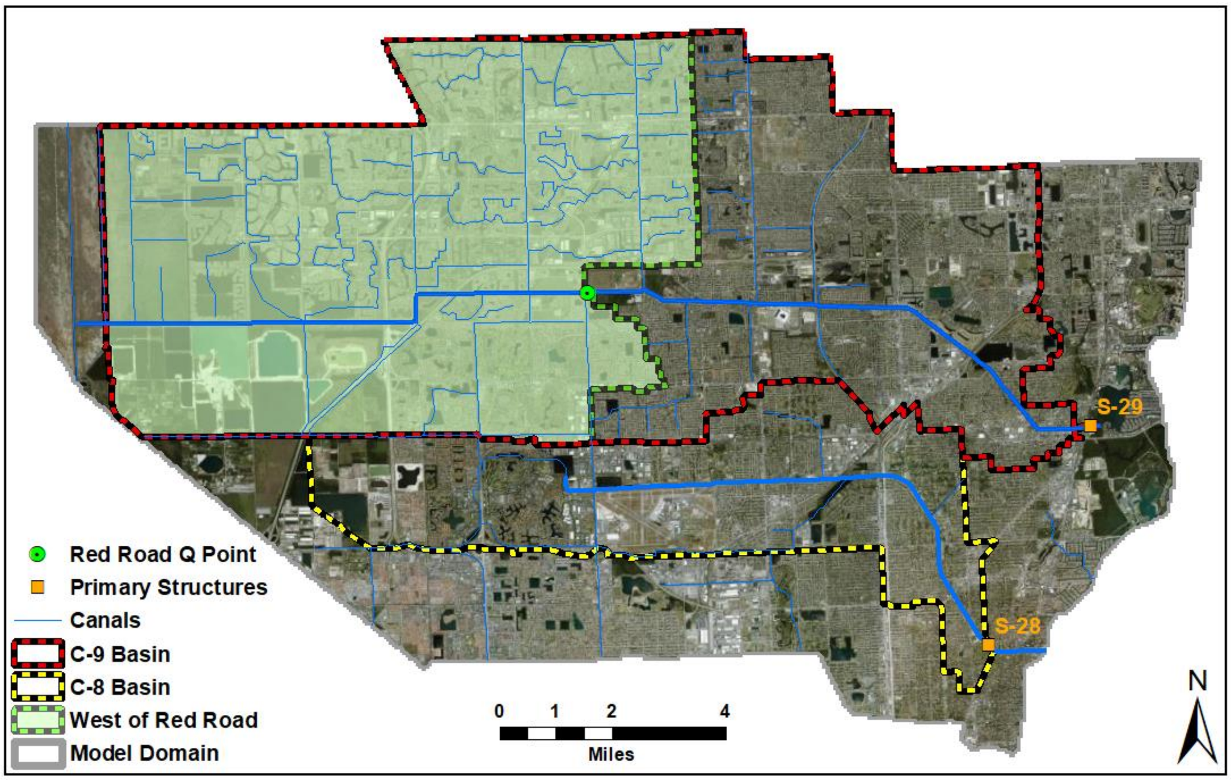

Figure 8.2-1: Catchment Areas for Calculating PM #2

Figure 8.2-2 through **Figure 8.2-5** present a visual comparison of the area-weighted discharge hydrographs for each canal segment with respect to the 72-hour 5-year, 10-year, 25-year, and 100-year design storms. Although the peak discharge during each design storm event are referred to in this section as the calculated discharge capacity, the true capacity of the canal segment is the net discharge corresponding to the largest design flood event that remains within the banks of the canal. Therefore, the results of PM #2 must be evaluated in conjunction with the results of PM #1 (Maximum Stage in Primary Canals) and PM #5 (Frequency of Flooding). As discussed in **Section 8.1**, peak stages in all canals exceeded the canal banks for the 100-year event. In several canal locations, a 10-year event was sufficient to cause water levels to exceed the canal bank elevations (see **Figure 8.1-3** and **Figure 8.1-4**) but these generally appear to be localized flooding instances that do not extend far from the canal banks. This is based on an examination of the PM #5 results (**Section 8.3**).

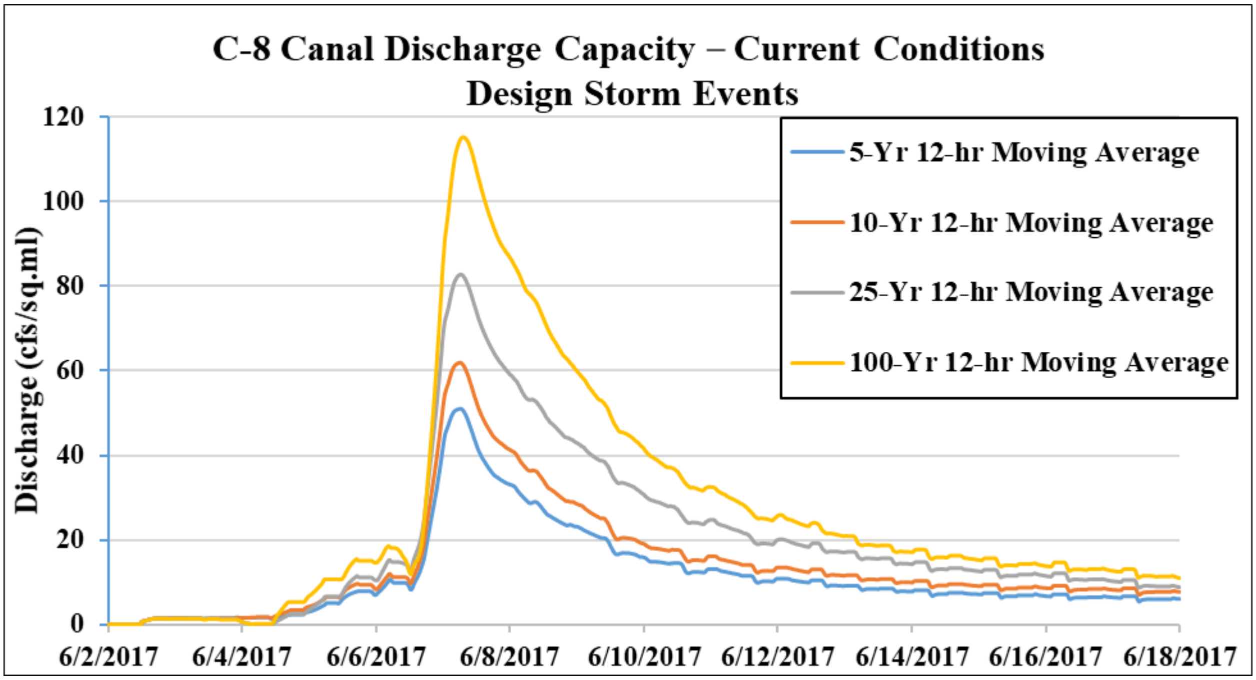

Figure 8.2-2: Area-Weighted Discharge Hydrograph for C-8 Canal Structure S-28

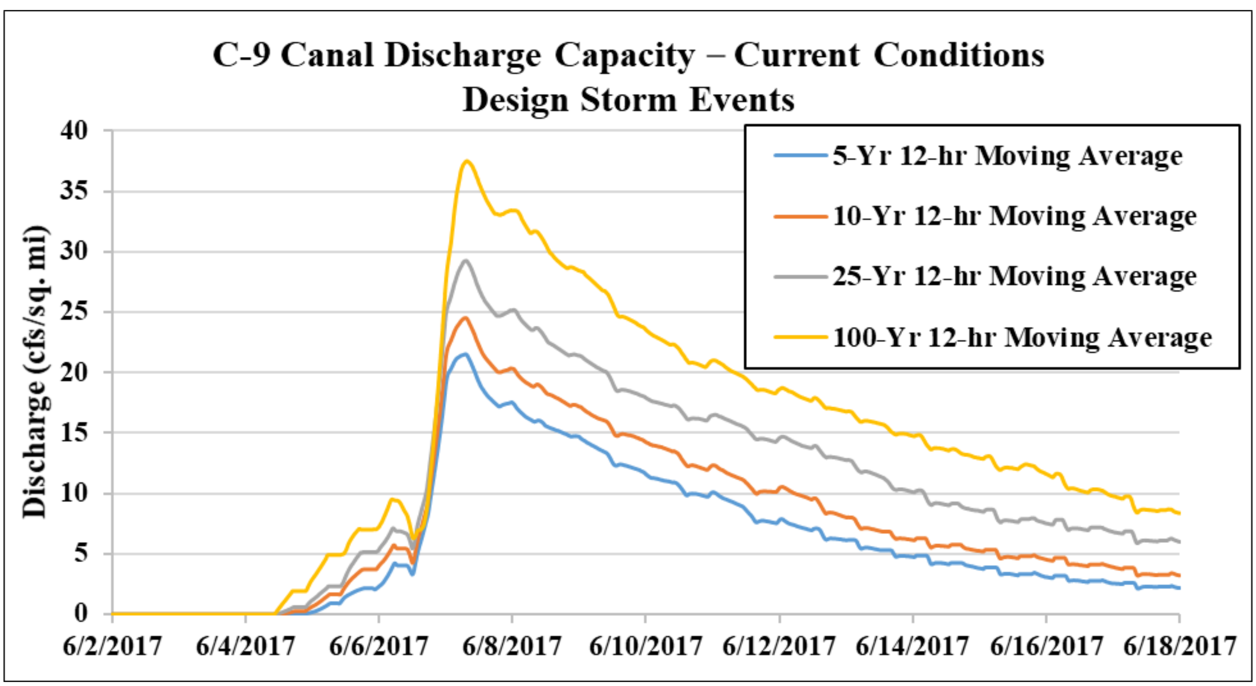

Figure 8.2-3: Area-Weighted Discharge Hydrograph for C-9 Canal Structure S-29

The C-8 canal is allowed "essentially unlimited inflow by gravity connections", as is the area draining to the C-9 Canal east of Red Road. Therefore, the only canal segment in the model that is subject to District discharge limitations is the area draining to the C-9 Canal west of Red Road, which has a limit of 20 CSM pumped. The peak discharge capacity of the C-9 Canal west of Red Road was 20.9 CSM for the 100-year design storm. However, it cannot be said that the area west of Red Road is exceeding the permitted allowance as there are several gravity connections contributing to that discharge capacity. Additionally, there are pumped connections east of Red Road that share a common drainage area with west of Red Road due to the interconnectivity of the drainage system. Therefore, the discharge capacity of the C-9 Canal, with respect to east or west of Red Road, is strictly an estimate and should not be used for regulatory purposes. With that said, the SBDD pump discharge and operation rules are based on their permitted allowance from the District. Considering there are gravity connections west of Red Road, the 100-year peak discharge capacity of 20.9 CSM compared to the permitted allowance of 20 CSM pumped sounds reasonable.

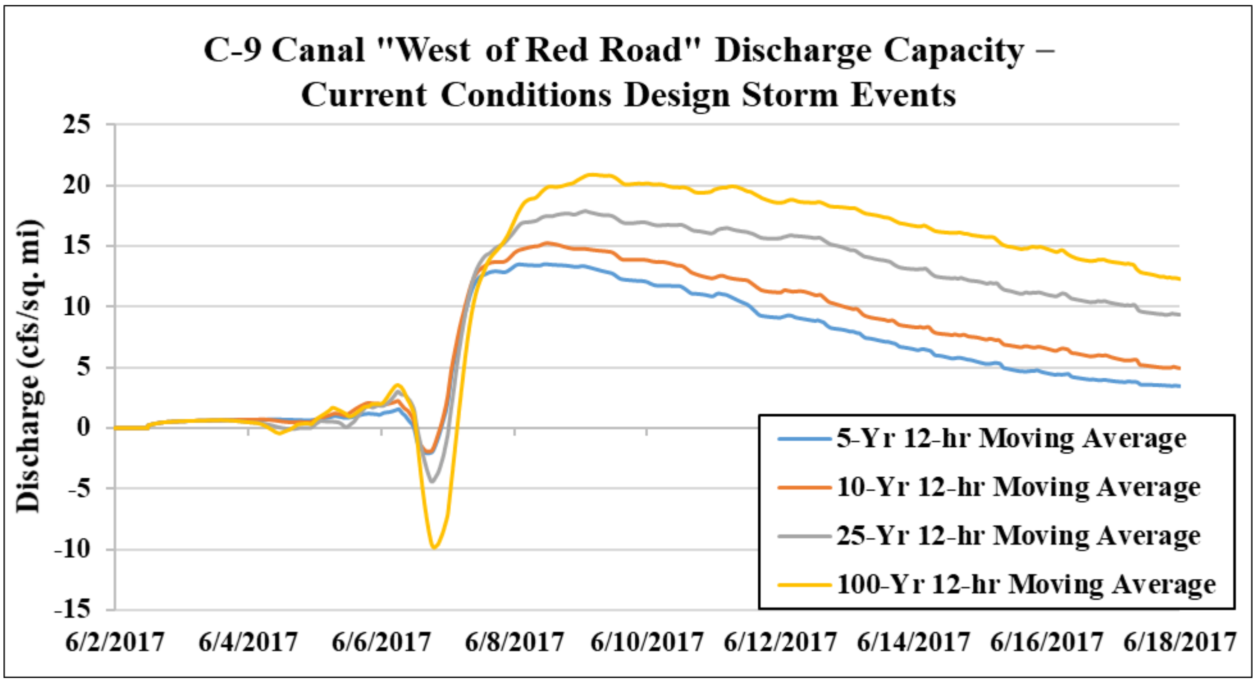

Figure 8.2-4: Area Weighted Discharge Hydrograph for C-9 Canal West of Red Road

Discharge west of Red Road is an estimate due to interconnected outfalls on both sides of Red Road

Figure 8.2-4 has negative discharge during peak rainfall. This occurs because there is a delayed response in the west side as there is a significant amount of dead storage (large lakes in SBDD). The storage in the west side is controlled by pumps that turn on at an elevation higher than control elevation. As the pumps turn on, the discharge becomes positive.

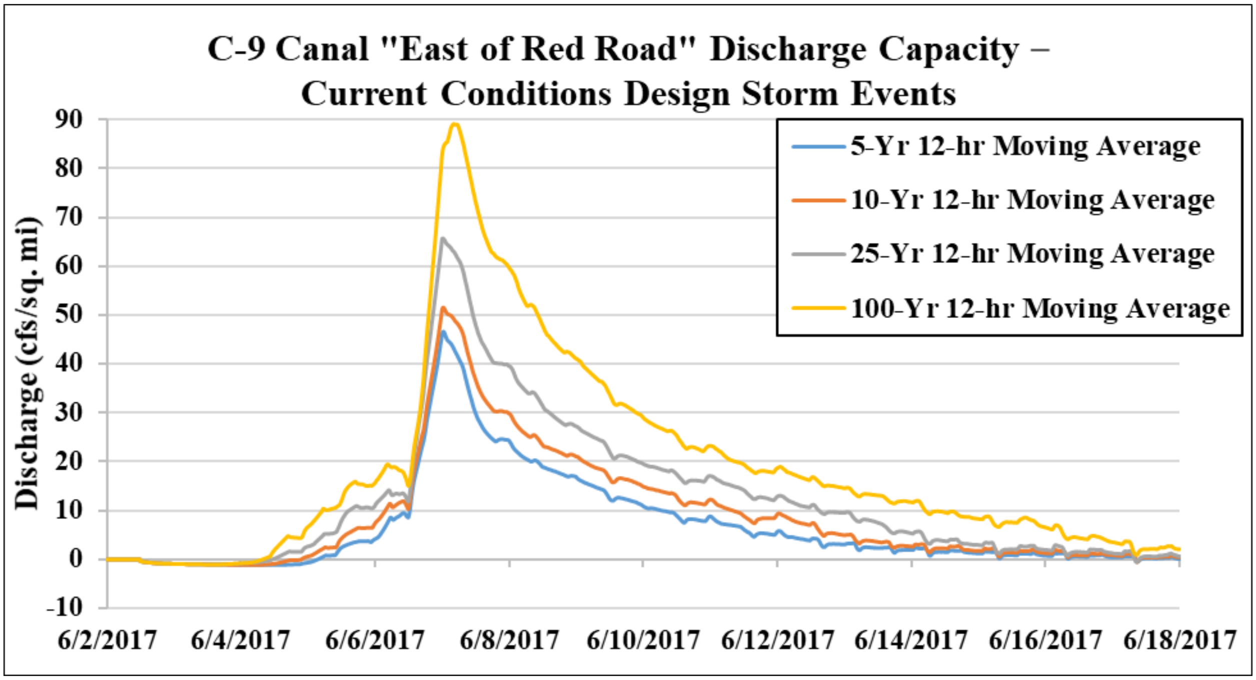

Figure 8.2-5: Area-Weighted Discharge Hydrograph for C-9 Canal East of Red Road

Discharge east of Red Road is an estimate due to interconnected outfalls on both sides of Red Road

Figure 8.2-6 shows the location of inter-basin connections, where discharge between the C-8 and C-9 watersheds occur, as well as between the C-8 and C-7 watersheds.

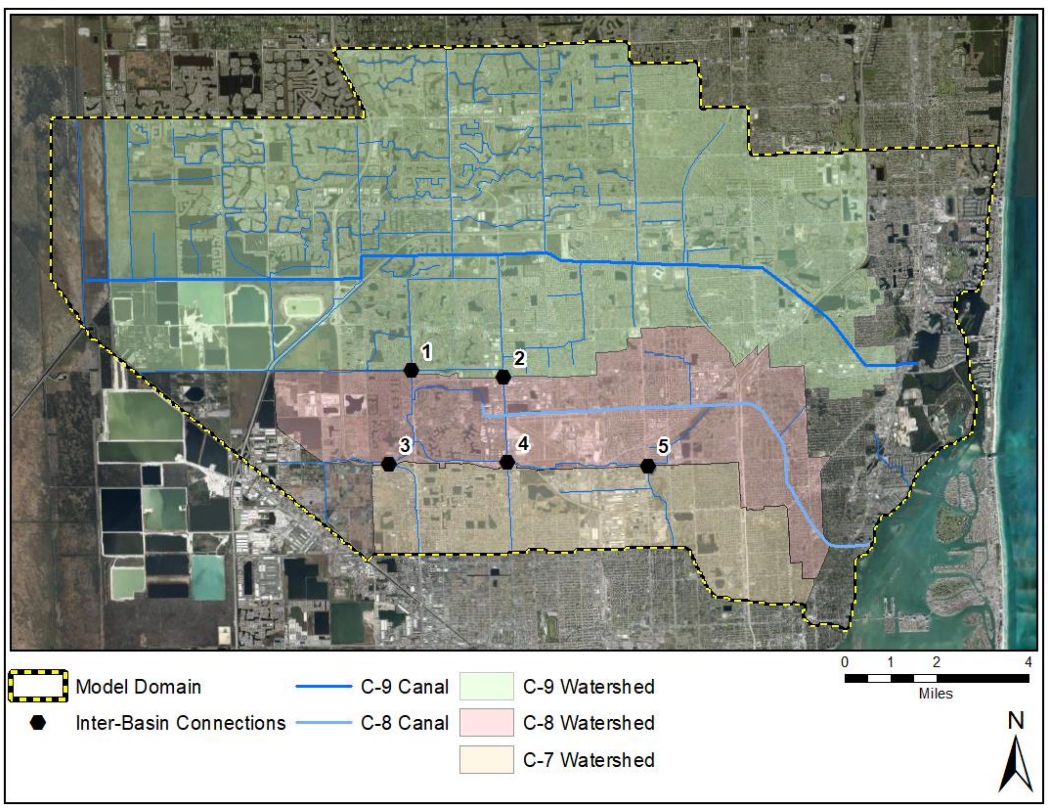

Figure 8.2-6: Location of Inter-Basin Connections

Connection 1 is a culvert under NW 78th Ave. **Figure 8.2-7** shows the inter-basin discharge, with positive values representing flow from the C-8 to the C-9 watershed and negative values indicating flow from the C-9 to the C-8 watershed. For the 100-year design storm, the peak discharge from C-8 to C-9 watershed at this inter-basin connection is about 60 cfs, whereas the peak discharge at Red Road on the C-9 Canal is around 1300 cfs. Relative to the flow in the C-9 Canal, this inter-basin exchange is small, contributing less than 5% of the peak discharge.

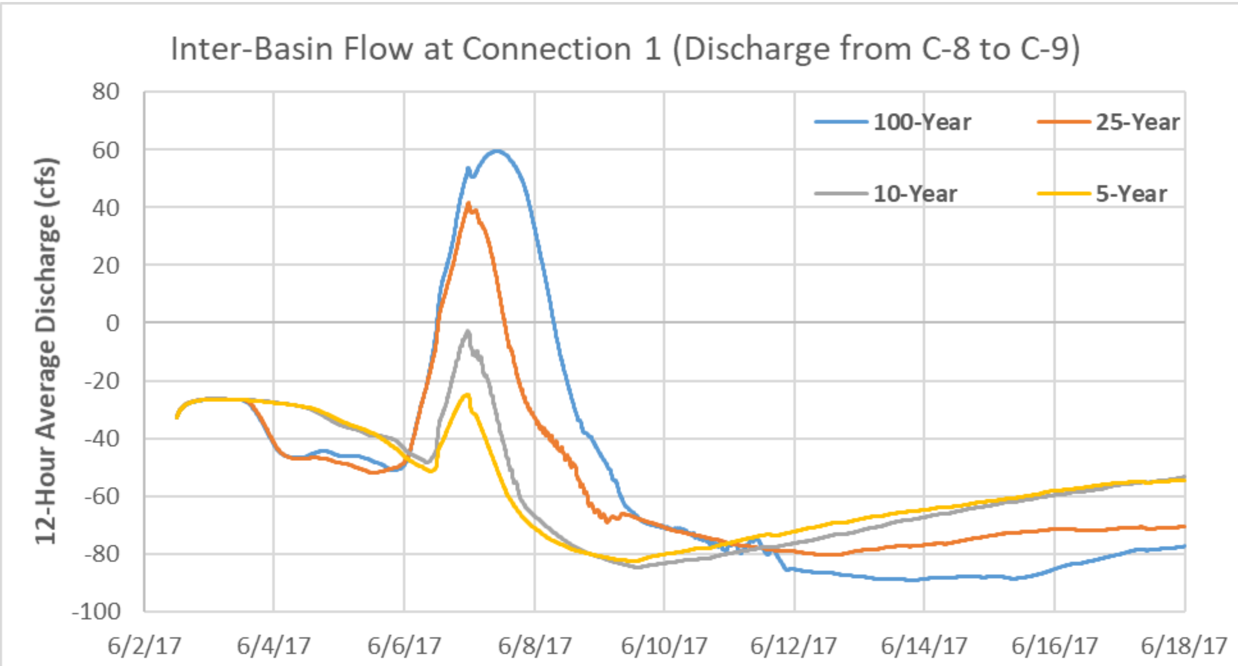

Figure 8.2-7: Inter-Basin Discharge Between C-8 and C-9 Watersheds at Connection 1

For the 100-year design storm, the peak discharge from C-9 to C-8 watershed at this inter-basin connection is about 90 cfs. However, this occurs several days after the peak discharge and does not contribute to peak discharge rates in the C-8 Canal.

Connection 2 is a culvert under Palmetto Expressway, just west of Red Road. **Figure 8.2-8** shows the inter-basin discharge, with positive values representing flow from the C-9 to the C-8 watershed and negative values indicating flow from the C-8 to the C-9 watershed. For the 100-year design storm, the peak discharge from C-9 to C-8 watershed at this inter-basin connection is about 125 cfs, however, it occurs several days after the peak discharge in the C-8 Canal. During the peak discharge at S-28, this basin interconnect is contributing a relatively small amount during the 25 and 100-year events. During the 5 and 10-year storms, the inter-basin flow during peak discharge at S-28 is more significant than during the 25 and 100-year storms, with approximately 10% and 8%, respectively.

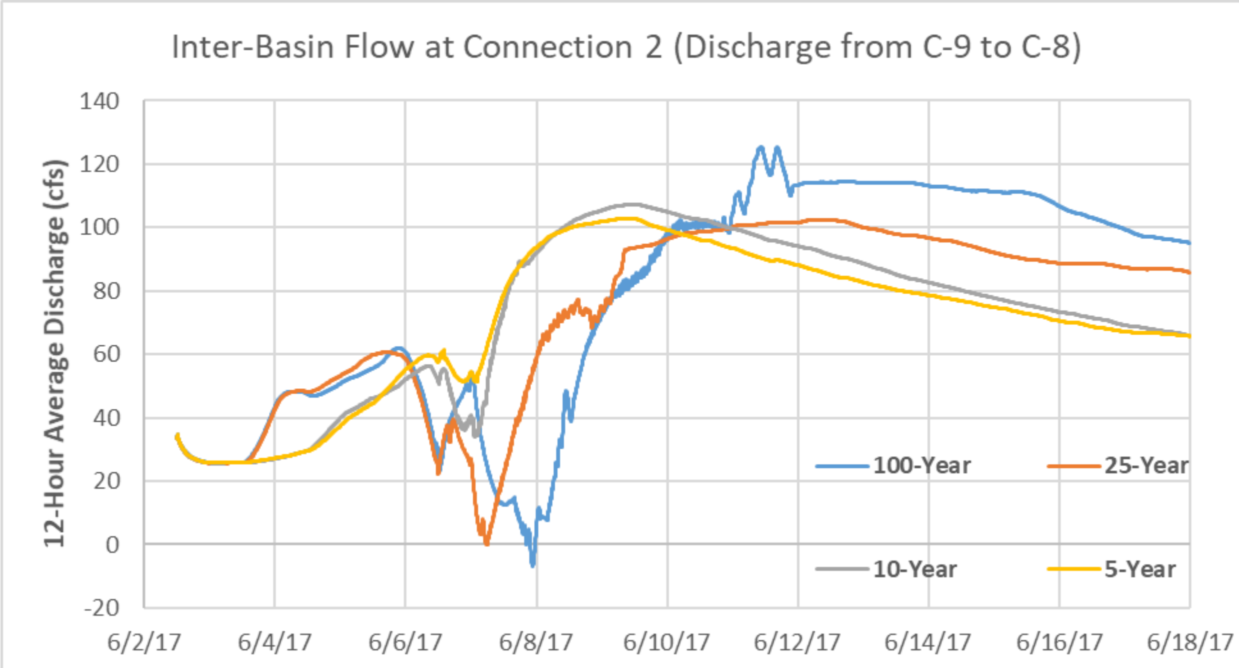

Figure 8.2-8: Inter-Basin Discharge Between C-8 and C-9 Watersheds at Connection 2

Connection 3 is a culvert under I75. **Figure 8.2-9** shows the inter-basin discharge, with positive values representing flow from the C-8 to the C-7 watershed and negative values indicating flow from the C-7 to the C-8 watershed. Flows from C-8 to C-7 watershed reduces the burden on the C-8 canal, peaking at about 100 cfs during the 25 and 100-year storms. During the 5 and 10-year storms, the discharge leaving the C-8 watershed is higher, at about 170 cfs. This relieves the C-8 canal system of some stress.

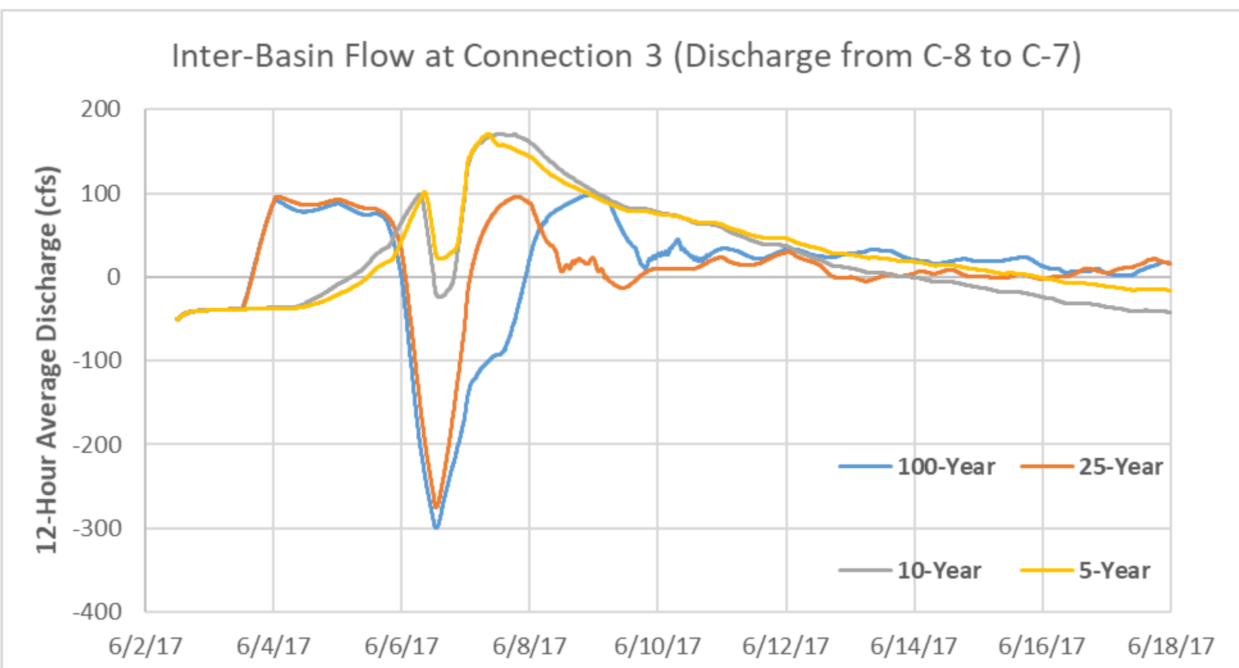

Figure 8.2-9: Inter-Basin Discharge Between C-8 and C-7 Watersheds at Connection 3

For the 25 and 100-year design storm, the peak discharge from C-7 to C-8 watershed at this inter-basin connection is about 300 cfs and occurs about 18 hours prior to peak discharge at S-28. Relative to the peak discharge at S-28, this inter-basin flow is about 9% for the 100-year event and 13% for the 25-year event. This adds stress to the C-8 Canal system.

Connection 4 is a culvert under NE 135th St at Red Road. **Figure 8.2-10** shows the inter-basin discharge, with positive values representing flow from the C-8 to the C-7 watershed and negative values indicating flow from the C-7 to the C-8 watershed. Flows from C-8 to C-7 watershed reduces the burden on the C-8 canal, peaking at about 50 cfs during the 100-year storm. This relieves the C-8 canal system of some stress.

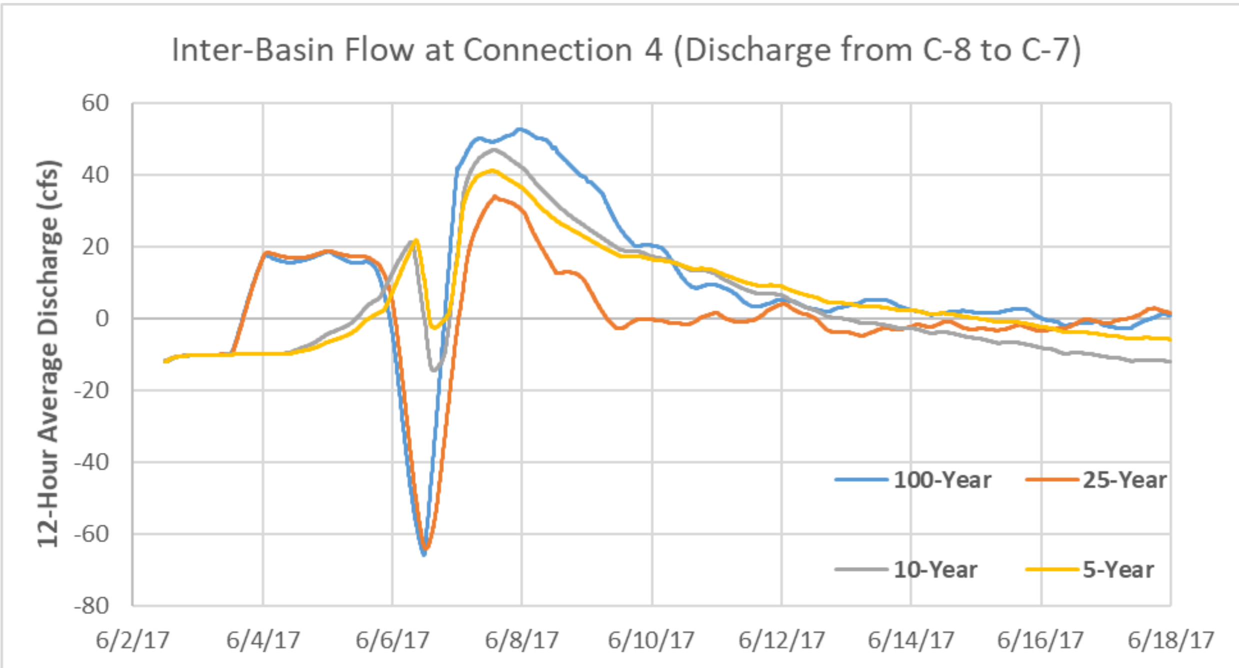

Figure 8.2-10: Inter-Basin Discharge Between C-8 and C-7 Watersheds at Connection 4

For the 25 and 100-year design storm, the peak discharge from C-7 to C-8 watershed at this inter-basin connection is about 65 cfs and occurs about 18 hours prior to peak discharge at S-28. Relative to the peak discharge at S-28, this inter-basin flow is rather insignificant, with about 2% for the 100-year event and 3% for the 25-year event.

Connection 5 is a culvert under NE 135th St just east of NW 27th Ave. **Figure 8.2-11** shows the inter-basin discharge, with negative values indicating flow from the C-8 to the C-7 watershed. Flows from C-8 to C-7 watershed reduces the burden on the C-8 canal, peaking at about 120 cfs during the 100-year storm. This relieves the C-8 canal system of some stress.

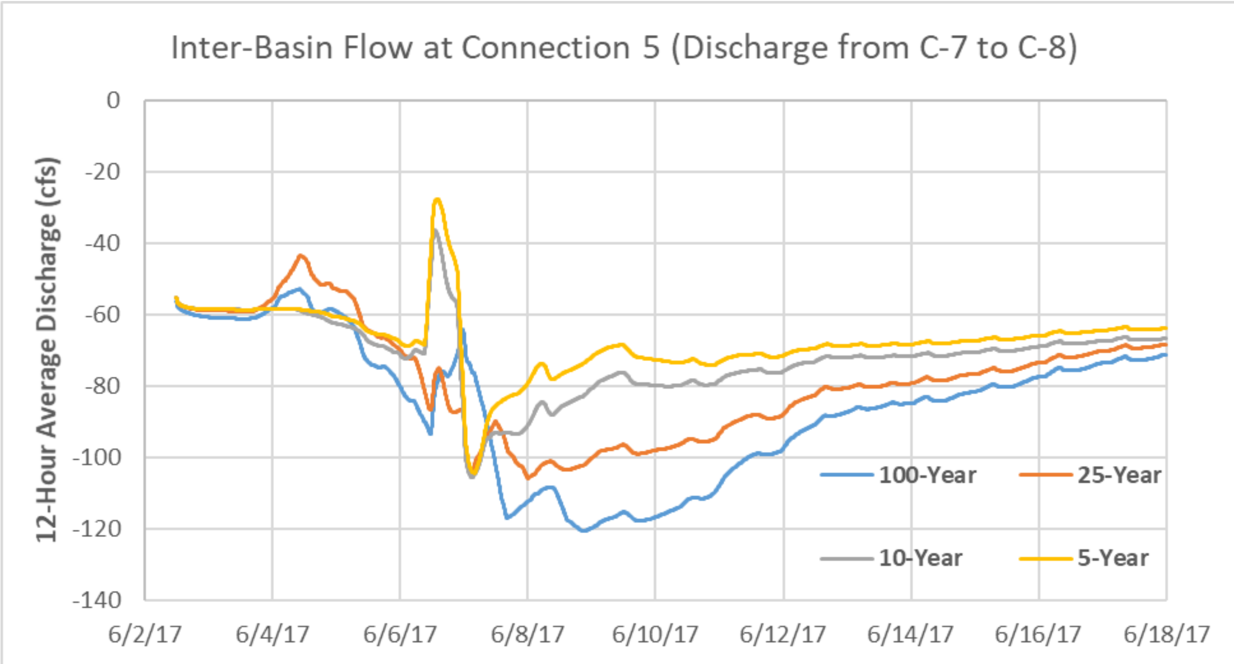

Figure 8.2-11: Inter-Basin Discharge Between C-8 and C-7 Watersheds at Connection 5

8.3 PM #3 – Structure Performance

PM #3 shows the effective capacity of a tidal structure. For this metric, structure discharge over a range of storm events and sea level rise scenarios is compared with the original static design condition. Future work in Phase 1B of this project will simulate three sea level rise scenarios, so this performance metric currently only evaluates current condition design storms with no sea level rise. This PM provides insight on the current structure performance. Phase 1B will evaluate the tidal structures in the same way to determine what degradation in performance occurs, if any, under sea level rise scenarios.

SFWMD has completed a similar evaluation for the S-28 and S-29 structures in reports titled, *The Effects of Sea Level Rise on S28 Performance* (Zhang, 2017) and *The Effects of Sea Level Rise on S29 Performance* (Zhang, 2017). In these evaluations, a simple hydraulic model was used with fixed headwater stage based on design headwater and a tailwater that oscillates tidally. To add to the work that has already been done, this PM is evaluated using the full MIKE SHE / MIKE HYDRO model results. Essentially, the main difference is that headwater is not forced, rather it is simulated using the fully dynamic model. Please note that this analysis is for informational purposes and is not intended to replace the previous work done by the District, but rather supplement it and analyze it using a different method.

Structure S-28 has a static design headwater and tailwater of 2.2 ft and 1.7 ft, respectively. The static design discharge is 3220 cfs based on 0.5 ft head gradient (Zhang, 2017). **Figure 8.3-1** and **Figure 8.3-2** show instantaneous values and 12-hour moving average values, respectively, for S-28 based on a 25-year design storm.

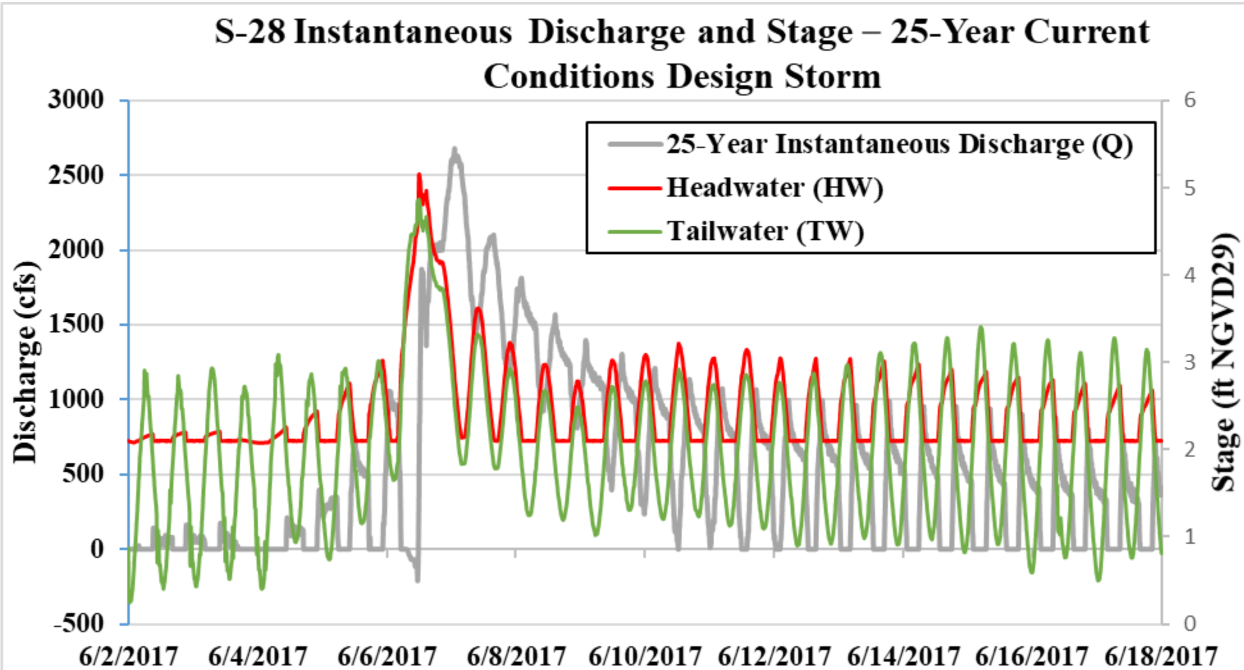

Figure 8.3-1: Instantaneous Discharge and Stage at S-28 Structure for 25-Year Current Conditions Design Storm

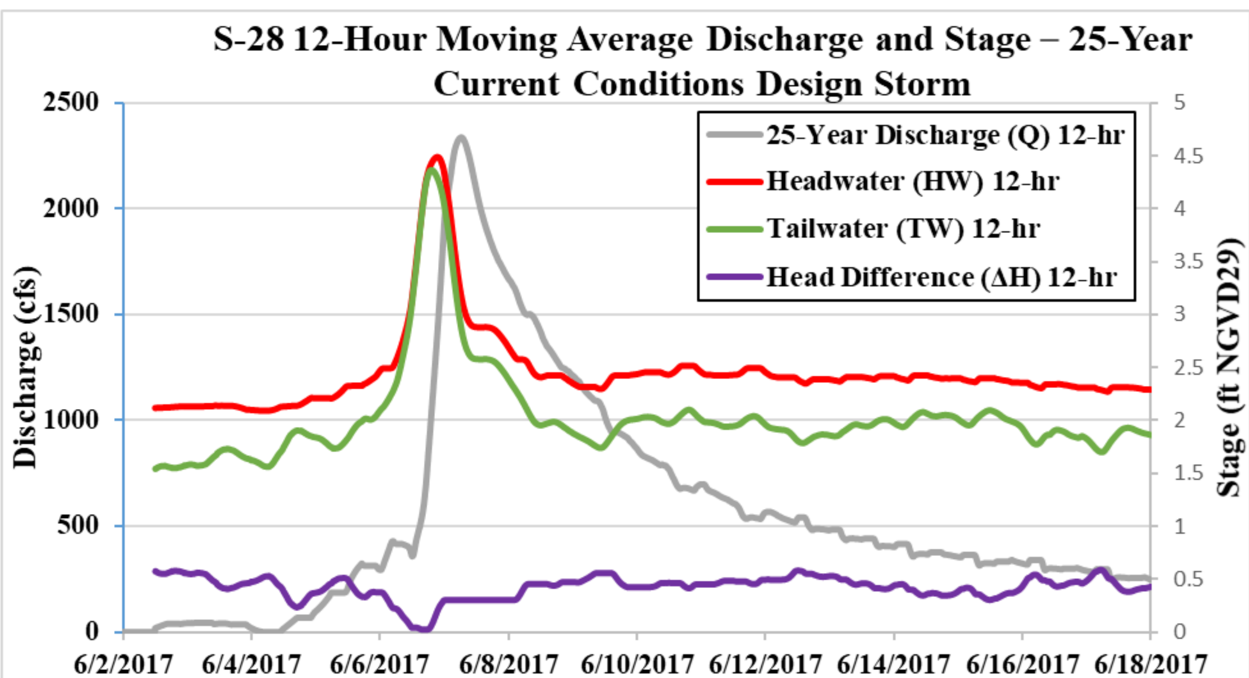

Figure 8.3-2: Tidally Averaged (12-hour) 25-Year Design Storm Discharge, Stage, and Head Gradient for Structure S-28

Figure 8.3-3 and **Figure 8.3-4** show instantaneous values and 12-hour moving average values, respectively, for S-28 based on a 100-year design storm.

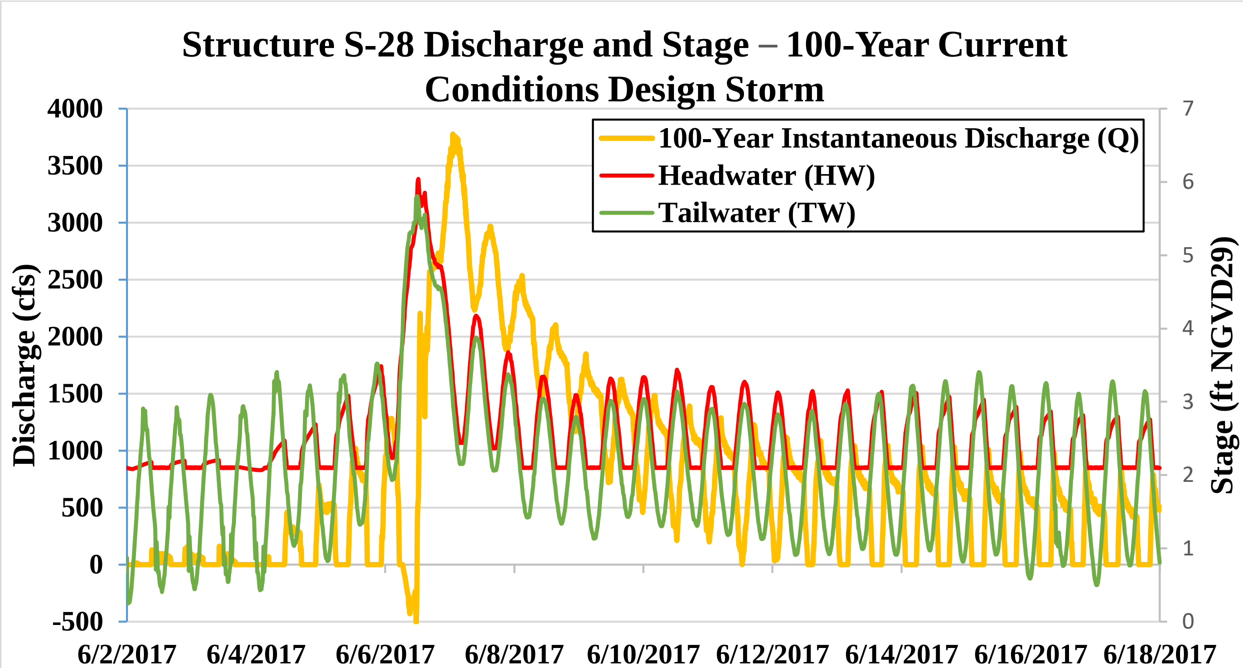

Figure 8.3-3: Instantaneous Discharge and Stage at S-28 Structure for 100-Year Current Conditions Design Storm

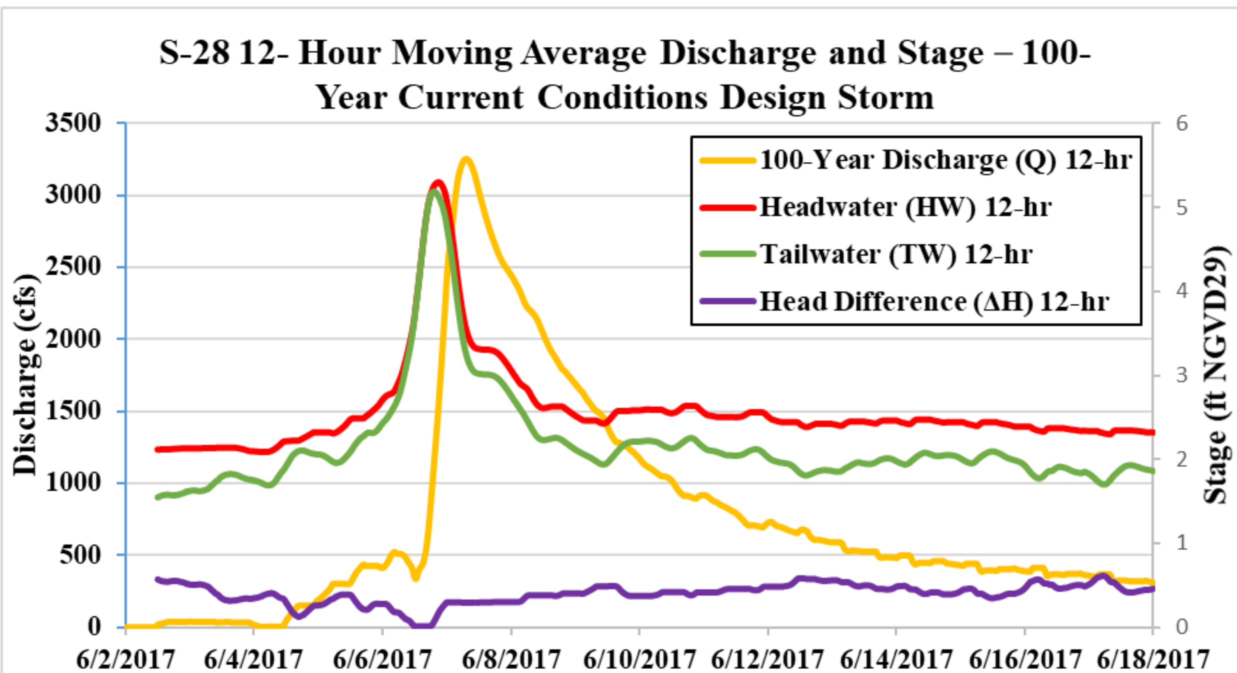

Figure 8.3-4: Tidally Averaged (12-hour) 100-Year Design Storm Discharge, Stage, and Head Gradient for Structure S-28

As shown in **Figure 8.3-4,** the S-28 structure slightly exceeds the design discharge of 3220 cfs, with a 12-hour moving average peak of 3250 cfs. While this discharge occurs with a 12-hour average head difference of only 0.3 feet, the design headwater assumption is violated. The assumed design headwater stage is 2.2 feet, while the predicted headwater is 3.5 feet. **Table 8-5** summarizes the simulated 12-hour moving average peak discharge, headwater, tailwater, and head differential for S-28, for each of the design storms.

Table 8-5: Summary of the 12-Hour Moving Average Discharge and Stage at S-28

S-28	12-Hour Moving Average			
	Peak Discharge (cfs)	Peak Headwater (ft NGVD29)	Peak Tailwater (ft NGVD29)	Head Differential (ft)
5-Year	1441	2.75	2.39	0.36
10-Year	1748	2.93	2.61	0.32
25-Year	2337	3.17	2.87	0.3
100-Year	3254	3.55	3.25	0.3

Structure S-29 has a static design headwater and tailwater of 2.4 ft and 1.9 ft, respectively. The static design discharge is 4780 cfs based on 0.5 ft head difference (Zhang, 2017). **Figure 8.3-5** and **Figure 8.3-6 s**how instantaneous values and 12-hour moving average values, respectively, for S-29 based on a 25-year design storm.

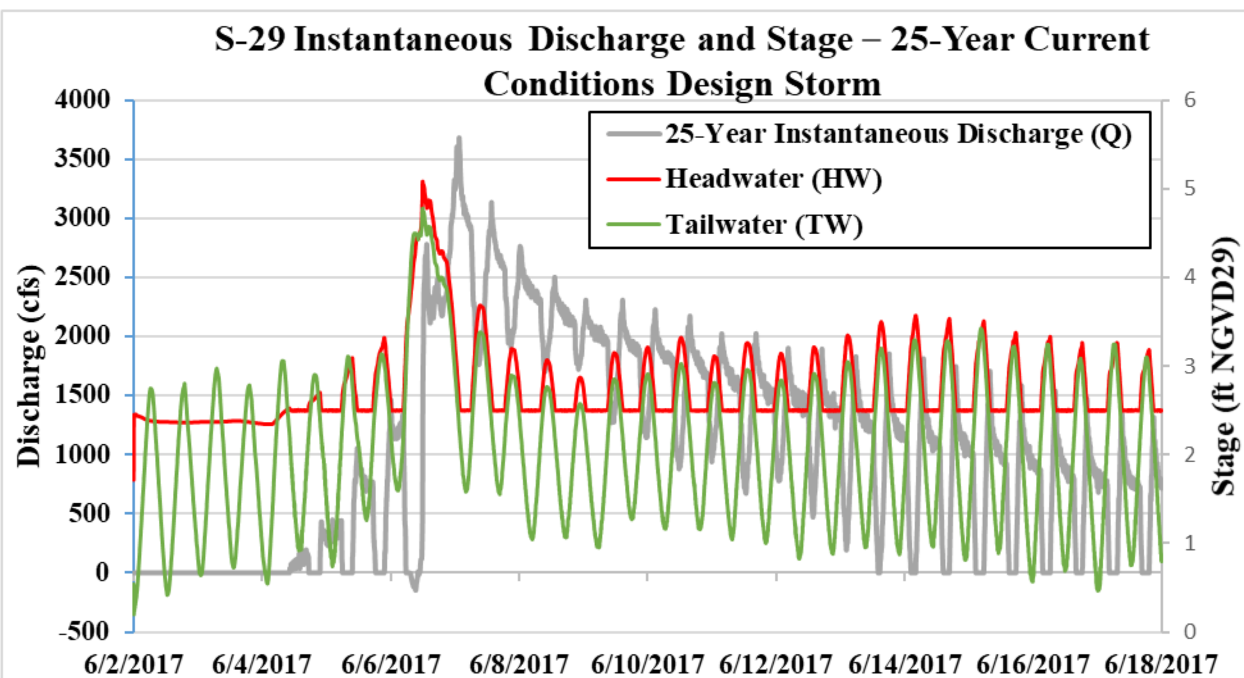

Figure 8.3-5: Instantaneous Discharge and Stage at S-29 Structure for 25-Year Current Conditions Design Storm

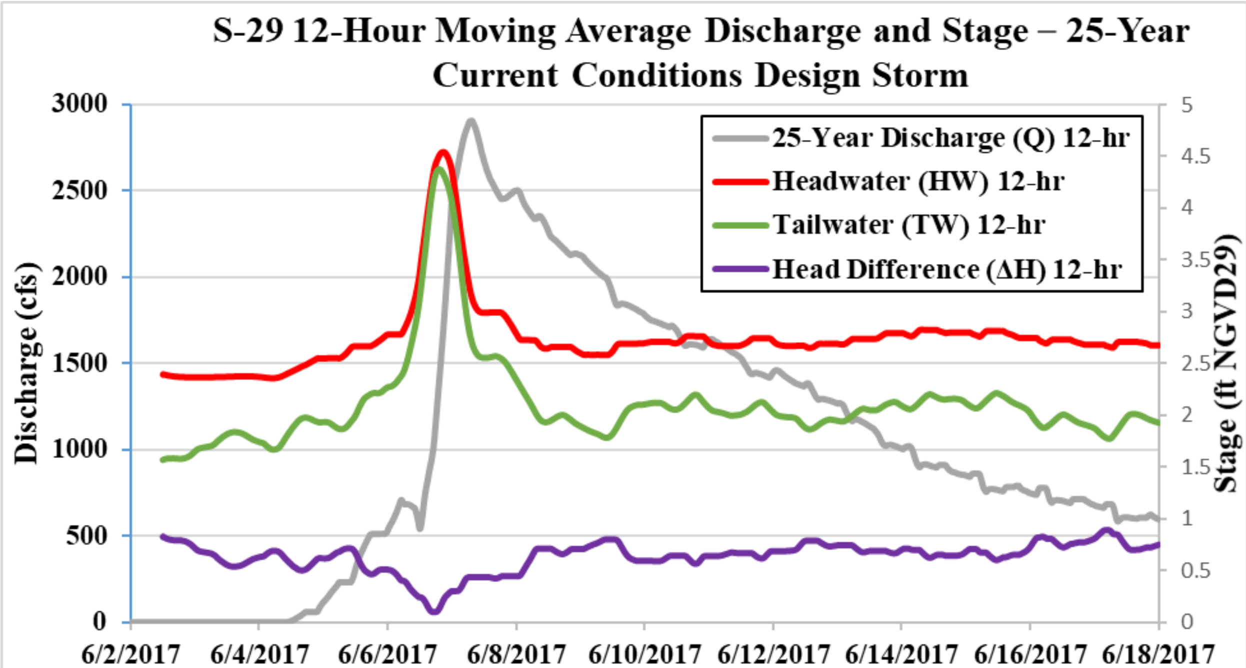

Figure 8.3-6: Tidally Averaged (12-hour) 25-Year Design Storm Discharge, Stage, and Head Gradient for Structure S-29

Figure 8.3-7 and **Figure 8.3-8** show instantaneous values and 12-hour moving average values, respectively, for S-29 based on a 100-year design storm.

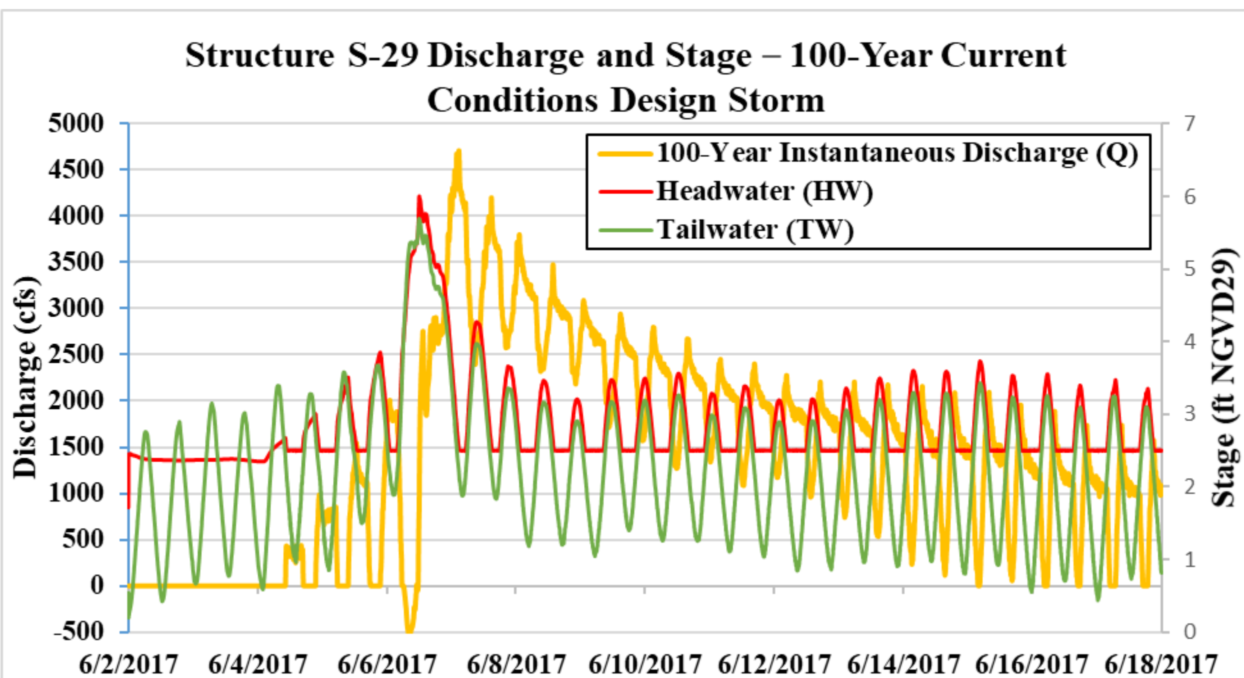

Figure 8.3-7: Instantaneous Discharge and Stage at S-29 Structure for 100-Year Current Conditions Design Storm

During the 100-year design storm, structure S-29 has an instantaneous peak discharge of 4710 cfs, which is just shy of the static design discharge of 4780. While this discharge occurs with an instantaneous head difference of 0.31 feet, the design headwater assumption is slightly violated. The assumed design headwater stage is 2.4 feet, while the predicted headwater is 2.5 feet.

As shown in **Figure 8.3-8**, the S-29 structure falls significantly short of the design discharge of 4780 cfs, with a 12-hour moving peak of just 3728 cfs. The 12-hour moving average head difference was only 0.35 ft, compared to 0.5 ft in the static design condition. This indicated that the current conditions storm surge was preventing S-29 from reaching its design condition. Additionally, the design headwater assumption is violated with a 12-hour average headwater elevation of 3.5 feet, compared to 2.4 feet for the static design condition assumption. Phase 1B of this project will determine if there would be any further degradation in performance under three sea level rise scenarios.

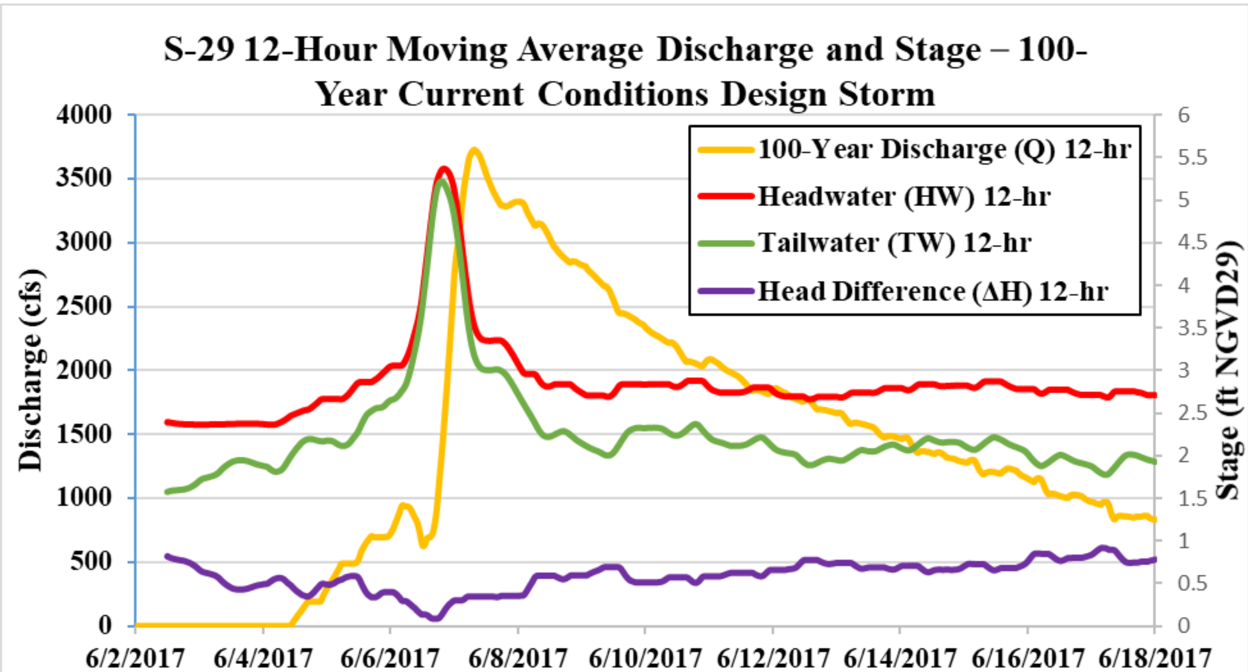

Figure 8.3-8: Tidally Averaged (12-hour) 100-Year Design Storm Discharge, Stage, and Head Gradient for Structure S-29

Table 8-6 summarizes the simulated 12-hour moving average peak discharge, headwater, tailwater, and head differential for S-28, for each of the design storms.

Table 8-6: Summary of the 12-Hour Moving Average Discharge and Stage at S-29

S-29	12-Hour Moving Average			
	Peak Discharge (cfs)	Peak Headwater (ft NGVD29)	Peak Tailwater (ft NGVD29)	Head Differential (ft)
5-Year	2140	2.84	2.27	0.57
10-Year	2437	2.95	2.44	0.51
25-Year	2908	3.14	2.71	0.43
100-Year	3728	3.52	3.17	0.35

8.4 PM #4 – Peak Storm Runoff

PM #4 is the maximum conveyance capacity of a watershed at the tidal structure for a range of design storms. It shows the maximum conveyance (moving 12-hr average) for a specific design storm and a specific tidal boundary condition. This metric will be evaluated during Phase 1B of this project, where three sea level rise scenarios will be simulated. **Figure 8.4-1** and **Figure 8.4-2** represent the design storm discharge at tidal structures S-28 and S-29, respectively. These discharge hydrographs, specifically the peak discharge, will be compared with the peak discharge under future sea level rise scenarios.

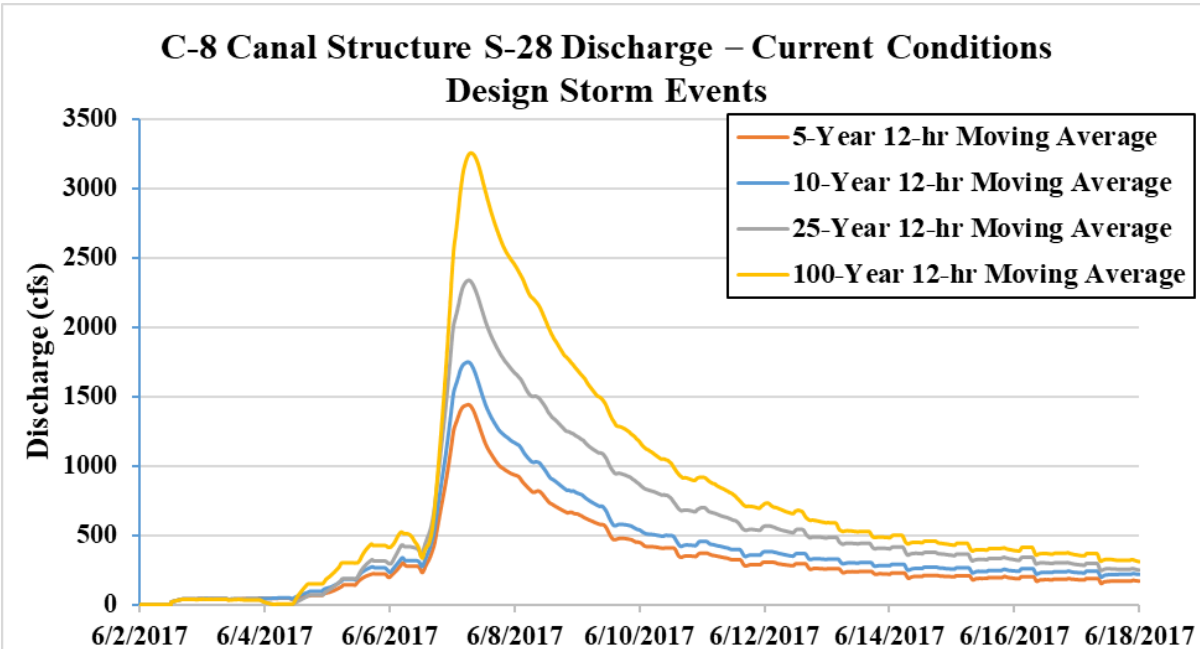

Figure 8.4-1: C-8 Canal Structure S-28 Discharge Hydrographs

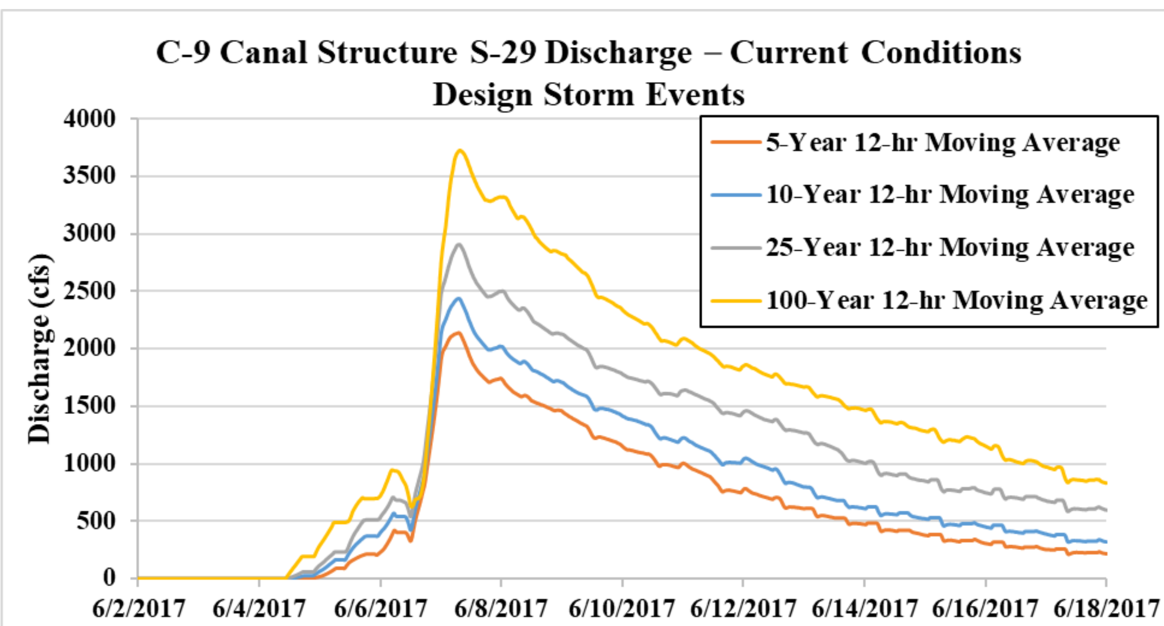

Figure 8.4-2: C-9 Canal Structure S-29 Discharge Hydrographs

Figure 8.4-3 shows the 12-hour average peak discharge versus the design storm return period for S-28 and **Table 8-7** shows the instantaneous and 12-hour average peak discharge. **Figure 8.4-3** will be used in the next phase (Phase 1B) to compare changes in peak discharge for each design storm under future conditions.

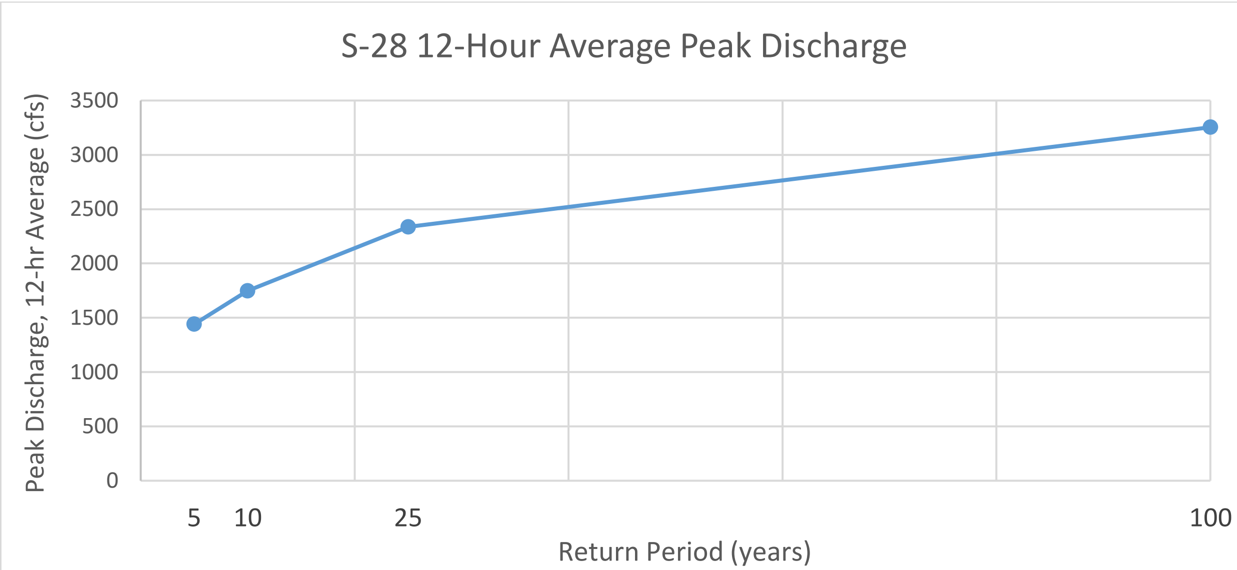

Figure 8.4-3: Structure S-28 12-Hour Average Peak Discharge

Table 8-7: S-28 Peak Discharge Summary

S-28	Peak Discharge (cfs)	
	Instantaneous	Moving Average (12-hr)
5-Year	1720	1441
10-Year	2059	1748
25-Year	2679	2337
100-Year	3777	3254

Figure 8.4-4 shows the 12-hour average peak discharge versus the design storm return period for S-29 and **Table 8-8** shows the instantaneous and 12-hour average peak discharge. **Figure 8.4-4** will be used in the next phase (Phase 1B) to compare changes in peak discharge for each design storm under future conditions.

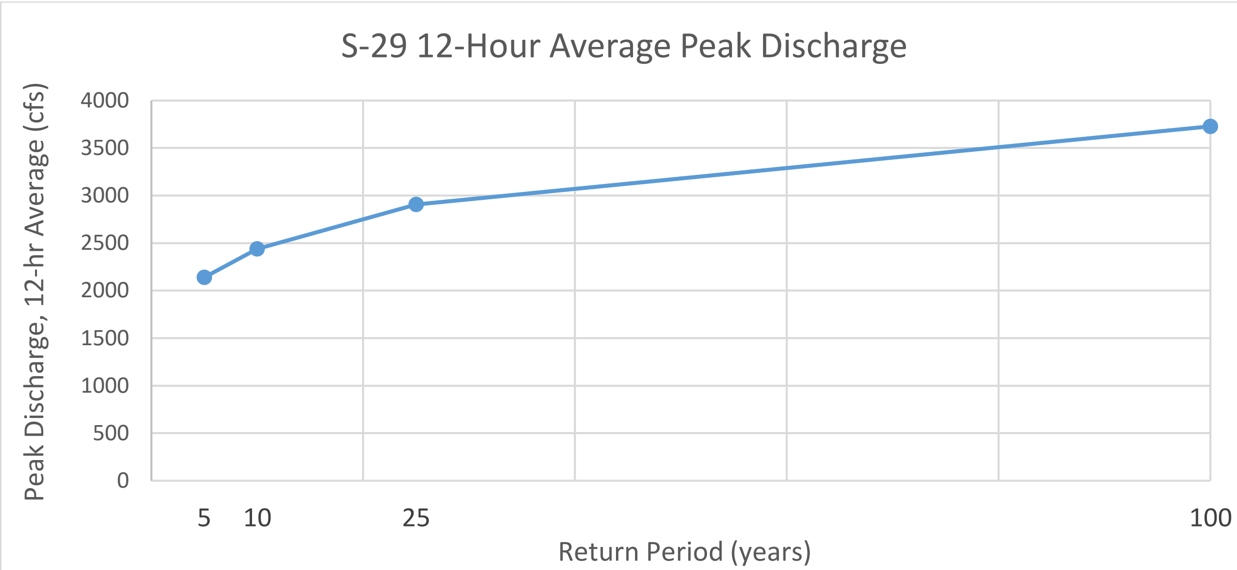

Figure 8.4-4: Structure S-29 12-Hour Average Peak Discharge

Table 8-8: S-29 Peak Discharge Summary

S-29	Peak Discharge (cfs)	
	Instantaneous	Moving Average (12-hr)
5-Year	2647	2140
10-Year	3052	2437
25-Year	3681	2908
100-Year	4710	3728

8.5 PM #5 – Frequency of Flooding

For this PM, the depths of overland flooding were evaluated for the 72-hour design storms with the return period of 5-year, 10-year, 25-year, and 100-year. These flood depths, or elevations, can be compared with elevations of features such as buildings and roadways, where such information exists. For the purposes of this C8/C9 FPLOS evaluation, flood inundation maps were prepared using MIKE SHE gridded model output for each storm event, in the form of depth of overland water. Flooding depths were representative of the overland water depths on the 125-ft grid. The resulting flood inundation maps over the entire model domain are shown in **Figure 8.5-1** through **Figure 8.5-4** for each of the four design storm events. **Figure 8.5-5** through **Figure 8.5-8 show** the flood duration maps for each of the design storm events for urban areas only. **Figure 8.5-9** through **Figure 8.5-11** show up close examples of flood duration along the C-8 Canal and **Figure 8.5-12** through **Figure 8.5-15** show up close examples of flood duration along the C-9 Canal.

The southwest portion of the C-9 Basin is undeveloped (as of the date of current condition model development, or year 2020), and thus were not served by stormwater collection and conveyance facilities. These undeveloped areas show the greatest extents and depths of flooding for the design storm events.

Notable developed areas also show flooding under PM #5. For example, residential areas along the C-8 Canal upstream and downstream of NE 135th St (CR 916), show extensive spatial extents of flooding in PM #5, which is most evident for the 25-year and 100-year events. This flooding is corroborated by PM #1 results, which show the south canal bank is exceeded for the 10-year event over a long segment upstream of CR916, while the north bank is exceeded for the 5-year event downstream of CR916.

In the C-9 Watershed, extensive flooding is shown along a 1-mile segment of the canal, on the south side of the canal west of Red Road (a.k.a. CR823 or 57th Ave.) for the 25-and 100-year events. However, PM #1 does not show a canal bank exceedance in this location. The flooding in this area could be due to the topography being lower than the canal bank and/or inadequate secondary drainage infrastructure. Other areas of flooding include residential areas further upstream, on the north side of the C-9 Canal upstream of the Ronald Reagan Turnpike. Again, the PM #1 results do not show a bank exceedance in this area. The flooding shown in this area could be from under-performing secondary/tertiary drainage systems.

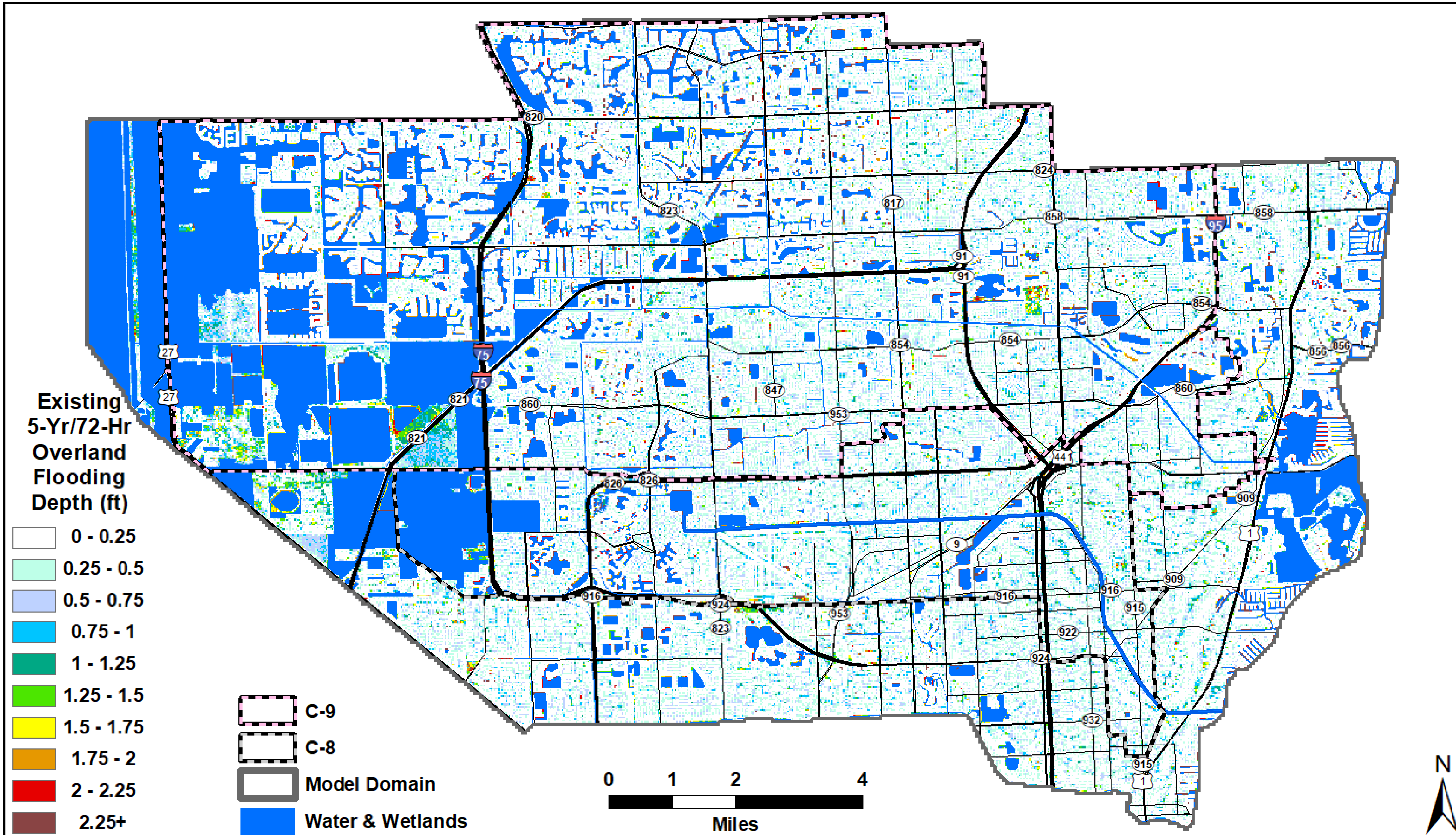

Figure 8.5-1: Flood Inundation Map for 5-Year Design Storm Event

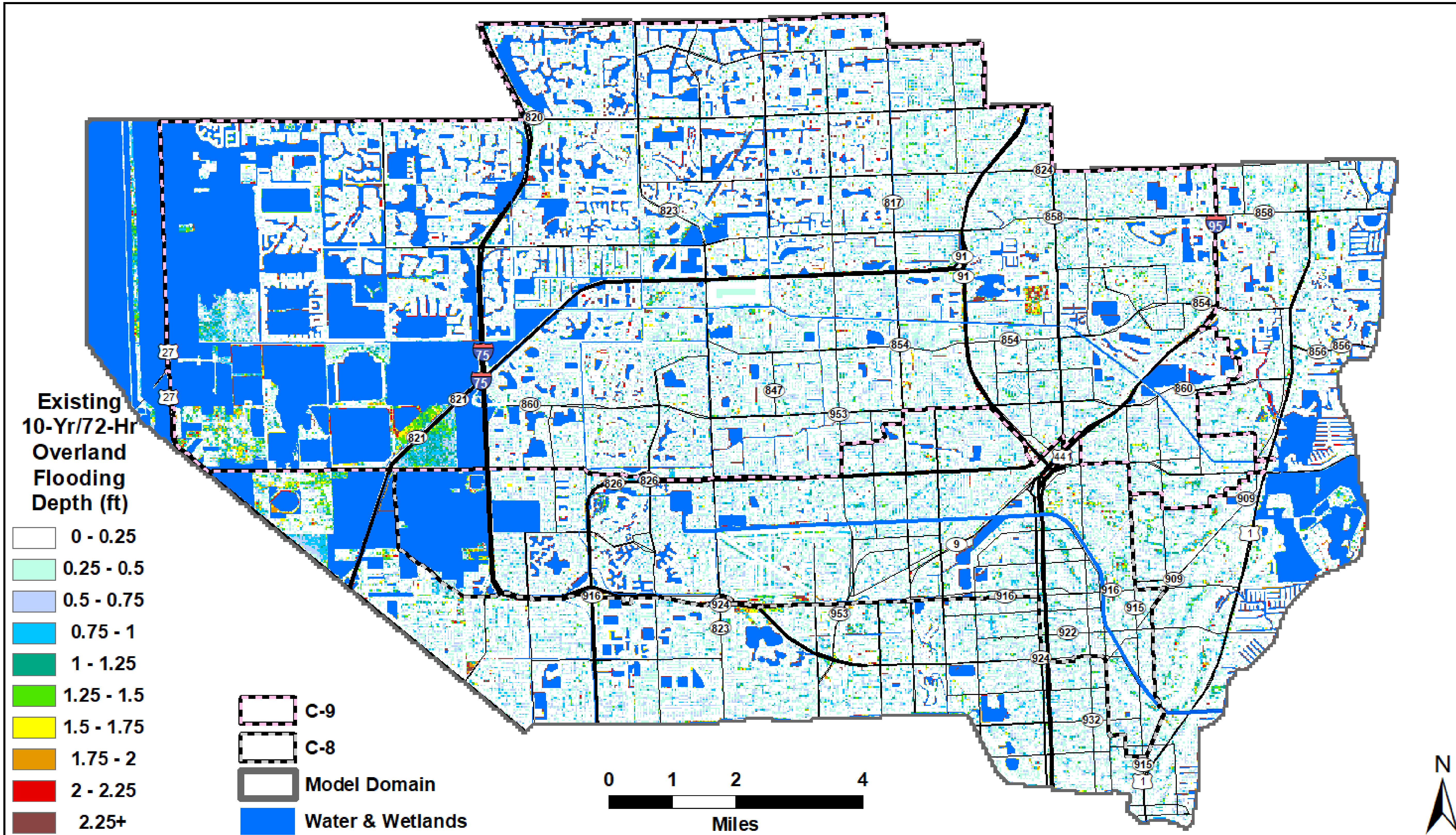

Figure 8.5-2: Flood Inundation Map for 10-Year Design Storm Event

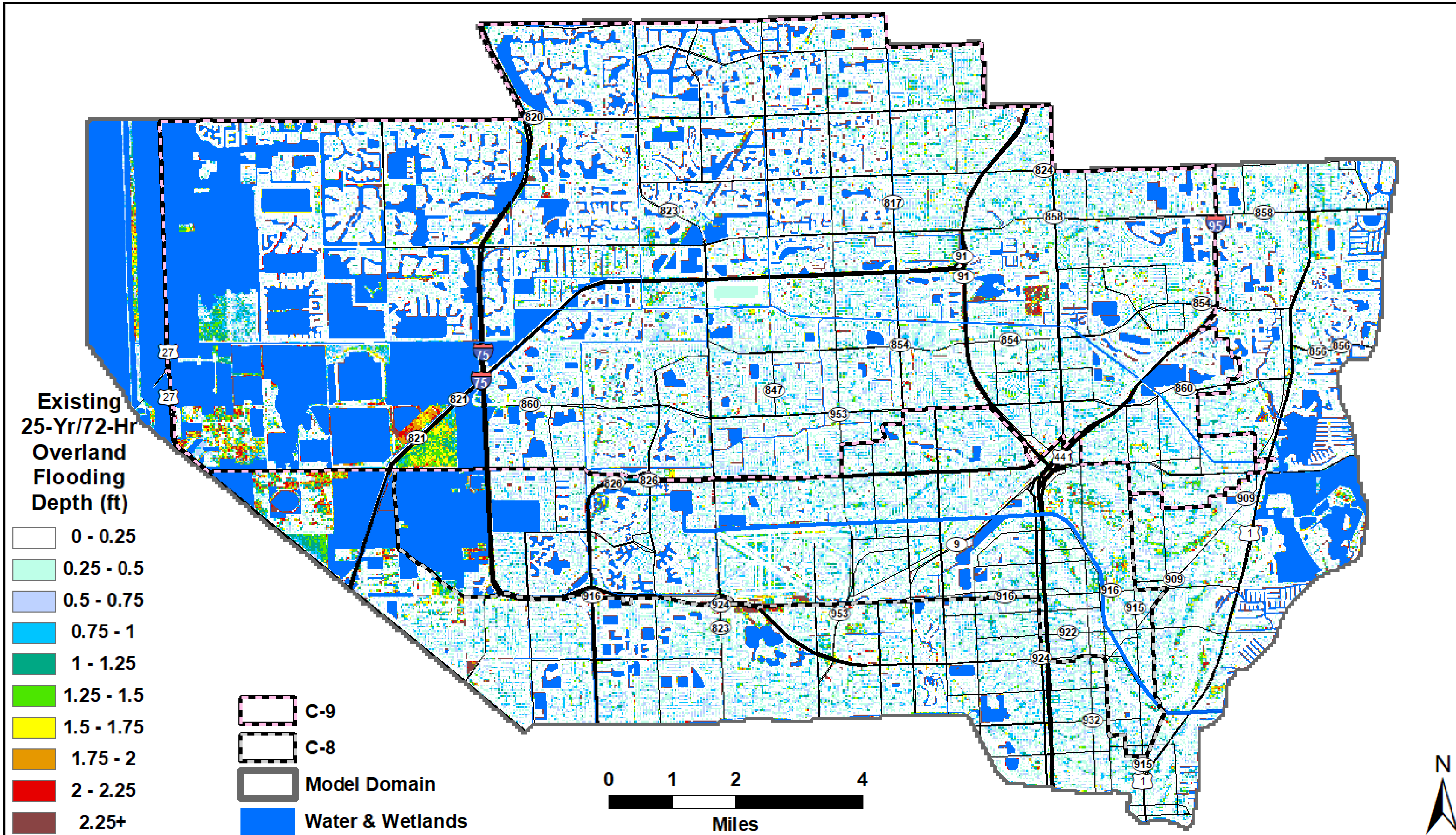

Figure 8.5-3: Flood Inundation Map for 25-Year Design Storm Event

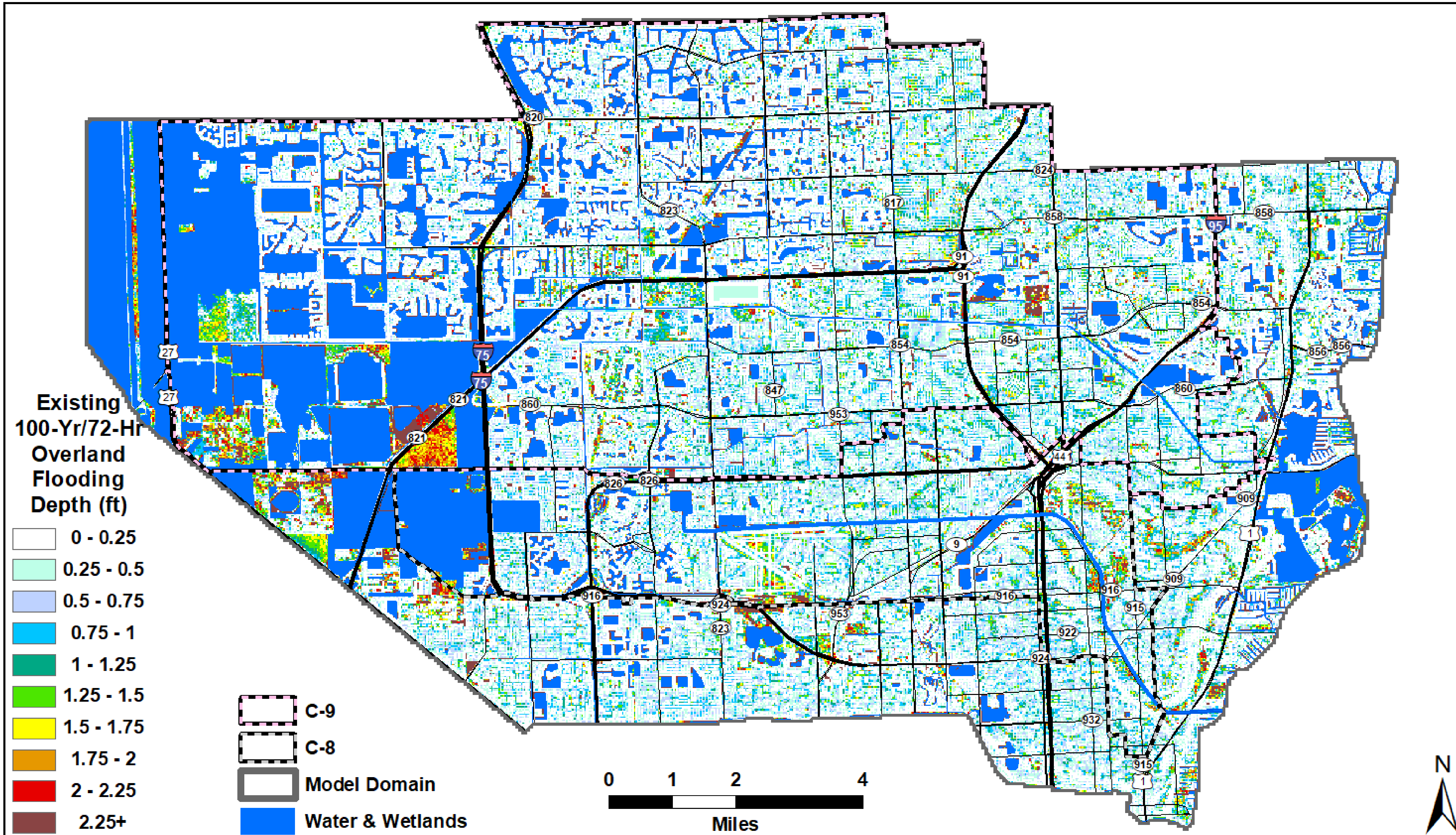

Figure 8.5-4: Flood Inundation Map for 100-Year Design Storm Event

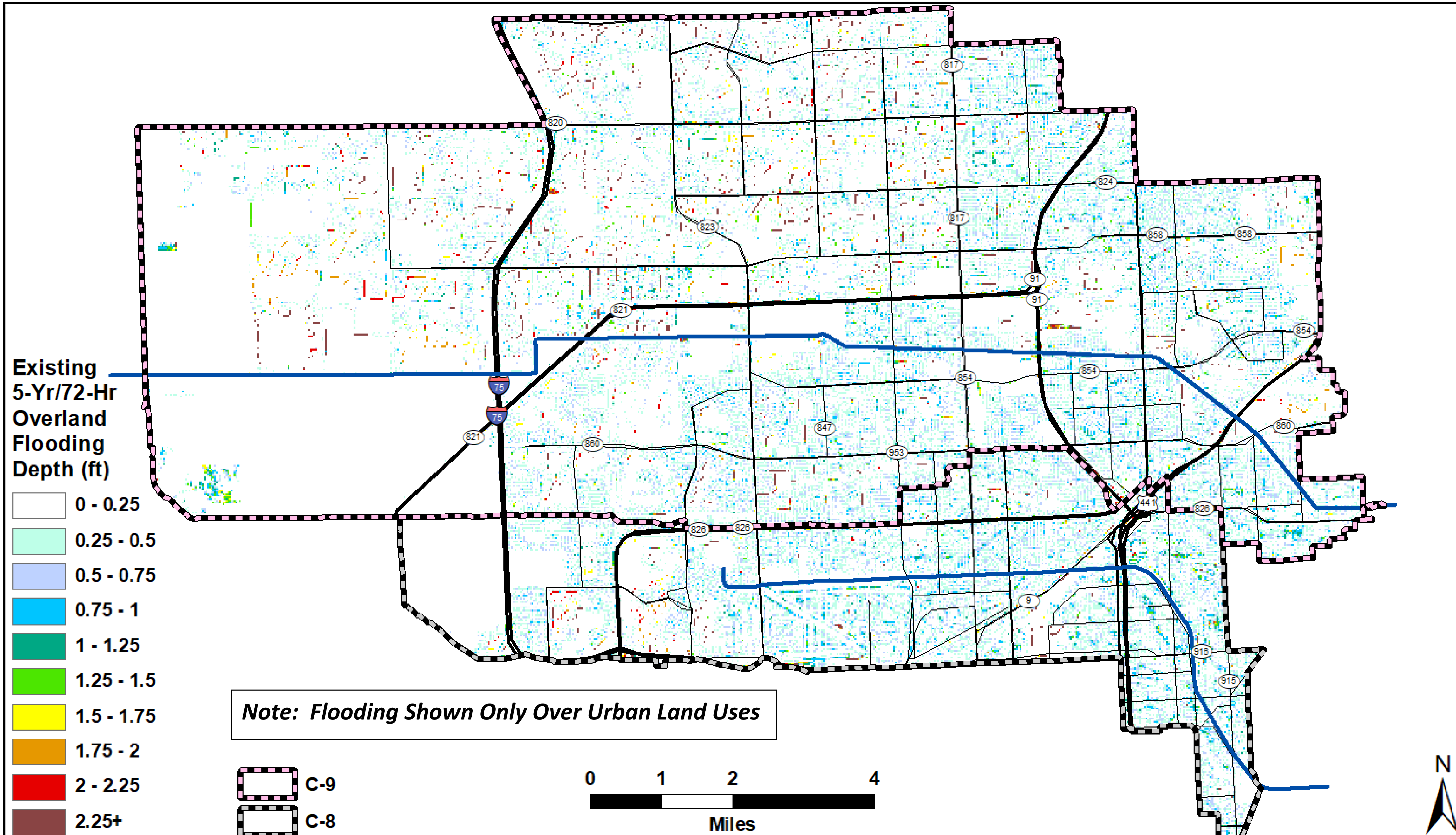

Figure 8.5-5: Flood Inundation Map for 5-Year Design Storm Event in Urban Land Use Areas

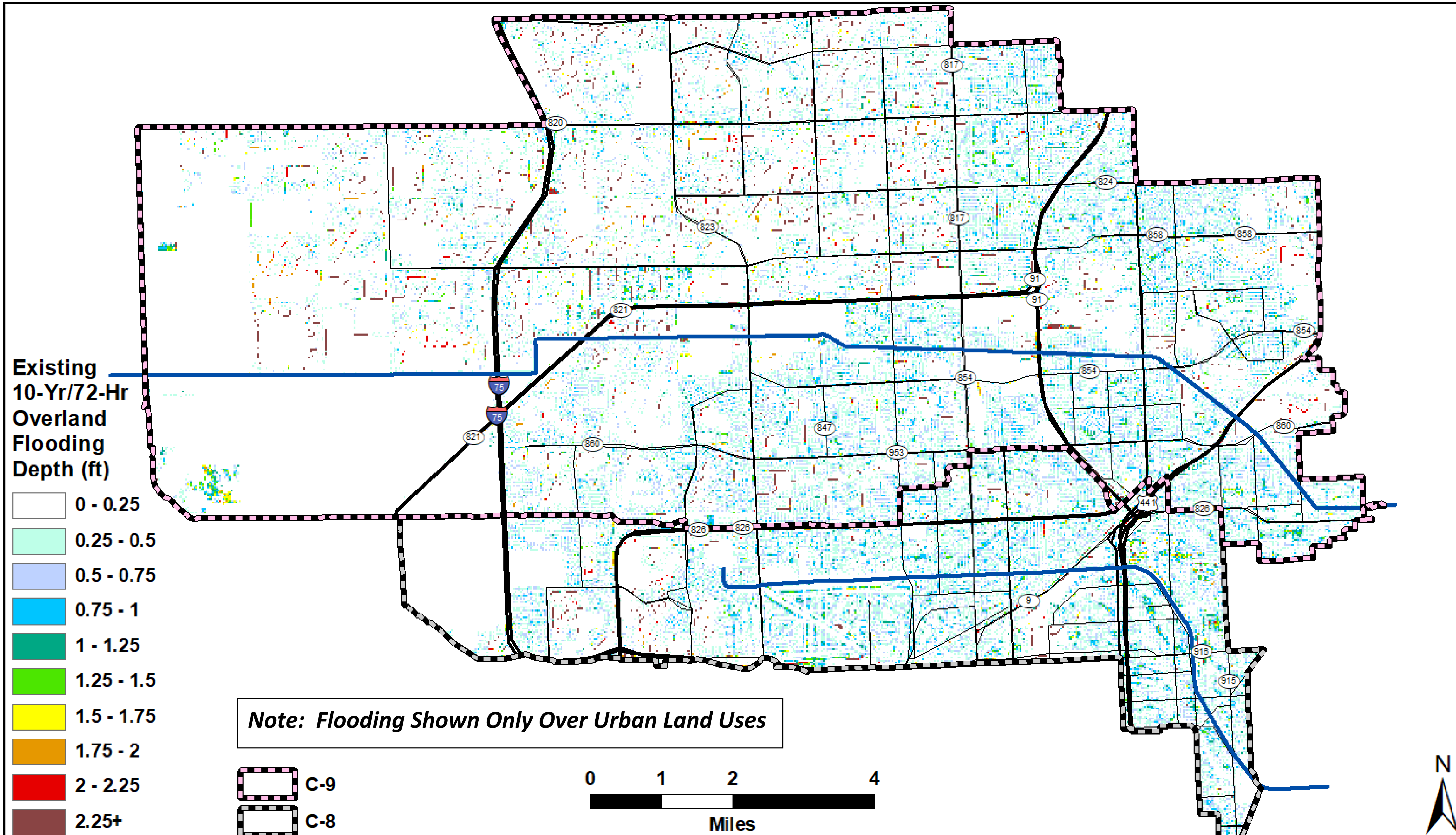

Figure 8.5-6 Flood Inundation Map for 10-Year Design Storm Event in Urban Land Use Areas

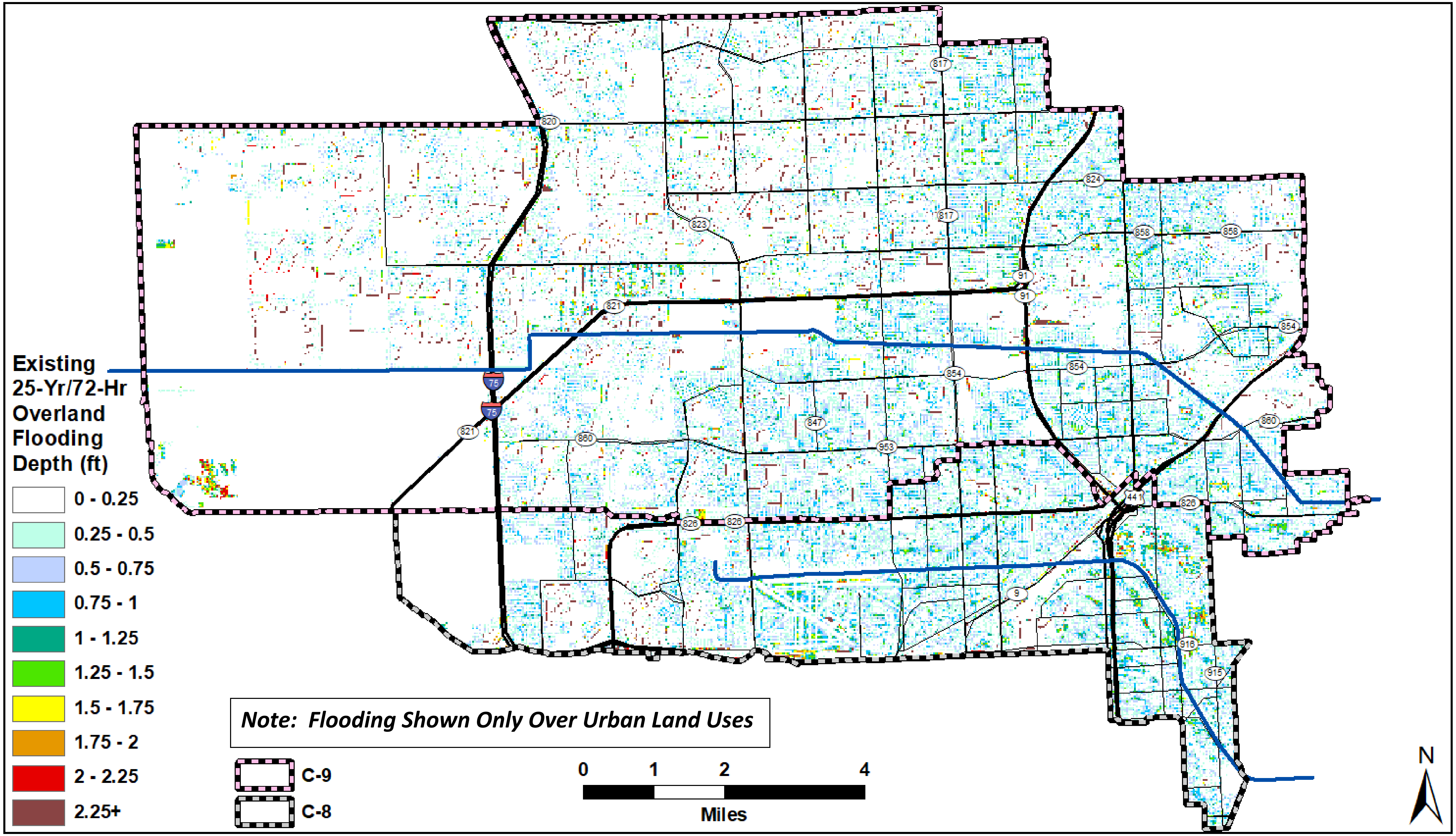

Figure 8.5-7: Flood Inundation Map for 25-Year Design Storm Event in Urban Land Use Areas

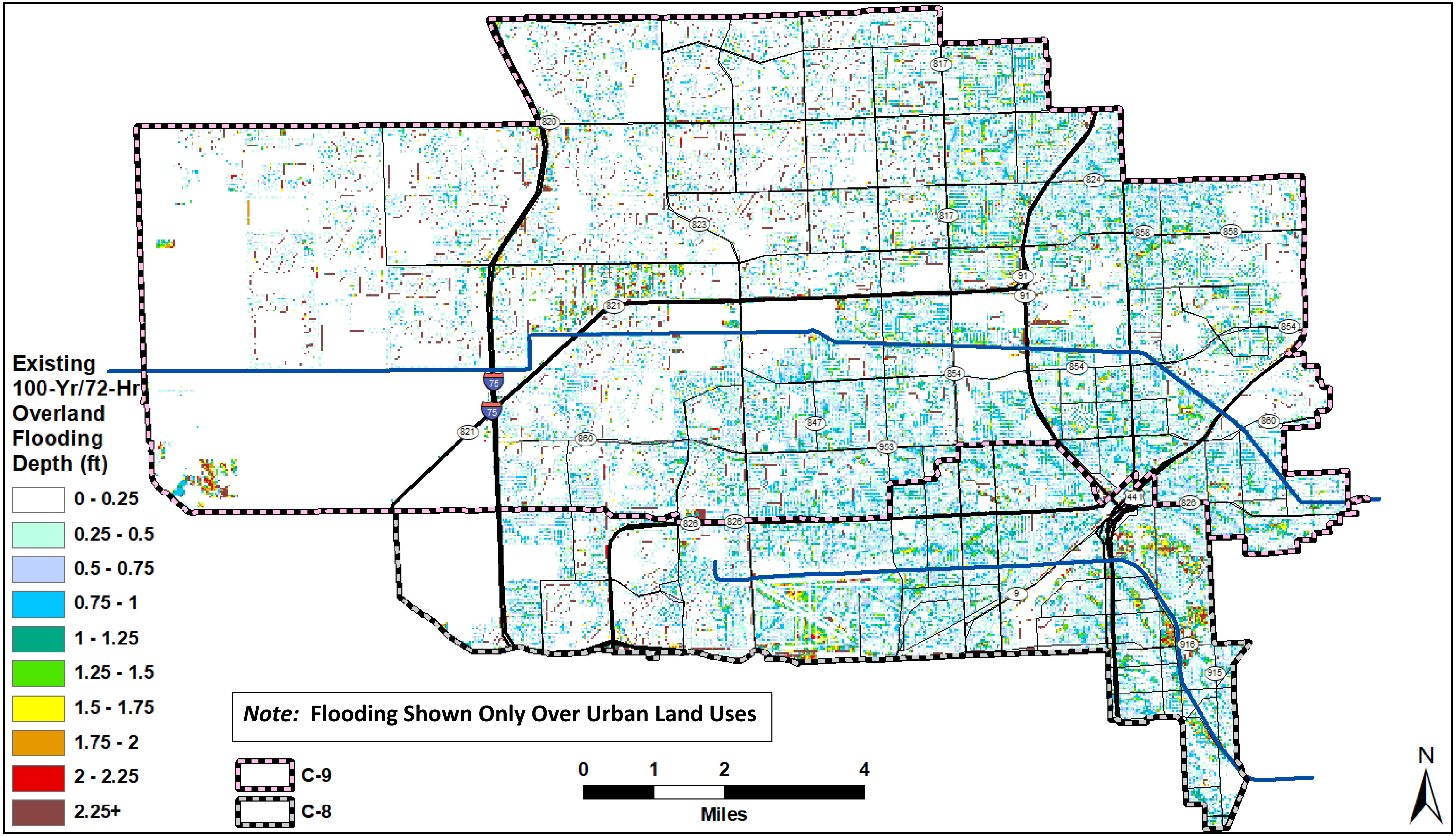

Figure 8.5-8: Flood Inundation Map for 100-Year Design Storm Event in Urban Land Use Areas

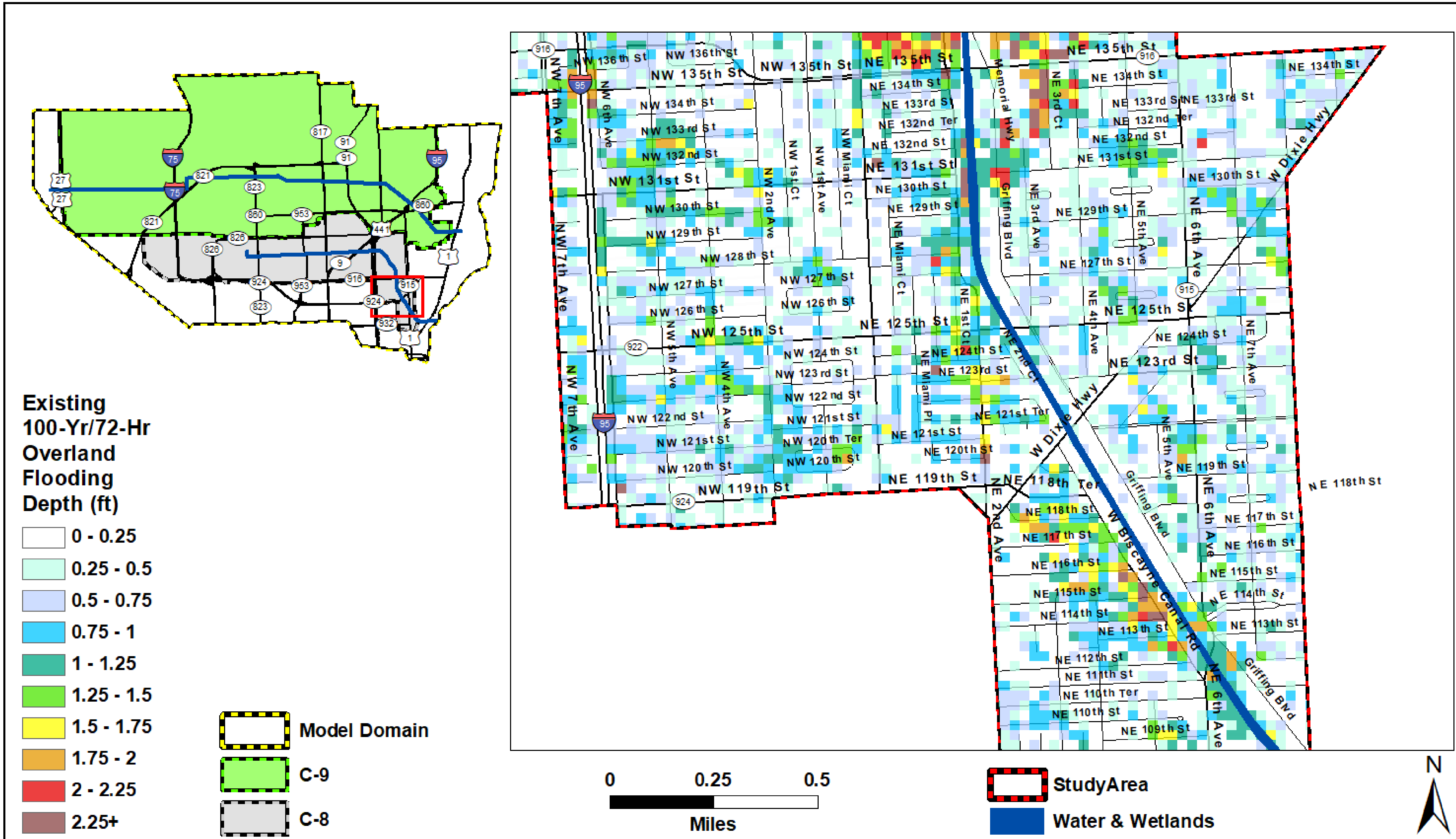

Figure 8.5-9: Up Close Flood Inundation Map for 100-Year Design Storm Event C-8 Canal Between and NE 135th St (CR916) and NE 6th Ave (CR915)

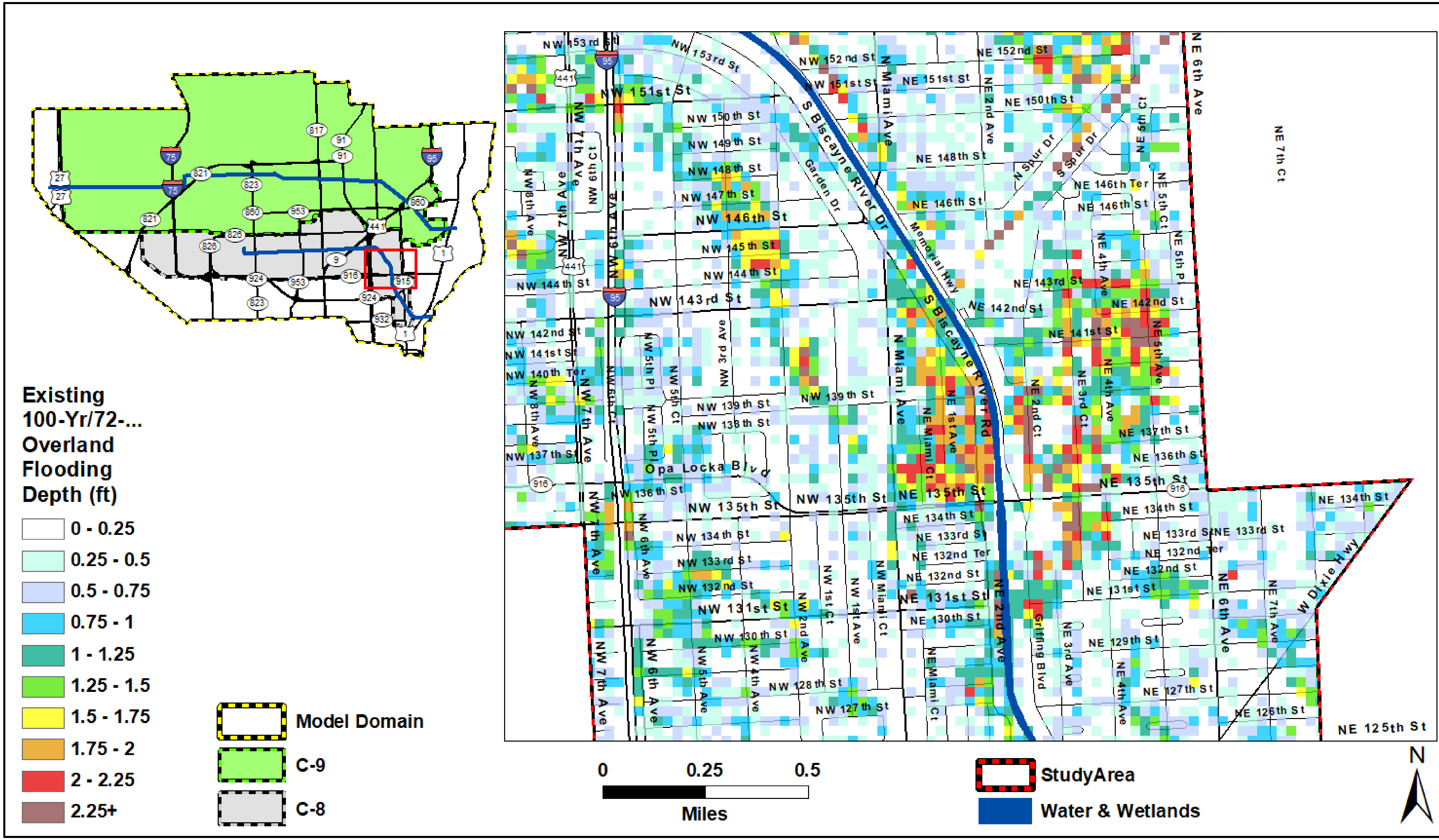

Figure 8.5-10: Up Close Flood Inundation Map for 100-Year Design Storm Event C-8 Canal Between North Miami Ave and NE 135th St (CR916)

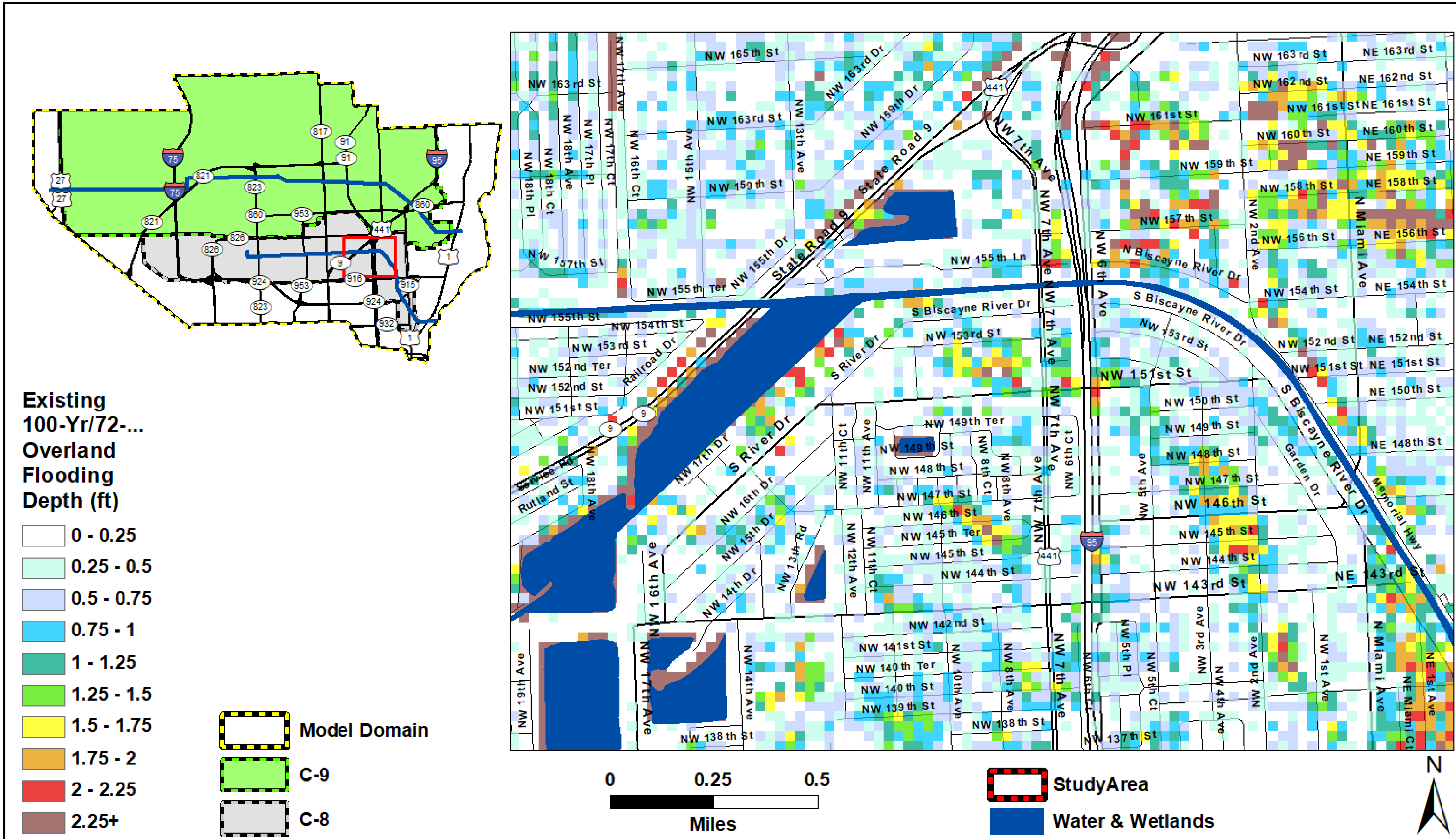

Figure 8.5-11: Up Close Flood Inundation Map for 100-Year Design Storm Event C-8 Canal Near Opa Locka Canal

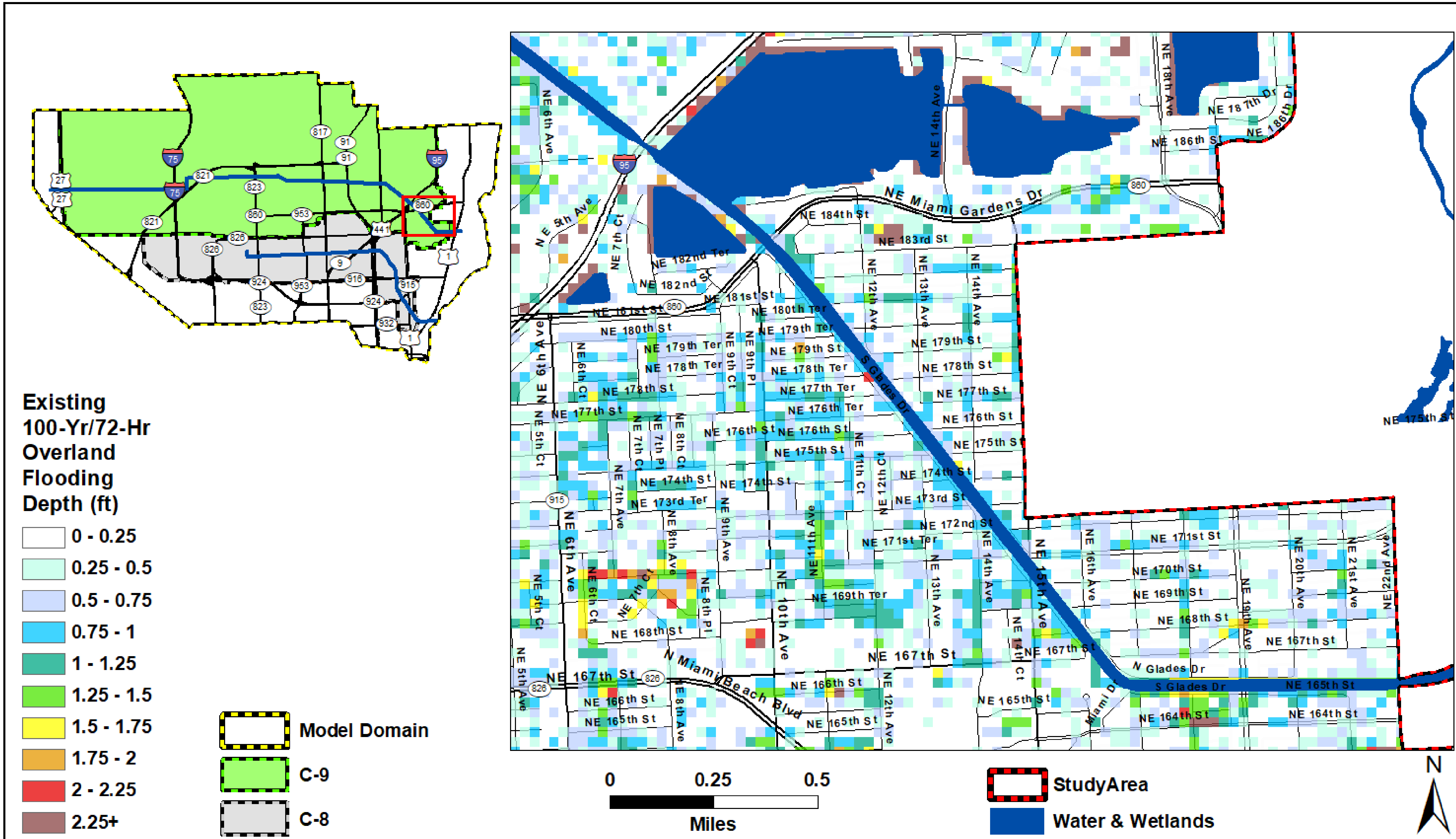

Figure 8.5-12: Up Close Flood Inundation Map for 100-Year Design Storm Event C-9 Canal Between I-95 and S-29

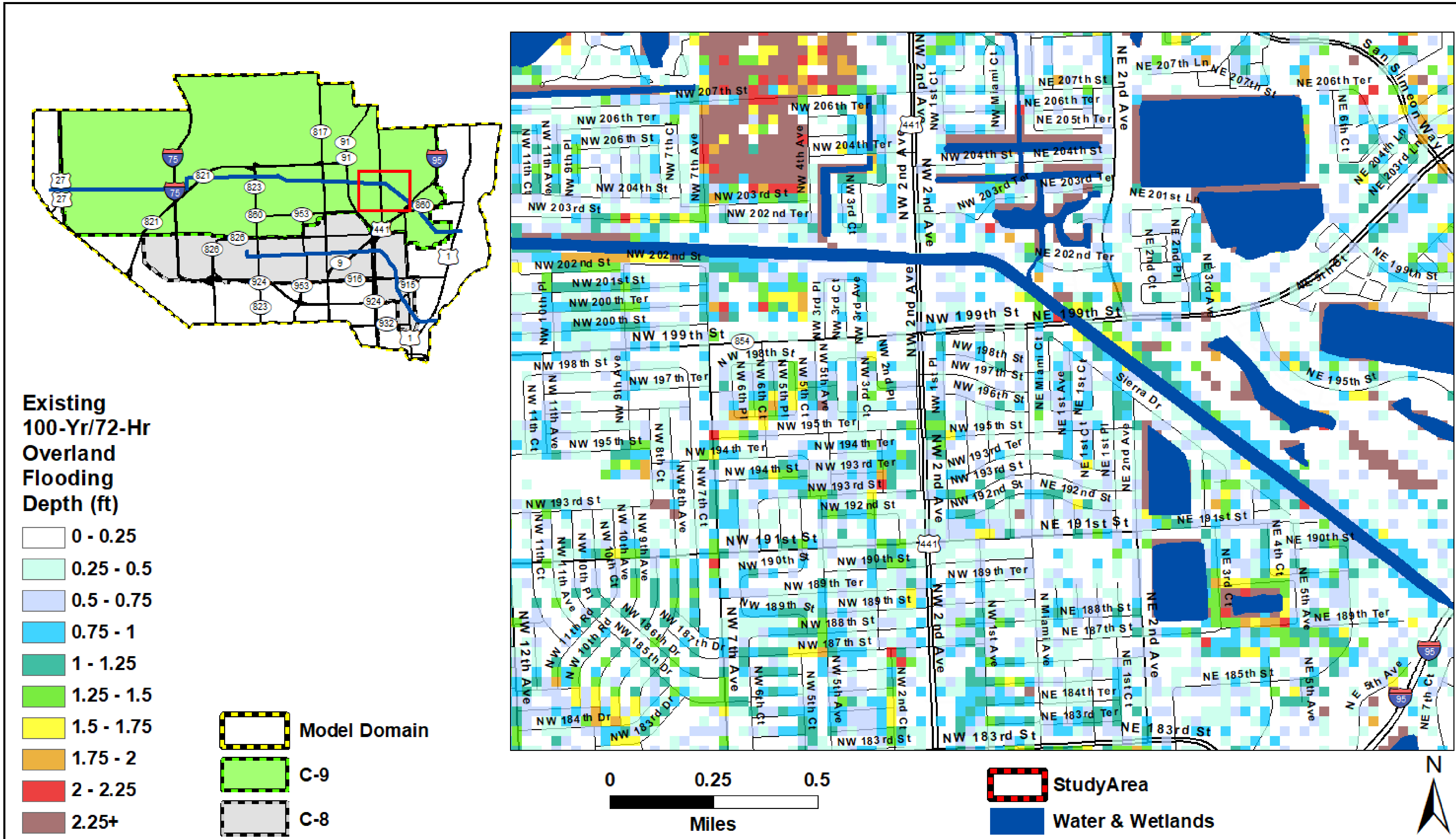

Figure 8.5-13: Up Close Flood Inundation Map for 100-Year Design Storm Event C-9 Canal Near US Hwy 441

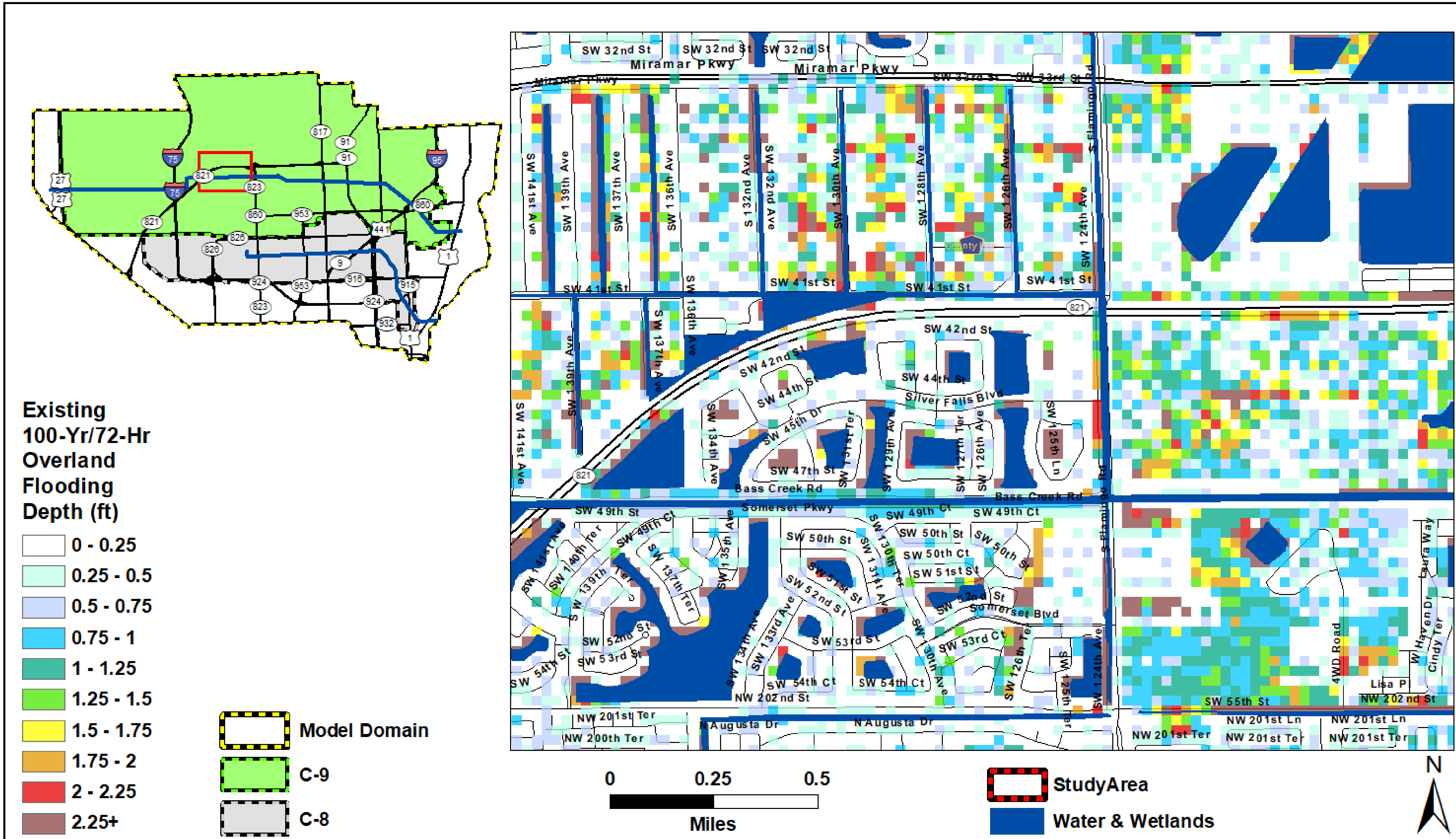

Figure 8.5-14: Up Close Flood Inundation Map for 100-Year Design Storm Event C-9 Canal Near Ronald Reagan Turnpike

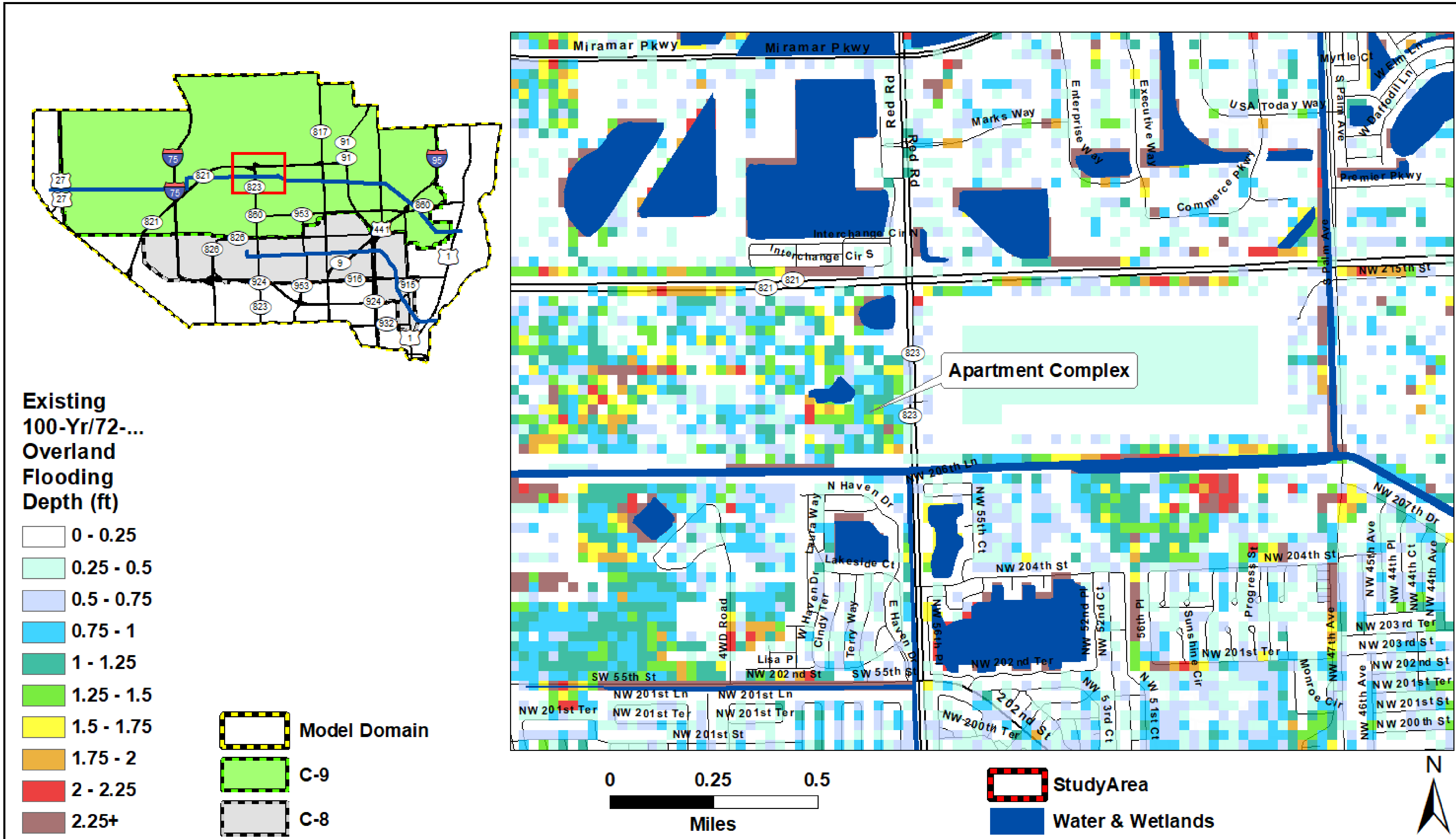

Figure 8.5-15: Up Close Flood Inundation Map for 100-Year Design Storm Event C-9 Canal Near Red Road

8.6 PM #6 – Duration of Flooding

For PM #6, the duration of flooding maps were developed by estimating the duration over which water depth exceeds a given threshold value. In this study, the duration of overland flooding was estimated using model simulated water depths and a threshold flooding depth of 0.25 ft. Additionally, the duration of flooding in the District Canals were estimated as the amount of time it takes for the water levels to return to target stage. The target stages of 3.6 ft for S-28Z and 3.5 ft for S-29Z were provided by the District (Email from Hongying Zhao, 5/12/2020). **Table 8-9** shows the duration of time taken for the headwater at S-28 and S-29 to return to target stage.

Table 8-9: Duration for Water Levels to Return to Target Stage

Design Storm	Duration to Return to Target Stage (hr)	
	S-28Z	S-29Z
5-Year	27	55
10-Year	40	92
25-Year	95	158
100-Year	140	242

The duration of overland flooding was estimated for all four design storm events based on the length of time the flood depth was predicted to exceed the threshold value (0.25 ft) within each MIKE SHE 125-ft grid cell using the statistics tool in MIKE ZERO. The flood duration maps for each of the design storm events are shown in **Figure 8.6-1** through **Figure 8.6-4** for the 5-year, 10-year, 25-year, and 100-year design storm events, respectively.

Based on model simulations, large areas were inundated for over 72 hours, even for the 5-year design storm (**Figure 8.6-1)**. These areas are comprised primarily of lakes and wetlands and other low-lying undeveloped areas. An increase in flooding extent and duration was observed as the magnitude of the design storms increased (**Figure 8.6-2** through **Figure 8.6-4**). A vast majority of the watershed was inundated for at least a small duration during the 100-year design storm. Developed areas with the largest flood duration generally tend to coincide with the highest depths of flooding determined from PM#5. **Figure 8.6-5** through **Figure 8.6-8** show the flood duration maps for each of the design storm events for urban areas only. **Figure 8.6-9** through **Figure 8.6-11** show up close examples of flood duration along the C-8 Canal and **Figure 8.6-12** through **Figure 8.6-15** show up close examples of flood duration along the C-9 Canal.

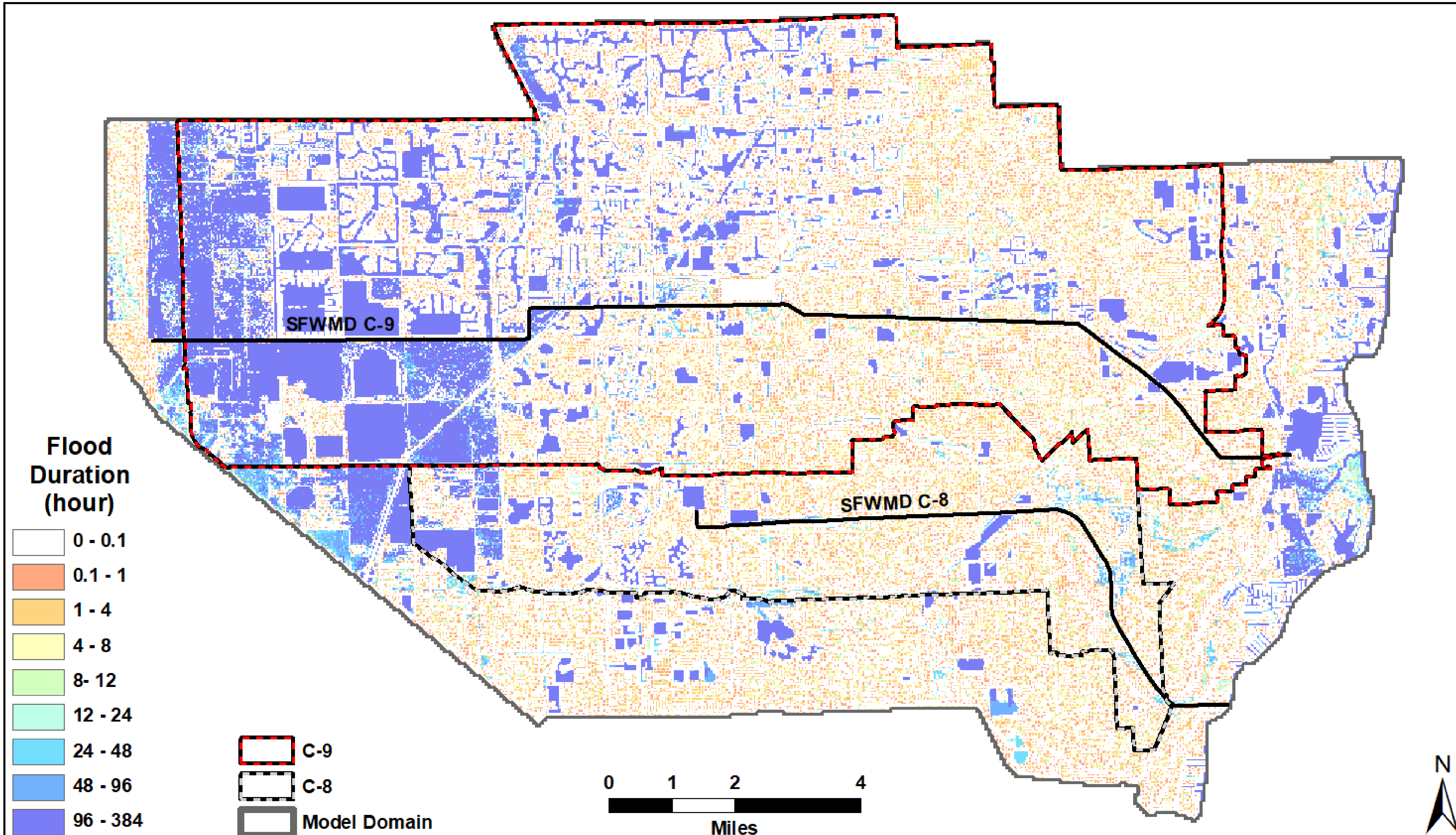

Figure 8.6-1: Flood Duration Map for 5-Year Current Conditions Design Storm Event

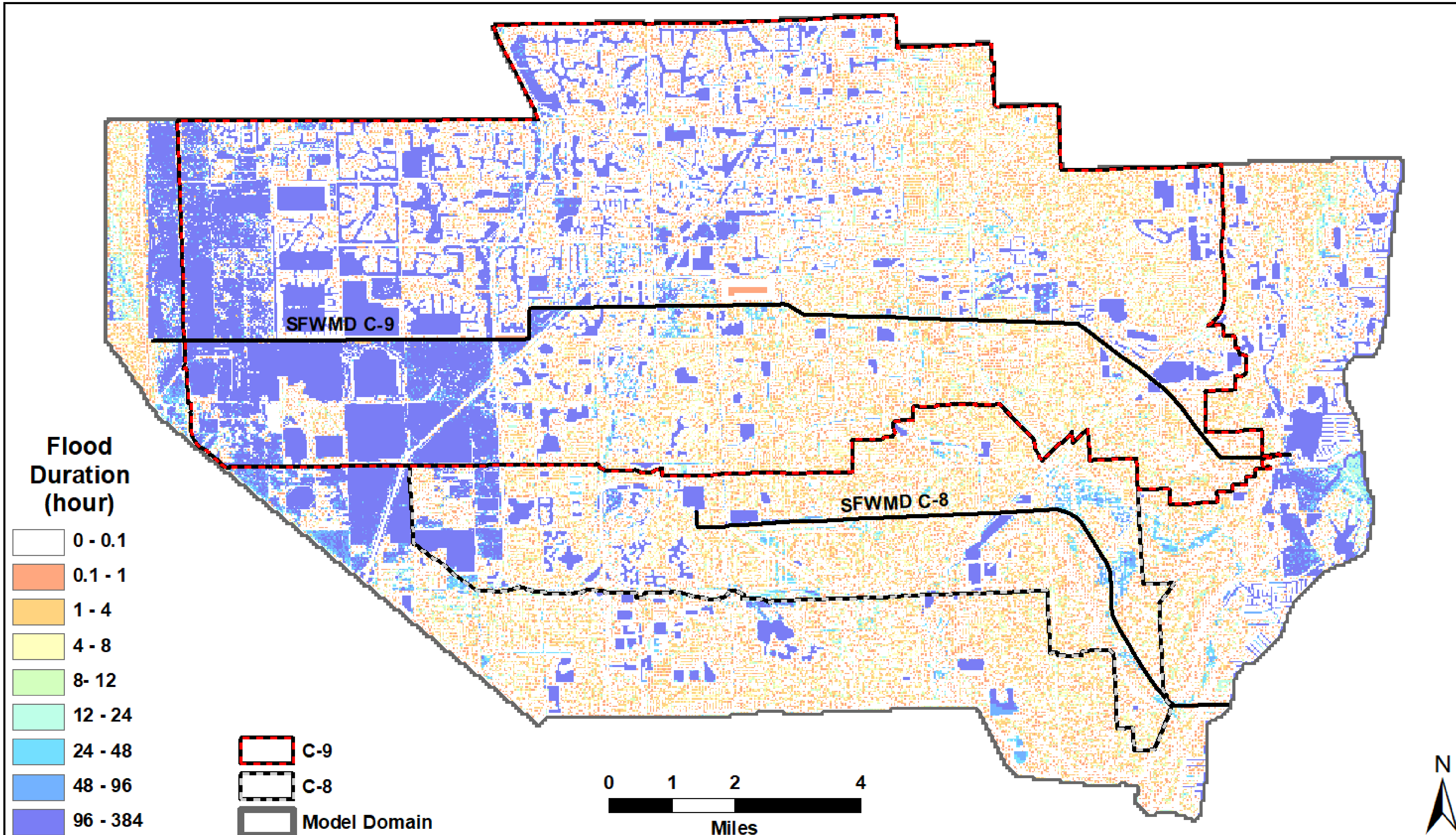

Figure 8.6-2: Flood Duration Map for 10-Year Current Conditions Design Storm Event

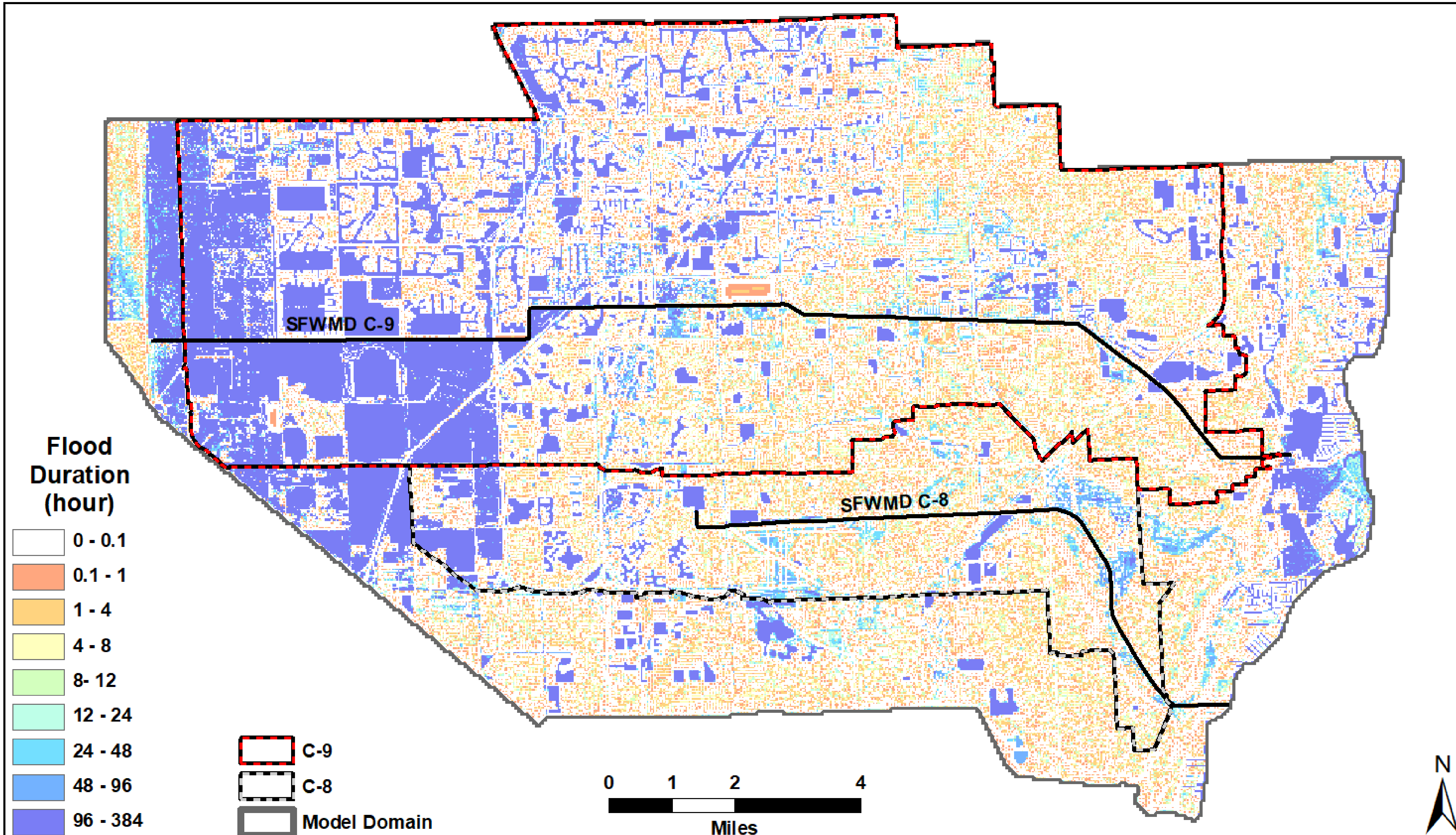

Figure 8.6-3: Flood Duration Map for 25-Year Current Conditions Design Storm Event

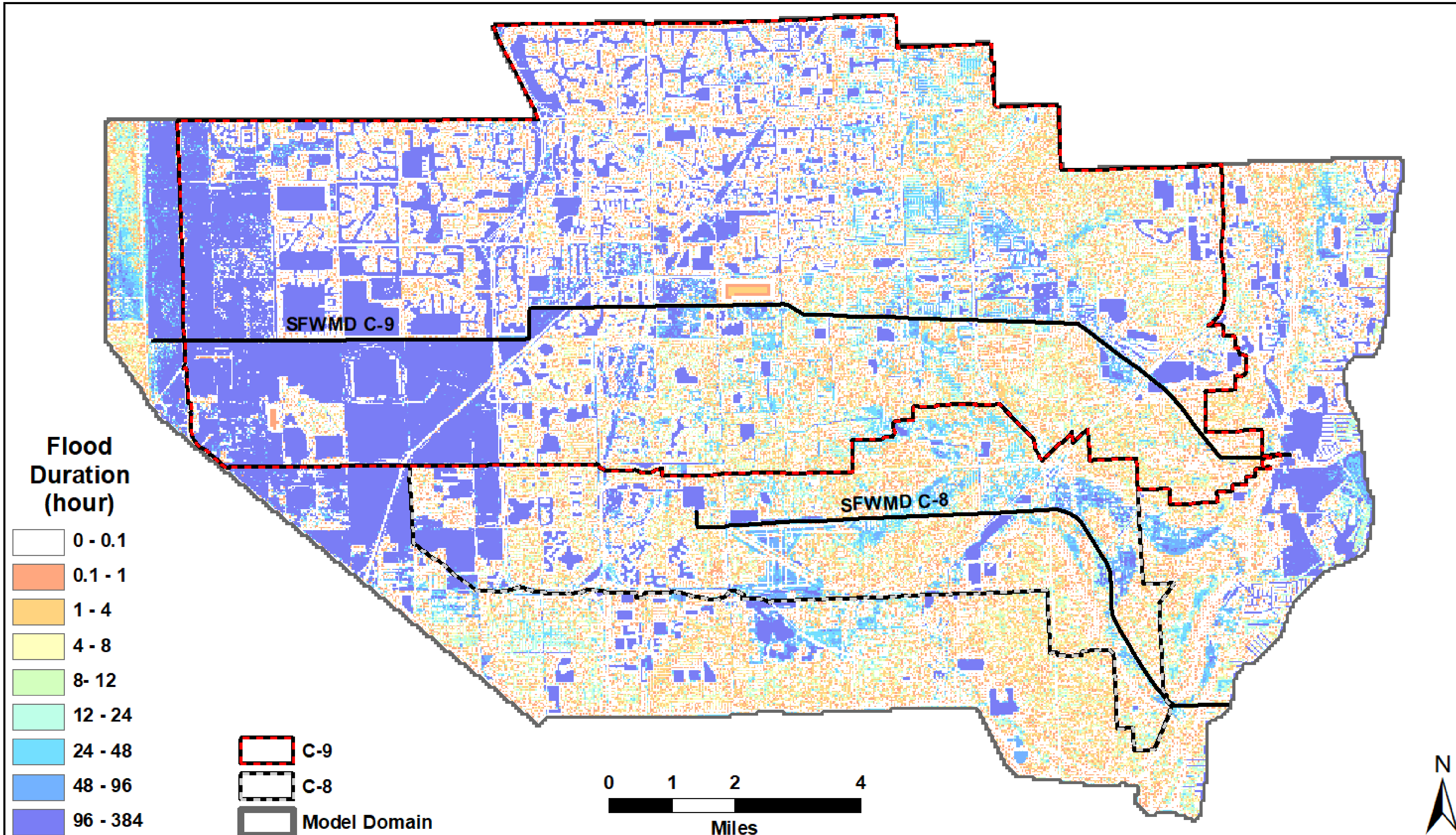

Figure 8.6-4: Flood Duration Map for 100-Year Current Conditions Design Storm Event

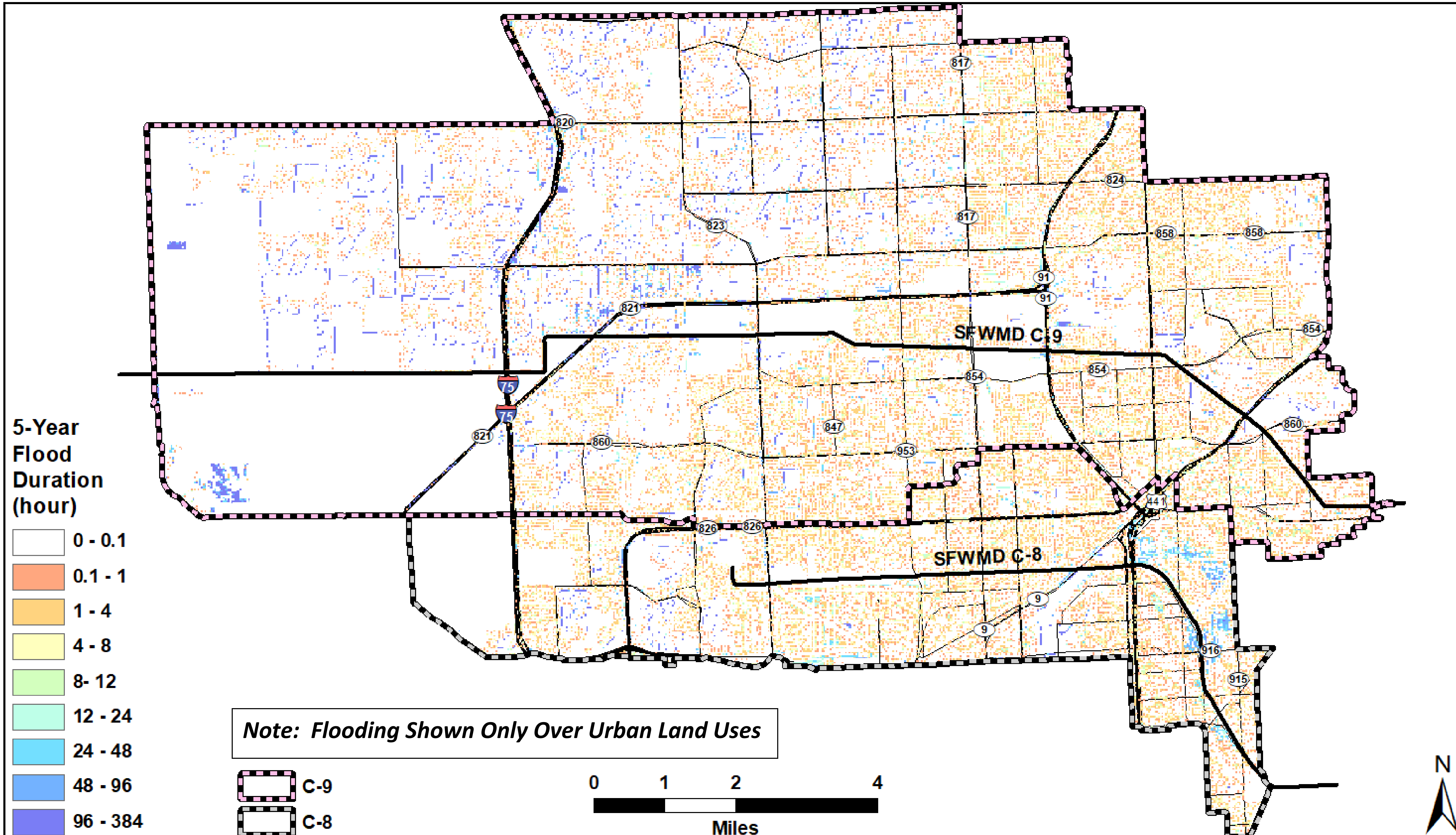

Figure 8.6-5: Flood Duration Map for 5-Year Design Storm Event in Urban Land Use Areas

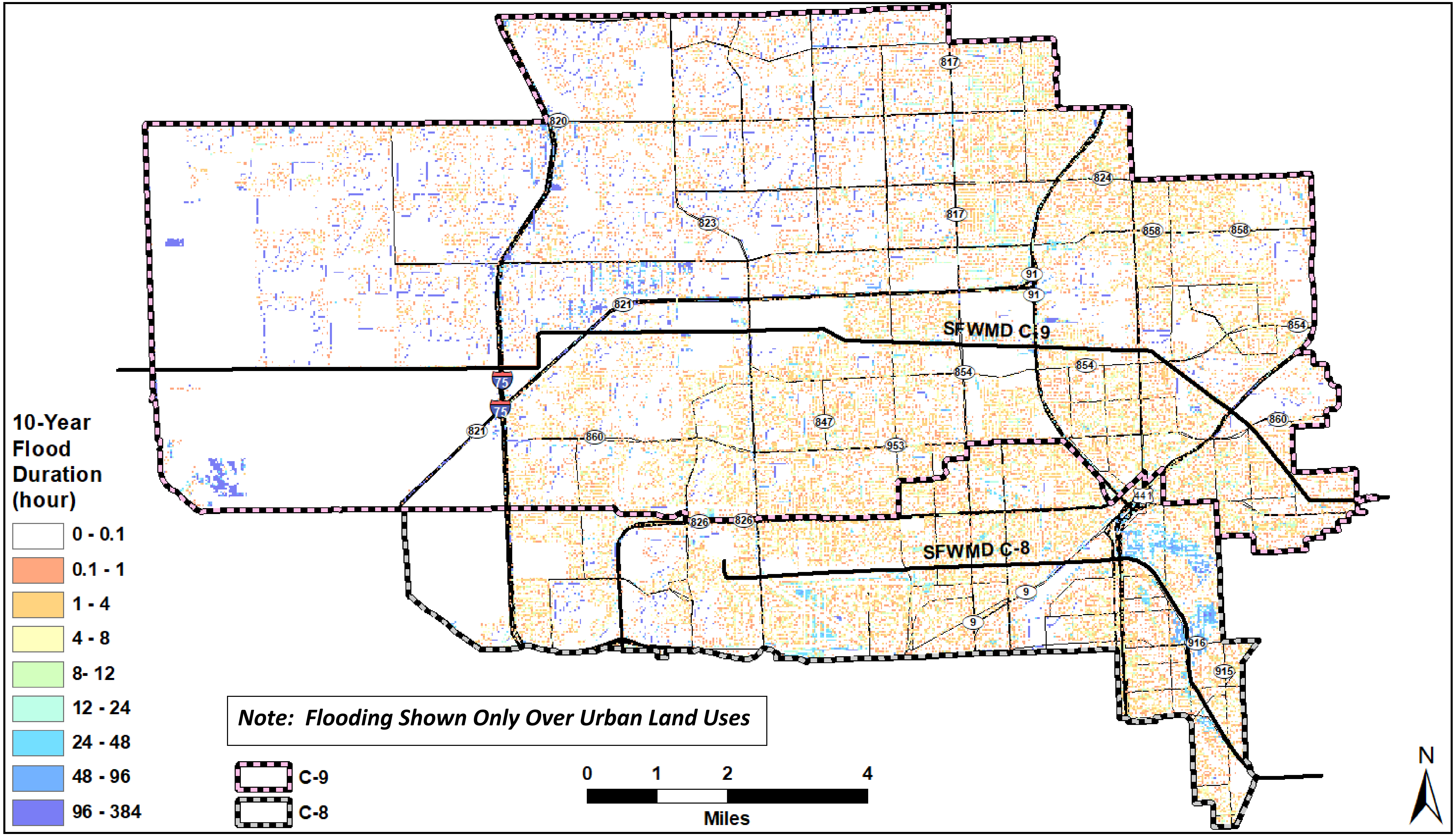

Figure 8.6-6 Flood Duration Map for 10-Year Design Storm Event in Urban Land Use Areas

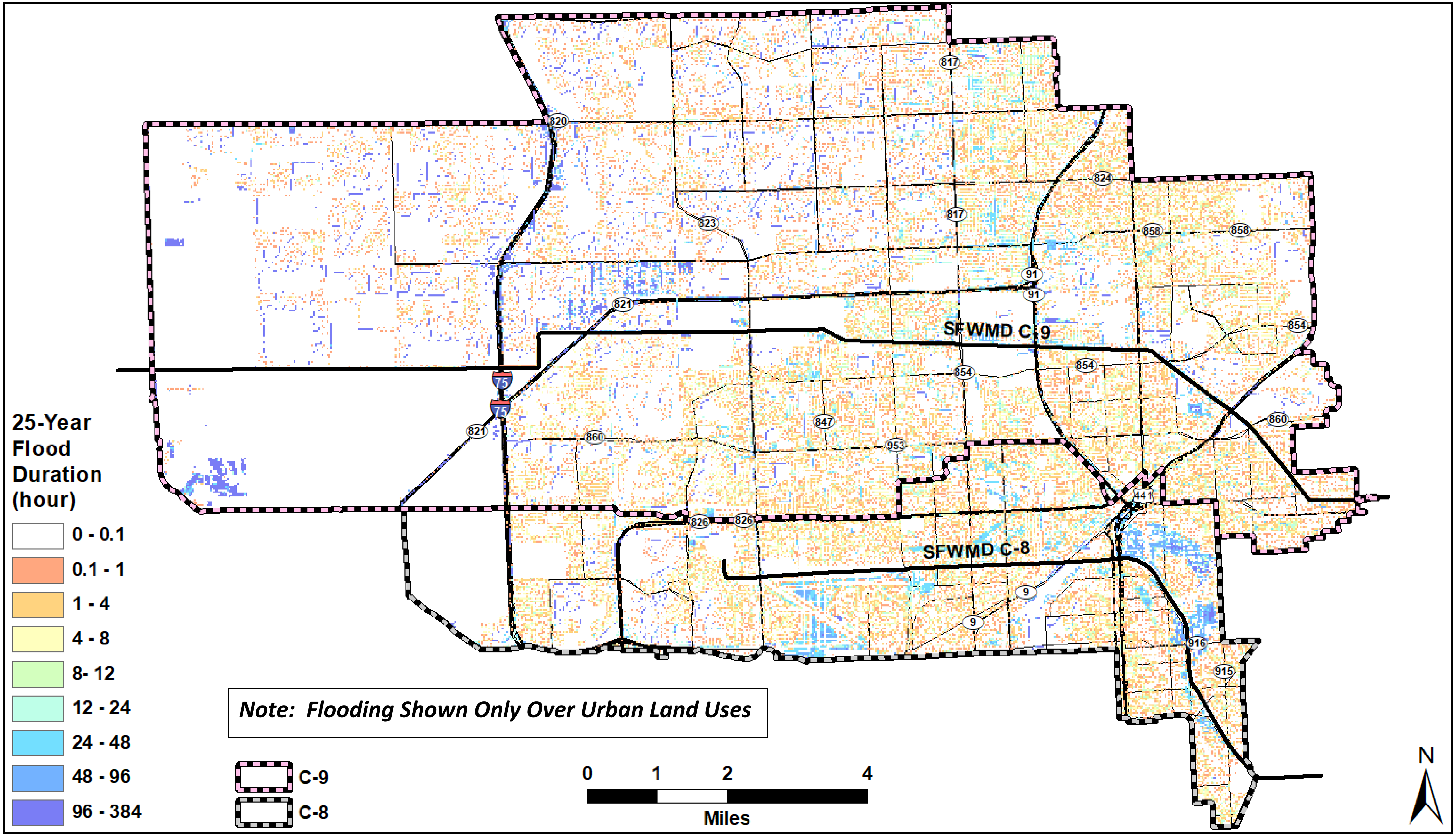

Figure 8.6-7: Flood Duration Map for 25-Year Design Storm Event in Urban Land Use Areas

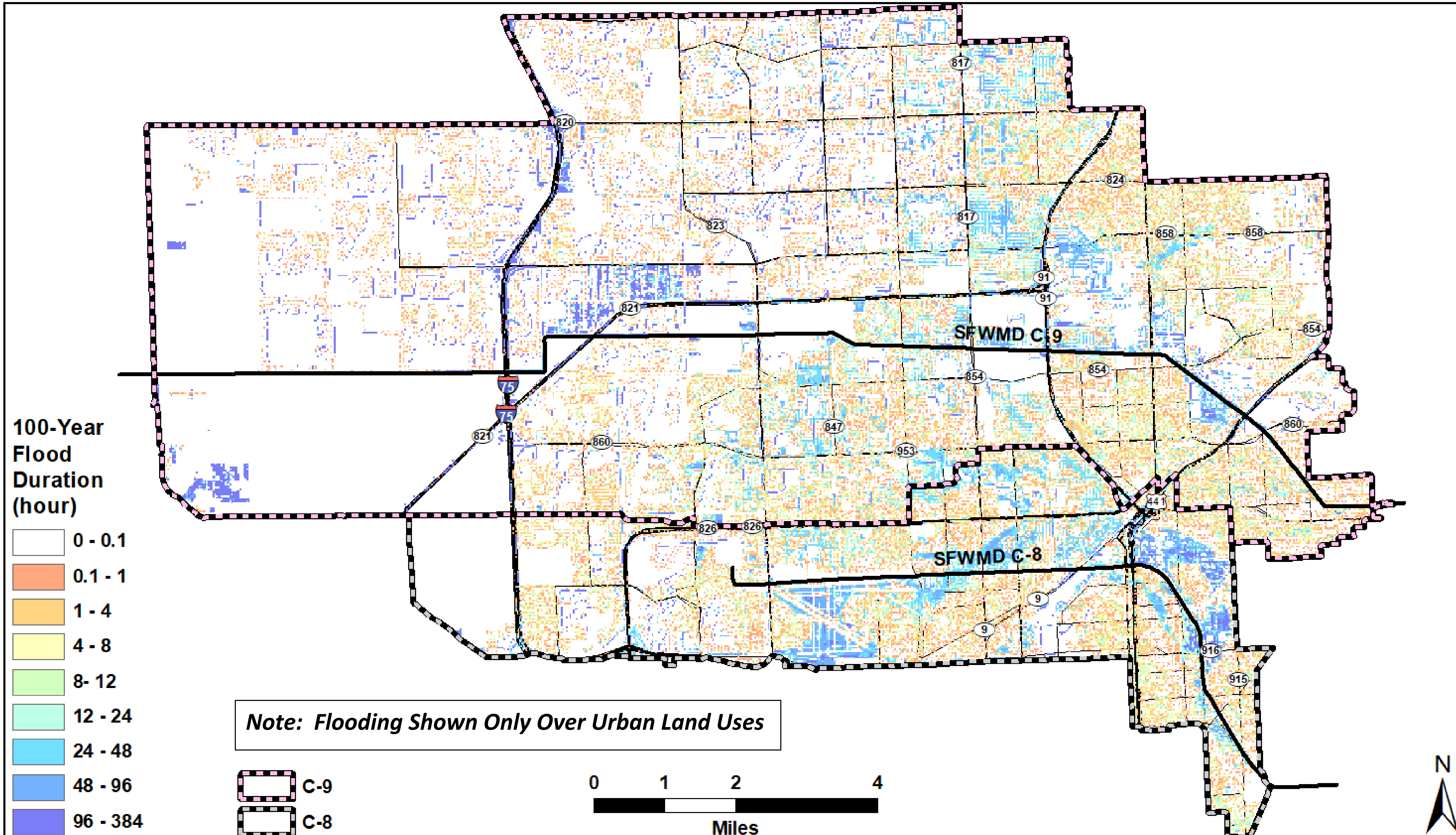

Figure 8.6-8: Flood Duration Map for 100-Year Design Storm Event in Urban Land Use Areas

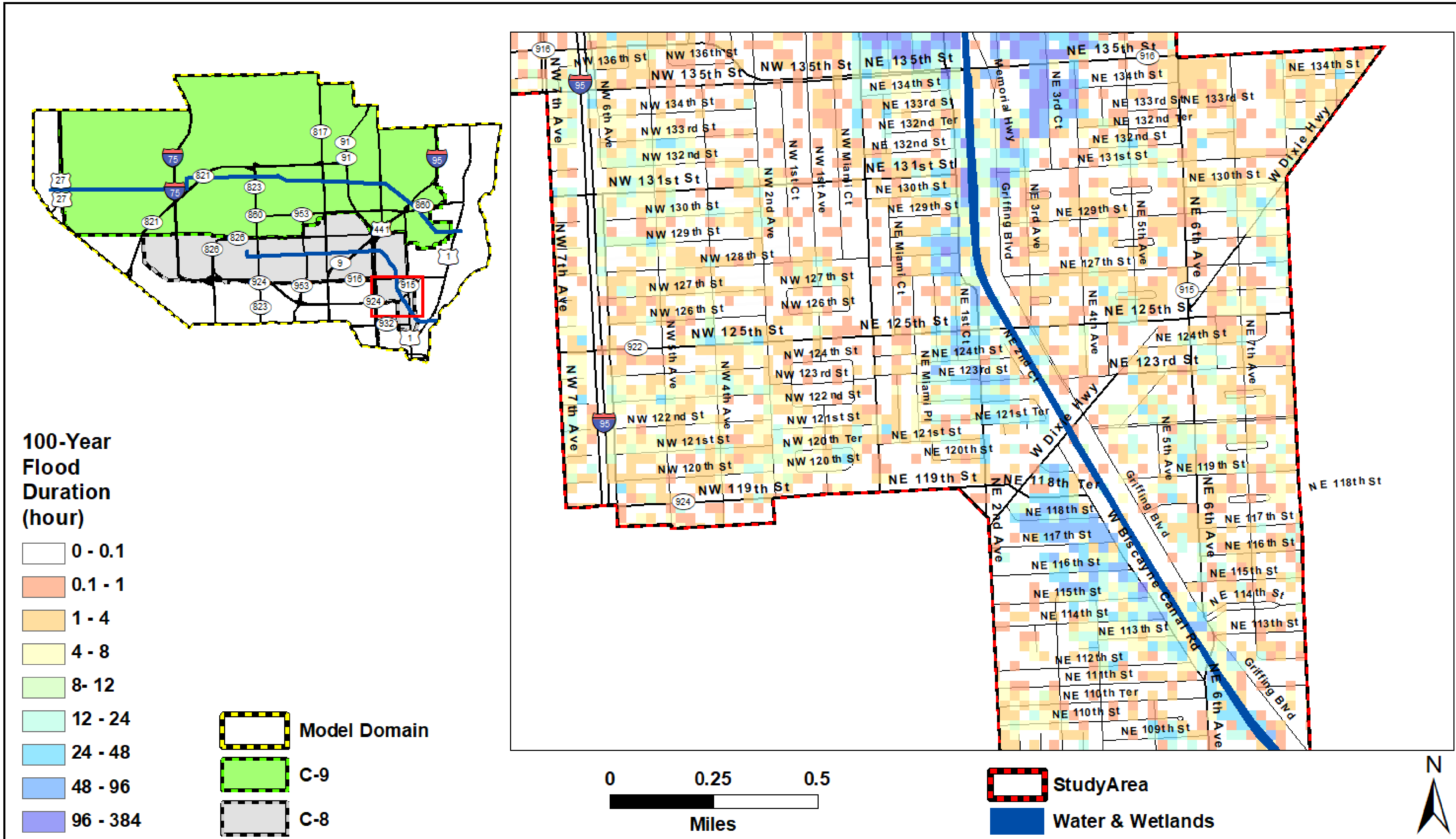

Figure 8.6-9: Up Close Flood Duration Map for 100-Year Design Storm Event C-8 Canal Between and NE 135th St (CR916) and NE 6th Ave (CR915)

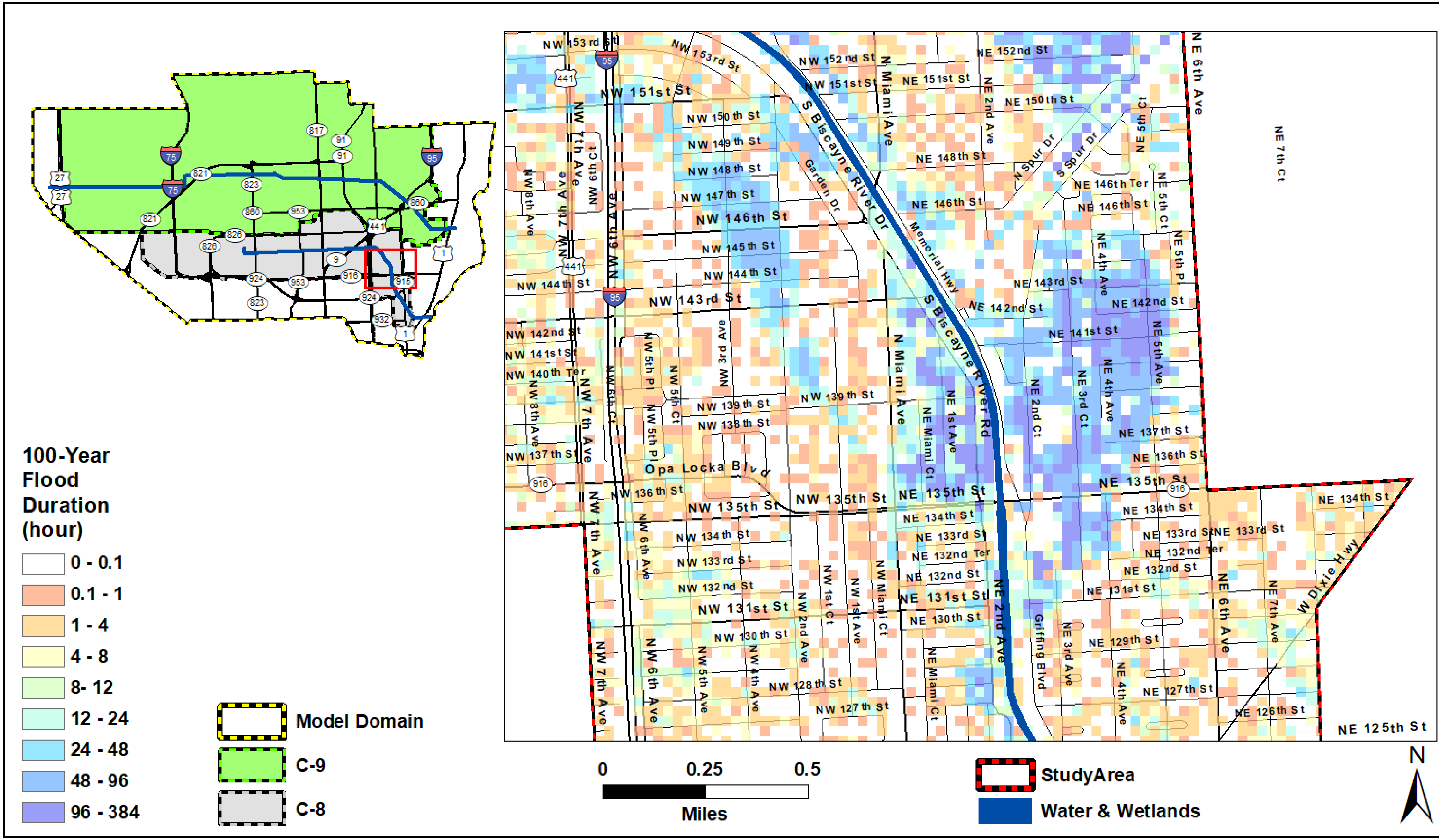

Figure 8.6-10: Up Close Flood Duration Map for 100-Year Design Storm Event C-8 Canal Between North Miami Ave and NE 135th St (CR916)

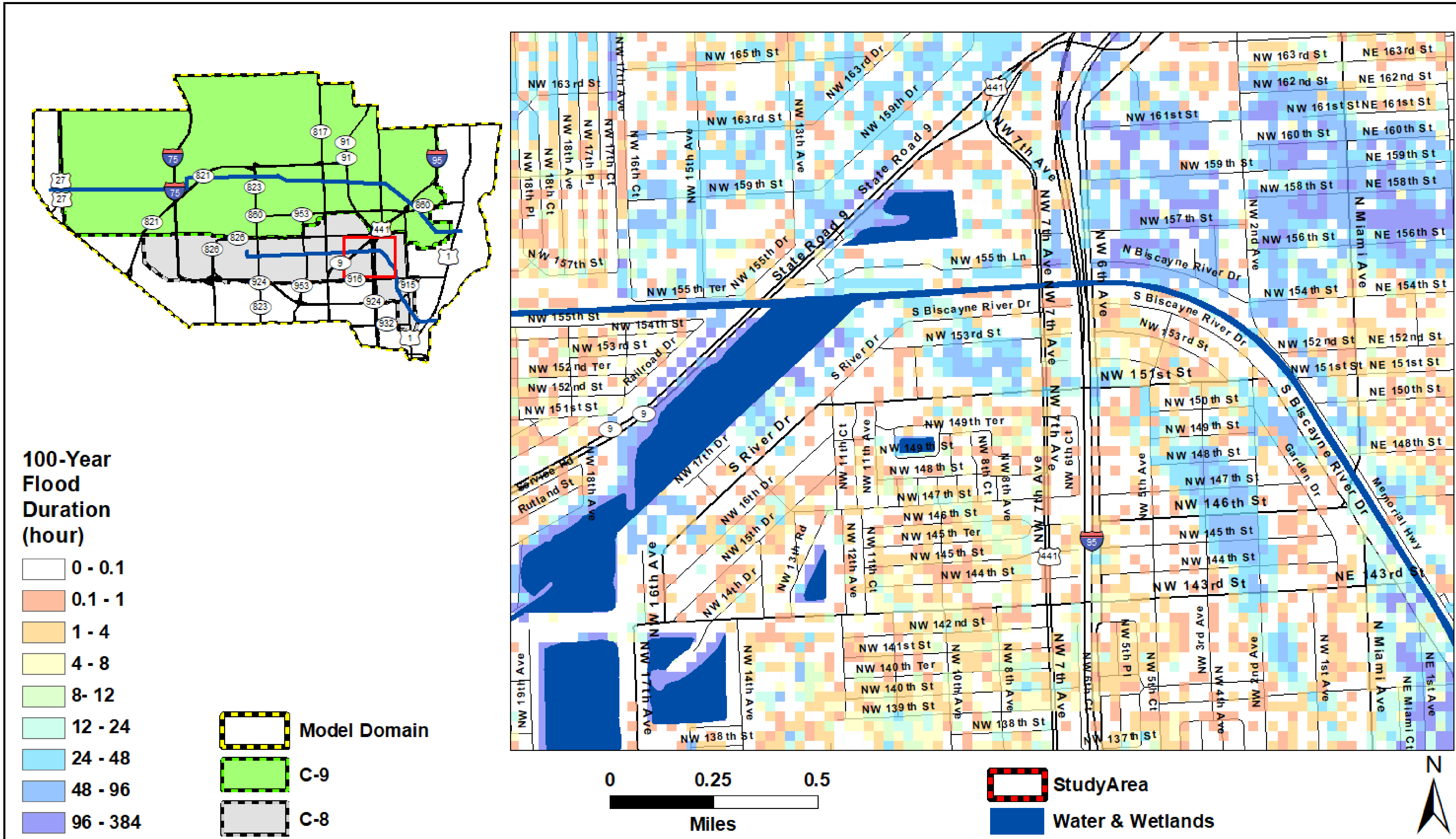

Figure 8.6-11: Up Close Flood Duration Map for 100-Year Design Storm Event C-8 Canal Near Opa Locka Canal

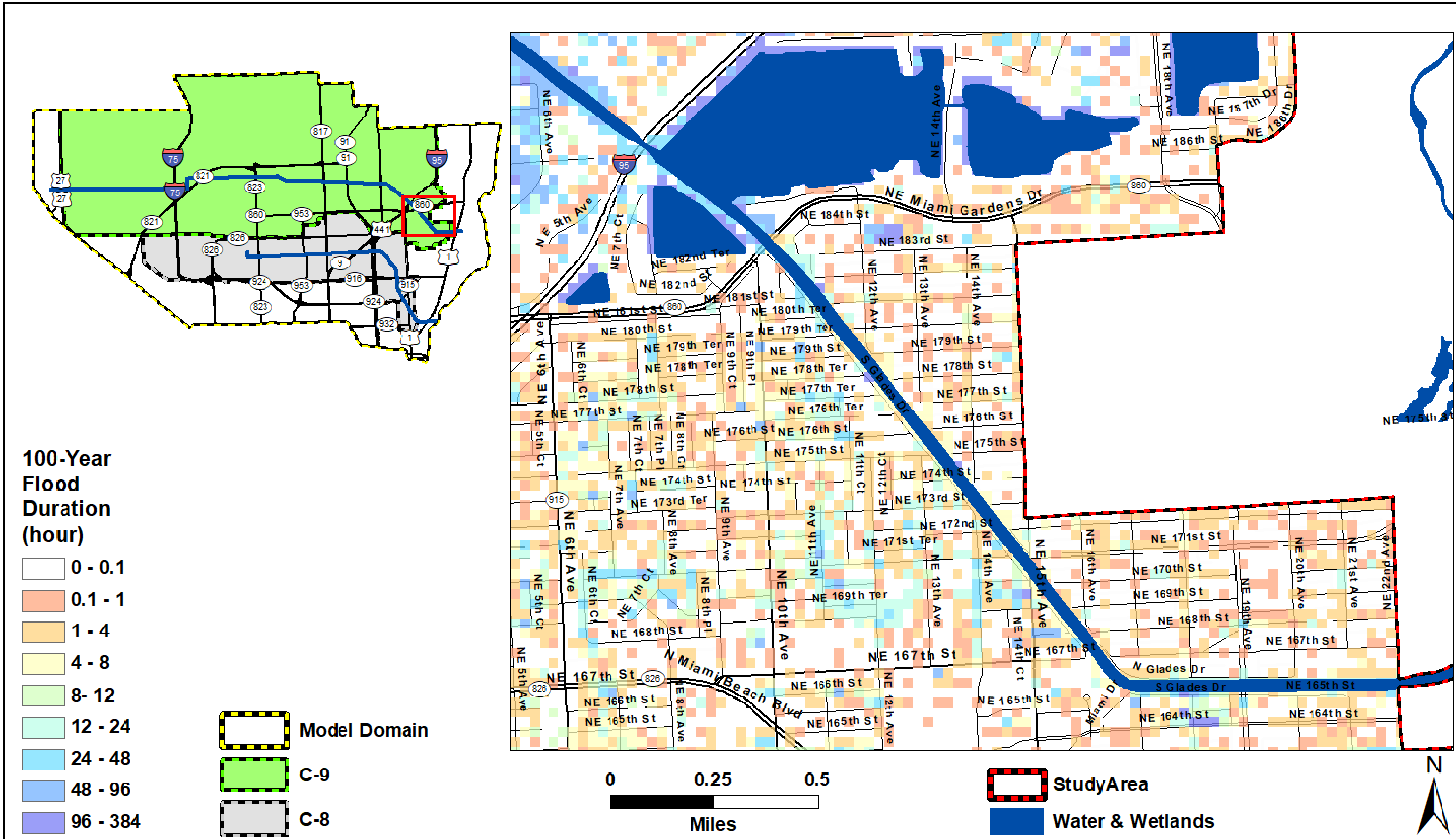

Figure 8.6-12: Up Close Flood Duration Map for 100-Year Design Storm Event C-9 Canal Between I-95 and S-29

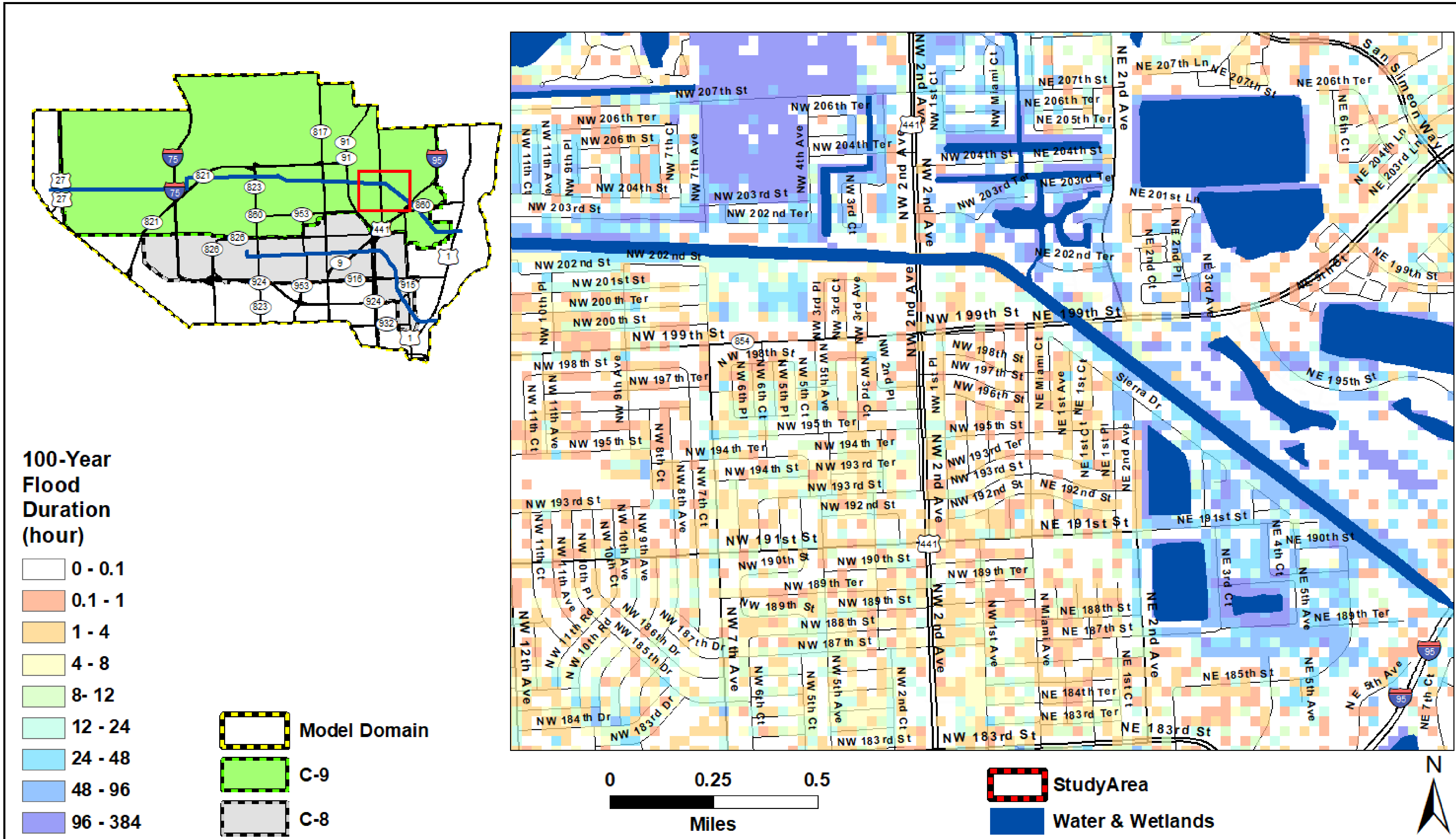

Figure 8.6-13: Up Close Flood Duration Map for 100-Year Design Storm Event C-9 Canal Near US Hwy 441

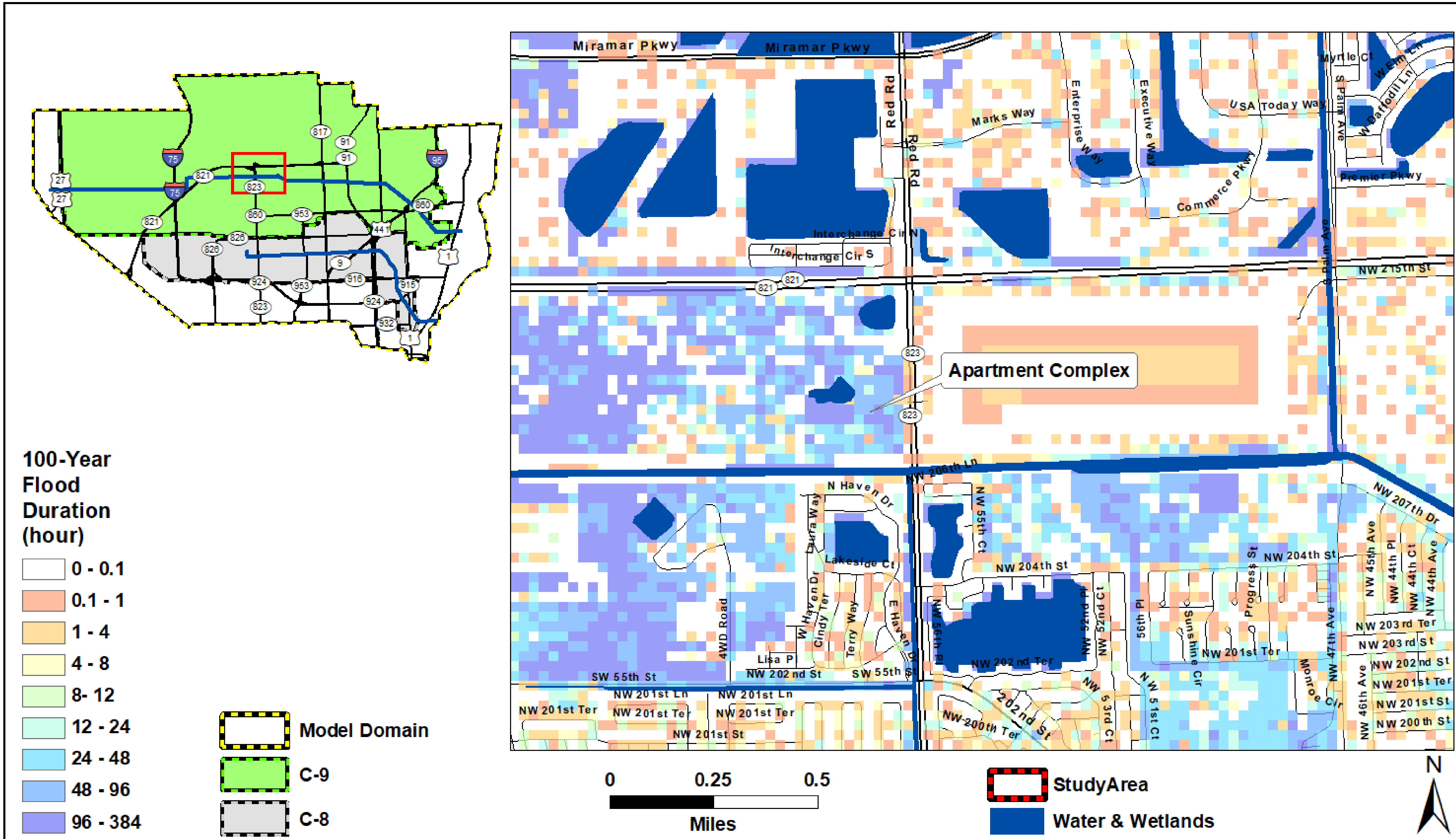

Figure 8.6-14: Up Close Flood Duration Map for 100-Year Design Storm Event C-9 Canal Near Red Road

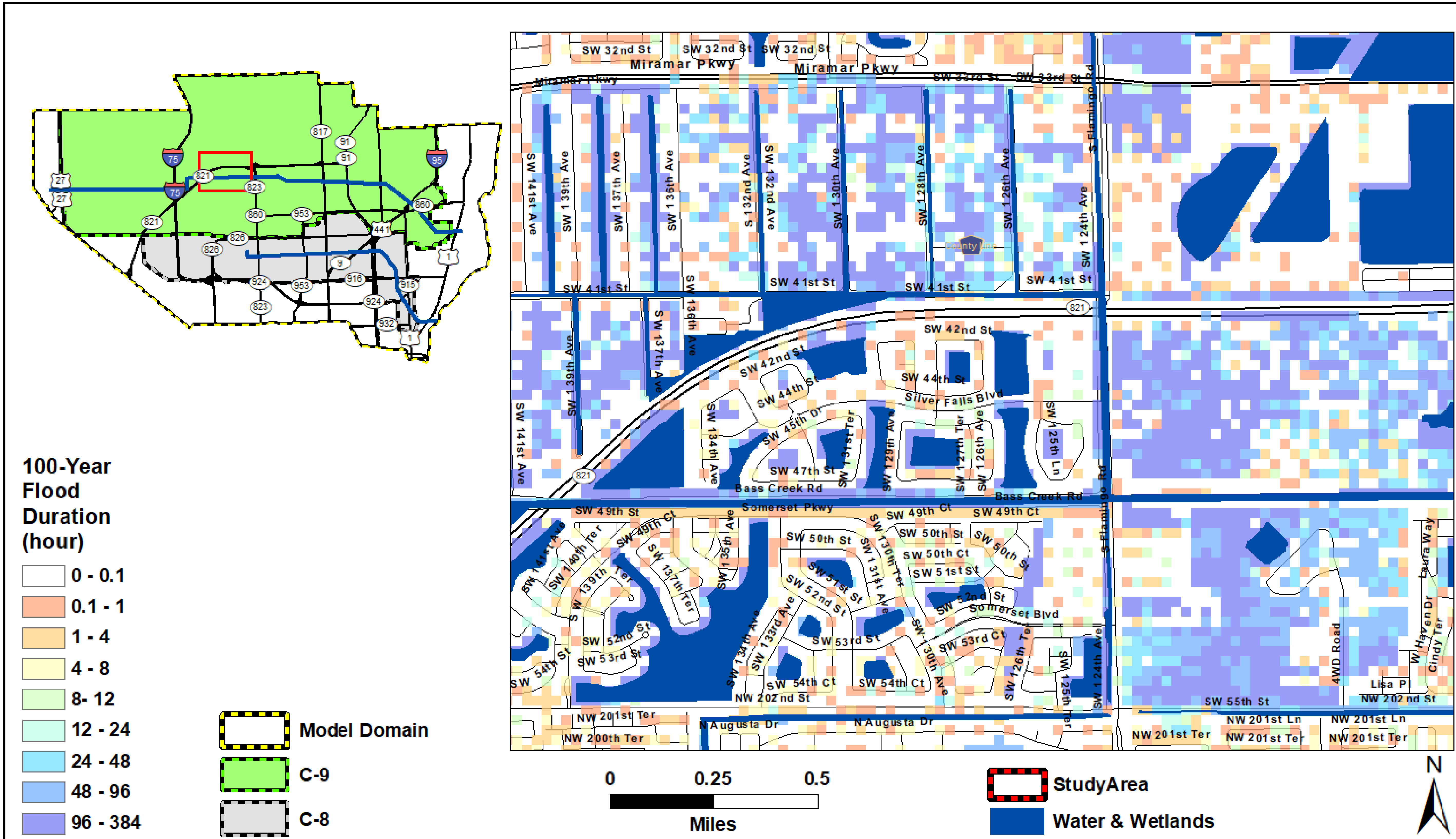

Figure 8.6-15: Up Close Flood Duration Map for 100-Year Design Storm Event C-9 Canal Near Ronald Reagan Turnpike

9 CONCLUSIONS

The current conditions design storm simulation results were evaluated using six performance measures. The analysis presented in this report provides a model-based assessment of the current level of flood protection provided by the C-8 and C-9 watershed's primary canal network and associated control structures. These results were used to determine potential FPLOS deficiencies by highlighting areas that failed multiple performance measures such as bank exceedances that corresponded to overland inundation (PM #5 and/or PM #6). In some cases, PM #1 bank exceedances did not manifest as significant overland inundation and thus were considered insignificant localized FPLOS deficiencies. In other cases, flooding was shown by PM #5 and PM #6 that did not correspond to bank exceedances in PM #1, suggesting that flooding could be due to problems with secondary and tertiary drainage systems.

It should also be noted that the model results are subjected to certain limitations associated with the scale of the 2-dimensional model grid. Although the model uses a 125-ft grid that is suitable for the sub-regional scale flood protection level of service evaluation, the results should not be extended to local-scale evaluations or regulatory determinations of flooding extents, where considerable variations in topography can occur within the area of each grid cell.

9.1 Current Conditions

9.1.1 C-8 Basin

Based on the results of this study, it appears that the C-8 canal generally provides a 10-year level of service, with some areas receiving a 25-year level of service or better. There were a few localized areas where the water levels exceeded the canal banks for the 5-year event as shown in PM #1 (**Figure 8.1-3)**, however, it does not correspond to a significant area of flood inundation as shown in PM #5 (**Figure 8.5-1).** For the 25-year design storm, the model results suggest that several segments of the C-8 Canal would be overwhelmed during peak flood conditions, with the western segment (west of Opa Locka Canal) generally performing better than the eastern segment. For the 100-year design storm, the model results suggest that most of the C-8 Canal would be overwhelmed during peak flood conditions, while most of the watershed would be inundated to some degree.

9.1.2 C-9 Basin

Based on the results of this study, it appears that the C-9 canal generally provides a 25-year level of service, with some areas receiving a 100-year level of service or better. There were a few localized areas where the water levels exceeded the canal banks for the 10-year event as shown in PM #1 (**Figure 8.1-4**), however, it typically does not correspond to a significant area of flood inundation east of Interstate I-75 as shown in PM #5 (**Figure 8.5-2**). West of Interstate I-75, the water level exceedance corresponds to a significant amount of area of flood inundation, although it is in undeveloped areas. For the 100-year design storm, the model results suggest that several segments of the C-9 Canal would be overwhelmed during peak flood conditions, while most of the watershed would be inundated to some degree. Some areas of this watershed appear to have deficiencies in secondary and/or tertiary drainage systems that result in flooding of developed areas, as these flooded areas generally do not correspond to canal bank exceedances.

REFERENCES

BDH Consulting Group. (2019). *Survey Work for C8 and C9 FPLOS Models*

Broward County. (2000). *Broward County Average Wet Season Water Table Map*. Broward County office of Environmental Services Water Management Division.

Environmental Protection Agency. (2015). *Storm Water Management Model User's Manual Version 5.1*.

DHI. (2017). *MIKE SHE User Guide v1*.

Fish, J.E., & Stewart, M.T. (1991). *Hydrogeology of the surficial aquifer system, Dade County, Florida*.

Florida Natural Areas Inventory. (2012). *Florida Land Cover Classification System Definitions for the Cooperative Land Cover Map v2.3*.

Hughes, J. D., & White, J. T. (2016). *Hydrologic conditions in urban Miami-Dade County, Florida, and the effect of groundwater pumpage and increased sea level on canal leakage and regional groundwater flow* (No. 2014-5162 Version 1.2 July 2016). US Geological Survey.

Miami-Dade County. (2017). *2015_ITD_LiDAR Project*; 5-ft Digital Elevation Model (DEM)

SBDD. (2013). *South Broward Drainage District Facilities Report and Water Control Plan*.

SFWMD LCLU. (2017). *South Florida Water Management District Land Cover Land Use 2014-2016 dataset*.

SFWMD H&H Bureau. (2015). *Flood Protection LOS Analysis for the C-4 Watershed, Appendix A: LOS Basic Concepts*.

Stoner and Associates. (2019). *Surveyors Report As-Built Survey*. For Project: Broward County 100 Year Flood Elevation Map & Associated Modeling

Taylor Engineering. (2019) *Broward County 100-Yr Flood Elevation Map & Associated Modeling Project*.

Taylor Engineering. (2019). *Broward County Current Conditions MIKE SHE and MIKE HYDRO Models*. Developed for Broward County 100-Year Flood Elevation Map & Associated Modeling Project.

Taylor Engineering. (2019) *Broward County Draft Model Update and Validation Report* (For Broward County 7/26/2019)

Taylor Engineering. (2019). *Deliverable 1.1, Data Availability Memorandum* (For SFWMD 8/26/2019)

Taylor Engineering. (2019). *Deliverable 1.2, C8-C9 Model Development Memorandum* (For SFWMD 11/4/2019)

Taylor Engineering. (2020). *Deliverable 2.1, C8-C9 Calibration and Validation Memorandum Final Draft* (For SFWMD 1/21/2020)

USGS. (2018) *Reference and Potential Evapotranspiration Reference and Potential Evapotranspiration*. https://www.usgs.gov/centers/car-fl-water/science/reference-and-potential-evapotranspiration?qt-science_center_objects=0#qt-science_center_objects.

Zhang. (2017). *The Effects of Sea Level Rise on S28 Performance*

Zhang. (2017). *The Effects of Sea Level Rise on S29 Performance*

List of Appendix Figures

List of Appendix Tables

APPENDIX A

From: Kevin Hart <kevin@sbdd.org>
Sent: Wednesday, January 2, 2019 2:32 PM
To: Mark Ellard <MEllard@Geosyntec.com>
Cc: John Loper <jloper@taylorengineering.com>; Zygnerski, Michael <MZYGNERSKI@broward.org>; Maran, Carolina <CMARAN@broward.org>; Luis Ochoa <luis@sbdd.org>
Subject: RE: Broward Future 100-Year Model Follow Up - SBDD

Mark,

Attached is the latest SFWMD permit for CS12, CS13, CS13-A, ICS12, ISC13 and ISC13-A.

Basically, the permit states the following:

- CS12, CS13, CS13-A are operated to allow the canal stages downstream of the intermediate gates to fluctuate with the C-11 Canal, but no lower that Elev. 3.00' NGVD (except with prior authorization from SFWMD).
- The maximum, combined discharge rate for CS12, CS13, CS13-A is 363 cfs.
- The intermediate gates (internal gate structures) are operated to maintain the permitted control elevation of 4.0' NGVD, within the upstream areas of the S-9/S-10 Basin (upstream of the gates). These gates are only opened when the tail water exceeds Elevation 4.0' NGVD.

The B-1 and B-2 pump stations are operated on a manual basis only. These two pump stations are operated by SBDD on an as-needed basis, and as determined by staff, during extreme rainfall events. Just as an FYI, neither station has operated during the past 7 years (except for maintenance purposes). Both stations have a gravity culvert connection to SBDD's C-1 Canal. For modeling purposes, the two pumps can be activated at Elevation 4.0' NGVD with a pumping capacity of 15,000 GPM. The pumps are used to reduce peak stages and durations within the sub-basins they serve.

The Silver Lakes Flood Gate is an emergency, basin inter-connect between Basins S-9/S-10 and S-5. This gate is operated to allow SBDD to move water from the C-11 Basin to C-9 Basin on an as-needed (emergency) basis. The operation of this gate is performed in conjunction with approval and authority from SFWMD. For modeling purposes, this gate should be closed. However, under adaptation strategies/scenarios, you are welcome to incorporate the use of this gate to manage stages between the C-11 and C-9 basin as applicable. As an FYI, there have been a handful of occasions where SFWMD has asked SBDD to discharge south through the S-5 Basin in order to limit discharges to the C-11 Canal.

The Nautica/Silver Lakes culvert (ID 408) is a basin inter-connect that is operated on an as-needed, emergency basis only. For modeling purposes, this gate should be closed. However, under adaptation strategies/scenarios, you are welcome to incorporate the use of this gate to manage stages between the S-4 and S-5 basins as applicable.

You're probably aware that SBDD has 2 other basin inter-connects that are operated on an as-needed, emergency basis only as well.......... between Basins S-3 and S-2.

On the pipe inverts, we do not have any additional information at this time. For modeling purposes, we suggest that you set the pipe inverts such that the top of pipe matches the Control Water Elevation (CWE), as that is SBDD's standard practice.

Let me know if you need any additional information.

Thanks.

Kevin Hart, P.E., CFM
District Director
South Broward Drainage District
6591 Southwest 160th Avenue
Southwest Ranches, FL 33331
954-680-3337 (office)
e-mail: kevin@sbdd.org

Figure A- 1: Email from SBDD

APPENDIX B

ENVIRONMENTAL RESOURCE PERMIT APPLICANT'S HANDBOOK VOLUME II
Effective: MAY 22, 2016

Appendix A: SFWMD - ALLOWABLE DISCHARGE FORMULAS

Canal	Allowable Runoff	Design Frequency
C-1	$Q = \left(\frac{112}{\sqrt{A}} + 31\right) A$	10 year
C-2	Essentially unlimited inflow by gravity connections southeast of Sunset Drive: 54 CSM northwest of Sunset Drive	200 year +
C-4	Essentially unlimited inflow by gravity connections east of S.W. 87th Avenue	200 year +
C-6	Essentially unlimited inflow by gravity connections east of FEC Railroad	200 year +
C-7	Essentially unlimited inflow by gravity connection	100 year +
C-8	Essentially unlimited inflow by gravity connection	200 year +
C-9	Essentially unlimited inflow by gravity connection east of Red Road; 20 CSM pumped, unlimited gravity with development limitations west of Red Road or Flamingo Blvd.	100 year +
C-10	---	200 year +
C-11	20 CSM west of 13A;40 CSM east of 13A	------------
C-12	90.6 CSM	25 year
C-13	75.9 CSM	25 year
C-14	69.2 CSM	25 year
C-15	70.0 CSM	25 year
C-16	62.6 CSM	25 year
C-17	62.7 CSM	25 year
C-18	41.6 CSM	25 year
C-19	57.8 CSM	------------
C-23	31.5 CSM	10 year

Figure B- 1: SFWMD ERP Allowable Runoff by Canal

APPENDIX C

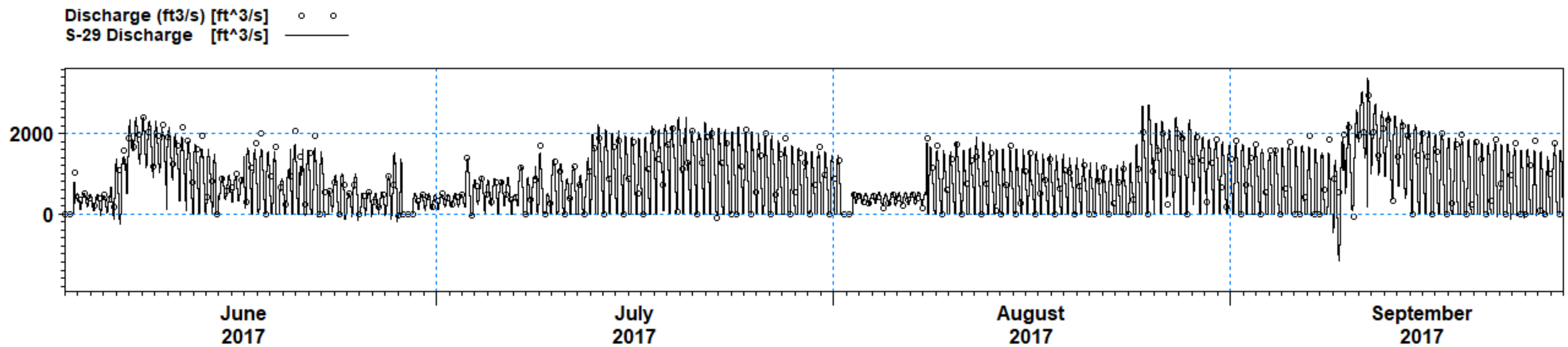

Figure C- 1: Simulated (line) vs Observed (dots) Discharge Comparison for SFWMD C-9 Structure S-29, June 2nd-September 27th, 2017

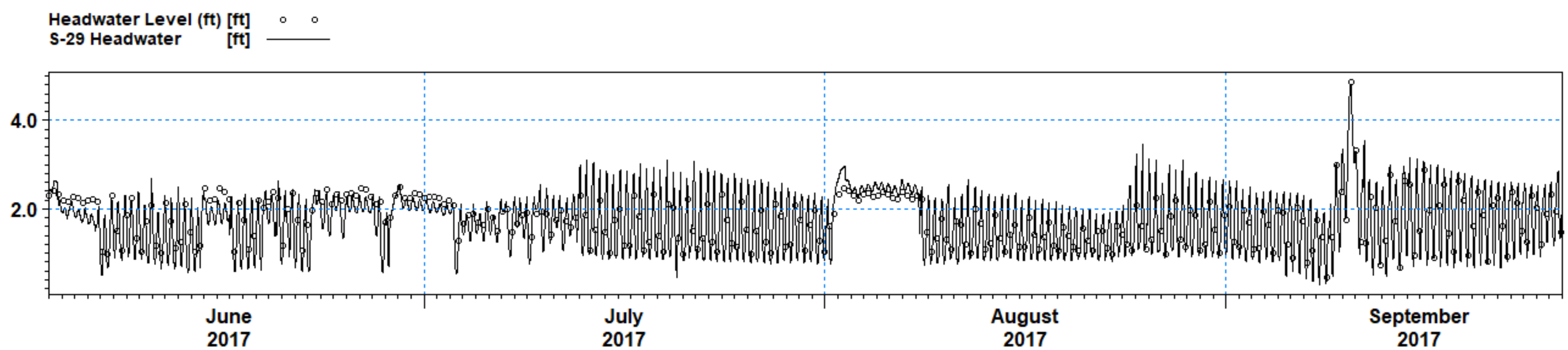

Figure C- 2: Simulated (line) vs Observed (dots) Headwater Comparison for SFWMD C-9 Structure S-29, June 2nd-September 27th, 2017

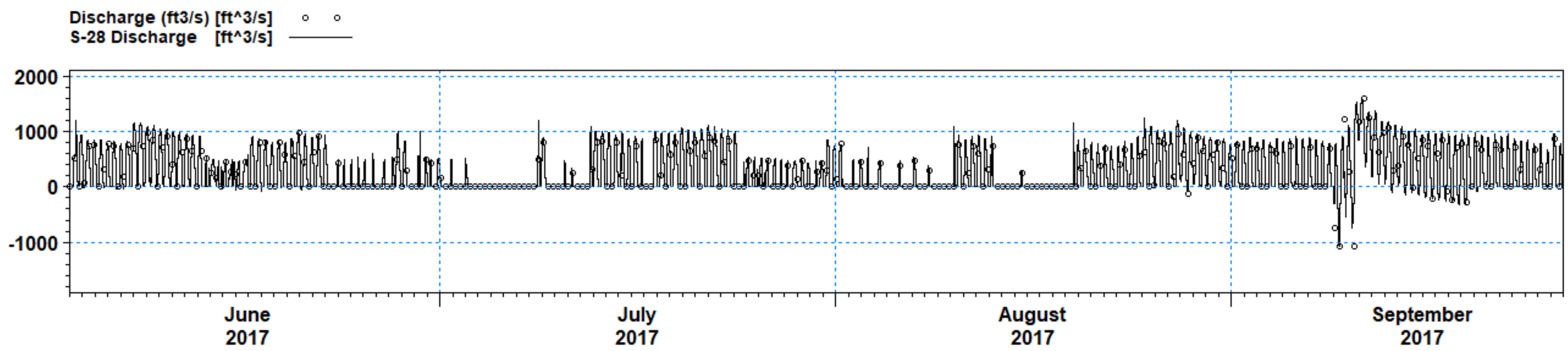

Figure C- 3: Simulated (line) vs Observed (dots) Discharge Comparison for SFWMD C-8 Structure S-28, June 2nd-September 27th, 2017

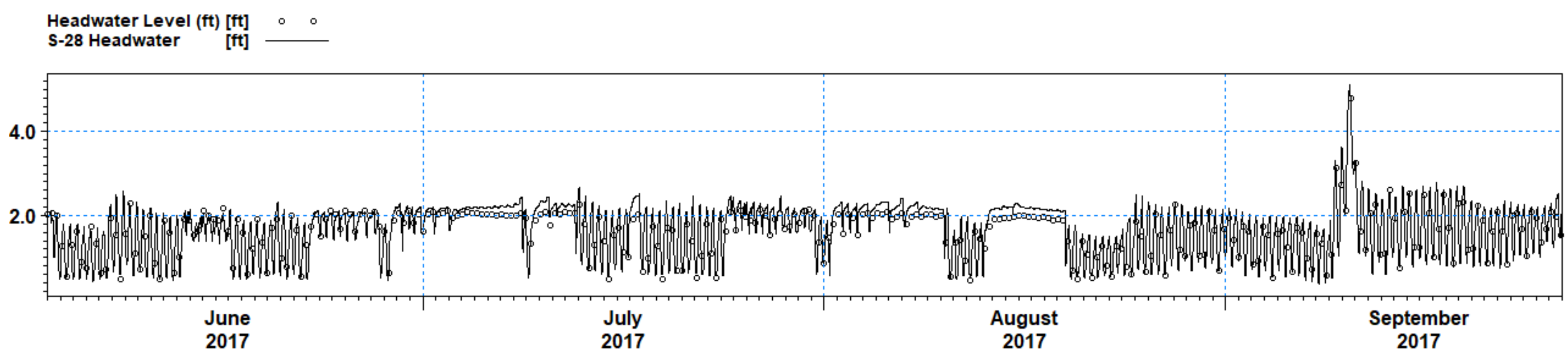

Figure C- 4: Simulated (line) vs Observed (dots) Headwater Comparison for SFWMD C-8 Structure S-28, June 2nd-September 27th, 2017

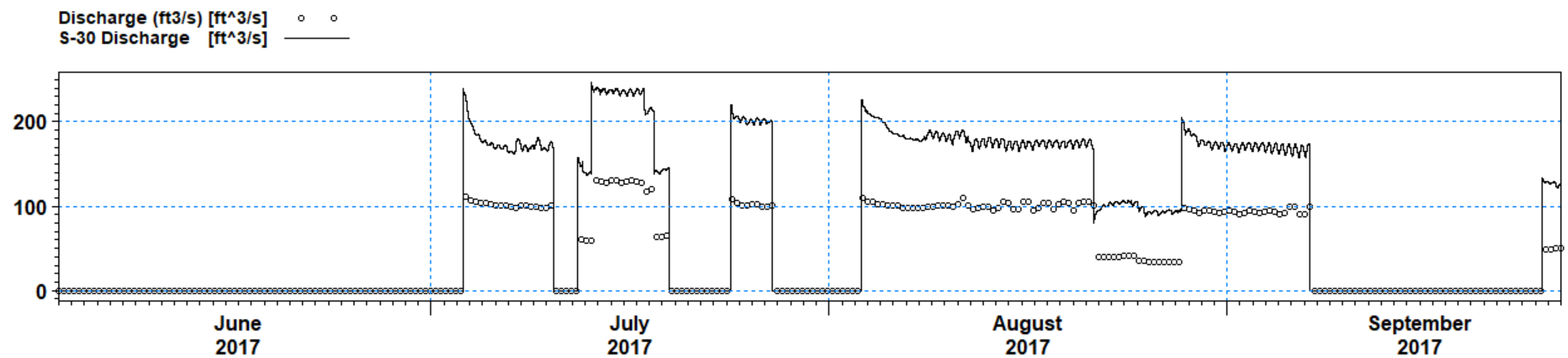

Figure C- 5: Simulated (line) vs Observed (dots) Discharge Comparison for SFWMD C-9 Structure S-30, June 2nd-September 27th, 2017

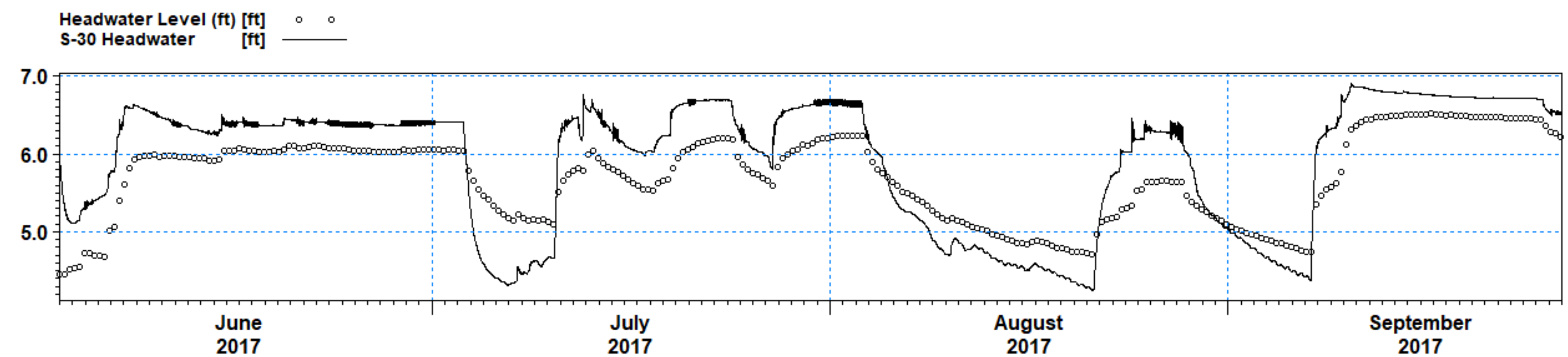

Figure C- 6: Simulated (line) vs Observed (dots) Headwater Comparison for SFWMD C-9 Structure S-30, June 2nd-September 27th, 2017

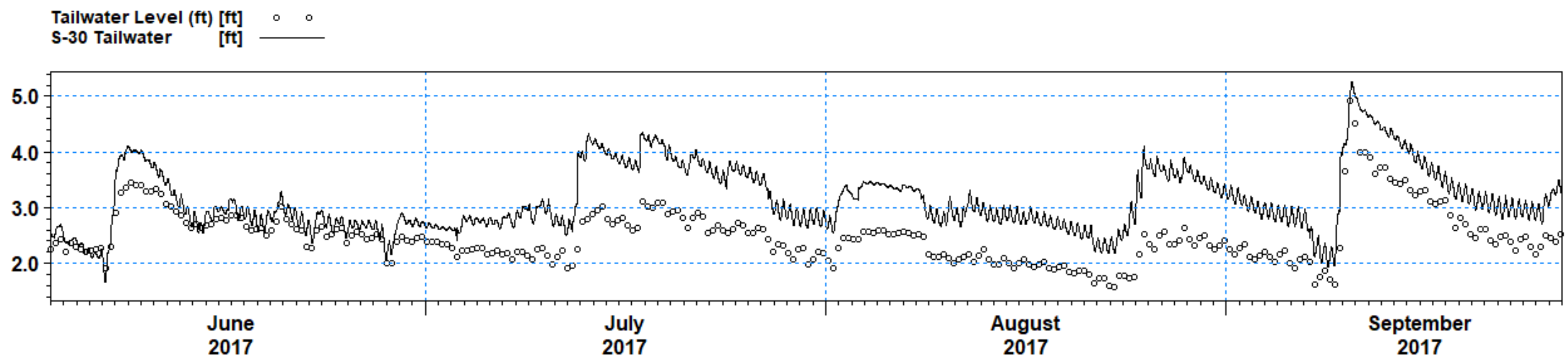

Figure C- 7: Simulated (line) vs Observed (dots) Tailwater Comparison for SFWMD C-9 Structure S-30, June 2nd-September 27th, 2017

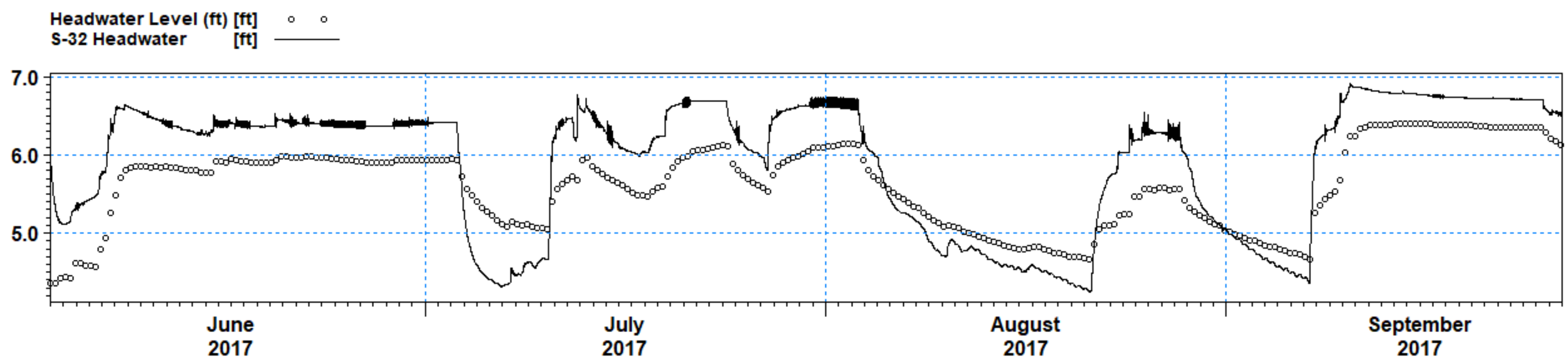

Figure C- 8: Simulated (line) vs Observed (dots) Headwater Comparison for SFWMD L-33 Structure S-32, June 2nd-September 27th, 2017

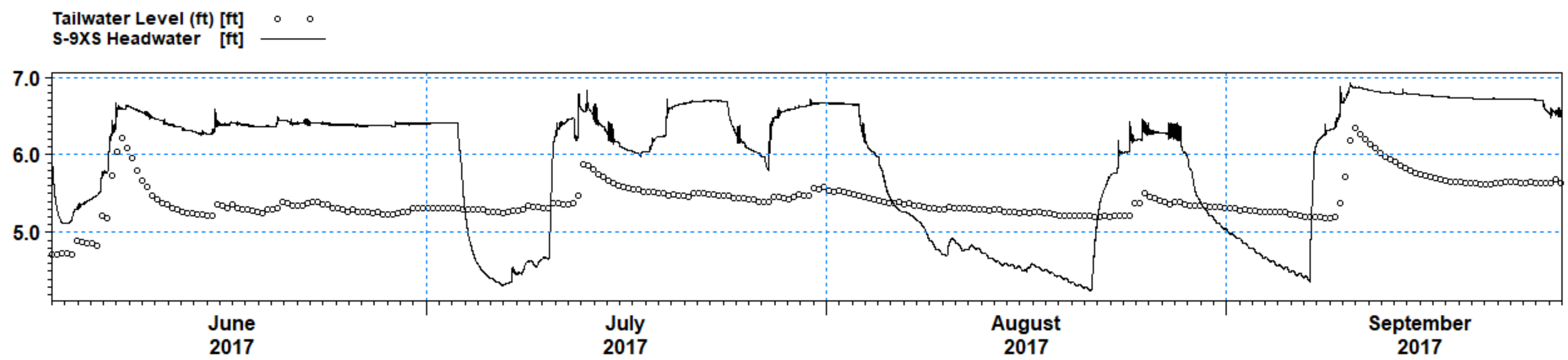

Figure C- 9: Simulated (line) vs Observed (dots) Headwater Comparison for SFWMD L-33 Structure S-9XS, June 2nd-September 27th, 2017

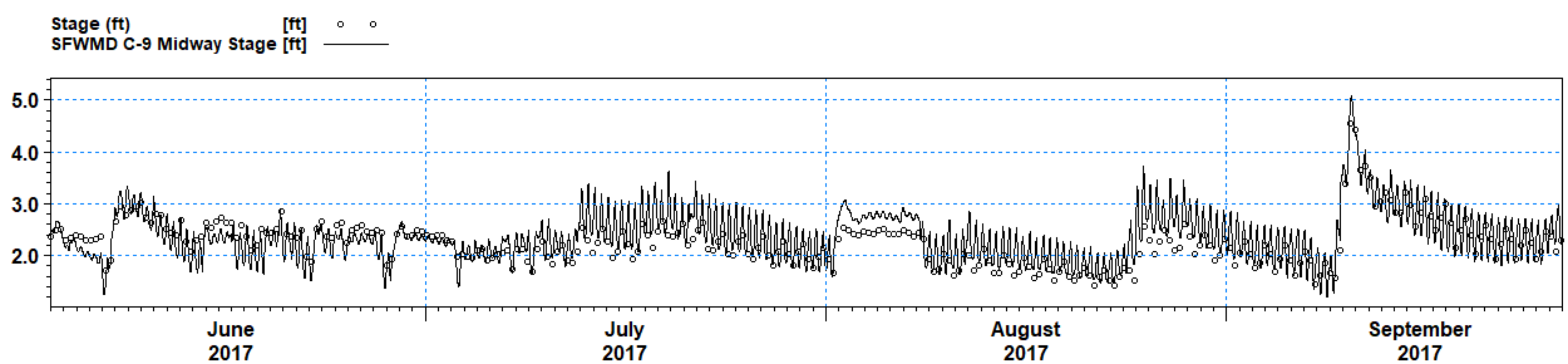

Figure C- 10: Simulated (line) vs Observed (dots) Stage Comparison for SFWMD C-9 Water Level Recorder S-29Z, June 2nd-September 27th, 2017

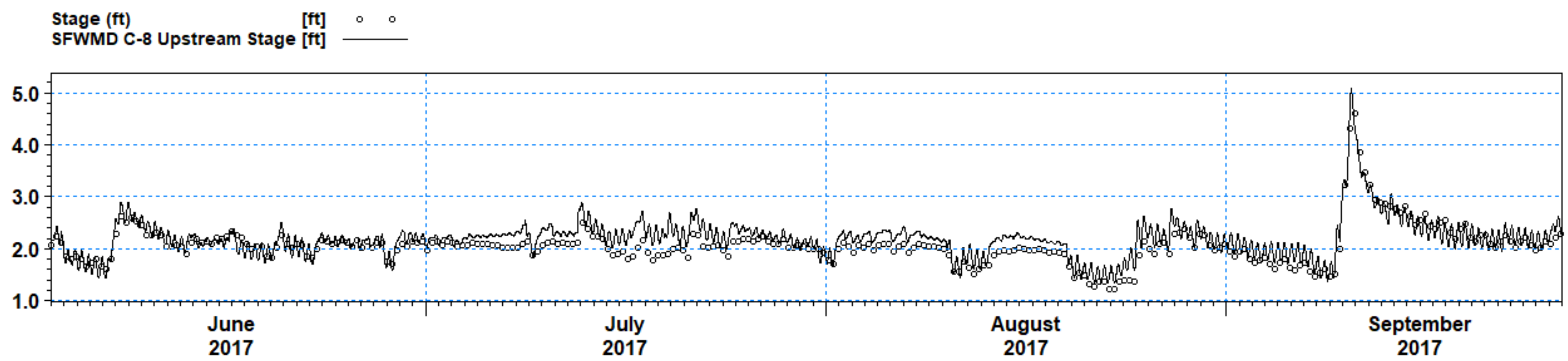

Figure C- 11: Simulated (line) vs Observed (dots) Stage Comparison for SFWMD C-8 Water Level Recorder S-28Z, June 2nd-September 27th, 2017

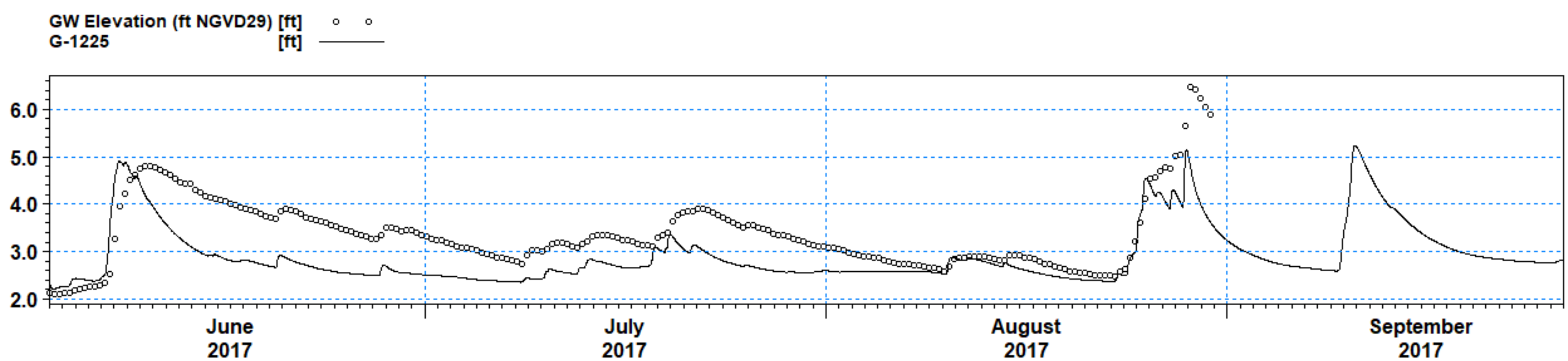

Figure C- 12: Simulated (line) vs Observed (dots) Groundwater Elevation Comparison for Well G-1225, June 2nd-September 27th, 2017

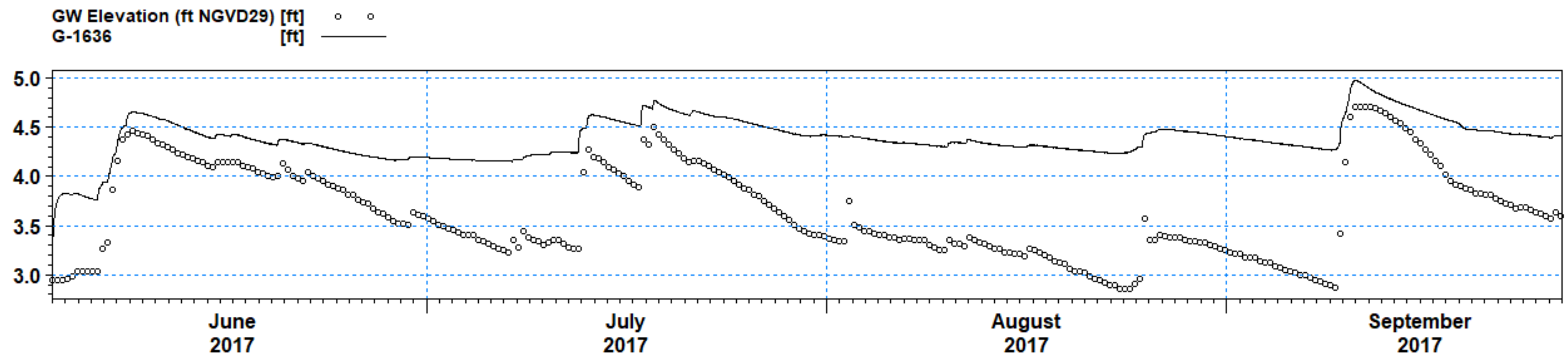

Figure C- 13: Simulated (line) vs Observed (dots) Groundwater Elevation Comparison for Well G-1636, June 2nd-September 27th, 2017

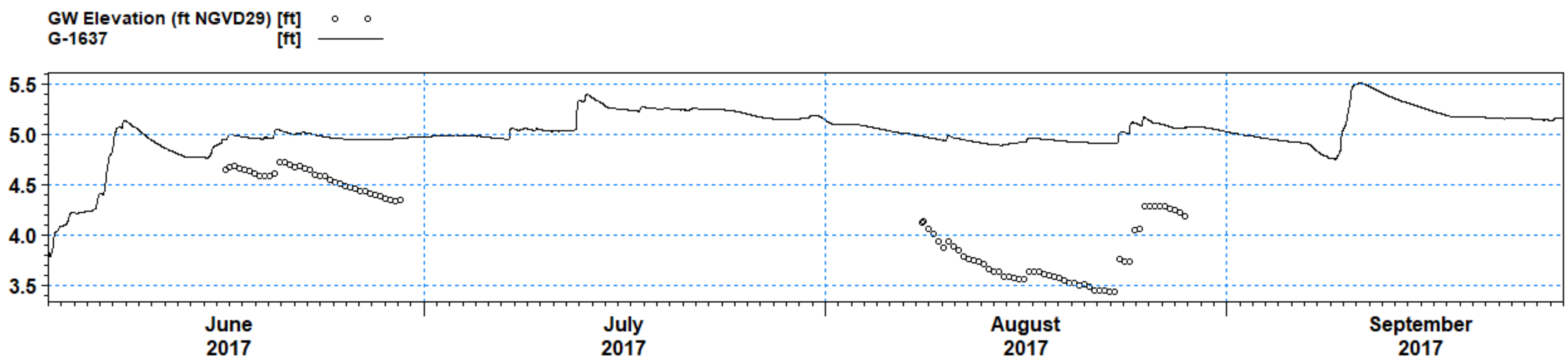

Figure C- 14: Simulated (line) vs Observed (dots) Groundwater Elevation Comparison for Well G-1637, June 2nd-September 27th, 2017

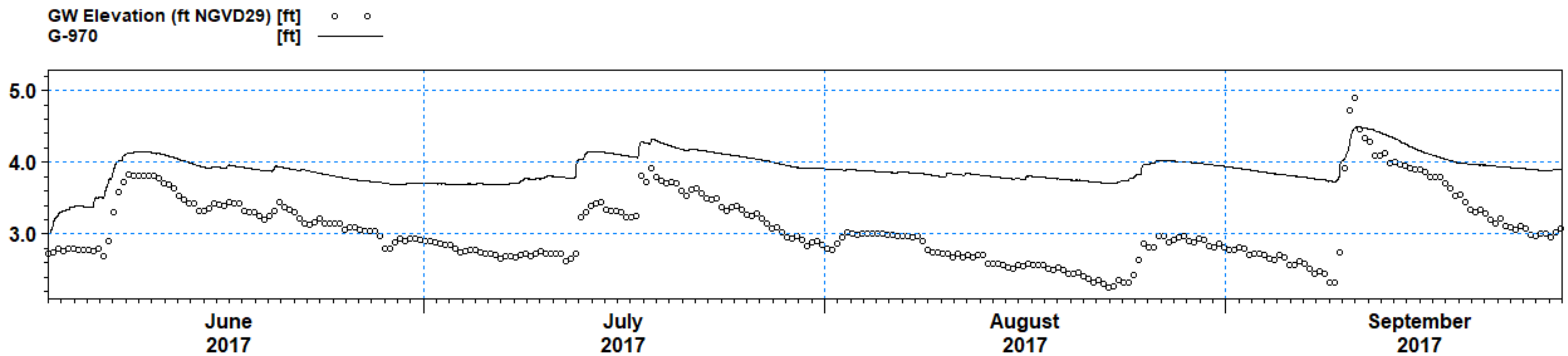

Figure C- 15: Simulated (line) vs Observed (dots) Groundwater Elevation Comparison for Well G-970, June 2nd-September 27th, 2017

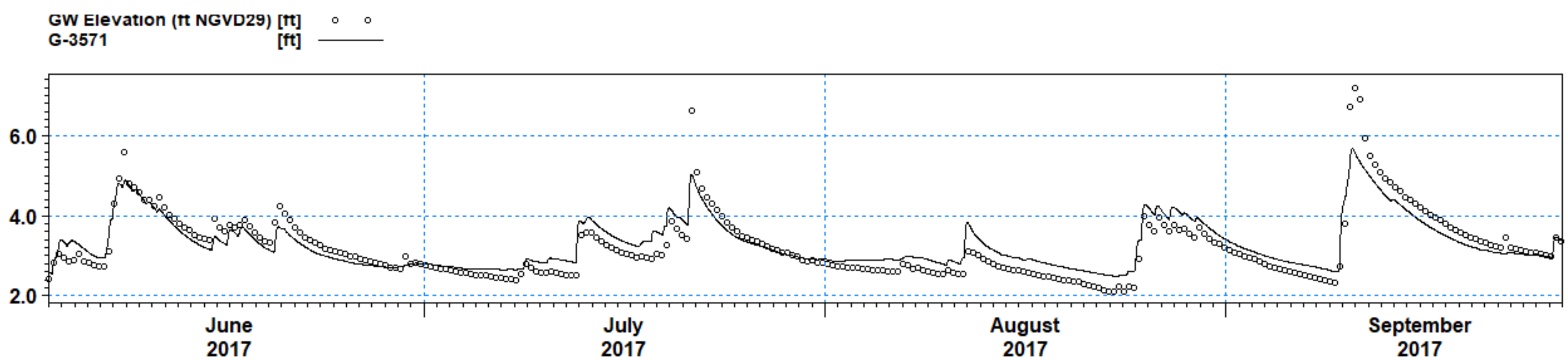

Figure C- 16: Simulated (line) vs Observed (dots) Groundwater Elevation Comparison for Well G-3571, June 2nd-September 27th, 2017

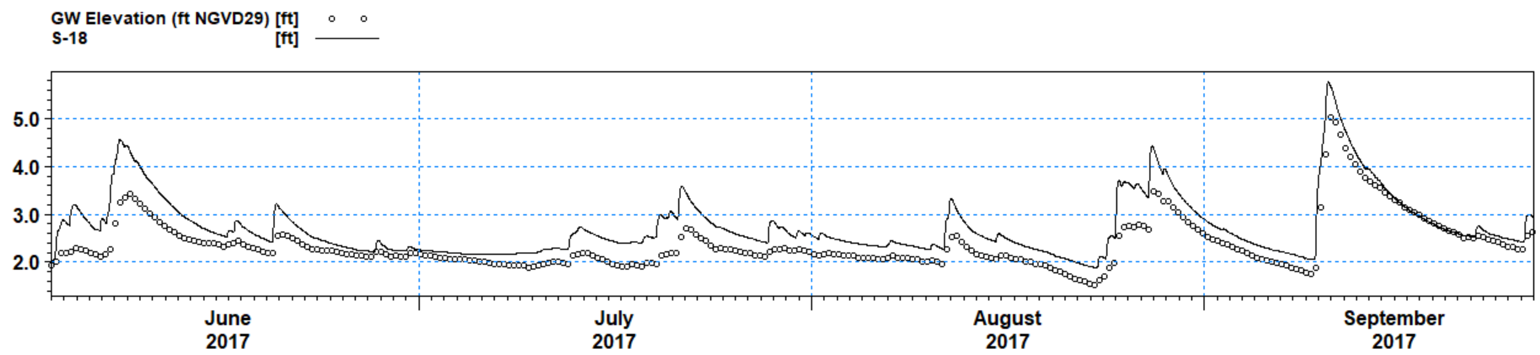

Figure C- 17: Simulated (line) vs Observed (dots) Groundwater Elevation Comparison for Well S-18, June 2nd-September 27th, 2017

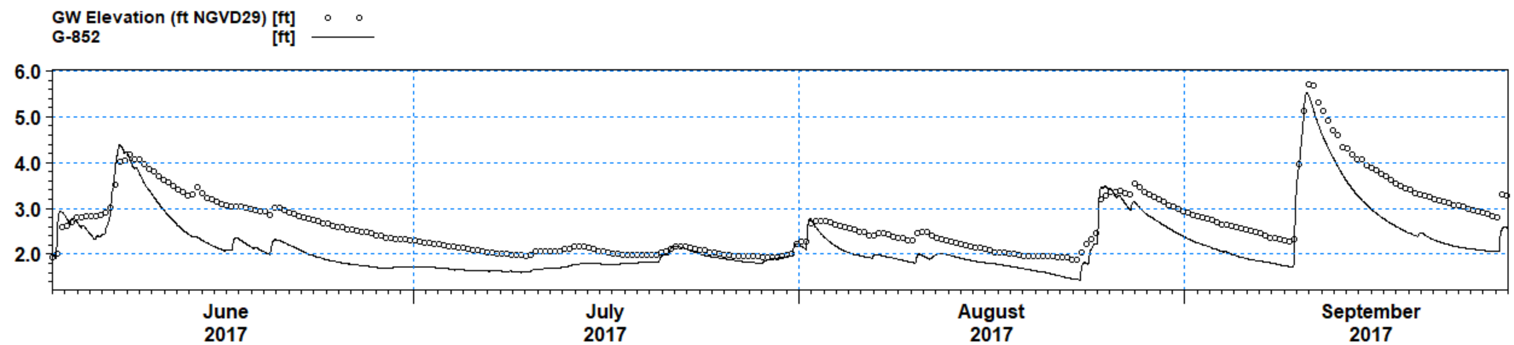

Figure C- 18: Simulated (line) vs Observed (dots) Groundwater Elevation Comparison for Well G-852, June 2nd-September 27th, 2017

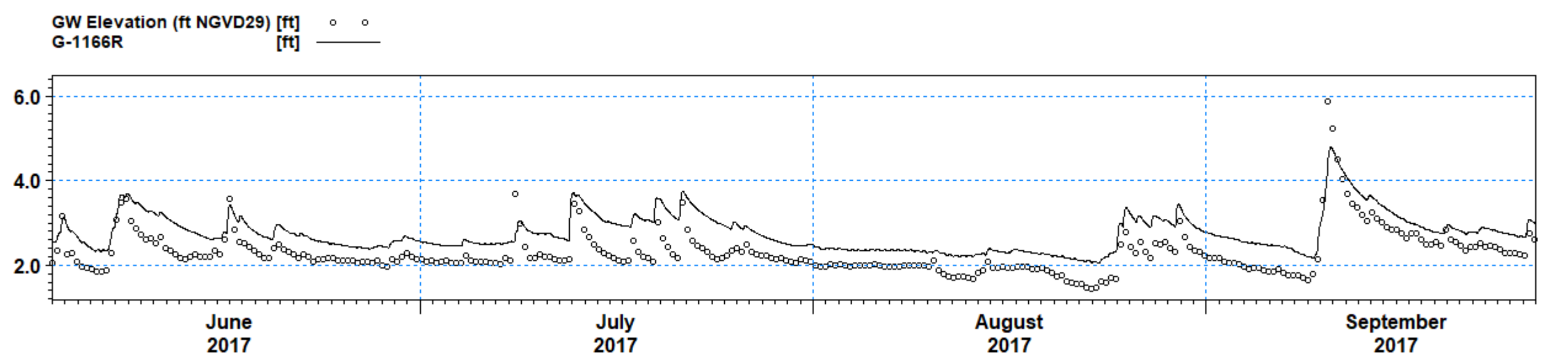

Figure C- 19: Simulated (line) vs Observed (dots) Groundwater Elevation Comparison for Well G-1166R, June 2nd-September 27th, 2017

APPENDIX D

Table D- 1: Peak Stage and Discharge Summary

Structure	Peak Stage (ft NGVD29)				Peak Discharge (cfs)			
	5-Year	10-Year	25-Year	100-Year	5-Year	10-Year	25-Year	100-Year
S-28	4.26	4.61	5.16	6.04	1721	2059	2679	3777
S-29	4.19	4.54	5.08	6.0	2647	3052	3681	4710
S-30 TW	4.87	5.23	5.49	5.97				

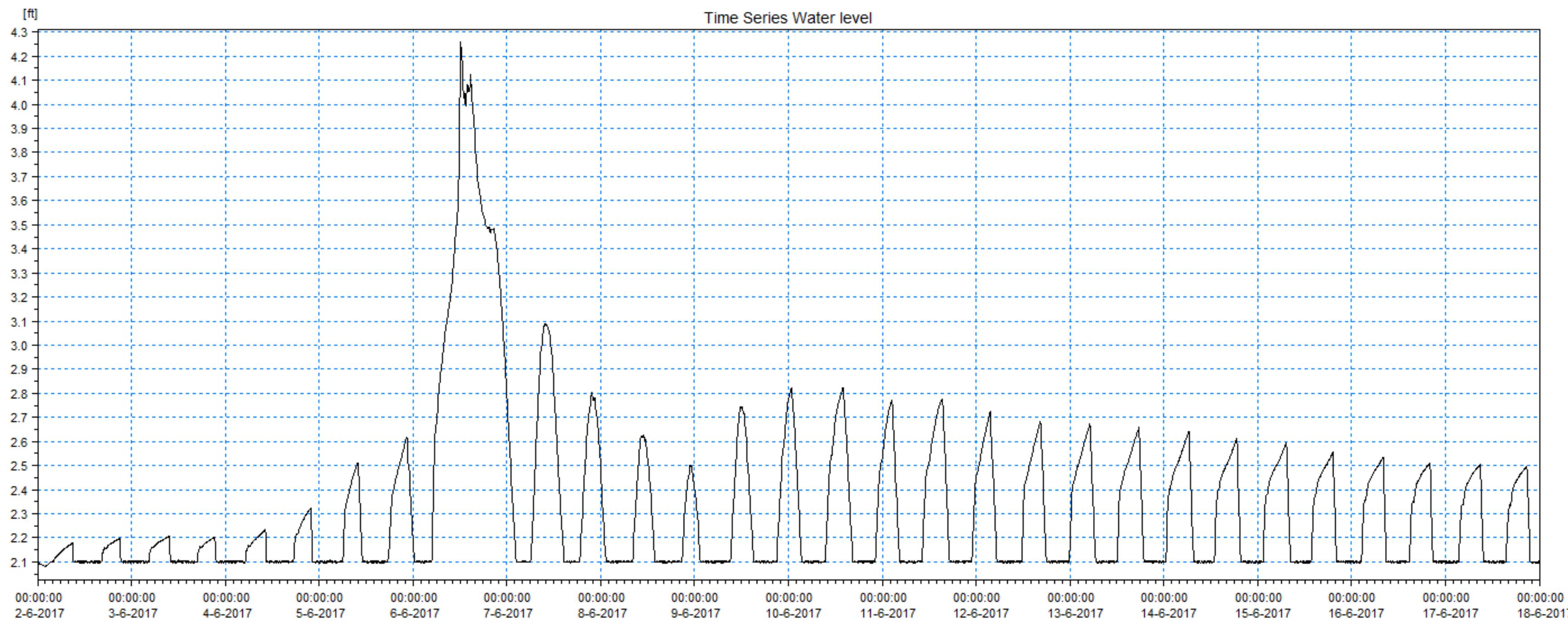

Figure D- 1: S-28 5-Year Design Storm Headwater Stage

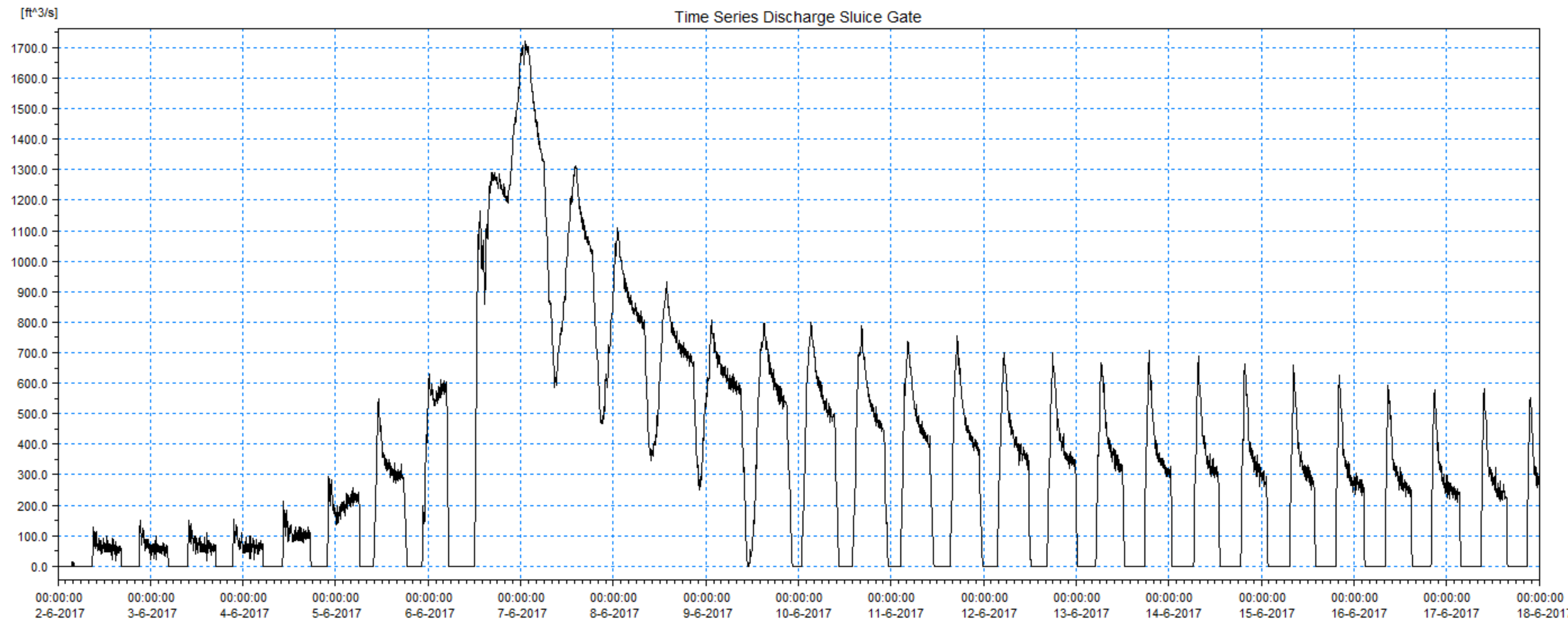

Figure D- 2: S-28 5-Year Design Storm Discharge (cfs)

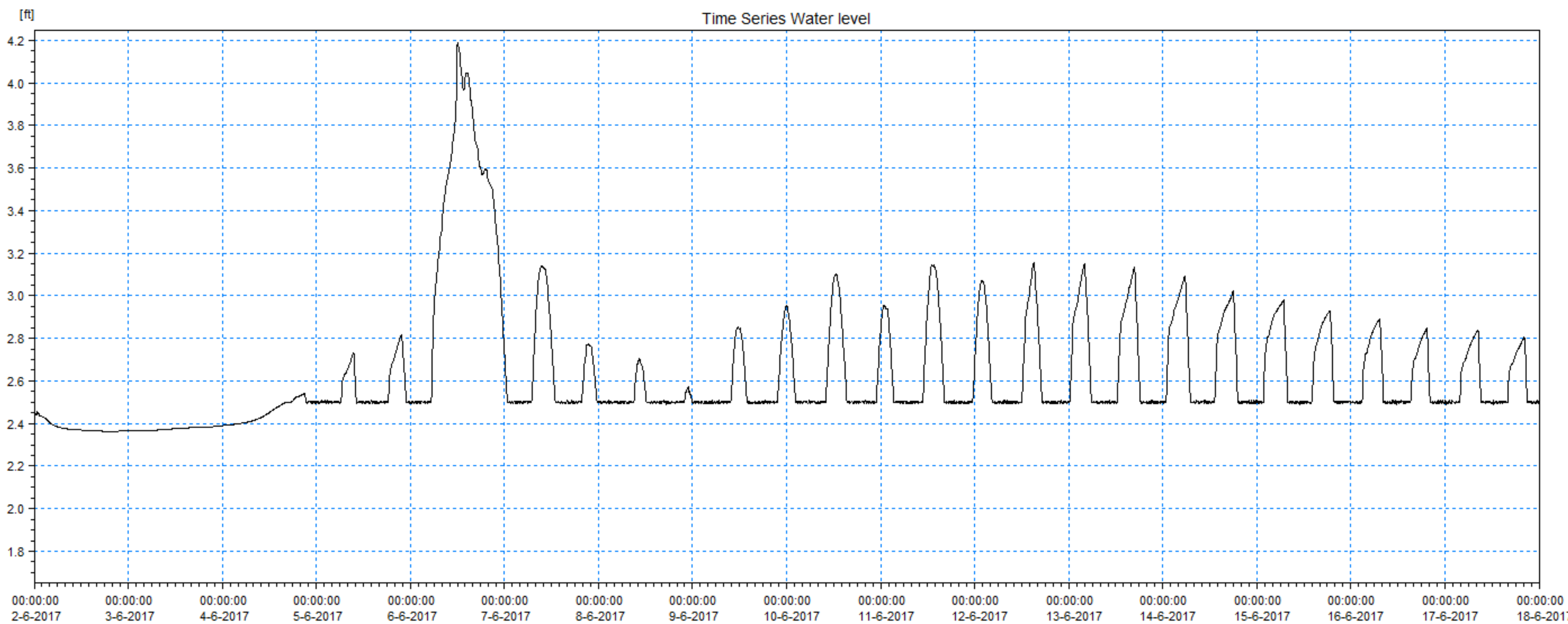

Figure D- 3: S-29 5-Year Design Storm Headwater Stage

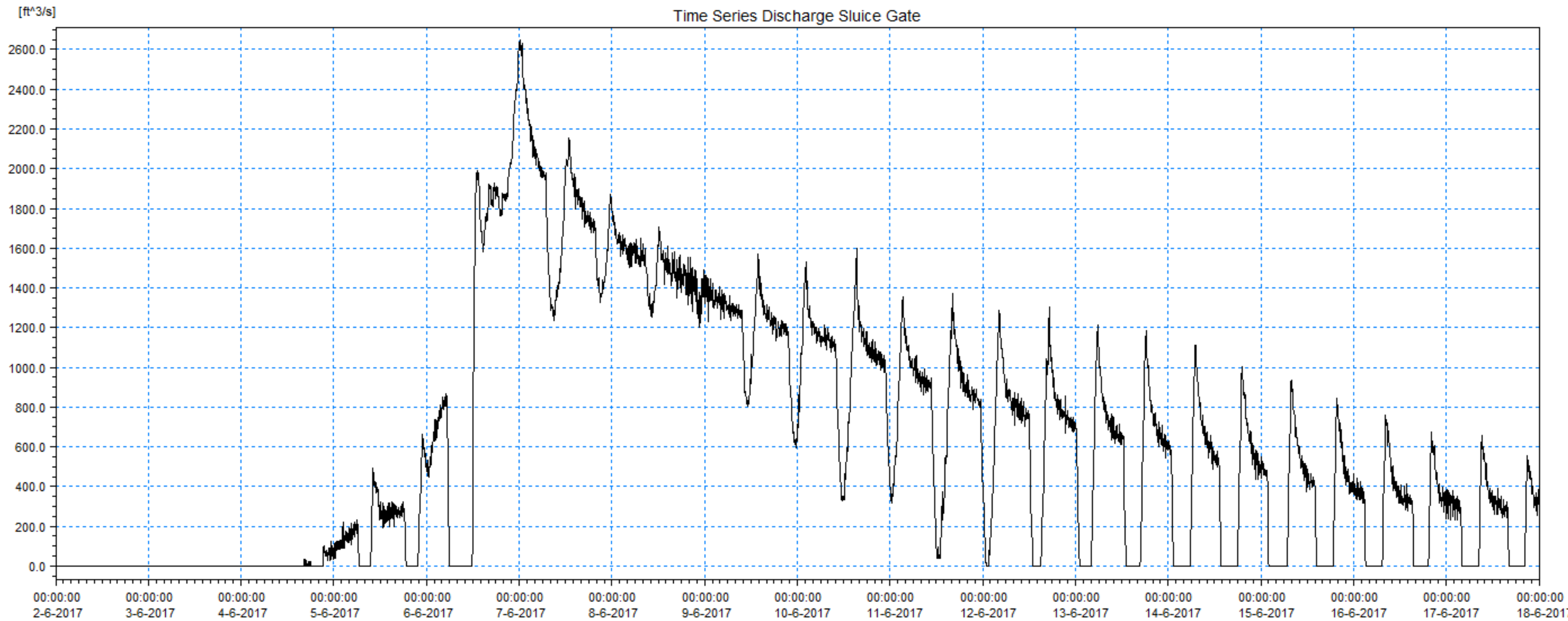

Figure D- 4: S-29 5-Year Design Storm Discharge (cfs)

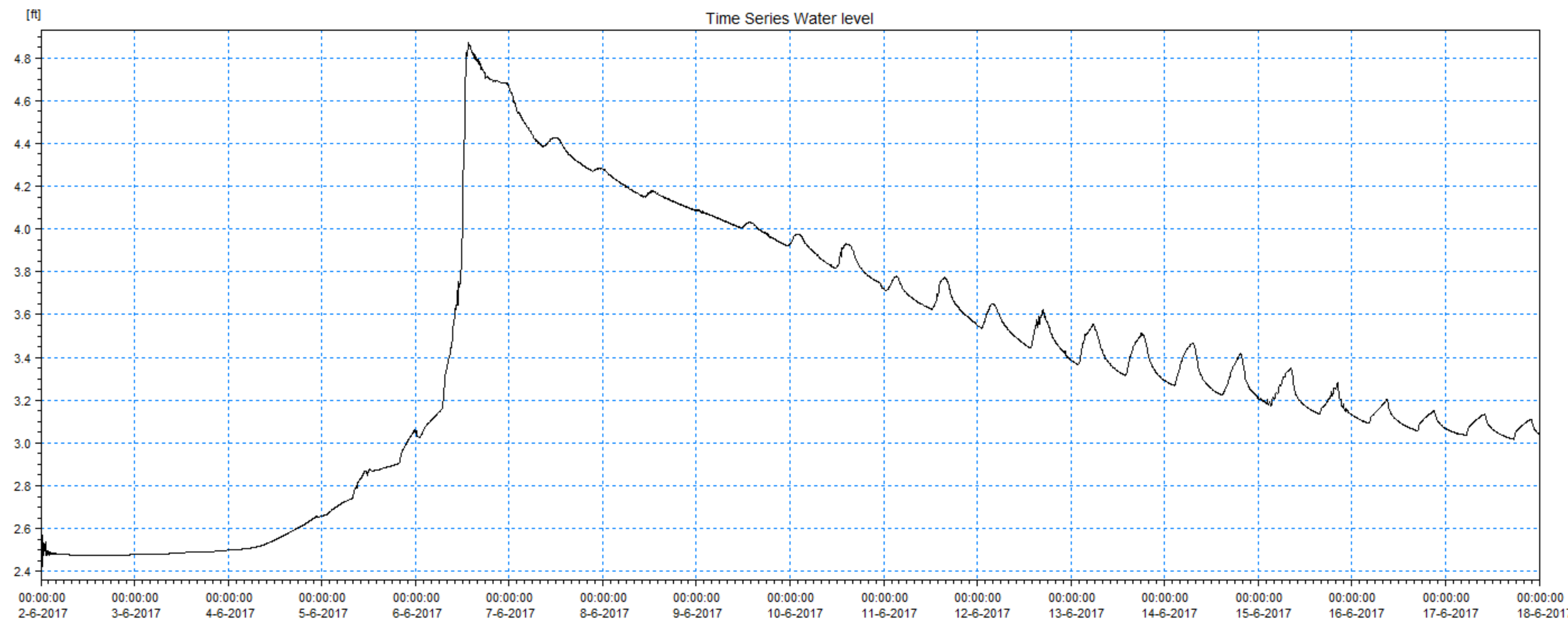

Figure D- 5: S-30 5-Year Design Storm Tailwater Stage

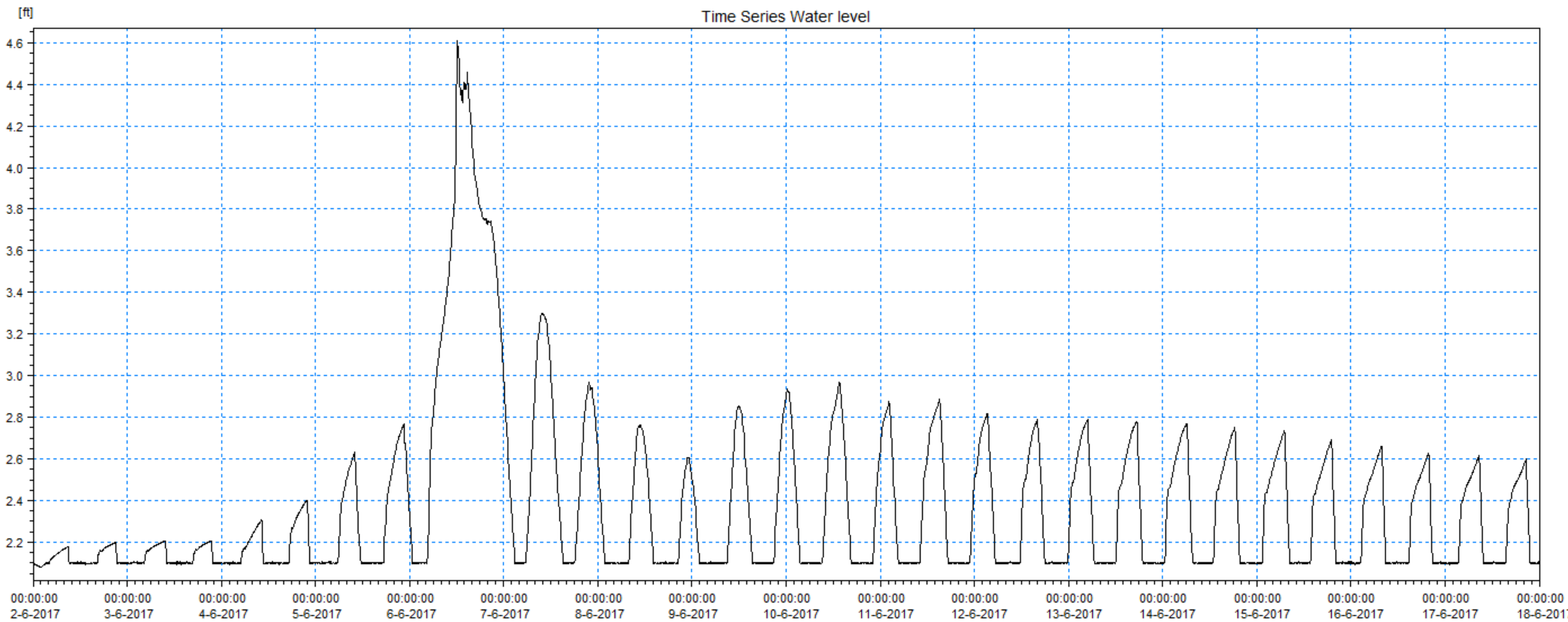

Figure D- 6: S-28 10-Year Design Storm Headwater Stage

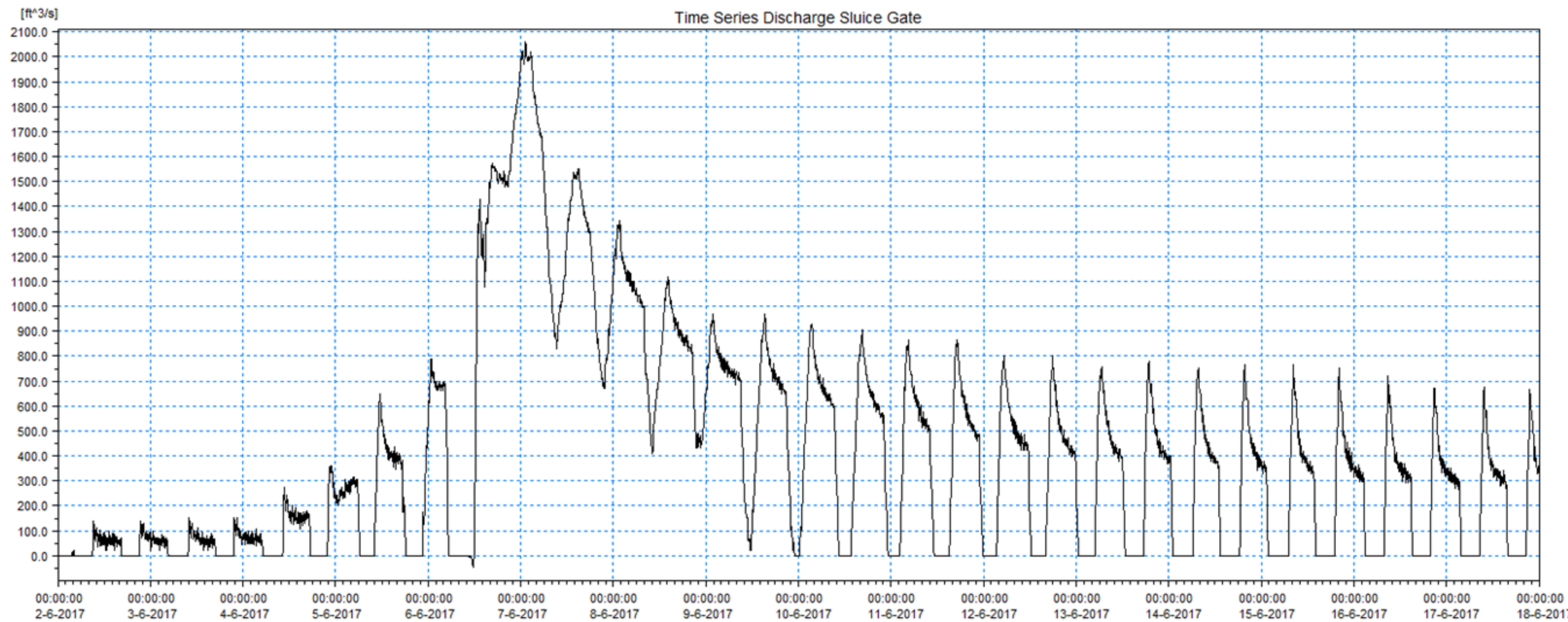

Figure D- 7: S-28 10-Year Design Storm Discharge (cfs)

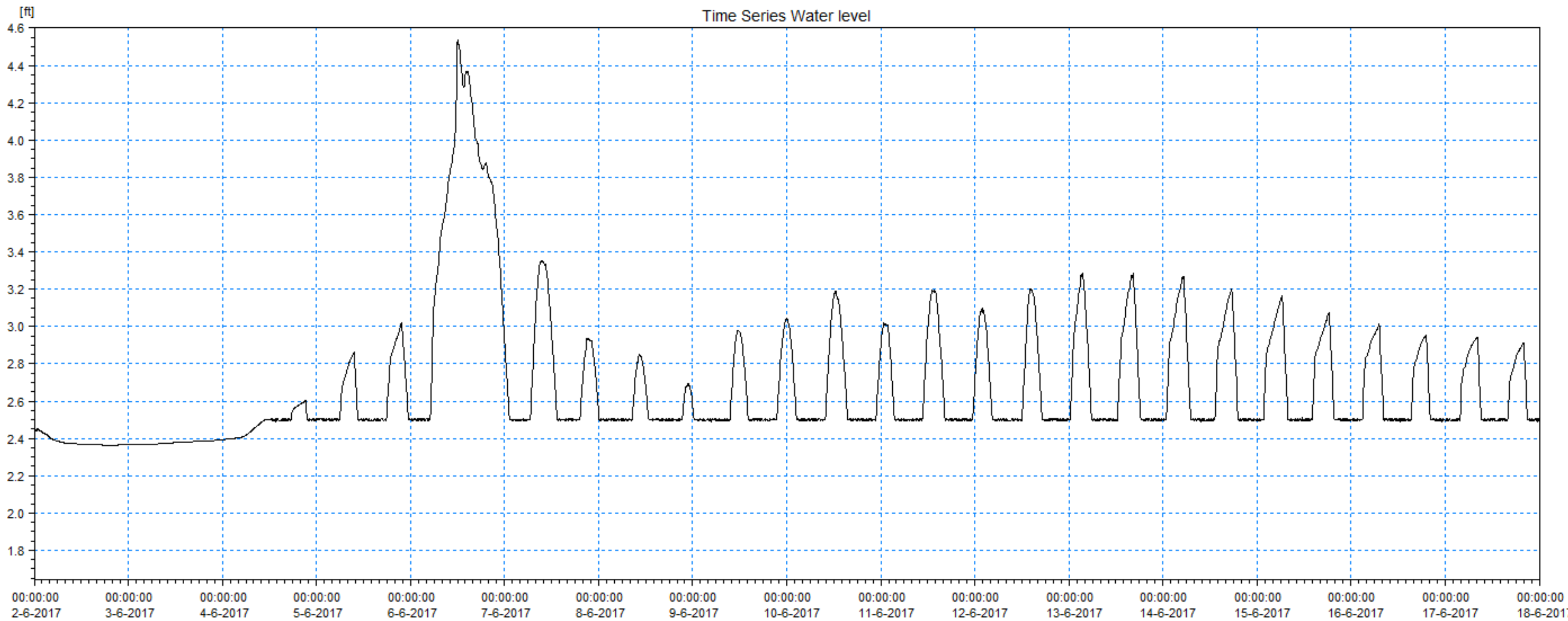

Figure D- 8: S-29 10-Year Design Storm Headwater Stage

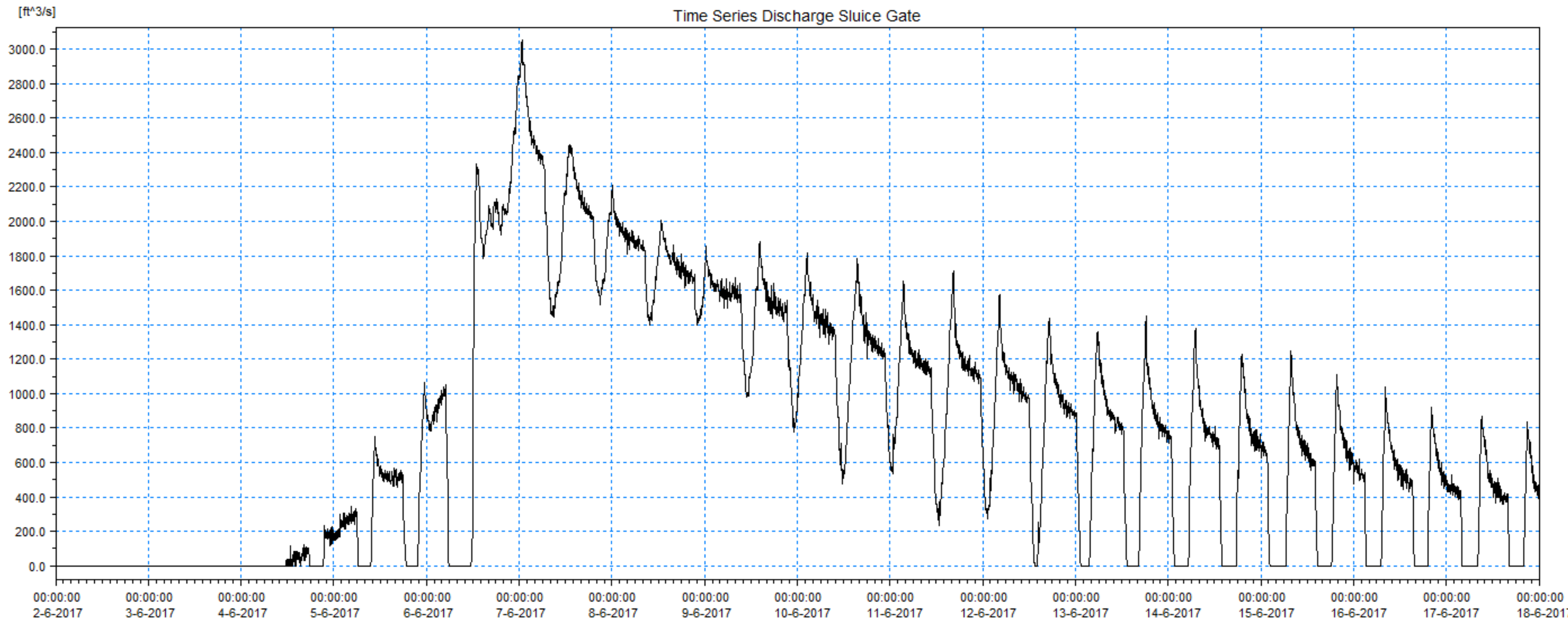

Figure D- 9: S-29 10-Year Design Storm Discharge (cfs)

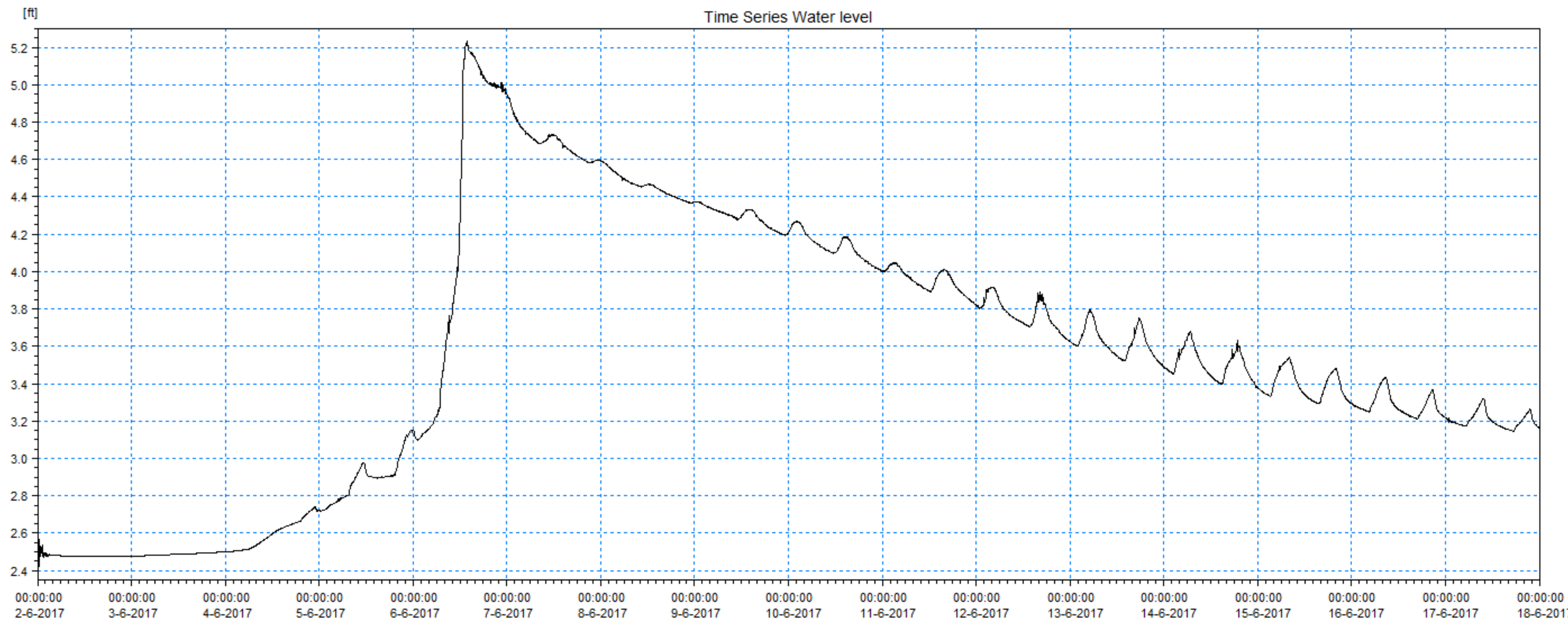

Figure D- 10: S-30 10-Year Design Storm Tailwater Stage

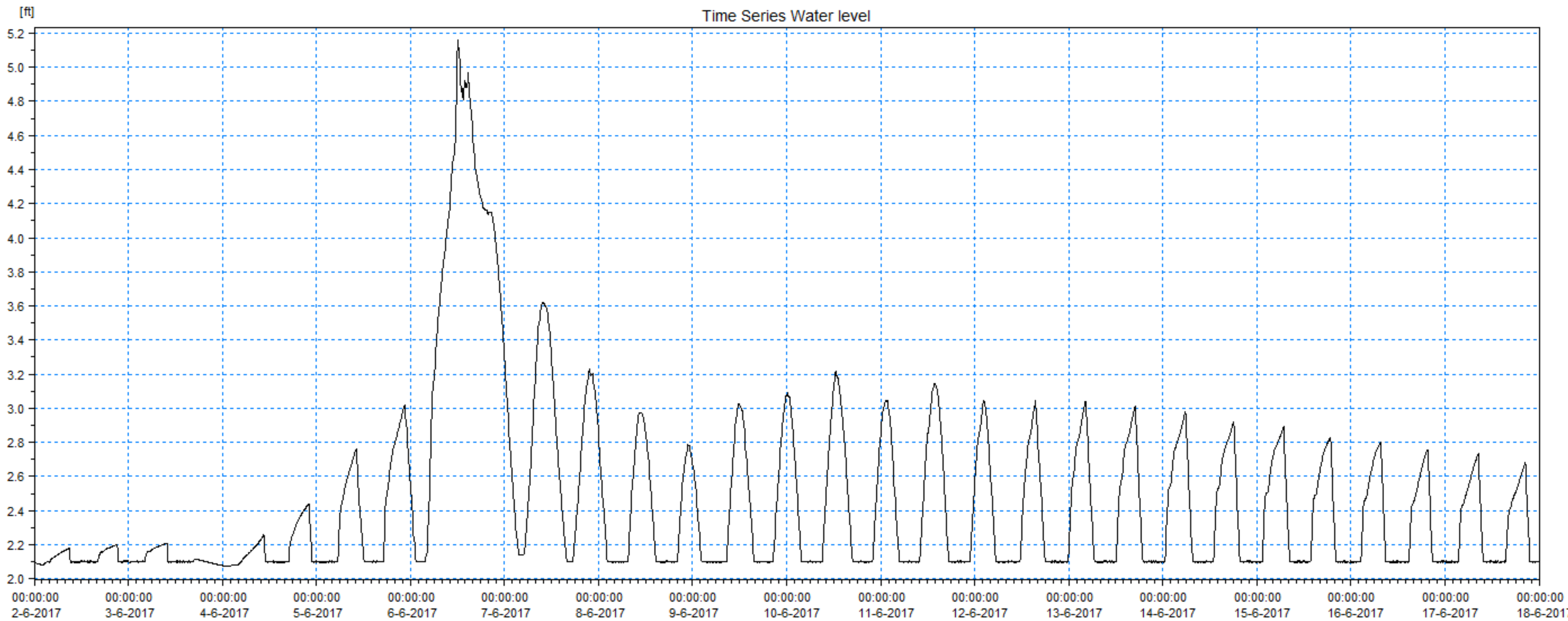

Figure D- 11: S-28 25-Year Design Storm Headwater Stage

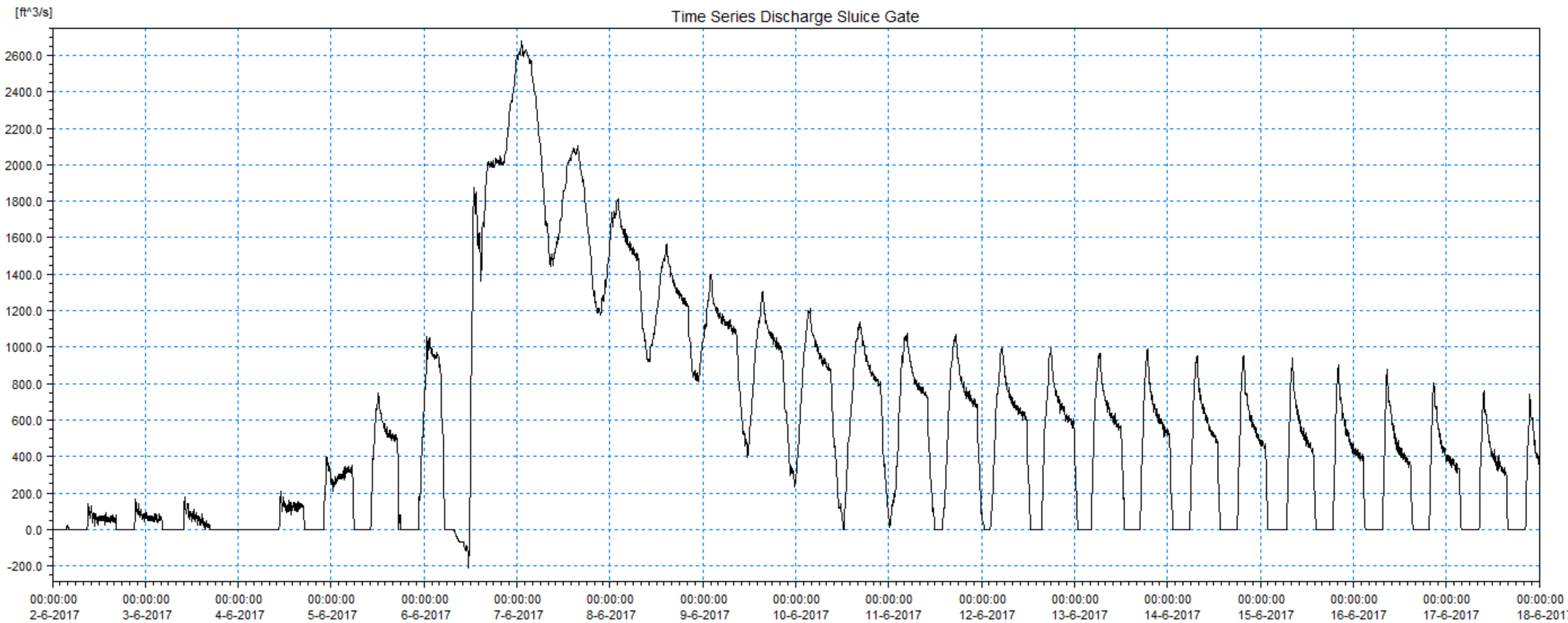

Figure D- 12: S-28 25-Year Design Storm Discharge (cfs)

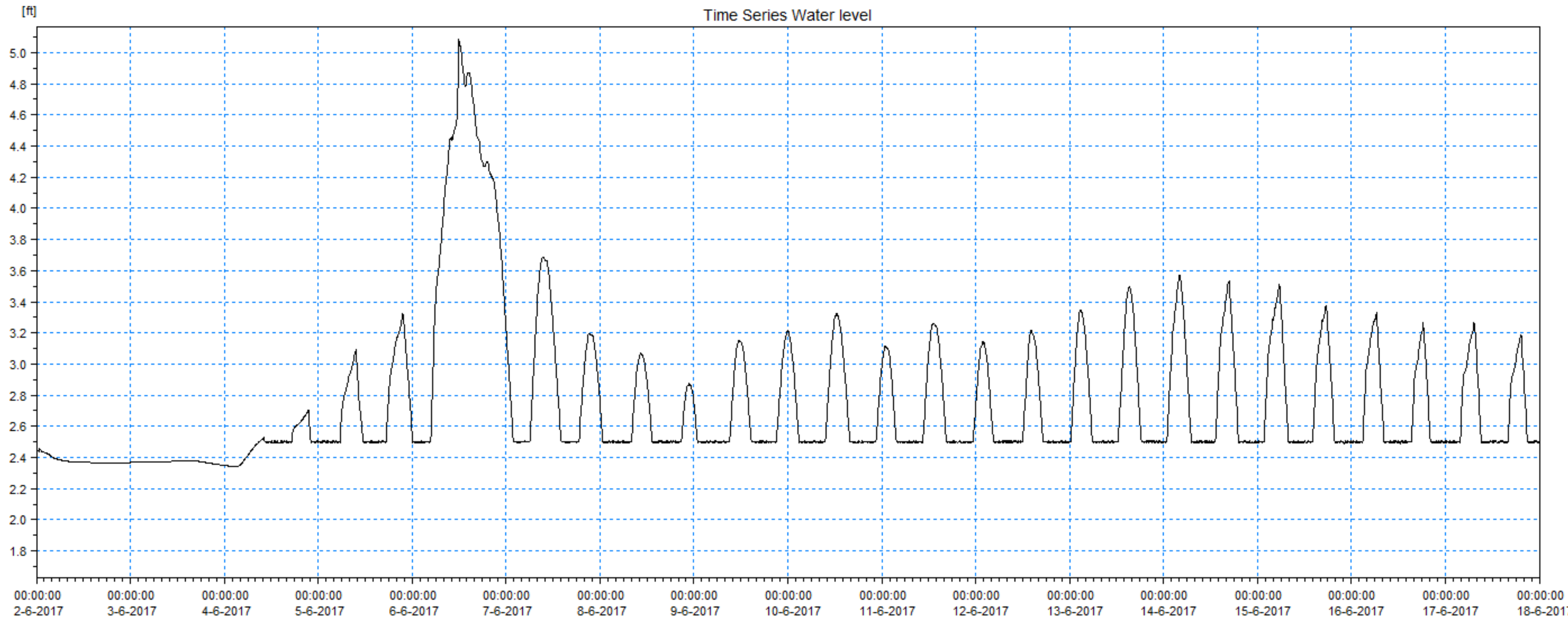

Figure D- 13: S-29 25-Year Design Storm Headwater Stage

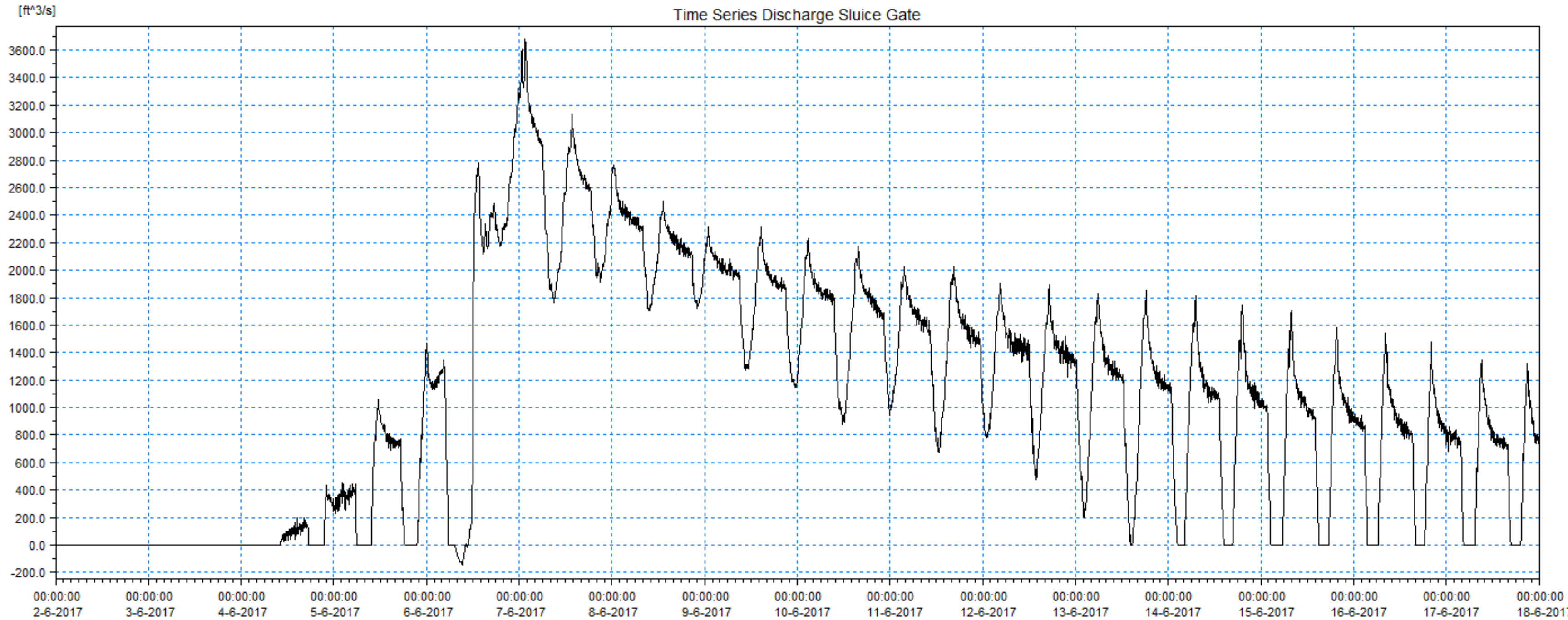

Figure D- 14: S-29 25-Year Design Storm Discharge (cfs)

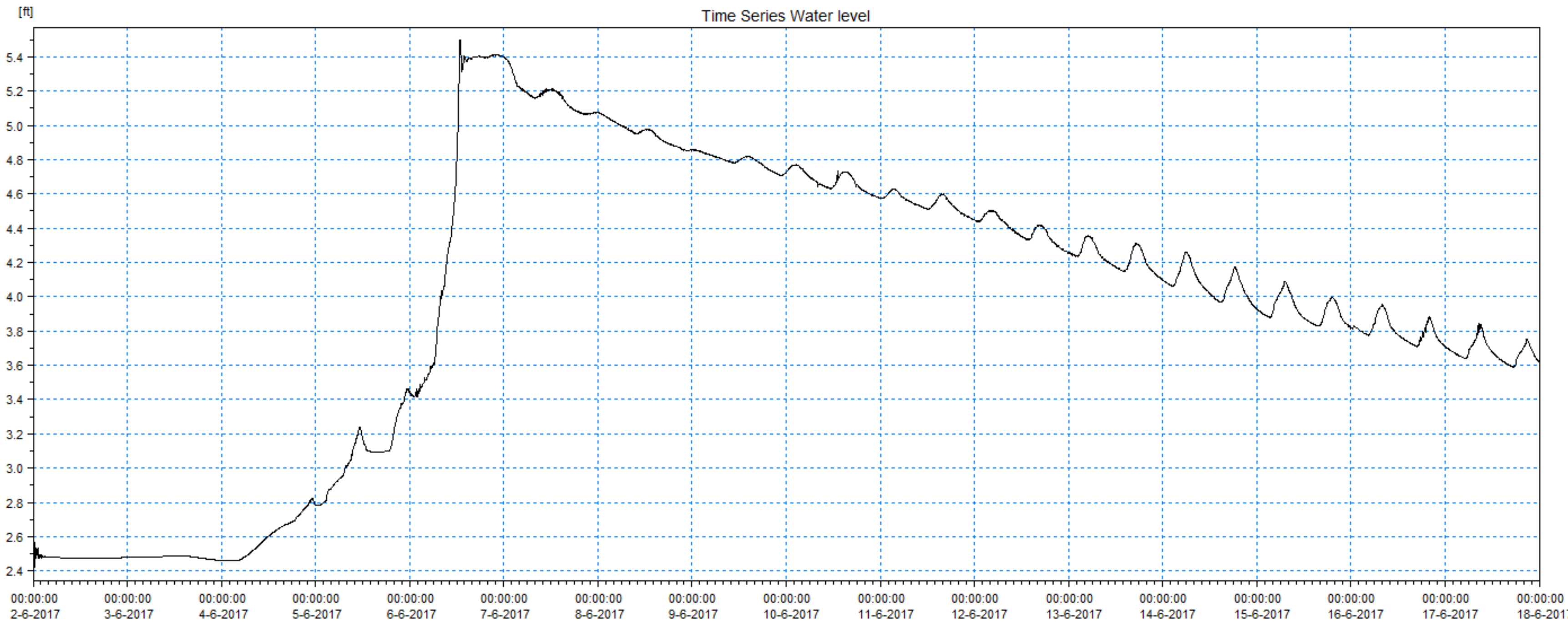

Figure D- 15: S-30 25-Year Design Storm Tailwater Stage

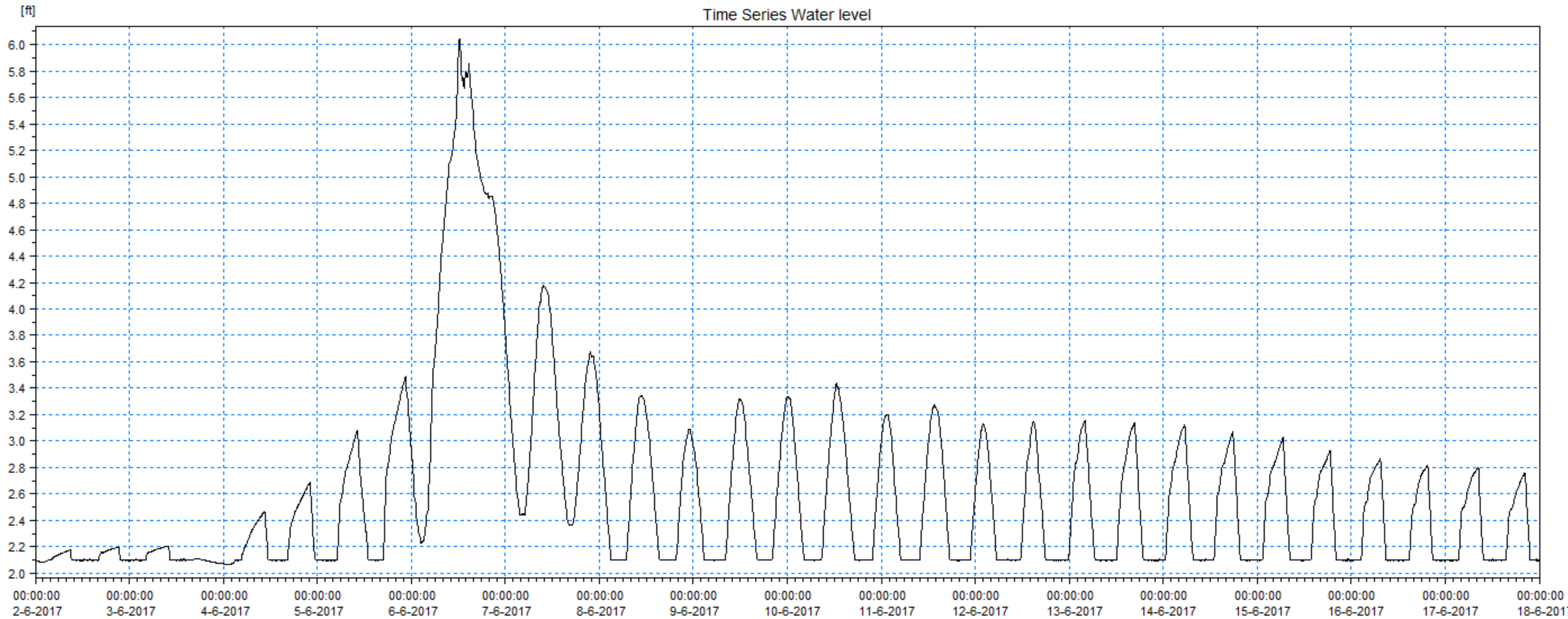

Figure D- 16: S-28 100-Year Design Storm Headwater Stage

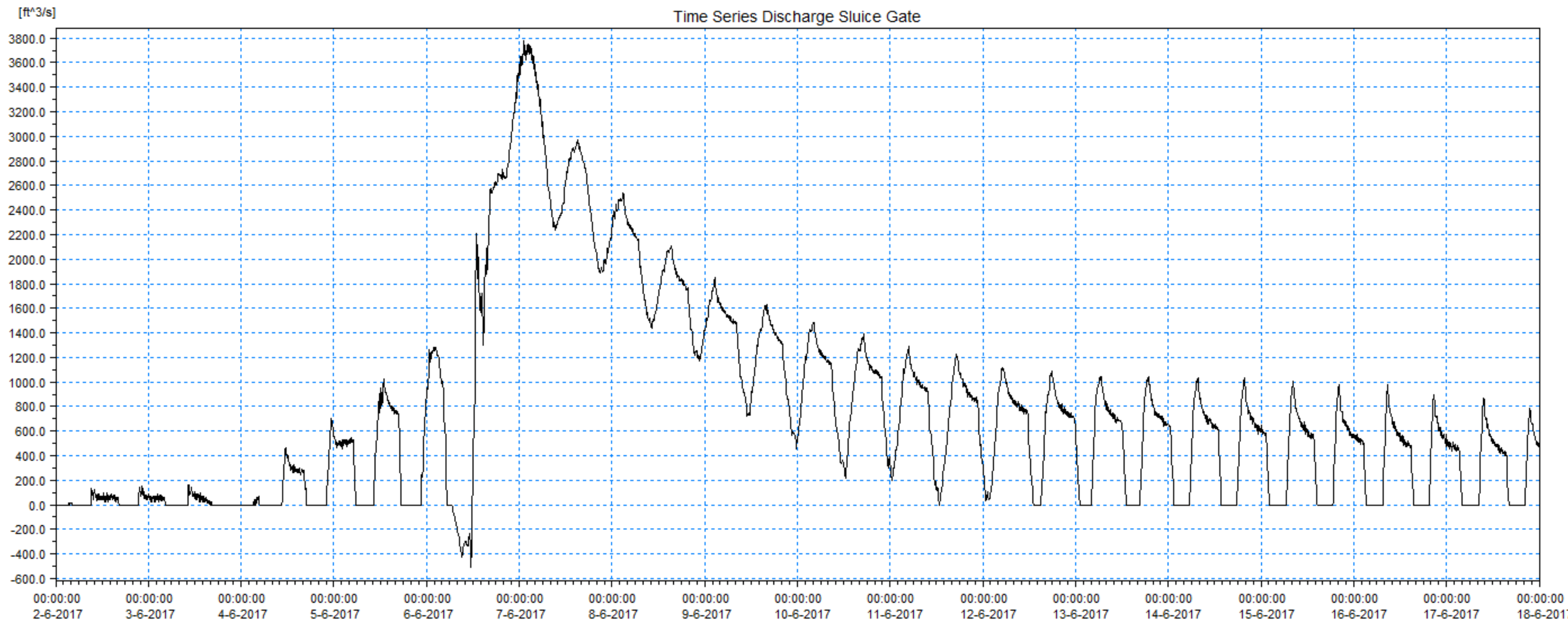

Figure D- 17: S-28 100-Year Design Storm Discharge (cfs)

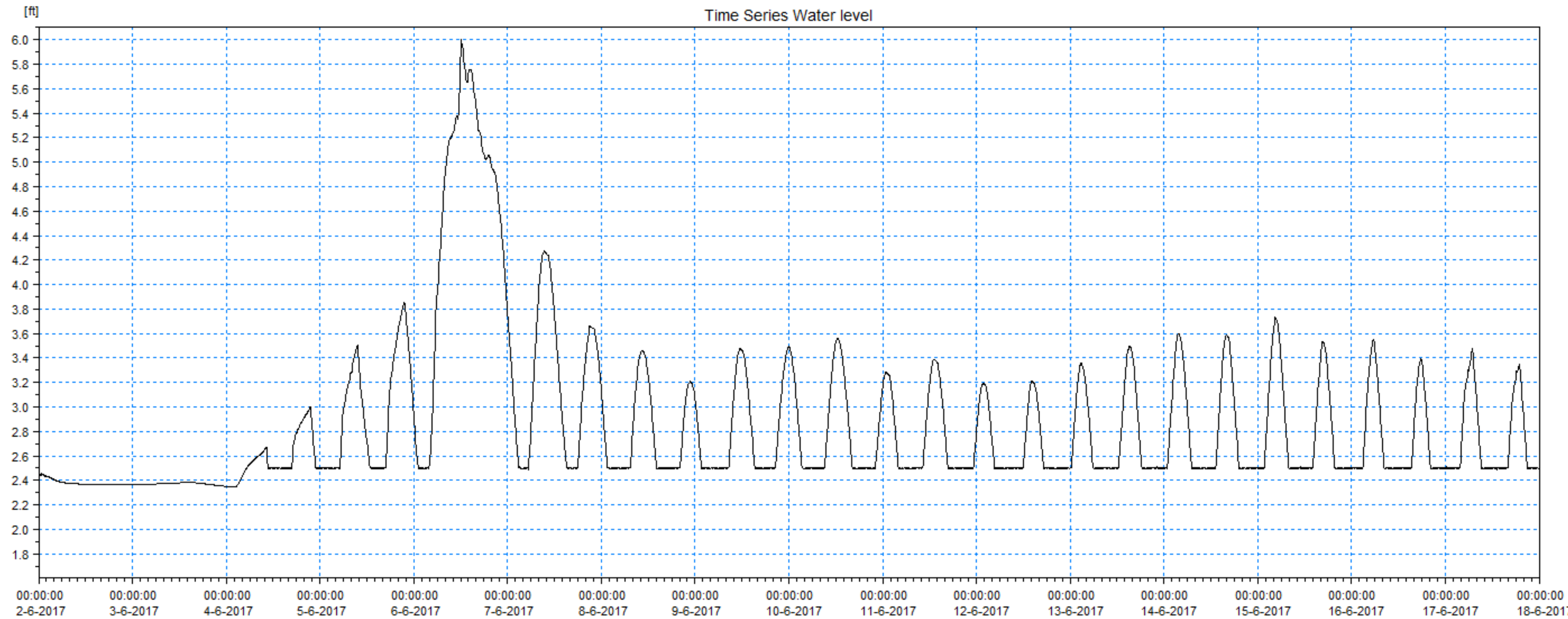

Figure D- 18: S-29 100-Year Design Storm Headwater Stage

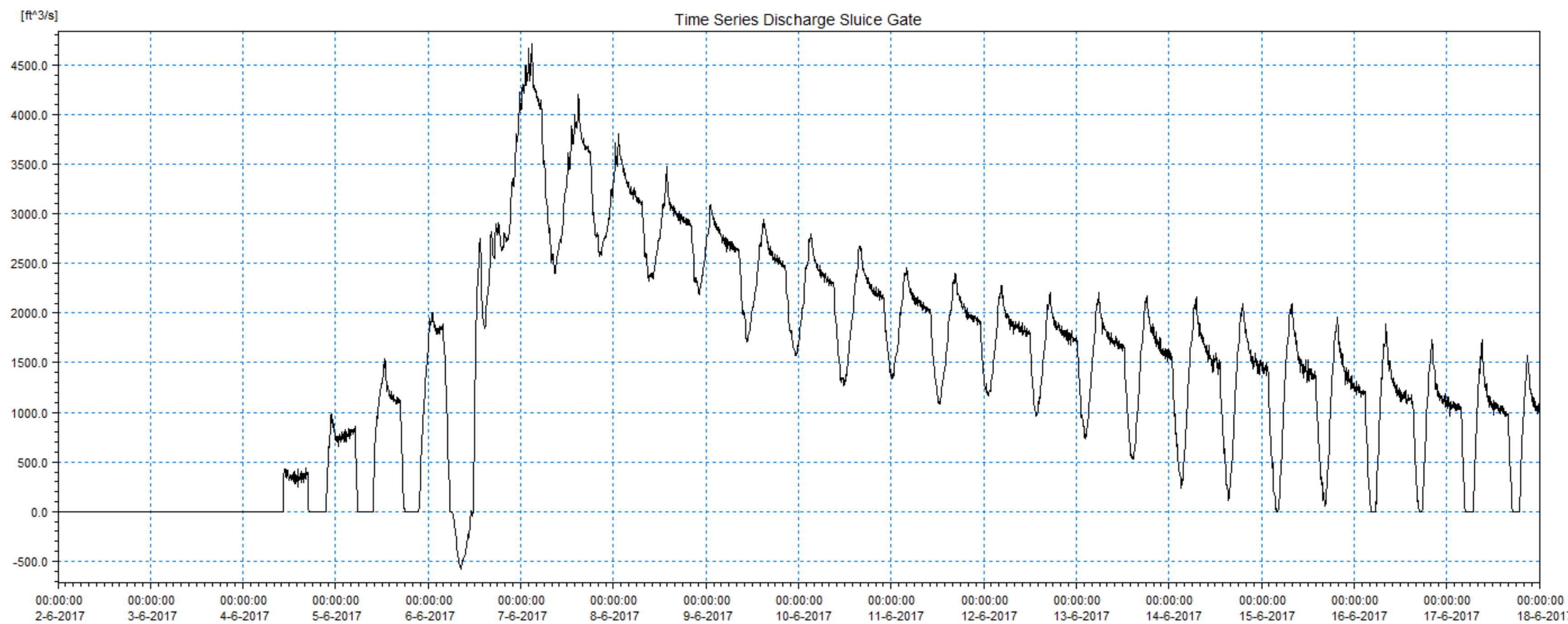

Figure D- 19: S-29 100-Year Design Storm Discharge (cfs)

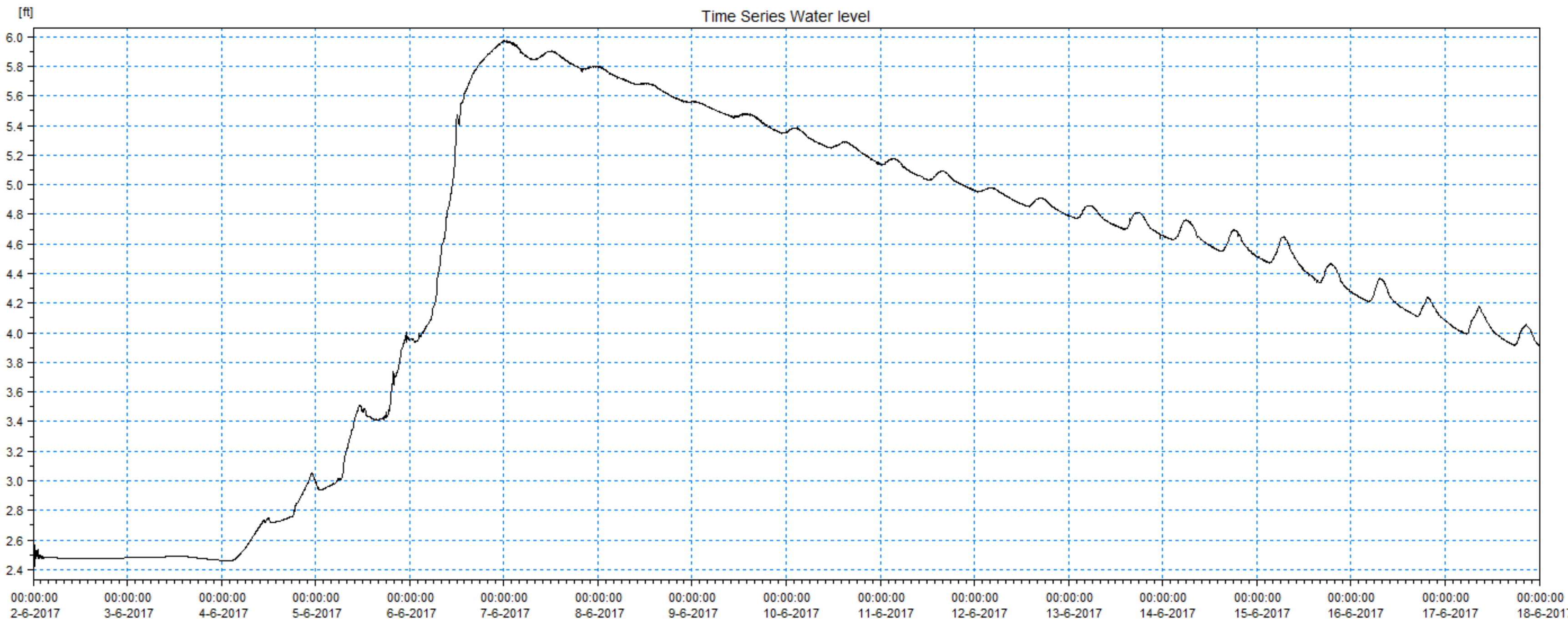

Figure D- 20: S-30 100-Year Design Storm Tailwater Stage

DRAFT Technical Memorandum (revised)

To: SFWMD

From: Taylor Engineering

Date: 7/30/2020

Re: Model Development for SFWMD C8-C9 Future Conditions FPLOS Study

1 INTRODUCTION

This memorandum documents the development and initial parameterization of the South Florida Water Management District (SFWMD) C-8 & C-9 Future Conditions MIKE SHE and MIKE HYDRO models. The developed models will be used in the C8-C9 future conditions flood protection level-of-service (FPLOS) study. Several model inputs and parameters used in the future condition model were obtained from the final version of the current conditions model. This memorandum will focus on the development and parameterization changes to the model to be used in future conditions simulations. For details on model development and setup of the existing conditions model, please refer to the report *Flood Protection Level of Service Provided by Existing Infrastructure for Current Sea Level Conditions in the C8 and C9 Watersheds* (Taylor Engineering, 6/17/2020).

2 RAINFALL

The design storms used in the future conditions model used the same NOAA Atlas 14 rainfall depths as used in the current conditions model. The design storms were temporally distributed based on the SFWMD 3-day distribution and spatially distributed based on Thiessen Polygons of the NOAA stations. The sensitivity run, to be completed only for the 10-year design storm, will have a 9% increase in rainfall. This increase comes from the Broward County DDF Change Factor Ensemble Analysis (Yin, Li, & Urich, 2019).

3 LAND USE

The future conditions land use map was developed by modifying the current conditions land use map to reflect projected future changes. Areas of future change were identified by comparing undeveloped, agricultural, and low development areas (such as low density residential) to future conditions land use maps from the Broward County Planning Council (2020) and Miami-Dade County (n.d.). The future conditions land use maps from these sources were generalized, whereas the current conditions land use map was very detailed. Therefore, by starting with the current conditions land use map and applying changes identified from the future land use map, there was no significant loss in spatial detail. The future land use changes were most often applied to areas classified as open land, recreational, cropland and pastureland, forests, and disturbed land. Areas classified as wetlands in current conditions were not changed due to their protected status.

Within the Broward County portion of the model, about 805 acres were changed to represent future land use conditions. Within the Miami-Dade County portion of the model, about 3180 acres were changed to represent future land use conditions. The areas with future land use changes are shown in **Figure 3-1**. The C-9 Impoundment area is represented as reservoir land use for future conditions.

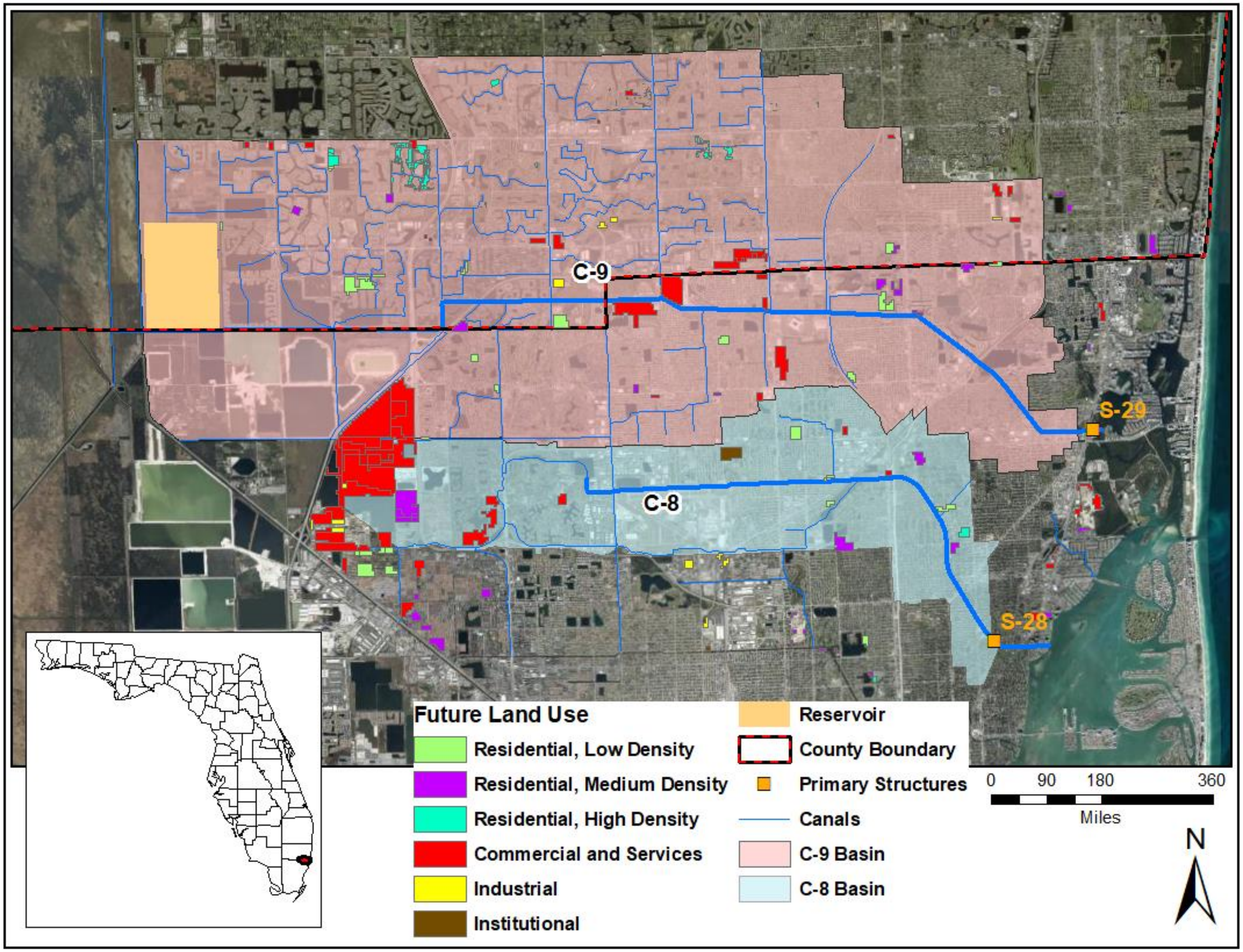

Figure 3-1: Areas of Future Land Use Changes

4 TOPOGRAPHY

The land surface elevation of the areas with future land use change were compared with the FEMA Base Flood Elevation (BFE) and increased where the current elevation is less than the BFE. For the larger areas with land use change that do not have storage explicitly modeled in the MIKE HYDRO model, a portion of the area will be lowered to account for floodplain compensation. Many of the areas with land use change were only a small cluster of grid cells, in which case it was not feasible or necessary to lower any of the grid cells once raised to BFE. These areas were relatively small and widely spread throughout the model domain, so they should have negligible hydrologic impact. Also, detention storage in these areas was accounted for in the overland flow module as discussed in **Section 5.2**. For the area of the C-9 impoundment (discussed in **Section 6.1.2**), the topography was adjusted so that the levees were accounted for (19.5 ft NGVD29) and the elevation inside the impoundment was set to the average impoundment ground elevation (4.5 ft NGVD29), per the Army Corps Project Implementation Report (USACE, 2012).

5 OVERLAND FLOW

In the current conditions model, most of the parameters in the overland flow module within Broward County were spatially varied by land use, while other parameters were spatially varied by land use within ERP permitted areas. Within Miami-Dade County, most of the parameters were spatially varied by land use, while other parameters were spatially varied by land use within areas that are internally drained. For the areas of land use that were changed to represent future conditions, the associated parameterization changes to the overland flow layers were applied the same way as in the current conditions. Refer to Section 3.7 in the C8 C9 FPLOS by Existing Infrastructure for CSL Conditions Draft Report (Taylor Engineering, 6/17/2020) for the specific details regarding parameterization of the overland flow module. For the purposes of this study, the following assumptions are applied:

- Each of the areas identified as having land use change is an "ERP permitted area" and must comply with the stormwater quality ordinance of retaining the greater of the first 1 inch of rainfall or 2.5 inches over the impervious area
- Within Broward County, the areas of land use change that are not considered Stormwater management category (SMC) 1 are considered SMC 3b (most conservative approach)
- Within Miami-Dade County, the areas of land use change have the same SMC classification as current conditions, such as internally drained or drains to branch
    - o Undeveloped internally drained areas that are now developed areas still drain internally unless explicitly modeled (such as the new Mega Mall)

A brief summary of the parameterization changes applied to the overland flow layers is provided in the following subsections.

5.1 Manning's Number

The Manning's roughness coefficient for the overland module was developed for the areas of land use change the same way as the current conditions model and was based on land use. Refer to Table 3-7 in the C8 C9 FPLOS by Existing Infrastructure for CSL Conditions Draft Report (Taylor Engineering, 6/17/2020) for the Manning's roughness coefficients based on land use by FLUCCS codes.

5.2 Detention Storage

The areas identified for land use change were assigned detention storage based on the new land use type. For the areas of land use change that were in areas directly controlled by operable structures represented in the model, no additional change to detention storage was made. For the areas of land use change that were not in areas directly controlled by operable structures, the detention storage was increased based on the assumption that all areas of future development will require an ERP. Therefore, detention storage in these areas of land use was increased the same way as in ERP areas (and internally drained areas within Miami-Dade County) in the current conditions model. This involved multiplying the paved area runoff coefficient (represents DCIA) by 2.5 inches and any of the resulting values which were less than 1” were increased to 1”.

5.3 Paved Area Runoff Coefficient

The areas identified for land use change were assigned a paved area runoff coefficient based on the new land use type. For the areas of land use change that were in areas directly controlled by operable structures, no additional change to the paved area runoff coefficient was made. For the areas of land use change that were not in areas directly controlled by operable structures, the paved area runoff coefficient was decreased based on the assumption that all areas of future development will require an ERP. Therefore, paved area runoff coefficients in these areas of land use were decreased the same way as in ERP areas (and internally drained areas within Miami-Dade County) in the current conditions study, which was to reduce the values by half. Refer to Table 3-7 in the C8 C9 FPLOS by Existing Infrastructure for CSL Conditions Draft Report (Taylor Engineering, 6/17/2020) for the runoff coefficients based on land use by FLUCCS codes.

6 RIVERS AND LAKES (1D MODEL)

6.1 1D Model Configuration Updates

In the future conditions model, two major changes to the 1D network were made, which are (1) explicitly representing the discharge from the two largest areas of land use change and (2) including the C-9 Impoundment. Although these two major changes are explicitly represented in the model, the specific details regarding the implementation are conceptual. These updates are discussed in the following two subsections.

6.1.1 Areas of Land Use Change

Based on the identified areas of land use change, it was decided that only the two largest areas would be explicitly modeled in the 1D network. **Figure 6-1** shows the location of the two largest land use change areas.

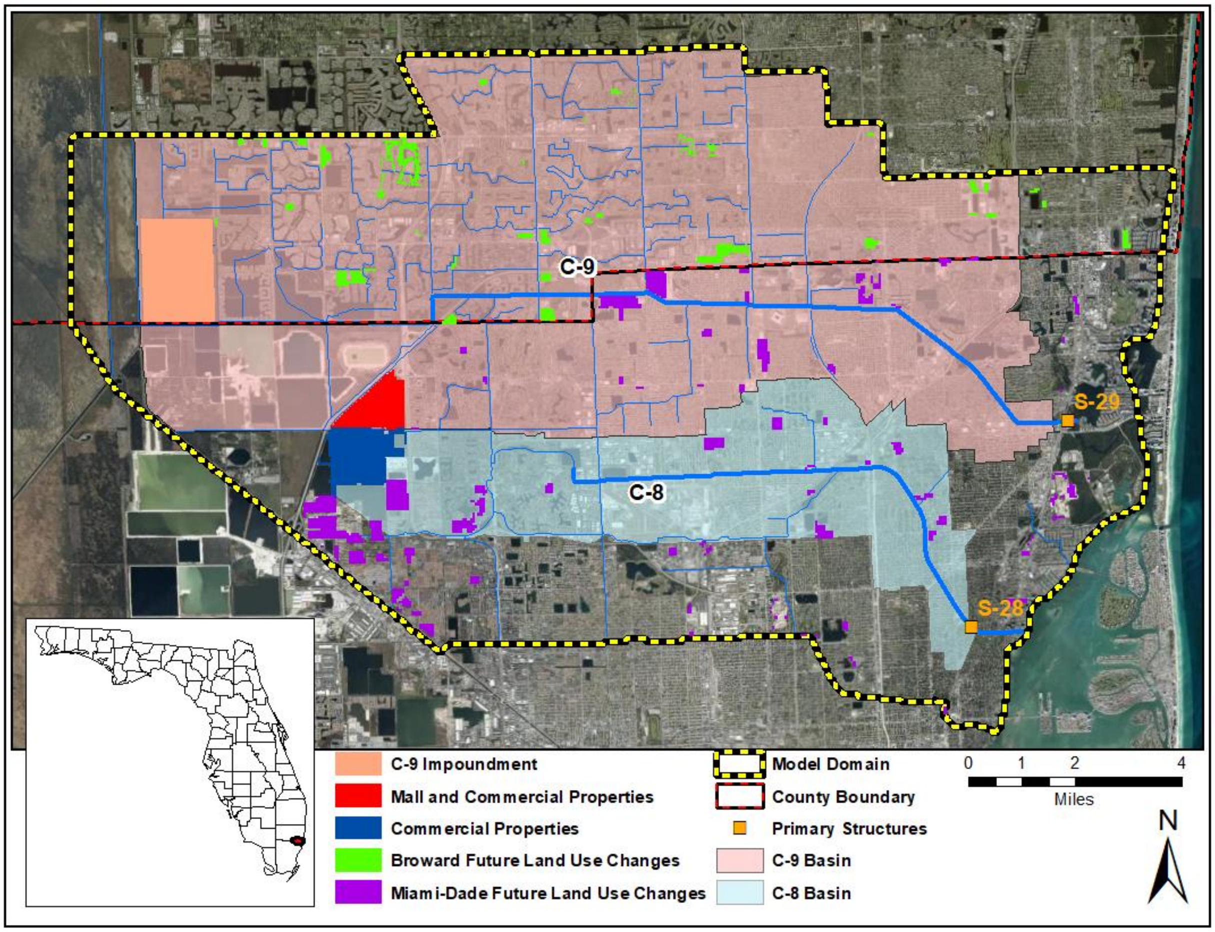

Figure 6-1: Areas of Land Use Change with Explicit MIKE HYDRO Changes

The first location (shown in red) is where the American Dream Miami Mall ("Mega Mall") and other commercial properties will be located. The second location (shown in blue) will be developed into other commercial properties. For these two locations, a conceptual MIKE HYDRO branch has been added to represent storage and to control discharge. To control the discharge, a pump that is limited to the District's CSM allowance is proposed. Although peak discharge from a developed property should not be greater than predeveloped conditions, these two areas are internally drained under current conditions. To be conservative, Taylor Engineering recommends representing these two areas as being controlled by a pump that limits the total discharge to the District's allowance, with the assumption that in future conditions these properties will have a positive outfall and ultimately drain to the C-9 Canal (area in red) and C-8 Canal (area in blue). Areas draining to the C-9 Canal have an allowance of 20 CSM pumped. There is currently no set allowance for areas draining to the C-8 Canal. For the purposes of this study, Taylor proposes to use the same discharge allowance for the area draining to the C-8 Canal as the area draining to the C-9 Canal. The proposed pumps will have an "on" elevation equal to 1 ft above the control elevation, which is proposed to be set at 0.5 feet below the existing property grade (40E-41.063 Conditions for Issuance of Permits in the Western Canal 9 Basin). Additionally, the pumps would be required to follow the same operating criteria as the pump stations in South Broward Drainage District, which requires the pumps to turn off when water levels in the C-9 Canal reach an elevation of 3.5 ft NGVD29 (Burns & McDonnell, 2006). The conceptual branch and lake will have an area equal to 20% of the land area being developed or have conceptual cross sections that represent storage between control and "pump on" elevation equal to the greater of 1" of rainfall over the entire area or 2.5" x the impervious area (based on runoff coefficient) of the land area being developed. For example, 400 acres of development requires storing the greater of 1"x 400 acres= 33.3 ac-ft or 2.5"x 0.72(runoff coefficient) x 400 acres= 60 ac-ft. Flood elevations will be compared to future topography, and volumes will be adjusted if necessary to reflect a realistic elevation in the lake.

6.1.2 C-9 Impoundment

The C-9 Impoundment is a project being designed with the intentions of capturing excess storm water. This will reduce the amount of water pumped to the water conservation areas and lost to tide and sometimes reduce water levels in the C-9 Canal. This project has the ability to reduce peak flood stages during major storms by pumping water from the C-9 Canal into an above-ground storage reservoir. The C-11 Impoundment is intended to operate the same way in the C-11 basin. These two projects are being designed to operate together in the future. The C-11 Impoundment project will have the ability to transfer water into the C-9 Impoundment, both for water management and for storm water control. However, the C-9 Impoundment project will only be able to "capture available storm runoff in the C-9 West Basin ***or*** to lift discharges from the C-11 West Basin (released from the C-11 Impoundment) to the C-9 Impoundment" (Burns & McDonnell, 2006). Therefore, it seems that during a major storm event, the two impoundments would operate independently, as the C-9 Impoundment will be pumping stormwater runoff from the C-9 basin. However, it is possible that the C-11 Impoundment could need to divert water to the C-9 Impoundment during a major storm. Instead of speculating on how to explicitly represent the interaction between the two projects, Taylor Engineering recommends not explicitly representing inter-impoundment transfer in the future conditions model and to represent it by limiting how long the C-9 Impoundment accepts water from the C-9 Basin.

The C-11 Impoundment project is planned to have a storage capacity of 4,592 ac-ft and a pumping rate of 1,050 cfs and the C-9 impoundment project is planned to have a storage capacity of 7,056 ac-ft and a pumping rate of 1,000 cfs (USACE, 2012). Therefore, if starting empty, the C-11 Impoundment could receive water at the maximum allowed rate for 53 hours and the C-9 Impoundment could receive water at the maximum allowed rate for about 85 hours. To simulate a reasonable worst case scenario, Taylor Engineering recommends assuming that both impoundments start at 50% capacity and that once full, the C-11 Impoundment diverts water to the C-9 Impoundment, at which point the C-9 Impoundment could no longer pump water from the C-9 basin. To eliminate the need to explicitly model the transfer of water from the C-11 Impoundment, Taylor Engineering proposes the following approach:

- Start the C-9 Impoundment at 50% capacity and assume the C-11 Impoundment is at 50% capacity (this means the C-11 could receive water for 26.5 hours before it is full)
- Allow the C-9 Impoundment to start receiving water from C-9 Canal when the water level in the western portion of the C-9 Canal reaches 3.5 ft NGVD29 (Burns & McDonnell, 2006)
- Stop the C-9 Impoundment from receiving water from C-9 Canal after 26.5 hours of pumping (assumes the C-9 and C-11 Impoundments would be pumping at the same time) (C-11 Impoundment full after 26.5 hours when starting at 50% capacity)

- The remaining volume is conceptual storage available for the water transfer from the C-11 Impoundment

This is a very simple and efficient way to represent the C-9 Impoundment in a worst case scenario, where it exists in future conditions but cannot be fully utilized. The explicit representation of water seepage from the C-9 Impoundment is not required as it can be assumed that any seepage that results from higher stages in the impoundment is captured and returned. Within MIKE HYDRO and MIKE SHE, the C-9 Impoundment components will be represented with low leakage coefficients. By setting the canal and overland leakage coefficients to low values, the seepage collection and return system can be left out as it is being conceptually represented by reducing or eliminating any seepage from occurring within the C-9 Impoundment area. As “The Savings Clause requires assurance that no negative impact will occur to existing levels of flood protection and is demonstrated in project design” (USACE, 2012), it can be assumed that the design of the Impoundment will have little to no negative impact, and reducing or eliminating the leakage is the simplest way to represent this complex system.

6.2 Boundary Conditions (1D Model)

The 1-D tidal boundaries (forced tailwater at tidal structures) used the SFWMD-provided design storm surge stage hydrographs. These are the same hydrographs from the current condition design storms, but increased by 1, 2, and 3 ft to represent various sea level rise scenarios. The design storm tidal boundaries for the future seal level rise scenarios are shown in **Figure 6-2** through **Figure 6-9**.

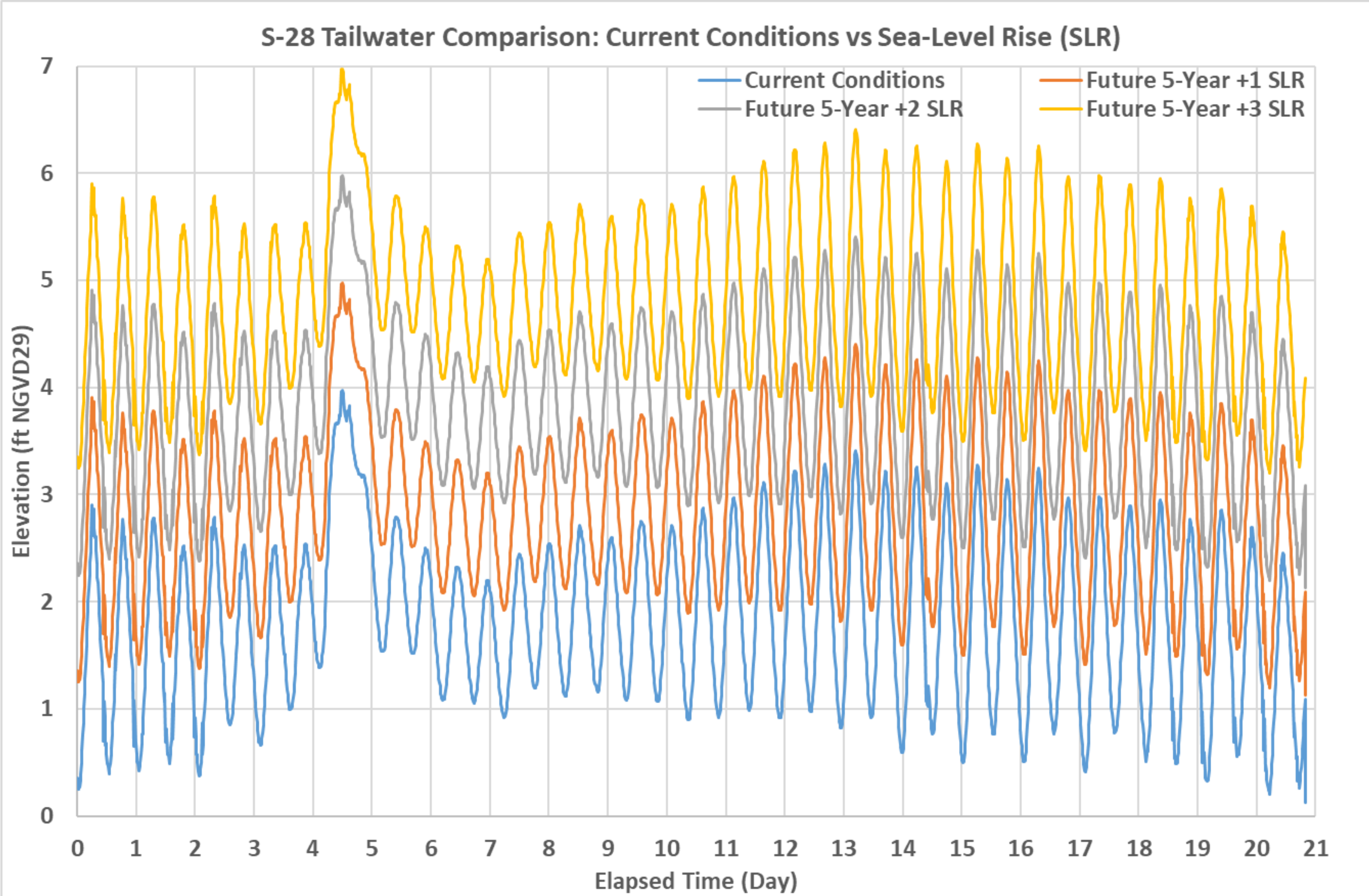

Figure 6-2: Future Conditions Sea Level Rise 5-Year Design Storm Tidal Boundary Stages for S-28

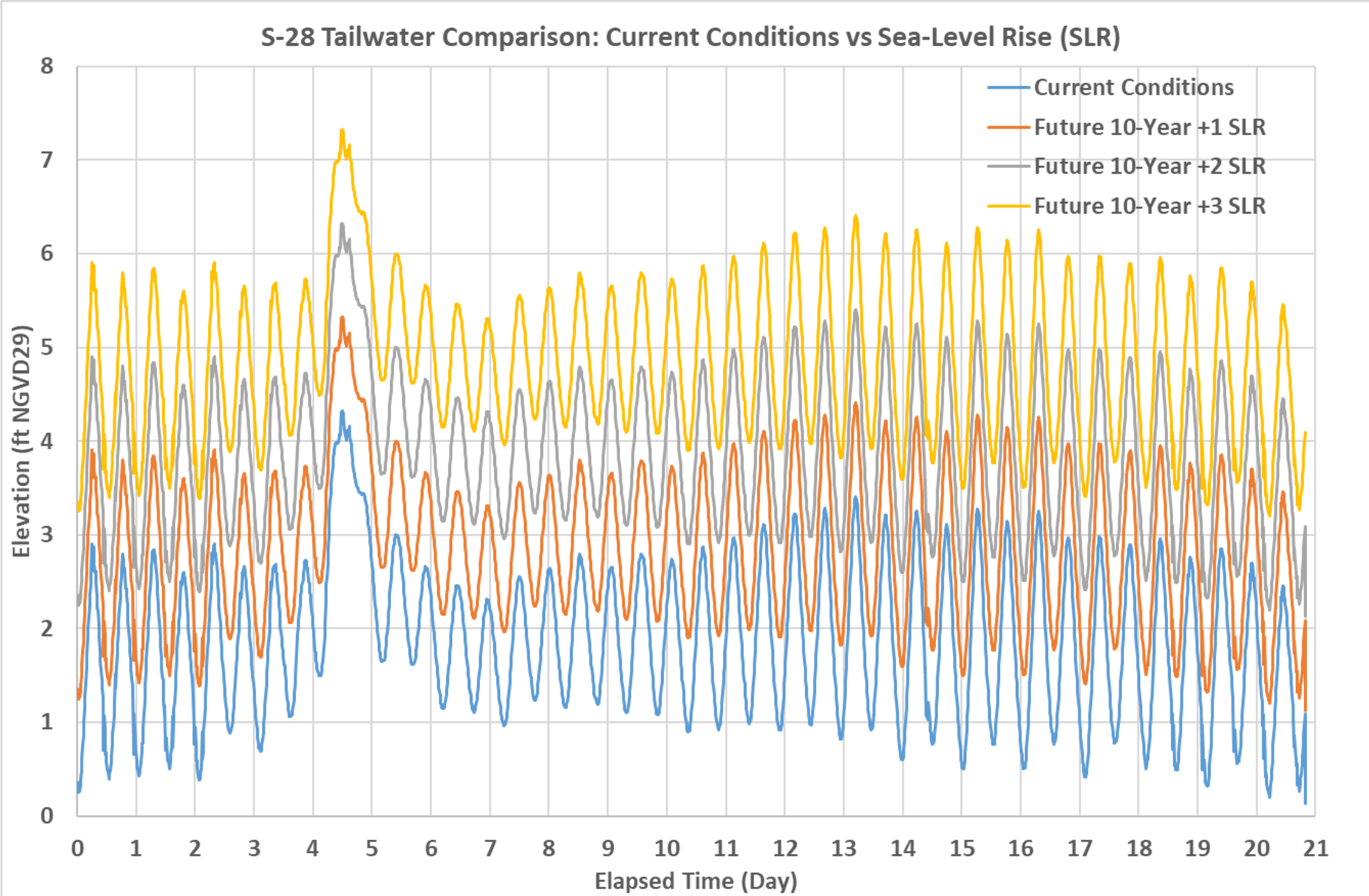

Figure 6-3: Future Conditions Sea Level Rise 10-Year Design Storm Tidal Boundary Stages for S-28

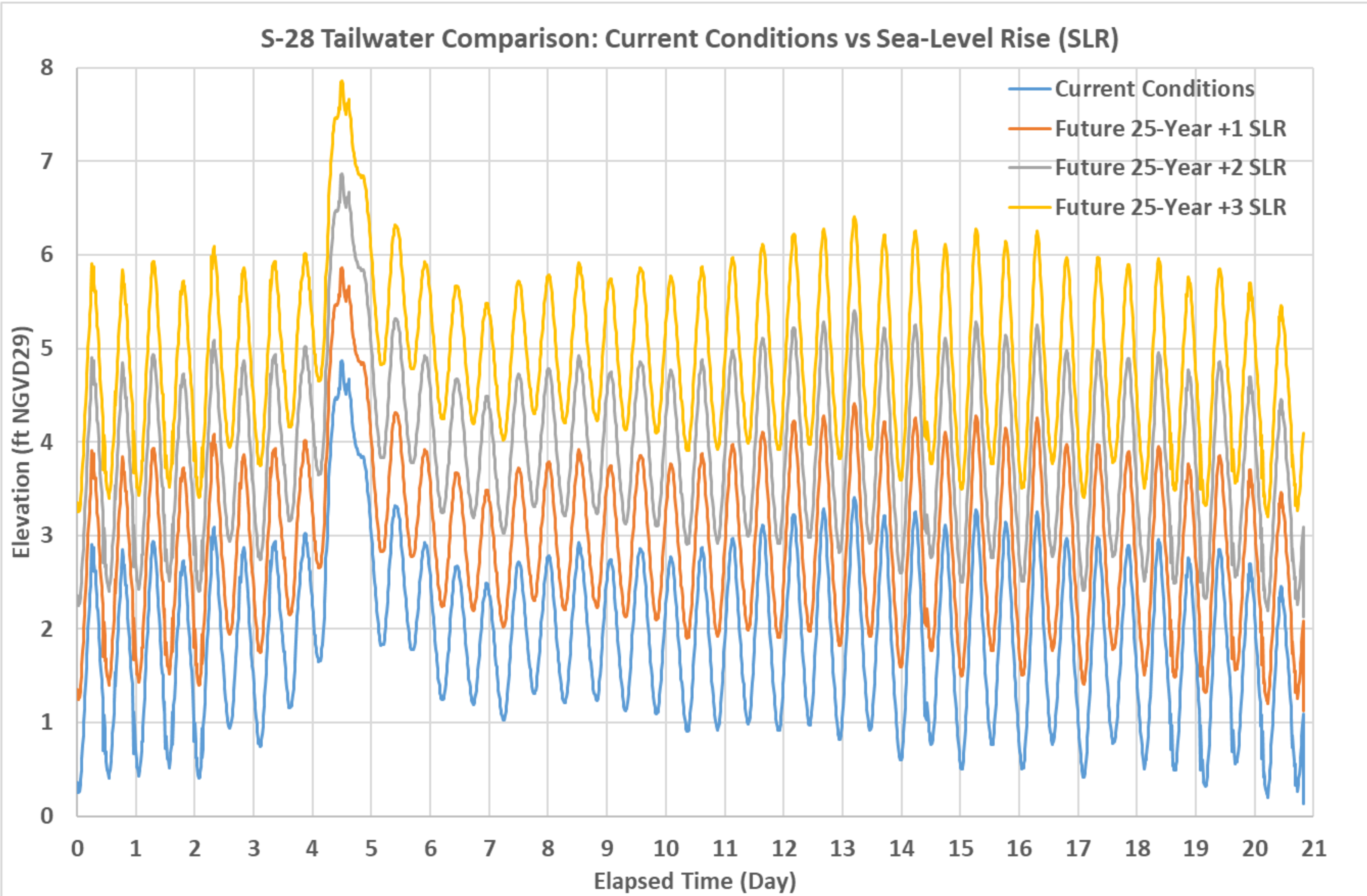

Figure 6-4: Future Conditions Sea Level Rise 25-Year Design Storm Tidal Boundary Stages for S-28

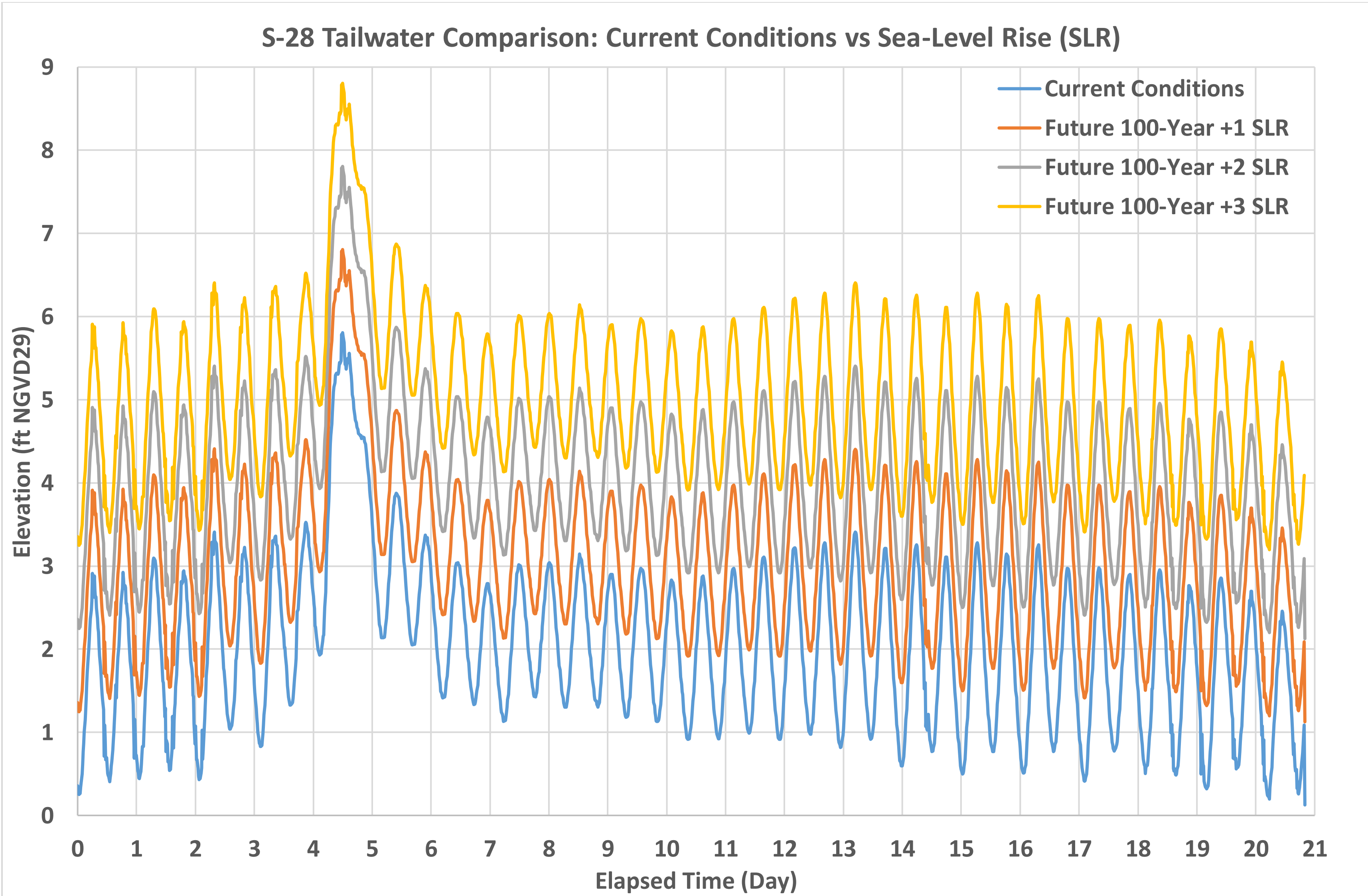

Figure 6-5: Future Conditions Sea Level Rise 100-Year Design Storm Tidal Boundary Stages for S-28

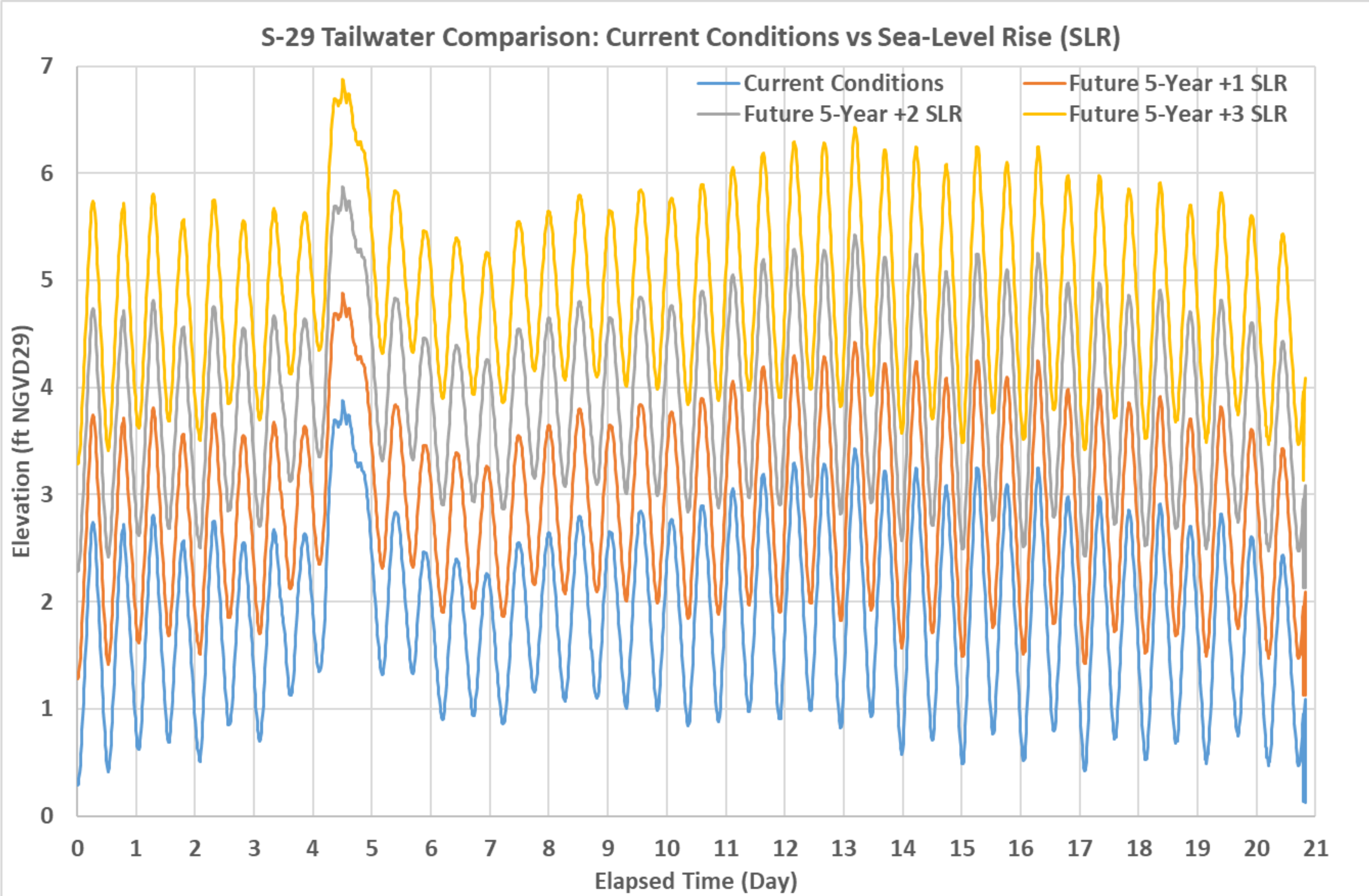

Figure 6-6: Future Conditions Sea Level Rise 5-Year Design Storm Tidal Boundary Stages for S-29

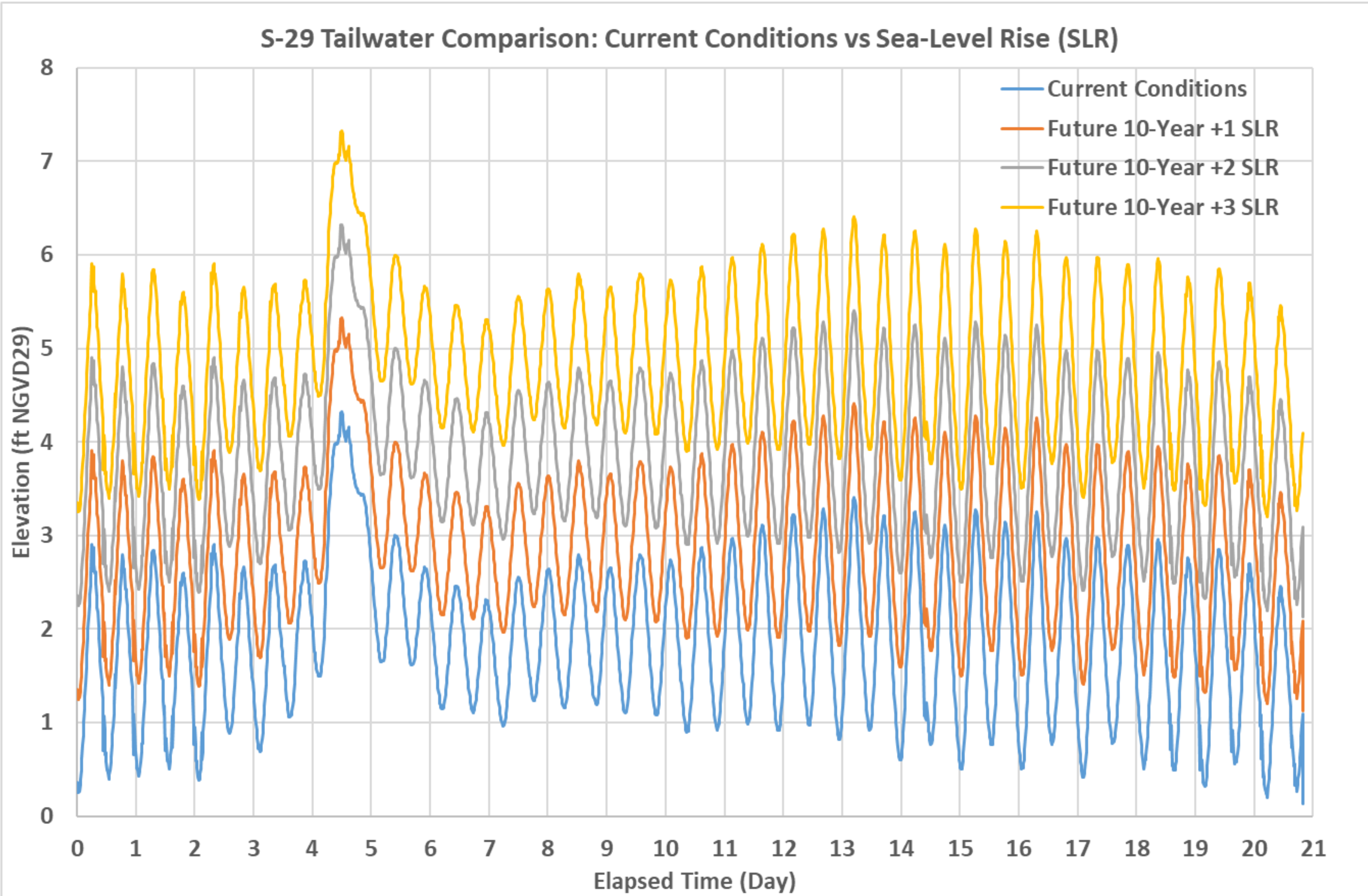

Figure 6-7: Future Conditions Sea Level Rise 10-Year Design Storm Tidal Boundary Stages for S-29

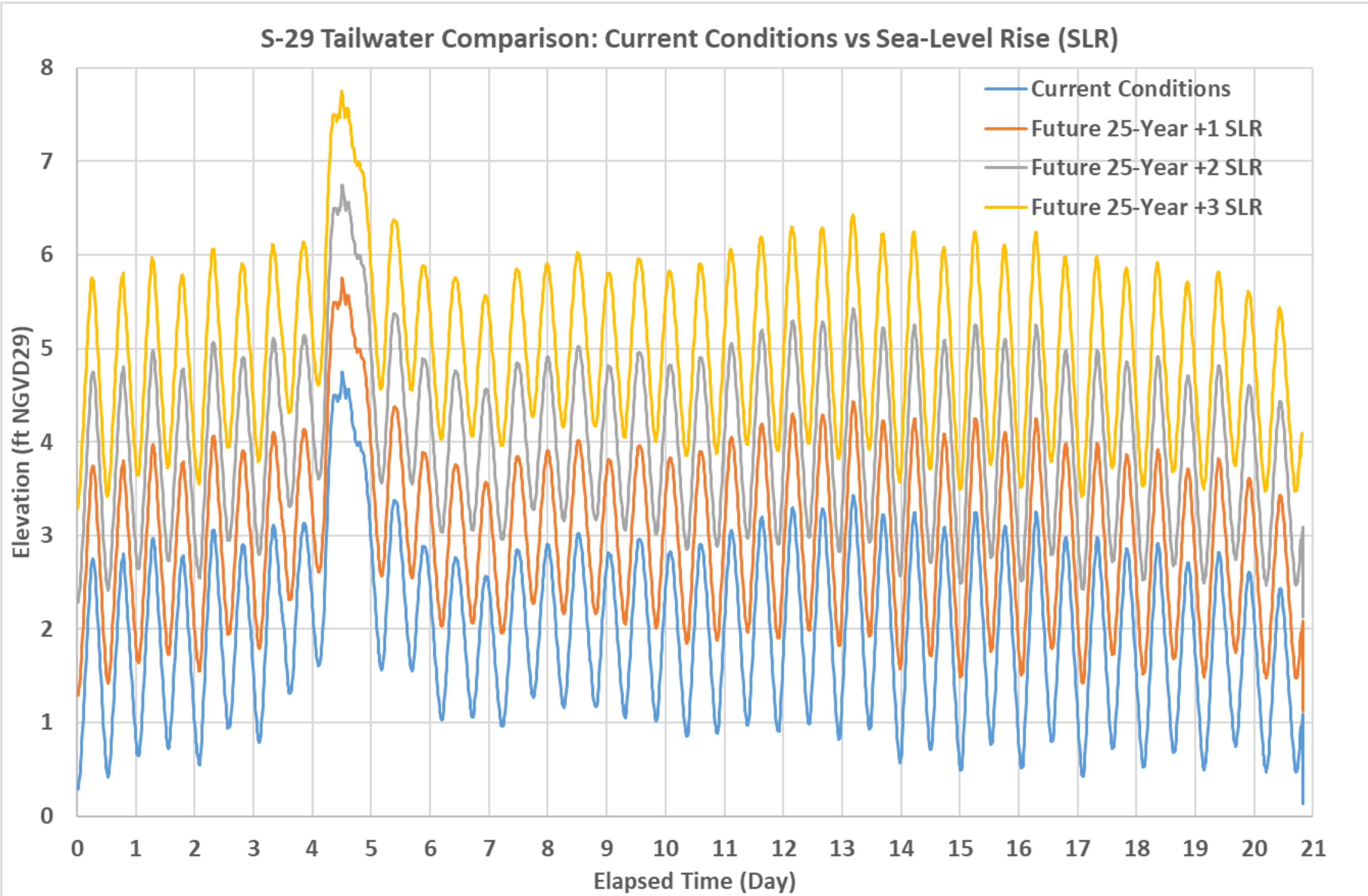

Figure 6-8: Future Conditions Sea Level Rise 25-Year Design Storm Tidal Boundary Stages for S-29

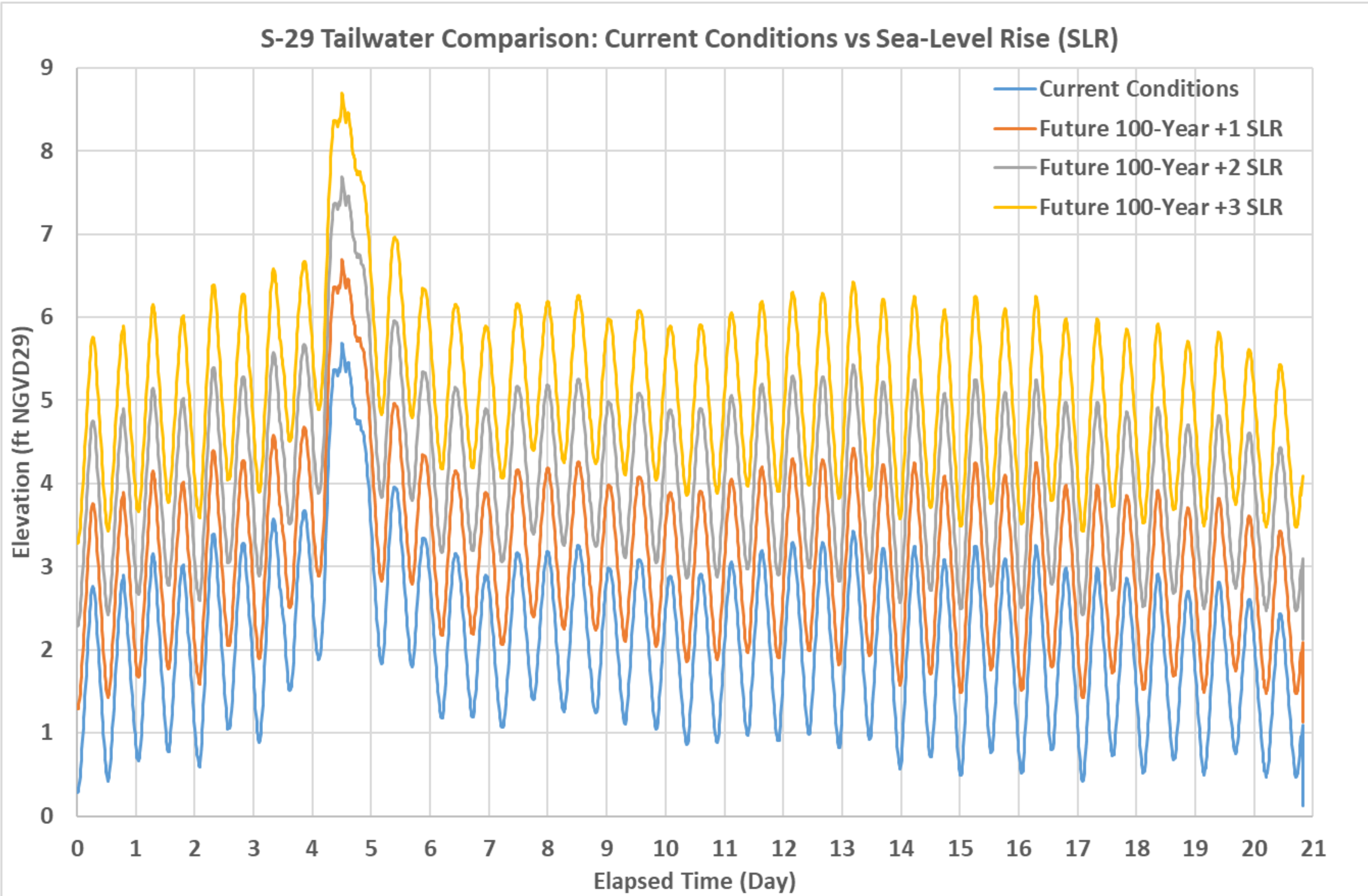

Figure 6-9: Future Conditions Sea Level Rise 100-Year Design Storm Tidal Boundary Stages for S-29

At the intercoastal waterway, water levels were forced based on the District-provided design storm surge stage time series data (**Figure 6-2** through **Figure 6-9**). On the southeast side of the model, the forced water levels (based on S-27 headwater) at the downstream boundary of the 1-D branches connecting to the C-7 Canals were updated to represent future conditions. Taylor Engineering proposed two methods for updating S-27 headwater to reflect the future conditions; (1) adding 1, 2, and 3 feet to the current conditions headwater (District's XPSWMM model simulated data) level to reflect the three sea level rise conditions while ensuring pre/post storm headwater is never lower than the low tide tailwater, and (2) increasing the headwater level by a factor determined through regression analysis of simulated future condition headwater levels based on the District's XPSMM model.

6.2.1 S-27 Headwater- Method 1

This method of developing future conditions headwater levels for the S-27 structure simply adds 1, 2, and 3 feet to the current condition's hydrograph, which was provided by the District (assumptions had to be made about pre/post storm water levels). As previously stated, this approach assumes that the S-27 structure maintains the same headwater/tailwater relationship that was observed in the District's XPSWMM current condition models. Adding 1, 2, and 3 feet to the current condition's headwater is the same as applying the current conditions headwater/tailwater ratio to the future conditions storm surge tailwater that includes 1, 2, and 3 feet of sea level rise. Slight adjustment to the pre/post storm water levels were made so that they do not drop below the minimum low tide tailwater elevation. This was done as it is unrealistic for a tidal spillway structure's headwater elevation to drop below the low tide tailwater elevation unless mitigation measures (i.e., a pump station) were to be implemented. An example of the proposed boundary condition hydrographs resulting from this method are shown in **Figure 6-10**.

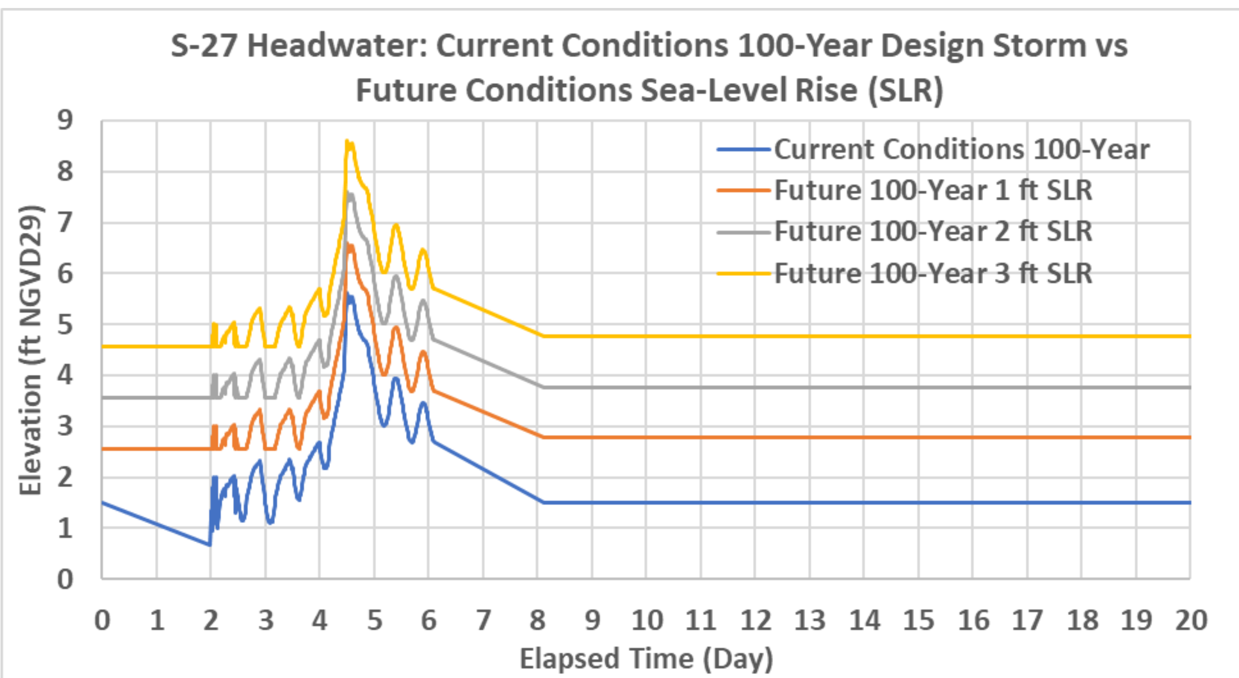

Figure 6-10: Example of S-27 Future Condition Headwater Stage Developed by Adding 1, 2, and 3 Feet to Current Conditions Stages

6.2.2 S-27 Headwater- Method 2

This method of developing future conditions headwater levels for the S-27 structure is based on a regression analysis of future conditions simulated data from the District's XPSWMM model. The District provided simulated future condition headwater levels for S-27 that for sea level rise scenarios of 0, 0.76, 1.09, and 2.21 feet, as shown in **Table 6-1**.

Table 6-1: SFWMD Future Conditions S-27 Peak Stage Under Various Sea Level Rise Conditions

Sea Level Rise in District's Future Conditions XPSWMM Model (ft)	Simulated Future Conditions Peak Water Level (ft NGVD29)
0 (base value)	5.941 (base value)
0.76	6.43
1.09	6.68
2.21	7.36

For this study, the sea level rise conditions are 1, 2, and 3 feet. Therefore, a regression analysis was conducted. The District's simulated future peak water levels were plotted against the amount of sea level rise and assigned the best-fitting trendline based on R^2 value, as shown in **Figure 6-11**.

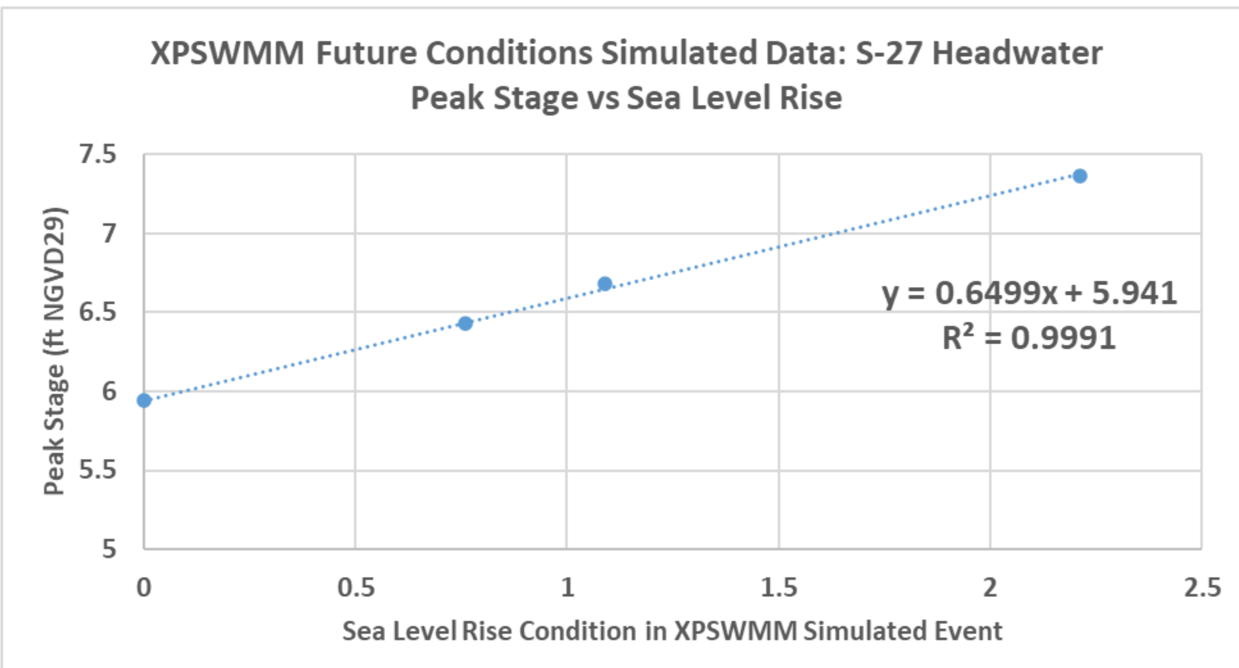

Figure 6-11: Regression Analysis of S-27 Future Conditions Headwater Stage vs Sea Level Rise

From the equation of the trendline, interpolated and extrapolated peak water levels for 1, 2, and 3 feet sea level rise were calculated. Then, a multiplication factor was calculated for each of the sea level rise conditions based on the simulated peak water level (peak water level with SLR divided by base peak water level), as shown in **Table 6-2**.

Table 6-2: Interpolated/Extrapolated Peak Water Levels from XPSWMM Future Conditions 100-Year Design Storm

Sea Level Rise Conditions (ft)	Interpolated/Extrapolated Peak Water Level based on XPSWMM Simulated Data (ft NGVD29)	Multiplication Factor
0 (base value)	5.94 (base value)	1.000
1	6.59	1.109
2	7.24	1.219
3	7.89	1.328

The multiplication factors shown in **Table 6-2** were multiplied with the current conditions headwater hydrograph for S-27. The peak water levels for S-27 headwater for future conditions sea level rise scenarios of 1, 2, and 3 feet are shown in **Table 6-3**. The S-27 headwater hydrographs for future condition sea level rise scenarios are shown in **Figure 6-12**.

Table 6-3: Peak Water Levels for S-27 Headwater for Future Conditions 100-Year Design Storms

Sea Level Rise Conditions (ft)	Current Conditions Peak Water Level	Multiplication Factor	Future Conditions Peak Water Level (ft NGVD29)
1	5.61	1.109	6.22
2		1.219	6.84
3		1.328	7.45

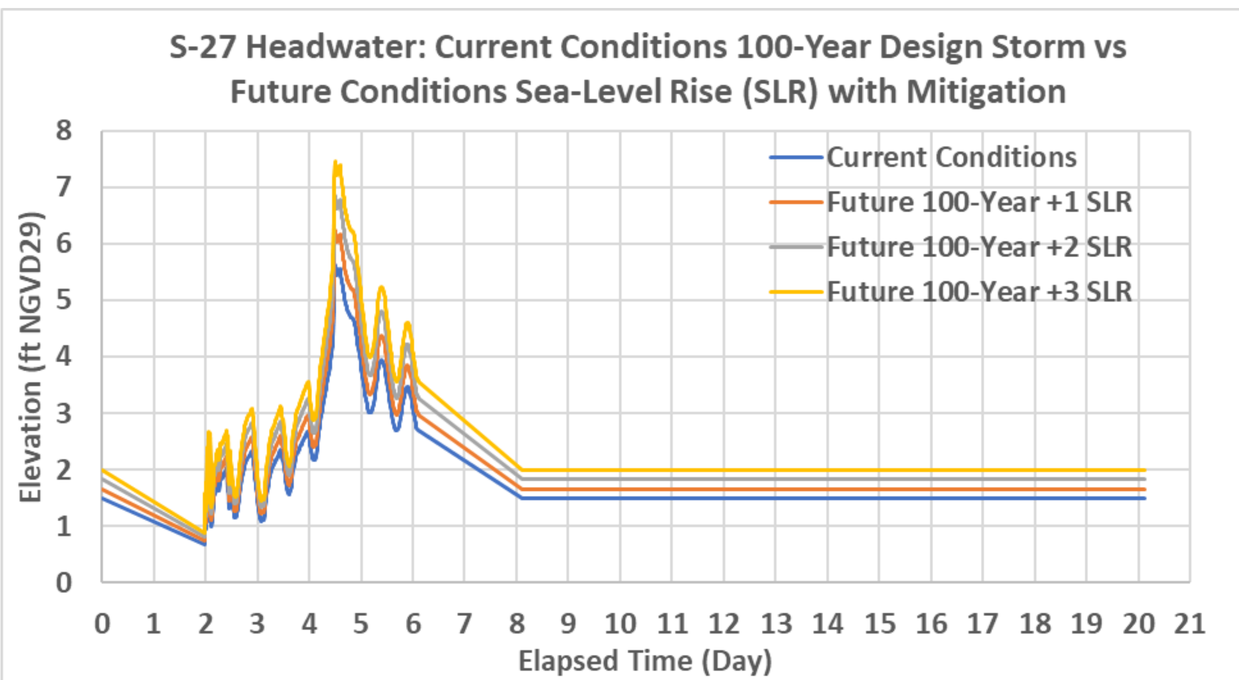

Figure 6-12: S-27 Future Conditions Headwater for 100-Year Design Storm Based on Regression Analysis of Future Conditions Simulated Data with Mitigation Measures

6.2.3 S-27 Headwater- Method Comparison and Sensitivity

The two methods of developing the S-27 headwater boundary represent different levels of conservativeness, with the higher boundary representing the most conservative scenario in terms of worst case flooding in the model. When this model was developed, the C-7 Canal was chosen as a boundary condition for two reasons: (1) There was observed data that was useful for calibrating/validating the model, and perhaps more importantly, (2) It was believed to be at a distance from the area of interest (C-8 basin/canal) such that any uncertainty in the boundary condition should have minimal effect on the outcome of the simulations. As there are two different levels of conservativeness that could be made for the future conditions water levels in the C-7 Canal, a sensitivity test was performed for the S-27 headwater boundary.

The sensitivity test was conducted using the current conditions model, with modified tailwater levels at S-28 and S-29 (to represent sea level rise) and the new headwater levels at S-27 headwater. The current conditions model was used so that the effects of the boundary condition could be determined without the effects of any other changes to the model such as land use and increased groundwater levels. Therefore, two model simulations were completed using the 100-year design storm with 3 ft of sea level rise. **Figure 6-13** shows the two S-27 headwater hydrographs and the respective tailwater hydrograph. The peak water level under the second method is about 1.2 ft lower than the more conservative approach of applying the current conditions headwater/tailwater ratio to the 3 ft storm surge tailwater hydrograph.

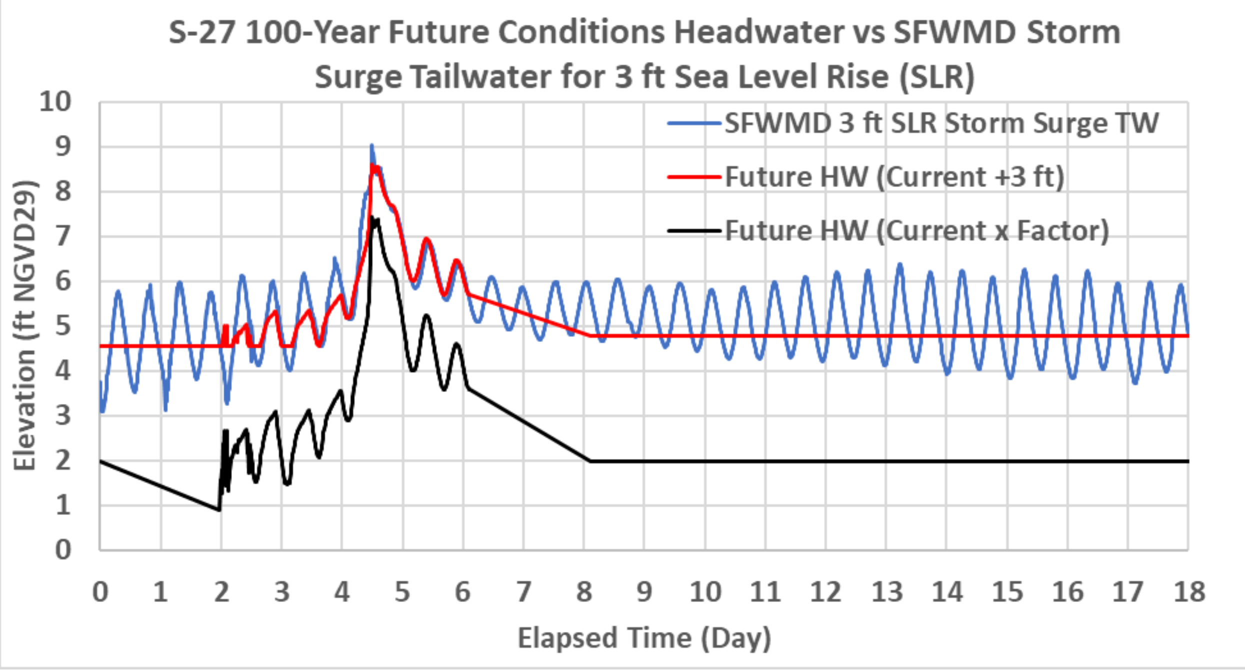

Figure 6-13: Comparison of the Developed 100-Year Design Storm S-27 Headwater Hydrographs and the SFWMD Storm Surge Design Storm Tailwater for 3 ft Sea Level Rise

Although the two approaches were significantly different, there was no significant difference indicated by the sensitivity test. The method of applying 3 ft to the current conditions hydrograph resulted in only 0.1 ft higher peak stages at S-28Z (upstream) and S-28 (downstream) of the C-8 Canal (**Figure 6-14** and **Figure 6-15**, respectively), when compared to the method of applying a multiplication factor. This small increase did not propagate into the C-9 Canal, which maintained the same levels. Additionally, there were no notable differences in duration of high-water levels in the C-8 Canal. The method of applying 3 ft to the current conditions hydrograph resulted in reduced inter-basin discharge from the C-8 to the C-7, when compared to the multiplication factor approach, although it was larger than under current conditions.

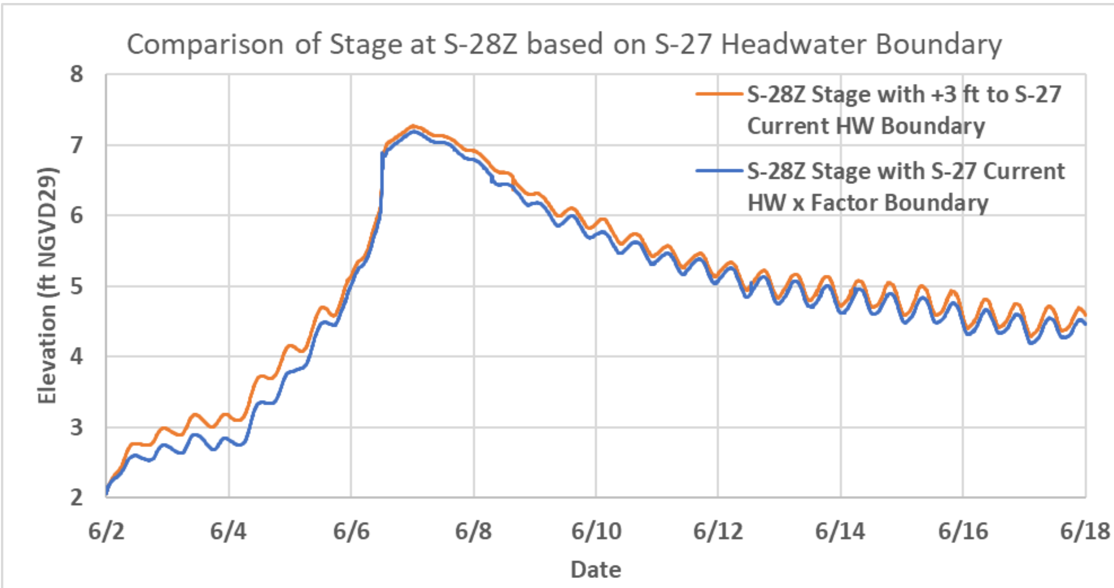

Figure 6-14: Headwater Stage Comparison at S-28 for Sensitivity Test

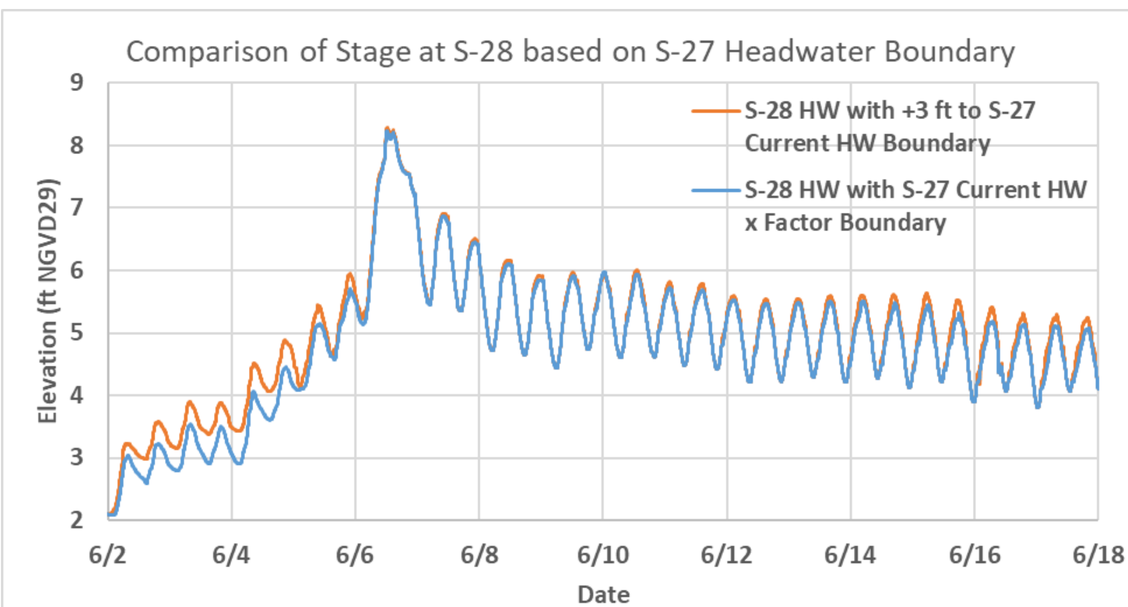

Figure 6-15: Stage Comparison at S-28Z for Sensitivity Test

The sensitivity test accomplished two things: (1) It demonstrated that either boundary could be used, as there was no significant difference in the C-8 model results and (2) It validated the assumption that the boundary was far enough from the area of interest that uncertainty in the boundary conditions had minimal effect on the outcome.

Both methods of developing future conditions headwater levels for S-27 are reasonable. Ultimately, the method selection should be based on the goal of the project. The purpose of the future conditions FPLOS study is to determine what could happen in the future in a worst-case scenario. Therefore, it is may be most appropriate to use the first method, which is just increasing the current conditions headwater by 1, 2, and 3 feet. The approach of just increasing the headwater based on the increase in tailwater is reasonable as the S-27 structure would likely be overtopped/bypassed for each sea level rise condition unless mitigative measures are implemented in the future.

As the model is not very sensitive to the S-27 headwater boundary, Taylor Engineering recommends using the method of applying 1, 2, and 3 ft to current conditions headwater, which aligns with the District's direction of using the most conservative approach.

6.2.4 S-27 Headwater Boundary

The recommended S-27 headwater boundary hydrographs for each of the design storms are shown in **Figure 6-16** through **Figure 6-19**.

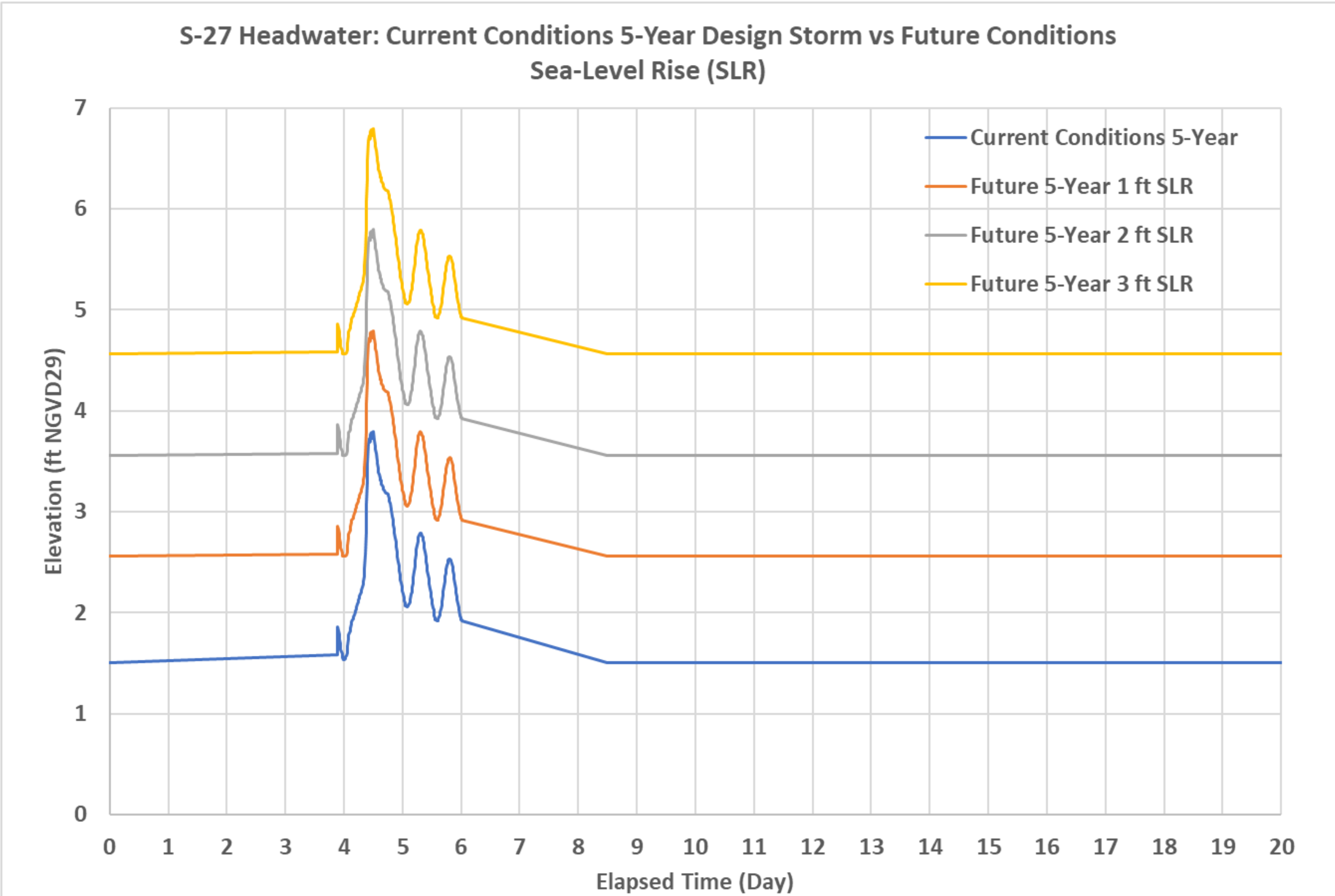

Figure 6-16: S-27 Future Condition Headwater Stages for 5-Year Design Storm under 3 Sea Level Rise Scenarios

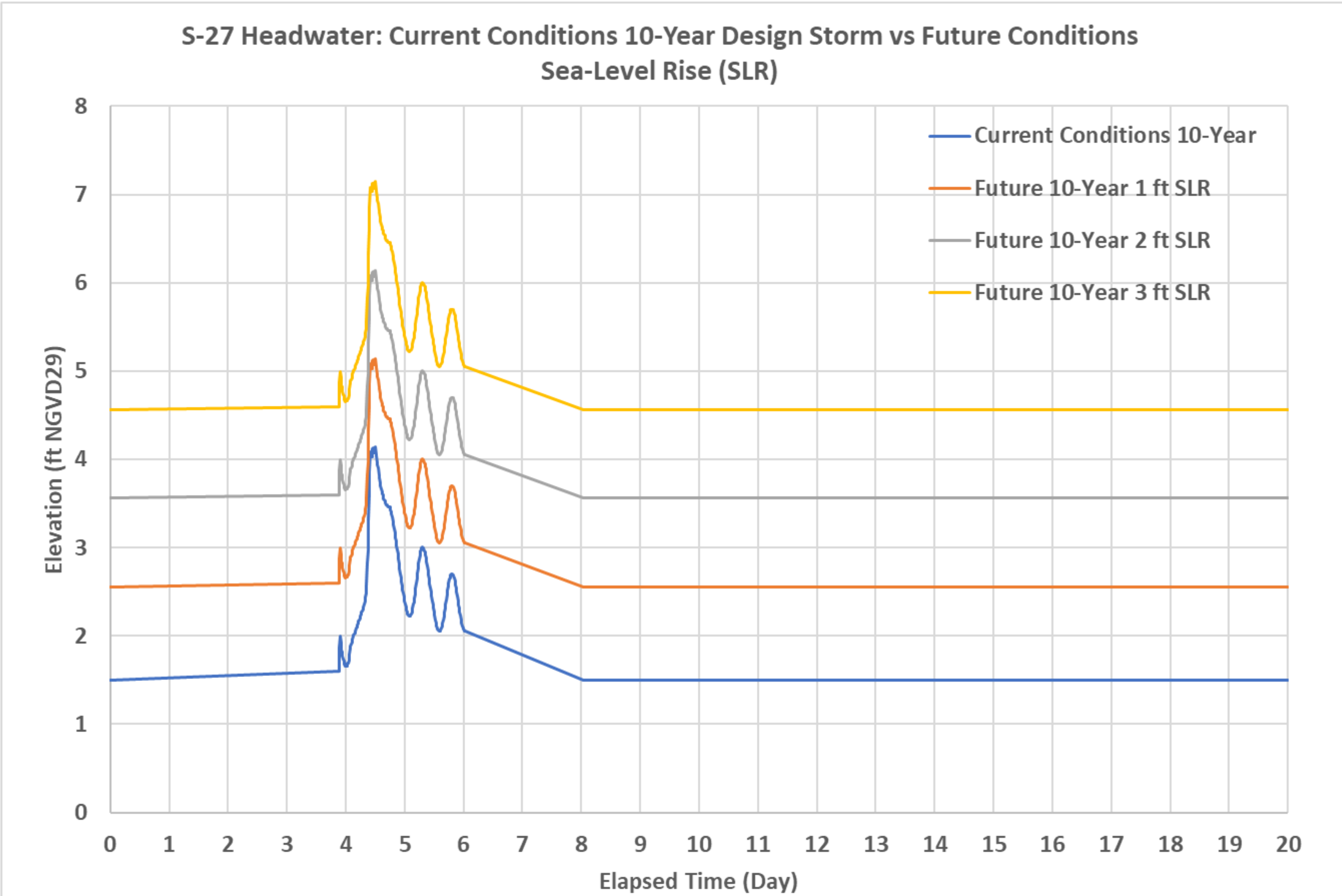

Figure 6-17: S-27 Future Condition Headwater Stages for 10-Year Design Storm under 3 Sea Level Rise Scenarios

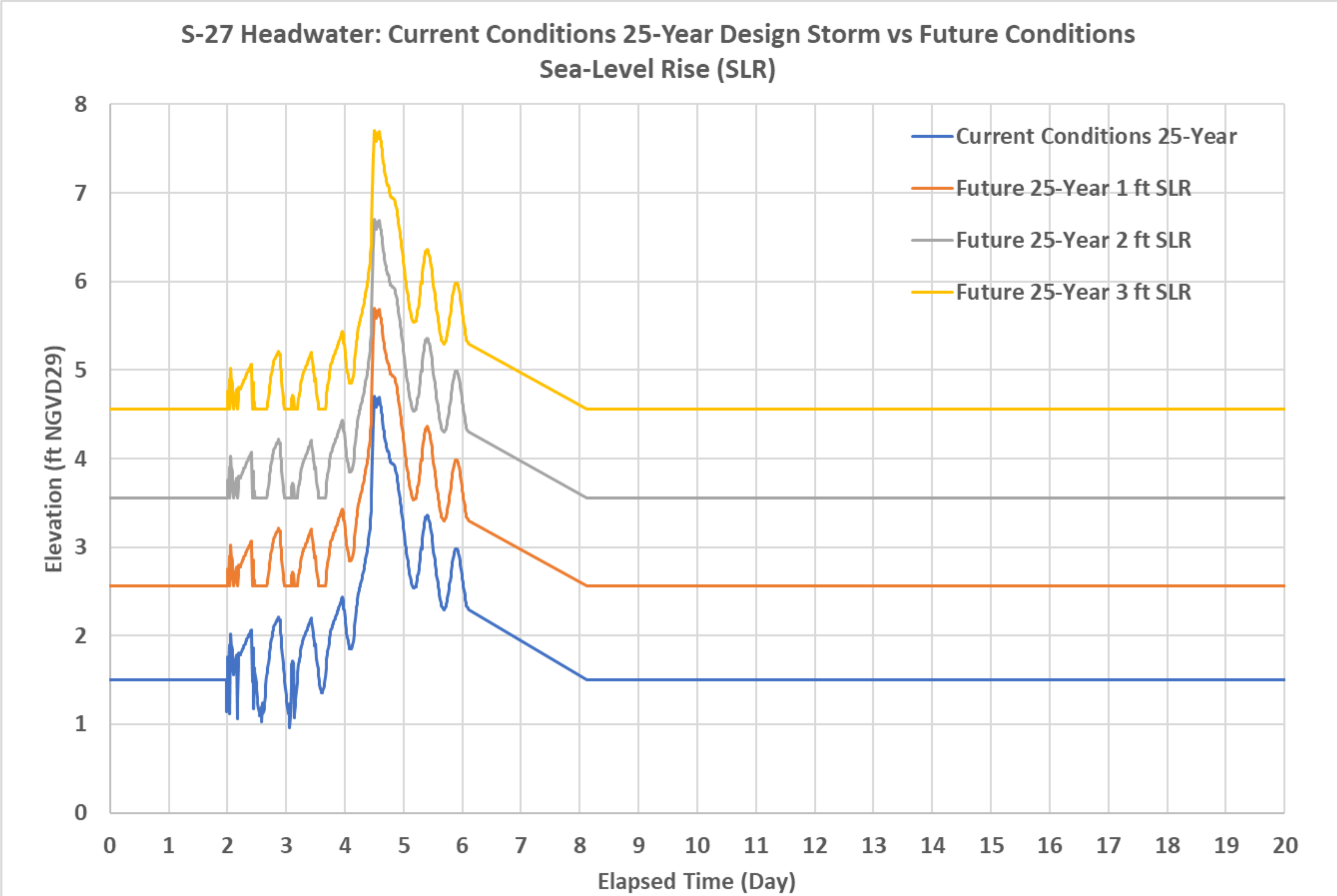

Figure 6-18: S-27 Future Condition Headwater Stages for 25-Year Design Storm under 3 Sea Level Rise Scenarios

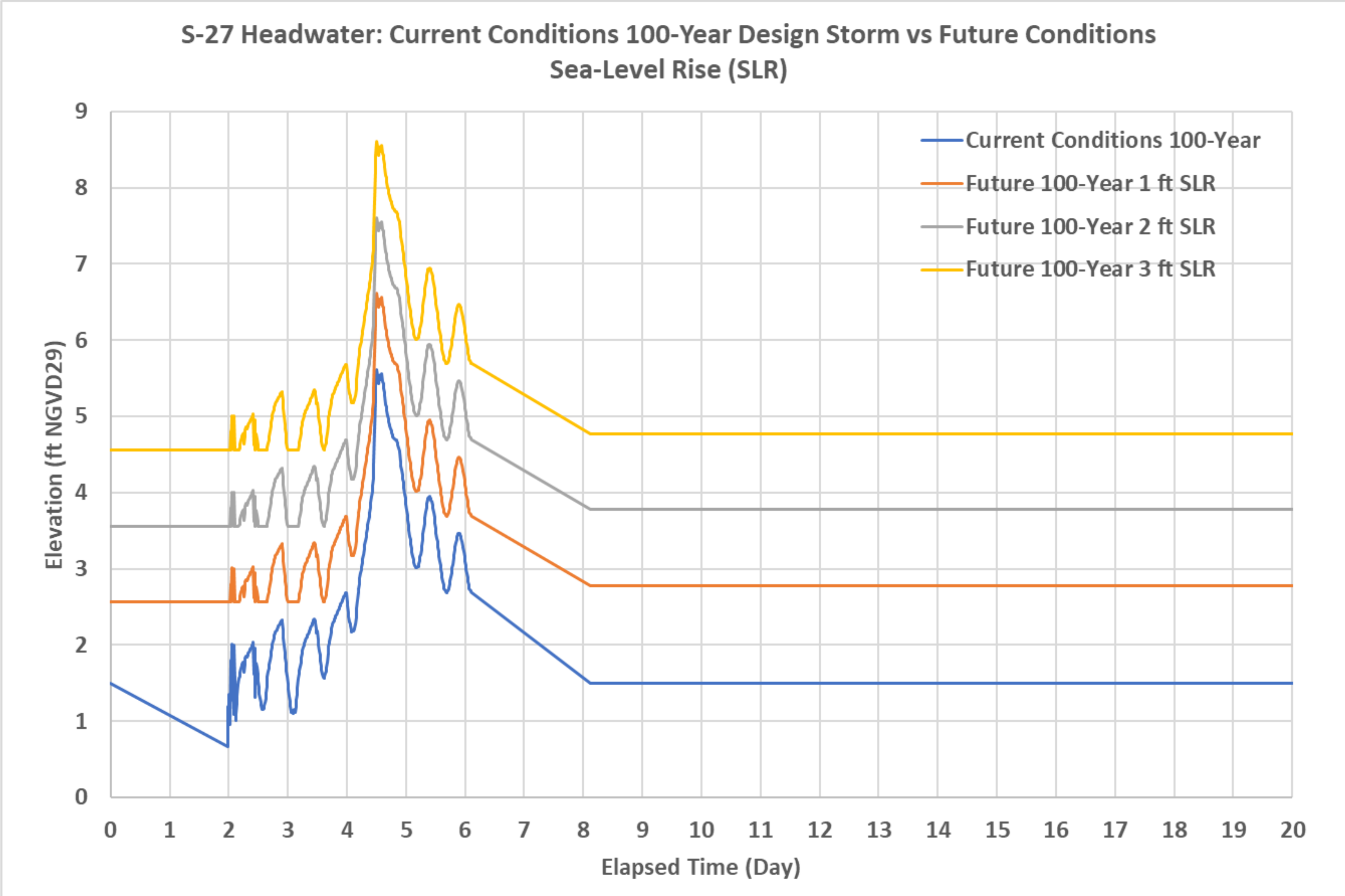

Figure 6-19: S-27 Future Condition Headwater Stages for 100-Year Design Storm under 3 Sea Level Rise Scenarios

7 INITIAL GROUNDWATER

For this study, the initial groundwater levels for future conditions were developed using the Broward County Future Groundwater Map (from the 2019 Broward County MIKE SHE Future Conditions 2060 model) and merging it with adjusted Miami-Dade potentiometric surface contours for the current conditions. Then, any area in the future conditions map that was lower than current conditions was replaced with the current condition groundwater level. The Broward County Future Initial Potential Head Map was based on a 26" of sea level rise. The Miami-Dade County potentiometric surface contours were adjusted by shifting the current condition contours to align with the contours created from the Broward County future conditions data. The Broward County Future Conditions Initial Potential Head Map covered the majority of the model domain.

As the Broward County data was based on 26" of sea level rise, the map described in the preceding paragraph was deemed appropriate to be used as the future conditions potentiometric surface map for the 2 ft sea level rise scenario. To develop the future potentiometric surface map for the 1 and 3 ft sea level rise scenarios, the current conditions groundwater surface elevation was subtracted from the future groundwater surface elevation for the 2 ft SLR scenario. The result of this was a difference map that showed how much the groundwater levels would increase from current conditions. This difference map was multiplied by 50%to represent the increase in groundwater due to 1 ft of sea level rise. To develop the future conditions potentiometric surface map for the 1 and 3 ft SLR scenario, the 50% difference map was subtracted and added to the 2 ft SLR future groundwater map, respectively. **Figure 7-1** through **Figure 7-3** show the future conditions initial potentiometric surface maps for each of the three sea level rise scenarios. Please note that the discontinuous groundwater elevations and checkered pattern are artifacts of the source data and the process of merging different datasets. These artifacts disappeared within the first few minutes of the simulation and there is a 2-day spin-up period prior to the design storms, which allows the groundwater to come to a dynamic equilibrium before the start of the design storm rainfall.

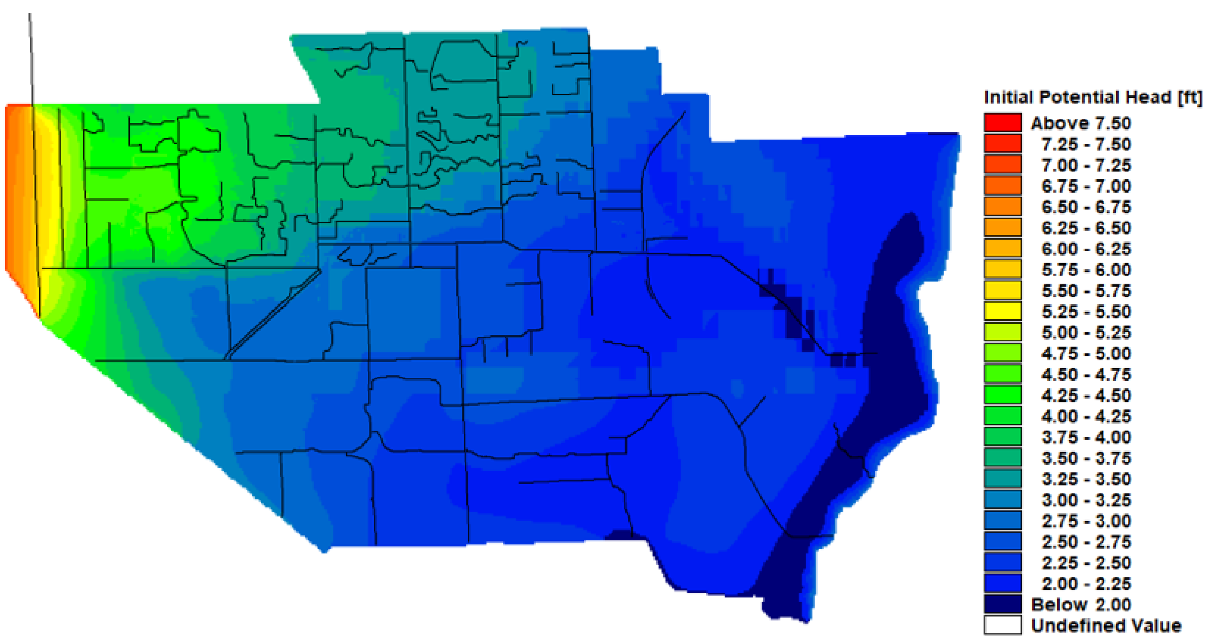

Figure 7-1: Future Conditions Initial Groundwater Levels for 1 ft Sea Level Rise

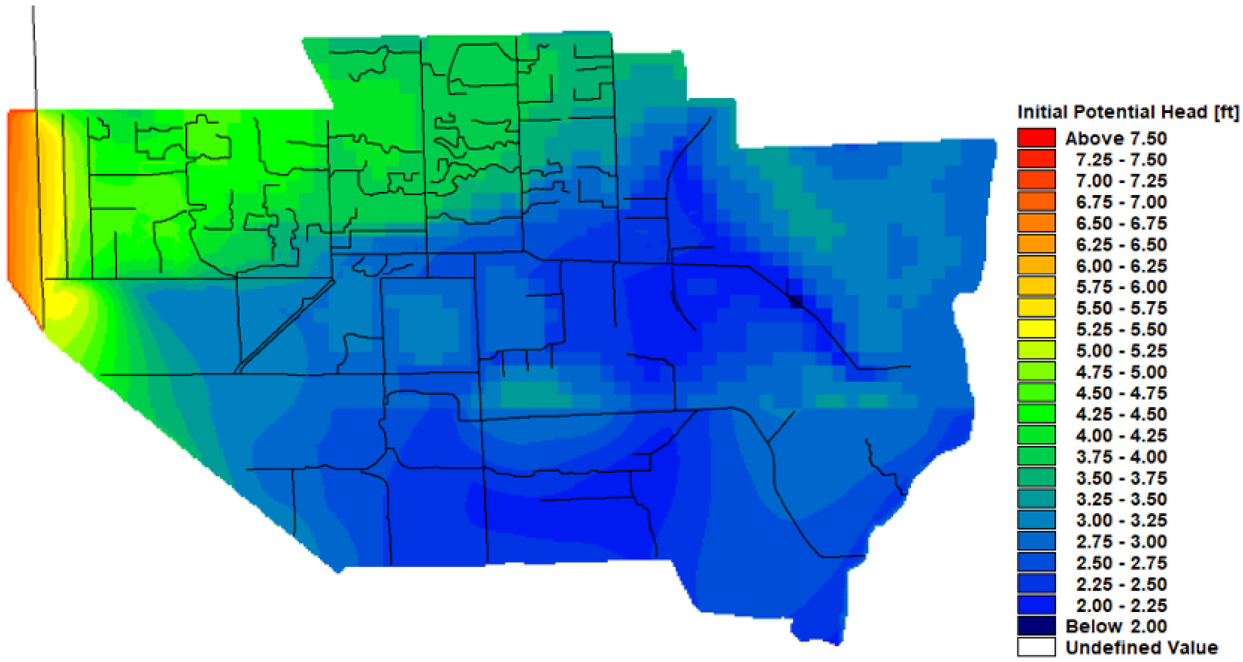

Figure 7-2: Future Conditions Initial Groundwater Levels for 2 ft Sea Level Rise

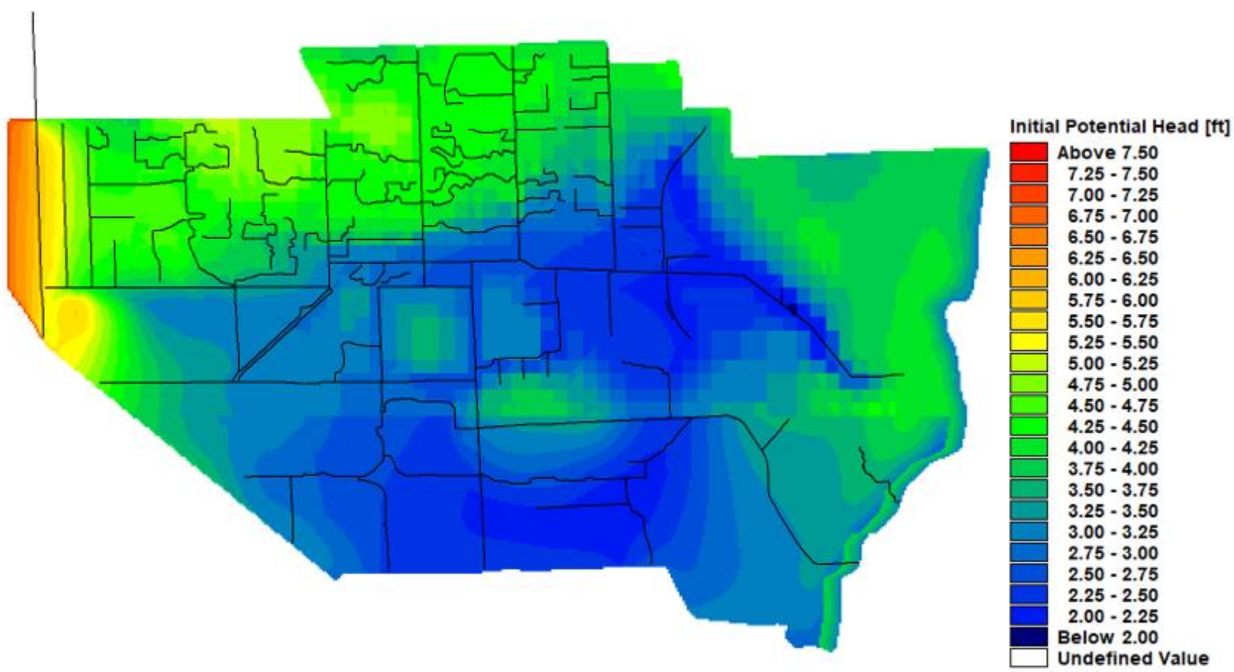

Figure 7-3: Future Conditions Initial Groundwater Levels for 3 ft Sea Level Rise

REFERENCES

Broward County Planning Council. (2020). *Broward County Future Land Use Plan (2040)* https://www.broward.org/PlanningCouncil/Pages/Maps.aspx

Burns & McDonnell. (2006). *Flood Protection Analysis for Broward County Water Preserve Areas C-11 and C-9 Impoundments (Final Report)*

Miami-Dade County. (n.d). *Miami Dade County Future Land Use (2030)*

Taylor Engineering. (2020). *Flood Protection Level of Service Provided by Existing Infrastructure for Current Sea Level Conditions in the C8 and C9 Watersheds*

USACE. (2012). *Central and Southern Florida Project Broward County Water Preserve Areas Revised Final Integrated Project Implementation Report and Environmental Impact Statement*

Yin, C., Li, Y., & Urich, P. (2019). *Broward County DDF Change Factor Ensemble Analysis*.

TAYLOR ENGINEERING, INC.

Flood Protection Level of Service Provided by Existing Infrastructure for Future Sea Level Conditions in the C8 and C9 Watersheds Final Report

Deliverables 4.2.2

CONTRACT 4600004085

Work Order 03

Submitted to:

South Florida Water Management District
3301 Gun Club Road
West Palm Beach, Florida 33406

Submitted 10/12/2020

14499 N. Dale Mabry Hwy, Suite 290,
Tampa, Florida 33618
813-963-6469 | www.taylorengineering.com

Table of Contents

List of Figures

List of Tables

List of Appendix Figures

List of Appendix Tables

1 INTRODUCTION

The South Florida Water Management District, herein referred to as SFWMD or District, is conducting a system-wide review of its regional water management infrastructure to determine the flood protection level of service (FPLOS) that could be provided under future conditions. The FPLOS describes the level of protection provided by the water management facilities within a watershed under both current and future conditions, where future conditions FPLOS considers sea level rise and future development. This information can be used by local governments, SFWMD, and other state and federal agencies to identify areas where improvements or upgrades of water management facilities are required, the appropriate entity or entities responsible for making improvements, and funding and technical resources available to support these efforts.

This report documents the future conditions model development and the FPLOS provided by existing infrastructure for the C-8 and C-9 Basins under future sea level conditions. Taylor Engineering has developed an integrated groundwater and surface water model of the C-8 and C-9 watersheds, using MIKE SHE and MIKE HYDRO, that was used to determine the flood protection level of service provided by existing infrastructure under future sea level conditions for the 72-hour design storm events of 1 in 5, 10, 25, and 100-year recurrence frequency. The flood protection level of service was determined through several metrics, the majority of which are derived from the outputs of the watershed-scale flood event modeling. The flood protection metrics are defined in **Section 3**.

2 MODEL DEVELOPMENT FOR FUTURE CONDITIONS FPLOS

This section documents the development and initial parameterization of the South Florida Water Management District (SFWMD) C-8 & C-9 Future Conditions MIKE SHE and MIKE HYDRO models. The developed models were used in the C8-C9 future conditions flood protection level-of-service (FPLOS) study. Several model inputs and parameters used in the future condition model were obtained from the final version of the current conditions model. This section focuses on the development and parameterization changes that were made to the model for the future conditions simulations. For details on model development and setup of the existing conditions model, please refer to the report *Flood Protection Level of Service Provided by Existing Infrastructure for Current Sea Level Conditions in the C8 and C9 Watersheds* (Taylor Engineering, 6/17/2020).

2.1 Rainfall

The design storms used in the future conditions model used the same NOAA Atlas 14 rainfall depths as used in the current conditions model. The design storms were temporally distributed based on the SFWMD 3-day distribution and spatially distributed based on Thiessen Polygons of the NOAA stations. The sensitivity run, to be completed only for the 10-year design storm, will have a 9% increase in rainfall. This increase comes from the Broward County DDF Change Factor Ensemble Analysis (Yin, Li, & Urich, 2019).

2.2 Land Use

The future conditions land use map was developed by modifying the current conditions land use map to reflect projected future changes. Areas of future change were identified by comparing undeveloped, agricultural, and lower density development areas (such as low density residential) to future conditions land use maps from the Broward County Planning Council (2020) and Miami-Dade County (n.d.). The future conditions land use maps from these sources were generalized, whereas the current conditions land use map was very detailed. Therefore, by starting with the current conditions land use map and applying changes identified from the future land use map, there was no significant loss in spatial detail. The future land use changes were most often applied to areas classified as open land, recreational, cropland and pastureland, forests, and disturbed land. Areas classified as wetlands in current conditions were not changed due to their protected status.

Within the Broward County portion of the model, about 805 acres were changed to represent future land use conditions. Within the Miami-Dade County portion of the model, about 3180 acres were changed to represent future land use conditions. The areas with future land use changes are shown in **Figure 2.2-1**. The C-9 Impoundment area is represented as reservoir land use for future conditions.

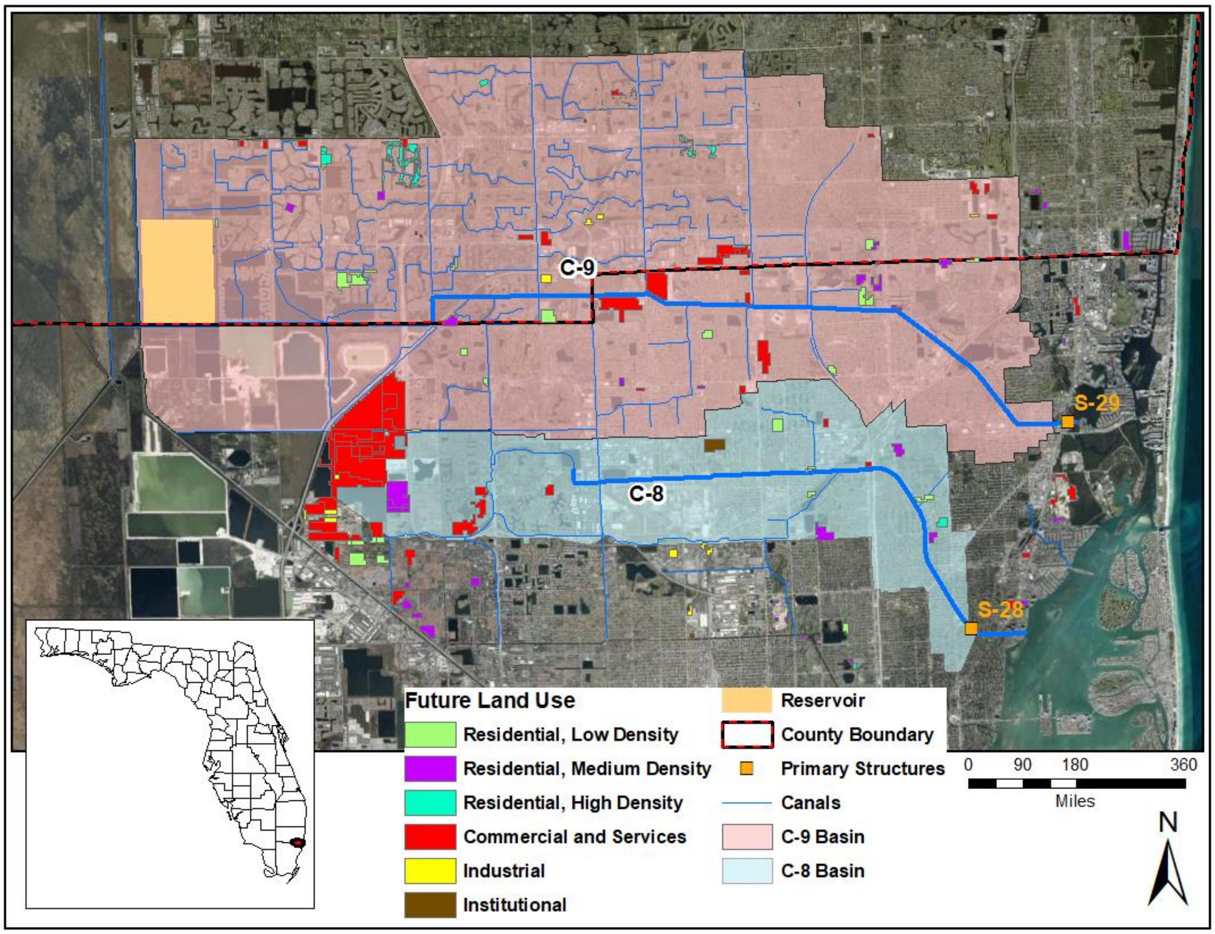

Figure 2.2-1: Areas of Future Land Use Changes

2.3 Topography

The land surface elevation of the areas with future land use change were compared with the FEMA Base Flood Elevation (BFE) and increased where the current elevation is less than the BFE. For the larger areas with land use change that do not have storage explicitly modeled in the MIKE HYDRO model, a portion of the area was lowered to account for floodplain compensation. Many of the areas with land use change were only a small cluster of grid cells, in which case it was not feasible or necessary to lower any of the grid cells once raised to BFE. These areas were relatively small and widely spread throughout the model domain, so they should have negligible hydrologic impact. Also, detention storage in these areas was accounted for in the overland flow module as discussed in **Section 2.4.2**. For the area of the C-9 impoundment (discussed in **Section 2.5.1.2**), the topography was adjusted so that the levees were accounted for (19.5 ft NGVD29) and the elevation inside the impoundment was set to the average impoundment ground elevation (4.5 ft NGVD29), per the Army Corps Project Implementation Report (USACE, 2012).

2.4 Overland Flow

In the current conditions model, most of the parameters in the overland flow module within Broward County were spatially varied by land use, while other parameters were spatially varied by land use within ERP permitted areas. Within Miami-Dade County, most of the parameters were spatially varied by land use, while other parameters were spatially varied by land use within areas that are internally drained (e.g., via exfiltration trenches, French drains, etc.). For the areas of land use that were changed to represent future conditions, the associated parameterization changes to the overland flow layers were applied the same way as in the current conditions. Refer to Section 3.7 in the C8 C9 FPLOS by Existing Infrastructure for CSL Conditions Draft Report (Taylor Engineering, 6/17/2020) for the specific details regarding parameterization of the overland flow module. For the purposes of this study, the following assumptions are applied:

- Each of the areas identified as having land use change is an "ERP permitted area" and must comply with the stormwater quality ordinance of retaining the greater of the first 1 inch of rainfall or 2.5 inches over the impervious area.
- Within Broward County, the areas of land use change that are not considered Stormwater management category (SMC) 1 are considered SMC 3b (most conservative approach)
- Within Miami-Dade County, the areas of land use change have the same SMC classification as current conditions, such as internally drained or drains to branch
    - o Undeveloped internally drained areas that are were developed still drain internally unless the drainage network was explicitly modeled in MIKE Hydro (such as the new Mega Mall)

A brief summary of the parameterization changes applied to the overland flow layers is provided in the following subsections.

2.4.1 Manning's Number

The Manning's roughness coefficient for the overland module was developed for the areas of land use change the same way as the current conditions model and was based on land use. Refer to Table 3-7 in the C8 C9 FPLOS by Existing Infrastructure for CSL Conditions Draft Report (Taylor Engineering, 6/17/2020) for the Manning's roughness coefficients based on land use by FLUCCS codes.

2.4.2 Detention Storage

The areas identified for land use change were assigned detention storage based on the new land use type. For the areas of land use change that were in areas directly controlled by operable structures represented in the model, no additional change to detention storage was made. For the areas of land use change that were not in areas directly controlled by operable structures, the detention storage was increased based on the assumption that all areas of future development will require an ERP. Therefore, detention storage in these areas of land use was increased the same way as in ERP areas (and internally drained areas within

Miami-Dade County) in the current conditions model. This involved multiplying the paved area runoff coefficient (represents DCIA) by 2.5 inches and any of the resulting values which were less than 1" were increased to 1".

2.4.3 Paved Area Runoff Coefficient

The areas identified for land use change were assigned a paved area runoff coefficient based on the new land use type. For the areas of land use change that were in areas directly controlled by operable structures, no additional change to the paved area runoff coefficient was made. For the areas of land use change that were not in areas directly controlled by operable structures, the paved area runoff coefficient was decreased based on the assumption that all areas of future development will require an ERP. Therefore, paved area runoff coefficients in these areas of land use were decreased the same way as in ERP areas (and internally drained areas within Miami-Dade County) in the current conditions study, which was to reduce the values by half. Refer to Table 3-7 in the C8 C9 FPLOS by Existing Infrastructure for CSL Conditions Draft Report (Taylor Engineering, 6/17/2020) for the runoff coefficients based on land use by FLUCCS codes.

2.5 Rivers and Lakes (1D Model)

2.5.1 1D Model Configuration Updates

In the future conditions model, two major changes to the 1D network were made, which are (1) explicitly representing the discharge from the two largest areas of land use change and (2) including the C-9 Impoundment. Although these two major changes are explicitly represented in the model, the specific details regarding the implementation are conceptual. These updates are discussed in the following two subsections.

2.5.1.1 Areas of Land Use Change

Based on the identified areas of land use change, it was decided that only the two largest areas would be explicitly modeled in the 1D network. **Figure 2.5-1** shows the location of the two largest land use change areas.

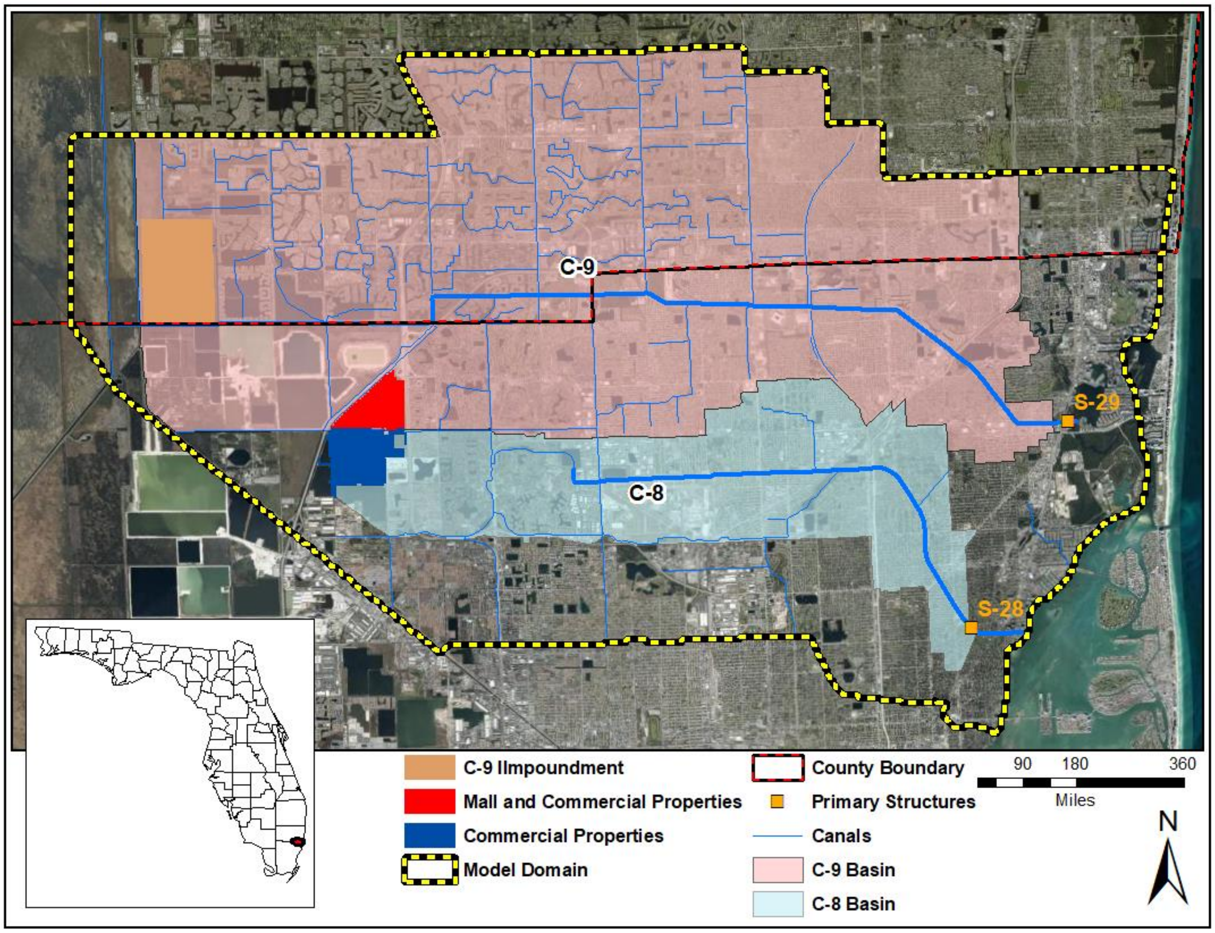

Figure 2.5-1: Areas of Land Use Change with Explicit MIKE HYDRO Changes

The first location (shown in red) is where the American Dream Miami Mall ("Mega Mall") and other commercial properties will be located. The second location (shown in blue) will be developed into other commercial properties. For these two locations, a conceptual MIKE HYDRO branch has been added to represent storage and to control discharge. To control the discharge, a pump that is limited to the District's CSM allowance is proposed. Although peak discharge from a developed property should not be greater than predeveloped conditions, these two areas are internally drained under current conditions. To be conservative, Taylor Engineering represented these two areas as being controlled by a pump that limits the total discharge to the District's allowance, with the assumption that in future conditions these properties will have a positive outfall and ultimately drain to the C-9 Canal (area in red) and C-8 Canal (area in blue). Areas draining to the C-9 Canal have an allowance of 20 CSM pumped. There is currently no set allowance for areas draining to the C-8 Canal. For the purposes of this study, Taylor used the same discharge allowance for the area draining to the C-8 Canal as the area draining to the C-9 Canal. The pumps have an "on" elevation equal to 1 ft above the control elevation, which was set at 0.5 feet below the existing property grade (Ref: 40E-41.063 F.A.C., Conditions for Issuance of Permits in the Western Canal 9 Basin). For the mall and commercial properties segment, the control elevation was 3.2 ft NGVD29 and the pump "on" elevation was set to 4.2 ft NGVD29. For the commercial properties segment, the control elevation was 3.4 ft NGVD29 and the pump "on" elevation was set to 4.4 ft NGVD29. The mall and commercial properties pump follows the same operating criteria as the pump stations in western South

Broward Drainage District, which requires the pump to turn off when water levels in the C-9 Canal reach an elevation of 6.8 ft NGVD29. Based on the 20 CSM allowance, the mall and commercial properties segment draining to the C-9 Canal has a discharge limit of 17.9 cfs and the commercial properties segment draining to the C-8 Canal has a discharge limit of 11.25 cfs.

The conceptual branches/lakes have an area equal to 20% of the property segment. The two large property segments were conceptually broken down into five categories for the purposes of determining the available storage. Each property was considered to have 20% lake, 20% parking, 10% road, 5% open space (10% by net area; total area minus lake, parking, and road) and 45% area available for development. Conceptually, the parking areas were assumed to be built on top of stormwater detention vaults at average topography elevation and are responsible for capturing the required runoff from the parking areas. The open space topography elevation was lowered to the average groundwater elevation.

For the mall and commercial properties segment, the average topography elevation was 3.7 ft NGVD29 and the average current condition groundwater elevation was 2.9 ft NGVD29. This provided 0.8 ac-ft of storage per acre of land that was converted to lake, parking area, and open space. For the commercial properties segment, the average topography elevation was 3.9 ft NGVD29 and the average current conditions groundwater elevation was 2.9 ft NGVD29. This provided 1 ac-ft of storage per acre of land that was converted to lake, parking area, and open space.

The amount of additional storage provided by the lake, under the parking areas, and in the open space was calculated by multiplying the area by the difference between the average topography elevation and average groundwater elevation. This storage volume (ac-ft) was divided by the difference between the FEMA BFE elevation and the average topography elevation, which resulted in the amount of land area (ac) that could be increased to the FEMA BFE. For the mall and commercial properties area draining to the C-9 Canal, only about 60 acres of the developed land could be raised to the FEMA BFE. For the commercial properties area draining to the C-8 Canal, about 120 acres of the developed land could be raised to the FEMA BFE. As this land segment was originally internally drained and draining to one of the nearby major lakes, it was assumed that part of the property would still drain internally in the future. With a large part of this property now being drained to the C-8 Canal, there is a reduced load on the lakes that were originally being drained to. Therefore, it was assumed that the remainder of the property segment lower than the FEMA BFE (about 50 acres) could be raised to the FEMA BFE without the need for additional compensation.

2.5.1.2 C-9 Impoundment

The C-9 Impoundment is a project being designed with the intentions of capturing excess storm water. This will reduce the amount of water pumped to the water conservation areas and lost to tide and sometimes reduce water levels in the C-9 Canal. This project has the ability to reduce peak flood stages during major storms by pumping water from the C-9 Canal into an above-ground storage reservoir. The C-11 Impoundment is intended to operate the same way in the C-11 basin. These two projects are being designed to operate together in the future. The C-11 Impoundment project will have the ability to transfer water into the C-9 Impoundment, both for water management and for storm water control. However, the C-9 Impoundment project will only be able to "capture available storm runoff in the C-9 West Basin ***or*** to lift discharges from the C-11 West Basin (released from the C-11 Impoundment) to the C-9 Impoundment" (Burns & McDonnell, 2006). Therefore, it seems that during a major storm event, the two impoundments would operate independently, as the C-9 Impoundment will be pumping stormwater runoff from the C-9 basin. However, it is possible that the C-11 Impoundment could need to divert water to the C-9 Impoundment during a major storm. Instead of speculating on how to explicitly represent the interaction between the two projects, Taylor Engineering did not explicitly represent inter-impoundment transfer in the future conditions model and instead represented it by limiting how long the C-9 Impoundment accepts water from the C-9 Basin.

The C-11 Impoundment project is planned to have a storage capacity of 4,592 ac-ft and a pumping rate of 1,050 cfs and the C-9 impoundment project is planned to have a storage capacity of 7,056 ac-ft and a pumping rate of 1,000 cfs (USACE, 2012). Therefore, if starting empty, the C-11 Impoundment could receive water at the maximum allowed rate for 53 hours and the C-9 Impoundment could receive water at the maximum allowed rate for about 85 hours. To simulate a reasonable worst case scenario, Taylor Engineering assumed that both impoundments start at 50% capacity and that once full, the C-11 Impoundment diverts water to the C-9 Impoundment, at which point the C-9 Impoundment could no longer pump water from the C-9 basin. To eliminate the need to explicitly model the transfer of water from the C-11 Impoundment, Taylor Engineering implemented the following approach:

- Start the C-9 Impoundment at 50% capacity and assume the C-11 Impoundment is at 50% capacity (this means the C-11 could receive water for 26.5 hours before it is full)
- Allow the C-9 Impoundment to start receiving water from C-9 Canal when the water level in the western portion of the C-9 Canal reaches 3.5 ft NGVD29 (Burns & McDonnell, 2006)
- Stop the C-9 Impoundment from receiving water from C-9 Canal after 26.5 hours of pumping at 1000 cfs (or equivalent volume) (assumes the C-9 and C-11 Impoundments would be pumping at the same time) (C-11 Impoundment full after 26.5 hours when starting at 50% capacity)
    - The remaining volume is conceptual storage available for the water transfer from the C-11 Impoundment

This is a very simple and efficient way to represent the C-9 Impoundment in a worst case scenario, where it exists in future conditions but cannot be fully utilized. The explicit representation of water seepage from the C-9 Impoundment is not required as it can be assumed that any seepage that results from higher stages in the impoundment is captured and returned. Within MIKE HYDRO and MIKE SHE, the C-9 Impoundment components will be represented with low leakage coefficients. By setting the canal and overland leakage coefficients to low values, the seepage collection and return system can be left out as it is being conceptually represented by reducing or eliminating any seepage from occurring within the C-9 Impoundment area. As "The Savings Clause requires assurance that no negative impact will occur to existing levels of flood protection and is demonstrated in project design" (USACE, 2012), it can be assumed that the design of the Impoundment will have little to no negative impact, and reducing or eliminating the leakage is the simplest way to represent this complex system.

Sensitivity tests were conducted for the 10-year 1 ft sea level rise and 100-year 2 ft sea level rise scenarios, in which the C-9 Impoundment was represented as only having 50% storage capacity, as well as 100% full. These four simulations showed that the C-9 Impoundment having 50% storage capacity has negligible effects on the overall FPLOS in the C-9 Basin. Although the model results were more sensitive to the C-9 Impoundment for the 10-year 1 ft sea level rise scenario that it was for the 100-year 2 ft sea level rise scenario, the sensitivity was not large enough to warrant not simulating potential storage in the C-9 Impoundment. For the 10-year 1 ft sea level rise C-9 Impoundment sensitivity test, there was a 0.15 ft stage reduction at the western side of the C-9 Canal (where the impoundment is) (**Figure 2.5-2**), 0.0 ft stage reduction at S-29 (**Figure 2.5-3**), and a total discharge difference of 8% at S-29 (**Figure 2.5-4**).

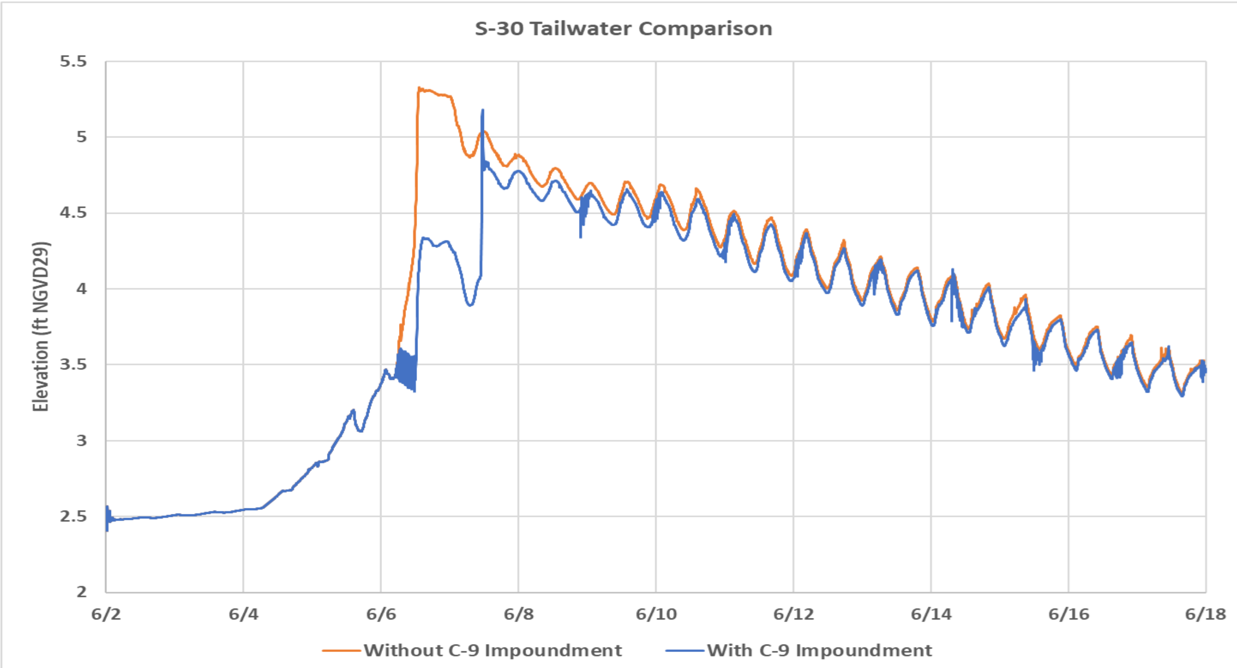

Figure 2.5-2: C-9 Impoundment Sensitivity Test for S-30 Tailwater During 10-Year Design Storm with 1 ft Sea Level Rise (with Impoundment= 50% Capacity)

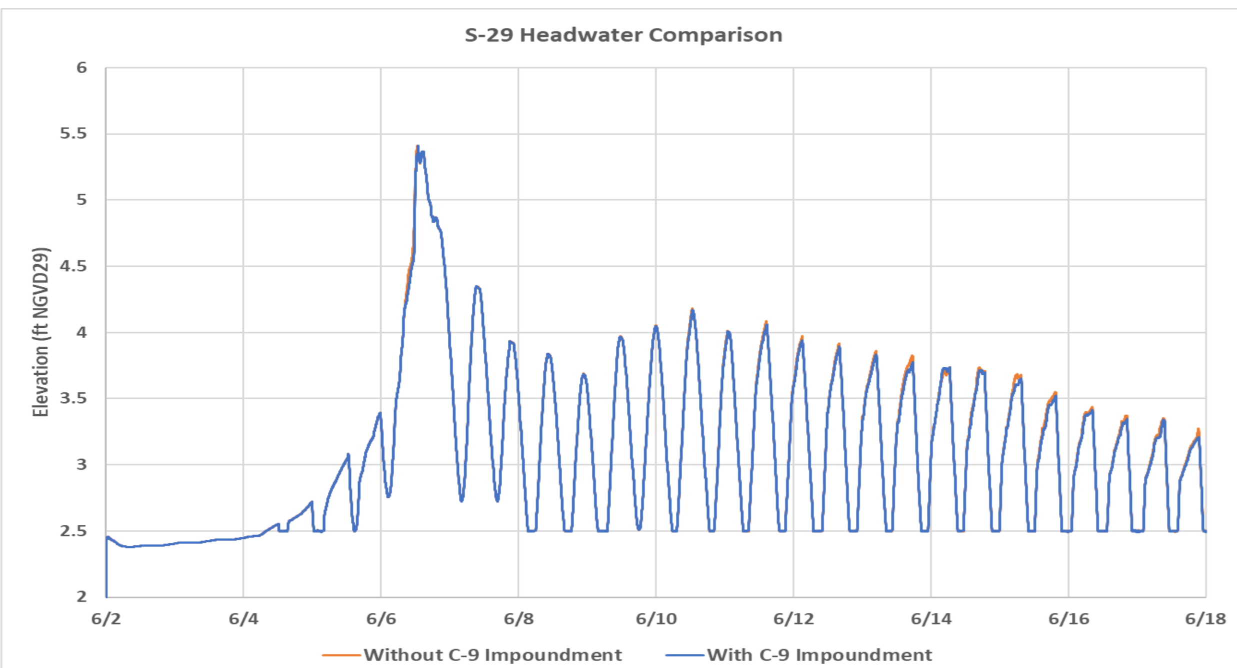

Figure 2.5-3: C-9 Impoundment Sensitivity Test for S-29 Headwater During 10-Year Design Storm with 1 ft Sea Level Rise (with Impoundment= 50% Capacity)

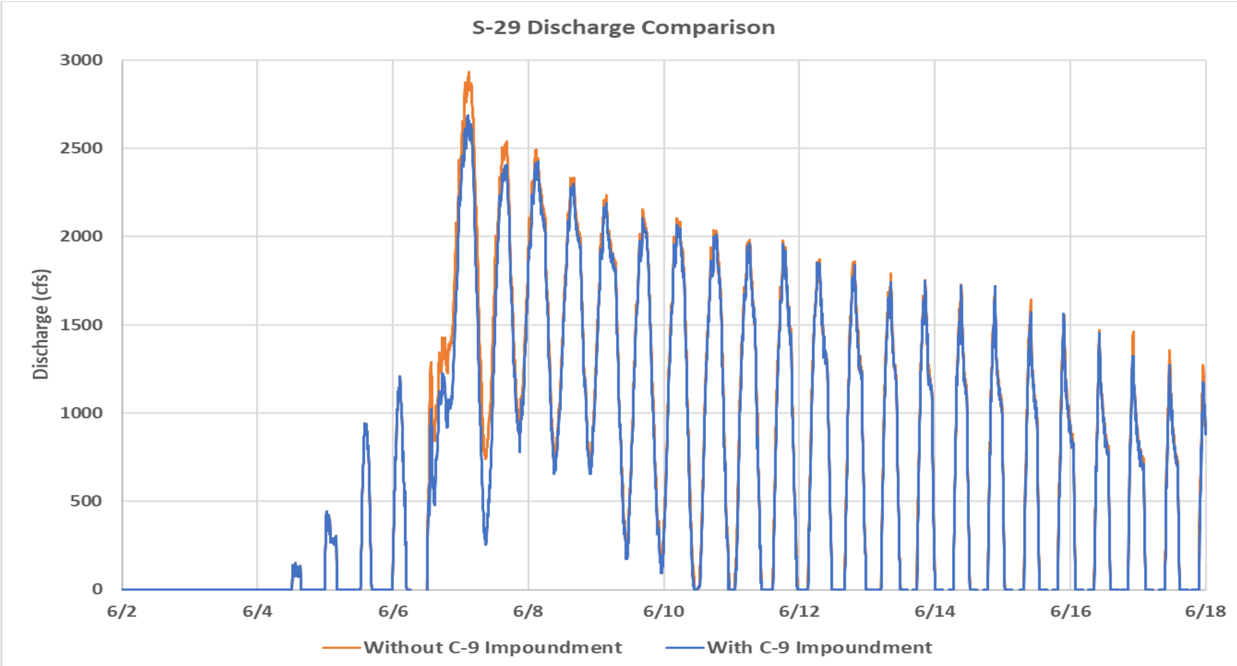

Figure 2.5-4: C-9 Impoundment Sensitivity Test for S-29 Discharge During 10-Year Design Storm with 1 ft Sea Level Rise (with Impoundment= 50% Capacity)

Comparatively, the 100-year 2 ft sea level rise scenario only had a 0.06 ft stage reduction at the western side of the C-9 Canal (**Figure 2.5-5**), 0.03 ft stage reduction at S-29 (**Figure 2.5-6**), and 1% total discharge difference at S-29 (**Figure 2.5-7**).

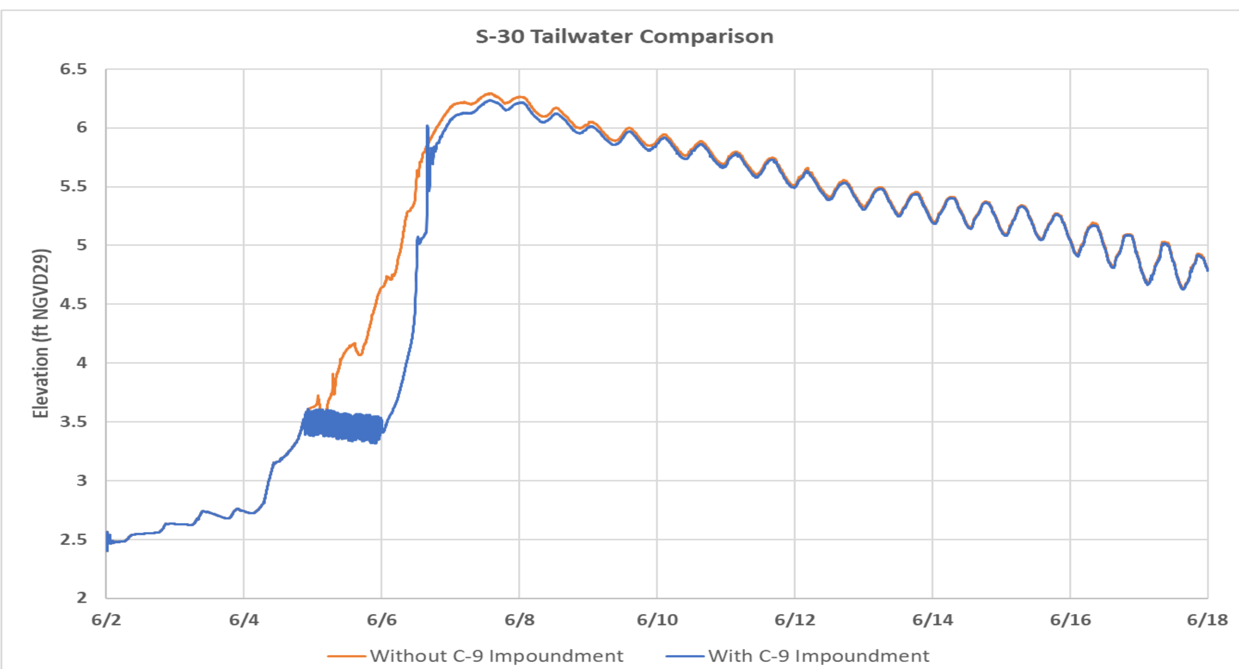

Figure 2.5-5: C-9 Impoundment Sensitivity Test for S-30 Tailwater During 100-Year Design Storm with 2 ft Sea Level Rise (with Impoundment= 50% Capacity)

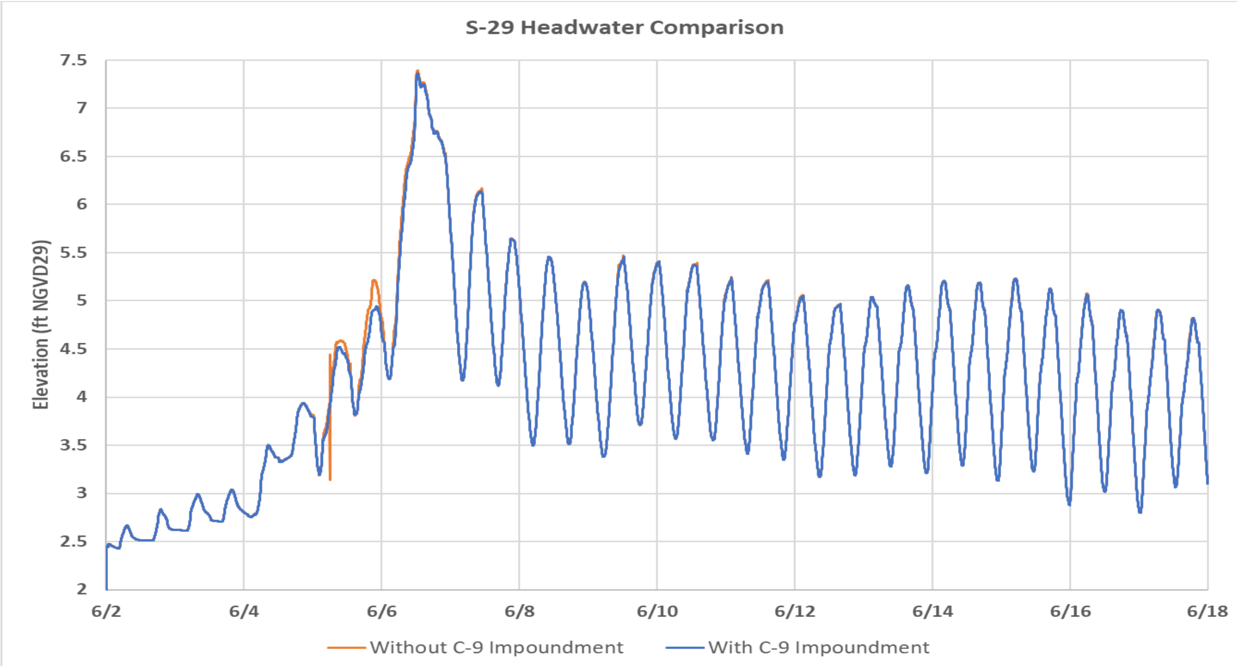

Figure 2.5-6: C-9 Impoundment Sensitivity Test for S-29 Headwater During 100-Year Design Storm with 2 ft Sea Level Rise (with Impoundment= 50% Capacity)

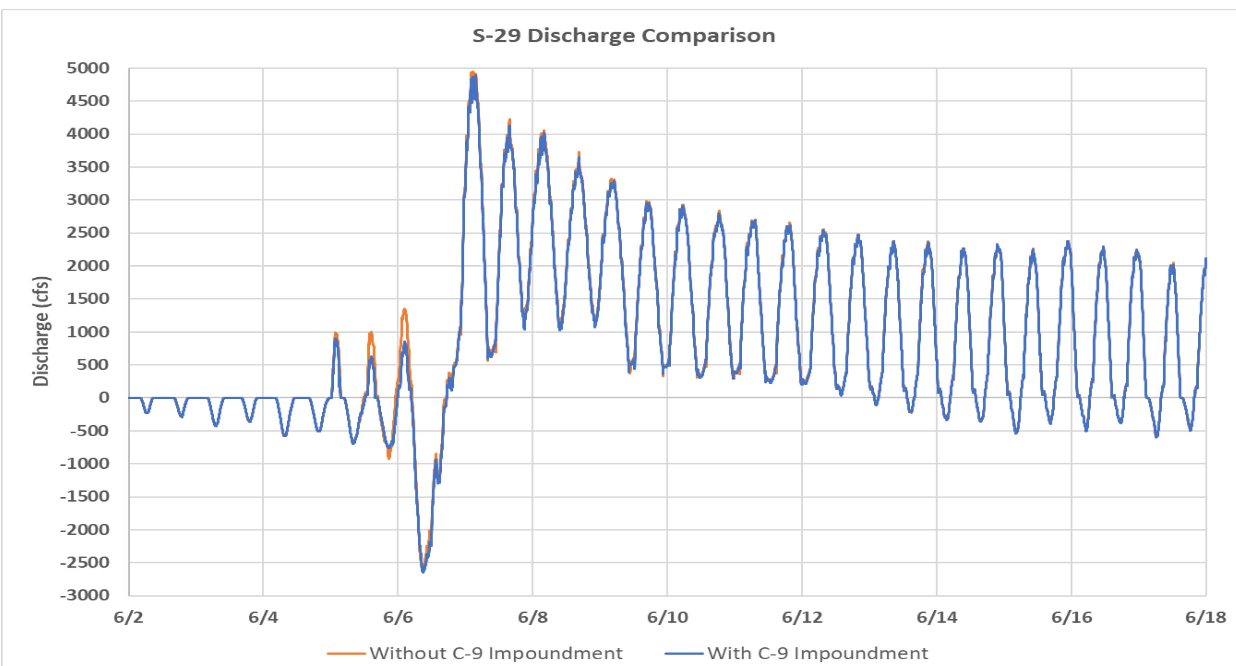

Figure 2.5-7: C-9 Impoundment Sensitivity Test for S-29 Discharge During 100-Year Design Storm with 2 ft Sea Level Rise (with Impoundment= 50% Capacity)

After analyzing the results of these sensitivity tests, Taylor Engineering suggested to keep the original recommendation of starting the C-9 Impoundment with 50% capacity, and the District agreed.

Comparatively, the 100-year 2 ft sea level rise scenario only had a 0.06 ft stage reduction at the western side of the C-9 Canal, 0.03 ft stage reduction at S-29, and 1% total discharge difference at S-29. After analyzing the results of these sensitivity tests, Taylor Engineering suggested to keep the original recommendation of starting the C-9 Impoundment with 50% capacity, and the District agreed.

2.5.2 Boundary Conditions (1D Model)

The 1-D tidal boundaries (forced tailwater at tidal structures) used the SFWMD-provided design storm surge stage hydrographs. These are the same hydrographs from the current condition design storms, but increased by 1, 2, and 3 ft to represent various sea level rise scenarios. The design storm tidal boundaries for the future seal level rise scenarios are shown in **Figure 2.5-8** through **Figure 2.5-15**.

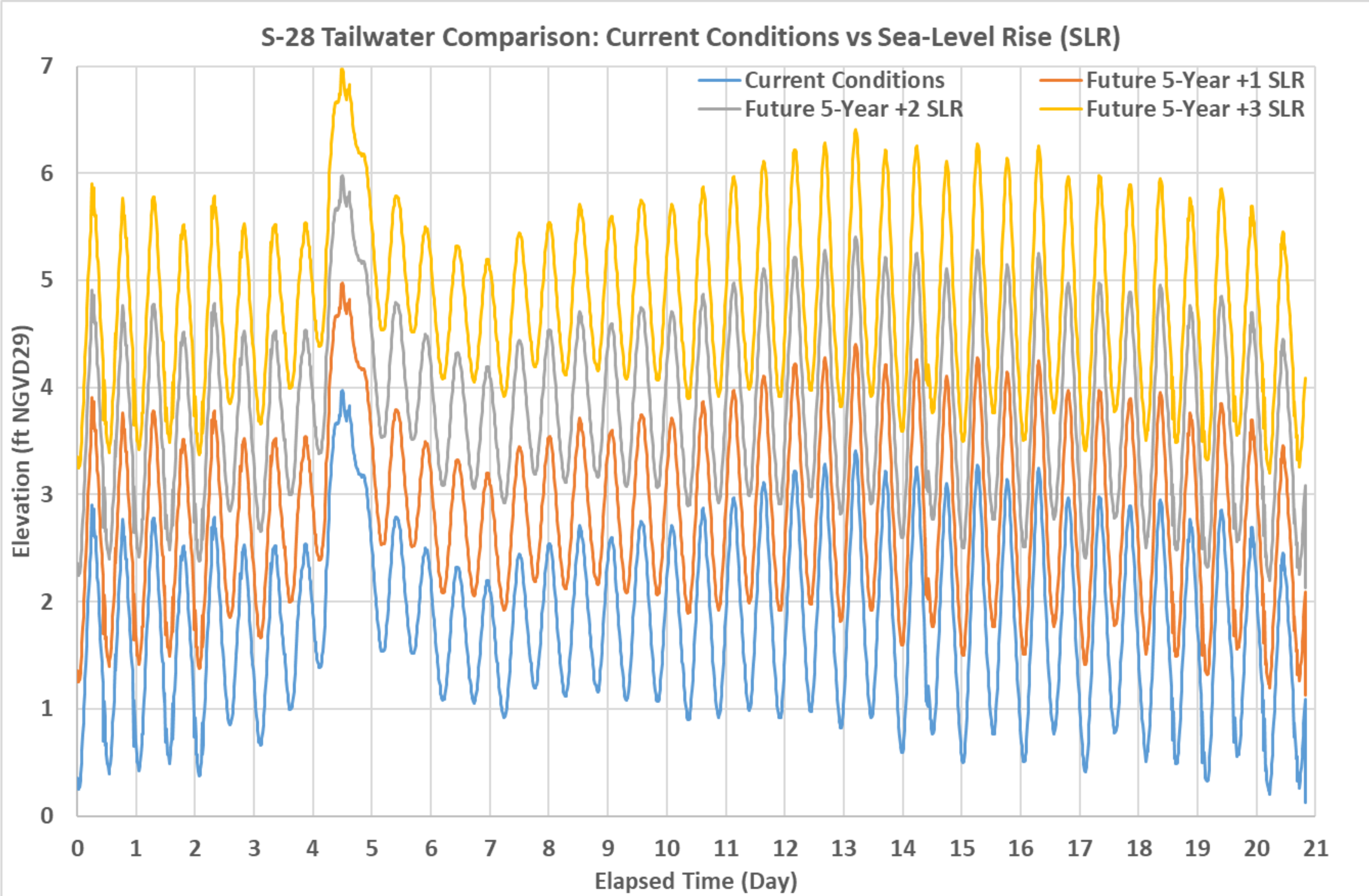

Figure 2.5-8: Future Conditions Sea Level Rise 5-Year Design Storm Tidal Boundary Stages for S-28

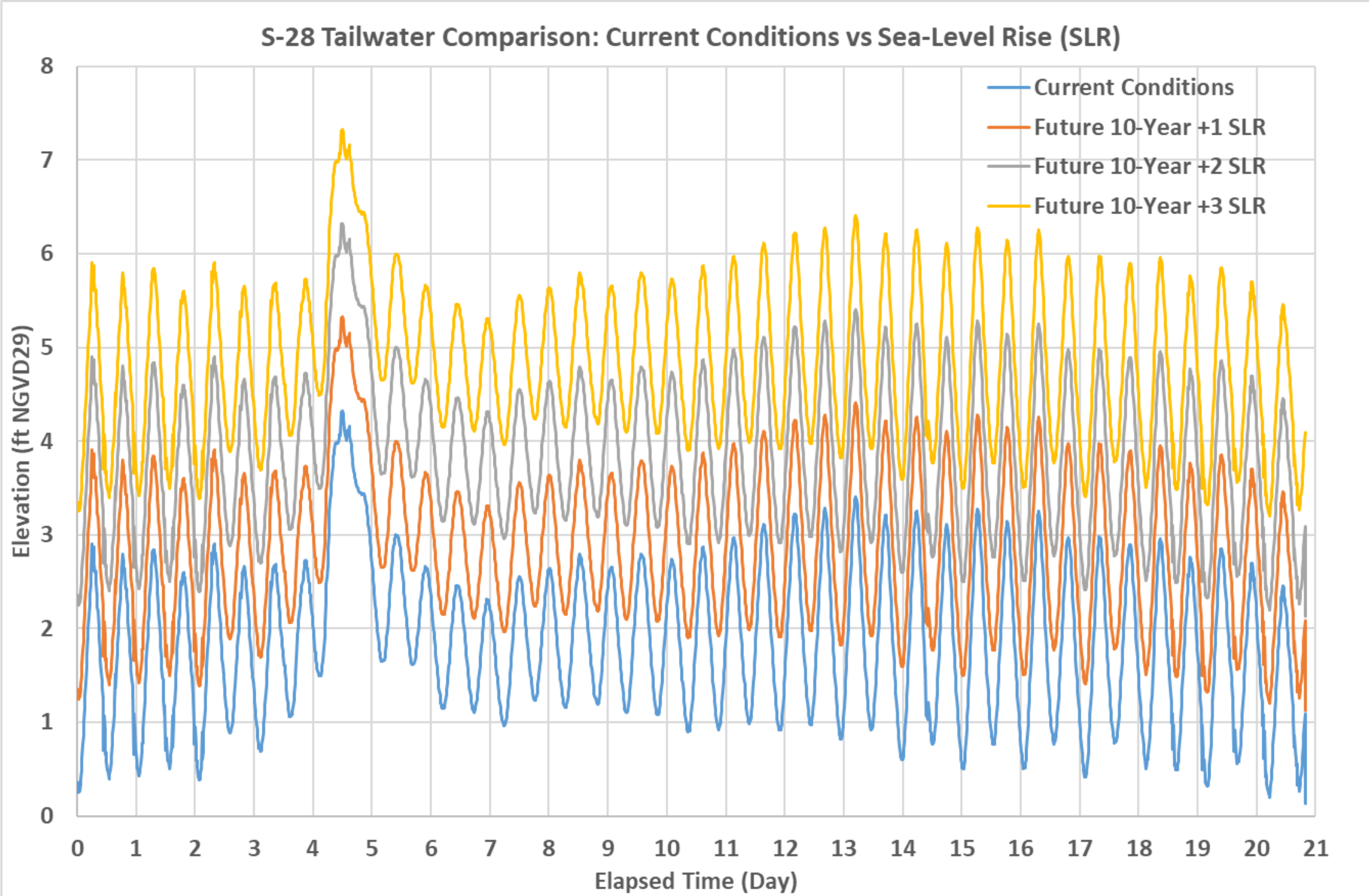

Figure 2.5-9: Future Conditions Sea Level Rise 10-Year Design Storm Tidal Boundary Stages for S-28

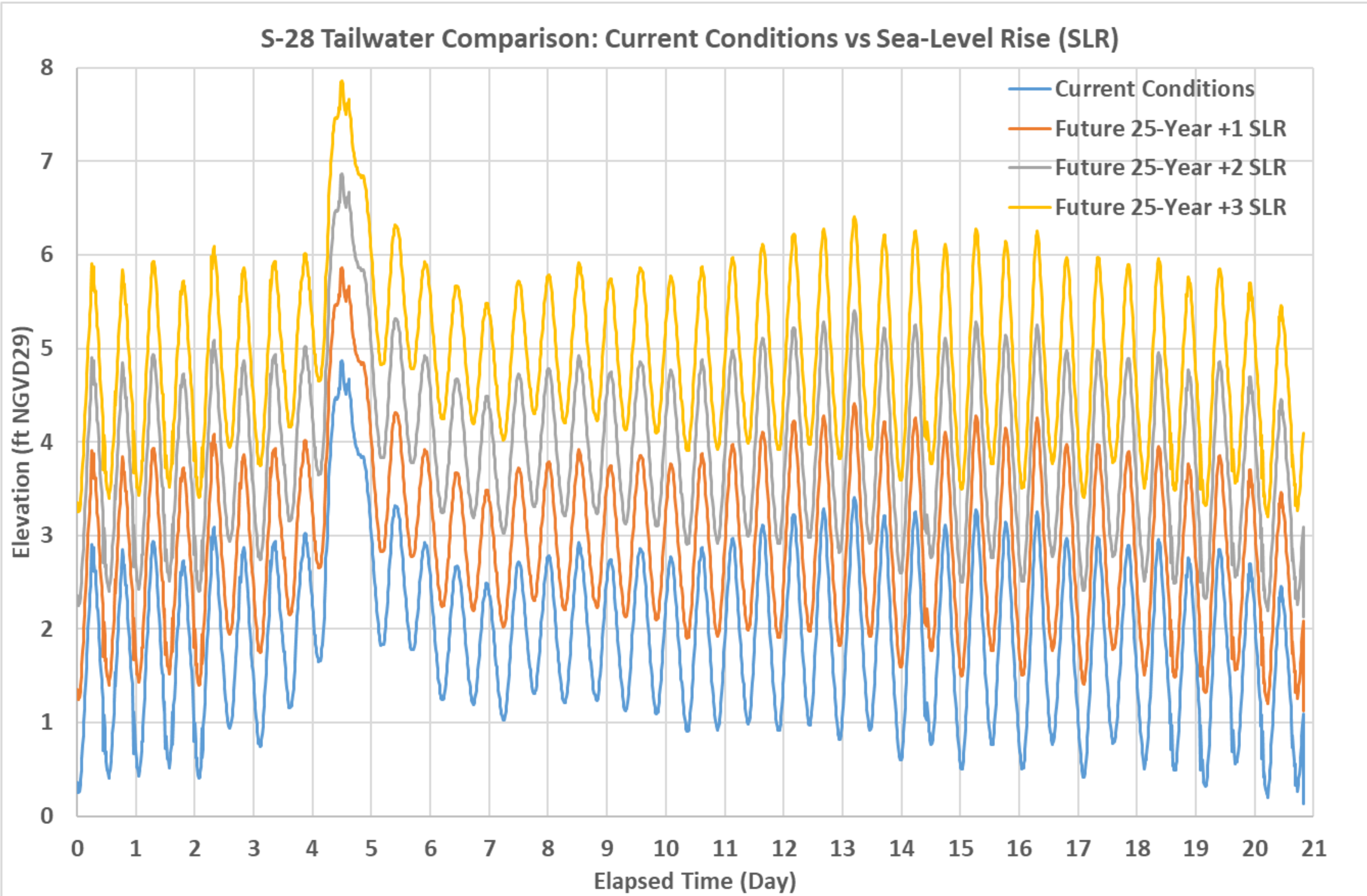

Figure 2.5-10: Future Conditions Sea Level Rise 25-Year Design Storm Tidal Boundary Stages for S-28

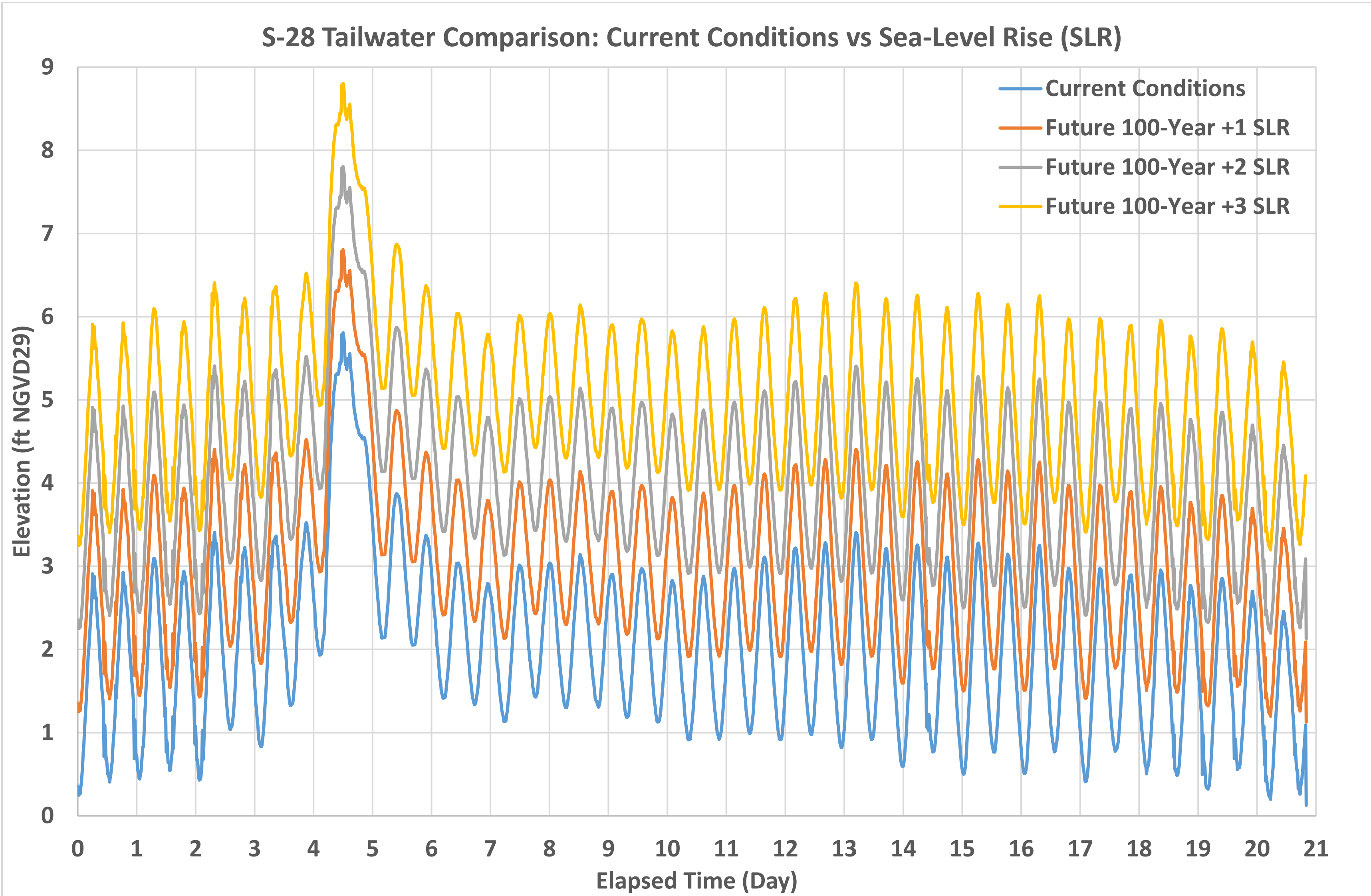

Figure 2.5-11: Future Conditions Sea Level Rise 100-Year Design Storm Tidal Boundary Stages for S-28

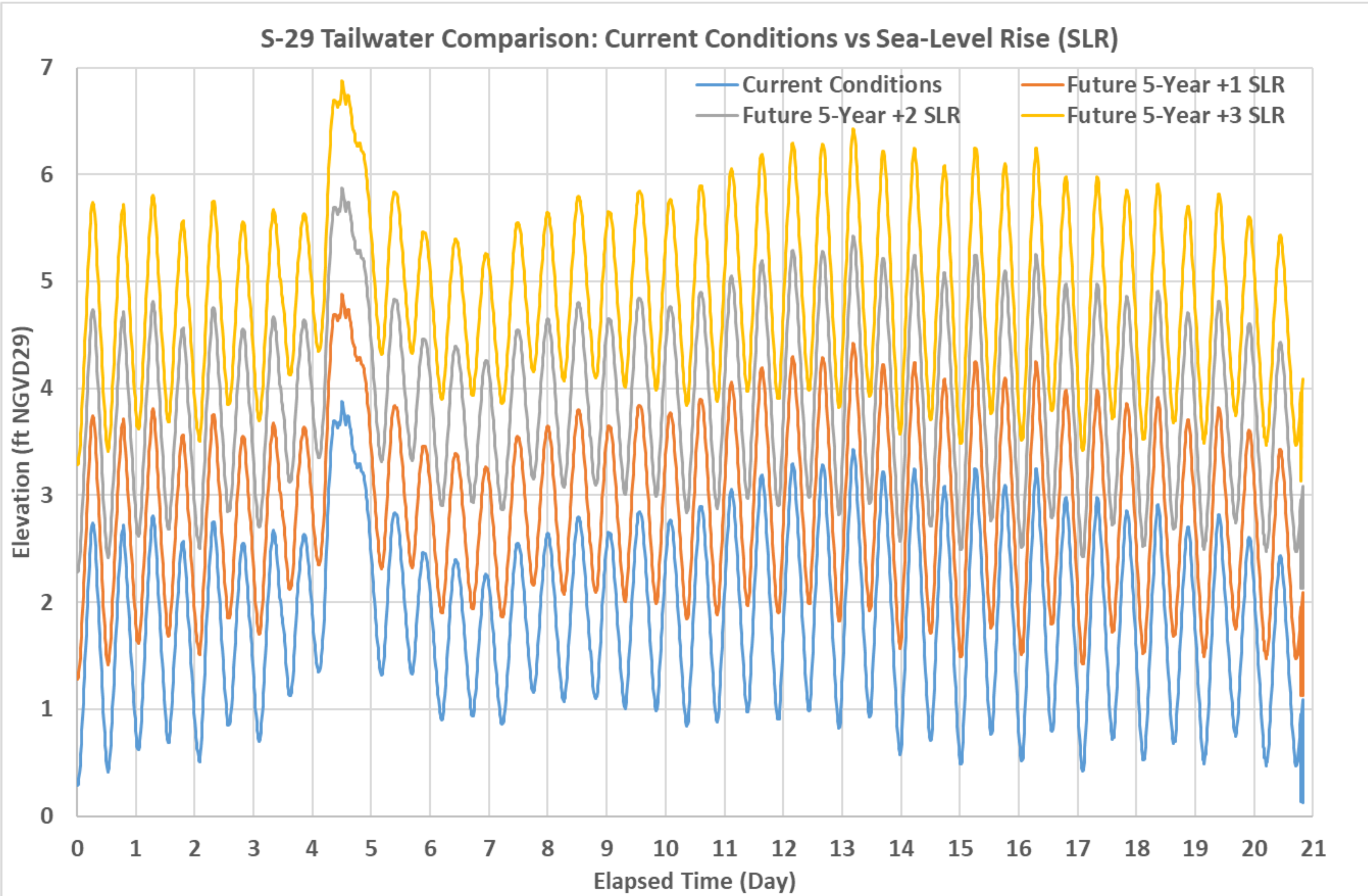

Figure 2.5-12: Future Conditions Sea Level Rise 5-Year Design Storm Tidal Boundary Stages for S-29

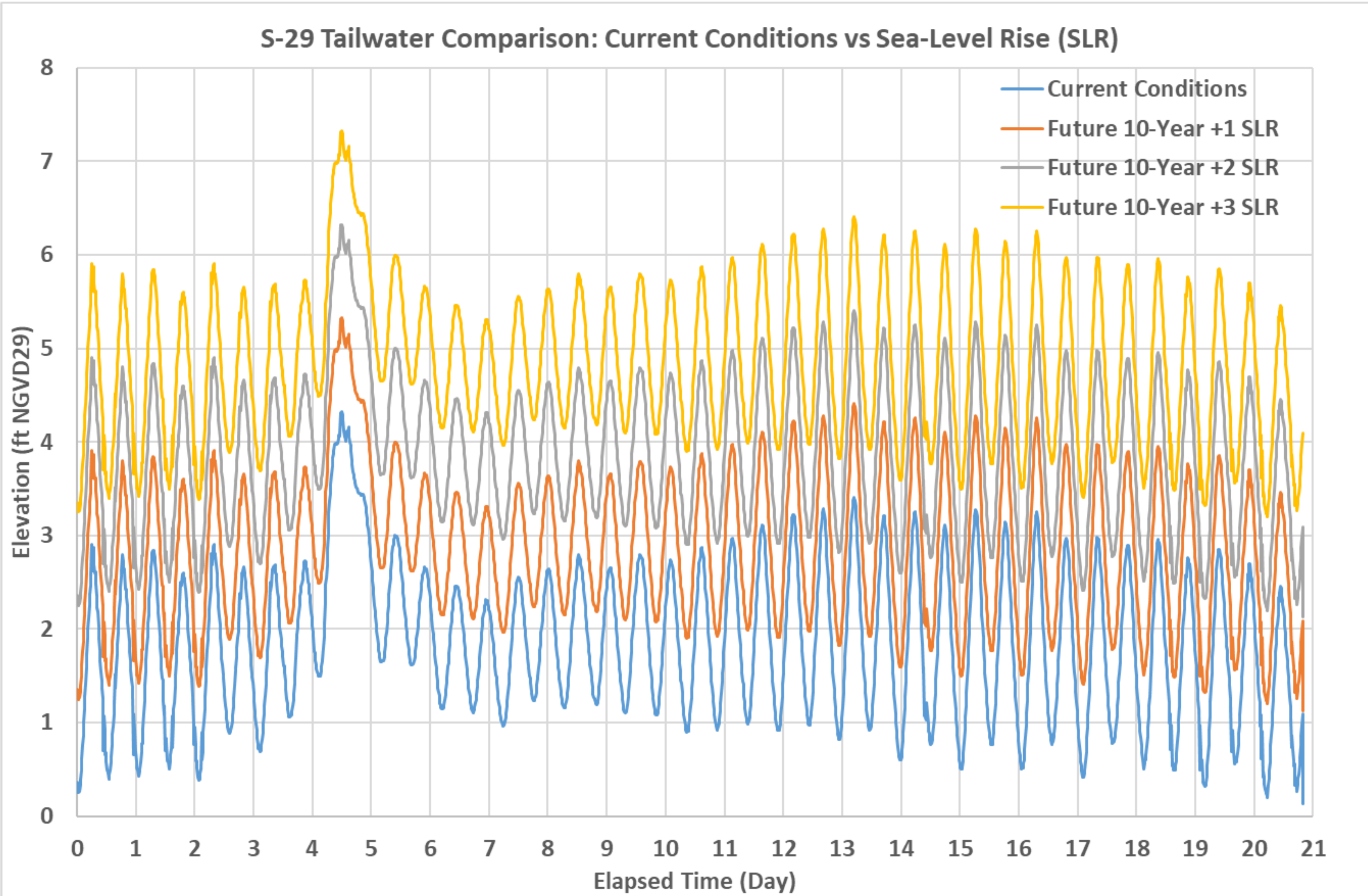

Figure 2.5-13: Future Conditions Sea Level Rise 10-Year Design Storm Tidal Boundary Stages for S-29

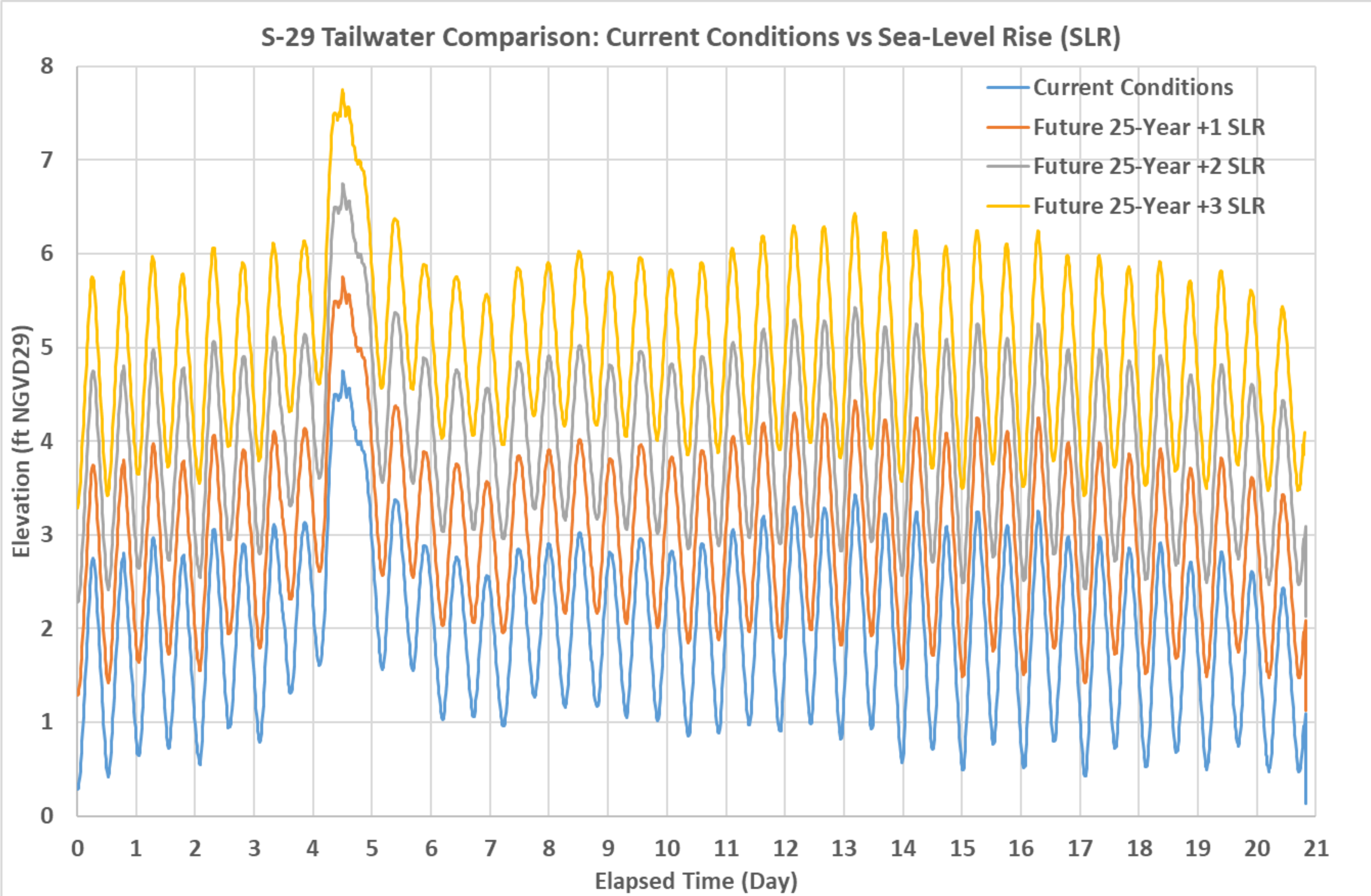

Figure 2.5-14: Future Conditions Sea Level Rise 25-Year Design Storm Tidal Boundary Stages for S-29

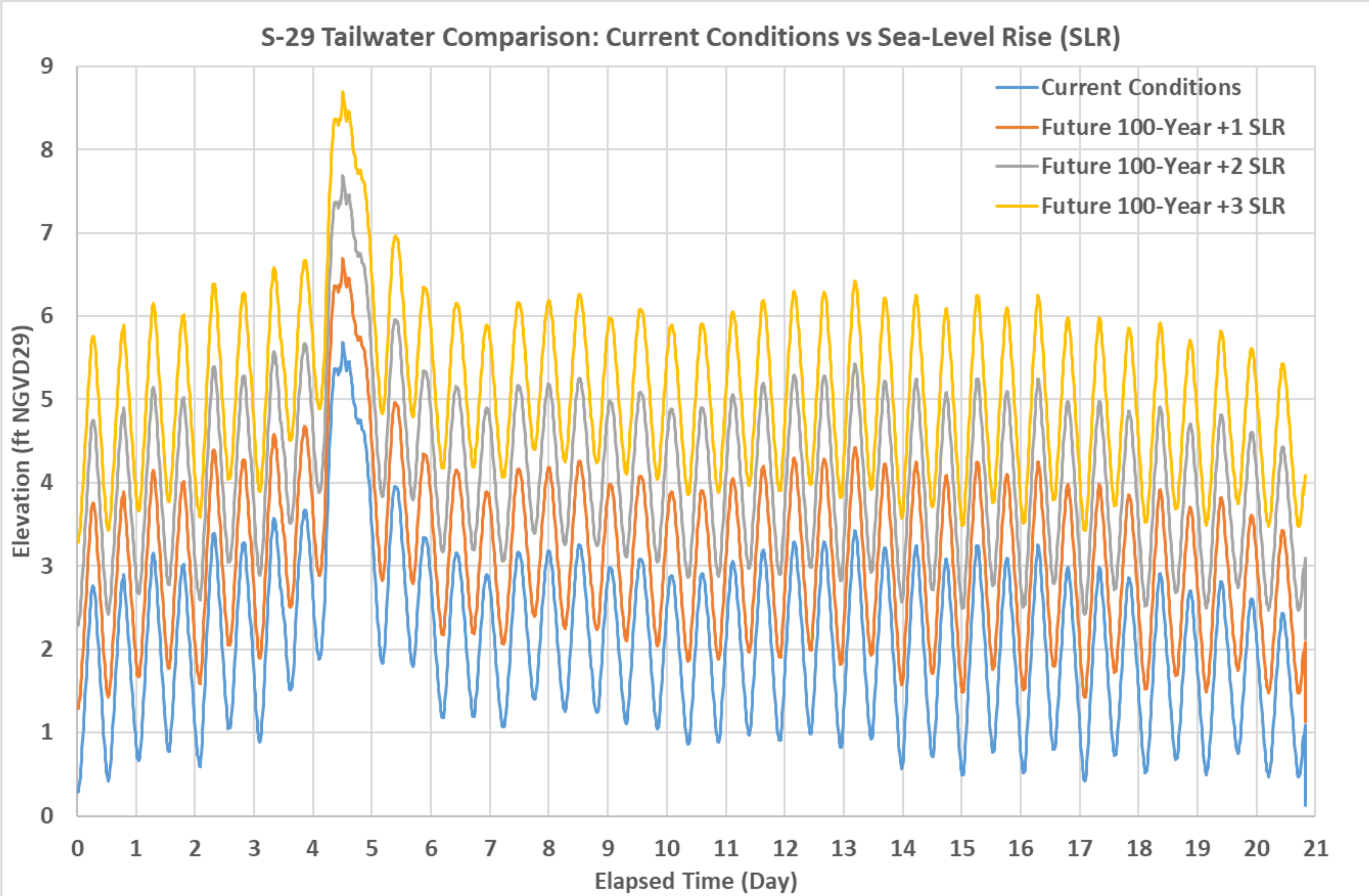

Figure 2.5-15: Future Conditions Sea Level Rise 100-Year Design Storm Tidal Boundary Stages for S-29

At the intercoastal waterway, water levels were forced based on the District-provided design storm surge stage time series data (**Figure 2.5-8** through **Figure 2.5-15**). On the southeast side of the model, the forced water levels (based on S-27 headwater) at the downstream boundary of the 1-D branches connecting to the C-7 Canals were updated to represent future conditions. Taylor Engineering proposed two methods for updating S-27 headwater to reflect the future conditions; (1) adding 1, 2, and 3 feet to the current conditions headwater (District's XPSWMM model simulated data) level to reflect the three sea level rise conditions while ensuring pre/post storm headwater is never lower than the low tide tailwater, and (2) increasing the headwater level by a factor determined through regression analysis of simulated future condition headwater levels based on the District's XPSMM model.

2.5.2.1 S-27 Headwater- Method 1

This method of developing future conditions headwater levels for the S-27 structure simply adds 1, 2, and 3 feet to the current condition's hydrograph, which was provided by the District (assumptions had to be made about pre/post storm water levels). As previously stated, this approach assumes that the S-27 structure maintains the same headwater/tailwater relationship that was observed in the District's XPSWMM current condition models. Adding 1, 2, and 3 feet to the current condition's headwater is the same as applying the current conditions headwater/tailwater ratio to the future conditions storm surge tailwater that includes 1, 2, and 3 feet of sea level rise. Slight adjustment to the pre/post storm water levels were made so that they do not drop below the minimum low tide tailwater elevation. This was done as it is unrealistic for a tidal spillway structure's headwater elevation to drop below the low tide tailwater elevation unless mitigation measures (i.e., a pump station) were to be implemented. An example of the proposed boundary condition hydrographs resulting from this method are shown in **Figure 2.5-16**.

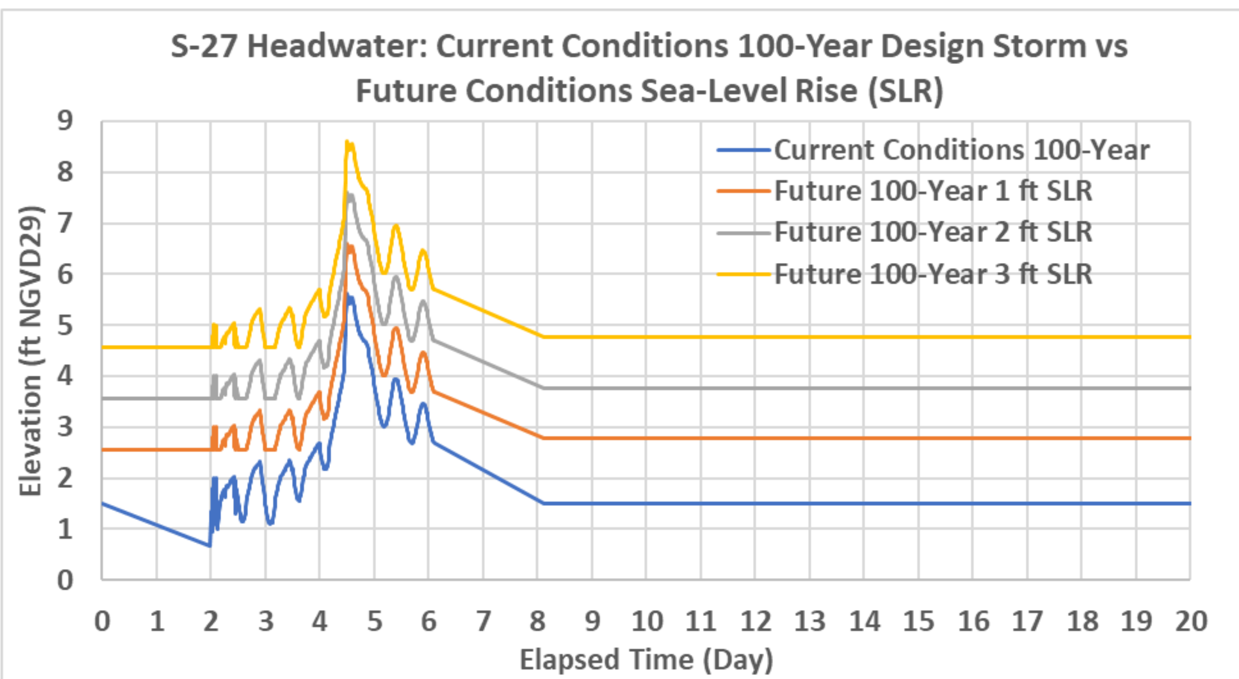

Figure 2.5-16: Example of S-27 Future Condition Headwater Stage Developed by Adding 1, 2, and 3 Feet to Current Conditions Stages

2.5.2.2 S-27 Headwater- Method 2

This method of developing future conditions headwater levels for the S-27 structure is based on a regression analysis of future conditions simulated data from the District's XPSWMM model. The District provided simulated future condition headwater levels for S-27 that for sea level rise scenarios of 0, 0.76, 1.09, and 2.21 feet, as shown in **Table 2-1**.

Table 2-1: SFWMD Future Conditions S-27 Peak Stage Under Various Sea Level Rise Conditions

Sea Level Rise in District's Future Conditions XPSWMM Model (ft)	Simulated Future Conditions Peak Water Level (ft NGVD29)
0 (base value)	5.941 (base value)
0.76	6.43
1.09	6.68
2.21	7.36

For this study, the sea level rise conditions are 1, 2, and 3 feet. Therefore, a regression analysis was conducted. The District's simulated future peak water levels were plotted against the amount of sea level rise and assigned the best-fitting trendline based on R^2 value, as shown in **Figure 2.5-17**.

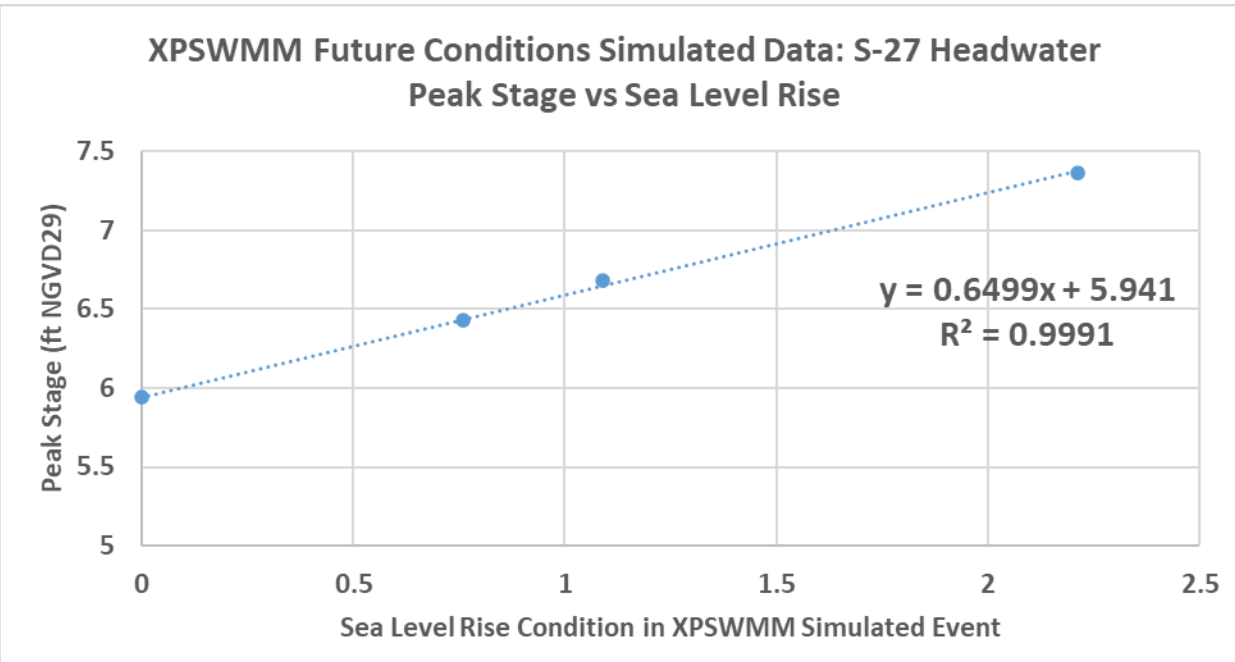

Figure 2.5-17: Regression Analysis of S-27 Future Conditions Headwater Stage vs Sea Level Rise

From the equation of the trendline, interpolated and extrapolated peak water levels for 1, 2, and 3 feet sea level rise were calculated. Then, a multiplication factor was calculated for each of the sea level rise conditions based on the simulated peak water level (peak water level with SLR divided by base peak water level), as shown in **Table 2-2**.

Table 2-2: Interpolated/Extrapolated Peak Water Levels from XPSWMM Future Conditions 100-Year Design Storm

Sea Level Rise Conditions (ft)	Interpolated/Extrapolated Peak Water Level based on XPSWMM Simulated Data (ft NGVD29)	Multiplication Factor
0 (base value)	5.94 (base value)	1.000
1	6.59	1.109
2	7.24	1.219
3	7.89	1.328

The multiplication factors shown in **Table 2-2** were multiplied with the current conditions headwater hydrograph for S-27. The peak water levels for S-27 headwater for future conditions sea level rise scenarios of 1, 2, and 3 feet are shown in **Table 2-3**. The S-27 headwater hydrographs for future condition sea level rise scenarios are shown in **Figure 2.5-18**.

Table 2-3: Peak Water Levels for S-27 Headwater for Future Conditions 100-Year Design Storms

Sea Level Rise Conditions (ft)	Current Conditions Peak Water Level	Multiplication Factor	Future Conditions Peak Water Level (ft NGVD29)
1	5.61	1.109	6.22
2		1.219	6.84
3		1.328	7.45

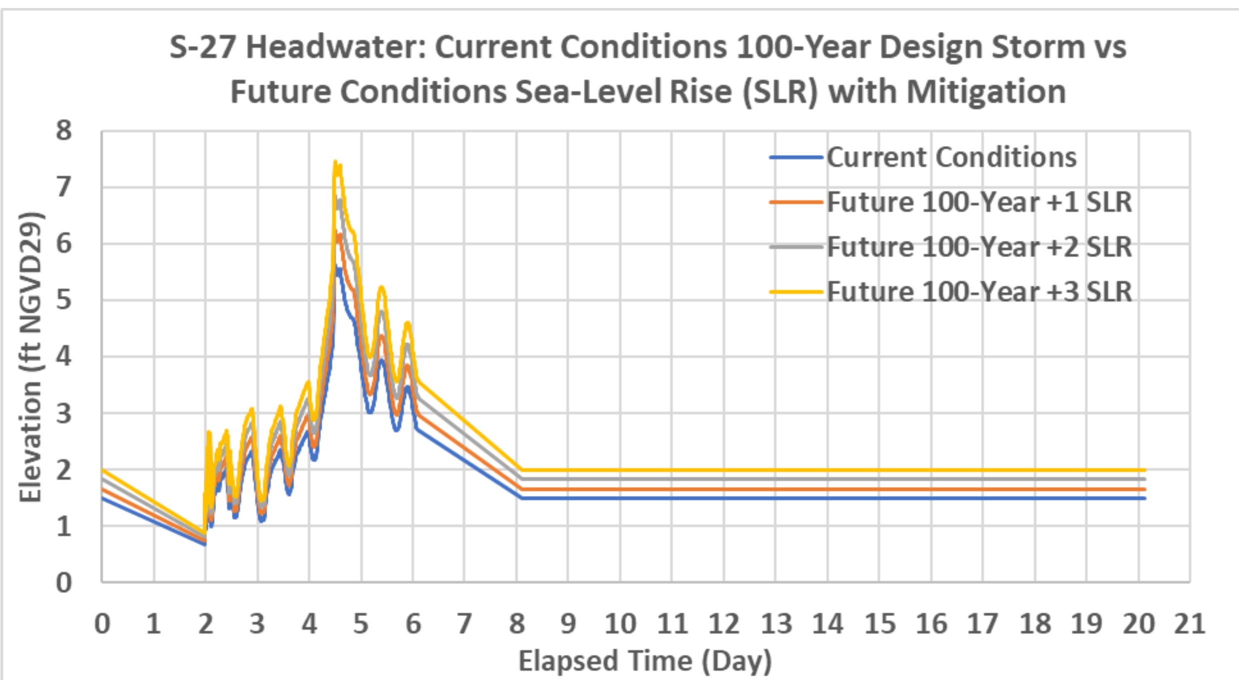

Figure 2.5-18: S-27 Future Conditions Headwater for 100-Year Design Storm Based on Regression Analysis of Future Conditions Simulated Data with Mitigation Measures

2.5.2.3 S-27 Headwater- Method Comparison and Sensitivity

The two methods of developing the S-27 headwater boundary represent different levels of conservativeness, with the higher boundary representing the most conservative scenario in terms of worst case flooding in the model. When this model was developed, the C-7 Canal was chosen as a boundary condition for two reasons: (1) There was observed data that was useful for calibrating/validating the model, and perhaps more importantly, (2) It was believed to be at a distance from the area of interest (C-8 basin/canal) such that any uncertainty in the boundary condition should have minimal effect on the outcome of the simulations. As there are two different levels of conservativeness that could be made for the future conditions water levels in the C-7 Canal, a sensitivity test was performed for the S-27 headwater boundary.

The sensitivity test was conducted using the current conditions model, with modified tailwater levels at S-28 and S-29 (to represent sea level rise) and the new headwater levels at S-27 headwater. The current conditions model was used so that the effects of the boundary condition could be determined without the effects of any other changes to the model such as land use and increased groundwater levels. Therefore, two model simulations were completed using the 100-year design storm with 3 ft of sea level rise. **Figure 2.5-19** shows the two S-27 headwater hydrographs and the respective tailwater hydrograph. The peak water level under the second method is about 1.2 ft lower than the more conservative approach of applying the current conditions headwater/tailwater ratio to the 3 ft storm surge tailwater hydrograph.

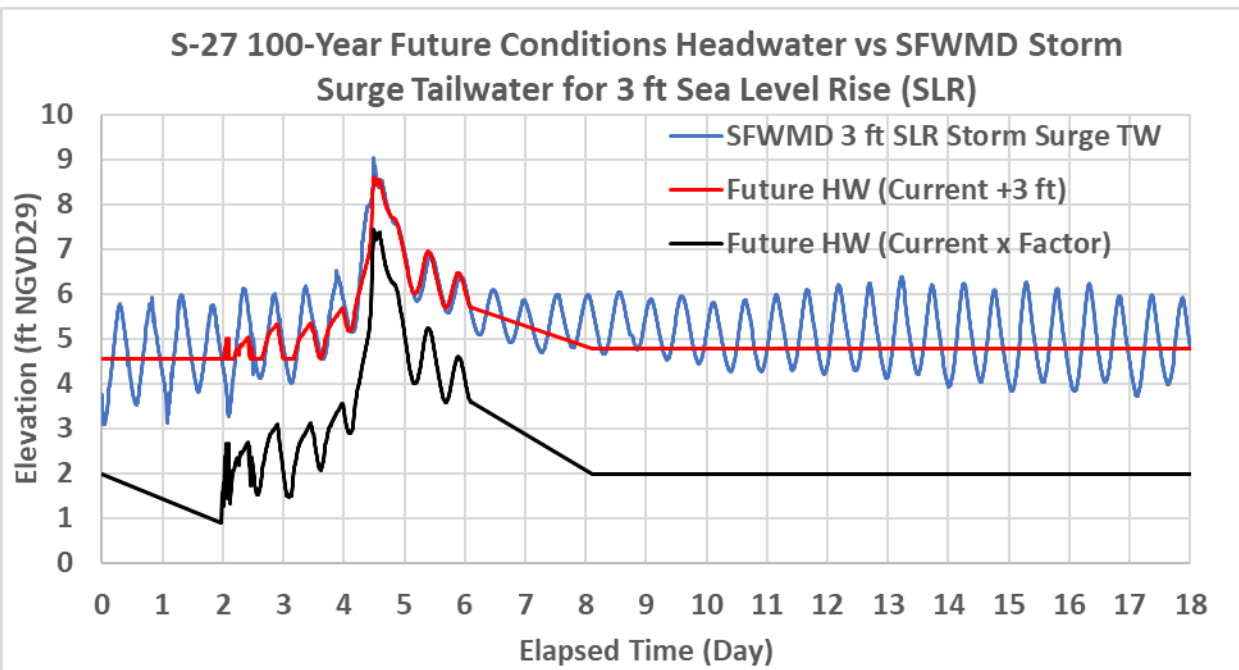

Figure 2.5-19: Comparison of the Developed 100-Year Design Storm S-27 Headwater Hydrographs and the SFWMD Storm Surge Design Storm Tailwater for 3 ft Sea Level Rise

Although the two approaches were significantly different, there was no significant difference indicated by the sensitivity test. The method of applying 3 ft to the current conditions hydrograph resulted in only 0.1 ft higher peak stages at S-28Z (upstream) and S-28 (downstream) of the C-8 Canal (**Figure 2.5-20** and **Figure 2.5-21**, respectively), when compared to the method of applying a multiplication factor. This small increase did not propagate into the C-9 Canal, which maintained the same levels. Additionally, there were no notable differences in duration of high-water levels in the C-8 Canal. The method of applying 3 ft to the current conditions hydrograph resulted in reduced inter-basin discharge from the C-8 to the C-7, when compared to the multiplication factor approach, although it was larger than under current conditions.

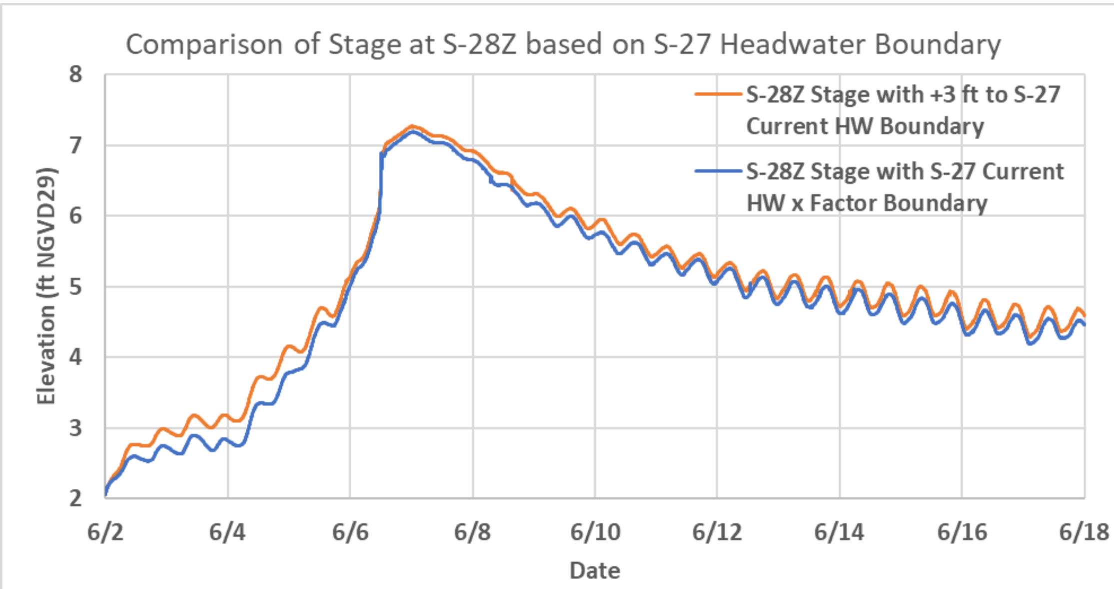

Figure 2.5-20: Headwater Stage Comparison at S-28 for Sensitivity Test

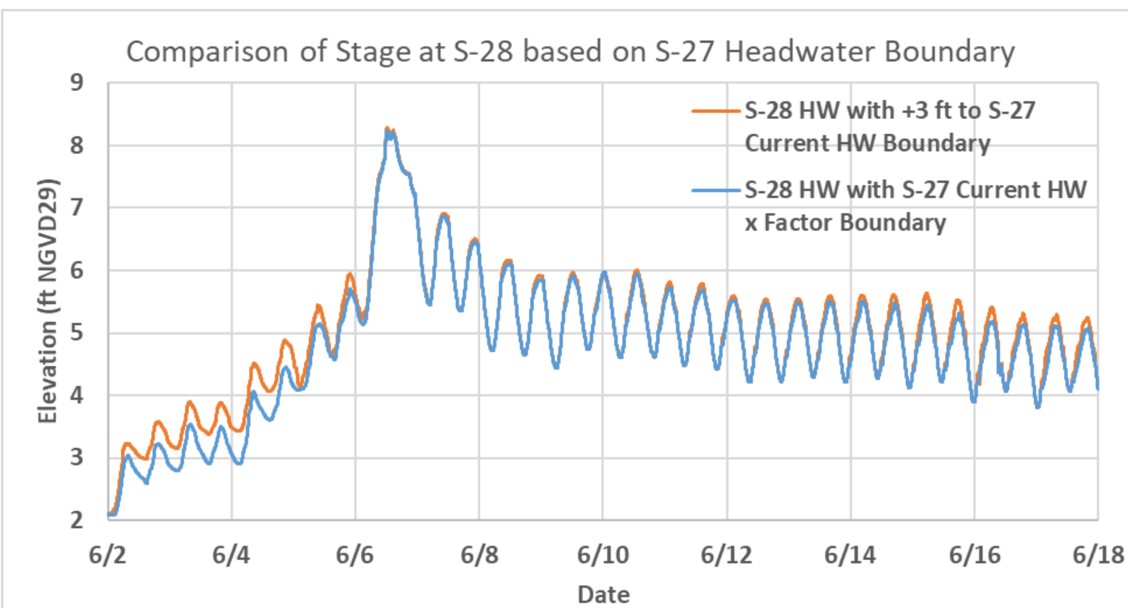

Figure 2.5-21: Stage Comparison at S-28Z for Sensitivity Test

The sensitivity test accomplished two things: (1) It demonstrated that either boundary could be used, as there was no significant difference in the C-8 model results and (2) It validated the assumption that the boundary was far enough from the area of interest that uncertainty in the boundary conditions had minimal effect on the outcome.

Both methods of developing future conditions headwater levels for S-27 were reasonable. Taylor Engineering, supported by the District, decided to use the first method, which increased the current conditions headwater by 1, 2, and 3 feet. This aligned with the District's direction of using the conservative approach. This approach was reasonable as it was believed that the S-27 structure would likely be overtopped/bypassed for each sea level rise condition unless mitigative measures are implemented in the future.

The recommended S-27 headwater boundary hydrographs for each of the design storms are shown in **Figure 2.5-22** through **Figure 2.5-25**.

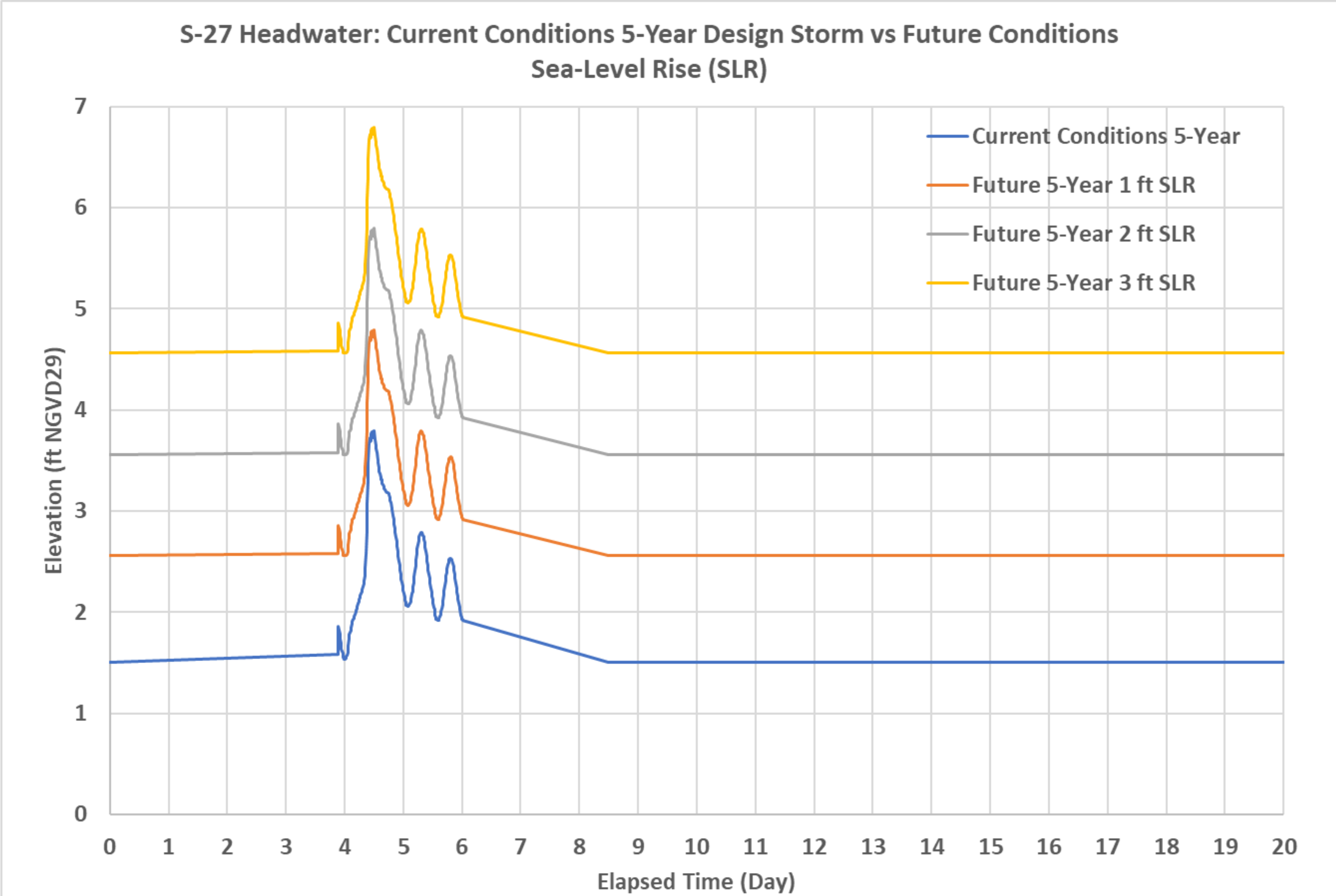

Figure 2.5-22: S-27 Future Condition Headwater Stages for 5-Year Design Storm under 3 Sea Level Rise Scenarios

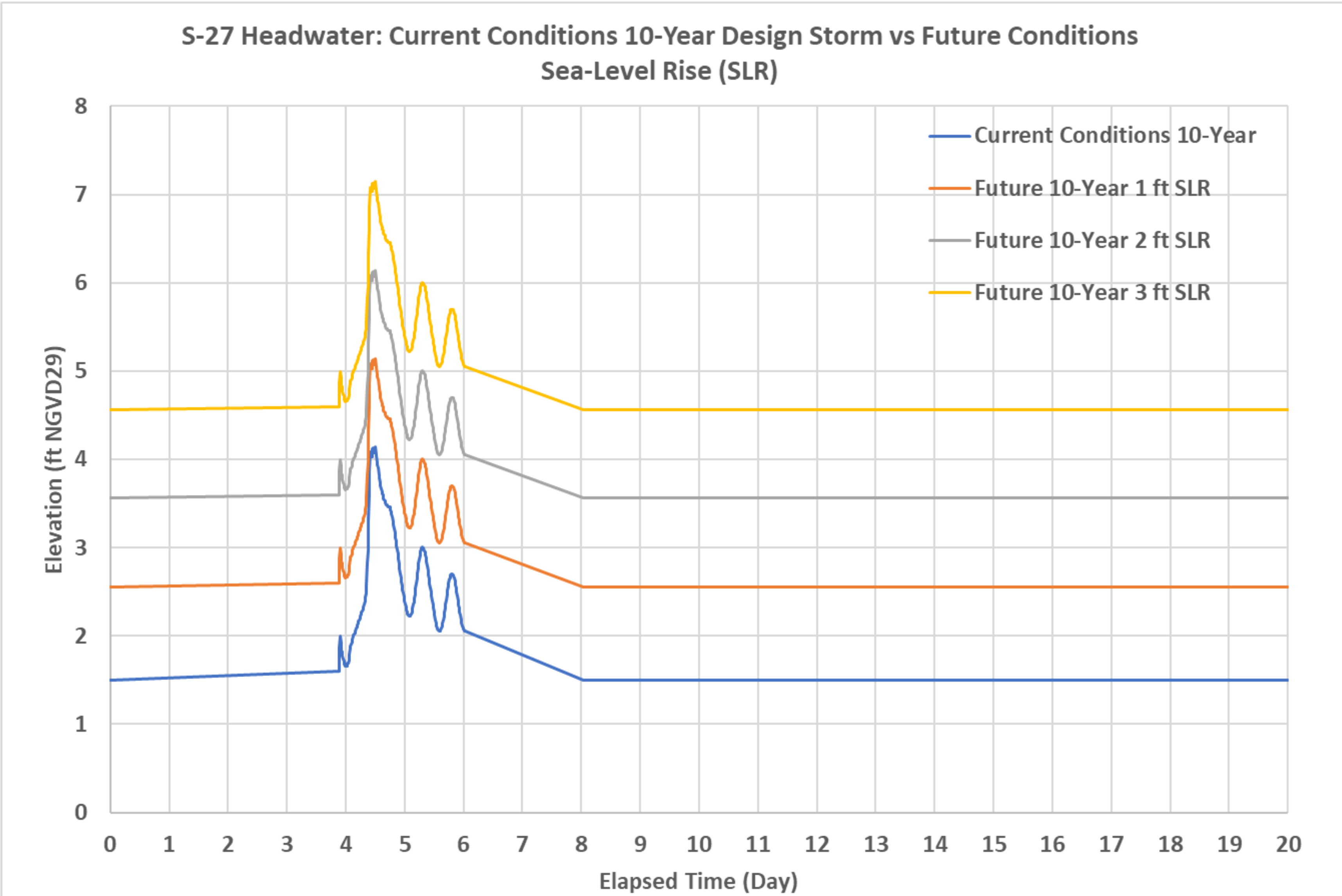

Figure 2.5-23: S-27 Future Condition Headwater Stages for 10-Year Design Storm under 3 Sea Level Rise Scenarios

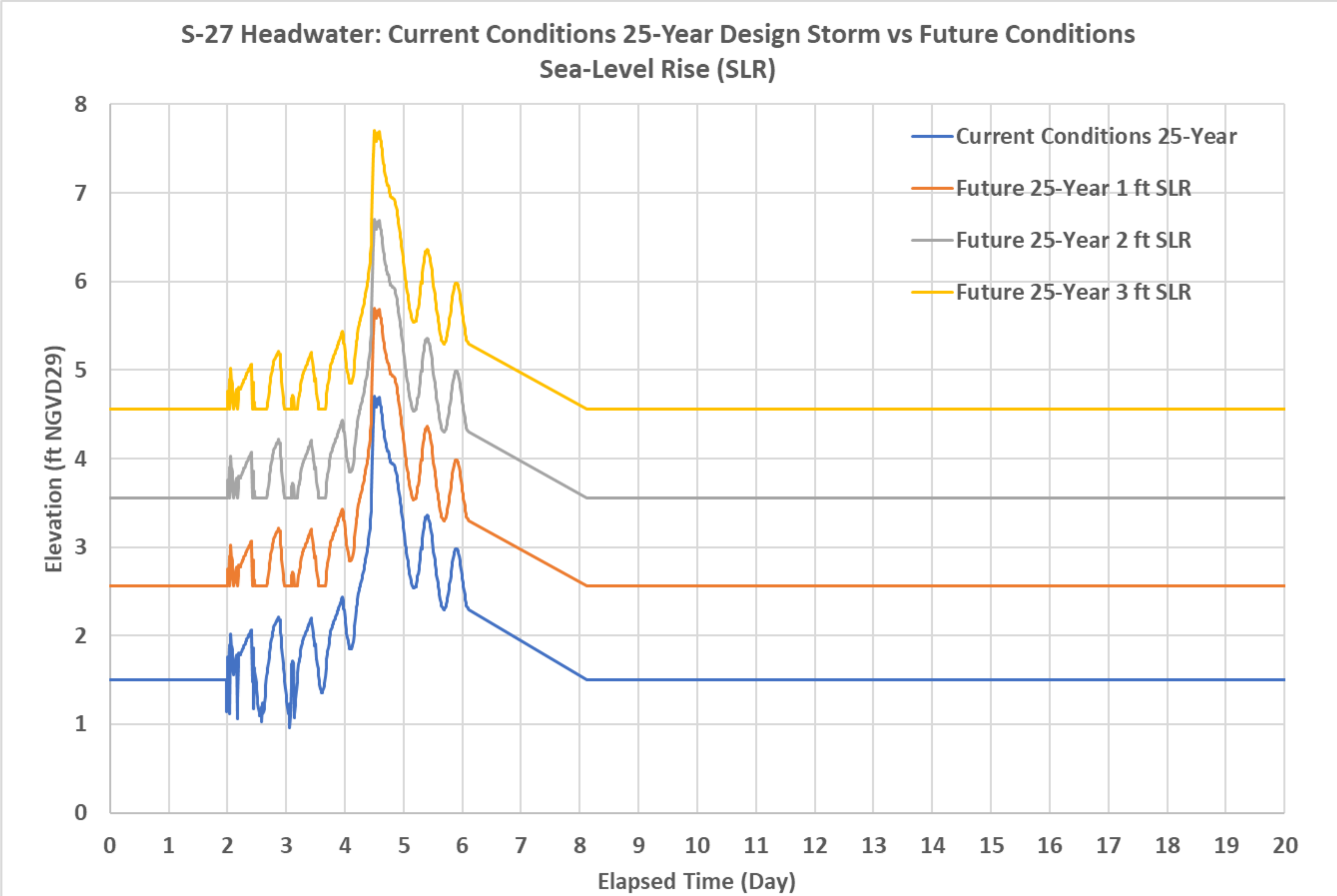

Figure 2.5-24: S-27 Future Condition Headwater Stages for 25-Year Design Storm under 3 Sea Level Rise Scenarios

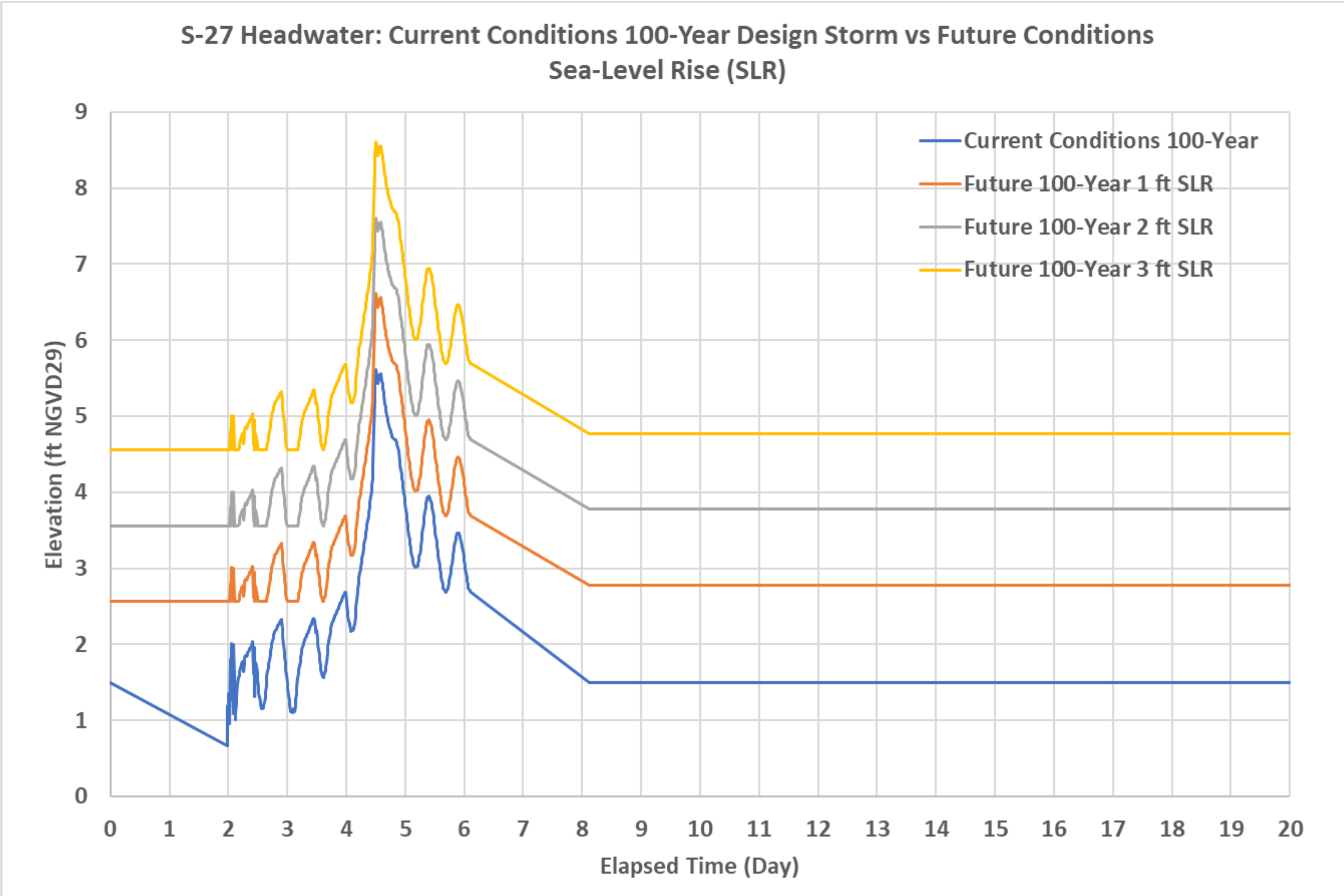

Figure 2.5-25: S-27 Future Condition Headwater Stages for 100-Year Design Storm under 3 Sea Level Rise Scenarios

2.6 Initial Groundwater

For this study, the initial groundwater levels for future conditions were developed using the Broward County Future Groundwater Map (from the 2019 Broward County MIKE SHE Future Conditions 2060 model) and merging it with adjusted Miami-Dade potentiometric surface contours for the current conditions. Then, any area in the future conditions map that was lower than current conditions was replaced with the current condition groundwater level. The Broward County Future Initial Potential Head Map was based on a 26" of sea level rise. The Miami-Dade County potentiometric surface contours were adjusted by shifting the current condition contours to align with the contours created from the Broward County future conditions data. The Broward County Future Conditions Initial Potential Head Map covered the majority of the model domain.

As the Broward County data was based on 26" of sea level rise, the map described in the preceding paragraph was deemed appropriate to be used as the future conditions potentiometric surface map for the 2 ft sea level rise scenario. To develop the future potentiometric surface map for the 1 and 3 ft sea level rise scenarios, the current conditions groundwater surface elevation was subtracted from the future groundwater surface elevation for the 2 ft SLR scenario. The result of this was a difference map that showed how much the groundwater levels would increase from current conditions. This difference map was multiplied by 50% to represent the increase in groundwater due to 1 ft of sea level rise. To develop the future conditions potentiometric surface map for the 1 and 3 ft SLR scenario, the 50% difference map was subtracted and added to the 2 ft SLR future groundwater map, respectively. **Figure 2.6-1** through **Figure 2.6-3** show the future conditions initial potentiometric surface maps for each of the three sea level rise scenarios. Please note that the discontinuous groundwater elevations and checkered pattern are artifacts of the source data and the process of merging different datasets. These artifacts disappeared within the first few minutes of the simulation and there is a 2-day spin-up period prior to the design storms, which allows the groundwater to come to a dynamic equilibrium before the start of the design storm rainfall.

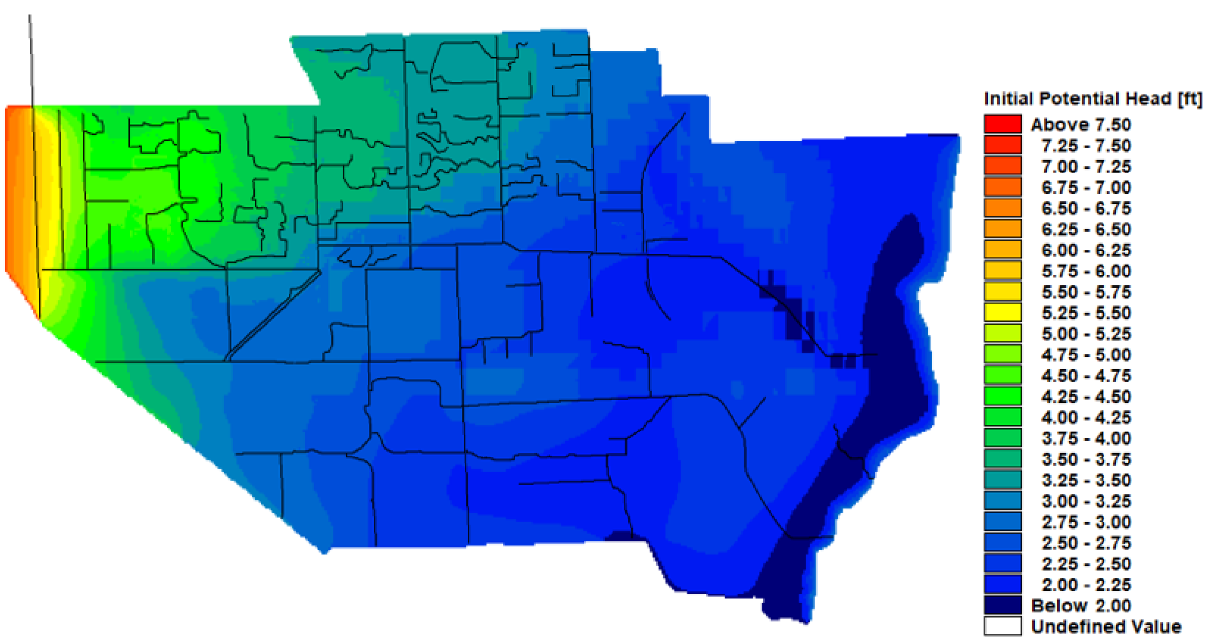

Figure 2.6-1: Future Conditions Initial Groundwater Levels for 1 ft Sea Level Rise

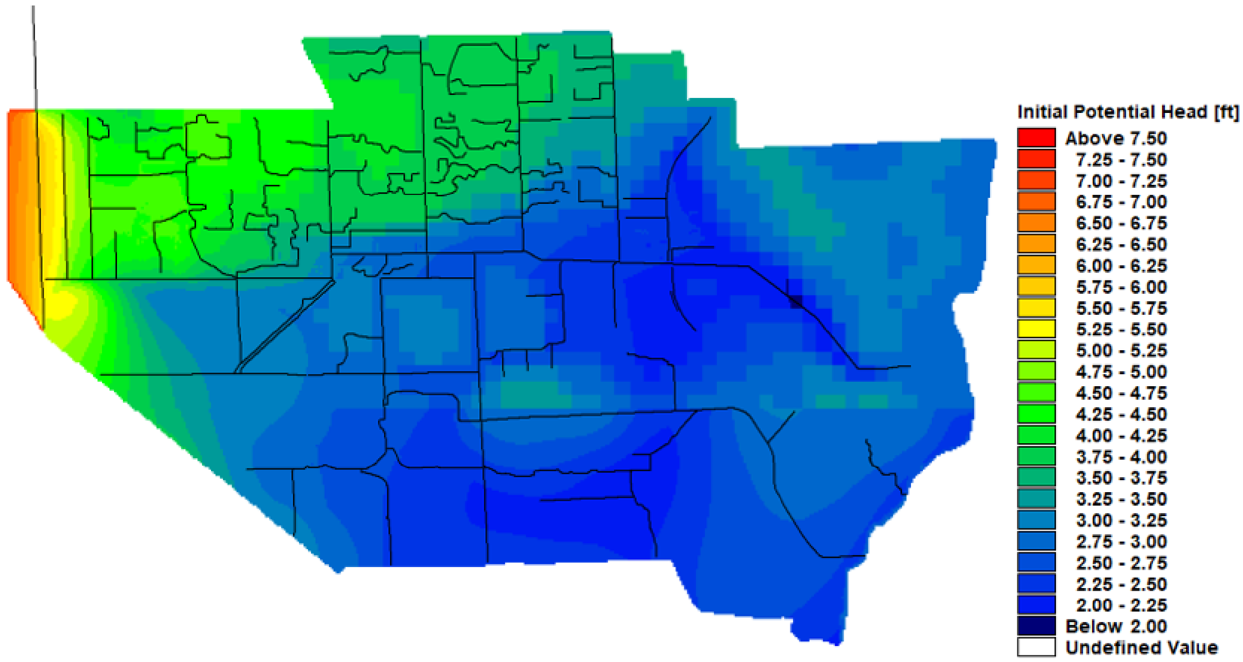

Figure 2.6-2: Future Conditions Initial Groundwater Levels for 2 ft Sea Level Rise

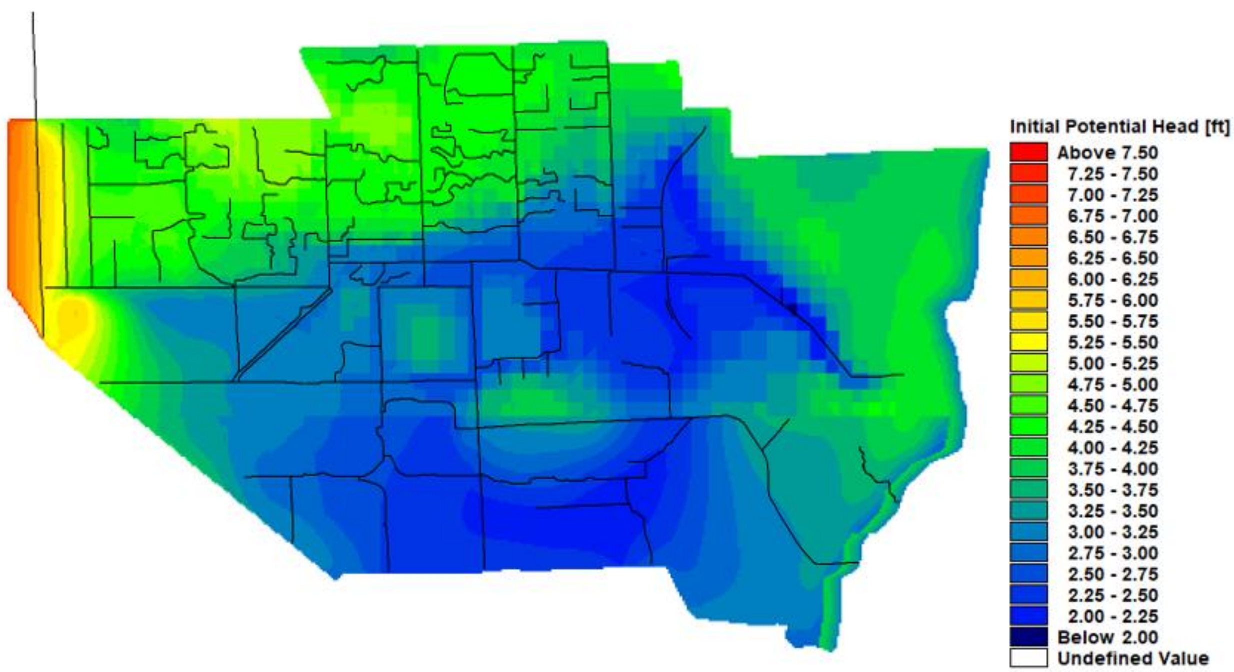

Figure 2.6-3: Future Conditions Initial Groundwater Levels for 3 ft Sea Level Rise

3 FLOOD PROTECTION LEVEL OF SERVICE METRICS

The District relies on six (6) formal performance metrics (PMs) to evaluate the flood protection level of service provided by the primary water management infrastructure. These metrics, defined briefly in this section, were initially derived from the District publication *Flood Protection LOS Analysis for the C-4 Watershed, Appendix A: LOS Basic Concepts* (SFWMD H&H Bureau, December 29, 2015) and later refined by Interflow Engineering and Taylor Engineering in the Big Cypress Basin FPLOS Study. **Section 4** provides the results of the FPLOS evaluation for future conditions with sea level rise.

PM #1 Maximum Stage in Primary Canals – This is the peak stage profile in the primary canal system. The profile is developed for the 72-hour duration, 5-year, 10-year, 25-year, and 100-year recurrence frequency design storms. The largest design storm that stays within the canal banks establishes the FPLOS of the primary canal system.

PM #2 Maximum Daily Discharge Capacity through the Primary Canals – This is the maximum discharge capacity throughout the primary canal network. Discharge is calculated as area weighted flow, in units of cubic feet per second per square mile of contributing area for the 25-year design event. Tidal effects are filtered by using a 12-hour moving average of discharge. Although the peak of the 25-year net discharge hydrographs are referred to in this report as the calculated discharge capacity, the true capacity of the canal segment is the net discharge corresponding to the largest design flood event that remains within the banks of the canal using the results of the 5-year, 10-year, 25-year, and 100-year events.

PM #3 – Structure Performance – Effects of Sea Level Rise – This metric shows the effective capacity of a tidal structure. It is comparable to the static design condition assumed in the original design but compares structure flow over a range of storm surge events and a range of sea level rise scenarios. Phase 1A of this project evaluated structure performance during current conditions, with no effects of sea level rise. For this Phase 1B of this project, the structure performance is evaluated under 1, 2, and 3 ft sea level rise.

PM #4 Peak Storm Runoff – Effects of Sea Level Rise – This is the maximum conveyance capacity of a watershed at the tidal structure for a range of design storms. It shows the maximum conveyance (moving 12-hour average) for a specific design storm and a specific tidal boundary condition. This metric examines the behavior of the system under severe stress and can be used to check if conditions exceed design limits. In evaluating this PM, it is assumed that design rainfall and design storm surge occur simultaneously, which maximizes stress on the structure. This metric was analyzed in Phase 1A of this project, in which current conditions were evaluated. For this project (Phase 1B), the future condition design storms were analyzed and the effects of sea level rise were compared with current conditions.

PM #5 Frequency of Flooding – Stage-based FPLOS for Subwatersheds – In this metric, the flood elevations or depths of overland flooding are evaluated for the 72-hour duration, 5-year, 10-year, 25-year, and 100-year recurrence frequency design storms. These flood depths/elevations can then be compared with elevations of build features such as buildings and roadways, where such information exists. For the purposes of this C-8 and C-9 FPLOS evaluation, flood inundation maps were developed from the model output for each storm event.

PM #6 Duration of Flooding – This metric quantifies the duration of flooding across the entire watershed. For this Study, the length of time the flood elevation is projected to be above a threshold depth of 0.25 ft was mapped over the entire study area using the multi-cell gridded model output files for the 2-D overland flow component.

4 FLOOD PROTECTION LEVEL OF SERVICE – FUTURE CONDITIONS SEA LEVEL

Future conditions with sea level rise was simulated for the 72-hour 5-year, 10-year, 25-year, and 100-year 3-day design storm events. For each design storm, three future sea level rise scenarios, 1, 2, and 3 ft, were simulated (SLR1, SLR2, and SLR3). The model setup for these scenarios was previously described in **Section 2**. **Appendix A** provides a summary of the model results at primary control structures. The remainder of this section describes the results of the FPLOS evaluations. For comparison purposes, figures in PM #1, #2, and #4 present future conditions results with the current conditions results.

4.1 PM #1 – Maximum Stage in Primary Canals

This is the peak stage profile in the primary canal system. The profile is developed for the 72-hour 5-year, 10-year, 25-year, and 100-year design storms. The largest design storm that stays within the canal banks establishes the FPLOS of the primary canal system.

To evaluate this PM under future conditions within the C-8 and C-9 watersheds, instantaneous peak stage profiles were prepared for the primary canals within the watersheds, which are the C-8 and C-9 Canals, respectively. Bank elevations on the profile figures are based on the MIKE HYDRO cross-section data. Also shown in the figures are major roadway landmarks, control structures, and primary canal junctions.

Table 4-1 through **Table 4-3** summarize the PM #1 results for SLR 1, SLR2, and SLR3, respectively, which are shown graphically in **Figure 4.1-2** through **Figure 4.1-9**. These tables list the maximum return period profile that is contained within the canal banks.

Although the C-8 Canal contained the 5-year and 10-year profiles along the majority of the canal length under current conditions, the banks were exceeded in several locations for the 5-year SLR1 event. Similarly, although the C-9 Canal contained the 10-year and 25-year profiles along the majority of the canal length under current conditions, the bank elevation was exceeded for the 5-year SLR1 event at a few locations. Therefore, if a strict interpretation of this criteria is used, then both the C8 and C9 Canal have less than a 5-year FPLOS. However, as summarized in the Conclusions, the determination of FPLOS should consider the results of all applicable performance metrics. With careful consideration of PM #1 and PM #5, the C8 and C9 Canals provide a 5-year and 10-year FPLOS for SLR1 and SLR2, respectively. For SLR3, both the C8 and C9 Canals provide less than a 5-year FPLOS. With respect to **Table 4-1** through **Table 4-3**, "FPLOS Localized" is the return period that any bank exceedances are noticed, even if it doesn't correspond to a significant area of flood inundation as shown in PM #5. FPLOS overall is the return period in which there are several bank exceedances and/or the bank exceedances correspond to a significant area of flood inundation as shown in PM #5.

Table 4-1: PM #1 Summary Results for Sea Level Rise 1

Canal Segment	Figure Number	FPLOS Localized	FPLOS Overall	Comment
C-8	**Figure 4.1-2**	5-year	5-Year	Overall FPLOS from **Section 6.1.1**
C-9	**Figure 4.1-3**	5-year	10-year	Overall FPLOS from **Section 6.1.2**

Table 4-2: PM #1 Summary Results for Sea Level Rise 2

Canal Segment	Figure Number	FPLOS Localized	FPLOS Overall	Comment
C-8	**Figure 4.1-2**	5-year	<5-year	Overall FPLOS from **Section 6.1.1**
C-9	**Figure 4.1-3**	5-year	10-year	Overall FPLOS from **Section 6.1.2**

Table 4-3: PM #1 Summary Results for Sea Level Rise 3

Canal Segment	Figure Number	FPLOS Localized	FPLOS Overall	Comment
C-8	**Figure 4.1-2**	5-year	5-year	Overall FPLOS from **Section 6.1.1**
C-9	**Figure 4.1-3**	5-year	5-year	Overall FPLOS from **Section 6.1.2**

The PM #1 performance of the C-8 Canal under future conditions is generally worse east of its confluence with the Opa Locka Canal compared to the western segment. Notable areas of bank exceedances as shown in **Figure 4.1-2** include:

- Downstream of NE 6th Avenue (CR915) south bank exceeded for 5-year SLR1 event.
- Just west of NE 6th Avenue (CR915), north and south bank exceeded for 5-year SLR1 event.
- Downstream of NE 135th St. (CR 916), north and south bank exceeded for 5-year SLR1 event.
- From North Miami Avenue to NE 135th St., south bank exceeded for 5-year SLR1-year event.
- Downstream of Opa Locka Canal, south bank exceeded for 5-year SLR1 event.
- Halfway between Marco Canal and State Highway 9, south bank exceeded for 5-year SLR1.

Under current conditions, the hydraulic grade line of the C-8 Canal typically had a positive gradient downstream towards the tidal structure. However, under future sea level rise conditions, this gradient becomes zero and often negative. The inflection point is the point at which the slope of the hydraulic grade line changes from positive to negative. For the 5-year SLR1 and SLR2 events, the hydraulic grade line becomes flat, or zero, in a few locations. This suggests that the effects of sea level rise are in equilibrium with the effects of increased initial groundwater elevations and higher runoff potential. However, for the 5-year SLR3 event, there is no inflection point as everything upstream of S-28 has a negative gradient. This suggests that the effects of 3 feet of sea level rise are more influential than the increase in initial groundwater and runoff potential, which is what causes the flow direction to shift from west to east (inland to tide) to east to west (tide to inland). A similar trend is shown for each design storm under the 3 ft sea level rise condition. For the 25-year 2 ft sea level rise event, the inflection point was shifted about 8000 ft upstream from NE 6th Ave for SLR1 to NE 135th St, compared to the 25-year SLR1 event.

The PM #1 performance of the C-9 Canal under future conditions is generally worse east of its confluence with Carol City Canal A compared to the western segment. Notable areas of bank exceedances in the C-9 Canal as shown in **Figure 4.1-3** include:

- Upstream of S-29, south bank exceeded for 5-year SLR1 event.
- Halfway between I-95 and S-29 to S-29, south bank exceeded for 5-year SLR1 event, north bank for the 5-year SLR2 event.
- Downstream of US Hwy 441, north bank exceeded for 10-year SLR1 event and 5-year SLR2 event, south bank exceeded for 10-year SLR3 event and 25-year SLR2 event
- From SBDD pumps S-4 and S-5 to Highway I75, south bank exceeded for the 5-year SLR3 event and 10-year SLR2 event.
- From SBDD pumps S-3 to the Ronald Reagan Turnpike, south bank exceeded for the 5-year SLR3 event and the 25-year SLR1 event

Under current conditions, the C-9 Canal typically had a positive gradient downstream towards the tidal structure for the 5-year and 10-year design storms. For both the 25-year and 100-year current condition design storms, inflection points could be seen in multiple locations, including near the SBDD S-4/S-5 pump stations and near the SBDD S-2 pump station. Under current conditions, these inflection points appear to be mostly caused by the discharge from the pump stations, causing localized high water levels that cause flow both west (towards inland) and east (towards tide). Under future conditions, although the pump discharge still contributes, the inflection points become influenced by the increase in sea level rise as well. Please note that the reason that SLR1 peak stage in the western C-9 Canal is lower than current conditions is because of the C-9 Impoundment pulling water from the western end of the C-9 Canal.

It is important to note that the maximum water levels presented in the maximum surface water profiles do not occur at the same time; they are the maximum stage at each location regardless of timing. For the 5-year and 10-year future conditions SLR1 design storms, an inflection point or dip in the profile between the SBDD S-4/S-5 pump stations and Highway I75 can be seen. **Figure 4.1-1** shows two instantaneous moments of the water surface profile for the C-9 Canal. The right side of the dip, between Highway I75 and SBDD S-7 pump station, occurs at the peak of the design storm, which has the highest rainfall and the highest storm surge levels (pink portion of the graph). At the peak of the design storm, the C-9 Impoundment is pumping which caused lower water levels in the western C-9 Canal. This results in a steep hydraulic grade line from east to west. About 24 hours later, the rainfall has finished, the maximum storm surge has passed, the C-9 Impoundment has stopped pumping, the S-29 structure is near peak discharge, and there is still discharge into the C-9 Canal. This causes the water levels in the western C-9 Canal to rebound and results in a steep hydraulic grade line from west to east (blue portion of the graph). At some point during the simulation, the water level where the two grade lines overlap were higher than it was during the two instantaneous moments captured in the figure, however, it was lower than current conditions. The dip in the profile, which is lower than current conditions, is in part a result of the two "extremes" causing lower levels in the canal.

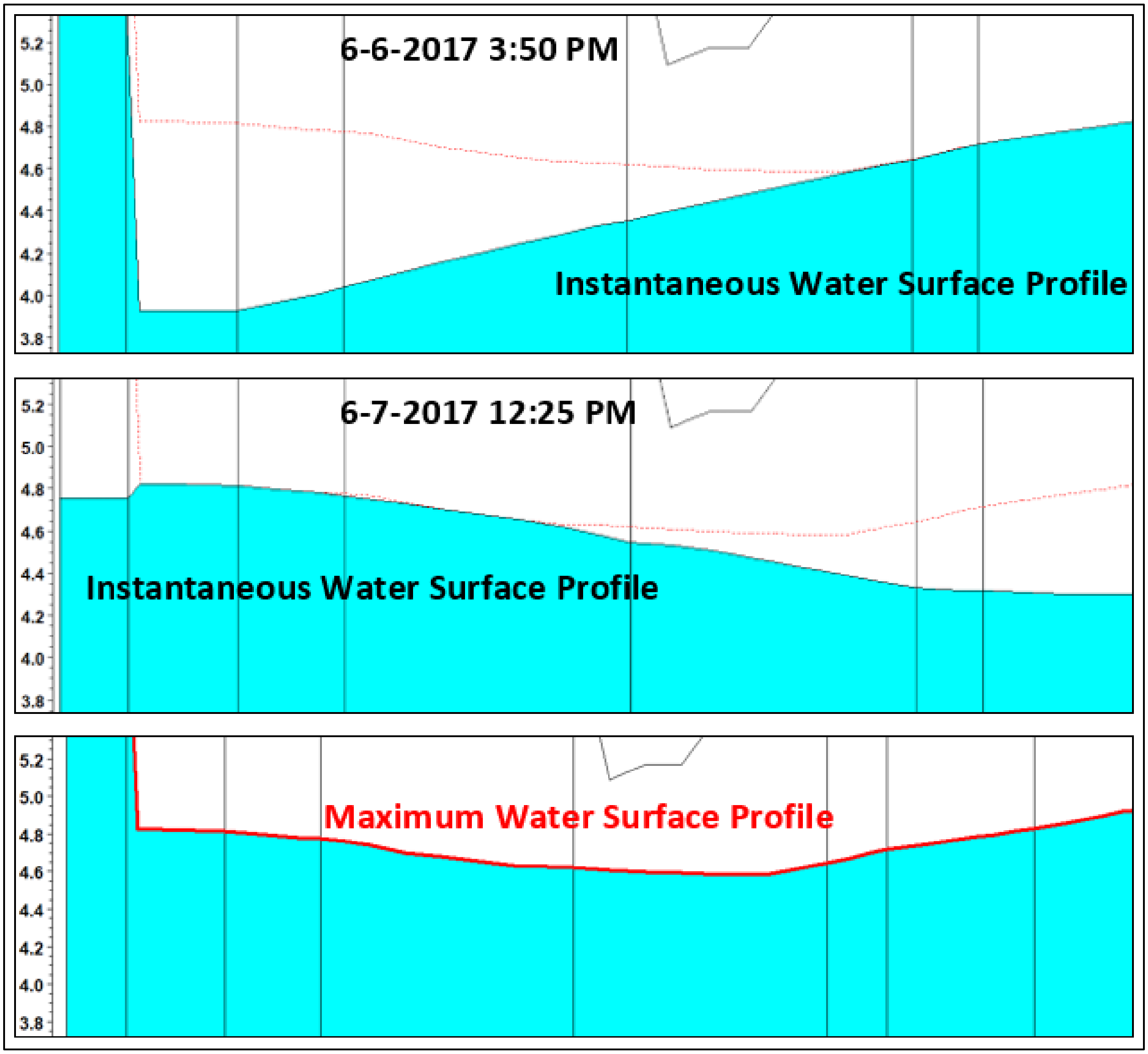

Figure 4.1-1: Visual representation of C-9 Canal Stage at Two Moments During the 5-Year SLR1 Event

For the 5, 10, and 25-year 1 ft sea level rise scenarios, the effects of the C-9 Impoundment appear to have more influence on the western C-9 Canal stages than sea level rise. This is not the case for the 100-year SLR1 scenario or any of the SLR2 or SLR3 scenarios. Like the C-8 Canal, the C-9 Canal mostly has a negative grade line for each design storm under the 3 ft sea level rise scenario. This shows that 3 ft of sea level rise is more influential than the increased initial groundwater levels and increased runoff potential for both canals.

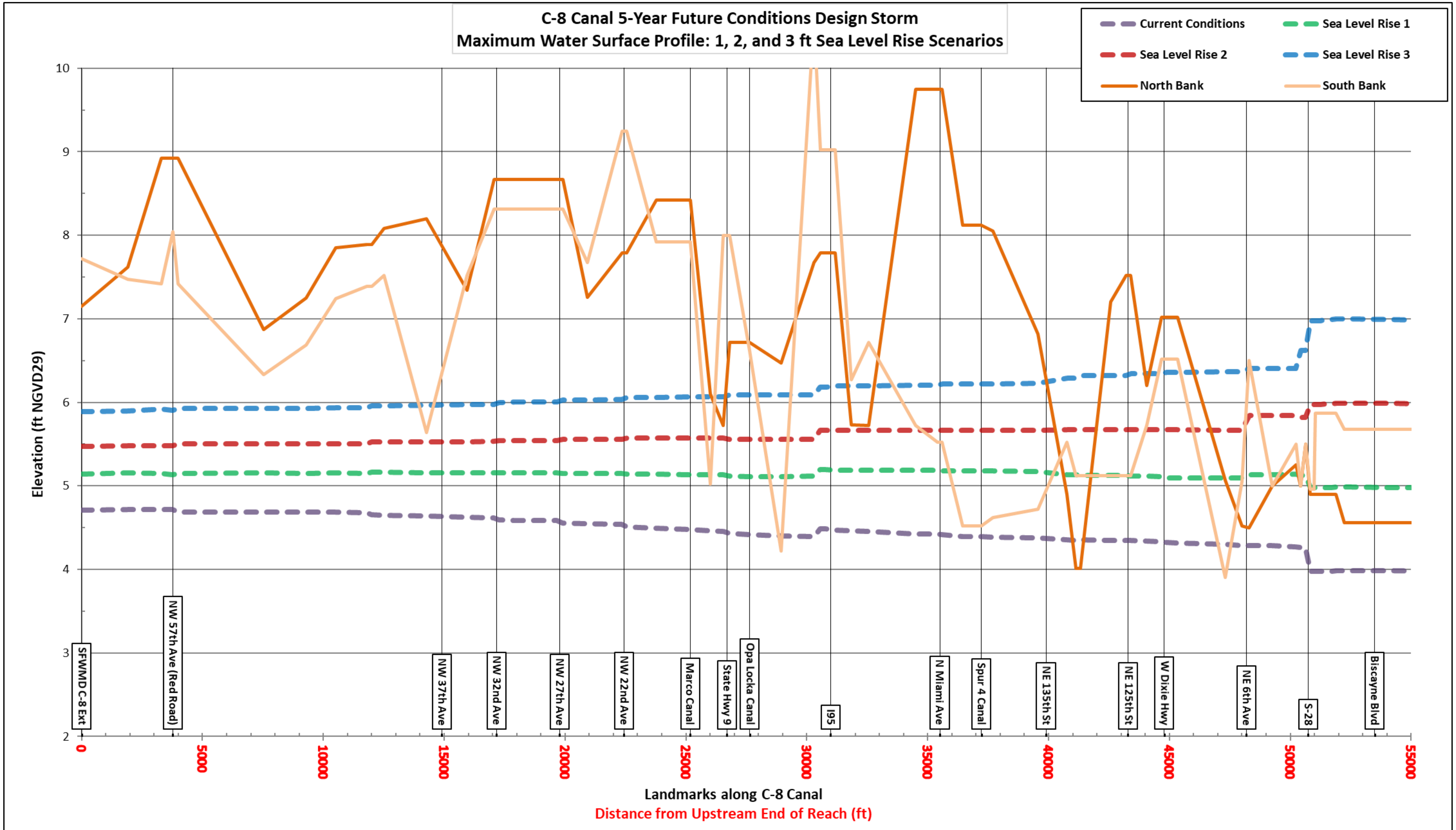

Figure 4.1-2: C-8 Canal Peak Stage Profiles for 5-Year Design Storm – Current vs Future Sea Level Rise Scenarios

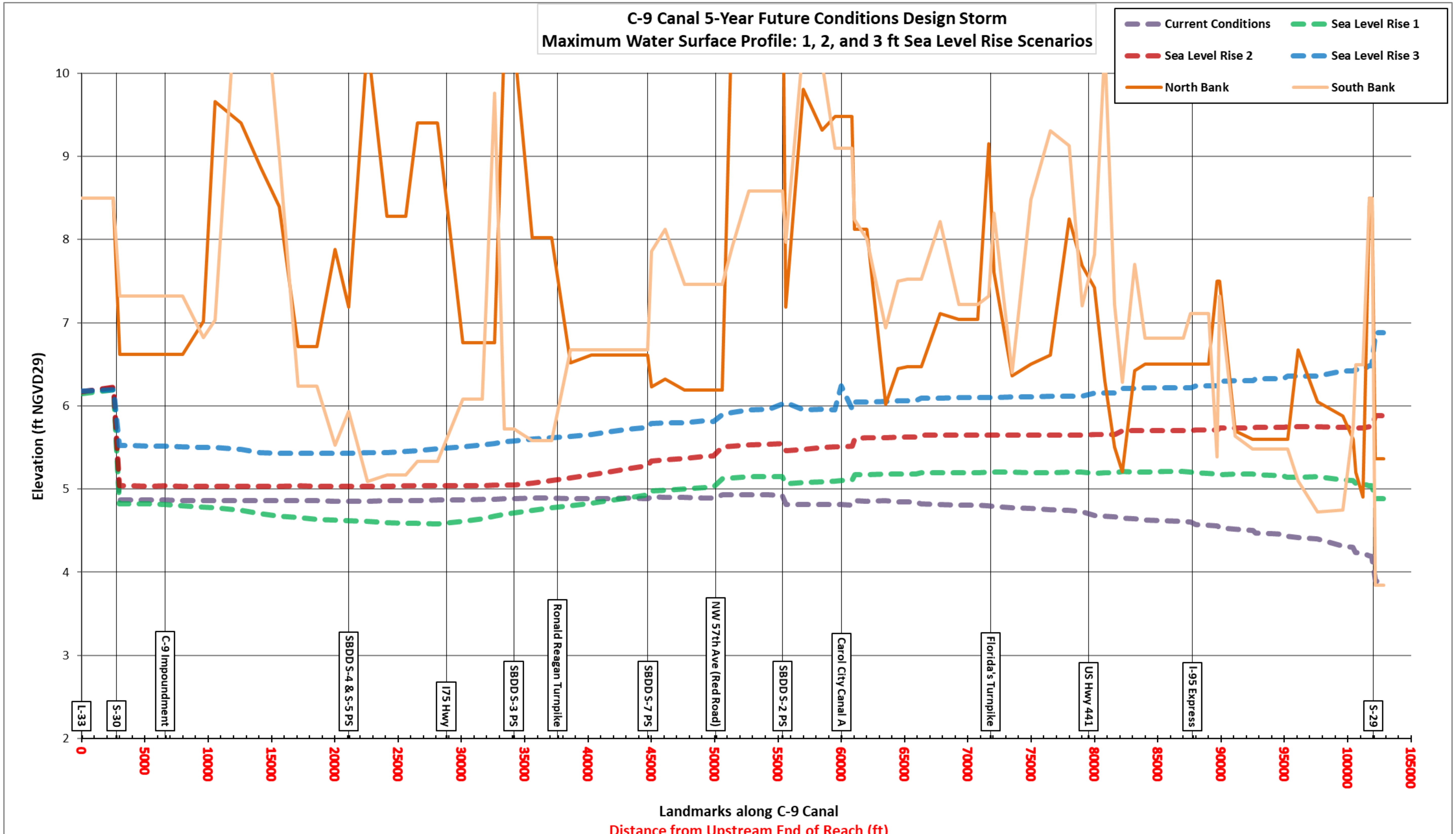

Figure 4.1-3: C-9 Canal Peak Stage Profiles for 5-Year Design Storm – Current vs Future Sea Level Rise Scenarios

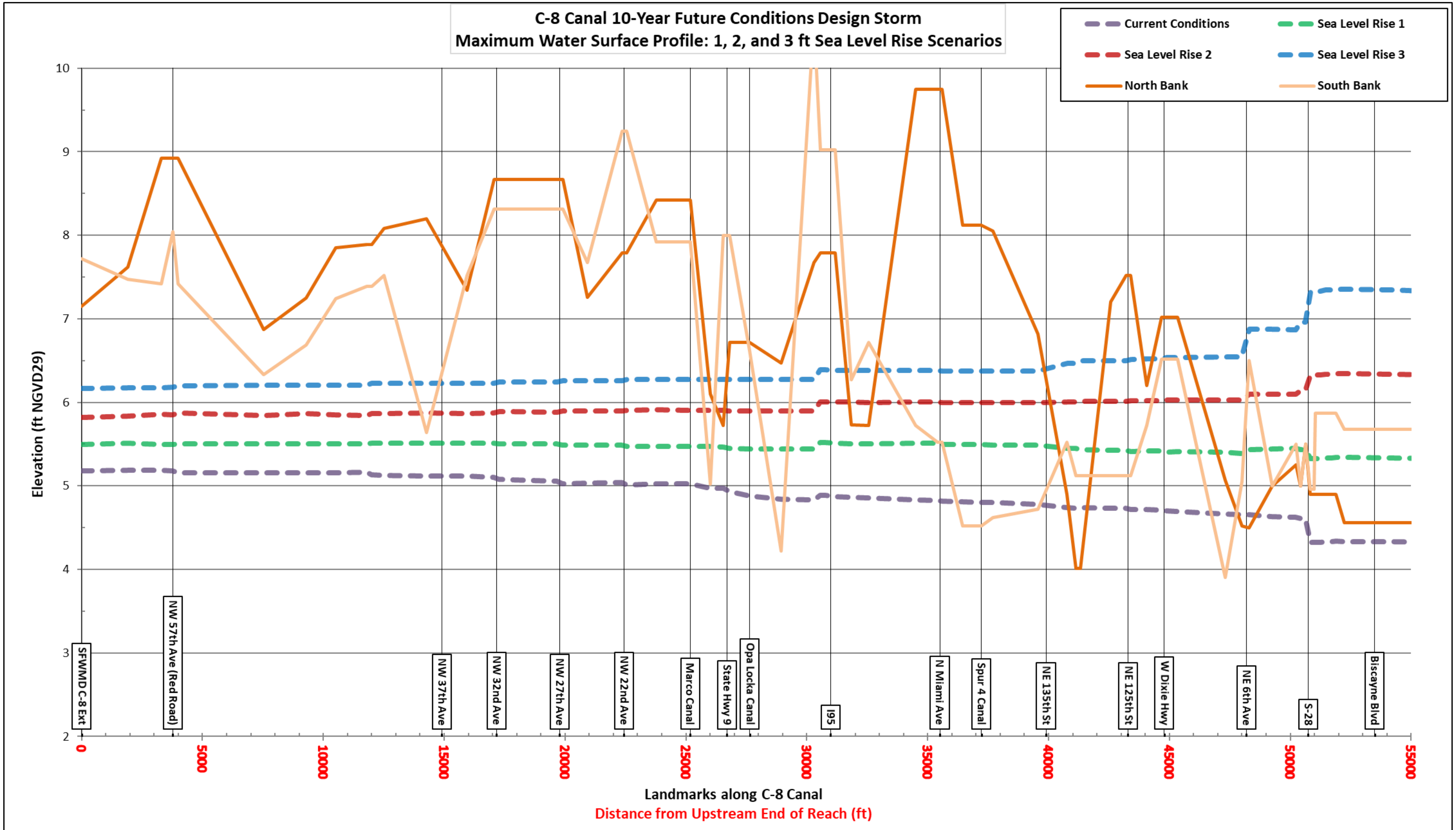

Figure 4.1-4: C-8 Canal Peak Stage Profiles for 10-Year Design Storm – Current vs Future Sea Level Rise Scenarios

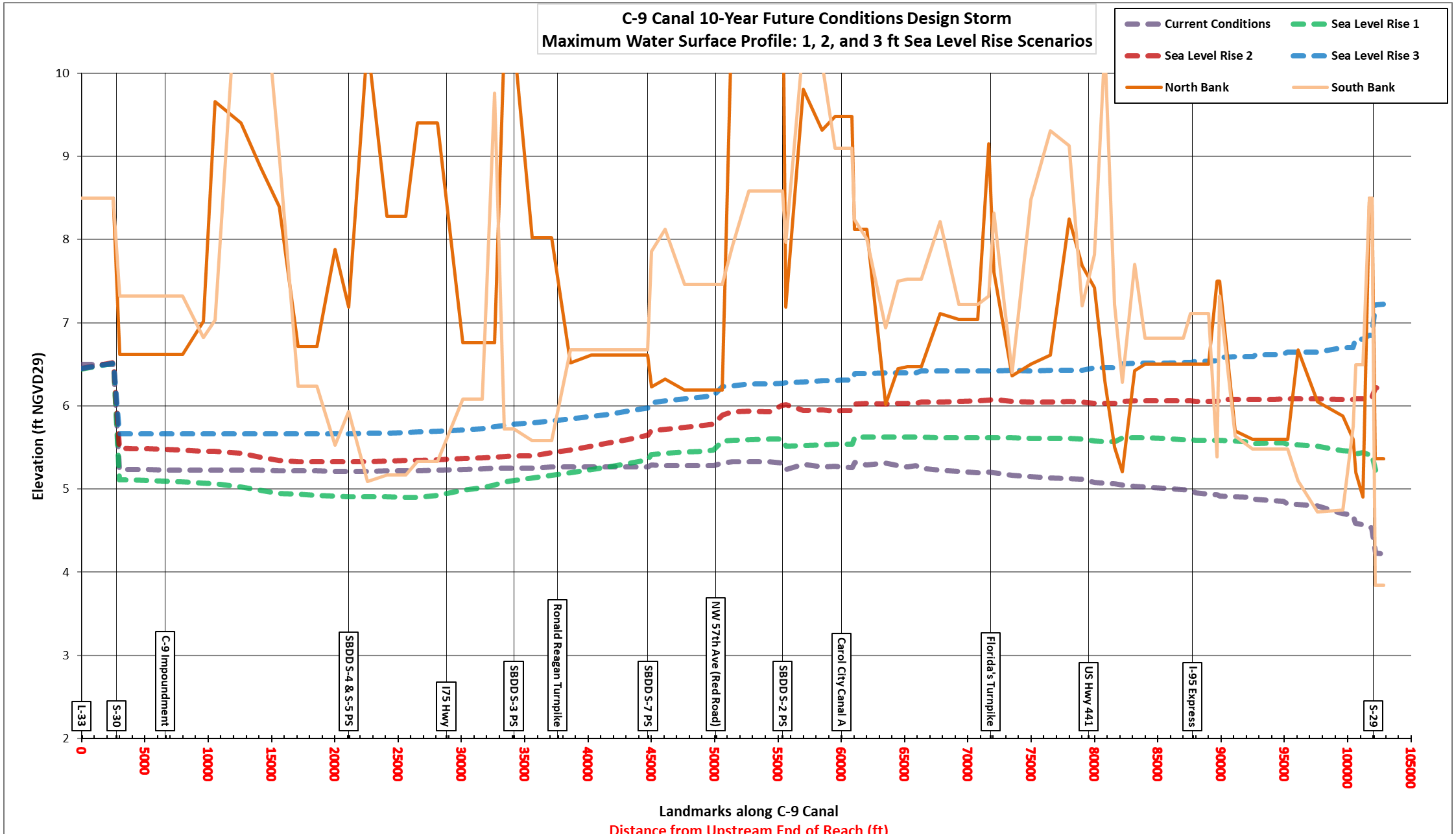

Figure 4.1-5: C-9 Canal Peak Stage Profiles for 10-Year Design Storm – Current vs Future Sea Level Rise Scenarios

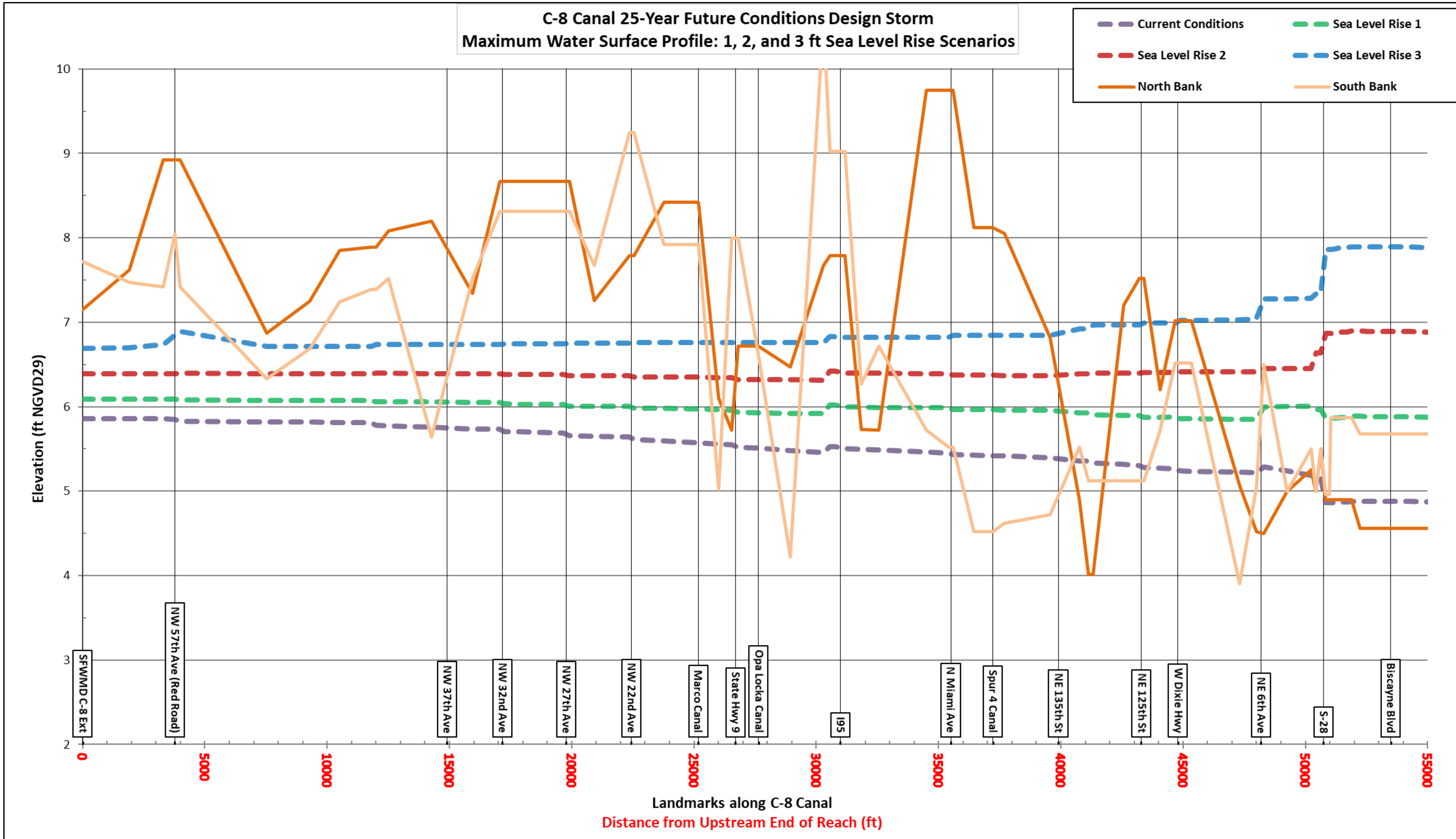

Figure 4.1-6: C-8 Canal Peak Stage Profiles for 25-Year Design Storm – Current vs Future Sea Level Rise Scenarios

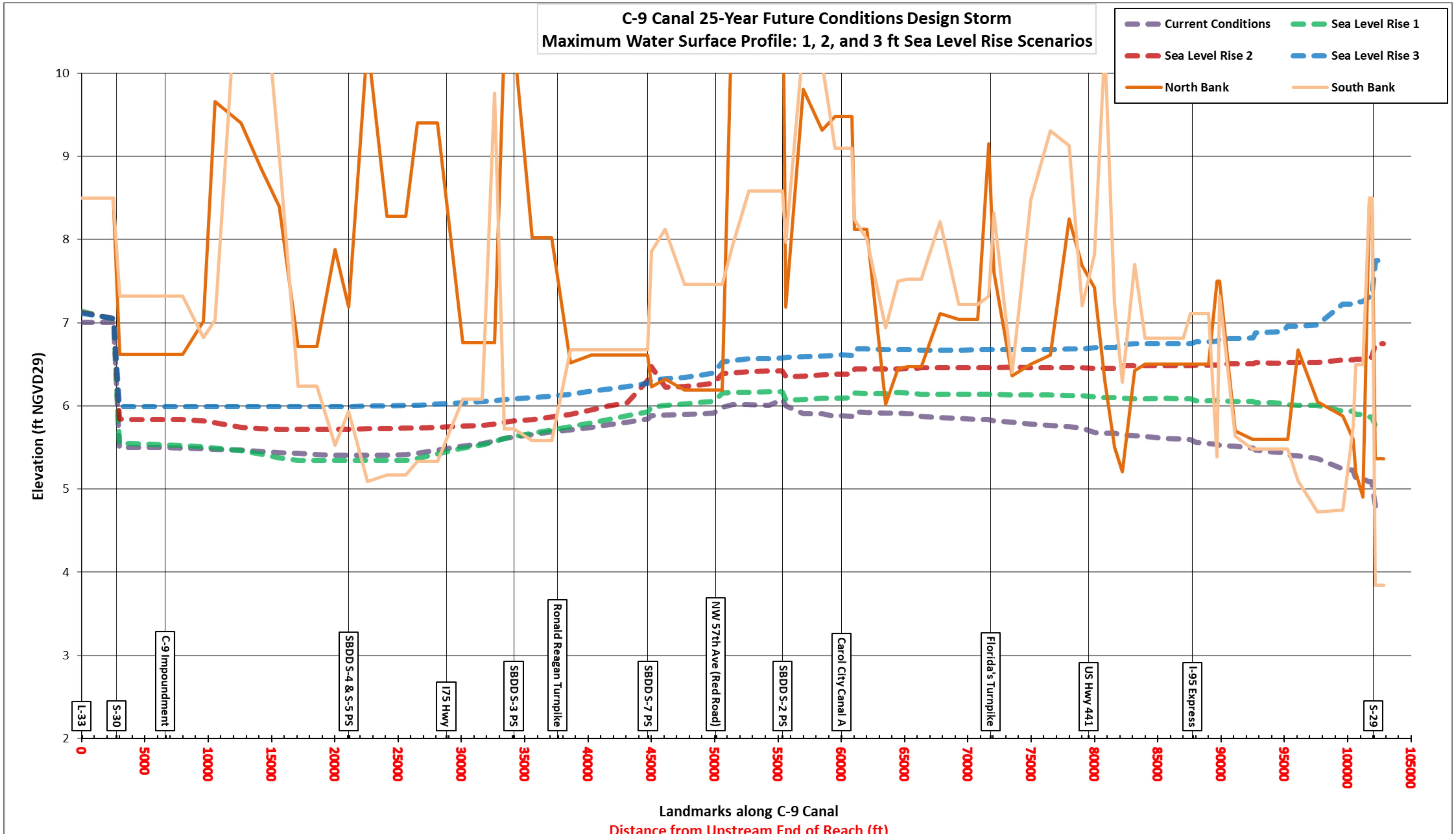

Figure 4.1-7: C-9 Canal Peak Stage Profiles for 25-Year Design Storm – Current vs Future Sea Level Rise Scenarios

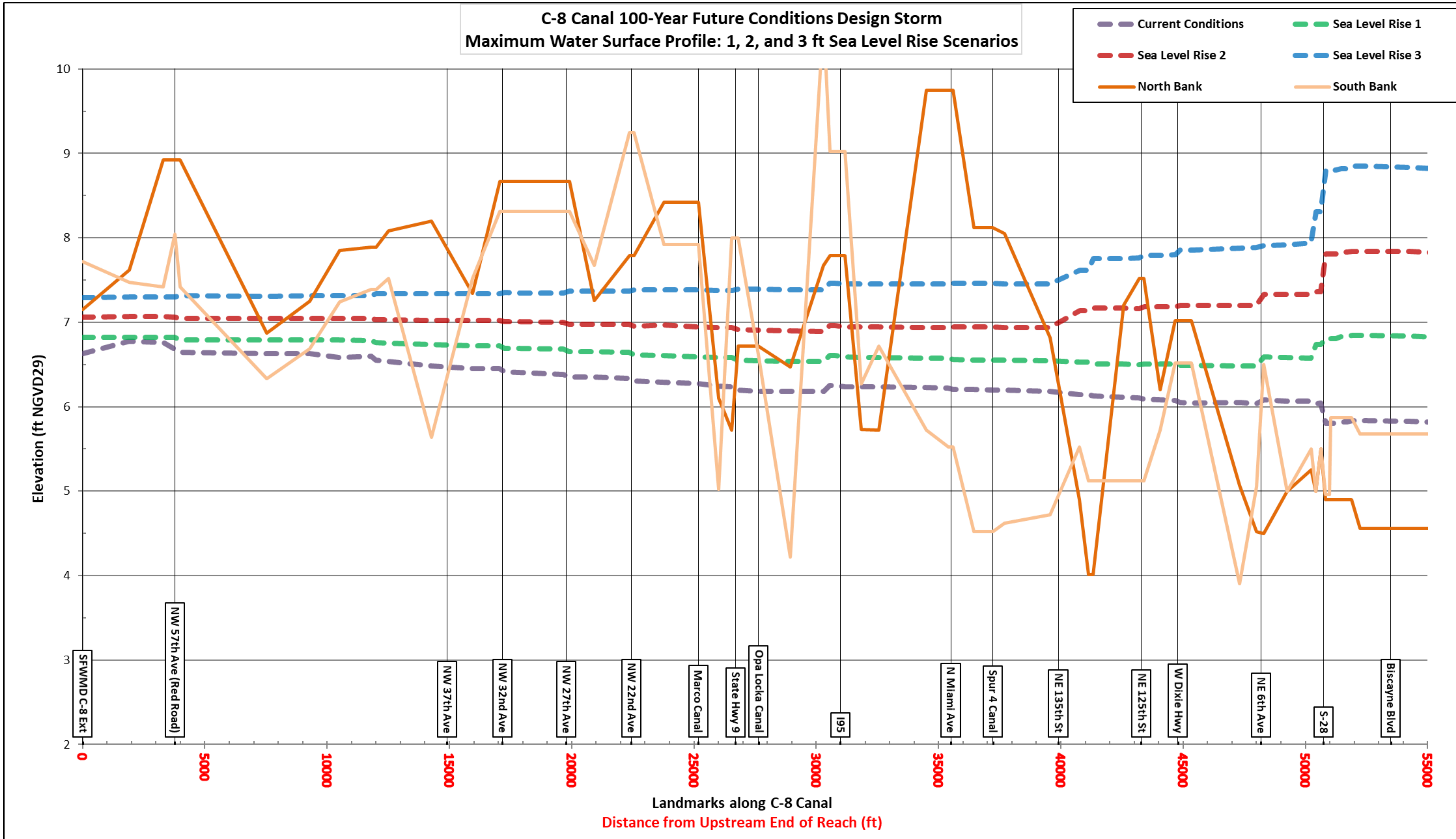

Figure 4.1-8: C-8 Canal Peak Stage Profiles for 100-Year Design Storm – Current vs Future Sea Level Rise Scenarios

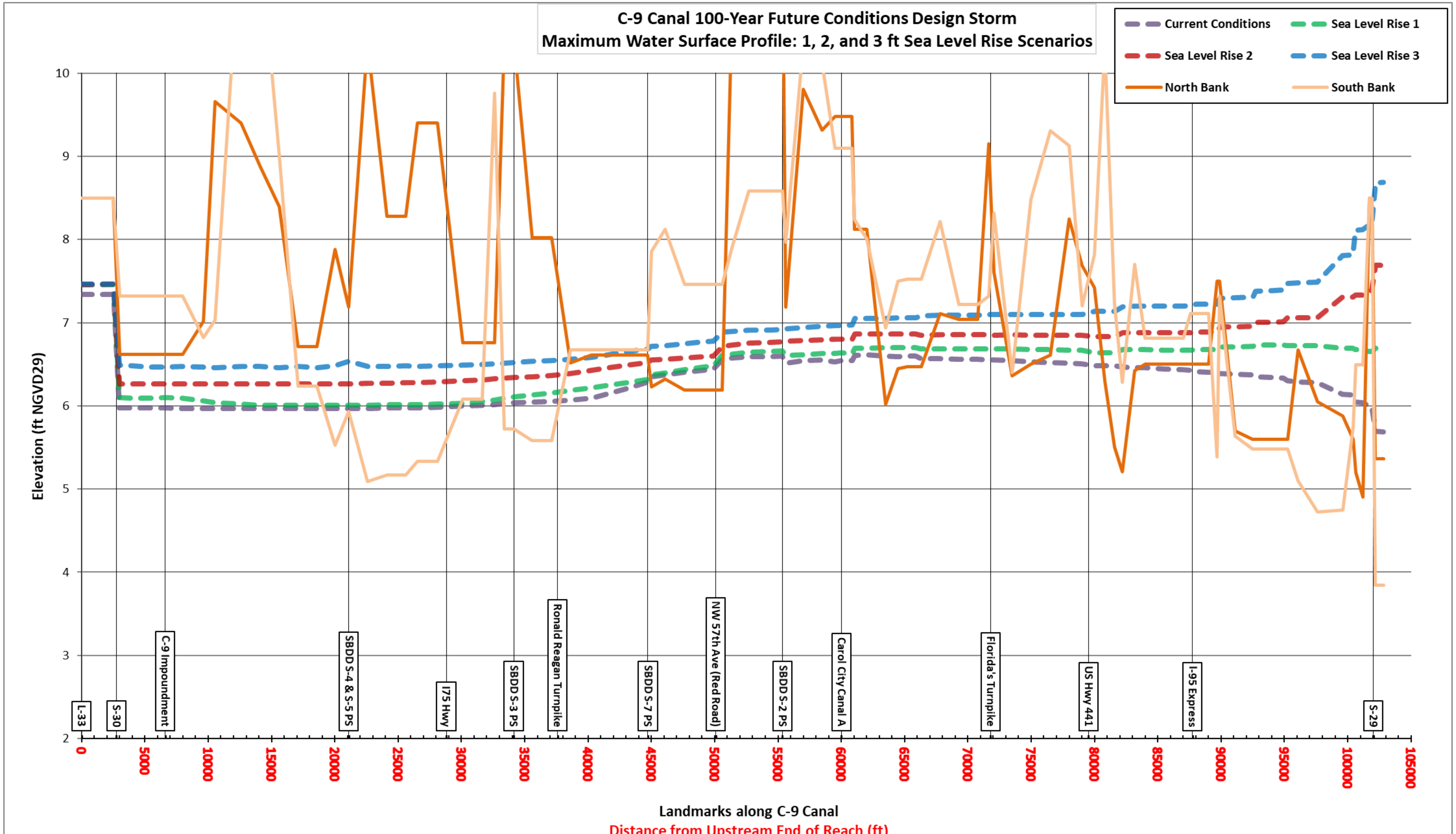

Figure 4.1-9: C-9 Canal Peak Stage Profiles for 100-Year Design Storm – Current vs Future Sea Level Rise Scenarios

Table 4-4 through **Table 4-6** show the peak stages at the major landmarks along the C-8 Canal for each of the future condition sea level rise scenario design storms. Bridge low cord elevations were specified where applicable. Although the water level in the C-8 Canal exceeded bank elevations in several locations for the various design storms, the water level did not get high enough to become restricted by the low cord elevation of any bridge for SLR1 and SLR2 scenarios. For the 100-year 2 ft sea level rise scenario, the water level in the C-8 canal was elevated enough to be within 0.02 ft of becoming restricted by the low cord of a bridge, as shown in orange in **Table 4-5**. Although not restricted in the model simulation, it is close enough and well within the error of margin that it should be considered at risk. For the 100-year 3 ft sea level rise scenario, the water level in the C-8 Canal exceeded bank elevations in several areas and became elevated enough to become restricted by the low cord elevation of two bridges, as shown in red in **Table 4-6**. None of the bridges were overtopped.

Table 4-4: C-8 Canal Peak Stage at Landmarks for SLR1

Landmark	Peak Stage (ft NGVD29)				Bridge Low Cord Elevation (ft NGVD29)
	5-Yr	10-Yr	25-Yr	100-Yr	
SFWMD C-8 Ext	5.14	5.49	6.09	6.82	
NW 57th Ave (Red Road)	5.14	5.5	6.09	6.82	9.2
NW 37th Ave	5.16	5.51	6.06	6.74	
NW 32nd Ave	5.16	5.5	6.03	6.69	9.18
NW 27th Ave	5.16	5.5	6.03	6.68	7.02
NW 22nd Ave	5.15	5.49	6	6.64	8
Macro Canal	5.14	5.47	5.97	6.59	
Rail Road / State Hwy 9	5.13	5.47	5.96	6.58	7.44
NW 7th Ave Bridge	5.11	5.45	5.93	6.54	8.53
I-95	5.2	5.52	6.02	6.61	8.05
North Miami Ave	5.19	5.51	5.99	6.58	9.62
Spur 4 Canal	5.18	5.49	5.96	6.55	
NE 135th St	5.17	5.49	5.96	6.55	7.38
NE 125th St	5.13	5.43	5.9	6.5	11.47
W Dixie Hwy	5.11	5.42	5.88	6.5	10.57
NE 6th Ave	5.13	5.43	6	6.59	9.02
S-28 (HW)	5.13	5.43	5.97	6.74	
Biscayne Blvd	4.98	5.34	5.88	6.84	

Table 4-5: C-8 Canal Peak Stage at Landmarks for SLR2

Landmark	Peak Stage (ft NGVD29)				Bridge Low Cord Elevation (ft NGVD29)
	5-Yr	10-Yr	25-Yr	100-Yr	
SFWMD C-8 Ext	5.48	5.82	6.39	7.06	
NW 57th Ave (Red Road)	5.48	5.85	6.39	7.06	9.2
NW 37th Ave	5.53	5.87	6.39	7.03	
NW 32nd Ave	5.55	5.89	6.38	7.0	9.18
NW 27th Ave	5.55	5.88	6.38	7.0	7.02
NW 22nd Ave	5.56	5.9	6.37	6.97	8
Macro Canal	5.57	5.91	6.35	6.95	
Rail Road / State Hwy 9	5.57	5.91	6.35	6.94	7.44
NW 7th Ave Bridge	5.56	5.89	6.32	6.9	8.53
I-95	5.66	6.01	6.42	6.96	8.05
North Miami Ave	5.67	6	6.39	6.94	9.62
Spur 4 Canal	5.67	6	6.37	6.94	
NE 135th St	5.67	6	6.37	6.94	7.38
NE 125th St	5.67	6.01	6.4	7.16	11.47
W Dixie Hwy	5.67	6.02	6.41	7.18	10.57
NE 6th Ave	5.84	6.1	6.45	7.33	9.02
S-28 (HW)	5.82	6.14	6.64	7.36	
Biscayne Blvd	5.99	6.34	6.89	7.84	

Table 4-6: C-8 Canal Peak Stage at Landmarks for SLR3

Landmark	Peak Stage (ft NGVD29)				Bridge Low Cord Elevation (ft NGVD29)
	5-Yr	10-Yr	25-Yr	100-Yr	
SFWMD C-8 Ext	5.89	6.17	6.69	7.29	
NW 57th Ave (Red Road)	5.9	6.18	6.84	7.3	9.2
NW 37th Ave	5.97	6.23	6.74	7.34	
NW 32nd Ave	6	6.25	6.75	7.35	9.18
NW 27th Ave	6	6.25	6.75	7.35	7.02
NW 22nd Ave	6.03	6.26	6.75	7.37	8
Macro Canal	6.06	6.28	6.76	7.38	
Rail Road / State Hwy 9	6.07	6.28	6.76	7.38	7.44
NW 7th Ave Bridge	6.09	6.27	6.76	7.39	8.53
I-95	6.18	6.39	6.83	7.46	8.05
North Miami Ave	6.2	6.38	6.82	7.45	9.62
Spur 4 Canal	6.22	6.37	6.84	7.46	
NE 135th St	6.23	6.37	6.84	7.46	7.38
NE 125th St	6.32	6.5	6.97	7.76	11.47
W Dixie Hwy	6.34	6.52	6.99	7.8	10.57
NE 6th Ave	6.41	6.87	7.28	7.91	9.02
S-28 (HW)	6.62	6.96	7.34	8.31	
Biscayne Blvd	7	7.35	7.89	8.85	

Table 4-7 through **Table 4-9** shows the peak stages at the major landmarks along the C-9 Canal for each of the design storms. Bridge low cord elevations were specified where applicable. For the 5-year and 10-year SLR1 design storm events, the water level in the C-9 Canal exceeded bank elevations in a couple locations (**Figure 4.1-3**) and the water level became high enough to become restricted by the low cord of one bridge, as shown in red in **Table 4-7.** For the 25-year and 100-year SLR1 design storms, the water level in the C-9 Canal exceeded bank elevations in several areas and became elevated enough to become restricted by the low cord elevation of three bridges, as shown in red in **Table 4-7**. Canal bank exceedances increased with both design storm frequency and sea level rise. For the sea level rise 3 scenario, the three bridges that became submerged under the 25 and 100-year SLR1 scenarios became submerged for each design storm, as shown in red in **Table 4-9**. It is unknown if any of the submerged bridges would become overtopped as the overflow elevations are unknown (these were not surveyed, and bridge decks were scrubbed from the DEM).

Table 4-7: C-9 Canal Peak Stage at Landmarks for SLR1

Landmark	Peak Stage (ft NGVD29)				Bridge Low Cord Elevation (ft NGVD29)
	5-Yr	10-Yr	25-Yr	100-Yr	
L-33	6.15	6.44	7.14	7.46	
S-30 (TW)	4.82	5.11	5.55	6.1	
SBDD S-4 & S-5 PS	4.62	4.91	5.34	6.01	
I75 Hwy	4.58	4.92	5.42	6.02	
SBDD S-3 PS	4.72	5.11	5.63	6.11	
Ronald Reagan Turnpike	4.77	5.17	5.71	6.16	
SBDD S-7 PS /Flaming Rd	4.93	5.35	5.93	6.32	9.76
NW 57th Ave (Red Road)	5.03	5.47	6.05	6.48	9.54
SBDD S-2 PS / NW 47th Ave	5.15	5.6	6.17	6.66	8.9
Carol City Canal A	5.1	5.54	6.1	6.64	
NW 37th Ave	5.11	5.54	6.1	6.63	8.6
NW 27th Ave	5.18	5.63	6.15	6.7	7.93
Florida's Turnpike	5.2	5.62	6.14	6.68	
US Hwy 441	5.19	5.58	6.11	6.64	7.53
NW 199th St	5.21	5.62	6.09	6.68	8.6
I-95 Express	5.2	5.58	6.06	6.68	8.43
Miami Gardens Dr	5.18	5.59	6.06	6.71	8.96
NE 15th Ave	5.14	5.54	6.01	6.72	8.87
NW 19th Ave	5.11	5.46	5.94	6.7	5.6
NE 22nd Ave	5.07	5.42	5.89	6.68	4.9
Rail Road at Biscayne Blvd	5.04	5.42	5.87	6.66	5.77
S-29 (HW)	5.04	5.42	5.87	6.65	

Table 4-8: C-9 Canal Peak Stage at Landmarks for SLR2

Landmark	Peak Stage (ft NGVD29)				Bridge Low Cord Elevation (ft NGVD29)
	5-Yr	10-Yr	25-Yr	100-Yr	
L-33	6.17	6.45	7.12	7.46	
S-30 (TW)	5.04	5.49	5.84	6.26	
SBDD S-4 & S-5 PS	5.03	5.33	5.72	6.26	
I75 Hwy	5.04	5.36	5.74	6.29	
SBDD S-3 PS	5.05	5.4	5.82	6.34	
Ronald Reagan Turnpike	5.1	5.44	5.86	6.37	
SBDD S-7 PS /Flaming Rd	5.28	5.64	6.31	6.52	9.76
NW 57th Ave (Red Road)	5.4	5.78	6.27	6.6	9.54
SBDD S-2 PS / NW 47th Ave	5.54	6	6.42	6.77	8.9
Carol City Canal A	5.51	5.95	6.38	6.8	
NW 37th Ave	5.51	5.94	6.38	6.8	8.6
NW 27th Ave	5.62	6.03	6.45	6.87	7.93
Florida's Turnpike	5.65	6.07	6.46	6.85	
US Hwy 441	5.66	6.03	6.45	6.84	7.53
NW 199th St	5.7	6.06	6.48	6.88	8.6
I-95 Express	5.71	6.05	6.49	6.89	8.43
Miami Gardens Dr	5.74	6.07	8.52	6.95	8.96
NE 15th Ave	5.75	6.08	6.52	7.06	8.87
NW 19th Ave	5.74	6.08	6.55	7.31	5.6
NE 22nd Ave	5.74	6.09	6.56	7.33	4.9
Rail Road at Biscayne Blvd	5.75	6.1	6.58	7.38	5.77
S-29 (HW)	5.75	6.1	6.58	7.38	

Table 4-9: C-9 Canal Peak Stage at Landmarks for SLR3

Landmark	Peak Stage (ft NGVD29)				Bridge Low Cord Elevation (ft NGVD29)
	5-Yr	10-Yr	25-Yr	100-Yr	
L-33	6.18	6.45	7.11	7.46	
S-30 (TW)	5.52	5.67	5.99	6.49	
SBDD S-4 & S-5 PS	5.43	5.67	5.99	6.54	
I75 Hwy	5.48	5.69	6.02	6.48	
SBDD S-3 PS	5.58	5.78	6.09	6.52	
Ronald Reagan Turnpike	5.62	5.82	6.11	6.55	
SBDD S-7 PS /Flaming Rd	5.75	5.97	6.27	6.69	9.76
NW 57th Ave (Red Road)	5.82	6.12	6.39	6.78	9.54
SBDD S-2 PS / NW 47th Ave	6.03	6.27	6.57	6.92	8.9
Carol City Canal A	6.24	6.31	6.61	6.97	
NW 37th Ave	5.96	6.31	6.61	6.97	8.6
NW 27th Ave	6.06	6.4	6.68	7.06	7.93
Florida's Turnpike	6.1	6.42	6.68	7.1	
US Hwy 441	6.15	6.46	6.7	7.14	7.53
NW 199th St	6.21	6.51	6.74	7.19	8.6
I-95 Express	6.24	6.54	6.77	7.22	8.43
Miami Gardens Dr	6.3	6.59	6.81	7.29	8.96
NE 15th Ave	6.36	6.65	6.96	7.47	8.87
NW 19th Ave	6.42	6.7	7.22	7.81	5.6
NE 22nd Ave	6.44	6.8	7.25	8.11	4.9
Rail Road at Biscayne Blvd	6.48	6.85	7.31	8.17	5.77
S-29 (HW)	6.48	6.85	7.31	8.17	

4.2 PM #2 – Maximum Daily Discharge Capacity through the Primary Canals

PM #2 is the maximum discharge capacity throughout the primary canals. Discharge is calculated for canals as area weighted flow, in units of cubic feet per second per square mile of contributing area. Canal segments are generally defined as areas between water control structures, however, there are no intermittent control structures along the C-8 and C-9 Canals. Therefore, the segment associated with structures S-28 and S-29, is the entire C-8 and C-9 Canals, respectively. This means that the contributing area for S-28 and S-29 is the entire C-8 basin and C-9 basin, respectively. Structure S-30, which is on the C-9 Basin boundary, was closed for the majority or entirety of the design storms (based on control rules), so there was negligible/no additional inflow into the C-9 basin. Within the C-9 Basin, there are two areas with different allowable runoff rates based on the District's ERP Handbook; (1) "essentially unlimited inflow by gravity connections east of Red Road", and (2) "20 CSM pumped and essentially unlimited inflow by gravity connections west of Red Road or Flamingo BLVD". Therefore, the C-9 Basin discharge capacity was estimated for the entire C-9 Basin, as well as for the respective areas east and west of Red Road. **Table 4-10** through **Table 4-13** lists the canal segments identified for this analysis, the contributing area for each canal segment, and the discharge capacity calculated for each segment associated with each design and sea level rise scenario.

Discharge capacity was calculated by dividing the 12-hour moving average peak of the discharge hydrograph by the canal segments contributing area. For structures S-28 and S-29, discharge capacity was calculated by dividing the peak 12-hour discharge by the entire basin area. For the C-9 Basin, two additional estimates were made for the respective areas east and west of Red Road. These two additional estimates were necessitated by the presence of two different allowable runoff rates within the C-9 Basin. For the drainage area west of Red Road, the peak discharge at the Q-point (model discharge calculation point) located at Red Road (shown as a green dot in **Figure 4.2-1**) was divided by the contributing drainage area (highlighted in green in **Figure 4.2-1**). For the drainage area east of Red Road, the peak discharge at the Q-point located at Red Road was subtracted from the peak discharge at structure S-29, and then divided by the contributing drainage area east of Red Road. Tidal effects were filtered by using a 12-hour moving average of discharge.

Table 4-10: Water Control Catchment Discharge Capacity for 5-Year Future Conditions Design Storms

Structure / Segment	Inflow	Outflow	Water Control Catchment Area (sq.mi)	5-Year Design Storm Peak Discharge Capacity (cfs/sq.mi)			
				Current	SLR1	SLR2	SLR3
S-28	Beginning of C-8	S-28	28.22	51	48.2	44.2	39
S-29	Beginning of C-9/ Structure S-30	S-29	99.37	21.5	16.7	11.7	9.1
C-9 west of Red Road	Beginning of C-9/ Structure S-30	Q-point at Red Road	61.24	13.5	10.6	7.3	3.9
C-9 east of Red Road	Q-point at Red Road	S-29	38.13	46.7	45.7	39.6	32.7

Discharge west and east of Red Road is an estimate due to interconnected outfalls on both sides of Red Road

Table 4-11: Water Control Catchment Discharge Capacity for 10-Year Future Conditions Design Storms

Structure / Segment	Inflow	Outflow	Water Control Catchment Area (sq.mi)	10-Year Design Storm Peak Discharge Capacity (cfs/sq.mi)			
				Current	SLR1	SLR2	SLR3
S-28	Beginning of C-8	S-28	28.22	61.9	60.3	57.4	50.5
S-29	Beginning of C-9/ Structure S-30	S-29	99.37	24.6	19.2	15.9	12.5
C-9 west of Red Road	Beginning of C-9/ Structure S-30	Q-point at Red Road	61.24	15.2	12.1	8.5	4.5
C-9 east of Red Road	Q-point at Red Road	S-29	38.13	51.3	51.5	47.9	45.5

Discharge west and east of Red Road is an estimate due to interconnected outfalls on both sides of Red Road

Table 4-12: Water Control Catchment Discharge Capacity for 25-Year Future Conditions Design Storms

Structure / Segment	Inflow	Outflow	Water Control Catchment Area (sq.mi)	25-Year Design Storm Peak Discharge Capacity (cfs/sq.mi)			
				Current	SLR1	SLR2	SLR3
S-28	Beginning of C-8	S-28	28.22	82.8	82	82	66.1
S-29	Beginning of C-9/ Structure S-30	S-29	99.37	29.3	25.2	21.7	16.6
C-9 west of Red Road	Beginning of C-9/ Structure S-30	Q-point at Red Road	61.24	17.9	15.3	11.9	7.6
C-9 east of Red Road	Q-point at Red Road	S-29	38.13	65.8	68	65.5	58

Discharge west and east of Red Road is an estimate due to interconnected outfalls on both sides of Red Road

Table 4-13: Water Control Catchment Discharge Capacity for 100-Year Future Conditions Design Storms

Structure / Segment	Inflow	Outflow	Water Control Catchment Area (sq.mi)	100-Year Design Storm Peak Discharge Capacity (cfs/sq.mi)			
				Current	SLR1	SLR2	SLR3
S-28	Beginning of C-8	S-28	28.22	115.3	115.5	103.4	82.6
S-29	Beginning of C-9/ Structure S-30	S-29	99.37	37.5	34	29.7	23.1
C-9 west of Red Road	Beginning of C-9/ Structure S-30	Q-point at Red Road	61.24	20.9	18.1	14.1	8.7
C-9 east of Red Road	Q-point at Red Road	S-29	38.13	89.1	90.9	88.7	80.9

Discharge west and east of Red Road is an estimate due to interconnected outfalls on both sides of Red Road

Figure 4.2-1 shows the contributing areas draining to each canal segment. The C-8 catchment polygon was based on the District's Arc Hydro Enhanced Database (AHED). The C-9 catchment polygons were based on both the District's AHED as well as SBDD and Miami-Dade County subbasins. It is important to note that the C-9 Basin is technically one drainage area and does not have a real drainage divide. The two drainage areas shown within the C-9 Basin represent the spatial variability in the District's allowable discharge rates within the C-9 Basin. The area-weighted discharge presented for the areas east and west of Red Road are an approximation due to the uncertainty in the exact location of this allowable runoff-based basin divide. Additionally, the drainage areas east and west of Red Road are interconnected. Although the drainage divide is specified as Red Road, the contributing drainage area on the north side of the C-9 Canal extends east of Red Road and has two outfalls that are interconnected, one east of Red Road and one west of Red Road. For this analysis, the discharge at Red Road was used, so some discharge from the contributing drainage area is not included as it discharges further downstream. It should be noted that comparing the discharge in the western half of the C-9 Canal to the permitted rates does not have significant meaning as there are several gravity connections to the C-9 Canal west of Red Road and two pumped connections east of Red Road.

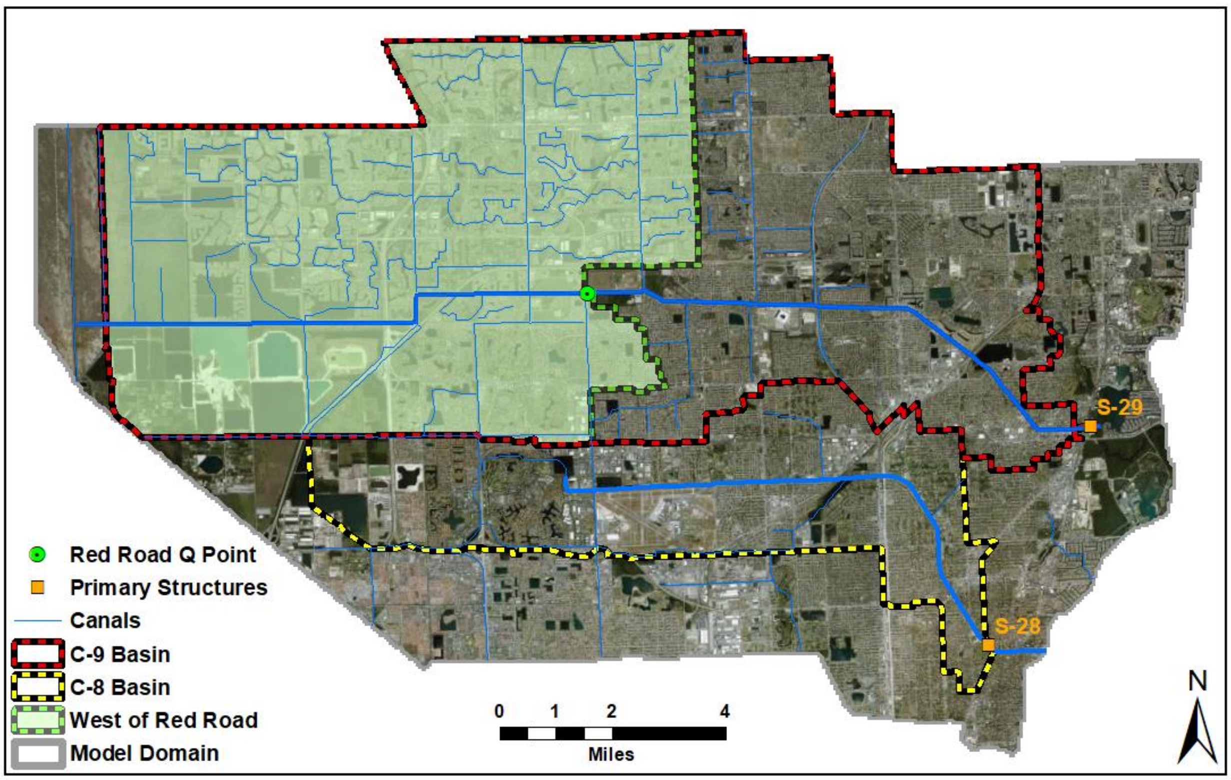

Figure 4.2-1: Catchment Areas for Calculating PM #2

The following figures present visual comparisons of the area-weighted discharge hydrographs for the C-8 and C-9 Canal for each design storm under three sea level rise conditions vs current conditions. An additional two hydrographs are presented for areas east and west of Red Road. Areas east of Red Road are allowed unlimited discharge by gravity and areas west of Red Road have a pumped discharge limitation equal to 20 CSM. It is important to note that the discharge capacity east and west of Red Road is approximate as there are several gravity connections west of Red Road and pumped connections east of Red Road. Additionally, there are pumped connections east of Red Road that share a common drainage area with west of Red Road due to the interconnectivity of the drainage system. Therefore, the discharge capacity of the C-9 Canal, with respect to east or west of Red Road, is strictly an estimate and should not be used for regulatory purposes.

Although the peak discharge during each design storm event are referred to in this section as the calculated discharge capacity, the true capacity of the canal segment is the net discharge corresponding to the largest design flood event that remains within the banks of the canal. Therefore, the results of PM #2 must be evaluated in conjunction with the results of PM #1 (Maximum Stage in Primary Canals) and PM #5 (Frequency of Flooding).

4.2.1 5-Year Design Storms

Figure 4.2-2 through **Figure 4.2-5** present a visual comparison of the area-weighted discharge hydrographs for each canal segment with respect to the 5-year 72-hour design storm for each sea level rise scenario.

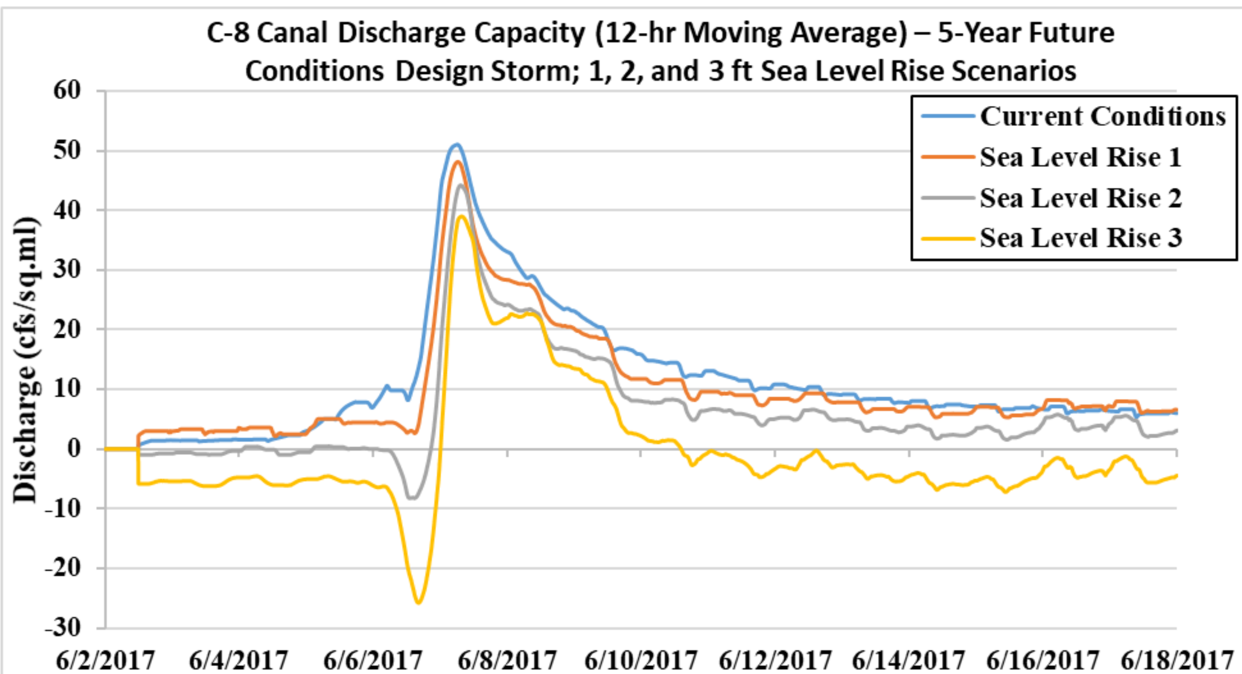

Figure 4.2-2: Area-Weighted Discharge Hydrograph for C-8 Canal (S-28) for 5-Year Design Storms

For both the C-8 and C-9 Canals, the discharge capacity for the 5-year design storm is reduced with the increase in sea level rise. This was expected as it was believed that the increased tidal water levels would reduce the structures ability to discharge and at some point, cause a flow reversal. Although the tidal structures are designed to prevent backwater through gate operation (gates are closed when tailwater stage is higher than headwater stage), the increase tailwater stages due to sea level rise allow the tidal water to overtop and/or bypass the structure. In the C-8 Canal, a flow reversal can be seen during the 5-year SLR2 scenario and is significantly larger during the SLR3 scenario.

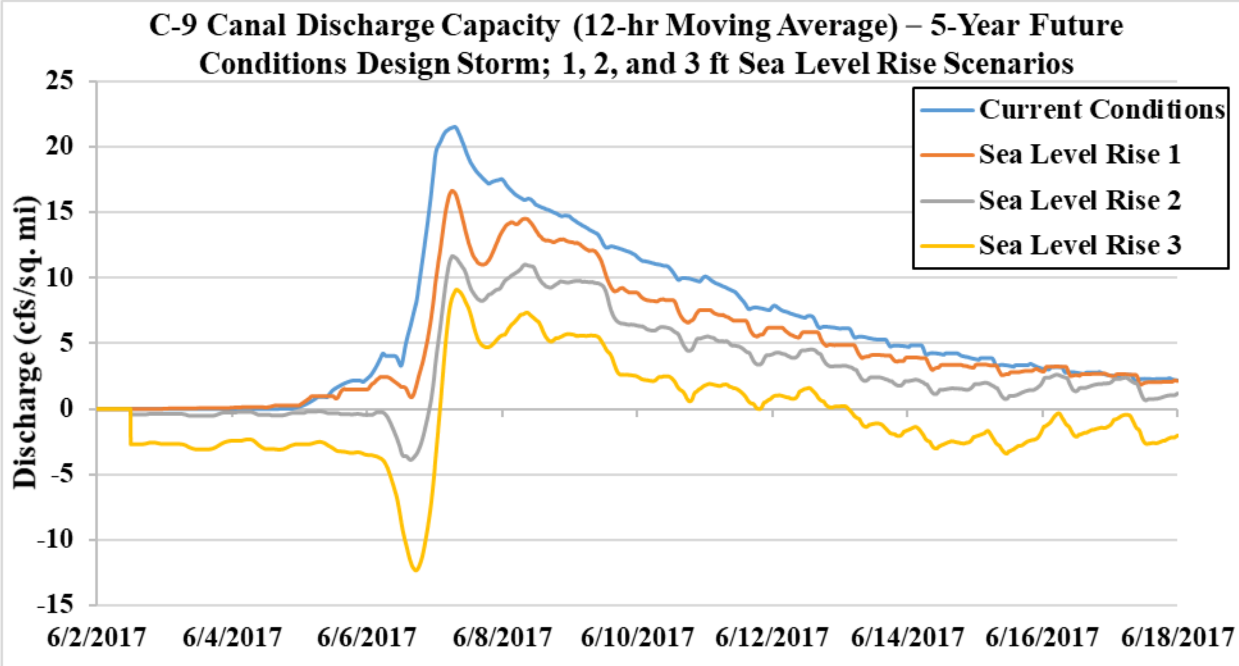

Figure 4.2-3: Area-Weighted Discharge Hydrograph for C-9 Canal (S-29) for 5-Year Design Storms

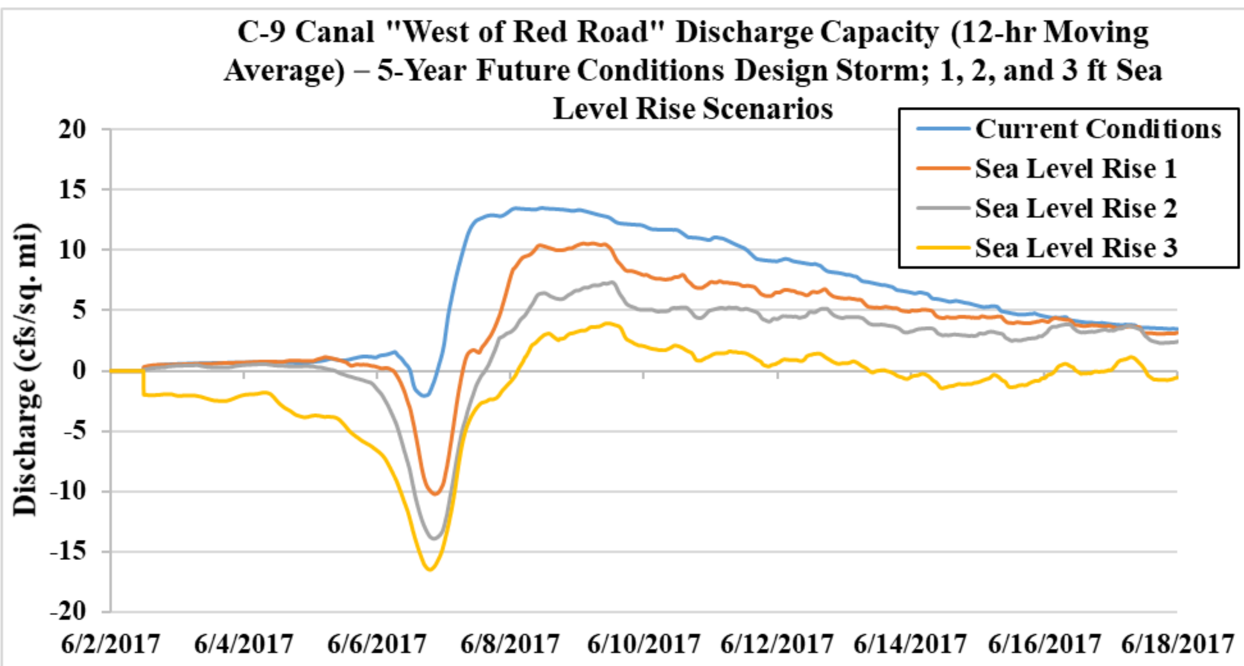

Figure 4.2-4: Area Weighted Discharge Hydrograph for C-9 Canal West of Red Road for 5-Year Design Storms

Discharge west of Red Road is an estimate due to interconnected outfalls on both sides of Red Road

The peak discharge capacity of the C-9 Canal west of Red Road was 13.5 CSM for the 5-year current conditions scenario and is further reduced for each sea level rise scenario, resulting in less than 5 CSM for SLR3. This reduction is caused by higher water levels east of Red Road, which is a result of sea level rise.

The western C-9 basin is drained by pumps on the secondary canals. Based on simulated stages in the C-9 canal, the future conditions pumping duration was not limited by current permit conditions requiring pumps to shut off when stages in C-9 reach a certain level (between 6.5 - 7.0 ft NGVD29, depending on location). Therefore the total discharge to the C-9 canal under future sea level rise scenarios would likely be greater than current conditions due to increased groundwater levels, which tends to increase runoff. This shows that the simulated reduction in discharge capacity of the C-9 Canal was not caused by a reduction in discharge to the canal but is caused by higher tailwater conditions in the eastern segment of C-9. The future discharge capacity is inversely related to sea level.

Figure 4.2-4 shows negative discharge during peak rainfall. This occurs because there is a delayed response in the west side of C-9 as there is a significant amount of dead storage (large lakes in SBDD) and because of the C-9 Impoundment, which is pulling water from the western C-9 Canal. The storage in the west side is controlled by pumps that turn on at an elevation higher than control elevation (See **Appendix B**) . As the pumps turn on and the C-9 Impoundment pumps turn off, the discharge becomes positive. For the area east of Red Road, as shown in **Figure 4.2-5**, a negative discharge during peak rainfall is seen during the SLR3 scenario. This indicates that under the 3 ft sea level rise scenario, the inflection point is shifted west, past Red Road, which can be seen in **Figure 4.1-3**. The inflection point is the point in which the slope of the hydraulic grade line changes from positive to negative.

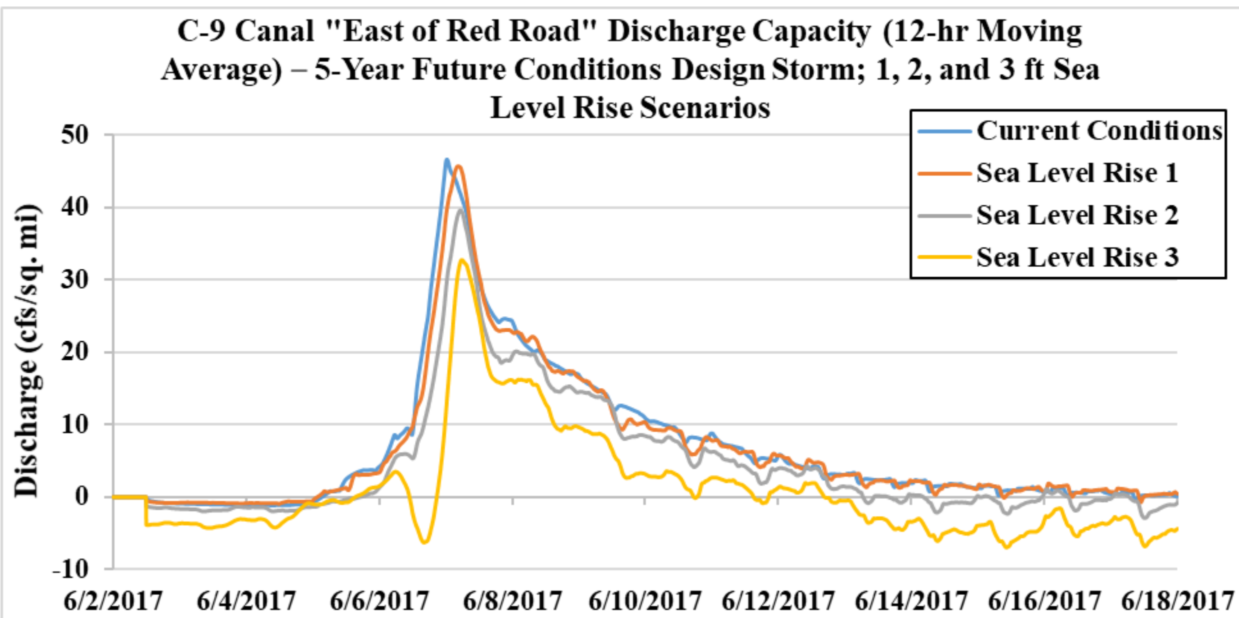

Figure 4.2-5: Area-Weighted Discharge Hydrograph for C-9 Canal East of Red Road for 5-Year Design Storms

Discharge east of Red Road is an estimate due to interconnected outfalls on both sides of Red Road

4.2.2 10-Year Design Storms

Figure 4.2-6 through **Figure 4.2-9** present a visual comparison of the area-weighted discharge hydrographs for each canal segment with respect to the 10-year 72-hour design storm for each sea level rise scenario.

For both the C-8 and C-9 Canals, the discharge capacity for the 10-year design storm is reduced with the increase in sea level rise. For both the C-8 and C-9 Canals, a flow reversal can be seen during the SLR2 scenario and is significantly larger during the SLR3 scenario.

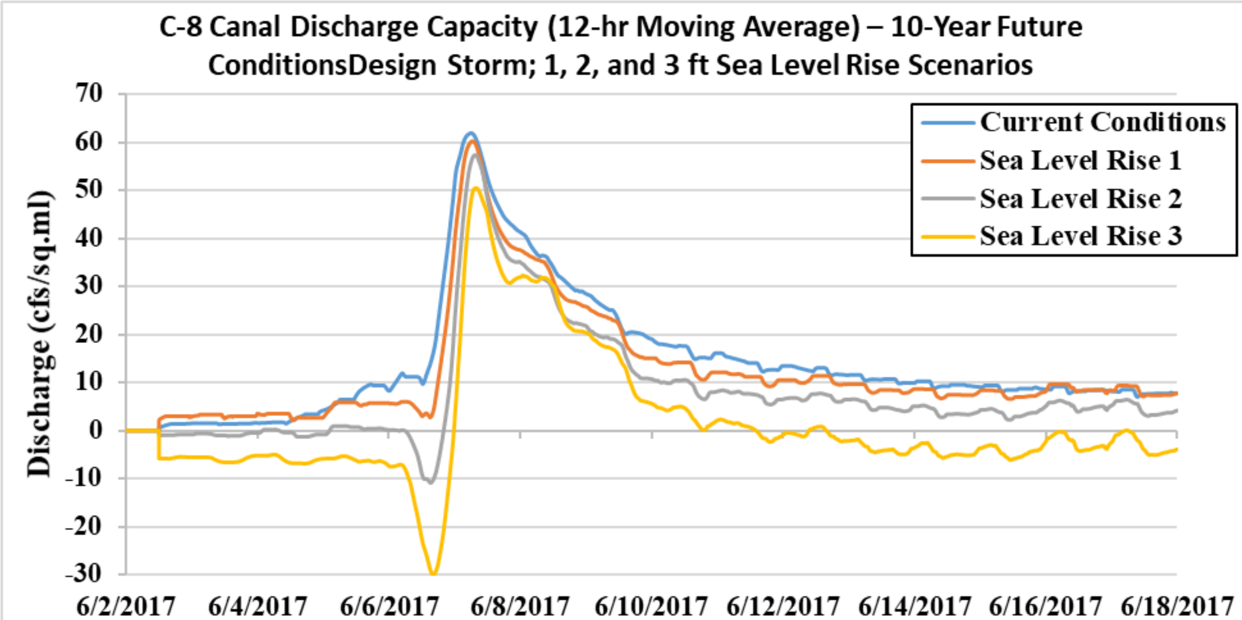

Figure 4.2-6: Area-Weighted Discharge Hydrograph for C-8 Canal (S-28) 10-Year Design Storms

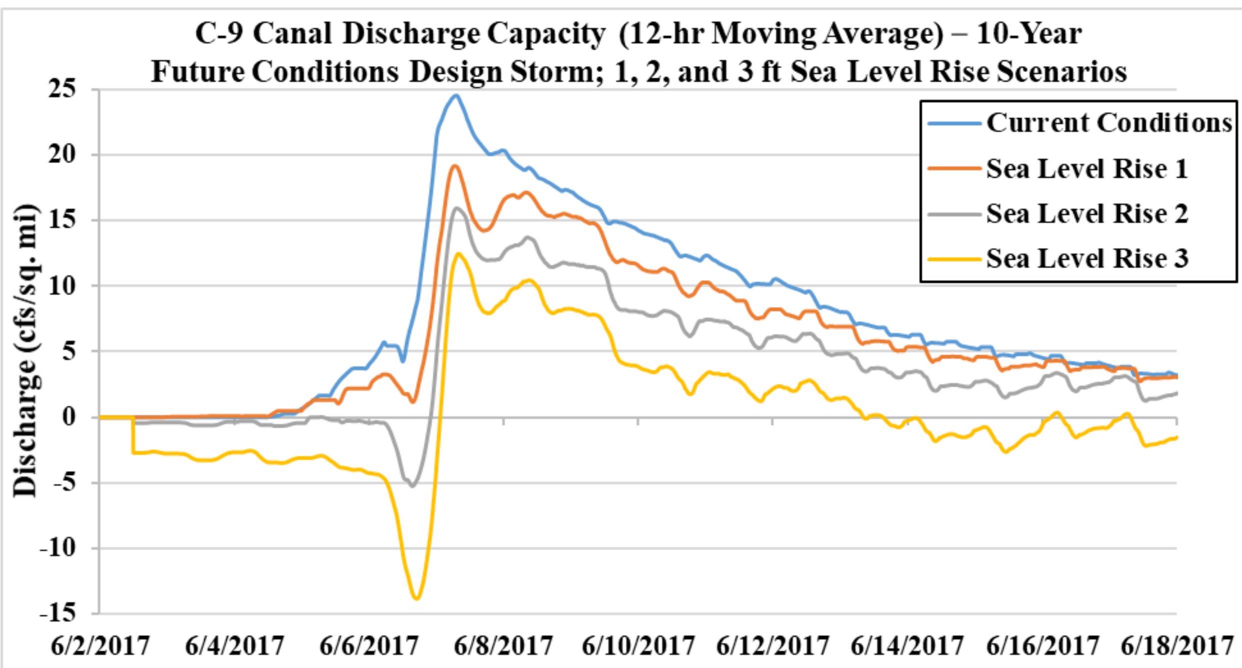

Figure 4.2-7: Area-Weighted Discharge Hydrograph for C-9 Canal (S-29) 10-Year Design Storms

The peak discharge capacity of the C-9 Canal west of Red Road was 15.2 CSM for the 10-year current conditions scenario and is further reduced for each sea level rise scenario, resulting in less than 5 CSM for SLR3. This reduction is caused by higher water levels east of Red Road, which is a result of sea level rise. The western C-9 basin is drained by pumps and based on simulated stages in the C-9 canal, the pumping duration was not limited, so total discharge to the C-9 canal under sea level rise scenarios were equivalent or greater than current conditions due to increased groundwater levels. This shows that the reduction in discharge capacity of the C-9 Canal was not caused by a reduction in discharge to the canal.

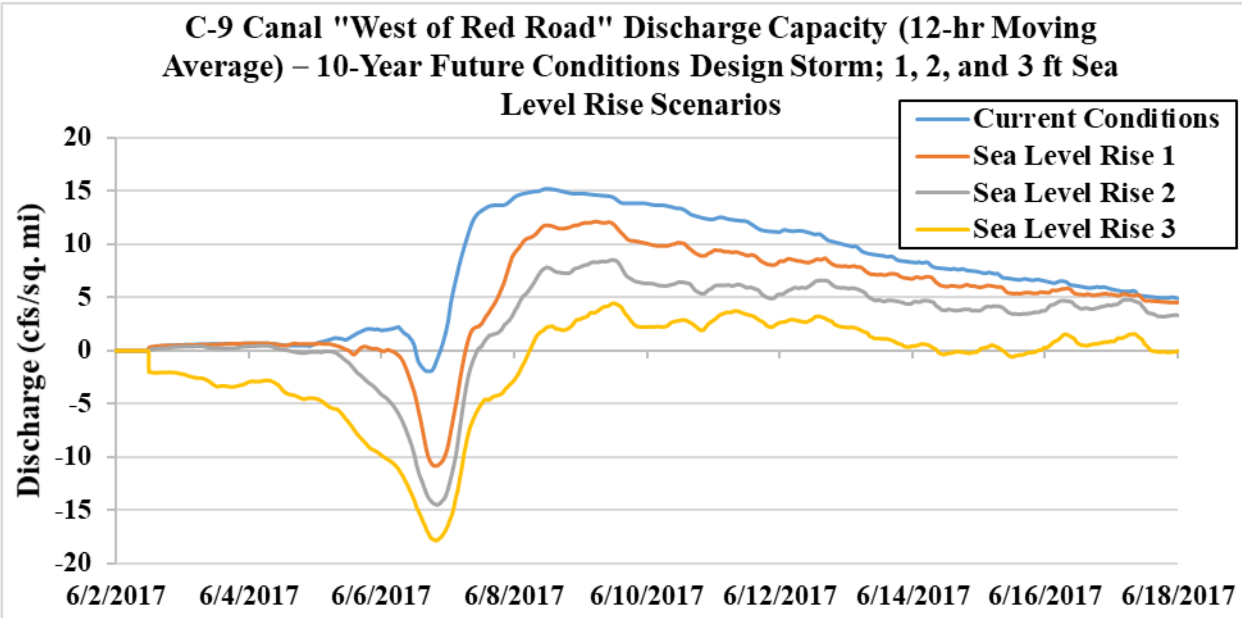

Figure 4.2-8: Area Weighted Discharge Hydrograph for C-9 Canal West of Red Road for 10-Year Design Storms

Figure 4.2-8 shows negative discharge during peak rainfall, similar to the 5-year storm results. Again, this occurs because there is a delayed response in the west side as there is a significant amount of dead storage (large lakes in SBDD) and because of the C-9 Impoundment, which is pulling water from the western C-9 Canal. The storage in the west side is controlled by pumps that turn on at an elevation higher than control elevation. As the pumps turn on and the C-9 Impoundment pumps turn off, the discharge becomes positive. For the area east of Red Road, as shown in **Figure 4.2-9**, a negative discharge during peak rainfall is seen during the SLR3 scenario. This indicates that under the 3 ft sea level rise scenario, the inflection point is shifted west, past Red Road, which can be seen in **Figure 4.1-5**.

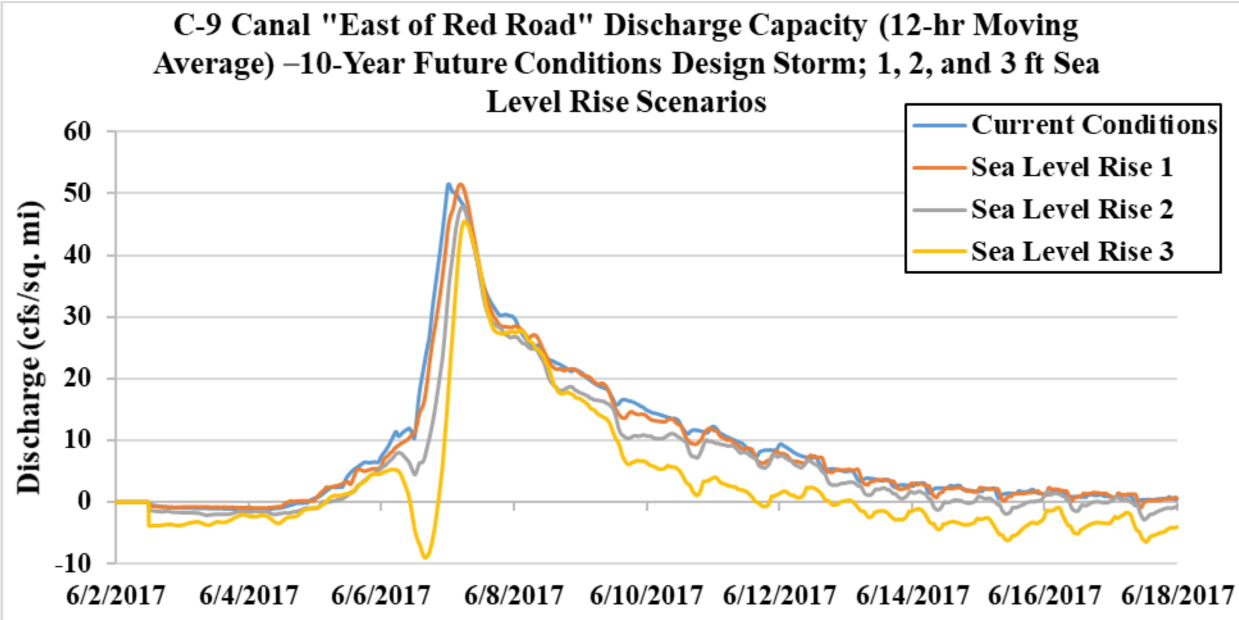

Figure 4.2-9: Area-Weighted Discharge Hydrograph for C-9 Canal East of Red Road for 10-Year Design Storms

4.2.3 25-Year Design Storms

Figure 4.2-13, and **Figure 4.2-14** present a visual comparison of the area-weighted discharge hydrographs for each canal segment with respect to the 25-year 72-hour design storm for each sea level rise scenario.

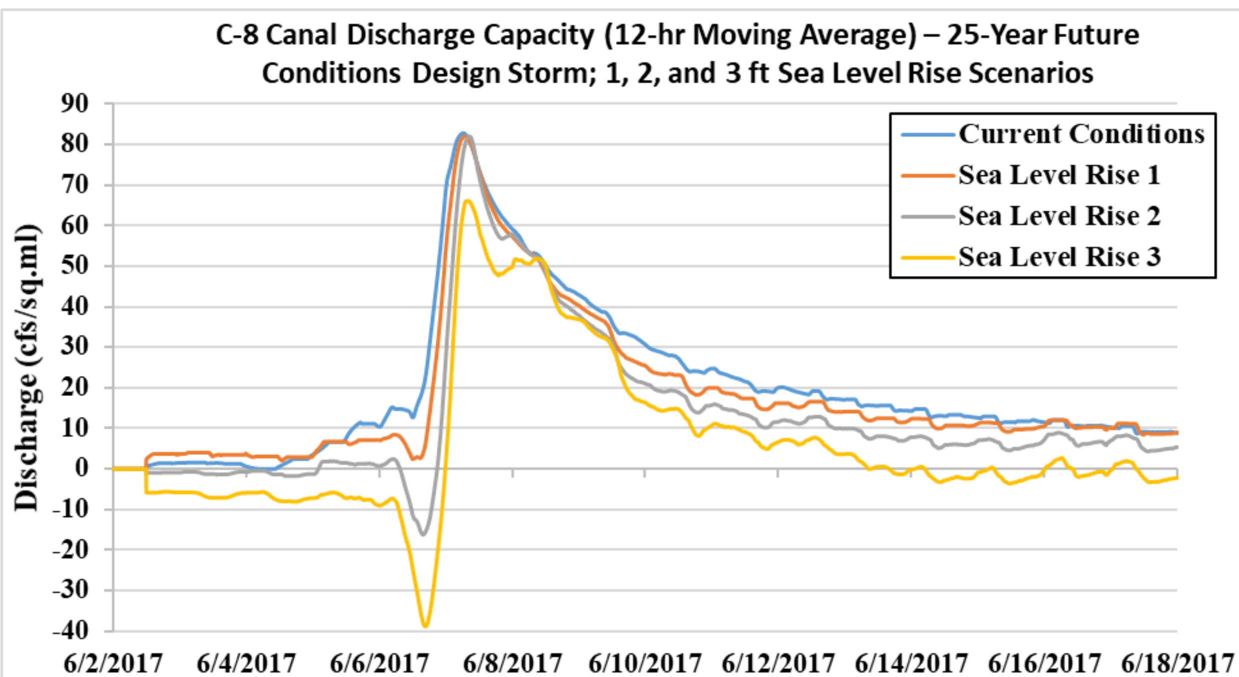

Figure 4.2-10: Area-Weighted Discharge Hydrograph for C-8 Canal (S-28) 25-Year Design Storms

For both the C-8 and C-9 Canals, the discharge capacity for the 25-year design storm is reduced with the increase in sea level rise. For both the C-8 and C-9 Canals, a flow reversal can be seen during the SLR2 scenario and is significantly larger during the SLR3 scenario.

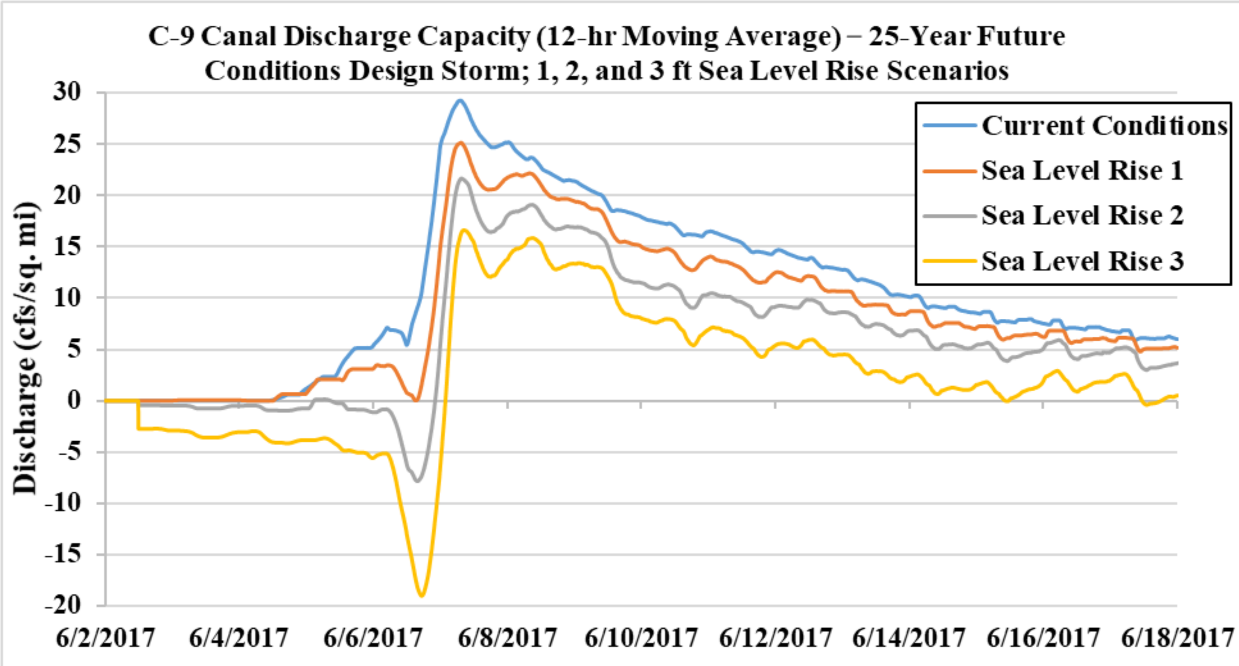

Figure 4.2-11: Area-Weighted Discharge Hydrograph for C-9 Canal (S-29) 25-Year Design Storms

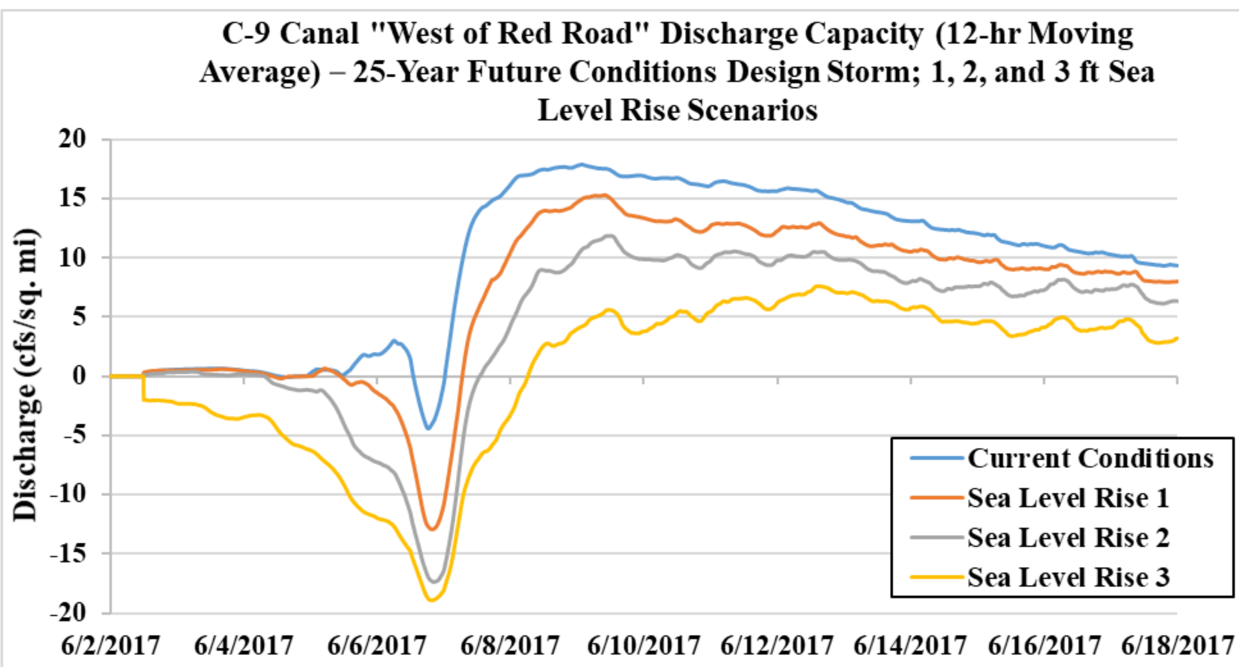

Figure 4.2-12: Area Weighted Discharge Hydrograph for C-9 Canal West of Red Road for 25-Year Design Storms

The peak discharge capacity of the C-9 Canal west of Red Road was 17.9 CSM for the 25-year current conditions scenario and is further reduced for each sea level rise scenario, resulting in less than 8 CSM for SLR3. This reduction is caused by higher water levels east of Red Road, which is a result of sea level rise. Like the 5-year and 10-year design storms, the drainage by pumps to the western C-9 canal was not limited by simulated stage, therefore, the reduction in discharge capacity was not caused by a reduction in discharge to the C-9 Canal.

Figure 4.2-12 shows negative discharge during peak rainfall. This occurs for the same reasons previously described in the discussion of the 5-year and 10-year storm events. For the area east of Red Road, as shown in **Figure 4.2-13**, a negative discharge during peak rainfall is seen during the SLR3 scenario. This indicates that under the 3 ft sea level rise scenario, the inflection point is shifted west, past Red Road, which can be seen in **Figure 4.1-7**. Interestingly, the peak discharge capacity for SLR1 is greater than current conditions, which could indicate that the changes in future conditions runoff potential and initial groundwater elevation is more influential than the increase in sea level for the 25-year design storm. For the 3 ft sea level rise scenario, there was 1 pump station east of Red Road that had limited pumping duration due to simulated stages in the C-9 Canal.

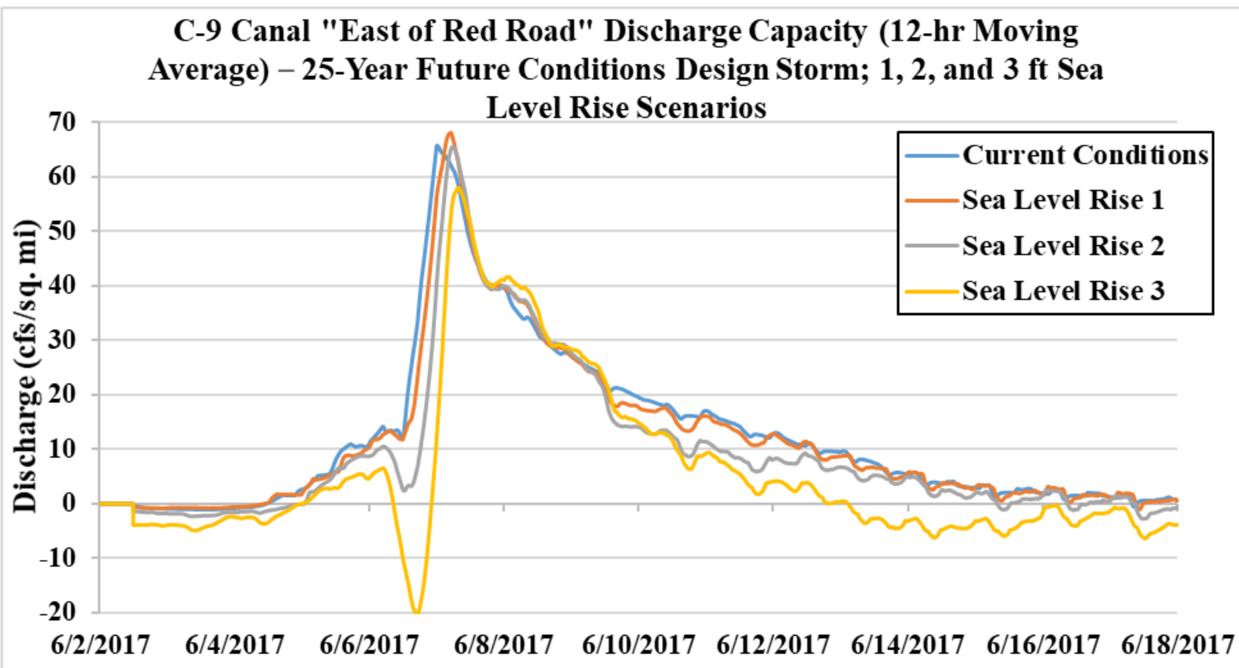

Figure 4.2-13: Area-Weighted Discharge Hydrograph for C-9 Canal East of Red Road for 25-Year Design Storms

4.2.4 100-Year Design Storms

Figure 4.2-14 through **Figure 4.2-17** presents a visual comparison of the area-weighted discharge hydrographs for each canal segment with respect to the 100-year 72-hour design storm for each sea level rise scenario.

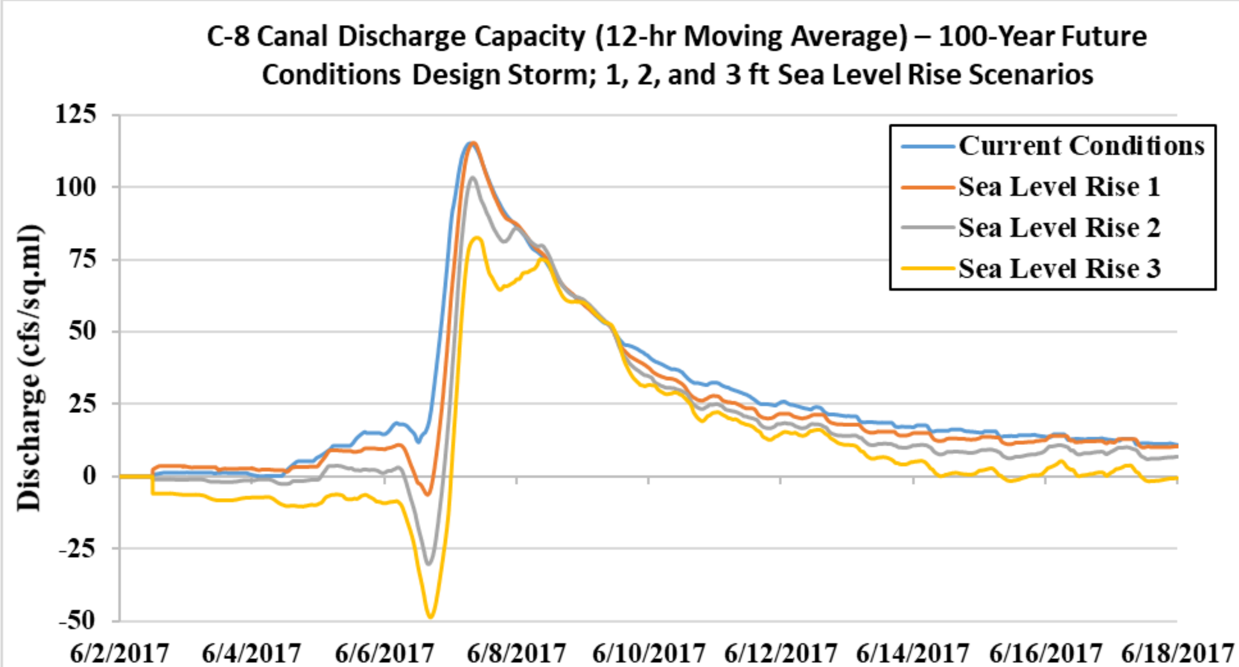

Figure 4.2-14: Area-Weighted Discharge Hydrograph for C-8 Canal (S-28) 100-Year Design Storms

For the C-8 Canal, the discharge capacity for the 100-year design storm is slightly higher (0.17 CSM) for the SLR1 scenario than current conditions but is reduced with further increase in sea level rise. For the C-9 Canal, the discharge capacity for the 100-year design storm is reduced with the increase in sea level rise. For both the C-8 and C-9 Canals, a flow reversal can be seen during the SLR1 scenario and is significantly larger during the SLR3 scenario.

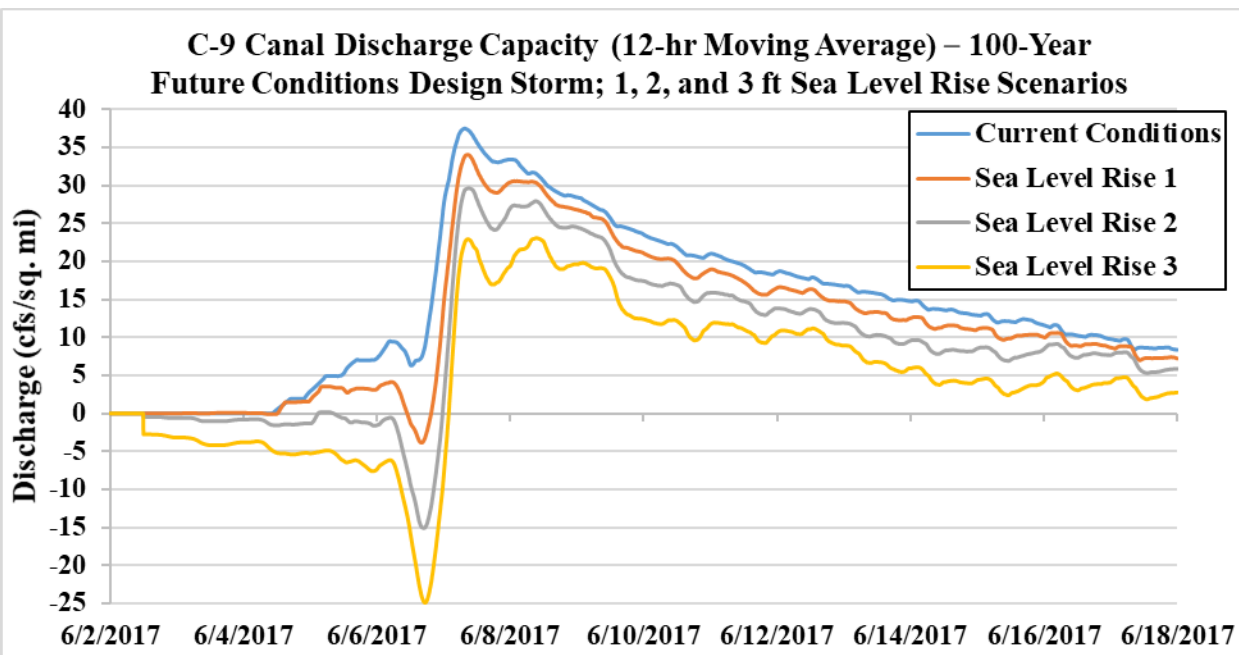

Figure 4.2-15: Area-Weighted Discharge Hydrograph for C-9 Canal (S-29) 100-Year Design Storms

The peak discharge capacity of the C-9 Canal west of Red Road was 20.9 CSM for the 25-year current conditions scenario and is further reduced for each sea level rise scenario, resulting in less than 9 CSM for SLR3.

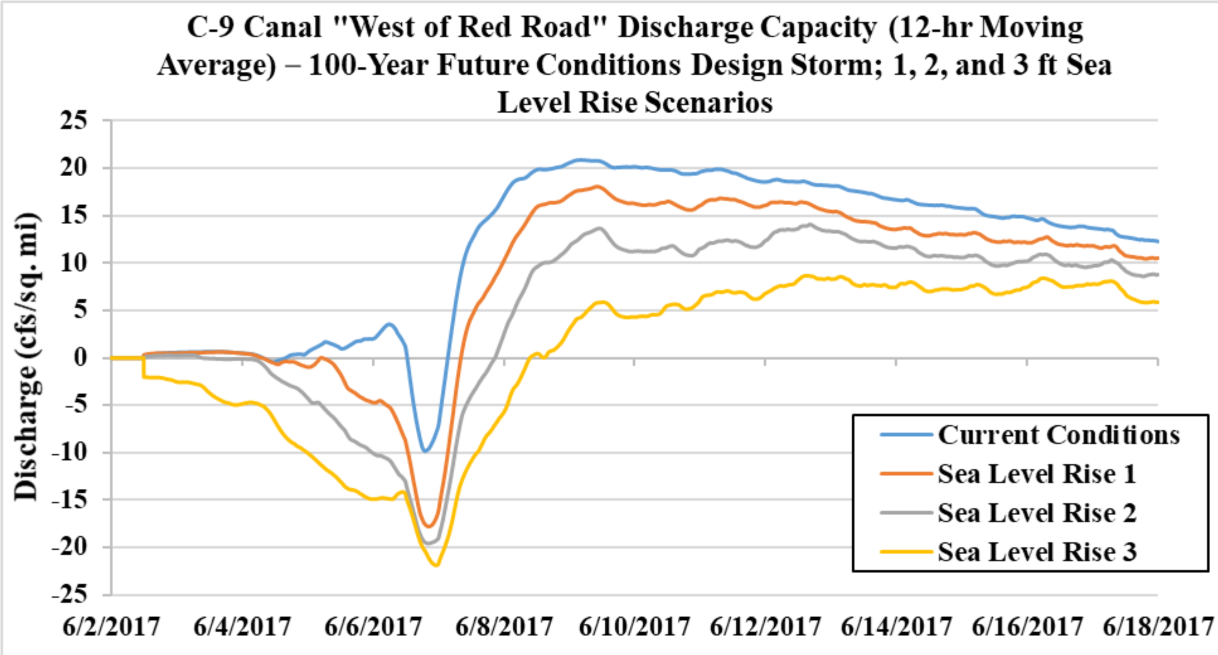

Figure 4.2-16: Area Weighted Discharge Hydrograph for C-9 Canal West of Red Road for 100-Year Design Storms

Figure 4.2-16 shows negative discharge during peak rainfall. This occurs for the same reasons previously described in the discussion of the 5, 10, and 25-year storm events.

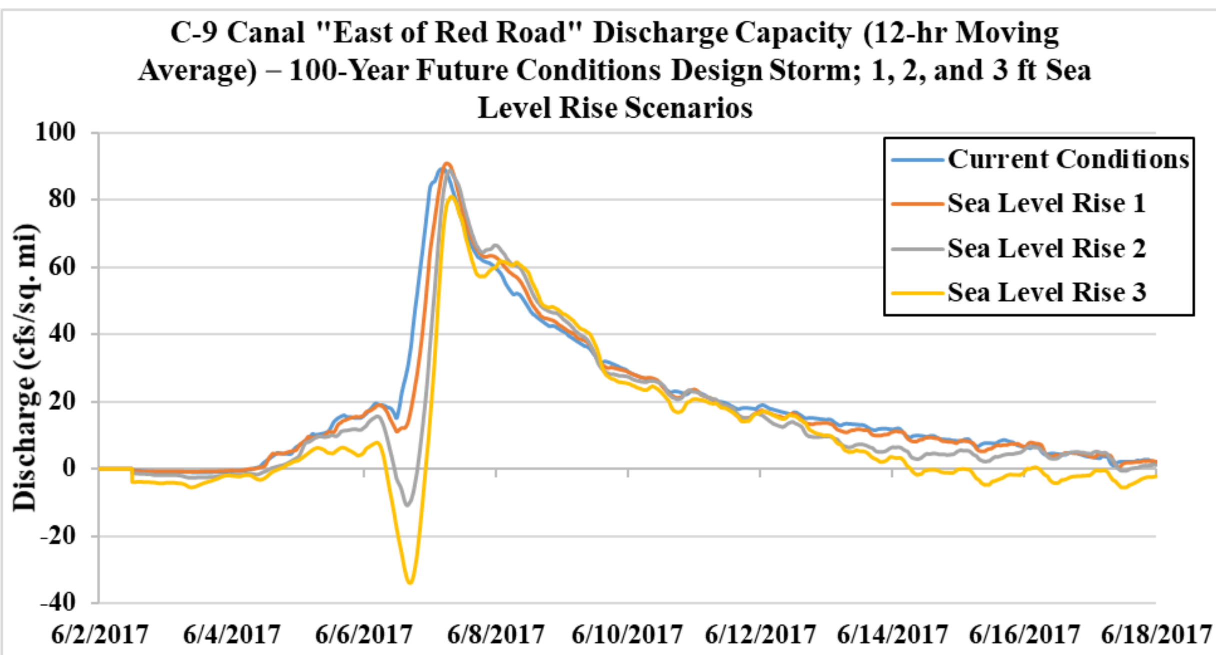

Figure 4.2-17: Area-Weighted Discharge Hydrograph for C-9 Canal East of Red Road for 100-Year Design Storms

For the area east of Red Road, as shown in **Figure 4.2-17**, a negative discharge during peak rainfall is seen during the SLR2 and SLR3 scenarios. This indicates that under the 2 ft and 3 ft sea level rise scenarios, the inflection point is shifted west, past Red Road, which can be seen in **Figure 4.1-9**. Interestingly, the peak discharge capacity for SLR1 is greater than current conditions, which could indicate that the changes in future conditions runoff potential (as a result of higher initial groundwater elevation) is more influential than the 1 ft increase in sea level for the 100-year design storm. For the 1 ft and 2 ft sea level rise scenarios, there was 1 pump station east of Red Road that had limited pumping duration due to simulated stages in the C-9 Canal. For the 3 ft sea level rise scenario, there were 2 pump stations east of Red Road that had limited pumping duration.

4.2.5 Inter-basin Discharge

Figure 4.2-18 shows the location of inter-basin connections, where discharge between the C-8 and C-9 watersheds occur, as well as between the C-8 and C-7 watersheds.

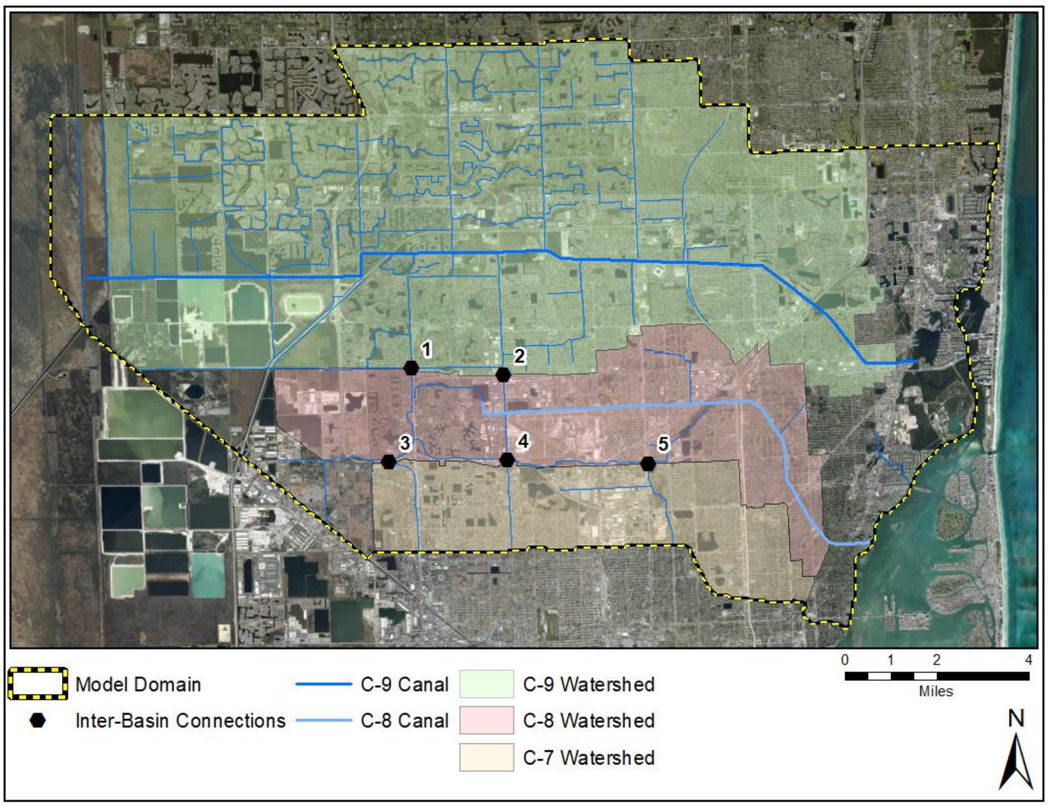

Figure 4.2-18: Location of Inter-Basin Connections

Connection 1 is a culvert under NW 78th Ave. **Figure 4.2-19** and **Figure 4.2-20** show the inter-basin discharge for the 5-year and 100-year design storms, with positive values representing flow from the C-8 to the C-9 watershed and negative values indicating flow from the C-9 to the C-8 watershed. For the 5-year current conditions design storm, there was no discharge from the C-8 to the C-9 Canal, as the flow direction was from the C-9 Canal to the C-8 Canal. Under all three future conditions sea level rise scenarios, there is inter-basin discharge in the direction from the C-8 to C-9 Canal. This is likely due to the C-9 Impoundment, which reduces stage in the C-9 Canal, which creates a head gradient from C-8 to C-9.

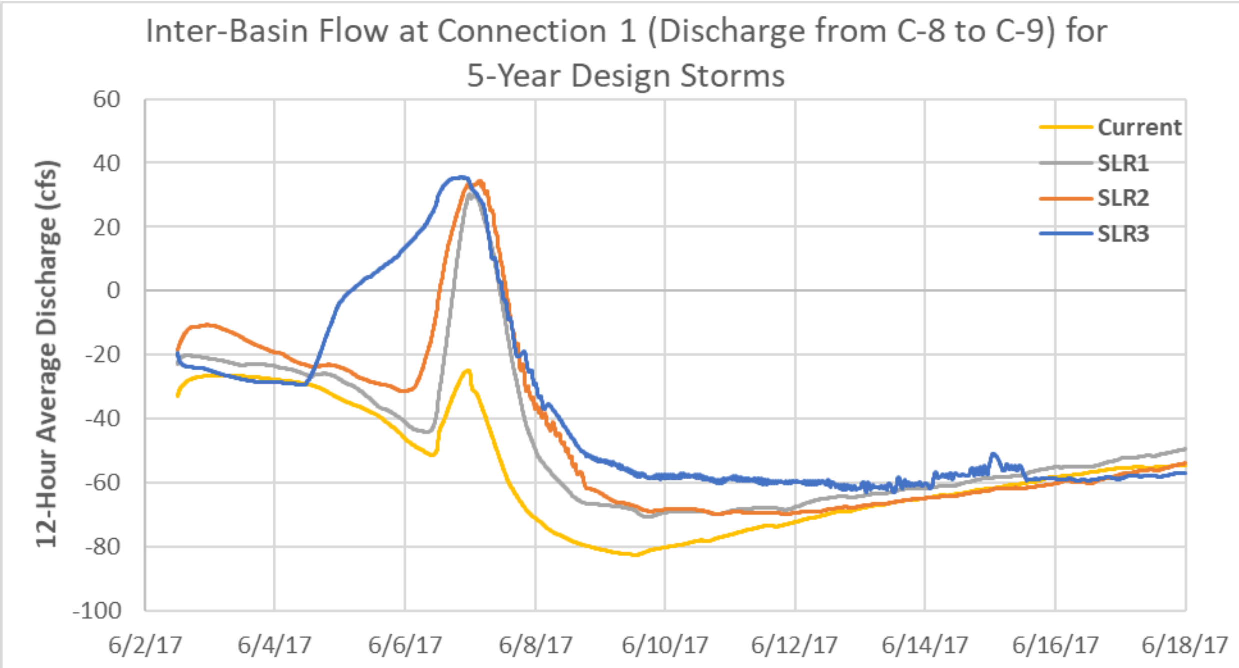

Figure 4.2-19: 5-Year Inter-Basin Discharge Between C-8 and C-9 Watersheds at Connection 1

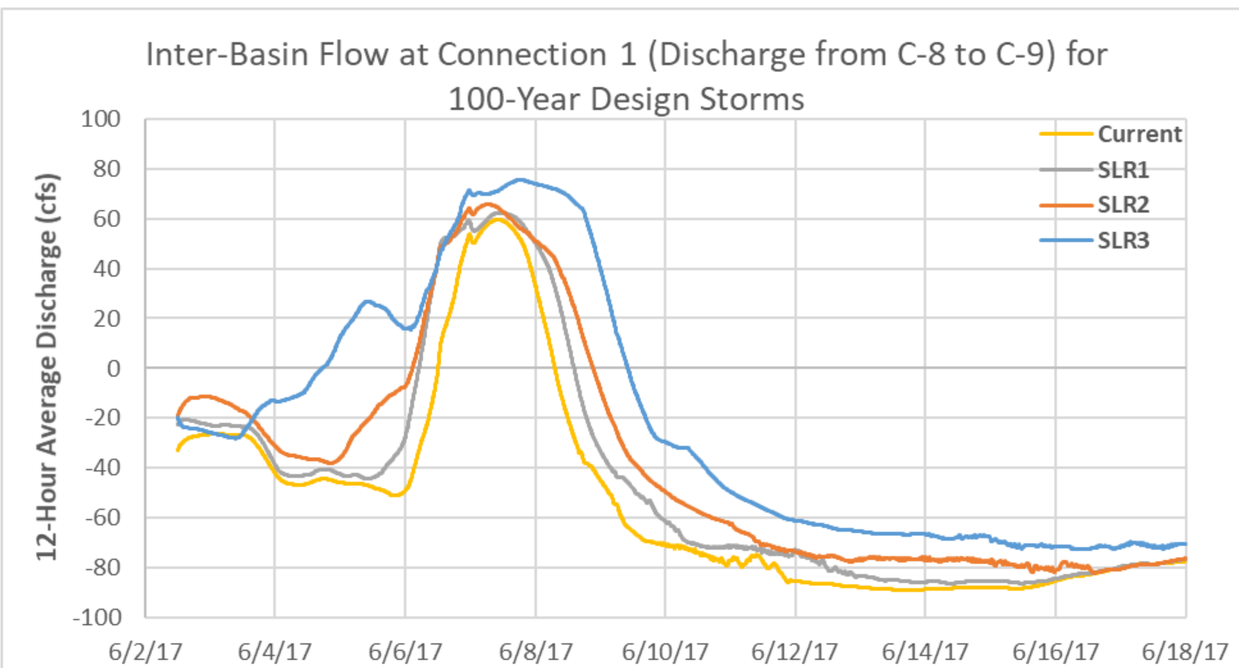

Figure 4.2-20: 100-Year Inter-Basin Discharge Between C-8 and C-9 Watersheds at Connection 1

For the 100-year future conditions design storms, the peak discharge from C-8 to C-9 watershed at this inter-basin connection doesn't change much compared to current conditions. Current conditions peak discharge was about 60 cfs, whereas the future conditions peak discharge for SLR1, SLR2, and SLR3 is 62, 66, and 76 cfs, respectively. Relative to the flow in the C-9 Canal at Red Road (1300 cfs for SLR1, 1200 cfs for SLR2, and 1100 cfs SLR3), this inter-basin exchange is small, contributing around 5-7%, respectively.

The peak discharge from C-9 to C-8 watershed at this inter-basin connection is reduced from about 90 cfs under current conditions to 70-86 cfs depending on SLR. However, this occurs several days after the peak discharge and does not contribute to peak discharge rates in the C-8 Canal.

Connection 2 is a culvert under Palmetto Expressway, just west of Red Road. **Figure 4.2-21** and **Figure 4.2-22** show the inter-basin discharge for the 5-year and 100-year design storms, with positive values representing flow from the C-9 to the C-8 watershed and negative values indicating flow from the C-8 to the C-9 watershed. For the 5-year design storm, the peak discharge from C-9 to C-8 watershed at this inter-basin connection was reduced from about 100 cfs under current conditions to about 70-90 cfs under future conditions sea level rise scenarios. The peak inter-basin discharge occurs several days after the peak discharge in the C-8 Canal. For the 5-year design storm, there was no discharge from C-8 to C-9 watershed at this inter-basin connection under current conditions, however, under SLR2 and SLR3, the peak inter-basin discharge is 30 cfs and 50 cfs, respectively. Relative to the peak flow in the C-9 Canal at Red Road (850 cfs for SLR2 and 620 cfs SLR3), this inter-basin exchange is small, contributing no more than 8%.

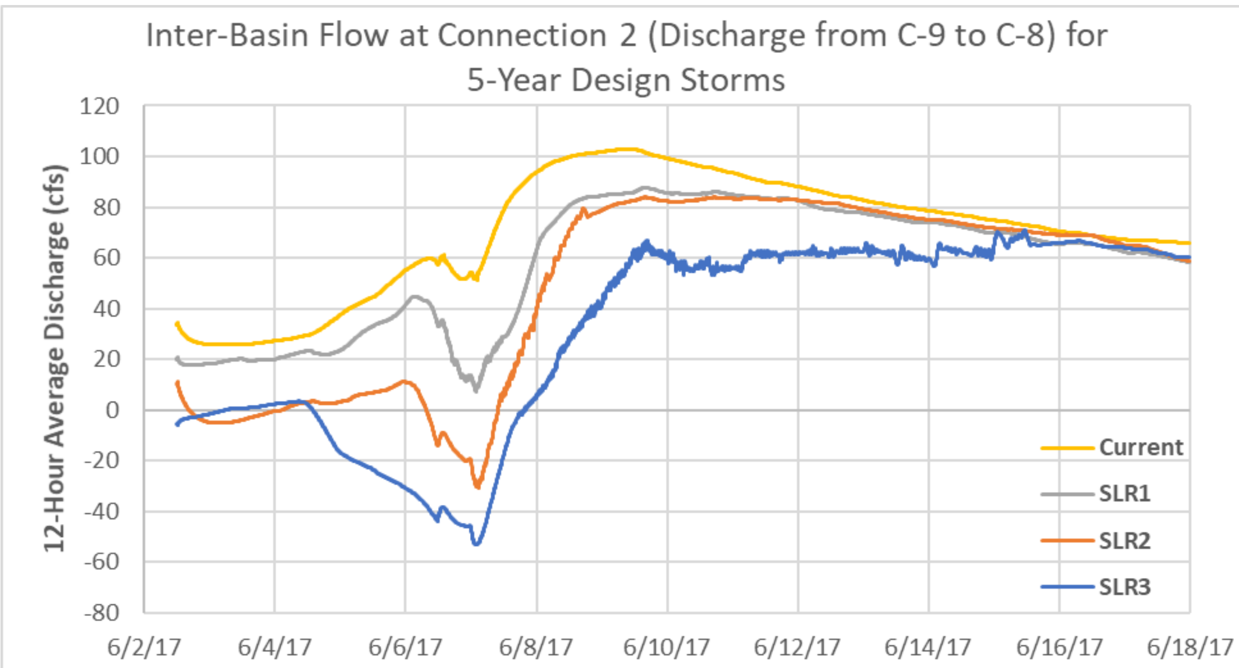

Figure 4.2-21: 5-Year Inter-Basin Discharge Between C-8 and C-9 Watersheds at Connection 2

For the 100-year design storm, the peak discharge from C-9 to C-8 watershed at this inter-basin connection was reduced from about 125 cfs under current conditions to about 80-110 cfs under future conditions sea level rise scenarios. The peak inter-basin discharge occurs several days after the peak discharge in the C-8 Canal. For the 100-year design storm, there was almost no discharge from C-8 to C-9 watershed at this inter-basin connection under current conditions, however, under all sea level rise scenarios, the peak inter-basin discharge is larger, between 30-50 cfs. Relative to the peak flow in the C-9 Canal at Red Road (1340 cfs for SLR1, 850 cfs for SLR2, and 620 cfs SLR3), this inter-basin exchange is small, contributing between 2% and 8%.

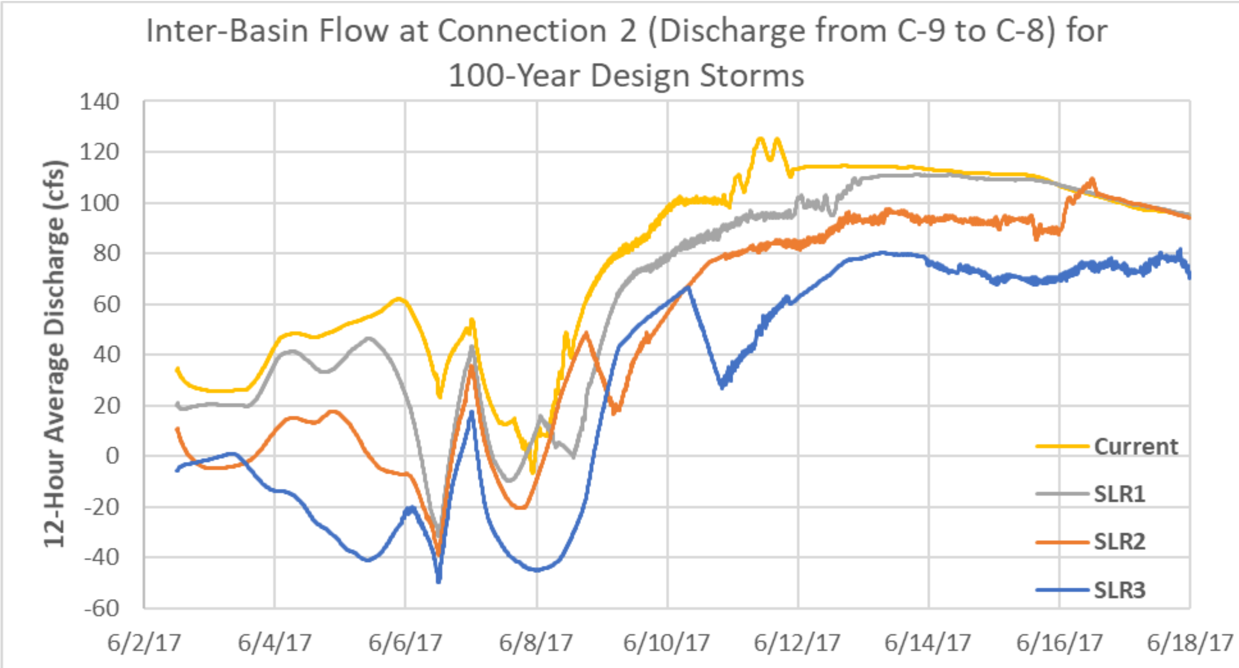

Figure 4.2-22: 100-Year Inter-Basin Discharge Between C-8 and C-9 Watersheds at Connection 2

Connection 3 is a culvert under I75. **Figure 4.2-23** and **Figure 4.2-24** show the inter-basin discharge for the 5-year and 100-year design storms, with positive values representing flow from the C-8 to the C-7 watershed and negative values indicating flow from the C-7 to the C-8 watershed. Flows from C-8 to C-7 watershed reduces the burden on the C-8 canal, peaking at 189 cfs, 237 cfs, and 266 cfs for SLR1, SLR2, and SLR3, respectively, compared to 171 cfs under current conditions.

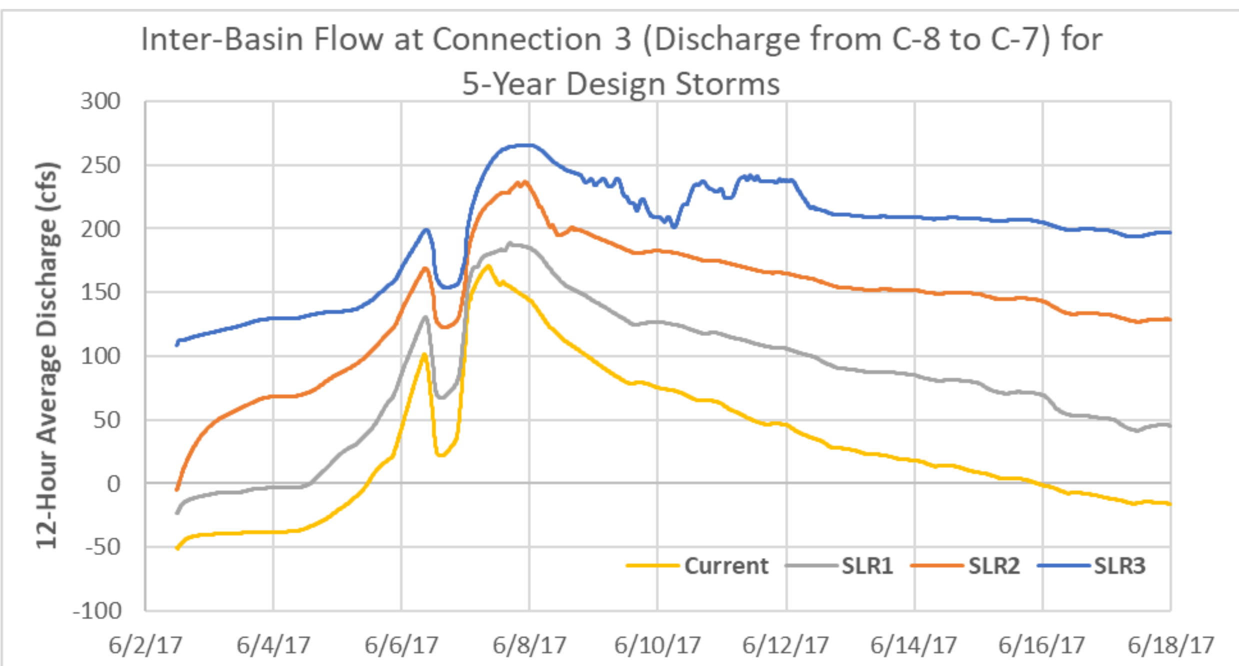

Figure 4.2-23: 5-Year Inter-Basin Discharge Between C-8 and C-7 Watersheds at Connection 3

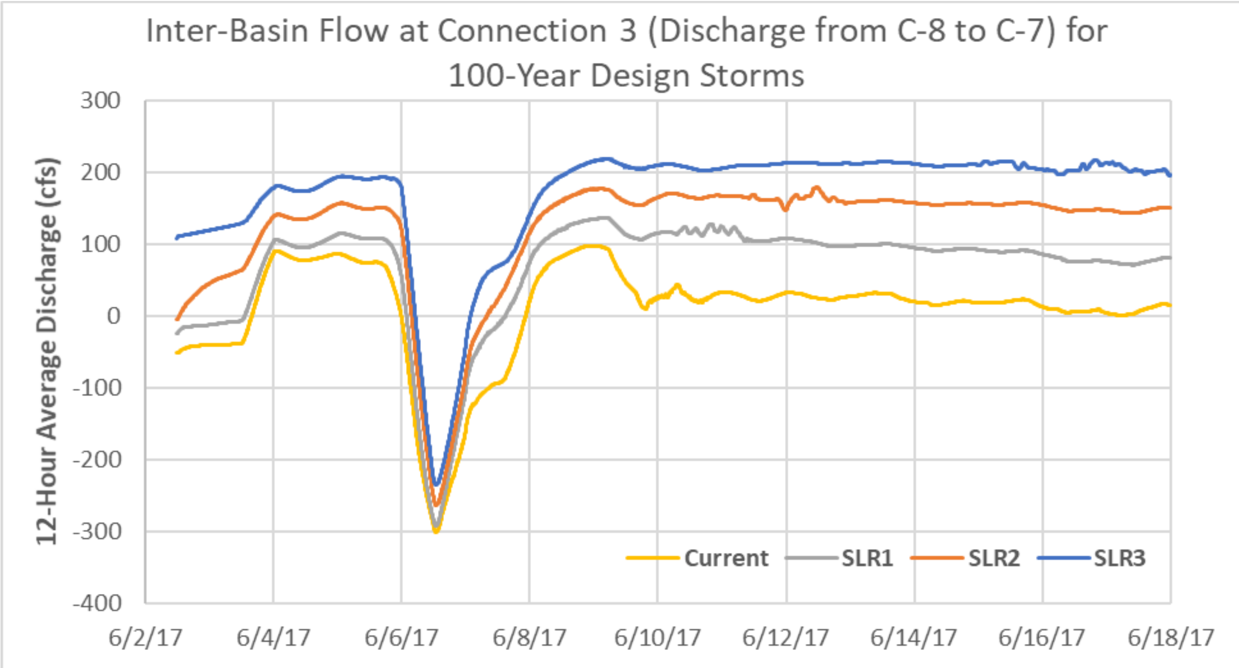

Figure 4.2-24: 100-Year Inter-Basin Discharge Between C-8 and C-7 Watersheds at Connection 3

For the 100-year design storm, the peak discharge from C-7 to C-8 watershed at this inter-basin connection was about 300 cfs for current conditions and occurs about 18 hours prior to peak discharge at S-28. For future conditions, the inter-basin discharge from C-7 to C-8 was reduced to 235 cfs for SLR1, 264 cfs for SLR2, and 291 cfs for SLR3. The reduced peak inter-basin discharge from C-7 to C-8 reduces the stress on the C-8 Canal system, as does the increased post-storm inter-basin discharge.

Connection 4 is a culvert under NE 135th St at Red Road. **Figure 4.2-25** and **Figure 4.2-26** show the inter-basin discharge for the 5-year and 100-year design storms, with positive values representing flow from the C-8 to the C-7 watershed and negative values indicating flow from the C-7 to the C-8 watershed. Flows from C-8 to C-7 watershed reduces the burden on the C-8 canal, peaking at about 50 cfs for SLR1, 60 cfs for SLR2, and 70 cfs for SLR3, compared to 40 cfs current conditions. This relieves the C-8 canal system of some stress.

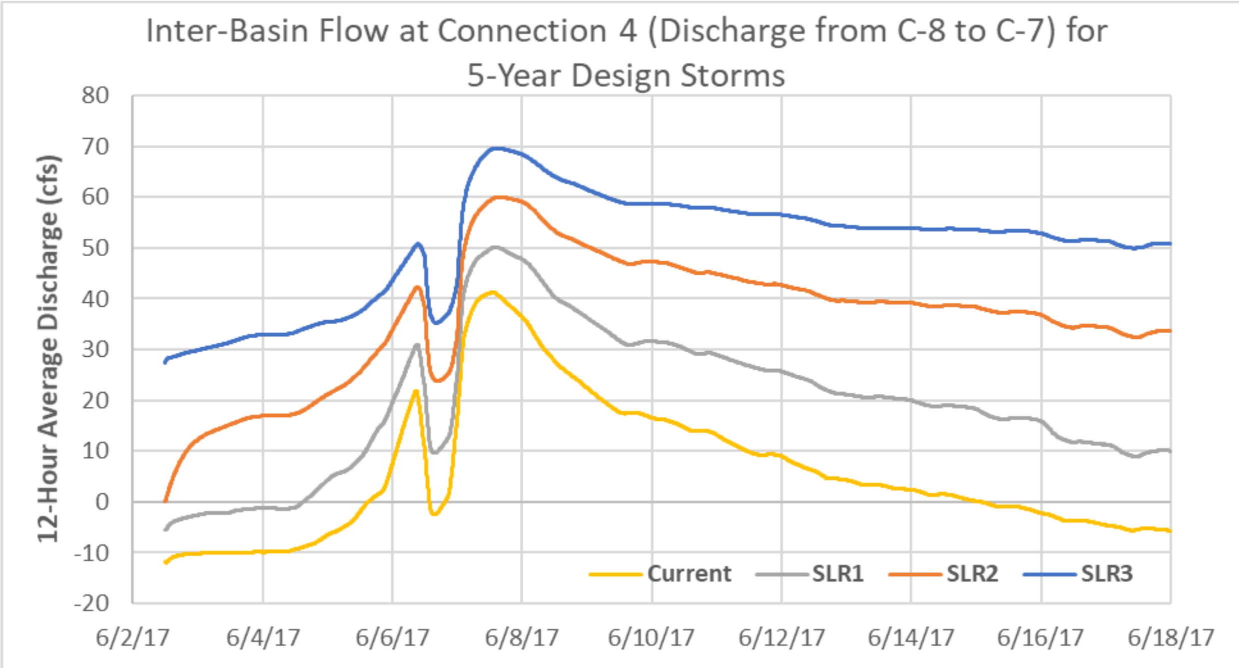

Figure 4.2-25: 5-Year Inter-Basin Discharge Between C-8 and C-7 Watersheds at Connection 4

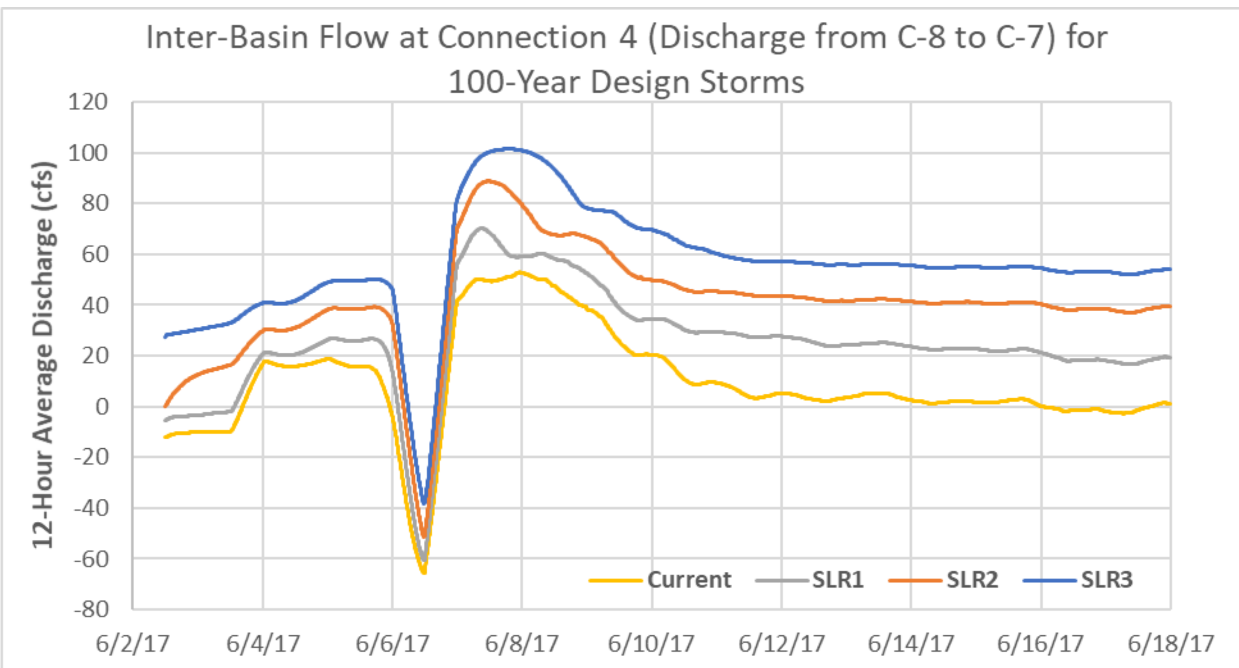

Figure 4.2-26: 100-Year Inter-Basin Discharge Between C-8 and C-7 Watersheds at Connection 4

For the 100-year design storm, the peak discharge from C-7 to C-8 watershed at this inter-basin connection was about 65 cfs for current conditions and occurs about 18 hours prior to peak discharge at S-28. For future conditions, the inter-basin discharge from C-7 to C-8 was reduced to 61 cfs for SLR1, 52 cfs for SLR2, and 39 cfs for SLR3. The reduced peak inter-basin discharge from C-7 to C-8 reduces the stress on the C-8 Canal system, as does the increased post-storm inter-basin discharge.

Connection 5 is a culvert under NE 135th St just east of NW 27th Ave. **Figure 4.2-27** and **Figure 4.2-28** show the inter-basin discharge for the 5-year and 100-year design storms, with negative values indicating flow from the C-8 to the C-7 watershed. Flow from C-8 to C-7 watershed reduces the burden on the C-8 Canal. For the 5-year design storms, there was not much change in inter-basin flow from the C-7 to C-8 Canal, staying around 100 cfs. For the 100-year SLR2 and SLR3 design storms, there was increased inter-basin flow from C-7 to C-8 during peak rainfall, which adds stress to the C-8 Canal system.

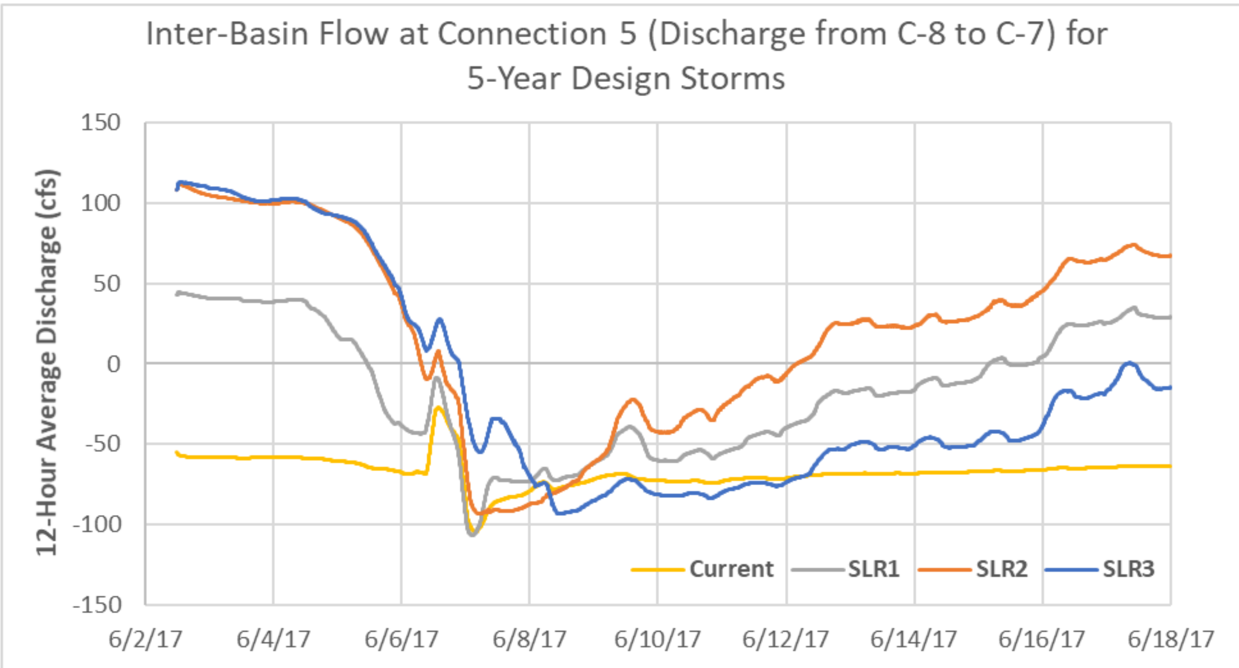

Figure 4.2-27: 5-Year Inter-Basin Discharge Between C-8 and C-7 Watersheds at Connection 5

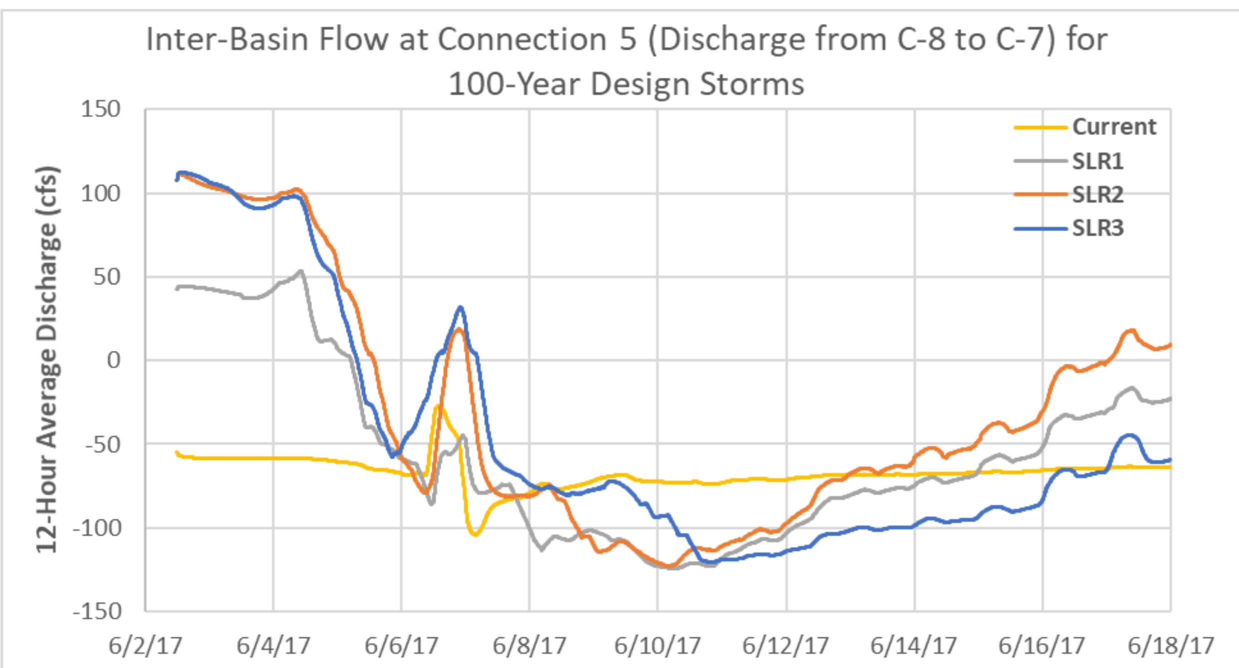

Figure 4.2-28: 100-Year Inter-Basin Discharge Between C-8 and C-7 Watersheds at Connection 5

4.3 PM #3 – Structure Performance

PM #3 shows the effective capacity of a tidal structure. For this metric, structure discharge over a range of storm events and sea level rise scenarios is compared with the original static design condition. Future condition design storms simulated three sea level rise scenarios. This PM provides insight on the structure performance under future sea level rise conditions and compares it with current conditions to determine what degradation in performance occurs, if any.

SFWMD has completed a similar evaluation for the S-28 and S-29 structures in reports titled, *The Effects of Sea Level Rise on S28 Performance* (Zhang, 2017) and *The Effects of Sea Level Rise on S29 Performance* (Zhang, 2017). In these evaluations, a simple hydraulic model was used with fixed headwater stage based on design headwater and a tailwater that oscillates tidally. To add to the work that has already been done, this PM is evaluated using the full MIKE SHE / MIKE HYDRO model results. Essentially, the main difference is that headwater is not forced, rather it is simulated using the fully dynamic model. Please note that this analysis is for informational purposes and is not intended to replace the previous work done by the District, but rather supplement it and analyze it using a different method.

4.3.1 S-28

Structure S-28 has a static design headwater and tailwater of 2.2 ft and 1.7 ft, respectively. The static design discharge is 3220 cfs based on 0.5 ft head gradient (Zhang, 2017). **Figure 4.3-1** and **Figure 4.3-2** show instantaneous values and 12-hour moving average values, respectively, for S-28 based on a 25-year design storm with 1 ft of sea level rise. Although the instantaneous peak discharge for the 25-year SLR1 is greater than current conditions, it is short lived.

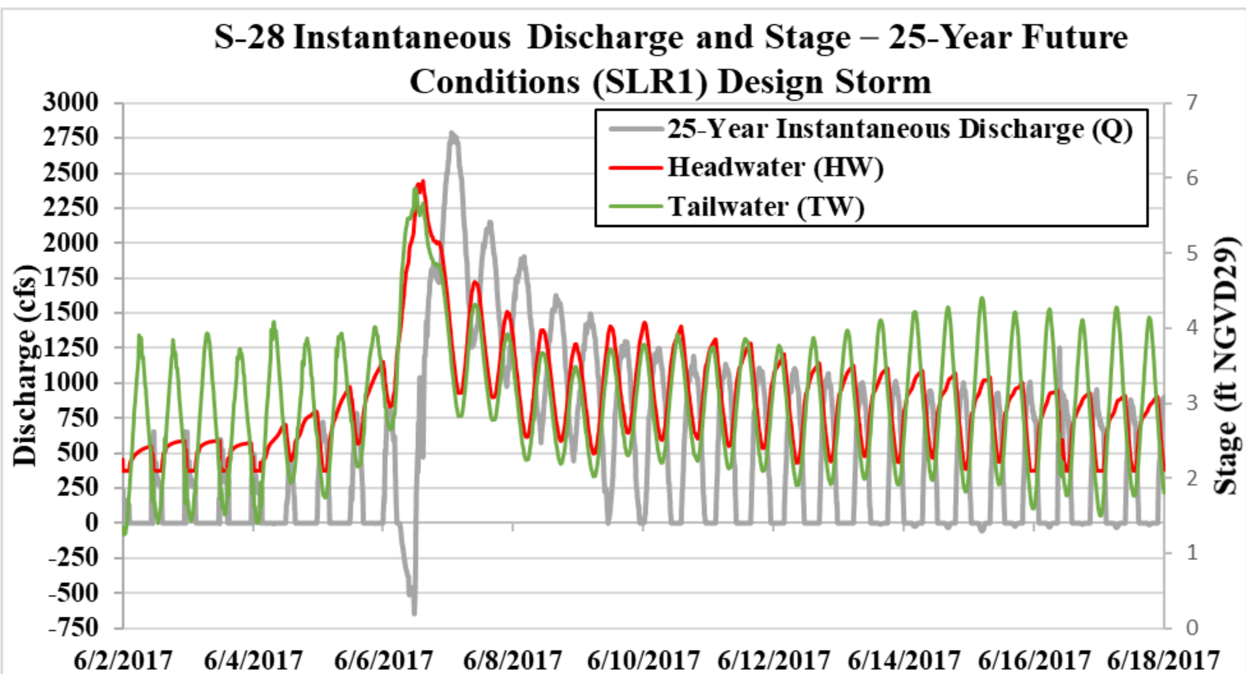

Figure 4.3-1: Instantaneous Discharge and Stage at S-28 Structure for 25-Year Future Conditions Sea Level Rise 1 Design Storm

At the peak of the storm, there is about 650 cfs of reversed flow, which is likely what caused the increased peak discharge, as there was more water "stacked" on the upstream side of the structure. Filtering out the effects of the tide reveals that the peak discharge decreased compared to current conditions.

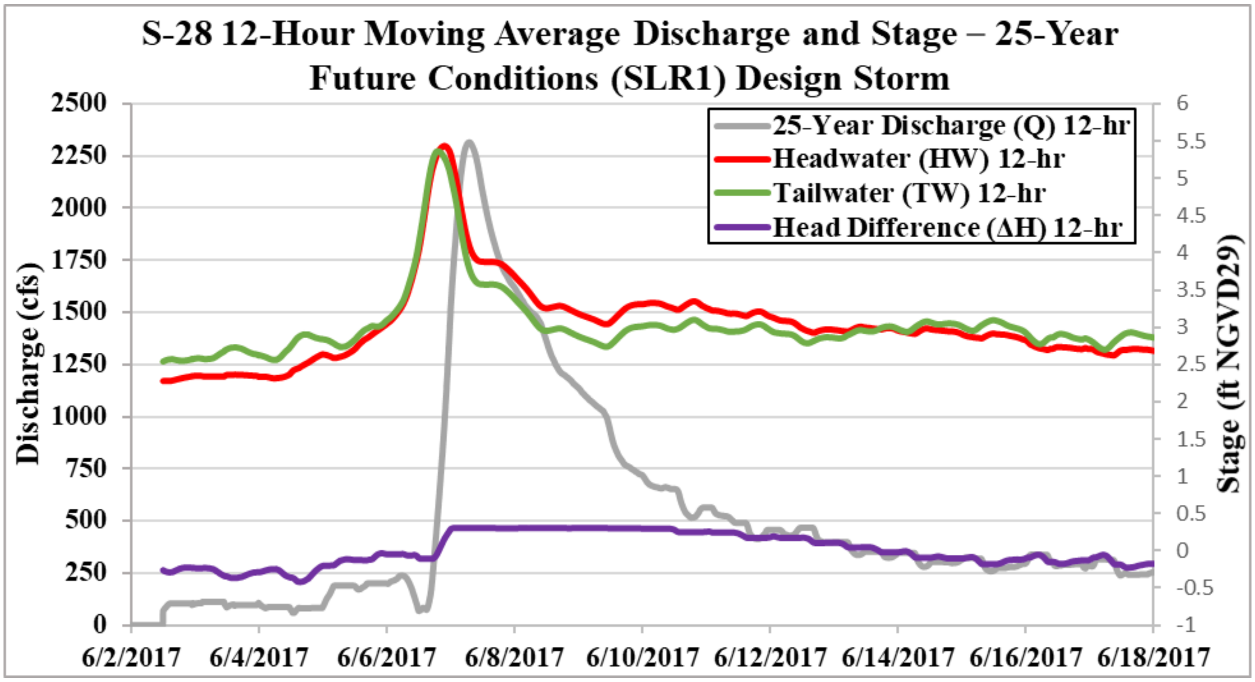

Figure 4.3-2: Tidally Averaged (12-hour) 25-Year Future Conditions Sea Level Rise 1 Design Storm Discharge, Stage, and Head Difference for Structure S-28

Figure 4.3-3 and **Figure 4.3-4** show instantaneous values and 12-hour moving average values, respectively, for S-28 based on a 100-year design storm with 1 ft of sea level rise. Although the instantaneous peak discharge for the 100-year SLR1 is greater than current conditions, it is short lived. At the peak of the storm, there is over 1,000 cfs of reversed flow, which is likely what caused the increased peak discharge, as there was more water "stacked" on the upstream side of the structure. Filtering out the effects of the tide reveals that the peak discharge slightly increased (5 cfs) compared to current conditions.

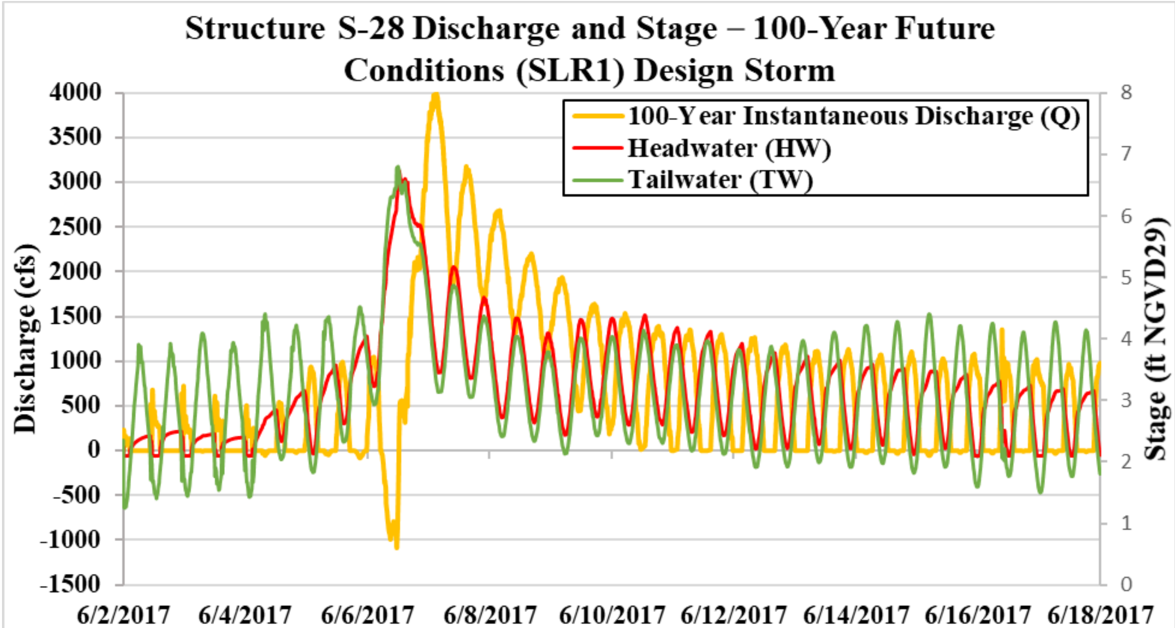

Figure 4.3-3: Instantaneous Discharge and Stage at S-28 Structure for 100-Year Future Conditions Sea Level Rise 1 Design Storm

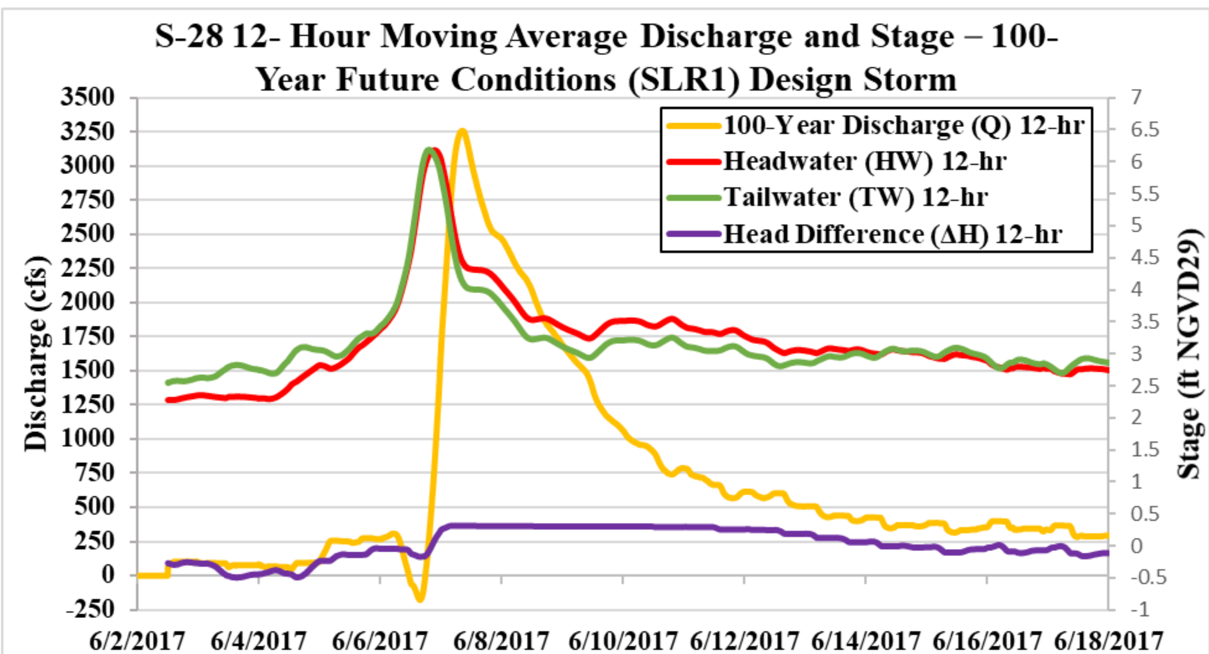

Figure 4.3-4: Tidally Averaged (12-hour) 100-Year Future Conditions Sea Level Rise 1 Design Storm Discharge, Stage, and Head Difference for Structure S-28

As shown in **Figure 4.3-4,** the S-28 structure slightly exceeds the design discharge of 3220 cfs, with a 12-hour moving average peak of 3260 cfs. While this discharge occurs with a 12-hour average head difference of only 0.31 feet, the design headwater assumption is violated. The assumed design headwater stage is 2.2 feet, while the predicted headwater is 4.4 feet at the time of peak discharge. Additionally, there is a flow reversal, peaking at 178 cfs due to a -0.17 ft headwater/tailwater gradient.

Figure 4.3-5 and **Figure 4.3-6** show instantaneous values and 12-hour moving average values, respectively, for S-28 based on a 25-year design storm with 2 ft of sea level rise. Although the instantaneous peak discharge for the 25-year SLR2 is about 500 cfs greater than current conditions, it is short lived. At the peak of the storm, there is nearly 1200 cfs of reversed flow, which is likely what caused the increased peak discharge, as there was more water "stacked" on the upstream side of the structure.

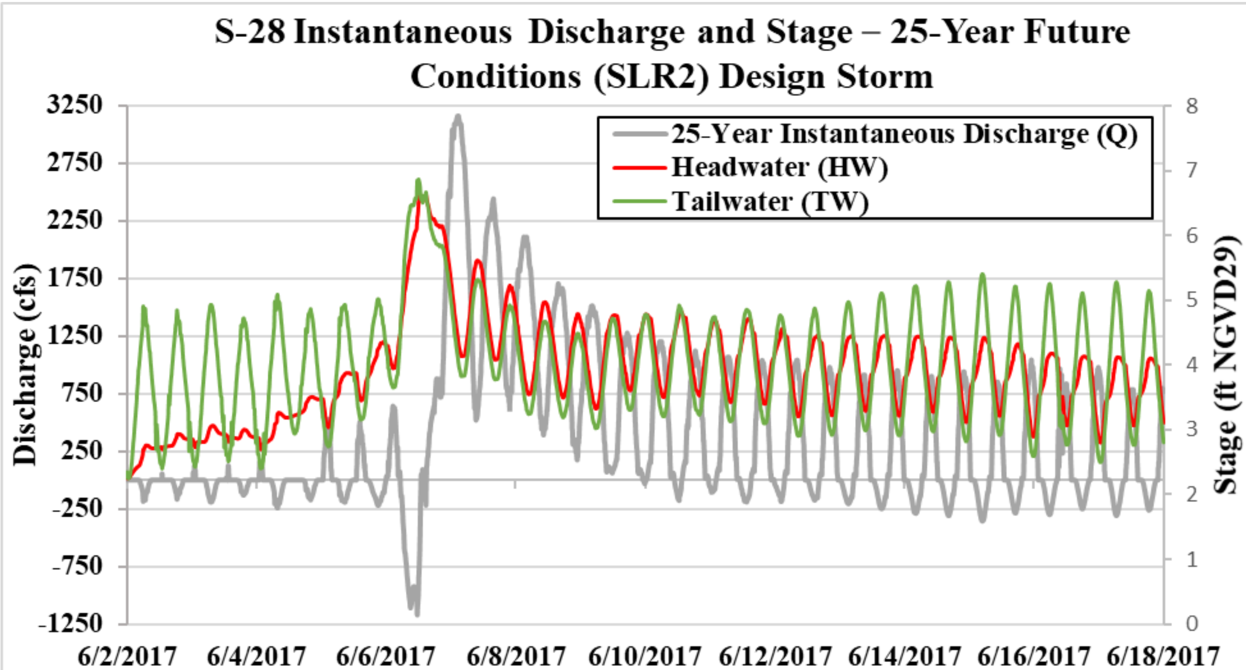

Figure 4.3-5: Instantaneous Discharge and Stage at S-28 Structure for 25-Year Future Conditions Sea Level Rise 2 Design Storm

Filtering out the effects of the tide reveals that the peak discharge decreased compared to current conditions.

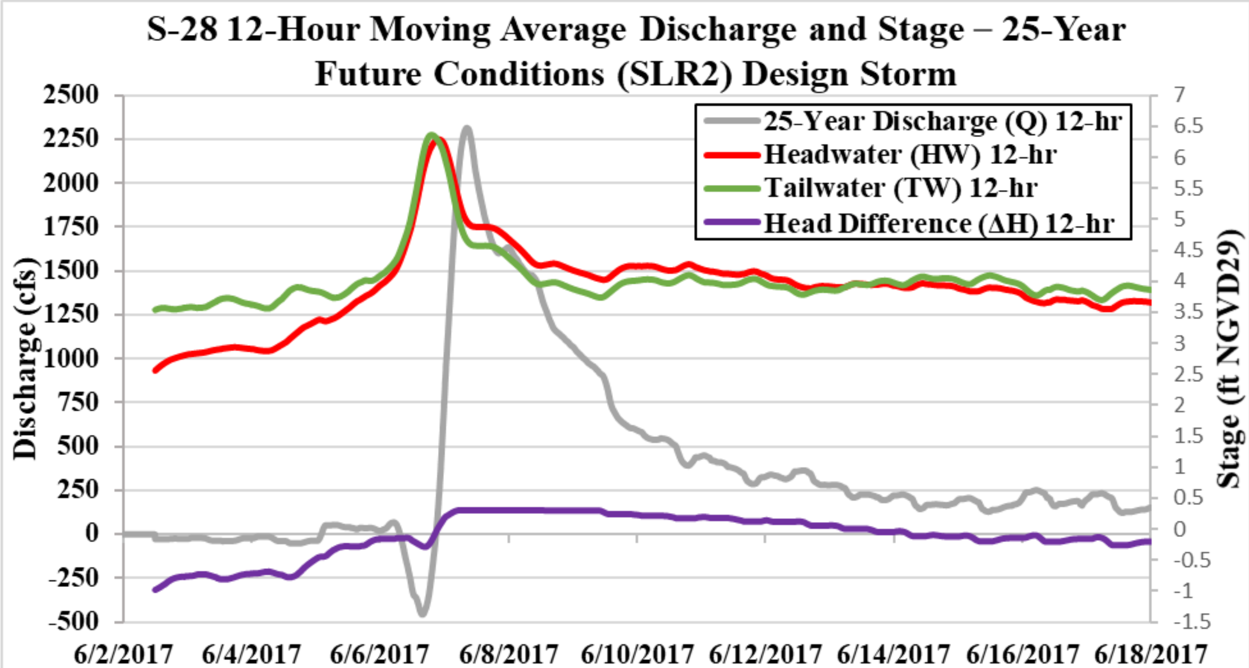

Figure 4.3-6: Tidally Averaged (12-hour) 25-Year Future Conditions Sea Level Rise 2 Design Storm Discharge, Stage, and Head Difference for Structure S-28

Figure 4.3-7 and **Figure 4.3-8** show instantaneous values and 12-hour moving average values, respectively, for S-28 based on a 100-year design storm with 2 ft of sea level rise.

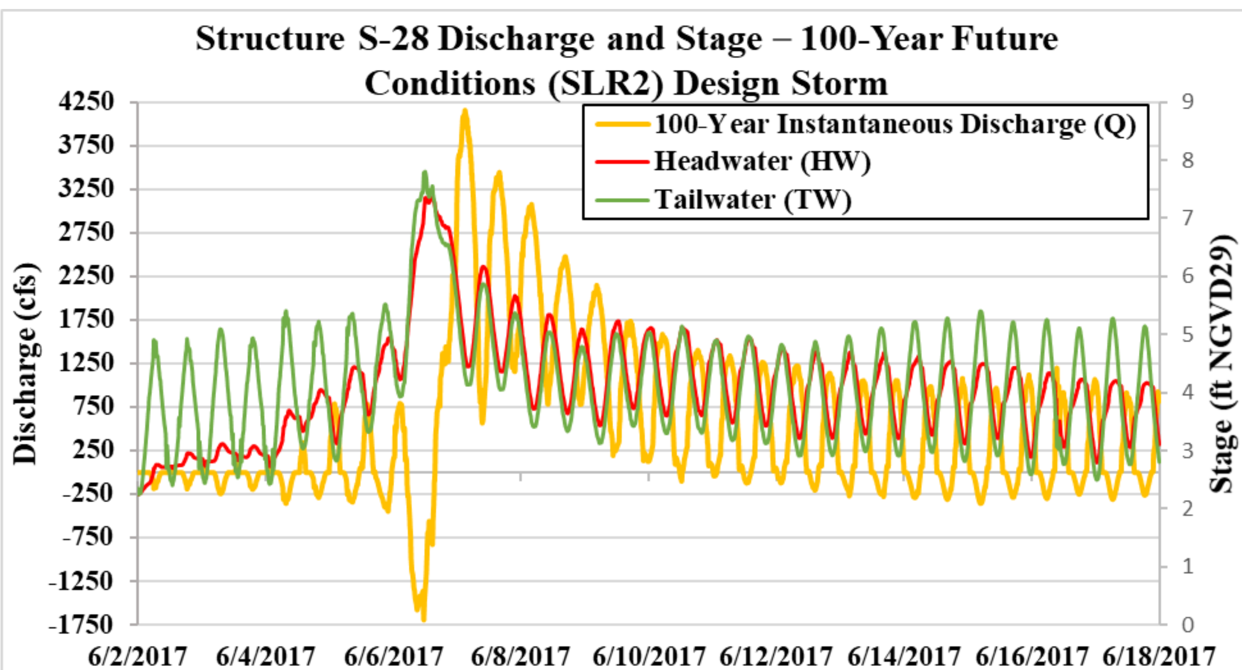

Figure 4.3-7: Instantaneous Discharge and Stage at S-28 Structure for 100-Year Future Conditions Sea Level Rise 2 Design Storm

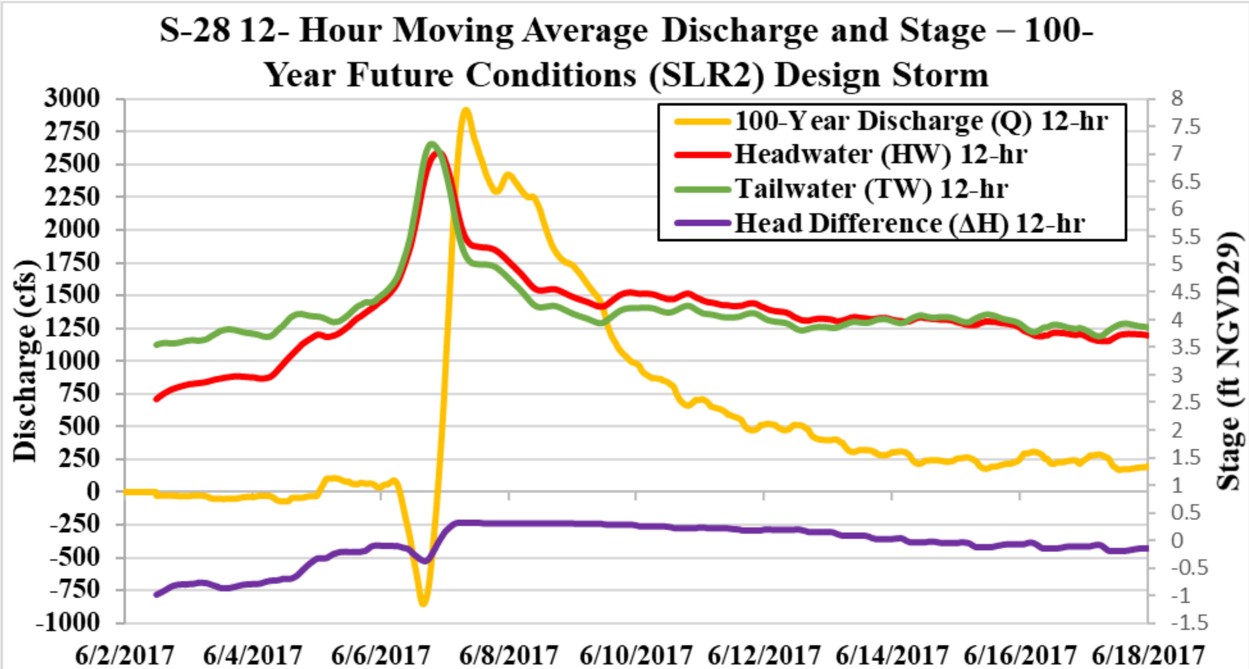

Figure 4.3-8: Tidally Averaged (12-hour) 100-Year Future Conditions Sea Level Rise 2 Design Storm Discharge, Stage, and Head Difference for Structure S-28

As shown in **Figure 4.3-8,** the S-28 structure is unable to reach the design discharge of 3220 cfs, with a 12-hour moving average peak of 2919 cfs. While this discharge occurs with a 12-hour average head difference of only 0.32 feet, the design headwater assumption is violated. The assumed design headwater stage is 2.2 feet, while the predicted headwater is 5.5 feet at the time of peak discharge. Additionally, there is a flow reversal, peaking at 855 cfs due to a -0.37 ft headwater/tailwater gradient.

Figure 4.3-9 and **Figure 4.3-10** show instantaneous values and 12-hour moving average values, respectively, for S-28 based on a 25-year design storm with 3 ft of sea level rise. Although the instantaneous peak discharge for the 25-year SLR3 is about 600 cfs greater than current conditions, it is short lived. At the peak of the storm, there is 1722 cfs of reversed flow. Filtering out the effects of the tide reveals that the peak discharge decreased.

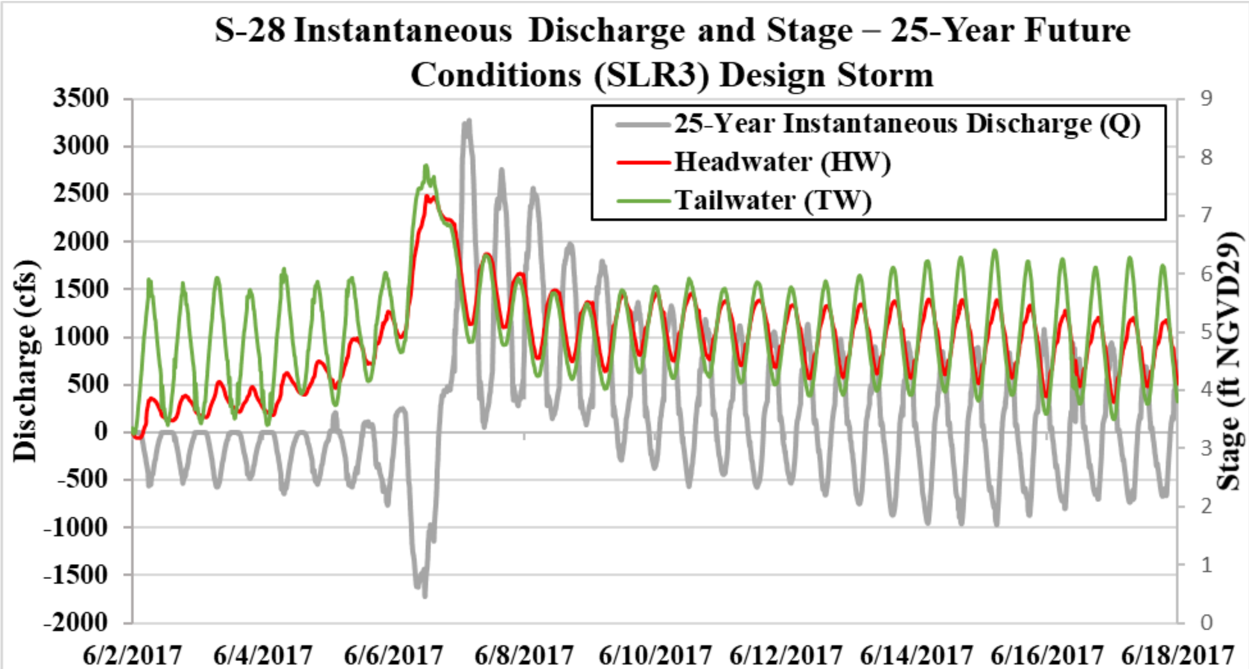

Figure 4.3-9: Instantaneous Discharge and Stage at S-28 Structure for 25-Year Future Conditions Sea Level Rise 3 Design Storm

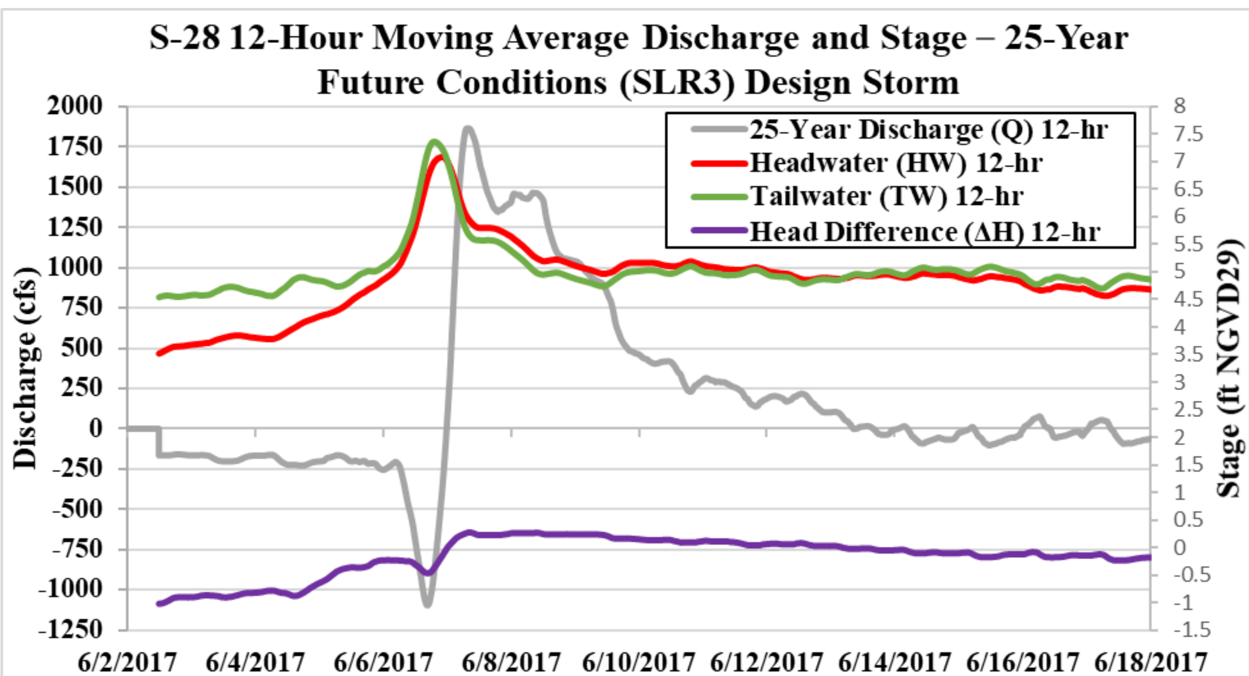

Figure 4.3-10: Tidally Averaged (12-hour) 25-Year Future Conditions Sea Level Rise 2 Design Storm Discharge, Stage, and Head Gradient for Structure S-28

Figure 4.3-11 and **Figure 4.3-12** show instantaneous values and 12-hour moving average values, respectively, for S-28 based on a 100-year design storm with 3 ft of sea level rise.

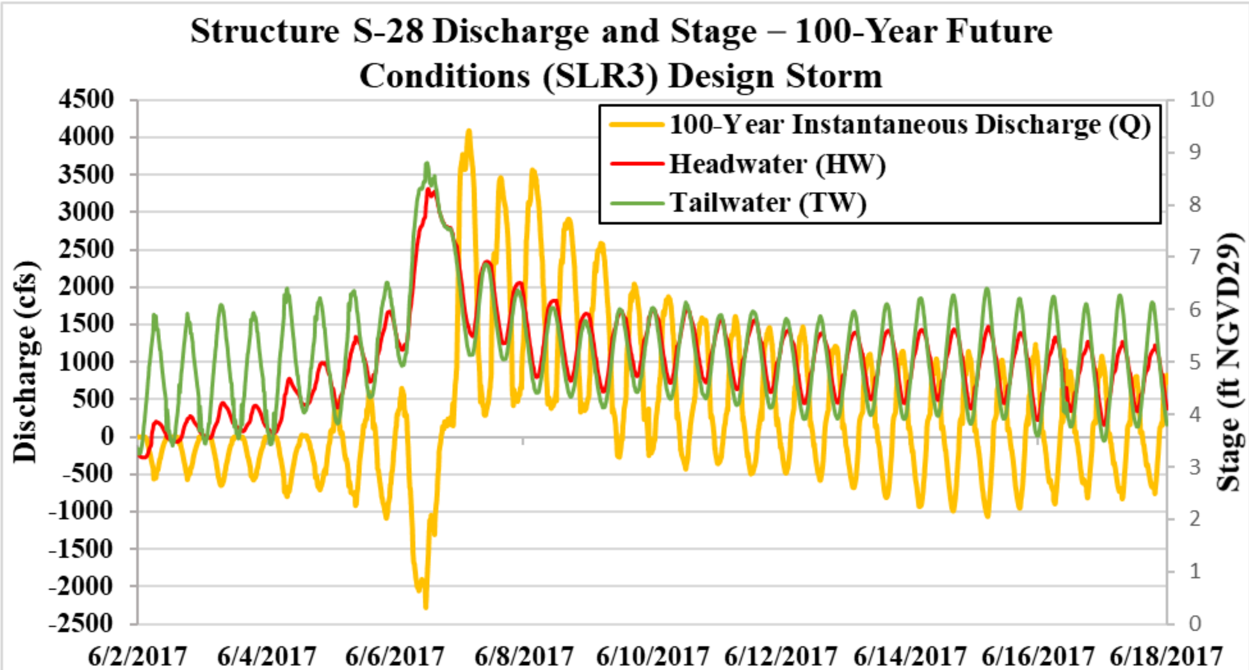

Figure 4.3-11: Instantaneous Discharge and Stage at S-28 Structure for 100-Year Future Conditions Sea Level Rise 3 Design Storm

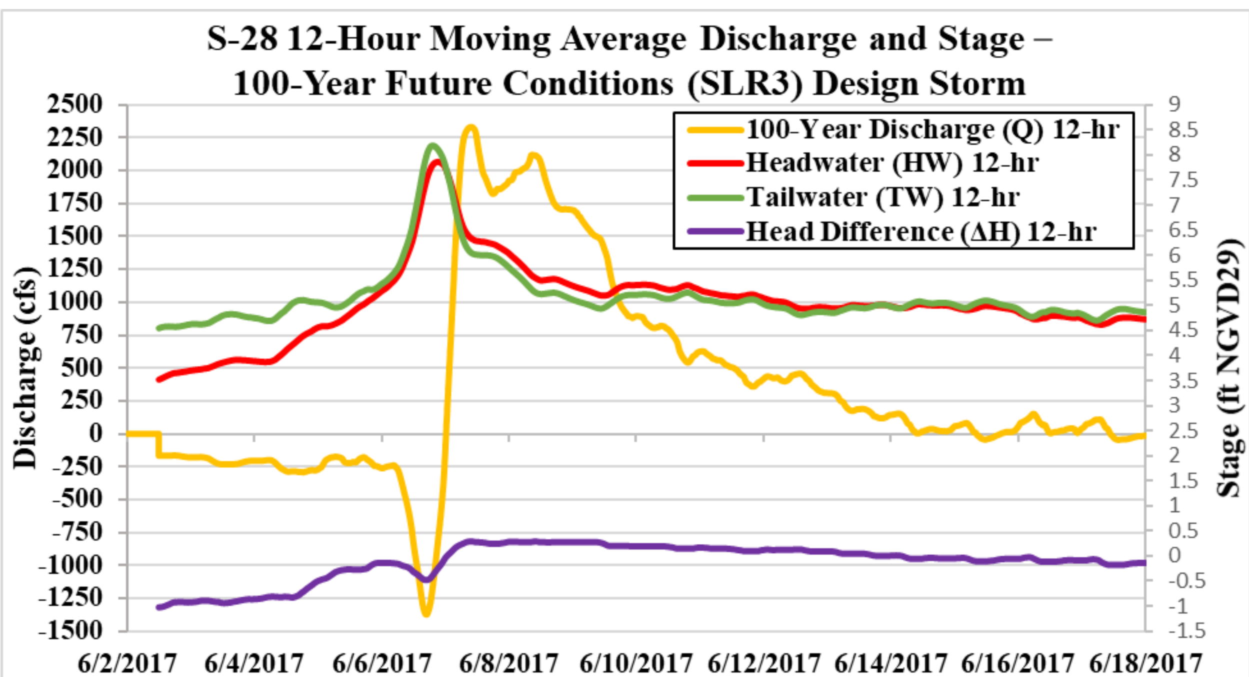

Figure 4.3-12: Tidally Averaged (12-hour) 100-Year Future Conditions Sea Level Rise 3 Design Storm Discharge, Stage, and Head Gradient for Structure S-28

As shown in **Figure 4.3-12,** the S-28 structure is unable to reach the design discharge of 3220 cfs, with a 12-hour moving average peak of 2331 cfs. While this discharge occurs with a 12-hour average head difference of only 0.29 feet, the design headwater assumption is violated. The assumed design headwater stage is 2.2 feet, while the predicted headwater is 6.4 feet at the time of peak discharge. Additionally, there is a flow reversal, peaking at -1374 cfs due to a -0.48 ft headwater/tailwater gradient.

Table 4-14 through **Table 4-17** summarize the simulated 12-hour moving average peak discharge, headwater, tailwater, and head differential for S-28, for each of the design storms. From the tables, an inverse relationship is evident between the peak discharge and rising sea level, which is to be expected.

Table 4-14: Summary of the 12-Hour Moving Average Discharge and Stage at S-28 for 5-Year Future Conditions Design Storms

Design Storm Scenario	5- Year Design Storm 12-Hour Moving Average at S-28			
	Peak Discharge (cfs) [Q	Headwater (ft NGVD29) at Peak Q	Tailwater (ft NGVD29) at Peak Q	Head Differential (ft) at Peak Q
Current	1441	2.75	2.39	0.36
SLR1	1359	3.68	3.38	0.30
SLR2	1248	4.58	4.28	0.30
SLR3	1101	5.5	5.26	0.24

Table 4-15: Summary of the 12-Hour Moving Average Discharge and Stage at S-28 for 10-Year Future Conditions Design Storms

Design Storm Scenario	10- Year Design Storm 12-Hour Moving Average at S-28			
	Peak Discharge (cfs) [Q]	Headwater (ft NGVD29)	Tailwater (ft NGVD29) at Peak Q	Head Differential (ft) at Peak Q
Current	1748	2.93	2.61	0.32
SLR1	1700	3.87	3.56	0.31
SLR2	1619	4.76	4.46	0.30
SLR3	1424	5.69	5.44	0.25

Table 4-16: Summary of the 12-Hour Moving Average Discharge and Stage at S-28 for 25-Year Future Conditions Design Storms

Design Storm Scenario	25- Year Design Storm 12-Hour Moving Average at S-28			
	Peak Discharge (cfs) [Q]	Headwater (ft NGVD29) at Peak Q	Tailwater (ft NGVD29) at Peak Q	Head Differential (ft) at Peak Q
Current	2337	3.17	2.87	0.30
SLR1	2315	4.09	3.78	0.31
SLR2	2315	4.96	4.66	0.30
SLR3	1865	5.96	5.69	0.27

Table 4-17: Summary of the 12-Hour Moving Average Discharge and Stage at S-28 for 100-Year Future Conditions Design Storms

Design Storm Scenario	100- Year Design Storm 12-Hour Moving Average at S-28			
	Peak Discharge (cfs) [Q]	Headwater (ft NGVD29) at Peak Q	Tailwater (ft NGVD29) at Peak Q	Head Differential (ft) at Peak Q
Current	3254	3.55	3.25	0.30
SLR1	3259	4.44	4.13	0.31
SLR2	2919	5.48	5.16	0.32
SLR3	2331	6.36	6.07	0.29

4.3.2 S-29

Structure S-29 has a static design headwater and tailwater of 2.4 ft and 1.9 ft, respectively. The static design discharge is 4780 cfs based on 0.5 ft head difference (Zhang, 2017). **Figure 4.3-13** and **Figure 4.3-14** **s**how instantaneous values and 12-hour moving average values, respectively, for S-29 based on a 25-year design storm with 1 ft sea level rise.

The instantaneous peak discharge for the 25-year SLR1 scenario is smaller than current conditions and is short lived. At the peak of the storm, there is nearly 750 cfs of reversed flow. Filtering out the effects of the tide reveals a more significant decrease in the peak discharge compared to current conditions.

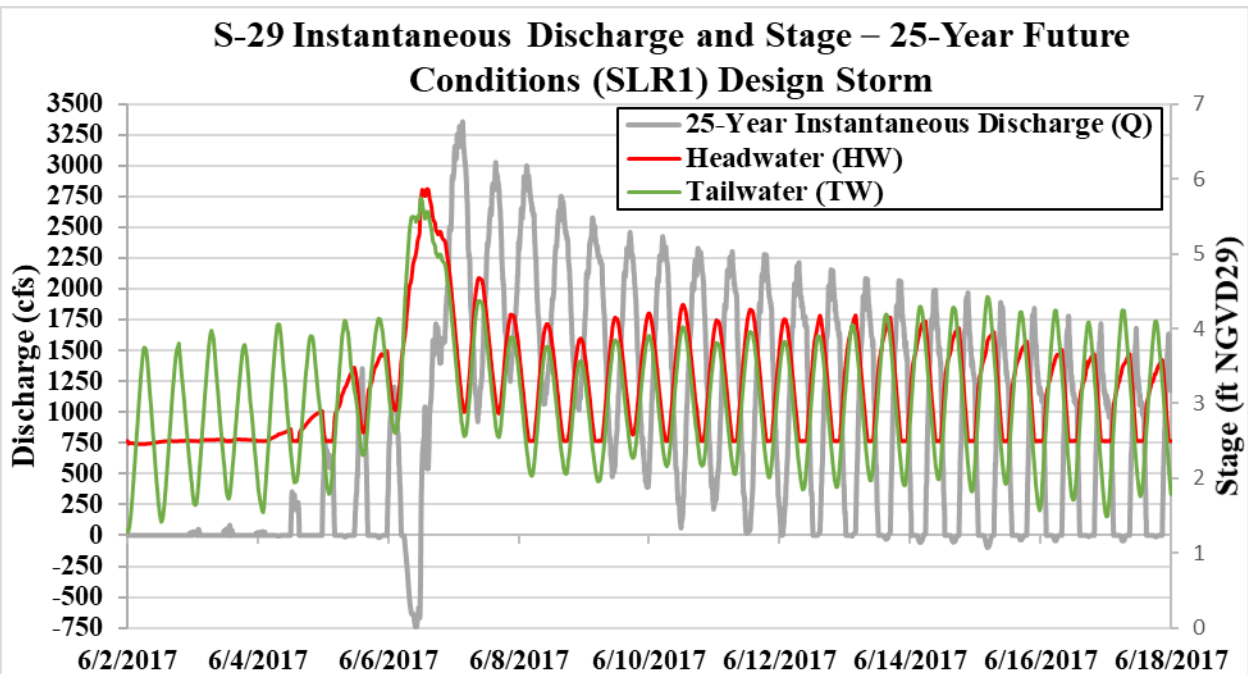

Figure 4.3-13: Instantaneous Discharge and Stage at S-29 Structure for 25-Year Future Conditions Sea Level Rise 1 Design Storm

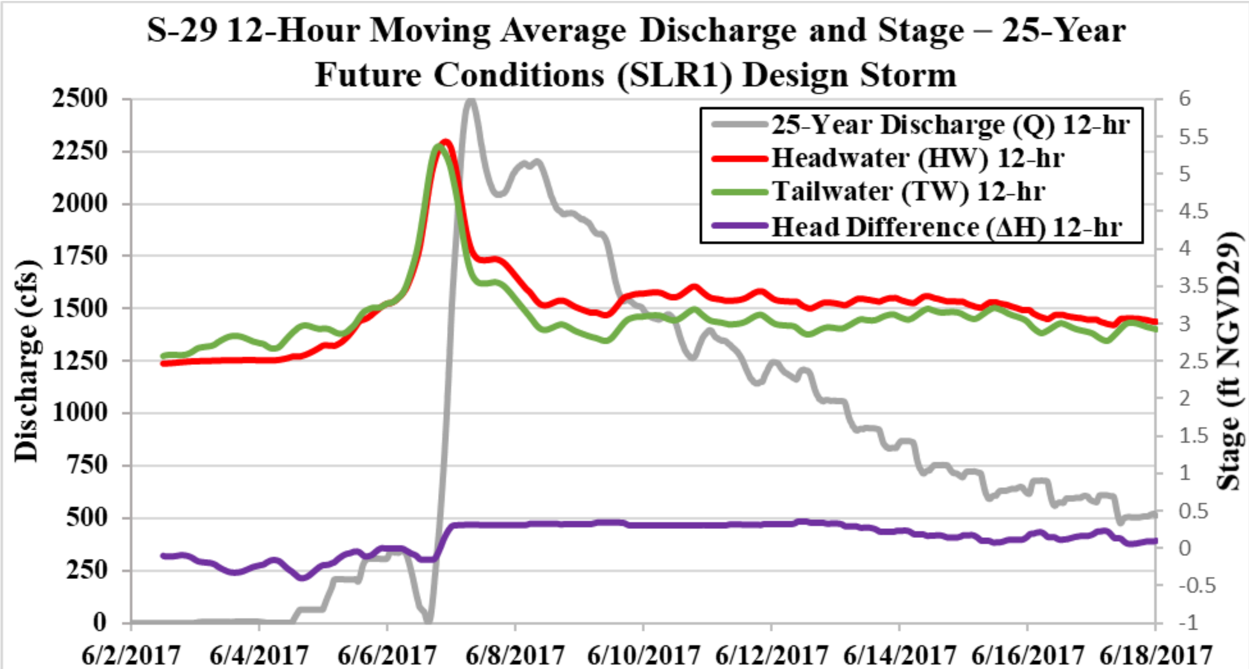

Figure 4.3-14: Tidally Averaged (12-hour) 25-Year Future Conditions Sea Level Rise 1 Design Storm Discharge, Stage, and Head Gradient for Structure S-29

Figure 4.3-15 and **Figure 4.3-16** show instantaneous values and 12-hour moving average values, respectively, for S-29 based on a 100-year design storm with 1 ft of sea level rise.

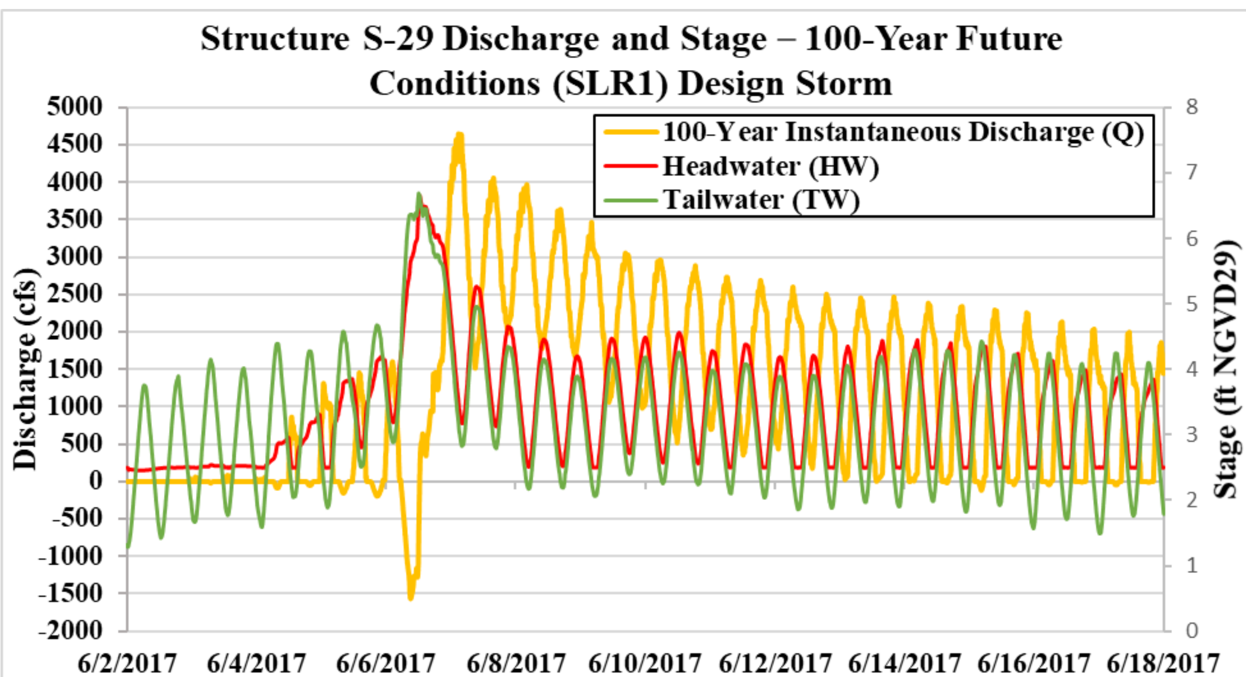

Figure 4.3-15: Instantaneous Discharge and Stage at S-29 Structure for 100-Year Future Conditions Sea Level Rise 1 Design Storm

The instantaneous peak discharge for the 100-year SLR1 scenario is smaller than current conditions and is short lived. At the peak of the storm, there is over 1500 cfs of reversed flow. Filtering out the effects of the tide reveals a more significant decrease in the peak discharge compared to current conditions.

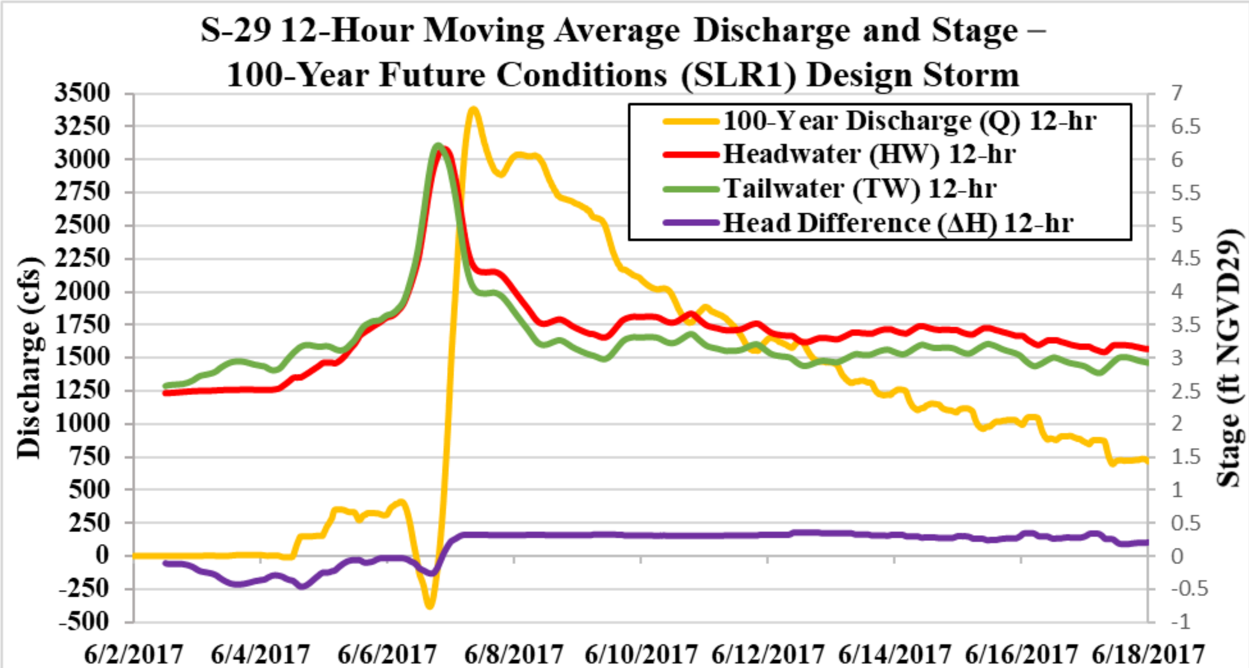

Figure 4.3-16: Tidally Averaged (12-hour) 100-Year Future Conditions Sea Level Rise 1 Design Storm Discharge, Stage, and Head Gradient for Structure S-29

As shown in **Figure 4.3-16,** the S-29 structure falls significantly short of the design discharge of 4780 cfs, with a 12-hour moving peak of just 3384 cfs. While this discharge occurs with a 12-hour average head difference of only 0.32 feet, the design headwater assumption is violated. The assumed design headwater stage is 2.2 feet, while the predicted headwater is 4.4 feet at the time of peak discharge. Additionally, there is a flow reversal, peaking at 384 cfs due to a -0.26 ft headwater/tailwater gradient.

Figure 4.3-17 and **Figure 4.3-18** show instantaneous values and 12-hour moving average values, respectively, for S-29 based on a 25-year design storm with 2 ft of sea level rise. The instantaneous peak discharge for the 25-year SLR2 is about 220 cfs smaller than current conditions. At the peak of the storm, there is nearly 1750 cfs of reversed flow. Filtering out the effects of the tide reveals a more significant decrease in the peak discharge.

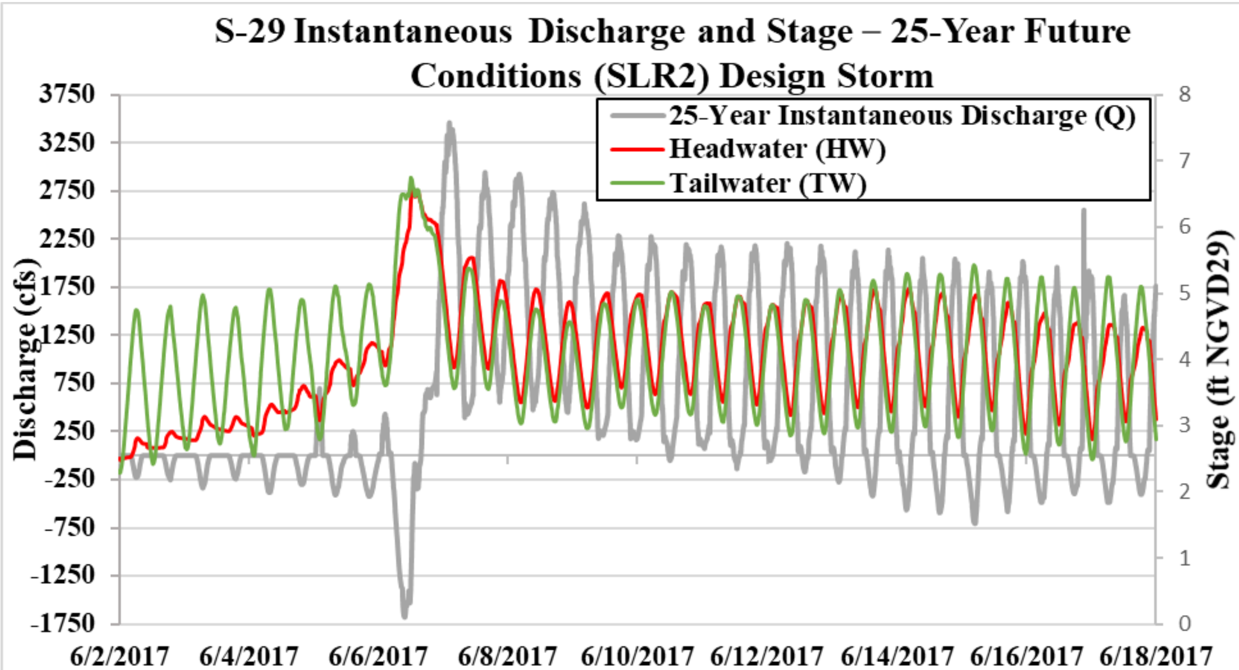

Figure 4.3-17: Instantaneous Discharge and Stage at S-29 Structure for 25-Year Future Conditions Sea Level Rise 2 Design Storm

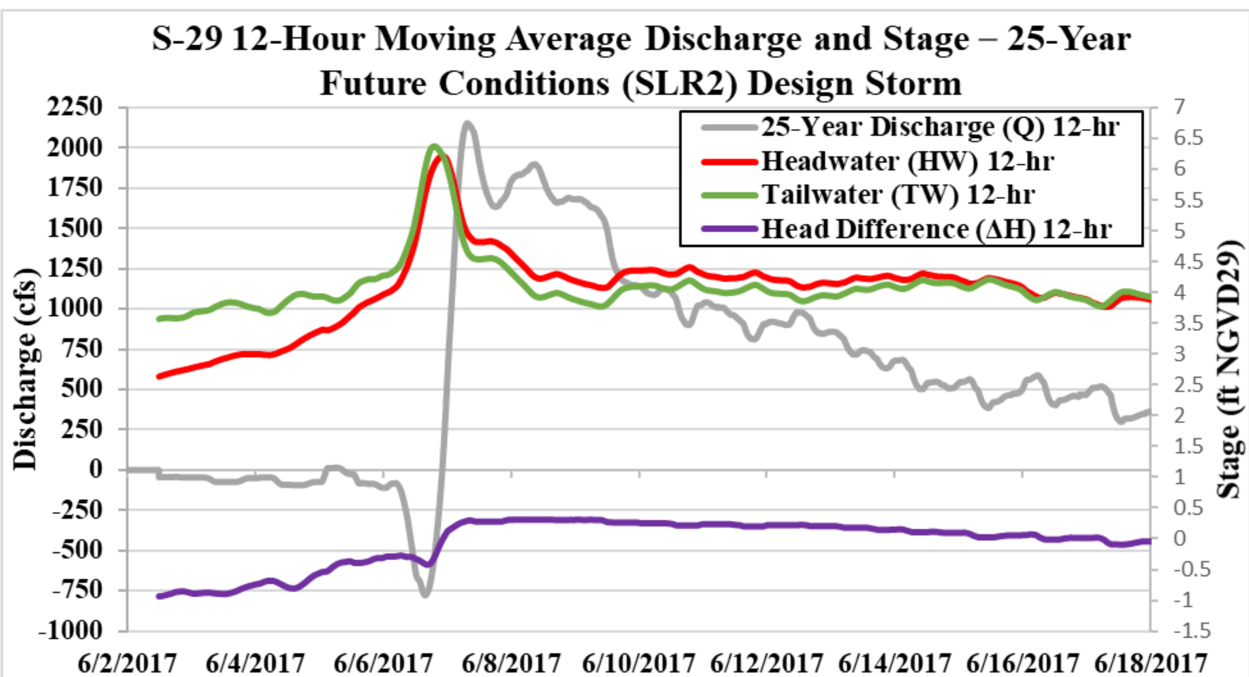

Figure 4.3-18: Tidally Averaged (12-hour) 25-Year Future Conditions Sea Level Rise 2 Design Storm Discharge, Stage, and Head Gradient for Structure S-29

Figure 4.3-19 and **Figure 4.3-20** show instantaneous values and 12-hour moving average values, respectively, for S-29 based on a 100-year design storm with 2 ft of sea level rise.

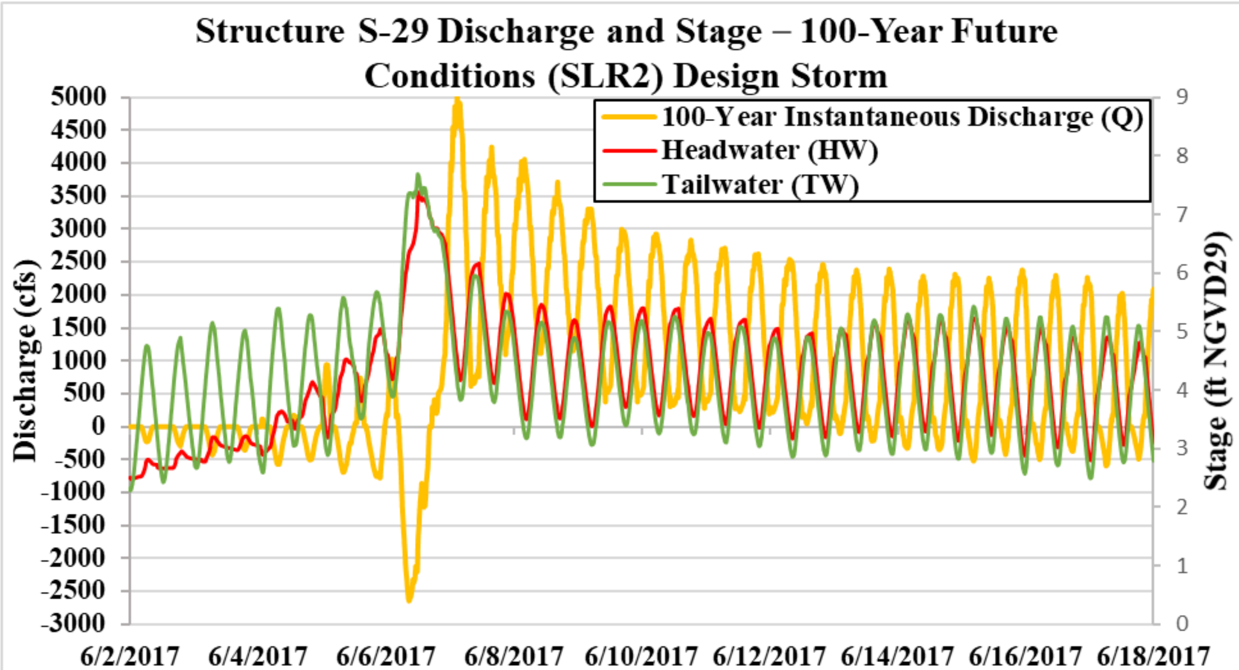

Figure 4.3-19: Instantaneous Discharge and Stage at S-29 Structure for 100-Year Future Conditions Sea Level Rise 2 Design Storm

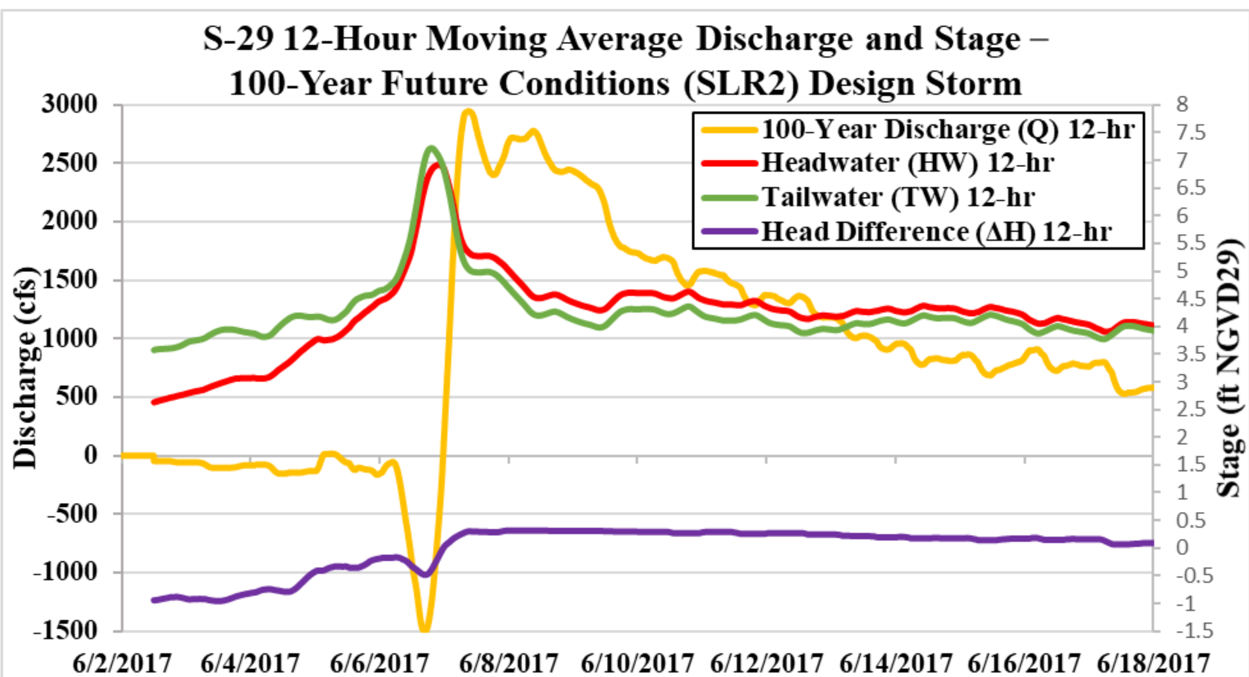

Figure 4.3-20: Tidally Averaged (12-hour) 100-Year Future Conditions Sea Level Rise 2 Design Storm Discharge, Stage, and Head Gradient for Structure S-29

As shown in **Figure 4.3-20,** the S-29 structure falls significantly short of the design discharge of 4780 cfs, with a 12-hour moving peak of just 2947 cfs. While this discharge occurs with a 12-hour average head difference of only 0.3 feet, the design headwater assumption is violated. The assumed design headwater stage is 2.2 feet, while the predicted headwater is 5.3 feet at the time of peak discharge. Additionally, there is a flow reversal, peaking at -1500 cfs due to a -0.48 ft headwater/tailwater gradient.

Figure 4.3-21 and **Figure 4.3-22** show instantaneous values and 12-hour moving average values, respectively, for S-29 based on a 25-year design storm with 3 ft of sea level rise. The instantaneous peak discharge for the 25-year SLR3 is only about 50 cfs smaller than current conditions, however, filtering out the effects of the tide reveals a more significant decrease in the peak discharge. At the peak of the storm, there is nearly 1900 cfs of reversed flow.

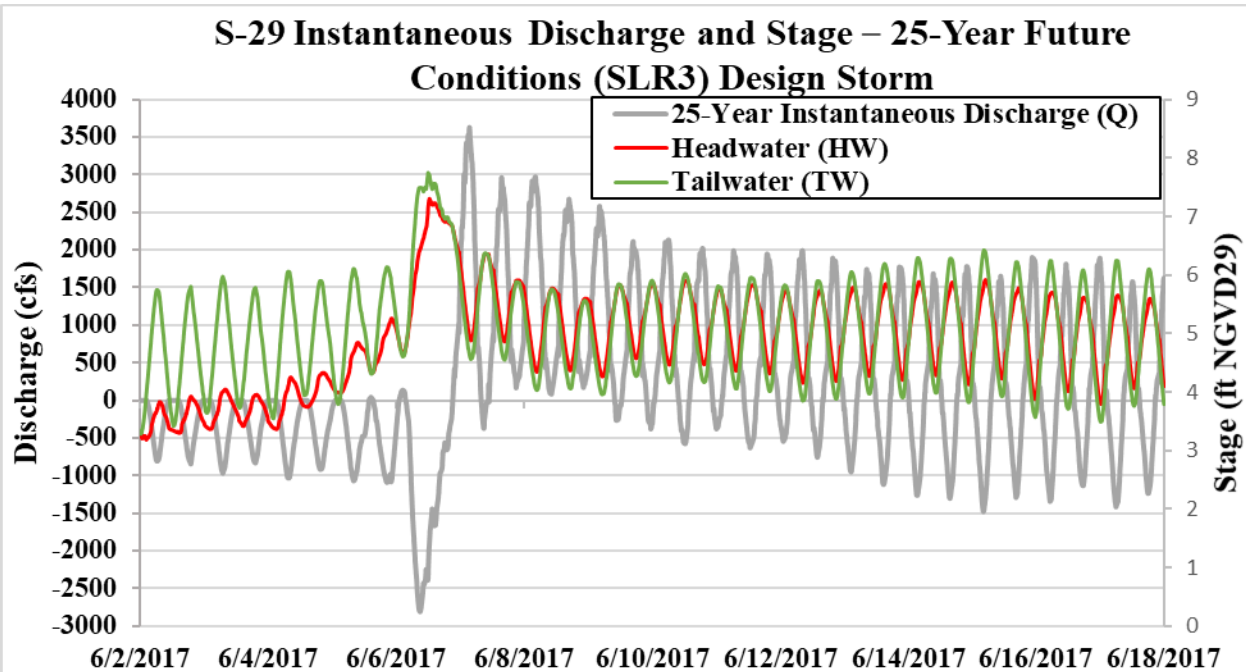

Figure 4.3-21: Instantaneous Discharge and Stage at S-29 Structure for 25-Year Future Conditions Sea Level Rise 3 Design Storm

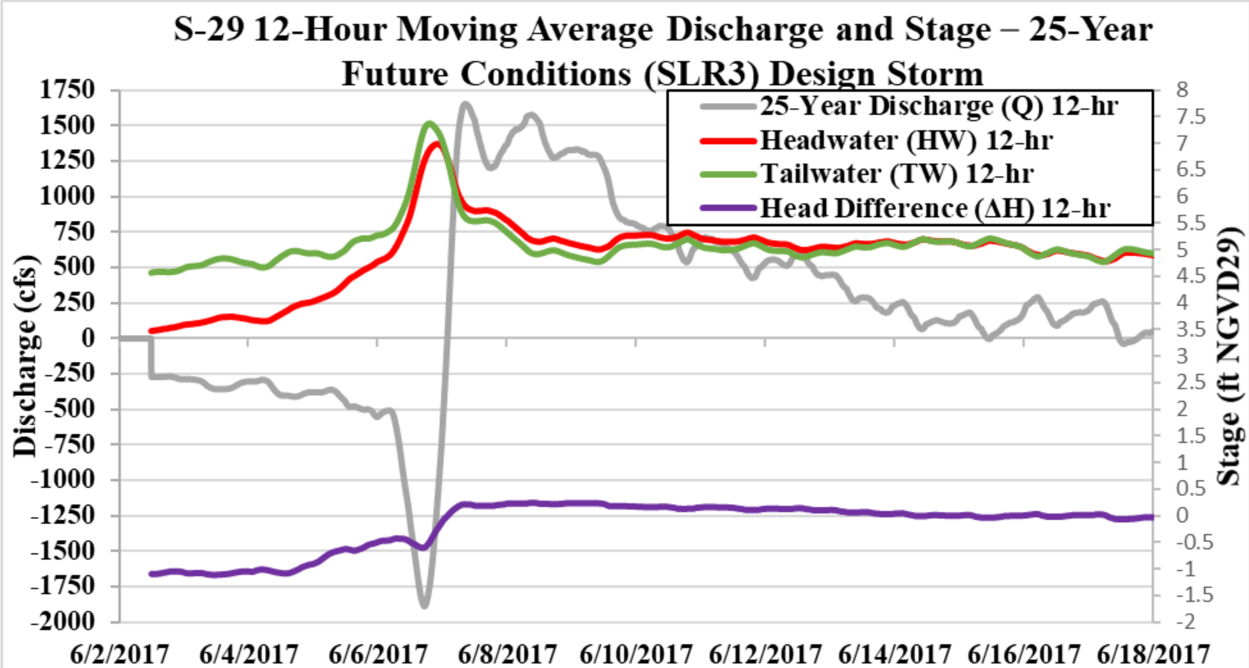

Figure 4.3-22: Tidally Averaged (12-hour) 25-Year Future Conditions Sea Level Rise 3 Design Storm Discharge, Stage, and Head Gradient for Structure S-29

Figure 4.3-23 and **Figure 4.3-24** show instantaneous values and 12-hour moving average values, respectively, for S-29 based on a 100-year design storm with 3 ft of sea level rise.

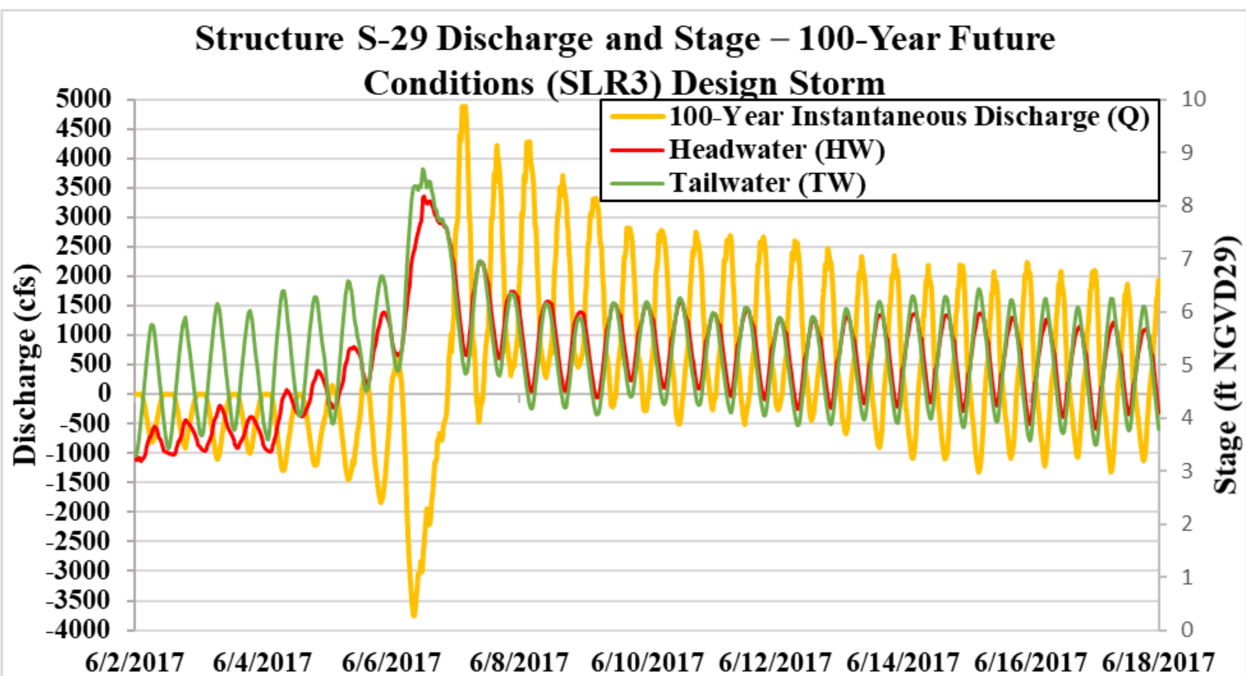

Figure 4.3-23: Instantaneous Discharge and Stage at S-29 Structure for 100-Year Future Conditions Sea Level Rise 3 Design Storm

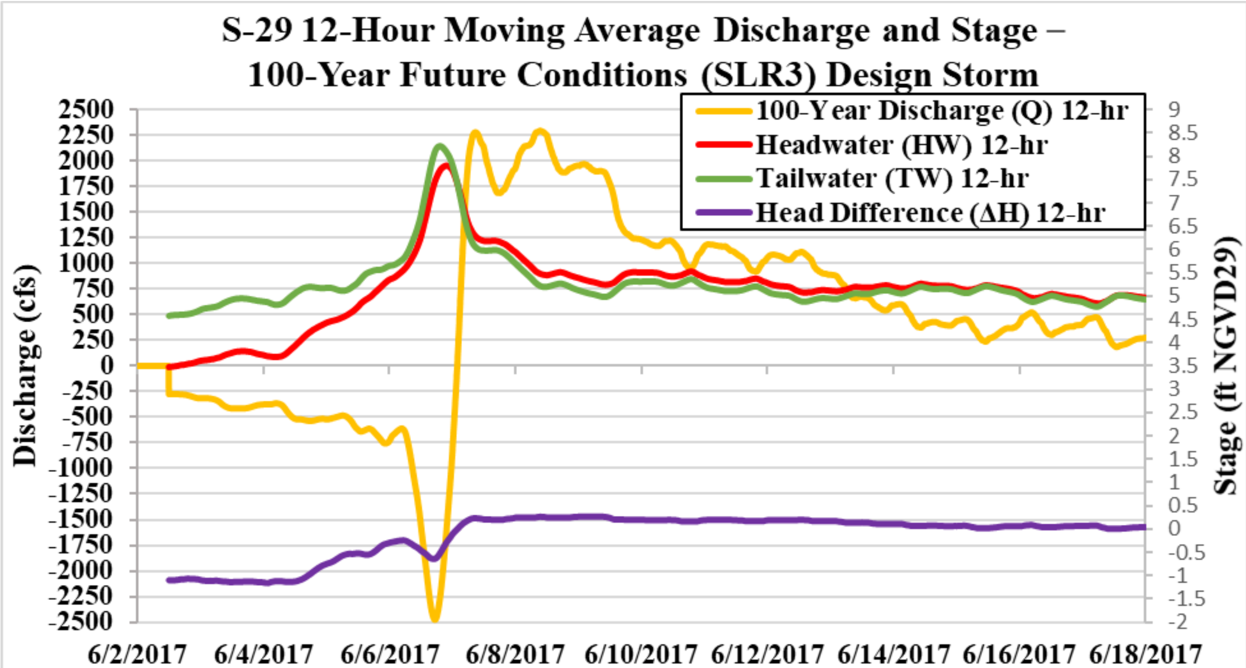

Figure 4.3-24: Tidally Averaged (12-hour) 100-Year Future Conditions Sea Level Rise 3 Design Storm Discharge, Stage, and Head Gradient for Structure S-29

As shown in **Figure 4.3-24,** the S-29 structure falls significantly short of the design discharge of 4780 cfs, with a 12-hour moving peak of just 2294 cfs. This discharge occurs with a 12-hour average head difference of only 0.26 feet and the design headwater assumption is violated. The assumed design headwater stage is 2.2 feet, while the predicted headwater is 5.5 feet at the time of peak discharge. Before the peak positive flow, there is a flow reversal, peaking at -2477 cfs (larger than the peak outflow) due to a -0.64 ft headwater/tailwater difference.

Table 4-18 through **Table 4-21** summarizes the simulated 12-hour moving average peak discharge, headwater, tailwater, and head differential for S-29, for each of the design storms. Similar to the trend at S-28, the numbers show an inverse relationship between sea level and peak discharge. However, this trend is even more pronounced at S-29 compared to S-28. This is partially due to the C-9 Impoundment providing some relief by pumping up to 1000 cfs out of the canal for a total of volume of about 713.6 million gallons.

Table 4-18: Summary of the 12-Hour Moving Average Discharge and Stage at S-29 for 5-Year Future Conditions Design Storms

Design Storm Scenario	5- Year Design Storm 12-Hour Moving Average at S-29			
	Peak Discharge (cfs) [Q]	Headwater (ft NGVD29) at Peak Q	Tailwater (ft NGVD29) at Peak Q	Head Differential (ft) at Peak Q
Current	2140	2.84	2.27	0.57
SLR1	1655	3.65	3.34	0.31
SLR2	1159	4.58	4.33	0.25
SLR3	905	5.39	5.21	0.18

Table 4-19: Summary of the 12-Hour Moving Average Discharge and Stage at S-29 for 10-Year Future Conditions Design Storms

Design Storm Scenario	10- Year Design Storm 12-Hour Moving Average at S-29			
	Peak Discharge (cfs) [Q]	Headwater (ft NGVD29) at Peak Q	Tailwater (ft NGVD29) at Peak Q	Head Differential (ft) at Peak Q
Current	2437	2.95	2.44	0.51
SLR1	1904	3.80	3.49	0.31
SLR2	1584	4.70	4.42	0.28
SLR3	1238	5.58	5.38	0.20

Table 4-20: Summary of the 12-Hour Moving Average Discharge and Stage at S-29 for 25-Year Future Conditions Design Storms

Design Storm Scenario	25- Year Design Storm 12-Hour Moving Average at S-29			
	Peak Discharge (cfs) [Q]	Headwater (ft NGVD29) at Peak Q	Tailwater (ft NGVD29) at Peak Q	Head Differential (ft) at Peak Q
Current	2908	3.14	2.71	0.43
SLR1	2500	3.99	3.68	0.31
SLR2	2153	4.96	4.67	0.29
SLR3	1653	5.82	5.61	0.21

Table 4-21: Summary of the 12-Hour Moving Average Discharge and Stage at S-29 for 100-Year Future Conditions Design Storms

Design Storm Scenario	100- Year Design Storm 12-Hour Moving Average at S-29			
	Peak Discharge (cfs) [Q]	Headwater (ft NGVD29) at Peak Q	Tailwater (ft NGVD29) at Peak Q	Head Differential (ft) at Peak Q
Current	3728	3.52	3.17	0.35
SLR1	3384	4.38	4.06	0.32
SLR2	2947	5.34	5.04	0.30
SLR3	2294	5.48	5.22	0.26

4.4 PM #4 – Peak Storm Runoff

PM #4 is the maximum conveyance capacity of a watershed at the tidal structure for a range of design storms. It shows the maximum conveyance (moving 12-hr average) for a specific design storm and a specific tidal boundary condition. **Figure 4.4-1** and **Figure 4.4-2** represent the 5-year design storm discharge at tidal structures S-28 and S-29, respectively. These discharge hydrographs, specifically the peak discharge, are evaluated under three future sea level rise scenarios and compared with current conditions. **Figure 4.3-3** through **Figure 4.3-8** present the discharge at tidal structures S-28 and S-29 for the 10, 25, and 100-year design storms.

4.4.1 5-Year Design Storm

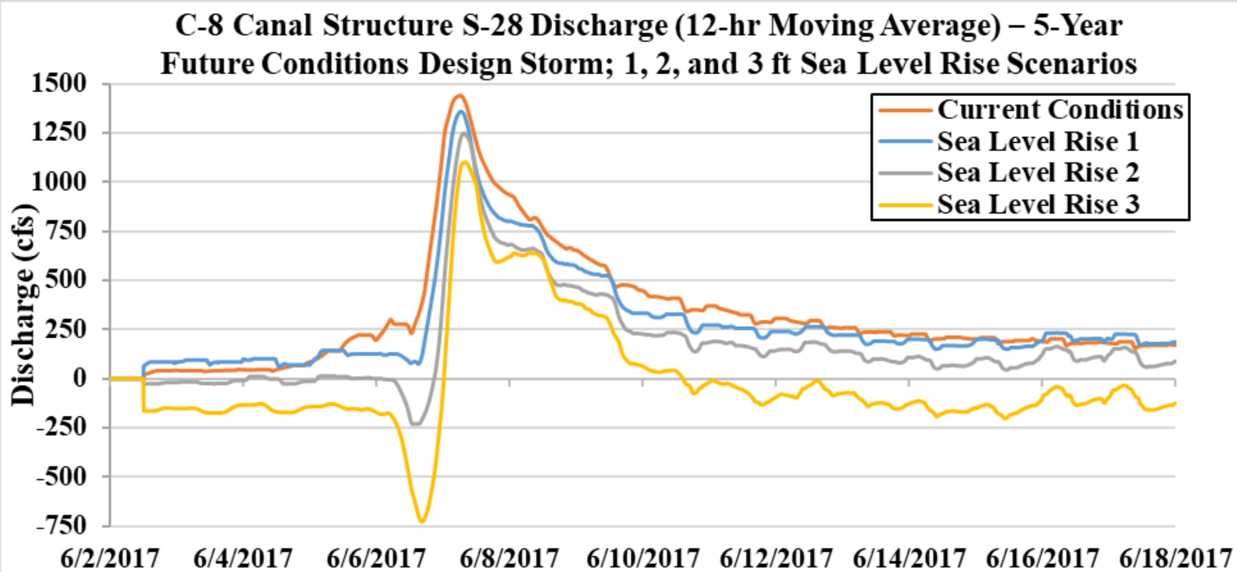

Figure 4.4-1: C-8 Canal Structure S-28 Discharge Hydrographs for 5-Year Design Storms

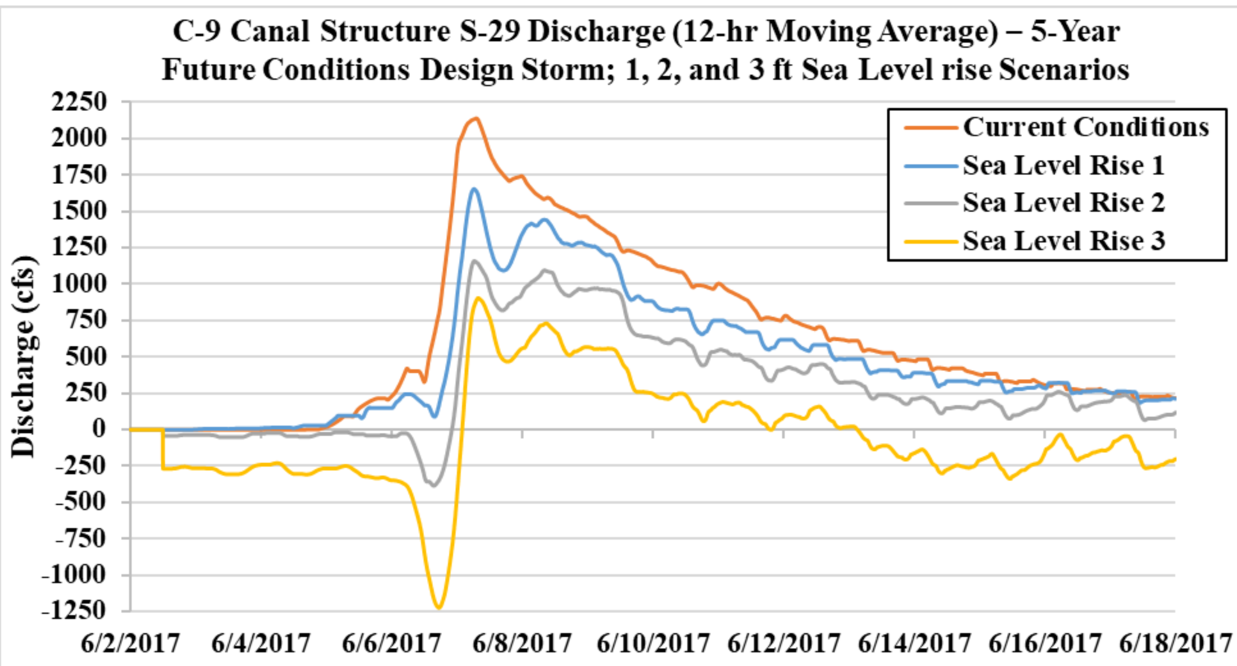

Figure 4.4-2: C-9 Canal Structure S-29 Discharge Hydrographs for 5-Year Design Storms

4.4.2 10-Year Design Storm

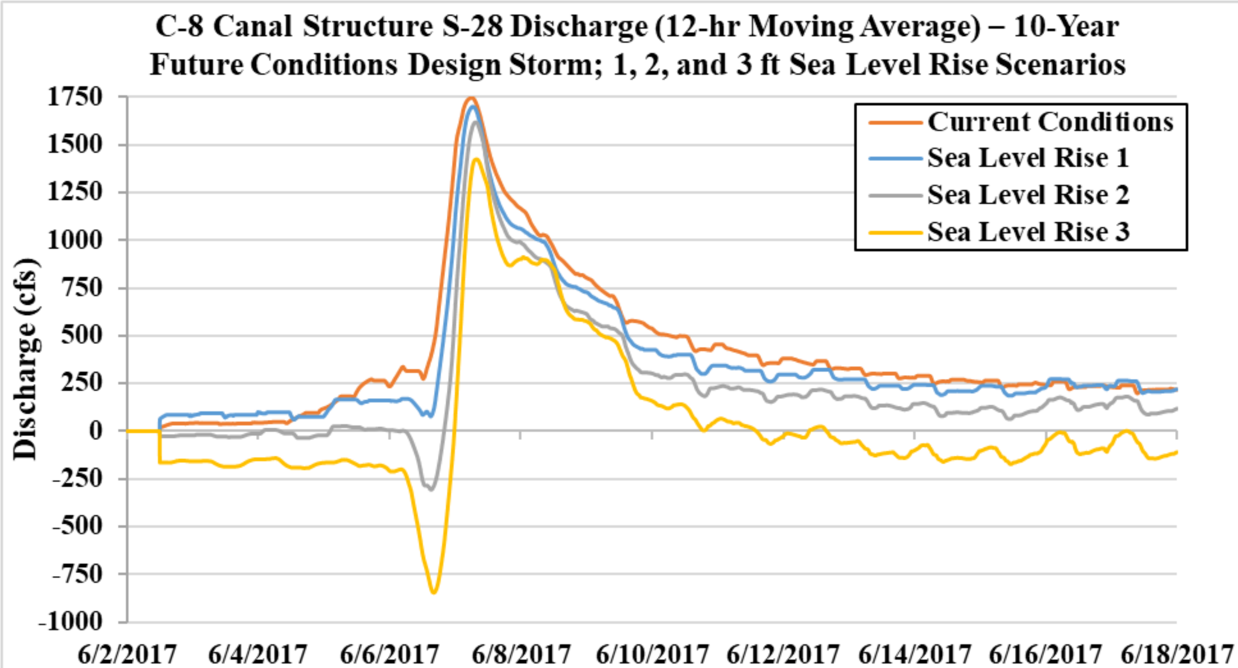

Figure 4.4-3: C-8 Canal Structure S-28 Discharge Hydrographs for 10-Year Design Storms

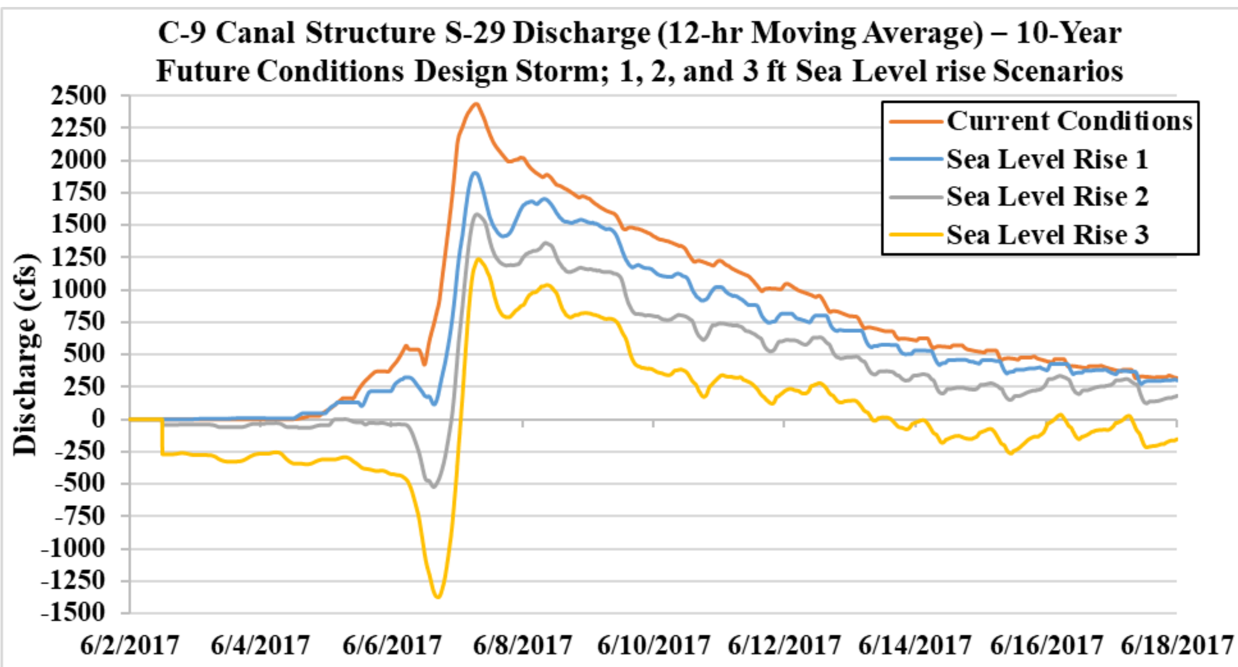

Figure 4.4-4: C-9 Canal Structure S-29 Discharge Hydrographs for 10-Year Design Storms

4.4.3 25-Year Design Storm

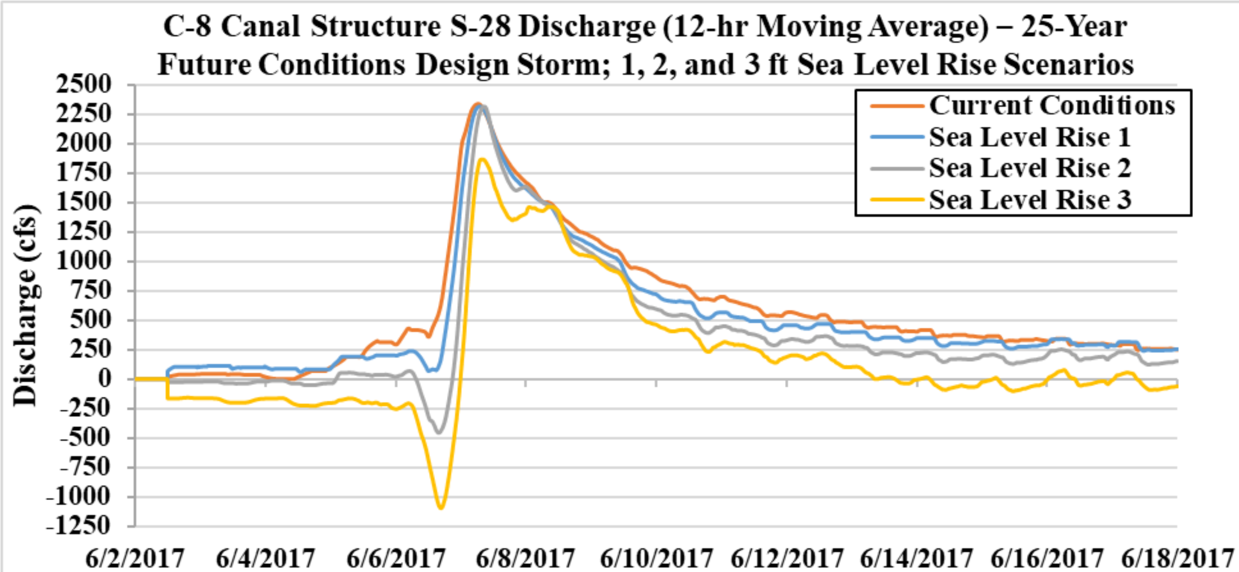

Figure 4.4-5: C-8 Canal Structure S-28 Discharge Hydrographs for 25-Year Design Storms

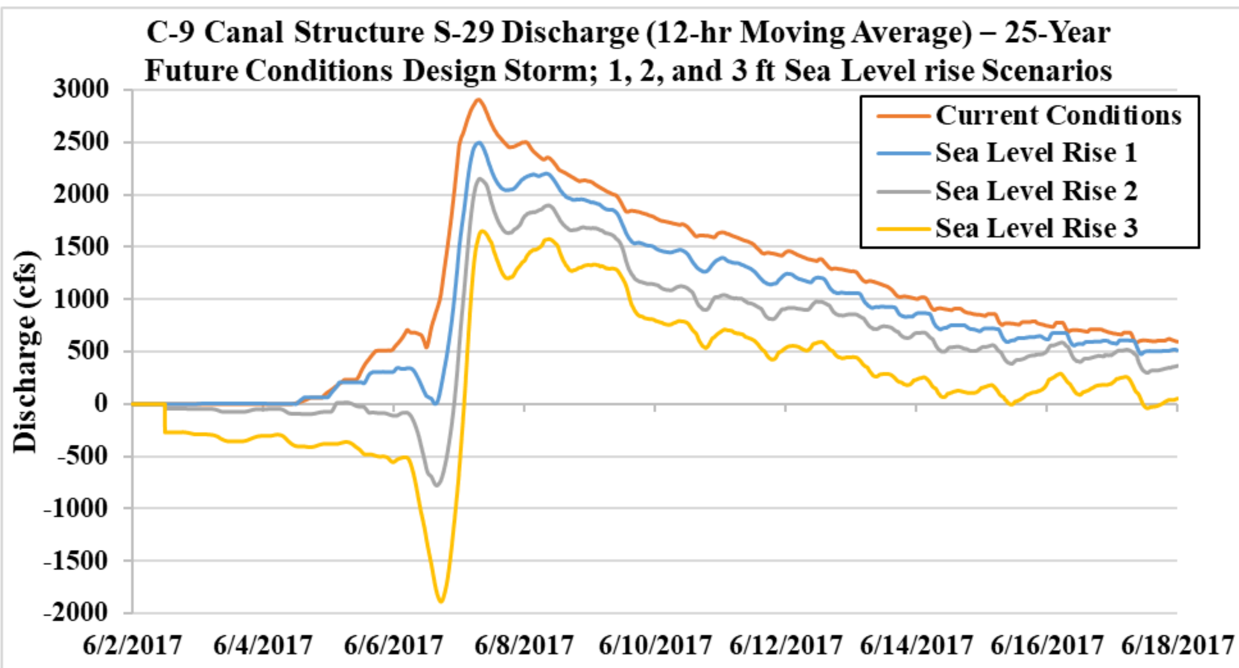

Figure 4.4-6: C-9 Canal Structure S-29 Discharge Hydrographs for 25-Year Design Storms

4.4.4 100-Year Design Storm

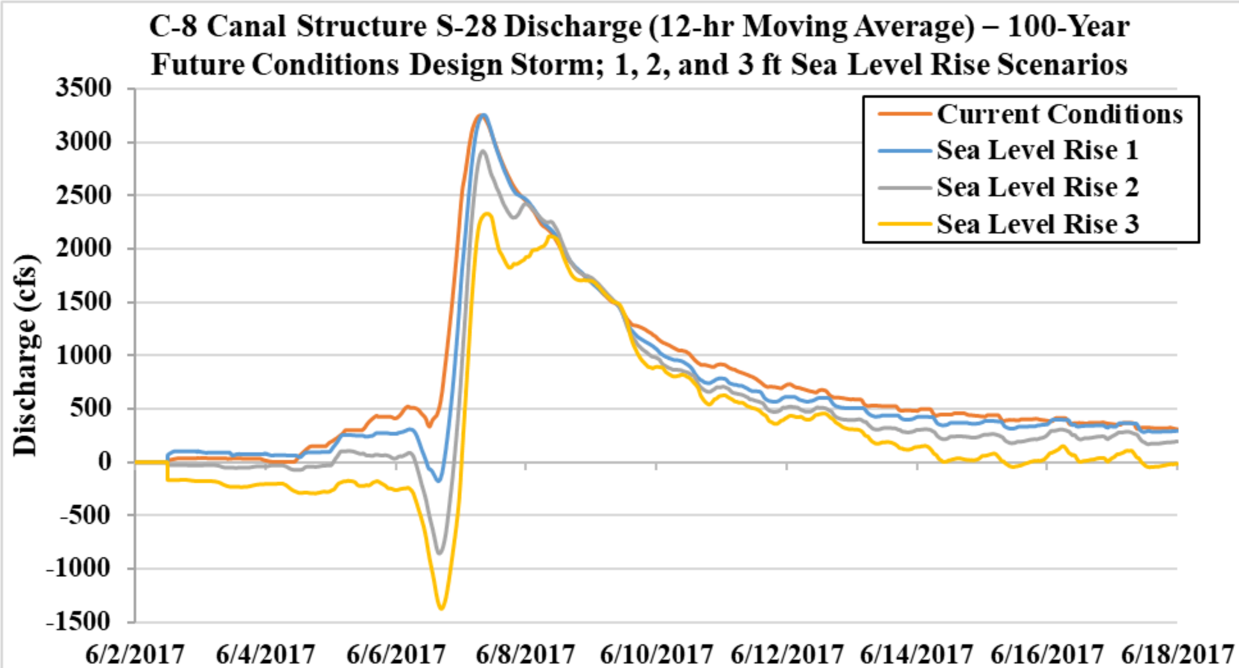

Figure 4.4-7: C-8 Canal Structure S-28 Discharge Hydrographs for 100-Year Design Storms

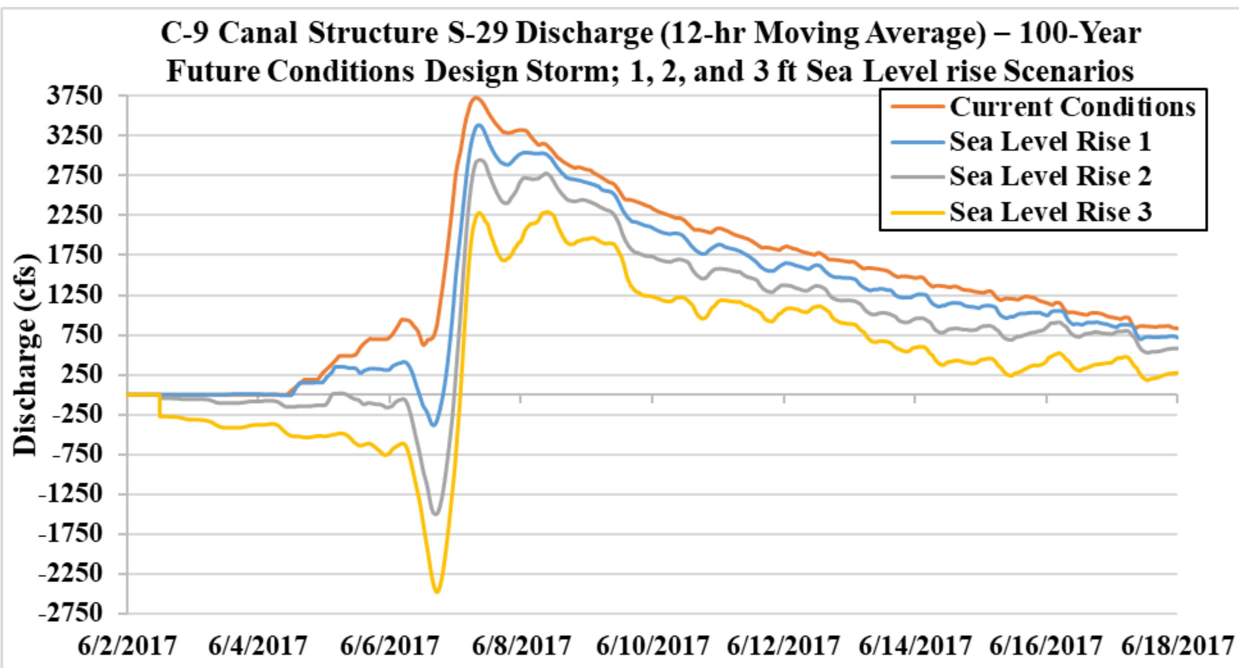

Figure 4.4-8: C-9 Canal Structure S-29 Discharge Hydrographs for 100-Year Design Storms

4.4.5 Peak Discharge Summary

Figure 4.4-9 shows the S-28 12-hour average peak discharge versus the design storm return period for three sea level rise scenarios. From the figure, it can be seen that the 5, 10, and 25-year 12-hour average peak discharges are relatively insensitive to sea level rise up to and including the 2 feet SLR scenarios. However, the discharges are all reduced significantly in the 3-foot SLR Scenario. **Table 4-22** through **Table 4-25** show the instantaneous and 12-hour average peak discharge for each design storm and sea level rise scenario.

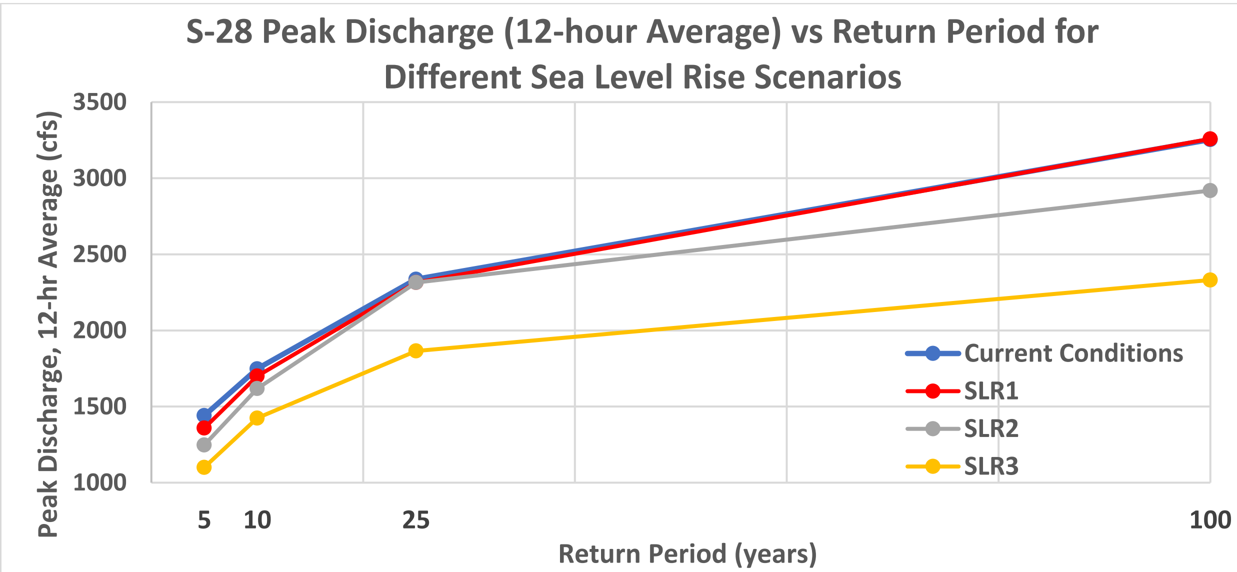

Figure 4.4-9: Structure S-28 12-Hour Average Peak Discharge for Different Sea Level Rise Scenarios

Table 4-22: S-28 Peak Discharge Summary for 5-Year Design Storms

Sea Level Rise Scenario	S-28 5-Year Design Storm Peak Discharge (cfs)		12-hr Moving Average Discharge Reduction Percentage
	Instantaneous	Moving Average (12-hr)	
Current	1720	1441	N/A
SLR1	1695	1359	5.7%
SLR2	1839	1248	13.4%
SLR3	2087	1101	23.6%

Table 4-23: S-28 Peak Discharge Summary for 10-Year Design Storms

Sea Level Rise Scenario	S-28 10-Year Design Storm Peak Discharge (cfs)		12-hr Moving Average Discharge Reduction Percentage
	Instantaneous	Moving Average (12-hr)	
Current	2059	1748	N/A
SLR1	2103	1700	2.7%
SLR2	2268	1619	7.4%
SLR3	2615	1424	18.5%

Table 4-24: S-28 Peak Discharge Summary for 25-Year Design Storms

Sea Level Rise Scenario	S-28 25-Year Design Storm Peak Discharge (cfs)		12-hr Moving Average Discharge Reduction Percentage
	Instantaneous	Moving Average (12-hr)	
Current	2679	2337	N/A
SLR1	2789	2315	0.9%
SLR2	3163	2315	0.9%
SLR3	3278	1865	20.2%

Table 4-25: S-28 Peak Discharge Summary for 100-Year Design Storms

Sea Level Rise Scenario	S-28 100-Year Design Storm Peak Discharge (cfs)		12-hr Moving Average Discharge Reduction Percentage
	Instantaneous	Moving Average (12-hr)	
Current	3777	3254	N/A
SLR1	3999	3259	-0.2%
SLR2	4157	2919	10.3%
SLR3	4094	2331	28.4%

Figure 4.4-10 shows the S-29 12-hour average peak discharge versus the design storm return period for three sea level rise scenarios. Unlike at S-28, the 12-hour peak discharges at S-29 for all storms are sensitive to all SLR scenarios, including the 1-foot SLR. This is partially due to the C-9 Impoundment and western lakes/prior mine pits attenuating the discharge.

Table 4-26 and **Table 4-29** shows the instantaneous and 12-hour average peak discharge for each design storm and sea level rise scenario.

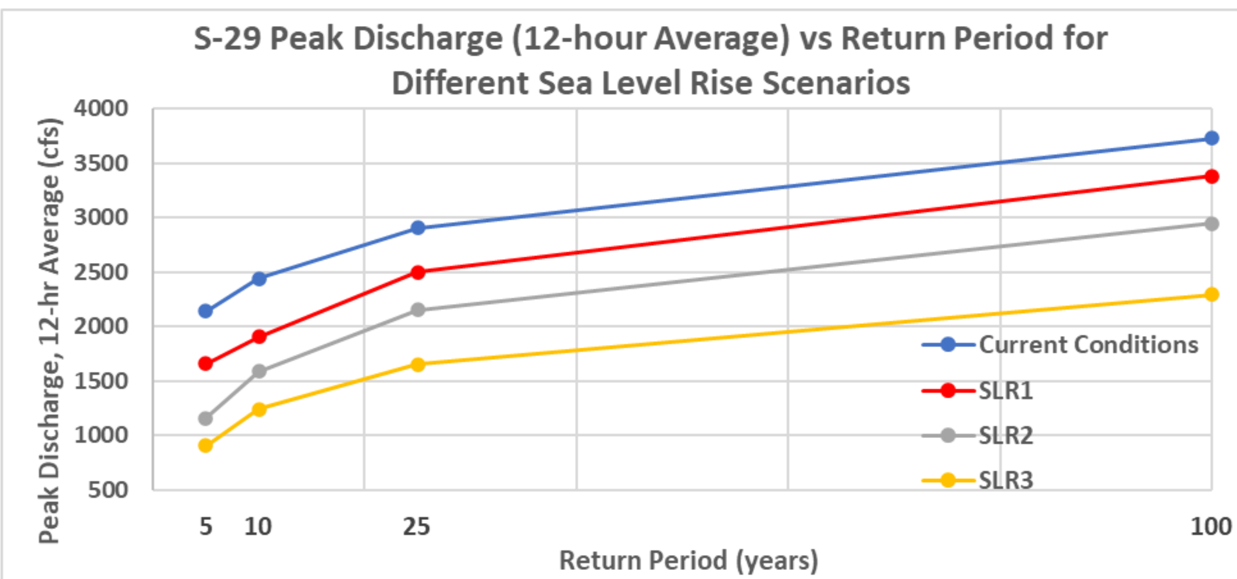

Figure 4.4-10: Structure S-29 12-Hour Average Peak Discharge for Different Sea Level Rise Scenarios

Table 4-26: S-29 Peak Discharge Summary for 5-Year Design Storms

Sea Level Rise Scenario	S-29 5-Year Design Storm Peak Discharge (cfs)		12-hr Moving Average Discharge Reduction Percentage
	Instantaneous	Moving Average (12-hr)	
Current	2647	2140	N/A
SLR1	2417	1656	22.6%
SLR2	2190	1159	45.8%
SLR3	2186	905	57.7%

Table 4-27: S-29 Peak Discharge Summary for 10-Year Design Storms

Sea Level Rise Scenario	S-29 10-Year Design Storm Peak Discharge (cfs)		12-hr Moving Average Discharge Reduction Percentage
	Instantaneous	Moving Average (12-hr)	
Current	3052	2437	N/A
SLR1	2698	1904	21.9%
SLR2	2526	1584	35.0%
SLR3	2631	1238	49.2%

Table 4-28: S-29 Peak Discharge Summary for 25-Year Design Storms

Sea Level Rise Scenario	S-29 25-Year Design Storm Peak Discharge (cfs)		12-hr Moving Average Discharge Reduction Percentage
	Instantaneous	Moving Average (12-hr)	
Current	3681	2908	N/A
SLR1	3360	2500	14.0%
SLR2	3460	2153	26.0%
SLR3	3632	1653	43.2%

Table 4-29: S-29 Peak Discharge Summary for 100-Year Design Storms

Sea Level Rise Scenario	S-29 100-Year Design Storm Peak Discharge (cfs)		12-hr Moving Average Discharge Reduction Percentage
	Instantaneous	Moving Average (12-hr)	
Current	4710	3728	N/A
SLR1	4645	3384	9.2%
SLR2	5074	2947	20.9%
SLR3	4883	2294	38.5%

4.5 PM #5 – Frequency of Flooding

For this PM, the depths of overland flooding were evaluated for the 72-hour design storms with the return period of 5-year, 10-year, 25-year, and 100-year with sea level rise conditions of 1, 2, and 3 ft. These flood depths, or elevations, can be compared with elevations of features such as buildings and roadways, where such information exists. For the purposes of this C-8/C-9 FPLOS evaluation, flood inundation maps were prepared using MIKE SHE gridded model output for each storm event, in the form of depth of overland water. Flooding depths were representative of the overland water depths on the 125-ft grid. The resulting flood inundation maps over the entire model domain are shown in **Figure 4.5-1** through **Figure 4.5-12** for each of the four design storm events and sea level rise scenarios. **Figure 4.5-13** through **Figure 4.5-24** show the flood inundation maps for each of the design storm and sea level rise scenarios for urban areas only within the C8 and C9 basins. **Figure 4.5-25** through **Figure 4.5-42** show up close examples of flood depth along the C-8 Canal and **Figure 4.5-43** through **Figure 4.5-66** show up close examples of flood depth along the C-9 Canal. **Figure 4.5-67** through **Figure 4.5-69** show the maximum overland water depth difference between future and current conditions for the 25-Year SLR1, SLR2 and SLR3 design storm events.

The southwest portion of the C-9 Basin is mostly undeveloped (even with future land use changes considered), and thus were not served by stormwater collection and conveyance facilities. These undeveloped areas show the greatest extents and depths of flooding for the design storm events.

Notable developed areas also show flooding under PM #5. For example, residential areas along the C-8 Canal upstream and downstream of NE 135th St (CR 916), show extensive spatial extents of flooding in PM #5, which is most evident for the 25-year and 100-year SLR3 events, but is also evident in 5-year and 10-year SLR2 events. This flooding is corroborated by PM #1 results, which show that both the north and south bank is exceeded for the 5-year SLR1 event over a long segment upstream and downstream of CR916. For the 100-year SLR 3 event, flood stage in this area is upwards of 3 ft higher than the bank elevations.

In the C-9 Watershed, extensive flooding is shown upstream of S-29 for the 10-year SLR3 event, as well as downstream of US Highway 441. This flooding is corroborated by PM #1 results, which show that both the north and south bank exceedances for 10-year SLR3 event over long segments. Under current conditions, there were localized areas such as west of Red Road and upstream of the Ronald Reagan Turnpike that showed flooding in PM #5 but did not show canal bank exceedances in PM #1. Flooding in these areas could be due to the topography being lower than the canal bank and/or inadequate secondary drainage infrastructure. However, under future conditions, particularly with 2 ft and 3 ft sea level rise, the canal stage does exceed the bank elevations in these locations. The canal banks exceedances exacerbate the localized flooding that was shown when canal stages were still in-bank.

Both the C-8 and C-9 Canal experience extensive flooding, upwards of 2 to 3 ft in depth, for several miles during the 25-year and 100-year 3 ft sea level rise scenarios. This was an expected result due to the low bypass elevation of the tidal outfall structures, as well as the relatively low canal bank elevations for many parts of the C-8 and C-9 Canals.

4.5.1 5-Year Design Storm Model-Wide Flood Depth Map

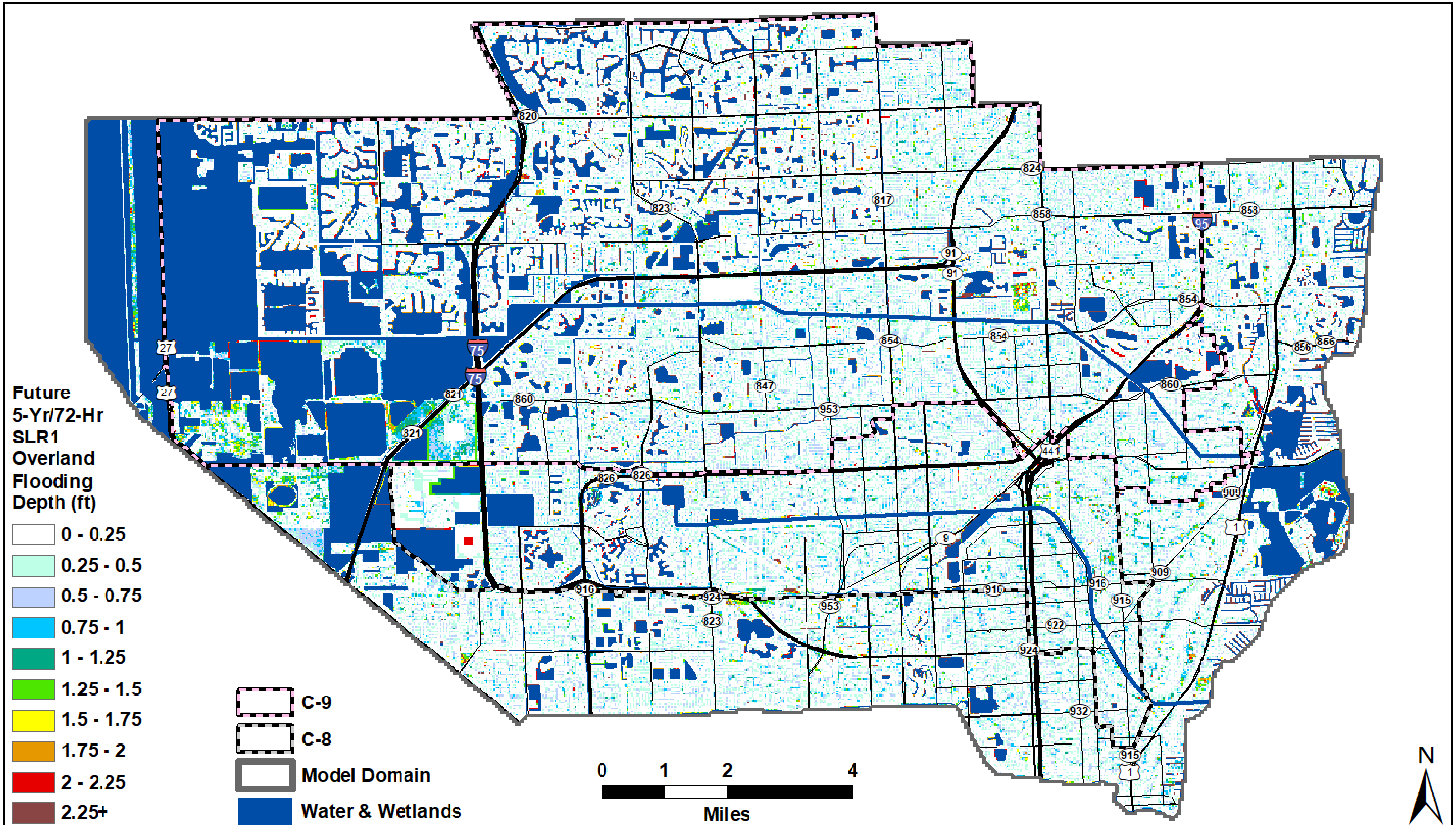

Figure 4.5-1: Flood Inundation Map for 5-Year Sea Level Rise 1 Design Storm Event

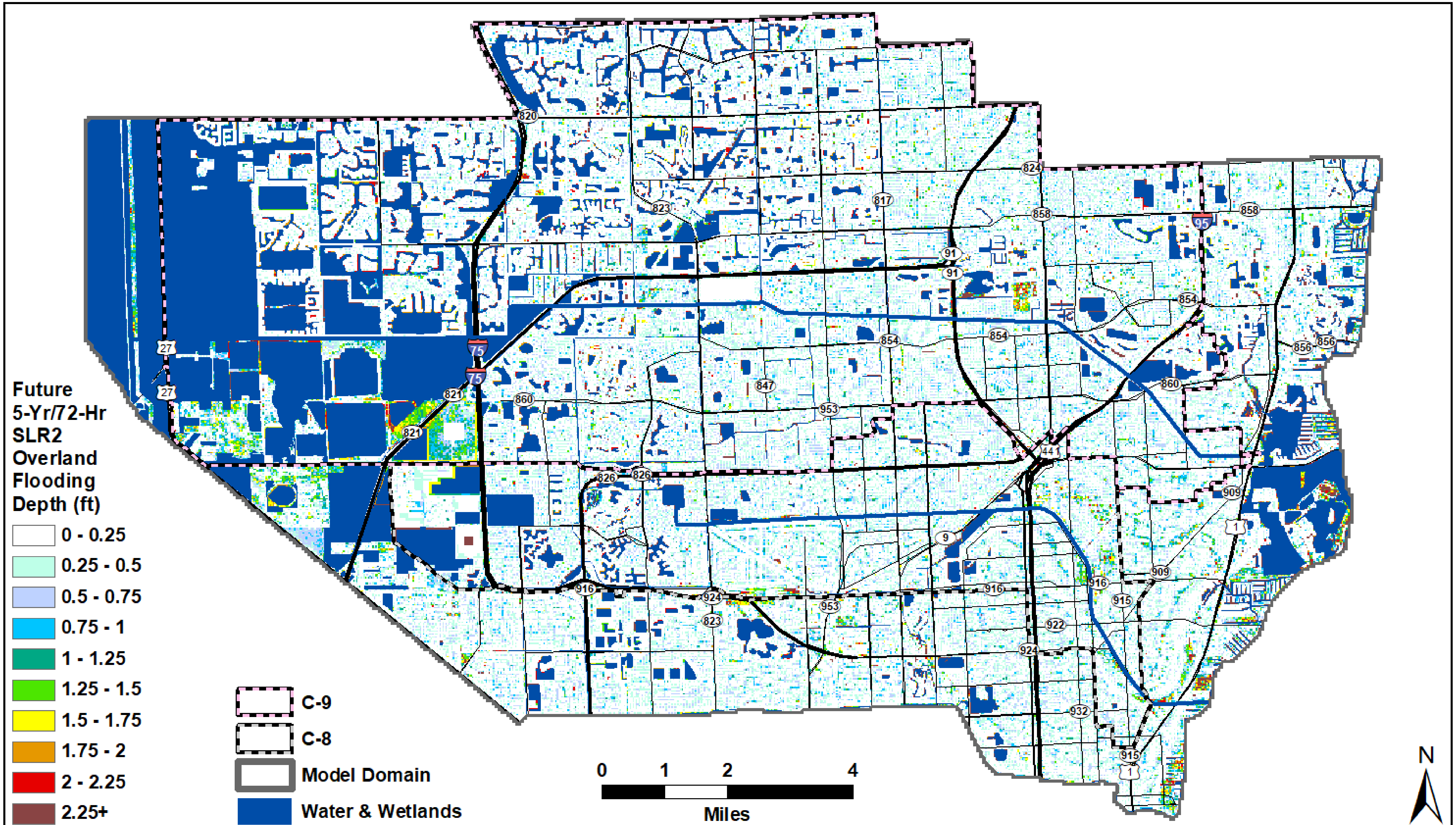

Figure 4.5-2: Flood Inundation Map for 5-Year Sea Level Rise 2 Design Storm Event

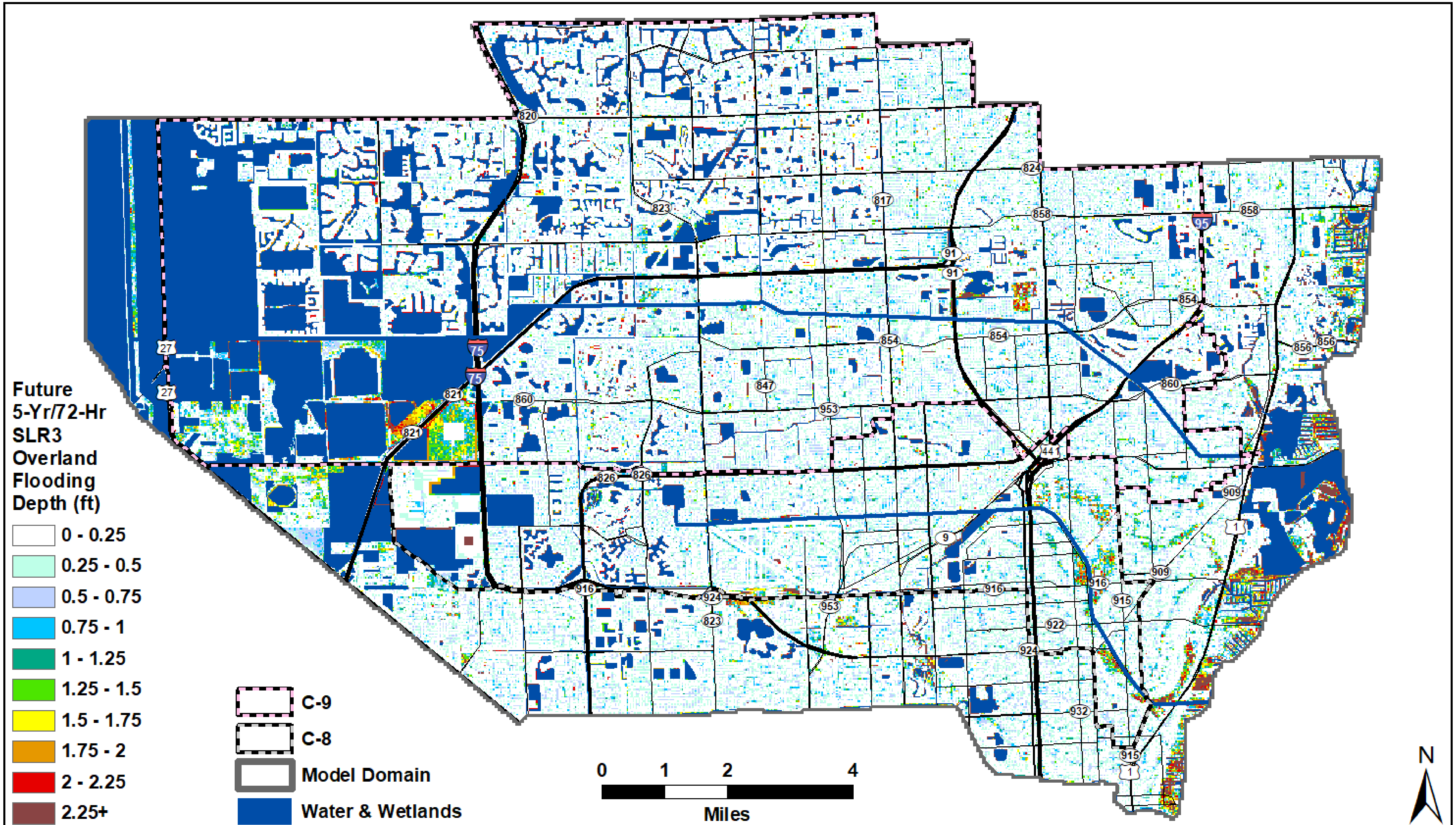

Figure 4.5-3: Flood Inundation Map for 5-Year Sea Level Rise 3 Design Storm Event

4.5.2 10-Year Design Storm Model-Wide Flood Depth Map

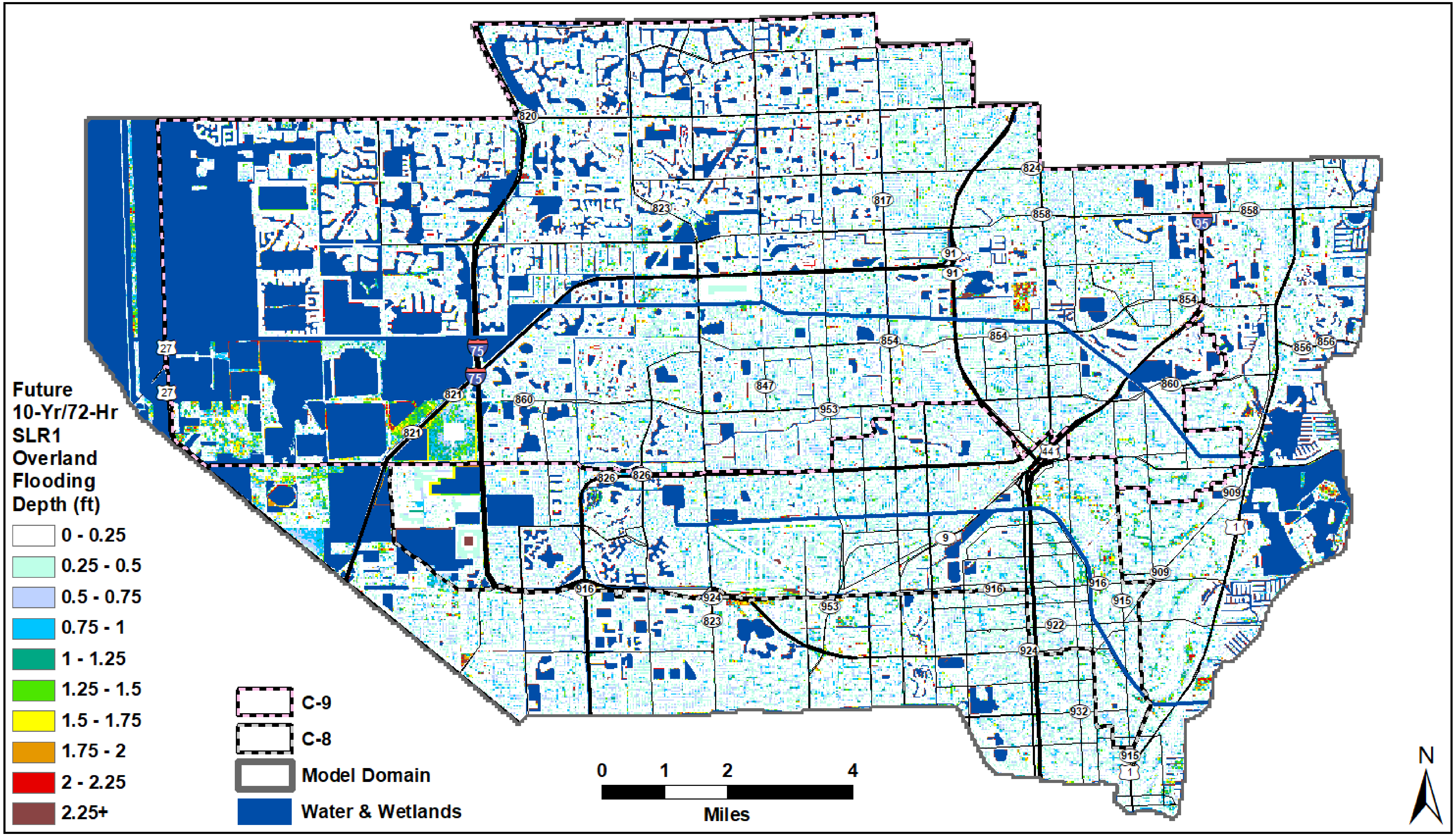

Figure 4.5-4: Flood Inundation Map for 10-Year Sea Level Rise 1 Design Storm Event

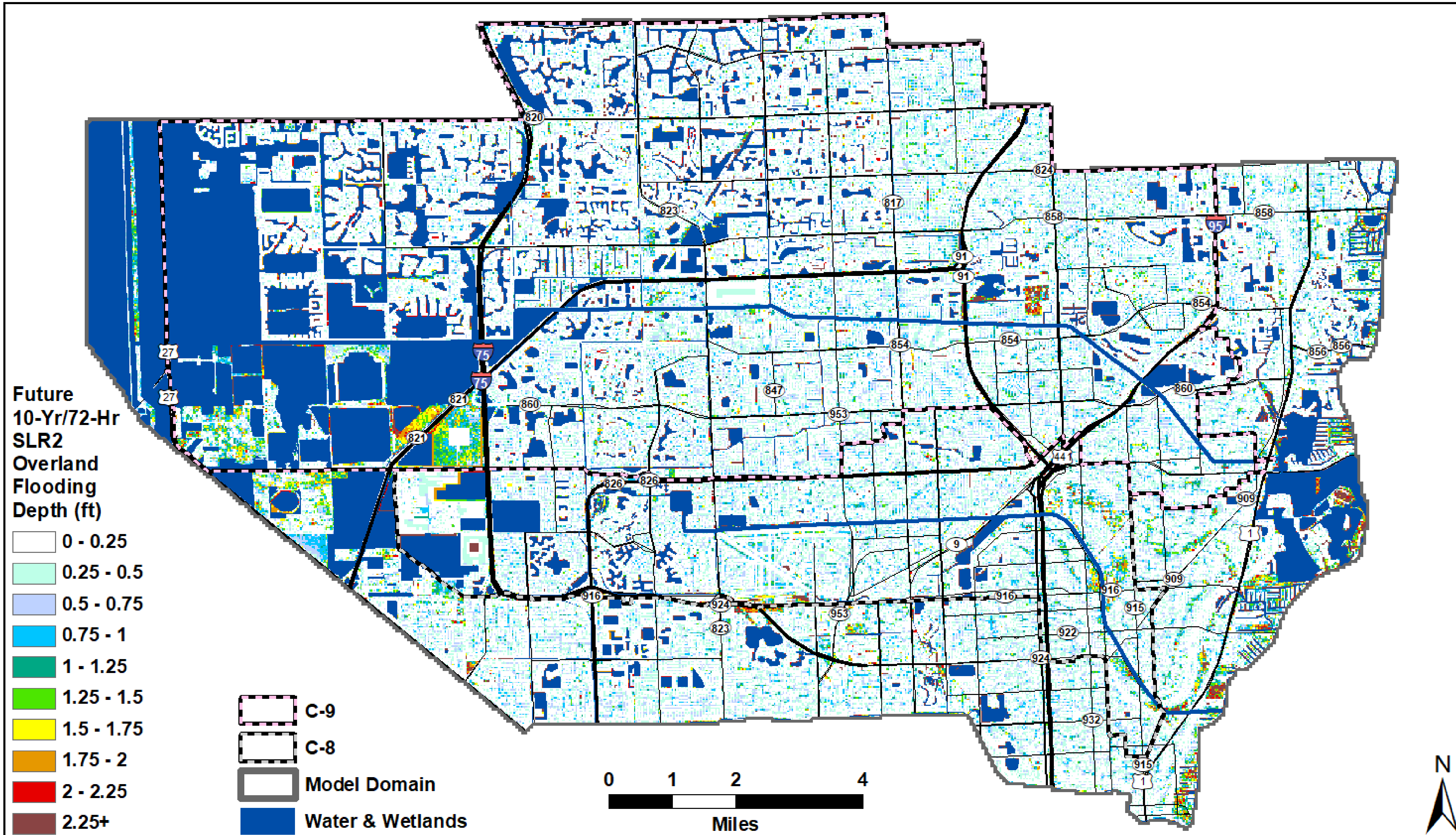

Figure 4.5-5: Flood Inundation Map for 10-Year Sea Level Rise 2 Design Storm Event

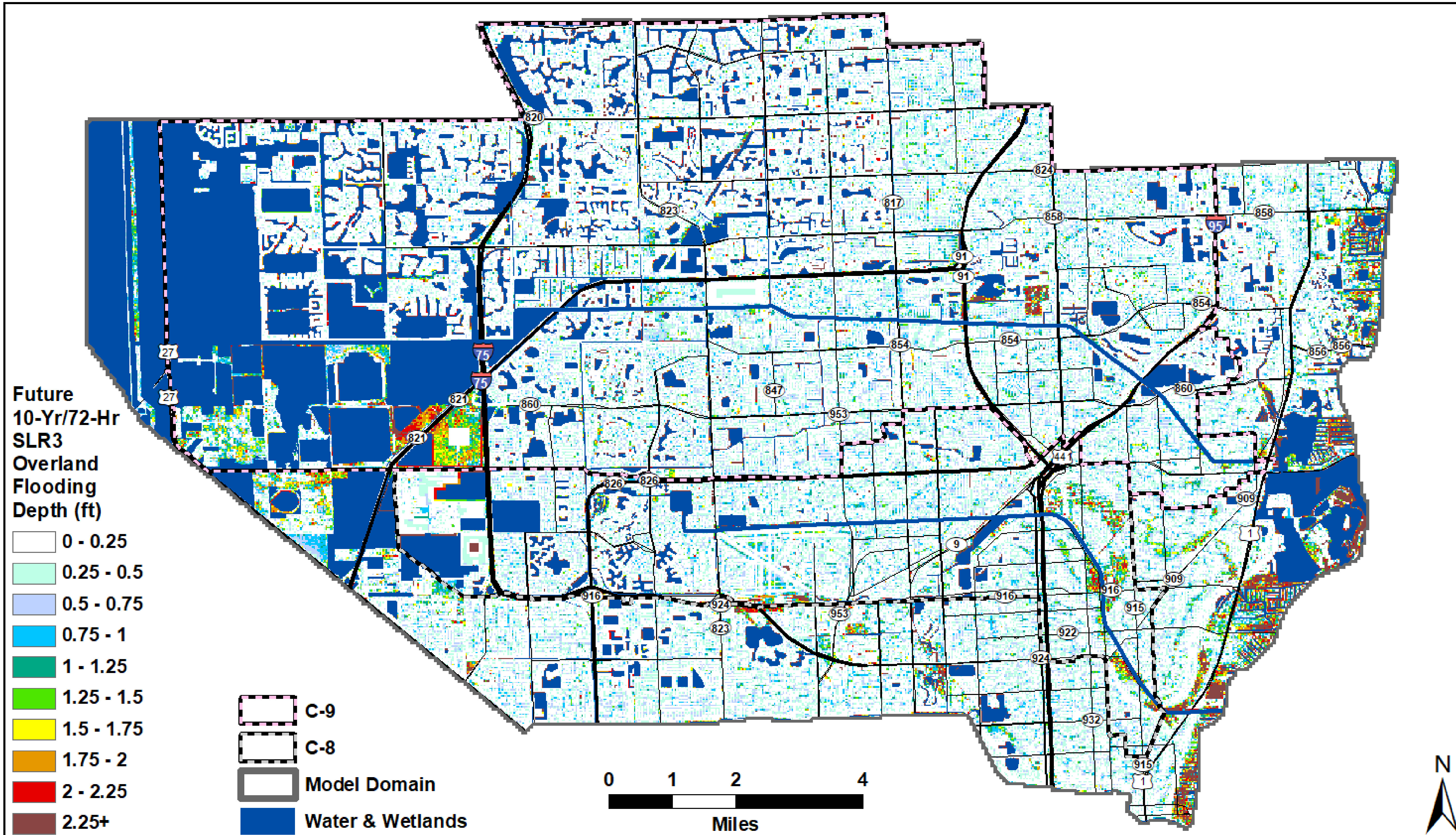

Figure 4.5-6: Flood Inundation Map for 10-Year Sea Level Rise 3 Design Storm Event

4.5.3 25-Year Design Storm Model-Wide Flood Depth Map

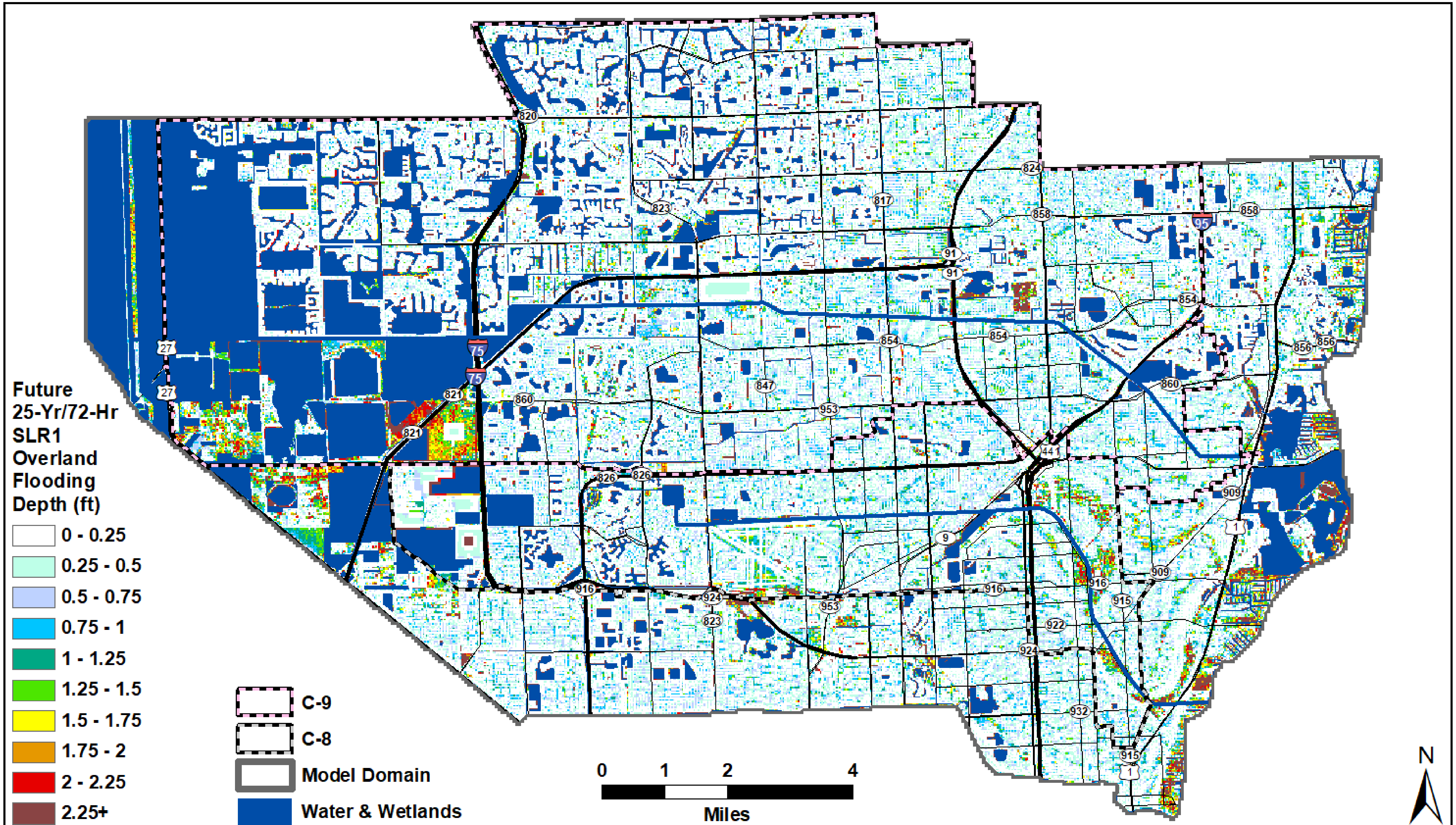

Figure 4.5-7: Flood Inundation Map for 25-Year Sea Level Rise 1 Design Storm Event

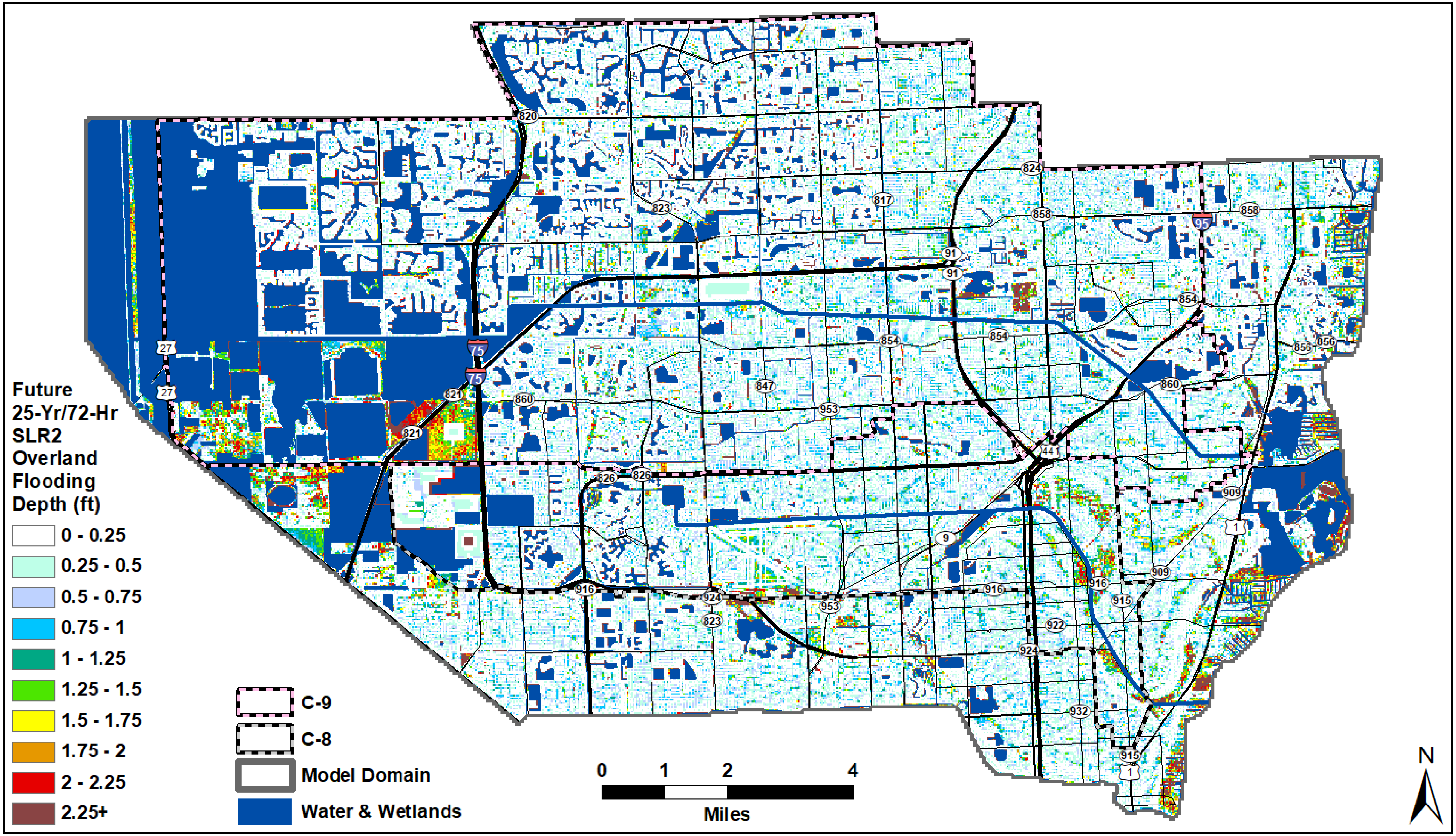

Figure 4.5-8: Flood Inundation Map for 25-Year Sea Level Rise 2 Design Storm Event

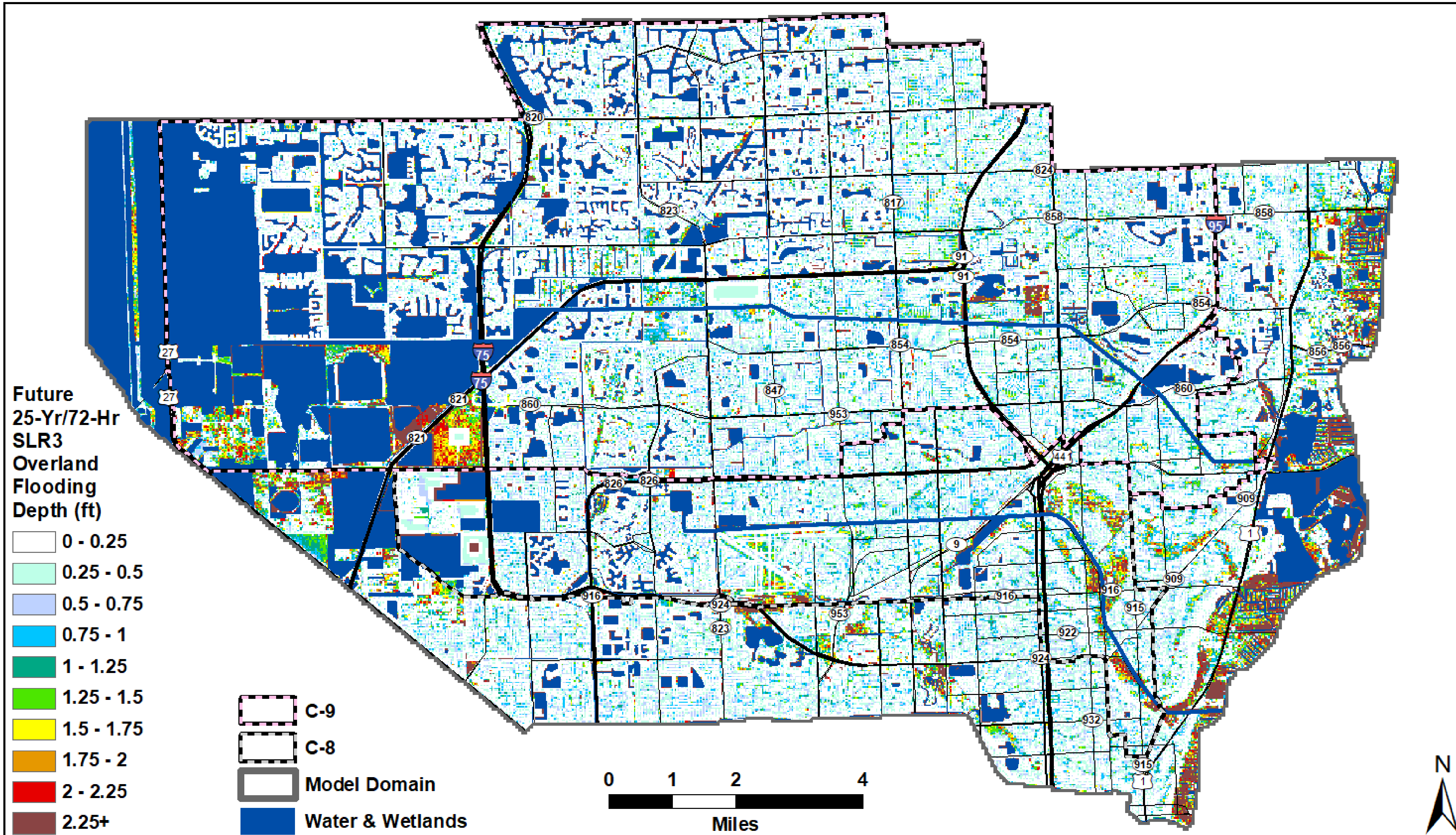

Figure 4.5-9: Flood Inundation Map for 25-Year Sea Level Rise 3 Design Storm Event

4.5.4 100-Year Design Storm Model-Wide Flood Depth Map

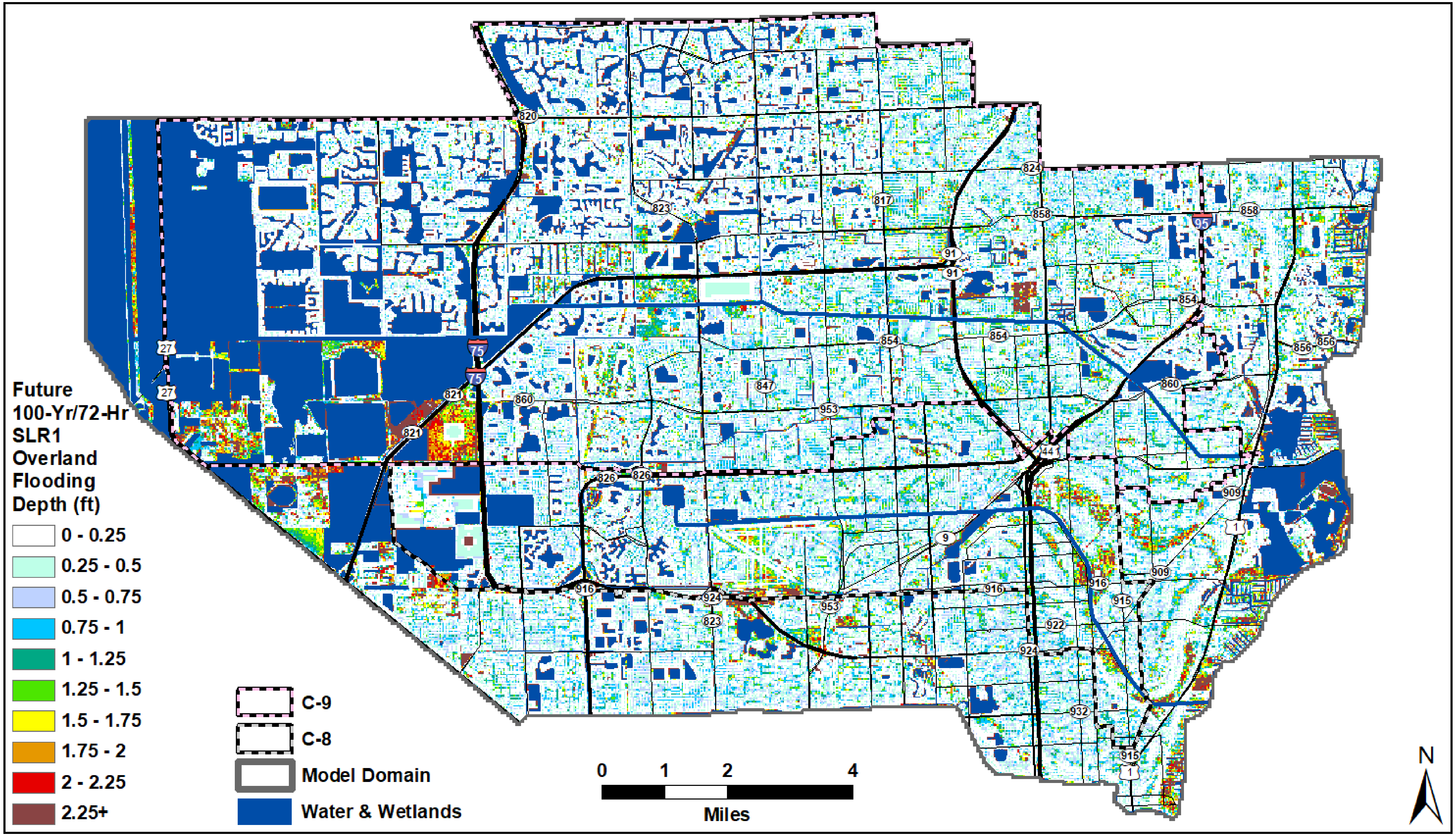

Figure 4.5-10: Flood Inundation Map for 100-Year Sea Level Rise 1 Design Storm Event

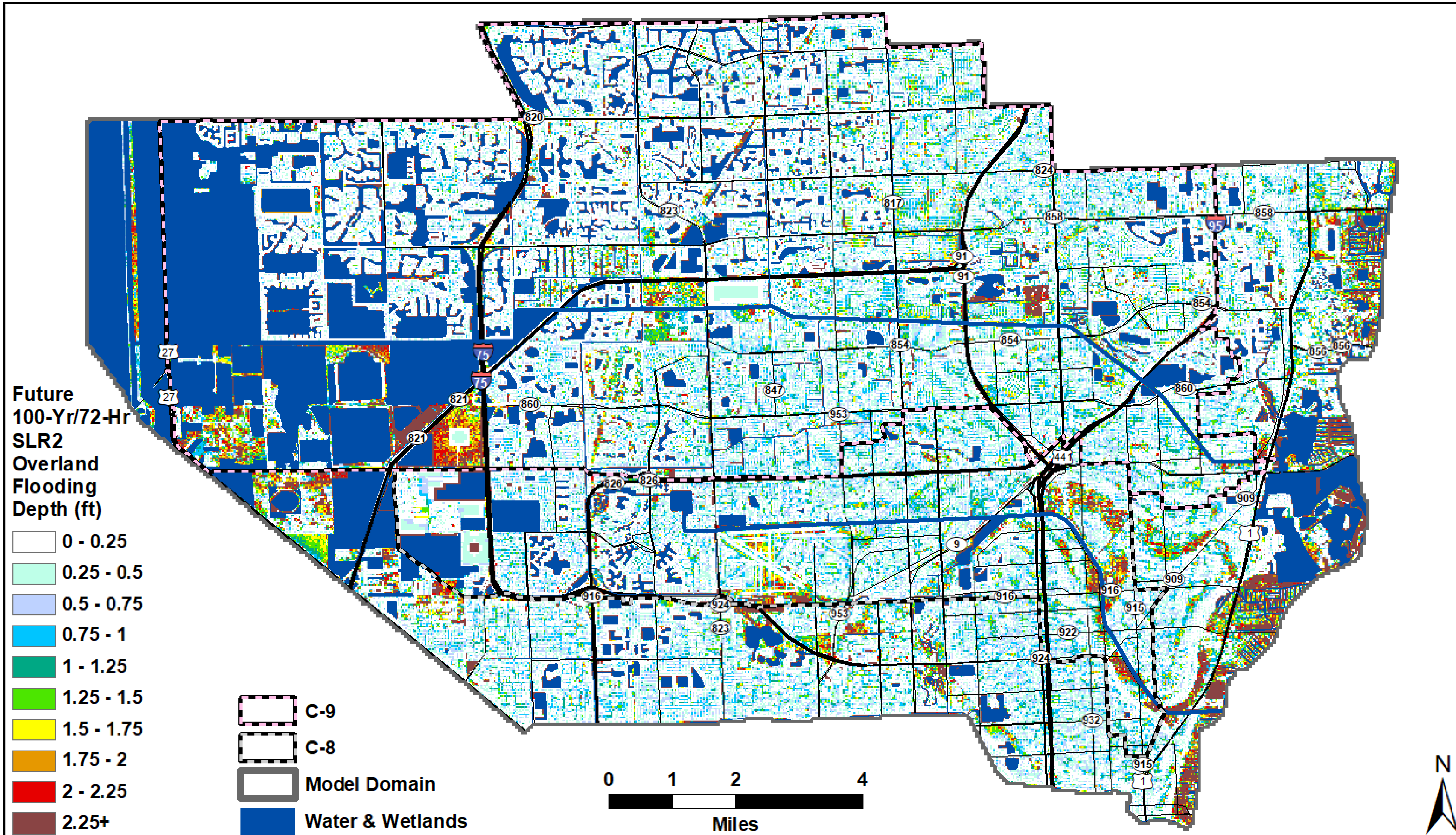

Figure 4.5-11: Flood Inundation Map for 100-Year Sea Level Rise 2 Design Storm Event

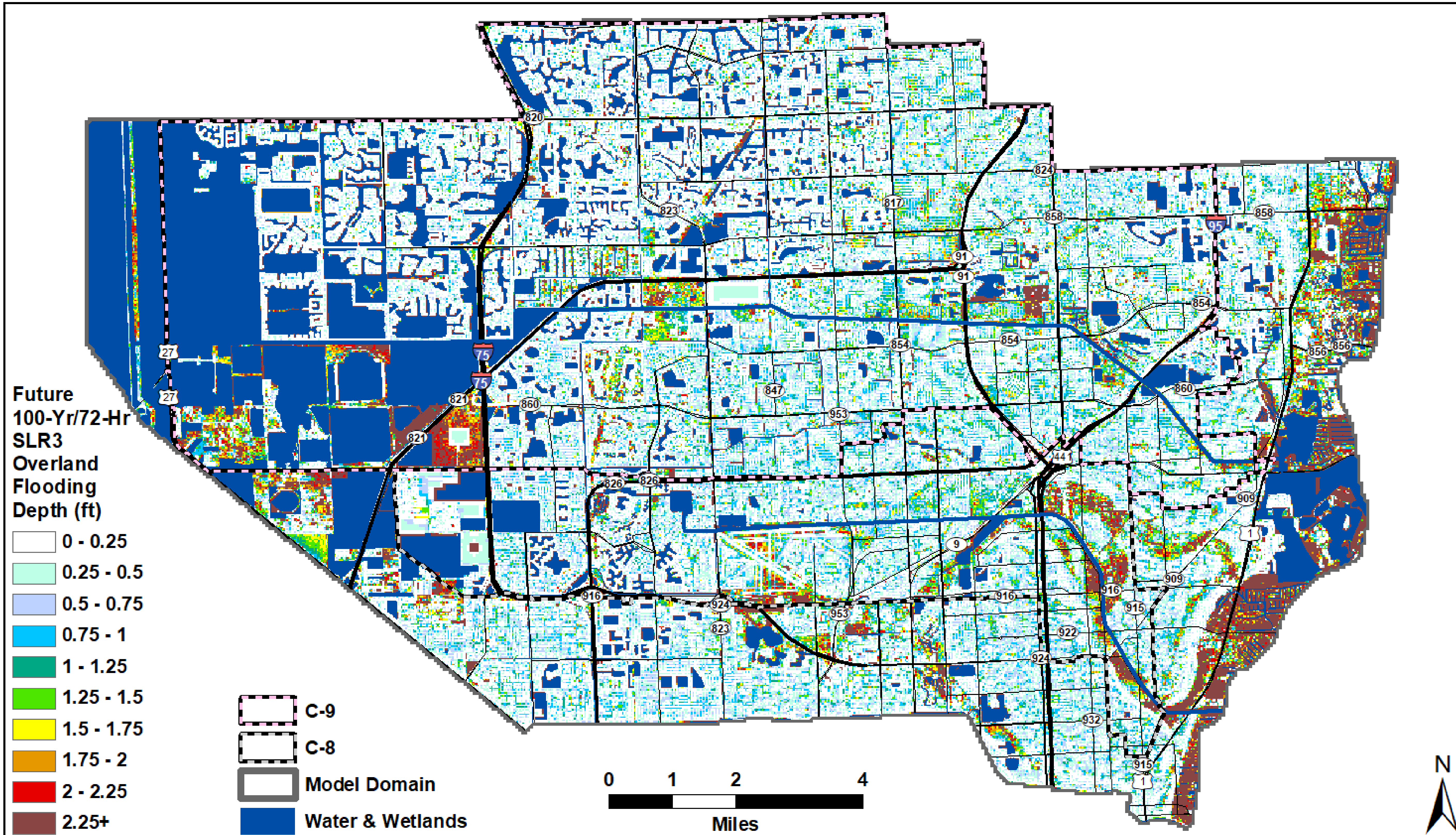

Figure 4.5-12: Flood Inundation Map for 100-Year Sea Level Rise 3 Design Storm Event

4.5.5 5-Year Design Storm Flood Depth Map for Urban Land Use Areas

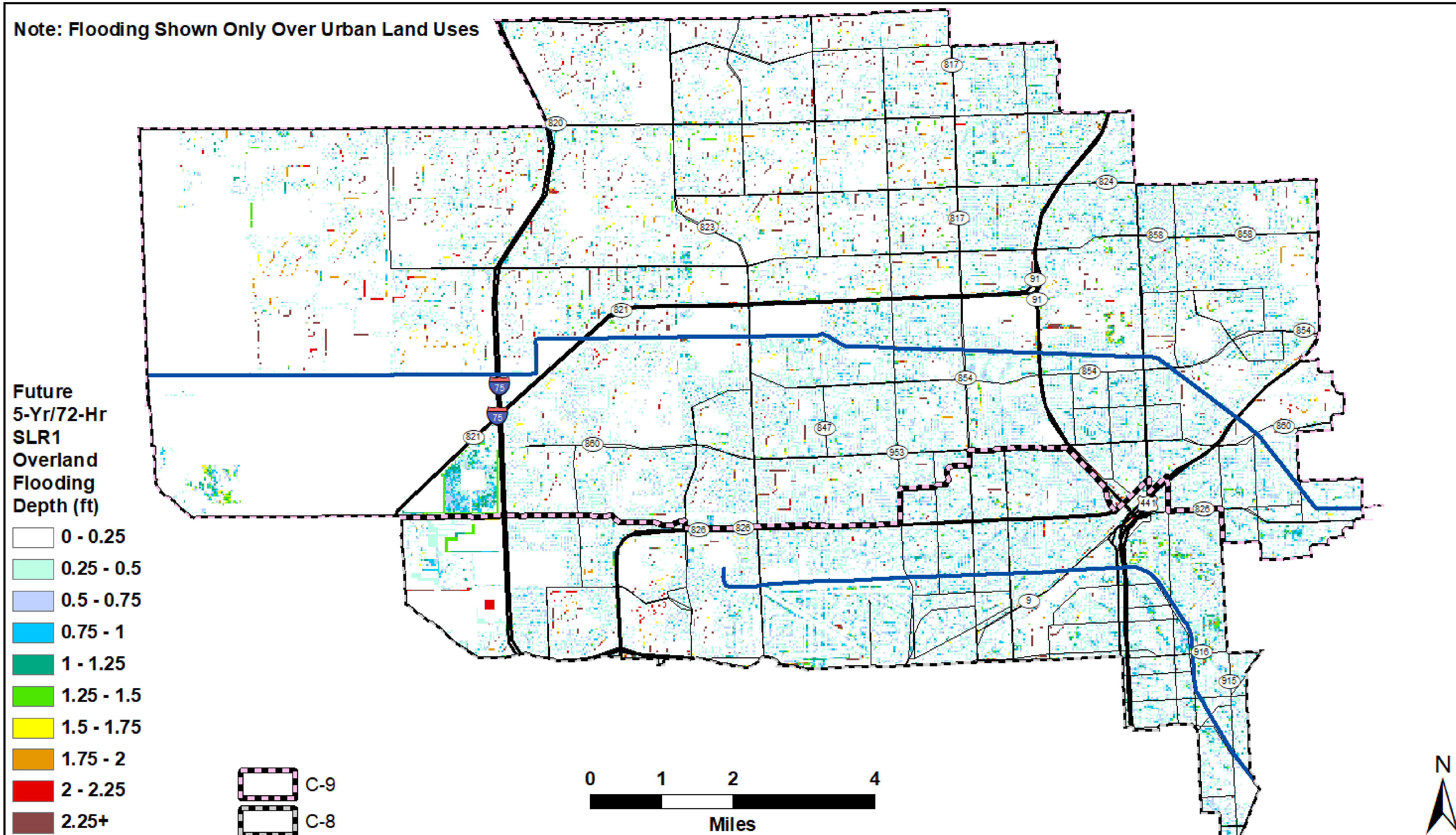

Figure 4.5-13: Flood Inundation Map for 5-Year Sea Level Rise 1 Design Storm Event in Urban Land Use Areas

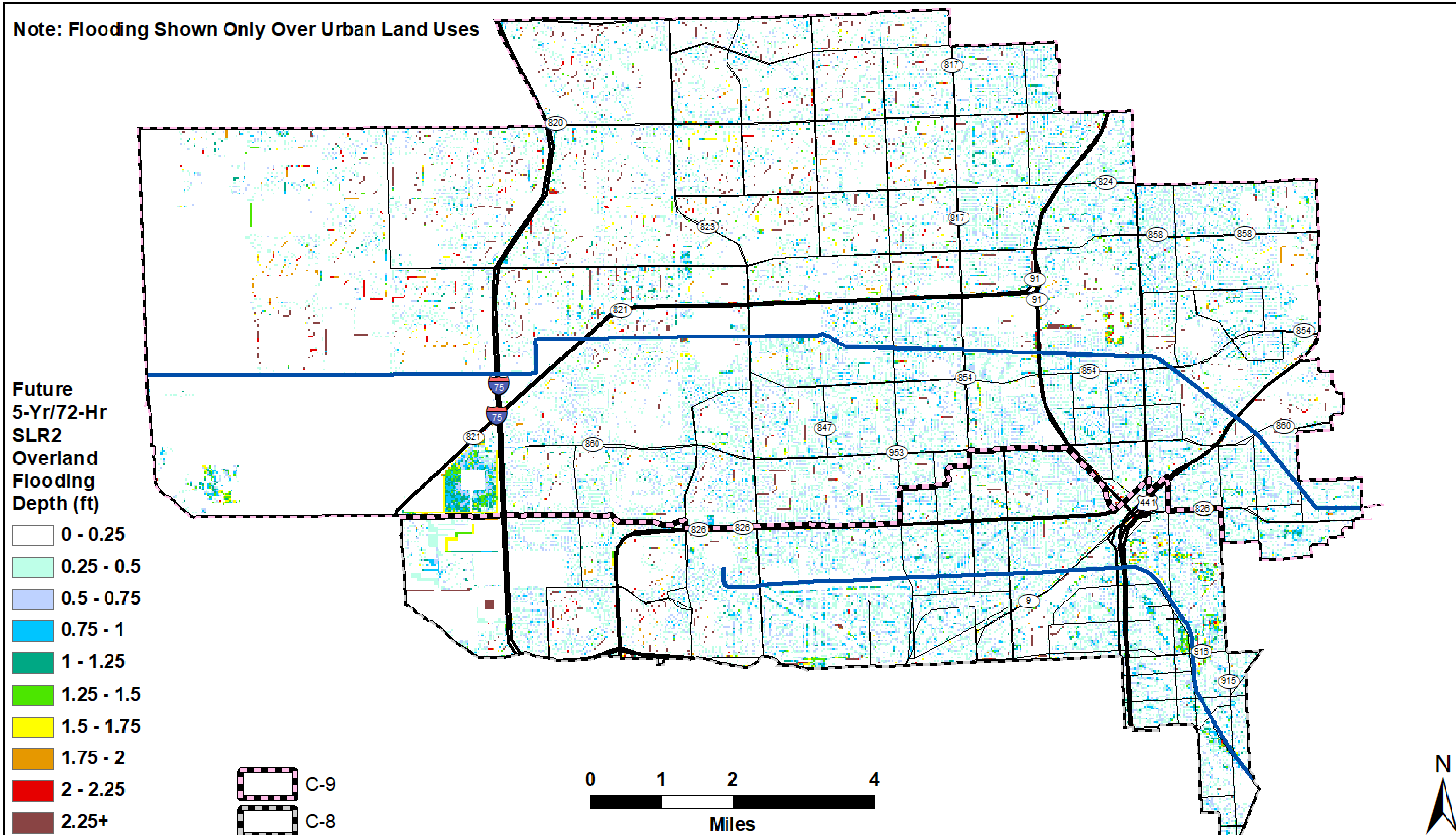

Figure 4.5-14: Flood Inundation Map for 5-Year Sea Level Rise 2 Design Storm Event in Urban Land Use Areas

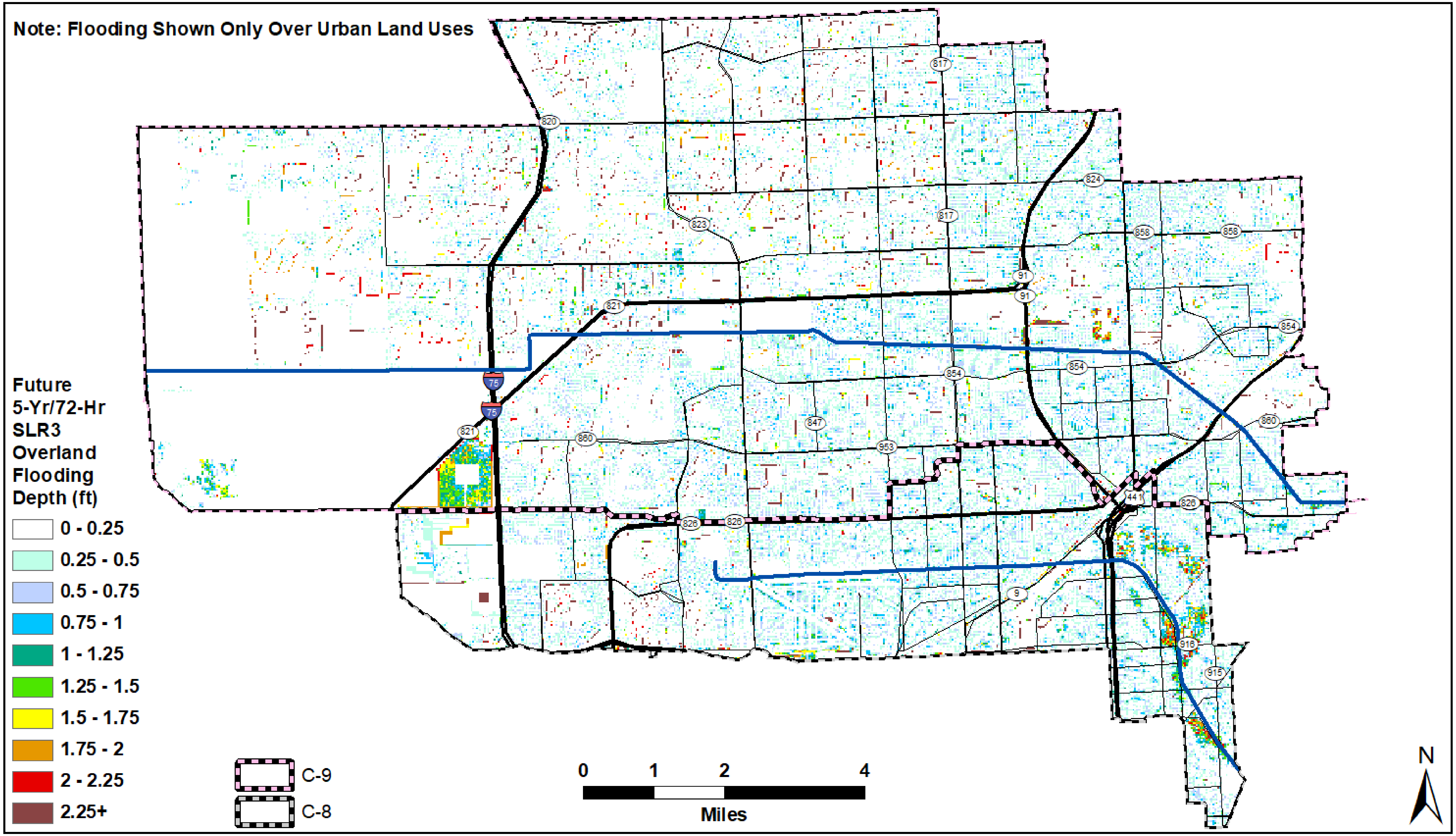

Figure 4.5-15: Flood Inundation Map for 5-Year Sea Level Rise 3 Design Storm Event in Urban Land Use Areas

4.5.6 10-Year Design Storm Flood Depth Map for Urban Land Use Areas

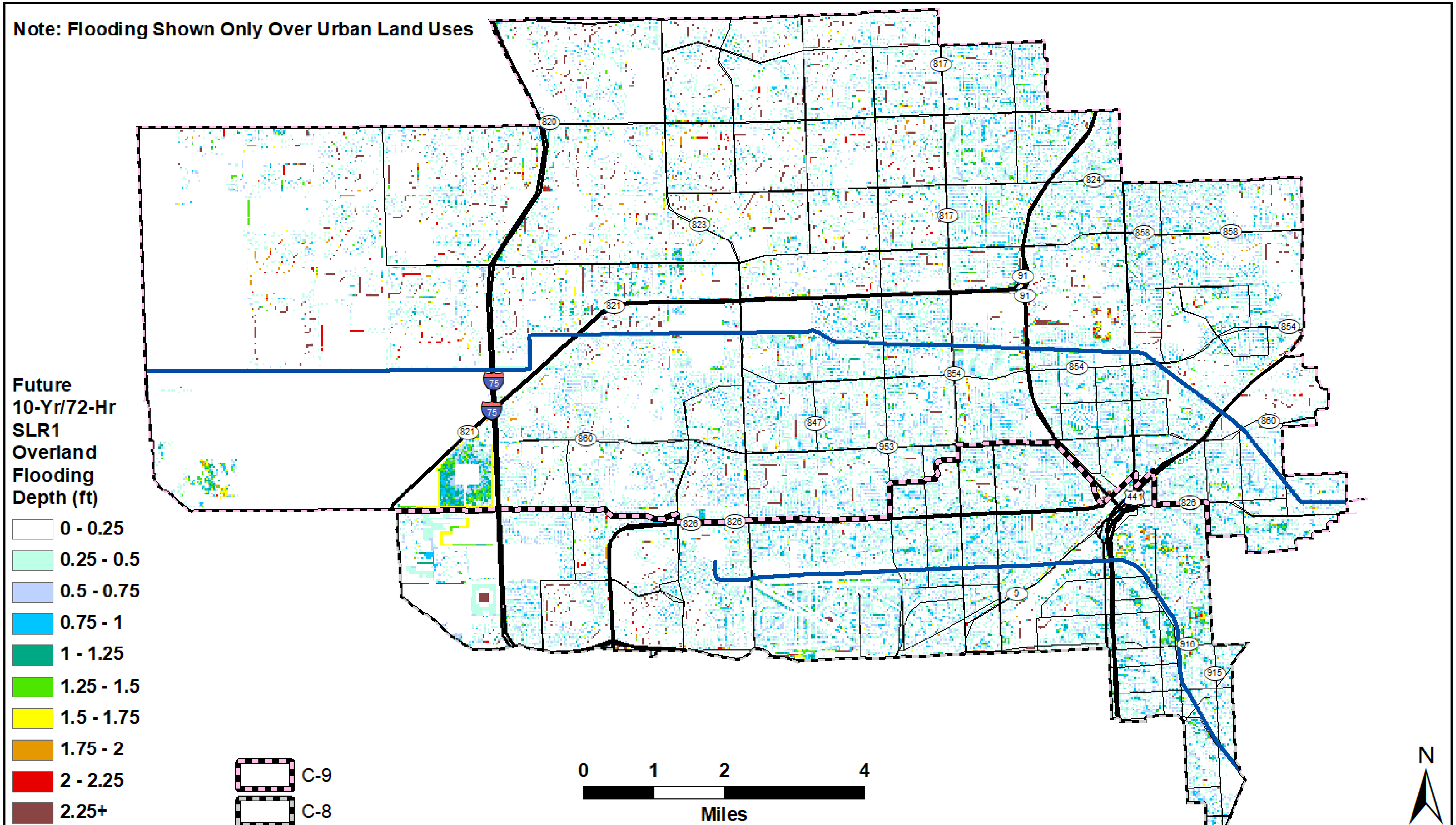

Figure 4.5-16 Flood Inundation Map for 10-Year Sea Level Rise 1 Design Storm Event in Urban Land Use Areas

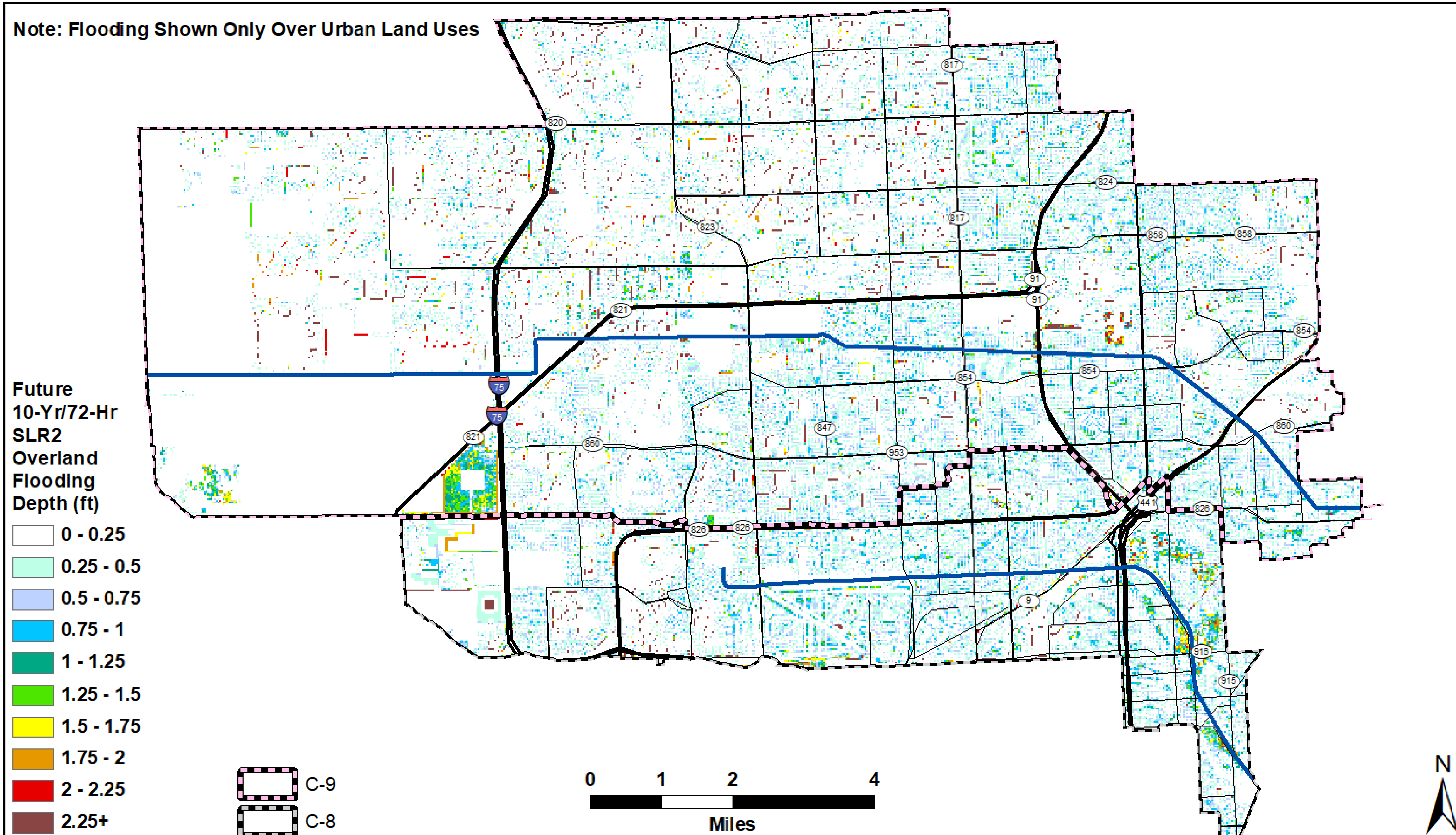

Figure 4.5-17 Flood Inundation Map for 10-Year Sea Level Rise 2 Design Storm Event in Urban Land Use Areas

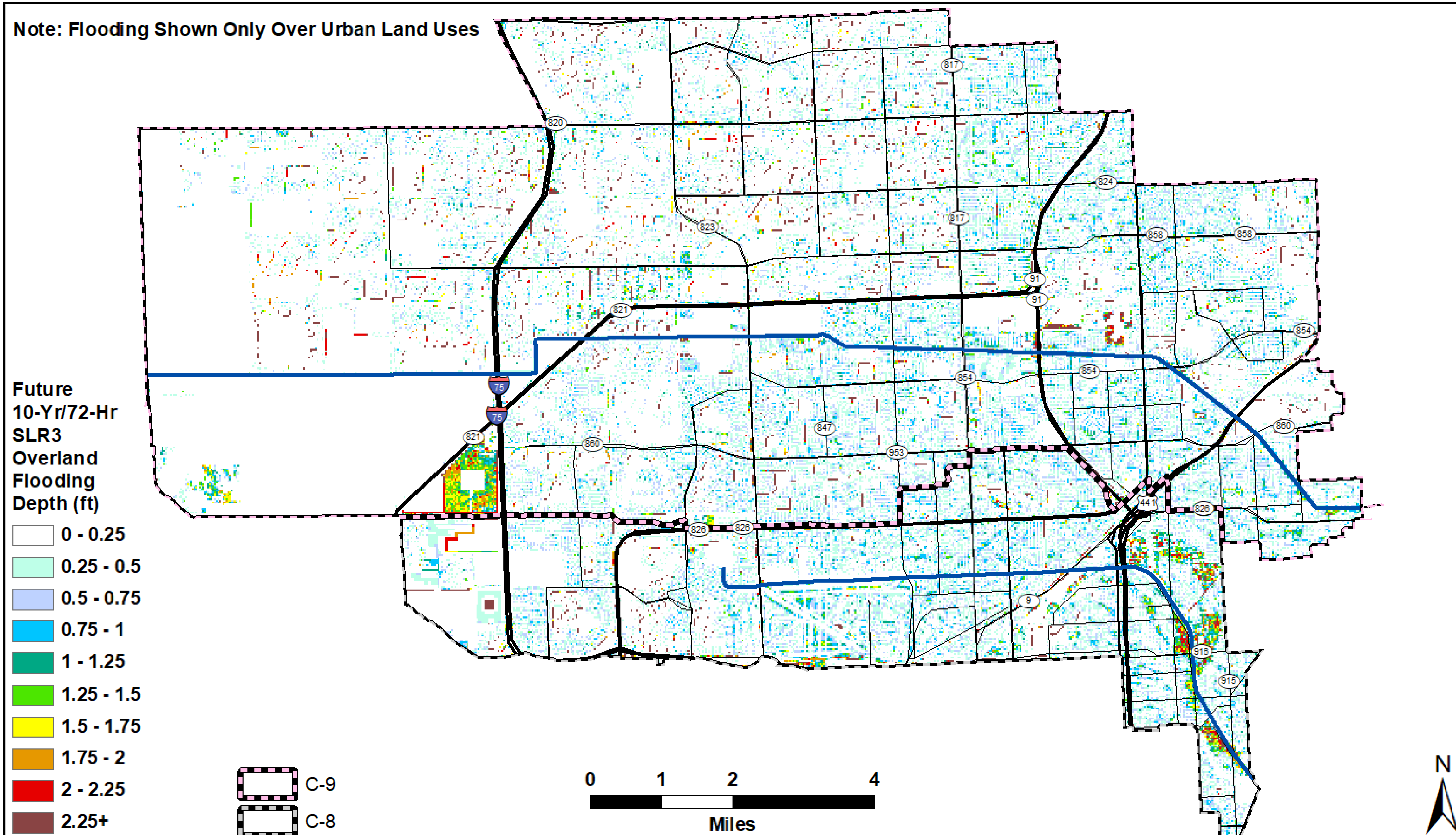

Figure 4.5-18 Flood Inundation Map for 10-Year Sea Level Rise 3 Design Storm Event in Urban Land Use Areas

4.5.7 25-Year Design Storm Flood Depth Map for Urban Land Use Areas

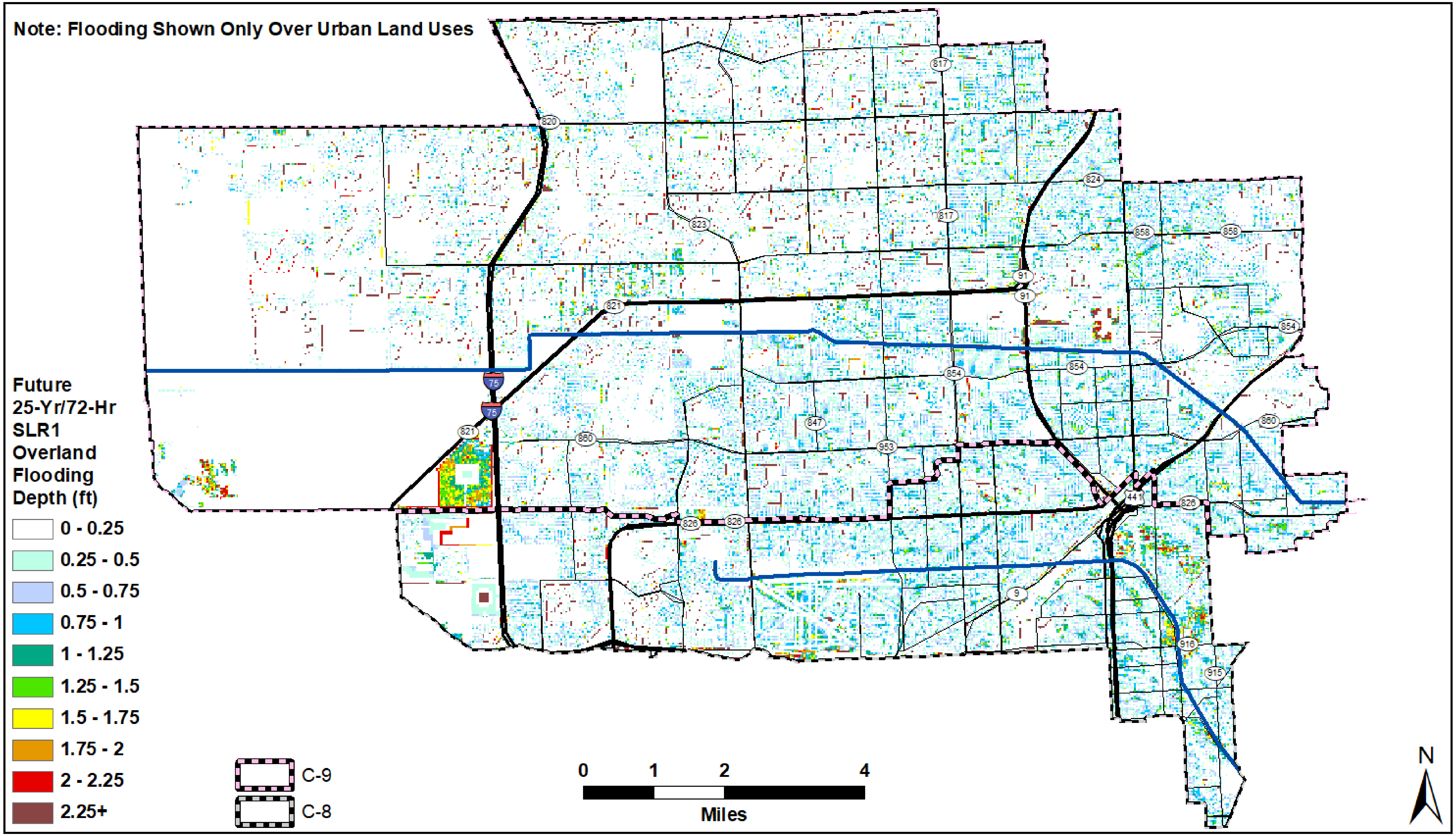

Figure 4.5-19 Flood Inundation Map for 25-Year Sea Level Rise 1 Design Storm Event in Urban Land Use Areas

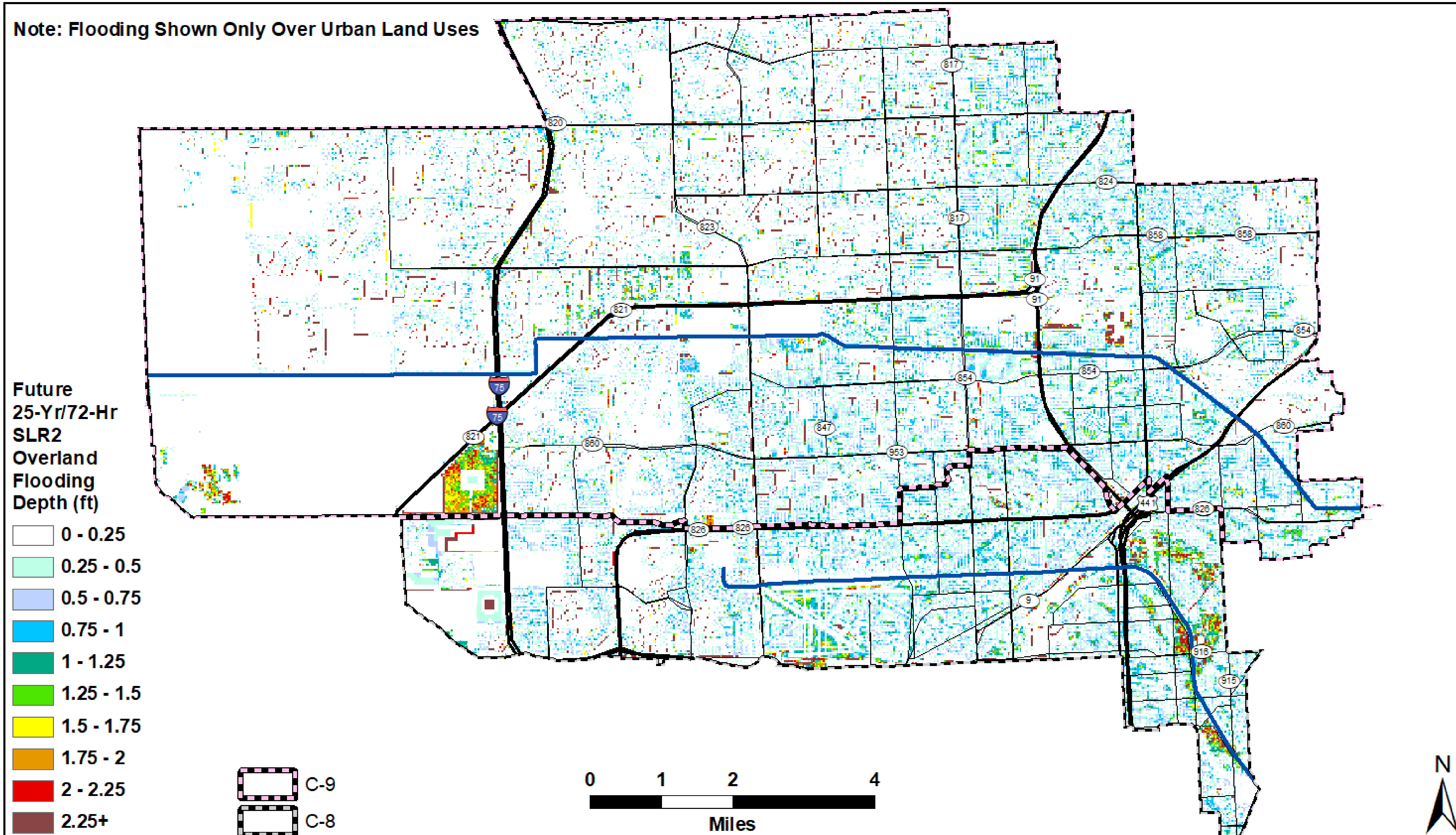

Figure 4.5-20 Flood Inundation Map for 25-Year Sea Level Rise 2 Design Storm Event in Urban Land Use Areas

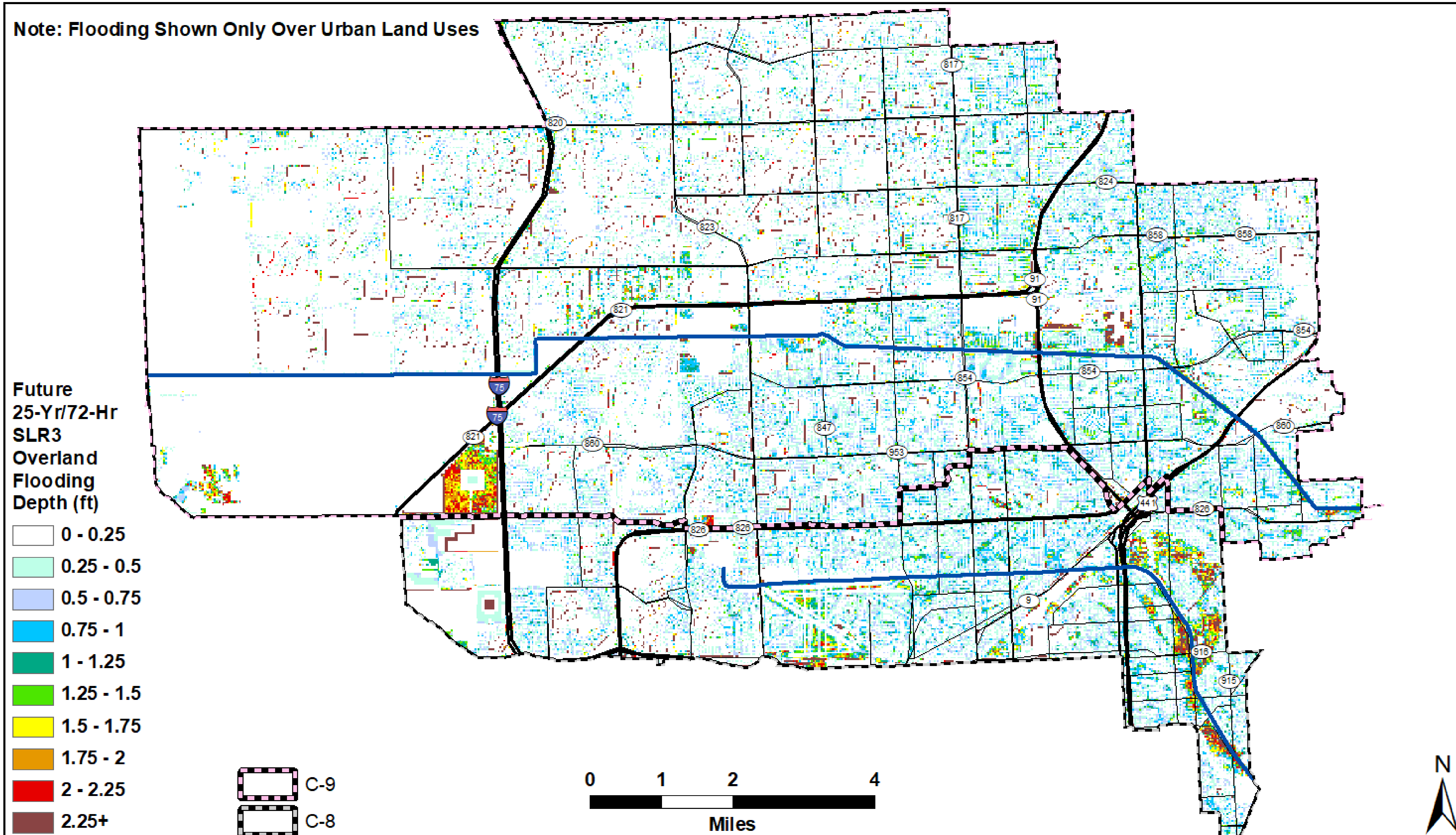

Figure 4.5-21 Flood Inundation Map for 25-Year Sea Level Rise 3 Design Storm Event in Urban Land Use Areas

4.5.8 100-Year Design Storm Flood Depth Map for Urban Land Use Areas

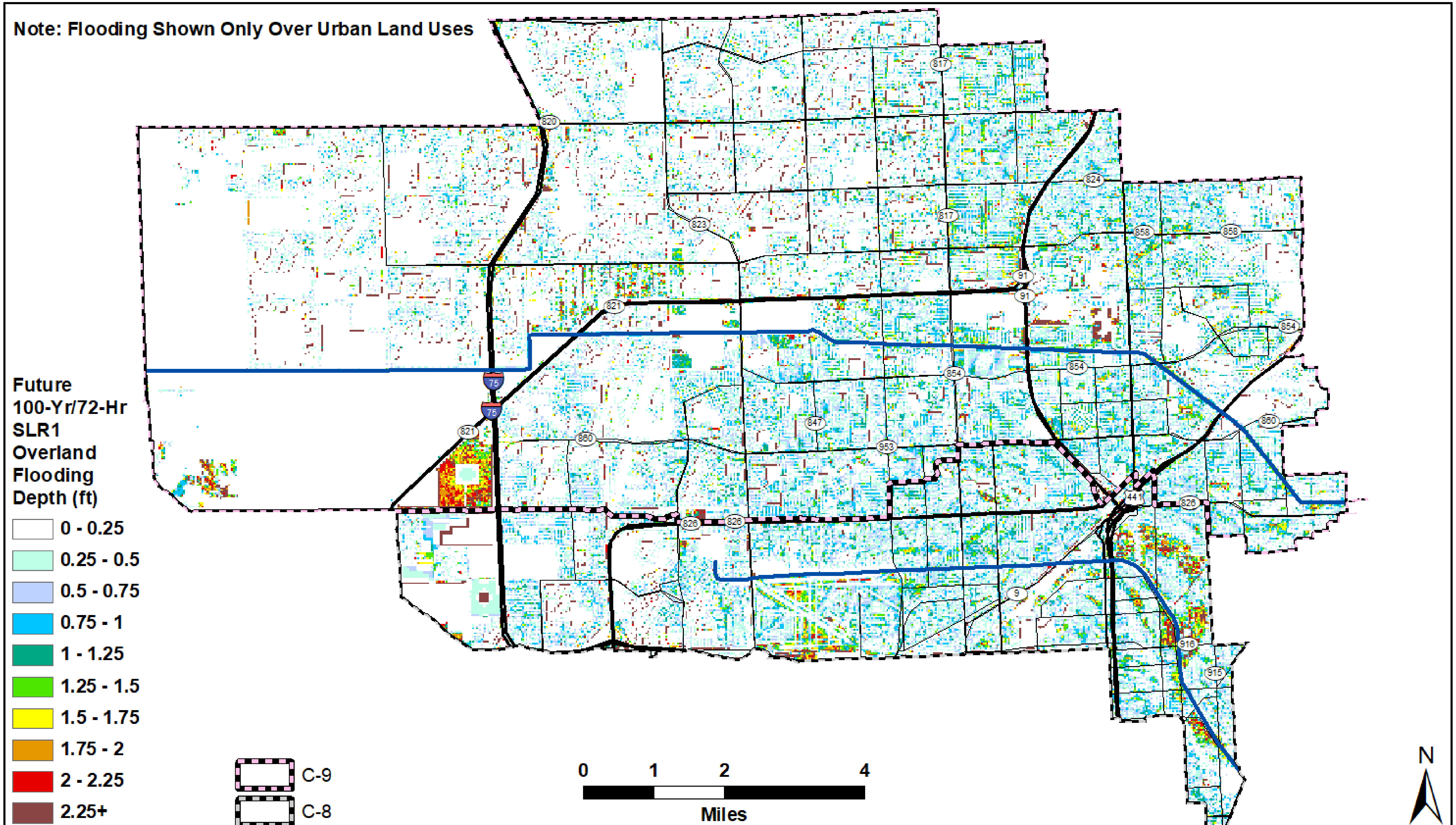

Figure 4.5-22 Flood Inundation Map for 100-Year Sea Level Rise 1 Design Storm Event in Urban Land Use Areas

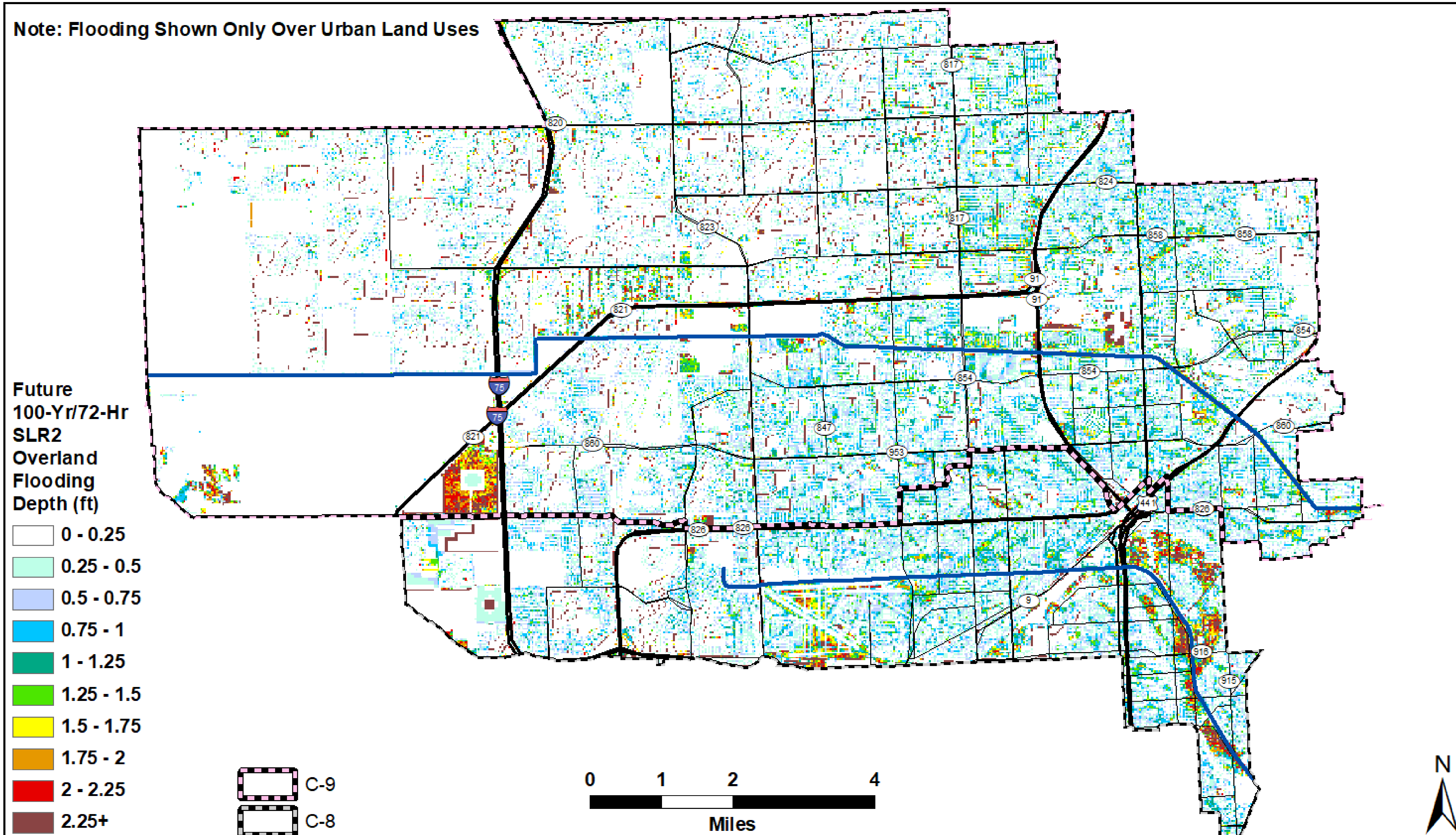

Figure 4.5-23 Flood Inundation Map for 100-Year Sea Level Rise 2 Design Storm Event in Urban Land Use Areas

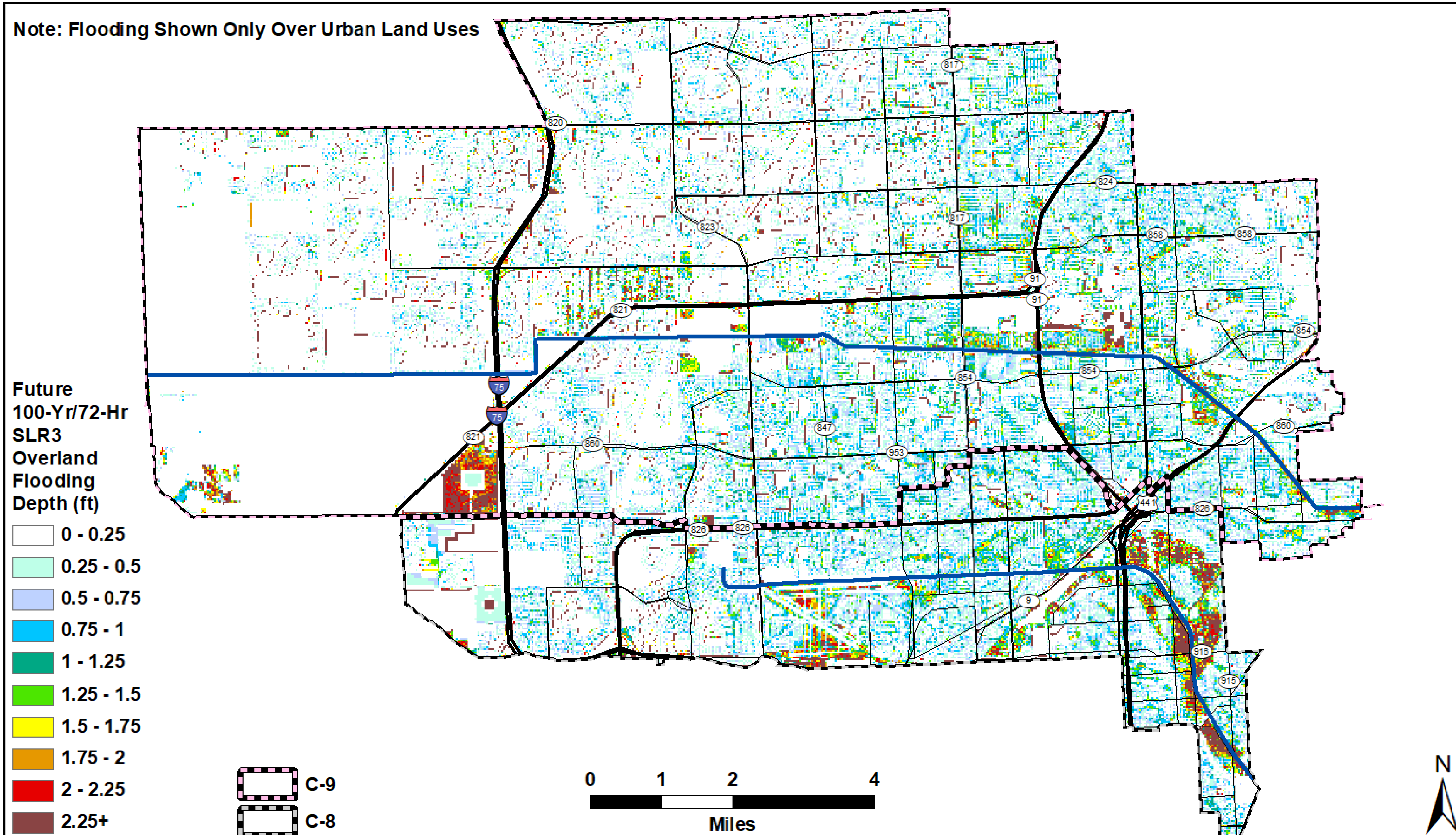

Figure 4.5-24 Flood Inundation Map for 100-Year Sea Level Rise 3 Design Storm Event in Urban Land Use Areas

4.5.9 Up-Close Flood Inundation Maps

For the C-8 Canal, bank exceedances seen in PM #1 caused by the future conditions 5-year design storm with various sea level rise correspond to a significant area of flood inundation as shown in PM #5. For the C-9 Canal, there are only a few areas of bank exceedance for the 5-year design storms, which do not correspond to significant areas of flood inundation, as shown in PM #5. However, the 10-year design storm with various amounts of sea level rise causes additional bank exceedances, some of which do correspond to a significant area of flood inundation. Therefore, for the "up-close" flood inundation maps shown in this section, the 5-year design storms will be shown for the C-8 Canal and the 10-year design storms will be shown for the C-9 Canal. Additionally, the 100-year design storms will be shown for both canals.

Under current conditions, increase in flooding was presented with respect to an increase in design storm rainfall volume and intensity. Intuitively, more rainfall increases the flooding potential under the same conditions. This is a well-established principle; therefore, future conditions results are presented with respect to an increase in sea level rise for a given design storm

For the C-8 Canal, each design storm intensity and sea level rise combination larger than the 5-year SLR1 event show an increase in flood inundation with respect to the increase in sea level. For example, in the lower reaches of C-8, the floodwaters start to come out of bank and flood the neighboring residential areas for the 5-year SLR2 event and become worse as design storm intensity and sea level rise increase.

Figure 4.5-25 through **Figure 4.5-27** show up-close flood inundation maps for the area between NE 135th St (CR916) and NE 6th Ave (CR915). For the 5-year SLR1 event, little to no flood inundation with respect to an overbank exceedance is shown, however, areas of flood inundation become more pronounced for the SLR2 event. Similarly, the area and depth of the SLR3 flood inundation significantly increases. For these three maps, the same rainfall is used, and the other difference is the amount of sea level rise and the initial groundwater levels that changed to represent the effects of higher tidal levels. **Figure 4.5-28** through **Figure 4.5-30** show the same location but for the 100-year design storm. Although significant flooding is shown for the SLR1 event, distinct increases in the area and depth of flood inundation is seen for the SLR2 and SLR3 events.

Figure 4.5-31 through **Figure 4.5-33** show up-close flood inundation maps for the area between North Miami Ave and NE 135th St (CR916). Localized flood inundation along the west bank is seen in a couple of locations for the 5-year SLR1 event, with significant increases in spatial extent and depth noted for the SLR2 and SLR3 events. Interestingly, there are areas of flood inundation in the SLR1 event that appear to be caused more by localized flooding than by bank exceedances that become worsened by bank exceedances under 2 ft and 3 ft of sea level rise. **Figure 4.5-34** through **Figure 4.5-36** show the same location but for the 100-year design storm. Again, although significant flooding is shown for the SLR1 event, distinct increases in the area and depth of flood inundation is seen for the SLR2 and SLR3 events.

Figure 4.5-37 through **Figure 4.5-39** show up-close flood inundation maps for the area near the Opa Locka Canal. Like the previous two areas, little to no flooding from bank exceedances are seen under SLR1 but become visible and increase in extent and magnitude as sea level rise increases. **Figure 4.5-40** through **Figure 4.5-42** show the same location but for the 100-yar design storm, which also experiences an increase in flood area and depth as sea level rise increases.

Typically, the C-9 Canal has higher bank elevations than the C-8 Canal, which meant less bank exceedances and less area and magnitude of flood inundation under current conditions. Although higher, they are not high enough to prevent flooding under sea level rise conditions. Notable bank exceedances were seen for the 10-year design storm, even with just 1 ft of sea level rise. Like the trend for the C-8 Canal, the extent and magnitude of the flood inundation increases with sea level rise. **Figure 4.5-43** through **Figure 4.5-45** show up-close flood inundation maps for the area between I-95 and S-29. For the 10-year SLR1 event, only a small area of flooding is seen upstream of S-29. For the SLR2 event, this area becomes further inundated and for the SLR3 event, the flooding extends nearly 2 miles upstream. **Figure 4.5-46** through **Figure 4.5-48** show the same location but for the 100-yar design storm.

Figure 4.5-49 through **Figure 4.5-51** show up-close flood inundation maps for the area near US Highway 441. For the 10-year SLR1 event, a notable area of flooding is seen both upstream and downstream of US Highway 441, however, only the segment downstream is caused by bank exceedance. For the SLR2 and SLR3 scenarios, the flooding downstream of US Highway 441 has significant increase in flooding extent and depth, while the area upstream has very little change. The upstream area not changing much with response to sea level rise makes sense as there is not a bank exceedance. **Figure 4.5-52** through **Figure 4.5-54** show the same location but for the 100-yar design storm, however, these figures do show an increase in flooding with response to sea level rise for the area upstream of US Highway 441 as the water level in the canal exceeds the bank elevations.

Figure 4.5-55 through **Figure 4.5-57** show up-close flood inundation maps for the area just west of the Ronald Reagan Turnpike. Like current conditions, this area shows some flooding in PM #5 while showing no bank exceedances in PM #1. The flooding in this area could be due to the topography being lower than the canal bank and/or inadequate secondary drainage infrastructure. For the 10-year design storms, regardless of 1, 2, or 3 ft sea level rise, the flooding in this location does not change much (small changes likely due to initial groundwater elevation differences). On the west side of this up-close example (Near Bass Creek Road), even the 100-year design storm 3-ft scenario does not cause bank exceedance, however, an increase in flood inundation is seen, shown in **Figure 4.5-58** through **Figure 4.5-60**. This is partially due to the increased canal stage limiting the gravity-based discharge from the surrounding area. On the east side of this up-close example, a significant increase in flooding is shown for the 100-year design storm as sea level rise increases, and the bank elevations become further exceeded.

Figure 4.5-61 through **Figure 4.5-63** show up-close flood inundation maps for the area near Red Road. Like the previous up-close example, this area shows flooding in PM #5 without bank exceedances in PM #1, both in current conditions as well as for the 10-year future condition design storms. However, for the 100-year design storm, the banks are exceeded, which leads to an increase in flood inundation as sea level rise increases as shown in **Figure 4.5-64** through **Figure 4.5-66**.

Sea level rise increases the stress on the drainage systems by reducing the discharge capacity of the tidal structures which leads to increased stages in the canals. Aside from making existing areas that exceed canal banks worse, sea level rise can cause new canal segments to exceed bank elevations, which will worsen any flooding that already exists. This section presents up-close examples of flood inundation as sea level rise increases.

4.5.9.1 Up-Close Flood Inundation Maps for the C-8 Canal Between NE 135th St (CR916) and NE 6th Ave (CR915)

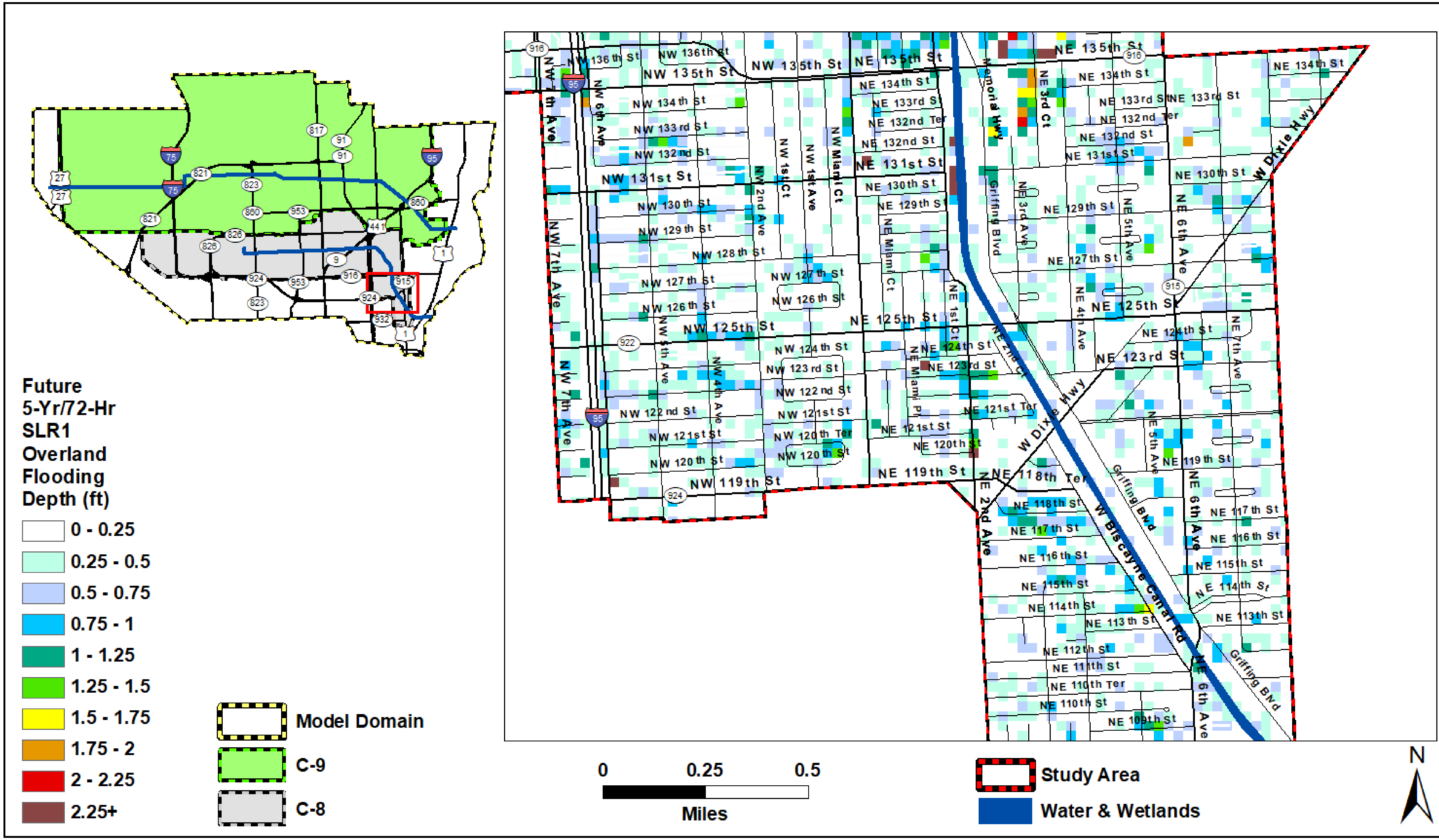

Figure 4.5-25: Up Close 5-Year Sea Level Rise 1 Flood Inundation Map for the C-8 Canal Between and NE 135th St (CR916) and NE 6th Ave (CR915)

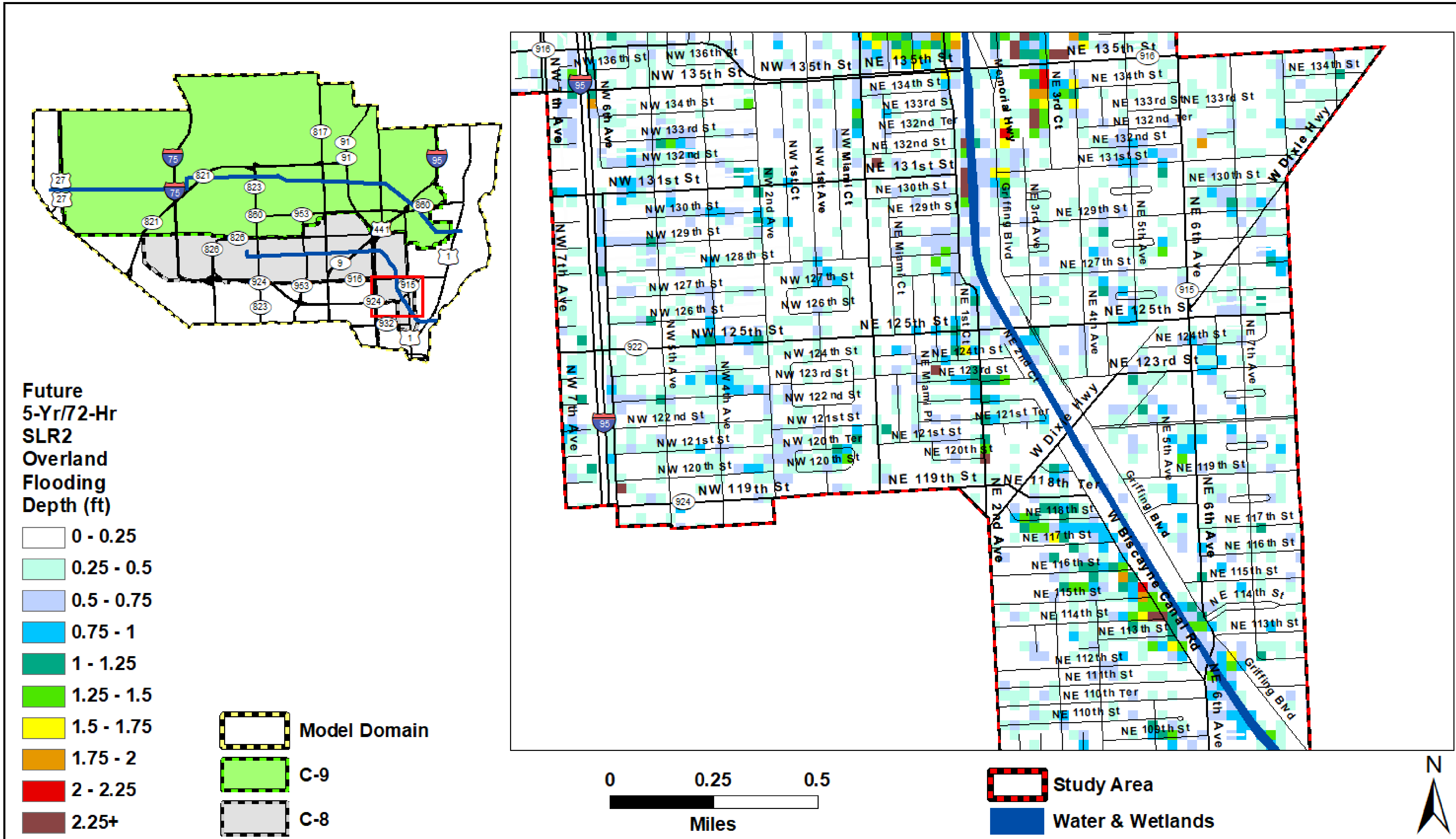

Figure 4.5-26: Up Close 5-Year Sea Level Rise 2 Flood Inundation Map for the C-8 Canal Between and NE 135th St (CR916) and NE 6th Ave (CR915)

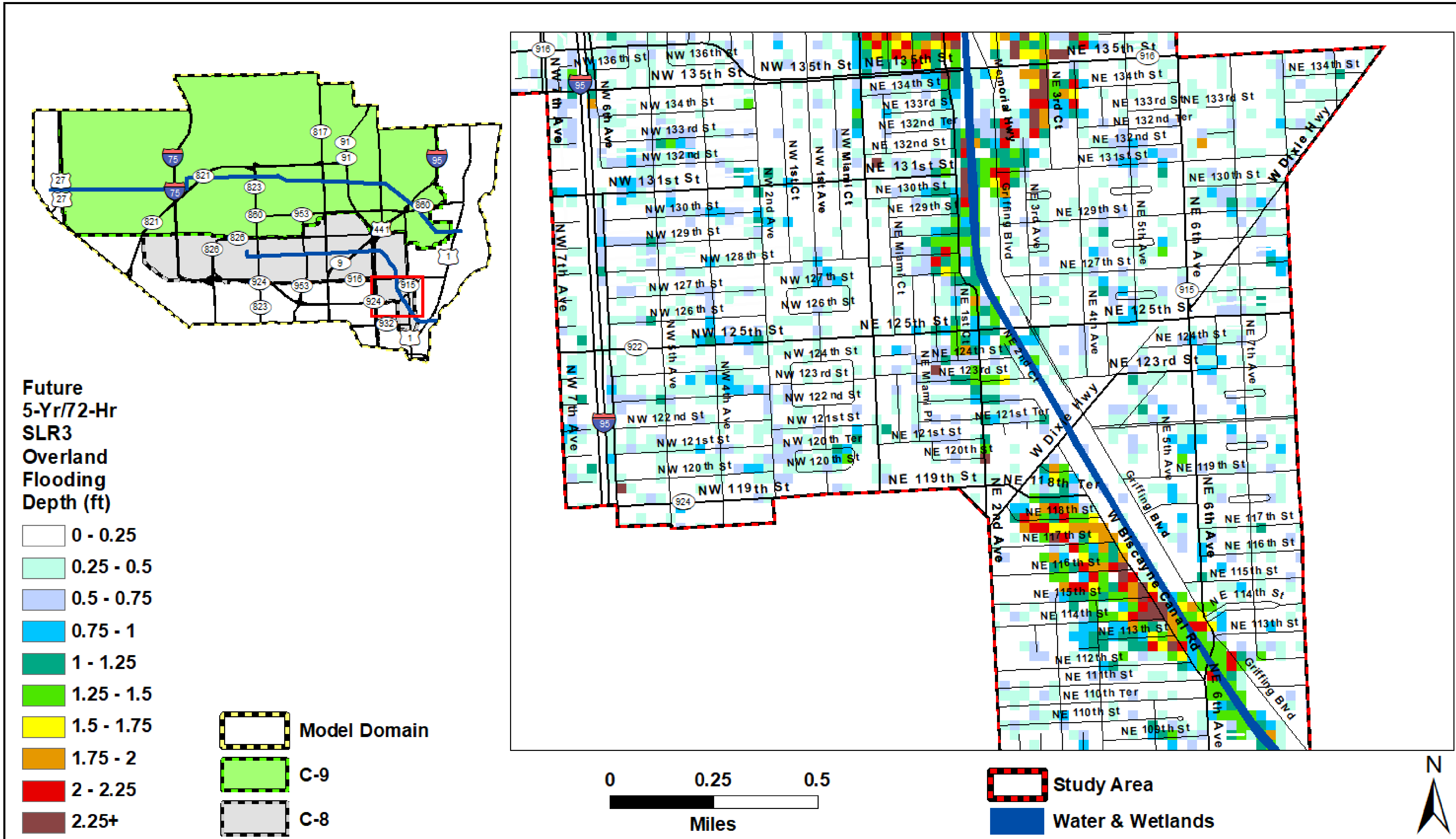

Figure 4.5-27: Up Close 5-Year Sea Level Rise 3 Flood Inundation Map for the C-8 Canal Between and NE 135th St (CR916) and NE 6th Ave (CR915)

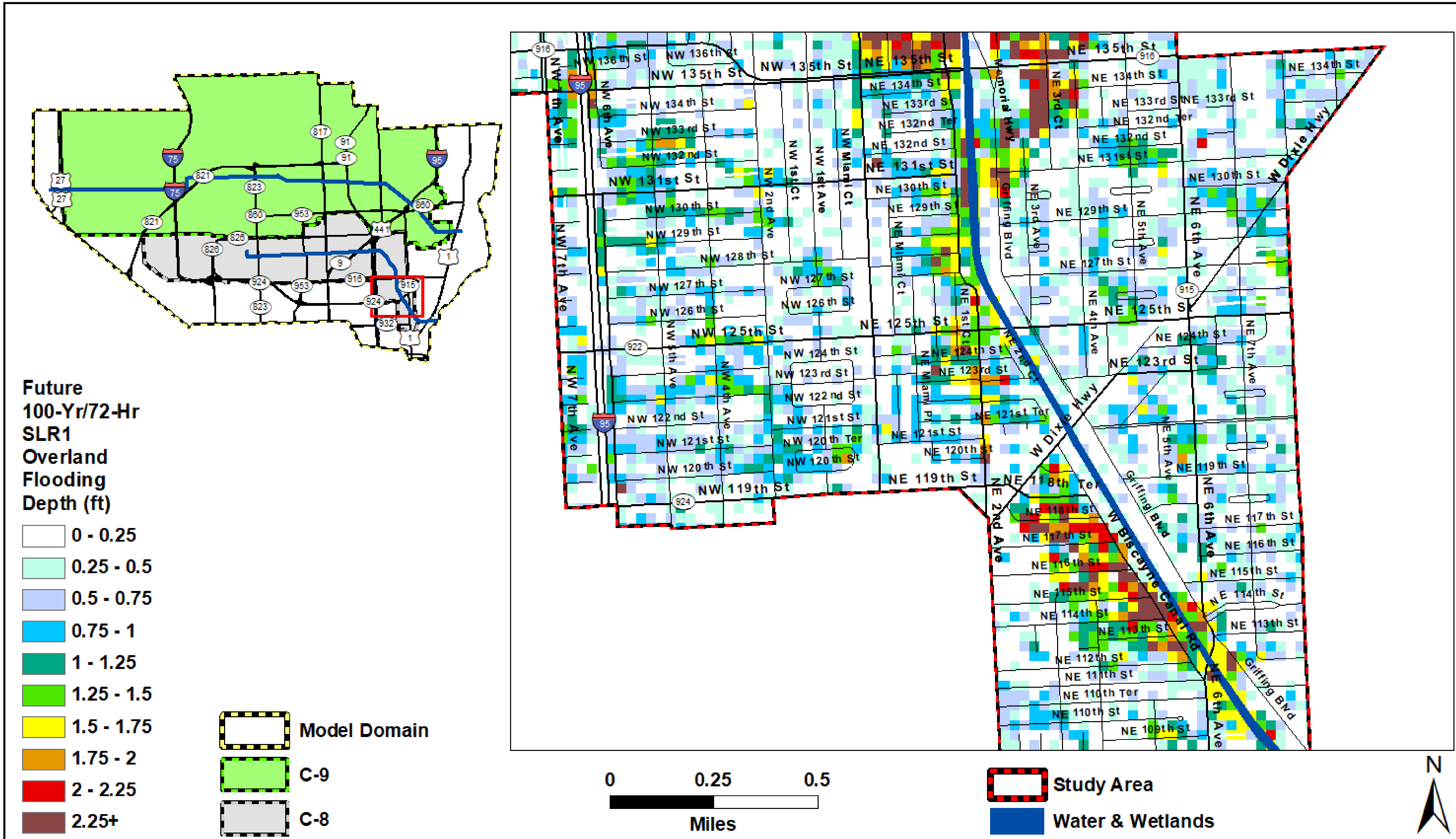

Figure 4.5-28: Up Close 100-Year Sea Level Rise 1 Flood Inundation Map for the C-8 Canal Between and NE 135th St (CR916) and NE 6th Ave (CR915)

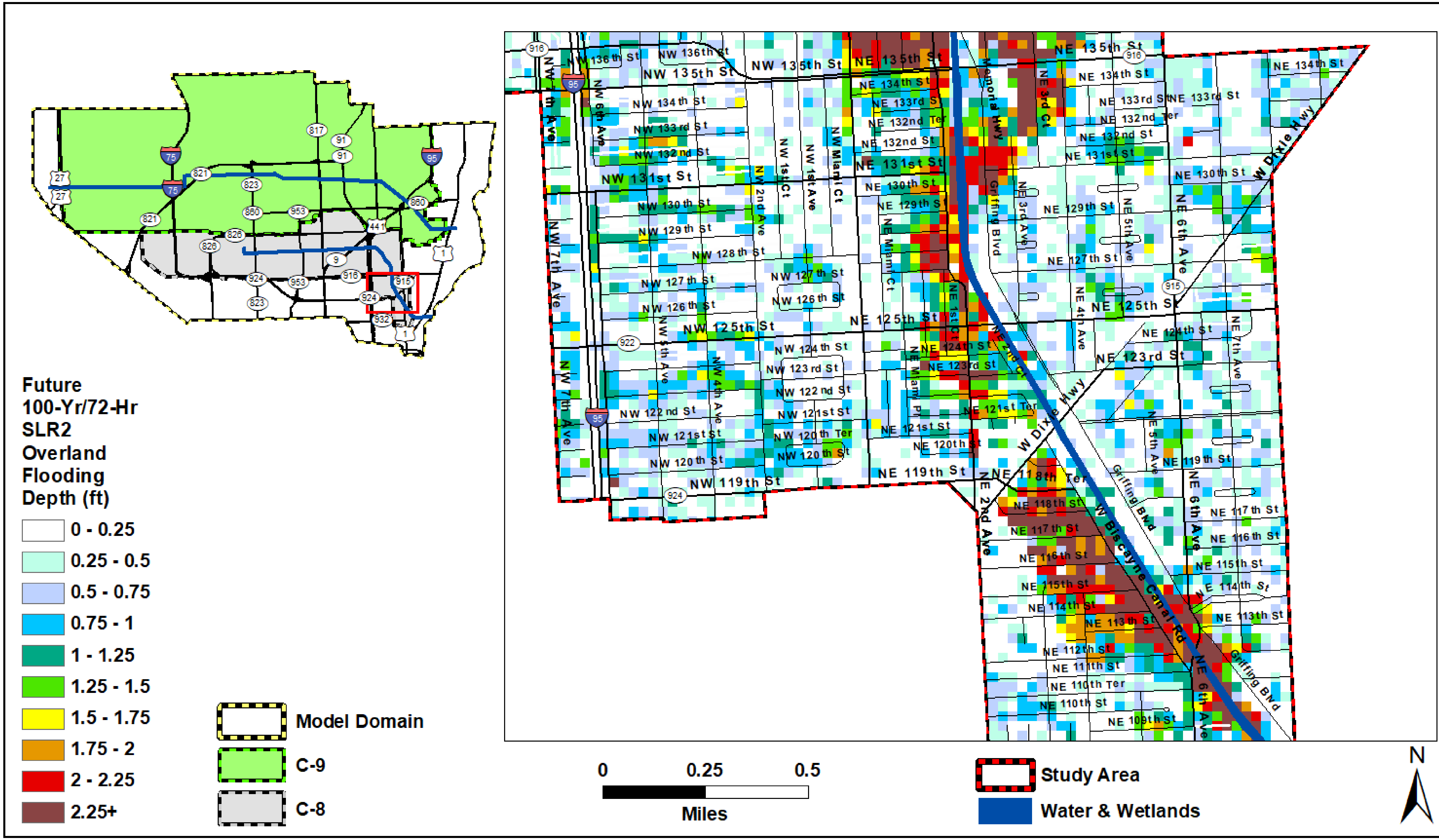

Figure 4.5-29: Up Close 100-Year Sea Level Rise 2 Flood Inundation Map for the C-8 Canal Between and NE 135th St (CR916) and NE 6th Ave (CR915)

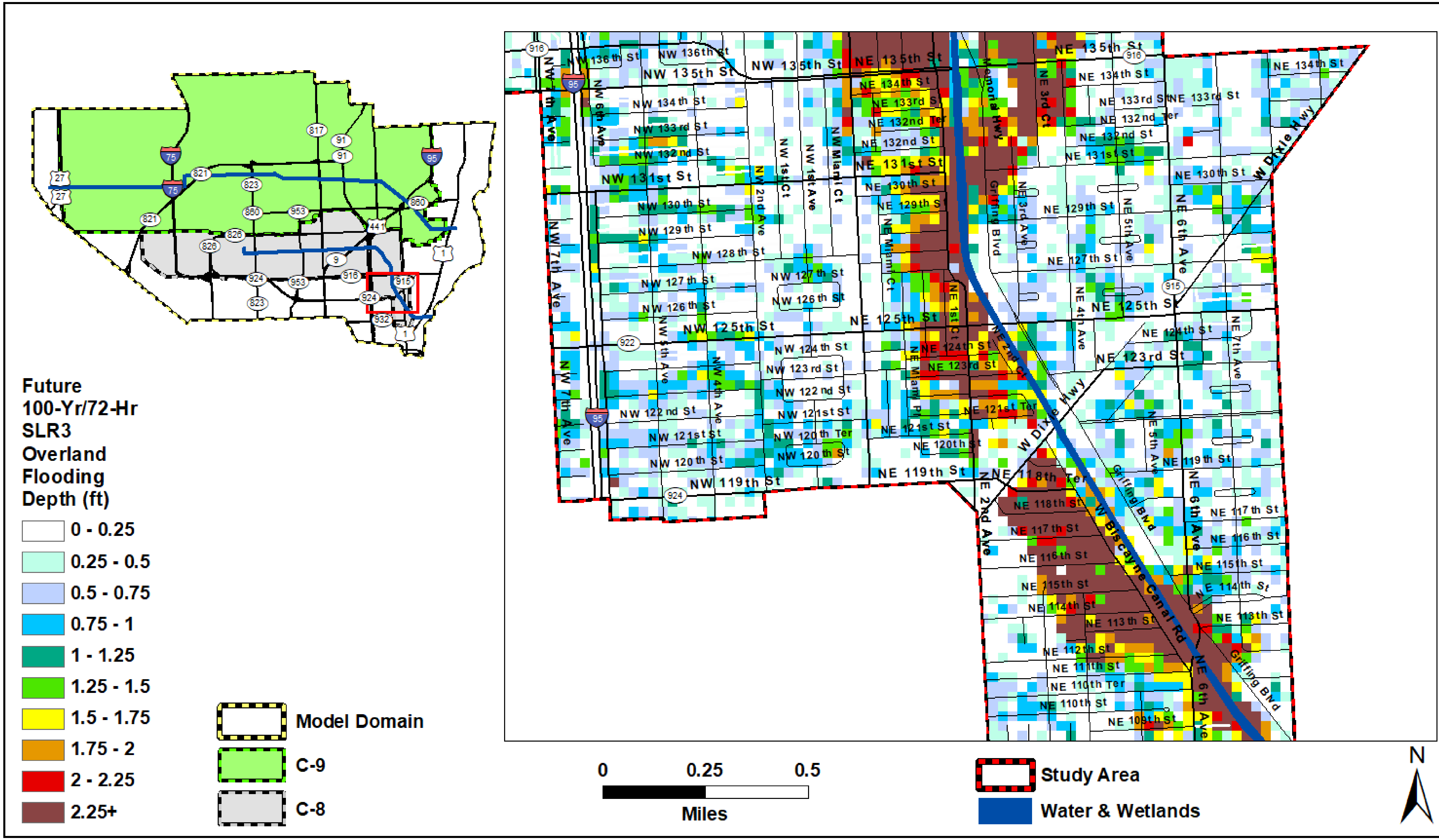

Figure 4.5-30: Up Close 100-Year Sea Level Rise 3 Flood Inundation Map for the C-8 Canal Between and NE 135th St (CR916) and NE 6th Ave (CR915)

4.5.9.2 Up-Close Flood Inundation Maps for the C-8 Canal Between North Miami Ave and NE 135th St (CR916)

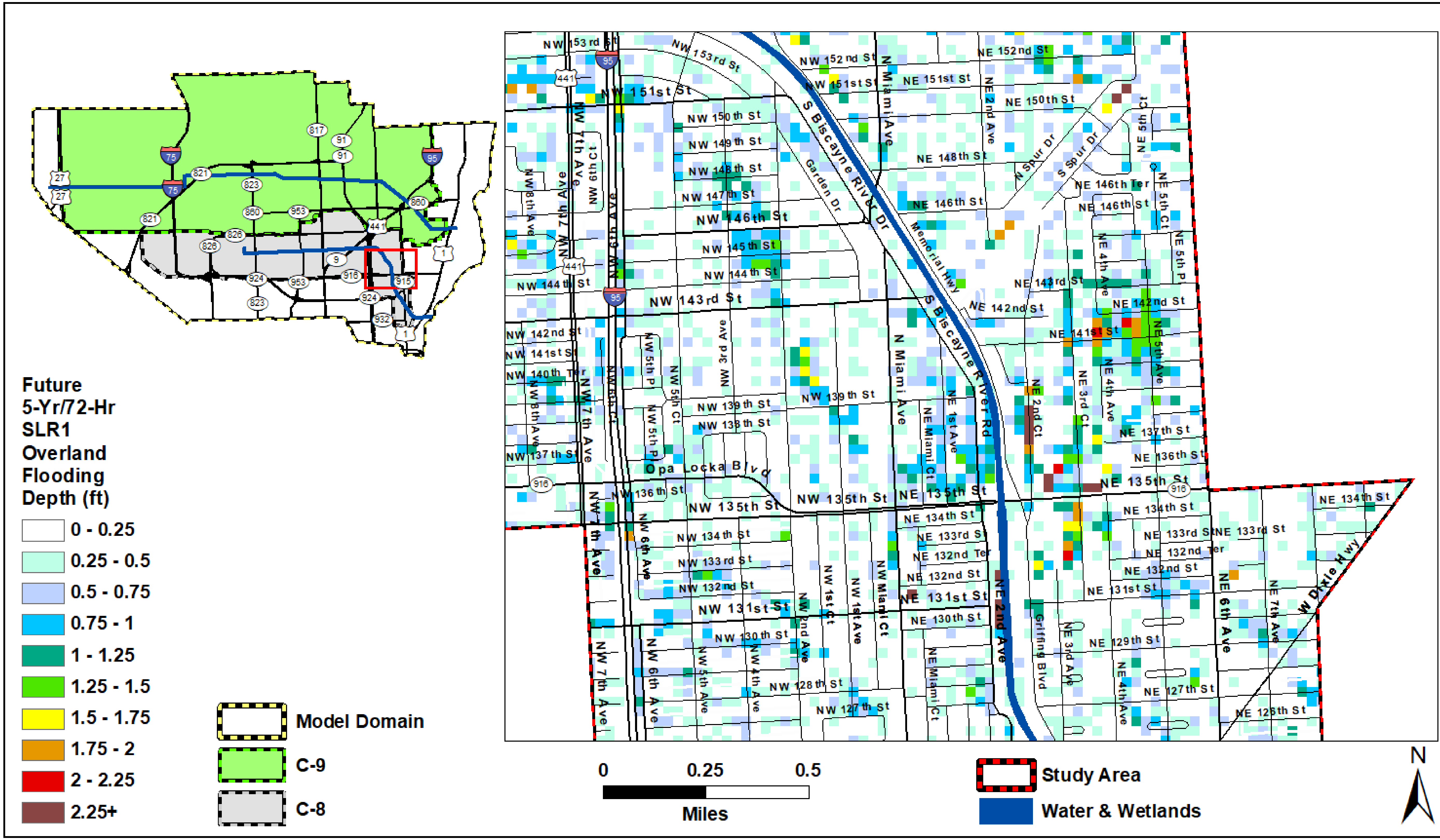

Figure 4.5-31: Up Close 5-Year Sea Level Rise 1 Flood Inundation Map for the C-8 Canal Between North Miami Ave and NE 135th St (CR916)

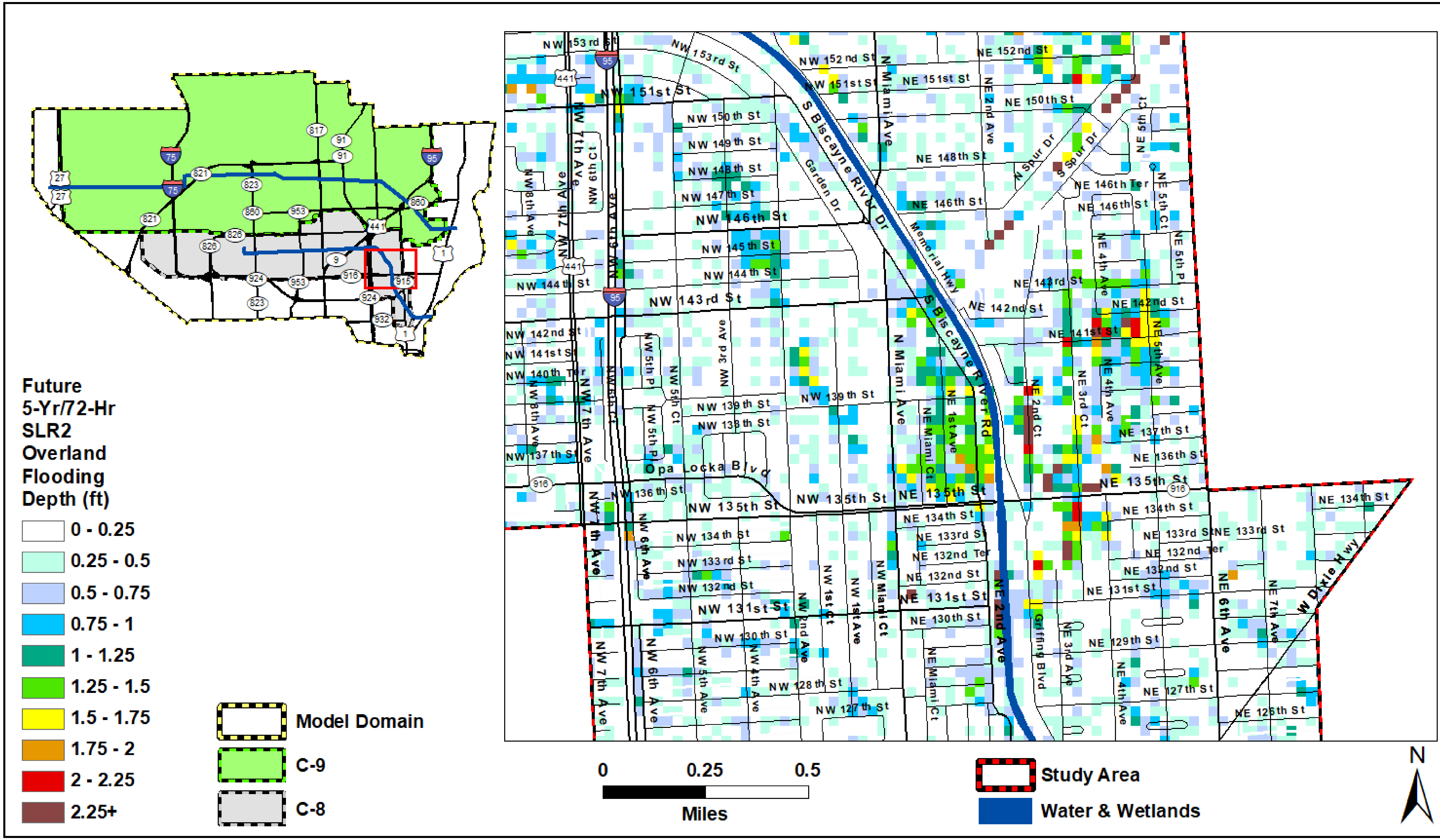

Figure 4.5-32: Up Close 5-Year Sea Level Rise 2 Flood Inundation Map for the C-8 Canal Between North Miami Ave and NE 135th St (CR916)

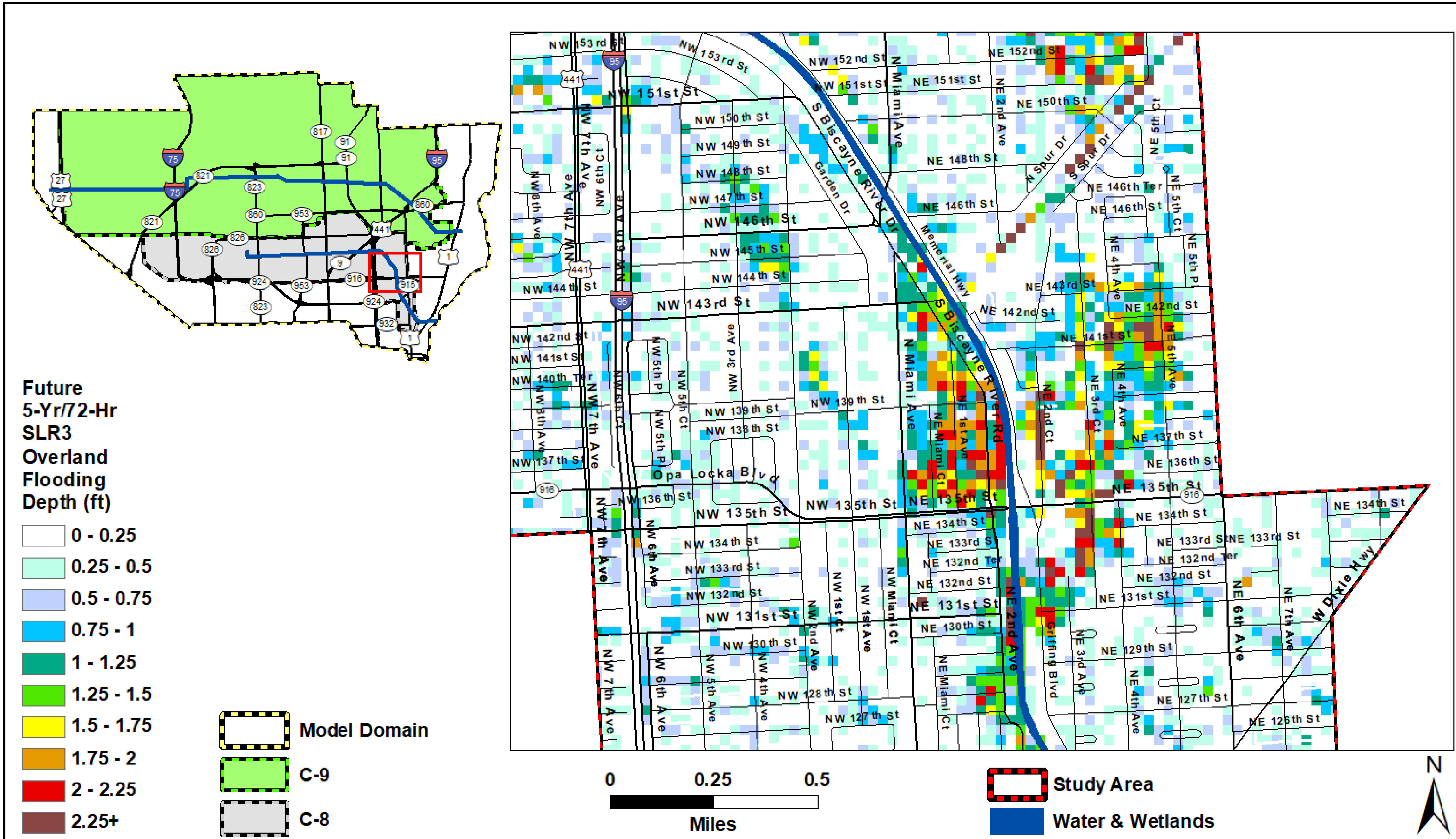

Figure 4.5-33: Up Close 5-Year Sea Level Rise 3 Flood Inundation Map for the C-8 Canal Between North Miami Ave and NE 135th St (CR916)

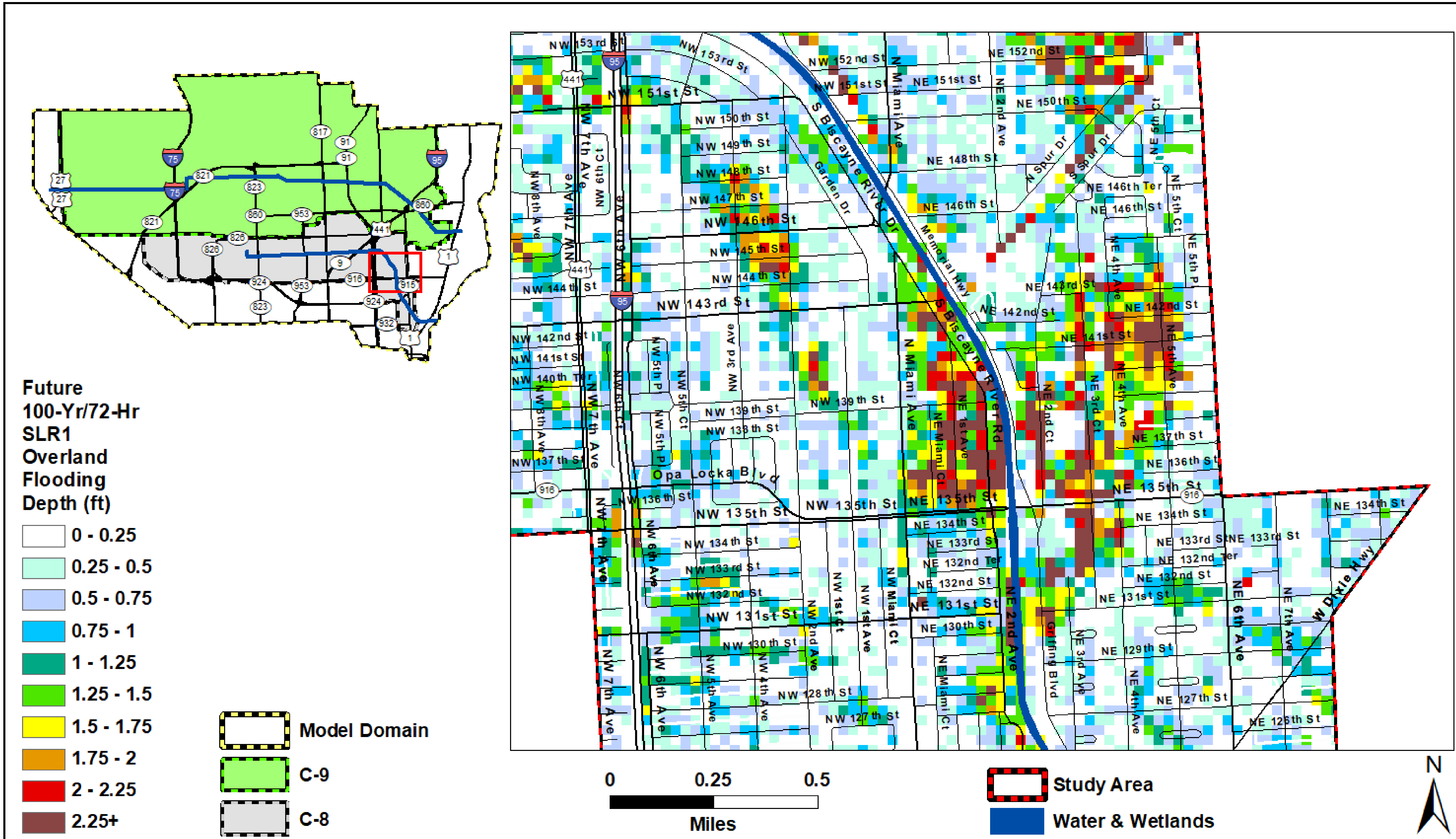

Figure 4.5-34: Up Close 100-Year Sea Level Rise 1 Flood Inundation Map for the C-8 Canal Between North Miami Ave and NE 135th St (CR916)

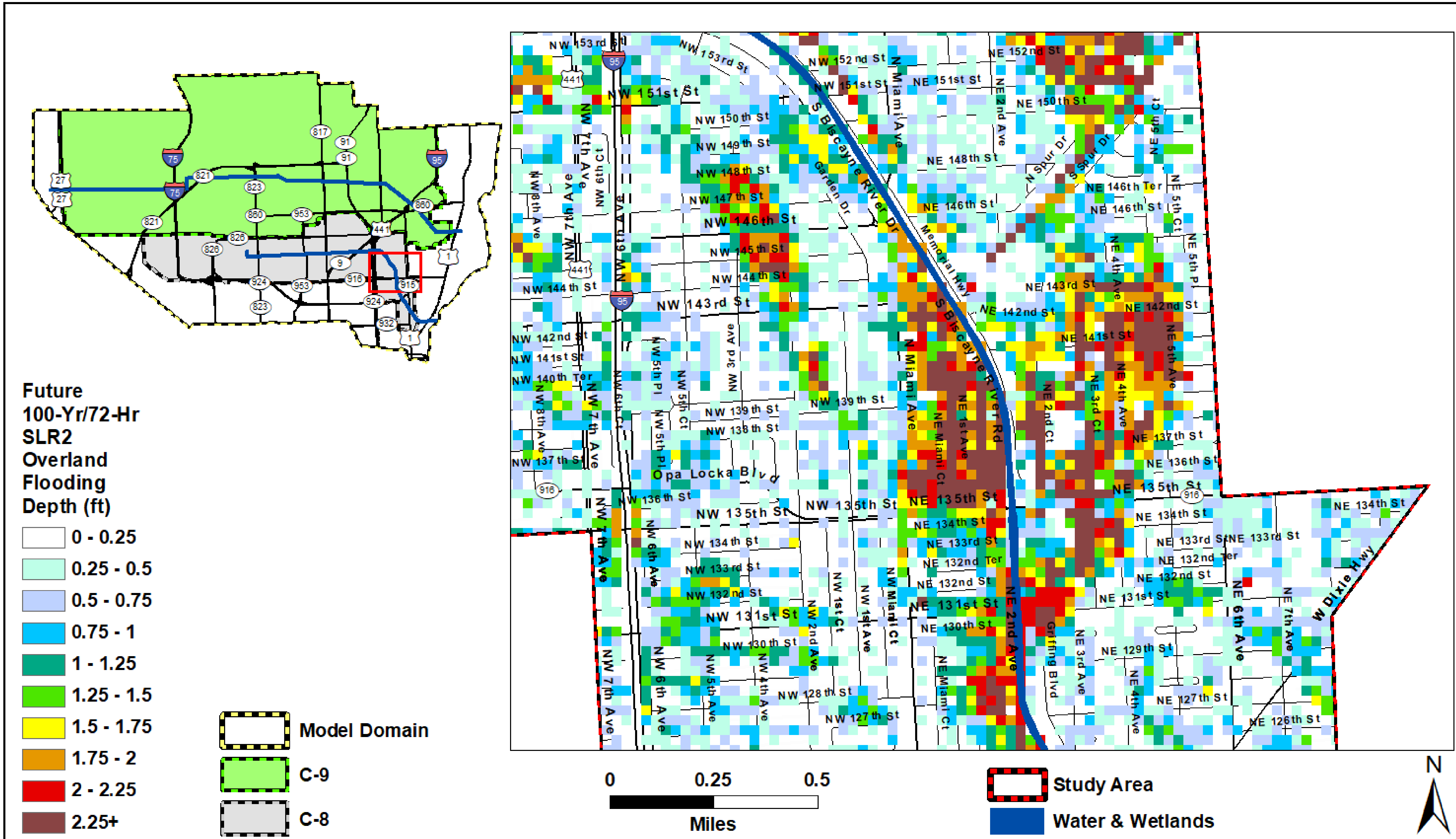

Figure 4.5-35: Up Close 100-Year Sea Level Rise 2 Flood Inundation Map for the C-8 Canal Between North Miami Ave and NE 135th St (CR916)

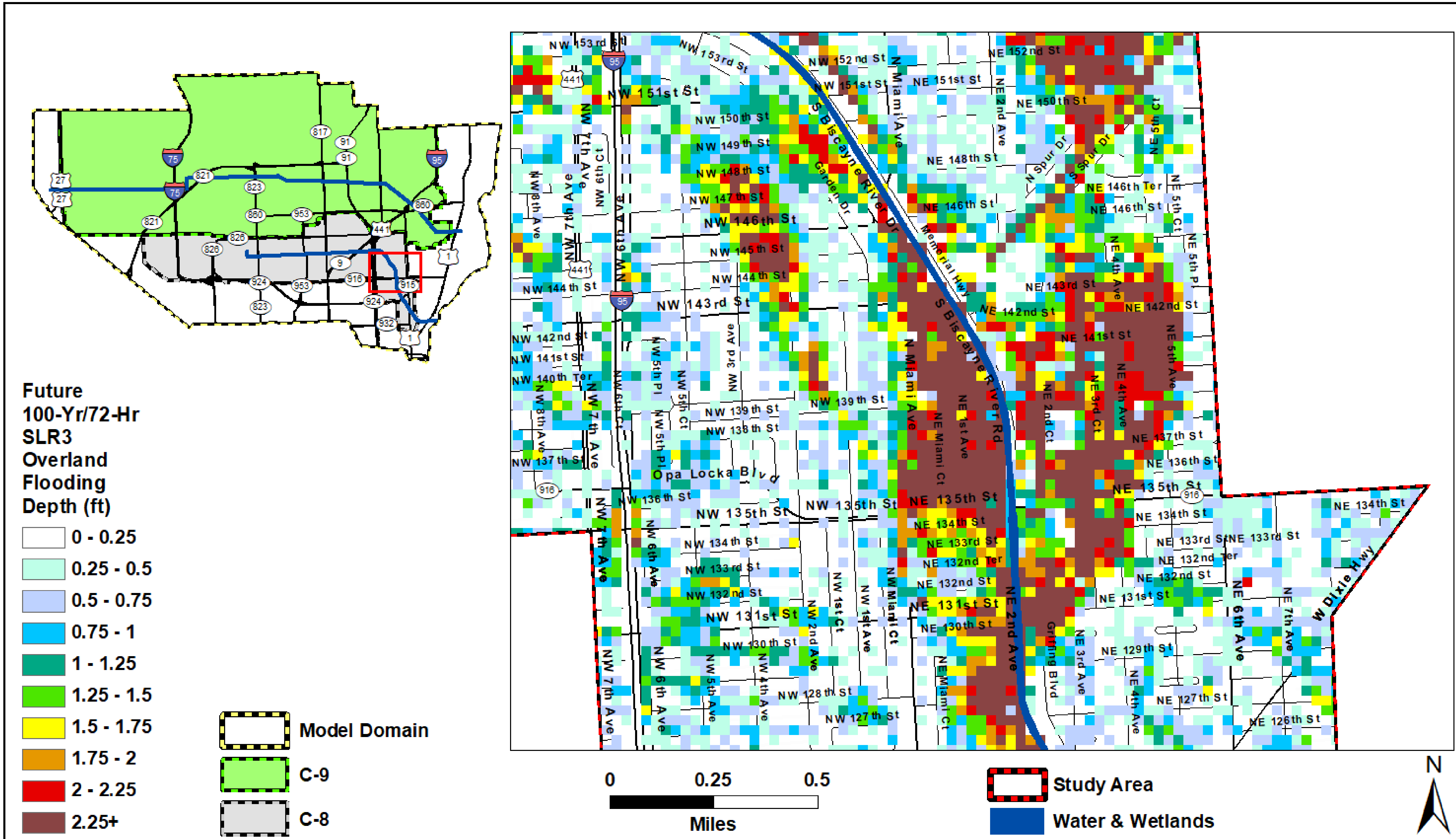

Figure 4.5-36: Up Close 100-Year Sea Level Rise 3 Flood Inundation Map for the C-8 Canal Between North Miami Ave and NE 135th St (CR916)

4.5.9.3 Up-Close Flood Inundation Maps for the C-8 Canal Near Opa Locka Canal

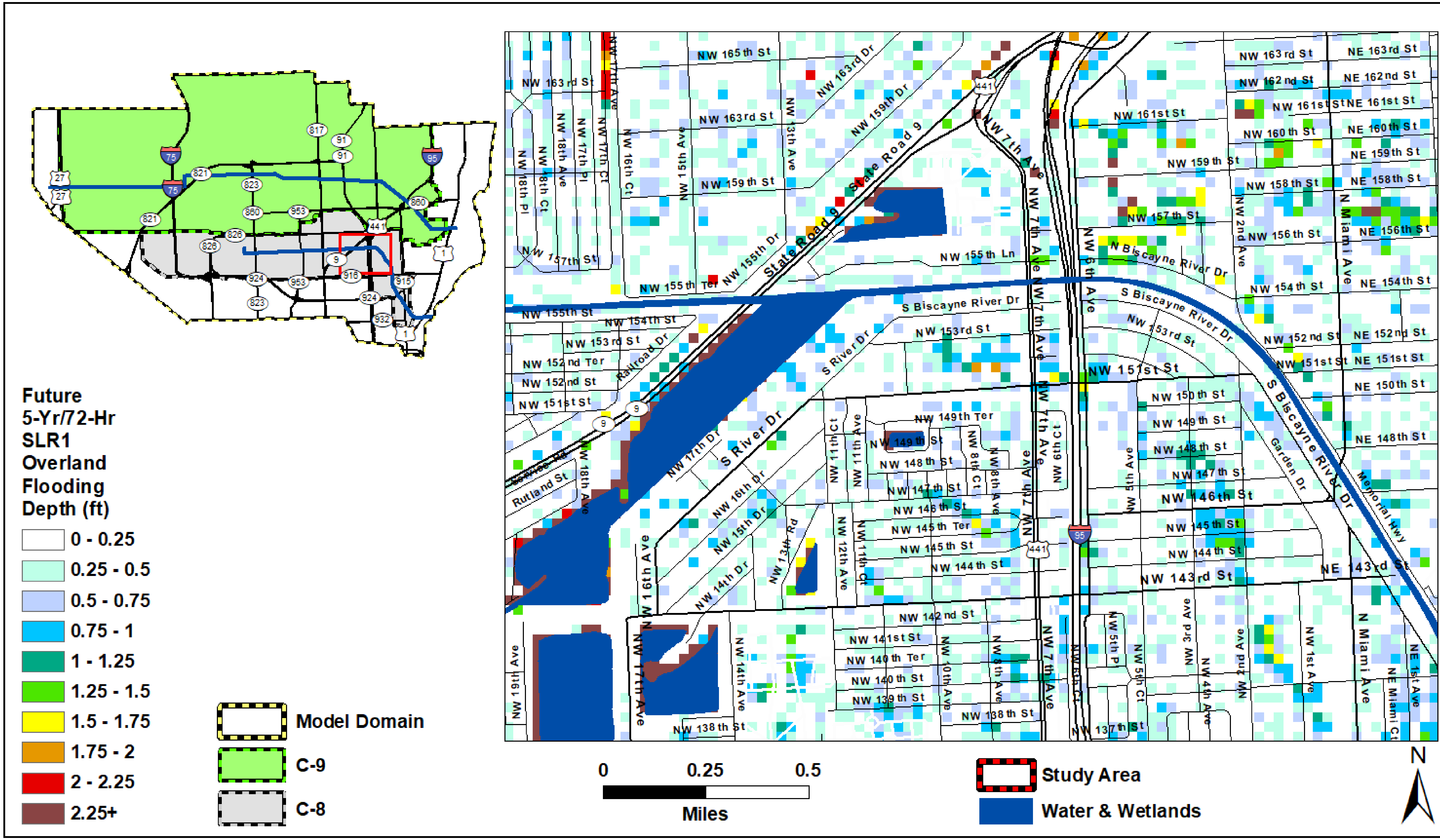

Figure 4.5-37: Up Close 5-Year Sea Level Rise 1 Flood Inundation Map for the C-8 Canal Near Opa Locka Canal

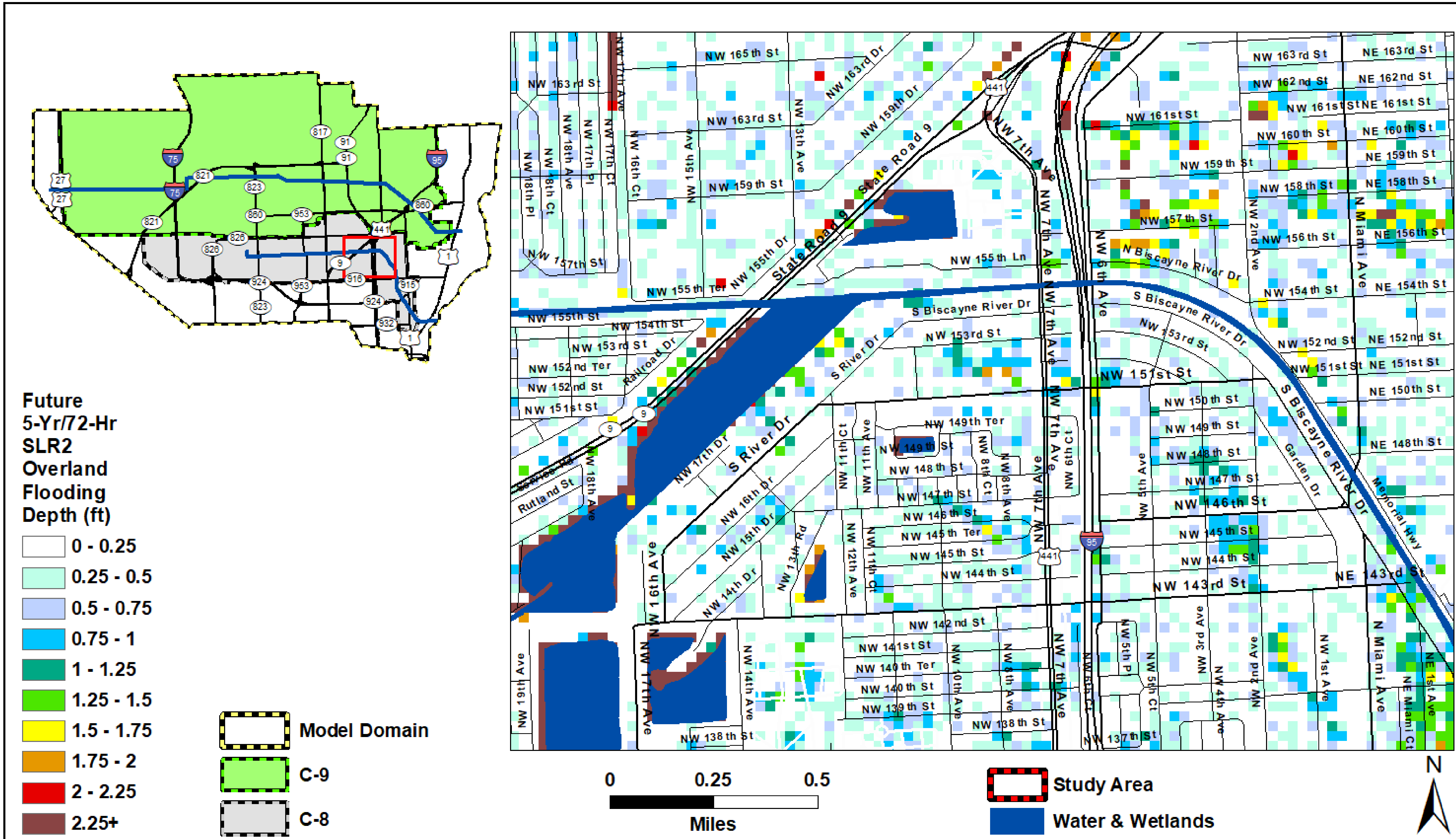

Figure 4.5-38: Up Close 5-Year Sea Level Rise 2 Flood Inundation Map for the C-8 Canal Near Opa Locka Canal

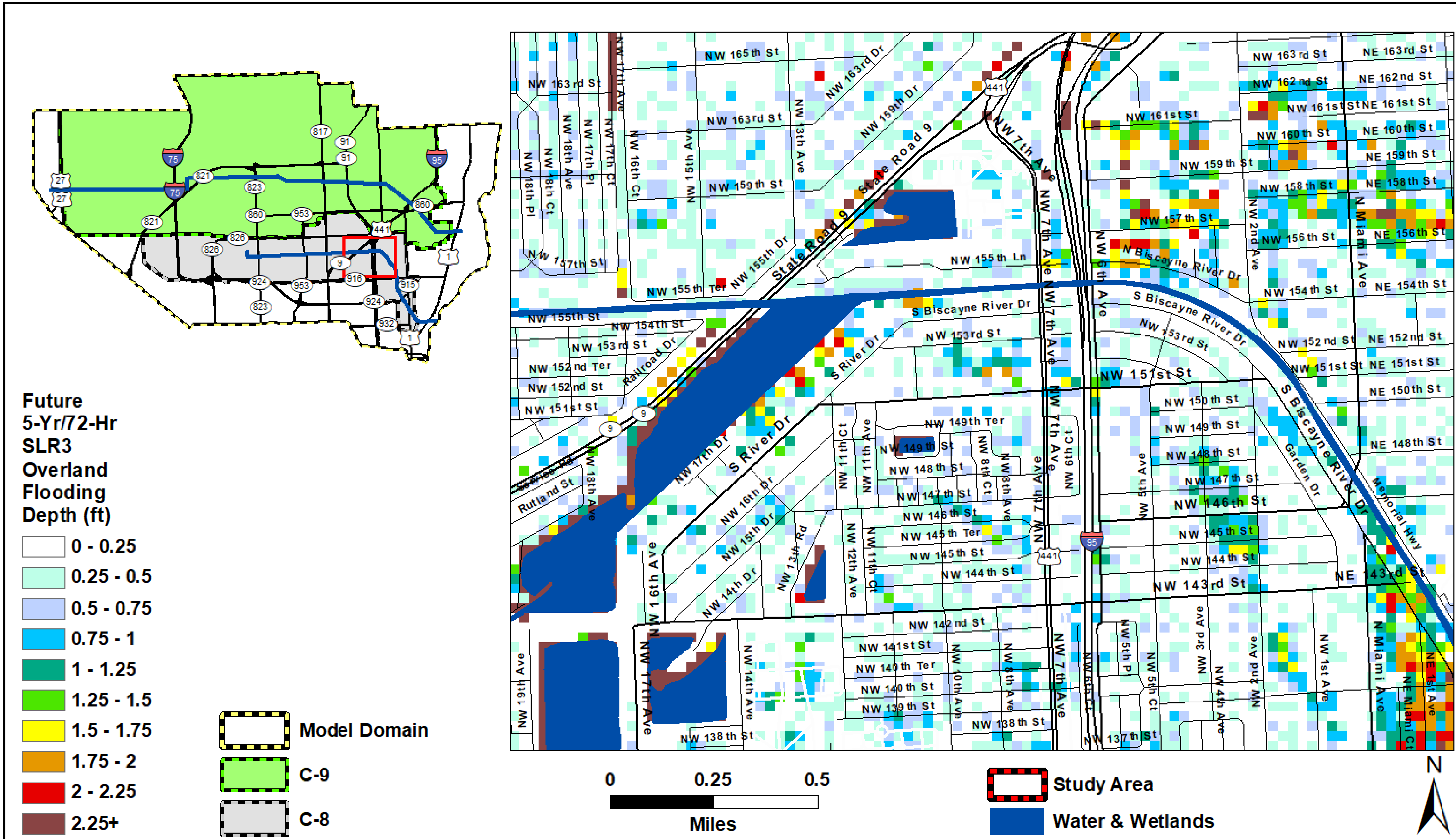

Figure 4.5-39: Up Close 5-Year Sea Level Rise 3 Flood Inundation Map for the C-8 Canal Near Opa Locka Canal

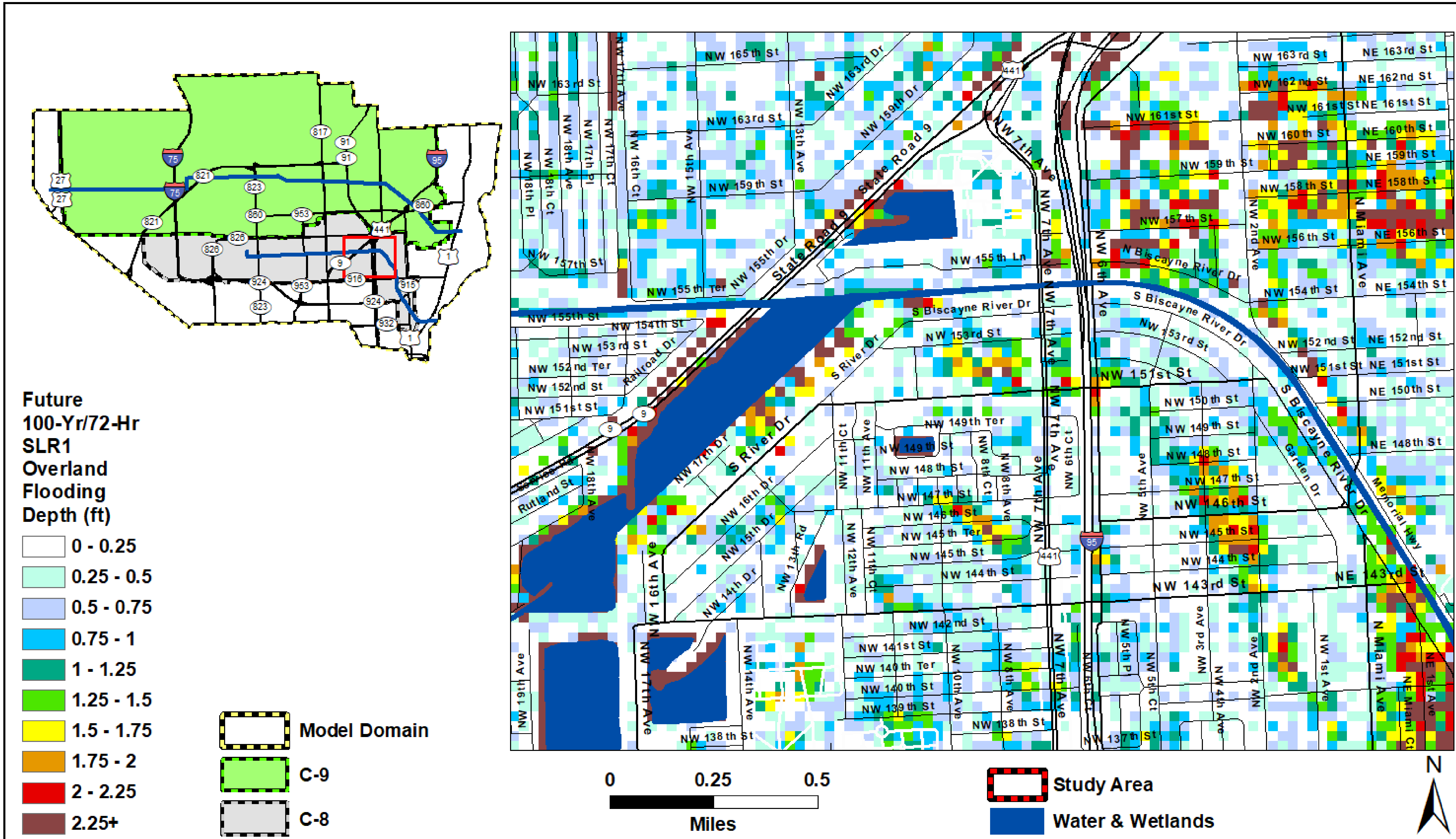

Figure 4.5-40: Up Close 100-Year Sea Level Rise 1 Flood Inundation Map for the C-8 Canal Near Opa Locka Canal

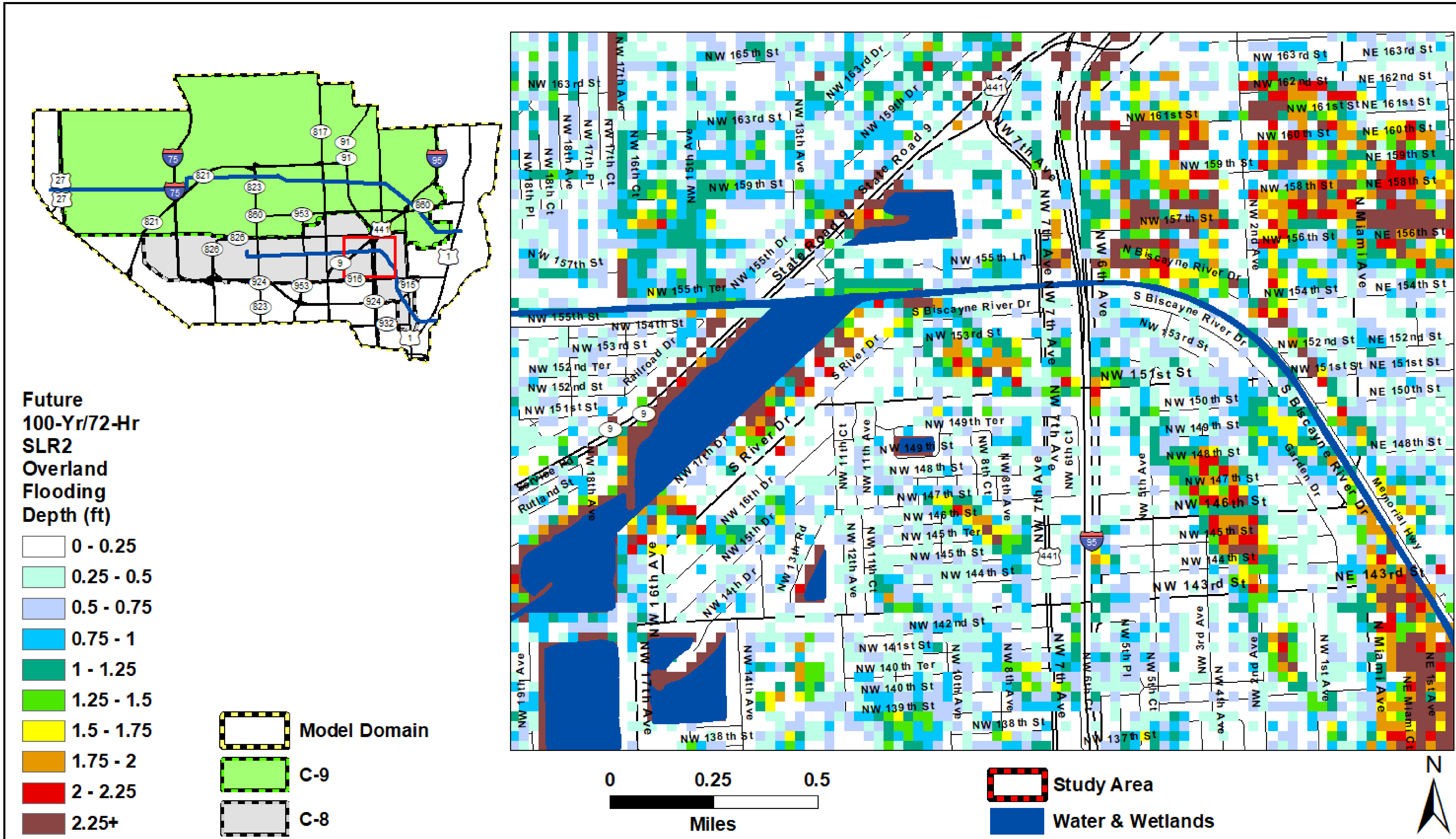

Figure 4.5-41: Up Close 100-Year Sea Level Rise 2 Flood Inundation Map for the C-8 Canal Near Opa Locka Canal

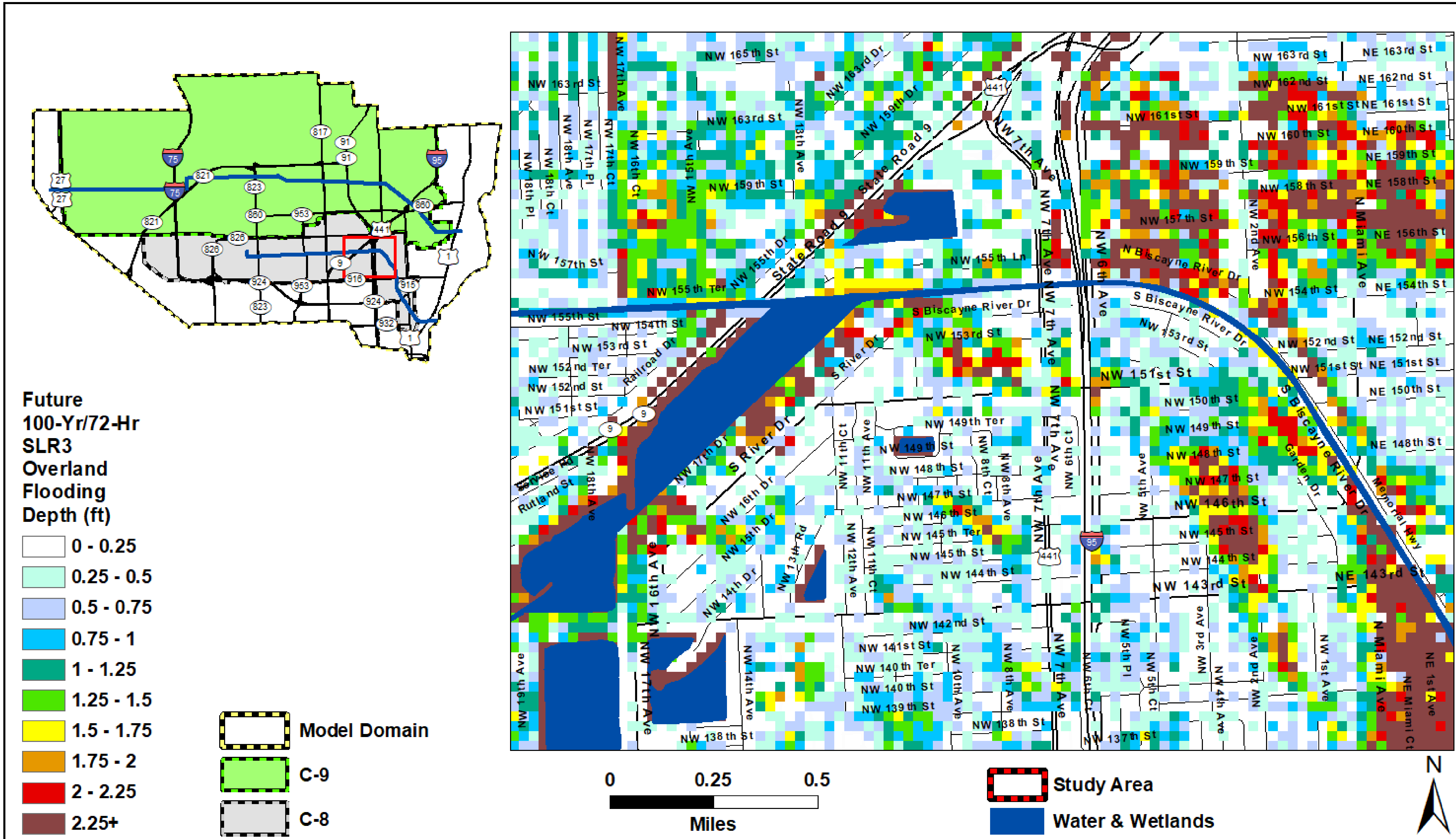

Figure 4.5-42: Up Close 100-Year Sea Level Rise 3 Flood Inundation Map for the C-8 Canal Near Opa Locka Canal

4.5.9.4 Up-Close Flood Inundation Maps for the C-9 Canal Between I-95 and S-29

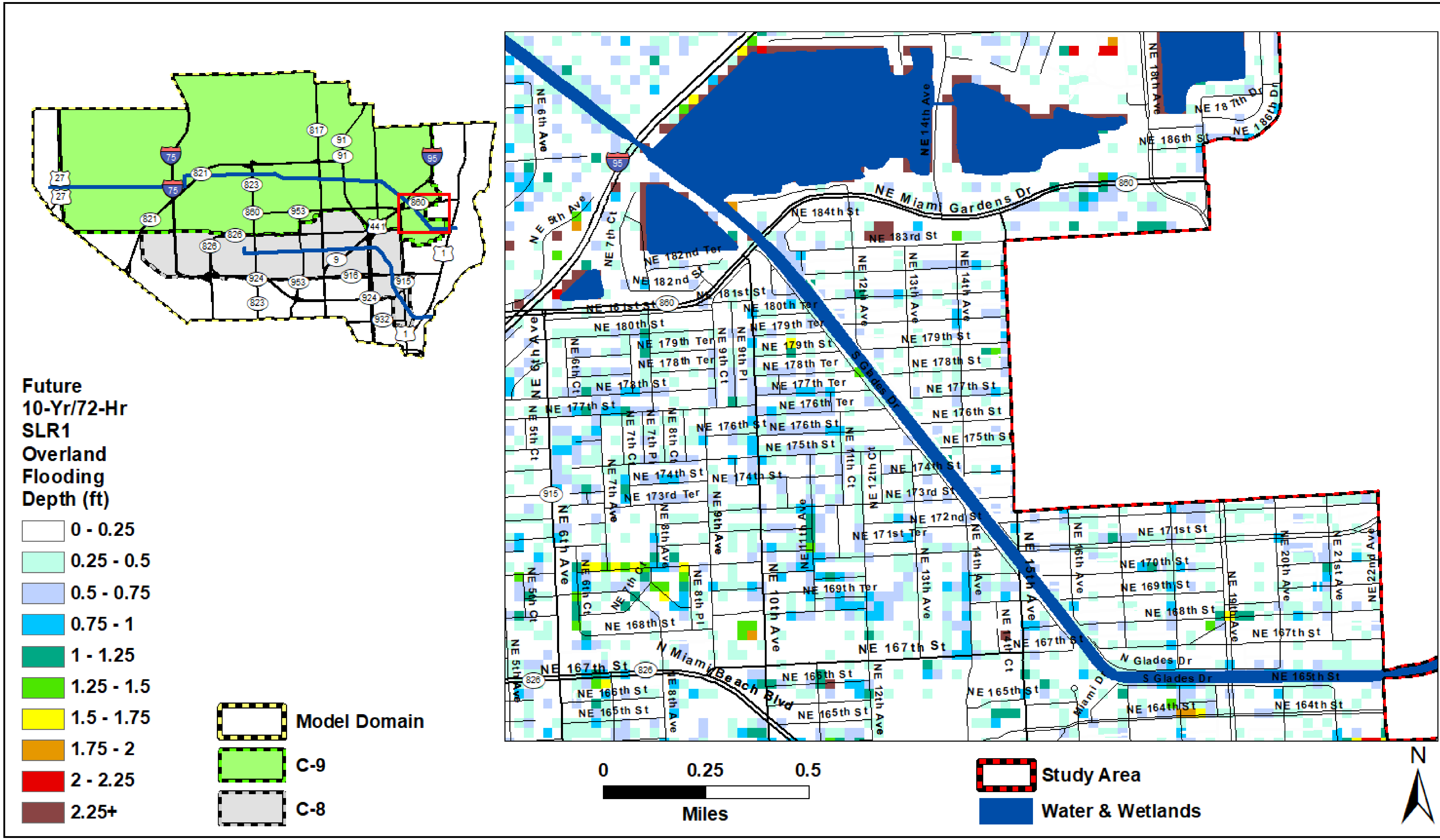

Figure 4.5-43: Up Close 10-Year Design Storm Sea Level Rise 1 Flood Inundation Map for the C-9 Canal Between I-95 and S-29

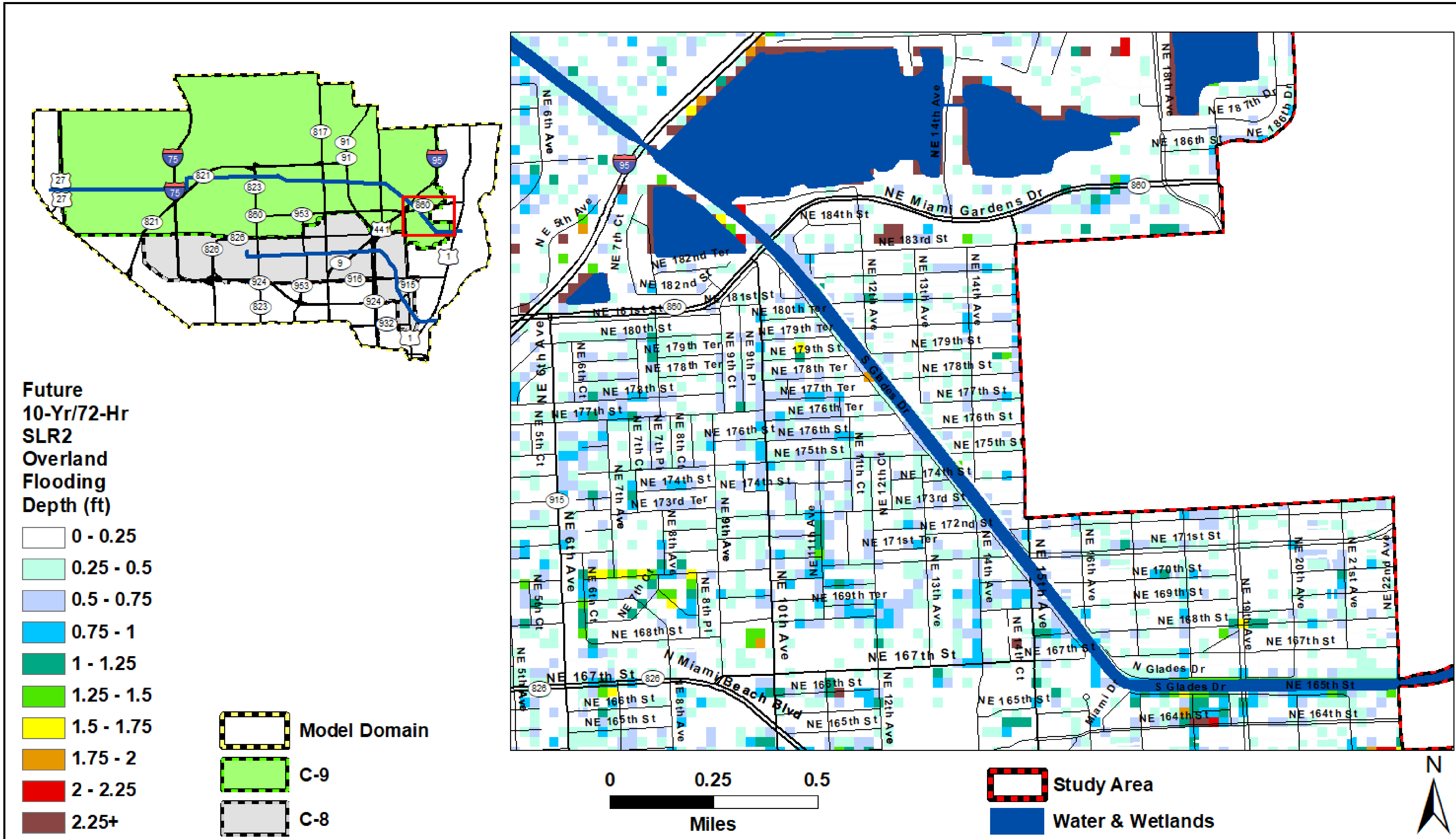

Figure 4.5-44: Up Close 10-Year Design Storm Sea Level Rise 2 Flood Inundation Map for the C-9 Canal Between I-95 and S-29

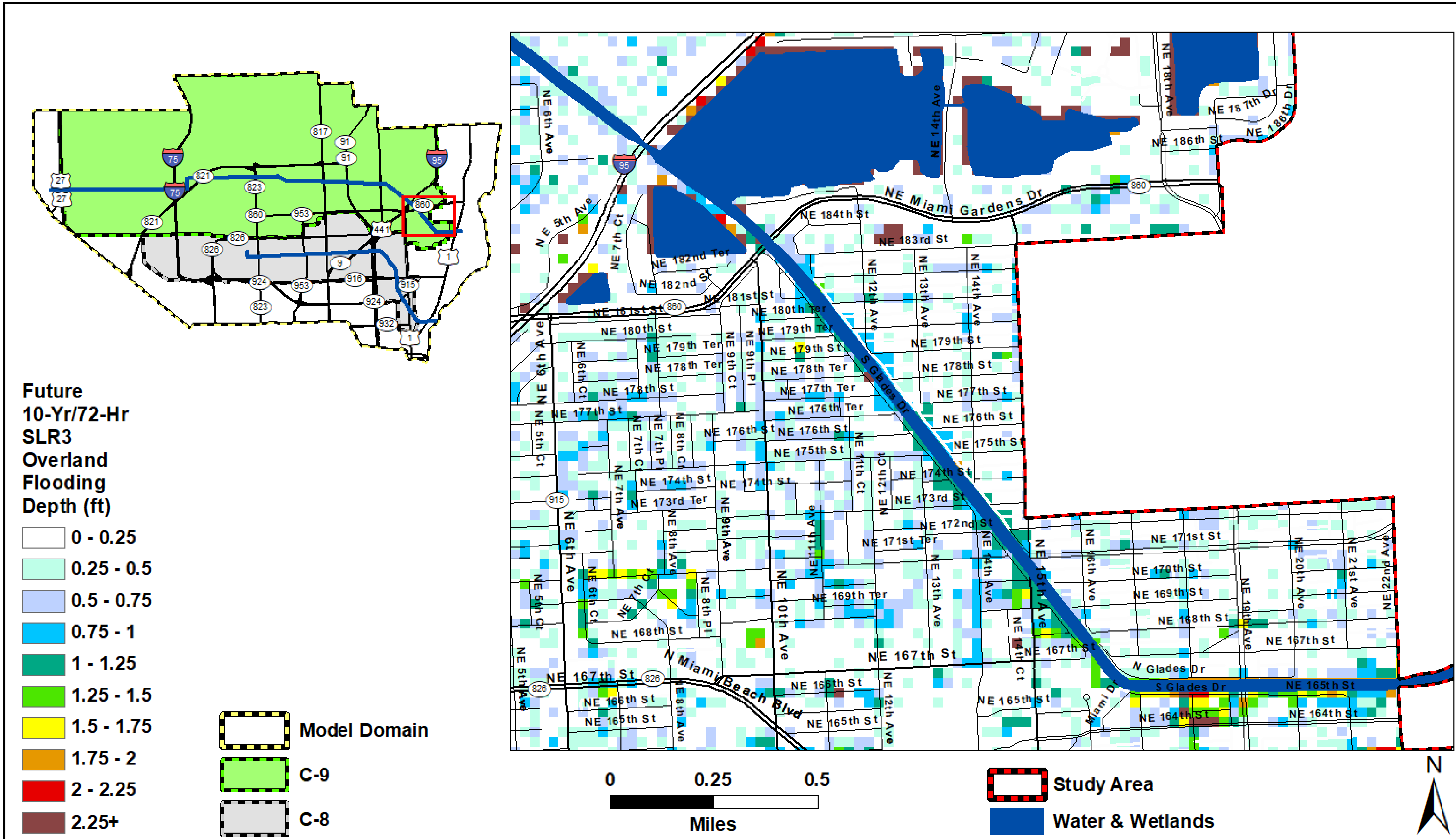

Figure 4.5-45: Up Close 10-Year Design Storm Sea Level Rise 3 Flood Inundation Map for the C-9 Canal Between I-95 and S-29

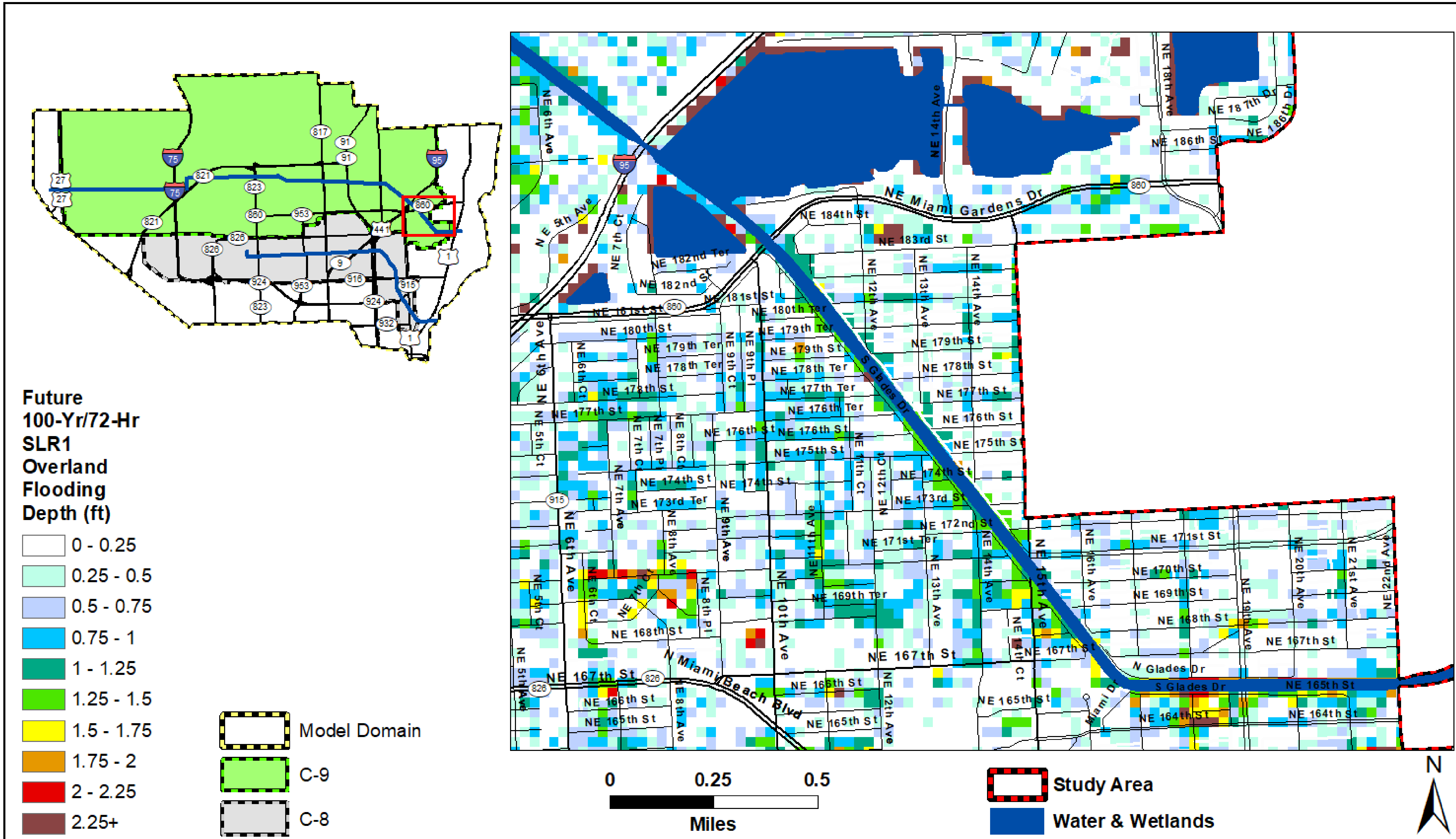

Figure 4.5-46: Up Close 100-Year Design Storm Sea Level Rise 1 Flood Inundation Map for the C-9 Canal Between I-95 and S-29

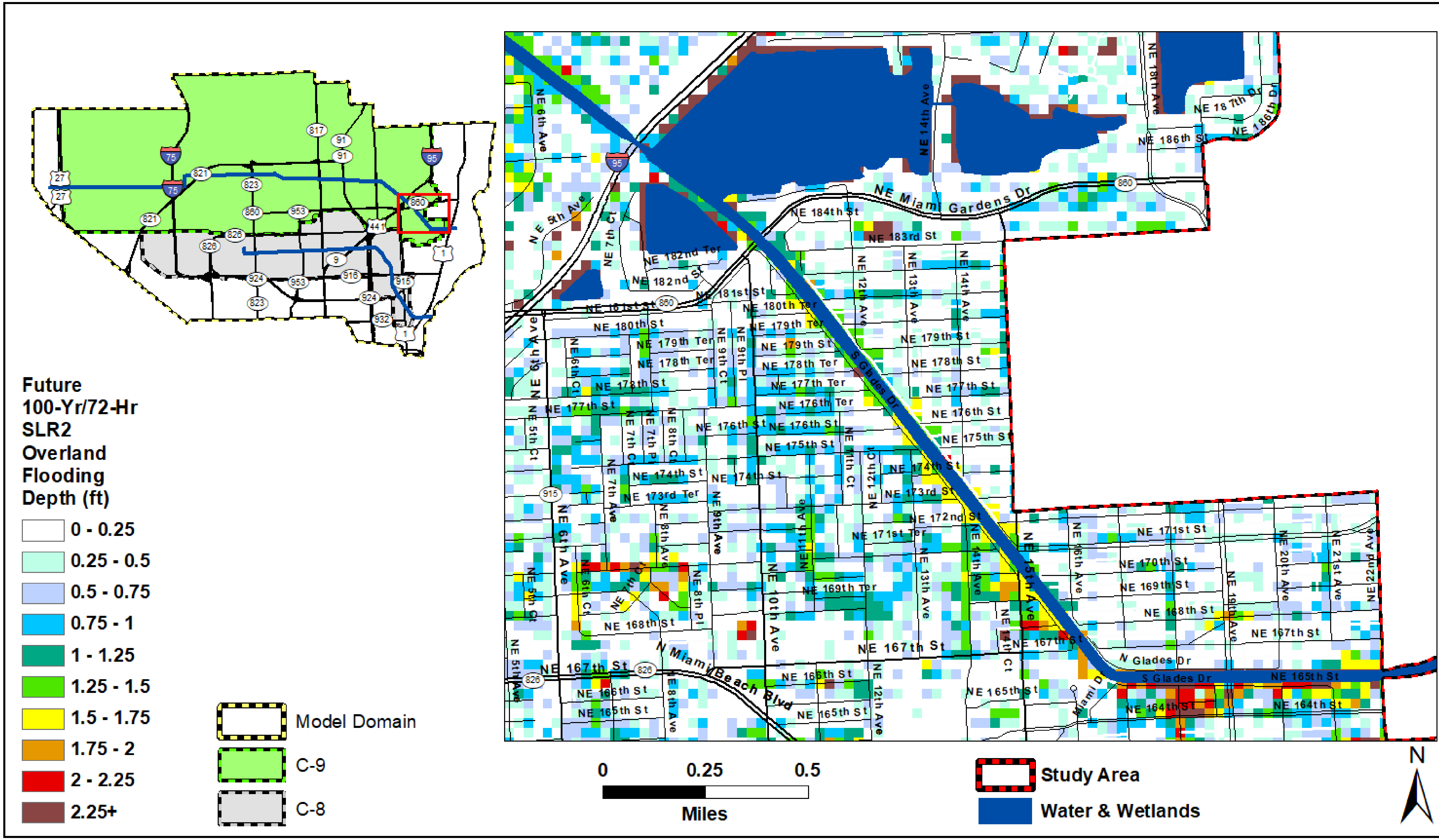

Figure 4.5-47: Up Close 100-Year Design Storm Sea Level Rise 2 Flood Inundation Map for the C-9 Canal Between I-95 and S-29

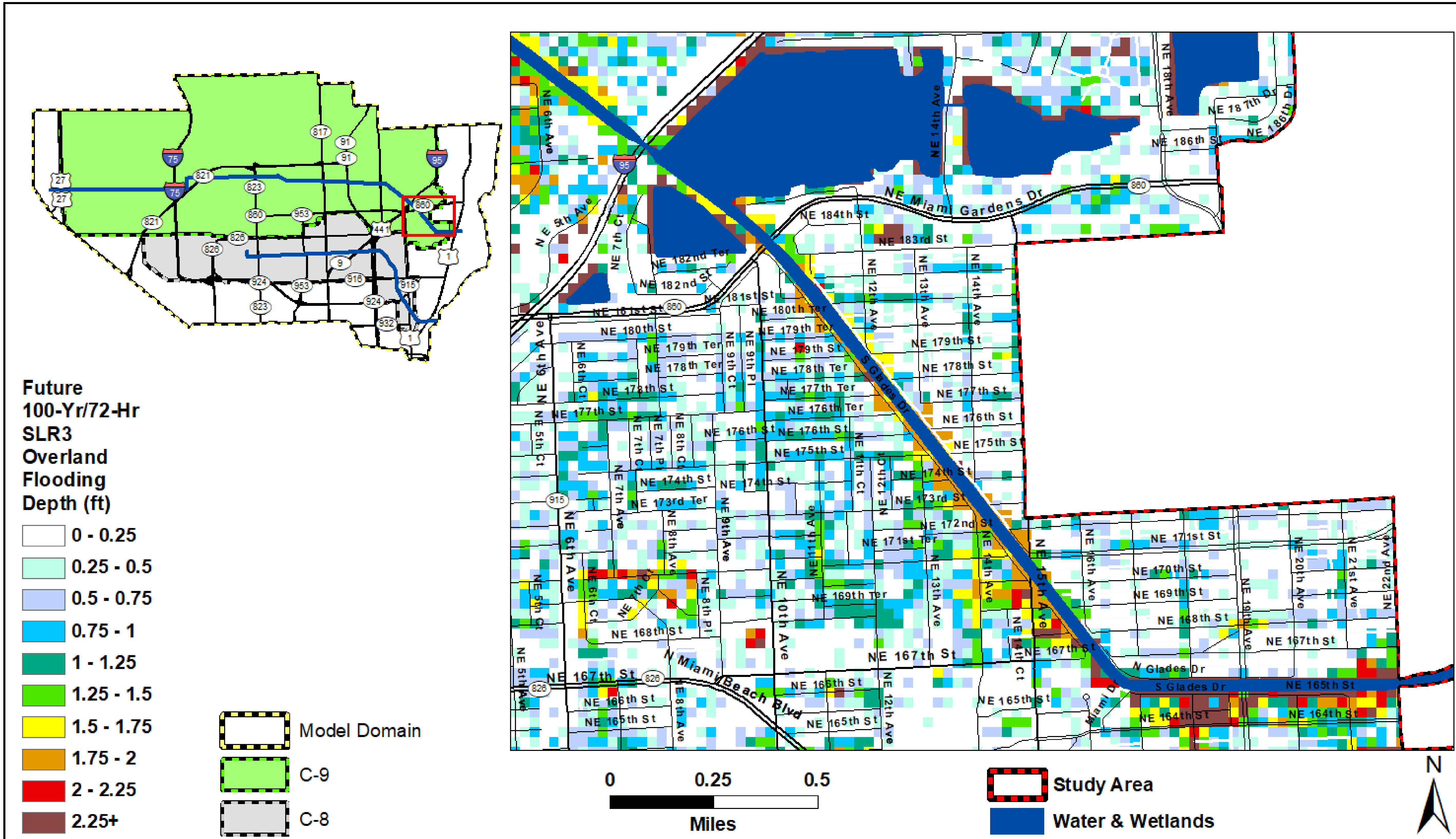

Figure 4.5-48: Up Close 100-Year Design Storm Sea Level Rise 3 Flood Inundation Map for the C-9 Canal Between I-95 and S-29

4.5.9.5 Up-Close Flood Inundation Maps for the C-9 Canal Near US Hwy 441

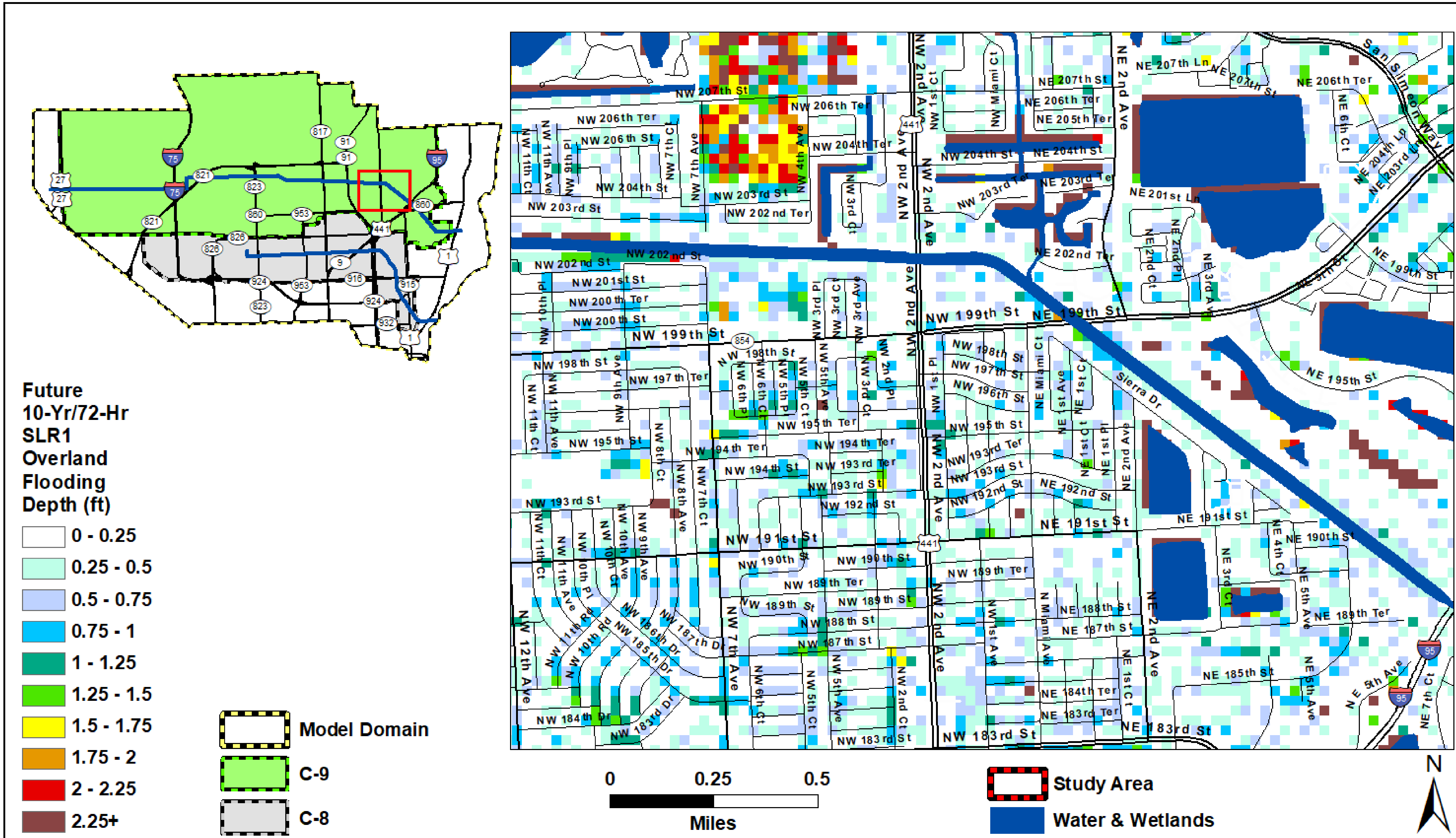

Figure 4.5-49: Up Close 10-Year Sea Level Rise 1 Flood Inundation Map for the C-9 Canal Near US Hwy 441

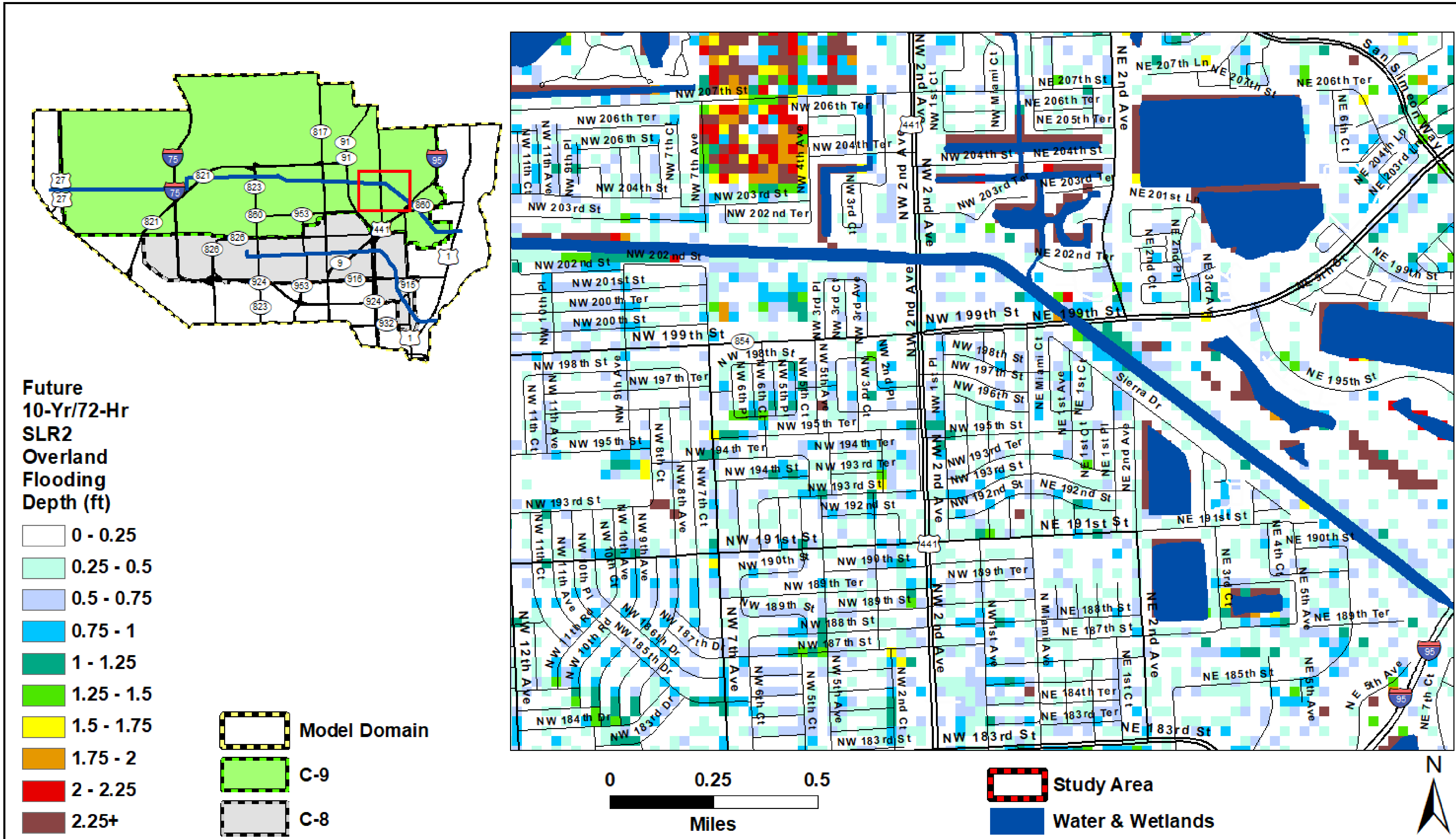

Figure 4.5-50: Up Close 10-Year Sea Level Rise 2 Flood Inundation Map for the C-9 Canal Near US Hwy 441

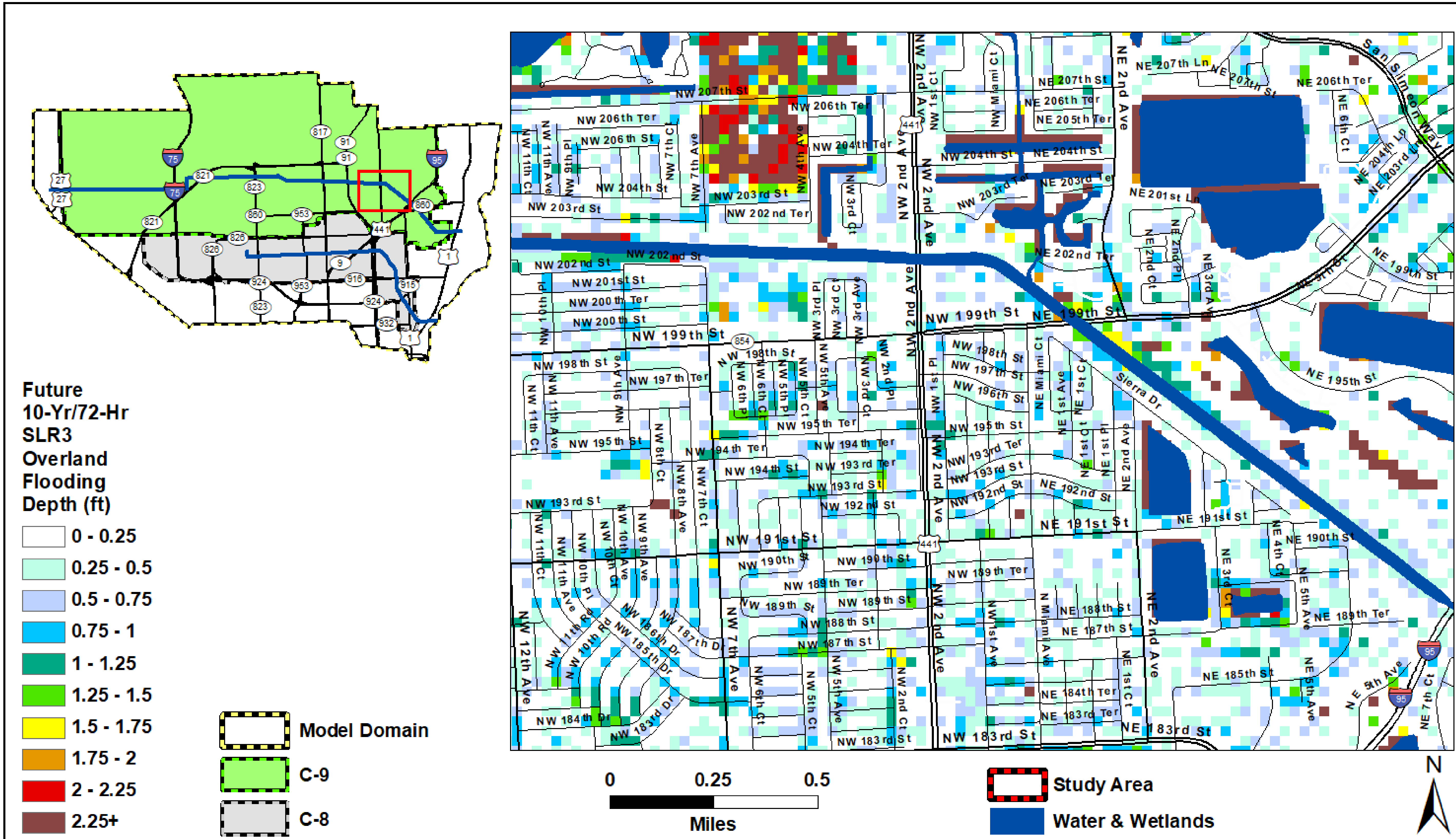

Figure 4.5-51: Up Close 10-Year Sea Level Rise 3 Flood Inundation Map for the C-9 Canal Near US Hwy 441

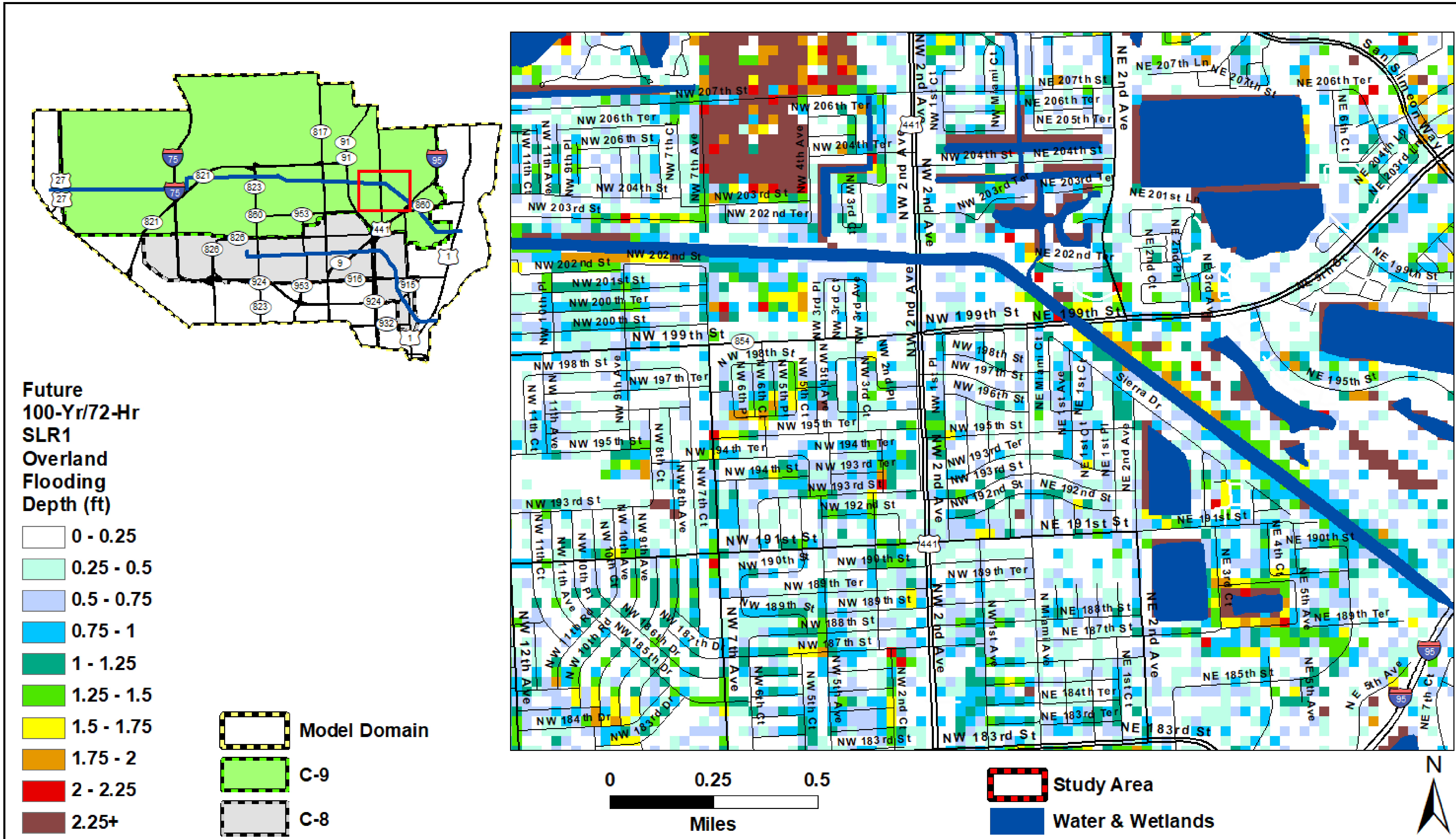

Figure 4.5-52: Up Close 100-Year Sea Level Rise 1 Flood Inundation Map for the C-9 Canal Near US Hwy 441

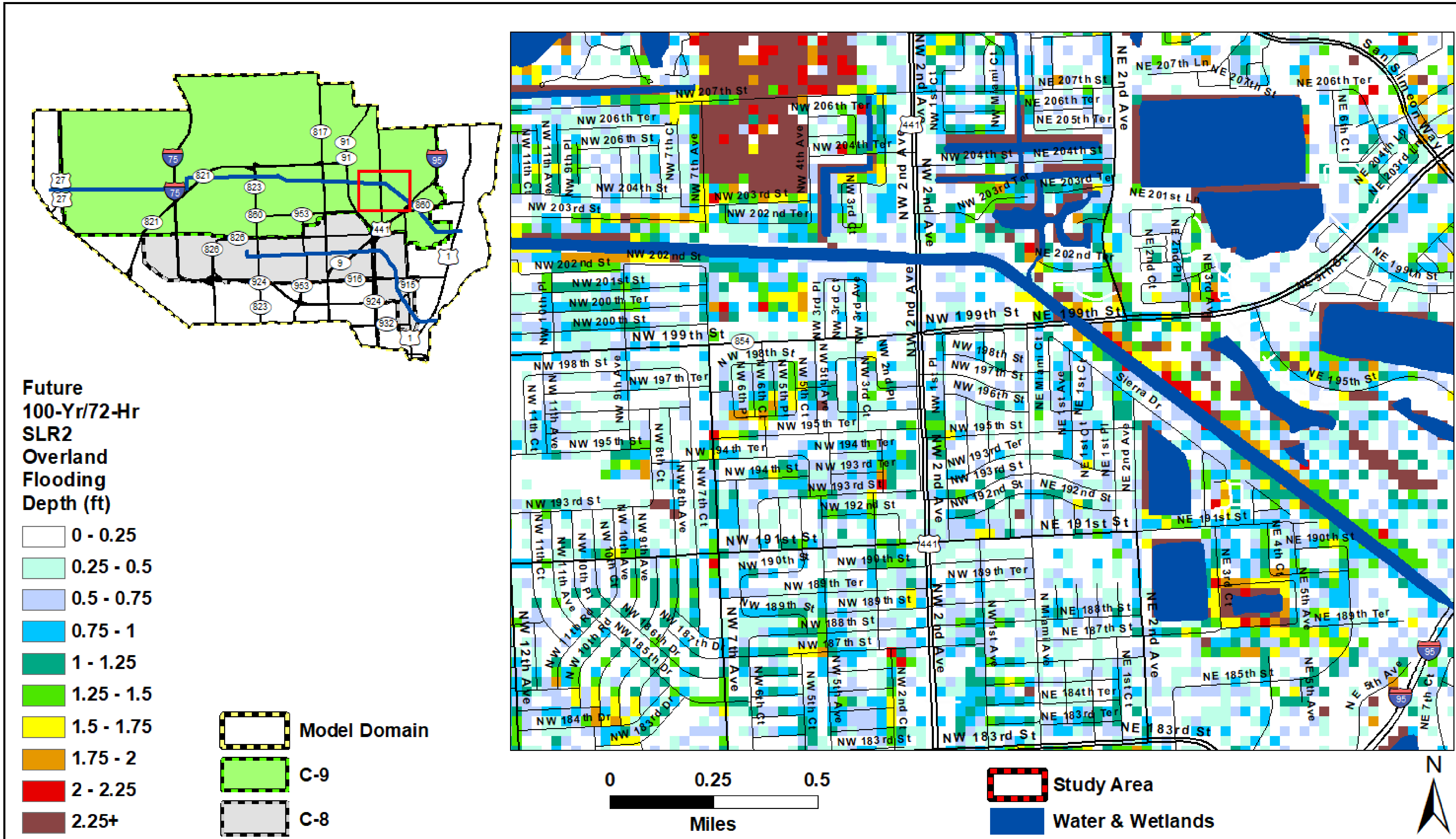

Figure 4.5-53: Up Close 100-Year Sea Level Rise 2 Flood Inundation Map for the C-9 Canal Near US Hwy 441

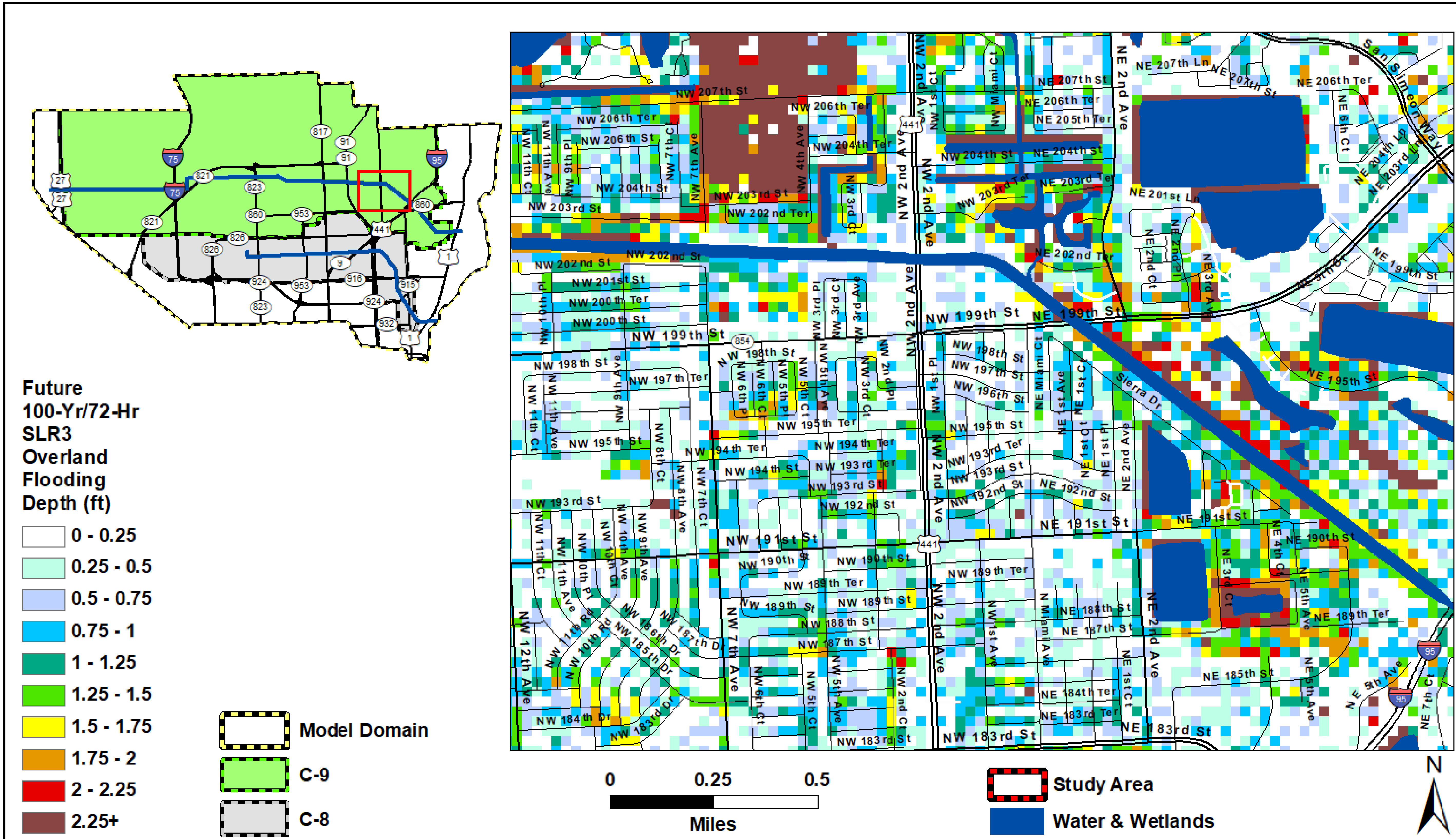

Figure 4.5-54: Up Close 100-Year Sea Level Rise 3 Flood Inundation Map for the C-9 Canal Near US Hwy 441

4.5.9.6 Up-Close Flood Inundation Maps for the C-9 Canal Near Ronald Reagan Turnpike

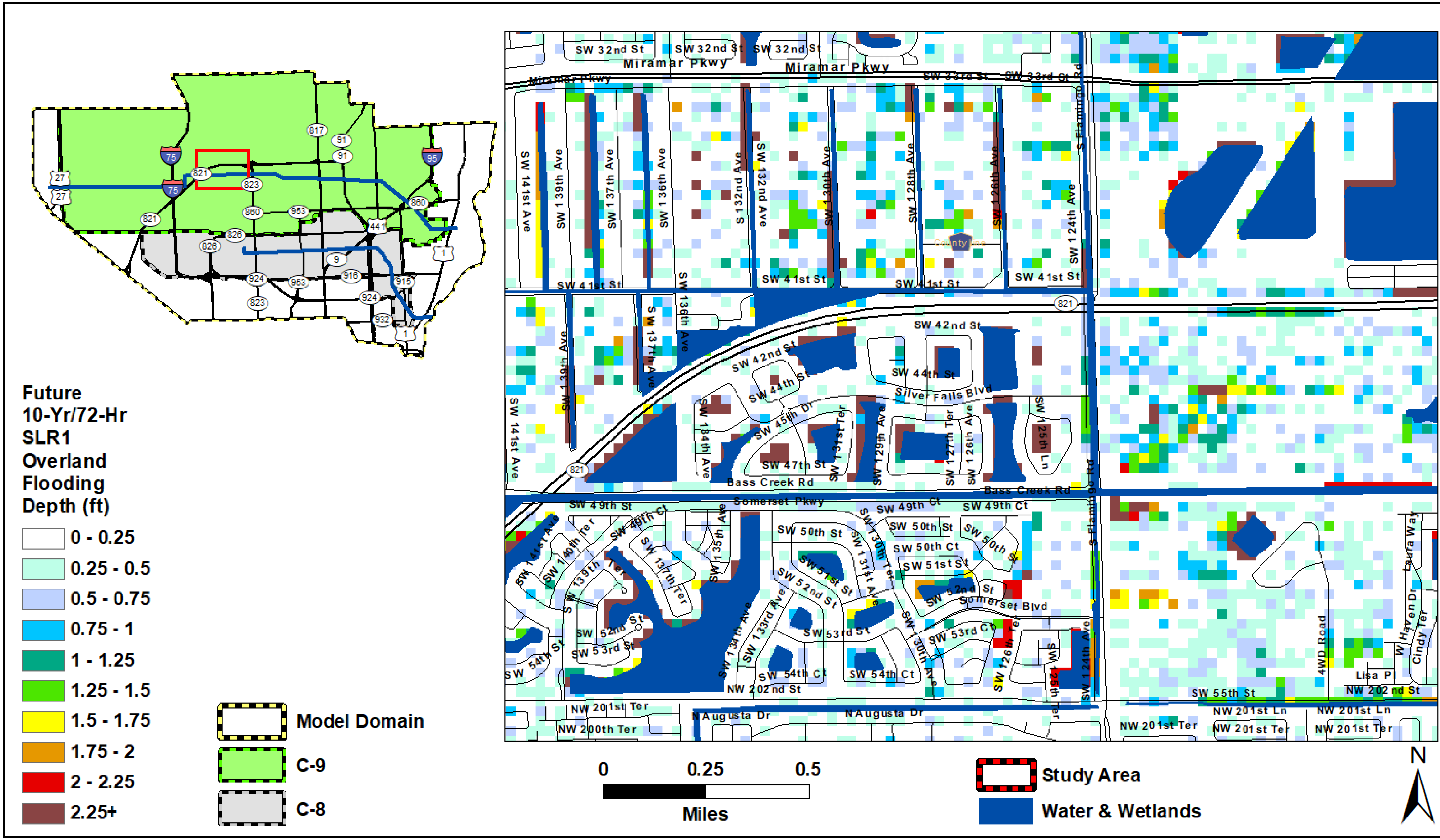

Figure 4.5-55: Up Close 10-Year Sea Level Rise 1 Flood Inundation Map for the C-9 Canal Near Ronald Reagan Turnpike

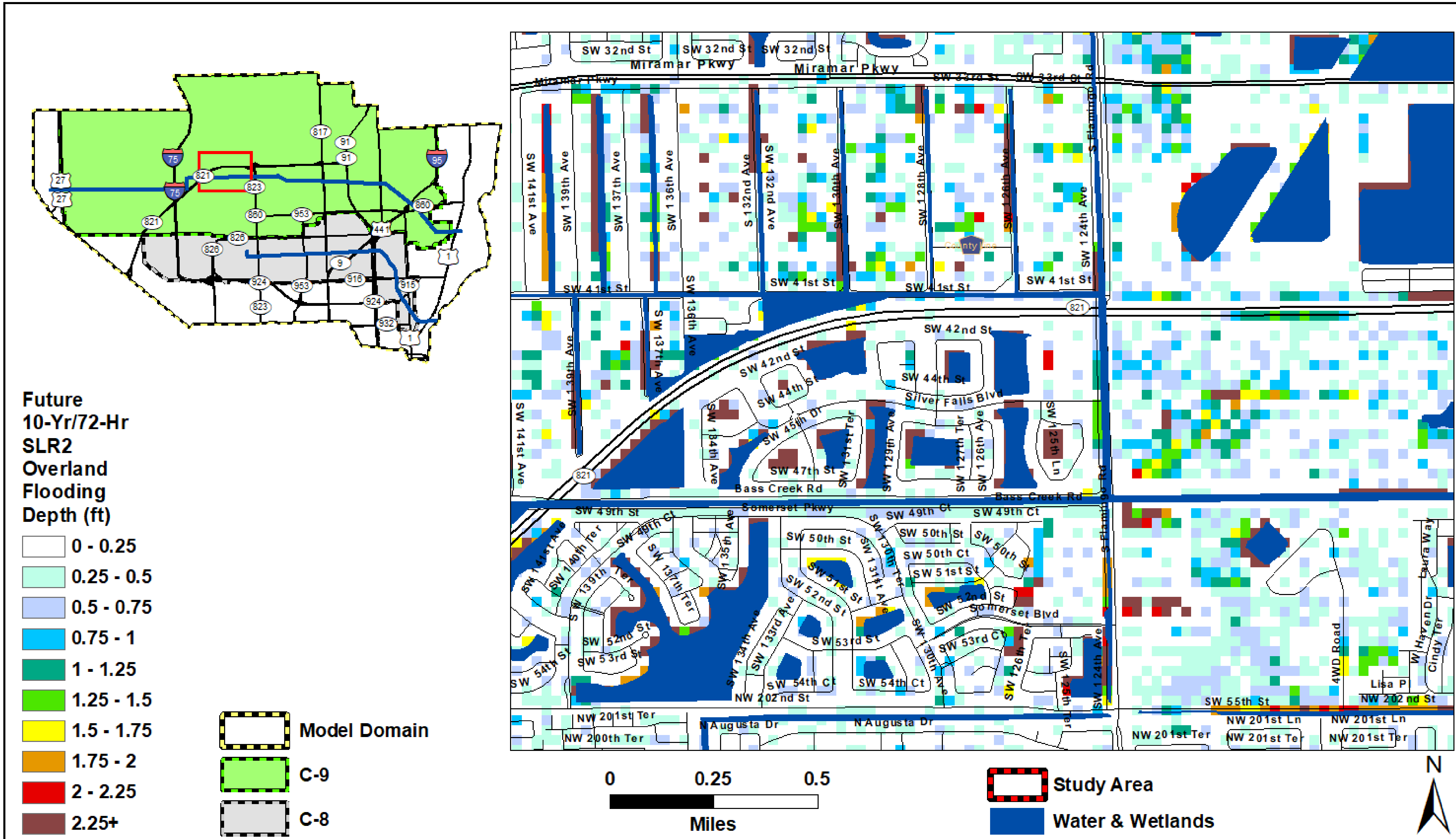

Figure 4.5-56: Up Close 10-Year Sea Level Rise 2 Flood Inundation Map for the C-9 Canal Near Ronald Reagan Turnpike

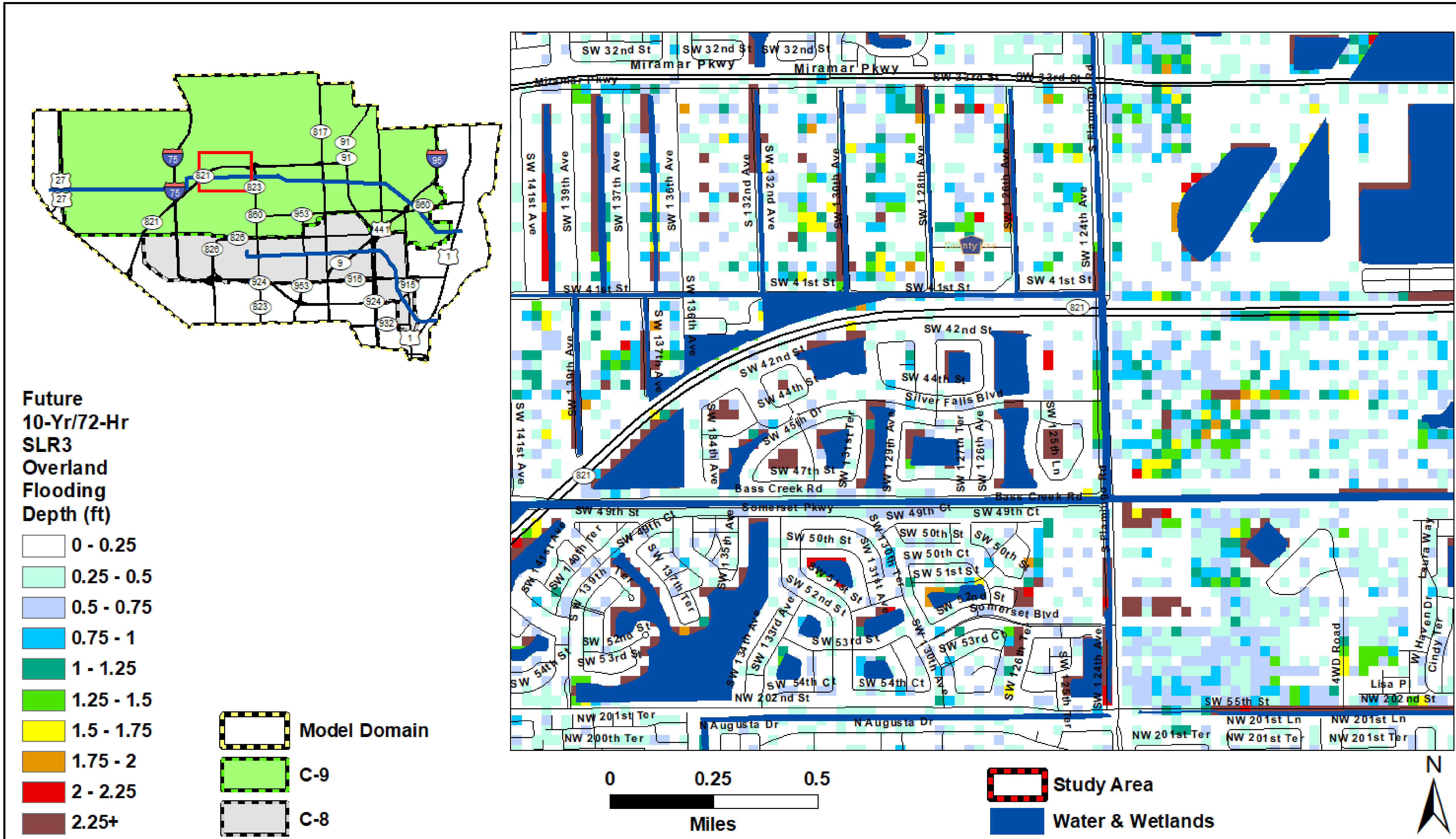

Figure 4.5-57: Up Close 10-Year Sea Level Rise 3 Flood Inundation Map for the C-9 Canal Near Ronald Reagan Turnpike

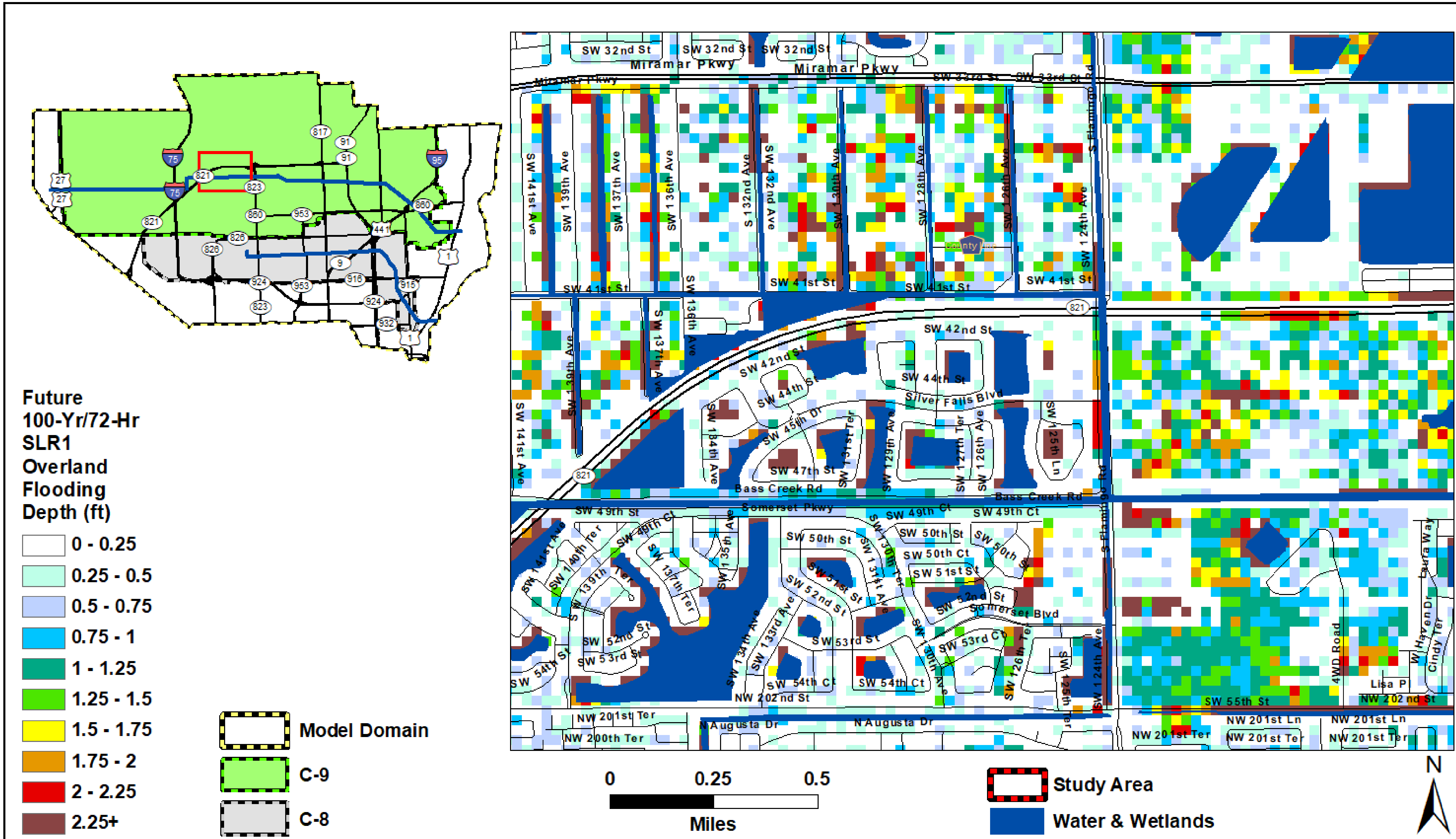

Figure 4.5-58: Up Close 100-Year Sea Level Rise 1 Flood Inundation Map for the C-9 Canal Near Ronald Reagan Turnpike

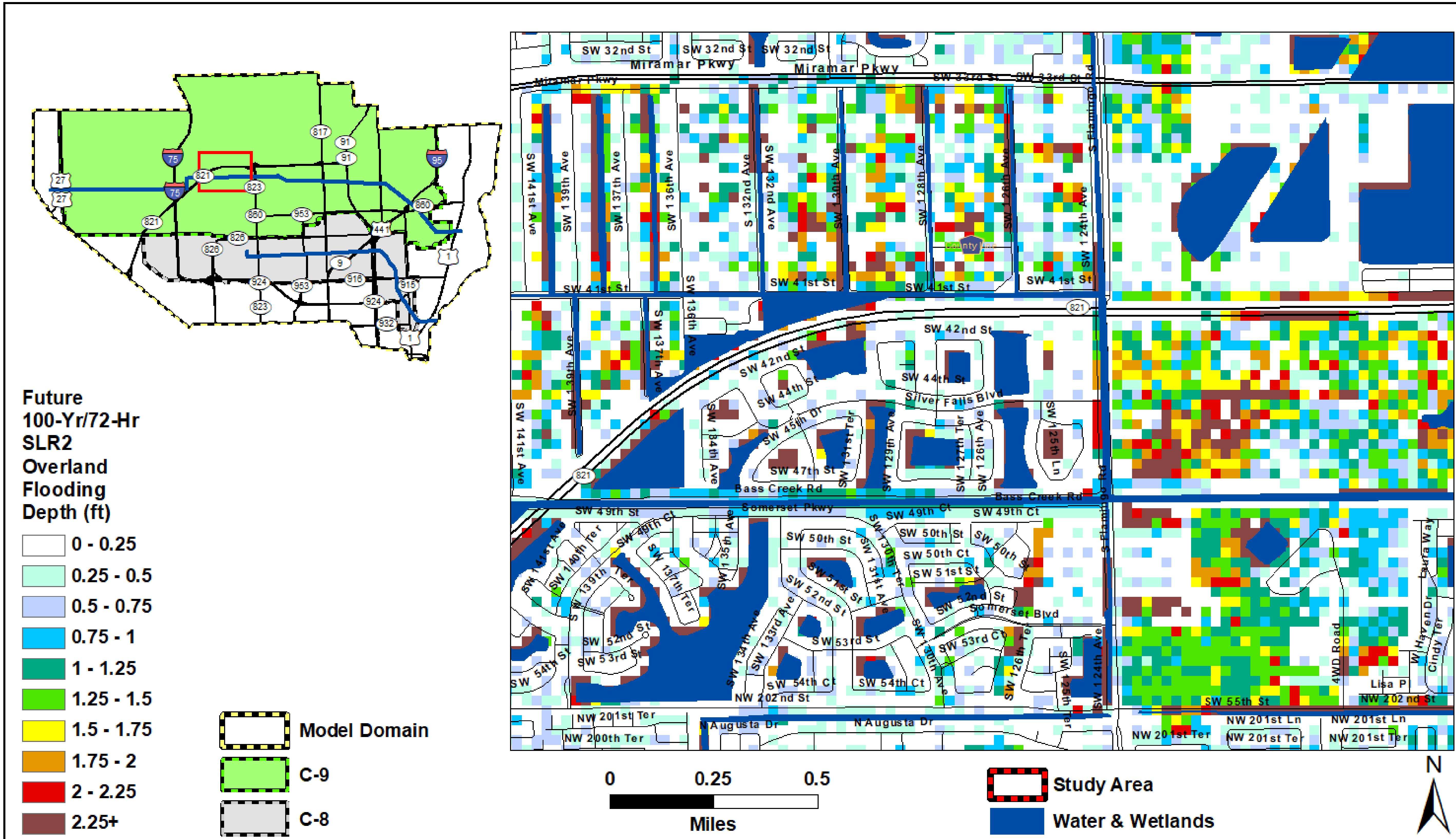

Figure 4.5-59: Up Close 100-Year Sea Level Rise 2 Flood Inundation Map for the C-9 Canal Near Ronald Reagan Turnpike

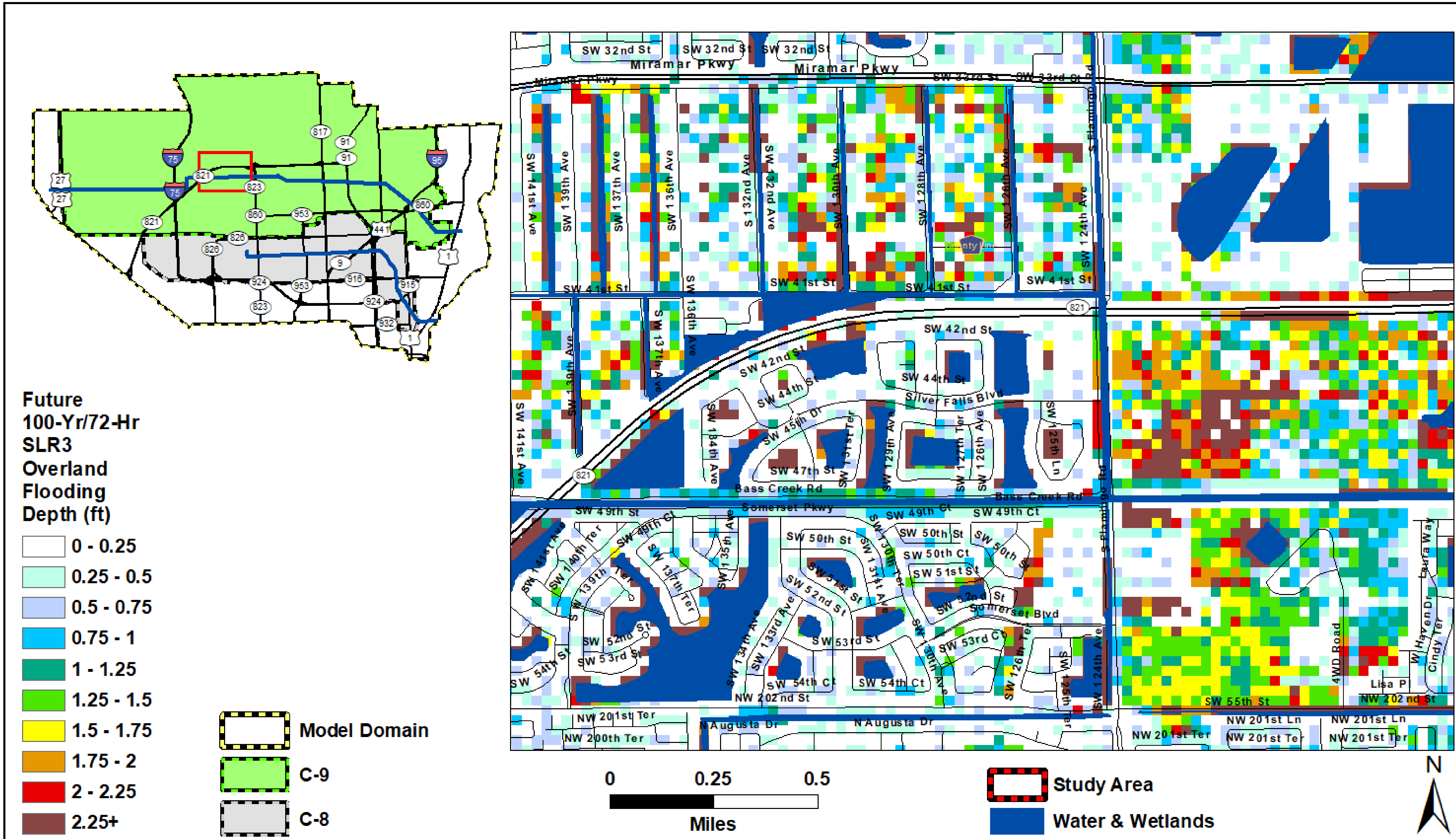

Figure 4.5-60: Up Close 100-Year Sea Level Rise 3 Flood Inundation Map for the C-9 Canal Near Ronald Reagan Turnpike

4.5.9.7 Up-Close Flood Inundation Maps for the C-9 Canal Near Red Road

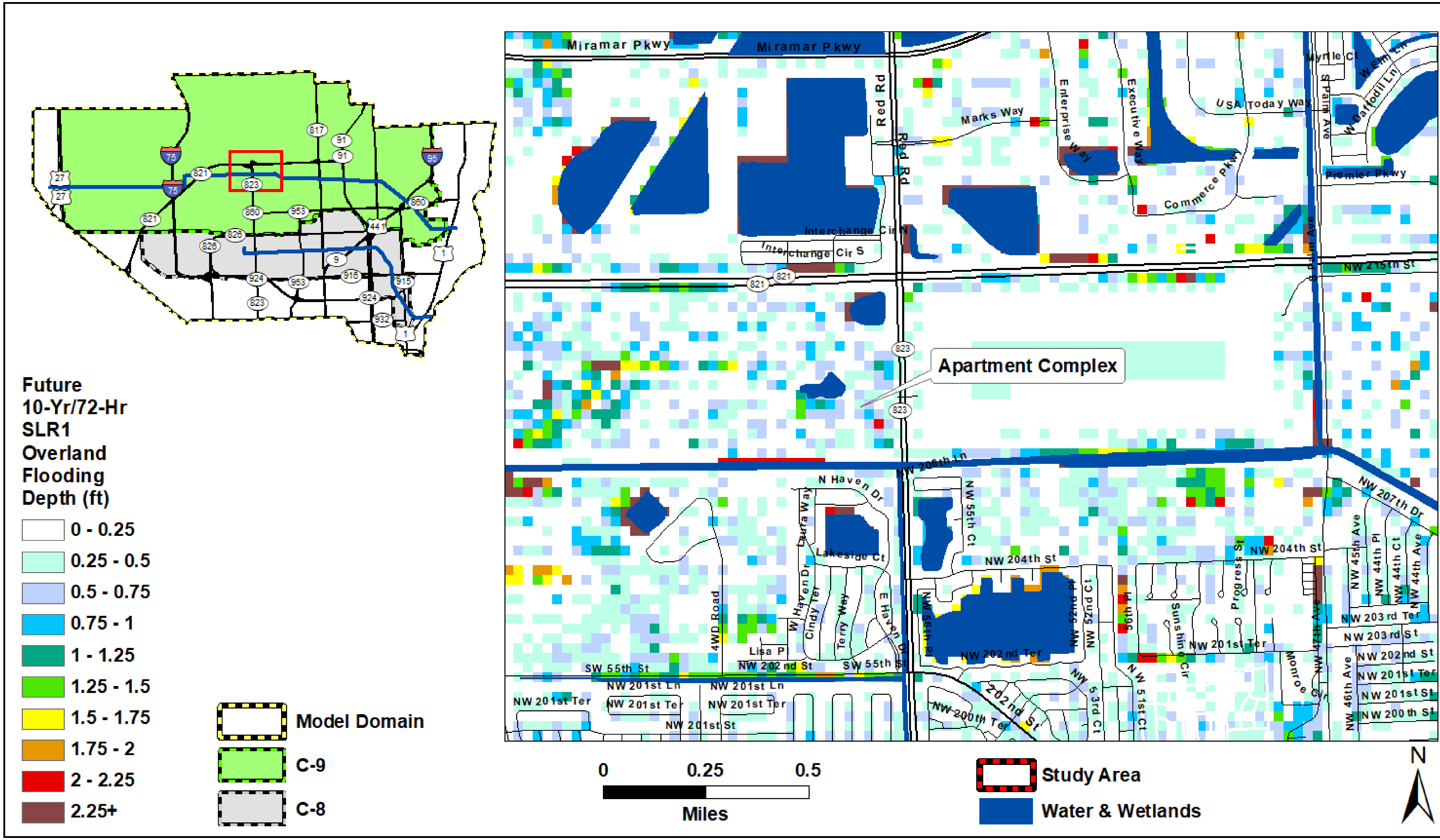

Figure 4.5-61: Up Close 10-Year Sea Level Rise 1 Flood Inundation Map for the C-9 Canal Near Red Road

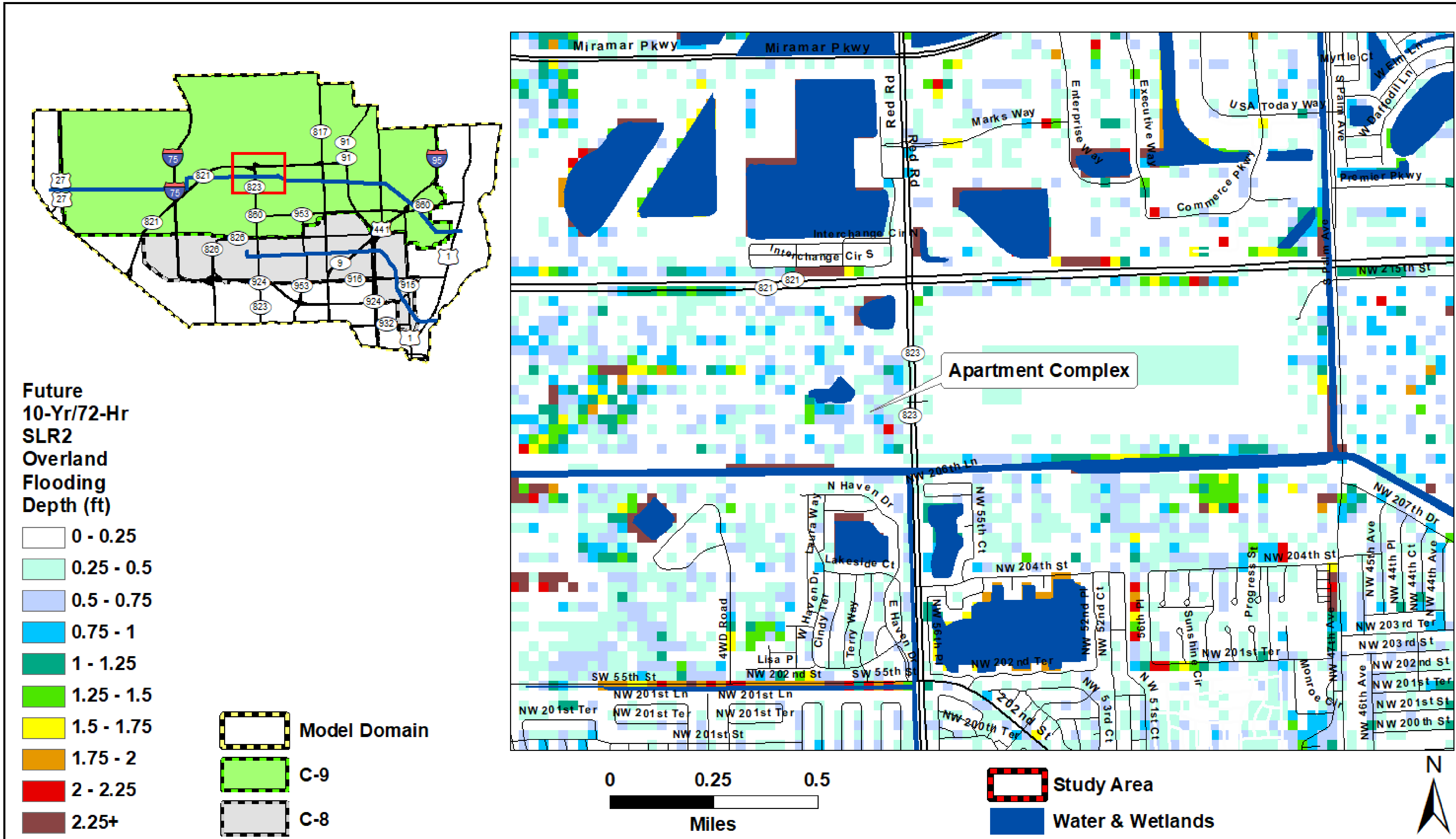

Figure 4.5-62: Up Close 10-Year Sea Level Rise 2 Flood Inundation Map for the C-9 Canal Near Red Road

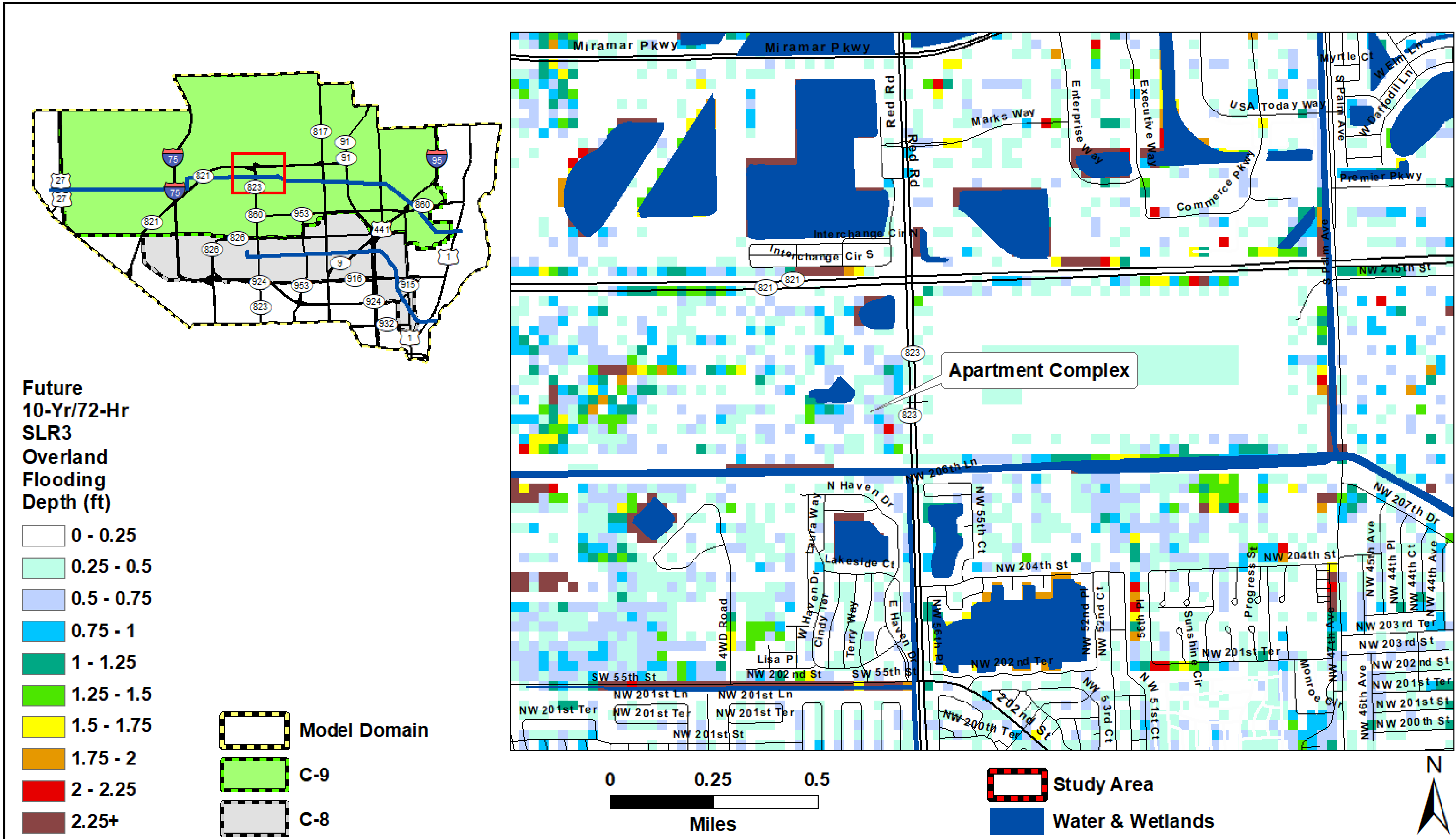

Figure 4.5-63: Up Close 10-Year Sea Level Rise 3 Flood Inundation Map for the C-9 Canal Near Red Road

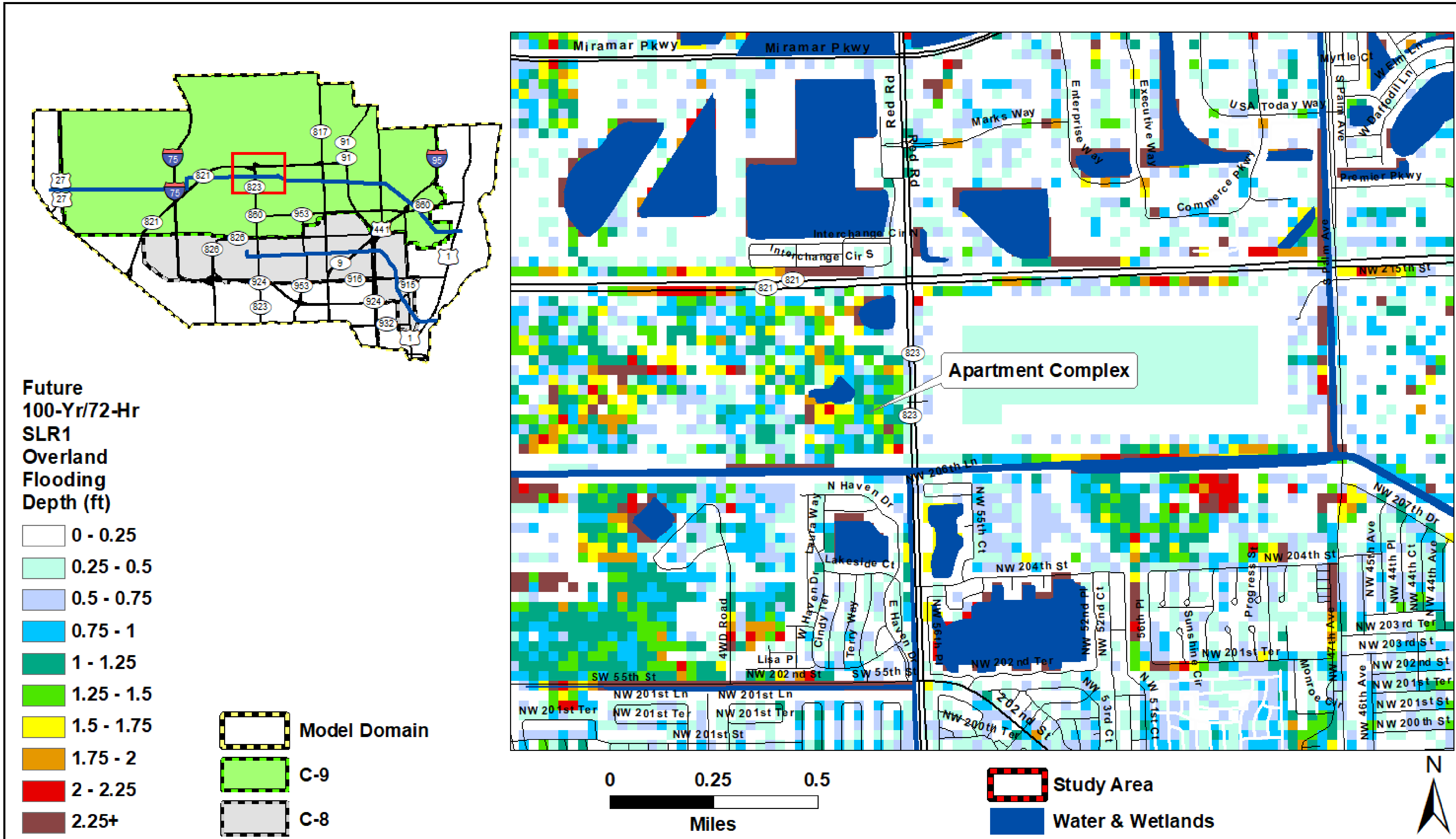

Figure 4.5-64: Up Close 100-Year Sea Level Rise 1 Flood Inundation Map for the C-9 Canal Near Red Road

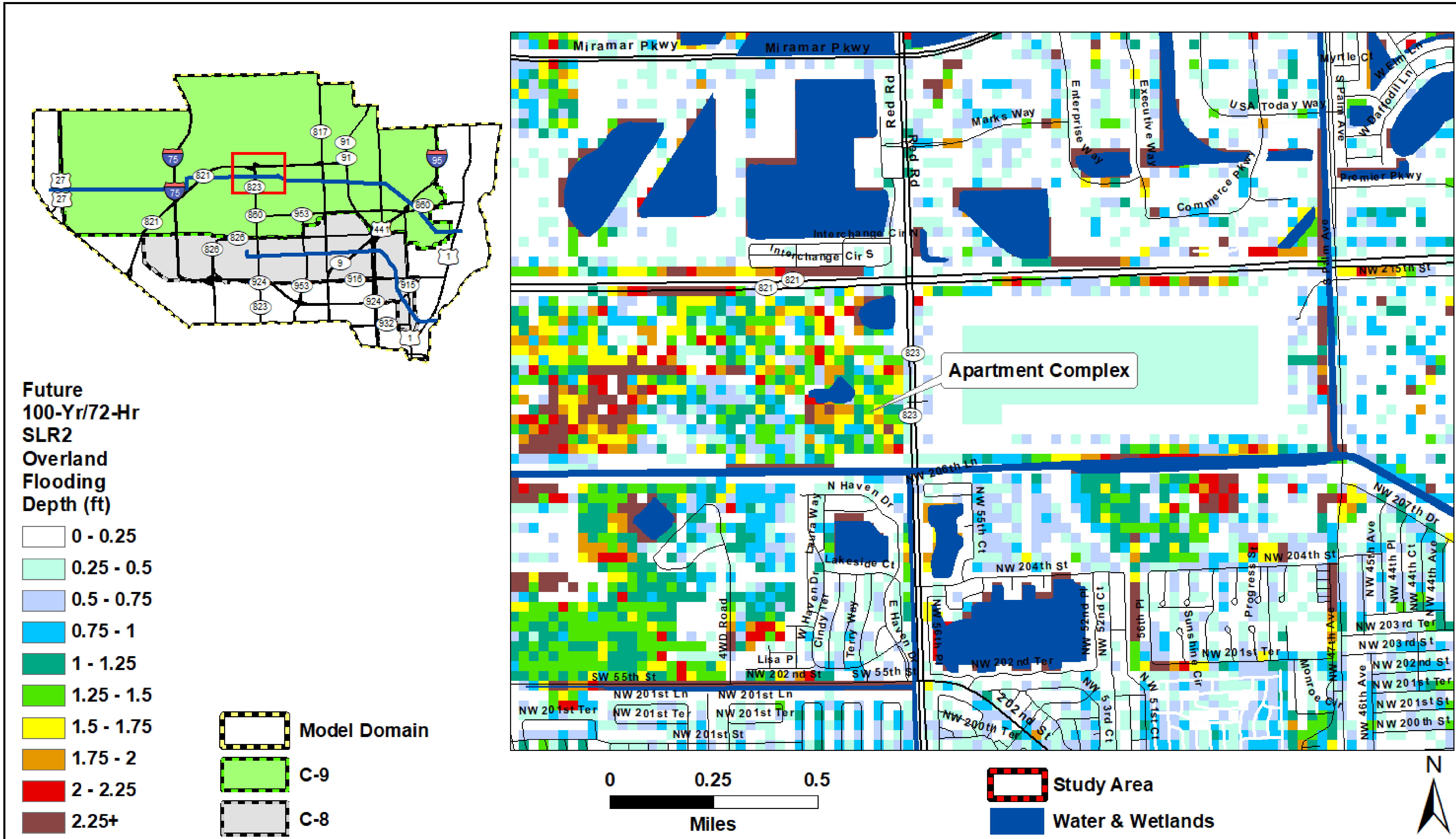

Figure 4.5-65: Up Close 100-Year Sea Level Rise 2 Flood Inundation Map for the C-9 Canal Near Red Road

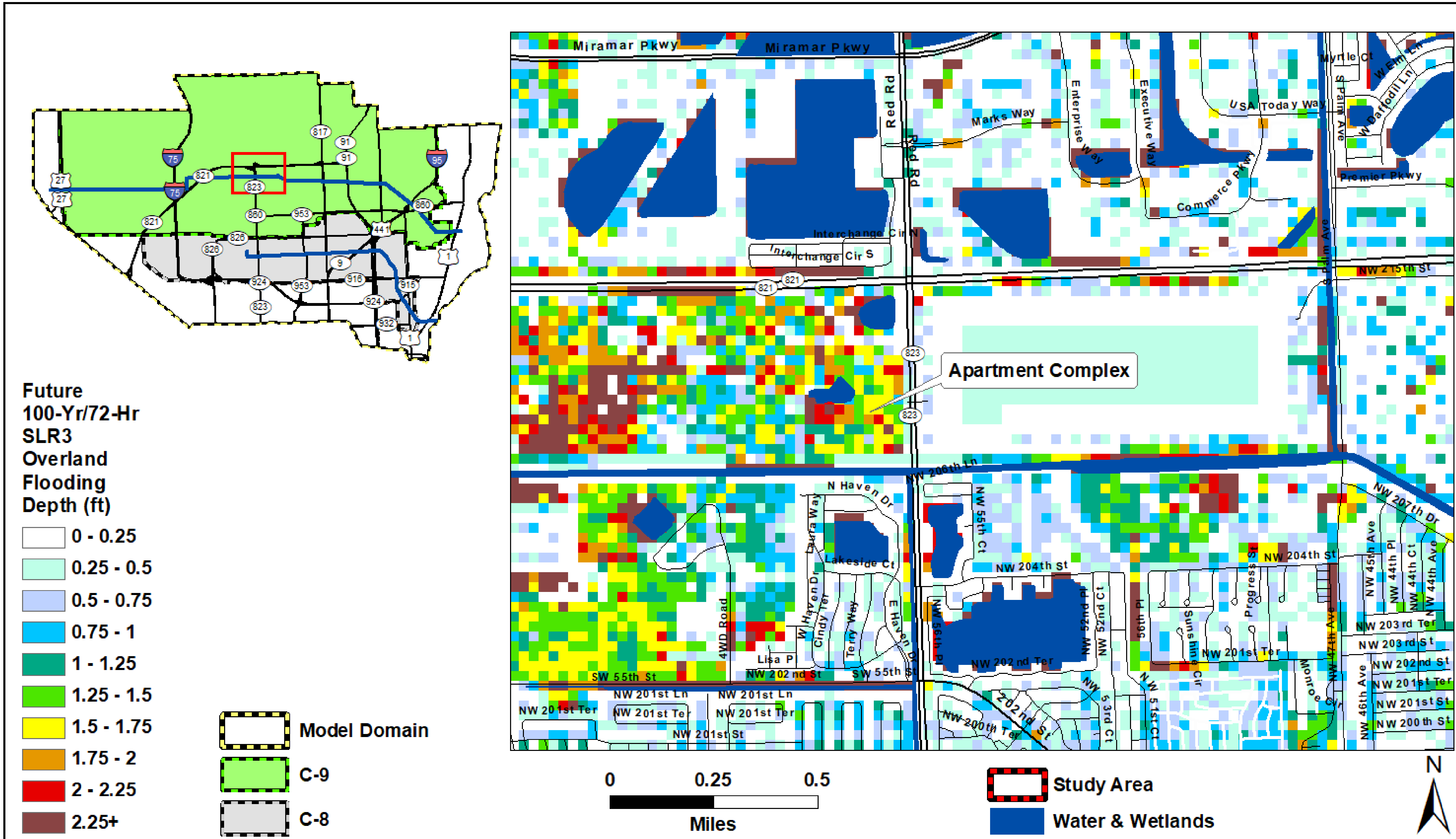

Figure 4.5-66: Up Close 100-Year Sea Level Rise 3 Flood Inundation Map for the C-9 Canal Near Red Road

4.5.10 Flood Inundation Difference Maps for Urban Land Use Areas

This section presents depth difference maps between the future conditions 25-year design storm with 1, 2, and 3 ft sea level rise and current conditions. These maps provide another way to interpret the PM #5 results by depicting the increases in flood elevations and extents that can be expected with increasing sea level. Under current conditions, increase in flooding was presented with respect to an increase in design storm intensity. Intuitively, more rainfall increases the flooding potential under the same conditions. This is a well-established principle; therefore, instead of presenting difference maps between two design storms of different intensities, future conditions results are presented with respect to an increase in sea level rise for a given design storm. For any given design storm (same rainfall), the effect of the increase in sea level rise does not necessarily act the same way as the increase in rainfall does. For instance, an increase in rainfall mostly leads to a model-wide increase in flood depth. However, an increase in sea level rise has varying effects on the area and depth of flood inundation. **Figure 4.5-67** through **Figure 4.5-69** show the maximum overland water depth difference between future conditions and current conditions for the 25-year design storm for all three sea level rise scenarios, for urban land use only. It is important to note that there is no difference in rainfall. It is also important to note that areas of future land use change that have increased topography elevation will mostly show up as negative values as they are no longer low points that accumulate water.

Figure 4.5-67 presents the difference in maximum water depth between the 25-year SLR1 and the current conditions 25-year design storm. Although there are changes in the maximum flood depth, the differences are typically in close proximity of the C-8 and C-9 Canal, or areas of topography elevation change. There is noticeably less flood depth difference in the C-9 basin than there is in the C-8 basin, which makes sense as the C-9 basin in drained by pumps and the C-8 basin is gravity-driven. This suggests that the C-8 basin *should* be more sensitive to sea level rise as any changes in the C-8 Canal stage directly correspond to a change in the ability for the C-8 basin to drain.

Figure 4.5-68 presents the difference in maximum water depth between the 25-year SLR2 and the current conditions 25-year design storm. Compared to the SLR1 difference, there are more changes in the maximum flood depth, with the largest differences still being in close proximity of the C-8 and C-9 Canal. Aside from the larger spatial extent of increased flood depths, the flood depths are also significantly higher, especially along the C-8 Canal. This was also observed in the maximum stage profiles in PM #1 and the up-close flooding in PM #5. Under SLR2, parts of the C-9 Basin, away from the C-9 Canal, are starting to show increases in flood depth.

Figure 4.5-69 presents the difference in maximum water depth between the 25-year SLR3 and the current conditions 25-year design storm. The changes in the maximum flood stage are significant, both in terms of extent and depth. Under SLR3, significant lengths of the C-8 and C-9 Canals, as well as inland areas, “feel the effects” of 3 ft of sea level rise. Increased flooding is seen in parts of Broward County that are normally drained by pumps. In the 3 ft sea level rise scenario, parts of the secondary system in eastern SBDD experience increased flooding as the SBDD pumps are forced to stop pumping due to the high water level in the C-9 Canal. Flooding in the C-8 Basin increases as stage in the C-8 Canal increase, as it is drained by gravity. Therefore, increases in stage in the C-8 Canal from increases in sea level rise will have a direct effect on flood levels in the C-8 Basin.

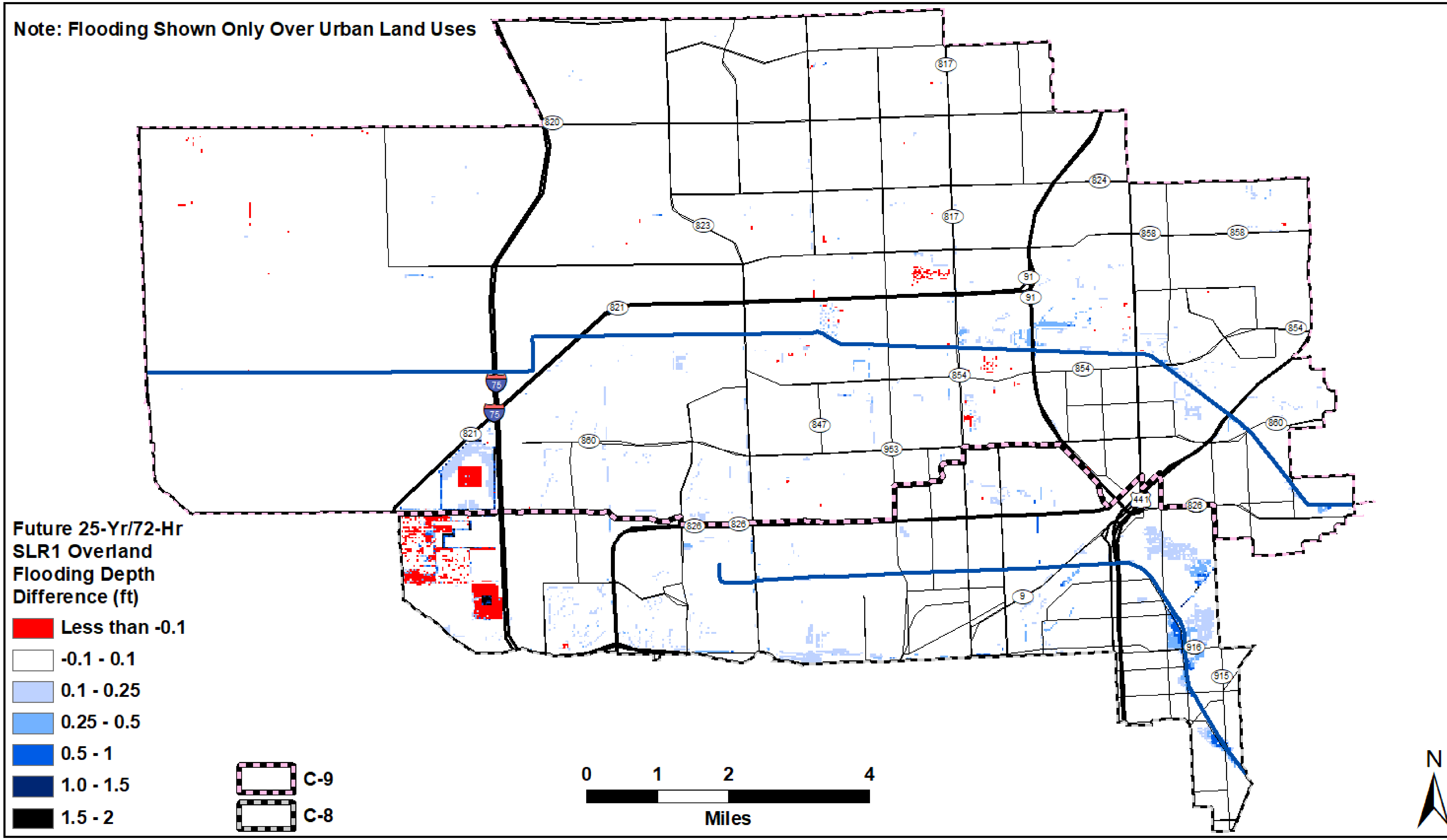

Figure 4.5-67: Flood Inundation Difference Map for 25-Year Sea Level Rise 1 Design Storm Event in Urban Land Use Areas (Future minus Current Conditions)

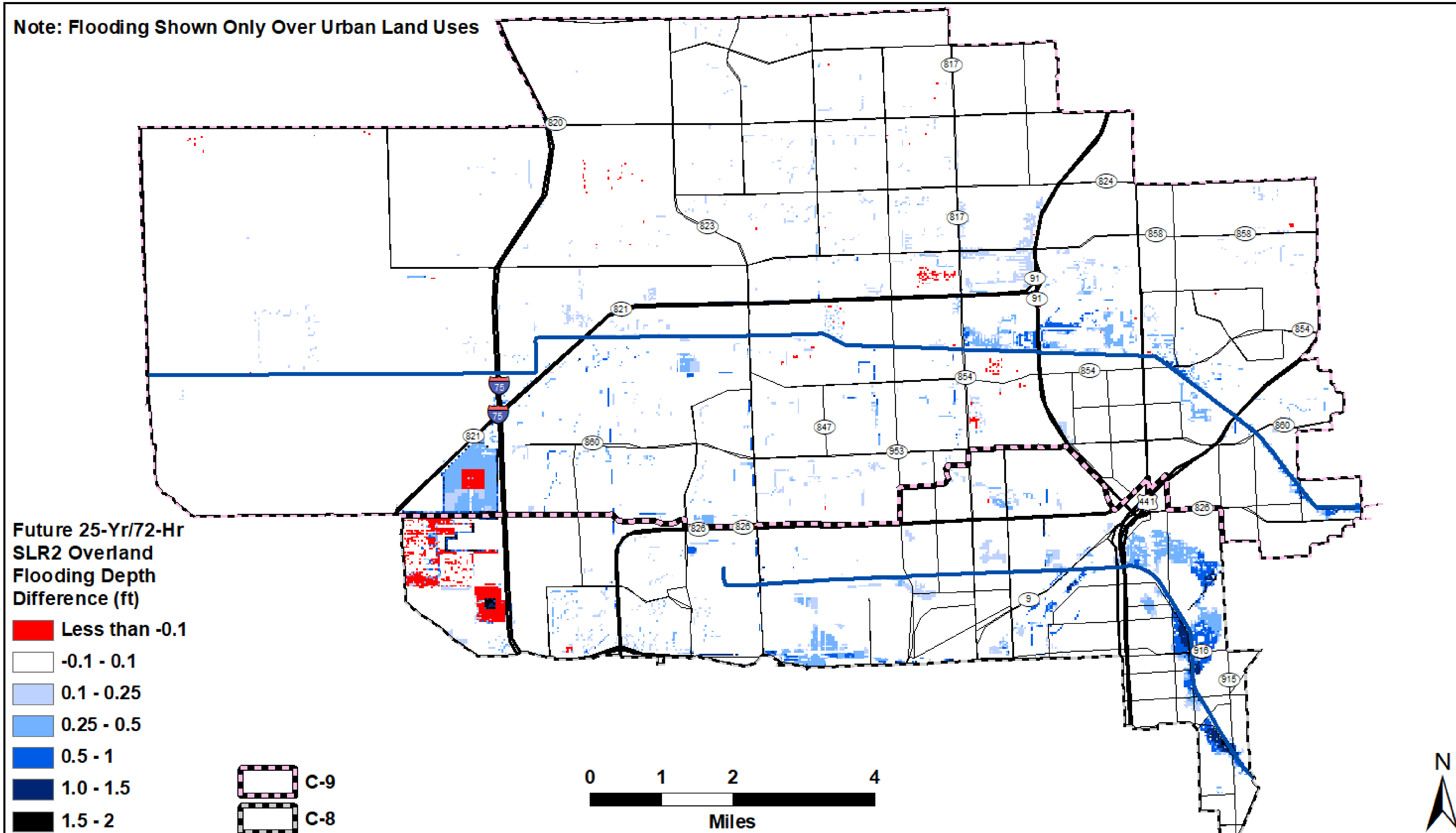

Figure 4.5-68: Flood Inundation Difference Map for 25-Year Sea Level Rise 2 Design Storm Event in Urban Land Use Areas (Future minus Current Conditions)

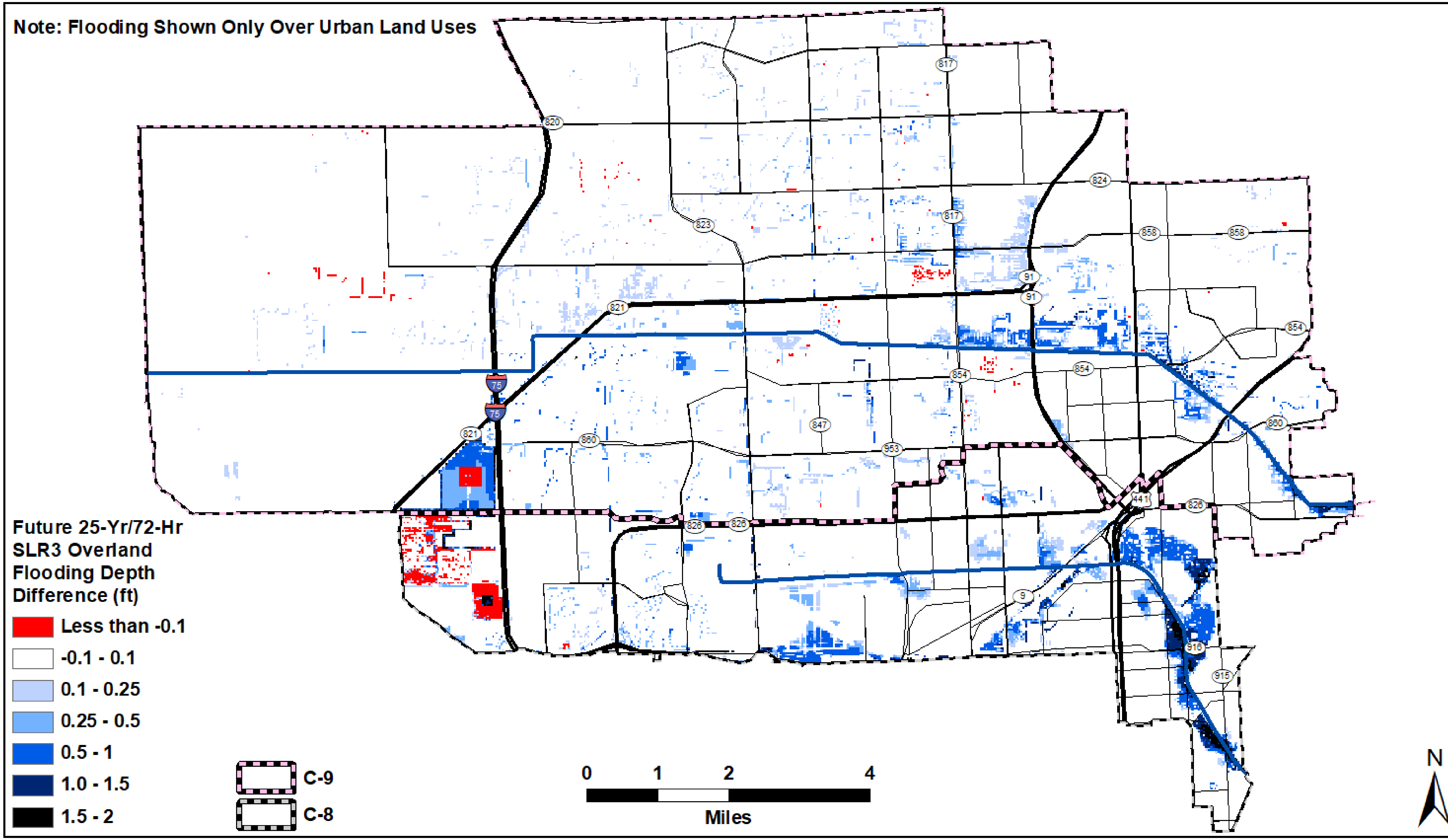

Figure 4.5-69: Flood Inundation Difference Map for 25-Year Sea Level Rise 3 Design Storm Event in Urban Land Use Areas (Future minus Current Conditions)

4.6 PM #6 – Duration of Flooding

For PM #6, the duration of flooding maps were developed by estimating the duration over which water depth exceeds a given threshold value. In this study, the duration of overland flooding was estimated using model simulated water depths and a threshold flooding depth of 0.25 ft. Additionally, the duration of flooding in the District Canals were estimated as the amount of time it takes for the water levels to return to target stage. The target stages of 3.6 ft for S-28Z and 3.5 ft for S-29Z were provided by the District (Email from Hongying Zhao, 5/12/2020). **Table 4-30** shows the duration of time taken for the water level in the C-8 and C-9 Canal to return to target stage, based on the first instance. For the 2 ft and 3 ft sea level rise scenarios, the C-8 and C-9 Canals do not return to target stage during the model simulation period if based upon the crest of the tidal signal. As shown in Table 4-30, even the lowest portion the tidal cycle is higher than target stage for the 3 ft sea level rise scenario.

Table 4-30: Duration for Water Levels to Return to Target Stage

Design Storm	Duration for S-28Z Return to Target Stage (hr)				Duration for S-29Z Return to Target Stage (hr)			
	5-Year	10-Year	25-Year	100-Year	5-Year	10-Year	25-Year	100-Year
Current	27	40	95	140	55	92	158	242
SLR1	44	60	128	181	60	98	182	247
SLR2	163	217	255	N/A	245	279	N/A	N/A
SLR3	N/A	N/A	N/A	N/A	N/A	N/A	N/A	N/A

N/A means that the stage did not return to target stage within the model simulation period

The duration of overland flooding was estimated for all four design storm events based on the length of time the flood depth was predicted to exceed the threshold value (0.25 ft) within each MIKE SHE 125-ft grid cell using the statistics tool in MIKE ZERO. The flood duration maps for each of the design storm events are shown in **Figure 4.6-1** through **Figure 4.6-12**.

Based on model simulations, large areas were inundated for over 72 hours, even for the 5-year sea level rise 1 design storm (**Figure 4.6-1**). These areas are comprised primarily of lakes and wetlands and other low-lying undeveloped areas. An increase in flooding extent and duration was observed as the magnitude of the design storms increased. Additionally, an increase in flooding extent and duration was observed as the magnitude of sea level rise increased, even across the same return period design storm. A vast majority of the watershed was inundated for at least a small duration during the 100-year SLR1 design storm, with notable increases for the 100-year SLR3 storm. Developed areas with the largest flood duration generally tend to coincide with the highest depths of flooding determined from PM#5. **Figure 4.6-13** through **Figure 4.6-24** show the flood duration maps for each of the design storm and sea level rise scenario for urban areas only. **Figure 4.6-25** through **Figure 4.6-42** show up close examples of flood duration along the C-8 Canal and **Figure 4.6-43** through **Figure 4.6-66** show up close examples of flood duration along the C-9 Canal. **Figure 4.6-67** through **Figure 4.6-69** show the maximum flood duration difference between future and current conditions for the 25-Year SLR1, SLR2 and SLR3 design storm events.

4.6.1 5-Year Design Storm Model-Wide Flood Duration Map

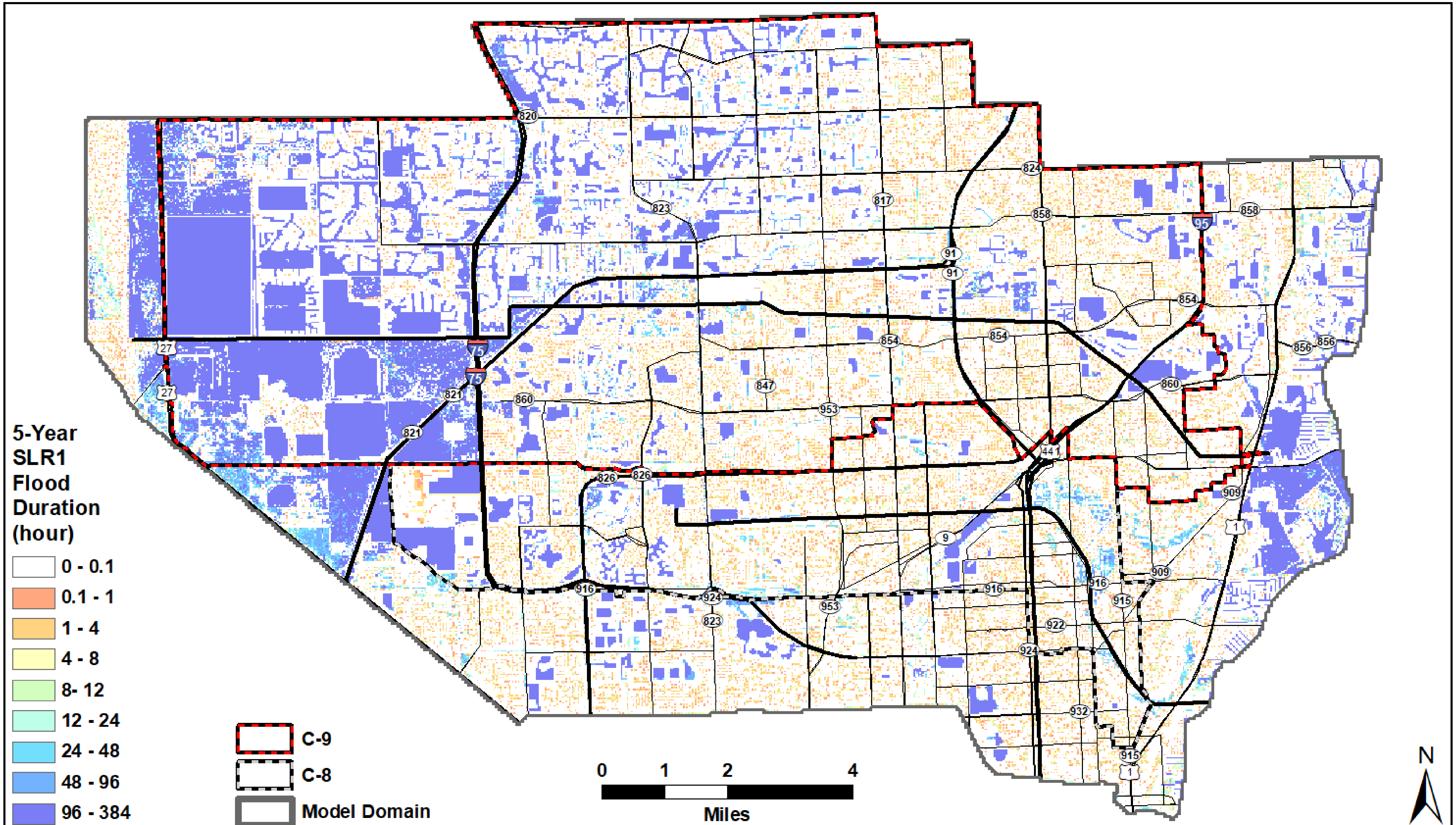

Figure 4.6-1: Flood Duration Map for 5-Year Sea Level Rise 1 Design Storm Event

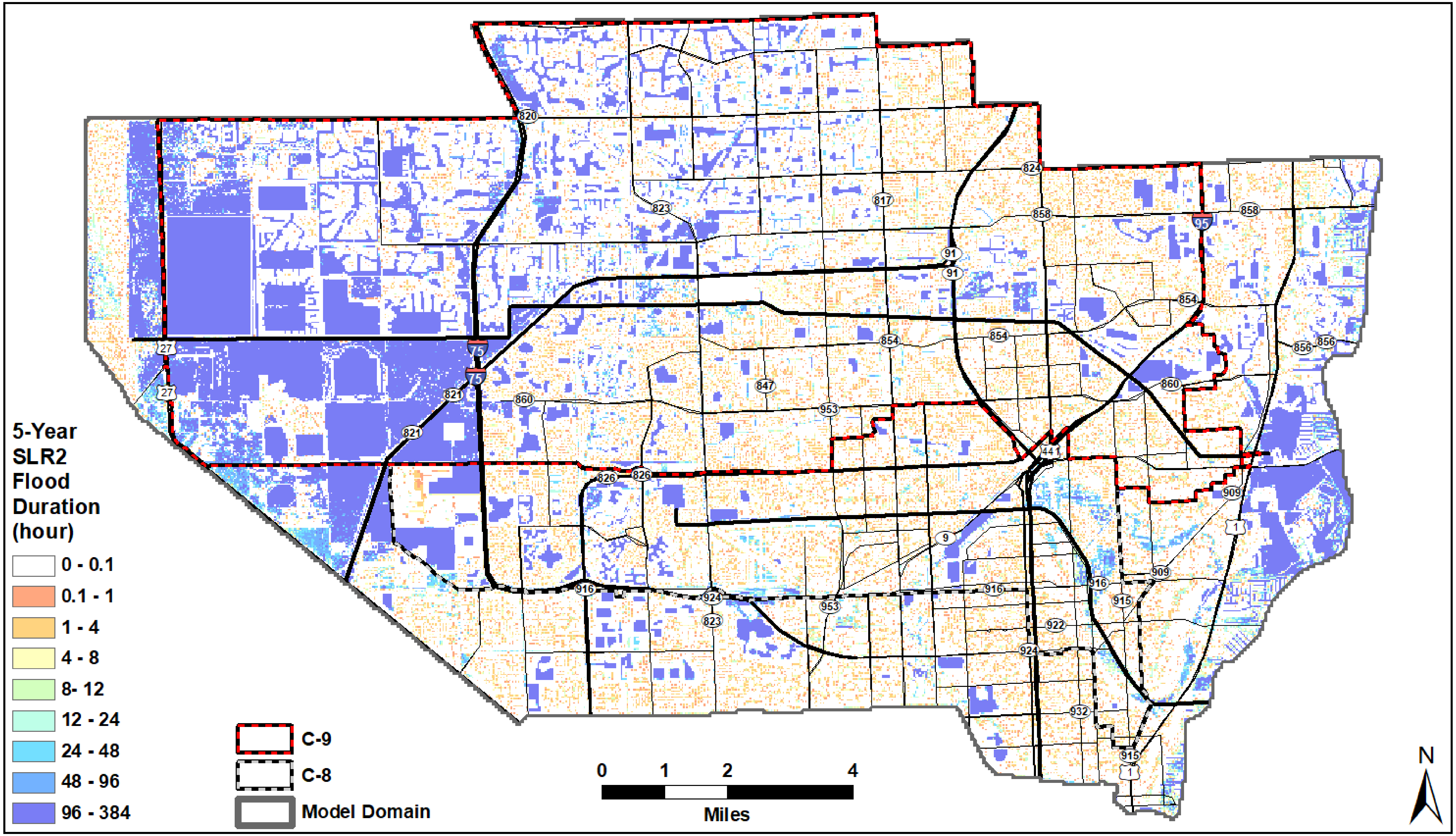

Figure 4.6-2: Flood Duration Map for 5-Year Sea Level Rise 2 Design Storm Event

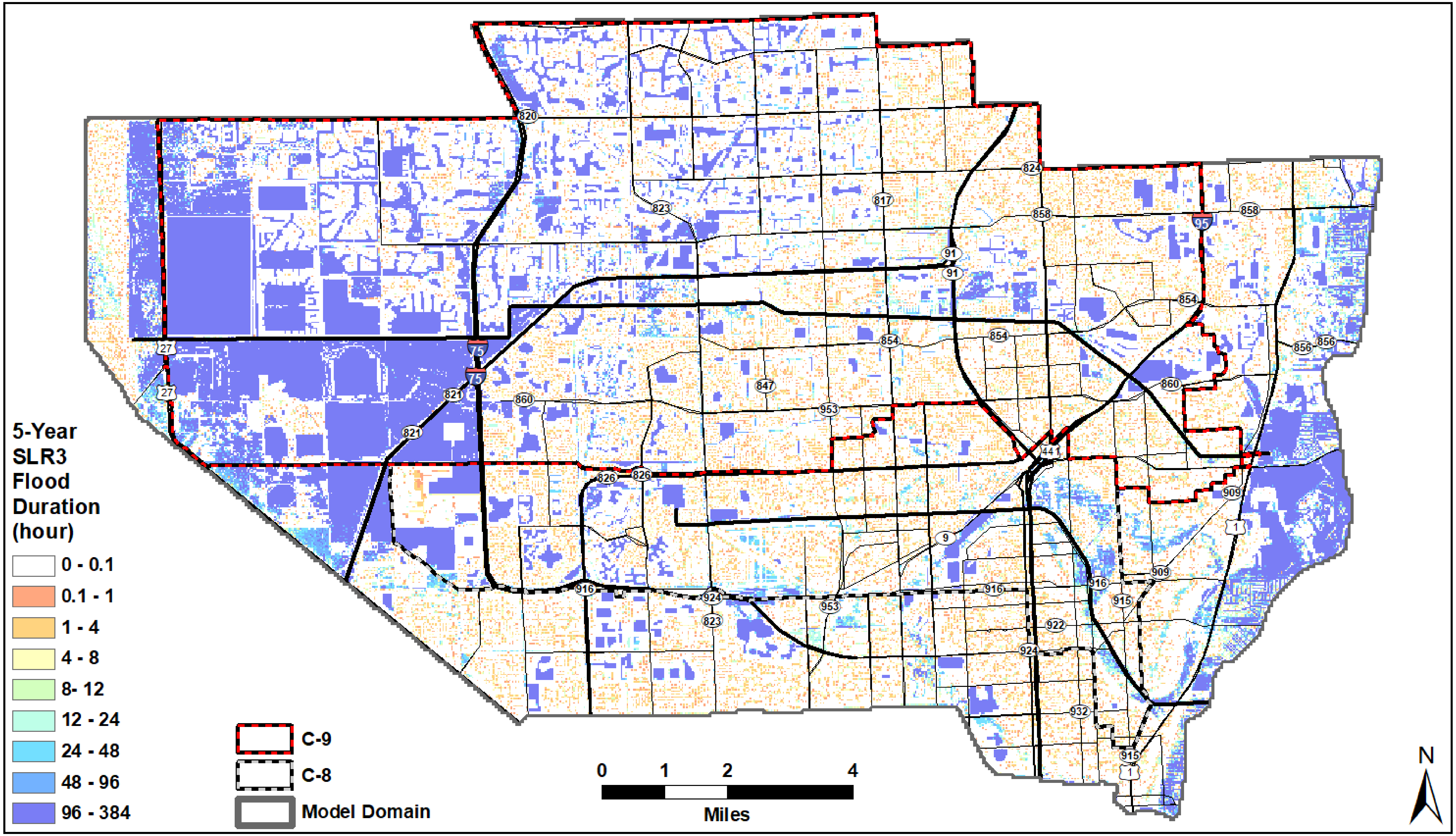

Figure 4.6-3: Flood Duration Map for 5-Year Sea Level Rise 3 Design Storm Event

4.6.2 10-Year Design Storm Model-Wide Flood Duration Map

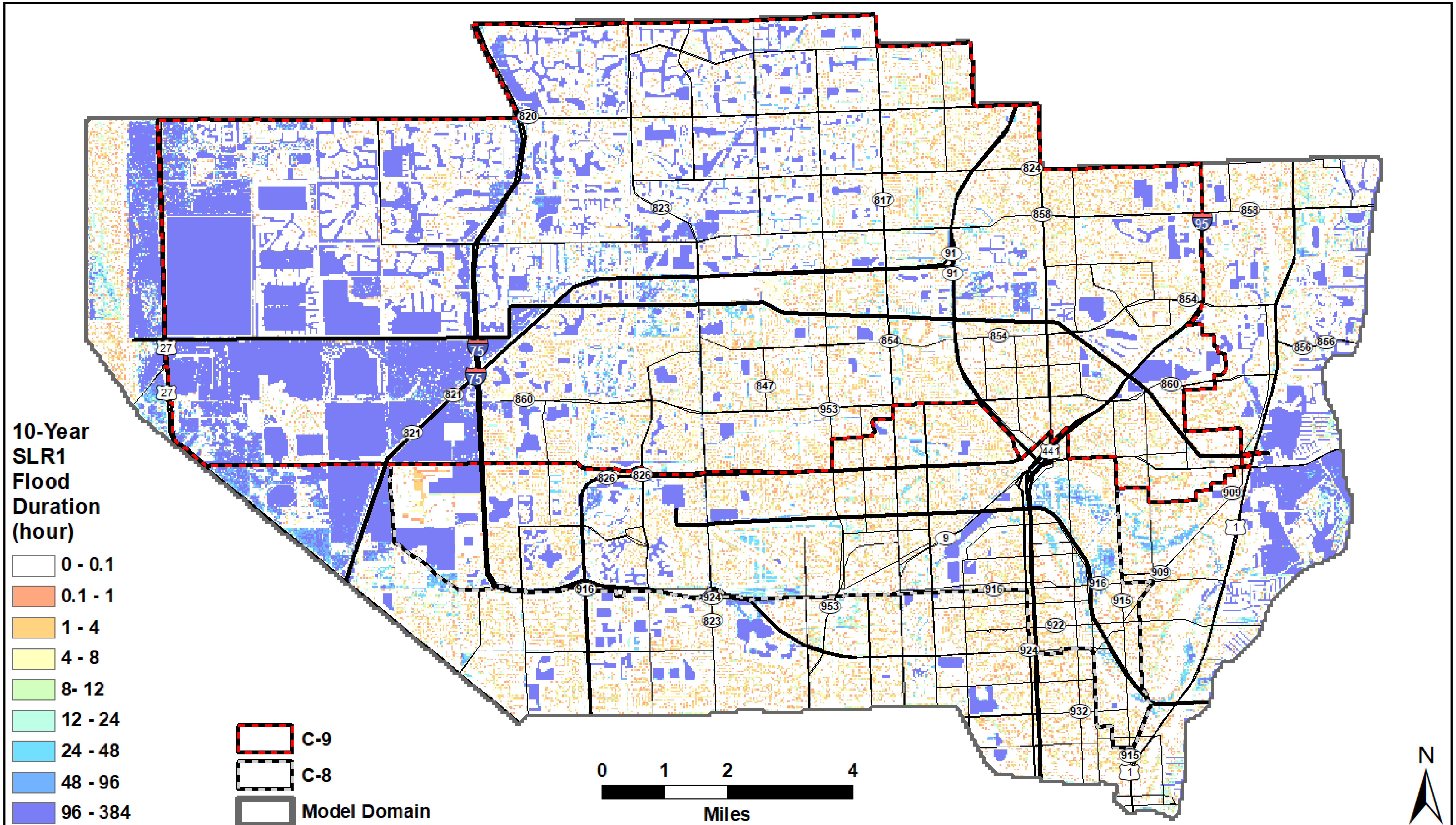

Figure 4.6-4: Flood Duration Map for 10-Year Sea Level Rise 1 Design Storm Event

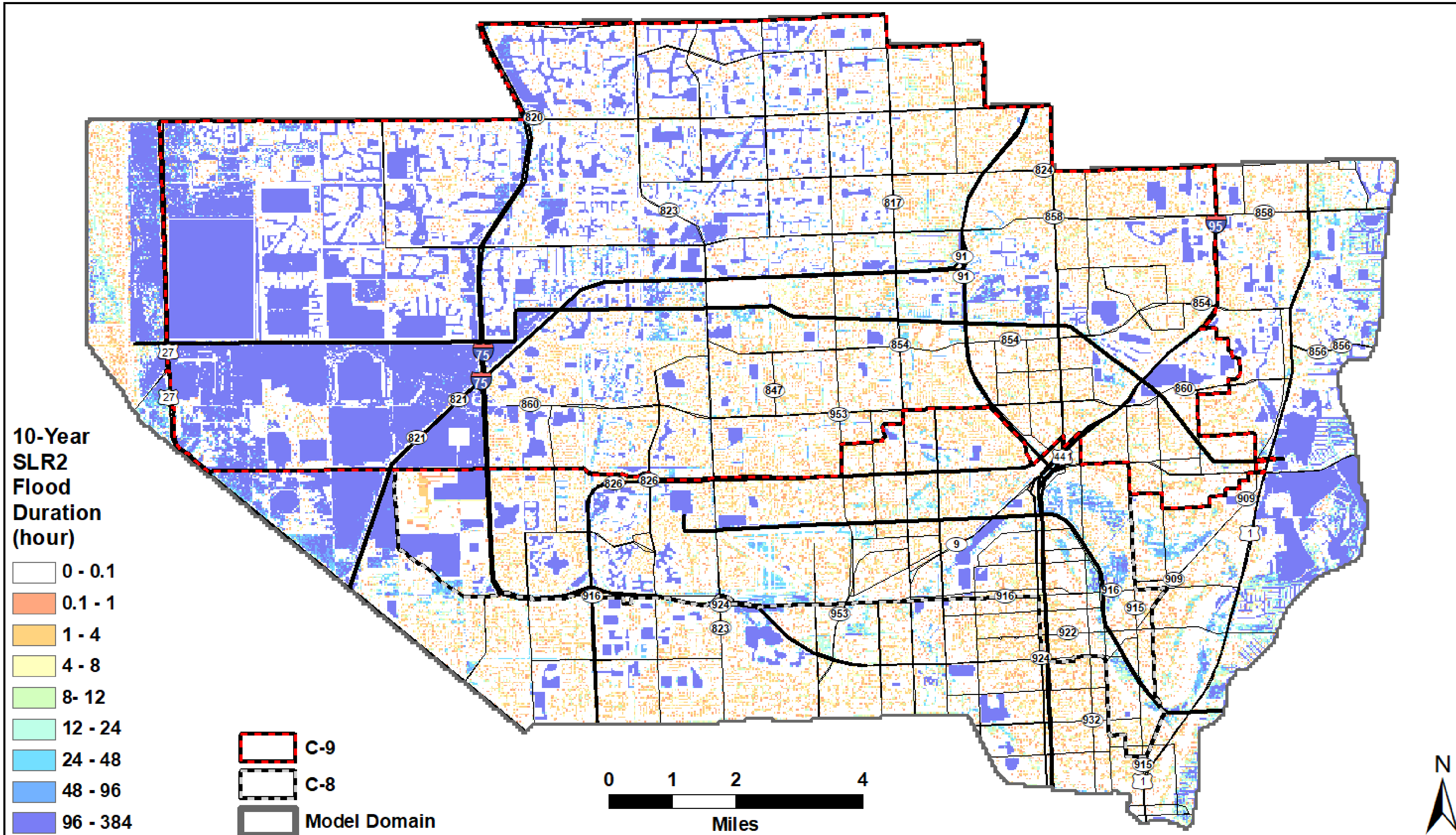

Figure 4.6-5: Flood Duration Map for 10-Year Sea Level Rise 2 Design Storm Event

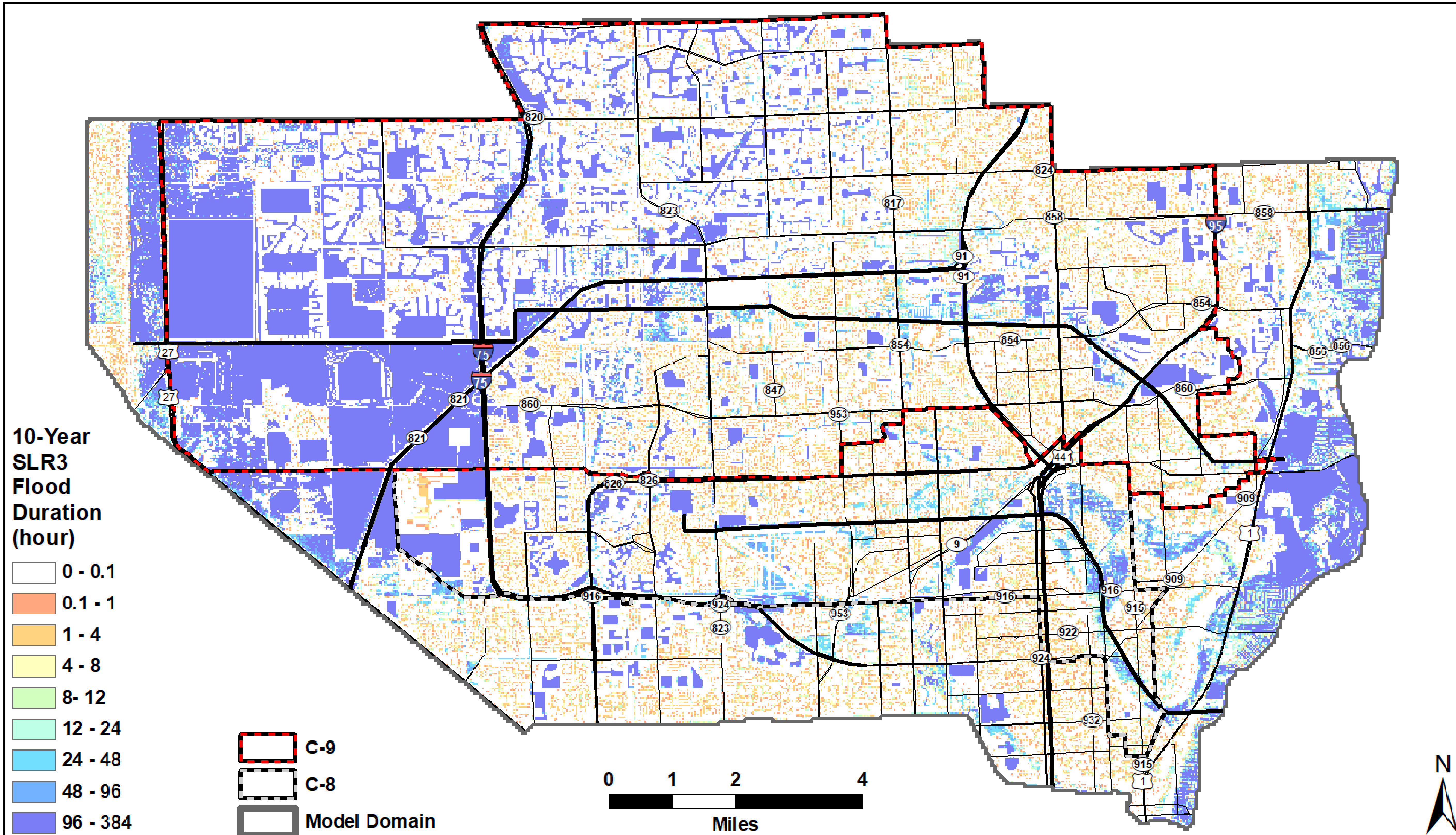

Figure 4.6-6: Flood Duration Map for 10-Year Sea Level Rise 3 Design Storm Event

4.6.3 25-Year Design Storm Model-Wide Flood Duration Map

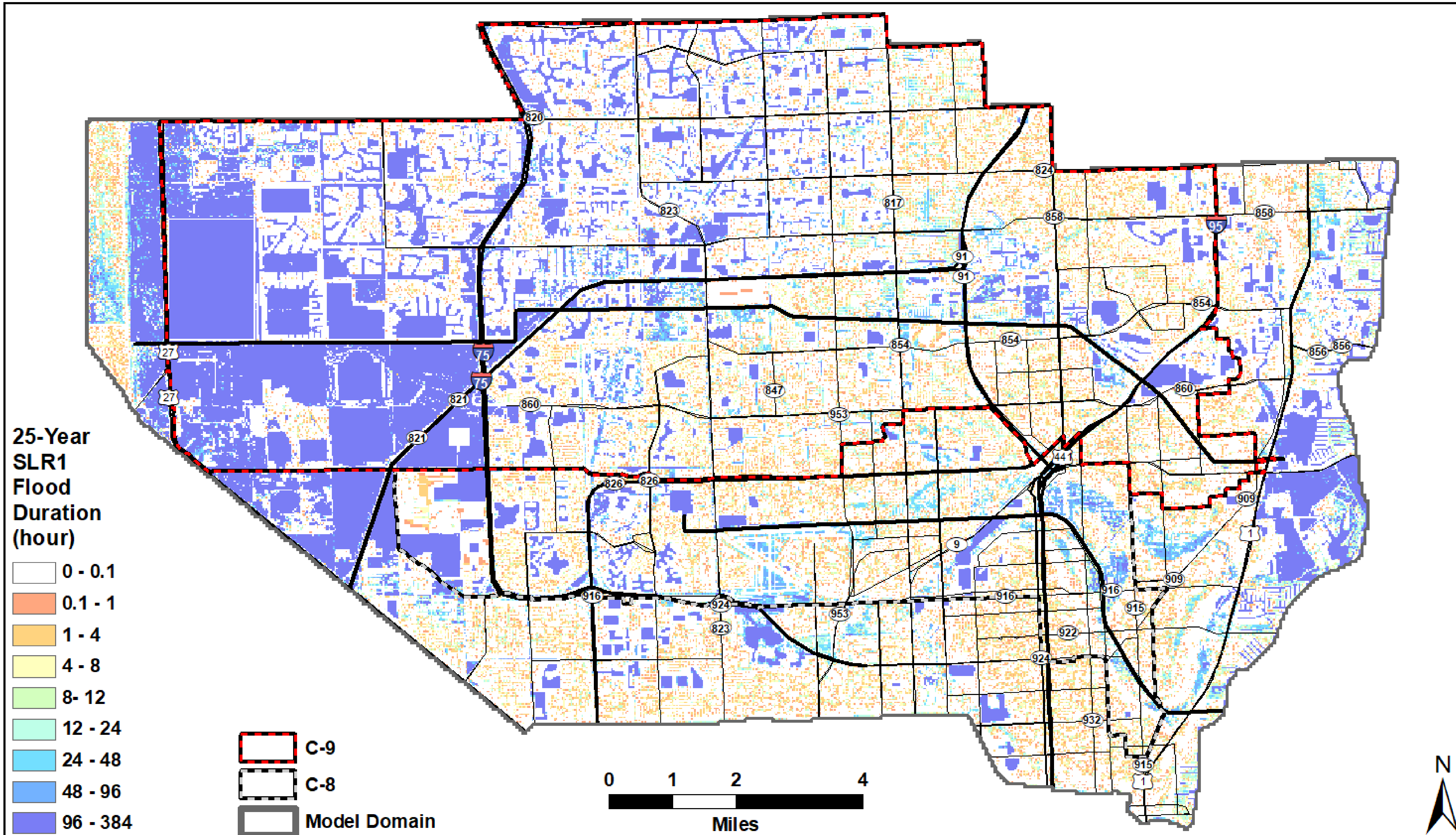

Figure 4.6-7: Flood Duration Map for 25-Year Sea Level Rise 1 Design Storm Event

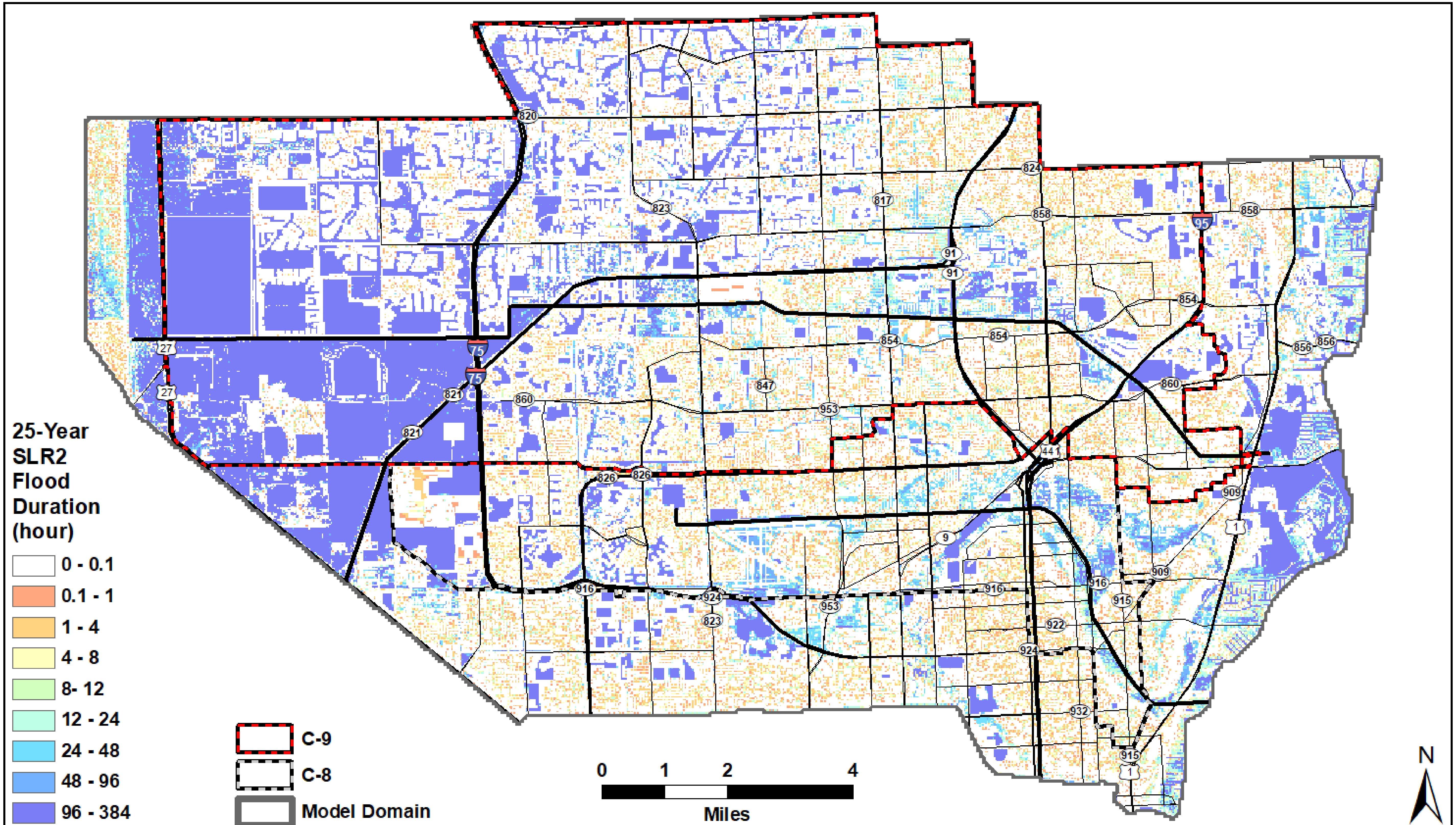

Figure 4.6-8: Flood Duration Map for 25-Year Sea Level Rise 2 Design Storm Event

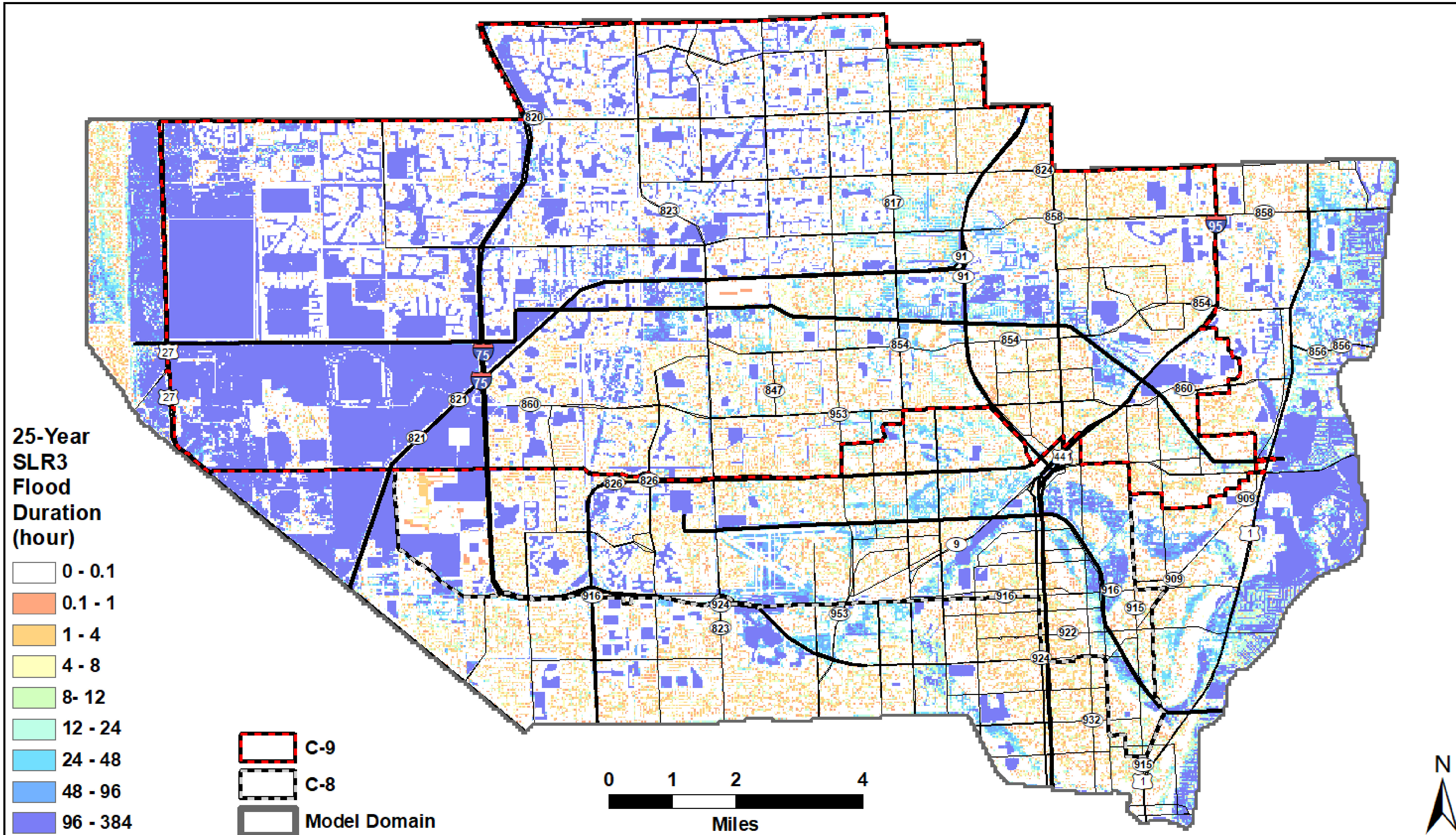

Figure 4.6-9: Flood Duration Map for 25-Year Sea Level Rise 3 Design Storm Event

4.6.4 100-Year Design Storm Model-Wide Flood Duration Map

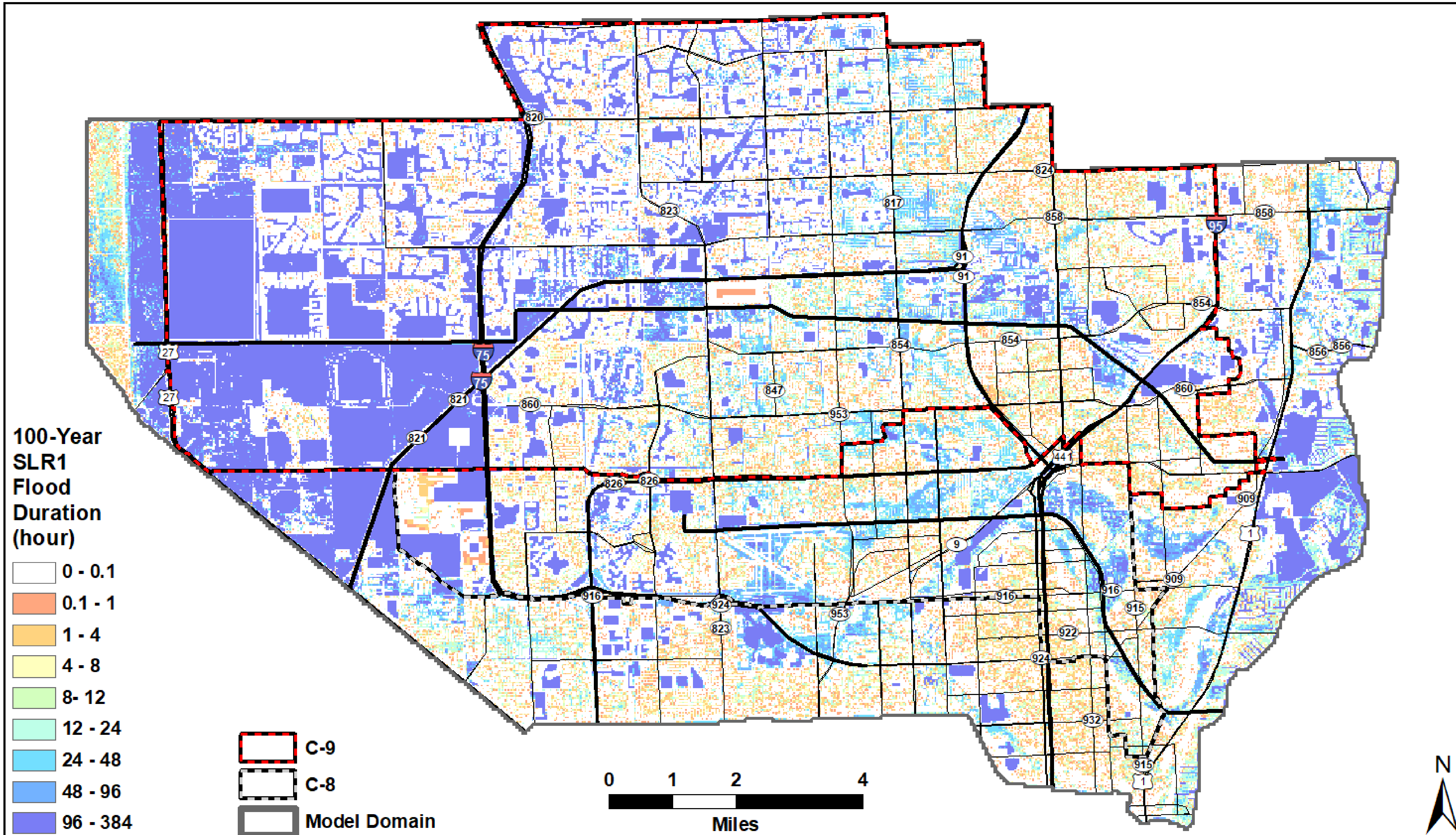

Figure 4.6-10: Flood Duration Map for 100-Year Sea Level Rise 1 Design Storm Event

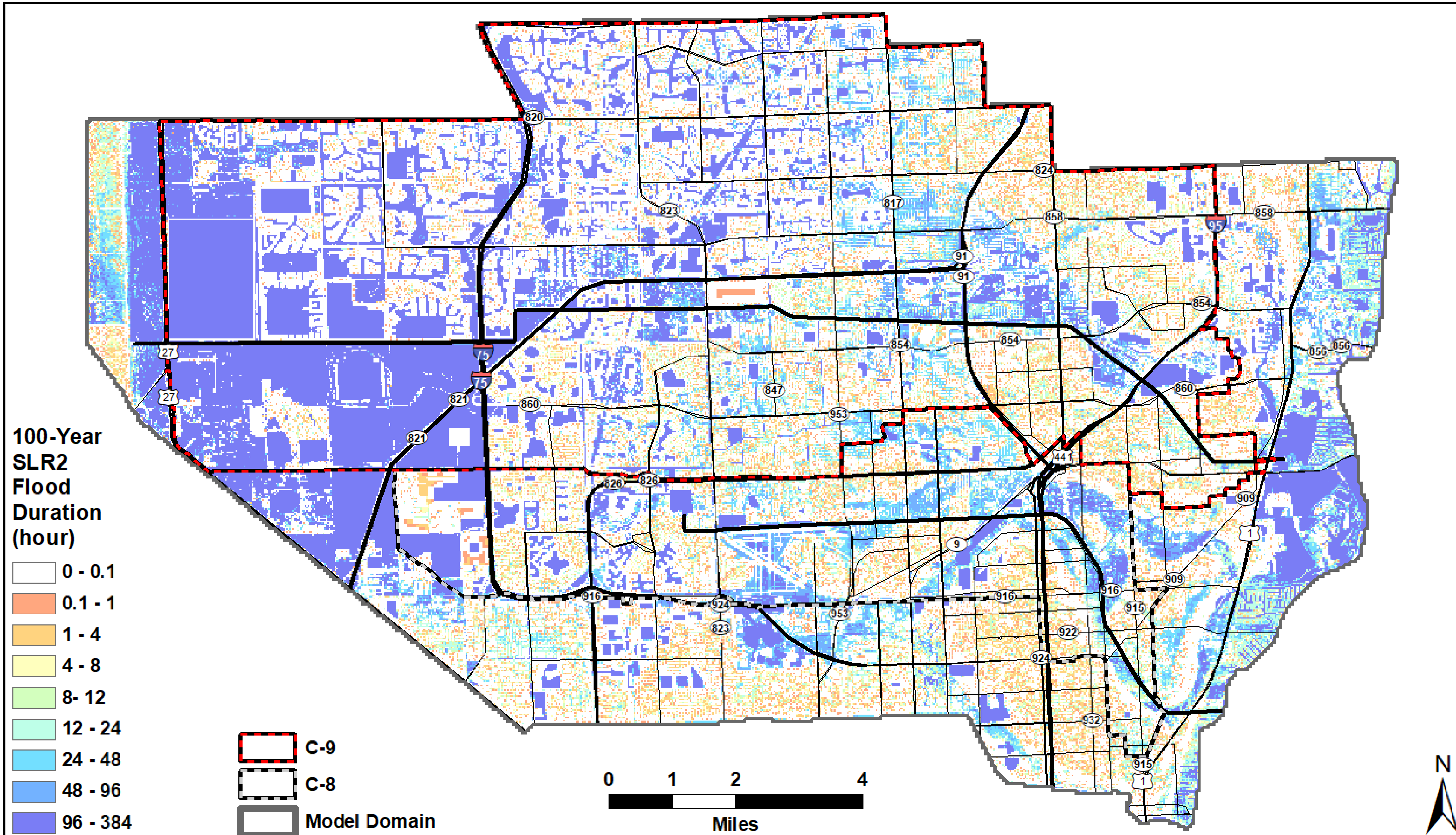

Figure 4.6-11: Flood Duration Map for 100-Year Sea Level Rise 2 Design Storm Event

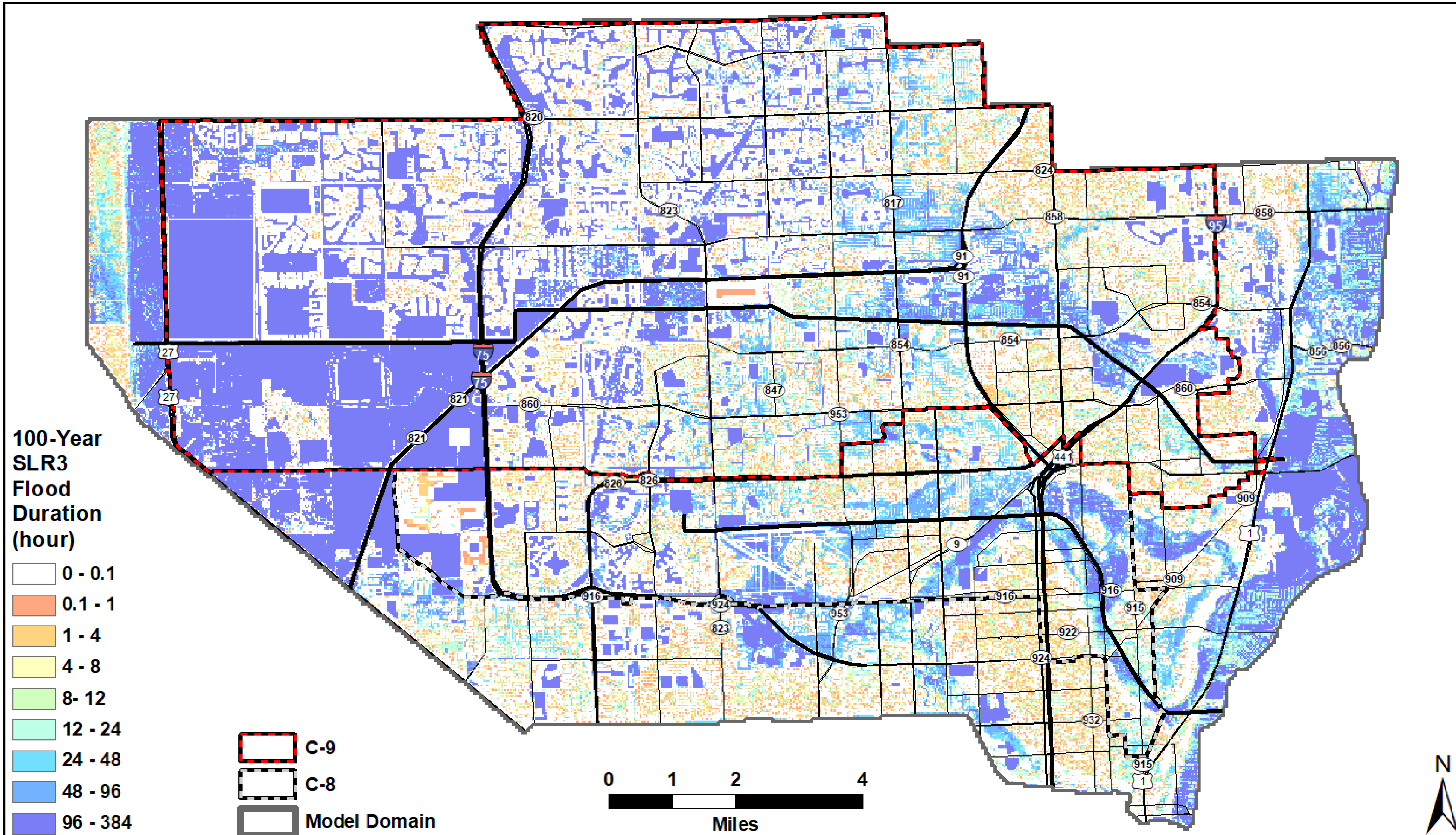

Figure 4.6-12: Flood Duration Map for 100-Year Sea Level Rise 3 Design Storm Event

4.6.5 5-Year Design Storm Flood Duration Map for Urban Land Use Areas

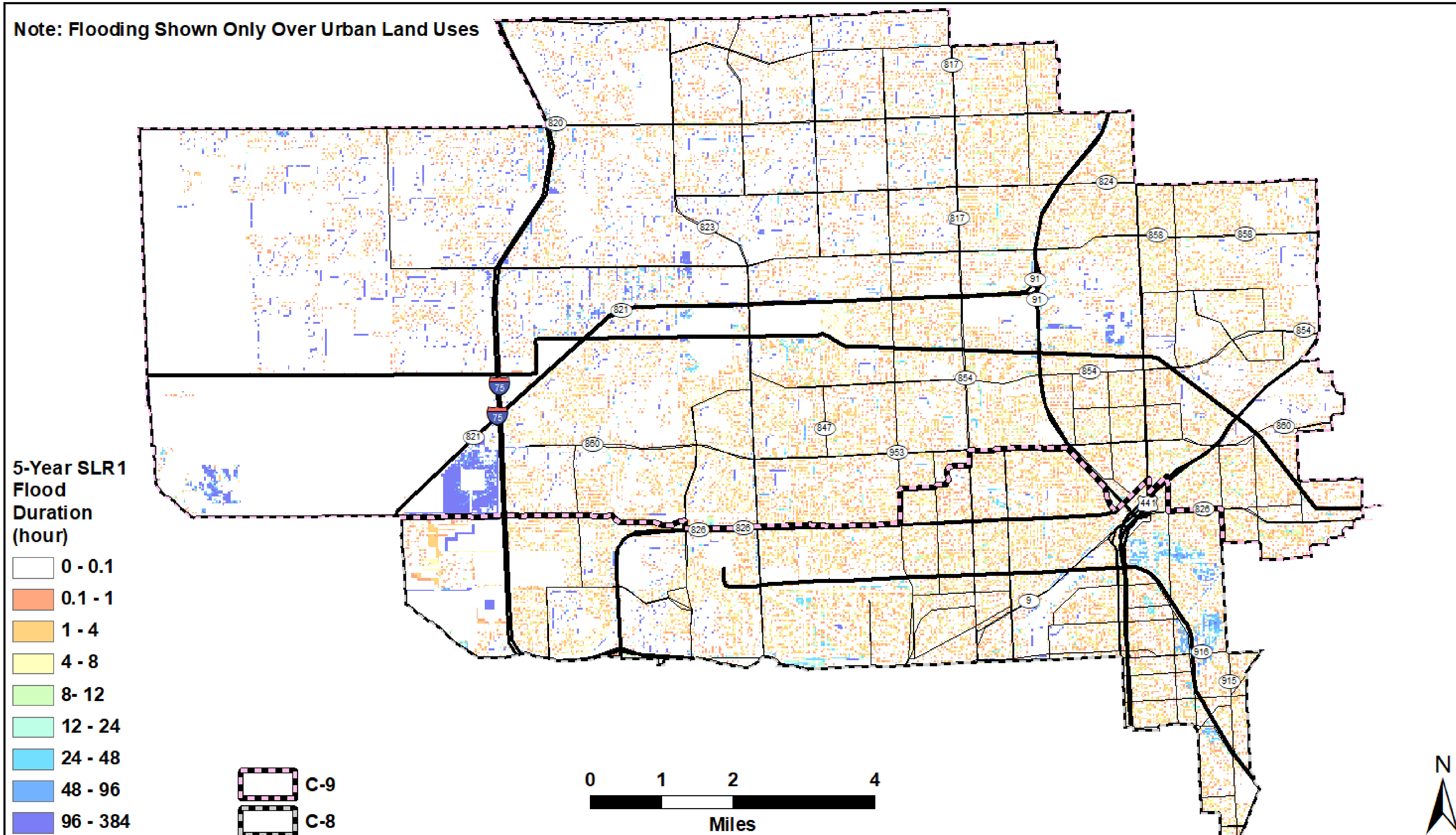

Figure 4.6-13: Flood Duration Map for 5-Year Sea Level Rise 1 Design Storm Event in Urban Land Use Areas

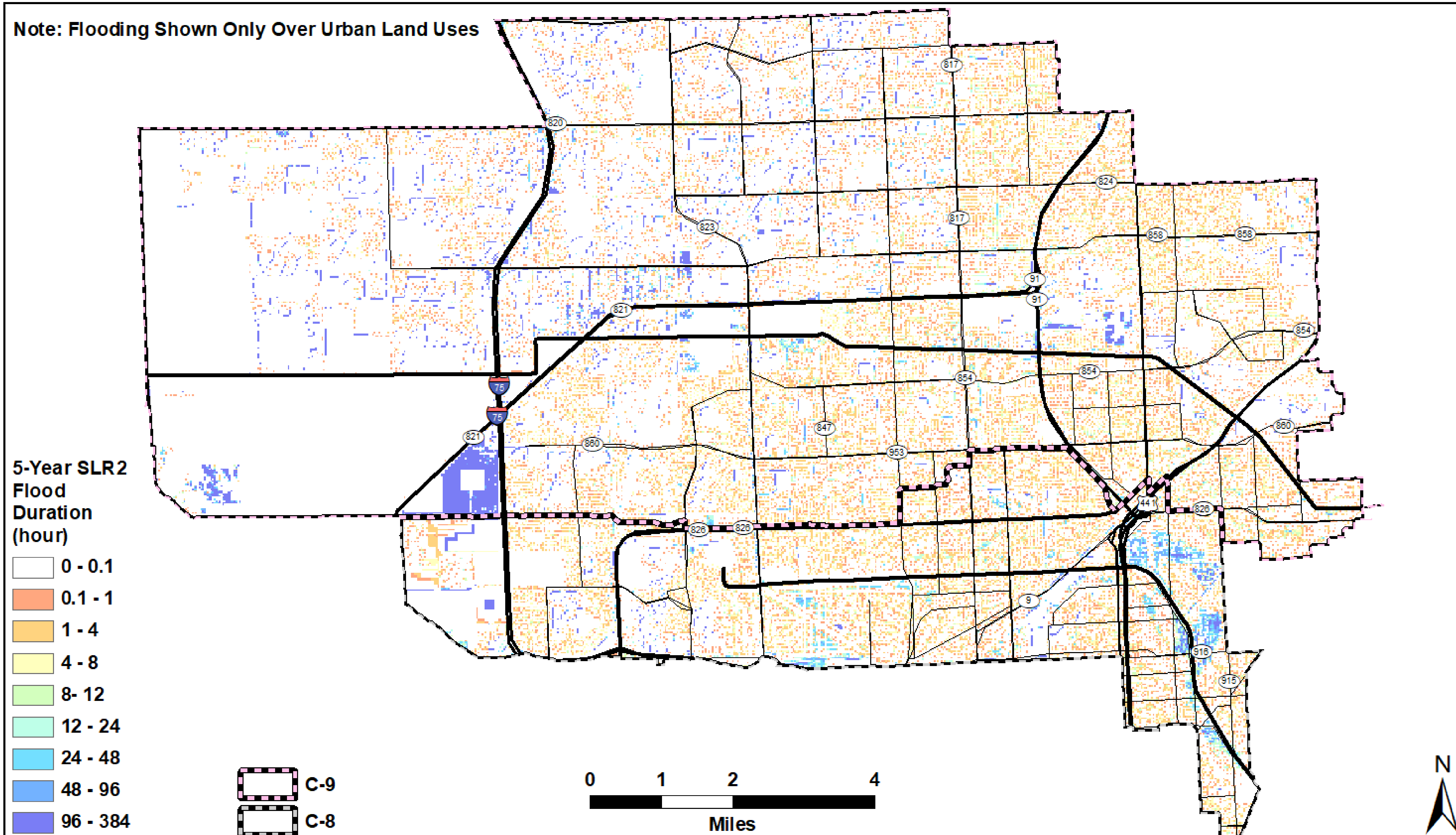

Figure 4.6-14: Flood Duration Map for 5-Year Sea Level Rise 2 Design Storm Event in Urban Land Use Areas

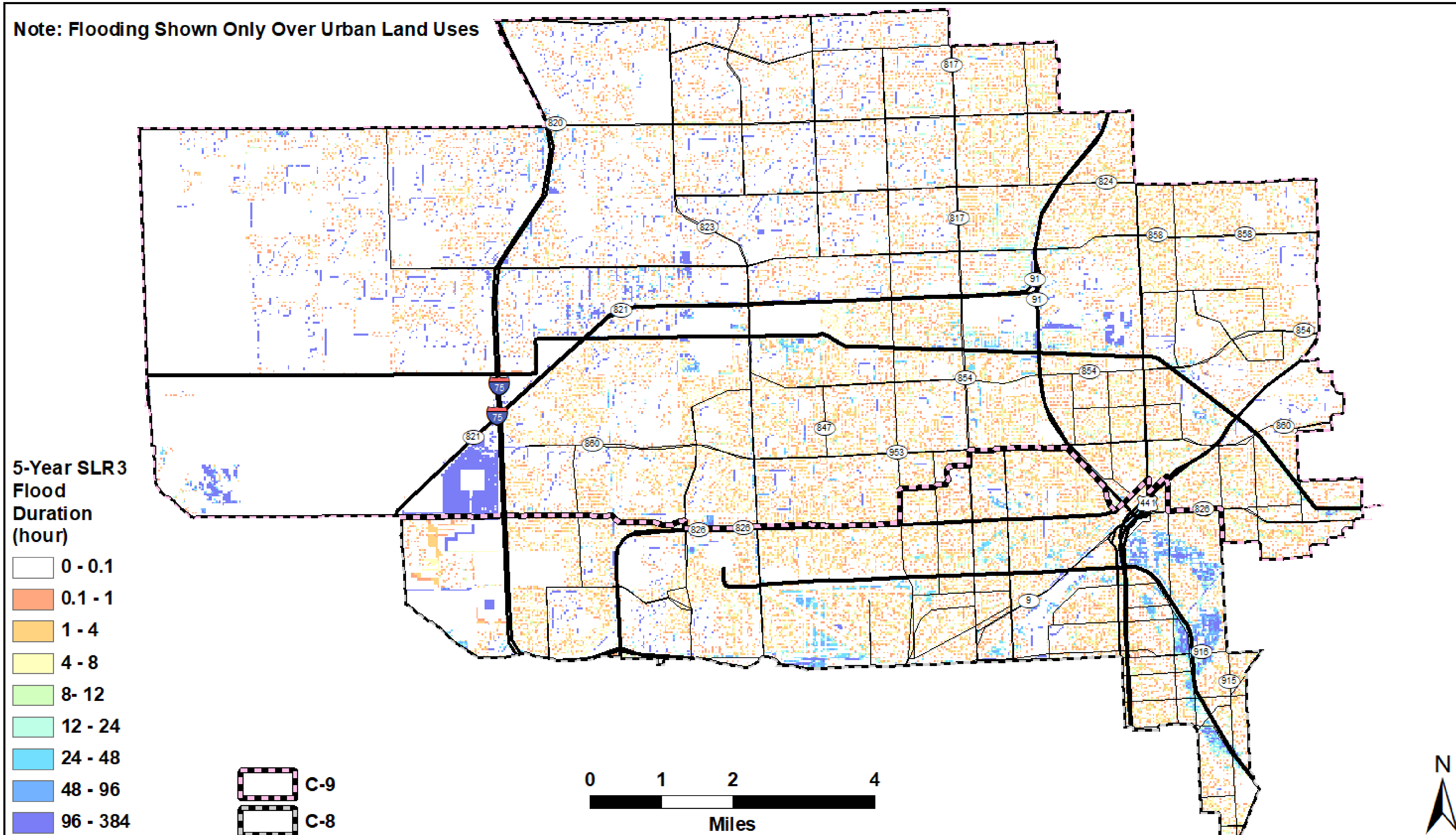

Figure 4.6-15: Flood Duration Map for 5-Year Sea Level Rise 3 Design Storm Event in Urban Land Use Areas

4.6.6 10-Year Design Storm Flood Duration Map for Urban Land Use Areas

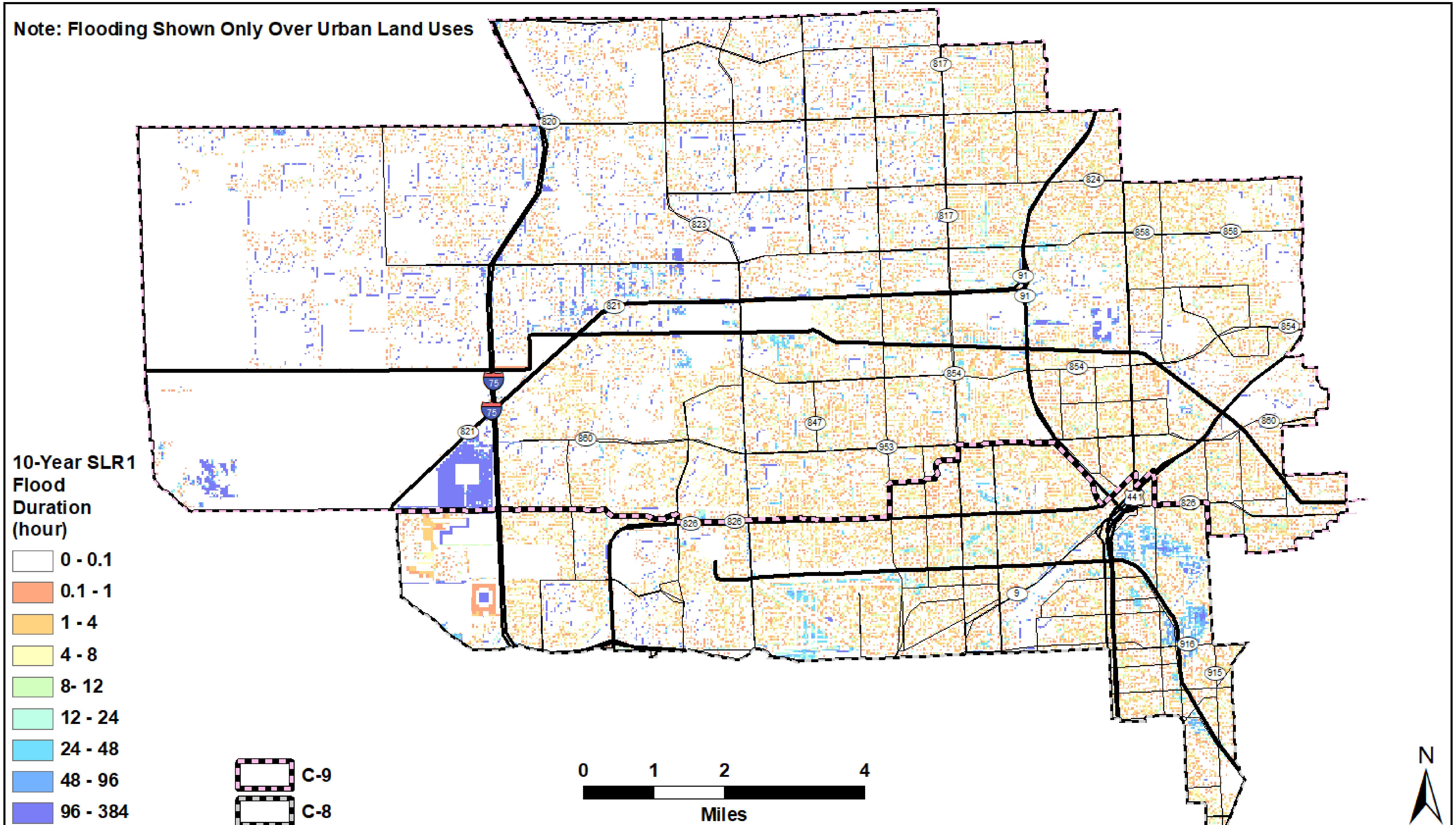

Figure 4.6-16: Flood Duration Map for 10-Year Sea Level Rise 1 Design Storm Event in Urban Land Use Areas

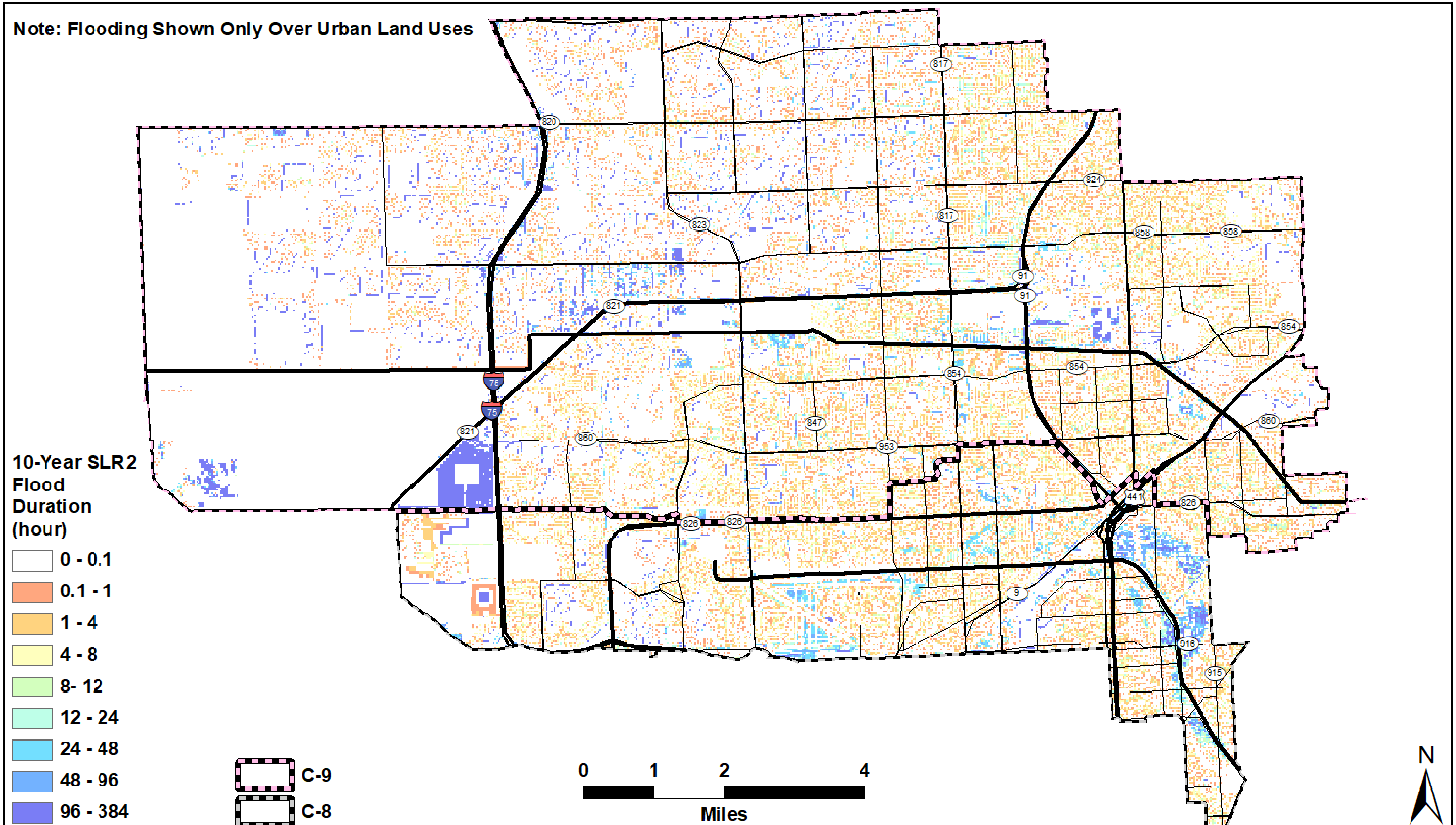

Figure 4.6-17: Flood Duration Map for 10-Year Sea Level Rise 2 Design Storm Event in Urban Land Use Areas

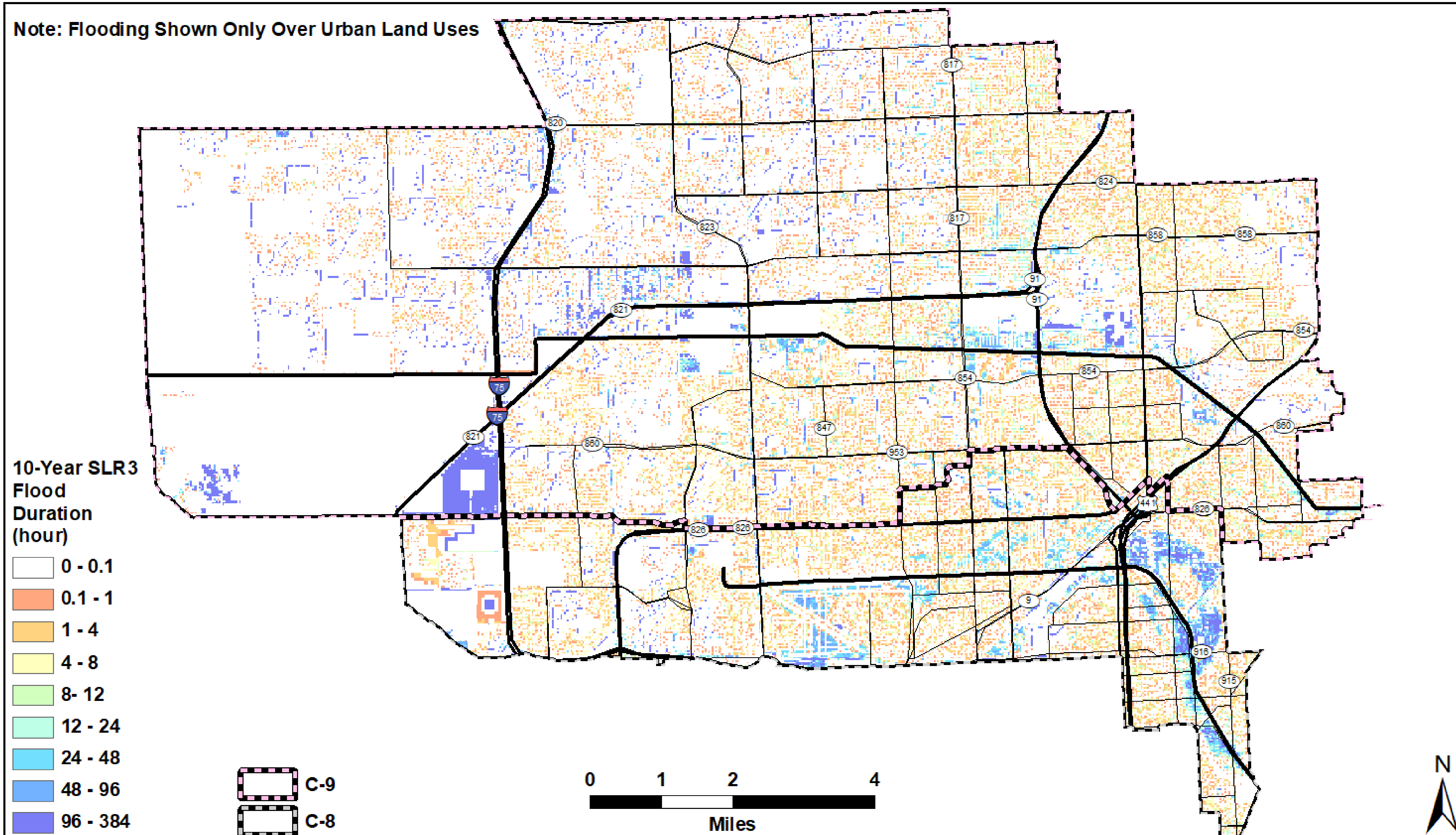

Figure 4.6-18: Flood Duration Map for 10-Year Sea Level Rise 3 Design Storm Event in Urban Land Use Areas

4.6.7 25-Year Design Storm Flood Duration Map for Urban Land Use Areas

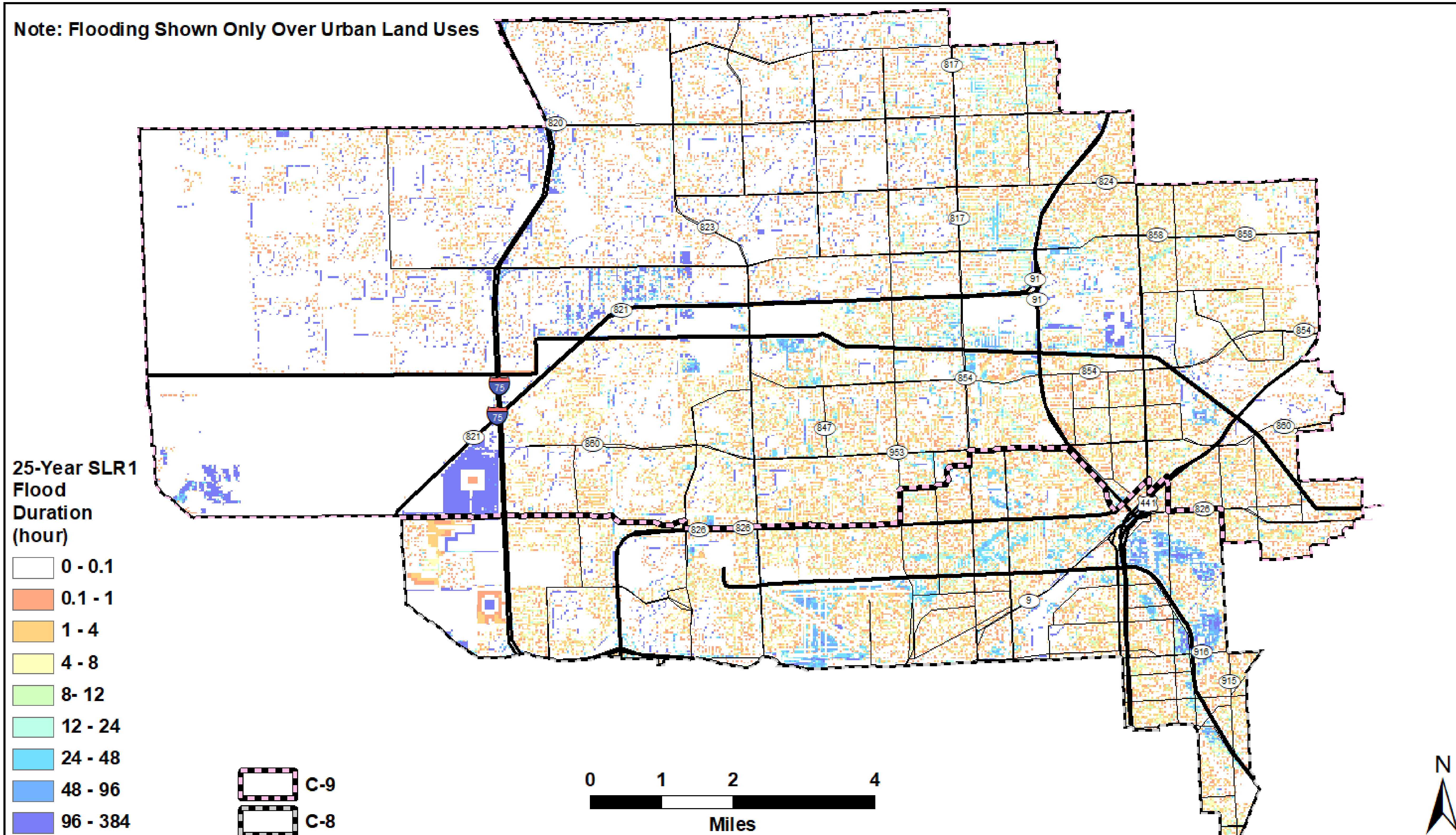

Figure 4.6-19: Flood Duration Map for 25-Year Sea Level Rise 1 Design Storm Event in Urban Land Use Areas

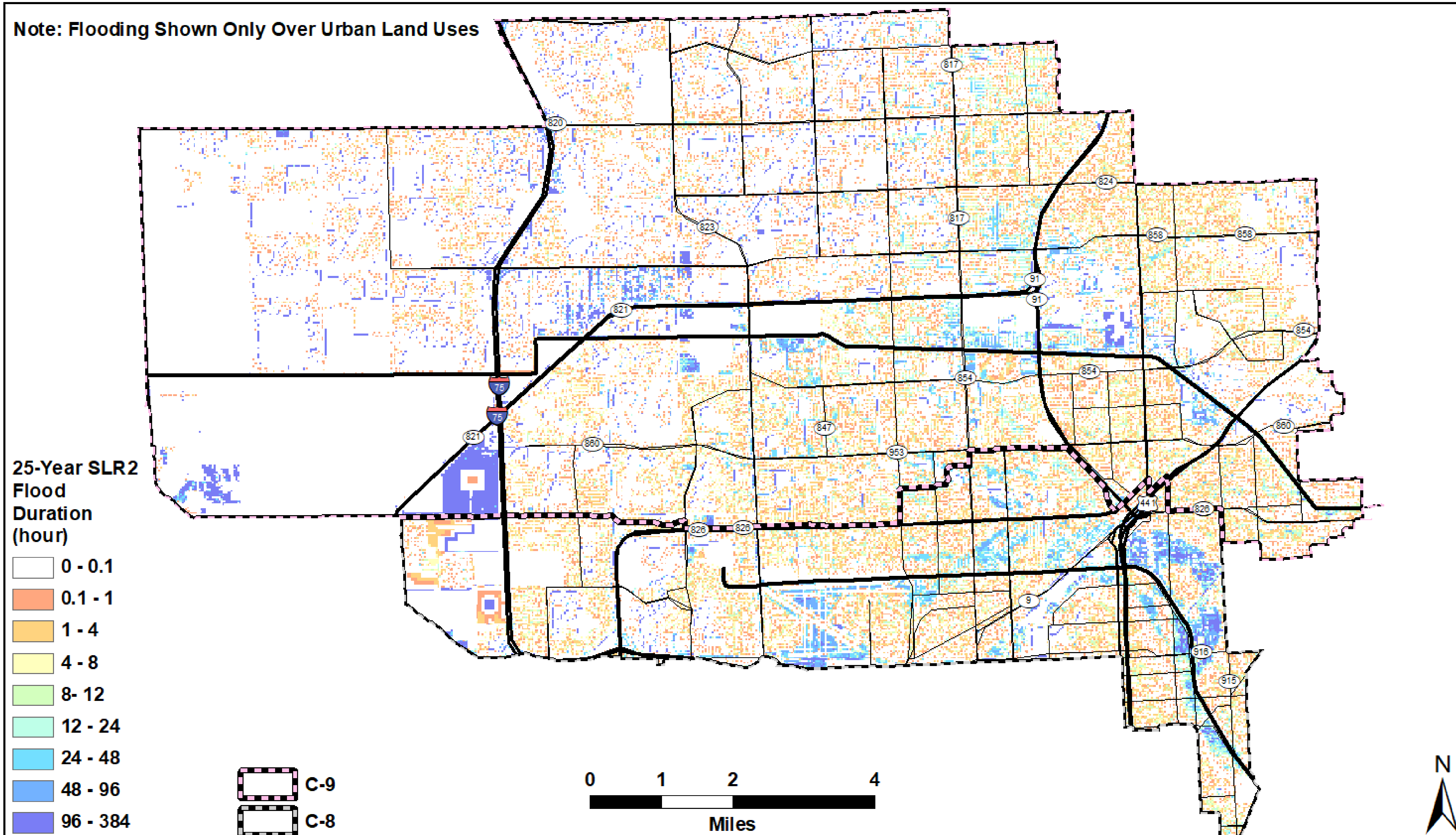

Figure 4.6-20: Flood Duration Map for 25-Year Sea Level Rise 2 Design Storm Event in Urban Land Use Areas

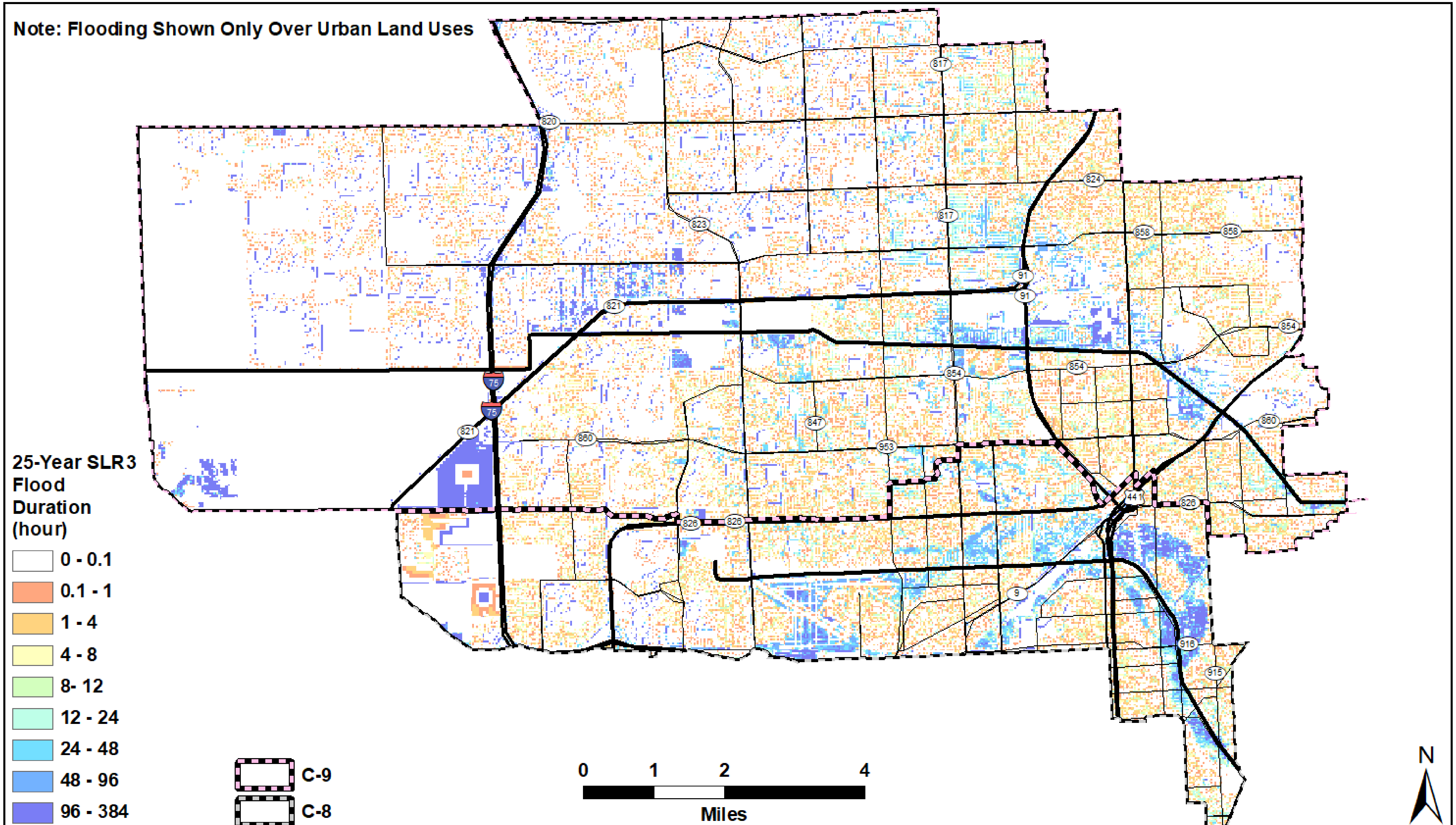

Figure 4.6-21: Flood Duration Map for 25-Year Sea Level Rise 3 Design Storm Event in Urban Land Use Areas

4.6.8 100-Year Design Storm Flood Duration Map for Urban Land Use Areas

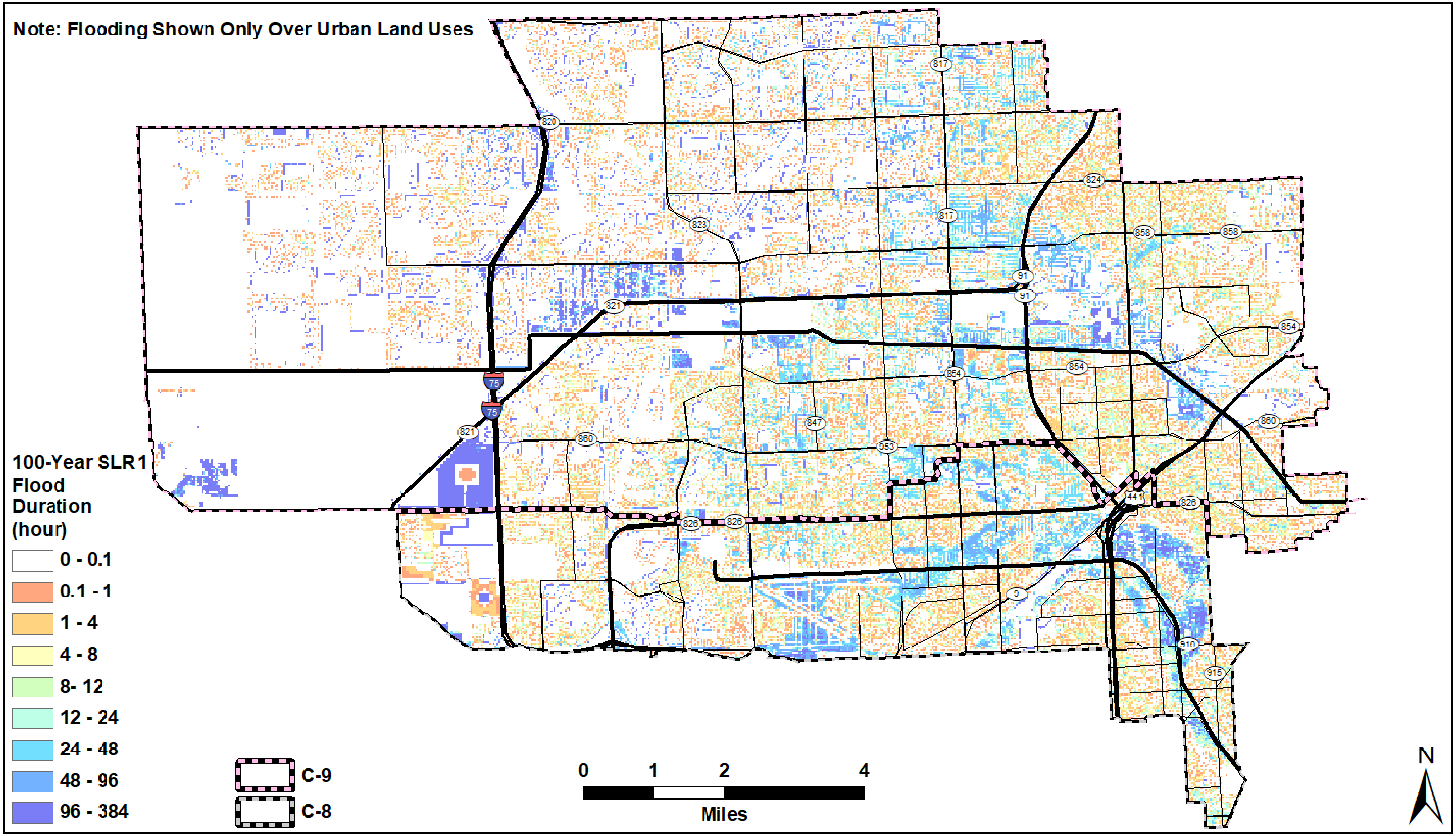

Figure 4.6-22: Flood Duration Map for 100-Year Sea Level Rise 1 Design Storm Event in Urban Land Use Areas

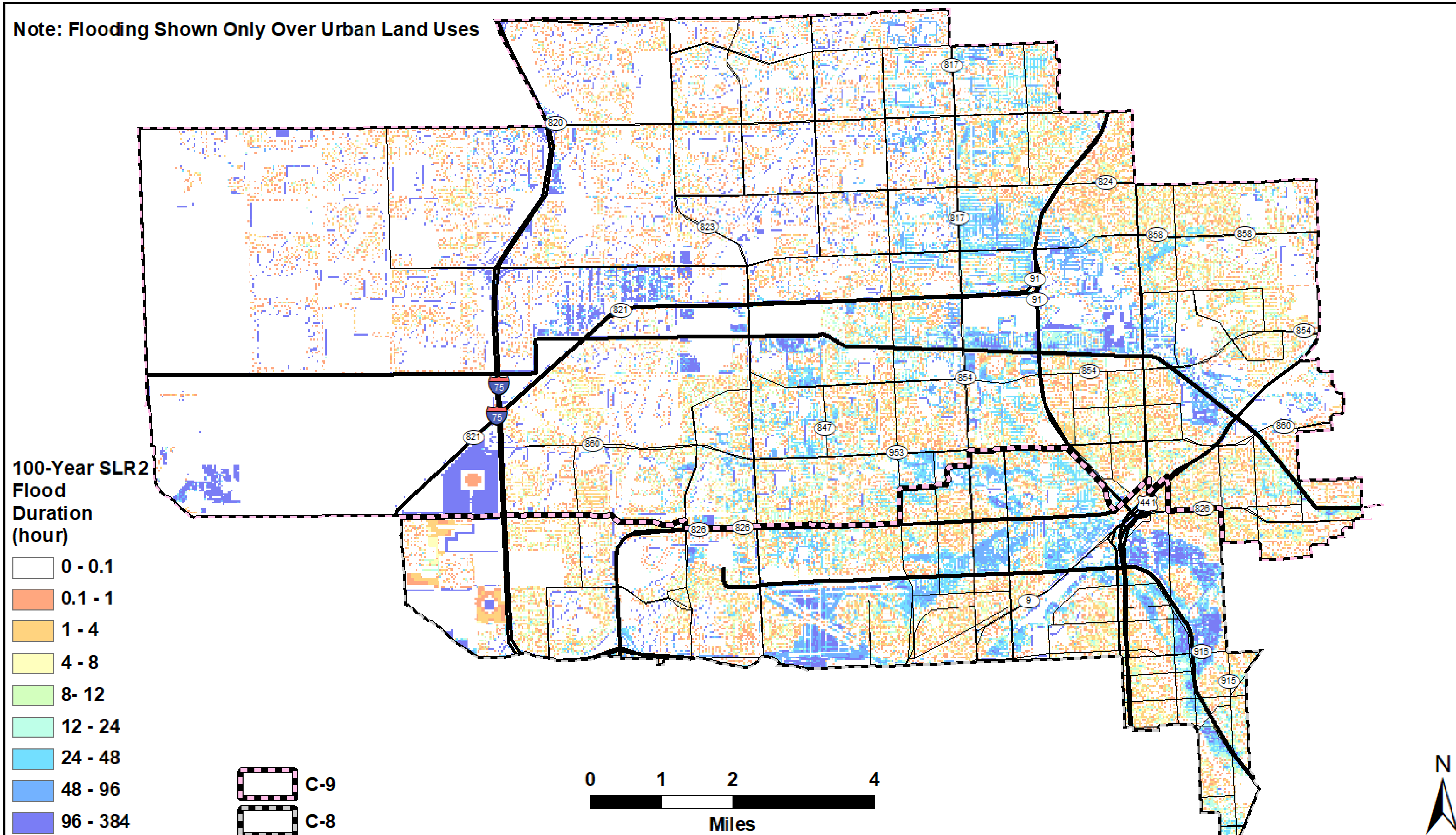

Figure 4.6-23: Flood Duration Map for 100-Year Sea Level Rise 2 Design Storm Event in Urban Land Use Areas

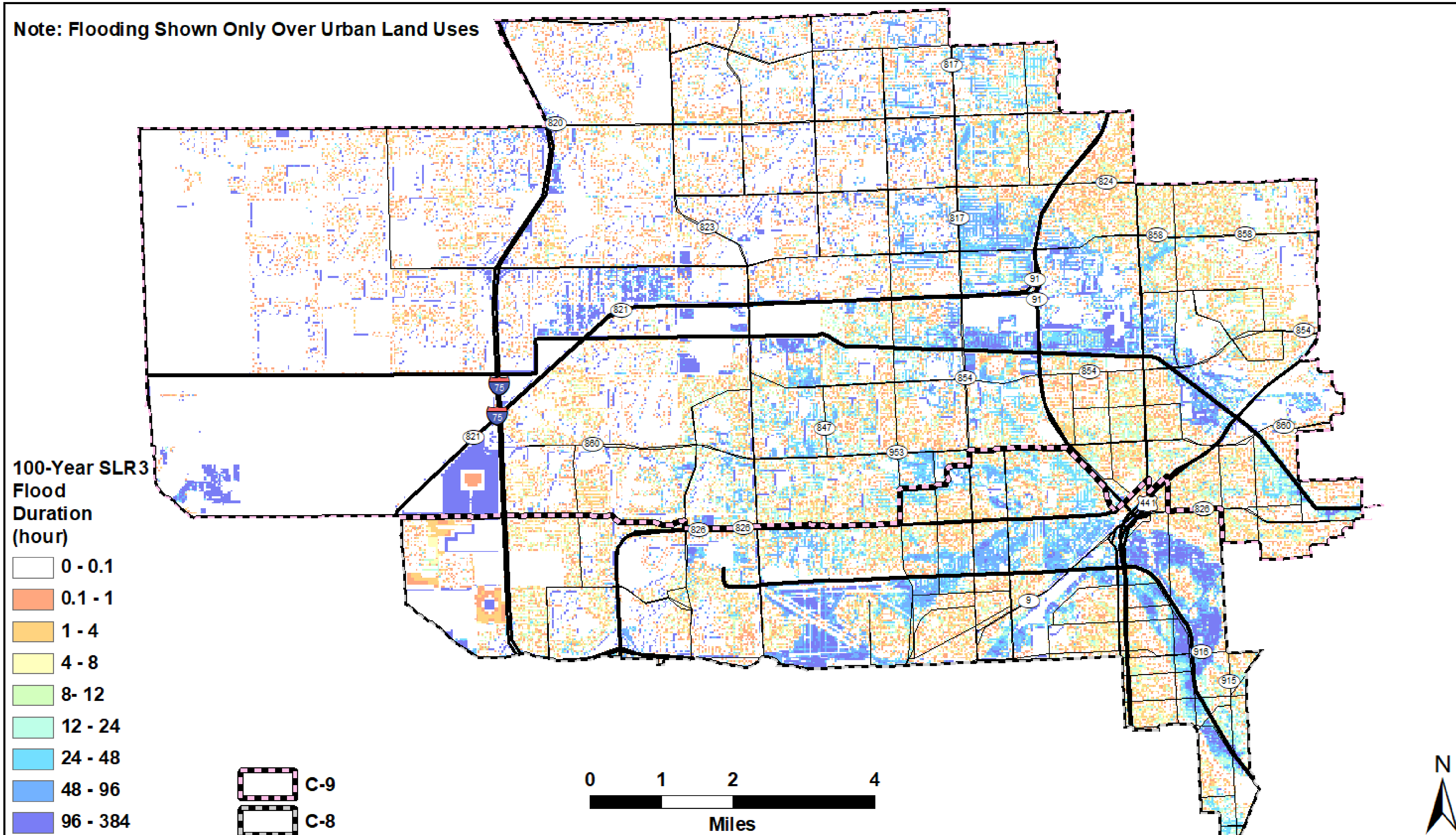

Figure 4.6-24: Flood Duration Map for 100-Year Sea Level Rise 3 Design Storm Event in Urban Land Use Areas

4.6.9 Up-Close Flood Duration Maps

4.6.9.1 Up-Close Flood Duration Maps for the C-8 Canal Between NE 135th St (CR916) and NE 6th Ave (CR915)

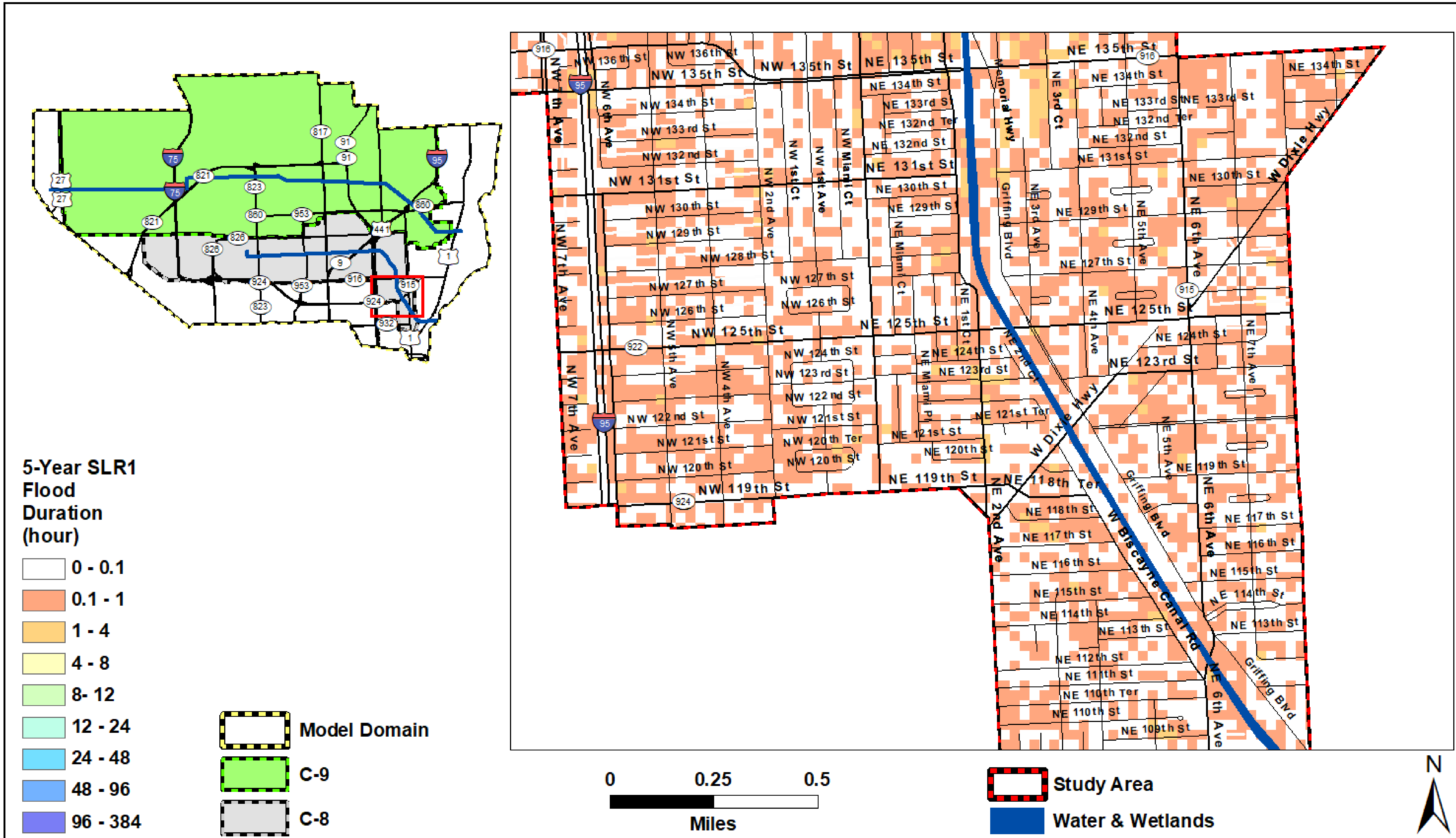

Figure 4.6-25: Up Close 5-Year Sea Level Rise 1 Flood Duration Map for the C-8 Canal Between and NE 135th St (CR916) and NE 6th Ave (CR915)

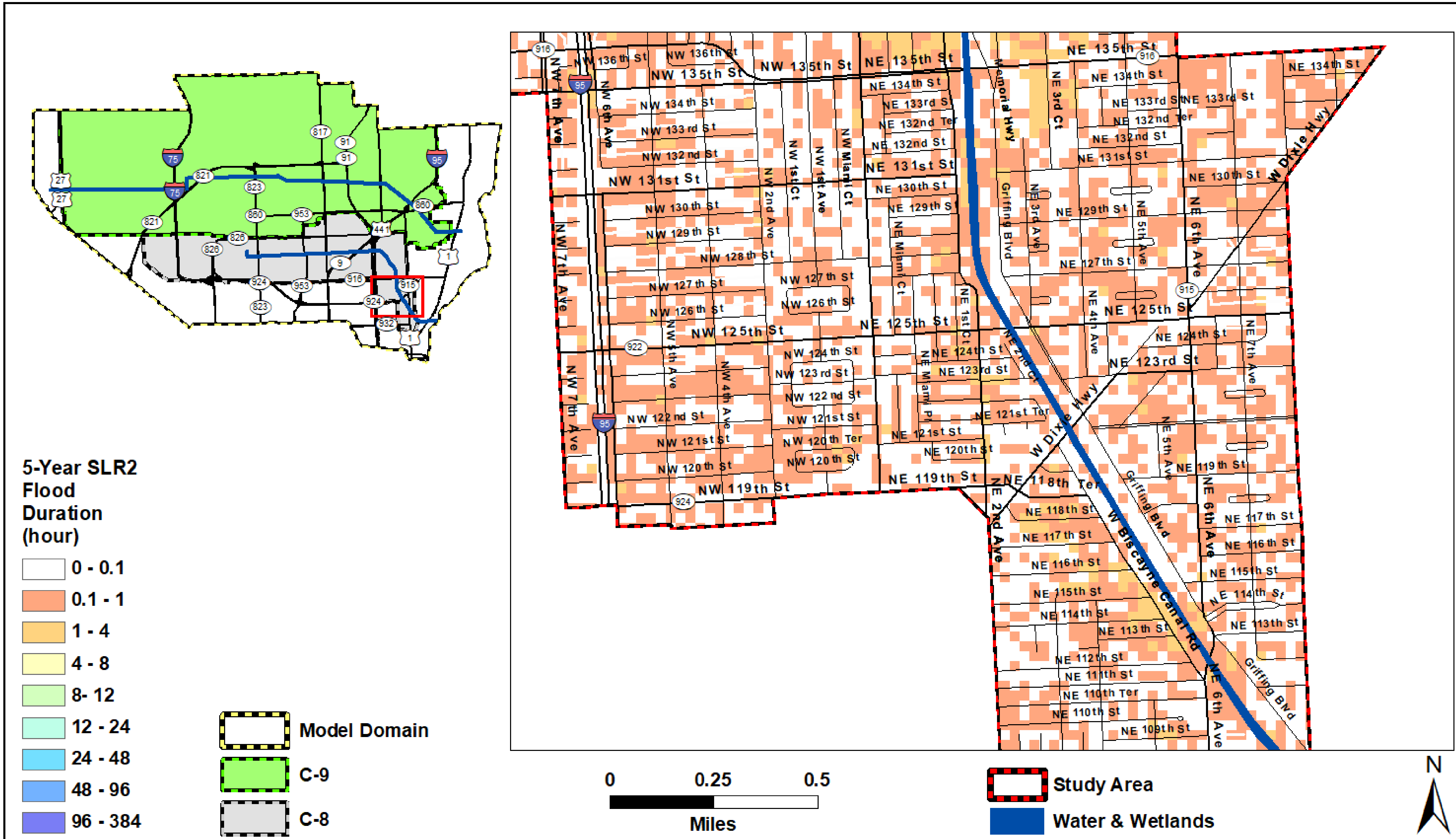

Figure 4.6-26: Up Close 5-Year Sea Level Rise 2 Flood Duration Map for the C-8 Canal Between and NE 135th St (CR916) and NE 6th Ave (CR915)

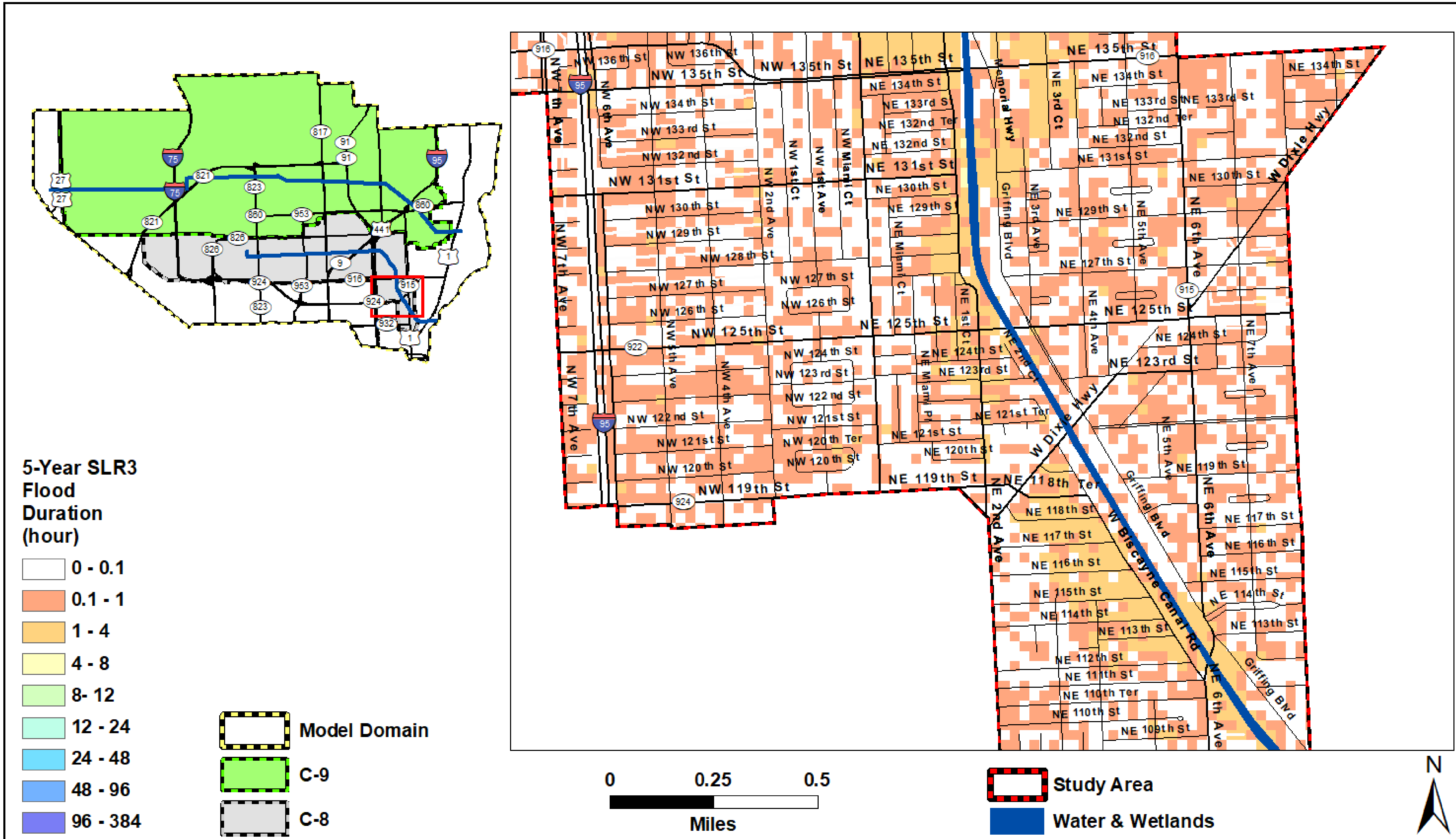

Figure 4.6-27: Up Close 5-Year Sea Level Rise 3 Flood Duration Map for the C-8 Canal Between and NE 135th St (CR916) and NE 6th Ave (CR915)

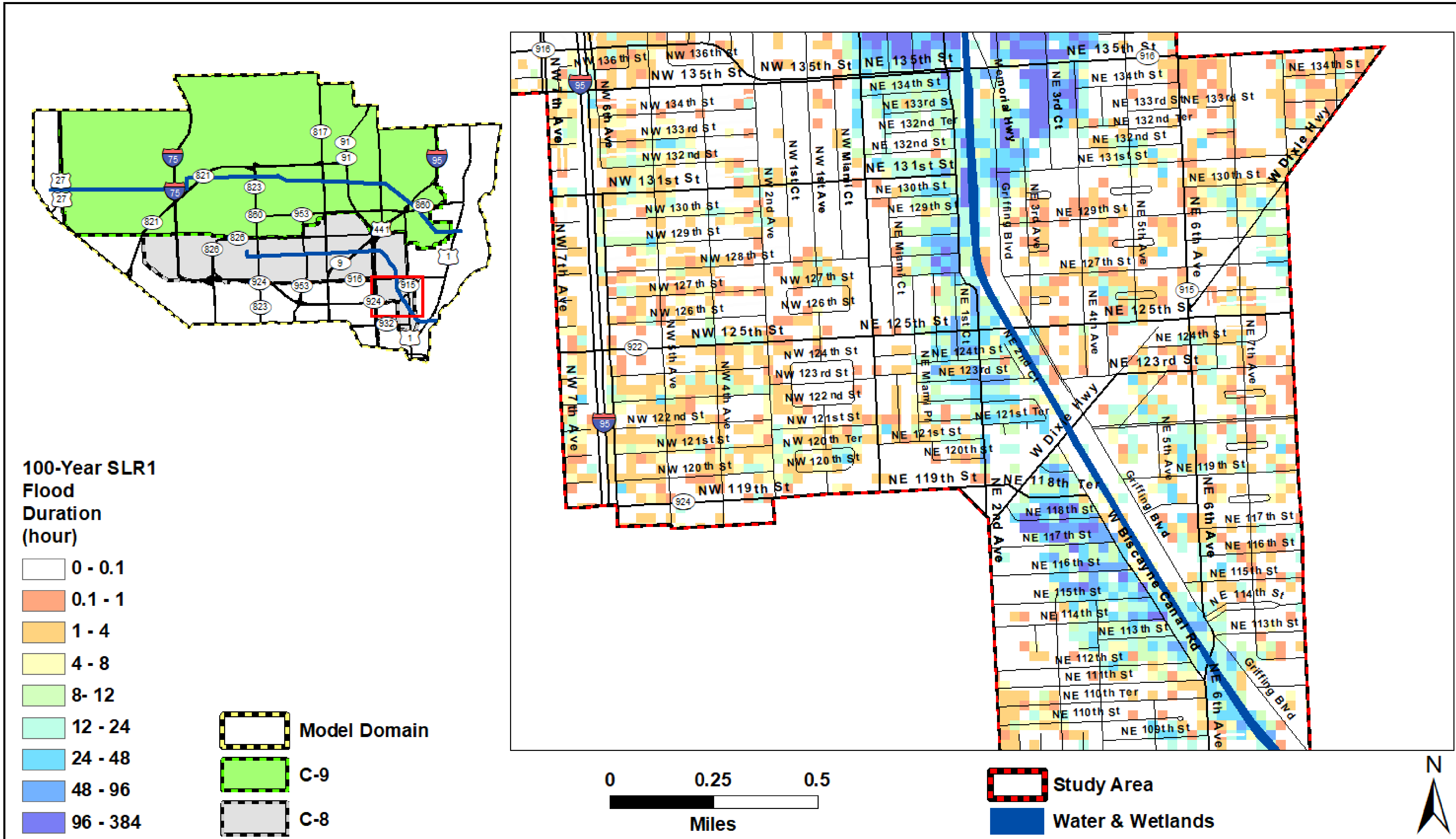

Figure 4.6-28: Up Close 100-Year Sea Level Rise 1 Flood Duration Map for the C-8 Canal Between and NE 135th St (CR916) and NE 6th Ave (CR915)

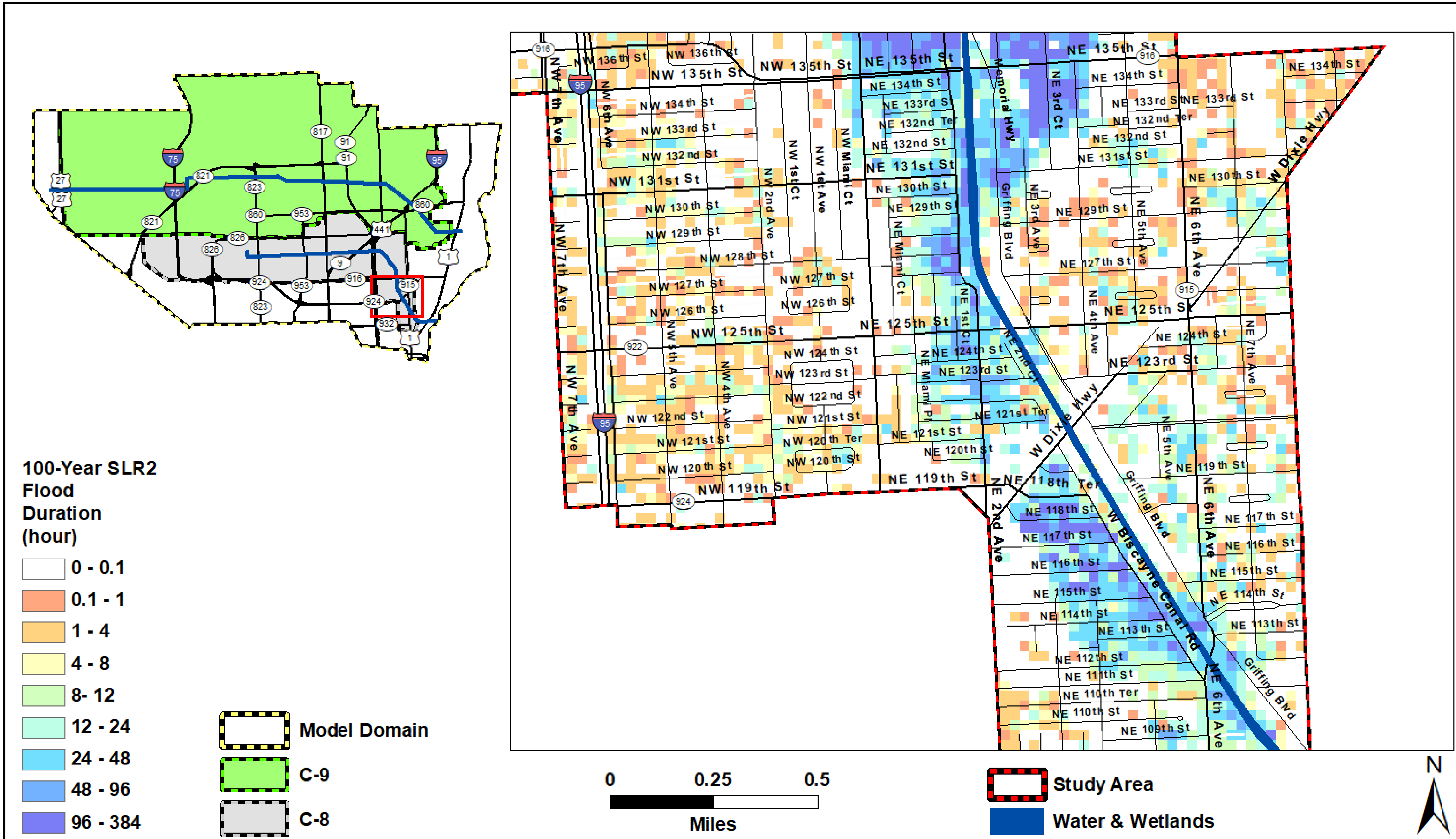

Figure 4.6-29: Up Close 100-Year Sea Level Rise 2 Flood Duration Map for the C-8 Canal Between and NE 135th St (CR916) and NE 6th Ave (CR915)

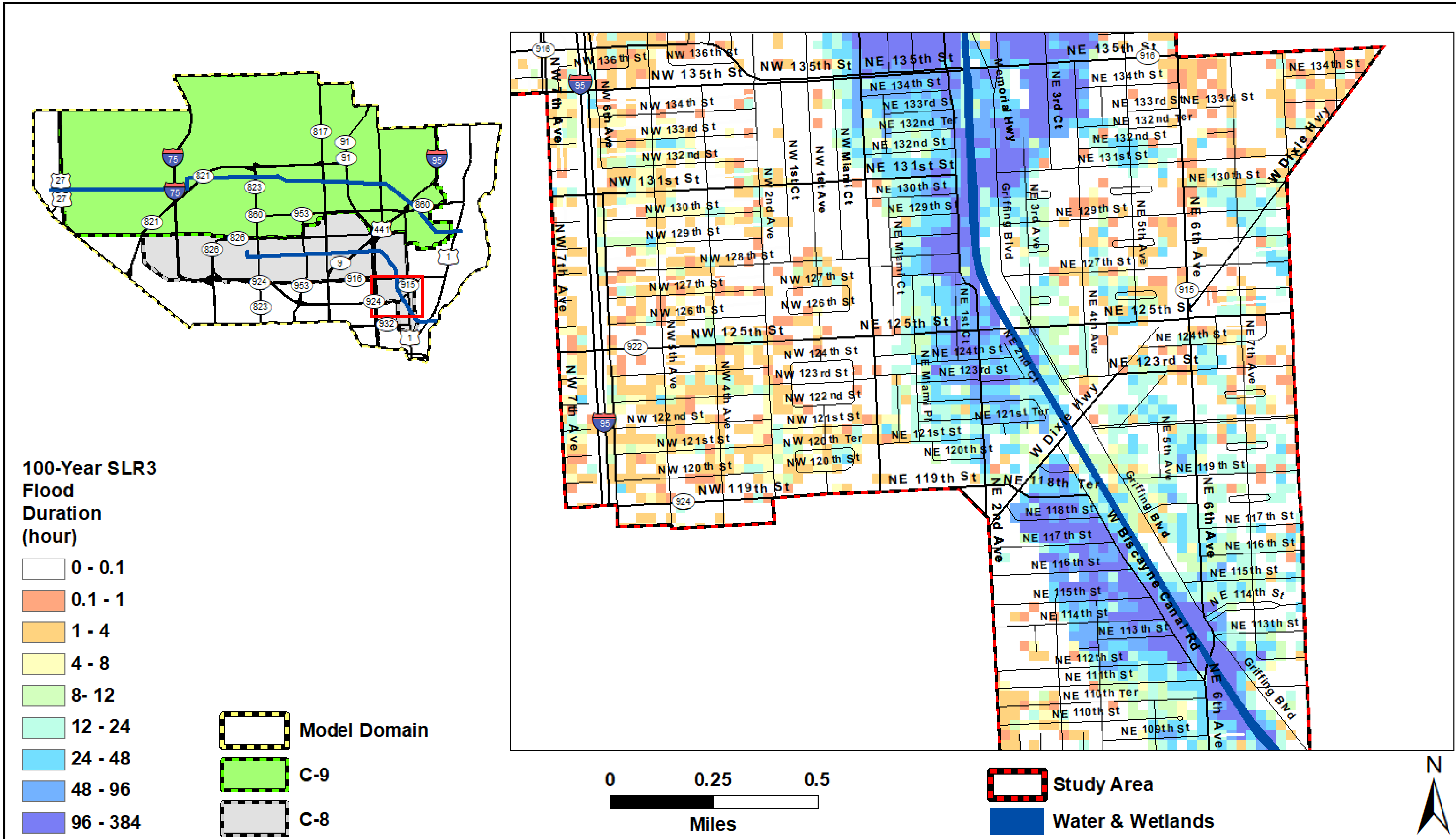

Figure 4.6-30: Up Close 100-Year Sea Level Rise 3 Flood Duration Map for the C-8 Canal Between and NE 135th St (CR916) and NE 6th Ave (CR915)

4.6.9.2 Up-Close Flood Duration Maps for the C-8 Canal Between North Miami Ave and NE 135th St (CR916)

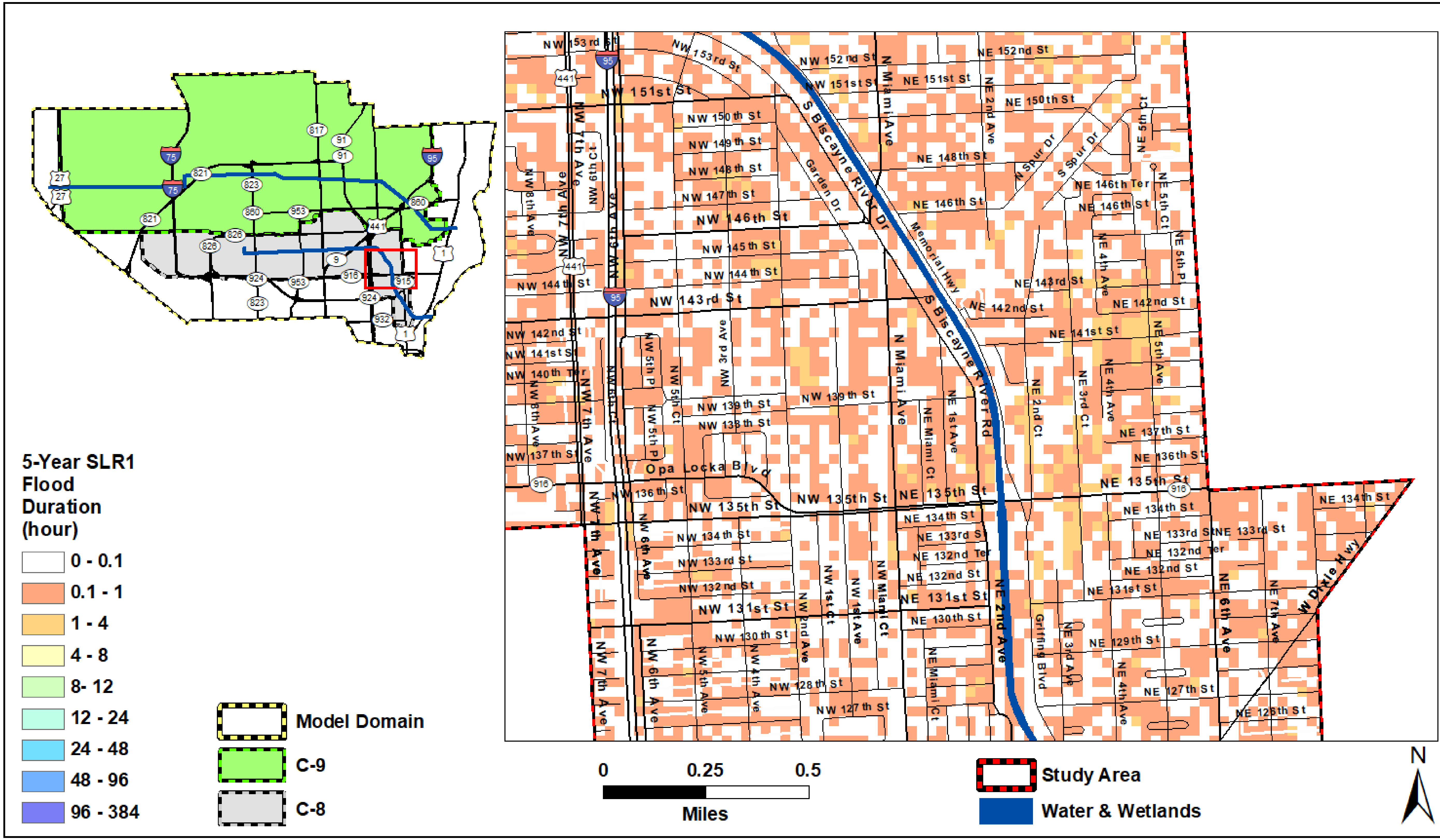

Figure 4.6-31: Up Close 5-Year Sea Level Rise 1 Flood Duration Map for the C-8 Canal Between North Miami Ave and NE 135th St (CR916)

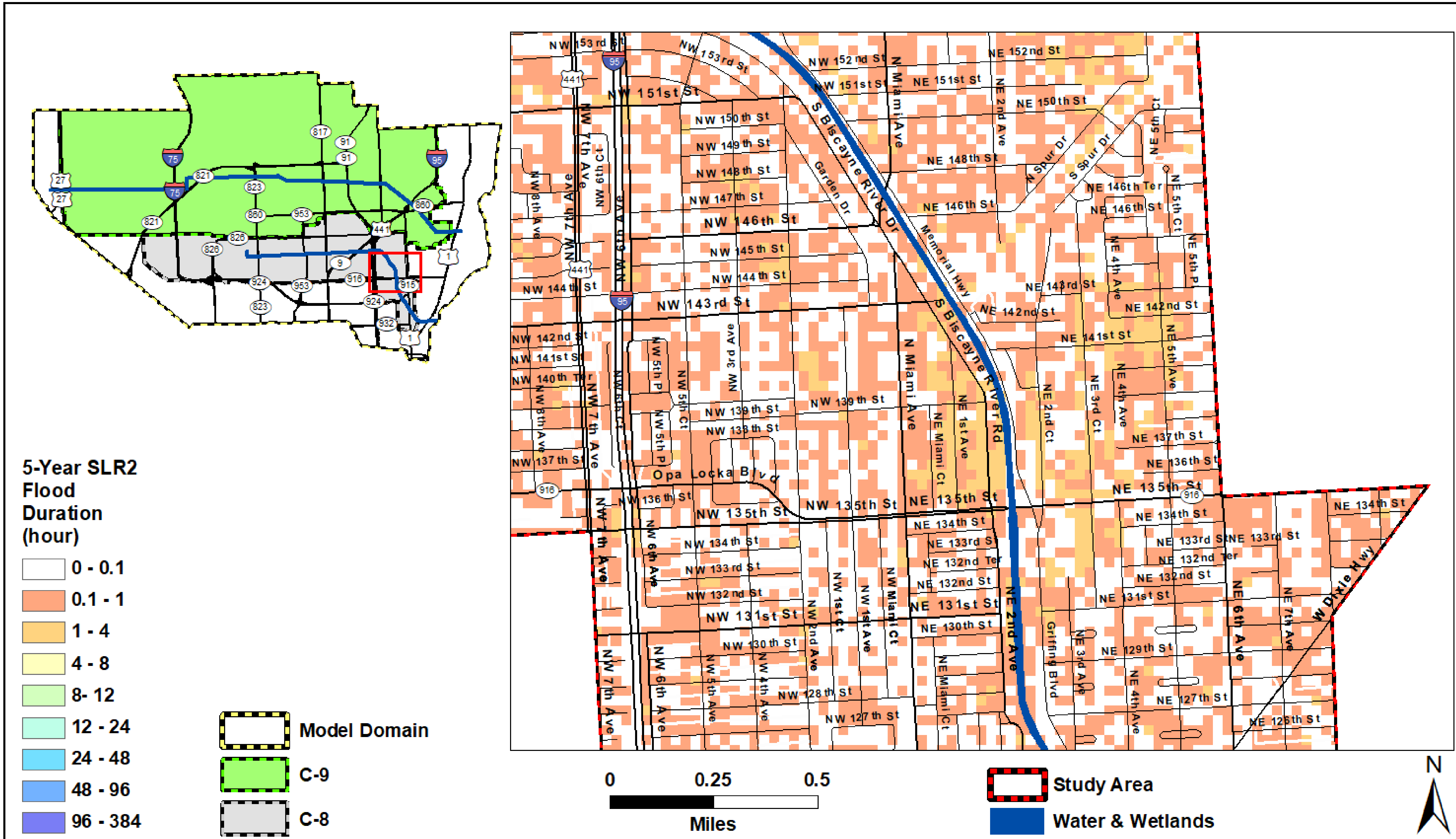

Figure 4.6-32: Up Close 5-Year Sea Level Rise 2 Flood Duration Map for the C-8 Canal Between North Miami Ave and NE 135th St (CR916)

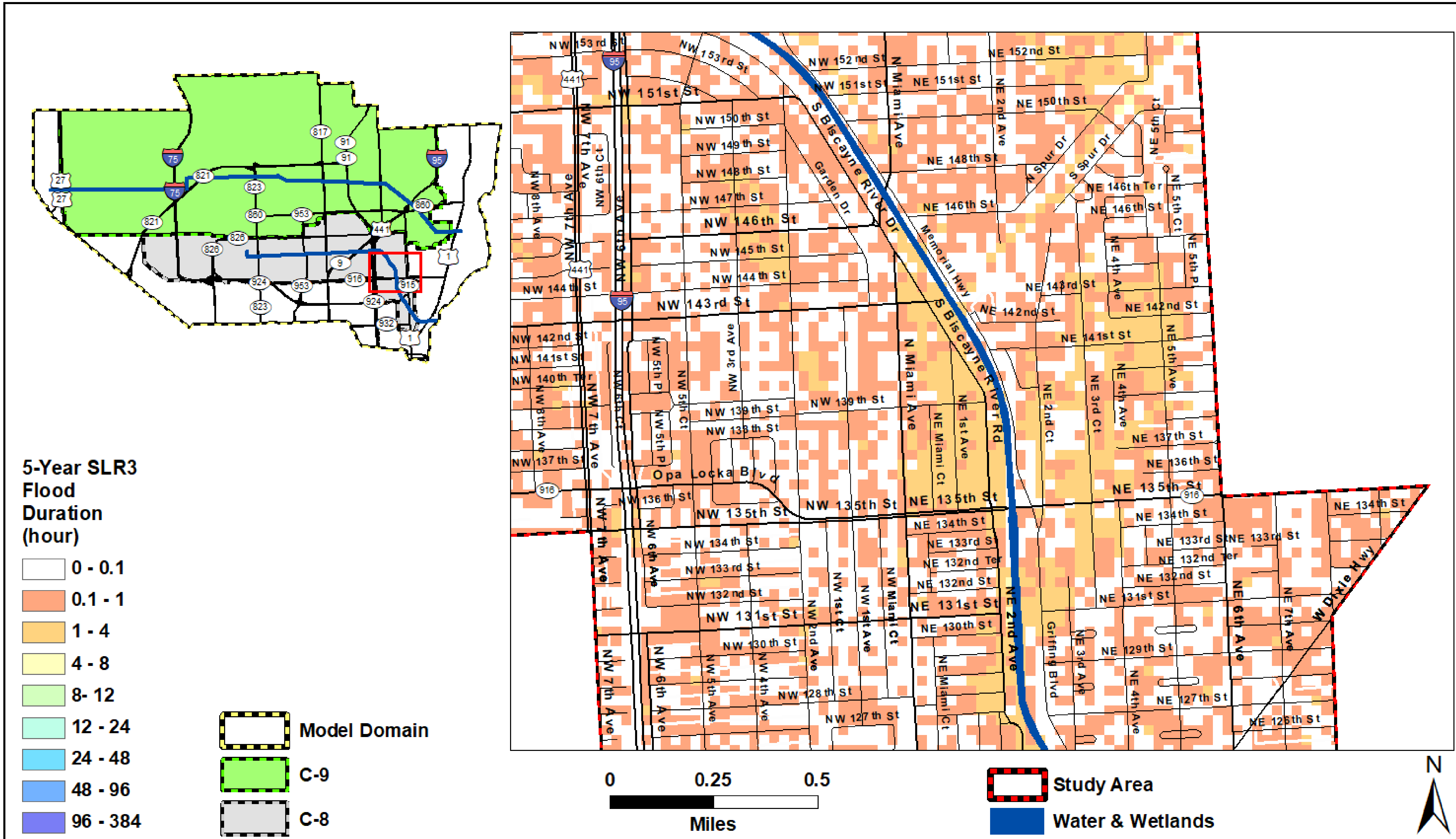

Figure 4.6-33: Up Close 5-Year Sea Level Rise 3 Flood Duration Map for the C-8 Canal Between North Miami Ave and NE 135th St (CR916)

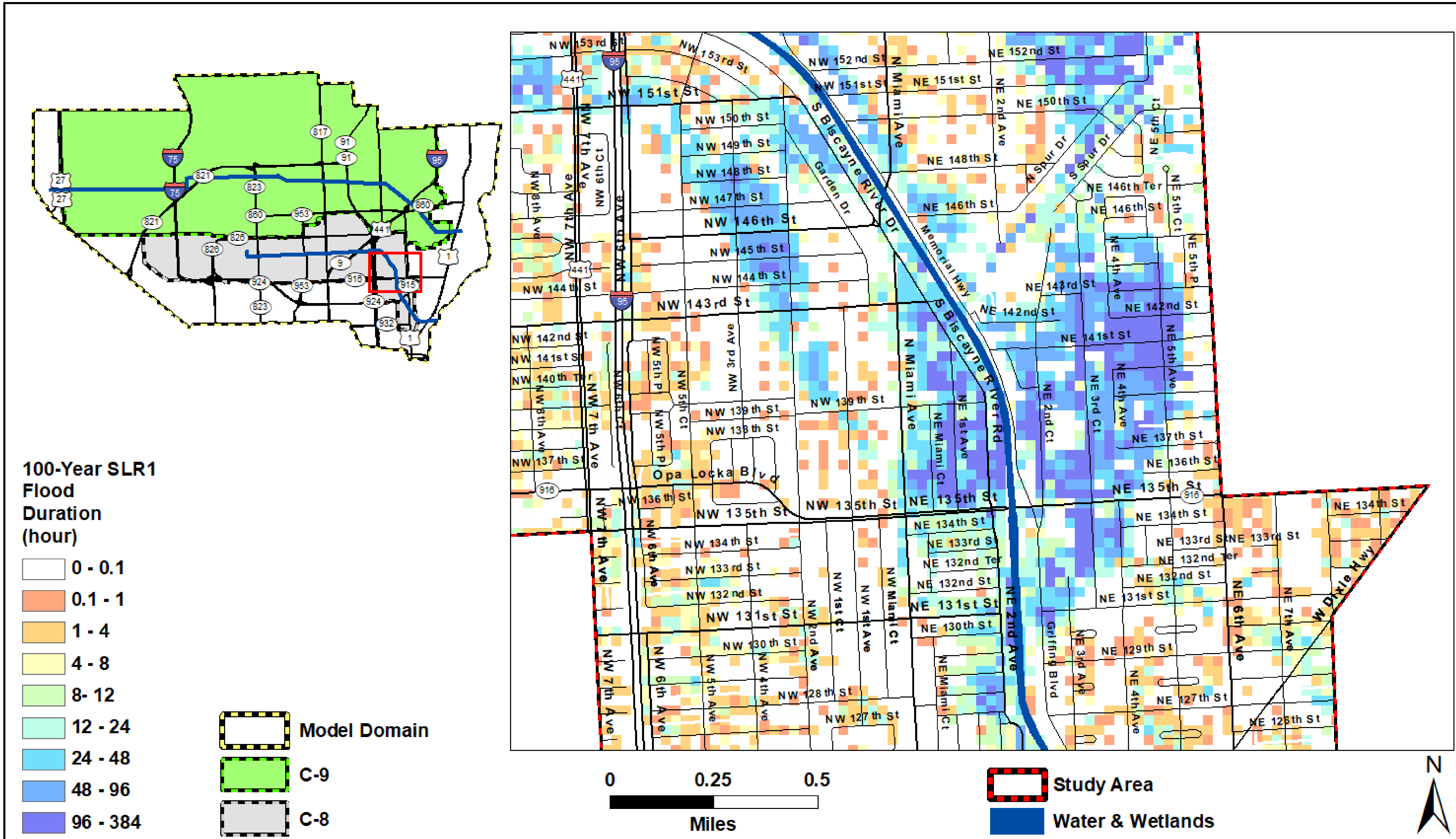

Figure 4.6-34: Up Close 100-Year Sea Level Rise 1 Flood Duration Map for the C-8 Canal Between North Miami Ave and NE 135th St (CR916)

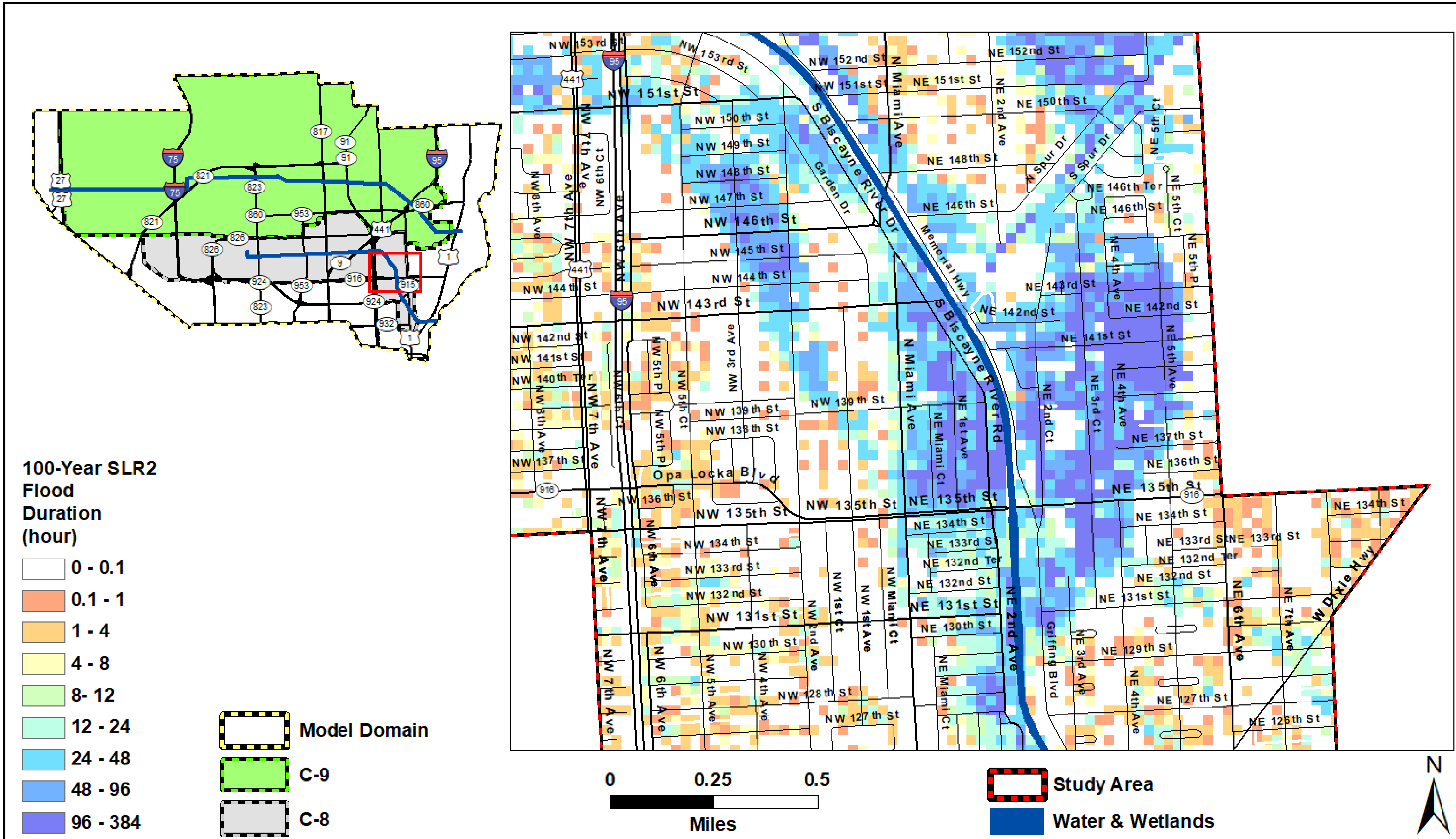

Figure 4.6-35: Up Close 100-Year Sea Level Rise 2 Flood Duration Map for the C-8 Canal Between North Miami Ave and NE 135th St (CR916)

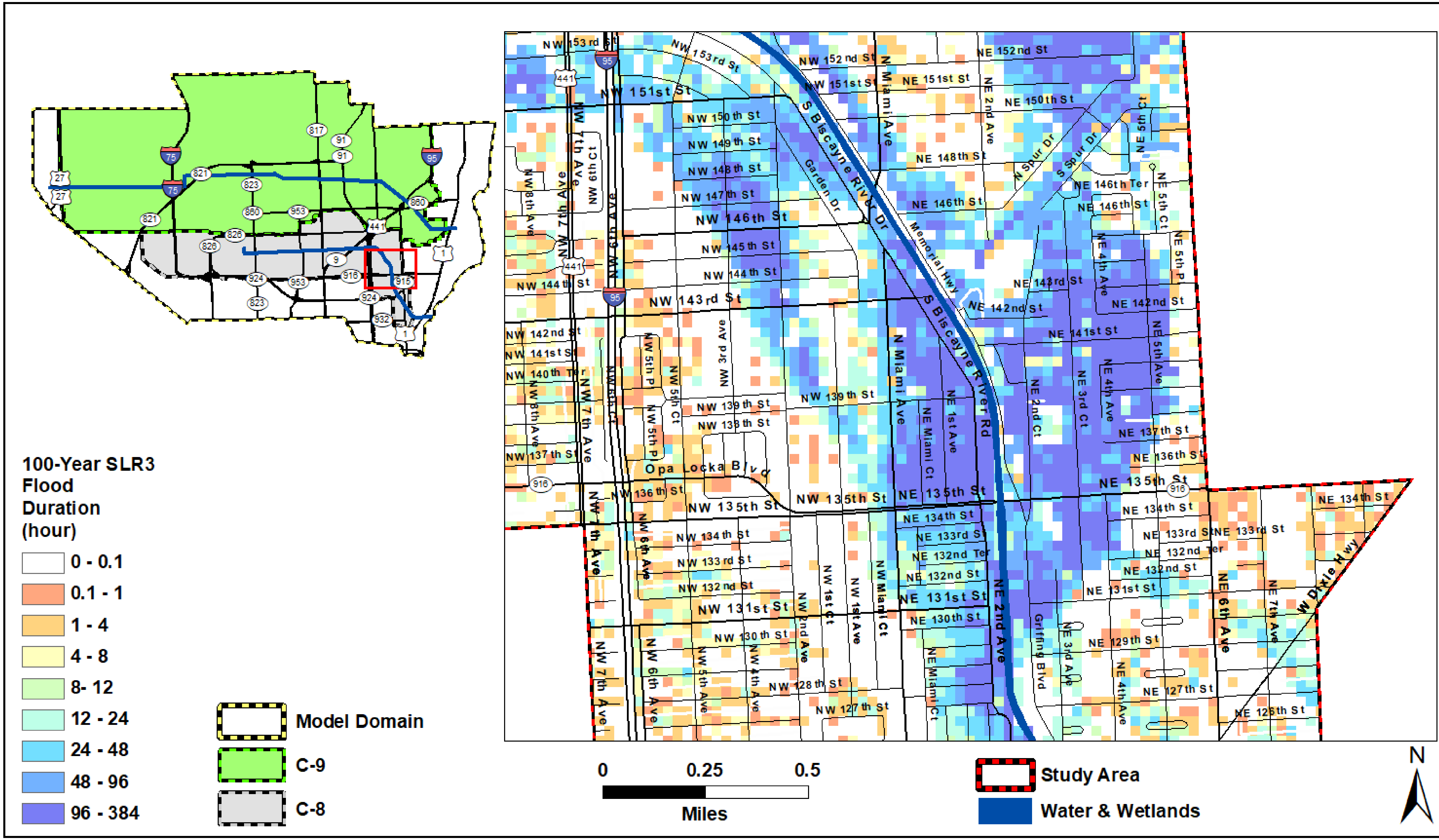

Figure 4.6-36: Up Close 100-Year Sea Level Rise 3 Flood Duration Map for the C-8 Canal Between North Miami Ave and NE 135th St (CR916)

4.6.9.3 Up-Close Flood Duration Maps for the C-8 Canal Near Opa Locka Canal

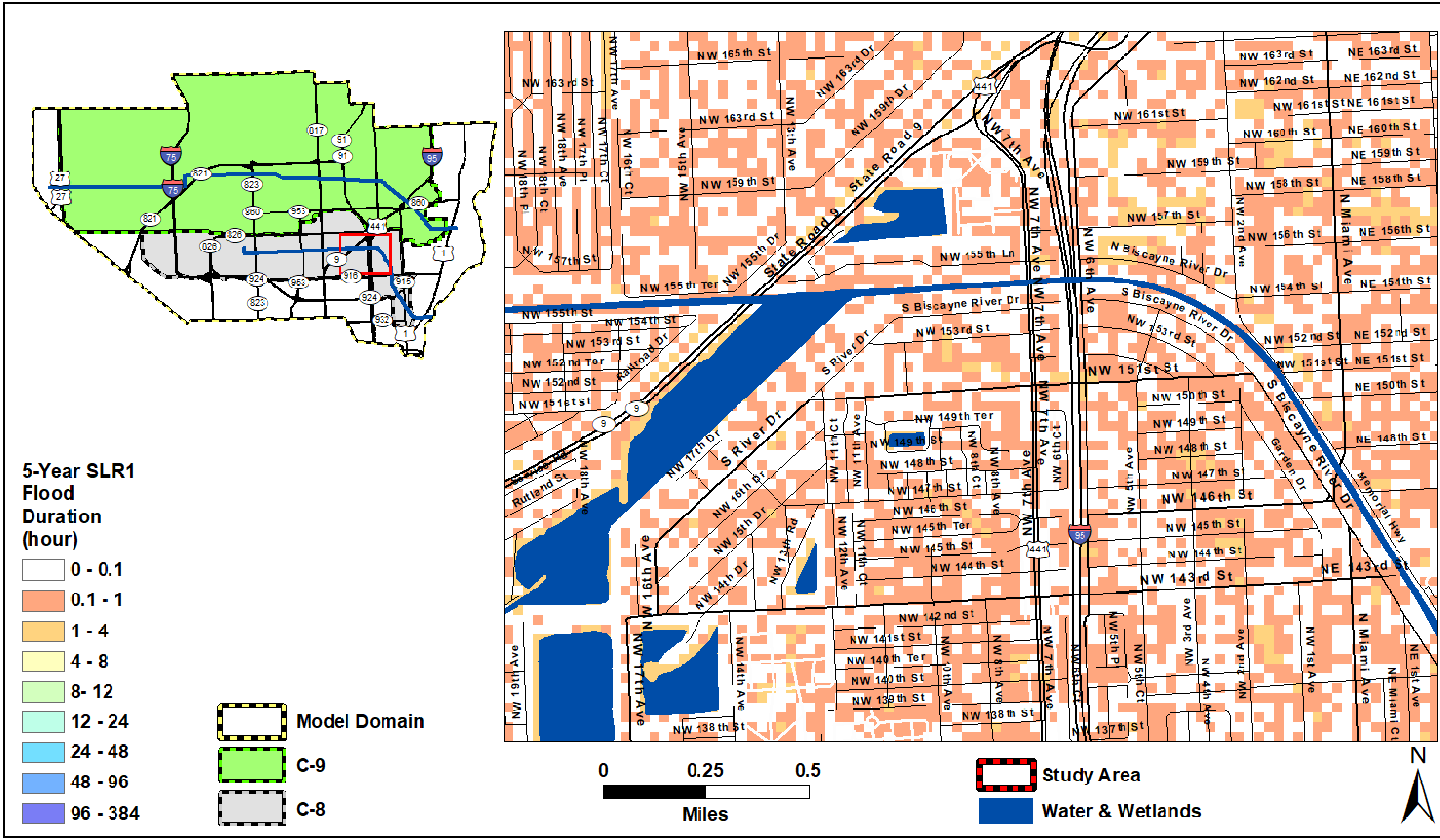

Figure 4.6-37: Up Close 5-Year Sea Level Rise 1 Flood Duration Map for the C-8 Canal Near Opa Locka Canal

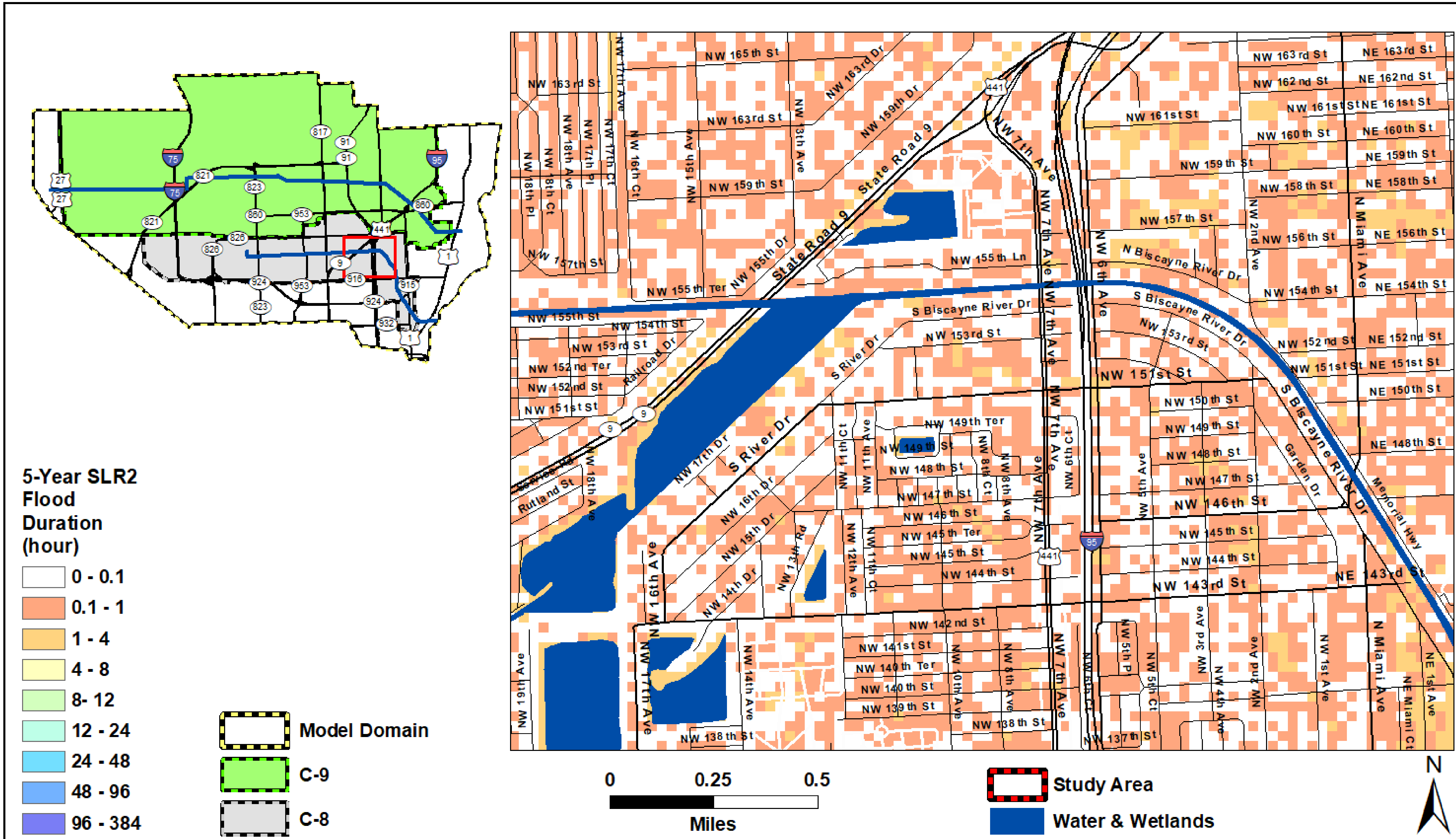

Figure 4.6-38: Up Close 5-Year Sea Level Rise 2 Flood Duration Map for the C-8 Canal Near Opa Locka Canal

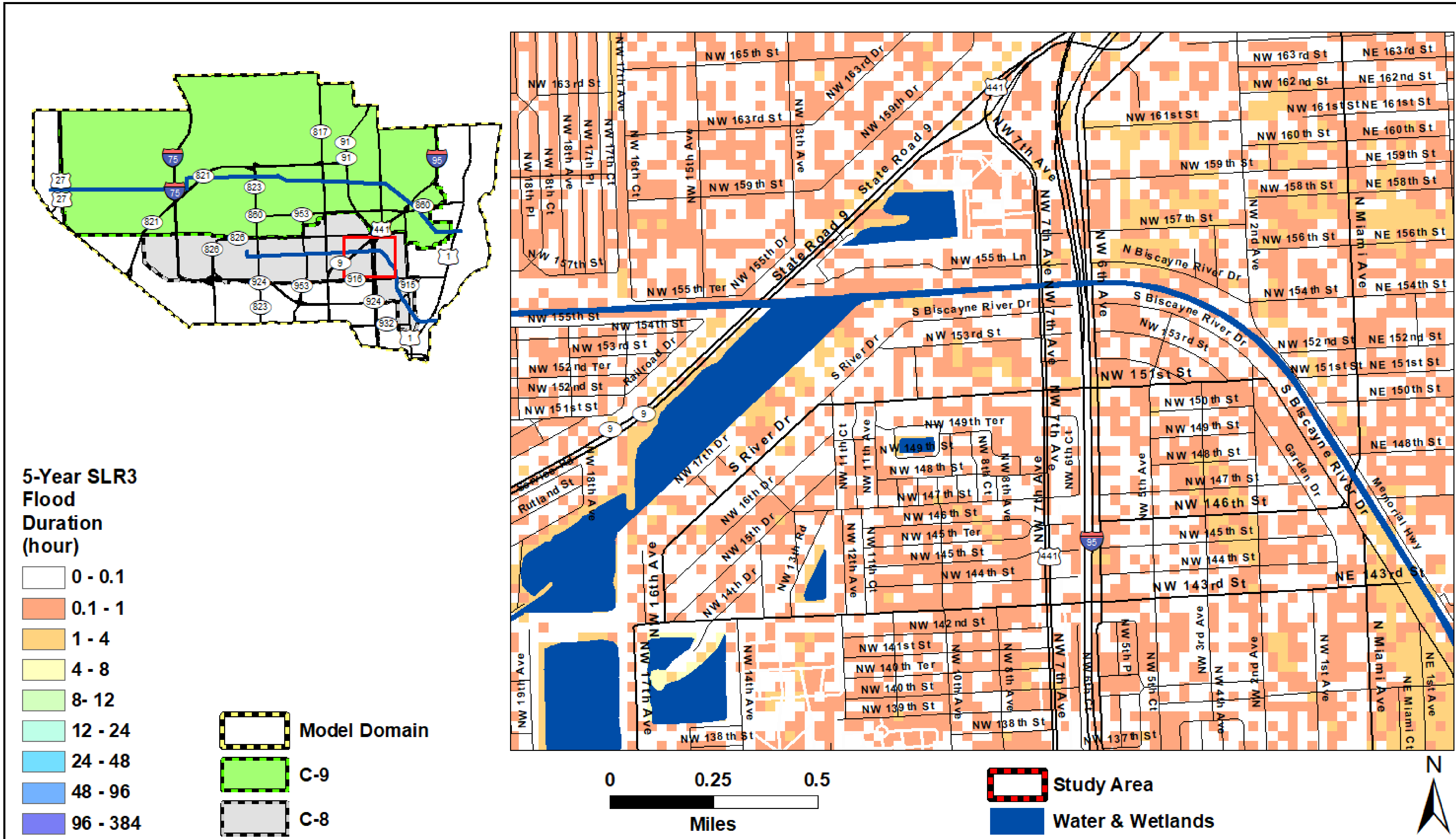

Figure 4.6-39: Up Close 5-Year Sea Level Rise 3 Flood Duration Map for the C-8 Canal Near Opa Locka Canal

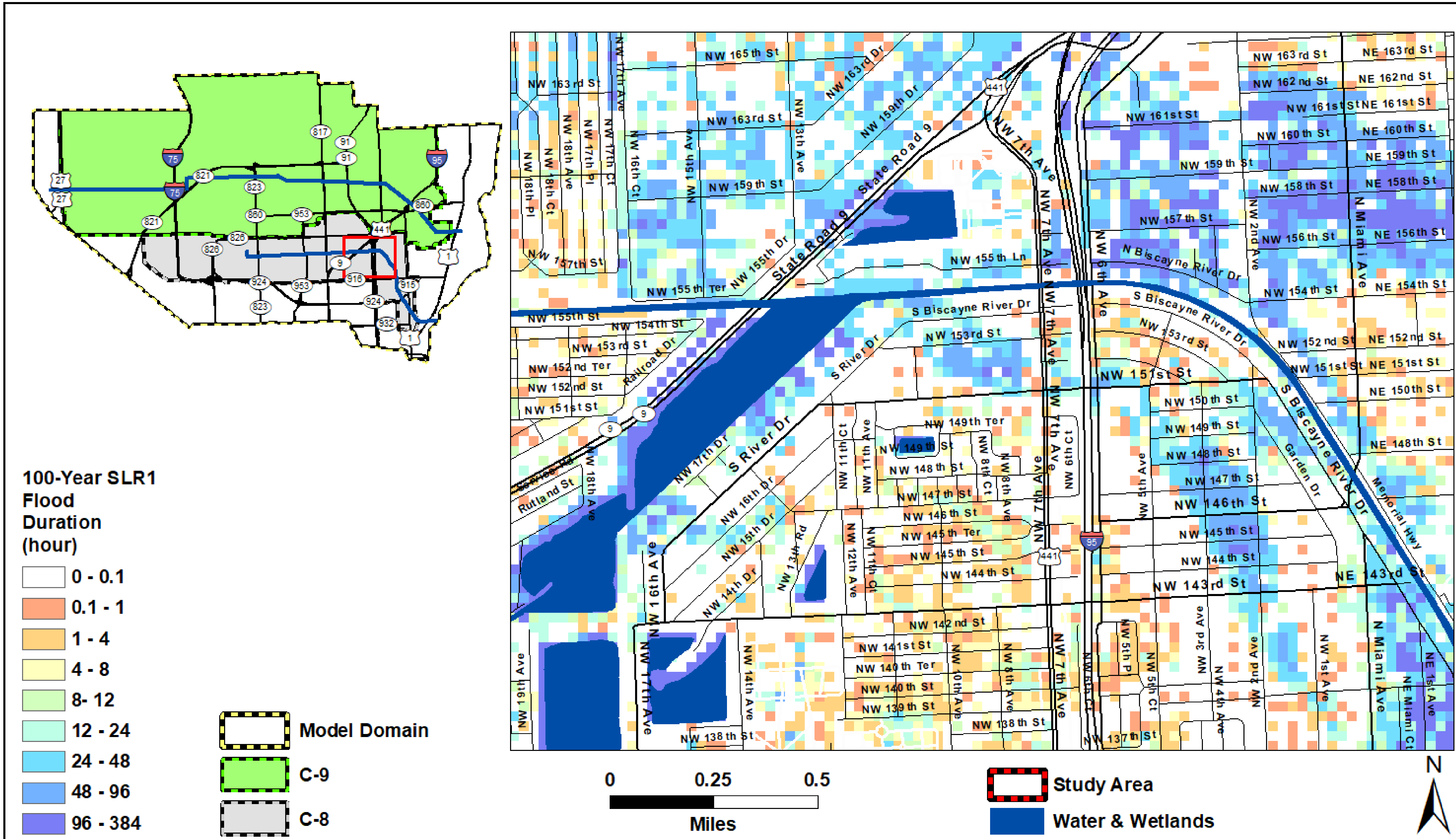

Figure 4.6-40: Up Close 100-Year Sea Level Rise 1 Flood Duration Map for the C-8 Canal Near Opa Locka Canal

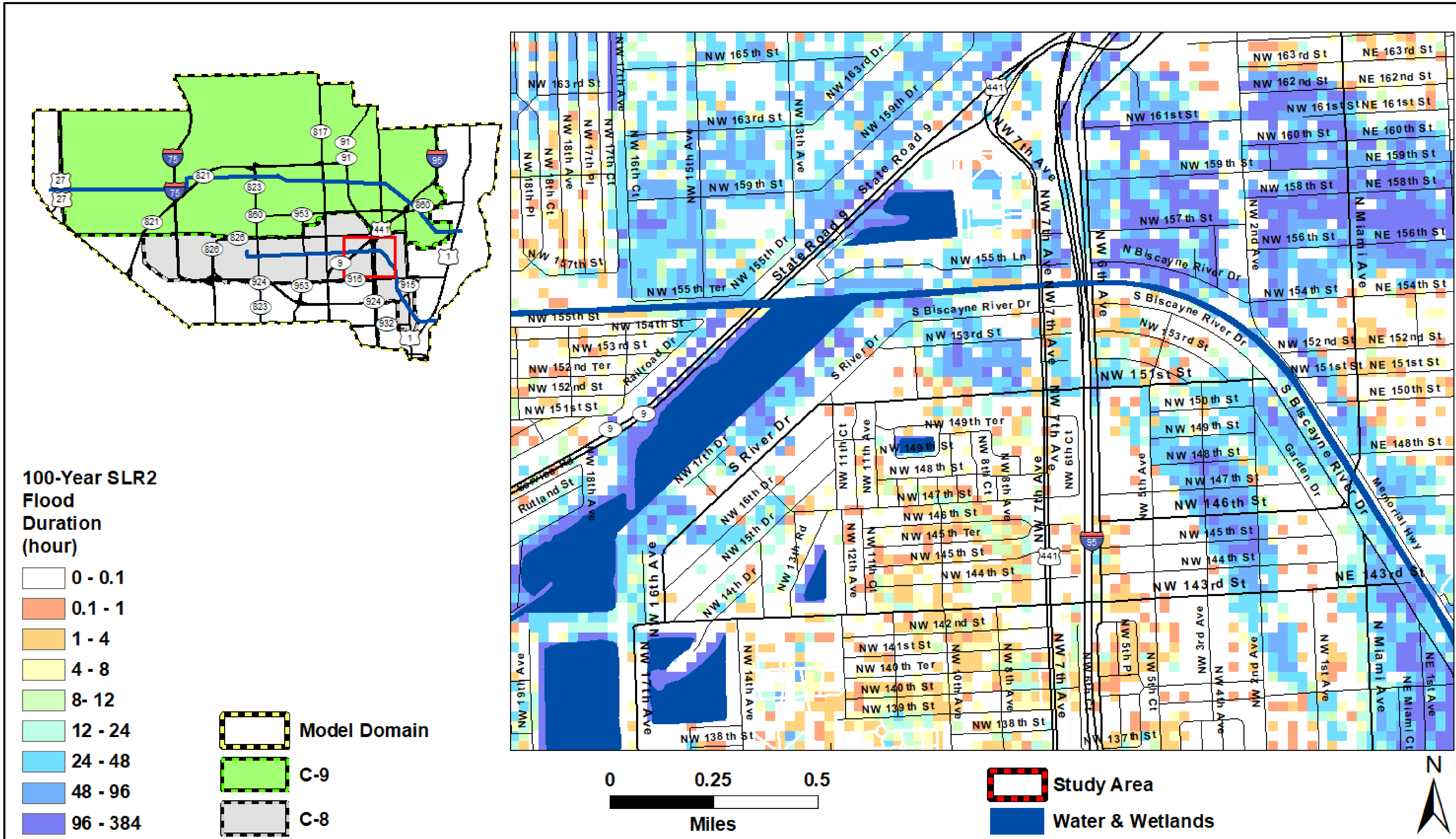

Figure 4.6-41: Up Close 100-Year Sea Level Rise 2 Flood Duration Map for the C-8 Canal Near Opa Locka Canal

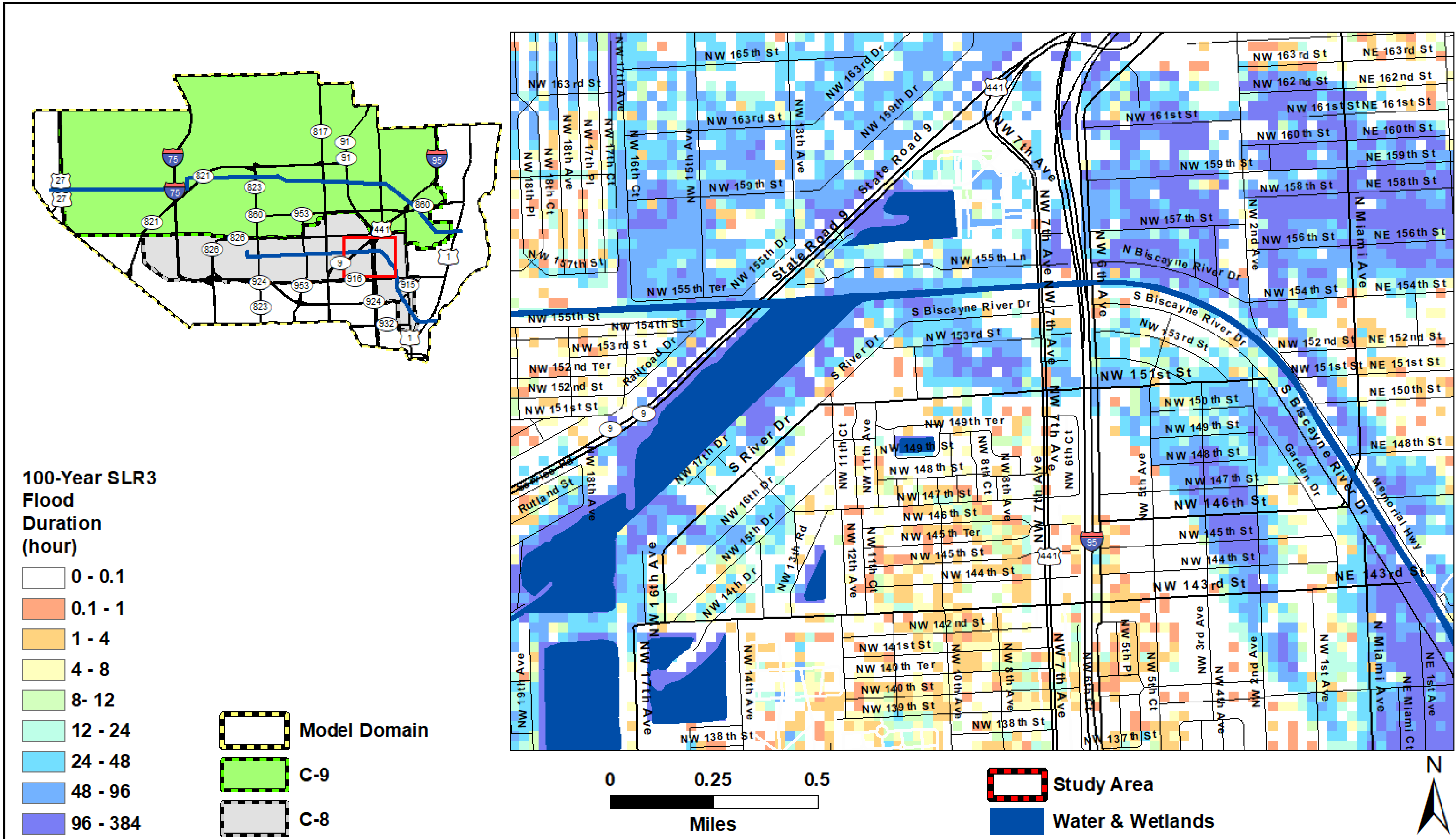

Figure 4.6-42: Up Close 100-Year Sea Level Rise 3 Flood Duration Map for the C-8 Canal Near Opa Locka Canal

4.6.9.4 Up-Close Flood Duration Maps for the C-9 Canal Between I-95 and S-29

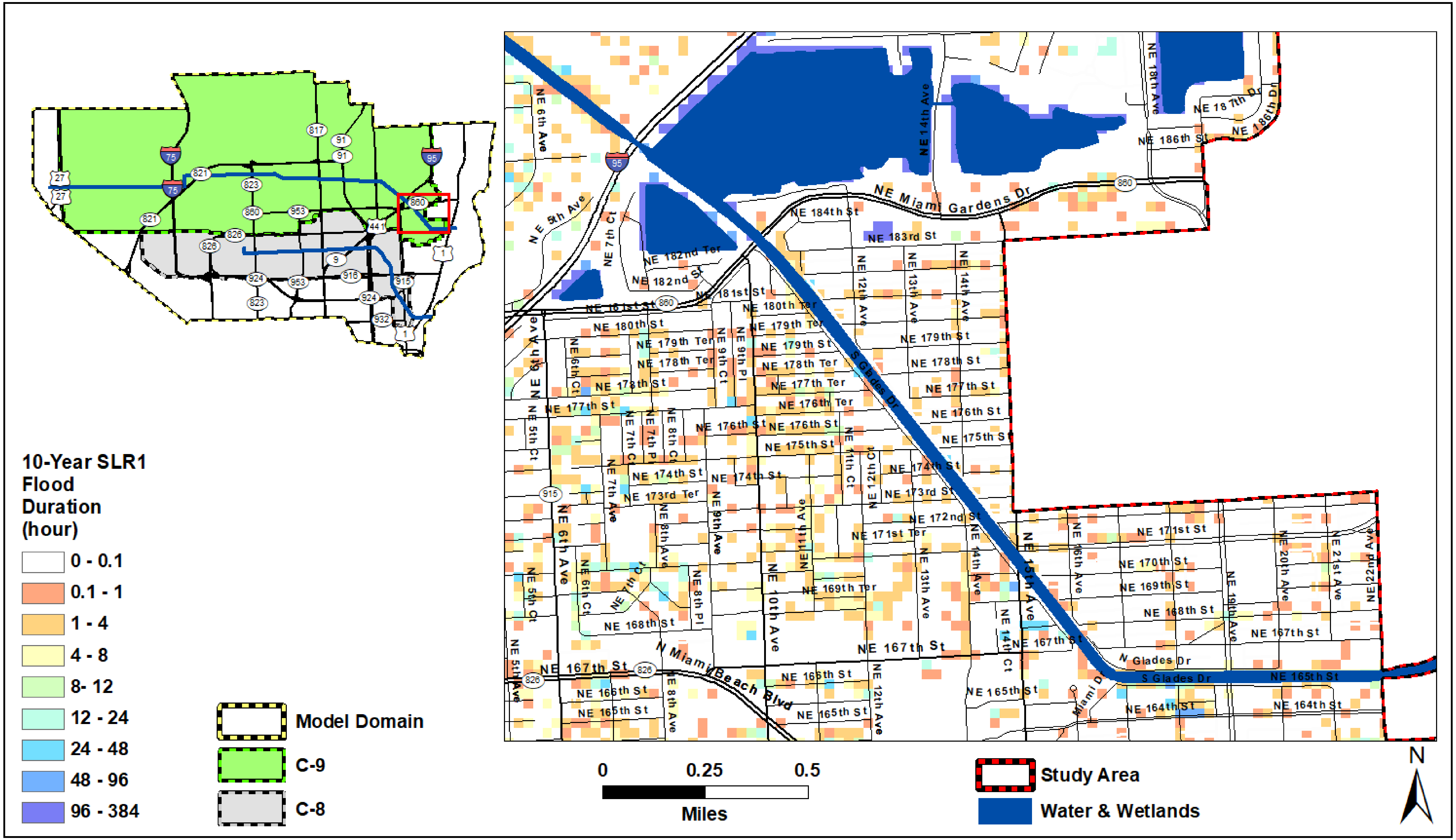

Figure 4.6-43: Up Close 10-Year Design Storm Sea Level Rise 1 Flood Duration Map for the C-9 Canal Between I-95 and S-29

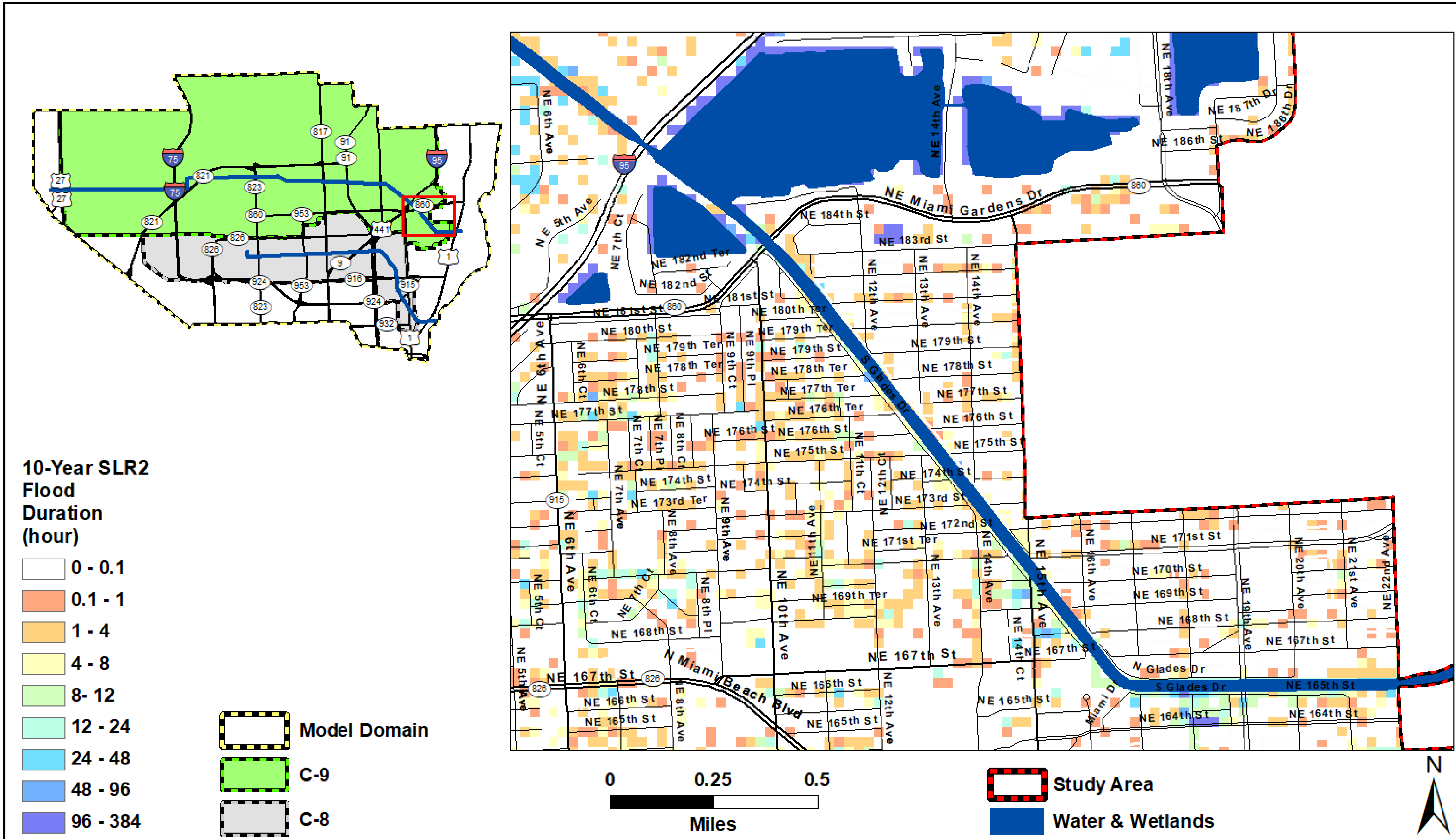

Figure 4.6-44: Up Close 10-Year Design Storm Sea Level Rise 2 Flood Duration Map for the C-9 Canal Between I-95 and S-29

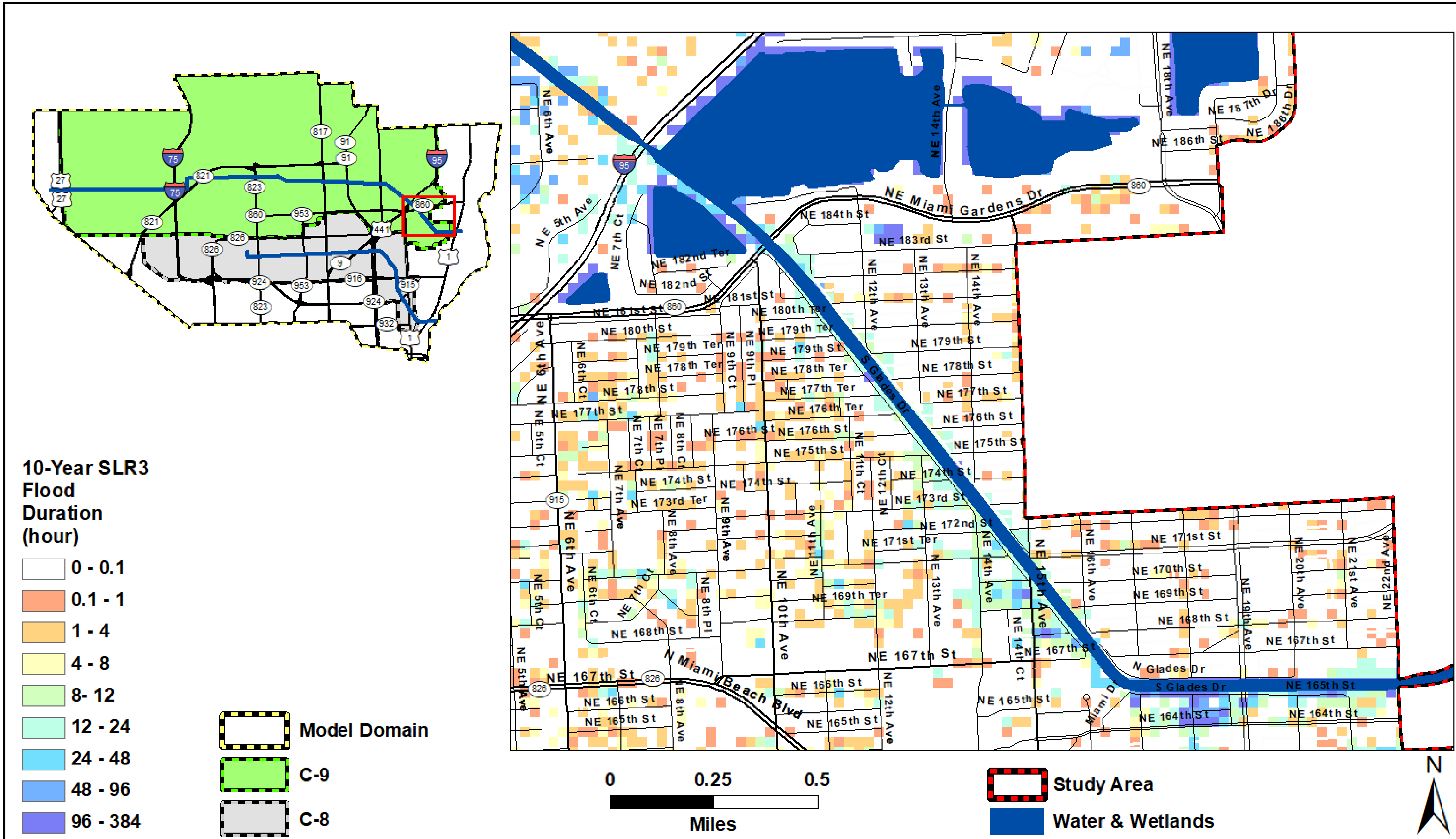

Figure 4.6-45: Up Close 10-Year Design Storm Sea Level Rise 3 Flood Duration Map for the C-9 Canal Between I-95 and S-29

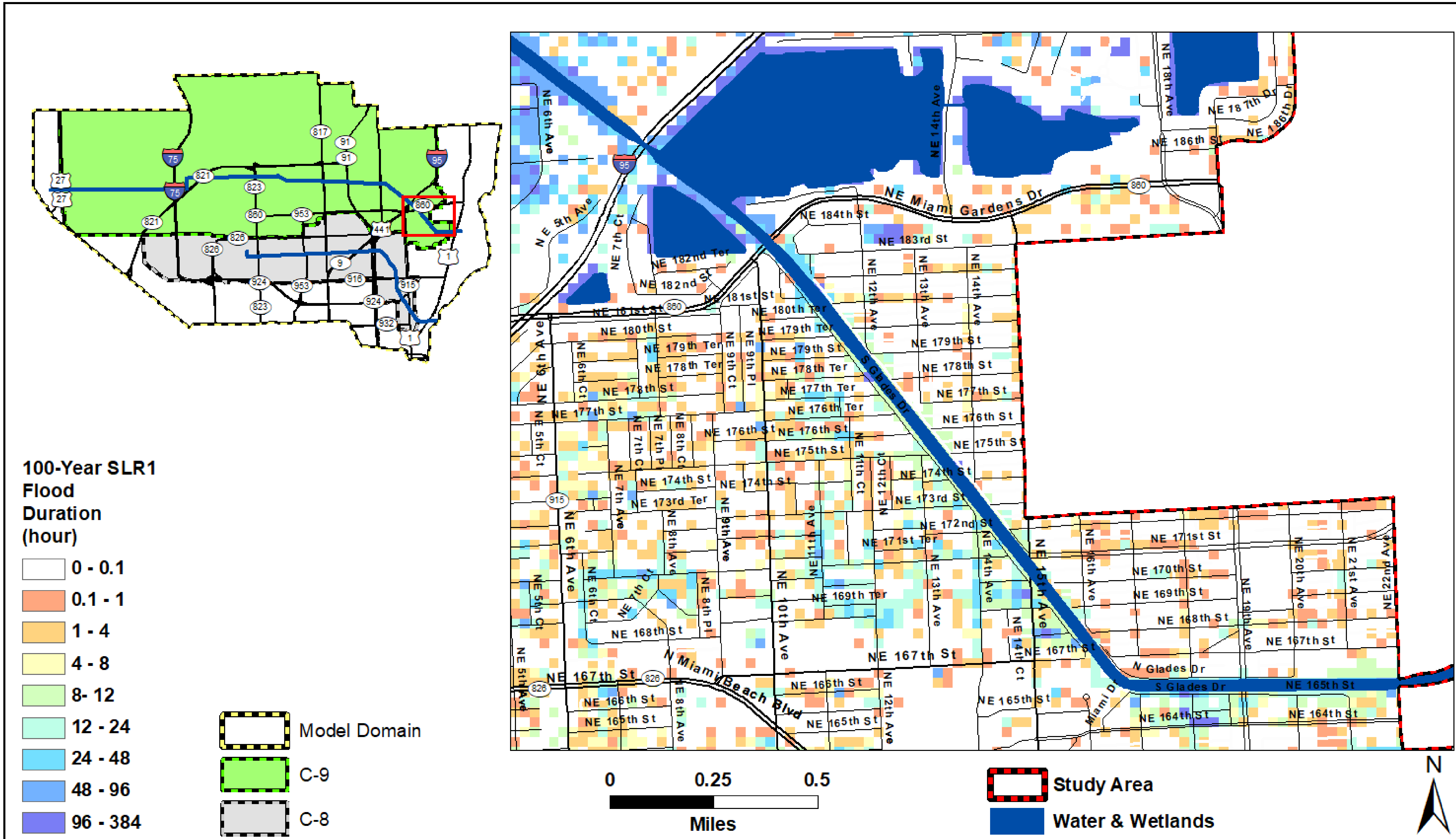

Figure 4.6-46: Up Close 100-Year Design Storm Sea Level Rise 1 Flood Duration Map for the C-9 Canal Between I-95 and S-29

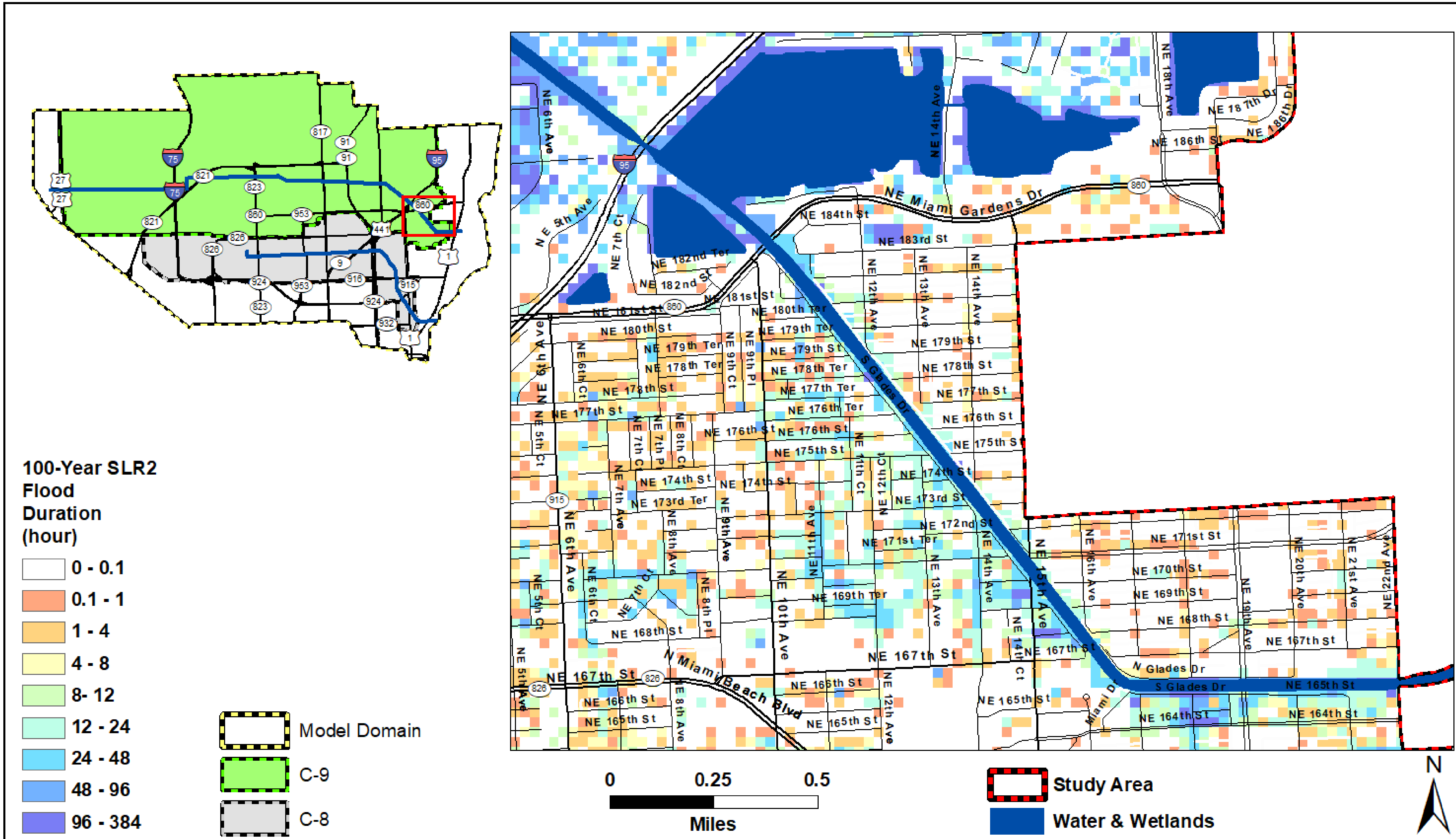

Figure 4.6-47: Up Close 100-Year Design Storm Sea Level Rise 2 Flood Duration Map for the C-9 Canal Between I-95 and S-29

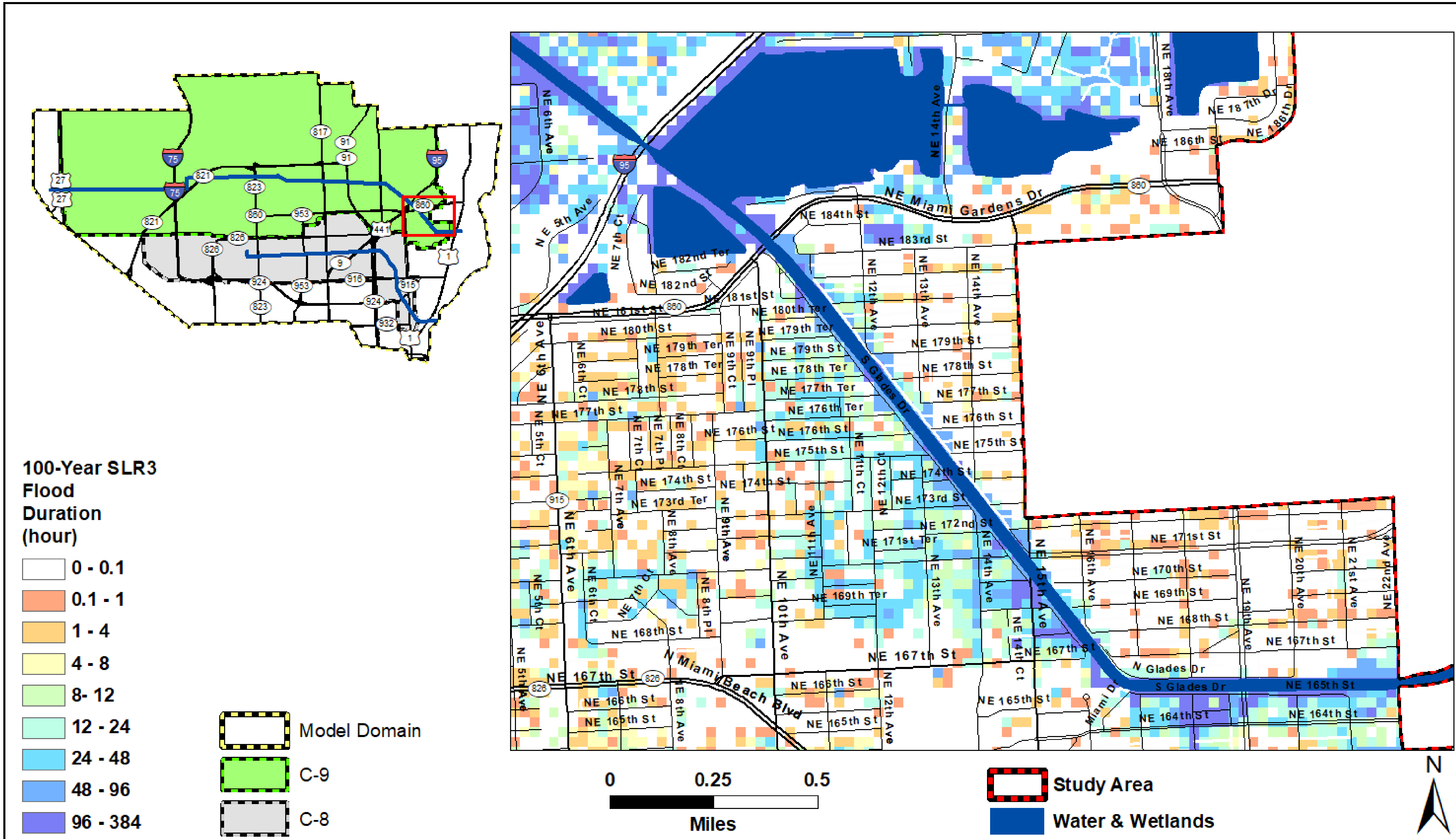

Figure 4.6-48: Up Close 100-Year Design Storm Sea Level Rise 3 Flood Duration Map for the C-9 Canal Between I-95 and S-29

4.6.9.5 Up-Close Flood Duration Maps for the C-9 Canal Near US Hwy 441

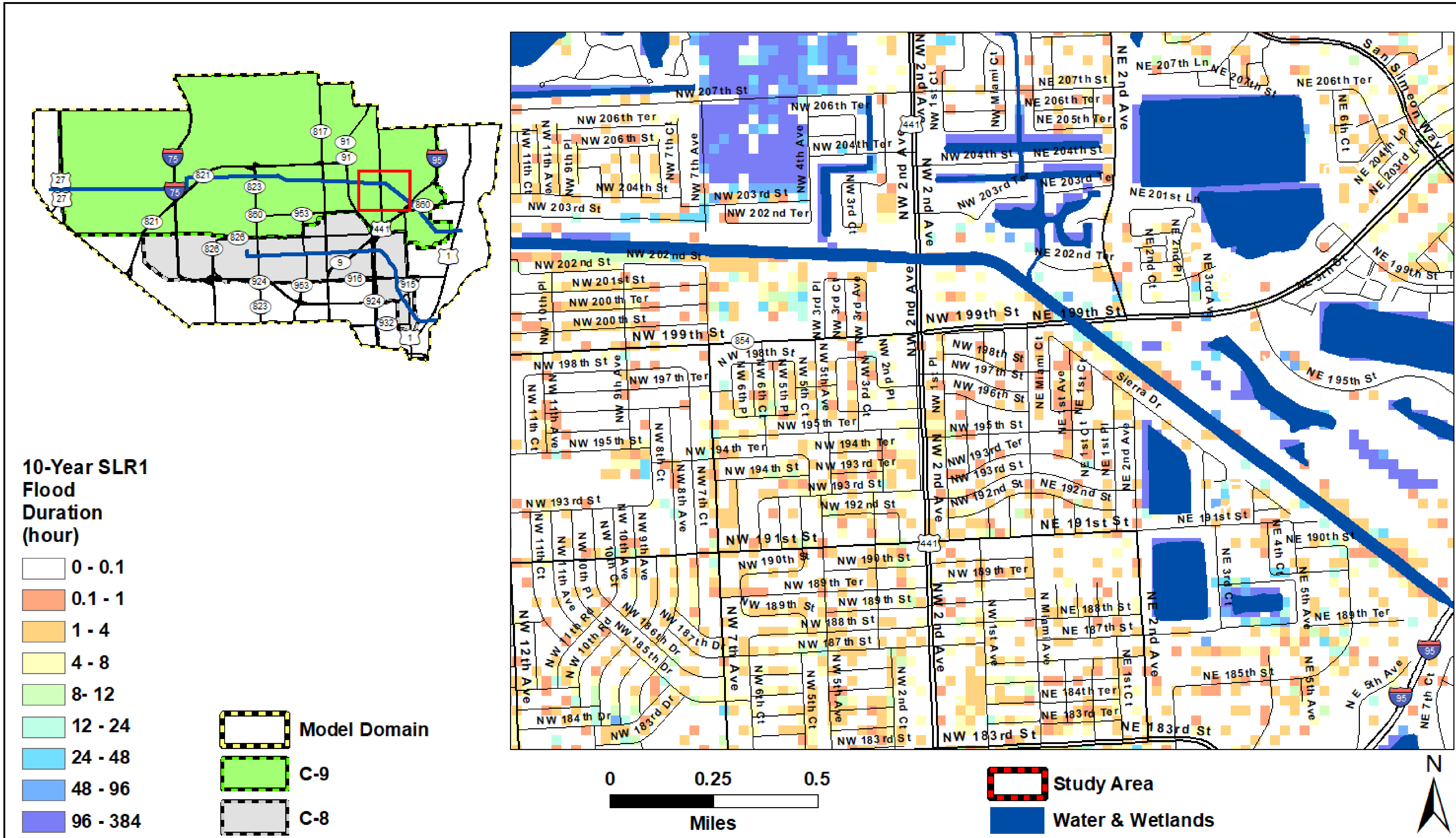

Figure 4.6-49: Up Close 10-Year Sea Level Rise 1 Flood Duration Map for the C-9 Canal Near US Hwy 441

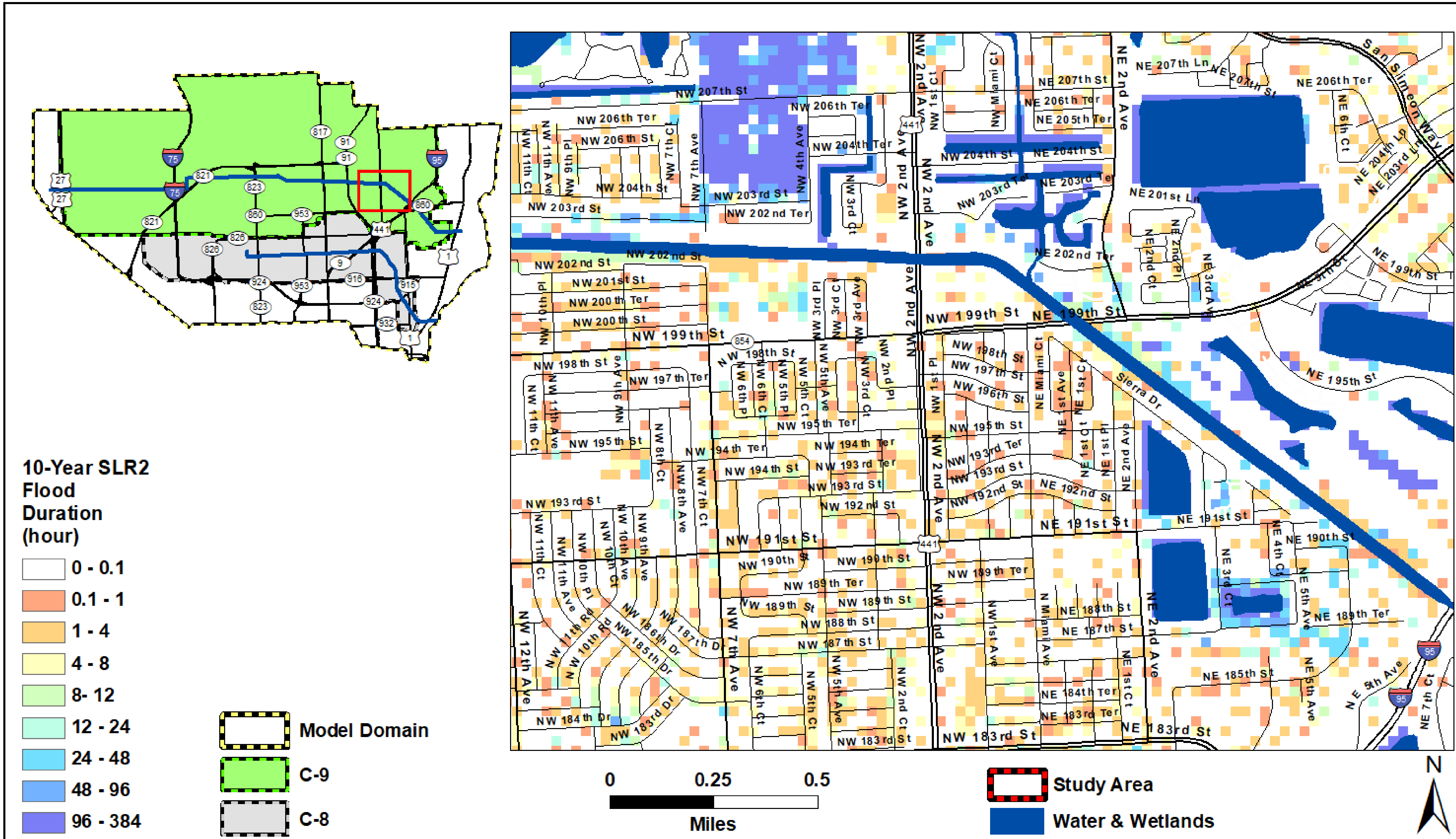

Figure 4.6-50: Up Close 10-Year Sea Level Rise 2 Flood Duration Map for the C-9 Canal Near US Hwy 441

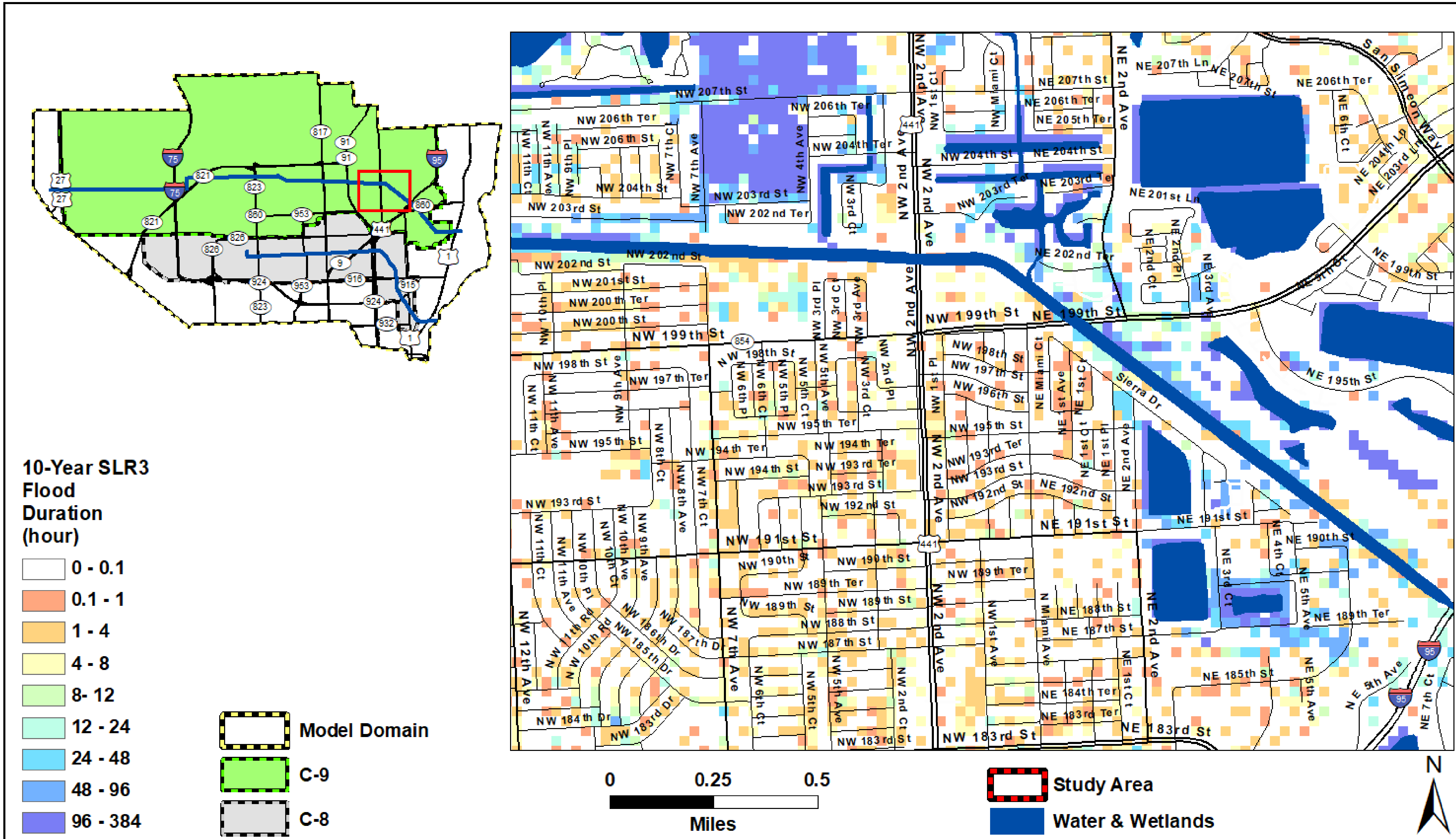

Figure 4.6-51: Up Close 10-Year Sea Level Rise 3 Flood Duration Map for the C-9 Canal Near US Hwy 441

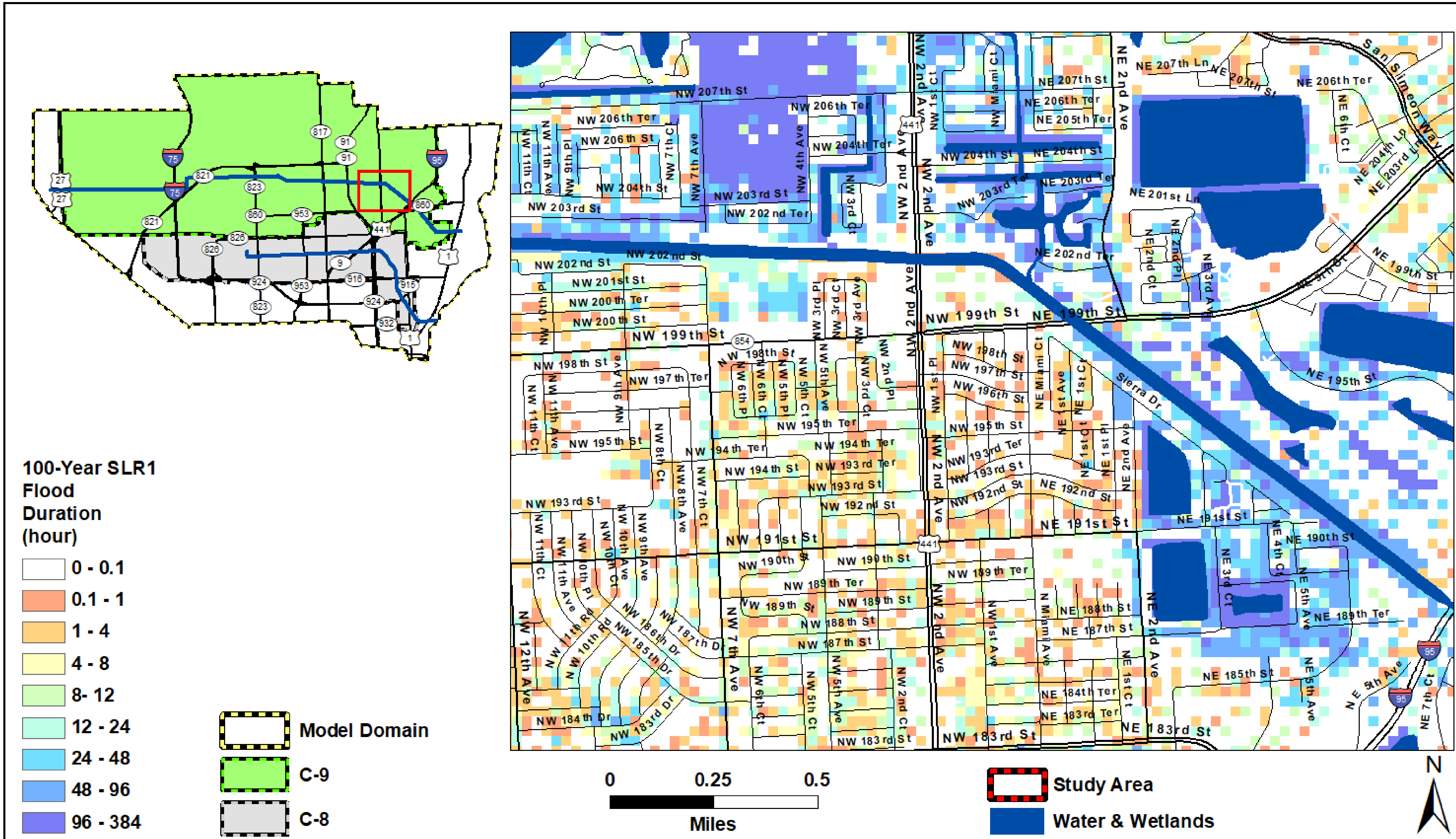

Figure 4.6-52: Up Close 100-Year Sea Level Rise 1 Flood Duration Map for the C-9 Canal Near US Hwy 441

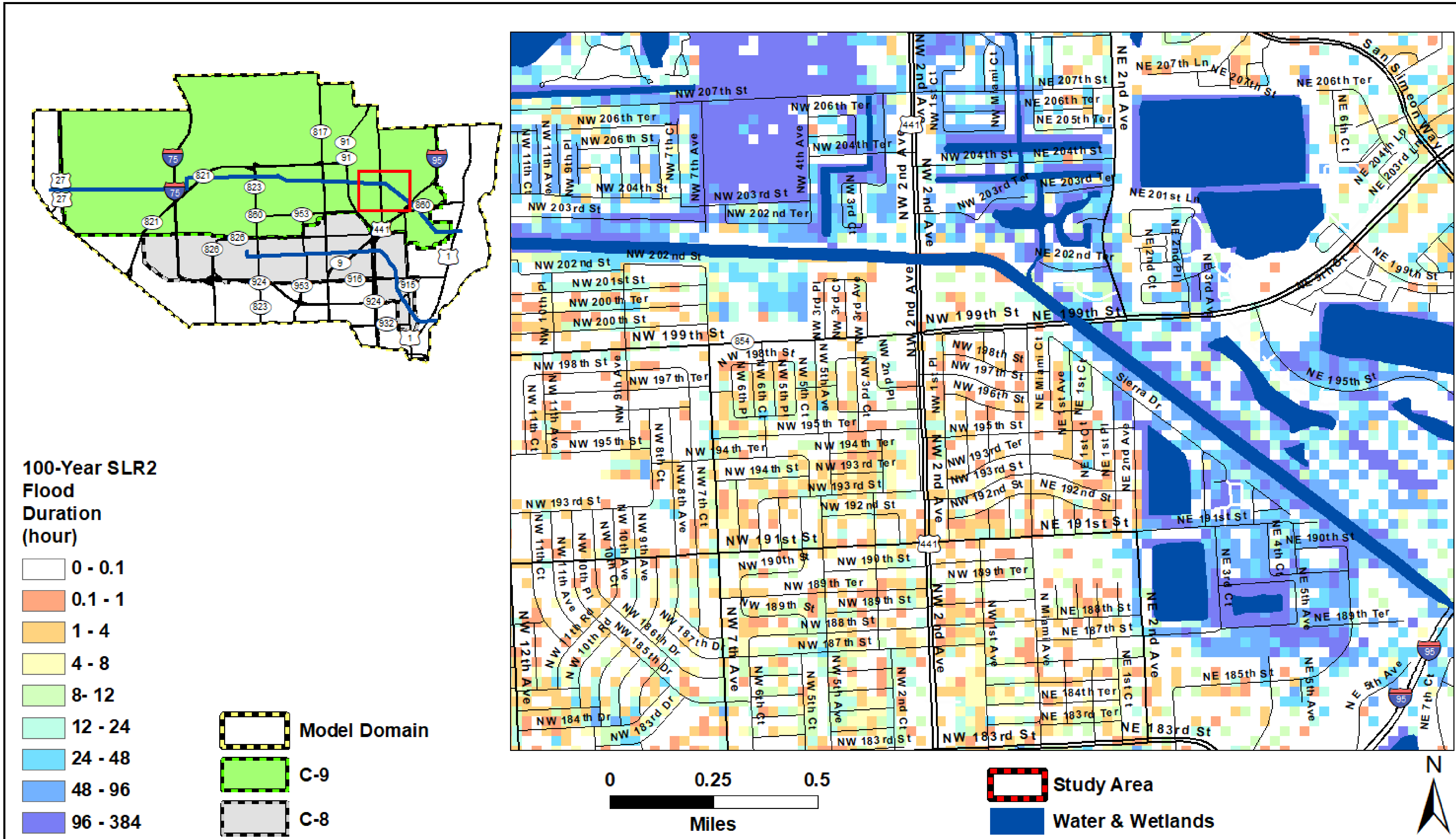

Figure 4.6-53: Up Close 100-Year Sea Level Rise 2 Flood Duration Map for the C-9 Canal Near US Hwy 441

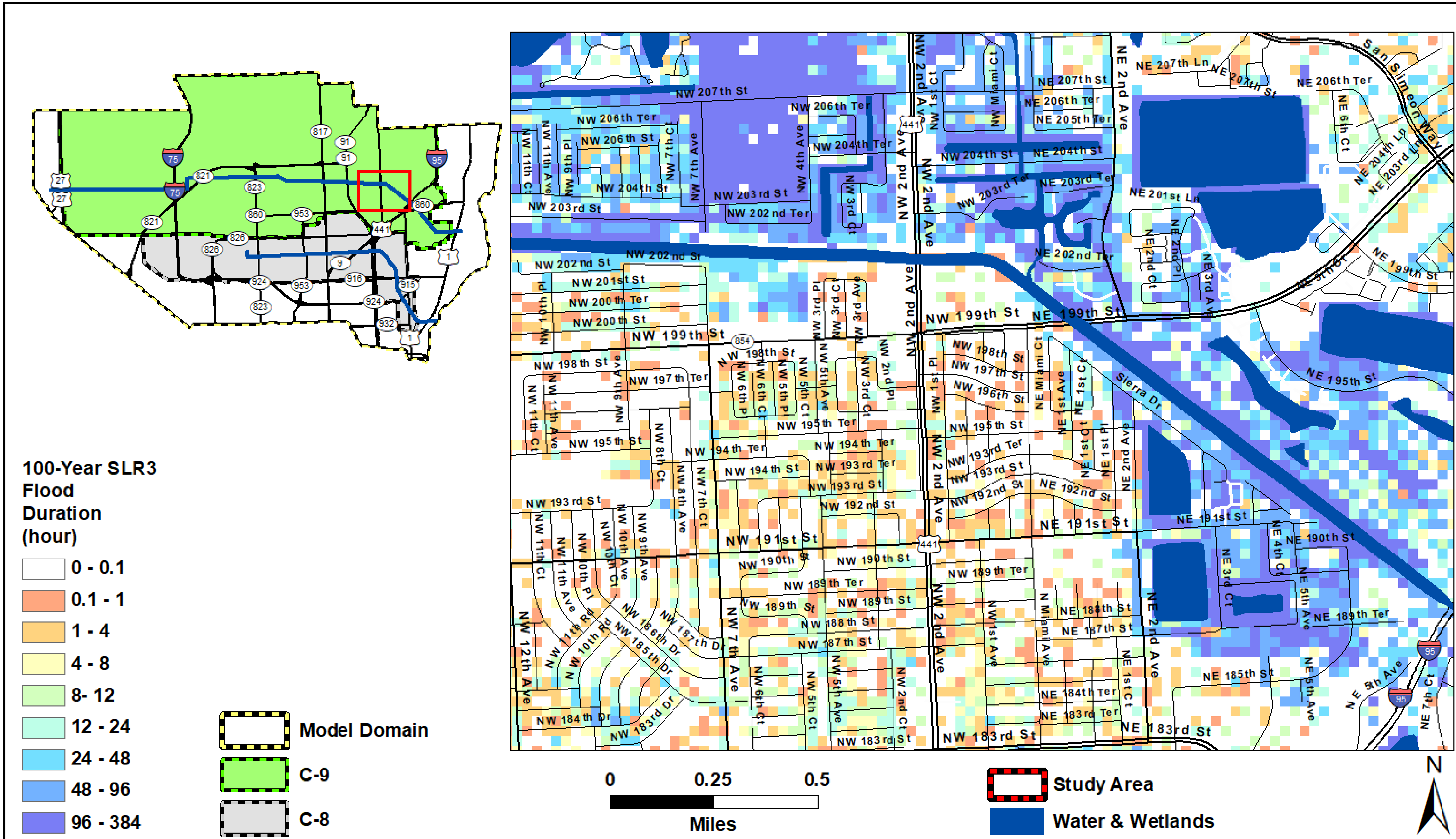

Figure 4.6-54: Up Close 100-Year Sea Level Rise 3 Flood Duration Map for the C-9 Canal Near US Hwy 441

4.6.9.6 Up-Close Flood Duration Maps for the C-9 Canal Near Ronald Reagan Turnpike

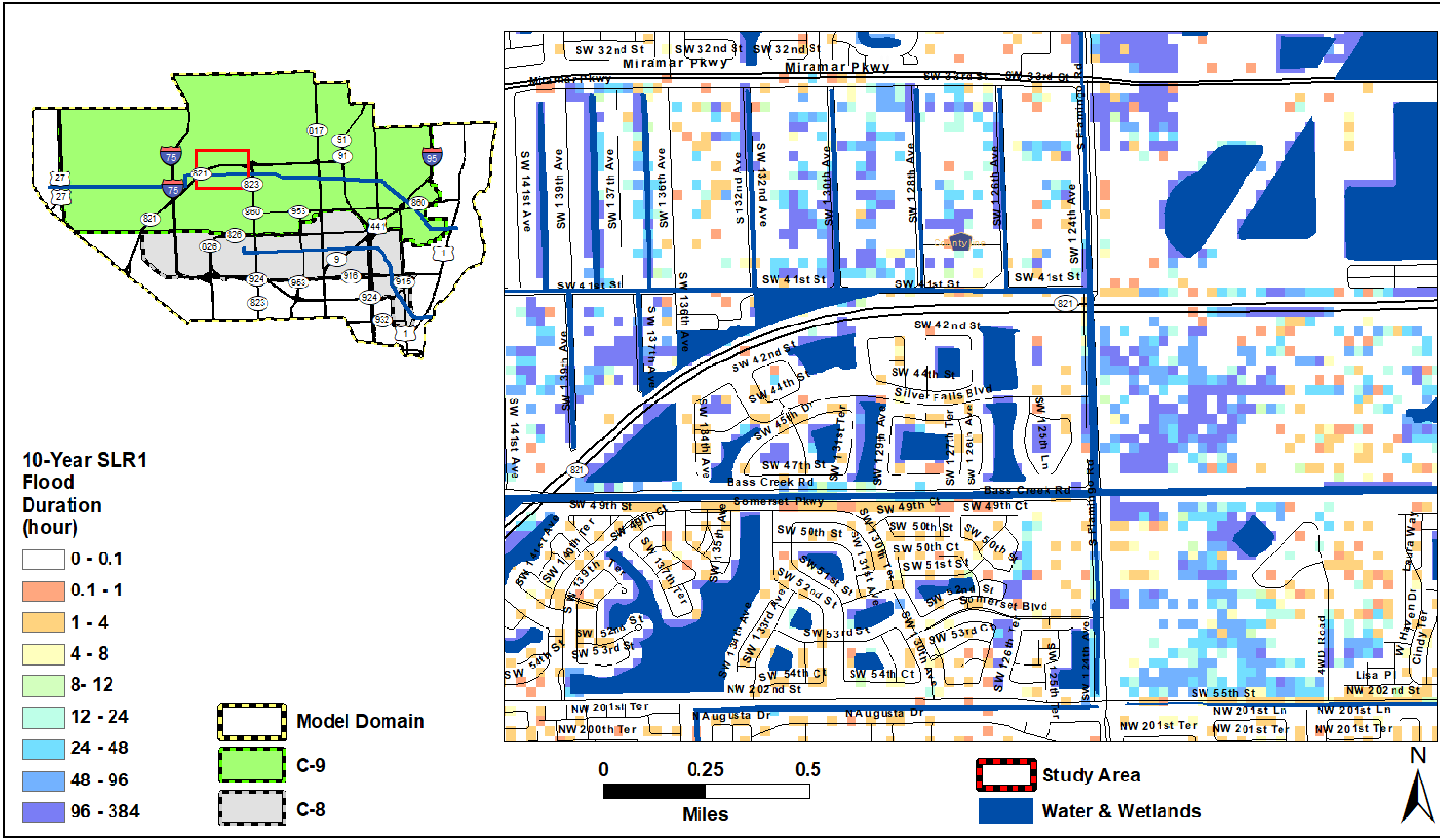

Figure 4.6-55: Up Close 10-Year Sea Level Rise 1 Flood Duration Map for the C-9 Canal Near Ronald Reagan Turnpike

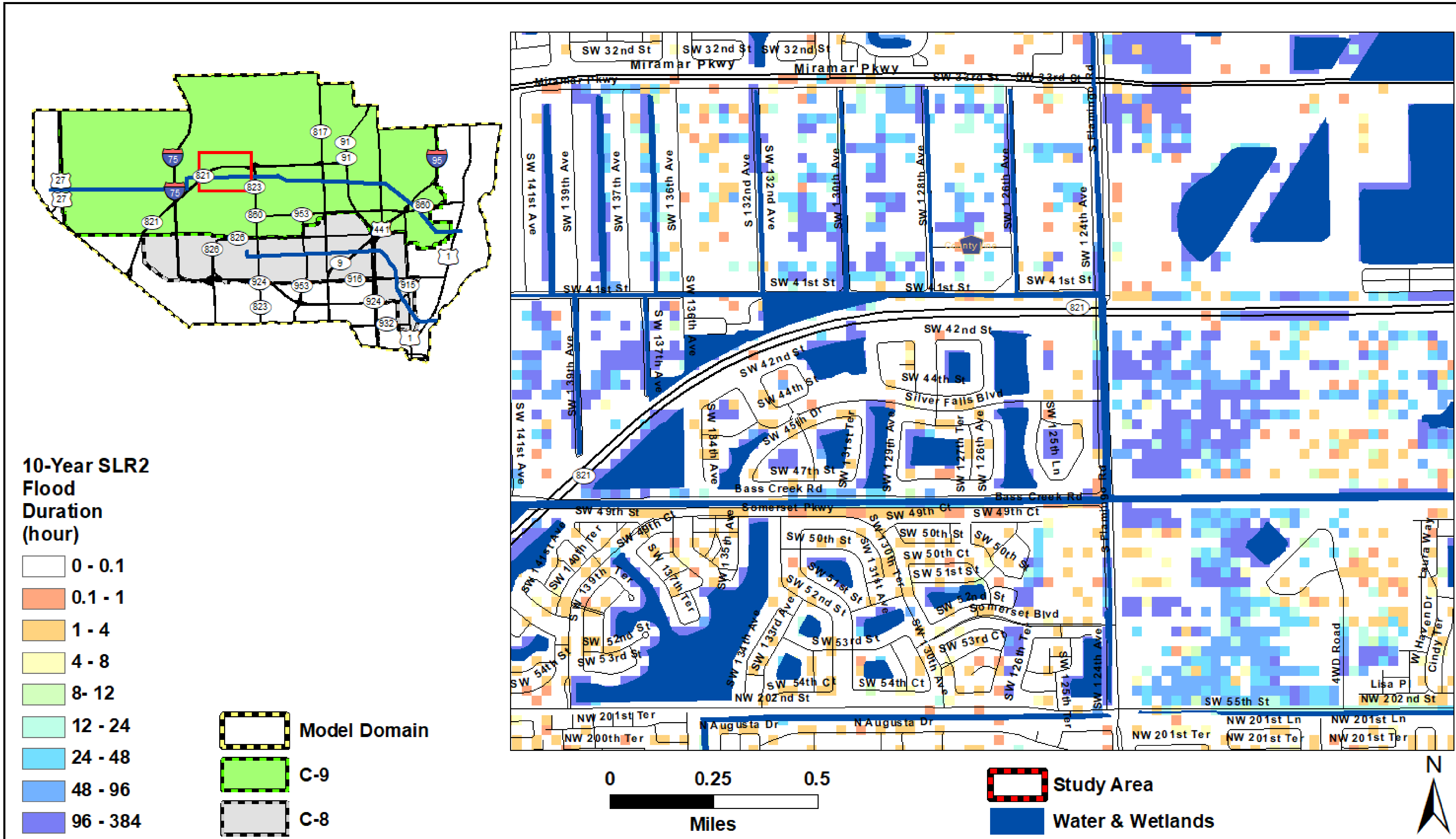

Figure 4.6-56: Up Close 10-Year Sea Level Rise 2 Flood Duration Map for the C-9 Canal Near Ronald Reagan Turnpike

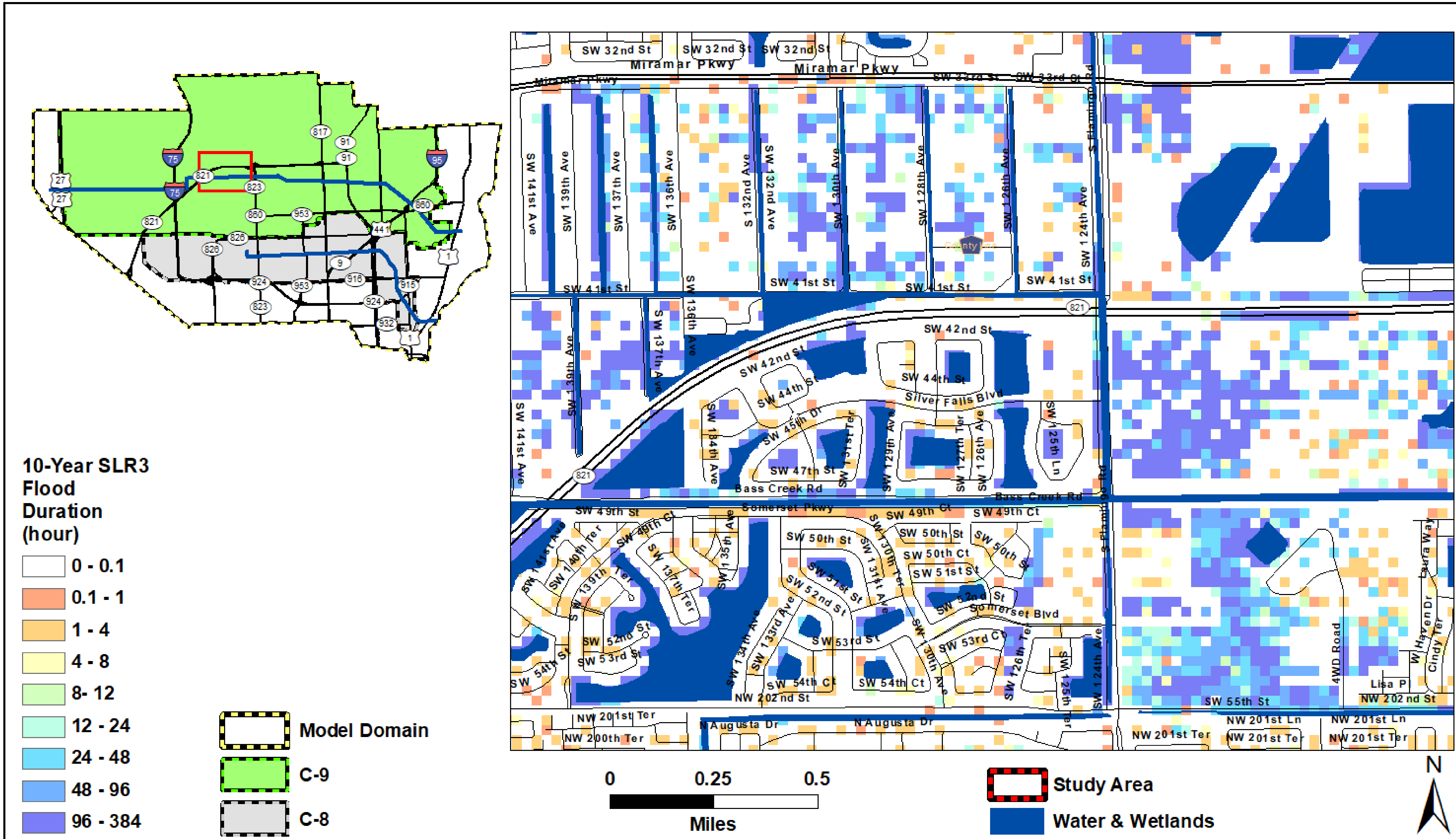

Figure 4.6-57: Up Close 10-Year Sea Level Rise 3 Flood Duration Map for the C-9 Canal Near Ronald Reagan Turnpike

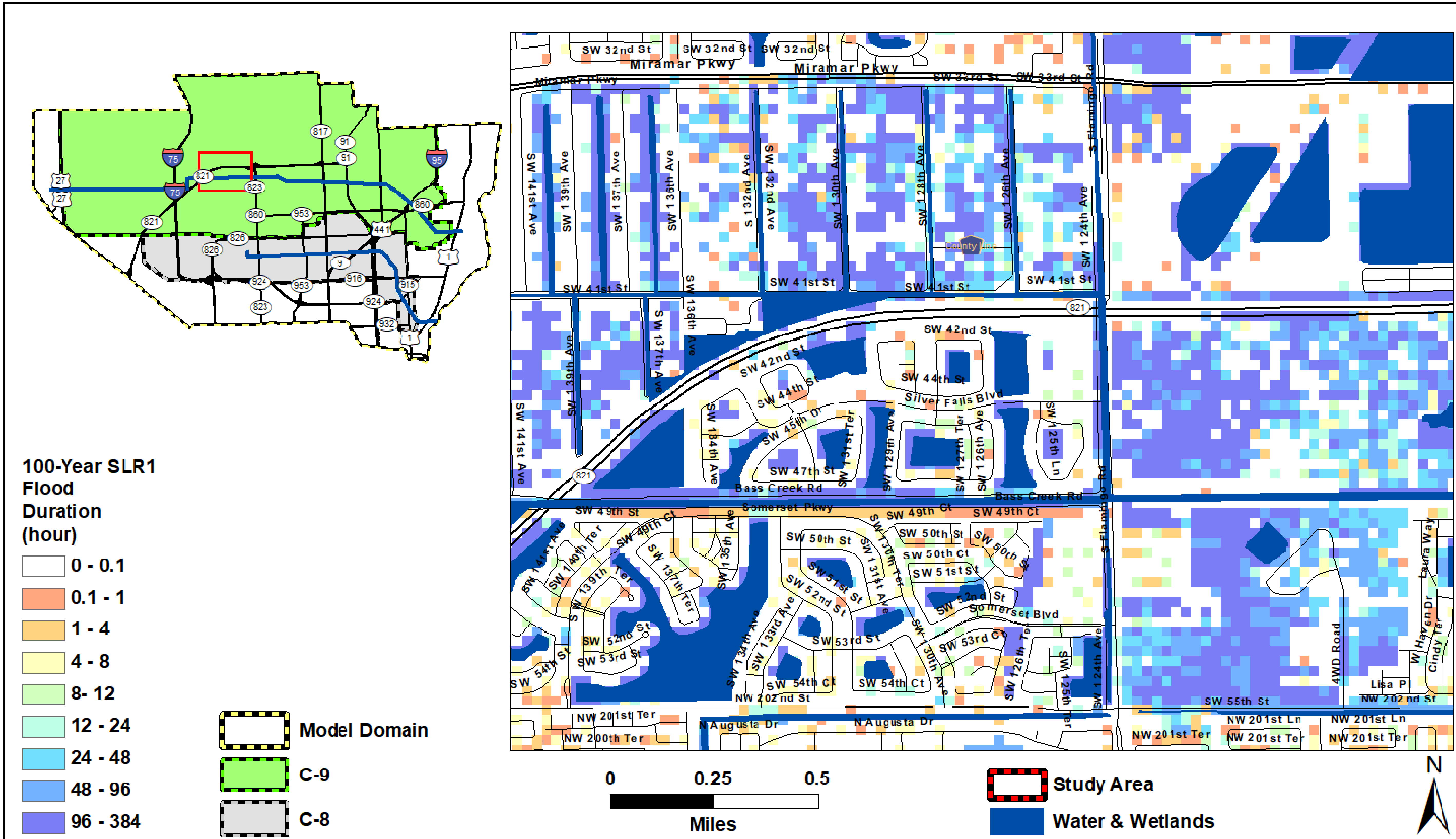

Figure 4.6-58: Up Close 100-Year Sea Level Rise 1 Flood Duration Map for the C-9 Canal Near Ronald Reagan Turnpike

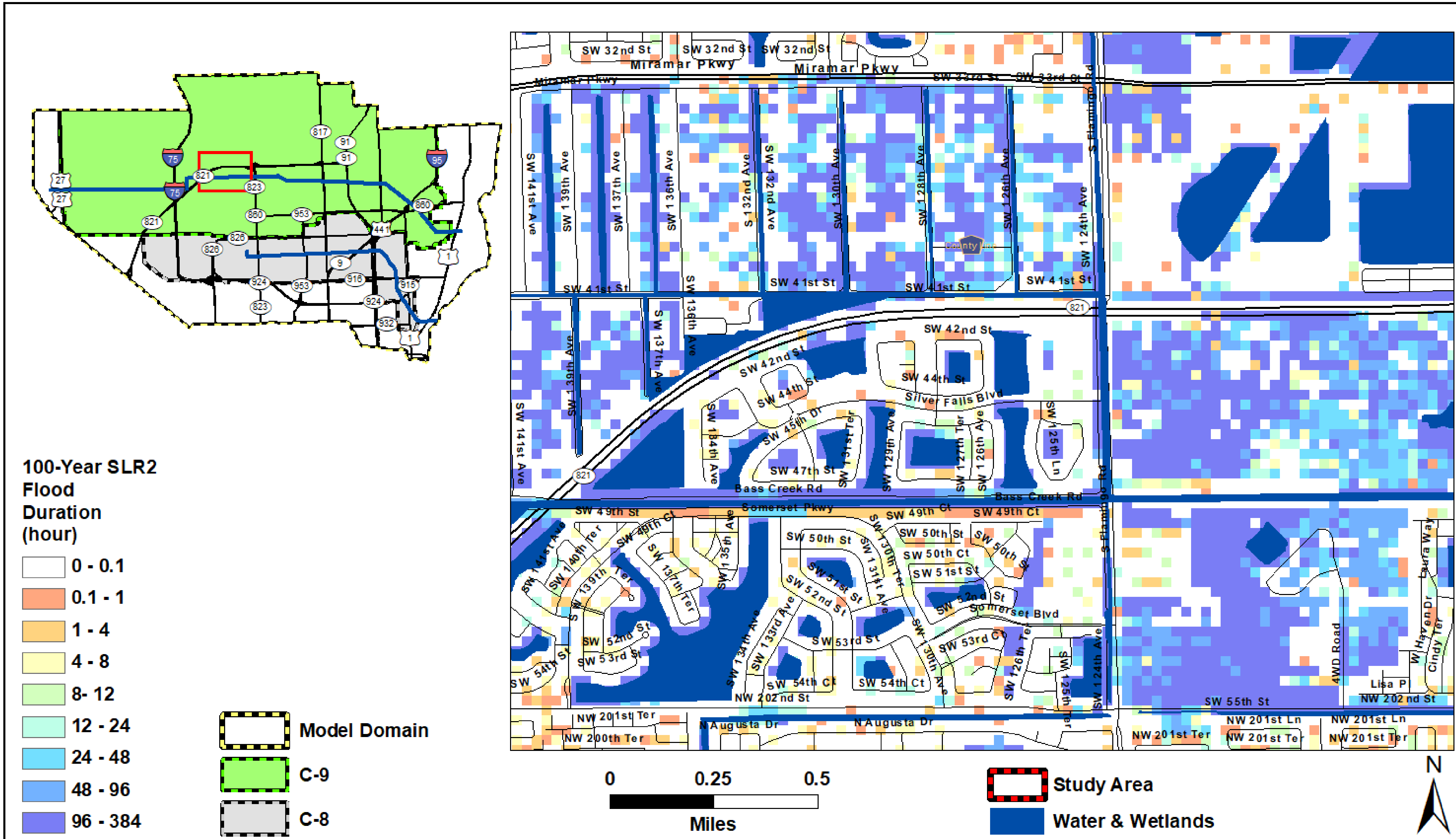

Figure 4.6-59: Up Close 100-Year Sea Level Rise 2 Flood Duration Map for the C-9 Canal Near Ronald Reagan Turnpike

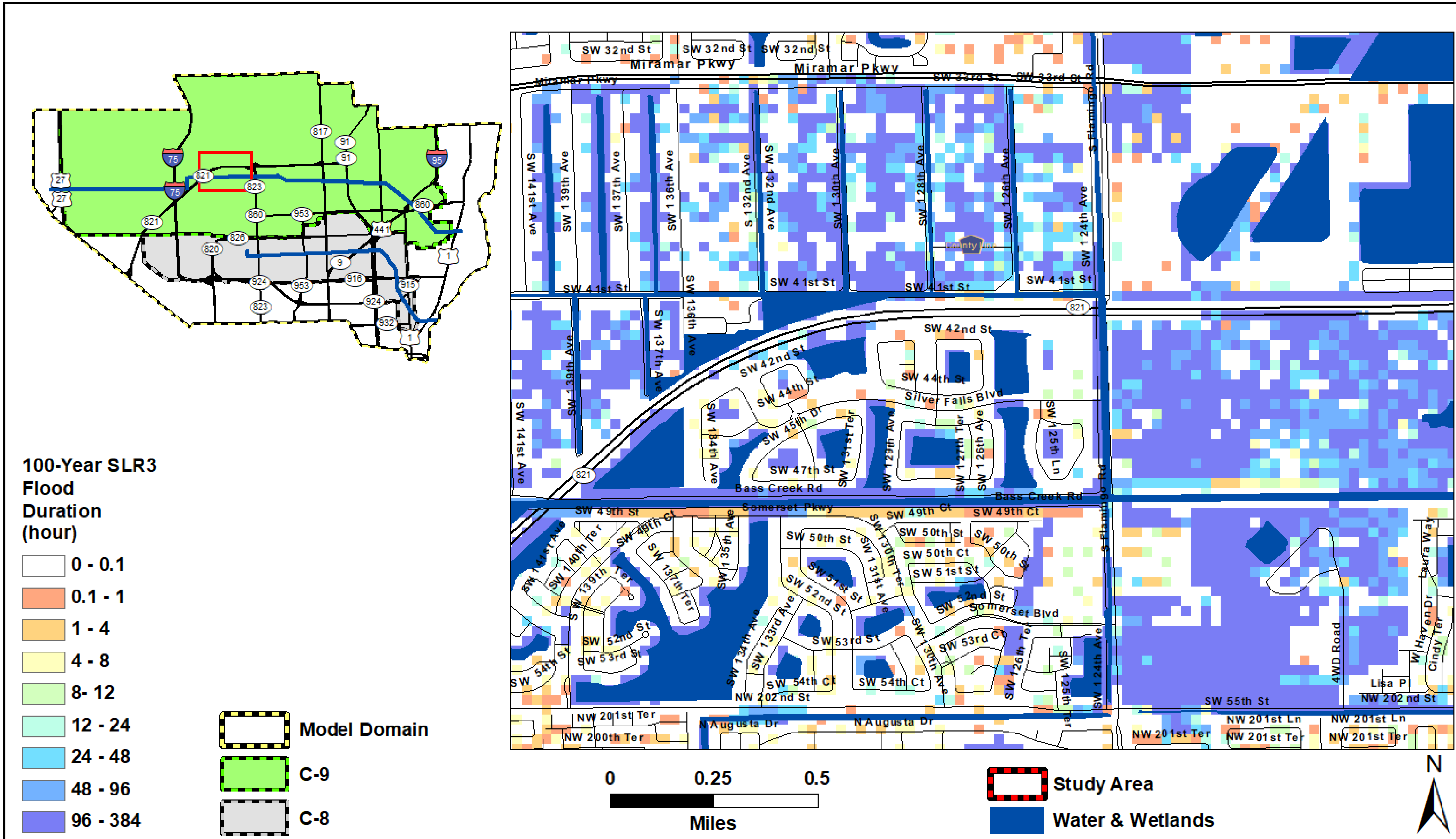

Figure 4.6-60: Up Close 100-Year Sea Level Rise 3 Flood Duration Map for the C-9 Canal Near Ronald Reagan Turnpike

4.6.9.7 Up-Close Flood Duration Maps for the C-9 Canal Near Red Road

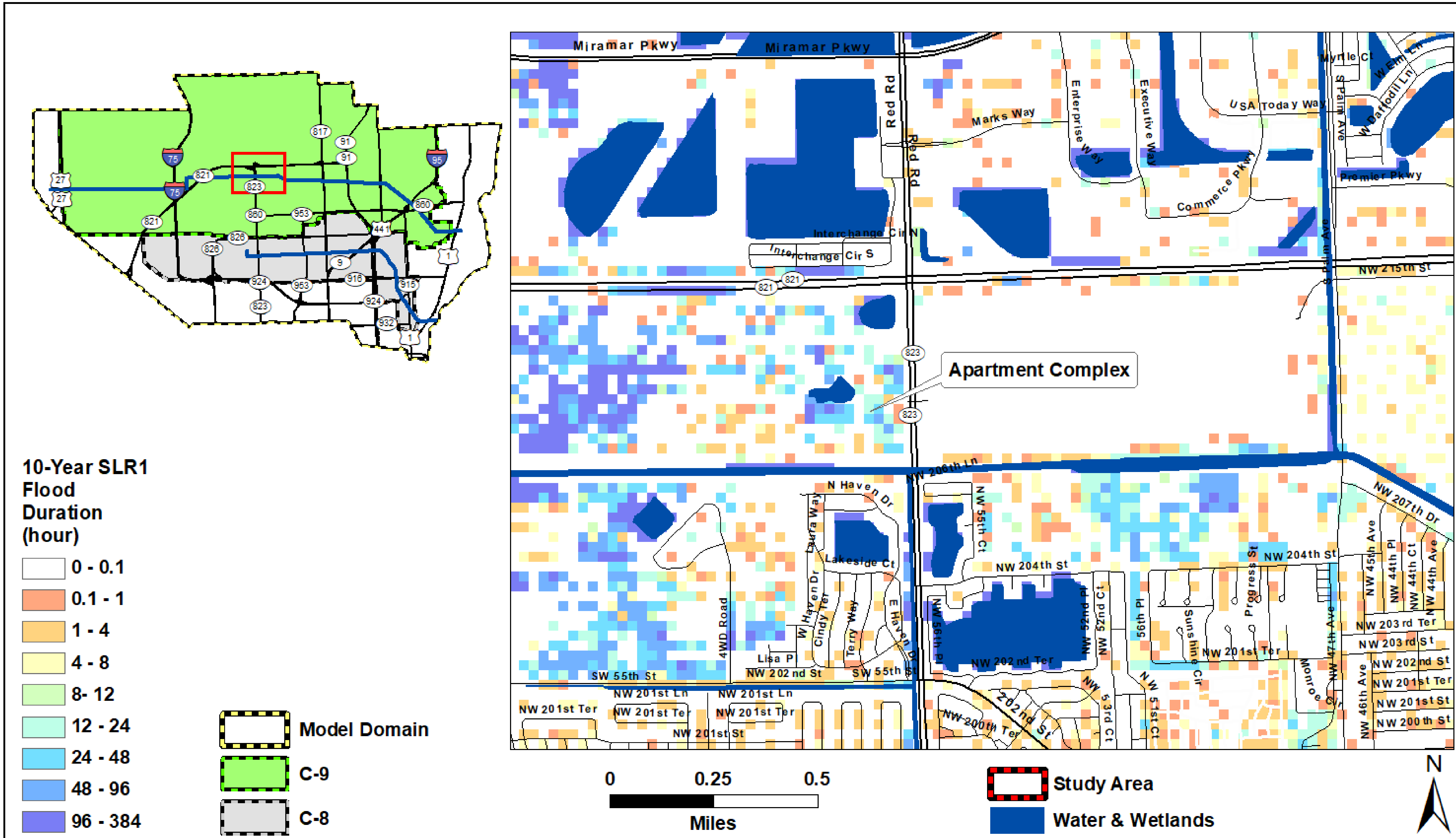

Figure 4.6-61: Up Close 10-Year Sea Level Rise 1 Flood Duration Map for the C-9 Canal Near Red Road

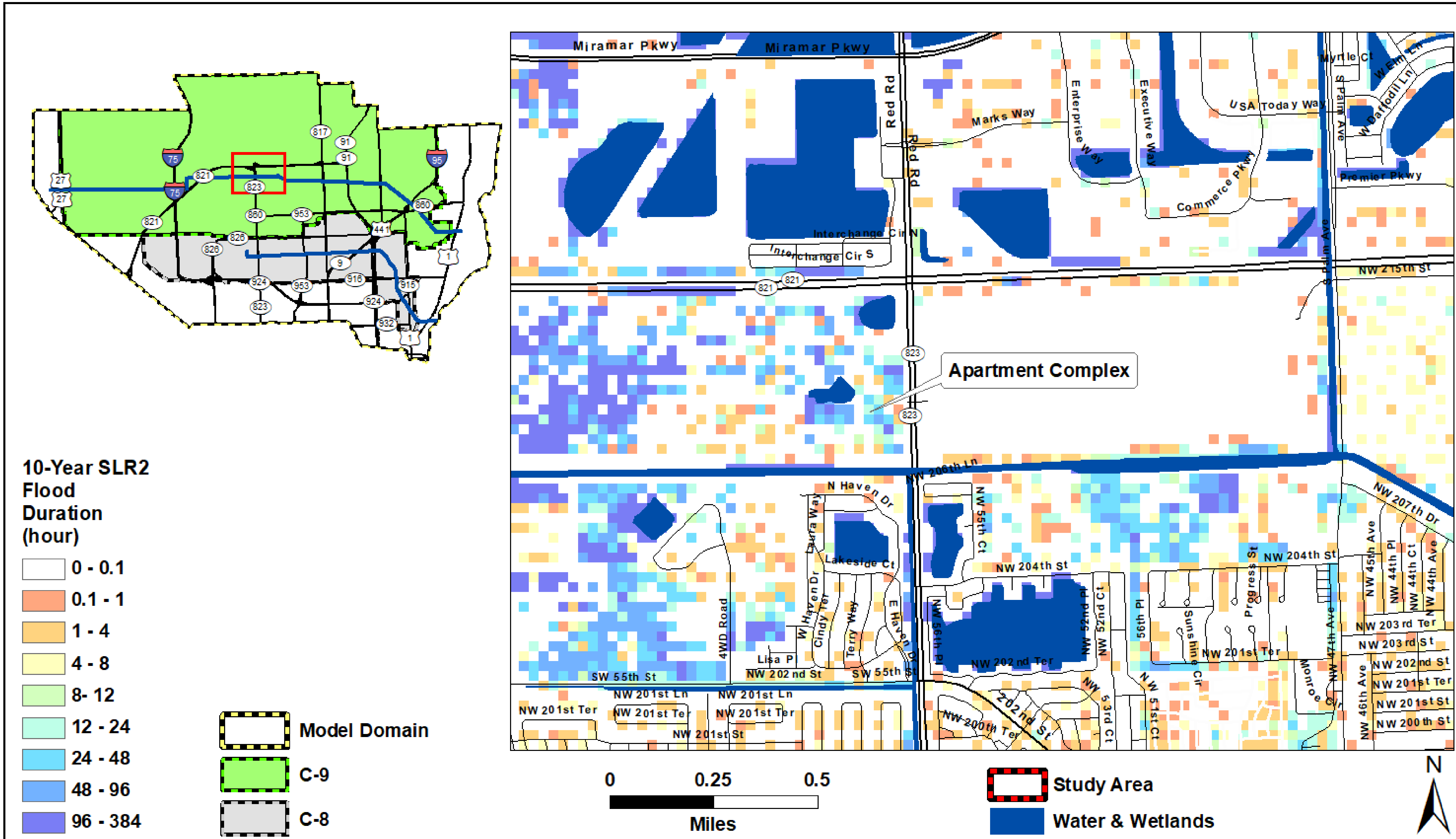

Figure 4.6-62: Up Close 10-Year Sea Level Rise 1 Flood Duration Map for the C-9 Canal Near Red Road

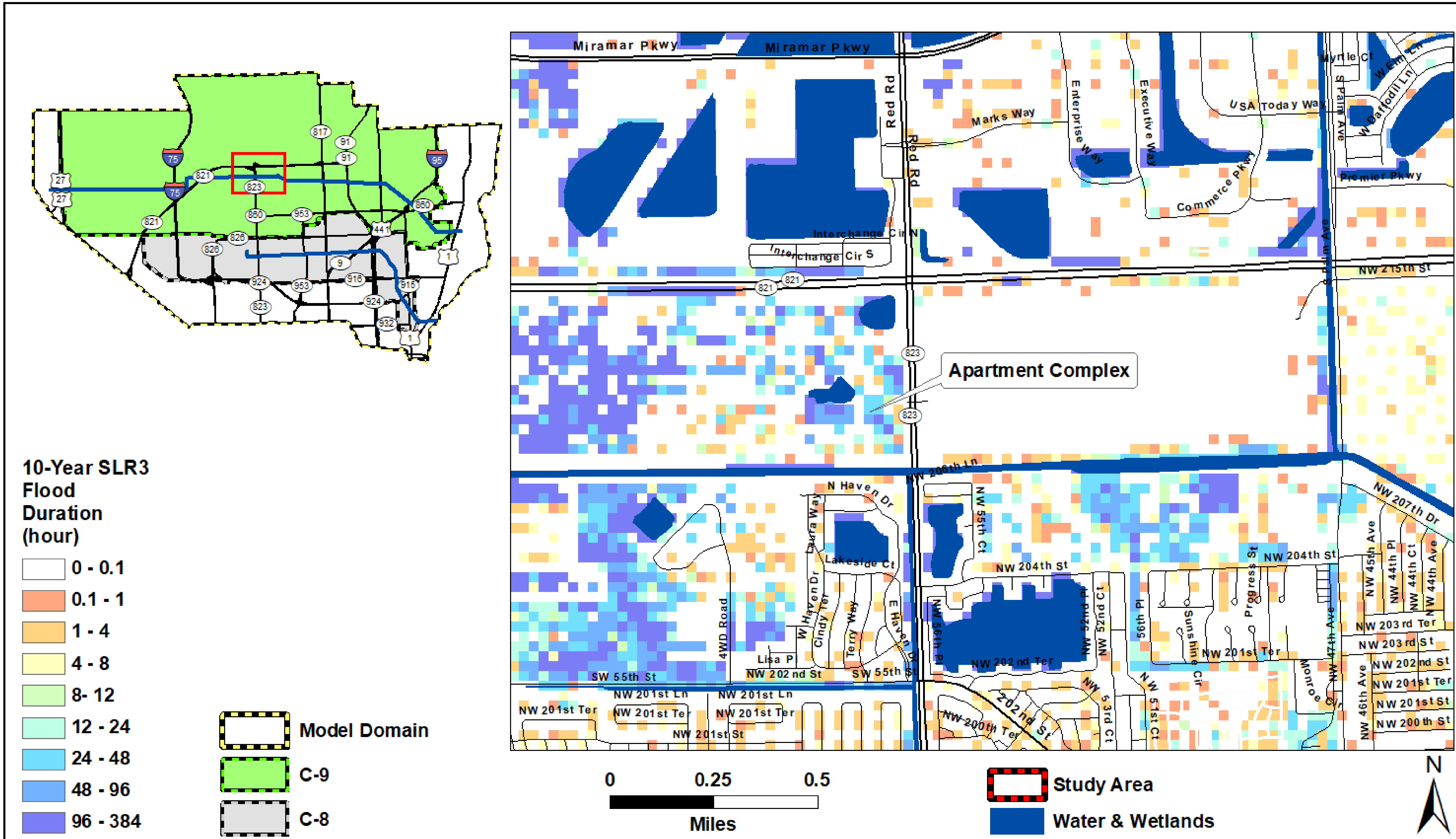

Figure 4.6-63: Up Close 10-Year Sea Level Rise 1 Flood Duration Map for the C-9 Canal Near Red Road

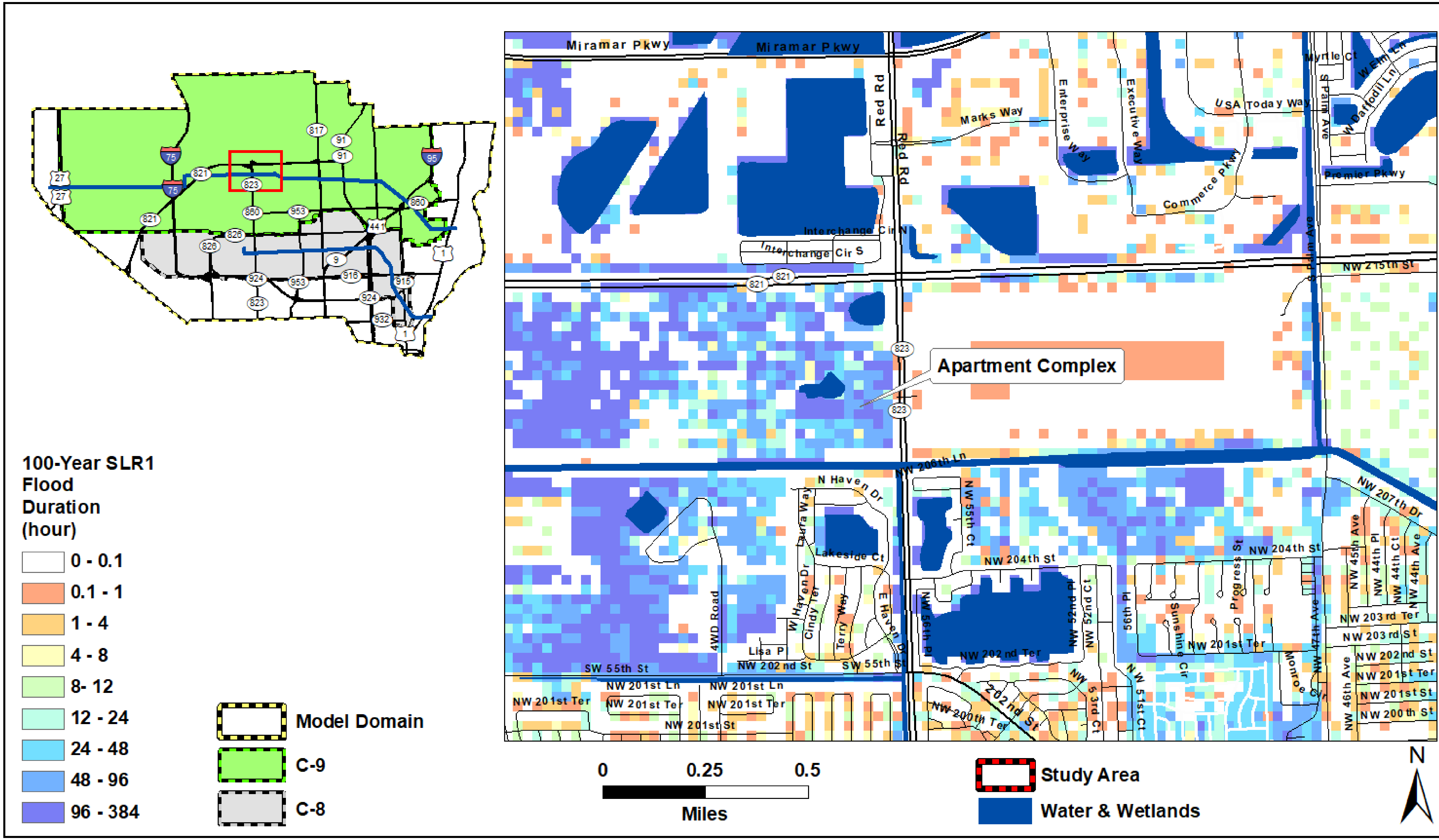

Figure 4.6-64: Up Close 100-Year Sea Level Rise 1 Flood Duration Map for the C-9 Canal Near Red Road

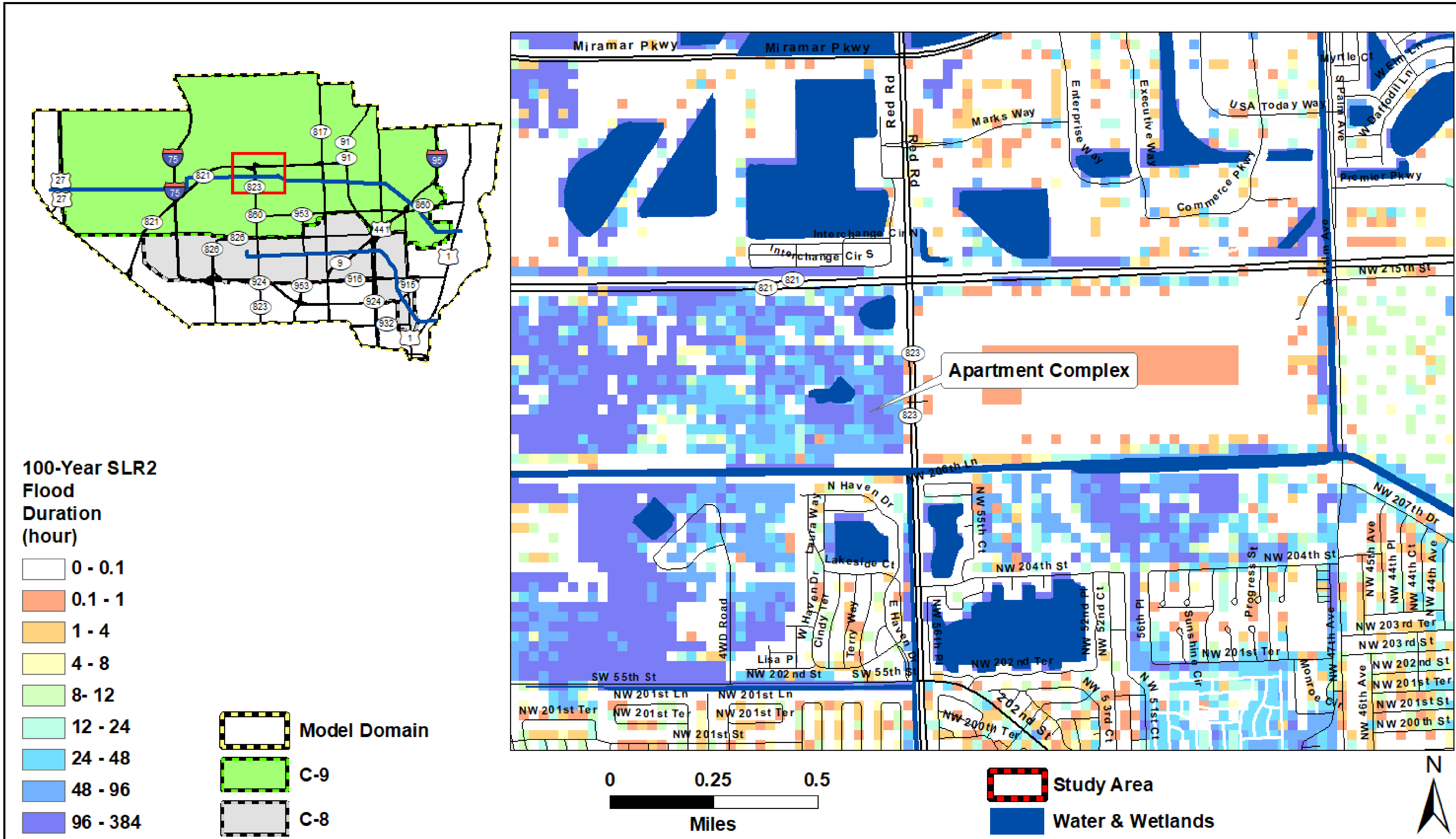

Figure 4.6-65: Up Close 100-Year Sea Level Rise 1 Flood Duration Map for the C-9 Canal Near Red Road

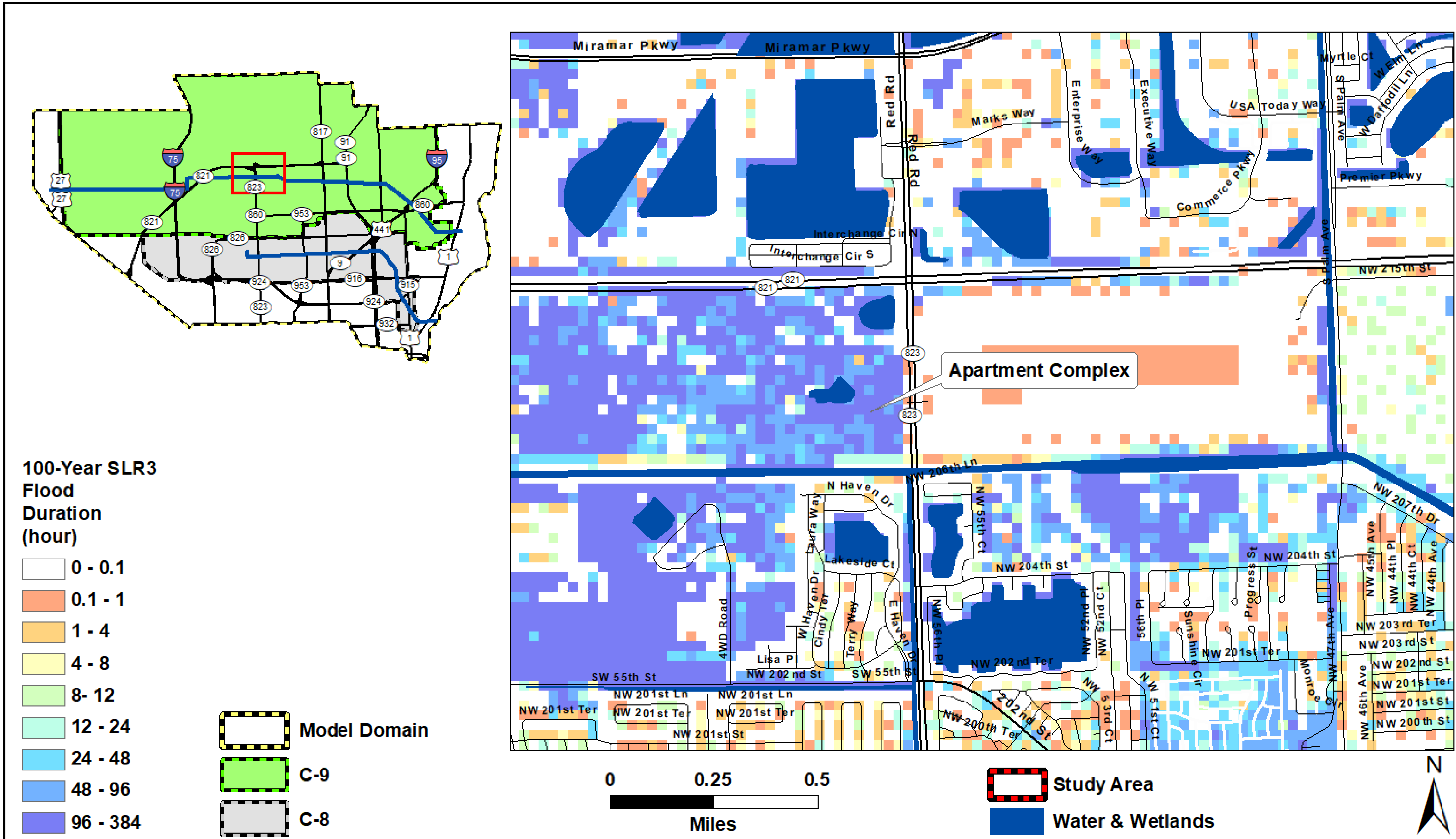

Figure 4.6-66: Up Close 100-Year Sea Level Rise 1 Flood Duration Map for the C-9 Canal Near Red Road

4.6.10 Flood Duration Difference Maps for Urban Land Use Areas

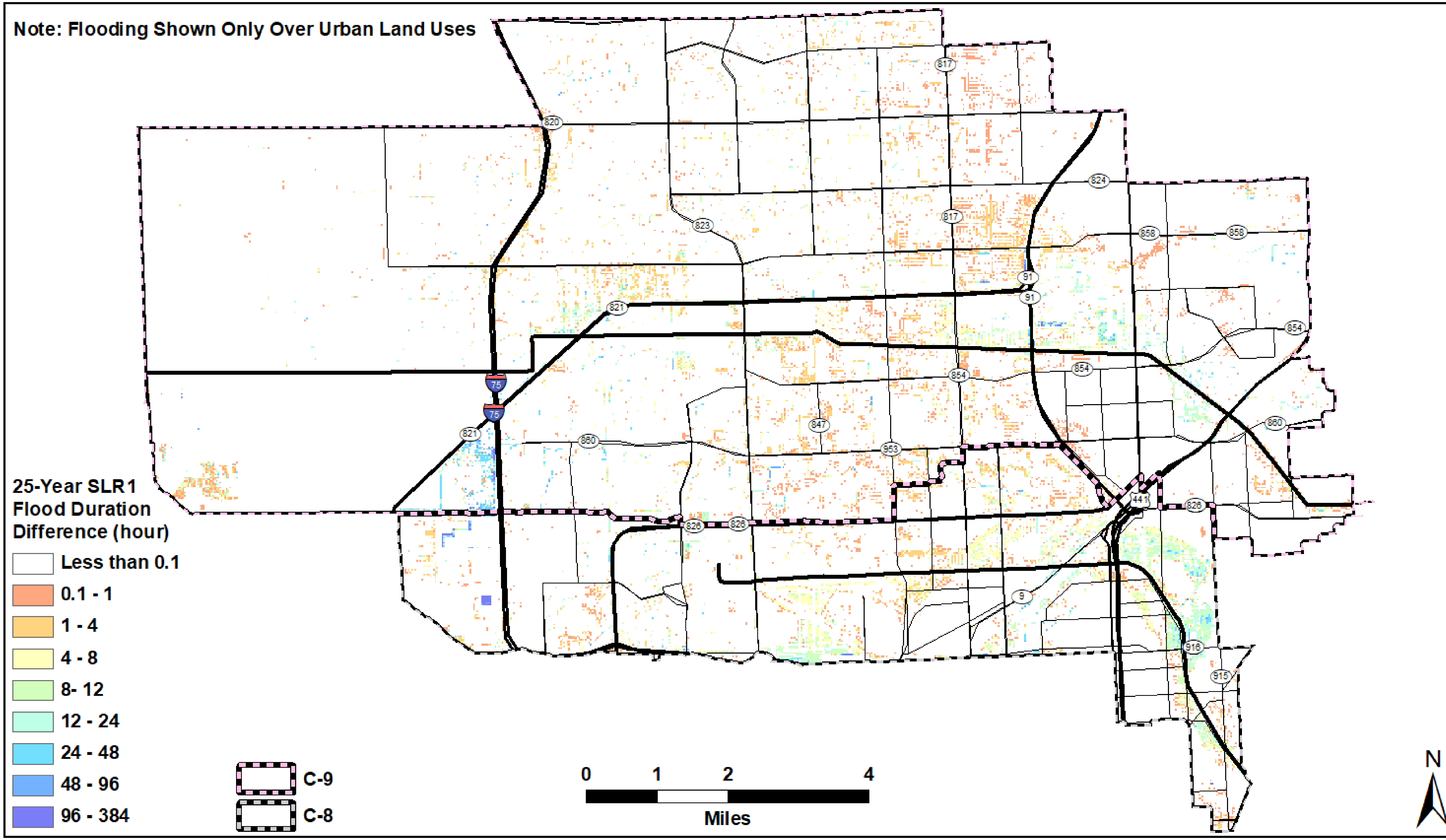

Figure 4.6-67: Flood Duration Difference Map for 25-Year Sea Level Rise 1 Design Storm Event in Urban Land Use Areas (Future minus Current Conditions)

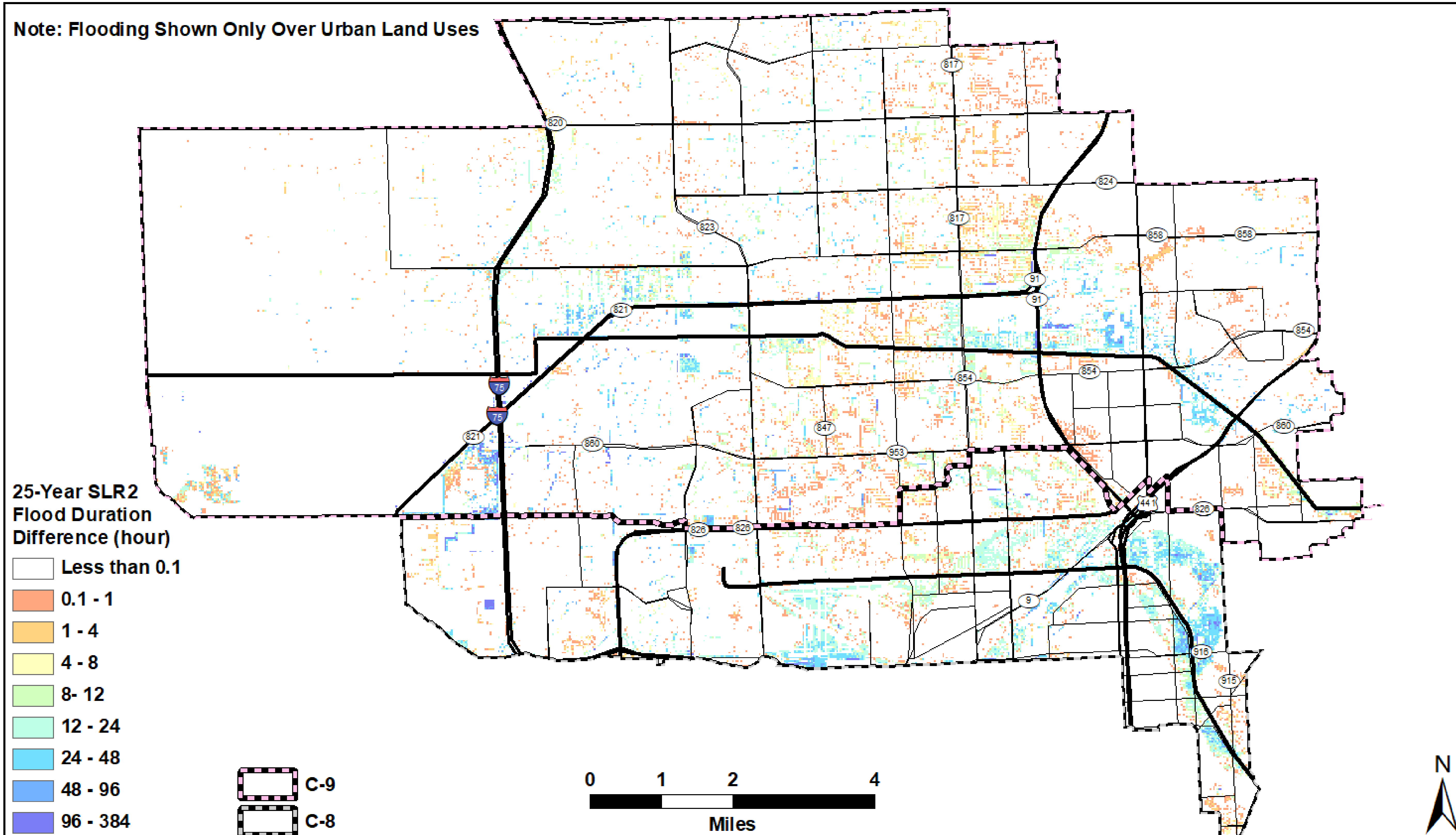

Figure 4.6-68: Flood Duration Difference Map for 25-Year Sea Level Rise 2 Design Storm Event in Urban Land Use Areas (Future minus Current Conditions)

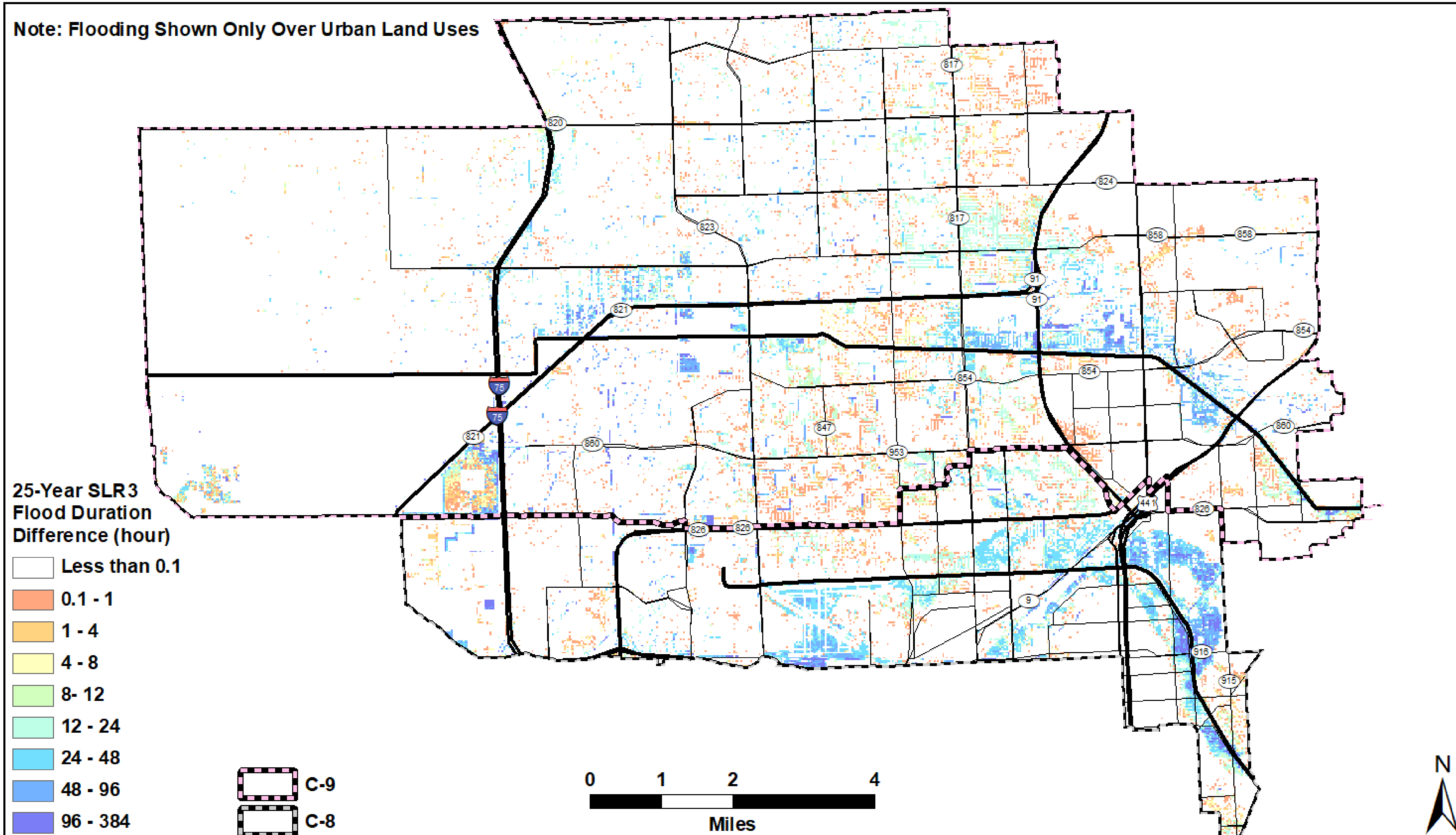

Figure 4.6-69: Flood Duration Difference Map for 25-Year Sea Level Rise 3 Design Storm Event in Urban Land Use Areas (Future minus Current Conditions)

5 RAINFALL SENSITIVITY TEST – 10-YEAR SLR1 DESIGN STORM

A rainfall sensitivity test was conducted for the future conditions design storms using the 10-year 1 ft sea level rise scenario. A 9% increase was applied to the NOAA Atlas 14 10-year rainfall depths based on the Broward County DDF Change Factor Ensemble Analysis (Yin, Li, & Urich, 2019). The sensitivity test used the same SFWMD 3-day temporal distribution and Thiessen Polygon spatial distribution used in the previous design storm simulations. The total rainfall depth was the only parameter change for the sensitivity test. The following subsections describe the applicable results of the FPLOS evaluation on the 10-year SLR1 rainfall sensitivity simulation.

5.1 PM #1 – Maximum Stage in Primary Canals

This is the peak stage profile in the primary canal system. The profile was developed for the 10-year 72-hour design storm with 1 ft sea level rise and a 9% increase in rainfall. To evaluate this PM under future conditions within the C-8 and C-9 watersheds, instantaneous peak stage profiles were prepared for the primary canals within the watersheds, which are the C-8 and C-9 Canals, respectively. Bank elevations on the profile figures are based on the MIKE HYDRO cross-section data. Also shown in the figures are major roadway landmarks, control structures, and primary canal junctions. **Figure 5.1-1** and **Figure 5.1-2** show the maximum stage in the C-8 and C-9 Canals, respectively.

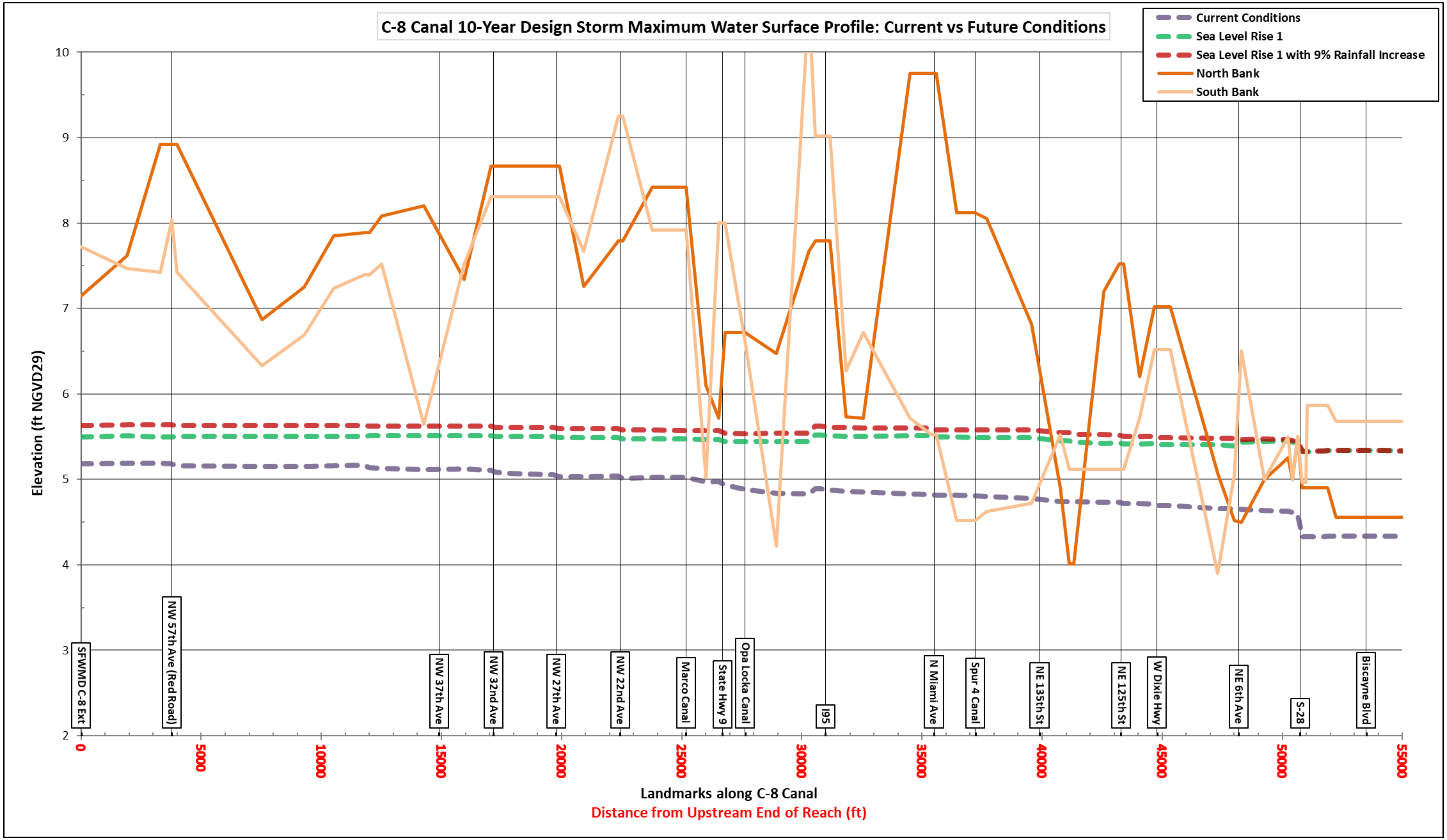

Figure 5.1-1: C-8 Canal Peak Stage Profiles for 10-Year Design Storm – Current vs Future Sea Level Rise and Rainfall Scenarios

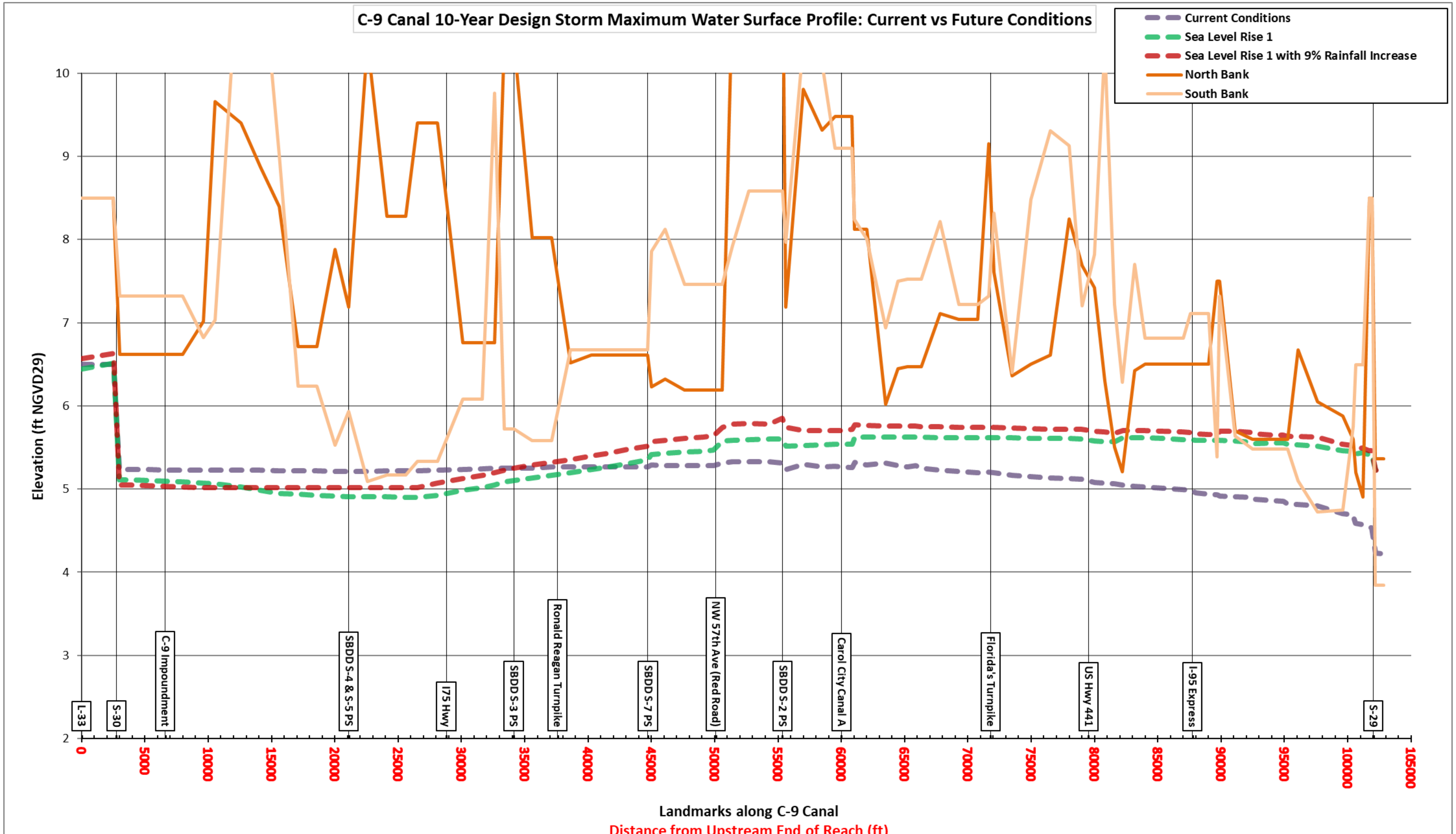

Figure 5.1-2: C-9 Canal Peak Stage Profiles for 10-Year Design Storm – Current vs Future Sea Level Rise and Rainfall Scenarios

5.2 PM #2 – Maximum Daily Discharge Capacity through the Primary Canals

Discharge capacity was calculated by dividing the peak of the discharge hydrograph by the canal segments contributing area. For structures S-28 and S-29, discharge capacity was calculated by dividing the peak discharge by the entire basin area. For the C-9 Basin, two additional estimates were made for the respective areas east and west of Red Road. These two additional estimates were necessitated by the presence of two different allowable runoff rates within the C-9 Basin. For the drainage area west of Red Road, the peak discharge at the Q-point located at Red Road (shown as a green dot in **Figure 4.2-1**) was divided by the contributing drainage area (highlighted in green in **Figure 4.2-1**). For the drainage area east of Red Road, the peak discharge at the Q-point located at Red Road was subtracted from the peak discharge at structure S-29, and then divided by the contributing drainage area east of Red Road. Tidal effects were filtered by using a 12-hour moving average of discharge.

Table 5-1 lists the canal segments identified for this analysis, the contributing area for each canal segment, and the discharge capacity calculated for each segment associated with each of the 10-year design scenarios analyzed.

Table 5-1: Water Control Catchment Discharge Capacity for 10-Year Future Conditions Design Storms

Structure / Segment	Inflow	Outflow	Water Control Catchment Area (sq.mi)	10-Year Design Storm Peak Discharge Capacity (cfs/sq.mi)		
				Current	SLR1	SLR1 w/ Rainfall Increase
S-28	Beginning of C-8	S-28	28.22	61.9	60.3	66.7
S-29	Beginning of C-9/ Structure S-30	S-29	99.37	24.6	19.2	21.2
C-9 west of Red Road	Beginning of C-9/ Structure S-30	Q-point at Red Road	61.24	15.2	12.1	13.0
C-9 east of Red Road	Q-point at Red Road	S-29	38.13	51.3	51.5	56.6

Discharge west and east of Red Road is an estimate due to interconnected outfalls on both sides of Red Road

The following figures present visual comparisons of the area-weighted discharge hydrographs for the C-8 and C-9 Canal for the future conditions 10-year design storm with 1 ft sea level rise and 9% increase in rainfall. An additional two hydrographs are presented for areas east and west of Red Road. With the higher rainfall, the structure discharge capacities increased by 6.4 cfs/sq.mi and 2.0 cfs/sq.mi for S-28 and S-29, respectively compared to SLR1 with current rainfall.

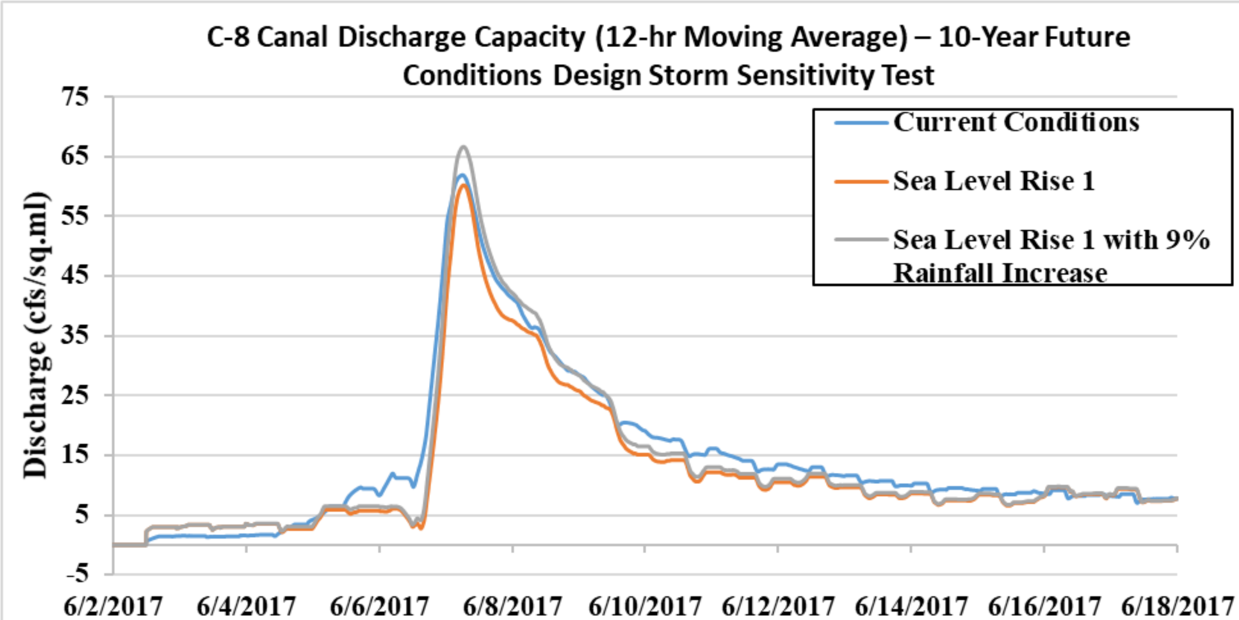

Figure 5.2-1: Area-Weighted Discharge Hydrograph for C-8 Canal (S-28) 10-Year Design Storm Sensitivity Test

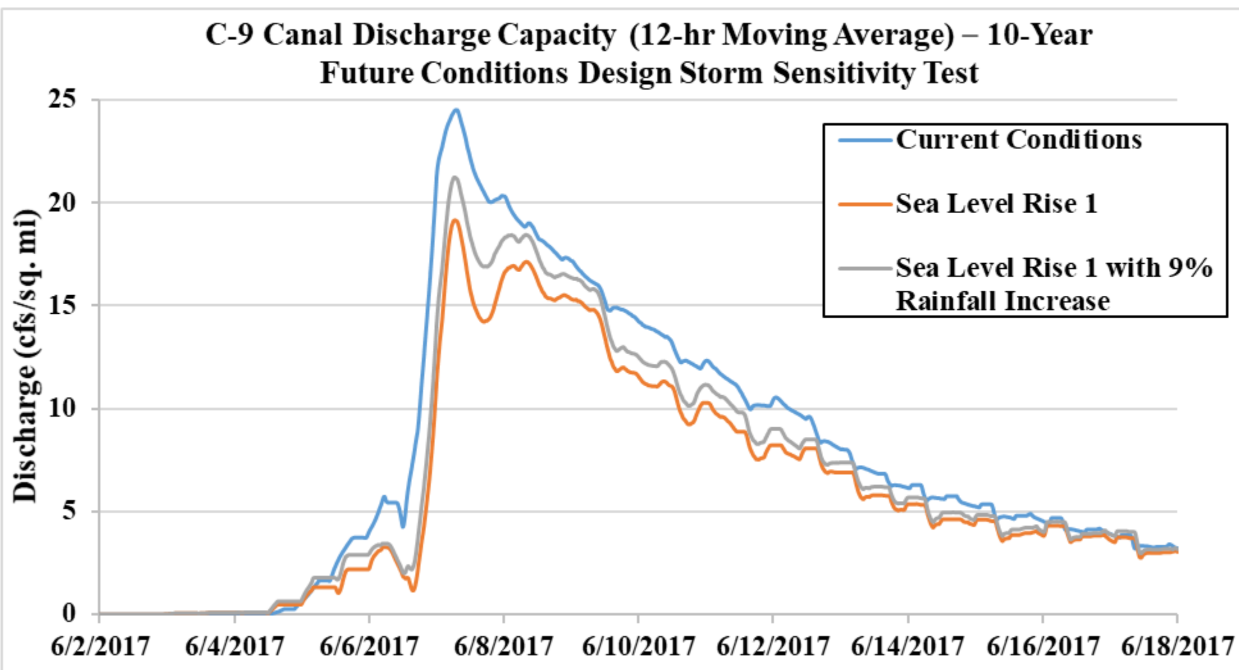

Figure 5.2-2: Area-Weighted Discharge Hydrograph for C-9 Canal (S-29) 10-Year Design Storm Sensitivity Test

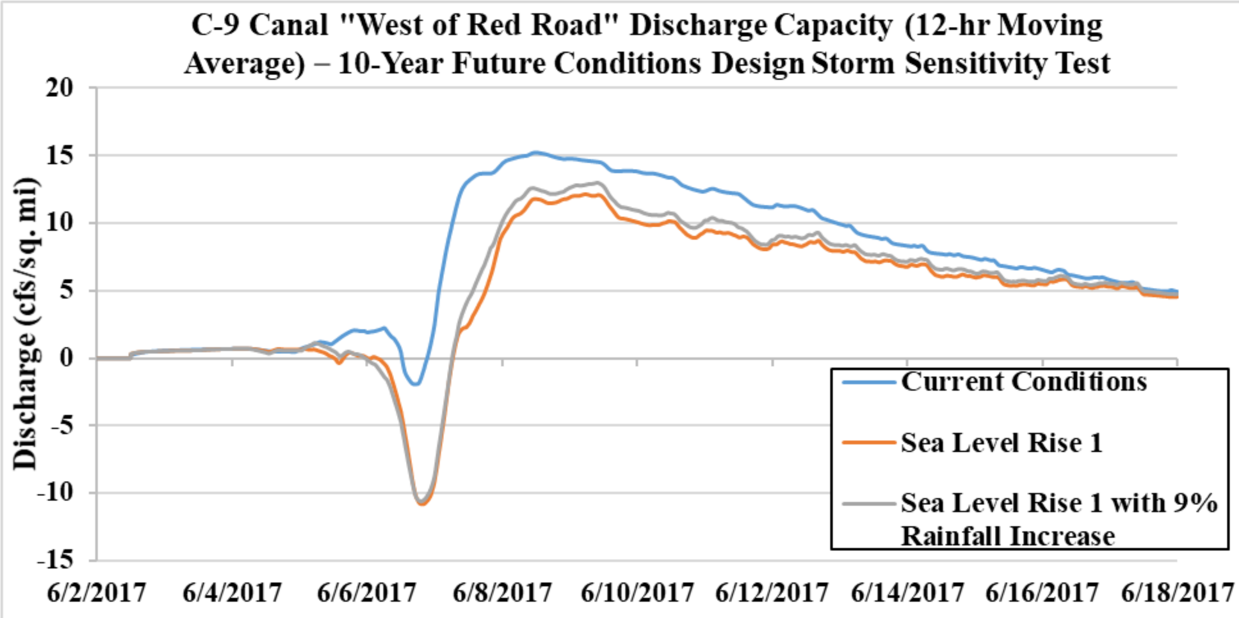

Figure 5.2-3: Area Weighted Discharge Hydrograph for C-9 Canal West of Red Road for 10-Year Design Storms

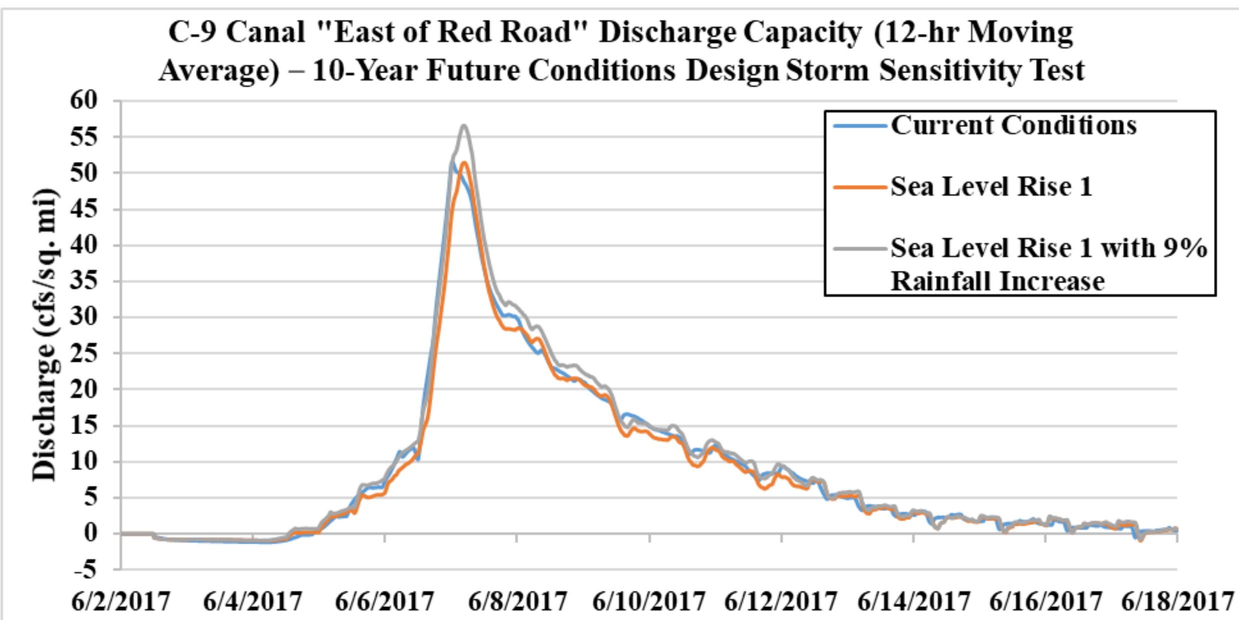

Figure 5.2-4: Area-Weighted Discharge Hydrograph for C-9 Canal East of Red Road for 10-Year Design Storms

5.3 PM #4 – Peak Storm Runoff

PM #4 is the maximum conveyance capacity of a watershed at the tidal structure. It shows the maximum conveyance (moving 12-hr average) for a specific design storm and a specific tidal boundary condition. **Figure 4.4-1** and **Figure 4.4-2** represent the design storm discharge at tidal structures S-28 and S-29, respectively. These discharge hydrographs, specifically the peak discharge, were evaluated for the 10-year future conditions SLR1 scenario with 9% increase in rainfall and compared with the current conditions and future conditions SLR1 design storm. With the higher rainfall, the peak structure discharge increased by 181 cfs and 207 cfs for S-28 and S-29, respectively, compared to SLR1 with current rainfall.

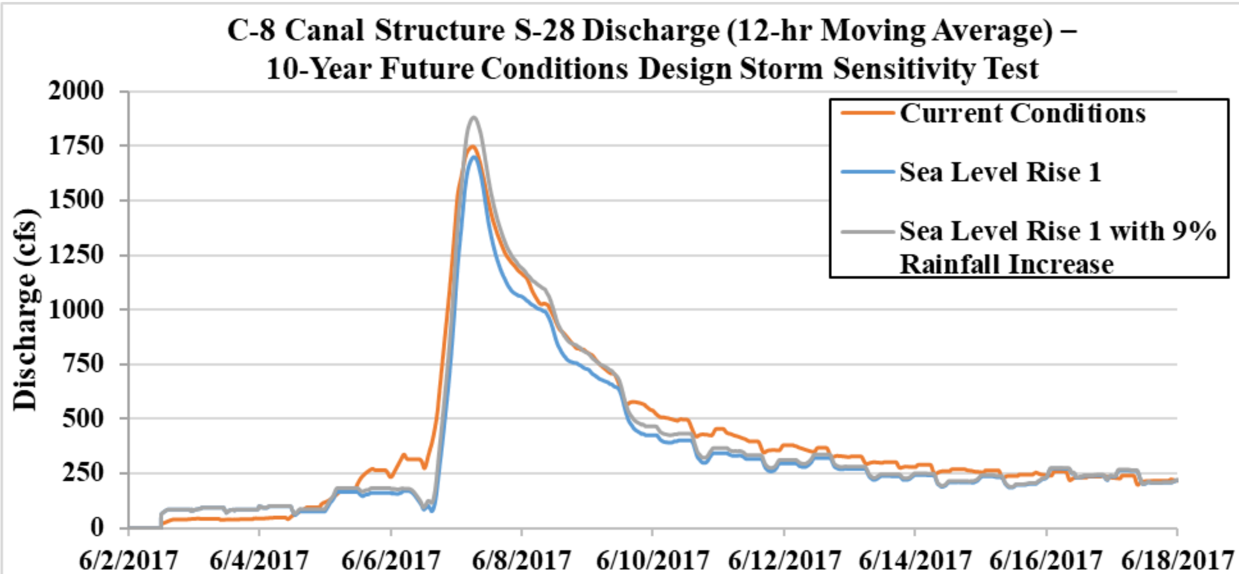

Figure 5.3-1: C-8 Canal Structure S-28 Discharge Hydrographs for 10-Year Design Storm Sensitivity Test

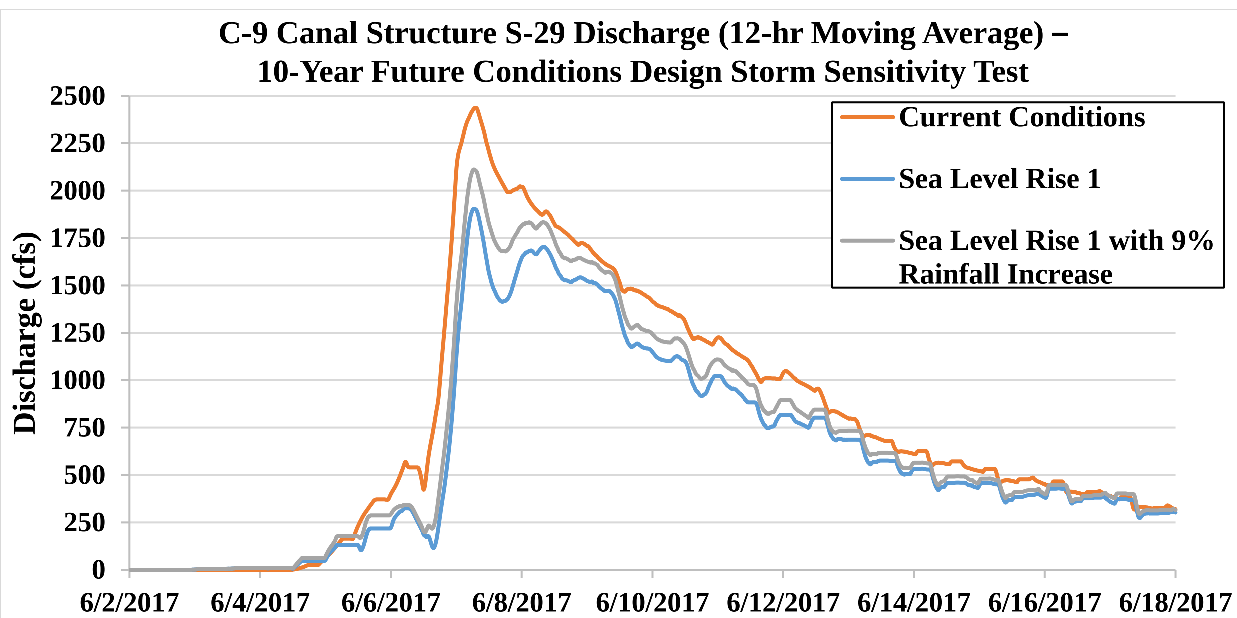

Figure 5.3-2: C-9 Canal Structure S-29 Discharge Hydrographs for 10-Year Design Storm Sensitivity Test

5.4 PM #5 – Frequency of Flooding

For this PM, the depths of overland flooding were evaluated for the 10-year design storm with 1 ft sea level rise and 9% increase in rainfall. These flood depths, or elevations, can be compared with elevations from the 10-year SLR1 design storm to see how sensitive the model is to changes in rainfall under future conditions. For the purposes of this C-8/C-9 FPLOS evaluation, flood inundation maps were prepared using MIKE SHE gridded model output for each storm event, in the form of depth of overland water. Flooding depths were representative of the overland water depths on the 125-ft grid. The resulting flood inundation map over the entire model domain is shown in **Figure 5.4-1** and the flood inundation map over urban areas only is shown in **Figure 5.4-2. Figure 5.4-3** shows the maximum overland water depth difference between future conditions with rainfall increase and future conditions without rainfall increase for the 10-Year SLR1, design storm events.

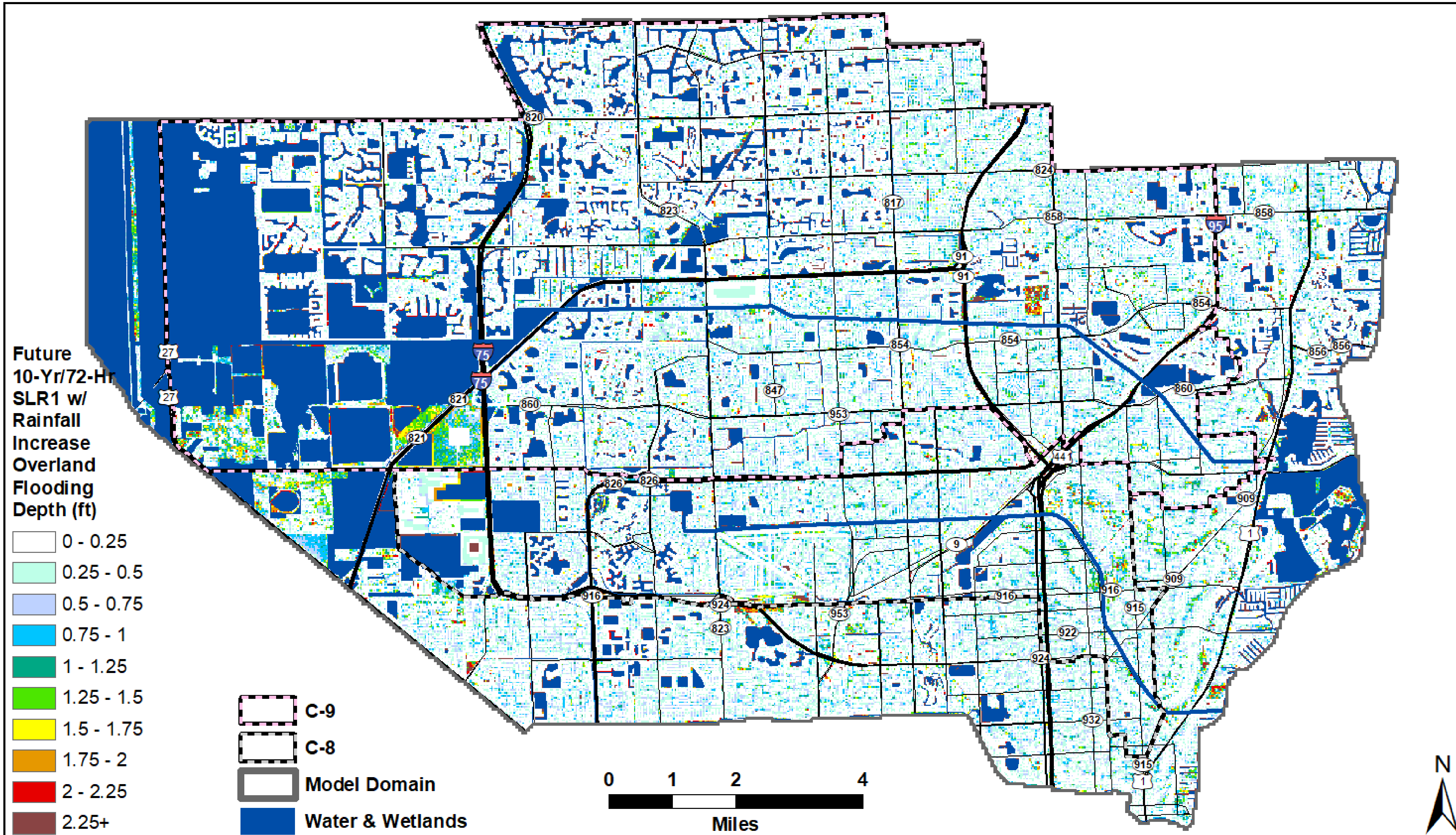

Figure 5.4-1: Flood Inundation Map for 10-Year Sea Level Rise 1 Design Storm Event with 9% Increase in Rainfall

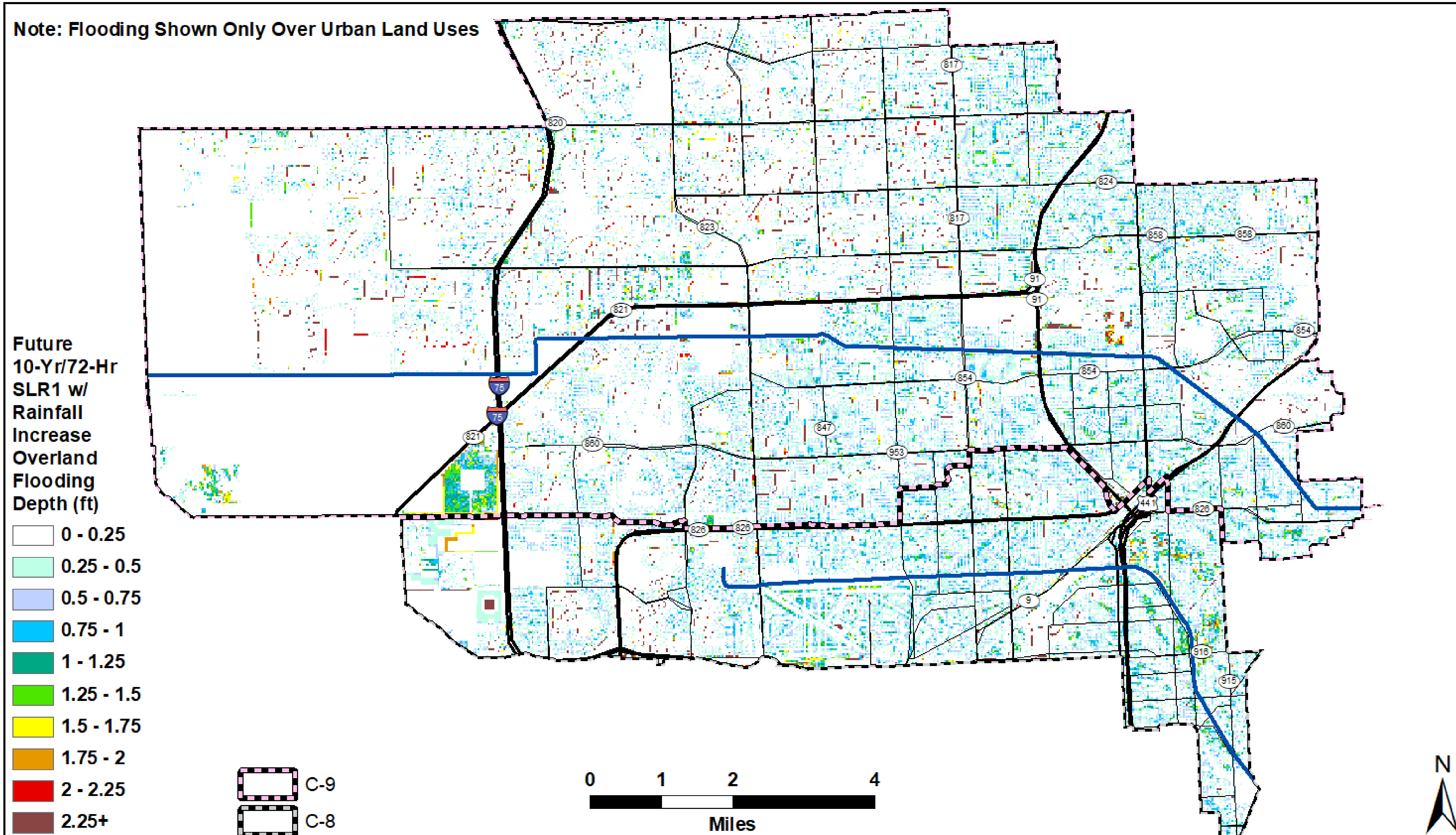

Figure 5.4-2: Flood Inundation Map for 10-Year Sea Level Rise 1 Design Storm Event with 9% Increase In Rainfall in Urban Land Use Areas

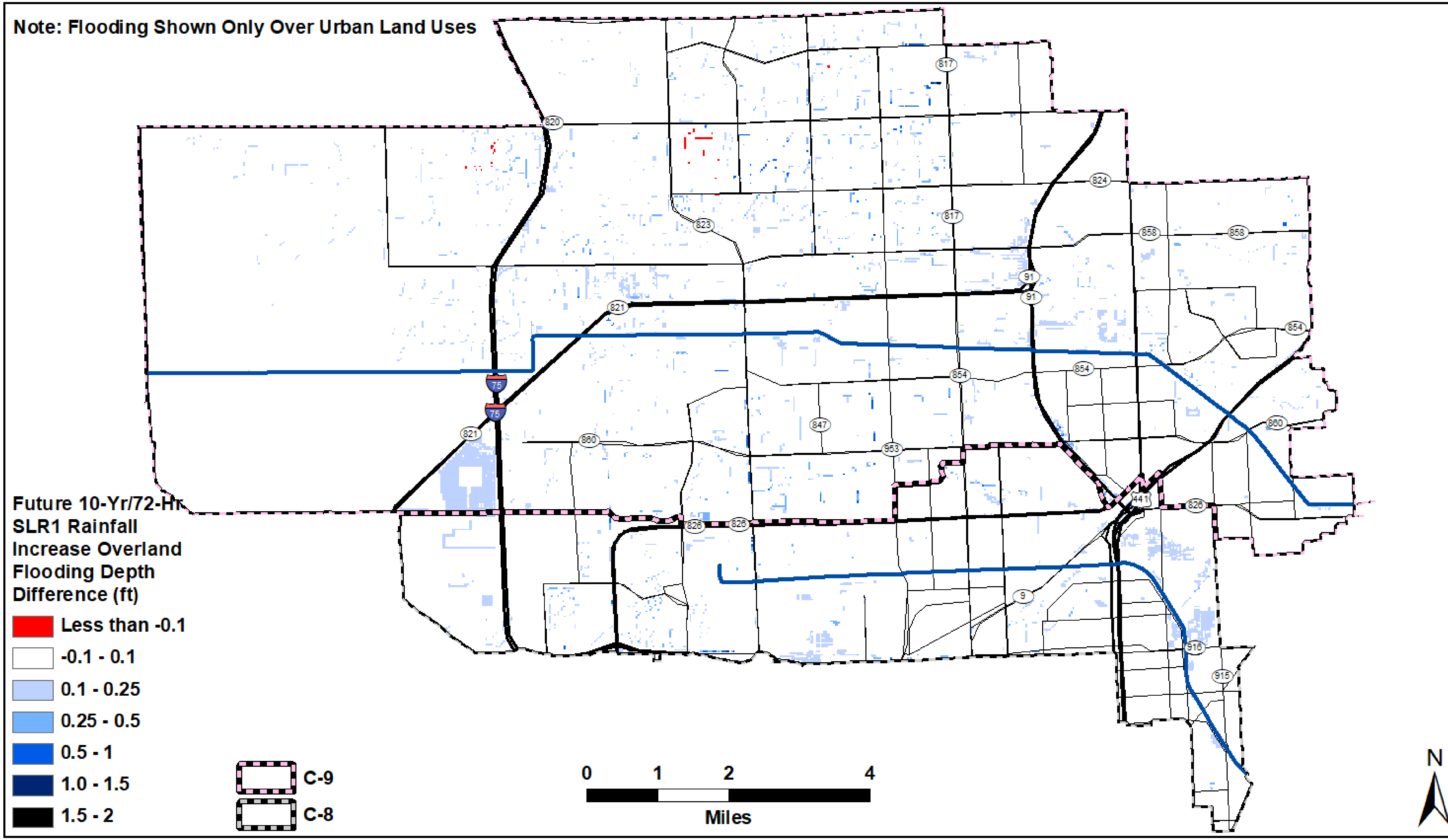

Figure 5.4-3: Flood Inundation Difference Map for 10-Year Sea Level Rise 1 Design Storm Event with Increased Rainfall, in Urban Land Use Areas (Future Conditions with Rainfall Increase minus Future Conditions without)

5.5 PM #6 – Duration of Flooding

For PM #6, the duration of flooding maps were developed by estimating the duration over which water depth exceeds a given threshold value. In this study, the duration of overland flooding was estimated using model simulated water depths and a threshold flooding depth of 0.25 ft. Additionally, the duration of flooding in the District Canals were estimated as the amount of time it takes for the water levels to return to target stage. The target stages of 3.6 ft for S-28Z and 3.5 ft for S-29Z were provided by the District (Email from Hongying Zhao, 5/12/2020). **Table 5-2** shows the duration of time taken for the water level in the C-8 and C-9 Canal to return to target stage, based on the first instance.

Table 5-2: Duration for Water Levels to Return to Target Stage for 10-Year Design Storms

Design Storm	Duration for S-28Z Return to Target Stage (hr) 10-Year	Duration for S-29Z Return to Target Stage (hr) 10-Year
Current	40	92
SLR1	60	98
SLR1 with 9% Rainfall Increase	70	123

The duration of overland flooding was estimated for all four design storm events based on the length of time the flood depth was predicted to exceed the threshold value (0.25 ft) within each MIKE SHE 125-ft grid cell using the statistics tool in MIKE ZERO. The flood duration map over the entire model domain for the 10-year SLR1 design storm with 9% increase in rainfall is shown in **Figure 5.5-1** and the flood duration map over urban area only is shown in **Figure 5.5-2. Figure 5.5-3** shows the flood duration difference between future conditions with rainfall increase and future conditions without rainfall increase for the 10-Year SLR1, design storm events.

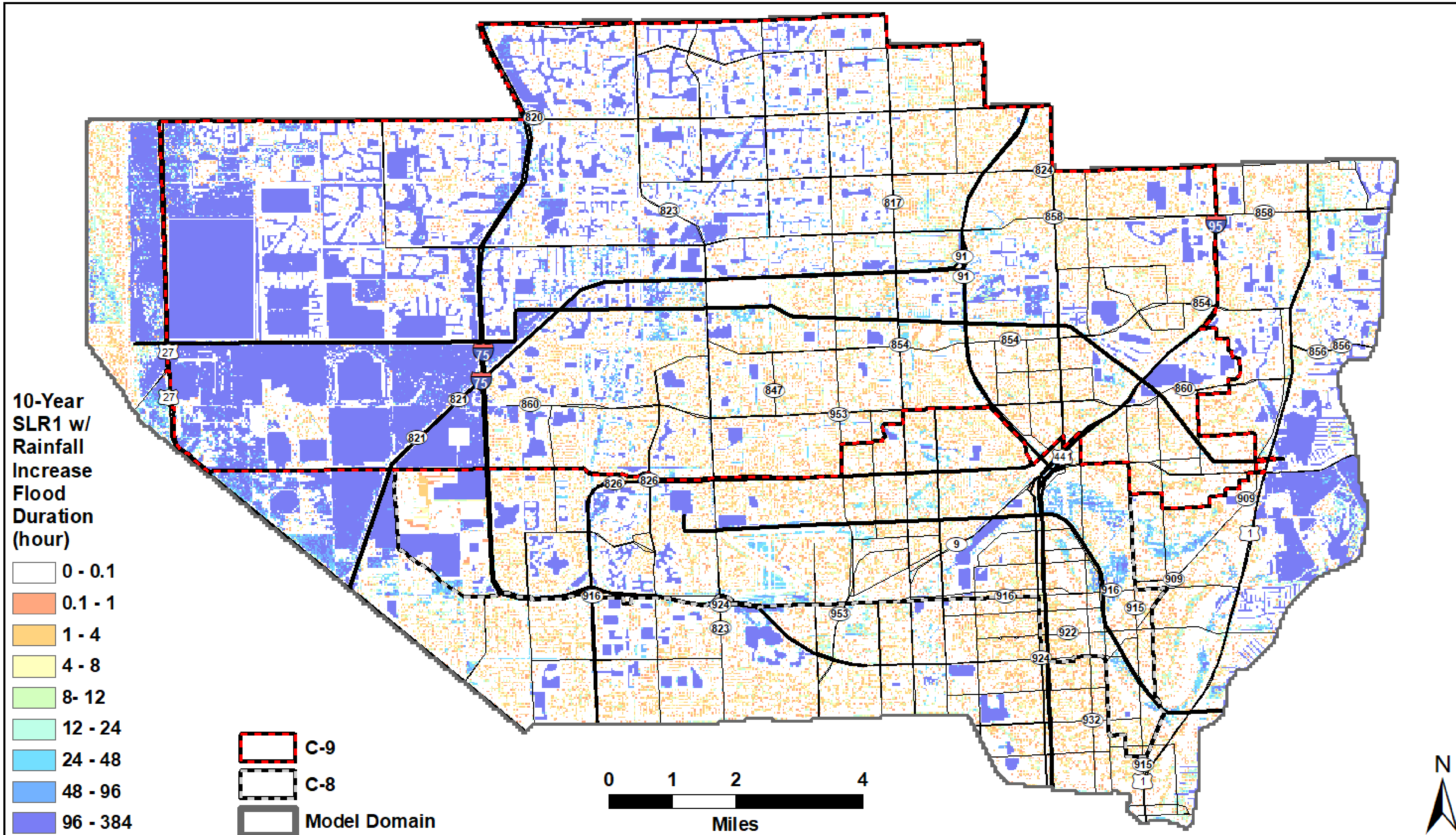

Figure 5.5-1: Flood Duration Map for 10-Year Sea Level Rise 1 Design Storm Event with 9% Increase in Rainfall

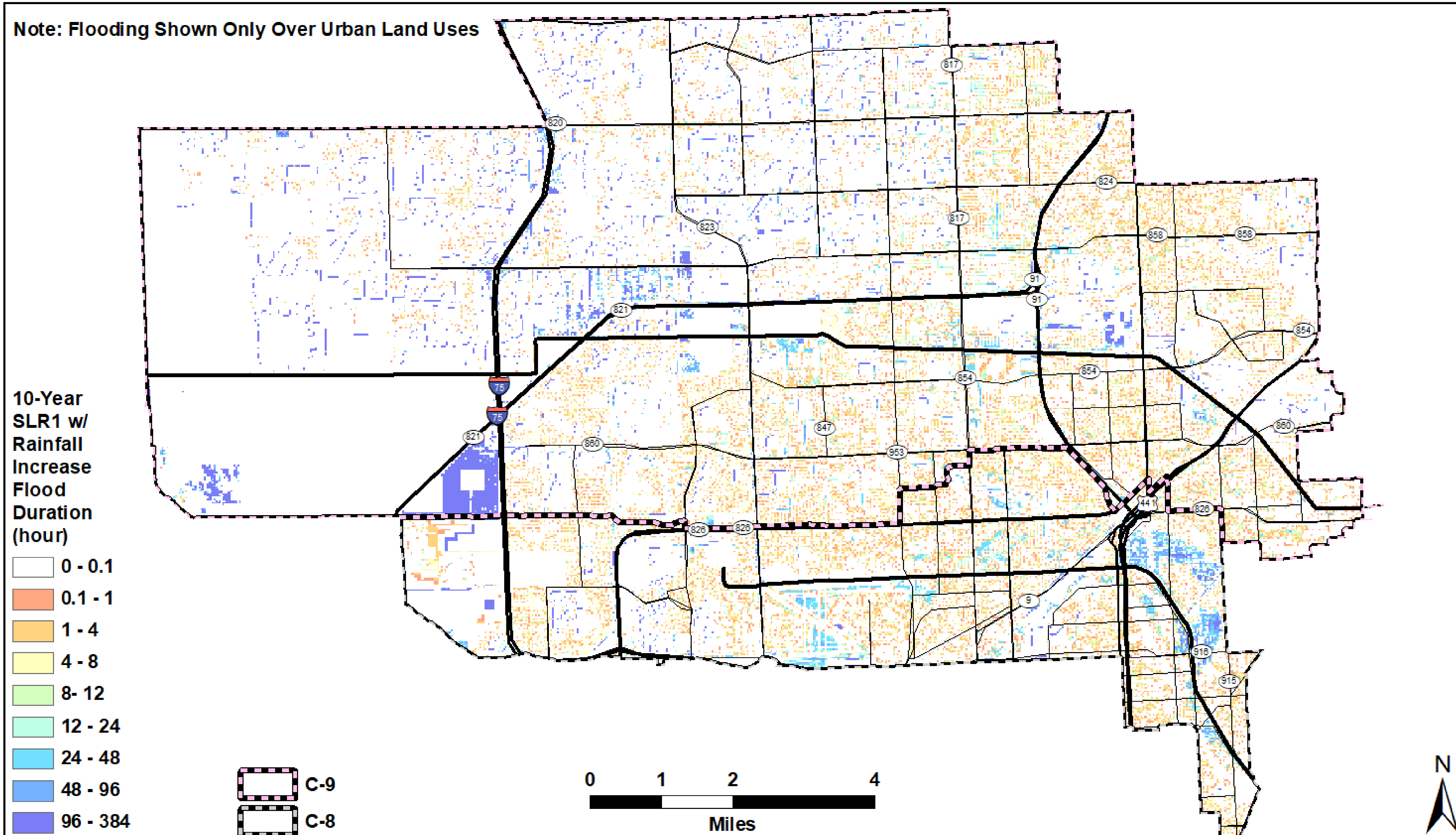

Figure 5.5-2: Flood Duration Map for 10-Year Sea Level Rise 1 Design Storm Event with 9% Increase in Rainfall in Urban Land Use Areas

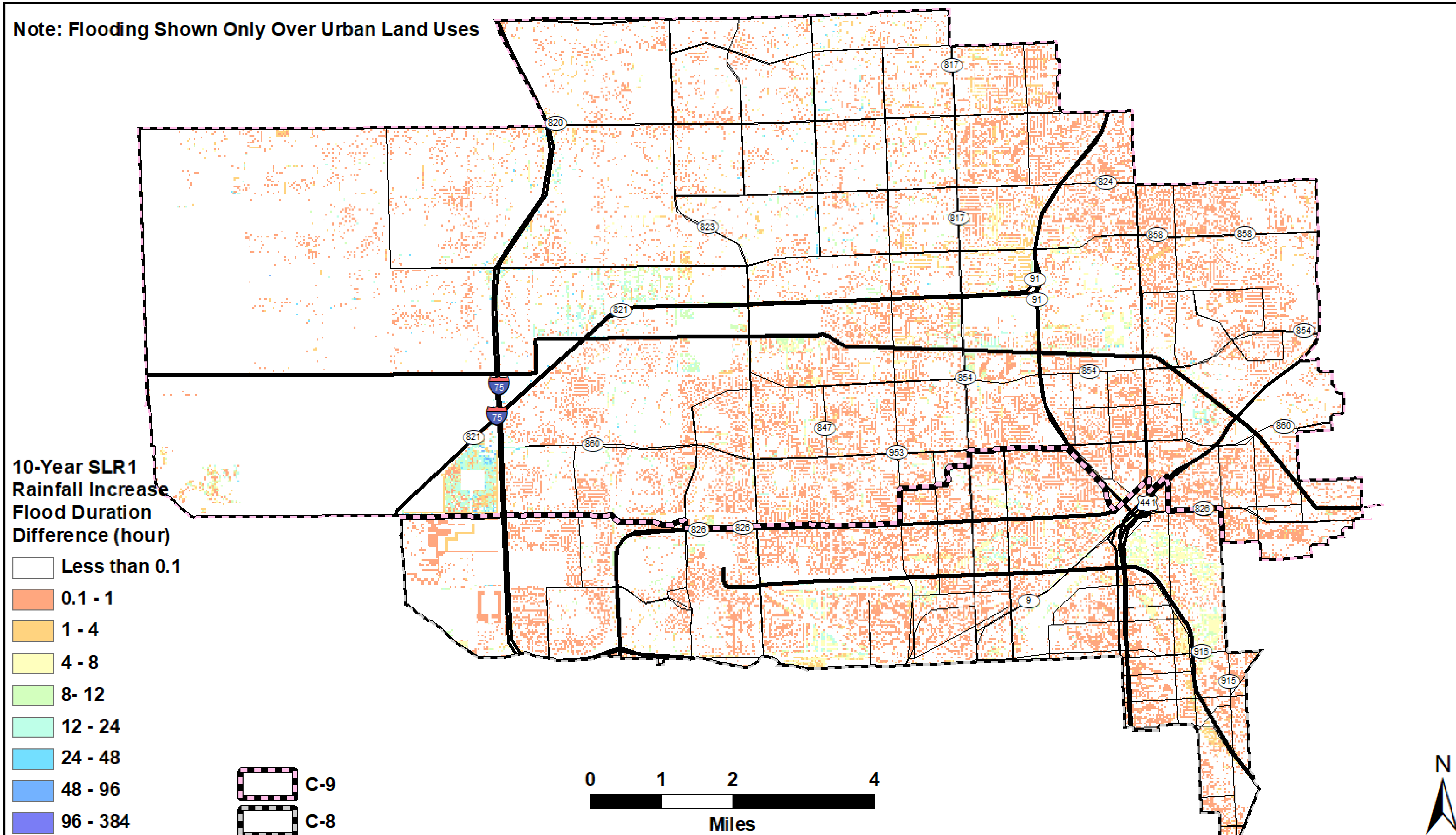

Figure 5.5-3: Flood Duration Difference Map for 10-Year Sea Level Rise 1 Design Storm Event with Increased Rainfall, in Urban Land Use Areas (Future Conditions with Rainfall Increase minus Future Conditions without)

6 CONCLUSIONS

The future conditions design storm simulation results were evaluated using six performance measures. The analysis presented in this report provides a model-based assessment of the future level of flood protection provided by the existing C-8 and C-9 watershed's primary canal network and associated control structures. These results were used to determine potential FPLOS deficiencies by highlighting areas that failed multiple performance measures such as bank exceedances that corresponded to overland inundation (PM #5 and/or PM #6). In many cases, PM #1 bank exceedances did manifest as significant overland inundation, shown in PM #5, and thus were considered significant localized FPLOS deficiencies.

It should also be noted that the model results are subjected to certain limitations associated with the scale of the 2-dimensional model grid. Although the model uses a 125-ft grid that is suitable for the sub-regional scale flood protection level of service evaluation, the results should not be extended to local-scale evaluations or regulatory determinations of flooding extents, where considerable variations in topography can occur within the area of each grid cell.

6.1 Future Conditions

6.1.1 C-8 Basin

Based on the results of this study, it appears that the C-8 canal generally provides a 5-year or less level of service, especially for the 2 ft and 3 ft sea level rise conditions. Although some localized areas have a 25-year level of service or better with respect to bank exceedances, the system as a whole is overwhelmed for the design storms of lower intensity. Under the 3 ft sea level rise scenario, even a 5-year design storm was enough to overwhelm a significant portion of the system. There were a few localized areas where the water levels exceeded the canal banks for the 5-year 1 ft sea level rise event as shown in PM #1 (**Figure 4.1-2)**, however, it does not correspond to a significant area of flood inundation as shown in PM #5 (**Figure 4.5-1).** For the 25-year design storm, regardless of the amount of sea level rise, the model results suggest that a significant portion of the eastern half of the C-8 Canal would be overwhelmed during peak flood conditions, with the western segment (west of Marco Canal) generally performing better. For the 100-year design storm, regardless of the amount of sea level rise, the model results suggest that most of the C-8 Canal would be overwhelmed during peak flood conditions, while most of the watershed would be inundated to some degree. The 100-year 3 ft sea level rise event was the worst-case scenario simulated, and it shows that nearly half of the C-8 Canal would be out-of-bank (**Figure 4.1-8)** and a significant portion of the watershed would inundated, with large areas experiencing over 2 feet of flood depth (**Figure 4.5-12**).

The C-8 Canal is overwhelmed in large segments for the majority of the design storm and sea level rise combinations, which can be in-part attributed to its low bank elevations. However, the S-28 tidal outfall structure also has a significant role in the performance of the C-8 Canal. Under future conditions sea level rise scenarios, the discharge capacity of the S-28 structure is reduced. Looking at the 12-hour moving average peak discharge, it becomes apparent that S-28 is unable to maintain design capacity under certain sea level rise conditions. Although peak discharge is not reduced drastically for the SLR 1 and 2 foot scenarios for design storms up to and including the 25-year event, the peak discharge is reduced by 24%, 19%, 20%, and 28%, from current conditions to the 3 ft sea level rise scenario for the 5, 10, 25, and 100-year design storms, respectively. The peak discharge response is different at S-29, which starts to "feel the effects" of sea level rise for even the 1 ft SLR scenario and for the smaller storm events (discussed in the next subsection). Interestingly, the instantaneous peak discharge is larger under future conditions, however, this is a result of the increased surge-induced reverse flow which is bypassing the structure and causing the water to "stack", which provides the opportunity for increased instantaneous discharge once the tide level falls. The design discharge of 3220 cfs was only reached during the 100-year design storm events, however, the design headwater assumption is violated by 2.2 ft. The assumed design headwater stage is 2.2 feet, while the predicted headwater is 4.4 feet at the time of peak discharge. Although the design discharge can be passed, the resulting increased headwater elevation causes flooding within the C-8 watershed.

6.1.2 C-9 Basin

Based on the results of this study, it appears that the C-9 canal generally provides a 10-year or less level of service for the 1 ft and 2 ft sea level rise conditions and a 5-year level of service for the 3 ft sea level rise scenario. Although some localized areas have a 25-year or 100-year level of service with respect to bank exceedances, the system as a whole is overwhelmed for the design storms of lower intensity. Under the 3 ft sea level rise scenario, a 10-year design storm was enough to overwhelm a significant portion of the system. There were a few localized areas where the water levels exceeded the canal banks for the 10-year 1 ft sea level rise event as shown in PM #1 (**Figure 4.1-5**), however, it does not correspond to a significant area of flood inundation as shown in PM #5 (**Figure 4.5-4**). For the 25-year design storm, regardless of the amount of sea level rise, the model results suggest that a large portion of the C-9 Canal would be overwhelmed during peak flood conditions, with the western segment (west of Carol City Canal A) generally performing better. For the 100-year design storm, regardless of the amount of sea level rise, the model results suggest that most of the C-9 Canal would be overwhelmed during peak flood conditions, while most of the watershed would be inundated to some degree. The 100-year 3 ft sea level rise event was the worst-case scenario simulated, and it shows that nearly half of the C-9 Canal would be out-of-bank (**Figure 4.1-9**) and a significant portion of the watershed would inundated, with large areas experiencing over 2 feet of flood depth (**Figure 4.5-12**).

The C-9 Canal is overwhelmed in localized segments for the majority of the design storm and sea level rise combinations, which can be attributed to its low bank elevations and higher tailwater conditions under sea level rise scenarios. The discharge capacity of the S-29 structure is reduced under all of the future sea level rise scenarios. Looking at the 12-hour moving average peak discharge, it becomes apparent that S-29 is unable to maintain design capacity under all sea level rise conditions. For the 5, 10, 25, and 100-year design storms, the peak discharge is reduced by 23%, 22%, 14%, and 9%, respectively, from current conditions to the 1 ft sea level rise scenario. Similarly, a reduction of 46%, 35%, 26%, and 21%, respectively, is seen for the 2 ft sea level rise scenario and 58%, 49%, 43%, and 38%, respectively, is seen for the 3 ft sea level rise scenario. These reductions are due to a combination of factors: (1) the C-9 Impoundment removing water from the western C-9 Canal will ultimately reduce the total volume discharged to tide, (2) discharge from some of the eastern SBDD pump stations will be limited due to stages in the C-9 Canal triggering "pump off" conditions required by permit, and (3) the storage characteristics of the western C-9 basin, namely the prevalence of large lakes (former mine pits) ,which have the ability to attenuate peak discharge rates and accommodate storm surge-induced flow reversals.

REFERENCES

Broward County Planning Council. (2020). *Broward County Future Land Use Plan (2040)* https://www.broward.org/PlanningCouncil/Pages/Maps.aspx

Burns & McDonnell. (2006). *Flood Protection Analysis for Broward County Water Preserve Areas C-11 and C-9 Impoundments (Final Report)*

Miami-Dade County. (n.d). *Miami Dade County Future Land Use (2030)*

SFWMD H&H Bureau. (2015). *Flood Protection LOS Analysis for the C-4 Watershed, Appendix A: LOS Basic Concepts*.

Taylor Engineering. (2020). *Flood Protection Level of Service Provided by Existing Infrastructure for Current Sea Level Conditions in the C8 and C9 Watersheds*

USACE. (2012). *Central and Southern Florida Project Broward County Water Preserve Areas Revised Final Integrated Project Implementation Report and Environmental Impact Statement*

Yin, C., Li, Y., & Urich, P. (2019). *Broward County DDF Change Factor Ensemble Analysis*.

Zhang. (2017). *The Effects of Sea Level Rise on S28 Performance*

Zhang. (2017). *The Effects of Sea Level Rise on S29 Performance*

Appendix A Instantaneous Stage and Discharge Summary

Table A- 1 Peak Stage and Discharge Summary for 5-Year Design Storms

Structure	Peak Stage (ft NGVD29)			Peak Discharge (cfs)		Minimum Discharge (cfs)	
	S-28	S-29	S-30 TW	S-28	S-29	S-28	S-29
Current	4.26	4.19	4.87	1721	2647	0	0
SLR1	5.12	5.04	4.82	1696	2417	-238	-323
SLR2	5.82	5.75	5.04	1839	2190	-773	-1057
SLR3	6.62	6.48	5.52	2087	2186	-1301	-1962

Table A- 2 Peak Stage and Discharge Summary for 10-Year Design Storms

Structure	Peak Stage (ft NGVD29)			Peak Discharge (cfs)		Minimum Discharge (cfs)	
	S-28	S-29	S-30 TW	S-28	S-29	S-28	S-29
Current	4.61	4.54	5.23	2059	3052	-45	-1
SLR1	5.43	5.42	5.11	2103	2698	-407	-489
SLR1 + 9% Rainfall	5.45	5.46	5.05	2268	2884	-430	-429
SLR2	6.14	6.10	5.49	2268	2526	-1016	-1215
SLR3	6.96	6.85	5.67	2615	2631	-1534	-2225

Table A- 3 Peak Stage and Discharge Summary for 25-Year Design Storms

Structure	Peak Stage (ft NGVD29)			Peak Discharge (cfs)		Peak Reverse Discharge (cfs)	
	S-28	S-29	S-30 TW	S-28	S-29	S-28	S-29
Current	5.16	5.08	5.49	2679	3681	-210	-146
SLR1	5.97	5.86	5.55	2789	3360	-647	-744
SLR2	6.64	6.58	5.84	3163	3460	-1171	-1680
SLR3	7.34	7.31	5.99	3278	3632	-1722	-2812

Table A- 4 Peak Stage and Discharge Summary for 100-Year Design Storms

Structure	Peak Stage (ft NGVD29)			Peak Discharge (cfs)		Peak Reverse Discharge (cfs)	
	S-28	S-29	S-30 TW	S-28	S-29	S-28	S-29
Current	6.04	6.00	5.97	3777	4710	-507	-578
SLR1	6.74	6.65	6.10	3999	4645	-1087	-1566
SLR2	7.36	7.38	6.26	4157	5073	-1692	-2649
SLR3	8.31	8.17	6.49	4094	4883	-2281	-3756

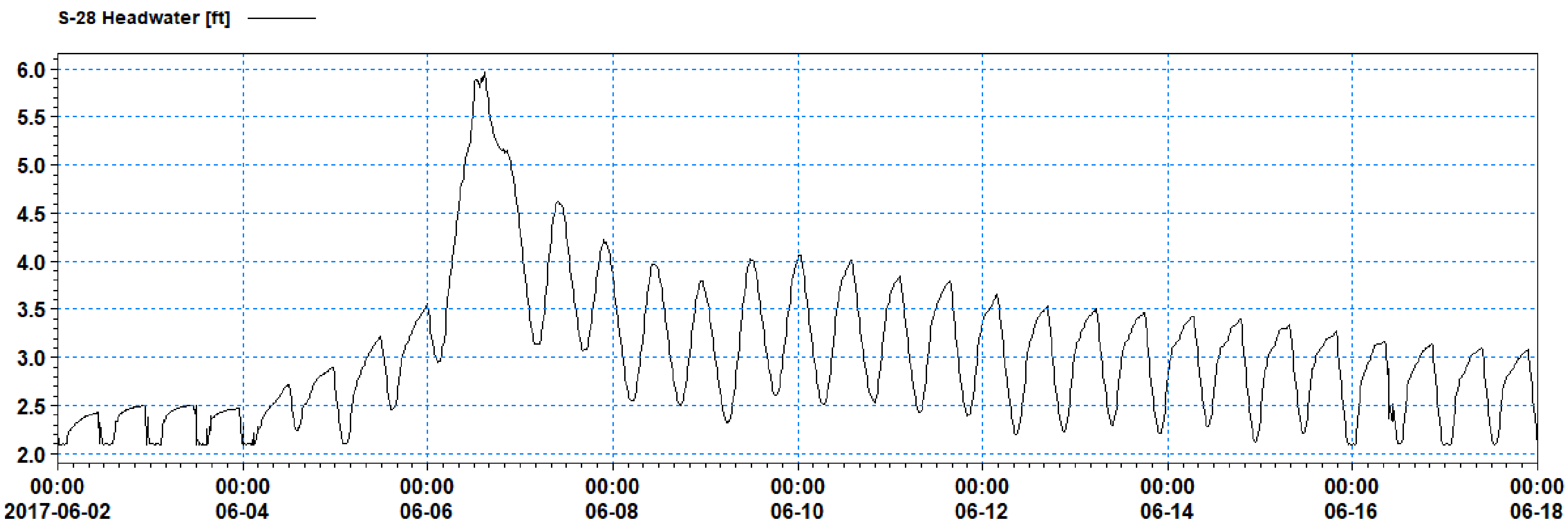

Figure A- 1: S-28 25-Year SLR1 Design Storm Headwater Stage

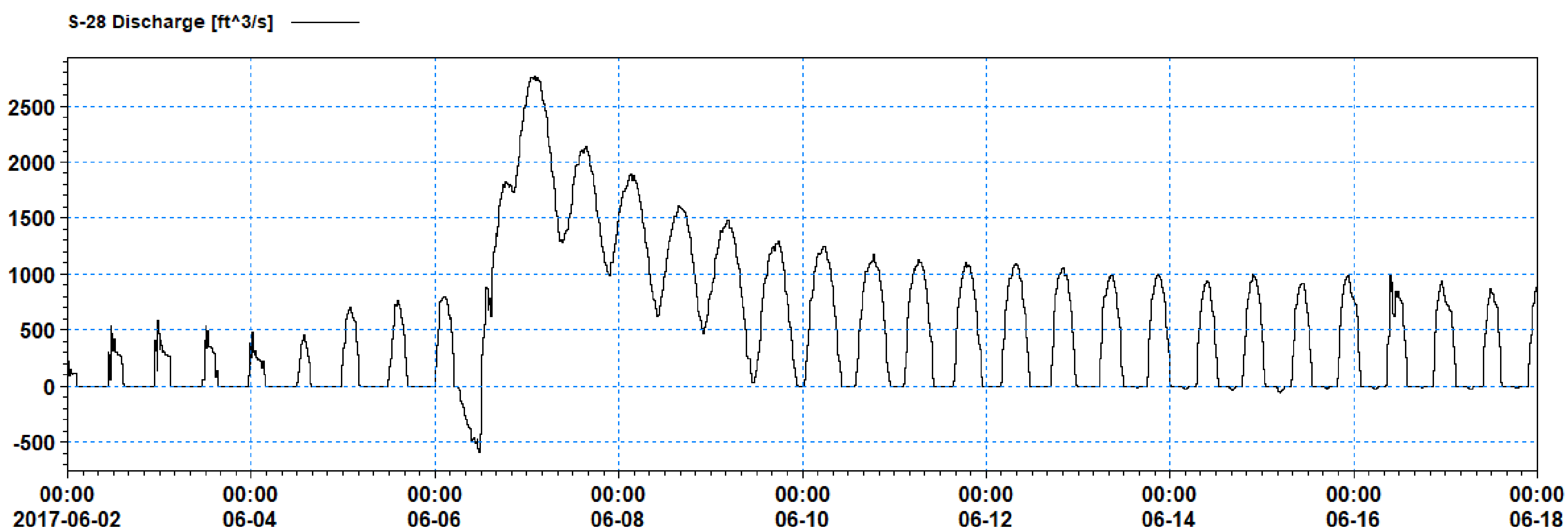

Figure A- 2: S-28 25-Year SLR1 Design Storm Discharge

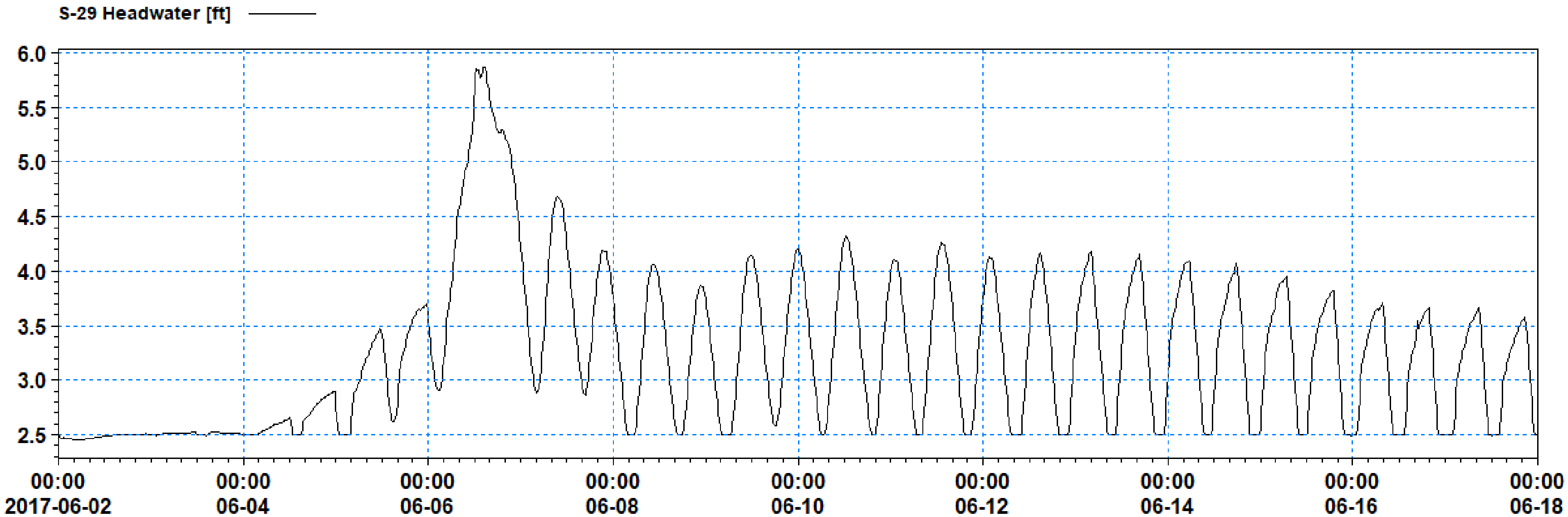

Figure A- 3: S-29 25-Year SLR1 Design Storm Headwater Stage

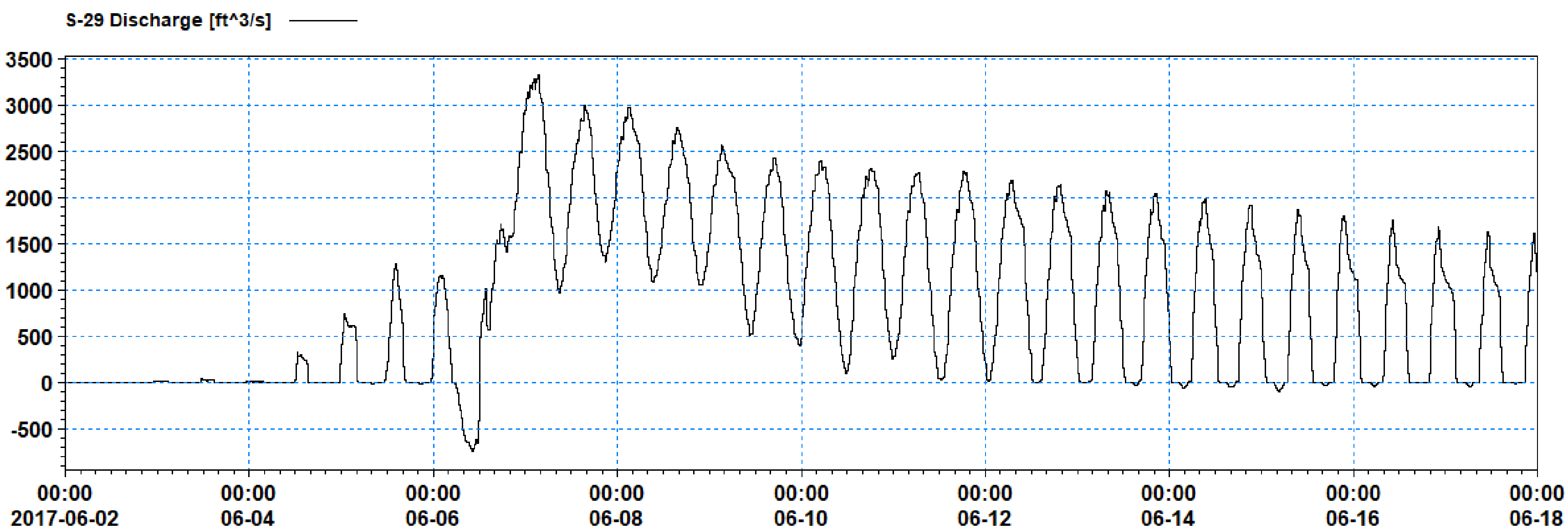

Figure A- 4: S-29 25-Year SLR1 Design Storm Discharge

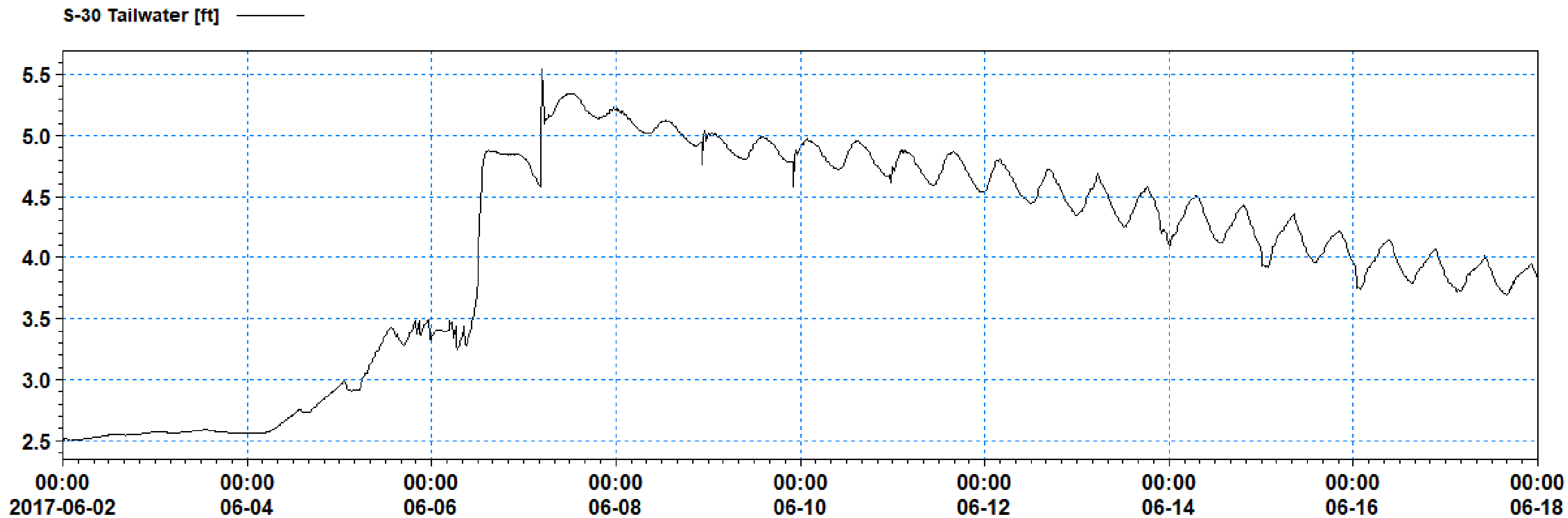

Figure A- 5: S-30 25-Year SLR1 Design Storm Tailwater Stage

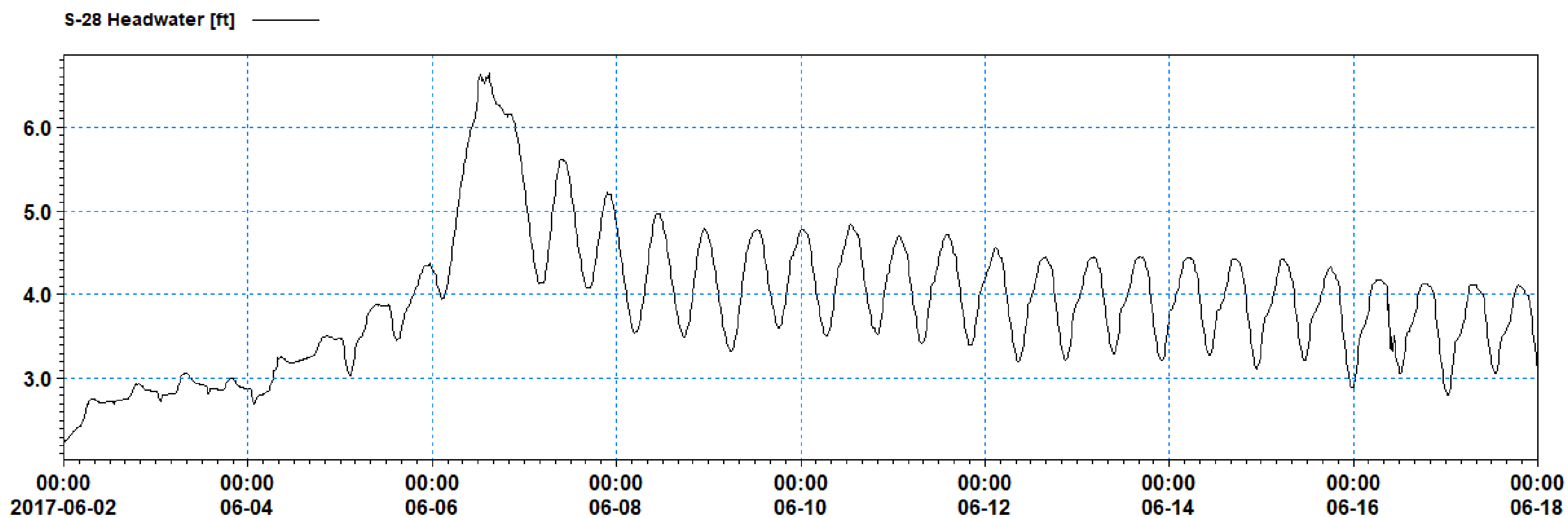

Figure A- 6: S-28 25-Year SLR2 Design Storm Headwater Stage

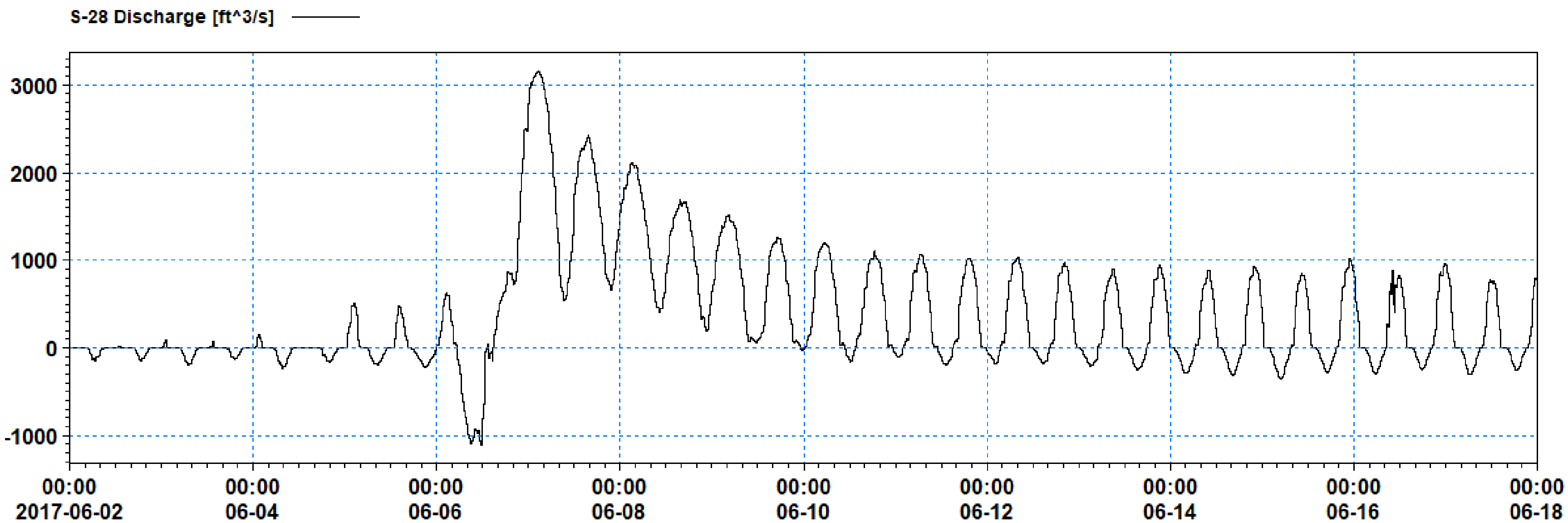

Figure A- 7: S-28 25-Year SLR2 Design Storm Discharge

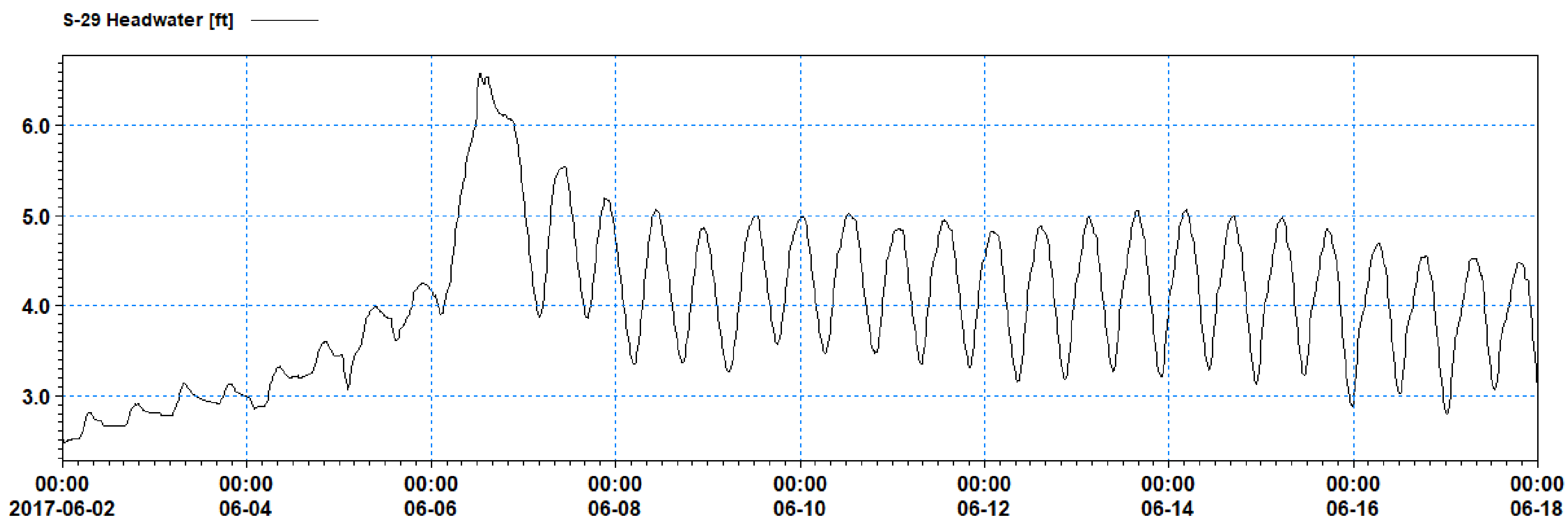

Figure A- 8: S-29 25-Year SLR2 Design Storm Headwater Stage

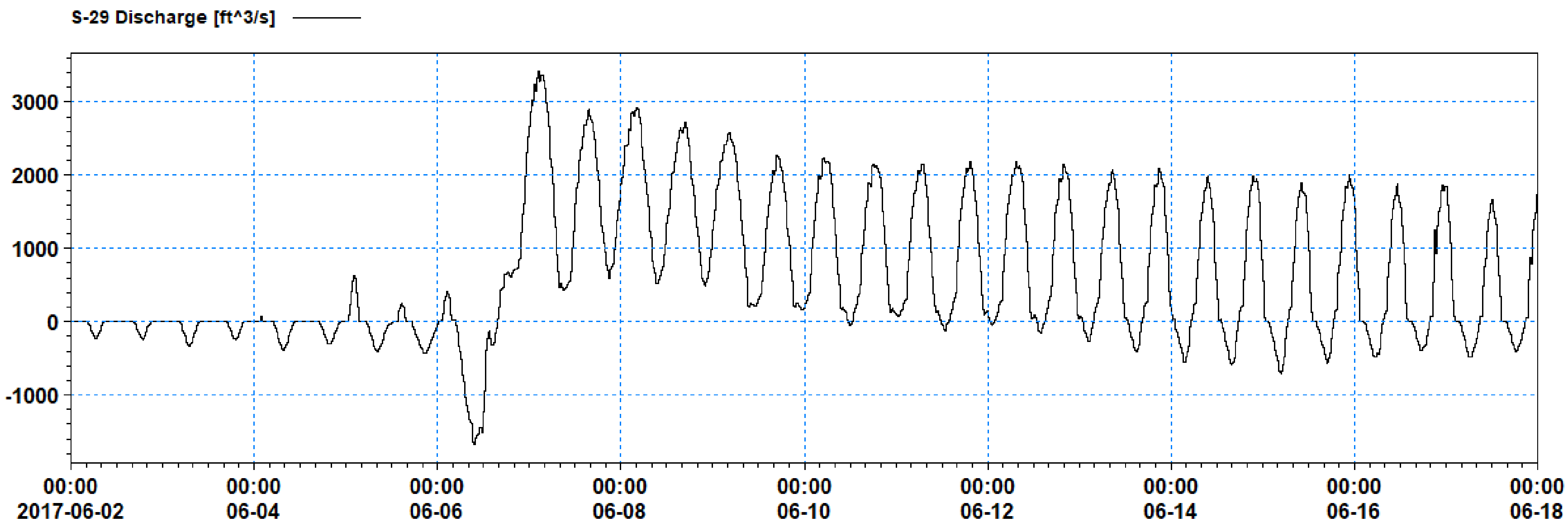

Figure A- 9: S-29 25-Year SLR2 Design Storm Discharge

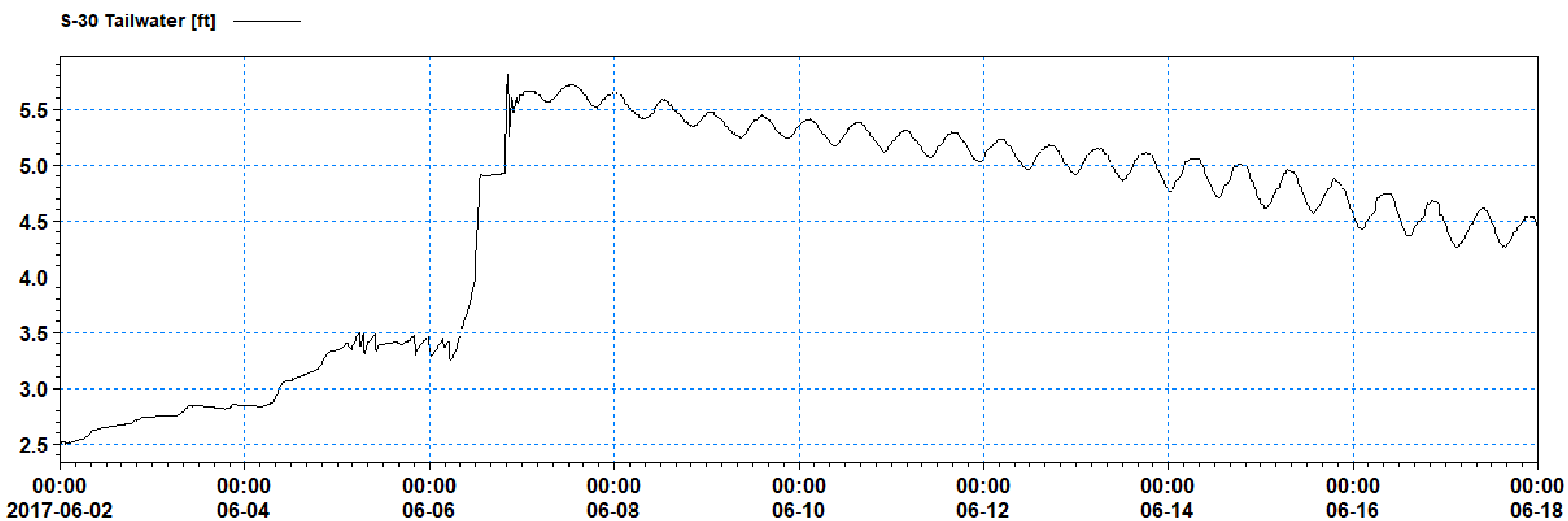

Figure A- 10: S-30 25-Year SLR2 Design Storm Tailwater Stage

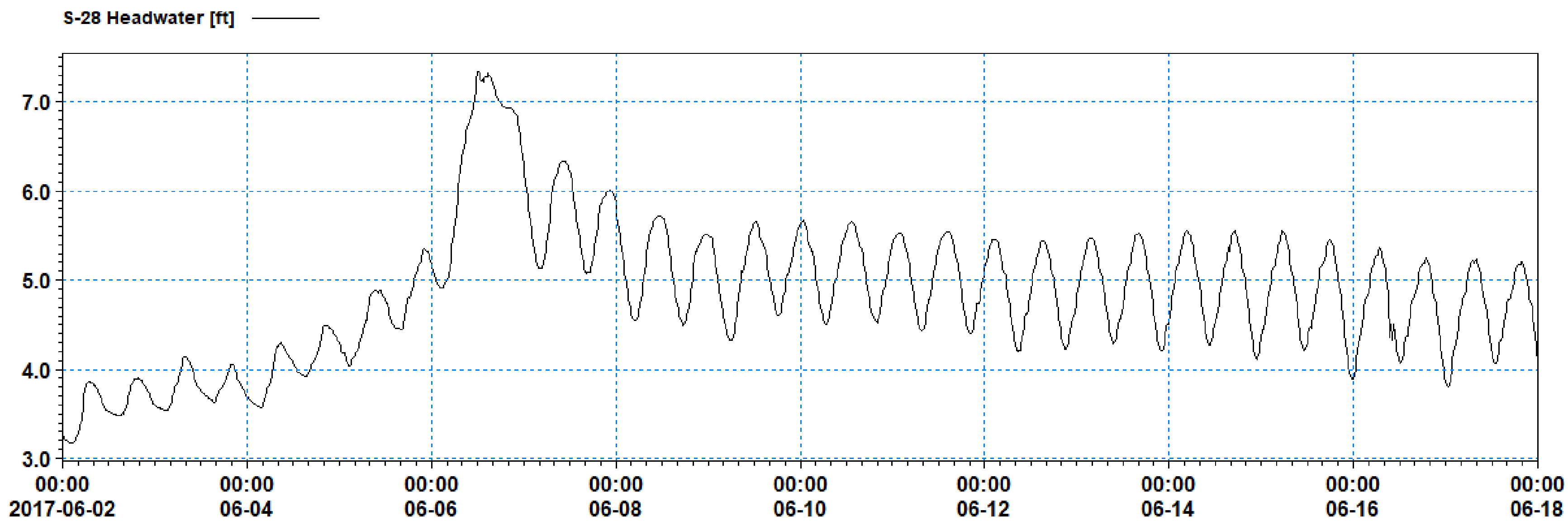

Figure A- 11: S-28 25-Year SLR3 Design Storm Headwater Stage

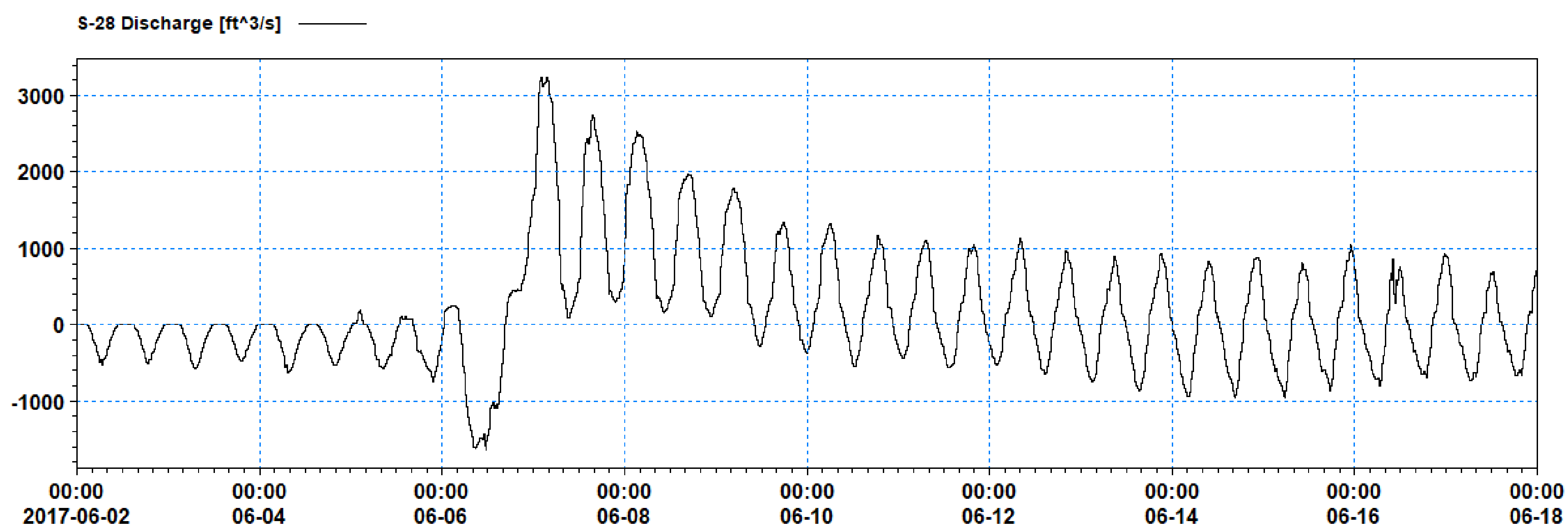

Figure A- 12: S-28 25-Year SLR3 Design Storm Discharge

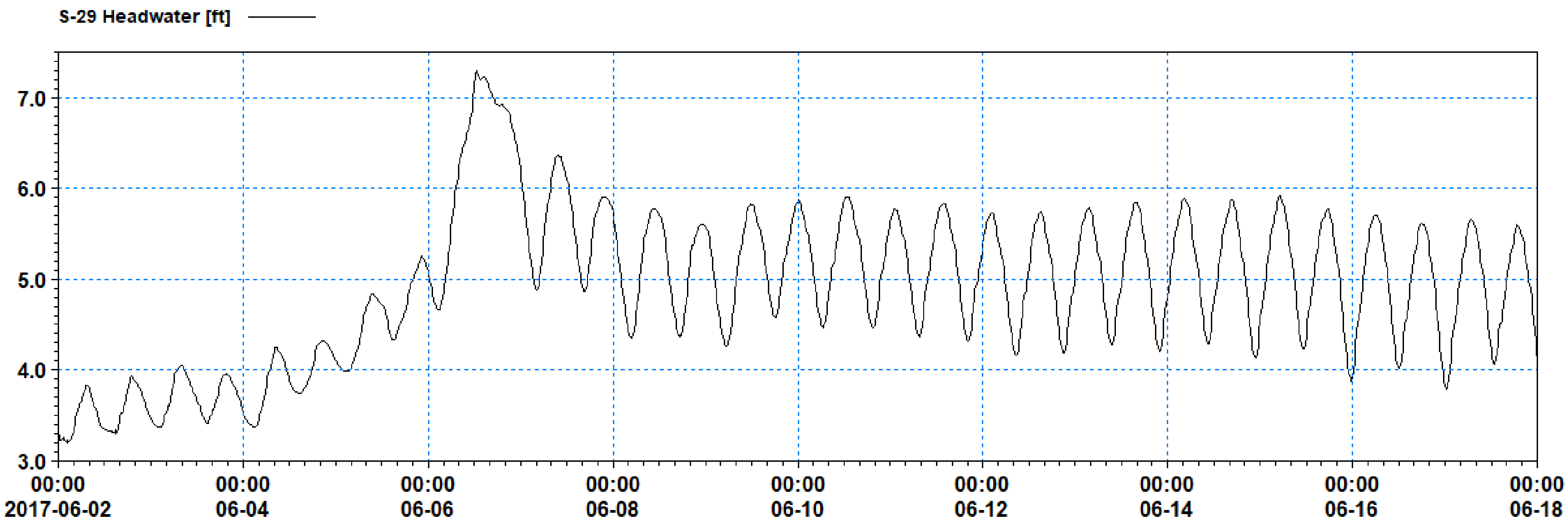

Figure A- 13: S-29 25-Year SLR3 Design Storm Headwater Stage

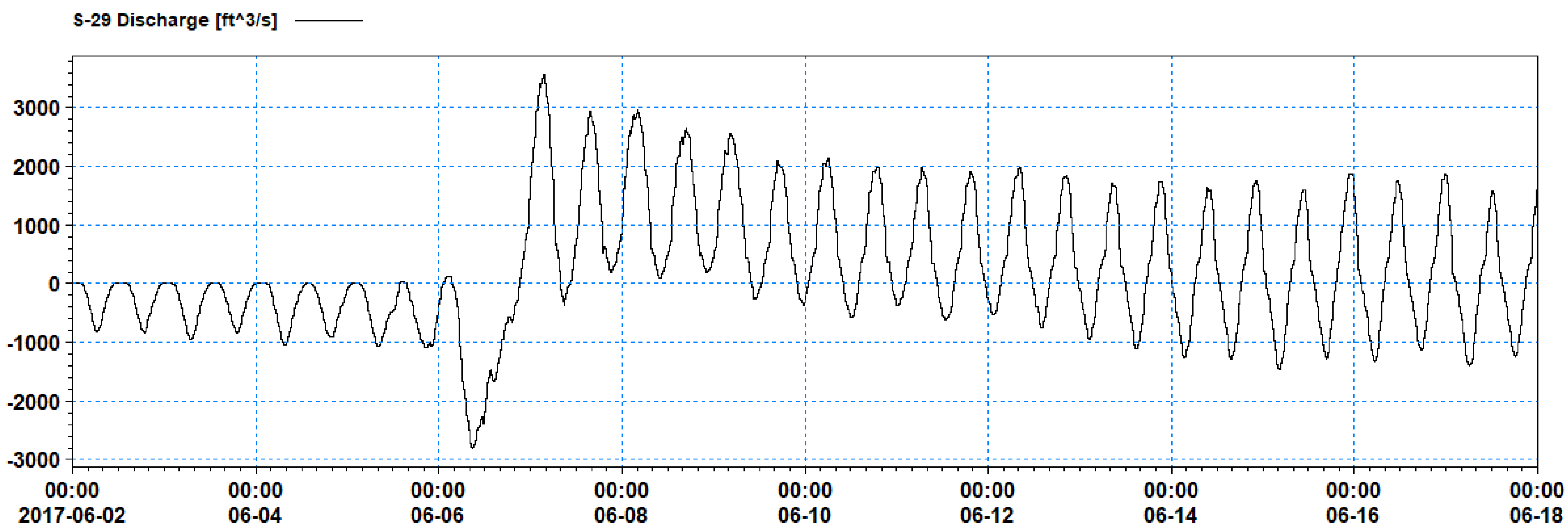

Figure A- 14: S-29 25-Year SLR3 Design Storm Discharge

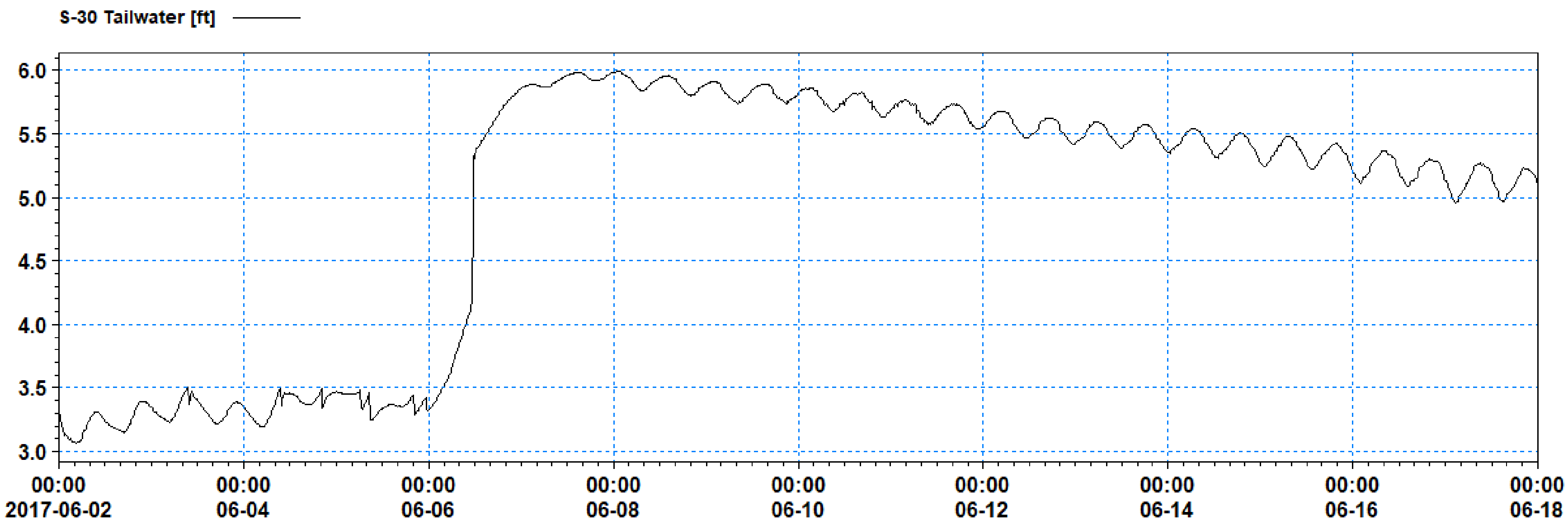

Figure A- 15: S-30 25-Year SLR3 Design Storm Tailwater Stage

Appendix B South Broward Drainage District Control Elevations and Pump-On Elevations

Per permit, here are SBDD's pump on elevations at all its stormwater pump stations:

Pump Station	CWE	Pump On Elevation	Pump Capacity	Total Allowable Q
S-1 - First Pump	2.50' NGVD	2.75' NGVD	47, 500 GPM	425 cfs (all pumps off at tailwater Elev. of 6.5' NGVD)
S-1 – Second Pump		3.00' NGVD	47, 500 GPM	
S-1 – Third Pump		3.00' NGVD	47, 500 GPM	
S-1 – Fourth Pump (spare)				
S-2 (3 pumps)	2.70' NGVD	3.30' NGVD	45,000 GPM EA.	524 cfs (S-2 & S-7 combined; pumping ceases when the C-9 Canal = Elev. 6.8' NGVD)
S-7 (3 pumps)	2.70' NGVD	3.30' NGVD	50,000 GPM EA.	524 cfs (S-2 & S-7 combined; pumping ceases when the C-9 Canal = Elev. 6.8' NGVD)
S-3 (3 pumps)	3.00' NGVD	3.60' NGVD	45,000 GPM EA.	200 cfs (pumping ceases when the C-9 Canal = Elev. 6.8' NGVD)
S-4 (2 pumps)	3.50' NGVD	4.00' NGVD	31,000 GPM	70 cfs (pumping ceases when the C-9 Canal = Elev. 6.8' NGVD)
S-5 (3 pumps)	4.00' NGVD (Sub-Basin 1) 4.25' NGVD (Sub-Basin 2) 4.50' NGVD (Sub-Basin 3)	4.50' NGVD	40,000 GPM EA.	180 cfs (pumping ceases when the C-9 Canal = Elev. 6.8' NGVD) Pumps Off at Elev 4.00' NGVD
S-8 – First Pump	3.50' NGVD	4.30' NGVD	75,000 GPM	167 cfs (from Elev. 4.3' – 4.55')
S-8 – Second Pump	3.50' NGVD	4.55' NGVD	75,000 GPM	334 cfs (from Elev. 4.55 to 5.70'; discontinue pumping when C-11 Canal = Elev. 5.7' NGVD)
S-8 – Third pump (spare)				

The pump off elevation at all pump stations is equal to the CWE unless otherwise noted. SBDD operates its pump stations such that the pumps/engines rotate and there is always one pump/engine that serves as a spare pump/engine.

Feel free to contact me with any questions.

Thanks.

Kevin Hart, P.E., CFM
District Director
South Broward Drainage District
6591 Southwest 160th Avenue
Southwest Ranches, FL 33331
954-680-3337 (office)
e-mail: kevin@sbdd.org

Figure B- 1: South Broward Drainage Control Elevations and Pump Station Information

Technical Memorandum

To: SFWMD

From: Taylor Engineering

Date: October 30, 2020

Subject: C8-C9 Potential Mitigation Strategies

Introduction

The purpose of this Technical Memorandum is to present a preliminary suite of potential flood mitigation strategies for investigation in a future phase of the C8 and C9 Flood Protection Level of Service (FPLOS) project. The focus of the mitigation strategies discussed in this memorandum is on structural improvements to the primary canals and control structures. However, improvements to the secondary conveyance systems, as well as non-structural improvements, may be contemplated in the future as complementary mitigation strategies and thus are also discussed briefly herein. No findings or opinions regarding the effectiveness, cost, or overall feasibility of any of the potential strategies are included in this document as those are topics for future analysis, beyond the scope of this document. This document is not intended to serve as an exhaustive listing of all potential mitigation strategies.

The objective of the flood mitigation strategies would be to increase the level of flood protection provided by the District's flood control infrastructure, both under current conditions and in anticipation of future conditions including land use changes and sea level rise (SLR). FPLOS for future conditions was characterized in the recently prepared Flood Protection Level of Service Provided by Existing Infrastructure for Future Sea Level Conditions in the C8 and C9 Watersheds Draft Report (Taylor Engineering, 2020).

Future analyses of the strategies discussed herein must consider several constraints including, but not limited to, the following:

- Projects intended to lower flood risk in a particular region must avoid increasing the flood risk in other places. Of particular concern are the regions downstream of the District's tidal outfall structures.
- Improvements must avoid or minimize impacts to navigation and recreation.
- Improvements must minimize impacts to sensitive habitat and listed species.
- Improvements must avoid adverse water quality impacts.
- The costs of improvements must be compared across alternatives to provide an acceptable level of flood protection at a minimum cost.

Potential Flood Mitigation Strategies for the C8 Basin

Mitigation Strategy #1: Canal Conveyance Improvements Conveyance improvements within the eastern segment of C8, downstream of its confluence with Marco Canal could help improve the current conditions FPLOS. As noted in the recent FPLOS report (Taylor, 2020), this canal segment has a number of bank exceedances, even for the more frequent (e.g., 10-year) design storm events. Dredging the C8 Canal to deepen and/or widen the cross section could reduce flood elevations and thus the frequency of bank exceedances. Although the effectiveness of this strategy would tend to diminish with increasing SLR and higher storm surge elevations, this strategy could be implemented in conjunction with mitigation strategy #2 to improve FPLOS in future SLR scenarios, which would serve to maintain manageable headwater elevations at S28.

Mitigation Strategy #2: S28 Structure Improvements Possible improvements to S28 include adding a pump station and re-building the gated structure to increase the heights of the platform and the gates in order to reduce frequency of overtopping. Tie-back levees or flood walls to tie the structure into higher ground, such as the nearby railroad embankment, would have to be a component of the structure improvements to reduce the potential for storm surge flanking the structure as shown on **Figure 1**.

Figure 1 – Potential Alignment of Tie-Back Levees for S28 structure Improvements

Mitigation Strategy #3: Flood Walls and Storm Surge Barrier Downstream of S28: Mitigation strategy #3 is somewhat similar to Mitigation strategy #2 but would be more comprehensive and could potentially provide a higher level of flood protection under the more extreme SLR and storm surge scenarios. This strategy would involve construction of a storm surge barrier (i.e., a miter gate or sector gate) downstream of S28 in the vicinity of U.S Highway 1 (Biscayne Blvd), along with a flood wall to tie the surge barrier back into high ground. According to the USACE Back Bay Study (USACE, 2020), the associated flood wall would have to be continuous with a flood wall and storm surge barrier in the C7 Watershed (**Figure 2**).

In order to be effective under the more extreme SLR scenarios, levees and/or flood walls may have to incorporate seepage barriers due to the extremely high permeability of the underlying Biscayne Aquifer. Without such barriers, the porous limestone of the Biscayne could provide a subsurface pathway for tidal waters to flow underground, seeping into the canals upstream of the floodwalls and surge barriers whenever the tides are higher than canal stages.

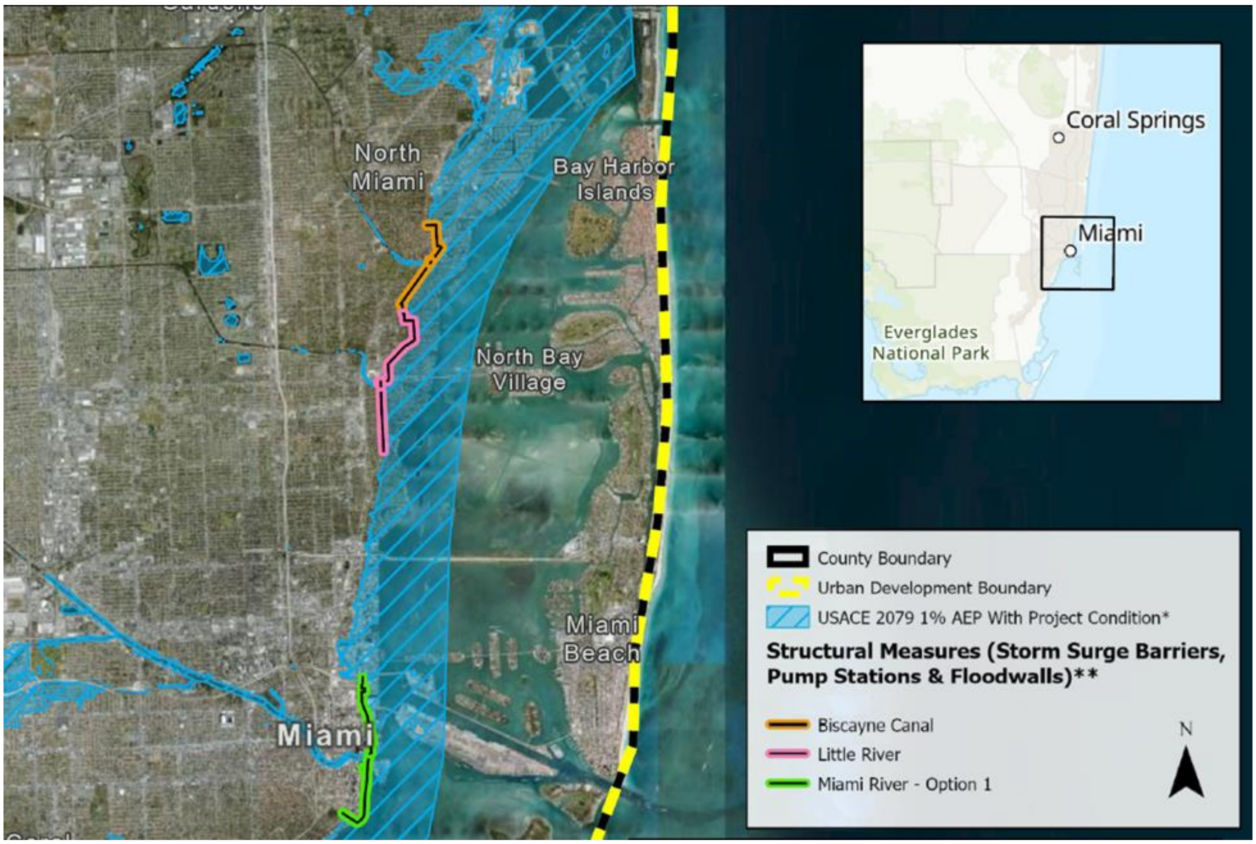

Figure 2 – Storm Surge Barriers and Flood Walls on C8, C7, and Miami River
(Adapted from USACE, 2020)

Assessing the feasibility of seepage barriers will require a detailed analysis of the site(s) geology. Seepage barriers are expected to be costly in this environment. Due to the limestone geology, sheet pile walls may not be feasible. Seepage cut-off walls could possibly be constructed using a sequence of drilled shafts or specialized bedrock-cutting equipment similar to that currently employed in the rehabilitation of the Herbert Hoover Dike (Bruce, 2009). Furthermore, this strategy may require additional seepage management infrastructure (seepage collection canals and pumps) on the inland side of the seepage barriers in order to collect and discharge fresh groundwater to tide.

Another possible refinement to this strategy would involve co-locating the surge barrier with the gated control structure (S28) and/or a forward pump station. The current plan presented in the USACE Back Bay study calls for a separate surge barrier some distance downstream of S28. If the surge barrier, rebuilt

S28, and forward pump station could all be co-located, there may be opportunities to improve the operational flexibility of the system over the current plan, such as having the ability to pump down C-8 when the surge barrier is closed. Thus the structure could serve dual purposes of conveying rainfall-induced runoff while protecting against storm surge.

Mitigation Strategy # 4: Raise levees along C-8 canal and add gates / pumps on the secondary branches. If, in the future SLR scenarios, it is no longer feasible or cost effective to maintain stages in the primary canals at acceptable levels, it may be necessary to consider raising the levees along the primary canals and constructing new gated structures and/or pumps on the secondary canals to achieve an acceptable level of flood protection. **Figure 3** shows the flood depth differences for the 25-year event with no mitigation measures (3-foot SLR minus current conditions), along with conceptual locations of potential new gated structures and pump stations on existing secondary canals at their confluence with the primary canals. Also shown on this figure are areas that currently drain directly to the primary canals. Because these areas would not be protected by improvements on secondary branches, they would require modifications to the stormwater collection system to either (a) re-route the drainage to a nearby secondary branch, or (b) re-route the drainage to new municipal pump stations (not shown). Although the extensive drainage modifications this would require may render this strategy infeasible basin-wide, this option was included for completeness or as an option to be considered for targeted areas.

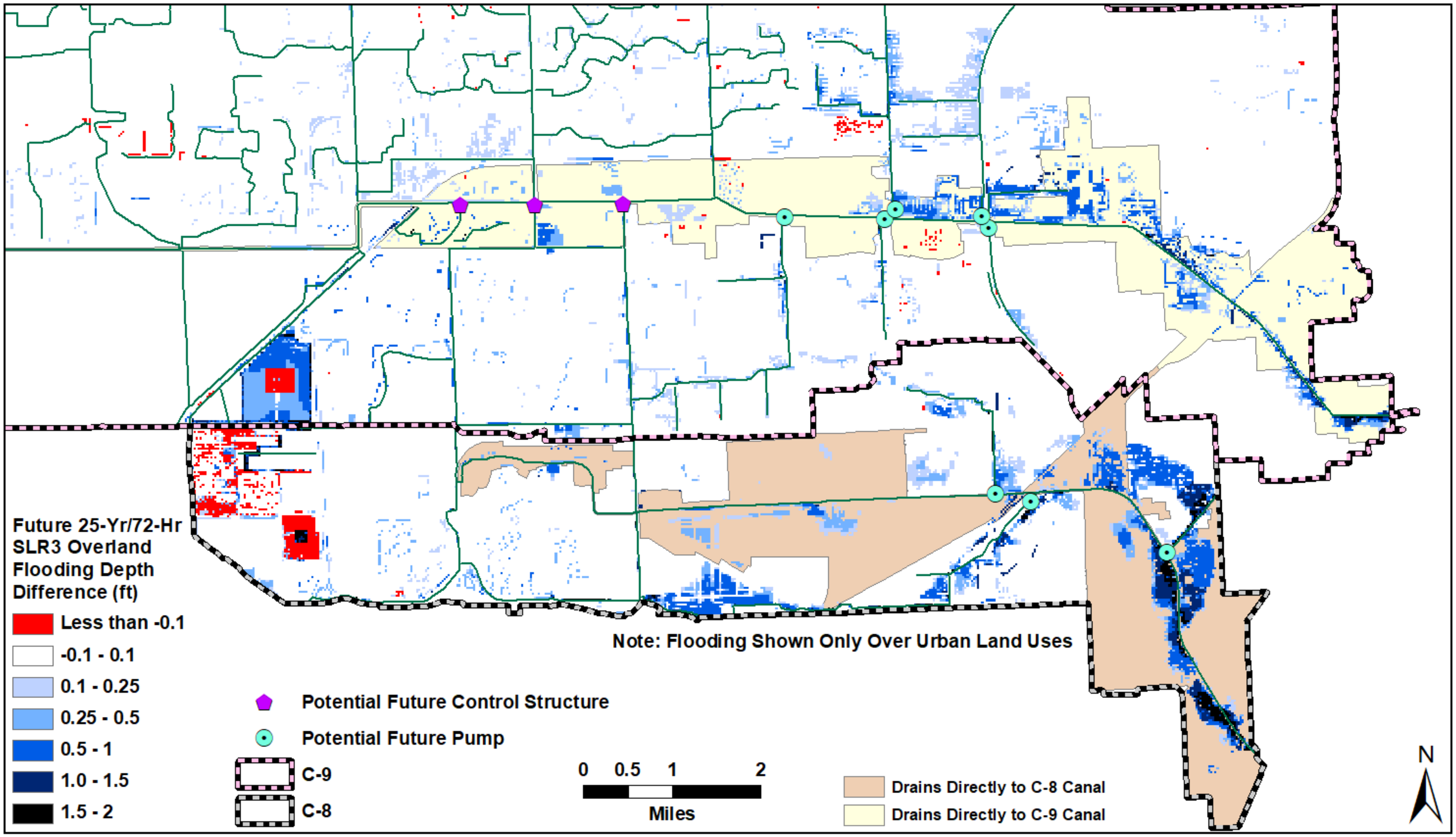

Figure 3 – Flood Difference Map (25-YR 3-ft SLR minus 25-Year Current Conditions) with Possible Locations of Future Control Structures and/or Pump Stations

Potential Flood Mitigation Strategies for the C9 Basin

Mitigation Strategy #1: Connect Western Mine Pits South of C9 Canal to the C9 Canal. This option would provide storage and attenuation of peak flood flows in the western C-9 Basin. This is currently an area of active mining. This project was identified by the USACE and SFWMD as an eventual CERP project, referred to as the North Lake Belt Storage Area. The project would be constructed after the mining operations have been completed and would complement the C9 and C11 Impoundments by providing additional storage capacity and operational flexibility (USACE and SFWMD, 2012). From Broward County (2000), the project is described as follows:

> *This component includes the construction of canals, pumps, water control structures and an in-ground storage reservoir in northwestern Miami-Dade County. The reservoir will have a storage capacity of over 29.3 billion gallons of water and will encompass approximately 4,500 acres. An underground seepage barrier around the reservoir's perimeter will enable drawdown during dry periods and prevent seepage losses. The purpose of this project is to capture and store stormwater runoff from western C-11 and C-9 Basins in Broward County and from the C-6 basin in Miami-Dade County. This will help maintain water levels in the C-9 Canal in Broward County and other canals in Miami-Dade County during the dry season.*

In addition to the benefits noted above, this strategy could have water quality benefits due to the potential for increasing residence time in the flood control system.

Mitigation Strategy #2: S29 Structure Improvements. This strategy would involve re-building the S29 structure and adding a forward pump station. The structure would be rebuilt to increase the heights of the platform and the gates in order to reduce frequency of overtopping. A levee and floodwall would be required to tie the structure into higher ground and reduce overtopping and potential for storm surge flanking the structure (**Figure 4**). This strategy would include a surge barrier on the Oleta River to the north of S29. The Oleta River barrier would cut off a potential pathway for storm surge to bypass the S29 and enter the C9 basin from the north and west through a swath of urbanized lowlands.

A more comprehensive (and more costly) version of this strategy that would provide a higher level of flood protection could also be considered for the C9 Basin. This would be similar to the strategy of flood walls and surge barriers discussed as Mitigation Strategy #3 for the C8 Basin.

Mitigation Strategy # 3: Raise levees along C-9 Canal and add gates / pumps on the secondary branches. This strategy is similar to mitigation strategy #4 in the C-8 basin. If, in the future SLR scenarios, it is no longer feasible or cost effective to maintain stages in the primary canals at acceptable levels, it may be necessary to consider raising the levees along the primary canals and constructing new gated structures and/or pumps on the secondary canals to achieve an acceptable level of flood protection. Referring again to **Figure 3,** conceptual locations of potential new gated structures and pump stations on existing secondary canals at their confluence with C-9. As in C-8, areas draining directly to C-9 would not be protected by improvements on secondary branches, and would require additional modifications to the stormwater collection systems to either (a) re-route the drainage to a nearby secondary branch, or (b) re-route the drainage to new municipal pump stations (not shown). Although the extensive drainage modifications this would require may render this strategy infeasible basin-wide, this option was included for completeness or as an option to be considered for targeted areas.

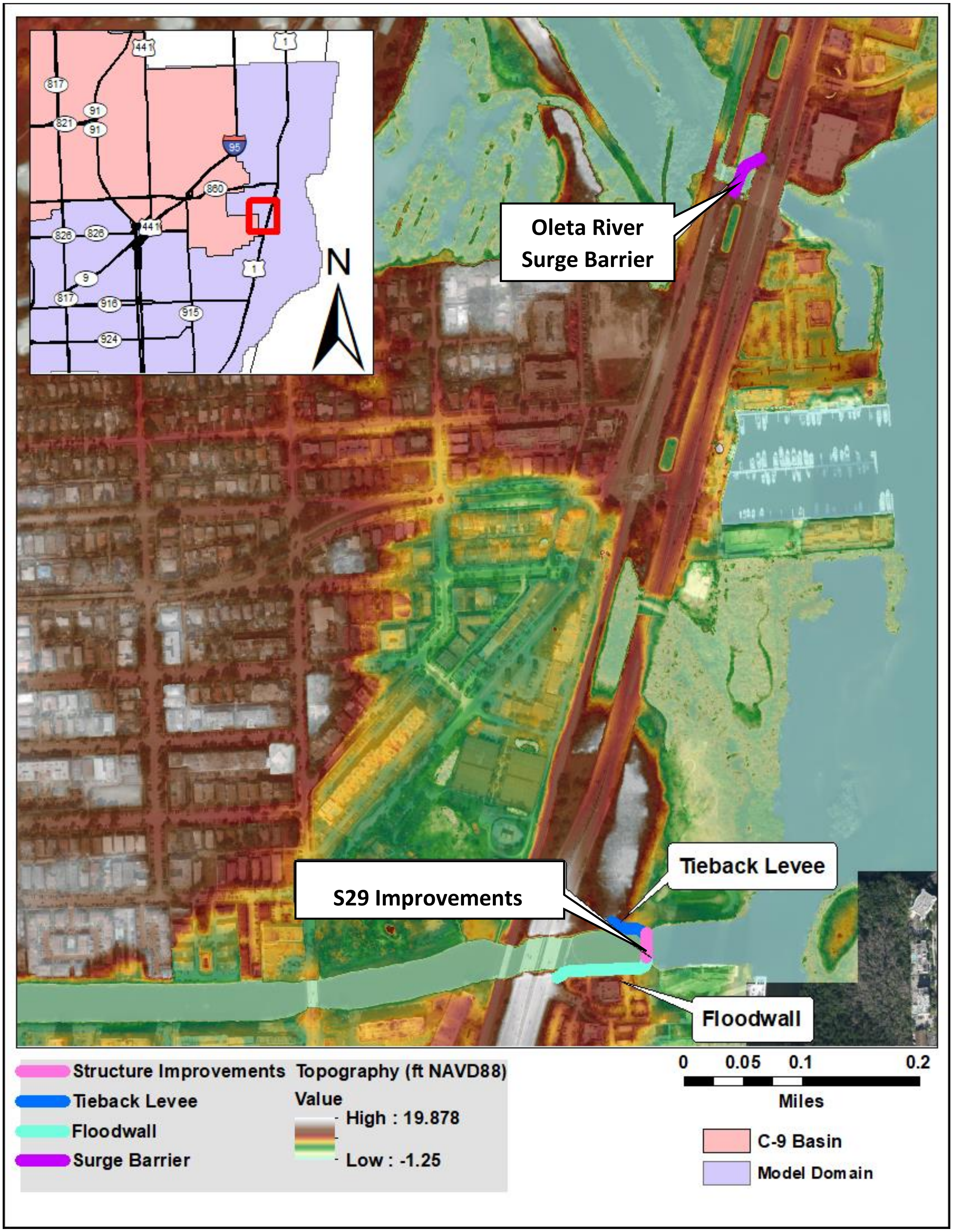

Figure 4 – Locations of S29 Improvements and Potential Oleta River Surge Barrier

Mitigation Strategy #4: Increase Connectivity Between C-9 and C-11: This strategy was identified by the South Broward Drainage District (SBDD) as a way to increase operational flexibility. In particular, enlarging the Silver Lake Control Structure would facilitate the movement of water into C-11 Basin from SBDD S5 Basin or vice versa depending on relative water levels within the two canals.

Non-Structural and Nature-Based solutions

The strategies discussed above could be implemented independently or in conjunction with non-structural measures and nature-based features to help further reduce flood risk within both the C-8 and C-9 basins. These may include, but are not limited to, the following:

- A flood warning system, to include real-time flood forecasting. This could buy time for evacuations and pre-storm drawdown of canals and lakes.
- Elevating, floodproofing, or acquiring and demolishing the most flood-susceptible structures
- Elevating roads
- Green infrastructure / low-impact development (LID) to increase infiltration, slow runoff, and improve water quality
- Nature based solutions (e.g., mangroves, dunes, and living shorelines) – For example, Taylor Engineering in coordination with the USACE, Jacksonville District (2018) utilized the 3-dimensional ADCIRC-SWAN Model to simulate coastal storm risk benefits of mangrove vegetation and dune restoration in Miami-Dade County. An array of potential storm forcing conditions were simulated to assess the effects of mangrove effects to storm surge-induced water heights. This study documented how mangroves can attenuate storm surge heights (from approximately 0.5 to 1.5 feet) along area of the shoreline and interior areas in Biscayne Bay.

References

Broward County, 2000. A Rationale for Supporting the Comprehensive Everglades Restoration Plan (C&SF Restudy), Staff Report to the Water Advisory Board through the Technical Advisory Committee.

Taylor Engineering Inc. 2018. ADCIRC Storm Event Modeling for the Miami-Dade County Surge Study. Draft Report Prepared for the U.S. Army Corps of Engineers, Jacksonville District.

Taylor Engineering, Inc., 2020. Flood Protection Level of Service Provided by Existing Infrastructure for Future Sea Level Conditions in the C8 and C9 Watersheds, Draft Report. Prepared for SFWMD.

USACE and SFWMD, 2012. Central and Southern Florida Project, Broward County Water Preserve Areas Revised Final Integrated Project implementation Report and Environmental Impact Statement.

USACE, 2020. Miami-Dade Back Bay Coastal Storm Risk Management Draft Integrated Feasibility Report and Programmatic Environmental Impact Statement, Draft Feasibility Study.